1001

Osteoblastic Oxygen Sensing Prolyl Hydroxylases Regulate Bone Homeostasis by Controlling both Osteoclastogenesis and Angiogenesis. Colleen Wu*[1], Erinn Rankin[1], Edward LaGory[1], Rebecca Andersen[1], Steven Rhodes[2], Tremika Wilson[3], Khalid Mohammad[3], Alesha Castillo[4], Theresa Guise[3], Ernestina Schipani[3], Amato Giaccia[2]. [1]Stanford University, USA, [2]Indiana University Medical School, USA, [3]University of Michigan, USA, [4]VA Palo Alto Health Care System, USA

The osteoblastic niche houses cells of osteoblastic and hematopoietic lineages across varying oxygen tensions. However, the contribution of this oxygen gradient to bone homeostasis is poorly understood. The prolyl hydroxylase enzymes (PHD 1-3) are oxygen sensors, which control hypoxic signaling. To elucidate the role of these crucial oxygen-sensing enzymes in the osteoblastic niche, we generated knockouts of each PHD isoform and isoform combination within osteoblasts. Using these genetic mouse models we demonstrate that PHD enzymes act as a molecular rheostat of HIF activation to differentially regulate two important aspects of bone physiology; cross talk between osteoblasts and osteoclasts and osteogenic/angiogenic coupling. Combined inactivation of Phd2 and Phd3 within osteoblasts leads to augmented synthesis and secretion of OPG resulting in a subsequent decrease in osteoclast numbers and an increase in trabecular bone volume. Unexpectedly, these changes in bone homeostasis were not associated with HIF- mediated neo-angiogenesis as vascular density was not altered in PHD2 and PHD3 deficient mice. Genetic deletion of Hif-2α caused the complete abrogation of PHD2 and PHD3 mediated suppression of bone turnover whereas constitutive activation of Hif-2α within osteoprogenitor cells phenocopied mice lacking functional osteoblastic PHD2 and PHD3. Thus, HIF-2α was both necessary and sufficient for osteoblast-mediated inhibition of osteoclastogenesis. In contrast, genetic loss of all three PHD isoforms in osteoblasts resulted extreme HIF signaling activation, leading to a series of deleterious effects including aberrant hematopoiesis, and extreme blood vessel formation associated with an excessive augmentation of trabecular bone volume. Importantly, loss of Phd2 and Phd3 protected ovariectomized mice against bone loss by normalizing the OPG to RANKL ratio. Taken together, we identify a previously unknown relationship between PHD/HIF signaling and RANK/RANKL/OPG axis, revealing a role for PHD/HIF signaling in the regulation of bone homeostasis that is independent of angiogenesis. Our findings have important clinical implications as the OPG/RANK/RANKL signaling axis is a key molecular driver of pathological bone loss and we demonstrate that precise regulation of hypoxic signaling through the selective rather than collective inactivation of PHD isoforms is required to modulate OPG to protect against osteoporosis and prevent potential tissue toxicity.

Disclosures: Colleen Wu, None.

1002

Vascular Smooth Muscle Cell LRP6 Inhibits Noncanonical Wnt Signaling and Arteriosclerotic Calcification In Diabetic LDLR-/- Mice. Su-Li Cheng[1], Bindu Ramachandaran[1], Abraham Behrmann[1], Jian-su Shao[2], Karen Krchma[1], Megan Mead[1], Lawrence Brill[1], Bart Williams[3], Dwight Towler*[4]. [1]Sanford-Burnham Medical Research Institute, USA, [2]MD Anderson Cancer Center, USA, [3]Van Andel Research Institute, USA, [4]Sanford-Burnham Medical Research Institute, USA

Msx-Wnt signaling regulates osteogenic differentiation during bone formation and the arterial calcification of type 2 diabetes. The canonical Wnt co-receptors LRP5 and LRP6 play overlapping roles in bone; however, contributions to vascular disease are poorly understood. Therefore, we generated SM22-Cre;LRP6(fl/fl);LDLR-/- mice to ablate the LRP6 gene in the vascular smooth muscle cell (VSMC) lineage of LDLR-/- mice – a background susceptible to high fat diet (HFD) -induced vascular calcification. As compared to LRP6(fl/fl);LDLR-/- controls, SM22-Cre;LRP6(fl/fl);LDLR-/- sibling cohorts exhibited significantly increased aortic calcification following 3 months of HFD-challenge (1.3-fold; p =0.002). No differences were noted in body composition, blood glucose, or lipids. Pulse wave velocity, an index of vascular stiffness, was increased by LRP6 deficiency. This paralleled increases in aortic and circulating osteopontin (OPN), a matrix cytokine that regulates arteriosclerotic disease. Survey of Wnt ligand and Fzd receptor expression in LRP6-deficient aortas revealed upregulation of Wnt7b and Wnt4 – two ligands supporting noncanonical signaling – along with Fzd10. Western blot and immunohistochemistry confirmed Wnt7b and Fzd10 protein accumulation. To better understand signaling mechanisms, we transfected HEK293T cells with OPN promoter – luciferase reporter constructs, mapping regulatory responses to LRP6 and Fzd10. Fzd10 expression significantly upregulated OPN promoter activity, and localized to a regulatory element between -135 and -45 relative to the start site of transcription. Induction was augmented by Wnt7b and Wnt5a, and completely inhibited by co-expression of LRP6. Fzd10 induction of NFAT-dependent transcription, a hallmark of noncanonical calcium signaling, was also inhibited by LRP6 and independent of LRP6 structural motifs required for canonical signaling. Using mass spectroscopy, complexes containing LRP5 and specific members of the protein arginine methyl transferase (PRMT) family were found to interact with LRP6. The nuclear-cytoplasmic distribution of PRMTs and arginine methylation were perturbed in LRP6-deficient aortas, and co-expression of specific PRMT family members differentially regulated LRP6-inhibited OPN promoter activity. Thus, loss of aortic LRP6 upregulates expression of noncanonical Wnt ligands, receptors, and signals in VSMCs, driving the expression of prosclerotic gene regulatory programs via PRMT-modulated relays.

Disclosures: Dwight Towler, None.

1003

Direct Transformation of Chondrocytes to Bone and Vessel Cells in Patients with Osteoarthritis (OA). Yan Jing*[1], Yinshi Ren[2], Baozhi Yuan[3], Joseph Borrelli[4], Yin Xiao[5], Ying Liu[2], Chuanju Liu[6], Ding Bai[7], Jian Feng[8]. [1]USA, [2]Texas A&M Baylor College of Dentistry, USA, [3]University of Wisconsin, USA, [4]Texas Health Physicians Group, Arlington, TX, USA, [5]Institute of Health & Biomedical Innovation, Queensland University of Technology, Brisbane, Australia, Australia, [6]New York University, USA, [7]State Key Laboratory of Oral Diseases (Sichuan University), Department of Orthodontics, West China Stomatology Hospital of Sichuan University, China, [8]Texas A&M Health Science Center, USA

Although OA is the most common degenerative skeletal disorder, there has been an intensive ongoing debate regarding the initial site of the disease: articular cartilage or subchondral bone. One commonly-held belief is that some chondrocytes directly form bone without going through endo-chondrogenesis, which is accelerated in OA, leading to osteosclerosis. To test this hypothesis, we use an immunostain assay to initially demonstrate that DMP1, a matrix protein highly expressed in osteocytes, is expressed in hypertrophic chondrocytes and osteocyte (Ocy)-like cells in calcified cartilage (Fig a). These Ocy-like cells remain in their original cartilage lacunae and distribute in pairs. Acid-etched SEM images in mice reveals that these directly-formed Ocys are round in shape with few dendrites lying on cement line (Fig b). The cell lineage tracing results from crossing Aggrecan-Cre[ER] & Rosa 26-lacZ mice demonstrate that the chondrocytes in the articular cartilage directly transform into bone cells (Fig c). We also obtain mRNAs from a 5-mon-old pig's non-calcified, calcified cartilage and subchondral bone respectively using laser capture technique. The quantitative RT-PCR data shows much higher levels of ALP (28- or 12.5-fold), TRAP (5.9- or 3.4-fold), and OSX (4.6- or 5-fold) in calcified cartilage compared to non-calcified cartilage and subchondral bone separately, indicating hypertrophic chondrocyte can remove mineral and future transform to bone cells. Finally, we extend the animal studies to directly address whether the above finding has clinical relevance in OA patients. Using FITC-confocal imaging techniques, we show sharp increased Ocy-like cells in calcified cartilage matrix from OA knee samples, which are round in shape with short deformed dendrites (Fig d). The combined histological (H&E, Safranin O and SEM) images show bone-like islands in non-calcified and calcified areas, which have no direct link with subchondral bone (Fig e-f). In those cartilage surrounded bone islands, some of Ocys are in paired and some of them directly surrounded by hypertrophic chondrocytes. Interestingly, some chondrocytes are TRAP positive and express VEGF and α-SMA, suggesting they can remove matrices and participate in angiogenesis (Fig g-i). Based on the above findings, we conclude that at least some of chondrocytes directly transform into Ocys in the normal articular cartilage, which is greatly accelerated in OA patients (Fig j). (Work supported by NIH DE018486 to JQF)
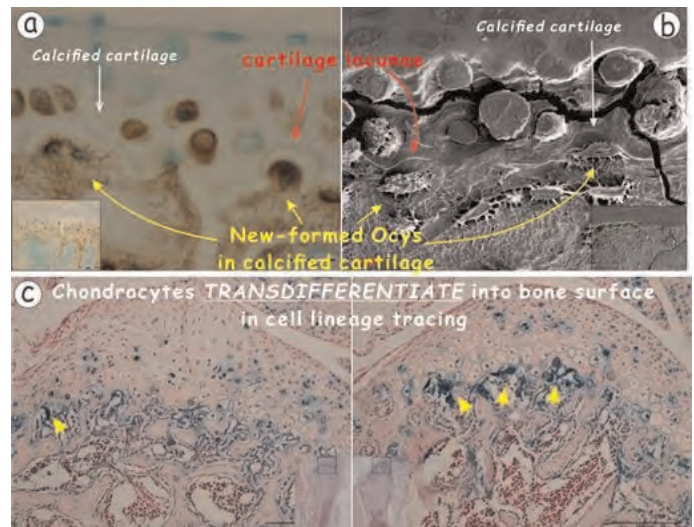

Fig a-c

Fig d-f

Fig g-i

Fig j

Disclosures: Yan Jing, None.

1004

Roles of Osteoblast-derived VEGF in Osteoblastic Differentiation and Bone Formation During Bone Repair. Kai Hu*[1], Bjorn Olsen[2]. [1]Harvard School of Dental Medicine, USA, [2]Harvard School of Dental Medicine, USA

Vascular endothelial growth factor (VEGF) plays pivotal roles in the communication between blood vessels and bone cells during bone turnover and repair. However, the precise mechanisms are not fully elucidated. To examine roles of osteoblast-derived VEGF in bone repair, a tibial monocortical defect (0.8 mm hole) was made in mice with Vegfa deleted from osteoblast precursors (Osterix-cre; Vegfa flox/flox, CKO mice) and WT littermates (Vegfa flox/flox). At D3 after surgery, CKO mice exhibited reduced numbers of vessels and macrophages. Strong correlation (R^2=0.877) between vessel density and macrophage number indicated that VEGF may be required for macrophage-mediated angiogenesis. At D7, intramembranous ossification (IO) occurred at injury holes while endochondral ossification (EO) was observed in the wounded periosteum. Within the injury hole, μCT showed less mineralization in CKO than in WT mice ($1.98 \pm 0.79\%$ vs. $10.74 \pm 2.47\%$ (BV/TV)), and aniline blue staining indicated reduced collagen accumulation ($17.56 \pm 2.56\%$ vs. $37.99 \pm 2.35\%$ (collagen area/total area)). Decreased mineralization/collagen ratio ($11.56 \pm 3.51\%$ vs. $30.45 \pm 6.6\%$) also suggested a delay in osteoblast maturation, in further support of compromised IO. To probe cellular mechanisms of IO in this injury model, a Cre-induced transgene, ZsGreen, was introduced. Although the number of ZsGreen+ cells, representing osteoblast precursors and their descendants, was not reduced at injury sites in CKO mice at D7, bone sialoprotein (BSP) and osteocalcin (OCN) levels were greatly decreased. In addition, CKO mice exhibited fewer blood vessels, and the vessel density was positively correlated with BSP and OCN levels. This suggested an association between angiogenesis and osteoblast differentiation. In areas of periosteal EO, WT mice showed gradual degradation of cartilage and recruitment of osteoclasts and blood vessels. In contrast, CKO mice exhibited delayed replacement of cartilage by bone. At D28, a new cortical layer appeared outside the original bone collar in both WT and CKO mice. A decrease in the callus thickness and bone volume in CKO mice, of $47.19 \pm 15.43\%$ and $55.44 \pm 6.23\%$, respectively, indicated a reduction in remodeling capability. In summary, VEGF produced in osteoblastic lineage cells is required at various stages of bone repair. The findings add to the understanding of VEGF functions and may contribute to the development of novel strategies to improve bone repair and regeneration.

Disclosures: Kai Hu, None.

1005

Erythropoietin reduces bone formation and stimulates bone resorption: new insights into endocrine regulation of bone remodeling. Sahar Hiram-Bab*[1], Tamar Liron[2], Naamit Deshet-Unger[3], Avi Salamon[2], Moshe Mittelman[4], Max Gassmann[5], Kristin Franke[6], Martina Rauner[7], Ben Wielockx[8], Drorit Neumann[3], Yankel Gabet[9]. [1]Department of Cell & Developmental Biology, Sackler Faculty of Medicine, Tel Aviv University, Israel, [2]Department of Anatomy & Anthropology, Sackler Faculty of Medicine, Tel-Aviv University, Israel, [3]Department of Cell & Developmental Biology, Sackler Faculty of Medicine, Tel-Aviv University, Israel, [4]Department of Medicine, Tel Aviv Sourasky Medical Center, Sackler Faculty of Medicine, Tel-Aviv University, Israel, [5]Institute for Veterinary Physiology, Vetsuisse Faculty & Zurich Center for Integrative Human Physiology (ZIHP), University of Zurich, Switzerland, [6]Institute of Pathology, Technische Universität Dresden, Germany, [7]Medical Faculty of the TU Dresden, Germany, [8]Institute of Pathology, Dresden University of Technology, Germany, [9]Department of Anatomy & AnthropologySackler Faculty of Medicine, Israel

The negative effect of hypoxia on bone metabolism is well established but its mechanism of action is not fully understood. Hypoxia triggers the production of erythropoietin (EPO), a hormone most recognized for its hematopoietic function. An increasing number of roles unrelated to red blood cell production, have been attributed to EPO, many of which are mediated by non-erythroid cells. In light of the controversy on the effect of increased serum levels of EPO on the skeleton, we investigated here the effect of the hormone on bone metabolism using EPO overexpressing (Tg6), and EPO-administered adult mice. In these models, the increase in EPO levels is similar to its physiologic increase at high altitude. Using microcomputed tomography, histology and serum markers we found that high EPO levels result in a severe trabecular bone loss, due to increased bone resorption and reduced bone formation. This bone loss consisted of reduced trabecular number, but not thickness, with no effect on the cortical bone compartment. A similar bone response was observed with high and low doses, with no difference between intermittent and continuous administration modes. Using FACS and specific surface markers, we found that EPO targets the monocytic lineage by increasing the number of monocytes/macrophages, pre-osteoclasts and mature osteoclasts in bones. In contrast with the attenuation of bone formation in vivo, EPO treatment in vitro did not inhibit osteoblast differentiation and activity, as demonstrated by RT-qPCR of marker genes and mineralization assays. However, EPO strongly stimulated osteoclastogenesis (TRAP staining) and pit resorption (measured in calcium-phosphate-coated wells) in a cell-autonomous manner. Furthermore, our data
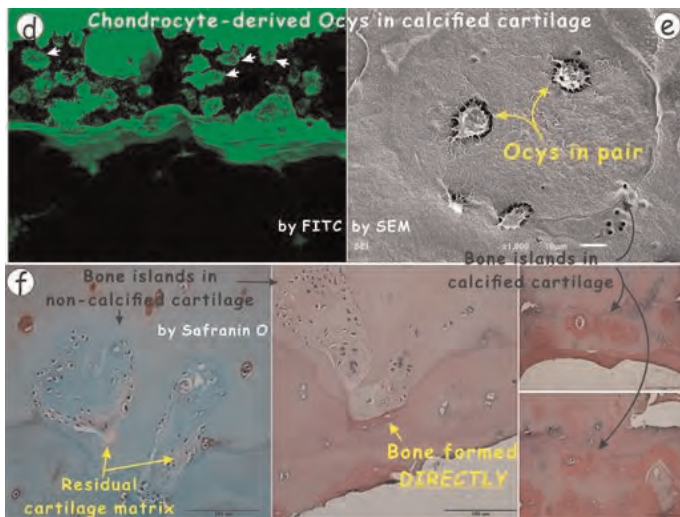
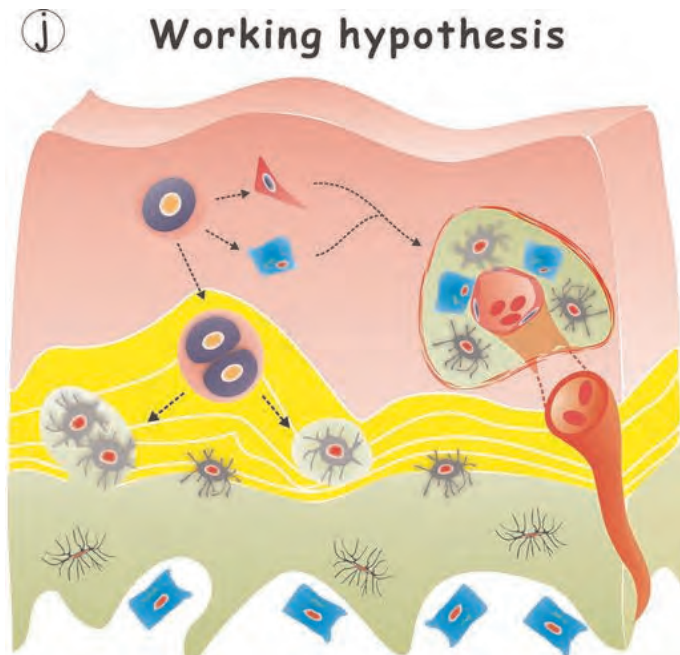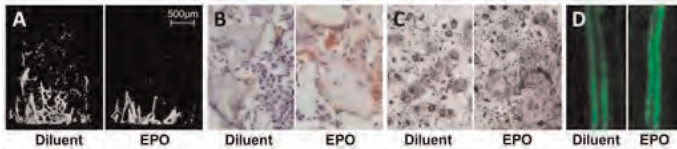indicate that EPO receptor signaling in osteoclast precursors involves the Jak2 and PI3K pathways, but is independent of the MAPK/MEK pathway. These findings demonstrate that EPO strongly regulates bone mass by stimulating osteoclastogenesis and propose a new mechanism for hypoxia-induced bone loss.

EPO induced trabecular bone loss (A, micro-CT), by stimulating osteoclastogenesis in vivo (B, histology) and in vitro (C, TRAP), and by attenuating bone formation (D, calcein-labeled histology).

Figure

Disclosures: Sahar Hiram-Bab, None.

1006

Loss of *Nf1* in Osteoprogenitors Affects Fracture Resistance at Multiple Levels of Bone Organization. Mathilde Granke*[1], Jean de la Croix Ndong[2], Sasidhar Uppuganti[2], Guillaume Vignaux[2], Alexander Makowski[3], Daniel Perrien[1], Florent Elefteriou[2], Jeffry Nyman[1]. [1]Vanderbilt University Medical Center, USA, [2]Vanderbilt University, USA, [3]Department of Veterans AffairsVanderbilt University, USA

Mutations in the *NF1* gene can cause skeletal abnormalities, including tibial bowing, fracture and pseudarthrosis. The reason why fractures occur in NF1 children remains unclear, in part because previous mouse models, based on *Nf1* ablation in the early mesenchymal lineage, are characterized by severe development phenotypes that complicate the interpretation of the bony phenotypes observed. In this study, we used inducible Tet[off]-based *Osx*-cre transgenic mice crossed to *Nf1*[flox/flox] mice (*Nf1*$_{Osx}$[-/-]) to assess how post-natal ablation of *Nf1* in osteoprogenitors affects bone's fracture resistance.

At 2 weeks of age, repression of cre activity was stopped by withdrawal of doxycycline from the drinking water, leading to *Nf1* ablation in post-natal osteoprogenitors. Mice were euthanized at 6 wks, 14 wks, and 34 wks of age (n≥7/age/genotype). Femoral midshafts were i) scanned with μCT to obtain tissue mineral density (TMD), porosity, and cortical thickness; ii) analyzed with ^{1}H NMR to assess bound water; and iii) subjected to 3pt bending to estimate strength and modulus. Reference point indentation (BioDent, 10 cycles at 0−2N) was performed on the tibiae (5 indents with 500μm spacing on the anterior side opposite to the tibiofibular junction) to obtain average creep indentation (avCID) and average loading slope (avLS).

Nf1 ablation in post-natal osteoprogenitors did not affect stature but inhibited the age-related increase in bone strength, with structural and material strength being significantly lower in *Nf1*$_{Osx}$[-/-] compared to WT mice at 34 wks (Fig). Compared to WT, *Nf1*$_{Osx}$[-/-] mice also had a thinner cortex and higher porosity at 34 wks (Fig). At the material level, *Nf1* deletion also impeded the age-related increase in TMD (Fig). Similarly, indentation resistance declined less in *Nf1*$_{Osx}$[-/-], with the probe tip penetrating deeper (higher avCID, lower avLS) in *Nf1*$_{Osx}$[-/-] compared to WT bone tissue (Fig). Finally, water bound to the matrix decreased from 6 to 14 wks of age in both genotypes, and was less in *Nf1*$_{Osx}$[-/-] versus WT bone at 34 wks of age (Fig).

Similar to observations from NF1 patient biopsies, loss of *Nf1* from osteoprogenitors in mice causes increased porosity and decreased mineralization. This study shows that this translates into a loss in fracture resistance at different levels of bone organization (structural and tissue), thus providing useful parameters to predict bone alteration in children with NF1, prior to overt bone bowing and fracture.

a: different from 6 wk; b: different from 14 wk
#: different from WT
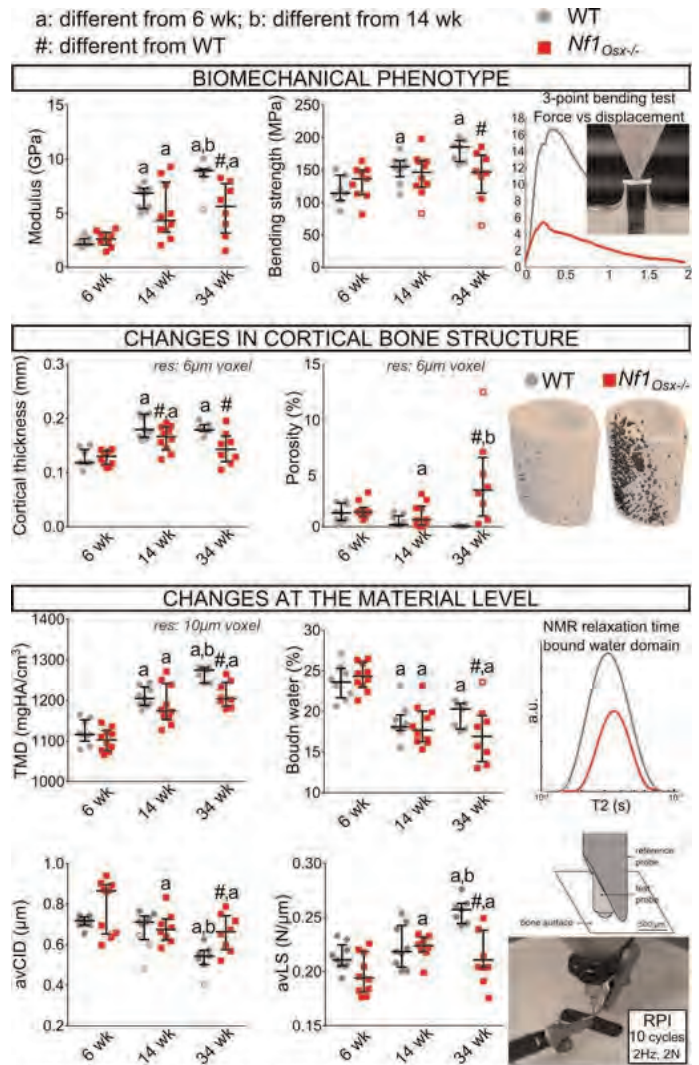
Bars represent the median with interquartile range. Outliers (as defined by the Thompson Tau method) are open symbols.

Fig

Disclosures: Mathilde Granke, None.

1007

Mechanical Signals Improve Bone Quality Compromised by Type 2 Diabetes, Potentially by Enhancing the Bone Marrow Mesenchymal Stem Cell Population and its Paracrine Regulation of Bone-forming Osteoblasts. M. Ete Chan*[1], Gregory Lee[1], Danielle Green[1], Benjamin Adler[1], Gabriel Pagnotti[1], Vihitaben Patel[1], Clinton Rubin[2]. [1]Stony Brook University, USA, [2]State University of New York at Stony Brook, USA

Type 2 diabetes (T2D) is clinically linked to an increased bone fracture risk. Previous studies have shown that low intensity vibration (LIV), acting as a surrogate for the mechanical components of exercise, significantly improves bone quality, an outcome associated with increased bone marrow mesenchymal stem cell (MSC) populations. However, it is not known if these stimuli can modulate bone in a model of T2D, or if these signals will influence the lineage selection of MSC in T2D model. Combining *in vivo* and *in vitro* approaches, this study investigates (1) the impact of LIV on bone mechanical strength in T2D, and (2) the role of MSCs, by themselves and in relation to other bone marrow cells, in responding to LIV. Using a murine model of T2D in an 8-week study, thirty 5w old male C57BL/6J mice were divided into 3 groups (n=10): regular diet (RD; 10kcal% fat), high fat diet (HF; 45kcal% fat) and high fat diet with LIV (HFv). LIV was delivered via a vertically oscillating plate (30min/day, 5 day/wk at 90Hz and 0.2g) to HFv, while HF and RD were sham-handled. Biomechanical testing showed that while the tibiae of HF had lower stiffness (-22%) and elastic modulus (-45%) than RD (p=0.03), LIV increased these properties in HFv by +27% and +108%, respectively, as compared to HF (p=0.02). LIV also increased cortical thickness (+2.1%, p=0.009) and bone marrow MSC populations (+53%, p<0.05). The effect of LIV on MSC proliferation was examined with isolated MSC (2,500 cells/1.9cm^2) in two groups (n=4): While one group received 30min of LIV, another group was sham handled (control). After 48hrs, the vibrated MSCs

proliferated 177% more than the non-vibrated MSCs (p=0.04). Further, conditioned medium from vibrated and non-vibrated MSCs were transferred to a distinct set of osteoblasts (OBs) (n=4). OBs with conditioned media from vibrated MSCs proliferated 70% more than the OB receiving control medium (p=0.03), implicating that signaling molecules secreted by MSCs modulated OB proliferation. In summary, T2D, induced by a high fat diet, compromised bone mechanical properties, while LIV improved mechanical strength despite T2D. The salutary impact of these mechanical signals may, in part, be achieved directly by increasing MSC proliferation, and indirectly via paracrine promotion of bone-forming OBs to promote osteogenesis.

Disclosures: M. Ete Chan, None.

1008

N-cadherin Restrains Parathyroid Hormone (PTH) Activation of Lrp6/β-catenin Signaling and Its Bone Anabolic Action. <u>Leila Revollo</u>*[1], <u>Jacqueline Kading</u>[2], <u>Jiemin Li</u>[2], <u>Sung Yeop Jeong</u>[2], <u>Gabriel Mbalaviele</u>[3], <u>Roberto Civitelli</u>[3]. [1]Washington University, Division of Bone & Mineral Diseases, USA, [2]Washington University, USA, [3]Washington University in St. Louis School of Medicine, USA

Formation of a complex between parathyroid hormone (PTH), PTH/PTHrP 1 receptor (PTH1R), and Lrp6 has been linked to PTH signaling and anabolic action. Since N-cadherin regulates canonical Wnt/β-catenin pathway by interacting with Lrp5/6 via axin, we hypothesized that N-cadherin may also modulate PTH signaling and osteoanabolic action by interfering with Lrp6. We tested this hypothesis in N-cadherin-ablated bone marrow stromal cells (BMSC) from mice with a selective deletion of the N-cadherin gene (*Cdh2*) in osteoprogenitors (*Cdh2$^{flox/flox}$::Osx-Cre; cKO*). Co-immunoprecipitation experiments using control BMSC from *Cdh2$^{flox/flox}$ mice* showed that PTH1R interacts with Lrp6, but not Lrp5 nor N-cadherin. This interaction was enhanced by exposure to PTH$_{1-34}$ in *cKO cells,* but not in control. In BMSC and MC3T3-E1 cells, PTH$_{1-34}$ promoted PKA-dependent β-catenin stabilization via C-terminus phosphorylation (S675), and Tcf/Lef transcriptional activity. PTH-induced phosphorylation of β-catenin at S675 was accentuated in *cKO* BMSC relative to control. Consistent with enhanced β-catenin stabilization, PTH$_{1-34}$ stimulated expression of Tcf/Lef target genes, *Lef1* and *Axin2*, to a larger degree in mutant cells compared to control. These suggests that *Cdh2*-ablated cells are more responsive to activation of β-catenin signaling by PTH. Increased PTH responsiveness in N-cadherin deficiency extends to PTH anabolic effect *in vivo*. Treatment with intermittent human PTH$_{1-34}$ (80μg/kg bw, sc, 5x/week, 4 weeks; iPTH) increased trabecular thickness and bone volume/tissue volume in *cKO* to a significantly larger extent than in control mice, assessed by μCT imaging. On bone histomorphometry, iPTH significantly increased mineral apposition rate and bone formation rate in *cKO* mice, contrasting with more modest changes in control mice. While osteoclast and osteoblast surface per bone surface were modestly affected, serum CTX increased to a similar extent in response to iPTH in mice from both genotypes, and serum P1NP was significantly increased in iPTH-treated *cKO* mice but not in control. These findings suggests that N-cadherin restrains PTH activation of bone formation, but not bone resorption. Since LRP6 is involved in osteoprogenitor differentiation and PTH anabolic effect, we propose that N-cadherin functions as a "buffer" for Lrp6 at the cell surface, thus modulating Lrp6/PTHR1 interaction and consequently the intensity of PTH-induced activation of Lrp6/β-catenin responses.

Disclosures: Leila Revollo, None.

1009

Androgens Reduce Skeletal Mechanoresponsiveness in Adult Male Mice. <u>Michaël Laurent</u>*[1], <u>Mieke Sinnesael</u>[1], <u>Ludo Deboel</u>[1], <u>Peter Delisser</u>[2], <u>Vanessa Dubois</u>[2], <u>Evelien Gielen</u>[3], <u>Lance Lanyon</u>[4], <u>Joanna Price</u>[2], <u>Geert Carmeliet</u>[1], <u>Frank Claessens</u>[2], <u>Dirk Vanderschueren</u>[1]. [1]Katholieke Universiteit Leuven, Belgium, [2]University of Bristol, United Kingdom, [3]University Hospitals Leuven, Belgium, [4]Royal Veterinary College, United Kingdom

Introduction: Testosterone and exercise synergistically induce muscle hypertrophy and can be used to treat cachexia in chronic diseases. Whether androgens also influence bone's response to mechanical loading or unloading is incompletely understood.

Methods: 16-week-old male C57Bl/6J mice were sham-operated or orchidectomized (ORX) and given placebo or anabolic doses of testosterone (T) or dihydrotestosterone (DHT) by s.c. silicone implants. These groups (n=7-11) received unilateral tibia loading (3x/w for 2 weeks, 40 cycles, 2400 με peak strain) started after 1 or 10 days, or unilateral Botox® injection on day 0 with 3 or 19 weeks follow-up.

Results: By two-way ANOVA, there was a significant interaction between androgen status and the osteogenic loading response. Cortical thickness was increased by T and DHT in control limbs but these groups partially (T) or completely (DHT) failed to exhibit the loading-related increase seen in sham and ORX. Trabecular bone volume also showed relatively larger load-related increases in ORX. T and DHT restored periosteal bone formation to sham levels but completely suppressed the load-related increase. Both loading and androgens suppressed skeletal RANKL/OPG mRNA ratios. ORX decreased and T increased the percentage of sclerostin-immunoreactive osteocytes (but not serum sclerostin), and loading no longer affected

osteocytic sclerostin expression in ORX and T. Botox and ORX synergistically induced trabecular bone loss at 3 weeks compared to internal control limbs, which was mitigated by androgens. The degree of muscle paralysis as well as calf muscle volumes and -weights were not affected by androgens. After 19 weeks, there was still a trabecular deficit in sham-Botox limbs, which was completely restored by T and DHT. Osteocyte-specific (Dmp1-Cre) androgen receptor knock-out mice showed identical skeletal responses to loading or disuse.

Conclusion: Androgens suppress both the osteogenic response to mechanical loading and disuse-related bone loss in adult male mice. This effect seems related to their antiresorptive actions and upregulation of sclerostin, independent of muscle volume. If confirmed in humans, our results suggest that androgens or loading may compensate the effect of each other's absence on bone loss; loss of both stimuli has a synergistic negative impact, while anabolic doses of both are unlikely to provide additive benefits.

Disclosures: Michaël Laurent, None.

1010

Synovial insulin resistance is linked to osteoarthritis in type 2 diabetes. <u>Sharon Ansboro</u>*[1], <u>Robert Maynard</u>[2], <u>Daisuke Hamada</u>[2], <u>Christopher Farnsworth</u>[2], <u>Robert Mooney</u>[3], <u>Michael Zuscik</u>[4]. [1]The Center for Musculoskeletal Research, USA, [2]Center for Musculoskeletal Research, USA, [3]University of Rochester Medical Center, USA, [4]University of Rochester School of Medicine & Dentistry, USA

Obesity induced type 2 diabetes (T2D) and associated systemic metabolic dysregulation is widely accepted as a risk factor for osteoarthritis (OA). Characteristic to T2D is resistance of tissues to insulin. We hypothesize that in OA, reduced insulin signalling attributed to insulin resistance in the synovium may initiate and exacerbate OA disease progression. We investigated insulin receptor (IR) expression and signalling in human fibroblast-like synoviocytes (FLSs) isolated from synovium of T2 diabetic and non-diabetic patients undergoing knee arthroplasty. A genetic approach was used to target insulin signalling in lubricin expressing (PRG4 positive) synovial tissues in obese, T2D mice to further to the hypothesis.

Human synovial tissue was analysed for IR expression via immunohistochemistry and for insulin activation of pAKT signalling via Western blotting. Effects TNFa and insulin on catabolic gene expression, and MMP1 and MMP13 protein levels were assessed in FLSs isolated from these tissues. To assess the role of FLS insulin signalling on spontaneous OA development in an obesity induced T2D model, male PRG4-Cre C57BL/6J mice were bred with IR fl/fl mice. Mice were placed on HF (60% kcal) or low-fat (10% kcal) diets at 5 weeks of age. After 16 weeks on diet, knee joint morphology was assessed via histology to visualize osteophytes and changes in articular cartilage.

Human FLSs were shown to be insulin responsive with dose dependent phosphorylation of IR and Akt. Synovial tissue harvested from T2D patients was insulin resistant, evidenced by a remarkable loss of AKT phosphorylation compared to synovium from non-diabetic patients (Fig. 1). TNFa, a pro-inflammatory cytokine elevated in T2D, markedly increased expression of cartilage degrading proteases in human FLSs including *ADAMTS4*, MMP13 and MMP1. Insulin treatment inhibited all of the TNFa responses by >50% (Fig. 2). Consistent with these findings, ablation of the IR in PRG4-Cre^{ERT2};IR$^{f/f}$ mice mimicked the knee joint changes that we have previously reported in HF mice. Compared to IR$^{f/f}$ controls, tamoxifen-induced PRG4-Cre^{ERT2};IR$^{f/f}$ mice showed spontaneous formation of osteophytes and early degenerative changes in the articular cartilage, effects that are observed in IR$^{f/f}$ HF mice (Fig. 3).

These notable changes in knee joint morphology suggest that loss of insulin signalling in PRG4-expressing FLSs disrupts the normal joint homeostasis and may initiate and exacerbate OA disease progression.
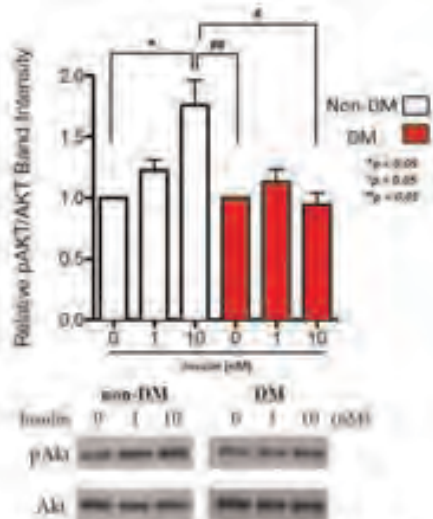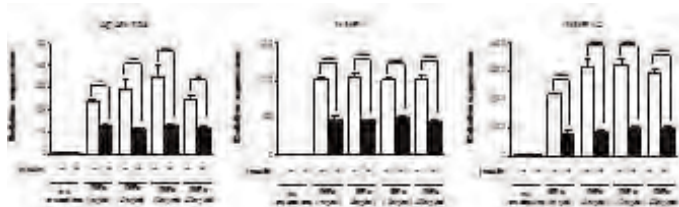
Fig 1: Phosphorylation of Akt following insulin treatment of human non-diabetic and diabetic synovial tissue

Fig. 1

Fig 2: Insulin-dependent suppression of cartilage-degrading enzymes in synoviocytes

Fig 2

Fig 3: Prg4 Cre targeted ablation of Insulin receptor (IR) in lean vs high fat, type 2 diabetic mice

Fig 3

Disclosures: Sharon Ansboro, None.

1011

Phase 2 Randomized, Double Blind, Placebo Controlled Trial of Anti-Myostatin Antibody LY2495655 in Older Fallers With Low Muscle Strength.

Clemens Becker*[1], Stephen Lord[2], Stephanie Studenski[3], Stuart Warden[4], Roger Fielding[5], Christopher Recknor[6], Marc Hochberg[7], Serge Ferrari[8], Hubert Blain[9], Ellen Binder[10], Yves Rolland[11], Leijun Hu[12], Qasim Ahmad[12], Kelli Pacuch[12], Elisa Gomez[12], Olivier Benichou[13]. [1]Robert-Bosch-Krankenhaus, Germany, [2]NeuRA, UNSW, Australia, [3]University of Pittsburgh (at the time the work was done), USA, [4]Indiana University School of Health & Rehabilitation Sciences, USA, [5]Jean Mayer USDA HNRCA At Tufts University, USA, [6]United Osteoporosis Center, USA, [7]University of Maryland School of Medicine, USA, [8]Geneva University Hospital & Faculty of Medicine, Switzerland, [9]Montpellier University Hospital, University Montpellier 1, MacVia-LR, France, [10]Washington University School of Medicine, USA, [11]Gérontopôle de Toulouse, Centre Hospitalo-Universitaire de Toulouse (CHU Toulouse), France, [12]Eli Lilly & Company, USA, [13]Eli Lilly & Company, France

Purpose: This trial was designed to test whether the anti-myostatin monoclonal antibody LY2495655 (LY) could increase appendicular lean body mass (aLBM) and improve physical performance in elderly fallers with low muscle strength. NCT01604408.

Methods: Subjects randomized (N=201) were aged ≥75 yrs, had ≥1 fall in past yr, low hand grip strength (≤37 kg [men]; ≤21 kg [women]) and low performance on a 5-time chair stand (5XCS) test without arms (≥12 s). LY 315 mg or placebo (pbo) was administered as 3 SC injections of 1.5 mL every 4 wks for 20 wks, followed by a 16 wk observational period. The primary objective was to assess the change from baseline to 6 months for aLBM for LY compared to pbo. Secondary and exploratory outcomes included 5XCS without arms (or with arms for subjects unable to do it without arms), 4-step stair climbing time and power (and same over 12-steps at equipped sites), fast and usual gait speed over 4 m, 6 min walking distance, isometric leg extension strength, hand grip strength, and incidence of falls. The 2-sided alpha level was set a priori at 0.05 for the primary analysis (ITT including all subjects with a baseline and ≥1 post baseline value) and 0.1 for all performance based measures (PBMs).

Results: Subjects were 70% women, aged 82 ± 5 yrs (mean $\pm$ SD), with BMI=26.5 ± 4 kg/m^2. Study groups were balanced for baseline aLBM (14.9 ± 2.2 kg [women]; 21.9 ± 3.1 kg [men]) and PBMs. LY subjects tended to have more pre-existing conditions and a higher risk of falls and fractures. Treatment was discontinued early in 19.6% of LY vs 14.1% of pbo arm. The change in aLBM from 0 to 6 months was +0.43 kg (SE 0.12; p<0.001) larger in LY than in pbo (+2.5%). Several power intensive PBMs (stair climbing, repeated chair stands, and fast gait speed) were improved in LY vs pbo subjects (Fig. 1). The incidence of falls per subject-yr was 1.6 (LY) vs 2.0 (pbo) (NS).

One death due to ischemic colitis occurred in an 87 yr old LY subject with a history of surgery for abdominal aortic aneurysm. At least 1 adverse event of fracture was reported in 6 pbo vs 10 LY subjects (NS). Injection site reactions were more frequent in the LY arm (30% vs 9%) and most often mild, requiring treatment discontinuation in 2 LY subjects. No safety issues related to muscle were observed.

Conclusions: In older fallers with low muscle strength, 6 months of LY treatment increased aLBM and consistently improved power intensive PBMs.
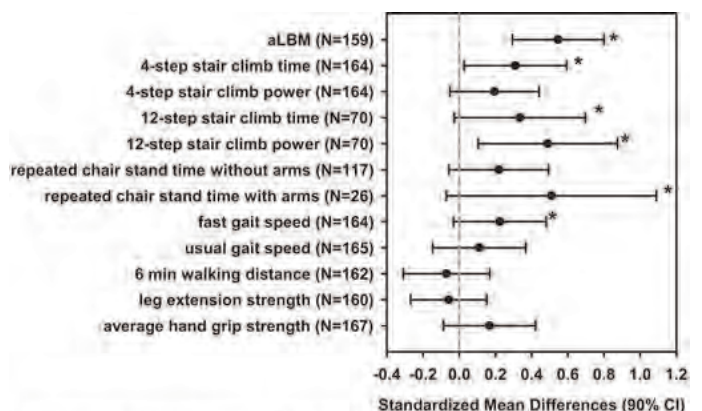
Standardized mean differences are for the difference between LY and placebo for the change from baseline to 6 months. A repeated measures mixed models for the changes from baseline was fitted for each endpoint. N=sample size of analysis for each measure including LY and placebo subjects. * p-value <0.1 for treatment effect including 3 and 6 month visits. Endpoints measured in seconds were multiplied by -1.

Figure 1. Summary of primary outcome and performance based measures.

1012

Fall Risk Assessment Predicts Fall Related Osteoporotic and Hip Fracture in Older Women and Men. Martin Nilsson*[1], Joel Eriksson[2], Anders Odén[3], Helena Johansson[4], Mattias Lorentzon[5]. [1]Centre for Bone & Arthritis Research At the Sahlgrenska Academy, Sweden, [2]Centre for Bone & Arthritis Research, Sweden, [3]Consulting Statistician, Sweden, [4]Geriatric Medicine, Department of Internal Medicine & Clinical Nutrition, Institute of Medicine, Sahlgrenska Academy, University of Gothenburg, Sweden, [5]Geriatric Medicine, Center for Bone Research at the Sahlgrenska Academy, Sweden

Purpose: Falls are one of the most common causes of disability in older adults. Only 1 in ten falls results in serious injury. Fall risk assessment instruments predict falls but it is unknown to what extent they predict serious health outcomes such as hip fracture.

Methods: Using the Senior Alert register, we identified 128,596 older patients (82.4 ± 7.8 years (mean $\pm$ SD), 59.6 % women) who had a fall risk assessment using the Downton Fall Risk Index (DFRI) at baseline. DFRI is a composite index (0-11) of established risk factors for falls. Fractures, resulting in a hospital visit, and mortality were investigated in the Swedish patient register and cause of death register. The predictive role of DFRI was calculated using a Cox proportional hazards model with age, sex, height, weight, and prevalent osteoporotic fracture as covariates, taking time to outcome or end of study into account.

Results: During the follow up (>80,000 patient years) 6,699 patients suffered an osteoporotic fracture. Among those patients, 2,557 sustained a hip fracture. The incidence of hip fracture was three times higher in patients with a high DFRI-score (7-11) (3.2%) compared to those with a low score (0 or 1) (1.1%, $p<0.001$). DFRI independently predicted osteoporotic fracture (Hazard Ratio, HR/per DFRI-step (95% confidence intervals) 1.06 (1.05-1.17)) and hip fracture (HR 1.14 (1.11-1.16)). DFRI more strongly predicted hip fracture (HR 1.33(1.26-1.40)) vs. 1.09(1.06-1.12)) in 70-year old than in 90-year old patients ($p<0.001$).

Conclusions: In conclusion, our data provide evidence that fall risk assessment using DFRI independently predicts fall-related hip fracture and other osteoporotic fractures in older men and women, indicating its clinical usefulness to identify patients who would benefit from interventions.

Disclosures: Martin Nilsson, None.

1013

The Influence of Exercise on the 3D distribution of Cortical and Trabecular Bone across the Proximal Femur: The HipHop Study. Sarah Allison*[1], Kenneth Poole[2], Graham Treece[2], Andrew Gee[2], Carol Tonkin[2], Winston Rennie[3], Jonathan Folland[1], Greg Summers[4], Katherine Brooke-Wavell[5]. [1]Loughborough University, United Kingdom, [2]University of Cambridge, United Kingdom, [3]University Hospitals of Leicester, United Kingdom, [4]Derby Hospitals NHS Foundation Trust, United Kingdom, [5]Loughborough University, United Kingdom

Regular exercisers have a lower fracture risk, despite exercise having only modest effects on aBMD. This discrepancy may be explained by exercise producing localised structural changes that are not captured by aBMD. We previously demonstrated that regular, but brief, multidirectional hopping exercise increased BMC at the femoral neck in the exercise leg (EL) versus the control leg (CL) of older men (The HipHop Study). The aim of the present study was to determine the distribution of cortical mass, thickness and density changes across the entire proximal femur, using the cortical bone mapping technique.

Fifty, healthy older men had hip QCT scans taken at baseline and after one year of performing short, daily bouts of single-legged hopping exercises (x50 multidirectional hops per session on the randomly allocated leg). Cortical bone mapping identified thickness, mass and density and nearby trabecular density distributions on each femur, which was then registered to an average femur. Statistical parametric mapping was used to identify changes of these parameters over time in the exercise leg (EL) and control leg (CL), and also significant differences between legs. Results were displayed as a 3D colour map over the surface of the proximal femurs. All hip QCT scans and map analyses were blinded to the leg allocation.

Of the fifty men that participated in the study, thirty-four (age 70 ± 4 years) exercised for 12-months, attending $92 \pm 9\%$ of prescribed exercise sessions. Throughout the femur, cortical mass increased significantly more in the EL (+2.7%) compared to the CL (+1.6%); P=0.0019, but substantially larger changes (over 6%) were evident at localised regions of the femoral neck and shaft (Figure 1). Trabecular density also increased noticeably more in the EL (+6.4) versus CL (+4.5%); P=0.0127, with the inferior region of the femoral neck increasing by over 12% with exercise. Cortical density increased in both the EL (+1.8%, P=0.0001) and the CL (+1.6%, P=0.0013), whereas the cortical thickness changes (EL +0.5%; CL -0.2%; P=0.1358) were not statistically significant.

Our findings show that brief bouts of single-legged hopping exercises can significantly increase cortical mass and trabecular density over a relatively short time frame, at regions of the femoral neck that may be important to structural integrity. These exercise induced changes were localised rather than being evenly distributed across the proximal femur.
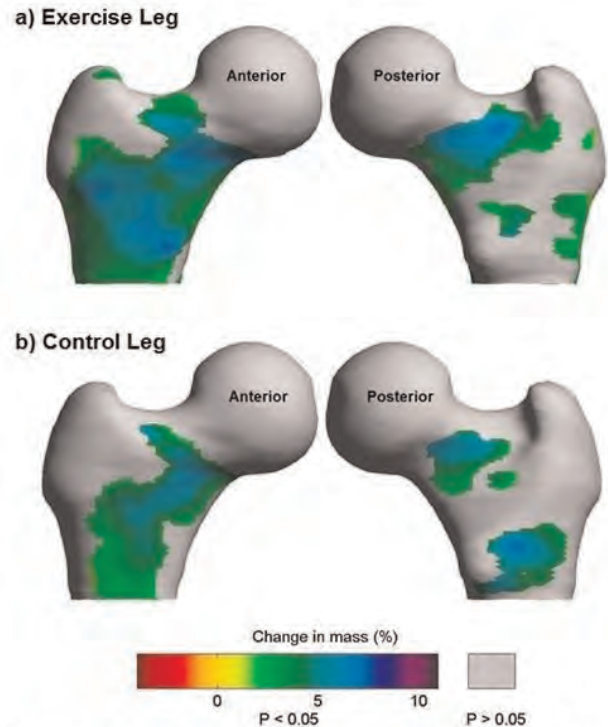
Figure 1. Change in cortical mass in the exercise leg (n=34) (a) and control leg (b), expressed as a percentage of baseline cortical mass

Figure1

Disclosures: Sarah Allison, None.

1014

Effects of Vitamin D and Multimodal Exercise on Prevention of Injurious Falls in Older Women. Kirsti Uusi-Rasi*[1], Radhika Patil[2], Saija Karinkanta[2], Kari Tokola[2], Pekka Kannus[2], Christel Lamberg-Allardt[3], Harri Sievanen[2]. [1]UKK Institute for Health Promotion Research, Finland, [2]The UKK Institute for Health Promotion Research, Finland, [3]University of Helsinki, Finland

This two-year randomized (double blind for vitamin D) placebo-controlled intervention trial assessed the effects of exercise and vitamin D on the risk of falls and injurious falls in older Finnish women. 409 women aged 70 to 80 years were randomly assigned into one of the four groups: 1) 20 µg vitamin D + exercise (D$^+$Ex$^+$), 2) 20 µg vitamin D + no exercise (D$^+$Ex$^-$), 3) placebo + exercise (D$^-$Ex$^+$), and 4) placebo + no exercise (D$^-$Ex$^-$). Included participants had at least one fall during the previous year, no use of vitamin D supplements, no regular exercise at baseline, and no contraindication to exercise. Multimodal supervised exercise training was given twice a week for 12 months, and once a week for the subsequent 12 months. In addition to monthly fall diaries, functional lower limb strength (5 times chair stand), dynamic balance (6.1 m backwards walking) and mobility (normal walking speed) were assessed at 6-month intervals. Cox-regression models were used to assess hazard ratios (HZ; 95% CI) for falls and injurious falls. Generalized linear mixed models and logistic regression models were used to estimate between-group differences in physical performance using age, height, and weight as covariates.

There was no difference in the rate of all falls between groups, but compared with the reference group (D$^-$Ex$^-$), D$^+$Ex$^+$ and D$^-$Ex$^+$ groups had less injurious falls requiring medical care (0.28; 0.10 to 0.76 and 0.17; 0.05 to 0.59, respectively), while D$^+$Ex$^-$ did not differ from D$^-$Ex$^-$ (0.84; 0.41 to 1.71). Chair-stand time improved in both Ex groups compared to the D$^-$E$^-$ group; for D$^+$Ex$^+$ (p=0.054), and more significantly for the D$^-$Ex$^+$ (p=0.027). Walking speed was maintained in the D$^-$Ex$^+$ group (p=0.007), while declined in other groups with no significant difference compared to D$^-$Ex$^-$. A combined analysis of the improvement either in time (for complete 6.1m walk) or distance (for incomplete walk) in backwards walking from baseline to the end was significantly greater in D$^+$Ex$^+$ compared to D$^-$Ex$^-$ (p=0.017).

Exercise was beneficial for balance and mobility, whereas vitamin D had no effect on these physical performance traits. Exercise was also associated with reduced risk for injurious falls requiring medical care, although the rate of all falls was similar in all groups.

Disclosures: Kirsti Uusi-Rasi, None.

1015

Use of Hypnotics and SSRI is Associated with Increased Risk of a Fall-Related Injury, Osteoporotic Fracture and Hip Fracture in Older Women and Men. Daniel Sundh*[1], Martin Nilsson[2], Joel Eriksson[3], Dan Mellstrom[4], Mattias Lorentzon[5]. [1]"institute of Medicine, Sahlgrenska Academy", Sweden, [2]Centre for Bone & Arthritis Research At the Sahlgrenska Academy, Sweden, [3]Centre for Bone & Arthritis Research, Sweden, [4]Sahlgrenska University Hospital, Sweden, [5]Geriatric Medicine, Center for Bone Research at the Sahlgrenska Academy, Sweden

BACKGROUND

The fracture risk assessment tool FRAX is used clinically to estimate 10-year risk of fracture, but only oral glucocorticoids can be entered as a risk medication. Hypnotics and selective serotonin re-uptake inhibitors (SSRI), have been linked to increased fall risk and risk of hip fracture, but whether or not this risk increase is independent of FRAX risk factors is unclear.

METHODS

Using the Senior Alert register, we identified 128,596 older patients (82.4 ± 7.8 years (mean$\pm$SD)) with information regarding age, sex, height, weight and prevalent fall-related injury at baseline. Incident fall-related injury, osteoporotic and hip fracture as well as prevalent fracture, diseases causing secondary osteoporosis and mortality were investigated in the Swedish patient- and cause of death register. Drug dispensation data was obtained from the Swedish prescribed drug register. Use of SSRI and hypnotics was investigated in relation to prevalent fall-related injury and fracture using χ^2 test. Cox proportional hazard models were used, taking time to outcome or end of study into account. Models with fracture as outcome were adjusted for FRAX-variables (age, height, weight, sex, prevalent fracture, secondary osteoporosis, rheumatoid arthritis and glucocorticoid use) while fall-related injury was adjusted for age, height, weight, sex and prevalent fall-related injury.

RESULTS

During the follow up (>80,000 patient years) 15,220 patients suffered a fall-related injury, 6,699 an osteoporotic fracture and 2,557 a hip fracture.

Both use of hypnotics and SSRI were associated with prevalent fall-related injury and fracture (Table 1A). Both medications predicted incidence of hip fracture and osteoporotic fracture independently of other risk variables in FRAX (Table 1B). SSRI and hypnotics predicted incident fall-related injury, also after adjusting for previous falls (Table 1B).

CONCLUSIONThe results of this study demonstrate that use of both SSRI and hypnotics is associated with increased risk of both osteoporotic and hip fracture, independent of FRAX risk factors, indicating that taking also these risk medications into account could improve fracture prediction in older women and men. Furthermore, our results suggest that the observed fracture risk increase is likely to be due to increased susceptibility to falls.

Table 1. Use of SSRI and hypnotics predict hip fracture

	SSRI		Hypnotics	
A	Yes (n=22,435)	No (n=106,161)	Yes (n=24,601)	No (n=103,995)
Prevalent fall-related injury (%)	11,393 (50.7)[c]	41,171 (38.8)	11,062 (45.0)[c]	41,502 (40.0)
Prevalent osteoporotic fracture (%)	5,033 (22.4)[c]	16,095 (15.2)	4,808 (19.5)[c]	16,320 (15.7)
Incident fall-related injury (%)	2,828 (12.6)[c]	12,471 (11.7)	3,115 (12.7)[c]	12,184 (11.7)
Incident hip fracture (%)	518 (2.3)[c]	2,039 (1.9)	546 (2.2)[f]	2,011 (1.9)
Incident osteoporotic fracture (%)	1,301 (5.8)[c]	5,429 (5.1)	13,66 (5.6)[b]	5,364 (5.2)
B	Hazard Ratio (95% CI)		Hazard Ratio (95% CI)	
Fall-related injury*	1.05 (1.01-1.10)[a]		1.11 (1.07-1.15)[c]	
Osteoporotic fracture[#]	1.10 (1.03-1.17)[b]		1.08 (1.02-1.15)[a]	
Hip fracture[#]	1.30 (1.18-1.43)[c]		1.21 (1.10-1.33)[c]	

[a]p<0.05, [b]p<0.01, [c]p<0.001

[f]Difference in distributions was investigated using χ^2 test.

* Cox proportional hazard model was adjusted for sex, age, height, weight and previous fall-related injury

[#] Cox proportional hazard model was adjusted for FRAX risk factors including sex, age, height, weight, secondary osteoporosis, prevalent osteoporotic fracture, p.o. glucocorticoid use and rheumatoid arthritis.

Table 1. Use of SSRI and hypnotics predict hip fracture

Disclosures: Daniel Sundh, None.

1016

Regulation of *Osteocalcin* expression and neuro-endocrine functions by HDAC4. Arnaud Obri*, Munevver Makinistoglu, Gerard Karsenty. Columbia University, USA

It was recently shown through genetic means that in the mouse and in humans, the bone-derived hormone osteocalcin regulates glucose metabolism and male fertility. Furthermore, in the mouse, undercarboxylated osteocalcin crosses the blood-brain barrier, binds to neurons of the hippocampus and is necessary for several cognitive functions, the most severely affected by the absence of osteocalcin being spatial learning and memory. The biological importance of the functions fulfilled by osteocalcin begs the question of the regulation of expression of this gene in osteoblasts. Since it is already known that this regulation involves transcription factors such as Runx2 and ATF4, we asked if it might also involve chromatin remodeling enzymes. Indeed, we show that the class II histone deacetylase, HDAC4 interacts tightly with the transcription factor ATF4. This interaction stabilizes ATF4, allows it to accumulate in the nucleus and enhances its ability to transactivate the *Osteocalcin* promoter. To verify the biological relevance of these molecular observations, we generated mice lacking *Hdac4* only in osteoblasts. *Hdac4$_{osb}$*-/- mice display low *Osteocalcin* expression, hypoinsulinemia with impaired insulin secretion, hypotestosteronemia, low sperm count, and infertility. Moreover, a Morris Water Maze test revealed a significant decrease in learning and memory in *Hdac4$_{osb}$*-/- mice. To verify that these functions are related to the interaction that was noted in vitro between HDAC4 and ATF4, we generated compound mutant *Hdac4$_{osb}$*+/-;*Atf4$_{osb}$*+/- mice. These *Hdac4$_{osb}$*+/-;*Atf4$_{osb}$*+/- mice also display a decrease in *Osteocalcin* expression, low circulating levels of undercarboxylated osteocalcin and hypoinsulinemia. By demonstrating that at least one chromatin remodeling enzyme affects *Osteocalcin* expression, this study identifies a second level of regulation of *Osteocalcin* expression and of its endocrine and cognitive functions.

Disclosures: Arnaud Obri, None.

1017

Analysis of Osteocalcin's Cognitive Function in WT Mice and of its Signaling in Neurons. Lori Khrimian*, Stylianos Kosmidis, Eric Kandel, Gerard Karsenty. Columbia University, USA

It was recently shown that in the mouse, the bone-derived hormone osteocalcin (OCN) is necessary for several cognitive functions such as the prevention of anxiety and depression, and to an even larger extent, learning and memory. Remarkably for this set of functions, osteocalcin does not rely on Gprc6a, which is not expressed in the brain. In view of these results, this study asked two questions: Is OCN sufficient to improve cognitive functions in wild type (WT) mice; and what is the signaling pathway that it uses in hippocampal neurons? To determine if OCN is sufficient to improve cognitive functions in young adult mice, WT 2-month old mice were implanted with pumps delivering vehicle or OCN intracerebroventricularly (ICV). After one month of infusion, animals were subjected to behavioral testing. Animals receiving OCN showed a significant decrease in anxiety-like behavior. In view of these findings, we next asked if OCN could improve cognition in older mice, by delivering ICV 10 ng/hr OCN in 16-month-old WT mice, for one month. At the end of this infusion period, we assayed for memory and other hippocampal functions through the Novel Object Recognition test. Mice that received OCN demonstrated a significant improvement in memory and all hippocampal functions. These results indicate that OCN is sufficient to improve cognition in WT mice regardless of their age. In an effort to uncover the mechanisms whereby osteocalcin signals in hippocampal neurons, we asked whether it uses the same signaling molecules it has been shown to use in other target cells. This analysis showed that phospho CREB (pCREB), which is essential for optimal spatial learning and memory in rodents, is markedly decreased in the hippocampus of *Ocn*-/- as compared to WT mice. Of note, the decrease in pCREB accumulation was more pronounced in *Ocn*-/- mice born from *Ocn*-/- mothers, which is consistent with the recently described influence of maternal OCN on brain development. Conversely, an acute stereotactic injection of uncarboxylated osteocalcin directly into the hippocampus of WT animals was sufficient to dramatically increase pCREB levels, compared to the hemisphere injected with vehicle. These results suggest that the receptor of OCN in hippocampal neurons might be a GPCR, as it is peripheral tissues.

Disclosures: Lori Khrimian, None.

1018

Defective Muscle-Bone Interplay Severely Impairs Bone Homeostasis in ALS Mice. Ke Zhu*[1], Jianxun Yi[2], Yajuan Xiao[2], Yumei Lai[1], Pingping Song[1], Wei Zheng[1], Hongli Jiao[1], Di Chen[1], Jingsong Zhou[2], Guozhi Xiao[1]. [1]Department of Biochemistry, Rush University Medical Center, USA, [2]Department of Molecular Biophysics & Physiology, Rush University Medical Center, USA

Skeletal muscle loading is a primary source of anabolic mechanical stimuli for bone throughout life. However, effects of muscle unloading on bone in diseases with muscle atrophy are poorly understood. Amyotrophic lateral sclerosis (ALS) is a neuromuscular disease characterized by progressive muscle atrophy. This study determined if and how the bone homeostasis is impacted in the G93A mice, a well-established ALS mouse model, before and after the onset of muscle atrophy. Results showed that four-month-old G93A mice with severe muscle atrophy displayed a dramatic reduction of bone mass compared to their sex- and age-matched wild type (WT) control mice. Bone formation was greatly impaired in G93A mice as demonstrated by defective activation of the AKT and ERK/MAPK signaling pathways in mesenchymal stromal cells, reduced formation and expansion of the osteoprogenitor population in bone marrow, and inhibited osteoblast differentiation and mineralization apposition rate in the G93A bones. In the meantime, osteoclast formation induced by M-CSF and RANKL was enhanced in G93A versus WT primary marrow monocyte cultures. In vivo osteoclast differentiation and bone

resorption were strikingly accelerated in G93A compared to WT mice. Furthermore, osteocytes embedded in the G93A bone matrix expressed elevated levels of sclerostin and RANKL proteins and reduced level of b-catenin protein. Finally, analyses of osteoblast and osteoclast parameters of 2-month-old G93A mice that did not display muscle atrophy revealed no significant impairment in bone remodeling. These results suggest that defective muscle-bone interplay in ALS mice severely impairs bone homeostasis by inhibiting bone formation and activating bone resorption.

Disclosures: Ke Zhu, None.

1019

PPARβ Deficiency Decreases Bone Formation Concomitantly to Increased Bone Marrow Fat Infiltration and Muscle Weakness. <u>Nicolas Bonnet</u>*[1], <u>He Fu</u>[2], <u>Beatrice Desvergne</u>[2], <u>Serge Ferrari</u>[3]. [1]University Geneva Hospital (HUG), Switzerland, [2]Center for integrative Genomics, Faculty of Biology & Medicine, University of Lausanne, Switzerland, [3]Geneva University Hospital & Faculty of Medicine, Switzerland

Pparß-/- mice have recently been reported to display characteristic features of muscle wasting and weakness as well as increased bone resorption and bone loss. Whether bone formation is also altered and which mechanisms couple bone and muscle deficiency in these mice however remains unclear. Body composition was evaluated in Pparß-/- and Pparß+/+ female mice from 1 to 18 months by DXA and bone forming indices and gene expression investigated by histomorphometry and qPCR at 18 month of age.

Compared to Pparß+/+, Pparß-/- had lower handgrip force and treadmill running distance, as well as decreased gastrocnemius mass, accompanied by a lower ratio of type I/II fibers and fat infiltrations. Muscle metabolic gene expression, i.e. Mip, Hif, Foxo3, was lower in Pparß-/- vs Pparß+/+, whereas Pparγ expression was increased (all p<0.05). Moreover, Mstn muscle expression was higher and circulating myostatin increased more with age in Pparß-/- than Pparß+/+ (+4.4 vs +2.9 fold, p<0.05).

From 1-to 18-months, TB lean and BMD gain were lower in Pparß-/- vs Pparß+/+ (+111.4% vs +156.2% and +58.6% vs +78.3%, respectively, p<0.01). At 18 months of age, Pparß-/- had lower endocortical and perioteal BFR (-44% and -100% vs PPARß+/+, p=0.09 & p<0.05, respectively) as well as significantly lower femoral BV/TV, CtTV, CtBV, and strength compared to Pparß+/+. In addition Pparß-/- accumulated more bone marrow fat with age (+217% of adipocyte volume vs Pparß+/+, p<0.05). Osteoblast differentiation (Runx2, Osterix, Coll1a, Ctnnb) and oxidative function (Foxo1, Hmox) were lower in Pparß-/- vs Pparß+/+. In addition, in vitro, primary osteoblast and mesenchymal stem cell from Pparß-/- bone marrow showed a lower proliferation and a higher differentiation into adipogenic lineage associated with high Pparγ and Fabp4 expression (+212% and +1032% vs Pparß+/+, p<0.001).

These results indicate that Pparß expression maintains muscle mass and bone formation with aging, while preventing fat infiltration in these tissues. These effects are mediated by an inhibition of myostatin and Ppar gamma expression, thereby enhancing differentiation of the osteoblastic lineage. These observations point to PParß as a potential target to prevent the age-related decline in musculo-skeletal functions.

Disclosures: Nicolas Bonnet, None.

1020

Targeting RANK/RANKL as a novel treatment for muscle weaknesses and dystrophic conditions. <u>Nicolas Dumont</u>[1], <u>Sébastien Dufresne</u>[1], <u>Patrice Bouchard</u>[1], <u>Éliane Lavergne</u>[1], <u>Charles Godbout</u>[1], <u>Antoine Boulanger-Piette</u>[1], <u>Sandrine-Aurélie Kake-Guena</u>[2], <u>Paul C. Pape</u>[2], <u>Renu Sarao</u>[3], <u>Josef M. Penninger</u>[3], <u>Jérôme Frenette</u>*[4]. [1]Université Laval, Canada, [2]Université Sherbrooke, Canada, [3]IMBA, Austria, [4]Université Laval, Can

Receptor-activator of nuclear factor kB (RANK), its ligand RANKL and the soluble decoy receptor osteoprotegerin (OPG) are the key regulators of osteoclast differentiation and bone. Although there is a strong association between osteoporosis and skeletal muscle atrophy/dysfunction, the functional relevance of a particular biological pathway that regulates synchronously bone and skeletal muscle physio-pathology is still elusive. One key determinant of muscle contractility is the Ca^{2+} pump called sarco/endoplasmic reticulum Ca^{2+} ATPase (SERCA) which transfers Ca^{2+} from the cytosol into the lumen of the SR, making Ca^{2+} available for the next contraction. Here we show that selective deletion of RANK in skeletal muscle greatly increases the activity of SERCA (> 200% increase) in fast-twitch *extensor digitorum longus* (EDL) but not slow-twitch *soleus* (SOL) muscles. The large increase in SERCA activity in denervated EDL muscle is likely to be associated with the significantly increased force production upon selective deletion of RANK in these muscles. Similarly, the inhibition of RANKL/RANK with OPG-Fc greatly increases force in muscles from dystrophic mdx mice compared to those from normal mice (233% gain in force relative to PBS-treated mdx mice) and prevents the loss of SERCA expression and activity. To understand more precisely the contribution of RANK in muscular dystrophy, we then generated a RANK/dystrophin double-deficient mouse model and showed that RANK deletion preserves muscle force, reduces significantly muscle damage and increases SERCA activity in dystrophic mice. RANK/RANKL interaction is thus a new and key actor in several models of muscle weaknesses and

myopathies and its inhibition represents a new therapeutic avenue for several muscular diseases.

Disclosures: Jérôme Frenette, None.

1021

Sarcopenia and Increased Body Fat in Sclerostin Deficient Mice. <u>Andrew Krause</u>*, <u>Toni Speacht</u>, <u>Peter Govey</u>, <u>Yue Zhang</u>, <u>Jennifer Steiner</u>, <u>Charles Lang</u>, <u>Henry Donahue</u>. Penn State College of Medicine, USA

While the absence of mechanical load results in muscle and bone loss, very little is known regarding the interaction of bone and muscle during the absence of mechanical load. To address this issue we examined changes in bone and muscle in mice deficient in Sost the gene that encodes sclerostin. Previous studies have shown Sost knockout (KO) mice were resistant to unloading induced by hind limb suspension (HLS) (1) as were mice given sclerostin antibody (2). To explore possible interactions between muscle and bone during unloading, we examined the hypothesis that both bone and muscle from Sost KO mice are resistant to HLS induced atrophy.

Mice (4m male C57Bl/6J) globally deficient in Sost since birth (Sost KO), and wild type (WT) controls were exposed to HLS or maintained in control cages for 2 weeks (4 groups, n=4-9/group). Mice were subjected to baseline and endpoint μCT scans. Total body weight and quadriceps weight were recorded and per cent muscle and fat quantified by 1H-NMR.

At baseline, Sost KO mice displayed significantly greater trabecular bone volume relative to WT. Loss of trabecular bone following 2 weeks of unloading was significantly attenuated in Sost KO (Fig.1). Sost KO displayed reduced loss of trabecular BV/TV (-4% vs. -47%, p<0.05), trabecular thickness (-2% vs. -41%, p<0.05), and trabecular number (+6% vs. -15%, p<0.05). All mice were of similar weight at the start of study; however, Sost KO displayed significantly more adipose tissue and less lean tissue than WT mice (Fig. 2). HLS resulted in a further gain of fat and loss of muscle in Sost KO. HLS resulted in decreased quadriceps weight in WT (Figure 3). Quadricep weight was decreased in Sost KO controls relative to WT controls but did not decrease further after HLS.

These are the first studies to examine skeletal muscle in Sost KO mice exposed to unloading. While Sost KO gained bone and were resistant to unloading, they displayed dramatic sarcopenia and increased adiposity. Previous studies did not observe sarcopenia in mice given anti sclerostin antibody for three weeks nor were these mice resistant to HLS-induced muscle loss. (2). Our results suggest that long term sclerostin deficiency, while having positive effects on bone, may have deleterious effects on muscle. If confirmed, these findings should be considered when developing therapeutic protocols using sclerostin antibody.

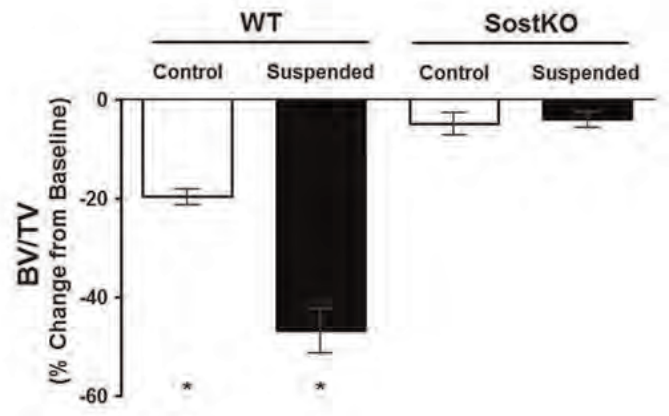References: 1. Lin et al. JBMR 24(10)1651; 2. Spatz et al. JBMR 28(4)856.

Figure 1. HLS-induced decreases in trabecular BV/TV are attenuated in Sost KO. *p<0.05 v. WT cont.

Figure 2. Baseline body composition in WT and Sost KO. *p<0.05 v. WT cont.

Figure 3. Both HLS and Sost KO results in decreased quadriceps weight. *p<0.05 v. WT cont.

Disclosures: Andrew Krause, None.

1022

HDAC5 Controls MEF2C-Driven Sclerostin Production by Osteocytes.
Marc Wein*[1], Jordan Spatz[2], Shigeki Nishimori[1], John Doench[3], David Root[3], Daniel Brooks[4], Mary Bouxsein[5], Paola Divieti Pajevic[6], Henry Kronenberg[1]. [1]Massachusetts General Hospital, USA, [2]Harvard-MIT Division of Health Sciences & Technology (HST), USA, [3]Broad Institute, USA, [4]Beth Israel Deaconess Medical Center, USA, [5]Beth Israel Deaconess Medical Center, Harvard Medical School, USA, [6]Massachusetts General Hospital & Harvard Medical School, USA

Osteocytes secrete paracrine factors that regulate the balance between bone formation and destruction. Among these molecules, sclerostin (encoded by the gene SOST) inhibits osteoblast function, and is an osteoporosis drug target. The molecular mechanisms underlying SOST expression remain largely unexplored. To investigate mechanisms controlling sclerositn production by osteocytes, we have developed a system in which lentiviral-mediated shRNA gene silencing can be used to interrogate candidate gene function in vitro using Ocy454 cells, a novel murine osteocytic cell line. Here, we report that HDAC5 negatively regulates sclerostin levels in osteocytes, both in vitro and in vivo. HDAC5 shRNA increases, whereas HDAC5 overexpression decreases SOST expression, as assessed by RT-qPCR and ELISA in Ocy454 cells. Micro-CT shows that 8 week old female global HDAC5-/- mice have 32.4% lower trabecular BV/TV in the distal femur than WT controls. The bones of the HDAC5-/- mice show increased levels of SOST mRNA (83% increase from calvarial RNA assessed by RT-qPCR compared to wild type littermates), a greater fraction of sclerostin-positive cortical osteocytes (61.4% positive in WT mice, 85.2% positive in HDAC5-/- mice), and decreased Wnt activity (based on RT-qPCR for for AXIN2 and

immunohistochemistry for non-phosphorylated beta-catenin). In Ocy454 cells, Hdac5 binds and inhibits the transcriptional activity of Mef2c, a transcription factor crucial for SOST expression, based on co-immunoprecipitation and luciferase reporter assays. HDAC5 deficiency leads to increased Mef2c association and histone 3 lysine 27 acetylation at a conserved SOST enhancer 45 kB downstream from the gene's transcription start site, as assessed by chromatin immunoprecipitation. MEF2C shRNA abrogates increased sclerostin secretion due to HDAC5 knockdown. Finally, endogenous Hdac5 associates with this same enhancer region by chromati immunoprecipitation in Ocy454 cells, suggesting direct regulation of SOST gene expression by Hdac5 in osteocytes. Taken together, these results demonstrate that HDAC5 functions in osteocytes as a negative regulator of MEF2C-driven sclerostin production. Studies are ongoing to determine the upstream signals that regulate HDAC5 function in these cells.

Disclosures: Marc Wein, None.

1023

Ift80 balances canonical and non-canonical hedgehog signaling pathways during osteoblast differentiation and bone development.
Xue Yuan*[1], Shuying Yang[2]. [1]University At Buffalo, USA, [2]State University of New York At Buffalo, USA

Increasing studies have shown that intraflagellar transport (Ift) proteins play crucial roles in bone development and remodeling. Ift80 is one of the Ift complex B proteins. Partial mutations of *Ift80* in humans cause two diseases: Jeune asphyxiating thoracic dystrophy and short rib polydactly type III with severe bone abnormalities. Our previous *in vitro* study demonstrated that Ift80 regulates osteoblast (OB) differentiation likely through the Hedgehog (Hh) signaling pathway. We further characterized the role and mechanism by which Ift80 regulates Hh canonical and non-canonical signaling pathways, OB differentiation and bone development *in vivo*. We generated *Ift80* conditional knockout mice (*Ift80^{flox/flox}*) and specifically deleted *Ift80* in OB precursor cells (OPCs) by using the *osterix-Cre* (*Osx-cre*) transgenic line. We found that the OB-specific deletion of *Ift80* resulted in apparent growth retardation, markedly lower bone mass and longer hypertrophic cartilage. About 70% of OPCs derived from the *Ift80^{flox/flox}*/*Osx-cre* calvaria bone had either lost or shorten cilia. Compared to the *Ift80^{flox/flox}* cells, *Ift80^{flox/flox}*/*Osx-cre* cells completely lost osteogenic capacity and had significantly less ALP activity. Deletion of *Ift80* dramatically reduced the expression of BMP2, Osx, osteocalcin and RUNX2. Ectopic expression of BMP2 or RUNX2 partially restored the osteogenic differentiation ability in *Ift80^{flox/flox}*/*Osx-cre* OPCs. Moreover, deletion of *Ift80* significantly inhibited the transcription of the Hh target genes Gli1 and Patched, and the signaling activity of Gli2, a critical transcriptional factor in Hh canonical signaling pathway; but dramatically elevated the activity of RhoA, the important downstream effector of non-canonical Hh signaling pathway. The cells with overactive RhoA had greater stress fiber density, which inhibited OB differentiation. Either the reorganization of the stress fibers with cytochalasin D or the inhibition of G$_{\alpha i}$ or phosphoinositide 3-kinase with pertussis toxin or LY294002, respectively, partially rescued the deficiency of osteogenic differentiation in *Ift80^{flox/flox}*/*Osx-cre* OPCs by blocking RhoA activation. Our results revealed a new mechanism through which Ift80 balances the Hh-Gli2 canonical and Hh-G$_{\alpha i}$-RhoA non-canonical pathways in OB differentiation using an *in vivo* genetic model. Thus, IFT80 could be a potential therapeutic target for the treatment of bone diseases.

Disclosures: Xue Yuan, None.

1024

A subset of mesenchymal stem/progenitor cells responds to stress and constitutes a major source of new osteoblasts during fracture repair *in vivo*.
Dongsu Park*[1], Joel A. Spencer[2], Charles P. Lin[2], David T. Scadden[3]. [1]Baylor College of Medicine, USA, [2]Wellman Center for Photomedicine & Center for Systems Biology, Massachusetts General Hospital, USA, [3]Center for Regenerative Medicine, Massachusetts General Hospital, Harvard Stem Cell Institute, USA

The constant remodeling of the mammalian skeleton has been long hypothesized to be dependent on the presence of mesenchymal stem cells (MSCs) with unknown *in vivo* identity. Despite recent progress in uncovering *in vivo* MSC markers, such as Nestin or αSMA, the substantial heterogeneity and wide tissue distribution of these markers hamper in vivo demonstration of stem cell identity and multi-lineage potential. In particular, the physiologic locations of true MSCs and their contribution to fracture repair have not been clearly elucidated. We have previously shown that transient activation of the *myxovirus resistance-1* (*Mx1*) promoter genetically marks MSC-like cells in vivo. While they meet the current definitions of MSC *in vitro*, the *Mx1*^{+} stem/progenitors exhibit osteo-lineage restricted i*n vivo*. Here, we demonstrate *in vivo* characteristics and dynamics of endogenous skeletal stem/progenitor cells (SSPCs) in bone repair. The combination of osteo-lineage cell tracing models and time-lapse intravital imaging of induced microfractures revealed the relocation of endogenous *Mx1*^{+} SSPCs to fracture sites during the first few days after injury, in which critical events in the early repair process occur. Notably, sequential *in vivo* imaging of SSPCs in the fracture site of *Mx1/Nestin-GFP* or *Mx1/αSMA-GFP* dual reporter mice revealed that *Mx1*^{+}*Nestin*− SSPCs rather than *Nestin*-GFP^{+} perivascular cells are the source of new osteoblasts during fracture healing *in vivo*. Surprisingly, these *Mx1*^{+} SSPCs are
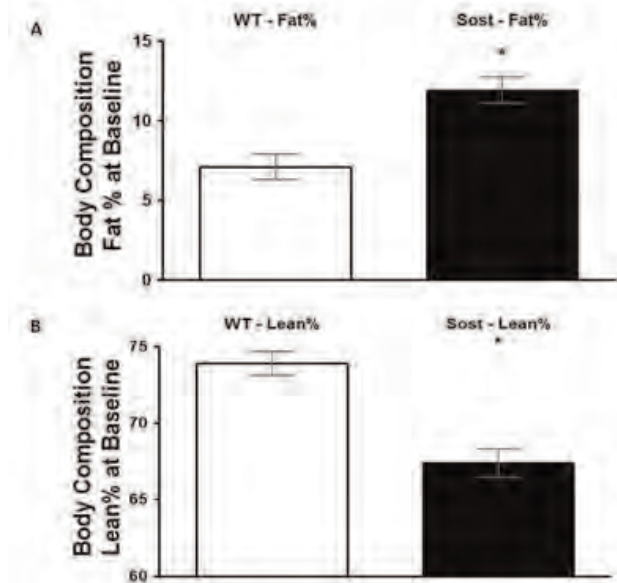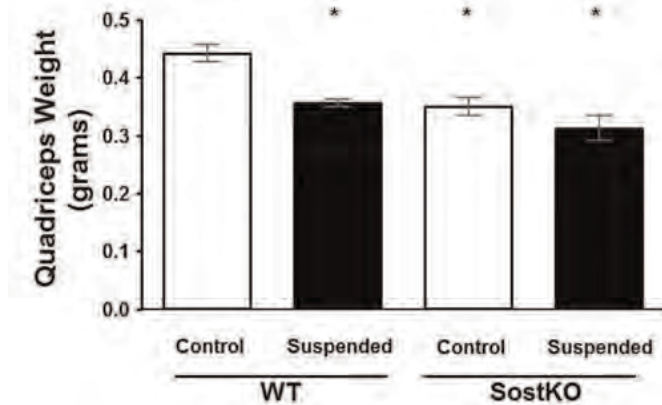
αSMA-GFP positive, suggesting that the combination of *Mx1* and *αSMA* distinguish endogenous SSPCs from other mesenchymal populations in bone marrow. Our findings further define *in vivo* identification of skeletal stem/progenitor cells with physiological roles in bone remodeling and regeneration. These data indicate that a subset of MSCs is much more dynamic than other populations and is highly influenced by physiologic selection pressures.

Disclosures: Dongsu Park, None.

1025

Diacylglycerol kinase Ñ (DGKÑ) is a critical regulator of bone homeostasis by modulating c-FOS levels in osteoclasts. <u>Ali Zamani</u>*[1], <u>Pamela Hesker</u>[2], <u>Justus Katungi</u>[3], <u>Roberta Faccio</u>[4]. [1]Department of Orthopedics, Washington University, St. Louis, Missouri, USA, [2]Washington University in St Louis School of Medicine, USA, [3]Washington University in St.Louis-Orthopaedic Surgery Department, USA, [4]Washington University in St Louis School of Medicine, USA

Although PLCγ2 is a critical modulator of osteoclast (OC) development under inflammatory conditions, its high homology with PLCγ1 renders PLCγ2 specific targeting difficult. In contrast, diacylglycerol (DAG), a downstream product of PLCγ2 catalytic activity, is strictly controlled by tissue specific diacylglycerol kinases (DGKs), which convert DAG into phosphatidic acid. Since we have previously shown that DAG controls OC functions, we sought to examine the role of DGKs in bone homeostasis. DGKζ was the most highly expressed isoform in bone marrow derived macrophages (BMMs) and OCs. Strikingly, DGKζ deficiency resulted in a substantial osteoporotic bone phenotype, with sparse trabecular pattern, thinning of the cortical bone, and a marked increase in periosteal OCs. The severity of the bone phenotype was exacerbated using the serum-induced model of arthritis, which led to extensive joint osteolysis in DGKζ-/- mice compared to WT. In vitro, DGKζ-/- BMMs formed higher number and larger OCs with increased resorptive capacity, as further documented by increased expression of markers associated with differentiation, fusion, and resorption. Surprisingly, while no differences in RANKL signaling were noted, M-CSF stimulation induced a significant increase in c-FOS protein levels in DGKζ-/-cells compared to WT. Because DGKζ deficiency leads to DAG accumulation, we hypothesized that M-CSF enhanced c-FOS levels via DAG. Indeed, MCSF induced a time dependent accumulation of DAG with significantly higher levels in DGKζ-/- cells compared to WT. To demonstrate the impact of DAG on c-FOS expression, we exposed WT cells to PMA, a DAG analog, and found dose-dependent elevation of c-FOS. Furthermore, a c-FOS luciferase reporter driven by the DAG responsive element (TRE) rapidly induced c-FOS expression. Finally, to demonstrate the relevance of M-CSF/DAG/c-FOS signaling in osteoclastogenesis, we turned to PLCγ2+/- BMMs, which have reduced DAG production and fewer OCs. We hypothesized that genetic deletion of DGKζ in PLCγ2+\- mice would rescue OC formation by restoring DAG levels. Indeed, the OC defect observed in PLCγ2+/- cultures was rescued by the deletion of DGKζ. To our knowledge, this is the first report demonstrating that DGKζ is a critical regulator of bone homeostasis by controlling c-FOS levels downstream of M-CSF. Together this data demonstrates that modulation of DGKζ activity could lead to new promising therapeutic strategies for pathological bone loss.

Disclosures: Ali Zamani, None.

1026

FoxO1 inhibits bone mass accrual through its expression in neurons of the locus coeruleus. <u>Daisuke Kajimura</u>*, <u>Gerard Karsenty</u>. Columbia University, USA

Congruent lines of investigation have identified the broadly expressed transcription factor FoxO1 as a mediator of multiple physiological processes in a wide variety of organs. Moreover, biochemical studies have shown that phosphorylation of FoxO1 in response to extracellular signals prevents its nuclear translocation and therefore decreases its transcriptional activity. This aspect of FoxO1 biology is relevant to the regulation of bone mass because the hormone adiponectin triggers the phosphorylation of FoxO1 in neurons of the locus coeruleus and it is thought that this may be one mechanism whereby adiponectin inhibits sympathetic nervous system output. To determine if it is the case and to elucidate how FoxO1 might regulate the sympathetic tone we generated and analyzed mice lacking FoxO1 only in neurons of the locus coeruleus (*FoxO1$_{LC-/-}$*). When compared to littermate controls, *FoxO1$_{LC-/-}$* mice demonstrate, at all time points analyzed, a marked decrease in the activity of the sympathetic nervous system as determined by measuring norepinephrine content in the brainstem, urinary elimination of epinephrine, and expression of *Ucp1* in brown adipose tissue. As a consequence of this decrease in the activity of the sympathetic nervous system, *FoxO1$_{LC-/-}$* mice experience a high bone mass phenotype because of a decrease in bone resorption and an increase in bone formation parameters. To understand how FoxO1 could exert such a significant influence on the sympathetic regulation of bone mass we performed a gene expression survey. This analysis identified *Dbh,* a locus coeruleus-specific gene that encodes the initial and rate-limiting enzyme in the synthesis of catecholamines, as being down regulated in the *FoxO1$_{LC-/-}$* mice. A molecular study showed that FoxO1 binds to and trans-activates the promoter of *Dbh*. These results uncover the first transcriptional mechanism

responsible for the sympathetic regulation of bone mass and identify a novel, long range, mechanism whereby FoxO1 regulates bone mass in vivo.

Disclosures: Daisuke Kajimura, None.

1027

Rare Protein-Coding Variants Are Associated with Osteoporotic Fracture: An Exome-Chip Analysis of 44,130 Adult Caucasians in CHARGE and GEFOS Consortia. <u>Yi-Hsiang Hsu</u>*[1], <u>Karol Estrada</u>[2], <u>Paul Leo</u>[3], <u>Alexander Teumer</u>[4], <u>Ching-Ti Liu</u>[5], <u>Emma Duncan</u>[6], <u>HouFeng Zheng</u>[7], <u>Ryan Minster</u>[8], <u>Leo-Pekka Lyytikäinen</u>[9], <u>Najaf Amin</u>[10], <u>Ruben Pengelly</u>[11], <u>Raquel Cruz Guerrero</u>[12], <u>Janja Marc</u>[13], <u>Carrie Nielson</u>[14], <u>Laura Yerges-Armstrong</u>[15], <u>Melina Claussnitzer</u>[16], <u>Ling Oei</u>[17], <u>NM van Schoor</u>[18], <u>Carolina Medina-Gomez</u>[19], <u>Yanhua Zhou</u>[20], <u>Chao-Ho Cheng</u>[21], <u>Yongmei Liu</u>[22], <u>Uwe Völker</u>[4], <u>Mika Kahonen</u>[23], <u>Cyrus Cooper</u>[24], <u>Andre Uitterlinden</u>[25], <u>Anke Hannemann</u>[26], <u>David Karasik</u>[27], <u>Simona Mencej-Bedrac</u>[28], <u>Jose Antonio Riancho Moral</u>[29], <u>John Holloway</u>[11], <u>Terho Lehtimäki</u>[9], <u>Rebecca Jackson</u>[30], <u>L Adrienne Cupples</u>[5], <u>Tamara Harris</u>[31], <u>Henri Wallaschofski</u>[32], <u>Fernando Rivadeneira</u>[33], <u>Brent Richards</u>[34], <u>Daniel Chasman</u>[35], <u>Matthew Brown</u>[36], <u>Douglas Kiel</u>[37]. [1]Hebrew SeniorLife Institute for Aging Research & Harvard Medical School, USA, [2]Analytic & Translational Genetics Unit, Massachusetts General Hospital, USA, [3]University of Queensland Diamantina Institute, Brisbane, Australia, Australia, [4]Interfaculty Institute for Genetics & Functional Genomics, University of Greifswald, Germany, [5]Biostatistics Dept. Boston University, USA, [6]Royal Brisbane & Women's Hospital, Australia, [7]Departments of Medicine, Human Genetics, Epidemiology & Biostatistics, McGill University, Canada, [8]Department of Human Genetics & Epidemiology, Graduate School of Public Health, University of Pittsburgh, USA, [9]Department of Clinical Chemistry, Fimlab Laboratories, Finland, [10]Department of Epidemiology, Erasmus Medical Center, Netherlands, [11]Human Genetics & Genomic Medicine, University of Southampton Faculty of Medicine, United Kingdom, [12]University of Santiago de Compostela, Spain, [13]Division of Clinical Biochemistry, University of Ljubljana, Slovenia, [14]Oregon Health & Science University, USA, [15]University of Maryland School of Medicine, USA, [16]Hebrew SeniorLife, Institute for Aging Research & Harvard Medical School, USA, [17]Erasmus University Medical Center, The Netherlands, [18]Department of Epidemiology & Biostatistics, the EMGO Institute of Health & Care Research, Netherlands, [19]Erasmus Medical Center, The Netherlands, [20]Boston University, USA, [21]Hebrew SeniorLife Institute for Aging Research, USA, [22]Center for Human Genetics, Division of Public Health Sciences, Wake Forest School of Medicine, USA, [23]Department of Clinical Physiology, University of Tampere School of Medicine, Finland, [24]University of Southampton, United Kingdom, [25]Rm Ee 575, Genetic Laboratory, The Netherlands, [26]Institute of Clinical Chemistry & Laboratory Medicine, University Medicine, Germany, [27]Hebrew SeniorLife; Bar Ilan University, USA, [28]Faculty of Pharmacy, University of Ljubljana, Slovenia, [29]Hospital U.M. Valdecilla-IFIMAV, University of Cantabria, Spain, [30]The Ohio State University, USA, [31]Intramural Research Program, National Institute on Aging, USA, [32]Institute of Clinical Chemistry & Laboratory Medicine, Institute for Community Medicine, University Medicine Greifswald, University of Greifswald, Germany, [33]Erasmus University Medical Center, The Netherlands, [34]McGill University, Canada, [35]Brigham & Women's Hospital & Harvard Medical School, USA, [36]Diamantina Institute of Cancer, Immunology & Metabolic Medicine, Australia, [37]Hebrew SeniorLife, USA

Osteoporotic fracture (FX) is heritable (BMD-adjusted heritability: 35%~69% in European descent Caucasians), suggesting that genetic variants contribute to FX risk independent of BMD. Among 56 previously reported BMD associated genome-wide significant (GWAS) loci, only 6 were also genome-wide significantly associated with FX risk. Most of these GWAS SNPs are likely to be in LD with un-genotyped causal variants responsible for underlying fracture susceptibility. Thus, identifying causal variants is a necessary step to study the underlying biology of FX risk. The availability of new exome genotyping chips with 235,933 protein-coding variants (non-synonymous, splice sites and stop altering SNPs selected from ~18,000 genes) provides a feasible way to identify causal variants in the exome. We conducted an exome-chip analysis to identify novel functional coding variants that are associated with FX risk. The exome-chip was genotyped in 10 Cohort studies comprising 44,130 adult Caucasians participants (8,781 FX cases and 35,349 controls; 86% female). FX (excluding fingers, toes, skull, pathological fractures and those resulting from high trauma) phenotypes were obtained by interview and confirmed in most studies through medical record review. Since observed MAF of most genotyped variants (78%) was ≤ 1%, we performed gene-based collapsing tests (allele-count and SKAT tests) in each study to identify rare coding variants (MAF ≤ 1%) associated with FX.

Covariates adjusted in the models included age, age^2, sex, weight, height, ancestral genetic background, sub-cohorts and estrogen use. For family-based studies, a kinship matrix was incorporated into test statistics to take into account within-family correlations. An inverse-variance fixed effect meta-analysis (seqMeta package) was used to combine results from 10 studies. The most significant association was found in the *PPM1J* gene (p=7.6x10^{-12}). Other novel associations that achieved genome-wide significance (p < 4.2x10^{-6}, Bonferroni correction) were found in *WAC*, *DAZL*, *MRPS23* and *SMPDL3B* genes. We also performed single variant association analysis for variants with MAF > 1%. The most significant, novel association was found for a missense variant, SNP K450E in SLFN14 gene (p=7x10^{-6}). Other strong associations (p < 5x10^{-5}) were found for previously reported loss-of-function variants V667M and A1330V in *LRP5* and a common variant in *SLC25A13*. In summary, our analysis identified novel, rare, missense variants associated with FX. A larger exome-chip meta-analysis with an additional ~20,000 samples is underway to increase the statistical power of identifying coding functional variants.

Disclosures: Yi-Hsiang Hsu, None.

1028

Osteoblast-specific Overexpression of Human WNT16 Increases both Cortical and Trabecular Bone Density and Improves Bone Structure in Mice. <u>Imranul Alam</u>*, <u>Mohammed Alkhouli</u>, <u>Rita O'Riley</u>, <u>Weston Wright</u>, <u>Dena Acton</u>, <u>Amie Gray</u>, <u>Michael Econs</u>. Indiana University School of Medicine, USA

Previous genome-wide association studies have identified common variants in genes associated with bone mineral density (BMD) and risk of fracture. Recently, we identified SNPs in WNT16 that were associated with peak BMD in premenopausal women. To further identify the role of WNT16 in bone mass regulation, we created transgenic (TG) mice over-expressing human WNT16 in osteoblasts on B6 background using 2.3-kb rat Col1α1 promoter. We compared bone phenotypes and performed serum biochemistry analysis between TG and wild-type (WT) mice. Compared to WT mice, WNT16-TG mice exhibited significantly higher (p<0.0001) whole body aBMD (16-21%) and BMC (16-28%) at 6 and 12 weeks of age in both male and females. μCT analysis of trabecular bone at distal femur revealed 3-fold (male) and 14-fold (female) higher (p<0.0001) BV/TV, 31% (male) and 74% (female) higher Tb.N, 52% (male) and 99% (female) higher Tb.Th but 29% (male) and 46% (female) lower Tb.Sp in TG mice compared to WT littermates (Figure 1). The cortical bone at midshaft femur also showed 22% (male) and 14% (female) higher (p<0.005) BA/TA and 14% (male) and 8% (female) higher cortical thickness in the TG mice (Figure 1). Serum biochemistry analysis at 12 weeks of age showed that both Ca and P levels were similar between male WT and TG mice but female TG mice had 11% higher P level and male TG mice had 20% higher serum ALP and 23% higher OC compared to WT mice. In addition, 14% (male) and 22% (female) lower CTX/TRAPc5b ratio was observed in TG mice compared to WT animals, suggesting that WNT16 affects both bone formation and resorption parameters. Also, expression of ALP and OC genes were upregulated in male TG mice compared to WT littermates. Our data indicate that WNT16 is critical for positive regulation of both cortical and trabecular bone mass and structure, and that this molecule can be targeted for therapeutic interventions to treat osteoporosis or other low bone mass and high bone-fragility conditions.
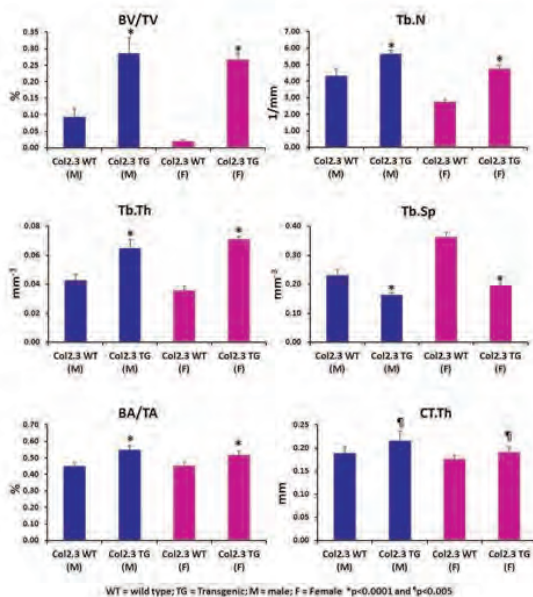

Figure 1

Disclosures: Imranul Alam, None.

1029

Gut Microbiota Plays a Pivotal Role in the Bone Loss Induced by Sex Steroid Deficiency. <u>Jau-Yi Li</u>*[1], <u>Benoit Chassaing</u>[2], <u>Michael Reott</u>[1], <u>Jonathan Adams</u>[1], <u>M. Neale Weitzmann</u>[1], <u>Andrew Gewirtz</u>[2], <u>Roberto Pacifici</u>[1]. [1]Emory University School of Medicine, USA, [2]Center for Inflammation, Immunity & Infection, Georgia State University, USA

Postmenopausal osteoporosis results, in part, from the chronic inflammatory state caused by sex-steroid deficiency. One of the involved mechanisms is increased production of TNFα by activated T cells but the nature of the antigens (Ags) driving T cell activation is unknown. The intestine contains trillions of microbes known as the microbiota. The microbiota is crucial for the induction, training, and function of the host immune system, contributes to inflammatory processes, and regulates bone mass accrual. To determine the role of microbiota to the bone loss of sex-steroid deficiency, germ-free (GF) mice and mice housed in standard conditions (control mice) were treated with vehicle or Leuprolide, a GN-RH agonist that blocks sex-steroid production mimicking ovariectomy, at 375 μg/month for 10 weeks starting at 10 weeks of age. Before euthanizing, fecal DNA was subjected to quantitative PCR to confirm GF status. Attesting to successful induction of hypogonadism, Leuprolide markedly decreased the weight of the uterus and ovaries in all mice. μCT analysis at sacrifice revealed that GF mice had a higher trabecular bone volume (BV/TV), and cortical bone volume (Ct.Vo) in the distal femur and the spine, as compared to controls. Demonstrating a role for gut microbiota, Leuprolide caused a greater bone loss in control mice than in GF mice in all regions of interest. The difference in Leuprolide-induced loss of bone volume between control and GF mice was ~20 % in the spine, ~27 % in the femoral metaphysis, ~30 % in the femoral epiphysis and ~38 % in the femoral cortex. Serum levels of CTX, a marker of bone resorption, were increased ~2-fold by Leuprolide in control but not in GF mice. GF mice had a ~50 % smaller increase in bone marrow (BM) cells than control mice in response to Leuprolide. Moreover, Leuprolide increased the frequency of TNFα+CD4+ and TNFα+CD8+ T cells in the BM in control mice but not in the BM of GF mice. In summary these findings demonstrate that gut microbiota plays a significant role in inducing bone loss and increasing bone turnover in sex-steroid deficient mice by providing the Ags required for BM T cell expansion and increased TNFα production. We suggest that the composition of gut microbiota may be involved in regulating the magnitude of bone loss experienced by postmenopausal women.

Disclosures: Jau-Yi Li, None.

1030

Blood-circulating microRNAs are indicative of Fractures at the Femoral Neck in post-menopausal Women. <u>Matthias Hackl</u>*[1], <u>Susanna Skalicky</u>[1], <u>Sylvia Weilner</u>[2], <u>Peter Dovjak</u>[3], <u>Peter Pietschmann</u>[4], <u>Johannes Grillari</u>[2]. [1]TAmiRNA GmbH, Austria, [2]Department of Biotechnology, University of Natural Resources & Life Sciences Vienna, Austria, [3]Salzkammergut-Klinikum Bad Ischl, Gmunden, Vöcklabruck, Austria, [4]Department of Pathophysiology & Allergy Research, Medical University of Vienna, Austria

Osteoporosis is characterized by a systemic reduction in bone mass leading to increased bone fragility and consequently elevated risk of bone fractures. Several guidelines have been introduced to assist the assessment of fracture risk, such as the integration of basic clinical parameters with bone mineral density (BMD). However, individualized fracture risk assessments based on genetic analyses have not yet been implemented in the clinical praxis.

Recently, microRNAs (miRNAs) have been identified to be secreted into the bloodstream from cells of various tissues, thus, possibly indicating local pathological processes. In addition, proof exists that miRNAs play an important role in the control of homeostasis between bone anabolism and catabolism ("osteomiRs"). However, it is not well established whether imbalances in bone remodeling are also reflected in the levels of circulating miRNAs, and could therefore be utilized as non-invasive biomarkers of osteoporosis.

In this study we describe the use of miRNA qPCR arrays for quantification of 175 microRNAs in serum samples obtained from 7 patients with recent osteoporotic fractures at the femoral neck (FN), and 7 age-matched control samples (C). Differential expression analysis was performed by non-parametric analysis and p-values were adjusted for multiple testing using BH false-discovery rate. Under these conditions 6 microRNAs reached significance of adj.p < 0.05 (Fig. 1), of which 4 have previously been described as osteomiRs. For example, miR-133b, which is known to regulate osteogenic differentiation by repression of RUNX2 transcription factor, was found down-regulated in recently fractured patients, while miR-10a, which is targeting inhibitors of osteogenesis, was found up-regulated.

The potential use of these microRNAs as markers of osteoporotic fractures was confirmed by ROC analyses and calculation of AUC values (Fig. 2). All miRNAs were further assessed by overexpression and knockdown in an in vitro model of osteogenic differentiation using adipose tissue-derived stem cells.

Overall, these data provide first proof that circulating microRNA levels are altered in post-traumatic patients suffering from osteoporosis, and that these microRNAs might be involved in the regulation of bone metabolism. Future studies will show, whether this knowledge can be used to improve current diagnostic methodologies to predict fracture risk and treatment response in osteoporosis patients.
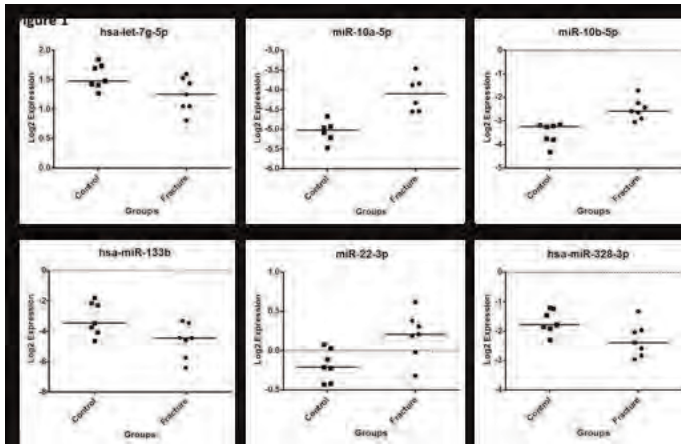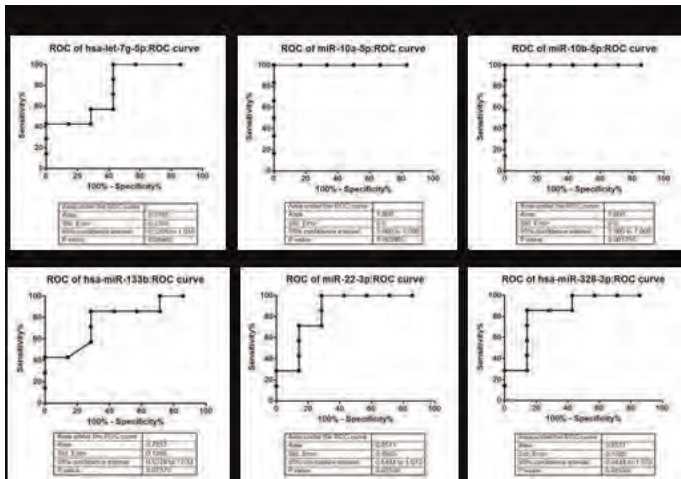
Figure 1

Figure 2

1031

Wnt-Lrp5 signaling regulates fatty acid metabolism in the osteoblast. Julie Frey[1], Zhu Li[1], Jessica Ellis[1], Charles Farber[2], Susan Aja[1], Michael Wolfgang[1], Thomas Clemens[3], Ryan Riddle*[1]. [1]Johns Hopkins University School of Medicine, USA, [2]University of Virginia, USA, [3]Johns Hopkins University, USA

The interaction of Wnt ligands with frizzled receptors and the closely-related Lrp5 and Lrp6 co-receptors is critical for many aspects of osteoblast function. In this study, we identify a previously unrecognized Wnt-dependent function unique to the Lrp5 co-receptor that enables osteoblasts to oxidize fatty acids. Mice lacking the Lrp5 co-receptor specifically in osteoblasts and osteocytes exhibit the expected reductions in postnatal bone mass but also develop an increase in body fat with corresponding reductions in energy expenditure. These changes in body composition and metabolism were not the result of deviations in glucose metabolism, as random fed and fasting glucose measurements, as well as formal glucose and insulin tolerance testing, revealed normal responses in the Lrp5 mutant mice. Rather, genetic ablation of Lrp5 in bone cells was associated with increased levels of plasma triglycerides and free fatty acids, without changes in the metabolic profile of the liver, muscle, or brown adipose. These phenotypes were not observed in mice lacking the Lrp6 co-receptor in osteoblasts and osteocytes. However, the development of visceral fat was correlated with the functional activity of Lrp5 in osteoblasts, as mice engineered to express a high-bone mass mutant Lrp5 allele (LRP5[G171V]) in bone are leaner than controls with reduced plasma lipid levels. In this context, Wnt-initiated signals downstream of Lrp5 regulate the expression of key enzymes required for fatty acid β-oxidation as microarray analysis of mRNA isolated from Lrp5-deficient calvarial osteoblasts and quantitative PCR analysis of samples collected from the long bones of mutant mice revealed reductions in the expression of *Acsl1, Acadl, Acads, Acadvl*, and *Cpt1b*, the rate-limiting enzyme in fatty acid oxidation. Moreover, oxidation of oleate was significantly reduced in cultures of Lrp5-deficient osteoblasts, while acute stimulation with Wnt10b or LiCl enhanced the expression of enzymatic mediators of fatty acid oxidation and the oxidation of oleate by wild-type osteoblasts *in vitro*. Together, our data suggest a direct link between bone cell metabolism and whole-body energy expenditure and that Wnt-Lrp5 signaling regulates basic cellular activities beyond

those associated with fate-specification and differentiation in bone. We speculate that therapeutic approaches designed to stimulate bone formation by targeting Wnt-Lrp5 signaling may also positively influence whole-body metabolism.

1032

The GABA_BR1 Modulates Skeletal Actions of Chronic Hyperparathyroidism by Controlling PTH Secretion and Ca²⁺-responsiveness of The Parathyroid Glands. Hanson Ho[1], Jenna Hwong[1], Alfred Li[1], Christian Santa Maria[1], Zhiqiang Cheng[1], Amanda Herberger[1], Chia-Ling Tu[1], Jean-Pierre Vilardaga[2], Wenhan Chang*[1]. [1]Endocrine Research Unit, Department of Veterans Affairs Medical Center, University of California San Francisco, USA, [2]University of Pittsburgh, School of Medicine, USA

To define the mechanisms underlying the enhanced PTH secretion and the right-shifted Ca^{2+} set-point in the inhibition of PTH secretion in the primary hyperparathyroidism (HPT), we generated a mouse model (PTC-CaSR-Het) with heterozygous knockout (KO) of the calcium-sensing receptor (CaSR) gene targeted specifically to parathyroid cells (PTCs). These mice showed elevated serum Ca^{2+} (sCa) and PTH (sPTH) levels and increased body weights and produced skeletal anabolism as indicated by increases in bone size (Tb.TV), trabecular (Tb) bone mass (Tb.BV/TV), and number (Tb.N) by micro-computed tomography (µCT) (see Table below). We further found that PTCs express the type B γ-aminobutyric acid (GABA) receptor 1 (GABA_BR1), which is another member of family C GPCR and has strong structural homology to the CaSR. By fluorescence resonance energy transfer (FRET) and bimolecular fluorescence complementation (BiFC) technologies, we confirmed that the CaSR and GABA_BR1 form strong heteromeric protein complexes in HEK-293 cells transfected with the cDNAs of the fluorescent protein-tagged receptors. To test whether the GABA_BR1 critically mediate PTH secretion and alter Ca^{2+}-responsiveness of PTCs at basal and HPT states, we compared sCa^{2+} and sPTH levels and skeletal phenotypes among PTC-CaSR-Het mice, PTC-GABA_BR1-Hom mice, which have both alleles of *Gabbr1* genes deleted in PTCs, double PTC-CaSR-Het/GABA_BR1-Hom KO (DKO) mice, and their control (Cont) littermates. The secretory capacities and Ca^{2+} set-points of parathyroid glands (PTGs) cultured from these mice were also assessed. Interestingly, the PTC-GABA_BR1-Hom mice showed reduced sCa and sPTH levels and decreases in body weight, bone size (Tb.TV), Tb bone mass (Tb.BV/TV), and thickness (Tb.Th) (Table below). Furthermore, the mineral and skeletal phenotypes of PTC-CaSR-Het and PTC-GABA_BR1-Hom mice were mutually alleviated in the DKO mice. PTGs cultured from the PTC-CaSR-Het mice showed a profound increase in the maximal secretion (3-4 fold) and a right-shift in Ca^{2+} set-points from 1.3 to 1.5 mM vs Cont PTGs (see Figure below), but these effects were completely abrogated by concurrent ablation of the *Gabbr1* genes in the PTGs of the DKO mice. Our data support the concept that the parathyroid GABA_BR1 critically control mineral and skeletal homeostasis at basal and HPT states by promoting PTH secretion and by inhibiting the Ca^{2+}-responsiveness of PTCs potentially by physically interacting with the CaSR.

Genotype	sPTH, pg/mL	sCa, mg/dL	Body wt gm	Tb. TV mm³	Tb.BV/TV %	Tb.N	Tb.Th µm
Cont	172±11	9.61±0.06	28.3±0.4	2.07±0.05	10.0±0.4	4.64±0.09	39.5 ± 0.7
CaSR-Het	219±19*	10.91±0.15**	30.3±0.9*	2.34±0.08**	13.0±1.2*	5.28±0.12**	42.3 ± 1.5
GABA_BR1-HOM	115±8**	9.42±0.04**	25.3±0.4**	1.66±0.03**	8.8±0.5*	4.80±0.17	35.5±0.7**
DKO	130±24	10.01±0.24*	29.6±1.2	2.04±0.05	10.3±0.1	4.28±0.17	38.8±1.4

* $p<0.05$; ** $p<0.01$ compared to control mice (Cont) DKO: PTC-CaSR-Het/GABABR1-Hom double KO mice
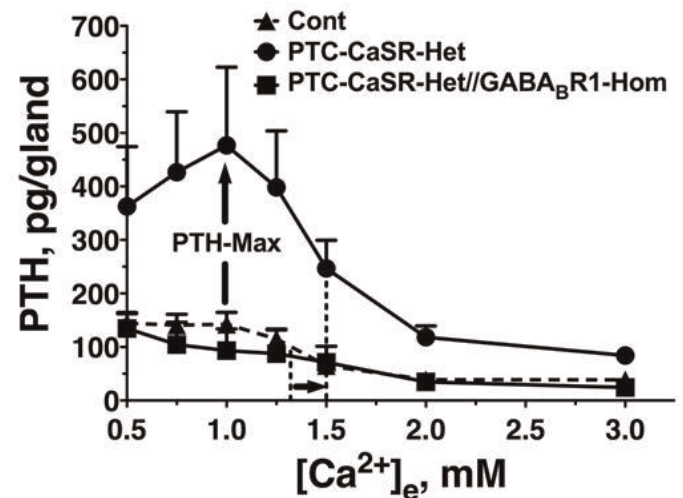
Table: Mineral and skeletal phenotypes of the PTC-specific gene KO mice.

Figure: PTH secretion and Ca dose response curves in cultured PTGs

1033

ERRalpha, a pro-Bone metastatic factor : Implication in metastatic Niche and prostate Cancer Stem Cells phenotype. Mathilde Bouchet[1], Anais Fradet[1], Carine Delliaux[2], Lamia Bouazza[1], Francesco Pantano[1], Xavier Leroy[3], Akeila Bellahcene[4], Vincent Castonovo[4], Philippe A.R. Clezardin[5], Martine Duterque-Coquillaud[2], Edith Bonnelye*[6]. [1]INSERM1033, France, [2]CNRS UMR8161, France, [3]Institut de Pathologie-Centre de Biologie-Pathologie, France, [4]University of Liege, Belgium, [5]INSERM & University of Lyon, France, [6]Faculte de Medecine RTH Laennec, France

Up to 80% of patients dying from prostate carcinoma have developed bone metastases that are incurable. Because we found the orphan nuclear receptor ERRa (Estrogen receptor related receptor alpha) expressed in bone metastases from prostate cancer patients, we modulated its expression in PC3 cells. We showed that human PC3 cells over-expressing wild-type ERRa (PC3-ERRa) increased rapidly and dramatically, in 3 weeks only, osteolytic bone lesions in SCID mice (n=10) $(1,20 \pm 0,34*$ for osteolysis (mm2) and $18,5 \pm 5,4**$ for skeletal tumor burden (TB/STV)(%)) compared to that observed with PC3-CT cells $(0,49 \pm 0,22$ (osteolysis) and $2 \pm 0,73$ (TB/STV)). Surprisingly bone destruction was combined with new bone formation, as 70% of the metastatic limbs that were bearing PC3-ERRa cells had mixed lesions compared with CT-PC3 that only developed osteolytic lesions. Osteoclasts were directly affected in vivo and in vitro which was associated with the stimulation of pro-osteoclastic factors mRNA of Cox2, MMP1, RANK, and Cathepsin K by PC3-ERRa. On the other hand, a statistical stimulation of bone formation in calvaria culture and in MC3T3 was observed when cells were co-cultured with PC3-ERRa compared to PC3-CT. That was combined with the up-regulation of ET1, Wnt3a and Wnt5a mRNA and protein by PC3-ERRa which may explain the occurrence of bone formation in the skeletal lesions. Interestingly, tumoral microenvironment was also affected by PC3-ERRa cells, as mouse periostin (POSTN), was over-expressed by the cancer-associated-fibroblasts in vivo which was probably due to the fact that TGFb2 was stimulated in PC3-ERRa cells in vitro and in vivo. Moreover, we found that over-expressing ERRa in PC3 inhibits spheres formation (in presence or absence of POSTN) which was associated with a decrease in the enforcers of the stem cell phenotype and pluripotency Nanog and Oct4 expression in vivo. Finally we showed that elevated expression of ERRa mRNA in prostate carcinoma (cohort of 60 patients) is also associated with high level of ET1, Cox2, POSTN and Wnt5a. In conclusion, our data provided for the first time evidence that ERRa can promote both osteolysis and osteosclerosis in animal models of prostate cancer bone metastases via the stimulation of pro-osteoclastic and pro-osteoblastic factors. These data also suggest an implication of ERRa in the stromal niche via the TGFb2/POSTN/Wnt signaling and in the inhibition of the self-renewal capacity and pluripotency of tumor cells.

Disclosures: Edith Bonnelye, None.

1034

WNT5A Inhibits Skeletal Metastases of Prostate Cancer in Mice and Is Associated with a Longer Patient Survival. Stefanie Thiele*[1], Andy Göbel[2], Sandra Hippauf[2], Tilman D. Rachner[2], Michael Muders[2], Susanne Fuessel[2], Ricardo Bernhardt[3], Franz Jakob[4], Martina Rauner[5], Lorenz Hofbauer[6]. [1]Germany, [2]Uniklinikum Dresden, Germany, [3]Technische Universität Dresden, Germany, [4]University of Würzburg, Germany, [5]Medical Faculty of the TU Dresden, Germany, [6]Dresden University Medical Center, Germany

Prostate cancer is the most common cancer type in elderly men and often metastasizes to bone in advanced stages. Early detection could therefore help to prevent cancer progression and skeletal metastases. Thus, it is important to find prognostic markers that predict the aggressiveness of prostate cancer. Wnt proteins are implicated in carcinogenesis and especially WNT5A has been discussed to influence the clinical outcome of various cancer types, including prostate cancer. In addition, WNT5A stimulates osteogenic differentiation. Hence, WNT5A may not only be involved in prostate cancer development, but also in the formation of subsequent skeletal metastases. Here, we determined the role of the WNT5A expression profile in prostate cancer *in vitro* and *in vivo*.

A tissue microarray was created using a cohort of 397 mainly high-risk prostate cancer patients who underwent radical prostatectomy, and was stained for WNT5A. Effects of WNT5A knock-down or overexpression on proliferation and apoptosis of prostate cancer cell lines (PC3, C42B, MDA-PCa-2b) were examined *in vitro*. In vivo, WNT5A was overexpressed in luciferase-labeled PC3 cells (PC3-Luc) which generate osteolytic lesions. To determine the impact of WNT5A on tumor growth PC3-Luc cells were injected subcutaneously, intratibially or intracardially into nude mice.

Expression of WNT5A was higher in prostate cancer patients as compared to patients with benign prostatic hyperplasia (p<0.05). Patients with high WNT5A levels had a higher probability for a longer survival than those with low WNT5A expression (p=0.025). *In vitro*, WNT5A overexpression in PC3 cells reduced proliferation by 39%, and simultaneously induced apoptosis 2-fold (as determined by caspase 3/7 activation, annexin V/PI-positive cells, PARP cleavage, and DNA fragmentation). Knock-down of WNT5A yielded opposite results. Similar effects were seen in C42B and MDA-PCa-2b. *In vivo,* subcutaneous tumor growth and tumor growth within the bone microenvironment was inhibited in nude mice injected with WNT5A-overexpressing

PC3-Luc cells compared to mice injected with PC3-Luc cells (-90% and -85%, p<0.05). Moreover, while 80% of the mice receiving PC3-Luc cells developed bone metastases and bone lesions, overexpression of WNT5A abolished this process.

These data indicate that WNT5A exhibits anti-tumor effects in prostate cancer and may be suitable as a prognostic marker and novel therapeutic target for prostate cancer and associated skeletal metastases.

Disclosures: Stefanie Thiele, None.

1035

Modeling osteogenic sarcoma: insight into tumor initiation and progression. Jianning Tao*, Brendan Lee. Baylor College of Medicine, USA

Osteogenic sarcoma (OS) is the most common malignant tumor of bone with a predilection for adolescents and young adults. Human OS occurs sporadically and bone tumor initiation and progression are poorly understood. We describe here the generation of characterization of a genetically engineered mouse model of OS based on conditional expression of truncated Notch1 protein. All animals spontaneously developed bone tumors including OS-like with 100% penetrance. The tumors, developed through Rbpj-dependent canonical pathway, model human OS including morphology, metastatic behavior, cytogenetic complexity, and genome-wide expression profiling. We demonstrated that Notch activation combined with p53 loss synergistically accelerates OS development in mice, though p53 driven OS is not dependent on canonical Notch signaling, revealing a dual dominance of Notch oncogene and p53 mutation in the development of OS. Because of similarity between murine OS and human OS, our authenticated model can be used not only to address cancer mechanisms of OS but also as a valuable platform for developing novel therapeutic strategies.

Disclosures: Jianning Tao, None.

1036

Runx2 Phosphorylation Increases Migration and Invasive Activity of Prostate Cancer Cells and is Associated with Metastatic Disease. Chunxi Ge*[1], Guisheng Zhao[2], Xiang Zhao[2], Yan Li[3], Hui Li[3], Binbin Li[5], Giuseppe Pannone[4], Pantaleo Bufo[4], Angela Santoro[4], Francesca Sanguedolce[4], Simona Tortorella[4], Marilena Mattoni[4], Silvana Papagerakis[5], Evan Keller[3], Renny Franceschi[3]. [1]Pom Univ of Michigan School of Dentistry, USA, [2]University of Michigan School of Dentistry, USA, [3]University of Michigan, USA, [4]University of Foggia, Italy, [5]University of Michigan School of Medicine, USA

The osteogenic transcription factor, Runx2, is abnormally expressed in prostate cancer where it stimulates expression of several metastasis-associated genes. During normal bone development, Runx2 transcriptional activity is activated by signals known to be hyperactive in prostate cancer including the ERK/MAP kinase pathway, which phosphorylates Runx2 at Ser 301 and Ser 319. This study examines the role of these phosphorylation sites in Runx2-dependent activation of metastasis-associated gene expression, *in vitro* migration and invasive activity of prostate cell lines as well as the relationship between Runx2 phosphorylation and tumor stage. Runx2 was preferentially expressed in more invasive prostate cancer cell lines (PC-3> C4-2B > LNCaP). Furthermore, the ratio of Runx2-S319-P/total Runx2 as well as P-ERK/ total ERK was greater in PC-3 and C4-2B versus LNCaP cells. Phosphorylated Runx2 had an exclusively nuclear localization and was enriched in PC3 cultures while total Runx2 had a cytoplasmic and nuclear distribution. Overexpression of wild type Runx2 increased *Mmp9*, *Vegfa* and *Spp-1* mRNA and increased *in vitro* migratory and invasive activity in PC-3 cells as well as the non-tumorigenic prostate cell line, RWPE1. In contrast, a phosphorylation-deficient Runx2 mutant (Runx2-S301A,S319A) had greatly reduced activity. Analysis of tissue microarrays from 129 patients revealed strong nuclear staining with a Runx2-S319-P-specific antibody in primary prostate cancers and metastases. P-Runx2 staining was positively correlated with Gleason score and occurrence of lymph node metastases. Little or no Runx2 phosphorylation was detected in normal prostate tissue, benign prostate hyperplasia or prostatitis indicating that Runx2 phosphorylation is closely associated with prostate cancer induction and progression towards an aggressive phenotype.

Disclosures: Chunxi Ge, None.

1037

Micro-RNA-mediated Targeting of Runx2 Reduces Breast Cancer Metastasis and Progression of Osteolytic Disease. Hanna Taipaleenmaki*[1], Gillian Browne[2], Jacquelin Akech[3], Andre Van Wijnen[4], Janet Stein[5], Eric Hesse[6], Gary Stein[7], Jane Lian[8]. [1]University Medica Center Hamburg-Eppendorf, Germany, [2]Department of Biochemistry & Vermont Cancer Center, University of Vermont College of Medicine, USA, [3]University of Massachusetts Medical School, USA, [4]Mayo Clinic, USA, [5]Vermont Cancer Center, University of Vermont College of Medicine, USA, [6]University Medical Center Hamburg-Eppendorf, Deu, [7]University of Vermont, College of Medicine, USA, [8]University of Vermont College of Medicine, USA

Progression of breast cancer to metastatic bone disease is associated with an aberrantly elevated expression of Runx2, which promotes the disease progression by activating many genes involved in the 'vicious cycle' of cancer-induced bone disease. Because transcription factors are not readily targetable for therapeutic intervention, our goal was to evaluate the potential clinical use of Runx2-targeting miRNAs to reduce tumor growth and bone metastatic burden. Expression analysis of a panel of miRNAs regulating Runx2 revealed a reciprocal relationship between the abundance of Runx2 protein and two miRNAs, miR-135 and miR-203. These miRNAs are highly expressed in normal breast epithelial cells where Runx2 is not detected, and conversely are absent in metastatic breast cancer cell lines and tissue biopsies that express Runx2. Reconstituting metastatic MDA-MB-231-Luc cells with miR-135 and miR-203 reduced the abundance of Runx2 and the expression of the metastasis-promoting Runx2 target genes IL-11, MMP-13, and PTHrP. Additionally, tumor cell viability decreased and cell migration was suppressed *in vitro*. *In vivo* implantation of MDA-MB-231-luc cells expressing miR-135 or miR-203 into the mammary gland, followed by additional intratumoral administration of the synthetic miRNAs reduced tumor growth and importantly, spontaneous metastasis to bone. Furthermore, intratibial injection of these miRNA-expressing cells impaired tumor growth in the bone environment, inhibited bone resorption and secondary metastasis to lung. We conclude that miRNAs targeting Runx2 are protective against metastasis, while deregulated expression of Runx2 in aggressive tumor cells is related to the loss of specific Runx2-targeting miRNAs. Our studies have also demonstrated for the first time that delivery of synthetic miRNAs is a viable therapeutic strategy to target transcription factors for the prevention of metastatic bone disease.

Disclosures: Hanna Taipaleenmaki, None.

1038

Intravital 2-photon imaging reveals tumour-associated macrophages as the cellular targets underlying the anti-tumour activity of bisphosphonates in vivo. Michael J Rogers*[1], Simon Junankar[1], Charles E McKenna[2], Shuting Sun[2], Tri Giang Phan[1]. [1]Garvan Institute of Medical Research, Australia, [2]University of Southern California, USA

Bisphosphonate (BP) drugs target rapidly to the skeleton and are the gold standard treatment to inhibit osteoclastic bone resorption in patients with metastatic bone disease. BPs also decrease tumour growth and metastasis outside the skeleton in mouse tumour models. In recent clinical trials, adjuvant treatment with zoledronic acid alongside standard therapy also increased disease-free survival, and reduced local tumour recurrence and soft tissue metastases in estrogen-deficient women with early breast cancer. However, the exact mechanisms underlying these anti-tumour effects of BPs are not known since BPs are generally considered to have little, if any, effect on cells in soft tissues outside the skeleton other than a transient effect on circulating monocytes. To finally answer this question we determined the cell types capable of internalising fluorescently-labelled BP in 4T1 mammary tumours in live mice. Within minutes of tail vein injection, intravital 2-photon imaging revealed the flow of BP into mammary tumours via the disorganised tumour vasculature. BP then diffused into mammary tumour tissue from leaky vessels and bound to microcalcifications that were rapidly engulfed by F4/80[+] tumour-associated macrophages. Intravital imaging of individual macrophages in tumours of live mice also revealed the uptake of BP by pinocytosis. Flow cytometric analysis of the mammary tumours 24 hours after iv injection of BP confirmed that cellular uptake of BP occurred predominantly by CD11b^{+}F4/80^{+} macrophages, but not by tumour cells or CD11b^{+}F4/80^{-} tumour-infiltrating leukocytes. BP did not accumulate in normal mammary tissue. These studies provide conclusive evidence that, under certain circumstances, BPs can be rapidly internalised by tumour-associated macrophages outside the skeleton. The disorganised and leaky vasculature of tumours facilitates the local diffusion of BP and uptake by macrophages, enhanced by the presence of microcalcifications. Given the important role of macrophages in promoting tumour progression and metastasis, our studies strongly suggest that the anti-tumour activity of BPs in vivo occurs via effects on tumour-associated macrophages rather than by direct effects on tumour cells.

Disclosures: Michael J Rogers, None.

1039

Reduced Cortical Bone Mass in Mice with B Lymphocyte-Specific Androgen Receptor Inactivation. Jianyao Wu*[1], Anna Borjesson[2], Anna Wilhelmson[3], Åsa Tivesten[3], Sofia Moverare Skrtic[4], Claes Ohlsson[4]. [1]Sahlgrenska Academy, University of Gothenburg, Sweden, [2]Center for Bone & Arthritis Research, Sahlgrenska Academy, Sweden, [3]Wallenberg Laboratory for Cardiovascular & Metabolic Research, Institute of Medicine, Sahlgrenska Academy, University of Gothenburg, Sweden, [4]Center for Bone & Arthritis Research at the Sahlgrenska Academy, Sweden

Sex steroids are chief regulators of gender differences in the skeleton, and male gender is one of the strongest protective factors against osteoporotic fractures. Male mouse models with general inactivation of the androgen receptor (AR) have reduced trabecular and cortical bone mass. Recent studies using cell-specific inactivation of the AR demonstrate that testosterone acting via the AR in osteoblast-lineage cells increases the trabecular bone mass. However, the AR expressing cell type mediating the effects of androgens on cortical bone is unknown. The immune system is a crucial regulator of bone homeostasis and it has been proposed that B and T lymphocytes are involved in the bone-sparing effect of sex steroids. We hypothesized that the AR in immune cells might mediate the effects of androgens on cortical bone mass. The aim of the present study was, therefore, to determine the possible role of the AR in B and T lymphocytes for cortical bone homeostasis using mouse models with cell-specific inactivation of the AR.

To assess the role of the AR in T lymphocytes, we generated T cell-specific male AR[-] mice (using LCK-Cre). However, these mice had unchanged cortical bone parameters (cortical thickness, area and volumetric bone mineral density) as analyzed by µCT in the mid-diaphyseal region of femur. To determine the role of the AR in B lymphocytes, we generated B cell-specific male AR[-] mice (using CD19-Cre, deleting the AR from the pre-B cell stage). Importantly, the B cell-specific AR[-] mice displayed significantly reduced cortical bone area (-13±3%, p<0.01) and thickness (-9±2%, p<0.01) compared with control mice. The reduced cortical thickness was mainly caused by reduced periosteal circumference. To validate these findings, we developed a second mouse model with B cell-specific inactivation of the AR using Mb1-Cre mice (deleting AR from the pro-B cell stage). These mice also had reduced cortical bone area (-10±3%, p<0.05) and thickness (-8±2%, p<0.01) compared with control mice. In contrast, osteoblast-specific inactivation of the AR (using Osx1-Cre) did not affect the cortical bone parameters in male mice, confirming the results from previous osteoblast-specific mouse models.

In conclusion, we demonstrate that B cell-specific AR inactivation results in reduced cortical bone mass. Based on these findings, we propose that the AR in B lymphocytes may, at least partly, mediate the stimulatory effects of androgens on cortical bone mass.

Disclosures: Jianyao Wu, None.

1040

T cell expression of CD40L potentiates the bone anabolic activity of PTH by promoting osteoblastogenesis and bone formation. Jerid Robinson*[1], Jau-Yi Li[2], Abdul Malik[2], Michael Reott[3], Lindsey Walker[1], Jonathan Adams[1], M. Neale Weitzmann[2], Roberto Pacifici[2]. [1]Emory University, USA, [2]Emory University School of Medicine, USA, [3]Emory University School of Medicine, USA

T cells are required for intermittent parathyroid hormone (iPTH) treatment to increase bone volume and strength. One of the involved mechanisms is increased production of the osteogenic Wnt ligand Wnt10b by bone marrow T cells. However, additional mechanisms might play a role. T cells provide proliferative and survival cues to SCs through CD40L, a surface molecule of activated T cells that induces CD40 signaling in SCs. Thus a cross-talk between T cells and SCs mediated by the CD40L contributes to maintain an adequate pool of osteoblastic cells. To investigate the role of CD40L in the anabolic activity of iPTH 6 week old WT and CD40L-/- mice were injected daily with vehicle or iPTH (80µg/kg/day) for 4 weeks. Femurs and spines were then harvested and analyzed by µCT scanning. iPTH induced a lower increase in bone volume (BV/TV) in CD40L-/- mice as compared to WT controls in both regions. Indices of bone structures were also improved less potently by iPTH in CD40L-/-mice than in WT mice. iPTH had similar effects in cortical bone in WT and CD40L mice, consistent with the fact that T cells potentiate the trabecular but not the cortical anabolic effects of iPTH. Mechanistic studies revealed that iPTH increased bone formation more potently in WT than in CD40L -/- mice. Moreover, iPTH increased the number of SCs, stimulated SC proliferation and differentiation, and blocked SC apoptosis in WT mice but not in CD40L-/- mice. To investigate the specific role of T cell expressed CD40L, T cell deficient TCRβ-/- mice were subjected to adoptive transfer of WT T cells and CD40L -/- T cells. Reconstituted mice were then treated with vehicle or iPTH for 4 weeks. We found that iPTH induced a significant increase in BV/TV, indices of bone structure, and bone formation in TCRβ-/- mice reconstituted with WT T cells. By contrast iPTH did not exert a significant anabolic activity in T cell deficient mice and mice with T cells lacking CD40L expression. In conclusion, our data show that T cell expressed CD40L potentiates the bone anabolic activity of iPTH. Activation of CD40 signaling in SCs by T cell expressed CD40L is required for iPTH to increase SC proliferation, differentiation and lifespan.

Disclosures: Jerid Robinson, None.

1041

Continuous PTH Treatment Induces Bone Loss through T Cells Produced IL17. Jau-Yi Li*[1], Lindsey Walker[2], Abdul Malik[1], Michael Reott[3], Jonathan Adams[4], M. Neale Weitzmann[1], Roberto Pacifici[1]. [1]Emory University School of Medicine, USA, [2]Emory University, USA, [3]Emory University School of Medicine, USA, [4]Emory University School of Medicine, USA

Hyperparathyroidism in humans and continuous PTH treatment (cPTH) in mice stimulate bone resorption and cause bone loss by regulating RANKL/OPG production by stromal cells (SCs) and osteoblasts. Reports have shown that T cells markedly potentiate the bone catabolic effect of cPTH by inducing CD40 signaling in SCs through their surface receptor CD40L. In addition, cPTH stimulate T cells to secrete the osteoclastogenic cytokine TNF, a factor that potentiates the osteoclastogenic activity of RANKL. A search for additional mechanisms by which T cells potentiate cPTH induced bone loss revealed that in vivo cPTH treatment for 2 weeks increased by ~2-3 fold the frequency of Th17 cells in the BM. Th17 are a highly osteoclastogenic population of CD4+ cells defined by the capacity to produce IL-17, a potent inducer of RANKL and TNF production. To investigate the mechanism by which cPTH expands Th17 cells we assessed Th17 cell differentiation, proliferation and homing. We found that cPTH increased the differentiation of naïve CD4+ cells into Th17 cells. However, cPTH did not regulate Th17 proliferation and homing. Th17 cell differentiation is induced by several cytokines including TGFβ, IL-6 and TNF. All of these factors are upregulated by cPTH. We found that cPTH increased the relative frequency of Th17 cells in the BM in WT mice, but not in TNF-/- mice. Moreover, cPTH increased IL-17A mRNA levels and the expression of the Th17-inducing transcription factors RORα and RORt in BM CD4+ T cells in WT but not in TNF-/- mice. These findings reveal that cPTH expands Th17 cells through TNF. To investigate the contribution of Th17 cells to cPTH induced bone loss, mice were treated with cPTH and either Irr. Antibody (Ab) or anti IL-17 Ab for 2 weeks. IL-17 Ab completely blocked the loss of trabecular and cortical bone (as measured by μCT), and the increase in bone resorption (as measured by histomorphometry and serum CTX). By contrast, treatment with Irr Ig did not antagonize the bone catabolic effects of cPTH. Furthermore, IL-17 Ab completely blocked the increase in SC production of TNFα and RANKL induced by cPTH, demonstrating that cPTH stimulates SC osteoclastogenic function through T cell produced IL17. In summary, these findings demonstrate that cPTH polarizes the differentiation of CD4+ cells toward the Th17 subset via TNF, and that cPTH induces bone loss through IL-17. Neutralization of IL-17 may thus represent a novel therapeutic strategy for hyperparathyroidism.

Disclosures: Jau-Yi Li, None.

1042

Tmem178 modulates bone homeostasis via a novel negative feedback loop targeting endoplasmic reticulum Ca^{2+} mobilization in osteoclasts. Corinne Decker*[1], Deborah Novack[2], Roberta Faccio[2]. [1]Washington University in St. Louis, USA, [2]Washington University in St. Louis School of Medicine, USA

PLCγ2 catalytic activity triggers Ca^{2+} fluxes leading to robust activation of NFATc1, the central transcription factor of osteoclastogenesis (OCG). Despite PLCγ2's essential role in promoting OC formation, its therapeutic targeting is impeded by high homology with the ubiquitously expressed PLCγ1. To identify specific mediators downstream of PLCγ2, we performed a gene array comparing WT and PLCγ2-/- OC precursors. Transmembrane protein 178 (Tmem178), an uncharacterized integral membrane protein, is a novel PLCγ2-dependent gene that is upregulated by RANKL in WT cells. In striking contrast to the osteopetrotic phenotype of PLCγ2-/- mice, Tmem178 deficiency leads to a significant 35% decrease in trabecular bone accompanied by enhanced OC numbers (KO 25.7+/-4.4, WT 12.5+/- 1.9). Tmem178-/- OC precursors are more sensitive to RANKL in vitro as shown by rapid induction of TRAP, DC-STAMP, and calcitonin receptor, suggesting that Tmem178 acts in a negative feedback loop downstream of RANKL-PLCγ2. As the addition of LPS or TNF to Tmem178-/- preOCs further exacerbates OCG, we tested Tmem178's role in restraining pathological bone loss using 2 models of inflammatory osteolysis: supracalvarial LPS and serum-transfer arthritis. In both conditions Tmem178 null mice suffer profound bone loss due to significant increase in OCs compared to WT mice. Thus, Tmem178 regulates OCG and bone mass in basal and pathological states. Increased OC numbers and responsiveness to RANKL are often associated with augmented NF-kB and MAPK activation. Remarkably, we found no changes in these pathways in Tmem178-/- preOC. Nevertheless, NFATc1 total protein levels and nuclear translocation are strikingly amplified in Tmem178-/- cells. To determine how Tmem178 controls NFATc1 levels we measured cytosolic Ca^{2+} in preOCs stimulated with RANKL and found a higher immediate spike and sustained increase in $[Ca^{2+}]$ in null cells compared to WT. By immunofluorescence and co-immunoprecipitation, we detected Tmem178 in the endoplasmic reticulum (ER) where it interacts with Stim1, a known regulator of Ca^{2+} mobilization during OCG. Importantly, ectopic Tmem178 suppresses thapsigargin-induced ER Ca^{2+} release and likewise dampens RANKL-stimulated NFATc1 and OCG. These findings suggest that Tmem178 is a previously unknown fine-tune regulator of ER Ca^{2+} stores. In sum, we define Tmem178 as a critical mediator of bone homeostasis via a novel negative feedback loop targeting the RANKL-Ca^{2+}-NFATc1 axis.

Disclosures: Corinne Decker, None.

1043

Inflammation-Induced Hypercytokinemia and Myeloproliferation Underlie Osteopenia in Scurfy Mice; the Animal Model For Heritable Autoimmune Disease IPEX. Yousef Abu-Amer[1], Tim Hung-Po Chen*[2], Gaurav Swarnkar[2], Gabriel Mbalaviele[1]. [1]Washington University in St. Louis School of Medicine, USA, [2]Washington University School of Medicine, USA

Immune surveillance through regulatory T cells (Tregs) plays a crucial role in bone homeostasis. The development and function of Tregs requires the Foxp3 gene product. The mouse model of autoimmune disease IPEX (Immune dysregulation, Polyendocrinopathy, Enteropathy, X-linked) syndrome, namely *Scurfy (Sf)*, bears a loss-of-function mutation in *Foxp3*. Both IPEX and Sf result in multi-organ inflammation. Herein, we report that *Sf* mice exhibit severe bone loss mediated by accelerated osteoclastogenesis (OCG). Biochemical studies suggest that Foxp3 deficiency results in upregulation of NEMO/IKKg gene in T helper cells through loss of Foxp3/NEMO interaction, thereby trigging NF-kB mediated over-production of pro-OCG cytokines (e.g. M-CSF, RANKL, IL-17 and TNF). In this study, we use molecular, cellular and pharmacological approaches to study how loss of Foxp3 prompts osteolysis. Using hematopoietic stem cell flow analysis of bone marrow cells (BMC), we observed a 2.5x increase of lin⁻Sca-1⁺c-kit⁺ hematopoietic stem cells (LSK HSCs) and 2x increase for granulocyte/macrophage progenitors (GMPs) in *Sf* relative to WT BMC. Interestingly, using *ex vivo* OCG assay, fluorescence-activated cell sorted LSK HSCs derived from *Sf* BMC exhibited significantly increased (5x) OCgenic potential than GMPs, implying that inflammatory condition in *Sf* mice affects osteoclast progenitors at very primitive stage. *Sf* LSK HSCs exhibited greater sensitivity to M-CSF signaling and contained 5x more PU.1+ *Sf* LSK HSCs than WT. *In vivo* administration of M-CSF neutralizing antibody (Ab) as well as crossing *Sf* hemizygous female with *Op* heterozygous male (half reduction of systemic M-CSF level) attenuated but not entirely reversed osteopenia in *Sf* and OCG *ex vivo* . Contrarily, *in vivo* administration of IL-17 neutralizing Ab or RORg inhibitor failed to reverse osteopenia, questioning the importance of IL-17 for autoimmune osteopenia in the context of Treg deficiency. Intriguingly, the immunosuppressive mTOR inhibitors, rapamycin and pp242, also had similar effect as the M-CSF Ab. Mechanistically, M-CSF antibody, M-CSF genetic ablation, rapamycin and pp224 all reduced GMP frequency in *Sf* BM, suggesting that they act either directly or indirectly at the HSC level. Taken together, our study suggests that Foxp3 deficiency leads to osteopenia owing to dysregulation of NF-kB and subsequent cytokine-mediated hyperproliferation of myeloid precursors and presents a target for therapeutic intervention.

Disclosures: Tim Hung-Po Chen, None.

1044

PARP1 is a Potent Negative Regulator of Bone Resorption. Chao Qu*[1], Samer Abu-Amer[2], Susan Grimston[3], Sheri Bonar[4], Jacqueline Kading[2], Gaurav Swarnkar[5], Monika Fey[5], Michael Hottiger[5], Yousef Abu-Amer[3], Roberto Civitelli[3], Gabriel Mbalaviele[3]. [1]Washington University in St Louis, USA, [2]Washington University School of Medicine, USA, [3]Washington University in St. Louis School of Medicine, USA, [4]Washington University in St. Louis, USA, [5]University of Zurich, Switzerland

Accumulating evidence indicates that poly(ADP-ribose) polymerase 1 (PARP1) regulates non-apoptotic functions, including transcriptional regulation. Evidence also shows that PARP1 undergoes various post-translational modifications, including caspase-mediated proteolytic cleavage at aspartate 214 (PARP1^{D214} site). To investigate PARP1 role in skeletal homeostasis, we characterized knock-in mice globally expressing non-cleavable PARP1 (PARP1$^{D214N/D214N}$ mice). Although PARP1$^{D214N/D214N}$ mice are grossly normal and fertile, bone volume/total volume (BV/TV) measured by μCT is significantly higher in 8 weeks old mutant mice compared to wild-type (WT) mice (0.35 ± 0.02 vs. 0.24 ± 0.03, p<0.005). Bones are also stiffer in mutant mice relative to WT mice (65.85 ± 16.17 N/mm vs. 42.51 ± 12.32 N/mm, p<0.05). To gain insights into the cellular mechanisms underlying this phenotype, we studied RANKL- and M-CSF-induced osteoclast (OC) differentiation of mouse bone marrow macrophages (BMMs). Intriguingly, a single allele of non-cleavable PARP1 (PARP1$^{+/D214N}$) is sufficient to suppress OC differentiation by >90%, and PARP1$^{D214N/D214N}$ arrests this process. During OC formation, PARP1, but not PARP1^{D214N}, is fully degraded, suggesting that this protein negatively regulates OC formation. To further test this hypothesis, we leveraged the fact that activation of NOD-like receptor (NLR) family, pyrin containing 3 (NLRP3) inflammasome targets PARP1 for cleavage at PARP1^{D214} site. We find that activation of the NLRP3 inflammasome promotes the cleavage of WT, but not PARP1^{D214N}; genetic or pharmacological inhibition of the NLRP3 inflammasome not only prevents PARP1 cleavage, but also inhibits of OC formation. Conversely, mice expressing constitutively activated NLRP3 (CA-NLRP3) inflammasome in myeloid cells, exhibit increased OC formation in vivo and decreased BV/TV compared to WT mice (0.24 ± 0.04 vs 0.12 ± 0.02, p<0.05). Furthermore, we find that PARP1 is barely detectable in BMMs expressing CA-NLRP3 inflammasome compared to WT cells. In summary, we find that PARP1 negatively regulates OC development, and its stability and abundance are at least in part controlled by the NLRP3 inflammasome during

osteoclastogenesis. Thus, we have uncovered a novel function of PARP1 in bone homeostasis.

1045

Bisphosphonate Drug Holiday and Fracture Risk. <u>Annette Adams</u>*[1], <u>John Adams</u>[2], <u>Marsha Raebel</u>[3], <u>Beth Tang</u>[2], <u>Jennifer Kuntz</u>[4], <u>Vinutha Vijayadeva</u>[5], <u>Elizabeth McGlynn</u>[2], <u>Wendolyn Gozansky</u>[3]. [1]Kaiser Permanente Southern California, USA, [2]Kaiser Permanente Center for Effectiveness & Safety Research, USA, [3]Kaiser Permanente Colorado, USA, [4]Kaiser Permanente Northwest, USA, [5]Kaiser Permanente Hawaii, USA

Purpose: Among women with ≥3 years exposure to bisphosphonates (BPs), we compared the incidence of osteoporosis-related fragility fractures in those who discontinued BPs for at least 12 months (drug holiday) to those who continued to use BPs (persistent use).

Methods: This retrospective cohort study included women aged ≥45 years from 4 Kaiser Permanente (KP) regions who initiated BP use between January 1, 1998 and December 31, 2009. Drug holiday was defined as ≥12 months with BP use at 0% adherence. Persistent use status required ongoing use at ≥50% adherence. The primary outcome of interest was the first occurrence of an incident clinical osteoporosis-related fragility fracture, identified from the electronic medical record (EMR) via ICD-9-CM codes. All subjects were followed until fracture, disenrollment from the health plan, death, or December 31, 2012. From the EMR, we collected information on the following potential confounders and effect modifiers: race/ethnicity; age; body mass index (BMI); comorbidities; history of previous fragility fracture; lowest T-score prior to cohort entry; fall risk; ten-year fracture risk; and prior/concomitant use of bone-active medications. Persistent users and drug holiday subjects were compared with regard to several demographic and clinical characteristics. Time-varying Cox proportional hazards models were used to compare osteoporosis-related fracture incidence between the two groups.

Results: The cohort of 28620 women, observed for 111997 person-years, included 17123 (59.8%) persistent BP users and 11497 (40.2%) drug holiday subjects. The drug holiday group had: fewer comorbidities, higher baseline T-scores, and lower fracture and fall risk scores. A total 3,571 osteoporosis-related fractures were observed. The unadjusted rate ratio (RR) for any osteoporosis-related fractures for drug holiday compared to persistent use was 0.87 (95% CI 0.81-0.94), but RR=1.0 (95% CI 0.9-1.2) for hip fractures only. The time-varying models suggested no differences in fracture risk (hazard ratio (HR) 0.90, 95% CI 0.80–1.00), after adjustment for baseline fall and fracture risk, comorbidities, and other bone-active medication use. Similarly, no difference in hip fracture risk was observed (HR 0.84, 95% CI 0.68–1.03).

Conclusion: Women who undertake a holiday from BP use are not at greater risk of osteoporosis-related fragility fractures, nor hip fractures specifically, than are women who continue to use BPs persistently.

1046

Effects of Two Years of Teriparatide, Denosumab and Combination Therapy on Peripheral Bone Density and Microarchitecture: The DATA-HRpQCT Extension study. <u>Joy Tsai</u>*[1], <u>Alexander Uihlein</u>[2], <u>Sherri-Ann Burnett-Bowie</u>[1], <u>Robert Neer</u>[1], <u>Yuli Zhu</u>[3], <u>Nicholas Derrico</u>[3], <u>Katelyn Foley</u>[3], <u>Hang Lee</u>[4], <u>Mary Bouxsein</u>[5], <u>Benjamin Leder</u>[6]. [1]Massachusetts General Hospital, USA, [2]Northwestern Memorial Faculty Foundation, USA, [3]Massachusetts General Hospital, Endocrine Unit, USA, [4]Massachusetts General Hospital, Biostatistics Center, USA, [5]Beth Israel Deaconess Medical Center, Harvard Medical School, USA, [6]Massachusetts General Hospital Harvard Medical School, USA
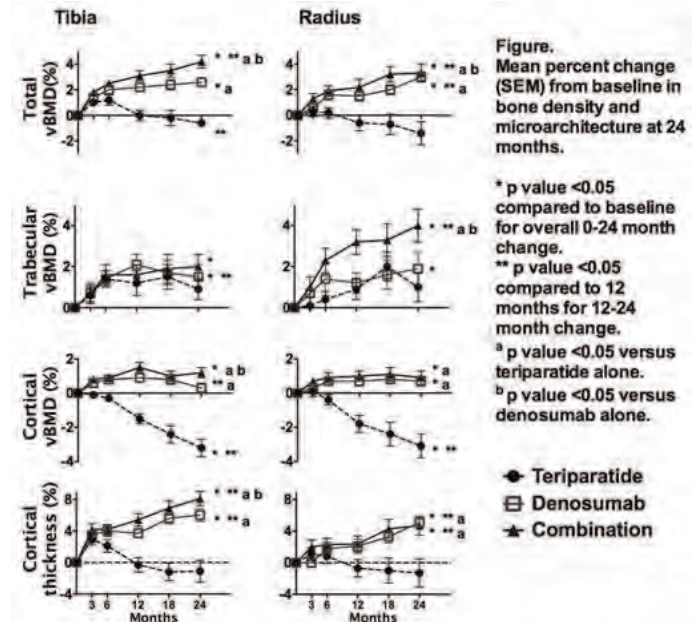
Background: In postmenopausal women, 24 months of combined denosumab (DMAB) and teriparatide (TPTD) increased hip and spine BMD more than either drug alone. The effect of combined DMAB and TPTD therapy on peripheral cortical and trabecular bone density and microarchitecture, however, is unknown.

Methods: We randomized 94 postmenopausal osteoporotic women ages 51-91 to receive TPTD 20-ug SC QD, DMAB 60-mg SC Q6 months, or both (COMBO) for 24 months. Women were excluded if they had ever used IV bisphosphonates (BPs) or oral BPs in the past 6 months. Total, trabecular and cortical density (Tot.vBMD, Tb.vBMD, Ct.vBMD), cortical thickness (Ct.Th) and trabecular microarchitecture were measured by high-resolution peripheral QCT of the distal radius and tibia at 0, 3, 6, 12, 18, and 24 months.

Results (Fig): At both the radius and tibia, Tot.vBMD and Tb.vBMD increased in the DMAB and COMBO groups but not in the TPTD group. The increase in Tot.vBMD in the COMBO group was greater than that in either monotherapy group at both sites (p<0.005 for all between-group comparisons). The increase in Tb.vBMD in the COMBO group was greater than in either monotherapy group at the radius (p<0.002 for both comparisons). Ct.vBMD decreased in the TPTD group but increased or was maintained in the DMAB and COMBO groups at both sites. The increase in tibial Ct.vBMD in the COMBO group was greater than in either monotherapy group (p<0.002 for both comparisons). Ct.Th did not change in the TPTD group but increased in the other groups at both sites. The increase in Ct.Th at the tibia was greater in the COMBO group than either monotherapy group (p<0.001 for both comparisons).Trabecular number increased in the COMBO group more than in the DMAB group (p=0.044). Changes during the 2nd year were notable for progressive increases in total vBMD and Ct.Th in the COMBO group. Ct.vBMD decreased linearly over 2 years in the TPTD group, which is in contrast to the observed changes in radius aBMD by DXA where the decline is limited to the first year.

Conclusions: Two years of combined DMAB and TPTD therapy increases radius and tibia total vBMD, increases radius Tb.vBMD, and increases tibia Ct.Th more than either drug alone. Furthermore, the TPTD-induced decrease in Ct.vBMD is fully prevented by DMAB co-administration. The combination of DMAB and TPTD results in the most favorable changes in peripheral bone density and geometry and may prove a useful intervention in women at high risk of fracture.

Figure

Figure. Mean percent change (SEM) from baseline in bone density and microarchitecture at 24 months.

* p value <0.05 compared to baseline for overall 0-24 month change.
** p value <0.05 compared to 12 months for 12-24 month change.
[a] p value <0.05 versus teriparatide alone.
[b] p value <0.05 versus denosumab alone.

● Teriparatide
□ Denosumab
★ Combination

1047

Denosumab Restores Cortical Bone Loss at the Distal Radius Associated With Aging and Reduces Wrist Fracture Risk: Analyses From the FREE-DOM Extension Cross-over Group. <u>John P. Bilezikian</u>*[1], <u>Claude Laurent Benhamou</u>[2], <u>Celia J.F. Lin</u>[3], <u>Jacques P. Brown</u>[4], <u>Nadia S. Daizadeh</u>[3], <u>Peter R. Ebeling</u>[5], <u>Astrid Fahrleitner-Pammer</u>[6], <u>Edward Franek</u>[7], <u>Nigel Gilchrist</u>[8], <u>Paul D. Miller</u>[9], <u>James A. Simon</u>[10], <u>Ivo Valter</u>[11], <u>Cristiano A.F. Zerbini</u>[12], <u>Cesar Libanati</u>[3]. [1]Columbia University, USA, [2]Orléans Hospital, France, [3]Amgen Inc., USA, [4]CHU de Québec Research Centre, Canada, [5]The University of Melbourne, Australia, [6]Medical University, Austria, [7]Medical Research Center Polish Academy of Sciences, Poland, [8]The Princess Margaret Hospital, New Zealand, [9]Colorado Center for Bone Research, USA, [10]George Washington University, USA, [11]CCBR, Estonia, [12]Centro Paulista de Investigação Clinica, Brazil

Purpose: The skeleton is 80% cortical bone, and cortical bone loss is a major determinant of increased fracture risk. Denosumab (DMAb) has been shown to increase BMD at sites of cortical bone, including the radius, a skeletal site not responsive to most osteoporosis treatments. DXA measurements over time allow for tracking changes in BMD and mass, known predictors of fracture risk. Here, we evaluated changes over time in radius BMD and wrist fracture incidence during 3 years of placebo (Pbo) and during 5 subsequent years of DMAb therapy in the FREEDOM and its Extension (EXT) trials.

Methods: We evaluated 2207 women who enrolled in the EXT and received Pbo during FREEDOM (3 years), and DMAb 60 mg Q6M during EXT (5 years) (Cross-over group); all women received daily calcium and vitamin D. A subset of these women (n=115) participated in a distal radius DXA substudy and were evaluated at baseline and during FREEDOM and EXT. Analysis of mean percentage changes in BMD over time from FREEDOM and EXT baselines consisted of a repeated measure model. Wrist fracture rates (per 100 subject-years), rate ratios, and 95% confidence intervals (CI) were computed.

Results: At FREEDOM baseline, the mean (SD) 1/3 radius T-score was –2.53 (1.18). During FREEDOM, daily calcium and vitamin D alone resulted in a

progressive and significant loss of BMD at the 1/3 radius (–1.2%); however, during EXT, DMAb halted and reversed bone loss (Figure). With 5 years of DMAb treatment, a significant gain in BMD (1.5% at EXT Year 5) was observed, compared with EXT baseline. The wrist fracture rate during the Pbo period in FREEDOM was 1.02 (0.80–1.29) per 100 subject-years. During the first 3 years of EXT, while BMD recovered to the original baseline levels in response to DMAb, the wrist fracture rate remained comparable to the FREEDOM Pbo rate (Table); and with 2 additional years, BMD increased further, and the wrist fracture rate declined to levels significantly lower than the FREEDOM Pbo rate (rate ratio=0.57, 95% CI=0.34–0.95; p=0.03).

Conclusion: In untreated women with postmenopausal osteoporosis, cortical bone density at the radius declined despite calcium and vitamin D supplementation. DMAb treatment for 3 years reversed this bone loss, and 2 additional years of treatment resulted in further BMD gains that translated to significantly lower wrist fracture rates. These data provide evidence, for the first time, of the clinical importance of reversing cortical bone loss.
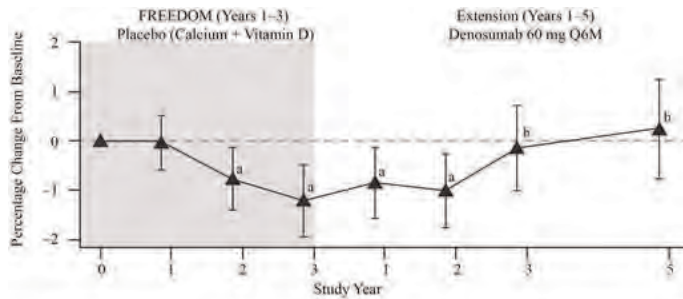
Figure. Distal Radius Percentage Change in Mean BMD From FREEDOM Baseline Through Extension Year 5

	FREEDOM (Years 1–3) Placebo (Calcium + Vitamin D)	Extension (Years 1–5) Denosumab 60 mg Q6M				
Denosumab exposure	NA	Year 1	Year 2	Year 3	Year 4	Year 5
Wrist fractures, n	67	58			19	
Fracture rate*	1.02 (0.80–1.29)	0.96 (0.74–1.25)			0.58 (0.37–0.90)	

*Wrist fracture rate (95% CI) per 100 subject-years

Table. Wrist Fracture Rates During FREEDOM and Through Extension Year 5 (N=2207 Cross-over Subjects)

1048

Teraparatide Stimulates Bone Formation Rapidly in the Human Femoral Neck.

Felicia Cosman*[1], David Dempster[2], Jeri Nieves[3], Hua Zhou[1], Marsha Zion[1], Catherine Roimisher[1], Yvonne Houle[4], Robert Lindsay[1], Mathias Bostrom[4]. [1]Helen Hayes Hospital, USA, [2]Columbia University, USA, [3]Columbia University & Helen Hayes Hospital, USA, [4]Hospital for Special Surgery, USA

Background: Teriparatide (TPTD) rapidly increases bone formation in cancellous and cortical bone of the iliac crest, ultimately increasing bone mass and reducing risk of vertebral and nonvertebral fractures. However, hip BMD improvements with TPTD are modest and there are no data confirming that TPTD reduces hip fracture risk because the study was underpowered for that outcome. Objective: In order to learn more about the effects of TPTD on the femur, we performed a double blind trial of TPTD vs Placebo (PBO) in patients about to undergo a Total Hip Replacement (THR) for osteoarthritis. Methods: Participants were randomized to receive daily TPTD or PBO for an average of 6.1 weeks prior to THR (range 4.6-11.8 weeks). After an average of 3 weeks of study medication, tetracycline labels were administered following standard protocol. During the THR, an intact sample of the femoral neck (FN) was procured, fixed, and sectioned transversely. Four envelopes (cancellous, endocortical, intracortical and periosteal) were analyzed. Mineralized surface (MS/BS) and mineral apposition rate (MAR) were measured and bone formation rate (BFR) calculated. Serum PINP and CTX levels were obtained at baseline and at THR. 39 individuals were enrolled and data are presented on the first 26 analyzed (16 postmenopausal women, mean age 72+9; 10 men, mean age 69.8+7.7). Results: The figure shows tetracycline uptake in cancellous bone from individuals on PBO and TPTD, with substantially more labeled surface in the TPTD-treated subject. Median BFR, MS/BS and MAR by treatment group for each bone envelope are shown in the Table. In both cancellous and endocortical bone, BFR and MS/BS were 2-4 fold higher in TPTD than in PBO (p<0.05). MAR was higher in both cancellous and intracortical envelopes in TPTD compared to PBO (p<0.05). In the periosteum, BFR was high in both groups (relative to other envelopes), without significant group differences. In TPTD treated subjects, PINP and OC increased by over 130%

(p<0.0004), while CTX did not increase significantly. PINP increments correlated with BFR (r=0.5; p<0.02). PINP and CTX did not change in PBO. Conclusions: TPTD stimulates bone formation rapidly in the femoral neck, with prominent effects in cancellous and endocortical envelopes. These findings provide a mechanistic basis for TPTD-mediated improvement in hip strength. This study is the first demonstration of the effect of an osteoporosis medication on cellular activity in the human femur.

Table. Bone Formation Indices in the Total Femoral Neck by Treatment Group, Median (interquartile range)

	BFR/BS (mm3/mm2/yr)		MS/BS (%)		MAR (um/d)	
	PBO	TPTD	PBO	TPTD	PBO	TPTD
Cancellous	0.004 (0.003-.009)	0.019 (0.014-.034)*	2.02 (1.03-3.67)	7.11 (5.82-14.01)**	0.84 (0.36-0.65)	0.69 (0.65-0.74)*
Endocortical	0.015 (0.009-0.030)	0.037 (0.024-079)*	7.81 (3.71-12.10)	16.66 (9.68-27.84)*	0.85 (0.57-0.71)	0.68 (0.57-0.73)
Periosteal	0.066 (0.021-0.093)	0.086 (0.072-0.117)	21.41 (8.48-29.47)	28.77 (21.24-35.09)	0.82 (0.67-0.85)	0.85 (0.70-0.94)
Intracortical	0.030 (0.010-0.042)	0.045 (0.027-0.086)	10.50 (4.60-16.9)	16.78 (9.48-21.92)	0.70 (0.65-0.74)	0.78 (0.74-0.84)*

p-values Wilcoxon rank-sum * p<0.05 ** p<0.01

Table
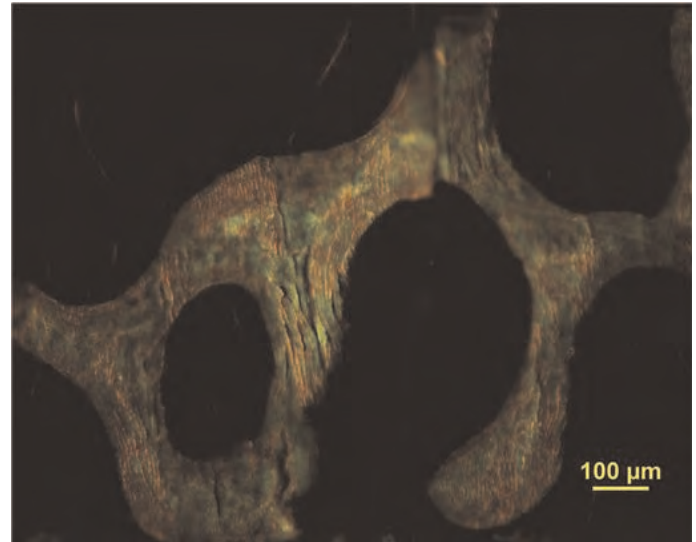
Figure
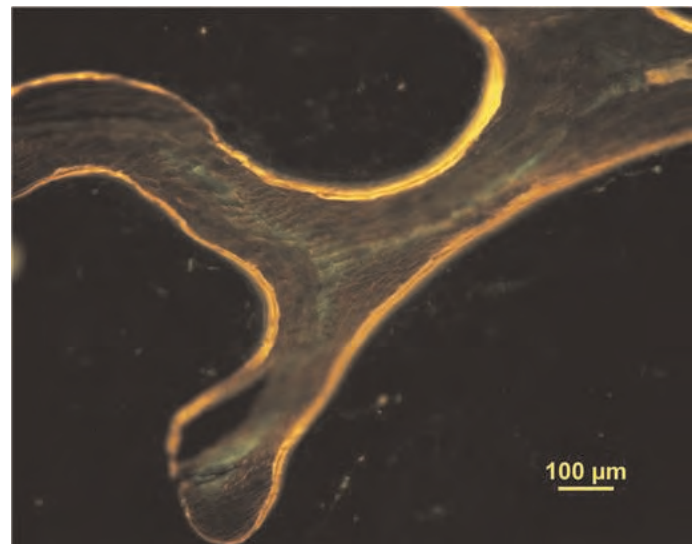
Figure

1049

Romosozumab and Teriparatide Effects on Vertebral Cortical Mass, Thickness, and Density in Postmenopausal Women With Low Bone Mineral Density (BMD). Tristan Whitmarsh*[1], Graham Treece[1], Andrew Gee[1], Michael Bolognese[2], Jacques P. Brown[3], Stefan Goemaere[4], Andreas Grauer[5], David Hanley[6], Carlos Mautalen[7], Christopher Recknor[8], Yu-Ching Yang[9], Cesar Libanati[6], Kenneth Poole[1]. [1]University of Cambridge, United Kingdom, [2]Bethesda Health Research Center, USA, [3]CHU de Québec Research Centre, Canada, [4]Ghent University Hospital, Belgium, [5]Amgen Inc., USA, [6]University of Calgary, Canada, [7]Centro de Osteopatías Médicas, Argentina, [8]United Osteoporosis Center, USA, [9]Amgen Inc., USA

Purpose: Romosozumab (Romo) is a monoclonal antibody that binds sclerostin and stimulates bone formation while decreasing bone resorption. Recently, 12 months of Romo was shown to increase DXA lumbar spinal BMD by 11.3% in a phase 2 international, randomized, placebo-controlled trial (McClung, *NEJM* 2014). DXA measurements, however, do not generally distinguish cortical versus trabecular changes, nor identify the location or distribution of added bone mass. We assessed cortical parameters from the L1 vertebral computed tomography (CT) scans obtained in that same clinical trial by mapping the vertebral bone surface and measuring the global and local changes.

Methods: We evaluated baseline and 12 month L1 CT scans from postmenopausal women treated with Romo (210 mg SC QM, n=17), teriparatide (TPTD, 20 µg daily, n=19), and placebo (n=20). Cortical measurements were performed, blinded to treatment, using the Stradwin software tool, which is able to measure and map cortical BMD (CBMD), trabecular BMD directly adjacent to the cortex (TBMD), cortical thickness (CTh), and cortical mass (CMass=$0.1 \times$ CTh $\times$ CBMD) (Treece, *Med Image Anal* 2010, 2012). Transferring these maps to a canonical vertebral surface allows evaluation and topographical illustration of longitudinal changes and determining differences between treatments.

Results: Treatment groups were balanced at baseline (Table). Romo resulted in a mean (95% CI) CTh increase of 11.2% (9.0 to 13.4), a CBMD increase of 1.6% (0.2 to 2.9), a TBMD increase of 22.2% (19.2 to 25.3), and a CMass increase of 12.7% (10.8 to 14.7). Cortical maps show the topographical locations of the increase in CTh, CMass, and TBMD compared with placebo (Fig). TPTD resulted in smaller changes: a CTh increase of 5.6% (3.9 to 7.4), a TBMD increase of 17.4% (12.2 to 22.6), a CMass increase of 4.6% (3.4 to 5.8), and a slight but not significant CBMD reduction of 0.5% (–1.8 to 0.7). The improvements in CTh (p<0.001), CBMD (p=0.04), and CMass (p<0.001) with Romo were significantly greater than those observed with TPTD. The only significant change in the placebo group was a reduction of 4.3% (–6.7 to –1.9) in TBMD.

Conclusion: Treatment with Romo was associated with significant improvements in cortical parameters of the vertebrae, which were greater compared with placebo or TPTD. This study confirms the robust bone forming effects of Romo and provides new insights into the cortical changes on the vertebra in response to Romo treatment.
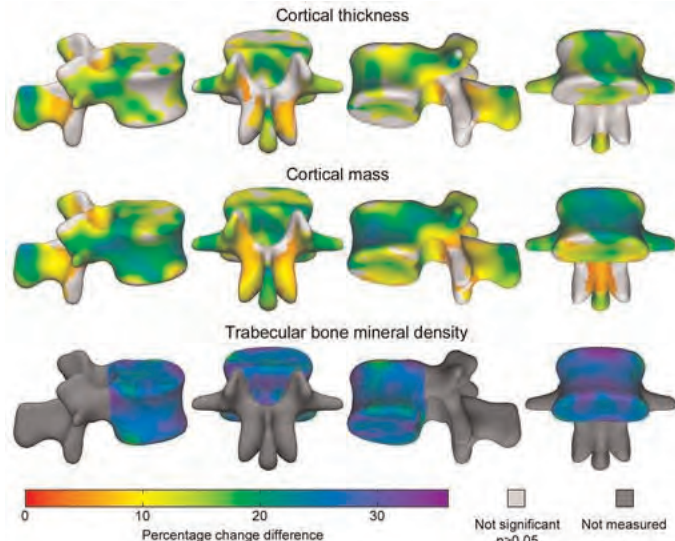

Fig. Cortical Parameter Increases in Response to a 12-Month Romo Treatment With Respect to Placebo

	Placebo (n=20)	Teriparatide (n=19)	Romosozumab (n=17)
Age (years)	67.2 ± 6.1	65.6 ± 6.1	64.6 ± 5.0
Mean CTh (mm)	0.94 ± 0.07	0.93 ± 0.07	0.90 ± 0.08
Mean CBMD (mg/cm³)	769.5 ± 63.5	780.6 ± 56.8	779.8 ± 53.3
Mean TBMD (mg/cm³)*	111.0 ± 18.4	117.9 ± 20.7	112.2 ± 25.2
Mean CMass (mg/cm²)	73.5 ± 9.3	73.5 ± 8.2	70.6 ± 4.6

*TBMD values are of the vertebral body only.

Table. Baseline Characteristics (Mean ˜ SD) With No Significant Between-Group Differences

1050

The Long Term Effects of Abaloparatide (BA058) On Micro-CT and Histomorphometry in Osteopenic Cynomolgus Monkeys. Aurore Varela*[1], Solomon Haile[2], Nancy Doyle[2], Susan Y. Smith[1], Robert Guldberg[3], Gary Hattersley[4]. [1]Charles River Laboratories, Canada, [2]Charles River, Canada, [3]School of Mechanical Engineering, Georgia Institute of Technology, USA, [4]Radius, USA

Abaloparatide (ABL) is a analog of PTHrP(1-34) being developed for osteoporosis treatment. This study evaluated the effects of ABL for 16 months in aged osteopenic, ovariectomized (OVX) monkeys. Four groups were OVX and one group underwent Sham surgery. After a 9-month bone depletion period, animals received daily SC injections of either vehicle (Sham and OVX controls) or ABL at 0.2, 1 or 5 µg/kg. Animals received calcein, 15 and 5 days prior to euthanasia. Cancellous bone histomorphometry was performed at the femoral neck and lumbar vertebra (L2) while cortical bone was evaluated at the femur mid-diaphysis. Micro-CT was performed on T12 vertebral body, L6 trabecular cores, distal femur and humeral cortical beam. In the cancellous bone of OVX control animals, 25 months post OVX, a slight decrease in BV/TV was observed with increases in osteoblast surface, wall thickness, double label surface (L2), mineralizing surface, osteoid volume, osteoid surface and bone formation rates. Effects of OVX were substantial in cortical bone dynamic parameters with increases in most label-derived parameters of bone formation, but with little effect on cortical structures. With micro-CT, similar slight decreases in BV/TV were noted at trabecular sites (distal femur -7%, T12 -14%, L6 core -26%) in OVX controls and minimal decreases in cortical vBMD were measurable (distal femur -4%, T12 -5%, beam 4%). At L2, ABL completely counteracted the OVX-related decrease in bone structural parameters (BV/TV) at ≥ 1 µg /kg, significantly increased wall thickness at all doses and increased the formation period. At the femoral neck, dose-dependent increases in BV/TV were noted. At L2 and femoral neck, minor increases in trabecular thickness and trabecular number contributed together to the bone gains. With micro-CT, similar increases in BV/TV were noted at trabecular sites (distal femur up to +19%, T12 +25%, L6 core +35%). At cortical sites, increases in endocortical labeled surfaces and endocortical bone formation rate were noted in animals administered 5 µg/kg with no effects on cortical geometry. Similarly with micro-CT, no significant changes were noted in cortical bone geometry, but importantly with no increase in cortical porosity. In summary, treatment with ABL at ≥ 1 µg /kg to OVX monkeys completely restored the OVX-induced cancellous and cortical bone loss at clinically relevant sites by increasing bone formation without affecting cortical porosity.

1051

Heterozygous deletion of Wntless in the osteoclast lineage causes osteopenia demonstrating that osteoclasts are a critical source of Wnt proteins in the developing skeleton. Megan Weivoda*[1], Ming Ruan[1], Christine Hachfeld[1], Larry Pederson[1], Rachel Davey[2], Jeffrey Zajac[3], Jean Vacher[4], Richard Lang[5], Bart Williams[6], Sundeep Khosla[7], Jennifer Westendorf[1], Merry Jo Oursler[1]. [1]Mayo Clinic, USA, [2]University of Melbourne, Australia, [3]Austin Hospital, Australia, [4]Institut De Recherches Cliniques De Montréal, Canada, [5]Cincinnati Children's Hospital Medical Center, USA, [6]Van Andel Research Institute, USA, [7]Mayo Clinic College of Medicine, USA

Wnt signaling is crucial for normal skeletal development and adult bone homeostasis. Although several cell types in the skeleton are known to produce Wnts, the contribution of these cellular sources to skeletal Wnt signaling is not clear. Osteoclasts secrete multiple Wnts including Wnt1, Wnt3a, and Wnt10b. We hypothesized that osteoclasts are a critical source of Wnts in skeletal development. The membrane-associated chaperone, Wntless (Wls), is required for intracellular Wnt transport and Wnt secretion. To assess the contribution of osteoclast-derived Wnts to skeletal development, transgenic Cd11b or cathepsin K (Ctsk) promoter Cre mice were crossed with Wls flox mice to obtain animals with heterozygous deletion of Wls in the osteoclast lineage (Cd11b/Wls^Het and Ctsk/Wls^Het). *In vivo* dual-energy X-ray

absorptiometry analysis showed Cd11b/Wls[Het] and Ctsk/Wls[Het] mice exhibited decreased bone mineral density in the spine and femur at 6 weeks of age. Animals were sacrificed at 8 weeks. Bone marrow was isolated for analysis of osteoclast Wls expression and Wnt protein secretion in vitro. Femurs were assessed by peripheral quantitative computed tomography (QCT), micro computed tomography (CT), and histomorphometry. Wls protein was significantly reduced in bone marrow osteoclast cultures from Cd11b/Wls[Het] and Ctsk/Wls[Het] animals as compared to littermate control cultures. Total protein secretion by Ctsk/Wls[Het] mature osteoclasts was unaltered compared to controls; however, Ctsk/Wls[Het] osteoclast secretion of Wnt1, Wnt3a, and Wnt10b was significantly reduced. Peripheral QCT analysis of Cd11b/Wls[Het] and Ctsk/Wls[Het] femurs showed significant reductions in cortical bone area, thickness, and density, as well as significant decreases in total and trabecular density. MicroCT analysis revealed a 60% reduction in cortical thickness in the cancellous region of the Ctsk/Wls[Het] femurs; trabecular microCT parameters were unchanged. Interestingly, endocortical osteoblast numbers were decreased by 70%, and osteoclast numbers were significantly increased. The decreased cortical phenotypes of Cd11b/Wls[Het] and Ctsk/Wls[Het] mice are strikingly similar to the decreased cortical phenotypes of mice with osteoblast specific deletion of Lrp5/Lrp6 or ß-catenin. This suggests that osteoclasts are a prime source of anabolic Wnts in the cortical region. These data demonstrate that osteoclast lineage-derived Wnts play an essential role in skeletal development.

Disclosures: Megan Weivoda, None.

1052

Deletion of LRP6 in Different Stages of Osteoblastic Lineage of Cells Impairs Bone Formation at Different Postnatal Stages. Changjun Li*[1], Hui Xie[2], Janet Crane[3], Xu Cao[3], Mei Wan[1]. [1]Johns Hopkins University School of Medicine, USA, [2]Johns Hopkins Medical Institution, USA, [3]Johns Hopkins University, USA

Bone-forming osteoblast lineage of cells is derived from bone marrow mesenchymal stem cells (MSCs).Low-density lipoprotein receptor-related protein 6 (LRP6) is a positive regulator for bone formation, and mutations in LRP6 are associated with human bone disorders. However, the role of LRP6 in different stages of osteoblast lineage of cells remains largely unknown. It was reported that transgenes that use control regions from the nestin gene mark bone marrow perivascular MSCs. In this study, we generated two mouse models, in which LRP6 was specifically deleted in either mature osteoblasts or in bone marrow MSCs by crossing *osteocalcin-Cre* or *nestin-Cre* mice with *LRP6[flox]* mice and investigated the changes of osteoblastogenesis and bone formation.

LRP6[f/f]::osteoclacin-Cre mice (named "*OC-KO*") had normal body weight and length compared with their wild type littermates, whereas *LRP6[f/f]::nestin-Cre* mice (named "*Nes-KO*") demonstrated reductions in body weight and length at 1 and 3 months of age. Bone architecture measured by μCT showed marginal changes in bone mass in the primary spongiosa area but a reduction in the secondary spongiosa of femurs at 3 month-old *OC-KO* mice. The remodeling area of *OC-KO* mice showed a decreased bone formation rate as detected by Goldner's Trichrome staining and calcein double labeling. On the contrary, *Nes-KO* mice exhibited a significant reduction in bone mass in both primary and secondary spongiosa area of femurs. The results suggest that LRP6 deficiency in osteoblasts primarily affected trabecular bone remodeling in adults, whereas LRP6 deficiency in MSCs impaired both postnatal bone acquisition and bone remodeling. Bone histomorphometric and immumohisto-chemical analysis showed that both *OC-KO* and *Nes-KO* mice exhibited significant reduction in the number of bone surface osteoblasts but marginal changes in the number of osteoclasts, indicating the primary role of LRP6 in regulating osteoblast lineage of cells. Further characterizing the cellular mechanisms of the reduced osteoblastogenesis in both mutant mice revealed that LRP6 deficiency in osteoblasts mainly impaired the differentiation of osteoblasts, whereas LRP6 deficiency in MSCs led to the reduced pool of osteoblast-forming osteoprogenitors due to the diminished survival and proliferative capacity of MSCs. Thus, LRP6 is a key positive regulator for osteoblastogenesis with distinct functions in different differentiation stages of osteoblastic lineage of cells.

Disclosures: Changjun Li, None.

1053

Hedgehog Induces Osteoblast Differentiation through IGF-mTORC2 Signaling. Yu Shi*[1], Jianquan Chen[2], Courtney Karner[3], Fanxin Long[3]. [1]Washington University in St. Louis, USA, [2]Washington University, USA, [3]Washington University School of Medicine, USA

Hedgehog (Hh) signaling critically regulates the endochondral bone formation in vivo. It is further known that Hh signaling directly induces osteoblast differentiation via the Gli family of transcription factors. However, the osteogenic effectors downstream of Gli are largely unknown. Here by RNA sequencing, we found that components of the Igf signaling pathway were induced by Hh activation during osteoblast differentiation in vitro. Moreover, Hh activated Igf-mTORC2-Akt signaling in a Gli-dependent manner. Knockdown of Igf2, Igf1r or the mTORC2-specific component rictor, similar to pharmacological inhibition of Akt, suppressed Hh-induced osteoblast differentiation in vitro. We further discovered that IGF synergized with Hh signaling via Akt-dependent Gli2 stabilization. To test the

physiological contribution of Igf signaling to Hh-induced osteoblast differentiation, we deleted Igf1r in the mouse embryo by using the Gli1-CreERT2 knockin allele that expresses CreERT2 (tamoxifen (TM)-inducible Cre) from the endogenous Gli1 genomic locus. TM-induced deletion of IGF1R in Gli1-expressing cells prior to osteoblastogenesis diminished bone formation without affecting cartilage development. Take together, these results support a model wherein Hh induces IGF signaling which in turn augments the Hh response to stimulate osteoblast differentiation. This study therefore establishes a cross-regulatory relationship between Hh and Igf signaling in bone.

Disclosures: Yu Shi, None.

1054

BMP-Alk3 signaling exerts opposite effects on trabecular versus cortical bone formation in postnatal mice. Joohyun Lim*[1], Fanxin Long[2]. [1]Washington University in St. Louis, USA, [2]Washington University School of Medicine, USA

Bone morphogenetic proteins (BMPs) were discovered for their ability to induce ectopic bone. Although it is well established that BMP signaling is essential for cartilage development during endochondral bone formation, how physiological BMP signaling directly regulates bone formation in postnatal mice remains unclear. To fill this knowledge gap, we conditionally deleted the type I BMP receptor Alk3 in osteoblast-lineage cells. Alk3 mutants were normal in size and weight but had thinner cortical diameter compared to littermate controls due to reduced osteoblast activity in the periosteum. This result therefore corroborates the anabolic function of BMP signaling in bone formation. Unexpectedly, however, Alk3 deletion significantly increased cancellous bone formation due to increased osteoblast numbers and mineralizing surface, without affecting osteoclast numbers and function. Furthermore, Alk3 deletion significantly increased BrdU-positive osteoblast precursors in the chondro-osseous junction, indicating that Alk3 negatively regulates the proliferation of osteoblast progenitors. Collectively, these results demonstrate that Alk3-dependent BMP signaling in osteoblast-lineage cells has opposing roles in cancellous versus cortical bone formation in postnatal mice. Because Alk3 deletion greatly suppressed Sost expression by osteocytes, we speculate that Alk3 normally restricts the proliferation of osteoblast progenitors in the trabecular bone region through Sost-mediated inhibition of Wnt signaling. To test whether Alk3 function is mediated by the Smad proteins, we deleted Smad4 in osteoblast-lineage cells by using the same genetic approach. Interestingly, Smad4 deletion also increased cancellous bone formation and reduced cortical diameter, but to a lesser degree than Alk3 removal. Thus, our data support a model in which BMP-Alk3 signaling exerts opposite effects on trabecular versus cortical bone formation in postnatal mice, and that these effects are mediated through both Smad-dependent and independent mechanisms.

Disclosures: Joohyun Lim, None.

1055

TGIF Is Required for Canonical Wnt Signaling-induced Bone Formation. Ming-zhu Zhang*[1], Eric Hesse[2], Celine Prunier[3], Mutsuko Ohnishi[4], Harikiran Nistala[5], Yun-feng Yang[6], Guang-rong Yu[7], Santosh Kumar[8], William Horne[9], Roland Baron[10], Azeddine Atfi[11]. [1]School of Medicine, Tongj Hospital, Tongji University, Chn, [2]Department of Oral Medicine, Infection & Immunity, Harvard School of Dental Medicine, Boston, United States, 02115, USA, [3]Laboratory of Cell Signaling & Carcinogenesis, INSERM UMRS938, 184 Rue du Faubourg St-Antoine, 75571, France, [4]Department of Oral Medicine, Infection & Immunity, Harvard School of Dental Medicine, 02115, USA, [5]Harvard University, USA, [6]Department of Orthopedics, Tongji Hospital, School of Medicine Tongji University, Shanghai, China,200065, China, [7]Department of Orthopedics, Tongji Hospital, School of Medicine Tongji University, Shanghai, China,200065, China, [8]Cancer Institute, University of Mississippi Medical Center, 2500 N. State St, Jackson, MS 39216., USA, [9]Harvard School of Dental Medicine, USA, [10]Harvard School of Medicine & of Dental Medicine, USA, [11]Department of Oral Medicine, Infection & Immunity, Harvard School of Dental Medicine, Boston, United States, 02115, USA

The homeodomain protein TGIF regulates several physiological processes and plays crucial roles in cell fate determination and tissue homeostasis. TGIF is phosphorylated in numerous cell systems, yet the responsible kinase(s) remains unidentified. In an effort to address this issue, we interrogated the Eukaryotic Linear Motif (ELM) database, and found that TGIF possesses a potential GSK3β phosphorylation site (T235 and T239). We then showed that indeed GSK3β can directly phosphorylate TGIF, as demonstrated by in vitro kinase assays and western blotting using an antibody that specifically recognizes TGIF phosphorylated at T235/T239. Functionally, we found that mutation of T235/T239 resulted in decreased TGIF turnover, providing an initial hint that phosphorylation by GSK3β might hinder TGIF stability. In fact, suppressing GSK3β activity through either genetic or chemical approaches triggered decreased TGIF polyubiquitination and clearance. Thus, similar

to β-catenin, phosphorylation of TGIF by GSK3β leads to its ubiquitination and degradation. As GSK3β is a key kinase in Wnt signaling, we then investigated whether TGIF played a physiological role in this pathway. Remarkably, expression of TGIF enhanced Wnt-induced gene expression, whereas TGIF deficiency elicited the opposite effects. Mechanistically, TGIF appeared to promote β-Catenin accumulation, interfering with the assembly of the β-Catenin destruction complex. Furthermore, activation of Wnt signaling induced the expression of TGIF itself in many cell lines, revealing an ability of TGIF to govern a feed-forward loop that sustains Wnt signaling.

Given that Wnt signaling is a potent regulator of osteoblast differentiation and bone formation, we then tested whether TGIF was capable to enhance this pathway in osteoblasts (OBs) and bone formation in vitro and in vivo. Expressing TGIF increased OB differentiation in the pre-OB cell lines, ST2 and C3H10T1/2 through Wnt signaling activation, as TGIF depletion was sufficient to blunt Wnt3a-induced osteoblast differentiation in these cell systems. In vivo, TGIF-/- mice display decreased osteoblast differentiation and low bone mass. More importantly, deletion of TGIF prevented the high bone mass phenotype seen in mice harboring heterozygote deletion of the Wnt signaling inhibitor DKK1. This study therefore establishes TGIF as a component of the Wnt signaling machinery that is required for efficient Wnt-induced osteoblast differentiation and bone formation.

Disclosures: Ming-zhu Zhang, None.

1056

PTH/PTHrP Receptor Signaling in Osteoprogenitors is Essential for B Lymphocyte Differentiation, Maturation, and Mobilization in Mice. <u>Cristina Panaroni</u>*[1], <u>Keertik Fulzele</u>[2], <u>Vaibhav Saini</u>[3], <u>Rhiannon Chubb</u>[4], <u>Paola Divieti Pajevic</u>[5], <u>Joy Wu</u>[6]. [1]Stanford University School of Medicine, USA, [2]Massachusetts General Hospital; Harvard Medical School, USA, [3]MGH, Harvard Medical School, USA, [4]Endocrine Unit, Massachusetts General Hospital, USA, [5]Massachusetts General Hospital & Harvard Medical School, USA, [6]Stanford University School of Medicine, USA

The osteoblast lineage is a major regulator of various hematopoietic lineages by providing specialized niches for their development in bone marrow (BM). We have previously demonstrated that ablation of Gsα in Osterix-positive (Osx) osteoprogenitors in mice results in osteopenia accompanied by developmental arrest of B-lymphocyte precursors in BM. Because PTH treatment has been shown to enhance osteoblast support of B lymphocyte differentiation *in vitro*, we hypothesized that PTH/PTHrP receptor (PPR) might be the G-protein coupled receptor upstream of Gsα in osteoprogenitors, mature osteoblasts, or osteocytes that regulates B lymphocyte maturation in the BM. Here we show that B lymphocyte development in BM is regulated by PPR signaling only in osteoprogenitors. No impaired B cell development was found when PPR was ablated in mature osteoblasts or osteocytes. On the contrary, and similar to mice depleted of Gsα in osteoprogenitors, Osx-PPR knockout (KO) mice exhibit a severe osteoporotic phenotype and a specific reduction in B cell precursors, as previously reported. Surprisingly, the overall number of total B lymphocytes in BM was not significantly reduced due to a 3-fold increase in mature B cells, which were mainly located along the endosteal bone. In case of BM failure, hematopoiesis can take place in the spleen. Therefore, we investigated the spleen of Osx-PPRKO mice but observed no extramedullary hematopoiesis, suggesting impaired maturation and retention of B cells in the BM of Osx-PPR KO mice. Intra-tibial injection of labeled B lymphocytes revealed a 27-fold increase in the number of labeled mature B cells in the BM and 6-fold decrease in labeled mature B cells in the spleen of Osx-PPR KO mice, further supporting increased retention of B cells in BM. We next examined the main adhesion molecules involved in B lymphocyte migration/adhesion. The integrin α4β1 is abundantly expressed on B lymphocytes and strongly interacts with its stromal ligand VCAM1 to increase adhesion to the microenvironment. Interestingly, we found a 3-fold increase in VCAM1 expression in bone, and *in vivo* treatment with VCAM1 neutralizing antibody reduced the frequency of mature B cells in the BM of Osx-PPR KO mice by 50%. In summary, PPR signaling in early osteoprogenitors, but not mature osteoblasts and osteocytes, is necessary for B cell differentiation, maturation, and mobilization.

Disclosures: Cristina Panaroni, None.

1057

FGF23 regulates bone mineralization in a vitamin D and Klotho-independent fashion. <u>Sathish Kumar Murali</u>*[1], <u>Paul Roschger</u>[2], <u>Ute Zeitz</u>[1], <u>Klaus Klaushofer</u>[3], <u>Olena Andrukhova</u>[1], <u>Reinhold Erben</u>[4]. [1]Dept. of Biomedical Sciences, University of Veterinary Medicine, Austria, [2]L. Boltzmann Institute of Osteology, Austria, [3]Hanusch HospitalLudwig Boftzmann Institute of Osteology, Austria, [4]University of Veterinary Medicine, Austria

Fibroblast growth factor-23 (FGF23) is a phosphaturic hormone secreted by osteoblasts and osteocytes in response to vitamin D and phosphate. Lack of Fgf23 or of Klotho (Kl), the co-receptor for FGF23, leads to severe impairment of bone mineralization in mice. However, the mechanisms underlying the Fgf23- and Klotho deficiency-associated defects in bone mineralization are still poorly understood. To examine the vitamin D independent role of FGF23 and Klotho in bone mineralization, we crossed Fgf23-/- or Kl-/- mice with mice expressing a non-

functioning vitamin D receptor (VDR$^{\Delta/\Delta}$). As expected, Fgf23-/- and Kl-/- mice were characterized by increased serum 1,25 (OH)$_2$D$_3$, and impaired bone mineralization as evidenced by μCT and histomorphometric analysis. The mineralization defect in Fgf23-/- and Kl-/- mice was associated with increased bone mRNA expression of ANK (progressive ankylosis), ENPP1 (ectonucleotide pyrophosphatase phosphodiesterase 1), ENPP3 (ectonucleotide pyrophosphatase phosphodiesterase 3), and osteopontin (OPN) as compared to wild-type and VDR$^{\Delta/\Delta}$ mice. In addition, we found increased pyrophosphate levels and OPN protein expression in bones of Fgf23-/- and Kl-/- mice. Ablation of vitamin D signaling in Kl-/-/VDR$^{\Delta/\Delta}$ compound mutants normalized serum Fgf23 levels, bone mineralization, bone pyrophosphate levels, and bony expression of ANK, ENPP1, ENPP3, and OPN, suggesting that the mineralization defect observed in Kl-/- mice is entirely due to 1,25(OH)$_2$D$_3$-driven upregulation of the mineralization inhibitor OPN, and of the pyrophosphate-regulating factors ANK, ENPP1, ENPP3. However, despite normalization of bone pyrophosphate levels, bone mineralization remained impaired and OPN protein expression remained increased in Fgf23-/-/VDR$^{\Delta/\Delta}$ compound mutants relative to wild-type and VDR$^{\Delta/\Delta}$ mice. Differentiated primary osteoblasts isolated from Fgf23-/- mice, but not those isolated from Kl-/- mice, showed cell autonomous increases in OPN mRNA and protein expression as compared to wild-type cells. In addition, treatment of differentiated primary osteoblasts isolated from wild-type mice with recombinant FGF23 decreased OPN protein expression. Taken together, our data suggest that Fgf23 but not Klotho has a vitamin D independent role in bone mineralization through direct regulation of OPN.

Disclosures: Sathish Kumar Murali, None.

1058

Deletion of PTH1R expression from limb mesenchyme affects systemic mineral ion homeostasis. <u>Yi Fan</u>*[1], <u>Beate Lanske</u>[2], <u>Tatsuya Kobayashi</u>[3], <u>Tadatoshi Sato</u>[1], <u>Michael Densmore</u>[4]. [1]Harvard School of Dental Medicine, USA, [2]Harvard School of Dental MedicineHarvard Medical School, USA, [3]Massachusetts General Hospital, USA

PTH is secreted by the parathyroid glands in response to low serum calcium and vitamin D levels. It signals through the parathyroid hormone 1 receptor (PTH1R) in kidney and bone to regulate mineral ion homeostasis and bone remodeling. We generated a viable novel mouse model, *Prx1Cre;PTH1R$^{fl/fl}$*, by ablating the PTH1R at the early limb bud stage in order to explore the contribution of PTH1R expression in long bones to modulate systemic mineral ion homeostasis. We confirmed efficient and specific deletion of PTH1R in adult limbs and calvaria. H/E & von Kossa staining showed reduced amounts of trabecular and cortical bone in *Prx1Cre;PTH1R$^{fl/fl}$* limbs at P0, 3 and 6 weeks of age. qPCR analyses revealed decreased expression of osteoblast and some osteocyte markers, with exception of *Mepe*, *Dmp1*, *Opn* and more importantly *Fgf23* mRNA. Also, normal FGF23 protein expression was detected in mutants by immunohistochemistry.

To examine changes in systemic mineral ion homeostasis we measured various biochemical parameters. Whereas serum Ca^{2+} and PTH levels were unchanged, serum Pi, 1,25(OH)$_2$D$_3$, and iFGF23 levels were significantly decreased in mutants. Notably, a marked reduction in *Galnt3 expression*, an enzyme required for O-glycosylation of FGF23, was detected in *Prx1Cre;PTH1R$^{fl/fl}$* bones, signifying that a failure in proper post-translational modification of FGF23 could be responsible for the lower circulating FGF23 levels.

Moreover, changes in the expression of renal genes involved in balancing mineral ion homeostasis, such as *Klotho*, *Napi2a*, *CalbindinD$_{28}$K,* were found in mutants. Interestingly, renal *1a(OH)ase* expression in mutants was normal but its expression in limbs was significantly decreased, indicating that the lower serum 1,25(OH)$_2$D$_3$ could be due to the local loss of PTH1R in limbs.

To further explore the regulation of FGF23 by PTH, 2-week old mutants and littermate controls were daily injected with hPTH(1-34) or vehicle for 1 week. FGF23 mRNA expression was upregulated in control limbs but remained unchanged in the mutants. Although controls responded with the expected increase in serum calcium and decrease in serum phosphate no changes in serum calcium were seen in the mutants, while serum phosphate significantly decreased.

In summary, our data suggest that PTH1R in limbs is required for induction of FGF23 mRNA and is essential to regulate systemic mineral ion homeostasis.

Disclosures: Yi Fan, None.

1059

Phosphate-induced signaling cascade is regulated by Trps1 in mineralizing cells. <u>Maria Kuzynski</u>[1], <u>Morgan Goss</u>[2], <u>Callie Mobley</u>[1], <u>Dobrawa Napierala</u>*[2]. [1]University of Alabama at Birmingham, USA, [1]University of Alabama at Birmingham, USA, [2]University of Alabama At Birmingham School of Dentistry, USA

The availability of phosphate is one of the critical factors regulating biomineralization. Phosphate supports biomineralization not only as a component of inorganic phase of mineralizing tissues, but also as a signaling molecule that acts on target cells and induces molecular changes supporting biomineralization. It has been demonstrated that phosphate-induced Erk1/2 activation is bi-phasic and promotes expression of mineralization-related genes. Many of these genes have promoters enriched in GATA consensus elements suggesting that GATA transcription factors

play role in regulation of gene expression in response to phosphate. Trps1 is a GATA-type transcription factor that is expressed during development of skeletal and dental tissues. Our previous data from Trps1-KO and Col1a1-Trps1 transgenic mice implicate Trps1 in biomineralization, however its precise role in this process is unknown. To understand how Trps1 regulates biomineralization, we generated odontoblastic cell lines deficient for Trps1 (Trps1-KD) and overexpressing Trps1 (Trps1-OE). Cellular and molecular analyses of these cell lines uncovered that Trps1-deficieny results in a loss of the mineralization potential, associated with decreased expression of Phospho1 and TNAP phosphatases, and Runx2 and Sp7 osteogenic transcription factors. In contrast, Trps1-overexpression results in delayed and decreased mineralization as well as decreased expression of genes regulated by phosphate. Analyses of phosphate-induced Erk1/2 activation uncovered disturbed second Erk1/2 activation peak in both Trps1-KD and Trps1-OE cells in comparison with controls. These data implicate Trps1 in phosphate-induced signaling cascade and suggest that Trps1 regulates the biomineralization process by controlling expression of a subset of phosphate-responsive genes.

Disclosures: Dobrawa Napierala, None.

1060

Mechanisms Underlying Ectopic Mineralization in a Mouse Model of Diffuse Idiopathic Skeletal Hyperostosis. Hisataka Ii[1], Sumeeta Warraich[1], Neil Tenn[1], Diana Quinonez[1], David Holdsworth[1], James Hammond[2], S. Jeffrey Dixon*[1], Cheryle Séguin[1]. [1]The University of Western Ontario, Canada, [2]University of Alberta, Canada

Equilibrative nucleoside transporter 1 (ENT1) mediates the passive flow of adenosine across cell membranes. We previously reported that mice lacking ENT1 (*ENT1*^{-/-}) exhibit progressive ectopic mineralization of spinal tissues including intervertebral discs (IVDs) – a phenotype resembling diffuse idiopathic skeletal hyperostosis (DISH) in humans. Our objective was to investigate the mechanisms underlying ectopic mineralization in *ENT1*^{-/-} mice. Intact IVDs were isolated from wild-type and *ENT1*^{-/-} mice at 2 months of age (prior to detection of disc mineralization), 4 and 6 months of age (when extensive mineralization was detected in IVDs). Tissues were processed for RNA extraction and real-time PCR, subjected to enzymatic dissociation for cell isolation and culture, or fixed for histological evaluation. Characterization of wild-type tissues demonstrated that, in contrast to brain and visceral organs, ENT1 is the primary nucleoside transporter expressed in the IVD. This observation was confirmed functionally by measuring uptake of [³H]2-chloroadenosine in cultures of IVD cells isolated from wild-type mice. No differences in candidate gene expression were detected in intact IVDs isolated from *ENT1*^{-/-} mice compared to wild-type mice at 2 or 4 months of age. However, at 6 months of age, expression of regulators of mineralization including *Mgp, Enpp1, Ank, Spp1* and *Alpl* were significantly reduced in *ENT1*^{-/-} mice compared to wild-type. To assess whether changes detected in *ENT1*^{-/-} mice were cell autonomous, cultures of annulus fibrosus cells were established. Cultures from *ENT1*^{-/-} IVDs demonstrated greater alkaline phosphatase activity than wild-type cells when isolated from mice at either 2 or 6 months of age. *ENT1*^{-/-} cultures also showed greater mineralization than wild-type cells at 2 months of age. Cultures of cells from 6-month-old *ENT1*^{-/-} mice exhibited significantly greater expression of *Ibsp, Enpp1, Spp1, Alpl* and *Runx2* than wild-type cultures. Interestingly, histological evaluation of intact IVDs demonstrated aberrant alkaline phosphatase activity in cells of the inner annulus fibrosus in *ENT1*^{-/-} mice. Together, these findings suggest that both cell-autonomous and systemic mechanisms disrupt expression of alkaline phosphatase and other regulators of mineralization, which in turn results in ectopic calcification of spinal tissues in *ENT1*^{-/-} mice. These observations may provide new clues as to the pathogenesis of DISH in humans.

Disclosures: S. Jeffrey Dixon, None.

1061

***Gli1* haploinsufficiency disrupts postnatal bone homeostasis under physiological and pathological conditions.** Yoshiaki Kitaura*[1], Hironori Hojo[2], Yuske Komiyama[3], Tsuyoshi Takato[3], Ung-Il Chung[4], Shinsuke Ohba[5]. [1], Japan, [2]The Center for Disease Biology & Integrative Medicine, USA, [3]The university of Tokyo, Japan, [4]University of Tokyo Schools of Engineering & Medicine, Japan, [5]The University of Tokyo, Japan

Hedgehog (Hh) signaling plays important roles in various development processes. The signaling exerts its biological effects through the Gli-mediated transcription of its target genes. In the mammalian skeleton, Hh input is required for the specification of *Runx2*-positive osteoblast precursors during endochondral ossification. In contrast to the established roles of Hh signaling in skeletal development, the evidence of its roles in adult bone homeostasis is not complete. In the present study, we aimed to identify roles of Gli1, a transcriptional activator induced by Hh signaling activation, in postnatal bone homeostasis. The body weights of the 8-week-old *Gli1*^{-/-} mice were approx. 20% lower than those of the WT and *Gli1*^{+/-} mice, which suggested systemic abnormalities by complete loss of *Gli1* gene. Therefore, we analyzed the skeletal system in *Gli1*^{+/-} male mice. *Gli1* haploinsufficiency caused decreased bone mass with reduced bone formation and accelerated bone resorption; that is, an uncoupling of the bone metabolism. Hh-mediated osteoblast differentiation was largely impaired in cultures of *Gli1*^{+/-} precursors, and the impairment was rescued by the *Gli1* expression by the adenoviral transduction. In addition, *Gli1*^{+/-} precursors showed premature

differentiation into osteocytes and increased ability to support osteoclastogenesis. These data suggest that the uncoupling of bone metabolism is caused by the premature differentiation of *Gli1*^{+/-} precursors into osteocytes that have greater capacities to support osteoclastogenesis. When we compared fracture healing between wild-type and *Gli1*^{+/-} adult mice, we found that the *Gli1*^{+/-} mice exhibited impaired fracture healing with insufficient callus formation by three-dimensional μ-CT analyses. In the histological analyses on sections stained with the hematoxyline-eosine (H-E) and alcian blue revealed that both of soft and hard callus were reduced in the *Gli1*^{+/-} mice compared to WT mice; both endochondral ossification and intramembranous ossification were affected by *Gli1* haploinsufficiency during the fracture healing process at a postnatal stage. Thus, we propose that Gli1 acting downstream of Hh input contributes to adult bone metabolism under both physiological and pathological conditions, in which this molecule not only promotes osteoblast differentiation but also acts as a repressor for osteoblast maturation toward osteocytes to maintain normal bone homeostasis.

Disclosures: Yoshiaki Kitaura, None.

1062

Prolonging JAK/STAT signaling by deletion of osteocytic SOCS3 results in a profound sex-divergent change in trabecular bone mass. Holly Brennan*[1], Rachelle Johnson[2], Emma Walker[1], Gordon Smyth[3], Nicos Nicola[3], T. John Martin[4], Natalie Sims[2]. [1]St Vincent's Institute of Medical Research, Australia, [2]St. Vincent's Institute of Medical Research, Australia, [3]Walter & Eliza Hall Institute, Australia, [4]St. Vincent's Institute of Medical Research, Australia

The SOCS (suppressor of cytokine signaling) family of proteins limit the duration of JAK/STAT cytokine signaling. SOCS3 binds directly to receptors that play key roles in bone metabolism, including glycoprotein 130 (gp130), leptin receptor and G-CSF receptor, thereby inhibiting receptor-associated JAK tyrosine kinase activity. SOCS3 expression in the osteoblast lineage is stimulated by parathyroid hormone (PTH), mechanical loading and IL-6/gp130 family cytokines, which all increase bone formation, at least in part, by acting on the osteocyte.

To investigate the role of osteocytic SOCS3 in bone remodeling, we examined the skeletal phenotype of mice with SOCS3 conditionally deleted in osteocytes (DMP1Cre.SOCS3f/f). Femora were analyzed by microCT, and tibiae by histomorphometry, during development (2-week-old), growth (6-week-old), and early and late adult bone remodeling (12- and 26-week-old).

DMP1Cre.SOCS3f/f mice demonstrated a sex-divergent phenotype in trabecular bone, after sexual maturation. At 2 weeks of age, trabecular bone volume (BV/TV) was significantly greater (3-fold, p<0.01) in male and female DMP1Cre.SOCS3f/f mice compared to age- and sex-matched controls (DMP1Cre.SOCS3w/w). Trabecular thickness and number were also significantly higher. This high bone mass phenotype was significant also at 6 weeks of age in both sexes. However, at 12 weeks of age, while both male and female DMP1Cre.SOCS3f/f mice demonstrated a high level of bone remodeling, including significantly greater osteoid surface and volume (p<0.01), osteoblast surface (p<0.0001) and osteoclast surface (p<0.05), the effect of SOCS3 deletion on trabecular bone mass was profoundly different between sexes. In 12-week-old female DMP1Cre.SOCS3f/f mice, BV/TV was increased 7-fold (p<0.0001), such that the marrow space was almost entirely filled with rapidly remodeling bone. In contrast, males exhibited a ~50% reduction in BV/TV (p<0.05) compared to age- and sex-matched controls. At 26 weeks, male mice retained their low BV/TV, and the high bone mass phenotype of the females completely resolved to wildtype levels.

These data indicate that SOCS3-mediated inhibition of osteocytic JAK/STAT signaling restrains both bone formation and resorption, with the balance being sex- and age-specific. The striking sexually divergent phenotype at 12 weeks indicates that osteocytic JAK/STAT signaling is a key influence that determines sexual dimorphism in adult trabecular bone remodeling and bone mass.

Disclosures: Holly Brennan, None.

1063

Plasma Sphingosine 1-Phosphate Levels and the Risk of Osteoporotic Fractures: The Ceor Study. Mohammed-Salleh Ardawi*[1], Abdulrahim Rouzi[2], Nawal Al-Senani[2], Mohammed Qari[3], Shaker Mousa[4]. [1]Center of Excellence for Osteoporosis Research & Department of Clinical Biochemistry & KAU Hospital, Faculty of Medicine, King Abdulaziz University, Saudi Arabia, [2]Center of Excellence for Osteoporosis Research & Department of Obstetrics & Gynecology & KAU Hospital, Faculty of Medicine, King Abdulaziz University, Saudi Arabia, [3]Center of Excellence for Osteoporosis Research & Department of Haematology & KAU Hospital, Faculty of Medicine, King Abdulaziz University, Saudi Arabia, [4]The Pharmaceutical Research Institute, Albany College of Pharmacy & Health Sciences, USA

Background: In vivo and in vitro studies showed that sphingosine 1-phosphate (S1P) to act as a coupling factor stimulating osteoclastogenesis and controlling the migration of osteoclast precusosrs between blood and bone compartments. Also, S1P is known to stimulate osteoblastss proliferation, migration and survival. We

hypothesized that postmenopausal women with elevated plasma S1P levels might be related to greater risk for osteoporosis-related fractures (ORFs).

Methods: We studied, the association between circulating S1P [measured by ELISA kit (Echelon Biosciences Inc., USA)] and ORF risk in 707 postmenopausal women (age $\geq$50 yrs), in a population-based study with a mean follow-up period of 5.2 ± 1.3 years. Multivariate Cox proportional-hazards regression models were used to analyze fracture risk, adjusted for age, body mass index, and other confounding risk factors.

Results: Plasma S1P levels (μmol/L) were significantly higher in women with ORFs (7.23 ± 1.79) than in those without ORFs (5.02 ± 1.51) (P<0.0001). High S1P levels were strongly associated with increased fracture risk. After adjustment for age and other confounders, the relative risk was >6.2-fold among postmenopausal women for each 1-SD increment increase in plasma S1P level. Women in the highest quartile of S1P levels had a 10-fold increase in fracture risk. Results were similar when we compared S1P at the 1-year visit to an average of 2-3 measurements. Fracture risk attributable to S1P levels was 31.5% in the highest quartile. Associations between S1P levels and fracture risk were independent of bone mineral density and other confounding risk factors.

Conclusions: High plasma S1P level appears to be a strong and independent risk factor for ORFs among postmenopausal women and could be a useful biomarker to improve fracture risk assessment.

Analysis	Continuous (per SD) Analysis HR (95% CI)	Quartile-Specific Analysis HR (95% CI)
Plasma sphingosine 1-phosphate:		
Unadjusted	6.22 (5.02 – 7.82)	10.41 (2.92 – 33.37)
Adjusted for age	6.07 (4.87 – 7.58)	9.92 (2.84 – 34.58)
Multivariate 1	6.12 (4.92 – 7.66)	9.89 (2.83 – 34.44)

Table 1: Hazard ratios for osteoporosis-related fractures by sphingosine 1-phosphate cut-off values

Disclosures: Mohammed-Salleh Ardawi, None.

1064

Bone Material Strength as measured by microindentation in vivo is decreased independently of BMD in patients with fractures. Frank Malgo*[1], Neveen Hamdy[2], Socrates Papapoulos[2], Natasha Appelman-dijkstra[3]. [1]Leiden University Medical Center, Netherlands, [2]Leiden University Medical Center, The Netherlands, [3]LUMC Centre for Bone Quality Dept of Endocrinology, The Netherlands

Background: Bone strength depends on bone mass, architecture and composition. Besides a decrease in Bone Mineral Density (BMD), altered microarchitecture and biomechanical properties of bone contribute to fracture risk. A new technique of microindentation has been introduced for the in vivo measurement of the biomechanical properties of bone. We hypothesized that Bone Material Strength (BMS) as measured by microindentation would be lower in patients with osteopenia or osteoporosis and a fracture compared to those without.

Methods: We performed microindentation in 65 men and women with (Fx+) or without fractures(Fx-) and with osteopenia or osteoporosis as measured by DXA. Patients with metabolic bone diseases were excluded. Microindentation was performed using the Osteoprobe® Reference Point Indenter(Active Life Scientific Inc., Santa Barbara,CA. USA) in the midshaft of the tibia.

Results: Fx+ patients were older (60.0 years $\pm$ 14.0 vs. 51.9 years $\pm$ 15.3; p=0.044) and used more alcohol than Fx- patients (21% of patients vs. 0%; p=0.033), but there was no significant difference in the number of patients who were active smokers, had type 2 diabetes or used corticosteroids, nor in mean BMD values, BMI, serum levels of calcium, PTH or 25-OH vitamin D between groups. After adjusting for age, alcohol use and type 2 diabetes, BMS was significantly lower in Fx+ patients than in Fx- patients (BMS 78.5$\pm$0.9 vs. 84.1$\pm$4.6; p=0.010). Separate analysis of subjects with osteopenia (n=41) showed that Fx+ patients with osteopenia had significantly lower BMS values than Fx- patients with osteopenia (BMS 79.3$\pm$0.9 vs. 86.0$\pm$1.5; p=0.004). BMS was comparable in Fx+ patients with osteopenia and in Fx + patients with osteoporosis, BMS 79.3$\pm$0.9 vs. 76.7$\pm$2.1 (p=0.267) respectively, in the presence of significant differences on both the lumbar spine 0.91 g/cm^2 $\pm$ 0.02 vs. 0.78 g/cm^2 $\pm$ 0.02 (p=0.001) and the femoral neck 0.72 g/cm^2 $\pm$ 0.01 vs. 0.56 g/cm^2 $\pm$ 0.03 (p<0.001).

Conclusion: This study is the first to show that Bone Material Strength is significantly lower in fracture patients with osteopenia and comparable to fracture patients with osteoporosis. Our data suggest an aspect of altered bone quality contributing to bone fragility independent of BMD. Further studies are required to establish the value of Bone Material Strength as a predictor of fracture risk, especially in patients with osteopenia.

Disclosures: Frank Malgo, None.

1065

Effect of Vertebral Artifact and Exclusions on Fracture Prediction from Lumbar Spine BMD and TBS (Trabecular Bone Score): The Manitoba BMD Cohort. William Leslie*[1], Suzanne Morin[2], Lisa Lix[1], Sumit Majumdar[3], Didier Hans[4]. [1]University of Manitoba, Canada, [2]McGill University, Canada, [3]University of Alberta, Canada, [4]Lausanne University Hospital, Switzerland

Background: Age-related spondylosis is common and degrades lumbar spine DXA scan quality. Spine TBS (trabecular bone score) may be less sensitive to spondylosis but has not been studied in relation to fracture outcomes.

Methods: Using a registry of all clinical DXA results for Manitoba, Canada, we identified women age >40y with baseline spine DXA (GE Prodigy) from years 1999-2011. Vertebral exclusions were identified by ISCD-certified physicians at the time of initial clinical reporting. Spine TBS was measured by researchers at the University of Lausanne blinded to clinical outcomes. BMD and TBS T-scores were derived for the total spine, individual vertebral levels, minimum/maximum, and (if there were vertebral exclusions) the non-excluded and excluded levels. Incident major osteoporotic fractures (MOFs) and clinical vertebral fractures (VFs) were identified from population-based health services data, and fracture discrimination estimated from area under the ROC curve (AUROC).

Results: 47,736 women met the inclusion criteria. 15,938 (33%) had vertebral exclusions and these varied by level: L4 98%, L3 63%, L2 14%, L1 10%. Vertebral exclusions had a large effect on the BMD T-score (non-excluded levels -1.6, excluded levels -0.4) and on the TBS T-score (non-excluded levels -1.4, excluded levels -0.5). AUROC for predicting MOF from total spine BMD T-score was 0.673 in women without vs 0.642 with vertebral exclusions; non-excluded levels had higher AUROC (change +0.016) but excluded levels had worse AUROC (change -0.007). AUROC for MOF from total spine TBS T-score was 0.644 in women without vs 0.613 with vertebral exclusions; non-excluded levels had higher AUROC (change +0.010) but excluded levels had worse AUROC (change -0.037). Similar results were seen for clinical VFs based upon BMD (AUROC change non-excluded levels +0.026, excluded levels -0.011) and TBS (AUROC change non-excluded levels +0.019, excluded levels -0.055). In women with vertebral exclusions, BMD or TBS T-score for L1 showed higher AUROC for MOF prediction than for any other vertebral level, and minimum T-score showed better MOF prediction than maximum T-score.Summary: Spine DXA artifacts requiring vertebral exclusions affect both spine BMD and TBS. Excluded levels had higher BMD and TBS and worse fracture prediction. Exclusion of levels affected by artifact improved fracture prediction. BMD reporting procedures excluding lumbar spine artifacts also appear to be applicable to TBS.

		Women without vertebral exclusions (N=31,798)			Women with vertebral exclusions (N=15,938)		
		T-score (mean)	AUROC MOF (Δ)²	AUROC VF (Δ)¹	T-score (mean)	AUROC MOF (Δ)²	AUROC VF (Δ)¹
BMD	Total spine (L1-4)	-1.11	0.673 (ref)	0.713 (ref)	-0.97	0.642 (ref)	0.688 (ref)
	Non-excluded levels	N/A	N/A	N/A	1.59	0.659 (+0.026)	0.715 (+0.026)
	Excluded levels	N/A	N/A	N/A	-0.36	0.636 (-0.007)	0.678 (-0.011)
	L1 alone	1.24	0.664 (-0.009)	0.703 (-0.010)	1.60	0.653 (+0.011)	0.703 (+0.015)
	L2 alone	1.31	0.671 (-0.002)	0.712 (-0.001)	1.53	0.638 (-0.005)	0.690 (+0.002)
	L3 alone	-0.87	0.668 (-0.004)	0.707 (-0.005)	-0.71	0.631 (-0.011)	0.671 (-0.018)
	L4 alone	1.21	0.664 (-0.009)	0.721 (+0.009)	-0.37	0.627 (-0.015)	0.668 (-0.021)
	Minimum	1.71	0.677 (+0.004)	0.721 (+0.009)	1.92	0.654 (+0.011)	0.706 (+0.018)
	Maximum	-0.62	0.664 (0.000)	0.699 (-0.013)	-0.05	0.627 (-0.015)	0.664 (-0.024)
TBS	Total spine (L1-4)	-0.78	0.644 (ref)	0.681 (ref)	1.03	0.613 (ref)	0.640 (ref)
	Non-excluded levels	N/A	N/A	N/A	1.41	0.623 (+0.010)	0.659 (+0.019)
	Excluded levels	N/A	N/A	N/A	-0.55	0.577 (-0.037)	0.585 (-0.055)
	L1 alone	1.91	0.653 (+0.009)	0.679 (-0.003)	-2.19	0.625 (+0.011)	0.662 (+0.022)
	L2 alone	-0.36	0.637 (-0.007)	0.674 (-0.007)	1.06	0.601 (-0.012)	0.632 (-0.008)
	L3 alone	-0.05	0.608 (-0.036)	0.644 (-0.038)	0.20	0.581 (-0.032)	0.593 (-0.047)
	L4 alone	-0.30	0.604 (-0.040)	0.636 (-0.045)	-0.65	0.570 (-0.044)	0.571 (-0.069)
	Minimum	-2.07	0.654 (+0.010)	0.685 (+0.003)	-2.40	0.625 (+0.012)	0.660 (+0.020)
	Maximum	0.38	0.612 (-0.032)	0.650 (-0.031)	0.21	0.588 (-0.025)	0.597 (-0.043)

¹,² p<.001 vs women without vertebral exclusions; ¹ all AUROC SE<.01; ² all AUROC SE <.02

Table: BMD and TBS T-scores, AUROC for incident MOF and AUROC for clinical VF

Disclosures: William Leslie, None.

1066

Prospective Association between Novel Biomarker of Oxidative Stress and Hip Fracture in Postmenopausal Women. Shuman Yang*[1], Diane Feskanich[2], Walter Willett[2], Heather Eliassen[2], Tianying Wu[3]. [1]University of Cincinnati, USA, [2]Departments of Nutrition & Epidemiology, USA, [3]Department of Environmental Health, USA

Background: Human studies suggest that oxidative stress is a risk factor for osteoporosis, but its relationship with fracture risk is poorly understood. The purpose of the present study was to investigate the association between biomarker of oxidative stress and hip fracture in postmenopausal women.

Methods: We conducted a prospective study in the Nurses' Health Study among 996 postmenopausal women aged 60 years or older at baseline blood collection in 1989-1990. Plasma fluorescent oxidation products (FlOP)_320 was measured at 320/420 nm (excitation/emission) wavelengths. FlOP_320 is formed when oxidation products such as lipid hydroperoxides, aldehyde, and ketones react with DNA in presence of metals. FlOPs generated from many different pathways (lipid, protein and DNA oxidation) reflect a global oxidation burden. FlOP assay is 10-100 times more sensitive than measurement of malondiadehyde (A specific lipid oxidation marker). We used Cox proportional hazards regression model to investigate the association between baseline FlOP_320 and risk of hip fracture, adjusting for age,

body mass index, history of osteoporosis, history of hypertension, prior fracture, physical activity, alcohol intake, postmenopausal hormone therapy, calcium intake, vitamin D intake, carotenoid intake, smoking status, fasting status, and time and month of blood draw.

Results: Forty four hip fractures (4.4%) were identified during the follow-up (Maximum = 23 years). In the multivariable model, the hazard ratios (HR) of hip fracture in the second and third tertiles of FlOP_320 were 2.17 (95% confidence interval [CI] = 0.90-5.26) and 2.80 (95% CI = 1.18-6.67), respectively, in comparison with the lowest tertile, and the risk increased linearly with increasing FlOP_320 (P for trend = 0.019). After stratifying our analysis by time of follow-up ($<$10 and $\geq$ 10 years), we found similar risk estimates of hip fracture in both time intervals as the overall association between FlOP_320 and hip fracture. As an oxidation marker, we did not find significant interaction of FlOP_320 with fasting status ($P = 0.358$), alcohol intake ($P = 0.126$), current smokers ($P = 0.955$) and history of hypertension ($P = 0.854$) in assessing risk of hip fracture.

Conclusions: In this prospective study, higher plasma FlOP_320 was an independent risk factor for hip fracture. The marker may help improve the assessment of hip fracture risk in postmenopausal women.

Table 1. Association between plasma fluorescent oxidation products and risk of hip fracture

	Tertile 1	Tertile 2	Tertile 3	P for trend
N	331	331	334	—
Range (FI/ml)	< 335	$\geq 335 - 546$	≥ 546	—
Median (FI/ml)	270	404	1337	—
Incidence of hip fracture (n, %)	9 (2.7%)	15 (4.5%)	20 (6.0%)	—
Adjusted for age	1 (ref)	1.81 (0.79, 4.14)	2.51 (1.14, 5.52)	0.012
Adjusted for age and hypertension	1 (ref)	1.78 (0.78, 4.06)	2.35 (1.07, 5.18)	0.015
Adjusted for multiple risk factors*	1 (ref)	2.17 (0.90, 5.26)	2.80 (1.18, 6.67)	0.019

Values are hazard ratios (95% confidence interval), unless otherwise specified. FIOP = Fluorescent oxidation products. FI = Fluorescent intensity units.
*Risk factors included age (continuous), history of hypertension (yes/no), body mass index (< 25, ≥ 25 and < 30, ≥ 30 and <35, and ≥ 35 kg/m²), fasting status (< 8 and ≥ 8 hours), time and month of blood draw, alcohol intake (in quartiles, 0, > 0 and <1, ≥ 1 and < 6.7, and ≥ 6.7 g/day), physical activity (in quartiles, < 5.2, ≥ 5.2 and < 12.7, ≥ 12.7 and < 25.9, and ≥ 25.9 MET-hours/week), total calcium intake (In quartiles, < 667, ≥ 667 and < 969, ≥ 969 and < 1347, and ≥ 1347 mg/day), total vitamin D intake (In quartiles, < 187, ≥ 187 and < 303, ≥ 303 and < 536, and ≥ 536 IU/day), total carotenoid intake (In quartiles, < 6.2, ≥ 6.2 and < 9.0, ≥ 9.0 and < 12.8, and ≥ 12.8 1000 IU/day), history of osteoporosis (yes/no), smoking status (current smokers, past smokers, non-smokers), postmenopausal hormone therapy (yes/no) and prior fracture (yes/no).

Table 1

1067

Beyond BMD: Trochanteric Soft Tissue Thickness Predicts Hip Fracture in Older Adults. <u>Alyssa Dufour</u>*[1], <u>Arunima Awale</u>[1], <u>Douglas Kiel</u>[1], <u>Ann Schwartz</u>[2], <u>Deborah Kado</u>[3], <u>Eric Orwoll</u>[4], <u>Mary Bouxsein</u>[5], <u>Marian Hannan</u>[6]. [1]Hebrew SeniorLife, USA, [2]University of California, San Francisco, USA, [3]University of California, San Diego, USA, [4]Oregon Health & Science University, USA, [5]Beth Israel Deaconess Medical Center, Harvard Medical School, USA, [6]HSL Institute for Aging Research & Harvard Medical School, USA

Hip fractures are disabling events and 25% of adults over 50 years will die in the year following fracture. Low BMD is a well-accepted major risk factor, yet up to half of those suffering a hip fracture do not have low BMD; alternative methods of assessing fracture risk are needed. To look beyond BMD, we examined the relation between factors that influence the load applied to the hip in a sideways fall and risk of hip fracture in men and women from the Framingham Osteoporosis Study.

In a nested case-control study, we measured trochanteric soft tissue thickness (STT, mm) of both hips from whole body DXA scans (Lunar DPX-L) done in 1996-2001 (baseline). Averages of right and left hip STT measurements were used for analyses. Factor-of-Risk (FoR) was defined as the ratio of attenuated force applied to the hip in a sideways fall divided by femoral strength. Attenuated force (N) was calculated from height (m) and weight (kg) and incorporated the cushioning effect of STT. Femoral strength (N) was estimated from femoral neck BMD using published cadaveric femoral strength testing. Incident hip fractures were confirmed by interview and review of medical records through 12/31/08. Hip fracture cases were matched to 4 non-fracture controls by sex and age $\pm$3 years. We used conditional logistic regression to calculate odds ratios (OR) and 95% confidence intervals (CI) for a 1 SD decrease in BMD and STT or a 1 SD increase in FoR and the risk of hip fracture. We adjusted for femoral neck BMD (g/cm^2) in STT models only. AIC indicated model fit (lower values=better).

In 190 participants, at baseline, average age was 69 years ($\pm$9, range 45-87), BMI was 28 kg/m^2 ($\pm$5.2), BMD was 0.801 g/cm^2 ($\pm$0.137) and 76% were female. There were 38 incident hip fractures over 9 ± 3.8 yrs follow-up (mean STT: 40.2mm $\pm$ 17.9) and 152 age- and sex- matched controls (mean STT: 50.6mm $\pm$ 21.5). Lower BMD predicted hip fracture (OR=2.9, p=.0002)(Table). Hip fracture risk increased 2.4-fold higher per 1 SD (21.21mm) decrease in STT, even after adjustment for BMD (OR=1.8). Increased FoR was also predictive of hip fracture (OR=2.9). Using the AIC statistic, we found that a model including STT and BMD was the best predictor of hip fracture.

These results show strong evidence that STT, easily measured from DXA scans, is predictive of hip fracture independent of BMD. Future work should consider this effect compared to FRAX score and, with larger numbers of hip fractures in both men and women.

OR and 95% CI for association between BMD, Trochanteric Soft Tissue Thickness and Factor of Risk with hip fracture per 1 standard deviation change.

	Mean (SD)	OR	95% CI	p-value	AIC[3]
BMD (g/cm^2)[1]					
BMD	0.800 (0.137)	2.88	(1.66, 5.00)	0.0002	106.993
Soft Tissue Thickness (mm)[1]					
STT	48.56 (21.21)	2.36	(1.33, 4.17)	0.0033	113.081
STT+BMD		**1.84**	**(1.01, 3.34)**	**0.0457**	**104.290**
Factor-of-Risk[2]					
FoR	1.01 (0.35)	2.92	(1.65, 5.17)	0.0002	108.108

[1]odds ratios per 1 standard deviation decrease
[2]odds ratios per 1 standard deviation increase
[3]lower AIC value = better model fit

Table

1068

Gene Panel Diagnostics for Disorders with Abnormal Bone Mass: Results From 50 Patients. <u>Uwe Kornak</u>*[1], <u>Ralf Oheim</u>[2], <u>Peter Krawitz</u>[1], <u>Tomasz Zemojtel</u>[3], <u>Michael Amling</u>[2], <u>Stefan Mundlos</u>[1], <u>Peter N. Robinson</u>[1]. [1]Charité-Universitaetsmedizin Berlin, Germany, [2]University Medical Center Hamburg-Eppendorf, Germany, [3]Labor Berlin - Charité Vivantes GmbH, Germany

Disorders with abnormal bone mass have their origin in skeletal development and/or homeostasis. Common consequences are reduced mechanical stability leading to bone deformation or fractures, as well as chronic pain and hematological, immunological, and neurological complications. The spectrum ranges from rare early-onset forms to the very common medical problem late-onset osteoporosis. While the role of common genetic polymorphisms for the susceptibility to late-onset osteoporosis has been extensively investigated the role of rare variants is still poorly defined. In order to offer comprehensive genetic testing at an affordable cost we developed a next-generation sequencing-based gene panel comprising coding and non-coding regions relevant for disorders with abnormal bone mass. We here present exemplary genotyping results of 50 patients with early-onset disorders as well as common late-onset osteoporosis. A special focus will be put on osteoporosis cases in which we unexpectedly identified bona fide mutations in the *FGFR1, LRP5, RUNX2, and WNT1* genes, respectively, thus proving the relevance of the rare-among-the-common hypothesis. In these cases genetic diagnostics can radically change the interpretation of disease phenotype, prognosis and recurrence risk and can be the basis for an optimal individualized therapeutic strategy.

1069

Suppression of osteoprotegerin by glucocorticoids may underlie their adverse effects on cortical bone mass. <u>Marilina Piemontese</u>*[1], <u>Jinhu Xiong</u>[2], <u>Rajamani Selvam</u>[1], <u>Priscilla Baltz</u>[1], <u>Stuart Berryhill</u>[1], <u>Erin Hogan</u>[1], <u>Robert Weinstein</u>[2], <u>Stavros Manolagas</u>[2], <u>Charles O'Brien</u>[2]. [1]University of Arkansas for Medical Sciences, USA, [2]Central Arkansas VA Healthcare System, Univ of Arkansas for Medical Sciences, USA

Glucocorticoid administration causes low bone mass by acting directly on osteoblasts and osteoclasts. However, most studies in mice have focused on the trabecular compartment and the effects of glucocorticoids on the cortical compartment are less well characterized. Here we have analysed the impact of glucocorticoids on cortical bone by treating mice with placebo or prednisolone (2.1 mg/kg/day) for 28 days. Prednisolone administration reduced femoral BMD as measured by DEXA, compared to placebo treated mice, but did not change body weight. Prednisolone also reduced cortical thickness and increased cortical porosity at the metaphysis of femur, as measured by microCT, and this was associated with a decline in strength, as assessed by 3-point bending. Histological analysis of tibial sections revealed elevated osteoclast number at the endocortical surface of prednisolone treated mice, compared to placebo treated mice. Consistent with these findings, expression of osteoclast specific genes, such as calcitonin receptor and tartrate resistant acid phosphatase, was increased in the cortical bone of prednisolone treated mice. These changes in osteoclasts were associated with reduced expression of osteoprotegerin (OPG) in osteocyte-enriched cortical bone. In contrast, expression of receptor activator of nuclear factor kappa-B ligand (RANKL) was unaffected by prednisolone. OPG protein in the bone marrow supernatants was also reduced by prednisolone. These results suggest that glucocorticoids increase osteoclast number in cortical bone by acting on osteoblast lineage cells. To determine whether glucocorticoid action directly on osteoclasts also contributes to the changes in cortical bone, we used mice in which osteoclasts are protected from the actions of glucocorticoids by transgenic expression of 11beta-hydroxysteroid dehydrogenase type 2, an enzyme that inactivates glucocorticoids. Administration of prednisolone to these mice or their control littermates resulted in similar amounts of cortical bone loss and strength. These findings suggest that the detrimental effects of glucocorticoids on the cortical bone compartment result from suppression of OPG production by osteocytes.

1070

Deletion of the androgen receptor in osteoblast progenitors (using Prx1-Cre) reduces bone mass and precludes the effects of orchidectomy in cancellous, but not cortical, bone. <u>Semahat Serra Ucer</u>*[1], Aaron Warren[2], Shoshana Bartell[3], Srividhya Iyer[3], Li Han[3], Julie Crawford[3], Charles O'Brien[3], Maria Jose Almeida[3], Stavros Manolagas[3]. [1]University of Arkansas for Medical Sciences, USA, [2]Center for Osteoporosis & Metabolic Bone Diseases, Central Arkansas Veterans Healthcare System, University of Arkansas for Medical Sciences, USA, USA, [3]Central Arkansas VA Healthcare System, Univ of Arkansas for Medical Sciences, USA

In males, androgens are critical for the acquisition of bone mass in both the cortical and cancellous bone compartment during growth and for its maintenance throughout life. Mice with global deletion of the androgen receptor (AR) exhibit low cortical and cancellous bone mass. On the other hand, targeted deletion of AR in osteoblasts or osteocytes results in lower cancellous bone mass, but it has no effect on the cortical compartment. And, as we report elsewhere in this meeting, AR deletion from osteoclasts (using LysM Cre) has no bone phenotype. It is still possible, however, that the effects of androgens on the cortical compartment result from actions on osteoprogenitors. We have, therefore, generated mice with conditional deletion of an AR allele in pluripotent mesenchymal progenitors, using Prx1-Cre (AR flox;Prx1-Cre). At 7 weeks of age, when androgen levels start to rise in mice, the skeletal phenotype of AR flox;Prx1-Cre male mice was indistinguishable from the AR flox littermate controls by micro-CT. At 12 and 26 weeks of age, however, the AR flox;Prx1-Cre exhibited a 30% and 45% decrease of cancellous bone volume, respectively; as well as lower trabecular number and connectivity. Cortical thickness was unaffected at all ages. We next sham-operated or orchidectomized (ORX) 20-week-old AR flox;Prx1-Cre and AR flox mice, and examined their skeletons 6 weeks later. ORX caused the expected decrease in BMD at the femur in AR flox mice as compared to the sham-operated littermates. In contrast, the effect of ORX on femoral BMD was completely abrogated in the AR flox;Prx1-Cre mice. ORX also decreased cancellous bone volume and trabecular number in the femur of control mice, while it had no effect in the AR flox;Prx1-Cre mice. In contrast to our findings in cancellous bone, both control and AR flox;Prx1-Cre mice lost similar amount of cortical bone with ORX. These results demonstrate that AR deletion in the osteoblast lineage recapitulates the effects of ORX in cancellous bone, indicating that the protective effects of androgen on cancellous bone result from AR-mediated effect of androgen in osteoblast progenitors or their descendants. The protective effects of androgens on cortical bone mass, on the other hand, must be mediated by cells other than those of the osteoblast or the osteoclast lineage.

Disclosures: Semahat Serra Ucer, None.

1071

Prolyl Hydroxylase 2 (PHD2) controls Bone Homeostasis through increasing Erythropoietin Production via HIF2α. <u>Martina Rauner</u>*[1], Kristin Franke[2], Lorenz Hofbauer[3], Ben Wielockx[2]. [1]Medical Faculty of the TU Dresden, Germany, [2]Technische Universität Dresden, Germany, [3]Dresden University Medical Center, Germany

Prolyl hydroxylase 2 (PHD2) regulates hypoxia-inducible factor α (HIFα) transcription factors and thus, erythropoietin (EPO) production. Under normoxic conditions, HIFα is constantly inactivated through hydroxylation by PHD2. Due to the embryonic lethality of PHD2 knock-out mice, its precise role in erythropoiesis and tissue homeostasis has long remained unknown. Recently, we generated a conditional knock-out (cKO) mouse lacking PHD2 in EPO-producing cells. These mice have high levels of EPO and an increased hematocrit, which is dependent on HIF2α. In this study, we determined the role of PHD2 in bone.

Total, trabecular, and cortical bone density at the femur was significantly decreased by 12%, 20%, and 5% in cKO as compared to wild-type (WT) mice. Results were confirmed using histomorphometry, showing a 38% decrease in bone volume in the tibia, accompanied by microarchitectural changes including fewer trabeculae (-33%) and an increased trabecular spacing (+59%) in cKO mice. Bone resorption was not affected, as determined using serum levels of C-terminal telopeptide of type I collagen and tartrate-resistant acid phosphatase, and the histological evaluation of osteoclasts. In addition, conditional knock-out of PHD2 using the lysM-cre and vav-cre lines did not result in an altered bone phenotype. In contrast, osteoblasts function was severely impaired. Serum levels of procollagen type I N-terminal propeptide and osteocalcin were decreased by 30-40% in cKO mice. In line with that, the mineralized surface, the mineral apposition rate, the bone formation rate, and the osteoblast surface were reduced by 35-50%. Because cKO are characterized by high serum EPO levels, we next assessed the bone phenotype in EPO-treated mice. Similar to cKO, mice treated with 3 U EPO per day for 28 days had a lower vertebral trabecular bone mineral density (-18%) and a lower local rate of bone formation (BFR: -29%). To further pinpoint which downstream signals are involved in the bone phenotype of cKO mice, we used PHD2/HIF1α (P2/H1) and PHD2/HIF2α (P2H2) double-knock-out (DKO) mice. While P2/H1 DKO mice, which also have high EPO levels, showed a similar bone phenotype as cKO, including decreased bone density and bone formation, bone density was restored in P2/H2 DKO mice, which have normal EPO levels.

Thus, PHD2 controls bone homeostasis at least in part through increasing HIF2α-dependent EPO production and thus, is a novel player in osteohematology.

Disclosures: Martina Rauner, None.
This study received funding from: DFG, CRTD, Elsbeth-Bonhoff foundation

1072

An O-glycosylation on Fibronectin Mediates Hepatic Osteodystrophy by Interacting with α4β1 Integrin. <u>Carla Sens</u>*[1], <u>Nina Kawelke</u>[1], <u>Anja von Au</u>[1], <u>Inaam Nakchbandi</u>[2]. [1]University of Heidelberg & Max-Planck Institute of Biochemistry, Germany, [2]Max-Planck Institute of Biochemistry & University of Heidelberg, Germany

Patients with autoimmune liver disease experience increased circulating levels of a fibronectin (FN) isoform that is characterized by the presence of O-glycosylation called oFN by 40% (p<0.05) compared to healthy controls. This isoform significantly inhibits osteoblast differentiation *in vitro* (as measured by nodule formation, alkaline phosphatase activity or osteocalcin). Injection of oFN in mice over two weeks results in decreased BMD by 17%, osteoblasts by 45% and BFR by 60% compared to vehicle-treated mice (all p<0.05). Enzymatic O-deglycosylation of oFN normalized nodule formation *in vitro*. Three possible O-glycosylation sites have been described in FN. Mutations in these three sites followed by transient transfection in primary newborn murine osteoblasts and evaluation of osteoblast differentiation were performed. This allowed localization of the responsible O-glycosylation site at AA 33 of the variable region. Indeed, simultaneous addition of oFN and an antibody that recognizes this O-glycosylation (glyc-Ab) normalized osteoblast differentiation. Further, oFN decreased pERK by 50%, while oFN+glyc-Ab normalized and the transfection with the mutated construct increased pERK two-fold. This suggests that oFN acts by inhibiting integrin-mediated signaling. The variable region of FN binds to α4β1 or α4β7 integrin. Differentiating osteoblasts express α4 and β1 but not β7 by flow cytometry. oFN decreased surface expression of α4β1 by 62%, while oFN+glyc-Ab normalized α4 expression. Based on these findings we hypothesized that α4β1 mediated oFN effects on osteoblasts. An antibody that binds to α4β1 (PS/2) was added to osteoblasts treated with oFN. Osteoblast differentiation *in vitro* and pERK normalized in the presence of oFN+PS/2 suggesting that α4β1 mediates the inhibition of oFN on the osteoblasts. To test this *in vivo* we injected oFN in mice in which β1 integrin was deleted in osteoblasts (col-α1(I)-cre β1^{fl/fl}). In these mice oFN failed to decrease BMD in contrast to controls. This suggests that b1 integrin on the osteoblasts is needed to mediate oFN effects.

In summary, oFN elevation in patients with hepatic osteodystrophy results in inhibition of osteoblast activity. An O-glycosylation in the variable region of fibronectin mediates this effect. This O-glycosylation acts by interfering with a4b1 integrin-mediated signaling. We have thus characterized the defect and the receptor mediating bone loss in patients with hepatic osteodystrophy.

Disclosures: Carla Sens, None.

1073

What generates porosity in cortical bone?. <u>Nicolai Lassen</u>*[1], <u>Thomas Andersen</u>[2], <u>Jean-Marie Delaisse</u>[3], <u>Søren Harving</u>[4], <u>Ellen Hauge</u>[5], <u>Gete Eschen</u>[6], <u>Jesper Thomsen</u>[7], <u>Annemarie Brüel</u>[8]. [1]Vejle Hospital, Denmark, [2]Vejle Hospital - Lillebaelt Hospital, IRS, University of Southern Denmark, Denmark, [3]Vejle Hospital, IRS, University of Southern Denmark, Denmark, [4]Department of Orthopaedic Surgery, Aalborg Hospital, Denmark, [5]Aarhus University Hospital, Denmark, [6]Department of Plastic Surgery, Aarhus Hospital, Denmark, [7]Aarhus University, Denmark, [8]University of Aarhus, Denmark

Cortical bone has a considerable, but often disregarded, contribution to the overall strength of bone. The physiological process greatly affecting bone strength is bone remodelling. A cortical bone remodeling unit is commonly described to involve a cutting cone of osteoclasts (OC) excavating a tunnel (called a Haversian canal), a reversal zone generating an osteogenic environment, and a closing cone where bone forming osteoblasts (OB) refill the canals until only a narrow canal remains. With age, not only the number but also the diameter of Haversian canals increases, resulting in increased porosity, which weakens the bone. Herein, we aim at identifying the biological activities leading to increased porosity.

We used therefore human bone specimens from five proximal femurs and two fibulae. We took benefit of sections cut in the longitudinal direction of the Haversian canals, making it possible to follow the sequential remodeling steps. Serial sections were immunostained for OC (TRAcP and cathepsin K) and OB (Runx2 and CD56) markers, thereby allowing 3D reconstructions of the distribution of OC and OB activities in a remodelling unit.

The analysis revealed that so-called "reversal" surfaces were not only lined by typical osteoprogenitor cells expressing Runx2 and CD56, but also by OCs exerting "secondary" resorption on the lateral surfaces of the canals, and thus widening them. In a 2D analysis, 35% of the detected reversal surfaces showed secondary resorption, but the systematic 3D analysis of 21 Haversian canals with remodeling events revealed that all reversal surfaces showed secondary resorption. Furthermore, the 3D analysis revealed that secondary resorption occurred mostly on early reversal surfaces (close to the cutting cone), where OCs and osteoprogenitors were closely interacting. Later reversal surfaces (close to the osteoid) were only lined with osteoprogenitors.

In conclusion, in cortical bone remodeling the reversal phase does not simply represent a switch turning off the resorption of the cutting cone and turning on pro-osteogenic activities, as would commonly be expected from a "reversal" phase. It rather appears as a bone remodeling step where OCs and OB-lineage cells compete, thereby determining how much bone will be removed laterally, and how soon the bone removed by the OC can be replaced by bone forming OBs.

Disclosures: Nicolai Lassen, None.

1074

Dysregulated innate immune responses mediate chronic inflammation leading to osteoarthritis. <u>Evangelia Kalaitzoglou</u>*[1], <u>Mary Beth Humphrey</u>[2]. [1]OUHSC, USA, [2]University of Oklahoma Health Sciences Center, USA

Obesity increases the risk of developing OA in weight-bearing and non-weight-bearing joints suggesting that both mechanical and non-mechanical factors associated with obesity increase the risk of OA. Chronic, low-grade inflammation may provide a critical link between obesity and OA. Abnormal innate immune responses in obesity, likely mediated via free fatty acid (FFA) activation of Toll-Like Receptor 4 (TLR4), increase pro-inflammatory mediators, such as tumor necrosis factor-α (TNFα), and contribute to the development of OA. TREM2, paired with DAP12, inhibits TLR-induced cytokine responses in macrophages and therefore may provide protection from high-fat diet induced OA. We hypothesize that high fat diet- induced OA is partly mediated by dysregulation of innate immune responses to FFA leading to increased pro-inflammatory cytokines driving abnormal cellular and tissue responses within joints resulting in OA. To test our hypothesis, macrophages derived from wild type (WT) and DAP12-deficient (DAP12 KO) mice were stimulated with endotoxin free FFA (palmitic and lauric acid) and proinflammatory cytokines, ERK and NFκB activation, as measured by IKBα degradation, were evaluated. WT and TREM2-deficient (TREM2 KO) mice were placed on a high fat diet for 3 months and knee joints evaluated histologically for OA changes. Our studies show that WT macrophages have dose and time-dependent ERK activation and IKBα degradation as well as TNFα production in response to palmitic acid and lauric acid. Compared to WT macrophages, DAP12 KO macrophages have increased TNFα production and ERK and NFκB activation in response to palmitic acid and lauric acid stimulation, indicating that DAP12 negatively regulates FFA-induced responses in macrophage. TREM2 KO mice on a high fat diet have increased histological changes of early knee osteoarthritis compared to WT mice. Ongoing studies with mice on a high fat diet will reveal whether TRL4 KO mice are protected from high-fat diet induced OA when compared to DAP12 KO mice that may have early or more severe osteoarthritis. In conclusion DAP12 and TREM2 signaling complex has an immunoregulatory function in FFA stimulated cytokine responses in macrophages. TREM2 KO mice have accelerated OA compared to WT mice on a high fat diet. By examining how high fat diet alters innate inflammatory and metabolic pathways associated with OA, we hope to develop novel therapeutic targets to prevent or suspend the progression of osteoarthritis.

Disclosures: Evangelia Kalaitzoglou, None.

1075

Increasing 25-hydroxyvitamin D levels over time: The Study of Women's Health Across the Nation (SWAN). <u>Deborah Mitchell</u>*[1], <u>Hang Lee</u>[2], <u>Gail Greendale</u>[3], <u>Jane Cauley</u>[4], <u>Sherri-Ann Burnett-Bowie</u>[1], <u>Joel Finkelstein</u>[1]. [1]Massachusetts General Hospital, USA, [2]Massachusetts General Hospital, USA, [3]University of California, Los Angeles, USA, [4]University of Pittsburgh Graduate School of Public Health, USA

The importance of vitamin D for bone health as well as its potential role in nonskeletal health has garnered much recent attention. Population-based studies investigating temporal trends in 25-hydroxyvitamin D (25OHD) have reported conflicting results. Our goal was thus to investigate changes in mean 25OHD levels over time and predictors of these changes in the Study of Women's Health Across the Nation (SWAN), a multi-center, racially and ethnically diverse cohort of women. 1582 women had 25OHD measured in 1998-2000 (at age 48 ± 3 years) and again in 2009-2011 (at age 60 ± 3 years). 25OHD was measured by liquid chromatography-tandem mass spectrometry in a single batch. Over this interval, the mean 25OHD level increased by 6.5 ng/mL (95% CI 5.9 to 7.0), from 21.5 ± 9.8 to 28.0 ± 11.5 ng/mL (p<0.001 after adjustment for age, BMI, menopausal status, study site, and season of blood draw). As expected, baseline mean 25OHD levels varied by race/ethnicity (14.0 ng/mL (African-American), 25.4 ng/mL (Caucasian), 19.8 ng/mL (Chinese), 18.3 ng/mL (Hispanic), and 24.0 ng/mL (Japanese) (p<0.001)). However, the magnitude of increase was similar among groups, ranging from 5.3 ng/mL (Caucasian) to 8.7 ng/mL (Chinese) (Figure 1). The observed increases in 25OHD did not vary by socio-economic status (SES), education level, or acculturation. At the 2009-2011 visit, 49% of subjects reported taking a multivitamin or vitamin D supplement; the adjusted increase in 25OHD was higher among supplement users (10.1 vs. 3.2 ng/mL, p<0.001). Using the Institute of Medicine definition of vitamin D deficiency as 25OHD < 20 ng/mL, the proportion of deficient women decreased from 43% to 24% (p<0.001) over the interval. Among those who reported using supplements at the 2009-2011 visit, the proportion deficient decreased from 35% to 6% (p<0.001) while the proportion decreased from 51% to 39% among non-users (p<0.001). Rates of 25OHD < 20 ng/mL were significantly lower among supplement users of all racial/ethnic groups (p<0.001 for all comparisons at the 2009-2011 visit) (Figure 2). In summary, we observed an increase in average 25OHD levels as well as a decrease in the proportion of subjects with vitamin D deficiency in this observational cohort over an approximately 11 year interval. Subjects of all races/ethnicities as well as of differing SES, level of education, and degree of acculturation had similar changes. Use of vitamin supplements was a major determinant of changes in 25OHD levels.

Figure 1
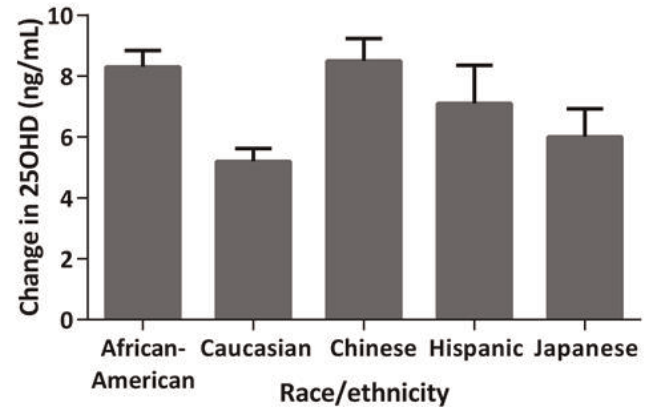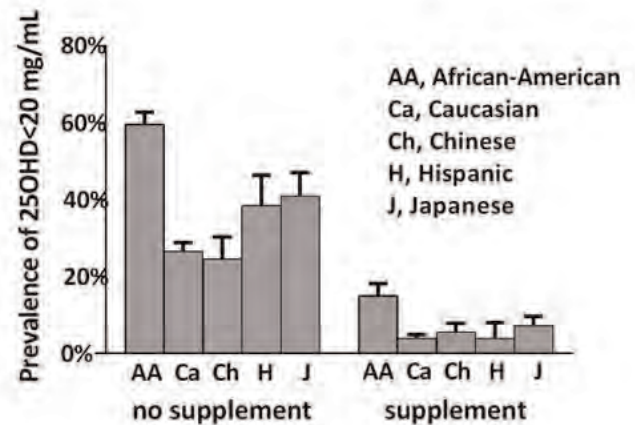
Figure 2

Disclosures: Deborah Mitchell, None.

1076

Serum 25 Hydroxyvitamin D (25(OH)D), Bone Mineral Density (BMD) and Fracture Risk across the Menopausal Transition: Study of Women's Health Across the Nation (SWAN). <u>Jane Cauley</u>*[1], <u>Gail Greendale</u>[2], <u>Kristine Ruppert</u>[3], <u>Yinjuan Lian</u>[3], <u>John Randolph</u>[4], <u>Joan Lo</u>[5], <u>Robert Neer</u>[6], <u>Sherri-Ann Burnett-Bowie</u>[6], <u>Joel Finkelstein</u>[6]. [1]University of Pittsburgh Graduate School of Public Health, USA, [2]University of California, Los Angeles, USA, [3]University of Pittsburgh, USA, [4]University of Michigan, USA, [5]Kaiser Permanente, USA, [6]Massachusetts General Hospital, USA

Circulating 25(OH)D has been linked to fracture risk but to our knowledge, there is no information on whether 25(OH)D predicts fracture over the menopausal transition or whether 25(OH)D is associated with changes in BMD over the menopausal transition. We studied 1620 women enrolled in the bone cohort of the Study of Women's Health Across the Nation (SWAN). Women attended up to 11 clinic visits for an average follow-up of 9.5 years. 25(OH)D was measured at the 02 clinic visit, 2 years after enrolling in SWAN. At this time, 1207 (74.5%), were pre or early perimenopausal; 116(7.2%) late perimenopausal, 77(4.8%) postmenopausal based on bleeding patterns. Menopausal status or had hysterectomy was unknown for 220 (13%). The mean 25(OH)D (ng/ml) was 21.6 but differed markedly by race/ethnicity; White, 25.2; Black, 14.1; Chinese, 20.1 and Japanese, 23.5, p<0.001); 703 (43%) had a value < 20ng/ml. The mean age of the women at time of 25(OH)D measure was 48.5 ± 2.7, with no difference by race/ethnicity. Body mass index (BMI) (kg/m²) was greatest in Black women, 31.8; lower in White women, 28.2 and lowest in Japanese, 23.5 and Chinese, 23.2 women. Incident non-traumatic fractures that occurred after visit 02 were ascertained at each annual visit initially by self-report and later, confirmed by radiographic report. A total of 88 women experienced an incident non-traumatic fracture. Cox proportional hazard models were used to calculate the hazard ratio (HR) (95% confidence interval (CI)). Each 10 ng/ml increase in 25(OH)D was associated with a 25% lower fracture risk, even after adjusting for BMI, BMD

and other important confounding variables, Table. Women with 25(OH)D >20 ng/ml had a 42% lower risk of fracture. Exclusion of women who were already postmenopausal at visit 02 had no effect. Longitudinal analyses of BMD across the menopausal transition were confined to the subset of 791 women for whom a final menstrual period (FMP) could be determined. The mean 25(OH)D level in this subgroup (21.2 ng/ml) was similar to the total population. We compared rates of spine and hip BMD changes in women from -5 to -1 yr before the FMP, 1 year before to 2 years after FMP and 2 to 5 years after FMP. We found no association between (25(OH)D and transmenopausal bone loss. We conclude that women with higher 25(OH)D levels at midlife have a lower risk of subsequent fractures. Vitamin D supplementation may be warranted in women with 25(OH)D <20 ng/ml.

Table: 25(OH)D and fracture over the menopausal transition		
25(OH)D	Base Model[1] HR(95% CI)	Multivariate Model[2] HR(95% CI)
per 10 ng/ml increase	0.75(0.58, 0.96)	0.75(0.57, 0.997)
≥ 20 vs <20 ng/ml	0.55(0.35, 0.86)	0.58(0.35, 0.96)
[1] Adjusted for age, site, race.		
[2] Base model + fracture history, prior and current hormone therapy, BMI, physical activity, education, total hip BMD, calcium and D supplements, corticosteroids, diabetes.		

table

Disclosures: Jane Cauley, None.

1077

Intestinal Calcium Absorption Decreases Dramatically After Gastric Bypass Surgery, Despite Optimization of Vitamin D Status. <u>Anne Schafer</u>*[1], <u>Deborah Sellmeyer</u>[2], <u>Connie Weaver</u>[3], <u>Amber Wheeler</u>[4], <u>Lygia Stewart</u>[5], <u>Stanley Rogers</u>[4], <u>Jonathan Carter</u>[4], <u>Andrew Posselt</u>[4], <u>Dennis Black</u>[4], <u>Dolores Shoback</u>[6]. [1]University of California, San Francisco & the San Francisco VA Medical Center, USA, [2]The Johns Hopkins Bayview Medical Center, USA, [3]Purdue University, USA, [4]University of California, San Francisco, USA, [5]San Francisco VA Medical Center & the University of California, San Francisco, USA, [6]VA Medical Center, USA

Roux-en-Y gastric bypass (RYGB) surgery has negative effects on the skeleton. RYGB can result in vitamin D malabsorption. Additionally, the bypassed duodenum and proximal jejunum are usual sites of active, transcellular calcium (Ca) uptake. However, Ca absorption occurs throughout the intestine, and those who have undergone RYGB might maintain sufficient Ca absorption, particularly if vitamin D status is optimal. We determined the effects of RYGB on fractional Ca absorption in the setting of optimized vitamin D status and recommended Ca intake, hypothesizing that these efforts would mitigate against post-op declines in Ca absorption and bone mass.

A prospective cohort of 33 obese men and women (body mass index 45 ± 7 kg/m^2) had serum 25-hydroxyvitamin D [25(OH)D] levels repleted and maintained at ≥30 ng/mL before and after RYGB. Total daily Ca intake of 1200 mg was maintained with individually-dosed Ca citrate supplements. Fractional Ca absorption was measured pre-op and 6 months post-op with a dual stable isotope method. Isotope enrichment was determined by inductively coupled plasma mass spectrometry. Laboratory measures and bone mineral density (BMD) by DXA were assessed. We report here the first 22 participants' pre- and post-op data.

Mean 6-month weight loss was 33 kg (Table). Fractional Ca absorption decreased from 0.33 ± 0.14 to 0.07 ± 0.04 (p<0.001), despite serum 25(OH)D levels of 41 (pre-op) and 38 (post-op) ng/mL. PTH level increased, and urinary Ca decreased. Bone turnover markers increased markedly, and BMD decreased at the total hip and femoral neck. Greater percentage weight loss and decreases in IGF-1 and IGF-binding protein 3 levels were correlated with larger percentage decreases in fractional Ca absorption (Spearman's ρ 0.51, 0.50, and 0.59, respectively; all p-values ≤0.04). Those with larger percentage decreases in fractional Ca absorption had greater increases in serum CTX, but changes in fractional Ca absorption and BMD were not correlated.

We conclude that even with maintenance of 25(OH)D levels ≥30 ng/mL, fractional Ca absorption decreases dramatically after RYGB. These findings suggest that in addition to addressing vitamin D deficiency, clinicians must ensure sufficient Ca intake post-op, although the approach to Ca supplementation needs to be established. Among RYGB patients, those who lose the most weight may have the most severe declines in Ca absorption. Strategies to avoid long-term skeletal consequences should be investigated.

Fractional Ca absorption and other parameters, before and after RYGB			
Variable	Pre-op	6 months post-op	p-value
Weight (kg)	127 ± 19	93 ± 15	<0.001
BMI (kg/m^2)	45 ± 8	33 ± 6	<0.001
Fractional Ca absorption	**0.33 ± 0.14**	**0.07 ± 0.04**	**<0.001**
25(OH)D (ng/mL)	41 ± 10	38 ± 13	0.21
24-hour urinary Ca (mg)	145 ± 96	105 ± 77	0.02
Serum Ca (mg/dL)	9.2 ± 0.3	9.2 ± 0.3	0.55
PTH (pg/mL)	47 ± 31	53 ± 21	0.04
Estradiol (pg/mL)	51 ± 24	57 ± 35	0.68
IGF-1 (ng/mL)	129 ± 46	134 ± 56	0.94
IGFBP-3 (ng/mL)	4220 ± 840	3785 ± 753	<0.01
CTX (ng/mL)	0.276 ± 0.119	0.999 ± 0.344	<0.001
P1NP (ng/mL)	31 ± 12	68 ± 23	<0.001
Total hip areal BMD (g/cm^2)	1.158 ± 0.149	1.112 ± 0.115	<0.01
Femoral neck BMD(g/cm^2)	0.967 ± 0.142	0.929 ± 0.117	<0.001

Fractional Ca absorption and other parameters, before and after RYGB

Disclosures: Anne Schafer, None.

1078

Vitamin K1 supplementation does not improve bone health even among postmenopausal women with low baseline serum vitamin K1: Secondary analyses from the ECKO trial. <u>Maryam Hamidi</u>*[1], <u>Hanxian Hu</u>[1], <u>Olga Gajic-Veljanoski</u>[1], <u>Judy Scher</u>[1], <u>Angela M. Cheung</u>[2]. [1]University Health Network, Canada, [2]University Health Network-University of Toronto, Canada

Background: Observational studies have shown associations between vitamin K1 insufficiency and impaired bone health status in postmenopausal women. However, the findings of clinical trials suggest that vitamin K1 supplementation in healthy postmenopausal women does not improve bone health. Conversely, clinical trials have shown vitamin K2 supplementation to be beneficial to bone health in frail and elderly women with osteoporosis. Therefore, it has been hypothesized that vitamin K supplementation may improve bone health in postmenopausal women, only if they have subclinical vitamin K deficiency. So far, no studies have examined the effect of vitamin K1 supplementation on bone health in postmenopausal women with low baseline serum vitamin K concentrations. Objectives: To examine whether vitamin K1 supplementation reduces bone loss, as measured by BMD, and bone turnover (BTM) in postmenopausal women with osteopenia and low fasting serum concentrations of vitamin K1. Methods: This is a secondary analysis of the ECKO trial including 161 women who had baseline fasting serum vitamin K concentrations ≤ 1 nmol/l. In the ECKO trial 440 postmenopausal women with osteopenia were randomized to receive vitamin K1 (5mg/d) or placebo for 2-4 years to examine the effect of vitamin K on bone health. All study participants were advised to maintain a total daily intake of 1500 mg of calcium and 800 IU of vitamin D throughout the study. BMD outcomes were 2-year change in lumbar spine, femoral neck, total hip and ultradistal radius BMD. BTM outcomes were 2-year change in osteocalcin, C-terminal telopeptide and percentage of under-carboxylated osteocalcin. We used two-sample t-test for all outcomes. A 2-sided p-value < 0.05 was considered statistically significant. All analyses were performed using SAS 9.3. Results: Median fasting serum vitamin K1 at 2-years was 17.4 (IQR:9-27.9) nmol/l for the treatment group, and 1.05 (IQR:0.6-1.75) nmol/l for the placebo group. There were no significant differences between the two groups in any of the bone health outcomes. There was a significant difference between 2-year change in serum concentrations of vitamin K1 between the two groups (p<0.0001). We found no interactions between group and 2-year change in 25-hydroxyvitamin D concentrations. Conclusion: Vitamin K1 supplementation (5mg/d) for 2 years does not improve bone health status in postmenopausal women with osteopenia who have low fasting baseline serum vitamin K concentrations.

Disclosures: Maryam Hamidi, None.

1079

Trabecular Plate-Rod Morphology and Connectivity are Abnormal and Associated with Reduced Bone Stiffness in Women Treated with Glucocorticoids. <u>Ji Wang</u>[1], <u>Bin Zhou</u>[1], <u>Kyle Nishiyama</u>[1], <u>Stephanie Sutter</u>[2], <u>X Guo</u>[1], <u>Emily Stein</u>*[3]. [1]Columbia University, USA, [2]Columbia University Medical Center, USA, [3]Columbia University College of Physicians & Surgeons, USA

Glucocorticoids (GCs) increase fracture risk through mechanisms distinct from their effects on bone density. We previously reported that postmenopausal women using oral GCs have lower volumetric bone density, cortical thickness and thinner, more widely and irregularly spaced trabeculae compared to controls. In this study, we further investigated structural mechanisms associated with fragility in these patients using individual trabecula segmentation (ITS)-based morphologic analysis. This three-dimensional model independent technique is based upon high-resolution peripheral quantitative CT scans and directly measures individual trabeculae, characterizing trabecular (Tb) type (plate vs. rod), orientation and connectivity. We hypothesized that GC treated women would have fewer Tb plates and less Tb connectivity compared to controls. Women treated with oral GCs for >3 months (n=30) were matched by age and race with women never exposed to GCs (n=60). Mean age was 68 yrs (67% Caucasian).

Among GC-treated subjects, 67% had rheumatologic disease, mean dose of prednisone was 8 mg/d, and treatment duration was 3 years. Areal BMD by DXA was similar at all sites. By ITS at the radius, GC subjects had significantly lower directly measured bone volume fraction (-13%;p<0.03), fewer Tb plates (-7%;p<0.03) and tended to have fewer Tb rods (-4%;p=0.08). They had significantly fewer axially aligned trabeculae (-16%;p<0.03), lower connectivity between plates (-19%;p<0.03) and between plates and rods (-17%;p<0.02). At the tibia, GC-treated women tended to have lower bone volume fraction (-8%;p=0.052), had significantly fewer Tb plates (-6%;p<0.02), fewer axially aligned trabeculae (-14;p<0.01) and less connectivity between plates (-14%;p<0.02). They tended to have less connectivity between plates and rods (-10%;p=0.06). Whole bone stiffness by finite element analysis, was lower among GC subjects at both radius (-16%;p<0.005) and tibia (-11%;p<0.02). Lower stiffness was associated with lower bone volume fraction, fewer plates, fewer axially aligned trabeculae, and less Tb connectivity (r=0.59-0.70;p<0.001 for all). The ITS images below, with plates in green and rods in red, show fewer Tb plates in GC-treated subjects. In summary, GC-treated women had fewer Tb plates, a less axially aligned Tb network and less Tb connectivity. These features were associated with lower stiffness and may be novel mechanisms for biomechanical compromise in postmenopausal women treated with GCs.
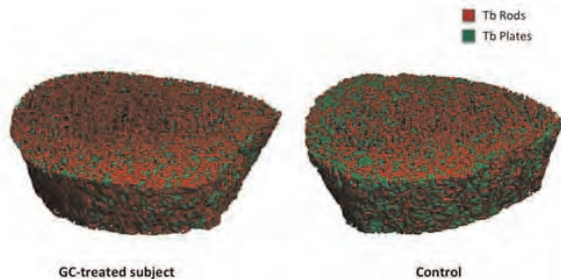
ITS Images at the Tibia of a GC-treated and Control Subject

Disclosures: Emily Stein, None.

1080

Medical Comorbidity and Osteoporosis Are Associated with Subsequent Initiation of Proton Pump Inhibitors. Laura Targownik*[1], Zoann Nugent[2], William Leslie[1]. [1]University of Manitoba, Canada, [2]University of Manitoba, Canada

Introduction: Observational studies have demonstrated an association between proton-pump inhibitors (PPI) use and the occurrence of fractures. Persons with greater frailty may be more likely to be prescribed PPIs, and frailty may also be associated with reduced bone mineral density (BMD) and fracture. Therefore, we aimed to determine whether either greater degrees of medical comorbidity and/or the presence of pre-existing osteoporosis is associated with subsequent prescription of PPIs.

Methods: We used the Manitoba BMD Database, which contains all DXA results for Manitoba, Canada, with linkages to population-based health services databases, to identify residents who underwent DXA testing from 2001-2011. Persons with a previous prescription for PPIs, prior history of fracture or prior osteoprotective medication use were excluded. Global comorbidity was assessed using Johns Hopkins Aggregate Diagnostic Groups (ADGs), which is an enumeration of health care visits for specific indications over the previous year. Osteoporosis and osteopenia were based on WHO criteria using femoral neck BMD. Subjects were followed for the next 5 years for becoming new PPI users (defined as pharmacy dispensations with >90 days continuous use). Cox proportional hazards modelling was performed to evaluate predictors of subsequent PPI initiation.

Results: Of the 27,028 persons meeting the inclusion criteria, 11.0% initiated PPIs over the next 5 years. Subjects with high medical comorbidity (>6 ADGs) were significantly more likely to be prescribed PPIs than those with low comorbidity (18.9 vs 6.1%, p<0.0001). Persons with osteoporosis were also more likely to be prescribed PPIs than those with normal BMD (13.5% vs. 10.3%, p=.0011). Multivariable regression showed that pre-existing osteoporosis, greater medical comorbidity, older age, and higher BMI were all independently predictive of future PPI use (Table).-Conclusions: Pre-existing osteoporosis and multiple medical comorbidities predict the future use of PPIs. As both osteoporosis and medical comorbidity are associated with an increased risk of fracture, this may represent an alternate explanation for the association between PPI use and fracture. Further work is required to determine whether PPI use remains a risk factor for future fracture when controlling for this increased propensity for PPI prescription among those at highest risk for fracture.

Table: Predictors of PPI Initiation Following Performance of DXA

Predictor	Hazard Ratio	95% CI Limits	
Total Subjects	27028		
Female vs Male	0.87	0.76	1.006
Normal	ref		
Osteoporosis (T-score < -2.5)	1.18	1.03	1.36
Osteopenia (-1 < T-score < -2.5)	1.08	0.98	1.18
Age			
50-59	ref		
60-69	1.28	1.15	1.42
70-79	1.53	1.37	1.70
80-89	1.68	1.45	1.94
Comorbidity			
Low (0-2 ADGs)	ref		
Moderate (3-5 ADGs)	1.75	1.57	1.94
Severe (6+ ADGs)	3.18	2.85	3.56
BMI			
<18 (Underweight)	0.81	0.57	1.14
18-25 (Normal BMI)	ref		
25-30 (Overweight)	1.32	1.21	1.45
>=30 (Obese)	1.60	1.45	1.78

Table

Disclosures: Laura Targownik, Takeda Canada, 3

1081

Asfotase Alfa: Sustained Improvements in Hypophosphatasia-related Rickets, Physical Function, and Pain During 3 Years of Treatment for Severely Affected Children. Katherine Madson*[1], Cheryl Rockman-Greenberg[2], Agustin Melian[3], Scott Moseley[3], Amy L. Reeves[4], Tatjana Odrljin[3], Michael Whyte[1]. [1]Shriners Hospital for Children-Saint Louis, USA, [2]University of Manitoba, Canada, [3]Alexion Pharmaceuticals Inc, USA, [4]Shriners Hospitals for Children, USA

Hypophosphatasia (HPP) is the rare inborn error of metabolism characterized by low alkaline phosphatase activity and defective skeletal and dental mineralization due to inactivating muta-tion(s) within the tissue-nonspecific alkaline phosphatase (TNSALP) gene. Our preliminary reports of severely affected children aged 5-12 yrs treated for 6 mos with asfotase alfa, a bone-targeted recombinant human TNSALP, demonstrated bone healing with improved skeletal mineralization as assessed by radiographic scales, DXA BMD Z-scores, and iliac crest biopsy.[1,2,3] Here, we report comprehensive data from 3 yrs of treatment with asfotase alfa in these patients. This multinational, open-label study assessed radiographic changes of rickets using a Radiographic Global Impression of Change (RGI-C) scale and a Rickets Severity Scale (RSS).[4] Data from patients treated for 3 yrs were compared to their baseline (BL), and compared to 2-yr historical control (HC) data. In addition, we evaluated BMD Z-scores, physical function (6-minute walk test [6MWT]), strength and agility (eg, one-legged stationary hop on the Bruininks-Oseretsky Test of Motor Proficiency [BOT-2]), comfort/pain (Pediatric Orthopedic Society of North America [POSNA] Pediatric Outcome Data Collection Instrument [PODCI]), and disability (Child Health Assessment Questionnaire [CHAQ]).

During this extension study, 12/13 pts (1 withdrew: elective surgery) received 3 yrs of therapy with asfotase alfa up to 6 mg/kg/wk SC. At BL, all patients had rachitic disease, abnormal gaits, and 8 (62%) had muscle weakness. With asfotase alfa treatment, significant improvement in rickets was observed during the first 6 mos, and was sustained at 2 yrs (RGI-C: p<0.0001 vs HC; RSS: p=0.0025 vs HC) and at 3 yrs (RGI-C: p=0.0078 vs BL). DXA BMD Z-scores improved (p=0.0875) through 3 yrs. The Table shows 6MWT, BOT-2 one-legged stationary hop, CHAQ disability, PODCI comfort/pain scores, and height Z-scores which all improved through 3 yrs. The most common adverse events (AEs) were injection site reactions. There were no deaths, serious AEs, or withdrawals due to AEs. 12 pts tested positive for anti-asfotase alfa antibodies; 2 pts had neutralizing antibodies without apparent effect on clinical efficacy. Severely affected children with HPP who received asfotase alfa experienced rapid and continued improvements including healing of rickets, physical function, and reduced pain and disability that are sustained through 3 years.

Table: Function and Growth Measures in Children with HPP Treated with Asfotase Alfa

	Baseline	6 months	2 years	3 years
6-Minute Walk Test: Distance Walked – Percent Predicted				
Median (Min, max)	61% (29%, 82%)	85% (52%, 100%)	83% (73%, 92%)	87% (82%, 96%)
p-value*	--	<0.0001	<0.0001	<0.0003
BOT-2 One-legged Stationary Hop (# hops)				
Median (Min, max)	0 (0, 29)	4 (0, 35)	19 (0, 35)	21 (9, 34)
p-value*	--	0.0006	0.0026	0.0030
CHAQ Disability (lower scores = less disability)				
Median (Min, max)	1.0 (0.0, 2.3)	0.3 (0.0, 0.5)	0.0 (0.0, 1.8)	0.0 (0.0, 1.5)
p-value*	--	0.0068	0.0019	0.0029
PODCI Comfort/Pain Scores (higher scores = less pain)				
Median (Min, max)	39 (18, 55)	55 (23, 57)	55 (42, 57)	56 (26, 57)
p-value*	--	0.0553	0.0080	0.0336
Height Z-scores (less negative value = improvement)				
Median (Min, max)	-1.3 (-6.6, -0.0)	-1.1 (-6.9, -0.1)	-0.8 (-6.5, -0.0)	-0.8 (-6.1, 0.1)

*p-value compared with baseline

[1] Whyte MP et al. Hypophosphatasia (HPP): Enzyme Replacement Therapy (EzRT) for Children Using Bone-Targeted, Tissue Nonspecific Alkaline Phosphatase. ENDO, 2010

[2] Whyte MP et al. Treatment of Children with Hypophosphatasia (HPP) with ENB-0040: Radiographic and DXA Outcomes After 6 Months of Therapy. ESPE, 2011

[3] Whyte MP et al. Hypophosphatasia (HPP): Iliac Crest Histomorphometry of Affected Children Given Subcutaneous Enzyme Replacement Therapy, ENB-0040. ASBMR,2011.

[4] Thacher J Trop Pediatr (2000) 46:132-9

Function and Growth Measures in Children with HPP Treated with Asfotase Alfa

1082

Efficacy and Safety of a Human Monoclonal Anti-FGF23 Antibody (KRN23) in Cumulative 4-Month Dose Escalation (KRN23-INT-001) and 12-Month Long-Term Extension Study (KRN23-INT-002) in Adult Subjects with X-Linked Hypophosphatemia (XLH).

Thomas Carpenter*[1], Xiaoping Zhang[2], Erik Imel[3], Mary Ruppe[4], Thomas Weber[5], Mark A. Klausner[2], Takahiro Ito[2], Maria Vergeire[2], Jeffrey S. Humphrey[2], Francis Glorieux[6], Anthony Portale[7], Karl Insogna[1], Munro Peacock[8]. [1]Yale University School of Medicine, USA, [2]Kyowa Hakko Kirin Pharma Inc, USA, [3]Indiana University School of Medicine, USA, [4]The Methodist Hospital, USA, [5]Duke University Medical Center, USA, [6]Shriners Hospital for Children & McGill University, Canada, [7]University of California San Francisco, USA, [8]Indiana University Medical Center, USA

Purpose: X-linked hypophosphatemia (XLH) is an inherited metabolic bone disease caused by mutations of PHEX, with abnormally elevated serum FGF23 resulting in low serum phosphorus (Pi), inappropriately normal 1,25 dihydroxyvitamin D [1,25(OH)$_2$D] levels, short stature and skeletal deformities. Single (IV and SC) and 4 monthly SC doses of KRN23 increased TmP/GFR, serum Pi, and 1,25(OH)$_2$D in adults with XLH. Here we report the long-term efficacy and safety of KRN23 using a monthly dosing regimen throughout the initial 4-month period and a subsequent 12-month extension of titrated dosing in adults with XLH.

Methods: 22 adults with XLH were treated with up to 16 doses of open-label SC KRN23 (0.05-1 mg/kg) every 28 days according to a dosing algorithm. Primary outcomes were the percentage of subjects attaining predetermined serum Pi ranges and safety. Biochemistry and immunogenicity were assessed periodically during each dosing interval and up to 81 days after the last dose.

Results: All subjects had baseline serum Pi <2.5 mg/dL. After 4 cumulative doses in the first study, mean serum Pi reached clinically meaningful level during the 12 dosing intervals in the extension study. Maximum serum Pi levels were reached 7-14 days after each of 12 doses. On Day 7, 44.4% to 71.3% of subjects achieved serum Pi levels in the target range of >2.5 to ≤3.5 mg/dL; 0-16.7% between 3.5 and 4.5 mg/dL, and none >4.5 mg/dL. TmP/GFR followed a similar pattern as serum Pi; 1,25(OH)$_2$D levels peaked at Day 7 post-dosing and tended to decrease with subsequent doses. KRN23 was well tolerated; there were no deaths, life-threatening AEs, or treatment-related serious AEs; 2 subjects were discontinued because of AEs (nephrolithiasis, restless leg syndrome). 14 subjects (63.6%) had treatment-related AEs, the most common being injection-site reactions (5), arthralgia (3), restless leg syndrome (2), injection-site pain (2), and decreased neutrophil count (2). There were no changes in renal ultrasound, ECG, safety laboratory parameters, or physical examinations; no subject developed anti-KRN23 antibodies. Mild hypercalcemia occurred intermittently in 2 subjects and 3 subjects had transient hypercalciuria.

Conclusions: Blocking FGF23 activity by SC administration of KRN23 every 28 days for an extended period of up to 16 months demonstrated a favorable safety profile and increased serum Pi, TmP/GFR and 1,25(OH)$_2$D.

1083

Deficits in Cortical Bone Density and Microstructure in Type 2 Diabetes: Framingham HR-pQCT Study.

Elizabeth (Lisa) Samelson*[1], Mary Bouxsein[2], Elana Brochin[3], Xiaochun Zhang[3], Ching-An Meng[3], Kerry Broe[3], Mary Hogan[3], Danette Carroll[3], Robert McLean[3], Marian Hannan[5], L. Adrienne Cupples[6], Caroline Fox[7], Douglas Kiel[8]. [1]Hebrew SeniorLife, Harvard Medical School, USA, [2]Beth Israel Deaconess Medical Center, Harvard Medical School, USA, [3]Institute for Aging Research, Hebrew SeniorLife, USA, [6]Hebrew SeniorLife Institute for Aging Research & Harvard Medical School, USA, [5]HSL Institute for Aging Research & Harvard Medical School, USA, [6]Boston University School of Public Health; NHLBI Framingham Heart Study, USA, [7]National Heart Lung & Blood Institute, National Institutes of Health, USA, [8]Hebrew SeniorLife, USA

Risk of fracture, particularly at the lower leg, is 2-fold higher in older adults with type 2 diabetes (T2D), despite having normal or increased areal BMD, relative to those without T2D. Since DXA underestimates fracture risk in T2D patients, new methods are needed to identify skeletal fragility in this vulnerable population. Evidence from small clinical studies of postmenopausal women suggests T2D is associated with deficits in cortical microarchitecture. We conducted a community based study of men and women to compare bone microarchitecture by HR-pQCT between those with and without T2D, and determine the association between bone microarchitecture and HbA1C level.

This study included 627 members (367 women, 260 men) of the Framingham Offspring Cohort, who attended a baseline examination (2005-08), including evaluation of T2D and A1C, and underwent HR-pQCT scanning at the tibia and radius 6 yr later. T2D was defined as glucose >126 mg/dl or use of T2D medication. A1C (%) was measured from morning fasting blood. Linear regression was used to calculate means and correlations for the association between volumetric bone density (vBMD), geometry, and microstructure indices of trabecular and cortical bone and T2D and A1C, adjusted for age, sex, and weight.

Mean baseline age was 65 yr (range, 45-84) and included 71 cohort members (40 men, 31 women) with T2D. At the tibia, total and trabecular vBMD and number were higher in those with T2D than those without T2D; however, the differences were not significant (TABLE). In contrast, persons with T2D had significantly lower cortical vBMD and higher cortical porosity. A similar pattern was seen with increasing A1C level: trabecular indices were better with increasing A1C but cortical bone indices were worse, although significance was limited to trabecular number. There were no other differences in HRpQCT bone indices in those with and without diabetes or by A1C level. At the radius, we found no significant association between bone HRpQCT indices and T2D or A1C.

In this community-based study of women and men, we showed that T2D and increased A1C are associated with deficits in cortical microstructure and density at the distal tibia. It remains unknown whether deficits in cortical bone explain increased fracture risk observed at the lower leg in diabetes. These results help to identify areas to target for investigation of the mechanism responsible for skeletal fragility in diabetic bone.

Association between volumetric bone density (vBMD), geometry, and microstructure indices of trabecular and cortical bone at the tibia and diabetes and HbA1C. Framingham HRpQCT Study (N=627)						
	Diabetes N=71		**No Diabetes** N=556		**HbA1C(%)** N=627	
	Mean[†]	±E	Mean[†]	SE	Correlation[†]	p
Total vBMD (mg/cm³)	291.06	6.61	284.53	2.27	0.30	0.05	0.20
Trabecular vBMD (mg/cm³)	184.13	4.50	175.09	1.55	0.08	0.07	0.09
Trabecular number (1/mm)	2.15	0.03	2.07	0.01	0.09	0.09	0.03
Cortical vBMD (mg/cm³)	796.74	9.02	814.00	2.76	0.04	-0.02	0.69
Cortical Porosity (%)	11.17	0.38	10.03	0.13	<0.01	0.07	0.07
Cross-sectional area (mm²)	749.56	14.77	776.41	5.08	0.17	-0.04	0.30
Endocortical perimeter (mm)	132.30	3.22	127.00	1.11	0.13	-0.02	0.68
Periosteal perimeter (mm)	103.61	2.45	106.64	0.84	0.45	-0.03	0.45

Adjusted for age, sex, and weight

TABLE.

1084

High Incidence of Osteoporotic Fractures Following Hematopoietic Stem Cell Transplantation.

Xerxes Pundole[1], Heather Lin[2], Andrea Barbo[2], Huifang Lu*[3]. [1]The University of Texas MD Anderson Cancer Center, USA, [2]UT MD Anderson.org, USA, [3]UT MD Anderson Cancer Center, USA

Background: Survivors following hematopoietic stem cell transplantation (HSCT) are increasing and rapid bone loss is common, but the incidence of fractures is unknown. Bone remodeling and the temporal sequence of bone loss following HSCT is complex and much remains unknown.

Methods: We performed a chart review of adult patients that underwent a HSCT at MD Anderson Cancer Center from January 1, 1997 to December 31, 2011 and followed them retrospectively to identify incident fractures. Fractures were identified by utilizing physician billing codes and confirmed by reviewing clinic notes and/or reports of radiologic evidence. Rates of fracture were compared with the US general

population using estimates from the 1994 National Health Interview Survey (NHIS). Gender, age at time of HSCT, indication and type of HSCT, were assessed as risk factors using regression analysis based on the Cox proportional hazard model.

Results: A total of 7,650 patients underwent a HSCT in the 15 year period. The mean age at the time of HSCT was 49.29 ($\pm$ 13.51) years with a median of 51 (range: 18 - 81) years. Forty-five percent of the patients were female. The most common reason for undergoing a HSCT was a hematological malignancy (89.5%). Approximately 8% (n=631) developed a fracture with about 11% (n=440) in those that received an autologous transplant and 5% (n=191) in those that received an allogeneic transplant. The median time to fracture hadn't been observed. By year 5, 12% of HSCT patients had experienced a fracture and 23% by year 15. A Cox proportional hazard model showed that those $\geq$ 50 years at the time of HSCT had a 1.9 times greater hazard of developing a fracture as compared to those < 50 years (Hazard Ratio (HR) = 1.9, p-value < .001); patients who received autologous HSCT had larger hazard of developing a fracture than those who received allogeneic HSCT (HR=1.58, p-value <.0001), after adjusting for sex and race. The Kaplan Meier plot showed that the time to develop a fracture was greater in those had underwent an allogeneic HSCT in comparison to autologous HSCT (log rank p-value <.0001). Age and gender specific fracture incidence rates following HSCT were significantly greater than that of the US general population in all sub groups. The striking difference was an approximately 10 times greater risk in 45-64 year old males and females and an even greater risk (approximately 15 times higher) in males >65 years of age at the time of HSCT. Males had more vertebral fractures (56%) and females had more (53%) non-vertebral fractures (X^2 = 5.07, p-value = 0.024).

Conclusion: Fractures rates following HSCT are increased, especially at age > 45 years and this corresponds to the increased hazard we observed in those > 50 years of age at the time of HSCT. This study is the first to quantify the magnitude of the problem. Evaluation of a comprehensive set of risk factors is necessary.

Disclosures: Huifang Lu, None.

1085

Bone Microarchitecture assessed by HR-pQCT as Predictor of Fracture Risk in Postmenopausal Women: The OFELY Study. <u>Elisabeth Sornay-Rendu</u>[1], <u>Stephanie Boutroy</u>[2], <u>François Duboeuf</u>[3], <u>Roland Chapurlat</u>*[4]. [1]INSERM UMR1033, Université de Lyon, France, [2]INSERM U1033 & Université de Lyon, France, [3]INSERM UMR1033 & Université de Lyon, France, [4]E. Herriot Hospital, France

Several cross-sectional studies have shown that alterations of bone microarchitecture (MA) contribute with low areal BMD to skeletal fragility but the independent contribution of cortical and trabecular (Tb) architecture to the risk of fracture has not been evaluated prospectively in women. The aim of this study was to prospectively investigate the prediction of fragility Fx by bone MA assessed by HR-pQCT in postmenopausal women.

We measured at the 14th annual follow-up of the OFELY study bone MA at the distal radius and tibia with HR-pQCT (XTreme CT, Scanco Medical AG, Bassersdorf, Switzerland) in addition to areal BMD with DXA in 588 postmenopausal women, mean(SD) age 68(9) yr.

During a median[IQ] 7.1[0.9] yr of follow-up, 101postmenopausal women sustained an incident fragility fracture including 61 women with a major osteoporotic Fx (MOP Fx: hip, clinical spine, shoulder or wrist). After adjustment for age, women who sustained Fx had significant alterations of total and Tb volumetric densities (vBMD) at both sites, cortical parameters (area and thickness at the radius, vBMD and porosity at the tibia), trabecular number (TbN), connectivity density, stiffness and estimated failure load at both sites, compared with control women.

After adjustment for age, prevalent Fx, T score hip, menopausal age and current tobacco use, each quartile decrease of several baseline values of bone MA at the radius was associated with significant increased fracture risk with adjusted hazard ratios [HR(95%CI)] of 1.28(1.02-1.64) for Tt.vBMD, 1.37(1.09-1.72) for Tb.vBMD and 1.28(1.02-1.61) for TbN. For MOP Fx, Tb.vBMD or TbN in the lowest quartile was associated with increased fracture risk with adjusted HR of 2.25(1.21-4.18) and 2.05(1.11-3.78) respectively. At the tibia, each quartile decrease of Tt.vBMD, stiffness and failure load was associated with adjusted HR of 1.47(1.06-2.04), 1.49(1.06-2.08) and 1.49(1.06-2.08) respectively for MOP Fx.

We conclude that alterations of bone MA predict the risk of fracture in postmenopausal women. Their assessment may play an important role in identifying women at high risk of fracture who could not be adequately detected by BMD measurement alone, and who may benefit from a therapeutic intervention.

Disclosures: Roland Chapurlat, None.

1086

Clinical Presentation of Primary Hyperparathyroidism: a Five-Year Study. <u>Cristiana Cipriani</u>*[1], <u>Federica Biamonte</u>[2], <u>Daniele Diacinti</u>[3], <u>Piergianni Biondi</u>[2], <u>Orlando Raimo</u>[4], <u>Sara Piemonte</u>[5], <u>Jessica Pepe</u>[6], <u>Elisabetta Romagnoli</u>[7], <u>John Bilezikian</u>[8], <u>Salvatore Minisola</u>[1]. [1]"Sapienza", University of Rome, Italy, [2]Department of Internal Medicine & Medical Disciplines, "Sapienza" University of Rome, Italy, [3]Department of Radiology, "Sapienza" University of Rome, Italy, [4]Department of Interla Medicine & Medical Disciplines, "Sapienza" University of Rome, Italy, [5]Department of Internal Medicine & Medical Disciplines, "Sapienza", Italy, [6]Department fo Internal Medicine & Medical Disciplines, "Sapienza" University of Rome, Italy, [7]"Sapienza", University of Rome, Italy, [8]Columbia University College of Physicians & Surgeons, USA

The clinical presentation of Primary hyperparathyroidism (PHPT) is characterized in most developed countries as asymptomatic. Assessment for kidney stones (KS) is not routinely conducted in subjects who do not have any history of signs of renal involvement. Similarly, assessment for vertebral fractures (VF) is not routinely conducted in subjects who do not have any previous history or symptoms. In this study, we evaluated the prevalence of KS, and VF in a cohort of patients diagnosed with PHPT over a 5-year period.

We studied 140 PHPT patients [127 women (18 pre- and 109 postmenopausal) and 13 men; mean age 63.2$\pm$11 yrs] consecutively referred to our Mineral Metabolism Unit, 2009-2013. All patients had abdominal ultrasound, 3-site DXA (Lumbar spine, femoral neck (FN),total hip (TH)] and distal 1/3 radius (R). Antero-posterior and lateral X-rays of thoracic and lumbar spine were performed in 131 patients.

KS were detected in 77/140 patients (55%); 16.4% of patients had bilateral KS. Spine X-ray showed vertebral fractures in 46/131 patients (35.1%): 19.1% of patients had one VF, 9.2% had two and 6.9% had more than two VF. 62.9% of patients had osteoporosis by T-score at any site, 31.4% had osteopenia alone, and only 5.7% had normal BMD. Among patients with VF, 25.9% had osteoporosis by DXA and 9.1% had osteopenia. Mean age of patients with only KS (57$\pm$13.7) was significantly younger than that of patients with only VF (69.3$\pm$6.5) and only osteoporosis (63.6$\pm$9.6)(p<0.05 for both)

The prevalence of asymptomatic patients was 54.3% [69 women (8 pre- and 61 postmenopausal) and 7 men; mean age 64.$\pm$11.3]. Among asymptomatic patients, 35.5% had KS, 33.3% had VF and 65.8% had osteoporosis. Table 1 shows the prevalence of the association between different complications in asymptomatic, symptomatic and the total cohort of patients.

Our data show that KS and VF are highly prevalent among PHPT patients, even in those classified as asymptomatic. While VF are frequent among older subjects even in absence of osteoporosis, KS are mostly observed in younger patients. To our knowledge, this is the first study that reports prevalence of target organ complications among so-called "asymptomatic patients". Our results emphasize the need of a thorough evaluation in asymptomatic patients, before classifying them as suffering from mild disease.

Table 1. Prevalence of the association between different complications among asymptomatic, symptomatic and the total cohort of patients

	ASYMPTOMATIC	SYMPTOMATIC	TOTAL
KS + VF + OP	8.3%	16.9%	12.2%
KS + VF	11.1%	22%	16.8%
KS + OP	21%	41.5%	30.7%

Table_1

Disclosures: Cristiana Cipriani, None.

1087

Osteosarcoma invasiveness and recurrence are controlled by exosome-induced tumor initiating cells. Paul Daft*[1], Majd Zayzafoon[2], Joan Cadillac[2]. [1]The University of Alabama At Birmingham, USA, [2]University of Alabama at Birmingham, USA

Osteosarcoma (OS) is the most common primary malignant bone cancer in children. Although the management of this devastating disease has improved in the last 20 years, its post-surgical recurrence and distant metastasis still pose a grim prognosis. It is thought that a small subset of invasive tumor cells called tumor-initiating cells (TICs) is associated with the most lethal characteristics of cancer. In OS, TICs were identified to express high levels of c-kit and Stro-1. We discovered that OS TICs also express high levels of α-CaMK-II. The genetic and pharmacologic inhibition of α-CaMK-II significantly decrease the number of TICs and result in 98% of OS cells being c-kit and Stro-1 negative, which we defined as Dormant Tumor Cells (DTCs). Furthermore, we discovered that TICs secrete large amounts of nanosized vesicles (exosomes). Therefore, we hypothesized that the growth and metastasis of osteosarcoma relies on α-CaMK-II controlled exosome release that regulates the development of tumor-initiating cells. Using fluorescence-activated cell sorting, we isolated TICs (CD117^{+}, Stro-1^{+}) and DTCs (CD117^{-} and Stro-1^{-}) from 143B OS cells. TIC-secreted exosomes were visualized by cryo-electron microscopy and measured to be 50–130 nM and confirmed by western blotting for their expression of flotillin-1 and CD63. NanoSight nanoparticle analysis demonstrated that TICs secret 75% more exosomes than DTCs and the pharmacologic inhibition of α-CaMK-II decreases exosome numbers by 60% when compared to control. Adding TIC-secreted exosomes to DTCs results in a 70% increase in Notch1 protein levels and transforms DTCs into TICs by significantly increasing CD117 (300%), Stro-1 (200%) and Nanog (200%) protein levels. Furthermore, we discovered that TIC-secreted exosomes contain significantly more (80%) of the Notch1 regulating miR-199b and miR146a when compared to DTC exosomes. Hind limbs-containing OS tumors were then amputated, and tumor recurrence was monitored. Pulmonary metastasis/recurrence in saline treated mice was 100% two months after amputation and decreases to 12% in mice treated with CaMKII inhibitors. TICs were the predominant cells in the metastatic and recurrent tumors as shown by their expression of Sox2 and NANOG. Finally, we intratibially injected TICs or DTCs into 6-week old mice. We show that 100% of mice injected with TICs develop tumors and only 25% of DTCs did so, while TIC tumors secrete 800% more exosomes in the blood than DTC tumors.

Disclosures: Paul Daft, None.

1088

Foxo1 Expressed in Osteoblasts Promotes the Leukemogenic Properties of β-Catenin by Activating Notch Signaling. Aruna Kode*[1], Ioanna Mosialou[1], Sanil J Manavalan[1], Julie Teruya Feldstein[2], Govind Bhagat[1], Ellin Berman[2], Stavroula Kousteni[1]. [1]Columbia University Medical Center, USA, [2]Memorial Sloan-Kettering Cancer Center, USA

Osteoblasts affect self-renewal and expansion of hematopoietic stem cells (HSCs) and homing of healthy hematopoietic and tumor cells into the bone marrow. Moreover, in the mouse, constitutive activation of β-catenin (Ctnnb1CAosb mice) in osteoblasts is sufficient to alter the differentiation potential of myeloid and lymphoid progenitors and to trigger the development of acute myeloid leukemia (AML). Because the same genetic event is associated with AML development in humans we sought to better understand its molecular bases. For that purpose we examined in vivo whether FoxO1, a transcription factor known to interact with β-catenin, affects its AML inducing properties. Deleting one allele of FoxO1 mice from the osteoblasts of leukemic Ctnnb1CAosb mice prevented the appearance of anemia, peripheral monocytosis, neutrophilia and lymphocytopenia that are otherwise observed in Ctnnb1CAosb mice. Similarly, FoxO1 haploinsufficiency in osteoblasts of Ctnnb1CAosb mice prevented the shift in the differentiation of HSCs to the myeloid lineage and the increase in the LSK+/CD150+/CD48- subset of long term repopulating HSC progenitors (LT-HSCs). Histological analysis showed that myeloid and megakaryocyte dysplasias observed in Ctnnb1CAosb mice and associated with their AML phenotype were also rescued in Ctnnb1CAosb;FoxO1osb+/- animals. As a result FoxO1 haploinsufficiency in osteoblasts prevented the early lethality of Ctnnb1CAosb mice since Ctnnb1CAosb;FoxO1osb+/- mice lived and were healthy for at least one year, the entire time that they were observed. At the molecular level FoxO1 interacts with β-catenin in osteoblasts to induce expression of the Notch ligand Jagged-1 which initiates the dysmyelopoiesis leading to AML. ChiP/Re-ChiP assays and transient transfection experiments showed that this interaction requires the formation of a β-catenin/FoxO1 complex at two distinct locations in the regions of the Jagged-1 promoter. It also leads to subsequent activation of Notch signaling in LT-HSC progenitors. These events induce the leukemogenic transformation of HSCs. These findings identify FoxO1 through its expression in osteoblasts as a factor affecting hematopoiesis and provide a molecular mechanism whereby the FoxO1/activated β-catenin interaction results in AML. They further support the notion that targeting the bone marrow niche may be a new strategy to treat leukemia and raise the prospect that FoxO1 oncogenic properties may occur in other tissues.

Disclosures: Aruna Kode, None.

1089

Large-scale Temporal Gene Expression Profiling Reveals Potential NOTCH1 Target Genes Responsible for Cartilage Fibrosis and Degradation. Zhaoyang Liu*[1], Anthony Mirando[2], Regis O'Keefe[2], Michael Zuscik[3], Matthew Hilton[4]. [1]University of Rochester Medical Center, USA, [2]Department of Orthopaedics & Rehabilitation, Center for Musculoskeletal Research, University of Rochester Medical Center, USA, [3]University of Rochester School of Medicine & Dentistry, USA, [4]Duke University Musculoskeletal Research Center, USA

Notch signaling is critical in regulating cartilage development and homeostasis. Recent studies have identified elevated levels of Notch signaling in osteoarthrits (OA) cartilage, however the downstream Notch targets responsible for OA development remain unclear. To address this issue, we developed several Notch gain-of-function (GOF) in vivo and in vitro models. We first generated two cartilage-specific Notch GOF in vivo mouse models: $Acan1Cre^{ERT2}$; $Rosa-NICD1$ and $Col2Cre$; $Rosa-rtTA^{fl+}$; $tetON-NICD1$ (tetON NICD1). Both animal models exhibit early and progressive OA-like phenotypes, including articular cartilage fibrosis and degradation, meniscus degeneration, and synovial tissue expansion as early as two months of age. Immunohistochemical analyses of the articular cartilage revealed significant induction of fibrotic and catabolic factors in the mutant articular cartilage, including COL3A1, MMP13, and Aggrecanase (NITEGE). Lineage tracing with $Acan1Cre^{ERT2}$; $R26R^{fl}$; $Rosa-NICD1^{fl+}$ mice revealed invasion of a non-$Acan1$ expressing fibrotic cell population at the surface of the mutant articular cartilage, likely originating from the synovium. Additionally, TUNEL staining in both mutant models demonstrated enhanced chondrocyte apoptosis. To identify novel early and late Notch responsive target genes in cartilage, we performed high throughput RNA-seq of P2 primary chondrocytes isolated from tetON NICD1 and control mice and induced Notch signaling with doxycycline treatments for 6h and 48h in vitro. Notch activation induced 451 genes at 6h and 1249 genes at 48h, including Notch pathway genes ($HeyL$, $Notch3$, $Jag1$, etc.), cartilage degradation enzymes ($Mmp13$, $Mmp9$, $Adamts4$, $Ctsc$, etc.), fibrous collagens ($Col3a1$, $Col4a1$, $Col5a1$, etc.), growth factors ($Pdgfb$, $Tgfb1$, $Tgfb2$, etc.), and cytokines/chemokines ($Il6$, $Ccl20$, $Cxcl1$, etc.). Notch activation also down-regulated the expression of 75 genes at 6h and 867 genes at 48h, including cartilage-related collagens ($Col2a1$, $Col9a1$, $Col11a1$, etc.) and chondrogenic genes ($Sox9$, $Sox5$, $Sox6$, $Acan1$, $Matn1$, etc.). Collectively, these data have identified novel Notch target genes in cartilage, and demonstrated that sustained Notch signaling suppresses the chondrogenic phenotype and promotes cartilage fibrosis and degradation, implicating the Notch signaling pathway as a potential therapeutic target for OA.

Disclosures: Zhaoyang Liu, None.

1090

Glut1-dependent glucose uptake in osteoblasts is necessary for bone formation before and after birth and whole-body glucose homeostasis. Jianwen Wei*, Junko Shimazu, Gerard Karsenty. Columbia University, USA

The regulation of insulin secretion and sensitivity by the bone-derived hormone osteocalcin naturally raises the following question: Why does bone regulate glucose metabolism? A first step in answering this question might be to define the functions of glucose in bone. We first showed through hyperinsulinemic euglycemic clamps that bone uptakes glucose, mostly in an insulin-independent manner, and that the amount of glucose up-taken by bone is nearly one fifth of what is up-taken by muscle, the organ up-taking the largest amount of glucose in the mouse. Moreover, studies conducted in isolated cells established that osteoblasts or osteoclasts uptake one third of the amount of glucose up-taken by myoblasts. Consistent with the insulin-independent nature of this process, the glucose transporter Glut1 appears to be 100 fold more abundant than any other glucose transporters in bone cells. Accordingly, in cell-based assays glucose uptake is decreased 70% in osteoblasts lacking $Glut1$ and is increased 20% in osteoblasts overexpressing modestly (2 fold) $Glut1$. Glycogen content is also decreased in $Glut1$-deficient osteoblasts. In vivo, the absence of $Glut1$ in osteoblast progenitors dramatically delays the onset of bone formation in mouse embryos and significantly decreases the size of embryos whereas the deletion of $Glut1$ in differentiated osteoblasts only, results in two distinct phenotypes. The first one is a decrease in all parameters of bone formation including the osteoblast number that leads to a low bone mass in adult $Glut1_{osb}$-/- mice. The second phenotype seen in adult $Glut1_{osb}$-/- mice is an osteocalcin-dependent glucose intolerance and insulin resistance. Conversely, mice overexpressing $Glut1$ in differentiated osteoblasts display a high bone mass because of an increase in bone formation parameters, and a better glucose tolerance and insulin sensitivity than control littermates. Molecular studies performed in wild type and mutant osteoblasts demonstrated that by limiting AMPK activity, glucose normally favors mTOR signaling in osteoblasts and thereby collagen synthesis and bone formation; osteocalcin synthesis and glucose metabolism. In summary, Glut1-dependent glucose uptake in cells of the osteoblast lineage is a significant regulator of bone formation pre and post-natally, and of whole-body glucose homeostasis. The extent of the functions of glucose in osteoblasts provides a rationale for the regulation of glucose metabolism by bone.

Disclosures: Jianwen Wei, None.

1091

Brown Adipose Tissue Indices a Bone Anabolic Effect Through an Uncoupling Protein 1- Mediated Elevation of Central Neuropeptide Y Expression and Reduced Sympathetic Tone. <u>Amy Nguyen</u>[1], <u>Herbert Herzog</u>[1], <u>Paul Baldock</u>*[2]. [1]Neuroscience Division, Garvan Institute of Medical Research, Australia, [2]Garvan Institute of Medical Research, Australia

Brown adipose tissue (BAT) remains a putative therapy for obesity, due to its ability to dissipate energy through the actions of uncoupling protein-1 (UCP-1), which is expressed in the mitochondria of brown adipocytes. Interestingly, a positive correlation between BAT and bone mass has been identified, linked to the bone anabolic effect of reduced sympathetic tone. However, several critical questions remain: i) what component of BAT is responsible for the bone anabolic effect, and ii) what is the pathway by which BAT activity regulates sympathetic tone. This study, for the first time, examines UCP-1, BAT and bone mass using a mouse model deficient in UCP-1 (UCP-1 KO), and identifies a central NPY circuit whereby UCP-1 activity regulates sympathetic tone.

Six week old male UCP-1 KO and wild type mice were housed for 10 weeks either at thermoneutrality (30℃), where UCP-1 is inactive, or under mild cold-stress (22℃), where UCP-1 would be activated for thermogenesis. At 30℃, no differences in cancellous or cortical bone parameters were apparent.

However, under conditions of permanent mild cold-stress (22℃), UCP-1 KO mice displayed reduced cancellous bone volume (21%, p<0.05), trabecular number, thickness mineralizing surface compared to wild type mice. UCP-1 KO mice also exhibited reduced femur length, and cortical periosteal and endosteal perimeters, with no differences in body weight.

A similar, although reduced, effect was also observed in female mice.

Critically, cold-stressed UCP-1 KO displayed reduced hypothalamic neuropeptide Y (NPY) expression compared to wild type. We have shown that cold-stress elevates NPY, which inhibits central tyrosine hydroxylase neurons in the hypothalamus, reducing sympathetic tone to protect bone during chronic stress (1). Thus the decrease in NPY in UCP-1 KO would release the sympathetic inhibition, raising sympathetic output as noted previously in the BAT-deficient Misty mouse (2).

Thus UCP-1 activity during mild cold-stress is protective of bone mass, indicating that thermogenesis initiated during cold-stress plays a positive role in bone mass. Moreover, we demonstrate that the central NPY/sympathetic circuit is involved in this BAT-Bone pathway.

1. Baldock P, Lin S et al. Neuropeptide Y Attenuates Stress-Induced Bone Loss Through Suppression of Noradrenaline Circuits. JBMR 2014 Epub.

2. Motyl KJ, Bishop KA et al. Altered thermogenesis and impaired bone remodeling in Misty mice. JBMR 2013 28:1885-97.

Disclosures: Paul Baldock, None.

1092

Exercise regulation of marrow fat in the setting of PPARγ agonist treatment. <u>Maya Styner</u>*[1], <u>Xin Wu</u>[2], <u>William Thompson</u>[3], <u>Gunes Uzer</u>[3], <u>Zhihui Xie</u>[2], <u>Buer Sen</u>[4], <u>Andrew Romaine</u>[2], <u>Gabriel Pagnotti</u>[5], <u>Clinton Rubin</u>[6], <u>Martin Styner</u>[2], <u>Mark Horowitz</u>[7], <u>Janet Rubin</u>[1]. [1]University of North Carolina, Chapel Hill, School of Medicine, USA, [2]University of North Carolina, USA, [3]University of North Carolina, USA, [4]University of North Carolina At Chapel Hill, USA, [5]Stony Brook University, USA, [6]State University of New York at Stony Brook, USA, [7]Yale University School of Medicine, USA

Marrow adipose tissue (MAT), associated with skeletal fragility and hematologic insufficiency, remains poorly understood. We have shown that exercise prevents MAT accumulation while promoting bone formation, a response that may depend on caloric expenditure. In contrast, we hypothesized that exercise would not be able to overcome the powerful adipogenic biasing of mesenchymal stem cells that accompanies PPARγ agonist therapy and leads to increased MAT. Thus, we tested the response of MAT and bone to running exercise in the setting of the PPARγ agonist rosiglitazone (Rosi). Eight week-old female C57BL/6 mice were treated with +/- Rosi 20 mg/kg/day incorporated into a regular chow diet (RD). Exercise groups were provided voluntary access to running wheels (RD-E, Rosi-E), running ~12 km/d. Femoral MAT and tibial bone quantity were assessed by μCT (lipid binder osmium) as previously described (Styner et al. *Bone* 2014). Total femur MAT was 4.5-fold higher in Rosi relative to RD (p<0.0001). As expected, exercise suppressed MAT in RD-E mice by half compared with RD (p<0.01). Surprisingly, MAT acquisition in Rosi fed mice also responded to exercise in all regions tested: epiphysis, metaphysis and diaphysis (figure 1), although MAT did not return to control levels (p<0.001 for total femur). Tibial mRNA in Rosi-treated mice demonstrated ≥ 3-fold increase in perilipin, fatty acid synthase (FASN) and fat-specific protein 27 (FSP27) compared to RD. While exercise attenuated Rosi-induced FASN, it failed to decrease lipid-droplet associated markers perilipin and FSP27. This suggests that while exercise can alter the metabolic usage of MAT, essentially burning calories, it cannot fully overcome adipogenic biasing of stem cells. Rosi decreased bone quantity as expected; importantly, exercise was not able to overcome bone deficit in Rosi-E group. In summary, Rosi induced MAT accumulation throughout the femur and, while exercise partially limited Rosi induction of MAT volume, perhaps through fuel usage, it was unable to overcome the negative effects of Rosi on bone quantity. Our results suggest that MAT supplies fuel for energy needs of exercise, but that exercise cannot overcome the pathologic effects of PPAR agonists on bone health.
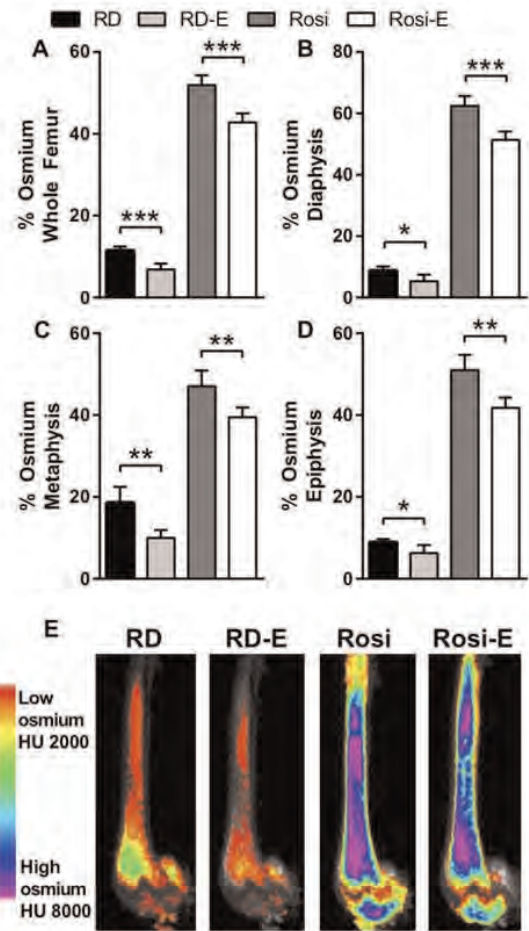
Figure 1. Exercise attenuates marrow adipose tissue in RD and Rosi treated mice. Eight-week-old C57BL/6 mice were treated with oral rosiglitazone (Rosi) or a regular diet (RD), and subdivided into voluntary running exercise groups for six weeks (RD-E, Rosi-E). **A-D,** Quantification of marrow adipose tissue (MAT) via μCT imaging of lipid-binder osmium as mm³ of osmium per femoral volume, in indicated regions. **E,** Each image represents an average of n=5 mice, color labeled to demonstrate distribution of MAT.

Figure 1

Disclosures: Maya Styner, None.

1093

Placental morphology is differentially related to offspring skeletal size and volumetric density assessed by pQCT.

Christopher Holroyd[1], Clive Osmond[1], David Barker[1], Susan Ring[2], Deborah Lawlor[2], J.H. Tobias[3], George Davey Smith[2], Cyrus Cooper[4], Nicholas Harvey*[5]. [1]MRC Lifecourse Epidemiology Unit, University of Southampton, Southampton, UK, United Kingdom, [2]MRC Integrative Epidemiology Unit, University of Bristol, Bristol, UK, United Kingdom, [3]Avon Orthopaedic Centre, United Kingdom, [4]University of Southampton, United Kingdom, [5]MRC Lifecourse Epidemiology Unit, University of Southampton, United Kingdom

We have previously demonstrated that placental size is positively related to indices of offspring skeletal size shortly after birth. It is not known if such associations persist into later postnatal life and whether placental size might be differentially associated with measures of bone size and density. We investigated relationships between placental morphology and bone size and volumetric density during adolescence in a population-based mother-offspring cohort.

The Avon Longitudinal Study of Parents and Children (ALSPAC) recruited women from the former region of Avon, UK. In 1991, from April to December, 12,942 babies were born at term. Placentas were preserved in formaldehyde, and in 2010 a sample of 1746 placentas were measured and photographed. At 15 years the children underwent a pQCT scan (Stratec XCT2000) in order to assess tibial size, geometry and volumetric density at the 50% site. Pubertal stage was assessed by Tanner Stage Questionnaire.

Complete placental, pQCT and pubertal assessment data were available for 421 children [mean (sd) age 15.5 (0.27) years]. After adjustment for sex, gestational age at birth, age and pubertal stage at pQCT scan, and mother's weight, height, age and parity, placental area was positively associated with endosteal circumference (r=0.24, p<0.001), periosteal circumference (r=0.19, p<0.001) and cortical area (r=0.09, p=0.06); in contrast placental area was inversely associated with cortical density (r=-0.14, p=0.004). Similar associations were documented for placental volume.

These findings confirm previous associations between placental size and offspring skeletal development and that these relationships persist into later childhood/adolescence. Furthermore, they support the concept that cortical density may be lower in larger cross-section tubular bones, most likely a mass reducing adaptation to the greater strength conferred by the distribution of material further from the centre of the bone.

Disclosures: Nicholas Harvey, None.

1094

The Choice of Pediatric Reference Database Changes Spine Bone Mineral Density Z-scores but Not the Relationship with Prevalent Vertebral Fractures.

Leanne M Ward*[1], Kerry Siminoski[2], Shayne Taback[3], Celia Rodd[3], Robert Stein[4], Annie M Sbrocchi[5], Josephine Ho[6], Ronald M Grant[7], Elizabeth A Cummings[8], Robert Couch[2], David A Cabral[9], Stephanie Atkinson[10], Nathalie Alos[11], Nazih Shenouda[1], Mary Ann Matzinger[1], Brian Lentle[12], Frank Rauch[5], Jinhui Ma[13], and the Canadian STOPP Consortium[14]. [1]University of Ottawa, Canada, [2]University of Alberta, Canada, [3]University of Manitoba, Canada, [4]University of Western Ontario, Canada, [5]McGill University, Canada, [6]University of Calgary, Canada, [7]University of Toronto, Canada, [8]Dalhousie University, Canada, [9]University of British Columbia, Canada, [10]McMaster University, Canada, [11]Université de Montréal, Canada, [12]University of British Columbia, Canada, [13]Children's Hospital of Eastern Ontario, Canada, [14]National Pediatric Bone Health Working Group, Canada

Aim and Objectives: To assess the disparity in lumbar spine BMD Z-scores (LS-BMDZ) generated by different reference databases and evaluate whether the relationship between LS-BMDZ and prevalent vertebral fractures (VF) varies with the choice of BMD reference database.

Patients and Design: 186 children with recently diagnosed leukemia underwent LS-BMD; Z-scores were generated on four reference databases. Prevalent VF were assessed by the Genant semi-quantitative method. Logistic regression assessed the association between VF (sustained in 15.6% of children)and LS-BMDZ (either as a continuous factor, or a binary risk factor at ± 2.0 SD). The prediction performance was assessed using both the area under the curve (AUC) for receiver operating characteristics and the net reclassification improvement (NRI) (compared to the Hologic version 12.3 normative database).

Results: The proportion of children with LS-BMDZ $\leq$ -2.0 ranged from 15% to 48%. Using the -2 SD cut-off, the logistic regression model assessing the relationship between LS-BMDZ and VF yielded odds ratios (OR) from 2.3 (95% CI: 1.0, 5.3) to 5.0 (95% CI: 2.0-12.4), AUC from 0.60 (95% CI: 0.51, 0.70) to 0.66 (95% CI: 0.56, 0.76), and NRI from -0.64 (95% CI: -1.02, -0.26) to -0.08 (95% CI: -0.35, 0.18). In contrast, with standardized LS-BMDZ used as a continuous risk factor, the ORs were distributed across a narrow range from 2.4 (95% CI: 1.6, 3.7) to 2.6 (95% CI: 1.6, 4.1), the AUC ranged from 0.71 (95% CI: 0.59, 0.82) to 0.72 (95% CI: 0.60, 0.83) and the NRI ranged from -0.17 (95% CI: -0.57, 0.22) to -0.06 (95% CI: -0.45, 0.33).

Conclusions: The use of a LS-BMDZ cut-off to define pediatric osteoporosis is problematic given the large variation in LS-BMDZ depending upon the choice of reference database that is used, as well as the variability in the association between LS-BMDZ (expressed as a binary variable) and prevalent VF, and in the prediction performance across different reference databases. On the other hand, if LS-BMDZ is used as a continuous variable, the association between vertebral fractures and LS-BMDZ across reference databases is not influenced by the choice of reference data.

This study was funded by the Canadian Institutes for Health Research

Disclosures: Leanne M Ward, None.

1095

Absence of ER cation channel *TMEM38B*/TRIC-B causes recessive osteogenesis imperfecta by dysregulation of collagen post-translational modification.

Wayne Cabral*[1], Elena Makareeva[2], Masaki Ishikawa[3], Aileen Barnes[1], MaryAnn Weis[4], Felicitas Lacbawan[5], David Eyre[6], Yoshihiko Yamada[3], Sergey Leikin[7], Joan Marini[8]. [1]Bone & Extracellular Matrix Branch, NICHD, NIH, USA, [2]Section on Physical Biochemistry, NICHD, NIH, USA, [3]Molecular Biology Section, NIDCR, NIH, USA, [4]Department of Orthopaedics & Sports Medicine, University of Washington, USA, [5]Department of Medical Genetics, Children's National Medical Center, USA, [6]University of Washington Orthopaedic Research Labs, USA, [7]National Institutes of Health, USA, [8]National Institute of Child Health & Human Development, USA

Recessive osteogenesis imperfecta (OI) is caused by mutations in genes encoding proteins involved in post-translational interactions with type I collagen. A novel form of recessive OI has recently been reported in Bedouins from Israel and Saudi Arabia, caused by a homozygous deletion of exon 4 and surrounding intronic sequence of *TMEM38B*. *TMEM38B* encodes TRIC-B, an integral ER membrane monovalent cation channel proposed to be involved in Ca^{++} release from intracellular stores. However, the molecular mechanisms through which this founder mutation causes an OI phenotype are unknown. We identified a 20 month-old girl with moderately severe OI who is the offspring of consanguineous parents from Saudi Arabia, and is homozygous for the *TMEM38B* founder mutation. She has recurring long bone fractures, ligamentous laxity and blue sclerae. Her fibroblasts were used to investigate the mechanism of OI caused by the *TMEM38B* deletion. *TMEM38B* transcripts are 25% of control level, and include six alternatively spliced forms. Although one minor transcript is in-frame, complete absence of TRIC-B protein was confirmed by immunoblot. Consequently, proband cells have decreased steady-state intracellular and ER luminal Ca^{++} concentrations. Furthermore, Ca^{++} stores were more rapidly depleted upon ATP-induced Ca^{++} flux from the ER in patient cells. We also identified alterations in proband type I collagen post-translational modification and conformation. Proband collagen has increased electrophoretic migration of alpha chains on SDS-Urea PAGE, consistent with a 30% reduction in collagen helical lysine hydroxylation, despite increased LH1 protein and transcripts. The detection of lower stability collagen species (comprising 30-40% of total collagen) on DSC and decreased procollagen pericellular processing indicate an abnormal procollagen conformation, as do increased intracellular levels of chaperones PDI and GRP/BiP. Extracellular matrix deposited by proband fibroblasts in culture contained only collagen with normal stability, resulting in a 30% reduction of collagen content. Further, FKBP65, which is stabilized by Ca^{++} and required for collagen telopeptidyl hydroxylation by LH2, as well as fibrillar crosslinking, was decreased in proband fibroblasts. These data support a role for TRIC-B in intracellular Ca^{++} mobilization. We propose that absence of TRIC-B causes OI by dysregulation of multiple collagen-specific chaperones and modifying enzymes in the ER through Ca^{++} modulation.

Disclosures: Wayne Cabral, None.

1096

Greater Bone Mineral Accrual after the Adolescent Growth Spurt Results in Stronger Bones in Young Adulthood: Evidence from 20-year follow-up of the Pediatric Bone Mineral Accrual Study.

Saija Kontulainen*, James Johnston, Hassanali Vatanparast, David Cooper, Adam Baxter-Jones. University of Saskatchewan, Canada

Introduction: The peak accrual rate for bone mineral content (BMC) occurs within the first year after the adolescent growth spurt (i.e., age of peak height velocity, PHV) in both sexes. It is unknown if BMC, fat or lean tissue accrual during this rapid skeletal development will have a longer-term impact on bone strength in adulthood. Our purpose was to assess the role of adolescent total body BMC, fat and lean tissue accrual after the age of PHV on adult bone strength at the radius and tibia.

Methods: Participants were from the Saskatchewan Pediatric Bone Mineral Accrual Study (1991-2011). Eligible participants had DXA-derived total body BMC, fat and lean tissue mass measured at 1-year post-PHV (n=98, 51 females) or change in these variables between PHV and 1-year post-PHV (n=75, 40 females), and pQCT-derived forearm and lower leg scans obtained in young adulthood (mean age 29.3, SD 2.3 years). We used linear regression to assess if BMC, fat or lean mass at 1-year post-PHV, or their changes, contributed to the prediction of validated pQCT bone strength

indices at the distal (4%) and shaft sites of radius (65%) and tibia (66%) in young adulthood, when controlling for adult body and muscle size.

Results: Total body BMC at 1-year post-PHV was an independent, positive determinant of adult bone strength in all measured sites (Table 1). Fat mass at 1-year post-PHV was negatively associated with adult bone strength at both sites of radius and at the tibia shaft (Table 1). Lean mass was excluded from the models due to multicollinearity (VIF>5). BMC gain from PHV was an independent predictor of adult bone strength at the distal radius and tibia (Table 1).

Conclusion: These unique longitudinal findings suggest that greater bone mineral accrual after the peak in the growth spurt may lead to greater bone strength in adulthood while higher fat mass at the same time point may hinder attainment of bone strength at the radius and tibia in young adulthood. This evidence highlights the importance of skeletal growth on adult bone strength and supports efforts aiming to optimize development in body composition in adolescence to enhance prevention of osteoporosis and bone fragility.

Table 1. Models predicting bone strength at the distal and shaft sites of radius and tibia in young adulthood (n= 88 in Models A and B, n=75 in Model C)

	Distal Radius Strength			Radius Shaft Strength			Distal Tibia Strength			Tibia Shaft Strength		
	Adj. R²	Beta (Std)	p-value	Adj. R²	Beta (Std)	p-value	Adj. R²	Beta (Std)	p-value	Adj. R²	Beta (Std)	p-value
Model A: Adult determinants	.71		<.001	.74		<.001	.62		<.001	.77		<.001
Sex		-.32	.003		-.03	.749		-.03	.749		-.27	<.001
Adult muscle area		.53	<.001		.67	<.001		.67	<.001		.17	.012
Adult height		.34	.579		.23	.002		.23	.002		.56	<.001
Model B: Adult + Adolescent (at 1-year post-PHV)	.76		<.001	.80		<.001	.66		.025	.83		<.001
Sex		-.28	.008		.01	.939		-.36	<.001		-.20	.008
Adult muscle area		.37	.001		.51	<.001		.31	<.001		.04	.334
Adult height		-.15	.074		.03	.684		-.25	.010		.33	<.001
Adolescent BMC		.42	<.001		.44	<.001		.51	<.001		.46	<.001
Adolescent fat mass		-.18	.006		-.17	.003		-.11	.122		-.10	.045
Model C: Adult + Adolescent BMC-gain	.71		.050	.72		.579	.60		.025	.76		.087
Sex		-.29	.019		-.10	.417		-.13	.003		-.25	.006
Adult muscle area		.49	.000		.60	<.001		.37	.001		.11	.192
Adult height		.01	.937		.20	.030		-.01	.917		.53	<.001
Adolescent BMC-gain in a year from PHV		.17	.000		.04	.579		.21	.025		.17	.087

Adj. R² = Adjusted coefficient of determination. Beta (Std)=Standard beta coefficient, BMC=bone mineral content, PHV=peak height velocity

Table 1.

1097

Improved Survival with Asfotase Alfa Treatment in Pediatric Patients with Hypophosphatasia at High Risk of Death. Michael Whyte*[1], Cheryl Rockman-Greenberg[2], Christine Hofmann[3], Edward C.W. Leung[2], Scott Moseley[4], Kenji P Fujita[4], Agustin Melian[5], David Thompson[5], Johannes Liese[3]. [1]Shriners Hospital for Children-Saint Louis, USA, [2]University of Manitoba, Canada, [3]University Children's Hospital, University of Wurzburg, Germany, [4]Alexion Pharmaceuticals, USA, [5]USA

Hypophosphatasia (HPP) is the rare metabolic bone disease caused by loss-of-function mutation(s) in the tissue-nonspecific alkaline phosphatase (TNSALP) gene. Mortality rates are considered to be 50%-100% in the infantile and perinatal forms of HPP[1]. Here, we report significantly better survival in severely affected, high-risk, pediatric HPP patients (pts) during treatment with asfotase alfa (an investigational bone-targeted TNSALP replacement) compared with untreated age-matched historical control (HC) HPP pts. Data were pooled from 2 multicenter, Phase 2, open-label, ongoing studies of asfotase alfa for perinatal and infantile HPP (n=37) and compared with data from a multicenter, retrospective, chart review study of untreated HC pts (n=48) matched for age and HPP severity. Enrollment criteria included: age ≤ 5 years, and history of rachitic chest deformity, and/or respiratory compromise, and/or pyridoxine-responsive seizures (HPP complications associated with a high risk of death[2]). Kaplan-Meier analyses of overall survival and invasive ventilation-free (IVF) survival included sensitivity analyses controlling for age at enrollment and calendar year of diagnosis. Baseline characteristics were similar between treated and HC pts. Abnormally shaped chest, respiratory distress, and pyridoxine-responsive seizures were documented in 81% vs. 83%, 73% vs. 83%, and 35% vs. 21% of treated vs. HC pts, respectively. Median age (min, max) at symptom onset was 1 (0, 5.5) vs. 0 (0, 5.9) months for treated vs. HC pts, respectively. Median duration of treatment was 1.8 (0, 5) years. Survival was significantly better in pts treated with asfotase alfa compared with HC (Figure 1). Over the analysis period, 89% (33/37) of treated pts survived vs. 27% (13/48) of HC pts (p <0.0001). Median survival time was 8.9 months for HC pts. In contrast, the high survival rate for treated pts at data cutoff precluded calculation of median survival time. IVF survival was also markedly improved in treated pts: 84% (21/25) required no invasive ventilation and survived, compared with 25% (12/48) of HC pts (p<0.0001). Better survival and IVF survival likely reflect improved mineralization of the rib cage and its influence on respiratory function[3]. Significance was retained in sensitivity analyses. Asfotase alfa treatment significantly improved survival and invasive ventilation-free survival in pediatric patients severely affected by HPP and at high risk of death.

Figure 1. Kaplan-Meier analysis of overall survival. Hypophosphatasia patients treated with asfotase alfa showed significantly greater survival compared to (untreated) historical control patients
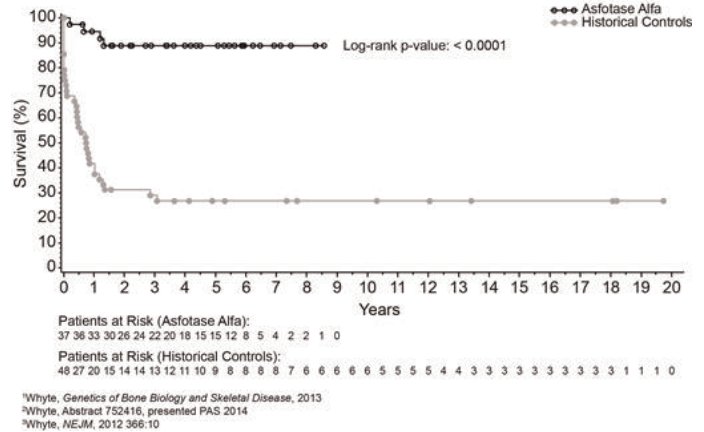
[1]Whyte, Genetics of Bone Biology and Skeletal Disease, 2013
[2]Whyte, Abstract 752416, presented PAS 2014
[3]Whyte, NEJM, 2012 366:10

Figure 1

1098

Bone Fractures in Children and Adults with Autism Spectrum Disorder. Ann Neumeyer[1], Julia O'Rourke[1], Alexandra Massa[1], Hang Lee[2], Elizabeth Lawson[3], Christopher McDougle[1], Madhusmita Misra*[4]. [1]Lurie Center for Autism, Massachusetts General Hospital & Harvard Medical School, USA, [2]Biostatistics Center, Massachusetts General Hospital, USA, [3]Massachusetts General HospitalHarvard Medical School, USA, [4]Pediatric Endocrine & Neuroendocrine Units, Massachusetts General Hospital & Harvard Medical School, USA

Purpose: We have previously reported lower bone mineral density (BMD) in peripubertal boys with autism spectrum disorder (ASD) than in typically developing controls. However, it is not clear whether lower BMD in ASD results in an increased risk for fracture.

Methods: In this study, we examined rates and types of fracture in a large sample of children and adults with ASD (n= 18,152 for children 3-22 years and 4,215 for adults 23-50 years) vs. those without ASD (n= 6,311,505 for children and 11,438,194 for adults), by querying a national database of ED visits (the National Emergency Department Sample 2010) over a one-year period. We hypothesized that those with a diagnosis of ASD would display higher rates of fractures at the hip and spine compared to those without a diagnosis of ASD both in children and adults (based on our previous data for bone density).

Results: In the 3-22 year old patient population, those with ASD had a higher risk of hip fracture than those without ASD [odds ratio (OR) 3.33, p<0.0001], and this difference was more marked in girls [OR 8.1 in girls with ASD (p=0.0005), and 2.0 in boys with ASD (p=0.06)]. In contrast, compared to those without ASD, upper extremity fractures were less common in boys with ASD (p<0.0001). Spine fractures were too few to be analyzed. Observed differences across groups persisted after controlling for age. Similar to our data in children with ASD, adults with ASD 23-50 years old had a higher OR for hip fractures than adults without ASD (OR 11.7, p<0.0001) in both men (OR 6.8, p<0.0001) and women (OR 24.8, p<0.0001). Also, adult men without ASD had a higher risk for upper extremity fractures than those with ASD, and no increase in the risk for spine fractures. In contrast, women with ASD compared with those without ASD had a higher OR for upper extremity fractures (OR 2.27, p=0.0038), and spine fractures (OR 10.61, p=0.0034). Children and adults with ASD were younger than those without ASD, and differences across groups persisted after controlling for age.

Conclusion: Previous reports of lower bone density in children with ASD compared with typically developing controls are concerning for a higher risk of fractures (particularly of the hip) in this population. This is worrisome given the high morbidity associated with hip fracture. Further studies are necessary to better understand the decreased bone density in autism and its implication for fracture development.

1099

Pentosidine and degree of mineralization are increased in bone from fractured-patients with type 1 diabetes mellitus. <u>Delphine Farlay</u>*[1], <u>Laura Armas</u>[2], <u>Evelyne Gineyts</u>[3], <u>Robert Recker</u>[2], <u>Georges Boivin</u>[4]. [1]INSERM, UMR1033; Université De Lyon, France, [2]Creighton University, USA, [3]INSERM U1033, Université de Lyon, France, [4]INSERM, UMR1033; Universite De Lyon, France

Type 1 diabetes (T1D) is associated with increased fracture risk, not explained by the measurement of bone mineral density (BMD). If T1D causes deterioration in "bone quality" rather than reduction in BMD (bone mass) is an important question and little investigated in human. The aim of this study was to analyze the bone matrix (organic and mineral) of iliac bone biopsies, from T1D patients with fragility fracture (FX, n=5), sex and aged-matched T1D patients without fracture (non-FX, n=5), and to compare them to controls (CTL, n=5). All the analyses were performed separately on cortical (cort) and trabecular (trab) bone. Data were then correlated with patient' information (Weight, Body mass index, duration of diabetes), and Laboratory data (HbA1c, 25(OH)D, creatinine, IGF-1). Non-enzymatic cross-links (pentosidine, PEN), and enzymatic cross-links (PYD and DPD) were examined by HPLC after extraction from embedded bone slices. Degree of mineralization (DMB) was assessed by quantitative microradiography, microhardness was measured by microindentation and bone material properties were obtained by FTIRM. We confirmed that trabecular bone from FX-T1D patients contained significantly higher levels of PEN than in CTL (p=0.04). In bone from non-FX T1D, PEN was not significantly increased but tended to be higher than CTL. PYD was not modified in either T1D group compared to CTL. DPD was decreased in non-FX, only in cortical bone. In trabecular bone from FX-T1D, PEN was higher compared to both CTL (p=0.04) and non-FX T1D (p=0.04). Microhardness tended to increase in non-FX and FX T1D, both in cortical and trabecular bone. Mineral maturity, crystallinity and carbonation were not modified, confirming the absence of an effect on bone remodeling activity. Interestingly, we found significantly positive correlations between HbA1c and PENtrab, HbA1c and DMBtotal, PENtrab and DMBtotal (Fig.). Correlations with DMB were confirmed by mineralization index measured by FTIRM. This suggested that in T1D, HbA1c can predict both accumulation in bone of pentosidine and lead to a higher DMB. Indeed, it appears that bone from FX-T1D is more mineralized than both non-FX T1D and CTL. In conclusion, we showed that high serum HbA1c impacts both organic and mineral matrix in bone biopsies. Increase in both Pen and DMB were observed in bone from FX-T1D. Association of both high PEN and degree of mineralization could stiffen bone matrix and lead to fractures.
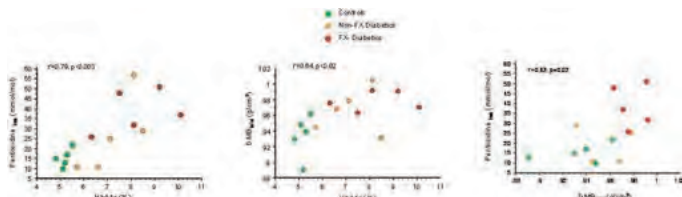

Figure: Spearman correlations between HbA1c, pentosidine and degree of mineralization

Disclosures: Delphine Farlay, None.

1100

Elevated Sphingosine 1-Phosphate Levels are Associated with Vertebral Fractures in Patients with Type 2 Diabetes Mellitus. <u>Mohammed-Salleh Ardawi</u>*[1], <u>Daad Akbar</u>[2], <u>Abdulrahim Rouzi</u>[3], <u>Nawal Senani</u>[4], <u>Ali Ahmad</u>[5], <u>Mohammed Qari</u>[6]. [1]Center of Excellence for Osteoporosis Research & Department of Clinical Biochemistry & KAU Hospital, Faculty of Medicine, King Abdulaziz University, Saudi Arabia, [2]Center of Excellence for Osteoporosis Research & Department of Internal Medicine & KAU Hospital, Faculty of Medicine, King Abdulaziz University, Saudi Arabia, [3]Center of Excellence for Osteoporosis Research & Department of Obstetrics & Gynaecology & KAU Hospital, Faculty of Medicine, King Abdulaziz University, Saudi Arabia, [4]Center of Excellence for Osteoporosis Research & Department of Obstetrics & Gynaecology, Faculty of Medicine & KAU Hospital, King Abdulaziz University, Saudi Arabia, [5]Center of Excellence for Osteoporosis Research, King Abdulaziz University, Saudi Arabia, [6]Center of Excellence for Osteoporosis Research & Department of Haematology & KAU Hospital, Faculty of Medicine, King Abdulaziz University, Saudi Arabia

Background: Patients with type 2 diabetes (T2DM) are at increased risk of vertebral fractures (VFs) compared with non-T2DM subjects, due to poor bone quality. Recent studies in non-diabetic subjects have demonstrated that high sphingosine 1-phosphate (S1P) levels are associated with VFs independent of bone mineral density (BMD). We investigated the changes in plasma S1P levels in relation to VFs among postmenopausal women with T2DM.

Methods: We assessed cross-sectionally 482 postmenopausal women with T2DM and 482 age-matched postmenopausal women without T2DM who were recruited at diabetic clinics and primary health care centers for inclusion in a bone health survey. The main outcome measures wereplasma S1P [measured by ELISA method (Echelon Biosciences Inc., USA)] (overnight fasting samples), BMD, and bone turnover markers. Lateral X-rays of the thoracic and lumbar spine were taken to diagnose VFs.

Results: Plasma S1P levels were increased among women with T2DM as compared with non-T2DM controls (P<0.001). Plasma S1P levels were higher when T2DM women were stratified by the number of VFs (P<0.001). Multiple logistic regression analysis showed that plasma S1P levels were positively associated with 1 VF (odds ratio [OR]=2.35, CI:1.12-4.26, P=0.012), 2 VFs (OR=2.61, CI:1.31-4.86, P=0.004), and ≥ 3 VFs (OR=6.62, CI:2.92-23.1) P<0.001). Plasma S1P levels were inversely correlated with BMD at various sites (P=0.011 to 0.023), whereas they were positively correlated with bone resorption markers (P=0.026 to 0.034).

Conclusions: Increased plasma S1P were associated with VFs among postmenopausal women with T2DM, suggesting that S1P may be involved in increased bone fragility in T2DM and could be potential markers of VF severity.

Disclosures: Mohammed-Salleh Ardawi, None.

1101

Does Diabetes Modify the Effect of FRAX Risk Factors for Major Osteoporotic and Hip Fracture Prediction? The Manitoba BMD Cohort. <u>William Leslie</u>*[1], <u>Suzanne Morin</u>[2], <u>Lisa M. Lix</u>[1], <u>Sumit Majumdar</u>[3]. [1]University of Manitoba, Canada, [2]McGill University, Canada, [3]University of Alberta, Canada

Background: Diabetes mellitus increases risk for major osteoporotic fractures (MOF) independent of factors that comprise the WHO Fracture Risk Assessment tool (FRAX). It is uncertain how best to consider the effect of diabetes in identifying high risk individuals. Therefore, we explored whether diabetes simply adds to, or modifies the effect of FRAX clinical risk factors on MOF and hip fracture risk.

Methods: Using a registry with all clinical DXA results for Manitoba, Canada, we identified women and men age >40 years undergoing baseline DXA in years 1996-2011. Population-based health services data were used to identify diabetes diagnosis, covariates required for FRAX, and incident MOFs. Since the effect of prior fracture is modified by anatomical site, prior fracture was stratified as clinical vertebral, hip, humerus, forearm, pelvis, and "other" (excluding head, neck, hands, feet). Cox proportional hazards models were used to test for interaction effects of diabetes with FRAX clinical risk factors (Model 1) and prior fracture site (Model 2).

Results: The study population included 62,413 individuals (age mean 64 years [SD 11], 91% women) of whom 6,455 (10%) had a diagnosis of diabetes. During mean follow-up 6 years, 492 (7.6%) with diabetes and 3726 (6.7%) without diabetes developed incident MOFs. Diabetes was a significant risk factor for fracture (adjusted hazard ratio [aHR] Model 1: 1.34 [95%CI 1.22-1.48]; Model 2: 1.16 [1.06-1.28]). FRAX risk factors showed significant associations with incident MOFs in one or more analyses. However, no significant interactions of diabetes with any FRAX risk factors were identified. Results were similar without BMD in the model except that higher BMI showed a stronger protective effect (aHR per 5 kg/m^2 0.83 with diabetes, 0.79 without diabetes; p-interaction 0.276). Prior fractures were risk factors for MOF, but again there were no significant interactions with diabetes diagnosis. For predicting hip fractures (1108 incident events), age was a significant modifier of diabetes-related risk (aHR age <60: 4.67 [95%CI 2.76-7.89], age 60-69: 2.68 [1.77-4.04], age 70-79: 1.57 [1.20-2.04], age >80: 1.42 [1.10-1.99]; p-interaction <.001).

Summary: Diabetes is an independent risk factor for MOFs but did not significantly modify the effect of FRAX risk factors or prior fracture site. However, diabetes exerted a stronger effect on hip fracture risk in younger versus older individuals. This has implications for fracture risk assessment in diabetes and for identifying high risk individuals.

	Non-diabetic (N=55,958)	Diabetic (N=6,455)	
MODEL 1: FRAX risk factors	HR (95% CI)	HR (95% CI)	P-interaction
Age (per 10y)	1.43 (1.38-1.47)	1.39 (1.27-1.53)	0.781
Sex (male vs female)	0.90 (0.79-1.02)	1.04 (0.79-1.34)	0.407
BMI (per 5 kg/m2)	0.98 (0.95-1.02)	0.90 (0.83-0.98)	0.080
Current smoking *	1.23 (0.98-1.54)	1.87 (1.13-3.07)	0.317
Glucocorticoid use	1.30 (1.14-1.48)	1.13 (0.83-1.54)	0.398
Rheumatoid arthritis	1.43 (1.24-1.64)	1.74 (1.21-2.49)	0.325
High alcohol use	2.02 (1.70-2.41)	1.98 (1.27-3.09)	0.941
Any prior fracture	1.62 (1.51-1.74)	1.72 (1.42-2.07)	0.588
Femoral neck T-score (per SD)	1.68 (1.61-1.75)	1.60 (1.44-1.79)	0.456
MODEL 2: Prior fracture site	HR (95% CI)	HR (95% CI)	P-interaction
Age (per 10y)	1.68 (1.63-1.73)	1.61 (1.47-1.76)	0.535
Sex (male vs female)	1.00 (0.88-1.14)	1.15 (0.86-1.52)	0.454
Prior vertebral fracture	2.33 (2.07-2.62)	2.67 (1.95-3.66)	0.420
Prior hip fracture	1.55 (1.30-1.85)	1.67 (1.08-2.58)	0.802
Prior humerus fracture	1.86 (1.61-2.14)	1.89 (1.33-2.68)	0.941
Prior forearm fracture	1.43 (1.29-1.60)	1.57 (1.15-2.14)	0.573
Prior pelvis fracture	1.67 (1.28-2.18)	0.81 (0.33-1.99)	0.130
Prior other fracture**	1.32 (1.19-1.46)	1.31 (1.02-1.69)	0.992

TABLE: Hazard ratios for incident major osteoporotic fracture.

Disclosures: William Leslie, None.

1102

Cortical Bone Laminar Analysis reveals Increased Midcortical Porosity in Type 2 Diabetics with History of Fragility Fractures. Ursula Heilmeier*[1], Karen Cheng[2], Robin Parrish[2], Jasmine Nirody[3], Janina Patsch[4], Thomas Baum[5], Andrew Burghardt[3], Gabby B. Joseph[3], Ann Schwartz[3], Thomas Link[3], Galateia Kazakia[3]. [1]University of California San Francisco, USA, [2]University of California, Berkeley, USA, [3]University of California, San Francisco, USA, [4]Medical University of Vienna, Austria, [5]Klinikum rechts der Isar, TU Muenchen, Germany

Diabetic bone disease is an increasingly recognized complication of Type 2 diabetes (T2D) characterized by paradoxically high fracture rates. Elevated cortical porosity was recently identified as a main factor contributing to this high fragility. However, the underlying mechanisms of diabetic cortical porosity remain elusive. Potential hypotheses include cortical trabecularization due to expansion of the bone marrow space, increased vascular infiltration, or both. The purpose of this study was to assess the nature and the spatial distribution of cortical porosity by determining pore number, size and radial distribution within endosteal, midcortical and periosteal layers of cortical bone in T2D women with fractures (DMFx) and compare them to fracture-free diabetics (DM), and non-diabetic controls with (Fx) and without (Co) fractures. 79 postmenopausal women (n=20 per group, DM: n=19) underwent high resolution peripheral quantitative computed tomography (HR-pQCT) of the distal tibia. HR-pQCT images were post-processed using our newly developed cortical bone laminar analysis (Fig. 1). Cortical bone contours and intracortical porosity were semi-automatically segmented, the cortex was divided into three layers of equal width, and each pore was assigned to a layer based on the location of its centroid. Total pore area (TPA), total pore number (TPN), and average pore area (APA) were calculated within each layer. Using ANOVA with post-hoc Tukey tests we found that DMFx subjects exhibited significantly elevated global porosity compared to DM subjects (+190%, p=0.001). Elevated porosity in DMFx vs DM patients was isolated to the midcortical layer (+271% TPA, p=0.030) (Fig. 2). High midcortical porosity in DMFx patients was associated with high TPN (DMFx: 21.2 vs. DM: 45.6; +126%; p=0.018) rather than APA (p>0.05). In all four groups, endosteal pores were generally larger (+135% APA p≤0.021) and more numerous (+319% TPN p≤0.001) than periosteal pores. We conclude that cortical pore laminar analysis is a helpful tool in investigating diabetic bone disease-related cortical porosity. Our finding of isolated high porosity in the midcortical layer suggests that this zone might be particularly susceptible to diabetic bone disease and that unique mechanisms may be acting within this midcortical region in T2D postmenopausal women with history of fragility fractures. However, longitudinal studies are needed to investigate the natural evolution of cortical porosity over time.

Figure 1. Assignment of pores in cortical bone laminar analysis. Left: Pores (black) are shown in full with lines depicting laminar region boundaries. Center: Pore skeletons are assigned to a single layer (endosteal pores in red, midcortical pores in blue, periosteal pores in green). Right: Full pores are assigned to a layer according to the location of their skeletons.
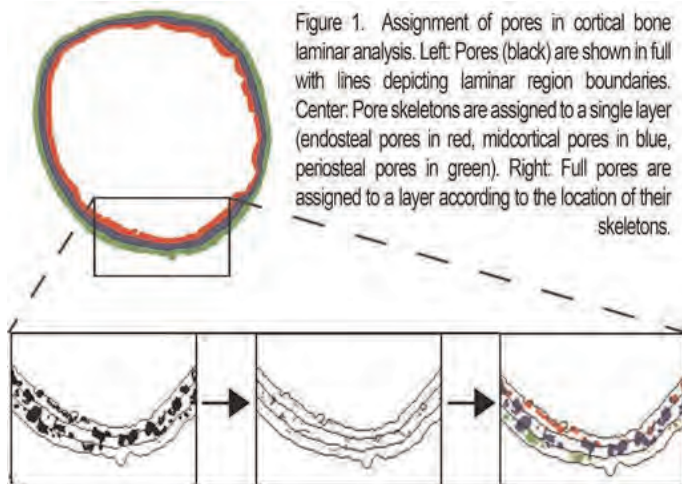
Figure 1

Figure 2 A-C. Results of cortical bone laminar analysis displayed by cortical layer and group (Co=Controls, Fx=women with history of fragility fractures, DM=type 2 diabetic women without fractures, DMFx= type 2 diabetic women with history of fragility fractures). ANOVA and post hoc Tukey tests revealed between-group differences as highlighted in white boxes. Elevated porosity in DMFx vs DM patients was isolated to the midcortical layer (+271% TPA, p=0.030), and driven by pore number rather than pore size (Fig.2 A and B). ** p≤ 0.001, * p≤ 0.05
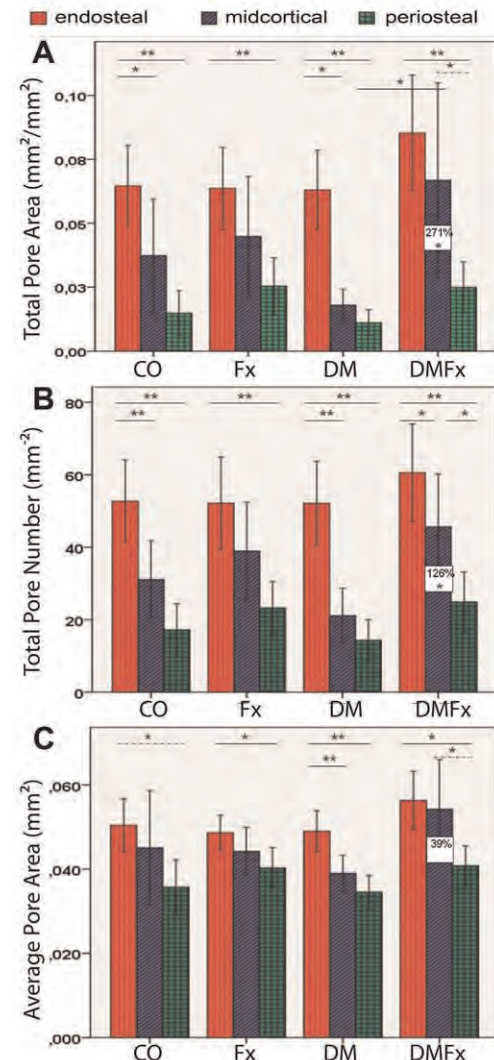
Figure 2

1103

Type 2 Diabetes and Obesity Each Contribute Separately to Adverse Skeletal Health: Adverse Effects on Cortical Bone Microarchitecture. Jessica Furst*[1], Laura Beth Anderson[2], Chiyuan Zhang[2], Kyle Nishiyama[2], Dorothy Fink[3], Shonni Silverberg[2], Mishaela Rubin[2]. [1]Columbia University Medical Center, USA, [2]Columbia University, USA, [3]NYP-Columbia, USA

Obesity and type 2 diabetes (T2D) are increasingly recognized to have adverse effects on skeletal health. Both disorders have a paradoxically elevated fracture risk despite the presence of normal to elevated bone mineral density (BMD) measurements. Although the two conditions often coexist, whether they have separate and specific contributions to bone fragility is unknown. To analyze the distinct effects of obesity and T2D on skeletal indices, we used dual energy X-ray absorptiometry (DXA; Hologic QDR4500, Waltham, Mass) and high resolution peripheral quantitative computed tomography (HRpQCT: Scanco, XtremeCT) with finite element analysis and cortical porosity assessment to examine 4 groups of postmenopausal women: normal weight, euglycemic controls (Cntrl n=6; BMI 22±1 kg/m2 and HbA1c 5.7%±1), obese euglycemic (Ob-NonDM n=5; BMI 36±2 kg/m2 and HbA1c 5.6%±1), nonobese type 2 diabetic (NonObDM n=8; BMI 24.4±1 kg/m2 and HbA1c 8.9%±1) and obese type 2 diabetic (ObDM n=9; BMI 35.6±1 kg/m2 and HbA1c 9.7%±1). The groups did not differ in age (mean overall age 59.4±1).

Generalized linear models were used with group status as the fixed effect to examine the difference in microarchitectural parameters.

We found that ObDM had higher BMD by DXA than Cntrl, Ob-NonDM and NonObDM at all sites. Similarly, by HRpQCT, trabecular bone volume and whole bone stiffness at the radius and tibia were greater in ObDM than in the other 3 groups. Cortical indices were worst in NonObDM (Table). Cortical BMD and thickness were lower and cortical porosity higher at both the radius and tibia and cortical area was lower at the tibia. Moreover, cortical porosity was highest in NonObDM at both the radius and tibia.

These data suggest that while the combination of T2D and obesity has a beneficial effect on densitometric indices, T2D in the absence of obesity has a deleterious effect on microarchitectural cortical parameters at both a weight-bearing and non-weight-bearing site. The cortical deficit is consistent with a decrease in volumetric bone density, and is likely due to increased cortical porosity, as well as a decrease in the overall amount of cortical bone. We conclude that T2D without obesity has a distinct adverse effect on cortical microarchitecture. This is the first study to provide insight into the separate contributions of diabetes mellitus and obesity to adverse skeletal health.

Group	Cortical BMD (Mg hydroxyapatite/cc)	Cortical Thickness (mm)	Cortical Area (mm²)	Cortical Porosity (%)
Radius				
Cntrl	923±21	0.808±0.05	48±3	4.7±.80
Ob-NonDM	882±22	0.760±0.06	46±3	6.5±.90
NonObDM	830±19[a,b]	0.646±0.05[a]	43±3[a]	8.1±.80[a,b]
ObDM	920±18	0.951±0.04[c]	59±2[b,c]	5.2±.70
Tibia				
Cntrl	847±30	0.972±0.09	92±7	9.4±1.5
Ob-NonDM	820±33	0.980±0.09	93±8	10.3±1.7
NonObDM	756±28[a,b]	0.736±0.08[a]	72±7[a,b,c]	13.7±1.5[a,b]
ObDM	861±26	1.199±0.07	123±6[b,c]	9.3±1.3

[a]p<0.05 vs ObDM
[b]p<0.05 vs control
[c]p<0.05 vs Ob-NonDM

HRpQCT Parameters at the Radius and Tibia

Disclosures: Jessica Furst, None.

1104

Effect of Denosumab on Fasting Glucose Concentrations in Postmenopausal Women with Osteoporosis: Results From Subjects With Diabetes or Prediabetes From the FREEDOM Trial. Nicola Napoli*[1], Eric Vittinghoff[2], Nicola Pannacciulli[3], Daria Crittenden[3], Jang Yun[4], Andrea Wang[4], Rachel Wagman[5], Ann Schwartz[6]. [1]University Campus Bio-Medico di Roma, Italy, [2]UCSF, USA, [3]Amgen, Inc., USA, [4]Amgen, Inc., USA, [5]Amgen, Incorporated, USA, [6]University of California, San Francisco, USA

High serum RANKL concentration was a predictor of incident type 2 diabetes (T2DM) in a population-based study, and blockage of RANKL signaling improved glucose tolerance by enhancing hepatic insulin sensitivity in mouse T2DM models (Kiechl et al. *Nature Med* 2013;19(3):358-366). Denosumab (DMAb) is a fully human monoclonal antibody that binds with high affinity and specificity to RANKL and prevents the formation, function, and survival of osteoclasts, and is associated with vertebral and nonvertebral fracture risk reduction. In a prior post-hoc analysis of the FREEDOM trial, a 3-year, randomized, double-blind, placebo (PBO)-controlled study that enrolled 7808 postmenopausal women with osteoporosis, DMAb had no effect on incident diabetes or fasting serum glucose (FSG) in women without diabetes at baseline. Based on the favorable effect of blockage of RANKL on glucose tolerance in mouse T2DM models, we tested the hypothesis that DMAb decreases FSG in FREEDOM subjects with diabetes or prediabetes.

Baseline diabetes status was ascertained by self-report, use of anti-diabetic medication (ADM), or an FSG ≥126 mg/dL. Prediabetes was defined as an FSG 100-125 mg/dL on no ADM. Average postbaseline FSG across visits was estimated using a repeated measures model and compared between DMAb and PBO. The model included treatment group; baseline FSG, body mass index, and age; visit; ADM use; treatment-by-visit interaction; and ADM use-by-visit interaction as fixed effects.

Baseline characteristics were similar between DMAb and PBO in both the subpopulations with diabetes and prediabetes. The estimated average postbaseline FSG across visits was not significantly different between DMAb and PBO in either women with diabetes or in women with prediabetes (p=0.20 and p=0.42, respectively); however, when censoring FSG values after ADM use in women with diabetes, estimated average postbaseline FSG across visits was lower with DMAb than PBO (p=0.02) (Table).

In this post-hoc analysis of postmenopausal women with osteoporosis, DMAb did not appear to affect FSG in the overall population with diabetes or prediabetes. There was evidence of FSG lowering with DMAb in women with diabetes who were not currently using any ADM. It remains to be determined whether blockage of RANKL has a clinically important effect on glucose metabolism.

Table

	Diabetes[1]		Prediabetes[2]		Diabetes (prior to ADM use)[3]	
	DMAb (N = 334)	PBO (N = 315)	DMAb (N = 628)	PBO (N = 640)	DMAb (N = 146)	PBO (N = 136)
Baseline FSG (mg/dL)[4]	136.9 (43.8)	138.9 (51.3)	106.3 (5.9)	106.3 (5.8)	125.5 (34.6)	122.3 (31.1)
Average post-baseline FSG (mg/dL)[5]	131.34 (128.20, 134.48)	134.24 (131.00, 137.48)	102.15 (100.93, 103.36)	101.79 (100.57, 103.00)	114.88 (110.84, 118.92)	121.69 (117.52, 125.85)
Difference (DMAb − PBO)[6]	−2.9 (7.3, 1.6)		0.3 (−0.5, 1.2)		−6.8 (−12.6, -1.0)	
P-value[7]	0.20		0.42		0.02	

N = Number of subjects who received ≥ 1 dose of investigational product and non-missing FSG at baseline
[1] All subjects with diabetes
[2] All subjects with prediabetes
[3] Subjects with diabetes on no ADM at baseline; on-study FSG values were censored after ADM use
[4] Data are mean (SD)
[5] Estimated average postbaseline FSG across visits using a repeated measures model including treatment group; baseline FSG, BMI, and age; visit; ADM use; treatment-by-visit interaction; and ADM use-by-visit interaction as fixed effects
[6] Data are LS mean (95% CI)
[7] P-value for difference in postbaseline FSG across visits between DMAb and PBO

Table_glucoseabstract

Disclosures: Nicola Napoli, None.

1105

Effective Hexa-D-Arginine Therapy of X-Linked Hypophosphatemia Occurs Through Biochemical Targeting of MicroRNA335. Baozhi Yuan*[1], Abigail Radcliff[2], Michael Johnson[1], Robert Blank[3], Marc Drezner[1]. [1]University of Wisconsin, USA, [2]University of Wisconsin-Madison, USA, [3]Medical College of Wisconsin, USA

Previously, we found that decreased osteoblast *Signe1* (7B2) mRNA expression is a pivotal abnormality underlying the pathogenesis of X-Linked Hypophosphatemia (XLH), and that Hexa-D-Arginine (D6R) treatment rescues the *HYP* phenotype by increasing 7B2 mRNA. Recently, we observed that *Hyp*-mouse bone has increased miR335-3P and -5P expression, which reduce 7B2 mRNA by targeting the 7B2-3'UTR region. However, it remains unknown if miR335-3P and -5P serve as biochemical targets for D6R rescue of the *HYP* phenotype. Thus, we studied D6R effects on the miR335 mediated decrease in 7B2 production. Dose-dependent D6R treatment of TMOb osteoblasts resulted in a maximal decrement in expression of miR-3P (0.25 ± 0.2 vs 0.94 ± 0.1 [relative expression (re)]; p<0.01) and -5P (0.42 ± 0.02 vs 0.94 ± 0.1 [re]; p<0.01). In accord, D6R treated TMOb cells exhibited increased 7B2 mRNA (2.59 ± 0.40 vs 1.09 ± 0.3 [re]; p<0.05), as well as the anticipated down-stream effects. To confirm miR335-3P and 5P were biochemical targets for D6R treatment of XLH, we assessed D6R effects on TMOb cells transfected with *Phex* siRNA. Transfected cells exhibited a significant increase in miR335-3P (3.0 ± 0.20 vs 1.2 ± 0.08 [re]; p<0.01) and -5P (4.15 ± 0.80 vs 1.7 ± 0.08 [re]; p<0.01). However, D6R treatment abolished the stimulatory effects of *Phex* siRNA, restoring normal expression of miR335-3P (1.26 ± 0.10 vs 1.2 ± 0.08 [re]) and -5P (1.35 ± 0.30 vs 1.25 ± 0.10 [re]). Thereafter, we treated normal and *Hyp*-mice for 5 weeks with vehicle or D6R (1.5 μmole/kg/day). Bones from vehicle treated *Hyp*-mice showed a significant increase, compared to normal mice, in miR335-3P (4.76 ± 0.80 vs 1.03 ± 0.09 [re]; p<0.001) and -5P (6.29 ± 0.99 vs 1.01 ± 0.08 [re]; p<0.001). In contrast, bones from D6R treated *Hyp*-mice, exhibited a dramatic reduction, to levels similar to those in treated normal mice, in miR335-3P (1.78 ± 0.16 vs 1.65 ± 0.31 [re]) and -5P (2.25 ± 0.37 vs 1.86 ± 0.95 [re]). In concert, in *Hyp*- mouse bone, 7B2 mRNA increased, while FGF-23 and β-catenin mRNA decreased, to normal, thereby normalizing phosphate homeostasis and bone mineralization. The D6R effects on miR335-3P and -5P were specific, as no inhibitory effects were observed *in vitro* and/or *in vivo* on the expression of other miRNAs (e.g. miR214, let-7e, miR218, miR126), many of which affect bone metabolism. These data confirm increased miR335-3P and -5P expression play a central role in the pathogenesis of XLH and provide a target for effective drug treatment of this disease.

Disclosures: Baozhi Yuan, None.

1106

Aptamer-Functionalized Lipid Nanoparticles (LNPs) Targeting Osteoblasts as a Novel RNA Interference-Based Bone Anabolic Strategy. Liang Chao*[1], Ge Zhang[2], Baosheng Guo[3], Heng Wu[4], Liangqiang Zhang[5], Aiping Lu[3]. [1]Hong Kong, [2]Ge Zhang' S Lab, Hong Kong, [3]Hong Kong Baptist University, Hong Kong, [4]HKBU, Hong Kong, [5]Beijing Proteome Research Center, China

Objective: Our previously developed osteogenic siRNA delivery system (AspSer-Ser)₆-liposome has concerns on efficacy and safety mainly due to lack of osteoblast-specific delivery at cellular level (Zhang G, Nat Med 2012; Wang X, Nat Med 2013). The objective of this project is to develop novel aptamer-functionalized LNPs directly targeting osteoblasts at cellular level for RNAi-based bone anabolic therapy.

Methods: Aptamers were screened by cell-SELEX with osteoblasts as target cells and hepatocytes and PBMCs as non-target cells. Osteoblast-specific aptamer was

conjugated to LNPs that encapsulated osteogenic *Plekho1* siRNA (Lu K, Nat Cell Bio 2008), *i.e.*, Aptamer-LNPs-siRNA. *In vitro* evaluation of Aptamer-LNPs-siRNA was conducted by cyto-TEM, flow cytometry and confocal imaging in terms of physicochemical properties, biological characteristics and cellular uptake mechanisms. *In vivo* studies from biophotonic imaging, immunohistochemistry, FACS, real-time PCR, microCT, bone histomorphometry and mechanical testing were performed to examine the selectivity, efficacy and safety of Aptamer-LNPs-siRNA, including tissue/cell-selective delivery, gene knockdown efficiency, dose-response pattern, persistence of gene silencing, bone anabolic action and toxicity.
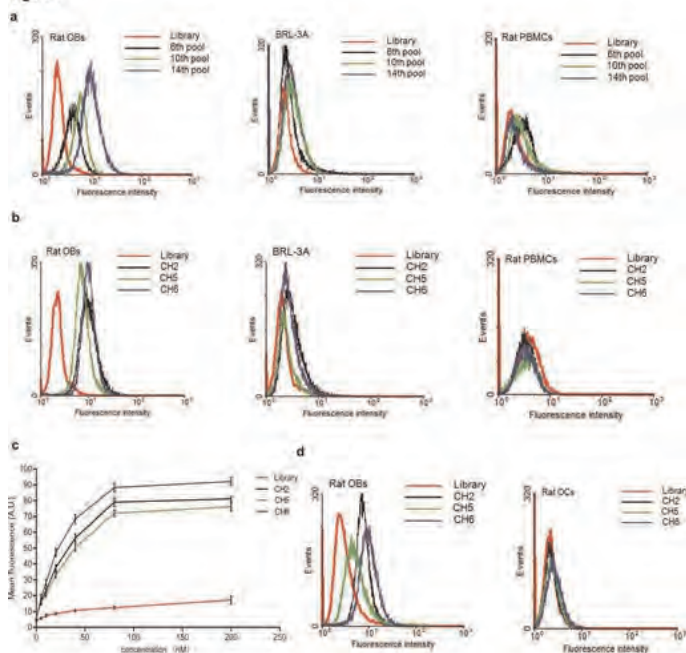
Results: We screened an aptamer (CH6) which could target osteoblasts but not hepatocytes and PBMCs (Fig. 1). Then, we developed CH6-functionalized LNPs encapsulating *Plekho1* siRNA, *i.e.*, CH6-LNPs-siRNA. *In vitro* data suggested that CH6 facilitated osteoblast-specific uptake of the encapsulated siRNA mainly *via* macropinocytosis (Fig. 2). Consistently, *in vivo* data further confirmed that CH6 facilitated skeleton/osteoblast-specific delivery of *Plekho1* siRNA (Fig. 3) and long persistence of gene knockdown (Fig 4), leading to promoted bone formation, improved bone micro-architecture (Fig. 5), increased bone mass and enhanced mechanical properties in osteopenic rats with no obvious toxicity.

Conclusion: CH6 aptamer-functionalized LNPs is a promising targeting system for directly delivering siRNA to osteoblasts, thus updates the targeted delivery systems from tissue level toward cellular level to facilitate clinical translation of RNAi-based bone anabolic strategy in efficiency and safety (N_HKBU435/12, NSFC 81272045, FRG2/12-13/027 and SCM-2013-SZTIC-001).
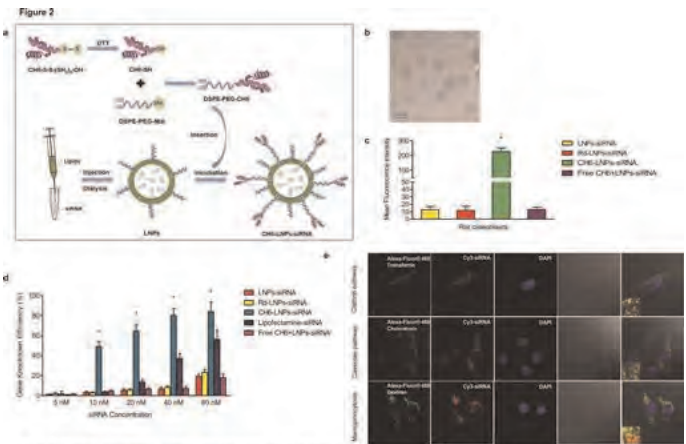
Reference

Lu K, et al. *Nat Cell Biol*. 10(8):994-1002. 2008
Zhang G, et al. *Nat Med*. 18: 307-14, 2012
Wang, X. *et al*, *Nat Med*. 19(1):93-100, 2013

Fig. 2 Preparation, morphology, cellular selectivity, knockdown efficiency and mechanism of cellular uptake (a) Preparation (b) Morphology: Cryo-TEM images of CH6-LNPs-siRNA. (c) Cellular selectivity (d) Gene knockdown efficiency (e) Pathway for cellular uptake: Intracellular co-localization of *Plekho1* siRNA encapsulated in CH6-LNPs and endocytic markers (dextran, transferrin and cholera toxin) in rat primary osteoblasts.

Fig. 2
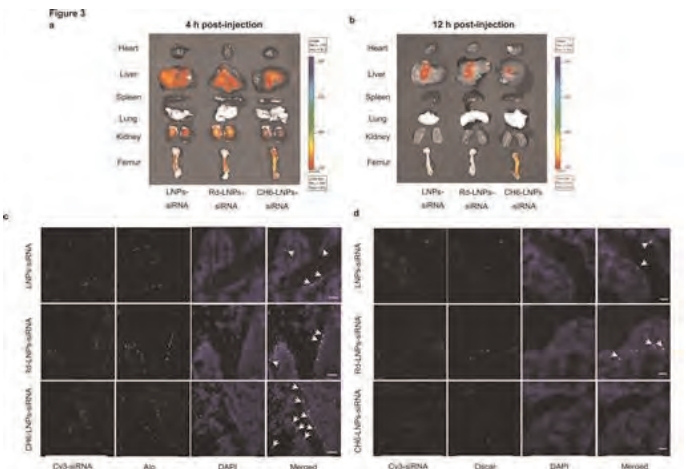
Fig. 3 Tissue distribution and cell-selective delivery *in vivo* (a, b) Tissue distribution: Localization of Cy3-labeled siRNA in rats administered with LNPs-siRNA, Rd-LNPs-siRNA or CH6-LNPs-siRNA by biophotonic imaging. (c, d) Cellular selectivity in bone: Fluorescence micrographs of cryosections of proximal tibiae after injection with LNPs-siRNA, Rd-LNPs-siRNA and CH6-LNPs-siRNA, respectively.

Fig. 3
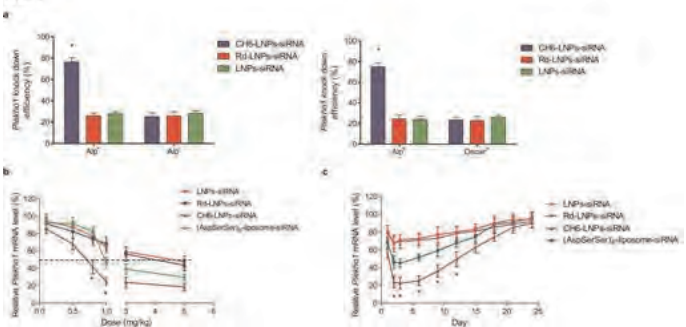
Fig. 4 Cell-selective gene knockdown efficiency, dose-response pattern and persistence of gene silencing *in vivo* (a) The knockdown efficiencies of *Plekho1* mRNA in Alp+, Alp- and Oscar+ cells after the administration of LNPs-siRNA, Rd-LNPs-siRNA or CH6-LNPs-siRNA detected by FACS in combination with real-time PCR (b) Dose-dependent gene silencing investigated by RT-PCR after tail vein injection of LNPs-siRNA, Rd-LNPs-siRNA, CH6-LNPs-siRNA or (AspSerSer)₆-liposome-siRNA at a single siRNA dose ranging from 0.1-5 mg/kg. (c) Persistence of gene silencing investigated by RT-PCR and normalized to the baseline after a single injection of LNPs-siRNA, Rd-LNPs-siRNA, CH6-LNPs-siRNA or (AspSerSer)₆-liposome-siRNA at the siRNA dose of 1 mg/kg. The data was presented as the mean ± standard deviation; n=6 per group. * P<0.05 for a comparison of CH6-LNPs-siRNA with LNPs-siRNA or Rd-LNPs-siRNA or (AspSerSer)₆-liposome-siRNA.

Fig. 4

Fig. 1 Cell-SELEX for identification of osteoblast-specific aptamers (a) The binding ability of the enriched pools to target cells (rat primary osteoblasts) and negative controls (rat hepatocyte cell line BRL-3A and PBMCs) (b) The binding ability of the FAM-labeled aptamer candidates (CH2, CH5 and CH6) to target cells and negative controls. (c) Flow cytometry to determine the binding affinity of the aptamer candidates for the target cells (d) The binding ability of the FAM-labeled, 2'-O-methyl-nucleotide substitutions modified aptamer candidates (CH2, CH5 and CH6) to rat primary osteoblasts (left) and osteoclasts (right) determined by flow cytometry. Rat OBs: rat primary osteoblasts; Rat OCs: rat osteoclasts; Rat PBMCs: rat peripheral blood mononuclear cells; BRL-3A: rat hepatocyte cell line.

Fig. 1

Fig. 5

Disclosures: Liang Chao, None.

1107

Efficacy of an Experimental small interfering RNA Therapy for Autosomal Dominant Osteopetrosis type 2 (ADO2). <u>Mattia Capulli</u>*[1], <u>Antonio Maurizi</u>[2], <u>Nadia Rucci</u>[2], <u>Anna Teti</u>[2]. [1]Department of experimental Medicine, University of L'Aquila, Italy, [2]University of L'Aquila, Italy

ADO2 patients experience high morbidity, including frequent fractures, osteomyelitis, hematological and neurological impairment. Reduced osteoclast activity is caused, in about 70% of cases, by heterozygous dominant negative mutations of the *CLCN7* gene, encoding the Cl^-/H^+ antiporter type 7 (ClC-7). Because of the dominant missense nature of the mutation, we hypothesized that small interfering (si)RNA could silence the mutant transcript without affecting the WT mRNA, thus mimicking a condition of aplosufficiency. The most frequent *CLCN7* gene mutation in humans is a ClC-7 p.G215R amino acid substitution. $CLCN7^{G215R}$-specific siRNA (100 nM) silenced by 85% transfected mutant mRNA/*EGFP* in HEK293 cells and in human osteoclasts generated from peripheral blood mononuclear cells (n=3; p=0.002; Student's t test). No change of $CLCN7^{WT}$ mRNA and no effect of scrambled siRNA on the mutant transcript were observed. Osteoclasts generated from the bone marrow of $Clcn7^{G213R}$ ADO2 mice, harboring the murine homolog of the human mutation, showed 70% reduced resorption pit formation (n=3; p=<0.0001 vs WT). This condition was 2.6-fold reverted by treatment with 100 nM $Clcn7^{G213R}$-specific siRNA (p=0.002 vs scrambled siRNA-treated ADO2 osteoclasts), rescuing bone resorption to 78% of WT osteoclasts. siRNAs were then made sticky by 3' dAdT overhangs and conjugated with the PolyPlus Transfection JetPEI® siRNA reagent, a linear polyethylenimine derivative providing effective and reproducible siRNA delivery *in vivo*, preventing inflammatory responses. Single i.p. injection in ADO2 mice of 2 and 4mg/Kg $Clcn7^{G213R}$-specific sticky siRNA/ JetPEI conjugate induced 67% and 95% silencing of tibia mutant mRNA, respectively, with maximal effect at 48 hours. Treatment of ADO2 mice, 3 times a week for 2 weeks, with 4mg/Kg $Clcn7^{G213R}$-specific siRNA induced a 1.46-fold increase of serum CXT (n=3-5; p=0.036), 20% decrease of tibia trabecular BV/TV (n=6-8; p=0.02), 13% decrease of TbN (p=0.03) and 7% decrease of TbTh (p=0.05), with an overall improvement of the osteopetrotic bone phenotype. Similar mRNA silencing was obtained with siRNAs against *CLCN7* mutations causing ClC-7 p.R767W and p.R286W amino acid substitutions. These results demonstrate that a siRNA-based experimental treatment of ADO2 is feasible, and underscore a translational impact for future strategy to cure this therapeutically neglected form of osteopetrosis (patent RM2014A000272).

Disclosures: Mattia Capulli, None.

1108

Therapeutic silencing intra-osseous *Ckip-1* for promoting bone formation in an aged rat model of male osteoporosis. <u>Baosheng Guo</u>*[1], <u>Baoting Zhang</u>[2], <u>Ge Zhang</u>[3]. [1]Hong Kong Baptist University, Hong Kong, [2]Price of Wales Hospital, The Chinese University of Hong Kong, Hong Kong, [3]Ge Zhang' S Lab, Hong Kong
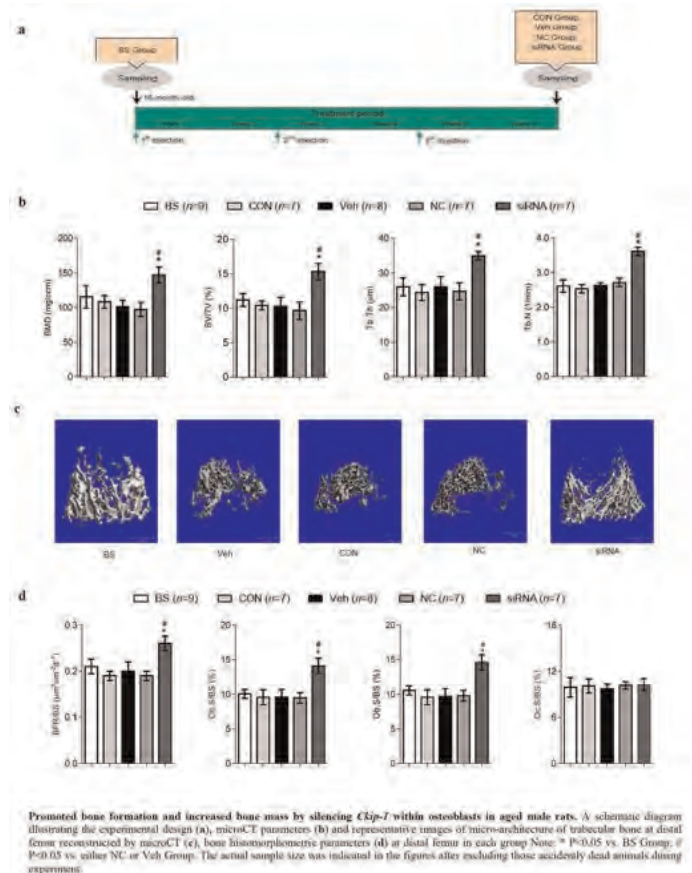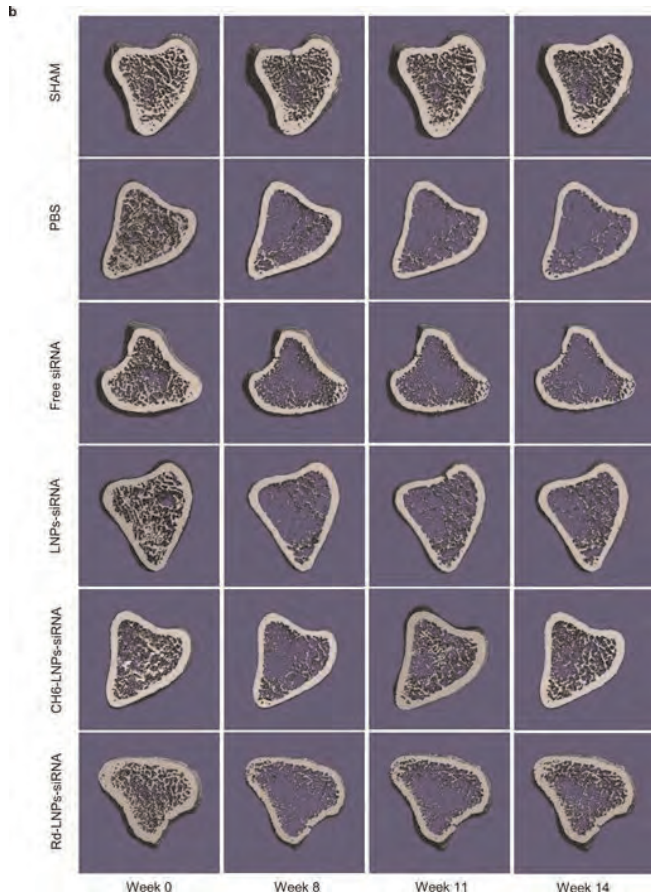
Introduction: *Ckip-1* is a newly discovered negative regulator gene of bone formation during bone development and bone maintenance without activating bone resorption (Lu K, et al, 2008). *Ckip-1* mRNA expression increased with age, whereas the bone formation decreased with age in the bone specimens from both the osteoporotic fracture patients and aged male rats (Guo B, et al, 2010. Thus, we hypothesized that *in vivo* administration of *Ckip-1* siRNA delivered by our previously developed (Asp-Ser-Ser)6-liposome (Zhang G, et al, 2012) could promote bone formation and improve trabecular architecture in aged osteoporotic men.

Objectives: We aimed to investigate the effects of *Ckip-1* siRNA delivered by (Asp-Ser-Ser)6-liposome on bone formation and trabecular architecture in the aged rat model of male osteoporosis.

Methodology: Ten 16-month-old male Sprague-Dawley rats were sacrificed at as baseline (BS group) before treatment. Thereafter, forty 16-month-old male rats were divided into siRNA treatment group (siRNA), Non-sense siRNA group (NC), vehicle control group (Veh) and age-matched control group (CON). The rats in above Group were given three periodic injections of *Ckip-1* siRNA (4 mg/kg), non-sense siRNA (4 mg/kg) encapsulated by osteoblast-specific delivery system, osteoblast-specific delivery system alone and PBS at an interval of two weeks, respectively. All the rats in each treatment group were sacrificed after six weeks of treatment (Figure a). After sacrifice, the bilateral distal femurs were subjected to microCT measurement and subsequent bone histomorphometric analysis.

Results: The microCT data revealed that the trabecular parameters in siRNA group were notably increased from baseline. The above microCT parameters were all obviously higher in siRNA Group than those in NC, Veh and CON groups (Figure b). Consistently, the better organized trabecular micro-architecture was also found in the rats from siRNA Group compared to the rats in BS, NC, Veh and CON groups (Figure c). The bone histomorphometric analysis data showed that the bone-formation-related parameters in siRNA Group were all significantly increased from baseline and higher than those in NC, Veh and CON groups, whereas the bone-resorption-related parameter (osteoclast surface) was unchanged among all the groups (Figure d).

Conclusion: Therapeutic gene silencing of *Ckip-1* in osteogenic cells could promote bone formation and improve trabecular architecture in aged rat model of male osteoporosis.

Promoted bone formation and increased bone mass by silencing *Ckip-1* within osteoblasts in aged male rats. A schematic diagram illustrating the experimental design (a), microCT parameters (b) and representative images of micro-architecture of trabecular bone at distal femur reconstructed by microCT (c), bone histomorphometric parameters (d) at distal femur in each group Note: * P<0.05 vs. BS Group, # P<0.05 vs. either NC or Veh Group. The actual sample size was indicated in the figures after excluding those accidently dead animals during experiment

Fig

1109

Decreased Optineurin Mediates MVNP Effects on Pagetic Osteoclast Formation. <u>Quanhong Sun</u>*[1], <u>Juraj Adamik</u>[1], <u>Jolene Windle</u>[2], <u>G. David Roodman</u>[3], <u>Deborah Galson</u>[1]. [1]University of Pittsburgh, USA, [2]Virginia Commonwealth University, USA, [3]Indiana University, USA

Paget's disease is characterized by abnormal osteoclasts (OCL) in pagetic lesions. Measles virus nucleocapsid protein (MVNP) has been reported to play a key role in the development of abnormal OCL in Paget's patients. In addition, MVNP expression targeted to OCL in transgenic mice induces pagetic-like lesions in vivo and aberrant OCL in vitro. MVNP induced upregulation of IL-6 is essential for the pagetic OCL phenotype. We have recently reported that MVNP activation of TBK1, an IKK family member, plays a critical role in mediating the effects of MVNP to generate aspects of the pagetic osteoclast phenotype, including elevated IL-6. Another IKK family member, optineurin (Optn), which is most closely related to IKKγ, has been shown to play a negative role in the innate immunity antiviral response by interacting with TBK1. Optn is a key player regulating various physiological processes including cell division and autophagy as well as the antiviral response. Interestingly, a non-coding SNP in the OPTN gene has recently been identified as a genetic risk factor for Paget's disease. We hypothesized that MVNP might prevent Optn repression of TBK1 function in OCL progenitors, thereby inducing a pagetic OCL phenotype. We have found that Optn mRNA and protein levels are decreased in OCL precursors from TRAP-MVNP mice as compared to wild-type OCL precursors. Similar results were observed in NIH3T3 cells stably or transiently transfected with MVNP cDNA compared to empty vector control cells. Optn over-expression inhibited IL-6-promoter luciferase reporter expression in HEK293 cells, and strikingly, even decreased endogenous IL-6 mRNA in the NIH3T3 cell line. Optn co-expression with MVNP blocked the MVNP stimulation of the IL-6 luciferase reporter in HEK293 cells and of endogenous IL-6 mRNA in NIH3T3 cells. Optn over-expression attenuated the p65 activation stimulated by MVNP or TBK1 in NIH3T3 cells. We found that TBK1 over-expression further decreased the Optn mRNA level in both TRAP-MVNP and wild-type OCL precursors, suggesting that there may be a positive feedback loop involved that potentiates the initial effects of MVNP activation of TBK1. Importantly, Optn over-expression in primary bone marrow monocytes decreased RANKL-stimulated OCL formation. These results suggest that the MVNP-induced decrease of Optn may mediate the effects of MVNP or TBK1 on the expression of IL-6, a key contributor to the pagetic OCL phenotype, and on OCL formation.

1110

The Histone Deacetylase Sirtuin 1 is a Transcriptional Modulator of the Neuronal Control of Bone Mass. <u>Na Luo</u>*[1], <u>Aruna Kode</u>[1], <u>Ioanna Mosialou</u>[1], <u>Mattia Capulli</u>[2], <u>Stavroula Kousteni</u>[1]. [1]Columbia University Medical Center, USA, [2]University of L'Aquila, Italy

A well-established mode of neuronal regulation of bone mass favors bone mass accrual by inhibiting the activity of the sympathetic nervous system (SNS). In this regulatory loop the transcriptional mechanisms regulating catecholamine synthesis are still poorly understood. In addressing this question we focused on Sirtuin 1 (Sirt1), a histone deacetylase that integrates intracellular networks and intercellular signaling to facilitate multiple physiological functions. We show that a generalized but modest increase in Sirt1 expression in transgenic mice (TgSirt1 mice), compromised bone mass by suppressing bone formation and by promoting bone resorption. The opposite effects of Sirt1 on the two compartments of bone remodeling correlated with an increase in the activity of the SNS. Two observations further implicated the SNS as a mediator of the skeletal actions of Sirt1. First, expression of Ucp1 in brown fat as well as levels of urinary epinephrine and norepinephrine increased in TgSirt1 mice. Second, expression of c-Myc, Creb and their target genes per1, per2, cry1, bmaI1 that are upregulated by SNS signaling and contribute to the SNS regulation of bone mass, increased in osteoblasts of TgSirt1 mice. Moreover, pharmacological inhibition of SNS signaling by daily administration of the beta adrenergic receptor inhibitor propranolol to TgSirt1 mice for 4 weeks fully restored osteoblast and osteoclast numbers and rescued the low bone mass phenotype of these animals. To determine if the high sympathetic tone in TgSirt1 mice was due to a central effect of Sirt1, we examined Sirt1 expression in the brain. Immunofluorescence analysis in coronal brain sections showed that Sirt1 is expressed in the serotonergic neurons of the brainstem and the locus coeruleus, from where sympathetic activity emanates. Lastly, we inactivated Sirt1 specifically in the brain by injecting 12-week-old mice carrying an allele of Sirt1 in which exon 4 is floxed in the third ventricle with an adenovirus expressing recombinant Cre. We verified that Sirt1 was efficiently inactivated in the entire brain including the brainstem, hypothalamus, midbrain. Sirt1 inactivation in the brain decreased SNS activity and as a result, it increased bone mass by increasing bone formation and suppressing bone resorption. These observations suggest that, besides its cell autonomous effects in osteoblasts and osteoclasts, Sirt1 controls bone mass by a mechanism that involves upregulation of SNS signaling.

1111

Convergence of transcriptional and epigenetic programs regulating osteogenic differentiation from mesenchymal stromal cells. <u>Jonathan Gordon</u>*[1], <u>Hai Wu</u>[1], <u>Troy Whitfield</u>[2], <u>Coralee Tye</u>[3], <u>Andre Van Wijnen</u>[4], <u>Janet Stein</u>[5], <u>Gary Stein</u>[6], <u>Jane Lian</u>[7]. [1]University of Vermont, USA, [2]Department of Cellular & Developmental Biology, University of Massachusetts Medical School, Worcester, MA, USA, [3]Vermont Cancer Center & Department of Biochemistry, University of Vermont, Burlington, VT., USA, [4]Mayo Clinic, USA, [5]Vermont Cancer Center & Department of Biochemistry, University of Vermont, Burlington, VT., USA, [6]University of VermontCollege of Medicine, USA, [7]University of Vermont College of Medicine, USA

Commitment to the osteoblast lineage is a complex process, utilizing a diverse cohort of DNA-binding regulatory molecules to initiate and sustain the stochastic progression of pluripotent mesenchymal cells to a tissue-specific terminally differentiated cell. These regulatory proteins may interact with chromatin directly through a DNA-binding domain, or through protein-protein interactions with DNA-bound proteins, functioning to modify gene expression and thereby providing a tissue-specific expression profile. To examine the mechanisms of osteoblast-related transcription factor regulation of lineage commitment, we have used a pure population of FACS-sorted vascular-associated aSMA+ MSCs to define genome-wide binding patterns of transcriptional regulators including Runx2, Dlx3 and several others during osteogenic differentiation. In addition we have compared these binding events with epigenetic modifications including H3K4me1, H3K4me3, H3K9me3, H3K9acetyl, H3K27me3, H3K27acetyl and H3K36me3. The patterns of transcription factor binding events present an overall picture as to regulation of gene expression during lineage specific commitment of MSC-derived osteoblasts. Using gene expression data derived from RNA-seq profiling, osteoblast-related transcription factor binding was correlated with differential gene expression and histone modification patterns to allow us to define gene regulatory networks contributing to osteogenesis. Using this analysis method, we have identified several gene regulatory pathways that include genes grouped by distinct functional roles such as: forkhead box family genes (FOX), chromatin regulators (e.g., Ezh2, Hdac10, Hdac2, Hdac3, Sirt1, Sirt6, Ncoa5, MLL3, DNMT1), nuclear co-receptors (e.g., VDR, Rarg, Nr1d2, Nr4a1, Rara, Nr2c1) and several zinc finger-related protein encoding genes. In addition, we have defined novel regulatory regions, denoted by histone modification marks and multiple transcription factor binding sites that may function as super enhancers critical for chromosomal organization leading to osteogenic differentiation. These data provide a global map of transcription factor binding and histone modifications during lineage commitment and define a comprehensive molecular signature of osteogenesis. This information can be further used to examine the role of specific transcriptional regulators and their involvement in osteoblast/bone development.

1112

***Dnmt3b* is a Critical Target Gene during the Development of Osteoarthritis.** <u>Jie Shen</u>*[1], <u>Cuicui Wang</u>[2], <u>Jason Meyers</u>[1], <u>John Ashton</u>[1], <u>Tzong-Jen Sheu</u>[1], <u>Jennifer Jonason</u>[1], <u>Regis O'Keefe</u>[1]. [1]University of Rochester, USA, [2]University of Rochester Medical Center, USA

Osteoarthritis (OA) is a degenerative disease of articular cartilage that is projected to afflict >50 million people in the US by the year 2020. Predispositions include joint injury, heredity, obesity, aging and environment factors. Recent human studies revealed that DNA methylation signature was significantly shifted between healthy and OA patients, suggesting DNA methyltransferase (Dnmt) may play a critical role during OA pathogenesis. Despite extensive work over the past 20 years to delineate the epigenetic mechanism(s) of OA, a full understanding of the role of Dnmt is yet to be achieved. There are there major Dnmts. Dnmt1 is ubiquitous and is involved in the whole genome methylation homeostasis. In contrast, two de novo Dnmts, 3a and 3b have tissue specific expression patterns and create unique methylation signatures. Our data showed that the expression of Dnmt3b, but not Dnmt1 or Dnmt3a was significantly decreased in several well-established OA models, including an aging model, MLI model, and obesity model. Articular cartilage IHC array, including 70 human OA cartilage and 14 healthy cartilage samples, confirmed that DNMT3b expression was reduced in OA patients. In vitro experiments showed that mechanical loading and inflammatory factors significantly decreased Dnmt3b expression in ATDC5 chondrocytes. To examine the effect of Dnmt3b in chondrocytes, we treated primary articular chondrocytes with Dnmt3b siRNA and found that loss of Dnmt3b dramatically stimulated chondrocyte hypertrophy by reducing TGF signaling and increasing BMP signaling. To further investigate the role of Dnmt3b during OA development, we generated Dnmt3b conditional knockout mice (Dnmt3b^{Agc1ER}), which were administrated with tamoxifen at 2-month-old of age. In 3-month-old Dnmt3b^{Agc1ER} mice, superficial zone articular chondrocytes had hypertrophy with high Type X Collagen expression. In 5-month-old Dnmt3b^{Agc1ER} mice, a severe OA-like phenotype was observed, including cartilage tissue degradation, subchondral sclerosis and osteophyte formation. RNA-seq and Methyl-seq were performed and an integrated analysis performed; the data confirmed Dnmt3b targets expression and methylation of multiple TGF signaling targets and other genes involved chondrocyte

maturation and osteoarthritis. In summary, multiple known risk factors of OA change the homeostasis of articular chondrocytes via down-regulation of the *Dnmt3b* gene and target several OA-related pathways such as TGF-b and BMP signaling.

Disclosures: Jie Shen, None.

1113

Histone Deacetylase 3 Suppresses Erk Phosphorylation and Subsequent Matrix Metalloproteinase (MMP)-13 Activity in Chondrocytes during Endochondral Ossification. Lomeli Carpio*, Elizabeth Bradley, Meghan McGee-Lawrence, Jennifer Westendorf. Mayo Clinic, USA

Histone deacetylase (Hdac) inhibitors are used extensively for treating cancer, arthritis, and epilepsy; however, these drugs inhibit multiple Hdacs, are teratogens, and have detrimental effects on the skeleton. Several Hdacs contribute to endochondral bone formation. In this study, we defined the cell autonomous role of Hdac3 in chondrocyte maturation by deleting it pre- and post-natally in type II collagen alpha 1 (Col2a1)-Cre expressing chondrocytes. Hdac3-CKO$_{Col2}$ mice rarely survived embryogenesis. The few that did survive were hypomorphic for Hdac3 expression, runted, and had severely reduced cancellous and cortical bone density. Postnatal Hdac3 deficiency was induced with a tamoxifen-inducible Col2a1 Cre model (Hdac3-CKO$_{Col2ERT}$). At 4-weeks of age, these animals had residual hypertrophic cartilage and increased osteoclast activity in the primary spongiosa. By 8 weeks, these animals had compromised bone architecture, with significant decreases in cancellous bone but increases in cortical bone thickness, which is a compensation for disrupted growth plate maturation during development. Phosphorylation of Erk1/2, as well as its substrate Runx2, was elevated in Hdac3-depleted immature mouse articular chondrocyte (IMAC) micromass cultures. Activated Erk and Runx2 directly stimulate matrix metalloproteinase (MMP)-13 gene expression. MMP-13 mRNA and active enzymatic levels were higher in Hdac3-deficent IMAC cultures, as measured by QPCR and type I collagen zymography of conditioned media, respectively. U0126, an ERK inhibitor, returned MMP-13 expression to control levels in Hdac3-deficient IMAC cultures. In control mice, phosphorylated Erk and MMP-13 expression are restricted to the pre-hypertrophic zone of chondrocytes. With Hdac3 deficiency, phosphorylated Erk and MMP-13 are prematurely and prominently expressed in proliferative, pre-hypertrophic and hypertrophic chondrocytes. Together, these results indicate that Hdac3 controls the temporal and spatial regulation of Erk phosphorylation and subsequent MMP-13 expression to ensure proper chondrocyte maturation and ossification during long bone development.

Disclosures: Lomeli Carpio, None.

1114

MicroRNA-140 provides robustness to the regulation of hypertrophic chondrocyte differentiation by the PTHrP-HDAC4 pathway. Garyfallia Papaioannou*[1], Fatemeh Mirzamohammadi[2], Shigeki Nishimori[1], Marc Wein[1], Henry Kronenberg[1], Eric N. Olson[3], Tatsuya Kobayashi[1]. [1]Massachusetts General Hospital, USA, [2]Massachusetts General Hospital & Harvard Medical School, USA, [3]University of Texas Southwestern Medical Center, USA

Growth plate chondrocytes go through multiple differentiation steps and eventually become hypertrophic chondrocytes. The parathyroid hormone (PTH)-related peptide (PTHrP) signaling pathway plays a central role in the regulation of hypertrophic differentiation, at least in part, by enhancing histone deacetylase 4 (HDAC4), a negative regulator of Mef2 transcription factors that drives hypertrophy. We have previously shown that loss of the chondrocyte-specific microRNA (miRNA), miR-140, alters chondrocyte differentiation with a phenotype that includes mild acceleration of hypertrophic differentiation. However the mechanism by which miR-140-loss regulates chondrocyte differentiation is not clear. In this study, we investigated the interaction between the miR-140 pathway and the PTHrP-HDAC4 pathway. Homozygous deletion of the PTHrP or HDAC4 gene causes premature hypertrophic differentiation and reduces endochondral bone growth, whereas heterozygosity of PTHrP or HDAC4 has virtually no effect, suggesting that one allele of PTHrP or HDAC4 is sufficient to maintain normal skeletal growth. However, we found that the bone growth of heterozygous PTHrP or HDAC4 mutant mice was substantially impaired in miR-140-deficiency. This finding demonstrates that miR-140 plays an important role when the PTHrP-HDAC4 function is partially impaired, suggesting that these molecules are components of a common pathway. We found that miR-140-deficient chondrocytes showed increased Mef2c expression with normal levels of total and phosphorylated HDAC4. This finding indicates that the miR-140 pathway merges with the PTHrP-HDAC4 pathway at the level of Mef2c expression. Since Mef2c is not a predicted target of miR-140, the Mef2c upregulation is likely an indirect effect of miR-140-deficiency. We found that miR-140-deficient primary chondrocytes showed greater activation of p38 mitogen-activated protein kinase (MAPK) to serum stimulation when compared with control. Inhibition of p38 MAPK *in vitro* reduced Mef2c expression in miR-140-null chondrocytes, suggesting that miR-140 suppresses p38 MAPK signaling to inhibit hypertrophic differentiation. These results demonstrate that miR-140 ensures the robustness of the PTHrP/HDAC4 regulatory system by suppressing Mef2c-inducing stimuli.

Disclosures: Garyfallia Papaioannou, None.

1115

Epigenetic control of skeletal development by the histone methyltransferase EZH2. Amel Dudakovic*[1], Fuhua Xu[2], Emily Camilleri[1], Meghan McGee-Lawrence[1], Eric Lewallen[1], Scott Riester[1], John R. Hawse[3], Gary Stein[4], Martin Montecino[5], Jennifer Westendorf[1], Andre Van Wijnen[1]. [1]Mayo Clinic, USA, [2]New Jersey Medical School, UMDNJ, USA, [3]Mayo Clinic College of Medicine, USA, [4]University of VermontCollege of Medicine, USA, [5]Universidad de Concepcion, Chile

Epigenetic control of gene expression is critical for normal development of fetal tissues including bone. Yet, chromatin related mechanisms that activate bone-specific programs have remained under-explored. Therefore, we investigated the expression profiles of a large cohort of epigenetic regulators (~400) during osteogenic differentiation of human mesenchymal stromal/stem cells (hMSCs) and mouse MC3T3 osteoblasts. We applied high-throughput RNA sequencing (RNASeq) analysis, robotic reverse-transcription quantitative polymerase chain reaction (RT-qPCR) analysis and western blotting. The molecular analyses establish that the polycomb group protein Enhancer of Zeste Homolog 2 (EZH2) is down-regulated during osteoblastic differentiation. EZH2 is the catalytic subunit of Polycomb Repressive Complex 2 (PRC2) and functions as a histone methyl-transferase. It suppresses gene transcription through modification of H3 lysine 27 by tri-methylation (H3K27Me3) and generates inaccessible chromatin. Knock-down (siRNA) of EZH2 protein levels or chemical inhibition of the enzymatic activity of EZH2 using a specific inhibitor (GSK126) during differentiation enhances the expression of osteoblast-specific histological and molecular biomarkers (e.g., Alizarin Red and AP staining, as well as ALPL, IBSP and BGLAP mRNAs). To understand the function of this epigenetic regulator during skeletal development, we examined a conditional knockout mouse (cKO) model for Ezh2. The Ezh2 gene was conditionally eliminated by Cre mediated excision in the mesenchymal lineage using the Prrx1 promoter. The resulting mice were examined for gross anatomy, radiology and μCT. Compared to wild type littermates, Ezh2 cKO mice exhibit stunted growth and malformation of forelimbs, paws, lumbar vertebrae and clavicles. Alterations are also observed in the epiphysis, the tibia-fibula junction and trabecular bone formation. Mutant mice have low bone mass as measured by DXA and μCT analysis. Several of these skeletal abnormalities resemble those observed in human patients with EZH2 mutations. Our data indicate that EZH2 is a critical epigenetic regulator for normal skeletal development and bone formation.

Disclosures: Amel Dudakovic, None.

1116

Formation of a Zinc finger protein 521-NuRD co-repressor complex is involved in osteoprogenitor commitment and Zebrafish skeletal development. Ken-ichi Takeyama*[1], Harikiran Nistala[2], William Addison[1], Satya Kota[1], Genri Kawahara[3], Louis Kunkel[3], Julian Mintseris[4], Steven Gygi[4], Francesca Gori[5], Roland Baron[6]. [1]Harvard School of Dental Medicine, USA, [2]Harvard University, USA, [3]Harvard Medical School, Boston Children's Hospital, USA, [4]Harvard Medical School, USA, [5]Harvard School of Dental Medicine, Massachusetts General Hospital, USA, [6]Harvard School of Medicine & of Dental Medicine, USA

The differentiation of mesenchymal stem cell (MSC) into osteoblast or chondrocyte is strictly controlled through gene regulation and epigenetic mechanisms with post-translational modifications on core histones. We have previously shown that the C2H2-type zinc finger protein 521 (Zfp521) plays important roles as a transcriptional repressor during osteoblastogenesis and chondrogenesis. Although HDAC-dependent repression of Runx2 or repression of Ebf1 are involved, the molecular mechanism(s) by which transcriptional repression by Zfp521 occurs still remains unclear.

To elucidate the transcriptional repressor function of Zfp521, we performed protein complex purification by stably expressing Zfp521 in HEK293A cells. We found all core components of the Nucleosome Remodeling and Deacetylase (NuRD) complex by mass spec analysis and validated the formation of a large complex (over 2 MDa) by glycerol gradient fractionation. Intriguingly, transglutaminase (TGase)3, which mediates protein-protein cross-linking, was also found in this complex. Endogeneous association of Zfp521 with NuRD and TGase3 was also observed in MEFs, W-20 and C3H10T1/2 cells, suggesting that Zfp521 regulates transcriptional repression through this complex during MSC differentiation. GST pull-down analysis demonstrated that RBBP4, a NuRD component that interacts with histone H4, binds directly to the N-terminal 13 amino acids (N13aa) of Zfp521 and to the catalytic region of TGase3. Furthermore, addition of N13aa peptides to the complex resulted in the disassembly of the Zfp521 and NuRD complex, whereas depletion of RBBP4 in HEK293A cells induced the dissociation of Zfp521 and TGase3.

To investigate the role of the Zfp521-NuRD complex in MSC differentiation in vivo, we depleted Zfp521 or RBBP4 homologs in Zebrafish and analyzed their skeletal phenotype. The mutant embryos (depleted Zfp521 or RBBP4) demonstrated similar developmental abnormalities including delayed cranial cartilage and bone development, and reduced expression of Sox9, Runx2 and Col II, suggesting that the Zfp521-NuRD complex plays a role in the suppression of genes involved in early skeletal development.

Taken together, our results suggest that 1) Zfp521 forms a large complex with NuRD and TGase3, and 2) the mechanisms by which Zfp521 exerts its transcriptional repression function to regulate MSC differentiation into osteoblast and chondrocyte involves epigenetic regulation via the recruitment of the NuRD complex.

Disclosures: Ken-ichi Takeyama, None.

1117

The molecular chaperone FKBP51 regulates energy metabolism and bone mass by controlling PPARg and p38 MAPK activities in adipocytes and marrow mesenchymal stem cells. <u>Lance Stechschulte</u>*[1], <u>Edwin Sanchez</u>[1], <u>Piotr Czernik</u>[2], <u>Beata Lecka-Czernik</u>[2]. [1]University of Toledo Health Science Campus, USA, [2]University of Toledo College of Medicine, USA

Nuclear receptor PPARγ controls energy metabolism and promotes differentiation of mesenchymal stem cells (MSC) to adipocytes at the expense of osteoblasts. In contrast, p38 MAPK promotes MSC differentiation to osteoblasts at the expense of adipocytes. Phosphorylation of p38 MAPK at Thr180/Tyr182 is required for its kinase activity, which in turn phosphorylates and activates the pro-osteoblastic factors Runx2 and Wnt10b, and inhibits PPARγ pro-adipocytic transcriptional activity through Ser112 phosphorylation. Our recent evidence suggests that FK506-binding protein-51 (FKBP51) negatively regulates p38 and positively regulates PPARγ activity. Overexpression of FKBP51 in COS7 cells increases rosiglitazone-induced PPARγ activity at a PPRE-luciferase reporter, while deficiency of FKBP51 decreases PPARγ activity. The latter result correlated with a simultaneous increase of PPARγ phosphorylation at Ser112 and p38 MAPK phosphorylation at Thr180/Tyr182. Animals with whole-body FKBP51 ablation (p51-KO) are lean, insulin sensitive, and protected from obesity, with greatly reduced adipose tissue mass. These animals also exhibit high bone mass. Trabecular bone mass is 30% higher in p51-KO vs. WT mice, mainly due to increased number of trabeculae. This is accompanied by increased activity of osteoblasts, as reflected by 40% larger mineralized surface, 20% higher mineral apposition rate, and 60% higher bone formation rate. Osteocytes isolated from cortical bone of femurs showed decreased SOST expression by 2-fold in p51-KO animals. Consistently, osteoblasts isolated from the surface of the same bone are highly activated, as measured by increased expression of Runx2, osterix, collagen and osteocalcin. When tested for their differentiation potential, marrow MSCs derived from p51-KO mice develop fewer adipocytic colony forming units (CFU), but the same number of CFUs in the osteoblastic lineage. Interestingly, calcium content was 2-fold higher in osteoblasts formed from the marrow of p51-KO animals. These results indicate that the FKBP51 chaperone regulates energy metabolism and bone mass by controlling the balance between PPARγ and p38 MAPK activities. Thus, FKBP51 activity is evidence for a common mechanism regulating MSC differentiation and energy maintenance. Targeting this mechanism may serve as a new pharmacological means for simultaneous treatment of obesity, diabetes and osteoporosis.

Disclosures: Lance Stechschulte, None.

1118

Glucocorticoid Signaling in Osteoblasts Mediates Age-Associated Changes in Glucose Metabolism and Body Composition in Mice. <u>Holger Henneicke</u>*[1], <u>Jingbao Li</u>[2], <u>Sylvia Jane Gasparini</u>[3], <u>Markus Seibel</u>[4], <u>Hong Zhou</u>[4]. [1]ANZAC Research Institute, The University of Sydney, Australia, [2]Key Laboratory for Space Bioscience & Biotechnology, Institute of Special Environmental Biophysics, Faculty of Life Sciences, Northwestern Polytechnical University, China, [3]Bone Biology Program, ANZAC Research Institute, The University of Sydney, Australia, [4]Bone Research Program, ANZAC Research Institute, University of Sydney, Australia

The physiological aging process is associated with changes in body composition and metabolism, including central obesity, diabetes and osteoporosis. The osteoblast has recently been identified as a mediator of GC-induced metabolic dysfunction in mice.[1] We therefore hypothesized that a mechanistic link exists between increased GC signaling in the osteoblast and changes in body composition and fuel metabolism during aging.

To test this hypothesis, we investigated the aging phenotype of transgenic (tg) mice in which glucocorticoid signaling had been selectively disrupted in osteoblasts/osteocytes via targeted overexpression of the glucocorticoid-inactivating enzyme, 11ß-hydroxysteroid dehydrogenase type 2 ('11ßHSD2-tg' mice). Body weight and composition, insulin sensitivity and glucose tolerance, serum corticosterone (CS) and osteocalcin levels as well as hepatic gene expression patterns related to glucose and lipid metabolism were assessed in female 11ßHSD2-tg mice and litter-matched wild-type (WT) controls at 2 and 18 months of age.

From 2 to 18 months of age, female WT mice gained more in body weight (WT: +32g vs tg: +16g, p<0.01) and overall fat mass (WT: +20.7g vs tg: +6.3g, p<0.01, Fig 1A) than their tg littermates. 18 months-old WT mice exhibited reduced insulin sensitivity and hepatosteatosis, while insulin responsiveness and hepatic lipid deposition remained normal in their tg littermates (Fig. 1B). Hepatic mRNA expression of lipogenic and gluconeogenic genes was higher in aged WT compared to aged tg mice (acetyl-coA-carboxylase, WT: 12.8 vs tg: 5.6 fold increase on respective young control, p=0.051 & glucose-6-phosphatase, WT: 8.1 vs tg: 3.3 fold increase on respective young control, p=0.09). Serum CS concentrations were similar in 18-

month-old WT and tg mice and ~3-fold higher than in 2-month-old mice (p<0.05). Serum osteocalcin concentrations declined during aging in both genotypes but remained significantly higher in tg mice at all time points (p<0.05).

Conclusion: Glucocorticoid signaling in osteoblasts is critically involved in the pathogenesis of age-related changes in glucose handling and body composition. Osteocalcin may act as a mediator of age-related metabolic dysfunction.

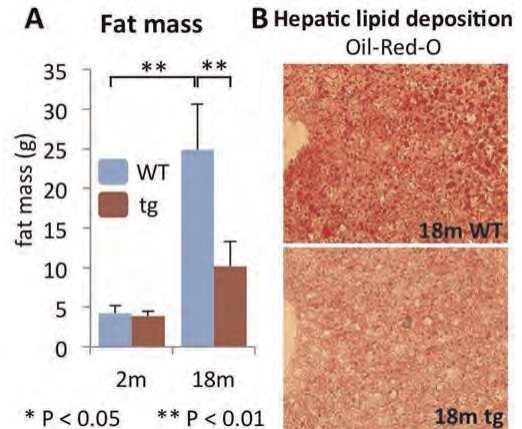1. Brennan-Speranza et al., J Clin Invest. 2012; 122(11): 4172-89

Figure 1: Fat mass (A) and hepatic lipid deposition (B) in WT and tg mice.

Disclosures: Holger Henneicke, None.

1119

Brown adipocyte-like cells from the peripheral nerve functionally contribute to heterotopic bone formation in a multifaceted manner. <u>Elizabeth Salisbury</u>*[1], <u>ZaWaunyka Lazard</u>[2], <u>Eric Beal II</u>[2], <u>Eleanor Davis</u>[2], <u>Alan Davis</u>[1], <u>Elizabeth Olmsted-Davis</u>[1]. [1]Baylor College of Medicine, USA, [2]Baylor College of Medicine, USA

We have previously developed an animal model of heterotopic ossification (HO), whereby delivery of bone morphogenetic protein 2 (BMP2) to the skeletal muscle of mice initiates a crucial neuro-inflammatory response that ultimately results in endochondral bone formation within the muscle. One major outcome of neuro-inflammation is the degranulation of mast cells, which release proteases that remodel the epineurial matrix of the nerve. Mast cells also release serotonin locally, resulting in a significant increase in noradrenaline and activation of sympathetic signaling within 2 days after delivery of BMP2. Immunohistochemical and FACS analysis indicated the activation and replication of perineurial fibroblasts expressing the β₃-adrenergic receptor (ADRB3), through which noradrenaline is known to signal. This population of ADRB3^{+} cells also expressed the neural migratory marker HNK1. By 4 days after exposure to BMP2, isolation and characterization of these ADRB3^{+} cells revealed their presence within the soft tissues surrounding the site of BMP2 delivery and their absence from the nerves, suggesting the migration of this cell population. These cells also expressed the brown adipocyte marker uncoupling protein 1 (UCP1), which enables uncoupled aerobic respiration, as well as markers of glucose lactate fermentation, which provides these cells unique metabolic properties. Suppression of mast cell degranulation and the pursuant sympathetic signaling by administration of cromolyn inhibited the generation of these brown adipocyte-like cells, ablating both UCP1 gene and protein expression at the site. Cromolyn administration also significantly reduced heterotopic bone formation, as indicated by microCT, and appeared to suppress cartilage formation. Immunohistochemistry revealed multiple fates for these brown adipocyte-like cells, as one subset expressed the neural guidance molecule reelin and another expressed vascular endothelial growth factors (VEGF-D) for proper vascularization of the new bone. Furthermore, using tracking animals, a portion of these cells appear to differentiate directly into chondrocytes. The data collectively suggest that BMP2 activates a population of perineurial cells within the nerve to expand, migrate, and differentiate into brown adipocyte-like cells that have multiple functions in guiding the formation of heterotopic bone.

Disclosures: Elizabeth Salisbury, None.

1120

Leptin is crucial for ventral hypothalamic FosB-mediated regulation of glucose and energy homeostasis but not for bone homeostasis. Kazusa Sato*[1], Anna Idelevich[2], Glenn Rowe[3], Francesca Gori[4], Roland Baron[5]. [1]Harvard School of Dental Medicine, USA, [2]Harvard University, USA, [3]Harvard Medical School, USA, [4]Harvard School of Dental Medicine, Massachusetts General Hospital, USA, [5]Harvard School of Medicine & of Dental Medicine, USA

The ventral hypothalamus (VHT) plays a key role in bone homeostasis as well as in energy balance and glucose metabolism, through endocrine and neuronal pathways. Leptin, a key adipokine signaling via both the VHT and the periphery affects positively energy and glucose metabolism whereas it has been reported to also affect bone.

ΔFosB is a naturally truncated form of FosB that opposes AP-1 transcriptional activity. ENO2 (enolase 2)-ΔFosB mice, in which the expression of ΔFosB is driven in bone, adipose tissues, and the VHT, have increased bone mass and energy expenditure, decreased fat mass and increased glucose tolerance and insulin sensitivity, despite lower levels of leptin. Moreover, viral-mediated expression of ΔFosB in the VHT, where leptin receptors are highly expressed, phenocopies all the bone, glucose and energy phenotypes of ENO2-ΔFosB mice. We have generated a ΔFosB transgenic model in leptin deficient ob/ob mice (ob/ob-ENO2-ΔFosB) to determine whether the bone and energy phenotypes were linked and whether leptin could be that link. Surprisingly, in this model the ΔFosB-mediated metabolic improvement was lost whereas the increased bone mass remained, despite the absence of leptin.

The present study was therefore performed to evaluate the contribution of leptin to ΔFosB-mediated regulation specifically in the VHT. To this end, C57BL/6 and ob/ob mice were stereotaxically injected in the VHT with adeno-associated virus encoding ΔFosB (AAV-ΔFosB) or GFP (AAV-GFP) as control.

AAV-ΔFosB injection in the VHT did not improve the severe obesity and adiposity of ob/ob mice. Whereas C57-AAV-ΔFosB mice had increased energy expenditure, as expected, ob/ob-AAV-ΔFosB mice failed to respond. Similarly, ob/ob-AAV-ΔFosB mice failed to correct the exacerbated glucose intolerance and insulin resistance together with hyperinsulinemia and hypertrophic pancreatic islets observed in ob/ob-AAV-GFP mice. In contrast, μCT analysis of distal femur revealed that the ob/ob-AAV-ΔFosB mice still showed the significant increases in BV/TV and trabecular numbers and a significant decrease in trabecular spacing compared to ob/ob-AAV-GFP.

Taken together, these results demonstrate that signaling from the VHT downstream of ΔFosB affects separately bone homeostasis and energy/glucose metabolism: expression of the AP1 antagonist ΔFosB in the VHT increases bone in a leptin-independent manner whereas its regulation of energy and glucose metabolism is leptin-dependent.

Disclosures: Kazusa Sato, None.

1121

DLK1 Exerts a Negative Feedback Regulation on The Osteocalcin-Insulin Loop. Basem Abdallah*[1], Nicholas Ditzel[2], Gerard Karsenty[3], Moustapha Kassem[2]. [1]Odense University Hospital, University of South Denmark, Denmark, [2]Odense University Hospital, Denmark, [3]Columbia University, USA

Several lines of evidence support the endocrine role of the skeleton in overall energy metabolism through the undercaboxylated form of osteocalcin (Glu-OCN) that acts on beta cells of the pancreas to increase their proliferation and the secretion of insulin. In turn insulin singals in osteoblasts favors in two-step pathways the decarboxylation and activation of osteocalcin. The nature of the negative regulatory signal of this loop remains unknown. DLK1/PREF-1/FA1 (Delta like 1/Pre-adipocyte factor-1/ fetal antigen-1), is a circulating factor produced by pancreatic β cells that co-localized with insulin in the secretory vesicles. Thus, we examined the role of DLK1 in insulin signaling in osteoblastic cells and its contribution to energy metabolism. Glu-OCN stimulated *Dlk1* gene expression by pancreatic islets. Insulin-induced osteoblast differentiation and osteocalcin expression were blocked in calvarial osteoblasts (OB) derived from osteoblast-specific *Dlk1* overexpressing mice (Col1-Dlk1) while it was significantly up-regulated in *Dlk1* null mice-derived OB (*Dlk1*^{-/-}OB). In addition, serum levels of Glu-OCN were reduced in Col1-Dlk1 mice by 43%, while it was elevated in *Dlk1*^{-/-}mice by 48% compared to WT controls. In vivo glucose metabolic studies revealed reduced insulin secretion and sensitivity in Col1-Dlk1 mice, while *Dlk1*^{-/-}mice showed increased insulin secretion and sensitivity. At the molecular levels, DLK1 antagonizes insulin signaling in OB by inhibiting the AKT phosphorylation of the forkhead transcription factor FoxO1 and also decreases osteocalcin expression. We propose that Glu-OCN-controlled production of DLK1 by pancreatic β cells acts as one negative feedback mechanism to counteract the stimulatory effects of insulin on osteoblast production of GLU-OCN, a mechanism preventing osteocalcin-induced hypoglycemia.

Disclosures: Basem Abdallah, None.

1122

Mitochondrial Etiology of Osteoporosis. Roman Eliseev*, Jerry Madukwe, Regis O'Keefe. University of Rochester, USA

Current views on the pathogenesis of osteoporosis are primarily centered on aging-associated hormone depletion. However, the loss of bone starts before the decline in hormones and is, in large part, due to increased oxidative stress in aging bone. Mitochondria are both a major source and major sensor of oxidative stress. Therefore, mitochondria are in the center of research efforts in various fields including cardiovascular pathology; however their role in the pathogenesis of bone diseases, such as osteoporosis, is unknown. Bone forming osteoblasts originate from mesenchymal stem cells (MSC). Undifferentiated MSCs primarily use glycolysis for energy production and switch to mitochondrial oxidative phosphorylation during osteogenic differentiation. Active mitochondria are required for MSC osteogenic differentiation. We hypothesized that mitochondrial function is disrupted in aged bone marrow (BM) MSCs leading to their decreased osteogenicity and bone loss. Our data indicate that aged mice showing signs of bone loss as measured with micro-CT and histology (Fig. 1), have decreased oxidative metabolism in bone tissue as measured with metabolomics mass spectroscopy, and decreased BM MSC mitochondrial function as measured with oxygen consumption rate assay.

Mitochondrial permeability transition (MPT) is the major mechanism of mitochondrial dysfunction in aging. The MPT is a non-selective mitochondrial pore regulated by cyclophilin D (CypD). CypD knock-out (KO) mouse is an established MPT loss-of-function model which shows protection from aging-associated mitochondrial dysfunction in various tissues. We have evaluated the effect of CypD KO on aged bone and BM MSCs. Our data indicate improved bone quality (Fig. 1) and biomechanical properties, and increased BM MSC mitochondrial function and osteogenic potential in aged CypD KO mice when compared to aged wild type mice.

Our study presents evidence of disruption of oxidative metabolism and mitochondrial function in aged bone, and suggests that the MPT plays a significant role in such a disruption. Protecting mitochondrial function in BM MSCs via inhibition of the MPT is, therefore, a promising new approach to improve aging bone.
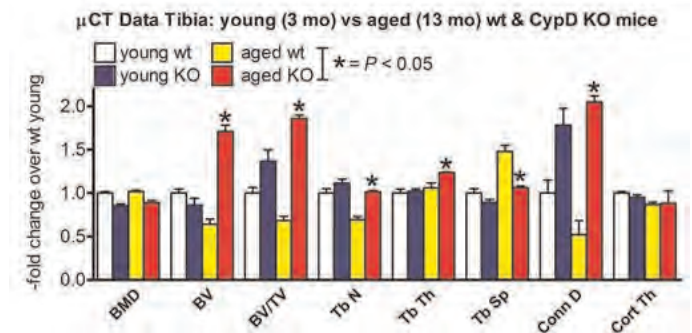

Figure 1

Disclosures: Roman Eliseev, None.

1123

Identification of Gremlin1 as A Catabolic Factor Induced by Mechanical Stress Loading in Articular Chondrocytes. Song Ho Chang*[1], Hiroshi Kobayashi[2], Keita Okada[1], Shurei Sugita[3], Tomotake Okuma[1], Sakae Tanaka[1], Taku Saito[4]. [1]The University of Tokyo, Japan, [2]The University of Tokyo Hospital, Japan, [3]Japan, [4]University of Tokyo, Graduate School of Medicine, Japan

Excessive mechanical stress loading on articular cartilage is one of the major factors of osteoarthritis (OA); however, the molecular mechanisms of cartilage degradation by such loading remain unclear. To know target genes in this process, we first examined gene expression profiles of articular chondrocytes under mechanical stress loading using a cell stretcher system, STB-140 (STREX). We applied a uni-axial cyclic cell stretch (0.5 Hz, 10% stretch) to primary articular chondrocytes from 5-day-old mouse knee joints for 30 min, and cultured them for an additional 24 h. Among 2,076 upregulated genes in microarray analysis, we focused on Gremlin1 (Grem1), which is one of the most highly expressed genes. Grem1 is known to be a secretory protein that regulates limb development, although its function in articular cartilage is unknown. Immunocytochemistry confirmed that Grem1 expression was increased in cytoplasm of articular chondrocytes by cyclic cell stretch. Grem1 mRNA expression also increased under the cyclic hydrostatic pressure (0.1 Hz, 20 MPa) to femoral heads obtained from 3-week-old mouse in our original programmable system. Immuno-fluorescence further revealed that Grem1 protein was enhanced on the cell surface of articular chondrocytes during OA development of the experimental mouse model. In primary culture of mouse articular chondrocytes, recombinant human (rh) Grem1 treatment induced the expressions of catabolic factors including *Mmp13* and *Adamts5*, and suppressed those of anabolic factors including *Col2a1*, *Aggrecan* and *Sox9*. In the organ culture of mouse femoral heads, rhGrem1 treatment increased aggrecan release into the medium in a dose-dependent manner. In the experimental mouse OA model, intraarticular injection of rhGrem1 exacerbated cartilage degradation. To further

examine the mechanism underlying the catabolic effect of Grem1, we focused on the NF-κB signal which was identified as a candidate by pathway analyses and gene ontology analyses. In the organ culture of femoral heads from conditional knockout mice of Rela, a representative transcription factor of the NF-κB signal, rhGrem1 did not induce the aggrecan release. We additionally confirmed that an IKK inhibitor (BMS-345541) treatment also diminished the increase of aggrecan release. In conclusion, Grem1 is induced by mechanical stress loading and exerts catabolic effects to articular cartilage through the NF-κB signal. Gremlin1 may provide a novel therapeutic target of OA.

Disclosures: Song Ho Chang, None.

1124

Cellular Tension Regulates TGFβ Receptor Spatial Organization and Induction of Chondrogenic Gene Expression. Joanna Rys*[1], Christopher DuFort[1], Michelle Baird[2], Michael Davidson[2], Tamara Alliston[1]. [1]University of California, San Francisco, USA, [2]National High Magnetic Field Laboratory & Department of Biological Science, Florida State University, USA

The extracellular microenvironment is rich in physical and biochemical cues that powerfully regulate cell behavior. Cells dynamically sense external physical cues through integrins and respond by modulating internal cellular tension and mechanotransduction pathways. Cell tension, generated in response to physical cues like substrate stiffness, calibrates the cellular response to biochemical signals through mechanisms that remain unclear. The growth factor TGFβ is a potent agonist of chondrocyte differentiation and is implicated in skeletal dysplasia and osteoarthritis. Previous work by our group demonstrated that substrate stiffness strongly enhances TGFβ-induced effector activity and chondrocyte gene expression (Allen 2012). To identify the molecular mechanisms by which physical cues modulate the cellular response to TGFβ, we are investigating the hypothesis that cellular tension regulates TGFβ receptor (TβRI and TβRII) spatial organization and function.

We utilized high-resolution quantitative imaging (total internal reflection fluorescence, TIRF) and novel fluorescently labeled TGFβ receptor subunits to visualize spatiotemporal regulation of signaling in mesenchymally-derived ATDC5 and NIH-3T3 cells. This innovative approach provided an unprecedented view of the cell surface and revealed that TβRII is excluded from focal adhesions, forming a peripheral ring that surrounds integrin α2 (Fig 1A-D). In contrast, both forms of TβRI (Alk1, Alk5) co-localize with integrin α2 at focal adhesion sites. This receptor organization pattern depends on cellular tension, as molecular inhibitors against both ROCK and myosin disrupt the exclusion of TβRII, and lead to co-localization with integrin α2 within 15 minutes of treatment (Fig 1E-H). To further elucidate the effect of cellular tension on TGFβ receptor dynamics, we created spatially resolved maps of individual receptors with single particle tracking photoactivation localization microscopy (sptPALM). These maps reveal distinct patterns of TβR localization with respect to focal adhesions. We utilized mass spectrometry coupled with co-immunoprecipitation to identify novel and specific protein-protein interactions with TβRI and TβRII, thus gaining insight into interactions that drive these mechanisms. This work elucidates the molecular mechanisms by which cells integrate physical and biochemical cues, insight that advances our understanding of development and disease progression in the skeleton and other tissues.
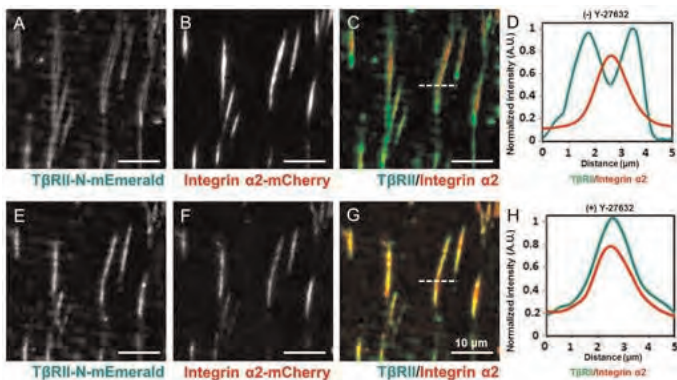

Figure 1

Disclosures: Joanna Rys, None.

1125

Muscle, Bone, and Nerve Differentially Interact to Achieve Trabecular and Cortical Bone Homeostasis. Steven Bain, Philippe Huber, Ronald Kwon, Laura Stoll, Ted Gross*. University of Washington, USA

Muscle atrophy precipitates rapid and frequently profound bone loss. The reduction in skeletal loading concomitant with sarcopenia has been presumed to be a primary mediator of bone catabolism. However, it is unclear whether diminished muscle function may modulate bone homeostasis independent of skeletal loading as in *vivo* models of muscle atrophy are invariably coupled with decreased skeletal loading. To address this question, we implemented three *in vivo* models of neuromuscular dysfunction intended to demonstrate differential gait dysfunction and muscle atrophy. We used gait kinetics and kinematics to quantify tibia mid-shaft normal strains and serial microCT imaging to quantify muscle, tibia trabecular and cortical bone atrophy in female C57 mice (16wk). Mice were randomly assigned to receive transient paralysis of the right calf (C) or quadriceps (Q) muscle groups (2U/100g Botulinum Toxin A, BTxA) or peripheral nerve injury (PNI) of the right sciatic nerve via a plastic sleeve (n=8/grp). Mice were assessed on d0, d5 and d12, with all measures normalized to d0 data. Gait-induced normal strains were more diminished by Q than C paralysis at d5 (-53.0 $\pm$ 4.9% vs -35.4 $\pm$ 3.1%; p=0.01), but were equivalently diminished by d12 (C: -37.0 $\pm$ 3.8%; Q: -40.6 $\pm$ 8.1%). PNI did not alter normal strains vs d0. By d12, calf muscle volume was diminished more by C (-32.2 $\pm$ 0.9%; p<0.01) than Q paralysis (-18.0 $\pm$ 2.4%), but not altered by PNI. C and Q paralysis significantly, but equivalently, degraded trabecular BV/TV at d5 (C:-21.4 $\pm$ 5.2%; Q:-33.8 $\pm$ 3.0%) and d12 (C:-69.1 $\pm$ 3.6%, Q:-72.0 $\pm$ 3.2%), while PNI induced less, but significant BV/TV loss at d12 (-26.5 $\pm$ 4.1%). C (8.4 $\pm$ 1.0%) and Q paralysis (11.7 $\pm$ 2.0%) induced significant (but equivalent) endocortical resorption at d12, while PNI did not. Diminished normal strains and decreased trabecular BV/TV were minimally correlated (r^2<0.19), but the relation between diminished normal strains and endocortical expansion was significant (r^2=0.62, p<0.01). In sum, these data suggest that cortical and trabecular bone are differentially regulated by muscle, bone and nerve interactions. For cortical homeostasis, muscle function was a potent modulator via gait-induced mechanical stimuli. However, the significant trabecular loss following PNI and the poor correlation between decreased gait-induced strains and BV/TV, suggest that neuronal pathways serve an essential role in trabecular homeostasis.

Disclosures: Ted Gross, None.

1126

The nuclear envelope mechanosome regulates mechanical activation of βcatenin and its nuclear transport. Gunes Uzer*[1], Buer Sen[2], William Thompson[1], Zhihui Xie[3], Sherwin Yen[3], Guniz Bas[3], Maya Styner[4], Clinton Rubin[5], Janet Rubin[4]. [1]University of North Carolina, USA, [2]University of North Carolina At Chapel Hill, USA, [3]University of North Carolina, USA, [4]University of North Carolina, Chapel Hill, School of Medicine, USA, [5]State University of New York at Stony Brook, USA

Mechanical signals generated during functional loading promote osteoblastogenesis at load bearing sites and this mechanically-induced MSC phenotype is supported by nuclear shuttling of βcatenin to nucleus, a process that is poorly understood. Mimicking exercise, high magnitude strain (HMS, ~2%) augments pro-osteogenic and anti-adipogenic programs in MSC through proximal activation of FAK/mTORC2/Akt that regulates the active βcatenin pool. Low intensity vibration (LIV, 0.7G x 90Hz) induces a phenotypic response similar to HMS inducing FAK and Akt phosphorylation and preventing βcatenin degradation. However, application of LIV generates virtually no substrate strain (0.001%), which suggests that cellular mechanosensing and signal initiation must differ from that of HMS, even though both induce nuclear βcatenin translocation. We found that disruption of the nuclear envelope LINC complex (Linker of Nucleoskeleton and Cytoskeleton), through delivery of DNKASH or siSUN, prevented LIV but not HMS induction of pFAK and pAkt (p<0.01) supporting the idea that mechanosensing of LIV and HMS is dissimilar. Further, inhibition of FAK or FAK's co-regulator Fyn, both essential for strain-induced Akt recruitment focal adhesions (FAs), did not interfere with Akt activation by LIV (p<0.05). As Akt is required for the phenotypic LIV response, and its activation required LINC, we hypothesized that LIV might activate Akt at the nuclear envelope to facilitate inward βcatenin transport. First, immunoprecipitation (IP) of the FA protein Vinculin revealed that LIV-induced pAkt was not found in the FAs. We next found that IP of Nesprin, a LINC complex protein in the nuclear envelope showed a strong association with pAkt and βcatenin. Interestingly, βcatenin-Nesprin association decreased after LIV treatment followed by an increase in nuclear βcatenin, implicating Nesprin, and thus the LINC complex, in enabling the distal mechanical event of βcatenin nuclear entry. Indeed, disrupting LINC function (DNKASH, siSUN) prevented *both* LIV and HMS-induced nuclear accumulation of βcatenin. In summary, our data show that while proximal mechanical signals differ – the FAK and Akt response to substrate strain requires the substrate/membrane interface while response to LIV requires the cytoskeletal/nuclear interface – their distal signaling converges at the nuclear envelope where nuclear-cytoskeletal coupling is required for mechanically induced βcatenin transport into the nucleus.

Disclosures: Gunes Uzer, None.

1127

Altered force sensing and cell-cell adhesion by mutant ACVR1/ALK2 FOP progenitor cells – implications for heterotopic ossification. Julia Haupt*, Brian Cosgrove, Claire McLeod, Andria Culbert, Robert L. Mauck, Eileen M. Shore. University of Pennsylvania, USA

In the rare genetic disease fibrodysplasia ossificans progressiva (FOP), progenitor cells are misregulated to differentiate to heterotopic bone in connective tissues. Rigidity of the microenvironment is a key modulator of lineage specification and

sufficient to direct cell fates. Soft substrates induce mesenchymal progenitors towards neuro-/adipogenic lineages while stiff substrates promote chondro-/osteogenesis. Pathologic stiffening of the microenvironment occurs in fibrotic diseases when damaged tissue aberrantly acquires increased rigidity during wound healing. Injury-induced early-to-intermediate stage FOP lesions similarly exhibit excessive fibroproliferation. Gain-of-function mutations in the BMP type I receptor ACVR1/ALK2 cause FOP, with R206H mutation most prevalent. Since BMP signaling regulates and is regulated by cell tensional force (with low signaling activity on soft vs. high activity on stiff substrates), altered ACVR1 signaling could influence mechanotransduction pathways. We hypothesized that the FOP mutation alters mechanical force sensing in progenitor cells, altering the perception of mechanical cues and lowering the threshold for bone formation. We used immortalized mouse embryonic fibroblasts (iMEFs) from an ACVR1^{R206H} knock-in embryo and WT littermate on varied matrix elasticity (soft: 5kPa; moderate: 15kPa, stiff: 55kPa) and analyzed morphological parameters (cell size, aspect ratio (AR), circularity, solidity) at low cell density. WT cells responded to increasing stiffness as expected with increased cell size and AR, and decreased circularity and solidity. However, FOP iMEF response to soft substrates was similar to WT on stiff substrates, and FOP cells were less responsive to substrate rigidity. Increased cell polarity and membrane extensions in FOP iMEFs correlated with enhanced migration and proliferation. FOP iMEFs also showed a loss of contact inhibition, reduced cell-cell contacts with failure in adherens junction formation, and β-catenin loss at cell membranes. Increased β-catenin degradation in FOP iMEFs was facilitated by overexpression of the destruction complex component Axin2. These data support that the combination of increased BMP signaling, misinterpretation of soft substrates, and overall reduced sensitivity to mechanical stimuli in FOP cells lowers their threshold for commitment to chondro-/osteogenic lineages, resulting in an aberrant tissue repair response that leads to ectopic bone formation.

Disclosures: Julia Haupt, None.

1128

Inner ear vestibular signals contribute to bone loss through the sympathetic nervous system. <u>Guillaume Vignaux</u>*, <u>Jean De La Croix Ndong</u>, <u>Florent Elefteriou</u>. Vanderbilt University, USA

Elderly is a population highly affected by bone loss and with high risk of fracture. The vestibular system is degenerating with age and is known to influence autonomic outflow. Since sympathetic nerve activation induces bone loss, we hypothesized that microgravity-induced bone loss in space may be, at least in part, caused by disturbance in vestibular signals. To address this hypothesis, we used a mouse model of vestibular lesion (VBX).

VBX animals were subjected to a bilateral transtympanic injection of sodium arsenilate whereas Sham animals were injected with PBS. One hundred and twenty 2-month old mice were divided in 12 groups: 1) WT groups±VBX±propranolol 2) global beta2 adrenergic receptor (b2AR) deficient groups±VBX 3) osteoblast specific b2AR deficient groups±VBX.

Vestibular syndrome was evaluated 3, 15 and 30 days after lesions. One month after lesions, micro-CT and histomorphometry analyses were performed on the femoral epiphysis. UCP1 gene expression in the brown adipose tissue and serum TNFα were respectively measured as a marker of sympathetic nervous system (SNS) outflow and systemic inflammation.

During the entire month of study, all VBX animals expressed a significant vestibular syndrome. Micro-CT analyses revealed a significant reduction in trabecular Bone Volume/Tissue Volume in the WT VBX group versus WT Sham group. This phenotype was accompanied with both a significant decrease in osteoblast surface/bone surface and a significant increase in osteoclast surface/bone surface ratio. Additionally, UCP1 expression was increased 2-times after VBX whereas serum TNFα levels were not affected, suggesting an increase in SNS outflow and absence of chronic inflammation. Pharmacological treatment with propranolol (a non-selective beta blocker) or b2AR deficiency (global and specific) completely blunted the vestibular-induced bone loss and changes in bone microarchitecture and cellular parameters.

We conclude that vestibular signals, transmitted via sympathetic nerves, modulate bone remodeling, and that vestibular dysfunction may contribute to bone loss occurring with aging, along with the decrease in mobility and hormones changes. These results may also shed a new light on patients with vestibular disease.

Disclosures: Guillaume Vignaux, None.

1129

Alternative NF-κB Controls Mitochondrial Biogenesis Independent of Osteoclast Differentiation. <u>Rong Zeng</u>*[1], <u>Deborah Novack</u>[2], <u>Chang Yang</u>[3]. [1]Washington University in St. Louis, USA, [2]Washington University in St. Louis School of Medicine, USA, [3]Washington University in St Louis School of Medicine, USA

The Osteoclast's (OC) role to resorb bone matrix is governed by many signaling pathways that control both differentiation and resorption, including the alternative NF-kB. Mitochondria are extremely abundant in OCs and likely provide ATP to ruffled membrane vATPases. During osteoclastogenesis (OCg) *in vitro*, mitochondria DNA copy number (mtCN) (a surrogate for mitochondria content) rises, but data are conflicting on whether it is obligate for differentiation. In this study we used mutations in the alternative NF-kB pathway proteins RelB and NIK to dissect the

relationship between mitochondrial biogenesis (MB) and OCg. When OC precursors from relb-/-, nik-/-, and CatK.NT3 (constitutively active NIK transgene driven by the Cathepsin K promoter) mice were cultured under osteoclastogenic conditions (M-CSF+RANKL), we found mtCN to be reduced in relb-/- and nik-/-, and increased in CatK.NT3 cultures. Likewise, expression of oxidative phosphorylation subunits, assayed by qRT-PCR and immunoblotting, were significantly blunted in relb-/- and nik-/- but increased in CatK.NT3 cells. Importantly, there were parallel functional changes in basal and maximal oxygen consumption rates. By transmission EM, both relB-/- and CatK.NT3 OCs have abnormal mitochondrial morphology. Cells lacking classical pathway subunit p65 did not recapitulate these differences, indicating the distinct role of alternative NF-kB pathway for MB. To deduce the mechanism for MB defects, we examined expression of several genes known to control MB. PGC-1β (but not PGC-1α, PRC, or PPARγ) was significantly decreased in relb-/- and nik-/- cells during OCg, with ChIP data showing PGC-1β as a direct RelB transcriptional target. Because PGC-1β has been suggested to positively regulate both MB and OCg in OCs, we retrovirally overexpressed PGC-1β in relb-/- cells and evaluated both processes. Surprisingly, PGC-1β had no effect on differentiation or NFATc1 expression, and only partially restored MB. To investigate whether a lack of differentiation prevented MB, we overexpressed NFATc1 in relB-/- precursors, which fully restored OCg but had no effect on MB. Bone resorption was improved, but did not reach levels in similarly transduced WT cultures, indicating resorptive defects independent of differentiation. We conclude that one distinct arm of alternative NF-kB controls OCg (via NFATc1) while the other controls MB (via PGC-1β and other targets), acting in concert to contribute to OC's role in bone resorption.

Disclosures: Rong Zeng, None.

1130

The actin-binding protein Cofilin and its interaction with cortactin are required for podosome patterning in osteoclasts and bone resorption in vivo and in vitro. <u>Detina Zalli</u>*[1], <u>Kenichi Nagano</u>[2], <u>Lynn Neff</u>[3], <u>Ken-ichi Takeyama</u>[2], <u>Walter Witke</u>[4], <u>Francesca Gori</u>[5], <u>Roland Baron</u>[6]. [1]USA, [2]Harvard School of Dental Medicine, USA, [3] Harvard School of Dental Medicine 188 Longwood Ave Boston MA 02115, USA, [4]Prof. Dr. Walter Witke Institute of Genetics University Bonn Karlrobert Kreiten Str. 13 D - 53115 Bonn/Germany, Germany, [5]Harvard School of Dental Medicine, Massachusetts General Hospital, USA, [6]Harvard School of Medicine & of Dental Medicine, USA

Osteoclast (OC) adhesion to and migration along bone surfaces and thereby bone resorption requires expansion of specific F-actin adhesion structures, the podosomes, into a ring and their dense packing into the sealing zone, to define and seal off the resorption compartment. We and others have shown that the OC-specific transition from podosome clusters to belt is dependent on microtubules (MTs). Proteins enriched at MT +ends interact with proteins in podosomes, allowing the physical interaction of podosomes and MTs to control podosome behavior, with the interaction of cortactin (CTTN) and MTs EB1 playing a key a role in belt formation. MT +ends regulate CTTN phosphorylation by Src and CTTN phosphorylation and acetylation are inversely related. CTTN-deleted OCs are accordingly defective in sealing-zone formation and bone resorption. In the present study we explored further the link between MTs, podosomes and bone resorption by deleting cofilin, an actin-binding protein highly expressed in OCs, testing the hypothesis that it may act downstream of the MT-EB1-CTTN axis.First, we deleted cofilin in OCs in mice by crossing Ctsk-Cre mice with cofilin (Cof)$^{fl/fl}$ mice. Ctsk-Cre:Cof$^{fl/fl}$ mice displayed a markedly increased trabecular BV with normal BFR, indicating decreased resorption. Cofilin-depleted OCs showed impaired cell migration in vitro. In addition, Cof-depleted OCs presented defective targeting of microtubules to, and patterning of, the podosome belt. MT stability was decreased, with low levels of acetylated tubulin. Our results show that dephosphorylation of cofilin is required to stabilize MTs and allow podosome belt formation. Conversely, MT disruption leads to increased cofilin phosphorylation at Ser3. We then investigated whether cofilin interacts with CTTN in podosomes. We found that cofilin interacts with CTTN, and that phosphorylation of either cofilin or CTTN disrupts this interaction. In contrast, acetylated CTTN, induced by treatment of OCs with the HDAC inhibitor TSA, led to increased interaction with cofilin. Moreover, the localization of cofilin was altered in CTTN-null cells and conversely, CTTN localization was altered in cofilin-null OCs. These findings suggest that in OCs, the patterning of podosomes into a sealing zone involves the interaction between cofilin and CTTN downstream of the MTs plus-end protein EB1 and that this interaction is critical for the functional organization of OCs.

Disclosures: Detina Zalli, None.

1131

A Role for the Proprotein Convertase Furin in the Regulation of Osteoclastic Bone Resorption. <u>Benjamin Ng</u>*[1], <u>Dian Teguh</u>[2], <u>Nathan Pavlos</u>[3], <u>Jennifer Tickner</u>[4], <u>Jiake Xu</u>[3]. [1]The University of Western Australia, Australia, [2]Research personnel, Australia, [3]University of Western Australia, Australia, [4]University of Western Australia, Australia

Osteoporosis is a devastating disease, leading to bone fragility and fracture which has significant physical, psychosocial, and financial consequences. Increased

osteoclast (OC) formation and bone resorption is a major pathological hallmark of osteoporosis. Using comparative microarray analysis between OCs and macrophage-progenitors, we recently uncovered a cluster of genes encoding nine members of a convertase protein family that regulate proteolytic maturation of proproteins. Among these, furin, a regulator of the proteo-cleavage of the V-ATPase proton pump subunit Ac45, was identified as the major RANKL-responsive isoform expressed in OCs. To address the physiological importance of furin in OC-mediated bone resorption, we generated conditional knockout mice specifically lacking furin in OCs (Furin$^{\Delta OC}$). MicroCT analysis of 12 week old female mice demonstrated a significant increase in trabecular bone volume in the femora of Furin$^{\Delta OC}$ mice compared to floxed controls (by 62.0 $\pm$ 28.0%; p=0.003). Interestingly, histomorphometric analysis revealed that specific deletion of furin did not significantly alter the number or surface area of OCs in vivo. Consistently, OC formation and fusion was unaffected by furin deletion in vitro. By comparison, OC bone resorptive function was significantly impaired in OCs lacking furin as determined by reduced CTX (by 31.8 $\pm$ 11.5%; p=0.04) and reduced bone resorption pit depth (by 51.7 $\pm$ 7.2%; p=0.002). Consistent with the role of furin as the primary processing enzyme of Ac45, the expression levels of mature Ac45 protein were reduced in OCs from Furin$^{\Delta OC}$ mice compared to control littermates. In line with reduced Ac45 maturation, intracellular acidification was significantly reduced (by 20.3 $\pm$ 8.4%; p=0.01) in Furin$^{\Delta OC}$ OCs. Collectively, these data imply that furin functions as a positive regulator of osteoclastic bone resorption during bone homeostasis, in part through the proteolytic processing of the V-ATPase accessory subunit Ac45. Furin may therefore serve as a potential new therapeutic target for the treatment of OC-mediated bone diseases.

Disclosures: Benjamin Ng, None.

1132

EBI2 guides osteoclast precursors to endosteal niches and regulates bone mass homeostasis. Erin Nevius*[1], Mark Horowitz[2], Masaru Ishii[3], Joao Pereira[2]. [1]Yale School of Medicine, USA, [2]Yale University School of Medicine, USA, [3]Graduate School of Medicine & Frontier Biosciences, Osaka University, Japan

Endosteal niches attract and regulate the activity of hematopoietic precursors, macrophages, osteoblasts, and osteoclasts. Osteoblasts and osteoclasts are essential regulators of skeletal integrity and are exclusively positioned in contact with endosteal surfaces. The purpose of this study was to characterize the mechanisms guiding these cells towards endosteal surfaces. The factors and mechanisms controlling this process are largely unknown. Here we show that the oxysterol 7α,25-dihydroxycholesterol (OHC) and its Gαi protein coupled receptor EBI2, direct monocyte/osteoclast precursor migration towards endosteal niches, promote cell fusion, and regulate osteoclast differentiation. We show that the dynamic motile behavior of osteoclast precursors is restricted in the absence of EBI2-signaling, and this defect directly reduces osteoclast differentiation. Using a novel two-photon microscopy procedure to examine and quantify the 3-dimensional network of bone-associated osteoclasts, we demonstrate that EBI2 and cholesterol 25 dihydroxylase (CH25H) deficient mice have reduced osteoclast number and size. Consequently, EBI2-signaling deficient mice have increased bone mass and are protected from age-, and estrogen deficiency-induced osteoporosis. Using real-time intravital microscopy we visualized single monocytic cells with osteoclast precursor properties being attracted to and fusing with preformed bone-lining osteoclasts. These data suggest that osteoclast precursors migrate in a directed manner towards bone-lining osteoclasts. Osteoclast precursors, osteoclasts and osteoblasts express oxysterol-synthesizing enzymes and secrete 7α,25-OHC, indicating that EBI2 ligands are secreted in bone-proximal niches. Therefore, we assessed the role of EBI2 in guiding osteoclast precursors towards bone surfaces and promoting osteoclast differentiation in vivo. We show that EBI2 signaling is sufficient to direct monocyte/osteoclast precursors to endosteal surfaces and potentiates osteoclast differentiation in vivo. These studies identify a novel mechanism for bone mass homeostasis that involves ligand- directed cell migration towards endosteal niches. Therapeutic strategies targeting oxysterols and EBI2 signaling may have considerable clinical potential for the treatment of skeletal disorders, including menopause-induced bone loss.

Disclosures: Erin Nevius, None.

1133

Gain of function of Jagged1 stimulates osteoclastogenesis leading to low bone volume. Yangjin Bae*[1], Hanqiu Zheng[2], Yuqing Chen[3], Terry Bertin[3], Yibin Kang[4], Brendan Lee[1]. [1]Baylor College of Medicine, USA, [2]Department of Molecular Biology, Princeton University, USA, [3]1Departments of Molecular & Human Genetics, Baylor College of Medicine, USA, [4]Princeton University, USA

The Notch pathway is highly conserved signaling system involving cell fate determination, proliferation, differentiation, and tissue maintenance and/or renewal of stem cells in adults. Activation of Notch signaling requires a direct cell- cell interaction of Notch receptors and ligands. The importance of Notch signaling has been shown in human diseases that are caused by mutations in Notch receptors and ligands. Among these, mutations in the Notch ligand Jagged 1 (JAG1) results in Alagille syndrome (AGS). AGS patients can have skeletal defects including hemivertebrae and frequent fractures. Furthermore, genome wide association

(GWA) studies have demonstrated an association between bone mineral density (BMD) and JAG1 polymorphisms. Hence, JAG1 is likely an essential Notch ligand for proper skeletal patterning and for postnatal skeletal homeostasis. Others have shown that JAG1 is highly induced ligand during fracture repair, suggesting the potential target to promote bone formation. Here, to understand the *in vivo* pathological consequence of gain of JAG1 function in bone, we generated *jag1* transgenic mouse driven by Col1a1 2.3kb promoter (*Col1a1-Jag1*). *Col1a1-Jag1* mice exhibit low bone mass. Interestingly, excessively trabecularized cortical bone was also observed suggesting the increased bone remodeling in cortex due to ectopic expression of *Jag1*. The osteoporotic phenotype was associated with increased osteoclast numbers that was confirmed with *in vitro* co-culture studies using transgenic osteoblasts. *In vivo*, mature osteoclast markers, *Trap* and *Ctsk*, were up-regulated. Overall, *Jag1* transgenic mouse share the osteoporotic phenotype of gain of function Notch1 in osteoblast. Our preliminary study of *Col1a1-Jag1* suggests that Jag1 plays an important role in bone homeostasis and remodeling.

Disclosures: Yangjin Bae, None.

1134

ADAMTS 18 is important regulator of post-natal skeletal development and bone remodeling. Sardar Uddin*[1], Zong Dong Li[2], Yi-Xian Qin[3], Chuanju Liu[4]. [1]New York University Medical Center, USA, [2]Stony Brook University, USA, [3]State University of New York at Stony Brook, USA, [4]New York University, USA

ADAMTS 18 (a distintegrin and metalloproteinase with a thrombospondin type motif, AD18) is a member of a secreted Zn-metalloproteinase ADAMTS family. ADAMTS 18 was identified as bone mass determination factor and associated with hip bone fractures in major human ethnic groups in a genome-wide association study (GWAS). The purpose of this project is to *determine the role of ADAMTS 18 in skeletal development and remodeling.*

The growth and weight curve for AD18 $^{-/-}$ mice were recorded for 3 months and injected with calcein and alirzain red for histomophometry analysis. Mice were euthanized at age of 14 weeks, trabecular bone at proximal tibia was analyzed using microCT and mechanical properties were accessed with four-point bending at fermal mid-diaphysis. Microarray studies were conducted and confirmed using real time PCR. The over expression and miRNA studies are being conducted to further delineate the underlying mechanism of AD18 in bone remodeling.

The phenotypic analysis of AD18$^{-/-}$ confirmed smaller structure of KO mice relative to litter mates at 14 weeks but the difference was not apparent at 2 weeks suggest that AD18 plays important role in post natal skeletal development. The high expression of AD18 in metaphysis and diaphysis with little or no expression in physis and fetal cartilage further indicates that AD18 plays an important role in bone remodeling rather with limited or no role in bone modeling.

AD18 $^{-/-}$ mice exhibit smaller tibia and growth plates with significantly compromised trabecular bone quality and quantity. Cortical bone does not show significant difference but mechanical testing show significant reduction in bone strength indicating potential disorientation of collagen fibers in bone matrix. AD18 expression and μCTdata collective suggest that AD 18 is important regulator of bone matrix classification as indicated by GWAS study.

AD18 deletion significantly inhibited genes associated with osteogenesis and activated genes associated osteoclastogensis. Over expression of AD18 in C2C12 confirmed increased Ssh1, Prrx 1, Runx 2 and Osterix and inhibited osteoclastogensis associated genes Lair 1 and Siglec-15 in RANK ligand treated RAW cells (figure 1).

In summary, the data from current study strongly implies that AD18 is an important and novel regulator of osteoclastogensis and osteogensis in bone remodeling with potential therapeutic implications for treatment of post natal dwarfish, osteopenia and osteoporosis.
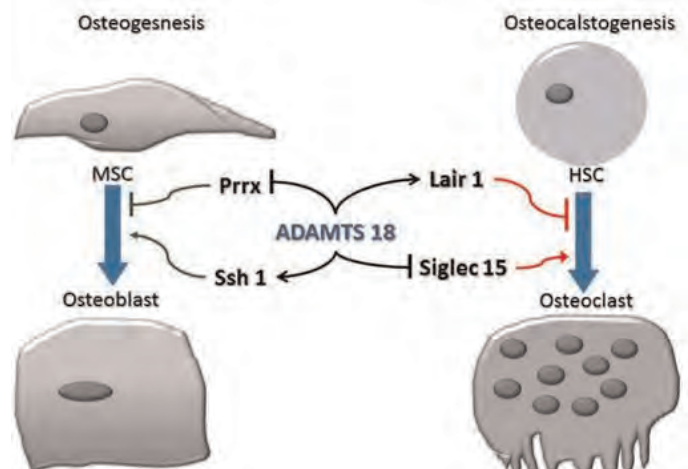

Figure 1: AD18 plays an important role in regulation of bone remodeling by inhibiting osteoclastogen

Disclosures: Sardar Uddin, None.

1135

Assessment and Intervention Thresholds for FRAX probabilities in the UK – An Evaluation of adjusting Thresholds in Older Postmenopausal Women.

Eugene McCloskey*[1], Helena Johansson[2], Anders Oden[3], Nicholas Harvey[4], Juliet Compston[5], John Kanis[6]. [1]University of Sheffield, United Kingdom, [2]Centre for Metabolic Bone Diseases, University of Sheffield Medical School, Sweden, [3]Consulting Statistician, Sweden, [4]MRC Lifecourse Epidemiology Unit, University of Southampton, United Kingdom, [5]University of Cambridge School of Clinical Medicine, United Kingdom, [6]University of Sheffield, Belgium

In postmenopausal women, the UK National Osteoporosis Guideline Group (NOGG) intervention threshold is set at the 10-year probability of major osteoporotic fracture (OP) in a woman with a prior fracture, and reaches 33% at 85 years. This high threshold is avoided in many older women as the guidance also advocates treatment in those with a prior fracture without the need for DXA, especially at older ages (e.g. >70-75 years). However, women without prior fracture are required to achieve the intervention threshold, with or without a BMD measurement. We wished to compare the impact of current assessment and intervention thresholds to that of an alternative strategy at older ages.

Using a simulated population of over 56,000 women aged 50-90 years in the UK, with a distribution of risk factors similar to that in FRAX derivation cohorts and age distribution matched to the current UK population, the current NOGG strategy was compared to a strategy whereby the intervention and assessment thresholds were identical to those in the current NOGG strategy up until the age of 70 years (major OP probability intervention threshold 20%), but thereafter remained constant with increasing age.

Under current guidance, 38% of women aged 50-90 years would be recommended for therapy, comprising 30.1% with prior fracture, 1.4% with high risk in the absence of fracture and 6.4% at high risk after DXA scanning. Under the alternative strategy, the proportion recommended for therapy would only increase slightly (40.8%) but the impact at older ages was more marked. For example, in women aged 80-84 years (see Table), only a small proportion (9%) were eligible for therapy in the absence of fracture and the average probabilities of major osteoporotic fracture and particularly hip fracture were substantially higher in such patients than those qualifying on the basis of prior fracture. Under the alternative strategy, more elderly women with non-fracture risk factors would qualify for treatment (21%) and fewer would need a DXA scan. The average probabilities of major osteoporotic fracture and hip fracture are similar in all women indicated for therapy, with or without a fracture.

We conclude that the alternative threshold equilibrates fracture risk, particularly hip fracture risk, across treatment groups in older women with improved use of DXA resources.

Table 1. Comparison of the current and alternative strategies in women aged 80-84 years. The numbers in parentheses represent the average 10 year probability of major osteoporotic or hip fracture, respectively.

Strategy	Prior fracture (%)	High risk (%)	DXA referred (%)	Treat post DXA (%)	Total treated (%)
Current	39 (27,13)	3 (35, 26)	19 (22, 12)	6 (33, 22)	47 (29, 15)
Alternative	39 (27, 13)	14 (26, 16)	11 (18, 9)	7 (22, 12)	59 (27, 13)

Table 1

Disclosures: Eugene McCloskey, None.

1136

Bone Mineral Density (BMD) at Multiple Sites and Risk of Multiple Types of Fracture: The Osteoporotic Fractures in Men (MrOS) Study.

Didier Chalhoub*[1], Eric Orwoll[2], Peggy Cawthon[3], Kristine Ensrud[4], Douglas Bauer[5], Steven Cummings[6], Jane Cauley[7]. [1]University of Pittsburgh, USA, [2]Oregon Health & Science University, USA, [3]California Pacific Medical Center Research Institute, USA, [4]University of Minnesota & Minneapolis VA Health Care System, USA, [5]University of California, San Francisco, USA, [6]San Francisco Coordinating Center, USA, [7]University of Pittsburgh Graduate School of Public Health, USA

Although many studies have examined the association between low bone mineral density (BMD) and fracture risk in older men, none have simultaneously studied the relationship between multiple sites of BMD and risk of multiple types of fractures or compared areal BMD (aBMD) with volumetric BMD (vBMD).

Using data from the Osteoporotic Fractures in Men (MrOS) study, we studied the association between multiple sites of aBMD and vBMD measurements, and risk of various fracture types during an average of 10.2 years of follow up. Hip and spine aBMD and vBMD were measured by dual-energy X-ray absorptiometry (DXA) and quantitative computed tomography (QCT), respectively. Information on fractures was

obtained through our postcard follow-up system. Postcards are mailed every 4 months; >97% of these contacts are complete. All fractures were confirmed by radiographic report. Risk of clinical fractures was assessed at the hip, wrist, spine, arm, rib/chest/sternum, pelvis/tailbone, leg, hand/finger, skull/face, shoulder, ankle/foot/toe, and any non-spine fracture. After excluding participants with pathological fractures, Cox proportional-hazards modeling was used to assess the risk of fracture in 5990 older men per one standard deviation decrease in BMD; aBMD was available in 5989 and vBMD, in 3554 men. Except for a higher proportion of minorities, the characteristics of men in the vBMD subset were similar to the overall population of men.

Lower femoral neck aBMD and trabecular vBMD were associated with an increased risk of fracture at the hip, wrist, spine, arm, rib/chest/sternum, pelvis/tailbone, shoulder, ankle/foot/toe, and any non-spine fracture with HRs ranging between 1.12 and 2.79. There was no association between aBMD or vBMD with skull/face fractures (figure 1 and 2). In contrast, there was little association between femoral neck cortical vBMD and fracture (figure 3). Similar findings were found between lumbar spine aBMD and trabecular vBMD and fracture (data not shown).

In older men, the risk of various types of fractures is higher with lower areal and volumetric BMD. The stronger associations observed for trabecular vBMD than cortical vBMD may reflect the higher rate of bone turnover in the trabecular compartment.
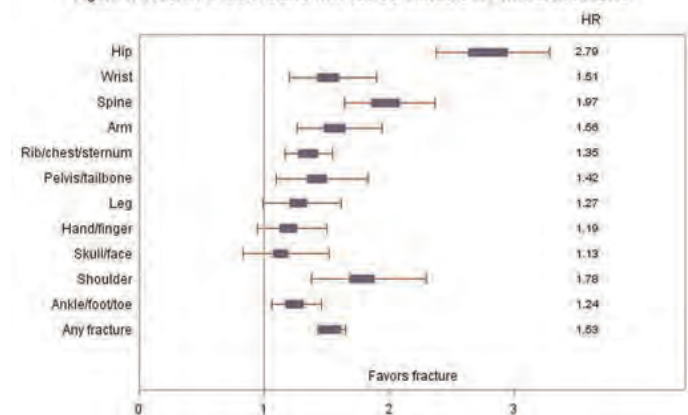

Figure 1. Fracture risk associated with one SD decrease in femoral neck aBMD
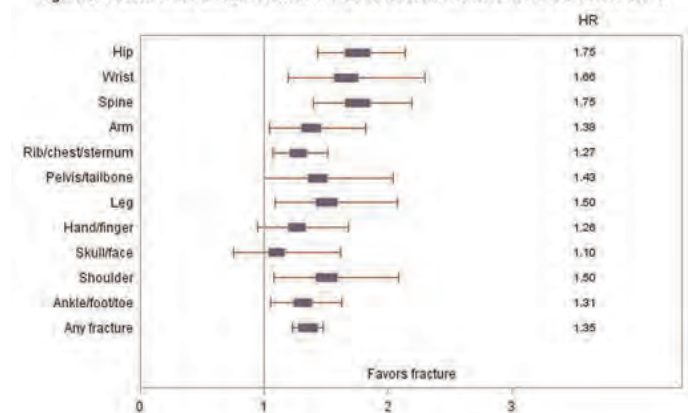

Figure 2. Fracture risk associated with one SD decrease in femoral neck trabecular vBMD

Figure 3. Fracture risk associated with one SD decrease in femoral neck cortical vBMD
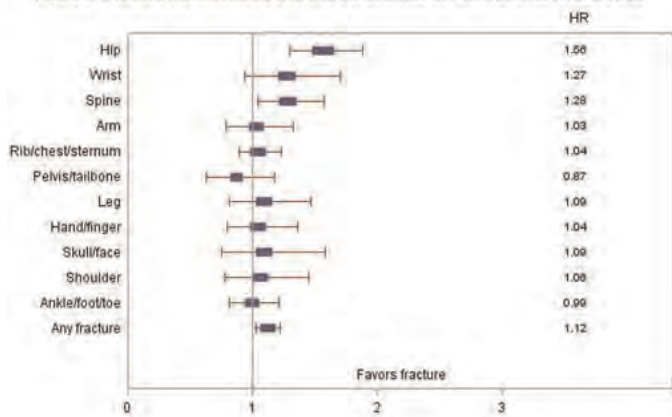
Disclosures: Didier Chalhoub, None.

1137

Risk and Cumulative Incidence of Subsequent Fractures Following an Initial Fracture: a Cohort Study with a Quarter Century Follow-up. Suzanne Morin*[1], Lin Yan[2], Lisa Lix[2], Sumit Majumdar[3], William Leslie[2]. [1]McGill University, Canada, [2]University of Manitoba, Canada, [3]University of Alberta, Canada

Background: Population-based data on long-term risk of subsequent fractures following an initial fracture are sparse.

Objective: To determine sex- and age-specific relative risk and cumulative incidence of hip (HF) and major osteoporotic fractures (MOF; hip, wrist, spine, humerus) over a 23-year period following any type of initial fracture.

Methods: Using comprehensive health care databases from Manitoba, Canada, we performed a retrospective matched cohort study of community-dwelling men and women aged 50 years and older with incident fracture 1986-2006 (n=62 491 fracture cases) with age and sex-matched controls (n=179 562). Annual crude and relative fracture rates to March 31st 2012 were determined according to initial fracture site and trauma intensity. Hazard ratios (HR) for subsequent fracture were estimated using relative survival analysis. Cumulative incidence rates for subsequent fractures were estimated after accounting for competing mortality. We performed a subgroup analysis in residents in long-term care (LTC) at the time of initial fracture (5600 cases and 14 180 controls, not matched on LTC status).

Results: We identified 11 694 wrist, 10 238 hip, 6211 humerus, 3793 spine, 28 718 other and 1837 traumatic fracture cases. The annual crude rates of subsequent of MOF or HF were highest during the first year, and following an initial fracture at the hip, humerus and spine in both men and women. The increased relative risk for subsequent MOF and HF was highest following initial humerus (HR 2.4; 95%CI: 2.2-2.5 and HR 2.2; 95% CI:2.0-2.4), spine (HR 2.4; 95% CI:2.2-2.7 and HR 2.1; 95% CI: 1.8-2.4) and hip fractures (HR 1.6; 95% CI:1.5-1.7 and HR 1.6; 95% CI 1.4 -1.7) and lowest following traumatic fractures. HRs were consistently higher in men than women, and in the younger age-groups (Table). Accounting for risk of competing mortality, the cumulative incidence of subsequent MOF and HF to 23 years was higher in fracture cases versus controls except in the oldest age category where this relationship reversed and was higher in controls than in cases (Figure). Controls also had a higher cumulative incidence of subsequent fracture than fracture cases who were LTC residents.

Conclusions: Long-term subsequent fracture risk following any type of initial fracture is considerable, particularly in the year post-fracture, though the risk is mitigated by competing mortality in the elderly. This suggests early interventions post-fracture are needed.

Table 1 Age-stratified Hazard Ratios (HR) and 95% Confidence Intervals (CI) of subsequent fractures (major osteoporotic fractures or hip fractures) by site of initial fractures

Age years	Subsequent Major Osteoporotic Fractures HR and 95% CI					
	Hip	Humerus	Other	Spine	Trauma	Wrist
50-59	4.6(3.2,6.5)	3.6(2.9,4.5)	2.0(1.8,2.2)	3.5(2.5,4.9)	1.6(1.1,2.3)	2.4(2.1,2.7)
60-69	3.0(2.4,3.6)	2.6(2.2,3.0)	1.7(1.6,1.8)	2.4(1.9,3.0)	1.5(1.1,2.2)	1.8(1.6,2.0)
70-79	1.9(1.7,2.1)	2.2(1.9,2.4)	1.5(1.4,1.6)	2.9(2.4,3.4)	1.3(1.0,1.7)	1.5(1.4,1.7)
80-89	1.3(1.2,1.4)	2.0(1.8,2.3)	1.4(1.3,1.5)	2.0(1.7,2.4)	1.3(0.9,1.9)	1.4(1.2,1.6)
90+	0.8(0.7,1.0)	1.3(0.9,1.9)	1.2(1.0,1.4)	1.7(1.1,2.6)	1.3(0.3,5.2)	1.2(0.9,1.7)
Age years	Subsequent Hip Fractures HR and 95% CI					
50-59	10.2(5.3,19.8)	4.6(3.0,7.1)	2.3(1.9,2.8)	3.1(1.6,6.1)	0.6(0.2,1.7)	2.2(1.6,3.1)
60-69	3.5(2.6,4.6)	2.6(2.0,3.3)	1.8(1.6,2.1)	1.9(1.3,2.8)	1.2(0.6,2.1)	1.5(1.3,1.9)
70-79	1.9(1.7,2.2)	1.9(1.6,2.2)	1.5(1.3,1.6)	2.5(2.0,3.1)	1.1(0.7,1.6)	1.5(1.3,1.7)
80-89	1.2(1.1,1.4)	1.8(1.6,2.1)	1.4(1.2,1.5)	1.8(1.4,2.2)	1.2(0.7,2.0)	1.3(1.2,1.5)
90+	0.7(0.6,1.0)	1.4(0.9,2.1)	1.1(0.9,1.4)	1.7(1.0,2.8)	1.6(0.4,6.7)	1.0(0.7,1.5)

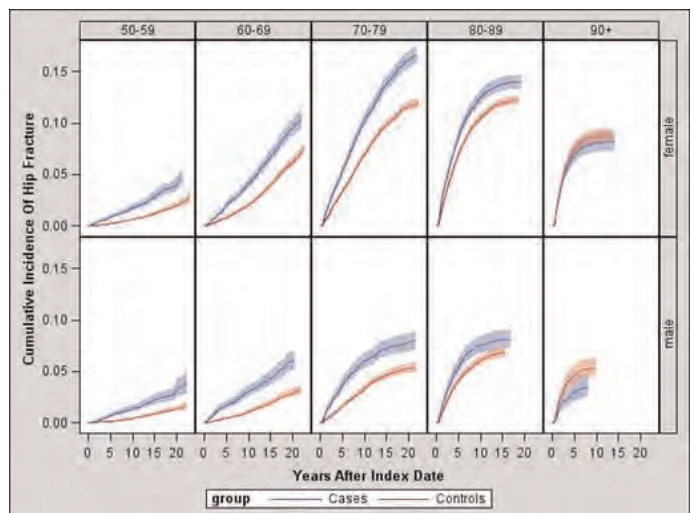Table 1 Age-stratified Hazard Ratios (HR) and 95% Confidence Intervals (CI) of subsequent fractures

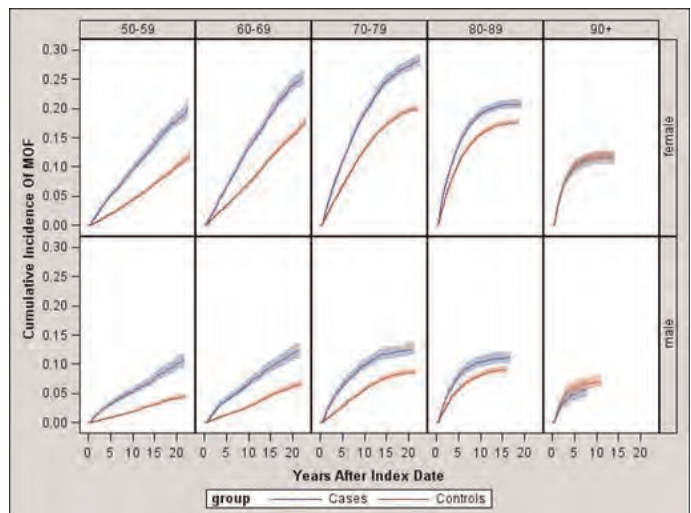Figure 1 Cumulative incidence competing risk of subsequent hip fractures

Figure 2 Cumulative incidence competing risk of subsequent major osteoporotic fractures

1138

Persistence with Osteoporosis Therapies among Osteoporotic Women at High Risk for Fracture within a Commercially-Insured Population in the United States. Emily Durden[1], Lung-I Cheng*[2], Elnara Eynullayeva[1], Larry Radbill[1], Paul Juneau[1], Leslie Spangler[3], Faisal Mirza[3], Bradley Stolshek[2]. [1]Truven Health Analytics, USA, [2]Amgen, Inc., USA, [3]Amgen, USA

PURPOSE: Several medications are effective at reducing fracture risk in osteoporotic patients. However, persistence and compliance with osteoporosis therapy are generally poor. Recently, new therapies with less frequent administration have become available. This study evaluates persistence and compliance with osteoporosis therapies over 12 months after therapy initiation among osteoporotic women at high risk for fracture in the U.S.

Methods: Females ≥ 50 years of age at high risk for fracture who newly initiated denosumab, raloxifene, teriparatide, or oral bisphosphonates (alendronate, ibandronate, or risedronate) between 1/1/2012 and 3/31/2012 were identified from the *MarketScan® Commercial* and *Medicare* databases (index date = qualifying claim date). High risk for fracture was indicated by one or more of the following: age ≥ 70, a pre-index fracture, or pre-index use of osteoporosis therapy which was discontinued at least 3 months prior to index. Patients were required to have ≥ 24 months of pre-index and ≥ 12 months of post-index continuous enrollment. Propensity score weighting was used to adjust for differences in baseline clinical and demographic characteristics. Persistence, indicated by continuous use of index therapy with no gap > 60 days; medication coverage ratio (MCR), indicated by the proportion of days covered by therapy; and compliance, defined by an MCR ≥ 0.80, were assessed during the 12-month follow-up. Logistic regression models were estimated to compare persistence and compliance between therapies.

Results: 6,187 women who newly initiated the index therapy (mean [SD] age: 71.9 [10.9] years) were identified. Propensity score weight-adjusted 12-month persistence with the index medication was highest among patients treated with denosumab (68.9%), followed by teriparatide (58.3%), raloxifene, (43.0%), alendronate (36.0%), ibandronate (33.4%), and risedronate (28.0%). The adjusted compliance varied from 70.3% for denosumab users, 51.1% for teriparatide users, 40.4% for raloxifene users, to 25.0 – 32.8% for oral bisphosphonate users. The odds of being persistent and compliant across treatments favored denosumab (odds ratios for persistence from 1.62 to 5.75, p<0.0001; for compliance from 2.36 to 7.25, p<0.0001).CONCLUSION: In this analysis of women with osteoporosis at high risk for fracture, persistence and compliance over 12 months were higher among patients who newly initiated denosumab compared to other osteoporosis therapies.

Table 1. Propensity Score Weight-Adjusted Persistence Rates, Medication Coverage Ratios (MCRs), and Compliance Rates with Index Therapy over 12 Months

	Persistence Rates		MCRs		Compliance Rates	
	n	%	Mean	SD	n	%
Denosumab (n=961)	662	68.9	0.83	0.21	676	70.3
Alendronate (n=2,820)	1,014	36.0	0.53	0.33	924	32.8
Ibandronate (n=1,062)	355	33.4	0.56	0.31	320	30.1
Risedronate (n=716)	200	28.0	0.47	0.32	179	25.0
Raloxifene (n=374)	161	43.0	0.59	0.33	151	40.4
Teriparatide (n=254)	148	58.3	0.65	0.32	130	51.1

Notes: Persistence is indicated by continuous use of index therapy with no gap > 60 days; medication coverage ratio (MCR) is indicated by the proportion of days covered by therapy; compliance is indicated by MCR ≥ 0.80.

Table 1. Propensity Score Weight-Adjusted Persistence and Compliance Rates

Table 2. Propensity Score Weight-Adjusted Odds Ratios and Associated 95% Confidence Limits from Logistic Regression Model[1]. Persistence and Compliance with Index Therapy over 12 Months

	Persistence Odds Ratios	95% CIs		Compliance Odds Ratios	95% CIs	
		Lower	Upper		Lower	Upper
Denosumab vs. Alendronate	3.97	3.39	4.65	4.93	4.20	5.81
Denosumab vs. Ibandronate	4.48	3.72	5.43	5.65	4.65	6.85
Denosumab vs. Risedronate	5.75	4.65	7.14	7.25	5.81	9.00
Denosumab vs. Raloxifene	2.94	2.30	3.77	3.53	2.75	4.53
Denosumab vs. Teriparatide	1.62	1.22	2.16	2.36	1.78	3.15

[1] Models adjusted for age, health plan type, US Census region, urban residency, patient out-of-pocket expenditure for the index therapy, and the following baseline/pre-index clinical characteristics: Charlson Comorbidity Index score, number of unique medications prescribed, diagnosis of osteoporosis, osteopenia, renal insufficiency, gastrointestinal side effects, coronary heart disease, and osteoporosis-related fracture.

Propensity Score Weight-Adjusted Odds Ratios from Logistic Regression Models

1139

Diagnostic pathways for the detection of incomplete atypical femur fractures: An economic evaluation. Olga Gajic-Veljanoski*[1], R Bleakney[2], Linda Probyn[3], Angela M. Cheung[4]. [1]University Health Network, Canada, [2]Mount Sinai Hospital, Canada, [3]University of Toronto, Sunnybrook HSC, Dept. of Medical Imaging, Canada, [4]University Health Network-University of Toronto, Canada

Purpose: We conducted a cost-effectiveness analysis to determine which combination of diagnostic tests leads to the most accurate, the least costly and the safest detection of incomplete atypical femur fractures (AFFs) in patients on long-term bisphosphonates.

Methods: We developed a probabilistic decision tree model to compare 43 diagnostic pathways including single alternatives (SE-femur by densitometer [DXA], conventional radiograph X-ray [XR], CT, bone scintigraphy or MRI) and the combinations of DXA or XR with other alternatives in all or in selected patients (18 DXA, 15 XR and 5 DXA & XR combinations). The base case was a 65-year-old woman with osteoporosis and leg pain, treated with long-term bisphosphonates. We assumed a health care payer's perspective (2013 CAD). The incidence of incomplete AFFs and accuracy of DXA vs. XR were based on the data of our screening study and the published literature. We assumed that DXA and XR incur the same costs (base case). The diagnostic properties of other tests, their costs and all effective radiation exposures were based on the literature. Our outcomes included accurate diagnosis of AFF (true positives and true negatives), costs, effective radiation dose (mSV) and incremental cost-effectiveness ratio ($/accurate diagnosis). We estimated second-order uncertainty using Monte Carlo simulations.

Results: The mean accuracy of the 43 pathways ranged from 0.71 to 0.994, the mean costs from $40.4 to $496.9 and the cumulative effective dose from 0mSV to 7.1mSV. In base case analysis, comparing 43 alternative pathways, the three XR pathways ranked best (Table). After excluding XR-related pathways, DXA alone and DXA combined with either CT or MRI in test-positive patients ranked best (Table). At low incidence of incomplete AFFs (<1/1000 patient-years), addition of bone scan to XR or DXA in test-positive was more cost-effective than their combination with MRI. In sensitivity analyses, when the cost of DXA was at least $11 cheaper than the cost of XR (<=$29), XR alone pathway was eliminated by extended dominance and DXA plus CT in test positive ranked as the second best alternative (mean costs and mean accuracy: $48.92 and 0.9919, $299.6/accurate diagnosis).

Conclusions: For the detection of incomplete AFFs, combinations of XR or DXA with CT in initially test-positive patients may represent reasonable case finding pathways.

Table. Cost-effectiveness of best diagnostic pathways for the detection of incomplete AFFs

Diagnostic pathway	Mean Costs ($)[§] (95% CrI)	Mean Accuracy (95% CrI)	Incremental Costs ($)	Incremental Accuracy	$/Accurate diagnosis
Analysis comparing all pathways (n=43)					
XR alone	40.37 (23.9-63.1)	0.9556 (0.89-0.99)			
XR plus CT in test positive	53.45 (33.1-83.2)	0.9936 (0.97-1.00)	13.08	0.0380	344.13
XR plus MRI in test positive	66.78 (38.6-110.2)	0.9942 (0.99-1.00)	13.33	0.0006	22 218.30
Analysis comparing pathways with SE-femur (DXA) as the initial test					
SE-femur (DXA) alone	40.37 (23.9-63.1)	0.9266 (0.88-0.96)			
SE-femur (DXA) plus CT in test positive	59.82 (38.2-88.1)	0.9914 (0.97-1.00)	19.41	0.0644	301.37
SE-femur (DXA) plus MRI in test positive	79.80 (48.9-121.6)	0.9925 (0.97-1.00)	19.98	0.0011	18 162.41

[§]Costs in 2013 CAD, discounted at 3% (t=1 year) ; 95% CrI denotes 95% credible interval; base case incidence of incomplete AFFs = 1/200.

Table

1140

Comparison of Fracture Risk Prediction by the U.S. Preventive Task Force Strategy and Two Alternative Strategies in Women 50-64 Years Old in the Women's Health Initiative. Carolyn Crandall*[1], Joseph Larson[2], Nelson Watts[3], Margaret Gourlay[4], Meghan Donaldson[5], Andrea Lacroix[6], Jane Cauley[7], Jean Wactawski-Wende[8], Margery L.S. Gass[9], John Robbins[10], Kristine Ensrud[11]. [1]University of California, Los Angeles, USA, [2]Fred Hutchinson Cancer Research Center, Seattle, WA, USA, [3]Mercy Health Osteoporosis & Bone Health Services, USA, [4]University of North Carolina, USA, [5]San Francisco Coordinating Center, USA, [6]Fred Hutchinson Cancer Research Center, USA, [7]University of Pittsburgh Graduate School of Public Health, USA, [8]University at Buffalo, USA, [9]The North American Menopause Society, USA, [10]University of California, Davis Medical Center, USA, [11]University of Minnesota & Minneapolis VA Health Care System, USA

Background: The United States Preventive Services Task Force (USPSTF) recommends osteoporosis screening for women younger than 65 years whose 10-year predicted risk of major osteoporotic fracture (MOF) is ≥9.3% using the Fracture Risk Assessment Tool (FRAX). Among postmenopausal women aged 50-64 years old, it is uncertain how the USPSTF screening strategy compares with the Osteoporosis Self-Assessment Tool (OST) and the Simple Calculated Osteoporosis Risk Estimate (SCORE) in discriminating women who will and will not experience osteoporotic fracture.

Objective: To assess the sensitivity, specificity, and area under the receiver operating characteristic curve of the three strategies for discrimination of incident MOF over 10 years of follow-up among postmenopausal women aged 50-64 years.

Design: Prospective study, follow-up 1993-2008

Setting and participants: 62,492 participants of the Women's Health Initiative Observational Study and Clinical Trials, aged 50-64, not taking osteoporosis medication. We did not exclude data from women taking menopausal hormone therapy.

Measurements: 10-year FRAX-predicted probability of MOF (clinical spine, hip, forearm, shoulder), OST risk score, SCORE risk score, 10-year (observed) incidence of MOF.

Results: For identifying women with incident MOF, sensitivity of the strategies ranged from 25.8 to 39.8, specificity ranged from 60.7 to 65.8 and AUC for the ROC curves ranged from 0.52 to 0.56. Among women aged 50-54 years, the sensitivity of the USPSTF strategy for identifying incident MOF was 4.7% (3.3-6.0). Adjusting the thresholds to improve sensitivity resulted in decreased specificity.

Conclusions: The USPSTF strategy only identified about one-quarter of women aged 50-64 years who went on to experience incident MOF. Our findings do not support use of the USPSTF strategy, OST, or SCORE to identify younger postmenopausal women at risk of fracture.

Sensitivity, specificity, and area under the receiver operating characteristic curve (AUC) for identifying major osteoporotic fracture[1] after 10 years, stratified by baseline age.

All participants (n=62492)	Osteoporotic Fracture		
	Sensitivity (95% CI)	Specificity (95% CI)	AUC (95% CI)
USPSTF (FRAX ≥9.3%)	25.8 (24.6-27.0)	83.3 (83.0-83.6)	0.56 (0.55-0.57)
SCORE (>7)	38.6 (37.3-39.9)	65.8 (65.4-66.2)	0.53 (0.53-0.54)
OST (<2)	39.8 (38.5-41.1)	60.7 (60.3-61.1)	0.52 (0.52-0.53)
Aged 50-54 years (n=14679)	**Osteoporotic Fracture**		
	Sensitivity (95% CI)	Specificity (95% CI)	AUC (95% CI)
USPSTF (FRAX ≥9.3%)	4.7 (3.3-6.0)	97.0 (96.8-97.3)	0.54 (0.52-0.55)
SCORE (>7)	18.5 (16.0-21.0)	78.8 (78.1-79.5)	0.54 (0.52-0.56)
OST (<2)	22.9 (20.1-25.6)	74.2 (73.5-74.9)	0.54 (0.52-0.56)
Aged 55-59 years (n=22363)	**Osteoporotic Fracture**		
	Sensitivity (95% CI)	Specificity (95% CI)	AUC (95% CI)
USPSTF (FRAX ≥9.3%)	20.5 (18.6-22.3)	86.3 (85.8-86.7)	0.55 (0.53-0.56)
SCORE (>7)	22.1 (20.2-24.0)	81.1 (80.5-81.6)	0.53 (0.51-0.54)
OST (<2)	36.7 (34.5-39.0)	63.9 (63.3-64.6)	0.52 (0.51-0.53)
Aged 60-64 years (n=25450)	**Osteoporotic Fracture**		
	Sensitivity (95% CI)	Specificity (95% CI)	AUC (95% CI)
USPSTF (FRAX ≥9.3%)	37.3 (35.4-39.1)	72.3 (71.7-72.9)	0.56 (0.55-0.57)
SCORE (>7)	57.6 (55.7-59.5)	44.4 (43.7-45.0)	0.53 (0.52-0.54)
OST (<2)	48.1 (46.2-50.1)	49.6 (48.9-50.2)	0.54 (0.52-0.55)

[1] The following fractures qualified as major osteoporotic fracture: clinical vertebral, hip, lower arm/wrist, and upper arm.

Table

Disclosures: Carolyn Crandall, None.

1141

MiR-17-92 Family MicroRNAs Play an Essential Role in Limb Development by Suppressing TGF-b Signaling. Fatemeh Mirzamohammadi*[1], Garyfallia Papaioannou[2], Elena Paltrinieri[3], Tatsuya Kobayashi[2]. [1]Massachusetts General Hospital & Harvard Medical School, USA, [2]Massachusetts General Hospital, USA, [3]Massachusetts General Hospital, USA

Small non-coding RNAs, microRNAs (miRNAs), regulate gene expression at the post-transcriptional level. Oncogenic miR-17-92 miRNAs promote cell proliferation by suppressing genes involved in specific signaling pathways including the transforming growth factor b (TGF-b) and phosphatidyl inositol 3 kinase (PI3K) pathways. Recent evidence suggests that miR-17-92 family miRNAs play an important role in skeletal development; hemizygous deletion of the miR-17-92 cluster miRNA gene causes Feingold syndrome type 2, whereas duplication of this gene has been found in patients with overgrowth and post-axial polydactyly type 2A. However, the mechanism by which miR-17-92 miRNAs regulate skeletal development is not known. In order to address this question, we conditionally deleted the miR17-92 gene and its paralogous miR106b-25 cluster miRNA gene in developing mouse limbs and the skull using Prx1-Cre transgenic mice. Conditional deletion of the miR-17-92 miRNA gene caused cutaneous syndactyly, brachydactyly, and delayed ossification of frontal bones in the skull. Additional deletion of the miR-106b-25 gene in miR-17-92 conditional knockout mice exacerbated the skeletal phenotype, suggesting that miR-17-92 and miR-106b-25 miRNAs play overlapping roles in limb development. In contrast, miR-17-92 overexpression caused limb overgrowth. miR-17-92 deficient limb bud and calvarial mesenchymal cells showed a dramatic reduction in proliferation. We found that miR-17-92 deficiency increased levels of TGF-b receptor II (Tgfbr2), a predicted miR-17 target gene, and phosphorylated Smad2, whereas there was no increase in the phosphorylated Akt level, indicating that miR-17-92 miRNAs suppress TGF-b but not PI3K signaling in skeletal mesenchymal cells. Treatment of miR-17-92 miRNA-deficient mesenchymal cells with the TGF-b receptor inhibitor, GW788388, ameliorated the proliferation defect. Furthermore, GW788388 treatment rescued the limb defects of miR-17-92/miR-106b-25 miRNA double conditional knockout mice. These data demonstrate that miR17-92 and miR106b-25 miRNAs promote proliferation of limb bud mesenchymal progenitor cells by suppressing cytostatic TGF-β signaling. In summary, we have shown that suppression of TGF-b signaling by miR-17-92 miRNAs is critical for mesenchymal cell proliferation and normal limb development. Our work provides a mechanistic insight into the pathoetiology of the Feingold syndrome.

Disclosures: Fatemeh Mirzamohammadi, None.

1142

Conditional ablation of MT1-MMP in SM22a-expressing cells identifies vascular- associated progenitors cells as essential for skeletal homeostasis. Joanne Shi*, Pamela Robey, Kenn Holmbeck. National Institute of Dental & Craniofacial Research, USA

Purpose: Extracellular matrix remodeling is essential in development. More so than in other tissues, the skeleton is extremely dependent on matrix turnover due to the continuous remodeling required for growth and mineral homeostasis. Membrane-type 1 matrix metalloproteinase (Mt1-Mmp) is a transmembrane molecule required for skeletal development and homeostasis. Accordingly, universal ablation of this enzyme leads to dramatic skeletal dysplasia with rampant bone erosion, arrested bone apposition and skeletal growth, which ultimately leads to early demise of mutant mice. To elucidate in greater detail from which cell and tissue specific compartment these defects emanate, we have performed selective ablation in a stage-specific manner to identify the temporal and spatial requirement for Mt1-Mmp activity in the skeleton

Methods: To selectively ablate the expression of *Mt1-Mmp* in vascular-associated cells, an *SM22a-Cre* expressing mouse strain was crossed to a mouse strain carrying a floxed allele of *Mt1-Mmp* to generate *SM22a-Cre; Mt1f/f* mice. Additionally the *SM22a-Cre* strain was mated to *Rosa-26-LacZ* reporter mice to track expression of the Cre recombinase. The latter demonstrated predominant expression of *SM22a-Cre* in vascular-associated cells, but also in sutures, endostea, periostea and osteocytes.

Results: Selective loss of *Mt1-Mmp* in *SM22a*-positive cells leads to dwarfism with progressive skeletal dysplasia, rampant bone erosion and numerous osteoclasts in all bony segments, coinciding with disruption of Rankl attenuation by proteolysis. μCT analysis of whole skeleton and femora documented progressive loss of bone in all morphometric indices and dynamic bone apposition measurements were consistent with diminished bone formation. To validate this finding further, heterotopic ossification was induced, in vivo, using rhBMP-2 containing-Gelfoamäcarrier implanted subcutaneously. The resulting ossicles from *SM22a-Cre; Mt1f/f mice* displayed extremely poor bone formation with absence of trabeculation and hematopoietic marrow.

Conclusion: Loss of *Mt1-Mmp* in *SM22a*-positive cells identifies vascular-associated cells as an essential progenitor pool required for basic skeletal growth, regulation of bone resorption and bone formation. In summary, we demonstrate that Mt1-Mmp-mediated proteolysis constitutes an indispensable skeletal progenitor function in vascular-associated cells, where it is required for normal skeletal development and homeostasis.

Disclosures: Joanne Shi, None.

1143

Characterization of aSMA Expressing Cells That Contribute To Muscle Heterotopic Ossification. Brya Matthews*[1], Elena Torreggiani[1], Danka Grcevic[2], Ivo Kalajzic[1]. [1]University of Connecticut Health Center, USA, [1]University of Connecticut Health Center, USA, [2]University of Zagreb, Croatia

Heterotopic ossification is formation of bone in atypical locations including muscle. Heterotopic ossification generally occurs as a result of aberrant BMP signaling. However, further studies are required to identify BMP-responsive cells in the muscle and understand how they contribute to heterotopic ossification. Alpha smooth muscle actin (αSMA) is a marker of perivascular cells and mesenchymal progenitors that contribute to bone growth and fracture healing. We aimed to evaluate whether αSMA+ cells can contribute to bone formation during heterotopic ossification.

To identify and trace cells we used αSMA promoter-driven inducible Cre (αSMACreERT2) combined with a Cre-activated tdTomato reporter Ai9 to generate SMA9 mice. Mature osteoblast/osteocytes were labeled with the Col2.3GFP reporter. To label muscle satellite cells we utilized Pax7CreERT2/Ai9 mice.

Pax7Cre/Ai9 labels cells below the basal lamina consistent with a satellite cell phenotype, while SMA9 labels similarly localized cells, in addition to perivascular cells. Pax7Cre/Ai9+ satellite cells are CD45/CD31-, Sca1- but SM/C2.6+. The SMA9+ cells are CD45/CD31- and ~60% express satellite cell marker SM/C2.6. 5% express MSC markers Sca1 and PDGFRα, and a larger proportion express PDGFRβ. During BMP2-induced heterotopic ossification, SMA9+ cells comprised 28% chondrocytes and 44% of Col2.3GFP+ osteoblasts, while Pax7Cre/Ai9+ satellite cells labeled only muscle fibers. Culture of sorted cells indicated that SMA9+ and Pax7Cre/Ai9+ cells differentiated into myotubes while the negative cells do not. SMA9+ cultured cells showed the highest upregulation of osteogenic gene expression after culture in the presence of BMP2. To clarify which subset of SMA9 cells possess osteogenic potential, we subdivided SMA9+ cells based on expression of SM/C2.6 and evaluated their ability to differentiate into osteoblasts after transplantation into muscle with BMP2. We observed osteogenic differentiation of SMA9/SM/C2.6+ cells suggesting that once the satellite cell population is removed from its niche they can exhibit osteogenic potential.

αSMA labels mesenchymal progenitor cells in the muscle that contribute to heterotopic ossification induced by BMP2. Our data indicate that the perivascular fraction of cells is responsible for heterotopic ossification, however, muscle satellite cells are capable of osteogenic differentiation after removal from their niche.

Disclosures: Brya Matthews, None.

1144

Interaction of RBP-J and Endogenous TGF-β Signaling Controls ITAM-Mediated Costimulation of Osteoclastogenesis and Bone Resorption. Christine Miller*, Susan Li, Xiaoyu Hu, Lionel Ivashkiv, Baohong Zhao. Hospital for Special Surgery, USA

Homeostatic osteoclastogenesis requires not only RANK signaling but also costimulatory signals from ITAM -containing receptors/adaptors, predominantly DAP12 and FcRγ in osteoclast precursors. The mechanisms by which costimulatory signals are regulated and integrated with RANK signaling are not well understood. In this study, we investigated whether RBP-J, a newly identified key inhibitory transcription factor for osteoclastogenesis, regulates ITAM-mediated co-stimulation and controls the crosstalk between ITAM and RANK signaling. To address these questions, we generated DAP12 and RBP-J double knockout (KO) mice ($Rbpj^{ΔM/ΔM}Dap12^{-/-}$) and DAP12, FcRγ and RBP-J triple KO mice (TKO). Strikingly, we found that RBP-J deficiency almost completely reversed the defects of osteoclast differentiation program and significantly rescued the osteopetrotic bone phenotype of *Dap12* KO or *Dap12/ Fcrg* double knockout (DKO) mice by bypassing the requirement for costimulation of osteoclastogenesis during bone homeostasis. In inflammatory settings, RBP-J deficiency enabled TNF-α to induce osteoclast formation and bone resorption in *Dap12* KO mice. Thus, RBP-J imposes a requirement for ITAM-mediated costimulation of RANKL or TNF-α induced osteoclastogenesis and bone resorption. Mechanistically, RBP-J suppressed induction of key osteoclastogenic factors NFATc1, Blimp1 and c-Fos by opposing ITAM-mediated expression and function of PLCγ2 and downstream calcium-CaMKK-Pyk2 signaling. Furthermore, we showed that the mechanism of PLCγ2 regulation is transcriptional, and then built upon the next generation high-throughput RNA sequencing experiments to identify a novel regulatory loop whereby RBP-J restrains the responsiveness of osteoclast precursors to endogenous TGF-β signaling, which in turn regulates transcription of PLCγ2 and downstream calcium oscillation. To the best of our knowledge, our results provide the first example of regulatory mechanisms of PLCγ2 expression and negative regulation of ITAM-signaling by RBP-J. These findings indicate that RBP-J plays an important role in suppressing ITAM-mediated costimulation, thereby limiting crosstalk between ITAM and RANK/TNFR signaling and fine tuning osteoclastogenesis during bone homeostasis and under inflammatory conditions. Environmental cues that regulate RBP-J expression/function would thus modulate the requirement for costimulatory signaling for osteoclast differentiation and bone remodeling.

Disclosures: Christine Miller, None.

1145

Ensuing Osteopetrosis in TAK1-Null Mice Owing to Defective NF-B and NOTCH Signaling. Gaurav Swarnkar*[2], Yousef Abu-Amer[1], Kannan Karuppaiah[3], Gabriel Mbalaviele[1]. [1]Washington University in St. Louis School of Medicine, USA, [2]Washington University School of Medicine, USA, [3]Washington University School of Medicine in St. Louis, USA

The protein kinase TGFβ activated kinase-1 (TAK1) is involved in activation of MAPK and NF-κB signaling pathways in response to inflammatory stimuli, and it has been reported to play a role in osteoclast (OC) survival. However, the physiological role and mechanism of TAK1 action in bone development has not been fully explored. In this study, TAK1 was conditionally deleted (cKO) in the myeloid lineage. TAK1cKO mice exhibited osteopetrosis, growth retardation and impaired tooth eruption, consistent with micro-CT and histological analysis parameters and with fewer osteoclasts compared with wild type mice. In vitro studies showed that bone marrow monocytes from TAK1cKO fail to differentiate into OC and expressed low levels of TRAP, Cathepsin-K, β3-integrin, and MMP9. This differentiation defect was corrected when WT-TAK1 was re-introduced retrovirally. We further found that activation of JNK, p38 and NF-κB in TAK1-deficient cells in response to RANKL was abrogated. To study the details of the mechanism underlying osteopetrosis in TAK1-null mice, we probed candidate pathways and found elevated levels of the transcription factor RBPjκ, a downstream target of NOTCH signaling, which has been reported to negatively regulate OC differentiation. Consistently, we observed significant reduction in the levels of NICD, a NOTCH cleaved peptide. More intriguingly, forced expression of exogenous NICD partially reversed the osteoclastogenic phenotype with concomitant changes in RBPjκ and NFATc1 levels. Surmising that activation of NF-κB is essential for complete rescue, expression of catalytically active IKK2, the immediate target of TAK1, restored NICD levels and completely recovered osteoclastogenesis. To further support this observation, we generated LysM-Cre-TAK1-RBPjκ for compound deletion of TAK1 and RBPjκ (DcKO) mice. In agreement with in vitro studies, we found that deletion of RBPjκ in the TAK1 null background significantly corrected the osteopetrotic phenotype. MicroCT and histology showed a complete rescue of the TAK1cKO phenotype as DcKO showed BV/TV, TB.Th, TB.N. and Tb.SP comparable to the WT mice with a significant increase in the OC numbers. In summary, our data establish that TAK1 is required for osteoclastogenesis and play an important role in bone development. We further provide evidence that the mechanism underlying the bone defect in TAK1-deficient condition is via coordinated regulation of NF-κB and NOTCH-RBPjκ signaling pathways.

Disclosures: Gaurav Swarnkar, None.

1146

Osteocalcin regulates muscle function and mass. Paula Mera*, Kathrin Laue, Gerard Karsenty. Columbia University, USA

A decrease in muscle function and mass or muscle wasting is a hallmark of the aging process and appears at the same time bone mass decreases. The fact that these two main manifestations of aging develop simultaneously has long raised the prospect that bone and muscle influence each other through means that need to be identified. To test the existence of the validity of this hypothesis from the bone point of view and since GPRC6A, a bona fide receptor for the bone-derived hormone osteocalcin, is expressed in fibers and satellite cells of the muscles; we asked if osteocalcin regulates muscle function and mass in the mouse. Here we show that, starting at 3 months of age *Osteocalcin null* mice (*Ocn-/-*) exhibit a decrease in muscle function as determined by either a gradual speed increase exercise or an endurance test performed in a treadmill apparatus designed to determine muscle fatigue. At the same time that this functional defect develops, muscle mass decreases in *Ocn-/-* mice. Conversely, in *Esp-/-* mice, a model of gain-of-function of osteocalcin, muscle function and mass are increased at 3 months of age. These functions of osteocalcin are mediated by GPRC6A, since mice lacking this receptor in all cells or in mycytes only display the same muscle phenotype than *Ocn-/-* mice. In searching for the molecular mode of action of osteocalcin in muscle we first demonstrated that, as previously seen in β-cells of the pancreas and Leydig cells of the testis, osteocalcin induces the activation of the cAMP/PKA pathway in mouse primary myotubes and that this activation is dependant on their expression of GPRC6A. We observed that osteocalcin, also in a GPRC6A-dependent manner, leads to the inhibition of the cellular energy sensor AMP-activated protein kinase (AMPK) in primary myotubes, this in turn promotes the activation of the mTOR complex, as demonstrated by the increase in the phosphorylation of its substrate S6K, a well-known activator of protein synthesis. Concomitantly, we found that osteocalcin promotes tyrosine incorporation into cellular proteins in wild type, but not in *Gprc6a-/-* primary myotubes. As expected given the nature of GPRC6A the effect of osteocalcin on AMPK-mTOR-S6K axis are dependant on the activity of PKA. Altogether, these data identify a novel function of osteocalcin as a regulator of muscle functions and mass and an additional signaling pathway affected by this hormone.

Disclosures: Paula Mera, None.

1147

Odanacatib Anti-Fracture Efficacy and Safety in Postmenopausal Women with Osteoporosis. Results from the Phase III Long-Term Odanacatib Fracture Trial (LOFT). Michael McClung*[1], Bente Langdahl[2], Socrates Papapoulos[3], Kenneth Saag[4], Silvano Adami[5], Henry Bone[6], Tobias de Villiers[7], Douglas Kiel[8], Annie Kung[9], Prasanna Kumar[10], Sung-Kil Lim[11], Xu Ling[12], Kurt Lippuner[13], Carlos Mautalen[14], Toshitaka Nakamura[15], Jean-Yves Reginster[16], Ian Reid[17], Jose Rodriguez Portales[18], Christian Roux[19], Jesus Walliser[20], Nelson Watts[21], Jose Ruben Zanchetta[22], Cristiano Zerbini[23], Andrea Rybak-Feiglin[24], Dosinda Cohn[24], Carolyn DaSilva[24], Rachid Massaad[25], Arthur Santora[26], Boyd Scott[26], Nadia Verbruggen[25], Albert Leung[27], Antonio Lombardi[23]. [1]Oregon Osteoporosis Center, USA, [2]Aarhus University Hospital, Dnk, [3]Leiden University Medical Center, The Netherlands, [4]University of Alabama at Birmingham, USA, [5]University of Verona, Italy, [6]Michigan Bone & Mineral Clinic, USA, [7]Stellenbosch University, South Africa, [8]Hebrew SeniorLife, USA, [9]Dr. Kung-Wai Chee Clinic, Hong Kong, [10]Bangalore Diabetes Centre, India, [11]Yonsei University, Korea, democratic people's republic of, [12]Peking Union Medical College Hospital, Peoples Republic of China, [13]Department of Osteoporosis, University Hospital & University of Berne, Switzerland, [14]Centro de Osteopatías Médicas, Argentina, [15]University of Occupational & Environmental Health, Japan, [16]CHU Centre Ville, Belgium, [17]University of Auckland, New Zealand, [18]Catholic University of Chile, Chile, [19]Hospital Cochin, France, [20]Bone Metabolism Clinic, Hospital Angeles del Pedregal, Mexico, [21]Mercy Health Osteoporosis & Bone Health Services, USA, [22]Instituto de Investigaciones Metabolicas (IDIM), Argentina, [23]Centro Pualista de Investigação Clinica, Brazil, [24]Merck & Co., Inc., USA, [25]MSD Europe Inc., Brussels, Belgium, [26]Merck & Co. Inc., USA, [27]USA

Odanacatib (ODN), a selective oral inhibitor of cathepsin K, is in development for the treatment of osteoporosis. The randomized, double-blind, placebo-controlled, event-driven, Phase III Long-Term Odanacatib Fracture Trial (LOFT; NCT00529373) and its pre-planned blinded extension, in which patients continue on their originally assigned treatment, evaluated the efficacy and safety of ODN 50 mg once-weekly to reduce fracture risk in postmenopausal women with osteoporosis. Primary endpoints of the trial were new morphometric vertebral (VFx), hip, and clinical non-vertebral fractures. Secondary endpoints included safety and tolerability, clinical VFx, spine and hip BMD, and bone turnover markers. LOFT enrolled women ⩾65 years of age with a BMD T-score ⩽−2.5 at the total hip (TH) or femoral neck (FN) or with a prior radiographic VFx and a T-score ⩽−1.5 at the TH or FN. Participants were randomized to either ODN or placebo (1:1) and received weekly vitamin D_3 (5600IU) and daily calcium supplements to ensure a total daily calcium intake of ~1200 mg.

Overall, 16,713 participants were randomized at 387 centers in 40 countries, 16,071 were included in the analyses, and 642 excluded from all analyses due to study site closure (n=483), duplicate randomization (n=3), or failure to take any study drug (n=156). At baseline, mean (SD) age was 72.8 (5.3) years, 57% were Caucasian, 46.5% had a prior VFx, and mean BMD T-scores were: lumbar spine -2.7, TH -2.4, and FN -2.7. A total of 237 patients with hip fracture were estimated to provide statistical power. A prespecified interim analysis was performed when ~70% of targeted events had accrued. An external Data Monitoring Committee (DMC) reviewed these data and recommended that the base study be closed early due to robust efficacy and a favorable benefit-risk profile. The DMC noted that safety issues remained in certain selected areas. Both safety and efficacy continue to be monitored in the ongoing blinded extension trial. Data from an average follow-up of 40.8 months have been accrued from the base and extension studies, with 7081 patients completing at least 4 years of follow-up. At the time this abstract was written, final data analysis was not complete. This presentation will summarize the efficacy of ODN on fractures and BMD and general safety from the blinded, placebo-controlled base and extension study periods of LOFT. A separate presentation will discuss in depth the safety profile for ODN from this trial.

1148

Safety and Tolerability of Odanacatib Therapy in Postmenopausal Women with Osteoporosis: Results from the Phase III Long-Term Odanacatib Fracture Trial (LOFT). Socrates Papapoulos*[1], Michael McClung[2], Bente Langdahl[3], Kenneth Saag[4], Silvano Adami[5], Henry Bone[6], Tobias de Villiers[7], Douglas Kiel[8], Annie Kung[9], Prasanna Kumar[10], Sung-Kil Lim[11], Xu Ling[12], Kurt Lippuner[13], Carlos Mautalen[14], Toshitaka Nakamura[15], Jean-Yves Reginster[16], Ian Reid[17], Jose Adolfo Rodriguez-Portales[18], Christian Roux[19], Jesus Walliser[20], Nelson Watts[21], Jose Ruben Zanchetta[22], Christiano AF Zerbini[23], Andrea Fybak-Feiglin[24], Dosinda Cohn[24], Carolyn A da Silva[24], Celine Le Bailly De Tilleghem[25], Arthur Santora[26], Boyd Scott[26], Nadia Verbruggen[27], Albert Leung[28], Antonio Lombardi[26], Deborah Gurner[26]. [1]Leiden University Medical Center, The Netherlands, [2]Oregon Osteoporosis Center, USA, [3]Aarhus University Hospital, Dnk, [4]University of Alabama at Birmingham, USA, [5]University of Verona, Italy, [6]Michigan Bone & Mineral Clinic, USA, [7]Stellenbosch University, South Africa, [8]Hebrew SeniorLife, USA, [9]Dr. Kung-Wai Chee Clinic, Hong Kong, [10]Bangalore Diabetes Centre, India, [11]Yonsei University College of Medicine, South Korea, [12]Peking Union Medical College Hospital, Peoples Republic of China, [13]Department of Osteoporosis, University Hospital & University of Berne, Switzerland, [14]Centro de Osteopatías Médicas, Argentina, [15]National Center for Global Health & Medicine, Japan, [16]CHU Centre Ville, Belgium, [17]University of Auckland, New Zealand, [18]Pontificia Universidad Católica de Chile, Chile, [19]Hospital Cochin, France, [20]Bone Metabolism Clinic, Hospital Angeles del Pedregal, Mexico, [21]Mercy Health Osteoporosis & Bone Health Services, USA, [22]Instituto de Investigaciones Metabolicas (IDIM), Argentina, [23]Centro Paulista de Investigações, Brazil, [24]Merck Sharp & Dohme Corp, USA, [25]MSD Europe Inc., Belgium, [26]Merck & Co., Inc., USA, [27]MSD Europe Inc., Belgium, [28]USA

Odanacatib (ODN), a selective oral inhibitor of cathepsin K, is in development for the treatment of osteoporosis. The randomized, double-blind, placebo-controlled, event-driven, Phase III Long-Term Odanacatib Fracture Trial (LOFT; NCT00529373) and its pre-planned blinded extension, in which patients continued on their originally assigned treatment, evaluated the efficacy and safety of ODN 50 mg once-weekly in reducing the risk of fractures in postmenopausal women with osteoporosis.

Women ⩾65 years with a BMD T-score ⩽-2.5 at the total hip (TH) or femoral neck (FN), or with a radiographic vertebral fracture and T-score ⩽-1.5 at the TH or FN were randomized (1:1) to ODN or placebo. Participants also received weekly vitamin D_3 (5600 IU) and daily calcium supplements to ensure a total daily intake of ~1200 mg. Primary endpoints were new morphometric vertebral, hip, and clinical non-vertebral fractures. Safety analysis used a multi-tiered approach on the All-Patients-as-Treated population. External Clinical Adjudication Committees evaluated the following adverse event (AE) categories: select dental, select skin, serious respiratory, delayed fracture union, atypical femoral fractures, atrial fibrillation/flutter, cardio-vascular and cerebrovascular.

Overall, 16,713 participants were randomized at 387 centers in 40 countries, 16,071 were included in the analyses, and 642 excluded from all analyses due to study site closure (n=483), duplicate randomization (n=3), or failure to take any study medication (n=156). Baseline mean (SD) age was 72.8 (5.3) years, 57% were Caucasian, and 46.5% had a prior vertebral fracture. Mean baseline BMD T-scores were: lumbar spine -2.7, TH -2.4, and FN -2.7.

The base study was closed early based on the recommendation of the independent Data Monitoring Committee (DMC) who reviewed a prespecified interim analysis and noted robust efficacy and a favorable benefit/risk profile. The DMC also noted that safety issues remained in certain selected areas. Both safety and efficacy continue to be monitored in the ongoing blinded extension.

Safety data from this large, long-term study will be presented, including the incidence of AEs in the ODN and placebo groups in the base study and its ongoing blinded extension. At the time this abstract was written, final data analysis was not complete. The results will be available for presentation at the ASBMR meeting.

1149

Randomized Controlled Trial to Assess the Safety and Efficacy of Odanacatib in the Treatment of Men with Osteoporosis. <u>Eric Orwoll</u>*[1], <u>Silvano Adami</u>[2], <u>Neil Binkley</u>[3], <u>Roland Chapurlat</u>[4], <u>Bente Langdahl</u>[5], <u>Steven Doleckyj</u>[6], <u>Hilde Giezek</u>[7], <u>Boyd Scott</u>[6], <u>Arthur Santora</u>[6]. [1]Oregon Health & Science University, USA, [2]University of Verona, Italy, [3]University of Wisconsin, Madison, USA, [4]E. Herriot Hospital, France, [5]Aarhus University Hospital, Dnk, [6]Merck & Co., Inc., USA, [7]MSD Europe Inc., Brussels, Belgium

Background

Osteoporosis in men is an important clinical problem, associated with significant morbidity, mortality, and societal expense. Odanacatib (ODN), a selective inhibitor of cathepsin K, is currently being investigated as a treatment for osteoporosis. In a Phase II study in postmenopausal women, treatment with ODN 50mg once-weekly resulted in increases in bone mineral density (BMD) at the lumbar spine (LS) (11.9%) and total hip (TH) (9.8%) over 5 years. This Phase III study investigated safety and efficacy of ODN in the treatment of men with osteoporosis.

Methods

This was a double-blind, randomized; placebo controlled 24-month trial. We enrolled men $\geq$40 and $\leq$95 years of age with idiopathic osteoporosis or osteoporosis due to hypogonadism. A LS or hip (TH, femoral neck (FN) or trochanter) T-score of $\leq$-2.5 to $\geq$-4.0 without prior vertebral fracture or $\leq$-1.5 to $\geq$-4.0 with one prior vertebral fracture was required. Participants were randomized (1:1) to 50mg of ODN or PBO orally once-weekly, and received weekly vitamin D_3 (5600IU) and daily calcium supplements (total including food ~1200mg daily). The primary outcome was the effect of ODN versus PBO on LS BMD assessed by DXA versus PBO at 24 months. Secondary outcomes included safety and tolerability and changes in BMD at the TH, FN, trochanter sites, and bone turnover markers.

Results

A total of 292 men were randomized and received at least one dose of study medication. The average age was 68.8 years, and 5.8% had total testosterone levels below 250ng/dL. BMD increases from baseline at 24 months in the ODN group at the LS and all 3 hip sites (TH, FN and trochanter) were 6.9%, 1.9%, 1.7% and 2.8% respectively, and all were greater vs. PBO (all p<0.01). Compared to PBO at 24-months, ODN significantly decreased the bone resorption markers u-NTx/Cr and s-CTx (68% and 77%, both p<0.001), and also decreased bone formation markers, s-P1NP and s-BSAP (16 and 8%, p=0.001 and p=0.019 respectively). The between group decrease of bone formation markers was maximal at 3 months, after which levels returned towards baseline by 24 months. The adverse events and overall safety profile were similar between ODN and PBO.

Conclusion

In this study, ODN increased spine and hip BMD in osteoporotic men. Changes in bone turnover markers suggest that ODN treatment decreases bone resorption while producing relatively small decreases in bone formation. ODN is a promising potential therapy for treatment of osteoporosis in men.

1150

The Transition from Denosumab to Teriparatide or from Teriparatide to Denosumab in Postmenopausal Women with Osteoporosis: The DATA-Switch Study. <u>Benjamin Leder</u>*[1], <u>Joy Tsai</u>[2], <u>Alexander Uihlein</u>[3], <u>Yuli Zhu</u>[4], <u>Katelyn Foley</u>[4], <u>Robert Neer</u>[2], <u>Sherri-Ann Burnett-Bowie</u>[2]. [1]Massachusetts General Hospital Harvard Medical School, USA, [2]Massachusetts General Hospital, USA, [3]Northwestern Memorial Faculty Foundation, USA, [4]Massachusetts General Hospital, USA

Introduction: Bisphosphonates (BPs) preserve and extend BMD increases achieved during a 2-year course of teriparatide (TPTD) and TPTD preserves and extends BP-induced BMD gains as well. This allows patients to transition from one treatment to another as clinically indicated. The effects of TPTD when used after denosumab (DMAB), however, and the effects of DMAB when used after TPTD are unknown. Defining the clinical consequences of these drug transitions is essential in guiding the management of osteoporosis over time.

Methods: Postmenopausal osteoporotic women completing the DATA study that assessed the effects of 2-years of DMAB (60-mg every 6-months), TPTD (20-μg daily), or both, were enrolled in DATA-Switch. In DATA-Switch, women who received DMAB for the first 2-years were switched to TPTD and women who received either TPTD or TPTD+DMAB were switched to DMAB alone. BMD was measured 6 and 12 months after switching treatments.

Results (Fig): In women switched from TPTD to DMAB (n=27), 12-months of DMAB increased spine BMD by an additional 5.7%, femoral neck (FN) BMD by an additional 3.5%, and total hip (TH) BMD by 3.1%, resulting in net 3-year BMD increases of 15.1% at the spine, 5.7% at the FN, and 5.3% at the TH. In women switched from DMAB to TPTD (n=24), spine BMD decreased by -1.5% after 6-months of TPTD but then rebounded, resulting in a 12-month change of +1.6% and a net 3-year change of 10.4%. One year of TPTD given after DMAB, however, decreased FN BMD by -1.6% and TH BMD by -2.7%, resulting in net 3-year BMD increases of 1.6% at the FN and 0.7% at the TH. In women switching from combination therapy to DMAB alone (n=21), spine BMD increased by an additional

2.7% while FN and TH increased only slightly, resulting in net 3-year increases of 15.0% at the spine, 7.2% at the FN, and 7.1% at the TH. After a total of 3-years of therapy, the increase in TH BMD remained greater in women who received combination therapy followed by DMAB than in either other groups (P=0.047).

Conclusions: DMAB prevents bone loss and increases BMD in women treated with TPTD. TPTD, however, does not fully prevent the bone loss that occurs after DMAB discontinuation, particularly at the hip. Thus, the use of TPTD immediately after DMAB may not be advisable, especially in women at very high fracture risk. Two years of combined TPTD and DMAB followed by DMAB alone results in the most favorable effects on hip BMD and may be a useful treatment approach in high-risk patients.
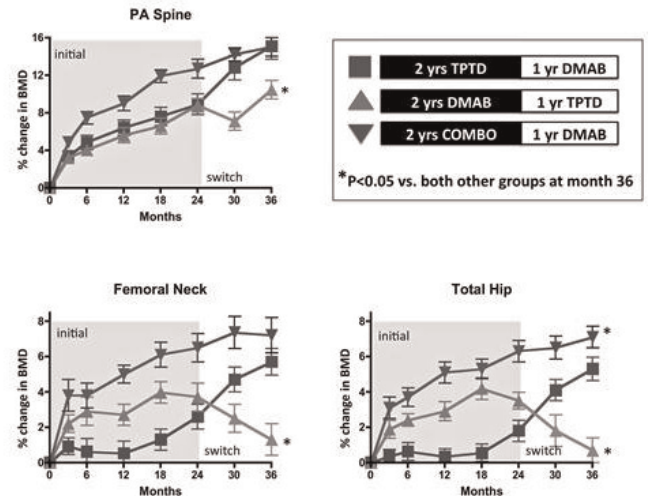
Figure

1151

Effect of Blosozumab on Bone Mineral Density: 52-Week Follow-up of a Phase 2 Study of Postmenopausal Women with Low Bone Mineral Density. <u>Charles Benson</u>*[1], <u>Alan Chiang</u>[1], <u>Leijun Hu</u>[1], <u>Alam Jahangir</u>[1], <u>Bruce Mitlak</u>[1], <u>Robert Recker</u>[2], <u>Deborah Robins</u>[1], <u>Hideaki Sowa</u>[3], <u>Adrien Sipos</u>[1]. [1]Eli Lilly & Company, USA, [2]Creighton University, USA, [3]Lilly Research Laboratories Japan, Eli Lilly Japan K.K., Japan

Purpose: Blosozumab (bmab) is a humanized anti-sclerostin monoclonal antibody being developed for the treatment of severe osteoporosis. A randomized, parallel-design, double-blind, placebo-controlled, Phase 2 study that assessed the safety and efficacy of different bmab doses found that 52 weeks of bmab treatment significantly increased lumbar spine bone mineral density (BMD) and was generally well tolerated. Based on bone biomarker data, the BMD increases seen in the Phase 2 study likely resulted from elevated bone formation not associated with increased resorption. Here, we report the 52-week follow-up data from the Phase 2 study. Methods: Postmenopausal women with low BMD (lumbar spine T-score -3.5 to -2.0) were randomized to 1 of 3 subcutaneous bmab treatments (180 mg every 4 weeks [Q4W] [n=31]; 180 mg every 2 weeks [Q2W] [n=30]; 270 mg Q2W [n=30] or placebo (n=29) for 52 weeks followed by a 52-week follow-up period during which patients did not receive bmab. Efficacy was assessed as BMD changes from baseline through Week 104 in lumbar spine, total hip, and femoral neck. BMD was measured by dual energy x-ray absorptiometry. Safety was also assessed. Results: Of the 120 women enrolled (mean baseline age 66 years; mean lumbar spine T-score -2.75), 106 completed the 52-week treatment and entered the 52-week follow-up; 88 completed the follow up. In general, bmab resulted in significantly greater increases in BMD for lumbar spine, total hip, and femoral neck at 52 weeks of treatment compared with placebo (Figure). Upon treatment discontinuation, a reduction in BMD was seen in all bmab groups. However, at the end of the follow-up period, lumbar spine, total hip, and femoral neck BMD for bmab 270-mg Q2W and lumbar spine and total hip BMD for bmab 180-mg Q2W remained significantly greater than placebo. Treatment-emergent adverse events (TEAEs) during the 52-week follow-up period were similar across treatment groups, with most due to infections and infestations (n=39). TEAEs reported during the 52-week follow-up did not appear to be due to bmab treatment. Conclusion: After 52-weeks of bmab treatment, lumbar spine, total hip, and femoral neck BMD increased significantly compared with placebo, as reported previously. During 52 weeks of post-treatment follow-up, BMD declined, but generally remained significantly greater than placebo for the 2 highest doses. These findings support the continued study of bmab to treat osteoporosis.
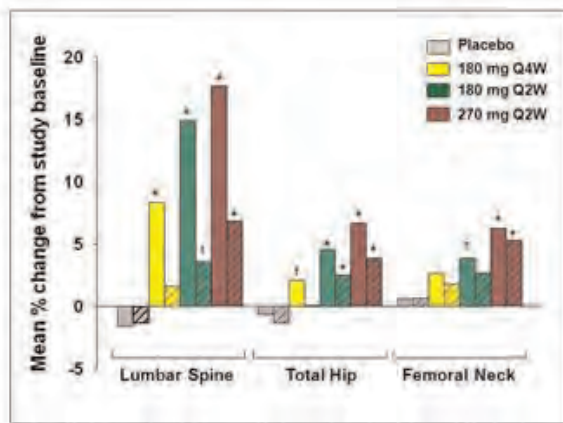
Figure legend: Open bars indicate mean % change from study baseline at 52 weeks of bmab treatment. Striped hatching indicates mean % change from study baseline through Week 104. *p<0.001, †p<0.05 compared with placebo. Abbreviations: Q4W= bmab every 4 weeks, Q2W= bmab every 2 weeks. P-values are corrected Dunnett's adjusted p-values.

Figure

1152

Effects of 2 Years of Treatment With Romosozumab Followed by 1 Year of Denosumab or Placebo in Postmenopausal Women With Low Bone Mineral Density.

MR McClung*[1], A Chines[2], JP Brown[3], A Diez-Perez[4], H Resch[5], J Caminis[6], Ma Bolognese[7], S Goemaere[8], HG Bone[9], JR Zanchetta[10], J Maddox[2], O Rosen[2], S Bray[11], A Grauer[2]. [1]Oregon Osteoporosis Center, USA, [2]Amgen Inc., USA, [3]Laval University & CHU de Québec Research Centre, Canada, [4]Autonomous University of Spain, Spain, [5]St. Vincent Hospital, Austria, [6]UCB, USA, [7]Bethesda Health Research Center, USA, [8]Ghent University Hospital, Belgium, [9]Michigan Bone & Mineral Clinic, USA, [10]Instituto de Investigaciones Metabólicas, Argentina, [11]Amgen Ltd., United Kingdom

Purpose: We previously reported that 1 year of treatment with the sclerostin antibody romosozumab (Romo) was associated with increased bone mineral density (BMD) and bone formation and with decreased bone resorption in postmenopausal women with low BMD (McClung *NEJM* 2014). Here, we report the results of 2 years of treatment with Romo followed by 1 year of denosumab (DMAb) or placebo.

Methods: This phase 2 study enrolled 419 postmenopausal women age 55 to 85 years with a lumbar spine, total hip, or femoral neck T-score $\leq$–2.0 and $\geq$–3.5. Women received 1 of 5 regimens of Romo (70 mg QM, 140 mg QM, 210 mg QM, 140 mg Q3M, 210 mg Q3M; data for the 210 mg QM group are shown in the figures) or placebo for 2 years. At the end of 2 years, eligible subjects entered a 1-year extension phase and were re-randomized 1:1 within their original treatment group to placebo or DMAb 60 mg Q6M. Only women who entered the extension were included in these analyses.

Results: Romo led to rapid and marked increases in lumbar spine and total hip BMD during year 1 and continued increases through year 2. The largest gains were observed with Romo 210 mg QM, with BMD increases of 15.7% (lumbar spine) and 6.0% (total hip) (Figures). Women receiving Romo 210 mg QM who transitioned to DMAb continued to accrue BMD at a rate similar to that in the second year of Romo; in those who transitioned to placebo, BMD returned towards pretreatment levels.

Romo induced rapid stimulation of bone formation (P1NP) and decreased bone resorption (CTX). Increases of P1NP were transitory, returning towards baseline within 6 to 12 months and remaining below baseline through year 2. CTX remained below baseline through year 2. In subjects receiving Romo 210 mg QM who transitioned to DMAb: P1NP and CTX decreased; for those who transitioned to placebo: P1NP gradually returned to pretreatment levels, while CTX initially increased above baseline and gradually returned towards baseline.

Adverse events were balanced between the placebo and Romo groups during the first 2 years of the study (with the exception of injection site reactions, most reported as mild) and in the placebo and DMAb groups during year 3.

Conclusion: Romo led to rapid and marked increases in lumbar spine and total hip BMD over 2 years, which continued with DMAb and resolved after transition to placebo. These data suggest that the treatment effects observed with Romo are further augmented by follow-on treatments like DMAb.
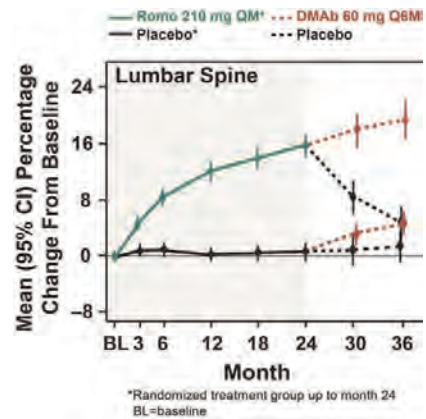
Figure 1
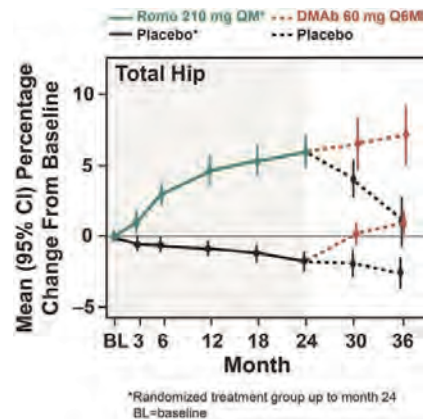
Figure 2

FR0002

Sclerostin and FGF-23 Protein Expression in Bone of Patients with Chronic Kidney Disease. Florence Lima*[1], Valentin David[2], Hanna Mawad[1], Hartmut Malluche[4]. [1]University of Kentucky, USA, [2]University of Miami, Miller School of Medicine, USA, [4]University of Kentucky Medical Center, USA

Purpose: Chronic kidney disease-mineral and bone disorder (CKD-MBD) develops early and progresses inexorably during loss of kidney function. Sclerostin and FGF23, both produced by osteocytes, are increased in blood in CKD-MBD. The aim of this study was to explore expression of sclerostin and FGF23 in bone and to establish correlations with blood levels and bone turnover.

Methods: In this IRB approved cross-sectional study, 45 patients with CKD stage 5 on dialysis underwent anterior iliac crest biopsies after double-tetracycline labeling. Undecalcified bone samples were evaluated by histomorphometry to assess turnover and for quantifying FGF23 and sclerostin expression by immunostaining. Serum sclerostin and FGF23 levels were measured by ELISA.

Results: Patients with low bone turnover had higher serum sclerostin levels than patients with high bone turnover (3.7 ng/mL ± 1.3 vs. 1.9 ng/mL ± 1.3, P<0.001). Serum FGF23 levels were lower in patients with low bone turnover (2475 pg/mL ± 4720 vs. 16169 pg/mL ± 13426, P<0.01). Expression of sclerostin in osteocytes was higher in patients with low bone turnover (P<0.01) and expression of FGF23 was higher in patients with high bone turnover (P<0.05; Table 1). Sclerostin positive osteocytes were more present in cortical bone (P<0.001) while FGF23 positive osteocytes were more present in trabecular bone (P<0.05) in both turnover groups. Sclerostin and FGF23 expression in trabecular and cortical bone correlated with serum levels (sclerostin: rho = 0.49 and 0.44, P<0.05; FGF23: rho = 0.69 and 0.68, P<0.001). Correlations between sclerostin and FGF23 blood levels as well as their expression in bone with histomorphometric bone parameters are shown in the Table 2. Serum sclerostin and its expression in bone were negatively correlated with bone formation rate and osteoid thickness. Serum FGF23 and its expression in bone were negatively correlated with mineralization lag time.

Conclusion: These results show different patterns of sclerostin and FGF23 expression in low and high bone turnover suggesting a role in the turnover abnormalities of patients with CKD stage 5 on dialysis.

	% scl+ocy		% FGF23+ocy	
	Trabecular bone	Cortical bone	Trabecular bone	Cortical bone
Low Turnover	17.1 ± 12.0	25.4 ± 11.3	1.7 ± 2.3	1.5 ± 2.5
High Turnover	1.0 ± 0.8	6.3 ± 7.0	7.4 ± 9.0	4.2 ± 3.4
Values represent mean ± standard deviation.				

Table 1. Percentage of osteocytes positive for sclerostin (%scl+ocy) and for FGF23 (%FGF23+ocy)

	sB sclerostin	%sB cl+ocy (trab)	%sB cl+ocy (cort)	sFGF23	%FGF23+ocy (trab)	%FGF23+ocy (cort)
BV	-0.18	-0.18	-0.21	0.49**	0.28	0.56**
BFR BS	-0.64**	-0.76**	-0.69***	0.41*	0.25	0.31
O.Th	-0.40*	-0.49*	-0.51**	0.15	-0.05	-0.01
MLT	0.00	0.21	0.11	-0.57**	-0.53**	-0.58**
Ac.F	-0.61**	-0.81**	-0.71**	0.50**	0.30	0.41*

** Correlation is significant at the 0.01 level (2-tailed)

* Correlation is significant at the 0.05 level (2-tailed)

Table 2. Correlation coefficients for sclerostin and FGF23 serum and their expression with bone hist

Disclosures: Florence Lima, None.

FR0003

Gfi1 Inhibits Osteoblast Differentiation in Multiple Myeloma by Inducing Epigenetic Repression of *Runx2* in Bone Marrow Stromal Cells. Juraj Adamik*[1], Quanhong Sun[1], G. David Roodman[2], Deborah Galson[1]. [1]University of Pittsburgh, USA, [2]Indiana University, USA

Multiple myeloma (MM), the most frequent cancer to impact the skeletal system, induces osteolytic bone lesions that rarely heal even after therapeutic remission. MM-induced alteration of the bone marrow microenvironment causes suppression of bone marrow stromal cell (BMSC) differentiation into functional bone-forming osteoblasts (OB) by repressing the key OB differentiation factor Runx2. We reported that MM cells upregulate the transcriptional repressor Gfi1 in BMSC, which can repress the *Runx2* gene. We examined if direct Gfi1 binding and recruitment of chromatin co-repressors alters the epigenetic state of the *Runx2* gene resulting in long term OB suppression. Co-culture experiments revealed that MM repression of *Runx2* mRNA is a direct result of inhibition of pre-loaded, promoter-bound paused and elongating (Ser2-phospho CTD) RNA Pol II. Kinetic ChIP analyses of MM-exposed

preosteoblast MC4 cells revealed that Gfi1 is recruited to the *Runx2* gene only after 24 h of MM treatment with increased occupancy at 36 and 48 h. Concomitantly, we observed recruitment to the *Runx2* gene of histone modifiers HDAC1, Co-REST, LSD1, and G9a along with reduction of the transcriptionally permissive euchromatin marks H3K4me3, H3K9ac, H3K12ac, H3K27ac, and H3K36me3. These changes persisted even after removal of MM cells making OB differentiation refractory to OB differentiation signals. The opposite changes were found on the *Il6* gene, which is upregulated in MM-exposed BMSC. Gfi1 over-expression studies demonstrated that full length Gfi1 binds to the endogenous *Runx2* promoter and recruits HDAC1 and G9a, repressing *Runx2*. However, the 239-423 Gfi1 DNA binding domain binds *Runx2* and recruits HDAC1, but not G9a, and does not repress *Runx2*, indicating that HDAC1 recruitment is not sufficient to repress *Runx2*. Additionally we showed that although Gfi1 knockdown in MC4 cells did not block the MM-induced rapid decrease of *Runx2* mRNA (within 3 h), it did prevent the sustained repression of *Runx2* following induction of OB differentiation for 2-4 d. This result fits with the observed delayed arrival of Gfi1 at *Runx2* and suggests that Gfi1 is a critical mediator of long term epigenetic suppression of the *Runx2* gene in the myeloma distorted BMSC microenvironment. The understanding of the mechanisms associated with the suppressive effects of Gfi1 may lead to development of therapeutics for various inflammatory diseases causing homeostatic imbalance in the bone microenvironment such as MM.

Disclosures: Juraj Adamik, None.

FR0007

Atypical Femoral Fractures: Radiographic and Histomorphometric Features in 19 Patients. Aliya Khan*[1], Angela M. Cheung[2], Osama Ahmed Khan[3], Mohammed Zohair Rahman[1], Ken Pritzker[4], Brian Lentle[5]. [1]McMaster University, Canada, [2]University Health Network-University of Toronto, Canada, [3]McMaster University, Canada, [4]University of Toronto, Canada, [5]University of British Columbia, Canada

Purpose

This study describes characteristics and histomorphometric and radiographic features of atypical femoral fractures (AFF) as seen in 19 cases referred for evaluation.

Methods

All patients referred for evaluation of AFF were reviewed.

Patients meeting the ASBMR criteria for AFF were further evaluated and tetracycline labeled bone biopsies were completed. Radiographs were reviewed by a musculoskeletal radiologist.

Results

All fracture lines were transverse or short oblique and 15 of 19 patients demonstrated thickened cortices on x-ray. We report 19 cases of AFF in patients on long term bisphosphonate (BP) therapy. 14 of 19 fractures occurred without a fall or direct trauma to the femur with 5 cases occurring after a fall from standing height. All patients were female; average age was 65 years (range 23-80 years). 4 of the 19 cases were of Chinese descent, 4 were East Indian, with 11 being Caucasian. Average BP durations of use was 9.8 years (range 6-15 years). 9 of 19 patients were on alendronate alone, 2 patients were on risedronate alone, 6 patients on a combination and 1 patient on a combination of pamidronate and alendronate. 1 patient was on a combination of alendronate and denosumab. Prodromal thigh or groin pain was seen in 12 of the 19 patients for 1 to 15 months prior to fracture. Proton pump inhibitor use was present in 6 patients. 2 patients were on prednisone for rheumatoid arthritis and 2 patients on prednisone for asthma. 1 patient had a diagnosis of osteogenesis imperfecta type IV with a history of multiple fragility fractures and had experienced a femoral fracture after 12 years of IV pamidronate with features consistent with an AFF. All patients had 25OH Vit D levels > 50nmol/L. 18 of the patients with radiographic features of AFF had been on a bisphosphonate for > than 6 years. 1 patient had been on alendronate for 5 months. 8 of 19 patients had bilateral femoral fractures.

Bone Biopsy Results

A large number of patients with radiographic features of an AFF had evidence of mineralization abnormalities on tetracycline labeled bone biopsy. Decreased osteoid surface and mean mineralized trabecular width was seen in 6 of 11 biopsies. Diffuse label was noted in 5 of 11 biopsies. Mineralization abnormalities were noted in a significant number of patients with radiographic features of AFF. All of the women had normal or mildly reduced serum vitamin D levels.

Conclusion

Histomorphometric features seen on bone biopsy in women sustaining an AFF in association with long term bisphosphonate use included evidence of mineralization abnormalities and decreased bone formation. 1 patient had features of decreased bone formation and mineralization abnormalities with only 5 months of bisphosphonate exposure. Improved understanding of the pathophysiology leading to these fractures may be gained with further histomorphometric data in larger numbers of patients.

Histomorphometry

Name	OS a) 16-22 b) 16-23	MOW	MMTW	ES/TS	Label	Banding (Single/Double/Mixed)
NR	15%	6 um	115 um	4%	N	None
DM					Y	Double
EP	22%	11 um	136 um	4%	Y	Double
WL	2%	13 um	188 um	1%	Y	Double
KSC	26%	9 um	171 um	2%	Y	Single
PW	36%	8 um	169 um	2%	Y	Mixed
JI	7%	5 um	129 um	2%	Y	Double
JD	9%	6 um	110 um	5%	Y	Mixed
MSC	4%	7 um	134 um	5 %	Y	Double
CD	7%	8 um	195 um		Y	Single

OS – Osteoid Surface MOW – Mean Osteoid Width MMTW – mean mineralized trabecular width ES/TS – Eroded Surface/Trabecular Surface

Atypical Femoral Fractures ASBMR 2014

FR0010

A Novel *VCP* Mutation in a Patient with Paget's Disease of Bone without Myopathy and Neurological Involvement. Omar Albagha*[1], Ranganath Lakshminarayan[2], Stuart Ralston[1]. [1]University of Edinburgh, United Kingdom, [2]University of Liverpool, United Kingdom

Missense mutations in *VCP* cause the rare disorder of Inclusion body myopathy, Paget's disease of the bone and frontotemporal dementia (IBMPFD) and some cases of amyotrophic lateral sclerosis. Mutations of VCP have not previously been reported in classical PDB in the absence of other features of IBMPFD. Here we describe a novel missense mutation in the *VCP* gene in a patient with classical PDB. The patient was diagnosed with polyostotic PDB at age 52 years affecting the pelvis, humerus, spine and skull and there was no family history of PDB, muscle or neurological disease. He died at age 92 and there were no signs of myopathy or dementia. The *VCP* mutation was detected as part of an exome sequencing effort to identify novel PDB-associated mutations. Exome capture was performed using Agilent SureSelectXT V5 target enrichment kit followed by DNA sequencing using the illumina Hiseq2000 platform with a 36X mean coverage. Sequence mapping, alignment and variant calling were performed using the Picard/BWA/GATK pipeline. Analysis of known PDB susceptibility genes identified a heterozygous mutation c.697A>G (p.I233V) in *VCP* which was not detected in the publicly available databases including 1000 Genome and NHLBI exome data. This mutation is located next to the previously reported p.A232E which causes severe IBMPFD and affects the D1 domain that provides the protein's main catalytic activity. This study illustrates that classical PDB may occur as the result of mutations in *VCP* and extends further the phenotypic spectrum of diseases caused by missense mutations in this gene

FR0012

NFAM1 Modulates Calcineurin-NFATc1 Signaling during Osteoclast Differentiation in Paget's Disease of Bone. Yuvaraj Sambandam*[1], Kumaran Sundaram[2], Takamitsu Saigusa[1], Sudhaker Rao[3], William Ries[1], Sakamuri Reddy[2]. [1]Medical University of South Carolina, USA, [2]Charles P. Darby Children's Research Institute, USA, [3]Henry Ford Hospital, USA

Paget's disease of bone (PDB) is a chronic focal skeletal disorder that affects 2-3% of the population over 55 years of age. The disease is characterized by abnormal osteoclasts with excess bone resorption activity and abundant poor quality new bone formation.We previously detected measles virus nucleocapsid protein (MVNP) transcripts in osteoclasts from patients with PDB. Also, MVNP stimulates pagetic osteoclast formation in vitro and in vivo. We identified that microarray analysis of human bone marrow derived preosteoclast cells transduced with MVNP increased (7-fold) NFAT activating protein with ITAM motif 1 (NFAM1) expression. NFAM1(also known as CNAIP) is a ~30 kDa transmembrane glycoprotein that contains an extracellular Ig domain and an intracellular immunoreceptor tyrosine-based activation motif (ITAM) bearing region, however, a functional role for NFAM1 in PDB is unknown. Therefore, we hypothesize that NFAM1 modulates MVNP induced pagetic osteoclast differentiation. We demonstrate that MVNP expression in normal human peripheral blood monocytes (PBMC) significantly increased (10-fold) NFAM1 mRNA expression without RANK ligand (RANKL) treatment. Western blot analysis further confirmed that MVNP increased (4.8-fold) NFAM1 expression in these cells. Also, bone marrow cells derived from patients with Paget's disease demonstrated elevated levels of NFAM1 mRNA expression. NFAM1 has been shown to induce ITAM phosphorylation and Syk recruitment. We showed that MVNP transduction into preosteoclast cells increased ITAM phosphotyrosine

activation (4.0-fold) and p-Syk (5.5-fold) levels without RANKL stimulation. Furthermore, MVNP expression upregulates calcineurin, a calcium-dependent serine-threonine phosphatase (8-fold) and NFATc1 (5-fold) transcription factor expression. We then measured intracellular Ca^{2+} concentrations in fura-2/AM loaded preosteoclast cells with dual-excitation wavelength fluorescence microscopy. MVNP transduced cells stimulated with RANKL showed elevated Ca^{2+} oscillations and intracellular levels. Interestingly, shRNA knock-down of NFAM1 expression significantly decreased MVNP induced calcineurin, p-Syk, NFATc1 expression and intracellular Ca^{2+} levels in preosteoclast cells. Furthermore, NFAM1 suppression inhibits MVNP induced osteoclast differentiation in mouse bone marrow cultures. Thus, our results suggest that NFAM1 modulation of calcineurin-NFATc1 signaling axis plays a critical role in pagetic osteoclast differentiation.

FR0013

Long-Term Effect of Recombinant Human Parathyroid Hormone, rhPTH(1-84), on Skeletal Dynamics in Patients With Hypoparathyroidism: One-Year Data From the Open-Label RACE Study. Bart L. Clarke*[1], Michael Mannstadt[2], Dolores M. Shoback[3], Tamara J. Vokes[4], Mark L. Warren[5], Michael A. Levine[6], Hjalmar Lagast[7], John P. Bilezikian[8]. [1]Mayo Clinic Division of Endocrinology, Diabetes, Metabolism, & Nutrition, USA, [2]Massachusetts General Hospital & Harvard Medical School, USA, [3]SF Department of Veterans Affairs Medical Center, University of California, USA, [4]University of Chicago Medicine, USA, [5]Endocrinology & Metabolism, Physicians East, USA, [6]Children's Hospital of Philadelphia, USA, [7]NPS Pharmaceuticals, Inc, USA, [8]College of Physicians & Surgeons, Columbia University, USA

Patients with hypoparathyroidism have reduced bone turnover, abnormally increased bone mineral density (BMD), and abnormal bone microarchitecture. Conventional therapy with oral calcium (Ca) and activated vitamin (Vit) D does not normalize skeletal metabolism and can cause hypercalcemia and hypercalciuria. The phase III, placebo-controlled REPLACE study demonstrated the safety and efficacy of 50, 75, or 100 µg rhPTH(1-84) in patients with hypoparathyroidism.[1] In REPLACE, treatment with rhPTH(1-84) improved mineral homeostasis, increased bone turnover markers (BTMs), and reduced BMD. The RELAY study showed that a lower dose (25 µg) of rhPTH(1-84) may be sufficient for some patients. A hypothesis of RACE, a study of patients previously treated in REPLACE and/or RELAY, is that long-term treatment with rhPTH(1-84) provides prolonged effects on skeletal turnover and maintains serum and urine mineral parameters.

Patients were started on 25 or 50 µg/d rhPTH(1-84) with titration up to 50, 75, or 100 µg/d if active Vit D and oral Ca could be reduced further. Bone turnover was assessed by: serum levels of bone-specific alkaline phosphatase, cross-linked C-telopeptide of type 1 collagen, aminoterminal propeptide of type 1 collagen, and osteocalcin. BMD was determined by DXA.

Of the 53 patients enrolled at 13 centers (83% female; mean $\pm$ SD age 48 ± 10 y; BMI 31 ± 7 kg/m^2; mean duration of hypoparathyroidism 16 ± 13 y), 49 are included in this interim analysis. 74% (95% CI, 59–85) met the efficacy endpoint ($\geq$50% reduction in oral Ca [or $\leq$500 mg/d] and $\geq$50% reduction in active Vit D [or $\leq$0.25 µg/d] at Week 52 while maintaining a serum Ca level $\geq$7.5 mg/dL). By Week 52, mean baseline Ca and active Vit D doses were reduced by $67\%\pm34\%$ and $73\%\pm44\%$, respectively. At Week 52, all BTMs had increased from low normal baseline levels (Table). BMD Z-scores at lumbar spine (LS), total hip (TH), femoral neck (FN), and distal one-third radius (DR) decreased toward normal at Week 52 (baseline mean $\pm$ SD): LS -0.05 (2.02 ± 1.49), TH -0.08 (1.44 ± 1.14), FN -0.12 (1.27 ± 1.28) and DR -0.20 (0.94 ± 0.81). Adverse event profile was similar to the REPLACE trial.[1]

Extended treatment with rhPTH(1-84) is associated with increases in BTMs, even when re-treated with rhPTH, and beneficial reductions in BMD. These findings also demonstrate that bone turnover remains stimulated with rhPTH(1-84) over 1 year, confirming results in shorter-term studies.

Mannstadt M, et al. *Lancet Diabetes Endocr.* 2013;1:275-83.

Table. Mean Change From Baseline in BTMs at Week 52

Parameter, Mean ± SD	Actual Value	Normal Values*	Percent Change From Baseline
BSAP, µg/L			
Baseline	9.7±3.3	3–30	
Week 52	19.5±10		113±103
CTX, ng/L			
Baseline	215.6±166	≤1040	
Week 52	637.3±382		309±328
OCN, µg/L			
Baseline	3.6±2	≤22	
Week 52	21.2±17		533±439
P1NP, µg/L			
Baseline	33.8±19	≤75	
Week 52	191.2±166		512±374

BSAP=bone-specific alkaline phosphatase; CTX= cross-linked C-telopeptide of type 1 collagen; OCN=osteocalcin; P1NP= aminoterminal propeptide of type 1 collagen.
*Reference ranges as reported by a central laboratory for different BTMs; normal ranges vary by age, gender, and menopausal status.

Table - Mean Change From Baseline in BTMs at Week 52

FR0014

Low Vitamin D Levels in Primary Hyperparathyroidism Affect Cortical Bone Density and Porosity but not Estimated Bone Stiffness. <u>Marcella Walker</u>*[1], <u>Kyle Nishiyama</u>[1], <u>Elaine Cong</u>[2], <u>James Lee</u>[3], <u>Anna Kepley</u>[1], <u>Chiyuan Zhang</u>[1], <u>X Guo</u>[1], <u>Shonni Silverberg</u>[1]. [1]Columbia University, USA, [2]Columbia Presbyterian Medical Center, USA, [3]Columbia University College of Physicians & Surgeons, USA

Data regarding the skeletal effects of vitamin D (25OHD) deficiency and insufficiency in primary hyperparathyroidism (PHPT) are limited. Patients with mild PHPT (n=100; 78% women, mean age $\pm$ SD 62$\pm$12 years, calcium 10.7$\pm$0.6mg/dl, PTH 83$\pm$41pg/ml; 25OHD 30$\pm$10ng/ml) were studied with bone markers, dual x-ray absorptiometry (DXA), high-resolution peripheral quantitative computed tomography (HRpQCT) and microfinite element analysis (µFEA). Low 25OHD levels were common (54%<30ng/ml, mean 21$\pm$6 ng/ml; 20%$\leq$20ng/ml, mean 14$\pm$4ng/ml). Those with 25OHD<30 vs. $\geq$30ng/ml (mean 38$\pm$6ng/ml) did not differ by PHPT duration, history of nephrolithiasis or fractures, renal function or race, but they were younger (58$\pm$13 vs. 67$\pm$9yrs, p=0.0001), more likely to be male (31 vs. 13%, p=0.06) and tended to have higher BMI (29.0$\pm$6 vs. 26.8$\pm$6kg/m^2, p=0.06). Before and after adjusting for age and BMI, those with 25OHD<30ng/ml had higher PTH (94$\pm$42 vs. 70$\pm$42pg/ml, p=0.01) but lower PO$_4$ (2.9$\pm$0.5 vs. 3.2$\pm$0.5mg/dl, p<0.01) and FGF-23 (98$\pm$114 vs. 146$\pm$114RU/ml, p=0.06) levels but serum calcium, 1,25-dihydroxyvitamin D, and bone turnover (CTX and BSAP) did not differ. Those with 25OHD<30ng/ml had lower age- and BMI-adjusted DXA T-scores at the 1/3 radius (-1.6$\pm$1.4 vs. -0.9$\pm$1.4; p=0.02) but not at other sites (spine: 1.0$\pm$0.2 vs. 0.9$\pm$0.2, p=0.73; FN: -1.1$\pm$1.0 vs. -1.3$\pm$1.0, p=0.66; total hip: -0.7$\pm$1.0 vs. -1.1$\pm$1.6, p=0.29). By HRpQCT, those with 25OHD<30ng/ml had 15% higher cortical porosity at the tibia (7.5$\pm$2.3 vs. 6.5$\pm$2.3%, p=0.05) but not the radius, and tended to have lower cortical density (radius: 801$\pm$83 vs. 832$\pm$83mgHA/cm^3 p=0.07; tibia: 756$\pm$67 vs. 783$\pm$68mgHA/cm^3 p=0.06). These differences did not affect µFEA-estimated whole bone stiffness (radius: 31.0$\pm$9.6 vs. 32.4$\pm$9.6kN/mm, p=0.51; tibia: 102.7$\pm$23.0 vs. 98.9$\pm$23.0kN/mm, p=0.45) or failure load. Trabecular indices did not differ by vitamin D status. Those with 25OHD$\leq$20ng/ml also had higher PTH ($\leq$ 20 vs. $\geq$30ng/ml: 113$\pm$40 vs. 70$\pm$42pg/ml, p<0.001; vs. >20ng/ml: 75$\pm$39pg/ml, p<0.001). Similar cortical trends were apparent in those with 25OHD$\leq$ 20 vs. $\geq$30, but these were less marked in those with 25OHD $\leq$ 20 vs. >20ng/ml. Results were similar in women only. In mild PHPT low 25OHD is associated with higher PTH levels, higher cortical porosity and modestly lower cortical BMD. These differences did not result in lower mechanical competence, suggesting that the current 25OHD thresholds do not have a major effect upon skeletal health in mild PHPT.

Disclosures: Marcella Walker, None.

FR0015

PTH(1-84) Treatment is Safe and Effective in Hypoparathyroidism for Six Years. <u>Mishaela Rubin</u>*[1], <u>Natalie Cusano</u>[2], <u>Laura Beth Anderson</u>[1], <u>Dinaz Irani</u>[3], <u>James Sliney</u>[1], <u>Elizabeth Levy</u>[1], <u>Wen-wei Fan</u>[1], <u>Donald McMahon</u>[2], <u>John Bilezikian</u>[2]. [1]Columbia University, USA, [2]Columbia University College of Physicians & Surgeons, USA, [3]Columbia University Medical Center, USA

Hypoparathyroidism (HypoPT) is a rare disorder in which PTH is absent. We found that 4 years of PTH(1-84) reverses the associated hypocalcemia, hyperphosphatemia, hypercalciuria and elevated bone mineral density (BMD). Yet the lifelong nature of HypoPT necessitates an extension of those findings. 27 HypoPT (47.7 $\pm$ 2 yrs; 20 female; 25 Caucasian) were studied (postsurgical: n=16; autoimmune: n=10; DiGeorge: n=1). Medications included calcium: 2858 $\pm$ 240 mg/d; calcitriol: 0.66 $\pm$ 0.1 µg/d; vitamin D: 13,389 $\pm$ 3,247 IU/d and HCTZ: 9 $\pm$ 3 mg/d. Serum calcium was 8.5 $\pm$ 1 mg/dL with undetectable PTH; BMD (g/cm^2) was lumbar spine 1.227 $\pm$ 0.05; femoral neck 0.968 $\pm$ 0.04, total hip 1.085 $\pm$ 0.04 and distal 1/3 radius 0.733 $\pm$ 0.01. PTH(1-84) was started at 100 µg qod and changed after 2-3 years to 50 µg/d (n=15); other doses ranged from to 25-100 µg/d. Decreases occurred in supplemental calcium (2858 $\pm$ 240 to 1250 $\pm$ 267 mg/d; p<0.001), calcitriol (0.66 $\pm$ 0.1 to 0.27 $\pm$ 0.1 µg/d; p<0.001) and vitamin D (13,389 $\pm$ 3,247 to 2045 $\pm$ 3,633 p=0.04); HCTZ did not change. Serum calcium was stable (8.5 $\pm$0.2 to 8.6 $\pm$0.2 mg/dl) while 24 hr urinary calcium decreased (273.0 $\pm$ 25 to 193.3 $\pm$ 27 mg; p=0.007). Serum phosphate (4.3$\pm$0.2 to 4.2 $\pm$0.2 mg/dl), creatinine (0.96 $\pm$ 0.1 to 0.96 $\pm$ 0.1 mg/dl), and 1,25(OH)2D (39.0 $\pm$ 4 to 33.8 $\pm$ 10) did not change, but 25(OH)D (79.7 $\pm$7 to 40.9 $\pm$ 19 ng, p=0.04) and Mg decreased (1.8 $\pm$0.1 to 1.7 $\pm$0.1 mg/dl; p=0.02), while alkaline phosphatase increased (65.3 $\pm$ 3 to 77.3 $\pm$ 4 IU/l; p=0.007). BMD (g/cm^2) increased 4% at the spine (1.22 $\pm$ 0.1 to 1.26 $\pm$ 0.1; p=0.004), 3% at the total hip (1.08 $\pm$ 0.1 to 1.10 $\pm$ 0.1; p=0.03), did not change at the femoral neck (0.97 $\pm$0.1 to 0.97 $\pm$0.1) and decreased 4% at the 1/3 radius (0.73 $\pm$ 0.1 to 0.71 $\pm$ 0.1; p<0.001). One kidney stone and 2 fractures (stress and toe) occurred. Hypercalcemia occurred 13 times out of 407 serum calcium measurements (6%). These data suggest that 6 years of PTH(1-84) treatment in HypoPT leads to sustained normalization in calcium metabolism. Urinary calcium excretion, calcium and calcitirol supplemental requirements persisted in being lower than baseline values, along with maintenance of normal serum calcium levels. BMD changes were site-specific, with a proclivity to increase at trabecular and decrease at cortical sites. These data, the longest-term clinical experience with PTH treatment available to date, suggest that PTH(1-84) treatment is a safe and effective long-term option in HypoPT.

Disclosures: Mishaela Rubin, NPS Pharmaceuticals, 7

FR0016

Skeletal Microstructure Continues to Improve Markedly Two Years After Parathyroidectomy in Primary Hyperparathyroidism. <u>Natalie Cusano</u>*[1], <u>Chiyuan Zhang</u>[2], <u>Wen-Wei Fan</u>[1], <u>Aline Costa</u>[2], <u>Elizabeth Levy</u>[1], <u>John Bilezikian</u>[1]. [1]Columbia University College of Physicians & Surgeons, USA, [2]Columbia University, USA

It is well known that BMD improves after parathyroidectomy in primary hyperparathyroidism but little is known about post-parathyroidectomy changes in skeletal microstructure. We previously reported our results in a cohort of subjects through 18 months and we now extend our findings through 2 years post-parathyroidectomy. We studied 28 subjects [age: 63 $\pm$ 14 years, duration: 7 $\pm$ 9 years, 19 women (17 postmenopausal), 93% Caucasian] with baseline and at least 6 month data. Of these participants, 19 were also assessed at 12 months, 15 at 18 months, and 9 at 24 months (5 women). Measurements were made at the distal radius and tibia using high resolution peripheral quantitative computed tomography (HRpQCT, Scanco Medical AG) to assess volumetric bone mineral density (vBMD) and bone microstructure. To evaluate changes after parathyroidectomy, we used a linear mixed model for repeated measures. At both the radius and tibia, there were significant increases in total vBMD; total, cortical, and trabecular area; and cortical thickness (Table). Additionally, there was a significant increase in cortical density at the tibia alone. The tibia experienced greater numerical improvements than the radius.

We also investigated sex-specific differences using sex as a covariate in the model. Age was similar (men: 57 $\pm$ 19 vs. women: 66 $\pm$ 10 years; p=0.13). Men demonstrated a trend towards shorter duration of disease (2 $\pm$ 5 vs. 9 $\pm$ 7 years; p=0.06). We found gender-specific differences at the tibia that remained significant after adjustment for age and disease duration in trabecular density (men: +3.4 $\pm$ 10% vs. women -0.3 $\pm$ 9%; p=0.006) and trabecular bone volume fraction (men: +3.2 $\pm$ 10% vs. women -0.3 $\pm$ 9%; p=0.009).

This report provides the longest post-parathyroidectomy results for HRpQCT to date, demonstrating clear improvement in geometric properties and vBMD at both the radius and tibia. Our results continue to demonstrate site-specific differences, with greater improvements at the tibia, a weight-bearing site. We also report gender-specific differences in trabecular microstructure at the tibia. The etiology for sex-specific differences in response to parathyroidectomy is unclear. The results help to establish that bone quality improves after parathyroidectomy and that there ar0e differences between men and women.

Table. Percentage change in cortical (Ct) and trabecular (Tb) HRpQCT parameters up to 24 months after PTX in PHPT subjects

Radius	6 months (%)	12 months (%)	18 months (%)	24 months (%)
Total vBMD	1.02 ± 3.9*	1.01 ± 6.1	1.83 ± 7.5*	2.32 ± 9.0*
Total Area	0.09 ± 0.5	0.21 ± 0.7†	0.26 ± 0.9†	0.29 ± 1.0†
Ct Area	1.38 ± 8.2	2.10 ± 9.6	2.78 ± 10.5	5.56 ± 12.9‡
Tb Area	-0.14 ± 1.3	-0.05 ± 1.6	-0.17 ± 1.7	-0.66 ± 2.1†
Ct Thickness	1.81 ± 8.5	2.40 ± 9.9*	3.04 ± 10.9*	5.82 ± 13.3‡
Ct Density	0.05 ± 2.6	-0.02 ± 4.0	-0.23 ± 4.7	0.51 ± 5.7
Tibia	6 months (%)	12 months (%)	18 months (%)	24 months (%)
Total vBMD	1.43 ± 3.2‡	2.36 ± 5.0‡	2.57 ± 6.3‡	3.09 ± 7.8‡
Total Area	0.12 ± 0.3†	0.15 ± 0.6‡	0.25 ± 0.6‡	0.33 ± 0.7‡
Ct Area	3.68 ± 8.5†	5.67 ± 13.4‡	9.44 ± 17.1‡	11.00 ± 21.4‡
Tb Area	-0.34 ± 0.7†	-0.62 ± 1.0‡	-0.56 ± 1.3‡	-0.83 ± 1.6‡
Ct Thickness	3.69 ± 8.9†	5.66 ± 14.0‡	9.89 ± 17.8‡	11.00 ± 22.2‡
Ct Density	0.51 ± 2.9	0.43 ± 4.6	1.47 ± 5.7*	1.89 ± 6.9*

Mean ± SD; vBMD, volumetric bone mineral density; *p<0.05, †p<0.01, ‡p<0.001 from baseline

Table

Disclosures: Natalie Cusano, None.

FR0020

Accurate Quantification of Bone Fragility Requires Inclusion of Pores of all Sizes. <u>Afrodite Zendeli</u>*[1], <u>Yohann Bala</u>[2], <u>Mariana Kersh</u>[3], <u>Ali Ghasem-Zadeh</u>[4], <u>Ego Seeman</u>[4], <u>Roger Zebaze</u>[5]. [1]Endocrine Centre, Austin Health, University of Melbourne, Australia, Australia, [2]University of Melbourne, Dept. of Medicine, Australia, [3]Department of Mechanical Engineering, Melbourne School of Engineering, University of Melbourne, Australia, Australia, [4]Austin Health, University of Melbourne, Australia, Australia, [5]Austin Health, University of Melbourne, Australia

Introduction: Intracortical remodeling during growth forms osteons with Haversian and Volkmann canals responsible for most cortical voids which are seen as 'pores' of ~50-80 µm. With age, unbalanced and accelerated remodeling upon canal surfaces enlarges them focally, some coalesce form large pores, while new canals may be excavated increasing canal density (number per unit volume). This increase in porosity causes 70% of all age-related bone loss and increases fragility exponentially. As porosity may generate stress concentrators and influence crack initiation, large numbers of small pores may reduce strength more than fewer large pores independently of the total void volume. As in vivo imaging devices like HRpQCT have a resolution of ~125 µm, we proposed that failure to include pores <125 µm

underestimates bone fragility by underestimating porosity and disregarding the stress risers so produced by small pores.

Methods: In scanning electron microscopy images of the anterior subtrochanteric region in 16 Caucasian women (age 29 – 87 years), we assessed pore number and diameter to determine the contribution of pores < 125 μm to total porosity. Finite element (FE) models were used to simulate loading the subtrochanteric cortex. Total porosity was kept constant at 25% varying pore size from 53 to 300 μm while applying a 250KN bending force along one edge of the cortex to quantify strain distribution.

Results: Limiting quantification of porosity to pores > 125μm excluded $77.2 \pm 9.4\%$ of all pores in the total cortex; $88.1 \pm 9.22\%$ of pores were missed in the compact-appearing cortex (CC), and $58.6 \pm 14.3\%$ were missed in the transitional zone (TZ) ($p < 0.001$). Thus, porosity was underestimated by 41.9 ± 17.4 % in the total cortex. The underestimation was almost three-fold greater in the CC than in the TZ (56.6 ± 20.2 % vs 18.1 ± 16.6 %; $p < 0.001$).

For a given level of porosity, although total strain was relatively constant, areas with highest strain increased with decreasing pore diameter ($R^2 = 0.72$; $p < 0.001$). When pore size was < 125 μm, the areas subjected to >2600 μstrain increased by 135% compared to models with pores > 125 μm.

Conclusion: Confining quantification of porosity to pores above the resolution of HRpQCT underestimates porosity by 50% and ignores the contribution of ~80% of all pores to fragility. Accurate quantification in the effects of ageing, diseases and therapies in bone fragility requires inclusion of all pores regardless of their size.

Disclosures: Afrodite Zendeli, None.
This study received funding from: NHMRC

FR0026

Consequences of acute estrogen deficiency on bone quality and biology and the effects of Low Intensity Vibrations for mitigating bone loss. <u>Divya Krishnamoorthy</u>*[1], <u>Clinton Rubin</u>[2], <u>Danielle Frechette</u>[3]. [1]SUNY Stony Brook University, USA, [2]State University of New York at Stony Brook, USA, [3]Stony Brook University, USA

Current drug and non-drug treatments for post-menopausal osteoporosis are not particularly effective at reversing the severe insult to bone quantity. This study investigates the responsiveness of skeletal remodeling in ovariectomized (OVX'd) mice to low intensity mechanical vibrations (LIV), which has been shown to be anabolic to bone. We aimed to identify the most effective period, either in the acute or chronic phases of OVX-induced bone loss, for the application of mechanical intervention. In just 2w following the cessation of estrogen, C57BL/6 female mice OVX'd at the age of 8w (n=5, OVX) revealed a significant 38% (p<0.05) reduction in trabecular BV/TV compared to sham controls (n=6, AC), along with a 19% increase and 18% decrease in trabecular spacing and number, respectively (both p>0.05). In addition to the immediate defect in bone quality, bone marrow cell populations also exhibited shifts within just 2w following OVX. The percent of B cells, T cells and myeloids show 44% increase (p>0.05) and 14% & 17% decrease (p>0.05) with respect to controls. Mice receiving just 2w of LIV (n=8, LIV) treatment (0.3g, 90Hz, 15min/day) immediately following cessation of estrogen exhibited only about half the decrease in BV/TV compared to shams as that of OVX (-20% in LIV (p>0.05) vs. -38% in OVX (p<0.05)). Bone marrow leukocyte populations showed no significant differences with LIV suggesting that, the partial mitigation of bone by LIV might actually be a protection of resident bone cells rather than an effect on the bone marrow cell populations. The application of LIV for 6w following the significant insult to bone that occurs in 2wks was in fact unsuccessful at both restoring trabecular bone and normalizing bone marrow leukocyte populations. These data not only reveal that the insult to the skeletal quality and biology is defected immediately upon estrogen deficiency but that the application of interventions would be more effective during menopause when bone remodeling is at its peak rather than post-menopause when bone loss it too severe to overcome.

Estrogen Deficiency results in a signifcant insult to trabecular BV/TV following 2 weeks and LIV treatment mitigates the loss
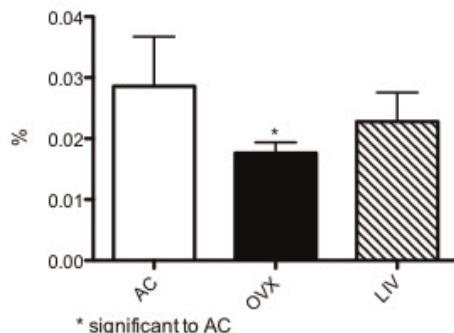
Estrogen Deficiency results in insult to BV/TV following 2w & LIV treatment mitigates the loss

Disclosures: Divya Krishnamoorthy, None.

FR0027

Cortical Tissue from Postmenopausal Women with Atypical Fractures Shows Reduced Heterogeneity in Nanomechanical Properties. <u>Ashley Lloyd</u>*, <u>Eve Donnelly</u>. Cornell University, USA

Bisphosphonates are the primary pharmacologic treatment for osteoporosis and reduce fracture risk by 30-50% in postmenopausal women. However, atypical femoral fractures, characterized by a transverse brittle morphology, have been associated with prolonged bisphosphonate treatment. Because bisphosphonates reduce bone remodeling, they have the potential to alter bone tissue material properties. However, the tissue material properties of atypical fractures are unknown.

Thus, the objectives of this study were (1) to compare the nanomechanical properties of bone tissue from patients with atypical femoral fractures to that of patients with typical fragility fractures, and (2) to correlate the nanomechanical properties with compositional properties.

Specimens of proximal femoral cortical bone adjacent to the fracture site were obtained from postmenopausal osteoporotic women during fracture repair surgery. The patients were allocated into three study groups: patients with atypical fractures, all of whom had a history of bisphosphonate use (+BIS Atypical: n=7, age 73+/-12y, bis 9.3+/-4y); and patients with typical fragility fractures with and without bisphosphonate use (+BIS Typical: n=4, age 88+/-6y, bis 9.5+/-6y; -BIS Typical: n=4, age 85+/-3y).

Raman microscopy was used to assess the mineral:matrix ratio, carbonate:phosphate ratio, and mineral crystallinity. Nanoindentation was used to assess the reduced modulus and hardness. The compositional properties were correlated with nanomechanical properties. Compositional heterogeneity was assessed through the full width at half maximum of parameter histograms.

Mean mineral:matrix ratio was 7.5% greater in atypical samples compared to pooled controls (+BIS Atypical: 1.57 vs. +BIS Typical: 1.33, p=.016; vs. –BIS Typical: 1.41, p=.086) (Fig. 1a). The distributions of tissue mechanical properties were narrower in atypical samples compared to pooled controls, with reduced modulus 15.9% narrower (p=.053) and hardness 12.4% narrower (p=.033) (Fig. 1b). Crystallinity was the best predictor of both hardness and reduced modulus across all groups.

The elevated tissue mineralization in atypical samples suggests increased tissue age and increased brittleness. The decrease in heterogeneity of mechanical properties is consistent with a reduction in overall bone toughness due to a loss of intrinsic toughening behavior and the transverse fracture morphology observed radiographically.

Fig. 1 Comparison of compositional and nanomechanical parameters for +BIS Atypical, +BIS Typical, and –BIS Typical groups. *p<0.05, #p<0.08 (a) Parameter means (b) Parameter distribution widths
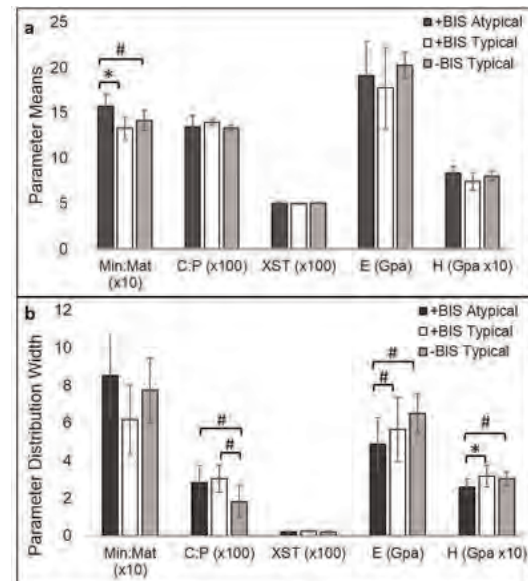
Comparison of parameter means and distribution widths across groups

Disclosures: Ashley Lloyd, None.

FR0036

Sequential Impact Loading and Zoledronic Acid Pre-Treatments Protect Against Disuse-Induced Bone Strength Loss in the Rat Femoral Neck. <u>Ray Boudreaux</u>*, <u>Jessica Brezicha</u>, <u>Scott Lenfest</u>, <u>Anand Narayanan</u>, <u>Susan Bloomfield</u>, <u>Harry Hogan</u>. Texas A&M University, USA

Disuse is a potent down-regulator of bone mass. Recent data demonstrate that bisphosphonates (BP) and exercise can mitigate bone loss, yet interactive effects when the two are combined are unclear. Zoledronic Acid (ZA) given as a yearly injection avoids the GI side effects of other BPs. This study used high impact loading (IL) to simulate exercise, followed by ZA just before a period of disuse. We hypothesized that this novel sequential pre-treatment would protect against disuse-induced losses in strength and densitometric properties at the femoral neck (FN). We further

hypothesized that the sequential combination of IL and ZA pre-treatment would be superior to either treatment alone.

Male Sprague-Dawley rats (6-mo) were block assigned by initial body weight to 1 of 6 groups (n=12/group): BC (baseline control), CC (cage control), HU (hindlimb unloaded), IL+HU (impact loading prior to HU), ZA+HU (ZA prior to HU), and IL+ZA+HU (IL followed by ZA prior to HU). IL took place 3x/wk, consisting of 25 free-fall drops per session from a height of 60 cm for 5 weeks. A single dose of ZA (60 µg/kg) was administered the day before the start of 28d of HU, achieved via the traditional tail suspension method. Femurs were collected at the end of HU, and *ex vivo* pQCT scans conducted followed by standard mechanical tests of the FN. For untreated HU rats, disuse caused significantly lower ultimate force (-20%) and absorbed energy (-35%) vs. CC, but all 3 treatments were effective countermeasures. At the end of HU, ultimate force was 21% higher than HU for IL+HU, 17% higher for ZA+HU, and 31% higher for the combination (IL+ZA+HU). Absorbed energy was also higher (by 34%, 30%, 49%, respectively). HU lowered total BMC (-11%) and vBMD (-6%) vs. CC. All 3 treatments had significantly higher vBMD than HU (by 5.8%, 6.9%, 8.3%, respectively). For BMC and bending strength index, however, only IL+ZA+HU led to significantly higher values vs. HU (by 14% and 15%, resp.).Our study demonstrated that monotherapy of IL or ZA was capable of mitigating HU-induced bone loss in the FN of skeletally mature rats, but the sequential combination of IL+ZA was better than either treatment alone for mechanical properties and selected densitometric variables. To our knowledge, this is the first study to document protection from disuse bone loss in rats via ZA and/or impact loading. The results provide encouraging support for the potential advantages to be gained from combination therapies.

Disclosures: Ray Boudreaux, None.

FR0042

Microdamage Formation In Osteocalcin and Osteopontin Deficient Mice. Stacyann Morgan*[1], Ondrej Nikel[1], Atharva Poundarik[2], Caren Gundberg[3], Deepak Vashishth[1]. [1]Rensselaer Polytechnic Institute, USA, [2]Rensselaer Polytechnic University, USA, [3]Yale University School of Medicine, USA

Fatigue-induced microdamage leads to bone resistance against stress and fragility fractures. We have recently shown that osteocalcin (OC) and osteopontin (OPN) acts as link proteins and enhances bone toughness[1]. However, the role of these proteins in energy dissipation during physiological cyclic loading is unknown. To address this question, here we studied microdamage formation in wild type (WT) and OC-OPN$^{-/-;-/-}$ mice subjected to cyclic loading.

Tibias from male 6 months old C57/BL6 mice (n=6) and their OC-OPN$^{-/-;-/-}$ littermates were obtained and stored in saline soaked gauze at -80C until use. The soft tissue was removed and a strain gauge (EA-13-015DJ-120, Vishay) was bonded on to the lateral surface. Each bone was loaded by a linear ramp in four point bending at 40N/sec until 5000µ² was achieved. The bones were subsequently loaded in fatigue between 1N and the predetermined maximum load at 2Hz. Cyclic loading was interrupted in the tertiary phase of the fatigue life at 70% stiffness loss. Samples were stained in 1% basic fuchsin and embedded in polymethyl methacrylate (PMMA). Transverse sections through the region of the gauge were created at 100 µm thickness. Diffuse damage and linear microcracks were observed using a confocal microscopy at 10x (Zeiss LSM 510Meta, Carl Zeiss,Germany). Linear microcrack density and diffuse damage area were assessed for each sample. Mann-Whitney Rank Sum test was used to determine differences between the groups.

Linear microcracks and diffuse damage was observed in both groups. However, diffuse damage was significantly higher in WTs (p=0.002) than OC-OPN$^{-/-;-/-}$ (WT=0.072$\pm$0.06 mm^2/ mm^2, OC-OPN$^{-/-;-/-}$ =0.003$\pm$0.07 mm^2/ mm^2). While OC-OPN$^{-/-;-/-}$ had higher number of linear microcracks (4.33$\pm$3.5 #LMC/ mm^2) compared to WTs (3.0$\pm$2.7 #LMC/ mm^2), the result was not significantly different (p=0.30). Differences in fatigue behavior between the two groups was consistent with microdamage data and also showed differences in post fatigue creep behavior. In summary, our study shows that the loss of OC and OPN from bone matrix, significantly reduces diffuse damage formation and affects fatigue behavior of bone. The results indicate that energy dissipation is largely governed by diffuse damage formation, as opposed to linear microcracks, and its absence decreases the resistance of bone to fatigue failure.

References: [1] Poundarik, et al (2012) Dilational Bone Formation in Bone. PNAS 109(47):19178-83

Disclosures: Stacyann Morgan, None.

FR0046

Lack of Adaptive Bone Response to Increased Mechanical Loading in a Mouse Model of Reduced Peripheral Sensory Nerve Function. Mollie Heffner*[1], Blaine Christiansen[2]. [1]UC Davis Medical Center, USA, [2]University of California - Davis Medical Center, USA

Sensory nerves in bone have traditionally been assigned the role of pain transmission, but recent insights into the interaction between neuropeptides and bone cells suggest a more direct role for nerves in bone. However, the role of sensory nerves in bone, especially under adaptive conditions such as increased mechanical loading, remains largely undefined. In this study, we used capsaicin-treated mice as a model of decreased peripheral sensory nerve function to study the role of sensory

nerves during adaptation of bone to anabolic mechanical loading. Mice were injected subcutaneously with capsaicin (50 mg/kg) on days 2 and 5 after birth; decreased sensory nerve function was confirmed in skeletally mature mice (12 weeks old) with a thermal stimulus sensitivity test. Capsaicin- (n = 10 male, 10 female) and vehicle-treated mice (n = 10 male, 8 female) were subjected to mechanical loading via tibial compression. The right lower leg of each mouse was compressed to a target compressive load of 3 N at 4 cycles/sec, 1200 cycles/day, 5 days/week for 2 weeks. Left tibiae served as internal controls. Bilateral tibiae were scanned using micro-computed tomography (SCANCO µCT 35). Trabecular bone was analyzed at lateral and medial compartments of the proximal tibial metaphysis. Cortical bone was analyzed at 10, 20, 30, 40 and 50% of the tibia length from the proximal end. Tibial compression resulted in increased bone structure in the loaded tibiae of vehicle-treated mice, particularly at the lateral metaphysis trabecular bone, and at proximal sites along the tibial length (10% and 20%). In contrast, we observed no differences in bone structure between the loaded and contralateral tibiae of capsaicin-treated mice. For example, male vehicle-treated mice had 5.5% greater trabecular thickness at the lateral region of the tibial metaphysis (p = 0.028), while male capsaicin-treated mice showed no significant change. Similarly, female vehicle-treated mice had 2.7-5.8% greater bone area in the loaded tibia compared to the contralateral tibia at 10% and 20% of the tibia length, while female capsaicin-treated mice showed no differences at these locations (Fig. 1). These findings suggest that bones of mice with reduced peripheral sensory nerve function are less sensitive to increased mechanical loading than sensory intact mice. These observations are potentially important when considering treatment options for bone disease in subjects with diminished sensory nerve activity.
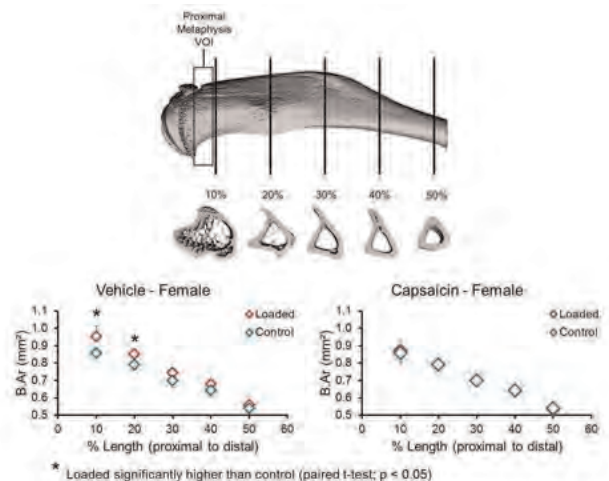
Cross-sectional bone area of loaded and control tibiae of vehicle and capsaicin-treated female mice.

Disclosures: Mollie Heffner, None.

FR0048

A School-based Seven Year Exercise Intervention Program in 6-9 Year Old Children Improve Skeletal Traits without Increasing the Fracture Risk – A Population-Based Prospective Controlled Study in 3534 Children. Jesper Fritz*[1], Magnus Karlsson[2], Bjorn Rosengren[2], Magnus Dencker[2], Caroline Karlsson[2]. [1]Sweden, [2]Skåne University Hospital Malmö, Lund University, Sweden

Purpose: Most prospective physical activity (PA) intervention studies in children are short-term and concerns for an increased fracture risk.

Method: We conducted a population based long-term prospective controlled exercise intervention study with 40 minutes of scheduled PA in school per day for 7 years in 619 girls and 720 boys aged 6-9 years at study start. An age matched control cohort of 1069 girls and 1126 boys continued with the Swedish standard of 60 minutes PA per school week. We registered incident fractures and calculated rate ratio (RR) with 95% confidence interval (95% CI). In a sub-sample of 63 girls and 91 boys in the intervention and 38 girls and 36 boys in the control group, we followed skeletal traits annually by dual X-ray absorptiometry (DXA) and at last follow-up also by peripheral quantitative computed tomography (pQCT). We calculated individual slopes and annual changes in bone mineral density (BMD; g/cm2), bone mineral content (BMC; g) and femoral neck area (cm2) and we also assessed volumetric BMD (vBMD; mg/cm3) between groups. Data are reported as mean gender-specific group differences with 95% CI within brackets.

Results: There were 25.2 fractures/1000 person-years in the intervention group and 23.4 fractures/1000 person-years in the control group, resulting in a RR of 1.08 (0.88, 1.31). Furthermore, there were no group differences in the gender specific fracture risk evaluations (data not shown). For girls the annual gain in spine BMD was 0.01g/cm2 (0.00, 0.01), in femoral neck BMC 0.07g (0.02, 0.11) and in femoral neck area 0.03cm2 (0.00, 0.06) greater in the intervention than in the control group. With DXA at last follow up, the intervention girls had 0.4g (0.0, 0.8) higher femoral neck BMC than the control girls. With pQCT at last follow up, the intervention girls had 13.7mm2 (0.4, 27.0) larger tibial cortical area, 16.4g (1.3, 31.4) higher tibial cortical BMC and

22.6mg/cm3 (4.1, 41.0) higher tibial trabecular vBMD than the control girls. The intervention boys had at last follow-up 18.5mg/cm3 (4.1, 32.9) higher radius cortical vBMD than the control boys while the other traits and annual gains were similar.

Conclusions: PA intervention for 7 years in school in at study start 6-9 year old children, improves in girls the gain in bone mass and bone structure and is in boys associated with higher bone mass without in neither of the genders increasing the fracture risk.

FR0051

Effects of History of Amenorrhea on Marrow Adiposity, Cortical Bone Mass and Distribution in Retired Elite Gymnasts. Rachel Duckham*[1], Timo Rantalainen[2], Gaele Ducher[3], Prisca Eser[3], Robin Daly[4]. [1]Deakin University, Aus, [2]University of Jyväskylä, Finland, [3]Deakin University, Australia, [4]Centre for Physical Activity & Nutrition Research, Deakin University, Australia

Purpose: Bones adapt to prevalent loading in a site-specific manner, which may be related to the preferential differentiation of bone marrow mesenchymal stem cells into osteoblasts rather than adipocytes. Given that amenorrhea (AME) can adversely affect bone health, the aims of this study were to examine: 1) the effects of history of athletic AME on exercise-induced changes in bone strength, geometry, cortical vBMD and its distribution in retired gymnasts; 2) examine whether bone marrow density, as an estimate of marrow adiposity, differs between retired gymnasts with contrasting menstrual histories, and 3) whether marrow density is an independent predictor of cortical bone mass, structure and strength.

Methods: 28 female retired gymnasts (mean$\pm$SD: age 23 ± 5 years; years retired 6 ± 4) reporting a history of AME (primary or secondary AG, n=10) were compared with former eumenorrhoeic gymnasts (EG, n=15) and controls (C, n=30, aged 26 ± 8 years). pQCT was used to assess marrow density, muscle CSA, total (ToA), cortical (CoA) and medullary area (MeA), strength strain index (SSIp) and total cortical and regional (endo-, mid- and peri-cortical) vBMD at the mid (66%) radius and tibia.

Results: Menarcheal age was delayed in AG compared to EG and C (17 vs 13 and 12 years, P<0.001). At the radius, SSIp was 22-29% (P<0.001) higher in AG and EG versus C, which was accompanied by 19-25% (P<0.001) greater ToA. CoA was not different between AG and C because of medullary expansion in AG. Radial cortical vBMD was 9-18% (P<0.05) lower at the endo- and mid-cortical regions in AG compared to C. At the tibia, AG had 18% (P<0.05) higher SSIp compared to C, which was accompanied by enhanced bone structure (12-13% greater ToA and CoA, P<0.05) but not cortical vBMD. Marrow density did not differ significantly between AG (tibia 0.967+0.006; radius 0.946$\pm$0.008), EG (tibia 0.959$\pm$0.006; radius 0.957$\pm$0.007) and C (tibia 0.954$\pm$0.004; radius 0.960$\pm$0.005). Moreover, there was no associations between marrow density and bone strength and its determinants in the subgroups or all women combined, even after adjusting for bone length, MeA and muscle CSA.

Conclusion: Former female gymnasts, irrespective of menstrual history, had greater cortical bone size and strength, but normal or lower vBMD, at peripheral sites compared to the non-active women. In contrast, there were no differences in marrow adiposity which suggests that it did not contribute to the observed differences in bone strength.

FR0054

Increased Physical Activity during Growth Improves Muscular Development without Affecting Fracture Risk – a Four-Year Prospective Controlled Exercise Intervention Study in 2 525 Children. Marcus Coster*[1], Jesper Fritz[1], Magnus Dencker[2], Susanna Stenevi-Lundgren[2], Jan-Ake Nilsson[2], Bjorn Rosengren[2], Magnus Karlsson[2]. [1]Sweden, [2]Skåne University Hospital Malmö, Lund University, Sweden

Short-term pediatric exercise intervention programs improve muscle strength. It is unknown whether these benefits remain with extended duration of intervention, and some concerns for higher fracture risk have been raised. We therefore evaluated the effects of a four-year exercise intervention on fracture risk and muscle strength.

We registered incident fractures in an intervention group of 391 girls and 468 boys, aged 6–9 years at study start, who received 40 minutes of physical activity (PA) per school day (200 minutes per week) during a four-year period, and in a control group of 815 girls and 851 boys who continued with the standard of 60 minutes of PA per week. In a sub-cohort of 236 children we annually estimated muscle strength as isokinetic Peak Torque (PT) of the knee extensors and flexors in the right leg at speeds of 60o/second and 180o/second by a computerized dynamometer. We also measured lean body mass by dual energy X-ray absorptiometry (DXA). We calculated the rate ratio (RR) for fracture risk and estimated annual change in muscle strength and lean body mass by linear regression in each individual. We adjusted group comparisons for baseline age, baseline value for the measured parameter, annual changes in height and Tanner stage at follow-up.

The fracture risk was similar in the intervention and control group [RR 1.10 (0.82, 1.47)]. The annual gain in PT flexion strength was greater in girls (p<0.05) and boys (p<0.01) in the intervention than in the respective control group, while the gain in lean body mass was similar. Girls in the intervention group also had greater gain in PT extension strength at 180 °/sec (p<0.05).

Our four-year exercise intervention program initiated in the prepubertal period improves the gain in leg muscle strength in both girls and boys without affecting the fracture risk.

FR0055

Novel "3-6" infant DXA scanning and analysis protocols to isolate movement and other artifacts. John Shepherd*[1], Bo Fan[1], Cassidy Powers[2], Lynda Stranix-Chibanda[3], Mary Glenn Fowler[4], Linda Dimeglio[5], Cynthia Mukwasi[6], Kathy George[7], George K Siberry[8]. [1]University of California, San Francisco, USA, [2]UCSF, USA, [3]Department of Paediatrics & Child Health College of Health Sciences University of Zimbabwe, Zimbabwe, [4]Makerere University(MU)-Johns Hopkins University(JHU) Research Collaboration, Uganda, [5]Indiana University School of Medicine, USA, [6]University of Zimbabwe, Zimbabwe, [7]FHI 360, USA, [8]NICHD/NIH, USA

Much progress has been made in prevention of mother to child transmission (PMTCT) of HIV by use of combination antiretroviral drugs (ARVs) given to the mother and infant during pregnancy and breastfeeding. However, some ARVs have been linked to decreased bone mineral density. Movement and artifacts in infant DXA scans are common, and may lead to scan invalidation. To date, standardized acquisition and analysis methods for infant spine and whole body DXA scans do not exist. We developed a "3-6" infant DXA protocol for up to 3 scan attempts and 6 analysis regions for whole body scans. The 3-6 protocol is designed to improve the odds of acquiring a motion-free scan, and a correction method using either reflection or multiscan imputation. We characterized the effectiveness of this protocol by measuring the precision and accuracy of the bone and soft tissue measures. Newborns received spine and whole body DXA scans with up to 3 attempts to acquire a motion free scan. All attempts were saved. A 6-region whole body analysis was used to allow for reflection analysis of arms and legs, and to isolate the head. We evaluated the difference in BMC for head and arm positioning. Regional precisions were estimated as root mean square errors (RMSE) or percent coefficients of variation (%CV) for scans with multiple valid results. Results from scans without movement were compared to estimated results from either reflection (whole body) or multiscan imputation (spine). To date, 533 infants have been sequentially recruited (198 male) with at least one valid whole body scan (82%) and spine scan (91%). An additional 11% of whole body and 7% of spine scans were recovered using reflection and multiscan imputation. Spine precision for paired scans was 3.2% (BMD) and 4.1% BMC (n=30 pairs). Whole body precision was 6.6% for BMC and 5.0% for BMD (n=5 pairs), and 1.9%, 3.2%, 2.7%, and 1.4% for lean, fat, % fat, and total mass respectively. Omitting one vertebrae did not significantly impact the total BMD. One-vertebra imputation resulted in < 1% total BMD change. The RMSE of total body measures using reflection was in all cases less than the precision for any single region. After adjusting for subtotal BMC, head turning caused an apparent increase in total BMC by 3.6%. Arm and leg bending showed no difference in the total BMC (p>0.3). We conclude that the 3-6 protocol is effective in improving the accuracy of infant DXA scans and provides good spine and whole body DXA precision.

Ideal positioning for an infant whole body scan with six regions of interest. Notice that there are no motion artifacts and no overlapping regions.

Infant whole body example of 3-6 protocol
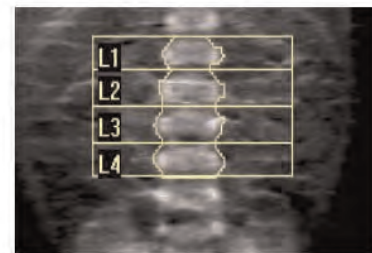
Fig.1: spine scan with no motion

Infant spine image for 3-6 protocol

FR0057

Determining Peak Bone Mineral Density in 16 to 24 year olds: A Longitudinal HR-pQCT Study. <u>Lauren Burt</u>*[1], <u>Sarah Manske</u>, <u>Jenn Bhatla</u>, <u>David Hanley</u>, <u>Steven Boyd</u>. University of Calgary, Canada

Peak bone mineral density (PBMD) occurs by late adolescence or early adulthood, and its timing has mainly been assessed using dual x-ray absorptiometry (DXA). PBMD measured with high-resolution peripheral quantitative computed tomography (HR-pQCT) may differ due to resolution or skeletal site differences. If HR-pQCT can be used as a clinical assessment tool, identifying individuals with osteoporosis and increased fracture risk, normative data illustrating PBMD is important to implement a T-Score classification system. In our population-based cohort we aimed to assess differences in PBMD between females and males by HR-pQCT compared with DXA.

Females (n=42, 21.5 yrs) and males (n=33, 21.6 yrs) from the Calgary youth cohort of the Canadian Multicentre Osteoporosis Study (CaMos) participated in a 2-year follow-up study. DXA (Hologic, USA) scans of the left hip provided areal bone mineral density (aBMD) of femoral neck (FN) and total hip (TH). Non-dominant radius and left tibia were scanned using HR-pQCT (Scanco Medical, Switzerland). To compare repeat scans, automated 3D image registration was conducted (IPL software) and masks of the common region were applied for data analysis. Total volumetric BMD (Tt.BMD), cortical BMD (Ct.BMD), trabecular BMD (Tb.BMD) and cortical porosity (Ct.Po) were assessed, and finite element analysis estimated apparent bone strength. A repeated measures ANOVA assessed age-related bone change over time.

Over 2-years, DXA-derived aBMD decreased at the FN and TH for females and males by -0.5 to -1% per year (p<0.01). At the radius, Tt.BMD increased by 1% per year for both females and males (p<0.01), Tb.BMD increased 0.8% per year for males (p<0.01) but did not increase for females. Ct.BMD increased by 0.7% for females and 1% per year for males (p<0.01). There were no significant changes in Ct.Po or apparent bone strength for females or males at the radius (p>0.05). At the tibia, there were no significant increases in BMD for females or males; however, Ct.Po increased 7% for females and 10% per year for males (p<0.01). Apparent bone strength did not change for females or males at the tibia (p>0.05).Our 2-year longitudinal study is consistent with known DXA peaks in aBMD occuring before 20 years at the FN and TH. Our 3D measures reflected an increase in HR-pQCT-derived BMD parameters at the radius, suggesting PBMD at the radius occurs at an age greater than 22 years in both females and males. At the tibia, all HR-pQCT-derived BMD parameters remained stable suggesting PBMD at this skeletal site may occur before 22 years in both females and males, similar to hip aBMD. Like DXA (hip vs. spine), timing of PBMD differs according to skeletal site (radius vs. tibia). Peak normative data for HR-pQCT should comprise of <22 year olds to capture PBMD at the tibia and ≥ 22 year olds to capture PBMD at the radius.

Disclosures: Lauren Burt, None.

FR0058

Does up to three years of exposure to recreational gymnastics between 4 and 12 years of age influence bone strength development at the radius and tibia?. <u>Marta Erlandson</u>*[1], <u>Stefan Jackowski</u>[1], <u>Rita Gruodyte-Raciene</u>[2], <u>Saija Kontulainen</u>[1], <u>Adam Baxter-Jones</u>[1]. [1]University of Saskatchewan, Canada, [2]Lithuanian Sports University, Lithuania

Introduction: Gymnastics training results in unique high mechanical loading to the skeleton. It therefore, provides an excellent model for assessing the effects of weight-bearing physical activity on bone development. Elite gymnasts have been found to display higher aBMD, BMC, and bone structrual strength both during active sports participation and after retirement. Recreational gymnasts have also been found to have greater bone parameters in cross-sectional studies compared to peers not exposed to gymnastics. What is unknown is the long-term consequence of early exposure to recreational, low-level, gymnastics on the subsequent development of bone strength. The purpose of this study was to investigate the influence of exposure to recreational gymnastics during childhood on bone properties and estimated strength development at the radius and tibia.

Methods: One hundred and twenty seven children (59 males, 68 females) between 4 and 9 years of age, involved in either recreational gymnastics (gymnasts) or other recreational sports (non-gymnasts) were recruited and followed for three consecutive years. Measures included demographics, anthropometrics, gymnastics participation, physical activity and peripheral quantitative computed tomography (pQCT) scans of the distal and shaft sites of forearm and lower leg. Multilevel random effects models were constructed to assess development of bone strength measures, controlling for age, limb length, weight, physical activity, muscle area, sex, and gymnastics exposure.

Results: Once age, limb length, weight, muscle area, physical activity and sex were accounted, it was observed that individuals exposed to recreational level gymnastics had significantly greater total bone area (18.0 ± 7.5 mm^2) and total bone content (6.0 ± 3.0 mg/mm) at the distal radius than individuals not exposed to recreational gymnastics (p<0.05). Gymnastics exposure was not a significant independent predictor for any bone measures at the radial shaft or at the tibia (p>0.05).

Conclusions: Exposure to recreational gymnastics provides skeletal benefits at the distal radius at all ages, suggesting that childhood recreational gymnastics exposure is advantageous to bone development at the wrist. As recreational gymnastics skills can be implemented into physical education programs, this type of training could potentially impact primary wrist fracture prevention. However, randomized controlled trials of recreational gymnastic exposure are required to further support these findings.

Disclosures: Marta Erlandson, None.

FR0059

The Association of Child Bone Measures Across Ages with Parent Bone Measures. <u>Steven Levy</u>*[1], <u>Elena Letuchy</u>[2], <u>Julie Eichenberger Gilmore</u>[3], <u>Kathleen Janz</u>[1], <u>Trudy Burns</u>[4], <u>James Torner</u>[5]. [1]University of Iowa, USA, [2]Univ. of Iowa Dept. of Epidemiology, USA, [3]Univ. of Iowa College of Medicine, USA, [4]Univ of Iowa College of Epidemiology, USA, [5]Univ. of Iowa Department of Epidemiology, USA

Purpose: This analysis characterized associations between parental bone and growth measures and those of their children from early childhood to late adolescence. These associations can indicate propensity for growth and bone accrual determined by familial influences. Methods: Iowa Bone Development Study examinations conducted every 2 to 3 years from age 5 to 17 years (6 waves) in boys and girls obtained measures of bone mineral content (BMC) and density (BMD) for hip, spine, and whole body from DXA (Hologic); and growth measures of height and weight. Parental measures were assessed once at the age 8 examinations. Parent-child correlations were estimated for: 1) "raw" bone and growth outcomes; 2) minimally adjusted outcomes (residuals and predicted values from gender- and wave-stratified linear regression models for children with height and weight (for bone) as predictors; parental models also included age); and 3) fully adjusted outcomes (models also included, e.g., physical activity). Analyses were done for children using all available data from each wave (n=120-240 per wave, varied by wave and parent/child gender) and again for those with measures at each examination (n=218). Results: The parent-child height association was stronger for maternal measures, and increased with child age (r=0.46 to 0.59 for daughters; r=0.40 to 0.59 for sons). Weight correlations showed a slight positive age trend for daughters, but not sons, and the strength of the association was not different for mothers vs. fathers. Spine BMC showed stronger maternal associations. The hip BMC and whole body (without head) BMC maternal associations were also stronger for daughters (r=0.5). For sons, there was no difference mothers vs. fathers (r=0.45). The strongest associations were for maternal-child spine BMC (r?0.6 for sons and daughters) at age 17. In general, there appear to be stronger maternal influences on bone measures; the strength is modified by covariate adjustment. Father-daughter associations are strongest for covariate-adjusted spine BMD and BMC; father-son associations are strongest for hip BMC and BMD. Analyses limited to children measured at all waves showed similar patterns. Conclusion: The strength of parent-child height, but not weight, associations was dependent on child age. Only spine measures showed stronger associations at older ages when adjusted for growth measures and other covariates, reflecting stronger parental influences.
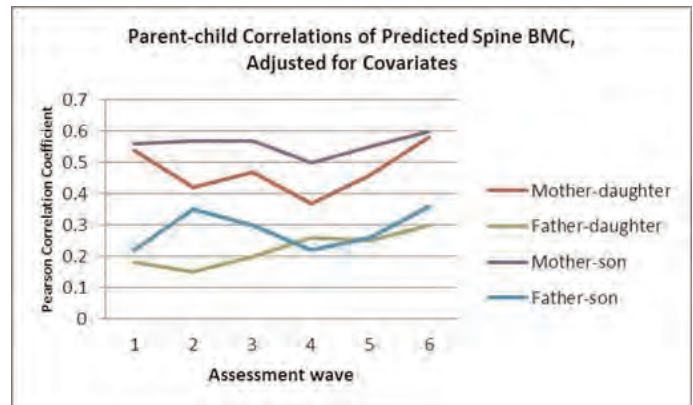
S Levy abstract figure

Disclosures: Steven Levy, None.

FR0060

The Longitudinal Relationship Between Visceral Fat and Bone Development: The Iowa Bone Development Study. <u>Natalie Glass</u>*[1], <u>James Torner</u>[1], <u>Elena Letuchy</u>[1], <u>Trudy Burns</u>[1], <u>Kathleen Janz</u>[1], <u>Janet Schlechte</u>[2], <u>Julie Eichenberger Gilmore</u>[1], <u>Steven Levy</u>[1]. [1]University of Iowa, USA, [2]University of Iowa Hospital, USA

Purpose: Greater visceral fat (VF) has been associated with with lower bone measurements in youth, though this relationship has not been evaluated long-itudinally. The purpose of this study was to determine if VF is negatively associated with bone parameters in overweight and obese adolescents from age 11-17.

Methods: Iowa Bone Development Study participants underwent peripheral quantitative computed tomography (pQCT) scans of the radius and tibia and whole body dual energy x-ray absorptiometry (DXA) scans every 2 years from age 11-17. Eligible participants were overweight or obese at age 11 according to CDC BMI

percentiles and had age 11 baseline scans and age 15 or 17 follow-up. VF area (cm^2) was estimated from whole body DXA scans using Apex 4.0.2 software (Hologic, Inc). Gender specific analyses evaluated the relationship between VF and bone development with growth models using biological age (visit age – age of peak height velocity) as the time variable adjusted for limb length and lean mass. Results are presented as standardized parameter estimates.

Results: Eligible participants included 42 girls(45% obese) and 52 boys (35% obese) with a mean age at baseline of 11.2 ± 0.3 years. In girls, greater VF was associated with thinner cortical bone and lower strength-strain index (SSI) at the radius (20% site), but not tibia (Table). In boys, greater VF was associated with lower density and strength at the trabecular bone site (4%) at the tibia but not radius. At the cortical site in boys (20%), greater VF was associated with thinner bones at the radius with no significant associations at the tibia. In sensitivity analyses restricted to obese participants, results remained relatively unchanged in girls. In boys, the relationship between VF and SSI (20% site) became significant (-0.12 ± 0.05, p=0.0260) while parameter estimates for associations at the 4% tibial site were attenuated and no longer reached significance (BMD: -0.14 ± 0.08, p=0.11; BSI: -0.17 ± 0.09, p=0.07).

Conclusions: Greater VF is associated with lower cortical bone strength at the non-weight-bearing radius but not at the tibia where greater mechanical loading may attenuate the negative relationship. Lower trabecular bone strength at the tibia with greater VF in boys may be a reflection of more rapid growth at that site. These results suggest the bone-fat relationship may vary depending on adiposity and bone site and explain previous, conflicting reports on this relationship.

Bone Measurement		Parameter Estimate±SE	p-value
Radius 4% site			
Bone Mineral Density	Girls	-0.03±0.08	0.76
	Boys	-0.05±0.06	0.39
Bone Strength Index	Girls	-0.04±0.08	0.59
	Boys	-0.006±0.04	0.88
Radius 20% site			
Bone Mineral Density	Girls	-0.03±0.05	0.50
	Boys	-0.03±0.06	0.66
Cortical Thickness	Girls	-0.21±0.07	<0.01
	Boys	-0.16±0.05	<0.01
Strength-Strain Index	Girls	-0.12±0.05	0.01
	Boys	-0.04±0.02	0.07
Tibia 4% site			
Bone Mineral Density	Girls	-0.04±0.08	0.62
	Boys	-0.19±0.05	<0.01
Bone Strength Index	Girls	-0.13±0.07	0.07
	Boys	-0.14±0.04	<0.01
Tibia 38% site			
Bone Mineral Density	Girls	-0.02±0.04	0.63
	Boys	-0.03±0.06	0.64
Cortical Thickness	Girls	-0.09±0.05	0.08
	Boys	-0.08±0.05	0.08
Strength-Strain Index	Girls	-0.05±0.04	0.15
	Boys	-0.03±0.02	0.21

Table: Relationship Between VF and Bone Development (Standardized Parameter Estimates˜SE)

Disclosures: Natalie Glass, None.

FR0063

CCL3 demonstrates sexually dimorphic regulation of skeletal homeostasis and the hematopoietic stem cell pool in the bone marrow. Benjamin Frisch*[1], Alexandra Goodman[1], Mary Georger[1], Michael Becker[1], Laura Calvi[2]. [1]University of Rochester School of Medicine & Dentistry, USA, [2]University of Rochester School of Medicine, USA

Hematologic malignancies are known to remodel the bone marrow microenvironment reducing support for normal hematopoiesis and increasing support for malignant hematopoiesis. One molecular mechanism that has been demonstrated to play a role in this microenvironmental remodeling is the chemokine CCL3. However under normal physiologic conditions the role of CCL3 in the maintenance of the skeleton and hematopoiesis is poorly understood. To study this we utilized mice that lack CCL3 (CCL3KO). CCL3KO mice demonstrate a marked increase in the frequency and number of phenotypic long-term hematopoietic stem cells (LT-HSCs) in the marrow by flow cytometric analysis (0.0053 $\pm$ 0.0005 vs. 0.0106 $\pm$ 0.0007 % of cells, WT vs. CCL3KO p≤0.0001 n=8 mice/group). A significant increase was also seen in short-term HSCs (ST-HSCs), but not in multipotent progenitors (MPPs) (data not shown), suggesting that in the HSC compartment CCL3 regulates the most immature hematopoietic cells. When separated by gender we observed that the LT-HSC phenotype, when compared to WT controls, was most severe in female CCL3KO mice with a 2.8 fold increase in LT-HSC frequency while male mice had a 1.5 fold increase in LT-HSC frequency, both were statistically significant. In the peripheral blood, monocytes, granulocytes, and red blood cells were all significantly decreased in CCL3KO mice (9.78 $\pm$ 0.3 vs. 8.06 $\pm$ 0.2 RBCs*10^6/μl, WT vs. CCL3KO p≤0.001 n=8 mice/group). This suggests that CCL3 not only regulates the most immature hematopoietic cells, but also the production of mature hematopoietic cells. When the skeleton was analyzed we found that male mice had no change in femoral trabecular (Tb) architecture, while female mice showed decreased Tb number (0.79 fold, p≤0.05

n=4 mice/group), decreased Tb connectivity density (0.62 fold, p≤0.05 n=4 mice/group), increased Tb thickness (1.17 fold, p≤0.01 n=4 mice/group), and increased Tb spacing (1.29 fold, p≤0.05 n=4 mice/group) in the femur when compared to WT controls measured by μCT. In femoral cortical bone male and female CCL3KO mice had opposite phenotypes when compared to WT controls measured by μCT. Males had decreased cortical thickness (0.87 fold, p≤0.05 n=4 mice/group) while females had increased cortical thickness (1.17 fold, p≤0.05 n=4 mice/group). These data support a gender specific role for CCL3 in the maintenance of the bone marrow microenvironment with sexually dimorphic effects on both the skeletal and hematopoietic systems.

Disclosures: Benjamin Frisch, None.

FR0064

Fibrillin-1 Regulates Marrow Stem Cell Lineage Commitment and Differentiation. Silvia Smaldone*[1], Francesco Ramirez[2]. [1]USA, [2]Icahn School of Medicine at Mount Sinia, USA

Previous characterization of osteopenia in mice with Marfan syndrome has implied that the extracellular protein fibrillin-1 restricts osteoblast maturation and osteoblast-dependent osteoclastogenesis. Here osteopenia progression was studied in mice with conditional inactivation of Fbn1 gene in the developing limbs (Fbn1$^{Prx1-/-}$ mice). Micro-computed tomography (μCT) analyses of Fbn1$^{Prx1-/-}$ mice revealed progressive decline of bone mass after the animals reached 1-month of age. Progressive osteopenia was associated with persistent bone resorption, due to elevated number of osteoclasts, and reduced bone formation rate (BFR) in spite of proper mineralization ability of bone marrow derived osteoblasts. Interestingly, a transient increase in the number of skeletal progenitor cells (SkP) concomitant with reduced number of mesenchymal stem cells (MSC) was observed in 3 months-old mice and it was followed by a dramatic decline in SkP frequency and mature osteoblasts number in 6-month-old Fbn1$^{Prx1-/-}$ mice. These results suggested that lack of functional fibrillin-1 in the bone marrow microenvironment accelerate MSC's rate of commitment leading to a premature, age-dependent, depletion of the stem pool and eventually bone forming cells. These changes were also accompanied by loss of marrow fat cells resulting from impaired plasticity of bone marrow progenitor cells towards adipogenesis. Consistent with enhanced TGFβ activity of bone marrow cell cultures, systemic treatment of Fbn1$^{Prx1-/-}$ mice with pan-TGFβ neutralizing antibody 1D11 mitigated both bone and MSC loss. Altogether, our data indicate that fibrillin-1 is a structural component of the bone marrow niche that regulates lineage commitment and differentiation of MSCs by modulating local TGFβ activity.

Disclosures: Silvia Smaldone, None.

FR0065

BMP-2 Exerts a Tight Control of CXCL12 Cellular, Temporal and Spatial Expression that is Essential in Fracture Repair. Helen Willcockson*[1], Timothy Myers[1], Lara Longobardi[2], Ping Ye[2], Tieshi Li[2], Joseph Temple[1], Alessandra Esposito[1], Billie Moats-Staats[3], Anna Spagnoli[2]. [1]University of North Carolina, USA, [2]University of North Carolina at Chapel Hill, USA, [3]University of North Carolina- Chapel Hill, USA

The molecular mechanisms through which bone morphogenic protein-2 (BMP2) exerts its essential role in fracture repair still need to be determined. Although there is compelling evidence that CXCL12 is involved in the regenerative response to injuries, its function in fracture repair has been scarcely investigated. Here, we report a functional interplay between BMP2 and CXCL12 during fracture repair. Using BMP2-LacZ reporter mice, we found that during the first 10 days after fracture, cellular expression of BMP2 and CXCL12 co-localize along the endosteum adjacent to the fracture site. To determine the possible regulation of CXCL12 by BMP2, we used control (BMP2$^{flox/flox}$) and Prx1Cre conditional BMP2 haploinsufficient fractured mice (BMP2$^{cKO/+}$) that have abnormal fracture healing. Fractured wild-type mice showed CXCL12 expressing cells (detected by immunohistochemistry and immunofluorescence) within the endosteum close to the fracture site and within the fractured bones that lasted up to 14 days post-fracture. This immunodetection was fracture-induced since CXCL12 signal within the endosteum was almost undetectable in unfractured mice. Compared to control (BMP2$^{flox/flox}$) fractured mice, we found higher levels of CXCL12 expression in BMP2$^{cKO/+}$ fractured mice that were maintained through day 21 after fracture. Remarkably, BMP2$^{cKO/+}$ showed a disorganized pattern of CXCL12 expression at the endosteal site as well as within the fractured bones, with an increase in endothelial-containing vascular formations that were PECAM positive. In apposition to these vascular structures, supportive pericytes expressing NG2 were associated with CXCL12 positive cells. Stem cell factor expression showed a similar distribution with CXCL12. To determine a functional relationship between CXCL12 and BMP2, we treated BMP2$^{cKO/+}$ and control mice with AMD3100, an antagonist of CXCL12 receptor(s) given IP (2.5 mcg/gm of body weight/2x/day) 2 days before and from day 2 to day 7 after fracture. We found that AMD3100 induced callus formation in BMP2$^{cKO/+}$ mice as determined by microCT, histological and in-situ hybridization analyses for bone/cartilage markers. Taken together our studies show that BMP2 exercises controlled regulation of CXCL12 expression in time, pattern and localization that is essential for fracture repair. This has far-reaching implications for our understanding of the fracture repair process and to promote healing by modulating these mechanisms.

Disclosures: Helen Willcockson, None.

FR0066

Bone Marrow Adipocytes are Distinct from White or Brown Adipocytes. <u>Mark Horowitz</u>*[1], <u>Ryan Berry</u>[2], <u>Rose Webb</u>[2], <u>Tracy Nelson</u>[2], <u>Yougen Xi</u>[2], <u>Casey R. Doucette</u>[3], <u>Jackie A Fretz</u>[2], <u>Chris D. Church</u>[2], <u>Clifford J. Rosen</u>[3], <u>Matthew S. Rodeheffer</u>[2]. [1]Yale University School of Medicine, USA, [2]Yale School of Medicine, USA, [3]Maine Medical Center Research Institute, USA

It has become evident that bone marrow (BM) adipocytes are more than " filler" in the BM. We have developed new techniques to quantitatively assess BM adipogenesis and lineage trace BM adipocyte progenitors (MAP) in mice. Using these techniques we have found that different mouse strains have different endogenous levels of marrow fat and BM adipogenesis. While increased marrow adipose tissue (MAT) has divergent affects on bone density, much remains to be discovered about the origin, ontology and function of BM adipocytes and their relationship to adipocytes in other depots.

We have found that C57BL/6 mice have very low constitutive marrow adipocytes that can be induced by feeding with rosiglitazone-containing diet, high-fat diet or irradiation. To determine the origin of BM adipocytes, we have performed lineage tracing using the fluorescent *mT/mG* reporter mouse in concert with various mouse models driving cre-recombinase from lineage specific promoters. In *mT/mG* mice, expression of cre-recombinase results in permanent removal of the targeted dTomato (mT) cassette and expression of the membrane targeted eGFP (mG) cassette, resulting in "flipping" from dTomato+ to eGFP+ cells. BM adipocytes within either the BM plug or decalcified frozen sections of long bones from cre:mT/mG mice can be visualized through fluorescent confocal microscopy.

All preformed brown adipocytes are traced in *Myf5-cre:reporter* mice. We have found that BM adipocytes are not lineage related to brown adipocytes as they are uniformly dTomato+ in *Myf5-cre:mT/mG* mice. In addition, all BM adipocytes are uni-locular, while brown adipocytes are multi-locular. WAT-APs have recently been shown to express PdgfRα leading to tracing all white adipocytes in *Pdgfra-cre:mT/mG* mice. However, only a subset of BM adipocytes is traced by *PdgfRα-cre*, regardless of the induction method, suggesting that MAPs and WAT-APs may be distinct. Consistent with this data, recent reports have shown that BM adipocytes are traced in *Osx1-cre:mT/mG* mice. We observe uniform dTomato+ vWAT, sWAT, BAT adipocytes and APs, while tracing a subset of cells on bone surfaces and osteocytes in this same model.

These experiments indicate that MAT is dynamic and changes in response to stress and that BM adipocytes/MAPs are distinct from white or brown adipocytes/APs. These data are some of the first to define the ontogeny of BM adipocytes/MAPs *in vivo* and indicate that BM contains a distinct fat depot.

Disclosures: Mark Horowitz, None.

FR0067

Elucidating the Osteoimmunology of Critical Defects with Longitudinal Intravital Microscopy in the Murine Cranial Window Model. <u>Longze Zhang</u>*[1], <u>Jason Inzana</u>[2], <u>Hani Awad</u>[3], <u>Regis J. O'Keefe</u>[1], <u>Xinping Zhang</u>[3], <u>Edward Schwarz</u>[1]. [1]University of Rochester, USA, [2]USA, [3]University of Rochester Medical Center, USA

Background: Reconstruction of critical defects remains a major challenge due to the host inflammatory and fibrotic response. Thus, elucidating the osteoimmunology responsible is essential towards a solution. Previously we found that intermittent teriparatide (rPTH) therapy facilitates structural femoral and calvarial allograft healing in mice via increased osteogenesis and host-allograft bony union, and significantly decreased fibrosis. We also discovered that it significantly decreased large vessel arteriogenesis and the accumulation of mast cells in the interfacial tissue between the host and allograft bone. As the functional significance of this finding is unknown, we utilized in vivo multiphoton laser scanning microscopy (MPLSM) in the murine chronic cranial defect window chamber model to test the hypotheses that: 1) mast cell appearance in a critical bone defect coincides with arteriogenesis; and 2) mast cells specifically accumulated proximal to large (>30 μm in diameter) vessels.

Methods: Chronic cranial defect windows were produced in 8-week-old C57B/6 mice, which were randomized to rPTH or placebo. FITC-conjugated anti-Mcpt-5 or anti-CD11b antibody, was administered i.v. with Texas Red-Dextran to image mast cells or monocytes/macrophages respectively, with the vasculature. Weekly MPLSM imaging was performed, and 3D-reconstruction of the z-stack images with Amira was used to quantify vessel thickness, vascular volume, total volume, and vascular volume fraction. We also quantified Mcpt-5+ and CD11b+ cell numbers and determined their mean distance from large vessels (>30μm) vs. small (<30μm) blood vessels.

Results & Discussion: rPTH significantly increased angiogenesis and decreased arteriogenesis, consistent with prior studies. While CD11b+ cells were present in the middle of the defect in large numbers (60+/- 20/field, 10X) as early as day 14, Mcpt-5+ cells first appeared in the ROI on day 28 with much fewer number (12 +/- 6/field, 10X). Moreover, while CD11b+ cells were significantly closer to small vs. large vessels (14.1+/- 4.1 μm vs. 98.9 +/- 19.0 μm; p <0.05), the opposite was true for Mcpt-5+ cells (61 +/- 3.7 μm vs. 26.9 +/- 14.6 μm; p <0.05). These novel findings suggest that coupled osteogenesis and angiogenesis at the healing edge of a critical defect is opposed by arteriogenesis and fibrosis within the defect, and that rPTH efficacy includes inhibitory effects on arteriogenesis and mast cell-induced fibrosis.

Disclosures: Longze Zhang, None.

FR0068

Roquin Is A Novel Regulator of Bone Homeostasis. <u>Bay Sie Lim</u>*, <u>Euphemie Landao</u>, <u>Shek Man (Jacky) Chim</u>, <u>Jennifer Tickner</u>, <u>Nathan Pavlos</u>, <u>Jiake Xu</u>. University of Western Australia, Australia

Many osteolytic diseases have highlighted the intimate relationship between the immune and skeletal system. However, the underlying mechanism of osteoimmunology remains poorly understood. To gain insights into the molecular genetics and mechanisms of osteoimmunology, we have employed a chemical (ENU) mutagenesis screen and identified a mouse line, San Roque (*san/san*), which carries a M199R mutation in the Roquin (Rc3h1) gene. *San/san* mice display an autoimmune disease consistent with Systemic Lupus Erythematosus with dysregulation of follicular helper T cells [1]. Preliminary X-ray analysis revealed that *san/san* mice exhibit a lower bone density in comparison to WT littermates. MicroCT and histological analyses confirmed a low bone mass phenotype in *san/san* mice with a significant reduced bone volume (BV/TV) as compared to WT littermates (Figure 1). Real-time PCR showed elevated RANKL expression in whole bone isolated from *san/san* mice relative to WT mice. Flow cytometry analysis revealed that the increased RANKL expression was accompanied by a significant expansion of putative osteoclast progenitor populations in the *san/san* mice relative to WT mice. Consistent with the observed increased in progenitors, we also observed enhanced osteoclastogenesis and osteoclast activity from bone marrow macrophages (BMMs) derived from *san/san* mice, accompanied by enhanced RANKL-mediated MAPK signaling. *In vivo* bone calcein labeling showed a reduction in bone mineral apposition rate in the *san/san* mice indicating that osteoblast activity was also affected. In keeping with this phenotype, *san/san* calvarial-derived osteoblast culture showed a reduction in bone nodule formation. Furthermore, co-culture experiments revealed that calvarial osteoblasts of *san/san* mice have a reduced ability to support osteoclastogenesis, suggesting an extrinsic contribution to the pre-priming effect of osteoclast progenitors within the bone marrow niche in *san/san* mice. Taken together, our data demonstrates that Roquin is an important regulator of bone homeostasis and osteoimmunology.Reference

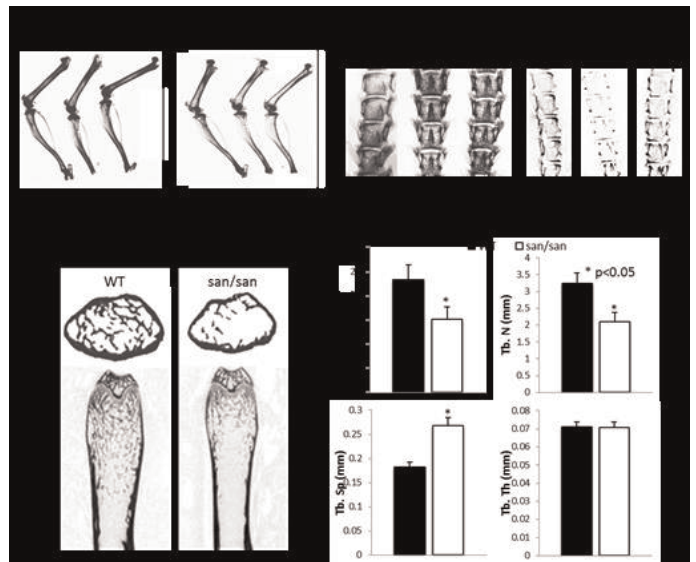1. Vinuesa, C.G., et al., Nature, 2005. 435(7041): p. 452-8.

Figure 1: (A) X-ray and (B) microCT images of wild type (WT) and San Roque (san/san) mutant mice.

Disclosures: Bay Sie Lim, None.

FR0069

Specificity protein-1 mediated SDF-1/CXCL12 synthesis is inhibited by Cbl-PI3K interaction in bone marrow reticular cells. <u>Naga Suresh Adapala</u>[1], <u>Vanessa Piccullio</u>[2], <u>Hector Aguila</u>[2], <u>Joseph Lorenzo</u>[2], <u>Archana Sanjay</u>*[3]. [1]Texas Scottish Rite Hospital for Children, USA, [2]University of Connecticut Health Center, USA, [3]UCHC, USA

The chemokine SDF-1/CXCL12 plays an important role in bone remodeling by influencing osteoclast precursor migration and osteoblast formation. However, the molecular mechanism(s) regulating SDF-1 synthesis are not well understood. The E3 ubiquitin ligase and adaptor protein Cbl, influences bone remodeling by regulating the cellular distribution and activity of phosphoinositide 3-kinase (PI3K). We previously reported that mice with a loss of Cbl-PI3K interaction, due to a tyrosine to phenylalanine mutation at the PI3K binding site of Cbl protein (CblY737F, YF knock-in mice) had uncoupling of bone resorption from bone formation. Loss of Cbl-PI3K complex formation also resulted in increased PI3K/AKT signaling and SDF-1 expression, which altered the cellular composition of the bone marrow. SDF-1 is predominantly produced by CXCL12 abundant reticular (CAR) cells and flow

cytometric analysis revealed that both numbers of CAR cells and their SDF-1 production were increased in the bone marrow of YF mice. We found that SDF-1 promoter activity in WT cells was attenuated by a PI3K inhibitor. Next, to understand the molecular mechanism of increased production of SDF-1 in YF mice, bone marrow reticular cells (CD45⁻Ter119⁻CD31⁻Sca1⁻) were treated with increasing concentrations of PI3K and AKT inhibitors. Basal SDF-1 gene expression was 2-fold higher in YF cells compared to WT cells. The degree of inhibition observed with 1μM concentrations of either inhibitor in WT cells was only seen with 10μM concentration in YF cells. There are several Specificity protein 1 (Sp1) transcription factor-binding sites in SDF-1 promoter. Compared to WT, higher Sp1 protein levels were detected in the nucleus of YF cells. Furthermore, treatments of WT cell with the PI3K inhibitor LY294002 at either 1 and 10μM markedly decreased Sp1 localization in the nucleus. However, decreased nuclear Sp1 levels were only detected in YF cells at higher concentrations of LY294002. Treatment of cells with Mithramycin A, which blocks Sp1 binding to GC-rich regions of the SDF-1 promoter, markedly reduced SDF-1 mRNA levels in WT cells. However, significantly less inhibition was seen in YF cells. Taken together, these data suggest that the YF mutation of Cbl results in increased-PI3K/AKT signaling which, in turn, increases SP-1-regulated SDF-1 expression in the bone marrow reticular cells. We conclude that Cbl-PI3K interaction in WT bone marrow reticular cells negatively regulates SP1-mediated SDF-1 synthesis.

Disclosures: Archana Sanjay, None.

FR0070

CTLA4-Ig Protects Against PTH Induced Bone Loss by Inhibiting T Cell Production of TNFα. <u>Abdul Malik</u>*[1], <u>Jerid Robinson</u>[2], <u>Jau-Yi Li</u>[1], <u>Michael Reott</u>[3], <u>Jonathan Adams</u>[4], <u>M. Neale Weitzmann</u>[1], <u>Roberto Pacifici</u>[1]. [1]Emory University School of Medicine, USA, [2]Emory University, USA, [3]Emory University School of Medicine, USA, [4]Emory University, USA

Continuous PTH (cPTH) treatment, a model of primary hyperparathyroidism, induces bone loss by stimulating the production of the osteoclastogenic cytokine TNFα (TNF) by bone marrow (BM) T cells. CTLA4-Ig (Abatacept) is an inhibitor of costimulation approved for rheumatoid arthritis that inhibits T cell activation and T cell cytokine production. In this study we investigated whether CTLA4-Ig prevents cPTH induced bone loss. 16 weeks old C57BL/6 female mice were infused with vehicle or cPTH (hPTH 1-34 at 80μg/kg/day) for four weeks using osmotic mini pumps. Mice were also treated with CTLA4-Ig or irrelevant-Ig (Irr.Ig) 100μg/mice IP, three times a week. cPTH induced a significant loss of trabecular bone in mice treated with Irr. Ig but not in those injected with CTLA4-Ig, demonstrating that CTLA4-Ig inhibits cPTH induced bone loss. CTLA4-Ig completely prevented the increase in serum levels of CTX (a marker of bone resorption) and osteocalcin (a marker of bone formation) induced by cPTH. Cultures of BM from mice treated with cPTH produced more osteoclasts (OCs), colony forming unit-alkaline phosphate (CFU-ALP) and miner-alization nodules than those from control mice. These changes were prevented CTLA4-Ig treatment. We also found that CTLA4-Ig inhibited the capacity of cPTH to increase T cell TNF production. In summary, we found that CTLA4-Ig protects against the bone loss and the increase in bone resorption induced by cPTH by blocking the production of TNF by T cells. These findings provide a proof of principle for utilizing CTLA4-Ig as a novel treatment for primary hyperparathyroidism.

Disclosures: Abdul Malik, None.

FR0071

A Novel Sequestosome-1 / p622 ZZ Domain Inhibitor Blocks TNFα Induced Suppression of OBL Differentiation in MM. <u>Rebecca Silbermann</u>*[1], <u>Jumpei Teramachi</u>[1], <u>Khalid Mohammad</u>[1], <u>Wei Zhao</u>[1], <u>Dan Zhou</u>[1], <u>Peng Yang</u>[2], <u>Julie L. Eiseman</u>[2], <u>Xiang-Qun Xie</u>[2], <u>G. David Roodman</u>[1], <u>Noriyoshi Kurihara</u>[1]. [1]Indiana University, USA, [2]University of Pittsburgh, USA

Multiple myeloma (MM) bone disease is marked by irreversible osteoblast (OBL) suppression and uncoupling of the bone resorption – formation process. We previously reported that the ZZ domain of sequestosome-1 (p62) is required for bone marrow stromal cell (BMSC) support of MM cell growth and serves as a platform for the formation of signaling complexes that result in NF-κB, p38 MAPK, and PI3K activation in MM patient BMSC. We developed a small molecule inhibitor, (XRK3F2), that blocks p62-ZZ domain mediated protein interactions, including TNFα mediated signaling in BMSC, and recently reported that intraperitoneal XRK3F2 treatment induced new cortical bone formation by μCT in C57BL/KaLwRij mice intratibially inoculated with the murine MM cell line 5TGM1-gfp, as compared with vehicle treated animals bearing MM. Histology confirmed the presence of new bone formation along the periosteal surface of the tibia, and animals that developed new bone formation had high-grade extra-tibial tumors without evidence of new bone formation in bones that had not been inoculated with MM cells.

We now report that XRK3F2 induces new cortical bone formation only in the presence of significant systemic MM tumor burden (defined by high IgG2b levels), and that in all cases new bone formation developed adjacent to tumor, as demonstrated by anti-GFP immunohistochemistry, suggesting that XRK3F2 modulates local MM cell and bone cell interactions. To evaluate if XRK3F2 alters MM production of OBL inhibitors or stromal cell differentiation under osteoblasto-genic conditions, we treated 5TGM1 cells, murine stromal cells (MC4), and 5TGM1 – MC4 co-cultures with doses of XRK3F2. XRK3F2 did not alter 5TGM1 production

of MC4 derived IL-7 or TNFα when MM cells were cultured alone, and did not affect MC4 differentiation in the absence of MM. Interestingly, XRK3F2 treatment of 5TGM1-MC4 co-cultures under osteogenic conditions resulted in significantly higher levels of RUNX2 than vehicle treated co-cultures. This effect was most pronounced at XRK3F2 doses similar to the IC₅₀ reached in vivo in our prior studies. XRK3F2 treatment in our co-culture system also blocked the over-expression of GFI-1, a transcriptional repressor of RUNX2 induced in MM cells by BMSC or TNFα. These results suggest that XRK3F2 may block GFI-1 or the TNFα induced suppression of OBL differentiation observed in MM cell-BMSC co-cultures, and that p62-zz domain blockade may serve as an anabolic agent in MM bone disease.

Disclosures: Rebecca Silbermann, None.

FR0072

Alternatively Activated Monocyte and Macrophage Efferocytosis Support Prostate Cancer Skeletal Metastasis. <u>Jacqueline Jones</u>*[1], <u>Fabiana Soki</u>[2], <u>Hernan Roca</u>[1], <u>Stefanie Thiele</u>[3], <u>Yusuke Shiozawa</u>[1], <u>Yugang Wang</u>[1], <u>Todd Morgan</u>[1], <u>Lorenz Hofbauer</u>[3], <u>Kenneth Pienta</u>[4], <u>Laurie McCauley</u>[2]. [1]University of Michigan, USA, [2]University of Michigan School of dentistry, USA, [3]Dresden University Medical Center, Germany, [5]Dresden University Medical Center, Germany, [4]John Hopkins University, USA

Macrophages play a vital role in maintaining tissue homeostasis by clearing foreign pathogens and apoptotic tumor cells through phagocytosis (termed efferocytosis). However, their functional role and pathophysiological contribution to the tumor microenvironment in skeletal metastases is unclear. The purpose of this study was to determine the efferocytic monocyte/macrophage type and its potential in supporting prostate cancer (PCa) skeletal metastasis through efferocytosis. FACS analysis of peripheral blood mononuclear cells isolated from patients with PCa skeletal metastasis showed significantly higher (20% increase) triple positive CD68+/CD14+/CD16+ (alternatively activated, M2) monocyte populations as compared with non-cancer controls (p<0.05), and significantly correlated with their PSA levels (p<0.05). Moreover, monocytes isolated from PCa skeletal metastasis patients presented a 2.5 fold increase in efferocytosis versus patients without cancer. To further confirm these findings, we analyzed tissue microarrays, which revealed malignant PCa tissue expressed significantly higher levels of MFG-E8, a known facilitator of efferocytosis, in invasive versus benign tissues (31.9 ± 1.3 and 4.9 ± 0.7 respectively). Co-localization of CD68+ phagocytic cells and MFG-E8 was significantly increased in malignant PCa tissue (p<0.05). To determine the molecular mechanisms, several *ex vivo* assays were performed. *Ex vivo* analysis of efferocytosis using murine bone marrow macrophages revealed that MHCII^low CD36+ and F4/80+ positive cells (M2 macrophages) are proficient at efferocytosis of apoptotic tumor cells and phospha-tidylserine coated apoptotic mimicry beads. Modulation of macrophage efferocytosis with resolvin D (stimulator), cytochalasin D (inhibitor) or placement at 4˚ (blunt inhibition) resulted in differential expression of pro-efferocytic and tumorigenic genes (TGF-β, MFG-E8, MERTK, and PPAR-γ). Cytokine stimulation using IL4 and M-CSF increased macrophage efferocytosis, which correlated with increased pro-tumorigenic, M2-like gene expression (YM1, TGF- β). More importantly, soluble factors released from macrophages during efferocytosis resulted in a 30% increase of PC-3 cell numbers in a transwell assay, compared to macrophages alone. Together, these studies suggest that M2 macrophages display an efferocytic behavior that promotes PCa growth. Targeting these subpopulations shows promise as a therapeutic approach for skeletal metastasis.

Disclosures: Jacqueline Jones, None.

FR0073

Critical role of Pim-2 in NF-κB-mediated suppression of osteoblastogenesis and stimulation of osteoclastogenesis: Therapeutic impact of Pim inhibition on myeloma bone disease. <u>Jumpei Teramachi</u>*[1], <u>Masahiro Hiasa</u>[2], <u>Asuka Oda</u>[3], <u>Ryota Amachi</u>[3], <u>Takeshi Harada</u>[3], <u>Shingen Nakamura</u>[3], <u>Kumiko Kagawa</u>[3], <u>Hirokazu Miki</u>[3], <u>Shiro Fujii</u>[3], <u>Keiichiro Watanabe</u>[4], <u>Itsuro Endo</u>[5], <u>Toshio Matsumoto</u>[5], <u>Masahiro Abe</u>[6]. [1]The University of Tokushima, Japan, [2]Indiana University School of Medicine, USA, [3]Department of Medicine & Bioregulatory Sciences, Institute of Health Biosciences, The University of Tokushima Graduate School, Japan, [4]Tokushima University Hospital, Japan, [5]University of Tokushima Graduate School of Medical Sciences, Japan, [6]University of Tokushima, Japan

Myeloma (MM) cells enhance osteoclastogenesis and suppress osteoblastogenesis to cause devastating bone destruction with rapid loss of bone. The NF-κB pathway is critically involved in tumor expansion and bone destruction in MM. The activation of the NF-κB pathway suppresses osteoblastogenesis while enhancing osteoclastogen-esis. We demonstrated that the activation of the NF-kB pathway up-regulated Pim-2 kinase levels in MM cells, and that blockade of Pim-2 induced MM cell death and ameliorated MM bone disease. However, the precise role of Pim-2 in bone metabolism still remains unknown. Therefore, the present study was undertaken to clarify the relationship between the Pim-2 and NF-κB pathways in bone metabolism on MM bone disease. TNF-α potently induced Pim-2 expression in bone marrow stromal cells

(BMSC) and MC3T3-E1, and also in monocytes and RAW264.7. The TNF-α-induced up-regulation of Pim-2 in these cells was mostly abolished by inhibitors of NF-κB. However, Pim inhibition did not affect the the activation of the NF-κB pathway in MC3T3-E1 induced by TNF-a, suggesting Pim-2 induction downstream of the NF-κB pathway. TNF-α potently suppressed mineralized nodule formation by BMP-2 in MC3T3-E1 and BMSC along with the activation of the NF-κB pathway; however, addition of the Pim-2 inhibitor SMI-16a as well as Pim-2 siRNA restored their mineralization. The Pim-2 inhibition enhanced the phosphorylation of Smad1/5 by BMP-2 while suppressing Smad2/3 phosphorylation by TGF-b in MC3T3-E1. The Pim-2 inhibition also suppressed the induction of NFATc1 and c-fos, critical factors for osteoclast differentiation, as well as osteoclastogenesis by TNF-α or RANKL. Histomorphometric analysis in bone lesions in mouse MM models showed that treatment with SMI-16a restored bone formation with mild amelioration of osteoclastogenesis. Consistently, the suppression of osteoclastogenesis *in vitro* required SMI-16a at doses over 10 μM, while 0.2 μM was enough to induce osteoblastogenesis, suggesting preferential induction of bone formation. Collectively, these results demonstrated that Pim-2 is a major downstream target of NF-κB signaling in both osteoblastic and osteoclastic lineage cells in addition to MM cells to cause the skewed bone metabolism in MM. Because different signaling pathways besides the NF-κB pathway also up-regulate Pim-2 expression in these cells, Pim-2 is suggested to be a pivotal therapeutic target for bone destruction and tumor progression in MM.

Disclosures: Jumpei Teramachi, None.

FR0075

Ubiquitin-specific peptidase 45 (USP45), a family member of de-ubiquitinating enzyme, controls epithelial-mesenchymal transition of breast cancer in bone. <u>Yuki Nagata</u>*[1], <u>Soichi Tanaka</u>[2], <u>Kenji Hata</u>[3], <u>Masahiro Hiasa</u>[4], <u>Riko Nishimura</u>[3], <u>Toshiyuki Yoneda</u>[4]. [1]Indiana University-Purdue University Indianapolis, USA, [2]Osaka University, Japan, [3]Osaka University Graduate School of Dentistry, Japan, [4]Indiana University School of Medicine, USA

Aggressive cancer cells undergo epithelial-mesenchymal transition (EMT) in which epithelial cancer cells trans-differentiate into mesenchymal fibroid cells and acquire increased invasiveness and metastasis. EMT is regulated by a variety of extracellular and intracellular molecules. TGFb is one of the most potent stimulators of EMT and Snail is a well-recognized transcription factor that promotes EMT by repressing the expression of the epithelial marker, E-cadherin. We found MCF-7 human breast cancer cells expressing GFP (MCF-7/GFP) underwent EMT with up-regulation of Snail and down-regulation of E-cadherin when inoculated in the tibial bone marrow in which TGFb is continuously released via bone resorption. Inhibition of bone resorption by zoledronic acid (ZA) inhibited osteolytic colonization of MCF-7/GFP cells with decreased Snail expression. To our surprise, Snail expression in MCF-7/GFP cells was decreased by ZA treatment of MCF7 cells *in vitro*, suggesting that ZA decreased Snail expression independent of bone resorption. The decrease of Snail by ZA was restored by the proteasome inhibitor lactacystin, suggesting that ZA decreases Snail expression via ubiquitin/proteasome degradation. Differential microarray analysis of untreated and ZA-treated mammary tumors identified the de-ubiquitinating enzyme, ubiquitin-specific peptidase 45 (USP45), as a candidate involved in proteasomal degradation of Snail. USP45 expression was increased in MCF-7/GFP tumors in bone compared with the tumor in the mammary fat pad. TGFb increased USP-45 as well as Snail. Overexpression of USP45 in MCF-7/GFP cells induced Snail expression and other mesenchymal markers including N-cadherin and vimentin, while E-cadherin expression was abolished. USP45 physically bound to Snail and specifically de-ubiquitinated Snail. *In vitro* de-ubiquitination assays showed Snail ubiquitination was inhibited by USP45. ZA inhibited USP-45 expression and its de-ubiquitinating activity, thereby promoting Snail degradation. Importantly, ZA prevented metastasis of breast cancer from bone to lung and liver, presumably by promoting Snail degradation via inhibition of USP 45. Thus, our results suggest that the bone microenvironment rich in TGFb stimulates EMT in breast cancer by preventing proteasomal degradation of Snail via up-regulation of the de-ubiquitinating enzyme USP45. USP45 may be a potential target for development of a novel therapeutic agent for bone metastasis of breast cancer.

Disclosures: Yuki Nagata, None.

FR0077

Targeting Dickkopf-related protein 1 (Dkk1) reduces extraskeletal tumor growth by novel immunomodulatory effects. <u>Lucia D'Amico</u>*[1], <u>Ali Zamani</u>[2], <u>Aude-Helene Capietto</u>[1], <u>Roberta Faccio</u>[3]. [1]Washington University School of Medicine, USA, [2]Department of Orthopedics, Washington University, St. Louis, Missouri, USA, [3]Washington University in St Louis School of Medicine, USA

Myeloid derived Suppressor Cells (MDSC) are potent inhibitors of anti-tumor T-cell responses involved in tumor progression. Downregulation of PLCγ2/β-catenin pathway occurs in MDSC from cancer patients and tumor-bearing mice and enhances their ability to suppress T cell activation and promote tumor growth. However, how β-catenin is reduced in MDSC during tumor progression is unknown. Dkk1 is an inhibitor of the Wnt/β-catenin pathway and is highly expressed in multiple myeloma patients with lytic bone disease. Although Dkk1 is known to modulate tumor growth

in bone by suppressing osteoblast differentiation, we propose the novel hypothesis that Dkk1 favors tumor progression via downregulation of β-catenin in MDSC. To avoid possible confounding results due to the function of Dkk1 on bone cells, we chose to study the immunomodulatory effects of Dkk1 using an extraskeletal tumor model consisting of mice bearing subcutaneous (s.c) Lewis Lung Carcinomas (LLC). While Dkk1 expression is barely detectable in LLC cells in vitro, Dkk1 level in the tumor is significantly upregulated 14 days after inoculation. Dissection of the tumor mass reveals that the Wnt inhibitor is mainly expressed by the tumor-associated fibroblasts but not by LLC cells. To investigate the effects of Dkk1 on extraskeletal tumor growth, α-Dkk1 or IgG control Abs (20 mg/kg) were administered 3x/week to WT mice at time of LLC s.c inoculation. Strikingly, tumor growth is significantly decreased in mice treated with α-Dkk1Ab compared to controls (p =0.019). While α-Dkk1Ab does not directly affect LLC proliferation or survival in vitro, Dkk1 neutralization significantly reduces % of MDSC in vivo. This finding suggests that Dkk1 promotes tumor growth by favoring MDSC expansion. To further investigate the effects of Dkk1 on MDSC accumulation, we turned to the PLCγ2-/- mice since PLCγ2 null MDSC display reduced β-catenin level and stronger immune-suppressive functions compared to WT. α-Dkk1Ab significantly reduces tumor growth in null mice compared to IgG (p = 0.006). % of MDSC in bone marrow, spleen and tumor site is reduced while % of CD4 and CD8 T cells are restored by α-Dkk1Ab. Importantly, Dkk1 neutralization rescues β–catenin expression in PLCγ2-/- MDSC. Taken together, we demonstrate that α-Dkk1 treatment reduces extraskeletal tumor growth by targeting MDSC. The novelty of this work consists in having identified an immunomodulatory role for Dkk1 independent of its effects on bone cells.

Disclosures: Lucia D'Amico, None.

FR0078

The unexpected role of Hemoglobin beta (HBB) in breast cancer. <u>Nadia Rucci</u>*[1], <u>Mattia Capulli</u>[1], <u>Luca Ventura</u>[2], <u>Patrizia Sanità</u>[3], <u>Simona Delle Monache</u>[3], <u>Adriano Angelucci</u>[3], <u>Anna Teti</u>[1]. [1]University of L'Aquila, Italy, [2]San Salvatore Hospital, Italy, [3]University of L'Aquila, Italy

Breast cancer (BrCa) patients with metastases restricted to bone (BO) show a longer overall survival compared to BrCa patients developing bone and visceral metastases (BV). Gene expression analyses revealed few genes whose expression was significantly different between the two groups of bone metastases. Among them, we found the hemoglobin beta (HBB) to be one of the most upregulated in BV vs. BO. We confirmed the HBB expression in 34 out of 57 human primary tumors analyzed. Moreover, the percentage of HBB positive cancer cells (HBB score) in ductal and lobular breast carcinomas was significantly higher in the invasive lesions than in the in situ counterpart (6-fold, P<0.05). Higher expression of HBB was also observed in ductal infiltrating carcinoma *vs.* the lobular invasive histotype (2.2-fold, P<0.05), while benign lesions, the in situ counterpart of lobular carcinoma and normal tissue were negative. Interestingly, a positive correlation (P<0.05) was observed between HBB and the score of the proliferation marker Ki67. In vitro, we evaluated HBB expression between poorly aggressive (MCF7, HCC1954) and highly aggressive (MDA-MB231) BrCa cells, finding a higher mRNA and protein expression in the latter (11-fold P<0.05). Forced HBB overexpression in MDA-MB231 cells (MDA-HBB) induced an increased ability to migrate and invade in vitro vs. control cells (MDA-Empty), accompanied by increased transcriptional and protein expression of MMP9, and by increased expression of several oxidative stress associated mRNAs, including NOS2, NOX5, DUSP1, PREX1 and LPO. In an in vitro tube formation assay, MDA-HBB conditioned medium induced tube formation better than MDA-Empty (1.5-fold increase P<0.05). In agreement, the in vivo growth rate of orthotopically implanted MDA-HBB was significantly higher (P<0.005) compared to MDA-Empty. Tumor weight was increased too (1.9 fold, P=0.002), while histology showed less fibrosis in MDA-HBB tumor sections (0.4 fold, P<0.001). Moreover, local recurrence and visceral metastases were observed in 60% of MDA-HBB implanted mice, while MDA-Empty tumor recurrence and relapse did not occur over the same timeframe. Intriguingly, primary human prostate cancers as well as the prostate cancer cell line PC3 did not express HBB, suggesting specificity for BrCa. In conclusion, the expression of HBB in BrCa is positively correlated with aggressiveness, implying that HBB expression in BrCa cells could represent a specific pivotal pro-tumoral event.

Disclosures: Nadia Rucci, None.

FR0079

CXCL14, an inhibitor of CXCL12/CXCR4 signaling, is upregulated in prostate cancer bone metastasis. <u>Alexander Dowell</u>[1], <u>Katrina Clines</u>[2], <u>Colm Morrissey</u>[3], <u>Shi Wei</u>[1], <u>Gregory Clines</u>*[4]. [1]University of Alabama at Birmingham, USA, [2]University of Michigan, USA, [3]University of Washington, USA, [4]University of Michigan, USA

Prostate cancer bone metastasis is present in 90% of men with advanced stage disease and is the principal source of morbidity and death. The discovery of novel drugs that target bone metastasis and biomarkers that identify men with early stage prostate cancer who are at risk for bone metastasis is of critical importance. An investigation by our group to uncover targets of endothelin-1, a factor involved in the osteosclerotic response of prostate cancer in bone, led to the identification of CXCL14. This 77 amino acid secreted protein is a member of the CXC chemokine

family. Chemokines play a pivotal role in prostate cancer cell homing to bone. CXCL14 represented an ideal target of interest due to its close homology with CXCL12 (also known as SDF-1). CXCL12 originating from bone promotes epithelial-mesenchymal transition and directs the migration of CXCR4-expressing circulating prostate cancer cells to bone. We hypothesized that CXCL14 modifies the action of CXCL12 during the metastasis of prostate cancer to the skeleton. In a human prostate cancer tissue microarray, the expression of CXCL14 was significantly upregulated in prostate cancer bone metastasis (H-Score mean 172.5, n=113) as compared to soft tissue metastasis (H-score mean 99.5, n=57, p<0.001), primary prostate cancer and normal prostate. CXCL14 expression in the prostate cancer xenograft line LuCaP 23.1 was increased in mouse tibia compared to subcutaneous implanted tumor. Similarly, CXCL14 was absent from the ARCaP$_M$ prostate cancer cell line, but was readily detected after intratibial inoculation. These data suggest that bone, but not other tissues, supplies prostate cancer cells with a unique signature of factors that increase CXCL14 expression. We next performed functional studies to uncover CXCL14 action in prostate cancer. CXCL14 blocked CXCL12-mediated *in vitro* chemotaxis of the ARCaP$_M$ prostate cancer cell line and is consistent with recent published data that CXCL14 binds to CXCR4 to block CXCL12-mediated activation of CXCR4. CXCL14 therefore opposes CXCL12 action and may be a critical factor in colonization of prostate cancer cells after CXCL12-mediated arrival to bone. Our model supports that bone-derived CXCL12 directs CXCR4-expressing prostate cancer cells to bone, and the bone microenvironment activates prostate cancer CXCL14 expression that reverses CXCL12 to halt further migration and promote colonization in bone.

Disclosures: Gregory Clines, None.

FR0080

Lysyl oxidase promotes survival and outgrowth of colon cancer cells in the bone marrow, enabling bone metastasis formation. Caroline Reynaud*[1], Laura Ferreras[2], Delphine Goerhig[2], Marie Brevet[3], Philippe A.R. Clezardin[4]. [1]INSERM Unité 1033UFR de Médecine Lyon-Est (domaine Laënnec), Fra, [2]INSERM U1033, France, [3]Hospices Civils de Lyon, France, [4]INSERM & University of Lyon, France

Lysyl oxidase (LOX) catalyzes the cross-linking of collagens and elastin in the extracellular matrix, thereby regulating the tensile strength of many tissues, such as in the bone. In cancer, LOX plays a critical role in facilitating tumor growth and metastasis formation in soft tissues. Whether tumor-derived LOX also enables bone metastasis is unknown. In this study, we first showed by immunohistochemistry using patient's tumor specimens, that *LOX* was expressed in the desmoplastic tumor stroma of pairs of colorectal carcinomas and their matching bone metastases. Preclinical experiments showed that *LOX* overexpression in different colon carcinoma cell lines enhanced the formation of osteolytic lesions in animals by promoting both skeletal tumor burden and osteoclast-mediated bone resorption. Additionally, exogenous LOX treatment of animals enhanced bone metastasis formation caused by parental colorectal carcinoma cells. Conversely, the pretreatment of animals with the LOX inhibitor b-aminopropionitrile or the silencing of *LOX* in colorectal carcinoma cells drastically reduced the formation of osteolytic lesions. *In vitro*, tumor-derived LOX indirectly promoted osteoclast differentiation by enhancing the secretion of osteolytic factors from colon cancer cells. LOX also directly enhanced the attachment of colon cancer cells to collagen (but not to fibronectin) and promoted cancer cell survival by activating interleukin-6 autocrine signaling pathways. In conclusion, our findings provide novel evidence that LOX endows colon cancer cells with the ability to thrive in the bone marrow microenvironment and stimulate osteoclast-mediated bone destruction.

Disclosures: Caroline Reynaud, None.

FR0081

Tumour-derived alkaline phosphatase promotes Epithelial-Mesenchymal Transition (EMT) and cell survival in bone metastatic prostate cancer; regulation by miR-373. Srinivasa Rao*, Ann Snaith, Patrick Kratschmer, Freddie Hamdy, Claire Edwards. University of Oxford, United Kingdom

Prostate cancer (PCa) bone metastases are often associated with mixed osteolytic/osteoblastic lesions. Identifying novel mechanisms that underlie this debilitating bone disease will ultimately reveal new therapeutic targets. We have identified differential expression of the key osteoblastic enzyme alkaline phosphatase (ALP) in a panel of PCa cell lines with increasing metastatic potential. Using a high-throughput screening approach, in vivo models of disease and pharmacological and molecular manipulation of ALP, the function and regulation of tumour-derived ALP in PCa bone metastasis was explored. ALP activity and mRNA expression were higher in osteoblastic ARCaPM cells than non-metastatic ARCaPE (p<0.001). ALP expression was lower in osteolytic PC3 cells, and undetectable in the majority of non-bone metastatic cell lines. Inoculation of ARCaPM cells into nude mice resulted in both osteolytic and osteoblastic lesions following microCT analysis, whereas PC3 cells resulted in purely osteolytic lesions. Lentiviral-mediated knockdown of ALP in ARCaPM cells resulted in ~50% decrease in cell viability and Mesenchymal-Epithelial Transition, evidenced by a change in morphology, increase in E-cadherin (p<0.001) and decreased migration. ALP knockdown in PC3 cells decreased cell viability (p<0.01). Inhibition of ALP by levamisole dose-dependently inhibited cell viability in a panel of bone

metastatic PCa cells. ALP activity also correlated with the ability of PCa cells to mineralize in vitro. We have undertaken two complementary approaches to study ALP regulation in PCa bone disease. RNA-seq identified microRNAs that were differentially expressed in ARCaPM cells as compared to ARCaPE cells. Transfection of ARCaPM cells with a microRNA mimic library followed by a high-throughput functional screen identified microRNAs that regulate ALP activity. From these data, we focused on miR-373, which has a 22-fold lower expression in ARCaPM cells compared to ARCaPE cells (p<0.05). Overexpression of miR-373 in ARCaPM cells resulted in a 60% reduction in ALP gene expression (p<0.05), a reduction in Runx2 expression, a 20% reduction in ALP activity (p<0.01), and a 60% reduction in mineralization of ARCaPM prostate cancer cells (p<0.01). Our study defines a novel mechanism whereby tumour-derived ALP induces EMT and survival of PCa cells, with ALP expression regulated by miR-373, so identifying ALP and miR-373 as mediators of PCa bone metastasis.

Disclosures: Srinivasa Rao, None.

FR0084

Integrin Alpha5beta1 is a Potential Therapeutic Target to Treat Experimental Breast Cancer Bone Metastasis. Francesco Pantano[1], Martine Croset[2], Keltouma Driouch[3], Edith Bonnelye[4], Michele Iuliani[1], Marco Fioramonti[1], Daniele santini[1], Giuseppe Tonini[1], Philippe A.R. Clezardin*[5]. [1]Medical Oncology Division, University Campus-Bio-Medico, Italy, [2]INSERM Research Unit U1033, University of Lyon1, France, [3]Institute Curie, France, [4]Faculte de Medecine RTH Laennec, France, [5]INSERM & University of Lyon, France

The fibronectin receptor, α5β1 integrin, is highly expressed in breast cancer cell lines and disseminated tumor cells (DTC) from bone marrow (BM) of breast cancer patients. The binding of α5β1 to fibronectin sustains tumor growth and contributes to the survival of breast cancer cells in BM. We have shown by *in-silico* analysis, using public microarray data sets, that high levels of α5 expression correlates with a short onset of bone metastasis (BonMet) in resected breast cancer patients. Quantitative real-time PCR analysis performed on primary tumors from 427 breast cancer patients showed that (1) high α5 levels correlated with metastatic status and clinical parameters and (2) α5 was an independent negative prognostic factor for BonMet relapse. Therefore, we studied the role of α5β1 in a mouse model of BonMet. We choose the breast cancer cell line B02, which highly expresses α5β1 and specifically metastases to bone, that we injected intra-arterially to mice in combinaison with the anti-human-α5β1 chimeric antibody (M200). *In vitro*, M200 blocked the adhesion and migration of B02 to fibronectin. To assess the role of α5β1 in early BM colonization by tumor cells, mice were treated with M200 (3 injections at 15mg/kg, starting the day prior to B02 inoculation to mice) or with vehicle. Seven days after tumor cell injection, the DTC number in the BM was significantly decreased in M200-treated mice, highlighting the anti-invasive properties of M200. Then, B02 tumor-bearing mice were treated with vehicle or M200 at 15mg/kg, 3 times a week during 28 days at which time, animals develop overt BonMet. M200 treatment delayed the onset of metastasis and decreased the extent of osteolytic lesions and tumor burden in metastatic mice. Additionally, M200 decreased human osteoclast differentiation *in vitro*, suggesting that α5β1 may also inhibit bone resorption *in vivo*. The lentiviral mediated-silencing of α5 expression in B02 reproduced the inhibitory effects obtained with M200 treatment of mice bearing BonMet. However, α5 silencing in MDA-MB-231 cells, which form metastases to BM and lungs, affected only DTC number in bone but not in lungs, indicating that the activity of α5β1 may be tissue-specific. Overall, we have shown that α5β1 mediates colonization of tumor cells in the BM and promotes the progression of bone metastasis *in vivo*, suggesting that the therapeutic targeting of α5β1 may be an effective strategy to treat bone metastasis.

Disclosures: Philippe A.R. Clezardin, None.

FR0085

Roundabout receptors mediate breast cancer bone metastasis formation and progression. Lise Clement-Demange*[1], Bénédicte Eckel[2], Vincent Gonin[2], Delphine Goehrig[2], Chantal Diaz-Latoud[2], Philippe A.R. Clezardin[3]. [1]France, [2]INSERM U1033, France, [3]INSERM & University of Lyon, France

Roundabout (ROBO) receptors regulate axon guidance. We did a comparative transcriptomic analysis of human MDA-MB-231 breast cancer cells with that of a cell subpopulation that only metastasizes to bone (referred to as B02) and demonstrated that Robo1 and Robo4 receptors were overexpressed in B02 cells. Interestingly, a high Robo4 expression in primary tumors from patients with breast cancer (n=254) correlated with poor prognosis and increased risk of relapse to bone. We therefore examined the functions of Robo1 and Robo4 in tumor outgrowth and bone metastasis formation.

Inoculation of Robo4-depleted cells in the mammary fat pad of mice led to a 50% reduction in tumor burden, whereas the outgrowth of Robo1-depleted tumors was substantially increased, compared with animals injected with mock-transfected B02 cells. Bone metastasis experiments were realized by injection of tumor cells into the caudal artery of mice and animals were analyzed by radiography on day 25 after tumor cell inoculation. The extent of osteolytic lesions was dramatically increased in

animals bearing Robo1-depleted tumors, when compared with animals bearing Robo4-depleted tumors.*In vitro*, the treatment of parental B02 breast cancer cells with anti-Robo1 antibody promoted invasiveness, whereas anti-Robo4 antibody dose-dependently inhibited B02 cell invasion. Altogether these results let us hypothesize that Robo4 might facilitate the engraftment of tumor cells in the bone marrow. To address this question, two experiments were set up. First, the bone marrow was flushed from the hind limbs of animals 7 days after tumor cell inoculation and cells cultured under antibiotic selection, enabling the selective growth of tumor cells. The number of colonies from the bone marrow of mice inoculated with Robo4-depleted cells was reduced by 75 to 80% when compared with Robo1-depleted cells. In the second experiment, B02 cells were first incubated with an anti-Robo4 antibody, one hour before intra-tibial inoculation. The incidence of colony appearance after bone marrow flush was reduced by 50% when B02 cells were incubated with the anti-Robo4 antibody and the number of colonies was dramatically reduced from 792 to 33 / mouse. These results provide strong evidence that axon guidance receptors Robo1 and Robo4 are involved in bone metastasis formation and that the use of an antibody directed against Robo4 receptor could lead to the development of innovative therapies to prevent bone metastasis.

Disclosures: Lise CLEMENT-DEMANGE, None.

FR0087

Chondrocyte-specific Deletion of *Sod2* Exacerbates Cartilage Degeneration Associated with Low Mitochondrial Membrane Potential in Mice. Masato Koike*[1], Nojiri Hidetoshi[2], Yusuke Ozawa[3], Kenji Watanabe[3], Isao Masuda[3], Yuta Muramatsu[4], Haruka Kaneko[2], Daichi Morikawa[2], Keiji Kobayashi[3], Yoshitomo Saita[5], Takahisa Sasho[4], Takuji Shirasawa[6], Koutaro Yokote[7], Kazuo Kaneko[2], Takahiko Shimizu[3]. [1]Chiba University Graduate School of Medicine, Japan, [2]Department of Orthopedics, Juntendo University Graduate School of Medicine, Japan, [3]Department of Advanced Aging Medicine, Chiba University Graduate School of Medicine, Japan, [4]Department of Orthopedics, Chiba University Graduate School of Medicine, Japan, [5]Department of Orthomedics, Juntendo University Graduate School of Medicine, Japan, [6]Department of Aging Control Medicine, Juntendo University Graduate School of Medicine, Japan, [7]Department of Clinical Cell Biology & Medicine Chiba University Graduate School of Medicine, Japan

Superoxide dismutase 2 (SOD2) is a major antioxidant enzyme localized mitochondria to diminish mitochondrial superoxide. Human studies have reported that SOD2 protein and *SOD2* gene expression were significantly decreased in osteoarthritic cartilage. However, pathophysiological role of SOD2 in chondrocytes has not been fully elucidated yet. Here, we generated a novel chondrocyte-specific *Sod2*-deficient (cKO) mouse using a Cre-loxp system to conclude whether SOD2 loss in chondrocytes enhances osteoarthritis (OA) progression. Dehydroethidium, a specific dye for superoxide detection, staining revealed that *Sod2* ablation significantly enhanced superoxide generation by 400% in isolated chondrocytes from the cKO mice. *Sod2* loss in chondrocytes of knee joint developed no obvious skeletal abnormalities during growth term, while the cKO mice significantly accelerated cartilage loss in the depth of tidemark at eight weeks after surgery. Moreover, *Sod2* deficiency spontaneously exacerbated OA pathologies at 12 months of age. *In vitro* experiments also revealed that *Sod2* depletion caused impaired mitochondrial membrane potential using JC-1 staining as well as swollen mitochondrial morphology associated with disrupted cristae using an electron microscope. Furthermore, gene expression analyses clarified that anabolic genes, including *Col2a1* and *Acan*, were significantly down-regulated, while catabolic genes, including *Mmp13* and *Adamts5*, were significantly up-regulated. Alcian blue staining confirmed a significant 80% decrease of proteoglycan in cKO chondrocytes. Taken together, these results demonstrated that *Sod2* deficiency in chondrocytes induced mitochondrial superoxide generation and mitochondrial dysfunction associated with decreased membrane potential resulted in cartilage degeneration and loss via impaired proteoglycan metabolism. Our findings revealed that SOD2 plays a protective role in OA pathogenesis regulating mitochondrial function in mice.

Disclosures: Masato Koike, None.

FR0088

HIF-1α is essential for articular cartilage homeostasis through induction of anabolic factors and suppression of catabolic factors. Keita Okada*[1], Song Ho Chang[1], Yoko Hosaka[2], Hiroshi Kobayashi[3], Shurei Sugita[4], Haruhiko Akiyama[5], Ung-Il Chung[6], Hiroshi Kawaguchi[7], Taku Saito[2]. [1]The University of Tokyo, Japan, [2]University of Tokyo, Graduate School of Medicine, Japan, [3]The University of Tokyo Hospital, Japan, [4], Japan, [5]Gifu University, Japan, [6]University of Tokyo Schools of Engineering & Medicine, Japan, [7]JCHO Tokyo Shinjuku Medical Center, Japan

Hypoxia-inducible factor-1α (HIF-1α) plays a crucial role in hypoxic conditions for cell survival in various tissues. In chondrocytes, previous studies have shown that HIF-1α is essential in endochondral ossification and for interzone formation in joint

development; however, the underlying molecular mechanisms remain unclear. Moreover, while HIF-2α regulates expression of various catabolic factors and osteoarthritis (OA), physiological and pathological functions of HIF-1α in articular cartilage are yet to be revealed. Here, we investigated the HIF-1α function in articular cartilage by analyzing surgical OA models and cartilage development using conditional knockout mice. When we created the experimental OA model one week after tamoxifen injection to *Col2a1-Cre^ERT2^;Hif1a^f/f^* mice, we found that OA development was markedly accelerated as compared to the control *Hif1a^f/f^* joints. We then examined articular cartilage formation in *Sox9-Cre;Hif1a^f/f^* embryos, and found a massive cavity continuing from the joint surface forming a trumpet-shaped epiphysis. Notably, apoptosis and Mmp13 expression were upregulated in both of these cKO mice. In addition, aggrecan release was increased when femoral heads from 3 week old cKO mice were cultured in IL-1β and decreased when WT mice were cultured with $CoCl_2$, a stabilizer of Hif-1α. To determine altered gene expression by HIF-1α deficiency, we carried out a microarray with cartilage samples from cKO mice. The catabolic factors Mmp13 and Mmp9, anabolic factors Sox9 and Col2a1 and the apoptosis related genes Bnip3 and Bnip3l showed marked fold changes. To confirm these results, we obtained articular chondrocytes from *Hif1a^f/f^* mice and introduced adenoviral vector expressing Cre recombinase or GFP. Real-time RT-PCR revealed increases of catabolic factors including *Hif2a*, *Mmp13* and *Mmp9*, and decreases of anabolic factors including *Col2a1* and *Sox9* by the deletion of HIF-1α under both normoxic and hypoxic (1% O_2) conditions. Similar results were also obtained by HIF-1α silencing in primary articular chondrocytes from WT mice using siRNA. When HIF-1α was lentivirally overexpressed in ATDC5 cells, the opposite results were obtained. In conclusion, HIF-1α is essential for articular cartilage homeostasis through its induction of anabolic factors and suppression of catabolic factors and HIF-2α. Elucidation of the molecular network related to HIF-1α may lead to an understanding of cartilage regeneration and subsequent OA treatment.

Disclosures: Keita Okada, None.

FR0089

PTHrP is a candidate marker of slowly replicating "resting" chondrocytes in the postnatal growth plate cartilage. Noriaki Ono*[1], Wanida Ono[2], Henry Kronenberg[2]. [1]University of Michigan School of Dentistry, USA, [2]Massachusetts General Hospital, USA

In endochondral bone development, chondrocytes in growth plate cartilage continue to proliferate postnatally, providing engines for bone lengthening. We hypothesize that slowly replicating cells of the growth plate are the sources of all other chondrocytes and show characteristics of postnatal stem cells. To isolate label-retaining cells (LRCs) (and therefore slowly replicating cells) from the growth plate, we generated mice harboring a Tet-Off system regulating expression of GFP linked to a histone (H2B-GFP) driven by type II collagen (Col2) promoter. In order to preferentially mark growth plate chondrocytes with tdTomato, we also included a *Col2-creER* transgene activating a *Rosa26*-tomato reporter (*Col2-tTA*; *TRE*-H2B-EGFP; *Col2-creER*; *R26R*-tomato). These mice were fed with doxycycline from 3 weeks of age for various periods to shut off GFP expression (chase), and injected twice with tamoxifen during 72 hours before being sacrificed. Dissected epiphyses were digested with collagenase to harvest chondrocytes for FACS analysis. Tomato$^+$ chondrocytes near the top of the growth plate retained a higher level of H2B-GFP expression. The fraction of a label-retaining population with $>10^4$ unit of GFP (GFP^{high}) within the Tomato$^+$ population gradually decreased as the chase period lengthened. LRCs and non-LRCs were FACS-sorted after 4 weeks of chase, when GFP^{high} represented ~10% of total Tomato$^+$ cells. RNA of both populations was amplified and subjected to Affymetrix cDNA microarray analysis. Upregulated genes in LRCs were listed and confirmed by qPCR using independent samples. Of these genes, we found that *PTHrP* mRNA was enriched in LRCs (x3.8). Analysis of *PTHrP-LacZ* knock-in mice revealed that PTHrP$^+$ chondrocytes were localized at the top of the postnatal growth plate. To ask whether these cells are slowly replicating, *PTHrP-LacZ* mice were pulsed with 9 serial injections of EdU from postnatal day 4 to 6 and chased thereafter for 3 weeks. While $17.9 \pm 2.7\%$ of EdU$^+$ cells were LacZ$^+$ shortly after the pulse at day 7, the fraction increased to $77.6 \pm 9.6\%$ after the chase at day 28, suggesting that LRCs were enriched among PTHrP$^+$ cells. Therefore, our data indicate that *PTHrP* is a candidate marker for slowly replicating "resting" chondrocytes of the postnatal growth plate, and will be instrumental in identifying characteristics of putative chondrocyte stem/progenitor cells. We are currently generating *PTHrP-creER* BAC transgenic mice to study the fate of these chondrocytes.

Disclosures: Noriaki Ono, None.

FR0090

Ablation of CypA Leads to Impaired Chondrogenesis by Inhibiting NF-κB-Sox9 Pathway. Mian Guo*[1], Jia Shen[2], Jinny Kwak[2], Xinli Zhang[2], Aaron James[3], Kevork Khadarian[2], Kang Ting[2], Chia Soo[4], Robert Chiu[5]. [1]Dental & Craniofacial Research Institute & Division of Oral Biology, School of Dentistry, University of California, Los Angeles; Department of Neurosurgery, the Second Affiliated Hospital of Harbin Medical University, USA, [2]Dental & Craniofacial Research Institute & Section of Orthodontics, School of Dentistry, University of California, Los Angeles, USA, [3]Department of Pathology & Laboratory Medicine, David Geffen School of Medicine, University of California, Los Angeles, USA, [4]Division of Plastic & Reconstructive Surgery, School of Medicine, University of California, Los Angeles; Department of Orthopedic Surgery, School of Medicine, University of California, Los Angeles, USA, [5]Dental & Craniofacial Research Institute & Division of Oral Biology, School of Dentistry, University of California, Los Angeles; Jonsson Comprehensive Cancer Center & Division of Surgical Oncology, University of California, Los Angeles, USA

Cyclophilin A (CypA) is a PPIase (peptidyl-prolyl cis-trans isomerase) that regulates protein folding, stability and translocation in diverse cellular processes. Recent studies have demonstrated skeletal malformations in mice with PPIase deficiency. This study aims to investigate the role of CypA in chondrogenesis and the potential involvement of the NF-κB-Sox9 signaling pathway.

First, the skeletal phenotypes of CypA wildtype (wt) and knockout (ko) mice were assessed by Alcian Blue/Alizarin Red whole mount staining, microCT, and immunohistochemistry. Next, we cultured E12.5 mouse limb bud cells (wt vs ko) and ATDC5 prechondroblastic cells (control vs stable knockdown) in 3D systems. The chondrogenic capacity of these cells was compared by immunostaining and RT-PCR of chondrogenic markers expression. Finally, the direct interaction between CypA and NF-κB/p65 was determined using co-immunoprecipitation. In addition, CypA regulation of NF-κB/p65-Sox9 signaling was analyzed by western blot, luciferase reporter assay and immunohistochemical staining.

Results showed that CypA ko mice were 10% shorter in body length at birth, and exhibited endochondral ossification defects in the skull, long bones and vertebrae. MicroCT analyses and Alcian Blue staining of femur and lumbar vertebrae revealed significantly decreased bone formation and cartilaginous matrix deposition in CypA ko mice. When assessing the long bone growth plate in developing mice, we observed a thinner growth plate, shorter chondrocyte columns, and reduced expressions of Col2 & Col10 in CypA null mice (Fig.1). The inhibition of chondrogenesis by down-regulating CypA was confirmed *in vitro* in mouse limb bud cells and ATDC5 cells. Alcian Blue staining for chondrocytes and the expression of several chondrogenic differentiation markers (Col2, Col10, Runx2 and Sox9) were all decreased in CypA ko or kd cells (Fig.2). Next, the involvement of NF-κB/p65-regulated Sox9 expression in CypA-mediated chondrogenesis was assessed. Results showed that CypA affects p65 stability by directly binding its N-terminal 170-176 amino acids. p65 levels and activity were significantly inhibited in CypA knockdown cells, which in turn led to the downregulation of Sox9 expression (Fig.3).

These findings suggest that CypA plays an important role in chondrogenic development via the regulation of the NF-κB/p65-Sox9 signaling pathway. Further study will focus on the mechanisms of CypA regulated endochondral ossification.

FIGURE 1

Fig.1

FIGURE 2

Fig.2

FIGURE 3
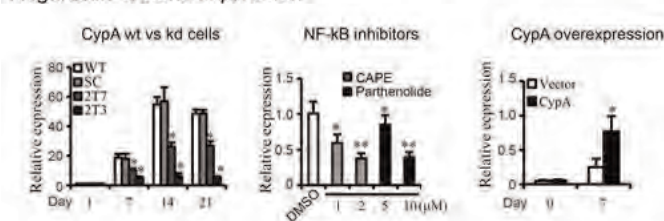
Fig.3

FR0092

Notch Inhibits Chondrogenic Differentiation of Mesenchymal Progenitor cells by Targeting Twist1. Martin Chang*[1], Ye Tian[2], Edward Schwarz[3], Matthew Hilton[4], Yufeng Dong[3]. [1]University of Rochester Medical Center, USA, [2]Shengjing Hospital, China Medical University, China, [3]University of Rochester, USA, [4]Duke University Musculoskeletal Research Center, USA

Recently we have demonstrated the importance of RBPjk-dependent Notch signaling in the regulation of mesenchymal progenitor cell (MPC) differentiation during chondrogenesis both *in vivo* and *in vitro*, although the exact molecular mechanisms remain unknown. Here we have performed Notch gain- and loss-of-function experiments to demonstrate for the first time that Notch suppression of MPC differentiation and chondrogenesis acts via up-regulation of the transcription factor *Twist1*. Notch activation, via Notch intracellular domain (NIDC1) over-expression, in micromass cultures of murine limb-bud MPCs displayed an inhibition of chondrogenesis. This was evidenced by significant decreases in the expression of chondrogenic marker genes, including *Col2a1* and *Acan1*, as well as decreased alcian blue staining. We further demonstrated that *Twist1* is exclusively expressed in MPCs at early stages of chondrogenesis during Notch activation and that inhibition of Notch signaling in these cells significantly reduced TWIST1 protein levels. In contrast, over-expression of NICD1 induced rapid TWIST1 expression in the nucleus and the effects of Notch on MPC differentiation was markedly reduced by knocking down of *Twist1* in MPC

micromass cultures (Fig. 1). Furthermore, luciferase assays demonstrate that constitutively active Notch signaling significantly enhanced *Twist1* promoter activity. Interestingly, mutation studies indicate that a putative NICD/RBPjk binding element TGGGAA (-1432/-1426) in the promoter region is required for the Notch-responsiveness of the *Twist1* promoter. Finally, chromatin immunoprecipitation assays using limb-bud MPCs further confirmed that the NICD influences *Twist1* transcription by directly binding to the *Twist1* promoter *in vivo* via the RBPjk binding site (Fig. 2). Taken together, our results indicate that RBPjk-dependent Notch signaling directly activates *Twist*1, and this likely contributes to the Notch-mediated repression of chondrogenesis and chondrocyte gene expression. These data provide novel insights into our understanding of the molecular mechanisms underlying Notch inhibition of chondrogenesis.
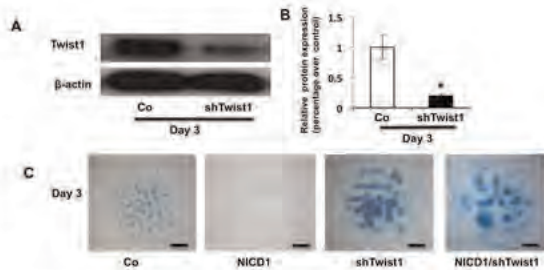
Fig. 1: Limb bud cells in micromass were infected with NICD1 or/and shTwist1 lentivirus for 3 days before being harvested for Western Blot and Alcian blue staining (A) Twist1 protein levels were significantly reduced by Twist1 shRNA lentiviral infection. (B) Quantification of Twist1 protein expression in Western blots. (C) A significant increase in chondrocyte nodule formation was observed in both shTwist1 infected cells with or without co-infection with NICD1, and a drastic reduction in chondrocyte nodule formation was seen in NICD1-expressing cells. Scale bars, 100 μm.

Fig. 1
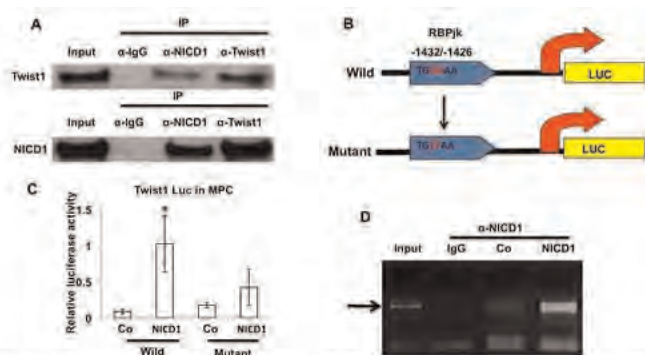
Fig. 2: (A) Immunoprecipitation assays (n=3) show that Twist1 protein interacts with NICD1. (B) RBPJK binding site-mutated promoter construct. Nucleotides that mutate from established consensus sequences are highlighted in red. (C) Twist1 promoter Luciferase assays. (D) Chromatin immunoprecipitation showed a specific fragment was detected between the RBPJK response element and Twist1 in control (Co) MPCs, and this fragment formation was enhanced by overexpression of NICD1 in MPCs.

Fig. 2

***Disclosures: Martin Chang**, None.*

FR0095

Smad2/3 Mediated TGFbeta Signaling Controls Postnatal Chondrocyte Proliferation and Differentiation by Inhibiting *Ihh* Transcription. <u>Weiguang Wang</u>*, <u>Karen Lyons</u>, <u>Teni Anbarchian</u>. University of California, Los Angeles, USA

TGF-β signaling exhibits important roles in joint development and articular cartilage (Ref1). However, it is not clear to what extent TGF-β mediates its effects through canonical Smad2/3 pathways vs. non-canonical pathways. To address this question, we generated mice with a conditional deletion of *Smad2* in chondrocytes using Col2cre (*Smad2cko*), mice with *Smad3* globally deleted (*Smad3-/-*), and the cross of these two strains to obtain mice with both *Smad2 & 3* deleted in chondrocytes (Double mutant mice). At P0, *Smad2cko*, *Smad3-/-* and double mutant mice exhibited an expansion of both non-hypertrophic and hypertrophic zones in growth plate. PCNA staining showed that there is an increase of proliferation in resting chondrocytes in all 3 types of mutant mice. These defects were much more severe in *Smad2/3* double mutant and *Smad2cko* than in *Smad3-/-* mice. *In situ* hybridization results demonstrated an increase of *Ihh* mRNA expression in prehypertrophic

chondrocytes in all 3 types of mutant mice, when compared with the WT(Fig. In addition, qPCR showed that TGF-β treatment inhibits *Ihh* transcription in rib primary chondrocytes of WT mice, but this inhibition is diminished in cells from all 3 types of mutant mice, and that this defect is more severe in double mutant and *Smad2cko* than in *Smad3-/-* cells. Moreover, luciferase reporter assay showed that Smad2 and Smad3 are required for inhibition of the 742bp *Ihh* promoter by TGF-β. Further examination of this *Ihh* promoter revealed 4 putative Smad2&3 binding elements (SBEs). Chip analysis using ATDC5 cells revealed that Smad2 only associates with SBE2, and Smad3 has high affinity with both SBE1 and SBE2, suggesting that Smad2 and Smad3 may have different functions in regulating expression of *Ihh*. Enhanced *Ihh* signaling is highly associated with osteoarthritis phenotype (Ref2). By 1 month, the double mutant mice developed early onset of osteoarthritis-like phenotypes. By 4 months, there was severe degeneration of articular cartilage, associated with elevated expression of Ihh, ColX and MMP13 in all these mutant mice. These observations suggest that TGF-β signaling mediated by both Smad2 and Smad3 is important for the regulation of postnatal growth plate chondrocyte proliferation, differentiation and maintenance of articular cartilage, and that Smads 2 & 3 may control these processes via inhibiting *Ihh* transcription.

References:
1. Wang et al., *Birth Defects Res C Embryo Today* 2014 Mar;102(1):37-51
2. Lin et al., *Nat Med.* 2010 Jan;16(1):129

Ihh (In Situ)

Figure. Increased *Ihh* expression in growth plates of *Smad2cko*, *Smad3-/-* and *Smad2/3* double mutant mice. In situ hybridization of P0 tibia sections. Note the increase of *Ihh* expression (Red) in prehypertrophic chondrocyte zones of *Smad2cko*, *Smad3-/-* and *Smad2/3* double mutant mice, when compared with the WT mice.

Increased Ihh expression in growth plates of Smad2cko, Smad3-/- and Smad2/3 double mutant mice

***Disclosures: Weiguang Wang**, None.*

FR0097

The novel transcription factor Zinc Finger Homeobox 4 (Zfhx4) is critical to late stage of endochondral ossification. <u>Eriko Nakamura</u>*[1], <u>Kenji Hata</u>[2], <u>Maokoto Wakabayashi</u>[3], <u>Yoshiaki Yura</u>[1], <u>Toshiyuki Yoneda</u>[4], <u>Riko Nishimura</u>[2]. [1]Osaka University Graduate School of Dentistry, Japan, [2]Osaka University Graduate School of Dentistry, Japan, [3]Asahi Kasei Pharma, Japan, [4]Indiana University School of Medicine, USA

Endochondral ossification is a unique and important biological event, temporally and spatially regulated by transcription factors, including Sox9, Runx2, and Osterix. Although our understanding of the transcriptional regulation of endochondral ossification is in progress, the precise regulatory mechanism still remains elusive. We examined whether yet-unidentified transcription factors contribute to endochondral ossification. To address this, we performed microarray analyses using mouse limb bud cells. Mcroarray analyses showed high expression level of Zfhx4, a gene putatively proposed to be responsible for 8q21.11 Microdeletion Syndrome., The syndrome is characterized by micrognathia, camptodactyly, and syndactyly. Consistent with the microarray, RT-qPCR showed that Zfhx4 was highly expressed in chondrocytes, long bones, and calvariae. To investigate the role of Zfhx4 in endochondral ossification, we generated the Zfhx4 floxed mice and subsequently mated them with CAG-Cre transgenic mice. The Zfhx4 conditional knockout (KO) mice died of respiratory failure within a day after birth. The skeletal preparation of the Zfhx4 KO mice at E15.5 exhibited trivialized thoracic cavity, malformation of skull, and dysplasia of femur, scapula, mandible and rib. Histological analyses indicated that endochondral ossification was arrested at hypertrophic zone in the femur of Zfhx4 KO mice at E15.5. We next examined expression of chondrogenic markers by performing immunohistochemical staining of femur of Zfhx4 KO and wild-type (WT) littermates at E15.5. Col2 and Col10 expression levels were equivalent in Zfhx4 KO and WT. In contrast, MMP13 expression was dramatically down-regulated in Zfhx4 KO mice compared with WT mice. Of note, calcification of cartilage matrices was markedly suppressed in Zfhx4 KO at E15.5 as demonstrated by von Kossa staining. Because the phenotype observed in Zfhx4 KO resembled Osterix KO, we examined interaction between Zfhx4 and Osterix. Fluorescent imaging analyses showed co-localization of Zfhx4 with Osterix, but not with Runx2. These results suggest that Zfhx4 is an important transcription factor, playing a role in degradation and calcification of cartilage matrices, presumably through interaction of Zfhx4 with Osterix. In conclusion, we identified Zfhx4 as a novel transcription factor that might be critical to the late stage of endochondral ossification.

***Disclosures: Eriko Nakamura**, None.*

FR0098

The transcription factor Foxc1 regulates chondrocyte hypertrophy in a synergistic cooperation with Runx2. Michiko Yoshida*[1], Kenji Hata[2], Sachiko Iseki[3], Teruko Takano-Yamamoto[4], Riko Nishimura[2], Toshiyuki Yoneda[5]. [1]Osaka University Graduate School of Dentistry, Japan, [2]Osaka University Graduate School of Dentistry, Japan, [3]Tokyo Medical & Dental University, Japan, [4]Tohoku University Graduate School of Dentistry, Japan, [5]Indiana University School of Medicine, USA

Endochondral ossification is spatially and temporally controlled by chondrogenic transcription factors. Given complexity and diversity of endochondral ossification, we attempted to identify an additional yet-unexplored transcription factor that contributes to the regulation of endochondral ossification. To this end, we performed FACS-assisted microarray profiling of transgenic mice overexpressing an improved-YFP, Venus, under the control of the *Col2a1* gene promoter and identified Forkhead Box c1 (Foxc1) that was selectively expressed in cartilage. Immunohistochemistry showed the evident expression of Foxc1 in proliferating and hypertrophic chondrocytes, suggesting a potential role of Foxc1 in endochondral ossification. Consistent with this notion, overexpression of Foxc1 strikingly increased *Col10a1* mRNA expression. DNA pull-down assay showed the direct binding of Foxc1 to a Foxc1-binding element in the *Col10a1* gene promoter. Of note, overexpression of Foxc1 together with Runx2, an essential transcription factor for chondrocyte hypertrophy, synergistically increased the expression of *Col10a1* and *MMP13*, both of which are well-known target gene of Runx2 in hypertrophic chondrocytes. Moreover, IP-western analysis demonstrated a physical association between Foxc1 and Runx2. These data collectively suggest that the interactions between Foxc1 and Runx2 play an important role in the regulation of chondrogenic gene expression associated with hypertrophy. Finally, we investigated the role of Foxc1 in vivo using spontaneous *Foxc1*-inactivated mutant mice (*Foxc1[ch]*). *Foxc1[ch/ch]* mice showed diverse skeletal abnormalities including dwarf phenotype and complete absence of the ossification center in the sternum. Histological analysis showed that there are reduced areas positive for Col10a1 and MMP13 in tibia of *Foxc1[ch/ch]* mice compared to that of WT mice at E15.5 days. Remarkably, Col10-positive hypertrophic chondrocytes were not detected in the sternum of *Foxc1[ch/ch]*. *Col10a1* mRNA expression was decreased in primary chondrocytes isolated from *Foxc1[ch/ch]*. However, Runx2 mRNA expression was not affected and overexpression of Foxc1 restored the expression of *Col10a1* in *Foxc1[ch/ch]* chondrocytes.

In conclusion, we identified the transcription factor Foxc1 that is selectively expressed in cartilage. Our results suggest that synergistic interactions of Foxc1 with Runx2 may regulate chondrocyte hypertrophy via the control of Col10a1 and MMP13 expression.

Disclosures: Michiko Yoshida, None.

FR0099

Absence of Cx37 leads to bone matrix modifications in mice: a potential explanation for why reduced cortical thickness is not followed by decreased mechanical strength. Rafael Pacheco Da Costa*[1], Eduardo Katchburian[2], Hannan Davis[3], Lilian Plotkin[4], Rejane Reginato[5]. [1]Indiana University/Universidade Federal de Sao Paulo - Brazil, Brazil, [2]Federal University of São Paulo, Brazil, [3]Indiana University School of Medicine, USA, [4]Indiana University School of Medicine, USA, [5]UNIFESP - Federal University of São Paulo, Brazil

Connexin (Cx) 37 is a gap junction protein expressed in all bone cell types, and its deletion leads to increased cancellous bone mass due to defective osteoclast maturation. In spite of reduced cortical thickness, Cx37-deficient mice (Cx37^{-/-}) exhibit higher mechanical strength in the femoral midshaft than Cx37^{+/+} littermates, suggesting changes in bone composition. We investigated here whether global deletion of Cx37 alters the composition of bone extracellular matrix. For this, mRNA isolated from vertebrae of 5-month-old Cx37^{-/-} mice and littermate Cx37^{+/+} wild type controls (N=7-10) was analyzed by qPCR. Cx37^{-/-} mice exhibited increased expression of Col3a1 (a gene involved in collagen formation), and Loxl2, Loxl3 and Loxl4 (genes that encode for enzymes associated with collagen maturation) compared to Cx37^{+/+} mice. Consistent with this, collagen fiber in the femoral midshaft analyzed in bone sections stained with picrosirius red and evaluated under polarization microscopy, showed that Cx37^{-/-} mice exhibit predominance of reddish birefringence, suggesting the presence of thicker fibrils and reduced bone remodeling. In addition, these mice showed more intense type II collagen immunostaining, which could explain the improved bone strength, and a slight decrease in biglycan, an indication of increased collagen maturation. On the other hand, decorin did not change. Sulfated glycosaminoglycans were slightly decreased in Cx37^{-/-} mice, as evidenced by alcian blue staining. On the other hand, expression of biglycan proteoglycan, Chsy1 and Chpf glycosaminoglycans, and of Has3, a gene associated with synthesis of low molecular weight hyaluronan, was increased in Cx37^{-/-} mice. MLO-Y4 osteocytic cells silenced for Cx37, using shRNA, which reduced Cx37 mRNA levels by 82% (N=6-9) and protein by 40% (N=3), exhibited increased Chsy1 and Chpf and decreased Has2 and Chsy3 mRNA expression. In addition, luminican and decorin mRNA levels were decreased in MLO-Y4 osteocytic cells lacking Cx37. Consistent with the *in vivo* results, Col1a1, Col3a1, Lox, Loxl1 and Loxl2 were increased in Cx37-silenced MLO-Y4 cells, suggesting that modifications in the bone matrix originate, at least in part, from changes in osteocytic gene expression. Our findings suggest that deletion of Cx37

increases bone strength through modification of extracellular bone matrix protein synthesis by osteocytes.

Disclosures: Rafael Pacheco Da Costa, None.

FR0102

ASXL2 Regulates Skeletal, Glucose and Lipid Homeostasis. Nidhi Rohatgi*[1], Takashi Izawa[2], Tomohiro Fukunaga[3], Qun-Tian Wang[4], Matthew Silva[5], Michael Gardner[6], Michael McDaniel[7], Clay Semenkovich[6], Wei Zou[5], Steven Teitelbaum[5]. [1]Washington University in St. Louis, USA, [2]University of Tokushima Grad Sch, Japan, [3]Washington University in St. Louis School of Medicine, USA, [4]UIC Biological Sciences, USA, [5]Washington University in St. Louis School of Medicine, USA, [6]Washington University School of Medicine, USA, [7]Washington Univerity School of Medicine, USA

ASXL2 is an ETP, transcription-regulating protein which is highly associated with bone mineral density in mouse and man. We find by cluster analysis that ASXL2 is expressed conjointly with genes governing myeloid differentiation suggesting it may participate in osteoclast differentiation. In fact, osteoclastogenesis of ASXL2-/- mice is arrested eventuating in a 400% increase in trabecular bone mass. Interestingly, ASXL2 regulates the osteoclast via two distinct but related signaling pathways. First, it induces osteoclast formation in a PPARγ /c-Fos-dependent manner. Thus, it is required for RANK ligand- and PPARγ agonist (thiazolidinedione)-induced bone resorption. Second, ASXL2 promotes osteoclast mitochondrial biogenesis and thus function in a c-Fos independent manner which is mediated by PGC-1β. Because PPARγ is a nuclear receptor and transcription factor which not only governs osteoclast formation but is key to maintaining whole body insulin sensitivity and glucose metabolism, we asked if ASXL2 impacts these metabolic events. Establishing such is the case ASXL2-deficient mice have type 2 diabetes (T2D) with impaired glucose homeostasis and global insulin resistance. As occurs in diabetic patients, fracture repair of ASXL2-/- mice is delayed. Similar to that attending PPARγ deficiency, Asxl2-/- mice are also lipoatrophic with significantly smaller subcutaneous and epididymal fat pads. The white adipose tissue of ASXL2-/- mice contains immature adipocytes and defects both in lipogenic and lipolytic markers. Our studies establish a link between skeletal biology and the metabolic syndrome and may provide insights into the reason thiazolidinedione-treated T2D patients are predisposed to poorly healing fractures.

Disclosures: Nidhi Rohatgi, None.

FR0103

Protein Phosphatase 5 (PP5) regulates both energy metabolism and bone mass by reciprocal regulation of PPARγ and Runx2 activities. Lance Stechschulte*[1], Chunxi Ge[2], Piotr Czernik[3], Edwin Sanchez[1], Renny Franceschi[4], Beata Lecka-Czernik[3]. [1]University of Toledo Health Science Campus, USA, [2]Pom Univ of Michigan School of Dentistry, USA, [3]University of Toledo College of Medicine, USA, [4]University of Michigan, USA

Nuclear receptor PPARγ represents a ligand-regulated transcription factor that translates metabolic, nutritional, and pathophysiological signals into adipocyte activities maintaining energy metabolism. PPARγ is also expressed in marrow mesenchymal stem cells (MSCs) and controls development of both osteoblasts (OB) and adipocytes (AD). PPARγ is subjected to posttranslational phosphorylation which determines its specific activities, including promotion of AD differentiation into white or beige phenotypes, and anti-OB activity. Upon PPARγ activation, Ser112 phosphorylation is decreased, promoting marrow MSCs commitment toward white-type AD and away from the OB lineage. The Runx2 transcription factor, a major regulator of MSC commitment to the OB lineage, is also controlled by phosphorylation. Increased phosphorylation at Ser319 is essential for its pro-OB effect. Because of their reciprocal effects on MSC differentiation toward OB and AD lineages, we hypothesized PPARγ and Runx2 activities are regulated by the same mechanism. PP5 phosphatase binds to both transcription factors and dephosphorylates Ser112 of PPARγ leading to increased pro-AD and anti-OB activity, and dephosphorylates Ser319 of Runx2 leading to decreased pro-OB activity. PP5 overexpression reduced Runx2 basal and MAPK-stimulated transcriptional activity, along with Ser319 phosphorylation. Interestingly, PP5 did not affect pERK levels, neither basal nor induced, indicating that Runx2 is a direct target for PP5. PP5-KO mice are characterized with reduced weight gain, reduced body fat, lower fasting glycaemia, improved glucose and insulin tolerance, augmented spontaneous locomotor activity and energy expenditure, and augmented bone mass with reduced marrow adiposity. Epidimal fat of PP5-KO mice is converted to beige fat characterized by increased expression of UCP1 and beige AD-specific markers. Marrow MSCs derived from PP5-KO mice have higher potential to develop colony forming units (CFU) of OB lineage, but lower potential to develop fat-laden CFUs of AD lineage. PP5 deficiency in marrow MSCs results in increased expression of pro-OB markers and markers of beige AD, including Wnt10b and IGFBP2. These results identify PP5 as a common regulator of PPARγ and Runx2 activities and implicate that improved energy metabolism synergizes with increased bone mass. Our observation may now form the basis for novel therapies that simultaneously target bone and fat metabolism.

Disclosures: Lance Stechschulte, None.

FR0104

Gsα-deficient osteoblasts and osteocytes induce beige adipogenesis and a lean phenotype via interactions with skeletal muscle. Keertik Fulzele*[1], Vaibhav Saini[2], Padrig Tuck[3], Xiaolong Liu[3], Christopher Dedic[3], Jenna Garr[3], Vladimir Zoubine[3], Pankaj Shah[3], Evan Rosen[4], Paola Divieti Pajevic[5]. [1]Massachusetts General Hospital; Harvard Medical School, USA, [2]MGH, Harvard Medical School, USA, [3]Endocrine Unit, Massachusetts General Hospital, Harvard Medical School, USA, [4]Division of Endocrinology, Diabetes, & Metabolism, Beth Israel Deaconess Medical Center, Harvard Medical School, USA, [5]Massachusetts General Hospital & Harvard Medical School, USA

Mice with induced osteocyte or osteoblast deficiency are significantly lean indicating a role of osteolineage cells in regulating body fat accumulation It has been reported that undercarboxylated osteocalcin (ucOC) secreted by mature osteoblasts, regulates glucose homeostasis; however, it could not rescue the lean phenotypes of osteoblast deficient mice suggesting other mechanism(s) for regulation of body adiposity. We found that mice lacking the stimulatory subunit of G-proteins, Gsα, in osteoblasts and/or osteocytes are lean similar to the osteoblast or osteocyte-deficient mice. DMP1-Cre or osteocalcin-Cre (OC-Cre) mice were mated with Gsα floxed mice to generate mice lacking Gsα only in osteocytes (DMP1-GsαKO) or both osteoblasts and osteocytes (OC-GsαKO). DMP1-GsαKO and OC-GsαKO mice had significantly decreased body weights by 9-weeks of age and continued to be leaner as compared to control littermates. DXA analysis revealed that the decreased body weight was due to significant decrease in body adiposity in DMP1-GsαKO (36%), and OC-GsαKO (10%) mice whereas the lean mass not changed. Gonadal and inguinal fat pads (GWAT and InWAT) were significantly decreased in DMP1-GsαKO (77%), and OC-GsαKO (35%) mice whereas brown adipose tissue (BAT), and pancreas were not changed. The lean phenotype of these mice was not dependent on ucOC, because serum insulin levels were not altered during fasting as well as in fed state and osteocalcin levels were reduced. Histological examination of GWAT and InWAT showed a significantly decreased adipocyte cell surface area and numerous multi-locular adipocytes suggesting brown-adipocyte-like adipogenesis in these WAT, called beige adipocytes. Immunostaining for uncoupling protein 1 (UCP1) revealed extensive beige adipogenesis in GWAT and InWAT of these mice along with increase in beige adipogenesis markers (PRDM16, Dio2, Cox5b, and Elvol3) as assessed by qPCR. Among the circulating factors that induce beige adipogenesis, we found that serum levels of irisin were significantly increased in DMP1-GsαKO, and OC-GsαKO mice. Moreover, we found that osteoblasts and osteocytes also expressed irisin and these levels were increased in Gsα-deficient osteoblasts and osteocytes as assessed by immunohistochemistry and qPCR. Taken together, our data show that Gsα-deficient osteoblasts and osteocytes leads to a lean phenotype primarily by increasing beige-adipogenesis, at least in part, via increased irisin from skeletal muscle.

Disclosures: Keertik Fulzele, None.

FR0107

Systematic integration of computational approaches and validation experiments reveals functionality beyond GWAS signals and identifies *ADCY5* as having genetic pleiotropy for Bone Mineral Density and Type 2 Diabetes. Melina Claussnitzer*[1], Luke D Ward[2], Xing Chen[3], David Karasik[4], Adrienne L Cupples[5], Hans Hauner[6], Douglas Kiel[7], Manolis Kellis[2], Yi-Hsiang Hsu[8]. [1]Hebrew SeniorLife, Institute for Aging Research & Harvard Medical School, USA, [2]Computer Science & Artificial Intelligence Laboratory, Massachusetts Institute of Technology (MIT), USA, [3]Harvard University, USA, [4]Hebrew SeniorLife; Bar Ilan University, USA, [5]Department of Biostatistics, Boston University School of Public Health, USA, [6]Else Kröner-Fresenius-Zentrum for Nutritional Medicine, Technical University Munich, Germany, [7]Hebrew SeniorLife, USA, [8]Hebrew SeniorLife Institute for Aging Research & Harvard Medical School, USA

Recent studies suggest genetic pleiotropy of bone mineral density (BMD) and metabolic syndrome risk factors, but the underlying genetic factors remain unknown. Genetic signals emerging from genome-wide association studies (GWAS) are frequently located in non-coding regions and have rarely been traced to the disease-causing variants. We recently developed Phylogenetic Module Complexity Analysis (PMCA), to infer regulatory variants in a region of disease association. PMCA tests variants by analyzing the flanking region for cross-species conserved motif modules, exploiting evolutionary information while allowing for transcription factor binding site turnover.

To systematically study pleiotropy, and to identify the underlying causal variants, we conducted the first multivariate GWAS of femoral neck BMD and metabolic risk factors in ~35,000 Caucasians, and identified 140 bivariate loci that achieved genome-wide significance or genome-wide suggestive significance. We then applied PMCA to the 140 bivariate signals and identified several potential pleiotropic causal variants. Among them, the intronic variant rs56371916 at the *ADCY5* locus (bivariate GWAS p-value = 1.9×10^{-9} for BMD with glucose levels). We report multiple lines of evidence supporting rs56371916 (C/T, MAF=0.14) to be causal for the genetic correlation: (1) it

harbors a functional regulatory SREBP motif based on conservation of a AP1-NKXH-SREBP-EVI motif cluster across species; (2) chromatin segmentations on the Roadmap reference epigenomes revealed rs56371916 to be located in an enhancer chromatin state; (3) using EMSA, we found allele-specific SREBP binding for adipocytes (2.3-fold, p<0.05) and osteoblasts (3.1-fold, p<0.05) nuclear extract; (4) luciferase assays show cell type-specific enhancer effects for osteoblasts (2.8-fold, p<0.05) and adipocytes (3.5-fold, p<0.05); (5) Lastly, we use SREBP-1 knockdown by siRNA to show that increase in *ADCY5* mRNA is dependent on rs56371916 (1.9-fold, p<0.05) and regulation by SREBP-1. We are currently undertaking CRISPR/Cas9 genome engineering in patient samples to assess osteoblast function and insulin sensitivity.

Our general approach for the computational discovery and experimental dissection of disease variants has important implications on the study of pleiotropy in particular, and complex traits more generally, which can help bridge the genotype-to-phenotype gap between genetic variants, molecular mechanisms, and cellular and organismal phenotypes.

Disclosures: Melina Claussnitzer, None.

FR0108

The Transient Receptor Potential Channel M8 (TRPM8) Regulates Mesenchymal Stromal Cell Lineage Allocation, Cortical Expansion and the Skeletal Response to Acute Cold Exposure in Mice. Katherine Motyl*[1], Phuong Le[1], Daniel Brooks[2], Casey Doucette[1], Mary Bouxsein[3], Clifford Rosen[4]. [1]Maine Medical Center Research Institute, USA, [2]Beth Israel Deaconess Medical Center, USA, [3]Beth Israel Deaconess Medical Center, Harvard Medical School, USA, [4]Maine Medical Center, USA

Recent data indicate a role for thermogenic brown adipose tissue (BAT) in regulating bone remodeling in humans and rodents. In particular, we have found that activation of BAT is associated with SNS-mediated trabecular bone loss. Deletion of TRPM8 causes reduced thermogenesis in response to the TRPM8 agonist icilin, which mimics cold-exposure. We sought to determine if TRPM8 plays a role in bone homeostasis and if *Trpm8-/-* mice would have altered thermogenesis and bone remodeling in response to cold. Utilizing mice with GFP-tagged TRPM8 expression, we found TRPM8 positive cells within bone marrow *in vivo* and *ex vivo*. BMSCs from -/- mice had reduced fibroblast colony forming units, alkaline phosphatase and Von Kossa staining during osteoblast differentiation compared to littermate controls. Interestingly, BMSCs from -/- mice also had reduced adipocyte differentiation (Oil Red O). This finding was further confirmed with ear mesenchymal stem cells (eMSCs) differentiated to adipocytes. Despite striking differences *in vitro*, -/- mice at 22°C have only subtle differences in trabecular micro-architecture of the femur. However, -/- mice have significantly lower total area and medullary area of the femur diaphysis (at 52 wks of age), suggesting impaired periosteal expansion and endosteal resorption. We next used cold-exposure to examine the effect of thermogenesis on bone. After 6 hr at 4°C, +/+ tibiae (including marrow) had reduced *Runx2*, increased *Rankl*, and increased *Ucp1* (thermogenic marker) expression compared to room temperature (RT) controls, a change which was prevented in -/- tibiae. When exposed to 4°C for 3 weeks (after 1 week acclimatization at 18°C), both +/+ and -/- mice lost trabecular bone compared to RT similarly, despite lower core temperature (T) of the -/- mice during the first 2 weeks. Core T then normalized in -/- mice, suggesting novel, undefined mechanisms are present to sense cold and activate thermogenesis. In summary, TRPM8 may be important for BMSC lineage allocation, which could explain why cooler extremities (i.e. long bones) have more marrow adiposity relative to axial bones. Further quantitation of marrow adiposity in the -/- mice by osmium μCT, and experiments examining the differential role of TRPM8 in acute vs. long-term cold exposure are underway. These studies will enhance our understanding of thermogenesis and the communication between adipose tissue and bone, and have implications for osteoporosis and obesity therapeutics.

Disclosures: Katherine Motyl, None.

FR0109

Effect of Prolonged Caloric Restriction on Bone Metabolism and Bone Mineral Density in Non-obese Younger Adults. Dennis Villareal*[1], Lugi Fontana[2], Sai Krupa Das[3], Leanne Redman[4], Steven Smith[5], Edward Saltzman[3], Connie Bales[6], James Rochon[7], Carl Pieper[6], Megan Huang[8], Michael Lewis[9], Ann V Schwartz[10]. [1]University of New Mexico School of Medicine, USA, [2]Washington University School of Medicine, USA, [3]5Jean Mayer USDA Human Nutrition Research Center on Aging at Tufts University, USA, [4]Pennington Biomedical Research Center, USA, [5]Florida Hospital & Sanford Burnham Medical Research Institute, USA, [6]Duke Universtiy School of Medicine, USA, [7]Rho Federal Systems, USA, [8]Duke Clinical Research Institute, USA, [9]University of Vermont College of Medicine, USA, [10]University of California San Francisco, USA

Importance: Although caloric restriction (CR) could delay biological aging in humans, it is unclear if this would occur at the cost of significant bone loss.
Objective: To evaluate the effect of prolonged CR on bone metabolism and bone mineral density (BMD) in young healthy adults.

Design: We conducted a two-year multicenter randomized, controlled trial.

Participants: Two-hundred eighteen normal weight or slightly overweight (body mass index: 25.1 ± 1.7 kg/m^2), young (age: 37.9 ± 7.2 yr) adults participated in the study.

Interventions: Participants were randomly assigned to 25% CR (CR group; n=143) or ad libitum (AL group; n=75).

Main outcomes and measures: Main outcomes for this study were BMD and markers of bone turnover. Other outcomes included body weight and composition, bone-active hormones, nutrient intake, physical activity (PA), and strength.

Results: Body weight (-7.5 $\pm$ 0.4 vs. 0.1 $\pm$ 0.5 kg), fat mass (-5.3 $\pm$ 0.3 vs. 0.4 $\pm$ 0.4 kg), and fat-free mass (-2.2 $\pm$ 0.2 vs. -0.2 $\pm$ 0.2 kg) decreased in the CR group, not in the AL group (all $p<0.001$). Compared with AL, the CR group had greater losses in BMD at 24 months: at the lumbar spine (-0.013 $\pm$ 0.003 vs. 0.007 $\pm$ 0.004 g/cm^2), total hip (-0.017 $\pm$ 0.002 vs. 0.001 $\pm$ 0.003 vs g/cm^2), and femoral neck vs. (-0.015 $\pm$ 0.003 vs. -0.005 $\pm$ 0.004 g/cm^2). Changes in bone turnover markers were greater at 12 months for C-telopeptide (0.098 $\pm$ 0.012 vs. 0.025 $\pm$ 0.015 µg/L), tartrate-resistant acid phosphatase (0.4 $\pm$ 0.1 vs. 0.2 $\pm$ 0.1 U/L), and bone-specific alkaline phosphatase (BSAP) (-1.4 $\pm$ 0.4 vs. -0.3 $\pm$ 0.1 vs. U/L) but not P1NP; at 24 months only BSAP differed between groups (-1.5 $\pm$ 0.4 vs. 0.9 $\pm$ 0.6). In addition to lower weight, the CR group had larger increases in cortisol and adiponectin and decreases in leptin and insulin, hormones associated with bone loss, compared with AL. However, 25-hydroxyvitamin D and IGF-1 changes did not differ between CR and AL groups. The CR group also had a larger reduction in PA. Multiple regression analyses revealed that the combination of changes in body composition, hormones, nutrient intake, and PA explained 10-31% of the variance in changes in BMD and bone markers in the CR group.

Conclusions and relevance: Bone loss at clinically important sites of osteoporotic fractures represents a potential limitation of prolonged CR. Further long-term studies are needed to determine the clinical significance of bone loss in healthy young adults with CR-induced weight loss.

Disclosures: Dennis Villareal, None.

FR0113

Sclerostin is associated with metabolic syndrome in older men from the MINOS cohort. Cyrille Confavreux*[1], Pawel Szulc[2], Olivier Borel[3], Annie Varennes[4], Joelle Goudable[5], Roland Chapurlat[6]. [1]INSERM UMR1033 - Universite de Lyon, France, [2]INSERM UMR 1033, University of Lyon, Hopital E. Herriot, Pavillon F, France, [3]INSERM U1033 - Université de Lyon, France, [4]Laboratoire Central de Biochimie, Hospices Civils de Lyon, France, [5]INSERM UMR1060 - Université de Lyon, Hospices Civils de Lyon, France, [6]E. Herriot Hospital, France

Rationale. Bone is an endocrine organ regulating energy metabolism. In mice, the metabolic syndrome (MetS) phenotype induced by the destruction of half osteoblasts was partially rescued by osteocalcin (OC) treatment suggesting that bone may secrete other metabolically active factors. Preliminary data show that serum sclerostin is increased in type 2 diabetic patients and is correlated positively with abdominal fat and weakly negatively with HDL-cholesterol level. Therefore, our aim was to study the association between serum sclerostin level and MetS in older men.

Materials and methods. Serum levels of sclerostin and OC were measured in 694 men aged 50 to 85 years. MetS was diagnosed according to the harmonized definition (Alberti. Circulation 2009). Serum sclerostin was measured using Teco® ELISA kit. We assessed the association between sclerostin level and MetS using logistic regression.

Results. Serum sclerostin was higher in 216 men with MetS than in the 478 without MetS (0.66 $\pm$ 0.21 vs 0.61 $\pm$ 0.19 ng/ml; p<0.005). In a logistic regression model adjusted for age, smoking, alcohol intake, physical activity and serum levels of 25OHD, OC and apparent free testosterone, higher sclerostin serum level was associated with higher prevalence of MetS (OR [95%CI]=1.28 per 1 SD increase [1.05-1.57]; p<0.05). Average serum sclerostin level increased across the increasing number of MetS components (p for trend <0.001) and was 15% (0.5 SD) higher in men with 4-5 MetS components compared with men without any MetS component. In contrast to OC, the strength of the relationship of sclerostin with mild (3 components) and moderate/severe (4/5 components) MetS was similar (OR=1.25 [1.01-1.55] and 1.33 [1.001-1.76] per 1 SD increase, respectively). After adjustment for confounders, MetS prevalence was two-fold higher in the highest sclerostin quartile (vs the lowest) and in the lowest OC quartile (vs the highest), respectively. After further adjustment for urinary total deoxypyridinoline, men who were simultaneously in the highest sclerostin quartile and the lowest OC quartile had higher MetS prevalence (OR=2.90 [1.51-5.55]; p<0.001) compared with men who were simultaneously in the three lower sclerostin quartiles and three upper OC quartiles.

Conclusion. In older Caucasian men, higher serum sclerostin was associated with MetS independently of OC, bone resorption rate and other confounders. Men with the "high sclerostin-low osteocalcin" profile had the highest MetS prevalence.

Disclosures: Cyrille Confavreux, None.

FR0114

The relationships between bone-derived proteins, osteocalcin and sclerostin, and atherosclerosis in subjects with coronary artery bypass grafting. Kyoung Min Kim*, Soo Lim, Jae Hoon Moon, A Ram Hong, Hak Chul Jang, Sung Hee Choi. Seoul National University Bundang Hospital, South Korea

Accumulating evidence recently suggests the systemic roles of bone-derived proteins, and severe human studies reported the relationships between osteocalcin (OCN) or sclerostin, and the atherosclerotic parameters. The aims of this study were to evaluate sclerostin and osteocalcin levels in subjects who underwent coronary artery bypass graft (CABG) surgery and to analyze its relationships with atherosclerosis.

This was an age- and sex- matched case-control study that included 61 male subjects who underwent CABG and identical number of controls. Forty-six subjects (37.7%) were diabetes and 62 hypertensive subjects (50.8%) were included. Serum sclerostin, uncarboxylated-osteocalcin (ucOCN) and carboxylated-osteocalcin (cOCN) were measured using a commercially available ELISA and were transformed logmatically for statistical analysis.

Serum sclerostin concentrations in CABG group were significantly higher than in the controls, whereas the levels of serum ucOCN in CABG group were significantly lower than in the controls (p<0.05, respectively). These statistical significances were maintained even after adjusting for confounding atherosclerotic risk factors. However, there was no difference in cOCN levels between CABG group and controls. When subjects were further divided according to the presence of diabetes, serum ucOCN concentrations in CABG group were significantly lower regardless of diabetic status (p<0.05 in both groups). In multiple logistic regression analysis, both higher sclerostin and lower ucOCN levels were independent predictors for atherosclerosis (OR 2.46, 95% CI 1.02-7.51, p<0.05 for sclerostin, OR 0.34, 95% CI 0.15-0.75, p<0.05 for ucOCN). In subjects who underwent CABG, serum sclerostin level was increased and ucOCN level was decreased compared to controls. Further studies are warranted to establish the precise roles of sclerostin or ucOCN in the pathogenesis of atherosclerosis.

Disclosures: Kyoung Min Kim, None.

FR0116

Phosphate Set Point Defect in *Dmp1* Knockout Mice. Shoji Ichikawa*[1], Rita Gerard-O'Riley[1], Amie Gray[1], Dena Acton[1], Jian Feng[2], Michael Econs[1]. [1]Indiana University School of Medicine, USA, [2]Texas A&M Health Science Center, USA

Inactivating mutations in the dentix matrix protein 1 (*DMP1*) gene cause an autosomal recessive form of hypophosphatemic rickets (ARHR). Hypophosphatemia in ARHR results from increased circulating levels of a phosphaturic hormone, fibroblast growth factor 23 (FGF23), which inhibits renal phosphate reabsorption and 1,25-dihydroxyvitamin D synthesis. Similarly, elevated FGF23 is responsible for X-linked hypophosphatemic rickets (XLH). Recently, we demonstrated that *Phex* mutations in a murine model of XLH create a lower set point for extracellular phosphate, where increased phosphorus further stimulates Fgf23 production to maintain low serum phosphorus levels. In this study, we tested the presence of the altered response to extracellular phosphate in a murine model of ARHR, *Dmp1* knockout mice. *Dmp1* knockout mice were crossed to *Galnt3* knockout mice, a murine model of familial tumoral calcinosis, to generate *Dmp1/Galnt3* double knockout mice. We then compared serum biochemistries of 12-week-old double knockout mice to those of controls, including *Dmp1* knockout mice, *Galnt3* knockout mice, and phenotypically normal double heterozygous mice. *Dmp1* knockout mice had 19 fold increase in intact Fgf23 levels, resulting in hypophosphatemia. In contrast, *Galnt3* knockout mice had 33% reduction in intact Fgf23 with consequent hyperphosphatemia. *Dmp1* knockout mice in the *Galnt3*-null background had almost complete correction of serum phosphorus with normal intact Fgf23 levels, but a 57 fold elevation in total Fgf23 concentrations. We also determined how loss of the Dmp1 function affects processing of Fgf23 protein. In normal mice, approximately 55% of Fgf23 existed as intact protein. Due to the lack of *O*-glycosylation to protect from proteolytic cleavage, only 1.5% of intact Fgf23 was secreted in *Galnt3* knockout mice. Interestingly, there was little proteolytic cleavage of Fgf23 in *Dmp1* knockout mice, while *Dmp1* knockout mice lacking normal *Galnt3* alleles had the same level of cleavage as in *Galnt3* knockout mice. In summary, *Dmp1* knockout mice had markedly elevated Fgf23 levels in part due to decreased proteolytic processing of Fgf23. Lack of *O*-glycosylation by *Galnt3* was able to normalize intact Fgf23, and thus, serum phosphorus, in *Dmp1* knockout mice. However, the increased Fgf23 production in the double knockouts suggests that similar to *Phex* mutant mice, *Dmp1* knockout mice may have a lower set point for extracellular phosphate.

Phosphorous (mg/dL)

Intact Fgf23 (pg/mL)

Total Fgf23 (pg/mL)

Intact/Total Fgf23
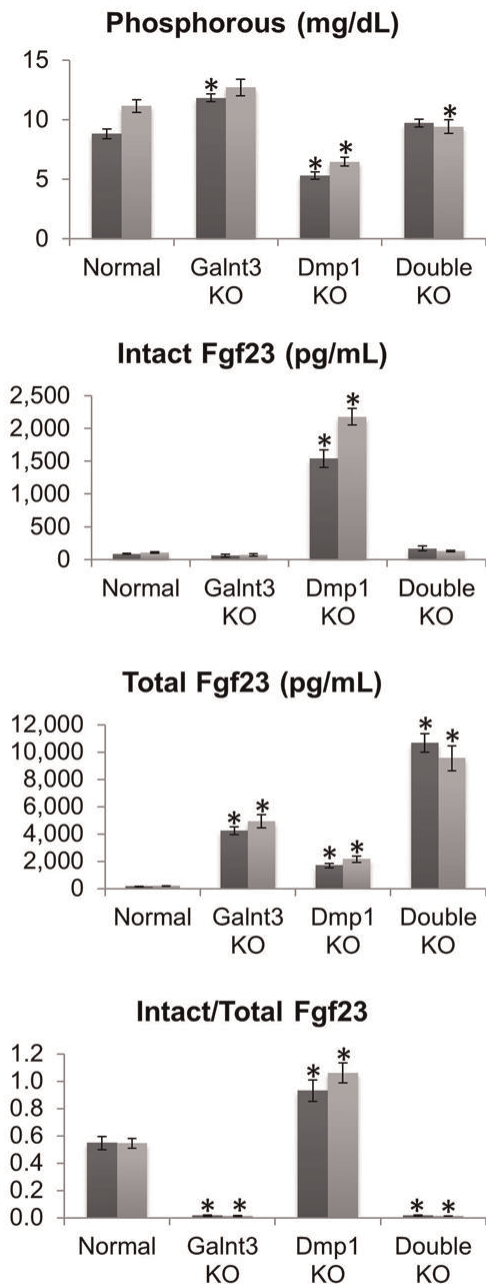
Dark gray, males; light gray, females.
Number of animals = 9-10 per group.
*Significant difference to same-sex normal littermates (unpaired t-test p-value < 0.05).

Serum biochemistries of Dmp1/Galnt3 double knockout mice and controls.

Disclosures: Shoji Ichikawa, None.

FR0118

SNORD116, a Non-translated, Imprinted Central Regulator of Bone Mass: Possible Role in Skeletal Abnormalities in Prader-Willi Syndrome. Ee-Cheng Khor[1], Bruce Fanashawe[1], Yue Qi[2], Peter Croucher[1], Herbert Herzog[2], Paul Baldock*[3]. [1]Osteoporosis & Bone Biology Division, Garvan Institute of Medical Research, Australia, [2]Neuroscience Division, Garvan Institute of Medical Research, Australia, [3]Garvan Institute of Medical Research, Australia

Our understanding of the central control of bone mass has increased markedly; however, much remains to be determined. Here we describe the first non-translated, imprinted pathway from the brain to bone, and its potential role in disease.S-NORD116 exists as a 29 copy cluster of unknown function; it is not translated but produces small non-translated nucleolar RNA's (snoRNA). SNORD116 is widely expressed in the brain in humans and is exclusively expressed in the brain of mice.SNORD116 resides within the Prader-Willi Critical Region, and is therefore imprinted, with the maternal copy silenced. Prader-Willi Syndrome (PWS) individuals display additional dysfunction and/or deletion of the non-silenced paternal allele. Loss of SNORD116 has recently been associated with PWS, which involves obesity, insatiable appetite, cognitive impairment, hormonal imbalance, short stature and osteoporosis.Snord116 KO mice were studied to determine whether SNORD116 may regulate bone mass and potentially the skeletal changes in PWS. Consistent with reduced stature in PWS, Snord116 KO mice showed delayed skeletal development, with reduced bone size and mass in femurs and vertebrae of both sexes. The osteopenia in Snord116 KO was due to reduced cortical bone volume and cortical mineral apposition rate, with no change in cancellous bone. Importantly, the reduced cortical bone formation was evident in skeletally mature mice, indicating ongoing suppression of osteoblast activity by loss of Snord116 expression in the brain, beyond developmental processes.These skeletal changes were consistent with diminished somato-tropic axis activity; with reduced serum IGF-1 levels in Snord116 KO mice.The site of Snord116 activity in bone was isolated to the hypothalamus, with viral-mediated over-supply of Snord116 in this region further reducing bone mass in Snord116 KO mice. Moreover, this response indicates that normal skeletal homeostasis requires a physiological range of Snord116 expression.In conclusion, SNORD116 deletion in mice recapitulates the short stature and low BMD and aspects of the hormonal imbalance of PWS individuals. Moreover, it demonstrates for the first time, that non-translated RNA, expressed solely within the brain can regulate bone mass in health and disease. Moreover, it illustrates the potential complexity of central regulation of bone mass.

Disclosures: Paul Baldock, None.

FR0119

The anti-osteoanabolic function of Sost is blunted in mice carrying the high bone mass mutation of Lrp5. Timur Yorgan*[1], Stephanie Boerms[2], Peggy Benisch[3], Franz Jakob[4], Michael Amling[5], Thorsten Schinke[6]. [1]University of Hamburg, University Medical Center Hamburg-Eppendorf, Germany, [2]Department of Osteology & Biomechanics, University Medical Center Hamburg-Eppendorf, Germany, [3]University of Wuerzburg, Germany, [4]Orthopedic Center for Musculoskeletal Research, University of Wuerzburg, Germany, [5]University Medical Center Hamburg-Eppendorf, Germany, [6]Department of Osteology & Biomechanics, University Medical Center Hamburg Eppe, Germany

Activating mutations of the putative Wnt co-receptor Lrp5 or inactivating mutations of the secreted molecule Sclerostin cause excessive bone formation in mice and humans. Previous studies have suggested that Sclerostin functions as an Lrp5 antagonist, yet clear *in vivo* evidence was still missing, and alternative mechanisms have been discussed. To address the question, if the anti-osteoanabolic function of Sclerostin, at least in mice, depends on Lrp5 interaction, we took advantage of two previously established mouse lines carrying different high bone mass alleles of Lrp5 (Lrp^{A123V} and Lrp^{G170V}). We additionally generated transgenic mice over-expressing *Sost* specifically in osteoblasts and crossed them into the Lrp^{A123V} and Lrp^{G170V} background. Using μCT-scanning and histomorphometry we found that transgenic over-expression of *Sost* under the control of a 2.3 kb *Col1a1* promoter fragment causes reduced bone formation and osteoporosis in the presence of intact Lrp5. Importantly however, this anti-osteoanabolic influence of *Sost* over-expression was fully abolished in mice homozygous for the Lrp^{A123V} or the Lrp^{G170V} allele, respectively. In contrast, osteoblast-specific over-expression of *Krm2*, encoding a transmembrane Wnt signaling antagonist, dramatically reduced bone mass on both, the wildtype and the mutant Lrp5 background. These data show that Krm2, a putative receptor for Dkk proteins, influences bone remodeling in an Lrp5-independent manner. Most importantly however, we were able to provide *in vivo* evidence showing that Sclerostin controls bone formation through interacting with the extracellular region of Lrp5.

Disclosures: Timur Yorgan, None.

FR0120

The Effects of Activin Receptor Type IIB Fusion Protein (ActRIIB-Fc) on Hindlimb Skeletal Muscles and Femoral Properties of Osteogenesis Imperfecta Model (*oim*) Mouse. Young Jeong*[1], Marybeth Brown[2], R. Scott Pearsall[3], Charlotte Phillips[4]. [1]University of Missouri, USA, [2]University of Missouri, USA, [3]Acceleron Pharma, USA, [4]University of Missouri-Columbia, USA

Osteogenesis imperfecta (OI) is a heritable connective tissue disorder primarily due to defects in the type I collagen genes. The clinical features of OI include low bone mass with reduced biomechanical strength, and frequent fractures in patients. Myostatin, a member of transforming growth factor- β (TGF-β) superfamily, is known to regulate muscle differentiation and growth by signaling through activin receptor type IIB (ActRIIB). Myostatin deficiency can lead to increased muscle mass,

which has been associated with increased bone mass and strength. In addition, Activin A, another member of TGF-β superfamily, is highly expressed in bone cells and known to promote osteoclastogenesis by signaling through the activin receptors. Recent studies using soluble activin receptor type IIB fusion protein [ActRIIB-Fc (RAP-031), Acceleron Pharma] were shown to prevent the effects of androgen deprivation and aging on bone quality; increasing muscle force production and bone mineral density. The ActRIIB-Fc functions as a molecular decoy receptor and binds to myostatin and activin A, preventing endogenous ActRIIB activation, leading to increased muscle and bone mass, respectively. In the following study, we investigated whether the use of ActRIIB-Fc would increase bone and muscle mass in the osteogenesis imperfecta mouse (*oim*) model. Bi-weekly injections (10mg/kg) of ActRIIB-Fc were given to Wt and *oim/oim* mice, beginning at 2 months of age. At 4 months, the mice were weighed, and the hindlimb skeletal muscles and bones were harvested. In treated mice, the overall body weights and the soleus, plantaris, tibialis anterior, and quadriceps muscle weights were increased compared to vehicle treated control mice regardless of gender and genotype. By µCT analysis, female Wt and *oim/oim* mice femora exhibited increased cortical bone width with ActRIIB-Fc treatment, as well as Wt female femora exhibited gains in polar moment of area with ActRIIB-Fc treatment. Our findings suggest that systemic administration of ActRIIB-Fc induced gains in hindlimb skeletal muscle weights in both genders of Wt and *oim/oim* mice, with improved femoral bone geometry in female Wt and *oim/oim* mice.

Disclosures: Young Jeong, None.
This study received funding from: Acceleron Pharma

FR0121

The F508DEL-CFTR Mutation Inhibits Osteoblast Differentiation and Function Through Constitutive Activation of Nf-Kb Signaling. Carole Le Henaff*, Rafik Mansouri, Dominique Modrowski, Pierre J. Marie. UMR-1132 Inserm, Paris, France & b Université Paris Diderot, Sorbonne Paris Cité, France

Cystic fibrosis (CF) is often associated with bone loss with significant clinical implications. The mechanisms underlying bone pathology in CF are poorly known. We recently showed that mice with the prevalent human F508del mutation in the CF transmembrane conductance regulator (CFTR) display vertebral osteopenia resulting from decreased bone formation and altered osteoblast activity in vivo. To identify the molecular mechanisms underlying the altered bone formation in CF, we characterized the osteoblast phenotype in F508del-CFTR mice and we determined the mechanisms involved in this phenotype. The analysis of bone marrow stromal cells (BMSCs) isolated from long bones in F508del-CFTR mice revealed a marked decrease in the expression of osteoblast genes (RUNX2, ALP, COL1A1, OC) associated with decreased in vitro matrix mineralization compared to WT mice. Mutant trabecular osteoblasts also displayed decreased ALP and COL1A1 mRNA levels compared to WT mice, indicating that the F508del-CFTR mutation mostly impacts osteoblast differentiation and function. In contrast, cell proliferation was not affected in BMSCs or in trabecular osteoblasts. The alteration in osteoblast function was related to the F508del-CFTR mutation since a CFTR corrector (miglustat) improved osteoblast gene expression in mutant osteoblasts. Mechanistically, we found that trabecular osteoblasts from F508del-CFTR mice had constitutively active NF-kB transcriptional activity compared to WT osteoblasts, as shown in a NF-kB reporter assay. Consistent with the increased NF-kB signaling, we found that both BMSCs and trabecular osteoblasts isolated from F508del-CFTR mice showed increased RANKL/OPG ratio compared to WT mice. Importantly, inhibition of NF-kB signalling by a specific pharmacological inhibitor improved osteoblast gene expression and reduced the RANKL/OPG ratio in F508del-CFTR osteoblasts. The data indicate that NF-kB signaling is exacerbated in F508del osteoblasts, which results in a marked alteration of osteoblast differentiation and function and increased expression of key modulators of osteoclastogenesis. This reveals a novel molecular mechanism underlying the osteoblast dysfunction induced by the F508del-CFTR mutation in mice, and suggests a molecular target to attenuate the abnormal osteoblast activity and decreased bone formation in this genetic disorder.

Disclosures: Carole Le Henaff, None.

FR0122

WNT1 is one of the major WNT ligands regulating bone homeostasis. Kyu Sang Joeng*[1], Yi-Chien Lee[2], Ming-Ming Jiang[2], Terry Bertin[2], Yuqing Chen[2], Annie Mary Abraham[3], Hao Ding[3], Xiaohong Bi[4], Catherine Ambrose[5], Brendan Lee[1]. [1]Baylor College of Medicine, USA, [2]Baylor College of Medicine, USA, [3]University of Texas Health Science Center at Houston, USA, [4]University of Texas Health Science Center at Houst, USA, [5]University of Texas Health Science Center at Houston, USA

We and other groups recently identified that various mutations in *WNT1* cause a recessive form of Osteogenesis Imperfecta (OI), characterized by brittle bones. To understand the function of WNT1 in bone homeostasis as well as the pathogenic mechanism of OI caused by *WNT1* mutations, we studied two mouse models; *swaying* mice carrying a spontaneous mutation in *Wnt1* (as a loss of function study) and *DMP1-Cre; Rosa26-Wnt1* mice (as a gain of function study). Interestingly, the swaying mice recapitulate the major features of OI patients, exhibiting spontaneous fractures (65% fracture rate) with severe osteopenia. Subsequent histomorphometric analyses showed that osteoblast activity

was significantly decreased in *swaying* mice without any changes in osteoclasts. The specific defects in osteoblasts prompted us to test the osteogenic potential of WNT1 using the gain of function mouse model. We overexpressed WNT1 in late osteoblasts/osteocytes by crossing *DMP1-Cre* transgenic mice with *Rosa26-Wnt1* knock-in mice. As we expected, the *DMP1-Cre; Rosa26-Wnt1* mice showed a dramatic increase in bone mass. Our *in vitro* study confirmed that WNT1 enhances osteoblast differentiation and mineralization. To understand the biomechanical and biochemical mechanism of the fracture incidence in *swaying* mice, we performed 3-point bending and Raman spectroscopy. *Swaying* mice exhibited reduced bone strength with decreased mineral composition in the bone matrix, which is different from other OI models that exhibit increased mineral composition in the bone matrix. Finally, we tested the therapeutic potential of sclerostin antibody (Scl-Ab) in OI caused by *WNT1* mutations by using swaying mouse. Interestingly, *swaying* mice treated with Scl-Ab from 2 to 8 weeks of age showed improved fracture incidence (10% fracture rate when compared to vehicle treated *swaying* mice (80% fracture rate). Subsequent analyses showed significantly increased bone mass in the Scl-Ab treated *swaying* mice. Based on these data, we conclude that 1) WNT1 is a major WNT ligand regulating bone homeostasis in both mice and humans, 2) the *swaying* mouse is a model of OI caused by WNT1 mutations, 3) the low bone mass phenotype in *swaying* mice is due to decreased osteoblast activity, 4) the biomechanical and Raman spectroscopic analyses suggest that the mechanism of bone fragility in OI due to *WNT1* mutations is distinct from other types of OI, and 5) Acl-Ab may be an effective treatment for OI patients with *WNT1* mutations.

Disclosures: Kyu Sang Joeng, Amgen provided Scl-Ab for this study, 10

FR0124

Discovery of Novel Models of Bone Disease using an Unbiased High-Throughput Phenotyping Screen of Transgenic Mice. Douglas Adams[1], Renata Rydzik[1], Li Chen[1], Seung-Hyun Hong[2], Dana Godfrey[3], Xi Jiang[1], Zhihua Wu[1], Vilmaris Diaz-Doran[1], Caibin Zhang[1], Dong-Guk Shin[4], David Rowe[1], Cheryl Ackert-Bicknell*[5]. [1]University of Connecticut Health Center, USA, [2]University of Connecticut, USA, [3]The Jackson Laboratory, USA, [4]University of Connecticut, USA, [5]University of Rochester, USA

Work is underway via the Knockout Mouse Program (KOMP) to generate knockout mice for all known genes and to conduct cursory phenotyping to identify the physiologic role(s) of these genes. However, for bone, this phenotyping includes only whole body areal bone mineral density (aBMD), a low-resolution measure lacking mechanistic dimension. A more comprehensive examination of bone is needed to capture the bone physiologic role of any gene; thus, we have developed a high-throughput pipeline to conduct such phenotyping. We will phenotype males and females of 80 KOMP lines per year over 4 years, plus controls. Our high-resolution µCT analysis is automated to provide rapid morphometric measurements of femora and vertebrae, and when this analysis identifies a bone phenotype, we conduct additional dynamic bone histomorphometry. We are using an automated cryo-sectioning method and a uniquely objective computational image analysis protocol to achieve precise, high-throughput measures indicative of bone formation and resorption. All skeletal phenotype data generated will be publically available via a devoted website. Our goal is to identify new genes with key roles in regulating bone physiology. One such example is cerebellin 3 precursor protein (*Cbln3*), a gene primarily studied for its role in neuronal synapses. By µCT we determined that female *Cbln3*^{-/-} mice present with no phenotype in femoral bone mass or geometry, whereas male mice exhibited 33% higher femoral trabecular bone mass (p=0.007) and 6% higher cortical mass (p=0.03), with no difference in femur length. Histomorphometry confirmed this sexual dimorphism in trabecular mass, as well as a characteristically higher BFR in females. Measurement of femoral aBMD confirmed a 7% increase in male *Cbln3*^{-/-} mice, whereas in females both BMC and bone area increased, resulting in a trend towards a net decrease in aBMD which complicates interpretation of bone phenotype if screened by aBMD alone. From these data, we conclude that *Cbln3* is a novel regulator of bone physiology. Our pipeline is poised to identify a number of such novel models as we are purposely choosing genes that are understudied in the context of bone biology. As we move towards personalized medicine, there is genuine need to define the genetic landscape of disease. This requires understanding the number of genes that impact skeletal disease and the degree and manner in which they do so, current gaps in knowledge that our study seeks to fill.

Disclosures: Cheryl Ackert-Bicknell, None.

FR0128

Novel Causes of Bone Dysplasias Identified through Whole Exome Sequencing. Emily Farrow*[1], Serdar Ceylaner[2], Zafer Bicakci[3], Ergun Cetinkaya[4], Melanie Patterson[5], Lisa Krivohlavek[5], Margaret Gibson[5], Katie Barger[5], Carol Saunders[5], Neil Miller[5], Neil Mardis[5], Stephen Kingsmore[5]. [1]Children's Mercy Hospital, USA, [2]Intergen Genetics Diagnosis & Research Centre, Turkey, [3]Pediatrics, Kafkas University, Turkey, [4]Pediatrics of Endomer, Turkey, [5]Children's Mercy Hospital, USA

Inherited bone dysplasias occur in approximately 1/5000 births. Often a molecular diagnosis, important not only for establishing recurrent risks but also for clinical treatment, is not made due to genetic heterogeneity. While individual inherited bone dysplasias are rare, their collective study has been important in identifying novel therapeutic targets for common multifactorial bone disorders, such as osteoporosis, which affects 30% of postmenopausal women.

Whole exome sequencing was performed on two patients with undiagnosed bone dysplasias. Previously, both patients had undergone extensive clinical testing that was negative. Exome sequencing of the probands identified likely causative mutations in two biologically plausible, novel candidate genes. The first patient, who died of osteopetrosis at 5 months of age, had a homozygous, premature stop variant in the gene encoding TNF receptor-associated factor 6 (TRAF6). The second patient had cleft palate, severe pectus excavatum, and mesomelic dysplasia and was found to have a homozygous frameshift variant in hyaluronan and proteoglycan link protein 1 (HAPLN1). Each variant is unique in the Center for Pediatric Genomic Medicine's warehouse of 1400 individuals tested, 1000 Genomes, and the Exome Variant Server. Clinical sequencing confirmed disease segregation with variant homozygosity in the two consanguineous families. In both patients, the bone dysplasia recapitulated the features of mice with null mutations of these loci. Taken together, these results demonstrate that next generation sequencing of probands is an effective diagnostic tool for the identification of novel genes for mendelian causes of bone dysplasia.

FR0132

Tissue Non-specific Alkaline Phosphatase Enzyme Therapy Prevents Abnormal Craniofacial Endochondral and Intramembraneous Bone Development in the $Alpl^{-/-}$ Mouse Model of Infantile Hypophosphatasia. Jin Liu[1], Hwa Kyung Nam[1], Cassandra Campbell[1], Kellen Da Silva Gasque[2], Jose Luis Millan[2], Nan Hatch*[1]. [1]University of Michigan, USA, [2]Sanford-Burnham Medical Research Institute, USA

Hypophosphatasia (HPP) is a rare metabolic disorder that features osteomalacia due to loss-of function mutations in the gene (Alpl) encoding tissue-nonspecific alkaline phosphatase (TNAP). Recent reports demonstrated that injection of a mineral-targeted form of TNAP in infants and children with debilitating HPP dramatically improves skeletal mineralization, yet a high incidence of craniosynostosis (the premature fusion of cranial bones) remains in these patients. Significantly, as more children with HPP survive due to enzyme replacement therapy, craniosynostosis has become a more pressing medical concern in this patient population. TNAP enzyme replacement has thus far been initiated weeks to years after birth in HPP patients. We hypothesize that the therapy must be initiated at an earlier developmental time point to prevent craniosynostosis and craniofacial skeletal abnormalities in HPP patients. We are utilizing the Alpl-/- mouse model of infantile HPP to establish mechanisms by which TNAP regulates craniofacial skeletal development and determine if earlier TNAP enzyme replacement can prevent craniofacial skeletal abnormalities. Results show that juvenile Alpl-/- mice exhibit histologic abnormalities of calvarial bones and the cranial base involving growth plates, cortical and trabecular bone that include poorly demarcated cortices, diminished marrow space and hypertrophic chondrocyte zone expansion. Craniosynostosis in the form of coronal suture fusion is present by three weeks after birth. Alpl-/- mice also feature significantly diminished cranial and cranial base bone mineralization, and an abnormal craniofacial shape. Here we also report for the first time that TNAP enzyme replacement starting in neonates rescues all craniofacial skeletal abnormalities seen in Alpl-/- mice. Micro-CT, histologic and digital caliper based analyses show that the skulls of treated P15 Alpl-/- mice (n=44) are significantly different than those of untreated Alpl-/- mice (n=44), but not significantly different than those of wild type mice (n=45). These findings demonstrate that post-natal TNAP enzyme replacement therapy is efficacious for preventing HPP-associated craniofacial skeletal abnormalities when initiated shortly after birth. Results presented here also indicate that the influence of TNAP on craniofacial skeletal development extends beyond that of promoting hydroxyapatite crystal growth, and includes both osteoblastic and chondrocytic differentiation mechanisms.

FR0133

A number of novel loci are implicated for height and bone density determination through integration of ESR1 DNA occupancy and SNP association data. Matthew Johnson*[1], Perry Evans[2], Mahdi Sarmady[2], Kurt Hankenson[3], Andrew Wells[4], Struan Grant[5]. [1]Children's Hospital of Philadelphia, USA, [2]The Children's Hospital of Philadelphia, USA, [3]University of Pennsylvania, USA, [4]Children's Hospital of Philadelphia, USA, [5]Children's Hospital of Philadelphia / University of Pennsylvania, USA

Genome-wide association studies (GWAS) have demonstrated that genetic variation at the *ESR1* (Estrogen Nuclear Receptor Alpha) locus is associated with BMD. ESR1 is a transcription factor known to regulate osteoclastogenesis. Given these observations, we hypothesized that ESR1 regulates the expression of a set of molecular pathways critical to skeletal function. Drawing on our laboratory and bioinformatic experience, we analyzed ChIP-seq data for ESR1 available via the ENCODE project to determine its global genomic binding and pathway pattern in order to gain clearer understanding of its role in bone homeostasis.

We aligned the ChIP-seq data generated for two different cell lines i.e. T-47D (derived from mammary ductal carcinoma) and ECC-1 (derived from endometrium

adenocarcinoma). Using HOMER set at an FDR of 1%, a comparable total of 5,729 and 5,530 binding sites were observed for T-47D and ECC-1, respectively, corresponding to 3,726 and 4,194 known genes, respectively.We then performed pathway analyses using Ingenuity. The category entitled 'Connective Tissue Development and Function, Tissue Development, Cancer' and 'Cardiovascular System Development and Function, Organ Morphology, Skeletal and Muscular System Development and Function' were ranked among the most significantly enriched for 'Associated Network Functions'. Furthermore, when considering 'Canonical Pathways', "Wnt/β-catenin Signaling" ($P= 2.84$x10^{-4}; T-47D) and "ERK/MAPK Signaling" ($P= 2.09$x10^{-4}; ECC-1) were significantly enriched. We also observed that ESR1 binding sites in T-47D were significantly enriched for GWAS-implicated loci for both endocrine and cancer traits, whereas for ECC-1 this significant enrichment was limited to just endocrine. Given these observations, we investigated if we could reveal novel BMD and height loci through a meaningful reduction of constraints of multiple testing by restricting association analyses of available genome wide genotyping data to just the genes yielded from this approach. To that end, we observed significant association with a number of loci, including *ITCH* ($P=5.37$x10^{-6}) and *MAP1LC3A* ($P=7.24$x10^{-6}), which survived correction for the number of multiple tests applied.

In conclusion, ChIP-seq data generated leveraging this GWAS-implicated transcription factor provided a biologically plausible method in which to limit multiple testing in assessment of genome-wide genotyping data to implicate novel trait-associated loci.

FR0135

Strong Correlation Between BMD Associated Transcripts in Postmenopausal Iliac Bone Biopsies and DNA Methylation Levels at Specific CpGs. Sjur Reppe*[1], Runa M. Grimholt[2], Robert Lyle[2], Ole K. Olstad[2], Vigdis T. Gautvik[3], Kaare M. Gautvik[4]. [1]Oslo University Hospital, Ullevaal, Norway, [2]Oslo University Hospital, Ullevaal, Norway, [3]University of Oslo, IMB, Norway, [4]Oslo University Hospital, Oslo Deacon Hospital, University of Oslo, Norway

Background DNA methylation affects expression of associated genes and may explain part of the "missing heritability" from GWAS studies in post-menopausal osteoporosis which is a multigenetic disorder. In spite of large population studies, single nucleotide polymorphisms (SNPs) can only account for ~6 % of the BMD variation. In bone biopsies from a well described cohort of post-menopausal women (50-85 years) presenting with a marked variation in T-score, we analyzed global mRNA expression and CpG DNA methylation data aiming to identify methylation patterns affecting transcript levels and thereby bone metabolism.

Methods We obtained global mRNA expression data from postmenopausal iliac bone biopsies through analysis on Affymetrix microchips. DNA was isolated from the same 80 bone biopsies, and global DNA methylation data on ~450 000 CpGs were obtained using Illumina 450 k beads.   In this study we analyzed CpG methylation levels in the genes that represent the mRNAs most significantly correlated to BMD.

Results We initially looked for CpGs in the 10 genes whose mRNA levels showed the highest correlation to BMD and detected that   *SOST* and *MEPE* contained several CpGs correlating to their mRNA levels as well as to BMD and the osteoporotic phenotype. Next, we correlated transcript levels of the 100 genes most significantly associated with BMD with in all 2600 CpG methylation sites present in these genes. We found 4 transcripts (MEPE, SOST, WIF1 and DKK1) highly correlated (r > |0.4|, p<0.0002) to >100 CpG methylation levels, while on average each of the 100 transcripts correlated only to 15 CpGs. We also identified 10 CpGs in which the methylation level correlated strongly with the osteoporotic phenotype.

Conclusions Our results suggest that in bone a relationship exists between DNA methylation and level of transcription in genes highly associated with BMD. Wnt associated genes which are known to affect bone metabolism, appear to especially lend themselves to regulation by CpG methylatio

FR0137

FGF23 Neutralizing Antibody Improves Bone Phenotype of HMWFGF2 Isoforms Transgenic Mice. Liping Xiao*[1], Collin Homer-Bouthiette[1], Erxia Du[1], Marja Marie Hurley[2]. [1]University of Connecticut Health Center, USA, [2]University of Connecticut Health Center School of Medicine, USA

Overexpression of nuclear high molecular weight isoforms of FGF2 (HMWTg) in osteoblastic lineage cells induces dwarfism, hypophosphatemia and osteomalacia in HMWTg mice via modulation of FGF23, FGF receptors (FGFR) and Klotho (Xiao & Hurley, 2010). HMW also has phosphate independent effects on bone formation in vitro mediated in part via FGF23. HMW inhibits bone marrow stromal cell (BMSC) mineralization through FGF23/FGFR/MAPK in vitro (Xiao & Hurley, 2013).

To determine the impact of FGF23 neutralization on bone homeostasis in HMWTg mice, 2-month old HMWTg or Vector control male mice were intraperitoneally injected with 10mg/kg FGF23-Ab or an isotype control antibody (IgG), 2 days/week, for 6 weeks. Bone mineral density (BMD) and bone mineral content (BMC) were monitored at 0, 2, 4, and 6 weeks post injection using a Piximus Mouse 11 densitometer. At 4 and 6 weeks post injection, serum and 24 hour urine

were collected to measure calcium (Ca++) and phosphorous (Pi). Urine creatinine was measured for normalization of urine Pi excretion. To assess femur length, Digital x-rays of the isolated femurs were obtained post sacrifice..

As previously reported, HMW mice were smaller than Vector mice. This decreased body size was not rescued by FGF23AB injection (Table 1). Serum phosphate was significantly decreased in HMWTg-IgG mice compared with Vector-IgG mice (Table 1). Six-week injection of the FGF23 antibody corrected the hypophosphatemia in HMWTg mice, accompanied by reduced urine phosphate wasting (Table 1). Serum Ca++ level was similar among the three groups of mice. As shown in Table 1, six-weeks of injection of the FGF23-Ab rescued the decreased vertebral BMD and BMC observed in HMWTg mice. Similar rescue was observed on femoral BMD and BMC. FGF23-Ab injection also partially corrected the shortened femur length observed in HMWTg mice (Table 1 and Figure 1). Widened growth plate in HMWTg mice was also partially normalized by FGF23-Ab injection. However, the dwarf phenotype was not corrected.

We conclude that excess actions of FGF23 underlie some of the phenotypic abnormalities such as hypophosphatemic rickets in HMWTg mice.

Table 1	Vector IgG	HMW IgG	HMW FGF23AB
Body Weight 6w (g)	24.02±0.11	19.88±0.49	19.77±0.51#
Serum Pi 6w (mg/dL)	8.51±0.56	6.27±0.31*	7.94±0.64@
Urine Pi/Cr 4w (mol/g)	0.10±0.01	0.13±0.03	0.11±0.01
Serum Ca 6w (mg/dL)	9.00±0.53	8.95±0.46	8.23±0.39
Vertebrae BMD 6w (g/cm2)	0.054±0.001	0.046±0.001*	0.051±0.003
Vertebrae BMD 6w (g)	0.036±0.001	0.030±0.001*	0.032±0.002
Femur BMD 6w (g/cm2)	0.063±0.002	0.054±0.001*	0.055±0.001#
Femur BMC 6w (g)	0.025±0.001	0.020±0.001*	0.023±0.001#@
Femur Length 6w (mm)	11.32±0.06	10.10±0.13*	10.58±0.07#@

*: Vector IgG vs. HMW IgG p<0.05

#: Vector IgG vs. HMW FGF23AB p<0.05

@: HMW IgG vs. HMW FGF23AB p<0.05

Table 1
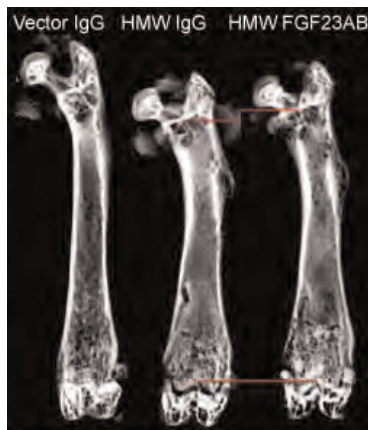
Figure 1. X-ray of the femur.

Figure 1

Disclosures: Liping Xiao, None.

FR0139

Role of XLαs in phosphate and vitamin D metabolism during early postnatal development. Qing He*[1], Cumhur Aydin[2], Braden Corbin[3], Regina Goetz[4], Moosa Mohammadi[4], Antonius Plagge[5], Murat Bastepe[3]. [1]Endocrine Unit, Department of Medicine, Massachusetts General Hospital & Harvard Medical School, USA, [2]Gulhane School of MedicineAnkara, TURKEY, Turkey, [3]Massachusetts General Hospital, Harvard Medical School, USA, [4]Department of Biochemistry & Molecular Pharmacology, New York University School of Medicine, USA, [5]Department of Cellular & Molecular Physiology, Institute of Translational Medicine, University of Liverpool, United Kingdom

The imprinted *GNAS* complex locus encodes several products including the alpha subunit of the stimulatory G protein (Gsα) and its extra-long variant XLαs. XLαs can mimic Gsα, which mediates the actions of PTH and plays important roles in skeletal development and mineral ion homeostasis. Since XLαs is expressed in bone and kidney, we aimed to investigate its role in the regulation of serum phosphate and calcium. In XLαs knockout mice (XLKO), we observed hyperphosphatemia (WT 10.3

± 0.2 mg/dl; KO 11.4 ± 0.4 mg/dl; p<0.05) and hypocalcemia (WT 1.48 ± 0.01 mmol/l; KO 1.42 ± 0.02 mmol/l; p<0.05) at postnatal day 2 (P2). These mice showed 2-fold elevated serum PTH (WT 65.25 ± 1.34 pg/mL; KO 138.10 ± 4.99 pg/mL; p<0.01), as well as significantly increased 1,25-dihydroxyvitamin D levels (WT 183.42 ± 4.64 pmol/L; KO 378.02 ± 6.86 pmol/L; p<0.001). Quantitative RT-PCR analysis of whole kidneys revealed about 5-fold and 2-fold increases of 25-hydroxyvitamin D 1-alpha hydroxylase (Cyp27b1) and vitamin D-24 hydroxylase (Cyp24a1) mRNA levels, respectively. P10 XLKO mice displayed a similar but milder phenotype than P2 XLKO mice. Western blot analysis and immunofluorescence staining of kidneys from P10 XLKO mice demonstrated increased levels of sodium-phosphate co-transporter Npt2a in brush border membranes of the proximal tubules. In response to PTH injection, the brush border levels of Npt2a decreased in both WT and XLKO kidneys, but the induction of Cyp27b1 was modestly blunted in XLKO. In addition, serum FGF23 levels in XLKO mice were significantly reduced (WT 524.11 ± 11.64 pg/mL; KO 158.86 ± 9.29 pg/mL; p<0.001 at P2; and WT 398.68 ± 10.14 pg/mL; KO 234.40 ± 10.50 pg/mL; p<0.01 at P10). FGF23 mRNA levels in XLKO femurs were also significantly reduced (38.86 ± 4.37%; p<0.05 at P10). Moreover, injection of a stable recombinant FGF23 mutant (FGF23R176Q) for 4 days from P6 to P10 into XLKO mice normalized the serum phosphorus levels (saline-injected WT 12.07 ± 0.10 mg/mL; saline-injected KO 13.64 ± 0.16 mg/mL; FGF23-injected WT 10.53 ± 0.17 mg/mL; FGF23-injected KO 11.62 ± 0.23 mg/mL), and significantly decreased renal Cyp27b1 mRNA levels. These results indicate that XLαs is essential for normal phosphate and vitamin D metabolism and plays a critical role in regulating FGF23 expression during early postnatal development.

Disclosures: Qing He, None.

FR0140

Effect of a Calcilytic Compound in Autosomal Dominant Hypocalcemia Model Mice. Bingzi Dong*[1], Itsuro Endo[1], Takeshi Kondo[2], Yukiyo Ohnishi[2], Masahiro Abe[2], Seiji Fukumoto[3], Tomoka Hasegawa[4], Norio Amizuka[5], Shin-ichi Aizawa[6], Toshio Matsumoto[1]. [1]University of Tokushima Graduate School of Medical Sciences, Japan, [2]University of Tokushima, Japan, [3]University of Tokyo Hospital, Japan, [4]Hokkaido University, Japan, [5]Hokkaido University School of Dentistry, Japan, [6]RINKEN Center for developmental biology, Japan

Background: Activating mutations of calcium sensing receptor (CaSR) gene cause autosomal dominant hypocalcemia (ADH). ADH develops hypocalcemia, hyperphosphatemia, and hypercalciuria, similar to hypoparathyroidism. Treatment of ADH with active vitamin D_3 aggravates urinary Ca excretion and renal insufficiency. PTH replacement cannot reverse all the abnormalities especially renal calcification and deranged bone mineralization. Thus, new therapeutic strategy is needed for ADH. Calcilytics are allosteric inhibitors of CaSR, and can stimulate PTH secretion and renal Ca reabsorption. Thus, calcilytics can become a specific therapeutic agent for ADH. Previously, we demonstrated that a calcilytic, JTT-305, suppressed the exaggerated response to extracellular Ca^{2+} in HEK cells transfected with CaSR genes bearing activating mutations. The present study was aimed to clarify whether JTT-305 can reverse the phenotypes of ADH in mutated CaSR gene knock-in mice in vivo.

Methods: We generated two strains of ADH model mice with activating mutations of human CaSR (C129S in the extracellular domain, A843E in the transmembrane domain) knocked-in (KI). A843E mutation has more severe phenotype in human. We treated these mice with JTT-305 or PTH, and investigated their effect on Ca and Pi metabolism.

Results: Both C129S and A843E KI mice exhibited hypocalcemia, hyperphosphatemia, hypercalciurea, renal calcification, and reduced serum 1,25(OH)$_2$D, urinary cAMP, and renal CYP27b1 mRNA encoding 1α-hydroxylase, mimicking almost all the features of human ADH. A843E KI mice exhibited more prominent phenotypes as in humans. Mutated CaSR KI mice showed increased BMD but low bone turnover with low serum PTH. JTT-305 treatment rapidly increased serum PTH, improved serum and urine Ca and Pi levels, and increased urinary cAMP and renal CYP27b1 mRNA expression in a dose-dependent manner. After long-term treatment with JTT-305, serum Ca recovered to normal range, and urinary Ca excretion decreased with no renal calcification. JTT-305 also increased BMD in both wild type and KI mice with higher bone remodeling. In contrast, PTH replacement improved serum Ca and Pi in KI mice, but urinary Ca remained elevated and renal calcification remained.

Conclusion: Mutated CaSR gene KI mice mimicked almost all the features of human ADH, and JTT-305 can reverse all the abnormalities in Ca and Pi parameters in these mice. JTT-305 can become a new therapeutic agent for ADH.

Disclosures: Bingzi Dong, None.

FR0143

Regulation of PTH-induced Bone Loss: A Role for Monocyte Chemoattractant Protein-1. Jawed Siddiqui*[1], Joshua Johnson[1], Joseph Tamasi[2], Nicola Partridge[3]. [1]New York University, USA, [2]Bristol-Myers Squibb, USA, [3]New York University College of Dentistry, USA

Parathyroid hormone (PTH) stimulates bone resorption as well as bone formation *in vivo*. The catabolic actions of PTH have been recognized in patients with hyperparathyroidism, or with acute infusion of hPTH(1-34). Our microarrays of

bone from rats injected with hPTH-(1-34) daily for 14 days showed a number of cytokines and chemokines were highly induced, in particular, RANKL, IL-6, and CCL2 (Monocyte Chemoattractant Protein-1, MCP-1). We also found that transient MCP-1 is essential for the anabolic effects of hPTH(1-34) on bone. To determine the role of MCP-1 in prolonged continuous PTH, as seen in hyperparathyroidism, we treated 8-week-old female WT and MCP-1$^{-/-}$ mice with continuous infusion of hPTH(1–34) or vehicle for 14 days, using Alzet osmotic pumps. To assess the differential effects of hPTH-(1-34) on cortical and trabecular bone, microcomputed tomography was utilized to analyze femurs harvested at death. Cortical bone showed that infusion with hPTH induced significant bone loss in WT mice with decreased bone volume/total volume (BV/TV), bone mineral density (BMD), mean cross-sectional area (B.Ar) and mean polar moment of inertia (MMI) when compared with the saline treated group. In addition, cortical thickness (Cs.Th) and total cross sectional area (T.Ar) were also found to be significantly lower in hPTH-infused WT mice. In contrast, hPTH did not cause significant cortical bone loss in MCP-1$^{-/-}$ mice. Further, μCT analysis of trabecular bone showed that compared with the saline group, the hPTH group had reduced trabecular thickness (Tb.Th), and structure model index in WT mice. Again, the MCP-1$^{-/-}$ mice were protected against PTH-induced bone loss. To establish whether MCP-1 is required for PTH to induce osteoclast formation in vitro, bone marrow macrophages (BMMs) from MCP-1$^{-/-}$ and WT mice were cultured with M-CSF and RANKL for 7 days and osteoclasts were counted. Data revealed that BMMs from MCP-1$^{-/-}$ mice showed decreased multinucleated osteoclast formation compared to WT mice. Further, mRNA analysis of the distal femurs of hPTH(1-34) infused mice showed that PTH induced the expression of NFAT, TRAP, carbonic anhydrase and cathepsin/K in WT mice but failed to demonstrate such changes in MCP-1$^{-/-}$ mice, indicating that MCP-1 is necessary for the recruitment of monocytes and pre-osteoclastic cells and assists in the formation of mature osteoclasts. Together these are the first data to show that MCP-1 is required for the catabolic response to PTH.

Disclosures: Jawed Siddiqui, None.

FR0153

Role of Interleukin-32 Gamma in Bone Formation in Ankylosing Spondylitis.
Chang Keun Lee*[1], Eun-Ju Lee[2], Eun-Jin Lee[3], Seokchan Hong[2], Bin Yoo[2], Tae-Hwan Kim[4], Soo-Hyun Kim[5], Eun-Ju Chang[3], Yong-Gil Kim[2]. [1]University of Ulsan College of Medicine, South Korea, [2]Department of Rheumatology, University of Ulsan College of Medicine, Asan Medical Center, South Korea, [3]Department of Biomedical Sciences, Cell Dysfunction Research Center & BMIT, University of Ulsan College of Medicine, Asan Medical Center, South Korea, [4]Hanyang University Hospital for Rheumatic Diseases, South Korea, [5]Department of Biomedical Science & Technology, Konkuk University, South Korea

Objective. To investigate the role of IL-32γ in osteoblast differentiation and its association with the pathogenesis of ankylosing spondylitis (AS).

Methods. The concentration and expression of IL-32γ were evaluated in synovial fluid and synovial tissue from patients with AS, rheumatoid arthritis (RA) and osteoarthritis (OA), using ELISA and immunohistochemistry. To establish whether IL-32γ affects bone formation in vivo, we used micro-CT to examine osteoblast differentiation from calvarial cells of IL-32γ transgenic (TG) mice and bone volume in these animals. To elucidate the mechanism of osteoblastogenesis, levels of regulators were assayed in IL-32γ TG mice and in human osteoblasts after IL-32γ stimulation.

Results. The IL-32γ levels were higher in the synovial fluid of AS patients compared with RA or OA patients. Expression of IL-32 was higher in AS synovia than in RA or OA synovia. IL-32γ TG mice showed higher rates of osteoblast differentiation than wild-type (WT) mice. Micro-CT analysis revealed that IL-32γ TG mice, particularly males, have a higher bone volume than WT mice. The constitutive expression of DKK-1, a negative regulator, was suppressed in calvarial cells from IL-32γ TG mice, and IL-32γ reduced DKK-1 expression in both WT precursor cells and human osteoblasts. IL-32γ increased the expression of receptor activator of nuclear factor kappa-B ligand (RANKL), but not osteoprotegerin (OPG), leading to a high RANKL/OPG ratio.

Conclusions. The elevated expression of IL-32γ in AS enhances osteoblast differentiation and increases bone volume in mice. Therefore, IL-32γ is a potential molecular target to prevent the progression of AS.

Disclosures: Chang Keun Lee, None.

FR0155

Pro-Resorptive Therapy for Heterotopic Ossification. Song Xue*[1], Roberto Fajardo[2], Kevin McHugh[1]. [1]University of Florida, USA, [2]UT Health Science Center, San Antonio, USA

Heterotopic ossification (HO) is the formation of bone in non-osseous tissues. HO is a frequent complication of orthopaedic surgery, especially following blast-trauma, with two thirds of patients developing painful and debilitating HO. There are currently no effective treatments for HO other than surgical excision of the ossified tissue which is an extremely difficult and involved procedure. Therefore, there is a significant unmet need for effective and non-invasive treatments of HO.

Bone metabolism is regulated by the local expression and ratio of the osteoclast (OC) inducer RANKL to the native OC inhibitor osteoprotegerin (OPG). We show that OPG expression is higher and OC numbers are much lower in HO bone, relative to native skeletal sites. We hypothesize that high OPG expression is required for HO, blocking OC formation and favoring maintenance of heterotopic bone. We propose that releasing the OPG blockade of OC formation, with function-blocking anti-OPG antibodies, will allow OC formation and prevent the development of HO. Importantly, due to the high OPG expression, HO will be a selective target of this pro-resorptive approach.

We employed a mouse model of HO in which transgenic mice harbor a Cre-inducible constitutively-active ALK2 receptor construct (caALK2)(a R220A mutant of the BMP receptor ALK2). Expression of the caALK2 gene is induced by intramuscular injection of adenoviral Cre (Ad-Cre). Following injection of Ad-Cre, animals reproducibly develop significant ectopic bone at the site of injection over a rapid 14 day time course. Systemic treatment is by intraperitoneal injection of anti-OPG antibody. HO production was demonstrated over time by a range-of-motion (ROM). MicroCT was used to quantify HO formation and contralateral native bone volume. Histology was used to characterize the HO and to identify TRAP positive OCs.

Systemic treatment with an inhibitory antibody against OPG results in an increase in OCs in ectopic bone. Statistically significant reduction of mineralized tissue in HO was seen with a concomitant and statistically significant improvement in ROM, compared to IgG treated controls. Notably, bone loss seen at ectopic sites was greater than loss at native skeletal sites in the same animal.

These studies indicate that osteoclastic resorption is likely inhibited in HO by OPG expression and if OPG function is blocked, HO is reduced. Therefore, novel pro-resorptive therapies for HO may have a significant impact on the treatment of HO.

Disclosures: Song Xue, None.

FR0156

Role of *sarA* in osteomyelitis pathogenesis in UAMS-1 and LAC clinical strains of *Staphylococcus aureus* . Dana Gaddy*, Nisreen Akel, Karen Beenken, Mark Smeltzer, Larry Suva. University of Arkansas for Medical Sciences, USA

Osteomyelitis is a serious bone infection typically caused by *Staphylococcus aureus*, the pathogenesis of which is poorly understood. The details of the cellular host responses of bone to the infection are specifically lacking. Biofilms play a clinically defining role in many forms of *S. aureus* infection, and can confer an intrinsic resistance to both conventional antibiotics and host defenses. Biofilm formation requires the staphylococcal accessory regulator (*sarA*), and its mutation limits the capacity of wildtype *S. aureus* to form a biofilm. Indeed, *sarA* mutations are correlated with an increased susceptibility to multiple antibiotics and a reduced capacity to cause bone and joint infections *in vivo*. We sought to determine the impact of *sarA* in a murine model of osteomyelitis, and determined the host bone response to infection using two contemporary genetically diverse clinical *S. aureus* isolates (UAMS-1) and a community-acquired strain (LAC), along with their isogenic *sarA* mutants. Mice were injected unicortically with vehicle control or *S. aureus* into the femoral diaphysis of adult mice. On day 14, serum was collected and injected limbs harvested and fixed in formalin. Serum inflammatory cytokine profiles demonstrated that wildtype *S. aureus* infection selectively diminished IL-1 receptor antagonist levels while increasing IP10/CXCL10. In contrast, injection of the *sarA* mutants resulted in lower IP10 induction. MicroCT analysis of all injected bones revealed extensive reactive periosteal new bone surface that extended proximally, distally and circumferentially. Non-infected bones healed within 14 days, whereas UAMS-1 and LAC infection caused extensive injection site osteolysis, and significant increases in new periosteal bone forming surfaces and reactive bone volume. Histomorphometry demonstrated that the increased new bone area/total area extended well beyond the localization of Gram+ bacteria. Injection of the biofilm-compromising *sarA* mutants, resulted in less injection site bone erosion and significantly decreased reactive new bone formation. Collectively, these data demonstrate the importance of *sarA* (and possibly biofilm formation) in the etiology and pathophysiology of osteomyelitis in *S. aureus* infections *in vivo,* and suggest that targeting this molecule for therapeutic inhibition may limit biofilm formation as well as the host bone response, thereby enhancing the efficacy of antibiotic therapy.

Disclosures: Dana Gaddy, None.

FR0159

Sparsely ionizing radiation exacerbates the effects of rat hindlimb suspension on the musculoskeletal system. Nisreen Akel*, Robert Griffin, Howard Hendrickson, Parimal Chowdhury, Maxim Dobretsov, Larry Suva, Dana Gaddy. University of Arkansas for Medical Sciences, USA

It is well known that spaceflight and disuse have deleterious effects on the musculoskeletal system. Since these effects could be attributed to either the microgravity (disuse) and/or radiation components, we determined the extent to which irradiation affects the well-characterized disuse-associated effects on muscle and bone loss. Having previously demonstrated that 2 weeks of hindlimb suspension (HLS) in adult 6 month old rats caused dramatic loss in both trabecular and cortical bone mineral density, as well as compromised soleus muscle mass and protein synthesis, we next determined if ionizing radiation exacerbated HLS. We compared the

musculoskeletal response in 4 groups of rats: control (CON), irradiated (IR), HLS, and irradiated plus suspended (IR+HLS) for 2 weeks. IR and IR+HLS groups were exposed to a 2Gy radiation per exposure every third day for a total radiation dose of 10Gy over 2 weeks. HLS, but not IR, resulted in soleus muscle atrophy. Although the proximal tibial trabecular bone mineral density (BMD) was not affected by IR, BMD was significantly diminished by HLS, and further significantly decreased by IR+HLS. Similarly, cortical midshaft BMD was unaffected by IR alone, but was compromised by HLS, an effect significantly exacerbated by IR. To address the mechanisms involved in the HLS+IR-dependent effects of the MSK system, a series of metabolomics analyses were performed. IR significantly increased soleus muscle Citrulline/Arginine (Cyt / Arg) ratio over CON. HLS+IR together further increased the soleus muscle Cyt / Arg ratio. Alterations in the bioavailability of citrulline are proposed to result in a compromised microvasculature. These effects lead to detrimental changes in nitric oxide (NO) production, thereby implicating the NO pathway in mediation of the observed MSK effects of both HLS and IR. The metabolomics approach revealed a significant decrease in the serum concentration for eleven amino acids following HLS, many of which are involved in NO synthesis. Collectively, these data demonstrate that HLS induces major physiological changes in the MSK system, some of which involve the NO pathway, and that these changes are exacerbated by exposure to irradiation. Such a scenario experienced in spaceflight and/or onboard ISS will require novel countermeasures that protect and/or reverse the effects.

Disclosures: Nisreen Akel, None.

FR0160

Tensile Force Induces Vascular Formation during the Eary Biomechanical Response of Cranial Sutures via ROCK2, CTGF, and ERK1/2 Dependent Mechanisms. <u>Nobuo Takeshita</u>*[1], <u>Masakazu Hasegawa</u>[2], <u>Kiyo Sasaki</u>[2], <u>Daisuke Seki</u>[2], <u>Shunrou Miyashita</u>[2], <u>Ikuko Takano</u>[2], <u>Yuuki Miyajima</u>[2], <u>Teruko Takano-Yamamoto</u>[1]. [1]Tohoku University, Japan, [2]Division of Orthodontics & Dentofacial Orthopedics, Department of Oral Health & Development, Tohoku University Graduate School of Dentistry, Japan

Sutures are fibrous tissues that connect bones in craniofacial skeletal complexes. Sutures are not only sites of craniofacial skeletal growth, but also transmit mechanical stresses that are loaded to the craniofacial skeleton. Tensile force induces vascular formation in sutures, and vascular formation may be one principal biological process that directs subsequent bone formation. However, the molecular regulatory mechanisms of this tensile force-induced vascular formation in sutures are not fully understood. In the present study, an *in vivo* analysis was performed to elucidate the molecular mechanisms of vascular formation during the early biomechanical response of sutures. We established a murine model to apply tensile force to cranial sagittal sutures. The expression of osteoblast markers decreased in a time-dependent manner in the early response of sutures. In contrast, tensile force upregulated the mRNA expressions of vascular factors, including VEGF and Hif-1α, endothelial cell markers, and MMPs in sutures. The expressions of ROCK2 and CTGF mRNA were also upregulated by tensile force, and administration of ROCK inhibitor Y-27632 and a CTGF neutralizing antibody abolished the tensile force-induced VEGF expression. The inactivation of CTGF also partially inhibited Hif-1α expression induced by tensile force. Moreover, tensile force activated ERK1/2 signaling in sagittal sutures, and ERK1/2 inhibitor U0126 partially inhibited the tensile force-induced CTGF expression. In conclusion, we demonstrate for the first time the gene expression dynamics that indicate induction of vascular formation during the early response of sutures to tensile force. Moreover, these data suggest that tensile force-induced vascular formation is regulated by complex molecular mechanisms orchestrated by ROCK2, CTGF, and, at least in part, by ERK1/2.

Disclosures: Nobuo Takeshita, None.

FR0165

Mechanotransduction from Dendritic Processes to Cell Body of Osteocytes through the Functional Interplay of Integrin Activation, PI3K Signaling and Connexin Hemichannels. <u>Manuel Riquelme</u>*[1], <u>Nidhi Batra</u>[2], <u>Jean Jiang</u>[3]. [1]University of Texas Science Center, San Antonio, USA, [2]University of Texas Health Science Center at San Antonio (UTHSCSA), USA, [3]University of Texas Health Science Center at San Antonio, USA

Connexin 43 (Cx43) hemichannel in osteocytes is a major portal for release of factors important for the anabolic effects of mechanical loading on bone. Mechanical stimulation in the form of fluid flow shear stress induces the opening of Cx43 hemichannels in MLO-Y4 osteocyte releasing prostaglandins, ATP and potentially other signaling molecules. We and others have previously shown that dendritic processes serve as a mechanical sensory part of the osteocyte. We also demonstrated that the interaction between integrin α5 and Cx43 on the cell body is essential for the opening of hemichannels by mechanical stress. However, how mechanical signals are transmitted from dendritic processes to cell body leading to the opening of Cx43 hemichannels remained unknown. Here, we show that integrin αVβ3 located at the dendritic processes is a primary mechanosensor that activates intracellular PI3K/AKT signaling, and integrin α5β1 and Cx43 hemichannels on the cell body. Integrin αV co-localized with integrin β3, but not Cx43 at the osteocytic dendritic processes. Upon

flow shear stress, both integrin α5β1 and αV were activated. Inhibition of integrin αV activation prevented the Cx43 hemichannel opening on the cell body. Ablation of integrin α5 by siRNA attenuated the hemichannel opening when dendrites were mechanically stimulated, suggesting the mechanical transmission from integrin αV to α5 in the opening of hemichannels. Moreover, the inhibition of flow shear stress-induced PI3K/AKT activation blocked integrin α5β1 activation and hemichannel opening. Interestingly, inhibition of the activation integrin αV, but not α5, attenuated the activation of PI3K-AKT upon mechanical loading. Under rest condition, the activation of PI3K/AKT pathway induced by insulin growth factor 1 increased the activity of Cx43 hemichannels; however it did not induce the activation of α5β1, suggesting that the phosphorylation by AKT is sufficient for the opening of Cx43 hemichannels. Moreover, hemichannel opening was only blocked by anti-integrin αV antibody at low, but not high FSS, suggesting that αV is a more sensitive mechanosensor than α5 in opening HC. Taken together, these results suggest that dendritic integrin αVβ3 senses mechanical stimulation that activates PI3K/AKT leading to the activation of integrin α5β1 and subsequently the opening of Cx43 HC with a release of important bone anabolic factors.

Disclosures: Manuel Riquelme, None.

FR0166

MiR-103a: a novel mechano-sensitive microRNA inhibits bone formation through targeting Runx2. <u>Bin Zuo</u>*[1], <u>JunFeng Zhu</u>[1], <u>Jiao Li</u>[2], <u>XiaoDong Chen</u>[1], <u>Xiaoling Zhang</u>[3]. [1]Department of Orthopedic Surgery, Xinhua Hospital, Shanghai JiaoTong University School of Medicine (SJTUSM), China, [2]The Key Laboratory of Stem Cell Biology, Institute of Health Sciences, Shanghai Institutes for Biological Sciences (SIBS), Chinese Academy of Sciences (CAS) & Shanghai Jiao Tong University School of Medicine (SJTUSM), China, [3]Institute of Health Sciences, Peoples Republic of China

Emerging evidence indicates that microRNAs (miRNAs) play essential roles in regulating osteoblastogenesis and bone formation. However, the role of miRNA in osteoblast mechanotransduction remains to be defined. In this study, we aimed to investigate if miRNAs regulate mechanical stimulation-triggered osteoblast differentiation and bone formation through modulation of Runx2, the master transcription factor for osteogenesis. We first investigated the role of mechanical loading both in a mouse model and in osteoblasts culture system and the outcomes clearly demonstrated that mechanical stimuli can regulate osteogenesis and bone formation both *in vivo* and *in vitro*. Using bioinformatic analyses and subsequently confirmed by quantitative Real-Time PCR (qRT-PCR), we identified miR-103a as a novel mechano-sensitive miRNA in human preosteoblast cell lines. Both miR-103a and its host gene PANK3 were downregulated during cyclic mechanical stretch-induced (CMS, 8% elongation, 0.5 Hz) osteoblast differentiation, whereas Runx2 protein expression was upregulated. Overexpression of miR-103a significantly decreased Runx2 protein level and inhibition of miR-103a increased Runx2 protein level, suggesting that miR-103a acts as an endogenous attenuator of Runx2 in osteoblasts. Mutation of putative miR-103a binding sites in Runx2 mRNA abolishes miR-103a-mediated repression of the Runx2 3'UTR luciferase reporter activity, suggesting that miR-103a binds to Runx2 3'UTR. Osteoblast marker genes profiling and osteogenic phenotype assays demonstrated that miR-103a negatively correlates with CMS-induced osteogenesis. Further, the perturbation of miR-103a also has a significant effect on osteoblast activity and matrix mineralization. More importantly, we found an inhibitory role of miR-103a in regulating bone formation in hindlimb unloading mice, and pretreatment with antagomir-103a partly rescued the osteoporosis caused by mechanical unloading. Taken together, our data suggest that miR-103a is the first identified mechano-sensitive miRNA that regulates osteoblast differentiation via directly targeting Runx2, and therapeutic inhibition of miR-103a may be an efficient anabolic strategy for skeletal disorders caused by pathological mechanical loading.

Disclosures: Bin Zuo, None.

FR0167

Osteoblast mechanoresponse: the role of Lipocalin 2. <u>Mattia Capulli</u>*[1], <u>Sara Gemini Piperni</u>[1], <u>Patrick Lau</u>[2], <u>Petra Frings-Meuthen</u>[2], <u>Martina Heer</u>[3], <u>Anna Teti</u>[1], <u>Nadia Rucci</u>[1]. [1]University of L'Aquila, Italy, [2]German Aerospace Center (DLR), Germany, [3]PROFIL - Institute for Metabolic Research GmbH, Germany

A global transcriptome analysis of mouse calvarial osteoblasts, subjected to simulated microgravity (0.008*g*), revealed Lipocalin2 (LCN2) to be the most upregulated gene in low loading condition. In this study we demonstrated that upregulation of LCN2 in mechanical unloading occurs in humans and mice. We evaluated LCN2 serum levels in 8 healthy male volunteers, subjected to head-down tilt bed rest and observed a progressive increase of LCN2 that achieved statistical significance after 12 days (R=0.31, P=0.01). Results obtained in humans were confirmed in three different mouse models of mechanical unloading: tail suspension, treatment with the muscle paralysis inducer Botox, and dystrophic MDX mice. In all these models, the unloading condition reduced the bone volume/tissue volume ratio and significantly increased the transcriptional expression of LCN2 in bone compared to control mice. A significant increase or LCN2 protein expression was also confirmed

in the femurs of Botox-treated mice. Moreover, increase of mechanical loading in MDX mice, obtained by treadmill physical exercise, reduced the LCN2 expression to 18% of untrained MDX (P<0.05), returning its level to that of WT (90% of WT, P=0.52). Interestingly, mouse osteoblasts expressed the LCN2 receptors megalin and 24p3r, thus indicating an autocrine-paracrine effect of LCN2 in this cell type. In agreement with our hypothesis, primary mouse osteoblasts transduced with LCN2-expression-vector (LCN2OBs) showed reduced Runx2, Osterix and Alp transcriptional expression compared to empty-vector transduced osteoblasts (emptyOBs) (28, 20 and 17% of control, respectively, P<0.04). Consistently, ALP activity was less prominent in LCN2OBs (54% of control, P=0.003). LCN2OBs also exhibited an increase of the Rankl/Opg ratio and IL-6 mRNA expression (8- and 5.3-fold, respectively, P<0.02), suggesting that LCN2 up-regulation could link osteoblast poor differentiation with enhanced osteoclastogenesis. Reliably, incubation of purified mouse bone marrow mononuclear cells with conditioned media from LCN2OBs, or their co-culture with LCN2OBs, enhanced osteoclast formation (5- and 2-fold, respectively, P<0.05). In conclusion, our in vivo and in vitro data indicate that LCN2 is involved in the osteoblast mechanoresponse and that its upregulation appears central to the loss of bone induced by low mechanical forces, contributing to both poor osteoblast differentiation and increased osteoblast-mediated osteoclastogenesis.

Disclosures: Mattia Capulli, None.

FR0170

PDGF Secreted by TRAP[+] Preosteoclasts Induces Angiogenesis for Bone Formation. Hui Xie*[1], Zhuang Cui[2], Long Wang[3], Lingling Xian[4], Zhuying Xia[5], Yin Hu[5], Changjun Li[1], Liang Xie[1], Janet Crane[6], Mei Wan[4], Gehua Zhen[7], Tao Qiu[4], Weizhong Chang[6], Maureen Pickarski[8], Le Duong[9], Xu Cao[6]. [1]Johns Hopkins Medical Institution, USA, [2]Department of Orthopaedic Surgery, Johns Hopkins University School of Medicine, USA, [3]Department of Orthopaedic Surgery, Johns Hopkins University School of Medicine, USA, [4]Johns Hopkins University School of Medicine, USA, [5]Institute of Endocrinology & Metabolism, Second Xiangya Hospital of Central South University, China, [6]Johns Hopkins University, USA, [7]The Johns Hopkins Hospital, USA, [8]Merck & Co., Inc., USA, [9]Merck Research Laboratories, USA

Angiogenesis is essential for new bone formation during bone modeling, remodeling and growth. Osteoblast bone formation requires transport of minerals, nutrients, oxygen and metabolic wastes through blood vessels, but regulation of angiogenesis for bone formation remains elusive. Here we report that TRAP[+] preosteoclasts secrete PDGF-BB to induce angiogenesis for the new bone formation. In brief, conditioned medium (CM) of TRAP[+] preosteoclasts significantly increased migration of epithelial progenitor cells (EPC) and MSCs and the neutralizing antibody for PDGF-BB abolished the migration. TRAP[+] preosteoclasts secrete PDGF-BB, but not mature bone resorptive osteoclasts. TRAP[+] lineage-specific PDGF-BB knockout mice ($Pdgfb^{-/-}$) show that bone mass of both trabecular and cortical bone were significantly decreased. Importantly, PDGF-BB levels in both bone marrow and peripheral blood were significantly decreased, and bone marrow VEGF level was also decreased, suggesting that angiogenesis in the bone marrow was affected. We found that vessel volume and surface in both bone marrow and periosteum were significantly decreased in $Pdgfb^{-/-}$ mice and the CD31^{+} EPCs were also decreased. Moreover, the osteoblast size was much smaller in $Pdgfb^{-/-}$ mice relative to their WT littermates, suggesting that PDGF-BB secreted by TRAP[+] preosteoclasts stimulates angiogenesis for osteoblast maturation and bone formation. Furthermore, phosphorylation of PDGFRβ and its downstream components PI3K, Akt and FAK was induced by preosteoclast CM. Notably, EPC and MSC migration induced by preosteoclast CM was abolished by each of the inhibitors for PDGFR, PI3K, Akt and PAK, indicating that PI3K/Akt/FAK signaling mediates the cell migration. Cathepsin K inhibitor (CatK), as a novel anti-osteoporosis drug for inhibition of osteoclast bone resorption, stimulates bone formation and increases TRAP^{+} cells. We found that PDGF-BB levels were increased significantly in both bone marrow and peripheral blood, and VEGF level was also increased in bone marrow. Blood vessel volume and surface in both bone marrow and periosteum were significantly increased in CatK KO mice and WT mice treated with CatK inhibitor L-235, and CD31^{+} EPCs were also increased. Taken together, PDGF-BB secreted by TRAP^{+} preosteoclasts stimulates angiogenesis to prepare transport minerals, nutrients, oxygen and other factors for osteoblastic bone formation during bone remodeling and cortical bone formation.

Disclosures: Hui Xie, None.
This study received funding from: Merck

FR0171

Role of the STING cytosolic DNA sensor pathway in bone remodeling. Rebecca Baum*[1], Shruti Sharma[1], Yukiko Maeda[1], Catherine Manning[1], Jason Organ[2], David Burr[2], Ann Rothstein[1], Kate Fitzgerald[1], Ellen Gravallese[1]. [1]University of Massachusetts Medical School, USA, [2]Indiana University School of Medicine, USA

Innate immune sensors such as cytosolic DNA sensors and toll-like receptors detect nucleic acid from viral and bacterial pathogens to clear infection, as well as endogenous nucleic acid from stressed or dying cells, contributing to the pathogenesis of autoimmune disease. Upon detection of DNA, cytosolic sensors trigger a signaling cascade that results in the production of proinflammatory cytokines and type I interferons. We have identified a potentially important role for cytosolic DNA sensor pathways in bone by studying a mouse lacking the lysosomal endonuclease DNaseII. In this model, DNA accumulates in lysosomes and in the cytosol, leading to polyarthritis and articular bone erosions, resembling that seen in human rheumatoid arthritis. Given the production of proinflammatory cytokines in this model, bone loss would also be expected in the axial and appendicular skeleton. Paradoxically, bone accumulates, resulting in almost complete replacement of the marrow cavity by bone at 16 mo. Total trabecular volume (femur) is significantly increased by 6 mo. in DNaseII deficient mice compared to controls (5.58 vs 4.51 mm^3; p=0.0018). CFU assays demonstrate the presence of increased numbers of osteoblast precursors, and osteoid production is also significantly increased. Furthermore, ectopic bone forms throughout the spleen, a site of extramedullary hematopoesis and probable DNA accrual. To understand mechanism, we sought to define the contribution of cytosolic DNA sensors in this model of bone accrual. Several cytosolic sensors signal through an ER-associated protein, stimulator of interferon genes (STING). Therefore, we generated mice deficient in both DNaseII and STING. As previously reported, arthritis is completely abrogated in these mice. We now show that STING deficiency also prevents the accrual of bone seen in the long bones and spleens of DNaseII deficient mice (bone density: 813.7 vs 846.9 mg HA/cm^3; p=0.002). To determine the contribution of STING in bone turnover, independent of DNaseII deficiency, we evaluated the bone phenotype in STING deficient mice. By 6 mo. of age, a significant decrease is seen in bone density (1059.8 vs 1088.9 mg HA/cm^3; p=0.0072) and BV/TV (0.46 vs 1.03%; p=0.0156) in STING deficient mice compared with controls. The discovery of a role for DNA sensor pathways in bone may provide insights into mechanisms of bone remodeling as well as new targets for the treatment of bone disorders.

Disclosures: Rebecca Baum, None.

FR0174

TIEG suppresses SOST expression and mediates the skeletal response to sclerostin antibody therapy. Anne Gingery*[1], Kevin S. Pitel[2], Gino W. Gaddini[3], Xiaodong Li[4], Hua Zhu Ke[5], Russell T. Turner[6], Nalini M. Rajamannan[7], Urszula T. Iwaniec[6], Thomas C. Spelsberg[8], Malayannan Subramaniam[8], John R. Hawse[9]. [1]Mayo Clinic School of Medicine, USA, [2]Mayo Clinic, USA, [3]Oregon State University, USA, [4]Amgen, Inc., USA, [5]Amgen, USA, [6]Oregon State University, USA, [7]Mayo Clinic, Rochester MN, USA, [8]Mayo Clinic, USA, [9]Mayo Clinic College of Medicine, USA

TGFβ Inducible Early Gene-1 (TIEG) is known to play important roles in skeletal development and its misregulation and mutation is associated with osteoporosis in humans. Furthermore, TIEG has recently been shown to be critical for optimal TGFβ, BMP and estrogen signaling in bone. Finally, TIEG knockout (KO) mice exhibit a female-specific osteopenic phenotype. In order to better understand the molecular basis for this phenotype, we determined gene expression changes in the cortical shells of long bones isolated from wildtype (WT) and TIEG KO mice. One of the most up-regulated genes in KO bone was sclerostin (Scl) which exhibited approximately a 12-fold increase relative to WT animals. Serum levels of Scl were also significantly elevated in KO mice and TIEG was shown to suppress Scl promoter activity in transient transfection assays. The use of TOPGAL reporter mice demonstrated that loss of TIEG expression resulted in a 3-fold decrease in canonical Wnt pathway activity in the skeleton relative to WT mice potentially due to elevated Scl levels. In order to determine the contribution of elevated Scl levels in the observed osteopenic phenotype of TIEG KO mice, we treated WT-TOPGAL and KO-TOPGAL animals with either vehicle control or a Scl neutralizing antibody (25 mg/kg, 1x/wk, s.c.) for 6 weeks (10 animals/treatment group). DXA, pQCT and microCT analyses revealed that deactivation of Scl resulted in significant increases in numerous cancellous and cortical bone parameters throughout the skeleton in both WT and KO mice. Overall, a more robust skeletal response was observed in TIEG KO mice following antibody administration. To understand potential differences in the response of WT and KO mice to Scl antibody administration, a Wnt signaling pathway PCR array was employed to monitor gene expression changes in the cortical shells of long bones. These data revealed that 15 and 17 genes were significantly up- or down-regulated following antibody exposure in WT and KO animals respectively, of which only 3 were commonly regulated in both genotypes. A number of positive regulators of Wnt signaling, such as Wnt1, Lef1, Wnt4 and Frzd6 were induced in TIEG KO mice but not WT animals following antibody treatment. These data demonstrate that elevated sclerostin levels in TIEG KO mice substantially contribute to the observed osteopenic phenotype and reveal that TIEG imparts significant effects on the response of the skeleton to Scl antibody therapy.

Disclosures: Anne Gingery, None.

FR0176

CHIP Is a Critical Regulator of Bone Remodeling. <u>Shan Li</u>*[1], <u>Wanqing Xie</u>[2], <u>Guozhi Xiao</u>[1], <u>Di Chen</u>[1]. [1]Rush University Medical Center, USA, [2]Rush University Medical Center, USA

The regulatory mechanism of bone remodeling is not fully understood. CHIP is an E3 ligase and regulates protein stability in immune and tumor cells. The role of CHIP in bone remodeling has not been reported. In this study, we found that $Chip^{-/-}$ mice had osteopenic phenotype. μCT analysis showed that bone volume, bone mineral density, trabecular numbers, trabecular thickness and connectivity density were significantly reduced (66, 59, 44, 33 and 75% decreases); while trabecular separation and structure model index were significantly increased (1.7- and 1.4-fold) in 1-month-old $Chip^{-/-}$ mice, indicating lower trabecular bone mass and more fragile bone in $Chip^{-/-}$ mice. Histology analyses showed that TRAP+ osteoclast numbers and osteoclast surface were significantly increased (1.6- and 1.5-fold) in $Chip^{-/-}$ mice. In vitro assays showed that osteoclast numbers (3.5-fold) and bone resorption area were significantly increased in osteoclast cultures derived from $Chip^{-/-}$ mice. Expression of $Cathepsin\ K$, $Mmp9$, and $Nfatc1$ was increased (7-, 16-, and 5-fold) after RANKL treatment in $Chip^{-/-}$ bone marrow cells. A significant increase in TRAF6 protein, but not mRNA, levels were observed in $Chip^{-/-}$ bone marrow cells, suggesting that CHIP regulates TRAF6 protein stability. In a series of in vitro studies we found that: 1) Interaction of endogenous CHIP with TRAF6 was detected in RAW264.7 cells. 2) The ubiquitination and proteosome degradation of endogenous TRAF6 protein was significantly reduced in $Chip^{-/-}$ bone marrow cells. 3) Mutation of CHIP in the site which is required for its E3 ligase activity completely abolished CHIP-induced TRAF6 degradation in 293 cells. 4) The phosphorylation of IKKα/β and IκBα was significantly increased in $Chip^{-/-}$ bone marrow cells treated with RANKL. 5) p65 nuclear translocation was enhanced in $Chip^{-/-}$ bone marrow cells treated with RANKL. 6) RANKL- or TRAF6-induced NF-κB activity was suppressed by CHIP in RAW264.7 cells. In addition to changes in osteoclast formation, we also found that bone formation rates were significantly reduced in 1-month-old $Chip^{-/-}$ mice. β-catenin protein levels, ALP activity and mineralized bone nodule formation were significantly decreased and expression of osteoblast marker genes, including $Runx2$, Osx, $Col1$, Opn, Bsp and OC, was down-regulated (43, 37, 67, 30, 60, and 45% decreases) in $Chip^{-/-}$ bone marrow stromal cells. Our studies demonstrated that CHIP is a critical regulator for bone remodeling.

Disclosures: Shan Li, None.

FR0184

Is MMP-13 the critical mediator for the effects of HDAC4 deletion in mice?. <u>Teruyo Nakatani</u>*[1], <u>Tiiffany Chen</u>[2], <u>Shoshana Yakar</u>[3], <u>Nicola Partridge</u>[4]. [1]New York University College of Dentistry, USA, USA, [2]New York University, USA, [3]New York University College of Dentistry, David B. Kriser Dental Center, USA, [4]New York University College of Dentistry, USA

Histone deacetylase 4 (HDAC4), which is expressed in prehypertrophic chondrocytes, regulates chondrocyte hypertrophy. $Hdac4^{-/-}$ mice are runted in size at birth and do not survive to weaning. Previously, we reported that HDAC4 is a repressor of MMP-13 transcription, and the absence of HDAC4 leads to increased expression of MMP-13 both in vitro (osteoblastic cells) and in vivo (hypertrophic chondrocytes and osteoblasts). MMP-13 is expressed in both these cells and is thought to be involved in endochondral ossification and bone remodeling. To identify whether the phenotype of $Hdac4^{-/-}$ mice is due to MMP-13 up-regulation, we generated $Hdac4^{-/-}/Mmp13^{-/-}$ double mutants. The $Mmp13^{-/-}$ mice have a similar body mass compared to wild type mice. The $Hdac4^{-/-}/Mmp13^{-/-}$ mice are significantly heavier and larger than the $Hdac4^{-/-}$ mice and their mean survival is longer ($Hdac4^{-/-}$: 7.3, $Hdac4^{-/-}/Mmp13^{-/-}$:16days). Histological examination showed that the double mutants recover the heights of their growth plate. Immunohistochemistry showed that the expression of osteocalcin and alkaline phosphatase increased in $Hdac4^{-/-}/Mmp13^{-/-}$ mice compared with $Hdac4^{-/-}$ mice. TRAP staining was decreased in $Hdac4^{-/-}$ mice but rescued in $Hdac4^{-/-}/Mmp13^{-/-}$ mice. Tibiae of 8 day old animals were subjected to microCT analysis. We found that $Hdac4^{-/-}$ mice have significantly decreased cortical bone mass compared with the wild type mice. In $Hdac4^{-/-}/Mmp-13^{-/-}$ mice, all these parameters recovered. In trabecular bone, ablation of HDAC4 caused an increase in BMD and Tb.Th which normalized in the $Hdac4^{-/-}/Mmp13^{-/-}$. Taken together, our findings indicate that the premature phenotype seen in the $Hdac4^{-/-}$ mice is partially derived from MMP-13 elevation and may be due to a bone remodeling disorder that influences tibial cortical bone mass, mineralization, trabecular thickness, BMD and connectivity.

Disclosures: Teruyo Nakatani, None.

FR0191

A Selective Androgen Receptor Modulator that favorably affects the bone muscle interface. <u>Venkatesh Krishnan</u>*[1], <u>Henry Bryant</u>[1], <u>Yanfei Ma</u>[1], <u>Charles Benson</u>[2], <u>Prabhakar Jadhav</u>[2], <u>Judith Henck</u>[2], <u>Nita Patel</u>[2], <u>Heather Bullock</u>[2], <u>Alan Chiang</u>[1], <u>Timothy Waterhouse</u>[2], <u>Masahiko Sato</u>[3], <u>George Zeng</u>[2], <u>Benjamin Yaden</u>[2], <u>Pamela Shetler</u>[2]. [1]Eli Lilly & Company, USA, [2]Lilly Research laboratories, USA, [3]Indiana University School of Medicine, USA

Testosterone supplementation increases skeletal muscle mass and maximal voluntary strength in healthy, androgen-deficient and eugonadal young and older men. However, administration of steroidal androgens is associated with a high frequency of dose-limiting adverse effects, such as erythrocytosis and prostate events. We developed a SARM with minimal androgenic activity in the prostate and no observable risk of erythrocytosis while maintaining muscle and bone anabolic activity. Daily oral treatment of LY2452473 resulted in a dose-dependent increase (ED_{90} 2.5 mg/Kg-d) in vertebral bone mineral content (BMC), cross-sectional area and bone mineral density (BMD) in the delayed rat ORX model accompanied by gains in cortical area (associated with increases in periosteal alkaline phosphatase activity) and recovery of mid-shaft and femoral neck biomechanical properties to the sham control animal levels. A significant but modest increase in levator ani muscle mass is seen with oral administration of LY2452473 in the delayed rat orchidectomy (ORX) model. No treatment related effects in the prostate or uterine endometrium were noted in the 8 week pharmacology model when using female or male gonadectomized rats up to 10 mg/kg/day (uterus) or 30 mg/kg/day (prostate). A significant gain in whole body muscle mass as measured by DEXA was seen in phase I studies in healthy volunteers at the 5 mg dose. A dose dependent increases in procollagen type 1 N-terminal (P1NP) and decreases in resorption markers were also observed in these trials. In addition using peripheral QCT we show a gain in calf muscle area in 4 weeks in both males and females. In contrast, LY treatment did not show changes in PSA in men and signs of virilization in females or changes in hematocrit at any of the doses. However, SARM treatment resulted in a dose dependent decrease in HDL (>20%) which was completely reversible after cessation of treatment. Collectively, the SARM molecule represents an oral agent with bone and muscle anabolic activities that is devoid of some of the classic risks associated with testosterone replacement.

Disclosures: Venkatesh Krishnan, Eli Lilly & Company, 4
This study received funding from: Eli Lilly and Company

FR0192

Activation of Prostaglandin E$_2$ EP4 signaling promotes primary myoblast proliferation via regulation of cell cycle progression and MyoD expression. <u>Chenglin Mo</u>*[1], <u>Lori Wetmore</u>[2], <u>Julian Vallejo</u>[3], <u>Leticia Brotto</u>[3], <u>Lynda Bonewald</u>[4], <u>Marco Brotto</u>[4]. [1]University of Missouri-Kansas City, USA, [2]William Jewell College, USA, [3]Muscle Biology Research Group, School of Nursing & Health Studies, University of Missouri-Kansas City, USA, [4]University of Missouri - Kansas City, USA

PGE_2 is produced by osteocytes and elevated in response to mechanical loading. Our previous studies showed the MLO-Y4 osteocyte-like cell conditioned media and a major component of this media, PGE_2, stimulated C2C12 myogenesis. To validate and extend these previous studies using cell lines, primary myoblasts isolated from mouse hindlimb muscles were used. All four PGE_2 receptors, EP1 to EP4, were detectable in primary myoblasts by real-time PCR. To identify the functional receptor, cells were treated with 50nM of PGE_2, 17-phenyl trinor PGE_2 (EP1/EP3 agonist), butaprost (EP2 agonist), or CAY 10598 (EP4 agonist). After 48h, cells were collected and counted. Treatment with PGE_2 or EP4 agonist CAY 10598 significantly increased myoblast number by 23.3±6.4% and 17.6±6.2% ($p<0.05$), respectively. However, EP1/EP3 or EP2 agonists did not have any significant effects. To confirm that EP4 signaling is important for primary myoblast proliferation, cells were then treated with 30μM of the EP4 antagonist L161,982 for 48h, which resulted in a 27.3±4.3% ($p<0.05$) decrease in proliferation. To study the molecular mechanisms behind the effect of PGE_2 signaling on primary myoblast proliferation, cell cycle analysis was conducted. Primary myoblasts were synchronized in G0/G1 phase by serum starvation with Ham's F-10 medium containing 1% fetal bovine serum (FBS) for 10h, then the medium was switched to complete growth medium (Ham's F-10 with 20% FBS) along with the addition of PGE_2, CAY 10598, or L161,982 for 12h. Cell cycle analysis showed that although no significant difference was observed between control and PGE_2 or CAY 10598 treated cells, L161,982 increased the number of cells in G0/G1 phase by 19.4±3.7% ($p<0.05$), suggesting that EP4 signaling could be important for G1-S phase transition. Next, MyoD protein expression, a muscle regulatory factor that plays a role in satellite cells activation and myoblast proliferation was measured using Western blot analysis. Compared with control, MyoD did not change after treatment with of PGE_2, CAY 10598, or L161,982 at 12h. However at 36 hrs, MyoD increased by 55.7% and 48.5% following PGE_2 and CAY 10598 treatments, whereas L161,982 reduced MyoD level to 43.1%. Taken together, these data suggest that PGE_2 signaling via EP4 receptor is important for the regulation of cell cycle progression and MyoD expression in primary myoblast proliferation.

Disclosures: Chenglin Mo, None.

FR0193

Establishment and characterization of a novel Tet-Off embryonic stem cell lines carrying ALK2. <u>Mai Fujimoto</u>*[1], <u>Satoshi Ohte</u>[2], <u>Masashi Shin</u>[2], <u>Katsumi Yoneyama</u>[3], <u>Kenji Osawa</u>[2], <u>Sho Tsukamoto</u>[2], <u>Arei Miyamoto</u>[4], <u>Takato Mizuta</u>[2], <u>Shoichiro Kokabu</u>[2], <u>Akihiko Okuda</u>[5], <u>Naoto Suda</u>[5], <u>Takenobu Katagiri</u>[24]. [1]Saitama Medical University Research Center for Genomic Medicine, Jpn, [2]Saitama Medical University Research Center for Genomic Medicine, Japan, [3]Saitama Medical Univercity Reserch Center fo Genomic Medicine, Japan, [4]Saitama Medical University,Research Center for Genomic Medicine, Japan, [5]Meikai University School of Dentistry, Japan

Fibrodysplasia ossificans progressiva (FOP) is a rare hereditary disease, which is characterized by postnatal progressive heterotopic endochondral ossification in skeletal muscle. Gain-of-function mutations of ALK2, one of type I BMP receptors, have been identified in patients with typical and atypical FOP. In the present study, we established and characterized murine embryonic stem (ES) cell lines, which express V5-tagged wild-type (WT) or mutant (R206H) ALK2 from the ROSA26 locus in a Tet-Off system. These cell lines did not express the V5-tagged exogenous ALK2 in the presence of Dox (Dox+). In contrast, the expression of WT or mutant ALK2 was turned on by removing Dox (Dox-) from the culture media. The mRNA and protein levels of WT and mutant ALK2 were confirmed in the Dox- cultures by quantitative real-time RT-PCR and Western blotting, respectively. In FACS analysis, both WT and mutant ALK2 were expressed on the cell surface in the Dox- cultures. The BMP-specific luciferase reporter activity was induced in both WT and mutant ALK2-carrying cells in response to BMP stimulation in the Dox+ cultures, although the reporter was induced without adding BMP in the Dox- cultures of mutant ALK2-carrying cells. The cells were maintained in Dox+, and then they were cultured in pellets in Dox+ or Dox- with or without adding TGF-β/BMP to induce chondrogenic differentiation. Simultaneous stimulation with TGF-β and BMP induced the mRNA expression of type II and type X collagens in both WT and mutant ALK2-carrying cells even in the Dox+ cultures. In contrast to WT ALK2-carrying cells, the mutant ALK2-carrying cells differentiated into chondrocytes in the Dox- cultures in the presence of TGF-β alone. Taken together, these findings suggested that mutant ALK2 found in FOP stimulates the capacity of chondrogenic differentiation in stem cells. This Tet-Off ES cells may be a useful model to examine molecular mechanisms of heterotopic ossification in patients with FOP.

Disclosures: Mai Fujimoto, None.

FR0194

The Age-Associated Rise in miRNAs from Muscle Target SDF-1 and Musculoskeletal Regulatory Genes is Reversed with Caloric Restriction and Leptin. <u>Sudharsan Periyasamy-Thandavan</u>[1], <u>Samuel Herberg</u>[2], <u>Phonepasong Arounleut</u>[3], <u>Sunil Upadhyay</u>[4], <u>Galina Kondrikova</u>[4], <u>Amy Dukes</u>[4], <u>Colleen Davis</u>[4], <u>Maribeth Johnson</u>[4], <u>Xing-Ming Shi</u>[4], <u>Carlos Isales</u>[4], <u>Mark Hamrick</u>[5], <u>William Hill</u>*[6]. [1]Georgia Regents University & Charlie Norwood VAMC, USA, [2]Case Western Reserve University, USA, [3]Georgia Regents University (formally Georgia Health Sciences University), USA, [4]Georgia Regents University, USA, [5]Georgia Health Sciences University, USA, [6]Georgia Regents University & Charlie Norwood VAMC, USA

MicroRNAs (miRNAs) have the potential to regulate broad changes in connected systems and pathways altering homeostatic gene expression. We have previously identified age-related changes in the expression profiles of miRNAs isolated from human bone marrow mesenchymal stem cells (BMSCs). These miRNAs targeted numerous genes associated with musculoskeletal development, maintenance, aging and osteoporosis. As well as, the chemokine SDF-1 (CXCL12), and its receptor CXCR4. The SDF-1 axis is critical in the migration, survival, and engraftment of stem cells, including BMSCs and muscle satellite cells (SCs). We have noted leptin can alter systemic and muscle SDF-1 levels in an age-related manner suggesting nutrient signaling may effect systemic, or tissue SDF-1 expression. We hypothesized that changes in nutrient signaling pathways may modulate specific miRNA in an age specific manner. In turn these miRNAs may alter SDF-1 and key osteogenic, or myogenic pathway genes. We tested this hypothesis by examining changes in miRNAs, we had previously identified as linked to aging in BMSCs, in muscles of mice aged 12 months and 20 months fed ad-libitum (AL) and mice 20 months on caloric restriction (CR). We also treated other mice aged 20 months on caloric restriction with recombinant mouse leptin for 10 days at 10 mg/kg body weight. Age-associated patterns of expression of miR-29b-1-3p, miR-29b-1-5p, miR-1244 & miR-141 in murine muscle (12 vs 20 months) mirrors that seen in human BMSCs between young (under 45 years of age) and older (over 65 years of age) subjects. In both cases the miRs 29b-1-5p, 1244 and 141 increased, while miR-29b-1-p3 did not change. Of interest the miR-29 family is well known to target musculoskeletal and extracellular matrix genes. CR reduced the miRs 29b-1-5p, 1244 and 141 in 20 month old mice to levels equal to that of 12 month mice while miR-29b-1-3p was not altered. Of interest CR with leptin treatment further reduced expression of miRs 29b-1-5p, 1244 & 141 well below that seen in the 12 month mice and surprisingly the amount of miR-29b-1-3p rose significantly. Therefore, it appears that food restriction is a potent regulator of

miRNAs, and suppresses miRNAs that target musculoskeletal gene systems in aged muscle. Leptin further drives this effect significantly below what is seen in younger muscle, which may induce an imbalance in gene expression that might itself impair the potential for muscle regeneration.

Disclosures: William Hill, None.

FR0195

The Effects of Combined Use of Glucocorticoids and Bisphosphonates on Musculoskeletal System in a Mouse Model of Duchenne Muscular Dystrophy. <u>Jane Mitchell</u>[1], <u>Sung-Hee Yoon</u>*[2], <u>Jinghan Chen</u>[3], <u>Ariana delaCruz</u>[2], <u>Kim Sugamori</u>[3], <u>Marc Grynpas</u>[4]. [1]University of Toronto, Canada, [2]University of Toronto, Canada, [3]Univeristy of Toronto, Canada, [4]Lunenfeld-Tanenbaum Research Institute of Mount Sinai Hospital, Canada

Duchenne Muscular Dystrophy (DMD) is an X-linked recessive genetic disorder occurring in 1 in 3500 boys. Due to mutations in the gene encoding dystrophin, a sarcolemmal protein critical in stabilizing the link between muscle fibers and dystrophin-associated glycoprotein complex in surrounding extracellular matrix, DMD patients show progressive muscle membrane fragility and muscle necrosis. Glucocorticoids (GC) are the only available treatment, having anti-inflammatory effects on muscles thus prolonging ambulation in patients with DMD. GC-induced osteoporosis (GIO) resulting in increased bone fragility and high prevalence of vertebral bone fractures is common in DMD patients. We hypothesized that the use of bisphosphonates (BP) at the initiation of GC treatment will ameliorate GIO development during growth, without harmful effects on dystrophic muscle. In this study, C57BL10ScSn-Mdx mice (Mdx), the a commonly used animal model for DMD, received continuous GC (prednisone) or placebo treatment from 5 to 13 weeks of age. Bisphosphonates (pamidronate) were given for the first two weeks of GC therapy in some mice and the effects of GC and combination therapy of GC and BP (GCB), on bones and muscles were examined. GC treatment significantly decreased femur length (p<0.001) compared to PL treated WT and Mdx mice. Areal bone mineral density (BMD) determined by dual energy X ray absorptiometry (DEXA) was significantly decreased in GC-Mdx (p<0.001) and this was ameliorated in mice treated with GC and bisphosphonate. MicroCT analysis of cortical bone in mid-diaphysis showed that GC treatment resulted in significantly decreased cortical thickness (p<0.001), and bone area (p<0.001) compared to PL treated mice. GCB-Mdx mice had significantly greater cortical thickness and bone area compared to GC-Mdx. GC therapy significantly improved muscle function as measured by fore-limb grip strength test, histological analysis of diaphragm, and serum creatine kinase (CK), and these improvements were also seen in mice treated with GC and bisphosphonate. Thus, early BP treatment at the initiation of long-term GC therapy is demonstrated to ameliorate GC-induced loss of cortical bone without any negative effects on dystrophic muscles in growing mice.

Disclosures: Sung-Hee Yoon, None.

FR0196

Effects of eldecalcitol on body weight, bone mineral density and skeletal muscle in glucocorticoid-treated rats. <u>Hayato Kinoshita</u>*[1], <u>Naohisa Miyakoshi</u>[2], <u>Michio Hongo</u>[2], <u>Yuji Kasukawa</u>[2], <u>Koji Nozaka</u>[2], <u>Yoichi Shimada</u>[3]. [1]Akita University, Japan, [2]Akita University Graduate School of Medicine, Japan, [3]Akita University Graduate School of Medicine Department of Orthopedics Surgery, Japan

Purpose: Prednisolone (PSL) causes secondary osteoporosis (OP) and myopathy, which is a risk factor for falls. It is reported that vitamin D prevents falls and fractures. However, the effects of a new vitamin D_3 analogue, eldecalcitol, on steroid-induced myopathy are still unclear. In this study, we examined whether eldecalcitol could inhibit PSL-induced myopathy or OP in rats.
Methods: Six-month-old female Wistar rats were randomized into the following four groups (n=14?16/group): 1) control group, administered eldecalcitol vehicle and PSL vehicle; 2) PSL group, administered PSL (10 mg/kg) and eldecalcitol vehicle; 3) E group, administered eldecalcitol (0.05 μg/kg) and PSL vehicle; and 4) PSL+E group, administered PSL and eldecalcitol. PSL, eldecalcitol and their vehicles were administered every day for 2 or 4 weeks. Body weight loss during the experiment was measured. Right calf muscle strength and fatigue were measured at the end of administration. Muscle strength and fatigue were obtained by electrically stimulating the right sciatic nerve. Sections from the left tibialis anterior (TA) muscle were stained by adenosine triphosphatase and the cross-sectional areas (CSAs) of the muscle fibers were measured. Bone mineral density (BMD) of the right femur was measured by dual-energy X-ray absorptiometry.
Results: Only after 4 weeks of treatment, weight loss in the PSL+E group was significantly higher than that in the control group (p<0.01) and muscle strength of the PSL+E group was significantly higher than that of the PSL group (p<0.05). Furthermore, CSAs in the E group and PSL+E group were significantly larger than those in the PSL group (p=0.0026 and p=0.0115). After 2 weeks of treatment, the distal femoral BMD of the E group was significantly higher than that of the PSL group (p=0.0261). After 4 weeks of treatment, the total, proximal, middle and distal femoral BMD of the PSL group was significantly lower than those of the control and

E groups (p=0.0005 and p<0.0001, respectively). Eldecalcitol significantly increased the total, proximal and distal BMD after treatment with PSL compared with the PSL group (p=0.0002, p=0.0069, and p<0.0001) after 4 weeks of treatment.

Conclusions: In the 4-week-treated rats, eldecalcitol prevented muscle atrophy of the TA and loss of femoral BMD, and increased calf muscle strength. Based on these results, we hypothesize eldecalcitol will inhibit steroid-induced OP and myopathy after 4 weeks administration.

Disclosures: Hayato Kinoshita, None.

FR0197

Mediation of SDF-1/CXCR4 signaling in aged skeletal muscle by the adipokine leptin. Samuel Herberg*[1], Sudharsan Periyasamy-Thandavan[2], Phonepasong Arounleut[3], Sunil Upadhyay[4], Amy Dukes[5], Colleen Davis[4], Galina Kondrikova[5], Maribeth Johnson[5], Carlos Isales[4], William Hill[2], Mark Hamrick[6]. [1]Case Western Reserve University, USA, [2]Georgia Regents University & Charlie Norwood VAMC, USA, [3]Georgia Regents University (formally Georgia Health Sciences University), USA, [4]Georgia Regents University, USA, [5]Georgia Regents University, USA, [6]Georgia Health Sciences University, USA

Aging is associated with a decline in both muscle and bone mass, which is thought to involve dysfunction in bone- and muscle-derived stem cells. The chemokine SDF-1 (CXCL12) and its receptor CXCR4 play important roles in the migration, survival, and engraftment of stem cells, including bone marrow stromal cells (BMSCs) and muscle satellite cells (SCs). Adult muscle constitutively expresses SDF-1, and CXCR4 expression in muscle is elevated during muscle regeneration. Previous work in mice has shown that, with food restriction, leptin levels are decreased while SDF-1 levels are increased, and the reverse is observed with diet-induced obesity. We therefore speculated that leptin and the SDF-1/CXCR4 axis may interact throughout adulthood to mediate musculoskeletal tissue repair and regeneration. We tested this hypothesis by examining SDF-1 and CXCR4 expression in muscles of mice aged 12 months and 20 months fed ad-libitum (AL) and mice 20 months on caloric restriction (CR). We also treated mice aged 20 months on caloric restriction with recombinant mouse leptin for 10 days at 10 mg/kg body weight. Serum SDF-1 was increased in the aged mice, but leptin treatment reduced serum SDF-1 to levels seen in the younger (12 month) animals. SDF-1alpha expression in muscle decreased with age, but was increased with caloric restriction, and leptin treatment reversed this increase. CXCR4 expression in muscle decreased slightly with age, but was increased almost four-fold with caloric restriction, and this increase was attenuated by leptin treatment. Together these data suggest that food restriction is a potent stimulus for SDF-1 and CXCR4 activation in aged muscle, and that leptin can antagonize this effect. Thus, while we have previously demonstrated that leptin can increase muscle mass and IGF-1 in leptin-deficient rodents, leptin may also impair the potential for muscle regeneration and satellite cell migration via its effects on SDF-1/CXCR4 interactions.

Disclosures: Samuel Herberg, None.

FR0199

Elevated TGF-β in Subchondral Bone Causes Joint Degeneration of Rheumatoid Arthritis and Osteoarthris. Xin Xu*[1], Liwei Zheng[2], Qin Bian[3], Xuedong Zhou[4], Xu Cao[5]. [1]Johns Hopkins University, Medical Institute, USA, [2]West China School of Stomatology, Sichuan University, Peoples Republic of China, [3]USA, [4]West China School of Stomatology, Sichuan University, China, [5]Johns Hopkins University, USA

Rheumatoid arthritis (RA) is an autoimmune disease that affects many tissues/organs including synovial joints, skin, lung, kidneys, vasculatures, etc. However, inadequate understanding of the pathogenesis of articular cartilage degeneration leads to insufficient treatment/prevention of this disease. Our previous study has shown that TGF-β-mediated subchondral bone alterations play an essential role in initiating cartilage degeneration of osteoarthritis (OA). Although rheumatoid arthritis and osteoarthritis have distinct clinical manifestations, both diseases are associated with bone marrow edema/lesions in the subchondral/subcortical bone. The current study was to delineate the mechanisms of TGF-β-mediated subchondral bone pathologies in the initiation of cartilage degeneration of RA-affected joint. By using both collagen-induced arthritis (CIA) mice model and spontaneous arthritis mice (TNF-α transgenic mice) model, we detected uncoupled bone remodeling phenotypes in the tibial subchondral bone of RA affected joint, accompanying with an excessive activation of TGF-β ligand and its down-stream signaling chronologically sequential to the increased osteoclastic bone resorption. Cellular clusters of osteoprogenitors and increased level of nestin positive Mesenchymal Stem Cells (MSCs) were also observed in the RA-affected subchondral bone marrow. By inhibition of TGF-β signaling with intraperitoneal administration of TβRI inhibitor (SB-505124), the abnormal bone phenotypes of CIA mice were rescued paralleled to the subsidence of MSCs/osteoprogenitors aggregation in the subchondral bone marrow, and the articular cartilage was protected. The cartilage protective effect of TGF-β blockade was also reproduced by local neutralization of TGF-β with pan-specific antibody (1D11) in the

tibial subchondral bone of CIA rat. Further conditional deletion of the gene encoding TGF-β receptor II (Tgfbr2) in nestin-positive MSCs also rescued the uncoupled bone remodeling phenotypes in the subchondral bone of CIA mice (Nestin-cre[T-M]Er::Tgfbr2flox/flox mice), and consequently protected the cartilage of RA. Hence, our data clearly demonstrate that excessive activation of TGF-β in subchondral bone initiates cartilage degeneration in RA, and the pathogenesis of OA and RA joint destruction converges on the TGF-β-mediated subchondral bone pathologies.

Disclosures: Xin Xu, None.

FR0200

Elucidating Molecular Mechanisms leading to Post Traumatic Osteoarthritis in Sost KO Mice. Jiun Chiun Chang*[1], Blaine Christiansen[2], Nicole Collette[3], Aimy Sebastian[4], Deepa Murugesh[5], Sarah Hatsell[6], Aris Economides[7], Craig Blanchette[8], Gabriela Loots[9]. [1]University of California, Merced, USA, [2]University of California - Davis Medical Center, USA, [3]Lawrence Livermore National Laboratory, USA, [4]University of California, Merced, USA, [5]Lawrence Livermore National Laboratories, USA, [6]Regeneron Pharmaceuticals, USA, [7]Regeneron Pharmaceuticals, Inc., USA, [8]Lawrence Livermore National Laboratories, USA, [9]Lawrence Livermore National Laboratory, UC Merced, USA

Sost was recently implicated in regulating chondrocyte function in osteoarthritis (OA). Sost levels were found to be elevated in regions of osteoarthritic cartilage in surgical models of OA. However, the role of *Sost* in OA and its involvement in regulating biomarkers such as MMPs, interleukins and collagens is unclear. We examined the progression of OA using a noninvasive tibial compression overload model of post traumatic osteoarthritis (PTOA) in mice overexpressing (*TG*) or lacking *Sost* (*KO*). OA development was examined histologically and by μCT at 6-, 12-, and 16- weeks post injury. KOs displayed a more severe cartilage loss relative to the wildtype (*WT*) littermates, while a less severe OA phenotype was observed in TGs. We also quantified subchondral trabecular bone in the femoral epiphysis and osteophyte formation by μCT. Injured knees of *WT* mice lost a significant amount of trabecular bone (~24%), while *KOs* exhibited no significant bone loss. Moreover, ~28% greater osteophyte volume was observed in the *KOs* and ~49% less in the *TGs* relative to *WTs* at 16 weeks post injury. Fluorescent MMPSense substrate was administered intravenously immediately post injury and MMP activity was quantified 3 days post injury. *KO* injured joints showed similar MMP activity levels as controls while *TG* had ~2-fold less MMP activity, suggesting that *SOST* overexpression inhibits the activity of proteolytic enzymes known to degrade articular cartilage matrix. Next we quantified gene expression using RNA sequencing (RNASeq) at 1 day post injury and compared injured and uninjured *KO* joints to injured and uninjured littermate controls. In this analysis, 84 and 78 transcripts were found to be up-regulated by more than 2-fold in *WT* and *KO* injured joints, respectively. Consistent with the MMPSense data, MMPs 2/3/13 transcripts were significantly up-regulated in both *KO* and control injured joints. Among the transcripts that were differentially expressed between *KO* and control injured joints we found CRABP-II 6-fold up-regulated exclusively in *WT* injured joints only, while RRAD was up-regulated 14-fold in *KO* injured joints and only 2-fold in injured controls, suggesting that these genes may play a role in the phenotypic differences observed between *WT* and *KO* injured joints. These results show that in mice which have developed in the absence of Sost, the response to traumatic joint injury is accentuated; in contrast, chronic overexpression of SOST appears to have a protective role.

Disclosures: Jiun Chiun Chang, None.

FR0201

Genetic Inhibition of FGFR1 in Cartilage at Adult stage Attenuates the Degeneration of Articular Cartilage in FGFR3 disruption mice. Yangli Xie*[1], Wei Xu[2], Junlan Huang[2], Xiaolan Du[2], Siru Zhou[2], Lin Chen[3], Zuqiang Wang[2]. [1]Center of Bone Metabolism & Repair,State Key Laboratory of Trauma, Burns & Combined Injury, Trauma Center, Institute of Surgery Research, Daping Hospital, Third Military Medical University, Chn, [2]Center of Bone Metabolism & Repair, State Key Laboratory of Trauma, Burns & Combined Injury, Trauma Center, Institute of Surgery Research, Daping Hospital, Third Military Medical University, China, [3]Daping Hospital, Peoples Republic of China

Study has shown that deletion of fibroblast growth factor receptor 3 (FGFR3) lead to spontaneous osteoarthritis (OA) in mice. We previously demonstrated that inducible disruption of FGFR1 in cartilage delays the progression of cartilage degeneration in spontaneous OA and destabilization of the medial meniscus (DMM) models. Previous work has suggested that the ratio of FGFR1 to FGFR3 in articular cartilage may infulence the maintenance of cartilage and development of OA. To study the relative role of FGFR1 and FGFR3 in the process of cartilage maintenance, we induciblly inactivated FGFR3 and FGFR1 in chondrocytes by injecting tamoxifen

(TM) into mice with floxed *Fgfr*1 alleles, floxed *Fgfr*3 alleles and Col2a1-CreERT2 allele (hereafter referred to as Fgfr1/3[Col2ER]) and compared them with Fgfr1[Col2ER], Fgfr3[Col2ER] and Cre-negative mice. All mice mentioned above were intraperitoneally injected with TM (1 mg/10 g body weight, × 5 days) at age of 8 weeks. DMM surgery was performed on the right knee joints of 10-week-old male mice, and sham surgery was performed with medial capsulotomy only. All knee joint specimens were analyzed by micro-computed tomography, histologic analysis, and real-time PCR at 8 weeks postoperatively or at 12 months.

Compared to Fgfr1[Col2ER], Fgfr3[Col2ER] and Cre-negative mice, Fgfr1/3[Col2ER] mice showed no significant gross phenotype. The length of tibia and femurs showed no remarkable changes. Histologically, Fgfr3Col2ER mice developed early-onset of DMM induced and age-related cartilage matrix loss and abnormal hypertrophy of chondrocytes in the knee cartilage compared with Cre-negative mice, while, Fgfr1/3[Col2ER] mice showed the similar process with Cre-negative mice. Immunohistochemical analysis demonstrated a significant reduction in matrix metalloproteinase 13 (MMP13) and Collagen 10 expression in the superficial chondrocytes above the tidemarks of Fgfr1/3[Col2ER] mice compared with that of Fgfr3Col2ER mice. Gene expression analysis demonstrated that inactivation of FGFR3 led to enhanced Collagen10,Mmp13 and Adamts5 expressions and depressed Col2, aggrecan expressions in knee cartilage, while inactivation of FGFR1 in FGFR3 [Col2ER] mice can alleviate these phenotype.

Our results indicate that deletion of FGFR3 in chondrocytes leads to early-onset degeneration of knee cartilage which can be partially rescued by deletion of FGFR1. These findings about the role of FGFR1 and FGFR3 in articular cartilage degeneration may provide experimental data for further mechanism studies, and for screening of therapeutic approaches for human OA.

Disclosures: Yangli Xie, None.

FR0202

3D Bone Microarchitectural Assessment in the Human Knee by Second Generation HR-pQCT – A New Tool for Early Osteoarthritis Detection?.
Sarah Manske*, Ying Zhu, Britta Jorgenson, Steven Boyd. University of Calgary, Canada

The sequence of events leading to osteoarthritis (OA) after joint injury such as anterior cruciate ligament (ACL) tears is poorly understood. Increasing evidence suggests that subchondral bone changes may precede cartilage loss. However, the nature of the bone changes that may be linked to OA progression is unclear as both high and low BMDs have been associated with radiographic OA.

High resolution peripheral quantitative computed tomography (HR-pQCT) scanners have become standard tools to assess bone microarchitecture *in vivo*, however, until recently, gantry size limited scan sites to distal peripheral limbs. The development of the second generation scanner (HR-pQCT2; XtremeCTII, Scanco Medical) with a larger field of view (FOV, 14 cm), longer gantry (115 cm), and increased scan length (20 cm) will permit examination of sites such as the knee and elbow. We sought to explore the capability of this cutting edge technology to examine bone microarchitecture in the knee.

We scanned two human cadaveric knees, and one participant (height = 178 cm, weight = 78 kg) *in vivo* five months following an ACL reconstruction in the HR-pQCT2. For the participant, we acquired a 6 cm long region of interest using the patient protocol (61 μm, 43 ms integration time (IT), 900 projections/180˚). In the cadaveric samples, we tested several protocols by varying spatial resolution, IT, and number of projections to optimize image quality and acquisition time. For 3D visualization, we filtered the images and applied a threshold to segment bone from soft tissue.

Qualitatively, we found that in the cadaveric scans we obtained sufficient image quality for microarchitectural analysis with a practical scan acquisition time using 61 μm, 100 ms IT and 900 projections/180˚ (Figure 1). In the participant scan, the knee and surrounding soft tissue fit in the gantry, although positioning in the centred FOV was a challenge. These initial *in vivo* data resulted in images that were noisier than radius scans using the same protocol. However, we could clearly visualize individual trabeculae, as well as the tunnels drilled during the ACL reconstruction.

Protocol optimization for participant scans is ongoing. Future work will involve defining subregions of analysis at various depths from the cartilage surface. We plan to use this new technology examine individuals at risk for developing knee OA to determine whether microarchitectural deterioration can be used as an early OA detection tool.

Figure 1. Sagittal view of cadaveric knee acquired at 61 μm, 100 ms integration time, and 900 projections/180° using HR-pQCT2.

Figure 1 - sagittal view of cadaver knee

Disclosures: Sarah Manske, None.

FR0207

The influence of osteophytes on femoral neck microcracks in osteoarthritis.
Gustavo Davi Rabelo[1], Jean-Paul Roux*[2], Nathalie Portero-Muzy[1], Stephanie Boutroy[3], Roland Chapurlat[4], Pascale Chavassieux[5]. [1]INSERM UMR1033, Université de Lyon, France, [2]INSERM, UMR 1033, Université de Lyon, France, [3]INSERM U1033 & Université de Lyon, France, [4]E. Herriot Hospital, France, [5]INSERM UMR1033, Université De Lyon, France

Structural changes of the femoral neck (FN) contribute to the risk of fracture. Patients with osteoarthritis (OA) seem protected against FN fracture, mostly related to cortical thickening. In relation to osteophytes, patients with osteophytic hip OA had higher BMD, wider femoral necks, and greater bone strength than those with atrophic OA or without OA. The aim of this study was to evaluate the microcrack density (Cr.N/BV) and length (Cr.Le) in hip OA and its relation with cancellous and cortical characteristics in the osteophyte region.

Samples were obtained during arthroplasty for hip OA in 18 women (66 ± 8 yrs). Calcein bulk-staining was performed to identify microcracks and Goldner staining for the histomorphometric analysis. 3D measurements were assessed by HR-pQCT (Scanco). The presence of microcracks was analyzed in the osteophyte area and in the remaining part. The texture analysis of the cortex was made separately in the quadrants of the osteophyte and the opposite part. Both a thresholded and an unthresholded methods were used in order to improve the 3D analysis obtained with the low resolution of the CT images (82 μm). From thresholded images, we measured cortical thickness (Ct.Th) and its heterogeneity (Ct.ThSD), porosity (Ct.Po) and Fractal Dimension (Ct.FDbin). From unthresholded images, we measured the Fractal Dimension (Ct.FDgray) and lacunarity.

Osteophytes were present in all samples, but microcracks were observed in only 3 of them. Cr.N/BV was significantly higher in cancellous than cortical bone (p<0.001) but Cr.Le tended to be higher in cortical than cancellous bone (p=0.07). Cr.N/BV was significantly lower in osteophytes than in the other part (p=0.02). The bone mass of the osteophytes was significantly higher than the other part (p<0.0005) but the microarchitecture was not better. Cortical fractal dimension was significantly higher in the osteophyte quadrant than the opposite quadrant (Ct.FDbin p<0.005, Ct.FDgray p=0.002), with higher Ct.Th (p<0.0001) and Ct.ThSD (p≤0.01). The lacunarity and Ct.Po were not significantly different.

In conclusion, these results showed that in hip OA, the microcrack formation was lower in the osteophytes. The osteophyte region presents a higher complexity (Fractal dimension) in bone structure when compared with the opposite part. These results suggest that the different organization of osteophyte bone may explain lower microdamage frequency, which is useful to understand microdamage occurrence in bone.

Disclosures: Jean-Paul Roux, None.

FR0209

Nuclear Factor of Activated T-Cells (Nfatc)2 Inhibits Osteoblast Function and Causes Osteopenia. <u>Stefano Zanotti</u>*, <u>Ernesto Canalis</u>. University of Connecticut Health Center, USA

Nuclear factor of activated T-cells (Nfat)c1 to c4 are transcription factors that regulate critical cellular events. Whereas Nfat proteins play an undisputable role in osteoclastogenesis, the function of Nfat in cells of the osteoblastic lineage is controversial. Constitutive activation of Nfatc1 and c2 in osteoblasts suppresses cell function, although study of Nfat proteins *in vivo* yielded conflicting results. To establish the consequences of Nfatc2 activation in osteoblasts, we generated FVB transgenic mice, where a 3.6 kilobase fragment of the collagen type I α1 promoter directs Nfatc2 expression (*Col3.6-Nfatc2*). The *Nfatc2* transgene harbors serine to alanine substitutions that render Nfatc2 constitutively active. The skeletal phenotype of *Col3.6-Nfatc2* mice of both sexes and of sex-matched littermate controls was studied by microcomputed tomography and histomorphometry. *Col3.6-Nfatc2* mice had no obvious phenotype, and bone extracts from transgenics exhibited *Nfatc2* mRNA levels 5 to 11 fold higher than controls. Femurs were slightly shorter in *Col3.6-Nfatc2* mice but the effect was transient and observed only at 1 month of age. One month old *Col3.6-Nfatc2* male and female mice exhibited pronounced osteopenia. Femoral cancellous bone volume was reduced by 40 to 50% and trabeculae were reduced in number and were more rod-like in relationship to control mice. In addition, *Col3.6-Nfatc2* female mice exhibited a thin and porous cortical bone. The mechanisms underlying the osteopenia differed between sexes. *Col3.6-Nfatc2* female mice had a 30% reduction in bone formation. In contrast, male transgenics had an increase in osteoblast number. This finding suggests incomplete osteoblast maturation, since bone formation was not enhanced, and is consistent with previously established effects of Nfatc2 on osteoblastogenesis mediated by interactions with osterix. Osteoclast number and bone resorption were not affected in either sex. To explore the cellular mechanisms responsible for the osteopenia, bone marrow stromal cells from *Col3.6-Nfatc2* and control mice were cultured. In agreement with the *in vivo* observations, Nfatc2 inhibited alkaline phosphatase activity and mineralized nodule formation. In conclusion, *in vivo* Nfatc2 activation in osteoblasts causes cancellous and cortical bone osteopenia and inhibits bone formation. This confirms previous work *in vitro* and establishes Nfatc2 as an inhibitor and not a stimulator of osteoblast function and bone formation.

Disclosures: Stefano Zanotti, None.

FR0210

Cannabinoid CB1 Receptor in Sympathetic Nerves Regulates Bone Mass. <u>Saif Deis</u>*[1], <u>Natalya Kogan</u>[1], <u>Lital Goldfine</u>[1], <u>Raj Kamal Srivastava</u>[2], <u>Saja Baraghithy</u>[1], <u>Esther Shohami</u>[1], <u>Beat Lutz</u>[1], <u>Itai Bab</u>[3]. [1]Hebrew University of Jerusalem, Israel, [2]Johannes Gutenberg University, Germany, [3]The Hebrew University, Israel

It is now established that the endocannabinoid (EC) system, including the cannabinoid receptors and EC metabolizing enzymes, have an important role in bone health. Retrograde cannabinoid CB1 receptor (CB1) signaling regulates synapse activity throughout the brain. In addition, CB1 expression has been demonstrated in sympathetic terminals in peripheral organs, including the skeleton, where it transmits retrograde signals that restrain norepinephrin (NE) release thus transiently stimulating bone formation following an acute challenge. In agreement with these findings we show here in MC3T3 E1 and newborn calvarial osteoblasts that isoproterenol, a β-adrenergic receptor agonist having NE-like activity, stimulates production of the major EC, 2-arachidonoylglycerol (2AG) by increasing the expression of its biosynthetic enzyme diacylglycerol lipase α. These findings are consistent with a 2AG-NE negative feedback circuit that regulates the synaptic-like activity between sympathetic terminals and osteoblasts. To assess the occurrence of this circuit *in vivo* we characterized the skeletal phenotype of mice with conditional deletion of CB1 in sympathetic nerves (*DBH-Cre/CB1f/f* mice). These mice have increased NE levels in the circulation and peripheral tissues. The CB1 deletion does not affect bone mass accrual determined by quantitative microcomputed tomography in the distal femoral metaphysis and vertebral bodies of young, 12-week old mice. By contrast, 35-week old *DBH-Cre/CB1f/f* mice have a marked high bone mass phenotype, representing a paradox based on previous reports that adrenergic signaling decreases bone formation and bone mass. Quantitative mRNA analysis in the same mice shows increased expression of β2 adrenergic receptor (β2AR) and monoacylglycerol lipase, the 2AG rate limiting enzyme. These findings suggest that chronic inactivation of sympathetic CB1 leads to disruption of the 2-AG-NE circuit with possible desensitization of osteoblastic β2AR and decreased 2AG levels with the consequent increase in bone mass. Thus, the emerging peripheralized CB1 antagonists may be useful for combating osteoporosis.

Disclosures: Saif Deis, None.

FR0211

Cyclooxygenase 2 deficiency impaired the bone regeneration capacity of muscle derived stem cells via cell autonomous and non-autonomous mechanisms. <u>Xueqin Gao</u>*[1], <u>Arvydas Usas</u>[1], <u>Aiping Lu</u>[1], <u>Ying Tang</u>[1], <u>Minakashi Poddar</u>[1], <u>Adam Kozemchak</u>[1], <u>James Cummins</u>[1], <u>Johnny Huard</u>[2]. [1]University of Pittsburgh, USA, [2]Orthopaedic Surgery, USA

Cycloxygenase-2 (COX-2) deficient mice have delayed and reduced bone fracture healing and we have observed that COX2 is expressed dynamically during muscle derived stem cell (MDSC) mediated bone healing. This study investigated the role that both donor and host COX-2 played in MDSC-mediated bone repair in a critical size calvarial defect model.

Experimental design: (1) Determine the role of host COX-2 in MDSC mediated bone healing. 5×10^5 BMP4/GFP transduced MDSCs were implanted into 5 mm critical size calvarial defects in COX-2KO and WT mice using fibrin sealant as a scaffold. Bone formation was monitored by μCT40 biweekly for 8 wks. (2) Determine the role of donor COX-2 in MDSC mediated bone healing. We isolated 3 populations of MDSCs from both WT and COX-2KO mice via the preplate technique. Cells were transduced with retro BMP4/GFP, implanted into skull defects created in CD-1 nude mice and bone formation was evaluated by μCT40 (biweekly), and Herovici's and GFP staining. (3) Determine the effect that donor cells have on host cells. 36 CD-1 nude mice were divided into WT MDSC/BMP4GFP and COX-2KOMDSC/BMP4/GFP groups. After implantation, mice were sacrificed at days 3, 7, and 14, and the skulls were harvested. Immunofluorescent staining for CD68, Gr-1, CD31, Ki67 was performed. Von Kossa staining was also performed at day 14. (4) In vitro pellet culture was used to determine the cells' osteogenic and chondrogenic capacities. (5) In vitro cells' oxidative stress resistance was determined using 250 and 400uM H_2O_2.

Results: (1) BMP4/GFP transduced MDSCs formed significantly less bone in COX-2KO mice than in WT mice. (2) COX2KO MDSCs/BMP4/GFP formed less bone in the CD-1 nude mice than WTMDSCs/BMP4/GFP. Histology showed less collagen type 1 and fewer GFP positive osteoblasts and osteocytes in the mice injected with COX2KO MDSC/BMP4GFP cells. (3) Fewer macrophages were recruited to the defect area by d3 and the resolution of inflammation was delayed in COX2KO MDSCs group; no effect was observed with Gr-1^{+} neutrophil infiltration or with CD31^{+} cell recruitment by d3 or d7. Fewer GFP^{+}Ki67^{+} cells were found in the COX-2KO MDSC group than the WT MDSC group. Von Kossa staining indicated less mineralized tissue formation in the COX-2KO MDSC group than the WT group. (4) COX2KO MDSCs formed smaller mineralized pellets as determined by μCT, Von Kossa and osteocalcin staining. COX-2KO MDSCs did not efficiently differentiate into chondrocytes compared to the WT MDSCs. (5) COX-2KO MDSCs showed decreased cell survival at both H_2O_2 concentrations compared to the WT MDSCs.

Conclusion: Our results indicate that both donor and host COX2 play important roles in MDSC mediated bone regeneration. The impaired bone regeneration capacity of COX2KO MDSCs was mediated, at least in part, to a poor cell proliferation and survival, reduction in osteogenic differentiation and the deleterious paracrine effect they had on host cells.

Disclosures: Xueqin Gao, None.

FR0212

Deletion of Rorβ, a Novel Regulator of Osteoblast Function, Slows Trabecular Bone Loss During Aging in Mice. <u>Qian Xing</u>[1], <u>Kristy Nicks</u>[1], <u>Joshua Farr</u>[1], <u>Daniel Fraser</u>[1], <u>Sundeep Khosla</u>[2], <u>David Monroe</u>*[3]. [1]Mayo Clinic, USA, [2]Mayo Clinic College of Medicine, USA, [3]Mayo Foundation, USA

The regulation of osteoblast differentiation requires the coordinate activities of numerous transcription factors. While factors such as Runx2 and osterix are essential, others act to fine-tune in response to external cues. One such factor is retinoic acid receptor-related orphan receptor beta (Rorβ). We have previously shown that Rorβ is as a negative regulator of osteoblast differentiation [*JBMR* 27(4):891-901, 2012] whose expression decreases throughout normal osteoblast differentiation. Sustained Rorβ expression inhibits mineralization and Rorβ also represses Runx2 transcriptional activity. Interestingly, Rorβ expression is highly elevated in bone marrow-derived osteoprogenitor cells during normal aging in mice and humans, suggesting that Rorβ may play a role during aging in bone. Collectively, these data suggest a model whereby Rorβ inhibits osteoblast differentiation through suppression of Runx2 activity in osteoprogenitors and that increased Rorβ expression has a negative impact on bone maintenance during aging. In order to test this hypothesis, we aged global Rorβ knockout (Rorβ^{-/-}) and wild-type littermate control mice and characterized both cortical and trabecular skeletal phenotypes at 6, 9 and 12 months using pQCT at the tibia. Trabecular vBMD at the tibial metaphysis was higher in Rorβ^{-/-} mice at 6 months (10.8%; p=0.042), 9 months (13.0%; p=0.044) and 12 months (15.8%; p=0.040). No change was observed in any cortical parameter. We also assessed bone microarchitecture following sacrifice (12 months) using μCt. As shown in the Figure, increased trabecular bone at the femoral metaphysis is evident in the Rorβ^{-/-} mice. A significant increase in BV/TV (20-fold; p=0.029) and trabecular number (44%; p=0.032), and a decrease in trabecular separation (-34%; p=0.0048) in the Rorβ^{-/-} mice was observed. Calculation of the structure model index (SMI), which estimates the plate-rod characteristics of the trabecular structure, demonstrated significantly more plate-like structures in the Rorβ^{-/-} mice (p=0.012). In summary, our data demonstrate the genetic loss of Rorβ in mice results in slowed trabecular bone loss during aging as compared to the bone loss in wild-type controls, in support of our hypothesis. These

data suggest that suppression of Rorβ activity during aging may represent a novel treatment for age-related bone loss.

Wild-type   Rorβ$^{-/-}$
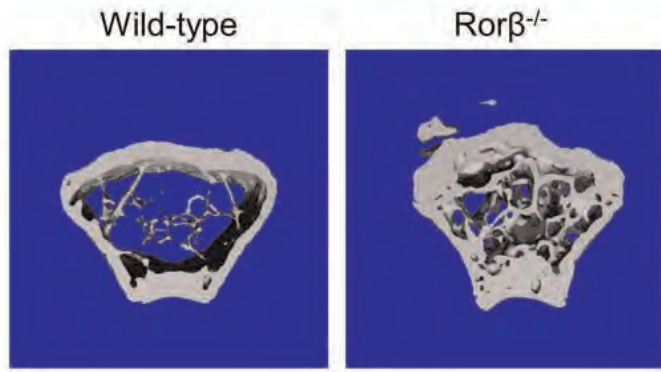
Figure

Disclosures: David Monroe, None.

FR0214

miR-874-3p expressed during weaning phase positively regulates skeletal mass and plays an important role in primary osteoporosis. <u>Priyanka Kushwaha</u>*[1], <u>Vikram Khedgikar</u>[2], <u>Jyoti Gautam</u>[2], <u>Anirudha Karvande</u>[2], <u>Nasser Ahmed</u>[2], <u>Deepika Mishra</u>[3], <u>Prabodh Kumar Trivedi</u>[3], <u>Ritu Trivedi</u>[2]. [1]Central Drug Research -CSIR, India, [2]CSIR-CDRI, India, [3]CSIR-NBRI, India

Emerging evidences indicates that microRNAs (miRNAs) have important role in regulation of osteoblast differentiation and bone formation. Thus far, no study has established the relationship between post-weaning phase of maternal skeletal metabolism with bone formation. Microarray profiling of bone marrow cells during lactation and post-weaning phase revealed that 8 microRNAs were hugelyand differentially regulated, out of which 5 miRNAs were up-regulated and 3 were down-regulated. These miRNAs were validated into primary osteoblast cells. Out of these the most promising miR-874-3p, is a well characterized tumor suppressive miRNA, whose expression was up-regulated during post-weaning and osteoblast mineraliza-tion stages. Identified miR-874-3p promoted osteoblast differentiation and miner-alization by repressing histone deacetylase-1 (HADC1) at post transcriptional level. Overexpression of miR-874-3p enhanced osteoblastogenesis whereas inhibition of miR-874-3p expression attenuated it. HADC1, an enhancer of Runt related transcription factor-2 (Runx2) degradation was confirmed by target validation. *In vivo* silencing of miR-874-3p led to decrease bone formation and reduced trabecular microarchitecture in sham and ovariectomized (OVx) mice. Our finding suggests that miR-874-3p is a potential miR and pharmacological inhibition of miR-874-3p reduced osteoblast mineralization, bone formation, trabecular bone and plays an important role in primary osteoporosis. miR-874-3p may provide potential therapeutic opportunity for treatment of primary osteoporosis.

Disclosures: Priyanka Kushwaha, None.

FR0217

***In Vivo* Maintenance of Cortical Bone Mass is Dependent on Estrogen Receptor Alpha Binding to Estrogen Response Elements in Mouse Osteoblasts.** <u>Kristy Nicks</u>*[1], <u>Daniel Fraser</u>[2], <u>Sundeep Khosla</u>[3], <u>David Monroe</u>[4]. [1]Mayo Clinic, USA, [2]Mayo Clinic, USA, [3]Mayo Clinic College of Medicine, USA, [4]Mayo Foundation, USA

Estrogen (E) is a key regulator of bone metabolism whose effects are primarily mediated by estrogen receptors (ER)-α and ERβ. ERs modulate transcription via either the "classical" pathway, which involves direct DNA binding to estrogen response elements (EREs) or the "non-classical" pathway, which is ERE-independent and acts through protein-protein interactions with other transcription factors. Our previous work demonstrated that mice expressing only an ERα that cannot bind EREs [non-classical ER knock-in (NERKI)] are osteopenic and have impaired bone formation associated with decreased osteoblast (OB) number. However, the interpretation of this data is potentially confounded by systemic hormonal changes (increased E and decreased IGF-1 levels) observed in the NERKI model that may have indirect effects on bone. To circumvent this issue, we selectively deleted ERα in OBs (ERα$^{\Delta OB}$) by crossing the osteocalcin (Oc)-Cre driver mouse with an ERα conditional allele (ERα$^{flox/flox}$). Throughout this study we used the Oc-Cre littermates as our normal control (denoted WT). In 3-month old ERα$^{\Delta OB}$ female mice, we observed a 9% decrease in total tibial bone mineral density (BMD) as measured by pQCT when compared to WT mice (P = 0.0001). To establish if ERE binding was necessary for recovery of this bone deficit, we determined whether transgenic re-expression of either WT ERα or NERKI in ERα$^{\Delta OB}$ mice improved BMD measurements. The deficit was not only prevented in ERα-replaced mice but was

increased by 16% (P < 0.0001), whereas the NERKI-replaced mice remained osteopenic (6% decrease), and had BMD measurements similar to ERα$^{\Delta OB}$ mice. These differences were associated with changes in cortical bone as there was a significant decrease in tibial cortical BMD in ERα$^{\Delta OB}$ mice compared to WT (P = 0.0015) that was prevented in ERα-replaced mice but not in NERKI-replaced mice. To ensure comparable transgenic ERα or NERKI expression, we isolated RNA from the femur diaphysis of all study mice and performed QPCR analyses using primers specific for the ERα or NERKI transgenes. No significant differences in expression levels of the transgenes were observed in either the ERα- or NERKI-replaced mice, demonstrating comparable ER replacement (WT or NERKI) in both groups. In summary, our data demonstrate that in osteoblasts, classical estrogen signaling is necessary for normal skeletal development in the cortical compartment.

Disclosures: Kristy Nicks, None.

FR0225

HDAC4 integrates PTH and sympathetic signaling in osteoblasts to regulate *Rankl* expression and osteoclasts differentiation. <u>Arnaud Obri</u>*, <u>Munevver Parla Makinistoglu</u>, <u>Gerard Karsenty</u>. Columbia University, USA

Both the parathyroid hormone (PTH) and the sympathetic nervous system can enhance *Rankl* expression in osteoblasts and thereby osteoclast differentiation by increasing cAMP production in these cells. PTH does so through yet unknown transcriptional mechanisms whereas the sympathetic tone recruits for that purpose the osteoblast enriched transcription factor ATF4 that binds to and trans-activate the *Rankl* promoter. These observations raise the following question: how two extracellular cues that use the same second messenger can elicit, in the same cell type, transcriptional events of different nature? We addressed this question through molecular means and the analysis of several osteoblast-specific mutant mouse strains lacking various transcription factors or chromatin remodeling enzymes. Our study shows that PTH signaling in osteoblasts favors *Rankl* expression because it triggers the polyubiquitination of HDAC4, a class II histone deacetylase in these cells. To achieve this function, PTH enhances the expression in osteoblasts of an E3 ubiquitin ligase that binds to HDAC4 only in the presence of PTH. This PTH-induced degradation of HDAC4 releases MEF2c that is now able to trans-activate the *Rankl* promoter following its binding to a MEF2 consensus binding site that is conserved in all vertebrate species analyzed. Unlike PTH, the sympathetic nervous system favors the accumulation of HDAC4 and promotes its association with ATF4 in osteoblasts. As a result of this association with HDAC4, ATF4 transcriptional activity is increased. We further show that, in vivo, the sympathetic tone disrupts the association that can occur in vitro between HDAC4 and Runx2 thus explaining why HDAC4 does not regulate Runx2 functions in osteoblasts as it does in chondrocytes. This study demonstrates that HDAC4 allows the integration, through different mechan-isms, of two distinct extracellular signals into the genome of the osteoblast; as a result it identifies *Hdac4* expression in osteoblasts as a major determinant of osteoclasts differentiation.

Disclosures: Arnaud Obri, None.

FR0226

Knockout of Nuclear HMWFGF2 Isoforms in Mice Modulates Bone and Phosphate Homeostasis. <u>Collin Homer-Bouthiette</u>*[1], <u>Marja Marie Hurley</u>[2], <u>Liping Xiao</u>[1]. [1]University of Connecticut Health Center, USA, [2]University of Connecticut Health Center School of Medicine, USA

Targeted overexpression of the Fibroblast Growth Factor 2 (FGF2) high molecular weight (HMW) isoforms in osteoblastic lineage cells in mice resulted in phenotypic changes, including dwarfism, rickets, osteomalacia, hypophosphatemia, increased serum PTH and increased levels of FGF23, in serum and bone. The current study examined the effects of genetically knocking out the HMWFGF2 isoforms (HMWKO) on bone and phosphate homeostasis in relation to wild type (WT) littermate mice as well as previously examined HMWTg mice versus Vector control. Two-month old male HMWKO mice were not dwarfed and had significantly increased bone mineral density (BMD) and bone mineral content (BMC) in femurs and lumbar vertebrae when compared to WT. Micro-CT and histomorphometry analysis of femurs revealed increased trabecular and cortical bone metrics consistent with improved bone mineralization. In vitro osteogenic bone marrow stromal cell cultures showed a significant increase in alkaline phosphatase positive colony number at 1 week and increased mineralization at week 3 in HMWKO. To assess the mechanism (s) for the observed bone phenotype in HMWKO, mRNA for genes important in osteoblast differentiation and matrix mineralization were determined in flushed tibiae of WT and HMWKO mice. In contrast to our published data in HMWTg in which type 1 collagen (Col1a1) was decreased, we observed increased Col1a1 in the HMWKO. In HMWKO, the mRNA for matrix-gla protein (Mgp) and matrix extracelluar phosphoglycoprotein (Mepe), negative regulators of matrix mineralization, were similar to WT in contrast to the profound increase observed in bones of HMWTg. Sclerostin (SOST), which regulates multiple downstream signaling pathways, was up regulated in bones of HMWTg, however, Sost mRNA was significantly decreased in the HMWKO. SOST can inhibit canonical Wnt signaling via binding of LRPs resulting in decreased osteoblast differentiation. SOST can also increase MEPE activity, which inhibits Phex activation of DMP1 thereby decreasing bone mineralization. Thus decreased Sost could contribute to the increased bone mass observed in HMWKO mice. We previously reported that increased FGF23 caused Pi

wasting via the bone/kidney axis in the HMWTg mice. In contrast, FGF23 mRNA was significantly decreased in HMWKO, which could contribute to normal serum Pi in HMWKO mice. This novel study demonstrates a significant negative impact of HMWFGF2 on biological functions in bone and phosphate homeostasis in mice.

Disclosures: Collin Homer-Bouthiette, None.

FR0229

Regulation of Bone Mass by Lrp4 and Secreted Wnt Antagonists.
Youngwook Ahn*[1], Jesús Fuentes-Antrás[1], Mark Dallas[2], Mark Johnson[3], Robb Krumlauf[1]. [1]Stowers Institute for Medical Research, USA, [2]University of Missouri, Kansas City Dental School, USA, [3]University of Missouri, Kansas City Dental School, USA

The Wnt/β-catenin signaling pathway plays a key role in bone mass acquisition and maintenance. The Wnt antagonists, sclerostin and Dkk1, control postnatal bone formation and resorption via their inhibitory interaction with Wnt co-receptors, Lrp5 and Lrp6. Lrp4 is related to Lrp5/6 and has emerged as a potential regulator of bone mass based on mutations identified in mice and humans and recent genetic association studies in humans. It has been reported that Lrp4 interacts with the Wnt antagonists *in vitro* and modulates Wnt/β-catenin signaling during limb and skin appendage development. In our study, we investigated the role for Lrp4 in bone growth using loss- and gain-of-function mouse models to explore underlying mechanisms of Lrp4 function with respect to its interaction with the Wnt co-receptors and antagonists. We generated transgenic reporter lines using a BAC clone covering the *Lrp4* genomic region and observed reporter expression mainly in osteoblast lineages in postnatal bone. MicroCT analyses of adult bones revealed changes in microstructure and bone mass including increased cortical thickness and decreased trabecular BV/TV in *Lrp4* deficient mice. Conversely, over-expression of *Lrp4* in osteoblast lineages lead to bone defects including rib fracture. Genetic interaction analysis suggests that Lrp4 is required for sclerostin to exert its function, but not for Dkk1 during limb patterning and bone growth. This observation was validated by *in vitro* reporter assays which support a synergy between Lrp4 and sclerostin in inhibition of Wnt/β-catenin signaling. We propose that Lrp4 plays a critical role in regulation of bone growth and homeostasis in part by mediating Wnt inhibitory function of sclerostin. Given the emerging role of sclerostin antibodies as an anabolic therapy for treating osteoporosis and facilitating fracture healing, we suggest that Lrp4 is a similar target for future therapy development.

Disclosures: Youngwook Ahn, None.

FR0233

Unique Distal Enhancers Linked to the Mouse *Tnfsf11* Gene Direct Tissue-Specific Expression and Inflammation induced Regulation of RANKL Expression.
Melda Onal*[1], Hillary St John[2], Allison Danielson[3], Charles O'Brien[4], J. Pike[1]. [1]university of wisconsin, USA, [2]University of Wisconsin-Madison, USA, [3]undergraduate student, USA, [4]Central Arkansas VA Healthcare System, Univ of Arkansas for Medical Sciences, USA

RANKL is a multifunctional TNF-like cytokine with diverse roles in organ development, immune function, and skeletal remodeling. The expression of this factor from its *Tnfsf11* gene locus is cell-specific and regulated by an array of local and systemic factors. Earlier studies indicate that these features of RANKL expression are mediated by a complex series of enhancers located up to 155 kb upstream of the gene's transcriptional start site. Several of these enhancers favor RANKL expression in mesenchymal lineage cells; others direct expression in immune cells. The impact of one upstream enhancer, termed D5 (DCR), has been explored through genomic deletion in mice (D5KO), confirming its importance in RANKL expression and in skeletal remodeling. Interestingly; however, several *Tnfsf11* enhancers located further upstream display unique cell type-specific and regulatory properties *in vitro*. To explore these control regions further, we prepared several additional *in vivo* murine enhancer deletion models and examined the consequence of these deletions as well as that of D5 on RANKL expression, regulation, and skeletal phenotype. The D5KO mouse manifests reduced RANKL expression and regulation by 1,25(OH)$_2$D$_3$, PTH and OSM in bone cells, and exhibits an age-exaggerated increase in BMD. In the D6KO mouse, however, basal RANKL expression was unaltered in bone cells and BMD levels were normal. Despite this, while RANKL induction by 1,25(OH)$_2$D$_3$ was retained, both *in vivo* and *ex vivo* responses to OSM and inflammatory LPS were lost. These observations are consistent with D6-mediated RANKL stimulation by cytokines in bone cells *in vitro*. Finally, while the T1KO mouse also manifested normal basal RANKL expression at skeletal sites and unaltered BMD, basal RANKL expression was strikingly reduced by 80% in the spleen, thymus and lung of growing and adult mice. This decrease was also identified in isolated B and T cells suggesting that RANKL expression is dependent upon the T1 enhancer early in the hematopoietic lineage. *Ex vivo* studies confirmed that RANKL expression in response to T cell activation was also blunted. Interestingly, this depletion of RANKL in immune tissue was also observed modestly in the D5KO as well. These murine models demonstrate that individual *Tnfsf11* enhancers exhibit unique capabilities relative to cell type-specific RANKL expression and regulation, and will be valuable in assessing the contribution of unique cell types to inflammatory bone loss.

Disclosures: Melda Onal, None.

FR0234

***Cfβ* promotes osteoblast lineage commitment and regulates the fate of mesenchymal stem cells by suppressing the expression of key adipocyte regulators and activating Wntl/β-catenin pathway** in vivo *and* in vitro.*
Mengrui Wu*[1], Wei Chen[2], Yi-Ping Li[2]. [1]The University of Alabama at Birmingham, USA, [2]University of Alabama at Birmingham, USA

How osteoblast (OB) lineage commitment is achieved is a fundamental question in bone biology. Despite recent insights gained from the effects of targeted deletion of OB regulator genes, the mechanism of OB lineage commitment from mesenchymal stem cells (MSCs) remains unclear. Core-binding factor, beta (Cfβ) plays an important role in skeletal development. However, the role of Cfβ in MSC lineage determination has not been clarified yet. To determine its role, we generated *Cfβ* conditional knockout mice using skeletal lineage-specific Cre-loxP systems. Oil red O staining showed that *Cfβ$^{f/f}$Prx1-Cre*, *Cfβ$^{f/f}$Col2α1-Cre*, and *Cfβ$^{f/f}$Osx-Cre* mice, but not *Cfβ$^{f/f}$Col1α1-Cre* mice, have dramatically decreased bone density and a pronounced accumulation of bone marrow adipocytes, which resembles osteoporosis in aging humans. Our findings indicate that the regulation of Cfβ in OB lineage commitment is cell lineage-specific. Calvarial cells derived from *Cfβ$^{f/f}$Osx-Cre* mice maintained strong adipogenic tendencies despite being cultured in osteogenic medium. qPCR and Western blot data demonstrated that compared to wild-type (WT) OBs, *Cfβ$^{f/f}$Osx-Cre* and *Cfβ$^{f/f}$Prx1-Cre* OBs highly expressed adipocyte regulator genes and marker genes (*e.g. Clebpα, PPARγ, FABP4*). Using chromosome immonoprecipitation (ChIP) analysis, we determined that Cfβ binds to both *Clebpα* and *PPARγ* promoters at the Cfβ/Runx binding sites near their transcription start sites. Promoter analysis data showed that Cfβ and Runx2 co-transfection, but not Cfβ alone, highly inhibited *Clebpα* promoter activity, indicating that inhibition functioned through the Cfβ/Runx2 complex. We also wondered how Cfβ promotes OB lineage commitment. Our data showed that although *β-catenin* mRNA expression was similar between WT and *Cfβ$^{f/f}$Osx-Cre* cells, non-phosphorylated (active form) β-catenin protein was dramatically increased, and β-catenin cell nucleus translocation was also increased in *Cfβ$^{f/f}$Osx-Cre* cells, indicating that Cfβ may promote MSC lineage commitment through Wnt/β-catenin signaling. In summary, we demonstrated that Cfβ regulates MSC differentiation toward osteoblastogenesis by inhibiting both *C/ebpα* and *PPARγ* expression at the transcriptional level and by activating Wnt/β-catenin signaling. Our study indicates that Cfβ regulates MSC lineage determination and can be a new therapeutic target of aging-related bone diseases (*e.g.* human age-related osteoporosis).

Disclosures: Mengrui Wu, None.

FR0235

Bone lining cells are a major source of osteoblasts during bone remodeling.
igor Matic*[1], Brya Matthews[2], Ivo Kalajzic[2]. [1]University of Connecticut Health Center, USA, [2]University of Connecticut Health Center, USA

During development osteoblasts are derived from multipotent mesenchymal stem cells. Similarly, during bone remodeling mesenchymal progenitor cells from bone marrow are thought to provide a continuous supply of mature osteoblasts. Osteoblasts can undergo apoptosis, or differentiate into osteocytes or quiescent bone lining cells (BLC). Activation of BLCs has been recently identified as a source of osteoblasts following intermittent PTH administration. The aim of this study was to determine if BLCs serve as a source of active osteoblasts during bone remodeling.

To selectively identify BLCs we utilized a transgenic approach in which osteoblasts and a subset of osteocytes are labeled using 10kb-Dmp1-CreERt2/Ai9 (DMP-Ai9) mice following tamoxifen treatment (Cre directed Tomato expression). Cell fate was determined histologically at time points where osteoblasts would be expected to either undergo apoptosis or differentiation.

By 40 days after labeling, matrix producing osteoblasts were still labeled, suggesting continuous activation of BLCs and supporting the idea that they could be a source of mature osteoblasts. To eliminate the possibility that osteoblasts lifespan is much longer than expected we selectively eliminated osteoblasts using a Col2.3?TK suicide gene. We introduced the Col2.3ΔTK into DMP-Ai9 mice to ablate preosteoblasts/osteoblasts while retaining BLCs. Following ganciclovir treatment, cuboidal osteoblasts were absent, while flat BLCs were labeled. Following 21 days of recovery, new osteoblasts form, and new areas of active bone surface are covered by DMP-Ai9 expressing osteoblasts. EdU staining demonstrated DNA synthesis in some of these labeled cells, suggesting their ability to divide. Bone marrow derived stromal cells do not generate DMP-Ai9 labeled bone nodules confirming that DMP1 is not expressed in marrow progenitors. To evaluate the contribution of BLCs in fracture healing, we injected DMP-Ai9 mice with tamoxifen 40 days before fracture. 14 days post-fracture we did not observe contribution of labeled cells to the fracture callus.

Our results define the bone lining cells as a source of proliferating and mature osteoblasts during bone remodeling, but not during fracture healing.

Disclosures: igor Matic, None.

FR0236

Chondrocytes Are a Major Source of Osteoblasts in Endochondral Bones *in Vivo*. Xin Zhou*[1], Stephen Henry[2], Benoit de Crombrugghe[3], Klaus von der mark[4], Henry adams[5]. [1]MD Anderson Cancer Center, USA, [2]University of Texas MD Anderson, USA, [3]UT MD Andrson cancer center, USA, [4]University of Erlangen-Nuremberg, Germany, [5]UT MD Anderson, USA

One of the crucial steps in endochondral bone formation is the replacement of a cartilage matrix produced by chondrocytes with bone trabeculae made by osteoblasts. However, the precise sources of osteoblasts responsible for trabecular bone formation have not been fully defined. To investigate whether cells derived from hypertrophic chondrocytes contribute to the osteoblast pool in trabecular bones, we genetically labeled either hypertrophic chondrocytes by *Col10a1-Cre* or chondrocytes by tamoxifen-induced *Agc1-CreERT2* using either *EGFP*, or *LacZ or Tomato* expression. Both Cre drivers were specifically active in chondrocytic cells not in perichondrium, in periosteum and in any of the osteoblast lineage cells. These *in vivo* experiments allowed us to follow the fate of cells labeled in *Col10a1* or *Agc1*-expressing chondrocytes. After the labeling of chondrocytes, abundant non-chondrocytic labeled cells were present in the primary spongiosa from the onset of primary ossification to after birth. These cells were distributed throughout trabeculae surfaces and after birth were present in the endosteum, and embedded within the bone matrix. Co-expression studies using osteoblast markers indicated that a proportion of the non-chondrocytic cells derived from chondrocytes labeled by *Col10a1-Cre* or by *Agc1-CreERT2* were functional osteoblasts. Our results thus indicate that *Col10a1* or *Agc1*-expressing chondrocytes have the capacity to undergo transdifferentiation to become osteoblasts. The osteoblasts derived from *Col10a1*-expressing hypertrophic chondrocytes represent about sixty percent of all mature osteoblasts in endochondral bones of one month old mice. In addition to cells in the periosteum, *Col10a1* and *Agc1*-expressing chondrocytes represent another major source of osteoblasts contributing to endochondral bone formation *in vivo*.

Disclosures: Xin Zhou, None.

FR0237

EP1 Deletion Enhances Mitochondrial Activity in Mesenchymal Stem Cell and Promotes Osteogenicity. Marina Feigenson*[1], Jennifer Jonason[2], Alayna Loiselle[2], Roman Eliseev[2], Regis O'Keefe[2]. [1], USA, [2]UNIVERSITY OF ROCHESTER, USA

Prostaglandin E2 (PGE2) is an important regulator of bone metabolism and is essential for bone regeneration. The function of the PGE2 receptor, EP1, in bone, however, is not well understood. We have recently demonstrated that *EP1*^{-/-} mice have enhanced fracture repair due to accelerated MSC osteoblastic differentiation, identifying EP1 as a negative regulator of bone formation. In the present study we sought to determine the cellular mechanisms through which loss of EP1 exerts a bone anabolic effect in mesenchymal stem cells (MSCs). Emerging evidence has identified mitochondrial function as a key factor in stem cell fate, while the loss of CD105 is associated with more committed stem cell populations. We tested the overall hypothesis that EP1 suppresses MSC osteoblastic differentiation and bone formation by inhibiting mitochondrial activity and increasing the population of CD105⁻ cells suggestive of more differentiated MSCs. Bone Marrow MSCs were isolated from wild type (WT) and *EP1*^{-/-} mice; the progenitor cell populations were assessed by flow cytometry and colony forming unit (CFU) assays, while mitochondrial activity was measured using the XF24 analyzer, and mitochondrial numbers and structure determined by electron microscopy.

EP1^{-/-} MSCs exhibited an increased CFU-F and CFU-O (8 and 10 times increase, respectively) and a 10 times increase in the CD45⁻CD31⁻Sca1⁺CD105⁻ population relative to WT controls (Figure 1). Additionally, *EP1*^{-/-} MSCs exhibited enhanced osteoblastic differentiation, supporting the concept of EP1 as negative regulator of bone formation. Also, we observed higher levels of mitochondrial activity as measured by levels of basal (6 times increase) and ATP-linked respiration (7 times increase) relative to WT controls (Figure 2). Electron microscopy showed *EP1*^{-/-} MSCs have mitochondria with more developed cristae. Moreover, blocking the oxidative phosphorylation inhibited the enhanced osteoblastic differentiation of *EP1*^{-/-} cells.

Taken together, these data identify PGE2/EP1 signaling as a negative regulator of bone formation, and suggest that EP1 maintains MSCs in an undifferentiated state by inhibiting the switch to oxidative phosphorylation. Conversely, loss of EP1 enhances mitochondrial activity, leading to more rapid osteoblastic differentiation and bone formation. These studies identify EP1 as a novel target to enhance bone regeneration, and suggest EP1 antagonism as a potential therapeutic mechanism.

Figure 1: EP1^{-/-} Bone marrow cells form more colonies (A) and have increased population of the C45⁻CD31⁻Sca1⁺CD105⁻ cells (B).

Figure 1

Figure 2: EP1^{-/-} bone marrow cells exhibit higher Oxygen Consumption Rate.
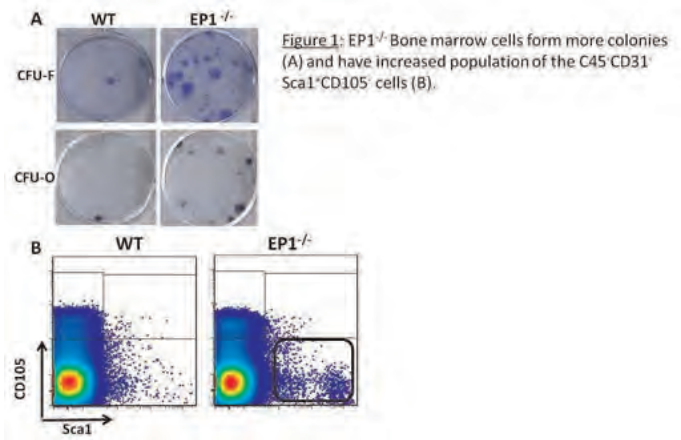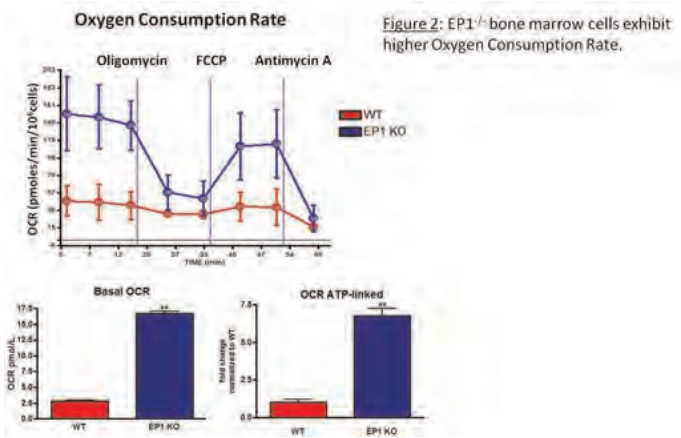
Figure 2

Disclosures: Marina Feigenson, None.

FR0238

ER Stress Signaling Molecule IRE1α Regulates Bone Develpment and Confers Genetic Risk for Human Osteoporosis. Shankar Revu*[1], Kai Liu[2], Fengming Wang[1], Konstantinos Verdelis[1], Mariana Bezamat[1], Alexandre Vieira[1], Hong-Jiao Ouyang[3]. [1]University of Pittsburgh, USA, [2], USA, [3]University of Pittsburgh, USA

The inositol-requiring enzyme 1α (IRE1α)/ X-box binding protein 1s (XBP1s) pathway is an evolutionarily conserved endoplasmic reticulum (ER) stress signaling and implicated in numerous physiological and pathological processes, such as the development of secretory organs and pathogenesis of inflammatory bowl disease, respectively. Upon ER stress, IRE1α acts through its endoribonuclease activity to generate spliced Xbp1 (Xbp1s) to maintain intracellular protein homeostasis. Osteoblasts are professional secretory cells. However, it remains essentially unknown whether IRE1α is required for bone development and homeostasis. To address this question, we performed a serial of functional and genetic studies as following. First, we, via immunohistochemical stains, observed that both IRE1α and XBP1 were highly expressed in osteoblastic cells of the developing bones. Further, it was observed that the endoribonuclease activity of IRE1α, as reflected by the ratio of Xbp1s vs. total Xbp1 (Xbp1t) mRNA, increased in bone tissues from post-natal day 14 to day 90. Moreover, ascorbic acid stimulated the gene expression of Sec61α, a XBP1s transcription target in osteoblastic MC3T3E1 cells. These results suggest that activation of IRE1α/XBP1s signaling is a physiological event intrinsic to osteoblast differentiation and bone development. Second, we generated mice lacking osteoblast-specific Ire1α (CKO) and their wild type littermates (WT) by breeding the Ire1αFlox/Flox mice with Osterix-Cre mice. It was observed that the Ire1α CKO mice exhibited reduced bone mass and increased marrow fat compared with the WT littermates, as shown by micro-qCT and histological analysis. Further, the CKO mice displayed reduced cell proliferation and dynamic bone formation of axial bones, as shown by calcein double labeling and BrdU immunostaining, respectively. These results demonstrate that the osteoblastic IRE1α is an important regulator for osteoblasto-genesis and bone marrow fat metabolism in vivo. Third, we performed association studies to detect over-representation of alleles in cases of human osteoporosis using common single nucleotide polymorphism (SNP) variants of IRE1α and XBP1s, and detected association between osteoporosis and IRE1 rs11655020 (p=5.0E-5) and XBP1 rs2097461 (p=0.004). Taken together, these findings, for the first time,

demonstrate that IRE1α is an essential regulator for bone development and a novel genetic risk factor for human osteoporosis.

Disclosures: Shankar Revu, None.

FR0241

Circulating Microvesicles from Elderly Donors impact on Osteogenic Differentiation of Mesenchymal Stem Cells. <u>Sylvia Weilner</u>[1], <u>Elisabeth Schraml</u>[1], <u>Matthias Wieser</u>[2], <u>Paul Messner</u>[3], <u>Andrea Maier</u>[4], <u>Heinz Redl</u>[5], <u>Peter Pietschmann</u>[6], <u>Matthias Hackl</u>[7], <u>Regina Grillari-Voglauer</u>[2], <u>Johannes Grillari</u>*[8]. [1]Department of Biotechnology, University of Natural Resources & Life Sciences Vienna, Austria, [2]Evercyte GmbH, Austria, [3]Department of Nanobiotechnology, University of Natural Resources & Life Sciences Vienna, Austria, [4]Department of Gerontology & Geriatrics, Leiden University Medical Center, Leiden, Austria, [5]Ludwig Boltzmann Institute for Experimental & Clinical Traumatology, AUVA Research Center, Austria, [6]Department of Pathophysiology & Allergy Research, Medical University of Vienna, Austria, [7]TAmiRNA GmbH, Austria, [8]University of Natural Resources & Life Sciences Vienna, Austria

Aging is a complex process that results in the decline of physiologic functions due to accumulation of damage in cells and tissues as well as in reduced repair capacities. The regenerative power of stem and progenitor cells has been found to decline with age and to be influenced by the systemic environment. In particular osteogenic differentiation capacity of mesenchymal stem cells (MSCs) has been shown to decrease with age thereby contributing to slowed down bone formation that might contribute to osteopenia or osteoporosis. Here, we set out to identify circulating factors of the aged systemic environment that influence the functionality of adult stem cells.

In order to identify such factors, serum of young versus elderly healthy individuals was tested for miRNAs and proteins. Indeed, we found miR-31 to be higher in elderly donors. As possible source we identified senescent endothelial cells that secrete miR-31 also in vitro, packaged into exosomes. Functionally characterizing miR-31 containing exosomes revealed that both, exosomes of senescent cells as well as exosomes of elderly donors, deliver miR-31 to mesenchymal stem cells and inhibit osteogenic differentiation. The effect of the vesicles can be rescued by antagonistic miR-31. One of the novel targets of miR-31 in this context is the Wnt ligand FZD3 whose knock-down leads to a similar inhibition of osteogenic differentiation as miR-31. In addition, we found that one microvesicular protein, Galectin 3 (Gal-3), that supports osteogenic differentiation is significantly decreased in the serum of elderly donors. Therefore, we postulate here that circulating microvesicles and their content might represent biomarkers and therapeutic targets whenever osteogenesis is a limiting factor, especially in age-related diseases like osteoporosis.
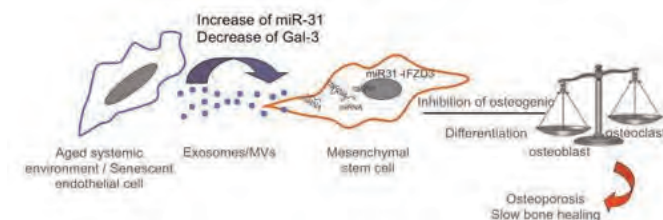
Figure 1

Disclosures: Johannes Grillari, Evercyte GmbH, 4

FR0245

iPS cell derived Endothelial Cells in Fibrodysplasia Ossificans Progressiva. <u>Emilie Barruet</u>*[1], <u>Wint Lwin</u>[2], <u>Marcela Morales</u>[2], <u>Ashley Urrutia</u>[2], <u>Hannah Kim</u>[2], <u>Christina Theodoris</u>[3], <u>Mark P. White</u>[4], <u>Deepak Srivastava</u>[5], <u>Edward Hsiao</u>[1]. [1]University of California, San Francisco, USA, [2]University of California, San Francisco, USA, [3]Gladstone Institute of Cardiovascular Disease, USA, [4]Gladstone Institute of Cardiovascular Disease, San Francisco, CA, USA, [5]Gladstone Institutes, USA

Musculoskeletal disorders affecting the bones and joints are major health problems for children and adults. Unfortunately, treatments for skeletal diseases are still rudimentary. The recent advent of human induced pluripotent stem cells (hiPSCs) provides an unparalleled opportunity to create human-specific models of human skeletal diseases. Patients with mutations in the Activin A Type I receptor (ACVR1), a BMP (bone morphogenetic proteins) receptor, develop the debilitating disease fibrodysplasia ossificans progressiva (FOP) showing progressive ossification of muscle and tendon. The majority of ACVR1 mutations occur in a single amino acid (R206H) that may increase ACVR1 signaling activity. Recent data suggest that human endothelial cells (ECs) carrying the ACVR1 R206H mutation may contribute to the formation of FOP lesions. Our overall hypothesis is that activated BMP signaling caused by the ACVR1 R206H mutation in ECs increases heterotopic bone

formation by increasing osteogenesis. In this study, we use a series of human iPSCs created from control and FOP donors to create iPS cell derived endothelial progenitor cells (iECs) as primary ECs cannot be isolated from FOP patients. CD31^{+}/KDR^{+} iECs formed at equal yields of 25% from both control and FOP iPS lines. FACS analysis of these CD31^{+}/KDR^{+} iECs showed that 95% of the cells expressed CD31^{+}/CD144^{+}, two markers found on mature ECs. We also found that FOP iPSCs could form iECs at lower BMP4 concentrations compared to control iPSCs, even in conditions lacking BMP4 (1% FOP vs 0.1% WT yield). Surprisingly, FOP endothelial cells showed little difference in mineralization using a 2D assay. However, a 3D protocol that recapitulates the endochondral bone formation through chondrogenic steps indicates that FOP iECs can form abundant chondrocytes by alcian blue staining. Here we show that FOP endothelial cells can have chondrogenic/osteogenic potential which may be critical for heterotopic ossification in FOP patients. These studies demonstrate the use of human iPSCs as a source for creating specific cell types to study their roles in human skeletal formation and diseases. The cellular mechanistic insights gained from these studies establish a foundation for understanding how endothelial cells contribute to heterotopic ossification and identifying new therapies not only for FOP but also other diseases of abnormal skeletal formation.

Disclosures: Emilie Barruet, None.

FR0246

Neural Origin of Osteoblasts during Heterotopic Ossification. <u>ZaWaunyka Lazard</u>*[1], <u>Elizabeth Salisbury</u>[1], <u>Eric Beal II</u>[2], <u>Elizabeth Olmsted-Davis</u>[1], <u>Alan Davis</u>[1]. [1]Baylor College of Medicine, USA, [2]Baylor College of Medicine, USA

Heterotopic ossification (HO) is a disease in which *de novo* bone formation occurs in non-skeletal tissues. Although the clinical etiology of HO is unclear, it often follows traumatic injury to skeletal bone and/or soft tissues associated or the nervous system. Recently, our laboratory demonstrated immediate structural changes to the local peripheral nerves, as well as both sensory and sympathetic signaling, within 48 hours of inducing HO through localized delivery of BMP2. Here we identify and characterize a unique cell population within the endoneurial compartment of peripheral nerves that replicates, migrates and undergoes osteogenic differentiation in response to the BMP2. Immediately upon delivery of BMP2, cells within the endoneurium start to express osterix protein. By 48 hours after delivery these cells are now observed outside the nerve, co-expressing claudin 5, a tight junctional protein on endothelial cells shown to be involved in regulating the "blood nerve barrier". In the presence of BMP2, these cells start to express the replication marker ki-67. Quantification of the claudin 5^{+} cells on day 0, 2, and 4, using fluorescence activated cell sorting (FACs) shows a significant increase in the number positive cells at 2 and 4 days after induction of HO. Isolation of these claudin 5 positive and negative populations confirmed expression of osterix[+] as well as dlx5[+] were found only in the positive population. Both markers are associated with osteogenesis in neural stem cell migration in the embryo. Interestingly, they also express the neural stem cell factor musashi, which is also associated with migrating neural crest stem cells. Immunohistochemical analysis of slides generated during each day of the HO process, suggests that these claudin 5^{+} cells maybe extravasating out of the nerve, through newly formed vasculature, to be later deposited between the muscle fibers, where they eventually form osteoblasts associated with the new bone. These cells also co-express PDGFRα, a key regulatory factor associated with glial cells and previously reported to be on the osteogenic stem cell for HO. The data collectively suggests that endoneurial compartment of peripheral nerves may house a unique stem-progenitor, that can rapidly expand and undergo osteogenesis during heterotopic bone formation.

Disclosures: ZaWaunyka Lazard, None.

FR0251

Choline Kinase Beta is an Important Regulator of Bone Homeostasis. <u>Jennifer Tickner</u>*[1], <u>Jasreen Kular</u>[2], <u>Nathan Pavlos</u>[3], <u>Tamara Abel</u>[4], <u>BaySie Lim</u>[5], <u>Ming Hao Zheng</u>[3], <u>Jiake Xu</u>[6]. [1]University of Western Australia, Australia, [2]University of Western Australia, Australia, [3]University of Western Australia, Australia, [4]Centre for Microscopy, Characterisation & Analysis, University of Western Australia, Australia, [5]University of Western Australia, Australia, [6]University of Western Australia, Australia

The maintenance of bone homeostasis requires tight coupling between the bone-forming osteoblasts and bone-resorbing osteoclasts. However, the precise molecular mechanism(s) underlying the activities of these specialized cells are still largely unknown. In search of novel molecules involved in bone homeostasis, we systematically screened a number of ENU-induced mutant mouse lines. Here we identify choline kinase beta (CHKB), a kinase involved in the biosynthesis of phosphatidylcholine, as a regulator of adult bone homeostasis. Choline kinase beta mutant mice (flp/flp) exhibit a systemic low bone mass phenotype comparable to osteoporosis. Consistently, osteoclast numbers and activity are elevated in flp/flp mice. Interestingly, although the area resorbed by flp/flp osteoclasts is not significantly different, pits are deeper, leading to increased CTX release in flp/flp cultures. Osteoclasts derived from flp/flp mice exhibit reduced sensitivity to excessive levels of extracellular calcium, a feature that allows them to persist at sites of bone resorption. We also demonstrated that, in addition to modulating osteoclast formation and function, a loss of CHKB also corresponds with a reduction in bone formation by

osteoblasts.1H-NMR spectroscopy revealed significant reductions in phosphocholine levels, the product of the choline kinase enzymatic reaction, in both osteoclasts and osteoblasts. Furthermore, levels of phosphatidylcholine, a major membrane phospholipid derived from phosphocholine were also reduced. Phosphocholine is an essential source of phosphate for biomineralisation by osteoblasts, we showed that osteoblasts from flp/flp mice had reduced phosphate release from matrix vesicles, consistent with their reduced phosphocholine levels. Supplementation of flp/flp mice with CDP-choline (Cytidine 5'-diphosphocholine) both *in vivo* and *in vitro*, a regimen which bypasses CHKB deficiency downstream of phosphocholine, restores osteoclast numbers to physiological levels, but does not restore osteoblast function. Taken together, these data posit CHKB as a new modulator of bone homeostasis through effects on both osteoclasts and osteoblasts.

Disclosures: Jennifer Tickner, None.

FR0252

Genetic Activation of *Nlrp3* Reveals NLRP3 Inflammasome Role in Osteoclast Activity. <u>Chao Qu*[1]</u>, <u>Samer Abu-Amer</u>[2], <u>Sheri Bonar</u>[3], <u>Jacqueline Kading</u>[4], <u>Yousef Abu-Amer</u>[5], <u>Roberto Civitelli</u>[5], <u>Gabriel Mbalaviele</u>[5]. [1]Washington University in St Louis, USA, [2]Washington University in St. Louis, USA, [3]Washington University in St. Louis, USA, [4]Washington University in St Louis, USA, [5]Washington University in St. Louis School of Medicine, USA

Autosomal-activating mutations in *NLRP3* cause excessive maturation of IL-1β by the NLRP3 inflammasome, ultimately promoting systemic inflammation and bone resorption in humans. Yet, skeletal anomalies in these patients continue to worsen even under treatment with IL-1β inhibitors, while other symptoms related to systemic inflammation are resolved, suggesting alternative mechanisms of inflammasome actions in the skeleton. To gain insights into the skeletal complications caused by hyper-active NLRP3, we engineered a *floxed-Nlrp3* allele for conditional activation of the NLRP3 inflammasome. We find that myeloid activation of this inflammasome by *LysM-Cre* causes approximately 60% lower bone mass associated with severe inflammation. However, mice with osteoclast (OC)-restricted inflammasome activation by *CatK-Cre* (CreK mice) are osteopenic (approximately 50% reduction relative to control mice) in the absence of inflammation. Serum CTX-1 levels are higher in *CreK* mice relative to wild-type (WT) mice (72.77±20.15 ng/ml vs. 42.93±9.52 ng/ml), but there is no difference in OC number on bone surfaces between the two genotypes. These results suggest increased cell autonomous OC activity in mutant mice, and strengthen the emerging concept that the NLRP3 inflammasome has cytokine-autonomous functions. *In vitro,* the number of OC forming from *CreK* and WT bone marrow macrophages treated with RANKL and M-CSF is comparable between both genotypes, findings consistent with *in vivo* results. In contrast, *CreK* OC display larger F-actin rings, and form larger resorption lacunae than WT OC (5236±502 μm² vs. 2623±725 μm², p<0.001), despite comparable number on bone slices, results corroborated by higher release of CTX-1 by mutant cells relative to WT cells (16.55±5.17 nM vs. 6.66±7.28 nM, p<0.05). Immunofluorescence show a punctuate patterns of NLRP3 expression in WT and mutant cells, reminiscent of active inflammasome, and indicative of active NLRP3 inflammasome even in WT OC. Thus, we have uncovered a novel mechanism whereby the NLRP3 inflammasome regulates OC activity in a cell autonomous manner independently of the inflammatory process.

Disclosures: Chao Qu, None.

FR0253

Osteoclast ruffled border formation and bone resorption require Plekhm1-regulated lysosomal secretion. <u>Toshifumi Fujiwara*[1]</u>, <u>Jian Zhou</u>[2], <u>Shiqiao Ye</u>[1], <u>Stavros Manolagas</u>[1], <u>Haibo Zhao</u>[1]. [1]Central Arkansas VA Healthcare System, Univ of Arkansas for Medical Sciences, USA, [2]UAMS, USA

Osteoclasts (OCs) resorb the mineralized bone matrix by secreting protons and cathepsin K (CTSK) through the ruffled border (RB) which is circumscribed by the sealing zone (actin-ring). While the mechanisms of how RANKL and integrin signaling activate actin-ring formation through c-Src have been well defined, it is unknown whether and how RANKL and integrins promote the secretory function of OCs. Genetic studies in humans and rodents with osteopetrosis have uncovered a central role of lysosomal pathways in OC function. However, it has remained unclear whether RB formation requires de novo biogenesis of lysosomes and/or their secretion. Plekhm1 (PLK1) is a lysosome-associated protein the mutations of which lead to osteopetrosis in humans and rats. Because of earlier evidence that PLK1 is indispensable for CTSK secretion, we studied here the role of lysosome trafficking in RB formation by crossing PLK1-floxed mice with LysM-Cre mice, thus, deleting PLK1 in myeloid cells. OC differentiation, actin-ring formation, and microtubule organization remained normal in PLK1^{-/-} cells. However, the resorptive capacity of PLK1^{-/-} OCs was markedly reduced as compared to control cells (Con). Reconstitution of PLK1^{-/-} OCs with wild type PLK1, but not PLK1 mutants of human and rat osteopetrosis , rescued CTSK secretion as well as RB formation and bone resorption. The morphology and function of the Golgi apparatus and endocytosis was unaffected by the loss of PLK1, as determined by immunofluorescent staining. Using an EGF receptor degradation assay - a classic readout of lysosome function- we determined that the degradation of this receptor was also unaffected; and so was autophagosome

formation, as measured by LC3-II/I ratio and ATG5-ATG12 conjugation. However, while the level of Lamp2, a lysosomal membrane protein, was similar between Con and PLK1^{-/-} OCs, loss of PLK1 caused an accumulation of enlarged lysosomes around the nuclei, as shown by live cell time-lapse imaging of actin-RFP and Lamp2-GFP expressing OCs. Furthermore, RB formation was completely absent in PLK1^{-/-} OCs, as determined by electron microscopic examination. Finally, using mass spectrometry we found that the PLK1 protein was bound to Rab7 and several components of the RANKL and integrin signaling complexes as well as microtubule motors. Collectively, these results demonstrate that PLK1 functions as an indispensible adaptor protein that bridges the RANKL and integrin signalings to lysosomal secretion.

Disclosures: Toshifumi Fujiwara, None.

FR0254

Snx10-dependent osteoclastic activity and gastric acidification is required for bone and calcium homeostasis. <u>Liang Ye*[1]</u>, <u>Leslie Morse</u>[2], <u>Li Zhang</u>[3], <u>Hajime Sasaki</u>[4], <u>Jason Mills</u>[5], <u>Greg Sibbel</u>[5], <u>Ariane Zamarioli</u>[6], <u>Ricardo Battaglino</u>[4]. [1]The Forsyth Institute & Harvard School of Dental Medicine, USA, [2]Harvard Medical School, USA, [3]The Forsyth Institute, USA, [4]The Forsyth Institute, USA, [5]Washington University School of Medicine, USA, [6]University of Sao Paulo, Brazil

Autosomal recessive osteopetrosis (ARO) is a heterogeneous genetic disease characterized by osteoclast failure and high childhood mortality. Approximately 25% of all human osteopetrosis cases are caused by mutations in unidentified genes. We previously identified Snx10 and demonstrated that this gene plays an essential role in osteoclast vesicle trafficking and bone resorption in vitro. Mutations in conserved residues in the human SNX10 were later described in patients with infantile osteopetrosis whose osteoclasts have altered endosomal pathways and reduced resorptive capacity. SNX10 is now known to account for ~4% of all cases of ARO. To study the role of Snx10 in bone homeostasis *in vivo*, we generated global and osteoclast-specific Snx10-deficient mouse strains. Global Snx10-deficient mice (Snx10 ins/ins) die prematurely at 3 weeks and exhibit a severe osteopetrosis with a superimposed mineralization defect. *Snx10 ins/ins* osteoclasts fail to endocytose dextran, form a ruffle border, or acidify the resorption lacuna. The mineralization defect, consistent with rickets, suggested that Snx10 is also required for calcium homeostasis. We found Snx10 to be also expressed in gastric zymogenic cells. Similar to osteoclasts, *Snx10 ins/ins* gut zymogenic cells exhibit a defect in secretory vesicle formation leading to hypochloridria and hypocalcemia. Osteoclast-specific Snx10 deficiency, on the other hand, has no effect on net calcium balance and consequently results in osteopetrosis with no rickets. *The global Snx10-deficient mice thus exhibit a complex phenotype that is a combination of osteopetrosis (due to impaired OC resorption) and rickets (impaired mineralization due to poor calcium absorption).* Finally, dietary supplementation with calcium gluconate rescues the rachitic phenotype and *dramatically extends life span* in Snx10-gobal deficient mice, suggesting that this may be a critical component of the clinical approach to Snx10-dependent human osteopetrosis that has previously gone unrecognized. We conclude that Snx10 is essential both for bone resorption and for gut acidification by regulating vesicular trafficking in both osteoclasts and gut zymogenic cells. Though the physiological links between the GI tract and bone have been known for decades, the current work is among the first to delineate the genetic mechanisms shared between these two tissues.

Disclosures: Liang Ye, None.

FR0255

Specific Ostm1 ablation in the hematopoietic mature osteoclast induce severe osteopetrosis. <u>Jean Vacher*[1]</u>, <u>Monica Pata</u>[2]. [1]Institut De Recherches Cliniques De Montréal, Canada, [2]IRCM, Canada

The spontaneous recessive mouse mutant grey-lethal (gl/gl) in the Ostm1 gene causes severe osteopetrosis and neurodegeneration. Ostm1 gene has a wide expression pattern particularly in hematopoietic lineages in the myeloid osteoclast and lymphoid cells. Cellular characterization of gl/gl hematopoiesis showed that multipotent cells can differentiate into all lineages and that the osteoclast lineage, from early progenitors to mature cells, is markedly stimulated. The mature gl/gl osteoclasts are in contrast poorly functional and display cytoskeletal defects. Importantly, targeting Ostm1 expression to committed osteoclast progenitors by TRAP-Ostm1 transgenic mice was insufficient to rescue mature osteoclast defects. However, full rescue of the gl hematopoietic defects in myeloid and lymphoid lineages including osteoclast, B and T cells, was attained when Ostm1 was expressed from a PU.1-BAC transgene in gl/gl mice establishing a probable hematopoietic crosstalk. To specifically address the role of Ostm1 in mature osteoclasts, we generated a conditional Ostm1 allele and induced specific mature osteoclast ablation using the CathepsinK-Cre deleter mouse. Specific recombination was concomitant with osteoclast maturation and loss of Ostm1 reached ~100% efficiency in fully mature OCLs produced ex vivo. In vivo loss of Ostm1 in mature osteoclasts resulted in a severe osteopetrotic phenotype as determined by a massive increase of bone mass with inefficient bone resorption, a lack of tooth eruption and early death around three weeks of age. All these features closely recapitulate the skeletal phenotypes that we characterized in the spontaneous germline Ostm1-null gl/gl mouse mutant. Taken together our studies demonstrate that

loss of Ostm1 in mature osteoclasts is sufficient to induce severe osteopetrosis as well as highlight the intricate role of Ostm1 on the hematopoietic cellular interactions.

FR0256

Targeting Cathepsin K to attenuate Toll-Like Receptor (TLR) signaling inhibits rheumatoid arthritis and periodontitis and reveals the critical function of Cathepsin K in osteoimmunology. <u>Liang Hao</u>*, <u>Wei Chen</u>, <u>Yi-Ping Li</u>. University of Alabama at Birmingham, USA

Despite many studies that have aimed to alleviate the effects of rheumatoid arthritis (RA) and periodontal disease, there is still an urgent need to improve the health of those suffering from these two inflammatory diseases. This study aims to discover new therapeutic targets and simultaneously reduce inflammation and bone resorption through a single target: Cathepsin K (Ctsk). The critical role of Ctsk in the immune response has not been established *in vivo* in RA and periodontitis. We hypothesized that RA and periodontitis may share the same immune response pathway. Thus, we explored the possible underlying mechanism using *Ctsk* knockout mice in the TNF-alpha overexpression-induced RA mouse model and the bacterial-induced periodontitis mouse model. Our data demonstrated that knockout of *Ctsk* can significantly reduce inflammation, meanwhile can inhibit cartilage destruction and bone resorption in both RA and periodontitis lesion areas. We also found that the number of macrophages, dendritic cells and T-cells were largely decreased in both lesion areas. Furthermore, knockout of *Ctsk* inhibited TLR4, 5 and 9 expressions in the gingival epithelial cell in periodontitis lesions and synovial fibroblast cells in RA lesions, indicating the innate immune response was also inhibited. Compared to wild-type (WT) dendritic cells (DCs) when stimulated by CpG DNA *in vitro*, the expression of inflammatory cytokines (*e.g.* TNFα, IL-1, and IL-6) in *Ctsk-/-* DCs was significantly impaired at both protein level and mRNA level. However, the expression of inflammatory c----ytokines in the *Ctsk-/-* DCs stimulated by Lipopolysaccharide (LPS) were not changed when compared to WT DCs. qRT-PCR analysis showed that the expression of *TLR4*, *5*, and *9* decreased in *Ctsk-/-* DCs when stimulated. However, knockout of *Ctsk* only affected TLR9 not TLR4 downstream signaling (*e.g. MyD88, TRAF6, IRAK1,* and *IRAK4*) when stimulated by CpG DNA and LPS. In summary, we demonstrated that Ctsk positively regulates immune responses in both RA and periodontitis disease models. Our data demonstrated that Ctsk promotes TLR4, 5 and 9 function and expression in immune cells both *in vivo* and *in vitro*. Inhibition of Ctsk can impair this immune response process, which may be a promising target to treat RA and periodontitis. Our study demonstrated the critical function of Ctsk in osteoimmunology and indicates that inhibition of Ctsk may have novel therapeutic functions in osteoclast and immune-related bone diseases.

FR0257

TRAP-Positive Multinucleated Cell Independent Bone Resorption in a Mouse Model of Inflammatory Bone Disease. <u>Mizuho Kittaka</u>*[1], <u>Tomoyuki Mukai</u>[2], <u>Teruhito Yoshitaka</u>[3], <u>Yasuyoshi Ueki</u>[4]. [1]University of Missouri-Kansas City School of Dentistry, USA, [2]University of Missouri - Kansas City, USA, [3]University Missouri-Kansas CitySchool of Dentistry, USA, [4]University of Missouri-Kansas City, School of Dentistry, USA

Osteoclasts are regarded as the exclusive bone-resorbing cells in pathological inflammatory bone destruction. This is based on observations that bone destruction is absent in osteoclast-free animal models of inflammatory bone disease such as TNF-α transgenic mice deficient in c-fos. Therefore, we hypothesized that ablation of osteoclasts would rescue the inflammatory bone destruction in *Sh3bp2^{KI/KI}* mice, a knock-in (KI) mouse model of cherubism (*Sh3bp2^{KI/KI}*). These mice exhibit TNF-α-dependent macrophage inflammation and increased RANKL-induced osteoclasto-genesis resulting in inflammatory bone destruction. To test this hypothesis, we created *Sh3bp2^{KI/KI}* mice on a c-fos-deficient background. Surprisingly, although the severity of bone erosion was less than on a *c-fos^{+/+}* background, bone erosion was still present in *Sh3bp2^{KI/KI}/c-fos^{-/-}* mice by microCT analysis. This bone erosion occurred even though no TRAP-positive (+) multinucleated cells were detected in *Sh3bp2^{KI/KI}/c-fos^{-/-}* mice. H&E staining showed inflammatory infiltrates surrounding joints and on the surface of long bones in *Sh3bp2^{KI/KI}/c-fos^{-/-}* mice, presumably responsible for the bone erosion. Inflammatory infiltrates were also observed in liver, stomach, and lymph nodes in addition to bone. Immunohistochemical staining with antibodies against F4/80 for macrophages and against matrix metalloproteinase (MMP)-9 showed that the cellular infiltrates at the eroded bone surfaces were positive for both. Real-time PCR analysis of spleen-derived M-CSF-dependent macrophages showed increased expression of MMP-9 (average 31-fold, n=2) and MMP-14 (average 46-fold, n=2) in *Sh3bp2^{KI/KI}/c-fos^{-/-}* macrophages compared to *Sh3bp2^{+/+}/c-fos^{-/-}* macrophages. Finally, *Sh3bp2^{KI/KI}/c-fos^{-/-}* M-CSF-dependent macrophages derived from fetal liver cells formed resorption pits on dentin slices when cultured with TNF-α and RANKL. These results suggest that *Sh3bp2^{KI/KI}/c-fos^{-/-}* mice develop TRAP+ multinucleated osteoclast-independent inflammatory bone resorption that is carried out by macrophages and that MMPs expressed in macrophages likely play a role in the bone resorption. In this model, macrophages gain functional competence to resorb bone via SH3BP2 gain of function. To our knowledge, the *Sh3bp2^{KI/KI}/c-fos^{-/-}* mouse

is the first *in vivo* model showing TRAP+ multinucleated osteoclast-independent inflammatory bone resorption.

FR0258

Cytosolic Calcium Flickers Orchestrate Steering during Osteoclast Migration. <u>Benjamin Wheal</u>*[1], <u>S. Jeffrey Dixon</u>[2], <u>Stephen M. Sims</u>[3]. [1]The University of Western Ontario, Can, [2]The University of Western Ontario, Canada, [3]The University of Western Ontario, Canada

Osteoclasts are multinucleated cells responsible for the resorption of bone and other mineralized tissues during development, physiological remodeling and pathological bone loss. Lamellipods are dynamic membrane protrusions at the perimeter of the osteoclast that advance the cell front during migration and are responsible for steering during chemotaxis. The purpose of this study was to investigate the subcellular Ca^{2+} signaling events underlying lamellipod dynamics, and how this signaling orchestrates turning in response to a chemotactic stimulus. We used ratiometric live-cell imaging to map $[Ca^{2+}]_i$ in real time within isolated rat osteoclasts. Vigilant regional analysis of multiple areas of interest revealed subcellular changes in $[Ca^{2+}]_i$. Osteoclasts that were not translating were still motile, as exemplified by the continuous ebb and flow of the lamellipod due to localized retraction and outgrowth. Ca^{2+} flickers − microdomains of elevated $[Ca^{2+}]_i$ lasting 25.5 ± 1.7 seconds – were observed sporadically within lamellipods. In most cases, Ca^{2+} flickers were followed promptly by local retraction of the lamellipod (72%) as opposed to outgrowth (20%, 25 different regions from 10 cells, p < 0.05). In keeping with this observation, regions of lamellipods exhibiting outgrowth most often did NOT exhibit Ca^{2+} flicker activity (79%, 24 different regions from 9 cells, p < 0.05). Furthermore, many lamellipod regions showed outgrowth until a flicker promptly triggered localized retraction. Attenuation of flickers by the intracellular Ca^{2+} chelator BAPTA promoted unchecked lamellipod outgrowth accompanied by impaired lamellipod retraction, creating highly elongated osteoclasts with a dendritic appearance. The role of Ca^{2+} flickers in steering osteoclasts during chemotaxis was investigated by creating a localized gradient of M-CSF. Directed migration induced by M-CSF promoted asymmetric Ca^{2+} flicker activity in lamellipods across the cell. Flicker activity was predominantly on the side of the lamellipod distant from the source of M-CSF, causing regional retraction (pruning). Thus, lamellipod retraction at distant sites underlies turning of the osteoclast towards the M-CSF. Here we show, for the first time, a role for exquisite spatiotemporal regulation of subcellular Ca^{2+} in the steering of migrating osteoclasts. Ca^{2+} flickers orchestrate osteoclast steering through lamellipod pruning, thereby encoding directional preference in response to a chemical cue.

FR0259

mTORC1 Activity in Osteoclasts is Regulated by Lysosomal pH. <u>Luciene Carraro-Lacroix</u>[1], <u>Yingwei Hu</u>[2], <u>Celeste Owen</u>[3], <u>Irina Voronov</u>*[4]. [1]Faculty of Dentistry, University of Toronto, Canada, [2]Institute of Dental Medicine, Qilu Hospital, Shandong University, China, [3]Centre for Modeling Human Disease, Samuel Lunenfeld Research Institute, Mt Sinai Hospital, Canada, [4]University of Toronto, Canada

During bone resorption, osteoclasts (OCs) utilize vacuolar H^+-ATPases (V-ATPases), multisubunit enzymes, to pump protons onto the surface that needs to be resorbed. We have a mouse model with a point mutation (R740S) in the V-ATPase *a3* subunit. These mice have defective V-ATPase activity resulting in mild osteopetrosis in heterozygous (+/R740S) and severe osteopetrosis in homozygous animals. OCs with R740S mutation have increased lysosomal pH and decreased *in vitro* OC differentiation.

To explain a connection between impaired OC-genesis in +/R740S cells and high lysosomal pH, we looked at autophagy, a lysosomal protein degradation pathway. Autophagy is activated in response to starvation (amino acid deprivation); in the presence of amino acids and growth factors, autophagy activation is inhibited by a complex containing Ser/Thr protein kinase mammalian target of rapamycin (mTOR), called mTORC1.

To assess autophagic flux, bone marrow-derived OCs were incubated with HBSS (starvation) for up to 2 hrs. Protein expression of two key molecules, microtubule-associated protein light chain 3 (LC3) and sequestosome 1 (p62/SQSTM1), was increased in +/R740S compared to +/+ cells, consistent with blocked autophagy. Immunofluorescence confirmed higher LC3 expression in +/R740S OCs. To investigate activation of mTORC1, the cells were incubated with HBSS for 60 min and then in fully supplemented media (recovery) for 30 min. Unexpectedly, mTOR protein levels as well as mTORC1 activity, as measured by phosphorylation of its substrate p-4E-BP1, were increased in +/R740S cells compared to +/+. mTORC1 is reported to be located on the lysosome, suggesting a link between lysosomal function and mTORC1 activity. To elucidate the mechanism of increased mTOR activity in +/R740S OCs, we hypothesized that upon amino acid signaling mTORC1 complex undergoes lysosomal degradation *via* the autophagy pathway. To test this hypothesis we treated OCs with lysosomal inhibitor chloroquine, known to elevate lysosomal pH. As a positive control, the cells were treated with proteasomal inhibitor MG132. Results demonstrated that 2 hour treatment with chloroquine increased mTOR protein levels

in +/+ OCs, confirming our hypothesis. mTOR protein levels in +/R740S OCs were not significantly affected by chloroquine, suggesting that a certain pH threshold is necessary for lysosomal protein degradation. These results show a novel molecular mechanism regulating mTOR protein levels and activity in OCs.

Disclosures: Irina Voronov, None.

FR0260

CHMP5 Is a Novel Risk Factor of Paget's Disease of Bone Regulating the NF-kB Pathway in Osteoclasts. <u>Jae Hyuck Shim</u>*[1], <u>Kwang Hwan Park</u>[2], <u>Matthew Greenblatt</u>[3]. [1]Weill Cornell Medical College, USA, [2]Yonsei University College of Medicine, USA, [3]Weill Cornell Medical College/Brigham & Women's Hospital, USA

Purpose of this study is to understand molecular mechanisms of a novel mouse model of Paget's Disease of Bone (PDB).

PDB is one of the most profound disorders of imbalanced bone homeostasis, characterized by a wave of increased lytic osteoclast activity followed by a wave of increased osteoblast activity, resulting ultimately in bone thickening, sclerosis and expansion. These increases in osteoblast function and bone formation are believed to be driven by altered osteoclast differentation. The classic secondary consequences of this process include local osteoarthritis and nerve entrapment, due to increased bone formation, as well as increased rates of osteosarcoma. While these clinical consequences make understanding mechanisms of PDB itself important, the dramatic increaes in osteoblast activity secondary to increased ostoclast activity seen in PDB must use molecular pathways of universal biological importance in regulating bone mass. Identification of these pathways of low bone mass such as osteoporosis and lytic bone tumors.

For decades attempts have been made to understand the pathogenesis of PDB. Recent advances include identification of genetic risk factors in the heritable form of PDB, including the autophagy/endocytosis-regulatory protein encoded by p62/SQSTM1 gene, and genes for valosin-containing protein (VCP), and optineurin. However, the mechanistic contribution of these genetic risk factors to the development of PDB remains to be elucidated. Recently, we have identified Chromatic Modifying Profein 5 (CHMP5) as a key regulator of NF-kB pathway and deletion of this gene increases NF-kB activity in osteoclasts in response to Receptor activator of nuclear factor kB ligand (RANKL). Accordingly, CHMP5 deletion enhances RANKL-induced osteoclast differentiation and mice lacking CHMP5 in mature osteoclasts using Cathepsin K (CTK)-cre mice (Chmp5-CTK mice) develop a severe, spontaneous disorder with nearly all the classic features of PDB, including the progressive deposition of osteoclast-rich periosteal bone with a typical "Pagetoid" appearance, gradual expansion of bones in both the axial and appendicular skeleton, enlarged osteoclasts with nuclear inclusion body, and increases in serum and histomorphometirc measurements of bone turnover. Therefore, understanding molecular mechanisms in this mouse model of PDB will contribute to identify novel therapeutic targets for the treatment of diseases of disordered bone remodeling and bone loss.

Disclosures: Jae Hyuck Shim, None.

FR0261

β-catenin deletion in Ctsk-expressing cells decreases bone mass. <u>Paula Ruiz</u>[1], <u>Marta Martin-Millan</u>[2], <u>Shoshana Bartell</u>[3], <u>Maria Jose Almeida</u>[3], <u>Marian Ros</u>[4], <u>Jesús Gonzalez-Macias</u>*[5]. [1]Fundación Instituto de Investigación Marqués de Valdecilla, Spain, [2]University of Cantabria, IDIVAL, HUMV, Spain, [3]Central Arkansas VA Healthcare System, Univ of Arkansas for Medical Sciences, USA, [4]Instituto de Biomedicina y Biotecnología de Cantabria, Spain, [5]University of Cantabria, HUMV, IDIVAL, RETICEF., Spain

It is well established that activation of Wnt/ß-catenin signaling in the osteoblast lineage leads to an increase in bone mass through a dual mechanism: increased osteoblastogenesis and decreased osteoclastogenesis. More recently, it has been shown that β-catenin in the osteoclast lineage decreases osteoclast formation. Specifically, removal of β-catenin from Lysozime-M expressing cells causes an increase in osteoclast numbers and decreases bone mass. We now examined if mature osteoclasts were the target of β-catenin by generating mice lacking β-catenin in Cathepsin-K;Cre expressing cells (here after ΔCatnb;CtsK). ΔCatnb;CtsK mice were born at the expected Mendelian ratio and had no significant changes in body weight than their littermate controls. Osteoclasts developed from non-adherent bone-marrow cells obtained from ΔCatnb;CtsK mice expressed significantly lower levels of β-catenin as determined by RT-PCR, while no differences were detected in macrophages. In line with our previous model, ΔCatnb;CtsK mice exhibited a significant decrease in bone mass. At 3 months of age, BMD was lower in vertebrae (female p=0.0007, male p=0.011) and femur (female p=0.007, male p=0.008) as determined by DEXA. Also, micro-CT showed a decreased BV/TV and a decreased trabecula number in vertebra and femur in both genders. However, in striking contrast to what was seen when β-catenin was deleted in osteoclast progenitors expressing Lysozime-M, ΔCatnb;CtsK animals exhibited a severe cortical bone phenotype in vertebrae, distal femur and proximal tibia, characterized by large holes which allowed the visualization of the bone marrow (Figure 1). These findings suggest that the absence of β-catenin in Ctsk-

expressing cells interferes with the physiological modeling process. In the mechanistic interpretation of these findings it must be taken into account that Cathepsin-K is expressed in cells other than osteoclasts, such as the perichondrial groove of Ranvier, which is considered to contain chondroprogenitors responsible for circumferential cartilage growth.
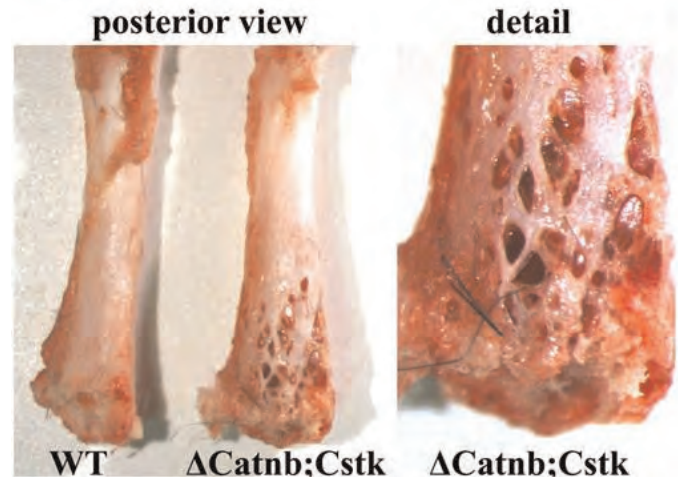
Figure 1

Disclosures: Jesús Gonzalez-Macias, None.

FR0264

Deletion of Wnt Receptors Lrp5 and Lrp6 or ß-catenin in osteoclast precursors differentially affects skeletal development. <u>Megan Weivoda</u>*[1], <u>Ming Ruan</u>[2], <u>Christine Hachfeld</u>[2], <u>Larry Pederson</u>[2], <u>Rachel Davey</u>[3], <u>Jeffrey Zajac</u>[4], <u>Yasuhiro Kobayashi</u>[5], <u>Bart Williams</u>[6], <u>Sundeep Khosla</u>[7], <u>Jennifer Westendorf</u>[1], <u>Merry Jo Oursler</u>[1]. [1]Mayo Clinic, USA, [2]Mayo Clinic, USA, [3]University of Melbourne, Australia, [4]Austin Hospital, Australia, [5], Japan, [6]Van Andel Research Institute, USA, [7]Mayo Clinic College of Medicine, USA

Mutations to proteins in the Wnt signaling pathway result in human bone phenotypes. Many studies have examined the role of anabolic Wnt signaling in osteoblasts and osteocytes; however, few have investigated the role of Wnt signaling in the osteoclast lineage. We determined that the early but not late addition of Wnt3a to osteoclast precursors (pOCs) inhibits differentiation *in vitro*. Therefore, we tested the hypothesis that Wnt signaling in pOCs is an important contributor to skeletal development. Rank promoter Cre or cathepsin K (Ctsk)-Cre animals were crossed with Lrp5/Lrp6 flox mice to impair Wnt receptor signaling in early (Rank/Lrp$^{del/+}$) and late (Ctsk/Lrp^{del}) pOCs. In addition, Ctsk- Cre mice were crossed with ß-catenin (ßcat) flox mice to impair canonical Wnt signaling in late pOCs (Ctsk/ßcat^{del}). Rank-Cre double knockout of Lrp5/Lrp6 was not achieved; therefore, Rank/Lrp$^{del/+}$ mice were analyzed for bone phenotypes. Six week femurs were assessed by peripheral quantitative computed tomography (pQCT) and micro computed tomography (μCT). Ctsk/ßcat^{del} mice had significant decreases in cortical bone in the cancellous region (see figure). Trabecular number (TbN) was significantly decreased, while structure model index (SMI), trabecular thickness (TbTh), and trabecular spacing (TbSp) were significantly increased. In contrast, Ctsk/Lrp^{del} femurs did not differ from littermates. However, Rank/Lrp$^{del/+}$ mice exhibited a significant decrease in bone density by pQCT, and significant decreases in bone volume, TbN, and TbTh, and increased TbSp by μCT analysis. The observed phenotype in the Rank/Lrp$^{del/+}$ mice and no phenotype with later Lrp deletion (Ctsk/Lrp^{del}) are consistent with our *in vitro* data demonstrating that early, but not late addition of Wnt3a to pOCs cultures inhibits osteoclast formation. In contrast to the Ctsk/ßcat^{del} mice, Rank/Lrp$^{del/+}$mice did not have altered cortical bone. This indicates that ßcat may have effects independent of canonical Wnt signaling in pOCs. Alternatively, Ctsk/ßcat^{del} may lead to a cortical phenotype through off target expression of Cre within the Groove of Ranvier. Because of these potential caveats to the Ctsk/ßcat^{del} model, we believe that evaluation of Rank/Lrp$^{del/+}$ is a better approach for studying the effects of Wnt signaling in osteoclast differentiation. Importantly, these data demonstrate that canonical Wnt receptor signaling in pOCs is important to skeletal development.
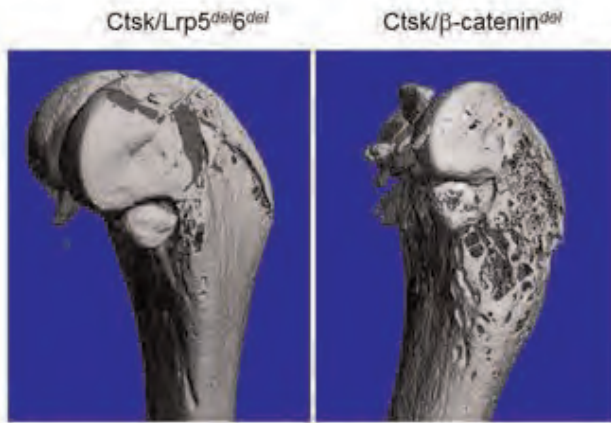
MicroCT images exhibit differential cortical phenotypes

Disclosures: Megan Weivoda, None.

FR0265

Inhibition of a cholesterol regulator, Srebp2, prevents bone loss induced by RANKL. Kazuki Inoue*[1], Yuuki Imai[2]. [1]Ehime University, Japan, [2]Ehime University, Japan

Clarification of the molecular mechanisms underlying osteoclastogenesis provides us new insights into both the physiology of bone metabolism and the pathophysiology of bone diseases. Recent studies revealed that osteoclastogenic transcription factors including *c-Fos,* and *Nfatc1*, sequentially and co-operatively facilitate the expression of osteoclast genes and determine osteoclast identity. However, there are still numerous other unidentified transcription factors involved in osteoclastogenesis.

To identify novel transcription factors in osteoclastogenesis, we performed a genome-wide analysis of open chromatin during RANKL-induced osteoclastogenesis using DNase-seq. As results from DNase-seq using RAW264 cells, we have successfully identified novel osteoclastogenic transcription factors including *Zscan10, Atf1, Nrf1,* and *Srebf2* (Inoue K and Imai Y. JBMR 2014 *in press.*). However, physiological and pathological functions of these transcription factors in bone metabolism remain unclear although osteoclastogenesis was impaired by knockdown of these factors. Among them, we focused on Srebp2 encoded by *Srebf2*, one of the master regulators of cholesterol regulation, because several studies reported a strong relationship between osteoclastogenesis and cholesterol homeostasis.

To investigate the *in vivo* functions of Srebp2, we treated RANKL-induced bone loss model mice with fatostatin, an inhibitor of Srebp2. Fatostatin was administered every day from 2 days before RANKL-injection. 48 hrs after RANKL-injection, the mice were sacrificed and the femora were harvested and analyzed by micro-computed tomography (μCT). As results of μCT analyses, fatostain treatment rescued the reduction of trabecular bone volume, bone mineral density, and trabecular number and the increase of trabecular separation in RANKL-treated mice. Moreover, fatostatin treatment suppressed osteoclast differentiation *in vitro*. These results suggested that fatostatin might affect osteoclast differentiation mediating through Srebp2 inhibition and inhibit RANKL-induced bone loss *in vivo*.

Taken together, our studies demonstrated that we succeed in identifying Srebp2 as a novel transcription factor regulating osteoclastogenesis by DNase-seq, and inhibition of Srebp2, such as fatostatin, might be a potential therapeutic strategy for osteoporosis. Further studies on Srebp2 functions will uncover more precise molecular mechanism underlying relationship between cholesterol homeostasis and bone metabolism.

Disclosures: Kazuki Inoue, None.

FR0266

Orphan Nuclear Receptor Nur77 Decreases Osteoclast Differentiation by Promoting NFATc1 Degradation via Ubiquitin E3 Ligase Cbl-b. Xiaoxiao Li*[1], Wei Wei[2], HoangDinh Huynh[2], Yihong Wan[3]. [1], USA, [2]UT southwestern, USA, [3]University of Texas Southwestern Medical Center, USA

Osteoclasts are the only cells that can degrade bone, and their over-activity has been implicated in many skeletal diseases such as post-menopausal osteoporosis, rheumatoid arthritis and cancer metastasis to the bone. In our lab's attempt to screen for genes that regulate osteoclast activity, we observed that Nur77 mRNA level increases continuously during osteoclast differentiation. Nur77 is an orphan nuclear receptor that has been shown to regulate apoptosis, inflammation, and carcinogenesis. However, its role in osteoclast differentiation has been previously unknown. The goal of my research is to characterize Nur77's role in osteoclast differentiation and bone metabolism, and identify the mechanisms by which Nur77 regulate osteoclast activity.

To study Nur77's effect on osteoclast, we obtained Nur77 -/- mice and found that osteoclasts derived from Nur77 -/- mice exhibited accelerated differentiation compared with WT mice. Furthermore, Nur77 -/- mice developed severe osteopenia due to increased osteoclast activity and unchanged osteoblast activity. In elucidating the mechanism by which Nur77 regulates osteoclast differentiation, we found that Nur77 can significantly decrease the activity of NFATc1, the master regulatory transcription factor in osteoclastogenesis, by promoting its degradation. Over-expression of Nur77 decreases NFATc1 protein level without affecting its mRNA level; while Nur77 -/- osteoclasts fail to downregulate NFATc1 at late stage of osteoclast differentiation. Furthermore, we discovered that Nur77 can transcriptionally up-regulate Cbl-b, an E3 ligase that has been shown to mediate NFATc1 ubiquitination and degradation. Over-expression of Nur77 increases Cbl-b expression, and loss of Nur77 leads to decreased Cbl-b level. Finally, we found that Nur77 over-expression can significantly increase Cbl-b promoter activity, and that mutating either one of the two putative Nur77 Response Elements in the Cbl-b promoter decreased its activity.

In summary, we've shown that Nur77 can decrease osteoclast differentiation by promoting NFATc1 degradation via upregulating Cbl-b. It is our hope that by understanding how Nur77 protects bone from excessive tissue loss, we can expand therapeutic options to treat osteoporosis, and other osteoclast related diseases.
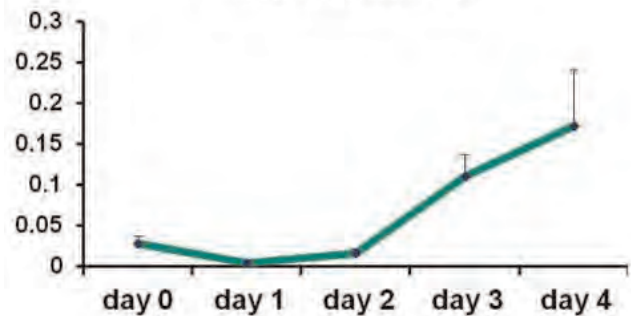
Nur77 mRNA increases during osteoclast differentiation
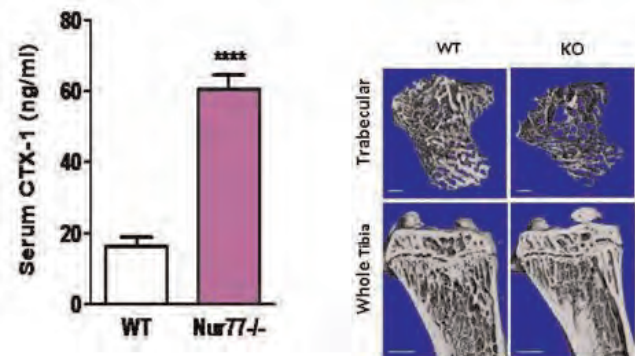
Loss of Nur77 increases osteoclast activity (CTX-1) and decreases bone density
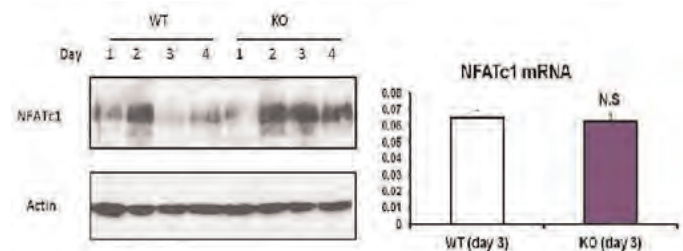
Nur77 KO mice derived osteoclasts fail to down regulate NFATc1 protein level
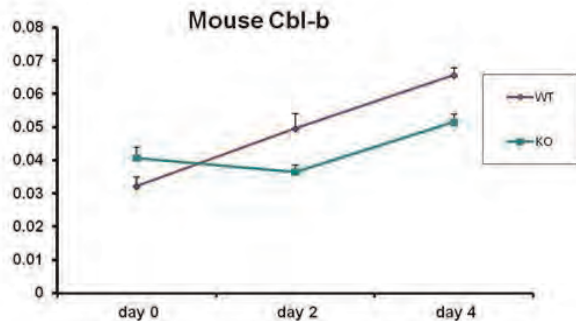
Nur77 KO mice derived osteoclasts have lower level of Cbl-b than WT

Cblb-luc-WT = AAATATCAgaacatcTGAGATGA
Cblb-luc-Mut1 = AACCAGCAgaacatcTGAGATGA
Cblb-luc-Mut2 = AAATATCAgaacatcTGCGACGC
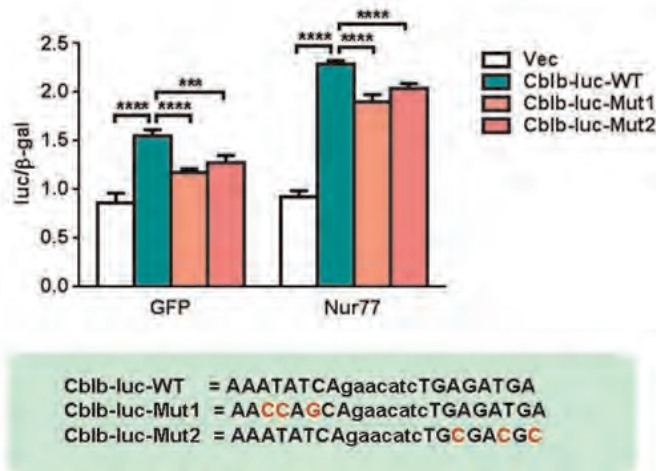
Nur77 increases WT Cbl-b promoter activity; Activity is Nur77 Response Element specific

Disclosures: Xiaoxiao Li, None.

FR0269

Sirtuin 1 suppresses mitochondrial ATP and osteoclastogenesis via FoxO-mediated stimulation of Heme oxygenase 1. Ha-Neui Kim*[1], Shoshana Bartell[2], Li Han[2], Aaron Warren[3], Srividhya Iyer[2], Rafael de Cabo[4], Stavros Manolagas[2], Maria Jose Almeida[2]. [1]Univ. Arkansas for Medical Sciences, Central Arkansas VA Healthcare System, USA, [2]Central Arkansas VA Healthcare System, Univ of Arkansas for Medical Sciences, USA, [3]Center for Osteoporosis & Metabolic Bone Diseases, Univ. Arkansas for Medical Sciences, & Central Arkansas Veterans Healthcare System, USA, [4]Translational Gerontology Branch, National Institute on Aging, National Institutes of Health, USA

Mitochondria-derived H_2O_2 stimulates osteoclast progenitor proliferation and potentiates osteoclastogenesis and is critical for bone remodeling under physiological and pathological conditions. The FoxO family of transcription factors restrains osteoclastogenesis by attenuating H_2O_2 accumulation. Sirt1 – an NAD+ dependent deacetylase – regulates FoxO1 and FoxO3 transcriptional activity. Deletion of Sirt1 in osteoclast progenitors, like deletion of FoxO1, FoxO3 and FoxO4, increases osteoclast number and decreases bone mass. Conversely, systemic Sirt1 stimulation by synthetic activators attenuates the loss of bone mass induced by unloading or aging. Here we examined whether FoxOs mediate the actions of Sirt1 in osteoclasts. Sirt1 activation by two different synthetic activators (SRT2104 and SRT3025) as well as resveratrol dose-dependently inhibited RANKL-induced osteoclast differentiation of bone marrow-derived macrophages. This effect was associated with decreased mRNA expression of several genes, including NFATc1, a key transcription factor for osteoclast generation. The inhibitory effect of Sirt1 stimulators on osteoclastogenesis was abrogated in cells lacking FoxO1, FoxO3 and FoxO4. Consistent with this finding, resveratrol increased the expression of several FoxO target genes, including heme oxygenase (Hmox) 1. Hmox1 catabolises heme, an essential cofactor for the stability and function of proteins of complexes III and IV of the electron transport chain. In line with this, Sirt1 activation reduced ATP production and mitochondrial DNA. In contrast, Hmox1 mRNA levels were strongly reduced by RANKL or FoxO deletion in osteoclast progenitors; while FoxO3 overexpression increased Hmox1 mRNA. Furthermore, deletion of FoxOs in osteoclast progenitors increased ATP production and prevented the suppressive effects of Sirt1 stimulators on mitochondria function. Our findings suggest that by inhibiting mitochondria function via stimulation of Hmox1, FoxOs decreased ATP production and H_2O_2 accumulation

and attenuate osteoclast progenitor proliferation. These effects of FoxO are stimulated by Sirt1. This mechanism of action might explain, at least in part, the positive effects of Sirt1 activators on bone mass.

Disclosures: Ha-Neui Kim, None.

FR0275

Osteocyte Lacunar Density is Breed Related in Mice. Brett Rosauer[1], Mohammed Akhter*[2], Donald Kimmel[3], Joan Lappe[2], Robert Recker[4]. [1]Creighton University, USA, [2]Creighton University Osteoporosis Research Center, USA, [3]Kimmel Consulting Services, USA, [4]Creighton University, USA

Breed-related differences in skeletal macroarchitecture, microarchitecture, strength, and bone adaptation response to mechanical stimuli have been well documented in mice. The osteocyte lacunar-canalicular (Ot.La) network may play a role in the response to mechanical loading. Ot.La density and volume in mice has not been well-studied. The objective of this project is to determine the three dimensional (3D) volume and density of osteocyte lacunae in three mouse breeds (DBA/2J [D2], C57BL/6 [B6], and C3H/HeJ [C3]), using the MicroXCT-200 (Carl Zeiss [aka Xradia], Pleasanton, CA USA) 3D X-ray microscope. 200μm thick cross-sections of the ulnar mid-shaft (3/breed) from 14wk old mice were scanned at 0.6μm voxel resolution using the 40X objective with 10 sec exposure time (28kV/5W), obtaining 400 projections. Each scan lasted ~2hrs. Voids within mineralized bone in each ulna were segmented and analyzed for void volumes (volume [μm³]) and number of voids within 100-200μm³ and 200-300μm³ ranges using AvizoFire™ software. The segmented voids (i.e., lacunae) from these ranges are shown, with and without surrounding hard tissue, in the ulnar mid-shaft of a B6 mouse (Figure 1). B6 mice appear to have greater lacunar density in both volume ranges, than either C3 or D2 mice (Table). In addition, lacunar density appeared highest in the posteromedial quadrant (Figure 1). The lacunar count in the ranges of 100-200mm³ and 200-300 mm³ are shown in Figure 2. B6 mice are known to be more responsive to mechanical stimuli than C3 and D2 mice (*Akhter et al. 1998; Pedersen et al., 1999*). Our data may suggest that the mechanotransduction response is positively related to the density of osteocytes in cortical bone tissue of the loaded bone. These are the first data to use 3D X-Ray microscopy to study the volume and density of osteocyte lacunae in relation to skeletal mechanosensitivity. Additional data will be presented and discussed.

Breed	D2	B6	C3
Average volume analyzed (mm³)	0.0195	0.0135	0.0113
Lacunar density #/mm³	2316	5704	3431

Table
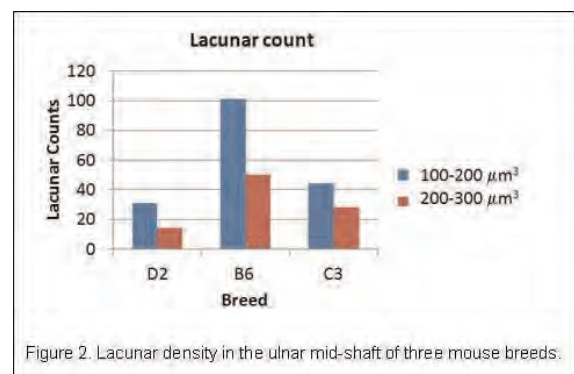
Figure 2. Lacunar density in the ulnar mid-shaft of three mouse breeds.

Figure-2
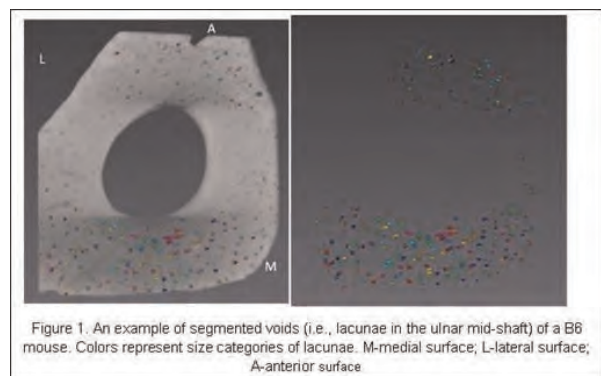
Figure 1. An example of segmented voids (i.e., lacunae in the ulnar mid-shaft) of a B6 mouse. Colors represent size categories of lacunae. M-medial surface; L-lateral surface; A-anterior surface

Figure-1

Disclosures: Mohammed Akhter, None.

FR0276

Osteocytes Produce Interferon-β as a Negative Regulator of Osteoclastogenesis. <u>Takuya Sato</u>*[1], <u>Chiyomi Hayashida</u>[1], <u>Junta Ito</u>[2], <u>Mai Nakayachi</u>[2], <u>Yoko Ohyama</u>[2], <u>Yoshiyuki Hakeda</u>[3]. [1]Meikai University School of Dentistry, Japan, [2]Meikai University School of Dentistry, Japan, [3]Meikai University School of Dentistry, Japan

Osteoclastogenesis is controlled by osteocytes, however, osteocytic regulatory molecules for osteoclastogenesis are largely unknown. We searched for such factors using newly developed culture methods. Our culture system mimics the three-dimensional cellular structure of bone, consisting of collagen gel-embedded osteocytic MLO-Y4 cells, stromal ST2 cells on the gel as bone lining cells, and bone marrow (BM) cells. The gel-embedded MLO-Y4 cells inhibited the osteoclastogenesis induced by $1,25(OH)_2D_3$ without modulating receptor activator of NF-kB ligand (RANKL) and osteoprotegerin (OPG) production by the ST2 cells, despite the gel-embedded MLO-Y4 cells supported osteoclastogenesis in the absence of ST2 cell layer. We next examined how co-cultures of MLO-Y4 cells in culture inserts affect osteoclastic differentiation of BM cells supported by ST2 cells or MLO-Y4 cells in the presence of $1,25(OH)_2D_3$. The presence of MLO-Y4 cells in the culture inserts inhibited osteoclastogenesis supported by either ST2 cells or MLO-Y4 cells, suggesting that although MLO-Y4 cells are capable of supporting osteoclastogenesis through cell contact with BM cells, MLO-Y4 cells produce humoral inhibitory factor(s) of osteoclastogenesis. In the BM cell culture, the conditioned medium from MLO-Y4 cells (MLO-Y4-CM) decreased the capability of osteoclastic differentiation from the cells induced by macrophage colony-stimulating factor (M-CSF). This decreased capability was concomitant with an increase in *protein kinase R* mRNA expression and an inhibition of c-Fos translation. These changes were partially normalized by the simultaneous addition of an anti-interferon (IFN)-β neutralizing antibody (α-IFN-β-Ab) to MLO-Y4-CM. To study primary osteocytes, we prepared non-osteocytic cell-free osteocyte-enriched bone fragments (OEBFs). When osteoclast precursors were induced by M-CSF in the presence of OEBFs, the generated cells exhibited a diminished capacity for osteoclastogenesis. OEBFs prepared from *OPG*-knockout mice exhibited a similar effect, indicating OPG-independent inhibition. The addition of α-IFN-β-Ab during the co-culture with OEBFs partially recovered the osteoclastogenic potential of the generated cells. The MLO-Y4 cells and OEBFs expressed *IFN-β* mRNA. Although osteocytic RANKL is known to be important for osteoclastogenesis, our data suggest that osteocytes also produce IFN-β as an inhibitor of osteoclastogenesis.

Disclosures: Takuya Sato, None.

FR0277

Parathyroid Hormone (PTH) Downregulates Notch2 Signaling in Osteocytes. <u>Stefano Zanotti</u>*, <u>Ernesto Canalis</u>. University of Connecticut Health Center, USA

Osteocytes are terminally differentiated osteoblasts residing within the bone matrix and targeting of these cells by PTH and Notch plays a critical role in bone remodeling. However, the interactions of PTH and Notch signaling in osteocytes are not known. PTH induces the expression of the Notch ligand *Jag1* in cells of the endosteal lining and in osteoblasts, but the consequences of this effect are understood poorly. Cultures of isolated osteocytes do not preserve the three-dimensional cellular network required for the regulation of bone remodeling and osteocytic cell lines do not replicate the gene expression profile of osteocytes *in vivo*. Therefore, we developed cultures of femoral cortical bone as a new model to investigate the interactions of PTH and Notch in osteocytes. Cortical bones were obtained from femurs of 6 week old C57BL/6 mice following removal of epiphyses and bone marrow and enzymatic digestion of the endosteal and periosteal linings. Cortical bone cultures expressed high levels of the osteocyte gene markers *Sost* and *Dmp1* and responded to PTH with a suppression of *Sost* and an induction of *Rankl* expression. These findings recapitulate the effects of PTH in osteocytes *in vivo* and validate cultures of cortical bone as a model to study osteocyte function. Although PTH induced *Jag1* mRNA levels in osteocyte cultures, PTH suppressed the expression of the Notch target genes *Hey1*, *Hey2* and *HeyL*, indicating that the induction of *Jag1* by PTH in osteocytes does not translate into activation of Notch signaling. To verify the inhibition of Notch signaling by PTH, the effects of PTH were investigated in a model of Notch2 gain of function. To this end, cortical femoral cultures from mice harboring a *Notch2* point mutation that leads to the expression of a stable Notch2 protein and increased Notch signaling, and from littermate controls, were used. Mutant mice exhibit a phenotype that recapitulates the Hajdu-Cheney syndrome, an incurable disease of increased NOTCH2 activity. Notch2 activation induced *Hey1* and *Hey2* mRNA levels and PTH downregulated *Hey1* and *Hey2* transcripts in osteocyte cultures from control and Hajdu-Cheney mice, indicating that PTH acts downstream of Notch2 to suppress *Hey1* and *Hey2* expression. In conclusion, PTH suppresses Notch signaling in osteocytes. Since Notch inhibits osteoblastogenesis and bone formation, downregulation of Notch signaling may be required to achieve an anabolic response to PTH.

Disclosures: Stefano Zanotti, None.

FR0281

Isolation of a hematopoietic cell-free preparation of highly purified DMP1-GFP+ osteocytes using fluorescence activated cell sorting (FACS). <u>Ling Yeong Chia</u>[1], <u>Nicole Walsh</u>[2], <u>T. John Martin</u>[3], <u>Natalie Sims</u>*[4]. [1]Department of Bone Cell Biology & Disease, Australia, [2]St Vincent's Institute of Medical Research, Australia, [3]St. Vincent's Institute of Medical Research, Australia, [4]St. Vincent's Institute of Medical Research, Australia

In order to identify specific genes expressed by osteocytes and thereby define their functions, osteocytes have commonly been isolated from bones of transgenic mice expressing GFP directed by the Dmp1 promoter (DMP1-GFP mice) using fluorescence activated cell sorting (FACS). However, while GFP-positive cells obtained in this manner express mRNA for known osteocyte genes, including *Sost*, *Dmp1* and *Mepe*, they have also been reported to express mRNA of genes associated with the osteoclast phenotype: *Dc-stamp*, *Oscar*, tartrate resistant acid phosphatase (*Acp5*) and calcitonin receptor (*Calcr*). This suggests either that osteoclasts and osteocytes share common genes and functions or that DMP1-GFP positive osteocyte populations contain osteoclasts.

To resolve this we isolated DMP1-GFP+ cells that were negative for hematopoietic and endothelial lineage markers by flow cytometry. This allowed us to isolate a population of DMP1-GFP expressing cells free of non-mesenchymal derived cell populations. Cells isolated by collagenase digestion from 7 day old DMP1-GFP calvariae were stained for hematopoietic lineage (Lin) surface markers (CD2, CD3e, CD4, CD45, CD5, CD8, CD11b, B220, Gr1, Ter119) and CD31 to identify myeloid, lymphoid and endothelial cells. Lin$^-$CD31$^-$ and Lin$^+$CD31$^+$ cell populations were then analyzed for GFP expression, and the four distinct populations isolated and assessed by quantitative real-time PCR.

Lin-CD31-GFP+ cells expressed mRNAs for osteocytic genes *Sost*, *Dmp1*, and *Mepe*, but not *Dc-stamp* or *Oscar*, confirming their identity as osteocytes and exclusion of osteoclasts by this method. *Dc-stamp* and *Oscar* mRNAs were restricted to hematopoetic (Lin$^+$CD31$^+$) cells, while *Calcr* and *Acp5* were readily detected in the purified osteocytes.

We also assessed the capacity of the purified osteocytes to support osteoclastogenesis. The purified osteocyte population expressed lower levels of RANKL mRNA compared to the osteoblast-enriched population (Lin$^-$CD31$^-$GFP$^-$). Furthermore, when the highly purified osteocytes were cultured with C57BL/6 bone marrow macrophages and stimulated with 1,25-dihydroxyvitamin-D3 no TRAP+ cells with >2 nuclei were formed.

In conclusion, our data demonstrates the utility and importance of hematopoietic lineage depletion to generate a highly purified osteocyte population from DMP1-GFP mice. These purified osteocytes express *Acp5* and *Calcr* but do not express other osteoclast markers, and are unable to fully support osteoclast formation in vitro.

Disclosures: Natalie Sims, None.

FR0282

Osteocyte Microvesicles in Cell-Cell Communication in Bone. <u>Kun Wang</u>*[1], <u>Andrew Keightley</u>[2], <u>Patricia Veno</u>[1], <u>Vladimir Dusevich</u>[2], <u>LeAnn Tiede-Lewis</u>[1], <u>Lynda Bonewald</u>[1], <u>Sarah Dallas</u>[1]. [1]University of Missouri - Kansas City, USA, [2]University of Missouri - Kansas City, USA

Microvesicles (100-1000nm) and exosomes (50-100nm) are membrane-bound particles shed by cells that function in intercellular communication by delivering their cargo to target cells. This cargo includes proteins, mRNAs and miRNAs that regulate target cell function. Using transgenic mice expressing a membrane-bound GFP in osteocytes (Dmp1-mem-GFPmice), we have previously shown that osteocytes shed GFP+ve microvesicles, which are either deposited in bone matrix or can be released into the marrow and circulation. Microvesicles from osteocyte-enriched primary calvarial and IDG-SW3 cell cultures were shown to potently stimulate osteoblast-to-osteocyte differentiation and had a protein cargo that included microvesicle markers, early and late osteocyte markers and RANKL. To further understand the mechanisms of intercellular communication by osteocyte microvesicles and their potential relevance in aging, we have analyzed their composition by proteomics and qPCR analysis and have determined whether they are produced in adult (5Mo) and aged (22Mo) mouse bones.

qPCR analysis showed that these microvesicles contained mRNA for osteocyte marker genes, including E11/gp38, Dmp1, PHEX as well as mRNA for OPG, RANKL, HIF1α and β-actin. Proteomic analysis showed a microvesicle proteome rich in membrane and cytoplasmic proteins that included proteins associated with the cytoskeleton/cell motility, membrane fusion/exocytosis, G-protein signaling, intracellular membrane trafficking, neurite outgrowth/axonal guidance and cell polarity. The proteome also included osteocyte markers, PHEX and voltage dependent ion channels. Matrix proteins such as fibronectin and periostin were also identified as well as some osteoblast proteins including type I collagen and alkaline phosphatase. By confocal microscopy we have previously shown abundant GFP+ve microvesicles in the matrix around osteocytes in neonatal Dmp1-mem-GFP mice. Since Dmp1 expression is reduced in aged mice, confocal microscopy was performed using DiI staining for lipid. Abundant vesicle-like structures were seen in bone matrix of adult and aged mice, suggesting that microvesicles are continually produced with aging. Together, our data suggest that osteocytes shed microvesicles with a protein and mRNA cargo that can alter the function of target cells in the osteoblast/osteocyte local environment and may also have effects on distant tissues. These functions of microvesicles may be relevant in the young and aged skeleton.

Disclosures: Kun Wang, None.

FR0283

Osteocytes directly communicate with sensory neuronal cells via cell-cell networks that are modulated under an acidic microenvironment. <u>Masahiro Hiasa</u>*[1], <u>Yuki Nagata</u>[2], <u>Jesus Delgado-Calle</u>[1], <u>Yohance M Allette</u>[2], <u>Matthew S Ripsch</u>[2], <u>Teresita Bellido</u>[1], <u>G. David Roodman</u>[3], <u>Fletcher A White</u>[2], <u>Toshiyuki Yoneda</u>[1]. [1]Indiana University School of Medicine, USA, [2]Indiana University, USA, [3]Indiana University, USA

Osteocytes form cell-cell networks by extending dendritic processes in mineralized cortical bone. During bone resorption, osteoclasts secrete protons to dissolve bone minerals via the a3 isoform vacuolar-H$^+$-ATPase in the ruffled borders, creating a localized acidic extracellular microenvironment. Thus, osteocytes are exposed to extracellular acidification at the proximal front end of osteoclastic bone resorption. We reasoned that the acidic microenvironment created by bone-resorbing osteoclasts affects osteocyte activity. Consistent with this hypothesis, Western analysis showed the expression of the acid sensing receptors, ASIC3, TRPV1 and TRPV4, on primary mouse calvarial osteocytes and the mouse osteocytic cell lines, MLO-A5 and MLO-Y4. Culture of primary osteocytes at pH 6.5 caused up-regulation of sclerostin expression and down-regulation of RANKL expression with activation of p65 NF-κB and IκB. These changes were inhibited by the specific ASIC3 antagonist, APETx2. These results suggest that osteocytes sense low pH via ASIC3 and consequently change their expression of genes associated with bone remodeling. Given that peripheral nerve fibers associated with cortical bone also sense acidic conditions via ASIC3 and are thought to control bone metabolism in which osteocytes play a central role, we next studied the functional communications between osteocytes and sensory neuronal cells in acidic conditions using the living dye transfer assay. We found that MLO-A5 osteocytic cells extended dendritic processes to contact the neurites of adjacent F11 sensory neuron-like cells and transferred the permeable living dye calcein to F11 cells. The gap junction inhibitors, 18α-glycyrrhetinic acid and GAP27, inhibited the calcein transfer, suggesting osteocytic cells and sensory neuronal cells develop direct cell-cell communications via gap junctions. Notably, extracellular acidification induced Ca^{2+} influx, an indicator for neuron cell excitation, in co-cultures of MLO-A5 cells and F11 cells. APETx2 inhibited this. In conclusion, our results demonstrate that osteocytes change their phenotype associated with bone remodeling in response to extracellular acidification, suggesting osteocytes are not only mechano-sensing but also acid-sensing cells. Our results also show that osteocytes communicate with and excite neighboring sensory neuron cells in acidic conditions, suggesting that osteocytes may relay acid-evoked pain signal to the sensory neurons innervating bone.

Disclosures: Masahiro Hiasa, None.

FR0284

Are Biochemical Markers of Bone Turnover Representative of Bone Turnover Assessed with Histomorphometry? An Analysis in a Sample of 370 Postmenopausal Women with Osteoporosis. <u>Pascale Chavassieux</u>*[1], <u>Nathalie Portero-Muzy</u>[2], <u>Jean-Paul Roux</u>[3], <u>Patrick Garnero</u>[4], <u>Roland Chapurlat</u>[5]. [1]INSERM UMR1033, Université De Lyon, France, [2]INSERM UMR1033, Université de Lyon, France, [3]INSERM, UMR 1033, Université de Lyon, France, [4]INSERM Research Unit, France, [5]E. Herriot Hospital, France

The levels of bone formation and resorption can be assessed at the tissue level by bone histomorphometry. This invasive method allows assessing the bone turnover at the basic structural unit. Systemic biochemical markers of bone turnover reflect the overall bone formation and resorption at the level of the entire skeleton but cannot discriminate the bone turnover changes in the different skeletal compartments. Postmenopausal osteoporosis is characterized by an imbalance between resorption and formation. The purpose of the study was to investigate the correlations between the serum biochemical markers of formation (bone alkaline phosphatase, Bone ALP; collagen type 1 N-propeptide, P1NP) and resorption (C-terminal crosslinking telopeptide of collagen type 1, sCTX) and osteoprotegerin (OPG) with histomorphometric parameters in a large population of postmenopausal women. 370 untreated postmenopausal osteoporotic women aged 50 to 84 yrs were selected with a lumbar T-score≤-2.5 SD or ≤-1 SD with at least one fracture. Transiliac bone biopsies were obtained after a double tetracycline labeling. The static (Ob.S/BS, OS/BS, OV/BV) and dynamic (MS/BS, BFR/BS, Acf) parameters of formation, and the parameters of bone resorption (ES/BS, Oc.S/BS, EV/BV, E.De) were measured. The mean values of biochemical markers were: Bone ALP 15.0±5.2 ng/ml; P1NP 56.2±21.9 μg/ml; sCTX 0.58±0.26 ng/ml; OPG 3.00±1.45 pmol/ml. Bone ALP and P1NP were significantly correlated with both the static and dynamic parameters of formation (0.13≤r≤0.34, 0.015≥p≥0.0001). sCTX was significantly correlated with all resorption parameters (0.13≤r≤0.28, 0.017≥p≥0.0001). In contrast, no correlation was found between OPG and histomorphometric parameters or the other biochemical markers. Serum PTH was weakly correlated only with osteoid parameters (r=0.15, p<0.005).

In conclusion, bone turnover markers except OPG, were significantly but modestly associated with bone turnover parameters measured in iliac cancellous bone. The iliac crest bone may not represent perfectly the whole bone turnover.

Disclosures: Pascale Chavassieux, None.

FR0285

Circulating Periostin: a Determinant of Cortical Bone Structure Heritability. <u>Nicolas Bonnet</u>*[1], <u>Claire Durosier</u>[2], <u>Emmanuel Biver</u>[2], <u>Thierry Chevalley</u>[3], <u>Rene Rizzoli</u>[4], <u>Serge Ferrari</u>[5]. [1]University Geneva Hospital (HUG), Switzerland, [2]Division of Bone Diseases, Geneva University Hospital & Faculty of Medicine, Switzerland, [3]University Hospitals of Geneva Division of Bone Diseases, Switzerland, [4]Geneva University Hospitals & Faculty of Medicine, Switzerland, [5]Geneva University Hospital & Faculty of Medicine, Switzerland

Periostin is a matricellular protein, which is mainly expressed by periosteal cells and osteocytes in cortical bone. Periostin down-regulates Sost gene expression and is necessary for the cortical bone response to loading and intermittent PTH. In mice receiving iPTH, circulating periostin (cPostn) levels increase and are correlated with cortical bone parameters. Recently, cPostn has been found to be a marker of fracture risk in postmenopausal women. We investigated the relationship between cPostn and bone microstructure in 65-yr old men and women and their offspring and calculated their heritability. We measured cPostn, sclerostin, bone turnover markers, areal bone mineral density (BMD) by DXA, bone trabecular (Tb) and cortical (Ct) parameters at the distal radius and tibia by HRpQCT (XtremeCT) in 84 parents aged 65.2±1.5SD years and 92 of their descendants aged 38.5±5.6SD. To test the association between cPostn and BMD, microstructure or turnover markers, we applied multiple regressions. Heritability (h2) by descent was estimated as twice the slope of the regression between parents and offspring. cPostn was higher in men compared to women. cPostn was negatively associated with age (r2=0.64, p<0.0001), Ct porosity (Ct.Po) and Ct pore diameter at distal radius (r2=0.26 & 0.15, p<0.0001) and tibia (r2=0.34 & 0.08, p<0.0001), but positively correlated with cortical area (Ct.area) and Ct thickness (Ct.Th) at distal radius (r2=0.17 & 0.15, p<0.0001) and tibia (r2=0.24 & 0.28, p<0.0001). These associations remained significant after adjustment for P1NP, CTX, and gender or age separately, but not after adjustment for both gender and age. In contrast, circulating sclerostin (cSost) was positively associated with BMD and BV/TV only but not with Ct.area or Ct.Po. H2 was 42-78% for BMD (depending of sites), 34-60% for Tb structure and 22-58% for Ct structure (depending of sites and parameters) (all p<0.05). For example, at the tibia, h2 was 58% for Ct.Perimeter and 26% for Ct.Po. H2 for cPostn and cSost was 50% and 40%, respectively (p<0.05). Radius Ct.Th in the offspring tended to be predicted by parents cPostn levels (r2=0.08, p=0.0632) after adjustment for P1PN, CTx and cSost. These results indicate that cPostn contributes to the age and gender-dependent alteration of the cortical bone compartment, independently of bone remodeling. Moreover, at least part of the heritability for cortical bone structure may be carried by additive genetic effects on cPostn.

Disclosures: Nicolas Bonnet, None.

FR0286

Automatic QCT quantification of the proximal femur: vBMD, bone volume, cortical bone thickness and finite element modeling. <u>Julio Carballido-Gamio</u>*[1], <u>Serena Bonaretti</u>[1], <u>Isra Saeed</u>[2], <u>Roy Harnish</u>[2], <u>Robert Recker</u>[3], <u>Andrew Burghardt</u>[1], <u>Joyce Keyak</u>[4], <u>Tamara Harris</u>[5], <u>Sundeep Khosla</u>[6], <u>Thomas Lang</u>[1]. [1]University of California, San Francisco, USA, [2]University of California, San Francisco, USA, [3]Creighton University, USA, [4]Department of Radiological Sciences, University of California, Irvine, USA, [5]Intramural Research Program, National Institute on Aging, USA, [6]Mayo Clinic College of Medicine, USA

QCT imaging is the basis for multiple assessments of bone quality, including compartmental vBMD analysis, finite element modeling (FEM), and statistical parametric modeling of vBMD and morphometry distribution. We integrated these approaches into an automated comprehensive proximal femoral QCT analysis. Here, we present a fully automated technique to segment hip QCT scans, which is used as a basis to: 1) prescribe volumes of interest for vQCT analysis, 2) map 3D variations in cortical bone thickness, and 3) assess FEM bone strength. In this study, we measured the accuracy of the segmentation technique and the reproducibility of the derived measurements.

This study used 179 hip vQCT scans from 2 vendors and 3 sites. Using a minimum deformation template (MDT) of the proximal femur, we developed an atlas-based segmentation algorithm consisting of 3 main steps: 1) poly-affine registration of the MDT to individual scans; 2) model-guided nonlinear registration; and 3) region growing and patch-based cleaning of the segmented boundaries obtained after applying the inverse of the registrations. Of the 179 scans, 49 were used for training of the segmentation in step 2, yielding 130 automatically segmented scans. Of these, 78 scans with manual segmentations were used for segmentation accuracy assessment, and 44 (22 scan-rescan pairs) for reproducibility of vQCT, FEM and cortical thickness measures. Cortical bone thickness was measured with a variant of the minimum line integral thickness approach: non-local fuzzy c-means was used to estimate the endocortical boundary, and cortical thickness was measured with minimum Euclidean distances, fuzzy logic, vBMD, and numerical integration. We evaluated inter-scan reproducibility (Fig. 1A) of vBMD, bone volume, cortical thickness, and nonlinear FEM strength in stance and posterolateral fall loading [Keyak Bone 2013] using RMS pairwise precision errors.

Segmentation accuracy and precision of derived measures are shown in Table 1. Figs. 1B and 1C respectively show representative examples of an automatic segmentation and scan-rescan cortical bone thickness maps.

Our automated hip segmentations had high fidelity to gold-standard manual segmentations, and were used to derive highly reproducible vQCT, FEM strength and cortical bone thickness measures. Our subjects were elderly, with scans obtained across multiple clinical sites and vendors, documenting the value of this approach for clinical trials and other multi-site studies.
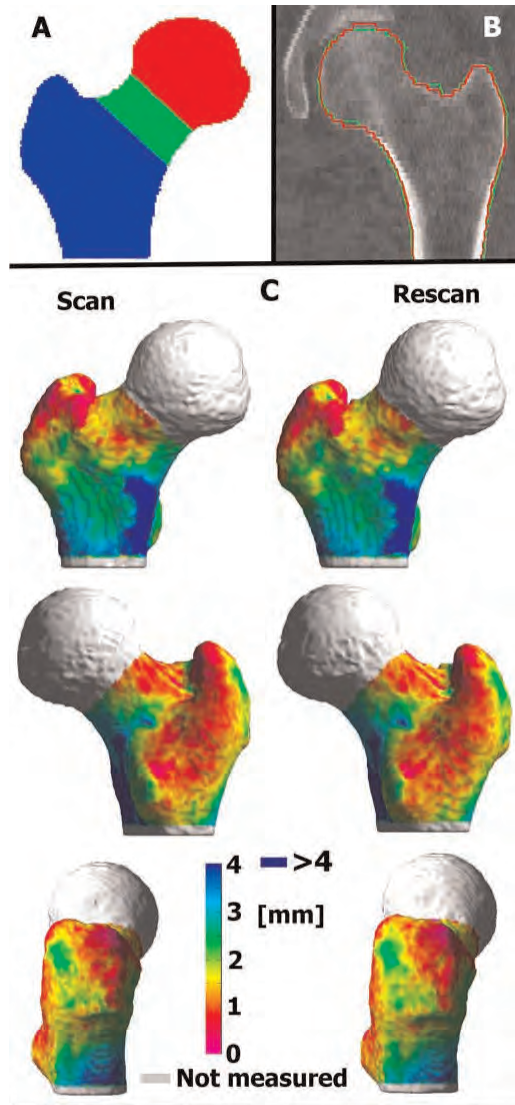
Fig. 1. A) Volumes of interest used in this study: head (red), neck (green), and trochanter (blue). B) Coronal cross-section of a representative automatic segmentation (red), also showing the manually derived contour (green). C) Anterior, posterior, and lateral views of a representative scan-rescan (left-right) 3D cortical bone thickness map.

Fig. 1

Table 1. Segmentation Accuracy and Reproducibility of Bone Measures

Accuracy (mean±SD) (n=78)		
DSC	FNR	SymDist [mm]
0.972±0.005	0.044±0.009	0.396±0.064

DSC = Dice similarity coefficient (a value of 0 indicates no overlap; a value of 1 indicates perfect agreement; higher numbers indicate that the results match the gold standard better)
FNR = False negative rate
SymDist = Average of minimum Euclidean distances between the automatically and the manually derived surface points
10 out of 130 scans failed locally: 8 in the head and 2 in the greater trochanter (7.7%). These scans were not part of the accuracy analysis

Reproducibility (RMS pairwise precision errors [%])						
vBMD (n=22)					Volume (n=22)	
T	I-Head	I-Neck	Tb-Neck	C-Neck	I-Troch	C-Troch
0.90	0.90	1.33	1.58	1.38	1.31	1.43
Cortical bone thickness (n=22)						
T		Neck			Troch	
0.78		1.89			0.76	
Finite element modeling strength (n=19)						
Nonlinear stance loading				Nonlinear FPL loading		
3.21				3.40		

T = Total; **I** = Integral; **Tb** = Trabecular bone; **C** = Cortical bone
Troch = Trochanter
FPL = Posterolateral fall

Table 1

Disclosures: Julio Carballido-Gamio, None.

FR0288

Cortical Bone Water in Renal Transplant Patients. Wenli Sun*[1], Mary Leonard[2], Hamidreza Saligheh Rad[3], Chamith Rajapakse[4], Felix Werner Wehrli[5]. [1]University of Pennsylvania, USA, [2]Stanford School of Medicine, USA, [3]Osteoporosis Research Center, Endocrinology & Metabolism Research Institute.Tehran University of Medical Sciences, Iran, [4]University of Pennsylvania School of Medicine, USA, [5]University of Pennsylvania Medical Center, USA

Renal Osteodystrophy (ROD) is a universal complication of end-stage renal disease. As renal disease progresses, excessive parathyroid hormone secretion results in abnormal trabecular bone connectivity, cortical bone thinning, and decreased cortical BMD. Noninvasive assessment of bone quality may evaluate fracture risk and guide therapy. In this study, we tested a new biomarker capable of evaluating cortical bone in ROD by measuring bone water concentration (BWC) using ultra-short echo time (UTE) MRI and compare the results with BMD measured by pQCT at the same anatomic site.

This prospective study involved 30 renal transplant recipients (16 males and 14 females; ages 25-60 years; BMI 16.2-38.0 kg/m^2) and 30 healthy controls matched one-to-one for race, sex, age (pair-wise mean difference < 3 years), and BMI (pair-wise mean difference < 4.8 kg/m^2). Micro-MR imaging was performed at 3T (Siemens Tim Trio, Erlangen, Germany) using an extremity quadrature bird-cage transmit/eight-channel receive (Invivo Corp., Orlando, FL). Transplant recipients were scanned within 2 weeks after renal transplantation (baseline) and 12 months later while the controls were examined at the baseline only. BWC was measured in the left tibial midshaft using a three-dimensional hybrid-radial UTE (3D HRUTE) sequence with slab-selective half-sinc pulse excitation.

Figure 1 shows BWC maps of a female transplant recipient and a matched control, superimposed on anatomic images. Transplant recipients had greater BWC than controls (25.2±3.6% versus 23.0±3.6%, +9.5%, $p<0.05$, paired t-test, Fig. 2) presumably secondary to greater porosity, which is a hallmark of renal disease. BMD measured by pQCT at the same site was only 1.8% lower in the patients compared to controls (1164.7±52.9 versus 1186.5±24.4 mg/cm^3, $p<0.05$). The greater BWC in patients is only partially explained by their lower BMD (Fig. 3). Data are suggestive of an increase in BWC 12 months post-transplantation (from 25.2±3.6% to 26.2±3.8%, +4.0%, $p=0.2$) as well as a slight increase in BMD (from 1162.3±52.9 to 1171.2±39.1 mg/cm^3, +0.8%, $p<0.05$). Data in larger cohorts will be needed as well as separation of

the BW measurements into collagen-bound and pore water, thereby eliminating the confounding effects of the two types of water that are known to change in opposite direction.
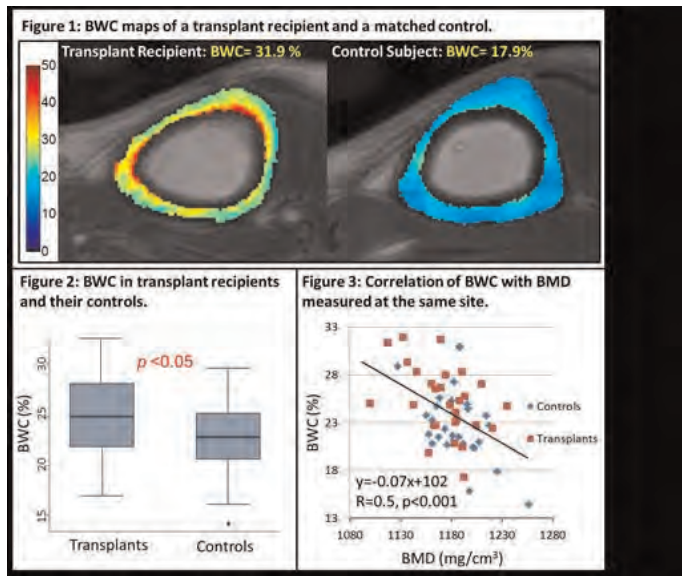
Figure

Disclosures: Wenli Sun, None.

FR0289

Impact of lumbar syndesmophyte on bone heath as assessed by Bone density (BMD) and Bone Texture (TBS) in men with axial spondyloarthritis.

Berengere Aubry-rozier*[1], Laura Wildberger[2], Vladimira Boiadjieva[3], Didier Hans[1], Nikolay Stoilov[3], Mariana Ivanova[3], Rumen Stoilov[3], Rasho Rashkov[3]. [1]Lausanne University Hospital, Switzerland, [2]Lausanne University Hospital, Switzerland, [3]Clinic of Rheumatology, University Hospital "St. Iv. Rilski", Bulgaria

Aim: Patients with spondyloarthritis (AS) have an elevated incidence of osteoporosis and are at increased risk of pathological vertebral fracture. Evaluation of bone by DXA has its limits in fracture prediction, already known in this population, probably because it only measures quantity, but not quality of bone. One hypothesis is that the presence of lumbar syndesmophyte could overestimate the spine BMD. Trabecular bone score (TBS) is a new texture measurement correlated with bone microarchitecture. Previous studies have shown that TBS is not impacted by osteoarthritis and thus could be a predictor of fracture better than spine BMD. We aimed to evaluate a male population of AS with BMD and TBS measurement and see the impact of lumbar syndesmophyte.

Method: Two cohorts of AS male patients (Lausanne, Sofia) with AS disease, clinical and bone parameters (femoral neck and total spine BMD + spine TBS) were merged. We compared BMD and TBS results regarding to the presence/absence of syndesmophyte and compared to young normative values (T-score for both BMD and TBS). T-tests were used to compare the two groups.

Results: Our study concerned 38 men (29 men with lumbar syndesmophytes (L1 to L4, $\geqslant$1), 9 without), all fulfilled the ASAS criteria, mean age 50 years old) and no difference in BMI (26.7 vs 25.3). Mean spine BMD T-score were 0.04+/-1.66 and -1.10+/-1.22 (p<0.05) respectively for AS men with and without syndesmophytes. Mean femoral neck BMD T-score were -1.32+/-1 and -0.96+/-0.78 (p<0.05) respectively for AS men with and without syndesmophytes. Mean TBS was 1.239+/-0.147 and 1.337+/-0.1(p<0.05) respectively for AS men with and without syndesmophytes.

Conclusions: The two populations (Lausanne and Sofia) had comparable BMD and TBS results, after exclusion of degenerative vertebrae and adjustment for the two DXA machines. As expected, the only "normal" result was spine BMD in AS men with syndesmophytes. Others results were lower than in a normal population. Interestingly, even if men with syndesmophyte had normal spine BMD results, they had lower TBS results than men without syndesmophyte and lower femoral neck BMD. All results are statistically significant. These results have to be confirmed in term of disease activity and fracture risk. In conclusion, spine BMD is erroneously influenced by syndesmophyte unlike spine TBS and femoral BMD. We can recommend to evaluate bone health in AS male population with syndesmophyte by measurement of spine TBS and femoral BMD.

Disclosures: Berengere Aubry-rozier, None.

FR0290

Microindentation in vivo captures elements of bone fragility independently of BMD.

Natasha Appelman-dijkstra*[1], Frank Malgo[2], Socrates Papapoulos[3], Neveen Hamdy[3]. [1]LUMC Centre for Bone Quality Dept of Endocrinology, The Netherlands, [2]Leiden University Medical Center, Netherlands, [3]Leiden University Medical Center, The Netherlands

Introduction: The strength of bone is determined by its mass, structure and material composition. Age is associated with loss and structural decay of bone but there is no information about changes in material properties. Recently a new technique has been made available for in vivo quantification of the resistance of bone to microindentation "Bone Material Strength" (BMS). The objective of our study was twofold. First we wanted to assess the relation between age and BMS, secondly to assess the relation between BMS and the calculated 10 year fracture risk by FRAX.

Methods: Treatment-naive subjects $\geqslant$ 40 years with osteopenia or osteoporosis. Clinical risk factors for fractures were collected and the FRAX-score was calculated. Microindentation was performed on the midshaft of the tibia with the Osteoprobe® Reference Point Indenter (Active Life Scientific Inc.,Santa Barbara, CA. USA).

Results: 58 patients (26 men) were included. Mean age was 60.3 ± 9.6 years (range 40.9-85.5 years). Mean BMI $24.7 \text{ kg/m}^2 \pm 4.5$ and 29(50%) had sustained a fracture. Eight patients had been or were currently treated with glucocorticosteroids, 11 used 3 or more units of alcohol a day and 11 patients were active smokers. 17 patients (29.3%) were diagnosed with osteoporosis. In fracture patients median FRAX-score was 7.0% (1.1-48.0) and 1.9 % (0.1-39.3) for major osteoporotic and hip fracture respectively. In non-fracture patients median FRAX-score was 3.6% (1.6-24.0) and 1% (0.2-8.6). Corrected for BMI and gender there was a significant correlation between Femoral Neck (FN) BMD and age. No relationship between FN-BMD and BMS was observed. There was a strong relationship between BMS and age (p=0.001) and furthermore, independently of BMD a significant correlation between BMS and the 10 year absolute fracture risk score by FRAX p<0.001.

Conclusion: Our findings demonstrate a significant relationship between Bone Material Strength and age as well as FRAX score. These data suggest that Bone Material Strength, as measured in vivo with microindentation, captures elements of bone fragility independently of BMD. Whether in clinical practice information about Bone Material Strength will improve the estimation of fracture risk warrants further investigation.

Disclosures: Natasha Appelman-dijkstra, None.

FR0291

Multi-modality in vivo Imaging Identifies Marrow and Vasculature within Pathological Cortical Porosity.

Robin Parrish*[1], Julien Rivoire[2], Misung Han[2], Anne Schafer[3], Thomas Link[4], Roland Krug[2], Galateia Kazakia[4]. [1]UC Berkeley, USA, [2]UC San Francisco, USA, [3]University of California, San Francisco & the San Francisco VA Medical Center, USA, [4]University of California, San Francisco, USA

Cortical bone porosity significantly impacts skeletal integrity. Pathological porosity is associated with decreased bone strength and increased fracture incidence. Importantly, pathological porosity and resulting strength deficits are modifiable. Therefore cortical porosity is an important and viable target for bone fragility treatment.

To develop treatments that prevent or reverse pathological porosity and associated bone fragility, we must understand the mechanisms driving pathological porosity. We hypothesize that pore space *content* will reveal systems driving pathological porosity. In this study, we aim to develop a multi-modal in vivo technique to visualize pore content using high resolution peripheral quantitative computed tomography (HR-pQCT) and magnetic resonance imaging (MRI).

Distal tibiae of two volunteers were imaged using HR-pQCT (Scanco Medical AG) to identify cortical pore space and 3T MR (GE Healthcare) to identify marrow and vessels within pore space. A FIESTA-C sequence was used to identify marrow, followed by an axial T1-weighted 2D FSE sequence. Gadolinium-based contrast agent was then injected, and post-contrast FSE imaging was performed using a multi-phase perfusion protocol to identify vessels.

Our results confirm that in vivo imaging can discriminate marrow from vessels within detectable pores (Fig. 1). Fat-sensitive FIESTA-C scans positively identified fatty marrow-filled pores while contrast-enhanced FSE scans positively identified vessel-filled pores. Using these sequences we captured images in cortices displaying exclusively vessel-filled pores (Fig. 1A) and both marrow- and vessel-filled pores (Fig. 1B). Vessel identification was confirmed by quantifying signal enhancement over the multiphase acquisition. Vessels enhanced while marrow maintained a constant signal (Fig. 2).

This technique lays the groundwork for mechanistic and therapeutic studies of pathological porosity and associated bone fragility. Differences between marrow- and vessel-filled pores in their response to stimuli will be important indicators of pore formation mechanisms. Marrow within new pores may indicate endocortical 'trabecularization' (marrow cavity expansion into the cortical envelope), dictating an intervention to direct mesenchymal cell differentiation towards osteoblastogenesis or regulate adipokines. Vascular components within new pores may indicate vascular network expansion, dictating modulation of vasoregulators or anti-angiogenic therapy.
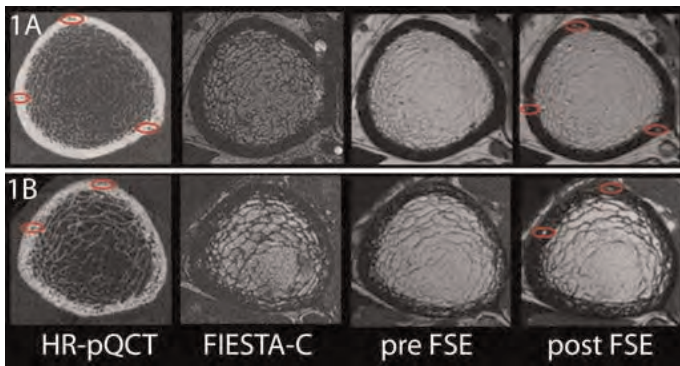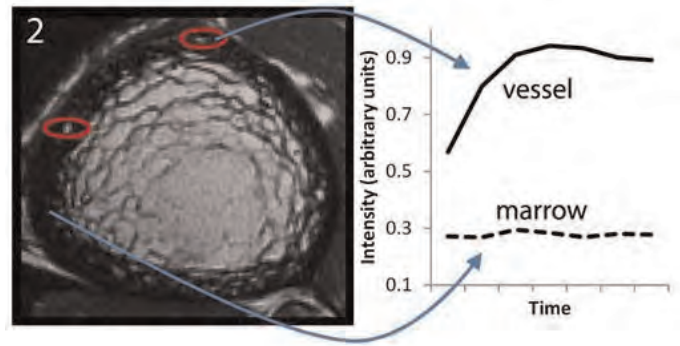
Figure 1

Figure 2

*Disclosures: **Robin Parrish**, None.*

FR0294

Clinical aspect of patients with and without vertebral fractures presenting at a fracture liaison service. <u>Sandrine Bours</u>*[1], <u>Tineke Van Geel</u>[2], <u>Joop Van Den Bergh</u>[3], <u>Sabine Landewe</u>[4], <u>Debby Vosse</u>[5], <u>Piet Geusens</u>[6]. [1]Maastricht University Medical Centre, The Netherlands, [2]Maastricht University, The Netherlands, [3]VieCuri MC Noord-Limburg & Maastricht UMC, The Netherlands, [4]Department of Internal Medicine, subdivision of Endocrinology, Maastricht University Medical Centre, Netherlands, [5]Department of Internal Medicine, subdivision of Rheumatology, Maastricht University Medical Centre, Netherlands, [6]University Hasselt, Belgium

Methods

Between May 2012 and October 2013, 1046 patients with a recent non-vertebral or clinical vertebral fracture (71.3% women and 28.6% men, mean age 65.8 ± 9.9 years) presented at the Fracture Liaison Service (FLS) of Maastricht University Medical Centre, the Netherlands. Of these patients, 89 (9.8%) presented with a clinical vertebral fracture. In all patients at the FLS, bone mineral density (BMD) measurement and laboratory tests (serum calcium, phosphate, 25(OH)D, protein electrophoresis, creatinine, PTH, TSH, and in men < 70 years with osteoporosis serum testosterone) were performed. Furthermore, assessment of prevalent vertebral fractures was performed, whether by Vertebral Fracture Assessment (VFA) or by conventional X-ray. A semi-quantitative scoring was performed according to Genant into grade 0 (<20%, no vertebral fracture), grade 1 (20-25%), grade 2 (25-40%) and grade 3 (>40%).

Results

In 997 (95.3%) of all patients assessment of prevalent vertebral fractures was performed. A prevalent vertebral fracture was found in 132 patients presenting with a non-vertebral fracture at baseline. Thus, a vertebral fracture (clinical and/or prevalent) was present in 221 (23.3%) patients presenting at the FLS with a recent fracture. The patients with a vertebral fracture (n=221) were compared to the patients without any vertebral fracture (n=726). Of the patients with a vertebral fracture, 94 (42.5%) had osteoporosis, 101 (45.7%) had osteopenia and 26 (11.8%) had a normal BMD, and in patients without a vertebral fracture these numbers were 205 (28.2%), 378 (53.1%) and 143 (29.7%), respectively (p < 0.001). Of the patients with a vertebral fracture, 61 (27.7%) had newly diagnosed contributors to secondary osteoporosis and bone loss (SECOB) compared to 162 (22.5%) of the patients without vertebral fracture (p=0.100). The prevalence of MGUS was not different in patients with and without vertebral fractures (9.6% vs. 9.4% respectively, p=0.879), and a multiple myeloma was diagnosed in 1 patient only.

Conclusion

At presentation at the FLS after a recent clinical fracture, nearly 25% of patients have a prevalent and/or clinical vertebral fracture. Patients with a vertebral fracture have a significantly lower BMD than patients without vertebral fractures. In patients with a vertebral fracture more frequently a newly diagnosed contributor to SECOB was found compared to patients without vertebral fracture, however this difference is not statistically significant.

*Disclosures: **Sandrine Bours**, None.*

FR0299

Clinical Performance of an Updated Version of Trabecular Bone Score in Men and Women: The Manitoba BMD Cohort. <u>William Leslie</u>*[1], <u>Renaud Winzenrieth</u>[2], <u>Sumit Majumdar</u>[3], <u>Lisa Lix</u>[4], <u>Didier Hans</u>[5]. [1]University of Manitoba, Canada, [2]Med-imaps, Hôpital X. Arnozan, PTIB, Pessac, France, France, [3]University of Alberta, Canada, [4]University of Manitoba, Canada, [5]Lausanne University Hospital, Switzerland

Lumbar spine TBS (Trabecular Bone Score) is a texture measurement from DXA that correlates with parameters of bone microarchitecture that can predict osteoporotic fractures independent of BMD. Limitations of the previous TBS algorithm (version 1.8), which was optimized for women of average body size, were identified when TBS was used in men or extremes of BMI due to prominent soft tissue effects. The current study evaluates an updated TBS algorithm (version 2.1) which was modified to address these technical issues.

Methods: From a clinical registry containing all DXA results for Manitoba, Canada, we identified women and men age >40 years with baseline spine DXA (GE Prodigy) from years 1999-2011. Spine TBS were measured using the previous (version 1.8) and updated TBS (version 2.1) algorithms by researchers at the University of Lausanne blinded to clinical outcomes. Incident major osteoporotic fractures (MOFs) and hip fractures (HFs) were obtained from population-based health services data. Descriptive statistics and correlations of both versions of TBS with age and BMI were determined. Fracture prediction was estimated from area under the ROC curve (AUROC). All analyses were sex-stratified.

Results (see tables): 47,736 women and 4348 men met the inclusion criteria. With the previous TBS algorithm, average TBS value for men appeared to be significantly lower than women. Under the updated algorithm, average values for men are slightly greater than for women. The updated algorithm is also minimally affected by BMI (Pearson r=0.01 in men, -0.01 in women). During mean follow up of 5 years in men there were 214 incident MOFs and 47 HFs; during 6 years in women there were 2895 incident MOFs and 694 HFs. Slight improvements in fracture prediction were seen with the updated TBS algorithm in both men (change in AUROC for MOFs +0.021, HFs +0.046) and women (change in AUROC for MOFs +0.012, HFs +0.020).

Summary: The updated TBS algorithm: (1) is less affected by soft tissue effects, (2) gives results for men that are consistent with their lower fracture risk, and (3) improves fracture prediction in both men and women compared with the previous algorithm.

	Men (n=4348) Mean±SD	Women (n=47,736) Mean±SD
Age (years)	64±12	63±11 *
BMI (kg/m²)	26.8±5.2	27.1±4.5 *
BMD L1-L4 (g/cm²)	1.128±0.200	1.047±0.181 *
Previous L1-L4 TBS (v1.7)	1.080±0.145	1.244±0.127 *
Updated L1-L4 TBS (v2.1)	1.360±0.132	1.318±0.123 *
Fracture prediction	AUROC (95%CI)*	AUROC (95%CI)*
MOF: L1-L4 BMD	0.637[0.601-0.672]	0.662[0.651-0.672]
MOF: Previous L1-L4 TBS (v1.7)	0.553[0.515-0.591]	0.628[0.618-0.638]
MOF: Updated L1-L4 TBS (v2.1)	0.574[0.535-0.614]	0.640[0.630-0.650]
HF: L1-L4 BMD	0.678[0.602-0.754]	0.677[0.656-0.698]
HF: HF: Previous L1-L4 TBS (v1.7)	0.623[0.544-0.703]	0.679[0.660-0.697]
HF: Updated L1-L4 TBS (v2.1)	0.669[0.585-0.753]	0.699[0.680-0.718]

* p<0,001

	Pearson correlations between	Previous L1-L4 TBS (v1.8)	Updated L1-L4 TBS (v2.1)
MEN	Age	-0.25*	-0.26*
	BMI	-0.40*	0.01*
	BMD L1-L4	0.14*	0.25*
	Previous L1-L4 TBS (v1.8)		0.77*
WOMEN	Age	-0.34*	-0.35*
	BMI	-0.18*	-0.01*
	BMD L1-L4	0.33*	0.38*
	Previous L1-L4 TBS (v1.8)		0.93*

* p<0,001

Tables-results2

*Disclosures: **William Leslie**, None.*

FR0301

Impaired trabecular bone microarchitecture improves after one year on gluten-free diet. A prospective HRp-QCT study in women with celiac disease.
Maria Belen Zanchetta*[1], vanesa longobardi[2], Florencia Costa[2], julio cesar bai[2]. [1]Instituto de Investigaciones Metabolicas (IDIM), Argentina, [2]md, Argentina

Background: We have recently identified a significant deterioration of trabecular and cortical microarchitecture in peripheral bones of patients with recently diagnosed celiac disease (CD) by using high resolution-peripheral quantitative computed tomography (HR-pQCT). Such affectation was mainly produced in the trabecular bone and might be primarily responsible for bone fragility fractures. Up to now, the effect of the gluten-free diet (GFD) on microstructural parameters of peripheral bones has not been assessed.

Aim: to explore one-year changes in bone microstructure produced by the instauration of a GFD in a prospective cohort of premenopausal women with newly diagnosed CD.

Methods: We prospectively enrolled 31 consecutive females with newly diagnosed CD. Up to now, 24 patients have been reassessed one year after diagnosis. Clinical and biochemical status, CD specific serology, bone densitometry and microstructural determinations (HR-pQCT) were performed at both time points. HR-pQCT bone volumetric and structural measurements were determined at the distal non-dominant radius and tibia in all patients.

Results: The microstructure of the trabecular compartment in the distal radius was significantly improved (BV/TV, trabecular density and trabecular thickness: $p<0.0001$) at the one-year time point. At the level of tibia, treatment was associated with significant increase of the total volumetric density ($p<0.01$), cortical density ($p<0.002$), trabecular density ($p<0.0001$), BV7TV ($p<0.0001$) and trabecular thickness ($p<0.002$). In contrast, in radius cortical thickness decreased significantly ($p<0.001$). (Table)

Conclusions: This is the first study exploring the one-year effect of the GFD on microstructural parameters measured by HR-pQCT in patients with newly diagnosed CD. Our study shows that trabecular parameters impaired at the time of diagnosis improved significantly with treatment. In contrast, cortical bone parameters may need more time on GFD to evidence positive changes. We postulate that trabecular bone microarchitecture improvement might be the substrate associated with the decreased risk of fractures observed after GFD in former studies.

	Basal	One-year	P
BMI (kg/m2)	23.2 ± 6.2	24.3 ± 6.4	0.0005*
(Rango)	(15.5 - 37.3)	(16.2 - 41.7)	
Distal radius			
Dcomp (mg HA/cm³)	865.4 ± 55.6	867.0 ± 48.5	0.65
Ct. Th (mm)	0.702 ± 0.142	0.672 ± 0.128	0.02
Dtrab (mg HA/cm³)	120.9 ± 25.0	133.2 ± 24.0	<0.0001
BV/TV (%)	10.1 ± 2.1	11.1 ± 2.0	<0.0001
Tb.N (1/mm)	1.72 ± 0.20	1.74 ± 0.21	0.54*
Tb.Th (mm)	0.059 ± 0.009	0.063 ± 0.006	0.0003
Distal tibia			
Dcomp (mg HA/cm³)	903.1 ± 48.7	916.7 ± 41.5	0.0007*
Ct. Th (mm)	1.08 ± 0.23	1.07 ± 0.21	0.49
Dtrab (mg HA/cm³)	130.0 ± 27.8	141.4 ± 28.1	<0.0001
BV/TV (%)	10.8 ± 2.3	11.8 ± 2.3	<0.0001
Tb.N (1/mm)	1.60 ± 0.30	1.58 ± 0.26	0.58
Tb.Th (mm)	0.068 ± 0.011	0.075 ± 0.012	0.0002

table

Disclosures: Maria Belen Zanchetta, None.

FR0309

Endochrondral ossification, mesenchymal stem cell and Wnt pathway specific loci predict differential skeletal effects in High Bone Mass.
Celia Gregson[1], John Kemp[2], Mhairi Marshall[3], Graeme Clarke[3], George Davey Smith[2], Matthew Brown[4], Emma Duncan[5], Jon Tobias*[6]. [1]University of Bristol, United Kingdom, [2]MRC Integrative Epidemiology Unit, University of Bristol, United Kingdom, [3]University of Queensland Diamantina Institute, Australia, [4]Diamantina Institute of Cancer, Immunology & Metabolic Medicine, Australia, [5]Royal Brisbane & Women's Hospital, Australia, [6]Musculoskeletal Research Unit, University of Bristol, United Kingdom

Introduction: Extreme high bone mass (HBM) may be monogenic (e.g. *LRP5* mutations) or polygenic, possibly from variants in the same genes that determine bone mineral density (BMD) in the general population where they explain 5.8% of variation in femoral neck (FN) BMD[1]. Having previously shown HBM cases carry excess variation in BMD-associated loci, we aimed to determine how variation in loci in different functional pathways, explains the phenotype of HBM.

Methods: 241 unexplained HBM cases (defined as lumbar spine (LS) L1 plus total hip Z-scores≥+4.4) were recruited from 15 UK centres, by screening 335,115 DXA

scans. Established *LRP5* mutations were excluded by Sanger sequencing (n=6). Infinium OmniExpress-12v1.0 genotypes were imputed to UK10K; 57 autosomal SNPs had certainty>0.8. Using Estrada's FN or LS Betas[1], we calculated weighted genetic risk scores (GRS^{FN}/GRS^{LS}) for total (n=57), Wnt (n=12), OPG-RANK-RANKL (n=3), endochrondral ossification (n=6) and mesenchymal stem cell (MSC) differentiation (n=4) annotated loci. GRS^{FN} were compared with total hip BMD (TH-BMD) and total body BMD (TB-BMD), GRS^{LS} with LS-BMD.

Results: A one SD increase in total GRS^{FN} was associated with a 0.13 SD [-0.01, 0.27], p=0.06, increase in TH-BMD and 0.13 [0.01, 0.25], p=0.04, increase in TB-BMD, explaining 1.6% and 3.2% phenotypic variance respectively; however, GRS^{LS} was independent of LS-BMD (0.12 [-0.05, 0.29], p=0.17, r²=0.8%)

Wnt GRS was associated with a 0.15 SD [0.01, 0.29], p=0.04, increase in TH-BMD (r²=2%), but was independent of TB-BMD (0.03 [-0.08, 0.15], p=0.57, r²=0.3%) and LS-BMD (-0.02 [-0.20, 0.15], p=0.79, r²=0%). Conversely, the endochrondral ossification GRS were independent of TH-BMD (0.01 [-0.13, 0.15], p=0.85, r²=0%) and LS-BMD (0.14 [-0.03, 0.31], p=0.11, r²=1.2%), but explained 2.3% of variance in TB-BMD (0.11 [-0.01, 0.23], p=0.08). Whereas, the MSC GRS was associated with a 0.19 SD [0.02, 0.37], p=0.03, r²=2.2%) increase in LS-BMD, but was independent of both TB-BMD and TH-BMD (p>0.8, r²=0%). All BMD sites were independent of OPG-RANK-RANKL GRS.

Conclusion: BMD in HBM appears driven by osteoblast rather than osteoclast pathways. A greater proportion of phenotypic variance in (i) hip BMD is explained by wnt pathway loci, (ii) total body BMD by endochrondral ossification loci and (iii) lumbar spine BMD by mesenchymal stem cell differentiation loci, suggesting differential genetic regulation of individual skeletal sites.[1]Estrada Nat Gen 2012

Disclosures: Jon Tobias, None.

FR0310

Changes in Bone Mineral Density and Trabecular Bone Score (TBS) as Indicators of On-Treatment Antifracture Effect: The Manitoba BMD Cohort.
William Leslie*[1], Sumit Majumdar[2], Suzanne Morin[3], Lisa Lix[4], Didier Hans[5]. [1]University of Manitoba, Canada, [2]University of Alberta, Canada, [3]McGill University, Canada, [4]University of Manitoba, Canada, [5]Lausanne University Hospital, Switzerland

BMD and TBS (with clinical risk factors) help identify individuals at high fracture risk and guide initiation of osteoporosis treatment (OSRx). Whether changes in BMD or TBS are useful indicators of on-treatment antifracture effect is unclear.

Methods: From a clinical registry of all DXA results for Manitoba, Canada, we identified women age >40 years not receiving OSRx at baseline with two DXA examinations. Linkage to health service records provided covariates for calculating FRAX major osteoporotic fracture (MOF) probability with BMD, OSRx use between the scan dates (as medication possession ratio [MPR]), and incident MOF (to March 31st 2011). Cox proportional hazards models for first MOF were used to estimate the hazard ratio (HR) per SD change in BMD (L1-4, total hip, femoral neck) or SD change in TBS (L1-4), adjusted for FRAX probability. Analyses were stratified by OSRx and considered two index dates: the first and the second DXA.

Results: Our criteria identified 9044 women, baseline age 62±10y, baseline FRAX MOF probability 9.4%±6.1%. During mean 7.7y follow up, 770 women developed one or more incident MOF (448 before and 296 after the second DXA). Between the two DXA scans (average interval 4.1y), 5083 women initiated OSRx (MPR<0.5 in 2044, MPR 0.5-0.8 in 1155, MPR >0.8 in 1884; bisphosphonate use 89-91%) while 3961 women received no OSRx. Change in BMD and TBS differed according to OSRx with larger changes seen in those with greater MPR (ANOVA p<.001). With first DXA as the index date, change in BMD or TBS did not predict fractures in untreated women (Table). For women initiating OSRx, there was greater antifracture effect for each SD increase in total hip BMD (decrease 20%, 95%CI 13-26%, p<.001) and femoral neck BMD (decrease 19%, 95%CI 12-26%), while decreases in BMD (exceeding LSC) were associated with higher fracture risk (total hip HR 1.52, 95%CI 1.21-1.90, femoral neck HR 1.70, 95%CI 1.27-2.27). In contrast, change in L1-4 BMD showed only a borderline effect in all treated women combined (decrease 9%, 95%CI 0-17%, p=.049) while change in L1-4 TBS showed no significant antifracture effect. With second DXA as the index date, no BMD or TBS change measures showed a significant association with subsequent MOF.

Summary: Greater on-treatment increases in total hip and femoral neck BMD are associated with lower fracture risk while BMD decreases are associated with higher fracture risk. In contrast, change in spine BMD or TBS were not good indicators of antifracture effect.

Table: HR (95%CI) for incident MOF according to change in BMD or TBS *.

Disclosures: William Leslie, None.

FR0312

Identification of Novel Serum Peptides and Proteins That Are Associated with Hip Bone Loss in Older Men. <u>Jian Shen</u>*[1], <u>Jodi Lapidus</u>[2], <u>Aaron Baraff</u>[2], <u>Christine Lee</u>[1], <u>Arie Baratt</u>[2], <u>Shannon McWeeney</u>[2], <u>Vladislav Petyuk</u>[3], <u>Douglas Bauer</u>[4], <u>Nancy Lane</u>[5], <u>Eric Orwoll</u>[1]. [1]Oregon Health & Science University, USA, [2]Oregon Health & Science University, USA, [3]Pacific Northwest National Laboratory, USA, [4]University of California, San Francisco, USA, [5]University of California, Davis Medical Center, USA

The mechanisms underlying bone loss remain incompletely understood, and there are few available biomarkers. We utilized a proteomics approach to identify serum peptides and proteins associated with bone loss in older men.

A subset of men (N=1875) were randomly chosen from the Osteoporotic Fracture in Men Study (age ≥65 yrs), after excluding users of osteoporosis medications. Men had 2-3 measures of femoral neck DXA BMD over an average follow-up at 4.6 years. Change in BMD was estimated from mixed effects regression models and categorized into three groups: maintenance (no decline), expected loss (loss rate up to 1 SD below the mean change) or accelerated loss (loss rate >1 SD of the mean change). A high-throughput LC-IMS-MS proteomics platform was used to identify and quantify serum peptides. Linear regression models adjusted for age, site and BMI were used to compare peptide abundance in baseline serum across three groups, with specific comparisons made between maintenance and accelerated loss groups via tests of contrasts. P-value and fold change from peptides within the protein were meta-analyzed to generate a significance level and fold change for proteins. The samples were divided into discovery (N=960) and replication cohorts (N=915). To identify networks and important hubs in the networks, we repeated analyses from the whole cohort and used peptides with FDR< 5% to build protein networks using the MetaCore.

We analyzed 3100 peptides that mapped to 325 proteins. 11 peptides in the discovery cohort and 5 peptides in the replication cohort were more abundant in men with accelerated loss compared to the maintenance group (FDR<5%). Meta analyses of peptides suggested 6 proteins were more abundant in both cohorts (FDR <10%), including RNAS1, C163A, CD14, SHBG, ENPP2 and IBP6 (Table). Using combined data from the whole cohort, the network analysis of 48 candidate proteins indicated highly connected hubs, such as CD44, Cystatin C and IBP6. The identified networks were enriched for key biological processes, such as complement activation and regulation of immune response.

Using proteomic methods in a large population of older men, we identified multiple serum proteins and potential biological processes associated with bone loss, including several previously linked to bone metabolism and thus with biological plausibility. These methods and our results provide an opportunity to better understand pathophysiology, and to develop new biomarkers for bone loss.

Table . Proteins differentially abundant in men with accelerated bone loss compared to men with maintained BMD in both cohorts

Protein	Description	Discovery cohort (N=960)			Replication cohort (N=915)		
		P-Value	FDR	Fold change	P-Value	FDR	Fold change
RNAS1	Ribonuclease pancreatic	2E-04	0.022	1.27	0.002	0.076	1.25
C163A	Scavenger receptor cysteine-rich type 1 protein M130	7E-04	0.022	1.35	0.004	0.076	1.3
CD14	Monocyte differentiation antigen CD14	0.012	0.055	1.12	<0.001	0.039	1.17
SHBG	Sex hormone-binding globulin	0.012	0.055	1.18	0.006	0.077	1.21
ENPP2	Ectonucleotide pyrophosphatase/ phosphodiesterase family member 2	0.016	0.055	1.18	0.01	0.089	1.19
IBP6	Insulin-like growth factor-binding protein 6	0.032	0.086	1.19	0.01	0.089	1.22

ASBMR2014_JShen_Table

***Disclosures: Jian Shen**, None.*

FR0316

Association of Incident Radiographic Vertebral Fracture with Back Pain Symptoms in Older Men: the Osteoporotic Fractures in Men (MrOS) Study. <u>Howard Fink</u>*[1], <u>Lynn Marshall</u>[2], <u>Jian Shen</u>[2], <u>Steven Cummings</u>[3], <u>Peggy Cawthon</u>[4], <u>Kristine Ensrud</u>[5], <u>Rena Singleton</u>[6], <u>Jane Cauley</u>[7], <u>Elizabeth Barrett-Connor</u>[8], <u>Nancy Lane</u>[9], <u>Deborah Kado</u>[8], <u>John Schousboe</u>[10]. [1]GRECC, Minneapolis VA Medical Center, USA, [2]Oregon Health & Science University, USA, [3]San Francisco Coordinating Center, USA, [4]California Pacific Medical Center Research Institute, USA, [5]University of Minnesota & Minneapolis VA Health Care System, USA, [6]University of Minnesota, USA, [7]University of Pittsburgh Graduate School of Public Health, USA, [8]University of California, San Diego, USA, [9]University of California, Davis Medical Center, USA, [10]Park Nicollet ClinicUniversity of Minnesota, USA

Incident radiographically-detected vertebral fractures (RVF) are associated with substantial back pain morbidity in older women. However, consequences of incident RVF on back pain symptoms in older men have not been examined prospectively.

To evaluate the association of incident RVF with subsequent back pain symptoms in older men, we used data from MrOS, a prospective cohort of community-dwelling men aged ≥65 years. At baseline (V1) and visit 2 (V2), about 4.6 years later, lumbar and thoracic spine x-rays were obtained, and men self-reported back pain symptoms

(any, severity, bother) and back pain-related daily activity limitation for the past 1 year. Prevalent (V1) and incident (V2) RVF were determined by Genant semi-quantitative grading criteria. V2 back pain severity, bother and activity limitation were the primary outcomes in 3 levels (Table). Frequencies and odds of these outcomes were compared between men with and without incident RVF using odd ratios (OR) and 95% confidence intervals (CI) from multinomial logistic regression. Analyses were adjusted for age, prevalent RVF, and V1 back pain (any, none).

Of 4383 men with complete V1 and V2 spine x-rays, 11% had a prevalent RVF at V1. During follow-up, 4.5% (196) of men had an incident RVF by V2. At V1, any back pain (61% vs. 67%, p=0.07) and bother most or all the time from back pain (p=0.04) were similarly or less common in men with versus those without a subsequent incident RVF. The two groups also had a similar V1 prevalence of moderate or severe back pain (p=0.22), and of activity limitation because of back pain (p=0.11). However, by V2, any back pain was reported significantly more often by men with incident RVF than by men without incident RVF (73% vs. 59%, p<0.0001). Further, for each back pain symptom, the percentage of men reporting the worst level was greater in men with incident RVF than in those without incident RVF (Table). Even after adjustment, ORs of all back pain symptom outcomes were significantly elevated.

In these older men, incident RVF were associated with large, statistically significant odds of severe, frequent, and activity limiting back pain at follow-up. However, residual confounding may affect these results. Further, because the exact dates of incident RVF are unknown, timing of changes in back pain symptoms relative to RVF occurrence cannot be determined. Incident RVF may be an important cause of new or worsened back pain symptoms in older men.

Back Pain Outcome	No new RVF	New RVF	OR (95% CI)*
Severity			
No back pain	40%	27%	1.0 (referent)
Mild	29%	30%	2.2 (1.5-3.3)
Moderate/Severe	31%	43%	3.0 (2.0-4.5)
Bother			
No back pain	40%	27%	1.0 (referent)
Rarely/Sometimes	46%	47%	2.2 (1.5-3.2)
Most of time/Always	13%	26%	4.6 (2.9-7.3)
Daily Activity Limitation			
No back pain	40%	27%	1.0 (referent)
Back pain-no related activity limitation	42%	35%	1.8 (1.2-2.7)
Back pain-with related activity limitation	18%	39%	5.2 (3.4-7.9)

*Adjusted for age, prevalent (V1) VF, and any V1 back pain.

Table. V2 Back Pain Outcome Frequency (%) by Incident Radiographic Vertebral Fracture (RVF) Status

***Disclosures: Howard Fink**, None.*

FR0317

Atypical femoral fractures: Sensitivity and specificity of radiographic characteristics. <u>Annette Adams</u>*[1], <u>Fei Xue</u>[2], <u>Jean Chantra</u>[3], <u>Richard Dell</u>[4], <u>Susan Ott</u>[5], <u>Stuart Silverman</u>[6], <u>Joseph Giaconi</u>[7], <u>Cathy Critchlow</u>[8]. [1]Kaiser Permanente Southern California, USA, [2]Amgen, Inc., USA, [3]Kaiser Permanente Southern California, USA, [4]Kaiser, USA, [5]University of Washington Medical Center, USA, [6]Cedars-Sinai/UCLA, USA, [7]Cedars Sinai Medical Center, USA, [8]Amgen Inc., USA

Purpose: To understand the real-world application of the 2013 ASBMR atypical femoral fracture (AFF) case definition criteria by summarizing the sensitivity and specificity of radiographic features for distinguishing AFF from other subtrochanteric or diaphyseal fractures among women enrolled in a large integrated health care organization.

Methods: We identified 55 physician-validated AFFs from years 2010-2012 and a sample of 39 non-AFF (nAFF) subjects from years 2009-2012, all with available radiographs. One fracture image was selected per subject for review by each of 4 independent reviewers, osteoporosis experts representing 4 different medical specialties: internal medicine, rheumatology, orthopedics, and radiology. Using a standardized data collection tool based on the 2013 revised AFF case definition, reviewers indicated the presence or absence of the following characteristics viewable on radiograph: subtrochanteric or diaphyseal fracture location, fracture pattern, non-comminution, periosteal and/or endosteal thickening, and cortical thickening. Sensitivity and specificity for each characteristic was calculated for each reviewer, and summarized across reviewers with the mean and range.

Results: The most highly sensitive factors for distinguishing between AFF and nAFF were subtrochanteric/diaphyseal fracture location (mean 99.4%, range 97.7-100%), lateral cortex transverse fracture pattern (mean 95.3%, range 90.2-97.7%),

medial cortex transverse or oblique fracture pattern (mean 94.0%, range 83.3-100%), and minimal or non-comminution (mean 94.2%, range 88.6-97.7%). Of these factors, specificity was greatest for lateral cortex transverse fracture pattern (mean 72.8%, range 69.6-76.0%), while medial cortex transverse or oblique pattern was least specific (mean 11.2%, range 0-42.6%). Localized endosteal/periosteal reaction and generalized increase in cortical thickness were only moderately sensitive and specific.

Conclusion: Fracture location and transverse fracture pattern in the lateral cortex were the most sensitive characteristics and were most highly agreed upon across reviewers in clinical settings. Other characteristics were less readily agreed upon across reviewers. Measurement of discrete combinations of individual characteristics may enhance sensitivity and/or specificity.

FR0318

Back Pain Is Associated with Increased Risk of Recurrent Falls Among Older US Women. Lynn Marshall*[1], Stephanie Harrison[2], Peggy Cawthon[3], Deborah Kado[4], Una Makris[5], Richard Deyo[6], Hans Carslon[6], Michael Nevitt[7]. [1]Oregon Health & Science University, USA, [2]San Francisco Coordinating Center, USA, [3]California Pacific Medical Center Research Institute, USA, [4]University of California, San Diego, USA, [5]University of Texas Southwestern Medical Center, USA, [6]Oregon Health & Science University, USA, [7]University of California San Francisco, USA

Falls among older adults are a major clinical and public health concern. Several fall risk factors, such as poor physical function, depression and prescription pain medication use, are more prevalent among older adults with back pain than in those without back pain. Whether back pain itself increases fall risk in elderly populations is unknown.

Our purpose was to determine the association of back pain to one-year risk of new falls among 6841 community dwelling U.S. women aged ≥65 years enrolled in the Study of Osteoporotic Fractures. On questionnaires at the second study visit, women reported any back pain in the past year, back pain severity, frequency of being bothered by back pain, and limiting their usual activities because of back pain. Every four months for the next 1 year, women reported numbers of falls on mailed questionnaires or phone calls. The primary outcome was recurrent falls defined as ≥2 falls. Risk of recurrent falls was compared between women with and without back pain symptoms using risk ratios (RR) and 95% confidence intervals (CI) from multivariable log-binomial regression. In the final model, RRs were adjusted for age, education, smoking history, fainting in the past year, hip pain, history of stroke, and Geriatric Depression Scale. During model building, factors assessed and found not to be potential confounders were prevalent radiographic vertebral fracture, difficulty with any instrumental activity of daily living, gait speed, grip strength, chair stand time, tandem stand time, and prescription medication use for pain, sleep problems or anxiety.

Most (61%) women reported any back pain in the past year. Of women with back pain, 58% reported moderate and 14% reported severe pain, 24% reported being bothered most or all of the time by back pain, and 22% reported limiting their usual activities because of back pain. During follow-up, 10% had recurrent falls. Any back pain was associated with a 50% increased risk of recurrent falls (adjusted RR=1.5, 95% CI: 1.3, 1.8). RRs for recurrent falls were of similar magnitude in all categories of back pain severity, frequency of bother, and for activities not limited by back pain (Table). The RR was highest for women who limited their activities because of back pain.Older community dwelling women with a recent history of back pain are at increased risk for recurrent falls. Whether back pain treatment reduces fall risk, or risk of injurious falls, in this population should be examined.

Table. Risk Ratios (RR) and 95% Confidence Intervals (CI) for Recurrent Falls in Relation to Back Pain Symptoms among Women Aged ≥65 Years

Back Pain Symptom	No.	Recurrent Falls, N (%)	Adjusted RR* (95% CI)
Severity			
No back pain	2,670	184 (7%)	1.0 (Referent)
Mild	1,174	121 (10%)	1.4 (1.1, 1.8)
Moderate	2,406	286 (12%)	1.6 (1.3, 1.9)
Severe	591	73 (12%)	1.5 (1.1, 1.9)
Frequency			
No back pain	2,670	184 (7%)	1.0 (Referent)
Rarely/Sometimes	3,160	347 (11%)	1.5 (1.2, 1.8)
Most/All of the time	1,011	133 (13%)	1.6 (1.3, 2.0)
Activities Limited by Back Pain			
No back pain	2,670	184 (7%)	1.0 (Referent)
No, activities not limited	3,240	339 (10%)	1.4 (1.2, 1.7)
Yes, activities limited	931	141 (15%)	1.8 (1.4, 2.3)

*Adjusted for age, education, smoking history, fainting in the past year, hip pain, history of stroke, and Geriatric Depression Scale.

Table.

FR0320

Fractures Increasing in Oldest Age Groups Despite Decreasing Fracture Rates: A Population-based Study. Susan Jaglal*[1], Gillian Hawker[1], Cathy Cameron[2], Ruth Croxford[3]. [1]University of Toronto, Canada, [2]Women's College Research Institute, Canada, [3]Institute for Clinical Evaluative Sciences, Canada

Many studies in developed countries have found that while the older population has been increasing, hip fracture rates in particular have been decreasing thereby offsetting the expected increase due to the aging population. We examined numbers and rates of common osteoporotic fractures including the hip, wrist, pelvis, shoulder and spine in the province of Ontario, Canada by age and sex from fiscal year 2002/03 to 2012/13. For hip fractures, the age-standardized rates have decreased but the absolute numbers have increased. The largest growth in the number of fractures has been in the oldest age groups 80+ and 90+ years. In 2002/03 the number of hip fractures in the 90+ age group was 1558 compared to 2226 in 2012/13. There was a 39.4% increase in the number of hip fractures among men aged 90+ and 27.3% increase among women aged 90+. Overall larger percent increases in fractures from fiscal year 2002/03 to 2012/13 were seen among men. Among those age 80+ the increase was 25.5% for men and 12.3% for women. For the other fractures large percent increases were also seen in the 80+ age group for both men and women. For wrist fractures there was a 36.7% increase in men age 80+ and 23.5% increase in women age 80+; for pelvis 49.4% in men age 80+ and 38.4% in women age 80+; for shoulder age 33.5% in men age 80+ and 25.3% in women age 80+; for spine 52% in men age 80+ and 41% in women age 80+. Fractures of the pelvis and spine had the largest percent increase in those aged 80+ followed by wrist, shoulder and hip across the time period. The percent increases were greater among men than women across all of the fracture types. Also steady yearly increases across the time period were noted. Overall these large percent increases in fractures in the oldest old in the midst of declining fracture rates have major implications on the cost of fractures to the health care system and the targeting of screening and treatment efforts. Factors may include increased comorbidity and less than optimal fall and fracture prevention particularly among men. Future research needs to characterize these fracture patients compared to the general elderly population and examine the reasons for the increase in fractures particularly among the oldest old.
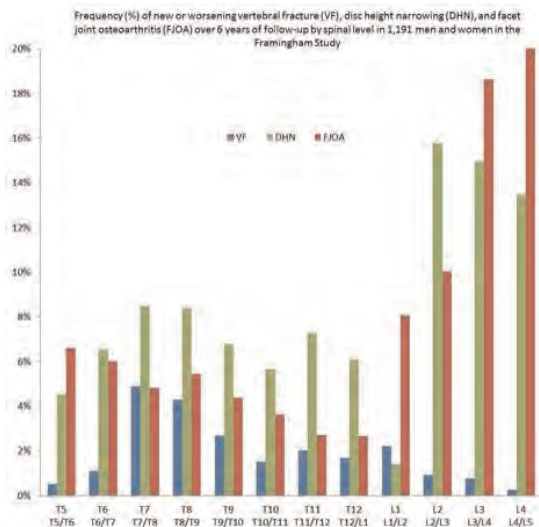
FR0323

Incidence and Worsening of Vertebral Fracture, Disc Height Narrowing, and Facet Joint Osteoarthritis Evaluated by Computed Tomography: The Framingham Study. Mohamed Jarraya*[1], Yanhua Zhou[2], L Adrienne Cupples[2], Ali Guermazi[3], Ching-An Meng[4], Elana Borchin[5], Douglas Kiel[6], Mary Bouxsein[7], Elizabeth (Lisa) Samelson[8]. [1]Boston University School of Medicine, USA, [2]Boston University School of Public Health, USA, [3]Boston University School of Medicine, USA, [4]Hebrew SeniorLife, USA, [5]Hebrew SeniorLife, USA, [6]Hebrew SeniorLife, USA, [7]Beth Israel Deaconess Medical Center, Harvard Medical School, USA, [8]Hebrew SeniorLife, Harvard Medical School, USA

Prior studies have not described degenerative features across the whole spine assessed by CT in non-clinical populations. We conducted a longitudinal study of new or worsening vertebral fracture (VF), disc height narrowing (DHN), and facet joint osteoarthritis (FJOA) over 6 yr in a community-based sample of men and women, and characterized these changes by spinal level, age and sex.

Participants included 1,191 cohort members of the Framingham Study (538 men, 653 women; mean age 61 yr; range 40-85) who had CT scans 6 yr apart. A radiologist scored VF, DHN, and FJOA at each spinal level (T5-L4) as grade 0=normal, 1=mild, 2=moderate, or 3=severe. We used chi-square tests to compare prevalence of VF (grade≥1), DHN (grade≥2), and FJOA (grade≥2) and frequency of new or worsening features (increase in ≥1 grade) in women and men, and to test for trends with age.

Prevalence of VF, DHN, and FJOA was 31, 68, and 87%. Prevalence of all 3 features increased with age (p<0.01). Frequency of new or worsening VF was similar in women (15%) and men (16%) and increased with age in women (p<0.01) but not men (p=0.41). Worsening of DHN increased with age (p<0.01) in women and men. Frequency of worsening DHN was higher in women than men at each age group (<60, 60-69, ≥70 yr; women 47, 64, 71%; men 38, 59, 60%), however, the difference between men and women was significant only for <60 yr (p=0.03). Worsening of FJOA did not increase with age in women (p=0.21) or men (p=0.15). However, women had greater frequency of FJOA worsening than men (p<0.01) in those <60 yr (54 vs 38%) and 60-69 yr (57 vs 39%), but not ≥70 yr (44 vs 46%, p=0.77). Frequency of new or worsening VF showed a bimodal distribution with peaks at the midthoracic and thoracolumbar spine, whereas worsening of DHN was greatest at the lumbar (13-16%, L2-L4), and midthoracic (8%, T7-T8) regions (FIGURE). Frequency of worsening of FJOA decreased from the upper to lower thoracic spine (from 7% at T5 to 3% at T12), but increased from the upper to lower lumbar spine (from 8% at L1 to 24% at L4).

We found that over 6 yr, more than half of men and women in this population experienced new or worsening of DHN and FJOA, and 1/6 had new or worsening VF. The high frequency of progression and distribution of these radiographic changes along the spine suggest that pathology in bone, disc, and joint may occur interdependently. Further work is needed to determine the sequence and etiology of these changes and impact on clinical outcomes.

FIGURE

Disclosures: Mohamed Jarraya, None.

FR0329

Serum Bioavailable Estradiol Adds Information Beyond FRAX® for Hip Fracture Reclassification in Elderly Swedish Men – MrOS Sweden. Liesbeth Vandenput[1], Maria Nilsson[2], Maria Nethander[3], Joel Eriksson[4], Osten Ljunggren[5], Andreas Kindmark[5], Mattias Lorentzon[6], Helena Johansson[7], Jodi Lapidus[8], Ying Wang[9], Eric Orwoll[9], Magnus Karlsson[10], Dan Mellstrom[11], Claes Ohlsson*[12]. [1]University of Gothenburg, Sweden, [2]Centre for Bone & Arthritis Research, Institute of Medicine, Sahlgrenska Academy, University of Gothenburg, Sweden, [3]Bioinformatics Core Facility, Sahlgrenska Academy, University of Gothenburg, Sweden, [4]Centre for Bone & Arthritis Research, Sweden, [5]Uppsala University Hospital, Sweden, [6]Geriatric Medicine, Center for Bone Research at the Sahlgrenska Academy, Sweden, [7]Centre for Metabolic Bone Diseases, University of Sheffield Medical School, Sweden, [8]Oregon Health & Science University, USA, [9]Oregon Health & Science University, USA, [10]Skåne University Hospital Malmö, Lund University, Sweden, [11]Sahlgrenska University Hospital, Sweden, [12]Center for Bone & Arthritis Research at the Sahlgrenska Academy, Sweden

Prospective cohort studies have reported that low serum estradiol (E2) and testosterone (T) and high sex hormone-binding globulin (SHBG) associate with increased fracture risk in men and that thresholds for these associations might exist. The aim of the present study was to determine the clinical utility of serum sex steroids for fracture risk prediction in men.

In the prospective population-based MrOS Sweden study, 2,542 men (69-80 years old) had baseline E2 and T analyzed by GC-MS and SHBG by RIA (exclusions; surgical or chemical castration, androgen treatment, anti-androgen treatment or not having all three serum parameters). Bioavailable (bio) E2 and bio T were calculated using law of mass equations. Incident X-ray verified hip (n=173, incidence 6.8%) and major osteoporotic (n=418, incidence 16.4%) fractures were evaluated (follow up @10 years). Discrimination was determined using C-statistics while net reclassification improvement (NRI) was used for reclassification analyses. The improvements of sex steroids as continuous parameters, as well as dichotomous parameters using predefined published thresholds (T < 300 ng/dl; bioT < 163.5 ng/dl; E2 < 16 pg/ml; bioE2 < 11.4 pg/ml; SHBG > 59.1 nM), were evaluated from base models of age (Model 1), age, BMI and BMD (Model 2), and FRAX®, including BMD (Model 3).

The improvements in fracture risk discrimination (AUC) from the different base models were minor for all sex steroids. However, when evaluated with the sensitive NRI, a significant improvement of all three base models was seen for low E2 (bio E2 < 11.4 pg/ml) both after 5 years (Model 1, 43%, p = 9.3x10^{-4}; Model 2, 42%, p = 1.7x10^{-3}; Model 3, 42%, p = 1.7x10^{-3}) and 10 years (p ≤ 1.1x10^{-3} for all three models) follow up for hip fractures. The increased NRI was mainly the result of a correct downward reclassification of those without a fracture. Similar significant improvements were observed for major osteoporotic fractures (p < 1x10^{-4}). Neither the different T nor SHBG parameters increased NRI significantly for hip fractures.

These findings demonstrate that low bio E2 (< 11.4 pg/ml) adds information beyond FRAX® for hip and major osteoporotic fracture reclassification in elderly Swedish men.

Disclosures: Claes Ohlsson, None.

FR0332

Associations of 25OHD and 1,25(OH)$_2$D with BMD, BMD Loss and Fracture. Christine Swanson*[1], Priya Srikanth[2], Christine Lee[1], Steven Cummings[3], Ivo Jans[4], Jane Cauley[5], Roger Bouillon[6], Dirk Vanderschueren[6], Eric Orwoll[1], Carrie Nielson[1]. [1]Oregon Health & Science University, USA, [2]Department of Public Health & Preventive Medicine, Oregon Health & Science University, USA, [3]San Francisco Coordinating Center, USA, [4]Laboratory of Diagnostic Medicine, KU Leuven, University of Leuven, Belgium, [5]University of Pittsburgh Graduate School of Public Health, USA, [6]Katholieke Universiteit Leuven, Belgium

Relationships between the biologically active vitamin D metabolite 1,25(OH)$_2$D and skeletal outcomes are uncertain. We examined the associations of 1,25(OH)$_2$D with BMD, BMD change, and incident fractures in a cohort of older men and compared them to those of 25OHD.

Using a case cohort design, we analyzed data from 1,000 men (age 74.6 ± 6.2 years) in the Osteoporotic Fractures in Men (MrOS) study, including 537 men that had DXA BMD obtained at baseline and at ~4.5 years of follow-up that were used for the longitudinal BMD change analyses. Incident non-spine fractures were ascertained. Cox proportional hazards models were used to test the association between vitamin D metabolite levels and non-vertebral and hip fractures. Linear regression models were used to estimate the association between vitamin D measures and baseline BMD and BMD change. Interactions between 25OHD and 1,25(OH)$_2$D were tested for each outcome.

There were 432 men with incident non-vertebral fractures and 81 with a hip fracture. As previously reported, higher 25OHD was associated with higher baseline BMD, slower BMD loss and lower hip fracture risk (Table). Conversely, men with

higher 1,25(OH)$_2$D had lower baseline BMD (Table). 1,25(OH)$_2$D associations with BMD loss and fracture were weaker than those for 25OHD and were usually not statistically significant (Table). However, the risk of hip fracture tended to be lower in men with higher 1,25(OH)$_2$D levels after adjustment for baseline hip BMD (HR 0.74, 95% CI 0.56-1.00), an effect that was similar in magnitude to that seen with higher 25OHD levels. There were no interactions between 25OHD and 1,25(OH)$_2$D on any outcome (all p $\geqslant$ 0.60). Adjustment of 1,25(OH)$_2$D data for 25OHD (and vice-versa) had little effect on the associations observed, however the protective effect of 1,25(OH)$_2$D on hip fracture seen after adjustment for baseline BMD was attenuated (Table).

In older men, higher 1,25(OH)$_2$D was associated with lower baseline BMD but was not related to the rate of bone loss or fracture risk. However, with BMD adjustment, a weakly protective association for hip fracture was seen with higher 1,25(OH)$_2$D. The associations of 25OHD with skeletal outcomes were generally stronger and independent of 1,25(OH)$_2$D.

Table. BMD and Fracture Associations with 25OHD and 1,25(OH)$_2$D

	Base Model[a]	Base Model[a] + BMD[b]	Base model[a] + BMD[b], Adjusted for the other Vit D[g]
Hip Fracture [HR, (95% CI)] per SD increase in Vitamin D			
25OHD	0.69 (0.52, 0.91)	0.69 (0.52, 0.93)	0.75 (0.54, 1.02)
1,25(OH)$_2$D	0.86 (0.66, 1.13)	0.74 (0.56, 1.00)	0.82 (0.60, 1.12)
Non-vertebral Fracture [HR, (95% CI)] per SD increase in Vitamin D			
25OHD	0.97 (0.87, 1.09)	1.01 (0.90, 1.13)	0.99 (0.88, 1.13)
1,25(OH)$_2$D	1.02 (0.92, 1.13)	0.99 (0.89, 1.11)	1.01 (0.90, 1.13)
Total Hip Baseline BMD (g/cm^2) [β (95% CI)] Mean = 0.96, SD = 0.14			
	Base Model[c]	Multivariable Model[d]	Multivariable Model[d], Adjusted for the other Vit D[g]
25OHD	0.02 (0.01, 0.03)	0.01 (0.00, 0.03)	0.02 (0.01, 0.03)
1,25(OH)$_2$D	-0.01 (-0.02, 0.00)	-0.02 (-0.03, -0.01)	-0.02 (-0.04, -0.01)
Annualized Total Hip BMD Change (%) [β (95% CI)] Mean = -0.49, SD = 0.95			
	Base Model[e]	Multivariable Model[f]	Multivariable Model[f], Adjusted for the other Vit D[g]
25OHD	0.09 (0.01, 0.18)	0.09 (0.00, 0.18)	0.10 (0.01, 0.20)
1,25(OH)$_2$D	0.03 (-0.05, 0.11)	0.00 (-0.08, 0.09)	-0.03 (-0.12, 0.06)

[a] age, race, site, season, physical activity, height, weight
[b] baseline total hip BMD
[c] age, race, site, season, BMI
[d] age, race, site, season, BMI, health status, smoking, alcohol, physical activity and inability to rise from chair
[e] age, race, site, season, BMI, baseline total hip BMD
[f] age, race, site, season, BMI, baseline total hip BMD, health status, smoking, alcohol, physical activity and inability to rise from chair
[g] That is, the 25OHD association is adjusted for 1,25(OH)$_2$D and vice versa

Table

FR0338

Visceral Adipose Tissue is Associated with Better Trabecular Density and Architecture but Increased Cortical Porosity: The Framingham Osteoporosis Study.

Douglas Kiel*[1], Kerry Broe[2], Adrienne Cupples[3], Serkalem Demissie[3], Caroline Fox[4], Marian Hannan[5], Yi-Hsiang Hsu[6], David Karasik[7], Ching-Ti Liu[3], Robert McLean[8], Ching-An Meng[9], Elizabeth (Lisa) Samelson[10], Xiaochun Zhang[9], Mary Bouxsein[11]. [1]Hebrew SeniorLife, USA, [2]Institute for Aging ResearchHebrew SeniorLife, USA, [3]Boston University School of Public Health, USA, [4]National Institutes of Health, USA, [5]HSL Institute for Aging Research & Harvard Medical School, USA, [6]Hebrew SeniorLife Institute for Aging Research & Harvard Medical School, USA, [7]Hebrew SeniorLife; Bar Ilan University, USA, [8]Hebrew SeniorLife Institute for Aging Research & Harvard Medical School, USA, [9]Institute for Aging Research, Hebrew SeniorLife, USA, [10]Hebrew SeniorLife, Harvard Medical School, USA, [11]Beth Israel Deaconess Medical Center, Harvard Medical School, USA

Obesity has been considered to protect against osteoporosis and fx because of mechanical and hormonal factors. Recently, body fat has been shown to be associated with lower BMD and increased risk for more fractures. Few studies have examined associations between VAT, BMD and microarchitecture in cortical and trabecular compartments. Thus, we performed a cross-sectional study of VAT and BMD and bone microarchitecture in 381 participants (60% women), avg age 57.6 $\pm$ 7.4 yrs from the Framingham Offspring cohort to determine whether cortical and trabecular BMD and microarchitecture differ according to the amount of VAT. VAT was measured from multidetector CT abdominal imaging by manually tracing its position beneath the abdominal muscular wall. BMD and microarchitecture were measured at the tibia and radius using HR-pQCT (Scanco Medical AG), focusing on six bone parameters: cortical porosity (CtPo,%), cortical thickness (CtTh, mm), cortical bone area fraction CtA/TtA, trabecular BMD (TbBMD, mg/cm^3), trabecular number (TbN, 1mm), and total BMD (TtBMD, mgcm^3). To isolate the contribution of VAT to BMD and architecture, we calculated the ratio of VAT to body weight (WT) and used ANCOVA to assess the association between quartiles of VAT/WT and BMD or microarchitecture. Analyses were repeated using quartiles of VAT. Analyses

adjusted for sex, age, ht (except for CtA/TtA), and in women, menopausal status. The average VAT was 1,977 $\pm$ 1013 cm^3. The average weight was 78 $\pm$ 16 kg. At the radius and tibia, CtTh and CtA/TtA increased across quartiles of VAT/WT (all p-trends <0.01). CtPo also increased by 8.2% at the radius (p-trend 0.06), but not the tibia (p-trend 0.43). TbBMD, TbN, and TtBMD increased with greater VAT/WT at the radius and tibia. When the analyses were repeated using quartiles of VAT, CtPo increased in the radius by 17% (p-trend 0.02) and in the tibia by 12% (p-trend 0.002) at the tibia. TbBMD and TbN generally increased while TtBMD did not. In conclusion, higher visceral adiposity is associated with greater total BMD, trabecular BMD and number, and greater cortical bone fraction, but also with greater cortical porosity. The finding that total density was positively associated with VAT/WT but not VAT may imply that weight increases total density while VAT affects cortical porosity. These complex effects on trabecular and cortical indices may partly explain why fractures occur at certain sites in obese persons such as the ankle and arm.

Association between visceral adipose tissue (VAT)/weight ratio and bone density and microarchitecture measures of the radius and tibia

	Bone Parameters	Q1 (N=83) (5.97 ± 2.10)	Q2 (N=87) (9.29 ± 1.95)	Q3 (N=92) (12.37 ± 2.15)	Q4 (N=87) (16.75 ± 3.31)	P-Trend
Radius (N=349)	CtPo (%)	3.67 ± 0.22	3.67 ± 0.21	3.46 ± 0.21	4.00 ± 0.22	0.06
	CtTh (mm)	0.716 ± 0.026	0.838 ± 0.025	0.843 ± 0.025	0.841 ± 0.026	0.02
	CtA/TtA**	0.196 ± 0.006	0.207 ± 0.006	0.208 ± 0.006	0.216 ± 0.006	0.02
	TbBMD (mg/cm^3)	140 ± 5.10	151 ± 4.94	147 ± 4.90	163 ± 5.16	0.03
	TbN (1/mm)	1.85 ± 0.05	1.90 ± 0.05	1.95 ± 0.05	2.10 ± 0.05	0.0002
	TtBMD (mg/cm^3)	271 ± 9.37	308 ± 9.07	308 ± 8.99	316 ± 9.48	0.01
	Bone Parameters	Q1 (N=94) (6.06 ± 2.11)	Q2 (N=93) (9.31 ± 1.96)	Q3 (N=95) (12.37 ± 2.13)	Q4 (N=93) (16.72 ± 3.33)	P-Trend
Tibia (N=375)	CtPo (%)	10.13 ± 0.41	10.37 ± 0.41	10.10 ± 0.40	9.88 ± 0.42	0.44
	CtTh (mm)	0.989 ± 0.031	1.094 ± 0.031	1.130 ± 0.030	1.134 ± 0.032	0.001
	CtA/TtA**	0.158 ± 0.004	0.170 ± 0.004	0.172 ± 0.004	0.179 ± 0.004	0.0007
	TbBMD (mg/cm^3)	149 ± 4.80	168 ± 4.76	161 ± 4.68	176 ± 4.92	0.001
	TbN (1/mm)	1.81 ± 0.05	2.00 ± 0.05	1.90 ± 0.05	2.15 ± 0.05	0.0001
	TtBMD (mg/cm^3)	244 ± 6.94	272 ± 6.88	272 ± 6.77	286 ± 7.11	<0.0001

*Adjusted for sex, age, height and menopause status (women)
**Adjusted for sex, age and menopause status (women)

Association between visceral adipose tissue (VAT)/weight ratio and bone density and microarchitectur

FR0339

How Long Does the Therapeutic Window of Opportunity Persist After a Fragility Fracture?.

François Cabana[1], Marie-Claude Beaulieu[2], Nathalie Carrier[1], Sophie Roux[3], Gilles Boire*[4]. [1]Centre hospitalier universitaire de Sherbrooke, Canada, [2]Université de Sherbrooke, Canada, [3]University of Sherbrooke, Canada, [4]Centre Hospitalier Universitaire De Sherbrooke, Canada

Objective: To determine how long an incident fragility fracture (FF) remains a strong incentive to initiate osteoporosis (OP) treatment.

Methods: The OPTIMUS program was implemented in fracture clinics to educate women and men over age 50 on the link between incident FF and OP and to empower Family Physicians (FPs) to diagnose and treat OP. The 1409 (1022 untreated) patients were included after sustaining a FF, and were assigned to usual care (Control Group; CG), or Minimal or Intensive interventions. In both interventions, baseline individualized letters were sent to FPs explaining the rationale to treat OP after most FF. Intensive patients also received more frequent follow-up (FU) phone calls during the first year and results from baseline blood tests were sent to their FP. Over the first year, reminder letters were sent to FPs of intervention patients who remained untreated upon FU, again suggesting to treat. At one year, untreated patients in both the CG and Minimal groups were offered an Intensive intervention. Phone FU was completed up to 48 months.

Results: Within Minimal and Intensive intervention patients, OP treatment initiation had occurred by 6 months in 31.7% of those initially untreated, and by 12 months, in 25% of those still untreated at 6 months. By 24, 36 and 48 months, rates had decreased to 14.1%, 2.5% and 0.7% of patients still untreated at 12, 24 and 36 months, respectively. The corresponding rates in CG patients were 13.8%, 5.6%, 17.8%, 5.2% and 5.4% by 6, 12, 24, 36 and 48 months, respectively.

Of the 114 untreated CG patients offered Intensive intervention at 12 months, 37 (32.5%) accepted the intervention and 20 (17.5%) initiated treatment. Following 12 months of Minimal intervention, 33/150 (22%) untreated patients accepted Intensive intervention but only 6 (4%) got treated over the next 36 months.

Conclusion: Individualized interventions targeting FF patients and their FPs were most successful to initiate OP treatment during the first 6 to 12 months after the initial FF, and their impact rapidly decreased thereafter. Even when offered an effective Intensive intervention, patients still untreated after 12 months of Minimal Intervention were unlikely to get treated, and treatment initiation rates after 12 months were slightly higher but remained low in untreated usual care patients. These findings suggest that, although a FF represents an ideal opportunity to start OP treatment, the window has already closed by 1 year.

FR0343

Validation of ICD-9 Codes or Self-report for Osteoporotic Fractures in Women Aged 45-60. Susan Ott*[1], Rebecca Hubbard[2], Belinda Operskalski[2], Do Peterson[2], Kelly Hansen[2], Andrea Lacroix[3], Delia Scholes[4]. [1]University of Washington Medical Center, USA, [2]Group Health Research Institute, USA, [3]Fred Hutchinson Cancer Research Center, USA, [4]Group Health CooperativeGroup Health Research Institute, USA

Fractures (fx) are an important outcome for epidemiological studies. Reviewing individual medical records is a more expensive method of collecting data than using automated electronic medical records or self-reported fx from questionnaires. We studied the validity of ICD-9 codes to identify clinical fx from osteoporotic locations (including ankles) in women aged 45-60 from a US health care system compared to physician-adjudicated medical record review. We also examined the concordance between self-report and validated fx.

Methods: After excluding for estrogen use, hysterectomy, or no encounters, we searched computerized records of 56021 women for an outpatient or inpatient fx code between 1/1/08 and 3/30/13. We identified 3178 potential cases and reviewed their charts. A random sample of 4374 women without a code were age-matched to those with a fx. Those with a confirmed fx and the random sample were telephoned by trained interviewers who were unaware of the fx status. Surveys were completed by 1186 women with a validated fx and 2301 without. We asked whether they had experienced a fx and which bone, if any, was broken. We then reviewed charts from the 52 women without a code but who self-reported a fx. We assumed that women without a code who self-reported no fx had not had a clinical fx.

RESULTS-Codes: Of 2529 validated fx, most common locations were: forearm (28%), ankle (21.8%), ribs (10.4%). The positive predictive value was 78% (women with an ICD-9 code who had a current clinical osteoporotic fx). Fx occurred in 0.91% without a code. Sensitivity of ICD-9 codes was 83.7%, specificity was 98.7%. Nine percent of the ICD-9 codes were for non-specific locations, and only half of them were osteoporotic (the rest were in hands/feet or >1yr prior to the code). Specific codes for other skeletal sites correctly identified fx between 62 and 100% of the time (Fig1). In those who had a fx and a site-specific ICD-9 code, the skeletal site was accurate in 97%. Self-report: 88% of women who had a valid fx reported the fx and, if so, the location was correct in 99%. Vertebral fx were the most commonly unreported fx (Fig2).

Conclusion: Either ICD-9 codes or self-report can be used to identify osteoporotic fx in middle-aged women using large datasets. The sensitivity is good with 83.7% for ICD-9 codes and 88% for self-report, but there will be some errors when evaluating fx of the spine or ankle.

Fig 2. Self-reported fractures according to confirmed fracture location

Disclosures: Susan Ott, None.

Fig1: Validated fractures according to ICD-9 codes

FR0344

Where the ball was dropped. Why do patients fall off Secondary Fracture Prevention Programs?. Manju Chandran*, Xiao Feng Huang, Matthew Tan. Osteoporosis & Bone Metabolism Unit, Singapore General Hospital, Singapore

Introduction: OPTIMAL (Osteoporosis Patient Targeted and Integrated Management for Active Living) is a clinician champion driven, case manager run multi-component secondary fracture prevention program set up in the public hospitals and polyclinics of Singapore. At Singapore General Hospital (SGH), the largest public tertiary teaching hospital in Singapore, the program was set up as a collaborative effort between multiple departments and in the 6 years since inception has gained international recognition amongst the osteoporosis community for its work on recruiting patients with fragility fractures. We have previously reported on the set up of the program and the good medication compliance rates amongst patients who completed 2 year follow up in the program [1, 2]. The aim of this study is to enumerate the patients who discontinued the program during the course of follow up and to evaluate the reasons for such discontinuation.

Methods: Retrospective review of the Centralized Computerized Recorded Data (CCRD) base of patients recruited into the OPTIMAL program at SGH.

Results: 1214 patients with fragility fractures have been recruited into the program. 302 patients have completed 2 years of follow up. 156 patients have been "right-sited" (discharged to follow up care with General Practitioners) and 483 patients are in current active follow up at the hospital. 104 patients withdrew from the program citing various reasons and 129 just stopped showing up for follow up visits. 29 patients had other reasons for stopping the program including development of other medical conditions such as renal failure, following up with specialists outside the hospital and thus being lost to follow up etc. 11 patients died during the course of follow up. The reasons cited by patients for withdrawal are shown in Table 1.

Discussion: It is important whilst implementing and running a fracture liaison service to periodically look back and evaluate where all "the ball was dropped". Willingness by patients to participate and comply with antiosteoporosis strategies is important to ensure disruption of the otherwise inevitable fracture cascade. Though our "drop out" rate was low, it is still large enough to be concerning and ensure that we do not rest on our laurels and make continued efforts to make the services beneficial to patients. Educating individuals with fracture and their families on the consequences and treatment of osteoporosis may help to make them more accepting of secondary preventive measures. Knowledge of the challenges faced by patients may be of use to stakeholders interested in developing fracture liaison services.

References:

Chandran M, Tan MZ et al. Secondary prevention of osteoporotic fractures-an "OPTIMAL" model of care from Singapore. Osteoporos Int. 2013 Nov;24(11):2809-17

Cheen MH, Kong MC et al. Adherence to osteoporosis medications amongst Singaporean patients. Osteoporos Int. 2012 Mar;23(3):1053-60

Reasons given for withdrawing from the program

Reason	N	Percentage
Too time consuming/ too frail and not having family member to accompany during hospital visits	50	48%
Osteoporosis Medications too expensive	35	33.6%
Do not think Osteoporosis is important problem or priority	11	10.5%
Fearful of Side Effects of medications or have experienced Side effects	6	5.7%

Table 1

Disclosures: Manju Chandran, None.

FR0345

Individual Characteristics that Predict Higher Health Care Costs After Hip Fracture. <u>John Schousboe</u>*[1], <u>Misti Paudel</u>[2], <u>Brent Taylor</u>[3], <u>Allyson Kats</u>[4], <u>Beth Virnig</u>[5], <u>Bryan Dowd</u>[5], <u>Kristine Ensrud</u>[6]. [1]Park Nicollet ClinicUniversity of Minnesota, USA, [2]Division of Epidemiology University of Minnesota, USA, [3]University of Minnesota, USA, [4]Chronic Disease Research Group, USA, [5]Division of Health Policy & Management, University of Minnesota, USA, [6]University of Minnesota & Minneapolis VA Health Care System, USA

Purpose: Health care costs after hip fracture are highly variable. Our purpose was to estimate the association of pre-fracture individual patient characteristics with costs attributable to hip fracture by linking the Study of Osteoporotic Fractures (SOF) participants' data with their Medicare claims.

Methods: For women enrolled in the SOF as of 1/1/1991 with a confirmed match to their Medicare claims (n=9,228), incident hip fractures were identified in Medicare Analysis and Provider Review (MedPAR) files by a hospital discharge diagnosis code of 820.0x or 733.14. Inpatient and outpatient costs were estimated from MedPAR, Carrier, Outpatient, and Home Health Care files. The association of pre-fracture participant characteristics with log of total costs of care for the first year after hip fracture were estimated with random effects regression models, adjusted for total costs of care the year before hip fracture and comorbidity.

Results: 738 women had a hip fracture (at mean age 83.7 years) between 1/1/1992 and 12/31/2009 while enrolled in Medicare Fee for Service. Median total costs (2010 U.S. dollars) the years before and after hip fracture were \$4,465 (IQR \$0 to \$14,066) and \$35,556 (IQR \$24,830 to \$50,903), respectively. Pre-fracture predictors significantly associated with total costs of care after hip fracture were body mass index, walk speed and depressive symptoms (table).

Model predicted total costs after hip fracture for those with BMI $\geq$ 30 kg/m2 compared to 20 to 24.9 kg/m2 were \$43,383 vs. \$33,916; for walk speed <1 m/sec vs. $\geq$ 1.0 m/sec, \$35,821 vs. 30,258; and for GDS score $\geq$ 6 vs. < 3, \$39,726 vs. \$33,208.

Age, bone density, grip strength, chair stand speed, health status, cognition (modified Mini-mental state exam score) and functional status (ability to perform IADLs) were not associated with total costs of care after hip fracture.

Conclusions: Pre-fracture obesity, slow walk speed, and depression are associated with higher health care costs after hip fracture, adjusted for comorbidity and health care costs the year before hip fracture.

Predictor (number of women)	Coefficient* (95% C.I.)
Body Mass Index < 20 kg/m² (80)	0.01 (-0.22 to 0.24)
20-24.9 (339)	Reference
25-29.9 (241)	0.04 (-0.12 to 0.19)
≥ 30 (78)	0.43 (0.20 to 0.66)
Walk Speed < 1.0 m/sec (644)	0.29 (0.08 to 0.50)
≥ 1.0 (94)	Reference
Geriatric Depression Scale Score <3 (418)	Reference
3 to <6 (206)	0.17 (0.01 to 0.32)
>=6 (114)	0.31 (0.12 to 0.51)

*Log(total costs) standard deviations change compared to reference

Table

FR0347

A longitudinal analysis of the impact of very low energy diets on bone mineral density. <u>Palak Choksi</u>*[1], <u>Amy Rothberg</u>[2], <u>Andrew Kraftson</u>[2], <u>Nicole Miller</u>[2], <u>Katherine Zurales</u>[2], <u>Charles Burant</u>[2], <u>Catherine Van Poznak</u>[3], <u>Mark Peterson</u>[2]. [1]University of Michigan, USA, [2]University of Michigan, USA, [3]University of Michigan Comprehensive Cancer Center, USA

Background The rising prevalence of obesity and concerns associated with co-morbidities and healthcare expenditures have led to greater clinical emphases on weight reduction. Very low energy diets are increasingly popular mainly due to the rapid weight loss without adverse effects associated with gastric bypass procedures. Body mass is also known to be an important determinant of bone mineral density (BMD), and rapid weight reduction is associated with decreases in BMD and potentially increased fracture risk. However, the effect of long-term weight loss maintenance, achieved through intensive caloric restriction on bone, is not well known. The purpose of this study was to examine the effects of a 12 week very low energy diet (800 calories/day) to promote a 15% loss in weight on changes in body mass, fat-free mass (FFM), and BMD over a period of 2 years.

Methods: Participants were adult men and women (50.6 $\pm$ 7.2 years) with a BMI >35 kg/m2, or having a BMI >32 kg/m2 and a clinical diagnosis of Type 2 diabetes mellitus. Changes in body mass, total body BMD, and FFM were examined after 15% of weight reduction and at the end of 2 years. The influence of absolute and rate of

weight reduction on BMD and FFM were assessed using general linear modeling, with baseline BMD (or FFM) as a covariate, and age, sex and change in body mass as model predictors.

Results Forty-nine subjects completed the 2-year study. The average weight loss was greater for men (23.51 $\pm$ 12.5 kg; 24.3%) than women (16.8 $\pm$ 19.2 kg; 19.2%) (p<0.05). At the end of 2 years, women lost greater FFM (8.2% vs. 5.0%; p<0.05), but not BMD (2.2% vs. 0.8%; p=0.13) than men. After adjusting for baseline BMD, age, and sex, there was a significant association between total weight loss and 2-year BMD (β = -0.001; p=0.01). Similarly, there was a significant independent association between total weight loss and 2-year FFM loss (β = -116.5; p=0.012). Age was an independent predictor of 2-year BMD (β = -0.002; p<0.01), but not FFM (p>0.05). Rapidity of weight reduction did not predict changes in BMD at 2 years; however it was independently associated with changes in FFM (β = -243.7; p=0.04).

Conclusions Diet-induced weight reduction may have deleterious effects on BMD and FFM. Although the clinical implications of these negative effects on bone and outcomes on fracture are unclear, these findings highlight the importance of focusing on bone health in individuals who are considering very low calorie diets.

FR0352

High Vitamin D is Associated with Low Fasting Insulin in Non-diabetic Men. <u>Anna Nilsson</u>*[1], <u>Ewa Waern</u>[2], <u>Mattias Lorentzon</u>[3], <u>Magnus Karlsson</u>[4], <u>Claes Ohlsson</u>[5], <u>Dan Mellstrom</u>[6]. [1]Sahlgrenska University Hospital, Sweden, [2]Sahlgrenska University Hospital, Sweden, [3]Geriatric Medicine, Center for Bone Research at the Sahlgrenska Academy, Sweden, [4]Skåne University Hospital Malmö, Lund University, Sweden, [5]Center for Bone & Arthritis Research at the Sahlgrenska Academy, Sweden, [6]Sahlgrenska University Hospital, Sweden

Vitamin D has been suggested as an important factor in glucose metabolism and vitamin D deficiency has been associated with insulin resistance. We have studied the covariation of vitamin D and fasting insulin levels in 1010 subjects participating in MrOS Gothenburg (a population-based study on randomly identified ambulant men aged 69 to 81 years). Fasting serum levels of 25-OH-vitamin D, adiponectin, leptin, insulin, parathyroid hormone, SHBG, and fasting plasma glucose were determined with commercially available kits. Season-adjusted z-scores of 25-OH-vitamin D levels were used for statistical calculations. All serum and plasma values except 25-OH-vitamin D and glucose were logarithmized after analysis of skewness. Patients with diabetes (n=148), defined as a previous diagnosis of diabetes mellitus or fasting plasma glucose levels above 7 mmol/L at the time of the blood sampling, were excluded prior to the statistical analysis leaving data from 822 non-diabetic men available for the statistical analysis. Mean age was 75.3 (SD: 3.2) years and mean BMI was 25.9 (SD: 3.3) kg/m2. A negative association was observed between 25-OH-vitamin D Z-scores and fasting insulin values (r=-0.13, p<0.001). Vitamin D levels were also negatively correlated to BMI (r=-0.12, p<0.001) and PTH (r=-016, p<0.001). Fasting insulin levels were negatively correlated to SHBG (r=-0.18, p<0.001) and adiponectin (r=-0.39, p<0.001) and positively correlated to BMI (r=0.46, p<0.001) and glucose (r=0.33, p<0.001). There was no association between fasting insulin and PTH levels (r=0.05). Adjustment for age did not change these linear correlations for insulin, nor did adjustment for age and BMI. Adjustment for age, BMI, and adiponectin eliminated any correlation between fasting insulin and SHBG (partial r=0.005) whereas vitamin D remained as a negative predictor of insulin (partial r=-0.10, p<0.01). Insulin levels were also positively correlated to leptin (r=0.51, p<0.001) and multiple regression showed that age, 25-OH-vitamin D, BMI, adiponectin, leptin and fasting plasma glucose explained 42 % of the variation of insulin levels (p<0.001). We conclude that there is a covariation in the concentrations of 25-OH-vitamin D and insulin in non-diabetic elderly men that is independent of age, PTH, SHBG, BMI, and adipocyte-derived hormones. The physiological explanation of this observation remains unclear, although previous studies suggest a possible insulin-sensitizing effect of vitamin D.

FR0354

Sex-specific effects of PTH, total 25OHD, and free 25OHD on femoral neck BMD. Lisa Langsetmo*[1], Claudie Berger[2], Brent Richards[3], Christopher Kovacs[4], William Leslie[5], David Hanley[6], Jonathan Adachi[7], Jerilynn Prior[8], Suzanne Morin[3], K. Shawn Davison[9], Stephanie Kaiser[10], Robert Josse[11], David Goltzman[3]. [1]Canadian Multicenter Osteoporosis Study, Canada, [2]CaMos, McGill University, Canada, [3]McGill University, Canada, [4]Memorial University of Newfoundland, Canada, [5]University of Manitoba, Canada, [6]University of Calgary, Canada, [7]St. Joseph's Hospital, Canada, [8]University of British Columbia, Canada, [9]University of Victoria, Canada, [10]Dalhousie University, Canada, [11]St. Michael's Hospital, University of Toronto, Canada

Serum 25-hydroxy vitamin D (25OHD) and parathyroid hormone (PTH) levels are inversely related and have been associated with changes in bone mineral density (BMD). Our objective was to examine relationships with femoral neck BMD of serum Total 25OHD (T-25OHD), Free 25OHD (F-25OHD), vitamin D binding protein (DBP) and PTH.

We measured levels in 3892 fasting serum samples taken during 1995-1997, 2000-02 and/or 2005-07 from 1902 women and 825 men (96% Caucasian) aged 25+ years in the longitudinal, population-based, Canadian Multicentre Osteoporosis Study. We used hierarchical models based on 10 years of longitudinal data to determine the associations between T-25OHD and PTH with femoral neck BMD. We considered pairwise interactions of T-25OHD, PTH, and antiresorptive use and adjusted for relevant covariates (see Figures). We also measured DBP concentrations and calculated F-25OHD levels in a subset of 1425 women and 605 men using only the most recent serum sample. We used linear regression models to determine the associations between F-25OHD, DBP and PTH with femoral neck BMD, considering similar interactions as above and adjusted for the same covariates.

Women with T-25OHD levels <50 nmol/L had lower femoral neck BMD values than those with T-25OHD between 50-75 nmol/L [0.008 g/cm^2 (95% C.I.: 0.002; 0.013) difference]. Higher PTH levels (> median) were also associated with lower femoral neck BMD [-0.010 g/cm^2 (-0.016; -0.003)] compared to women in the 1st quartile (Q) of PTH. Men with T-25OHD levels >75 nmol/L and with low PTH levels [1st Q] had femoral neck BMD higher by 0.020 g/cm^2 (0.006; 0.035) than men in the 1st Q of PTH with T-25OHD of 50-75 nmol/L. When using the subset with measured DBP in women, femoral neck BMD was determined predominantly by quartiles of PTH, with a significant effect of F-25OHD only at the highest and lowest quartiles of PTH (Figure 2). Exclusion of DBP from the model did not modify PTH and F-25OHD estimates. F-25OHD and DBP were not associated with femoral neck BMD in men.

In summary, our results suggest a greater effect of PTH than 25OHD on femoral neck BMD with possible modification of effect by F-25OHD or T-25OHD level. DBP levels did not alter the relationship of PTH with BMD in either women or men.

Figure 1: Femoral neck BMD estimates by PTH and Total 25OHD levels in men (using serum measures at multiple times).

Covariates included were age group, education, race, BMI, height, calcium intake, antiresorptive use, regular physical activity, regional centre.
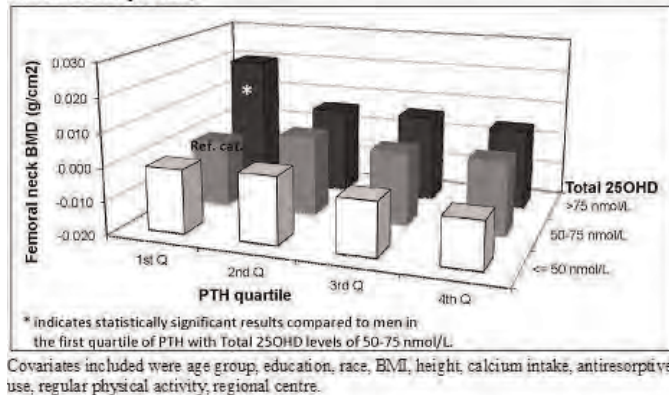
Figure 1: Femoral neck BMD estimates by PTH and Total 25OHD levels in men

Figure 2: Femoral neck BMD estimates by PTH and Free 25OHD levels in women (from linear regression: one measure per participant).

* indicates statistically significant results compared to women in the first quartile of PTH with Free 25OHD levels > median.

Covariates included were age group, education, race, menopause, BMI, height, calcium intake, antiresorptive and corticosteroid use, regular physical activity, regional centre.
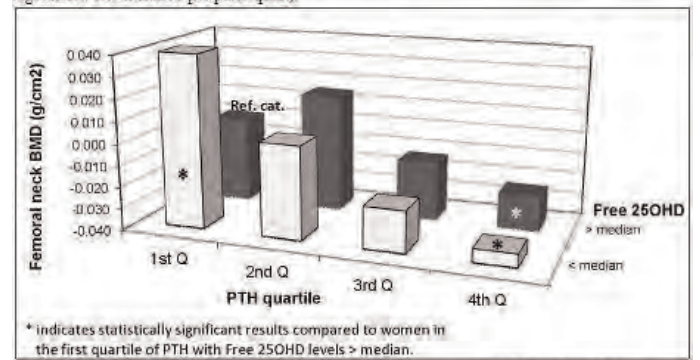
Figure 2: Femoral neck BMD estimates by PTH and Free 25OHD levels in women

Disclosures: Lisa Langsetmo, None.

FR0357

Bone Anabolic Effect in Ovariectomized Mice by low-dose RANKL Mediated by FoxP3^{+} CD8 T-Cells. Reggie Aurora*[1], Zachary Buchwald[2], Chang Yang[3], Suman Nellore[2], Elena Sashkova[2], Deborah Novack[4], Richard Di Paolo[2]. [1]Saint Louis University University, USA, [2]Saint Louis University School of Medicine, USA, [3]Washington University in St Louis School of Medicine, USA, [4]Washington University in St. Louis School of Medicine, USA

Estrogen loss at menopause increases effector T-cells that produce low-levels of proinflammatory cytokines in the bone marrow. These cytokines lead to a lower bone density and a higher risk of bone factures because they promote bone resorption, osteoclastogenesis and a deficit in new bone formation. Estrogen loss also increases levels of Receptor Activator of NF-κB ligand (RANKL), which promotes differentiation and bone resorption by osteoclasts. To treat osteoporosis, anti-RANKL therapy has been shown to be efficacious. Remarkably, we found while all doses of RANKL promote osteoclast activity in estrogen-replete mice, in ovariecto-mized (OVX) mice low-dose RANKL treatment ameliorated osteoporosis. Twelve week-old OVX mice were treated on two consecutive days, two weeks post-OVX, with 0.125 mg/kg RANKL. In addition to measuring bone resorption by serum CTX, mice were sacrificed and bones were harvested at ten days post-treatment for analysis by μCT, bone histomorphometry and FACS of bone marrow. We will present data that low-dose RANKL activates osteoclasts to induce FoxP3 expression in CD8 T-cells. FoxP3^{+} T-cells suppress the aberrant activation of self-reactive T-cells and promote the resolution of inflammation. We refer to these FoxP3^{+} CD8 T-cells as osteoclast-induced Tc$_{REG}$ (OC-iTc$_{REG}$). We have previously demonstrated that OC-iTc$_{REG}$ suppress osteoclast activity to form a novel feedback loop. We also have shown that OC-iTc$_{REG}$ are bifunctional, in addition to suppressing osteoclasts, they suppress the proliferation of CD4 and CD8 T-cells by dendritic cells. The effect of low-dose RANKL was superior to bisphosphonate treatment because it reduced levels of proinflammatory effector T-cells in the bone marrow allowing for new bone formation. We also demonstrate that proinflammatory cytokines (e.g. TNFα and IL-17) repress Tc$_{REG}$ induction, but a pulse of low-dose RANKL restores Tc$_{REG}$ induction by osteoclasts. Our studies therefore provide the mechanism by which low-dose RANKL leads to anabolic effect on the bone. Indeed, this anabolic effect of low-dose RANKL could not have been anticipated but can be explained by the negative feedback loop between osteoclasts and CD8 T-cells. These studies therefore extend the purview of Osteoimmunology by providing new insights into the effects of T-cells on osteoclasts and the effect of osteoclasts on regulating T-cells.

Disclosures: Reggie Aurora, None.

FR0358

Hyperlipidemia-induced Loss of Bone Mass is Caused by Decreased Bone Formation and is Associated with an Inflammatory Response in the Marrow: Evidence from the ApoE$^{-/-}$ Mouse Model of Atherosclerosis. Yu Liu*[1], Annick DeLoose[2], Kanan Vyas[2], Michela Palmieri[2], Amanda Hunt[2], Robert Weinstein[1], Charles O'Brien[1], Stavros Manolagas[1], Robert Jilka[1]. [1]Central Arkansas VA Healthcare System, Univ of Arkansas for Medical Sciences, USA, [2]Central Arkansas VA Healthcare System, Univ of Arkansas for Medical Sciences, USA

Atherosclerosis and osteoporosis are epidemiologically linked. However, a common mechanism that may underlie these conditions has not been elucidated. In the ApoE$^{-/-}$ mouse model of atherosclerosis, high fat (HF) diet causes hyperlipidemia and subendothelial accumulation of low density lipoprotein (LDL), which is oxidized in macrophages by reactive oxygen species (ROS) and the lipoxygenase Alox15.

Oxidized LDL and ROS then initiate a pathogenetic inflammatory response, similar to the disease in humans. Because HF diet also causes loss of bone mass in this model, we investigated whether the loss of bone is associated with an inflammatory response. Four-month-old female ApoE-/- mice fed a HF diet (37.1% kcal from fat) exhibited progressive loss of DEXA BMD in both the spine and femur over a 12 week period, as compared to mice fed a control diet (17% kcal from fat). The loss of BMD was accompanied by a decrease in trabecular bone volume due to a reduction in trabecular thickness, as well as decreased cortical thickness and increased cortical porosity, as determined by microCT. In vertebral cancellous bone sections, both osteoblast and osteoclast number were reduced by 2-fold and bone formation rate was reduced by 7-fold. Indices of lipid oxidation and ROS levels measured in bone marrow supernatants and bone marrow cells, respectively, were also increased. The number of monocyte/macrophages in the marrow was 30-40% higher, as measured by flow cytometry of anti-CD11b cells, whereas T cell (CD3+) and B cell (CD19+) number was unaffected. Nonetheless, transcript levels of the inflammatory cytokines IL-1β, TNF, IL-6 and MCP-1 were increased by 2-10 fold in all three hematopoietic cell types, as determined by qPCR analysis of cells purified with magnetic beads. The pro-osteoclastogenic RANKL was increased by 2-fold in T cells and by 5 fold in B cells; but so was the anti-osteoclastogenic IFNγ in T cells (2-fold). Alox15 expression was detected only in monocytes/macrophages, but its level was unaffected by the HF diet. These results suggest that hyperlipidemia induces an inflammatory response in the bone marrow of ApoE-/- mice, caused by ROS- and Alox15-mediated lipid oxidation. Furthermore, our results reveal that the loss of bone mass caused by HF diet is the result of decreased bone formation, not increased bone resorption.

Disclosures: Yu Liu, None.

FR0359

Eldecalcitol, a new-generation vitamin D$_3$ analog, increases trabecular bone via "minimodeling" in ovariectomized cynomolgus monkeys. Tomoka Hasegawa*[1], Saito Mitsuru[2], Doyle Nancy[3], Chouinard Luc[3], Smith Susan[3], Yamamoto Tomomaya[4], Oda Kimimitsu[5], Saito Hitoshi[6], Amizuka Norio[4]. [1]Hokkaido University, Japan, [2]Jikei University School of Medicine, Japan, [3]Charles River Laboratories, Canada, [4]Hokkaido University, Japan, [5]Niigata University, Japan, [6]Chugai Pharmaceutical Co., Ltd., Japan

Eldecalcitol, a new-generation vitamin D$_3$ analog, seems to be more bone anabolic compared with its predecessor alfacalcitol. Eldecalcitol inhibits osteoclast formation and bone resorption. It also promotes "minimodeling", a focal "budding" of new bone shown in the ovariectomized (OVX) rat model (Bone, 2011). Minimodeling is a type of bone formation independent of bone resorption: resting osteoblasts begin to deposit new bone onto existing bone surfaces without prior osteoclast-driven bone resorption. The objective of this study was to examine if eldecalcitol inhibits osteoclast formation and promotes minimodeling in a more complex animal model, the ovariectomized cynomolgus monkeys.

Twenty female cynomolgus monkeys of at least nine years of age were ovariectomized, and administered eldecalcitol (0.3μg/kg/day, ELD group) or vehicle (OVX group) for six months. All animals were injected with calcein prior to anesthesia. Femora and vertebrae were processed for histological examinations and collagen crosslinking evaluations. ELD bones showed increases in the number and thickness of femoral and vertebral trabeculae. OVX bones featured a relatively broader bone resorption area with several osteoclasts and rougher bone surfaces compared to those seen in ELD bones. Calcein labeling in ELD bones appeared as convex lines in the new bone buds deposited atop smooth arrest lines. Thus, eldecalcitol appears to induce minimodeling in cynomolgus monkeys. We also examined the occurrence of enzymatic cross-linking of collagen fibrils. Fractionated trabecular bone samples from both groups were separated in low-density (< 2.0 mg/mL) and high-density (⩾ 2.0 mg/mL) fractions through stepwise centrifugation. In the OVX group, differences in the degree of enzymatic crosslinking between fractions was not evident, while in the ELD group higher enzymatic collagen crosslinking was verifiable in the high density fraction, suggesting the occurrence of bone formation despite inhibition of bone resorption. In summary, eldecalcitol appears to inhibit osteoclast formation and induce new bone formation by means of minimodeling in cynomolgus monkeys as well as rats.

Disclosures: Tomoka Hasegawa, None.
This study received funding from: Chugai Pharmaceutical Co., Ltd.

FR0360

Pregnancy and Lactation Bone Loss Cause Long-Lasting Structural Deterioration of the Maternal Skeleton that Accumulates over Multiple Reproductive Cycles. Chantal De Bakker*[1], Allison Altman[1], Connie Li[2], Wei-Ju Tseng[2], Xiaowei Liu[1]. [1]University of Pennsylvania, USA, [2]University of Pennsylvania, USA

Maternal bone undergoes dramatic changes during reproduction, as the mother's skeleton forms a source of calcium for the fetus and newborn. However, the extent of pregnancy bone loss and recovery post-weaning remain controversial, leading to important questions regarding the effect of multiple reproductive cycles and the precise roles of pregnancy, lactation, and weaning in maternal bone health. In this

study we tracked changes in trabecular bone microarchitecture in the same rats (n=5) across 3 reproductive cycles (between ages 4-12 mo) using *in vivo* μCT (10.5 μm, Scanco vivaCT40). Each cycle consisted of a 3-wk pregnancy, 3-wk lactation, and 3-6 wk post-weaning recovery. 6 age-matched, virgin controls were used.

In the first reproductive cycle, trabecular structure declined rapidly during pregnancy and lactation (Fig 1A). At parturition, bone volume fraction (BV/TV) and trabecular number (Tb.N) were 46% and 24% lower than baseline, respectively, and after lactation, BV/TV, Tb.N, and Tb.Th were 82%, 56%, and 34% below baseline (p<0.05). After weaning, BV/TV recovered back to pre-lactation, but not to pre-pregnancy values, Tb.N did not recover, and Tb.Th recovered fully to baseline values. Serum TRACP 5b levels decreased 67% after weaning (p<0.05), but were not significantly different among control, lactation, and pregnancy rats. μCT-based *in vivo* bone dynamic histomorphometry indicates that bone resorption rate was highly elevated during pregnancy and lactation, and decreased 90% after weaning (p<0.05); bone formation rate increased 209% after weaning (p<0.05).

Subsequent reproductive cycles showed less total deterioration of BV/TV, Tb.N, and Tb.Th than the first cycle. Changes during pregnancy were less dramatic in later cycles but the effects of lactation and weaning remained pronounced (Fig 1C). For each cycle, recovery was incomplete, resulting in a net bone loss (Fig 1B). At the end of the study, trabecular structure of reproductive rats was substantially different from controls.

This study is the first longitudinal assessment of trabecular microstructure during multiple reproductive cycles. Each cycle induced a persistent, net bone loss, due to incomplete recovery after weaning. Comparison of the 3 cycles demonstrates decreased bone loss during later cycles, likely due to a reduction of bone lost during pregnancy. The first reproductive cycle causes significant pregnancy bone loss, which may have a long-lasting negative impact on bone quality.

Fig 1. (A) Representative renderings of the trabecular compartment at baseline, after pregnancy, after lactation, and 6 weeks after weaning during the first reproductive cycle. The effect of multiple cycles is demonstrated by (B) a profile plot showing changes in the percentage of the baseline BV/TV that remains at each reproductive stage, and (C) percent change in BV/TV occurring during pregnancy, lactation, and weaning during each reproductive cycle. *: different from previous time point (p<0.05), #: trend towards difference from previous time point (p<0.1), a: Cycle1 ≠ Cycle2 (p<0.05), b: Cycle1 ≠ Cycle3 (p<0.05).

Fig 1

Disclosures: Chantal De Bakker, None.

FR0361

Chronic Stress Induces Bone Loss via Glucocorticoid Signaling in Osteoblasts. Holger Henneicke*[1], Jingbao Li[2], Sylvia Jane Gasparini[3], Markus Seibel[4], Hong Zhou[4]. [1]ANZAC Research Institute, The University of Sydney, Australia, [2]Key Laboratory for Space Bioscience & Biotechnology, Institute of Special Environmental Biophysics, Faculty of Life Sciences, Northwestern Polytechnical University, China, [3]Bone Biology Program, ANZAC Research Institute, The University of Sydney, Australia, [4]Bone Research Program, ANZAC Research Institute, University of Sydney, Australia

Chronic stress and depression are risk factors for low bone mineral density and increased fracture risk. However, the mechanisms underlying stress-induced bone loss are ill defined. We hypothesised that endogenous hypercortisolism and its effect on osteoblast function play a central role in stress-induced bone loss. The present study aimed to define the effects of chronic mild stress (CMS) on the skeletal phenotype of young adult mice.

Methods: We used a transgenic (tg) mouse model in which glucocorticoid signaling had been selectively disrupted in osteoblasts and osteocytes via targeted over-expression of the glucocorticoid-inactivating enzyme 11ß-hydroxysteroid dehydrogenase type 2. Eight-week old tg mice and their wild type (WT) littermates were exposed to CMS for the duration of 4 weeks. Stressors included restraint stress, exposure to hot and cold, tilted cages and overnight illuminations. At endpoint, corticosterone serum concentrations were determined by LCMS and both the L3-vertebra and tibia were analyzed by micro-CT and dynamic histomorphometry.

Results: Compared to non-stressed control mice, serum corticosterone levels increased ~3-fold in stressed WT and tg mice. Exposure to CMS resulted in loss of vertebral trabecular bone mass in WT but not tg mice when compared to their respective non-stressed controls (BV/TV WT: -16%; tg: +3%, p<0.01). This was mainly due to a decrease in trabecular number (WT: -14%; tg: +1%; p<0.05) and a corresponding increase in trabecular separation (WT: +12%; tg: +1%; p<0.04) in WT mice only. While trabecular bone in the tibia was unaffected in both WT and tg mice exposed to CMS, tibial cortical volume (WT: -9%; tg: +1%; p<0.05) as well as cortical thickness (WT: -6%; tg: +2%; p<0.05) were reduced in stress-exposed WT but not in stress-exposed tg mice. Dynamic histomorphometry of the tibia revealed reduced endocortical (WT: -14%; tg: +42%; p=0.055) and pericortical bone formation rates (WT: -86%; tg: -3%; p=0.062) in stressed WT mice only.

Conclusion: In mice, CMS induces loss of both trabecular (vertebra) and cortical bone (tibia) via increased glucocorticoid signaling in osteoblasts and osteocytes.

Disclosures: Holger Henneicke, None.

FR0362

Deletion of TRAF3 Specifically in Mesenchymal Progenitor Cells Results in Age-related OsteoporosisThrough Effects on both Osteoblasts and Osteoclasts. Jinbo Li*[1], Zhenqiang Yao[2], Yan Xiu[3], Xiaoxiang Yin[4], Lianping Xing[2], Brendan Boyce[3]. [1], USA, [2]University of Rochester, USA, [3]University of Rochester Medical Center, USA, [4]University of Rochester Medical Center, USA

TNF receptor–associated factor 3 (TRAF3) negatively regulates non-canonical NF-κB signaling and thus limits RANKL- and TNF-induced osteoclast (OC) formation. However, it is not known if TRAF3 plays a role in osteoblast (OB) lineage cells. To study this question, we deleted TRAF3 specifically in mesenchymal precursor cells (MPCs) by crossing *Traf3^{f/f}* mice with *Prx-1^{cre}* mice to generate *Traf3^{f/f};Prx-1^{cre}* conditional knockout (cKO) mice and examined tibiae from 3- and 9-m-old cKO and *Traf3^{f/f}* control (Ctl) mice by µCT and histology. TV/BV and bone formation rates were normal in 3-m-old cKO mice, but these were significantly decreased in 9-m-old cKO mice (BV/TV: 3.6 ± 0.6 vs $15\pm3\%$ in Ctl; and BFR: 1.03 ± 0.05 vs 1.62 ± 0.16 µm³/µm²/d in Ctl; p<0.01). Interestingly, cKO OC numbers in growth plate were increased at both ages (231 ± 26 vs 109 ± 16 and 270 ± 35 vs 143 ± 17/mm² tissue area in 3- and 9-m Ctl, respectively). MPCs from 3-m-old cKO mice had higher proliferation (% BrdU⁺ cells in CD45⁻CD105⁺Scal⁺ cells: 23% vs 8% in Ctl), but reduced OB differentiation (% ALP⁺ cells in CFU-ALP⁺ colonies: 43 ± 4 vs $79\pm6\%$ in Ctl). In contrast, MPCs from 9-m-old cKO mice had reduced proliferation (% BrdU⁺ cells: 3% vs 8% in Ctl) and OB differentiation (% ALP⁺ cells: 21 ± 3 vs $80\pm8\%$ in Ctl). Bone-derived MPCs from both 3- and 9-m-old cKO mice had more than 3-fold higher RANKL expression levels. Calvarial cells from neonatal cKO mice induced significantly more OCs from both cKO and Ctl spleen cells than cells from WT mice (TRAP⁺ area: 2.7 ± 0.15 vs 1.3 ± 0.4mm² and 2.3 ± 0.4 vs 0.8 ± 0.2mm², respectively). To investigate if TRAF3 is involved in age-related bone loss, we examined TRAF3 protein levels in bone samples from 2- and 18–m-old WT mice and found that they were 80-90% lower than in young mice. In addition TGFb1 (which is released from bone resorption sites) induced TRAF3 ubiquitination and degradation. In summary, deletion of TRAF3 in MPCs results in osteoporosis as mice age due to increased RANKL-induced bone resorption and reduced OB formation and activity. We conclude that TRAF3 plays critical roles not only in OCs, but now also in MPCs to protect against age-related bone loss by limiting bone resorption and enhancing bone formation. Prevention of TRAF3 degradation in osteoblastic cells could be a new therapeutic approach for osteoporosis.

Disclosures: Jinbo Li, None.

FR0363

Heterozygosity for *TGFβR3* Alters Osteoblast and Osteoclast Differentiation and Signaling, Increases Peak Bone Mass, and Sensitizes Mice to OVX-Induced Bone Loss. Nicole Fleming[1], Vanessa Bray[2], James Butler[3], Tristan Fowler[4], Joey Barnett[5], Dana Gaddy[6], Erick Fleming[1], Jeffry Nyman[7], Rashmi Pandey[3], Daniel Perrien*[7]. [1]VUIIS, Vanderbilt University, USA, [2]Dept of Orthopaedic Surgery & Rehabilitation, Vanderbilt University, USA, [3]Department of Orthopaedic Surgery & Rehabilitation, Vanderbilt University, USA, [4]Universität Wien, Aut, [5]Department of Pharmacology, Vanderbilt University, USA, [6]University of Arkansas for Medical Sciences, USA, [7]Vanderbilt University Medical Center, USA

TGFβ-superfamily ligands and their Type I and Type II receptors have established roles in bone. However, the role of the Type 3 TGFβ Receptor (TβR3/Betaglycan) in bone metabolism has not been reported. Deletion of *TβR3* in endothelial cells increases sensitivity to TGFβ and impairs sensitivity to BMP. Hence, we hypothesized that *TβR3*+/- bone cells would display altered sensitivity to these ligands. Bone marrow from TβR3+/- mice cultured in osteogenic media produced fewer alkaline phosphatase-positive (AP+) colonies and lower %AP+ colonies than wild-type (WT) marrow. Furthermore, TβR3+/- cells were >10-fold more sensitive to inhibition of differentiation by TGFβ1 and significantly less sensitive to enhancement by BMP2. However, TGFβ- or BMP2-induced phosphorylation of Smads, p38, or Erk1/2 was unaltered in TβR3+/- Ob. In contrast, bone marrow or splenocytes cultured with M-

CSF and RANKL produced significantly more osteoclasts (OCL) and OCL differentiation was enhanced by TGFβ more in TβR3+/- than in WT. These data led us to examine the bone phenotype of TβR3+/- mice. MicroCT analysis of trabecular bone in the tibial metaphysis and L4 vertebra (VB) showed that 6-mo old male and female TβR3+/- mice (n=9-12/grp) had significantly greater bone volume fraction (BV/TV) and improved trabecular structure (Tb.N, Tb.Th, and Tb.Sp) compared to WT mice (p<0.05) in both genders. Because TGFβ-family ligands have been implicated in the development of osteoporosis, 4-mo old WT and TβR3+/- mice on a C57BL6 background underwent gonadectomy and were harvested 9 weeks later. Consistent with previous data, female WT C57BL6 mice were resistant to OVX-induced bone loss, as only Tb.Th was significantly lower than WT-Sham in either bone (p<0.002 for both). However, OVX caused significant trabecular bone loss in the tibia [BV/TV (p<0.005); Tb.N, Tb.Th, and Tb.Sp (all p<0.05)] and VB (BV/TV, Tb.Th; both p<0.01) of TβR3+/- OVX mice vs. TβR3-Sham. In contrast, ORX in male mice significantly decreased trabecular BV/TV and structural properties in both WT and TβR3+/- compared to male Sham mice of the same genotype (p<0.05 for all). These data demonstrate that haploinsufficiency of *TβR3* alters OB and OCL differentiation and sensitivity to TGFβ1 and BMP2 (possibly through a non-Smad mediated pathway), and confers a high bone volume phenotype in mice and sensitizes female mice to OVX-induced bone loss, establishing an important role for TβR3 in bone metabolism and the response to OVX.

Disclosures: Daniel Perrien, None.

FR0364

High Cortico -Trabecular Junctional Zone Porosity and Reduced Trabecular Density in Persons with Stress Fractures. Afrodite Zendeli*[1], Christian Muschitz[2], Minh Bui[3], Lukas Fischer[4], Wolfgang Schima[5], Fritz Lomoschitz[6], Norbert Laimer[7], Ali Ghasem-Zadeh[8], Roger Zebaze[9], Ego Seeman[8]. [1]Endocrine Centre, Austin Health, University of Melbourne, Australia, Australia, [2]St. Vincent's Hospital, Austria, [3]Centre for Epidemiology & Biostatistics, Melbourne School of Population & Global Health, University of Melbourne, Australia, Australia, [4]Computational Imaging Research Lab, Department of Biomedical Imaging & Image-guided Therapy, Medical University of Vienna, Austria, Austria, [5]5 Department of Diagnostic & Interventional Radiology - St. Vincent Hospital Vienna, Austria, Austria, [6]Department of Diagnostic & Interventional Radiology - St. Vincent Hospital Vienna, Austria, Austria, [7]Medical Department II - St. Vincent Hospital Vienna - The VINFORCE Study Group, Austria, Austria, [8]Austin Health, University of Melbourne, Australia, [9]Austin Health, University of Melbourne, Australia

Introduction Stress fractures associated with repetitive loading are usually not accompanied by deficits in areal bone mineral density (aBMD). Metaphyseal cortical bone is formed by condensation or 'corticalization' of trabeculae as they arise from the periphery of the growth plate. Adjacent trabeculae coalesce by bone formation upon their surfaces while central trabeculae form trabecular bone.

Methods To determine whether bone fragility is due to abnormalities in bone microstructure high resolution peripheral quantitative computed tomography (HR-pQCT) images of the distal radius and distal unfractured tibia of 26 cases (11 females, 15 males; mean age 37.1 ± 3.1 years) with stress fractures in their lower limb were compared with measurements obtained in 62 age-matched healthy controls (38 females, 24 males; mean age 35.0 ± 1.6 years).

Results In men, relative to controls, at the radius, cases had 11.4% smaller cortical cross sectional area (CSA) (p = 0.012). Porosity was higher in the outer transitional zone (OTZ) (6.9%, p = 0.006), inner transitional zone (ITZ) (2.4% p = 0.043) and the compact-appearing cortex (CC) (13.4% p = 0.023). Trabecular vBMD was 22.0% lower (p = 0.002). Similarly, at the distal tibia, cases had a 9.7% smaller cortical CSA (p = 0.008). Cortical porosity was higher in the OTZ (3.4%, p = 0.058), ITZ (0.8%, NS), CC (7.4%, p = 0.09). Trabecular vBMD was 17.3% lower (p = 0.001). In women, relative to controls, at the distal radius, cases had higher porosity of the OTZ (5.3%, p = 0.028), ITZ (2.3%, p = 0.030) and CC (11.4%, p = 0.054). Trabecular vBMD was 27.4% lower (p = 0.041). At the distal tibia, porosity was higher in the OTZ (5.9%, p = 0.035), ITZ (3.3%, p = 0.009) and CC (12%, NS). For both sexes, the odds ratio (OR) of porosity in CC, OTZ and ITZ at distal radius and distal tibia ranged between 1.24 and 3.13. A higher trabecular vBMD was associated with a lower OR for fracture, ranged between 0.24 and 0.5.Conclusion We suggest that individuals sustaining stress fractures may have impairment of trabecular 'corticalization' during growth. Thinner and more widely spaced trabeculae emerging from the growth plate may fail to corticalize leaving transitional zone porosity and a lower trabecular density.

Disclosures: Afrodite Zendeli, None.

FR0365

Pulsatile delivery of parathyroid hormone from an implantable device promotes bone regeneration in vivo. <u>Ming Dang</u>*[1], <u>Amy Koh</u>[2], <u>Laurie McCauley</u>[3], <u>Peter Ma</u>[4]. [1]Macromolecular Science & Engineering Center, University of Michigan, USA, [2]Department of Periodontics & Oral Medicine, University of Michigan, USA, [3]University of Michigan School of Dentistry, USA, [4]Department of Biologic & Materials Sciences, University of Michigan, USA

Objective: Pulsatile administration of parathyroid hormone (PTH) is known to improve bone architecture, bone mineral density and strength. PTH is currently the only anabolic agent clinically used in the US for the treatment of osteoporosis, but requires daily injection, making patient compliance inconvenient and an obstacle to effective treatment. In this study, an implantable multi-layer device loaded with PTH was developed and the anabolic actions of the PTH released from the device were evaluated in mice.

Methods: Biodegradable and biocompatible three-component polyanhydrides composed of sebacic acid, 1,3-bis(p-carboxyphenoxy)propane and poly(ethylene glycol) were synthesized and used as isolation layers. The device was fabricated by stacking the polyanhydrides isolation layers and PTH-loaded drug layers alternately, then sealing the frame of the device with PCL (polycaprolactone). Biologic activity of the released PTH was confirmed using a cell based cAMP binding assay. BSA (bovine serum albumin) loaded devices were prepared as the control group. The BSA protein release profile was measured using a MicroBCA protein assay in vitro. PTH and control devices were subcutaneously implanted in C57B6 mice (10d) for 3 weeks. The mice were then euthanized and vertebrae harvested for histological analyses.

Results: Polyanhydrides with various chemical composition exhibited typical surface erosion behavior and the erosion rate was controlled by the composition. Multi-pulse (more than 21) protein release was achieved using the multi-layer device and the interval time between two adjacent pulses was modulated by the thickness of the polyanhydride isolation layers. PTH release devices stimulated cAMP in human osteoblasts in a pulsatile fashion. Implantation devises delivering PTH increased vertebral bone area compared to control BSA devices measured by histomorphometric analyses. Histological staining of the capsule tissue surrounding the device showed an absence of significant invasion of inflammatory cells, suggesting low toxicity .

Conclusion: An implantable device capable of delivering PTH in a programmed pulsatile manner was developed. The PTH released from the device resulted in anabolic actions in vivo, thus promoting bone regeneration. The implantable device holds promise for treatment of conditions of bone loss without the burden of daily injection.

*Disclosures: **Ming Dang**, None.*

FR0366

Site-specific Effects of Spaceflight on Cancellous Bone Architecture in Ovariectomized Rats with Established Osteopenia. <u>Jessica Keune</u>*, <u>Dawn Olson</u>, <u>Urszula T. Iwaniec</u>, <u>Russell T. Turner</u>. Oregon State University, USA

Site-specific reductions in bone mass are commonly observed in both male and female astronauts who are physically fit and have normal bone density. However, it is less clear whether spaceflight results in further bone loss in already osteopenic individuals. The goal of this study was to determine the effects of spaceflight on cancellous bone mass and microarchitecture in the ovariectomized (ovx) rat model with established osteopenia. Rats were ovx at 10 weeks of age, divided into two groups (ground control and flight, n = 12/group), and starting at 12 weeks of age flown aboard the Space Shuttle (STS-62) for 14 days. The rats were sacrificed on day of landing and cancellous bone mass and microarchitecture was evaluated in distal femur, distal humerus, and 2nd lumbar vertebral body using micro-computed tomography. Compared to ground controls, rats flown in space had lower cancellous bone volume fraction in distal femur metaphysis, distal femur epiphysis, and lumbar vertebra (Table). Significant differences in cancellous bone volume fraction were not detected in distal humerus. The lower cancellous bone volume fraction in the distal femur metaphysis in flight rats was associated with lower connectivity density and trabecular number and higher trabecular spacing; significant differences in trabecular thickness were not detected with treatment. In contrast, the lower cancellous bone volume fraction in the distal femur epiphysis was associated with lower connectivity density, trabecular number and trabecular thickness and higher trabecular spacing. The lower cancellous bone volume fraction in the vertebral body was associated with lower trabecular number and trabecular thickness and higher trabecular spacing; significant differences in connectivity density were not detected with treatment. In summary, the effects of spaceflight on bone microarchitecture in rats with low circulating estrogen levels differ with location, from no measured effect (e.g., distal humerus) to net loss of cancellous bone with variable effects on trabecular connectivity density and thickness (e.g., distal femur metaphysis and lumbar vertebra). These findings suggest that: 1) spaceflight aggravates bone loss associated with estrogen deficiency, and 2) interventions to prevent detrimental skeletal effects of spaceflight need to take into consideration that bone loss may be localized and site-specific.

Effects of spaceflight on cancellous bone volume fraction (bone volume/tissue volume, BV/TV) in distal femur, distal humerus, and lumbar vertebral body.

Anatomical Site	Ground Control (BV/TV, %)			Flight (BV/TV, %)			t-test p-value
Distal femur metaphysis	6.7	±	0.3	4.9	±	0.3	< 0.0007
Distal femur epiphysis	28.2	±	0.2	24.1	±	0.4	< 0.0001
Distal humerus	32.6	±	0.5	32.6	±	0.3	0.9135
2nd lumbar vertebra	20.9	±	0.4	16.9	±	0.8	< 0.0005

Data are mean ± SE

Table

*Disclosures: **Jessica Keune**, None.*

FR0367

GILZ Protects TNF-alpha-induced Bone Loss in Mice. <u>Nianlan Yang</u>*[1], <u>Babak Baban</u>[1], <u>William Hill</u>[2], <u>Mark Hamrick</u>[3], <u>Carlos Isales</u>[1], <u>Xing-Ming Shi</u>[4]. [1]Georgia Regents University, USA, [2]Georgia Regents University & Charlie Norwood VAMC, USA, [3]Georgia Health Sciences University, USA

Background: Tumor necrosis factor-alpha (TNF-α) plays a key role in the pathogenesis of inflammatory diseases such as rheumatoid arthritis (RA). It is known that chronic inflammation causes bone loss. We showed previously that glucocorticoid (GC)-induced leucine zipper (GILZ), a GC anti-inflammatory effect mediator, can enhance osteogenic differentiation of bone marrow mesenchymal stem cells (MSCs), and antagonize the inhibitory effect of TNF-α on MSC differentiation. However, it is not known whether GILZ will have the same effects in vivo and thus serve as a potential new anti-arthritis drug candidate.

Methods: We created TNF-a:GILZ double transgenic mice by crossing a human TNF-a-expressing transgenic mouse with a GILZ transgenic mouse, in which the expression of GILZ is under the control of a 3.6kb type I collagen promoter fragment (Col3.6). The expression of TNF-α and GILZ in double transgenic mice was confirmed by RT-PCR, Western blot and ELISA, and the bone protective effects of GILZ were assessed with standard bone biology and histology techniques.

Results: Overexpression of GILZ blocked TNF-α-mediated bone loss in double transgenic mice as demonstrated by a significantly increased bone mineral density (BMD) in the femur (+13.5%, p<0.01), tibia (+12.9%, p<0.05) and vertebra (+14.5%, p<0.05) compared with that in the TNF-α transgenic mice. GILZ also reduced the expression levels of IL-6 mRNA and serum levels of RANKL, as well as the levels of overexpressed human TNF-α. Furthermore, GILZ antagonized the inhibitory effect of TNF-α on osteocalcin expression in GILZ-TNF-α double transgenic mice. As predicted, the TNF-α transgenic mice developed poly arthritic symptoms between week 8-9 along with significant body weight loss and bone loss. The double transgenic mice, somehow, showed little effect on inflammatory arthritic symptoms compared with the TNF-α transgenic mice. This could be due to the restricted GILZ transgene expression in osteoblastic lineage cells and ubiquitous and high level of TNF-α transgene expression in double transgenic mice because significant reductions of TNF-α was only observed in bone marrow mesenchymal lineage cells (-43.5%) but not in hematopoietic (or osteoclastic) lineage cells.Conclusion: Overexpression of GILZ in osteoprogenitor cells protects bone loss in mice with chronically elevated levels of proinflammatory cytokines such as TNF-α.

*Disclosures: **Nianlan Yang**, None.*

FR0368

Kinin receptor B1 and B2 knockout are resistant to the bone losing effects of glucocorticoid treatment. <u>Charlles Castro</u>[1], <u>Marina Eloi</u>*[2], <u>Daniela Horvath</u>[2], <u>João Carlos Ortega</u>[2], <u>João Bosco Pesquero</u>[2], <u>Vera Szejnfeld</u>[3]. [1]Universidade Federal de São Paulo, Brazil, [2]Universidade Federal de São Paulo, Brazil, [3]UNIFESF/EPM, Brazil

Glucocorticoid-induced osteoporosis (GIO), the most common form of secondary osteoporosis is frequently observed in patients with chronic inflammatory diseases. The role of kinins and their receptors B1 and B2 in acute and chronic inflammatory process is well established. On the other hand, the pro-inflammatory effect of kinins on bone remodeling has not been well studied. The present study was designed to investigate the effect of the deletion of the kinin receptors B1 and B2 genes in an animal model for GIO. C57BL/6 mice (both wild type, WT and kinin receptors B1 and B2 double-knockouts, B1B2KO mice) 16 weeks of age (10 animals per group) were treated for 5 weeks with prednisolone (5 mg/kg daily injections intraperitoneally) or saline. *In vivo* BMD measurements were performed at baseline, 2 and 5 weeks of treatment, while static and dynamic bone histomorphometry and serum bone markers were measured at the end of the protocol. As expected, densitometric data have shown that prednisolone treatment was associated with bone and lean mass loss and increased fat mass in WT mice (p<0.01). As described, B1B2KO mice had whole body BMD similar to WT controls at baseline and exhibited reduced fat mass from baseline to 5 weeks of the protocol when compared to their WT controls. Interestingly, B1B2KO mice did not lose bone with glucocorticoid treatment. B1B2KO mice had

preserved bone mass after 5 weeks of treatment with prednisolone (baseline BMD 0.0678 ± 0.0026 g/cm2, 5-week BMD 0.0673 ± 0.0021 g/cm2; p=0.536). Fat and lean mass during treatment with prednisolone did not differ from WT controls treated in the same manner. Hystomorphometric analyzes will evaluate whether the glucocorticoid effect on bone formation and resorption are modulated by the expression of B1 and B2 kinin receptors. Our data demonstrated that B1B2KO mice have normal bone mass with reduced adiposity. These mice present resistance to the adverse effect of glucocorticoid on bone homeostasis and that suggests that kinins may play a significant role in the setting of glucocorticoid-induced bone loss.

Disclosures: Marina Eloi, None.

FR0369

Vascular Defects Detected by Micro-MRI in the Femoral Head of Glucocorticoid Treated Mice: A Potential Early Diagnostic Predictor of Osteonecrosis. Robert Weinstein*[1], Erin A. Hogan[2], Marilina Piemontese[3], Jinhu Xiong[1], Charles A O'Brien[2], Stavros Manolagas[1]. [1]Central Arkansas VA Healthcare System, Univ of Arkansas for Medical Sciences, USA, [2]Central Arkansas VA Healthcare System, Univ of Arkansas for Medical Sciences, USA, [3]University of Arkansas for Medical Sciences, USA

Osteonecrosis of the hip develops in up to 40% of patients receiving long-term systemic therapy with glucocorticoids but the sequential pathological abnormalities that precede joint collapse remain obscure. Published evidence indicates that the primary adverse skeletal effects of glucocorticoid excess are directly on osteoclasts, osteoblasts, and osteocytes, prolonging the lifespan of the osteoclasts while decreasing the lifespan of osteoblasts and osteocytes. Furthermore, decrements in bone vascularity, blood flow, and water content contribute to the glucocorticoid-induced decrease in bone strength that occurs before and disproportionate to the decline in bone mass. The femoral head may be particularly susceptible to these effects because of the applied load and constrained blood supply. In support of this contention, in mice receiving placebo, the bone formation rate and expression of both the receptor activator of nuclear factor-κB ligand (RANKL) and vascular endothelial growth factor (VEGF) were higher in the cancellous bone of the femoral head than in the distal femur or lumbar vertebra. In C57BL/6 mice, 28 days after implantation of 2.1 mg/k·d slow-release prednisolone pellets, the cancellous bone volume, compression strength, and expression of osteocalcin, RANKL, and VEGF in the femoral head decreased but these changes did not occur in vertebral or distal femoral bone. In addition, the normal branching vascular tree of the femoral head was converted to dilated sinusoids as determined after infusion of lead chromate. Likewise, the trabecular canalicular circulation was diminished as revealed by injection of Procion red. To further investigate the role of changes in bone water in the pathogenesis of the loss of strength of the femoral head, a 7 Tesla Bruker magnetic resonance image scanner (MRI), custom-made surface coils, and 3D fast low angle short (FLASH) imaging were used to enhance T1 contrast of water protons in the murine femoral head, a site with only a 0.5 mm radius. The MRI results indicate that glucocorticoids cause a striking redistribution of marrow water and represent the first in vivo demonstration of glucocorticoid-induced damage to the femoral head. If translated to humans, application of MRI protocols designed to intensify T1 signaling could better identify patients at risk of osteonecrosis.

Disclosures: Robert Weinstein, None.

FR0370

Estradiol: Endocrine or Autocrine Regulator of Bone? Insights from Mass Spectrometry in Male Mouse Models. Michaël Laurent*[1], Ivo Jans[2], Marco Blokland[3], Frederike van Tricht[3], Saskia Sterk[3], Leen Antonio[4], Brigitte Decallonne[4], Geert Carmeliet[1], Geoffrey Hammond[5], Frank Claessens[4], Dirk Vanderschueren[1]. [1]Katholieke Universiteit Leuven, Belgium, [2]University Hospitals Leuven, Belgium, [3]RIKILT, Wageningen UR, Netherlands, [4]Katholieke Universiteit Leuven, Belgium, [5]University of British Columbia, Canada

Estrogens regulate peak bone mass and age-related bone loss in men. Recent studies in humans have shown that immunoassays have insufficient specificity compared to mass spectrometry to measure low serum sex steroid concentrations, especially estradiol (E2). Despite their importance as a preclinical osteoporosis model, mice lack circulating sex hormone-binding globulin (SHBG), and their steroid metabolism may differ from humans.

We measured sex steroid concentrations in serum, urine and bone homogenate extracts from 2- or 6-month-old wildtype (WT) or transgenic mice overexpressing human SHBG using liquid chromatography tandem mass spectrometry. In a pilot study, SHBG or WT mice (n=5/group) were orchidectomized and given continuous release testosterone (T) or E2 for 4 weeks.

Male WT mice had undetectable circulating E2 (<LOQ i.e. 1.3 pg/ml). Male SHBG mice still only had E2 in the pg/ml range despite SHBG levels >100-fold than normal for human males, and >100-fold higher T and DHT than WT male mice. E2 was detectable in female mice or males given E2, and increased by SHBG. Continuous T did not increase E2 in SHBG or WT males. Steroid profiling revealed estradiol-3-sulphate and other catabolites in urine in equal amounts in WT and SHBG males. E2 was detected in appendicular bone of WT and SHBG male and female mice, even after

bone marrow was flushed out. Weights of the androgen-sensitive seminal vesicles were lower and levator ani weights unaffected in SHBG males under both high T and basal conditions, and intraskeletal E2 was significantly decreased in T-treated SHBG mice.

We conclude that serum E2 is undetectable in male mice, in contrast to the vast majority of previous reports based on immunoassays. This absence can be explained by the known lack of aromatization in murine adipose tissue; lack of circulating SHBG and fluctuating T levels are not important explanations. SHBG raises total concentrations of active androgens and estrogens (when present) but restricts their bioavailability and activity in a tissue-specific manner. The presence of estrogen catabolites in urine even in WT males with undetectable serum E2 suggests that it acts as a local hormone (aromatization within tissues). This was confirmed by reliable intraskeletal E2 concentration, even in male WT mice with undetectable E2 in serum. Our results support the use of male mice as a model for estrogen regulation of male bone metabolism, albeit via mostly autocrine and not endocrine mechanisms.

Disclosures: Michaël Laurent, None.

FR0371

H_2O_2 generation in osteoclast mitochondria is indispensible for endocortical, but not cancellous, bone resorption in estrogen or androgen deficiency. Shoshana Bartell*[1], Li Han[1], Aaron Warren[2], Julie Crawford[2], Semahat Serra Ucer[3], Srividhya Iyer[1], Maria Jose Almeida[1], Stavros Manolagas[1]. [1]Central Arkansas VA Healthcare System, Univ of Arkansas for Medical Sciences, USA, [2]Central Arkansas VA Healthcare System, Univ of Arkansas for Medical Sciences, USA, [3]University of Arkansas for Medical Sciences, USA

Loss of bone mass following estrogen or androgen deficiency is caused by increased resorption of the cancellous compartment and of the endosteal surface of the cortex. Nonetheless, osteoclast (Oc) ERα mediates the protective effects of estrogens in the cancellous, but not the cortical, compartment. In contrast, the ERα of osteoblast (Ob) progenitors is required for normal periosteal bone accrual as well as the maintenance of cortical bone mass, but plays no role on cancellous bone. The Oc AR, on the other hand, has no effect on bone in males, whereas the Ob AR is required for the maintenance of cancellous bone. An increase in oxidative stress and phosphorylation of p66[Shc]– an isoform of the growth factor adapter Shc that plays a critical role in mitochondrial metabolism, oxidative stress, and apoptosis – have been implicated in the increased bone resorption associated with estrogen or androgen deficiency. Here, we examined the role of p66[Shc] in ovariectomy (OVX)-induced bone loss using a mouse model of global deletion of p66[Shc]. The loss of cortical and cancellous bone was similar in both the wild-type control and p66[Shc] KO mice, suggesting that p66[Shc] does not play a role in the anti-resorptive effects of estrogens. We next examined the role of mitochondria-derived H_2O_2 in cells of the Oc lineage by generating transgenic mice expressing human catalase targeted to the mitochondria, using the LysM-Cre strain. MitoCAT mice exhibited increased cortical and cancellous bone mass due to a decrease in Oc number. Six weeks following OVX of 12-week-old female mice, oxidative stress (including an increase in the phosphorylation of p66[Shc]) and serum CTx were increased and DEXA BMD was decreased at the spine and femur in the LysM-Cre littermate controls. All of these changes were abrogated in the mitoCAT mice. Furthermore, the mitoCAT mice were protected against the OVX-induced cortical bone loss and increased porosity; but not the loss of cancellous bone, as determined by micro-CT. Similar to the females, orchidectomized (ORX) 18-week-old male mitoCAT mice were protected against cortical but not cancellous ORX-induced bone loss. These results indicate that both estrogens and androgens (or perhaps estrogens alone in both females and males) decrease bone resorption at the endocortical surface via an effect that is mediated by cells of the Ob lineage – perhaps suppression of an osteoclastogenic cytokine – and leads to reduced H_2O_2 generation in osteoclasts.

Disclosures: Shoshana Bartell, None.

FR0373

Bone Mineral Density Changes Among Women Initiating Proton Pump Inhibitors or H2 Receptor Antagonists: Results from the SWAN Bone Study. Daniel Solomon*[1], Susan Diem[2], Kristine Ruppert[3], YinJuan Lian[3], Chih-Chin Liu[4], Alyssa Wohlfarht[4], Gail Greendale[5], Joel Finkelstein[6]. [1]Harvard Medical School, USA, [2]University of Minnesota, USA, [3]University of Pittsburgh, USA, [4]Brigham & Women's Hospital, USA, [5]University of California, Los Angeles, USA, [6]Massachusetts General Hospital, USA

Background: Proton pump inhibitors (PPIs) have been associated with diminished bone mineral density (BMD) and an increased risk of fracture, however prior studies have not yielded consistent results and many have sub-optimal ascertainment of both PPI use and BMD.

Purpose: We used the Study of Women's Health Across the Nation (SWAN) longitudinal cohort to examine the association between annualized BMD changes and new use of PPIs compared with new use of Histamine 2 receptor antagonists (H2RAs) or neither.
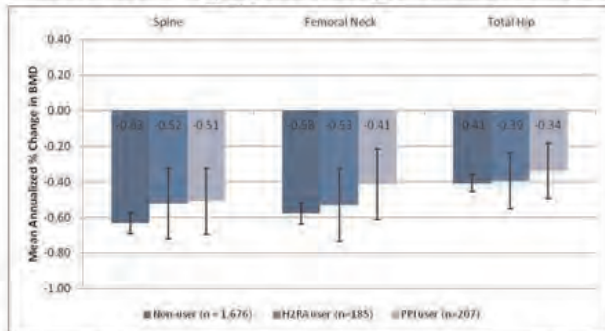
Methods: We compared the longitudinal changes in BMD among new users of PPIs, H2RAs and non-users using regression analyses. Mixed linear regression models

included recognized risk factors for osteoporosis, including demographics, menopausal transition stage, BMI, lifestyle factors, as well as comorbidities and concomitant medications. To test these methods, we also examined the effects of hormone therapy (HT) on BMD as a "positive control".

Results: We identified 207 new users of PPIs, 185 new users of H2RAs and 1,676 non-users. Study subjects had a mean age of 50 years and were followed for a median of 9.9 years. Adjusted models found no difference in the annualized BMD change at the lumbar spine, femoral neck or total hip comparing PPI users to H2RA users or non-users (see Figure A). These results were robust to sensitivity analyses. As well, an analysis of HT found that new users of these drugs did gain BMD compared with non-users supporting the validity of our study design (see Figure B).

Conclusions: These longitudinal analyses, plus similar prior studies, argue against an association between PPI use and BMD loss.

Figure A

Figure B

FR0375

Risedronate Prevents Anastrozole-Induced Bone Loss In The IBIS-II Prevention Trial.

Ivana Sestak*[1], Shalini Singh[2], Jack Cuzick[3], Glen Blake[4], Rajesh Patel[5], Rob Coleman[6], Mitch Dowsett[7], John F. Forbes[8], Anthony Howell[9], Richard Eastell[10]. [1], United Kingdom, [2]Centre for Cancer Prevention, United Kingdom, [3]Centre for Cancer Prevention, Wolfson Institute of Preventive Medicine, Queen Mary University of London, United Kingdom, [4]King's College London, United Kingdom, [5]Imperial College London, United Kingdom, [6]Department of Oncology, Cancer Clinical Trials Centre, Academic Unit of Clinical Oncology, United Kingdom, [7]Royal Marsden Hospital, United Kingdom, [8]University of Newcastle, Calvary Mater Hospital, Australia, [9]Paterson Institute for Cancer Research, United Kingdom, [10]University of Sheffield, United Kingdom

Background: Aromatase inhibitors, such as anastrozole (A), have been shown to prevent breast cancer in postmenopausal women at high risk of the disease, but these drugs have been associated with accelerated bone loss. Here, we analyse the effect of risedronate (R) on bone mineral density (BMD) after 3 years of follow-up in the IBIS-II trial, which is a randomised, placebo-controlled trial of A in postmenopausal women at increased risk of breast cancer.

Methods: 1410 postmenopausal women were enrolled in the bone sub-study and stratified into three strata according to their baseline T-score at spine or femoral neck (stratum I (N=761): T-score>-1.0; stratum II (N=500): -1.0<T-score>-2.5; stratum III (N=149): -2.5<T-score>-4.0 or/and two fragility fractures). All women received regular monitoring by DXA scans. The primary objective of this analysis was to compare the effect of R versus placebo (P) in osteopenic women in stratum II who were randomised to A in the main study. Secondary objectives included investigating the effect of A on BMD in women not receiving R and furthermore in osteoporotic women all receiving R. All results are presented as mean % BMD changes (95% CI) between baseline and 3 years of follow-up.

Results: Baseline and 3-year BMD data was available for a total of 892 women (stratum I=493, stratum II=296, stratum III=103). 146 women in stratum II were randomised to A (A/R=74, A/P=72). 3-year mean % BMD change at the spine for women receiving A/R was 1.3 (95% CI 0.3 to 2.9) compared to -2.6 (95% CI -3.9 to -1.3) for those on A/P (P<0.0001, Figure). Similar results were seen for mean % BMD change at the total hip (Figure). Women in stratum I and/or II not receiving R had a significant BMD decrease at the spine and total hip when randomised to A compared to P after 3 years of follow-up (spine: -3.9% vs. -1.2%, P<0.0001, total hip: -3.9% vs. -1.8%, P<0.0001). Osteoporotic women all received R and a significant increase in BMD at the spine, but not total hip was seen for women randomised to P but also for those on A (spine: 3.9% vs. 1.3%, P=0.009; total hip: 1.6% vs. 0.3%, P=0.1).

Conclusions: Our results show that women with osteopenia on A and receiving R showed a highly significant increase in BMD at the spine and total hip compared to those not receiving R. Women with healthy bone or osteopenia receiving A showed a large BMD decrease when compared to P, but our results show that BMD loss due to A can be controlled with bisphosphonate treatment.

Figure
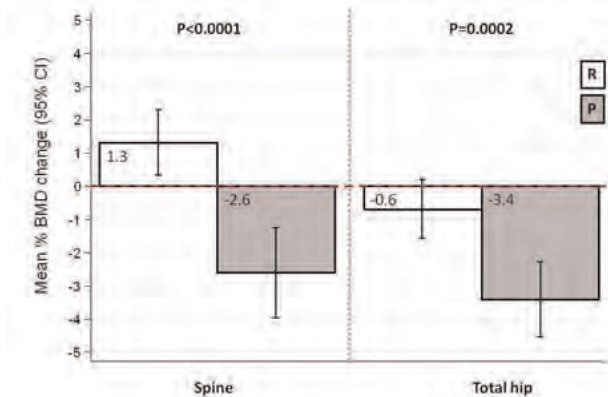
FR0377

Acute Skeletal Effects of PTH in Combination with Denosumab or Alendronate.

Joy Tsai*[1], Hang Lee[2], Yuli Zhu[3], Katelyn Foley[3], Sherri-Ann Burnett-Bowie[1], Robert Neer[1], Benjamin Leder[4]. [1]Massachusetts General Hospital, USA, [2]Massachusetts General Hospital, Biostatistics Center, USA, [3]Massachusetts General Hospital, Endocrine Unit, USA, [4]Massachusetts General Hospital Harvard Medical School, USA

Background: In contrast to the combination of bisphosphonates (BPs) and teriparatide (TPTD), the combination of TPTD and denosumab (DMAB) increases BMD at the spine and hip more than either drug alone. Furthermore, DMAB, unlike BPs, fully inhibits the stimulation of bone resorption induced by TPTD 20-mcg. We aimed to better define the resorptive properties of TPTD in the absence or presence of an antiresorptive drug, as well as the comparative capacity of DMAB and BP to inhibit TPTD-induced bone resorption even in the setting of high dose TPTD (40-mcg).

Methods: 18 postmenopausal osteoporotic women ages 52 to 81 who had not used oral BPs within 1-year were randomized to 2 treatment groups. At baseline, serum CTX, OC, and P1NP were measured both immediately prior to and 4-hours after a single 8 AM 40-mcg SC TPTD injection. When the 4-hour sampling was complete, subjects in group 1 received DMAB 60 mg SC and subjects in group 2 started oral weekly alendronate (ALN) 70 mg. 8-weeks later, CTX, P1NP, and OC were again measured in all subjects immediately before and 4-hours after a TPTD 40-mcg injection. Subjects were fasting at all visits. The within and between-group change in each marker at each visit was assessed by paired and unpaired t-test. The between-group difference between the TPTD-induced change at week 8 versus baseline was compared by ANCOVA.

Results (Fig): At baseline, TPTD induced a significant and similar increase in mean CTX in both treatment groups (ALN 47±13%, DMAB 49±17%). After 8

weeks of antiresorptive therapy, baseline CTX decreased by $63 \pm 18\%$ in the ALN group and by $90 \pm 5\%$ in the DMAB group (P=0.001 ALN versus DMAB). In the ALN group, TPTD maintained its ability to increase CTX ($44 \pm 34\%$) but TPTD had no effect on CTX in the DMAB group (P=0.002 ALN vs DMAB). At baseline, TPTD had no effect on OC or P1NP in either group. At week 8 in the DMAB group, OC and P1NP decreased by $8.3 \pm 8.9\%$ and $12.4 \pm 10.4\%$, respectively (P<0.04 for both).

Summary: In untreated women, a single 40-mcg SC injection of TPTD increases CTX within 4 hours. 8 weeks of DMAB, but not ALN, fully inhibits this high-dose TPTD–induced increase in CTX. The difference in the capacity of DMAB and ALN to inhibit the pro-resorptive effects of TPTD may, in part, explain the observed differences in TPTD combination therapies. These results suggest that combining DMAB with higher doses of TPTD may be an effective osteoporosis treatment strategy.
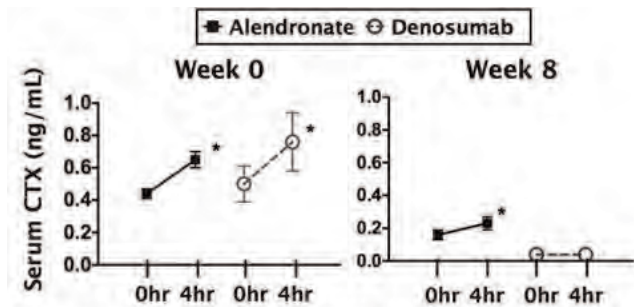
Figure. Serum CTX levels (mean ± SEM) before and 4 hours post-teriparatide injection in the alendronate-treated group and denosumab-treated group. *P<0.04 for the within-group increase.

Figure

FR0379

Responder Analysis of the Effects of Abaloparatide and Teriparatide on Bone Mineral Density in Postmenopausal Women With Osteoporosis. <u>Benjamin Leder</u>*[1], <u>Kathleen Banks</u>[2], <u>Louis O'Dea</u>[2], <u>C.R. Lyttle</u>[2], <u>John Yates</u>[3], <u>Gary Hattersley</u>[4]. [1]Massachusetts General Hospital Harvard Medical School, USA, [2]Radius, USA, [3]Radius Health, USA, [4]Radius, USA

Introduction and Methods: The lack of early gains in hip BMD among patients treated with the anabolic agent teriparatide (TPTD) is of potential clinical concern, especially in patients at high risk of hip fracture.

In a 24-week phase 2 study of postmenopausal women aged 55-85 with a T-score <-2.5 at the spine or femoral neck or a T-score of ≤-2.0 with either a prior low-trauma fracture, age >65, or a maternal history of osteoporosis, the PTHrP analog, abaloparatide (ABL, 80-μg SC daily) increased lumbar spine (LS), total hip (TH), and femoral neck (FN) BMD more than TPTD 20-μg SC daily and PBO (all subjects were also treated with calcium and vitamin D supplementation per local practice). To determine if women treated with 24-weeks of ABL 80-μg (n=35) were more likely to experience BMD gains than those treated with either TPTD 20-μg (n=38) or PBO (n=41), we performed a responder analysis comparing the percentage of subjects experiencing BMD gains of >0% and >3% at the TH, FN, LS, or at all three anatomic sites. Between group differences were compared by 2-sided Chi-square test.

Results: Over 24-weeks, TH BMD increased in 80%, 53% and 63% of women in the ABL, TPTD and PBO groups, respectively (p=0.014 ABL vs. TPTD). Similarly, FN BMD increased in 86%, 58% and 54% of women in these three groups, respectively (ABL vs. TPTD p=0.009; ABL vs PBO p=0.003). Almost all women in the ABL (94%) and TPTD (93%) groups experienced BMD gains at the LS whereas 33% lost bone in the PBO group (PBO vs. both ABL and TPTD p<0.004). More patients experienced BMD gains at all three anatomic sites in the ABL group (66%) than in the TPTD (40%) and PBO (29%) groups (p<0.03 ABL vs. both TPTD and PBO). More ABL-treated women had a >3% TH BMD gain (37%) than those treated with TPTD (16%) or PBO (15%) (ABL p<0.04 vs. both TPTD and PBO). 43% of ABL-treated women had a >3% FN BMD gain compared to 29% in both the TPTD and PBO groups (p=NS). The percentage of subjects with a >3% BMD gain at the LS was higher in ABL (89%) than PBO (41%) (p<0.001) but not TPTD (73%) (p=0.073).

Summary: In postmenopausal women with osteoporosis, more subjects treated with ABL experienced BMD increases at the LS, FN, TH, or all 3 sites compared to those treated with TPTD or PBO. Additionally, more subjects treated with ABL experienced a >3% BMD increase at the TH compared to TPTD or PBO. The overall high responder rate of ABL, particularly at the TH and FN as compared to TPTD, provides a strong rationale for its clinical development as an anabolic treatment for postmenopausal osteoporosis.
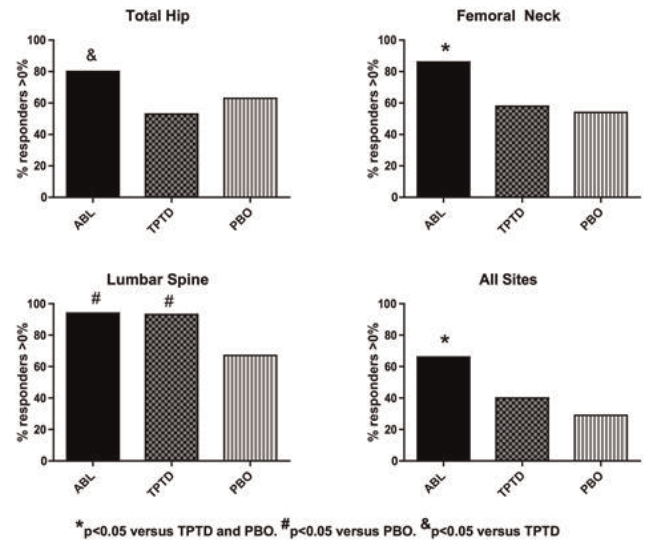
*p<0.05 versus TPTD and PBO. #p<0.05 versus PBO. &p<0.05 versus TPTD

Figure

FR0380

Romosozumab Significantly Improves Vertebral Cortical Bone Mass and Structure Compared With Teriparatide: HR-QCT Analyses of Randomized Controlled Trial Results in Postmenopausal Women with Low BMD. <u>T Damm</u>*[1], <u>C Libanati</u>[2], <u>J Peña</u>[1], <u>G Campbell</u>[1], <u>R Barkmann</u>[1], <u>Da Hanley</u>[3], <u>S Goemaere</u>[4], <u>Ma Bolognese</u>[5], <u>C Recknor</u>[6], <u>C Mautalen</u>[7], <u>YC Yang</u>[2], <u>CC Glüer</u>[1]. [1]Christian-Albrechts-Universität zu Kiel, Germany, [2]Amgen Inc., USA, [3]University of Calgary, Canada, [4]Ghent University Hospital, Belgium, [5]Bethesda Health Research Center, USA, [6]United Osteoporosis Centers, USA, [7]Centro de Osteopatias Medicas, Argentina

Purpose: Understanding the effect of therapies in the vertebral compartments is relevant to bone biology and clinical practice. We developed an improved technique using cortical shell segmentation-based layering of high resolution quantitative computed tomography (HR-QCT) scans of T12 vertebral bodies to evaluate compartment-specific changes in bone mineral density (BMD) and microstructure.

Methods: In an international, randomized, phase 2 study (McClung et al., *N Engl J Med.* 2014), postmenopausal women with low BMD supplemented with calcium and vitamin D received romosozumab (210 mg SC QM), teriparatide (20 mcg SC QD), or placebo (PBO). A subset of these women received HR-QCT scans of T12 (N=11 romosozumab, 12 teriparatide, 8 PBO) at baseline and month 12. For cortical HR-QCT analysis (blinded to treatment assignment), adjacent 200 micron thin films of the cortical shell were evaluated to determine changes from the outer soft tissue bordering the vertebrae to the medullary spongiosa (Figure). In addition to the standard cancellous compartment variables previously described (Graeff et al., *JBMR.* 2007), this improved method allows accurate determination of cortical variables in the subregions, including apparent and corrected (deconvolved) cortical thickness, bone mineral content (BMC), and BMD. Changes in cortical thickness are modeled assuming an average 50% mineralization of newly added matrix.

Results: At baseline, mean (SD) apparent cortical thickness of 1.37 (0.13) mm was corrected to a cortical thickness of 0.29 (0.05) mm. At month 12, romosozumab significantly improved cortical BMC and BMD from baseline and in comparison to teriparatide or PBO (all *P*≤0.0003; Table). These gains were attained by both endosteal and periosteal bone matrix apposition. Improvements in cancellous BMD were similar between romosozumab and teriparatide. Conclusion: Using HR-QCT scans of the spine, it is possible to evaluate changes across the cortical shell of the vertebral bodies and determine alterations in the endosteal and periosteal regions. The anatomical location and magnitude of these changes could impact changes in bone strength and thus affect fracture risk. Romosozumab administration was associated with significant increases in cortical thickness and improvement in all measured cortical parameters at 12 months compared with teriparatide or PBO. The clinical effect of romosozumab to reduce fractures is being evaluated in an ongoing phase 3 clinical program.
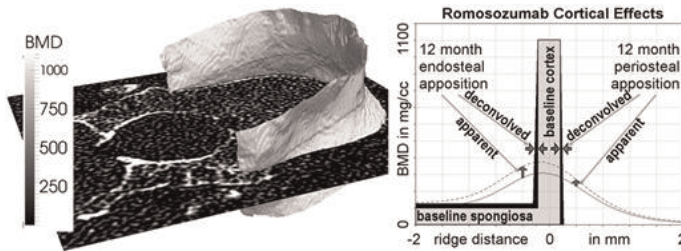
Figure. 3D Visualization of Vertebral Cortex (left) and Schematic Drawing of Bone Apposition (right)

Region	Romosozumab N = 11	Teriparatide N = 12	Placebo N = 8
Deconvolved cortical thickness (microns)	157 (12)*†	61 (12)‡	10 (14)
Cortical BMC (% of baseline)	22 (2)*†	11 (2)‡	−1 (2)
Apparent cortical BMD (mg/cm³)			
Periosteal apposition at 0.2 to 0. 6 mm from ridge	37 (4)*†	16 (4)‡	0 (5)
Endosteal apposition at −0.2 to −0.6 mm from ridge	59 (6)*†	19 (6)	0 (7)
Subcortical apparent BMD (mg/cm³)	28 (3)†	22 (3)‡	1 (4)
Spongiosa apparent BMD (mg/cm³)	20 (3)†	19 (3)†	−4 (3)

Values are mean (SD).
*P value ≤ 0.0003 compared with teriparatide.
†P value < 0.0001 compared with placebo.
‡P value < 0.05 compared with placebo.

Table. Changes From Baseline in Cortical Thickness, BMC, and BMD at Month 12

FR0383

Atypical subtrochanteric fracture is a rare phenomenon in osteoporotic patients treated with bisphosphonates. Christian Muschitz*[1], Hans Peter Dimai[2], Roland Kocijan[3], Heinrich Resch[4], Peter Pietschmann[5], Martina Kostic[6], Alexandra Kaider[7], Michael Szivak[8], Matthias Schilling[9], Heinrich W. Thaler[10]. [1]St. Vincent's Hospital, Austria, [2]Medical University of Graz – Department of Internal Medicine, Division of Endocrinology & Metabolism, Austria, [3]St. Vincent Hospital Vienna, Austria, [4]Medical University Vienna, Austria, [5]Department of Pathophysiology & Allergy Research, Medical University of Vienna, Austria, [6]St. Vincent Hospital – Medical Department II - Academic Teaching Hospital of Medical University of Vienna, Austria, [7]Center for Medical Statistics, Informatics & Intelligent Systems, Medical University of Vienna, Austria, [8]Austrian Trauma Insurance Agency (AUVA), Austria, [9]Institute for Medical Radiology, Diagnostics, Intervention; Clinical Center of Lower Austria, Austria, [10]Trauma Center Meidling, Austria

Purpose: Atypical femoral fractures (AFF) are fractures in the subtrochanteric region of the femur with characteristic appearance. Although an AFF is generally a rare event, several studies indicated a potential link between AFF and long-term bisphosphonate (BP) use. However, studies evaluating a possible interaction differed in study design and diagnostic criteria of AFF.

The aim was to investigate the incidence of AFF and a potential association of this fracture type with BP use and other medications over a period of 9 years (2002-2010).

Methods: We retrospectively analyzed the overall incidence of AFF and a potential association of this fracture type with BP use at one of the largest Austrian trauma hospitals with a catchment area of approximately 1.9 million people in the capital city Vienna. The incidence of hip fracture in this center was comparable to the incidence of hip fracture across Austria.

Results: A total of 5.322 patients who had sustained a de novo osteoporotic hip fracture were treated at this hospital. Subtrochanteric fractures were extracted from the database using ICD codes; every retrieved fracture case was radiographically analyzed by a blinded radiologist. 128 patients with a de novo low-traumatic subtrochanteric fracture were identified: 101 typical, 17 atypical and 10 borderline fractures. Median age of patients with typical femoral fractures and borderline fractures was 83.0 yrs. Patients with atypical fractures had a median age of 81.0 yrs. Female patients with a subtrochanteric femoral fracture were significantly older, with a median of 84.0 vs. 74.0 yrs (p<0.0001). Of the 6 patients with subtrochanteric fractures receiving bisphosphonates there was one female patient with an atypical fracture (oral bisphosphonate therapy for 29 months) and 5 patients had typical fractures and bisphosphonate therapy between 6 and 60 months. Comparison of the three fracture types showed no significant difference in medication use – neither with proton pump inhibitors nor tricyclic antidepressants or selective serotonine reuptake inhibitors - with the exception of phenprocoumon. This anticoagulant was used in 2%, 11.8% and 30% of patients with typical, atypical and borderline fractures, respectively (p<0.002).

Conclusions: Our data strongly indicate that cases of AFF are rare, even in patients with osteoporotic hip fractures. However, we did not detect an association of AFF and bisphosphonate use in this study group.

FR0384

Withdrawn

FR0387

Evaluation of Invasive Oral Procedures and Events in Women With Postmenopausal Osteoporosis Treated With Denosumab: Results From the Pivotal Phase 3 Fracture Study Extension. Nelson B. Watts*[1], John T. Grbic[2], Michael McClung[3], Socrates Papapoulos[4], David Kendler[5], Christence S. Teglbjaerg[6], Lawrence O'Connor[7], Rachel B. Wagman[7], Eric Ng[7], Nadia S. Daizadeh[7], Pei-Ran Ho[7]. [1]Mercy Health, USA, [2]Columbia University, USA, [3]Oregon Osteoporosis Center, USA, [4]Leiden University Medical Center, Netherlands, [5]University of British Columbia, Canada, [6]CCBR, Denmark, [7]Amgen Inc., USA

Purpose: Osteonecrosis of the jaw (ONJ) is a rare but serious adverse event of some antiresorptive therapies, including denosumab (DMAb), and invasive oral procedures and events (OPEs) are suggested to be an important risk factor (Ruggiero, *J Oral Maxillofac Surg* 2009). The incidence of positively adjudicated ONJ in the DMAb bone loss clinical program is rare (between ≥ 1 and < 10 per 10,000). In this study, we assessed the occurrence of invasive OPEs through Year 5 of the ongoing, 7-year FREEDOM Extension (EXT) trial.

Methods: In FREEDOM, women were randomized to receive DMAb 60 mg SC or placebo every 6 months for 3 years. Those who missed ≤ 1 dose of investigational product and completed the Year-3 visit were eligible for the open-label FREEDOM EXT; women in the EXT long-term group (N = 2343) received DMAb in FREEDOM and EXT, and women in the EXT cross-over group (N = 2207) received placebo in FREEDOM and DMAb in EXT. Women who reached the EXT Year-3 visit were asked to chronicle their history of invasive OPEs (eg, dental implants, tooth extraction, natural tooth loss, or scaling or root planing [extensive subgingival cleaning]) during the EXT. Every 6 months thereafter, women were asked to document their oral health history since the last visit. Jaw surgery information was collected starting from month 30 of the EXT.

Results: The majority of women (78%) participated in the survey. Over 5 years of the EXT, 42.4% of these women reported an invasive OPE; the incidence of the 5 individual OPEs reported were similar between groups (Table). ONJ incidence was 0.4% (7/1500 subjects) in women reporting invasive OPEs and 0.05% (1/2036 subjects) in women reporting no invasive OPEs. The actual number of invasive OPEs may be underestimated due to limited capture of OPEs in medical charts and due to recall bias by subjects of events that occurred in the first 3 years of the EXT. During the EXT (Years 1–5), the exposure-adjusted incidence of ONJ was 4.2 per 10,000 patient-years. Of the 8 ONJ cases, 6 have resolved, 1 is ongoing and continues to be followed, and the final outcome of 1 is unknown, as consent was withdrawn.

Conclusion: While invasive OPEs were common in this group of DMAb-treated women with postmenopausal osteoporosis, ONJ incidence was low. Invasive OPEs will continue to be queried prospectively in the EXT to characterize the long-term background rate.

	FREEDOM Extension Years 1–5		
	Long-term (N = 1827) n (%)	Cross-over (N = 1709) n (%)	All (N = 3536) n (%)
Age in years, mean (SD)	74.4 (4.7)	74.2 (4.8)	74.3 (4.8)
Any invasive oral procedure or event	763 (41.8)	737 (43.1)	1500 (42.4)
Scaling or root planing	500 (27.4)	481 (28.1)	981 (27.7)
Tooth extraction	387 (21.2)	354 (20.7)	741 (21.0)
Dental implant	88 (4.8)	79 (4.6)	167 (4.7)
Natural tooth loss	59 (3.2)	57 (3.3)	116 (3.3)
Jaw surgery	11 (0.6)	9 (0.5)	20 (0.6)

N = Number of subjects who received ≥ 1 dose of investigational product in FREEDOM Extension and responded to ≥ 1 oral event questionnaire related to FREEDOM Extension. n = Number of subjects with ≥ 1 invasive oral procedure or event.

Table: Summary of Invasive Oral Procedures and Events

FR0388

Findings from Denosumab (Prolia®) Post-marketing Safety Surveillance for Atypical Femoral Fracture, Osteonecrosis of the Jaw, Severe Symptomatic Hypocalcemia, and Anaphylaxis. <u>M Geller</u>[1], <u>RB Wagman</u>*[1], <u>PR Ho</u>[1], <u>S Siddhanti</u>[1], <u>C Stehman-Breen</u>[1], <u>NB Watts</u>[2], S Papapoulos[3]. [1]Amgen Inc., USA, [2]Mercy Health Osteoporosis & Bone Health Services, USA, [3]Leiden University Medical Center, Netherlands

Purpose: We characterize the Prolia post-marketing experience for 4 adverse drug reactions (ADRs): atypical femoral fracture (AFF), osteonecrosis of the jaw (ONJ), severe symptomatic hypocalcemia (SSH), and anaphylaxis.

Methods: The Amgen post-marketing database undergoes continual assessment of adverse events reported by health care providers, patients, and other sources. AFF and ONJ cases were assessed and adjudicated by independent committees. SSH and anaphylaxis prompted further review by Amgen Global Safety because causality due to Prolia could not be excluded.

Results: As of September 2013, estimated Prolia exposure was 1,252,566 patient-years. Four post-marketing reports were adjudicated as consistent with the AFF ASBMR definition (Shane *JBMR* 2010). All patients had used bisphosphonate (BP); 2 subjects healed and 2 had no follow-up information. For ONJ, 32 post-marketing reports were adjudicated as consistent with the AAOMS definition (Position Paper *AAOMS* 2009). Risk factors included ≥ 1: glucocorticoids, chemotherapy, prior BP use, older age, and invasive dental procedures. One-third of reports indicated resolution, 1/3 were ongoing, and the remainder were unknown. Routine pharmacovigilance in 2011 showed 8 reports of medically confirmed SSH that included symptoms of seizures and/or tetany; 7 of 8 patients had chronic kidney disease, a risk factor for hypocalcemia; most events occurred within 30 days of Prolia administration and responded to IV/PO calcium/vitamin D. Routine pharmacovigilance in 2012 showed 5 reports of medically confirmed anaphylaxis that included hypotension, dyspnea, throat tightness, facial and upper airway edema, pruritus, and/or urticaria. Most events occurred within 1 day of the first Prolia dose; emergency room treatments included antihistamines and IV/PO steroids with no fatal outcomes. Amgen assessment of SSH and anaphylaxis as possibly related to Prolia led to product labeling updates.

Conclusion: These Prolia post-marketing events have not shown any unexpected findings; the benefit/risk profile remains favorable. Ongoing safety surveillance continues through clinical studies and pharmacovigilance activities.

FR0391

Percentage of Women Achieving Non-osteoporotic BMD T-scores at the Spine and Hip Over 8 Years of Denosumab Treatment. <u>S Ferrari</u>*[1], <u>C Libanati</u>[2], <u>CJF Lin</u>[2], <u>S Adami</u>[3], <u>JP Brown</u>[4], <u>F Cosman</u>[5], <u>C Czerwiński</u>[6], <u>LH de Gregório</u>[7], <u>J Malouf</u>[8], <u>J-Y Reginster</u>[9], <u>NS Daizadeh</u>[2], <u>A Wang</u>[10], <u>RB Wagman</u>[10], <u>EM Lewiecki</u>[11], <u>S Cummings</u>[12]. [1]Geneva University Hospital, Switzerland, [2]Amgen Inc., USA, [3]University of Verona, Italy, [4]Laval University & CHU de Québec Research Centre, Canada, [5]Helen Hayes Hospital, USA, [6]Krakow Medical Center, Poland, [7]CCBR, Brazil, [8]Universitat Autònoma de Barcelona, Spain, [9]University of Liège, Belgium, [10]Amgen Inc., USA, [11]New Mexico Clinical Research & Osteoporosis Center, USA, [12]San Francisco Coordinating Center, CPMC Research Institute, & UCSF, USA

Purpose: Guidelines for the treatment of chronic conditions such as hypertension and diabetes include specific biomarker targets. This differs from osteoporosis treatment guidelines, which currently do not define treatment targets or goals. In general, absence of BMD loss and fracture are considered treatment successes. This is far from ideal because success defined by the lack of a negative outcome does not set a real goal for therapy. Potential goals for osteoporosis treatment might include reaching a BMD T-score value somewhere above –2.5 that represents an acceptable level of fracture risk. To provide insight into T-score values achieved over time with denosumab (DMAb), we report on the percentage of women who achieved a range of possible target BMD T-scores at both the lumbar spine and total hip over 8 years of treatment.

Methods: For these analyses, women received 3 years of DMAb (60 mg SC Q6M) during FREEDOM and 5 years of DMAb during the Extension for a total of 8 years of continued treatment. The percentage of women with T-scores >-2.5, >-2.2, >-2.0, and >-1.8 at both the lumbar spine and total hip, and T-scores >-2.5 at either the lumbar spine or total hip at baseline and over 8 years of DMAb treatment were determined. The influence of baseline T-score on subsequent T-score improvement was also explored.

Results: At FREEDOM baseline, mean (SD) lumbar spine and total hip T-scores were -2.83 (0.67) and -1.85 (0.79), respectively, for the DMAb Extension participants (N=2343). The percentage of women with T-scores >-2.5, >-2.2, >-2.0, and >-1.8 at both the lumbar spine and total hip progressively increased from baseline over 8 years of DMAb treatment as follows: 11% to 82% (>-2.5), 4% to 65% (>-2.2), 2% to 53% (>-2.0), and 1% to 39% (>-1.8) (Fig. 1). At individual sites, the percentage of women with a T-score >-2.5 increased from baseline over 8 years of DMAb treatment from 19% to 86% (lumbar spine) and from 75% to 94%

(total hip). Baseline T-scores by quartile remained largely consistent throughout the 8 years of DMAb treatment, which showed similar trajectory in BMD across subjects regardless of initial BMD (not shown).

Conclusion: DMAb enables a substantial proportion of women with osteoporosis to achieve non-osteoporotic T-scores. The data reported here contribute insightful information to discussions on the topic of treatment goals for osteoporosis.

Fig. 1. Percentage of Women Achieving a Particular T-score at Both the Lumbar Spine and Total Hip
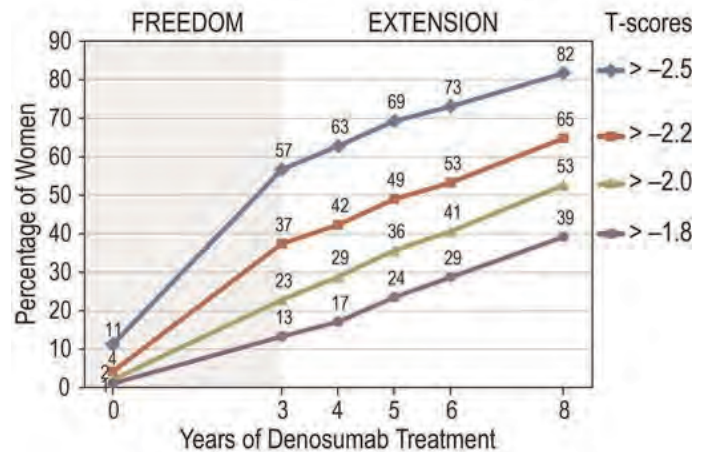
Fig. 1

FR0396

The Extent of Symmetry on Images of Bilateral Atypical Femoral Fractures. <u>Linda Probyn</u>*[1], <u>Angela M. Cheung</u>[2], <u>Jonathan Adachi</u>[3], <u>Leon Lenchik</u>[4], <u>Aliya Khan</u>[5], <u>Earl Bogoch</u>[6], <u>Robert Josse</u>[7], <u>Catherine Lang</u>[8], <u>R Bleakney</u>[9]. [1]University of Toronto, Sunnybrook Health SC, Dept. Medical Imaging, Canada, [2]University Health Network-University of Toronto, Canada, [3]St. Joseph's Hospital, Canada, [4]Wake Forest University, USA, [5]McMaster University, Canada, [6]St. Michael's Hospital, Canada, [7]St. Michael's Hospital, University of Toronto, Canada, [8]University of Toronto, Canada, [9]Mount Sinai Hospital, Canada

Purpose: Atypical Femoral Fractures (AFFs) are commonly bilateral. The purpose of this study is to evaluate bilateral AFFs and to determine if the imaging features of both fractures are similar.

Materials and Methods: Imaging studies of 76 patients with bilateral AFFs from the Ontario AFF cohort were retrospectively reviewed (3 men, 73 women, age range 31.1 to 91 years, mean age 67.3 years). The time interval between fracture diagnoses was determined. For each fracture, the following imaging features were evaluated: location of fracture, femoral angle, length of cortical thickening, comminution, medial spike (proximal or distal fragment) and fracture orientation (superior/inferior). Associations between imaging findings on pairs of bilateral fractures were assessed with Spearman's correlation (r_s) and the Kappa (κ) statistic.

Results: Bilateral fractures (62 incomplete and 14 complete) are diagnosed within 12 months of each other in 59/76 cases (77.6%). Average time between fracture diagnoses was 10.2 months. 90% of bilateral fractures was diagnosed within 2.9 years of each other (range 0 to 120 months). There was a strong correlation between fracture location (r_s =0.68) with 58/76 cases (76.3%) of bilateral fractures occurring within a distance of less than 5 cm. 41/76 cases (53.9%) had a distance of less than 2.5 cm between bilateral fractures. There was moderate correlation between femoral angles (r_s=0.4) and weak correlation between length of cortical thickening (r_s=0.28). There was substantial agreement for medial spike location (κ=0.67) and fracture orientation (κ=0.62) and moderate agreement for lack of comminution (κ=0.42). These findings were independent of time between fractures.

Conclusion: Patients with bilateral AFFs are likely to be diagnosed with the second one within the first year of presentation of the first one. Bilateral fractures are likely to have similar imaging findings and location along the femur, regardless of the time interval between fractures.
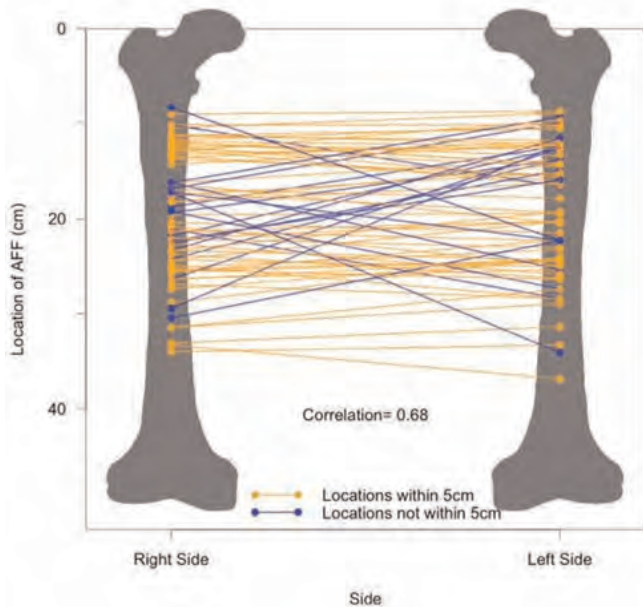
Bilateral Location image

Disclosures: Linda Probyn, None.

FR0397

Virtual Twin Estimates: Continued New Vertebral and Nonvertebral Anti-Fracture Efficacy Through 8 Years of Treatment With Denosumab. <u>SR Cummings</u>*[1], <u>E Vittinghoff</u>[2], <u>NS Daizadeh</u>[3], <u>M Austin</u>[3], <u>A Wang</u>[3], <u>RB Wagman</u>[3]. [1]San Francisco Coordinating Center, CPMC Research Institute, USA, [2]University of California San Francisco, USA, [3]Amgen Inc., USA

Purpose: Ethical concerns curtail duration of placebo (PBO) treatment in randomized clinical trials, which limits the ability to evaluate the efficacy of new therapies over the very long term. While open-label extensions with participants of the original trial permit long-term assessment, these subjects may be healthier and more persistent with treatment than those who dropped out of the original study or did not enroll in the extension. The virtual twin method addresses such limitations by simulating long-term PBO subjects ("virtual twins") with identical characteristics to the subjects in the extension (Vittinghoff et al., *Stat Med.* 2010). The pivotal phase 3 fracture trial (FREEDOM) evaluated denosumab (DMAb) vs PBO for 3 years (Cummings et al., *N Engl J Med*. 2009) and has been extended with open-label DMAb for an additional 7 years for all subjects who missed no more than 1 dose of investigational product during the FREEDOM study, completed the 36-month visit, and agreed to enroll in the Extension. We used the virtual twin method to assess fracture risk reduction after 8 years of DMAb treatment (ie, 3 years in FREEDOM and 5 additional years in its Extension) relative to long-term virtual twin PBO.

Methods: Models were developed to simulate fracture outcome for a hypothetical long-term PBO-treated population (ie, virtual twin PBO group) with identical baseline characteristics predictive of fracture risk (ie, BMD, fracture history, BMI, and age) as long-term DMAb subjects, using FREEDOM data from subjects who received PBO in FREEDOM and enrolled in the Extension. Estimates of the relative risks (RRs) between the observed long-term DMAb and the virtual twin PBO groups with bootstrap 95% confidence intervals were calculated.

Results: After 5 years of the Extension, representing 8 years of continued treatment with DMAb, the observed new vertebral fracture incidence in the long-term DMAb-treated group (5.5%) was significantly lower than the estimated incidence in the virtual twin PBO group (9.2%; RR: 0.60; 95% CI: 0.44–0.81; Figure). The observed incidence of nonvertebral fracture in long-term DMAb-treated subjects also was significantly below the estimated incidence in the virtual twin PBO group (RR: 0.54; 95% CI: 0.42–0.70; Figure).

Conclusion: The virtual twin analysis suggests that 8 years of DMAb continued to significantly reduce the risk of new vertebral and nonvertebral fractures.

RR = relative risk of fracture for long-term DMAb group compared with virtual twin PBO group
n = number of long-term DMAb-treated subjects with ≥ 1 fracture
N = number of subjects who were evaluable for fracture assessment at the beginning of the Extension
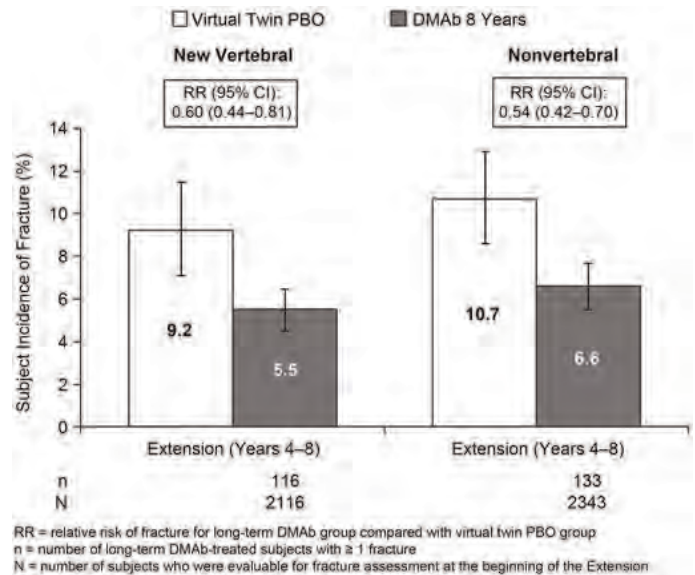
Figure. Subject Incidence of New Vertebral and Nonvertebral Fractures

Disclosures: SR Cummings, Amgen, Lilly, Merck, 3
This study received funding from: Amgen Inc.

FR0398

Zoledronic Acid in Frail Elders to Strengthen Bone: Three Year Results from ZEST Trial. <u>Susan Greenspan</u>*[1], <u>Mary Anne Ferchak</u>[1], <u>Subashan Perera</u>[2], <u>Dave Nace</u>[2], <u>Neil Resnick</u>[3]. [1]University of Pittsburgh, USA, [2]University of Pittsburgh, USA, [3]Univeristy of Pittsburgh, USA

Background: Although nearly 85% of frail seniors residing in long term care facilities have osteoporosis, the pivotal osteoporosis trials have systematically excluded fragile, functionally-impaired women. As a result, the vast majority are not treated even though they are at the greatest risk for fracture. The goal of the ZEST trial (Zoledronic acid in frail Elders to STrengthen bone) was to examine the safety and efficacy of a single dose of zoledronic acid over 2 years with a 1 year extension.

Methods: This double-blind, randomized controlled trial included women residents of a nursing home or assisted living facility, who were not on an antiresorptive agent despite having osteoporosis (BMD or fracture) and had a vitamin D level >20 ng/dL. We included residents with cognitive impairment, immobility, and multiple diseases and medications. All subjects (or their proxies) provided informed consent, and all received a single dose of zoledronic acid 5 mg or placebo IV, in addition to daily calcium (1200 mg) and vitamin D (800 IU). Participants were reconsented for the 1 year extension. The primary outcomes for the extension were the 36 month hip and spine BMD changes and safety. We measured BMD in a mobile unit and collected serious adverse events (AE) with an electronic surveillance system. We used linear mixed models for analyses.

Results: 181 women were randomized and 141 agreed to the one year extension. Mean age was 85.4 and there were no baseline differences between groups in age, BMI, calcium/vitamin D intake, BMD, activities of daily living, or cognitive or mental health status. The active treatment group included more women with diabetes, falls history, and slow gait speed. 92% of subjects completed 12 months; 67% completed 24 months and 49% completed 36 months. At 3 years, BMD percent changes at the total hip, femoral neck and spine were significantly greater in the active treatment group compared to placebo (all p< 0.01, table), with the adjusted differences of 5.4 percentage points at the total hip, 6.2 at the femoral neck and 4.5 at the spine. There were no significant differences in AEs during the third year.

Conclusions: This trial of single dose zoledronic acid for osteoporosis in cognitively impaired, frail osteoporotic women is the first to demonstrate that it is safe and effective in preserving/improving skeletal integrity over 3 years. Future studies are needed to determine if BMD improvement translates into fracture reduction.

Table: Percent change ± standard error in bone mineral density at the total hip, femoral neck and spine at 36 months

Skeletal site	Active (N=89)	Placebo (N=92)	P-value (between group difference)
Total hip	1.9±0.6**	-3.0±1.0**	p<0.0001
Femoral neck	1.7±1.3	-4.5±1.0**	p<0.0001
Spine	5.4±0.9**	0.7±0.8	p<0.0001

*p<0.05, ** p< 0.01 within group change from baseline

Table

Disclosures: Susan Greenspan, Eli Lilly, Amgen, 7

FR0405

Teriparatide Accelerates Healing of Bisphosphonate-Associated Atypical Femoral Fractures in Patients with Osteoporosis. Naohisa Miyakoshi*[1], Toshiaki Aizawa[2], Satoshi Sasaki[3], Shigeru Ando[4], Shigeto Maekawa[5], Hiroshi Aonuma[1], Hiroyuki Tsuchie[6], Hiroshi Sasaki[7], Yuji Kasukawa[1], Yoichi Shimada[8]. [1]Akita University Graduate School of Medicine, Japan, [2]Northern Akita Municipal Hospital, Japan, [3]Higashinaruse National Health Insurance Clinic, Japan, [4]Yamamoto-Kumiai General Hospital, Japan, [5]Ogachi Central Hospital, Japan, [6]Nakadori General Hospital, Japan, [7]Akita University School of Medicine, Japan, [8]Akita University Graduate School of Medicine, Japan

Introduction: Use of bisphosphonates, particularly long-term exposure, is associated with an increased risk of atypical femoral fracture (AFF). Teriparatide (TPTD) treatment may promote healing of AFFs, but few controlled studies have examined TPTD effects on healing of bisphosphonate-associated AFF. The aim of this study was therefore to compare fracture healing between patients with and without TPTD treatment after sustaining bisphosphonate-associated AFFs.

Methods: We retrospectively reviewed the medical records of 45 consecutive AFFs in 34 patients who had been prescribed oral bisphosphonates (alendronate or risedronate) for osteoporosis before AFF and with follow-up $\geq$12 months (range, 12-90 months). Thirty-seven complete or incomplete AFFs (82%) were treated surgically and eight incomplete AFFs (18%) were treated conservatively. Bisphosphonates were stopped at diagnosis. Based on the non-use or use of TPTD after each fracture, AFFs were divided into a non-TPTD control group (n=24) and a TPTD group (n=21). Time to fracture healing and rate of delayed or non-union were compared between groups.

Results: Fracture type (complete or incomplete) and treatment (surgical or conservative) did not differ significantly between groups. The TPTD group showed significantly faster fracture healing (mean ($\pm$standard deviation), 5.9 ± 3.1 months) than the non-TPTD group (8.8 ± 4.8 months; P=0.025). Rate of delayed or non-union was significantly lower in the TPTD group than in the non-TPTD group (p=0.015); in the TPTD group, 19 AFFs (90.5%) achieved normal union and two (9.5%) showed delayed union; in the non-TPTD group, 14 (58.3%) achieved normal union, nine (37.5%) showed delayed union, and one (4.2%) showed non-union. Subanalyses for surgically treated AFFs yielded similar results.

Conclusions: These results suggest that TPTD treatment significantly shortens the time to fracture healing and reduces rates of delayed or non-union after bisphosphonate-associated AFF.TPTD appears useful for treating bisphosphonate-associated AFF.

Disclosures: Naohisa Miyakoshi, None.

FR0408

A novel approach to inhibit bone resorption: ectosite inhibitors against cathepsin K. Preety Panwar*[1], Kent Soe[2], Haoran Cui[3], Xin Du[4], Jean-Marie Delaisse[5], Dieter Bromme[6]. [1]University of British Columbia, Canada, [2]Vejle Hospital, University of Southern Denmark, Denmark, [3]Department of Oral Biological & Medical Sciences, University of British Columbia, Canada, [4]Department of Oral Biological & Medical Sciences, University of British Columbia, Canada, [5]Vejle Hospital, IRS, University of Southern Denmark, Denmark, [6]The University of British Columbia, Canada

Accelerated osteoclastic bone resorption plays an important role in the pathogenesis of osteoporosis. Cathepsin K (CatK) is the predominant collagenase in osteoclasts and thus an important target for the inhibition of bone resorption. Currently available active site inhibitors block the collagenase activity of CatK but also inhibit its other proteolytic activities. Various non-skeletal abnormalities observed in CatK knockout mice raise the concern of adverse effects, and therefore, it is important to find alternative approaches to inhibit bone resorption. Previous studies have postulated that the collagenase activity of CatK depends on the formation of protease oligomers in the presence of glycosaminoglycans. Therefore, we propose to use inhibitors of CatK complex formation, which specifically block the collagenase activity of CatK without interfering with its other functions. We call these inhibitors: ectosite inhibitors.

Ectosite inhibitors were screened from various drug and natural product libraries using florescence assays, and further selected based on their ability to inhibit collagen degradation. The best candidate was tested for its efficacy to inhibit bone resorption by human osteoclasts seeded on bone discs. The inhibition of bone resorption was evaluated based on resorption surface, number of resorption events, their depth, proportion of resorption pits and trenches, CTX release, and number of osteoclasts.

Dihydrotanshinone I (DHTI) was the most promising ectosite inhibitor of CatK with an IC$_{50}$ ~10μM for collagen degradation. Docking experiments revealed the binding of DHTI in a protein-protein interface of CatK complexes. When DHTI was tested in bone resorption cultures in parallel to the active site inhibitor odanacatib, at optimum concentrations, DHTI was found to be a powerful inhibitor of resorption, comparable to odanacatib for all endpoints. The inhibitions induced by 10 μM DHTI

and 50 nM odanacatib were respectively: 47 and 40 % for resorption surface, 43 and 50% for resorption depth, and 83 and 61% for CTX. Notably both inhibitors almost completely abolished resorption trenches (long excavations reflecting aggressive resorption). Metabolic activity and number of osteoclasts were unaffected.

Collectively, our observations show that an ectosite inhibitor of CatK can effectively inhibit bone resorption to a similar extent compared to odanacatib. Thus ectosite inhibitors appear to be an attractive approach for anti-resorptive therapy.

Disclosures: PREETY PANWAR, None.

FR0410

Effects of Odanacatib on Bone Structure and Quality in Postmenopausal Women with Osteoporosis: Results from the Phase III Long-Term Odanacatib Fracture Trial (LOFT). Robert Recker*[1], David Dempster[2], Tobias de Villiers[3], Bente Langdahl[4], Paul Miller[5], Ivo Valter[6], Cristiano AF Zerbini[7], Dosinda Cohn[8], Steven Doleckyj[8], Le Duong[9], Boyd Scott[10], Nadia Verbruggen[11], Arthur Santora[12]. [1]Creighton University, USA, [2]Columbia University, USA, [3]Stellenbosch University, South Africa, [4]Aarhus University Hospital, Dnk, [5]Colorado Center for Bone Research, USA, [6]CCBR, Estonia, [7]Centro Paulista de Investigações Clínicas, Brazil, [8]Merck & Co., Inc., USA, [9]Merck Research Laboratories, USA, [10]Merck & Co., Inc., USA, [11]MSD Europe Inc., Belgium, [12]Merck & Co. Inc., USA

Odanacatib (ODN) is a selective oral inhibitor of cathepsin K in development for the treatment of osteoporosis. Unlike other osteoporosis treatments that reduce both bone resorption and formation, ODN reduces bone resorption with limited reduction of bone formation.[1] Bone histology in non-clinical and clinical studies indicates normal bone formation during ODN treatment. [2,3]

The skeletal benefits of once-weekly ODN were investigated in the event-driven, Phase III Long-Term ODN Fracture Trial (LOFT; NCT00529373). Postmenopausal women $\geq$65 years of age with a BMD T-score of $\leq$-2.5 at the total hip (TH) or femoral neck (FN), or with prior vertebral fracture and T-score of $\leq$-1.5 at the TH or FN, were randomly assigned (1:1) to either 50 mg of ODN or placebo once-weekly. Participants also received weekly vitamin D$_3$ (5600 IU) and daily calcium supplements to ensure a total daily calcium intake of ~1200 mg. Primary efficacy outcomes were the effect of ODN on the risk of new morphometric vertebral, hip, and clinical non-vertebral fractures. Additional endpoints included the effects of ODN on bone histology and histomorphometry, and skeletal structure.

LOFT randomized 16,713 postmenopausal women (mean [SD] age 72.8 [5.3] years) at 387 centers in 40 countries, with 16,071 included in analyses. Mean baseline BMD T-scores were: lumbar spine -2.7, TH -2.4, and FN -2.7. Transilial bone biopsies were obtained from consenting patients at baseline, and at 12, 24 and 36 months, and assessed by qualitative histology, 2D histomorphometry and 3D micro-computed tomography. A total of 341 biopsy specimens were obtained from 272 participants. Forty biopsies were obtained at baseline and 301 at the following time points: 12 months (n=2), 24 months (n=219) or 36 months (n=80). Paired biopsies (baseline and follow-up) were obtained in 17 patients, and 52 patients had biopsies performed at both Months 24 and 36.

Analyses of these data will provide information on the effects of ODN on bone remodeling and the incidence of qualitative abnormalities of bone formed during treatment, further elucidating ODN's mechanism of action. At the time this abstract was written, final data analysis was not complete. The results will be available for presentation at the ASBMR meeting.

References
Langdahl B et al. J Bone Miner Res 2012; 27: 2251-2258
Cusick T et al. J Bone Miner Res 2012; 27: 524-537
Bone HG et al. J Bone Miner Res 2010; 25: 937-947

FR0411

Inhibition NF-κB Signaling Pathway by Partial Ablation of the P65 Subunit Leads to Improved Bone Quality without Interfering with Bone Healing. Hongshuai Li*[1], Aiping Lu[2], Nicholas Oyster[2], Ying Tang[2], Bing Wang[2], Johnny Huard[3]. [1]University of Pittsburgh, USA, [2]University of Pittsburgh, USA, [3]Orthopaedic Surgery, USA

Background: Studies indicate that NF-κB antagonists hold great promise for the treatment of metabolic bone diseases such as osteoporosis; however, concerns about the inhibition of the NF-κB signaling pathway may also impair bone healing through the influence of inflammatory processes [1]. Therefore, exploring more specific targets in the NF-κB signaling pathway that could inhibit bone loss without affecting the bone healing process, remains important for developing novel and improved strategies for treating osteoporosis and inflammatory bone diseases. Materials: The mice lacking one allele of the NF-κB subunit p65 (p65+/–) and wild type (WT) mice at 1 year of age were used in this study. Results: Micro-CT revealed that p65+/– mice displayed more

dense bone tissues both in the lumber vertebra and the mid-shaft of their femurs compared to their WT littermates (Fig. 1 & Fig. 2). In vivo dynamic histomorphometric analysis revealed no significant differences in MAR (mineral apposition rate), MS (mineralizing surface), and BFR (bone formation rate) between the WT and p65+/– mice, both in their vertebra and skull (Fig. 3); however, p65+/– mice exhibited significantly decreased TRAP staining throughout their vertebra compared to WT mice (Fig. 4). A 1mm diameter unicortical bone defect was created on the medial side of the proximal tibia. The bone healing process was monitored with Micro-CT scanning and histology. At weeks 1 and 2 after surgery, X-ray radiographs and histology showed evidence of callus formation at the defect areas in both the p65+/– and WT mice. No significant differences were found in either of the groups regarding the volume of callus, BMD (Fig. 5), collagen deposition and calcification. Conclusion: Our results demonstrated that the specific inhibition of the NF-κB signaling pathway by partial ablation of the p65 subunit leads to improved bone quality without impairing bone healing. The improved bone quality is due, at least in part, to the reduction of osteoclastogenesis. These findings suggest that p65 subunit may represent an important therapeutic target for developing novel and improved strategies for treating osteoporosis and inflammatory bone diseases without interfering with the bone healing process.

References:

1. Chang, J., et al., Inhibition of osteoblastic bone formation by nuclear factor-kappaB. Nat Med, 2009. 15(6): p. 682-9.
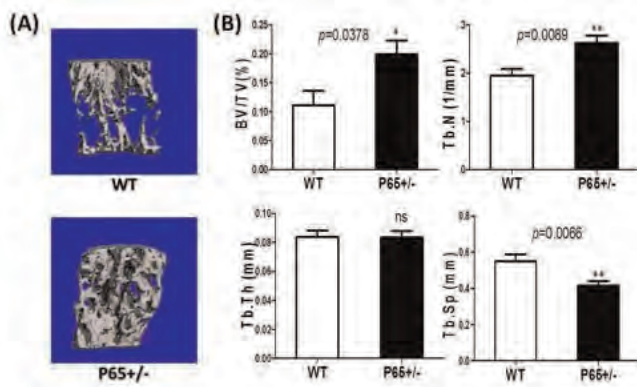
Fig. 1: Micro-CT analysis of the L6 vertebrae
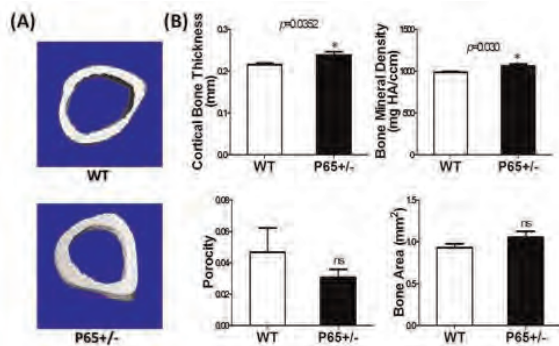
Fig. 2: Micro-CT analysis of the mid-shaft of femur
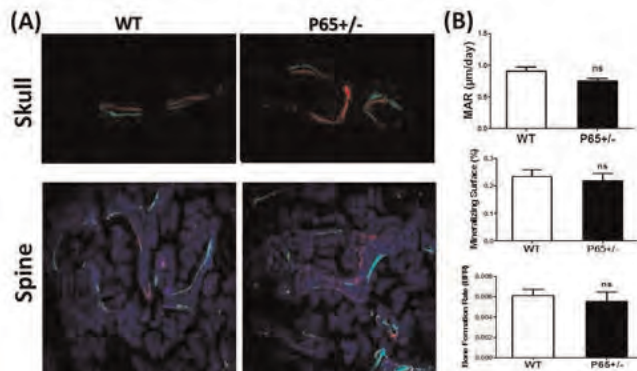
Fig. 3: Dynamic bone morphologic analysis on skull and spine
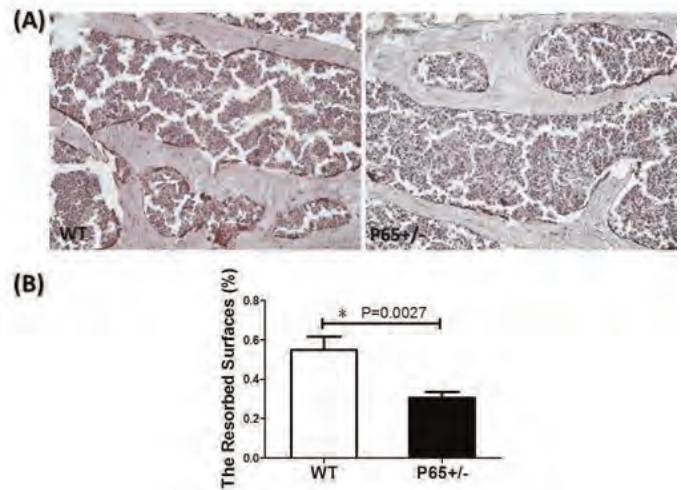
Fig. 4: TRAP staining
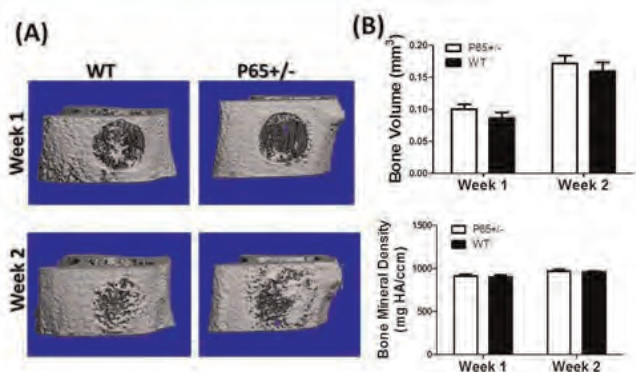
Fig. 5: Quantitative evaluation on bone defect healing on tibia

Disclosures: Hongshuai Li, None.

FR0414

Bone Properties in Type 2 Diabetes are Associated with the Advanced Glycation Endproduct Pentosidine.

Dorothy Fink*[1], Jessica Furst[2], Chiyuan Zhang[3], Laura Beth Anderson[3], Hongfeng Jiang[4], Serge Cremers[3], Kyle Nishiyama[3], Hua Zhou[5], David Dempster[6], Atharva Poundarik[7], Shonni Silverberg[3], Deepak Vashishth[8], Mishaela Rubin[3]. [1]NYP-Columbia, USA, [2]Columbia University College of Physicians & Surgeons, USA, [3]Columbia University, USA, [4]Columbia University College of Physician & Surgeons, USA, [5]Helen Hayes Hospital, USA, [6]Columbia University, USA, [7]Rensselaer Polytechnic University, USA, [8]Rensselaer Polytechnic Institute, USA

Fractures are a newly appreciated complication of type 2 diabetes (T2D) yet are not accounted for by bone mineral density (BMD). An explanation for this paradox may be accumulation of advanced glycation endproducts (AGEs) in bone matrix collagen and increased cortical porosity. Yet whether there is a relationship between AGEs and cortical porosity in T2D is unclear. We hypothesized that levels of the AGE pentosidine would be associated with cortical porosity and biomechanical indices in T2D.

We studied postmenopausal women with T2D (T2D; n=21) and postmenopausal healthy controls (C; n=28). There was no difference in age (T2D 59.4 ± 3 vs C 56.6 ± 0.9), or number of fractures (T2D: 4 vs C: 5) or BMD at the spine (T2D: 0.970 ± 0.07 vs C: 0.922 ± 0.02g/cm^2), or 1/3 radius (T2D: 0.674 ± 0.01 vs C: 0.655 ± 0.01g/cm^2), although femoral neck was greater in T2D (0.777 ± 0.06 vs 0.705 ± 0.02g/cm^2; p=0.03). HbA1c was higher in T2D (8.6 ± 0.9 vs 5.7 ± 0.07%; p<0.01) as was BMI (32 ± 3 vs 28 ± 1 kg/m^2; p=0.06). High resolution peripheral quantitative computed tomography (HRpQCT) was performed and pentosidine was measured in urine by UPLC/MS/MS. Tetracycline double-labeled iliac crest bone biopsies were performed in a random subset (6 T2D and 6 C). Bone strength was measured by reference point indentation as the total indentation distance (TID), or the distance that a test probe was able to be inserted into the bone biopsy sample.

Pentosidine levels did not differ between T2D and C (T2D: 90.8 ± 9 vs C: 84.2 ± 9 pmol/mg Cr, p=0.62). However, HRpQCT analysis revealed that pentosidine was associated with cortical porosity at the radius only in T2D (r=0.474, p=0.04). Histomorphometric analysis similarly revealed that pentosidine was associated with

the percent of cortical porosity area only in T2D (r=.896, p=0.04) and inversely associated with osteoid surface only in T2D (r= -0.97, p=0.006). Finally, microindentation showed that pentosidine was associated with greater TID (r=0.99, p=0.03) only in T2D.

These data provide proof of concept that pentosidine is related to cortical porosity in T2D. Accumulation of AGEs such as pentosidine in T2D may lead to impaired bone formation, as evidenced by low osteoid surface, and to the development of cortical porosity and compromised biomechanical indices. Further studies of skeletal organic matrix and bone microarchitecture properties are needed to shed light on the increased fracture risk associated with type 2 diabetes.

Disclosures: Dorothy Fink, None.

FR0415

Effect of Teriparatide in Patients with Osteoporosis and Type 2 Diabetes Mellitus. Ann Schwartz*[1], John Krege[2], Jahangir Alam[3], Dara Schuster[3]. [1]University of California, San Francisco, USA, [2]Eli Lilly & Company, USA, [3]Eli Lilly & Company, USA

Purpose: To examine the effect of teriparatide (TPTD) on the incidence of nonvertebral (NONVERT) fragility fractures, bone density, and safety in the subgroup of patients with osteoporosis and Type 2 diabetes mellitus (T2D) enrolled in the DANCE study. Methods: This was a post hoc analysis of patients with vs. without T2D, excluding Type 1 diabetes, treated with TPTD 20 µg/day for ≤2 years enrolled in the DANCE open-label, prospective, observational study. Incident rates of new fragility NONVERT fracture (traumatic fractures excluded) after 6-24 months vs. 0-6 months of TPTD therapy within groups were compared using a Poisson regression model. Time to new NONVERT fracture was compared using Kaplan-Meier analysis. Mixed model repeated measures analysis was used to evaluate bone density changes. Results: Of 4044 patients who received ≥1 dose of TPTD, 293 reported T2D. Patients with vs. without T2D at baseline had similar age (mean [SD] age, 69.2 [11.1] vs. 67.8 [11.9] years) and history of prior NONVERT fractures (59.0% vs. 55.8%), but higher L1-L4 T-scores (- 2.14 [1.45] vs. -2.51 [1.37], p<0.001) and more baseline clinical conditions (3.5 [1.6] vs. 1.7 [1.3], p<0.001). Mean TPTD exposure was similar (514.0 [290.1] vs. 544.4 [290.1] days). Over 18 months, bone density in the spine and total hip increased similarly in patients with vs. without T2D (both p-values>0.1); at the femoral neck, average increase was greater in T2D (p=0.01). There were 13 NONVERT fractures in the T2D group and 150 in the group without T2D. In the patients with T2D, the incidence of NONVERT fractures was 4.70 in the first 6 months vs. 2.11 per 100 patient years in months 6-24. In the patients without T2D, the incidence of NONVERT fracture was 3.54 in the first 6 months vs. 2.14 per 100 patient years during months 6-24. Fracture incidence declined 55% and 40% in those with and without T2D, respectively. The reduced incidence of NONVERT fracture over the 2 time periods was consistent (time by subgroup interaction p=0.56) in subjects with versus without T2D. There was no difference in the time to a new NONVERT fracture (p=0.94). Teriparatide was well tolerated and no new significant safety findings were observed. Conclusion: Patients with osteoporosis and diabetes receiving teriparatide showed similar increases in bone density at the spine and total hip and similar reductions over time in the incidence of nonvertebral fracture compared with osteoporosis patients without diabetes.

Disclosures: Ann Schwartz, Merck, 3
This study received funding from: Eli Lilly and Company

FR0416

Predictors of mortality subsequent to a fracture in diabetes mellitus patients. Jakob Linde*[1], Søren Gregersen[2], Peter Vestergaard[3]. [1]Aarhus University Hospital, Denmark, [2]Aarhus University Hospital, Denmark, [3]Aalborg University Hospital, Denmark

Background: Diabetes Mellitus is associated with an increased fracture risk and perhaps an increased risk of mortality subsequent to a fracture.
Aim: To investigate the association between diabetes related drugs and mortality.Methods: A nested case-control study was conducted. Cases were patients with DM who subsequently to a fracture died; controls were surviving DM patients. Using the Danish National Hospital Discharge Register (1977-2011), we included DM patients with information on date of DM diagnosis, date of fracture and comorbidities, from the Danish Cause of Death Register the date of mortality was collected (2008-2011). From the Central Region of Jutland, Denmark, medication use was collected (2008-2011). Medication use was defined as having collected a prescription prior to fracture. Analysis was performed by unconditional logistic regression.
Results: 2,621 diabetes patients with a fracture subsequent to diabetes diagnosis and with information on medication use were included. Of these 229 died. In multivariate analysis statin use (odds ratio (OR)= 0.54, 95 % confidence interval (CI): 0.37-0.80) decreased the risk of dying subsequent to a fracture. 1,106 (42 %) received statin treatment. Male gender (OR=1.43, 95 % CI: 1.05-1.95), increasing age at diabetes diagnosis (OR=1.06, 95%CI 1.05-1.08), a diagnosis of retinopathy (OR=2.49, 95 % CI: 1.44-4.28), a diagnosis of peripheral artery disease (OR = 1.63, 95 % CI: 1.10-2.42), and use of glucocorticoids (OR=1.97, 95 % CI: 1.26-3.09) all increased the risk of death. None of the antidiabetics; biguanides, glucagon-like receptor agonists, β-cell stimulants, glitazones, and insulin were significantly associated with altered mortality.

Conclusion: Co-morbidity reflected by late onset complications, heart failure and glucocorticoid use were associated with an increased risk of mortality subsequent to a fracture. Statin use may reduce mortality subsequent to a fracture in diabetes patients, clinical trials should decide whether diabetes patients suffering from a fracture should start in statin treatment irrespective of current recomendations.

Disclosures: Jakob Linde, None.

FR0417

The Risk of Hip Fracture Is Increased in Subjects with Late-Onset Autoimmune Diabetes (LADA): Results from the HUNT Study. Hanne Gulseth*[1], Lisa Forsen[2], Mari Hoff[3], Arnulf Langhammer[4], Siri Forsmo[5], Berit Schei[6], Kristian Midthjell[4], Haakon E. Meyer[7]. [1]Norwegian Institute of Public Health/ Oslo University Hospital, Norway, [2]Norwegian Institute of Public Health/University of Oslo, Norway, [3]Department of Public Health & General Practice, Faculty of Medicine, Norwegian University of Science & Technology, Norway, [4]HUNT Research Centre, Department of Public Health & General Practice, Faculty of Medicine, Norwegian University of Science & Technology, Norway, [5]Norwegian University of Science & Technology, Norway, [6]Women's Health, Department of Community Medicine, Norwegian University of Science & Technology/ Department of Obstetrics & Gynaecology St. Olavs Hospital Trondheim University Hospital, Norway, [7]Norwegian Institute of Public Health/ University of Oslo, Norway

Late-onset autoimmune diabetes in adults (LADA) is present in 5-10% of the diabetes population. LADA has an autoimmune nature, but shares the type 2 diabetes characteristic of insulin resistance. Our aim was to investigate, for the first time, whether hip and forearm fractures were increased in subjects with LADA compared to the general population.
We used data from the Norwegian population-based Nord-Trøndelag Health Study (HUNT2). Baseline assessments were done in 1995-1997 and fractures were retrieved from a registry covering all hip and forearm fractures in the county of Nord-Trøndelag from August 15th, 1995 to December 31th, 2012. All fractures were verified in medical records. The current analysis was restricted to participants ≥ 40 years at screening (n= 43 004), and LADA were defined in 126 subjects (diabetes onset at age ≥40 years; no insulin treatment during the first year after diagnosis). They were distinguished from type 2 diabetes by the presence of serum glutamic acid decarboxylase (GAD) autoantibodies. Hazard ratios adjusted for age, sex, and BMI were calculated with Cox regression.
During follow-up, 2271 persons sustained a hip fracture and 2806 persons sustained a forearm fracture. Participants with LADA had a doubled risk of hip fracture (HR = 2.2 (95% CI 1.4 – 3.4)) compared to those without diabetes. Additional adjustments for BMI did not change the results substantially. The hip fracture risk increased by disease duration, and those with duration ≥10 years had a HR = 2.5 (95% CI 1.4 - 4.6) , whereas those with disease duration < 10 years had a HR = 1.9 (95% CI 0.98 – 3.6). The risk of forearm fracture was however not increased in those with LADA (HR = 0.41 (95% CI 0.13 – 1.26)). In conclusion, subjects with LADA had increased risk of hip, but not forearm, fractures.

Disclosures: Hanne Gulseth, None.

FR0418

Type 1 Diabetes Mellitus Effects on Bone: Results of Histomorphometric Analysis. Laura Armas*, Robert Recker. Creighton University, USA

Diabetes Mellitus has a detrimental effect on the body's microvascular system effecting the kidneys, eyes and nerves. The effect on bone is less well known. Patients with Type 1 diabetes have a higher fracture risk than the general population, but this is not thought to be exclusively a result of lower bone mass. The effect of diabetes on bone micro-architecture and turnover is not well elucidated. We report here results of 29 subjects (16 females, 13 males, age 19-50) with Type 1 diabetes (diagnosed~ 19 years before) and their age and sex matched controls. The subjects were otherwise healthy without diabetic complications and the females were premenopausal. Six diabetic subjects had experienced low trauma fractures. A transilial bone biopsy was obtained after tetracycline labeling. The biopsy specimens were fixed, embedded, sectioned, and evaluated as previously described by Baron et al. Two sections, >250 µm apart, were read from the central part of each biopsy. Wilcoxon signed ranks test was used to compare the results between pairs and Mann Whitney U test to compare between fracturing subjects and controls. Structural measures such as bone volume (BV/TV) and trabecular thickness (TbTh) were no different between the 29 diabetic subjects and their matched control. The dynamic data also showed no differences in mineralizing surface, mineral apposition rate, bone formation rate or activation frequency. The six subjects who had experienced low trauma fractures had slightly lower BV/TV and TbTh than healthy controls, but the only significant difference in measures of dynamic histomorphometry was a shorter mineralization lag time (Mlt) in the diabetics with fracture. Healthy diabetics without complications have no identifiable structural or dynamic differences on histomorphometric analysis compared to age and sex matched controls. However, diabetics who have sustained low trauma fractures have subtle differences in structure and mineralization than

either healthy controls or diabetics without fracture.

Variable	Diabetic w/ Fracture	Control	P value
Bone Volume (BV/TV %)	16.3(14.2-23.7)	21.9(17.6-25.5)	0.076
Trabecular Number (1 /mm)	1.5(1.2-2.0)	1.7(1.5-1.9)	0.480
Trabecular Thickness (mm)	107(101-133)	128(108-152)	0.093
Trabecular Separation (mm)	638(489-824)	589(522-656)	0.454
Mineralizing Surface (%)	7.4(2.4-11.3)	6.6(2.8-10.7)	0.983
Mineral Apposition Rate (µm/d)	0.55(0.46-0.63)	0.53(0.44-0.58)	0.356
Osteoid Thickness (µm)	5.8(4.8-7.4)	6.5(6.0-7.7)	0.454
Osteoid Surface (OS/BS %)	3.4(2.2-10.2)	11.2(3.9-16.4)	0.134
Mineralization lag time (day)	9.2(4.6-14.6)	19.6(11.9-26.1)	0.007

Table

FR0419

Type 2 Diabetics with and without Fragility Fractures show characteristic Differences in their Serum MicroRNA Profiles that may be used for Fracture Risk Prediction. Ursula Heilmeier*[1], Matthias Hackl[2], Susanna Skalicky[3], Janina Patsch[4], Thomas Baum[5], Andrew Burghardt[6], Ann Schwartz[6], Johannes Grillari[7], Thomas Link[6]. [1]University of California San Francisco, USA, [2]TAmiRNA GmbH, Austria, [3]TAmiRNA GmbH, Austria, [4]Medical University of Vienna, Austria, [5]Klinikum rechts der Isar, TU Muenchen, Germany, [6]University of California, San Francisco, USA, [7]University of Natural Resources & Life Sciences Vienna, Austria

Type 2 diabetic (T2D) individuals are at increased risk for fragility fractures that is not fully captured by the current gold standard Dual X-ray absorptiometry. MicroRNAs (miRNAs) are small noncoding RNAs that master-regulate posttranscriptional gene expression and modulate various cell and disease processes, including the formation of extracellular matrix, oxidative stress, and angio- and osteogenesis. The purpose of this study was to determine and compare the serum miRNA expression levels in T2D women with history of fragility fractures (DMFx) and in fracture-free diabetics (DM) in order to identify miRNA candidates that could be used for fracture risk prediction in T2D. Serum from 38 postmenopausal T2D women (DM and DMFx, n=19 per group, similar eGFR) was used who were otherwise free of bone affecting diseases or medications. 375 circulating miRNAs were analyzed aside with standard quality controls by quantitative PCR using 384-well qPCR arrays. Ct values were corrected for background and technical variation and normalized. miRNAs with presence calls < 50% were excluded. Mann-Whitney-U testing identified 18 miRNAs with evidently small p-values (Table 1). Although these p-values did not survive Benjamini-Hochberg adjustments due to the small group sizes, the exploratory study design (false discovery rate of 0.2) revealed that 14 out of these 18 raw p-values can be regarded as significant and thus constitute potential novel markers to differentiate fracture status in T2D. Additional ROC analysis showed area under curve values (AUC) in the range of 0.76 to 0.85 for several miRNAs including the let-7 family, miR-148b-5b, miR-141-3p, miR-16-2-3p, and miR 340-3 (Fig.1). Interestingly, some of these miRNAs have previously been found to be upregulated during bone mineralization resulting in the repression of collagen expression (let-7 family), to regulate the activity of osteoclast inhibitors (miR-148), and to play a role in mesenchymal stem cell aging and oxidative stress response (miR-141-3p). We conclude, that T2D postmenopausal women with and without fragility fractures show characteristic differences in their serum miRNA profiles that may be used for fracture risk assessment in T2D. Differential miRNA profiling may also provide further insights in molecular mechanisms associated with diabetic bone disease. However, further validation studies are needed to replicate our findings and to establish definitive miRNA signatures for fracture risk assessment.

Table 1: List of 18 most promising miRNAs showing differential expresssion between T2D women with fractures (DMFx) and fracture-free T2D women (DM). Unadjusted p-values are provided in the left column, Benjamini-Hochberg-adjusted p-values at the right. With a False Discovery rate of 20 % only 3-4 of the listed miRNAs bear the risk of demonstrating a false positive raw p-value.

miRNA name	unadjusted p-Value	BH FDR 0.2
hsa-let-7g-5p	0.0018	0.1965
hsa-let-7e-5p	0.0022	0.1965
hsa-miR-148b-5p	0.0028	0.1965
hsa-let-7i-5p	0.0048	0.1965
hsa-miR-141-3p	0.0048	0.1965
hsa-miR-16-2-3p	0.0048	0.1965
hsa-miR-340-3p	0.0075	0.1965
hsa-miR-376c-3p	0.0078	0.1965
hsa-miR-106a-5p	0.0082	0.1965
hsa-let-7b-5p	0.0094	0.1965
hsa-miR-106b-5p	0.0098	0.1965
hsa-miR-339-5p	0.0102	0.1965
hsa-miR-500a-5p	0.0108	0.1965
hsa-miR-136-5p	0.0111	0.1965
hsa-miR-532-3p	0.0116	0.1965
hsa-miR-376a-3p	0.0142	0.2094
hsa-miR-181b-5p	0.0144	0.2094
hsa-miR-92a-3p	0.0148	0.2094

Table 1

Figure 1. Reiver operating characteristics (ROC curves) for several representative serum miRNAs showing significant classification of DMFx and DM subjects. Other miRNAs of this 18 miRNA subset did also show significance (data not shown). X-axis delineates the specificity (%), the y-axis shows the sensitivity (%) of the tested miRNA as a predictive biomarker for fracture status in T2D. Significance is given as p<0.05.
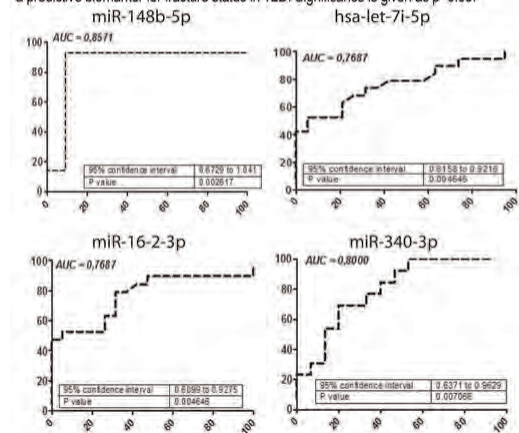
Figure 1

FR0420

HR-pQCT Detects Abnormal Cortical and Trabecular Bone Density and Structure in Young Adults with Cystic Fibrosis. Kyle Nishiyama*[1], Anna Kepley[1], Fernando Rosete[2], Claire Keating[2], Emily DiMango[2], Elizabeth Shane[3]. [1]Columbia University, USA, [2]Columbia University, USA, [3]Columbia University College of Physicians & Surgeons, USA

The median life expectancy for patients with cystic fibrosis (CF) is now in the early forties. However, the incidence of premature osteoporosis in patients with CF is much higher than the general population and increases with advancing age. Many studies have shown that CF patients have lower bone mineral density (BMD) than healthy controls. However, most used DXA, a 2D measurement of areal BMD (aBMD) that is confounded by bone size. The true extent of the bone deficit is unclear as CF patients are generally smaller in stature, and in many studies, differences in aBMD do not persist after adjusting for their smaller bone size. We used high-resolution peripheral quantitative computed tomography (HR-pQCT) to measure true volumetric BMD (vBMD) and bone microarchitecture at the peripheral skeleton in 15 patients with CF (age 27±6yrs) and 15 age- and sex-matched controls (age 27±4yrs). We scanned participants both at the standard HR-pQCT measurement sites and at a subject-specific variable site based on 4% of the limb length to determine whether differences in bone size affected the outcome. CF patients did not differ significantly in height from controls but had lower BMI (-12%, p=0.03). CF patients had significantly (p<0.05) lower aBMD at the spine (-13%), total hip (-15%), femoral neck (-14%), and ultradistal radius (-17%). At the standard site (Table), total vBMD was lower in CF patients than controls at the radius (-22%) and tibia (-20%). In the trabecular compartment, trabecular vBMD was significantly lower at the tibia (-20%)

with a trend at the radius (-20%, p=0.07). There was evidence of trabecular structure deterioration in CF patients, although the differences were not significant. Within the cortical compartment, cortical area, thickness and vBMD were markedly lower in CF patients at both the radius and tibia. Using the 4% variable site, we found a similar pattern of differences to the standard site, but the differences were of greater magnitude, particularly in measurements of area and cortical thickness (Figure). To our knowledge, this is the first study to apply HR-pQCT to patients with CF. We conclude that there are significant deficits in bone structure and density in patients with CF that are independent of bone size. Both the cortical and trabecular regions of the peripheral skeleton are affected. Compared to the variable site, the standard HR-pQCT measurement site may not fully capture the deterioration in bone structure in patients with CF.

	RADIUS			TIBIA		
	CF	Controls	p	CF	Controls	p
Total Area (mm2)	282.3±55.7	290.8±68.9	0.713	703.5±150.5	759.5±103.8	0.246
Tb Area (mm2)	232.0±49.0	226.5±66.4	0.801	589.6±133.2	613.3±91.3	0.574
Ct Area (mm2)	50.3±16.4	64.3±16.5	0.028	113.9±40.1	146.2±29.2	0.018
Total vBMD (mgHA/cm^3)	292.1±62.5	357.2±61.6	0.008	279.1±57.5	334.8±41.7	0.005
Tb.vBMD (mgHA/cm^3)	157.6±42.1	189.6±50.0	0.068	162.1±46.7	200.2±43.9	0.029
Ct.vBMD (mgHA/cm^3)	839.2±59.3	889.8±59.3	0.027	865.1±37.4	894.8±29.8	0.023
Ct.Th (mm)	0.70±0.19	0.89±0.20	0.013	1.08±0.32	1.34±0.23	0.017
Tb BV/TV	0.13±0.04	0.16±0.04	0.070	0.14±0.04	0.17±0.04	0.029
Tb.N (1/mm)	2.11±0.23	2.13±0.26	0.829	2.00±0.22	2.18±0.29	0.075
Tb.Th (mm)	0.062±0.015	0.074±0.017	0.051	0.067±0.016	0.076±0.011	0.077
Tb.Sp (mm)	0.418±0.054	0.403±0.059	0.481	0.438±0.058	0.390±0.070	0.055

Mean¯SD for CF patients and controls for trabecular (Tb) and cortical (Ct) HR-pQCT measurements.
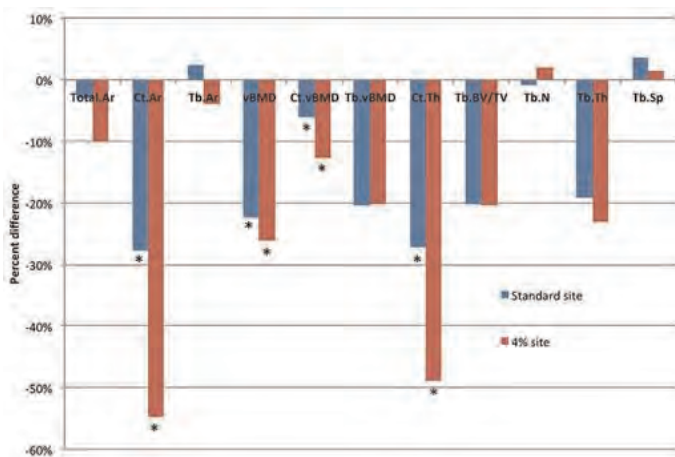
% diff. between patients with CF and controls at the standard and variable site. *p<0.05

Disclosures: Kyle Nishiyama, None.

FR0429

IGF Signaling in Periosteal Cells Plays a Crucial Role in Callus Formation and Bone Fracture Repair. Ping Ye*[1], Timothy Myers[2], Alessandra Esposito[3], Joseph Temple[3], Tieshi Li[1], Helen Willcockson[2], Billie Moats-Staats[4], Lara Longobardi[1], Anna Spagnoli[1]. [1]University of North Carolina at Chapel HIll, USA, [2]University of North Carolina, USA, [3]The University of North Carolina at Chapel Hill, USA, [4]University of North Carolina-Chapel Hill, USA

Bone fracture is one of most common injuries to skeletal tissue. Increasing experimental data, both in vivo and in vitro, has shown that periosteal cells play a critical role in fracture healing, at least in part, by contributing to the cellular callus formation. Previous studies also indicate that during development insulin-like growth factor (IGF) signaling is essential to the normal bone formation and growth by influencing cell proliferation, survival and calcification. We believe that IGF signaling in periosteal cells could play a key role in callus formation, thus, promoting bone fracture healing. To test our hypothesis, we, using the Cre-ER-LoxP strategy, generated and studied a new line of conditional mutant mice (igf1rPrx1KO mice), in which the expression of the type I IGF receptor (IGF1R) is specifically ablated in PRX1-positive periosteal cells in adult mice. At the age of 12-16 weeks, male mutant mice, as well as their male littermate controls, were given tamoxifen to induce IGF1R ablation, followed by tibia fracture. Following fracture, the number of Prx1-CreER transgene labeled cells gradually increased in the callus, positively correlating with the increased expression of callus Prx1 mRNA, suggesting that in the callus Prx1-positive cells are abundantly derived from the periosteum. Based on micro-CT analyses, the callus size was reduced in igf1rPrx1KO mice by 47% 10 days after fracture. With an

increase in recovery time, the volume of callus was increased in both control mice and igf1rPrx1KO mice. However, the magnitude of the increase was much smaller in igf1rPrx1KO mice, leading to a further reduction (by 54%) in the callus volume at 14 days after fracture. Similar to its reduction in total callus volume, igf1rPrx1KO mice also exhibited a significant reduction in the volume of soft tissue and new bone in the callus. As compared to that in control mice, the volume of soft tissue and new bone in the callus of igf1rPrx1KO mice was reduced by 44% and by 56% at 10 and 14 days post fracture, respectively. Our data strongly indicate that IGF1R mediated signaling in Prx- positive periosteal cells is required for normal callus formation. Our study also provides important insight into the molecular mechanism of bone fracture recovery, which might help to develop a strategy to utilize IGF to treat bone fracture.

Disclosures: Ping Ye, None.

FR0433

RANKL Inhibition in the Pathogenesis and Treatment of Fibrous Dysplasia. Andrea Burke*[1], Howard Wang[2], Jeffrey Tsai[3], Nisan Bhattacharyya[4], Alison Boyce[5], Rachel Gafni[1], Andrea Estrada[1], Alfredo Molinolo[4], Pamela Robey[6], Michael Collins[1]. [1]National Institutes of Health, USA, [2]University of Maryland, USA, [3]SUNY Buffalo, USA, [4]NIH, USA, [5]Children's National Medical Center, USA, [6]National Institute of Dental & Craniofacial Research, USA

Purpose: Fibrous dysplasia (FD) is a benign skeletal disease in which osteogenic precursors proliferate and replace normal bone with fibrous tissue. A somatic mutation in *GNAS* results in constitutive activation of Gs-alpha and elevated cAMP. Osteoclasts are prominent in FD, and receptor activator of nuclear factor kappa-B ligand (RANKL), a regulator of osteoclastogenesis, is overexpressed in an *in vitro* model of FD. RANKL expression is stimulated by cAMP, and its activity is inhibited by osteoprotegerin (OPG). Denosumab is a human monoclonal antibody to RANKL approved for treatment of osteoporosis and bone metastases. Limited experience in treating FD with Denosumab suggests its efficacy. We aim to investigate RANKL expression in FD and its inhibition with Denosumab.

Methods: Soluble RANKL and OPG were measured in serum of FD subjects and correlated with FD skeletal burden. FD tissue specimens were assessed for RANKL, RANK and Ki-67 by immunohistochemistry. RANKL expression was assessed in primary cultures of Vitamin D3/PGE2-stimulated control and patient-derived bone marrow stromal cells (BMSCs) by RT-PCR and ELISA. Control/FD BMSCs were co-cultured with M-CSF-stimulated human monocytes in the presence of Denosumab or isotype control IgG2 to study osteoclastogenesis. Effects on proliferation and cAMP levels were assessed.

Results: Patients had higher levels of circulating RANKL, lower OPG, and a higher RANKL/OPG ratio, which correlated with FD skeletal burden. FD tissue showed robust RANKL expression in highly proliferative, Ki-67 positive regions with RANK-positive giant cells. Primary cultures of FD BMSCs expressed more RANKL mRNA and protein in basal and stimulated state compared to controls. Stimulated FD BMSCs induced osteoclast differentiation in a co-culture system. Denosumab blocked osteoclastogenesis but had no effect on control/FD BMSC proliferation.

Conclusions: Increased levels of RANKL in FD specimens and *in vitro* systems supports the hypothesis that RANKL plays a role in FD pathogenesis, and that inhibition by Denosumab is a potential therapy. The effect of Denosumab on FD BMSC proliferation requires further study. Experiments are ongoing in a murine heterotopic ossicle model, which will provide a way to study molecular mechanisms of Denosumab in FD.

Disclosures: Andrea Burke, None.

FR0434

Adult Hypophosphatasia: Clinical Presentation and Diagnostic Findings. Lothar Seefried*[1], Franca Genest[2], Christine Hofmann[3], Sebastian v. d. Assen[2], Maximilian Rudert[2], Franz Jakob[2]. [1]Orthopedic Center for Musculoskeletal Research, Germany, [2]Orthopedic Center for Musculoskeletal Research, Germany, [3]University Childrens Hospital, Germany

Hypophosphatasia (HPP) is a rare, genetically determined metabolic disorder marked by deficient activity of Tissue-Nonspecific Alkaline Phosphatase (TNAP). The clinical spectrum of disease manifestations is very heterogenuous, especially in adults ranging from asymptomatic carriers to severely affected individuals with debilitating limitations and a high burden of disease.

To provide an overview of the frequency of distinctive disease symptoms, we extracted clinical, laboratory and genetic findings from the medical records of our cohort of affected adults. Analysis included patients with a documented mutation within the gene for ALPL and/or a coincidence of lowered ALP values combined with clinical symptoms of the disease.

In total 119 persons (77 females, 42 males) were identified meeting these criteria. Mean age of the individuals was 45.5 years (range 19-80y). In those persons where data could be obtained, antopometric data were (mean height/ BMI) 163.7 cm / 25.15 for women and 169.3 cm / 27.25 for men. The most frequent clinical symptom reported was musculoskeletal pain in 52 persons, followed by dental issues in 37 patients. Lab results showed Hypercalcaemia in 10 out of 70 persons, hyperpho-

sphatemia was present only in 6 out of 67. Serum-creatinine was elevated in 19 out of 68 patients. Vitamin D deficiency, defined als levels below 20ng/ml, was present in 35/60 patients. Renal issues were documented in nine of the patients. Results of genetic testing with documented ALPL-gene mutation was available for 75 of these patients with 54 of them having only one mutation thus being heterozygously affected and 21 harbouring at least two mutations. Distribution of the mutations over the 12 exons showed that Exon 6 was affect in 35 patients, while mutations in Exon 2 and 8 were only detected once, respectively.Due to the wide catchment area of included patients, together with their sometimes limited mobility, not all of the patients have been assessed personally. However, this analysis provides a preliminary insight in the frequency of widely accepted hallmarks of the disease, even in heterozygously affected patients which often prove to be not only asymptomatic carriers but rather experience reproducible symptoms and health limitations, especially in cases with dominant-negative mutations. Further evaluation of adult HPP patients is required to fully understand their burden of disease and develop respective therapeutic strategies, including non-medical, supportive measures as well as pharmacological interventions and adapted surgical procedures.

FR0435

Enzyme-Replacement Therapy in Life-Threatening Hypophosphatasia: The 3-Year Experience with Asfotase Alfa. Michael Whyte*[1], Jill H. Simmons[2], Richard E. Lutz[3], Scott Moseley[4], Agustin Melian[5], Tatjana Odrljin[4], Nicholas Bishop[6]. [1]Shriners Hospital for Children-Saint Louis, USA, [2]Vanderbilt Children's Hospital, USA, [3]Nebraska Medical Center, USA, [4]Alexion Pharmaceuticals Inc, USA, [5]Alexion Pharmaceuticals Inc, USA, [6]University of Sheffield, Academic Unit of Child Health, United Kingdom

Hypophosphatasia (HPP) is the rare, life-threatening when severe, disorder caused by mutation(s) in the tissue-nonspecific alkaline phosphatase (TNSALP) gene. In 2012[1], we detailed significant improvement in skeletal mineralization and developmental milestones in patients (pts) with perinatal and infantile HPP treated for 48 wks with asfotase alfa, a bone-targeted recombinant human TNSALP. We now report the comprehensive experience of these pts following 3 yrs of treatment. This is a multicenter, phase 2, open-label trial of asfotase alfa (SC, 1-3mg/kg, 3x/wk). Skeletal disease was assessed by a Radiographic Global Impression of Change (RGI-C) scale[1] and a Rickets Severity Scale (RSS)[1,2]. We also evaluated survival, respiratory status, growth, gross motor function (Bayley Scales of Infant Development [BSID-III] subscale), adverse events (AEs) and anti-asfotase alfa antibodies. Data are reported as medians (min, max; n). Age at baseline (BL)[1] was 6.8 mos (2.9 wks, 3 yrs). 9/11 pts completed 3 yrs of treatment (1 pt died at 7.5 mo treatment [sepsis unrelated to asfotase alfa]; 1 pt withdrew after 1st dose)[1] At 3 yrs, pts showed sustained improvement in rickets (RGI-C +2.5 [+1.7, +3], $p = 0.008$; change in RSS -6.3 [-9.5, 0], $p = 0.016$; n=8, 1 pt missing data). Of the 3 pts who still required respiratory support at 1 yr of treatment (2: mechanical ventilation [MV]; 1: supplemental oxygen $[O_2]$)[1], 2 were weaned from any support and 1 improved from MV to O_2 at last assessment (>3 yrs). Height/length Z-score,-3.7 (-9.2, -0.7; n=11) at BL, improved by a median change of +2.3 (-1.4, +4.1; n=8) at 3 yrs. BSID-III scaled score improved from 1 (1, 8; n=5) at BL/first assessment to 6 (2, 8; n=3) at 3yrs (mean for healthy peers=10). The most common AEs were mild/moderate injection-site reactions and upper respiratory infections (each in 6 pts). 3 serious AEs were considered possibly related to study drug (craniosynostosis, conductive deafness [same pt], and chronic hepatitis [1 pt]). Anti-asfotase alfa antibodies were detected in 6/10 pts; 4 pts tested positive for neutralizing antibodies without apparent effect on clinical efficacy. At 3 yrs, pts with perinatal and infantile HPP treated with asfotase alfa showed sustained improvement in bone mineralization, growth, motor function, and respiratory status. No definite drug-related serious AEs were reported. All 9 pts continue treatment.[1] Whyte *NEJM* (2012) 366:904-13 [2] Thacher *J Trop Pediatr* (2000) 46:132–9

FR0436

Hypophosphatasia: Clinical Nosology In Childhood Validated From 25 Years Experience With 174 Pediatric Patients. Michael Whyte*[1], Fan Zhang[2], William McAlister[3], Deborah Wenkert[4], Karen Mack[5], Marci Benigno[2], Stephen P. Coburn[6], Susan Wagy[2], Donna M. Griffin[2], Karen Erickson[6], Steven Mumm[7]. [1]Shriners Hospital for Children-Saint Louis, USA, [2]Shriners Hospital for Children-Saint Louis, USA, [3]Department of Pediatric Radiology, Mallinckrodt Institute of Radiology at St. Louis Children's Hospital, Washington University School of Medicine, USA, [4]Amgen, Inc., USA, [5]Shriners Hospital for Children-Saint Louis, USA, [6]Department of Chemistry, Indiana University – Perdue University, USA, [7]Washington University School of Medicine, USA

Hypophosphatasia (HPP) is the inborn-error-of-metabolism caused by inactivating mutation(s) within the gene that encodes the "tissue-nonspecific" isoenzyme of alkaline phosphatase (TNSALP). Inorganic pyrophosphate, an inhibitor of

mineralization and substrate for this cell-surface phosphohydrolase, accumulates extracellularly and can cause tooth loss, calcium crystal arthropathies, and rickets or osteomalacia. The remarkably broad expressivity of HPP, ranging from stillbirth due to profound skeletal hypomineralization to dental problems without bone disease in childhood or adult life, is largely explained by autosomal dominant versus recessive transmission of several hundred known *TNSALP* mutations. This expressivity has been codified primarily by patient age at presentation and diagnosis, but the extant classification scheme has not been validated.

To assess this nosology of HPP during childhood, we reviewed our 25 years of experience with 174 pediatric patients classified traditionally according to diminishing severity as perinatal, infantile, childhood, or odonto HPP, and with childhood HPP also designated severe or mild. Data came exclusively from inpatient investigations and focused on demographic, clinical, and DXA parameters as contrasted to healthy American children, and then compared among the patient groups.

The 174 patients comprised 13 survivors of infantile HPP, 96 with childhood HPP (58 severe, 38 mild), and 65 with odonto HPP. None was a survivor of perinatal HPP or an HPP "carrier". *TNSALP* mutation analysis has been positive in all but two of the 107 probands, with a gene dosage effect that reflected HPP severity. All assessed parameters (e.g., height, weight, number and age of premature tooth loss, grip strength, and spine and hip BMD) became more aberrant as the HPP severity classification increased, but with overlap between successive groups. For the 58 patients with severe childhood HPP, 42 were boys and 16 girls (p = 0.006), perhaps reflecting parental concern for reduced stature and strength in the boys versus girls.

Classification of pediatric HPP into infantile, severe and mild childhood, and odonto HPP organizes the disorder's remarkable expressivity, and will help to define its natural history and prognosis, and to evaluate emerging medical therapies.

FR0437

Unrecognized Mild Hypophosphatasia in Adults. Leyre Riancho-Zarrabeitia[1], Mayte García-Unzueta[2], Juan Gomez-Gerique[2], Jose Riancho*[3]. [1]Hospital U.M.Valdecilla, Spain, [2]Hospital U.M. Valdecilla, Spain, [3]University of Cantabria, Spain

Severe forms of hypophosphatasia are usually diagnosed during infancy and childhood. Adult forms have less severe manifestations and may go unrecognized. In order to get a better knowledge of its clinical spectrum, we performed a computerized search of low total alkaline phosphatase. Bone alkaline phosphatase, serum pyridoxal phosphate (PLP) and urine phosphoetanolamine (PEA) were measured in selected individuals.

Results.- Among 12,103 determinations of total alkaline phosphatase in a 31 month period, we identified 130 individuals with at least one result below 26 u/l. After reviewing the clinical records, unexplained persistently low levels were found in 50 individuals. Forty two who could be localized and accepted to participate were included (10 men, 32 women). Age range was 20-77 yr (mean 51). Total alkaline phosphatase levels were positively correlated with bone alkaline phosphatase (r=0.52, p<0.001), and negatively with serum calcium (r=-0.38, p=0.012), PLP (r= -0.51, p=0.001) and urine PEA (r= -0.49, p=0.001). Serum PLP was positively correlated with serum phosphorus and urine PEA, and inversely with bone alkaline phosphatase. Ten individuals (24%) had PLP levels above the reference range of 175 nmol/l. In comparison with those with PP<175, they had lower levels of bone alkaline phosphatase (6.2 ± 1.6 vs 8.6 ± 2.1, p=0.003) and higher levels of serum phosphorus (4.3 ± 0.5 vs 3.4 ± 0.5, p<0.001) and urine PEA (41.3 ± 22.8 vs 14.9 ± 11.0, p<0.001). Likewise, these individuals had higher frequency of hypertension (50 vs 12%, p=0.02) and premature teeth loss (70 vs 19%, p=0.005).

Conclusion.- About one in four individuals with persistent low levels of total alkaline phosphatase had increased levels of PLP, consistent with hypophosphatasia. Most patients have mild disease. However, they may have an increased risk of hypertension and premature teeth loss.

FR0438

Efficiency of whole exome sequencing for determining genetic origins of hypophosphatemic rickets patients without identified PHEX mutations. Catherine Brownstein*[1], Matthew Bainbridge[2], Meghan Towne[3], Nicholas Marinakis[3], Pankaj Agarwal[3], Alan Beggs[3], David Margulies[3], Gang-Qing Yao[4], Karl Insogna[4], Thomas Carpenter[4]. [1]Boston Children's Hospital & Harvard Medical School, USA, [2]Codified Genomics, USA, [3]Boston Children's Hospital, USA, [4]Yale University School of Medicine, USA

Introduction: Many genes are linked to phosphate homeostasis, and single gene sequencing is expensive (often over $400 per gene). Costs of whole exome sequencing (WES) has dropped exponentially, and annotation pipelines are increasingly accessible. We exome-sequenced 4 individuals who were diagnosed with hypopho-

sphatemic rickets on clinical grounds, however, sequencing of the coding regions of PHEX, DMP1, and FGF23 revealed no mutations.

Methods: Patients and family members were enrolled in The Manton Center for Orphan Disease Research. WES was performed at the Baylor School of Medicine Human Genome Sequencing Center, and sequences were run through pipelines at Claritas Genomics and at Codified Genomics.

Results: One de novo PHEX mutation missed during initial Sanger sequencing was identified (NM_000444:exon22:c.T2243G:p.L748R). Another patient and her affected son had heterozygous mutations in SLC9A3R1 (SLC9A3R1:NM_004252:exon2:c.G458A:p.R153Q), although neither patient exhibited the characteristic nephrolithiasis seen with that mutation.

Analysis of a fourth patient found two frameshifts in CYP27B1: (NM_000785:exon8:c.1326_1327insCCCACCC:p.P442fs and exon7:c.1160delA:p.N387fs). Interestingly, different pipelines had differing success rates in finding the CYP27B1 changes, and even Sanger confirmation results were not uniform for this sample .

Conclusion: PHEX is a large gene (215,558 bp), with 22 exons and multiple splice variants, and therefore mutations having escaped detection by pre-NGS methods is not surprising. However, NGS is not without issue- only 1 out of 2 pipelines identified both CYP27B1 frameshifts,

Our preliminary data suggests that WES is an efficient method to identify genetic basis of disease when a variety of candidate genes are possible causes of the condition. Multiple confirmatory pipelines may be necessary to achieve certainty in interpretation for difficult regions of the exome or genome. Investment in such approaches via WES for such unexplained cases may be important as more effective and appropriate therapies can be implemented .

The approach is likely to be a cost-effective method of determining genetic causes of newly diagnosed hypophosphatemia as well.

Disclosures: Catherine Brownstein, None.

FR0442

Loss of ERK1 and ERK2 in osteochondro progenitor cells causes metachondromatosis by enhancing chondrogenesis. <u>Zhijun Chen</u>*[1], <u>Susan X. Yue</u>[2], <u>Guang Zhou</u>[1], <u>Edward Greenfield</u>[1], <u>Shunichi Murakami</u>[1]. [1]Case Western Reserve University, USA, [2]Department of Orthopaedics, Case Western Reserve University, USA

Metachondromatosis, a human skeletal disorder caused by mutations in the *PTPN11* gene, is a rare hereditary disorder characterized by the formation of exostoses and enchondromas. Recently, conditional deletion of *Ptpn11* in skeletal cells has been shown to cause metachondromatosis-like phenotype in mice. However, the pathologic mechanisms whereby Ptpn11 deficiency leads to the development of metachondromatosis remain to be indentified. Ptpn11 encodes a tyrosine phosphatase Shp2 that plays an important role in ERK MAPK signaling. Our genetic study in mice has shown that ERK inactivation in the limb mesenchyme causes ectopic cartilage formation. In the present study, we therefore asked whether the inactivation of the ERK MAPK pathway in osteochondro progenitor cells can also lead to the metachondromatosis-like phenotype. We used *Prx1CreER-GFP* and *Osx-Cre* transgenes to inactivate *ERK2* in osteochondro progenitor cells of *ERK1*-null mice postnatally. Radiographic and histologic analyses indicated the formation of exostoses and enchondroma-like lesions in multiple bones, including the phalanges, metatarsals, and long bones in the limbs, in all of the 25 *Prx1CreER-GFP; ERK1⁻ᐟ⁻; ERK2^{flox/flox}* mice that were treated with tamoxifen. *Osx-Cre; ERK1⁻ᐟ⁻; ERK2^{flox/flox}* mice (3 out of 3) also showed multiple cartilaginous exostoses and enchondromas. Furthermore, *Prx1CreER-GFP; ERK1⁻ᐟ⁻; ERK2^{flox/flox}* mice showed ectopic cartilage formation in and around the muscles, tendons, knee menisci, and bony eminences, such as tibial, gluteal, and deltoid tuberosities. Lineage tracing experiment using the *ROSA26-LacZ* reporter revealed that the *Prx1CreER-GFP* transgene drives Cre-loxP-mediated recombination in multiple cell populations, including cells in the tendons, muscles, the perichondrial groove of Ranvier, and at the bone-ligament interface. Since those locations correspond to the ectopic cartilage formation, it is likely that ERK1/2 inactivation in these osteochondro progenitor cells induces chondrogenic differentiation leading to the development of exostoses. Immunostaining of ERK1/2 showed that the cartilaginous exostoses consisted of both ERK1/2-null and ERK1/2-positive chondrocytes, suggesting that ERK1/2-null cells signal to ERK1/2-positive cells and induce their chondrogenic differentiation. Collectively, our observations strongly suggest that ERK1/2 inactivation in osteochondro progenitor cells causes a metachondromatosis-like phenotype through enhancing chondrogenesis.

Disclosures: Zhijun Chen, None.

FR0448

Increased peripheral vascular flow and aortic stiffness are associated with higher lean mass but lower muscle quality in middle-aged and older adults: the Framingham Heart Study. <u>Shivani Sahni</u>*[1], <u>Na Wang</u>[2], <u>Alyssa Dufour</u>[3], <u>Douglas Kiel</u>[3], <u>Emelia Benjamin</u>[4], <u>Joanne Murabito</u>[5], <u>Joseph Vita</u>[6], <u>Marian Hannan</u>[7], <u>Paul Jacques</u>[8], <u>Robert McLean</u>[9], <u>Roger Fielding</u>[10], <u>Vasan Ramachandran</u>[11], <u>Gary Mitchell</u>[12], <u>Naomi Hamburg</u>[6]. [1]Hebrew SeniorLife, Institute for Aging Research & Harvard Medical School, USA, [2]Boston University School of Public Health, USA, [3]Hebrew SeniorLife, USA, [4]Framingham Heart Study, Boston University School of Public Health, Boston University School of Medicine, USA, [5]Framingham Heart Study & Boston University School of Medicine, USA, [6]Boston University School of Medicine, USA, [7]HSL Institute for Aging Research & Harvard Medical School, USA, [8]Jean Mayer USDA HNRCA, Tufts University, USA, [9]Hebrew SeniorLife Institute for Aging Research & Harvard Medical School, USA, [10]Jean Mayer USDA HNRCA At Tufts University, USA, [11]Framingham Heart Study, Boston University School of Medicine, USA, [12]Cardiovascular Engineering, Inc., USA

Impaired vascular function and increased aortic stiffness with aging is related to decreased physical function and performance of activities of daily living. Only one clinical study has reported the association of systemic vascular function with lower-limb muscular power in older adults with mobility limitations. We sought to evaluate whether alterations in peripheral blood flow and aortic stiffness may relate to muscle dysfunction in a large community-based cohort.

We examined the cross-sectional associations of peripheral vascular flow [resting flow velocity (RFV)] and aortic stiffness [carotid-femoral pulse wave velocity (CFPWV)] with arm lean mass, grip strength and arm muscle quality in 2,691 men and women from the Framingham Study Offspring Cohort (1998-2001). We further examined if RFV and CFPWV have interactive effects on muscle measures.

RFV was evaluated via high-resolution ultrasound and Doppler. CFPWV was evaluated using arterial tonometry and inverse transformed prior to analysis. Arm lean mass (both arms, kg) was measured using whole body DXA and grip strength (kg) was measured by isometric hand dynamometer (max. of 3 trials/hand). Arm muscle "quality" was calculated as the ratio of grip strength to arm lean mass. Multivariable linear regression was used to calculate the association of RFV and CFPWV with muscle measures, adjusting for sex, age; and height. Interaction between RFV and CFPWV was tested. If significant (P<0.10), adjusted least square means of muscle measures were calculated within sub-groups of RFV and CFPWV (dichotomized at median).

Mean age was 61 ± 10y (range 33-88). Mean arm lean mass, grip strength, arm muscle quality were: 5.0 ± 1.6 kg, 33 ± 12.9 kg, 6.31 ± 1.72, respectively. Higher RFV ($\beta \pm$SE: 0.124 ± 0.02, P<0.0001) and CFPWV ($\beta \pm$SE: 0.139 ± 0.03, P<0.0001) were associated with greater arm lean mass. The vascular measures were not significantly associated with grip strength (P range: 0.59-0.70). However, both higher RFV ($\beta \pm$SE: -0.178 ± 0.05, P=0.0006) and CFPWV ($\beta \pm$SE: -0.161 ± 0.07, P=0.01) were associated with lower arm muscle quality.

For muscle quality, a significant interaction was observed between RFV and CFPWV (P=0.09). Upon stratification, participants with lower RFV and lower CFPWV had higher muscle quality compared to those with either higher RFV (P=0.03) or higher CFPWV (P=0.06) or both (P=0.09, Figure).

These results suggest that high peripheral vascular flow, which may reflect aging-related metabolic disease, and high aortic stiffness are associated with greater muscle mass and with reduced muscle quality. Our findings are consistent with the possibility that altered vascular flow in conjunction with abnormal aortic stiffness induces microvascular damage in muscle tissue that adversely affects muscle function.
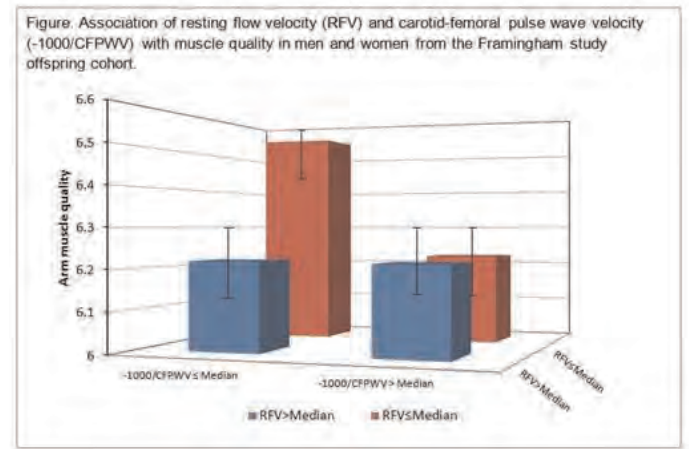
Figure

Disclosures: Shivani Sahni, Unrestricted research grants from General Mills Bell Institute of Health and Nutrition, 7

FR0449

Long-term bisphosphonate users have relatively lower skeletal muscle mass around the femur with increased serum pentosidine concentrations. Shigeharu Uchiyama*[1], Shota Ikegami[1], Keijiro Mukaiyama[2], Yukio Nakamura[3], Mikio Kamimura[4], Hiroyuki Kato[2]. [1]Shinshu University, School of Medicine, Japan, [2]Department of Orthopaedic Surgery, Shinshu University School of Medicine, Japan, [3]Dept of Orthopaedic Surgery Shinshu University School of Medicine, Japan, [4]Kamimura Clinic, Japan

One of the concerns regarding long-term use of bisphosphonate is the possible development of atypical femoral fractures(AFFs). AFFs show features consistent with stress or insufficiency fractures. We conducted a retrospective study to determine if the femurs of long-term bisphosphonate users could be exposed to excessive stress, which in turn could lead to AFFs. We recruited 31 female patients who had taken bisphosphonates for more than 3 years. Sixty-six female healthy volunteers matched with age, BMI, and DXA-derived BMD of the proximal femur, served as controls. We measured the skeletal muscle area around the proximal thigh and indices of the bone strength of the proximal femur with quantitative CT; we also measured several biochemical markers of bone metabolism. While no significant differences of the biomechanical indices of the proximal femur derived from qCT were detected, significant difference in the skeletal muscle area of the proximal thigh was observed between long-term bisphosphonate users and the controls (79 cm2 vs. 89 cm2, p = 0.0005). Furthermore, serum pentosidine levels were significantly greater in the bisphosphonate users than in the controls. The results suggest that long-term bisphosphonate users had a lower skeletal muscle mass around the femur, which had accumulated pentosidine. In such patients, repetitive load on the leg would not be well absorbed by the skeletal muscles. This would subject the brittle femur to excessive stress, leading to stress or insufficiency fractures.

	BP	Control	p-value
N	31	66	
Age years	72.6(9.4)	73.3(6.7)	0.714
BMI	20.4(2.8)	21.6(2.7)	0.053
DXA derived BMD g/cm²			
Lumbar Spine	0.932 (0.206)	0.906 (0.157)	0.499
Total hip	0.676 (0.112)	0.695 (0.090)	0.372
qCT			
femoral neck cortical thickness mm	1.6(0.5)	1.8(0.6)	0.20
femoral neck Buckling ratio	11.8(5.0)	10.8(5.2)	0.615
diaphysis cortical area cm²	1.00(0.1)	1.10(0.0)	0.257
Skeletal muscle area cm²	79.5(13.7)	89.3(12.4)	0.0005
Fat area cm²	8.3(3.2)	10.8(4.5)	0.039
BAP µg/L	10.6(3.6)	16.4(6.0)	< 0.0001
TRACP-5b mU/dL	296(127)	431(170)	0.0003
Homocystein nmol/mL	9.4(2.4)	8.6(2.7)	0.149
serumPentosidine µg/mL	0.0463(0.0189)	0.0269(0.0119)	< 0.0001
urine Pentosidine µg/mg CRE	0.1290(0.4060)	0.0411(0.0396)	0.061

Table

Disclosures: Shigeharu Uchiyama, None.

FR0451

Novel Mass Spectrometry Measurements of Circulating Myostatin Levels in Relation to Sarcopenia, Lean Mass and Bone Parameters in Women and Men. Joshua Farr*[1], Patrick Vanderboom[2], H. Robert Bergen[2], Sundeep Khosla[3], Nathan LeBrasseur[1]. [1]Mayo Clinic, USA, [2]Mayo Clinic, USA, [3]Mayo Clinic College of Medicine, USA

Over 50 yrs ago, circulating tissue-specific growth inhibitors were hypothesized to explain how tissue sizes are controlled. Since that seminal hypothesis, numerous such inhibitors have been discovered, including myostatin, a secreted protein that is derived from skeletal muscle and negatively regulates its mass. To date, however, conflicting data exist on how circulating myostatin levels change with aging and in patients with sarcopenia, possibly owing to poor assay validity.

Thus, we used high-performance liquid chromatography with tandem mass spectrometry to measure serum levels of myostatin as well as two of its key circulating inhibitors, follistatin-related gene protein (FLRG) and growth and serum protein-1 (GASP-1), in a population-based sample of 120 women and 120 men (within each sex: 40 younger subjects [mean age $\pm$ SD: 32.6 $\pm$ 4.7 yrs], 40 normal elderly subjects [age 75.4 $\pm$ 7.9 yrs] and 40 elderly subjects with sarcopenia [age 78.7 $\pm$ 7.5 yrs]). Myostatin levels were higher in men than women (8.6 $\pm$ 3.7 versus 6.7 $\pm$ 3.3 ng/mL, P<0.001) and were positively associated with total body lean mass (TBLM) in younger women and men (r = 0.34 and r = 0.36, respectively, P<0.05), but not in elderly subjects. Further, in patients with sarcopenia, the ratio of myostatin inhibitors (FLRG + GASP-1) to myostatin was significantly higher as compared to sex-matched normal elderly women (by 1.3-fold, P<0.01) and men (by 2.3-fold, P<0.01). Finally, after adjusting for age and sex in all subjects, serum myostatin levels relative to TBLM were negatively associated with hip and spine QCT-derived bone density (r = -0.16 and r = -0.15, respectively, P<0.05) and spine section modulus (r = -0.21; P=0.001).

Our data thus demonstrate that (1) circulating myostatin levels increase markedly with greater TBLM in younger adults, but not in the elderly population; (2) compared to healthy subjects of a similar age, patients with sarcopenia have higher levels of myostatin inhibitors for a given myostatin level; and (3) higher myostatin levels for a given amount of TBLM may have negative consequences for bone. These findings suggest that myostatin functions in a homeostatic regulatory mechanism to prevent excess skeletal muscle hypertrophy, and that in individuals with sarcopenia, natural inhibitors of myostatin are upregulated to limit further muscle wasting. Additional studies are needed to test this hypothesis as well as the potential role of myostatin in mediating bone loss.

Disclosures: Joshua Farr, None.

FR0453

Relationship of Muscle Function and Mass with the Health Assessment Questionnaire. Bjoern Buehring*[1], Sheeva Marvdashti[2], Christina C Lemon[2], Kaitlin R Chambers[2], Erin Johnson[2], Karen Hansen[3]. [1]University of Wisconsin, Madison, USA, [2]Department of Medicine, University of Wisconsin School of Medicine & Public Health, USA, [3]University of Wisconsin, USA

Introduction: The Health Assessment Questionnaire (HAQ) is a well validated, reliable and commonly used tool to assess physical function rheumatic diseases. It assesses 8 domains of function: Dressing / Grooming, Hygiene, Arising, Reach, Eating, Grip, Walking, and Common Daily Activities. Any of these activities requires not only good joint function but also different degrees of muscle strength and power. Sarcopenia, the age-related loss of muscle function and mass, is associated with a greater risk of falls, fractures and disability. This study aims to examine the relationship between muscle function/mass and HAQ scores obtained in a cohort of ambulatory, community-dwelling women. We hypothesized that muscle mass and function would correlate with HAQ scores, and that muscle function would more closely associate with HAQ scores than with muscle mass.

Methods: Subjects were 231 postmenopausal women (mean $\pm$ SD age 61$\pm$ 6 years) participating in a double-blind, randomized, placebo controlled trial evaluating treatment of vitamin D insufficiency. Baseline data was used for the analysis. Participants underwent whole body DXA (GE Lunar) testing, completed a 4–day diet diary and underwent the Timed up and go test (TUG) and 5 sit to stand test (STS). They also had a blood draw to measure various parameters and filled out the Physical Activity of the Elderly (PASE) Questionnaire and HAQ. The HAQ has a score from 0-3 with 0 indicating no disability and 3 indicating severe disability. Descriptive analysis, correlations and regressions were performed using the HAQ as a continuous and a dichotomous measure (score 0 or >0).

Results: 26% of participants had a HAQ score >0. Those with elevated HAQ scores were older, had higher BMI and ALM/Ht² and lower TUG, STS, and PASE scores (Table). In a step-wise, multi-variate regression model using parameters significant in univariate analysis only STS, TUG, BMI and caffeine intake remained associated with HAQ (all p < 0.05). STS and TUG were also significant when using HAQ scores as a continuous variable.

Conclusion: In ambulatory postmenopausal women, decreased TUG and STS scores and higher BMI were associated with increased HAQ scores. Results underscore that decreased muscle function and obesity negatively affect physical function. Additionally, our results suggest that these factors might elevate HAQ scores, independent of rheumatologic disease. The relationship of caffeine intake and HAQ deserves further investigation.

	HAQ score				p-value
	0 (n = 171)		> 0 (n = 59)		HAQ 0 vs. > 0
	Mean	SD	Mean	SD	
Age [years]	60	5.5	62	6.5	**0.028**
Height [m]	1.63	5.99	1.63	5.42	0.807
Weight [kg]	78.6	15.8	90.7	23.1	**<0.001**
BMI [kg/m²]	29.6	5.7	34.3	8.61	**<0.001**
Current smoker [%]	9	n/a	8	n/a	0.882
ALM/height² [kg/m²]	7.14	1.01	7.73	1.41	**0.004**
Timed Up and Go - time [s]	7.8	1.38	9.2	2.07	**<0.001**
Repeated chair rise time [s]	9.5	2.29	11.6	2.99	**<0.001**
PASE score	175	88.3	154	82.4	0.097
Lowest Hip DXA BMD T-score	-1.0	0.8	-0.86	0.75	0.221
Vitamin 25(OH)D [ng/ml] (n = 156/52)	20.2	4.9	19.1	5.61	0.207
PTH [pg/ml] (n =125/46)	49	16.9	52	18.1	0.426
Protein intake [g/day]	75	19.4	76	18.4	0.662
Fat intake [g/day]	76	26.5	79	32.8	0.532
Carbohydrate intake [g/day]	223	66.3	227	63.5	0.666
Alcohol intake [g/day]	6.7	14.6	4.9	9.9	0.312
Caffeine intake [mg/day]	189	169	122	84.9	**<0.001**

Table: Differences between participants with or without elevated HAQ scores

Table

Disclosures: Bjoern Buehring, None.

FR0455

Simple Functional Tests Predict Hip Fracture and Mortality in Postmenopausal Women; A 15 – Year Follow-Up. <u>Toni Rikkonen</u>*[1], <u>Kenneth Poole</u>[2], <u>Joonas Sirola</u>[3], <u>Reijo Sund</u>[4], <u>Risto Honkanen</u>[5], <u>Heikki Kroger</u>[6]. [1], Finland, [2]University of Cambridge, United Kingdom, [3]University of Eastern Finland / Kuopio, Finland, [4]University of Helsinki, Finland, [5]University of Eastern Finland, Finland, [6]Kuopio University Hospital, Finland

Aim

The earliest detectable sings of physical deterioration that predict hip fracture and mortality are not established. The aim of the study was to investigate the association of simple functional tests in relation to fracture risk and mortality in 15 year prospective follow-up.

Methods

Functional capacity and femoral neck bone mineral density (FN BMD) were measured in the population-based Osteoporosis Risk Factor and Prevention Study (OSTPRE) among 2791 women with a mean age of 59.1 years (range 53.2–65.6). Three physical tests were carried out and treated as dichotomous risk factors for functional decline; Ability to squat down (SQ) and touch the floor (y/n), ability to stand on one leg (SOL) for 10 seconds (y/n) and being ranked to the weakest grip strength (GS) quartile (y/n). FN BMD was measured with dual x-ray absorptiometry. Fractures and life style variables were recorded from self-reported questionnaires at baseline. Hip fractures (femoral neck, trochanteric and subtrochanteric) were verified from hospital discharge registry, deaths were recorded from national cause of death registry. Fracture risk and mortality were estimated by Cox proportional hazards model, with a mean follow-up time of 13.1 years and 13.8 years, respectively.

Results

A total of 578 fractures, including 35 hip fractures, were observed. Overall mortality during the follow-up was 9.2% (n=258). Altogether 56.9% (n=1587) of the women had none of the risk factors (SQ,SOL,WG) at baseline and were regarded as a reference group. Women with any of the risk factors acquired (n=1204) had higher risk for hip fracture, mortality and any fracture, with hazard ratios (HR) of 4.6 [95% confidence interval (CI) 2.1–10.1, $p<0.001$], 1.5(1.2-1.9, p=0.001), 1.5(1.2-1.7, $p<0.001$), respectively.

The strongest single determinant for hip fracture among tests was failed SOL, followed by failed SQ and weak GS, with their respective HR of 8.4(3.1-23.4, $p<0.001$), 5.2(2.3-11.8, $p<0.001$) and 4.3(1.8-10.3, p=0.001). Combinations of the risk factors only modestly increased the HR's. Adjusting fracture risks for FN BMD and age, or mortality for BMI and smoking did not alter the results.

Conclusion

Simple functional tests provide tools for risk assessment of the hip fracture, overall fractures and mortality. They also demonstrate the magnitude of frailty as an important predictor in hip fracture outcome.

Disclosures: Toni Rikkonen, None.

FR0456

The effect of acute exercise on undercarboxylated osteocalcin and insulin sensitivity in obese men. <u>Itamar Levinger</u>*[1], <u>George Jerums</u>[2], <u>Nigel Stepto</u>[3], <u>Lewan Parker</u>[3], <u>Fabio Serpiello</u>[3], <u>Glenn McConell</u>[3], <u>Mitchell Anderson</u>[3], <u>David Hare</u>[2], <u>Elizabeth Byrnes</u>[4], <u>Peter Ebeling</u>[5], <u>Ego Seeman</u>[6]. [1]Institute of Sport, Exercise & Active Living (ISEAL), Victoria University, Australia, [2]Austin Health, Australia, [3]Institute of Sport, Exercise & Active Living (ISEAL), Victoria University, Australia, [4]PathWest QEII Medical Centre, Australia, [5]Department of Medicine, School of Clinical Sciences, Monash University, Australia, [6]Austin Health, University of Melbourne, Australia

Background: Acute exercise improves insulin sensitivity for hours after the exercise is ceased. The skeleton contributes to glucose metabolism and insulin sensitivity via osteocalcin (OC) in its undercarboxylated (ucOC) form in mice. We tested the hypothesis that improvement in insulin sensitivity following exercise is partly mediated via ucOC in human subjects.

Methods: Eleven middle-aged (58.1 ± 2.2year mean$\pm$SEM), obese (BMI=33.1 ± 1.4kgm-2) non-diabetic men completed a euglycaemic-hyperinsulinaemic clamp at rest (Rest-Control) and at 60 min post-exercise (44 min of cycling at 95% of HRpeak). Insulin sensitivity was determined by glucose infusion rate relative to body mass (GIR, ml·kg^{-1}·min^{-1}) as well as GIR per unit of insulin (M-value). Blood samples and 5 muscle biopsies were obtained; two at the Resting-control session, one before and one after clamping, and three in the Exercise session, at rest, 60min post-exercise and after the clamp.

Results: Exercise increased serum ucOC ($6.4 \pm 2.1\%$, p= 0.013) but not total OC (p>0.05). Blood glucose was ~6% lower and insulin sensitivity ~35% higher post-exercise compared with control (both p<0.05). P-AKT was higher after exercise and insulin compared to exercise alone (no insulin, ~2 fold, p=0.006,) and insulin alone (no exercise, ~1.8 fold, p=0.029). In a multiple-linear regression model that included BMI, age and aerobic fitness, ucOC was an independent predictor for whole body insulin sensitivity at rest and post-exercise (b=0.59, p=0.023 and b= 0.66, p=0.005, respectively) as was BMI.

Conclusions: Acute exercise partly mediates its beneficial effects on insulin sensitivity via ucOC in obese men. Whether ucOC has a direct effect on skeletal muscle insulin sensitivity after exercise is yet to be determined.

Disclosures: Itamar Levinger, None.

FR0461

Hdac3 regulates osteoblastic glucocorticoid and lipid metabolism during aging. <u>Meghan McGee-Lawrence</u>*[1], <u>Lomeli Carpio</u>[1], <u>Ryan Schulze</u>[2], <u>Mark McNiven</u>[2], <u>Sundeep Khosla</u>[3], <u>Merry Jo Oursler</u>[1], <u>Jennifer Westendorf</u>[1]. [1]Mayo Clinic, USA, [2]Mayo Clinic, USA, [3]Mayo Clinic College of Medicine, USA

Histone deacetylase 3 (Hdac3) removes acetyl groups from lysine residues in histones and other proteins to epigenetically regulate gene expression. Hdac3 interacts with skeletal transcription factors and is essential for bone development and maintenance. We previously reported that conditional deletion of Hdac3 (Hdac3 CKO) in osteochondral progenitors, using Osx1-Cre, caused osteopenia and increased marrow adiposity, both hallmarks of an aging skeleton. Here we demonstrate that Hdac3 mRNA expression is reduced in bone cells from elderly women and primary bone marrow stromal cells (BMSC) and osteocytes from aged mice. More significantly, phosphorylation of S424-Hdac3, an event that stimulates deacetylase activity, is suppressed in osseous cells from old (22-26 months) mice as compared to young (1-2 months) animals. Lipid droplet formation was prevalent in the aged wildtype cultures as well as in osteogenic cultures of young Hdac3-depleted BMSCs. Gene expression analyses revealed insignificant changes in mRNA levels of Ppar gamma and fatty acid synthase, but Hdac3 CKO cultures demonstrated 10- to 20-fold increases in expression of genes related to lipid storage (Cidec, Perilipin1) and 2 to 3-fold changed in genes regulating glucocorticoid metabolism (11β-hydroxysteroid dehydrogenase type 1 (Hsd11b1)), suggesting that Hdac3 regulates local osteoblastic activation of glucocorticoids and lipid storage. In support of this hypothesis, lipid-containing cells in the Hdac3 CKO cultures expressed Runx2. In vitro lipid droplet formation was dependent on glucocorticoid signaling, as lipid storage and gene expression returned to near wildtype levels when dexamethosone (Dex) was excluded from the culture medium. Hdac3 attenuated Dex-induced activation of the glucocorticoid-responsive MMTV-luciferase reporter. Taken together, our data suggest that suppression of Hdac3 activity in bone cells contributes to reductions in bone density and increases in marrow adiposity that are associated with aging and long-term glucocorticoid treatment.

Disclosures: Meghan McGee-Lawrence, None.

FR0462

Loss of Progranulin Increases Bone Mass in Adult Mice in a Gender Dependent Manner. <u>Liping Wang</u>*[1], <u>Theresa M. Roth</u>[2], <u>Thi A. Nguyen</u>[3], <u>Ping Zhou</u>[3], <u>Jiasheng Zhang</u>[4], <u>Mary Nakamura</u>[5], <u>Eric J. Huang</u>[6], <u>Robert V. Farese Jr.</u>[7], <u>Robert Nissenson</u>[8]. [1]VA Medical Center, San Francisco, USA, [2]Endocrine Unit, VA Medical Center, USA, [3]Gladstone Institute of Cardiovascular Disease, USA, [4]Pathology, University of California, USA, [5]University of California, San Francisco/San Francisco VA Medical Center, USA, [6]Pathology, University of California / Pathology Service, VA Medical Center, USA, [7]Gladstone Institute of Cardiovascular Disease / Medicine & Biochemistry & Biophysics, University of California, USA, [8]VA Medical Center & University of California, San Francisco, USA

Progranulin (PGRN) is highly expressed in neurons and microglial cells. PGRN haploinsufficiency causes frontotemporal dementia and homozygous mutation causes neuronal ceroid lipofuscinosis, a disease linked to defective lysosomal function, in humans. Recent studies have suggested that PGRN promotes heterotopic ossification and skeletal repair by serving as a downstream effector of BMP signaling. However, the role of PGRN in normal skeletal homeostasis has not been studied. We studied skeletal phenotypes of 6 month old PGRN null (KO) and wild type (WT) mice. μCT assessment revealed that female mice lacking PGRN maintained much greater fractional bone volume (BV/TV, %) (WT vs. KO, 6.89 ± 0.42 vs. 13.82 ± 1.79, p<0.01) at distal femur (DF) and increased cortical thickness (Ct.Th, mm) at the tibio-fibular junction (TFJ) (WT vs. KO, 0.218 ± 0.005 vs. 0.237 ± 0.004, p<0.05). In contrast, no statistically significant difference was seen in cancellous BV/TV or Ct.Th between male KO and WT mice (WT vs. KO, BV/TV: 18.48 ± 0.66 vs. 15.84 ± 1.34; Ct.Th: 0.234 ± 0.002 vs. 0.231 ± 0.009). To gain further insight into the role of PGRN in bone structure, histomorphometry was performed in the same bones. Compared to WT mice, there was a 45.6% increase in trabecular width (p<0.05), 59.3% increase in trabecular number (p<0.01), and a 41.5% decrease in trabecular separation (p<0.001) at DF in the female KO mice. R493X, the most common mutation worldwide in humans, causes loss of functional PGRN and therefore dementia in humans. We assessed the bone phenotype of the mice with R493x mutations (R493X) using μCT. Similarly to the findings with PGRN KO, mice bearing the R493X PGRN mutation displayed a striking increase in cancellous BV/TV (WT vs. R493X, 6.51 ± 0.85 vs. 12.17 ± 1.09, p<0.01) at DF and in Ct.Th at TFJ (WT vs. R493X, 0.228 ± 0.003 vs. 0.245 ± 0.003, p<0.01) in the 6-month-old female mice, while the age-matched male mice had no effect on cancellous BV/TV at DF (WT vs. R493X: 12.62 ± 0.91 vs. 13.45 ± 1.23), but increased Ct.Th (WT vs. R493X, 0.247 ± 0.007 vs. 0.266 ± 0.004, p<0.05) at TFJ. Bone marrow mononuclear cells from

PGRN null mice were found to be defective in osteoclastogenesis in vitro, producing fewer and smaller osteoclasts, suggesting that an osteoclast defect may contribute to the skeletal phenotype. In conclusion, PGRN is important in maintaining bone homeostasis in adult female mice and might serve as a useful therapeutic target for preventing age-related bone loss in humans.

Disclosures: Liping Wang, None.

FR0463

Nox2-dependent ROS signaling protects against skeletal ageing. <u>Jin-Ran Chen</u>*[1], <u>Oxana P. Lazarenko</u>[2], <u>Kelly Mercer</u>[3], <u>Michael L. Blackburn</u>[3], <u>Thomas M. Badger</u>[3], <u>Martin J. J. Ronis</u>[4]. [1]University of Arkansas for Medical Science, Arkansas Children's Nutrition Center, USA, [2]Arkansas Children's Nutrition Center & The Department of Pediatrics, University of Arkansas for Medical Sciences, USA, [3]Arkansas Children's Nutrition Center, & The Department of Pediatrics, University of Arkansas for Medical Sciences, USA, [4]Arkansas Children's Nutrition Center, USA

Bone remodeling is age-dependently regulated and changes dramatically during the course of development. Progressive accumulation of reactive oxygen species (ROS), including superoxide, hydrogen peroxide, and hydroxyl radicals has been suspected to be the leading cause of many inflammatory and degenerative diseases and underlie the effects of ageing. In contrast, how reduced ROS signaling regulates inflammation and remodeling in bone remains unknown. Here, we utilized a p47phox knockout mouse model, in which an essential cytosolic co-activator of Nox2 is lost, to characterize bone metabolism at 6 weeks and 24 months of age. Using peripheral quantitative CT (pQCT), μCT and femur three point bending, and histomorphometric analyses, we show that bone mass and strength were all significantly higher in 6 weeks old p47$^{phox -/-}$ mice, but these were reversed in 24 month old p47$^{phox -/-}$ mice compared to their age-matched wild type controls. Increased bone formation with decreased bone resorption in 6 week old p47$^{phox -/-}$ mice, and decreased bone formation in 24 months old p47$^{phox -/-}$ mice reflected bone mass at these ages. Flow cytometric and Amplex Red hydrogen peroxide/peroxidase assays showed decreases in ROS generation in bone marrow cells and Nox2 signaling in osteoblastic cells from p47$^{phox -/-}$ mice compared to those from control wild type mice. Knocking down the Nox4 gene in neonatal osteoblastic cells from p47$^{phox -/-}$ mice in *ex vivo* blunted increased osteoblast differentiation. Expression of proinflammatory cytokines such as TNFα, IL6, RANKL and MMP9 in bone were all significantly increased in 24 month old p47$^{phox -/-}$ mice compared to their wild type controls, while we did not observe any differences in proinflammatory cytokine expression in 6-week-old p47$^{phox -/-}$ mice compared to wild type mice. These *in vivo* findings were mechanistically recapitulated in *ex vivo* cell culture of primary fetal calvarial cells, showed accelerated premature cell senescence accompanied by increased inflammation in cells from p47$^{phox -/-}$ mice. These data indicate that the observed age-related switch of bone mass in p47phox deficient mice occurs through an increased inflammatory milieu in bone and that Nox2-dependent physiological ROS signaling is redundant for osteoblast differentiation in early development, but it is required for suppression of inflammation in ageing bone. *Supported in part by ARS CRIS #6251-51000-005-03S (JRC) and R01 AA18282 (MJJR)*

Disclosures: Jin-Ran Chen, None.

FR0465

Hip Fracture And Sarcopenia: A Model Of Osteoporosis-Related Muscle failure. <u>Umberto Tarantino</u>*[1], <u>Jacopo Baldi</u>[2], <u>Eleonora Piccirilli</u>[2], <u>Maurizio Feola</u>[2], <u>Cecilia Rao</u>[2], <u>Elena Gasbarra</u>[2]. [1]Università degli Studi di Roma Tor Vergata, Italy, [2]Università degli Studi di Roma "Tor Vergata", Italy

Introduction: The widespread increase in life expectancy is accompanied by an increased prevalence of physical diseases such as osteoporosis which is associated with loss of muscle bulk and power. Objectives: Aim of this study was to evaluate the degree of muscular atrophy in the vastus lateralis muscle of patients with osteoporosis and to determine the role of IGF-1/PI(3)/Akt signaling pathways in the genesis of a specific type II osteoporosis-related muscle atrophy. Moreover we investigate the microstructural features in muscles of osteoporotic by using diffusion tensor imaging (DTI). Methods: We performed vastus lateralis biopsy in 25 women with osteoporosis (OP) undergoing surgery for hip fracture and in 25 age matched women undergoing arthroplasty for hip osteoarthritis (OA). All patients gave informed consent. Muscle fibers were counted, measured and classified. A Magnetic Resonance (MR) operating at 9.4T equipped with a micro-imaging probe with a maximum gradient strength of 1200 mT/m was used to investigate muscle samples. We evaluated the Fractional Anisotrophy (FA), the mean Diffusivity (MD) and the three eigen values (λ1>λ2>λ3). All computation was made using an homemade script in MATLAB®. Mean values and standard deviation were obtained for each variable for OP and OA subjects, p values<.05 were considered statistically significant. Results: Our findings revealed a high percentage of atrophic type II fibers (37%) in OP, whereas in OA lower figures were observed (12%). Furthermore, we show that: 1) in OP, atrophic type-II fibers a) are 3-fold more frequent than atrophic type-I fibers (p<.01), b) significantly correlate with the degree of op (p<0.05); 2) in OA, type II fibers atrophy is 1.5-fold more frequent than type-I (p<0.001), correlates fiber atrophy, disease duration, pain and functional impairment hip joint. FA was higher compared to (p=-0.936) while MD, λ2 λ3 were compare (p=0.022), respectively. No significant difference λ1 found between linear correlation OP subjects only. Conclusions: This study shows in

osteoporosis a preferential and diffuse type II fiber atrophy, that seems to be related to disease severity. FA is lower in OP when compared to OA. This outcome suggests that OP muscle has a more isotropic microstructure indicating that the micro-architetural alteration due to osteoporosis disease causes a higher radial diffusivity

Disclosures: Umberto Tarantino, None.

FR0467

Asxl1 loss alters histone methylation status, leading to skeletal deficits. <u>Feng-Chun Yang</u>*[1], <u>Peng Zhang</u>[2], <u>Zhaomin Li</u>[3], <u>Yongzheng He</u>[3], <u>Lihn Nguyen</u>[3], <u>Jiapeng Wang</u>[3], <u>Khalid S. Mohammad</u>[3], <u>Theresa A. Guise</u>[3], <u>Mingjiang Xu</u>[4]. [1]Indiana University, USA, [2]Indiana Univeristy, USA, [3]Indiana University, USA, [4]Indiana University School of Medicine, USA

Epigenetic mechanisms are critical in the tissue-specific regulation of gene expression. Histone methylation is one of the most important epigenetic modifications. However, whether histone methylation underlies the physiology and pathobiology of bone remodeling is not well established. *Additional sex combs* like 1 (*Asxl1*) has been shown to play an important role in both activation and silencing of *Hox* genes through interacting and regulating multiple histone modifying enzymes. Importantly, *ASXL1* is mutated in patients with Bohring-Opitz syndrome (BOS), characterized by severe bone deformities and other developmental deficits. Here, using an *Asxl1*-targeted mouse model, we challenged if *Asxl1* loss dysregulates critical genes controlling osteoblasto-genesis and bone remodeling through altered histone modifications. Using *Asxl1:GFP* reporter knock-in strategy, we found that *Asxl1* loss lead to skeletal developmental defects in vivo, including dwarfism and hypoplastic supraorbital ridges. Dual energy X-ray absorptiometric analysis indicated a significantly lower bone mineral density in these mice. MicroCT confirmed decreased bone volume and reduced trabecular bone volume in these mice compared to WT controls. *Asxl1* loss resulted in markedly decreased frequency of bone marrow mesenchymal stem progenitor cells (MSPCs) with impaired osteoblast differentiation and much higher adipocyte differentiation compared to control MSPCs. The skewed MSPC differentiation was associated with the alteration of expression of multiple genes controlling osteoblastic and adipocytic differentiation, such as *Runx2, Bglap, Sp7, Alpl, Parg, Cebpa,* and *Lpl*. Furthermore, the loss of *Asxl1* dramatically altered the H3K4me3 levels in MSPCs. Importantly, re-expression of *Asxl1* restored both the cellular phenotypes and gene expression levels in *Asxl1* deleted cells. Collectively, these results indicate that *Asxl1* loss impaired skeletal development through dysregulation of histone methylation states, which in turn altered gene expression in MSPCs. This study demonstrated a pivotal role of histone modification in bone homeostasis.

Disclosures: Feng-Chun Yang, None.

FR0468

Dissociation of cortical and trabecular bone parameters in mice with conditional deletion of Solute carrier family 4 (anion exchanger), member 2 (SLC4A2) in mesenchymal cells. <u>William O'Brien</u>*[1], <u>Julia Charles</u>[2], <u>Kelly Tsang</u>[3], <u>Kenichi Nagano</u>[4], <u>Gary Shull</u>[5], <u>Roland Baron</u>[6], <u>Antonios Aliprantis</u>[1]. [1]Brigham & Women's Hospital, USA, [2]Brigham & Women's Hospital & Harvard School of Medicine, USA, [3]Brigham & Women's Hospital, USA, [4]Harvard School of Dental Medicine, USA, [5]University of Cincinnati College of Medicine, USA, [6]Harvard School of Medicine & of Dental Medicine, USA

Solute carrier family 4 (anion exchanger), member 2 (SLC4A2) regulates the intracellular pH of osteoclasts and is necessary for this cell to resorb bone. Osteoclast-specific deletion of *Slc4a2* however only partially recapitulates the severe osteopetrotic phenotype observed in germline *Slc4a2$^{-/-}$* mice. Thus, we hypothesized that SLC4A2 also regulates bone mass through effects on mesenchymal lineage cells. To test this hypothesis, we used *Prx1-Cre* to delete a conditional allele of *Slc4a2* in the early limb bud mesenchyme (*Slc4a2^{Prx1Cre}*). Twelve-week-old male *Slc4a2^{Prx1Cre}* mice were compared to sex-matched, littermate *Slc4a2$^{fl/fl}$ Prx1-Cre$^-$* (WT) controls. By micro-CT, femurs of *Slc4a2^{Prx1Cre}* mice displayed increased cortical bone (Cortical thickness 0.26 vs. 0.18mm, p<0.05) and decreased trabecular bone (BV/TV 4.2 vs. 14.7%, p<0.05). Histomorphometry confirmed both of these differences, and identified reduced osteoblast numbers and osteoid volume in the femoral trabecular compartment of the mutants. A trend towards decreased BFRs was also observed in *Slc4a2^{Prx1Cre}* mice at this site. Furthermore, trabecular bone resorption activity (ES/BS 3.4 vs. 1.3%, p<0.05) and osteoclastogenesis (Oc.S/B.Pm 2.7 vs. 1.1%, N.Oc/B.Pm, 1.1 vs. 0.37/mm, p<0.05 for both) were increased in *Slc4a2^{Prx1Cre}* mice. In cortical bone, histomorphometry identified increased periosteal bone formation parameters in the mutants (Ps.BFR/BS 225 vs. 102um^3/um^2/day, Ps.BFR/BV 554 vs. 198%/year, p<0.05 for both). To test for systemic effects of our deletion strategy, we analyzed vertebral trabecular bone by micro-CT and found *Slc4a2^{Prx1Cre}* mice were indistinguishable from WT. This is consistent with the restricted expression of *Prx1* to limb bud mesenchyme. In summary, deletion of *Slc4a2* in limb bud mesenchyme increases cortical bone by elevating bone formation, and decreases trabecular bone mostly by promoting osteoclastic bone resorption. Thus, in addition to its previously appreciated function in osteoclasts, SLC4A2 also regulates bone remodeling through a direct function in mesenchyme-derived cells. The phenotype of *Slc4a2^{Prx1Cre}* mice is a rare example of dissociation of cortical and trabecular bone

mass and may provide insight into how bone remodeling is differentially regulated at these sites.

Disclosures: William O'Brien, None.

FR0469

Dullard/Ctdnep1 regulates endochondral ossification via suppression of TGF-ß signaling. Tadayoshi Hayata*[1], Yoichi Ezura[2], Makoto Asashima[3], Ryuichi Nishinakamura[4], Masaki Noda[5]. [1]Organization for Educational Initiatives, University of Tsukuba, Japan, [2]Tokyo Medical & Dental University, Medical Research Insititute, Japan, [3]Research Center of Stem Cell Engineering, National Institute of Advanced Industrial Science & Technology (AIST), Japan, [4]Department of Kidney Development, Institute of Molecular Embryology & Genetics, Kumamoto University, Japan, [5]Tokyo Medical & Dental University, Japan

Transforming growth factor (TGF)-ß signaling plays critical roles during skeletal development and its excessive signaling causes genetic diseases of connective tissues including Marfan syndrome and acromelic dysplasia. However, the mechanisms underlying prevention of excessive TGF-ß signaling in skeletogenesis remain unclear. We previously reported that *Dullard/Ctdnep1* encoding a small phosphatase is required for nephron maintenance after birth through suppression of bone morphogenetic protein (BMP) signaling. Unexpectedly, we found that *Dullard* is involved in suppression of TGF-ß signaling during endochondral ossification. Conditional *Dullard*-deficient mice in the limb and sternum mesenchyme by *Prx1-Cre* displayed impaired growth and ossification of skeletal elements leading to postnatal lethality. *Dullard* was expressed in early cartilage condensations and later in growth plate chondrocytes. Dullard deficiency enhanced the early cartilage condensation and differentiation, but impaired cartilage mineralization in micromass culture system, both of which was restored by treatment with TGF-ß type I receptor kinase blocker LY-364947. Protein levels of both phospho-Smad2/3 and total Smad2/3 were upregulated in Dullard-deficient micromass cultures, while Smad2/3 mRNA levels were not increased, suggesting that Dullard affects Samd2/3 protein stability. Response to TGF-ß signaling was also enhanced in Dullard-deficient primary chondrocyte cultures at late, but not early, time point. The phospho-Smad2/3 was upregulated in perichondrium and hypertrophic chondrocytes in *Dullard*-deficient embryos. Moreover, perinatal administration of LY-364947 ameliorated the skeletal deformity caused by Dullard deficiency in vivo. Thus, we identified Dullard as a new negative regulator of TGF-ß signaling in endochondral ossification.

Disclosures: Tadayoshi Hayata, None.

FR0470

Challenging the dogma of BMP canonical signaling in the absence of Smad4. Diana Rigueur*[1], Karen Lyons[2]. [1]Graduate Student, USA, [2]University of California, Los Angeles, USA

BMP signaling plays essential roles in the development and maintenance of bone and cartilage. However, the mechanisms by which BMP signaling regulates proliferation, differentiation, and apoptosis have yet to be completely elucidated. In the canonical BMP signaling pathway, the intracellular R-Smads 1, 5, and 8, transduce the signal by translocating to the nucleus with common Smad4 to activate BMP target genes. The majority of studies to date indicate that Smad4 is an essential component of canonical BMP signaling. However, there is some evidence in Drosophila that R-Smads transduce a limited amount of signaling in the absence of Smad4. To date, this has not been clearly demonstrated in vertebrates. Our recent findings provide evidence that Smad1/5/8-dependent, Smad4-independent BMP signaling does occur in vertebrates, and in the context of the cartilage growth plate, may be a major mode of BMP signaling. We find that cartilage specific loss of Smads1/5 in mice leads to a severe chondrodysplasia, yet cartilage-specific Smad4-knockout mice are viable and display a much milder cartilage phenotype. Through immunofluorescence, western blot analysis, and quantitative RT-PCR we show that transducers of the BMP pathway, both receptor activated Smads 1/5/8 and the non-canonical pathway, are ectopically elevated in the absence of Smad4. Moreover, a well-characterized BMP target gene, IHH, albeit reduced, responds to BMP stimulation in isolated Smad4 deficient primary chondrocytes. Through CHIP analysis, we show that Smads 1/5/8 are able to bind to the IHH promoter, although, at diminished levels in Smad4 deficient chondrocytes. Overall, these data exemplify that Smad4 may be required for canonical BMP transduction in many or most tissues; however, Smad4 may be dispensable for other systems, calling for a re-evaluation of the putative BMP canonical pathway and the extent of BMP signaling.

Disclosures: Diana Rigueur, None.

FR0471

Contrasting Skeletal and Molecular Phenotypes in Mice Lacking Prolyl Hydroxylase Domain-containing Protein 2 (PHD2) Gene in Chondrocytes Versus Osteoblasts. Shaohong Cheng*[1], Weirong Xing[2], Sheila Pourteymoor[3], Subburaman Mohan[4], Jan Schulte[3], Bo Liu[3]. [1]VA Loma Linda Health Care Systems, USA, [2]Musculoskeletal Disease Center, Jerry L. Pettis Memorial Veteran's Admin., USA, [3]1Musculoskeletal Disease Center, Jerry L Pettis VA Medical Center, USA, [4]Jerry L. Pettis Memorial VA Medical Center, USA

Ascorbic acid (AA) is indispensable for osteoblast (OB) maturation as mutant mice lacking GULO, an enzyme required for AA biosynthesis, develop spontaneous fractures due to impaired bone formation (BF). In our studies on the mechanism for AA effects on OBs, we found that the AA effect on osterix (Osx) expression is dependent on PHD2. Accordingly, we recently reported that conditional knock out (cKO) of PHD2 in OBs results in decreased bone size, BMD and BF rate and premature death at 12-14 weeks of age. Since AA is also known to regulate chondrocyte (CC) functions, we evaluated the role of PHD2 in CCs in this study by crossing Phd2 floxed mice with transgenic Col2α1-Cre mice. In contrast to the osteopenia phenotype of OB-specific PHD2 cKO mice, PHD2 disruption in CCs increased areal BMD by >20% (P<0.05) in femur, tibia and vertebra of 4 week old mice. Micro-CT analysis revealed a 118% and 42% (p<0.001) increase in trabecular BV/TV of femur and vertebra. The femur cortical BV/TV was also increased by 10% (p<0.001) in the cKO mice. While the femur length and size were reduced by 20% and 7% respectively, the increased trabecular and cortical bone BMD were maintained at 12 weeks of age. Histomorphometric analyses revealed that while BFR was unaffected, the TRAP positive osteoclast surface to bone surface was reduced by 14% (p<0.05) in the trabecular bone of cKO mice. Quantitative RT-PCR revealed that PHD2 expression was reduced by >60% in growth plate CCs. Surprisingly, loss of PHD2 in growth plate CCs increased Osx expression which is in contrast to reduced Osx expression in bones of OB-specific cKO mice. Since PHD2 is a key regulator of HIF1α that is required for chondrocyte survival and differentiation, we examined the VEGF mRNA level, a marker for HIF1α signaling. Indeed we found an 80% increase of VEGF mRNA level in the growth plate CCs of the cKO mice, suggesting up-regulation of the HIF1α pathway in the CCs of PHD2 cKO growth plates. CCs-derived from PHD2 floxed mice were infected with adenoviral (Ad)-Cre to delete the PHD2 gene or Ad-GFP control. AA reduced Osx expression in Ad-GFP but not in Ad-Cre CCs. Based on these data and our published data that Osx is required for terminal differentiation of CCs, we conclude that PHD2 negatively regulates chondrocyte maturation and endochondral BF in part by inhibiting Osx and VEGF expression, which is in sharp contrast to its role as a positive regulator of differentiation and Osx expression in OBs.

Disclosures: Shaohong Cheng, None.

FR0474

RECQL4 regulates p53 function *in vivo* during skeletogenesis. Linchao Lu*[1], Karine Harutyunyan[2], Weidong Jin[3], Jianhong Wu[3], Tao Yang[4], Yuqing Chen[3], Kyu Sang Joeng[1], Yangjin Bae[1], Jianning Tao[1], Brian Dawson[3], Ming-Ming Jiang[3], Brendan Lee[1], Lisa Wang[1]. [1]Baylor College of Medicine, USA, [2]University of Texas M. D. Anderson Cancer Center, USA, [3]Baylor College of Medicine, USA, [4]Van Andel Research Institute, USA

RECQL4 is a DNA helicase and functions in DNA replication, homologous recombination and DNA damage repair. Mutations in *RECQL4* are associated with three human disorders: Rothmund-Thomson syndrome (RTS), RAPADILINO, and Baller-Gerold syndrome (BGS). All three syndromes have prominent skeletal abnormalities, including radial ray abnormalities, foreshortened limbs, and cranio-synostosis.

To study the function of *RECQL4* in skeletogenesis *in vivo*, we generated a mouse *Recql4* conditional allele (*Recql4^{fl/fl}*) by gene targeting. *Recql4^{fl/fl}* mice were crossed with *Prx1-Cre* transgenic mice to inactivate *Recql4* in mesenchymal progenitor cells. *Recql4^{fl/fl};Prx1-Cre+* mice had short, abnormally shaped limbs, missing digits, and cranial suture synostoses. H&E staining of E18.5 growth plates showed reduced chondrocyte density and increased cell size. Growth plates of 3 week old *Recql4^{fl/fl};Prx1-Cre+* mice displayed abnormal cell morphology and disorganized cells leading to reduced ossification. Furthermore, crossing *Recql4^{fl/fl}* mice with *Col2a1-Cre* transgenic mice resulted in offspring with small, abnormally shaped rib cages and perinatal lethality. Growth plates from these mice displayed similar chondrocyte defects as those in *Recql4^{fl/fl};Prx1-Cre+* mice. TUNEL and BrdU incorporation assays showed increased apoptosis and decreased cell proliferation in the growth plates from both mouse models. Real-time RT-PCR revealed that transcripts of p53 target genes, including *CDKN1A/p21* and *Bax*, were significantly up-regulated in tissues from both models. Immunoblot analysis demonstrated dramatically increased p53 serine15 phosphorylation and elevated p21 protein levels in forelimb tissues of E13.5 *Recql4^{fl/fl};Prx1-Cre+* embryos. Conditional deletion of both *Recql4* and *p53* partially rescued the skeletal defects observed in *Recql4* single mutants, indicating that *Recql4* genetically interacts with *p53 in vivo* during skeletal development.

The skeletal phenotypes in *Recql4^{fl/fl};Prx1-Cre+* and *Recql4^{fl/fl};Col2a1-Cre+* mice recapitulate the major skeletal findings in the *RECQL4* spectrum of disorders. Our *in vivo* findings suggest that: 1) deletion of *Recql4* causes p53 activation which leads to

increased apoptosis and reduced cell proliferation in skeletal progenitor cells; 2) *Recql4* is required for normal skeletogenesis by modulating p53 function during development; and 3) p53 response contributes to the pathogenesis of developmental bone anomalies in patients with *RECQL4* mutations.

Disclosures: Linchao Lu, None.

FR0476

The homeoboxgene *DLX4* promotes generation of human induced pluripotent stem cells. <u>Naritaka Tamaoki</u>*[1], <u>Kazutoshi Takahashi</u>[2], <u>Hitomi Aoki</u>[3], <u>Kazuki Iida</u>[1], <u>Tomoko Kawaguchi</u>[1], <u>Daijirou Hatakeyama</u>[1], <u>Masatoshi Inden</u>[4], <u>Naoyuki Chosa</u>[5], <u>Akira Ishisaki</u>[5], <u>Takahiro Kunisada</u>[3], <u>Toshiyuki Shibata</u>[1], <u>Naoki Goshima</u>[6], <u>Shinya Yamanaka</u>[2], <u>Ken-Ichi Tezuka</u>[7]. [1]Department of Oral & Maxillofacial Science, Gifu University Graduate School of Medicine, Japan, [2]Center for iPS Cell Research & Application, Japan, [3]Department of Tissue & Organ Development, Gifu University Graduate School of Medicine, Japan, [4]Laboratory of Medical Therapeutics & Molecular Therapeutics, Gifu Pharmaceutical Universit, Japan, [5]Division of Cellular Biosignal Sciences, Department of Biochemistry, Iwate Medical University, Japan, [6]Biomedicinal Information Research Center, National Institute of Advanced Industrial Science & Technology, Japan, [7]Gifu University Graduate School of Medicine, Japan

(Background) Potential tumorigenicity is a problem in the application of induced pluripotent stem cells (iPSCs) to regenerative medicine. Therefore, it is important to improve the efficiency of iPSC generation without using proto-oncogenes, such as c-MYC. In a previous study, we established more than 150 dental pulp cells (DPC) lines isolated from extracted wisdom teeth and evaluated the potential of DPCs for iPS cell banking. In this study, we hypothesized that the reprogramming efficiencies of DPCs are affected by the developmental stages of donor teeth. Next, we attempted to identify new reprogramming factors to promote human iPSCs generation without c-MYC by using gene expression profiling between DPCs isolated from immature and mature teeth. (Methods and Results) Firstly we evaluated the reprogramming efficiencies of 9 DPC lines isolated from various developmental stages of third molar teeth, and introduced *OCT3/4*, *SOX2*, *KLF4*, and *c-MYC* (OSKM) into them by retroviral gene delivery. We found that all immature teeth DPC lines showed significantly higher reprogramming efficiency than mature teeth DPC lines. Our result indicated that immature teeth DPCs were much more amenable to reprogramming than mature teeth DPCs, and prompted us to compare these two groups of DPCs for gene expression profiling to identify genes up-regulating the reprogramming efficiencies of DPCs. Among the 28 genes significantly up-regulated by more than five-fold in immature teeth DPCs, we focused a homeobox gene *DLX4*. Real-time PCR assay showed that the expression levels of *DLX4* in DPCs isolated from immature teeth were much higher than those of mature teeth DPCs. We next studied whether ectopic expression of *DLX4* could increase the reprogramming efficiency of DPCs. We observed a synergistic increase in the number of iPSC colonies when *DLX4* was co-introduced with *OCT3/4*, *SOX2*, and *KLF4* (OSKD), and the number of iPSC colonies obtained from both immature and mature teeth DPCs with OSKD was similar to the number obtained using OSKM. As observed in DPCs, the OSKD cocktail also increased the reprogramming efficiency in human dermal fibroblasts to the same level observed using OSKM. (Conclusion) Here we reported the screening of genes differentially expressed in immature and mature teeth DPCs, and found that DLX4 significantly enhanced human iPSC colony formation in combination with OSK. Our finding suggests that DLX4 may be used to replace c-MYC in the derivation of human iPSCs to generate safer iPSCs.

Disclosures: Naritaka Tamaoki, None.

FR0478

Znf9 plays an indispensable role in skeletal development by upregulating the expression of Indian hedgehog (Ihh) and multiple limb development regulator genes. <u>Yun Lu</u>*[1], <u>Guiqian Chen</u>[2], <u>Wei Chen</u>[3], <u>Guochun Zhu</u>[4], <u>Yi-Ping Li</u>[3]. [1], USA, [2]University of Alabama at Birmingham, USA, [3]University of Alabama at Birmingham, USA, [4]The University of Alabama at Birmingham, USA

Znf9 is a cellular nucleic acid binding protein (CNBP) that is highly conserved among vertebrates and implicated in vertebrate craniofacial development. However, due to early embryonic lethality, the function of Znf9 in skeletal development and its molecular targets remain elusive. Hence, we generated $Znf9^{Loxp/Loxp}$ ($Znf9^{f/f}$) mice and then crossed $Znf9^{f/f}$ mice with the *Prx1*-Cre mice to generate mesenchymal stem cell-specific Znf9-deficient ($Znf9^{f/f}Prx1$-Cre) mice to study the role of Znf9 in limb, cartilage, and bone development. *Znf9* gene deletion was verified in the limb mesenchyme by qPCR and immunohistochemistry (IHC) in E14.5 $Znf9^{f/f}Prx1$-Cre embryos. Our data showed that at E17.5, depletion of Znf9 in the limb mesenchyme resulted in the extreme shortening of limbs. Histological analysis showed there is a significant decrease in chondrocyte proliferation. In addition, the transition from prehypertrophic to hypertrophic cells was severely impaired and the expression of osteopontin (*Opn*) and osterix (*Osx*) was largely decreased, indicating abnormal osteogenesis. The Heterozygous mice survived to adulthood, but exhibited very short limbs with malformations. However the Homozygous mice died at birth. 7-day-old $Znf9^{fl+}Prx1$-Cre mice, the resting zone was dramatically elongated, the proliferation zone and hypertrophic zone of the growth plates were drastically shortened and disorganized, and trabecular bone formation was reduced. Moreover, in one-month-old $Znf9^{fl+}Prx1$-Cre mice, the growth plates and long bone were severely deformed. In addition, *Znf9* deficiency impaired intramembranous bone formation. Interestingly, while the expression of indian hedgehog (*Ihh*) was largely reduced, the expression of parathyroid hormone-related protein (*PTHrP*) receptor (*PPR*) was dramatically increased in the $Znf9^{fl+}Prx1$-Cre mice growth plate, indicating that *Znf9* deficiency disrupted the Ihh-PTHrP negative regulatory loop. Furthermore, qRT-PCR revealed a significant reduction of limb development regulator genes (*e.g. Sox9, BMP2, Bmpr1b, Fgfr3, Runx2,* and *Shh*) in $Znf9^{fl+}Prx1$-Cre E17.5 mutant embryos when compared with WT embryos. Notably, Znf9 binding site analysis showed that there are Znf9 binding sites in the regulator gene promoter regions. Taken together, our study reveals that Znf9 is essential for limb development and that Znf9 regulates limb and growth plate development by upregulating the expression of multiple limb and growth plate development regulator genes.

Disclosures: Yun Lu, None.

SA0001

In Postmenopausal Women with Stage 3 CKD, Fractures are Associated with Abnormalities in Both Trabecular and Cortical Bone. <u>Emily Stein</u>*[1], <u>Kyle Nishiyama</u>[2], <u>Thomas Nickolas</u>[1], <u>Stephanie Sutter</u>[3], <u>Donald McMahon</u>[1], <u>X Guo</u>[2], <u>Elizabeth Shane</u>[1]. [1]Columbia University College of Physicians & Surgeons, USA, [2]Columbia University, USA, [3]Columbia University Medical Center, USA

Although evidence is accumulating that fracture risk is higher in postmenopausal (PM) women with mild stage 3 CKD than those with normal renal function, the pathogenesis has not been elucidated. Microarchitectural abnormalities have been reported in fracture patients with more severe CKD, but not in women with fractures and mild CKD. We hypothesized that among PM women with stage 3 CKD, those with fragility fractures would have higher PTH, worse cortical microarchitecture and lower stiffness. We enrolled 50 PM women with stage 3 CKD (age 72 ± 8yrs, 72% Caucasian), 25 with a history of low trauma fracture after menopause (FX) and 25 non-fractured controls. All had areal BMD (aBMD) of lumbar spine (LS), total hip (TH), femoral neck (FN), and 1/3 radius by DXA. Trabecular (Tb) and cortical (Ct) volumetric BMD (vBMD) and Tb microarchitecture were measured by high resolution peripheral computed tomography (HRpQCT, voxel size ~82 µm) of the distal radius and tibia and whole bone stiffness was estimated by finite element analysis. Groups were similar with respect to age, race, BMI and years since menopause. Mean eGFR by MDRD (46 ml/min) and iPTH (60 pg/ml) did not differ. Forearm (40%), spine (28%) and ankle (16%) fractures were most common. Mean DXA T-scores, well above the osteoporotic threshold in both groups, were lower in FX subjects at LS, TH, FN (all p<0.05) but not 1/3R. There were substantial differences in vBMD and microarchitecture at both radius and tibia (Table). At both sites, bone size (cross-sectional area) was similar. At the radius, FX subjects had lower total vBMD, lower Ct area, thickness and density. They also had lower Tb vBMD and number, higher Tb separation and tended to have more heterogeneity. At the tibia, FX subjects had lower total vBMD, lower Ct area and thickness, lower Tb density and thickness and tended to have greater Tb separation. Whole bone stiffness was substantially lower in FX subjects at both sites. In summary, PM women with stage 3 CKD and fractures have both cortical and trabecular abnormalities and lower stiffness compared to those with no history of fracture. Contrary to our hypotheses, abnormalities in FX subjects were not confined to cortical bone, nor did PTH differ by fracture status. Our results suggest that both cortical and trabecular bone losses may be important mechanisms of fracture in the burgeoning population of PM women with mild CKD.

	RADIUS	p-value	TIBIA	p-value
Total Density (mgHA/cm³)	-17	<0.01	-18	<0.003
Ct Area (mm²)	-17	<0.01	-19	<0.02
Ct Density (mgHA/cm³)	-4	<0.05	-4	0.13
Ct Thickness (mm)	-18	<0.009	-20	<0.03
Tb Area (mm²)	+9	0.13	+9	0.12
Tb Density (mgHA/cm³)	-20	<0.04	-18	<0.006
Tb Number (1/mm)	-14	<0.05	-8	0.14
Tb Thickness (mm)	-7	0.17	-13	<0.009
Tb Separation (mm)	+26	<0.04	+12	0.08
Heterogeneity (mm)	+44	0.09	+11	0.33
Whole bone stiffness (kN/mm)	-16	<0.03	-16	<0.003

Microarchitecture in women with CKD with and without FX (% difference)

Disclosures: Emily Stein, None.

SA0002

See Friday Plenary Number FR0002.

SA0003

See Friday Plenary Number FR0003.

SA0004

Assessment of C3-Epi-25-Hydroxyvitamin D concentration in adult serum: LC-MS/MS determination using [²H₃] 3-epi-25OHD₃ internal standard and NIST traceable commercial 3-epi-25OHD calibrators. <u>Jonathan Tang</u>*[1], <u>Christopher Washbourne</u>[2], <u>Isabelle Piec</u>[3], <u>William Fraser</u>[2]. [1]University of East Anglia, Norwich, UK, United Kingdom, [2]University of East Anglia, United Kingdom, [3]BioAnalytical Facility, University of East Anglia, United Kingdom

Background: The C-3 Epimer of 25 Hydroxyvitamin D_3 (3-Epi-25OHD₃) is produced in the liver by the epimerisation pathway of 25-hydroxy vitamin D_3. It differs from 25OHD₃ in configuration of the hydroxyl group at the third carbon (C-3) position. Despite the fact that little is known regarding its clinical significance, concerns have been raised that isobaric interference may result in over-estimation of total 25OHD when measured by liquid chromatography tandem mass spectrometry (LC-MS/MS).

Objective: The aim of the study was to assess the occurrence of 3-Epi-25OHD₃ in adult serum samples. A LC-MS/MS technique was developed to resolve and quantify 3-Epi-25OHD₃ from 25OHD₃. The newly available NIST (SRM972a) traceable 3-Epi-25OHD commercial standards were used to ensure assay accuracy.

Method: Serum was precipitated with zinc sulphate and acetonitrile containing [²H₃]-3-epi-25OHD₃ as internal standard. The extract was chromatographed using a 2.6µm 100 x 2.1mm I.D. solid core particle column. Mass detection and quantification were performed by positive electrospray ionization with MS/MS in multiple reaction monitoring mode.

Results: The method was able to fully resolved 3-Epi-25OHD₃ from 25OHD₃. The intraassay CVs for the epimer were 6.3% and 4.1% at 25.4 and 62.1 nmol/L respectively; and interassay CVs were 8.3% and 6.5% at 27.6 and 63.2 nmol/L, respectively. In our sample cohort with 25OHD₃ ranged between 3.4 – 165 nmol/L, 3-Epi-25OHD₃ was detected in 91.9% of samples (mean = 3.8 nmol/L). No detectable 3-Epi-25OHD₂ was found in our sample study. One patient sample had total 25OHD₃ of 187 nmol/L that was shown to contain 141 nmol/L of 25OHD₃ and 44 nmol/L of 3-Epi-25OHD₃. This patient was receiving a high dose of vitamin D supplementation.

Conclusion: Using [²H₃]-3-epi-25OHD₃ as internal standard and NIST aligned calibrators enabled us to obtain an accurate assessment of 3-epi-25OHD concentration in adult serum. Although the concentration of serum 3-epi-25OHD₃ was found to be low the presence was observed in the majority of our samples. The findings in this study showed that 3-epi-25OHD₃ contributed to the overestimation of 25OHD₃ that could potentially resulted in misinterpretation of total vitamin D status.

Disclosures: Jonathan Tang, None.

SA0005

Vitamin D and Calcium Supplement Diminish Bone Pain and Improves Self-Rated Health in Pre-menopausal Vitamin D Deficient Patients. <u>Darshana Durup</u>*[1], <u>Peter Schwarz</u>[2], <u>Lona Christrup</u>[1], <u>Bent Lind</u>[3], <u>Anne-Marie Heegaard</u>[4]. [1]Department of Drug Design & Pharmacology, Faculty of Health & Medical Sciences, University of Copenhagen, Denmark, [2]Glostrup Hospital, Denmark, [3]The Elective Laboratory of the Capital Region, Denmark, [4]Faculty of Health & Medical Sciences, University of Copenhagen, Denmark

Purpose: The aim was to 1) quantify and 2) characterize bone pain in vitamin D deficient pre-menopausal women suffering from bone pain. Furthermore, to investigate the effect of vitamin D and calcium treatment on bone pain and self-evaluated health. Hopefully this will help with earlier diagnosing of vitamin D associated bone pain, which can be very disabling without proper treatment

Methods: Sternum and medial tibia was subjected to mechanical stimuli using computer connected pressure algometry with electronic VAS allowing continuous measurement. Pressure pain threshold was the first pressure pain endpoint. Moderate to severe pain (VAS 7) was the second endpoint. Two probe sizes were used; 1 cm2 (diameter: 10 mm), which is the most widely used in the literature and a smaller 0.03 cm2 (diameter: 2 mm) that has shown to have least influence from skin nociceptors. Characterization of the pain was estimated using pain and health questionnaires (McGill Pain Questionnaire, Brief Pain Inventory and SF-36). Patients were tested and filled out questionnaire at baseline and additional after 1, 3, 6 and 12 month on vitamin D (76 µg/day) and calcium (800 mg/day) treatment

Results: Pressure pain threshold was significantly lower in 22 vitamin D deficient patients, both with the bigger probe at medial tibia: 130 mN (SD 90) vs. 405 mN (SD 180) (p < 0.0001) and sternum: 77 mN (SD 47) vs. 146 mN (SD 73) (p < 0.001) and with the smaller probe at medial tibia: 75 mN (SD 37) vs. 101 mN (SD 41) (p < 0.05) and sternum 51 mN (SD 30) vs. 92 (SD 43) (p < 0.001). Moderate to severe pain was also experienced at lower pressure levels. Serum 25-hydroxyvitamin D and parathyroid hormone normalized after 1 month on vitamin D and calcium supplement and an increase in pressure pain threshold was observed but never raised to the same level as the control group. Self-rated health assessed by SF-36 was poorer in all dimensions (p < 0.0001). The most frequently chosen pain words were tingling, taut and tiring

Conclusions: Vitamin D deficient pre-menopausal patients suffering from bone pain had lower pressure threshold. The bone pain was characterized as tingling, taut and tiring and the patients had lower self-rated health. Vitamin D and calcium supplement normalized serum 25-hydroxyvitamin D and parathyroid hormone within

a month and bone pain was diminished and quality of life was improved. However still significantly lower compared to healthy controls even after 12 month of treatment

SA0006

Is Strontium Ranelate a Therapeutic Option to Treat CRPS?. Manfred Herold*[1], Malgorzata Brunner-Palka[2]. [1]Innsbruck Medical University, Austria, [2]physician, Austria

CRPS (Complex regional pain syndrome) also referred to as reflex sympathetic dystrophy (RSD), Sudeck's atrophy or algodystrophy is a chronic painful condition with allodynia and hyperalgesia. An evidence based treatment is not known[1].

A 66-year old female was first time seen at the rheumatology unit in February 2013. She was unable to use the right hand in case of immobility in the metacarpo- and proximal interphalangeal joints and suffered from pain in the right hand. Sudeck's atrophy of the right hand was diagnosed 1995 after distal radius fracture. Several therapeutic interventions including physical therapy had been tried without success. Chronic pain remained and immobility was rapidly progressing.

Strontium ranelate 2 grams daily orally was started immediately. Fingertip hand distance, SF-SACRAH[2] and a visual analogue scale (VAS) of 100 mm (0=no pain) were used to document disease activity.

Already 6 weeks after first intake of strontium ranelate first improvements were reported. At the last visit in May 2014 the fingertip hand distance was 7 mm (70 mm at the beginning) and the right hand could again be used for easy working. According to the clinical improvement since February 2013 SF-SACRAH decreased from 6,2 to 2,0 and VAS from 80 to 22 mm.

CRPS is difficult to treat and usually results with major disability and pain. With strontium ranelate we observed an impressive improvement in hand motion, increase in functionality and decrease of pain. We suppose that the effect is based on strontium ranelate's dual mechanism of action with increasing bone formation and decreasing bone resorption.

Literature:

1 O'Connell NE et al. Cochrane Database Syst Rev. 2013 Apr 30;4. doi: 10.1002/14651858.CD009416.pub22 Rintelen B et al. Osteoarthritis Cartilage. 2009;17:59-63

SA0007

See Friday Plenary Number FR0007.

SA0008

Evaluation of Serum Sclerostin in Postmenopausal Women with Type 2 Diabetes Mellitus. Larissa Pimentel*[1], Francisco Bandeira[2], Sirley Vasconcelos[3], Luiz Griz[4], Vanessa Machado[5]. [1], Brazil, [2]University of Pernambuco, Brazil, [3]Hospital Agamenon Magalhães - Recife, Brazil, [4]Endocrinology & diabetes Uinit of Agamenon Magalhães Hospital, University of Pernambuco, Recife-PE-Brasil, Brazil, [5]Endocrinology & Diabetes Unit of Agamenon Magalhães, Brazil

Introduction: In type 2 diabetes mellitus (T2DM) there is an increased risk of fractures despite the elevated bone mineral density values. Several mechanisms have been proposed to explain the effect of glycemia control on bone. Few studies have evaluated serum sclerostin levels in patients with T2DM. The sclerostin is involved in the signaling pathway Wnt / β –catenin, which regulates the gene transcription essential for osteoblast cells. The study of this pathway led to the subsequent discovery of inhibitors of Wnt signaling secreted by osteocytes. These include sclerostin (SCL) and Dickkopf protein 1 (DKK1), which block the binding of the Wnt protein 5 to the related lipoprotein receptor (LDL -5) , thereby inhibiting osteoblastic stimulation.

Methods: This is a cross-sectional study comprising a population of 57 postmenopausal women with T2DM to evaluate serum sclerostin levels and correlate them to a control group of healthy young individuals. Serum sclerostin levels were assessed using a quantitative sandwich ELISA from Biomedica (Biomedica Gruppe, Vienna, Austria), with intra-assay and interassay value coefficients of 4 and 5.5%, respectively. This assay uses a polyclonal goat antihuman sclerostin antibody as a capture antibody and a biotin-labeled mouse monoclonal antisclerostin antibody for detection. Control and patient samples were run together.

Results: Mean age was 62,89 $\pm$ 8,9 years; duration of T2DM:12.99 9 $\pm$ 19 years; BMI: 30.16 $\pm$ 4.8 kg/m2; abdominal circumference: 103.11 $\pm$ 13.01cm; HDL-C : 51.19 $\pm$ 10.59mg/dL; LDL-C 118.63 $\pm$ 4.89; fasting plasma glucose 154.96 $\pm$ 74.17mg/dL; HBA1c:14.06 $\pm$ 2.94%; 25OHD 25.74 $\pm$ 11ng/dL. The mean age of the control group was 27.6 $\pm$ 3.6 years. Fifty percent of T2dm patient had SCL above the upper limit of normal. The mean serum sclerostin was 29.14 $\pm$ 12.29 pmol/L in the postmenopausal women with T2DM and 23.50 $\pm$ 6.62 pmol/L in the control group (p=0.031).

Conclusion: Our data demonstrated that T2DM patients have higher serum SCL concentrations and it may contribute to bone quality deterioration and an increased fracture risk.

SA0009

Progressive diffuse osteosclerosis in systemic lupus erythematosus. Nuria Guanabens*[1], Steven Mumm[2], Laia Gifre[3], Silvia Ruiz-Gaspà[4], Michael P. Whyte[5]. [1]Universitat De Barcelona, Spain, [2]Washington University School of Medicine, USA, [3]Hospital Clinic Barcelona, Spain, [4]CIBERehd. IDIBAPS, Spain, [5]Shriners Hospital for Children-Saint Louis, USA

Diffuse osteosclerosis is an unusual radiographic finding. We report a 38-year-old woman with idiopathic progressive diffuse osteosclerosis (PDO) of the central skeleton and focal sclerosis of proximal long bones. Systemic lupus erythematosus (SLE) was diagnosed in adolescence, and then well controlled. She had no history of intravenous drug abuse or hepatitis C, never fractured or taken antiresorptive therapy, and her family had low bone mass. Her first BMD measurement by dual photon absorptiometry was at age 17 years when she was receiving glucocorticoid treatment. Her lumbar BMD then was 79% of average age-matched normal values. Subsequent DXAs showed increasing lumbar BMD Z-scores (from +3.8 to +7.9), and increasing femoral neck BMD Z-scores from -1.1 to -0.7 from age 30 to 37 years. Serum calcium and phosphate levels were normal, with low urinary calcium excretion perhaps reflecting her positive bone balance. Serum 25OHD was <20 ng/mL and PTH slightly increased. eGFR was 41 – 48 mls/min. Serum multiplex biomarker profiling (SMBP) indicated normal bone remodeling (bone ALP, osteocalcin, sCTX, and TRAP5b were normal), without disturbances in levels of RANKL, OPG, FGF-23 or TGFb1. However, serum sclerostin was high (1241 pg/mL) (see Figure), as were matrix metalloproteinases MMP-3 (52 ng/mL) and MMP-7 (2126 pg/mL). Bone marrow biopsy revealed increased numbers of trabeculae and reticulum fibrosis in some areas, but no collagen fibrosis. Undecalcified transiliac bone showed increased numbers of thick trabeculae, few osteoclasts, absence of peritrabecular fibrosis, and scarce and irregular unmineralized osteoid with single diffuse fluorescent labels. Mutation analysis of LRP5 and SOST was negative. Our patient with SLE and PDO of unknown etiology showed increased circulating sclerostin in the absence of overt alterations in biochemical indices of bone remodeling, and no mutations in two candidate genes. Perhaps resistance to sclerostin accounts for her bone acquisition.
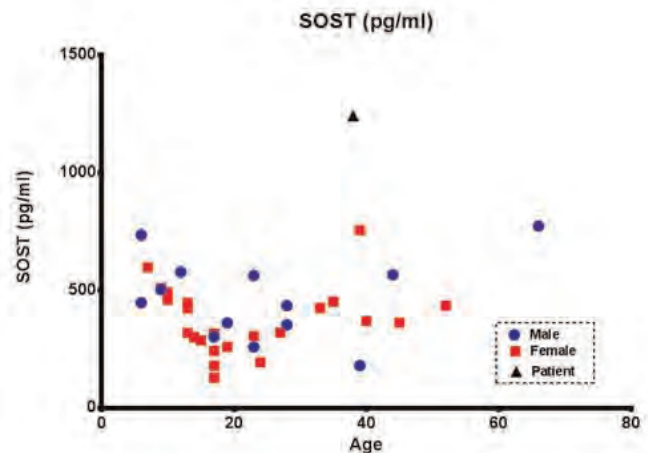
Serum sclerostin level in the patient and healthy controls

SA0010

See Friday Plenary Number FR0010.

SA0011

Gene-gene Interactions in Paget's Disease of Bone. Sabrina Guay-Bélanger*[1], David Simonyan[2], Edith Gagnon[2], Jean Morissette[3], Jacques P. Brown[4], Laetitia Michou[5]. [1]Centre de recherche du CHU de Québec-CHUL, Canada, [2]CHU de Québec Research Centre, Canada, [3]CHU de Québec Research Centre, Canada, [4]CHU de Québec Research Centre, Canada, [5]Université Laval, Canada

Purpose: Paget's disease of bone (PDB) is a uni or plurifocal metabolic bone disorder transmitted, in one third of cases, in an autosomal-dominant mode of inheritance with incomplete penetrance. To date, only the *SQSTM1* gene has been linked to the disease, with more than 20 mutations identified so far. Overall, these mutations are present in 40% of familial cases, and 10% of unrelated patients with PDB. Several other loci have been associated with the disease in patient non-carriers of a *SQSTM1* mutation, but these single nucleotide polymorphisms (SNPs) have a minor effect on PDB. The objective of this study was to investigate gene-gene interactions in PDB to determine whether these interactions could predict the PDB phenotype in patient non-carriers of a *SQSTM1* mutation.

Methods: We selected 31 SNPs previously reported in PDB, and located in 13 different loci. Every SNP was genotyped by Sequenom or Sanger sequencing in 244 PDB patients (French-Canadian and French populations) and 293 healthy individuals (French-Canadian population), all non-carriers of a *SQSTM1* mutation. We analyzed gene-gene interactions between all SNPs combined two by two. Statistical analyses included Fisher's exact tests or Chi-square tests, followed by a logistic regression analysis to search the interactions that were significantly associated with PDB. For all tests, a *p* value ≤ 0.05 was considered statistically significant.

Results: SNPs located in *EPS8L3*, *OPG*, *OPTN*, *DKK1* ($p<0.0001$) and *RANK* ($p=0.0005$) genes interacted together within the same gene, although they were not in linkage disequilibrium. There was also interactions between *KIAA1468*, *RPL17P14* and *PIGN* genes ($p<0.0001$), all located at the *18q21* locus. We also observed an interaction between *RANK* (*18q22*) and *RPL17P14* (*18q21*) genes ($p<0.0001$). Finally, the logistic regression analysis confirmed a statistically significant interaction between two SNPs in *OPG* ($p=0.0227$), and between *RANK* and *RPL17P14* ($p=0.0424$).

Conclusion: This preliminary study supports the existence of gene-gene interactions in PDB. The functional role of these interactions remains to be studied and may contribute to the PDB phenotype in absence of *SQSTM1* mutations.

Disclosures: Sabrina Guay-Bélanger, None.

SA0012

See Friday Plenary Number FR0012.

SA0013

See Friday Plenary Number FR0013.

SA0014

See Friday Plenary Number FR0014.

SA0015

See Friday Plenary Number FR0015.

SA0016

See Friday Plenary Number FR0016.

SA0017

Vitamin D Deficiency is Less Common in Mild Primary Hyperparathyroidism. Elaine Cong*[1], Marcella Walker[2], Anna Kepley[2], Chiyuan Zhang[2], Donald McMahon[3], Shonni Silverberg[2]. [1]Columbia Presbyterian Medical Center, USA, [2]Columbia University, USA, [3]Columbia University College of Physicians & Surgeons, USA

With the widespread use of vitamin D supplements in the general population, there are reports that the prevalence of vitamin D deficiency has declined. Whether this trend is also seen in patients with primary hyperparathyroidism (PHPT) is unclear. The prevalence of vitamin D deficiency (defined by 25-hydroxyvitamin D [25OHD] ≤20 ng/ml; profound deficiency <10) and insufficiency (25OHD<30) was assessed in 2 cohorts of PHPT patients recruited over twenty years apart at the same institution.

The two cohorts included 103 patients enrolled in a longitudinal natural history study of mild PHPT between 1984 and 1991 (79% female, 86% white, 16% Hispanic,

age (mean±SD) 55±12 years, BMI 26±6 kg/m2), and a recently recruited cohort of 100 patients enrolled between 2010 and 2014 (78% female, 87% white, 17% Hispanic, age 62±12 years, BMI 28±6 kg/m2). The cohorts did not differ in gender, race, ethnicity or BMI, but the 1984-1991 cohort enrolled younger patients (p<0.002). Mean 25OHD levels were 26% higher in the recent cohort (29±10 vs. 23±10 ng/ml, p<0.0001). While 25OHD deficiency and insufficiency were very common in the older cohort (6% < 10 ng/ml; 46%≤20 ng/ml; 82%<30 ng/ml; see Table), the current cohort had a lower prevalence of vitamin D deficiency and insufficiency (4%<10 ng/ml; 20%≤20 ng/ml; 54%<30ng/ml). Notably, none of the patients in the 1984-1991 cohort took vitamin D supplements, while 64% of the current cohort (and 80% of those with 25OHD>30 ng/ml) were taking vitamin D upon presentation (mean dose 1414±1489 IU/day [range 71-7143 IU]). The 1984-1991 cohort also had 35% higher PTH levels (127±69 vs. 83±41 pg/ml, p<0.0001), while serum calcium levels did not differ (10.6±0.6 vs. 10.7±0.6 mg/dl, p=0.13).

In summary, over the last two decades, the prevalence of vitamin D deficiency in patients with mild PHPT in the northeastern United States has declined by over 50%, while vitamin D insufficiency has decreased by over 30%. Today approximately half of our patients present with 25OHD levels >30 ng/ml. These changes are likely due to vitamin D supplementation. Vitamin D deficiency is thought to exacerbate PHPT. In our older cohort, the PTH elevations due to PHPT were most likely heightened by coexisting vitamin D deficiency. We conclude that differences in vitamin D status may underlie the observed 35% lower PTH concentration in the more recent, more vitamin D replete cohort of patients with mild PHPT.

Measurement (Mean±SD)	1984-1991 Cohort (N=103)	2010-2014 Cohort (N=100)	P-value
25OHD<10 (N/%)	10 (6%)	4 (4%)	0.55
25OHD (ng/ml)	7±2.5	8.3±1.5	0.28
PTH (pg/ml)	185±113	121±41	0.32
25OHD≤20 (N/%)	47 (46%)	20 (20%)	<0.0001
25OHD (ng/ml)	15±28	13.8±0.5	0.05
PTH (pg/ml)	148±76	111±36	0.05
25OHD<30 (N/%)	84 (82%)	54 (54%)	<0.0001
25OHD (ng/ml)	19±9	21±7	0.03
PTH (pg/ml)	132±74	92±44	0.0009

Prevalence of Vitamin D Deficiency and Insufficiency in Two PHPT Cohorts

Disclosures: Elaine Cong, None.

SA0018

A Novel Model to Predict Bone Mineral Density (BMD) in Cerebral Palsy (CP) Patients. Abdulhafez Selim*[1], Abeer Hegazy[2]. [1]Center for Chronic Disorders of Aging, PCOM, USA, [2]Agoza Rehabilitation Center, Egypt

Poor growth and nutrition in children with CP is a complex problem. Babies with CP may not gain weight at the same rate as other babies at their age. Multiple aspects of skeletal growth and development, including skeletal maturation, are frequently altered in children with moderate to severe CP. It is highly likely that certain growth pattern combinations are at high risk of developing severe osteoporosis. Clinicians need to able to predict those subgroups at high risk in order to prevent serious osteoporosis-related complications.

A cross-sectional study was conducted in order to study the correlation and interaction between various risk factors. The study included thirty patients with CP of both genders, between 5 and 8 years of age. Case record forms were used to capture full medical history. Full general medical and neurological examination was conducted for the selected group during the first visit. Evaluation of anthropometric measures including height weight and body mass index was also conducted. Patients were graded according to the Gross Motor Functional Classification (GMFC) for their level of affection. The current BMD scores were obtained using DXA scans. The collected data was organized, tabulated, and then analyzed.

A significant negative correlation was observed between the weight percentile rank and the BMD scores (0.8, P-value <0.001). On the other hand, a strong positive correlation was observed between quantitative values of calcium levels and the BMD Z scores (0.6, P-value = 0.001). Several other significant positive and negative correlations were also observed. Below normal BMI, height, severe spasticity, scoliosis, epilepsy, grade 4 GMFC, and anti-epileptic drugs had significant negative correlations with the BMD scores. Interaction analyses demonstrated that combination of more than two of these risk factors was associated with very low BMD (< -3.0). Regression analysis yielded a novel model to predict the BMD score in those patients. The model is based on the serum calcium and weight ranking data. The model is demonstrating high accuracy with p-value of 0.001. This model may provide a good tool to predict the BMD scores in those patients. This model had several advantages: quick, cheap, and without risk of radiation exposure.

Disclosures: Abdulhafez Selim, None.

SA0019

Accuracy of MRTA Measurements of Ulna Bending Stiffness and Strength in Cadaveric Human Arms. <u>Lyn Bowman</u>*, <u>Emily R. Ellerbrock</u>, <u>Gabrielle C. Hausfeld</u>, <u>Margeaux J. Dennis</u>, <u>Timothy D. Law, Jr.</u>, <u>John R. Cotton</u>, <u>Anne B. Loucks</u>. Ohio University, USA

Osteoporosis is characterized by reduced bone strength, but no medical device measures bone strength directly *in vivo*. Bone strength and stiffness are strongly associated ($r \geq 0.95$), but no clinical method measures bone stiffness in vivo either. The reference method for directly measuring bone stiffness and strength is Quasistatic Mechanical Testing (QMT), but QMT cannot be employed *in vivo*.

Type 2 osteoporosis affects cortical bone, where 80% of fractures in men and women after age 60 occur. Cortical bone comprises 95% the shafts of long bones, the mechanics of which are well assessed by bending tests. Mechanical Response Tissue Analysis (MRTA) is a minimal-risk, non-invasive, radiation-free, vibration analysis technique for making immediate, direct, functional measurements of the bending stiffness of long bones in humans *in vivo*. MRTA systems have been used for research for more than 25 years, but are not commercially available and little has been published about their accuracy.

To compare bones of different length (L), bending stiffness (k_B) is converted to flexural rigidity ($EI = k_B \times L^3/48$). Recently, we reported that the relationship between our MRTA and QMT measurements of EI were indistinguishable from the identity line in artificial human ulnas ($R^2 = 0.999$) and in cadaveric human ulnas *in vitro* ($R^2 = 0.99$), and that our MRTA measurements of EI in cadaveric human ulnas *in vitro* accurately predicted QMT measurements of bending strength (Strength = $18.1 \times$ EI_MRTA, $R^2 = 0.99$, SEE = 63 N). Here we report how our MRTA measurements of ulna EI in cadaveric human arms *in situ* are related to QMT measurements of ulna EI and bending strength.

20 cadaveric human arms from men and women age 48 to 96 yrs with BMI 14 to 40 kg/m^2 were obtained from a human tissue bank. Ulna EI was measured by MRTA *in situ*, and ulna EI and bending strength were measured by QMT *in vitro*. Ulnas were supported over the same span and centrally loaded in both tests.

The relationship between ulna EI_MRTA *in situ* and EI_QMT *in vitro* (Figure 1) was steeper than the identity line ($p = 10^{-4}$): EI_MRTA = $1.24 \times$ EI_QMT ($R^2 = 0.99$), but EI_MRTA still predicted ulna bending strength (Figure 2): Strength = $14.8 \times$ EI_MRTA, $R^2 = 0.99$, SEE = 71 N. We conclude that *in situ* the ulna is stiffened by other tissues, perhaps the radius bone via tension in the interosseous ligament. Nevertheless, MRTA measurements of ulna EI *in situ* accurately predict ulna bending strength measured by QMT.
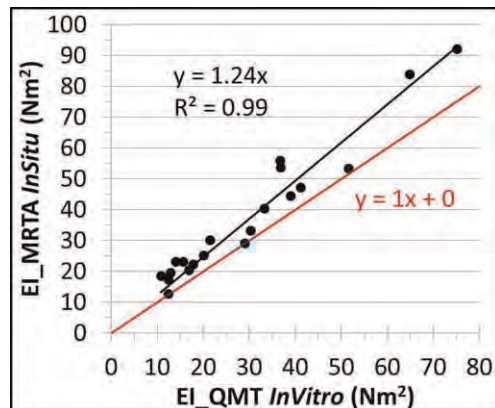
Figure 1. Ulna EI_MRTA in situ vs EI_QMT in vitro
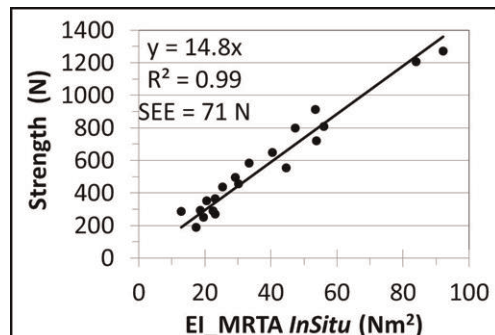
Figure 2. Ulna Strength vs EI_MRTA in situ

Disclosures: Lyn Bowman, *None.*

SA0020

See Friday Plenary Number FR0020.

SA0021

Age-related changes in bone biomechanical parameters in African ancestry men. <u>Pallavi Jonnalagadda</u>*[1], <u>Ryan Cvejkus</u>[2], <u>Joseph Zmuda</u>[3], <u>Clareann Bunker</u>[2], <u>Yahtyng Sheu</u>[3], <u>Alan Patrick</u>[4], <u>Christopher Gordon</u>[5], <u>Victor Wheeler</u>[4]. [1]Pitt Public Health, University of Pittsburgh, USA, [2]University of Pittsburgh, USA, [3]University of Pittsburgh Graduate School of Public Health, USA, [4]Tobago Health Studies Office, Trinidad & tobago, [5]McMaster University, Canada

Very little is known about the patterns and correlates of skeletal changes with aging in men of African ancestry. The purpose of these analyses was to examine the annualized percentage changes in bone strength parameters in 1608 African ancestry men aged 40 years and over during an average follow-up period of 6.2 years. We measured changes in axial stress strain index (SSIx) and polar stress strain index (SSIp) using quantitative computed tomography at the 4% and 33% sites in the radius and tibia corresponding to trabecular and cortical bone respectively. There was a 0.31% (IQR: -0.9 to 0.19) and 0.08% (IQR: -0.53 to 0.34) decrease every year in SSIp at the 4% and 33% radial sites respectively ($p < 0.0001$). The annual decrease in radial SSIx was 0.62 % (IQR: -1.37 to 0.12) and 0.1% (IQR: -0.68 to 0.49) at the 4% and 33% sites respectively ($p < 0.001$). In the tibia, there was a 0.58% (IQR: -1.15 to -0.12) and 0.33% (IQR: -0.82 to 0.02) decrease every year in SSIp at the 4% and 33% sites respectively ($p < 0.0001$). The annual decrease in SSIx in the tibia was 0.65% (IQR: -1.29 to -0.06) and 0.37% (IQR: -0.85 to 0.02) at the 4% and 33% sites respectively ($p < 0.0001$). Age at baseline was negatively correlated with the rate of decline in all biomechanical parameters in both limbs at the trabecular sites. In contrast, age at baseline was not correlated with any biomechanical parameters at the cortical sites. We conclude that advancing age is associated with an accelerated rate of decline in trabecular but not cortical bone strength parameters in African ancestry men.

Disclosures: Pallavi Jonnalagadda, *None.*

SA0022

An Exploratory Study on Bone Densitometric and Micro-Architectural Changes During Distal Radius Fracture Healing: the Fractured vs. the Non-Fractured Region. <u>Joost De Jong</u>*[1], <u>Paul Willems</u>[2], <u>Jacobus Arts</u>[2], <u>Sandrine Bours</u>[3], <u>Peter Brink</u>[4], <u>Piet Geusens</u>[5], <u>Bert van Rietbergen</u>[6], <u>Joop van den Bergh</u>[7]. [1]Maastricht University Medical Center, The Netherlands, [2]Department of Orthopaedics & CAPRHI, Maastricht University Medical Center, Netherlands, [3]Department of Internal Medicine, Maastricht University Medical Center, Netherlands, [4]Department of Surgery, Maastricht University Medical Center, Netherlands, [5]Department of Internal Medicine & CAPHRI, Maastricht University Medical Center, Netherlands, [6]Faculty of Biomedical Engineering, Eindhoven University of Technology, Netherlands, [7]Department of Internal Medicine & NUTRIM, VieCuri Venlo & Maastricht University Medical Center, Netherlands

High resolution peripheral quantitative computed tomography (HR-pQCT) is a promising tool to assess in vivo metaphyseal fracture healing.[1,2] However, subtle changes in bone density and micro-architecture parameters in the fracture region might be averaged out if the whole distal radius is assessed.[1] A more localized approach in which the region of interest (ROI) only covers the fracture line is therefore desired. The purpose of this exploratory study is to test a novel algorithm that enables the automatic detection and separate analyses of the fractured and non-fractured region.

In 6 post-menopausal women with a stable distal radius fracture, treated by cast immobilization, HR-pQCT images of the fracture were obtained at 1-2 (baseline), 3-4, 6-8 and 12 weeks post-fracture. The fractured region was identified automatically as the region in which low mineralized bone was present in the HR-pQCT images at 6-8 week post-fracture (Fig. 1). The remaining region within the periosteal boundary was selected as non-fractured region. Both ROI's were transposed on the images at 1-2, 3-4 and 12 weeks post-fracture. Standard bone mineral density (BMD) and micro-architectural parameters were calculated for the total, fractured and non-fractured region at each visit. A linear mixed-effect model was used to test whether parameters significantly changed from baseline.

In the fractured region, the percent changes from baseline peaked at 6-8 weeks post-fracture: total BMD was increased by 29% (p=0.02); trabecular BMD, number and thickness were increased by 60%, 33% and 22%, respectively; and trabecular separation was decreased by 34% (all $p \leq 0.01$). Cortical thickness did not change significantly. In the total region, percent changes from baseline did not reach significance at any time-point for all parameters, except total and trabecular BMD at 3-4 wks post-fracture with 8% and 6%, respectively. In the non-fractured region, only trabecular BMD was changed significantly at 3-4 wks post-fracture with 6%.

In addition to our previous studies[1,2] we now demonstrate that it is feasible to study the fractured and non-fractured region in distal radius fractures separately.

Changes in BMD and micro-architecture were significant and more pronounced in the fractured area compared to the total and non-fractured area. We thus expect that this approach can lead to a more accurate and sensitive evaluation of the bone healing process.

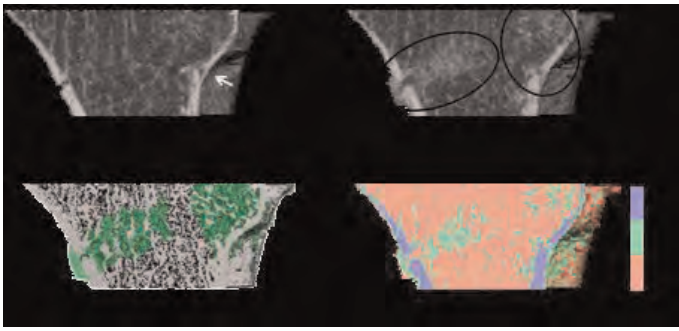[1]de Jong et al. Bone (2014)
[2]Meyer et al. JBMR (2014)

Figure 1

Disclosures: Joost De Jong, None.

SA0023

Atlas-based Correlation of Local Trabecular Directionality and Deformation with Serum Markers of Bone Turnover in Lung Transplant Recipients in a Longitudinal Setting. <u>Lukas Fischer</u>[1], <u>Alexander Valentinitsch</u>[2], <u>Thomas Gross</u>[3], <u>Daniela Kienzl</u>[1], <u>Claudia Schueller-Weidekamm</u>[1], <u>Franz Kainberger</u>[1], <u>Janina Patsch</u>[4], <u>Georg Langs</u>[1], <u>Matthew DiFranco</u>*[4]. [1]Medical University of Vienna, Austria, [2]Klinikum rechts der Isar, Technische Universität München, Germany, [3]Technical University of Vienna, Austria, [4]Medical University of Vienna, Austria

Non-invasive assessment of changes in bone microarchitecture over time can be performed by high-resolution peripheral quantitative computed tomography (HRpQCT). The aims of this pilot study were to develop a methodology for the quantification of trabecular reorganization beyond standard morphometry and to investigate the relation between trabecular reorganization, bone strength as captured by finite element analysis, and serum markers of bone turnover.

HRpQCT baseline and follow-up scans of the distal radius from lung transplant (LuTX) patients were obtained (n=33, 15 ± 5 month mean interval). Serum markers (CTX, OCN) were captured at each time point. Finite element analysis (FEA) was employed to measure stiffness (k), failure force (F_{max}), bone strength (σ_{max}). Manufacturer-provided standard bone morphology parameters were also acquired.

Baseline and follow-up scans were rigidly registered and deformation maps were obtained for each case[1]. Three parameters related to local changes in trabecular orientation and the direction of deformation were obtained: entropy of directionality (ED), entropy of Jacobian (EJ), and symmetric Kullback-Leibler divergence (KLD). All derived parameters were then correlated to the serum, FEA and morphology values on 3D grid-based regions of an atlas generated from the entire study population.

Significant (p<0.05) localized negative correlations between EJ and changes in BMD, k, F_{max} and σ_{max} were seen. OCN at baseline showed significant localized correlations with ED (negative) and KLD (positive). CTX at baseline showed localized positive correlations (non-significant) with EJ.

The OCN to ED negative correlation suggest that within the LuTX cohort, region-specific dominant trabecular directionality is observed where OCN, a formation marker, is elevated. The positive OCN to KLD correlation suggests that trabecular thickening is occurring without a decrease in dominant orientation. A positive CTX to EJ correlation could indicate that direction-independent bone loss is observed in conjunction with elevated CTX, a resorption marker.

We have proposed a methodology for discovering localized correlations between image-derived measures of trabecular reorganization and various bone metabolism, biomechanical and morphology markers. Application of this method to a LuTX cohort reveals correlations between trabecular directionality and both local systematic bone turnover and bone strength.

[1] DiFranco M. ASBMR 2013/SA0072

Corr: EJ to ΔBMD   Corr: EJ to CTX baseline   Corr: ED to OCN baseline   Corr: KLD to OCN baseline

Corr: EJ to Δk   Corr: EJ to ΔFmax   Corr: EJ to Δσmax

Figure 1: Regional maps of atlas-based correlations between derived measures of local trabecular changes and serum markers, BMD and finite element analysis parameters. A star represents statistical significance (p<0.05). Each map is based on the middle slice of the HRpQCT atlas volume (9 mm depth), and each grid region represents a 3D volume. White signifies too little information for a correlation.

Atlas-based region correlation maps

Disclosures: Matthew DiFranco, None.

SA0024

Can bone quality markers predict nonunion?. <u>Koji Nozaka</u>*[1], <u>Naohisa Miyakoshi</u>[1], <u>Michio Hongo</u>[1], <u>Yuji Kasukawa</u>[1], <u>Hiroshi Aonuma</u>[1], <u>Hiroyuki Tsuchie</u>[2], <u>Kentaro Ohuchi</u>[1], <u>Hayato Kinoshita</u>[3], <u>Chie Sato</u>[4], <u>Masashi Fujii</u>[4], <u>Yoichi Shimada</u>[4]. [1]Akita University Graduate School of Medicine, Japan, [2]Nakadori General Hospital, Japan, [3]Akita University, Japan, [4]Dept.of Orthopedic Surgery, Akita University Graduate School of Medicine, Japan

Background: The ability to predict susceptibility to nonunion would enable measures to be taken at an earlier stage, such as performance of more rigid fixation before surgery. Although low-intensity pulsed ultrasound (LIPUS) has been used for nonunion, bone union is not always achieved even with this method. While blood homocysteine (Hcy) and urinary pentosidine (Pen) levels have been reported as useful predictive markers of fracture, relationships to nonunion have not been elucidated.

Objective: To retrospectively investigate bone quality markers, specifically uncarboxylated osteocalcin (ucOC) (reference value, <4.50 ng/ml), blood Hcy (reference range, 3.7-13.5 nmol/ml), and urinary Pen (reference range, 0.019-0.070 μg/mg?Cr) in patients with nonunion and to clarify relationships to nonunion.

Subjects: Subjects comprised 26 patients (18 men, 8 women; mean age, 55.7 years; range, 29-84 years) who underwent additional treatment due to lack of porosis with LIPUS alone among the 63 patients who provided consent for measurement of bone quality markers among the 278 patients who underwent LIPUS for nonunion after osteosynthesis (Exclusions: diabetes, renal failure, steroid use, warfarin use, infections, fracture gap distance ≥9 mm).

Results: Elevated levels of bone quality markers were seen in all 26 patients, with elevated ucOC in 8 patients (mean, 6.91 ng/ml), Hcy in 10 (mean, 16.4 nmol/ml), and Pen in 18 (mean, 0.089 μg/mg?Cr)(including cases of overlap). Additional pharmacotherapy (e.g., PTH drug, vitamin K2, vitamin B12, etc.) was given to all 26 patients, and bone union tended to progress in many patients. In addition, further surgery was performed for 8 patients and combination with electric stimulation therapy was given for 2 patient.

Discussion: Management of nonunion involves many factors. However, causes of nonunion are often unclear. Bone quality markers may serve as predictors of nonunion. For further investigation, a comparison study with the group who had bone union with LIPUS alone is necessary.

Disclosures: Koji Nozaka, None.

SA0025

Characterization of Bone Quality in Rat Femur Performed Combination Therapy with PTH$_{1-34}$ and Vitamin K$_2$ Using FTIR Imaging. <u>Teppei Ito</u>*[1], <u>Tomohiro Shimizu</u>[2], <u>Masahiro Todoh</u>[3], <u>Masahiko Takahata</u>[4], <u>Hiromi Kimura-Suda</u>[1]. [1]Chitose Institute of Science & Technology, Japan, [2]Department of Orthopedic Surgery, School of Medicine, Hokkaido University, Japan, [3]Division of Human Mechanical Systems & Design, Faculty of Engineering, Hok kaido University, Japan, [4]Hokkaido University, School of Medicine, Japan

Teriparatide (PTH$_{1-34}$) has been shown to increase bone mass and promote skeletal repair, and vitamin K has been known to affect bone mineralization. We previously demonstrated that vitamin K influenced the efficacy of PTH$_{1-34}$ therapy for bone repair using a rat osteotomy model: The combination therapy with PTH$_{1-34}$ and vitamin K$_2$ improved mechanical properties and the bone mineral tissue density of fracture callus of the femur after the surgery. There are few reports written about the relationship between recovery of mechanical strength and bone quality in the skeletal site; however, the bone strength is determined by bone density and bone quality. In

this study, bone quality of the femur in the osteotomy model performed the combination therapy with PTH_{1-34} and Vitamin K_2 was characterized using FTIR imaging to investigate consequence for the bone strength. Twelve-week-old female Sprague-Dawley rats underwent a mid-shaft transverse femoral osteotomy were divided into four groups: Vehicle, PTH_{1-34} (daily 30 µg/kg/day subcutaneous injection) + solvent (p.o., three times a week), PTH_{1-34} + warfarin (0.4 mg/kg/day p.o., three times a week), and PTH_{1-34} + vitamin K_2 (menatetrenone, 30 mg/kg/day p.o., three times a week). The rats were subjected to the combination therapy for 8 weeks after the surgery, and then the femur was removed after euthanasia and was embedded in PMMA to prepare long-axial cross section for FTIR imaging. In three point bending test, the bone strength of the femur was determined in the following order: PTH_{1-34} + vitamin K_2 > PTH_{1-34} + solvent > PTH_{1-34} + warfarin > Vehicle. In FTIR images, the calcification of the femur underwent therapy with PTH_{1-34} + vitamin K_2 was higher than that of other groups, and the crystallinity of all PTH administrated groups slightly showed high level. The carbonate to phosphate ratio and the collagen cross-linking did not differ significantly between groups. The tendency of the bone strength was not coincident with that of the calcification, the crystallinity, the carbonate to phosphate ratio, and the collagen cross-linking. However, the collagen orientation was determined by FTIR imaging in the following order: PTH_{1-34} + vitamin K_2 > PTH_{1-34} + solvent > PTH_{1-34} + warfarin > Vehicle. We demonstrated that the collagen orientation significantly affected the bone strength in the rat osteotomy model.

SA0026

See Friday Plenary Number FR0026.

SA0027

See Friday Plenary Number FR0027.

SA0028

Discriminants of Prevalent Fragility Fractures in Chronic Spinal Cord Injury.
William Edwards*[1], Narina Simonian[2], Karen Troy[3], Thomas Schnitzer[4]. [1]University of Calgary, Canada, [2]Northwestern University, USA, [3]Worcester Polytechnic Institute, USA, [4]Northwestern University, USA

Spinal cord injury (SCI) is characterized by marked bone loss at regions below the neurological lesion. Within the first 2 to 3 years of SCI, some 50% of the bone mineral at the distal femur and proximal tibia is resorbed. The clinical consequence of this bone loss is a high incidence of low-energy fractures, most commonly observed at regions of the knee. Our purpose in this study was to identify and quantify clinical and bone-specific parameters that would discriminate prevalent fracture in chronic SCI.

Forty-two adults with SCI from 2.8 to 50.0 yrs of duration were recruited as part of a larger prospective intervention trial. Prior to treatment, computed tomography data were acquired for the proximal most 15cm of the non-dominant tibia. Bone mineral content (BMC) and volumetric bone mineral density (vBMD) were determined. Proximal tibia torsional strength (T_{ult}) was quantified using validated patient-specific finite element modeling procedures. The cause, location, and time of any lower-extremity fragility fractures that had occurred after SCI, and prior to treatment, were verified through medical records. The ability of SCI level and severity, BMC, vBMD, and T_{ult} to classify groups with and without fractures was determined using discriminant analyses.

Of the 42 participants, 14 had at least one prevalent fracture of the lower-extremity. The mean duration of SCI prior to first fracture was 15.8 yrs (range 3-38 yrs). SCI level and severity were not significant discriminants of individuals with and without prevalent fractures. The overall independent classification accuracy for T_{ult}, BMC, and vBMD were 71.4%, 69.0%, and 61.9%, respectively. On average, T_{ult} values were 33% lower for individuals with fractures compared to individuals without fractures (Figure 1). BMC and vBMD values were 25% and 17% lower for individuals with fractures compared to individuals without fractures. In summary, measures of bone mineral and strength, but not SCI level or severity, were significant discriminators of prevalent lower-extremity fragility fractures in individuals with chronic SCI. These preliminary findings suggest a critical need for the assessment of bone mineral and strength after SCI, which is currently not the standard of care for this population. Recruitment for our prospective intervention trial is still ongoing, and we anticipate that larger numbers of participants will allow us to more accurately predict individuals at high risk for fracture after SCI.

Figure 1. Mean ($\pm$95% CI) T_{ult} for the no fracture and prevalent fracture groups.
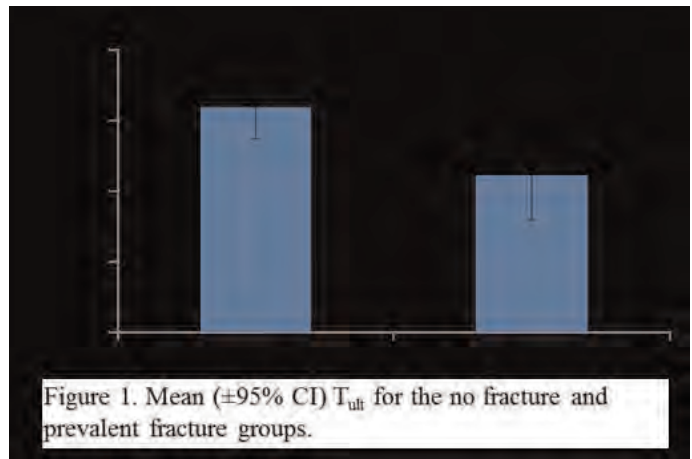
Figure 1

SA0029

Effect of Variations in Tissue-Level Ductility on Femoral Strength. Shashank Nawathe*[1], Nasim Barzanian[2], Mary Bouxsein[3], Tony Keaveny[4]. [1]University Of California at Berkeley, USA, [2]University of California, Berkeley, USA, [3]Beth Israel Deaconess Medical Center, Harvard Medical School, USA, [4]University of California, Berkeley, USA

The ductility of bone tissue, which describes the ability of bone tissue to deform before it eventually breaks and fractures, is a unique element of bone quality and varies with age and across the population. However, little is known about how typical population-variations in tissue-level ductility influence femoral strength, and whether such variations in ductility are more influential for the cortical or trabecular bone — potentially important factors in the etiology of age-related hip fractures. To provide insight, we conducted a parameter study using micro-CT-based finite element analysis of four human proximal femurs (ages 66–68 years) subjected to a sideways fall loading, each model having a voxel-element size of 82 microns and containing up to 120 million elements. For each femur, we varied the assumed value of the tissue-level ultimate strain — the strain at which tissue-level cracking and fracture occurs — and all other tissue-level properties were kept constant, including the elastic modulus (E=7.3 GPa) and yield strains (0.81% in compression; 0.33% in tension). Nine combinations of tissue ultimate strains were simulated for each femur: the mean value and the mean $\pm$ 1SD value, separately for the cortical (2.2$\pm$0.9%; McCalden, JBJS, 1993) and trabecular (8.8$\pm$3.7%; Hernandez, Bone, 2005) bone. Using non-linear finite element analysis, the strength of each femur, for each of the nine cases of tissue-level ductility, was defined as the maximum force from the computed force-deformation curve. Across the four bones, there was only a 10–12% variation in the femoral strength when the cortical and trabecular bone tissue ultimate strains were simultaneously varied by $\pm$ 1 SD about their mean values (Figure). Altering only the cortical ultimate strain by $\pm$1 SD about its mean varied the femoral strength by 4$\pm$1%, whereas, a $\pm$1 SD variation in only the trabecular tissue ultimate strain altered the femoral strength by 7$\pm$1%. These results indicate that typical population variations in tissue-level ductility account for only 10–12% of femoral strength during a sideways fall, typical variations in trabecular ductility having a larger effect than typical variations in cortical ductility. Given that femoral strength can vary multiple-fold at any age across the population due to variations in bone geometry and mass, these effects are relatively modest. However, it remains to be seen if tissue-level ductility is particularly low in some individuals who fracture their hip.
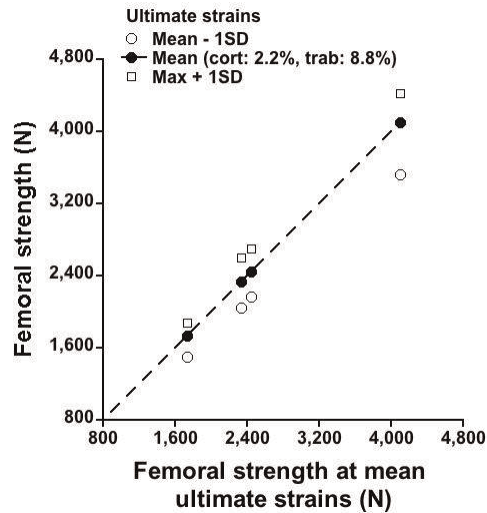
Variation in the femoral strength with simultaneous ~1 SD variation in cort & trab ultimate strains.

Disclosures: Shashank Nawathe, None.

SA0030

Glycation alters material properties of diabetic mice at multiple length scales. <u>Atharva Poundarik</u>*[1], <u>Grazyna Sroga</u>[2], <u>Mishaela Rubin</u>[3], <u>Deepak Vashishth</u>[2]. [1]Rensselaer Polytechnic University, USA, [2]Rensselaer Polytechnic Institute, USA, [3]Columbia University, USA

The ability of bone to resist fracture is determined not only by bone mineral density but also architecture and the quality of its organic extracellular matrix (ECM). Type-I collagen comprises over 90% of the organic matrix imparts bone, ductility and toughness [1]. Non-enzymatic glycation (NEG) of collagen, in the bones of aging or diabetic individuals, results in the formation of advanced glycation endproducts (AGEs). Studies have shown that non-enzymatic glycation and AGE accumulation not only deteriorates post-yield material properties but also increases stiffness and brittleness in bone. Furthermore, AGEs can increase up to five times with age, and have been strongly associated with an increased fracture risk [2].

Femora from the non-diabetic and diabetic mice (n=5-6 for each group) were harvested, notched in the anterior mid-diaphyseal region and stored in saline at -80°C prior to mechanical testing. Bending tests were done on a custom made fixture in the displacement feedback mode (Elf 3200, EnduraTEC), at cross-head rate of 0.001mm/s until fracture. The load-displacement curves were used to calculate the propagation toughness [3]. Subsequently, reference point indentation was performed on the anterior surface of the bones. This technique has recently been used to distinguish bone quality between fracture and non-fracture groups in humans [4]. Indentations were performed with a maximum applied load of 3 N for 10 cycles with a frequency of 2 Hz. Quantitative measures of indentation distance increase (IDI) were used in the analyses. Finally, a fluorescent AGE assay [2] was conducted to evaluate the presence of AGE in each the non-diabetic and diabetic group.

Fracture mechanics data showed that propagation toughness of the non-diabetic group (4.72 ± 0.79 MPa.m$^{0.5}$) was higher than the diabetic group (3.38 ± 0.58 MPa.m$^{0.5}$, p=0.012). Reference point indentation measurements revealed the indentation depth increase (IDI) in non-diabetic group ($6.84 \pm 1.07\mu$m) was greater than in diabetic group ($9.04 \pm 1.89\mu$m, p=0.033). AGE measurements showed a near significant difference between the non-diabetic and diabetic groups (p=0.072). Thus, diabetes induced post-translational modifications like AGEs, increase the propensity of fracture at multiple length scales.

References:
[1]: Wang et al. JOR, Vol. 19, 2001
[2]: Vashishth et al. Bone, Vol. 28, 2001
[3]: Takahashi, Intl J Press Vessels Pip, Vol. 79, 2002
[4]: Diez-Perez et al. Bone, Vol. 25, 2010

Disclosures: Atharva Poundarik, None.

SA0031

MRI-derived porosity index provides quantitative insight into cortical pore architecture. <u>Mahdieh Bashoor-Zadeh</u>*[1], <u>Chamith Rajapakse</u>[2], <u>Cheng Li</u>[3], <u>Wenli Sun</u>[1], <u>Mona Al Mukaddam</u>[1], <u>Alexander Wright</u>[1], <u>Felix Werner Wehrli</u>[4]. [1]University of Pennsylvania, USA, [2]University of Pennsylvania School of Medicine, USA, [3]University of Pennsylvania Health System, USA, [4]University of Pennsylvania Medical Center, USA

Small changes in cortical bone (CB) pore network exert a more pronounced influence on bone mechanical properties than do similar changes in trabecular bone. Microstructure of CB pores cannot be resolved even with the state-of-the-art human bone imaging modalities *in vivo*. Ultra-short echo time (UTE) MRI allows the assessment of CB through the detection of proton signal arising from mobile water residing in pores (pore water) and water bound to collagen matrix (bound water). The aim of our study was to develop a clinically feasible method to assess CB pore network by measuring the signal decay at only two echo times (TE) as part of a single 3D UTE MRI scan, the idea being that the first echo contains essentially all water and the second predominantly pore water.

Whole-cross section bone covering 36mm axially, centered at the site of maximum CB thickness were harvested from the tibial diaphysis of 16 cadavers (ages 27-97 years). First, the CB specimens underwent 3D UTE MRI generating images at TE=50 and 2000μs and reconstructed to isotropic 0.5mm voxel size. A porosity index (PI), defined as the ratio between a long and short-TE image intensities, was computed pixel by pixel. A segmented μCT image (8.6μm) from center of each specimen was selected. Cross sectional area of pores was calculated and averaged for each specimen. Each pore was categorized into four groups (Fig.1a). The contribution of each group to the total pore space was calculated as the ratio of area occupied by each group over total pore space area (area fraction). MRI-derived PI was compared with area fraction and average pore area derived from μCT.

Increased CB pore size is visually apparent in the μCT images of the CB obtained from older donors compared to younger donors (Fig.1a). The contribution of normal pores in total pore area decreased with age, while that of giant pores increased (Fig.1b). Average pore area was found to increase with age (R^2=0.69, Fig.2a).PI correlated positively with area fraction occupied by giant pores (R^2=0.68), and negatively with area fraction occupied by normal pores (R^2=0.78, Fig.1c). Average pore area showed strong positive association with PI (R^2=0.81, Fig.2b). The data provides compelling evidence that the age-related increase in porosity is the result of expansion of existing pores rather than creation of new pores. Data suggest that the MRI PI provides a new biomarker that provides insight into pore size distribution of CB *in vivo*.
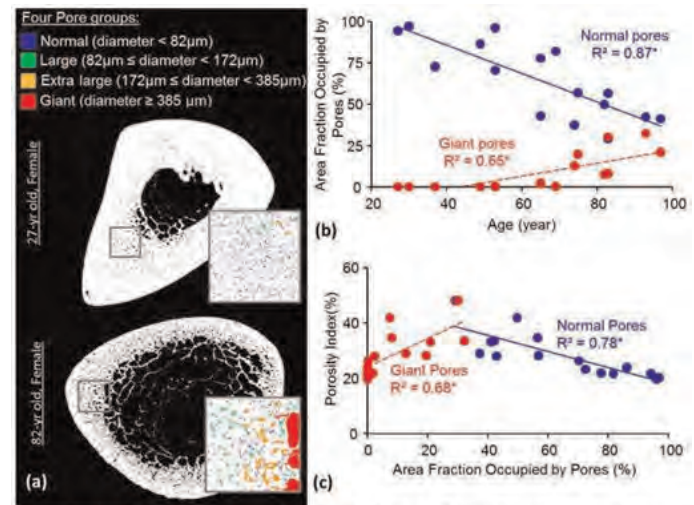

Figure1. a) μCT images obtained from cortical bone of two donors, with pore types color-coded (see magnification); b) association between age and area fraction occupied by normal and giant pores; c) correlation between porosity index and area fraction occupied by normal and giant pores (* indicates p<0.0005).
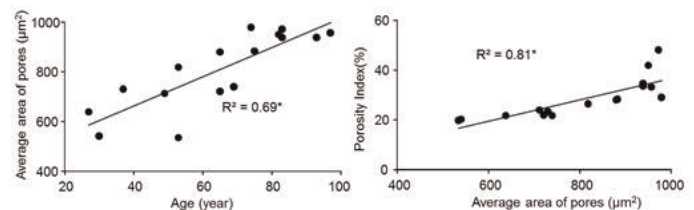
figure1.png

Figure 2. a) association between age and area fraction occupied by normal and giant pores; b) correlation between porosity index and area fraction occupied by normal and giant pores; (* indicates p<0.0005).

figure2

Disclosures: Mahdieh Bashoor-Zadeh, None.

SA0032

Nanomechanical Behavior of Extrafibrillar Matrix in Bone. Xiaodu Wang*[1], Liqiang Lin[2], Xiaowei Zeng[3], Haoran Xu[2], Anne Sheldrake[4], Jean Jiang[5]. [1]UTSA, USA, [2]Mechanical Engineering, UTSA, USA, [3]Mechanical Engineering, UTSA, USA, [4]Biomedical Engineering, UTSA, USA, [5]University of Texas Health Science Center at San Antonio, USA

In the hierarchy of bone, lamellae serve as the basic building unit for both human and animal bones. They are a sheet-like biocomposite of mineralized collagen fibrils embedded in an extrafibrillar matrix [1] and dictate, to large extent, the mechanical behavior of bone[2]. The structure and mechanical properties of mineralized collagen fibrils have been extensively studied, whereas only limited information is available regarding the role of the extrafibrillar matrix in bone mechanical behavior. In this study, a novel nanomechanical model of extrafibrillar matrix was proposed to assess its contribution to bone behavior from ultrastructural perspectives.

In this model, we assumed that the extrafibrillar matrix consists of hydroxyapatite (HA) polycrystals that are bounded through an organic interface of non-collagenous proteins (NCPs). This organic interface may facilitate relative sliding between individual mineral crystals, thereby imparting to bone more capability of dissipating energy during bone deformation and failure process. A novel cohesive finite element (FE) approach was used in this study to simulate the mechanical behavior of extrafibrillar matrix in both tension and compression modes. The polycrystals FE model was generated using Voronoi tessellation techniques with an average crystal size in the range of 22.5∼0.87nm. The inter-crystal interface was simulated using a cohesive zone model with exponential traction-separation laws for defining both opening and sliding deformation/failure at the interface.

The simulation results indicated that this model was able to capture the following behaviors of bone as reported in experimental studies [3]: 1) the maximum strain of mineral phase in both tension and compression modes observed in synchrotron X-ray scattering studies; 2) the sudden drop of strain in the mineral phase at the bulk yielding of bone under both tension and compression; 3) the cross-hatch damage (shear band) formation in compression; 4) the upper bound of the in situ elastic modulus of bone; and more importantly, 5) the effect of the organic interface integrity on the mechanical behavior of extrafibrillar matrix in bone, which was verified by testing bone specimens with and without enzyme induced interruption of organic interface in nanoscratch experiments.

In summary, the proposed model has shown a great potential in assessing the ultrastructural contributions to bone fragility.

Reference
1. Ziv, V., et al., Transitional structures in lamellar bone. Microsc Res Tech, 1996. **33**(2): p. 203-13.
2. Wang, X., et al., Cancellous bone lamellae strongly affect microcrack propagation and apparent mechanical properties: Separation of patients with osteoporotic fracture from normal controls using a 2d nonlinear finite element method (biomechanical stereology). Bone, 2008. **42**(6): p. 1184-92.
3. Giri, B., et al., In situ mechanical behavior of mineral crystals in human cortical bone under compressive load using synchrotron x-ray scattering techniques. Journal of the mechanical behavior of biomedical materials, 2012. **14**: p. 101-12.

Figures
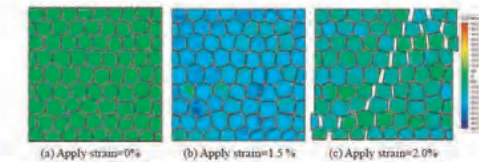
Fig 1 Deformation evolution of extrafibrillar matrix in compression from FE simulations
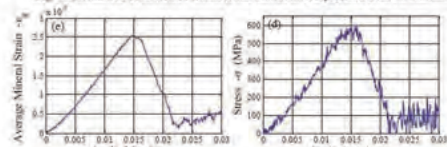
Fig 2 The measured mineral stress and strain vs. applied strain(a) strain(b) stress
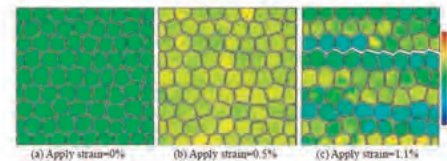
Fig 3 Deformation evolution of extrafibrillar matrix in tension from FE simulations
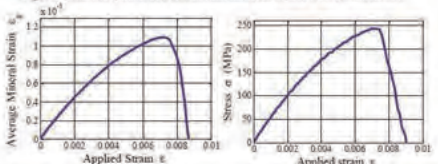
Fig 4 The measured mineral stress and strain vs. applied strain(a) stress (b) strain

References and Figures

Disclosures: Xiaodu Wang, None.

SA0033

Comparing Proximal Tibia Bone Stiffness and Structural Efficiency in Spaceflight and Hind Limb Unloading with a Sclerostin Antibody Countermeasure. Taylor Comte*[1], Anthony Lau[2], Eric Livingston[3], Rachel Ellman[4], Jordan Spatz[5], Louis Stodieck[6], Mary Bouxsein[7], Virginia Ferguson[6], Ted Bateman[8]. [1]UNC Chapel Hill, USA, [2]University of North Carolina at Chapel Hill, USA, [3]Department of Biomedical Engineering, University of North Carolina, USA, [4]Beth Israel Deaconess Medical Center, USA, [5]Harvard-MIT Division of Health Sciences & Technology (HST), USA, [6]University of Colorado, USA, [7]Beth Israel Deaconess Medical Center, Harvard Medical School, USA, [8]Univesity of North Carolina, USA

Unloading during spaceflight alters the microstructure of bone resulting in a significant reduction in bone health. Hind Limb Unloading (HLU) in mice is used to mimic microgravity conditions by suspending the mouse by the tail. Bone stiffness and structural efficiency have not been investigated in the HLU model. Finite Element Analysis (FEA) of the proximal tibia was performed on a HLU study mimicking the profile of space shuttle mission STS-135 (13-days of spaceflight). This allowed a detailed comparison of structural bone health between HLU and spaceflight in terms of bone stiffness and structural efficiency as well as their response to Sclerostin antibody (Scl-Ab).

Meshes were made from microCT Scans of 1.0mm thick cross sections of proximal tibias just inferior to the growth plate. Bone was segmented out and imported into ABAQUS for FEA to determine the stiffness and structural efficiency of the bone. The stiffness was determined by a applying a 0.5% compressive displacement on the superior face of the bone while the inferior face was constrained. The stiffness was the measured resultant force from the applied displacement, and the structural efficiency was calculated as the stiffness per amount of bone present.

HLU resulted in a decrease in BV (-17%) and Stiffness (-22%) when compared to ground control as measured by FEA. The reduction in BV (-17%) from unloading was the same as that found from spaceflight. However, spaceflight caused a greater decrease in stiffness (-34%). Scl-Ab prevented this loss of BV (+48%) and stiffness (+61%) in the HLU mice when compared to vehicle groups. Structural efficiency in the HLU vehicle group decreased a small amount (-5%) when compared to ground control, whereas the spaceflight model showed a greater decrease in structural efficiency (-22%) between the flight vehicle and ground control groups. The difference in structural efficiency from unloading can be attributed to the incomplete unloading in HLU. Future studies should investigate the mechanisms resulting in the changes in structural efficiency to further characterize differences in the HLU model and microgravity in spaceflight.

In conclusion, HLU resulted in reductions in BV and stiffness that were similar to reductions seen in the spaceflight model. Scl-Ab caused BV and stiffness to increase similar to the spaceflight model. In addition, HLU resulted in a smaller reduction in structural efficiency compared to the spaceflight model.
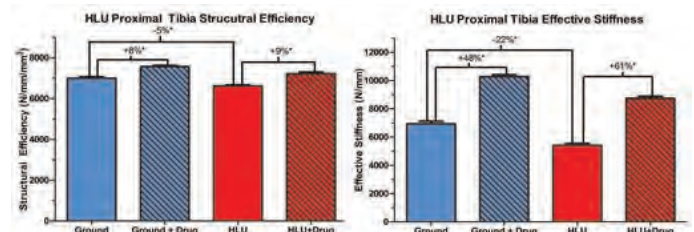
Effective stiffness and structural efficiency of HLU proximal tibia determined by Finite Elements.

Disclosures: Taylor Comte, None.
This study received funding from: AMGEN

SA0034

Differential Patterns of Bone Loss in the Femur and Vertebra of CD44^{-/-} Mice during Hindlimb Unloading. Jeyantt Srinivas Sankaran*[1], Sherin Kuriakose[2], Weidong Zhang[3], Leah Rae Donahue[4], Stefan Judex[1]. [1]Stony Brook University, USA, [2]Stony Brook University, USA, [3]The Jackson Laboratory, USA, [4]Jackson Laboratory, USA

The extent of bone loss between astronauts varies greatly, highlighting the contribution of genetic make-up to musculoskeletal health during unloading in space as well as on Earth. In a recent mouse linkage study, we identified the specific locations of chromosomal regions (Quantitative Trait Loci or QTL) that modulate bone's response to the removal of weightbearing. A potential candidate gene within one of the QTL included CD44, a well-established marker of bone marrow mesenchymal stem cells. CD44 has been associated with cell-cell and cell-extracellular matrix interactions. It may also play a role in osteoclast fusion and formation of multinucleated cells. To test the skeletal functions of CD44 during unloading, 9wk old, female CD44 knockout (CD44^{-/-}, n=26) and wild type (WT, n=34) mice were assigned to baseline control, age matched control, or subjected to 2wk of hindlimb

unloading (HLU). At baseline and compared to WT B6 mice, CD44^{-/-} mice had 40%, 17% and 14% (all P<0.005) lower trabecular bone volume fraction (BV/TV), trabecular number (Tb.N), and trabecular thickness (Tb.Th) in the femoral metaphysis. Cortical thickness, cortical area, periosteal and endosteal circumference were also different between CD44^{-/-} mice and WT at baseline (P<0.05). In the fifth lumbar vertebral body, CD44^{-/-} mice had 54% less BV, 26% less BV/TV, and 17% smaller Tb.Th (all P<0.05) while connectivity density and trabecular number were similar compared to WT mice. Upon unloading, changes in femoral trabecular indices were similar between CD44^{-/-} and WT mice but vertebrae of CD44^{-/-} mice when compared to their respective ambulatory controls were more sensitive to unloading than WT, with greater losses in Tb.N (14% in CD44^{-/-} Vs. 2% in WT), connectivity density (21% decrease in CD44^{-/-} Vs. 15% increase in WT) and an increase in trabecular separation (17% in CD44^{-/-} Vs. 2% in WT) (Tb.Sp) (Gene*HLU, P<0.05). Cortical bone architecture of CD44^{-/-} mice was also more sensitive to hindlimb unloading in the metaphysis, reflected by an increase in porosity (82% in CD44^{-/-} Vs. 46% in WT) and pore size (72% in CD44^{-/-} Vs. 37% in WT) and decrease in Ct.Th (11% in CD44^{-/-} Vs. 7% in WT). These data indicate the importance of CD44 as a regulator of bone quantity and architecture both during habitual load bearing as well as during unloading.

Disclosures: Jeyantt Srinivas Sankaran, None.

SA0035

Remodeling of Distribution of Elastic Modulus Gradients as Predictors of Early Stage Osteopenia. Kartikey Grover*[1], Minyi Hu[1], Liangjun Lin[2], Jesse Muir[3], Yi-Xian Qin[2]. [1]STONY BROOK UNIVERSITY, USA, [2]State University of New York at Stony Brook, USA, [3]STONY BROOK UNIVERSITY, USA

The objective of this study is to investigate remodeling in cortical bone due to functional disuse by measuring elastic modulus gradients in different regions by nano-indentation, and bone strain distribution.

Left tibial bone samples were obtained from 5-month old virgin female Sprague Dawley rats, including 1) baseline control (n=9), and 2) hind limb suspended (HLS) (4 weeks, n=9). 2mm segments were cut from the mid-shaft in the transverse plane, embedded in epoxy resin and elastic modulus measured by Nano indentation (Hysitron Triboindenter, Minneapolis). Three additional control rats were sacrificed and hind limbs axially loaded, from knee to the foot joint, (Bose Corporation, Minneapolis) using 6-10N at 1Hz. Strains at three rosette strain gauge sites around the mid-tibia (National Instruments Strain acquisition box) were measured for total of nine-channels. Bones were then scanned in micro-CT scanner (SCANCO Inc.) at 36μm resolution. Using linear beam theory MATLAB codes were built to find planar strain distribution.

Results: Elastic modulus gradient from periosteum to endosteum is much higher in the anterior and posterior regions (2.6GPa) than the medial regions (0.2GPa), in the control (Fig.1). In the same group, strain (peak to peak) distribution further showed similar higher strain gradient in the anterior-posterior directions(45με) but reduced to 5με in the lateral medial direction (Fig.2). Correlation between elastic modulus and strain gradient is significant (r^2>0.95, Fig.3). In the disuse group, however, the elastic modulus gradient in the anterior posterior regions reduced to 1.2GPa and increased in the medial, 2.7GPa (Fig.4).

The presence of elastic modulus gradient in the direction of strain gradient (r^2>0.95) in the control shows that material property of bone may be strongly influenced by overall strain magnitude. Under disuse condition, due to diminished mechanical loading, the nano-mechanical modulus gradient difference is decreased between different regions, implying progressive bone remodeling occurs during functional unloading. It is suggested that the variations in nano-mechanical gradients among different regions can serve as a predictor for early stage of osteopenia or bone weakening.

KEYWORDS- Remodeling, disuse, nano-indentation, Strain, elastic modulus
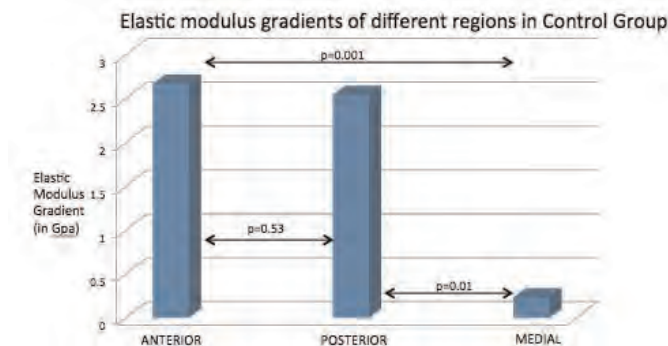
Fig 1-Elastic Modulus gradient in different regions in control group

2D MATLAB PLOT OF STRAIN DISTRIBUTION IN TRANSVERSE SECTION OF RAT TIBIA
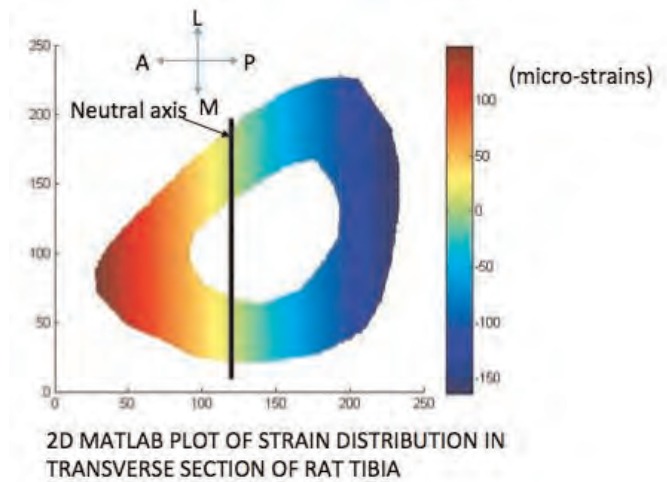
Fig 2-2D Matlab Plot of Strain Distribuiton in transverse section of rat left tibia
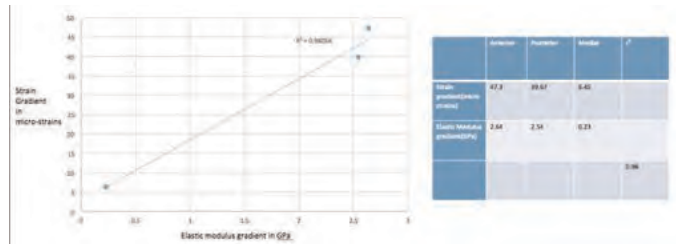
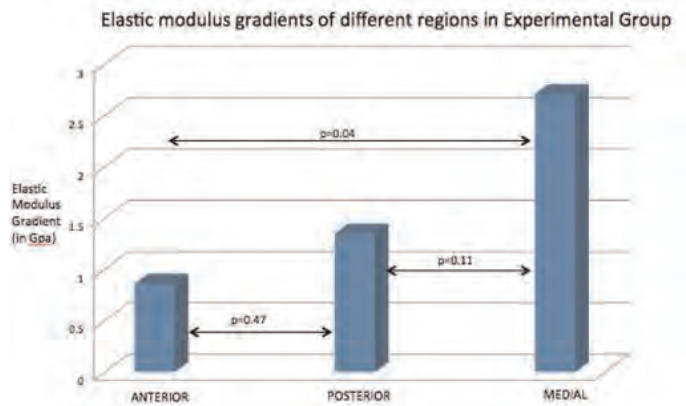Fig 3-Correlation between elastic modulus and strain gradients

Fig 4-Elastic Modulus gradient in different regions in disuse group

Disclosures: KARTIKEY GROVER, None.

SA0036

See Friday Plenary Number FR0036.

SA0037

Bone quality after filling of the maxillary sinus with a bioactive glass. Brigitte Burt-Pichat*[1], Sebastien Rizzo[1], Julie Hemar[2], Laurent Venet[3], Thierry Sauvigne[3], Estelle Franca[4], Georges Boivin[5]. [1]INSERM UMR 1033, Université de Lyon, France, [2]Université de Lyon, France, [3]Centre Hospitalier Lyon Sud, France, [4]Noraker, France, [5]INSERM, UMR1033; Universite De Lyon, France

Our main purpose was to assess bone quality in patients having a filling of maxillar sinus with a bioactive glass 45S5 (GlassBONE®, Noraker, Villeurbanne, France). Nine patients (4 women and 5 men aged 57 ± 10 yrs) were included in the study for a total of 17 bone samples located at the posterior maxilla. Samples were taken 6 months after bone filling, during implantation. Undecalcified samples were embedded in methyl methacrylate. Bone quality was assessed by histomorphometry (measurement bone volume and bone remodeling) on 8 μm-thick sections stained with Goldner's

trichrome, by microindentation (1) on surfaced blocks to calculate the Vickers microhardness (Hv, kg/mm^2), and by quantitative microradiography (1) on 100 ± 1 μm-thick sections to measure the degree of mineralization (DMB g/cm^3) and the heterogeneity index of mineralization (HI, g/cm^3). Histology showed bone structures composed of cortical and cancellous bone, a well vascularized marrow rich in bone cells. The residual bone was identified by its lamellar texture and the presence of bone marrow adipocytes. The newly-formed bone was characterized by a woven texture and the persistence in medullary cavity of biomaterial partially degraded. Bioactive glass 45S5, a bioceramic made of silicon, sodium, calcium, phosphorus, was well tolerated and caused no foreign-body reaction (inflammation, rejection). New bone volume varied between 4.4 and 54.4 % and the volume of residual bone was between 4.3 and 27.6 %. The bioactive glass increased bone formation stimulating osteoblast proliferation. Microhardness of new bone (38.96 ± 4.47 kg/mm^2) was closed to that of residual bone (42.54 ± 5.60 kg/mm^2). DMB were similar in newly-formed (1.02 ± 0.13 g/cm^3) and residual bone (0.91 ± 0.20 g/cm^3). HI was more heterogeneous in new bone (0.32 ± 0.16 g/cm^3) than in residual bone (0.27 ± 0.20 g/cm^3). The bioactive glass 45S5 was well osteointegrated and degraded with the formation of new bone. This biomaterial guided bone remodeling from the residual bone and promoted formation and mineralization of bone. Mineralization and microhardness of new bone were physiologically normal. Our data suggests the formation of bone tissue of good quality to secure the placement of the implant. Our results demonstrated the efficiency of bioactive glass 45S5 to fill maxillary sinus.[1]Boivin et al. 2008, Bone, 43:532-8.

SA0038

Combinatorial cassettes, a high-throughout approach for the assessment of bone formation *in vivo*. Luis Fernandez De Castro*[1], Subdhadip Bodhak[2], Sergei Kuznetsov[3], Tina Kilts[3], Marian Young[4], Sheng Lin-Gibson[2], Carl Simon[2], Pamela Robey[5]. [1]NIDCR (NIH), Spain, [2]NIST, USA, [3]NIH, USA, [4]National Institutes of Health, USA, [5]National Institute of Dental & Craniofacial Research, USA

Models of subcutaneous transplantation in immunocompromised mice have been shown to be useful for a wide variety of purposes, including cancer research, cell therapy and biomaterial and drug screening. In bone regeneration, subcutaneous transplantation is the most reliable tool to assay the osteogenic potential of cells, molecules and biomaterials, because the existing in vitro models lack predictive value in assessing osteogenic differentiation *in vivo*. However, the subcutaneous transplantation assays also present some handicaps, such as their long duration, low yield of samples (up to 4 per mice), uncontrolled transplant shape and mouse to mouse variability in bone formation.

To address these issues, we designed two hexagonal Teflon combi-cassettes of 15x15x3 mm with different numbers and sizes of cylindrical slots for sample testing. One contained 7 slots of 44 mm^3 (3 mm height and 4.3 mm diameter) and the other contained 19 slots of 14 mm^3 (3 mm height and 2.4 mm diameter), and used them to test the osteogenic potential of normal human bone marrow stromal cells (hBMSCs) loaded on a hydroxyapatite/tricalcium phosphate (HA/TCP) scaffold in vivo. Cassettes were implanted subcutaneously at the lower back of the mice, centered over vertebrae L5-L6 to S2-S3 and a positive and a negative control were included, by making 'traditional' HA/TCP transplants with or without cells in subcutaneous pockets placed bilaterally at the upper back, over ribs T5 to T10. Also, as internal negative controls, some slots were filled with unloaded scaffold. Eight weeks after implantation, transplants were harvested, fixed and processed for histochemistry.

Transplants from the cassettes formed abundant bone with some areas of lamellar structure, high vascularization and host hematopoiesis when compared to 'traditional' transplants.

In this study, we have developed a cassette transplantation system that will allow for the assessment of bone formation of up to 19 samples, addressing some of the current weaknesses of subcutaneous bone transplantation models, as it increases in almost 5-fold the number of transplants produced per animal and standardizes the size and shape of the transplants. In future experiments, we plan to test other cell populations in this system, such as murine BMSCs loaded into a gelatin sponge scaffold and ectopic bone formation induced by BMP2.

SA0039

Genetic regulation of skeletal robustness. Lauren Smith*[1], Erin M.R. Bigelow[2], Bonnie T. Nolan[2], Meghan Faillace[3], Joseph H. Nadeau[4], Karl Jepsen[5]. [1]Department of Orthopaedic Surgery, The University of Michigan, USA, [2]Department of Orthopaedic Surgery, The University of Michigan, USA, [3]GE Inspection Technologies, USA, [4]Pacific Northwest Research Institute, USA, [5]University of Michigan, USA

Skeletal robustness, a measure of how much a bone grows in width relative to length, is an important mechanical trait as variation in robustness accounts for 50-180% of the variation in bone strength among healthy adult men and women, depending on the bone site. This natural variation in strength is 5-10 times greater than the difference in bone strength reported between fracture and non-fracture groups, and may explain why individuals with slender bones show greater fracture

incidence throughout life. Our goal is to better understand the genetic and environmental factors contributing to the variation in robustness.

An individual's skeletal robustness is established as early as 2 years in humans and 2 weeks in mice. Although we know this trait is genetically regulated, we know very little about the mechanisms by which this genetic variation arises. We previously reported an analysis of 16 week old male C57BL/6J – Chr$^{A/J}$/NaJ chromosome substitution strains (CSS), a panel of mice where individual B6 (robust bone) chromosomes are replaced by the corresponding A/J (slender bone) chromosome. Herein, we analyzed male B6, A/J and CSS at 4 weeks (n=9-40/strain; N$_{ttl}$ = 250/age) to better understand how these genetic perturbations affect robustness during growth. Femora were imaged using nanoComputed Tomography (8 μm) to quantify cross-sectional morphology. CSS were compared to B6 using General Linear Model, adjusting for body size (body mass x femur length).

Fifteen CSS had similar robustness at both 4 and 16 weeks. Six strains (CSS-5, 8, 10, 12, 17, 18) were significantly more slender than B6 at both time points (p<0.05). However, five strains (CSS-1, 4, 11, 15, 19) showed different robustness phenotypes at 4 and 16 weeks. Of these, three were slender at 16 weeks but with normal robustness at 4 weeks (CSS-1, 15, 19); one was more robust at 16 weeks but had normal robustness at 4 weeks (CSS-4); and one had normal robustness at 16 weeks but was slender at 4 weeks (CSS-11).

The CSS showing similar alterations in robustness at both ages suggested that the genetic perturbation exerted its affect early during growth. In contrast, the CSS showing differences between 4 and 16 weeks indicate that the genetic perturbation exerted its effects much later during growth. This analysis showed that, robustness, a fairly simple trait, is under complex genetic regulation. Future work will examine how this variable genetic regulation of robustness affects mechanical function.

CSS -#	1	2	3	4	5	6	7	8	9	10	11	12	13	14	15	16	17	18	19	X	Cumulative CSS effect	A/J
4 week	-0.4	-0.2	2.9	-0.5	-.6	-0.2	-3.4	-6.4	0.2	-9.*	-*.1	-9.3	1.1	3.4	2.3	2.6	-5.4	-8.5	-4.2	-0.9	-51.3	-30.2
16 week	-8.1	4.6	3.9	11.6	-11.3	-.5.2	1.5	-10.2	-6.1	-8.9	-0.*	-*.2	-3.9	4.0	-8.0	-2.8	-11.9	-8.0	-*.*	1.8	-*.2	-33.2

Table 1.% difference between CSS and B6

SA0040

Kinetics of Maillard Reaction in Mineralized Human Bone. Grazyna Sroga*[1], Alankrita Siddula[2], Deepak Vashishth[1]. [1]Rensselaer Polytechnic Institute, USA, [2]Rensselaer Polytechnic Institute, USA

Advanced glycation end products (AGEs) accumulate with age due to non-enzymatic reaction between proteins and glucose or other reducing sugars. This post-translational modification process, termed glycation occurs under *in vivo* and *in vitro* conditions [1, 2]. To better understand glycation process of bone matrix proteins, we used *in vitro* glycation approach. The goal of the current work was to look for potential differences in the fluorescent AGEs formation in cortical and cancellous bones from human tibias glycated under glucose- or ribose-based conditions.

We determined that both sugars led to the formation of higher levels of AGEs and pentosidine (PEN) in cancellous than cortical bone originating from all tested donors (young, middle-age and elderly men and women). More efficient glycation of bone matrix proteins in cancellous bone most likely depended on a higher porosity of this tissue, which facilitated better accessibility of sugars to matrix proteins. Typically, the AGEs levels in glycated cortical bone from older donors were much higher than in young ones. Interestingly, the levels of PEN differed pronouncedly between glucose- vs. ribose-based glycation. Ribosylation generated primarily PEN (approx. 5- vs. 3-fold higher PEN level in the ribosylated than glucosylated bone samples).

Our studies on the kinetics of AGEs and PEN formation in human cortical and cancellous bone matrix revealed that after approx. one day of an induction period (a lag phase), the formation of fluorescent AGEs displayed steady increase in cortical as well as cancellous bone. Depending on the *in vitro* glycation conditions, the half-time of sugar conversion into AGEs varied from 6 to 7 days for ribose and 20 to 22 days for glucose. The corresponding half-time for PEN was approx. 5 to 6.5 days for ribose and approx. 15 to 17 days for glucose under the used *in vitro* glycation conditions.

In summary, our results show that *in vitro* glycation using glucose leads to the formation of lower levels of AGEs including PEN, whereas ribosylation appear to favor a pathway toward PEN formation. Our studies may help to understand differences in the progression of bone pathologies related to protein glycation by different sugars, for example, in osteoporosis, diabetes and aging.

[1] Bank et al, Biochem. J. 330(1998) 345-351.
[2] Vashishth et al, Bone 28(2001) 195-201.

SA0041

Mandibular reconstructed bone quality after filling of defects with dental bone substitutes in beagles. Sebastien Rizzo*[1], Augusto André Baptista[2], Brigitte Burt-Pichat[1], Capucine Rondot[3], Antoine Alves[4], Catherine Wittmann[3], Christian Gagnieu[5], Patricia Forest[3], Georges Boivin[6], Jean-Pierre Bernard[7]. [1]INSERM UMR 1033, Université de Lyon, France, [2]Faculté d'Odontologie, Université de Lorraine, France, [3]Biom'up, France, [4]NAMSA, France, [5]MATEIS, INSA de Lyon, Université Claude Bernard Lyon1, France, [6]INSERM, UMR1033 ; Universite De Lyon, France, [7]Faculté de Médecine, Division de Stomatologie Chirurgie Orale et Radiologie Dentaire et Maxillofaciale, Université de Genève, Switzerland

In dental implantology, bone substitutes are increasingly used as an alternative to autogenous bone grafts, long considered as the gold standard material for bone augmentation. Three biomaterials BS1, BS2 and BS3 (MATRI™BONE MAX, Biom'Up, Saint-Priest, France) are evaluated in a canine model of mandibular defects in comparison to deproteinized bovine bone mineral (DBBM, Bio-Oss Collagen®, Geistlich, France), to particulated autogenous bone (positive control) or to coagulum (negative control). The purpose of this study was to evaluate the mechanical quality of reconstructed bony defects by measuring the microhardness of the newly formed bone. The healing time period was 12 weeks. A total of 36 mandibular bone samples were obtained from 6 beagles (6 different graft sites per dog). Undecalcified bone samples were fixed, dehydrated and then embedded in methyl methacrylate (Namsa, Chasse/Rhône, France). The blinded bone microhardness evaluation (kg/mm^2) was performed on blocks surfaced by microindentation (1). Vickers indenter was used at a load of 25 g for 10 s. Twenty indentations were performed in the newly formed bone, 5 in the native cancellous bone and 5 in the native cortical bone, to obtain a total of 30 measurements per bone sample. Under the experimental conditions, the microhardness of newly formed bone in groups BS1, BS2, BS3, DBBM, positive control and negative control were respectively 39.27 ± 2.28; 36.74 ± 3.48; 39.17 ± 2.73; 38.97 ± 3.78; 40.27 ± 3.16; 40.36 ± 3.55 kg/mm^2, without any significant difference between groups. Except for the negative control, in all groups, the microhardness of the newly formed bone was significantly lower than the one of native cancellous bone (41.00 to 46.05 kg/mm^2) and than the one of The native cortical bone (50.96 to 54.61 kg/mm^2). The microhardness is correlated to bone mineralization, itself influenced by the age of bone tissue (1). Differences of ageing between the newly formed bone tissue and the native one could explain differences in bone microhardness. After 12 weeks of implantation, the microhardness of newly formed bone in defects filled with MATRI™BONE MAX is similar to the one of defects filled with autogenous particulated bone.1 - Boivin et al. 2008, Bone 43:532-8

SA0042

See Friday Plenary Number FR0042.

SA0043

Tissue Mineral Density Dependent Mechanical Properties of Individual Trabecula Plates and Rods Do Not Differ in Anatomic Directions but Individual Trabecular Directions. Eric Yu*, Ji Wang, Bin Zhou, X Guo. Columbia University, USA

Trabecular bone, susceptible to osteoporosis, consists of individual trabecular plates and rods, which are distributed distinctly along the longitudinal, transverse, or oblique anatomic directions of the skeleton (Fig.1). In each anatomic direction, mechanical properties of bone tissue are also expected to differ in (axial) or against (lateral) the direction of individual trabeculae, *i.e.*, anisotropic mechanical properties. However, anisotropic mechanical properties of individual trabeculae along various anatomic directions are currently not available. Objectives of this study are: to measure anisotropic tissue modulus and TMD of individual trabeculae; to examine their dependence on trabecular types and anatomic directions; and to determine the relationship between anisotropic tissue modulus and TMD of individual trabeculae.

Twelve cylindrical human trabecular bone samples from proximal femurs were imaged with hydroxyapatite density calibration phantoms at 25 μm resolution by μCT. Individual trabecular types and their anatomic directions were determined using individual trabecula segmentation (ITS) technique. On the embedded samples, microindentation tests were performed under wet condition on both axial and lateral cross-sections (Fig 1.C) of selected plates and rods in longitudinal (L), transverse (T), and oblique (O) directions, respectively (Fig 1.D). The point-by-point registered grayscale values of the μCT image at the indentation sites were converted to TMD using calibration phantoms.

The tissue modulus and the co-localized TMD of trabecular plates were significantly higher than those of trabecular rods (Fig. 2A, B). The axial tissue modulus of individual trabeculae was significantly higher than the lateral tissue modulus (Fig. 2C). The tissue modulus correlated strongly with TMD. These correlations do not differ significantly between plates and rods or different anatomic directions. However, the axial modulus correlation was significantly different from the lateral modulus correlation (Fig. 2D).

We measured anisotropic elastic modulus of individual trabecular plates and rods of different anatomic directions. Surprisingly, the heterogeneous tissue modulus correlated with TMD similarly regardless of trabecular types and anatomic directions. The correlation only differs in the axial and lateral trabecular directions. It remains to be seen how this heterogeneous anisotropic tissue property plays a role in whole bone mechanical competence.
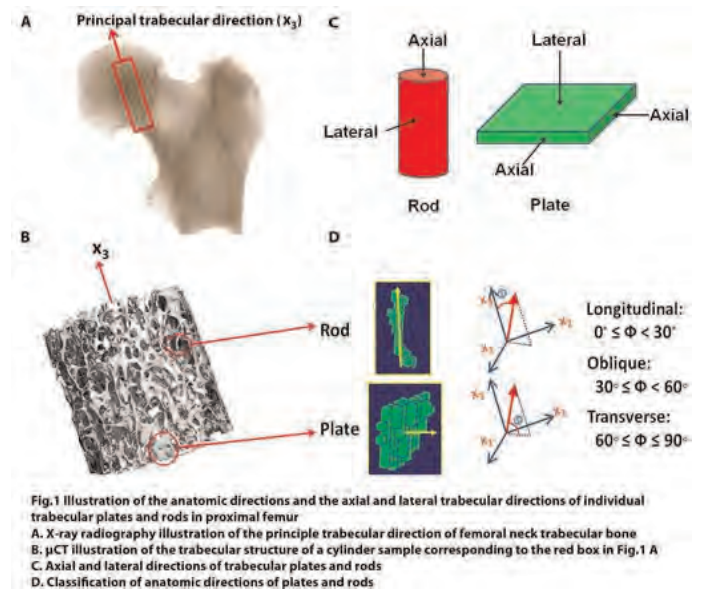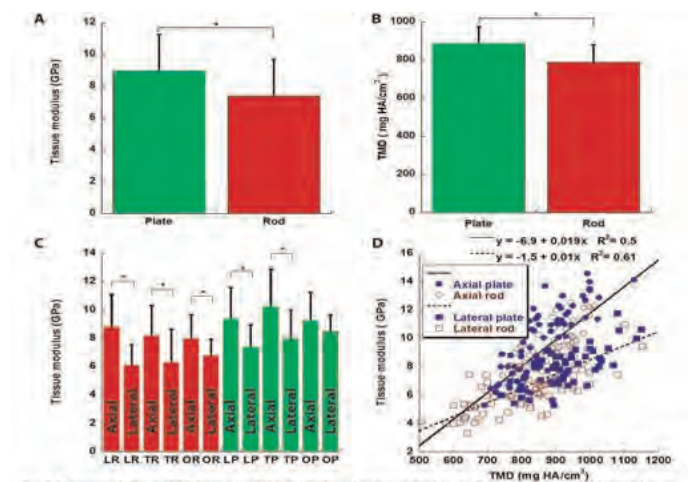

Fig.1 Illustration of the anatomic directions and the axial and lateral trabecular directions of individual trabecular plates and rods in proximal femur
A. X-ray radiography illustration of the principle trabecular direction of femoral neck trabecular bone
B. μCT illustration of the trabecular structure of a cylinder sample corresponding to the red box in Fig.1 A
C. Axial and lateral directions of trabecular plates and rods
D. Classification of anatomic directions of plates and rods

Figure 1

Fig.2 Tissue modulus and TMD vary in different trabecular types, anatomic directions and individual trabecular directions. (Plate: n=216; rod: n=216)
A. Plates have higher tissue modulus than rods. *p<0.05;   B. Plates have higher TMD than rods. *p<0.05
C. Tissue modulus in axial direction is higher than in lateral direction. *p<0.05. P and R denote plate and rod. L, T, O denote longitudinal, transverse and oblique. (p=0.53 for OP_axial vs. OP_lateral)
D. Tissue modulus closely correlates with TMD. However, the correlations differ between axial and lateral directions. *p<0.05

Figure 2

SA0044

Using Atomic Force Microscopy and Nanoindentation to Characterize Matrix Integrity of Mineralized Bone from Perlecan/HSPG2 Hypomorphic Mice. Jerahme Martinez*[1], Ben Morgan[2], Lewis Francis[3], Mary Farach-Carson[1], Liyun Wang[4], Ashutosh Parajuli[5]. [1]Rice University, USA, [2]College of Medicine Swansea University, United Kingdom, [3]College of Medicine Swansea University, Uzbekistan, [4]University of Delaware, USA, [5]University of Delaware College of Engineering, USA

Schwartz-Jampel Syndrome (SJS) is a rare human skeletal disorder with pleiotropic abnormalities in bone formation and stability. Common symptoms include a shortened stature, joint contractures, osteoporosis and disruption of both endochondral and membranous bone. SJS results from mutations to the perlecan gene, *HSPG2*, on chromosome 1p36, that reduces the amount of normal full-length perlecan deposited in the extracellular matrix (ECM); SJS thus can be considered a hypomorphic syndrome. Perlecan, a large multi-domain heparan sulfate proteoglycan (HSPG), functions as a key structural component of musculoskeletal tissue.

Reduction of perlecan diminishes ECM function at tissue interfaces, such as the chondro-osseous junction (COJ) of developing bones, and disrupts the lacunar canalicular system (LCS) of mineralized bone where perlecan is part of the mechanosensing pericellular matrix (PCM) surrounding the osteocytic processes that preserve fluid flow throughout mineralized bone. Our work here focuses on perlecan's mechanical role within newly mineralized bone ECM, where we hypothesized that a reduction of perlecan creates the SJS bone phenotype at least in part due to a change in matrix stiffness and loss of bone quality. We chose to examine the mechanical properties of calvaria. Tissues were collected from a perlecan mouse hypomorph model mimicking the SJS phenotype. To evaluate tissue stiffness we performed nanoindentation by atomic force spectroscopy (AFM). Surface topography images along with force data sets were generated for each tissue sample, revealing a high resolution map of the calvarial surface. The Young's modulus, determined by the Hertz model, was used to evaluate differences in matrix properties in SJS and normal mice. Our initial findings suggest that a reduction of perlecan does not directly impact bone stiffness in newly formed bone, thus the functional changes observed in SJS bone in older mice are likely to be due to altered bone stability.

Disclosures: Jerahme Martinez, None.

SA0045

Insulinogenic sucrose+amino acids mixture ingestion immediately after resistance exercise has an anabolic effect on bone compared with non-insulinogenic fructose+amino acids mixture in growing rats. Takuya Notomi*[1], Ikuaki Karasaki[2], Yuichi Okazaki[3], Nobukazu Okimoto[4], Yushi Kato[2], Kiyoshi Ohura[5], Masaki Noda[6], Toshitaka Nakamura[7], Masashige Suzuki[2]. [1]Department of Pharmacology, Osaka Dental University, Japan, [2]University of Tsukuba, Japan, [3]University of Occupational & Environmental Health, Japan, [4]Okimoto Clinic, Japan, [5]Department of Pharmacology, Osaka Dental University, Japan, [6]Tokyo Medical & Dental University, Japan, [7]National Center for Global Health & Medicine, Japan

Maximizing peak bone mass is an important factor in osteoporosis prevention. Resistance exercise increases bone mass and strength, while nutritional supplements have beneficial effects on bone loss reduction. We have previously shown that the combined intake of sucrose and amino acids (AA), which is strongly insulinogenic, efficiently increased muscle protein synthesis in dogs. To investigate the effects of sugar and an AA solution immediately after resistance exercise, we compared insulinogenic sucrose and non-insulinogenic fructose combined with an AA solution with or without resistance exercise in growing rats.

Squat jumping is used as the resistance exercise model. The rats were divided into 4 groups (sucrose with/without sucrose, fructose with/without exercise). Sucrose intake immediately after resistance exercise increased the trabecular bone mass and compressive maximum load compared with fructose+AA intake after exercise. Additionally, combined sucrose+AA and exercise increased trabecular bone formation and decreased bone resorption more than combined fructose and exercise. Without exercise, no parameters differed between the fructose and sucrose with AA intake groups. Serum insulin levels were greatly increased by sucrose+AA intake with exercise. In culture experiments, neither sugar+AA affected osteoblast and osteoclast differentiation. In a gene expression study, sucrose+AA intake after resistance exercise was shown to upregulate the Runx2 expression level and decrease RANKL/OPG ratio.

These results suggest that the combined intake of sucrose and an AA solution immediately after resistance exercise exerts anabolic effects on bone by altering gene expression related to bone remodeling. Although translation of our bone remodeling findings from animal to human studies has been challenging, our findings suggest that exercise with sugar+AA intake may contribute to improved bone health.

Disclosures: Takuya Notomi, None.

SA0046

See Friday Plenary Number FR0046.

SA0047

Spaceflight Compromises the Bending Strength of Murine Spinal Segments. Britta Berg-Johansen*[1], Alan Hargens[2], Jeffrey Lotz[3]. [1]University of California, San Francisco, USA, [2]University of California, San Diego, USA, [3]University of California, San Francisco, USA

Background/Purpose: Microgravity adversely affects the human spine, increasing the risk for low back pain and injury. The risk of intervertebral disc herniation in astronauts is increased more than 4-fold following spaceflight [1]. Bending motions are significant contributors to disc herniation [2], yet the effects of microgravity on the bending properties of the spine are unknown. The purpose of this study was to determine the effects of microgravity on the bending properties of murine spinal segments, with the hypothesis that bending properties are reduced.

Methods: Murine tails were obtained through NASA's Biospecimen Sharing Program from mice that had returned from a 30-day Bion M1 mission (flight, n=6)

and from vivarium controls (control, n=8). The C3-C4 caudal motion segment was isolated from each tail, radiographed to estimate disc height, and placed in a mechanical load frame (ElectroForce 3200). Motion segments were tested in four-point bending using a custom 3D-printed jig that applied bending in the ventral-dorsal plane (lower span = 7.5 mm; upper span = 2.5 mm). Loading consisted of 5 cycles of preconditioning (0-5 mm) at 0.05 mm/sec, followed by a ramp to failure at 0.006 mm/sec. Force-displacement data were analyzed for the following parameters: the toe region was defined as the displacement corresponding to an applied force of 1 N, the stiffness was defined as the slope of the linear region, and the strength was defined as the maximum force reached before failure.

Results: Microgravity reduced bending strength by 18% (6.17 $\pm$ 0.94 vs. 7.53 $\pm$ 1.13 N, p < 0.05) and reduced the toe region by 31% (0.53 $\pm$ 0.14 vs. 0.77 $\pm$ 0.21 mm, p = 0.05). Bending stiffness was not significantly different between groups (p > 0.25). Microgravity also tended to reduce disc height by 17% (0.24 $\pm$ 0.03 vs. 0.29 $\pm$ 0.04 mm, p = 0.06).

Conclusions: The adverse effect of microgravity on bending strength supports our hypothesis that reduced bending properties may be an important factor for explaining the increased herniation risk following spaceflight. Interestingly, microgravity also reduced the toe region. This is consistent with reports of decreased range of motion in astronauts, and together these findings motivate future work to investigate the underlying biochemical and structural mechanisms.

References: 1. Johnston et al. 2010 *Aviation, space, and environmental medicine* 81.6: 566-574; 2. Veres et al. 2009 *Spine*. 34(21): 2288-96.
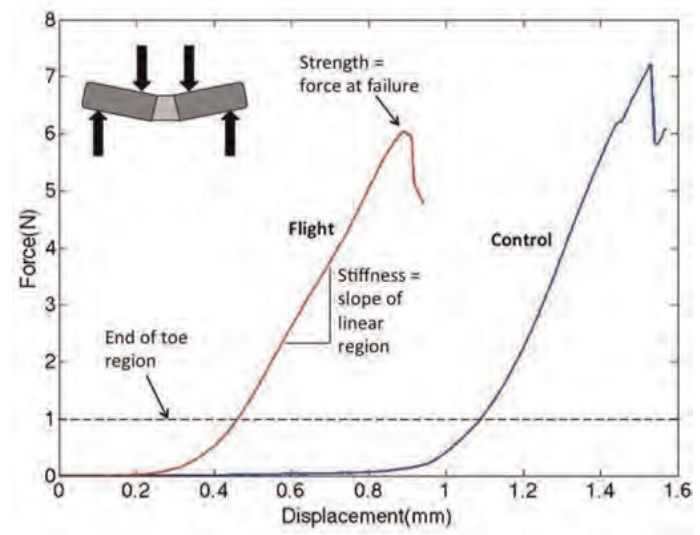

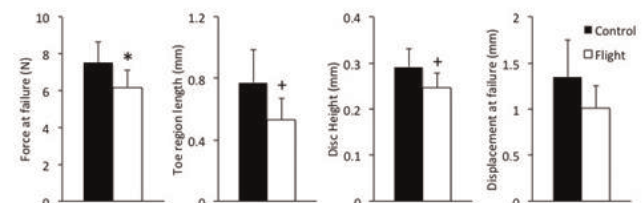Figure 1: Flight mice have reduced bending strength and disc flexibility (curve shifted to left)

Figure 2: Bending properties are reduced for spaceflight mice. *p<0.05, +p<0.06, paired t-test

Disclosures: Britta Berg-Johansen, None.

SA0048

See Friday Plenary Number FR0048.

SA0049

A study on the effect factors on BMD of affected femur neck in patients with hemiplegia. Yun Kyung Jeon*[1], Young Beom Shin[2], Myung Jun Shin[2], Chang Jae Hyeok[2]. [1]Pusan National University Hospital, South Korea, [2]Pusan National University Hospital, South Korea

The aim of this study was to investigate BMD of affected femur in patients with hemiplegic stroke. Medical records of 153 patients with stroke who admitted a rehabilitation clinic from January 2011 to March 2013 were retrospectively reviewed. We excluded the patients with non-hemiplegia, diseases which can affect the BMD such as diabetes mellitus, thyroid disease and anti-epileptic drugs. We also excluded

the patients who did not check both femur BMD. Total 68 subjects were finally enrolled in the study (38 males, 30 postmenopausal females). We measured BMD at affected and unaffected femur using dual energy X-ray absorptiometry, bone turnover markers and activity levels. The influences of factors on affected femur neck BMD were investigated by linear regression test. 31 subjects showed decreased BMD of affected femur neck (45%). In 16 males (61.9 $\pm$ 10.5 years), the mean duration after stroke was 51.3 $\pm$ 31.5 days, body mass index (BMI) was 22.4 $\pm$ 3.5 (kg/m2) and wheel chair ambulators were 12. The BMD ratio of affected and unaffected femur neck was 0.915 $\pm$ 0.07. The 25-hydroxy vitamin D was 8.2 $\pm$ 12.3 (ng/mL), serum osteocalcin was 5.25 $\pm$ 6.67 (ng/mL) and serum CTX was 0.315 $\pm$ 0.42 (ng/mL). In 15 postmenopausal females (68.3 $\pm$ 10.4 years), the mean duration after stroke was 31.1 $\pm$ 19.7 days, BMI was 22.6 $\pm$ 3.0 and wheel chair ambulators were 8. The BMD ratio of affected and unaffected femur neck was 0.926 $\pm$ 0.083. The 25-hydroxy vitamin D was 10.6 $\pm$ 10.5, serum osteocalcin was 7.81 $\pm$ 8.23 and serum CTX was 0.44 $\pm$ 0.56. In linear regression test, ambulation classification was a only effect factor on the BMD ratio of affected and unaffected femur neck (ß=0.38, p=0.034). The femur neck BMD of hemiplegic side were not decreased in all stroke patients. This study showed BMD changes in affected femur neck were link to ambulation classification than bone turnover marker.

Disclosures: Yun Kyung Jeon, None.

SA0050

Bone mineral density in osteopenic men is increased afte resistance training or plyometric exercise. Pam Hinton*[1], John Thyfault[2], Peggy Nigh[2], Melissa Carter[2], Nantian Lin[2], Jun Jiang[2]. [1]University of Missouri, USA, [2]University of Missouri, USA

The purpose of this study was to test the efficacy of exercise-based interventions to increase bone mass in osteopenic men. This randomized clinical trial examined the effects of 12 months of resistance training (RT, 2x/wk, N= 19) or plyometric exercise (PLY, 3x/wk, N= 19) on bone mineral content (BMC) and density (BMD) in physically active ($\geq$4hr/wk) men (mean age: 44 $\pm$ 2 y) with osteopenia of the hip or spine (i.e., -2.5<total hip or lumbar spine T-score£-1.0). Both the RT and PLY interventions were designed to load the hip and spine and to maximize the osteogenic response. All exercise training sessions were supervised by study personnel; and, participants rated pain and fatigue following each session on a scale of 0-100 with 100 being the highest fatigue or pain. Participants were provided daily supplemental calcium (1200 mg) and vitamin D (10 µg). Bone area, BMC, and BMD were measured at baseline and after 6 and 12 months of RT or PLY using dual-energy X-ray absorptiometry scans of the whole body (WB), hip and lumbar spine (LS). Serum 25(OH) vitamin D (25OHD) concentrations were measured at 0 and 12 months using ELISA. The effects of RT or PLY on changes in WB, hip, and LS BMC, BMD and 25OHD concentrations were evaluated using 2x2 repeated measures ANOVA (time, group). This study was conducted in accordance with the Declaration of Helsinki and was approved by the University of Missouri IRB. RT significantly increased muscular strength by 86, 118, 74, 45% for squat, lunge, deadlift, and military press, respectively; PLY significantly increased vertical jump by 8%. Thirty-six of 38 participants were vitamin D sufficient (25OHD>20 ng/ml) at baseline, and 25OHD did not differ between groups; 25OHD increased by 1.4 $\pm$ 1.2 ng/ml in RT and 4.4 $\pm$ 1.2 ng/ml in PLY at 12 months. WB and LS BMC and BMD significantly increased after 6 months of RT or PLY; hip BMC and BMD increased only in RT. Similar results were observed after 12 months of RT or PLY: WB and LS BMC and BMD increased after RT or PLY; hip BMD increased after RT only. The significant increases in BMC and BMD ranged from 0.8-1.6%. Pain ratings during the RT or PLY sessions were <10 at all timepoints, and fatigue ratings were <30 at all timepoints. In conclusion, resistance training or plyometric exercise, which appears safe and feasible, effectively increased bone mineral of the whole body and lumbar spine, while resistance training also increased BMD of the hip, in osteopenic men.

Disclosures: Pam Hinton, None.

SA0051

See Friday Plenary Number FR0051.

SA0052

Fracture History in Oligo-amenorrheic Athletes, Eumenorrheic Athletes, and Non-athletes: Correlations with Bone Density and Microarchitecture. Kathryn Ackerman*[1], Natalia Cano Sokoloff[2], Giovana Maffazioli[3], Vibha Singhal[4], Meghan Slattery[5], Hannah Clarke[5], Nicholas Derrico[6], Madhusmita Misra[7]. [1]Division of Sports Medicine, Department of Orthopedics, Boston Children's Hospital & Harvard Medical School & Neuroendocrine Unit, Massachusetts General Hospital & Harvard Medical School, USA, [2]Neuroendocrine Unit, Massachusetts General Hospital & Harvard Medical School, USA, [3]Neuroendocrine Unit, Massachusetts General Hospital & Medical School, USA, [4]Neuroendocrine Unit, Massachusetts General Hospital & Harvard Medical School & Pediatric Endocrine Unit, Massachusetts General Hospital for Children & Harvard Medical School, USA, [5]Neuroendocrine Unit, Massachusetts General Hospital & Harvard Medical School, USA, [6]Endocrine Unit, Department of Medicine, Massachusetts General Hospital, USA, [7]Neuroendocrine Unit, Massachusetts General Hospital & Pediatric Endocrine Unit, Massachusetts General Hospital for Children, Harvard Medical School, USA

Purpose: To compare fracture prevalence in oligo-amenorrheic athletes (OA), eumenorrheic athletes (EA), and non-athlete controls (C) and determine if bone mineral density (BMD) and microarchitectural parameters predict fracture risk.
Methods: 164 females (101 OA, 34 EA, and 29 C) 14-25 yo were studied cross-sectionally. Lifetime fracture history was recorded by a physician during participant interviews. Areal BMD was assessed by DXA at the spine, hip and whole body. Bone structure was assessed by HRpQCT at the radius and tibia, and strength by finite element analysis.
Results: OA, EA, and C did not differ in age, sexual maturity, or height. OA had lower BMI, older menarcheal age, and longer duration since last menses than EA and C (p$\leq$0.001 for all). Hours of exercise/week were similar in both athlete groups. Lifetime fracture risk was higher in OA than EA and C (47.5%, 23.5%, 17.2%, p=0.002). BMD Z-scores were lower in OA vs. EA at the total hip, femoral neck, spine, and whole body (p$\leq$0.005). BMD Z-scores were lower in C vs. EA at the total hip, femoral neck, and whole body (p$\leq$0.004). At the radius, OA had lower total volumetric BMD (vBMD), cortical (Ct) thickness and % Ct area, and greater Ct porosity and % trabecular (Tb) area than C (p<0.05). At the tibia, total and Tb area and Ct porosity were greater in both athlete groups vs. C (p<0.05). EA, but not OA, had greater Ct area than C (p<0.05). Stiffness and failure load were lower in OA than EA at both sites (p$\leq$0.05). Within athletes, those with fracture had lower BMD Z (all sites) (p$\leq$0.02), radial Tb vBMD and thickness (p$\leq$0.01), and tibial Tb vBMD (p=0.008) than those without fracture. Within OA, those with fracture had lower whole body BMD Z (p=0.02) and radial Tb thickness (p=0.03) than those without fracture.Conclusion: While weight-bearing athletic activity increases BMD, it may increase fracture risk in those with menstrual dysfunction. With repetitive loading, BMD is enhanced, and the weight-bearing tibia develops greater moment of inertia (expansion of total area) to protect against loading forces. Athletes with menstrual dysfunction lack some bone building benefits of exercise. Within athletes, Tb vBMD and thickness differentiate those with and without a history of fracture. This is the first study to examine bone structure in relation to fractures in female athletes. Prospective studies are needed to better assess bone parameters as predictors of fracture prevalence in this population.

Disclosures: Kathryn Ackerman, None.

SA0053

High Vitamin D and Physical Activity Status in Community-Dwelling Older Adults: Associations with Body Composition and Muscle Function Changes Over Five Years. David Scott[1], Peter Ebeling*[2], Kerrie Sanders[3], Dawn Aitken[4], Tania Winzenberg[5], Graeme Jones[6]. [1]The University of Melbourne, Australia, [2]Department of Medicine, School of Clinical Sciences, Monash University, Australia, [3]NorthWest Academic CentreThe University of MelbourneWestern Health, Australia, [4]Menzies Research Institute, University of Tasmania, Australia, [5]Menzies Research Institute Tasmania, Australia, [6]Menzies Research Institute, Australia
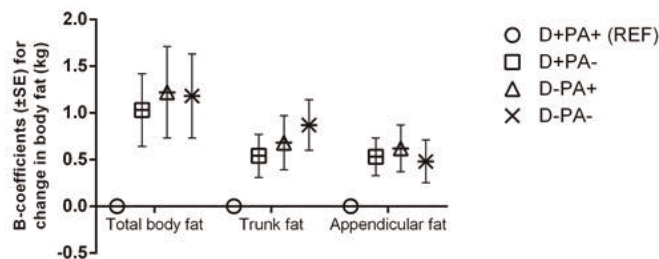
PURPOSE: Higher vitamin D and physical activity (PA) levels have been independently associated with improved body composition and muscle function. Greater fat oxidation and improvements in physical performance in response to exercise may also occur in older adults with higher serum 25-hydroxyvitamin D (25OHD) levels. We investigated the effects of combined high vitamin D and PA status on changes in body composition and muscle function in a prospective study of older adults over five years.
METHODS: 615 community-dwelling volunteers (61.3 $\pm$ 6.9 [mean $\pm$ SD] years; 52% female) were categorised according to baseline serum 25OHD ($\geq$ or <50nmol/L) and PA ($\geq$ or <10,000 pedometer-determined steps/day) levels into the following groups: high 25OHD and high PA (D+PA+; N=148), high 25OHD and low PA (D+PA-; N=225), low 25OHD and high PA (D-PA+; N=80), low 25OHD and low PA (D-PA-; N=162). Changes in DXA-assessed total body, trunk and appendicular

(AFM) fat mass, and appendicular lean mass, and changes in lower-limb strength (LLS; assessed by dynamometer) and muscle quality (LLS normalised to DXA-assessed lower-limb lean mass), were determined over 5.1 ± 0.5 years. Multivariable linear regression analyses adjusting for potential confounders including age, sex, comorbidities, and season of 25OHD/PA assessment compared the change in outcome variables between groups.

RESULTS: Compared with D+PA+, all other groups had significantly greater total body fat, trunk fat and AFM, and D-PA- had lower muscle quality, at baseline (all $P<0.05$). The other groups also had had significantly greater increases in total body fat, trunk fat and AFM over five years compared with D+PA+, as demonstrated in the Figure. Significant interactions were observed and revealed that baseline PA was negatively associated with the change in total body fat (β=-0.23; P=0.001) and AFM (β=-0.25; P=0.001) over five years for participants with high 25OHD, but not those with low 25OHD (β=-0.06 and β=-0.09; both P>0.05).

CONCLUSIONS: Older adults with both higher 25OHD and PA status had significantly smaller increases in body fat over five years, but no differences were observed for muscle mass or function. PA was negatively associated with age-related increases in body fat only in those with high baseline 25OHD status at baseline, suggesting correction of vitamin D deficiency may be important for older adults commencing exercise interventions in order to optimise fat loss.

Change in body fat over five years according to vitamin D and physical activity status at baseline.

Disclosures: Peter Ebeling, None.

SA0054

See Friday Plenary Number FR0054.

SA0055

See Friday Plenary Number FR0055.

SA0056

Withdrawn

SA0057

See Friday Plenary Number FR0057.

SA0058

See Friday Plenary Number FR0058.

SA0059

See Friday Plenary Number FR0059.

SA0060

See Friday Plenary Number FR0060.

SA0061

WNT16 genetic variation in fracture-prone children. Minna Pekkinen*[1], Sara Mäkitie[2], Suvi Vallius[2], Mervi Mäyränpää[3], Outi Mäkitie[4]. [1]Folkhälsan Institute of Genetics, University of Helsinki, Finland, [2]Folkhälsan Research Center, Biomedicum Helsinki, Finland, [3]Children's Hospital, Helsinki University Central Hospital & University of Helsinki, Finland, [4]Folkhälsan Research Center, Biomedicum Helsinki, Department of Molecular Medicine & Surgery, Karolinska Institutet, Stockholm, Sweden, Department of Clinical Genetics, Karolinska University Hospital, Stockholm, Sweden, Finland

Introduction: *WNT16* has been shown to associate with bone mineral density (BMD), bone strength, and osteoporotic fractures in several genome-wide association studies. WNT signaling stimulates the differentiation of osteoblast precursors and plays a major role in skeletal development and homeostasis. WNT16, a ligand to the signaling pathway, has a crucial role in cortical bone homeostasis. The deletion of *Wnt16* specifically affects cortical bone in mice by increasing sclerostin and RANKL/OPG ratio and leading to increased cortical bone resorption and porosity, and to decreased thickness. Decreased cortical bone density is associated with non-vertebral osteoporotic fractures. We therefore wanted to explore the role of WNT16 genetic variation in fracture-prone children.

Subjects and methods: During a 12-month period we recorded fracture history for all children (n=1412) who were treated for an acute fracture at Helsinki University Hospital. All apparently healthy children over 4 years of age, who had sustained: (1) at least one vertebral fracture; (2) two long-bone fractures before age 10 years; or (3) three long-bone fractures before age 16 years, were recruited. A total of 72 (5.2%) children fulfilled these inclusion criteria. *WNT16* gene exons were Sanger sequenced in 62 of these fracture-prone children and in 95 healthy controls.

Results: In the fracture-prone children we found seven different *WNT16* polymorphisms: c.1-4insCCCA (rs72099717) and c.66C>G (rs35391640) in exon 1, c.214C>T, p.G72R (rs2908004) and c.270 C>A, p.T90V (rs17143291) in exon 3, c.600G>A, p.R200R (rs17143296), c.601A>C, p.Q201K (rs74389152) and c.758C>T, p.T253I (rs2707466) in exon 4. Genotypes among the fracture-prone subjects were were for c.1-4ins -/- (63%), -/ins (34%) and ins/ins (3%); for c.66 C/C (86%) and C/G (15%); for c.214 C/C (32%), C/T (55%), and T/T (13%); for c.270 C/C (98%) and C/A (2%); for c.600 G/G (95%) and G/A (5%); for c.601 A/A (98%) and A/C (2%); and for c.758 C/C (35%), C/T (52%) and T/T (13%). However, all these polymorphisms were also found in healthy controls and genotype frequencies did not differ between the fracture-prone children and healthy controls.Conclusions: Despite recent observations demonstrating that *WNT16* genetic variation impacts cortical bone thickness, BMD, bone strength, and risk of fractures in mice and humans, our findings indicate that *WNT16* mutations or variations are not a common cause of increased fractures in children.

Disclosures: Minna Pekkinen, None.

SA0062

Effect of Long-Term Intravenous Bisphosphonate Treatment in Children with Osteogenesis Imperfecta. Telma Palomo De Oliveira*[1], Francis Glorieux[2], Frank Rauch[3]. [1]UNIFESP Sao PauloShriners Hospital for Children, McGill University, Canada, Brazil, [2]Shriners Hospital for Children & McGill University, Canada, [3]Shriners Hospital for Children, Montreal, Canada

Cyclical intravenous bisphosphonate therapy is widely used to treat children with osteogenesis imperfecta (OI), but little is known about long-term treatment outcomes. We therefore performed a retrospective chart review on 39 children (female: n=22 male:17) with OI who started intravenous bisphosphonate therapy before 5 years of age (median, 2.2 years; range, 5 weeks to 4.8 years),and who had a subsequent follow up period of at least 10 years (median,14.8 years; range 10.7 to 18.2 years) during which they had received intravenous bisphosphonate treatment (pamidronate or zoledronate) for at least 6 years. During follow-up, the lumbar spine areal bone mineral density z-score increased from -5.0 (SD:1.59) to -2.7(SD:1.25) and weight z-score increased from -3.2 (1.3) to -1.8 (1.8) (p<0.001 each). Height z-scores increased (p=0.04) from -5.2 (2.9) to -4.0 (2.0) in OI type IV (n=24), but did not change in OI-III (n=14). Patients had a median of 6 femur fractures (range, 0 to 18) and 4 tibia fractures (range, 0 to 17) during the follow-up period, and underwent a median of 9 (range, 0 to 24) intramedullary rodding procedures (upper and lower extremity segments combined). Spinal fusion surgery was performed in 17 patients. The median Cobb angle in the 22 patients who did not undergo spinal fusion was 21 degrees (range, 0 to 56). In conclusion,long-term intravenous bisphosphonate therapy was associated with higher z-scores forlumbar spineareal bone mineral density, weight and, in OI type IV, height, but the disease burden remains very high. More effective treatment approaches are required.

Disclosures: Telma Palomo De Oliveira, None.
This study received funding from: Shriners Hospital for Children

SA0063

See Friday Plenary Number FR0063.

SA0064

See Friday Plenary Number FR0064.

SA0065

See Friday Plenary Number FR0065.

SA0066

See Friday Plenary Number FR0066.

SA0067

See Friday Plenary Number FR0067.

SA0068

See Friday Plenary Number FR0068.

SA0069

See Friday Plenary Number FR0069.

SA0070

See Friday Plenary Number FR0070.

SA0071

See Friday Plenary Number FR0071.

SA0072

See Friday Plenary Number FR0072.

SA0073

See Friday Plenary Number FR0073.

SA0074

Letrozole and Ovariectomy Cause Bone Loss, Muscle Weakness and Increased Breast Cancer Bone Metastases in Mice. Laura Wright*[1], Ahmed Harhash[2], David Waning[3], Khalid Mohammad[1], Andrew Marks[4], Theresa Guise[1]. [1]Indiana University, USA, [2]Indiana University, USA, [3]Indiana University School of Medicine, USA, [4]Columbia University, USA

Adjuvant endocrine therapy using an aromatase inhibitor (AI) is a standard treatment for postmenopausal women with estrogen receptor (ER)-positive breast cancer. Unfortunately, 50% of women treated with an AI develop musculoskeletal complications. Previous studies in our laboratory have demonstrated bone loss and muscle weakness in ovariectomized (OVX) mice. We therefore hypothesized that complete estrogen deprivation using the AI letrozole would cause more profound muscle weakness and bone loss than OVX alone, and that this high bone turnover state could accelerate the progression of breast cancer bone metastases and negatively impact muscle function.

To test this, four-week female athymic nude mice underwent OVX or sham surgery and were treated daily with vehicle or AI (10μg/day; n=20/group). Two weeks after surgery and onset of treatment, bone mineral density was reduced in OVX-AI mice relative to vehicle-shams (p<0.01) as assessed by dual energy X-ray absorptiometry. Using bone micro-computed tomography (SCANCO viva40CT), trabecular bone volume fraction (BV/TV) of the proximal tibia was reduced by 53% is OVX-vehicle mice (p<0.001) and by 67% in OVX-AI mice (p<0.001) relative to vehicle-sham.

After confirming bone loss, the same animals were inoculated with ER-negative MDA-MB-231 human breast cancer cells into the left cardiac ventricle and were followed for osteolytic lesion formation (n=10-15/group). Since MDA-MB-231 is ER-negative, effects of complete estrogen deprivation should be indirect. Five weeks after inoculation, osteolytic lesion area was larger in OVX-AI mice relative to sham-vehicle (p=0.0215), while OVX or AI alone did not alter lytic lesion area. Skeletal muscle function was assessed by ex vivo measurement of maximal contractile specific-force of the extensor digitorum longus muscle. At 200Hz maximal contractile force in sham-letrozole and OVX-vehicle mice was reduced by 7% (p<0.05) and reduced by 12% in OVX-AI mice (p<0.001) relative to sham-vehicle.

Our murine studies confirm that AI treatment induces bone loss and skeletal muscle weakness, recapitulating effects in cancer patients. As hypothesized, the severe bone loss resulting from AI-induced estrogen depletion may prime the bone microenvironment for the development of breast cancer metastases to bone and potentiate muscle weakness. This model serves as an excellent tool to study the mechanisms of underlying musculoskeletal defects in cancer patients and assess potential therapeutics.

Disclosures: Laura Wright, None.

SA0075

See Friday Plenary Number FR0075.

SA0076

VEGF/HGF Inhibitor Cabozantinib Decreases RANKL Expression in Osteoblastic Cells and Inhibits Osteoclastogenesis and PTHrP-Stimulated Bone Resorption. Paula Stern*[1], Keith Alvares[2]. [1]Northwestern University Feinberg School of Medicine Department of Molecular Phar, USA, [2]Northwestern University, USA

Cabozantinib, a small molecule inhibitor of vascular endothelial growth factor (VEGF) and hepatocyte growth factor (HGF) signaling, has elicited impressive effects to decrease bone lesions in patients with prostate cancer metastases. To determine direct effects of the drug on bone, effects of the agents were examined on resorption in neonatal mouse bone organ cultures and on gene epxression, cell proliferation and phenotypic markers in osteoblast and osteoclast cell lines. Cabozantinib, 0.3 and 3 uM, prevented PTHrP-stimulated calcium release from neonatal mouse calvaria. The inhibitory effects were significant at 48 hr and sustained in longer cultures. 3 uM, but not 0.3 uM, inhibited calcium release from unstimulated bones. Since the effect on resorption culd reflect either effects on osteoblasts to prevent osteoclast activation, or direct inhibition of osteoclasts, responses in osteoblastic and osteoclast precursor cell lines were examined. 24 hr ptreatment of osteoblastic MC3T3-E1 cells with 3 uM cabozantinib results in decreased expression of receptor activator of NFkB ligand (RANKL) and alkaline phosphatase with no change in osteoprotegerin. 48 hr treatment of MC3T3-E1 cells with 3 uM cabozantinib resulted in inhibition of cell proliferation and decreased MTT activity. These effects of cabozantinib are consistent with earlier findings that VEGF promotes osteoblast survival and RANKL expression in MC3T3-E1 cells. Effects on alkaline phosphatase activity were biphasic, with small stimulatory effects from concentrations below 3 uM. When RAW 264.7 osteoclast precursor cells were differentiated with 20 ng/ml RANKL and c0-treated for 24 hr with 3 uM cabozantinib, there was no effect on the expression or RANK, TRAP, cathepsin K, alpha v or beta 3 integrin, or NFATc1. 5-day treatment of RANKL-treated RAW 264.7 cells with 3 uM cabozantinib decreased TRAP and MTT activity. These effects of cabozantinib are consistent with effects of VEGF to promote RANKL-stimulated osteoclast formation. The results suggest that the osteoblast could be the initial target for the effects of cabozantinib, with subsequent direct and indirect effects on osteoclastogenesis leading to decreased bone resorption. The multiple effects of cabozantinib on the bone microenvironment are consistent with the effectiveness of the drug in reducing the lesions resulting from prostate cancer metastases.

Disclosures: Paula Stern, Exelixis, 7
This study received funding from: Exelixis

SA0077

See Friday Plenary Number FR0077.

SA0078

See Friday Plenary Number FR0078.

SA0079

See Friday Plenary Number FR0079.

SA0080

See Friday Plenary Number FR0080.

SA0081

See Friday Plenary Number FR0081.

SA0082

Withdrawn

SA0083

Estrogen-related receptor alpha confers Methotrexate resistance via attenuation of *reactive oxygen species* **production and p53 apoptosis pathway in osteosarcoma U2OS cells.** <u>Peng Chen</u>*[1], <u>Haibin Wang</u>[2], <u>Zhijian Duan</u>[3], <u>June X Zou</u>[3], <u>Hongwu Chen</u>[3], <u>Wei He</u>[2], <u>Junjian Wang</u>[3]. [1]First School of Clinical Medicine, Guangzhou University of Chinese Medicine/Cancer center, University of California at Davis, USA, [2]First Affiliated Hospital of Guangzhou University of Chinese Medicine, China, [3]Cancer center, University of California at Davis, USA

Osteosarcoma (OS) is a malignant tumor mainly occurring in children and adolescents. Methotrexate (MTX), chemotherapy agent, is widely used in treating OS. However, treatment failures are common due to acquired chemoresistance, for which the underlying molecular mechanisms are still unclear. In this study, we reported that overexpression of estrogen-related receptor alpha (ERRα), an orphan nuclear receptor, promoted cell survival and blocked MTX-induced cell death in U2OS cells. We showed that MTX induced ROS production in MTX-sensitive U2OS cells and that ERRα can effectively block the ROS production and ROS associated cell apoptosis. Our further studies demonstrated that ERRα suppressed ROS induction of tumor suppressor P53 and its target genes NOXA and XAF1, mediators of P53-dependent apoptosis. In conclusion, this study demonstrated that ERRα plays an important role in the development of MTX resistance through blocking MTX induced ROS production and attenuating the activation of p53 mediated apoptosis signaling pathway, and points to ERRα as a novel target for improving osteosarcoma therapy.

The purpose of this study is trying to elucidate the underlying molecular mechanisms of the development of MTX-resistance in osteosarcoma and improve the osteosarcoma therapy

Disclosures: Peng Chen, None.

SA0084

See Friday Plenary Number FR0084.

SA0085

See Friday Plenary Number FR0085.

SA0086

Zinc Finger Protein 521 regulates retinoblastoma protein-dependent cell-cycle progression: Potential implications for osteosarcoma. <u>Harikiran Nistala</u>*[1], <u>Coco Roening</u>[2], <u>Serhan Zenger</u>[3], <u>Ken-ichi Takeyama</u>[3], <u>Francesca Gori</u>[4], <u>Roland Baron</u>[5]. [1]Harvard University, USA, [2]Massachusetts College of Pharmacy & Health Sciences, USA, [3]Harvard School of Dental Medicine, USA, [4]Harvard School of Dental MedicineMassachusetts General Hospital, USA, [5]Harvard School of Medicine & of Dental Medicine, USA

Zinc finger protein 521 (Zfp521) has been implicated in lineage determination of mouse ES cells and in the maintenance of precursor cells within the neuronal, mesenchymal and hematopoietic lineages. Zfp521 regulates chondrocyte and osteoblast maturation and represses adipocyte lineage determination. More recently, we demonstrated that Zfp521 interacts with the nucleosome remodeling deacetylase (NuRD) complex via retinoblastoma binding protein 4 (Rbbp4) in conjunction with nuclear transglutaminases (Tgm1 and Tgm3). Furthermore, we established that this effector complex regulates mesenchymal cell-fate determination and maintenance of pluripotency using the murine teratoma formation and somatic cell reprogramming assays respectively.

Instructive and permissive signals regulate mesenchymal stem cell fate between differentiation and self-renewal. It has become increasing clear that Zfp521 in association with lineage specific transcription factors mediates cell-fate determination. However, the role of Zfp521 in self-renewal and implicitly in the maintenance of pluripotency remains unknown.

In the present study, we demonstrate that Zfp521 interacts with the retinoblastoma protein (pRb/p110), thereby regulating G1/S transition within the cell cycle. In particular, in-silico bioinformatic analyses showed that Zfp521 shares a conserved LXCXQ motif (within zinc-finger 15) similar the LXCXE motif that several viral onco-proteins employ for high-affinity binding and inhibition of pRb. Site-specific mutagenesis resulting in the deletion of the zinc-finger domain spanning the LXCXQ motif or substitution of the Cys residue resulted in the loss of interaction between Zfp521 and pRb and a concomitant de-repression of E2F-dependent transcription in luciferase assays. Germline deletion of Zfp521 or knockdown of Zfp521 in various primary cell lines including human mesenchymal stem cells resulted in a significant reduction in BrdU incorporation despite unremarkable changes in PCNA labeling suggesting a block in G1/S transition. Taken together, these results suggest a possible oncogenic role of Zfp521 in retinoblastoma and osteosarcoma. Mouse models overexpressing Zfp521 should provide a valuable platform for investigating the molecular genetics of osteosarcoma and for developing novel therapeutic targets.

Disclosures: Harikiran Nistala, None.

SA0087

See Friday Plenary Number FR0087.

SA0088

See Friday Plenary Number FR0088.

SA0089

See Friday Plenary Number FR0089.

SA0090

See Friday Plenary Number FR0090.

SA0091

Natural Large-scale Regeneration of Rib Cartilage in a Mouse Model. <u>Marissa Srour</u>*[1], <u>Kent Yamaguchi</u>[1], <u>Jennifer Fogel</u>[1], <u>Aaron Montgomery</u>[1], <u>Aaron Misakian</u>[1], <u>Stephanie Lam</u>[1], <u>Daniel Lakeland</u>[1], <u>Francesca Mariani</u>[2]. [1]University of Southern California, USA, [2]University of Southern California, USA

The clinical need for methods to repair and regenerate large cartilage and bone lesions persists. One way to make new headway is to study skeletal regeneration when it occurs naturally. Cartilage repair is typically slow and incomplete. However, an exception to this observation can be found in costal cartilages where complete repair has been reported in humans but the cellular and molecular mechanisms have not been characterized. In this study, we establish a novel animal model for cartilage repair using the mouse rib costal cartilage. We further identify the perichondrium, the dense connective tissue that surrounds the cartilage, as a tissue essential for repair. Our results show that full replacement of the resected cartilage occurs quickly (within 1-2 months) and properly differentiates, but that repair occurs only in the presence of the perichondrium. During the healing period, the perichondrium changes its morphology, and when ectopically placed can support the formation of new cartilage. We hypothesize that the rib perichondrium contains a special niche that houses chondrogenic progenitors that possess qualities particularly suited for mediating repair. In support of this idea, label-retaining cells can be found within the perichondrium that appear to give rise to new chondrocytes. In conclusion, we have successfully established a model for hyaline cartilage repair in the mouse rib, which should be useful for a more detailed understanding of cartilage generation and ultimately for developing methods to improve cartilage and bone repair in other parts of the skeleton.

Disclosures: Marissa Srour, None.

SA0092

See Friday Plenary Number FR0092.

SA0093

A Time Course of FoxO Transcription Factor Activation in a Binge Model of Alcohol-Induced Deficient Bone Fracture Repair. <u>Philip Roper</u>*[1], <u>John Callaci</u>[2]. [1]Loyola University Medical Center, USA, [2]Loyola University of Chicago, USA

Alcohol abuse has known deleterious effects on bone health. Binge drinking has become increasingly prevalent and the predominant alcohol abuse pattern associated

with traumatic orthopedic injury and fracture. Proper fracture healing relies on coordinated differentiation of mesenchymal stem cells (MSC) into osteoblasts and chondrocytes to form the callus. MSC differentiation is driven by the canonical Wnt signaling pathway, which activates the transcription factor β-catenin. β-catenin is also a necessary cofactor for the family of FoxO transcription factors, which are activated by oxidative stress. Oxidative stress is elevated by alcohol abuse, and contributes to much of the pathogenesis related to alcohol abuse. We hypothesize that the systemic administration of alcohol will inhibit fracture healing in mice by inducing systemic oxidative stress, activating FoxO-mediated oxidative stress signaling and concomitant antagonism of Wnt signaling.

7-8 week old male C57BL/6 mice received intraperitoneal injections of ethanol (2g/kg) or saline for three consecutive days per week for two weeks. One hour after the last injection, the left tibia was stabilized with an intramedullary pin and surgically fractured. Animals continued with daily ethanol injections until sacrifice. Fracture callus tissue was isolated for histology or homogenized for protein expression and activation assays.

At day 6 and 9 post fracture gross deficiencies in callus formation and fracture healing are seen in alcohol treated animals, with significant decreases in callus volume, chondrocyte maturation, and endochondral ossification (p<0.05). These time points are also marked by an increase in FoxO expression (p<0.05) and activation (p<0.05), with a parallel decrease in β-catenin activation (p<0.05).

These results support our hypothesis and begin to elucidate the mechanism of alcohol-induced deficient fracture repair. Alcohol administration increases FoxO signaling within the callus tissue while decreasing β-catenin activation. These changes coincide with drastic fracture callus malformations. Since Wnt signaling is required for MSC differentiation toward an osteo-chondro lineage, alcohol-related activation of FoxO signaling could antagonize necessary Wnt-mediated differentiation leading to this suppression of callus formation.

Disclosures: Philip Roper, None.

SA0094

Histone Deacetylase 7 Suppresses Chondrocyte Proliferation and β-Catenin Activity during Endochondral Ossification. <u>Elizabeth Bradley</u>*[1], <u>Lomeli Carpio</u>[1], <u>Eric Olson</u>[2], <u>Jennifer Westendorf</u>[1]. [1]Mayo Clinic, USA, [2]University of Texas Southwestern Medical Center, USA

Histone deacetylases (Hdacs) are emerging as important regulators of endochondral ossification due to their ability to suppress gene transcription and modulate cellular responses to growth factors and cytokines. We previously showed that Hdac7 suppresses Runx2 activity and osteoblast differentiation. In this study, we examined the role of Hdac7 in chondrocyte differentiation. Hdac7 was highly expressed in proliferating chondrocytes within the growth plate. Pre-natal deletion of Hdac7 in type 2a1 collagen (Col2a1)-expressing chondrocytes produced few Hdac7-deficient animals, indicating partially penetrant embryonic lethality. To overcome this, we crossed Hdac7^{fl/fl} mice with animals expressing a tamoxifen-inducible Col2a1-Cre transgene and administered tamoxifen at postnatal day 5. These Hdac7-deficient mice displayed low bone density but enhanced chondrocyte proliferation. Immunohistochemistry showed higher levels of active β-catenin within proliferative chondrocytes of the growth plates of Hdac7-deficient animals. Active β-catenin levels were also higher in ex vivo cultured Hdac7-depleted chondrocytes, whereas total levels of β-catenin remained constant. Transcripts of Lef1 and Axin2, downstream β-catenin target genes, were also elevated in Hdac7-deficient cells. Igf1 and insulin, two potent chondrogenic mitogens, induced proteasome-mediated degradation of Hdac7, increased active β-catenin levels and enhanced β-catenin transcriptional activity. These data demonstrate that Hdac7 suppresses chondrocyte proliferation rates and b-catenin stability during endochondral ossification.
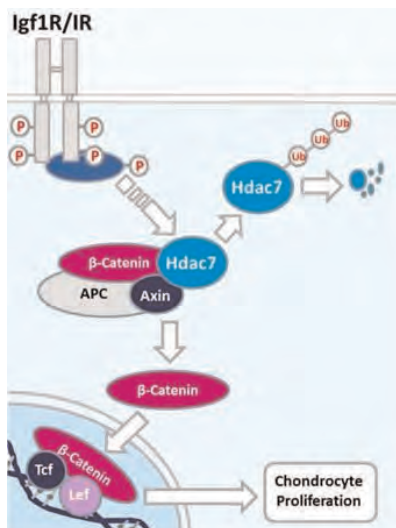
Bradley_Abstract Figure

Disclosures: Elizabeth Bradley, None.

SA0095

See Friday Plenary Number FR0095.

SA0096

The Notch target genes, *Hes1* and *Hes5*, regulate chondrogenesis and chondrocyte maturation by modulating *Sox9* expression. <u>Timothy Rutkowski</u>*[1], <u>Anat Kohn</u>[2], <u>Anthony Mirando</u>[3], <u>Deepika Sharma</u>[2], <u>Ryoichiro Kageyama</u>[4], <u>Michael Zuscik</u>[5], <u>Matthew Hilton</u>[6]. [1]University of Rochester, USA, [2]Graduate Student, USA, [3]Lab Manager, USA, [4]Collaborator, Japan, [5]University of Rochester School of Medicine & Dentistry, USA, [6]Duke University Musculoskeletal Research Center, USA

We have demonstrated that RBPjk-dependent Notch signaling suppresses chondrogenesis and induces chondrocyte maturation potentially via the repression of *Sox9*, however the molecular mechanisms remain unclear. Many of the HES/HEY transcriptional repressors are RBPjk-dependent Notch target genes. We have identified *Hes1, Hes5, Hey1,* and *HeyL* as Notch-regulated genes in mesenchymal progenitor cells (MPCs) and chondrocytes during cartilage development. Analyses of MPCs with *Hey1* and *HeyL* knock-down or of *Hey1^{-/-};HeyL^{-/-}* mutant embryos demonstrated no significant change in chondrogenesis and chondrocyte maturation *in vitro* or *in vivo*, suggesting that HEY factors may not be important for cartilage development. Interestingly, knock-down and over-expression of *Hes1* and/or *Hes5 in vitro* altered chondrogenesis and chondrocyte maturation in a manner consistent with RBPjk-dependent Notch loss-of-function (LOF) and gain-of-function (GOF), respectively. To determine whether HES1 and HES5 are necessary for limb cartilage development *in vivo*, we analyzed HES1 and HES1/5 LOF (*Prx1Cre;Hes1[f/f]* and *Prx1Cre;Hes1[f/f];Hes5^{-/-}*) mice at E11.5, E12.5, E13.5, E14.5, and E18.5. Histology, *in situ* hybridization, immunohistochemistry, and qPCR analyses of HES1/5 LOF limbs revealed accelerated chondrogenesis and delayed chondrocyte maturation with elevated and persistent SOX9 expression, a phenotype consistent with RBPjk-dependent Notch LOF models. Later stages of chondrocyte terminal maturation were only mildly delayed, suggesting that terminal chondrocyte hypertrophy and matrix turnover may be only partially HES-dependent. We also developed and analyzed HES1 GOF mice (*Prx1Cre;Rosa-Hes1[f/f]*) using a similar approach. Interestingly, we observed delayed or reduced chondrogenesis without a significant decrease in early *Sox9* expression. Therefore, to determine whether HES5 is sufficient to suppress *Sox9*, we performed *in vitro* HES5 GOF studies that caused reduced chondrogenesis and reduced *Sox9* expression. Using a 1kb *Sox9* luciferase construct, we observed a significant decrease in *Sox9* luciferase activity when HES5 was over-expressed *in vitro*. Lastly, chromatin immunoprecipitation (ChIP) analyses showed HES5 binding to the *Sox9* promoter in MPCs. Collectively, these data demonstrate that the downstream RBPjk-dependent Notch targets, HES1 and HES5, are important regulators of chondrogenesis and chondrocyte maturation, and that HES5 is the likely direct Notch target suppressing *Sox9*.

Disclosures: Timothy Rutkowski, None.

SA0097

See Friday Plenary Number FR0097.

SA0098

See Friday Plenary Number FR0098.

SA0099

See Friday Plenary Number FR0099.

SA0100

Withdrawn

SA0101

Thrombospondin-2 contributes to whole bone mechanical properties through its effects on collagen fibrillogenesis, lysyl oxidase activity and mineralization. <u>Eugene Manley, Jr.</u>*[1], <u>Joseph Perosky</u>[1], <u>Basma Khoury</u>[2], <u>Kenneth Kozloff</u>[3], <u>Andrea Alford</u>[1]. [1]University of Michigan, USA, [2]University of Michigan, USA, [3]University of Michigan Department of Orthopaedic Surgery, USA

The matrix protein, thrombospondin-2 (TSP2) affects collagen fibrillogenesis in a variety of physiologic contexts. Given the importance of type I collagen for the biologic and mechanical integrity of the skeleton, our objectives were to determine the effects of TSP2-deficiency on structural and mechanical properties at the whole-bone

level and on markers of collagen matrix formation at the cellular level. Left femora of 6-week old male TSP2+/+ (n=3) and -/- (n=5) C57/B6 mice were imaged by microCT and subjected to 4-pt bending. Slivers of tibial diaphyseal cortical bone were viewed by transmission electron microscopy (TEM). Additional 6-week old male mice (n=6-8 per genotype) were used to establish primary marrow-derived MSC-osteoblast cultures. Data are mean $\pm$ SD. TSP2-/- femora demonstrated a brittle phenotype, reflected by reduced post-yield displacement (0.56 $\pm$ 0.18 vs. 0.73 $\pm$ 0.18 mm), with PYD assessed as the total displacement between yield load and when load decreased 25% after ultimate load. Despite a reduced bending moment of inertia in TSP2-/-, (0.079 $\pm$ 0.018 vs 0.094 $\pm$ 0.004 mm4), both genotypes displayed comparable stiffness (94.5 $\pm$13.7 vs 97.8 $\pm$3.7 N/mm). To identify possible tissue-level mechanisms by which TSP2-deficiency affects whole-bone mechanics, we examined mineralization by microCT and collagen fiber morphology by TEM. Tissue mineral density was higher in TSP2-/- bones (919.7 $\pm$ 13.09 vs 902.2 $\pm$ 15.0 mg/cc). TSP2 -/- collagen fibers captured in cross-section were large and had diffuse borders, and those captured longitudinally lacked the characteristic periodicity of collagen-rich tissues. To elucidate the mechanisms by which TSP2 might contribute to collagen fibrillogenesis and skeletal tissue function, we examined markers of collagen matrix formation in primary MSC-osteoblasts. On Western blot, relative levels of liberated lysyl oxidase (LOX) pro-peptide were significantly reduced in TSP2 -/- cultures at day 10 (402 $\pm$ 123 vs 1859 $\pm$ 296 pixels, p<0.01) and day 14 (402 ? 334 and 6080 ? 4785 pixels, p<0.05). Concurrently, LOX activity was reduced in TSP2 -/- cultures at day 14 (15.4 $\pm$ 8.5 vs 28.3 $\pm$ 13.3 nmoles/μl/min, p<0.05). LOX conducts the final step of collagen fibrillogenesis by catalyzing crosslinks between collagen fibrils and fibers. Together our data suggest that TSP2 contributes to normal bone tissue composition and function by facilitating LOX-mediated cross-linking and mineralization.

Disclosures: Eugene Manley, Jr., None.

SA0102

See Friday Plenary Number FR0102.

SA0103

See Friday Plenary Number FR0103.

SA0104

See Friday Plenary Number FR0104.

SA0105

Lipoprotein lipase links systemic lipid transport to bone matrix and bone marrow fatty acid composition. Alexander Bartelt[1], Till Koehne[1], Till Koehne[2], Reimer Rudolph[3], Brigitte Mueller[2], Joerg Heeren[2], Ludger Scheja[4], Andreas Niemeier*[5]. [1]University Medical Center Hamburg-Eppendorf, Germany, [2]University Medical Center Hamburg-Eppendorf, Germany, [3]Heinrich Pette Institut Hamburg, Germany, [4]UKE Hamburg, Germany, [5]University Medical Center Hamburg-Eppendorf, Germany

Adipocytes are key regulators of energy homeostasis. Although the contribution of classical brown and white adipose tissue (BAT or WAT) to glucose and fatty acid metabolism are well characterized, the metabolic role of adipocytes in bone marrow remains elusive.

The purpose of this study was to characterize skeletal fatty acid metabolism and its contribution to systemic nutrient glucose and lipid handling in mice.

Whereas in parts of the skeleton the specific amount of fatty acids taken-up from the circulation was lower than in other metabolically active tissues such as BAT or liver, the overall contribution of the skeleton as a whole organ was quantitatively important, placing the skeleton among the top organs involved in systemic glucose as well as fatty acid clearance. We show that, especially in the bone marrow of the tibia, the fatty acid profile resembles classical BAT and WAT. Using a mouse model lacking a master regulator of plasma lipid turnover, lipoprotein lipase (LPL), specifically in adipocytes, we show that impaired fatty acid flux leads to reduced amounts of dietary essential fatty acids in both bone marrow and cortical bone while there was a profound increase in de novo produced fatty acids in both bone marrow and cortical bone.

In summary, we demonstrate that systemic fatty acid metabolism is intricately linked to local fatty acid metabolism in bone marrow and bone matrix.

Disclosures: Andreas Niemeier, None.

SA0106

Osteocalcin and Markers of the Metabolic Syndrome in Overweight Children within the IDEFICS Study. Bojan Tubic*[1], Per Magnusson[2], Staffan Mårild[3], Monica Leu[4], Verena Schwetz[5], Isabelle Sioen[6], Diana Herrmann[7], Barbara Obermayer-Pietsch[8], Lauren Lissner[4], Diana Swolin-Eide[9]. [1]Gothenburg University, Sweden, [2]Linkoping University,Sweden, Sweden, [3]Department of Pediatrics, The Queen Silvia Children's Hospital, Sweden, [4]Department of Public Health & Community Medicine, University of Gothenburg, Sweden, [5]Division of Endocrinology & Metabolism, University of Graz, Austria, [6]Department of Public Health, Ghent University, Belgium, [7]Leibniz Institute for Prevention Research & Epidemiology , Bremen, Germany, [8]Medical University Graz, Austria, [9]Queen Silvia Children's Hospital, Sweden

Purpose: Interactions between bone tissue and energy metabolism have not been thoroughly investigated during early childhood. This study was designed to investigate undercarboxylated osteocalcin (ucOC) and carboxylated osteocalcin (cOC) and their association with metabolic parameters and anthropometric characteristics in normal and overweight children.

Methods: A subsample of the Swedish subjects (n=108) participating in the 2007-2008 baseline survey of the IDEFICS (Identification and prevention of Dietary- and lifestyle-induced health Effects In Children and infantS) Study was included. A total of 62 overweight children of whom 46 were matched with 46 normal weight children aged 2-9 years, with respect to age, gender and month in which blood samples were collected. Subjects were categorized into weight categories according to International Obesity Task Force, Cole, 2012. Serum OC was measured with an electrochemiluminescence immunoassay on a Cobas instrument (Roche). The carboxylated fraction of OC was also determined in serum and was separated from ucOC samples by adsorption on hydroxyapatite. Insulin, glucose, HbA1C levels were measured and HOMA index was calculated. Mann-Whitney test were used for group comparisons and Spearman test for correlations.

Results: For the normal weight and overweight group mean (SE), height was 124.5 cm (1.89); 125.9 cm (1.67) P=0.55, weight 24.7 kg (0.84); 31.3 kg (0.93) P<0.0001, Body Mass Index – Standard Deviation Score (BMI-SDS) 0.05 (0.09); 1.80 (0.07) P<0.0001, respectively. Normal weight children had significantly higher cOC levels, mean 75.6 μg/L compared with overweight children, mean 69.1 μg/L, P<0.05. Overweight children had mean ucOC levels of 7.9 μg/L and normal weight children had mean levels of 7.0 μg/L, P=0.067. No difference was found for total OC between the normal- and overweight group, mean 82.6 μg/L respectively 77.0 μg/L, P=0.11. Total OC and cOC correlated inversely with HbA1C ($r=$ -0.28, P=0,03); ($r=$-0,3, P=0.02), respectively. Total OC, cOc and ucOC did not correlate with HOMA index, insulin, glucose levels or BMI-SDS score in the two subject groups.CONCLUSION: Carboxylated OC levels were lower in overweight young children. A tendency in increased uOC was found in overweight compared to normal weight children. Total OC and cOC was inversely correlated with HbA1C. Larger studies are warranted to explore the possible metabolic role of cOC in children.

Disclosures: Bojan Tubic, None.

SA0107

See Friday Plenary Number FR0107.

SA0108

See Friday Plenary Number FR0108.

SA0109

See Friday Plenary Number FR0109.

SA0110

Involvement of Sclerostin and FGF23 on Cardiovascular Disease in Men with or without type 2 Diabetes. Daniela Merlotti*[1], Luigi Gennari[1], Domenico Rendina[2], Konstantinos Stolakis[3], Claudio Corallo[3], Riccardo Muscariello[2], Stefano Rotatori[3], Maria Beatrice Franci[3], Barbara Lucani[3], Stefano Gonnelli[1], Nicola Giordano[3], Piero Tanganelli[4], Carlo Setacci[3], Pasquale Strazzullo[2], Ranuccio Nuti[1]. [1]University of Siena, Italy, [2]Department of Clinical & Experimental Medicine, Federico II University, Italy, [3]Department of Medicine, Surgery & Neurosciences, University of Siena, Italy, [4]Department of Medical biotechnologies, University of Siena, Italy

Sclerostin (SCL) and FGF23 are osteocyte-secreted factors which exert a major role in bone formation and mineral homeostasis. Recently, variations in their circulating levels were described in patients with diabetes (DM) and/or cardiovascular

disease (CVD). Moreover, both FGF23 and SCL are expressed in calcifying vascular smooth muscle cells in mice, suggesting an up-regulation of key osteocytic molecules during the vascular calcification process. In order to provide further insight on the relationship between these 2 osteocyte-derived factors and cardio-metabolic disorders we assessed their levels in a well characterized sample of 253 elderly DM and non-DM men from the Olivetti Heart Study cohort (an ongoing nationwide survey on the prevalence of cardiovascular risk factors) matched for age and BMI. Moreover, serum and tissue samples of 28 patients (11 DM and 17 non DM) who underwent carotid endarterectomy were collected and analyzed. Serum SCL levels significantly decreased with age in all subjects, and were inversely associated with renal function. The correlation was maintained when the 39 cases with renal impairment (GFR<60 mL/min) were excluded. Conversely, FGF23 levels were inversely associated with renal function only in patients with renal impairment. Both SCL and FGF23 levels were slightly but not significantly increased in DM vs non-DM patients, while a significant increase in SCL was observed in DM patients with CVD vs DM patients without CVD. On the opposite, FGF23 levels were increased in CVD patients irrespective of DM status. Importantly, SCL but not FGF23 levels were significantly affected by antidiabetic treatment, being reduced in metformin users and enhanced with insulin or sulphonylurea treatment. Finally, both SCL and FGF23 were significantly higher in patients with mild to severe abdominal aortic calcification (assessed by ultrasonography) than in subjects without calcifications. Consistent with the clinical data, a preliminary immunohistochemistry analysis of carotid plaques demonstrated SCL staining in most samples, particularly in calcifying smooth muscle cells and fibrotic tissue. Increased expression levels were observed in diabetic vs non-diabetic patients. Taken together these data indicate that both FGF23 and SCL play a role in the mechanisms of vascular calcification with a different impact in DM vs non-DM patients. Prospective studies are needed to evaluate the predictive power of these 2 osteocyte-derived markers on CVD.

Disclosures: Daniela Merlotti, None.

SA0111

Low Osteocalcin Levels are associated with Bone Marrow Transplant, more than Insulin Resistance, in Adult Survivors of Childhood Cancer. <u>Christopher White</u>*[1], <u>Jan Walker</u>[2], <u>Richard Cohn</u>[3], <u>Kristen Neville</u>[2]. [1]Prince of Wales Hospital, Australia, [2]Sydney Children's Hospital Randwick, Australia, [3]Sydney Chidlren's Hospital Randwick, Australia

Bone marrow fat may regulate bone mineral metabolism. Bone marrow transplant (BMT[+]) demonstrates early adipogenic change[1]. Survivors of childhood cancer develop insulin resistance[2]. Osteocalcin (OC) has been shown to influence insulin insensitivity in mice. We explored the association between insulin resistance and bone mineral metabolism in a study of survivors of childhood cancer who underwent BMT[+].

Methods: OC and P1NP were measured in 99 adult survivors almost 20 years after the treatment of their primary cancer in childhood. Diagnoses included haematological malignancies, neuroblastoma, Wilms tumour, bone and soft tissue and brain tumours. Nineteen had BMT[+] and 12 received total body irradiation (TBI) for conditioning. Adults were overweight/obese if BMI was $\geq$25kg/m^{2}. Abdominal adiposity (AA[+]) was defined as a waist:height ratio >0.5. Hyperinsulinemia (HI) was defined as a fasting insulin $\geq$20mU/L or peak insulin during OGTT $\geq$150mU/L and abnormal glucose tolerance (aGT) included those with either impaired glucose tolerance (IGT) or Diabetes Mellitus (DM) based on WHO criteria.

Results: BMT[+] is more insulin resistant than BMT[-] despite lower BMI (Table 1). While BMT[+] is more likely to be male and slightly shorter these differences were not significant. In both groups AA[+] was associated with significantly lower OC but BMI and markers of insulin resistance (HI+aGT) had no significant effect. Following adjustment for age, gender and abdominal adiposity BMT[+] was associated with significantly lower levels of OC than BMT[-] (Table 2) A similar but non-significant trend was seen for PINP.

Conclusions: Survivors of childhood cancer, particularly BMT[+], develop insulin resistance. OC, more so than the bone formation marker PINP, is reduced following BMT[+] and is associated with abdominal adiposity but not BMI nor a composite of HI, IGT or DM in adults surviving childhood cancer. These cross-sectional data suggest that the BMT[+] effect on OC is a consequence of engraftment; more so than from changes in insulin sensitivity though a contribution from AA[+] could exist. A longitudinal study of childhood cancer survivors will give greater insight into the factors that influence sequential changes in carbohydrate and bone mineral metabolism in this cohort.

1) Naveiras O. et al Nature 460:259-64. 2009
2) Neville K. et al JCEM 91: 4401–07, 2006

TABLE 1	BMT[+] (n= 19)	BMT[-] (n= 80)	p-value
Age	24 [18-38]	25 [18-39]	0.32
Years Since First Diagnosis	16.0 [10.2-32.5]	19.7 [6.3-33.6]	0.22
TBI	12 (63%)	0	
Sex (M/F)	14/5	41/39	0.08
Height SDS	-1.2 ±1.4	-0.8 ±1.2	0.22
Waist (cm)	82.2 ±10.5	84.5 ±14.2	0.53
BMI (kg/m^{2})	22.9 ±3.7	25.6 ±5.2	0.03
Waist/Ht ratio	0.49 ±0.06	0.51 ±0.08	0.42
AA[+]	9 (47%)	39 (49%)	0.91
Insulin (fasting) mU/L	18 [3-103]	7 [<2-61]	0.02
Glucose (fasting) mmol/L	5.1 ±1.6	4.7 ±0.5	0.05
HOMA mU.mmol/L[2]	2.6 [0.6-55.9]	1.5 [0.2-16.5]	0.004
HI+aGT	9 (47%)	6 (8%)	<0.001
aGT (IGT or DM)	7 (37%)	3 (4%)	<0.001
OC (ng/ml)	21.0 ±8.0	25.6 ±12.7	0.14
PINP (ng/ml)	62.2 ±29.2	67.6 ±36.0	0.55
25 OHD (nmol/L)	63.6 ±34.0	58.7 ±22.4	0.44

TABLE 2	BMT+	BMT-	β	95%CI	p value
OC (ng/ml)	21.0	25.6 ±12.7	7.7	2.4 - 12.9	0.004
	AA[+]	AA[-]	β	95%CI	p value
OC (ng/ml)	21.0	25.6 ±12.7	4.6	0.1 – 9.0	0.04

Osteocalcin, Bone Marrow Transplant and Insulin Resistance in Adult Survivors of Childhood Cancer

Disclosures: Christopher White, None.

SA0112

Mechanisms of Mitochondrial Remodeling in Bone loss during Hyperhomocysteinemia: A therapeutic aspect of Hydrogen Sulfide. <u>Anuradha Kalani</u>*[1], <u>Pradip K Kamat</u>[2], <u>Neetu Tyagi</u>[3]. [1]PhD, USA, [2]Univeristy of Louisville, USA, [3], USA

Hyperhomocysteinemia (HHcy, elevated levels of homocysteine) is the risk factor for osteoporotic fracture. Additionally, bone quality and strength is compromised by HHcy due to negative impact on collagen maturation by homocysteine (Hcy) coupling, a process called homocysteinylation. Thiol (–SH) group of Hcy is readily oxidized and generated reactive oxygen species (ROS) that lead to mitochondrial (mito-) oxidative stress. Hydrogen sulfide (H2S), a gasotransmitter, is endogenously synthesized and exerts a regulatory impact on many physiological and pathophysiological processes. Hence, the objective of this study was to evaluate the effect of H2S on mitochondrial remodeling that mitigates bone pathology during HHcy. We hypothesize that Hcy induces mitochondrial dysfunction, in part by altering mitochondrial fission and fusion events while H2S mitigates altered mito-dynamic events and improve bone quality. To test this hypothesis we employed wild-type (WT) males ages 8-10 weeks, WT, WT+NaHS (precursor of hydrogen sulfide,15 μM/kg body weight, intraperitoneal route, 15 days) CBS+/-, CBS+/-+NaHS. The mice were tested for biomechanical, X-ray, bending, micro CT tests. The bones were isolated and proteins were extracted along with pure mitochondrial preparations. Mitochondria were subjected for determination of mitochondrial fission (DRP-1) and fusion (Mfn-2) markers using Western blot, quantitative PCR and immunohistochemical analysis. The extent of collagen cross-linking with Hcy was determined with immunoprecipitation. Alkaline phosphatase and tartrate-resistant acid phosphatase assays were performed to check osteoclast expression in the bone. Our results determined CBS+/-bone weak and less stiffed using bending and x-ray tests. Micro CT analysis confirmed increased bone loss in CBS+/- bone as compared to other groups. In context with micro CT, histomorphometry analysis determined anomaly of bone cells in CBS+/-mice as compared to WT and WT+NaHS groups. Further molecular and immuno-localization studies revealed increased DRP-1 and decreased Mfn2 expression in CBS+/- mitochondrial fractions as compared to WT and WT+NaHS. Interestingly, the treatment of NaHS in CBS+/- mice significantly alleviated the bone deformities and increased bone strength. In conclusion, these results suggest our understanding of the pathogenesis of bone disease that included mito-dynamic events. The study also paves the way for development of new treatment options in bone deformity during HHcy.

Disclosures: Anuradha Kalani, None.

SA0113

See Friday Plenary Number FR0113.

SA0114

See Friday Plenary Number FR0114.

SA0115

Phosphate and calcium phenotype of GLUT2-/- mice, an animal model for Fanconi-Bickel-Syndrome. <u>Ruiye Bi</u>*[1], <u>Wenping Zhao</u>[1], <u>Hiroko Segawa</u>[2], <u>Bernard Thorens</u>[3], <u>Michael Mannstadt</u>[4]. [1]Massachusetts General Hospital, USA, [2]University of Tokushima Graduate School, Japan, [3]University of Lausanne, Switzerland, [4]Massachusetts General Hospital Harvard Medical School, USA

Purpose: Fanconi-Bickel Syndrome (FBS), an autosomal-recessive disease caused by loss-of-function mutations in the glucose-transporter GLUT2, is characterized by renal tubulopathy and can be associated with severe hypophosphatemic rickets. To investigate the mechanisms leading to phosphaturia, we characterized a mouse model of FBS.

Methods: Mice homozygous for the deletion in GLUT2 (GLUT2-/-) were rescued from early lethality by allowing glucose-stimulated insulin secretion through the transgenic expression of the related GLUT1 in the pancreas (tgGLUT2-/-). We studied the phosphate and calcium phenotype of mice homozygous (tgGLUT2-/-) or wildtype (tgGLUT2+/+) for the Glut2 ablation.

Results: Similar to patients with FBS, and consistent with previous reports, tgGLUT2-/- mice show significant glycosuria and mild hypoglycemia. tgGLUT2-/- mice further exhibit a modest increase in urinary fractional excretion of phosphorus (1.25 ± 0.13 dl/mg) compared to tgGLUT2+/+ mice (0.75 ± 0.08) (p<0.01) but no difference in serum phosphate. Western blot analysis using kidney brush border membranes revealed a profound 60% reduction of Npt2c in tgGlut2-/- compared to tgGLUT2+/+ mice. Surprisingly, Npt2a was significantly increased by 45%, which we confirmed by immunohistochemical evaluation of kidney sections. This observation argues against a general transporter dysfunction in the proximal tubule. tgGlut2-/- mice, compared with tgGlut2+/+, displayed lower circulating PTH (41 ± 8 vs 168 ± 31 pg/ml, p<0.01), lower 1,25(OH)2D3 (22 ± 4 vs 60 ± 12 pmol/dl, p<0.01) levels, hypercalciuria, but indistinguishable blood ionized calcium levels. Increased bone resorption, as evidenced by higher serum CTX in tgGLUT2-/- mice compared to tgGLUT2+/+ mice (51 ± 2 vs 39 ± 3 ng/ml, p<0.01), is likely the cause for this finding and could explain the lower bone density (Piximus X-ray).

Conclusions: tgGLUT2-/- mice exhibit profound downregulation of Npt2c, increased urinary phosphate excretion, but normal serum phosphate levels, contrary to humans with GLUT2 mutations, who can develop severe hypophosphatemia. This might reflect the different roles of Npt2c in mice, where almost no phenotype is observed when deleted, compared to humans where Npt2c mutations lead to rickets (HHRH). The intriguing calcium phenotype (low PTH, low 1,25(OH)2D3, normal serum and high urinary calcium) is likely due to increased bone resorption. The reason for the increased bone resorption is to be determined.

***Disclosures: Ruiye Bi**, None.*

SA0116

See Friday Plenary Number FR0116.

SA0117

Raman Micro-spectroscopic Analyses of Compositional Heterogeneity in Osteogenesis Imperfecta Mouse Bone. <u>Xiaomei Yao</u>*[1], <u>Charlotte Phillips</u>[2], <u>Yong Wang</u>[1]. [1]University of Missouri-Kansas City, USA, [2]University of Missouri-Columbia, USA

Osteogenesis imperfecta (OI) is characterized by bone fragility and skeletal deformities due to mutations in collagen resulting in abnormal collagen production or function. It remains unclear how collagen and mineral are altered at the molecular level or distributed at the tissue level. Raman micro-spectroscopy is a powerful non-invasive technique that allows *in vitro* studies on the organic and inorganic composition and distribution of mineralized tissues. Application of multivariate analysis can extract additional biochemical information from the high complexity of Raman spectra. Our goal was to investigate the molecular changes and distribution of the matrix and mineral in the *oim/oim* femoral cortical bone using Raman micro-spectroscopic analyses. The left femurs were dissected from 4-month-old male wild-type (*wt*) and homozygous (*oim/oim*) mice (n=3/group). Femurs were transversely sectioned using a diamond saw at the mid-shaft regions. Raman spectra were recorded with a JASCO NRS 2000 Raman spectrometer equipped with a 60X Olympus lens from medial region of the cross section. Over 300 spectra per group were collected and used for univariate spectral analysis and multivariate principle component analysis (PCA). PCA tests were performed in SPSS (v13.0). Raman spectra of *oim/oim* showed noticeable changes in the amide I and III spectral regions compared to *wt*. The collagen crosslinks (1660 cm^{-1}/ 1690 cm^{-1} peak heights) were 28% higher in *oim/oim* than *wt*, with a Standard Deviation (SD) that was 2500% greater in *oim/oim* than *wt*. The ratio of 1268 cm^{-1} / 1244 cm^{-1} of amide III peak increased 11% in *oim/oim* compared with *wt*, which suggests the lipid or α-helix content in the matrix is increased in *oim/oim*, and the *oim/oim* SD was 200% greater than *wt*. The phosphate-to-matrix ratios increased 20% in *oim/oim* compared to wt, with the *oim/oim* SD increased by 57% relative to *wt* SD. The mineral crystallinity increased 2% in *oim/oim* compared to wt, and its SD was 4% less in *oim/oim* than *wt*. PCA of Raman spectra clearly discriminates *oim/oim* and *wt* bones. Analysis of different principle components revealed which tissue component contributed to the spectral discrimination. *Oim/oim* femurs have increased bone collagen crosslinks and mineral-to-matrix

ratios with greater heterogeneity in bone matrix content and structure than *wt* femurs. The univariate and multivariate methods are powerful tools for the analysis of Raman spectra of the mineralized tissue.

***Disclosures: Xiaomei Yao**, None.*

SA0118

See Friday Plenary Number FR0118.

SA0119

See Friday Plenary Number FR0119.

SA0120

See Friday Plenary Number FR0120.

SA0121

See Friday Plenary Number FR0121.

SA0122

See Friday Plenary Number FR0122.

SA0123

TRAPPC9 Regulates BMP2-mediated Osteoblast Differentiation through Down-Regulation of NF-kB Activation. <u>Fayez Safadi</u>[1], <u>Thomas Mbimba</u>*[2], <u>Gregory Sondag</u>[3], <u>Fouad Moussa</u>[3], <u>Samir Abdelmagid</u>[1]. [1]Northeast Ohio Medical University, USA, [2]Kent State University, USA, [3]Northeast Ohio Medical University, USA

Intellectual disability (ID) is a serious disorder of the central nervous system with a prevalence of 1-3% in the general population. Recent studies identified different nonsense mutations in the trafficking protein particle complex (TRAPPC9) gene in consanguineous and nonconsanguineous families. These patients exhibit severe bone phenotypes such as short stature, polydactily, craniofacial deformity and micro-cephaly. TRAPPC9 is known to bind NFkB inducing kinase (NIK) and IkB kinas-beta (IKKbeta) and enhances cytokine-induced NFkB activation by increasing the kinase activities of IKK2 (IKKbeta) and NIK. It thus plays a role in the canonical and non-canonical NFkB signaling. Recent studies have identified NF-kB as a major negative regulator of osteoblast proliferation and differentiation that binds and suppresses Runx2 activation. Bone morphogenetic proteins (BMPs) are a group of growth factors and cytokines capable of inducing bone and cartilage formation. Two biochemical pathways are known to be activated by BMPs, one mediates the intracellular signal transduction through type I receptor phosphorylation of Smad1, Smad5 and Smad8. The second mediates the p38/MAPK pathways downstream of TAK1 pathways. TAK1 regulation mediates NF-kB activation through phosphor-ylation of IKK kinases. We hypothesize that TRAPPC9 regulates BMP2-mediated activation of NF-kB through Samd/p38/MAPK activation. We first examined TRAPPC9 expression and localization in bone by qPCR, Western blot and immuneprecipitation, which confirmed its expression in both osteoclasts and osteoblasts. Co-immunoprecipitation studies confirmed TRAPPC9 binding to both NIK and IKK2 in osteoblasts. To examine TRAPPC9 role during osteoblast differentiation, we performed loss- and gain-of-function studies in both MC3T3 and Bone marrow-derived MSCs using shRNA viral system. TRAPPC9 down-regulation showed a marked increased in all osteogenic markers such Runx2, Osx, Ocn, ALP, ColA1A which were suppressed in cells overexpressing TRAPPC9. TRAPPC9 down-regulation increases matrix maturation and mineralization shown by an increase in ALP staining and activity, Von Kossa and Alizarin red staining. Next, we showed that TRAPPC9 down-regulation mediates an increase in Smad1,5,8 and p38 MAPK activation associated with NF-kB down-regulation. Taken together, these data suggest that TRAPPC9 enhances osteoblast differentiation through Smad1,5,8 and P38 activation by suppressing of NF-kB signaling.

***Disclosures: Thomas Mbimba**, None.*

SA0124

See Friday Plenary Number FR0124.

SA0125

Hyperactive *RAS* Mutations in the Bone have an Intrinsic Negative Effect on Mineralization in Cutaneous-Skeletal-Hypophosphatemia Syndrome. Diana Ovejero*[1], Nisan Bhattacharyya[2], Andrea Burke[1], Laura Tosi[3], Larry Fisher[4], Edward McCarthy[5], Young Lim[6], Keith Choate[7], Michael Collins[1]. [1]National Institutes of Health, USA, [2]National Institutes of Health, USA, [3]Children's National Medical Center, USA, [4]National Institute of Dental & Craniofacial Research, USA, [5]Johns Hopkins Medical Institutions, USA, [6]Yale University School of Medicine, USA, [7] Yale University School of Medicine, USA

Congenital mosaic cutaneous disorders, such as epidermal and large congenital melanocytic nevi, are associated rarely with fibroblast growth factor 23 (FGF23)-induced hypophosphatemic rickets. In such cases, concomitant segmental dysplastic skeletal lesions are consistently observed. We have designated this spectrum of systemic findings as cutaneous-skeletal hypophosphatemia syndrome (CSHS). Although FGF23 is physiologically generated in bone, the source of its excess in this disorder has not been identified to date. In a previous report we described five CSHS individuals. Sequencing of their nevi and their bone lesions identified somatic hyperactive *RAS* mutations, absent in healthy tissues. To increase our understanding of these mosaic disorders, an iliac crest biopsy was obtained from one of the subjects. The obtained specimen corresponded to an area that had a dysplastic appearance on x-ray imaging. Goldner trichrome staining of the biopsy revealed severe osteomalacia out of proportion to the relatively mild degree of hypophosphatemia. This prompted us to investigate the potential inhibitory role of hyperactive RAS in the mineralizing abilities of human bone marrow stromal cells (hBMSC) and its relationship with FGF23 production. Wild type (WT) and mutant colonies of *HRAS* G13R hBMSC colonies were isolated and cultured in osteogenic media for 21 days. Alizarin red staining revealed a significantly lower mineralizing capacity in cells that carried the mutation. FGF23 was not detectable in the media of either WT or mutant cells. To further investigate the role of hyperactive RAS in FGF23 production, WT hBMSCs were transduced with adenovirus carrying WT or mutant Q61R *NRAS*. FGF23 protein was not detectable in either media or cellular lysates by ELISA, nor was FGF23 mRNA detectable by qPCR. We speculate that, independent of the systemic effects of hypophosphatemia, hyperactive *RAS* mutations in dysplastic tissue have an intrinsic effect on mineralization in CSHS.

Disclosures: Diana Ovejero, None.

SA0126

Identification of Gene Sets Dysregulated by Mutant ACVR1 Gene Causing A Rare Intractable Disease, Fibrodysplasia Ossificance Progressiva. Yoshihisa Matsumoto*[1], Makoto Ikeya[2], Takanobu Otsuka[3], Junya Toguchida[4]. [1]Kyoto University, Japan, [2]Kyoto University, Japan, [3]Nagoya city university, Japan, [4]Kyoto university, Japan

Fibrodysplasia Ossificans Progressiva (FOP) is a rare genetic disease characterized by progressive ectopic ossification. The responsible gene for FOP is the *ACVR1* gene, which is one of type I receptors for BMP. Mutant ACVR1 protein found in patients over-transduces the BMP signal upon ligand binding. This causes ectopic ossification in soft tissues after the initiation of BMP signal transduction triggered by unknown factors. Harvesting target tissues from patients is strictly prohibited because tissue damage accelerates the ectopic ossification. This issue now can be overcome by using iPSC derived from patients.

We have established iPSCs from patients with FOP and analyzed the difference between wild type iPSCs and FOP-iPSCs during osteogenesis and chondrogenesis. FOP-iPSCs show increased mineralization and chondrogenesis. We have, however, observed considerable clonal difference in terms of the differentiation property among clones in wild type and also in FOP-iPSCs. To overcome this problem, we have established rescued FOP iPSCs to replace mutant allele of ACVR1 gene in FOP iPSCs with wild type allele using homologous recombination technique. These rescued FOP iPSCs have identical genetic information except the mutation in ACVR1 and considered as an identical control iPSCs. We confirmed that rescued FOP-iPSCs showed reduced mineralization and chondrogenic properties compared with original FOP-iPSCs.In summary, FOP-iPSCs showed enhanced differentiation property in both osteogenic and chondrogenic lineages, and the results of rescued FOP-iPSCs indicated that these enhanced differentiation property was due to ACVR1 mutation.

Disclosures: Yoshihisa Matsumoto, None.

SA0127

Identification of the Third *LRP4* Mutation in a Patient Diagnosed with Sclerosteosis. Igor Fijalkowski*[1], Eveline Boudin[2], João Silva[3], Wim Van Hul[4]. [1]University of Antwerp, Belgium, [2]University of Antwerp, Belgium, [3]Instituto de Genética Médica, Portugal, [4]University of Antwerp, Belgium

Sclerosteosis is a rare, monogenic disorder characterized by a marked increase of bone mineral density, especially prominent at the skull and tubular bones. In addition, sclerosteosis patients present with tall stature, widened mandible and syndactyly.

Typically, this autosomal recessive disorder is caused by mutations in the *SOST* gene encoding the sclerostin protein- a potent Wnt signaling inhibitor. However, we were able to show that this condition is genetically heterogeneous. Mutations in the gene encoding low density lipoprotein receptor-related protein 4 (LRP4) were found in two sclerosteosis patients. The protein has been shown to facilitate the inhibitory action of sclerostin. Identified mutations impaired the binding between LRP4 and sclerostin, thus mimicking the phenotype of *SOST* loss of function.

Here, we report the identification of a third *LRP4* mutation in a 48 year old Portuguese patient presented with hyperostosis and sclerosis of the calvarium and tubular bones, tall stature, bilateral syndactyly of 3rd and 4th finger and hearing loss. Genomic DNA of the patient was obtained from peripheral blood mononuclear cells and subjected to mutation screening with the use of sanger sequencing techniques. All coding exons and exon-intron boundaries of the *LRP4* gene were screened. The mutation found, c.G3509A affects the same amino acid (p.Arg1170) that was previously found to be mutated in another sclerosteosis patient. The biological relevance of the mutation (p.Arg1170Gln) was confirmed with the use of dual luciferase assay. Hek293T cells were transfected with either WT or mutant LRP4 construct together with luciferase reporter constructs. Previously described mutation (p.Arg1170Trp) was used as a control. This experiment revealed that both mutated constructs present an impaired response to sclerostin addition (at two different concentrations) as compared to the WT protein (Figure 1).

Based on the data presented we conclude that the novel *LRP4* mutation, p.Arg1170Gln, is causative for the patient phenotype.
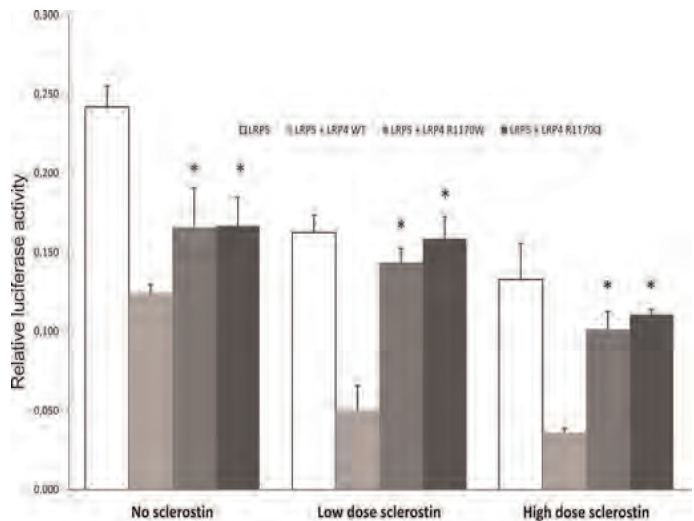

Figure 1: Sclerosteosis causing mutations in LRP4 result in a decreased inhibitory action of sclerostin on canonical Wnt signaling. In HEK293T cells Topflash, renilla and WT or mutant LRP4 constructs are transiently cotransfected with canonical Wnt signaling inducing plasmids (Wnt1 + LRP5) and different amounts of sclerostin. (* p<0,05)

Figure 1

Disclosures: Igor Fijalkowski, None.

SA0128

See Friday Plenary Number FR0128.

SA0129

Novel Mutations in the Osteoprotegerin Gene *TNFRSF11B* in Two Patients with Juvenile Paget's Disease. Dorit Naot*[1], Ally Choi[2], David Musson[3], Pelin Özlem Simsek Kiper[4], Gulen Eda Utine[4], Koray Boduroglu[4], Munro Peacock[5], Linda Dimeglio[6], Tim Cundy[7]. [1]University of Auckland, New Zealand, [2]University of Auckland, New Zealand, [3]University of Auckland, New Zealand, New Zealand, [4]Hacettepe University, Turkey, [5]Indiana University Medical Center, USA, [6]Indiana University School of Medicine, USA, [7]Faculty of Medical & Health Sciences University of Auckland, New Zealand

Juvenile Paget's disease (JPD) is a rare genetic bone disorder characterized by progressive skeletal deformities, fractures and deafness. There is considerable variation in the phenotype of JPD patients, from presentation in infancy with severe progressive deformity through to presentation in late childhood with minimal deformity. JPD is caused by recessive inactivating mutations in *TNFRSF11B*, the gene encoding osteoprotegerin (OPG). When OPG activity is deficient, the regulation of RANK/RANKL interaction is impaired and osteoclastic bone resorption is pathologically high. So far, approximately 10 different OPG mutations have been described in JPD patients. The current study presents two novel OPG mutations that were identified in patients with JPD.

Case 1 was a 27 year old man with a history of numerous fractures, bone pain and hearing loss. Case 2, a 9 months old male infant, had bone deformity and very high levels of alkaline phosphatase (1692 U/L). In order to determine the genetic cause of

disease in these patients, DNA samples were amplified with primers for intronic regions flanking the five exons of *TNFRSF11B* and PCR products were sequenced. Patient 1 carried a homozygous missense mutation A>C in exon 2, producing a threonine to proline substitution at position 76 (T76P). In patient 2, only exon 1 of *TNFRSF11B* was present, and a large deletion spanning approximately 260Kbp was identified between intron 1 and a region downstream of the gene.

Taken in conjunction with previously published cases, these results are consistent with the hypothesis that a genotype-phenotype association exist in JPD. The most severe phenotypes are caused by major gene deletions and by mutations affecting cysteine residues in OPG ligand-binding domain. In our study, the patient with the large deletion was diagnosed at a very early age, whereas the patient with the missense mutation had a less severe phenotype. The two novel mutations provide further evidence for the causative role of OPG mutations in JPD and for an association between genotype-phenotype in this disease.

Disclosures: Dorit Naot, None.

SA0130

Ossified Auricles: A New Feature Of Osteoprotegerin Deficiency Juvenile Paget's Disease. Gary Gottesman*[1], Katherine Madson[1], William McAlister[2], Angela Nenninger[3], Steven Mumm[4], Michael Whyte[1]. [1]Shriners Hospital for Children-Saint Louis, USA, [2]Washington University School of Medicine, USA, [3]Shriners Hospital for Children-Saint Louis, USA, [4]Washington University School of Medicine, USA

We report two of three unrelated patients with osteoprotegerin (OPG) deficiency juvenile Paget's disease (JPD) (OMIM #239000) who have auricular ossification, establishing this finding as a new feature. The "ossified auricle" describes rigid pinnae (sparing the ear lobe) from ectopic calcification or ossification due to various etiologies. Trauma and frostbite are the most common causes of dystrophic calcification of the auricle, but it also occurs in metabolic disorders including alkaptonuria, acromegaly, Addison's disease, diabetes mellitus, hypopituitarism, and hypothyroidism. Metastatic calcification of the auricle can occur when hypercalcemia or hyperphosphatemia cause hydroxyapatite deposition in multiple soft tissues as in hyperparathyroidism, pseudohypoparathyroidism, tumoral calcinosis, sarcoidosis, milk-alkali syndrome, and vitamin D intoxication. JPD is a rare heritable disorder featuring markedly elevated serum alkaline phosphatase activity with bone pain and deformity from generalized rapid skeletal turnover. Loss-of-function mutations within *TNFRSF11B*, encoding OPG, are the most common cause of JPD. OPG deficiency also leads to generalized vascular microcalcification that can result in retinopathy with blindness, and perhaps cerebral aneurysms or coronary artery occlusion.

Our 2007 report of a 60-year-old man with JPD recorded bisphosphonate treatment since his 41st year. He described hardening of his external ears by his mid-40s (JBMR 22:938). Recently, during examination of our three patients with OPG deficiency JPD (each with distinct mutations in *TNFRSF11B*), we found the pinnae to be rigid in the 17-year-old boy and 14-year-old girl, yet pliable in the 10-year-old boy. The girl's sleep was disrupted by pain from her inflexible pinnae. The boys had been treated with pamidronate for several years, whereas the girl had been treated with alendronate. Cranial imaging and radiographs demonstrated ossification within the external ears of the teenagers, apparently containing cortical bone with medullary spaces (Figure). Auricular biopsies were not performed. Ossification of other sites of elastic cartilage (external auditory canal, Eustachian tube, epiglottis, arytenoid) was not apparent radiographically. Our findings indicate ossification of the auricular elastic cartilage is a new feature of OPG deficiency JPD and warrants evaluation and understanding in this disease.

Panel A: Cranial CT (17-year-old boy) shows increased radiodensity within the external ears (arrows) apparently containing cortical bone with medullary spaces.

Panel B: Skull radiograph (14-year-old girl) coned down for soft-tissue assessment of the ears shows radiodensity similar to neighboring bone, with linear densities surrounding a medullary zone suggesting ossification (arrows).

OPG Ear

Disclosures: Gary Gottesman, None.

SA0131

Rapid Turnover Skeletal Disease Caused By A Multiple-Exon Duplication of *TNFRSF11A* Encoding RANK. Steven Mumm*[1], Felicity Collins[2], Shenghui Duan[3], Margaret Huskey[3], William McAlister[3], David Sillence[4], Michael Whyte[5]. [1]Washington University School of Medicine, USA, [2]The Children's Hospital at Westmead & Sydney University Medical School, Australia, [3]Washington University School of Medicine, USA, [4]The Children's Hospital at Westmead & Sydney University Medical School, Australia, [5]Shriners Hospital for Children-Saint Louis, USA

Mendelian disorders of constitutive RANK activation are caused by in-frame 12, 15, 18, or 27-bp duplications in exon 1 of *TNFRSF11A* encoding the signal peptide of RANK. The similar rapid bone turnover disorder juvenile Paget's disease (JPD) is due to deactivating mutations in *TNFRSF11B* encoding OPG. We report a rapid turnover skeletal disease in a mother and fetus from a novel RANK defect.

The 38-year-old proposita is the child of nonconsanguineous parents. Family history was negative for fractures or deafness. She wore hearing aids for deafness at age 15 months. Brittle teeth were noted at age 3 years. Secondary tooth loss began at age 9 years. At age 10 years, she was non-dysmorphic and without bone pain or fractures. Bone scintigraphy showed increased uptake in the long bones, and CT revealed hypoplastic ossicles and semicircular canals and no cochleas. A skeletal survey revealed thickened cortices of tubular bones, but a normal skull. Biopsy of a tibia and ileum showed unremarkable lamellar bone, slightly increased vascularity, numerous osteoblasts, and normal marrow. Serum alkaline and acid phosphatase were elevated. An atypical form of JPD was diagnosed. At age 14 years, she had normal stature, slight knock-knee deformity, and fractured major limb bones. She received calcitonin and then a bisphosphonate. At age 16 years, biopsy of the maxilla and jaw showed areas resembling cementifying fibroma, irregular woven bone, and marked osteoblastic and osteoclastic activity in a highly cellular fibrovascular stroma resembling osteolytic Paget's disease. Teeth were eroded and replaced by osteocementum and fibrous tissue. She was edentulous by age 27 years. At age 30 years, she had a prominent forehead and nasal bridge, deep set eyes, and anterior tibial bowing. Then, ultrasound of her first pregnancy at 18 weeks showed abnormal fetal bones with angulated femurs.

Sequencing of coding exons and adjacent mRNA splice sites of the RANK and OPG genes of the mother and abortus was negative. However, in both, microarray-based copy number analysis showed amplification of exons 4-9 of the RANK gene. Confirmatory qPCR showed 3 copies of exons 4-9 in the mother, and >3 in the fetus. An in-frame tandem duplication of exons 4-9 creates a RANK fusion protein of one extracellular RANKL-binding domain combined with double intracellular activation domains. Thus, we have identified a new genetic basis within the family of disorders featuring constitutive RANK activation.

A) At age 20 years, the mother's femurs are wide, bowed, and with areas of cortical thickening and patchy osteopenia.

B) The mother's fractured left humerus is expanded with patchy areas of osteopenia and osteosclerosis.

C) The 19 week abortus has short and laterally bowed femurs with wide medullary cavities. The right tibia is bowed, and both are widened.
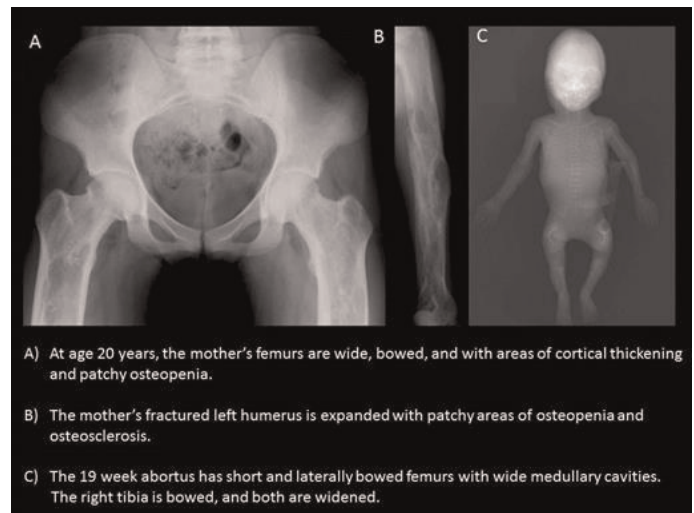
FEO figure

Disclosures: Steven Mumm, None.

SA0132

See Friday Plenary Number FR0132.

SA0133

See Friday Plenary Number FR0133.

SA0134

Genotype and Phenotype Analyses Suggest a Distinct Molecular Signature of Giant Cell Tumor Occurring in Paget's Disease of Bone. <u>Luigi Gennari</u>*[1], <u>Domenico Rendina</u>[2], <u>Maria De Lucia</u>[3], <u>Laetitia Michou</u>[4], <u>Daniela Merlotti</u>[1], <u>Stuart Ralston</u>[5], <u>Giuseppina Divisato</u>[3], <u>Laura Pazzaglia</u>[6], <u>Maria Serena Benassi</u>[6], <u>Riccardo Muscariello</u>[2], <u>Gianpaolo De Filippo</u>[2], <u>Ranuccio Nuti</u>[1], <u>Pasquale Strazzullo</u>[2], <u>Teresa Esposito</u>[3], <u>Fernando Gianfrancesco</u>[7]. [1]University of Siena, Italy, [2]Department of Clinical & Experimental Medicine, Federico II University, Italy, [3]Institute of Genetics & Biophysics, National Research Council of Italy, Italy, [4]Université Laval, Canada, [5]University of Edinburgh, United Kingdom, [6]Laboratory of Experimental Oncology, Rizzoli Orthopaedic Institute, Italy, [7]National Research Council of Italy, Italy

Giant cell tumor (GCT) is a rare but well-recognized neoplastic complication of Paget's disease of bone (PDB), accounting for a proportion of all neoplasms arising from pagetic tissue. In order to provide further insight on the phenotype of GCT in PDB we performed a systematic review of 117 GCT cases complicating PDB described to date. PDB patients who developed GCT were more likely to be polyostotic (93%), showed an higher male/female ratio (2.1), an increased prevalence of familial PDB (59%) and an earlier age at diagnosis of PDB (52 ± 12 yrs) compared with a reference cohort of 1483 pagetic patients without GCT. These GCT cases were also remarkably different from GCT described in non-pagetic patients. The latter mainly occurs in Asiatic subjects (while pagetic GCT affect white Caucasian patients in up to 83% of cases) is rarely multifocal (<1% vs 25% in pagetic GCT) and is more prevalent in females (male/female ratio 0.66) between the 2nd and 4rd decades of age. The skeletal localization of GCT was also different between pagetic and non pagetic patients, with involvement of the axial skeleton in 75% vs 15% of cases, respectively. Moreover, mortality rates were remarkably higher in PDB-GCT patients (with up to 50% mortality within 5 years from diagnosis of GCT) than those with GCT occurring in non-PDB patients or in PDB cases without GCT. Then we went on to investigate the molecular basis of pagetic and non-pagetic GCT. To this aim we collected the tumoral tissue samples from 8 and 44 pagetic and non-pagetic patients and peripheral blood samples for DNA analysis of a large PDB-GCT pedigree (with 14 affected relatives) and of 7 unrelated PDB-GCT cases. While 89% of non pagetic GCT tissues showed a recurrent somatic mutation of *H3F3A* gene (which is consistent with a previous report), we did not evidence any *H3F3A* variation in pagetic GCT tissue or in constitutive DNA from the unrelated GCT-PDB cases. A further genetic screening excluded the presence of somatic and germline mutations in *SQSTM1* or other genes known to be associated with PDB or PDB-related syndromes. Whole exome sequencing of the large PDB-GCT pedigree identified 3 variations in 2 candidate genes, in chromosome 1. Therefore, we conclude that the GCT associated with PDB recognizes a distinct molecular signature than GCT occurring in non-pagetic patients. Mutational analysis is being extended to the 7 unrelated PDB-GCT patients in order to identify the gene associated with GCT degeneration in PDB.

Disclosures: Luigi Gennari, None.
This study received funding from: Telethon grant GGP11119 to L.G.

SA0135

See Friday Plenary Number FR0135.

SA0136

Withdrawn

SA0137

See Friday Plenary Number FR0137.

SA0138

Induction of FGF23 expression in IDG-SW3 osteocytes by inflammatory stimuli. <u>Nobuaki Ito</u>[1], <u>Asiri Wijenayaka</u>[2], <u>Matthew Prideaux</u>[3], <u>Masakazu Kogawa</u>[4], <u>Renee Ormsby</u>[2], <u>Lynda Bonewald</u>[5], <u>David Findlay</u>[6], <u>Gerald Atkins</u>*[6]. [1]The university of Adelaide, Australia, [2]Centre for Orthopaedic & Trauma Research, University of Adelaide, Australia, [3]Centre for Orthopaedic & Trauma Research, University of Adelaide, Azerbaijan, [4]The University of Adelaide, Australia, [5]University of Missouri - Kansas City, USA, [6]University of Adelaide, Australia

Certain sepsis patients experience transient hypophosphatemia, of unknown origin but suggesting the involvement of pro-inflammatory cytokines. Osteocyte-derived fibroblast growth factor-23 (FGF23) has been recognised as the key physiological regulator of phosphate (Pi) homeostasis, although the regulatory mechanisms of FGF23 synthesis are not fully understood, in part due to the lack of suitable cell models. In the current study, we used the IDG-SW3 osteocyte-like cell line to investigate the effect of pro-inflammatory cytokines and lipopolysaccharide (LPS) on

FGF23 production. In differentiated IDG-SW3 cultures, basal *Fgf23* mRNA was markedly up-regulated by tumour necrosis factor-α (TNF), interleukin-1β (IL-1β), TNF-related weak inducer of apoptosis (TWEAK) and LPS, in a dose-dependent manner. Similar effects were observed in human trabecular bone samples cultured *ex vivo*. TNF and IL-1β induced *Fgf23* expression was reversed by the NF-κB signalling inhibitor, BAY11-7082. Indicative of a coordinated response, mRNA encoding negative regulators of FGF23, phosphate regulating endopeptidase homolog, X-linked (*Phex*), dentin matrix protein 1 (*Dmp1*) and ectonucleotide pyrophosphatase/phosphodiesterase I (*Enpp1*), were suppressed by TNF, IL-1β, TWEAK and LPS, independent of NF-κB signalling. Conversely, UDP-N-acetyl-alpha-D-galactosamine:polypeptide N-acetylgalactosaminyltransferase 3 (*Galnt3*), which protects intact FGF23 protein from cleavage by furin/furin-like proprotein convertases, slightly increased at certain time points and concentrations of these treatments. C-terminal FGF23 fragments in the media were robustly increased. However, there was no significant change in intact FGF23 protein levels except in the presence of Furin inhibitors. These observations confirm that cellular cleavage of intact FGF23 critically determines active FGF23 production. These results suggest that pro-inflammatory stimuli may contribute to hypophosphatemia during sepsis and likely other inflammatory conditions, by inducing the synthesis of FGF23 in osteocytes. IDG-SW3 is a suitable and unique cell line for the study of FGF23 regulation.

Disclosures: Gerald Atkins, None.

SA0139

See Friday Plenary Number FR0139.

SA0140

See Friday Plenary Number FR0140.

SA0141

Identification and Functional Characterization of a Novel Activating Mutation in the Human Calcium-sensing Receptor Gene, Responsible for Autosomal Dominant Hypocalcemia. <u>Anne Qvist Rasmussen</u>*[1], <u>Peter Schwarz</u>[2], <u>Niklas Jorgensen</u>[3]. [1]Capital Region of Denmark, Denmark, [2]Glostrup Hospital, Denmark, [3]Copenhagen University Hospital Glostrup, Denmark

Introduction: The human calcium homeostasis is very exact responding to even small fluctuations in the extracellular calcium-ion concentration. One of the keys to the regulation of this homeostasis is the calcium-sensing receptor (CASR). Functionally important mutations in the gene of CASR have been shown to cause calcium metabolic disorders such as hypercalcemia when an inactivating CASR mutation or hypocalcemia when activating mutation as in patients with autosomal dominant hypocalcemia (ADH). It has been shown that activating CASR mutations can increase the receptor sensitivity, increase the maximal signal transduction and interfere with the gradient of the CASR protein expression at the cell surface.

Patients and methods: The proband, a 42 years old woman, and two of her three children were clinically diagnosed with ADH. The proband and two children were genotyped in order to determine if there is an association between genotype and phenotype in this family. Functional characterization of the specific mutant CASR gene was evaluated by extracellular Ca^{2+} stimulated phosphoinositide (PI) hydrolysis as well as intracellular Ca^{2+}-release in transient transfected HEK-293 cells. The expression level of the mutant receptor protein on the cell surface membrane was evaluated by immunoblot analysis.

Results: Genotyping showed a heterozygous missense mutation of the CASR gene revealing a higher basal response in PI hydrolysis and in intracellular calcium release compared to wild-type (WT) CASR gene, without a left-shifted calcium set-point. The maximal response was not significantly changed by increased Ca^{2+} stimulation corresponding to a decreased sensitivity of the mutant CASR. Additionally, the CASR expression at the cell surface was reduced related to the WT receptor corresponding to an abnormality in the maturating process of the receptor protein which still remains to be clarified.

Conclusion: In the present study we have identified a novelactivating mutation in the CASR gene. The novel identified D126V mutation is a rare constitutive activating mutation in a known hotspot in the CASR gene. The mutation in the CASR gene identified in these three related patients co-segregate with the phenotype of the ADH diagnosis.

Disclosures: Anne Qvist Rasmussen, None.

SA0142

PTHrP Stimulates Skeletal Growth And Osteoblastic Bone Formation in An Intracrine Manner By Inhibiting P16-Rb And P19-P53-P21 Signal Pathways Mediated By Bmi1. Yongli Han*[1], Ruilei Teng[1], Ying Zhang[1], Zhen Gu[1], Lin Chen[2], Baojie Li[3], David Goltzman[4], Andrew Karaplis[4], Dengshun Miao[5]. [1]Nanjing Medical University, China, [2]Daping Hospital, Peoples Republic of China, [3]Shanghai Jiao Tong University, Peoples Republic of China, [4]McGill University, Canada, [5]Nunjing Medical University, Peoples Republic of China

We previously demonstrated that mice with a deletion of the parathyroid hormone–related peptide (PTHrP) nuclear localization sequence (NLS) and C-terminal region (*Pthrp* KI) displayed skeletal growth retardation and defective osteoblastic bone formation with down-regulation of Bmi1 and up-regulation of p16 and p21; however, it is unclear whether PTHrP stimulates skeletal growth and osteoblastic bone formation in an intracrine manner by inhibiting the p16-Rb and p19-p53-p21 signal pathways mediated by Bmi1. To answer this question, we generated compound mutant mice that are homozygous for the *Pthrp* KI mutation and either *p16* or *p53* deletion (*Pthrp* KI *p16*^{-/-} or *Pthrp* KI *p53*^{-/-}, respectively), and compared them with *p16*^{-/-}, *p53*^{-/-}, *Pthrp* KI, and WT littermates. Phenotypes were analyzed by histopathological, immunohistochemical, cellular and molecular approaches. Deletion of p16, but not p53 in *Pthrp* KI mice resulted in a longer lifespan. At 2 weeks of age, skeletal growth parameters, including length of long bones, size of epiphyses and PCNA positive chondrocytes, osteoblastic bone formation parameters, including BMD, trabecular bone volume, osteoblast numbers, and ALP, type I collagen and osteocalcin positive areas were increased in *p16*^{-/-} and *p53*^{-/-} mice, and reduced in *Pthrp* KI, *Pthrp* KI *p16*^{-/-}, and *Pthrp* KI *p53*^{-/-} mice compared to WT mice; however these parameters were increased in *Pthrp* KI *p16*^{-/-} and *Pthrp* KI *p53*^{-/-}mice compared to *Pthrp* KI mice. As well, the mRNA expression levels of Runx2, ALP, and type I collagen and the numbers of total CFU-f and ALP positive CFU-f generated from bone marrow cell cultures were increased significantly in *p16*^{-/-} and *p53*^{-/-} mice compared to WT mice and in *Pthrp* KI *p16*^{-/-}and *Pthrp* KI *p53*^{-/-}mice compared to *Pthrp* KI mice. Apoptotic osteoblasts and osteocytes were increased with the down-regulation of Bmi1 and Bcl-2 and the up-regulation of Caspase-3 at protein expression levels in *Pthrp* KI mice compared to WT mice and these alterations were rescued partially by deletion of either p16 or p53 in *Pthrp* KI mice. Our results demonstrate that deletion of either p16 or p53 in *Pthrp* KI mice can partially rescue defects in skeletal growth and osteoblastic bone formation by enhancing endochondral bone formation and osteogenesis. These studies therefore indicate that PTHrP can stimulate skeletal growth and osteoblastic bone formation in an intracrine manner through inhibiting p16-Rb and p19-p53-p21 signal pathways mediated by Bmi1.

Disclosures: Yongli Han, *None.*

SA0143

See Friday Plenary Number FR0143.

SA0144

Stapled Peptides as Long-Acting, Selective Parathyroid Hormone Antagonists. Manoj Samant*[1], Karen Olson[1], Aditi Mukherjee[1], Hubert Chen[2], Thomas Gardella[3], Allen Annis[4]. [1]Aileron Therapeutics, Inc., USA, [2], USA, [3]Massachusetts General Hospital, USA, [4]Aileron Therapeutics, Inc., USA

Stapled Peptides utilize an optimized hydrocarbon cross-linking chemistry that lock, or "staple", peptides into α-helices to mimic native protein structures and confer resistance to proteolysis. The resulting molecules exhibit extended plasma half-life after either intravenous or subcutaneous administration, while retaining molecular target specificity and potency of the underlying native protein structures. We have generated potent Stapled Peptide parathyroid hormone (PTH) antagonists as a novel and efficacious therapy for hyperparathyroidism. In SaOS-2 osteosarcoma cells (Figure 1), Stapled Peptide PTH antagonists (ATSP-10814 and ATSP-11302) inhibited PTH(1-34)-induced cAMP production at nanomolar and picomolar concentrations, up to 10,000-fold more potent than a PTH antagonist previously tested in the clinic (BIM-44002). Receptor binding assays using isolated PTHr1-containing membrane preparations correlated with cellular potency. Stapled Peptide PTH antagonists demonstrated equipotent activity against the native hormones PTH(1-34), full-length PTH(1-84), and PTH-related protein (PTHrP), and agonist activity was not measured at ≤10 µM in SaOS-2 cells. Stapled Peptide ATSP-10814 demonstrated a low plasma clearance of 231 mL/hr/kg, and a half-life of 1.6 hr following intravenous administration in Sprague-Dawley rats. Dose-dependent, statistically significant, and clinically relevant changes in serum calcium were detected in rats, with the maximal effect at 2 hr post-dose and lasting up to 7 hrs post-dose. To confirm the on-mechanism, calcium-lowering effects of Stapled Peptide PTH antagonists, we dosed thyroparathyroidectomized rats with vehicle or ATSP-10814, followed by PTH infusion at 1.25 µg/kg/h. ATSP-10814 markedly reduced PTH-induced increases in total and ionized serum calcium, whereas vehicle had no discernible effects. Collectively, these results demonstrate that Stapled Peptide PTH antagonists have enhanced pharmacokinetic and pharmacological properties relative to existing molecules, and the continued development of Stapled Peptides is warranted as a potential therapy for all major types of hyperparathyroidism.
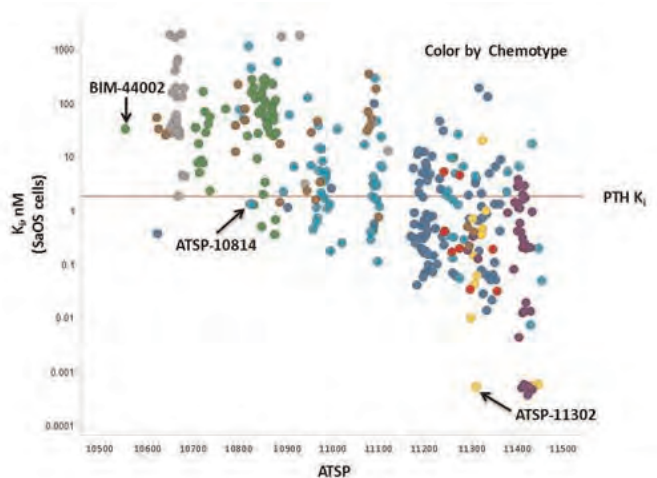
Stapled Peptide PTH Antagonists Potency Plot

Disclosures: Manoj Samant, *Aileron Therapeutics, Inc., 4*

SA0145

TSH elevation as first laboratory evidence for pseudohypoparathyroidism type Ib (PHP-Ib). Harald Jueppner[1], Angelo Molinaro*[2], Dov Tiosano[3], William Russell[4], Dionisios Chrysis[5], Outi Makitie[6], Rieko Takatani[7], Massimo Tonacchera[8]. [1]Massachusetts General Hospital, USA, [2]Endocrine Unit, Massachusetts General Hospital, USA, [3]Division of Pediatric Endocrinology, Meyer Children's Hospital, Rambam Health Care Campus, Israel, [4]Division of Pediatric Endocrinology & Diabetes, Vanderbilt University School of Medicine, USA, [5]Division of Endocrinology, Department of Pediatrics, Medical School, University of Patras, Greece, [6]Children's Hospital, Helsinki University Central Hospital, Finland, [7]Massachusetts General Hospital & Harvard Medical School, USA, [8]Endocrinology Unit, Department of Internal Medicine, University of Pisa, Italy

Objective: Pseudohypoparathyroidism type Ib (PHP-Ib) is caused by *GNAS* methylation changes that occur either in association with maternally inherited deletions within *GNAS* or *STX16*, or as a sporadic disorder. PHP-Ib patients typically present with isolated resistance towards PTH in the proximal renal tubules, which leads hypocalcemia and hyperphosphatemia. However, some individuals affected by this disorder show also resistance towards other hormones, particularly TSH. We now wanted to determine whether TSH elevations can be the first evidence for PHP-Ib.
Patients: Four patients developed PTH-resistant hypocalcemia 3-20 years after establishing the diagnosis of idiopathic hypothyroidism (IH) during childhood and were found to show *GNAS* methylation changes, thus establishing the diagnosis of PHP-Ib. We also searched in adult IH patients without evidence for calcium and phosphate abnormalities for similar epigenetic changes.
Results: In genomic DNA from three pediatric patients, who developed hypothyroidism before the onset of PTH-resistance, we observed broad epigenetic *GNAS* abnormalities, including loss of methylation at the exons AS, XL and A/B, and gain of methylation at exon NESP55; these findings are consistent with sporadic PHP-Ib. In the fourth patient, an isolated loss of methylation at *GNAS* exon A/B led to the identification of the 3 kb deletion in *STX16* gene as the cause of PHP-Ib. DNA from the patient's healthy mother revealed the same deletion. No *GNAS* methylation changes were observed in IH patients.
Conclusions: PHP-Ib can present initially only with TSH elevation and the onset of PTH-resistance can be delayed by many years. No methylation *GNAS* change were observed in our adult patients with TSH elevation, indicating that adult-onset hypothyroidism is not or only rarely associated with epigenetic changes at the *GNAS* locus. Our findings indicate that silencing of Gs-alpha transcription from the paternal allele can be more pronounced in the thyroid than in the proximal renal tubules, and it will therefore be important to screen pediatric patients with hypothyroidism for extended periods of time for changes in calcium, phosphate, and PTH to prevent symptomatic hypocalcemia and associated complications.

Disclosures: Angelo Molinaro, *None.*

SA0146

Co-expression Network Analysis Identifies Alpha-Synuclein (*Snca*) as a Mediator of Ovariectomy-induced Bone Loss. Gina Calabrese[1], Larry Mesner[2], Patricia Foley[3], Clifford Rosen[4], Charles Farber*[5]. [1], USA, [2]University of Virginia, USA, [3]University of Virginia, USA, [4]Maine Medical Center, USA, [5]University of Virginia, USA

Estrogen deficiency during the postmenopausal period leads to substantial bone loss. This loss is initiated, in part, by alterations in transcriptomic networks. Here, we utilized variation in global gene expression driven by natural genetic variation across inbred strains of mice to identify networks of co-expressed genes in bone that differ in response to OVX. Bilateral ovariectomy (OVX) or sham surgeries were performed in three inbred mouse strains (BALB/cJ, C3H/HeJ and C57BL/6J). MicroCT imaging of lumbar vertebrae and femora revealed significant effects of genotype on basal bone mass as well as the magnitude of bone loss after OVX. Global gene expression profiling of vertebrae and femora identified substantial transcriptomic differences due to genotype, with more subtle changes attributed to the effects of OVX. Across strains, surgical groups and skeletal sites, we identified 21 modules of co-expressed genes. The overall expression state of two of the 21 modules was significantly (P<0.002) different as a function of OVX. Intramodular connectivity, a measure of network connectedness, was highly correlated with the magnitude of differential gene expression due to OVX in one (L5-M13) of the two modules, suggesting that highly connected genes in this module play an important role in OVX-induced bone loss. The expression of all L5-M13 genes was decreased in OVX mice across all three strains and this module was enriched for genes involved in the response to oxidative stress. The most highly connected L5-M13 hub gene was alpha-synuclein (*Snca*). Mice deficient for *Snca* had less trabecular bone loss at the lumbar spine after OVX and this protection was associated with the specific disruption of the expression of L5-M13 genes and transcripts belonging to a separate module enriched for genes involved in neuronal function. These data, in general, highlight the power of co-expression network analysis for novel gene discovery and, specifically, identifies *Snca* as a key hub gene involved in coordinating transcriptomic networks in bone in response to estrogen deficiency.

Disclosures: Charles Farber, *None.*

SA0147

Withdrawn

SA0148

A bone-testicular interaction for the maintenance of male steroidogenesis. Daniela Hofer[1], Julia Münzker[2], Matthias Ulbing[2], Philipp Stiegler[3], Karla Hutz[4], Richard Zigeuner[4], Thomas Pieber[2], Helmut Müller[3], Barbara Obermayer-Pietsch*[5]. [1]Division of Endocrinology & Metabolism, Medical University Graz, Austria, Austria, [2]Department of Internal Medicine, Division of Endocrinology & Metabolism, Medical University Graz, Austria, Austria, [3]Department of Surgery, Division of Transplantation Surgery, Medical University Graz, Austria, Austria, [4]Department of Urology, Medical University Graz, Austria, Austria, [5]Medical University Graz, Austria

Introduction: Significant interactions of androgens and bone metabolism have recently been proposed in rodents via the involvement of osteocalcin (OC).
In humans, we have shown a strong association of testosterone and vitamin D and their parallel seasonal variation in more than 2200 men. Our aim was to investigate the molecular mechanisms of vitamin D (1,25D) and osteocalcin in male androgen synthesis in a primary testicular cell culture model.
Methods: Human testicular cells were isolated from testes of braindead organ donors. After addition of different concentrations of either LH (luteinizing hormone), IGF-1 (insulin-like growth factor 1), 1,25D and OC alone or in combination, RNA was isolated and the expression of selected genes of the male androgen and steroid metabolism were studied by real time quantitative PCR at baseline compared to hormonal treatment. Testosterone and 5a-dihydrotestosterone (DHT) were measured by immunoassay in cell culture supernatants initially and after hormonal stimulation.
Results: In isolated human testicular primary cells, addition of physiological doses of LH, as well as the combination of LH with IGF-1, did not significantly change the gene expression pattern of the selected genes compared to baseline. Addition of 1,25D significantly raised testosterone delivery in human primary testicular cells, compared to baseline and treatment with LH. Treatment with osteocalcin increased testosterone as well as DHT levels in cell culture supernatants dose-dependently. A combined treatment of LH, IGF-1 together with 1,25D and OC resulted in a significant increase of mRNA levels of selected genes of androgen synthesis and metabolism pathways, namely cholesterol side-chain cleavage enzyme (CYP11A1), 3b-hydroxysteroid dehydrogenase (HSD3B2), aromatase (CYP19A1) and cytochrome P_{450} 3A4 (CYP3A4).
Conclusion: We have shown a reproducible and dose-dependent involvement of vitamin D and osteocalcin in human male steroid- and androgen-synthesis. Our results support the recent view of bone as an endocrine organ. Considering osteocalcin and vitamin D as important players in male steroidogenesis might open up new clinical approaches for hypogonadism and osteoporosis.

Disclosures: Barbara Obermayer-Pietsch, *None.*

SA0149

Model-based Meta-analysis for Development of a Population-Pharmacokinetic (PPK) Model for Vitamin D3 and its 25OHD3 Metabolite. Alanna Ocampo*[1], Marc Gastonguay[2], Joseph Lorenzo[3], Matthew Riggs[4]. [1]University of Connecticut, USA, [2]Metrum Research Group LLC, USA, [3]University of Connecticut Health Center, USA, [4]Metrum Research Group LLC, USA

Purpose: Association of Vitamin D3 (D3) and its metabolite (25OHD3) levels with various diseases has become an active research focus in several areas, including bone health, diabetes, and cancer. Inherently, clinical studies investigating these relationships with D3 and 25OHD3 vary in dosing regimen, assays, demographics, and control of exogenous D3 production. This leads to uncertain and conflicting exposure-related associations with D3 and 25OHD3. To elucidate this parent-metabolite system, a PPK model was developed to predict D3 and 25OHD3 exposure from varied doses and administration routes to identify and understand sources of exposure variability within the complex network of D3-related physiology.
Methods: Specific search criteria were used in PUBMED to identify public source PK data pertaining to D3 and 25OHD3 in healthy or osteoporotic populations. Overall 77 studies with 12094 individuals were selected; this included 62 individual-level profiles as well as grouped data. Both IV, oral, single and multiple dose data were used, with D3 and 25OHD3 dosing (400-100000 IU/d and 15-1000 ug/d, respectively). A nonlinear mixed effects model was developed to simultaneously model the PK of D3 and 25OHD3 (NONMEM v7.2). Model development included consideration of 1- and 2-compartment (CMT) models with first-order absorption rate constant (ka) and linear or nonlinear clearance (CL). Random effects were weighted by arm sample size. Diagnostic plots and predictive checks assessed model adequacy.
Results: D3 and 25OHD3 dispositions were best described by 2-CMT models with nonlinear and linear clearances, respectively. D3 model estimates, relative to bioavailability (F) were: maximum rate of metabolism (Vmax, 1.15nmol/h), central volume of distribution (Vc, 11L/h), intercompartmental clearance (Q, 0.189L/h), peripheral volume of distribution (Vp, 1500L/h), and baseline concentration (Dbase, 5nmol/L). For 25OHD3: CL=0.0148 L/h, Vc=4.44 L, Vp=7.61 L, Q=0.0494 L/h, and Dbase=32.7nmol/L. Relative fraction of D3 conversion to 25OHD3 was described nonlinearly as 0.7*[D3/40]^0.169 (for D3 400-5600 IU/d). The same ka for D3 and 25OHD3 was assumed (0.323h-1).
Conclusions: The PK of D3 and 25OHD3, described by two CMT models with first order oral absorption, with nonlinear parent and linear metabolite CL, suggests that estimation of nonlinear CL may be important when considering comparisons of D3 and 25OHD3 exposures across studies and dosing regimens.
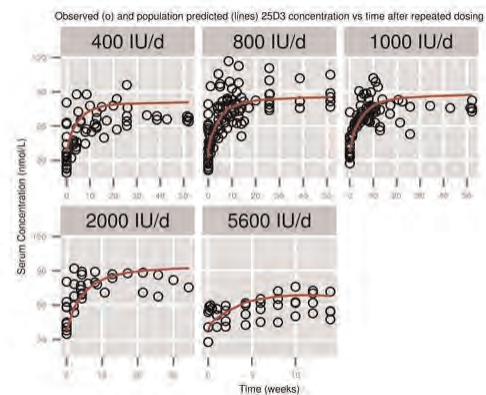
PPK Model Results for 25OHD3 Metabolite Concentrations

Disclosures: Alanna Ocampo, *None.*

SA0150

Renal CYP27B1 is essential to maintain circulating 1,25 dihydroxyvitamin D, and calcium and bone homeostasis. Yingben Xue*[1], Rene St-Arnaud[2], David Goltzman[3]. [1]Calcium Research Lab, McGill University, Canada, [2]Shriners Hospital for Children & McGill University, Canada, [3]McGill University, Canada

Although mainly expressed in kidney, CYP27B1, which converts 25 hydroxyvitamin D [25(OH)D] to 1,25 dihydroxyvitamin D [1,25(OH)₂D], is also expressed in other tissues, however, the physiological role of extrarenal CYP27B1 remains controversial. To study the impact of reducing renal CYP27B1 on circulating 1,25(OH)₂D, calcium and bone homeostatasis, we used a Tet-On system, in which rtTA is under the control of a Pax8 promoter, allowing inducible inactivation of a floxed CYP27B1 allele in renal tubules. We treated Pax8rtTA;tetOcre;OH$^{flox/flox}$ mice with dietary doxycycline (DOX) (870mg/kg) for 4 weeks after weaning to induce conditional CYP27B1 KO mice; DOX treated non-responsive mice (Pax8rtTA;OH$^{flox/flox}$, tetOcre;OH$^{flox/flox}$ and OH$^{flox/flox}$) were used as controls. We found that renal

CYP27B1 mRNA and protein were decreased by 65%, CYP24 mRNA was decreased by 62%, serum 1,25(OH)$_2$D was decreased by 49% and 25(OH)D was increased by 40% in KO mice. 1,25(OH)$_2$D biosynthesis was also decreased in vitro in cultured primary renal tubule cells of KO mice. KO mice showed normal serum calcium, secondary hyperparathyroidism and hypophosphatemia. Although CYP27B1 was expressed in intestine, intestinal CaBP9K and TRPV6 mRNA were decreased by 56% and 63%, respectively, suggesting that local CYP27B1 can not compensate for the deletion of renal CYP27B1 in regulating intestinal calcium transporter gene expression. We also confirmed expression of CYP27B1 in bone, however, in KO mice bone turnover was increased due to hyperparathyroidism, and bone mineral density (BMD) and bone mineral content (BMC) were decreased. To examine the response of KO mice to a low calcium (LCa) diet, mice were fed a DOX diet for 4wks after weaning followed by a LCa diet for 4 wks. In control mice, renal CYP27B1 mRNA levels were 2-fold higher after LCa diet stress; however, there was no change in KO mice. After LCa stress, CYP24 mRNA levels were decreased by 37% and 66% in control and KO mice, respectively. Serum 1,25(OH)$_2$D was increased from 71.6 pmol/L to 238.3 pmol/L in KO mice and from 140.4 pmol/L to 415.6 pmol/L in control mice. After LCa, bone turnover was significantly increased in control mice; BMD and BMC were decreased by 16% and 20%, respectively. In KO mice bone turnover did not change; BMD and BMC were decreased by only 6% and by 8%, respectively. We conclude that renal CYP27B1 is essential to maintain circulating 1,25(OH)$_2$D levels and normal calcium and bone homeostasis.

Disclosures: Yingben Xue, None.

SA0151

Withdrawn

SA0152

Vitamin D3 Regulates Frizzled 1 Expression in Osteoblasts. <u>Shibing Yu</u>[1], <u>Yanxia Chu</u>[2], <u>Joseph Zmuda</u>[3], <u>Yingze Zhang</u>*[4]. [1]University of Pittsburgh Medical Center, USA, [2]University of Pittsburgh Department of Medicine, USA, [3]University of Pittsburgh Graduate School of Public Health, USA, [4]University of Pittsburgh, USA

Frizzled 1 (FZD1) is a co-receptor for Wnt signaling and plays a role in osteoblast differentiation and mineralization. The expression of FZD1 is regulated by multiple transcription factors including Egr1 and E2F1. However, very little is known about the potential endocrinologic regulation of FZD1 expression. Vitamin D3 (1a,25-dihydroxy vitamin D3) plays an important role in bone mineralization and metabolism via direct actions on osteoblasts. It is well established that vitamin D3 and its receptor-VDR regulate gene expression in osteoblasts through interaction with a number of other genes, such as the Wnt co-receptor LRP5. To determine whether vitamin D regulates the expression and function of FZD1, we transfected FZD1 promoter constructs containing two promoter variants rs2232157 and rs2232158 in Saos2 cells for 12 hours and further treated the cells with control, 1nM, 5nM, 10nM and 100nM vitamin D3 for 24 hours. We demonstrated that vitamin D3 at the concentration of 100nM significantly suppressed FZD1 promoter activity independent of the polymorphisms. We further performed time course experiments for 2-, 6- and 24-hour treatment with 100nM vitamin D3 in Saos2 cells transfected with wild type FZD1 promoter. Interestingly, FZD1 promoter activity was significantly increased by 31% at 2 hours of vitamin D3 treatment, followed by a significant decrease by 27.5% at 24 hours after treatment. Quantitative PCR and Western blot confirmed altered expression levels of FZD1 mRNA and protein at 2- and 24-hour Vitamin D treatment. Taken together, our study demonstrates that vitamin D3 has a biphasic effect on FZD1 expression with an early increase and later decrease between 2 hour and 24 hour. Additional studies are needed to dissect the molecular mechanisms underlying this novel regulatory effect on FZD1.

Disclosures: Yingze Zhang, None.

SA0153

See Friday Plenary Number FR0153.

SA0154

Adenovirus 36, Adiposity and Inflammatory-Related Markers in Children. <u>Paige Berger</u>*[1], <u>Emma Laing</u>[1], <u>Norman Pollock</u>[2], <u>Stuart Warden</u>[3], <u>Kathleen Hill Gallant</u>[4], <u>Dorothy Hausman</u>[5], <u>Ralph Tripp</u>[5], <u>Linda McCabe</u>[6], <u>George McCabe</u>[6], <u>Connie Weaver</u>[4], <u>Munro Peacock</u>[7], <u>Richard Lewis</u>[1]. [1]The University of Georgia, USA, [2]Georgia Regents University, USA, [3]Indiana University School of Health & Rehabilitation Sciences, USA, [4]Purdue University, USA, [5]The University of Georgia, USA, [6]Purdue University, USA, [7]Indiana University Medical Center, USA

Purpose: Infection with a common respiratory virus, human adenovirus 36 (Ad36), may induce adipogenesis over osteogenesis, triggering obesity development at the expense of bone. Systemic inflammation may be partially responsible for this obesogenic effect. This study investigated the association of the serum human Ad36

antibody titer with markers of adiposity and inflammation in 291 children ages 9-13 years (50% female, 49% black, 21% obese). Methods: In this cross-sectional study, fasting blood samples were measured for Ad36-specific antibodies and inflammatory-related markers [tumor necrosis factor-alpha (TNF-α), interleukin-6 (IL-6), vascular endothelial growth factor (VEGF), and monocyte chemoattractant protein-1 (MCP-1)] using ELISA and multiplex assays, respectively. Obesity was defined as having a body mass index (BMI)-for-age ≥95th percentile, and dual-energy X-ray absorptiometry was used to measure body fat percentage (BF%). Results: Of the 291 children, 42% were positive for Ad36-specific antibodies [Ad36(+)]. There were no significant differences between Ad36(+) versus Ad36(−) groups in BMI-for-age percentile (64.8 vs. 72.1, P=0.13) or BF% (30.2% vs. 31.4%, P=0.30) after adjusting for age, sex and race. Binary logistic regression, also adjusted for BF%, revealed that the odds for being Ad36(+) were greater for the following serum inflammatory-related markers: highest TNF-α tertile (≥12.0 pg/mL) versus lowest (<8.2 pg/mL) (OR: 2.3; 95% CI: 1.2, 4.2), highest IL-6 tertile (≥1.7 pg/mL) versus lowest (<1.0 pg/mL) (OR: 2.3; 95% CI: 1.4, 4.0) and highest VEGF tertile (≥313 pg/mL) versus lowest (<136 pg/mL) (OR: 2.0; 95% CI: 1.1, 3.7). There was no relationship between Ad36(+) and MCP-1. Conclusions: Our data in children show that Ad36(+) is associated with several inflammatory-related markers, but not with greater adiposity.

Disclosures: Paige Berger, None.

SA0155

See Friday Plenary Number FR0155.

SA0156

See Friday Plenary Number FR0156.

SA0157

Calcium-release activated calcium channel inhibitors suppress acute arthritis in vivo by blocking osteoclast development. <u>Lisa Robinson</u>[1], <u>Jonathan Soboloff</u>[2], <u>Harry Blair</u>*[1], <u>John Barnett</u>[3]. [1]University of Pittsburgh, USA, [2]Temple University, USA, [3]West Virginia University School of Medicine, USA

Our in vitro studies show that osteoclast maturation is suppressed when calcium-release activated calcium currents (CRAC) are blocked by siRNA or by a CRAC antagonist, 3,4-dichloropropionaniline (DCPA). This is consistent with work showing that Ca^{2+}-activated NFATc is required for transcription of osteoclastic proteins. Further, studies of mice deficient in the plasma membrane Ca^{2+} channel Orai1, a key component of CRAC, have reduced, but not absent, bone degradation. As such, we reasoned that responses to stimuli that cause pathological bone resorption might be suppressed by CRAC antagonists without severe side effects. Therefore, we did a trial of treating acute collagen-induced arthritis in mice using 10 µM DCPA. This *dramatically suppressed the development of arthritis* over five weeks. Findings included significant reduction in bone and cartilage damage in sections of feet of the animals, and reduction in overall swelling of joints. All of this analysis was done using blinded observers, with 10-12 replicates of CIA and treated CIA. This response did not affect anti-collagen titers. There were no adverse effects in the treated group on animal weight or activity, consistent with low toxicity, which also has been noted in humans exposed to DCPA. Inflammatory arthritis is a disabling condition that affects many thousands of people in the US each year; it occurs in adults and children, after trauma, and secondary to infections (e.g., *Borrelia*), but typically it is idiopathic. Millions of adults live with chronic rheumatoid arthritis, which has similar features. Inflammatory arthritis often requires treatments with dangerous side effects. This new approach, based on an inhibitor of osteoclast maturation, may thus be applicable to treating acute arthritis. While the crossover from inhibiting bone degradation to inhibiting acute arthritis was not initially expected, other agents show similar broad spectrum effects on bone turnover and arthritis, including TNFα antagonists. Specifically, targeting CRAC might be appropriate to manage acute arthritis with less risk than steroids, metabolic inhibitors, or TNFα antagonists.

Disclosures: Harry Blair, None.

SA0158

Mouse Forearm Loading – Experimental Strain Quantification using a Digital Image Correlation Technique. <u>Mark Begonia</u>[1], <u>Mark Dallas</u>[1], <u>Mark Johnson</u>[2], <u>Ganesh Thiagarajan</u>*[3]. [1]University of Missouri Kansas City, USA, [2]University of Missouri, Kansas City Dental School, USA, [3]University of Missouri - Kansas City, USA

Gene expression in individual osteocytes in response to whole bone strain is heterogeneous. It has been hypothesized that gene expression is related to the actual strain on the individual osteocyte and its lacuna. In order to begin to correlate strain with biological response, we have performed a number of strain gage and Digital Image Correlation (DIC) studies to build finite element (FE) models approximating the strain fields experienced by osteocytes during loading. A 2D-DIC technique has been developed using two cameras to capture videos of both the medial and lateral

sides of the mouse forearm during compressive loading and a MATLAB based software employing a cross-correlation technique to quantify the displacement, strain histories, and strain contours in several distinct regions of the bone. Each ex vivo loading test was performed at multiple camera lens magnifications (2x, 3x and 4x). This methodology offers many advantages since; a) no additional stiffness is introduced by the adhesive between the strain gages and bones, b) the radius and ulna can be analyzed simultaneously using the same video, c) strain patterns can be studied in various regions of interest in either or both bones, and d) the medial and lateral strains in the forearm can be quantified simultaneously. At a magnification of 2x, the strain magnitudes were -3894 $\pm$ 1485 uε in the medial ulna, 2642 $\pm$ 551 uε in the lateral ulna,-2772 $\pm$ 507 uε in the medial radius, and 1841 $\pm$ 191 uε in the lateral radius. As the camera lens magnification increased to 3x and 4x, the strain magnitudes measured in the same region were higher in the lateral ulna (1.6x and 1.1x), lateral radius (1.7x and 1.8x), and medial radius (1.1x and 1.4x). Conversely, the medial ulna exhibited lower strain magnitudes (0.94x and 0.94x) with increasing magnification. This change is attributed to the increased sensitivity of the displacement magnitudes and consequently the strain magnitudes. This DIC method can be extended to in vivo testing to facilitate quantification of in situ strains and to avoid the calibrations required using existing ex vivo techniques. The eventual goal of this project is to use this data to build FE models to map macro strains on the bone surface and use them to build micro FE models that map actual locations of osteocytes to explain osteocyte activation in response to loading.

Disclosures: Ganesh Thiagarajan, None.

SA0159

See Friday Plenary Number FR0159.

SA0160

See Friday Plenary Number FR0160.

SA0161

Endoplasmic Reticulum Calcium Handling in Osteocyte Mechanobiology.
Genevieve Brown*[1], X. Edward Guo[2]. [1]Columbia University, USA, [2]Columbia University, USA

Osteocytes (OCY) exhibit spike-like oscillations in cytosolic calcium (Ca^{2+}) in response to mechanical stimuli both *in vitro* and *ex vivo*, whereas osteoblasts (OB) demonstrate fewer, weaker responses [Lu 2012; Jing 2014]. Previous work demonstrated the initial response of both cells relied on extracellular Ca^{2+}, while inhibitor studies implicated release of Ca^{2+} from endoplasmic reticulum (ER) stores as being critical to subsequent responses. Depletion of ER stores by thapsigargin or interruption of purinergic signaling all effectively abolished the multiple Ca^{2+} responses of OCY. Thus, it is possible the mechanisms of Ca^{2+} release and reuptake by the ER are important to OCY mechanobiology.

We sought to visualize the dynamics of Ca^{2+} signaling within bone cells under fluid flow by simultaneously monitoring Ca^{2+} separately in the cytosolic ($[Ca^{2+}]_{cyt}$) and endoplasmic ($[Ca^{2+}]_{ER}$) spaces using the cytosolic calcium indicator Fura Red and the ER-localized cameleon FRET biosensor D1ER, respectively [Palmer 2004]. In OCY, elevations of $[Ca^{2+}]_{cyt}$ coincided with depression of $[Ca^{2+}]_{ER}$, with subsequent peaks occurring after recovery of $[Ca^{2+}]_{ER}$ levels (Fig. 1A). In OB, only a single $[Ca^{2+}]_{cyt}$ response was observed, and while the ER contributed to this response, it did not refill in the time course of the experiment (Fig. 1B). Previous studies also implicated T-type voltage sensitive channels (VSCC) in regulating OCY Ca^{2+} oscillations. We explored the interaction between T-type VSCC and ER stores by treating OCY and OB with the inhibitor NNC 55-0396 prior to depleting the ER with thapsigargin (Fig. 2A). In OB, T-type inhibition had no effect on the depletion characteristics of the ER, consistent with its limited role in OB Ca^{2+} signaling. In OCY, treatment with the T-type inhibitor caused the ER to deplete faster than untreated controls, suggesting T-type channels are involved in ER Ca^{2+} release. Under flow, OCY pretreated with the inhibitor demonstrated fewer $[Ca^{2+}]_{cyt}$ spikes, corresponding to delayed recovery of $[Ca^{2+}]_{ER}$ (Fig. 2B).

These studies demonstrate the ER is more intimately involved in OCY calcium signaling than previously considered and support the hypothesis that OCY are capable of generating characteristic multiple responses by an ability to refill the ER stores. Future studies will further explore the role of VSCC and other channels on release and reuptake dynamics of ER Ca^{2+} trafficking in OCY, which may contribute to their mechanobiological function.
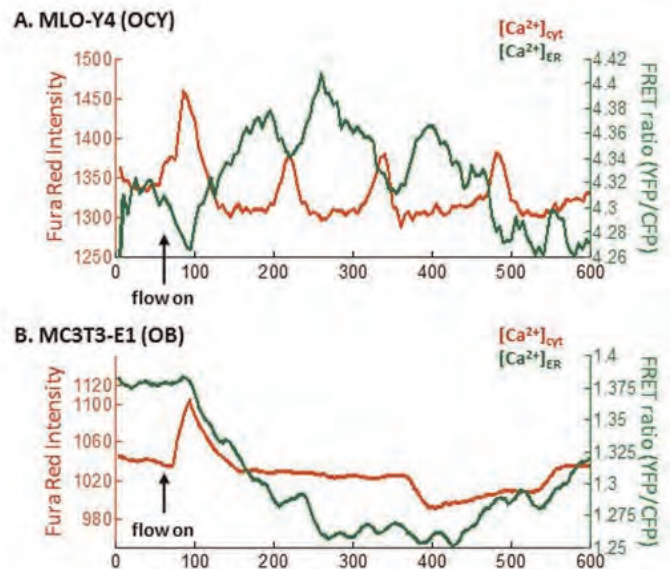
Figure 1
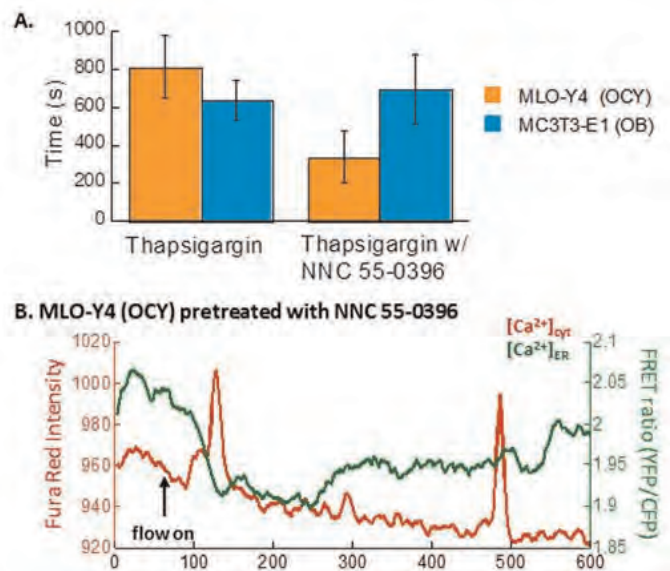
Figure 2

Disclosures: Genevieve Brown, None.

SA0162

Polycystin-1 Mediates Mechanical Strain-Induced Osteoblastic Mechanoresponses via Potentiation of Intracellular Calcium and Akt/β-Catenin Pathway.
Hua Wang*[1], Wen Sun[2], Junqing Ma[3], Yongchu Pan[3], Lin Wang[3], Wei-Bing Zhang[4]. [1]Institute of Stomatology, Nanjing Medical University, Peoples Republic of China, [2]Nanjing Medical UniversityThe Research Center for Bone & Stem Cells, Peoples Republic of China, [3]Institute of Stomatology, Nanjing Medical University, China, [4]School of Stomatology, Nanjing Medical University, Nanjing, China, USA

Mechanical regulation of bone formation involves a complex biophysical process, yet the underlying mechanisms remain poorly understood. Polycystin-1 (PC1) is postulated to function as a mechanosensory molecule mediating mechanical signal transduction in renal epithelial cells. To investigate the involvement of PC1 in mechanical strain-induced signaling cascades controlling osteogenesis, PKD1 gene was stably silenced in osteoblastic cell line MC3T3-E1 by using lentivirus-mediated shRNA technology. Here, our findings showed that mechanical tensile strain sufficiently enhanced osteogenic gene expressions and osteoblastic proliferation. However, PC1 deficiency resulted in the loss of the ability to sense external mechanical stimuli thereby promoting osteoblastic osteogenesis and proliferation. The signal pathways implicated in this process were intracellular calcium and Akt/β-catenin pathway. The basal levels of intracellular calcium, phospho-Akt, phospho-GSK-3β and nuclear accumulation of active β-catenin were significantly attenuated in PC1

deficient osteoblasts. In addition, PC1 deficiency impaired mechanical strain-induced potentiation of intracellular calcium, and activation of Akt-dependent and Wnt/β-catenin pathways, which was able to be partially reversed by calcium ionophore A23187 treatment. Furthermore, applications of LiCl or A23187 in PC1 deficient osteoblasts could promote osteoblastic differentiation and proliferation under mechanical strain conditions. Therefore, our results demonstrated that osteoblasts require mechanosensory molecule PC1 to adapt to external mechanical tensile strain thereby inducing osteoblastic mechanoresponse, partially through the potentiation of intracellular calcium and downstream Akt/β-catenin signaling pathway.

Disclosures: Hua Wang, None.

SA0163

Examining the Effects of Migration on Bone Quantity and Microarchitecture in Migratory Landbirds. Maria Squire*[1], Robert Smith[2], Jennifer Owen[3]. [1]Department of Biology, The University of Scranton, USA, [2]The University of Scranton, USA, [3]Michigan State University, USA

Bone is a dynamic tissue and continuously remodels its structure in response to changes in mechanical loading. For example, it is well established that when chickens are exposed to increased mechanical loading, bone quantity increases significantly within a few weeks. What happens in the bones of migratory landbirds, who as part of the annual cycle increase mechanical loading on their wing bones as they fly thousands of miles during both spring and fall migration, is not well characterized. In the current study we examined how the events associated with migration may have affected the quantity and microarchitecture of bone in Veery (*Catharus fuscescens*) and Wood Thrush (*Hylocichla mustelina*). We used high-resolution (10 μm) micro-computed tomography scanning to examine trabecular bone in the proximal humeri. Specifically, birds from both species were collected during spring migration (in LA), on the breeding grounds (in PA), and during fall migration (in AL). The parameters measured included trabecular bone volume fraction (BV/TV), trabecular thickness (TbTh), and tissue mineral density (TMD). The results suggest a trend towards greater BV/TV in AL Veerys as compared to LA (+23%) and PA (+26%), though the differences were not statistically significant. AL Veerys had 17% and 20% greater TbTh (p=0.05 and p<0.02, respectively) but 17% and 21% less TMD (p<0.01 each) as compared to LA and PA, respectively. For Wood Thrush, again the results suggest a trend toward greater BV/TV in AL birds as compared to LA (+10%) and PA (+13%), though not statistically significant. Additionally, AL Wood Thrush had 26% greater TbTh but 9% less TMD as compared to the LA (p<0.02 and p=0.05, respectively), and 16% greater TbTh and 8% less TMD in comparison to the PA (p=0.07 and p=0.09, respectively). Analysis of the effects of migration on cortical bone in the mid-diaphysis of the humerus in these birds is on going. Importantly, the current data suggest that, despite no change or a potential increase in bone volume fraction, birds from both species have less mineralized bone during fall migration. Consequently, we hypothesize that the events associated with fall migration increase bone quantity but also have a detrimental effect on degree of mineralization. Additional work is needed to examine a larger sample size in order to gain further insight into the mechanisms influencing changes in bone quantity and microarchitecture associated with migratory events in these birds.

Disclosures: Maria Squire, None.

SA0164

Mechanical Vibration Potentializes the Effect of Estrogen Hormone Replacement Therapy in Osteopenic Females Mice. Márcio Moura Moura*[1], Marise Lazaretti Castro[2], Helena Bonciani Nader[2], Ana Paula Mayumi Kawachi[2], Keico Okino Nonaka[3], Rejane Reginato[4]. [1]Luis Alves MouraAna lina de Almeida Moura, Brazil, [2]Federal University of São Paulo, Brazil, [3]Federal University of São Carlos, Brazil, [4]UNIFESP - Federal University of São Paulo, Brazil

Hormone replacement therapy is used to prevent bone loss during menopause. However, it is unknown whether this therapy can be enhanced when associated with mechanical vibration. The aim of this study was investigate the effects of estrogen hormone replacement therapy associated with low-intensity and high-frequency mechanical vibration on bone tissue of osteopenic female mice. Fifty, 3-month-old female Swiss mice were ovariectomized (OVX) or sham-operated (Sham). After 4 months, the animals were randomly separated into five groups (n=10): GI (Sham); GII (control) - OVX and treated only with vehicle solution (sunflower oil subcutaneously injected-7 days a week); GIII - OVX and submitted to mechanical vibration 60 Hz with acceleration of 0.6g for 60 days (30 min/day, 5 days/week) plus vehicle solution (7 days/week); GIV - OVX and treated with 10 μg/kg/day of 17β-estradiol subcutaneously injected (7 days/week); GV - OVX and submitted to mechanical vibration 60 Hz/0.6g for 60 days (30 min/day, 5 days/week) and treated with 10 μg/kg/day of 17β-estradiol subcutaneously injected (7 days/week). Bone mineral density (BMD) was performed before the ovariectomy, 120 days after OVX and at the end of the treatment. The animals were euthanized and femora were collected for the following analysis: histomorphometry, biochemistry, TRAP, Picro-Sirius red, immunohistochemical for caspase-3 and calcium quantification. The results showed that all groups increased BMD compared to GII. Trabecular bone area was increased in GIV and GV, but there was no difference in the cortical bone thickness. The highest concentration of hyaluronic acid and condroitin sulfate was observed in

GV. Furthermore, GV exhibited the highest number of osteoclasts and intense greenish birefringence of collagen fibers on the cortical and cancellous bone. On the other hand, the number of osteocytes positive for caspase-3 decreased in GV, as revealed by immunohistochemistry. In addition, the group that received the combined therapy was the only one that showed calcium concentration similar to the sham group. Taken together, our results indicate that mechanical vibration potentiates the estrogen hormone replacement therapy by accelerate the bone remodeling process. The combined treatment demonstrated positive effect on bone tissue constituents, improving bone microarchitecture and bone mineral density, as well modifying the profile of glycosaminoglycans and collagen on bone tissue of osteopenic female mice.

Disclosures: Márcio Moura Moura, None.

SA0165

See Friday Plenary Number FR0165.

SA0166

See Friday Plenary Number FR0166.

SA0167

See Friday Plenary Number FR0167.

SA0168

Research of bone mass change by PTH administration to OPN-KO mice neurectomy. Takayuki Yamada*[1], Yoichi Ezura[2], Tadayoshi Hayata[3], Kiyoshi Harada[4], Masaki Noda[1]. [1]Tokyo Medical & Dental University, Japan, [2]Tokyo Medical & Dental University, Medical Research Insititute, Japan, [3]Organization for Educational Initiatives, University of Tsukuba, Japan, [4]Tokyo Medical & Dental University, Japan

Mechanical stimulations, the exercise or gravity from the earth, are known as a factors to maintain bone mass. In environments, such as bedridden state or flight to the space, bone mass decreases.

Osteopontin (OPN) is necessary for unloading induced enhancement of bone resorption and suppression of bone formation in vivo. OPN plays a key role in conveying the effect of mechanical stress to osteoclasts and osteoblasts.

In addition, it has been reported that the sympathetic nervous system is the dominant, bone loss is induced. However, molecular mechanisms of bone metabolic are not completely known.

Currently, about 13 million people are suffering from osteoporosis in Japan.

In the case of elderly people, especially woman, the risk of becoming bedridden due to lumbar fracture is high. Parathyroid hormone (PTH) is one of the bone anabolic drug.

Thus, we performed neurectomy to OPN-KO mice, and made an unloading condition. Then we researched bone mass and changes of bone metabolic markers by PTH administration.

We used Male wild-type and OPN-KO mice in a C57BL/6J background (17 week old). They were performed neurectomy to right legs and sham surgery to left legs for 4 weeks. During unloading condition, we administrated PTH (80 μg/kg) or Vehicle 5 times per week.

There was no change in body weight and tibiae length by Neurectomy, We found that neurectomy induced decreasing of bone mineral density (BMD) in wild type tibiae, but PTH administration suppressed it mildly. However, in the absence of OPN, changes in BMD due to PTH and neurectomy was not observed BV/TV changed in a similar manner with BMD.

In mineralized nodule formation, there was no difference by Neurectomy, but PTH promoted mineralization in wild type.

These data suggest that a apossible interaction between neurectomy, OPN and PTH regarding maintenance of bone mass.

Disclosures: Takayuki Yamada, None.

SA0169

Loss of N-cadherin in Osteoblasts Enhances the Osteo-Anabolic Effects of Lrp5/6 Signaling. Cynthia Brecks*[1], Valerie Salazar[2], Susan Grimston[3], Leila Revollo[4], Marcus Watkins[3], Gabriel Mbalaviele[3], Roberto Civitelli[3]. [1]Washington University In St Louis, USA, [2]Harvard School of Dental Medicine, USA, [3]Washington University in St. Louis School of Medicine, USA, [4]Washington UniversityDivision of Bone & Mineral Diseases, USA

It has been shown that N-cadherin negatively regulates canonical Wnt/β-catenin signaling in osteoblasts through physical interaction with low density lipoprotein receptor-related protein-5 or 6 (Lrp5/6) and Axin. To understand the biological significance of this function of N-cadherin, we tested in vivo whether loss of the

N-cadherin gene (*Cdh2*) alters the ability of osteogenic cells to build bone in response to Lrp5/6 signaling. First, we activated Lrp5/6 in vivo by systemic administration of a Dickkopf-1 (Dkk1) neutralizing antibody (αDkk1) to mice with osteoblast-specific *Cdh2* ablation driven by the 2.3 *Col1A1* promoter (*Col1-Cdh2* cKO). At the dose of 20 mg/kg i.p., 3 times/week for 4 weeks, αDkk1 increased trabecular bone volume/total volume (BV/TV; by μCT) in both wild type (WT) and *Col1-Cdh2* cKO mice (0.536 ± 0.130 vs. 0.475 ± 0.117% at study end; p>0.10). However, a 4-fold lower dose of the antibody (5 mg/kg) was ineffective in WT mice, but resulted in a 2-fold increase of BV/TV (0.496 ± 0.085% at study end; p<0.01 vs. baseline) in *Col-Cdh2* cKO mice. αDkk1 increased cortical thickness and dynamic indices of bone formation in both genotypes, without affecting bone resorption. In a second study, we induced high bone mass (HBM) by using *Osx1-Cre* to activate a Dkk1-resistant *Lrp5^{A214V}* allele, and evaluated whether HBM was affected by compound conditional ablation of *Cdh2*. Consistent with increased anabolic response of *Col1-Cdh2* mice to αDkk1, BV/TV was higher in *Lrp5^{A214V};Cdh2* double mutants relative to *Lrp5^{A214V}* HBM mice. At the molecular level, bone marrow stromal cells (BMSCs) from *Col1-Cdh2* cKO mice expressed higher Lrp5, but not Lrp6 mRNA relative to WT BMSCs. Immunoblot analysis revealed Lrp5 and b-catenin proteins were more abundant in *Cdh2-cKO* versus WT BMSCs. And *Col1-Cdh2* cKO mice injected with a single dose of αDkk1 exhibited accelerated accumulation of β-catenin in bone relative to WT mice. In summary, our results demonstrate that mice lacking osteoblast *Cdh2* are hyper-responsive to bone anabolic effects of antibody-mediated Dkk1 inhibition or Lrp5 gain-of-function mutation, and suggest *Cdh2*-deficient osteoblasts are primed to respond to canonical Wnt signaling, most likely because of increased Lrp5 and b-catenin levels. These observations provide supporting evidence and assign biological significance with a skeletal outcome to a previously proposed model where N-cadherin negatively regulates Lrp5/6 signaling.

Disclosures: Cynthia Brecks, None.

SA0170

See Friday Plenary Number FR0170.

SA0171

See Friday Plenary Number FR0171.

SA0172

The bone anabolic potential of canonical WNT signaling requires epigenetic priming of endogenous BMP2 production: *in vitro, in vivo* and *in silico* studies. <u>Young dan cho</u>*[1], <u>Kyung mi woo</u>[2], <u>Jeong hwa baek</u>[2], <u>Young Ku</u>[3], <u>van Wijnen Andre J.</u>[4], <u>Hyun mo ryoo</u>[2]. [1]Seoul National University, South Korea, [2]Department of Molecular Genetics, School of Dentistry, Seoul National University, South Korea, [3]Department of Periodontology, School of Dentistry, Seoul National University, South Korea, [4]Departments of Orthopedic Surgery & Biochemistry & Molecular Biology, Mayo Clinic, USA

Bone loss is treated with anti-resorptive therapeutics (e.g., bisphosphonates) that inhibit bone-degrading osteoclasts or anabolic drugs that stimulate bone-depositing osteoblasts (e.g., BMP2, teriparatide and antibody inhibition of WNT antagonists). Activation of the WNT pathway can enhance BMP2 signaling, but only in cells primed to become osteoblasts. We solve this observation by showing that the osteogenic potential of BMP2 is epigenetically blocked by CpG methylation of the BMP2 gene promoter in non-osteogenic cells (e.g., adipocytes and fibroblasts). Data with methylation PCR, ChIP assay and in silico analysis by Next Generation Sequencing (NGS) showed that hypomethylation of this promoter by DNA methyltransferase (DNMT) inhibitor or histone deacetylase (HDAC) inhibitor enables WNT3A stimulation of autocrine BMP2 production in the non-osteogenic cells. In addition, direct injection to the bone marrow of DNMT inhibitor and WNT3A increased bone mass in the yellow marrow of 15 month old mouse.

Taken together, absence of epigenetic barrier allows WNT mediated induction of tandemly arranged autocrine loops that sustain endogenous BMP2 production. These findings clarify the potent bone anabolic activities of new antibody-based drugs that block the WNT inhibitor sclerostin. Furthermore, our data indicate that modulation of CpG methylation permits direct programming of non-osteogenic cells into osteoblasts for bone tissue-engineering applications.

Disclosures: YOUNG DAN CHO, None.

SA0173

The flavonoid fisetin promotes osteoblasts differentiation through Runx2 transcriptional activity. <u>Cedric Darie</u>*[1], <u>Laurent Léotoing</u>[2]. [1], France, [2], France

Scope: Flavonoids represent a group of polyphenolic compounds commonly found in daily nutrition with proven health benefits. Among this group, the flavonol fisetin has been previously shown to protect bone by repressing osteoclast differentiation. In the present study, we investigated the role of fisetin in regulating osteoblasts physiology.

Methods and results: In vivo mice treated with LPSs exhibited osteoporosis features associated with a dramatic repression of osteoblast marker expression. In this model, inhibition of osteocalcin and type I collagen alpha 1 transcription was partially countered by a daily consumption of fisetin. Interestingly, in vitro, fisetin promoted both osteoblast alkaline phosphatase activity and mineralization process. To decipher how fisetin may exert its positive effect on osteoblastogenesis, we analyzed its ability to control the runt-related transcription factor 2 (Runx2), a key organizer in developing and maturing osteoblasts. While fisetin did not impact Runx2 mRNA and protein levels, it upregulated its transcriptional activity. Actually, fisetin stimulated the luciferase activity of a reporter plasmid driven by the osteocalcin gene promoter that contains Runx2 binding sites and promoted the mRNA expression of osteocalcin and type I collagen alpha 1 targets.

Conclusion: Bone sparing properties of fisetin also rely on its positive influence on osteoblast differentiation and activity.

Disclosures: Cedric Darie, None.

SA0174

See Friday Plenary Number FR0174.

SA0175

Carbon-containing Polyhedral Boron-cluster Carborane BA321 acts on bone tissues as selective androgen receptor modulator (SARM). <u>Tsukasa Tominari</u>[1], <u>Chiho Matsumoto</u>[2], <u>Michiko Hirata</u>[3], <u>Masaki Inada</u>[2], <u>Chisato Miyaura</u>*[2]. [1]Tokyo University of Agriculture & Technology, Japan, [2]Tokyo University of Agriculture & Technology, Japan, [3]Tokyo University of Agriculture & Technology, Japan

Carboranes are a class of carbon-containing polyhedral boron-cluster compounds having exceptional hydrophobicity, and their features allow a new medical application as a biologically active molecule that interacts with steroid hormone receptors. We have reported carborane BE360 having carborane structure with two phenols, binds to estrogen receptor and exhibits estrogenic action in bone but not in uterus as selective estrogen receptor modulator (SERM). We have challenged to design new carborane compounds having high affinity with androgen receptor (AR) and synthesized them to search effective compounds for osteoporosis in the male as selective androgen receptor modulator (SARM). Among several carborane compounds, we noticed carborane compound BA321 as a putative AR antagonist, in which a benzene ring with electron-withdrawing group (-NO$_2$) and a hydroxyl group are placed at the opposite vertices of the hydrophobic carborane cage. In this study, we report that the effects of BA321 on bone tissues in the presence or absence of endogenous androgen in male mice. To examine the effects of BA321 on bone tissues in the absence of androgen, male mice were orchidectomized (ORX) and some of mice were treated with BA321 (10, 30 μg/day/mouse) subcutaneously for 4 weeks. ORX mice showed severe bone loss due to androgen deficiency measured by femoral BMD and three dimensional micro-CT, and the bone loss was completely recovered by the treatment with BA321. The weight of seminal vesicle, male sex organ, was reduced in ORX mice, and not influenced by the treatment of BA321. Therefore, BA321 did not exhibit androgenic action in sex organ whereas BA321 increased bone mass in the male mice. We further examined the effects of BA321 in the normal mice, with having endogenous androgen. When normal male mice were treated with BA321 (10, 30 μg/day/mouse) subcutaneously, BA321 significantly increased femoral BMD, and the weight of seminal vesicle was significantly suppressed. Therefore, BA321 binds to AR and acts on bone tissues as androgen and on sex organs as anti-androgen. Carborane BA321 may utilize to the treatment for osteoporosis in men as a SARM.

Disclosures: Chisato Miyaura, None.

SA0176

See Friday Plenary Number FR0176.

SA0177

Combination Therapy with Ibandronate and Eldecalcitol Enhances Bone Strength with upregulation of minimodeling in Aged Ovariectomized Rats. <u>Sadaoki Sakai</u>*[1], <u>Satoshi Takeda</u>[2], <u>Masanori Sugimoto</u>[3], <u>Masaru Shimizu</u>[4], <u>Koichi Endo</u>[4]. [1]Chugai Pharmaceutical Co., Ltd., Japan, [2]Chugai Pharmaceutical Co., Ltd., Japan, [3]Taisho Pharmaceutical Co., Ltd, Japan, [4]Chugai Pharmaceutical Co., Ltd., Japan

Ibandronate (IBN), a nitrogen-containing bisphosphonate, and eldecalcitol (ELD), an active vitamin D$_3$ derivative, are used for osteoporosis treatment. Active vitamin D$_3$ derivatives have been often used in combination therapy, however, there are no reports on the effects of combined IBN and ELD treatment.

Eight-month-old Wistar-Imamichi rats were ovariectomized and treated for 12 weeks with either vehicle, IBN (3 µg/kg/4week), ELD (15 ng/kg/day), or a combination of IBN and ELD.

Urinary DPD (deoxypyridinolin) was higher in vehicle control group than sham operated group and recovered in each monotherapy group. The combination treatment showed further suppression in DPD compared to each monotherapy group. Serum osteocalcin was higher in vehicle treated group and there were no differences between in all therapy groups versus in the sham group.

Lumbar BMD was higher in the monotherapy groups than in the vehicle control group, and was higher in the combination group than in both monotherapy groups. A mechanical strength of lumbar was improved in monotherapy groups and in the combination group. The maximum load was higher in the combination group than in the IBN monotherapy group.

In femurs, BMD was increased in both monotherapy groups, and was higher in the combination therapy group than in both monotherapy groups. The maximum load of femurs was higher in the combination group than in the vehicle control group.

Bone histomorphometry analysis revealed that combination therapy result in additive effects on reduction of ES/BS in cancellous and endosteal cortical bone in femurs, but bone formation parameters such as MS/BS or BFR/BS were not less than sham level. To elucidate this uncoupling of combination effect on bone formation and resorption, we focused on "minimodeling". The minimodeling in lumbar spine was significantly higher in ELD group than vehicle treated group. The combination treatment with IBN and ELD showed additional effect on elevation of minimodeling than ELD alone group.

This study suggests the additive effects of IBN and ELD combination therapy on the mechanical strengths of the lumbar vertebrae and femur. These effects may be induced by increased BMD via reduction of bone resorption without severe suppression of bone formation. The effect of combination treatment on minimodeling may play a part in maintaining bone formation at sham level with additive effect on reduction of bone resorption.

SA0178

OPG-Fc but not Zoledronic Acid Discontinuation Reverses Radiographic and Histologic Indices of Osteonecrosis of the Jaws (ONJ) in a Mouse Model.
Rafael De Molon*[1], Hiroaki Shimamoto[2], Olga Bezouglaia[2], Flavia Pirih[1], Sara Dry[3], Paul Kostenuik[4], Denise Dwyer[5], Rogely Waite Boyce[6], Tara Aghaloo[7], Sotirios Tetradis[7]. [1]UCLA School of Dentistry, USA, [2]UCLA School of Dentistry, USA, [3]UCLA School of Medicine, USA, [4]Amgen Inc., USA, [5]Amgen Inc, USA, [6]Amgen Inc, USA, [7]University of California, Los Angeles, USA

Osteonecrosis of the jaws (ONJ) is a significant complication of antiresorptive medications such as bisphosphonates and denosumab. Local risk factors include oral surgical procedures, dental infection, and poor-fitting dentures. Discontinuation of antiresorptives prior to tooth extraction to reduce ONJ risk or after ONJ occurrence to promote healing has been proposed, but is largely controversial. Here, we investigated whether antiresorptive discontinuation alters radiographic and histologic features of established ONJ in a mouse model employing high doses zoledronic acid (ZA) or OPG-Fc and periapical disease. Mice were pre-treated with veh, ZA or OPG-Fc for 3 weeks (wk), right mandibular molars were drilled to induce periapical infection and treatment continued for 8 wk. Then, antiresorptives were discontinued for 6 or 10 wk. Both agents significantly decreased TRACP-5b levels by 11 wk. TRACP-5b rose above baseline by 4-6 wk post-OPG-Fc withdrawal and returned to baseline by 10 wk. TRACP-5b progressively returned to baseline by 10 wk post-ZA withdrawal. µCT showed periapical bone loss, widening of the periodontal ligament (PDL) space, loss of lamina dura and thinning of the lingual cortical plate in the diseased site of veh group. OPG-Fc and ZA prevented these changes. After OPG-Fc discontinuation all µCT measurements were similar to the veh group. In contrast, ZA discontinuation did not alter µCT findings. TRAP staining showed increased osteoclast numbers in the diseased site of veh animals. No TRAP+ cells were seen in the OPG-Fc group, while TRAP+ cells detached from the bone with pyknotic nuclei were noted in the ZA group. After OPG-Fc withdrawal, TRAP+ cell numbers rose above baseline at 6 wk and returned to baseline by 10 wk. No significant change in TRAP+ cell number was seen after ZA withdrawal. Epithelial to alveolar crest distance increased in the diseased site of veh animals, denoting bone loss. This distance was preserved in OPG-Fc and ZA animals. Additionally, empty osteocytic lacunae and areas of osteonecrosis were present in the diseased site of OPG-Fc and ZA but not veh animals, consistent with ONJ. OPG-Fc, but not ZA, discontinuation increased the epithelial-alveolar crest distance at 6 and 10 wk and decreased the number of empty osteocytic lacunae and osteonecrotic area by 10 wk. These data collectively demonstrate that OPG-Fc but not ZA discontinuation reverses radiographic and histologic features of osteonecrosis in a mouse ONJ model.

SA0179

The inhibitory effect of zoledronate on early-stage osteoinduction by recombinant human bone morphogenetic protein 2 in an osteoporosis model.
Jae Hyup Lee*[1], Kyung Mee Lee[2], Hae-Ri Baek[2], Hyun-Kyung Lee[2]. [1]Seoul National University, College of Medicine, South Korea, [2]Department of Orthopedic Surgery, College of Medicine, Seoul National University, South Korea

This study aims to understand the effect of the combined treatment of zoledronic acid(ZA) and rhBMP-2 on osteogenesis in an osteoporosis model. Bone marrow-derived stem cells of osteoporosis patients were cultured and divided into the following groups: Control, Induction, B50 (rhBMP-2 50 ng), B100 (rhBMP-2 100 ng), ZA (ZA 10-7 M), ZB50 (rhBMP-2 50 ng+ZA 10-7 M), and ZB100 (rhBMP-2 100 ng+ZA 10-7 M). The cells were subjected to alkaline phosphatase (ALP) staining assay, an ALP activity assay, an Alizarin red (AR)-S staining assay, and RT-PCR to test the expression levels of ALP, runx-2, osteopontin (OPN), bone sialoprotein (BSP), and collagen genes. Ovariectomy was performed on SD rats, and a calvarial defect model was generated. The groups treated with rhBMP-2 and/or ZA showed a higher ALT activity than the Induction group, with no statistical significance, and the level was similar between the rhBMP-2 groups and the ZA+rhBMP-2 groups. Compared to the Control group, the other groups showed stronger ALP staining and AR-S staining. Using an ovariectomized rat calvarial defect model, the experimental animals were intravenously injected with either saline or 0.08mg/kg of ZA. Each treatment group was further subdivided based on rhBMP-2 5 µg treatment status. New bone formation was then evaluated 4 or 8 weeks after the treatments using micro-CT. The rhBMP-2 group showed a significantly higher calvarial defect coverage ratio compared to the ZA+rhBMP-2 group at both 4 and 8 weeks after the treatment, and the calvarial defect coverage ratio was significantly higher in the ZA+rhBMP-2 group than in the ZA group at 8 weeks. In addition, the ZA treatment lowered bone formation indices, such as the percent bone volume and trabecular number, and the trabecular thickness induced by rhBMP-2 after 4 weeks of treatment. Eight weeks of ZA treatment also decreased the trabecular thickness induced by rhBMP-2. The ZA+rhBMP-2 group showed significantly higher bone formation and bone quality compared to the ZA group. However, the initial bone formation and bone quality of the ZA+rhBMP-2 group were significantly lower compared to those of the rhBMP-2 group, and the negative effect induced by ZA treatment was alleviated as time passed. Thus, the combined application of rhBMP-2 and ZA significantly increased bone formation, but the initial bone formation was lower compared to the treatment with rhBMP-2 only.

SA0180

BMP2 and ibandronate combination therapy improves bone healing during non-weight bearing treatment of ischemic osteonecrosis of the femoral head.
Olumide Aruwajoye*[1], Justin Du[2], Nobuhiro Kamiya[3], Harry Kim[4]. [1]Texas Scottish Rite Hospital, USA, [2]Texas Scottish Rite Hospital, USA, [3]Texas Scottish Rite Hospital for Children, USA, [4]Scottish Rite Hospital for Children, USA

Ischemic osteonecrosis of the femoral head in children (Perthes disease) results in a flattening deformity of the femoral head due to excessive resorption of the necrotic bone without accompanying new bone formation. The main goal of treatment is to prevent deformity of the femoral head. Our previous studies using a piglet model of ischemic osteonecrosis showed that local non-weight bearing (NWB) treatment prevented the flattening deformity by mechanically unloading the joint but was ineffective in preventing excessive bone resorption or in promoting new bone formation. Since a balance of bone resorption and formation determines net bone loss, we studied the effect of treatment with BMP2 and bisphosphonate (ibandronate) that may increase bone formation and decrease bone resorption respectively, during NWB treatment in piglets. In this study, the right femoral head was surgically induced with ischemia and an above knee amputation of the right hindlimb was performed to prevent weight bearing. The piglets received either NWB alone or NWB along with a single intra-osseous infusion of BMP2 (BMP) or BMP2+ibandronate (BMP+IB) in the femoral head 1-2 weeks post-ischemia induction. The non-operated left hindlimb was used as the control (n=6 piglets/group). NWB minimized flattening deformity of the femoral head in all groups at 8 weeks post-ischemia induction as observed by radiographic analysis. Furthermore, evaluation of the bone volume by microCT analysis revealed significantly higher bone volume in the BMP+IB vs BMP (p<0.03) or BMP+IB vs NWB groups (p<0.001), (BV/TV%: Control 16.9±1.9, NWB 3.3±1.7, BMP 11.8±3.7, BMP+IB 19.7±6.5). The mean trabecular number was also significantly higher in the BMP+IB group vs BMP or NWB group (p<0.01) (Tb.N/mm: Control 2.1±0.2, NWB 0.4±0.2, BMP 1.1±0.6, BMP+IB 2.3±0.7). The increase in bone volume due to treatment with BMP+IB was confirmed by histomorphometry. In addition, the number of osteoclasts were significantly lower in the BMP+IB vs NWB group (p<0.01) (N.Oc/BS/mm: Control 2.0±0.8, NWB 4.7±3.0, BMP 2.0±1.4, BMP+IB 0.9±0.6) while the mineral apposition rate and the bone formation rate were significantly increased in the BMP and BMP+IB groups compared to NWB group (p<0.01). These results suggest that the local administration of BMP2 and ibandronate increases the bone volume by increasing bone formation

and decreasing bone resorption thereby enhancing bone healing during NWB treatment ischemic osteonecrosis of femoral head.

Two Dimensional microCT images from Control and treated femoral heads after ischemia induction with non-weight bearing (NWB), NWB+BMP2 (BMP), and NWB+BMP2+ibandronate (BMP+IB)
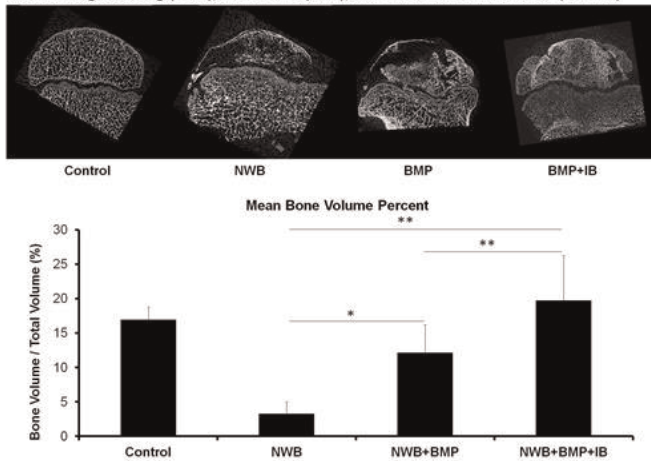
Bone Volume within Control and Treated Femoral Heads

SA0181

Brain-Specific PTEN Deletion Induces Abnormal Skeletal Activity in Mice.

Marjorie Thompson*[1], Philippe Huber[2], Gregory Smith[3], Andrew Holley[3], Steven Bain[4], Edith Gardiner[4], Joaquin Lugo[3], Ronald Kwon[4]. [1], USA, [2]University of Washington, USA, [3]Baylor University, USA, [4]University of Washington, USA

The broad association of epilepsy, autism, and related neurological disorders with dysfunctional bone metabolism [1] suggests a potential neural link between the cerebral cortex and bone that may underlie these deficits. In NS-Pten mice (neuronal subset-specific; Gfap-Cre;Pten$^{loxp/loxp}$), PTEN deletion induces an overactive PI3K-Akt-mTOR pathway, resulting in macrocephaly, hypertrophic cortical neurons, and epileptiform activity with persistent seizures [2]. In this study, we present evidence that brain-specific knockout of the PTEN gene induces abnormal bone metabolism in growing mice. 6wk NS-Pten mice exhibited forelimb clonus, spontaneous seizures, and hyperactivity in open field testing (p<0.001), as observed in previous studies [2,3]. NS-Pten mice also exhibited impaired motor learning, as indicated by decreased rotarod test performance (p<0.001). MicroCT analysis in 8wk NS-Pten mice (Fig 1) revealed increased total volume in the proximal tibia (p<0.001) and mid-diaphysis (p<0.001), respectively, while TMD was lower in both locations (p<0.001). Effects of PTEN deletion were localized and compartment specific, as evidenced by the lower trabecular bone volume in the proximal tibia (p<0.05) but higher cortical area (but normal cortical thickness) in the mid-diaphysis (p<0.05). NS-Pten mice were recently shown to exhibit decreased hippocampal levels of the Kv4.2 potassium channel [3], which is associated with increased neuron excitability and seizure susceptibility [4]. MicroCT analysis of Kv4.2 knockout mice revealed no significant bone phenotype, suggesting that decreased Kv4.2 is not sufficient to alter skeletal activity. Collectively, these studies identify diverse morphological and densitometric bone alterations in mice with brain-specific PTEN deletion that is not attributable to decreased physical activity (an etiological factor broadly ascribed to account for low bone mass in epilepsy patients). Given the association of brain-specific PTEN deletion with aberrant cortical brain activity, as well as the known influence of autonomic and sensory nerves on bone cell function, these studies provide an essential first step toward understanding the role of the cerebral cortex in the central regulation of bone metabolism.

References: 1. Samaniego EA et al., 2007, Semin Pediatr Neurol 14:196-200; 2. Ljungberg MC et al., 2009, Dis Model Mech 7-8:389-398; 3. Lugo JN et al., 2014, Front Mol Neurosci, In Press; 4. Lugo JN et al., 2012, Learn Mem, 19:182-189
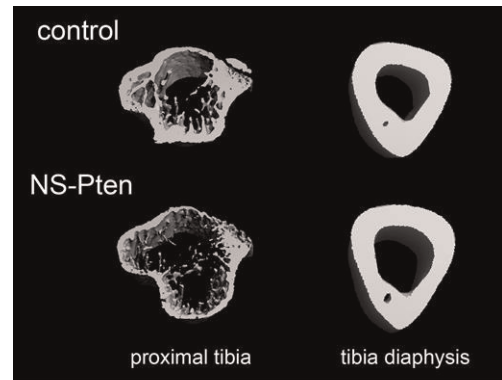
Fig. 1: MicroCT reconstructions of proximal tibia and mid-diaphysis in control and NS-Pten mice.

Figure 1

SA0182

Effects of Circulating Osteocalcin on Bone Remodelling.

Tara Brennan-Speranza*[1], Katharina Blankenstein[2], Hong Zhou[3], Markus Seibel[3]. [1]University of Sydney, Australia, [2]Bone Research Program, ANZAC Research Institute, University of Sydney, Australia, [3]Bone Research Program, ANZAC Research Institute, University of Sydney, Australia

Aim: Osteocalcin (OCN) is a protein synthesized solely by osteoblasts. While circulating OCN may play a role in regulating glucose metabolism, its functional role in bone is unclear. As osteocalcin knock-out mice display increased bone formation[1], we hypothesized that an increase in circulating OCN would lead to decreased bone formation.

Methods: Using in-vivo gene therapy [2], we transfected a wild-type osteocalcin (wtOCN) or a mutant osteocalcin construct (mOCN) which cannot be carboxylated into hepatocytes of 7-week-old mice. Empty vector (EV) was used as control. Tibiae were harvested at d21 post-transfection for mCT, histomorphometry and gene expression analysis.

Results: Compared to EV, total serum OCN levels were increased by 30% (wtOCN) and 40% (mOCN) on d21. BV/TV decreased from $17.9 \pm 1.8\%$ in EV to $11.5 \pm 1.2\%$ and $9.4 \pm 1.1\%$ in wtOCN and mOCN receiving mice, respectively (p<0.01). While trabecular spacing was increased, trabecular number and cortical thickness were significantly decreased by both OCN vectors. Trabecular thickness was unchanged. Histomorphometry revealed that compared to EV controls, both osteoblast and osteoclast surfaces were significantly increased in wtOCN and mOCN vector receiving mice. Furthermore, hepatic expression of the mOCN vector was associated with significant increases in Runx2 (1.5-fold), osterix (2-fold), BMP-4 (1.5-fold increase), BMP-7 (1.7-fold increase) and osteocalcin (1.5-fold) mRNA expression. . RANKL mRNA expression was significantly increased in both OCN vector-receiving mice. OPG remained unchanged.

Conclusion: Increasing circulating osteocalcin via gene therapy is associated with bone loss and accelerated bone turnover in mice.

Ducy, P et al., *Increased bone formation in osteocalcin-deficient mice.* Nature, 1996. 382(6590): p. 448-452.

Brennan-Speranza, TC et al., *Osteoblasts Mediate the Adverse effects of Glucocorticoid on Fuel Metabolism.* JCI, 2012. 122(11)89:4172-89

SA0183

Enhanced fracture healing following selective abrogation of Runx3 in the perisoteum.

Do Yu Soung[1], Vanessa Piccullio[1], Archana Sanjay[2], Marc Hansen[3], Hicham Drissi*[3]. [1]University of Connecticut Health Center, USA, [2]UCHC, USA, [3]University of Connecticut Health Center, USA

Fracture healing of long bones occurs through both endochondral and intramembranous ossification. The absence of the periosteum was shown to impair fracture callus formation, rendering this source of progenitor cells necessary for the healing process. We previously demonstrated a role for the Runx family member of transcription factors, Runx1 in mediating chondrogenic differentiation during development and soft callus formation. Additionally, the Runx1 homologue, Runx3 was shown to mediate early and late stages of chondrocyte differentiation in vitro. However, the role of Runx3 during skeletal development is understudied and its function in bone repair remains unknown. We crossed Runx3 floxed mice (Runx3F/F) withPrx1-Cre transgenic mice to generate mice in which Runx3 was conditionally abrogated Runx3 expression in mesenchymal progenitors (Prx1-Cre;Runx3F/F). While Runx3 was not necessary for normal limb development, periosteal cultures from Prx1-Cre;Runx3F/F revealed decreased Runx3 expression, which was concomitant with decreased markers of

chondrogenic differentiation. However, bone mineral density of femurs harvested from these mice was enhanced as measured by DEXA scanning.

To examine if Runx3 plays a role during bone repair, we performed femoral fracture in Prx1-Cre;Runx3F/F mutants. Mice with 100% Runx3 activity (Runx3F/+) were used as controls. Radiographic analyses of the fractured bones showed smaller calluses during bone repair in the Prx1-Cre;Runx3F/F mutants. Histological and histomorphometric analyses revealed that Prx1-Cre; Runx3F/F calluses contained significantly reduced amounts of cartilaginous tissue at day 7 post-fracture compared to Runx3F/+. However, bone tissue content was also increased in Prx1-Cre; Runx3F/F at day 21 post-fracture. Gene expression of chondrogenic and osteogenic markers using RNA extracted from callus tissue harvested by laser capture microdissection confirmed these findings. Further examination of histological sections from fractured limbs showed that osteoblast surface over bone surface was enhanced at day 21 while the number of osteoclasts remained unchanged between both genotypes. Conditional deletion of both Runx1 and Runx3 revealed dose-dependent decrease of cartilage in early calluses of fractured bones. The data indicate that selective abrogation of Runx3 in periosteal progenitor cells results in accelerated fracture healing and suggest a redundant function between Runx1 and Runx3 in early fracture repair.

Disclosures: Hicham Drissi, None.

SA0184

See Friday Plenary Number FR0184.

SA0185

Lead Induced Differences in Bone Properties in Osteocalcin +/+ and -/- Female Mice. <u>Terry Dowd</u>*[1], <u>Adele Boskey</u>[2], <u>Caren Gundberg</u>[3], <u>Marjolein Van Der Meulen</u>[4], <u>Olga Berezovska</u>[5]. [1]Brooklyn College of the City University of New York, USA, [2]Hospital for Special Surgery, USA, [3]Yale University School of Medicine, USA, [4]Cornell University, USA, [5]Department of Chemsitry Brooklyn College, USA

Introduction: Lead (Pb) toxicity is a major health problem in children and older adults. Bone is the major reservoir for Pb and serves as an endogenous source of exposure. We have shown in mature female mouse femora that Pb has detrimental effects on bone mineral properties ((Bone 47:888 2010). Osteocalcin (OC) has been reported to inhibit bone formation (Nature 382:448, 1996) and to impair remodeling (Bone 23:187, 1998)) while Pb has been shown to increase bone turnover. Purpose: To determine whether OC plays a role in the detrimental effects of Pb on bone by comparing bones from Pb sufficient and Pb deficient OC +/+ and OC -/- mice. Methods: Two month old female OC +/+ and OC-/- mice, generously provided by G. Karsenty, were exposed to Pb in the drinking water (0 or 250 ppm, blood Pb of 20 μg/dl) for 4 months. Bone mineral properties from 6 mo old femora were assessed by Fourier Transform Infrared Imaging (FTIRI), Micro-computed tomography (uCT), bone biomechanical measurements and serum turnover markers (P1NP, CTX). Results: As in previous studies, the turnover markers in OC-/- mice showed a significantly higher bone formation rate and no change in bone resorption vs +/+ mice. Lead significantly enhanced formation in both -/- and +/+ mice and resorption in +/+ mice, with a trend toward an increase in -/- mice. A significantly lower mineral to matrix ratio was seen in the Pb-free -/- mice compared to +/+ mice, suggesting increased matrix retention in OC -/- bones. This was supported by a decrease in cortical bone stiffness in both Pb-free and Pb exposed -/- mice but not in +/+ mice . There was increased mineral to matrix ratio and crystal size in Pb treated -/- mice compared to untreated -/- mice, both of which are consistent with increased resorption. In contrast to +/+ mice, Pb increased cortical thickness, bone mineral density and decreased stiffness in cortical bones of -/- mice. Conclusions: These results suggest that osteocalcin, through regulation of formation and resorption plays a role in the detrimental effects of Pb by increasing turnover, leading to decreased cortical thickness, BV/TV and increased marrow area/total area. This study sheds light on the molecular mechanism of Pb toxicity in bone and on the function of osteocalcin.

Disclosures: Terry Dowd, None.

SA0186

Muramyl dipeptide enhances Lipopolysaccharide-induced osteoclast formation and bone resorption by enhance of RANKL expression. <u>Masahiko Ishida</u>*[1], <u>Hideki Kitaura</u>[2], <u>Keisuke Kimura</u>[3], <u>Jafari Saeed</u>[4], <u>Haruki Sugisawa</u>[5], <u>Haruhiko Takada</u>[6], <u>Teruko Takano-Yamamoto</u>[7]. [1]Tohoku UniversityGraduate School of Dentistry, Japan, [2]Tohoku University, Japan, [3]Tohoku university, Japan, [4]Tohoku University Graduate School of Dentistry, Japan, [5] Tohoku University, Japan, [6]Tohoku University, Japan, [7]Tohoku University, Japan

Lipopolysaccharide (LPS) is a major component of cell wall of gram-negative bacteria that is able to induced osteoclast formation and pathological bone resorption. In addition, peptidoglycan is also a major component of cell membrane of gram-negative and gram-positive bacteria. Muramyl dipeptide (MDP) is the minimal essential structural unit responsible for the immunoadjuvant activity of peptidogly-cans. It has also been reported that MDP synergistically enhanced LPS-induced

proinflammatory cytokine production in human monocyte cells. In this study, we investigated that effect of MDP in LPS-induced osteoclast formation and bone-resorption. C57BL6/J mice were injected LPS, with or without MDP into supracalvariae. Animals were sacrificed, and fixation and demineralization were performed. Histological sections of calvaria were stained for tartrate-resistant acid phosphatase (TRAP), and osteoclast numbers were determined. The expression levels of mRNA for cathepsin K and TRAP in mice calvariae were quantified by real-time PCR. The number of osteoclasts and the level of mRNA for cathepsin K and TRAP in mice administrated both LPS and MDP were higher than that in mice administrated only LPS or MDP. The level of tartrate-resistant acid phosphatase form 5b (TRACP5b), as a marker of bone resorption, in mice administrated both LPS and MDP was also higher. Microfocal computed tomography was used to clarify the bone resorption pit in the calvariae. The ratio of the bone destraction area in the LPS and MDP administrated group was significantly higher than that in only LPS or MDP administrated group. Furthermore, LPS induced RANKL expression in the part of injection. MDP also enhanced LPS-induced RANKL expression in vivo and enhanced expression of RANKL in LPS activated stromal cell in vitro. Moreover, LPS induced TLR4, which is LPS receptor, expression and MDP enhanced LPS-induced TLR4 expression in vivo. Parathyroid hormone (PTH) was administrated with or without MDP. PTH induced osteoclast formation. However, MDP did not affect to PTH-induced osteoclast formation. These results suggested that MDP might enhance LPS-induced osteoclast formation through RANKL expression.

Disclosures: Masahiko Ishida, None.

SA0187

Scleraxis modulates fracture healing and callus formation. <u>Megan L Killian</u>*[1], <u>Jennifer A McKenzie</u>[2], <u>Evan G Buettmann</u>[2], <u>Benjamin D Havelka</u>[3], <u>Matthew J Silva</u>[2], <u>Michael J Gardner</u>[2]. [1], USA, [2]Washington University School of Medicine, USA, [3]Saint Louis University, USA

Scleraxis (Scx) is an important transcription factor for the development of tendons and has been identified as a modulator of bone morphogenetic protein-4 (BMP-4) during bone modeling (e.g., bone ridge formation) [1]. Periosteal colocalization of Scx- and Sox-9-positive progenitors, regulated by TGF-β, segregates tendon attachment units from bone during skeletogenesis [2]. While downstream factors of Scx, such as BMPs, are important for fracture healing, the role of Scx in fracture healing has not been explored. We hypothesized that Scx is upregulated during fracture healing, with its expression localized to the callus, and that loss of Scx in limbs would impair fracture healing.

Wildtype (C57BL6 WT with or without ScxGFP; N=8) and conditional knockouts (cKO: PRX1 Cre, Scx-floxed, N=10) were generated [3] and closed unilateral fractures were created and fixed in right femurs [4]. Five cKO mice had irreparable fractures and were immediately sacrificed. Left cKO femurs had greater mineral density (1136 ± 56 mgHA/cm³) than WT femurs (1046 ± 38 mgHA/cm³) but WT and cKO femurs were of comparable size. In WT mice, Scx was upregulated (p=0.04) and BMP-4 was downregulated (p=0.001) at 24hr post-fracture compared to contralateral limbs (2^-deltaCT, 18s ref; N=5, paired t-test). ScxGFP expression was localized to WT callus at 2wk post-fracture. While WT fracture healed well by 2wk (Fig1A-B'), cKO fracture healed non-uniformly (Fig1D-E'). Callus organization was impaired in cKO fracture (Fig1F) compared to WT fracture (Fig1C). cKO callus volume was smaller (11.0 ± 4 mm³) compared to WT mice (17.5 ± 3 mm³, p=0.07), and cKO mice had lower callus density (Fig 1E', 229 ± 15 mg HA/cm³) than WT mice (260 ± 23 mg HA/cm³, p=0.06).

This is the first study to demonstrate the role of Scx in fracture healing. Previously, others have identified contributions of Sox9+ periosteal cells in soft callus formation [5]. It is possible that Scx- and Sox9-expressing cells coordinate during the fracture healing process, as they do in development, and that both factors are required for robust callus formation. Future work is needed to identify 1) time course of fracture healing without Scx expression and 2) downstream and coordinated molecular cues, mediated by Scx, whose function(s) in callus formation and mineralization may be pharmacologically recovered.

Ref: 1.Blitz, Dev Cell, 2009; 2. Zelzer, Embryo Today, 2014; 3. Murchison, Dev, 2007; 4. Bonnarens & Einhorn. JOR, 1984; 5. Murao, JBMM, 2013
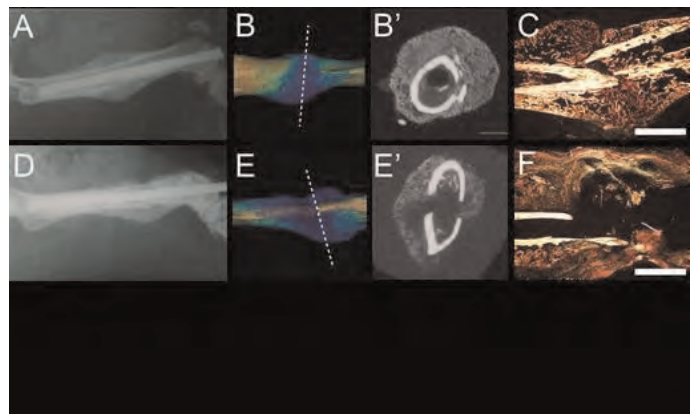

Figure 1

Disclosures: Megan L Killian, None.

SA0188

Serotonin Reuptake Inhibitors Inhibit Osteoclast Differentiation And Function Through A Serotonin-Independent And Nfatc1-Dependent Mechanism. <u>María José Ortuño</u>*, <u>Patricia Ducy</u>. Columbia University, USA

Selective Serotonin Reuptake Inhibitors (SSRIs) are a class of drugs widely used for a variety of psychiatric conditions and in a broad spectrum of patients. It is now clear that a long-term treatment with SSRIs can have deleterious consequence on bone mass through yet poorly understood mechanisms. In an effort to determine whether SSRIs exert any function on bone cells we treated mouse primary osteoblasts and osteoclasts with fluoxetine, one of the most frequently prescribed SSRI. To our surprise fluoxetine did not have any overt effect on osteoblasts. In contrast, even a low dose of fluoxetine impaired the differentiation and function of osteoclasts as determined by quantification of TRAP activity, cell fusion and bone resorbing ability. This inhibitory effect was observed with all SSRIs tested. That the SSRIs inhibition of osteoclast differentiation and function occurred to the same extent in osteoclasts derived from wild-type, Tph1-deficient, Tph2-deficient and 5Htt-deficient mice indicated that it is independent of the known effect of this drug on serotonin reuptake. To elucidate how fluoxetine could affect so profoundly osteoclast biology we then surveyed the expression of a large number of transcription factors in osteoclasts and found that Nfatc1 expression was regulated by fluoxetine. Consequently, the expression of all NFATC1 target genes tested including Cathepsin K, DC-STAMP, Clcn7 and Tcirg1 was decreased thus explaining the multifaceted inhibitory effect of fluoxetine on osteoclast biology.

Next, we extended these studies in vivo by treating wild-type mice with fluoxetine for different lengths of time. While long-term regimens elicited a bone loss, a shorter treatment caused an increase in bone mass due to an isolated decrease in bone resorption, thus confirming the observations made in cell culture. A gene expression analysis performed in the bones of these mice identified the same regulatory bases for this effect than the ones we defined in vitro. These studies provide a molecular explanation for the decrease in resorption parameters associated with a short exposure to SSRIs in young depressed patients.

Disclosures: María José Ortuño, None.

SA0189

Strontium ranelate leads to bone matrix modifications and increases bone formation in ovariectomized and osteopenic rats. <u>Jenifer Campos</u>*[1], <u>Mariana Freitas</u>[2], <u>Keico Okino Nonaka</u>[3], <u>Helena Nader</u>[4], <u>Eduardo Katchburian</u>[4], <u>Marise Lazaretti-Castro</u>[2], <u>Rejane Reginato</u>[5]. [1]Universidade Federal de São Paulo, Brazil, [2]Federal University of São Paulo, Brazil, [3]Federal University of São Carlos, Brazil, [4]UNIFESP, Brazil, [5]UNIFESP - Federal University of São Paulo, Brazil

Strontium ranelate (SrR) has been used for the treatment of severe osteoporosis in some countries. However, the effects of this drug on bone tissue constituents are still not entirely elucidated. We investigated the effects of different doses of strontium ranelate on bone tissue of osteopenic female rats. Thirty 6-month-old female Wistar rats were ovariectomized and after 3 months were randomly divided into 3 groups (n=10): GI (control) - gavage with water, GII - gavage with 300 mg/kg/day of SrR and GIII - gavage with 625 mg/kg/day of SrR for 90 days. The animals were submitted to DEXA analysis before and after the treatment. Next, the distal femora were processed for histomorphometry, picrosirius red, TUNEL and TRAP method, physical properties, mechanical resistance and quantification of glycosaminoglycans and calcium/phosphorus. Independently of the dose, the SrR administration modified the profile of some bone matrix components and increased cortical thickness. Sulfate chondroitin and phosphorus concentration decreased in all SrR-treated groups. Calcium quantification is significantly increased in GIII. Moreover, hyaluronic acid is highly concentrated in distal femora of GII when compared with GIII as revealed by ELISA test. There was a predominance of reddish birefringence in cortical bone of GIII whereas greenish birefringence was increased in GII when compared to others groups as evidenced by picrosirius red, suggesting that SrR acts on collagen maturation, in a dependent-dose fashion. The highest BMD was observed in GIII as evaluated by DEXA. In addition, GIII exhibited also the highest mechanical strength and BV/TA higher than GI. The number of TUNEL-positive osteocytes decreased in all treated groups compared to control, while the group that received the lower dosage had the highest number of TRAP-positive cells. Taken together, our findings show that strontium ranelate in the highest dose improve bone microarchitecture, modifying the bone matrix constituints, leading to increase bone strength and have mainly anabolic effect in bone tissue of ovariectomized and osteopenic rats.

Disclosures: Jenifer Campos, None.

SA0190

The whole-body analysis employing RANKL -/- and OPG -/- medaka fish reveals the in vivo bone resorption system. <u>Masahiro Chatani</u>*[1], <u>Yoshiro Takano</u>[2], <u>Takeshi Todo</u>[3], <u>Akira Kudo</u>[1]. [1]Tokyo Institute of Technology, Japan, [2]Tokyo Medical & Dental University, Japan, [3]Osaka University, Japan

Introduction: Bones have a variety of shapes in the body for supporting various organs, mainly nerves and blood vessels. The bone shapes are regulated by osteoclasts that are bone resorptive cells. Osteoclast precursors express RANK (Receptor Activator of Nuclear Factor Kappa-B) which binds to RANKL (RANK Ligand) to differentiate osteoclasts, while OPG (osteoprotegerin) binds to RANKL to inhibit osteoclast differentiation. However, it is unclear how RANKL and OPG co-operatively regulate bone resorption in a whole body in vivo. We previously established the live imaging system using medaka fish, which allowed observations of osteoclast behavior in a whole body (Chatani et al., 2011).

Aim: To clarify the mechanism how RANKL and OPG regulate bone resorption in a whole body during development using medaka as an experimental model.

Methods: RANKL-deficient (RANKL -/-) medaka and OPG-deficient (OPG -/-) medaka were established by using the Tilling (Targeting induced local lesions in genomes) and TALEN (*Transcription activator-like effector nucleases*) method, respectively. RANKL was specifically overexpressed in osteoblasts by using the osterix promoter-RANKL-2A-GFP vector. Osteoclasts were live-imaged by using the TRAP promoter-fluorescein protein transgenic line. Bone tissues were stained by Alizarin Red or ALC (alizarin complexone).

Results:RANKL -/- medaka survived to adulthood and generated offspring, and we found existence of a few osteoclasts in this fish. Due to a smaller number of osteoclasts in RANKL -/- medaka, the diameter of neural and hemal canals in the vertebral column became narrower as it grew, resulting in abnormal organogenesis in later development. Next, using the osterix promoter, TRAP-DsRed positive osteoclasts were induced around RANKL positive osteoblasts. Whereas no osteoclasts existed on the vertebral body under the normal condition, in OPG -/- medaka, numerous osteoclasts were induced around the vertebral column, including the vertebral body (Figure 1). OPG -/- medaka showed a short body (littermate +/?; 9.7 ± 0.46 mm, -/-; 4.6 ± 0.29 mm total length, p<0.0001, n=13, 22-29 days after hatch), due mostly to resorption of the vertebral column (Figure 2).

Conclusion: Bone resorption in RANKL-/- medaka was not properly regulated during development because of dysfunction of osteoclasts. Osteoclast precursors were forced to differentiate to osteoclasts with overexpressed RANKL from osterix positive osteoblasts. Loss of OPG induced numerous osteoclasts that destroyed the vertebral body, accompanied with a defect of body growth. These data suggest that the numerous osteoclast progenitors exist around the whole skeletal system and determine the appropriate level of total bone resorption under the regulation of RANKL and OPG.
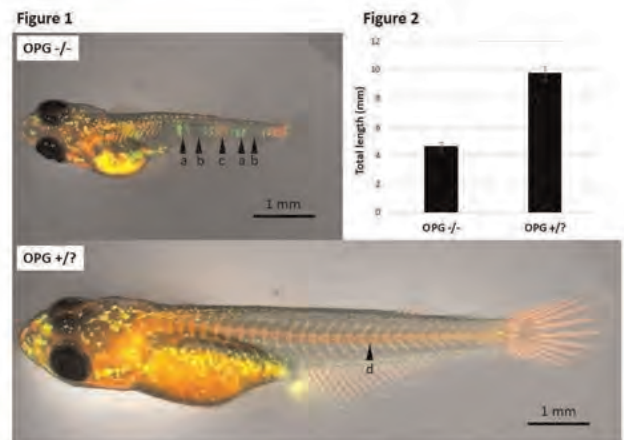
Figure 1. Whole images of OPG -/- and OPG +/? Medaka, crossed with TRAP-GFP transgenic line. Bone tissues were stained with ALC at days 23. Numerous osteoclasts (arrowhead a) completely resorbed the vertebral body in some areas, followed by the ALC negative regions (arrowhead b). There still remained some vertebral columns (arrowhead c). An arrowhead d shows the normal vertebral column.

Figure 2. Comparison of total body length between OPG -/- and OPG +/?. (littermate +/?; 9.7 ± 0.46 mm, -/-, 4.6 ± 0.29 mm, p<0.0001, n=13, 22-29 days after hatch)

Figure

Disclosures: Masahiro Chatani, None.

SA0191

See Friday Plenary Number FR0191.

SA0192

See Friday Plenary Number FR0192.

SA0193

See Friday Plenary Number FR0193.

SA0194

See Friday Plenary Number FR0194.

SA0195

See Friday Plenary Number FR0195.

SA0196

See Friday Plenary Number FR0196.

SA0197

See Friday Plenary Number FR0197.

SA0198

A Longitudinal Study of Articular Cartilage and Subchondral Bone During Spontaneous Osteoarthritis in Dunkin-Hartley Guinea Pigs. Weiwei Zhao*[1], Ting Wang[2], Qiang Luo[3], Chunyi Wen[3], Haobo Pan[2], Songlin James Peng[4], KwongYuen Chiu[3], Xu Cao[5], William Lu[3]. [1]The University of Hong Kong, Hong Kong, [2]Centre for Human Tissues & Organs Degeneration, Shenzhen Institutes of Advanced Technology, Chinese Academy of Sciences, China, [3]Department of Orthopaedics & Traumatology, The University of Hong Kong, China, [4]Shenzhen People's Hospital, Jinan University School of Medicine, Peoples Republic of China, [5]Johns Hopkins University, USA

Osteoarthritis (OA) is a degenerative disease affected the whole joint. Current researches advocate the imbalance of adaptations between cartilage and subchondral bone contributes to the progression of osteoarthritis.The kinetics of the bone-cartilage unit during naturally-occurring OA in Dunkin-Hartley (DH) guinea pig has not been well characterized. The first aim of this study is to investigate the correlation between cartilage damage and sunbchondral bone alterations in DH guinea pigs. Besides, transforming growth factor-β (TGF-β) has been demonstrated as a potential treatment target for OA, however, the spatiotemporal alteration of TGF-β during spontaneous OA has not been studies. The second aim is to evaluate the role of TGF-β in subchondral bone of DH guinea pig.

Micro-CT and histological analysis were adopted to obtain the morphological parameters of subchondral bone and the grade of cartilage degeneration. Their correlation was analyzed by partial correlation test with age as controlling variance. The number of osteoprogenitors and the activity of TGF-β was measured through immunostaining of osterix and pSmad2/3.

There was a time lag between the increase of the bone mineral density and thickness of subchondral plate, whereas the bone volume fraction displayed an initial increase followed by a decline along with the elevation of the porosity. With age, the trabeculae increased in bone mineral density, volume fraction, thickness and became less connective and anisotropic. However, different alterative patterns of structure model index and trabecular pattern factor were found between the lateral and medial sides. The cartilage degeneration was purely correlated with the volume fraction (γ = 0.290, P = 0.021) and thickness (γ = 0.301, P = 0.017) of subchondral trabeculae. The number of osteoprogenitors was highest at 6 months and sharply decreased after then. Their distribution is heterogeneous, that the peripheric bone marrows own more while the central bone marrows own less. The spatiotemporal alteration of pSmad2/3+ cells follows the similar pattern.

This study indicated the abnormal micro-architecture changes of subchondral bone may influence its mechanical properties and the overlying cartilage. The similarity of the spatiotemporal alterations between osteoprogenitors and active TGF-β suggests TGF-β activity may affect the elevated bone formation during spontaneous OA in DH guinea pig.
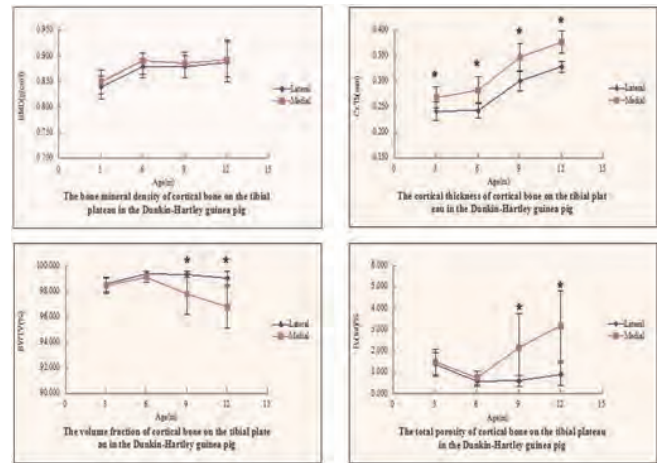
Fig. 1 Quantitative analysis of micro-architectural parameters in subchondral plate
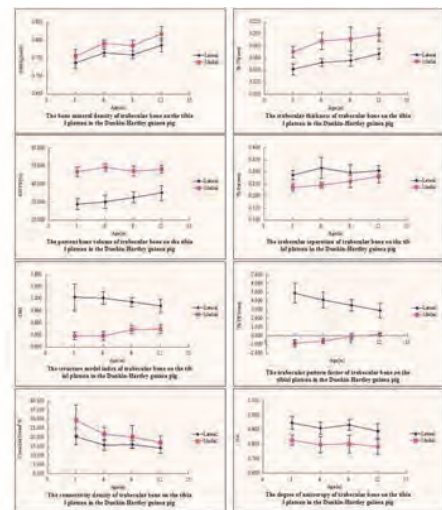
Fig. 2 Quantitative analysis of micro-architectural parameters in subchondral trabecular bone
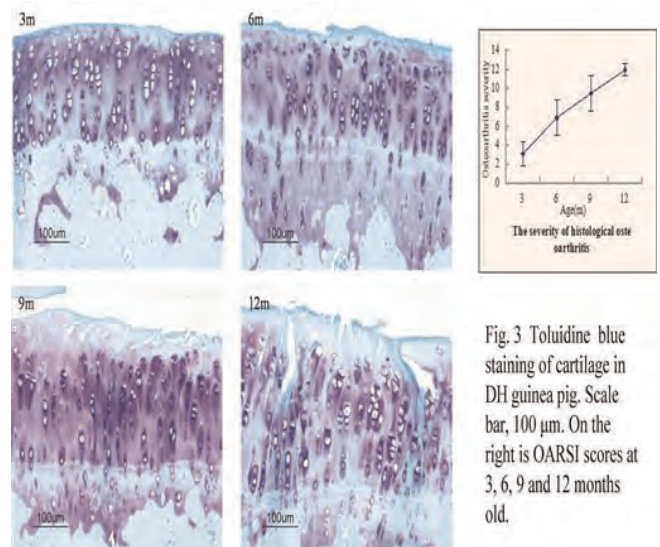
Fig. 3 Toluidine blue staining of cartilage in DH guinea pig. Scale bar, 100 μm. On the right is OARSI scores at 3, 6, 9 and 12 months old.

Fig. 3 Toluidine blue staining of cartilage in DH guinea pig

Fig. 4 Osterix staining in DH guinea pig tibial subchondral bone. Scale bar, 50 μm. On the bottom is a quantitative analysis of the number of OSX+ cells per bone marrow area (mm²).
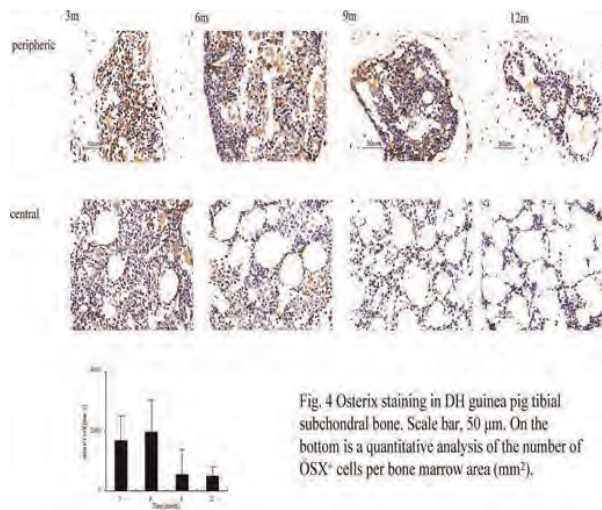
Fig. 4 Osterix staining in DH guinea pig tibial subchondral bone

Fig. 5 pSmad2/3 staining in DH guinea pig tibial subchondral bone. Scale bar, 50 μm. On the bottom is a quantitative analysis of the number of pSmad2/3+ cells per bone marrow area (mm²).
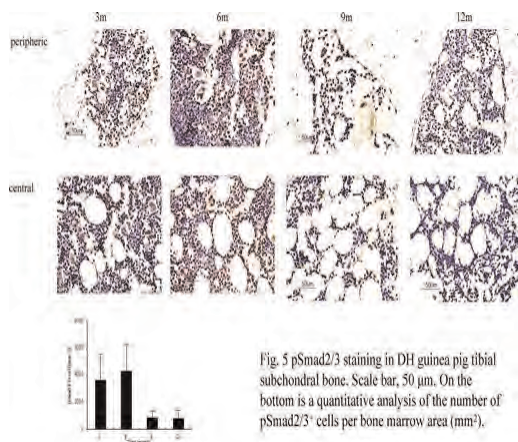
Fig. 5 pSmad2/3 staining in DH guinea pig tibial subchondral bone

Disclosures: Weiwei Zhao, None.

SA0199

See Friday Plenary Number FR0199.

SA0200

See Friday Plenary Number FR0200.

SA0201

See Friday Plenary Number FR0201.

SA0202

See Friday Plenary Number FR0202.

SA0203

Characterization of Skeletal Phenotype of Smurf2-Deficient Mice and the Potential Role of Smurf2-inhibition in Mitigating Osteoarthritis. <u>Henry Huang</u>*[1], <u>Eric Veien</u>[2], <u>Hong Zhang</u>[2], <u>David Ayers</u>[3], <u>Jie Song</u>[1]. [1]University of Massachusetts Medical School, USA, [2]University of Massachusetts Medical School, USA, [3]UMass Memorial Medical Center, USA

Background: Osteoarthritis (OA) is a degenerative joint disease leading to articular cartilage loss, osteophyte formation and subchondral bone thickening. OA is a leading cause of disability and is a significant socioeconomic burden. There is no effective disease modifying drugs for OA. Previously, it was shown that Smad

ubiquitin regulatory factor (Smurf) 2 is expressed in human OA cartilage and that overexpression of Smurf2 in mouse chondrocytes leads to OA-like changes[1]. It is unclear whether Smurf2 is required for normal skeletal development or OA pathogenesis. Here we examined age-dependent skeletal phenotypes of Smurf2-deficient mice. We also compared changes in the joint of young, skeletally mature mice after surgical destabilization of the medial meniscus (DDM), an established model for OA[2].

Methods: A previously reported[3] C57BL/6 Smurf2-deficient MT and WT mice were used. Using microCT, we quantitatively compared femoral cortical bone and tibial subchondral bone of young (4 months) and old (18-22 months) male WT and MT mice (n=6). We also compared gender differences in the lumbar vertebrae between old mice (n=5). Using a semi-quantitative histology scoring system[4], Safranin O-stained femoral and tibial sections (≥5) of each knee joint were blindly scored by 7 trained examiners. DMM surgery was carried out on 2-month old male WT and MT (n=13), and the cartilage and subchondral bone were examined 2 months post-op.

Results: No difference in cortical bone, trabecular bone or knee joint between WT and MT of a given age was detected. Age and gender-related changes such as trabecular bone loss and roughening of cartilage surface were comparable between genotypes. After DMM, 2/3 of WT developed moderate to severe OA (varying degrees of erosion from calcified cartilage down to subchondral bone), whereas majority of Smurf2 MT remained normal or developed mild OA (small superficial fibrillations with focal loss of proteoglycan staining), and only 1/3 exhibited moderate OA symptoms. Subchondral bone thickening after DMM was also detected, but no difference was detected between genotypes.

Conclusion: Smurf2 deficiency does not cause a detectable phenotypic change in skeletal tissues under normal development. However, under a pathological state such as DMM-induced OA, Smurf2 deficiency attenuated the severity of OA cartilage, suggesting a potential role of Smurf2 in modulating OA onset / progression or cartilage repair.

[1] Wu Q, et al. *Arthritis & Rheumatism*. 2008
[2] Glasson S, et al. *OsteoArthritis and Cartilage*. 2007
[3] Ramkumar C, et al. *Cancer Research*. 2012
[4] Glasson S, et al. *OsteoArthritis and Cartilage*. 2010

Disclosures: Henry Huang, None.

SA0204

Hypoxia and vitamin D contribute to leptin and DKK2 production in human osteoarthritic subchondral bone osteoblasts. <u>Béatrice Bouvard</u>[1], <u>Elie Abed</u>*[2], <u>Mélissa Yéléhé-Okouma</u>[3], <u>Arnaud Bianchi</u>[4], <u>Didier Mainard</u>[5], <u>Patrick Netter</u>[5], <u>Jean-Yves Jouzeau</u>[5], <u>Daniel Lajeunesse</u>[6], <u>Pascal Reboul</u>[7]. [1]UMR 7365, CNRS-Université de Lorraine, IMoPA, France, France, [2]Crchum-hôpital Notre-dame, Canada, [3]UMR 7365, CNRS-Université de Lorraine, IMoPA, France, France, [4]UMR 7365, CNRS-Université de Lorraine, IMoPA, France, France, [5]Centre Hospitalier Universitaire, Nancy, France, France, [6]CRCHUM, Canada, [7]UHP Nancy 1 / CNRS UMR7561, France

Introduction: Bone remodelling and increased subchondral densification are important in Osteoarthritis (OA) pathology. Modifications of bone vascularisation parameters, which lead to ischemic episodes associated with hypoxic conditions, have been suspected to play a role in OA. Hypoxia drives several pathways in bone tissue such as growth and regeneration, and can lead to diseases. Among several factors potentially involved in OA pathogenesis, leptin and DKK2 are good candidates since they are produced by normal osteoblasts (Ob) and are up-regulated in OA Ob. The regulation of leptin expression by hypoxia seems to be cell specific- or cell environment- dependent in most tissues, whereas the regulation of DKK2 has not yet been described. Here, we investigated the hypothesis that hypoxia may be driving the expression of leptin and DKK2 in OA Ob. Methods: Human OA subchondral Ob from the scleric portion of the tibial plateaus was cultured either under 20% or 2% oxygen tension in the presence or not of VitD3. The expression of VEGF, Sirt1, TGF-β1, leptin, osteocalcin, DKK2, Hif-1α and -2 α was measured by qRT-PCR, and leptin production by ELISA. Gene expression was reduced using siRNA technique, and Hif-2α stabilization measured by WB. MAPK signaling was investigated using several inhibitors. Results: Hypoxia stimulated the expression of VEGF, Sirt1, TGF-β1, leptin and DKK2 expression in OA Ob. VitD3 stimulated leptin and DKK2 expression 2- and 4.2-fold under normoxia, and 28- and 6.2-fold under hypoxia. The hypoxia-induced leptin production was confirmed by ELISA, particularly in presence of VitD3. Silencing Hif-2α (siHif-2α),?inhibited VitD3-stimulated leptin mRNA and protein levels by 70% and 60% respectively, while it failed to significantly alter the expression of DKK2. SiHif-1α failed to alter the expression of either leptin or DKK2. Immunoblotting showed that VitD3 greatly stabilized Hif-2α at the protein level under hypoxic condition. The increase in leptin expression under hypoxia was also regulated, in addition to the role of Hif-2α, by p38 MAPK and PI-3 kinase. Finally, we evaluated if the expression of leptin and DKK2 were both related to each other under hypoxia. Silept under hypoxia had no effect on the expression of DKK2. Likewise, siDKK2 did not alter the expression of leptin. Conclusions: Hypoxic conditions trigger Ob to produce leptin particularly under VitD3 stimulation whereas DKK2 is mainly regulated by VitD3 rather than hypoxia

Disclosures: Elie Abed, None.

SA0205

Inhibition of TGFb activity in Nucleus Pulposus Attenuate Disc Degeneration. Qin Bian*[1], Liwei Zheng[2], Xin Xu[2], Amit Jain[2], Khaled Kebaish[2], Gehua Zheng[2], Hui Xie[3], Janet Crane[4], Mei Wan[5], Paul Sponseller[2], zhengdong zhang[6], Edward Guo[6], Lee Riley[2], Yongjun Wang[7], Xu Cao[4]. [1], USA, [2]Johns Hopkins University, USA, [3]Johns Hopkins Medical Institution, USA, [4]Johns Hopkins University, USA, [5]Johns Hopkins University School of Medicine, USA, [6]Bone Bioengineering Laboratory, Columbia University, USA, [7]Othopedic Surgery, Peoples Republic of China

Degenerative disc disease (DDD) is a common cause of disability and functional limitation worldwide. Coordination of the activity of each component in the spine is essential in maintenance of disc homeostasis. However, little is known about how the notochordal cells maintain disc function and homeostasis in response to mechanical loading. We examined how altered mechanical loading in the spine leads to DDD using a spinal instability mouse model (SI) by resection of the L3-L5 spinous processes. Mid-sagittal images of ?CT scan revealed that the space between L4 and L5 vertebral bodies significantly narrowed in SI mice. 3D images of L4-5 endplates showed substantial decrease of disc space in SI. The spaces continued to decrease significantly from week 2 to 8 in SI mice. Both cranial and caudal endplates were significantly increased post-surgery with accelerated ossification of both cranial and caudal endplate. Endplates undergoes calcification and ossification in SI mice with significant increase of endplate score and Trap positive osteoclast numbers. Expansion and sclerosis of endplates in response to the alteration of mechanical loading decreased IVD space and may generate static compression force on disc contents. Temporal-spatial activation of latent TGFβ has been shown to maintain tissue homeostasis including bone and articular cartilage. We then examined the potential role of TGFβ in the notochordal cell morphologic changes and its potential contribution to disc degeneration with decreased IVD space. Phosphorylated Smad2/3 (pSmad2/3+) cells were significantly increased post-surgery and aggrecan expression was also increased. Furthermore, high protein levels of TGFβ1 were also observed in the discs from DDD patients. Importantly, neutralizing antibody against TGFβ was applied to an ex vivo IVD compression loading model. TGFβ?antibody inhibited loading-induced phosphorylation of Smad2/3 in notochordal cells and maintained their morphology relative to vehicle treatment. Finally, TGFβ type I receptor (TβRI) inhibitor (1 mg/kg) was systemically injected in the SI mice. As expected, pSmad2/3+ cells were reduced by TβRI inhibitor. Degeneration of IVD was prevented as assessed by IVD score and expression of aggrecan was maintained. Thus, narrowing of IVD space leads to aberrant activation of TGFβ and ultimately disc degeneration. Attenuation of activation of excess TGFβ may represent a therapeutic target for degenerative disc disease.

Disclosures: *Qin Bian, None.*

SA0206

Intra-Articular Treatment with Recombinant Human Bone Morphogenetic Protein 7 (rhBMP-7) Attenuates the Development of Post-Traumatic Osteoarthritis in Rats. Jukka Morko*[1], Zhiqi Peng[1], Katja Fagerlund[1], Yvonne Konkol[2], Jukka Rissanen[1], Jenni Bernoulli[2], Jussi Halleen[3]. [1]Pharmatest Services Ltd, Finland, [2]Pharmatest Services Ltd, Finland, [3]Pharmatest Services Ltd, Fin

Recombinant human bone morphogenetic protein 7 (rhBMP-7) is a bone-inducing agent used in spinal fusions and during fracture repair in clinical practice. In knee joints, rhBMP-7 has been shown to attenuate the development of degenerative changes induced by anterior cruciate ligament transection in rabbits and by excessive running in rats and to repair cartilage damage in several species. In this study, we characterized the effects of intra-articular rhBMP-7 on the development of post-traumatic osteoarthritis (OA) in male Lewis rats. Unilateral OA was induced in rat knee joints by surgical medial meniscal tear (MMT) and medial collateral ligament transection (MCLT). Treatment was started one week after the operation and continued once a week for 5 weeks. Rats were treated intra-articularly with rhBMP-7 at 0.25 μg/wk or vehicle. Treatment effects on body weight, static weight bearing and static mechanical allodynia were followed during the study. After 6 post-surgery weeks, rats were terminated and treatment effects on knee joints were determined histologically following the recommendations of the OARSI histopathology initiative. Paw weight bearing and paw withdrawal threshold were decreased in operated hind limbs before the start of treatment indicating knee joint discomfort and pain. Intra-articular rhBMP-7 improved paw weight bearing and increased paw withdrawal threshold. Microscopic OA assessment demonstrated from mild to marked degenerative changes in the medial compartment of operated knee joints treated with vehicle. These changes included the loss of chondrocytes, proteoglycans and collagen matrix from superficial layer down to tidemark in medial tibial plateau and the presence of large osteophytes and moderate synovial inflammation. The loss of chondrocytes and collagen matrix was pronounced on the outer 1/3 of the plateau. Almost similar lesions were observed in the middle 1/3 and less severe lesions in the inner 1/3. From non-generation to marked degenerative changes were identified in the medial compartment of operated knee joints treated with rhBMP-7. The treatment attenuated the width of significant cartilage degeneration in medial tibial plateau and the severity of chondrocyte and collagen matrix lesions in the middle and inner 1/3 of the plateau. This study demonstrated a chondroprotective activity for intra-articular

rhBMP-7 treatment in the rat MMT+MCLT model and supported the development of rhBMP-7 as a potent disease modifying OA drug.

Disclosures: *Jukka Morko, Pharmatest Services Ltd, 4*

SA0207

SA0208

The role of FoxA factors in the onset and development of Osteoarthritis. Andreia Ionescu*[1], Lin Xu[2], Elena Kozhemyakina[3], Klaus Kaestner[4], Yefu Li[2], Andrew Lassar[3]. [1]Harvard Medical School, USA, [2]HSDM, USA, [3]HMS, USA, [4]University of Pennsylvania, USA

We have recently identified FoxA transcription factors as key regulators of chondrocyte hypertrophy in the developing skeleton (Dev.Cell 22(5),2012).Therefore, we next asked whether the Fox A family is involved in the onset and development of osteoarthritis (OA) in the adult cartilage.To evaluate the expression of FoxA2 in postnatal articular cartilage, we employed a tamoxifen-inducible Cre driver knocked-into the 3' UTR of the FoxA2 gene. After crossing this mouse line into the ROSA26 reporter line, we observed that FoxA2 expression was highest in the knee and the femoral cap articular cartilage of one-month old animals, it precipitously declined at 3 months of age and remained at this low level through at least 1 year. To evaluate whether FoxA family members are necessary for cartilage degradation, we conditionally deleted FoxA2 in the articular cartilage of FoxA3 -/- mice, using a tamoxifen-inducible CRE recombinase driven by the Prg4 (Lubricin) regulatory sequences. Subsequently, we performed surgical destabilization of the medial meniscus on either the tamoxifen treated $Prg4^{CreERt2/+};FoxA2^{fl/fl};FoxA3^{-/-}$ mice or control $C57BL/6$ animals. While the wild-type $C57BL/6$ mice that have undergone surgery developed significant cartilage degradation (OARSI score 5.87 ± 0.12), the tamoxifen treated $Prg4^{CreERT2/+};FoxA2^{fl/fl};FoxA3^{-/-}$ mice showed very little sign of articular cartilage damage (OARSI score 1.45 ± 0.26). I next asked whether overexpression of FoxA2 in murine articular cartilage cells is sufficient to accelerate cartilage degradation. To drive exogenous FoxA2 expression in articular chondrocytes, I have generated mice containing the FoxA2 transgene driven by a reiterated reverse tetracycline transactivator (rtTA) response element (*TREtight-FoxA2*). This transgenic animal was in turn mated to a mouse containing rtTA knocked into the ROSA 26 locus downstream of a "floxed" STOP transcription cassette. Tissue specific expression of rtTA was achieved with the tamoxifen-inducible $Prg4^{CreERt2/+}$line. Control mice, lacking the FoxA2 transgene, that have undergone surgery developed mild symptoms of the disease (OARSI score 1.37 ± 0.33). In contrast, triple transgenic mice that have undergone surgery developed far more cartilage damage with more lesions on the articular cartilage (OARSI score 2.63 ± 0.43). These findings imply that the FoxA transcription factors are crucial regulators of osteoarthritis following surgically induced joint destabilization.

Disclosures: *Andreia Ionescu, None.*

SA0209

SA0210

SA0211

SA0212

SA0213

GPR40, a free fatty acid receptor, differentially impacts osteoblast behavior depending on differentiation stage and environment. Claire Philippe*. INRA, France

Scope: GPR40 is a free fatty acid receptor that has been recently shown to impact bone remodeling. This receptor protects skeleton by inhibiting bone resorbing osteoclast differentiation. Consistent with GPR40 expression on bone forming cells, we assumed that this receptor may also influence osteoblast activity.

Methods and results: To further investigate this hypothesis, biological effects of GW9508, a synthetic agonist for GPR40, was first tested on osteoblast differentiation

parameters. Assays were performed in two different cell models: the MC3T3-E1 osteoblastic cell line and primary bone marrow cultures extracted from *wild-type* and *GPR40 knock-out* mice. Both models showed a dual role of GPR40 on osteoblasts. Although receptor stimulation induced early stimulation of differentiation marker expression, it finally led to inhibition of mineralization process during late differentiation stages. To further elucidate this discrepancy, mice were ovariectomized to induce bone loss and received GPR40 agonist by gavage. Data revealed a weak influence of GPR40 agonist on osteoblast markers expression. Nevertheless, a significant increase in OPG expression was observed upon GW9508 treatment that contribute to explain the GPR40-related osteoporosis prevention.

Conclusion: To conclude, our results confirm the relevance of this new opportunity in the management of bone loss.

SA0214

See Friday Plenary Number FR0214.

SA0215

Possible role of RANKL-RANK signal in osteoblast differentiation. Midori Nakamura[1], Teruhito Yamashita[2], Yuko Nakamichi[1], Yuriko Furuya[3], Hisataka Yasuda[4], Nobuyuki Udagawa*[1]. [1]Matsumoto Dental University, Japan, [2]Matsumoto Dental University, Japan, [3]Oriental Yeast Co.,Ltd, Japan, [4]Oriental Yeast Company, Limited, Japan

A RANKL-binding peptide WP9QY (W9) is known to inhibit mouse osteoclastogenesis. In addition, W9 showed an anabolic effect on cortical bone in mice in vivo. W9 bound RANKL and differentiated osteoblasts with production of autocrine factors like BMP. In this experiment, effects of W9 on differentiation of osteoblasts and osteoclasts in mouse co-culture system of primary osteoblasts prepared from newborn mouse calvariae derived from RANKL-deficient or wild-type (WT) mice with WT-derived bone marrow mononuclear cells cultured in the presence of M-CSF for 24h. W9 strongly inhibited TRAP-positive multinucleated osteoclast formation as well as strikingly stimulated alkaline phosphatase (ALP)-positive osteoblast differentiation in the co-cultures of WT-derived osteoblasts and bone marrow cells in the presence of 1,25-dihydroxyvitamin D_3 or PTH. In contrast, RANKL-deficient osteoblasts had no osteoclastogenesis in co-cultures with bone marrow cells derived from WT mice in the presence of bone-resorbing factors. Importantly, W9 had weak activity of ALP-positive osteoblast differentiation in the co-cultures with RANKL-deficient osteoblasts even in the presence of W9, PTH or BMP-2. These experimental results indicate that W9 inhibited osteoclast formation via RANKL signaling in osteoblasts and directly stimulated osteoblast differentiation via RANKL signaling-mediated autocrine factors. Our findings suggest that the reverse signal from RANK on osteoclasts to RANKL on osteoblasts, and the forward signal from RANKL to RANK, could play an important role in the coupling between bone-formation and bone resorption.

1
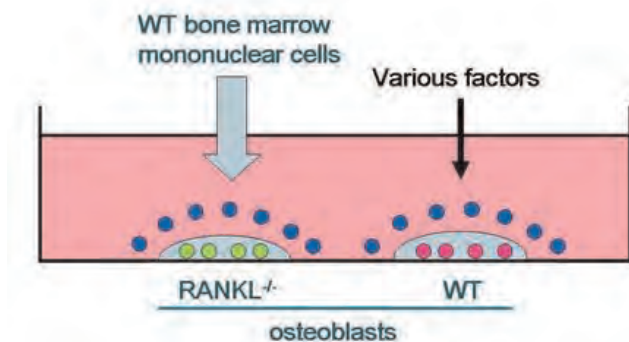
SA0216

The role of MACF1 in migration, proliferation and differentiation of preosteoblast and the screening of the natural antisense transcripts of MACF1. Airong Qian*[1], Lifang Hu[2], Yulong Sun[3], Dijie Li[2], Zhihao Chen[2], Peng Shang[4], Ge Zhang[5]. [1]Northwestern Polytechnical University, Peoples Republic of China, [2]Northwestern Polytechnical University, China, [3]Norhtwestern Polytechnical University, China, [4]Northwestern Polytechnical University, Peoples Republic of China, [5]Ge Zhang' S Lab, Hong Kong

Introduction: Microtubule-actin crosslinking factor 1 (MACF1), also referred to as actin cross-linking factor 7 (ACF7), is a member of plakin family. Based on previous studies, the role of MACF1 in osteoblast's function was investigated in this study. Moreover, the natural antisense transcripts (NATs) of MACF1 (MACF1-AS) were also screened.Materials and methods: MC3T3-E1 preosteoblasts were transfected with the recombinant lentivirus vector LV3-shRNA-MACF1 for knocking down MACF1 and cells transfected with the control recombinant lentivirus vector LV3-shRNA-NC was the negative control. After confirming the efficiency of LV3-shRNA-MACF1 and LV3-shRNA-NC by real time PCR and western blot. Real time PCR was used to detect the mRNA expression of osteogenic genes including runt-related transcription factor 2 (*Runx2*), type I collagen α1 (*Col Iα1*) and alkaline phosphatase (*ALP*). After induction of osteogenic differentiation for 17 d and 21 d, the mineralized nodules formation was detected by alizarin red s staining. The cell proliferation and migration were examined by cell counting with Vi-CELL cell viability analyzer and transwell assay, respectively. Moreover, with the aid of online NATs database, 6 MACF1-AS were obtained and the expression of MACF1 and MACF1-AS in primary pre-osteoblasts cultured under random position machine (RPM) was also evaluated by Real-time PCR.Results: After transfection with the recombinant lentivirus vector LV3-shRNA-MACF1, the expression of MACF1 in MC3T3-E1 was dramatically down-regulated . Real time PCR results showed that the mRNA expressions of *Runx2*, *Col Iα1* and *ALP* were all significantly down-regulated in LV3–shRNA-MACF1 transfected cells compared with the blank control cells. After 17 d and 21 d's osteogenic differentiation, the mineralized nodules formed in LV3-shRNA-MACF1 cells were significantly less than in LV3-shRNA-NC and blank cells. Besides, cell counting results showed that cell proliferation was significantly decreased in LV3–shRNA-MACF1 group. In addition, cell migration was also inhibited with low expression of MACF1 after 18 h transwell detection (Fig 1). Moreover, RPM exposure led to significantly down-regulation of MACF1 and MACF1-AS expression in primary pre-osteoblasts.

Conclusions: These findings show that MACF1 deficiency inhibits osteoblast migration, proliferation and differentiation, suggesting a key role of MACF1 in the osteoblast's function. Moreover, efficient MACF1-NATs were acquired.
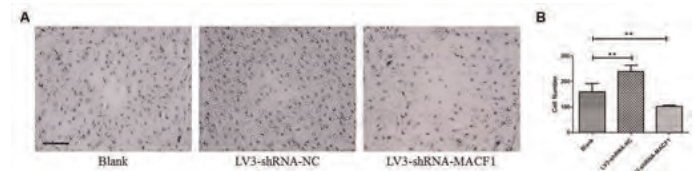

Fig.1 MACF1 deficiency inhibited the cell migration. A: microscope images. Bar: 200 çm.

SA0217

See Friday Plenary Number FR0217.

SA0218

Administration of PTH and Tob deficiency in mice synergistically enhances the levels of both cancellous and cortical bone mass. Shuichi Moriya*[1], Tadayoshi Hayata[2], Toru Suzuki[3], Takayuki Yamada[4], Jumpei Shirakawa[5], Kazuo Kaneko[6], Tadashi Yamamoto[3], Yoichi Ezura[7], Masaki Noda[4]. [1]Department of Orthopaedics, Juntendo University School of Medicine, Japan, [2]Organization for Educational Initiatives, University of Tsukuba, Japan, [3]Okinawa Institute of Science & Technology Graduate University, Japan, [4]Tokyo Medical & Dental University, Japan, [5]Tokyo medical & dental university, Japan, [6]Department of Orthopedics, Juntendo University School of Medicine, Japan, Japan, [7]Tokyo Medical & Dental University, Medical Research Insititute, Japan

Administration of PTH enhances bone formation and increases bone mass. However, its mechanisms are not fully understood especially in the newborn animals where vigorous bone formation is taking place. Tob (Transducer of ErbB2) is an inhibitor of BMP-Smad signaling in osteoblasts while its role in the regulation of PTH actions in bone is not known. Here, we investigated the effects of intermittent PTH on newborn mice in the absence or the presence of Tob to examine the possible interaction. First, PTH(1-34) (human) enhanced the expression of Tob messenger RNA levels in MC3T3-E1 osteoblastic cells in a time and dose dependent manner. PTH enhanced Tob mRNA expression at least in part via transcriptional events without requirement for new protein synthesis, thus this effect is a direct one. PTH enhancement of Tob protein expression was confirmed based on western blot analysis. To examine such PTH effects are also seen *in vivo*, single injection into C57BL/6 male mice was conducted. This PTH treatment enhanced Tob mRNA in the long bones in a time and dose dependent manner. To further test the in vivo significance of Tob in PTH actions in osteoblasts, intermittent administration of PTH was conducted in newborn Tob KO and wild type mice for ten days. Intermittent PTH treatment (100 µg/kg) increased cancellous bone mass (BV/TV) about two fold (9% vs. 18%) in wild type newborn mice. Tob deficiency alone minimally affect bone mass compared to wild type (9% vs. 10%). In contrast to wild type, Tob deficiency enhanced PTH-induced increase in bone mass about three fold (10% vs. 27%). To analyze the molecular mechanism operating under the interaction between PTH and Tob deficiency, we examined the phosphorylation levels of a PTH-target transcription

factor CREB (cAMP Response Element Binding Protein) based on western blotting. In control, PTH enhanced pCREB protein levels as known before. In contrast, when endogenous Tob was knocked-down by using si-RNA, PTH-induced phosphorylation of CREB protein was further significantly increased. These observations indicate that Tob acts as a novel endogenous negative feedback regulator of PTH anabolic action and at least one of the regulatory points for the interaction between PTH and Tob deficiency would be at the levels of CREB regulation.

Disclosures: Shuichi Moriya, None.

SA0219

Expression of Glucose Transporters during Osteoblast Differentiation. Anna-Reeta Virta[1], Milja Arponen[1], Kaisa Ivaska*[2]. [1]University of Turku, Finland, [2]University of Turku, Finland

Cellular uptake of glucose is mediated by a family of facilitative glucose transporters (Glut), which carry sugar across plasma membrane into cells. Bone remodeling should require a large amount of energy and osteoblast-like cells have been shown to express some of the members of the glucose transporter family. Glucose sensing, uptake and utilization in primary osteoblasts are, however, still poorly understood. The purpose of this study was to evaluate the expression of glucose transporters during proliferation, differentiation and maturation of osteoblasts from their bone marrow progenitors, the mesenchymal stromal cells (MSCs).

Bone marrow cells were isolated from rat long bones and the plastic-adherent MSC population was differentiated to osteoblasts using culture medium supplemented with ascorbic acid and sodium beta-glycerophosphate. Osteoblast differentiation was verified by the expression of osteoblast marker genes (such as alkaline phosphatase and osteocalcin) by qPCR during differentiation. The expression of Glut1, -2, -3 and -4 were evaluated by qPCR in MSCs and at various time points during osteoblast differentiation. The expression of genes involved in glucose metabolism, such as insulin receptor, as well as glucose uptake were also evaluated. We also analyzed the effect of high glucose on the expression of glucose transporters.

Rat MSCs and osteoblasts expressed clearly detectable levels of Glut1, Glut3 and Glut4 whereas Glut2 was not detected. The expression of Glut1 was highest in MSCs and relatively constant during osteoblast differentiation. Glut3 and insulin receptor were also expressed at all time points analyzed. The expression of Glut4 increased during differentiation and appeared to be highest in the mature osteoblasts. Glucose uptake was also increased together with osteoblast maturation. Long-term exposure to high extracellular glucose levels appeared to suppress the expression of Gluts in osteoblasts.

In conclusion, primary rat osteoblasts express Glut1, Glut3 and Glut4 throughout osteoblast differentiation and the expression of Gluts is modulated by high glucose levels. Osteoblasts thus express mechanisms for glucose sensing and uptake, which may play a role in peripheral glucose disposal and in skeletal responses to hyperglycemia.

Disclosures: Kaisa Ivaska, None.

SA0220

IGF-I Regulation of MicroRNA Expression in Osteoblasts. Chandrasekhar Kesavan*, Jon Wergedal, Subburaman Mohan. Jerry L. Pettis Memorial VA Medical Center, USA

The role of osteoblast produced IGF-I in regulating skeletal growth and mechanical strain effects on bone are well-established. However, little is known regarding the immediate downstream targets of IGF-I that mediate the IGF-I biological effects on bone cells. Because individual microRNA (miR)s can target multiple signaling pathways by influencing a number of mRNAs and because aberrant miR expression have been implicated in several disease states, we predicted miRs to be important mediators of IGF-I action in osteoblasts. To test this prediction, we first evaluated the expression levels of eight miRs that are known to be regulated and play important roles in regulating cellular processes in other tissues by real time RT-PCR using total RNA extracted from the bones of IGF-I conditional knockout (cKO) mice and corresponding wild type (WT) mice. We found that expression levels of miR92, miR20a, miR16, miR146a and miR222 were decreased by two to eight-fold (P<0.05) while the expression level of miR93 was increased by 70-fold in the bones of mice with a disruption of the IGF-I gene in type I collagen expressing osteoblasts compared to corresponding WT mice. To determine if IGF-I directly modulated the expression of these miRs, serum free cultures of MC3T3-E1 osteoblasts were treated with (100 ng/ml) or without IGF-I for 24 or 72 hours and expression levels were determined by real time RT-PCR. Expression levels of miR20a and miR146a were increased by 2- and 7-fold, respectively, at 24 hours while that of miR93 was decreased by 2-fold at 72 hours. By contrast miR93 expression was increased (1.5-fold, P<0.05) in response to IGF-I treatment in ATDC5 chondrocytes. Based on our data, we conclude that IGF-I both up regulates and down regulates miR expression levels in osteoblasts to mediate its biological effects.

Disclosures: Chandrasekhar Kesavan, None.

SA0221

PTH promotes the transcription of members of the LGR/Rspondin family in bone. Nicoletta Bivi*[1], Jonathan Lucchesi[2], Matthew Hamang[2], Qianqiang Zeng[2], Rick Cain[2], Mary Adrian[2], Masahiko Sato[3], Venkatesh Krishnan[4], Yanfei Ma[4]. [1]Eli Lilly & Co., USA, [2]Eli Lilly & Co., USA, [3]Indiana University School of Medicine, USA, [4]Eli Lilly & Company, USA

The LGR/Rspondin (RSPO) pathway is emerging as a novel modulator of Wnt signaling and recent data have suggested that members of the LGR/RSPO pathway may play a role in bone; however, little is known on the ability of the pathway to be regulated in osteoanabolic conditions. We sought to determine by qPCR whether an anabolic regimen of PTH(1-38) alters the levels of members of the LGR/RSPO pathway *in vivo* during fracture repair and in intact bone. Osteopenic rats (8 month old, 2 months post-ovaryectomy) were subjected to unilateral femoral osteotomy, in which a 1mm-gap was created and stabilized with external fixators. Rats were injected sc with 66 µg/kg hPTH(1-38) 3X/wk, starting from day 7 post-surgery, necropsied at 7, 14 or 21 days post-first dose. RNA was isolated from a portion of the femur encompassing the osteotomy site. At the fracture site, the most abundant transcripts were found to be LGR4 and RSPO1. Moreover, PTH(1-38) enhanced the levels of LGR6 6X at day 7 and 4X at day 14, while it diminished the levels of LGR4 at day 14. RSPO2 levels increased 3X at day 14 and day 21, while the levels of RSPO1 and RSPO3 were unchanged. Salmon calcitonin, injected at the concentration of 51 µg/kg 3X/wk, increased c-fos 2.4X at day 21, but did not affect members of the LGR/RSPO family, suggesting that a rise in cAMP is not sufficient to trigger the response, which requires activation of PTHR1. Of note, none of the members of the LGR/RSPO pathway was affected during fracture repair process in vehicle-treated animals. Messenger RNA was also analyzed in the metaphysis of the distal femur of young, intact rats. Human PTH(1-38) at the dose of 70 µg/kg was injected sub-cutaneously and femur metaphysis were collected 3 h and 8 h after. Also in intact metaphysis, LGR6 was increased, while LGR4 was decreased and only RSPO3 was found to be decreased 8 h post-injection by PTH(1-38). In UMR 106 cells, 100 nM PTH(1-38) increased RSPO2 mRNA levels after 24h. Furthermore, 100 nM PTH(7-34) or PTH(1-84) had no effect and a 100-fold excess of PTH(3-34) blocked the increase in RSPO2, suggesting that PTH(1-38) modulates the LGR/RSPO pathway at least in part through cAMP/PKA. Moreover, lack of activation of RSPO2 by PTH(1-84) could explain its known reduced effect compared to PTH(1-38) *in vivo*. In summary, the LGR/RSPO signaling could in turn play a role in the bone anabolic effects of PTH through the modulation of Wnt signaling.

Disclosures: Nicoletta Bivi, Eli Lilly and Company, 4

SA0222

***Rest/Nrsf* Suppresses Osteoblast Differentiation by Down Regulating *Osterix* Expression.** Subburaman Mohan[1], Bo Liu*[2], Shaohong Cheng[3], Sheila Pouteymoor[2]. [1]Jerry L. Pettis Memorial VA Medical Center, USA, [2]VALLHCS, USA, [3]VA Loma Linda Health Care Systems, USA

Runx2 and Osterix (Osx) are two master transcription factors that control osteoblast differentiation and the bone formation process. Identifying molecules that regulate activities of these transcription factors could provide a means to regulate osteoblast function and, thereby, new bone formation. Here we report a novel negative regulator of osteoblast differentiation - Rest (RE1-silencing transcription factor), also known as the neuron restrictive silencing factor or Nrsf. Rest/Nrsf was initially identified as a master negative regulator of neuronal differentiation. We found that Rest/Nrsf is abundantly expressed in osteoblasts including MC3T3-E1 cells, bone marrow stromal (BMS) cells, and calvarial osteoblasts (COB). Treatment of MC3T3-E1 osteoblasts with differentiation media containing 50 µg/ml ascorbic acid (AA) and 10mM β-glycerophosphate for 24 hrs caused a 47% (P<0.05) reduction in Rest/Nrsf mRNA expression compared to cells treated with control media. By contrast, the Osx mRNA level was increased by 1.9 fold (p<0.05) in the AA treated cells. Down regulation of Rest/Nrsf expression induced by osteoblast differentiation media was also confirmed by western blot analysis. To further test the function of Rest/Nrsf in osteoblast differentiation, we knocked down Rest/Nrsf expression by 88% (p<0.01) in MC3T3-E1 cells using Rest/Nrsf specific lentiviral shRNA. The Rest/Nrsf knockdown cells showed a 1.5 fold increase (p<0.05) in Osx mRNA level compared to scramble shRNA control cells. ALP mRNA level was also increased by 2.4 fold (p<0.05) after Rest/Nrsf knockdown. Accordingly, ALP activity in cellular extracts of Rest/Nrsf knockdown MC3T3-E1 cells was increased by 1.4 fold (p<0.05) compared to scramble shRNA control cells. Based on these data, we conclude that Rest/Nrsf is a negative regulator of Osx expression and osteoblast differentiation.

Disclosures: Bo Liu, None.

SA0223

Carbamazepine Inhibits Native Sodium Currents In Murine Osteoblasts.
Sandra Petty*[1], Carol Milligan[2], Marian Todaro[3], Terence O'Brien[3], John Wark[4], Eleanor Mackie[5], Steven Petrou[2]. [1]The University of Melbourne, Australia, [2]The Florey Institute of Neuroscience & Mental Health, Australia, [3]The University of Melbourne, Australia, [4]University of Melbourne Department of Medicine, Australia, [5]University of Melbourne, Australia

PURPOSE: It is well-established that patients with epilepsy have an increase in fracture risk. However, the mechanism for this association is less well defined. We hypothesised that osteoblasts express ion currents, which could be inhibited by anti-epileptic medication. We aimed to investigate whether: (1) mouse primary calvarial osteoblasts expressed voltage-activated sodium current, and (2) the anti-epileptic medication carbamazepine (CBZ) inhibited this current.

Methods: Primary osteoblasts isolated from the calvariae of neonatal C57BL/6 mice were used to examine the impact of CBZ on whole-cell current recordings produced using Patchliner, an automated planar patch-clamp system (Nanion, Germany). Currents were elicited using a voltage protocol stepping from -100 mV to +60 mV in 10 mV increments, for 20 ms, from a holding potential of -80 mV or -60 mV. CBZ (50 µM) was applied to the cells in the continued presence of external Tetraethylammonium (10 mM) and internal Cs+. Following washout of CBZ, 10 µM tetrodotoxin (TTX) a known voltage-gated sodium channel blocker was applied.

Results: Robust voltage-activated inward currents were elicited and external application of CBZ (50 µM) resulted in a significant inhibition of current amplitude 31.6 ± 5.9 % (n = 7; p<0.001), which was partially reversed upon washout. Subsequent application of TTX (10 µM) produced almost complete inhibition of current amplitude 89.96 ± 2.14 % (n = 6; p<0.0001).

CONCLUSIONS: Here we demonstrate that mouse osteoblasts express native voltage-activated sodium channels, which are sensitive to CBZ. To our knowledge this is the first study to utilise a Patchliner to examine native primary osteoblast sodium currents, and to demonstrate an inhibitory effect of CBZ. Further study is required to determine whether the effects on ion channel activity observed here, translate to clinically-relevant changes in bone signaling and bone quality.

Disclosures: Sandra Petty, None.

SA0224

Cbfβ upregulates Atf4 promoter activity and plays an indispensable role in skeletal development and homeostasis. Guochun Zhu*[1], Wei Chen[2], Junqing Ma[3], Mengrui Wu[4], Matthew McConnell[3], Joel Jules[2], Christie Paulson[3], Yi-Ping Li[2]. [1]The University of Alabama at Birmingham, USA, [2]University of Alabama at Birmingham, USA, [3]University of Alabama at Birmingham, USA, [4]The University of Alabama at Birmingham, USA

Activating transcription factor 4 (Atf4) is a key factor which mediates osteoblast formation and function. However, how *Atf4* is regulated at the transcriptional level remains unclear. We hypothesized that the Core-binding factor, beta (Cbfβ)/Runt-related transcription factor 2 (Runx2) complex upregulates *Atf4* expression at the transcriptional level during osteoblast differentiation and that dysfunction of this regulation may result in skeletal disease, such as cleidocranial dysplasia (CCD). To test this hypothesis, we first performed GeneChip (microarray) analysis. The data showed that *Atf4* mRNA expression increased 15 folds during osteoblast differentiation. The increase in *Atf4* expression is similar to the gene expression of several osteoblast markers. The dramatic increase in *Atf4* mRNA expression was confirmed by quantitative RT-PCR analysis using total RNA from mouse calvarial osteoblast differentiation cell cultures. Notably, an increase in *Atf4* mRNA expression during osteoblast differentiation was not shown by qPCR analysis using total RNA from *Cbfβ[f/f] Osx-Cre* mouse calvarial cell cultures, indicating that Cbfβ may be the key regulator of *Atf4* expression. To address the question of whether Cbfβ directly regulates *Atf4* expression at the transcriptional level by regulating *Atf4* promoter activity, we analyzed the *Atf4* promoter region. We found several Cbfβ/Runx complex binding sites in the *Atf4* promoter region (-4000/+80) and designed primers accordingly for chromatin immunoprecipitation (ChIP) assays. DNA was pulled down using the anti-Cbfβ antibody and analyzed using ChIP. The resulting data showed that Cbfβ binds near the transcription start site in the *Atf4* promoter region, indicating that Cbfβ upregulates *Atf4* expression directly by associating with the *Atf4* promoter in *cis*. The promoter luciferase assay showed that luciferase activity driven by *Atf4* promoter segments is almost lost in *Cbfβ[f/f] Osx-Cre* mouse calvarial cells and that the binding site is critical to *Atf4* promoter activity. Importantly, our data showed that mice with *Cbfβ* ablation via *Osx*-Cre exhibit severe skeletal dysplasia with a phenotype recapitulating the clinical features of CCD and a dramatic reduction in *Atf4* expression both in mRNA and protein levels. Overall, our study demonstrates that Cbfβ upregulates *Atf4* promoter activity and revealed that Cbfβ plays an indispensable role in skeletal development and homeostasis by upregulating *Atf4* promoter activity in osteoblasts.

Disclosures: Guochun Zhu, None.

SA0225

See Friday Plenary Number FR0225.

SA0226

See Friday Plenary Number FR0226.

SA0227

MEKK2 promotes osteoblast activity via phosphorylation and stabilization of β-catenin. Matthew Greenblatt*[1], Dong-Yeon Shin[2], Hwanhee Oh[3], Dou Liu[4], Bo Zhai[5], Sutada Lotinun[6], Roland Baron[7], Steven Gygi[8], Laurie Glimcher[2], Bing Su[9], Jae Hyuck Shim[10]. [1]Weill Cornell Medical College/ Brigham & Women's Hospital, USA, [2]Weill Cornell Medical College, USA, [3]Weill Medical College of Cornell University, USA, [4]Yale University, USA, [5]Harvard University, USA, [6]Chulalongkorn University, Thailand, [7]Harvard School of Medicine & of Dental Medicine, USA, [8]Harvard Medical School, USA, [9]Yale University, USA, [10]Weill Cornell Medical College, USA

Emerging evidence points to proper tuning of β-catenin activity in osteoblasts as a key determinant of both bone mass and hematopoietic niche functions. Here, we demonstrate that the mitogen-activated protein kinase kinase kinase (MAP3K) MEKK2 (MAP3K2) promotes osteoblast differentiation and bone formation both *in vitro* and *in vivo* via an unexpected activity to directly phosphorylate β-catenin at serine 675. This phosphorylation event stabilizes β-catenin by recruiting the deubiquinases OTUD4 and USP15, which prevents the basal turnover of β-catenin by inhibiting ubiquitin-dependent proteasomal degradation. A screen of several ligands acting on osteoblasts demonstrates that FGF2 activates MEKK2, and MEKK2 in turn mediates the ability of FGF2 to synergize with WNT stimulation to activate β-catenin and promote osteoblast differentiation. Lastly, genetic interaction studies between *Mekk2* and β-catenin (*Ctnnb1*) null alleles confirm that this pathway is an important physiologic regulator of bone mass *in vivo*. Thus, a FGF2/MEKK2 crosstalk pathway tunes β-catenin activity in osteoblasts, in turn tuning the rate of bone formation *in vivo*.

Disclosures: Matthew Greenblatt, None.

SA0228

Pin1 promotes nuclear stay of β-catenin and controls Wnt3a-induced osteoblast differentiation. Hea-rim Shin*[1], Taegyung Lee[2], Han-sol Bae[1], Young-Dan Cho[3], Won-Joon Yoon[2], Hyun-Mo Ryoo[4]. [1]Seoul National University, South Korea, [2]School of Dentistry Seoul National University, Korea, democratic people's republic of, [3]Seoul National University, South Korea, [4]Seoul National University School of Dentistry, South Korea

Canonical Wnt signaling plays an important role in osteoblast differentiation, in which β-catenin is the key mediator. Pin1 (Peptidylprolyl cis/trans isomerase, NIMA-interacting 1) isomerizes only phophorylated Ser/The-Pro motif. It regulates the conformational change of β-catenin, which is known to be associated with increased cancer risk, because of increased β-catenin level in the nucleus. Canonical Wnt signaling is also very important in osteoblast differentiation, however, association of Pin1 in this signal transduction pathway is still unknown. The specific aim of this study was to investigate if Pin1 is involved in the Wnt-induced osteogenesis. We found that Pin1 KO mouse showed reduction of β-catenin levels in the proximal tibial osteoblasts. So, using TOP Flash in Pin1 WT/KO mouse embryonic fibroblast (MEF) cells, we identified that Pin1 can control Wnt-induced transactivation activity. Inhibition of Pin1 activity by Juglone treatment repressed Wnt3a-induced osteoblast differentiation and bone marker gene expression in C2C12 cells. In contrast, overexpression of Pin1 stimulated osteoblast differentiation by Wnt3a administration. The transcriptional synergy including TOP Flash and ALP promoter activity was observed with Pin1 and Wnt3a. We demonstrated that Pin1 binds to β-catenin in the nucleus and Pin1 activity increased nuclear stay of β-catenin, not stimulated translocation of β-catenin to nucleus. Because isomerized β-catenin couldn't bind to APC which is β-catenin export protein as tumor suppressor. Consequently, Pin1 increases retention of β-catenin in the nucleus, which may explain the increased reporter activity and protein levels in vivo. Taken together, our results reveal that Pin1 is a novel regulator that promotes osteoblast differentiation through structural modification and stabilization of β-catenin in the nucleus. These results provide us a great insight about the importance of Pin1 and isomerization of β-catenin by Pin1 in bone development.

Disclosures: Hea-rim SHIN, None.

SA0229

See Friday Plenary Number FR0229.

SA0230

Smad8 negatively regulats BMP signaling in a dominant negative fashion. <u>Sho Tsukamoto</u>*[1], <u>Takato Mizuta</u>[2], <u>Mai Fujimoto</u>[3], <u>Satoshi Ohte</u>[2], <u>Kenji Osawa</u>[2], <u>Arei Miyamoto</u>[4], <u>Katsumi Yoneyama</u>[2], <u>Eiko Murata</u>[5], <u>Eijiro Jimi</u>[6], <u>Shoichiro Kokabu</u>[7], <u>Takenobu Katagiri</u>[1]. [1]Saitama Medical University Research Center for Genomic Medicine, Japan, [2]Saitama Medical University Research Center for Genomic Medicine, Japan, [3]Saitama Medical University Research Center for Genomic Medicine, Jpn, [4]Saitama Medical University,Research Center for Genomic Medicine, Japan, [5]Faculty of Health & Medical Care, Saitama Medical University, Japan, [6]Kyushu Dental College, Japan, [7]Kyushu Dental College, Japan

The intracellular signaling of bone morphogenetic proteins (BMPs) is regulated by receptor-regulated Smads (R-Smads), Co-Smads and inhibitory Smads (I-Smads). BMP-regulated R-Smads, namely Smad1, Smad5 and Smad8, are activated by phosphorylation by ligand-bound type I receptor kinases. We examined the specific role of each R-Smad in BMP activity by establishing constitutively active Smad1, Smad5 and Smad8 by substituting the C-terminal phosphorylation sites. Over-expression of Smad8 showed less BMP activity than Smad1 and Smad5, even though it associated with Smad4 and bound to the target DNA. The linker region of Smad8 suppressed the transcriptional activity in the chimeric Smads constructed among Smad1, Smad5 and Smad8. The mRNA expression levels of Smad8 were upregulated by BMP signaling, similar to the I-Smads, Smad6 and Smad7. Moreover, overexpression of Smad8 suppressed BMP activity in vitro. In contrast to the I-Smads, however, Smad8 did not inhibit the phosphorylation of Smad1 by type I receptors and suppressed the constitutively active Smad1. Smad8 formed complexes with Smad1 and bound to the DNA but suppressed the transcription of the target gene in a dominant negative fashion. Taken together, our findings suggest that Smad8 negatively regulates BMP signaling in a dominant negative fashion. Thus, it was also suggested that Smad8 is a novel type of transcriptional regulator in BMP signaling.

Disclosures: Sho Tsukamoto, *None.*

SA0231

The cooperation of CREB and NFAT is required for PTHrP-induced RANKL expression in mouse osteoblastic cells. <u>Jeong-Hwa Baek</u>*[1], <u>Hyun-Jung Park</u>[2], <u>Kyunghwa Baek</u>[3], <u>Hyung-Ryong Kim</u>[4]. [1]Seoul National University, School of Dentistry, South Korea, [2]Department of Molecular Genetics, Seoul National University School of Dentistry, South Korea, [3]Gangneung-Wonju national university, School of dentistry, South Korea, [4]Department of Dental Pharmacology, School of Dentistry, Wonkwang University, South Korea

Parathyroid hormone-related protein (PTHrP) is known to induce the expression of receptor activator of NF-κB ligand (RANKL) in stromal cells/osteoblasts. However, the signaling pathways involved remain controversial. In the present study, we investigated the role of cAMP/protein kinase A (PKA) and calcineurin/NFAT pathways in PTHrP-induced RANKL expression in C2C12 and primary cultured mouse calvarial cells. PTHrP-mediated induction of RANKL expression was significantly inhibited by H89 and FK506, an inhibitor of PKA and calcineurin, respectively. PTHrP upregulated CREB phosphorylation and the transcriptional activity of NFAT. Knockdown of CREB or NFATc1 blocked PTHrP-induced RANKL expression. PTHrP increased the activity of the RANKL promoter reporter that contains approximately 2 kb mouse RANKL promoter DNA sequences. Insertions of mutations in CRE-like element or in NFAT-binding element abrogated PTHrP-induced RANKL promoter activity. Chromatin immunoprecipitation assays showed that PTHrP increased the binding of CREB and NFATc1/NFATc3 to their cognate binding elements in the RANKL promoter. Inhibition of cAMP/PKA and its downstream ERK activity suppressed PTHrP-induced expression and transcriptional activity of NFATc1. CREB knockdown prevented PTHrP induction of NFATc1 expression. Furthermore, NFATc1 and CREB were co-immunoprecipitated. Muta-tions in CRE-like element completely blocked NFATc1-induced transactivation of the RANKL promoter reporter; however, mutations in NFAT-binding element partially suppressed CREB-induced RANKL promoter activity. Overexpression of CREB increased NFATc1 binding to the RANKL promoter and vice versa. These results suggest that PTHrP-induced RANKL expression depends on the activation of both cAMP/PKA and calcineurin/NFAT pathways, and subsequently, CREB and NFAT cooperate to transactivate the mouse RANKL gene.

Disclosures: Jeong-Hwa Baek, *None.*

SA0232

Ucma, a downstream target gene regulated by both Runx2 and Osterix, promotes osteoblast differentiation. <u>Yeon Ju Lee</u>[1], <u>So-Jeong Lee</u>*[1], <u>Eun-Hye Lee</u>[1], <u>Yeo Hyang Kim</u>[2], <u>Je-Yong Choi</u>[3], <u>Jung-Eun Kim</u>[4]. [1]Kyungpook National University School of Medicine, South Korea, [2]Kyungpook National University Hospital, South Korea, [3]Kyungpook National University, School of Medicine, South Korea, [4]Kyungpook National University School of Medicine, South Korea

Runx2 and Osterix (Osx) are known as master transcription factors for bone formation. However, genes acting downstream of both Runx2 and Osx have yet to be fully characterized. To investigate Runx2 and Osx downstream target genes, DNA microarray analysis was conducted on calvaria of wild-type, Runx2 heterozygous, Osx heterozygous, and Runx2/Osx double heterozygous mice. During osteogenesis, many genes were regulated by both Runx2 and Osx. The expression of unique cartilage matrix-associated protein (Ucma) was decreased in Runx2 heterozygous and Osx heterozygous mice and was further decreased in double heterozygous mice. In contrast, Ucma expression was increased in osteoblasts overexpressing either Runx2 or Osx and was further increased upon overexpression of both Runx2 and Osx. To examine Ucma expression during osteoblast differentiation, MC3T3-E1 osteoblastic cells were cultured for 30 days in a medium supplemented with ascorbic acid and β-glycerophosphate. Ucma expression initiated mid-way through osteoblast differentia-tion and continued throughout the differentiation process. To investigate whether Runx2 and Osx modulate the transcriptional activity of Ucma, an Ucma reporter construct was co-transfected with Runx2 and/or Osx expression plasmids into MC3T3-E1. The transcriptional activity of the Ucma promoter was increased upon transfection of both Runx2 and Osx expression vectors. Within the Ucma promoter, two Sp1-binding sites and three Runx-binding sites were identified. Runx2- and Osx-mediated activation of the mouse Ucma promoter was directly regulated by Runx2-and/or Sp1-binding sites. During osteoblast differentiation, the formation of mineralized nodules in an Ucma-overexpressing stable clone was earlier and more increased than that of the mock-transfected control. Mineralized nodule formation was highly augmented in MC3T3-E1 cultured in a medium containing Ucma proteins secreted from Ucma-overexpressing cells. Collectively, the results of this study suggest that Ucma is a novel downstream target gene regulated by both Runx2 and Osx and has a positive effect on osteoblast differentiation and nodule formation.

Disclosures: So-Jeong Lee, *None.*

SA0233

See Friday Plenary Number FR0233.

SA0234

See Friday Plenary Number FR0234.

SA0235

See Friday Plenary Number FR0235.

SA0236

See Friday Plenary Number FR0236.

SA0237

See Friday Plenary Number FR0237.

## SA0238

See Friday Plenary Number FR0238.

SA0239

Sensory Neuron Differentiation Enhances Osteoblast Differentiation Through Soluble Factors. <u>Leah Worton</u>*[1], <u>Brandon Park</u>[2], <u>Anthony Redidoro</u>[2], <u>Edith Gardiner</u>[1], <u>Ronald Kwon</u>[1]. [1]University of Washington, USA, [2]University of Washington, USA

Sensory nerves are known to regulate osteogenesis in conditions of bone formation such as fracture repair, heterotopic ossification and growth. Though significant innervation accompanies these processes understanding the osteo-anabolic potential of sensory nerves and their ability to directly guide osteoblast differentiation in these

physiologies is challenging. In this study we developed a novel *in vitro* model of sensory nerve-bone cell interaction using F11 sensory neuron-like and MC3T3 osteoblastic cells to examine the potential for sensory neuron differentiation to drive osteoblast differentiation through soluble factors. F11 cells differentiated with dibutyryl cAMP for 24h exhibited elongated morphology and neurite formation, compared to the rounded cell morphology of undifferentiated controls (Fig 1). Conditioned media (CM) from these F11 cells was then used to treat differentiating MC3T3 cells, and expression analysis performed. These cells had increased mRNA levels of signaling molecules, transcription factors and osteoblast differentiation markers which appeared to be expressed in a temporally relevant manner. Firstly, there were increased levels of AP-1 component genes including c-Fos (Fig 2A) in cells treated with CM from differentiated F11 cells for 24 and 48 h, compared to cells treated with media or with CM from undifferentiated F11 cells. Further evidence of altered signaling was seen with increased expression of VEGF (Fig 2B) and Cox2 after treatment with differentiated F11 CM at 48h. Regulation of osteoblast transcription factors Runx2 (Fig 2C), Dlx5 and Osx was also observed, though Runx2 expression did not differ between time-points and was similar with both types of F11 CM. Finally, for osteoblast differentiation markers, there was elevated OPN in MC3T3 cells after treatment with CM from both undifferentiated and differentiated F11 cells at 24h, though this up-regulation was not observed at 48h with undifferentiated F11 CM (Fig 2D). ALP mRNA was not detected after 24h of treatment, but was elevated at 48h in cells treated with CM from differentiated F11 cells (Fig 2E).These results demonstrate the potential for CM from F11 sensory neuron-like cells to directly enhance osteogenic gene expression in MC3T3 cells in the absence of cellular intermediaries or nerve-bone synaptic transmission. Thus, these studies provide a foundation for elucidating neural factors mediating crosstalk between sensory neurons and bone cells during osteogenesis.
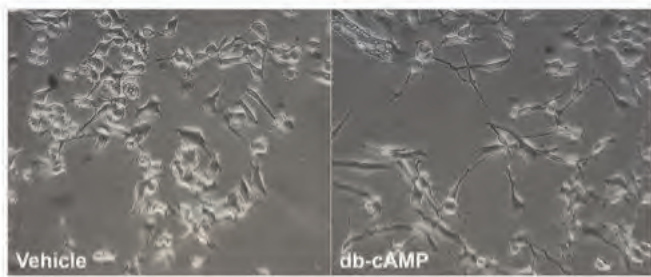
Figure 1. db-cAMP stimulates neuronal differentiation in F11 cells. Phase contrast images of F11 cells treated with vehicle (left) and db-cAMP (right) reveal enhanced neurite formation and more elongated morphology in db-cAMP-treated cells.
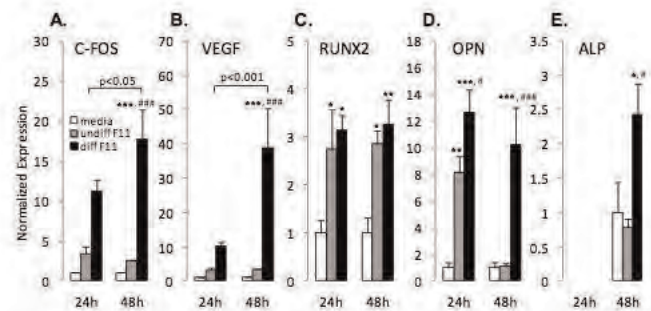
Figure 2. Conditioned media from F11 cells enhances MC3T3 gene expression in regard to signaling pathway components, osteoblastic transcription factors, and markers of osteoblastic differentiation. Shown are results for (A) c-Fos, (B) VEGF, (C) Runx2, (D) OPN, (E) ALP mRNA following treatment with F11 CM. *: p<0.05, **: p<0.01, ***: p<0.001 vs. media; #:p<0.05, ##:p<0.01, ###:p<0.001 vs. undifferentiated F11 CM.

Figure

Disclosures: Leah Worton, None.

SA0240

Signaling by matrix-bound VEGF controls the lineage commitment of multipotent mesenchymal progenitors. Fiona Louis*[1], Sylvie Peyroche[2], Marie-Thérèse Linossier[2], Laurence Vico[3], Alain Guignandon[2]. [1]Unit of Integrative Biology of Bone Tissue, INSERM U1059, France, [2]Unit of Integrative Biology of Bone Tissue, INSERM U1059, France, [3]University of St-Etienne, France

Cell lineage commitment of multipotent progenitors is determined by their mechanical properties. Cellular tension is mainly controlled by Rho family GTPases (RhoA & Rac1). Elevated RhoA (=high cell tension) is often associated with osteogenesis (OS) while low RhoA causes commitment towards adipogenesis (AD). Among several signaling pathways controlling RhoA and Rac1 activities, VEGF signaling appears of first importance since Liu *et al.* (JCI, 2012) suggested that VEGF/KDR translocation in stem cell nuclei (intracriny) activates Runx2 (OS) and inhibits PPARG2 (AD) transcription. In this context, we studied the evolution of RhoA/Rac1 activity, the expression of VEGF-A variants and receptors during AD and OS in a 3D culture of murine multipotent C3H10T1/2 cells (MMC).

OS was induced by growing MMC in 5 mM strontium on apatite and collagen coated microbeads. AD was induced by 1μM rosiglitazone. We observed that AD was characterized by a significant reduction in RhoA and Rac1 activities (-25% and -70% respectively) while both were stimulated during OS (+100% and +30% respectively). These unexpected results suggest that conventional Rac1/AD and RhoA/OS associations need to be revisited. Interestingly, the dual stimulation of RhoA & Rac1 in OS fits nicely with the requirement of active fibrillogenesis (RhoA dependent) and β-catenin translocation (Rac1 dependent) during this process.

High soluble VEGF secretion was observed during AD, while OS is associated with increased expression of the matrix-bound VEGF188 isoform (VEGFm). Both Flt1 and KDR expressions decreased dramatically with AD (-75% and -50% respectively) and increased in OS (+50% and +40% respectively), suggesting a specific VEGFm role in osteoblast differentiation. To assess the importance of this signaling, we immobilized VEGF165 on microbeads and showed its ability to stimulate RhoA and Rac1 in MMC. In contrast VEGF165 in a soluble form did not display this ability when incubated with MMC cultivated on microbeads.

Interestingly, the ability of mechanical stresses to direct stem cells commitment might be explained by their known stimulatory effect on VEGFm production.

We proposed that production and immobilization of VEGFm in skeletal stem cells niches trigger RhoA and Rac1 activations leading to their commitment toward osteoblastogenesis.

Disclosures: Fiona Louis, None.

SA0241

See Friday Plenary Number FR0241.

SA0242

Early Embryonic Stem Cell Markers are Commonly Induced in Both Fracture and in Ectopically Induced Bone Formation. Beth Bragdon*[1], Kyle Lybrand[2], Louis Gerstenfeld[3]. [1]Boston University School of Medicine Department of Orthopaedics, USA, [2]Boston University Dept of Orthopaedic Surgery, USA, [3]Boston University School of Medicine, USA

Introduction: Bone formation can be induced ectopically in muscle by Demineralized Bone Matrix (DBM) or BMPs suggesting that osteochondral progenitors may be found in non-skeletal tissues. A number of studies also show that osteochondral progenitor cells located in both the periosteum and surrounding skeletal muscles around a fracture site can contribute to the developing fracture callus. However, little is known regarding the earliest transcriptional regulators within the progenitor cell populations within these separate tissues that give rise to cells that contribute to early fracture healing or ectopic bone formation.

Methods: Human DBM was obtained from Medtronics Inc with an MTA. To generate ectopic bone formation, DBM (50mg) was implanted on the periosteum of the femur in male B6,129S7-Rag1tm1Mom/J mice. Implants were harvested at 2, 4, and 8 days post-operatively. Closed stabilized transverse fractures were generated in the right femora of male C57BL/6J mice. The callus was harvested at 1, 2, 3, and 5 days post-fracture. Total RNA was isolated and mRNA expression for embryonic stem cells (Sox2, Nanog, Oct4), muscle satellite cells (Pax7), and periosteal osteochondral progenitor cells (Prx1) were evaluated with real time qPCR.

Results: The embryonic stem cell markers showed increased expression in both the DBM-induced ectopic bone formation and fracture callus compared to the non-operative femurs. Sox2 and Nanog showed the most robust induction with over 100 fold increase expression in the ectopic bone while fracture repair was able to induce these genes over a 10 fold increase. Expression of these genes peaked in the DBM-induced ectopic bone formation at post-operative day 2 and subsequently decreased to base line levels by 5 days post fracture. Interestingly Prx1 and Pax7 were co induced with Nanog and Sox2 but showed more prolonged expression through day 5 and day 8 respectively in fracture callus and ectopic bone.

Conclusions: The robust induced expression of early embryonic stem cell markers during both ectopic bone formation and fracture repair is suggestive that these transcriptional regulators may be functional in postnatal skeletal stem cells. The expression of transcriptional regulators that have been separately associated with

periosteum and muscle suggests that these factors are not exclusively restricted to these tissues but may also be more generally functional in axial skeletal stem cell that contribute to bone repair.
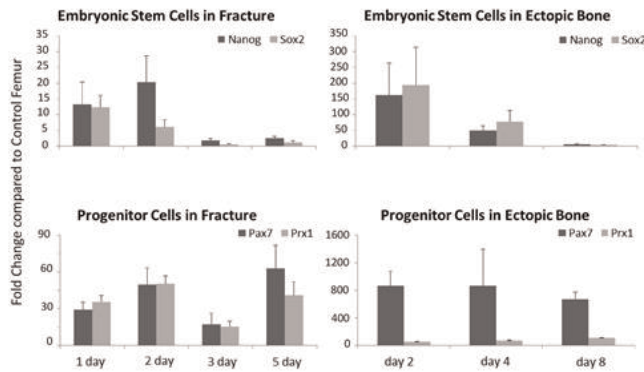

Figure 1. Embryonic and progenitor cell gene expression in fracture and ectopic bone formation

Disclosures: Beth Bragdon, None.

SA0243

Genome-wide Global Chromatin Landscape during Bone Differentiation from Normal and Osteogenesis Imperfecta iPS Cells. Lyuba Varticovski[1], Bethtrice Thompson*[2], Songjoon Baek[3], Jay Shapiro[4], Gordon Hager[3]. [1]NCI, National Institutes of Health, USA, [2]Howard U, USA, [3]LRBGE, NCI, NIH, USA, [4]Kennedy Krieger Institute, Johns Hopkins, USA

BACKGROUND: Although bone undergoes life-long remodeling, there is a substantial lack of information on the molecular basis of Mesenchymal Stem Cells (MSC) differentiation into osteoblast and key regulators of this process. We investigated genome-wide changes in chromatin landscape changes in iPS cells during MSC and osteoblast (OB) lineage differentiation, and how these changes affect gene expression. We compared these changes with OB differentiation of cells from a patient with Type III Osteogenesis Imperfecta (OI) who has a mutation in COL1A1. METHODS: Both iPS cell types were generated by retroviral transduction with 4 stem cell transcription factors: SOX2, OCT4, KLF4 and MYC. To investigate changes in chromatin landscape, we used DNase I or Benzonase, an alternative DNA cutting enzyme, combined with deep sequencing to detect DNA hypersensitivite sites (DHS) which, by definition, are not protected by histones and thus are accessible to transcription factors (TF) binding. RESULTS: Normal and OI-derived iPS cells readily differentiated into MSC, and osteoblast or adipose lineages as detected by alizarin red and oil red staining, disappearance of stem cell markers by flow cytometry, and gene expression. Analysis of sites hypersensitive to DNA cutting enzymes exposed key regulatory elements, including sites in promoters of known OB genes, such as COL1A1, RUNX2, as well as changes in sites not previously known to be associated with bone formation. Comparison between normal and OI-derived iPS cells confirmed significant differences between 76,223 DHS in normal and 40,932 in OI iPS with only 25,310 overlapping sites. These data underscore significant genome-wide chromatin landscape differences between normal and OI iPS cells, and indicate constrained chromatin landscape in OI derived iPS cells. Analysis of TF motifs most frequently modified during differentiation showed disappearance of motifs associated with TFs initially used to derive iPS cells: SOX2, OCT4 and KLF4, and appearance of new TF motifs for AP-1 and TEAD during final OB differentiation. CONCLUSIONS: Analysis of genome-wide chromatin landscape reveals chromatin changes in known osteogenesis-related genes as well as significant modifications in promoters and enhancers of genes that have not been previously associated with OB differentiation. This analysis offers an unprecedented view of chromatin modifications during OB differentiation and genes involved in this process..

Disclosures: Bethtrice Thompson, None.

SA0244

Identifying Markers in Pre-Implantation hES and iPS-Derived Progenitor Cells for In Vivo Skeletal Tissue Formation. Xiaonan Xin*[1], Kyle Shin[2], Xi Jiang[3], Liping Wang[1], Nathaniel Dyment[2], Mark Kronenberg[1], Jianping Huang[2], David Rowe[1], Alexander Lichtler[1]. [1]University of Connecticut Health Center, USA, [2]University of Connecticut Health Center, USA, [3]University of Connecticut Health Center, USA

Many studies that demonstrate in vitro MSC like differentiation from hES or iPS cells based on a CD profile lack evidence that these markers are predictive of in vivo bone or cartilage differentiation. We have reported a novel protocol, EB-EGM, for differentiation of hESC or iPSC into MSC-like cells, which form human cartilage and bone in a murine in vivo calvarial defect model. Histological analysis suggested that the implanted cells undergo endochondral-like bone formation. Flow cytometry analysis of the pre-implantation cells demonstrated that more then 95% of the cells at passage 3 expressed MSC surface marker proteins, CD44, CD73, CD90 and CD166, while only 1 or 2 % cells are positive for the endothelial marker CD31 or the hematopoietic markers CD34 and 45. However, in our hands, this panel of markers is not predictive of in vivo differentiation. To further characterize our EB-EGM protocol, we extracted RNA at different differentiation stages. We demonstrated that the cells undergo an epithelial/mesenchymal transition (EMT) by RT-PCR for E-cadherin and vimentin mRNA expression. We also wished to identify a gene expression signature that can distinguish hES and iPS-derived MSC-like cells that have the potential to form skeletal tissues in our in vivo model from similar MSC-like cells, also derived from hES or iPS cells but using different protocols, that do not form bone in our model. Initially, we used an osteogenesis low density array plate to compare hESC-derived EB-EGM-MSC with non-differentiated hESC, hESC-derived MSC produced using an EB-based protocol in non-EGM medium, which has shown no cartilage or bone formation in our in vivo mouse model, and adult bone marrow MSC. We saw differential expression of several genes, including Msx2. Currently, these RNA samples are undergo deep sequencing, which will allow an in depth study of the genes that may be potentially related to skeletal tissue formation. We have also applied this protocol to control human iPS cells derived from both fibroblasts and blood cells and shown robust cartilage and bone formation, with histological evidence for endochondral-like bone formation. We are working to develop more specific evidence for this using antibody staining and molecular markers. Our studies further support the utility of our protocol or analyzing the pathophysiology of genetic skeletal diseases, and provide the basis for refining protocols from differentiating iPS cells for therapy of skeletal diseases.

Disclosures: Xiaonan Xin, None.

SA0245

See Friday Plenary Number FR0245.

SA0246

See Friday Plenary Number FR0246.

SA0247

Osteogenic commitment of mesenchymal stem cells is driven by epigenetic mechanisms characterized by dynamic changes in histone modifications. Hai Wu*[1], Jonathan Gordon[1], Troy Whitfield[2], Phillip Tai[3], Andre Van Wijnen[4], Gary Stein[5], Janet Stein[6], Jane Lian[7]. [1]University of Vermont, USA, [2]3Department of Cell & Developmental Biology, University of Massachusetts Medical School, USA, [3]University of Vermont College of Medicine Department of Biochemistry, USA, [4]Mayo Clinic, USA, [5]University of Vermont College of Medicine, USA, [6]Department of Biochemistry, University of Vermont College of Medicine, USA, [7]University of Vermont College of Medicine, USA

Changes in histone post-translational modifications are fundamental events for chromatin remodeling and gene expression, leading to cell lineage commitment from pluripotent stem cells. Multipotent bone marrow stromal cells (BMSCs) are crucial for supporting bone tissue homeostasis. To address the underlying epigenetic mechanisms for osteogenesis, we profiled gene expression and histone modifications by RNA-Seq and ChIP-Seq respectively in the primary BMSCs committing to the osteoblast lineage at four stages: proliferation, early commitment/preosteoblasts, matrix deposition and maturation, and mineralization. From our profiling data, we selected 6 distinct patterns associated with osteoblast differentiation that had most biological relevance (for example, genes continuously upregulated, downregulated, and peaked at commitment). These gene sets were then correlated with 7 histone modifications to define signatures of histone modifications for developmentally expressed osteoblast-related genes. Seventy-five highly upregulated genes peaking at mineralization (eg.,Ocn, Bsp, Sost, Dkk1, Mepe, Enpp6, Bmp2) continuously acquired marks H3K9ac and H3K27ac, both reflecting transcriptional activation at promoters. At the same time, this gene set lost two repressive marks of transcription (H3K27me3 and H3K9me3). One gene set characterized by peak expression at commitment followed by a substantial decrease in expression is comprised of 291 genes, including many growth factors, transmembrane proteins and signaling mediators. This gene group exhibited an initial increase of H3K36me3 (transcription elongation mark) followed by a rapid decrease of this mark, closely correlating with the gene expression pattern. This observation suggests that gaining H3K36me3 is a prime indicator of transient gene upregulation. In conclusion, our data identifies distinct histone codes for different gene expression categories that are important drivers to establish osteoblast lineage.

* HW and JAG contributes equally to the work

Disclosures: Hai Wu, None.

SA0248

Paracrine effects of hematopoietic cells on human mesenchymal stem cells. Shuanhu Zhou*. Brigham & Women's Hospital, USA

A progressive decline in the ability of stem cells to maintain normal adult tissues or to repair injured tissues contributes aging. We and others uncovered that there are age-related intrinsic changes in human mesenchymal stem cells (hMSCs). Several lines of evidence indicate that the decline in stem cell function during aging can involve both cell intrinsic and extrinsic mechanisms. The bone and blood formation are intertwined in bone marrow, therefore hematopoietic cells and bone cells could be extrinsic factors for each other in bone marrow environment. In this study, by using an *in vitro* transwell co-culture platform, we assessed the paracrine effects of hematopoietic cells on hMSCs. Our data showed that hematopoietic cells stimulate proliferation and osteoblast differentiation and inhibit senescence in hMSCs. To determine the paracrine factors that are responsible for the effects of hematopoietic cells on hMSCs, gene profiles of growth factors, Wnts and cytokines were assessed in both hematopoietic cells and hMSCs. Results showed that TNF-α, PDGF-β and Wnt-related factors, *e.g.* Wnt1, 4, 6, 7a, and 10a, sFRP-3 and sFRP-5, are dominantly expressed in hematopoietic cells. We next determined the role of TNF-α and Wnt signaling pathways in the paracrine interactions during aging. There was an age-related increase in gene expression of TNF-α in hematopoietic cells and decrease in gene expression of TNF receptor 2 in hMSCs; TNF-α treatment induced cell death and senescence, reduced proliferation and osteoblast differentiation and stimulated NF-κB signaling in hMSCs. There was an age-related increase of β-catenin protein levels and TNF-α stimulated β-catenin signaling in hMSCs. Kockdown β-catenin by siRNA reduced SA-β-Gal$^+$ cells in hMSCs, implying that TNF-α *via* NF-κB as well as Wnt/β-catenin signaling performed as negative factors in paracrine actions of hematopoietic cells on hMSCs. In conclusion, our data demonstrate that there are paracrine actions of hematopoietic cells, *via* soluble factors, such as TNF-α, PDGF-β or Wnts etc., on hMSCs; the age-related increase of TNF-α in hematopoietic cells suggests that immunosenescence, *via* the actions of hematopoietic cells on mesenchymal stem cells, may be one of the extrinsic mechanisms of skeletal stem cell function decline during human skeletal aging.

Disclosures: Shuanhu Zhou, None.

SA0249

Regulation of skeletal stem cell multipotency by MT1-MMP. Jason Horton*[1], Heba Degheidy[2], Steven Bauer[2], Pamela Robey[3], Kenn Holmbeck[4]. [1]National Institutes of HealthNational Cancer Institute, USA, [2]Laboratory of Stem Cell Biology, Division of Cell & Gene Therapies, Center for Biologics Evaluation & Research, Food & Drug Administration, USA, [3]National Institute of Dental & Craniofacial Research, USA, [4]National Institute of Dental & Craniofacial Research, USA

Plasticity of the skeletal stem/progenitor cell lineage is an essential homeostatic mechanism initiated by skeletal injury or insult. Under normal circumstances, these primitive cells re-establish a bone/marrow organ with the proper balance of osteoprogenitors, hematopoietic-supportive stromal cells and marrow adipocytes, but in some cases the balance of these elements is disrupted. The mechanisms that govern skeletal stem cell activation and plasticity have yet to be defined in great detail, but are likely to involve both autocrine and paracrine cell-signaling, as well as interactions with extracellular matrix molecules. MT1-MMP has been identified as an indispensable modulator of mesodermal cell behavior and differentiation, and global deletion results in a severe skeletal phenotype. Conditional deletion of *Mt1-Mmp* from mature osteoblastic cells expressing osteocalcin (Ocn^{Cre}; $Mt1^{f/f}$) results in osteopenia, spontaneous fracture, and a dramatic conversion of red marrow to yellow marrow. This adipogenic shift is thought to arise from a failure to block the differentiation of skeletal stem/progenitor cells in the stromal-vascular compartment into adipocytes. Consistent with this notion, Ocn^{Cre}; $Mt1^{f/f}$ mice display abnormalities of fracture repair, characterized by generation of a thin mineralized cortex, failure to locally reconstitute hematopoietic marrow and expansion of yellow marrow throughout the fracture site. These results demonstrate that Mt1-MMP is a critical factor expressed by mature osteoblastic cells that governs marrow adiposity, and suggests interaction with a protease-dependent regulatory ligand that opposes adipose differentiation of the skeletal stem/progenitor cells.

Disclosures: Jason Horton, None.

SA0250

Understanding the periosteal response to mechanical load and injury. Candice GT Tahimic*[1], Tao Wang[2], Alicia T. Menendez[2], Chak Fong[2], Yongmei Wang[2], Shunichi Murakami[3], Daniel Bikle[1]. [1]Endocrine Research Unit, Division of Endocrinology UCSF & VAMC, USA, [2]Endocrine Research Unit, Division of Endocrinology UCSF & VAMC, USA, [3]Case Western Reserve University, USA

The periosteum is a multilayer structure that serves as a niche for stem and osteochondroprogenitor cell populations and a repository for molecules that contribute to bone formation. The long-term goal of our study is to understand the key cell populations and the molecular mechanisms by which a healthy periosteum is able to respond with robust bone formation during mechanical loading or injury. Towards this goal, we performed gene expression analysis of primary periosteal cell cultures from normal three month old ambulatory animals as they underwent directed differentiation into the osteogenic lineage. Differentiating periosteal-derived cells, like bone marrow stromal cells, display a similar trend in the progression of osteogenic markers such as alkaline phosphatase and osteocalcin. Periostin, a molecule that is commonly associated with periosteal cells was found to be upregulated in the later stages of periosteal differentiation consequent with downregulation of Prx-1 expression. By day 21, these periosteal cells display modest Alizarin red staining with significant mineralization occurring at day 28. We are currently examining the effect of mechanical loading on this differentiation process. To further understand the role of subsets of cell populations in the periosteum during the response to loading state or injury, we developed a double transgenic animal carrying a Rosa tdtomato reporter and a tamoxifen-inducible Cre-Prx1 transgene. This model allows cell fate tracing studies on the subset of Prx-1 expressing periosteal osteochondroprogenitors. Tamoxifen-treated three month-old animals exhibited increased tomato red labeling in the periosteum during the reloading phase after a period of skeletal unloading. In a fracture model, robust labeling was observed in early stage of callus formation. Moreover, derivatives of Prx1 osteochondroprogenitors persist in vivo as shown by the incorporation of the label into cortical bone. This finding is consistent with our in vitro studies wherein cultures of periosteal tissue from these transgenic animals show tomato red labeling from the early to late stages of osteogenic induction. In conclusion, major similarities exist between the differentiation program of BMSCs and periosteal-derived cells, although the timing of periostin expression distinguishes the periosteal cultures. In the adult, progeny of Prx1-expressing osteochondroprogenitors comprise a persistent subset of periosteal cells that are capable of responding to mechanical stimuli and fracture injury.

Disclosures: Candice GT Tahimic, None.

SA0251

See Friday Plenary Number FR0251.

SA0252

See Friday Plenary Number FR0252.

SA0253

See Friday Plenary Number FR0253.

SA0254

See Friday Plenary Number FR0254.

SA0255

See Friday Plenary Number FR0255.

SA0256

See Friday Plenary Number FR0256.

SA0257

See Friday Plenary Number FR0257.

SA0258

See Friday Plenary Number FR0258.

SA0259

See Friday Plenary Number FR0259.

SA0260

See Friday Plenary Number FR0260.

SA0261

See Friday Plenary Number FR0261.

SA0262

Arctigenin Inhibits Osteoclastogenesis by Suppressing Both Calcineurin-Dependent and Osteoblastic Cell-Dependent NFATc1 Pathways. <u>Teruhito Yamashita</u>*[1], <u>Shunsuke Uehara</u>[2], <u>Nobuyuki Udagawa</u>[3], <u>Feng Li</u>[4], <u>Shigetoshi Kadota</u>[4], <u>Hiroyasu Esumi</u>[5], <u>Yasuhiro Kobayashi</u>[2], <u>Naoyuki Takahashi</u>[1]. [1]Matsumoto Dental University, Japan, [2]Matsumoto Dental University, Japan, [3]Matsumoto Dental University, Japan, [4]University of Toyama, Japan, [5]Tokyo University of Science, Japan

Arctigenin, a lignan-derived compound, is known as an anti-inflammatory and anti-tumor reagent. Arctigenin was previously shown to inhibit osteoclastogenesis; however, this inhibitory mechanism has yet to be elucidated. Here, we showed that arctigenin inhibited the activity of nuclear factor of activated T-cells, cytoplasmic 1 (NFATc1), a key transcription factor for osteoclastogenesis. NFATc1 in osteoclast precursors was activated through two distinct pathways: the calcineurin-dependent and osteoblastic cell-dependent pathways. Arctigenin strongly inhibited receptor activator of nuclear factor κB ligand (RANKL)-induced osteoclast formation in mouse bone marrow macrophage (BMM) cultures, in which the calcineurin-dependent NFATc1 pathway was activated. Arctigenin suppressed neither the activation of NF-κB and MAP kinases nor the up-regulation of c-Fos expression in BMMs treated with RANKL. However, arctigenin suppressed RANKL-induced NFATc1 expression and its target genes. Interestingly, the treatment of osteoclasts with arctigenin converted NFATc1 into a lower molecular weight species, which was translocated into the nucleus even in the absence of RANKL. Nevertheless, arctigenin as well as cyclosporin A (CsA), a calcineurin inhibitor, suppressed the NFAT-luciferase reporter activity induced by ionomycin and PMA in BMMs. Chromatin immunoprecipitation analysis confirmed that arctigenin inhibited the recruitment of NFATc1 to the promoter region of the NFATc1 target gene. Arctigenin, but not CsA suppressed osteoclast formation in co-cultures of osteoblastic cells and bone marrow cells, in which the osteoblastic cell-dependent NFATc1 pathway was activated. The forced expression of constitutively active NFATc1 rescued osteoclastogenesis in BMM cultures treated with CsA, but not that treated with arctigenin. Arctigenin also suppressed the pit-forming activity of osteoclasts cultured on dentin slices. These results suggest that arctigenin induces a dominant negative species of NFATc1, which inhibits osteoclast differentiation and function by suppressing both calcineurin-dependent and osteoblastic cell-dependent NFATc1 pathways.

Disclosures: Teruhito Yamashita, None.

SA0263

Caspase-2 Plays a Role in Osteoclastogenesis by Regulating Reactive Oxygen Species. <u>Danielle Callaway</u>*[1], <u>Manuel Riquelme</u>[2], <u>Jean Jiang</u>[1]. [1]University of Texas Health Science Center at San Antonio, USA, [2]University of Texas Science Center, San Antonio, USA

Loss of caspase-2 in mice results in an osteopenic phenotype characterized by increased numbers of osteoclasts in vivo. However, the role of caspase-2 within the osteoclast as well as how loss of caspase-2 may contribute to increased osteoclast numbers has not yet been established. In this study, we showed that caspase-2 is present throughout the differentiation process, but caspase-2 protein levels become significantly reduced. Next, we sought to identify whether loss of caspase-2 led to an increase in osteoclast numbers in vitro due to enhanced osteoclast differentiation from macrophage precursors. RAW 264.7 cells were treated with siRNA against caspase-2, which led to an increase in osteoclast numbers as well as TRAP activity when siRNA was added at the beginning of the experiment or at day 2 of differentiation. Cells from *Casp2⁻/⁻* animals treated with RANKL similarly induced increased osteoclast numbers as well as TRAP activity compared to wild-type (WT) controls. In addition, *Casp2⁻/⁻* osteoclasts exhibited increased fusion, were larger than the control, and had increased protein levels of NFATc1. In order to evaluate whether caspase-2 loss had an effect on early differentiation, bone marrow macrophages (BMMs) from WT and *Casp2⁻/⁻* animals were assessed for the activation of downstream signaling pathway following RANKL addition, but no significant differences were found. Combined, the data from *Casp2* knockdown as well as from primary cells suggests that loss of caspase-2 did not appear to be involved in regulating the earlier stages of differentiation, but had a greater consequence on later stages involving preosteoclast fusion. In order to assess the mechanism behind the effects of caspase-2 loss on differentiation, the total and mitochondrial levels of reactive oxygen species (ROS) were evaluated since ROS has been characterized as a crucial component of osteoclastogenesis and that loss of caspase-2 is associated with increased ROS levels. During osteoclastogenesis, both total and mitochondrial ROS were increased in cells lacking caspase-2 but only after RANKL administration with a concomitant reduction in FoxO3a-regulated enzymes catalase and SOD2. Because mitochondrial ROS has been identified to be a possible regulator of the later stages of differentiation, the heightened levels in *Casp2⁻/⁻* cells could be the predominant mechanism that results in increased precursor fusion and osteoclast numbers.

Disclosures: Danielle Callaway, None.

SA0264

See Friday Plenary Number FR0264.

SA0265

See Friday Plenary Number FR0265.

SA0266

See Friday Plenary Number FR0266.

SA0267

Pathway analysis of microRNA profile during early, mid and late osteoclastogenesis. <u>Neha Dole</u>*[1], <u>Tiziana Franceschetti</u>[1], <u>Catherine Kessler</u>[2], <u>Sun-Kyeong Lee</u>[1], <u>Anne Delany</u>[1]. [1]University of Connecticut Health Center, USA, [2]University of Connecticut Health Center, USA

An understanding of the molecular mechanisms regulating the complex process of osteoclastogenesis is critical for the design of novel therapeutics for bone loss. Osteoclast formation and function are tightly regulated by transcriptional, post-transcriptional and post-translational mechanisms. Bone homeostasis requires such stringent regulation, to prevent excessive or insufficient bone resorption. microRNAs (miRNAs) are key post-transcriptional regulators of osteoclastogenesis. They bind to their target mRNAs to repress expression; controlling proliferation, differentiation, and apoptosis. Disruption of miRNA-mediated regulation alters osteoclast formation and bone resorption. Previous studies profiled miRNA expression in mouse osteoclast precursors treated with RANKL for 24 hours. However, a more complete miRNA signature, encompassing early, mid and late stages of osteoclastogenesis, is wanting.

Here, we analyzed miRNA expression in an enriched population of murine bone marrow osteoclast precursors (depleted of B220+ and CD3+ cells) undergoing 1, 3, or 5 days of RANKL-driven differentiation. The Agilent microarray platform was used to analyze expression of mature miRNAs. 93 miRNAs showed >2 fold-change during these early, mid, and late stages. Remarkably, many of these miRNAs were detected for the first time in osteoclasts. We identified 7 clusters of differentially expressed miRNAs, and validated the expression of selected miRNAs by qRT-PCR. Computational analyses predicted several recurring pathways that could be targeted by the miRNA clusters. These include mTOR, PI3 kinase/AKT, cell-matrix interactions, actin cytoskeleton organization, focal adhesion and axon guidance. This suggests that many miRNA clusters differentially expressed during osteoclastogenesis converge on the regulation of some key functional pathways. For example, cytoskeletal remodeling is crucial for osteoclast precursor migration, maturation, and bone resorption. Genes important for cytoskeletal remodeling are potential targets for abundantly expressed miRNAs such as miR-27b, miR-29 and let7 family members.

Overall, our study is unique in that we identified miRNAs differentially expressed during early, mid, and late osteoclastogenesis in a population of primary mouse bone marrow cells enriched for osteoclast progenitors. This novel data set contributes to our understanding of the molecular mechanisms regulating the complex process of osteoclast differentiation.

Disclosures: Neha Dole, None.

SA0268

Rhinacanthin C Inhibits RANKL-induced Osteoclast Differentiation by Suppressing MAPKs/NF-κB/NFATc1 Pathways through Preventing TRAF6-TAK1 Formation. <u>Mineko Tomomura</u>*[1], <u>Ryuichiro Suzuki</u>[2], <u>Yoshiaki Shirataki</u>[2], <u>Hiroshi Sakagami</u>[3], <u>Akito Tomomura</u>[4]. [1]Meikai University School of Dentistry, Japan, [2]Faculty of Pharmaceutical Sciences, Josai University, Japan, [3]Divisions of Pharmacology, Meikai University School of Dentistry, Japan, [4]Meikai University, School of Dentistry, Japan

The shrub *Rhinacanthus nasutus* (L.) Kurz (Acanthaceae) is widely distributed in Southeast Asian countries and used for the treatment of pneumonia, diabetes, hypertension and skin diseases. In search of anti-osteoclastogenic activity from plants, we found the ethyl acetate (EtOAc) extracts of root of *Rhinacanthus nasutus* inhibited the osteoclastogenesis stimulated by receptor activator of nuclear factor-κB ligand (RANKL) in RAW 264.7 cells. To investigate further the anti-osteoclastogenic constituents of *Rhinacanthus nasutus*, we isolated five components (rhinacanthin C, G, N and Q, and rhinacanthone) from the EtOAc-soluble fraction of this plant. Among

them, rhinacanthin C most potently inhibited the RANKL-stimulated osteoclasto-genesis from the mouse bone marrow macrophage (BMM) cultures. Rhinacanthin C dose-dependently inhibited tartrate-resistant acid phosphatase-positive multinuclear cell formation and pit formation without cell toxicity. Rhinacanthin C suppressed RANKL-stimulated c-Fos and NFATc1 expression, a master transcription factor for osteoclastogenesis. RANKL-induced phosphorylation of ERK, JNK and NF-κB were significantly inhibited by rhinacanthin C. Furthermore, rhinacanthin C inhibited RANKL-induced TRAF6-TAK1 complex formation, an upstream signaling event that is important for activation of MAPKs and NF-κB. This study suggests that rhinacanthin C may be the natural compound responsible for anti-osteoclastgenic activity of *Rhinacanthus nasutus* and it might be an alternative medicine for the prevention of osteoporosis.

Disclosures: Mineko Tomomura, None.

SA0269

See Friday Plenary Number FR0269.

SA0270

Soluble silica: an osteoclast-macrophage linage regulator in early RAW264.7 osteoclastogenesis. Pamela Uribe-Trespalacios*[1], Zivko Mladenovic[2], Kaveh Shahabi[3], Anders Johnasson[3], Maria Ransjo[4]. [1]University of Gothenburg, Sweden, [2]Gothenburg University, Sweden, [3]Umeå University, Sweden, [4]University of GothenburgSahlgrenska academy, Sweden

Diet and dietary supplements play an important part in osteoporosis treatment and prevention. Beyond calcium and vitamin D, an emanating number of studies have in recent years suggested that dietary silicon/soluble silica (Si) plays an important part of normal development of the skeleton and connective tissue. From in vitro cell culture studies on osteoblasts it has been reported that Si stimulates proliferation and acts on collagen synthesis/stabilization. It has also been demonstrated that Si inhibits osteoclast formation and bone resorption. The molecular mechanisms of Si on bone cells are however still unclear. The purpose of the present study was to further investigate the role of Si in osteoclastogenesis. Using neutral red uptake assay it could be established that Si concentrations ranging from 0-125µg/ml did not have any adverse effects on RAW264.7 cells. Next we used flow cytometry to analyze if Si would promote the RAW264.7 cells towards the macrophage or the osteoclastic lineage. We also studied how Si would alter gene expressions associated with osteoclastogenesis using quantitative real-time PCR. Our results suggest that Si dose dependently alters the expression of F4/80 and RANK as well as gene expressions associated with osteoclast fusion making Si a potentially important regulator in osteoclastogenesis.

Disclosures: Pamela Uribe-Trespalacios, None.

SA0271

A possible role of DMP1 as a negative regulator of FGF23 production in functional heterogeneity osteocytes: Three-dimensional morphological approaches. Ji-Won Lee*[1], Akira Yamaguchi[2], Tadahiro Iimura[3]. [1]Ehime University, Proteo-Science Center (PROS), Japan, [2]Tokyo Medical & Dental University, Japan, [3]Ehime University, Proteo-Science Center (PROS), Japan

FGF23 and dentin matrix protein (DMP1) are predominantly expressed in osteocytes in bone, regulating bone mineralization and phosphate metabolism, respectively. However, the mechanisms underlying the actions of DMP1 as a local factor regulating FGF23 and bone mineralization are not well understood. We first observed spatially distinct distributions of FGF23-and DMP1-positive osteocytic lacunae in rat femurs using immunohistochemistry. Three-dimensional immunofluor-escence morphometry further demonstrated that the distribution and relative expression levels of these two proteins exhibited reciprocally reversed patterns especially in midshaft cortical bone. These *in vivo* findings suggest a direct role of DMP1 in the regulation of FGF23 expression in osteocytes. We next observed that the exogeneous treatment of recombinant DMP1 in UMR-106 osteoblast/osteocyte-like cells and long-cultured MC3T3-E1 osteoblastic cells showed significant down-regulation of the FGF23 production. Moreover, exogenous DMP1 affect cellular morphological changes by increasing the number of focal adhesion points in both cells measured by 3D-reconstructed images. Consistently, the levels of phosphorylated FAK, ERK and p38 were significantly elevated, indicating that exogenous DMP1 is capable of activating FAK-mediated MAPK signaling. Our findings suggest that DMP1 is a local, direct and negative regulator of FGF23 production in osteocytes through in the FAK-mediated MAPK pathway, thus proposing a relevant pathway that coordinates the extracellular environment of osteocytic lacunae and phosphate metabolism.

Disclosures: Ji-Won Lee, None.

SA0272

Compartment-, Age-, and Disease-Specific Variability in the Architecture of Osteocyte Lacunar-Canalicular System. Xiaohan Lai*[1], Shannon Modla[2], Catherine B. Safran[3], Christopher Price[1], Liyun Wang[1]. [1]University of Delaware, USA, [2]DBI Bioimaging Center, University of Delaware, USA, [3]Department of Biological Sciences, University of Delaware, USA

Introduction: Osteocytes form an interconnected network through the lacunar-canalicular system (LCS). The LCS structure affects not only how osteocytes perceive external mechanical stimulation via fluid flow (outside-in signaling) but also how signaling molecules move from cell to cell (inside-out signaling). The LCS architecture is recently shown to correlate with tissue mineralization. Due to the large length scales spanning the LCS from the entire bone (~mm) to the canalicular annulus (~100nm), quantifying the LCS structure is challenging and data are lacking. The objective of this study was to quantify the compartment, age, and disease specific LCS variations in wildtype and two disease models (perlecan deficient Schwartz-Jampel Syndrome and Akita type I diabetes), which showed attenuated bone response to *in-vivo* loading and potential alterations in the osteocyte functions.

Methods: Right tibiae from male mice (Table 1) of either C57BL/6J (WT), perlecan deficiency (C1532Yneo), or Akita background with age of 15-32 weeks (N=3 mice/group) were stained in basic fuchsin, and embedded in plastic for confocal examination. Sagittal sections (50 mm thick) of both diaphyseal cortical bone and metaphyseal trabecular bone were imaged using a confocal. Osteocyte LCS architecture of individual lacunae and associated canaliculi was measured from the z-stack images using VOLOCITY and AMIRA software (Fig. 1). Low magnitude (10X) images were used to derive lacuna density. Diaphyseal and metaphyseal segments (~1mm) from the left tibiae were prepared for TEM microscopy. Ultrathin sections (~100nm thick) were post-stained and imaged at 6,300X magnification. LCS ultrastructure was quantified by tracing osteocyte lacunae, cell bodies, canaliculi, and cell processes in Adobe Photoshop (Figs. 2&3) and measured using BoneJ plugin in Image J. Student t-tests were performed for various comparisons with significance set at p<0.05. Results: Compartment and age did not affect the LCS structures significantly in the confocal-based measurements (lacunar size and canalicular/lacunar number density, Table 1) but altered the pericellular gaps between cell body to lacunar and canalicular walls under the TEM (Table 2). Perlecan deficiency and diabetes altered both the confocal and TEM measures of the LCS compared with WT (Tables 1, 2). These LCS anatomical alterations could partially account for the attenuated bone responses to mechanical forces observed in vivo.
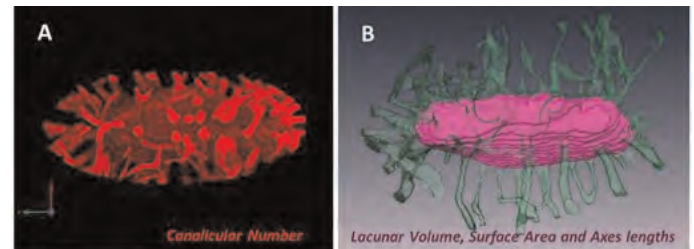

Fig. 1. Representative 3D renderings built from z-stack confocal images of lacunae and associated canaliculi were used to quantify (A) canalicular number in VOLOCITY ®and (B) lacunar volume, surface area and major and minor radii in AMIRA®.

Figure 1
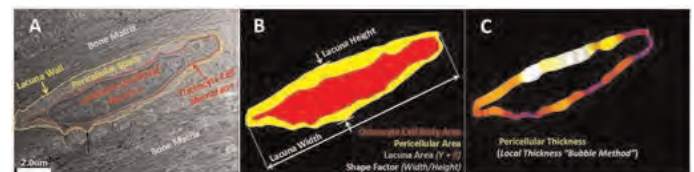
Fig. 2. The ultrastructural measurements of ostecyte lacunae were obtained from TEM images by (A) tracing the lacunar wall and cell body in Photoshop® and (B) thresholding, segmenting, and quantifying the shape of the lacuna (width/height), the cross-sectional areas of lacuna, cell body, and the pericellular annulus in Image J, (C) The mean thickness of the pericellular annular gap was measured using the Bubble method implemented in the BoneJ plug in

Figure 2
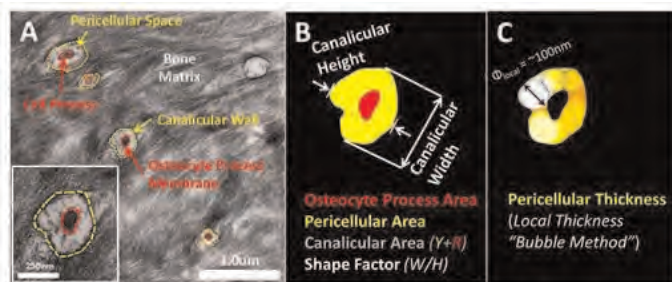
Fig. 3. The ultrastructural measurements of ostecyte canaliculi were obtained from TEM images by (A) tracing the canalicular wall and cell process in Photoshop® and (B) thresholding, segmenting, and quantifying the shape of the canaliculi (width/height), the cross-sectional areas of canalicular wall, cell process, and the pericellular annulus in Image J. (C) The mean thickness of the pericellular annular gap was measured using the Bubble method implemented in the BoneJ plug in. Canaliculi with the shape factor larger than 2.5 were excluded from the analysis to avoid errors from including oblique sections of the canalicular channels.

Figure 3

Table 1

Table 2

Disclosures: Xiaohan Lai, None.

SA0273

Mechanical Loading and High Glucose Modify the Chemokine Secretion Profile of Osteocytes Affecting Osteoclast Differentiation and Activity.

Arancha Gortazar*[1], Maria Teresa Portoles[2], Maria Concepcion Matesanz[2], Javier Linares[2], Maria Jose Feito[2], Daniel Arcos[3], Maria Vallet[4], Lilian Plotkin[5], Pedro Esbrit[6]. [1]Universidad San Pablo-CEU School of Medicine Madrid Spain, Spain, [2]Department of Biochemistry & Molecular Biology I, Faculty of Chemistry, UCM, Spain, [3]Department of Inorganic & Bioinorganic Chemistry, Faculty of Pharmacy, UCM, Instituto de Investigación Sanitaria Hospital 12 de Octubre i+12, Spain, [4]Department of Inorganic & Bioinorganic Chemistry, Faculty of Pharmacy, UCM, Instituto de Investigación Sanitaria Hospital 12 de Octubre i+12, Spain, [5]Indiana University School of Medicine, USA, [6]Instituto de Investigación Sanitaria (IIS)-Fundación Jiménez Díaz, Spain

Osteocytes, the most abundant cell type in bone, are buried in the mineralized bone matrix but regulate bone remodeling by altering osteoblast and osteoclast function. Osteocytes undergo apoptosis and recruit osteoclasts under conditions such as mechanical unloading, fatigue loading, and ovariectomy. Diabetes mellitus induces deleterious effects in bone, although the underlying mechanisms are not completely understood. Here, we aimed to evaluate the influence of high glucose (HG) exposure on the capacity of mechanical stimulation to affect osteoclast migration, differentiation and activity. To this end, MLO-Y4 cells were subjected or not (static control) to mechanical stimulation by fluid flow (FF, 10 dyn/cm^2, 15 min) following pre-treatment with HG or normal glucose for 48 h. Cell medium was changed, cells were cultured for additional 18 h and cell-conditioned medium (CM) was then collected. We first analyzed the secretion of various known chemokines: GM-CSF, IL-6, MCP-1, MIF-1a, MIF-1b, RANTES and VEGF in the CM, by Luminex multiplex assays. Both FF and HG, significantly inhibited chemokine secretion, compared to non-stimulated/static control osteocytes. We next exposed pre-osteoclastic RAW 264.7 cells to osteocyte CM for 14 d (renewing this medium every three days). Cell morphology, proliferation, reactive oxygen species (ROS) content and resorptive activity on hydroxyapatite disks in the presence of RANKL (40 ng/ml) and M-CSF (25 ng/ml) were determined. We found that the CM of static control osteocytes inhibited cell proliferation and ROS production in RAW 264.7 cells, but increased osteoclast differentiation and resorptive activity. Exactly opposite results were obtained when CM of FF stimulated osteocytes was added to RAW 264.7 cells. Interestingly, CM of osteocytes treated with HG, did not affect proliferation and ROS content, although induced the formation of multinucleated but inactive osteoclasts, in both FF and static control conditions. In conclusion, our in vitro findings demonstrate that osteocytes can change their chemokines secretion profile in response to mechanical stimulation and HG to control osteoclast differentiation and activity.

Disclosures: Arancha Gortazar, None.

SA0274

Microdamage and Mechanical Loading Have an Interactive Effect on Remodeling Signals Produced by Osteocyte.

Chao Liu*[1], Xiaoqing Zhang[2], Michael Wu[2], Lidan You[3]. [1]University of Toronto, Canada, [2]University of Toronto, Canada, [3]Mechanical & Industrial Engineering, University of Toronto, Canada

Introduction: Microdamage in bone triggers remodeling with resorption and bone formation along the damage site [1]. Osteocytes are cells distributed throughout the bone. They have been observed to be physically damaged by microdamage [2]. Interestingly, microdamage-induced remodeling requires mechanical loading in vivo [3]. Since osteocytes are the mechanosensors of bone [4], they could react to mechanical loading at the same time to microdamage. We hypothesize that osteocyte damaged by physical trauma similar to microdamage would produce increased levels of remodeling-related molecules; and this response is mechanically regulated.

Methods: Osteocyte Microdamage model: MLO-Y4 cells on glass slides were damaged by tungsten needles (1 µm tip) mounted on a frame with horizontally travel, and adjustment of vertical position (Fig 1). The cell culture was damage to have ~15% dead cells. Cell damage was assessed with Trypan Blue and Live/Dead assay. Fluid shear stress treatment: parallel flow chambers were used to apply fluid shear stress. The flow was oscillatory with sinusoidal profile at frequency of 1 Hz, with peak shear stress of 2 Pa for 1 hr. Gene quantification: Reverse transcription real-time PCR was used to measure IL-6, TNFα, COX-2, RANKL, and OPG mRNA levels, normalized to 18s. Soluble signals: PGE$_2$ and VEGF concentration were measured using EIA and ELISA.

Results: Significant number of dead cells was observed near the damage sites, ranges from 1-10 µm (Fig 2). COX-2 and VEGF mRNA levels increased 24 hrs after cell damage (Fig 3). Other measured mRNA levels was not changed. Concurrent fluid shear stress and physical damage induced higher COX-2 and VEGF mRNA (Fig. 4) and released molecule level (Fig. 5) than the effect from each individual stimulus.

Conclusions: The cell damage system produced osteocytes resembling those exposed to fatigue loading in vivo [5]. Mechanical loading likely supported the targeted bone remodeling to microdamage by enhancing inflammatory and angiogenic gene and protein expression levels in osteocytes. But osteocytes are not responsible for the changes in RANKL, OPG, IL-6, TNF-α that were observed in fatigue damaged bone in vivo [1].

References
1 Kidd, L. J. et al. Bone 46, 369-378 (2010)
2 Hazenberg, J. G. et al., J. Biomech. 39, 2096-2103 (2006)
3 Waldorff, E. I. et al., J. Bone Miner. Res. 25, 734-745
4 You, L., et al. Bone 42(1) 172-179 (2008).
5 Kennedy, O. D., et al., Bone 50 1115-1122 (2012)
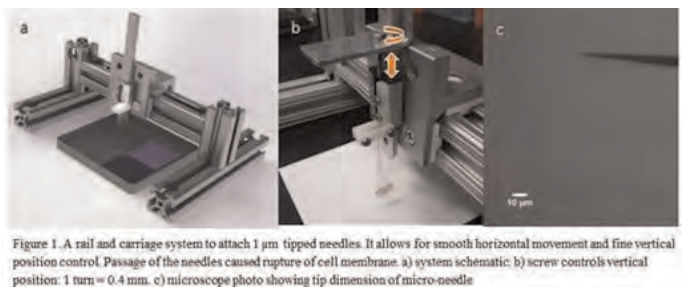
Figure 1. A rail and carriage system to attach 1 µm tipped needles. It allows for smooth horizontal movement and fine vertical position control. Passage of the needles caused rupture of cell membrane. a) system schematic; b) screw controls vertical position: 1 turn = 0.4 mm. c) microscope photo showing tip dimension of micro-needle
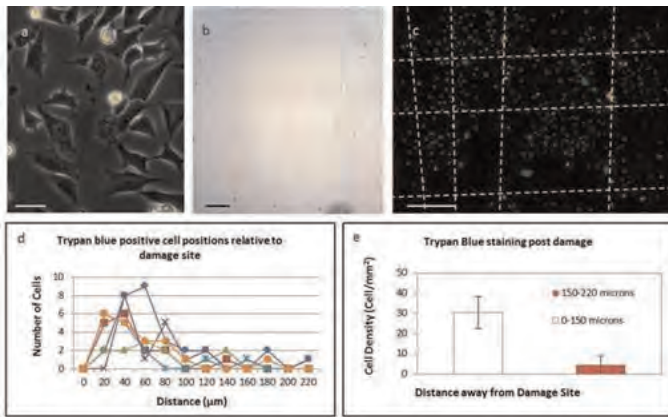
Figure 1.

Figure 2. a) MLO-Y4 cells damaged by the micro needle showing damage to cell body. b) Trypan Blue staining showed uptake of the dye near the damage sites (labeled with lines). c) LIVE/DEAD staining of damaged MLO-Y4 cells was used to quantify the percentage of cells that have sustained damage. Live and dead cells are labeled green and red respectively. d) e)Trypan Blue-positive cell density was quantified vs. distance to closest damage sites. (a bar = 50 µm, b, c bar = 250 µm)
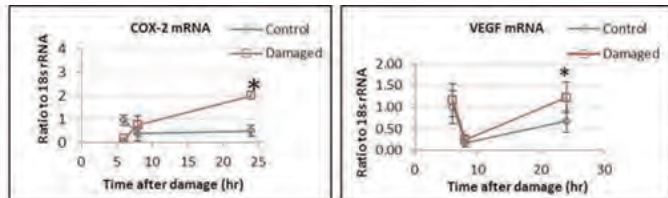
Figure 2.

Figure 3. Time-point response of MLO-Y4 cells to physical damage without fluid shear stress (n = 6). mRNA levels of VEGF and COX-2 are elevated 24 hrs after damage in MLO-Y4 cells.
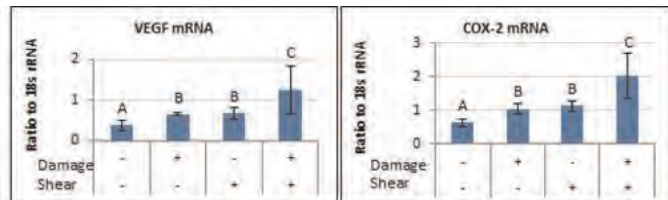
Figure 3.

Figure 4. MLO-Y4 cell response to the combinations of physical damage and fluid shear stress in terms of mRNA expression of VEGF and COX-2 (n = 3). Means that do not share a letter are significantly different.
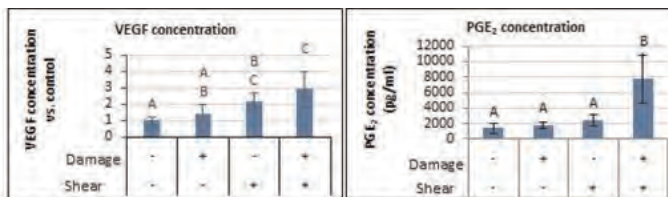
Figure 4.

Figure 5. MLO-Y4 cell response to the combinations of physical damage and fluid shear stress in terms secreted VEGF and PGE₂ 24hr after damage (n = 3). Means that do not share a letter are significantly different.

Figure 5.

Disclosures: Chao Liu, None.

SA0275

See Friday Plenary Number FR0275.

SA0276

See Friday Plenary Number FR0276.

SA0277

See Friday Plenary Number FR0277.

SA0278

The Importance of Activated Vitamin D for the Mineralization by the Osteocyte in Patients with Renal Hyperparathyroidism. <u>Aiji Yajima</u>*[1], <u>Ken Tsuchiya</u>[2], <u>Kosaku Nitta</u>[2], <u>Masaaki Inaba</u>[3], <u>Yoshihiro Tominaga</u>[4], <u>Norio Amizuka</u>[5], <u>Akemi Ito</u>[6], <u>Hironari Shindo</u>[7]. [1]Otsuki Municipal Central Hospital, Japan, [2]Tokyo Women's Medical University, Japan, [3]Osaka City University, Japan, [4]Nagoya Second Red Cross Hospital, Japan, [5]Hokkaido University School of Dentistry, Japan, [6]Ito Bone Histomorphometry Institute, Japan, [7]Otsuki Municipal Central Hospital, Japan

Introduction;

Whether vitamin D is important for the mineralization by the osteocyte or not is controversial. High dose of activated Vitamin D_3 (VD_3) suppresses the mineralization by the osteocyte in the mouse (Lieben L, et al. J Clin Invest 2012). However, activated VD_3 is administered to the patients after parathyroidectomy for renal hyperparathyroidism (PTX) to avoid tetany, leading to an increase of bone mineral density. Low mineralized bone area was evaluated in patients with or without VD_3 after the neck surgery to investigate the importance of VD_3.

Methods;

Fifteen patients (Group I; Age; 56.1 ± 9.3, Duration of Hemodialysis (HD); 13.8 ± 7.3 years) received high doses of 1α-hydroxyvitamin D_3; alfacalcidol (2.0-3.0 µg/day) after PTX and four patients (Group II; Age 56, 63, 67 and 67, Duration of HD, 19, 15, 25 and 15 years, respectively) did not receive VD_3 at all. Iliac bone biopsies were performed before and at 2-4 weeks after PTX in Group I and before and 4 weeks in Group II. Histomorphometric parameters were as follows; osteoclast surface (Oc.S/BS;%), Osteoblast surface (Ob.S/BS;%), osteoid volume (OV/BV;%), fibrous volume (Fb.V/TV;%) bone formation rate (BFR/BS; mm²/mm³/years) and low mineralized bone volume (LMV/BV;%). BFR/BS was measured only after PTX.

Results;

Group I; Oc.S/BS decreased from 4.9 ± 3.8 to 0.1 ± 0.6 (P<0.001), OV/BV increased from 10.8 ± 7.9 to 19.9 ± 8.8 (P=0.002), Fb.V/TV decreased from 6.1 ± 4.8 to 0.4 ± 1.4 (P<0.001) and LMV decreased from 10.3 ± 6.4 to 2.5 ± 1.8,but Ob.S/BS didn't change. BFR/BS (0.011 ± 0.009) was lower as compared with the normal value after PTX, meaning the development of low turnover osteomalacia.

Group II; Oc.S/BS and Fb.V/TV decreased and OV/BV increased in all patients, and Ob.S/BS didn't. In addition, BFR/BS was also lower in all patients in Group II. However, LMV/BV increased from 10.4 to 16.0 in Patient 1, 4.4 to 16.4 in Patient 2, 7.7 to 9.1 in Patient 3 and 1.4 to 15.9 in Patient 4 in this Group.

Conclusion; Bone formation rate was lower, meaning that mineralization by osteoblast decreased after PTX in both Groups although VD_3 was administered. By the way, the ability of mineralization by the osteocyte was surprisingly activated in patients receiving VD_3 because mineralization deficiency by the osteocyte leads to increased low mineralized bone volume. Therefore, VD_3 should be very important for the mineralization by the osteocyte, but not osteoblast in human being with renal insufficiency.

Disclosures: Aiji Yajima, None.

SA0279

Identification of miRNAs Involved in the Differentiation Process from Osteoblasts to Osteocytes. <u>Laura De Ugarte Corbalán</u>*[1], <u>Nicholas H. Farina</u>[2], <u>Matt Prideaux</u>[3], <u>Gary Stein</u>[4], <u>Jane Lian</u>[5], <u>Lynda Bonewald</u>[6]. [1]University of Missouri, Kansas City, USA, [2]University of Vermont College of Medicine, USA, [3]University of Adelaide, Australia, [4]University of VermontCollege of Medicine, USA, [5]University of Vermont College of Medicine, USA, [6]University of Missouri - Kansas City, USA

Bone formation and osteoblast differentiation are now appreciated to be regulated by miRNAs which support the coordination of many key signaling pathways essential for the onset of osteogenesis and for maintaining bone mass. However little is known about the molecular regulation of osteoblast to osteocyte differentiation. To begin to understand the role of miRNAs in this process, we performed miRNA array analyses of the different stages of IDG-SW3 cells from late osteoblast to early osteocyte to mature osteocyte. Total RNA was extracted at 0, 3, 7, 14, 21 and 28 days of culture to perform miRNA qPCR based global expression profiling arrays (Fluidigm). QC, PCA and hierarchical clustering were performed to verify biological replicates and a threshold was set at ≥2 fold change for comparison of expression levels. From 133 detected miRNA, 39 were significant to p<0.05, while 17 miRNAs were highly significant (p < 0.01). Included in 10 upregulated miRNAs (p<0.01), was miR-146b-5p, known to be elevated during osteogenic differentiation of muscle derived progenitor cells (Oishi et al, PLOS, 2014). Among the 7 downregulated miRNAs (p<0.01), miR-351-5p was identified, known to promote myogenesis (Chen et al, Physiol Gen, 2012). Multiple miRNAs were validated by the SYBR Green qPCR approach using primary osteoblasts and osteocytes isolated from 2 mo old murine long bones which replicated the results observed with the osteoblastic stage of IDG-SW3 cells (days 3-7) and late osteocyte stage IDG-SW3 cells (days 21-28). The DAVID v6.7 database was used to identify enriched KEGG pathways involved with

the genes predicted to be targeted by the 17 (significantly up or down regulated miRNAs) between day 0 and day 28. Pathways with established functions in osteoblast to osteocyte differentiation, such as Wnt signaling, were predicted targets of these miRNAs. In addition, several previously uncharacterized biological pathways potentially relevant to osteocyte cell structure, such axon guidance, were revealed. We propose that osteocytes have a unique subset of miRNAs consistent with their known properties, as well as revealing potentially novel activities.

Disclosures: Laura De Ugarte Corbalán, None.

SA0280

Morphological analysis of Dentin Matrix Protein 1 (DMP1) phosphorylation by Fam20C in the bone. <u>Kaori Oya</u>*[1], <u>Sunao Sato</u>[2], <u>Satoru Toyosawa</u>[3]. [1]Osaka University Dental Hospital, Japan, [2]Osaka University Graduate School of Dentistry, Japan, [3]Osaka University, Japan

[Background]: DMP1 is one of the acidic phosphoproteins that are specifically expressed in osteocytes. DMP1 has abundant acidic domains, which are negatively charged at physiological pH. It also contains a large number of phosphorylation sites, and these regions become another highly negative-charged domain after phosphorylation. The highly phosphorylated, negative-charged DMP1 may play an important role in the bone mineralization by recruiting calcium ion and subsequent mineral deposition. Most recently, it has been reported that Fam20C was expressed in the bone tissue and phosphorylated DMP1 in vitro. In this study, to clarify in situ phosphorylation event of DMP1 by Fam20C in the bone, we verified the localization of phosphorylated DMP1 and Fam20C in the rat bone by immunohistochemical methods.[Materials and methods]: Wistar rats (days 28 of postnatal life) were used in this study. Tibiae were fixed with 4% paraformaldehyde in PBS and then demineralized in buffered 10% EDTA and embedded in paraffin. Serial sections of 4-μm thickness were cut and they were used for immunostaining or double immunofluorescence staining. Phosphorylated DMP1 was estimated by overlapping immunostainings of DMP1 and phosphoserine.

[Results and Discussion]: We described the localization of each protein according to osteocyte classification (osteoblastic-, osteoid-, young-, old-OCs) as previously reported. Double immunofluorescence staining with DMP1 and phosphoserine showed that osteoblastic- and osteoid-OCs had an accumulation of DMP1 without phosphorylation in the Golgi area. On the other hand, young-OCs had phosphorylated DMP1 in intracytoplasmic Golgi area and perilacunar and pericanalicular mineralized bone matrix. Further, old-OCs had phosphorylated DMP1 in perilacunar and pericanalicular mineralized bone matrix, but had no immunoreaction of DMP1 and phosphoserine in intracytoplasmic area. Fam20C (Golgi kinase) was highly expressed in osteoid- and young-OCs and it was colocalized with DMP1 in their Golgi apparatus. These findings suggest that DMP1 begins to be phosphorylated in the Golgi apparatus of osteoid-OCs and phosphorylated DMP1 is secreted into extracellular matrix by young-OCs.

Disclosures: Kaori Oya, None.

SA0281

See Friday Plenary Number FR0281.

SA0282

See Friday Plenary Number FR0282.

SA0283

See Friday Plenary Number FR0283.

SA0284

See Friday Plenary Number FR0284.

SA0285

See Friday Plenary Number FR0285.

SA0286

See Friday Plenary Number FR0286.

SA0287

Bone Microstructure Analysis in Men by HR-pQCT: Associations with Age, Body Mass Index, and Androgens. <u>Narihiro Okazaki</u>*[1], <u>Andrew Burghardt</u>[1], <u>Ko Chiba</u>[2], <u>Makoto Osaki</u>[3], <u>Sharmila Majumdar</u>[1]. [1]University of California, San Francisco, USA, [2]Nagasaki University School of Medicine, Japan, [3]Nagasaki University, Japan

Objective: Male osteoporosis has been recognized as a major clinical problem because the number of men with osteoporosis is increasing as the elderly population increases. In addition, men with hip fractures have significantly higher morbidity and mortality rates compared to women. High-resolution peripheral quantitative computed tomography (HR-pQCT) allows high-resolution bone microstructure analysis in vivo for peripheral skeletal sites. The aim of this study was to investigate the relationship between bone microstructure measured by HR-pQCT and age, body mass index (BMI), and serum androgen levels which are considered as primary risk factors of male osteoporosis.

Methods: Subjects included 49 healthy males (mean age 60.1 ± 7.1, range 50-78 years). The distal radius and distal tibia were scanned using HR-pQCT with an isotropic voxel size of 82μm. The following bone microstructure parameters were measured: bone volume fraction (BV/TV), trabecular thickness (Tb.Th), trabecular number (Tb.N), trabecular separation (Tb.Sp), trabecular bone mineral density (Tb.BMD), cortical thickness (Ct.Th), cortical porosity (Ct.Po), cortical pore diameter (Po.Dm), and cortical bone mineral density (Ct.BMD). The relationships between the bone microstructure parameters and age, BMI, serum calcium, vitamin D, and testosterone were analyzed.

Results: In distal tibia, age had significant positive correlations with Ct.Po, Po.Dm, and had a significant negative correlation with Ct.BMD. In distal radius, age had a significant positive correlation with Ct.Po. However, age did not have a relationship with trabecular bone parameters. In addition, BMI, serum calcium, vitamin D, and testosterone were not correlated with either trabecular or cortical bone parameters.

Conclusion: Cortical bone microstructure, but not trabecular bone, changed significantly with aging, especially at the tibia - a weight bearing site. However, no relationship between BMI or testosterone and bone microstructure was observed.

Disclosures: Narihiro Okazaki, None.

SA0288

See Friday Plenary Number FR0288.

SA0289

See Friday Plenary Number FR0289.

SA0290

See Friday Plenary Number FR0290.

SA0291

See Friday Plenary Number FR0291.

SA0292

Osteoporotic women with clinical vertebral fractures have lower trabecular bone scores than controls matched by lumbar spine T-scores and age. <u>Albrecht Popp</u>*[1], <u>Nadshathra Varathan</u>[2], <u>Helene Buffat</u>[3], <u>Christoph Röder</u>[4], <u>Didier Hans</u>[5], <u>Kurt Lippuner</u>[1]. [1]Department of Osteoporosis, University Hospital & University of Berne, Switzerland, [2]Department of Osteoporosis, University Hospital & University of Berne, Switzerland, [3]Department of Osteoporosis, University Hospital & University of Berne, Switzerland, [4]Institute for Evaluative Research in Orthopaedic Surgery, University of Berne, Switzerland, [5]Lausanne University Hospital, Switzerland

Introduction:

The Trabecular Bone Score (TBS) is a grey-level texture measurement reflecting bone micro-architecture (MA) based on the quantification of the variogram from a given lumbar spine scan by dual energy X-ray absorptiometry (DXA). TBS has proven predictive value on fracture risk, partially independent of clinical risk factors and bone mineral density (BMD). The aim of this study is to evaluate its impact on clinical vertebral fracture risk in women with osteoporosis.

Methods:

Consecutive women who underwent vertebroplasty after clinical vertebral fracture(s) (cases) at the University Hospital of Berne, Switzerland, were compared with lumbar spine T-score and age matched, osteoporotic women without prevalent

clinical vertebral fracture (controls). Exclusion criteria were BMI <15 or >35 kg/m^{2} for all women, any non-osteoporotic metabolic bone disease, traumatic or malignant origin of the vertebral fracture for the cases and prevalent morphometric severe vertebral fractures in the control group. Lumbar spine (with at least two assessable vertebrae) and hip BMD were assessed by DXA (Hologic™, USA) and remained blinded for MA evaluation by TBS (Medimaps™, France). From initially 281 cases and 720 controls, 136 women of each group remained after matching for lumbar spine T-scores and age. Finally, seventeen women were pairwise excluded due to missing data. Mann-Whitney U-test was applied to compare differences between the groups (SPSS™).

Results:

The characteristics of the patients are given below:

Conclusion:

In this nested case-control study, osteoporotic women with clinical vertebral fractures had lower trabecular bone scores than controls matched by lumbar spine T-scores and age.

	Cases n=119	Controls n=119	p
Age (years)	70.9±8.5	70.1±7.9	0.363
BMI (kg/m2)	24.7±3.7	22.8±3.7	<0.001
LS T-score (SD)	-2.96±0.7	-2.97±0.7	0.969
Neck T-score (SD)	-2.28±0.8	-2.17±0.8	0.315
TBS	1.156±0.100	1.201±0.107	0.001

Clin VFx_table.png

Disclosures: Albrecht Popp, None.

SA0293

Age-Related Changes in Lumbar Spine Trabecular Bone Score in Chinese-American Men. <u>Barbara Silva</u>*[1], <u>Rajeev Babbar</u>[2], <u>George Liu</u>[2], <u>Chiyuan Zhang</u>[3], <u>Donald McMahon</u>[4], <u>Wen-Wei Fan</u>[5], <u>Didier Hans</u>[6], <u>John Bilezikian</u>[4], <u>Marcella Walker</u>[3]. [1]Federal University of Minas Gerais, Brazil, Brazil, [2]Weill Cornell Medical college, NYP Lower Manhattan Hospital, USA, [3]Columbia University, USA, [4]Columbia University College of Physicians & Surgeons, USA, [5]Columbia University Medical Center, USA, [6]Lausanne University Hospital, Switzerland

Trabecular bone score (TBS) is an indirect index of trabecular microarchitecture that can be derived from the lumbar spine (LS) DXA image. LS TBS is associated with vertebral and non-vertebral fractures in postmenopausal women and men. While TBS is readily available from LS DXA images through the application of specific software, normal TBS values across age, gender and race remain to be defined. It has been shown that Chinese-Americans (CH) women and men have lower areal bone density (aBMD) but similar or lower fracture rates than their Caucasian counterparts. More favorable bone microarchitecture has been observed in CH, which helps to explain their lower risk of fracture. TBS could be a useful adjunct to aBMD as determined by DXA for assessing fracture risk in this population. To this end, we investigated age- related changes in LS TBS and relationships between testosterone and TBS in a cohort of CH men.

We enrolled CH men of full Chinese descent, aged 20 to 90 years, with current residence in the US. Subjects who had sustained a hip fracture or those with conditions or medications known to affect bone metabolism were excluded. Additionally, we excluded individuals with BMI < 15 or > 35 kg/m². DXA of LS and hip sites (Hologic) as well as demographic, medical, and familial data were obtained. Serum total testosterone and 25OHD levels were measured. Site-matched LS TBS was extracted from the DXA image using TBS iNsight software (version 1.8).

We studied 341 CH men, mean age 56.1 $\pm$ 16.2 years, and mean BMI 24.3 $\pm$ 3.0 kg/m² (range 16.9- 34.7 kg/m²). Mean duration of residence in the US was 18.1 $\pm$ 12.0 years. Serum testosterone levels were normal (466 $\pm$ 176 ng/dL); mean 25OHD serum concentration was 26.5 $\pm$ 8.6 ng/mL. The mean LS TBS in the entire population was 1.387 $\pm$ 0.084, and ranged from 1.073 to 1.586. TBS was weakly associated with testosterone levels (r= 0.140; p=0.01). As expected, there was a negative correlation between TBS and age (r= -0.344; p<0.0001). Figure 1 shows mean BMD and LS TBS values for each 10-year age group.

LS TBS, which reflects bone microarchitectural texture, decreases with advancing age and testosterone levels in CH men. The changes observed in TBS are similar to age-related changes in BMD at the hip, but not the LS. While further research is needed to establish the association between TBS and fracture risk in CH men, TBS may aid in the clinical evaluation of bone microarchitectural deterioration in CH men.

Figure 1: Mean (±SD) lumbar spine trabecular bone score (LS TBS) and BMD at the LS, total hip (TH) and femoral neck (FN) for each 10-year age group:
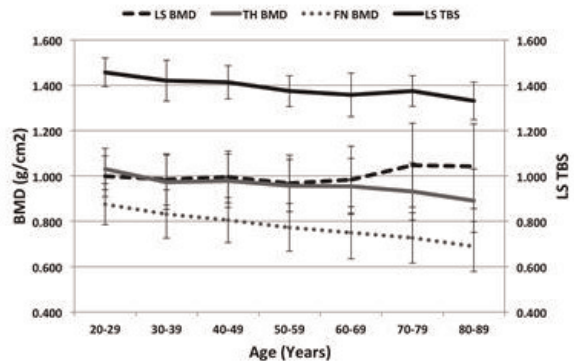
Figure 1

Disclosures: Barbara Silva, None.

SA0294

See Friday Plenary Number FR0294.

SA0295

Unusual Cause of Increased Lumbar Bone Mineral Density - Case Report. <u>Miro Cokolic</u>*[1], <u>Matej Rakusa</u>[2]. [1]medical doctor, Slovenia, [2], Slovenia

A 78 - year old female with known osteoporosis was reassessed for bone mineral density (BMD) measurement in december 2013. She was treated with calcium supplements, cholecalciferol 7000 IE per week and bisphosphonate. Her baseline BMD and T-score of lumbar spine (L1-L4), measured 9 years before were 0.699 g/cm2, -3.5 SD and Echinococcal cyst wasn't seen. The treatment was successful and the BMD was stable. On last control dual x-ray absorptiometry scan (DXA) of lumbar spine and hip, BMD of total lumbar spine was 0.910 g/cm2, T-score was -1.2 SD. BMD and T-scores for each lumbar vertebrae were: L1 1.384 g/cm2, +4.2 SD; L2 0.667 g/cm2, -3.3 SD; L3 0.654 g/cm2, -3.9 SD; L4 0.785 g/cm2, -3.0 SD. The BMD and T-score of the neck were 0.463 g/cm2, -3.5 SD and of the total hip were 0.590 g/cm2, -2.9 SD. On examining of the picture, we identified a calcified mass in the projection of L1 vertebra. We repeated the analysis of DXA scan and excluded the calcified formation and L1 vertebra. BMD of analyzed lumbar spine (L2-L4) was 0.701 g/cm2, T-score was -3.4 SD. BMD and T-scores were: L2 0.614 g/cm2, -3.8 SD; L3 0.642 g/cm2, -4.0 SD; L4 0.785 g/cm2, -3.0 SD.

We checked her previous examinations. Eleven months before she had CT of abdomen because of suspected gastric carcinoma. Three centimeters large calcified Echinococcal cyst was found, which was previously unnoticed. On the last DXA scan echinococcal cyst was probably projected to the L1 vertebra because of developement of kyphosis and consequently reduction of height.

Discussion

Artifacts can interfere with BMD measurements. The study showed that bra wires and calcium carbonate pills positioned lateral to the spine can change BMD. Several medical conditions, such as osteophyte formation, osteoarthritis, ankylosing spondylitis, vertebral fractions, aortic calcifications, can also increase BMD. However after examining the literature on Pubmed, to our knowledge there was no cases of falsely increased BMD of lumbar spine because of calcified Echinococcal cyst.

Disclosures: Miro Cokolic, None.

SA0296

Volumetric Bone Mineral Content changes assessed by 3D-DXA after two years of Alendronate Treatment. <u>Luis Del Rio</u>*[1], <u>Silvana Di Gregorio</u>[2], <u>Ludovic Humbert</u>[3], <u>Yves Martelli</u>[4]. [1]Cetir Centre Medical, Spain, [2]MD, Spain, [3]PhD, Spain, [4]Eng, Spain

3D-DXA is a new application that provides a 3D reconstruction of the proximal femur from a 2D DXA standard acquisition of the hip. This reconstruction method is based on a statistical model incorporating both the femoral shape and the 3D BMD distribution. A 3D personalized model is acquired by registering the statistical model onto the 2D DXA image of the patient so that the projection of the model matches the DXA image.

Objective: Measuring the bone mineral content changes in trabecular and cortical regions in patients after a 24-months treatment with alendronate.

Method: A group of 27 women with osteoporosis were included in this study. All the patients had alendronate treatment during two years. None of the patients had calcium or Vit D supplementation.

3D-DXA reconstruction was performed from images taken at baseline and 24-month follow-up visit. Bone changes were measured at the proximal femur region (excluding the femoral head). Bone mineral content (BMC) was measured in the cortical and trabecular bone in each 3D-DXA volumetric reconstruction. T-test was used to assess the differences between analyses at baseline and follow-up scans.

Results: We measured a 4.60% increase of proximal femur BMC (trabecular + cortical) (p=00001). The most significant change was observed in the trabecular region (increase of 5.53%, p=0.001). An increase of 2.9% was measured at the cortical bone (p=0.052).Conclusion: This method presents a high potential for clinical routine use, by providing 3D patient-specific reconstructions from a standard DXA acquisition and allowing for the assessment of the individual response to antifracture therapy.

Disclosures: Luis Del Rio, *None.*

SA0297

Assessing Age, Sex, and Racial Differences in Cortical Porosity Requires Adjustment for Site-Specific Variation in the Selected Region of Interest. <u>Ali Ghasem-Zadeh</u>*[1], <u>Andrew Burghardt</u>[2], <u>Afrodite Zendeli</u>[3], <u>Serena Bonaretti</u>[2], <u>Ashild Bjornerem</u>[4], <u>Xiao-Fang Wang</u>[5], <u>Yohann Bala</u>[6], <u>Galateia Kazakia</u>[2], <u>Roger Zebaze</u>[7], <u>Ego Seeman</u>[1]. [1]Austin Health, University of Melbourne, Australia, [2]University of California, San Francisco, USA, [3]Endocrine Centre, Austin Health, University of Melbourne, Australia, Australia, [4]UiT The Arctic University of Norway, Norway, [5]University of Melbourne, Austin Health, Australia, [6]University of Melbourne, Dept. of Medicine, Australia, [7]Austin Health, University of Melbourne, Australia

High-resolution peripheral quantitative computed tomography (HR-pQCT) measures micro-architecture in a region of interest (ROI) at the distal radius and tibia. Bone width and micro-architecture vary slice by slice along the length of a bone so differences in micro-architecture by age, pubertal stage, sex and racial group may be the result of differences in the placement of the ROI rather than the characteristics of the subjects.

To assess the slice-by-slice variation in cortical porosity of radius, 18 radii scanned as standard ROI and extended to 9.02 mm distally and 18.04 mm proximally(440 slices).We used Strax 1.0 software to assess slice by slice of total cortex, compact cortex, and transitional zone porosity for whole 440 slices.

We found 1 mm replacing ROI distally, in comparison with standard ROI, produce 2.02, 3.49, and 0.61% increment on the measured porosity of total cortex, compact cortex and transitional zone, respectively, however replacing 1 mm proximally produce 2.8, 4.8, and 0.50% reduction.

We infer that a more distal ROI has a significant effect on cortical porosity measurement particularly compact cortex porosity which may result in erroneous age, sex and racial differences being reported. This variation needs to be considered when interpreting data in persons who differ in bone length.

Key words cortical porosity, bone structural variability, micro-architecture
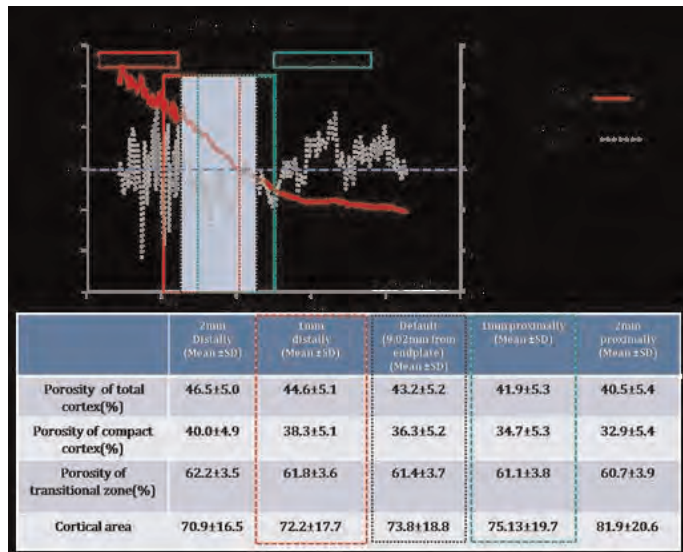
ID A14012945- Ali Ghasem-Zadeh asbmr2014

Disclosures: Ali Ghasem-Zadeh, *None.*

SA0298

Assessing the performances of the Trabecular Bone Score (TBS) on EOS[TM] images for the discrimination of osteoporotic fractures. <u>Karine Briot</u>*[1], <u>Anabela Darbon</u>[2], <u>Adrien Etcheto</u>[3], <u>Renaud Winzenrieth</u>[4], <u>Sami Kolta</u>[5], <u>Franck Michelet</u>[6], <u>Nor-Eddine Regnard</u>[7], <u>Antoine Feydy</u>[8], <u>Christian Roux</u>[9]. [1]Paris Descartes University, Cochin hospital, Rheumatology Hospital, France, [2]EOS imaging, R&D, Paris, France, France, [3]Hopital Cochin, France, [4]Med-imaps, Hôpital X. Arnozan, PTIB, Pessac, France, France, [5]Centre D'Evaluation, Des Maladies Osseuses, France, [6]Med-Imaps, Plateforme Technologique d'Innovation Biomédicale (PTIB), France, [7]EOS imaging, R&D, Paris, France, France, [8]Université Paris Descartes,. Service de Radiologie, Hôpital Cochin. INSERM U 1153, France, [9]Hospital Cochin, France

Introduction
The EOS[TM] X-ray imaging system allows full body frontal and lateral scans to be acquired simultaneously in the upright position, at low dose (~125 µSv). The trabecular bone score (TBS) was shown to relate to the bone architecture and fracture risk, using DXA imaging. A new prototype version of TBS has been developed for the EOS[TM] system. The aim of this study was to assess the discriminative value of the TBS measured on EOS[TM] images (TBS_{EOS}) for osteoporotic fractures.
Methods
We conducted a case-control study to assess the diagnostic value of TBS_{EOS} on a sample of patients aged $\geq$ 50 years, receiving no antiosteoporotic treatment. The sample consisted of 26 patients with severe osteoporotic fractures (11 vertebrae, 10 humeri, 2 hip and 3 proximal tibia fractures) and 51 patients without fracture. The TBS was computed on full-body EOS[TM] images, focusing on the lumbar spine region, blinded from clinical parameters. The patients were also scanned with a DXA bone densitometer (Hologic) and the Spine, Total hip and Femoral neck areal BMD (aBMD) were computed. Association of the TBS_{EOS} and aBMD (in g.cm^{-2}) with the fractures was assessed using ROC curves analysis (AUCs).
Results
Patients with fractures were significantly older than patients without fractures (mean age 68.5 vs 64.4 years, p=0.04) and had similar mean BMI (23.6 vs 22.6 kg/m^2, p=0.19). Prevalence of osteoporosis was similar in fracture and non-fracture groups (68 % vs 78.4%, p=0.97). aBMD measurements were also similar at lumbar spine (0.78 vs 0.79, p=0.92), total femur (0.73 vs 0.71, p=0.26) and femoral neck (0.60 vs 0.61, p=0.75). TBS_{EOS} values were significantly lower in fractured patients compared to non-fractured patients (0.646 vs 0.734, p=0.03). TBS_{EOS} was associated with the presence of fractures as reported by a significant AUC of 0.665.
Conclusion
This case-control study, based on a prototype version of the TBS_{EOS}, demonstrated the feasibility of TBS on low-dose EOS[TM] imaging devices. Results show that the TBS_{EOS} was successful in discriminating patients with osteoporotic fractures from controls independently of aBMD.

Disclosures: Karine Briot, *None.*

SA0299

See Friday Plenary Number FR0299.

SA0300

Concordance in Paired QCT and DXA at the Lumbar Spine. <u>Gabriel Bodeen</u>[1], <u>Alan Brett</u>*[2], <u>Perry Pickhardt</u>[3]. [1]Mindways Software, USA, [2]Mindways Software, Inc., USA, [3]University of Wisconsin, USA

Purpose: Quantitative CT (QCT) of the lumbar spine is used for diagnosis of osteoporosis and osteopoenia. The upper thresholds for these classifications are bone mineral densities (BMD) of 80 and 120 mg/cc, respectively, according to guidelines of the American College of Radiology (ACR). World Health Organization (WHO) standards for interpretation of DXA use T-Scores of -2.5 and -1 as thresholds for the same classifications. A study by Cann indicated that these QCT thresholds lead to the same rates of osteoporosis and osteopoenia in the population as the WHO thresholds. We investigated whether paired DXA and QCT measurements have similar thresholds as rate-based studies.
Methods: DXA and CT imaging of 58 subjects was completed at vertebrae L1 and L2, for 116 total vertebrae. Subject ages ranged from 49 to 86 years (mean 59 $\pm$ 8.7 SD). In each case, the time between DXA and CT imaging was less than 10 months (mean 72 days $\pm$ 57 SD). DXA imaging and analysis was done on a Lunar Prodigy (GE, Madison, WI). CT was collected on a LightSpeed Ultra and LightSpeed 16 (GE) and analyzed using asynchronous calibration data with QCT Pro (Mindways Software, Austin, TX). QCT T-Scores were calculated by linearly transforming the BMD thresholds to match the WHO thresholds.
Results: Equal rates for QCT and DXA occur in this cohort below BMD thresholds of 90 mg/cc for osteoporosis and 125 mg/cc for osteopoenia. (BMD estimates have been rounded to the nearest 5 mg/cc.) Concordance of classification at these thresholds by weighted Cohen's κ is κ=0.54. Maximum concordance is κ=0.58 and occurs nearest 75 – 130 mg/cc; the figure shows this as a scatterplot of QCT versus DXA T-Scores. Green curves at left and bottom show the projected distribution envelopes of the QCT and DXA, respectively. Horizontal and vertical red lines at -2.5

(solid) and -1 T-Scores (dashed) show regions with matched or unmatched classification. The cyan line is the line of best fit by Deming regression, which is equivalent to thresholds 75 – 120 mg/cc; a dotted black line is shown at unity for comparison.

Conclusions: For this cohort, concordance-based thresholds differ markedly from rate-based thresholds at the osteoporosis threshold, but they overlap at the osteopoenia threshold. The one-sided difference is explained by the variances around the best-fit line and the higher skewness of the DXA in this cohort (0.45 versus 0.13 for QCT). Concordance-based thresholds in this paired study support the ACR guidelines.
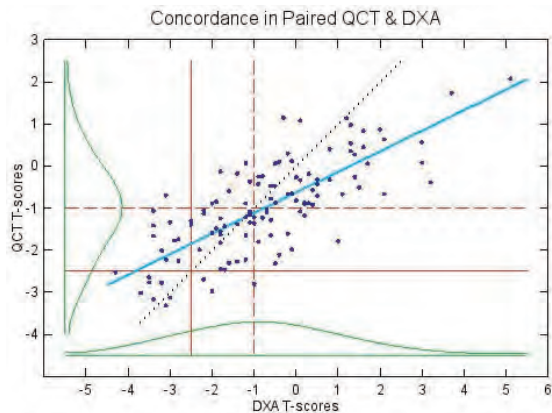
QCT_DXA_concordance

SA0301

See Friday Plenary Number FR0301.

SA0302

Osteoporosis treatment decision based on combining Bindex® and FRAX®.

Janne Karjalainen*[1], Ossi Riekkinen[2], Juha Töyräs[3], Jukka Jurvelin[3], Heikki Kroger[4]. [1]Bone Index Finland Ltd., Finland, [2]Bone Index Finland, Ltd., Finland, [3]University of Eastern Finland, Finland, [4]Kuopio University Hospital, Finland

According to National Osteoporosis Foundation (NOF) guidelines[1], treatment is recommended for osteoporotic patients and patients with osteopenia and high fracture probability (FRAX® with BMD over 3% for hip and/or over 20% for other fractures). In this study, a pocket size pulse-echo (PE) ultrasound (US) device, Bindex® and FRAX® with BMI is used in treatment pathway analysis and compared to NOF guidelines.

Elderly Caucasian woman (n = 427, age = 69 $\pm$ 9 years) under osteoporosis suspicion were examined using Bindex® device. Bindex® reports a diagnostic parameter, Density index, DI[2]. Previously, the 90% sensitivity and specificity thresholds for DI were determined along ISCD and NOS guidelines[3,4] in diagnostics of osteoporosis (the triage approach). By using these thresholds, subjects were classified as healthy (green), osteoporotic (red) or in need of DXA examination to verify diagnosis (yellow). Further, bone mineral density of the femoral neck and total hip were determined with axial DXA. Osteoporosis was diagnosed in individuals with T-score lower than -2,5 at the total hip or femoral neck. In addition, FRAX® scores with BMD (FRAX$_{BMD}$) and with BMI (FRAX$_{BMI}$) were determined.

A total of 173 subjects (73 osteoporotic) were selected to be treated along NOF guidelines. FRAX$_{BMI}$ was analyzed for patients with DI value in yellow or green area. Subjects with red DI value and yellow DI value with FRAX$_{BMI}$ over 3%/20% were selected to be treated. The subjects with yellow or green DI value and FRAX under 3%/20% were considered healthy. Only the subjects with green DI value and FRAX$_{BMI}$ over 3%/20% were selected for additional DXA measurement. In the proposed diagnostic pathway, the sensitivity and specificity of treatment decisions compared to NOS guideline were 94% and 80%, respectively. Only 23% of the patients were found to require additional DXA measurement to verify the treatment decision. The present results demonstrate that the ultra-portable US instrument with FRAX$_{BMI}$ shows strong agreement (86%) with treatment decisions using NOF guidelines. In addition, by using the triage approach and the pocket size technology with no ionizing radiation the treatment of OP would significantly increase.

[1] National Osteoporosis Foundation, Clinician's Guide, 2014, [2] Karjalainen, Osteoporos Int., 2012, [3] Hans, J Clin Densitom., 2008, [4] Patel, NOS practical guide, 2011.

SA0303

Performance Characteristics of Heel Quantitative Ultrasound (QUS) for the Assessment of Fracture Risk; an Individual-level Meta-analysis.

Nicholas Harvey*[1], Helena Johansson[2], Anders Oden[3], Douglas Bauer[4], Claus-C Glueer[5], Didier Hans[6], Stephen Kaptoge[7], Marc-Antoine Krieg[8], Timothy Kwok[9], Fernando Marin[10], Alireza Moayyeri[11], Terry O'Neill[12], Eric Orwoll[13], John Kanis[14], Eugene McCloskey[15]. [1]MRC Lifecourse Epidemiology Unit, University of Southampton, United Kingdom, [2]Centre for Metabolic Bone Diseases, University of Sheffield Medical School, Sweden, [3]Consulting Statistician, Sweden, [4]University of California, San Francisco, USA, [5]Christian Albrechts Universitaet zu Kiel, Germany, [6]Lausanne University Hospital, Switzerland, [7]University of Cambridge Bone Research Group, United Kingdom, [8]University Hospital, Switzerland, [9]The Chinese University of Hong Kong, Hong Kong, [10]Eli Lilly & Company, Spain, [11]King's College London, United Kingdom, [12]University of Manchester, United Kingdom, [13]Oregon Health & Science University, USA, [14]University of Sheffield, Belgium, [15]University of Sheffield, United Kingdom

Quantitative ultrasound (QUS) has an established role in screening for osteoporosis and/or assessing fracture risk. The aim of this meta-analysis was to undertake a more detailed examination of the relationships between QUS parameters and the risk of fracture using individual-level data.

In 9 prospective cohorts from Asia, Europe and North America, broadband ultrasonic attenuation (BUA dB/Mhz) and speed of sound (SOS m/sec) were measured at baseline in men and women subsequently followed for incident fractures. The latter were documented by self-report and in some cohorts confirmed by radiography. Measurements of femoral neck BMD were also available in a subset of individuals. Values of QUS and BMD were converted to z-scores within each cohort. An extension of Poisson regression was used to examine the relationship between fracture risk and BUA or SOS adjusted for age and time since baseline in each cohort. The results were merged and weighted according to the variance.

Baseline measurements of QUS were available in 46,124 men and women, mean age 70 years and 3018 osteoporotic fractures (including 787 hip fractures) occurred during a total follow up of 214,000 person-years. The summary gradient of risk (GR, hazard ratio per 1 SD) was 1.4 (95% CI: 1.4-1.5) for osteoporotic fracture for both BUA and SOS. For hip fracture the GR was 1.7 (95% CI: 1.6-1.8) for BUA and 1.6 (95% CI: 1.5-1.7) for SOS. The predictive value of QUS was the same for all ages (p>0.20) and across genders (p≥0.1) and remained significant following adjustment for BMD. However the GR was significantly higher for both fracture outcomes the lower the baseline BUA and SOS (p<0.001); for example, when BUA was below a z-score of 0, the GR was 2.0 (95% CI 1.8, 2.3) but above 0 it was 1.2 (95% CI 1.0-1.4). For the outcome of osteoporotic fracture, but not hip fracture, the predictive value of QUS (both BUA and SOS) decreased with time since baseline (p=0.018 and p=0.010, respectively). Results were similar in the subset (n-19,473) with concurrent BMD measurements; the GR for BMD for osteoporotic and hip fractures remained stable with time since baseline.

Quantitative ultrasound is an independent predictor of fracture for men and women particularly at low QUS values, but the predictive value for osteoporotic fracture risk decreases with time from baseline. These observations should be taken into account if incorporating QUS into fracture risk algorithms.

SA0304

Prediction of fracture risk by trabecular bone score (TBS).

Tuan Nguyen*[1], Didier Hans[2], Jacqueline Center[1], John Eisman[1]. [1]Garvan Institute of Medical Research, Australia, [2]Lausanne University Hospital, Switzerland

TBS is bone texture index that reflects bone microarchitecture. The present study sought to determine the association between TBS and fracture, and to define its prognostic value in terms of fracture prediction in the elderly.

The study was designed as a population based prospective cohort of 1688 women aged 60 years and above. The women were recruited between 1989 and 1993. Baseline anthropometric and demographic characteristics were ascertained at baseline by a structured questionnaire. BMD at the femoral neck and lumbar spine was measured by DXA (GE-LUNAR Corp, Madison, WI). TBS was analyzed blindly from clinical outcome by TBS iNsight® software v1.9 (Medimaps SASU, Pessac, France). Low trauma and non-pathological fractures were ascertained from X-ray reports during the follow-up (from study entry till 31/12/2013).

During the follow-up period, 418 women had sustained a fragility fracture. Women with fracture were significantly older, had lower femoral BMD and lower TBS than those without a fracture. Each standard deviation lower TBS (0.12) was associated with a 67% increase in the odds of fracture (odds ratio [OR] 1.67; 95%CI 1.43-1.96). However, TBS was correlated with femoral neck BMD (r = 0.38, P < 0.001) and age (r = -0.18; P < 0.001). After adjusting for FNBMD and age, the association between TBS and fracture risk was weaker but remained statistically significant (OR 1.37 (95%CI 1.15-1.64). Further adjustment for covariates, which we have shown to predict fracture risk, i.e. fall, quadriceps strength and prior fracture) did not significantly alter the result. Among women without osteoporosis, i.e. no

BMD in the osteoporotic range, lower TBS was also significantly associated with increased risk of fracture (OR 1.72; 95%CI 1.43-2.17) independent of femoral neck BMD. The proportion of variance in fracture risk that could be attributed to variation in TBS was ~4%.

These results suggest that lower TBS is associated with an increase in fracture risk, and that TBS could improve the accuracy of fracture prediction over and above that of femoral neck BMD and other recognised risk factors.

Disclosures: Tuan Nguyen, None.

SA0305

Trabecular bone score improves prediction accuracy of FRAX® for major osteoporotic fractures in elderly Japanese men: The Fujiwara-kyo Osteoporosis Risk in Men (FORMEN) Cohort Study. Masayuki Iki*[1], Yuki Fujita[2], Junko Tamaki[3], Yuho Sato[4], Renaud Winzenrieth[5], Katsuyasu Kouda[6], Akiko Yura[6], Jong Seong Moon[7], Nozomi Okamoto[8], Norio Kurumatani[8]. [1]Kinki University Faculty of Medicine, Japan, [2]Kinki University Faculty of Medicine, Japan, [3]Department of Hygiene & Public Health, Osaka Medical College, Japan, [4]Jin-ai University, Japan, [5]Med-Imaps, France, [6]Department of Public Health, Kinki University Faculty of Medicine, Japan, [7]Kio University, Japan, [8]Department of Community Health & Epidemiology, Nara Medical University School of Medicine, Japan

Aims: To evaluate whether trabecular bone score (TBS) improves the prediction accuracy achieved by FRAX® for major osteoporotic fractures (MOFx) in elderly Japanese men.

Methods: 2012 community-dwelling men aged 65 years and older completed the baseline study of the Fujiwara-kyo Osteoporosis Risk in Men (FORMEN) Cohort Study comprising areal bone mineral density (aBMD) measurements at the spine and hip (QDR4500A, Hologic, USA), height and weight measurements, and interviews covering clinical risk factors required to estimate 10-year absolute risk of MOFx (hip, spine, distal forearm and proximal humerus) by the Japanese version of FRAX® (v.3.8). The risk from FRAX® was adjusted to each participant's duration of follow-up. TBS was calculated at baseline in the same vertebrae for aBMD using TBS iNsight software (Med-Imaps, France). Incident MOFx during the follow-up were identified by interviews or supplemental mail and telephone surveys. Prediction accuracy improvement of the logistic model incorporating TBS plus the fracture risk from FRAX® in comparison with FRAX® alone model was evaluated by integrated discrimination improvement (IDI) and net reclassification improvement (NRI) in addition to the area under receiver operating characteristic curve (AUC).

Results: We identified 20 incident MOFx (2.5/1000 person-years (PY)) during total follow-up of 7986 PY (median follow-up, 4.5 years) for 1868 men (mean age, 73.0 ± 5.1 years at baseline). Participants with the MOFx had significantly lower femoral neck aBMD (0.681 ± 0.124 vs 0.740 ± 0.114, p=0.0182) and TBS (1.137 ± 0.089 vs 1.193 ± 0.083, p=0.0024) and higher risk of MOFx estimated by FRAX® ($3.0 \times \div 1.6\%$ vs $2.4 \times \div 1.7\%$), p=0.0407) than those without. Observed MOFx risk increased significantly with the increase in expected risk by FRAX® (p<0.0001). The numbers of observed MOFx in tertile groups of participants classified by the expected risk were smaller than the numbers of MOFx expected, but the difference was not significant (p=0.0918). AUC of FRAX® plus TBS model (0.699) for prediction of MOFx was not significantly different from AUC of FRAX® alone (0.671). However, NRI showed a significant increase in classification accuracy of FRAX® plus TBS model compared with FRAX® alone, (NRI: 47.4%, (95% confidence interval (CI): 4.2, 90.5)), and IDI showed a more modest but similar result (IDI: 0.003 (95% CI: 0.000, 0.012).

Conclusions: TBS improved prediction accuracy of FRAX® for MOFx in community-dwelling elderly Japanese men.

Disclosures: Masayuki Iki, None.

SA0306

Trabecular bone score predicts fracture incidence in non-osteoporotic older Chinese men, independently of hip Bone Density. Timothy Kwok*. Hong Kong

Kwok T, Leung J, Aubry-Rozier A, Hans D
Department of Medicine & Therapeutics, the Chinese University of Hong Kong
Jockey Club Centre for osteoporosis care and control, the Chinese University of Hong Kong
Department of Bone and Joint, Center of Bone diseases, Lausanne University Hospital, Lausanne, Switzerland
Email: Berengere.Aubry@chuv.ch and didier.hans@ascendys.ch

Background

Trabecular bone score (TBS) based on secondary analysis of pixel gray-level variations in DXA images of the lumbar spine is an indirect novel surrogate marker of global bone microarchitecture. There are cross sectional and prospective data to suggest that TBS is independently associated with fracture. There is however a lack of prospective data to confirm its role in fracture prediction in Chinese population and whether such role remains in non-osteoporotic subjects.

Subject and method

2000 men and 2000 women aged 65 years or more were recruited in 2001-3 for predictors of osteoporotic fractures. At baseline, comprehensive health assessment was performed. Bone mineral density (BMD) of hip and spine was measured by Hologic dual energy X ray absorptiometry. All subjects were followed up for an average of ten years for incidence of fractures primarily by electronic medical record system of the public hospitals in Hong Kong. Cox regression was performed to examine the association between baseline TBS scores (as assessed by TBS iNsight, Medimaps SA) and the incidence of major osteoporotic fractures over ten years. Femoral neck BMD was used as covariate. The subjects with osteoporosis as defined by T-score $\leq$ -2.5 at either hip or spine were excluded from analysis.

Result

1665 men and 1071 women had BMD within the normal and osteopenia range at baseline. Out of these, 91 men and 91 women had major osteoporotic fractures over ten years. Out of these 41 men and 19 women had hip fractures. Cox regression after adjustment for hip BMD and age showed that TBS score was significantly associated with major osteoporotic fracture in older men, but not in women (p=0.025 and 0.112 in men and women respectively). In contrast, TBS predicted hip fracture in older women but not in older men (p=0.048 and 0.393 respectively). Similar results were obtained when FRAX score was used as covariate.

Conclusion

TBS of lumbar spine was predictive of major osteoporotic fracture in older Chinese men without osteoporosis independently of clinical risk factors and hip BMD. The role of TBS in predicting osteoporotic fractures in non-osteoporotic older women requires a larger study.

Disclosures: Timothy Kwok, None.

SA0307

Unexpected Distinct Fall of Dental Alveolar Bone Density Measured by Computerized Microradiography (Bone Right) in Response to Teriparatide in Contrast to Its Bisphosphonate-Induced Rise. Yoshitomo Takaishi*[1], Takuo Fujita[2], Mutsumi Ohue[3], Tsuyoshi Jotoku[4], Yoshio Fujii[5], Akimitsu Miyauchi[6], Yasuyuki Takagi[7]. [1]Takaishi Dental Clinic, Japan, [2]Katsuragi Hospital, Japan, [3]Katsuragi Hospital, Japan, [4]Department of Orthopedic Surgery, Japan, [5]Calcium Research Institute Kobe Branch, Japan, [6]Miyauchi Medical Center, Japan, [7]National Hyogo Chuo Hospital, Japan

Background: Osteoporosis and periodontal disease, both quite prevalent in aging, appear to be closely related. Low values in computerized microdensitometry (Bone Right) was useful in predicting osteoporotic fracture (Takaishi et al., Adv Ther 2013), whereas very high values were pointed out around the lesions of osteonecrosis of the jaw (Takaishi et al 2010).

Methods: From among postmenopausal women attending Osteoporosis and Osteoarthritis Clinic of Katsuragi Hospital, 16 osteoporotic subjects consenting to participate the study were randomly divided into 2 groups, T and B. In Group T, 56? teriparatide (TP) was injected once a week and alendronate or minodronate (BP) was administered in Group B. Alverolar bone density (alBMD) was measured by computerized microdensitometry and lumbar bone mineral density (LBMD) and femoral neck bone mineral density (FNBMD) by DXA(Prodigy: GE Healthcare) before and after the treatment.

Results: In Group B, alBMD increased by $21.3 \pm 17.9\%$ (Mean $\pm$ SD). In group T, in contrast, it decreased by $18.9 \pm 20.9\%$ with a highly significant difference between the 2 Groups (p=0.0011). LBMD($+2.6 \pm 4.9\%$ and $-0.4 \pm 6.3\%$, p=0.3018) and FNBMD($+4.4 \pm 5.5\%$ and $+4.1 \pm 5.3\%$, p=0.9087) failed to change significantly in response to BP and TP.

The Responses of alBMD to BP and TP were significantly different from those of LBMD and FNBMD in both B (p=0.0213 for LBMD and p=0.0331 for FNBMD) and T Groups (p=0.0428 and p=0.0170) indicating exaggerated responses of alBMD to therapeutic agents compared to those of LBMD and FNBMD.Conclusion: Bisphosphonate increases alBMD more effectively than LBMD and FNBMD. Teriparatide, on the contrary, distinctly decrease alBMD, but not LBMD and FNBMD. In view of the very high alBMD around the lesion of BRONJ, this may explain the therapeutic effect of teriparatide on osteonecrosis of the jaw.

Disclosures: Yoshitomo Takaishi, None.

SA0308

A large-scale whole genome sequence-based analysis discovered novel genetic variants influencing bone mineral density: Results from the GEFOS and UK10K Consortia. Hou-Feng Zheng*[1], Vince Forgetta[2], Yi-Hsiang Hsu[3], Karol Estrada[4], Paul Leo[5], Jonathan Tobias[6], Charles Kooperberg[7], Ching-Ti Liu[8], Alberto Rosello-Diez[9], Daniel Evans[10], Carrie Nielson[11], Ulrika Pettersson-Kymmer[12], Joel Eriksson[13], Tony Kwan[14], Klaudia Walter[15], Yasin Memari[15], Shane McCarthy[15], Josine Min[6], Jie Huang[15], Petr Danecek[15], Beth Wilmot[16], Rui Li[2], Wen-Chi Chou[17], Lauren Mokry[2], Alireza Moayyeri[18], Melina Claussnitzer[19], Chia-Ho Cheng[20], Warren Cheung[16], Carolina Medina-Gomez[21], Bing Ge[2], Shu-Huang Chen[14], Kwangbom Choi[22], Ling Oei[23], James Fraser[2], Robert Kraaij[24], Matthew Hibbs[22], Celia Gregson[25], Denis Paquette[2], Albert Hofman[24], Carl Wibom[26], Mhairi Marshall[5], Brooke Gardiner[27], Paul Auer[28], Li Hsu[7], Sue Ring[29], Nathalie van der Velde[24], Beatrice Melin[26], John Kemp[5], Adrian Sayers[6], Yanhua Zhou[30], Sophie Calderari[31], Matthew Maurano[32], Jeroen van Rooij[24], Chris Carlson[7], Ulrike Peters[7], Soizik Berlivet[2], Josée Dostie[2], Claes Ohlsson[33], Andre Uitterlinden[34], David Goltzman[1], Tomi Pastinen[2], Elin Grundberg[14], Dominique Gauguier[31], Eric Orwoll[11], David Karasik[35], Chitra Dahia[36], George Davey-Smith[6], Nicholas Timpson[6], Nicole Soranzo[15], Richard Durbin[37], Scott Wilson[38], Matthew Brown[39], Tim Spector[18], L Adrienne Cupples[8], Celia Greenwood[2], Cynthia Loomis[40], Cheryl Ackert-Bicknell[41], Alexandra Joyner[42], Rebecca Jackson[43], Emma Duncan[44], David Evans[5], Fernando Rivadeneira[45], Douglas Kiel[17], Brent Richards[1]. [1]McGill University, Canada, [2]McGill University, Canada, [3]Hebrew SeniorLife Institute for Aging Research & Harvard Medical School, USA, [4]Analytic & Translational Genetics Unit, Massachusetts General Hospital, USA, [5]University of Queensland Diamantina Institute, Australia, [6]University of Bristol, United Kingdom, [7]Fred Hutchinson Cancer Research Center, USA, [8]Boston University School of Public Health, USA, [9]Sloan-Kettering Institute, USA, [10]California Pacific Medical Center, USA, [11]Oregon Health & Science University, USA, [12]Clinical Pharmacology, Sweden, [13]Centre for Bone & Arthritis Research, Sweden, [14]McGill University & Genome Quebec Innovation Centre, Canada, [15]Wellcome Trust Sanger Institute, United Kingdom, [16]Oregon Health & Science University, USA, [17]Hebrew SeniorLife, USA, [18]King's College London, United Kingdom, [19]Hebrew SeniorLife, Institute for Aging Research & Harvard Medical School, USA, [20]Hebrew SeniorLife, USA, [21]Erasmus Medical Center, The Netherlands, [22]The Jackson Laboratory, USA, [23]Erasmus University Medical Center, The Netherlands, [24]Erasmus Medical Center, Netherlands, [25]University of Bristol, United Kingdom, [26]Umeå University, Sweden, [27]niversity of Queensland Diamantina Institute, Australia, [28]University of Wisconsin, USA, [29]niversity of Bristol, United Kingdom, [30]Boston University, USA, [31]Cordeliers Research Centre, France, [32]University of Washington, USA, [33]Center for Bone & Arthritis Research at the Sahlgrenska Academy, Sweden, [34]Erasmus Medical Center, Canada, [35]Hebrew SeniorLife; Bar Ilan University, USA, [36]Hospital for Special Surgery, USA, [37]Wellcome Trust Sanger Institute, United Kingdom, [38]University of Western Australia, Australia, [39]Diamantina Institute of Cancer, Immunology & Metabolic Medicine, Australia, [40]New York University School of Medicine, USA, [41]University of Rochester, USA, [42]Sloan-Kettering Institute, USA, [43]The Ohio State University, USA, [44]Royal Brisbane & Women's Hospital, Australia, [45]Erasmus University Medical Center, The Netherlands

Previous studies have identified common genetic variants associated with BMD; whether low-frequency (minor allele frequency [MAF] between 1-5%) or rare (MAF ≤1%) variants influence BMD in the general population has not been established. Here we aim to identify novel low-frequency and rare genetic variants influencing BMD variation in 13 population-based cohorts of European ancestry. Through a large-scale meta-analysis of these cohorts (Ntotal=31,508), using whole-genome sequencing data from the UK10K consortium (N=2,868), whole-exome sequencing (N=2,320) and deep imputation (N=26,320) of rare variants using a combined UK10K/1000Genomes reference panel from GEFOS consortium, we identified a novel low-frequency variant with large effect size near EN1, mapping to 2q14.2, (MAF=1.7%, effect size= +0.24 standard deviations [SD], P=4.1 x 10-9). Variants at this locus overlapped a DNase1 hypersensitivity site (DHS) in osteoblasts which resides in a topological domain that includes EN1. We detected En1 expression during osteoblastogenesis in developing and mature cultured murine calvarial osteoblasts, Next, we analysed the bones of En1lacZ/+ knock-in mice and detected En1 positive cells in adult vertebrae and long bones which co-localized with alkaline phosphatase activity, confirming expression of this gene in situ. We generated conditional En1Cre/flox mutants (n= 3) and demonstrated that mutants have higher trabecular number, higher tissue mineral density. We also identified a novel rare variant with large effect for forearm BMD mapping to 7q31.31 (MAF=0.9%, effect size= -0.47 SD, P=9.3 x 10-9) and demonstrated that this variant overlaps a DHS that appears to mark an enhancer of WNT16. We tested these newly identified variants for their effect on any type of fracture risk in a large dataset (Ncases=10,459, Ncontrols=27,581, 76.2% of these samples overlap the BMD samples). Finally, In addition to rare and low-frequency described above, we also identified common variants but across known BMD loci, including 3 genome-wide significant loci for forearm BMD, 14 for lumbar spine, 17 for femoral neck. These findings provide an example for gene-discovery through a sequencing-based approach with subsequent imputation to identify low-frequency and rare variants scrutinized for the first time for association with BMD in a large–scale setting.

Disclosures: Hou-Feng Zheng, None.

SA0309

See Friday Plenary Number FR0309.

SA0310

See Friday Plenary Number FR0310.

SA0311

Correlates of Heel Bone Mass in Young Adults: The Role of Cholesterol Over 20 Years from Childhood to Early Adulthood. Benny Samuel Eathakkattu Antony*[1], Changhai Ding[2], Alison Venn[2], Terence Dwyer[3], Graeme Jones[4]. [1]Menzies Research Institute Tasmania, University of Tasmania, Australia, Australia, [2]Menzies Research Institute Tasmania, University of Tasmania, Australia, Australia, [3]Murdoch Childrens Research Institute, Australia, [4]Menzies Research Institute, Australia

Purpose: The association between lipids and bone mass in adult life is controversial and there is limited evidence in childhood. The aim of this study was to describe the association between lipids measured in childhood and young adult life and bone mineral density (BMD) in younger adults.

Methods: Subjects broadly representative of the Australian population (n=1431, female=52%, age=26-36) were selected from the Australian Schools Health and Fitness Survey of 1985. They underwent various measurements including leg strength, standing long jump, and physical work capacity (PWC$_{170}$). Physical activity, smoking and alcohol history were recorded using questionnaires. Fasting lipid profiles were assessed in childhood and 20 years later in adulthood. A single Sahara bone ultrasound densitometer was used to determine heel bone mass in adulthood.

Results: In multivariable analysis, childhood High Density Lipoprotein (HDL) was positively (β: 0.056 g/cm^2, 95% CI: 0.005, 0.108) and total cholesterol (TCH, β: -0.042 g/cm^2, 95% CI: -0.081, -0.003) and Low Density Lipoprotein (LDL, β: -0.019 g/cm^2, 95% CI: -0.039, 0.000) were negatively associated with BMD in adulthood. Similarly, adulthood TCH (β: -0.007 g/cm^2, 95% CI: -0.015, -0.001) and LDL (β: -0.011 g/cm^2, 95% CI: -0.019, -0.003) were negatively associated with adult life BMD. Subjects who remained in the abnormal category of TCH from childhood to adulthood had the least bone mass compared to other category changes.

These results were independent of gender, alcohol consumption and duration of follow-up from childhood to adulthood. The other potential confounders included in this analysis were age (negatively associated with BMD, β: -3.58 mg/cm^2 per year, 95% CI: -6.14, -1.01), smoking (β: -18.34 mg/cm^2, 95% CI: -27.35, -9.34), physical activity (vigorous activity, β: 0.04 mg/cm^2 per min/week, 95% CI: 0.01, 0.08) and BMI in childhood and adulthood (both positively associated with BMD). BMD were positively associated with PWC$_{170}$, leg muscle strength and long jump.

Conclusions: HDL in childhood was beneficially and high TCH was detrimentally associated with adulthood BMD. LDL and TCH in adulthood were detrimentally associated with BMD. These associations were independent of the potential confounders including physical activity. The effect of childhood HDL was independent of the adulthood HDL levels. These results indicate that cholesterol may have long-term effects on bone mass from childhood to adulthood.
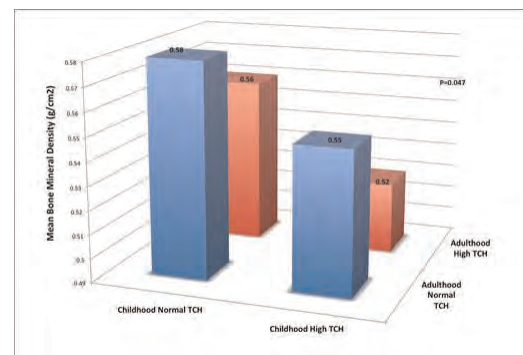
Mean BMD of subjects classified by their change in TCH levels from childhood to adulthood

Disclosures: Benny Samuel Eathakkattu Antony, None.

SA0312

See Friday Plenary Number FR0312.

SA0313

No Association Between BMD and Telomere Length in Healthy Women aged 25-93 Years. Barbara Rubek Nielsen*[1], Peter Schwarz[2], Allan Linneberg[3], Kaare Christensen[4]. [1]Research Centre of Ageing & Osteoporosis, Department of Medicine, Copenhagen University Hospital, Glostrup, Denmark, Denmark, [2]Research Centre of Ageing & Osteoporosis, Department of Medicine, Faculty of Health Sciences, University of Copenhagen, Copenhagen, Denmark, Denmark, [3]Research Centre for Prevention & Health, Capital Region of Denmark, Glostrup, Denmark, Denmark, [4]Danish Aging Research Center, University of Southern Denmark, Denmark

Introduction: Telomere length and bone mineral density (BMD) are considered phenotypes of ageing since both declines with age. Further, both are affected by inflammatory processes.

The aim of our study, of 460 healthy randomly selected women, was to assess the association between BMD and telomere length.

Method: BMD was evaluated by DXA at the lumbar spine and both hips. Telomere length was analyzed by qPCR, which is a quantitative measurement, where relative average telomere length is proportional to a T/S-ratio. We analysed DNA samples on two separate days (duplicates) and samples were run in triplicates.

Results: We found the association between telomere length and chronological age highly significant estimated by linear regression and correlation (P< 0.0001). For the regression analysis the covariates hormone therapy, menopause, physical activity during leisure time, smoking and alcohol habits and HbgA₁C were evaluated and showed no influence. R^2 of the linear model was 0.050, and the regression coefficient back transformed estimated that T/S were shortened 0.45% for every year in the range of 0.27%-0.64%.

By multiple regression analysis, the association between BMD and chronological age was estimated at the femoral neck, total hip and at the lumbar spine. For hip measurements, age was highly associated to BMD (P< 0.0001) whereas we found no association at lumbar spine. All analyzes were adjusted for BMI, menopause, physical activity as well as alcohol and smoking habits.

The association between BMD and telomere length was estimated by linear regression and showed only significance at left femoral neck. The association was further explored in a series of regression models successively adjusted for age, BMI, menopause, leisure time physical activity level and smoking and alcohol habits.

At all hip sites age and BMI were highly significant covariates, but at lumbar spine only BMI was highly significant (P<0.0001). Further, physical activity and menopause were at most sites significant covariates.

Conclusion: The prerequisites – that age is associated with telomere length and BMD – were met (except at the lumbar spine). We found no significant association between BMD and telomere length, but regression coefficients for all hip sites showed a positive trend.

Disclosures: Barbara Rubek Nielsen, None.

SA0314

Determinants of bone outcomes in obese and normal-weight young adults. Heli Viljakainen*[1], Helena Valta[2], Marita Lipsanen-Nyman[3], Tero Saukkonen[4], Eero Kajantie[5], Sture Andersson[3], Outi Makitie[6]. [1]University of Helsinki, Finland, [2]Hospital for Children & Adolescents, University of Helsinki, Helsinki Finland, Finland, [3]Children's Hospital, Helsinki University Central Hospital, University of Helsinki, Finland, [4]Novo Nordisk Pharma Oy, Finland, [5]National Institute for Health & Welfare, Diabetes Prevention Unit, Finland, [6]Children's Hospital, Helsinki University Central Hospital, Finland

Background: In children obesity associates with higher areal BMD yet leads to increased risk for peripheral fractures. We aimed to determine the contribution of lifestyle factors for bone outcomes in obese young adults and in normal-weight matched controls.

Methods: The study included 68 obese subjects with early-onset severe obesity and 73 normal-weight controls. History on physical activity (PA), data on dietary pattern, smoking and alcohol consumption were collected with a questionnaire. A food-based healthy eating index (HEI) was constituted based on nutrition recommendations. Bone characteristics were measured with DXA from central and with pQCT from peripheral sites; body composition was analyzed by DXA.

Results: The obese and control subjects were similar in age (mean 19.6 ± 2.6 yrs) and height but BMIs differed (39.7 and 22.6 kg/m²). Obese subjects reported a shorter time (median 31-70% shorter) of total and supervised PA during primary and secondary school and currently than controls (p<0.01). Obese subjects were more likely to smoke (34% vs 14%), had lower HEI (27 and 31 of the maximum value 50; p=0.007) but similar alcohol consumption. All crude bone outcomes were higher in obese subjects. Body composition differed between groups (p<0.001). Lean mass (LM) and trunk fat mass (FM) were independent determinants for bone outcomes. Interestingly, together with sex and height, these explained a smaller part of the variation in bone outcomes in obese subjects than in controls: adjusted r² were on 0.6

times smaller. Relative to LM bone outcomes were similar between the groups, while relative to LM + trunk FM all bone outcomes were 30% lower in the obese. In linear regression, lifestyle factors associated more likely with bone outcomes in the controls than in the obese subjects. In the obese, only the amount of supervised PA (ln transformed) during secondary school associated with cortical thickness in tibia and hip BMD: 0.299 (95% CI: 0.103;0.495) and 0.145 (-0.043;0.33). In the controls, total PA during secondary school and currently, HEI and alcohol consumption contributed to the bone outcomes.

Conclusions: Early-onset obesity is accompanied by unhealthy lifestyles. Supervised PA during secondary school associated with bone outcomes in obese subjects, while in controls determinants included also current PA, HEI and alcohol consumption. As lifestyle explains a smaller part of the variation of bone outcomes in obese subjects than in controls, the role of endocrine factors for bone health in obesity remains to be investigated.

Disclosures: Heli Viljakainen, None.

SA0315

Vitamin D status in Young Adults is associated with gender, educational level and living. Rune Tønnesen*. Center of ageing & osteoporosis, Denmark

Background & Purpose: Vitamin D status might influence the risk of osteoporosis later in life. The level of circulating vitamin D was tested in healthy young adults.Characterize 25-hydroxyvitamin D [vitamin D] status in young adults (18-25 y/o) and examine if it's associated with gender, education and living.

Material & Methods: We present data from a cross sectional study from winter period (from 15th October to 15th April) examining vitamin D, education (the education the participant studies), gender, living among 18 to 25 years old students attending their educational institutions in the Copenhagen area. Education was grouped in four categories according to type of education and length of education after primary school; Vocational and trade school 2-3 years [VTS], Gymnasium 3 years [G], College level 4-6 years [CoL], College or University 7-9 years [CoU].

Results: 536 students participated; 261 females and 277 males. Female students had a 20.4%higher vitamin D status (p=0.0001), 95% CI[9.6%, 32.1%] than male students. Students living at their own had a 15.9% higher vitamin D (p=0.0073), 95% CI[4.1%, 29.1%] compared to students living at their parents home. Students studying at CoL had a Vitamin D status that was 32.2% (p=0.0014) 95% CI [11.4%, 56.8%] higher than students studying at VTS. Students studying at CoU had a Vitamin D status that was 23.9% (p=0.0021) 95% CI [8.1%, 41.9%] higher than students studying at VTS.

Conclusion: The Vitamin D level in young adults is associated with educational level, gender and living. In order to focus campaigns for increasing the vitamin D level in the population, strategies ought toconsider the differencesof the recipients, most of all gender, living situation and educational level.
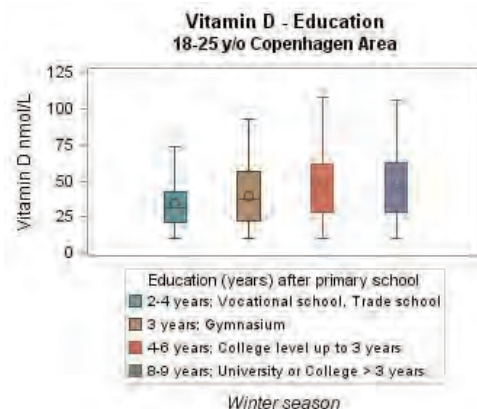
Vitamin D status & Educational level

Disclosures: Rune Tønnesen, None.

SA0316

See Friday Plenary Number FR0316.

SA0317

See Friday Plenary Number FR0317.

SA0318

See Friday Plenary Number FR0318.

SA0319

Dose Trabecular Bone Score (TBS) Improve the Predictive Ability of FRAX® ? : The Japanese Population-based Osteoporosis (JPOS) Cohort Study. Junko Tamaki*[1], Masayuki Iki[2], Yuho Sato[3], Renaud Winzenrieth[4], Etsuko Kajita[5], Sadanobu Kagamimori Kagamimori[6], Yoshiko Kagawa[7], Hideo Yoneshima[8]. [1]Department of Hygiene & Public Health, Osaka Medical College, Japan, [2]Kinki University Faculty of Medicine, Japan, [3]Department of Domestic Sciences, Jin-ai University, Japan, [4]Center of Bone diseases, Lausanne University Hospital, Lausanne, Switzerland, France, [5]Department of Public Health & Home Nursing, Nagoya University School of Health Sciences, Japan, [6]University of Toyama, Japan, [7]Kagawa Nutrition University, Japan, [8]Shuuwa General Hospital, Japan

Objectives: The aim was to investigate whether or not trabecular bone score (TBS) improves the predictive ability of FRAX® for osteoporotic fractures in Japanese women.

Methods: Participants were 1541 women aged 40 years or older without medications for osteoporosis at the baseline survey in 1996. A major osteoporotic fracture defined as a clinical fracture of the hip, vertebra, distal forearm, or proximal humerus that occurred without strong external force during the 10-year follow-up period were ascertained in the follow-up surveys or mail questionnaires in the JPOS Cohort Study. TBS at the baseline survey was calculated at the first to fourth vertebrae. The goodness-of-fit of models to data was compared between logistic models incorporating absolute fracture risk from FRAX® alone and the fracture risk from FRAX® and TBS by using integrated discrimination improvement (IDI) and net reclassification improvement (NRI) in addition to area under receiver operating characteristic curve (AUC) and Akaike's information criterion (AIC).

Results: The major osteoporotic fracture events (N=67) were ascertained during the median follow-up time of 10.0 years (total person-years, 15306 PY). The incidence rates of the major osteoporotic and hip fracture events were 4.38 women/1000PY and 0.72 women /1000PY, respectively. The women with major osteoporotic fractures had significantly lower TBS than those with no fractures (1.122 ± 0.098 vs. 1.187 ± 0.117, p<0.001). The AUC of a model incorporating fracture risk from FRAX® and TBS combined for major osteoporotic fractures prediction was not significantly greater than the AUC of FRAX® alone. According to AIC, a model incorporating fracture risk from FRAX® using femoral neck (FN) BMD and TBS [adjusted odds ratio; FRAX®, 1.35 (95%CI, 1.09-1.67); TBS, 1.46 (95%CI, 1.08-1.98)] afforded significantly better fit to the data than did a model obtained FRAX® using FN BMD alone. The NRI values showed a significant increase of about 30% in prediction accuracy for major osteoporotic fractures achieved by the FRAX® and TBS model compared with FRAX® alone, although the IDI showed no significant increase. Neither IDI nor NRI showed significant increase in prediction accuracy for hip fracture achieved by the FRAX® and TBS model compared with FRAX®.

Conclusions:TBS might improve risk classification for major osteoporotic fractures using FRAX® among Japanese women.

Disclosures: Junko Tamaki, None.

SA0320

See Friday Plenary Number FR0320.

SA0321

FRAX (Aus) as a predictor of falls risk in men. Kara Holloway*[1], Mark Kotowicz[2], Stephen Lane[3], Sharon Brennan[4], Julie Pasco[4]. [1]Barwon Health, Australia, [2]Deakin University School of Medicine, Australia, [3]Barwon Health Biostatistics Unit, Australia, [4]Deakin University, Australia

Purpose: The FRAX score utilises clinical risk factors to estimate the probability of sustaining a fracture over a 10-year period. Although falls increase the risk for fracture they are not incorporated into the FRAX. The aim of our study was to investigate if the 10-year probability of fracture determined by use of the Australian-specific FRAX is associated with falls risk in a cohort study of Australian men.

Methods: Clinical risk factors were documented for 469 men (age 40-90 years) assessed at the 5-year follow-up (2006-2010) of the Geelong Osteoporosis Study (GOS). The probability of osteoporotic fracture was calculated using the FRAX (Aus) tool that included femoral neck BMD. Self-reported incident falls were documented from questionnaires returned approximately one year later (median time of follow-up 13 months, IQR 12-14). Two multivariable analyses were performed: (i) the cross-sectional association between the FRAX scores and a falls risk score (Elderly Falls Screening Test, EFST[1]) using a linear regression model and (ii) the prospective relationship between the FRAX score and the time to a fall, using a Cox proportional hazards model.

Results: EFST scores were correlated with FRAX scores (= 0.03, p<0.003); however, after adjusting the EFST scores for age, the relationship was not significant (= 0.00, p=0.77). Among 469 men, 82 (17%) had fallen during the previous 12 months and 78 (17%) reported at least one incident fall during follow-up. The risk of incident falls increased with increasing FRAX score (HR for one percentage point increase in FRAX = 1.06, 95% CI 1.02, 1.09). However, after adjusting for age, the relationship between FRAX score and incident falls risk was not significant (HR = 1.02, 95% CI 0.97, 1.07).

Conclusion: The positive association between the FRAX scores and falls found in both the cross-sectional analysis with EFST and the time-to-event hazard function of incident falls was explained by increasing age. These data provide insufficient evidence for excluding falls from fracture risk assessment.

1 Cwikel, J., et al., *Disability and rehabilitation*, 1998. 20(5): p. 161-167.

Disclosures: Kara Holloway, None.

SA0322

Glucocorticoid Exposure and Fracture Risk in a Large Cohort of Commercially-Insured Rheumatoid Arthritis Patients Under Age 65. Akhila Balasubramanian*[1], Sally Wade[2], Robert Adler[3], Celia Lin[4], Michael Maricic[5], Cynthia O'Malley[6], Kenneth Saag[7], Jeffrey Curtis[7]. [1]Amgen Inc., USA, [2]Wade Outcomes Research & Consulting, USA, [3]McGuire VA Medical Center, USA, [4]Amgen, USA, [5]Catalina Pointe Rheumatology, USA, [6]Amgen, Inc, USA, [7]University of Alabama at Birmingham, USA

Systemic glucocorticoids (GCs) use can increase fracture risk, although dose-specific effects are incompletely understood, especially in younger adults. Underlying diseases (e.g., rheumatoid arthritis [RA]) can confound these associations. This study evaluated the impact of GC exposure on risk of fragility fracture (FF) in RA patients.

The 42,034 study patients identified in the MarketScan® claims database were newly treated for RA (index date) between 1/1/2005 and 12/31/2011, age 18-64 years at index, had benefits coverage for ≥12 months pre-index and no pre-index cancer. Patients with pre-index GC use were GC-free for ≥ 12 months prior to their first GC pharmacy claim, and had continuous benefits coverage from first GC claim to index date. GC use (any, cumulative dose [CD], peak dose, average daily dose [DD], cumulative days exposed, percent days exposed, days of continuous exposure, days since most recent use) was assessed for each patient-day and censored at the earliest of post-index FF, cancer diagnosis, or end of follow-up. Exposures were converted to prednisone equivalents and cumulative measures included pre-index use. Patient demographics at index and pre-index clinical characteristics were assessed. Incidence rates (IR) per 1,000 person-years for post-index FF were stratified by GC exposure. Cox's proportional hazards models estimated age- and sex-adjusted fracture risk by exposure level.

Patients averaged 738 (standard deviation [sd] 615) post-index follow-up days. Most patients (82%) had GC exposure during the study (43% with CD < 675 mgs; 73% had peak dose ≥ 15 mg/day). Exposed and unexposed patients were demographically similar (74% female; mean age 49.4 [10.7] and 49.8 [10.2] years); 1% had pre-index fracture. IRs (95% confidence intervals) for FF were 5.1 (4.6, 5.6) at 0 mg/day DD, 16.8 (11.4, 24.0) at DD ≥ 15 mgs/day, 4.8 (3.8, 6.0) at 0 mg CD, and 13.7 (10.6, 17.4) at CD ≥ 5400 mgs. Among patients ever-exposed to GCs, fracture risk was significantly elevated at CD > 2700 mg and DD ≥ 15 mg/day (Table). Following GC discontinuation, fracture risk (adjusted for age, sex, and CD) was 32% lower at 60-181 days since last exposure versus current exposure. Analyses restricted to patients younger than 50 years showed similar results.

In this large, relatively young cohort of RA patients, fracture risk increased by 2- to 3-fold at high levels of daily and cumulative GC dose, and began to decline within months of GC discontinuation.

Table: Risk of Post-Index Fragility Fracture among Rheumatoid Arthritis Patients Ever-Exposed to Systemic Glucocorticosteroids

		Hazard Ratio	95% C.I.	P-Value
Sex	Male (n=31,104)	ref		
	Female (n=10,930)	1.71	(1.33, 2.20)	<.0001
Age (years)	18 to 39 (n=7,230)	ref		
	40 to 44 (n=4,360)	1.81	(0.99, 3.31)	0.0524
	45 to 49 (n=6,168)	2.45	(1.44, 4.17)	0.0009
	50 to 54 (n=7,995)	2.94	(1.78, 4.86)	<.0001
	55 to 59 (n=8,736)	3.86	(2.37, 6.29)	<.0001
	60 to 64 (n=7,545)	5.57	(3.43, 9.04)	<.0001
Cumulative dose (mg)*†	> 0 to < 675	ref		
	675 to < 1350	1.07	(0.80, 1.44)	0.6504
	1350 to < 2700	1.00	(0.74, 1.36)	0.9854
	2700 to < 5400	1.41	(1.03, 1.93)	0.0317
	>= 5400	2.34	(1.68, 3.26)	<.0001
Average daily dose (mg/day)*†	0	ref		
	> 0 to < 5	1.43	(0.92, 2.23)	0.1091
	5 to < 7.5	1.00	(0.64, 1.55)	0.9891
	7.5 to < 15	1.21	(0.82, 1.80)	0.3439
	>= 15	2.67	(1.78, 3.99)	<.0001

*Exposure metrics were quantified on a person-time basis so patient numbers are not available.
†As the analysis represented in this table was restricted to patients ever-exposed to systemic glucocorticosteroids, all cumulative dose values are greater than zero. Average daily dose could have a value of zero during unexposed periods for this ever-exposed population.

Risk of post-index fracture among RA patients ever-exposed to systemic glucocorticosteroids

SA0323

See Friday Plenary Number FR0323.

SA0324

Low Risk for Hip Fracture Ten Years Before and After Total Hip Replacement Surgery in the Entire Swedish Population. Cecilie Vala*[1], Johan Kärrholm[2], Sabine Sten[3], Magnus Karlsson[4], Maria Vretemark[5], Valter Sundh[1], Mattias Lorentzon[6], Dan Mellstrom[7]. [1]Department of Geriatrics, Sweden, [2]department of orthopedic surgery, Sweden, [3]Department of Archaeology & Ancient History, Sweden, [4]Skåne University Hospital Malmö, Lund University, Sweden, [5]Västergötland Museum, Sweden, [6]Geriatric Medicine, Center for Bone Research at the Sahlgrenska Academy, Sweden, [7]Sahlgrenska University Hospital, Sweden

Background: Studies have shown that hip osteoarthritis (OA) is associated with high bone mass and that hip OA is uncommon in patients with hip fracture. We therefore studied the risk for having a hip fracture during the ten years before and after total hip replacement and investigated the mortality rates after these outcomes.

Method: We followed the total Swedish population born 1902-1952 (n=4 546 820) during the period 1987-2002. We identified from the patient register coordinated by the Swedish National Board of Health patients with diagnosis and surgical code for total hip replacement due to primary osteoarthritis (n=78 573), hip fracture (n=200 522), and both total hip replacement and hip fracture (n=2886). These data was linked with information from national census registers (Statistics Sweden) on mortality, marital status, migration, living place, professional occupation, income and education level. The risk time analyses are based on a Poisson regression model. Data is reported as mean with 95% confidence interval within brackets.

Results:The relative risk (RR) for patients with hip OA to have sustained a hip fracture during the ten years preceding the total hip replacement was 0.43 (0.40-0.46) and during the ten year after the surgery 0.42 (0.40-0.44). The lower risk of hip fracture before and after total hip replacement remains after adjustment for income, education, occupation and latitude. The RR for mortality the first year after a total hip replacement was 0.59 (0.56-0.62) and the first 10 years 0.71 (70-0.73) while the RR for mortality after a hip fracture during the first year was 4.00 (3.95-4.05) and during the first 10 years 2.05 (2.04-2.06).

Conclusion: Individuals with a total hip replacement due to primary OA had a low risk for hip fracture both the decade before and after surgery. This is probably explained by the association between primary hip OA and high bone mass. While the mortality rate the decade after a hip fracture is high, it is low after total hip replacement surgery. This could partly be explained by selection bias in that hip fracture is associated with morbidity and that patients with hip OA and serious morbidity is not referred to surgery.

Disclosures: Cecilie Vala, None.

SA0325

Secular Decline In Fracture Incidence Is Not Associated With Better Post-fracture Outcomes. Dana Bliuc*[1], Mei Chan[2], Tuan Nguyen[1], John Eisman[1], Jacqueline Center[1]. [1]Garvan Institute of Medical Research, Australia, [2]Osteoporosis & Bone Biology, Australia

The last decade has been characterised by an improvement in the health of the elderly population. Hip fracture incidence has declined and life expectancy has improved. However, it is unclear whether the outcomes following osteoporotic fracture have changed accordingly. The aim of this study was to compare re-fracture risk and excess mortality following osteoporotic fracture between two cohorts with similar ages but separated in time.

Study participants comprised women and men 60+ participating into DOES1 (recruited from 1989 and born prior to 1930) and DOES2 (recruited from 2000 and born between 1930 and 1945). Femoral neck BMD was measured at baseline. All fractures excluding head fingers and toes were recorded. Mortality data was obtained from funeral directors and local Dubbo media records. Age-standardized fracture incidence and mortality rates were calculated. The difference in excess mortality between the 2 cohorts was assessed using standardized mortality ratios calculated for each study cohort using time-specific population mortality rates.

The prevalence of osteoporosis declined between the 2 cohorts in both women (24% in DOES1 and 10% in DOES2) and men (12% in DOES1 and 6% in DOES2). Correspondingly, the standardized fracture incidence also declined by approximately a third in both women and men. Although absolute re-fracture rates also declined in DOES2 compared to DOES1, after accounting for the reduction in initial fracture rates the relative risk of re-fracture was similar for the 2 cohorts [women age-adjusted RR 2.0 (95% CI, 1.6-2.5) in DOES1 and 1.9 (95% CI, 1.7- 2.3) in DOES2 and men, 3.5 (95% CI, 2.7-4.8) in DOES1 and 3.4 (95% CI, 2.7- 4.5) in DOES2]. Similarly, crude mortality rates decreased during study follow-up. However, after taking into account the difference in general population life expectancy during the study periods (a decline in mortality rates of 1.3%/yr), the excess mortality post-fracture was similar for the 2 cohorts [women, age-adjusted SMR 2.2 (95% CI, 1.9- 2.7) in DOES1 and 2.0 (95% CI, 1.5- 2.7) in DOES2, and men, 2.2 (95% CI, 1.7- 2.8) in DOES1 and 2.4 (95% CI, 1.8-3.3) in DOES2].

This study has demonstrated that despite a reduction in the prevalence of osteoporosis and fracture incidence during the last 2 decades, re-fracture risk as well as the fracture-associated excess mortality was similar. Whether this is due to differences between the fracture populations remains to be explored.

Disclosures: Dana Bliuc, None.

SA0326

Temporal Trends in high- and low-trauma Hip, Femur and Pelvic Fracture Rates and Selected Quality of Care Indicators in Québec, Canada. Suzanne Morin*[1], Edward Harvey[2], Etienne Belzile[3], Jacques P. Brown[4], Sonia Jean[5]. [1]McGill University, Canada, [2]McGill University, Canada, [3]Université Laval, Canada, [4]CHU de Québec Research Centre, Canada, [5]Institut National De Santé Publique Du Québec, Canada

Purpose: Incidence rates of low-trauma (LT) fractures, particularly of the hip, have been noted to be decreasing. However, data on temporal trends in high-trauma (HT) fractures of the hip, femur and pelvis are lacking.

Methods: Using the hospital discharge database of the province of Québec, Canada, we performed a retrospective cohort study of men and women aged 50 years and older who sustained an incident hip, femur or pelvic fracture between1991-2010. Fractures and trauma intensity were identified using ICD-9-CM or ICD-10-CM diagnosis codes in medical records. We calculated age-standardized LT and HT fracture rates at each site and estimated time trends for fracture rates and selected quality of care indicators.

Results: Over 20 years, we identified 103 313 hip, 14 281 pelvic and 7 421 femur fractures of which 10%, 27% and 26% were HT fractures, respectively. Patients who sustained HT fractures were younger, were more frequently of male sex, and of worse social deprivation strata (p<0.001). (Table 1) Those with a HT pelvic or femur fractures were more likely to undergo surgical repair compared with LT fractures at similar sites (p<0.05 and <0.001, respectively). Mean surgical delay was similar in patients with LT and HT pelvic and hip fractures, but significantly shorter in patients with HT compared to LT femur fractures (p<0.001). Mean length of stay (LOS) was significantly shorter and mortality rates lower in patients with HT compared to LT fractures at any site (p<0.001). Overtime, the number of HT and LT fractures increased at all sites in the population. Age-standardized incidence rates of HT and LT fractures of the pelvis and femur increased significantly while LT fractures of the hip decreased and HT hip fractures remained stable. (Figure 1) Average age at the time of any LT fracture increased (p<0.01) and so did the proportions of patients with dementia and multiple comorbidities. Mean LOS decreased significantly following all fractures (p<0.001) and in-hospitality death remained stable following any pelvic fractures but decreased over time following LT femur fractures (p<0.05) and any hip fractures (p <0.001). The proportion of patients discharged to LTC following LT pelvic and hip fractures increased but not after HT fractures.

Conclusion: HT and LT fractures are associated with different patient characteristics, interventions and clinical outcomes; healthcare policies should address these distinctions to develop targeted care paths.

Table 1 Characteristics of patients and outcomes related to HT and LT fractures, Québec, Canada 1991-2010

Characteristic	Pelvis Fracture (N=14 281)		P-value	Femur Fracture (N=7 421)		P-value	Hip fracture (N=103 313)		P-value
	LT	HT		LT	HT		LT	HT	
Prevalence (n, %)	10 428 (73)	3 853 (27)		5 471 (74)	1 950 (26)		93 146 (90)	10 167 (10)	
Patients Characteristics									
Females (n, %)	8 421 (81)	3 853 (49)	**	4 328 (79)	1 051 (54)	**	70 495 (76)	6 247 (61)	**
Mean Age (SD)	81 (9)	69 (12)	**	77 (11)	68 (12)	**	81 (10)	74 (11)	**
Social deprivation index (Quintile)									
1-2 (favourable)	2 495 (27)	1 366 (38)	**	1 369 (29)	670 (37)	**	21 139 (27)	3 009 (32)	**
3 (neutral)	1 709 (19)	697 (19)		896 (19)	396 (22)		14 789 (19)	1 837 (20)	
4 -5 (unfavourable)	4 988 (54)	1 580 (43)		2 441 (60)	764 (42)		41 759 (54)	4 525 (48)	
Dementia (%)	826 (8)	58 (2)	**	295 (5)	23 (1)	**	6 996 (8)	244 (2)	**
Osteoporosis (%)	1 596 (15)	220 (6)	**	581 (11)	113 (6)	**	7067 (8)	563 (6)	**
Outcomes									
Means length of stay, days (SD)	22.4 (26)	19.7 (20)	**	22.7 (30)	19.7 (24)	**	20.3 (31)	17.1 (22)	**
In-hospital mortality (n, %)	558 (5)	97 (3)	**	349 (6)	57 (3)	**	8 287 (9)	409 (4)	**
Final Discharge destination (n, %)									
Home	7 381 (75)	3 059 (81)	**	3 138 (61)	1 359 (72)	**	48 173 (57)	7 143 (73)	**
Long-term care	1 787 (18)	252 (6.7)		1 135 (22)	201 (11)		22 585 (26.6)	1 104 (11)	
Discharged to the same milieu (n, %)	7 284 (70)	2 845 (74)	**	3 290 (60)	1 302 (67)	**	54 774 (59)	7 101 (70)	**

<0.05, **<0.001, NS: not significant

Table 1 Characteristics of patients and outcomes related to High and Low trauma fractures

Figure 2: Average annual percent change (AAPC) in age-standardized* incidence rates according to site and type of fracture; Québec, Canada 1991-2010

Pelvis and Femur

Hip
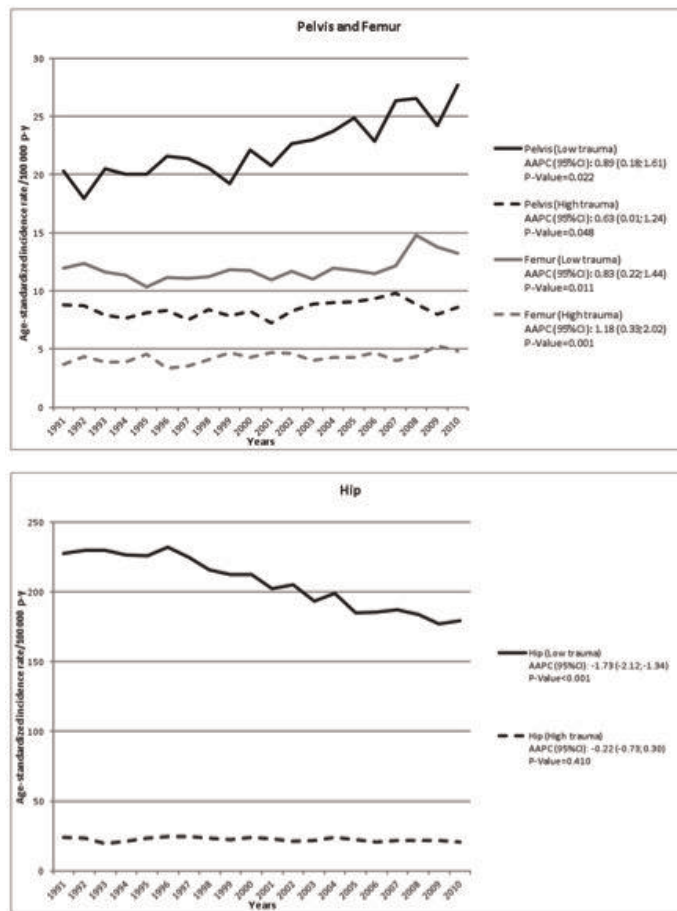
* Standardized to the 2001 age-structure of the Quebec population

Figure1 Average Annual % Change in Incidence Rates of fractures

Disclosures: Suzanne Morin, Amgen, 3; Amgen,; Eli Lilly, 3; Merck, 3; Eli Lilly,; Merck,

SA0327

Temporal Trends in Pelvic Fracture Rates and Selected Quality of Care Indicators in Québec, Canada. Sonia Jean*[1], Edward Harvey[2], Etienne Belzile[3], Jacques P. Brown[4], Suzanne Morin[5]. [1]Institut National De Santé Publique Du Québec, Canada, [2]McGill University, Canada, [3]Université Laval, Canada, [4]CHU de Québec Research Centre, Canada, [5]McGill University, Canada

Purpose: Like other major osteoporotic fractures, pelvic fractures are associated with recurrent fractures, reduced autonomy and excess mortality. Data depicting temporal trends and health outcomes associated with these fractures remain scarce.

Methods: Using the hospital discharge database of the province of Québec, Canada, we performed a retrospective cohort study of men and women aged 50 years and older who sustained an incident pelvis fracture between April 1, 1991, and March 31, 2010.

Fractures were identified using ICD-9-CM or ICD-10-CM diagnosis codes in medical records. We calculated age- and sex-specific rates and estimated time trends for fracture rates and selected quality of care indicators.

Results: Over 20 years, we identified 15 088 pelvic fractures (mean age 80 (SD 10) years in women, 72 (SD12) years in men, 73% women), of which 69% were low-trauma fractures and 52% were treated in a trauma center. (Table 1) Few patients (5%) underwent surgery; however the mean surgical delay was $\geq$ 2 days in 61% of those who required surgery. The average length of stay (LOS) in acute care was 22 (SD 25) days, and the in-hospital mortality was 4% in women and 6 % in men (p <0.001). Discharge destination was home in 77%, long-term care (LTC) in 15% and rehabilitation in 8 %, and 70% returned to their initial residential setting following discharge. There were 133 (1%) readmissions to the hospital associated with a pelvic fracture diagnostic ICD code within 6 months following discharge. Overtime, the number of pelvic fractures increased in the population, but age-standardized incidence rates remained stable, except in men and women $\geq$80 years where there was a linear average annual increase of 2.2% (95% CI: 1.6 -2.7). (Figure 1) Average age at the time

of fracture increased (p<0.0001) and so did the proportions of patients with dementia and multiple comorbidities. Mean LOS decreased by 9 days (p<0.0001) and in-hospitality death and re-admissions remained stable. The proportion of patients discharged to their home decreased by 6% (p<0.0001) due to an increase in discharge destination to LTC and rehabilitation.

Conclusion: Pelvic fractures rates are increasing in the older and frail population, and are associated with negative clinical outcomes. Care models should be reviewed to ensure adequate resources are provided to healthcare providers to offset the expected increase in demand resulting from ongoing changes in patients' characteristics.

Table 1: Characteristics of patients and outcomes related to pelvic fractures

Characteristic	Pelvis Fracture			P-value*
	Cohort	Women	Men	
Number of fracture (%)	15 088	10 975 (73)	4 113 (27)	NA
Patients and hospitals Characteristics				
Mean Age (SD)	78 (11)	80 (10)	72 (12)	<0.0001
Number of Comorbidities (%)				
0-1	10 930 (72)	7 914 (72)	3 016 (73)	0.1859
2-3	2 907 (19)	2 126 (19)	781 (19)	
$\geq$4	1 251 (8)	935 (9)	316 (8)	
Dementia (%)	894 (6)	740 (7)	154 (4)	<0.0001
Fractures and treatments Characteristics				
% of fracture considered as				
Traumatic	3 853 (26)	1 889 (17)	1 964 (48)	<0.0001
Fall	10 428 (69)	8 421 (77)	2 007 (49)	
Not specified	807 (5)	665 (6)	142 (4)	
% of fracture with surgical treatment	717 (5)	215 (2)	502 (12)	<0.0001
Surgical delays				
$\geq$2 days	434 (60)	128 (60)	306 (61)	
Outcomes				
Means acute care length of stay, days (SD)	22 (25)	22 (25)	22 (23)	<0.0001
In-hospital mortality N, (%)	691 (5)	463 (4)	228 (6)	0.0005
Final Discharge destination N, (%)				
Home	11 038 (77)	8 008 (76)	3 030 (78)	<0.0001
Long-term care	2 156 (15)	1 720 (16)	436 (11)	
Re-admission rate with principal diagnosis of pelvic fracture, 6 months N, (%)	133 (1)	110 (1)	23 (1)	0.0095

* Chi-square test for proportions comparison, ANOVA for continuous normally distributed variables, Wilcoxon and Kruskal-Wallis test for nonnormal continuous variables.

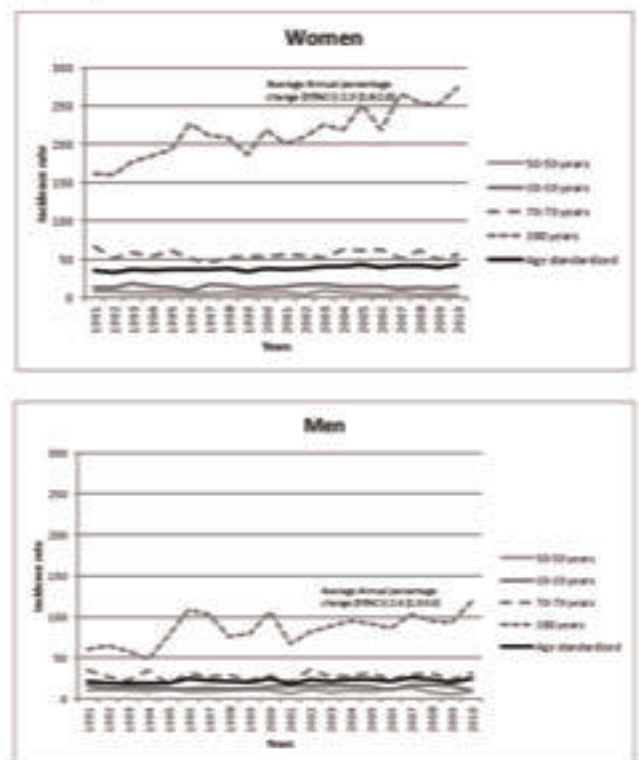Table 1 Characteristics of patients and outcomes related to pelvic fractures

Figure 1: Trends in age-specific and age-standardized incidence rates in women and men; Quebec, Canada 1991-2010

Women

Men

Figure1 Trends in Incidence Rates of pelvic fractures

Disclosures: Sonia Jean, None.

SA0328

The Influence of Lean Mass and Fat Mass on Fracture Outcome in a Prospective Community-Dwelling Korean Cohort. <u>Jung Hee Kim</u>*[1], <u>Hyung Jin Choi</u>[2], <u>Sang Wan Kim</u>[3], <u>Nam H. Cho</u>[4], <u>Chan Soo Shin</u>[1]. [1]Seoul National University College of Medicine, South Korea, [2]Chungbuk National University Hospital, South Korea, [3]Seoul National University College of Medicine, Boramae Hospital, South Korea, [4]Ajou University School of Medicine, South Korea

Lean mass (LM) and fat mass (FM) is known to be associated with osteoporosis. However, there are few studies regarding body composition and fracture outcome. We aimed to elucidate the effect of LM and FM on incidence of fractures in a prospective community-based Korean cohort.

We included 2,186 men and 2,750 women in a prospective community-dwelling cohort. LM and FM were measured by the bioelectrical impedance analysis at baseline (2001-2002). Fracture events included self-reported clinical fractures and low-trauma fractures at the hip, vertebrae, proximal humerus and radius sites during the follow-up period (mean duration, 9.4 years).

Mean age was 55.5 ± 8.8 years. The incidence of fracture events was 3.5% (77/2,186) in men and 7.8% (215/2,750) in women. When we compared the highest tertile with the lowest tertile of LM in men and women, the adjusted hazard ratios (95% CIs) of fracture were 0.158 (0.068-0.369) and 0.790 (0.547-1.141), respectively. Men within the highest tertile of FM had a lower risk fracture than those within the lowest tertile (adjusted HR [95% CI], 0.400 [0.211-0.758]). However, in women, higher FM did not reduce the fracture risk significantly (adjusted HR [95% CI], 1.162 [0.824-1.637]). In the composite analyses using LM and FM simultaneously, men within the highest tertile of LM and the lowest tertile of FM reduced the fracture risk by 91% compared with the lowest tertile of LM and FM. In women, subjects within the lowest tertile of LM and the highest tertile of FM showed a two-time higher risk for fracture than the lowest tertile of LM and FM.

Fat mass after removing mechanical loading components may be associated with increased fracture risk. High lean mass and low fat mass may protect against fracture.

Disclosures: Jung Hee Kim, None.

SA0329

See Friday Plenary Number FR0329.

SA0330

Sex hormones and radiographic vertebral fractures in older men. <u>Peggy Cawthon</u>*[1], <u>John Schousboe</u>[2], <u>Kristine Ensrud</u>[3], <u>Dennis Black</u>[4], <u>Jane Cauley</u>[5], <u>Steven Cummings</u>[6], <u>Erin LeBlanc</u>[7], <u>Gail Laughlin</u>[8], <u>Carrie Nielson</u>[9], <u>Deborah Kado</u>[10], <u>Andrew Hoffman</u>[11], <u>Elizabeth Barrett-Connor</u>[10], <u>Eric Orwoll</u>[9]. [1]California Pacific Medical Center Research Institute, USA, [2]Park Nicollet ClinicUniversity of Minnesota, USA, [3]University of Minnesota & Minneapolis VA Health Care System, USA, [4]University of California, San Francisco, USA, [5]University of Pittsburgh Graduate School of Public Health, USA, [6]San Francisco Coordinating Center, USA, [7]Kaiser, USA, [8]UCSD, USA, [9]Oregon Health & Science University, USA, [10]University of California, San Diego, USA, [11]Stanford, USA

Previous reports have shown that low bioavailable estradiol (bioE) and high sex hormone binding globin (SHBG) are associated with increased non-spine fracture risk in men. However, there are few reports of the association between sex hormones and vertebral fractures, particularly in men.

MrOS is a prospective cohort study of 5,994 ambulatory men aged ≥65 yrs at baseline of whom 1608 were randomly selected for measure of sex hormones. Estradiol (E2) and testosterone (T) were analyzed by spectrometry/ chromatographic methods and SHBG by automated immunoassay. Bioavailable estradiol (bioE2) and testosterone (bioT) were calculated using mass action equations. At baseline and again 4.6 years later, lateral spine films were obtained and radiographic vertebral fractures were identified using semi-quantitative (SQ) grading. Likelihood of prevalent fracture (SQ≥2) and likelihood of new or worsening fracture (change in SQ grade ≥1) was estimated by logistic regression models adjusted for covariates (see Table footnote). Sex hormones and SHBG were analyzed as continuous variables with odds ratio expressed per 1 SD increase. Complete fracture, sex hormone and covariate data were available for cross sectional analyses for 1451 men (mean age: 72.8 years) at baseline of whom 137 (9.4%) had a prevalent vertebral fracture. Complete data for prospective analyses were available for 1049 men during 4.6 years of follow-up, of whom 55 (5.2%) had a new or worsening vertebral fracture.

In cross-sectional analyses, each SD increase in bioE2 was associated with an 18% decreased likelihood of prevalent vertebral fracture, while each SD increase in SHBG was associated with a 20% increased likelihood of prevalent fracture (Table). E2, bioT and T were not associated with prevalent fracture.

In prospective analyses, each SD increase in SHBG was associated with a 29% increased likelihood of incident vertebral fracture; however there were no significant associations for E2, bioE2, T or bioT

Similar results were seen when analyses were limited to new radiographic vertebral fractures only; when results were adjusted for total hip BMD rather than lumbar spine BMD; and when SHBG results were adjusted for E and T or for bioE and bioT.

In summary, higher SHBG was associated with increased likelihood of prevalent and incident radiographic vertebral fractures in older men. However, we did not observe strong associations between E2, T, bioE2 or bioT and radiographic fracture in men.

Table. Likelihood of radiographic vertebral fracture (Odds ratio, 95% CI) by SD increase of sex hormone

	SD	Fracture	
		Prevalent (SQ≥2)	Incident (change SQ≥1)
E2	7.9 pg/ml	0.86 (0.71, 1.04)	1.09 (0.85, 1.41)
T	161.3 ng/dl	0.95 (0.78, 1.15)	1.06 (0.80, 1.39)
BioE2	4.pg/ml	0.82 (0.67, 0.99)	1.15 (0.84, 1.58)
BioT	64.9 ng/dl	0.83 (0.68, 1.01)	0.88 (0.66, 1.17)
SHBG	19.8 nM	1.20 (1.01, 1.43)	1.29 (1.00, 1.67)

*adjusted for age, race, clinical center, smoking, height, weight, fall history, # prescription medications, inability to rise from chair, physical activity and lumbar spine BMD (by Hologic 4500 DXA)

Table

Disclosures: Peggy Cawthon, None.

SA0331

A good self-estimated health lowers hip fracture risk independent of FRAX and BMD. <u>Hans Lundin</u>*[1], <u>Maria Sääf</u>[2], <u>Lars-Erik Strender</u>[3], <u>Sven Nyrén</u>[3], <u>Helena Salminen</u>[4]. [1]Karolinska Institutet, Sweden, Sweden, [2]Karolinska University Hospital Solna, Sweden, [3]Karolinska Institutet, Sweden, [4]Karolinska Institutet, Sweden

Bone mineral density (BMD) measured with DXA at the femoral neck is a well documented and very strong predictor of hip fracture risk. FRAX is the most used fracture prediction tool worldwide and includes BMD along with eleven other risk factors for hip fracture. The aims of this study was to see if self-estimated health measured with a visual analog scale (VAS) was associated with the risk of a hip fracture.This was a population-based prospective cohort study on 351 Swedish women aged 69-79 years at inclusion. These women self-estimaed their health and were assessed with FRAX including bone mineral density (BMD) at inclusion between 1999-2001. Global health was self-estimated with a visual analog scale (VAS) by writing an "x" on a 10 centimeter line drawn between "worst possible health" and "best possible health". The distance from "worst possible health" was measured in centimeters. Follow up was performed ten years later through Swedish medical records. The main outcome was a hip fracture. No participant was lost to follow up.The age adjusted ten-year hip fracture risk was decreased by 19% with every one cm better self-estimated health (Hazard ratio (HR) 0.81, 95% confidence interval (CI) 0.70-0.92). This relation was independent of BMD, FRAX-risk, previous fractures, parents low energy fractures, and the presence at baseline of ischaemic heart disease, diabetes mellitus, hypertension or any type of present or previous cancer.To have a self-estimated health below four centimeters compared to over four centimeters, resulted in a 2.3 times greater risk of a hip fracture after adjustment for femoral neck BMD (HR 2.3, 95% CI 1.1-4.8). This HR was not altered significantly after adjustment for any of the risk factors mentioned above. Self-estimated health thus seems to be able to identify high risk individuals not identified by any of the clinically most often considered risk factors. A low self-estmated health was not associated with the presence of any of several different common chronic diseases.

Disclosures: Hans Lundin, None.

SA0332

See Friday Plenary Number FR0332.

SA0333

Cardiovascular risk factor analysis in patients with a recent fracture at the Fracture Liaison Service. Caroline Wyers*[1], Lisanne Vranken[2], Robert Van Der Velde[3], Heinrich Janzing[4], Wim Morrenhof[5], Piet Geusens[6], Joop Van Den Bergh[7]. [1]Maastricht University, The Netherlands, [2]VieCuri Medical Centre, The Netherlands, [3]VieCuri Medical Center Venlo, the Netherlands, The Netherlands, [4]VieCuri Medical Centre, Department of Surgery, Netherlands, [5]VieCuri Medical Centre, Department of Orthopedic Surgery, Netherlands, [6]University Hasselt, Belgium, [7]VieCuri MC Noord-Limburg & Maastricht UMC, The Netherlands

Purpose: Patients with osteoporosis have an increased risk of cardiovascular diseases (CVD) and venous tromboembolic events (VTE). Medications such as NSAID's, strontium ranelate and raloxifene have a contra-indication for prescription in patients with a history of CVD, VTE or hyptertension (HT). The aim of this study was to investigate the prevalence of CVD, VTE, HT and diabetes mellitus type (DM2) in medical history in patients with a recent clinical fracture visiting the Fracture Liaison Service (FLS).

Methods: Retrospective chart review of all consecutive patients aged ≥ 50 years presenting with a recent clinical fracture, who visited the FLS for fracture risk assessment including evaluation of medical history. A contra-indication is defined as having CVD or VTE or HT in medical history. Data were analysed using Chi-square tests, Fisher's Exact Test and logistic regression analysis adjusting for age, sex, BMD (normal vs. osteopenia vs. osteoporosis) and fracture classification according to Center (finger & toe vs. minor vs. major vs. hip).

Results: 1359 patients with a recent clinical fracture were included (72% women; mean age 65 years). Osteoporosis was diagnosed in 30% of patients, osteopenia in 47% and normal BMD in 23%. Based on medical history, 30% of patients had a history of CVD (14%), VTE (2%), HT (15%) and DM2 (7%) or a combination. The presence of CVD, VTE, HT and DM2 increased with increasing age (21% in patients aged 50-59 years to 48% in patients aged >80 years; p=.000) and was higher in men (36% vs 27% women, respectively; p=.001), but independent of BMD and fracture type. In patients aged ≥ 70 years, 35% had a contra-indication and it was higher in men (46% vs. 33% women p=.000), but independent of BMD and fracture type. After adjustments, only men contributed significantly for having a contra-indication in the total study population (p=.000). In patients aged ≥ 70 years, men and hip fracture contributed significantly for having a contra-indication (p=.012, p=.044 respectively).

Conclusion: In patients presenting with a recent fracture, 30% have a history of either CVD, VTE, HT or DM2; and 29% in patients diagnosed with osteoporosis. A contra-indication was more frequently present in men. Although NSAIDS, strontium ranelate and ralofixene can be described safely in the majority of patients, careful evaluation of medical history with respect to CVD, VTE and HT should be performed before starting treatment with these medications.

Disclosures: Caroline Wyers, None.

SA0334

Direct and Indirect Effects of Frailty on Fractures: Potential Roles of Muscle and Bone. Andy Kin On Wong*[1], Courtney Kennedy[2], George Ioannidis[3], Karen Beattie[2], Christopher Gordon[2], Laura Pickard[2], Alexandra Papaioannou[4], David Goltzman[5], Jerilynn Prior[6], Heather Macdonald[6], Maureen Ashe[6], Leigh Gabel[6], Danmei Liu[6], Saija Kontulainen[7], Andrew Frank[7], Wojciech Olszynski[8], K. Shawn Davison[9], Lora Giangregorio[10], Robert Josse[11], Eva Szabo[12], Marta Erlandson[7], Tassos Anastassiades[13], Norma MacIntyre[2], Angela M. Cheung[14], Jonathan Adachi[15]. [1]McMaster UniversityUniversity Health Network, Canada, [2]McMaster University, Canada, [3]McMaster University, Canada, [4]Hamilton Health Sciences, Canada, [5]McGill University, Canada, [6]University of British Columbia, Canada, [7]University of Saskatchewan, Canada, [8]University of Saskatchewan, Canada, [9]University of Victoria, Canada, [10]University of Waterloo, Canada, [11]St. Michael's Hospital, University of Toronto, Canada, [12]University Health Network, Canada, [13]Queen's University, Canada, [14]University Health Network-University of Toronto, Canada, [15]St. Joseph's Hospital, Canada
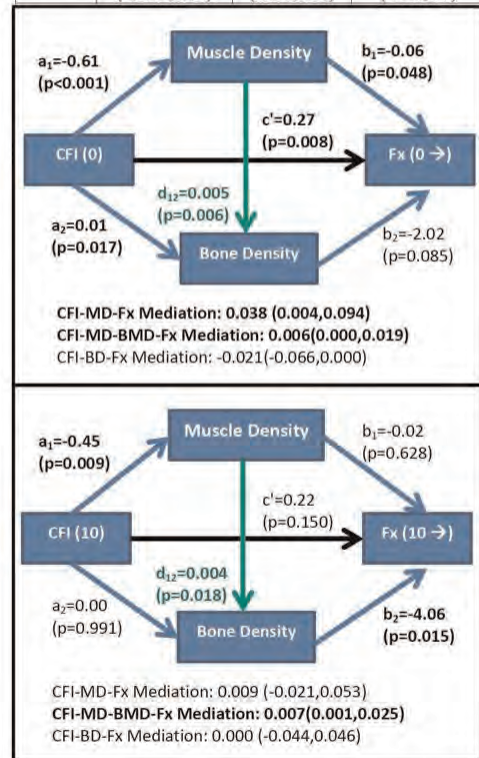
Objective: To explore the potential role of muscle and bone properties as independent and serial mediators in the causal pathway from frailty to fractures.

Methods: Women 60-85 years old within the Canadian Multicentre Osteoporosis Study (CaMOS) completed peripheral quantitative computed tomography (pQCT) (20 mm/s, 38 kVp) scans at 66% of the tibial length (at year 15). Muscle and cortical bone densities, mass, and area were derived. Comorbidities, cognition, energy, function and mobility questions obtained at baseline and year 10 were used to compute the CaMOS frailty index (CFI). Incident fractures were ascertained and categorized as fractures since baseline and fractures since year 10. A path analysis was performed with fractures regressed on frailty at baseline or at year 10, with each bone and muscle property as potential independent or serial mediators, adjusting for age, body mass index (BMI) and education. Direct, indirect and total effects were quantified using Hayes' mediation analysis models. All analyses were performed using PROCESS in SAS v9.3.

Results: Among 377 women (mean age: 65.6 ± 6.6 years; BMI: 26.84 ± 4.88 kg/m², 179(47.5%) with fractures since baseline, 48 (12.7%) with fractures since year 10), baseline and year 10 CFI significantly related to muscle but only marginally to bone properties (Table I). Baseline CFI was related to fractures (rate ratio: 2.78(95%CI: 0.06,5.50)) with direct effects significant only for the lower two tertiles of age and BMI. Significant indirect effects were mediated by muscle density but not by bone properties. Year 10 CFI was only associated with fractures as mediated by muscle mass. In the serial mediators' path analyses (Figure 1), the indirect effect of baseline CFI on fractures was significant only through muscle density without any serial contribution from bone. The direct effect of baseline CFI on fractures was larger than the total indirect effects through muscle or bone density. Year 10 CFI did not exhibit significant direct effects on fractures, but indirect effects through muscle mass or area on fractures was evident. The serial mediations of muscle and bone densities and areas on the year 10 CFI and fracture relation were significant.Conclusions: Frailty experienced earlier remains a lingering influence on incident fractures years later. Frailty experienced more recently may impact bone fragility through its more immediate association with muscle, and in part muscle's relation to bone.

Table I. Effects of baseline and year 10 CFI on muscle and bone properties. Models adjusted for age, BMI and education

Muscle	Mass (mg)	Density (mg/cm³)	Area (mm²)
Baseline	-16.08 (-24.13,-8.03)	-0.36 (-0.79,0.08)	-191.9 (-303.1,-807.9)
Year 10	-16.13 (-23.98,-8.28)	-0.19 (-0.61,0.24)	-210.4 (-318.3,-102.4)

Bone	Mass (mg)	Density (mg/cm³)	Area (mm²)
Baseline	-1.94 (-9.29,5.41)	0.01 (0.00,0.02)	-12.8 (-25.1,-0.5)
Year 10	-6.39 (-13.53,0.75)	0.00 (-0.01,0.01)	-9.5 (-21.6,2.5)

a_1=-0.61 (p<0.001) · Muscle Density · b_1=-0.06 (p=0.048)
c'=0.27 (p=0.008)
CFI (0) · Fx (0 →)
d_{12}=0.005 (p=0.006)
a_2=0.01 (p=0.017) · Bone Density · b_2=-2.02 (p=0.085)

CFI-MD-Fx Mediation: 0.038 (0.004,0.094)
CFI-MD-BMD-Fx Mediation: 0.006(0.000,0.019)
CFI-BD-Fx Mediation: -0.021(-0.066,0.000)

a_1=-0.45 (p=0.009) · Muscle Density · b_1=-0.02 (p=0.628)
c'=0.22 (p=0.150)
CFI (10) · Fx (10 →)
d_{12}=0.004 (p=0.018)
a_2=0.00 (p=0.991) · Bone Density · b_2=-4.06 (p=0.015)

CFI-MD-Fx Mediation: 0.009 (-0.021,0.053)
CFI-MD-BMD-Fx Mediation: 0.007(0.001,0.025)
CFI-BD-Fx Mediation: 0.000 (-0.044,0.046)

Figure 1. Path analysis examining direct influence of frailty on fractures (Fx) and its indirect effect through muscle (MD) and bone densities (BMD). All arrows indicate association as measured by a regression coefficient estimate.

Table I. Figure 1.

Disclosures: Andy Kin On Wong, None.

SA0335

Increased risk for hip fracture after bereavement. <u>Dan Mellstrom</u>*[1], <u>Valter Sundh</u>[2], <u>Magnus Karlsson</u>[3], <u>Claes Ohlsson</u>[4], <u>Mattias Lorentzon</u>[5], <u>John Kanis</u>[6], <u>Boo Johansson</u>[7], <u>Anders Odén</u>[8]. [1]Sahlgrenska University Hospital, Sweden, [2]Department of Geriatrics, Gothenburg University, Sweden, [3]Skåne University Hospital Malmö, Lund University, Sweden, [4]Center for Bone & Arthritis Research at the Sahlgrenska Academy, Sweden, [5]Geriatric Medicine, Center for Bone Research at the Sahlgrenska Academy, Sweden, [6]University of Sheffield, Belgium, [7]Department of Psychology, Gothenburg University, Sweden, [8]Department of biostatistics, Chalmers University, Sweden

Bereavement is associated with increased mortality and broken heart syndrome. The question arises whether bereavement also is related to broken hip.

We studied the Swedish population in 1986 with birth years 1902-1942, and followed 904,394 married couples from 1987 to 2002 in national research and census registers, coordinating information on mortality, hospital care, civil status, income, education and place of living. The relative risk of hip fracture incidence was estimated with Poisson risk time models, separately for each gender. Married individuals whose spouse did not die during the 16 year follow-up defined the reference group. Age during risk exposure was a covariate in all models.

The number of fractures 0-10 years after bereavement was 6,303 in men and 20,404 in women. The total years of risk in the bereaved group amounted to 601,787 in men and 1,679,773 in women. The sixteen-year morality was 24% in women and 41% in men. The excess risk (Hazard Ratio, HR) for hip fracture during the first 3 months after bereavement was 1.82 (CI = 1.62 – 2.05) for men and 1.54 (CI = 1.42 – 1.68) for women. The absolute risk decreased significantly over time during the first 3 years, but remained stable thereafter at a significantly elevated level compared to non-bereaved individuals for 10 years in both sexes (Table 1). There was also seen an increased risk during the years prior to death of spouse, which indicate a pre-mortality stress load on the partner.

Conclusion: We demonstrate a novel finding that bereavement is associated with an increased risk of hip fracture in both sexes, and that this is more marked in men than in women. The increased risk is most apparent during the first 3 months after bereavement, but even though there is a slow decrease during the next few years, an excess risk seems to remain at a significantly high level for several years thereafter.

Table 1. Increased risk for hip fracture after bereavement versus non-bereaved.
Time after bereavement HR women HR men
0 – 3 years 1.34 (1.30 – 1.38) 1.59 (1.53 – 1.66)
3 – 6 years 1.26 (1.22 – 1.30) 1.36 (1.30 – 1.43)
6 –10 years 1.25 (1.22 – 1.30) 1.38 (1.30 – 1.46)

Disclosures: Dan Mellstrom, None.

SA0336

Persistent low grade inflammation is associated with bone loss in elderly women. <u>Kristina Akesson</u>[1], <u>Sofia Berglundh</u>*[2], <u>Linnea Malmgren</u>[3], <u>Fiona McGuigan</u>[4], <u>Paul Gerdhem</u>[5], <u>Holger Luthman</u>[6]. [1]Skåne University Hospital, Malmö, Sweden, [2]Skåne University Hospital, Malmö, Sweden, [3]Skane University Hospital, Sweden, [4]University of Lund, Malmö, Skane University Hospital, Sweden, [5]Karolinska Institutet, Sweden, [6]Lund University, Sweden

Introduction: Evidence suggests inflammation may contribute to the pathophysiology behind impaired bone metabolism. Systemic inflammation negatively affects bone mass in rheumatoid arthritis patients but an inverse correlation between C-reactive protein (CRP), a marker of inflammation and bone mineral density (BMD) has also been observed. The aim of this study was to investigate the association between persistently elevated CRP levels and BMD, bone loss, fractures and mortality in 1044 women from the OPRA cohort of 75 year old Swedish women.

Method: CRP was measured at baseline, and at age 80 and differences in BMD and bone loss were compared. To capture the effect of inflammation over an extended period, we also classified women according to CRP levels at BOTH ages as follows: Group 1 CRP <3mg/L at 75y AND 80y; Group CRP 2 ≥3mg/L at 75y OR 80y; Group 3 CRP ≥3mg/L at 75y AND 80y.

Result: Women in the highest quartile of CRP (mean 5.74 mg/L) had significantly higher BMD at total hip (0.871 vs. 0.809 g/cm^2, p<0.001) and femoral neck (0.778 vs. 0.737 g/cm^2, p=0.007) compared to the lowest (mean 0.63 mg/L). CRP level at age 75 was not associated with BMD or bone loss. However, women with CRP ≥3mg/L at BOTH BL and at the 5 yr follow-up had higher bone loss compared to women with CRP<3mg/L at total hip (-0.125 vs. -0.085 g/cm^2, p=0.018) and FN (-0.127 vs. -0.078 g/cm^2, p=0.005) during 10 yrs of follow-up. Women in the highest quartile of CRP had a lower risk of major osteoporotic fractures (HR 0.76 (95 % CI 0.52-0.98) compared to the lowest, even after adjusting for weight and BMD. CRP was not associated with hip fracture or mortality.Conclusion: This study suggests that CRP is not indicative of osteoporosis or fracture risk in elderly women, however, in women with persistently elevated CRP there seems to be an increased rate of bone loss.

Disclosures: Sofia Berglundh, None.

SA0337

Sex-specific Associations Between Income and Incident Major Osteoporotic Fractures: A Population-based Analysis. <u>Sharon Brennan</u>*[1], <u>Lin Yan</u>[2], <u>Lisa Lix</u>[2], <u>Suzanne Morin</u>[3], <u>Sumit Majumdar</u>[4], <u>William Leslie</u>[5]. [1]Deakin University, Australia, [2]University of Manitoba, Canada, [3]McGill University, Canada, [4]University of Alberta, Canada, [5]University of Manitoba, Canada

Purpose: Lower income has been associated with increased fracture incidence at the hip. However, few studies have examined associations between income and fractures at other sites. We investigated sex-specific associations between income and incident fractures of the hip, wrist, humerus, and spine.

Methods: Incident fractures were identified from administrative health data for all residents (age 50+ yrs) of Manitoba, Canada, 2000-2007. Mean neighborhood (postal code area) annual household incomes were extracted from 2006 census files and categorized into quintiles. Age-adjusted and sex-stratified fracture incidences (per 100,000 person years) across income quintiles were calculated. We used a generalized linear model with a negative binomial distribution to estimate the relative risks (RR) of fracture for income quintile 1 (lowest income) vs. income quintile 5.

Results: A total of 15,094 incident fractures (4,736 hip; 3,012 humerus; 1,979 spine; and 5,367 wrist) were identified in 3,866 males and 11,228 females. For males, a negative linear association was observed between age-adjusted fracture incidence at major osteoporotic sites and income quintile; 646.6 vs. 397.3 for males in the lowest vs. highest income quintile, respectively (quintile 1 vs. quintile 5 RR 1.63, 95%CI 1.42-1.87) (Table). Similar negative linear associations were seen for males when stratified by skeletal site. Compared to the highest income quintile, men with the lowest income had a much greater age-adjusted RR of fracture at the hip (1.62, 95%CI 1.30-2.02), spine (1.65, 95%CI 1.28-2.13), humerus (1.97, 95%CI 1.59-2.43) and wrist (1.41, 95%CI 1.23-1.62). For females, we observed a weak negative linear association between overall fracture incidence and increasing income quintile (p-trend=0.029, lowest vs. highest income quintile RR 1.14, 95%CI 1.01-1.28). The only individual site to show a significant association with income was the wrist (p-trend=0.015, lowest vs. highest income quintile RR 1.09, 95%CI 1.01-1.28).

Conclusions: We report a consistent linear association between decreasing income quintile and higher fracture incidence in men, with a much smaller association in women. Men in the lowest income quintile had a 1.5-2 fold increased risk of fracture at the major osteoporotic sites compared to men in the highest income quintile. These data provide evidence that men with lower income may be an important target population for intervention to reduce the burden of fracture.

Table: Age-adjusted fracture incidence per 100,000 person years (SE) and RR (95% CI) according to income quintile.

	Quintile 1*	Quintile 2	Quintile 3	Quintile 4	Quintile 5	p-linear trend	RR Q1 vs. Q5
Males							
Hip	190.3 (16.8)	137.2 (5.1)	122.0 (6.4)	118.1 (8.9)	117.6 (8.5)	<.0001	1.62 (1.30, 2.02)
Humerus	135.3 (11.0)	84.4 (7.9)	71.7 (5.6)	73.6 (4.8)	68.7 (5.6)	0.0001	1.65 (1.28, 2.13)
Spine	115.1 (6.7)	103.9 (8.1)	90.5 (5.5)	92.1 (8.7)	69.7 (8.1)	<.0001	1.97 (1.59, 2.43)
Wrist	144.9 (8.9)	120.4 (7.9)	115.2 (6.9)	111.9 (7.2)	102.7 (5.1)	<.0001	1.41 (1.23, 1.62)
All sites	646.6 (33.1)	491.3 (11.6)	440.7 (16.9)	437.8 (16.8)	397.3 (19.2)	<.0001	1.63 (1.42, 1.87)
Females							
Hip	236.9 (18.4)	194.2 (9.2)	200.5 (10.4)	198.1 (10.9)	206.7 (17.5)	0.1542	1.15 (0.93, 1.41)
Humerus	264.4 (10.3)	193.5 (9.9)	206.9 (10.2)	198.5 (11.4)	200.3 (19.9)	0.0849	1.10 (0.98, 1.24)
Spine	104.0 (5.6)	105.9 (9.2)	104.4 (4.3)	98.5 (5.6)	94.4 (4.8)	0.0629	1.23 (0.99, 1.53)
Wrist	423.3 (12.2)	389.6 (9.0)	376.2 (9.3)	368.7 (13.4)	389.6 (10.5)	0.0155	1.09 (1.01, 1.17)
All sites	1,149.2 (44.3)	995.3 (18.3)	1,005.4 (25.9)	978.9 (23.3)	1,011.5 (47.2)	0.0291	1.14 (1.01, 1.28)

* Lowest income quintile Significant results in boldface.

Age adjusted fracture incidence per 100,000 person years according to income quintiles

Disclosures: Sharon Brennan, None.

SA0338

See Friday Plenary Number FR0338.

SA0339

See Friday Plenary Number FR0339.

SA0340

Implementation of FLS in the Province of Quebec (Canada): perseverance and creativity. <u>Marie-Claude Beaulieu</u>*[1], <u>Hélène Corriveau</u>[2], <u>Isabelle Gaboury</u>[2], <u>François Cabana</u>[3], <u>Gilles Boire</u>[4]. [1]Université de Sherbrooke, Canada, [2]Université de Sherbrooke, Canada, [3]CHUS, Canada, [4]Centre Hospitalier Universitaire De Sherbrooke, Canada

In the early 2000's, despite existing guidelines and recommendations, gaps in care after a fragility fracture (FF) persisted. To address these gaps, the OPTIMUS program was implemented in the Estrie area of the Province of Quebec, to foster inter-professional collaboration and to facilitate the involvement of Family physicians in the care of FF patients. The results in over 1400 consecutive patients were strongly positive, with treatment after a FF increasing from less than 20% to more than 50%. Family physicians, as well as family medicine and orthopedic residents, have been

trained to respond to a FF and now actively collaborate to their patients' treatment. A provincial interdisciplinary group called FOCUS (Fractures = Osteoporosis Care for US) has been working since 2011 to improve FF care and to implement Fracture Liaison Services (FLS) across the Province, in various centers including urban and rural regions. FOCUS includes physician champions in various disciplines (family medicine, internal medicine, rheumatology and orthopedics) as well as nurses. Meetings and exchanges have been made with regional health agencies and the Ministry of Health. A FLS system is now in place for post-hip FF care in Sherbrooke as well as in 3 hospitals in Montréal. OPTI-FRAC, a CIHR-supported research program, integrates locally adapted FLS systems with fall prevention in 5 areas of the Province. Members of the group share their algorithms of treatment, tools and other materials including a website. One team member was involved in the Canadian group on FLS implementation by Osteoporosis Canada and in the French translation of the pamphlet 'Make the first break the last with FLS.' This is now being circulated among clinicians, knowledge users and bureaucrats. Multiple local and regional initiatives are under way, following the FLS 2i and 3i models. Collective orders for nurses, personnel training, webinar for family physicians, pharmacists, nurses, physical therapists and a workshop for family medicine residents are concrete results of the group's work. We now work on the implementation of FLS across the province (according to local needs and resources), and on the integration of inpatients with FF of the proximal humerus, pelvis, wrist and vertebra into the FLS currently in place. By remaining creative and perseverant, with collaboration and adaptation to local realities, we develop efficient but low cost programs.

Disclosures: Marie-Claude Beaulieu, None.

SA0341

Osteoporosis in Female Type 1 Diabetic Patient at the Veterans Affairs Medical Center. Foiqa Chaudhry*[1], Kwame Ntim[2]. [1]University of Florida, USA, [2]University of Florida, USA

Objective: To highlight the importance of thorough secondary workup of osteoporosis in a young Type 1 diabetic female presenting after fracture.

Case: This patient is a twenty nine year old female who presented to the endocrinology department at the VA Hospital for initial consultation regarding management of her uncontrolled Type 1 diabetes mellitus. She had been diagnosed at age 18 and had since developed retinopathy, gastroparesis and neuropathy. Her most recent A1c was 11.1%. In obtaining her complete history, it was stated that she suffered a fall from sitting height and sustained a rib fracture a few months prior. This was followed up with a DXA scan which revealed a spine L1-L4 T score -2.0, Z score -2.0, BMD 0.83 grams per centimeter squared and left femoral neck T score -2.6, Z score -2.6, and BMD 0.56 grams per centimeter squared. She was told the osteoporosis was due to her poor diabetes control and plans were to start her on oral bisphosphonate therapy. On further questioning, patient revealed that she had not had a menstrual cycle in over 3 years. Laboratory data also showed 25-OH vitamin d level of 18.57 ng/mL nearly two years ago with no current supplementation. Though diabetes is a risk factor for osteoporosis, a lengthy discussion was undertaken to discuss possible secondary causes of her condition including primary ovarian failure and celiac disease. FSH and LH were ordered and patient referred to GI for bowel biopsy.

Discussion: Secondary causes are commonly considered when osteoporosis is found in a young patient. When receiving care in a VA setting however, causes such as premature menopause may be overlooked given the skewed population demographics, i.e. mostly male patients. Also, associated autoimmune conditions such as Celiac disease and primary ovarian failure should always be considered when managing a patient with Type 1 diabetes mellitus. These conditions may be the underlying cause of osteoporosis and should be addressed before considering bisphosphonate therapy.

Disclosures: Foiqa Chaudhry, None.

SA0342

Physicians' Attitudes to Contemporary Issues on Osteoporosis Management in Korea. Young-Kyun Lee*[1], Yong-Ki Min[2], Hyoung-Moo Park[3], Deog-Yoon Kim[4], Ho-Yeon Chung[5], Yong-Chan Ha[6]. [1]Seoul National University Bundang Hospital, South Korea, [2]Samsung Medical Center, South Korea, [3]Chung-Ang University College of Medicine, South Korea, [4]Kyung Hee University Hospital, South Korea, [5]Kyung Hee University, South Korea, [6]Chung-Ang University Hospital, South Korea

Background: Recently, several concerns here have been raised in management of osteoporosis. The current issue included the utilization of DXA and FRAX, screening of vitamin D deficiency and secondary osteoporosis, and long-term use of bisphosphonate and calcium supplements. There was no study on physicians' attitude on these current issues in Korea. Therefore, we investigated the physicians' attitude on these issues by survey.

Methods: We administered a 30-item questionnaire to all members of Korean Society for Bone and Mineral Research by email survey form. One hundred participants answered the questionnaire. The questionnaire included the questions about the physicians' attitude to current issues and the barriers to osteoporosis treatment in Korea.

Results : Most physicians use bone densitometry devices (99 %) and, central DXA was the most accessible device (95 %). Eighty-eight percent were aware of FRAX®,

but among them, only 19.3 % used it. The main reason for not using FRAX® was the lack of time in their proactive (76%) (Figure 1). Screening for vitamin D status and secondary osteoporosis was performed by 59% and 52 % of the respondents, respectively. The lack of awareness among patients and high costs of medication were perceived as the most important barriers to osteoporosis management in Korea (Figure 2).

Conclusion : This study provides physicians' perspective to the current issue for diagnostic and treatment of osteoporosis in Korea. To further improve osteoporosis management, educational programs for patients and doctor, and the improvement of reimbursement system should be considered in Korea.
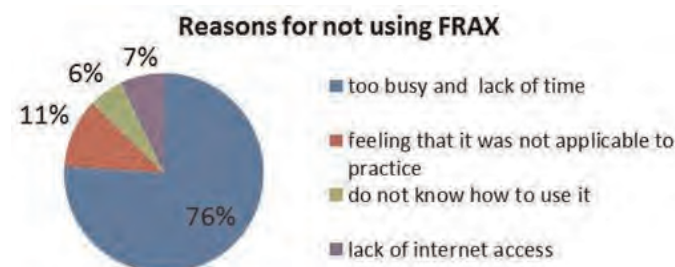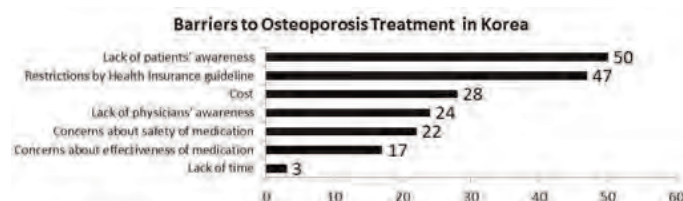

Figure 1

Figure 2

Disclosures: Young-Kyun Lee, None.

SA0343

See Friday Plenary Number FR0343.

SA0344

See Friday Plenary Number FR0344.

SA0345

See Friday Plenary Number FR0345.

SA0346

Factors Associated With Early Functional Outcome After Hip Fracture Surgery. Matthew Cohn*[1], Ting Cong[2], Benedict Nwachukwu[3], Minda Patt[4], Pingal Desai[5], Kara Gasiorowski[4], Jin Chen[3], Jonathan Jo[6], Joseph Lane[5]. [1]Weill Medical College of Cornell University, USA, [2]Weill Cornell Medical College, USA, [3]Hospital for Special Surgery, USA, [4]NewYork Presbyterian-Weill Cornell Medical Center, USA, [5]Hospital for special surgery, USA, [6]Weill Cornell Medical College, Hospital for Special Surgery, USA

Background: Hip fractures are common among patients with osteoporosis and as the U.S. population ages they are likely to be more prevalent. Early functional status is an indicator of longer-term outcome, predictors of functional recovery after hip fracture surgery have not been well studied. The purpose of this study was to determine the impact of surgical delay beyond 48 hours, after-hours surgery and ancillary support staff on early functional outcome after hip fracture surgery.

Methods: Ninety-nine consecutive patients underwent hip fracture surgery by a single surgeon between 2009 and 2013. Surgery after 48 hours was deemed as surgical delay and surgery after 5pm was deemed as after-hours. Ancillary staff experience was determined by experts from our institution as well as documented level of training. Functional status was determined by independent ambulation on post-operative day 3.

Results: Our study consisted of 99 patients (62 females). The mean age of our population was 79 ($\pm$12.6) years with a mean American Society of Anesthesiologists (ASA) classification of 2.8 ($\pm$0.59). Sixty-two patients experienced no delay and 72 patients received surgery during daytime hours. On post-operative day three, 49 of 63 patients (78%) with no delay were ambulating whereas only 14 of 36 patients (39%) with delayed surgery were able to ambulate (p < 0.001). This relationship persisted

when adjusted for ASA classification. No delay in patients over 80 (OR, 6.91 95% CI 2.16, 22.10) and females (OR, 7.05 95% CI 2.34, 21.20) was associated in greater chance of early ambulation. After-hours surgery was not associated with ambulation (p=0.35). Anesthesiologist and circulating nurse experience had no impact on patient's ambulatory status however non-orthopaedic scrub technicians were associated with worse functional status (OR 7.50, 95% CI, 1.46, 38.44, p = 0.01).

Conclusions: Surgical delay and non-orthopaedic scrub technicians are associated with worse early functional outcome after hip fracture surgery. Surgical delay should be avoided in older patients and women. More work should be done to understand the impact of surgical team composition on outcome.

Disclosures: Matthew Cohn, None.

SA0347

See Friday Plenary Number FR0347.

SA0348

Daily intake of high-dose vitamin D-enriched milk in healthy postmenopausal women: A randomized, controlled and double-blind nutritional trial (The EFICALCIO Study). Rebeca Reyes-Garcia*[1], Manuel Muñoz-Torres[2], Antonia Garcia-Martin[3], Santiago Palacios[4], Nancy Salas[4], Nicolas Mendoza[5], Miguel Quesada-Charneco[6], Federico Lara-Villoslada[7], Juristo Fonolla[8]. [1]Bone Metabolic Unit (RETICEF), Endocrinology Division, Hospital Universitario San Cecilio, Instituto de Investigación de Granada. Endocrinology Unit. Hospital General Universitario Rafael Mendez, Lorca, Murcia., Spain, [2]Bone Metabolic Unit (RETICEF), Endocrinology Division, Hospital Universitario San Cecilio, Instituto de Investigación de Granada., Spain, [3]Bone Metabolic Unit (RETICEF), Endocrinology Division, Hospital Universitario San Cecilio, Instituto de Investigación de Granada. Endocrinology. Hospital Comarcal del Noroeste, Caravaca de la Cruz, Murcia., Spain, [4]Palacios Institute of Women's Health, Spain, [5]Department of Obstetrics & Gynecology, University of Granada, Spain, [6]Endocrinology Division, Hospital Universitario San Cecilio, Spain, [7]Departamento de Investigación y Desarrollo. Lactalis Puleva, Spain, [8]Nutrition Department, Biosearch S.A, Spain

Background: Vitamin D deficiency is highly prevalent and can be associated with adverse health outcomes. Few studies have evaluated the effects of daily consumption of milk fortified with a high dose of vitamin D in a large cohort of healthy postmenopausal women.

Aims: To determine the effect of daily intake of milk enriched with vitamin D [with or without fructooligosaccharides (FOS)] on vitamin D status, bone mass and cardiovascular risk factors.

Patients and methods: This was a 2-year randomized controlled study in which five hundred healthy postmenopausal women (mean age 58.1 ± 4.8 years) were assigned to receive 500 ml/day of a dairy product to one of three groups: Control group (C) with skimmed milk (120 mg/100 ml calcium and vitamin D 0.75 ug/100 mL), group A with skimmed milk enriched with calcium and vitamin D (180 mg/100 mL and 3 ug/100 mL) and group B with skimmed milk enriched with calcium and vitamin D (180 mg/100 mL and 3 ug/100 mL) and FOS (5 g/L). We evaluated serum levels of 25-OH-vitamin D. We also measure anthropometric parameters, biochemical data of glucose metabolism and lipid prolife, body composition by electrical impedance and bone mineral density by DXA.

Results: After 24 months, changes in vitamin D in the control group (n=150) were non-significant (22.0 ± 7.3 vs 22.6 ± 7.3 ng/ml, p= 0.1). In group A (n=152) and group B (n=150) we observed a significant increase in vitamin D (Group A 21.3 ± 6.8 vs 26.6 ± 6.4 ng/ml; Group B 21.9 ± 9.5 ng/ml vs 25.2 ± 6.2 ng/ml, p<0.001 for both). The increase in vitamin D concentrations showed no differences according to the group of treatment (A or B). However, the changes observed in both groups of treatment were significantly higher compared to control group. In groups A (85.2%) and B (81.7%) a high percentage of women reached vitamin D levels>20 ng/ml, compared with the control group (53.9%), p < 0.01 for the comparison with control group.

Conclusions: Our data data confirms that daily intake of milk highly enriched with vitamin D, with or without FOS, in postmenopausal healthy women induces a significant improvement in vitamin D status.

Disclosures: Rebeca Reyes-Garcia, None.

SA0349

Eldecalcitol, a second generation active vitamin D analog, increases lumbar spine BMD in osteoporotic patients treated with alendronate regardless of their pretreatment levels of bone turnover. Akinori Sakai*[1], Masako Ito[2], Tatsushi Tomomitsu[3], Hiroshi Tsurukami[4], Satoshi Ikeda[5], Fumio Fukuda[6], Hideki Mizunuma[7], Tomoyuki Inoue[8], Hitoshi Saito[9], Toshitaka Nakamura[10]. [1]University of Occupational & Environmental Health, Japan, [2]Nagasaki University Hospital, Japan, [3]Department of Radiological Technology, Kawasaki College of Allied Health Professions, Japan, [4]Tsurukami Clinic of Orthopedics & Rheumatology, Japan, [5]Ken-Ai Memorial Hospital, Japan, [6]Kitakyushu General Hospital, Japan, [7]Department of Obstetrics & Gynecology, Hirosaki University School of Medicine, Japan, [8]Taisho Pharmaceutical Co., Ltd., Japan, [9]Chugai Pharmaceutical Company, Limited, Japan, [10]National Center for Global Health & Medicine, Japan

Purpose: In order to maximize the efficacy of bisphosphonate (BP), and to prevent negative calcium balance, osteoporotic patients on the BP therapy are generally recommended to take native vitamin D plus calcium concomitantly. In Japan, active vitamin D analog is often prescribed with BP for the same purpose. In this study, we compared the clinical efficacy and safety of concomitant use of a newly developed active vitamin D analog, eldecalcitol (ELD), with those of native vitamin D plus calcium supplementation, in patients with primary osteoporosis treated with alendronate (ALN).

Methods: A total of 219 patients were randomly assigned 1:1 to receive daily oral 0.75mg ELD plus weekly oral 35mg ALN, the licensed dose in Japan (ELD+ALN group; n=110), or daily oral vitamin D 400IU + calcium 610mg plus ALN (VitD/Ca+ALN group; n=109) for 48 weeks. The primary endpoint was percent change in lumbar spine BMD at the patient's last visit. Bone turnover markers and others were also evaluated.

Results: Compared with baseline, lumbar spine BMD increased 7.3% in the ELD+ALN group, 6.5% in VitD/Ca+ALN group in 48 weeks. There was no statistically significant difference between the two groups. All the bone turnover markers (serum BAP, P1NP, TRACP-5b, CTX and urinary NTX) measured were significantly reduced from the baseline in both groups. Reduction of the bone turnover markers was significantly greater in the ELD+ALN group than in the VitD/Ca+ALN group. Patients were then stratified by the pretreatment levels of each bone turnover marker. In patients with high pretreatment level of bone turnover markers (higher than upper normal limit), lumbar spine BMD significantly and equally increased from the baseline in both ELD+ALN and VitD/Ca+ALN groups. However, in patients with low or normal pretreatment level of bone turnover markers, the increases in lumbar spine BMD were blunted in the VitD/Ca+ALN group, on the other hand, treatment with ELD+ALN increased lumbar spine BMD comparable to those in patients with high pretreatment level of bone turnovers. No new safety concerns as well as no serum and urinary calcium abnormality were observed in both groups.Discussions: ELD increases lumbar spine BMD regardless of pretreatment levels of bone turnover markers in osteoporotic patients treated with ALN. Combination of ALN and ELD may be most beneficial in patients with low or normal baseline bone turnover.

Disclosures: Akinori Sakai, None.

SA0350

Evaluating the Effects of High-Dose Supplemental Vitamin D on Bone Density and Structure: Design of the VITamin D and OmegA-3 TriaL (VITAL). Amy Yue*[1], JoAnn Manson[2], Julie Buring[2], Nancy Cook[2], Patricia Copeland[1], Meryl Leboff[3]. [1]Brigham & Women's Hospital, USA, [2]Brigham & Women's Hospital Professor of Medicine, Harvard Medical School, USA, [3]Brigham & Women's HospitalProfessor of Medicine, Harvard Medical School, USA

Despite enthusiasm for the use of vitamin D supplements for bone health, it is uncertain whether supplemental vitamin D *alone* or in high doses has beneficial effects on bone health measures. Previous clinical trials have been limited by the inability to separate the effects of supplemental calcium from vitamin D, small sample size, and lack of measured 25-hydroxyvitamin D [25(OH)D] levels. To test whether high-dose supplemental vitamin D vs. placebo prevents bone loss, and improves bone structure and the balance of bone remodeling, we are conducting an ancillary study to the *VIT*amin D and Omeg*A*-3 Tria*L* (VITAL). VITAL is a 2x2 factorial, double-blind, placebo-controlled trial testing the benefits and risks of daily supplemental vitamin D_3 (cholecalciferol; 2000 IU/d) and/or omega-3 fatty acids (EPA+DHA; 1 g/d) in the primary prevention of cancer and cardiovascular disease among ~26,000 men aged ⩾50 and women aged ⩾55 years in the U.S. A sub-cohort of >1000 VITAL participants in the New England region were enrolled for detailed, in-person assessments at baseline and year 2 post-randomization at Harvard Catalyst, the NIH-sponsored Clinical and Translational Science Center (CTSC). Among CTSC participants not using bone active medications at baseline, we measured bone mineral density (spine, hip, and total body) and body composition (total and regional fat and

lean tissue) by dual X-ray absorptiometry (DXA), bone turnover biomarkers (serum procollagen type I N-terminal propeptide, osteocalcin, C-terminal telopeptide levels) and bone structure at the distal radius and tibia by peripheral quantitative computed tomography (pQCT). DXA and pQCT assessments were completed in 778 (exceeding target of 600) and 684 participants, respectively. Baseline levels of 25(OH)D, calcium, and PTH were collected in VITAL. All CTSC-based measures will be repeated 2 yrs post-randomization. We will also obtain bone architecture measures by high-resolution pQCT at year 2 post-randomization. This ancillary bone study will determine whether high-dose, supplemental vitamin D confers protective effects on bone density, structure and turnover, has effects on body composition, and whether achieved 25(OH)D levels affect these outcomes and vary according to body mass index and body composition. Results from this study will fill gaps in knowledge and elucidate the mechanisms through which high-dose vitamin D alone may prevent age-related fractures and have beneficial effects on bone health.

Disclosures: Amy Yue, None.

SA0351

Exposure to direct sunlight biodegrades vitamin D in milk. R. C. Hamdy, R. Mohseni, C. Magallanes, B. Som, T. Piggee. East Tennessee State University, Johnson City, TN 37614. <u>Ronald Hamdy</u>*. East Tennessee State University, USA

Vitamin D is essential for all phases of bone health. Its deficiency is very prevalent and one of the major causes of osteoporosis which affects about half the Caucasian female population over the age of 50 years. The mortality and morbidity associated with osteoporosis have profound psycho-socio-economic implications. Given that milk is fortified with vitamin D (cholecalciferol) and is considered a major source of this vitamin, we were concerned that direct exposure to sunlight would enhance its biodegradation and therefore lull consumers into a false sense of security regarding their dietary vitamin D intake.

The purpose of this study was to assess the effect of direct sunlight exposure on milk vitamin D content. The study was conducted on October 9, 2013 on a sunny day in North East Tennessee, average temperature 15°C/59°F. Commercially available skim milk (Kroger brand) within the recommended period of its 'Best used by date' was utilized. Two subsamples of milk were transferred to clear glass containers. One was placed under direct sunlight and the other in an adjacent shaded area. The tops were placed on the containers to avoid particulate matters getting in the containers. At 0, 15, 60, 120, and 180 minutes samples were taken from each container and transferred to clear glass vials. The modified AOAC Official Method 992.26 was utilized to extract vitamin D_3 (cholecalciferol). To validate the method, calibration curves were examined every time prior to analyzing the extracts. A sample of milk was also spiked with vitamin D_3 standard to validate the extraction procedure. The linear correlation between cholecalciferol concentration (range of 0.025-0.40 ppm) and peak area (R^2= 0.9986) confirms the validity of our methodology.

Our data show that about 65% of cholecalciferol in milk biodegrades within 15 minutes of exposure to direct sunlight. By 60 minutes only 17% of the original cholecalciferol remains in milk exposed to direct sunlight whereas 97% is still available in the sample kept in shade. These results have significant implications. Glass containers do not protect against cholecalciferol biodegradation.

Percent vitamin D content in milk
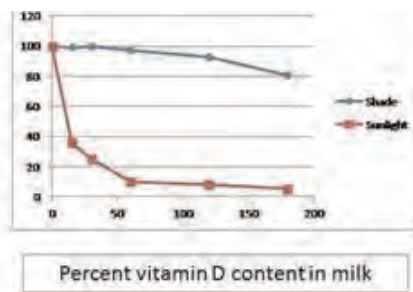
Biodegrad.D

Disclosures: Ronald Hamdy, None.

SA0352

See Friday Plenary Number FR0352.

SA0353

Rising Trend in Vitamin D Status in Ireland from 1993 to 2013: Concerns for the Future. <u>Malachi McKenna</u>*[1], <u>Barbara Murray</u>[2], <u>Myra O'Keane</u>[3], <u>Mark Kilbane</u>[3]. [1]St. Michael's Hospital, Ireland, [2]St. Michael's Hospital, Ireland, [3]St. Vincent's University Hospital, Ireland

Background. Concern has been expressed regarding the prevalence of vitamin D deficiency but also regarding unsubstantiated claims regarding benefit of high oral intakes. The Institute of Medicine (IOM) 2011 Report revised upwards dietary reference vitamin D intakes but cautioned against exceeding recommended intakes. They also specified corresponding 25-hydroxyvitamin D (25OHD) levels of 40 nmol/L (16 ng/mL) as the estimated average requirement (EAR) and 50 nmol/L (20 ng/mL) as the recommended daily allowance (RDA).

Objectives. We sought (1) to examine change in 25OHD over the last 20 years, (2) to create a model for trends in 25OHD from the dataset, and (3) to forecast levels of 25OHD based on the current trend.

Methods. We collated all 25OHD results from May 1993 until December 2013. The total number of results extracted was 69,012. After trimming the database to one sample per person, the total number was 43,997. We conducted a time series analysis that was analysed using a 4253H smoother, which is a running median smoothing function. We used the auto-regressive integrated moving average (ARIMA) model to examine trend, seasonality and cycles. The model was rebuilt excluding the final 3 years followed by comparison of the forecasted values with the actual values. Using the ARIMA model, forecasting 25OHD levels was extended to 2016. A single linear regression model was fitted to the last 6 years of the data in order to represent the moving average over time.

Results. The yearly average 25OHD increased from 30.6 nmol/L in 1993 to 50.8 nmol/L in 2013. The time series analysis using the 4253H smoother demonstrated seasonality of the data, as expected, and an upward trend without any cycles. The ARIMA model showed a close fit between the model and the data; the mean value of the errors was close to zero; the variance was least in the last 5 years; the error terms were normally distributed; and the rebuilt model performed well in predicting the values through 2011 to 2013. The forecast model up to 2016 showed an upward trend and seasonality. The regression equation was: 25OHD in nmol/L=month*0.057+43, indicating a yearly increase in average 25OHD of 0.68 nmol/L.

Conclusions. We noted a steady and consistent improvement in vitamin D status over the past 20 years such that the yearly average in 2013 at 50 nmol/L exceeded the IOM EAR of 40 nmol/L. This trend shows no sign of abating. There is now a dual concern about vitamin D depletion and overreplacement.

Disclosures: Malachi McKenna, None.

SA0354

See Friday Plenary Number FR0354.

SA0355

The Impact of 25(OH) Vitamin D Reference Method Procedure (RMP) Alignment on Measurements Obtained with the IDS Chemiluminescent-based Automated Analyzer Assay. <u>Christine Simpson</u>*[1], <u>Anna Maria Cusano</u>[2], <u>Karl Insogna</u>[1]. [1]Yale University School of Medicine, USA, [2]Yale University School of Medicine, USA

To address uncertainty in measuring 25(OH) vitamin D, the Vitamin D Standardization Program (VDSP) was established by the NIH, NIST, the CDC, and Ghent University. This program identified ID-LC-MS/MS as the 25(OH) vitamin D Reference Measurement Procedure (RMP). This ID-LC/MS/MS method is traceable to NIST Standard SRM2972. As manufacturers align their product to the RMP, the concern is that results obtained in aligned assays will be divergent from those obtained with pre-alignment assays. This may result in confusion among clinicians and consumers. IDS offers a chemiluminescent assay for 25(OH) vitamin D on its iSYS platform which has recently been harmonized to the RMP. Using single donor human serum samples with RMP target values, supplied by the VDSP, IDS calibrated their master human serum samples library. This library was used to value-assign the internal calibrators to define the assay's master curve and kit lot-specific calibrators. The predefined master curve is adapted to the analyzer using kit lot-relevant calibrators. To determine the impact of standardization on results obtained with iSYS reagents, 120 single donor serum samples were analyzed in two non-standardized and one standardized iSYS assay. As summarized in the graph, regardless of disease category or metabolite concentration, there was excellent agreement in results obtained in all three assays. For all 120 samples the $M\pm SD$ for the two non-standardized assays were 43.8 ± 22 and 44.3 ± 22 as compared to a mean value of 45.8 ± 23 ng/mL in the standardized assay. These initial data provide confidence that the move to NIST standardized assay will have little impact on results obtained with the iSYS platform.

25(OH) D Measurements in Eight Disease Categories Using Standardized and Non-standardized Reagents

Disclosures: Christine Simpson, None.

SA0356

Vitamin D Levels in Young Women with Anorexia Nervosa during Nutritional Rehabilitation and Relationship with Bone Mass. <u>Anna Svedlund</u>*[1], <u>Bojan Tubic</u>[2], <u>Cecilia Pettersson</u>[2], <u>Per Magnusson</u>[3], <u>Björn Wettergren</u>[4], <u>Diana Swolin-Eide</u>[5]. [1], Sweden, [2]Queen Silvia Children's Hospital, Sweden, [3]Linkoping University,Sweden, Sweden, [4]Paediatric Primary Care, Sweden, [5]Queen Silvia Children's Hospital, Sweden

Purpose: Anorexia nervosa (AN) may result in permanent low bone mass. The aim of this study was to investigate relationship with vitamin D and bone mineral density (BMD), bone mineral content (BMC) and body mass index (BMI) in young women hospitalized for severe anorexia nervosa.

Methods: Seventeen female patients with AN admitted to a specialised eating disorder inpatient unit (20.0 $\pm$ 2.5 years, BMI 15.5 $\pm$ 0.8 kg/m^2) were included. Six patients had vitamin D supplements daily before study entry. Patients underwent nutritional rehabilitation for 12 weeks with an extra high energy diet, starting at median 75 kcal/kg/day and gradually declining to 48 kcal/kg/day during the study. The mean intake of vitamin D and calcium was 26 μg resp. 2700 mg daily at start. Serum 25-hydroxyvitamin D (25(OH)D) was assessed by an electrochemiluminescence assay (Roche Diagnostics). BMD, BMC and body composition were measured by dual-energy X-ray absorptiometry (DXA) (Lunar Prodigy). Tibia volumetric BMD and muscle area were measured by peripheral quantitative computed tomography (pQCT) (Stratec).

Results: The mean weight gain was 9.2 kg and mean BMI 18.8 $\pm$ 1.0 kg/m^2 after 12 weeks, p<0.0001. No patient was vitamin D deficient (<25 nmol/l) and 24 % of the patients had vitamin D levels <75 nmol/l at start. The median serum 25(OH)D was 84 nmol/l at baseline and 75 nmol/l after 12 weeks (no significant change). At baseline the total body BMD (TBBMD) Z-score was above -1 in 13 patients, and 2 patients had Z-scores less than -2. There was no significant difference in TBBMD. TBBMD Z-score was significantly lower after 12 weeks, p<0.01. No difference in lean mass was observed. The adipose tissue increased from 12.2 $\pm$ 5.1% to 26.3 $\pm$ 5.0%, p<0.0001. Total BMC was significantly higher after 12 weeks, p<0.001. Trabecular and cortical bone mass, assessed by pQCT, were significantly lower after 12 weeks. We found no significant associations between serum 25(OH)D and BMD, BMC or BMI.*Conclusion:* On a positive note, none of the patients were vitamin D deficient at the start of this study. 25(OH)D levels did not decrease during the study although very little exposure to sunlight. We suggest that the adequate vitamin D status could be explained by sufficient vitamin D levels prior to study start and the high content of vitamin D in the diet. The increased BMC values suggest a positive effect on bone mass but further longitudinal studies are required to determine the long-term effect on BMD.

Disclosures: Anna Svedlund, None.

SA0357

See Friday Plenary Number FR0357.

SA0358

See Friday Plenary Number FR0358.

SA0359

See Friday Plenary Number FR0359.

SA0360

See Friday Plenary Number FR0360.

SA0361

See Friday Plenary Number FR0361.

SA0362

See Friday Plenary Number FR0362.

SA0363

See Friday Plenary Number FR0363.

SA0364

See Friday Plenary Number FR0364.

SA0365

See Friday Plenary Number FR0365.

SA0366

See Friday Plenary Number FR0366.

SA0367

See Friday Plenary Number FR0367.

SA0368

See Friday Plenary Number FR0368.

SA0369

See Friday Plenary Number FR0369.

SA0370

See Friday Plenary Number FR0370.

SA0371

See Friday Plenary Number FR0371.

SA0372

A double-blind, randomized, Phase III, multicenter study in 300 pediatric subjects receiving isotretinoin therapy therapy demonstrate no effect on pediatric bone mineral densityPurpose:. Kevin Hoover*[1], Colin Miller[2], Craig Langman[3], Rick Gilbert[4], Jason Gross[5]. [1]Virginia Commonwealth University, USA, [2]BioClinica, Inc., USA, [3]Ann & Robert H Lurie Childrens Hospital of Chicago, USA, [4]TKL Research, USA, [5]Cipher Pharmaceuticals, Canada

Abstract

Purpose: Isotretinoin (13-cis-retinoic acid) is a treatment for recalcitrant nodular acne with a purported effect on bone mineral density (BMD) in the spine and proximal femur. The side effects of isotretinoin were evaluated in a recent study to assess the safety of a new FDA-approved isotretinoin formulation: Lidose-isotretinoin (CIP-Iso).

Methods: This double-blind, randomized, Phase III, active control, parallel-group, multicenter study evaluated the safety and efficacy of CIP-Iso compared to a marketed isotretinoin in patients with severe recalcitrant nodular acne. To ensure optimum DXA assessments the following were excluded at screening: those with metal prosthetics in the spine, hip, or femur; fewer than 3 evaluable lumbar vertebrae between L1 and L4; or BMD Z-score < -2.0. 300 pediatric male and female patients aged between 12 and 17 years with documented Tanner stages were enrolled. Female patients were carefully screened and monitored to avoid pregnancy. Patients underwent 20 weeks of treatment with doses of 0.5-1.0 mg/kg/d and baseline and post-treatment DXA measurements of the spine were obtained utilizing either Hologic or GE (Lunar) scanners. 127 of the 300 subjects had heights documented and height adjusted Z-scores (HAZ) calculated.

Results: Z-Scores on the 300 subjects at baseline and post-treatment were not different in the treatment groups. The mean overall Z-score at baseline was 0.39 (1.09) and post-treatment of 0.34 (1.08) (Figure 1) (p=.25). The change in Z-score after treatment showed a dependence on Tanner Stage (p < 0.05). In the subset of patients in whom HAZ could be calculated, there was no dependence on Tanner stage. A statistically insignificant mean rise in HAZ was identified after treatment.

Conclusion: Two formulations of isotretinoin do not demonstrate a statistically significant effect on BMD or difference from one another. Trial patients demonstrated mean positive baseline Z-scores at study entry, likely due of the excluding patients with Z-scores of < 2.0. Z-scores demonstrated a statistically insignificant decline in bone mineral density that disappeared in those patient scores adjusted for height. The data from this clinical trial suggests that there is not a clinically meaningful effect on BMD on pediatric subjects taking isotretinoins for up to 6 months to treat recalcitrant nodular acne.
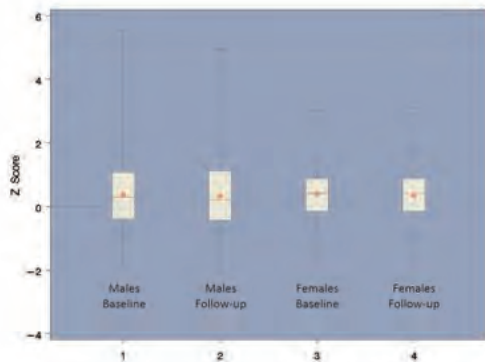

Fig. 1 Z-scores before and after treatment

SA0373

SA0374

Effects of long-term thyrotropin-suppressive therapy on bone mineral density and fracture prevalence in elderly women with differentiated thyroid carcinoma. Sabine Weidner[1], Albrecht Popp*[2], Sandra Grifone[3], Helene Buffat[3], Christian Boy[1], Thomas Krause[1], Kurt Lippuner[2]. [1]Department of Nuclear Medicine, Inselspital, University Hospital Berne, Switzerland, [2]Department of Osteoporosis, University Hospital & University of Berne, Switzerland, [3]Department of Osteoporosis, University Hospital & University of Berne, Switzerland

Introduction:
Patients with differentiated thyroid carcinoma (DTC) are commonly treated with thyroxine-based long-term thyrotropin (TSH)-suppressive therapy resulting in a state of chronic subclinical hyperthyroidism. Reported effects of TSH-suppressive therapy on bone are inconsistent. The aim of the present study was to determine the effects of TSH-suppression on areal bone mineral density (BMD) and fracture status in a homogeneous group of elderly women with DTC.

Methods:
Case-control study with consecutive women (>65 years) with DTC under current long-term TSH-suppressive therapy (>3 years) followed at the University Hospital of Berne, Switzerland, (cases) and age-matched healthy women from a representative age-matched population sample (controls). BMD was measured at lumbar spine (LS), hip (FN/TH), radius (rad 1/3), tibial diaphysis (T-DIA), and tibial epiphysis (T-EPI) by Dual Energy X-ray Absorptiometry (Hologic Discovery C[TM]; Hologic, Bedford, MA, USA). Vertebral fracture assessment (VFA) was performed and the individual history of previous clinical fragility fractures collected. Fractures were categorized into major osteoporotic fractures (MOF at the hip, spine, distal radius, and proximal humerus) and non-MOF. Significances were assessed by Mann-Whitney U-test.

Results:
Of 61 cases, 40 could be matched with controls. Mean ($\pm$ SD) age was 75.7$\pm$3.9 vs. 75.3$\pm$3.8 years, respectively. Mean duration of TSH-suppression was 10.9$\pm$5.7 years. Mean BMD T-scores by DXA were not significantly different between cases and controls: LS -0.7/-1.0; FN -1.3/-1.1; TH -0.9/-0.6; rad 1/3 -1.6/-1.4; T-DIA -0.6/-0.5; and T-EPI -1.2/-1.4. Similarly, the prevalence of morphometric vertebral fractures assessed by VFA, MOF, and non-MOF were not significantly different between groups.

Conclusion:
In elderly women with DTC under long-term thyrotropin-suppressive therapy, BMD T-scores at major skeletal sites and fragility fracture prevalence were not significantly different from those in age-matched healthy controls.

SA0375

SA0376

A risk factor for fracture in patients with rheumatoid arthritis is not the disease itself but the use of glucocorticoid–the third year results of the TOMORROW study-. Tatsuya Koike*[1], Yuko Sugioka[2], Kenji Mamoto[3], Tadashi Okano[3], Masahiro Tada[3], Kentaro Inui[4]. [1]Search Institute for Bone & Arthritis Disease (SINBAD), Japan, [2]Center for Senile Degenerative Disorder, Osaka City University Medical School, Japan, [3]Orthopaedic Surgery, Osaka City University Medical School, Japan, [4]Osaka City University Medical School, Japan

Background: Patients with rheumatoid arthritis (RA) who have muscle weakness and stiff or painful joints might be at increased risk of falling and fracture. The present study prospectively determines the incidence of falls, fractures, and their risk factors in patients with RA who participated in the TOMORROW study that began in 2010.

Methods: We evaluated anthropometric parameters, bone mineral density, disease activity and the occurrence of falls and fractures for a period of three years in 202 patients with RA (58 years) and 202 age- and gender-matched healthy volunteers (controls, 57 years).

Results: There is no difference in incidence of falls/fractures between RA patients (37%/9.4%) and controls (30%/7.4%) during three years. The patients with RA fell significantly more frequently than controls (2.76 vs. 1.91 falls/three years; p = 0.03). After adjusting for risk factors for falls and fractures, including age, sex, smoking and body mass index, multiple regression analysis revealed that a history of falls was the most significant parameter associated with the incidence of falls (odds ratio [OR], 3.59; 95% confidence interval [CI], 1.61–8.00; p = 0.002) in controls. However, a history of falls was not significantly associated in patients with RA (OR, 1.93; 95% CI, 0.99–3.77; p = 0.005). The total amount of glucocorticoid (GC), the average erythrocyte sedimentation rate (ESR) during the three years and anti- cyclic citrullinated peptide antibody (CCP) levels at entry were apparently related to the number of falls after adjusting for fall risk factors among the patients (GC, β = 0.158; p = 0.028; ESR, β = -0.211, p = 0.005; CCP, β = 0.295, p < 0.001). After adjusting for the same risk factors described above and RA, GC medication at entry (OR, 4.412, p = 0.004) and prevalence of vertebral fracture (OR, 3.14, p=0.005) were only associated with the incidence of fractures in whole population of this study.

Conclusions: The incidence of falls and fractures did not significantly differ between patients with RA and controls during a period of three years; however, more patients than controls fell repeatedly. Medicating RA with GC was apparently associated with the incidence of fractures and high doses of GC were associated with an increased frequently of falls among patients with RA.

SA0377

See Friday Plenary Number FR0377.

SA0378

Intermittent PTH (1-34) Administration Enhances Endothelium-Dependent Vasodilation of the Femoral Principal Nutrient Artery in Aged Rats and Alters the Marrow Microenvironment such that Vasodilation is Improved in its Presence. <u>Seungyong Lee</u>*[1], <u>Ashley Bice</u>[2], <u>Brianna Hood</u>[2], <u>Rhonda Prisby</u>[1]. [1]University of Delaware, USA, [2]University of Delaware, USA

BACKGROUND: Age-related declines in bone mass coincide with vascular dysfunction as evidenced by reduced vasodilation of the femoral principal nutrient artery (PNA), the primary conduit for blood flow to long bones (Prisby et al., 2007, Dominguez et al., 2010). In the presence of marrow, vasodilation of the PNA was impaired in young ($p<0.05$) and old (p=0.07) rats (Prisby et al., 2013a), suggesting a detrimental influence of marrow on bone vascular function. Young rats had augmented bone volume and vasodilation of the PNA following 15 days of intermittent parathyroid hormone (PTH) 1-84 administration (Prisby et al., 2013b). Accordingly, we sought to determine the influence of PTH 1-34 on 1) bone volume, 2) vasodilation of the PNA and 3) the marrow microenvironment as a function of age. *METHODS:* Young (4-6 mon) and old (22-24 mon) male Fisher-344 rats were grouped accordingly: 1) young control (CON; n=10), 2) young PTH (n=9), old CON (n=9) and old PTH (n=8). Rats received 43 μg/kg/day of PTH 1-34 or 100 μl/day of PBS for 15 days. Right femoral PNAs were isolated, cannulated and given cumulative doses of acetylcholine (ACh; $10^{-9} – 10^{-4}$ M) and DEA NONOate (DEA; 10^{-10}-10^{-4} M) in the absence and presence of marrow. Right distal femora (n=4/group) were scanned by μCT to obtain BV/TV (%), Tb.Th (μm), Tb.N (/mm^2) and Tb.Sp (μm). *RESULTS:* Body mass was higher ($p<0.05$) in old vs. young rats and marrow mass was similar among groups (range: 51-73 mg). BV/TV was higher (p=0.053) in young CON (37 ± 2%) vs. old CON (28 ± 1%), whereby Tb.N was augmented and Tb.Sp reduced. BV/TV was not enhanced with PTH treatment (young PTH; 38 ± 2% and old PTH; 29 ± 3%). Vasodilation of the PNA to ACh was diminished ($p<0.05$) 38% in old rats and, in the presence of marrow, vasodilation was reduced ($p<0.05$) by 44% in young rats. Interestingly, PTH augmented endothelium-dependent vasodilation of the PNA in old rats in the absence (11%; p=0.07) and presence (15%; $p<0.05$) of marrow. In contrast, PTH had no influence on vasodilation or the marrow microenvironment in young rats. Vasodilation to the endothelium-independent factor DEA did not change with age, PTH or marrow exposure. *CONCLUSION:* Age-related declines in endothelium-dependent vasodilation with advanced age may be partially restored with intermittent PTH administration. In addition, intermittent PTH administration alters the marrow microenvironment in aged rats such that vasodilation in its presence is enhanced following treatment.

Disclosures: SEUNGYONG LEE, None.

SA0379

See Friday Plenary Number FR0379.

SA0380

See Friday Plenary Number FR0380.

SA0381

Teriparatide Treatment for Sacral Insufficiency Fractures. <u>Yuji Kasukawa</u>*[1], <u>Naohisa Miyakoshi</u>[1], <u>Toshihito Ebina</u>[2], <u>Michio Hongo</u>[1], <u>Koji Nozaka</u>[1], <u>Yoshinori Ishikawa</u>[3], <u>Daisuke Kudo</u>[3], <u>Hayato Kinoshita</u>[4], <u>Kentaro Ohuchi</u>[1], <u>Masashi Fujii</u>[3], <u>Chie Sato</u>[3], <u>Yoichi Shimada</u>[3]. [1]Akita University Graduate School of Medicine, Japan, [2]Dept. of Orthopedic Surgery, Kakunodate General Hospital, Japan, [3]Akita University Graduate School of Medicine, Japan, [4]Akita University, Japan

Purpose: Until now, we have treated sacral insufficiency fractures with vitamin D or vitamin K in combination with low-intensity pulsed ultrasound at our institution. However, the clinical outcomes did not translate into sufficient improvement of activities of daily living (ADL). Teriparatide is expected to stimulate bone repair in cases of insufficiency sacral fractures owing to its effect on bone formation. The purpose of this study was to evaluate the effects of teriparatide on clinical outcomes and radiological findings of sacral insufficiency fractures.

Methods: We enrolled seven women (average age: 76 years) with sacral insufficiency fractures who received teriparatide treatment (subcutaneous daily injection in five patients and weekly in two patients) during 3 months or more. We evaluated comorbidities, time elapsed from pain onset to diagnosis, ADL, radiological findings, and visual analog scale (VAS) both pre- and post-treatment.

Results: Six patients had comorbidities, including hypertension, rheumatoid arthritis, liver cirrhosis, diabetes mellitus, muscle dystrophy, and acoustic nerve tumor. Average time elapsed from onset of pain to diagnosis of sacral insufficiency fracture was 17 days (3 to 20 days). Six out of seven patients (86%) could not walk or

sit because of severe pain at their first visit to our hospital. Computed tomography (CT) images revealed a fracture on the sacral wing in six patients, and a bone scintigram showed a bilateral H-shaped uptake over the sacral wings in one patient. All patients underwent teriparatide treatment after the diagnosis of sacral insufficiency fractures. Average VAS before treatment (87 mm, 69–100 mm) was significantly reduced after the 3-month teriparatide treatment (19 mm, 0–37 mm) (p=0.007). Five patients could walk after the 3-month treatment, and two patients were able to mobilize by themselves using a wheel chair. Six patients lived in their own homes, and one patient lived in an elderly care home. After the 3-month treatment, three patients presented bone union and four patients presented sclerotic changes (evidenced by CT images) at the fracture site.

Conclusion: We administered teriparatide treatment to seven elderly women with sacral insufficiency fractures within 30 days after the onset of pain. The pain was significantly improved and six patients showed bone union or sclerotic changes at the fracture site by 3 months of teriparatide treatment.

Disclosures: Yuji Kasukawa, None.

SA0382

Antiresorptive Therapy – Yes, It is Sometimes 'Too Late'. <u>Roger Zebaze</u>[1], <u>Cherie Chiang</u>[2], <u>Sandra Iuliano-Burns</u>[3], <u>Yohann Bala</u>[4], <u>Afrodite Zendeli</u>[5], <u>Negar Shahmoradi</u>[6], <u>Yu Peng</u>[7], <u>Ali Ghasem-Zadeh</u>[3], <u>Ego Seeman</u>*[3]. [1]Austin Health, University of Melbourne, Australia, [2]Austin Health, Australia, [3]Austin Health, University of Melbourne, Australia, [4]University of Melbourne, Dept. of Medicine, Australia, [5]Endocrine Centre, Austin Health, University of Melbourne, Australia, Australia, [6]Department of Endocrinology, Austin Health, Australia, [7]Straxcorp Pty Ltd, Australia

The aim of treatment of bone fragility is to prevent fractures. However, current antiresorptive therapies reduce non-vertebral fracture (NVF) risk by only 20%. Even in the settings of randomized trials ~ 80% of treated patients sustain NVF despite compliance with therapy. The reason for treatment failure is not fully understood.

Antiresorptive do not restore bone structure, they reduce the size of the reversible remodeling transient. We propose that if structural decay is too advanced (i.e., severe porosity), fragility will remain at its precarious level despite compliance with therapy. Thus, there is porosity value indicative of a structural deterioration so severe that treatment does not reduce fracture risk in people with such deterioration.

To test this hypothesis, we studied 69 postmenopausal women of whom 37 sustained a NVF despite being compliant with therapy; and 32 who remain fracture free with therapy. Patients with fracture, and fracture-free ones were matched by age ((71.2 ± 1.2 vs. 73.6 ± 1.64 years; NS) type, and duration of therapy (5.3 ± 0.56 vs. 4.7 ± 0.8; NS). Images were collected at the distal radius using HRpQCT and micro-structure was quantified using StrAx1.0. The sample was stratified into groups based on the percent porosity of the compact-appearing cortex (CC): Porosity >25% (entire population); >30%; >35%; >40%; 45%; >50%; >55%, and >60%

In groups with porosity below 45%, fracture rate was unchanged and independent of porosity (Fig, right panel). In groups with porosity >45%, fracture rate increased exponentially with increasing porosity (R^2=0.97; p<0.0001) and was 1.6 fold higher than that observed in those with porosity <45% (66.7 vs 41.6%; p=0.05). The OR for fracture according to groups followed the pattern, increasingly exponentially to reach 2.8 in patients with porosity>45% (fig Left panel) (OR similar to that observed in a similar population of untreated women[1]. About half (47.2%) of women treated with antiresorptives had a porosity >45%.

We infer that there is a level of structural deterioration (porosity >45%) above which antiresorptive therapy is ineffective. Whether or not anabolic therapy would be efficacious in such circumstances is unclear. Nevertheless, this calls into question the use of antiresorptives as first line therapy in all patients.

1.Bala et al, JBMR 2014.
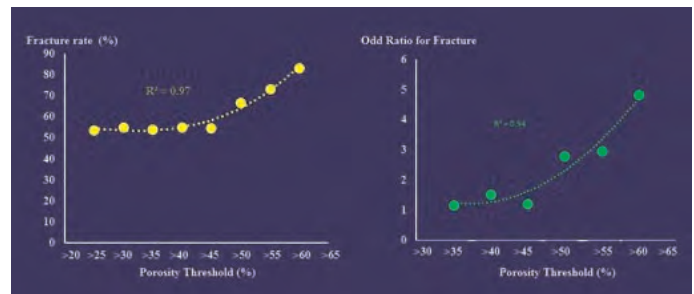
fig_treatment failure

Disclosures: Ego Seeman, Straxcorp Pty Ltd, 8

SA0383

See Friday Plenary Number FR0383.

SA0384

Withdrawn

SA0385

Brand-Name vs. Generic Oral Bisphosphonate Medications: Prescribing Patterns and Variations over Eleven Years. Lisa-Ann Fraser*[1], Jordan Albaum[2], Mina Tadrous[3], Andrea Burden[3], Salimah Shariff[4], Suzanne Cadarette[3]. [1]Western University, Canada, [2]University of Toronto, Canada, [3]University of Toronto, Canada, [4]University of Western University, Canada

Purpose: Alendronate and risedronate have proven fracture reduction efficacy and are considered first-line osteoporosis therapies. In Ontario Canada these medications are covered for those aged 65 and older by the Ontario Drug Benefit (ODB) plan. ODB has a generic substitution policy resulting in dispensing of generic versions of drugs when available. However, there is controversy as to the efficacy and safety of generic bisphosphonates. We studied oral bisphosphonates dispensed province-wide by ODB over 11 years with the aim of describing prescribing patterns in relation to brand-name vs. generic medications.

Methods: We identified all prescriptions for alendronate and risedronate dispensed through ODB from April 2001 to December 2012. Individuals who used these medications prior to 2001 were excluded, as were bisphosphonate doses used to treat conditions other than osteoporosis. Patients who reside in long-term care (LTC) are clearly identified in ODB, and therefore we divided our sample into community-dwelling vs. LTC users. The number of prescriptions dispensed per month were plotted, separately for community and LTC patients, in order to identify trends over time.

Results: We found a rapid switch from brand-name to generic bisphosphonate equivalents immediately after the generic was available, with >88% of drug dispensed being the generic version by 2 months after the release of the generic in all cases. Despite the generic substitution policy of ODB, a small population of patients remained on brand-name drug over time. There was a reduction in the number of generic drugs dispensed when new brand-name alternatives were introduced: there was a decrease in generic alendronate when Fosavance (alendronate plus vitamin D3) became available. Similarly, there was a decrease in generic weekly risedronate when monthly Actonel became available, and again when Actonel DR came out. The dispensing trends were similar in the community and in LTC.

Conclusions: The ODB generic substitution policy has resulted in rapid up-take of generic oral bisphosphonates in seniors in Ontario. However, there seems to be a preference for name-brand bisphosphonates as evidence by a drop in generics dispensed each time a new proprietary drug becomes available. Similarly, there is a small population of patients who remain on a name-brand bisphosphonate over time despite the availability of a generic equivalent.

Disclosures: Lisa-Ann Fraser, None.

SA0386

Dynamic analysis of short-term effects of bisphosphonates by using intravital two-photon microscopy. Junichi Kikuta*[1], Mai Shirazaki[2], Masaru Ishii[3]. [1]Graduate School of Medicine, Osaka University, Japan, [2]Graduate School of Medicine, Osaka University, Japan, [3]Graduate School of Medicine & Frontier Biosciences, Osaka University, Japan

Background/Purpose: Bisphosphonates have been clinically used for treatment of bone disorders such as osteoporosis. There have been many studies about the pharmacological properties of bisphosphonates, but most of them were analyzed by conventional methods such as micro-CT and histological analysis. These methods do not enable us to observe living mature osteoclasts. Thus, how bisphosphonates affect osteoclast dynamics *in vivo* remains elusive. This study aimed to investigate the short-term effects of bisphosphonates on the function of mature osteoclasts in living bone tissues by using intravital two-photon microscopy.

Methods: For visualizing mature osteoclasts, we utilized the mice expressing GFP under the promoter of a vacuolar type H^+-ATPase a3 subunit that were abundantly expressed in differentiated osteoclasts (a3-GFP mice). We observed calvaria bone tissues of a3-GFP mice by using an advanced imaging system for visualizing living bone tissues with intravital two-photon microscopy that we have originally established. For examining the short-term effects of bisphosphonates, risedronate (10 μg/kg), alendronate (20 μg/kg), or minodronate (4 μg/kg), was administered intravenously during imaging, and images were acquired consecutively.

Results: In control condition, we identified different populations of living mature osteoclasts in terms of their motility and function, i.e., 'static – bone resorptive (R)' and 'moving – non resorptive (N)'. Less than 1 hour after intravenous injection of risedronate, we found that many static osteoclasts changed their shapes and became moving cells, suggesting R to N functional switching without any change in the total number of mature osteoclasts. We also found that some osteoclasts had morphological signs suggestive of osteoclast apoptosis within several hours after risedronate administration. Furthermore, we could demonstrate that treatment of alendronate or minodronate also induced R to N conversion of mature osteoclasts on the bone surface.

Conclusion: By visualizing *in vivo* behaviors of mature osteoclasts, we found that bisphosphonates could change osteoclast morphology and inhibit bone resorption in living bone tissues within a short period.

Disclosures: Junichi Kikuta, None.

SA0387

See Friday Plenary Number FR0387.

SA0388

See Friday Plenary Number FR0388.

SA0389

Lack of Clinically Important Gender Differences in the Pharmacokinetics and Exposure-Response Relationship of Odanacatib. Julie Stone*[1], David Jaworowicz[2], Stefan Zajic[1], Rebecca Humphrey[3], Arthur Santora[4], Aubrey Stoch[5]. [1]Merck Research Laboratories, USA, [2]Cognigen Corporation, USA, [3]Cognigen Corporation, USA, [4]Merck & Co. Inc., USA, [5]Merck & Co., Inc., USA

Odanacatib is a selective cathepsin K inhibitor in development for the treatment of osteoporosis. A model-based analysis of pooled data from Phase 1, 2, and 3 clinical studies was undertaken to characterize the influence of gender on odanacatib exposures and the exposure-response relationship for the resorption biomarker uNTx/Cr, and for effects on lumbar spine bone mineral density (lsBMD).

A male population pharmacokinetic (PK) model was developed from pooled data from two Phase 1 studies, one Phase 2b study, and one Phase 3 study (918 plasma odanacatib concentrations from 180 men) and compared to a historical female PK model (Ref 1). The PK/PD dataset consisted of 1508 u-NTx/Cr values and 1269 lsBMD values from 283 men (n=126 receiving placebo) and 4999 u-NTx/Cr values and 4744 lsBMD values from 657 postmenopausal women from two Phase 2 studies. A semi-mechanistic PK/PD bone turnover model previously developed based on data from postmenopausal women was applied to the pooled male/female dataset (Ref 1). This model related odanacatib exposures to drug effects on resorption and osteoclast pharmacology to describe both uNTx/Cr and BMD longitudinal response data as a function of underlying formation and resorption rates and drug effects. The potential for gender differences in model parameters was tested using alpha 0.001 to account for the multiple evaluations applied.

The PK of odanacatib in men can be described by a one compartment model with first order absorption, dose dependent bioavailability, and linear elimination (apparent clearance of 0.976 L/hr, volume 116 L). The PK model parameter estimates in men were similar to those previously obtained in postmenopausal women with osteoporosis. Clearance in men with low testosterone levels (<250 ng/dL, n=8) was decreased 47% (95% CI 36-58%) relative to that in men with normal levels.

There were no statistically significant differences in the PK/PD relationship for anti-resorptive effects and effects on osteoclast pharmacology between men and women. Gender effects were identified on the bone formation rate component which is applied to both active and placebo subjects to reflect transient response to calcium and Vitamin D supplementation. This finding may reflect differences in diet or supplement usage by gender prior to study entry. No gender differences in endogenous bone resorption and formation rates were identified in the model suggesting that the underlying biology of turnover was not meaningfully different between male and female patients with similar disease severity.

In these analyses, no clinically important gender differences in the pharmacokinetics or exposure-response relationship of odanacatib were identified. These results support the evaluation of the same 50 mg odanacatib once-weekly dosing regimen in men and women for treatment of osteoporosis.Ref 1: Zajic et al. ASMBR 2010 Annual Meeting in Toronto, Canada

Disclosures: Julie Stone, Merck, 8; Merck, 4
This study received funding from: Merck & Co, Inc.

SA0390

Mechanically improved femoral bone strength by risedronate in postmenopausal women with breast cancer taking aromatase inhibitors : 2-year-longitudinal data. Su Jin Lee*[1], JO EUN Kim[2], Sung-Kil Lim[2], Yumie Rhee[3]. [1]Yonsei University Health System, South Korea, [2]Yonsei University College of Medicine, South Korea, [3]Department of Internal Medicine, College of Medicine, Yonsei University, South Korea

Objective: Risedronate has been proven to prevent aromatase inhibitor-induced bone loss (AIBL) assessed by 2D dual X-ray absorptiometry. We hypothesized that bisphosphonate treatment would also have benefit in the longitudinal changes in volumetric bone mineral density (vBMD) and geometric parameters in postmenopausal women with breast cancer taking aromatase inhibitors. We used quantitative computed tomography (QCT).

Methods: We retrospectively analyzed endocrine-responsive breast cancer patients who had undergone QCT measurement twice over 2 years and used propensity score analysis for matching age between two groups. All patients had been taking AIs and calcium carbonate 1250 mg plus 1000 IU as cholecalciferol. Among these patients, we classified them into two groups according to risedronate administration; calcium and vitamin D only administered group as the control (n=24), and risedronate-treated group as the RIS (n=26). The bone mineral density and cortical geometry parameters of neck, trochanter, intertrochanter, and total hip of the proximal femur were analyzed.

Results: Average age of all patients was 58.1 $\pm$ 4.7 years. Average of duration of risedronate was 633 days. CT data were obtained at baseline and follow-up scans were performed at almost 2 years. Risedronate blunted the decrease in vBMD and buckling ratio. Mean 2-year percent change from baseline in total vBMD was -0.98% (vs. -5.9% in control, p=0.022), +1.47% (vs. -2.3% in control, p=0.015), +0.1% (vs. -1.9% in control, p=0.202) and +0.77% (vs. -2.8% in control, p=0.016) in RIS group at the femoral neck, trochanter, intertrochanter, and total hip, respectively. We also found that risedronate treatment to breast cancer patients taking AIs significantly increased cortical thickness of total hip +0.3% (vs. –8.1% in control group, p=0.007) and decreased cortical buckling ratio compared to the patients taking AI only without risedronate at neck, trochanter and total hip. (Figure 1.)

Conclusion: This study shows preventive effects of oral risedronate on bone geometry as well as volumetric bone mineral density at the proximal femur by using QCT in postmenopausal women with endocrine responsive breast cancer taking AIs which can deteriorate the bone quality.
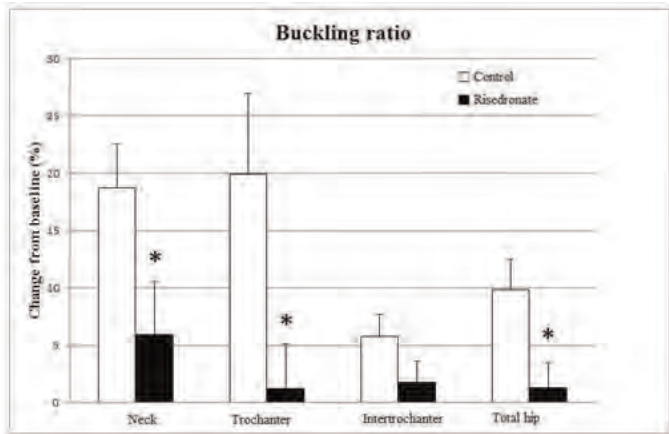

Figure 1. Percenta change from baseline of buckling ratio

SA0391

See Friday Plenary Number FR0391.

SA0392

Response in Subgroups based on Baseline 25-Hydroxyvitamin D and Bone Turnover Markers: Alendronate Sodium/Vitamin D$_3$ versus Calcitriol for Treatment of Osteoporosis in Chinese Women. <u>Zhen Lin Zhang</u>*[1], <u>Er Yuan Liao</u>[2], <u>Weibo Xia</u>[3], <u>Hua Lin</u>[4], <u>Qun Cheng</u>[5], <u>Li Wang</u>[6], <u>Yong Qiang Hao</u>[7], <u>De Cai Chen</u>[8], <u>Hai Tang</u>[9], <u>Yong De Peng</u>[10], <u>Li You</u>[10], <u>Liang He</u>[11], <u>Zhao Heng Hu</u>[12], <u>Chun Li Song</u>[13], <u>Fang Wei</u>[14], <u>Jue Wang</u>[14], <u>Lei Zhang</u>[14], <u>Arthur Santora</u>[15]. [1]Shanghai Sixth People's Hospital, Shanghai Jiaotong University School of Medicine, China, [2]The Second Xiangya Hospital, Central South University, China, [3]Peking Union Medical College HospitalDepartment of Endocrinology, Chn, [4]Peking Union Medical College Hospital, China, [5]Huadong Hospital Affiliated to Fudan University, China, [6]TianJin Hospital, China, [7]Shanghai Ninth People's Hospital, China, [8]West China Hospital, West China School of Medicine, Sichuan University, China, [9]Beijing Friendship Hospital, Capital Medical University, China, [10]Shanghai First People's Hospital, China, [11]Beijing Jishuitan Hospital, China, [12]Peking University People's Hospital, China, [13]Peking University Third Hospital, China, [14]MSD China, China, [15]Merck & Co. Inc., USA

Purpose: Postmenopausal osteoporosis co-morbid with vitamin D insufficiency is a health concern in China. A previous 6-month, randomized, open-label study (plus 6-month extension) demonstrated superior efficacy of alendronate 70mg/vitamin D$_3$ 5600 IU weekly (ALN/D5600) vs calcitriol 0.25μg daily on BMD and 25-hydroxyvitamin D [25(OH)D] increases and bone turnover marker (BTM) decreases in Chinese osteoporotic women. Our aim was to further investigate the relationship between BMD increases and baseline 25(OH)D and BTM and thus identify subgroup(s) with greater BMD increases during ALN/D5600 treatment.

Methods: In the original study, 219 women were randomized to ALN/D5600 weekly (n=111) or calcitriol 0.25μg daily (n=108) for 12 months. BMD, BTM (s-CTX/P1NP) and 25(OH)D were measured at baseline, Month 6 and 12. A post-hoc analysis was performed to assess BMD percent changes at month 12 in the ALN/D5600 group based on baseline 25(OH)D (tertiles) and BTM (median). Longitudinal data analysis was applied to model the correlation among repeated measurements. Analyses were based on the FAS with no missing data imputation. In addition, the relationship between baseline and Month 12 25(OH)D was further explored.

Results: In the ALN/D5600 group, baseline 25(OH)D tertile cut-offs were 16ng/mL and 23ng/mL. At month 12, the lumbar spine (LS) BMD percent changes were 5.34$\pm$0.69% in the 1st tertile, (n=29), 5.00$\pm$0.62% in the 2nd tertile (n=36), and 4.49$\pm$0.65% in 3rd tertile (n=32). Baseline median P1NP and s-CTx were 47.1μg/L and 533ng/L. The LS BMD changes were 5.79$\pm$0.52% above P1NP median (n=48) and 4.09$\pm$0.51% below median (n=49); and 5.18$\pm$0.54% above s-CTx median (n=47) and 4.70$\pm$0.52% below median (n=50). Post-hoc repeated measures in BMD percent changes suggested a statistical non-significance for all comparisons (p>0.05) between baseline 25(OH)D tertiles by ALN/D5600 treatment at the LS, femoral neck and total hip. However, significant differences in BMD percent change in subgroups between P1NP above and below median were seen at the LS (1.70$\pm$0.7%, 95%CI: 0.26, 3.15, p=0.02) and total hip (2.69$\pm$0.68%, 95%CI: 1.35, 4.03, p=0.0001). At Month 12, women in 2nd and 3rd baseline 25(OH)D tertiles had significantly higher 25(OH)D levels (mean>30ng/mL, p<0.05) vs. 1st tertile.

Conclusions: A 12-month ALN/D5600 treatment, increased BMD more in osteoporotic women with higher baseline BTMs and increased 25(OH)D more in women with vitamin D insufficiency at baseline.

SA0393

Risk factor for the Non-Responder of Bisphosphonates and Active Vitamin D Analog for the Treatment of Osteoporosis. <u>Mayuko Kinoshita</u>*[1], <u>Muneaki Ishijima</u>[2], <u>Yuko Sakamoto</u>[3], <u>Hidetoshi Nojiri</u>[4], <u>Liu Liz</u>[5], <u>Haruka Kaneko</u>[6], <u>Ryo Sadatsuki</u>[1], <u>Shinnosuke Hada</u>[1], <u>Kazuo Kaneko</u>[1]. [1]Department of Orthopaedics & Motor Organ, Juntendo University Graduate School of Medicine, Tokyo, JAPAN, Japan, [2]Juntendo University Graduate School of Medicine, Japan, [3]Department of Orthopaedics, Juntendo Nerima Hospital, Tokyo, JAPAN, Japan, [4]Juntendo University, School of Medicine, Japan, [5]University Graduate School of Medicine, Tokyo, JAPAN, Japan, [6]Department of Orthopaedics & Motor Organ, Juntendo University Graduate School of Medicine, Tokyo, JAPA, Japan

It has been revealed that vitamin D insufficiency is common in the community, especially for patients with osteoporosis. We have revealed that vitamin D insufficiency impaired the increase in lumber spine bone mineral density (LS-BMD) by bisphosphonates (BPs) without active vitamin D analogs for the patients with osteoporosis (CTI 2009). Combination with BPs and active vitamin D analog for osteoporosis treatment haa become widespread in Japan. We speculated that a "non-responder" for this combination therapy may exist in patients with osteoporosis. The aim of this retrospective study was to find out the factors related to the "non-responder" in this combination therapy. This study was approved by the institutional ethical review committee. During 2002 to 2012, 261 patients with osteoporosis were started to use BPs. As the 168 were excluded, the remaining 93 female patients were included in the study. BPs used in the study were alendronate, risedronate or minodronate. Active vitamin D analogs used were alfacalcidol and eldecalcidol. Multiple regression analysis was used to find the risk factors at first visit those affect %LS-BMD. A p value < 0.05 was considered to be statistically significant. LS-BMD of the patients was significantly increased by the combination therapy (p<0.001, 5.4% in average). Serum levels of iPTH were significantly decreased by the treatment (p<0.002), while serum levels of calcium were significantly increased by the treatment (p<0.001). When the patients were divided into four groups in terms of the %LS-BMD (Q1; -1.74%, Q2; 1.64%, Q3; 3.28%, Q4; 10.86%), no significant differences of the baseline characteristics of the patients were observed [e.g.; age, BMI, LS-BMD, sCa (adjusted), sPi, s25(OH)D, iPTH]. Multiple regression analysis revealed that the factor that affects the %LS-BMD was serum levels of calcium (sCa) at first visit (r^2=0.234, p=0.003). When sCa (reference range; 8.8 to 10.5 mg/ml) was 8.8-9.0 mg/ml, odds ratio for the decrease in %LS-BMD by the combination therapy for two years was 4.0 (95%CI: 1.41 to 11.38). In conclusion, when the osteoporotic patients were treated by the combination therapy for two years, the lower quarter of the patients with osteoporosis could be a "non-responder" (%LS-BMD; -1.74%). Lower serum levels of calcium at baseline, even in the reference range, is a risk factor for the "non-responder" for the treatment by the combination with BPs and active vitamin D analog.

SA0394

Sustained P1NP suppression with monthtly 150 mg risedronate treatment of postmenopausal women with low bone mass during 1 year treatment.

Gregorio Riera-Espinoza*[1], Yamila Cordero[2], Sandra Mendoza[3], Yuneci Gonzalez[3], Jeny Ramos[3]. [1]Unidad Metabolica. CEAM, Venezuela, [2]Unidad Metabolica., Venezuela, [3]Unidad Metabolica, Venezuela

Objective. It is to evaluate response of risedronate 150 mg once-a-month on P1NP, a highly specific marker of bone formation and its correlation with another high specific marker of bone resorption, C telopeptide after 1 year treatment in women with low bone mass. This two measurements has been suggested by IOF and IFCC as a reliable, specific and reproductible bone markers

Material and Methods. N-terminal propeptide of procollagen type I (P1NP) and serum Beta-CrossLaps (CTx) were evaluated in 80 postmenopausic Venezuelan women with low bone mass (T-score below -1.5) either at lumbar spine(LS) or femoral neck(FN) (Lunar Prodigy Advance, CV 1.5%). P1NP and CTx were measured on fully automated Cobas e411 (Electro-chemiluminescent immunoassay analyzer).

Results. Age was 59.8 ± 8.3, age of menopause 46.8 ± 6.3, 26% had received HRT for a mean of 2.99 years. BMD increased at lumbar spine 3.58% and 3.45% at femoral neck . P1NP reduction was: 46.3% and 54.3% at 3 and 12 months. Serum P1NP decreased more than 10% in 94.7% and 95.8% of patients at 3 and 12 months respectively

Conclusion. Risedronate 150 mg once-a-month suppressed bone remodeling into normal premenopausal reference range measured by 46.3% reduction on P1NP at 3 months and 54.3% at 12 months. CTx decreased 48% and 42% at 3 and 12 months respectively. Serum P1NP decreased more than 10% in 94.7% and 95.8% of patients at 3 and 12 months respectively . BMD increases 3.58% at lumbar spine and 3.45% at femoral neck. Our data support the use of changes in P1NP as a good indicator of effectiveness during, early 3 months or sustained 12 months, treatment of postmenopausal women with low bone mass with risedronate 150mg once-a-month

	Initial	3 months	12 months	p
DMO LS gr/cm2	0.889±0.1		0.918±0.1	<0.000
DMO FN gr/cm2	0.768±0.08		0.794±0.08	<0.000
Ca serum (mg-dl)	9.66 ± 0.37	9.72 ± 0.38	9.66±0.41	ns
P serum (mg-dl)	3.82 ± 0.46	3.78 ± 0.41	3.91±0.43	ns
Creat serum (mg/dl)	0.93 ± 0.1	0.86 ± 0.1	0.88±0.14	ns
Alkaline phosphatase (UI)	49.8 ± 13.4	42.6 ± 11.5	36.05±9.06	<0.000, initial v 3 and 12 mo <0.000 3 vs 12 mo
P1NP (ng/ml)	59.06 ± 22.3	31.01 ± 17.8	25.19±14.32	<0.000, initial vs 3 and 12 mo <0.000 3 vs 12 mo
CTx (ng/ml)	0.45 ± 0.18	0.21 ± 0.14	0.22±0.13	<0.000 initial vs 3 and 12 mo ns 3 vs 12 mo
Urinary Ca/creat	0.19 ± 0.1	0.17 ± 0.1	0.15±0.07	ns

Table 1

SA0395

The Effect of Monthly i.v. Ibandronate Injections on Japanese Patients with High-Risk Primary Osteoporosis: Subgroup Analysis of the Phase III MOVER Study.

Hiroshi Hagino*[1], Toshitaka Nakamura[2], Masako Ito[3], Tetsuo Nakano[4], Junko Hashimoto[5], Masato Tobinai[6], Hideki Mizunuma[7]. [1]Tottori University, Japan, [2]National Center for Global Health & Medicine, Japan, [3]Nagasaki University Hospital, Japan, [4]Tamana Central Hospital, Japan, [5]Chugai Pharmaceutical Corporation Limited, Japan, [6]Chugai Pharmaceutical Co. Ltd., Japan, [7]Hirosaki University, Japan

Purpose: The MOVER study compared the efficacy and safety of monthly i.v. ibandronate (IBN) with oral risedronate (RIS) in patients (pts) with primary osteoporosis. The aim was to show non-inferiority of IBN vs RIS in the incidence of non-traumatic vertebral fractures over 3 yrs. We present 3-yr subgroup data on the incidence of new/worsening vertebral fractures in pts with prevalent vertebral fractures (1 or >1, and ≥3) and femoral neck (FN) bone mineral density (BMD) T-scores ≥−2.5 or <−2.5, and <−3.0 at baseline.

Methods: MOVER was a randomized, double-blind study in ambulatory pts aged ≥60 yrs with fragile bone fracture, BMD of the lumbar spine L2–L4 or proximal femur (hip and FN) <80% of the young adult mean (T-score: –1.7, –1.6, and –1.4), and 1–5 vertebral fractures in the thoracic and lumbar spine. 1265 pts were randomized to receive i.v. IBN 0.5 or 1mg/month + oral daily placebo, or oral RIS 2.5mg/day (licensed Japanese dose) + monthly i.v. placebo.

Results: The per-protocol set comprised 1134 pts (IBN 0.5mg n=376; IBN 1mg n=382; RIS n=376). Baseline characteristics were balanced. Over 3 yrs, cumulative incidences of new/worsening vertebral fractures were 19.9% (95% CI 15.6–24.1) for IBN 0.5mg, 16.1% (95% CI 12.2–19.9) for IBN 1mg, and 17.6% (95% CI 13.6–21.6) for RIS. Both IBN doses were non-inferior to RIS (non-inferiority limit 1.55): 0.5mg, hazard ratio (HR) 1.09 (95% CI 0.77–1.54); 1mg, HR 0.88 (95% CI 0.61–1.27). The incidence of new/worsening vertebral fractures in any subgroup was lower with IBN 1mg than with RIS over 3 yrs. The fracture incidence in pts with 1 or >1 prevalent vertebral fractures was 11.2% and 20.4%, respectively, in the IBN 1mg group and 12.6% and 22.1%, respectively, in the RIS group. The fracture incidence in pts with FN BMD T-score ≥−2.5 or <−2.5 was 13.7% and 16.4% in the IBN 1mg group, and 15.0% and 19.1% in the RIS group. The fracture incidence in pts with ≥3 prevalent vertebral fractures or FN BMD T-score <−3.0 at baseline was 25.2% and 21.4% with IBN 1mg, and 31.3% and 22.2% with RIS. The fracture incidence in high risk pts was consistently lower with IBN 1mg than with RIS.Conclusions: Monthly i.v. IBN is non-inferior to oral RIS in reducing the incidence of vertebral fractures in Japanese pts with osteoporosis. IBN 1mg showed a lower numerical incidence of fractures than RIS; subgroup analyses were consistent with these findings. Monthly i.v. IBN appears to be most beneficial in pts with high fracture risk.

SA0396

SA0397

SA0398

SA0399

Effective secondary fracture prevention: a global quality exercise.

Muhammad Javaid*[1], Carey Kyer[2], Charlotte Moss[3], Paul Mitchell[4], Dominique Pierroz[5], Judy Stenmark[2], Kristina Akesson[6], Cyrus Cooper[7], and the IOF Fracture Working Group[8]. [1]University of Oxford, United Kingdom, [2]IOF, Switzerland, [3]MRC Lifecourse Epidemiology Unit, United Kingdom, [4]Synthesis Medical, New Zealand, [5]International Osteoporosis Foundation, Switzerland, [6]Skåne University Hospital, Malmö, Sweden, [7]University of Southampton, United Kingdom, [8]International Osteoporosis Foundation, Switzerland

Despite robust evidence for the effectiveness of secondary fracture prevention using a range of pharmaceutical agents, translation in the real world setting remains disappointing. One key aspect is whether the adopted the service delivery model will deliver effective case finding, assessment, treatment initiation and adherence at the population level. To support local initiatives across the globe, the International Osteoporosis Foundation developed Best Practice Framework standards providing a quality benchmark. We now report findings after the first 12 months of implementation.

30 hospitals across 5 continents submitted their questionnaires. The hospitals served populations from 100,000 to 1.3 million and were a mix of private and publicly funded. Fourteen services were led by orthopedics/ trauma, 8 by rheumatology, 4 by endocrinology and one by each of gynecology, geriatrics, radiology and rehabilitation. Each hospital managed 181 to 2530 fragility fracture patients per year with a total of 26,214 patients across all sites. Overall, 16 hospitals scored gold, 8 silver and 4 bronze. The pathway for the hip fracture patients had the highest proportion of gold grading, with vertebral fracture the lowest (figure).

In the first 12 months, we have successfully tested the implementation of the tool in a range of health settings across the globe. Initial findings confirm a significant heterogeneity in service provision and highlight the importance of a global approach to ensure high quality secondary fracture prevention services.
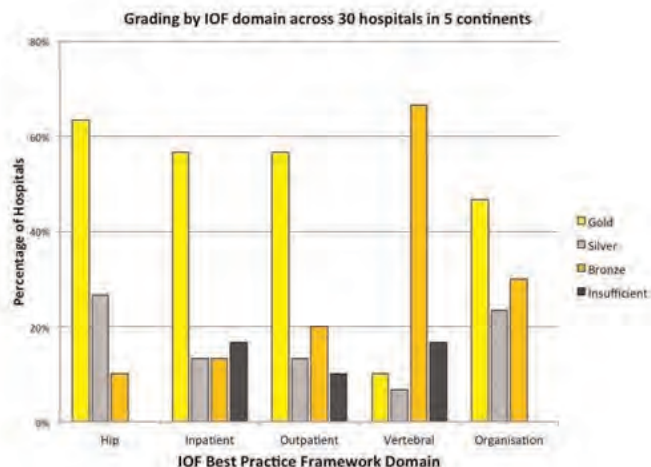
Figure 1

SA0400

Factors Associated with Sub-optimal Adherence to Bisphosphonate Therapy among Patients with Postmenopausal Osteoporosis. <u>Maral DerSarkissian</u>[1], <u>Cynthia O'Malley</u>*[2], <u>Irene Ferreira</u>[3], <u>Stuart Silverman</u>[4], <u>Deborah Gold</u>[5], <u>Rachel Wagman</u>[6], <u>Andreas Grauer</u>[7]. [1]Amgen Incorporated, USA, [2]Amgen, Inc, USA, [3]Amgen Limited, United Kingdom, [4]Cedars-Sinai/UCLA, USA, [5]Duke University Medical Center, USA, [6]Amgen, Incorporated, USA, [7]Amgen Inc., USA

Introduction: Patients are often sub-optimally adherent with bisphosphonates (BPs), which may result in diminished treatment effectiveness and increased risk of fracture. To explore why patients fail to adhere to prescribed therapies, we used patient-reported data to assess patient characteristics and beliefs associated with sub-optimal adherence to BP therapy.

Methods: We used a convenience sample of women aged ⩾ 55 with postmenopausal osteoporosis screened for 2 clinical trials in Europe, Australia, and North America from 2009-2010 who were still on daily or weekly oral BPs at the time of screening. Patients were classified as adherent if they scored 6 or greater on the Osteoporosis Specific-Morisky Medication Adherence Scale (OS-MMAS) or sub-optimally adherent if they scored less than 6. Self-reported baseline demographics, medical history, clinical characteristics, health behaviors, and patient reported outcomes were evaluated as predictors of sub-optimal adherence. Multivariable logistic regression was used to derive odds ratios (OR) and 95% confidence intervals (CI) to assess the association of factors on sub-optimal adherence.

Results: Of the 377 women included in our analysis, 93 (24.7%) were classified as adherent and 284 (75.3%) were classified as sub-optimally adherent. North American women were 3 times more likely to be sub-optimally adherent compared to women from Europe and Australia (OR = 3.00, 95% CI: 1.43, 6.32). Compared with women aged ⩾ 75, women between the ages of 55-64 (OR=0.63 95% CI: 0.31-1.28) and 65-74 (OR=0.39 95% CI: 0.17-0.89) had lower odds of sub-optimal adherence. Beliefs about both the ability to take medication appropriately and the convenience of medication were also significantly associated with decreased odds of sub-optimal adherence. The odds of sub-optimal adherence increased with increasing number of reported comorbidities, but decreased with greater consumption of alcohol compared to no daily consumption of alcohol.

Conclusion: Our results suggest there are significant differences in self-reported adherence to oral BPs by geographic region. In addition, addressing women's beliefs about their ability to use medications appropriately and their perceived convenience of medication use may help improve adherence as these factors were significant predictors of adherence.

SA0401

More Than 90% Two Year Adherence to 6-MonthlyDenosumab Injections in Patients with Different Forms of Osteoporosis. <u>Johann Ringe</u>*[1], <u>Parvis Farahmand</u>[2]. [1]Klinikum Leverkusen, University of Cologne, Germany, [2]West German Osteoporosis Center (WOC), Klinikum Leverkusen, University of Cologne, Germany

Introduction:
Bisphosphonate treatment in osteoporosis is discontinued in almost 50% of patients within the first year after starting application. Denosumab's longer dosing interval with its administration every 6 months as an s.c. injection might result in a better real life treatment adherence than weekly or monthly oral bisphosphonate treatment regimens.
Methods:
In an open investigator-initiated prospective observational study in routine clinical practice we investigated whether a careful medical explanation of treatment results every 6 months after the respective denosumab injections focussing on no or only mild and probably not drug related AE as well as on improvements of back pain and significant BMD increases have positive effects on patients' drug perception and its related future adherence to subsequent denosumab injections. We included 142 patients (69 with postmenopausal, 41 with male, and 32 with glucocorticoid-induced osteoporosis).
Results:
In the first year patients reported only 11 AEs (=7.6%) in the second year 9 AEs (=6.7%). All AEs were mild to moderate, disappeared without intervention and were obviously not drug related. Patients were very impressed by demonstrating them the original DXA-protocols every six months. After two years there were average increases of 9-11% at the lumbar spine and 5-6% at the total hip for the 3 groups. In parallel we found a significant decrease in back pain in the majority of patients and an average rate of new vertebral plus non-vert. fractures per patient year below 0.1. All together this resulted in a very low number of drop outs. At month 24 still 135 of the initially 142 patients accepted a fifth injection of denosumab, which is 95%.
Conclusion:
Results indicate that the reduced dosage frequency together with the rarity of adverse events as well as a consistency of rapid and highly significant increases in BMD during therapy used as a positive reinforcement during doctor-patient interactions had a significant, positive impact on osteoporotic patient's adherence to continue with the 6-monthly s.c. denosumab injections.Key words: osteoporosis, denosumab, treatment adherence, positive feedback

SA0402

National Bone Health Alliance: A Multi-SectorPublic-Private Partnership Working Together to Improve America's Bone Health. <u>Debbie Zeldow</u>[1], <u>David Lee</u>*[2]. [1]National Bone Health Alliance, USA, [2]NBHA, USA

The National Bone Health Alliance (www.nbha.org) is a public-private partnership launched in late 2010 that brings together the expertise and resources of its members to collectively promote bone health and prevent disease; improve diagnosis and treatment of bone disease; and enhance bone research, surveillance and evaluation.

NBHA currently includes 56 participating organizations (35 non-profit member organizations, 17 member companies and liaisons representing CDC, FDA, NASA and NIH).

The concept for NBHA stems from the 2004 Bone Health and Osteoporosis: A Report of the Surgeon General and the June 2008 Summit for a National Action Plan for Bone Health.

NBHA's "20/20 vision" is to reduce the incidence of hip and other bone breaks 20% by the year 2020.

NBHA provides a platform for its collective voice to weigh in on subjects important to bone health, particularly vitamin D, calcium, bone mineral density reimbursement and utilization and the risks and benefits of the use of bone health therapies; communication among organizations interested in bone health; shared priorities to become reality through pooled funding; and working together towards the goals and recommendations of the National Action Plan.

Activities for 2014 include:

Fracture Prevention CENTRAL (www.FracturePreventionCENTRAL.org) provides tools to health professionals, health insurers, hospitals and other sites interested in implementing this model of care.

NBHA Clinical Diagnosis of Osteoporosis Working Group position paper recently published online by *Osteoporosis International*.

Bone Turnover Marker Standardization Project: NBHA is leading the effort to standardize U.S. bone marker sample collection procedures, establish a U.S. reference range for one bone formation and one bone resorption marker and standardize bone turnover marker assays.

FLS Demonstration Study: The Bone Health Collaborative has launched a cloud-based study that will provides study sites with the FLS model of care and a cloud-based platform, to assess adoption and implementation of a fracture liaison service.

2Million2Many Public and Health Professional Awareness Campaign is educates about the 2 million bone breaks in the U.S. each year that are not accidents but signs of osteoporosis.

SA0403

Real-World Evidence on Treatment Initiation and Discontinuation in Canadian Osteoporotic Patients. <u>Marie-Claude Meilleur</u>*[1], <u>Martin Cloutier</u>[2], <u>Jimmy Royer</u>[3], <u>Arun Krishna</u>[4]. [1]Merck Canada Inc., Canada, [2]Analysis Group Inc., Canada, [3]Analysis Group Inc. & Université de Sherbrooke, Canada, [4]Merck, USA

OBJECTIVES: Patients with osteoporosis (OP) have several treatment options for the prevention of fragility fractures and treatment of OP. This study aims to assess rates of treatment initiation with antiresorptive agents (AAs) among Canadian patients with OP and a fragility fracture, and to assess discontinuation rates in patients treated with AAs.

METHODS: Patients ≥50 years of age with an OP-related event, defined as either a diagnosis for OP, a diagnosis for a fragility fracture, or a prescription fill for an AA were identified in Quebec's healthcare database, Régie de l'assurance maladie du Québec (RAMQ) between 06/2005 and 06/2013. Patients with a diagnosis for Paget's disease or a neoplasm were excluded. The index date was defined as a patient's first OP-related event date for the treatment initiation analysis and as a patient's first prescription fill date for an AA for the treatment discontinuation analysis. Patients were observed from their index date until the end of their continuous RAMQ healthcare plan enrollment or end of data availability (observation period). A treatment discontinuation was defined as a gap of ≥60 consecutive days between the last day of supply of the first AA initiated and the next prescription for this AA or the end of the observation period. Treatment initiation and discontinuation rates were measured using Kaplan Meier (KM) survival analyses. Patients were censored at the end of their observation period.

RESULTS: A total of 86,435 patients met the sample selection criteria. The sample was composed of 80.3% of females and 64.8% of patients ≥ 65 years old. Patients were observed for a median period of 4.7 years following their first OP-related event. Over the observation period, 45.2% of the patients initiated an AA. Among the 23,260 patients with a fragility fracture as their first OP-related event, 23.6% initiated an AA over their observation period; treatment initiation rates were 7.9% at 3 months and 13.5% at 12 months. Among the 37,291 patients who initiated an AA, a majority of patients had a treatment discontinuation (60-month KM rate: 66.4%) over their observation period; 15.5% of patients discontinued their treatment during the first month and 39.8% during the first 12 months following a treatment initiation.

CONCLUSIONS: Following a fragility fracture, less than 1 in 4 patients initiated an AA and about 2 in 5 patients who initiated an AA discontinued treatment within the first 12 months.

Disclosures: Marie-Claude Meilleur, Merck, 8; Merck Canada Inc., 4
This study received funding from: Merck Canada Inc.

SA0404

Effects of combination therapy of zoledronic acid plus teriparatide [rhPTH(1–34)] for fracture healing in mice. <u>Tsuyoshi Sugiura</u>*[1], <u>Masafumi Kashii</u>[2], <u>Kazuma Kitaguchi</u>[3], <u>Masayuki Furuya</u>[4], <u>Tokimitsu Morimoto</u>[4], <u>Yohei Matsuo</u>[5], <u>Takahiro Makino</u>[4], <u>Kousuke Ebina</u>[3], <u>Takashi Kaito</u>[4], <u>Motoki Iwasaki</u>[4], <u>Hideki Yoshikawa</u>[6]. [1]Faculty of Medicine, Graduate School of Medicine, Osaka University, Japan, [2]Osaka University Graduate School of Medicine, Japan, [3] Faculty of Medicine, Graduate School of Medicine, Osaka University, Japan, [4]Faculty of Medicine, Graduate School of Medicine, Osaka University, Japan, [5], Japan, [6]Osaka University Graduate School of Medicine, Japan

Introduction: Intermittent administration of teriparatide (TPTD) has a potent stimulatory effect on bone remodeling, and stimulates fracture healing. Clinical data suggest combination therapy with bisphosphonates and TPTD blunt the anabolic effect of TPTD, but animal models suggest that infrequently administered bisphonates interact differently. Recent clinical study also reported that the combination therapy of TPTD and zoledronic acid (ZOL) provided an additive effect on BMD of either spine or hip compared with ZOL or TPTD monotherapy. However, the effect of this combination therapy on fracture healing is unknown. The purpose of this study is to elucidate the individual and combined effects of TPTD and ZOL on fracture healing in mice fracture model.

Materials and Methods: Left femur was fractured and stabilized using intramedullary nail in eight-weeks-old female C57BL/6N mice. They were assigned to 4 different groups to receive 0.9% saline (0.1ml, five times per week, subcutaneous injection, Control group: n=5), ZOL alone (50 µg/kg single subcutaneous injection just after fracture, ZOL group: n=5), TPTD alone (40 µg/kg/day, 5 times per week, subcutaneous injection for 4 weeks, TPTD group: n=5), or ZOL plus TPTD (ZOL+TPTD group: n=5). Time-course microstructural analysis of fractured femur was performed using in vivo micro-CT at 0, 2, 3 and 4 weeks after fracture. Mice were euthanized 4 weeks after fracture. Volumetric BMD (vBMD) measurement of lumber spine (L4) was performed using micro-CT, and histological examination of fractured femur and lumber spine and biochemical examination including bone turnover markers were performed.

Results: Callus volume increased and reached its peak at 2 weeks after fracture in TPTD group and at 3weeks in the other three groups. Compared with TPTD or ZOL group, BV/TV and TbTh tended to be greater and TbSp tended to be smaller in ZOL+TPTD group at 4 weeks after fracture, but there were no statistical significant differences. Bony union rate increased over time, and reached to 100% in Control and

TPTD group and to 80% in ZOL and ZOL+TPTD group at 3weeks after fracture. L4 vBMD was significantly greater in ZOL+ TPTD group than in other three groups (+13.7% vs Control, +4.5% vs ZOL, +18.6% vs TPTD)

Conclusion: Combined treatment of TPTD and ZOL had additive effects on BMD of lumbar spine as previously reported, but there were not obvious effects in fracture healing of mice compared with individual treatment.

Disclosures: Tsuyoshi Sugiura, None.

SA0405

See Friday Plenary Number FR0405.

SA0406

The effect of teriparatide against pain and vertebral collapse after fresh osteoporotic vertebral fracture. <u>Hiroyuki Tsuchie</u>*[1], <u>Naohisa Miyakoshi</u>[2], <u>Yuji Kasukawa</u>[2], <u>Tomio Nishi</u>[3], <u>Hidekazu Abe</u>[3], <u>Toyohito Segawa</u>[4], <u>Yoichi Shimada</u>[5]. [1]Nakadori General Hospital, Japan, [2]Akita University Graduate School of Medicine, Japan, [3]Ugo Municipal Hospital, Japan, [4]Akita University Graduate School of Medicine, Japan, [5]Akita University Graduate School of Medicine, Japan

Purpose: Vertebral fracture is often seen in aged osteoporotic patients, and it causes a decline in activities of daily living. Teriparatide is expected to promote bone union after fracture. Therefore, we evaluated the analgesic action of and vertebral collapse prevention by administering teriparatide to fresh vertebral fracture patients.

Methods: Thirty-three patients with fresh osteoporotic vertebral fracture (48 vertebrae) hospitalized for treatment (male/female: 4/29, mean age: 82 years) participated in the present study. They were administered either teriparatide (daily or weekly) or risedronate for osteoporosis treatment based on their choice, and 9 patients (19 vertebrae) were administered teriparatide daily (Daily group), 11 patients (15 vertebrae) were administered teriparatide weekly (Weekly group), and 13 patients (14 vertebrae) were administered risedronate (RIS group). We compared serum cross-linked N-telopeptide of type I collagen, bone-specific alkaline phosphatase, calcium, inorganic phosphorus, the visual analogue scale (VAS), hospitalization period, vertebral collapse rate and local kyphotic angle of fractured vertebrae compared to that at the initial visit, and the frequency of the cleft in the vertebrae. In addition, we evaluated 22 fresh osteoporotic vertebral fracture patients (25 vertebrae) who did not take any osteoporotic medicines before and after hospitalization (Control group, male/female: 4/18, mean age: 82 years).

Results: At the start of treatment, there was no significant difference in the age, laboratory examinations, bone mineral density, VAS, vertebral collapse rate, or local kyphotic angle between the 4 groups. At 8 and 12 weeks after the initial visit, VAS scores in the Daily and Weekly group were significantly lower than in the RIS group (P<0.05). At 8 and 12 weeks after the initial visit, the differences in the vertebral collapse rate and local kyphotic angle in the Daily group were significantly lower than in the RIS and control groups (P<0.01 and P<0.05, respectively), and those in the Weekly group were significantly lower than in the control groups (P<0.05). The frequency of the cleft in the fractured vertebrae in the Daily group was significantly lower than in the RIS group (P<0.05). There was no significant difference in the hospitalization period.

Conclusion: Teriparatide is promising for the prevention of vertebral collapse progression after fresh osteoporotic vertebral compression fracture.

Disclosures: Hiroyuki Tsuchie, None.

SA0407

A Multicenter, Randomized, Double-blind, and Placebo-controlled Study of Chinese Medicine Zuogui Pill and Yougui Pill for Improving Bone Mineral Density. <u>Dezhi Tang</u>*[1], <u>Chenguang Li</u>[2], <u>Xuejun Cui</u>[2], <u>Dongfeng Zhao</u>[2], <u>Xiaofeng Li</u>[2], <u>Qin Bian</u>[2], <u>Bing Shu</u>[2], <u>Jing Wang</u>[2], <u>Weiwei Da</u>[2], <u>Wen Mo</u>[2], <u>Qi Shi</u>[2], <u>Yongjun Wang</u>[3]. [1]Longhua Hospital, Shanghai University of Traditional Chinese Medicine, Peoples Republic of China, [2]Longhua Hospital, Shanghai University of Traditional Chinese Medicine, China, [3]Othopedic Surgery, Peoples Republic of China

Natural herbal therapy offers an attractive alternative for the treatment of osteoporosis. The objective of this study is to evaluate the efficacy and safety of Chinese herbs, Zuogui Pill (ZGP) and Yougui Pill (YGP), for use in patients to improve bone mineral density (BMD). In this study, 200 subjects were included double-blindly and randomly allocated into two groups, treatment and control. All subjects were diagnosed with low bone mineral density and kidney deficiency in Traditional Chinese Medicine (TCM). Subjects in treatment group were treated for 6 months with either ZGP or YGP based on clinical characters of TCM, while control group received placebo for the same period of time. Primary outcome was lumbar spine BMD as determined by using dual-energy X-ray absorptiometry. Secondary outcomes included visual analogue scale (VAS), quality of life (ECOS-16), and serum markers of bone metabolism. Adverse effects were documented for safety assessment. Follow-ups were performed at regular intervals during a one-year period. We found that, in ZGP group, lumbar spine BMD was increased by 4.1% immediately after the

treatment from the baseline (P=0.047) and by 4.7% from the baseline at the end of the additional 6-month follow-up (P=0.055). Bone anabolic marker was also significantly improved after treatment (P<0.05). In YGP group, the VAS and ECOS-16 scores were also significantly reduced after treatment (P<0.05). Furthermore, bone resorption marker was significantly suppressed after treatment in YGP group (P<0.05), and bone anabolic marker was significantly increased (P<0.05), respectively. No severe adverse effects were observed in either ZGP group or YGP group. Taken together, ZGP and YGP are effective and safe therapeutic drugs for osteoporosis, which improve lumbar spine BMD, reduce pain intensity, alleviate bone resorption, and stimulate bone formation. This study was supported by the National Basic Research Program of China (2010CB530400), the Development Program of Innovation Team of Ministry of Education (1RT1270), the Program of Natural Science Foundation of China (81102604), the Scientific Research Innovation Project of Shanghai Education Committee (14YZ051), and Outstanding Young Talent Training Plan of Shanghai Health System (XYQ2013085).

Disclosures: Dezhi Tang, None.

SA0408

See Friday Plenary Number FR0408.

SA0409

Animal Models of Osteoporosis Correlate with Clinical Bone Marker Data in Women Treated with Ospemifene. <u>Ginger Constantine</u>*[1], <u>Shelli Graham</u>[2]. [1]EndoRheum Consultants, USA, [2]Shionogi Inc, USA

SERMs have been shown to prevent osteoporosis and reduce fracture risk. Ospemifene 60 mg/day is a nonhormonal, oral, selective estrogen receptor modulator (SERM) approved for the treatment of moderate to severe dyspareunia in postmenopausal women with vulvovaginal atrophy (VVA). It has shown bone-preserving effects in rats, including inhibition of OVX-induced decreases in ash weight at the femoral and tibial epiphyses, increases in tibial stiffness, improvement in bone markers and BMD changes, similar to the effects of estrogen treatment. Ospemifene 1-10 mg/kg reduced bone markers indicative of collagen degradation in a dose-dependent manner. The S-ICTP was reduced by 67 -82% compared with OVX rats (p < 0.05), equivalent to the effects of raloxifene.

Two randomized phase II clinical trials of ospemifene on serum bone markers in postmenopausal women have been performed. Ospemifene 30, 60 and 90 mg/day was compared with raloxifene 60 mg/day (the approved dose for osteoporosis) over 12 weeks. Markers of bone resorption (urinary N- and serum C-terminal cross linking telopeptides of type I collagen (NTX and CTX), and markers of bone formation (serum osteocalcin, bone-specific alkaline phosphatase [bone ALP], and procollagen type 1 N and C peptides [P1NP and P1CP]) were measured in 118 postmenopausal women with a mean age of ~57 years. Changes in bone markers were comparable in the ospemifene 60 and 90 mg/day and raloxifene groups. A similarly designed second phase II randomized clinical trial evaluated ospemifene 30, 60, and 90 mg/day versus placebo on bone turnover markers. Ospemifene reduced bone markers in a dose-dependent manner in this study of 176 healthy post-menopausal women (mean age of ~57 years). NTX decreased in all dosage groups, whereas CTX decreased in the 90 mg/day group. Formation markers (P1NP, P1CP, and bone ALP) were significantly decreased in all treatment arms and P1NP and bone ALP statistically differed from placebo.

Correlating animal models with human disease is often unreliable. However, in this large pre-clinical and clinical program OVX-rats treated with ospemifene had similar reductions in markers of bone turnover as did post-menopausal women treated with ospemifene. Bone turnover markers have been shown to correlate with fracture outcomes, thus the totality of the animal and human data support further evaluation of ospemifene as a treatment option for women desiring treatment of VVA and osteoporosis prevention.

Disclosures: Ginger Constantine, Shionogi Inc., 3
This study received funding from: Shionogi Inc.

SA0410

See Friday Plenary Number FR0410.

SA0411

See Friday Plenary Number FR0411.

SA0412

Melatonin improves bone mineral density (BMD) at the femoral neck in post-menopausal women with osteopenia: A randomized controlled trial. <u>Anne-Kristine Amstrup</u>*[1], <u>Tanja Sikjaer</u>[2], <u>Leif Mosekilde</u>[3], <u>Lars Rejnmark</u>[3]. [1]Aarhus University, Denmark, [2]Department of Medicine & Endocrinology, MEA Aarhus University Hospital, Denmark, [3]Aarhus University Hospital, Denmark

Background: Melatonin is known for its regulation of circadian rhythm, however over the recent years, in vivo and vitro studies with melatonin have shown that melatonin also may affect bone by increasing osteoblast differentiation and inhibiting osteoclast activity. Melatonin levels normally peaks around midnight, but the amplitude of the peak is attenuated with age. It is unknown whether decreased melatonin levels in the elderly may be associated with increased bone loss.

We aimed to investigate whether treatment with melatonin may improve BMD.

Method and design: In a double-blind placebo-controlled investigator initiated study, we randomized 81 healthy post-menopausal women with osteopenia to one-year of treatment with melatonin in a daily dose of 1 mg (N=20), or 3 mg (N=20), or similar placebo (N=41). Tablets were administrated at bedtime. All participants also received a daily supplement of 800 mg of calcium and 20 mg of vitamin D3. BMD was measured by DXA (Hologic Discovery scanner) at baseline and after 12 months of treatment

Results: Our studied women had a mean age of 63 years (range 56-73) years. Compared with placebo, BMD at the femoral neck increased by 1.4% in response to melatonin (p<0.05). A dose-response relationship was present (p<0.01) as femoral neck BMD decreased by 1.5% in the placebo group, by 1.0% in the 1 mg melatonin group, whereas BMD increased by 0.9% in the 3 mg melatonin group. At total hip, 3 mg melatonin increased BMD by 1.7% (p=0.01) compared to 1 mg melatonin. Treatment did not affect BMD significantly at the lumbar spine, or whole body. Melatonin did not change body weight, but did affect body composition. Compared with placebo, melatonin decreased fat mass by 6.9% (p<0.02), while lean body mass tended to increase by 2.4% (p=0.06). Treatment was well tolerated. Effects on biochemical bone markers are being analyzed and will presented at the meeting.

In conclusion: One year of treatment with melatonin improved BMD dose-dependently at femoral neck and showed beneficial effects on body composition in terms of a reduced fat mass. Large scaled studies are needed to further investigate whether melatonin may protect against fractures.

Disclosures: Anne-Kristine Amstrup, None.

SA0413

Hepatitis C Co-infection is Associated With Lower Areal and Volumetric BMD and Abnormal Trabecular Microarchitecture in HIV-infected Post-menopausal Minority Women. <u>Michael Yin</u>*[1], <u>Chiyuan Zhang</u>[1], <u>Susan Olender</u>[2], <u>David Ferris</u>[3], <u>Mariana Bucovsky</u>[1], <u>Ivelisse Colon</u>[4], <u>Nientara Anderson</u>[3], <u>Cosmina Zeana</u>[5], <u>Elizabeth Shane</u>[6]. [1]Columbia University, USA, [2]Columbia University, USA, [3]Mt Sinai St Lukes & Mt Sinai Roosevelt, USA, [4]Columbia University Medical Center, USA, [5]Bronx Lebanon Hospital Center, USA, [6]Columbia University College of Physicians & Surgeons, USA

Introduction: Fracture incidence is higher in HIV-infected patients with HCV-co-infection (HIV+/HCV+) than those with HIV infection alone (HIV+). Therefore, we hypothesized that HIV+/HCV+ women would have lower bone mineral density (BMD) and worse microarchitecture than HIV+ women.

Methods: We measured areal BMD (aBMD) by DXA at the spine (LS), femoral neck (FN), total hip (TH), distal 1/3 radius (1/3R) and ultradistal radius (UDR) and volumetric BMD of the distal radius and tibia by high-resolution peripheral quantitative CT (HR-pQCT) in 171 African American or Hispanic postmenopausal women, 44 HIV+/HCV+ and 127 HIV+. Data are presented as Mean + SEM. GLM was used with group status as a fixed effect, and age, BMI, and race entered as covariates.

Results: HIV+/HCV+ women were similar to HIV+ women with regard to age (57 vs 57) and BMI (28 vs 30 kg/m2), both p>0.05. HIV+/HCV+ women were more likely to be African American than Hispanic (59% vs 43%), but the difference was not significant (p=0.06). HIV+/HCV+ women had lower aBMD T scores (ranging from 0.40 to 0.48 SD lower) at the LS, TH, UDR (p<0.05); differences remained significant at TH and UDR, but not at the LS (p=0.08) after adjustment for age, race/ethnicity and BMI. Prevalence of osteoporosis tended to be higher in HIV+/HCV+ than HIV+ women (67% vs 33%, p=0.19). There were no group differences in HR-pQCT measures at the radius. At the tibia, however, HIV+/HCV+ women had lower total vBMD (227 $\pm$ 8 vs 253 $\pm$ 5 mgHA/cm^3; p<0.05) than HIV+ women. Cortical vBMD and thickness were similar between groups, while trabecular vBMD (113 $\pm$ 5 vs 123 $\pm$ 4 mgHA/cm^3) and trabecular thickness (61 $\pm$ 2 vs 69 $\pm$ 1 mm) were significantly lower in HIV+/HCV+ than HIV+ women, before and after adjustment for group differences in age, race/ethnicity and BMI (p<0.05).

Conclusion: Areal BMD by DXA is significantly lower in HIV+/HCV+ than HIV+ postmenopausal minority women at the hip and radius. By HR-pQCT, BMD deficits were confined to the trabecular compartment and to the tibia, a weight-bearing site. These data suggest that the higher fracture rates observed in HIV+/HCV+ than HIV+ individuals are due in part to true deficits in areal and volumetric bone density, that are more severe in trabecular than cortical bone.

Disclosures: Michael Yin, None.

SA0414

See Friday Plenary Number FR0414.

SA0415

See Friday Plenary Number FR0415.

SA0416

See Friday Plenary Number FR0416.

SA0417

See Friday Plenary Number FR0417.

SA0418

See Friday Plenary Number FR0418.

SA0419

See Friday Plenary Number FR0419.

SA0420

See Friday Plenary Number FR0420.

SA0421

Network-based Proteomic Analysis for Postmenopausal Osteoporosis in Caucasian Females. <u>Lan Zhang*</u>, <u>Yingchun Zhao</u>, <u>Hong-Wen Deng</u>. Tulane University, USA

As one of the crucial physiological events in female's life, menopause occurs during women's late 40s or early 50s. Transition of menopause status is accompanied with fluctuations in hormone levels and increasing risk for numerous health problems like cardiovascular disease and osteoporosis. Peripheral blood monocytes (PBM), well known as the potential osteoclast precursors, can differentiate into various cell types closely related to immune response, and produce cytokines important for osteoclast activity. By using the quantitative proteomics methodology LC-nano-ESI-MS^E, we performed protein expression profiles of PBM in 42 postmenopausal females with discordant bone mineral density (BMD) level. Traditional comparative analysis showed proteins encoded by 4 genes (LOC654188, PPIA, TAGLN2, YWHAB) and 3 genes (LMNB1, ANXA2P2, ANXA2) were significantly down- and up regulated in extremely low BMD group, and these results were consistent with previous research evidence. To study network pattern of the detected proteins, we performed weighted gene co-expression network analysis (WGCNA) and gene set enrichment analysis (GSEA). WGCNA showed that the module including annexin gene family (ANXA1, ANXA2, ANXA5, and ANXA6) was most significantly correlated with low BMD group and enriched GO categories in this module shared similar molecular functions associated with proinflammatroy cytokines in postmenopausal osteoporosis. GSEA revealed some complementary evidence of probable gene set involved in the regulation of monocyte activities. In this study, we evaluate the application of network-based analysis to quantitative proteomic data and the findings promote our understanding of biological function of important gene and protein clusters in postmenopausal osteoporosis.

Keywords: Circulating monocyte, GSEA, Menopause, LC-MS, WGCNA

Disclosures: Lan Zhang, None.

SA0422

Osteoporosis Treatment and Chronic Kidney Disease as Measured by Creatinine Clearance and Estimated Glomerular Filtration Rate. <u>Brian Decker*[1]</u>, <u>Ziyue Liu[2]</u>, <u>Allison Martin Nguyen[3]</u>, <u>Marc Rosenman[1]</u>, <u>Joel Martin[4]</u>, <u>Katie Allen[5]</u>, <u>Siu Lui Hui[6]</u>, <u>Erik Imel[6]</u>. [1]Indiana University School of Medicine, USA, [2]Department of Biostatistics, Indiana School of Medicine & Public Health, USA, [3]Merck & Co, USA, [4]Regenstrief Institute, USA, [5]Regenstrief Institute, USA, [6]Indiana University School of Medicine, USA

Chronic kidney disease (CKD) increases osteoporosis (OP) and fracture risks. Due to lack of data, bisphosphonates (BIS) are not recommended when creatinine clearance (CrCl) is <30 ml/min (risedronate, ibandronate) or <35ml/min (alendro-nate, zoledronate). Renal function assessment can differ between estimated CrCl or glomerular filtration rate (GFR), but clinical labs often report GFR. The objectives were to estimate the percent of OP treatment candidates with CKD, CKD rates using estimated CrCl vs. GFR, and frequency of BIS in these patients.

Candidates for OP treatment were identified from a multi-system health information network from 2000-2012. Patients were included if age 50+ and BMD via DXA or ICD9 code indicated OP; or osteopenia with fracture ICD9 codes; and had ≥2 creatinine values ≥90 days apart. GFR via the CKD-EPI and CrCl via the Cockcroft-Gault equations were estimated. "Persistent low" GFR or CrCl was defined as values <35 for ≥90 days without resolving; "transient low" was defined as values <35 which resolved.

Of 71293 patients (85% female, 90% white, 9% black) identified as OP treatment candidates, 27% (n=19273) had transient GFR <35 and 4.6% (n=3280) had persistent GFR <35. In the subset with both GFR and CrCl (21.2%, n=15102), transient values <35 occurred in 40.7% (GFR) and 55.7% (CrCl); while persistent values <35 occurred in 7.5% (GFR) and 21% (CrCl). In the persistent low CrCl group, only 33.4% had GFR <35 at the start of CrCl <35. In contrast, of those with persistent low GFR, 96.4% had CrCl <35 at the start of GFR <35.

Of the total sample, 29.4% received any OP treatment and 27.2% BIS. The closest GFR before treatment was <35 in 709 patients (3.4%) initiating any OP treatment; and 508 patients initiating BIS (3.0%). Among those with persistent low GFR, 5.4% continued previous OP treatment and an additional 5.9% initiated OP treatment after reaching GFR<35 (collectively 11.4%). Most of these were BIS (4.8% continuing, 4.5% initiating). Among those with persistent low CrCl, 6.1% continued and 15.6% initiated OP treatments after CrCl<35. Most were BIS (5.4% continuing, 13.5% initiating).

Nearly 5% of OP treatment candidates had persistent GFR below BIS recommendations and 27% had transient GFR <35. Of note is that GFR underestimated the prevalence of CKD relative to the CrCl estimate. Low GFR/CrCl occurs frequently in OP patients; new OP treatments for CKD patients are needed.

Disclosures: Brian Decker, None.
This study received funding from: Merck, Sharp & Dhome

SA0423

Risk and Prevalence of Vertebral Fractures among Breast Cancer Survivors in China. <u>Evelyn Hsieh*[1]</u>, <u>Qin Wang[2]</u>, <u>Renzhi Zhang[2]</u>, <u>Chun-Wu Zhou[2]</u>, <u>Youlin Qiao[2]</u>, <u>Liana Fraenkel[3]</u>, <u>Weibo Xia[4]</u>, <u>Karl Insogna[5]</u>, <u>Jennifer Smith[6]</u>, <u>Pin Zhang[2]</u>. [1]Yale School of Medicine, Section of Rheumatology, USA, [2]Cancer Institute & Hospital, Chinese Academy of Medical Sciences, China, [3]Section of Rheumatology, Yale School of Medicine, USA, [4]Peking Union Medical College HospitalDepartment of Endocrinology, Chn, [5]Yale University School of Medicine, USA, [6]Gillings School of Public Health, University of North Carolina, USA

Background/Purpose: Osteoporotic fractures lead to significant morbidity and mortality worldwide. Women with breast cancer (BC) are at high risk for fracture due to the deleterious impact of BC therapies on bone density. In China, BC survival is improving as screening, diagnosis and treatment programs expand, however the long-term impact of BC therapy on fracture risk among Chinese women remains unknown and no guidelines exist to prevent BC treatment induced bone loss. We designed a pilot study to evaluate the scope of this problem among BC survivors at a large cancer referral hospital in Beijing.

Methodology: BC survivors receiving care at the Cancer Institute and Hospital of the Chinese Academy of Medical Sciences between April-December 2013 were invited to participate. Women were eligible if they were between the ages of 50-70 years of age, had initiated treatment for BC at least 5 years prior to enrollment, and had no evidence of metastatic bone disease. Study procedures included a self-administered questionnaire regarding risk factors for and personal history of fracture and a thoracolumbar x-ray to assess for presence of vertebral fractures.

Results: 100 women were enrolled with a mean age of 57 ± 5 years, and BMI of 26.6 ± 4.8 kg/m^2. Mean years since BC diagnosis was 6.0 ± 0.8. The majority of cases were stage I or II at diagnosis (79.2%) and estrogen and/or progesterone receptor positive (87%). In total, 12 vertebral fractures were identified via thoracolumbar x-ray. In terms of risk factors for fracture, average reported lifetime height loss was 1.7 ± 1.1 cm, 11% reported a parental history of fracture, 9% reported a personal history of fracture, and 22% of women reported falling within the past year. Forty-five percent of all participants reported taking calcium supplements, but only 4% reported taking vitamin D supplements. Only 25% of women reported having a bone density scan since being diagnosed with BC and 14.4% had been told by a provider they had low bone density or osteoporosis.

Conclusions: Prevalence of fracture among our cohort of Chinese BC survivors was 12%, much higher than recently reported rates among age-matched healthy Chinese women in Beijing of less than 5%. Chinese women undergoing BC therapy should be routinely evaluated for osteoporotic fracture risk. Larger studies are necessary to identify sub-groups at particularly high risk in order to inform screening and prevention guidelines.

Disclosures: Evelyn Hsieh, None.

SA0424

Teriparatide (PTH1-34) treatment effectively increases bone mineral density in patients with pregnancy and lactation associated osteoporosis. <u>JO EUN Kim</u>*[1], <u>Su Jin Lee</u>[2], <u>Sung-Kil Lim</u>[1], <u>Yumie Rhee</u>[3]. [1]Yonsei University College of Medicine, South Korea, [2]Yonsei University Health System, South Korea, [3]Department of Internal Medicine, College of Medicine, Yonsei University, South Korea

Pregnancy and lactation-associated osteoporosis (PLO) is a rare disease characterized by the occurrence of fragility fracture(s), most commonly vertebral, in late pregnancy or the early postpartum period. The etiology and treatment of PLO is not established yet. Although bone turnover rate is increased in PLO patients, long-term treatment of bisphosphonate could be often inappropriate. Because most of the patients are young women in their late twenty to early thirty, and primiparas, so they want subsequent pregnancies. Thus in this study, we report demographic data of 36 PLO patients and the effect of 12~16 months-teriparatide therapy in 15 patients. Mean age of 36 patients was 30.5 years and they all had low traumatic fracture during postpartum. Mean fracture number was 3.8, and most prevalent fracture site was thoracic and/or lumbar vertebrae (94.4%). Z-score of lumbar spine was -2.8 ± 0.8 (mean $\pm$ SD) and serum β-CTx was slightly increased as 0.618 ± 0.359 ng/mL (premenopausal reference <0.573). After a 12~16 months of teriparatide treatment in 15 patients, their lumbar spine BMD (median, interquartile range) (g/m^2) increased from baseline of 0.725 (0.716 ~ 0.786) to 0.852 (0.772 ~ 0.897) (17.0 % increase, p=0.004) and Z-score was increased from -2.6 (-3.1 ~ -2.5) to -1.4 (-2.3 ~ -0.9) (p=0.002). Total hip BMD was increased from 0.678 (0.597 ~ 0.731) to 0.732 (0.653 ~ 0.778)(7.7% increase, p= 0.031) and Z-score increased from -1.7 to -1.1 (p=0.001). Serum β-CTx (ng/mL) was reduced from 0.683 (0.242 ~ 0.988) to 0.358 (0.271 ~ 0.484)(p=0.198) and osteocalcin (ng/mL) remained slightly elevated state from 24.71 (18.44 ~ 33.08) to 31.71(22.09 ~ 44.18)(p=0.109). Most patients experienced low back pain relief during one or two months of initial teriparatide treatment. In conclusion, teriparatide was effective to increase in lumbar spine and total hip BMD significantly, even though in PLO patients with high bone turnover. Teriparatide could be a good option as treatment for PLO patients with multiple vertebral fractures, alleviating long term accumulation of bisphosphonates, since most patients were primiparas.

Disclosures: JO EUN KIM, None.

SA0425

Long-term Changes in Bone Mineral Density in Kidney Transplant Recipients. <u>Kyla Naylor</u>*[1], <u>Amit Garg</u>[2], <u>Anthony Hodsman</u>[1], <u>David Rush</u>[3], <u>William Leslie</u>[4]. [1]Western University, Canada, [2]Western University, Canada, [3]University of Manitoba, Canada, [4]University of Manitoba, Canada

Background: Alterations in bone mineral metabolism occur when kidney function declines and often continue post-transplant. We investigated long-term changes in bone mineral density (BMD) among kidney transplant recipients undergoing routine clinical BMD monitoring and management.

Methods: We identified all adults receiving a kidney transplant in Manitoba, Canada (1996-2011) who had ≥2 post-transplant DXA examinations. BMD tests have been standard practice in the Manitoba renal transplant program since 1997. All BMD results were captured through the population-based Manitoba BMD program and were linked with health service records to identify medication use. BMD was expressed as sex- and age-matched Z-scores. Predictors of BMD change (g/cm^2/year) between successive scans were modeled using generalized estimating equations (GEE) stratified by prior osteoporosis treatment status (candidate predictors age, sex, baseline body mass index [BMI], change in BMI, osteoporosis treatment and glucocorticoid treatment).

Results: 326 kidney transplant recipients were included (mean age 45 years, 61% men). Recipients were followed for an average of 8.2 years (326 baseline and 766 follow-up DXA measurements). At baseline (first scan, median 0.5 years post-transplant) bone density was slightly below average for age and sex (mean Z-scores: lumbar spine -0.4 $\pm$ 1.6; femoral neck -0.7 $\pm$ 1.1; total hip - 0.7 $\pm$ 1.1). At the second scan (mean 2.7 years after first scan) mean bone density Z-scores had increased (lumbar spine -0.2 $\pm$ 1.6; femoral neck -0.6 $\pm$ 1; total hip -0.6 $\pm$ 1.1; matched P <0.01 at all sites). Even after restricting the analysis to recipients who had not received osteoporosis treatment, final mean bone density (mean 8.2 years after first scan) was average for age and sex (mean Z-scores: lumbar spine +0.7 $\pm$ 1.6; femoral neck - 0.1 $\pm$ 1.1; total hip 0.0 $\pm$ 1.1). Change in osteoporosis medication use in the year after a DXA scan occurred in 19% of recipients, with most of this (16%) representing initiation of osteoporosis treatment and only a small component (3%) stopping treatment. The only factor associated with significant BMD change at all sites from GEE was osteoporosis treatment (BMD increase). Greater glucocorticoids exposure was not associated with a significant change in BMD regardless of osteoporosis treatment status (P >0.05).

Conclusions: With routine BMD monitoring and management, post-transplant bone density typically remains stable or improves with mean values that are average for age and sex.

Disclosures: Kyla Naylor, None.

SA0426

Withdrawn

SA0427

Monocyte Chemotactic Protein-1 (MCP-1) is a Key Regulator of Remodeling Activation. <u>Mark Forwood</u>*[1], <u>Gemma Diessel</u>[2], <u>Andy Wu</u>[3], <u>Wendy Kelly</u>[2], <u>Nigel Morrison</u>[4]. [1]Griffith University, Australia, [2]Griffith University, Australia, [3]Mater Medical Research Institute, Australia, [4]Griffith University, Gold Coast Campus, Australia

Monocyte chemotactic protein-1 (MCP-1) belongs to the CC chemokine super-family (CCL2). It plays a critical role in recruitment and activation of leukocytes during acute inflammation, and has the highest level of gene induction in bone following anabolic PTH treatment[1]. We reported that MCP-1 is also specifically regulated during bone remodeling that is activated to repair stress fracture[2]. We hypothesized that MCP-1 is a necessary regulator of recruitment and activation of osteoclasts required for skeletal repair and remodeling. We used the ulnar stress fracture model, allowing scrutiny of focal remodeling with a known time course and precise anatomical location. Within 4 hours of stress fracture initiation, we observed significant increases in MCP-1 gene expression (P < 0.01), followed by increased serum levels within 24h (P < 0.05). To test our hypothesis, we used a plasmid DNA encoding a dominant negative mutant of MCP-1 (7ND) to specifically inhibit MCP-1 in vivo. Stress fracture was created in the right ulna of Wistar rats using cyclic end-loading. Unloaded animals were used as a control. 24 h prior to loading, 7ND plasmid vector, saline or empty vector control (pcDNA3.1), were injected in the thigh muscle to overexpress 7ND protein, effecting its secretion into systemic circulation. Rats were euthanized 4h (n=5/group) or 2 weeks (n=10/group) after loading for gene expression or histomorphometric analysis, respectively. Using qPCR analysis, there was 33-fold increase in MCP-1 expression 4h after loading (P<0.001), which was abolished by 7ND treatment. At 2 weeks, there was a profound suppression of osteoclast number (61%), resorption area (50%) and new bone formation (60%) in basic multicellular units that initiate remodelling of the stress fracture (P < 0.05). Conversely, 7ND treatment had no effect on formation of periosteal woven bone. MCP-1 is markedly upregulated by stress fracture, but also by intermittent PTH treatment[1]. We therefore conclude that MCP-1 is a critical regulator of chemotaxis and osteoclast differentiation during initiation events of bone remodeling.

1. Li et al., J Biol Chem 282: 33086-33097, 2007
2. Wu et al., Calcif Tissue Int 92:566–575, 2013

Disclosures: Mark Forwood, None.

SA0428

sCSF-1 Maintains Cortical Bone Thickness During Aging. <u>Ramaswamy Sharma</u>*[1], <u>Diane Horn</u>[2], <u>Kathleen Woodruff</u>[2], <u>Jean Jiang</u>[3], <u>Roberto Fajardo</u>[4], <u>Sherry Abboud Werner</u>[3]. [1]University of Texas Health Sciences Center At San Antonio, USA, [2]University of Texas Health Science Center at San Antonio, USA, [3]University of Texas Health Science Center at San Antonio, USA, [4]UT Health Science Center, San Antonio, USA

CSF-1 is a key regulatory molecule for bone homeostasis. Osteoblasts express CSF-1 isoforms/CSF-1R and are essential for maintaining bone mass. Studies indicate that expression of the soluble form of CSF-1 (sCSF-1) in osteoblasts of transgenic mice increases cortical bone thickness. However, the effect of sCSF-1 on bone remodeling during aging has not been explored. We established transgenic mice expressing human sCSF-1 driven by the osteocalcin promoter (sCSF-1Tg) and examined the bone phenotype at 3.5 months and 1 year of age using μCT, histology and histomorpho-metry. At 3.5 months, sCSF-1Tg mice showed elevated human CSF-1 levels in serum and bone. Trabecular bone in sCSF-1Tg mice was similar to WT littermates, whereas the diaphysis, although normal in diameter, showed increased cortical thickness and BMD. Sections of the diaphysis showed increased intracortical remodeling due to increased osteoclast activity and osteoblastic bone formation, resulting in a slightly more porous cortex. Fluorochome labeling revealed enhanced BFR along the endocortical surface that contributed to increased cortical thickness. At one year, trabecular bone in sCSF-1Tg mice was preserved, with BV/TV and BFR similar to that in WT mice, whereas the diameter of the femur and tibia mid-diaphysis was increased. Total cross-sectional area was 28% higher and cortical thickness and cortical bone area were increased in sCSF-1Tg mice. The BFR along both the periosteal and endocortical surface was increased and new bone along the endocortical surface resulted in narrowing of the marrow cavity. Osteoclasts in CSF-1Tg mice were identified along the endosteum, with some tunneling into the subendocortical region. The diaphysis in sCSF-1Tg mice showed persistent intracortical remodeling with cavities covered with osteoid and lined by osteoblasts and osteoclasts. Results suggest that sCSF-1, released by osteoblasts, likely mediates its effect via an autocrine and/or paracrine manner. These findings are novel and indicate that sCSF-1 expression during aging preserves cancellous bone volume and stimulates bone formation and turnover within cortical bone. Although remodeling created a slightly more porous cortex, this was overridden by apposition of new periosteal and endocortical bone, which increased diaphyseal thickness. Importantly, strategies to sustain sCSF-1 expression in bone during aging may be useful for preventing bone loss and enhancing cortical bone integrity.

Disclosures: Ramaswamy Sharma, None.

SA0429

See Friday Plenary Number FR0429.

SA0430

Stimulating the release of soluble Rankl by osteoblasts is a unique property of PTH. <u>Timo Heckt</u>*[1], <u>Johannes Keller</u>[2], <u>Athena Chalaris</u>[3], <u>Stefan Rose-John</u>[3], <u>Michael Amling</u>[4], <u>Thorsten Schinke</u>[5]. [1]University Medical Center Hamburg-Eppendorf, Germany, [2]Department of Osteology & Biomechanics, University Medical Center Hamburg-Eppendorf, Germany, [3]Biochemical Institute, University of Kiel, Germany, [4]University Medical Center Hamburg-Eppendorf, Germany, [5]Department of Osteology & BiomechanicsUniversity Medical Center Hamburg Eppe, Germany

Rankl, representing the major pro-osteoclastogenic cytokine, is synthesized as a transmembrane protein that can be cleaved by specific endopeptidases to release a soluble form into the circulation. We have previously reported that interleukin-33 (IL-33) induces expression of *Tnfsf11*, the Rankl-encoding gene, in primary osteoblasts, but we failed to detect Rankl in the medium of these cells following IL-33 administration. Based on this surprising observation we treated primary osteoblasts with various molecules (PTH, IL-33, 1,25-(OH)-Vitamin D3, TNFa, IL-11 and IL-17) for 6 hours, and found that all of them significantly induced *Tnfsf11* expression to a similar extent. Importantly however, only treatment with PTH, but not with any of the other cytokines, resulted in detectable Rankl concentrations in the medium, thereby uncovering a unique property of PTH, which does not only stimulate RANKL production, but also the release of its soluble form. To uncover the potential underlying mechanism we first monitored expression of *Adam10*, *Adam17* and *Mmp14*, encoding three putative Rankl-processing enzymes, but we failed to detect differential expression in response to PTH. We next applied genome-wide expression analysis to identify direct transcriptional targets of PTH in an unbiased approach. We thereby confirmed some of the transcriptional effects of PTH previously established in other systems, and we additionally identified few genes encoding putative endopeptidases that were significantly increased by PTH treatment of primary osteoblasts for 6 hours. A subsequent qRT-PCR expression analysis identified three genes of the Adam/Adamts family that were significantly induced by PTH, but not by IL-33. Taken together, our results demonstrate that transcriptional effects on *Tnfsf11* expression are not predicting an increased Rankl-release into the circulation and provide a basis to identify a Rankl-specific endopeptidase in a physiologically relevant setting.

Disclosures: Timo Heckt, *None.*

SA0431

PTH-Stimulated β-Catenin Signaling via PKA in Osteoblasts Is Blocked by a Factor Secreted by Osteoclasts. <u>Thomas Estus</u>*[1], <u>Shilpa Choudhary</u>[2], <u>Carol Pilbeam</u>[2]. [1]University of Connecticut, USA, [2]University of Connecticut Health Center, USA

Parathyroid hormone (PTH) is anabolic when given intermittently but catabolic when given continuously. Previous in vitro studies in our lab have shown that prostaglandins produced by cyclooxygenase-2 (Cox-2) can inhibit PTH-stimulated osteoblast differentiation. This inhibition was mediated by a factor secreted by bone marrow macrophages (BMMs) that had been treated with RANKL to commit them to the osteoclast lineage. We also found that continuous infusion of PTH was anabolic in Cox-2 knockout (KO) mice but not in wild type (WT) mice and increased expression of Wnt target genes, such as Wnt10b, Wisp1 and BMP-2, only in KO bone, not WT bone. The goal of this study was to test the hypothesis that the inhibitory factor secreted by BMMs blocks the osteogenic effects of PTH in vitro by inhibiting PTH-stimulated protein kinase A (PKA) signaling and, as a consequence, the phosphorylation of β-catenin at Ser552 and Ser675. Phosphorylation at these two sites has been shown to promote the transcriptional activity of β-catenin. Conditioned media (CM) was collected from WT and KO BMMs treated for 3 days with RANKL (30 ng/ml). Primary osteoblasts (POBs) were isolated from neonatal calvariae of Cox-2 KO mice and grown for 5 days before addition of WT or KO CM for 1.5 hours and treatment with PTH (10 nM) or vehicle for the last 20 minutes. PTH increased cAMP production in the presence of KO, but not WT, CM. PTH stimulated phosphorylation of β-catenin at both Ser552 and Ser675 sites in the presence of KO, but not WT, CM. Addition of H89, a PKA inhibitor, inhibited PTH-stimulated β-catenin phosphorylation. Similar results were obtained with forskolin, a direct activator of adenylyl cyclase. To rule out effects of protein kinase C (PKC), we treated with a specific PKC inhibitor, GF109203X, and found no effect on PTH-stimulated β-catenin phosphorylation. We conclude that the inhibitory factor made by RANKL-treated WT BMMs blocks PTH-stimulated β-catenin phosphorylation by inhibiting cAMP production and subsequent PKA activation. We speculate that some of the effects of this factor on PTH-stimulated osteoblast differentiation are due to inhibiting the Wnt signaling pathway.

Disclosures: Thomas Estus, *None.*

SA0432

Wnt Signaling Does Not Affect Inflammatory-driven Bone Resorption in Experimental Periodontal Disease. <u>Sabrina Garcia Aquino</u>[1], <u>Morgana Rodrigues Guimaraes</u>[1], <u>Ligia Araujo Barbosa</u>[2], <u>Bruna C S Rodrigues</u>[2], <u>Debora Emy Miyazaki Lopes</u>[2], <u>Carlos Rossa</u>*[3]. [1]School of Dentistry at Araraquara-Univ Estadual Paulista (UNESP), Brazil, [2]School of Dentistry at Araraquara - Univ Estadual Paulista (UNESP), Brazil, [3]School of Dentistry at Araraquara - Univ Estadual Paulista (UNESP), Brazil

The role of Wnt signaling on bone development is extensively studied; however its impact on bone turnover associated with inflammation is largely unknown. Periodontal disease is the most prevalent lytic disease of bone in humans and represents an interesting model to study bone resorption associated with inflammation. The hypothesis we test in this study is that modulation of Wnt signaling influence bone resorption in the LPS-induced experimental periodontal disease model by affecting the host response. We used Balb/c mice and induced periodontal disease by injections of 3 μL of a 10 mg/mL LPS suspension in the palatal mucosa adjacent to the first molars. These injections were performed 3 times/week for 4 weeks under inhalation anesthesia. Controls received injections of the same volume of PBS diluent. Injections of 2 μL of mouse recombinant proteins Wnt3a (40 μg/mL) or of its inhibitor DKK-1 (100 μg/mL) were performed 2x/week during the 4 weeks on the same anatomical sites in alternating days with the LPS/PBS injections. Negative controls received injections of the vehicle (0.1% BSA). All animals were euthanized 30 days after the start of the LPS or PBS injections. The maxillae were dissected, fixed in 10% buffered formalin for 24 h and transferred to 70% ethanol. Bone resorption was assessed by microcomputer tomography using 18 μm slices in a standardized region of interest (ROI) of 3,200 μm3. Stereometric analysis assessed the inflammatory cell infiltrate in H/E stained semi-serial sections. We used ELISA to determine OPG and RANKL levels in the gingival tissues. LPS injections resulted in significant (p<0.05) bone loss, which was not affected by concomitant activation of Wnt signaling and only attenuated (not significantly) by inhibition of Wnt signaling with DKK-1. Interestingly, Wnt3a injection in animals without periodontal disease induction (PBS-injected) also resulted in significant bone resorption. Stereometric analysis of the gingival tissues indicated that injections of either Wnt3a or DKK-1 aggravated the inflammatory cell infiltrate. The decrease on OPG/RANKL ratios in the tissues injected with LPS was not affected by concomitant injections of Wnt3a or DKK-1. We conclude that Wnt signaling does not affect the inflammatory infiltrate and the inflammatory-driven bone resorption in the LPS-induced periodontal disease model. Activation of Wnt signaling increased (p<0.005) alveolar bone resorption in the absence of LPS-induced inflammation

Disclosures: Carlos Rossa, *None.*

SA0433

See Friday Plenary Number FR0433.

SA0434

See Friday Plenary Number FR0434.

SA0435

See Friday Plenary Number FR0435.

SA0436

See Friday Plenary Number FR0436.

SA0437

See Friday Plenary Number FR0437.

SA0438

See Friday Plenary Number FR0438.

SA0439

Altered pyrophosphate homeostasis contributes to NF1 hyperosteoidosis and bone fragility. Jean De La Croix Ndong*[1], Alexander Makowski[2], Sasidhar Uppuganti[3], Guillaume Vignaux[3], Koichiro Ono[4], Daniel Perrien[5], Simon Joubert[6], Serena R. Baglio[7], donatella granch[7], david A. stevenson[8], Jonathan J. Rios[9], Jeffry Nyman[5], Florent Elefteriou[1]. [1]Vanderbilt University, USA, [2]Department of Veterans AffairsVanderbilt University, USA, [3]Vanderbilt university, USA, [4]Center for Bone Biology, USA, [5]Vanderbilt University Medical Center, USA, [6]Alexion Montreal Corp, Canada, [7]Laboratorio di Fisiopatologia Ortopedica e Medicina Rigenerativa, Istituto Ortopedico Rizzoli Via di Barbiano 1/10, Italy, [8]Department of Pediatrics, Division of Medical Genetics, University of Utah, USA, [9]Sarah M. & Charles E. Seay Center for Musculoskeletal Research, Texas Scottish Rite Hospital for Children, USA

Children with neurofibromatosis type I (NF1) can present with long bone and vertebral dysplasiae. The etiology of these skeletal complications is unclear, thus their clinical management remains difficult. Hypomineralization has been observed in bone biopsies from individuals with NF1 and from mouse models of NF1 skeletal dysplasia, but the contribution of this defect to the suboptimal bone mass, strength and poor healing associated with NF1 remains unclear. We show here that Nf1-deficient chondrocytes and osteoprogenitors are characterized by an ERK-dependent increase in Ank and PC1/Enpp1 expression, leading to accumulation of extracellular pyrophosphate and poor matrix mineralization. Nf1-deficient osteoprogenitors also exhibit impaired differentiation caused by an ERK-dependent blunted response to BMP2, hence reduced alkaline phosphatase (TNSALP) activity and low pyrophosphate catabolism. Consistent with these observations, bone mineralization and mechanical properties are reduced in mice lacking Nf1 in chondrocytes or osteoprogenitors. Importantly, a bone-targeted form of TNSAP (sALP-FcD10), which increases pyrophosphate catabolism, has significant beneficial effects on bone growth, mineralization, structure and mechanical properties in these mice. Bone mineralization and pyrophosphate homeostasis are thus dependent of proper control of the RAS-MAPK pathway by NF1, and sALP-FcD10 may represent a therapeutic avenue to prevent bone fracture in individuals with NF1.

Disclosures: Jean De La Croix Ndong, None.

SA0440

Challenges in localizing the tumor in tumor-induced osteomalacia with whole body venous sampling. Su Jin Lee*[1], Sung-Kil Lim[2], Yumie Rhee[3]. [1]Yonsei University Health System, South Korea, [2]Yonsei University College of Medicine, South Korea, [3]Department of Internal Medicine, College of Medicine, Yonsei University, South Korea

Tumor-induced osteomalacia (TIO) is a rare disease characterized by hypophostphatemia with impaired renal tubular phosphate reabsorption generally via increased fibroblast growth factor-23 (FGF-23). Thus, complete resection of the tumor is utmost important. As systemic whole body venous sampling for FGF-23 has been reported as a helpful tool to confirm preoperative diagnosis of TIO, we performed 5 cases of systemic venous sampling in patients who had negative findings in whole body magnetic resonance imaging (MRI) and In111 Octreotide scan. Blood samples were collected from 18-19 sites per patient and were analyzed by using FGF-23 ELISA KIT (Kainos Laboratories, Inc., Tokyo, Japan). There were no complications caused by whole body venous sampling. We classified into 8 sections as head and neck, right arm, left arm, intra-abdomen, right lower leg, right upper leg, left lower leg and left upper leg. After whole body venous sampling, the section of the highest FGF-23 level were further evaluated by MRI of the regions of interest.

All 5 patients had single dominant vein which showed the highest FGF23 levels. However, only two cases were successful of localizing the tumor responsible for TIO. The location of tumor corresponded to the highest FGF23 levels of single dominant vein in two cases. FGF23 level in all patients ranged from 78.16 pg/mL up to 1435.56 pg/mL, however, the higher FGF23 level did not mean the higher chance of finding the origin of the tumor. We also compared the ratio of FGF23 level of the highest section to that of the lowest of all the sections. The ratio was 1.54 in the first case and 1.34 in the second case. The ratio of failed cases was 1.78, 1.60 and 1.32, respectively. The ratio was not that higher even in successful cases compared to the failed cases. Previous report by N. Ito *et al.* had done total 10 cases of whole body sampling with a successful rate of localization, 80%. The average ratio of the highest level to the lowest level in these 8 successful cases was 1.83 ± 0.59 pg/mL (range 1.24 - 2.89 pg/mL).

To resect the tumor responsible for TIO properly, accurate localization is important. Systemic venous sampling based on a distinguished lesion with high level of FGF23 could give a clue for finding a tumor but not all tumors as our results, therefore, it has still limitation in identifying the tumor in TIO.

Disclosures: Su Jin Lee, None.

SA0441

Clinical Characterization of a Cohort of Patients with Familial Tumoral Calcinosis. Mary Ramnitz*[1], Pravitt Gourh[2], Jaydira Del Rivero[2], Diana Ovejero[1], Nisan Bhattacharyya[2], Lori Guthrie[2], Raphaela Goldbach-Mansky[2], Felasfa Wodajo[3], Shoji Ichikawa[4], Erik Imel[4], Michael Econs[5], Kenneth White[4], Brian Kirmse[6], Adele Boskey[7], Alfredo Molinolo[2], Rachel Gafni[1], Michael Collins[2]. [1]National Institutes of Health, USA, [2]National Institutes of Health, USA, [3]Virginia Hospital Center, USA, [4]Indiana University School of Medicine, USA, [5]Indiana University, USA, [6]Children's National Medical Center, USA, [7]Hospital for Special Surgery, USA

Introduction: Familial tumoral calcinosis (FTC)/hyperostosis-hyperphosphatemia syndrome (HHS) is an autosomal recessive disorder caused by mutations in *FGF23*, *GALNT3*, or *KLOTHO*. The result is a deficiency in, or resistance to, intact FGF23 causing hyperphosphatemia, increased renal tubular reabsorption of phosphorus (TRP), and elevated or inappropriately normal 1,25-dihydroxyvitamin D_3 (1,25-D_3). Affected individuals may develop ectopic calcifications and/or diaphyseal hyperostosis. Methods: Seven patients with FTC/HHS were evaluated. Radiographic, biochemical, histologic, and genetic analyses were performed and therapeutic interventions were attempted. Results: Clinical manifestations ranged from asymptomatic to multiple, large disabling calcifications. All patients had hyperphosphatemia, increased TRP, and elevated or inappropriately normal 1,25-D_3. C-terminal FGF23 was elevated while intact FGF23 was low in all patients. Two patients had overwhelming systemic inflammation (C-reactive protein (CRP) > 80 mg/L, nl <3.0). Radiographic findings ranged from diaphyseal thickening alone to massive calcification. All subjects tested to date had *GALNT3* mutations (2 siblings homozygous, 4 patients compound heterozygous). Sperm analyses were normal in one patient, but abnormal in his sibling. Histologic analyses of resected tissue showed chronic inflammation, and not only ectopic calcification, but also ossification. Fourier transform infrared spectroscopy revealed hydroxyapatite crystals of varying size and composition. Low phosphate diet and combinations of phosphate-lowering therapy were attempted with variable response. One patient experienced complete resolution of a calcific mass after 13 months of medical treatment. In patients with systemic inflammation, treatment with an IL-1 antagonist decreased CRP with a decrease in peri-lesional edema in one patient and improvement in both patients' well-being. Conclusion: This cohort expands the phenotypic and genotypic understanding of FTC/HHS and demonstrates the range of clinical manifestations despite similar biochemical profiles and genetic mutations and backgrounds. Two patients had overwhelming systemic inflammation which had not been described previously in FTC/HHS; their response to IL-1 antagonists suggests that anti-inflammatory treatment may be a useful adjuvant. Importantly, this is the first description of true ectopic ossification reported in FTC/HHS, possibly driven by the adjacent inflammation.

Disclosures: Mary Ramnitz, None.

SA0442

See Friday Plenary Number FR0442.

SA0443

Measurement of autoantibodies against osteoprotegerin in adult human serum: Development of a novel ELISA assay. Isabelle Piec*[1], Jonathan Tang[2], Christopher Washbourne[3], Emily Fisher[4], Julie Greeves[5], Sarah Jackson[6], Stuart Ralston[7], Philip Riches[8], William Fraser[3]. [1]BioAnalytical Facility, University of East Anglia, United Kingdom, [2]University of East Anglia, Norwich, UK, United Kingdom, [3]University of East Anglia, United Kingdom, [4]University of East Anglia, United Kingdom, [5]HQ Army Recruiting & Training Division, United Kingdom, [6]MOD, United Kingdom, [7]University of Edinburgh, United Kingdom, [8]Rheumatoic Disease Unit, Institute of Genetics & Molecular Medecine, United Kingdom

Introduction: In 2009, neutralizing autoantibodies against OPG (α-OPGAb) blocking the inhibitory effect of OPG on RANK signaling pathway were identified in a man with celiac disease associated with severe osteoporosis. Although this finding was not reproduced in thirty patients presenting coeliac disease and low bone mineral

density, Hauser *et al* (2013) recently detected the presence of α-OPGAb in patients presenting Rheumatoid Arthritis, Systemic Lupus Erythematosus, Spondyloarthritis and Osteoporosis. There is a growing focus on OPG autoantibodies as primary cause of high bone turnover in disorders with unknown etiology.

Objective: To develop an enzyme linked immunosorbent assay (ELISA) for detection and quantification of α-OPGAb in patient serum samples.

Method: A full-length human recombinant OPG is immobilized on a plate to allow capture of the antibodies from the sera. In a two-step reaction, the αOPGAb is detected using a biotinylated antibody and a horseradish peroxidase-labelled streptavidin. Substrate is incubated in a timed reaction and color development measured in a spectrophotometric microtiter plate reader. The concentration of human α-OPGAb in the samples is determined directly from a 4PL-fit standard curve.

Results: Intra-assay imprecision was <5% at 274.4 ± 18.8 and 98.5 ± 2.9 ng/mL. Inter-assay imprecision was <20% at 324.2 ± 53.3 and 166.8 ± 30.6 ng/mL. Linear range was 0-500ng/mL. Lower and upper limit of quantification were 3.9 and 500 ng/mL. Cross reactivity was assessed against human sera containing raised thyroid antibody and RANKL to ensure assay specificity. Using the method presented, we established that the adult population would be considered positive with a titer above the cut-off limit (95%) of 68ng/mL. Our preliminary data suggested that 14% of our sample population (n=136) presented elevated α-OPGAb.

Conclusion: We presented a novel ELISA assay for the detection and measurement of anti-OPG autoantibodies in human serum. The validated method showed excellent assay characteristics and is suitable for use in research and clinical hospital laboratories. In patients with severe form of osteoporosis, measurement of OPG autoantibodies could help clinicians identify appropriate treatment options for this particular subgroup of patients.

Disclosures: Isabelle Piec, None.

SA0444

Serum Levels of Amino-terminal Propeptide of C-type Natriuretic Peptide may Predict Growth Response to Growth Hormone Treatment in Patients with Achondroplasia/hypochondroplasia. <u>Takuo Kubota</u>*[1], <u>Kohji Miura</u>[2], <u>Wei Wang</u>[2], <u>Keiko Yamamoto</u>[3], <u>Makoto Fujiwara</u>[4], <u>Yasuhisa Ohata</u>[5], <u>Makiko Tachibana</u>[4], <u>Taichi Kitaoka</u>[6], <u>Yoko Miyoshi</u>[4], <u>Noriyuki Namba</u>[6], <u>Keiichi Ozono</u>[7]. [1]Osaka University Graduate School of Medicine & Dentistry, Japan, [2]Osaka University Graduate School of Medicine, Japan, [3]Osaka University Graduate School of Medicine, Japan, [4]Osaka University Graduate School of Medicine, Japan, [5]Osaka University Graduate School of Medicine, Japan, [6]Osaka University Graduate School of Medicine, Japan, [7]Osaka University Graduate School of Medicine, Japan

C-type natriuretic peptide (CNP) plays a vital role in endochondral growth and its derivative is on clinical trial to improve the growth of patients with achondroplasia. The amino-terminal propeptide of CNP (NT-proCNP) is an equimolar product of CNP biosynthesis and has a longer half-life in serum than CNP. NT-proCNP has been proposed as a biomarker of linear growth in healthy children and patients with growth hormone (GH) deficiency. However, the usefulness of serum NT-proCNP levels in patients with achondroplasia (ACH)/hypochondroplasia (HCH) remains to be elucidated. In this study, we studied serum NT-proCNP levels in untreated patients with ACH/HCH (n = 20: ACH 14; HCH 6), and compared with those in idiopathic short stature (ISS) (n = 24). All the patients with HCH have the N540K mutation in the fibroblast growth factor receptor 3 gene. The mean age and height SD score (SDS) are 3.1 years old and −4.5 in the patients with ACH/HCH, respectively, and 5.6 years old and −2.4 in the patients with ISS, respectively. Serum NT-proCNP levels inversely correlated with ages of patients with ISS in infancy and childhood. There were no obvious differences in NT-proCNP levels between patients with ACH/HCH and ISS at the age of 3 years despite a difference in height SDS. ACH/HCH patients with height SDS below −2.5 were treated with 0.35 mg/kg/week of GH. The mean height SDS significantly increased from −4.8 to −4.3 with one-year GH treatment. NT-proCNP levels in patients with ACH/HCH were increased 3 months following GH treatment. A similar response was observed in serum insulin-like growth factor I (IGF-I) SDS and alkaline phosphatase (AP) levels. When the patients with ACH/HCH were divided into halves regarding an increase in NT-proCNP levels: the upper half and the lower half, a gain of height SDS was significantly larger at the year after GH treatment in the upper half (+0.8 SDS) than in the lower half (+0.3 SDS). In contrast, an increase in IGF-I SDS and AP levels had no correlation with a gain of height SDS. These results indicate that GH increases height by stimulating the production of CNP and that unlike IGF-I SDS and AP levels, serum NT-proCNP levels may predict growth response to GH treatment in patients with ACH/HCH.

Disclosures: Takuo Kubota, None.

SA0445

Assessment of physical performance in patients with a recent clinical fracture at the Fracture Liaison Service. <u>Lisanne Vranken</u>*[1], <u>Caroline Wyers</u>[2], <u>Kenneth Meijer</u>[3], <u>Robert Van Der Velde</u>[4], <u>Heinrich Janzing</u>[5], <u>Wim Morrenhof</u>[6], <u>Piet Geusens</u>[7], <u>Joop Van Den Bergh</u>[8]. [1]VieCuri Medical Centre, The Netherlands, [2]Maastricht University, The Netherlands, [3]Department of Human Movement Sciences, NUTRIM , Maastricht University, Netherlands, [4]VieCuri Medical Center Venlo, the Netherlands, The Netherlands, [5]VieCuri Medical Centre, Department of Surgery, Netherlands, [6]VieCuri Medical Centre, Department of Orthopedic Surgery, Netherlands, [7]University Hasselt, Belgium, [8]VieCuri MC Noord-Limburg & Maastricht UMC, The Netherlands

Purpose

To assess physical performance and muscle function in patients presenting with a recent fracture (fx) evaluated at the Fracture Liaison Service (FLS).

Methods

All consecutive patients presenting with a recent fx (including VF), who had fx risk assessment (DXA at lumbar spine, femoral neck and hip) were evaluated for physical performance (Chair Stand Test (CST), Timed Up & Go Test (TUG), 6 minutes walking test (WD) and handgrip strength (HGS) at the FLS. Data were analysed using linear regression, Spearman's correlation and multiple regression adjusting for age, sex, BMD (normal vs. osteopenia vs. osteoporosis) and fx classification (finger & toe vs. minor vs. major vs. hip).

Results

372 consecutive patients (≥50 yrs) were evaluated (70% women; mean age 66 yrs), 61% with a minor, 22% major, 7% hip and 10% finger or toe fx. Osteoporosis was diagnosed in 28%, osteopenia in 51% and 20% had a normal BMD. At the CST women did 12 (2-26) rise and sit repetitions, men 13 (2-22) (p=.001). Lower CST performance was found with higher age (p=.000), lower BMD (p=.010) and severity of fx (p=.046). 38% had a CST below sex and age specific normative scores. TUG took 8s for women (4-33s), 8s for men (5-31s) (p=.018). Time to perform TUG increased with age (p=.000), lower BMD (p=.012) and severity of fx (p=.003). WD was lower in women (380m (60-673m) vs. 423m (134-674m) men p=.000), decreased with age (p=.000), with lower BMD (p=.000) and severity of fx (p=.000). HGS in women was 20kg (2-46kg), in men 38kg (18-60kg) (p=.000), decreased with age (p=.000), lower BMD (p=.004) and severity of fx (p=.024). 64% had HGS below sex and age specific normative values. After adjustments, age and hip fx were significant predictors for TUG and WD; age and sex for HGS and age for CST. In adjusted analyses for both sexes separately age was a significant predictor for all tests, hip fx in women for TUG and hip fx in men for TUG and WD. 94% performed all tests, 89% had a result below normative values for at least one test (51% 1, 35% 2, 3% 3 tests).

Conclusion

Assessment of physical performance in patients with a recent fx showed that 94% of patients were able to perform the tests. 89% of these patients had a score below normative values for at least one assessment. After adjustments, age, sex and hip fx were significant predictors for WD; age and sex for HGS; age and hip fx for TUG and only age for CST (with lower scores at older age, in women and after hip fx respectively).

Disclosures: Lisanne Vranken, None.

SA0446

Fall risk assessment using body composition, muscle strength and physical performance in hospitalized adults. <u>Hideki Tsuboi</u>*[1], <u>Jun Hashimoto</u>[2]. [1]Osaka Minami Medical Center, Japan, [2]National Hospital Organization, Osaka Minami Medical Center, Japan

Introduction; Falls in elderly are problems associated with increased morbidity and disability. Falls are also severe problem in hospitalized adults. In many hospitals, the fall risks are assessed by questionnaires provided by their medical safety committees. Therefore, the purpose of this study is to investigate the possibility to assess fall risks by body composition, muscle strength and physical performance.

Materials and Methods; 103 patients (69 male, 34 female) were enrolled in the study. The patients had a mean age of; male, 68.8 (43-87) years and female, 69.8 (39-88) years. All patients were classified in three groups at the time of admission using fall risk assessment questionnaire provided by medical safety committee in our hospital, A; high risk group, B; moderate risk group, C; low risk group. In addition, the body composition of the muscle mass in lower extremity was measured using by BIA (Bioelectrical Impedance Analysis; MC190,Tanita, Tokyo, Japan) method and muscle strength was assessed by hand grip strength. Moreover, physical performance assessment was evaluated measuring timed up and go test (TUG).

Results; 10 patients (4 male, 6 female) were assessed in Group A, 54 patients (38, 16) were assessed in Group B and 39 (27, 12) were group C. In Group A, muscle mass of lower extremities were 12.9±2.7 kg in male and 11.0±1.6 kg in female respectively. In Group B, 16.1±2.1 and 11.5±2.3 respectively, and in Group C, 16.5±2.3 and 11.4±1.5 respectively. Hand grip strength in Group A were 25.8±2.5 kg in male and 11.8±7.3 kg in female respectively, in Group B;25.9±8.5 and 15.5±4.9 respectively, and in Group C; 30.5±8.3 and 17.2±6.6 respectively. TUG in Group A were 9.3±2.0 sec. in male and 21.5±16.5 sec. in female respectively, in Group B; 9.5±4.6 and 10.8±3.4 respectively, and in Group C; 8.2±2.6 and 7.0±1.9 respectively.

Discussions; This study shows that results of muscle mass in lower extremities, hand grip strength and TUG were tend to decrease as the assessment for fall risks was worse. In male, muscle mass were reflected more clearly in fall risks, on the other hand, hand power strength and TUG were reflected more clearly in fall risks in female.

Conclusion; The examination of the combination among body composition, muscle strength and TUG may be useful as a screening test for assessment for fall risk in hospitalized adults.

Disclosures: Hideki Tsuboi, None.

SA0447

Gender and Race Disparities in Body Composition: an Analysis of National Health and Nutrition Examination Survey (NHANES) Data. <u>Didier Chalhoub*[1]</u>, <u>Hussein Abu Daya</u>[2], <u>Robert Boudreau</u>[3], <u>Jane Cauley</u>[4]. [1]University of Pittsburgh, USA, [2]University of Pittsburgh Medical Center (UPMC), USA, [3]University of Pittsburgh, USA, [4]University of Pittsburgh Graduate School of Public Health, USA

Body composition changes occur with age. However, gender and race differences in muscle and fat mass are not very well understood. We propose to study the patterns of muscle and fat distribution based on age, gender, and race.

The study population consisted of 15,356 white, black, and Hispanic individuals age ≥20. Data was obtained from the National Health and Nutrition Examination Surveys (NHANES) from 1999-2006. Subjects were stratified by gender, race, and age group. Appendicular lean mass (ALM) and appendicular fat mass (AFM) were calculated based on whole body dual-energy X-ray absorptiometry (DXA) scans results. The mean and standard deviation of the ALM, AFM, trunk fat, and total body fat were calculated.

Men had a higher appendicular lean mass (kg) (mean=26.8±0.1) compared to women (mean=17.8±0.1). In both genders, blacks had the highest ALM (men=29.4±0.2, women=21.0±0.1) followed by whites (men=26.9±0.1, women=17.6±0.1) and Hispanics (men=24.6±0.1, women=16.7±0.1). The ALM was lower in older age groups (figure 1). The total body fat (kg) was higher in women (mean=31.0±0.2) compared to men (25.5±0.2). In men, whites had the highest total body fat and trunk fat, whereas in women, blacks had the highest levels. Total body fat and trunk fat had a similar pattern increasing across age groups until age 70. Those >age70 old had lower total body fat and trunk fat compared to younger age groups (figure 2). In women, AFM followed a similar pattern. Despite having the highest total and trunk fat, white men had similar AFM to black men (figure 3).

Gender and race differences exist in body composition. Such differences should be accounted for while assessing muscle and fat mass.
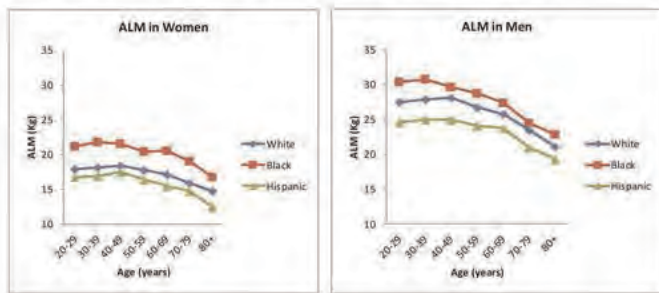
Figure 1. Appendicular lean mass
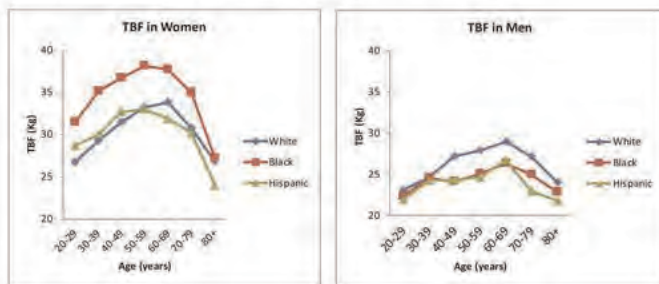
Figure 2. Total body fat

Figure 3. Appendicular fat mass

Disclosures: Didier Chalhoub, None.

SA0448

See Friday Plenary Number FR0448.

SA0449

See Friday Plenary Number FR0449.

SA0450

Muscle, Fat and Bone tissues in Patients with Hip Fracture. <u>M José Montoya*[1]</u>, <u>Mercè Giner</u>[2], <u>M Angeles Vázquez</u>[3], <u>Marta Rey</u>[4], <u>Aurora Gil-Bernal</u>[3], <u>David García-Romero</u>[3], <u>M Carmen Cañamero</u>[5], <u>Presentación Zambrano</u>[5], <u>Ramón Pérez-Cano</u>[6]. [1]University of Seville, Spain, [2]Bone Metabolism Unit, Internal Medicine, ''Virgen Macarena'' University Hospital, Spain, [3]Medicine Department, University of Seville, Spain, [4]Viamed Sta. Angela de la Cruz Hospital, Spain, [5]Traumatology & Orthopae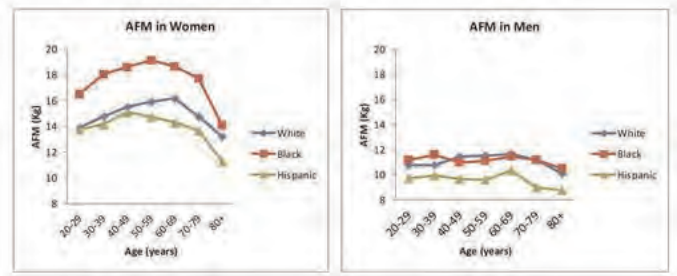dic Unit, ''Virgen Macarena'' University Hospital, Spain, [6]Bone Metabolism Unit, Internal Medicine, ''Virgen Macarena'' University Hospital / Medicine Department, University of Seville, Spain

Sarcopenia-related falls and fractures are becoming an emerging problem as a result of rapid aging worldwide. We aimed to evaluate the prevalence of sarcopenia in patients with hip fracture, testing the muscle mass of the arms and legs and the relationship among sarcopenia, bone mass, fat tissue and risk of falls.

M&M This cross-sectional study examined 88 patients immediately after a hip fracture. We carried out whole-body dual energy X-ray absorptiometry to analyze skeletal muscle mass (MM), total fat (TF), skeletal muscle mass index (SMI), appendicular skeletal muscle mass index (appendicular SMI), bone mineral density, neck BMD and hip BMD. Also, we analyzed bone parameters (PTH, 25(OH)Vitamin D, β-Crosslaps and PINP).

Sarcopenia was defined according to the criteria reported by Baumgartner: appendicular SMI below 7.26 kg / m2 in men and below 5.45 kg/m2 in women.

Statistical analysis of the results was conducted using the T-student test and correlations between variables were assessed with the Pearson correlation coefficient (SPSS 21.0).

Results:

Age, TF, SMI, appendicular SMI and neck BMD were similar in both groups. Women showed higher BMI (body mass index),(28.5 ± 5.5 vs 25.6 ± 4.8 kg/m2), lower MM (37.3 ± 5.2 vs 44.1 ± 5.7 kg) and worst hip BMD value (0.73 ± 0.11 vs 0.80 ± 0.14 gHA/cm2) than men, in all cases p< 0.05.

The prevalence of sarcopenia in men was higher, 70.6 % (12/17), than in women 16.4% (11/67), OR = 4.3, (95% CI 2.31 to 8), p = 0.0001. Sarcopenia risk increased with age in men (62.5% in <80 years old and 77.8% in > 80 years old), while it decreased in women (21.7 % vs 13.6%).

92% of women and 61% of men had insufficient levels of 25(OH)vitD (below 20 ng/mL), and we observed correlation between 25(OH)vitD levels and hip BMD (r= 0.333; p= 0.018) and with vitD and PTH (r= - 0.446; p= 0.0001).

The frequency of falls was not related with SMI and appendicular SMI.

We observed correlation between hip BMD or neck BMD with MM (r = 0.42; p = 0.0001/ r = 0.291; p = 0.10)Conclusions: The prevalence of sarcopenia in hip fracture patients is higher in men than in women, mainly above 80 years old. Muscle tissue influences in bone mass values. The majority of patients with hip fracture has insufficient levels of 25(OH)vitD.

Disclosures: M José Montoya, None.

SA0451

See Friday Plenary Number FR0451.

SA0452

Precision and Monitoring Time Intervals for Muscle Area and Density in Older Adults: A Comparison of Stratec and BoneJ Analyses. <u>Andrew Frank</u>*[1], <u>Wojciech Olszynski</u>[2], <u>Saija Kontulainen</u>[1]. [1]University of Saskatchewan, Canada, [2]Saskatoon Osteoporosis & Arthritis Infusion Centre, Canada

Introduction: Peripheral quantitative computed tomography (pQCT) is commonly applied to measure muscle area and density (a surrogate of inter- and intramuscular adipose infiltration). Precision and follow-up data can be used to calculate the monitoring time interval (MTI); an estimate of the time required between measurements where 50% of population will demonstrate a significant age-related change. MTI's assist to inform and optimize pQCT-based study designs in aging populations. We previously reported muscle precision and MTI values for older adult images analyzed using the commonly reported manufacturer's pQCT analysis software. Our purpose was to determine and compare the precision error and MTIs for pQCT-derived muscle area and density analyzed using Stratec XCT 6.00 (manufacturer's software) and BoneJ (a freely available software plugin for ImageJ).

Methods: Women (N=115) age 60 to 90 (mean 73.9, SD 7.9y) were recruited from the Saskatoon Cohort of the Canadian Multicentre Osteoporosis Study. Repeat pQCT scans were acquired an average of 347 (SD 15) days apart at 65% of forearm and 66% of lower leg length. A randomly selected subsample (n=35, mean age 73.7, SD 7.7y) were randomly selected for the calculation of short-term precision error from duplicate scans measured 9.7 (SD 3.6) days apart. Precision error was calculated as a root mean square coefficient of variation (CV_{rms}%). Paired t-tests compared software precision on log-transformed absolute mean differences. MTIs were calculated as the least significant change ($2.77*CV_{rms}$%) divided by the median annual percent change.

Results: The precision error for forearm area 2.2% vs 2.4%, and density 1.4% vs 1.3%, did not differ between Stratec and BoneJ respectively. Precision error for lower leg area 3.6% vs 2.5%, and density 1.9% vs 0.7%, differed (P=0.047 and P=0.006) between Stratec and BoneJ. For the Stratec vs BoneJ analyses the resulting MTIs were both 3yrs for area and 18 vs 45yrs for density in the forearm, and 18 vs 4yrs for area and 7 vs 3yrs for density in the lower leg.

Conclusion: Precision errors for muscle properties were comparable in the forearm and smaller in the lower leg when assessed with BoneJ versus Stratec. Researchers can reasonably expect to detect changes in forearm muscle area, and lower leg muscle area and density within 3-4 years when utilizing BoneJ to analyze pQCT-derived muscle outcomes in older adults.

Disclosures: Andrew Frank, None.

SA0453

See Friday Plenary Number FR0453.

SA0454

Serological peptide biomarkers derived from intramuscular connective tissue collagens are biomarkers of muscle mass. <u>Anders Nedergaard</u>*[1], <u>Ulrik Dalgas</u>[2], <u>Hanne Primdahl</u>[3], <u>Jørgen Johansen</u>[4], <u>Jens Overgaard</u>[5], <u>Kristian Overgaard</u>[2], <u>Kim Henriksen</u>[6], <u>Simon Lønbro</u>[2]. [1]Nordic Bioscience, Denmark, [2]Department of Public Health - Sport Science, Aarhus University, Denmark, [3]Department of Clinical Medicine - The Department of Oncology, Denmark, [4]Department of Oncology, Odense University Hospital, Denmark, [5]Dept. Experimental Clinicall Oncology, Aarhus University Hospital, Denmark, [6]Nordic Bioscience A/S, Denmark

Background
Cancer or iatrogenic cachexia are important clinical complications in clinical practice and improved biomarkers are needed to monitor and predict muscle loss. Our group has previously shown that the collagen fragment biomarkers ProC3 and IC6 are markers of muscle mass in young men and that the biomarker C6M is an indicator of anabolic response to reloading following unloading in the same group. Furthermore we found that the IC6/C6M ratio may also be related to muscle mass. In this study we set out to validate and expand our previous findings to recovering cancer patients and an age and gender matched control group.

Methods
Recovering head and neck cancer subjects from the DAHANCA25B cohort and age- and gender-matched controls were included in the study. Subjects in the DAHANCA cohort were randomized to resistance training either in the first or last 3 months (out of 6) after coming out of therapy and being habitually physically active in the remaining period. Subjects had blood drawn and muscle mass measured at baseline and the intervention subjects were also sampled at 3 and 6 months.

Results
We found that the biomarkers ProC3, IC6 and the IC6/C6M biomarker ratio all correlated significantly with muscle mass in the control group only. We also found that the C6M biomarker was not related to change in muscle mass in the intervention groups.

Conclusions
We have confirmed that the serological peptide biomarkers ProC3, IC6 and the IC6/C6M ratio are significantly correlated with muscle mass in healthy adults of both genders, but not in recovering head and neck cancer patients. Unfortunately, we were unable to extend our previous results where C6M was correlated to change in muscle mass to this cohort. The reason that these correlations are absent in the patient population is likely due to pathology-induced extra-muscular biomarker production.

Disclosures: Anders Nedergaard, None.
This study received funding from: Nordic Bioscience

SA0455

See Friday Plenary Number FR0455.

SA0456

See Friday Plenary Number FR0456.

SA0457

Caloric Restriction and the Adipokine Leptin alter the SDF-1 signaling axis and autophagy in Bone and MSCs. <u>Sudharsan Periyasamy-Thandavan</u>*[1], <u>Samuel Herberg</u>[2], <u>Phonepasong Arounleut</u>[3], <u>Sunil Upadhyay</u>[4], <u>Amy Dukes</u>[5], <u>Colleen Davis</u>[4], <u>Maribeth Johnson</u>[5], <u>Mark Hamrick</u>[6], <u>Carlos Isales</u>[4], <u>William Hill</u>[7]. [1]Georgia Regents University & Charlie Norwood VAMC, USA, [2]Case Western Reserve University, USA, [3]Georgia Regents University (formally Georgia Health Sciences University), USA, [4]Georgia Regents University, USA, [5]Georgia Regents University, USA, [6]Georgia Health Sciences University, USA, [7]Georgia Regents University & Charlie Norwood VAMC, USA

Within the bone marrow (BM), both osteogenic and adipogenic lineage cells originate from multipotent mesenchymal stromal/stem cells (MSCs). MSCs are a major source of the secreted chemokine stromal cell-derived factor-1 (SDF-1), which is critical in MSC differentiation and BM residence, largely via its receptor CXCR4. A major factor in age-associated osteoporosis is the fate of MSCs. Growing evidence suggests that SDF-1 is critical in regulating MSC differentiation resulting in either a pro-osteogenic fate, or an adipogenic one that leads to reduced bone mass and mineral density, as well as increased BM adipocytes. Leptin, a cytokine-like hormone is secreted in large part by adipocytes, exhibits anti-osteogenic effects via hypothalamic receptors. However, peripheral administration of leptin can demonstrate bone protective effects. Previous studies in mice suggest that dietary restriction decreases circulating leptin while increasing serum SDF-1 levels similar to the effect of aging. In contrast, the opposite occurs with diet-induced obesity. This study investigates the effects of caloric restriction (CR) and leptin on the SDF-1/CXCR4 axis in bone and BM tissues. For *in vivo* studies, we collected bone, BM cells and BM interstitial fluid from 12 and 20 month-old C57Bl6 mice fed ad-libitum (AL), and 20 month-old mice on CR with, or without, leptin for 10 days (10mg/kg body weight). To mimic conditions of CR *in vitro*, murine BM derived MSCs were treated with 1) *control (Ctrl):* normal proliferation medium, 2) *CR:* low glucose, low serum medium, or 3) *CR+leptin:* low glucose, low serum medium + 100 ng/ml rmLeptin for 6-72 h. Both SDF-1 and CXCR4 protein and mRNA expression in MSCs were increased by CR and CR + leptin. In contrast, the alternate SDF-1 receptor CXCR7 was decreased, this supports a change in SDF-1 signaling due to a shift in receptor availability. Additionally, autophagic flux was increased with CR and attenuated with the addition of leptin. However, mRNA isolated from bone shows SDF-1 and CXCR4 & 7 increase with age and this is reversed with CR, but addition of leptin returns this to the "aged" level. This suggests that in bone CR and leptin alter the nutrient signaling pathways in different ways to affect autophagy and the osteogenic cytokine SDF-1's local action. Studies focusing on the molecular interaction between nutrient signaling and autophagy mediated by CR, leptin and SDF-1 axis may help to address age-related musculoskeletal changes

Disclosures: Sudharsan Periyasamy-Thandavan, None.

SA0458

Aged-related Bone Loss (Osteopenia) in Old Male Mice Results From Diminished Activity and Availability of TGF-b and WNT Signaling. <u>Shen-chin Hsu</u>[1], <u>I-HUI Shu</u>[2], <u>Shanshan shi</u>*[3], <u>Hsin-chu Ho</u>[4], <u>Tzong-Jen Sheu</u>[5], <u>Wei Hsu</u>[6], <u>J. Edward Puzas</u>[7]. [1]Chung Shan Medical University Hospital Dept of Pharmacy, Taiwan, [2]Fanglio General Hospital, Taiwan, [3]University of Rochester, USA, [4]Wan-Chuan Clinics, Fangliao General Hospital, Taiwan, [5]University of Rochester, USA, [6]University of Rochester Medical Center, USA, [7]University of Rochester School of Medicine, USA

Both TGFb and WNT signaling are important for the development and maintenance of the skeletal system from embryogenesis till the whole life. TGFb can corss-talk and activate the WNT signaling with the establishment of extracellular

morphogens gradients, formation the smad/b-catenin-LEF protein complex in the nucleus. There are several groups who used different TGF-b and WNT-signaling pathway genetic modified mice to describe and demonstrate the importance of both signaling pathways in skeletal system. We used TGF-b reporter mice and in-vivo images these mice with luciferase substrate injection to understand which tissues had active TGF-b signal at varied postnatal stages. Most of the positive signals located in the calvaria and spine region especially in the tail area. In the twelve months old, the signals started to fade significantly if we kept the same sensitivity setting. This fade TGF-b signaling can be rescued with TGF-b ligand injection. We also used micro-ct to scan the bone density and ELISA to monitor the serum TGF-b amount at different time points (every two months till 14 months old). TGF-bRII is the only TGFb receptor that is capable of accepting all of three TGFb isoforms and eliciting functional signaling. Therefore, its ablation allows the study of Tgfb signaling while avoiding the functional redundancy of the ligands. Several other groups also reported different skeletal related tissues targeted TGFb-RII knockout mice. These TBRII knockout mice were either embryonic lethal or dead at birth and all showed skeletal malformation. Thus we decide to generate inducible-osteoblast-specific (Collagen-I-cre ERT2) TGF-bRII knockout mice and observe the bone loss phenotype of these mice. Both wild type (without Tamoxifen-TAM) and TGF-bRII (Het+TAM) did not have significant morphology changes under X-ray image and m-CT scan. The TGF-bRII (Homo+TAM) had significant bone loss. Other groups ever reported similar finding several years ago but just diminished activity and availability of TGF-b cannot explain the bone loss phenotype. WNT is the downstream signaling of TGF-b signaling pathway. There were several negative WNT regulators, ex FRZb, DKK, AXIN, SOST. We screened these four molecules and checked their expression level in wt(CRE), Col1-cre-ERT-TAM TBRII-het and homo mice. SOST had the highest expression level in TGF-bRII knockout mice and other three molecules did show significant change. We used SOST knockout mice to rescue this osteoblast-specific TGF-bRII caused bone loss and demonstrated the both TGF-b and WNT signalling were important to maintain the spine skeletal morphology integrity.

Disclosures: Shanshan shi, None.

SA0459

Aromatic Amino Acids Ameliorate Ovariectomy Induced Bone Loss. <u>Kehong Ding</u>*[1], <u>Aleena Lakhanpal</u>[2], <u>Qing Zhong</u>[1], <u>Wendy Bollag</u>[2], <u>Jianrui Xu</u>[2], <u>William Hill</u>[3], <u>Xing-Ming Shi</u>[1], <u>Mona El Refaey</u>[1], <u>Monte Hunter</u>[2], <u>Mark Hamrick</u>[4], <u>Carlos Isales</u>[1]. [1]Georgia Regents University, USA, [2]Georgia Regents University, USA, [3]Georgia Regents University & Charlie Norwood VAMC, USA, [4]Georgia Health Sciences University, USA

Postmenopausal bone loss is a major cause of osteoporosis in women. It has been proposed that estrogens may protect from bone loss in part by amelorating reactive oxygen species and oxidative stress induced damage to osteoblasts which occurs in postmenopausal states. Recently, our laboratory has shown that dietary aromatic amino acids have antioxidant properties, and when fed to aged C57Bl6 mices prevenst age-induced bone loss. However, the anabolic properties of aromatic amino acids on bone mass has not been investigated in low estrogen states. Based on these findings we hypothesized that endogenous antioxidants in the form of dietary supplements (aromatic amino acids) could prevent hypoestrogenic-induced bone loss. To address this question we placed three-month-old mice on a standard (18%) or low (8%) protein diet with/without aromatic amino acids supplements for four weeks after ovariectomy (OVX; n=10/group). Efffectiveness of the OVX was confirmed by uterine weight at the end of the experimental period. After four weeks the animals were sacrificed and analyzes included: bone densitometry (DXA), µCT, bone histomorphometry and serum markers of bone turnover. We found that OVX resulted in both trabecular and cortical bone loss (as measured by DXA and µ CT). Both cortical and trabecular bone loss was significantly ameliorated by the addition of aromatic amino acids (p<0.03; p<0.05 respectively). Further the OVX associated increase in PYD (a marker of bone breakdown) was inhibited by the aromatic amino acid supplement. Biomechanically, OVX was associated was associated with a decrease in ultimate force and stress at break and in Young's modulus, all significantly improved by the dietary aromatic amino acids. Taken together these data demonstrate that dietary aromatic amino acids significantly ameliorate OVX induced bone loss and that part of this protective effect may be through their antioxidant properties.

Disclosures: Kehong Ding, None.

SA0460

Effects of aging on bone turnover markers and bone density regulating hormones in cynomolgus monkeys. <u>Rana Samadfam</u>*, <u>Susan Y. Smith</u>. Charles River Laboratories, Canada

Values for bone turnover markers and hormones regulating bone density, including parathyroid hormone (PTH) and 1,25-dihydroxyvitamin D3 (VD3) in monkeys, can vary significantly depending on diet, kit supplier, origin of animals, time of day for sample collection, age and/or gender. This study investigated the effect of aging on biochemical markers of bone turnover and hormones in male and female monkeys originating from Mauritius and China. The variability was minimized by using the same diet, the same time of day for sample collection and the same kit supplier. Serum samples were collected for measurement of bone formation markers: bone specific alkaline phosphatase (BAP), osteocalcin and P1NP, PTH and VD3 and

bone resorption markers: C telopeptide (urinary and serum), urinary N-telopeptide and urinary Deoxypyridinoline (DPD). Urine markers were corrected for urinary creatinine. Serum and urine samples were collected in the morning from food deprived animals. Monkeys ranged in age from 12 months to over 15 years. Although the same suppliers were used for each kit, the lot number was different depending on the kit availability. The analyses for each parameter were carried out on separate occasions, months or years apart. Serum total calcium and phosphorus were also evaluated. All evaluated bone formation and bone resorption markers decreased with age. PTH levels did not decline with age however decreases were noted for VD3. Aging had no effect on serum total calcium levels although a trend for a decline was noted for serum phosphorous. No marked differences were noted between Mauritius and China origin animals or between males and females. The sharpest declines (2 to 6-fold) were noted between 6 to 9 years of age consistent with skeletal maturation (6 years). Values were the lowest and generally stable after the age of 9 years old (age of peak bone mass). In conclusion age-related decreases in serum and urinary bone turnover markers, serum phosphorous and VD3 were noted for cynomolgus monkeys.

Disclosures: Rana Samadfam, Charles River, 4

SA0461

See Friday Plenary Number FR0461.

SA0462

See Friday Plenary Number FR0462.

SA0463

See Friday Plenary Number FR0463.

SA0464

Sirtuin1 increases ATP production, Wnt signaling, osteoblastogenesis, and bone mass in mice via a FoxO-mediated mechanism. <u>Srividhya Iyer</u>*[1], <u>Li Han</u>[1], <u>Shoshana Bartell</u>[1], <u>Ha-Neui Kim</u>[2], <u>Aaron Warren</u>[3], <u>Julie Crawford</u>[4], <u>Igor Gubrij</u>[5], <u>Charles O'Brien</u>[1], <u>Stavros Manolagas</u>[1], <u>Maria Jose Almeida</u>[1]. [1]Central Arkansas VA Healthcare System, Univ of Arkansas for Medical Sciences, USA, [2]Univ. Arkansas for Medical Sciences, Central Arkansas VA Healthcare System, USA, [3]University of Arkansas for Medical Sciences, & Central Arkansas Veterans Healthcare System, USA, [4]University of Arkansas for Medical Sciences, USA, [5]Central Arkansas Veterans Healthcare System, Division of Pulmonary & Critical Care, University of Arkansas for Medical Sciences, USA

FoxOs attenuate bone formation by binding to β-Catenin and preventing β-Catenin/TCF mediated transcription in osteoblast progenitors. The transcriptional activity of FoxOs is modulated by several post-translational modifications including deacetylation by Sirt1 – a NAD^+ dependent deacetylase. Based on this and evidence that Sirt1 activation by synthetic molecules attenuates the age-dependent loss of bone mass, we investigated whether the anabolic effects of Sirt1 on bone are mediated by FoxOs. To this end, we generated mice in which a Sirt1 floxed allele was deleted using an Osx1-Cre transgene (Sirt1$^{\Delta Osx1}$). Sirt1$^{\Delta Osx1}$ mice exhibited lower femoral and vertebral cortical bone mass as compared to Osx1-Cre littermate controls. In addition, bone marrow-derived osteoprogenitors from the Sirt1$^{\Delta Osx1}$ mice showed an increase in the association between FoxO3 and β-Catenin, as measured by co-immunoprecipitation assays. In line with this latter finding, the expression of the Wnt-target genes axin2 and cyclinD1 was decreased, as was the proliferation of osteoprogenitors as well as osteoblastogenesis, measured by Alizarin Red staining. In contrast, FoxO-mediated transcription (measured by the activity of a FoxO-luciferase reporter construct), as well as the mRNA levels of the FoxO-target genes Nocturnin, RhoE and hemeoxygenase (Hmox) 1, were increased. Hmox1 degrades heme – an essential cofactor for the stability and function of complexes III and IV of the electron transport chain – and thereby decreases ATP production. Consistent with evidence that ATP promotes cell growth and proliferation, osteoprogenitors from mice lacking FoxO1, 3 and 4 in Osx1-Cre expressing cells had lower Hmox1 expression, increased ATP production, and higher proliferation. Conversely, reconstitution of FoxO activity in an osteoprogenitor cell line (established from bone marrow of the mice lacking FoxO1, 3 and 4), increased Hmox1 mRNA, decreased ATP levels, and decreased proliferation. Taken together with evidence that NAD^+ and Sirt1 activity decline with age, our results suggest for the first time that the age-associated decline of bone formation is due, at least in part, to a FoxO-mediated increase in Hmox1 and the suppression of mitochondria ATP production. Stimulation of Sirt1 with synthetic activators antagonizes this effect and can explain the positive effects of these small molecules on bone formation.

Disclosures: Srividhya Iyer, None.

SA0465

See Friday Plenary Number FR0465.

SA0466

Testosterone and its derivatives for the treatment of Sarcopenia in elderly males: A systematic review and Meta-analysis. <u>Sara Mursleen</u>*[1], <u>Sultan Alamri</u>[2], <u>Alexandra Papaioannou</u>[3]. [1]McMaster University, Canada, [2]King Abdulaziz University, Saudi Arabia, [3]Hamilton Health Sciences, Canada

Background: The incidence and burden of disease inflicting the elderly, such as Sarcopenia, is increasing with the aging demographic. The prevalence of Sarcopenia is 5-13% among individuals 60-70 years of age, and it increases to 11-50% among individuals 80 years and older. In 2010, the European Working group on Sarcopenia in older people reached a consensus on the definition of sarcopenia, which is a generalized loss of skeletal muscle mass and in addition a loss of either skeletal muscle strength or function.

Objective: To determine the impact of the administration of testosterone or testosterone-derivatives on muscle mass, strength, and function in elderly men.

Methods: A comprehensive and exhaustive search strategy was developed with a research librarian to identify randomized controlled trails which used testosterone/ derivatives as an intervention for men 50 years and older, with outcomes including muscle mass, strength, function, quality of life (assesed by using the Aging Male Symptoms Scale), and adverse events.

Results: 58 studies were identified for inclusion in the systematic review. A meta-analysis was completed on 8 studies up to date, with 50 studies pending. A statistically significant improvement in the intervention group was observed for muscle strength (SMD=0.37(95% CI 0.08,0.65) p=0.01). Muscle mass (SMD=0.38 (95% CI -0.19, 0.96), p=0.19), muscle function (SMD=0.04 (95% CI -0.14, 0.21), p=0.68),Somatic QoL (MD=-0.66 (95% CI -2.14, 0.83), p=0.39), Psychological QoL (MD=-0.71 (95% CI -1.47, 0.05), p=0.07), and Sexual QoL (MD=0.07 (95% CI -3.20, 3.34), p=0.97) did not yield statistically significant changes. There was no difference between groups in terms of major adverse events (OR=1.03 (0.72, 1.46), p=0.88).

Conclusion: Testosterone and its derivatives may be an important clinical intervention to increase muscle strength in sarcopenic individuals. Completion of meta-analysis of all 50 studies may provide greater insight into efficacy of remaining outcomes.

Disclosures: Sara Mursleen, None.

SA0467

See Friday Plenary Number FR0467.

SA0468

See Friday Plenary Number FR0468.

SA0469

See Friday Plenary Number FR0469.

SA0470

See Friday Plenary Number FR0470.

SA0471

See Friday Plenary Number FR0471.

SA0472

FGFR Inhibition Partially Corrects Size Abnormalities in $Nf1_{Col2}$[-/-] Mice. <u>Matthew Karolak</u>*, <u>Xiangli Yang</u>, <u>Florent Elefteriou</u>. Vanderbilt University, USA

Endochondral bone formation is a fascinating yet complex process by which long bones elongate during development and heal in adults. Genetic diseases and pathophysiological conditions can disrupt this process, causing various forms of dwarfism or fracture healing defects (non-union), for which therapeutic options are limited. Understanding how bones grow and mineralize with the proper speed and proportion during development should provide directions to design novel therapies promoting harmonious bone formation toward a functional skeleton and preventing cases of non-union. The chondrocyte is central to endochondral bone formation and repair, as the formation of a cartilage anlage/callus is a requisite first step in both processes and requires precise, spacio-temporal interactions. Patients with Neurofi-

bromatosis Type 1 (NF1) can present with bowing of the tibia, fracture and impaired fracture healing, characterized by the presence of fibrotic, cartilaginous pseudoarthrosis (PA) tissue, suggesting that inactivating mutations in *NF1* negatively alters mesenchymal stem cells differentiation and chondrocyte differentiation/function during fracture healing. Our past work in mice lacking *Nf1* in *Col2a1*-positive cells ($Nf1_{Col2}$[-/-]) showed that neurofibromin (the RAS/GTPase-activating protein encoded by *Nf1*) is required for normal growth plate formation and elongation. Mouse/human bone phenotypes associated by constitutive FGFR1 activation closely match with mouse models of *Nf1* loss-of-function in bone. Also, *Nf1* and *Fgfr1* expression overlaps in the growth plate. We thus hypothesized that neurofibromin is a negative regulator of FGFR1 signaling, and loss of FGFR1 in the growth plate would rescue the growth plate defects observed in $Nf1_{Col2}$[-/-] mice. We present here data indicating that genetic deletion of *Fgfr1* and *Nf1* together in *Col2a1*-positive cells does not rescue the defects observed in the $Nf1_{Col2}$[-/-] growth plates, including increased matrix catabolism at the osteochondral border and shortened hypertrophic zone length. These results suggest that pharmacological targeting of FGFR1 to treat NF1 PA may not be warranted. However, when $Nf1_{Col2}$[-/-] mice were treated with a pan-FGFR inhibitor (BGJ398), a partial correction of naso-anal length was observed after 18 days of treatment. Current studies are underway to determine the mechanism for this partial correction, including determining whether *Fgfr3* is ectopically expressed in the context of *Nf1* and/or *Fgfr1* deletion.

Disclosures: Matthew Karolak, None.
This study received funding from: Childrens Tumor Foundation

SA0473

IGF-I Signaling in Osterix-expressing Cells Is Required for Secondary Ossification Center Formation during Postnatal Bone Development. <u>Yongmei Wang</u>*[1], <u>Alicia Menendez</u>[2], <u>Chak Fong</u>[3], <u>Daniel Bikle</u>[4]. [1]Endocrine Unit, University of California, San Francisco/VA Medical Center, USA, [2]Endocrine Unit, University of California, San Francisco/ Veterans Affairs Medical Center, USA, [3]Endocrine Unit, University of California San Francisco/Veterans Affairs Medical Center, USA, [4]Endocrine Research Unit, Division of Endocrinology UCSF & VAMC, USA

Secondary ossification center (SOC) formation is an important event during postnatal bone development, but its regulating mechanism is unclear. Our previous studies demonstrated that global insulin-like growth factor-I (IGF-I) knockout (KO) mice had delayed SOC formation. In the current study, we use bone and cartilage specific IGF-I receptor (IGF-IR) KO mice ([OSX]IGF-IRKO) [floxed IGF-IR mice X GFP labelled osterix (OSX) promoter driven cre ([OSX]GFP-cre]. At Day 2 after birth (P2), [OSX]GFP-cre was highly expressed in the osteoblasts (OBs) in the bone surface of the metaphysis and in the prehypertrophic chondrocytes (PHCs) and inner layer of perichondral cells (IPCs). From P7, [OSX]GFP-cre was highly expressed in PHCs, IPCs, cartilage canals (CCs) and OBs in the epiphyseal SOC, but was only slightly expressed in the OBs in the metaphysis. H&E staining demonstrated that at P2, only cartilaginous tissue was found in the proximal epiphysis of the tibia in the [OSX]IGF-IRKO and their control littermates. In both mice, the perichondrium at the top of the epiphysis was getting thicker, but the small invaginations of the thickened perichondrium were observed only in the controls. At P7, in both mice, invaginations of the perichondrium invaded into the surrounding cartilage matrix and began to form the CCs, but the CCs formed in the [OSX]IGF-IRKOs were smaller and less in number. At P14, in both mice, canals excavated into the center of the cartilage generating the marrow space forming the SOC, but a smaller marrow space, less bone matrix, and more cartilage matrix were observed in the [OSX]IGF-IRKOs compared to the controls. Compared to the controls, the number of vessels and VEGF expression were less in the [OSX]IGF-IRKOs, as indicated by immunohistochemistry using antibodies against CD31 and VEGF, respectively. Ephrin B2, a regulator of VEGF production, was decreased in the [OSX]IGF-IRKOs compared with the controls. Quantitative real-time PCR revealed that the mRNA levels of the matrix degradation markers, MMP-9, 13 and 14 were decreased by 50%, 59% and 58%, respectively, in the [OSX]IGF-IRKOs compared to the controls. Our data indicate that during postnatal bone development, IGF-I signaling in OSX-expressing cells promotes cartilage matrix degradation and increases ephrin B2 production to stimulate VEGF expression and vascularization. These processes are required for normal CC formation in the establishment of the SOC.

*Disclosures: Yongmei Wang, None.*

SA0474

See Friday Plenary Number FR0474.

SA0475

Rotopol and MicroCT Imaging in the Regenerating Zebrafish Fin for BMD Therapeutic Discovery. Ronald Kwon*[1], Anthony Recidoro[2], Werner Kaminsky[2]. [1]University of Washington, USA, [2]University of Washington, USA

Osteoporosis is defined by low bone mineral density (BMD), an integrated measure of bone mass and mineralization that is associated with fracture risk. Though in vivo chemical and genetic screens hold unique potential to identify new therapeutic targets for enhancing BMD, they are challenged by the lack of models that are amenable to high-throughput approaches. Recently, we have initiated efforts to utilize the regenerating zebrafish tail fin, a model of rapid osteogenesis that recapitulates the major phases of human bone formation, for BMD therapeutic discovery. However, a major hurdle to such efforts is the lack of quantitative modalities for mineralization analysis in the zebrafish skeleton. Thus, our goals were to assess the correspondence between Rotopol microscopy (a quantitative form of birefringence imaging) and microCT in the regenerating fin, and to determine whether Botulinum toxin (BTx), a paralytic neurotoxin associated with mammalian osteogenic dysfunction, impairs bone mineralization in zebrafish. For Rotopol imaging, we implemented a custom polarized light microscope to synchronously acquire images under a stepwise rotating polarizer. By applying the appropriate relations [1], this enabled birefringence to be decoupled from transmittance and orientation, directly enabling quantitative analysis. Similar to our previous studies [2], BTx-injected fish exhibited reduced bone regrowth following tail fin amputation relative to saline-injected fish (p<0.001, d9). Rotopol and microCT imaging in regenerated bone rays revealed birefringence and TMD were highly correlated (R2=0.88, Fig 1AB), with correspondence occurring over the entire bone ray except near joints in non-regenerated tissue (due to birefringence from the fibrous inter-joint ligaments). In BTx-treated fish, Rotopol analysis revealed decreased birefringence (p<0.05 relative to saline controls) in the regenerated (but not non-regenerated) bone tissue (Fig 1C), suggesting that BTx impaired late-stage mineralization and/or secondary bone apposition but did not systemically induce demineralization in intact bone. Together, these studies establish sensitive and quantitative assays for bone mineralization analysis in the regenerating zebrafish fin, an essential first step toward integrating high-content microscopy with quantitative mineralization imaging for large-scale, systems-based screens of BMD accrual.

Refs: 1. Glazer et al., Proc R Soc A 1996 452; 2. Recidoro et al., JBMR 2013 28(S1)
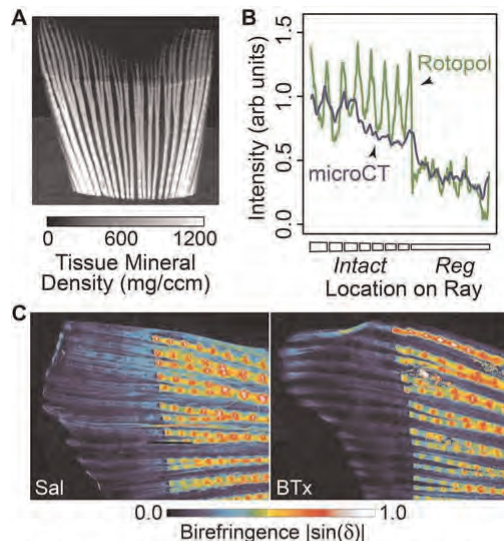
Fig 1: Mineralization imaging in the regenerating zebrafish fin using microCT and Rotopol microscopy. (A) microCT image of regenerated tail fin. Newly regenerated bone beyond the amputation plane is clearly visible. (B) Birefringence and TMD are closely correlated in both intact and regenerated bone, except for within inter-joint ligaments. (C) Rotopol imaging reveals decreased birefringence in the regenerate of BTx-injected fish.

Figure 1

Disclosures: Ronald Kwon, None.

SA0476

See Friday Plenary Number FR0476.

SA0477

Use of Quantitative Micro-computed Tomography for Assessment of Skeletal Growth and Whole-body Composition in Mice. Kim Beaucage*[1], Steven I. Pollmann[2], Stephen M. Sims[2], S. Jeffrey Dixon[1], David Holdsworth[1]. [1]The University of Western Ontario, Canada, [2]The University of Western Ontario, Canada

Micro-computed tomography (micro-CT) is the gold standard technique for quantification of radio-opaque tissue mass in small animal models. Our goals were: i) to evaluate repeated in vivo micro-CT imaging as a means for monitoring whole-body composition in short and long-term studies of growth and development in mice; and ii) to establish reference values for normative comparisons. Male C57BL/6 mice from 2 to 52 weeks of age were anesthetized and imaged using an eXplore Locus Ultra and/or eXplore speCZT micro-CT scanner (GE Healthcare Biosciences). Micro-CT images were reconstructed into 3D volumes with nominal isotropic voxel spacing of 100, 150 or 154 μm. We assessed changes in whole-body composition (WBC) including adipose tissue (AT), lean tissue (LT) and skeletal tissue (ST) volumes, and bone mineral density (BMD) and content (BMC). Signal-intensity thresholds were used to classify each voxel as adipose, lean or skeletal tissue, and tissue masses were calculated from assumed densities of 0.95 (adipose), 1.05 (lean), and 1.92 (skeletal) g/cm^3. Images revealed changes in tissue distribution with aging, such as the mineralization of caudal vertebrae, loss of subcutaneous fat and increase in visceral adipose tissue. Quantification showed biphasic increases in total volumetric body mass, LT and ST masses and BMC, consisting of rapid increases between 2 and 8 weeks of age, followed by slow linear increases to 52 weeks. On the other hand, BMD rapidly increased to a stable plateau at ~14 weeks of age, doubling from 171 ± 7 at 2 weeks to 340 ± 6 mg HA/cm^3 at 52 weeks of age. In contrast, AT mass increased exponentially with age. A micro-CT-derived total mass was calculated for each mouse and compared with the gravimetrically measured mass, which differed on average by less than 3%. Body composition parameters were highly reproducible for mice of the same age, but variability increased slightly with age. There was also good agreement in parameters obtained from the same group of mice scanned on the eXplore Locus Ultra and eXplore speCZT systems. This study provides reference data for researchers using the C57BL/6 mouse model. As well, it demonstrates the ability of in vivo single-energy micro-CT scans to quantify whole body composition in high-throughput studies of development and aging in mice.

Disclosures: Kim Beaucage, None.

SA0478

See Friday Plenary Number FR0478.

SU0001

Bone Mineral Density Predicts Fractures in Predialysis Chronic Kidney Disease. Sarah West*[1], Charmaine E Lok[2], Roxana Bucur[3], Angela M. Cheung[4], Eva Szabo[2], Dawn Pearce[5], Sophie Jamal[6]. [1]University of Toronto, Canada, [2]University Health Network, Canada, [3], Canada, [4]University Health Network-University of Toronto, Canada, [5]St Michael's Hospital, Canada, [6]The University of Toronto, Canada

Fractures are common in chronic kidney disease (CKD). We utilized data from our cohort of 130 men and women with predialysis CKD to determine if low bone mineral density (BMD) by dual energy X-ray absorptiometry (DXA; at the lumbar spine, total hip, 1/3 and ultradistal radius), or high resolution peripheral quantitative computed tomography (HRpQCT; at the radius) at baseline would increase the risk of fractures over 2 years of follow-up.

Subjects were recruited from 3 predialysis clinics in the Greater Toronto Area. We included men and women aged 18 and older with stages 3 to 5 CKD estimated by the CKD-EPI formula. We excluded subjects taking bone active agents and those with prior renal transplants. We used T-tests to determine if BMD measures (by HRpQCT and DXA) and the annual percent loss of BMD differed by fracture status.

The mean age of the 130 subjects was 61.6 $\pm$ 2.4 years, mean weight was 73.9 $\pm$ 2.3 kg, most subjects were Caucasian (71%) and the number of subjects were equally divided into stages 3, 4 and 5 CKD. The most common cause of CKD was diabetes (56%) and the mean duration of CKD was 92 months. Over 2 years there were 101 fractures (61 morphometric vertebral) in 59 subjects. Compared to those without incident fractures, those with incident fractures were more likely to report falls at baseline (34% vs. 77%) and were more likely to have had a prevalent vertebral fracture (12% vs. 83%). BMD by DXA at baseline was significantly lower at the lumbar spine, total hip, 1/3 and ultradistal radius among those with incident fractures compared to those without. For example, the mean BMD at the total hip was 0.83 g/cm^2 (95% Confidence Interval (CI): 0.79 to 0.86) for the entire cohort, 0.86 g/cm^2 (95% CI: 0.82 to 0.91) in those without fractures and 0.79 g/cm^2 (95% CI: 0.75 to 0.84) in those with incident fractures. Similarly, all baseline HRpQCT measures were lower in those with incident fracture compared to those without. For example, volumetric BMD by HRpQCT at the radius was 273.07 mg HA/cm^3 (95% CI: 256.94 to 289.21) for the entire cohort, 304.45 mg HA/cm^3 (95%CI: 280.69 to 328.22) in those without fractures and 246.82 mg HA/cm^3 (95% CI: 227.06 to 266.58) in those with incident fractures. Bone loss, by DXA and HRpQCT occurred in all subjects over 2 years, but was statistically significantly greater among those with incident fractures.Our data suggest that low BMD by DXA and HRpQCT is a risk factor for fracture in predialysis CKD.

Disclosures: Sarah West, None.

SU0002

Effect of parathyroid function and bone turnover on bone structural and material properties in dialysis patients. Junichiro Kazama*[1], Ichiei Narita[2], Yoshiko Iwasaki[3], Masafumi Fukagawa[4]. [1]Niigata University Medical & Dental Hospital, Japan, [2]Niigata University, Japan, [3]Oita University of Nursing & Health Sciences, Japan, [4]Tokai University School of Medicine, Japan

[Background] A fracture risk in patients with chronic kidney disease (CKD) is remarkably high. Although abnormalities in parathyroid function and bone turnover are common found among CKD patients, their influence on bone microscopic structural properties and/or material properties remain obscure.

[Methods] Biopsied iliac bone samples obtained from 48 stable dialysis patients were subjected for the analyses. Quantitative histomorphometric studies were performed in the virtual 3-dimensional space generated from the serial micro-CT sections. Semi-quantitative analyses of bone material properties were performed with a Raman spectrometric method. The data were compared with the biochemical and tetracycline labeling–based 2-dimensional histomorphometric results.

[Results] Both the trabecular pattern factor and the structural model index showed significant inverse correlations with bone formation rate, whereas none of the marrow cavity star volume, the connection density, or the number of nodes showed significant correlation with it. Circulating intact PTH levels showed a significant inverse correlation with cortical bone thickness, whereas none of above 5 cancellous bone structural parameters showed correlation with parathyroid function. None of the pentosidine/collagen ratio, mineral /matrix ratio, maturity of physiological crosslinks, maturity of crystal showed significant association with bone turnover or parathyroid function. [Conclusions] In dialysis patients, cancellous bone structure becomes more like plate-shaped pattern with uneven surface, along with increased bone turnover. However, this morphological change did not directly link to altered cancellous bone connectivity. Although bone material changes are commonly found among dialysis patients, we could not detect any factors dependent on parathyroid function or bone turnover. Cortical bone thinning was the only likely findings related to parathyroid function, which would potentially increase fracture risk.

Disclosures: Junichiro Kazama, None.

SU0003

Inflammation and iron deficiency stimulate FGF23 production. Valentin David*[1], Aline Martin[2], Kimberly Zumbrennen-Bullough[3], Chia Chi Sun[3], Herbert Lin[3], Tamara Isakova[4], Jodie Babitt[3], Myles Wolf[5]. [1]University of Miami,Miller School of Medicine, USA, [2]University of Miami, USA, [3]Massachusetts General Hospital, USA, [4]Feinberg School of Medicine, Northwestern University, USA, [5]Feinberg School of Medicine, Northwestern University, USA

Iron deficiency and inflammation are common in CKD, and associated with elevated circulating levels of fibroblast growth factor-23 (FGF23). We tested the hypothesis that iron deficiency and inflammation regulate FGF23 production.

To investigate the effects of inflammation on FGF23 production, wild-type (WT) mice were injected with heat-killed Brucella abortus (BA), interleukin-1B (IL1B) or saline (control). To test the effects of iron deficiency, WT mice were fed low-iron or normal diets for 3 weeks.

Inflammation decreased serum iron levels 6 hours after injection of both BA and IL1B mice compared to control mice. In BA mice, inflammation was accompanied by increased FGF23 mRNA expression in bone and a 9-fold increase in serum C-terminal FGF23 levels (cFGF23, which detects both intact FGF23 and its inactive C-terminal cleavage fragments). IL1B-injected mice demonstrated a comparable 3.5-fold and 8-fold increase in cFGF23 at 3 and 6 hours post-injection, respectively. No acute changes in intact FGF23 (iFGF23) levels were observed during the early post-injection period in either model, suggesting that FGF23 production and cleavage initially increase in parallel in response to inflammation. By 4 days post-injection, serum iFGF23 levels increased by 1.4-fold in IL1B mice compared to controls. Consistent with increased bioactive FGF23, mRNA expression of renal Cyp24a1 increased 4–fold, Cyp27b1 decreased 3-fold, and Npt2a decreased 2-fold, resulting in increased urinary phosphate excretion. Sustained iron deficiency induced by a low iron diet mimicked the effects of inflammation and resulted in a 2.5-fold increase in cFGF23, a 3-fold increase in osseous FGF23 mRNA expression, and a 2-fold increase in iFGF23.

Inflammation and iron deficiency stimulate FGF23 production but secretion of the intact protein is overridden initially by a simultaneous increase in proteolytic cleavage of FGF23. Chronic inflammation and sustained iron deficiency, however, lead to increased intact FGF23. These data suggest that iron deficiency and inflammation may contribute to elevated FGF23 levels in CKD.

Disclosures: Valentin David, None.

SU0004

Parathyroidectomy and serum leptin levels in stage 5 CKD patients. Ningning Wang*[1], Jingjing Zhang[2], Xiaoming Zha[2], Jianling Bai[3], Lina Zhang[2], Guang Yang[2], Changying Xing[2]. [1]Nanjing Medical University, Peoples Republic of China, [2]First Affiliated Hospital of Nanjing Medical University, China, [3]Nanjing Medical University, China

Background and objectives: Serum leptin is related to bone-mineral metabolism, nutrition and hematopoiesis in stage 5 chronic kidney disease (CKD) patients. Change of serum leptin level and its effects in CKD patients are controversial. This study aimed to evaluate the correlation between serum leptin with clinical and laboratory parameters and longitudinal changes of serum leptin after parathyroidectomy (PTX) in stage 5 CKD patients.

Methods: This cross-sectional study included 113 stage 5 CKD patients together with 76 controls, and a follow-up of two subgroups classified as successful (n=23) and unsuccessful (n=4) PTX from March of 2011 to October of 2013. Biochemical indices and serum leptin levels were measured.

Results: There was no difference between serum lnleptin (leptin values have been expressed as natural logarithms) levels in stage 5 CKD patients and healthy subjects(Table 1). Serum lnleptin in patients with stage 5 CKD was positive with BMI,serum triglyceride and albumin levels in males; BMI, hemoglobin, hematocrit and serum triglyceride level in females. However, serum lnleptin has a negative relationship with serum HDL (high density lipoprotein) and serum lniPTH (intact parathyroid hormone) in males, and serum HDL in females(Table 2). Compared with baseline, successful PTX subgroup had significant improvement in serum lnleptin level with a median follow-up of 5.70 months. Lnleptin change is positive related to weigt change, hemoglobin change and hematocrit change, while negative to lniPTH change. There was no significant change of serum lnleptin level in unsuccessful parathyroidectomy group with a median follow-up of 5.65 months(Table 3). From Table 4, serum lnleptin change correlated significantly with weight change(r=0.44, P=0.032), hemoglobin change(r=0.55, P=0.007), hematocrit change(r=0.51, P=0.013), and lniPTH change(r=0.44, P=0.034) in successful PTX group.

Conclusions: Serum lnleptin level has no difference between stage 5 CKD patients and healthy subjects. Serum lnleptin level is associated with bone-mineral metabolism, nutrition and hematopoiesis indexes in stage 5 CKD patients. Successful parathyroidectomy contributes to increased serum lnleptin level. Serum lnleptin change is positively related to weigt change, hemoglobin change and hematocrit change, while negatively to serum lniPTH change in successful PTX group.

Table 1. Baseline clinical and laboratory characteristics

Variable	Control (n=76)	Stage 5 CKD Patients (n=113)	P	Non-PTX Group (n=86)	PTX group (n=27)		
					Successful PTX Follow-Up (n=23)	Unsuccessful PTX Follow-Up (n=4)	Total (n=27)
Demographics							
Age (yr)	45.9±12.2	48.9±13.2	0.118	50.8±13.5	43.8±11.3	38.0±3.9	43.0±10.7[a]
Men/women	31/45	62/51	0.058	45/41	13/10	4/0	17/10
BMI (kg/m2)	23.3±2.7	21.9±3.1	0.001	22.1±3.0	21.3±3.3	19.8±2.9	21.1±3.2
Systolic BP (mmHg)	119.7±15.0	145.8±26.1	0.000	147.9±26.7	135.7±22.1	150.0±25.8	137.8±22.7
Diastolic BP (mmHg)	77.7±11.1	88.3±14.5	0.000	88.9±14.9	85.7±13.9	90.0±8.2	86.3±13.1
Dialysis mode, n(%)							
Predialysis	0(0.0)	31(27.4)	0.000	31(36.0)	0(0.00)	0(0.0)	0(0.00)
Hemodialysis	0(0.0)	66(58.4)	0.000	39(45.3)	23(100.0)	4(100.0)	27(100.0)[a]
Peritoneal dialysis	0(0.0)	25(22.1)	0.000	23(26.7)	0(0.0)	0(0.0)	2(7.4)[b]
Dialysis vintage (mo)	0(0.0-0.0)	10(0.0-72.5)	0.000	5(0.0-25.5)	96(48.0-108.0)	119(87.0-143.5)	96(50.0-120.0)[a]
Comorbidities, n(%)							
Diabetic mellitus	0(0.0)	15(13.3)	0.001	15(17.4)	0(0.0)	0(0.0)	0(0.0)[b]
Hypertension	8(10.5)	95(84.1)	0.000	74(86.0)	18(78.3)	3(75.0)	21(77.8)
Cause of ESRD, n(%)							
Glomerulonephritis	0(0.0)	82(72.6)	0.000	57(66.3)	21(91.3)	4(100.0)	25(92.6)[a]
Diabetic nephropathy	0(0.0)	9(8.0)	0.012	9(10.5)	0(0.0)	0(0.0)	0(0.0)
Hypertensive nephropathy	0(0.0)	6(5.3)	0.041	6(7.0)	0(0.0)	0(0.0)	0(0.0)
Polycystic kidney disease	0(0.0)	7(6.2)	0.027	6(7.0)	1(4.3)	0(0.0)	1(3.7)
Others	0(0.0)	9(8.0)	0.012	7(8.1)	1(4.3)	0(0.0)	1(3.7)
Anti-hypertension drugs, n(%)							
Calcium channel blocker	1(1.3)	67(59.3)	0.000	57(66.3)	9(39.1)	1(25.0)	10(37.0)[a]
ACEI or ARB	1(1.3)	29(25.7)	0.000	20(23.3)	6(26.1)	3(75.0)	9(33.3)
β-Receptor blocker	0(0.0)	39(34.5)	0.000	30(34.9)	8(34.8)	1(25.0)	9(33.3)
Other drugs	0(0.0)	23(20.4)	0.000	18(20.9)	5(21.7)	0(0.0)	5(18.5)
Laboratory values							
Hemoglobin (g/L)	142.3±16.3	92.9±20.7	0.000	89.9±20.8	101.2±18.0	108.3±17.9	102.2±17.8[a]
Hematocrit (%)	42.5±4.4	28.5±6.3	0.000	27.4±6.3	31.5±5.3	33.6±5.5	31.8±5.3[a]
Glucose (mmol/L)	5.2±0.4	4.8±1.2	0.002	5.0±1.3	4.2±0.4	3.9±0.5	4.2±0.4[a]
Creatinine (mmol/L)	69.1±15.0	903.8±349.4	0.000	894.2±379.4	925.7±228.1	984.1±289.0	934.3±232.7
Urea (mmol/L)	5.8±1.4	25.1±8.8	0.000	25.6±9.2	23.9±8.0	21.9±0.1	23.6±7.4
HDL cholesterol (mmol/L)	1.5±0.3	1.1±0.3	0.000	1.1±0.3	1.0±0.3	1.0±0.3	1.0±0.3
LDL cholesterol (mmol/L)	2.7±0.6	2.8±0.8	0.681	2.9±0.8	2.5±0.7	2.7±0.5	2.5±0.7
Total cholesterol (mmol/L)	5.0±0.8	4.5±1.1	0.000	4.6±1.1	4.1±1.0	4.2±0.9	4.1±1.0[b]
Triglyceride (mmol/L)	1.4±1.6	1.6±1.2	0.243	1.6±1.3	1.5±0.5	1.5±0.5	1.5±0.5
Albumin (g/L)	48.2±2.6	37.5±4.4	0.000	37.4±4.8	38.2±2.9	36.4±2.8	37.9±2.9
Calcium (mg/dl)	9.4±0.4	9.2±1.4	0.163	9.0±1.3	9.9±1.4	9.2±0.5	9.8±1.3[a]
Phosphorus (mg/dl)	4.8±0.7	7.9±2.3	0.000	7.6±2.2	8.9±2.8	7.7±1.2	8.7±2.6[b]
ALP (u/l)	73.4	94.6	0.000	83.5	585.3	840.1	606.8
	(60.0-87.1)	(75.55-180.0)		(68.4-114.3)	(215.0-1144.1)	(253.2-1100.9)	(295.0-1144.1)[a]
iPTH (pg/ml)	35.8	355.0	0.000	275.6	1876.4	2086.4	1904.3
	(28.3-50.9)	(192.0-1149.1)		(135.5-525.4)	(1334.3-3073.5)	(898.6-3083.6)	(1334.3-3073.5)[a]
lniPTH	1.6±0.2	2.7±0.7	0.000	2.4±0.4	3.3±0.2	4.4±2.5	3.5±1.0[a]
Leptin (pg/ml)	5264.1	5308.2	0.987	4571.0	6729.4	1189.3	8005.40
	(2723.2-9890.9)	(1707.6-13756.3)		(1572.6-15851.4)	(4758.2-12008.8)	(288.3-6278.6)	(2166.0-9983.2)
Ln leptin	3.7±0.4	3.7±0.6	0.842	3.7±0.6	3.7±0.4	2.8±0.7	3.7±0.6

Data are mean ± standard deviation (SD) or median (25th-75th percentile) as appropriate. Test of significance was by independent samples orWilcoxon rank sum test for continuous variables and chi-squared or Fisher exact test for categorical variables. BMI, body mass index; CKD, chronic kidney disease; PTX, parathyroidectomy; BMI, Body mass index; ESRD, end stage renal disease; ACEI, angiotensin-converting enzyme inhibitors; ARB, angiotensin receptor blocker; HDL, high density lipoprotein; LDL, low density lipoprotein; ALP, alkaline phosphatase; iPTH, intact parathyroid hormone.
[b]0.01 versus non-PTX group.
[a]0.05 versus non-PTX group.

Table-1

Table2. Correlation between serum lnleptin levels and variables in patients

Variable	Men		Women	
	R	P value	R	P value
Age	0.09	0.509	0.01	0.925
BMI	0.43	0.000	0.51	0.000
Dialysis vintage (mo)	0.03	0.817	-0.07	0.623
Hemoglobin (g/L)	0.02	0.856	0.36	0.010
Hematocrit (%)	0.07	0.610	0.32	0.024
Glucose (mmol/L)	0.31	0.013	0.21	0.136
HDL cholesterol (mmol/L)	-0.49	0.000	-0.36	0.009
LDL cholesterol (mmol/L)	-0.07	0.617	0.23	0.105
Total cholesterol (mmol/L)	-0.17	0.179	0.19	0.183
Triglyceride (mmol/L)	0.27	0.031	0.36	0.010
Albumin (g/L)	0.30	0.018	0.09	0.525
Calcium (mg/dl)	0.16	0.229	0.04	0.760
Phosphorus (mg/dl)	0.12	0.346	-0.07	0.632
ALP (u/l)	-0.13	0.330	-0.14	0.332
iPTH (pg/ml)	-0.13	0.326	-0.12	0.389
lni PTH	-0.27	0.035	-0.10	0.490

BMI, Body mass index; HDL, high density lipoprotein; LDL, low density lipoprotein; ALP, alkaline phosphatase; iPTH, intact parathyroid hormone.

Table-2

Table3. Clinical characteristics and Laboratory values in severe secondary hyperparathyroidism patients before and after parathyroidectomy

Variable in Two Subgroups	Baseline	After PTX	Mean Difference	P
Successful PTX follow-up (n=23)[a]				
Weigt(kg)	59.1±14.0	60.7±14.1	1.6±3.0	0.019
Hemoglobin (g/L)	102.1 ±18.3	122.8±16.4	20.7±21.3	P<0.001
Hematocrit (%)	31.9±5.4	38.5±5.2	6.6±6.5	P<0.001
HDL cholesterol (mmol/L)	1.0±0.3	1.0±0.3	0.0±0.2	0.672
LDL cholesterol (mmol/L)	2.5±0.7	2.7±1.0	0.2±0.6	0.179
Total cholesterol (mmol/L)	4.1±1.0	4.5±1.4	0.3±0.8	0.057
Triglyceride (mmol/L)	1.5±0.54	1.9±0.9	0.4±0.8	0.038
Albumin (g/L)	38.2 ±2.9	45.3±4.0	7.1±4.1	P<0.001
Calcium (mg/dl)	10.1±1.0	8.1±1.0	-2.0±1.4	P<0.001
Phosphorus (mg/dl)	8.9±2.8	4.4±1.8	-4.5±2.7	P<0.001
ALP (u/l)	708.1±550.2	217.6±172.0	-490.5±441.3	P<0.001
LniPTH	3.3±0.2	1.8±0.5	-1.5±0.4	P<0.001
Ln leptin	3.8±0.5	3.9±0.4	0.2±0.3	0.038
Unsuccessful PTX follow-up (n=4)[b]				
Weigt(kg)	56.8±8.3	58.8±16.2	2.0±8.4	0.665
Hemoglobin (g/L)	108.3±17.9	125.8±21.2	17.5±18.7	0.158
Hematocrit (%)	33.6±5.5	38.9±6.5	5.3±5.7	0.161
HDL cholesterol (mmol/L)	1.0±0.3	1.0±0.1	-0.1±0.3	0.776
LDL cholesterol (mmol/L)	2.7±0.5	2.2±0.7	-0.5±0.6	0.221
Total cholesterol (mmol/L)	4.2±0.9	4.3±0.2	0.1±1.1	0.900
Triglyceride (mmol/L)	1.5±0.5	1.8±1.5	0.3±1.2	0.623
Albumin (g/L)	36.4±2.8	45.8±3.8	9.3±3.1	0.009
Calcium (mg/dl)	9.2±0.5	8.8±1.8	-0.4±1.9	0.673
Phosphorus (mg/dl)	7.7±1.2	5.4±2.0	-2.4±1.8	0.075
ALP (u/l)	731.4±465.1	540.9±252.4	-190.5±610.5	0.577
LniPTH	3.1±0.5	3.0±0.3	-0.2±0.7	0.655
Ln leptin	3.0±0.7	3.1±0.7	0.1±0.4	0.727

Data are mean ± standard deviation (SD).
HDL, high density lipoprotein; LDL, low density lipoprotein; ALP, alkaline phosphatase; iPTH, intact parathyroid hormone.
[a]Patients were followed up for a median period of 5.70months.
[b]Patients were followed up for a median period of 5.65 months.

Table-3

Table 4. Correlation between lnleptin change with clinical and biochemical parameters (n=23)

Variable		Lnleptin Change
Weigt change (kg)	0.44	0.032
Hemoglobin change (g/L)	0.55	0.007
Hematocrit change (%)	0.51	0.013
HDL cholesterol change (mmol/L)	0.031	0.889
LDL cholesterol change (mmol/L)	0.22	0.318
Total cholesterol change (mmol/L)	-0.02	0.943
Triglyceride change (mmol/L)	0.09	0.680
Albumin change (g/L)	0.37	0.087
Calcium change (mg/dl)	0.01	0.967
Phosphorus change (mg/dl)	-0.28	0.201
ALP change (u/l)	-0.14	0.519
LniPTH change	0.44	0.034

HDL, high density lipoprotein; LDL, low density lipoprotein; ALP, alkaline phosphatase; iPTH, intact parathyroid hormone

Table-4

SU0005

Procollagen type-1 N-terminal propeptide (P1NP) levels by Elecsys assay correlate with bone formation rate in Chronic Kidney Disease.

Serge Cremers*[1], David Dempster[2], Hua Zhou[3], Elzbieta Dworakowski[4], Mafo Kamanda-Kosseh[1], Thomas Nickolas[5]. [1]Columbia University, USA, [2]Columbia University, USA, [3]Helen Hayes Hospital, USA, [4]Columbia University Medical Center, USA, [5]Columbia University College of Physicians & Surgeons, USA

Renal osteodystrophy is characterized by a spectrum of bone turnover ranging from adynamic bone disease to osteitis fibrosa cystica. Bone turnover assessment is an absolute required for treatment and is currently determined by tetracycline double-labeled transiliac crest bone biopsy. Non-invasive turnover determination in CKD is controversial because most bone turnover markers (BTMs) are renally cleared. P1NP is a bone formation marker, circulating in a mono- and a trimeric form, which are cleared both renally and non-renally. Our group reported that higher total levels of P1NP predict bone loss in pre-dialysis and dialysis-dependent CKD patients. We

hypothesized that in CKD levels of total P1NP would correlate with bone formation rate (BFR) measured by biopsy.

In 22 patients (male=8; female=14; mean age $\pm$ SD 68 ± 11 years,) with CKD stages 2-5D, fasting morning blood was collected within 6-months of double tetracycline double-labeled transiliac bone biopsy. Total serum P1NP was measured by ECLIA (Elecsys 2010, Roche Diagnostics, Indianapolis, IN). Reference range was 20-100 ug/L. BFR (μm^3/ μm^2/day) was determined histomorphometrically in trabecular, endocortical and intra-cortical bone from biopsy using ASBMR criteria. Data is presented as mean $\pm$ SD. P1NP and BFR were log transformed prior to analysis and relationships were determined by Pearson correlations.

Results: Five patients were on hemodialysis (HD) and mean estimated GFR in pre-dialysis patients was 36 ± 17 mL/min. Mean BFR at trabecular, endocortical and intracortical regions were 0.018 ± 0.031, 0.019 ± 0.035 and 0.030 ± 0.038 respectively and there were no significant differences in BFR between pre-dialysis and HD patients. P1NP for the total, pre-dialysis and HD cohorts was 332 ± 585ug/L, 98 ± 51ug/L and 1125 ± 878ug/L respectively. P1NP levels were significantly greater in HD compared to pre-dialysis (p=0.004) and there were no significant relationships between P1NP and eGFR among pre-dialysis patients. There were significant, moderate and direct associations between P1NP and BFR in the three envelopes (R^2 0.41, 0.34 and 0.34, all p<0.05 for trabecular, endocortical and intracortical bone, respectively).

These data suggest that measurement of serum P1NP by the Elecsys assay correlates well with BFR in CKD. Larger studies are needed in CKD populations to validate this finding, and to determine whether P1NP predicts future fracture and can be used to guide treatment to protect against bone loss and fracture.
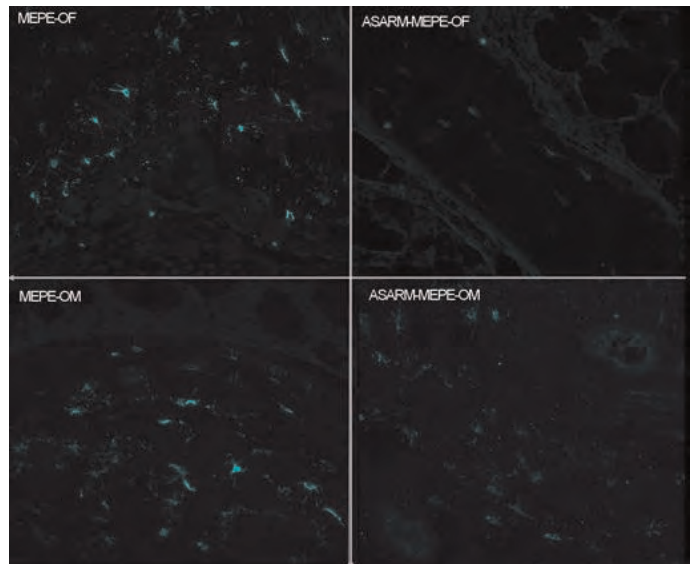
SU0006

The increased expression of ASARM-MEPE by osteocytes is associated with bone mineralisation defect in hemodialysed patients.

Martin Jannot*[1], Vasili Gnyubkin[1], Myriam Lessard[2], Norbert Laroche[1], Christophe Mariat[3], Luc Malaval[4], Laurence Vico[5], Marie-Helene Lafage-Proust[6]. [1]INSERM-U1059, France, [2]Hôpital du Sacré-Coeur , Service de Néphrologie, France, [3]Service de Néphrologie-CHU, France, [4]INSERM U1059-Université de Lyon-Université Jean Monnet, Saint-Etienne, France, [5]University of St-Etienne, France, [6]INSERM Unit 1059, France

Renal osteodystrophy (ROD) observed in chronic kidney disease (CKD) include 4 types of bone lesions according to the level of bone remodeling (high: osteitis fibrosa -OF- or low: adynamic bone disease -ABD) and mineralisation (osteomalacia -OM- and mixed uremic osteopathy). While high bone turnover is mostly linked to increased PTH serum levels, the pathophysiology of mineralisation defects and ABD remains obscure. DMP-1 and MEPE, two osteocyte matrix proteins of the SIBLINGs family are involved in bone mineralisation, indirectly (via DMP1-controlled FGF23 expression) and directly, their cleavage leading to the release of ASARM fragments which are both potent local inhibitors of mineralisation and phosphatonins. Furthermore, serum levels of sclerostin, another osteocyte protein which inhibits bone formation are highly increased in CKD. In this context, our working hypothesis was that osteocyte expression of these proteins might differ according to the ROD type.

Material and Methods: 26 iliac crest resin-embeded bone biopsies from hemodialysed patients (17 men, 10 women, mean age 59 ± 14 yrs) performed after double tetracycline labeling where selected and included: 5 ABD, 8 OF of various severity, and 13 patients with a mineralisation defect (OM or MUO). ROD type diagnosis was established according to bone histomorphometric criteria using Bone Formation Rate and mineralisation parameters (Osteoid volume and thickness and Mineralisation Lag Time). A control group consisting in bone biopsies from 10 non uremic osteoporotic patients or patients with normal bone histology was also analysed. We studied quantitatively, via semiautomatic image analysis, and qualitatively, the osteocyte expression of DMP1 , MEPE, ASARM-MEPE and sclerostin using indirect immunofluorescence after bone section decalcification and deplastification.

Results: MEPE was expressed in most of the osteocytes in both OF and OM lesions. In contrast, ASARM-MEPE was mainly observed in osteocytes of OM and MUO patients. (Fig-1:b: bone, m: marrow, arrow: immunolabelled osteocytes). While sclerostin was only present in osteocytes located at the center of trabeculae of OF and OM patients, a higher number of sclerostin-positive osteocytes were found in ABD. Finally, compared to non uremic bone, a dramatic increase in DMP-1 positive osteocytes was observed in all uremic patients.

Our results suggest that ASARM MEPE and Sclerostin may be involved in the pathophysiology of OM and ABD, respectively.

Figure 1

SU0007

Uremia exacerbates bone mechanical property in chronic kidney disease model rats with secondary hyperparathyroidism.

Yoshiko Iwasaki[1], Junichiro Kazama[2], Masafumi Fukagawa*[3]. [1]Oita University of Nursing & Health Sciences, Japan, [2]Niigata University Medical & Dental Hospital, Japan, [3]Tokai University School of Medicine, Japan

Bone fragility has been demonstrated often in patients with chronic kidney disease (CKD) including dialysis patients. High turnover bone induced by elevated parathyroid hormone (PTH) could be a possible cause of reduced bone volume. However, relationship between bone fragility and PTH has not been clearly shown except for those with very high PTH level. In order to elucidate the mechanisms underlying bone fragility in CKD patients with secondary hyperparathyroidism, we analyzed property of bone from animal model. Rats underwent 5/6 partial nephrectomy (Nx) or sham operation (Sham). After 8 weeks, these Nx rats were divided into two groups. One group was treated with the oral adsorbent AST-120 (4g/kg body weight admixed in animal feed) (CKD Trt rats), which decreases the accumulation of uremic toxins in sera such as indoxyl sulfate, and the other group was treated with vehicle (CKD rats). All rats were sacrificed at 16weeks after Nx, then serum and femur were obtained. Value of femoral storage modulus in CKD rats assessed by dynamic mechanical analysis was lower than that of Sham rats. The degree of reduction reached to 60% of sham value. Bone chemical composition measured by raman spectroscopy, that mineral matrix ratio, the ratio of physical crosslinks, and apatite crystallinity was reduced whereas pentosidine to matrix ratio increased in CKD rats. In addition, cortical area and thickness decreased in CKD rats compared with that of sham rats. Administered oral adsorbent treatment suppressed the reduction of storage modulus. Chemical composition parameters in CKD Trt rat were similar to that of in sham rats. The levels of PTH concentration, the values of cortical area, and cortical thickness were not different in CKD rats either with or without adsorbent treatment. These results suggest that the accumulation of uremic toxins facilitate deteriorating mechanical properties through changes of material properties independent of bone micro structural changes in CKD with secondary hyperparathyroidism.

SU0008

What is the Threshold of Renal Function that Influences the Measurement of Biochemical Markers of Bone Turnover among Postmenopausal Women with Osteoporosis?.

Pascale Chavassieux*[1], Jean-Paul Roux[2], Nathalie Portero-Muzy[3], Patrick Garnero[4], Roland Chapurlat[5]. [1]INSERM UMR1033, Université De Lyon, France, [2]INSERM, UMR 1033, Université de Lyon, France, [3]INSERM UMR 1033, Université de Lyon, France, [4]INSERM Research Unit, France, [5]E. Herriot Hospital, France

Some biochemical markers of bone turnover are excreted by the kidney. Consequently their serum concentration can be increased by renal failure, although the threshold of glomerular filtration rate (GFR) at which their concentration starts to rise is unknown. Abnormalities of bone remodeling are also observed when the renal function is declining (osteodystrophy), which also confounds the increase in

serum markers. The purpose of this study was to evaluate the relationship between the GFR and the bone remodeling assessed either by serum biochemical markers (bone alkaline phosphatase, Bone ALP; collagen type 1 N-propeptide, P1NP) and resorption (C-terminal crosslinking telopeptide of collagen type 1, sCTX) and osteoprotegerin (OPG) or the gold standard bone histomorphometry, in a large population of postmenopausal women with osteoporosis. 370 untreated postmeno-pausal osteoporotic women aged 50 to 84 yrs were selected. The creatinine clearance was estimated by the CKD-EPI equation. Transiliac bone biopsies were obtained after a double tetracycline labeling. The static (Ob.S/BS, OS/BS, OV/BV) and dynamic (MS/BS, BFR/BS, FP, Omt, Mlt, Acf) parameters of formation, and the parameters of bone resorption (ES/BS, Oc.S/BS, EV/BV, E.De) were measured.

In patients with CKD-EPI > 60 ml/min/1.73m2, the markers of formation (Bone ALP, P1NP) and of resorption (sCTX) were significantly correlated with the histomorphometric parameters of formation and resorption, respectively, but no significant correlation was observed between CKD-EPI and the biochemical markers or the histomorphometric parameters of bone turnover. In contrast, in patients with an altered renal function (CKD-EPI<60 ml/min/1.73m2), significant and negative correlations were observed between CKD-EPI and the histomorphometric parameters of formation (OS/BS, OV/BV, O.Th, FPa, Omt): -0.59<r<-0.43, 0.03>p>0.002, but no correlation was found between the biochemical markers and the histomorpho-metric parameters.

These results suggest that when the renal function is normal or moderately impaired (CKD-EPI>60 ml/min/1.73m2), serum levels of bone markers are not influenced and reflect the bone turnover. In contrast, when the renal function is impaired more importantly (CKD-EPI<60 ml/min/1.73m2) the serum biochemical bone markers reflect the renal function rather than the bone turnover itself.

Disclosures: Pascale Chavassieux, None.

SU0009

No significant change in Bone mineral density after vitamin D supplementa-tion in young and elderly women : Results from 2 randomized trials. SRI HARSHA Tella*[1], J. Christopher Gallagher[2], Lynette Smith[3]. [1]Creighton University School of Medicine, USA, [2]Creighton University Medical Center, USA, [3]University of Nebraska, USA

BACKGROUND: Vitamin D is often recommended for use with calcium supplements to increase bone mineral density (BMD) and prevent osteoporosis, however there are few systematic studies on effect of different doses of vitamin D supplementation on BMD.

METHODS:We conducted two randomized, placebo-controlled trials in women with vitamin D insufficiency (serum 25-hydroxyvitamin D ≤20 ng/dl/50 nmol/liter). Subjects in one trial were aged 25–45 years (198 Caucasian and African American) and in the other were aged 57-90 years (273 Caucasian and African American women). Older women were randomly assigned to placebo, vitamin D3 400, 800, 1600, 2400, 3200, 4000, or 4800 IU daily; calcium supplements were given to maintain total calcium intake of 1200-1400 mg/d. Younger women were randomized to placebo, 400, 800, 1600 and 2400IU/d and calcium intake was increased to 1000mg/d. Statistical difference between groups was tested by ANOVA.

RESULTS: In the older women the mean percent change in all subjects for BMD at 12 months was; total body, 0.62%(+2.72), there was no difference between Caucasian and African Americans (p=0.74). The percent change in femoral neck was 0.59% (+3.58) and there was no difference between races (p=0.64). The percent change in spine was 0.43% (+2.80) and there was no difference between the races. There was no significant difference in BMD at any site between various vitamin D doses and placebo.In the younger women the percent change in all subjects for BMD at 12 months was; total body 0.57% (+2.09),there was no difference between Caucasian and African Americans (p=0.70). The percent change in femoral neck was 0.79% (+3.02) ,there was no difference between races (p=0.62). the percent change in spine was 1.22% (+2.41) and no difference between races(p=0.60). There was no significant effect of vitamin D on BMD at any site between various doses of vitamin D and placebo.

CONCLUSION: The increase in total body, spine and hip BMD in young and elderly women given vitamin D doses between 400 and 4800 IU daily and calcium supplementation is small and is not different from placebo. It remains to be seen whether there is any effect on fractures in these populations.

Disclosures: SRI HARSHA TELLA, None.

SU0010

Withdrawn

SU0011

Large genomic deletions inactivate the MEN1 gene in Multiple Endocrine Neoplasia (MEN1) families. Filomena Cetani*[1], Elena Pardi[2], Simona Borsari[2], Federica Saponaro[2], Chiara Banti[2], Edda Vignali[3], Antonella Picone[2], Antonella Meola[2], Claudio Marcocci[4]. [1]University Hospital of Pisa, Italy, [2]Department of Clinical & Experimental Medicine, University of Pisa, Italy, [3]University Hospital of Pisa, Italy, [4]University of Pisa, Italy

MEN1 is an autosomal dominant disorder characterized by tumours in multiple endocrine glands, most commonly parathyroid, enteropancreatic and anterior pituitary glands. To date, germline mutations in the MEN1 gene have been identified in about 70–80% and 30% in familial and sporadic MEN1 cases, respectively. The MEN1 gene exons spans 9 kb of the genome encoding the menin protein with tumor suppressor function. More of 2/3 of MEN1 mutations, spread across the coding region, lead to a truncated protein, confirming a loss-of-function mechanism. A lack of a genotype-phenotype correlation has been observed. Approximately 20–30% of MEN1 patients do not have MEN1 mutations detected with conventional mutation screening methods. Up to date 12 large germline MEN1 deletions have been reported in unrelated MEN1 probands, accounting for around 3% of MEN1 cases analyzed.

The aim of this work was to evaluate if the MEN1 mutation detection rate can be increased by the occurrence of large monoallelic MEN1 gene deletions. We used Multiplex Multiplex Ligation-dependent Probe Amplification (MLPA) assay to identify gene copy number variations in a group of 25 MEN1 index cases (7 familial and 18 sporadic) negative for MEN1 mutations on direct sequencing. These cases belong to a cohort of 54 MEN1 probands, 33 of whom with a family history of the disease. At MEN1 sequencing analysis we found 29 germline mutations (54%), 26 of whom occurring in familial cases (79%). 72% of all detected mutations were frameshift, nonsense or affecting splice site junctions. MLPA experiments were performed on DNA obtained by patients' blood samples, using the SALSA MLPA probemix kit P244-B1 (MRCHolland), according to the manufacturer's instructions.

We found four MEN1 large deletions; a deletion spanning the whole gene in 2 kindreds, one encompassing the 5'UTR region, exons 1 and 2 in one sporadic case, and a deletion of exons 9-10 in a familial case.

We established that in our study alteration of the MEN1 gene can explain around 90% of MEN1 familial cases of Italian origin, since MEN1 large deletions account for 10% of all germline MEN1 mutations in MEN1 kindreds. We didn't observe any association between the type of mutations and the clinical characteristics of the disease. We recommend to include MLPA assay in the routine analysis for MEN1 mutations, especially in families without detected germline mutations, as this type of large MEN1 deletions were detected in 40% of MEN1 mutation negative cases.

Disclosures: Filomena Cetani, None.

SU0012

Urinary Calcium Excretion in Postmenopausal Women of African Ancestry. Mageda Mikhail*[1], shahidul islam[2], Albert Shieh[3], John Aloia[4]. [1]Winthrop University Hospital, USA, [2]winthrop university hospital, USA, [3]University of California, Los Angeles, USA, [4]Winthrop University Hospital, USA

PURPOSE: African Americans have lower urinary calcium excretion than white Americans. The primary purpose of this study was to develop a reference range for calcium excretion in postmenopausal black women and compare it to white women. A secondary objective was to evaluate the reliability of the fasting urinary calcium/creatinine ratio in predicting 24-hour urinary calcium excretion.

METHODS: Baseline data collected in 7 studies at one site for research purposes in 1,042 healthy black and white postmenopausal women were analyzed. In some studies, only fasting urinary calcium/creatinine ratio was available whereas in others, 24-hour urinary calcium excretion was measured as well. Reference ranges were calculated for 24-hour urinary calcium and fasting urinary calcium/creatinine ratio in each ethnic group. Correlations with demographics and selected laboratory values were calculated. Multiple linear regression model was developed to determine the predictors of the 24-hour urinary calcium excretion. Sensitivity-Specificity and agreement analyses were employed to determine the usefulness of fasting urinary calcium/creatinine ratio compared to 24-hour urinary calcium for detecting hypercalciuria and hypocalciuria.

RESULTS: Reference intervals for the 24-hour urinary calcium and for the fasting urinary calcium/creatinine ratio were 16 -180 mg /24 hours and 0.008 - 0.16 for African American women compared to 25 - 212 mg/24 hours and 0.026 - 0.23 in white women, respectively. Urinary creatinine excretion was higher in African Americans consistent with their higher muscle mass. Fasting urinary calcium/creatinine ratio was not a reliable predictor of 24-hour urinary calcium in either ethnic group.

CONCLUSION: Clinicians should be aware of the lower calcium excretion in African American women. In particular, the lower reference range should be considered when evaluation is made for hypocalciuria disease. The fasting urinary calcium/creatinine ratio should not be used as a substitute for 24-hour urinary calcium excretion.

Disclosures: Mageda Mikhail, None.

SU0013

A mutation in the TRAF6-binding domain of SQSTM1/p62 associated with Paget's disease of bone is associated with hyper-activation of signalling.

Sarah Rea*[1], Melanie Sultana[2], John Walsh[3], Nathan Pavlos[4], Jiake Xu[4], Lynley Ward[2], Robert Layfield[5], Thomas Ratajczak[2]. [1]Sir Charles Gairdner Hospital, Australia, [2]Dept Endocrinology & Diabetes, Sir Charles Gairdner Hospital, Australia, [3]University of Western Australia, Australia, [4]University of Western Australia, Australia, [5]University of Nottingham, United Kingdom

Introduction: Paget's disease of bone (PDB) is characterised by focal areas of increased bone remodelling, thought to be initiated by increased bone resorption by hyperactive osteoclasts and exacerbated by abnormal bone formation. Mutations in the SQSTM1/p62 gene are a common genetic cause of PDB and commonly affect the ubiquitin associated (UBA) domain region of the protein.

Methods: We assessed mutational effects on NF-κB and activator protein 1 (AP-1) activity using the Dual Luciferase assay (Promega). To assess mutational effects on TRAF6 ubiquitination, we co-transfected cells with expression plasmids for Ubiquitin, TRAF6 and SQSTM1/p62. Cells were lysed with RIPA buffer, clarified and subjected to immunoprecipitation with FLAG antibody. Antibody and bound proteins were bead-captured and following extensive washes bound proteins were eluted with SDS sample buffer and separated by SDS-PAGE, followed by Western blot analysis.

Results and Discussion: We report a non-conservative change (K238E) that manifests within the TRAF6-binding domain of SQSTM1/p62 that co-segregates with PDB in a family that displays a severe disease phenotype. Over-expression of this mutant protein leads to increased basal activity of NF-κB and AP-1, important mediators of osteoclast formation. These transcription factors are induced by upstream activation of TRAF6 (via auto-ubiquitination).

SQSTM1/p62 is required for TRAF6 ubiquitination, yet also mediates negative regulation of NF-κB and osteoclastogenesis by linking the de-ubiquitinating enzyme CYLD with TRAF6 at the proteasome. We find that K238E expression leads to a marked increase in the amount of poly-ubiquitinated TRAF6 observed. This finding is consistent with the increased signalling we routinely observe with this and other SQSTM1/p62 mutant proteins, and is thought to contribute to increased osteoclasts and bone resorption in PDB lesions.

Conclusions: We find that mutant SQSTM1/p62 expression leads to increased activation of transcription factors important for osteoclast signaling. This is associated with increased levels of ubiquitinated TRAF6, which may partially explain the molecular mechanisms of increased osteoclast activity in SQSTM1/p62 associated PDB.

SU0014

A Prospective Study on Juvenile Primary Hyperparathyroidism Population.

Federica Saponaro*[1], Federica Cacciatore[2], Elena Pardi[2], Simona Borsari[2], Claudio Marcocci[3], Filomena Cetani[4]. [1]M.D., Italy, [2]U.O. Endocrinology 2, Italy, [3]University of Pisa, Italy, [4]University Hospital of Pisa, Italy

Primary hyperparathyroidism (PHPT) is generally an adult disease and features of PHPT in juvenile population (J-PHPT) are still unclear.

The aim of the study was to evaluate the clinical, biochemical, densitometric and hystological characteristics in patients with J-PHPT, comparing sporadic (S) and familiar (F) J-PHPT.

We conducted a monocentric prospective study in 154 patients with ≤40 years and a median follow-up of 2 years (1-8). We compared the clinical presentation, the changes of biochemical, densitometric, histological parameters at diagnosis and at the last follow-up visit, between S and F-JPHPT.

One hundred-twelve patients had S-J-PHPT (neuroendocrine markers, calcitonin, pituitary hormones and serum calcium in relatives were in the normal range). Thirty-one patients had Multiple Endocrine Neoplasia type 1 (MEN1) syndrome and 11 Familiar Isolated Hyperparathyroidism (FIHP). Symptomatic nephrolitiasis was observed in 69.44% of S-J-PHPT and in 48.4% of F-J-PHPT.

Ninety S-J-PHPT and 27 F-J-PHPT underwent PTx. The histology showed in S-J-PHPT and F-J-PHPT respectively: a single adenoma in 85 and 7 patients, hyperplasia in 2 and 19 patients , carcinoma in 2 S - JPHPT and white cervicotomy was observed in one S-JPHPT and one F-JPHPT.

Ionized serum calcium and PTH significantly decreased after PTx in both S and F-JPHPT. Eleven (15%) patients with S-PHPT had persistence/recidive of PHPT and included one with white cervicotomy, one with hyperplasia and 9 with single adenoma. The persistence/recurrence rate was higher (n=10, 52.63%) in F-JPHPT compared with S-PHPT.

In both groups a more severe disease in term of serum Ca++ (S-PHPT p=0.039, F p=0.027), PTH (S p= 0.045, F p= 0.7) and radial Z score (S p= 0.001, F p=0.002) was observed in males compared with females.

Age was not significantly correlated with the severity of disease in term of Ca++, PTH and Z score in both groups; basaline serum Ca++ was significantly associated with PTH levels and severity of bone disease (Z score)

When the patients were stratified for age ≤25 and > 26 years, there was no statistical difference in the overall group or when comparing F-JPHPT and S-JPHPT.

In conclusion, J-PHPT seems to be a sintomatic disease confirming literature's data. J-PHPT is more severe in male than in females and has a higher rate of persistence/recurrent disease, even in S-J-PHPT patients. The severity of disease is independ from age and the clinical characteristic between S and F patients are similar.

SU0015

Beneficial Effects of PTH(1-84) in Hypoparathyroidism as Determined by Trabecular Bone Score (TBS).

Cristiana Cipriani*[1], Barbara Silva[2], Natalie Cusano[3], Aline Costa[4], Dinaz Irani[5], Alice Abraham[4], Donald McMahon[3], Laura Beth Anderson[4], Elizabeth Levy[6], Mishaela Rubin[4], John Bilezikian[3]. [1]"Sapienza", University of Rome, Italy, [2]Federal University of Minas Gerais, Brazil, Brazil, [3]Columbia University College of Physicians & Surgeons, USA, [4]Columbia University, USA, [5]Columbia University Medical Center, USA, [6]Columbia University, USA

Trabecular bone score (TBS) is a texturral index reflecting trabecular micro-architecture, as seen more directly by μCT and HRpQCT measurements. We have shown previously that TBS is normal in hypoparathyroid (HypoPT) patients, that PTH(1-84) improves TBS in premenopausal (PreM) women, and that PTH(1-84) preserves it in postmenopausal (PostM) women and men over a 4-year treatment period. Yet, no data are available on the effects of PTH(1-84) using TBS in HypoPT over a longer period of time. In this report, we provide new data on the effects of PTH(1-84) on TBS in HypoPT patients over an average of 5.5 years.

We studied 29 HypoPT subjects [22 women (10 PreM and 12 PostM) and 7 men; mean age 48.2 ± 13.4 yrs] treated with PTH(1-84) for a mean follow-up time of 69 ± 16 months (range 48-102). Site-matched LS TBS data were extracted from the DXA image (Hologic) using TBS iNsight software. Linear mixed model for repeated measures was performed to assess the % change in TBS relative to baseline by evaluating sex-specific differences and all results are adjusted for weight.

PreM women were younger than postM (35.6 ± 8 and 56.4 ± 8.9; p<0.0001) and men (52.1 ± 13.5; p<0.01). Mean TBS value was normal (1.428 ± 0.138; normal ≥1.35) but lower in PostM (1.358 ± 0.136) than in PreM women (1.491 ± 0.105; p<0.05) at baseline. In the entire cohort, PTH(1-84) improved TBS throughout the entire follow-up period (p<0.0001). In particular, there was a significant increase from 42 ($+2.25 \pm 0.94\%$; p<0.02) to 60 months ($+2.85 \pm 1.02\%$; p<0.01). The mean gain at 102 months was $1.73 \pm 3.55\%$. TBS significantly increased in PreM women by $2.96 \pm 1.25\%$ (p<0.02) at 36 and up to 84 months ($+5.38 \pm 2.17\%$; p<0.05), and in PostM women at 42 ($+3.66 \pm 1.53\%$; p<0.02) and 48 months ($+4.24 \pm 1.5\%$; p<0.01), while no changes were observed in men. Percent TBS changes were different among the 3 groups at 72 months (male vs PreM and PostM:p<0.05; PreM vs PostM:p<0.0001). A positive correlation between the % changes in TBS and LS BMD was observed at 24, 36 (r=0.4;p<0.05), 48 (r=0.4;p<0.01), 60 and 66 months (r=0.5 and 0.6;p<0.02).

In this study, we have shown that PTH(1-84) improves TBS in hypoPT over a period of time that exceeds any previous experience with long term use of PTH(1-84). In PreM women, TBS continues to increase for up to 7 yrs, thus confirming that microstructural improvements due to PTH(1-84) are particularly evident in younger individuals. There were no safety issues associated with long-term administration of PTH(1-84).

SU0016

Parathyroidectomy-Associated Thyrotoxicosis: A Prospective Cohort Study.

Lisa-Ann Fraser*[1], Stan Van Uum[2], Terri Paul[3], John Yoo[2]. [1]Western University, Canada, [2]University of Western Ontario, Canada, [3]St. Joseph's Health Centre, Canada

Purpose: Reports exist describing transient thyroid hormone elevation occurring after parathyroidectomy. We aimed to describe, in detail, changes in thyroid function occurring around the time of parathyroidectomy.

Methods: Consecutive adult patients with hyperparathyroidism who underwent parathyroidectomy were studied. Pre-operative bloodwork measured TSH, free T4, free T3, 25-hydroxyvitamin D, parathyroid status, and thyroid auto-antibodies. The type of surgery performed, and extent of thyroid manipulation was documented. Patients had blood work repeated on post-operative days 1, 3, 7, and 14. Between post-operative day 7 and 14 an Endocrinologist administered a standardized questionnaire and physical assessment and continued follow up out to 2 months.

Results: Nine consecutive patients were reviewed, 6 females and 3 males, 4 (females) were excluded due to pre-existing hypothyroidism. Of the 5 patients followed, all underwent 4-gland exploration, and 4(80%) developed hyperthyroidism in the post-operative period as documented by elevated serum free T3 and/or free T4. Two patients (40%) experienced symptomatic thyrotoxicosis. Free T3 was the first hormone to move outside of the normal range; it was found to be elevated as early as the first post-operative day. Free T4 showed maximal elevation at post-operative day 3. By post-operative day 14 all levels had fully normalized and remained normal when checked 1 month, and 2 months post-surgery. Symptomatic patients reported that symptoms lasted for approximately 2 weeks after their operation and then resolved completely. There was no association between pre-operative calcium level severity and

the subsequent development of post-operative hyperthyroidism. Similarly, vitamin D insufficiency did not predict thyroid hormone changes. No patient tested positive for anti-thyroid antibodies either pre or post-operatively, and none had recent iodine exposure or family history of hyperthyroidism.

Conclusions: Hyperthyroidism, including symptomatic thyrotoxicosis, occurs commonly after parathyroidectomy for hyperparathyroidism. Thyroid hormone levels seem to peak early in the first week after the operation, but stay elevated for up to 14 days. It may be prudent for physicians to warn their patients about this potential complication of surgery, and possibly consider adding beta-blockers during the first two weeks post-op in patients who are at high risk of cardiac complications from thyrotoxicosis.

Disclosures: Lisa-Ann Fraser, None.

SU0017

Protein Expression of Fibroblast Growth Factor Receptor/α-klotho, Vitamin D Receptor, CYP24A1 and CYP27B1 in Parathyroid Adenoma. A Ram Hong*[1], Jung Hee Kim[2], Chan Soo Shin[2], Seong Yeon Kim[1], Hye Sook Min[1], Sang Wan Kim[3]. [1]Seoul National University Hospital, South Korea, [2]Seoul National University College of Medicine, South Korea, [3]Seoul National University College of Medicine, Boramae Hospital, South Korea

Objective: Parathyroid hormone (PTH) secretion from parathyroid gland is regulated by circulating 1,25(OH)2D3, FGF23 and extracellular calcium. We aimed to investigate the role of FGFR, α-klotho, VDR, CYP24A1 and CYP27B1 in the pathogenesis of primary hyperparathyroidism (PHPT).

Methods: We included 66 patients who underwent parathyroidectomy for PHPT and 29 control patients with normal parathyroid in Seoul National University Hospital from January 2001 to December 2011. All patients diagnosed with PHPT had parathyroid adenomas. We evaluated the protein expression of FGFR, α-klotho, VDR, CYP24A1 and CYP27B1 in parathyroid gland using tissue microarray.

Results: FGFR, CYP24A1 and CYP27B1 were mainly expressed in cytoplasm, whereas α-klotho and VDR were expressed both in nucleus and cytoplasm. Nuclear and overall VDR expressions were significantly reduced in PHPT compared with the control group (P<0.001 and P=0.012, respectively). There were no significant differences in FGFR, α-Klotho, CYP24A1 and CYP27B expressions between the PHPT and the control. Nuclear VDR negatively correlated with serum levels of PTH (R=-0.229, P=0.033). There was negative correlation between α-klotho expression and serum levels of PTH (R=-0.429, P<0.001), whereas positive correlation was found between α-klotho expression and serum 25(OH) vitamin D3 levels (R=0.452, P=0.015).

Protein expression of α-Klotho, VDR, CYP24A1 and CYP27B1 were positively correlated in both PHPT and control group. Interestingly, FGFR expression was positively correlated with CYP24A1 expression only in PHPT group (R=0.224, P=0.036).

Conclusion: The protein expression of VDR was reduced in patients with parathyroid adenoma. Moreover, it was negatively correlated with serum PTH levels. This study showed low VDR and interaction among VDR, FGFR/α-klotho and enzymes involved in vitamin D metabolism may contribute to development of parathyroid adenoma.

Disclosures: A Ram Hong, None.

SU0018

A Semi-Automated Method for Defining Cortical Bone Breaks in Cadaveric Finger Joints using High-Resolution peripheral QCT and MicroCT. Michiel Peters*[1], Andrea Scharmga[2], Astrid Van Tubergen[3], Joop Van Den Bergh[4], Chris Arts[3], Bert Rietbergen[5], Piet Geusens[6]. [1]Maastricht University, The Netherlands, [2]Maastricht University, Netherlands, [3]MUMC, Netherlands, [4]VieCuri MC Noord-Limburg & Maastricht UMC, The Netherlands, [5]Eindhoven University of Technology, The Netherlands, [6]University Hasselt, Belgium

Radiography is considered the gold standard for visualizing bone erosions in rheumatic diseases. Detection of these erosions at an early stage may be relevant for clinical practice. Cortical breaks, which may be the first signs of erosions, cannot be seen on radiographs but are visible on High-Resolution peripheral QCT (HR-pQCT) and microCT (μCT). Visual scoring for these scans is laborious and inaccurate though.

To develop a semi-automatic algorithm for detection of cortical breaks in interphalangeal joints based on HR-pQCT and μCT scans and compare the results with visual scoring.

Fifteen interphalangeal joints from 8 female cadaveric index fingers were scanned by HR-pQCT (82 μm) and μCT (18μm). A semi-automated algorithm was applied twice by 2 independent readers to the HR-pQCT and once to the μCT scans. First, the periosteal surface of the bone structure was contoured. Second, a constant thickness of 0.25mm was chosen to identify the cortical bone. Last, breaks <0.5mm were discarded from this cortical bone structure. Separately, cortical breaks were visually scored from μCT images by 2 independent readers. A cortical break was defined as an interruption of cortical bone seen on 8 consecutive slices in two orthogonal planes. Descriptives and intraclass correlation coefficients (ICC) were calculated.

When applying the algorithm for the HR-pQCT scans, 252 cortical breaks (mean ± SD; 16.8 ± 13.5 per joint) were found by reader 1 and 249 (16.6 ± 14.3 per joint) by reader 2, with an ICC of .962, p<.001. The total number of cortical breaks found on the μCT was 491 (32.7 ± 27.1 per joint) with the algorithm and 225 (15.0 ± 5.0 per joint) with visual scoring, with an ICC of .012, p=.488. The ICC for comparison of μCT with HR-pQCT when applying the algorithm was .728, p=.001. The ICC between reader 1 and 2 with visual scoring on μCT was .563, p=.054.

Although some user input is still needed, a high inter observer reliability with the algorithm was found for the HR-pQCT. A good correlation was found between the HR-pQCT and μCT with the algorithm, although the number of cortical breaks detected by μCT was about twice as high with respect to HR-pQCT. The correlation between visual scoring and the algorithm was poor. In conclusion, the use of a semi-automated algorithm is a promising tool in the early detection of cortical breaks. Further research is needed for clarification of the difference in visual scoring and the algorithm.
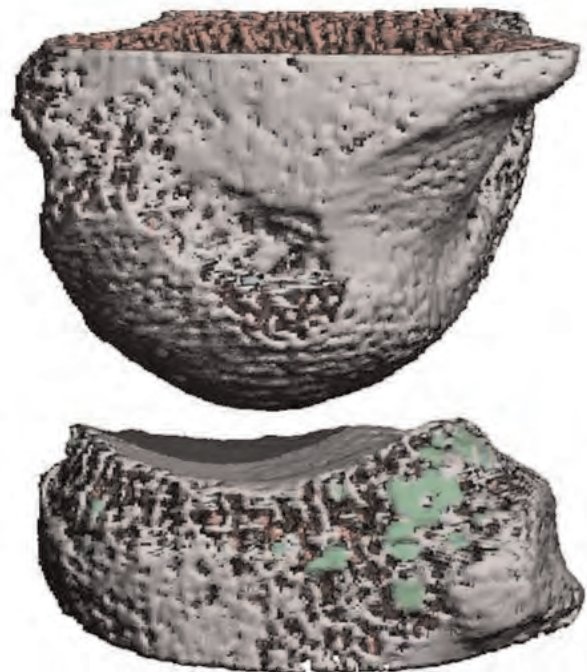

Figure 1. Shown is an example of a 3D reconstruction of a finger joint of a HR-pQCT scan. Shown in different colors are the different bone compartments as obtained by the algorithm. White: cortical bone structure. Red: trabecular bone structure. Green: cortical breaks >0.5mm

3D reconstruction of a finger joint by the semi-automated algorithm

Disclosures: Michiel Peters, None.

SU0019

Age Related Changes in the Structure, Composition and Properties of Porcine Cortical Bone. Iwona Jasiuk*[1], Michael Chittenden[2]. [1]University of Illinois at Urbana-Champaign, USA, [2]University of Illinois, USA

Composition-structure-property relations of bone provide fundamental understanding of bone quality. In this paper we report on the age dependent changes in the composition, structure, and mechanical properties of porcine femoral cortical bone at the mid-diaphysis region from six age groups (1, 3.5, 6, 12, 30 and 48 months). This study was motivated by the fact that limited date is available in the literature on porcine cortical bone during development. Porcine bone was chosen because its biology is similar to human bone. Scanning electron microscopy was used to quantify changes in the ultrastructure of bone at different quadrant positions. High resolution microscopy was used to measure the porosity and visualize three dimensional void structures (canals, resorption cavities and lacunae). Ash and water content tests were performed to measure water and organic and mineral contents of bone as a function of age. The mineral content increased with age while the porosity decreased. Nanoindentation technique with Berkovich fluid tip was employed to measure the elastic modulus and hardness at the nanoscale. Individual lamellae were indented in the longitudinal direction of bone in differetn structural components (osteonal, interstitial and plexiform bone). We found that the elastic modulus and hardness increased with age but at different rates in each microstructural component. Finally, reference point indentation was used to measure the average stiffness (Avg US), indentation distance increase (IDI), total indentation distance (TID), average energy dissipated (Avg ED), and creep indentation distance (CID) as a function of anatomical position within the femoral cross-section and as a function of loading direction (transverse and longitudinal). The Avg US increased, while IDI, TID, Avg

ED, and CID decreased with age on both transverse and longitudinal surfaces. The transverse surface measurements generally exhibited higher Avg US and lower IDI and TID compared to those measured on the subperiosteal surface. This research provides new insights on the composition, structure and properties changes in cortical bone at early ages.

Disclosures: Iwona Jasiuk, None.

SU0020

Association Between Reference Point Indentation Measures and Cortical Bone Composition, Bending Properties, and Fracture Toughness. <u>Lamya Karim</u>*[1], <u>Nathalie Portero-Muzy</u>[2], <u>Daniel Brooks</u>[3], <u>Evelyne Gineyts</u>[2], <u>Pascale Chavassieux</u>[4], <u>Roland Chapurlat</u>[5], <u>Mary Bouxsein</u>[1]. [1]Beth Israel Deaconess Medical Center, Harvard Medical School, USA, [2]Universite de Lyon, France, [3]Beth Israel Deaconess Medical Center, USA, [4]INSERM UMR1033, Université De Lyon, France, [5]E. Herriot Hospital, France

Assessment of cortical bone tissue mechanical properties both *in vivo* and *in vitro* is now possible by reference point indentation (RPI, Active Life Scientific) [1,2]. Clinical studies show worse cortical bone properties in women with hip fracture and type II diabetes [3,4]. Yet, little is known regarding the factors that influence RPI measurements and whether RPI measurements are associated with bone mechanical properties assessed by standard testing protocols [5]. Thus, we aimed to determine factors that may influence RPI measurements and the ability of RPI to reflect traditional mechanical properties using cortical bone specimens from sheep.

Sixteen sheep (age 8.1 ± 0.4 years) were randomly assigned to receive a vehicle or zoledronic acid for 3 months [6]. Two cortical beam specimens (~3.4 x 2.8 x 36.1 mm) per sheep were excised from the femoral posterior-lateral and posterior-medial quadrants. Cortical tissue mineral density (TMD) and cortical porosity (Ct.Po) were assessed by microCT, and indentation properties by RPI (9 N, 2 Hz, 10 cycles). Then one beam per animal was tested to failure by 4-point bending and the other by fracture toughness testing. A portion of cortical bone was used to quantify pentosidine, an advanced glycation end-product (AGE), using HPLC.

There were no differences between ZOL and VEH-treated specimens, so they were pooled for all analyses. RPI variables worsened with increasing Ct.Po and decreasing TMD (Table 1). Indentation distances were greater with increasing pentosidine content (r=0.44-0.67). Bending work-to-failure correlated positively with RPI-assessed average energy dissipation, whereas fracture initiation and propagation toughness values correlated negatively with RPI-derived loading and unloading slopes. No other RPI variables were associated with bending or fracture toughness properties.

In summary, our results indicate that increased porosity, decreased mineralization, and increased AGE content are associated with worse cortical bone indentation properties. Moreover, stiffer bone, as assessed by RPI, has less resistance to crack initiation and propagation. These findings provide insight into the factors that influence RPI measurements, as well as the interpretation of RPI measurements with respect to standard bending and fracture toughness tests.

References: [1] Bridges et al, 2012; [2] Hansma et al, 2008; [3] Diez-Perez et al, 2010; [4] Farr et al, 2013; [5] Jepsen and Schlecht, 2014; [6] Portero-Muzy et al, 2012

Table 1. Correlation coefficients between RPI measures, cortical TMD, porosity, mechanical testing variables, and pentosidine content for all specimens. P-value is shown in parentheses.

	Indentation distance (μm)	Total indentation distance (μm)	Indentation distance increase (μm)	Creep indentation distance (μm)	Average energy dissipation (μJ)	Average unloading slope (N/μm)	Average loading slope (N/μm)
Microcomputed tomography							
Cortical porosity (%)	0.49 (<0.01)	0.50 (<0.01)	0.29	0.33 (=0.08)	0.37 (=0.06)	-0.37 (=0.06)	-0.40 (<0.05)
Cortical TMD (mgHA/ccm)	-0.61 (<0.01)	-0.62 (<0.01)	-0.55 (<0.01)	-0.57 (<0.01)	-0.53 (<0.01)	0.49 (<0.01)	0.47 (<0.01)
Bending properties							
Yield Stress (MPa)	0.04	0.05	0.15	0.02	-0.22	-0.15	-0.01
Bending modulus (MPa)	-0.37	-0.35	0.17	-0.18	-0.14	-0.20	0.22
Work-to-failure/area (mJ/mm²)	0.05	0.05	0.15	0.24	0.80 (<0.01)	-0.06	-0.43
Flexural strength (MPa)	-0.19	-0.18	-0.01	-0.09	0.42	0.13	-0.12
Fracture toughness							
Initiation toughness (MPa√m)	-0.13	-0.10	0.09	-0.13	0.14	-0.65 (<0.01)	-0.50 (=0.07)
Propagation toughness (MPa√m)	-0.16	-0.13	0.12	-0.16 (<0.05)	0.18	-0.68 (<0.01)	-0.56 (<0.05)
Collagen crosslinks							
Pentosidine (mmol/mol collagen)	0.44 (<0.05)	0.47 (<0.01)	0.67 (<0.01)	0.66 (<0.01)	0.64 (<0.01)	-0.02	-0.13

Table 1

Disclosures: Lamya Karim, None.

SU0021

Brittle Bone Explained?: Multivariate Polarization Raman Spectroscopy for Assessing Bone Toughness. <u>Alexander Makowski</u>*[1], <u>Sasidhar Uppuganti</u>[2], <u>Meredith Huszagh</u>[2], <u>Ahbid Zein-Sabbato</u>[2], <u>Anita Mahadevan-Jansen</u>[2], <u>Jeffry Nyman</u>[3]. [1]Department of Veterans AffairsVanderbilt University, USA, [2]Vanderbilt University, USA, [3]Vanderbilt University Medical Center, USA

The age related decrease in human bone toughness is more severe than the age related loss of strength, yet current X-ray based diagnostics focus on the link between mineral and strength, ignoring collagen and subsequently toughness. Raman spectroscopy (RS) may complement existing tools, but RS for bone has been limited to peak ratios of composition. These represent only a fraction of the Raman spectra, ignoring subtle changes in shoulders or band widening, both seen in polarization changes that infer mineral and collagen organization. Here we present for the first time that full spectrum analysis including polarization information increases RS's ability to explain toughness differences in a mouse model of altered osteoblast differentiation.

Femurs were harvested from 20wk male mice (9 Atf4-/-, 15 Atf4+/+), and midshafts were μCT scanned at 12 μm voxels. RS was obtained using a confocal microscope (785nm diode; 50x NA=.75). Polarization RS parallel and orthogonal to the bone's long axis were acquired from the anterior midshaft for peak ratio intensity of mineral to collagen ratios (MCR). Full spectrum (300-1800cm⁻¹) principal components analysis (PCA) was used to find signatures that identify the Atf4-/- phenotype. Peak ratios and components significantly separating genotype (Mann Whitney; $p<0.05$) were classified by Sparse Multinomial Logistic Regression (SMLR). Bones from Atf4-/- have 74% lower toughness than Atf4+/+ mice, but no TMD difference. Polarization sensitive MCR *v*1 phosphate/AmideI significantly separates genotype but only explains 32% of variance and SMLR misclassifies all 9 Atf4-/- mice. Moreover, *v*1/AmideI correlation v. toughness is only significant for longitudinal orientation (R^2=27.3%, p<0.01). Gradually adding more RS information improves classification accuracy: full spectrum PCA at either orientation accurately classifies at most 70.8%; the average of both orientations achieves 75%, while including both orientations separately classifies 79.2%.Performing PCA of full Raman spectra improves classification and also allows analysis of subtle spectral components weighted in the explanation of toughness. The primary direction of RS variance (26%, PC1) was the only PC to significantly separate genotype ($p=0.001$; figure) and explain toughness, heavily weighting polarization sensitive wavenumbers. PCA of spectra collected at orthogonal polarization angles adds organization sensitivity, possibly improving RS assessments of fracture resistance.
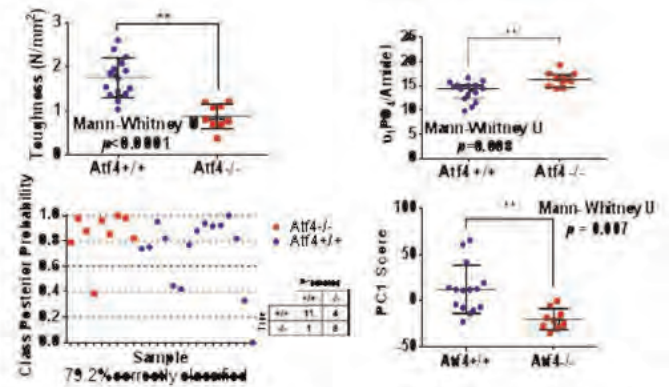
(A) Atf4-/- mice demonstrate significant toughness loss. (B) Polarization sensitive MCR separate tough from brittle bones.(C) SMLR correctly classified 75% of bones using PC1. (D) PC1 scores significantly separate brittle from tough bones

Classification of Brittle Bone

Disclosures: Alexander Makowski, None.

SU0022

Clinical Applicability of Trabecular Microarchitecture Class (TMAC) Assessement using Multi-Detector Comptuted Tomography. <u>Alexander Valentinitsch</u>*[1], <u>Lukas Fischer</u>[2], <u>Janina Patsch</u>[3], <u>Jan Bauer</u>[4], <u>Franz Kainberger</u>[2], <u>Georg Langs</u>[5], <u>Matthew DiFranco</u>[3]. [1]Klinikum rechts der Isar, Technische Universität München, Germany, [2]Medical University of Vienna, Austria, [3]Medical University of Vienna, Austria, [4]Klinikum rechts der Isar, Technische Universität München, Germany, [5]Medical University of Vienna, Computational Imaging Research Lab, Austria

Computational trabecular microarchitecture assessment in high-resolution peripheral quantitative computed tomography (HR-pQCT) has recently proposed the clustering of voxels into one of three trabecular microarchitectural classes (TMACs) using pattern recognition methods applied to textural and orientation features.

Motivated by promising clinical applications of TMACs in osteoporotic women and lung transplant recipients, we extend the method to multi-detector CT (MDCT) images in order to validate their reproducibility at lower, anisotropic resolutions, which can be acquired during clinical routine.

Twelve right forearms were obtained from human cadavers of males (n=4) and females (n=8). Imaging was performed on these fresh frozen specimen using the standard in vivo protocol of the HR-pQCT scanner (isotropic resolution 82μm). MDCT images were acquired using a 64-slice scanner with two optimized protocols, differing only in tube current-time product (UH1: 150mAs; UH2: 300mAs; both with spatial resolution 130x130x500μm). TMACs were calculated and visualized via "bone quality maps" for each of the 12 cadaver specimens for both modalities. To assess variability between TMACs from different modalities and protocols, cluster volume fraction (CL.V/TV) was calculated and compared using a repeated measures ANOVA with subsequent Bonferroni correction. The overlap statistics of the TMACs were quantified with the Dice coefficient (DC).

Post hoc tests revealed that both MDCT scan protocols resulted in a reduction of CL.V/TV for TMAC1 as compared to HR-pQCT, but it was not statistically significant (UH2: −8.8%,p=0.175; UH1: −9.1%, p=0.166). No significant differences were found for TMAC2 (UH2: +2.2%, p > 0.5; UH1:−0.4%, p >0.5). However, for TMAC3, a significant increase in CL.V/TV was seen for UH1 (+16.2%, p=0.005). When considering radiation dose, we noted that MDCT protocol UH2 outperformed UH1 in terms of overall Dice score by <2%, but effective dose (ED) was 81.8μSv for UH1 and 163.5μSv for UH2. This result also suggests that TMAC-based maps can be reliably generated at lower doses.

We demonstrated that TMAC mapping, initially validated for HR-pQCT, is applicable to MDCT. TMACs show good agreement despite MDCT having poorer spatial resolution, lower contrast and diminished sharpness. Future work should focus on in-vivo validation, possibly including central skeletal sites.
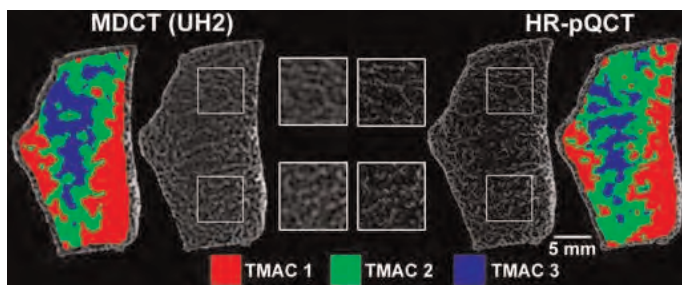

Fig. 1: Representative of differences in the trabecular microarchitecture and the TMAC distribution.

Disclosures: Alexander Valentinitsch, None.

SU0023

Differences in Assessment of Micro-Indentation Resistance between BioDent and OsteoProbe. <u>Mathilde Granke</u>*[1], <u>Sasidhar Uppuganti</u>[2], <u>Mary Katherine Manhard</u>[2], <u>Mark Does</u>[2], <u>Donald Lee</u>[2], <u>Daniel Perrien</u>[1], <u>Jeffry Nyman</u>[1]. [1]Vanderbilt University Medical Center, USA, [2]Vanderbilt University, USA

As a potential tool to improve fracture risk assessment, reference point indentation (RPI) directly measures the resistance of a patient's bone to microindentation. There are two clinically viable RPI techniques (both from ActiveLife Scientific, Inc.) using 20 cycles of loading in force control at a peak 10 N (BioDent) or a one-time impact load at ~45 N (OsteoProbe). As the loading mechanisms and presumably depth of penetration differ between OsteoProbe (~200 μm) compared to BioDent (~70 μm), we hypothesized that indentation resistance by OsteoProbe is more sensitive to the underlying microstructure than the BioDent. To test the hypothesis, we indented the tibia midshaft, a clinically viable site, as well as the distal radius and proximal humerus, near typical fracture sites, from 10 cadavers (>70 yo; male and female). First, 8 indents were performed per bone using the OsteoProbe (Fig). The indent depth was normalized by mean depth into a PMMA standard to give so-called bone material strength (BMS). Next, 8 neighboring indents were performed with the BioDent. Outcomes included total indentation distance (TID), indentation distance increase (IDI), creep indentation distance (avgCID), and unloading slope (avgUS). UTE MRI provided bulk pore water (i.e., cortical porosity), and μCT (10 μm voxel) was used to determine local porosity in the region below indents (diaphysis). RPI properties from the BioDent did not vary among the neighboring 8 indent locations in all bones, but BMS was lower in the thinner metaphyseal than in the thicker diaphyseal cortex of the forearm bones (Fig). Mean BMS was lower for both forearm bones than for the tibia (Fig), whereas TID (Fig) and AvgCID were higher for just the humerus compared to the tibia. There were no anatomical differences in IDI or avgUS. The avgCID was the only BioDent property correlated with BMS in the tibia (r=0.75, p=0.017). The expected inverse correlation between TID and BMS existed for only the radius with nominal significance (r=-0.56, p=0.096). As an explanation of the anatomical differences in BMS, this property correlated with bulk pore water (r=-0.69, p<0.001) and local intracortical porosity (r=-0.69, p<0.001), although not for tibia alone (Fig). None of the BioDent properties correlated with pore water and porosity. The assessment of indentation resistance likely differs between BioDent and OsteoProbe in that the latter may be sensitive to the underlying microstructure in addition to tissue properties.
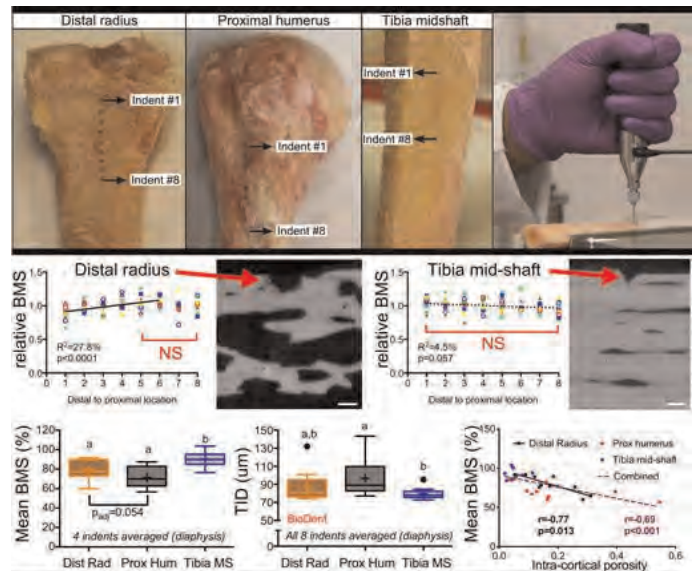
Rereference point indentation was performed at 8 locations using the hand-held OsteoProbe (top panel) and the bench-top BioDent (neighboring surface). Dividing each BMS value by the mean BMS among 8 locations per bone, relative BMS varied for the forearms bones (proximal humerus not shown) but did not for the tibia mid-shaft. Averaged among indentation locations on the diaphysis, BMS was less for the forearm bones than for the tibia, while TID (effectively the inverse of BMS) was greater for proximal humerus than for the tibia. Box and wiskers with mean at '+'; Difference between groups if letters are different.

Figure: Location of indentations and results

Disclosures: Mathilde Granke, None.

SU0024

Do Contralateral Femora Differ in Strength? A Multicentric Finite Element Study in Post-menopausal Women. <u>Enrico Schileo</u>*[1], <u>Cristina Falcinelli</u>[2], <u>Luca Balistreri</u>[3], <u>Fabio Baruffaldi</u>[3], <u>Sigurdur Sigurdsson</u>[4], <u>Vilmundur Gudnason</u>[5], <u>Roswitha Dietzel</u>[6], <u>Gabriele Armbrecht</u>[7], <u>Stephanie Boutroy</u>[8], <u>Fulvia Taddei</u>[3]. [1]Istituto Ortopedico Rizzoli, Bologna, Italy, Italy, [2]Istituto Ortopedico Rizzoli & University of Rome Tor Vergata, Italy, [3]Istituto Ortopedico Rizzoli, Italy, [4]Icelandic Heart Association, Iceland, [5]Icelandic Heart Association Research Institute, Iceland, [6]Charité, Germany, [7]Centre of Muscle & Bone Research, Charite-CBF, Germany, [8]INSERM U1033 & Université de Lyon, France

Introduction: the diagnosis of osteoporosis usually involves unilateral aBMD measurements. Conversely, small but significant asymmetries between contralateral proximal femora were reported for anatomy [1] and aBMD [2]. Finite Element (FE) models of bone strength, which combine anatomy and densitometry, recently improved aBMD classification of bone fracture risk [3], but so far neglected laterality.

Aim: to investigate the asymmetry in proximal femur strength as assessed by FE models from QCT data, in stance and sideways fall loading conditions, in a homogeneous cohort of post-menopausal women.

Methods: 198 QCT scans of intact proximal femora were obtained from three studies on osteoporotic fractures: AGES-Reykjavik (71 cases); Emilia-Romagna Regional Project on Osteoporosis (33); VPHOP European Project (94). A CT-based FE model of both proximal femora was generated [4]. Linear analyses were performed adopting a maximum principal strain criterion to define strength for each loading direction (validated with R^2=0.90 and RMSE 15%, against experimentally measured strength in 14 femora). The minimum strength among a range of loading directions mimicking the in-vivo variability of hip reactions (stance) and accidental conditions (fall) was determined for each femur. Femoral strength results in stance and fall were analysed separately.

Results: the average femoral strength was 5063 ± 1292N in stance and 2814 ± 626N in fall. Contralateral differences in stance and fall were comparable: only fall results are reported for brevity. Right femora were on average stronger (4.5%, p<0.005) but such difference might be close to model repeatability and is of little biomechanical relevance. The most relevant result was the large scatter observed, independently from the magnitude of strength, in Bland-Altman plots (95% CI: +37%, -28%). The mean absolute difference between contralateral bones was 14% (p<0.0001), close to the only similar existing study [5], performed in vitro on a smaller sample size. In summary the observed difference between contralateral femur strength is significant (exceeds 15% in 32% of subjects) and points to further studies to verify possible misclassification issues.

References:
[1] Auerbach and Ruff, J Hum Evol 50:203-18, 2006
[2] Hamdy et al., Osteoporos Int. 17:1772-80, 2006
[3] Kopperdahl et al., J Bone Miner Res. 29:570-80, 2014
[4] Schileo et al., J Biomech 41:356-67, 2008[5] Eckstein et al., J Bone Miner Res, 19: 379-385, 2004

Disclosures: Enrico Schileo, None.

SU0025

Evaluation of Bone Quality and Mechanics in a Mouse Model of Pseudoachondroplasia. Hao Ding*[1], Xiaohong Bi[2], Annie Abraham[1], Catherine Ambrose[3], Karen Posey[1], Jacqueline Hecht[1]. [1]University of Texas Health Science Center at Houston, USA, [2]University of Texas Health Science Center at Houst, USA, [3]University of Texas Health Science Center at Houston, USA

Mutations in the cartilage oligomeric matrix protein (COMP) gene cause pseudoachondroplasia (PSACH), a severe dwarfing condition associated with short limbs, pectus carinatum, joint laxity and an attractive face. Using an inducible system to express D469del-COMP in mice (MT-COMP), we have generated an *in vivo* model that replicates the critical cellular and clinical features of PSACH including intracellular retention of MT-COMP and reductions in long bone growth (12-18%). Although alterations in the growth plate and articular cartilage have been reported, there has been little research investigating the effects of MT-COMP on bone material properties and composition. Here, we report bone quality and mechanical properties from the femurs of the MT-COMP mouse.

Femurs from 4 week old male MT-COMP and wildtype (WT) mice were assessed by three-point bending mechanical tests. Both extrinsic and intrinsic mechanical properties of bones were then calculated using beam theory and geometric data from µCT analysis. Bone composition was determined by analyzing Raman spectra acquired from the broken femurs. Statistical analyses were performed to determine which parameters were significantly different between the two groups and to identify significant correlations between the mechanics and composition.

The MT-COMP bones were significantly less stiff, and withstood less loads before yield and failure. After accounting for the significantly smaller size of the bones, the intrinsic properties of MT-COMP bones were not significantly different from WT, indicating that anatomical geometry accounts for the variation in the mechanical function of mutant mice. The MT-COMP animals did not demonstrate any significant difference in terms of bone composition when compared to WT, which is in agreement with the outcome from mechanical testing. Correlation evaluation between bone composition and material properties revealed that collagen density correlated positively and significantly to bone elasticity (ie, pre-yield displacement, toughness and strain) while the mineral/matrix ratio correlated significantly to post-yield energy. In summary, the impaired bone mechanical function of MT-COMP mice arose from the smaller limb size but not the intrinsic material properties or bone composition. PSACH therapies that promote bone growth should improve the bone quality.

Disclosures: Hao Ding, None.

SU0026

Finite Element Analysis Accurately Reflects the Improvements in Vertebral Strength with Denosumab in Ovariectomized Cynomolgus Monkeys. David Lee*[1], Paul Hoffmann[2], Aurore Varela[3], Paul Kostenuik[4], Michael Ominsky[4], Tony Keaveny[5]. [1]O.N. Diagnostics, USA, [2]O.N. Diagnostics, USA, [3]Charles River Laboratories, Canada, [4]Amgen Inc., USA, [5]University of California, Berkeley, USA

Finite element analysis of clinical-resolution computed tomography scans of the hip and spine provides non-invasive measures of bone strength that are now cleared by the FDA for clinical use in assessing fracture risk and monitoring treatment. However, the accuracy of such clinical-type strength estimates for predicting true hip or spine strength has not yet been established in bones after treatment with osteoporosis therapeutic agents. To determine whether such clinical-type finite element analysis can correctly quantify changes in bone strength after treatment with denosumab, vertebrae from ovariectomized cynomolgus monkeys (cynos) treated with denosumab (DMab) were subjected to mechanical testing and finite element analysis. After 16 once-monthly injections, T12 vertebral specimens were prepared from the cynos in three groups: Sham (n=17), OVX+vehicle (n=20), and OVX+DMab (50 mg/kg, n=17). These samples were micro-CT scanned (34 µm voxel size) and tested in compression to failure. To produce clinical-type finite element analyses, the images were coarsened to 300 µm resolution and converted into continuum models having about 30,000 elements, and were then analyzed in a blinded manner using the VirtuOst finite element software. After unblinding, both sets of strength data were then normalized to the mean of the Sham group, to estimate strength changes from baseline and to account for potential human-cynos differences in BMD-strength relationships. We found that denosumab significantly increased bone strength as determined by both mechanical testing ($50 \pm 9\%$) and finite element analysis ($46 \pm 9\%$) as compared to the Sham group, which in turn was not significantly different from the OVX group (Figure). Correlation analysis indicated excellent agreement in normalized strength as measured by mechanical testing and finite element analysis (R^2=0.97,

$p<0.0001$, $Y=X$ type of agreement) with no significant differences between the two measurements for any group. These results validate this continuum type of finite element analysis for quantifying treatment effects of denosumab on vertebral strength in this monkey model of postmenopausal osteoporosis. Since this same continuum approach is used clinically, these results also support its use to estimate strength in patients treated with denosumab, while demonstrating that denosumab-induced improvements in bone strength are driven primarily by the features captured in these models, namely, bone mass and its distribution.
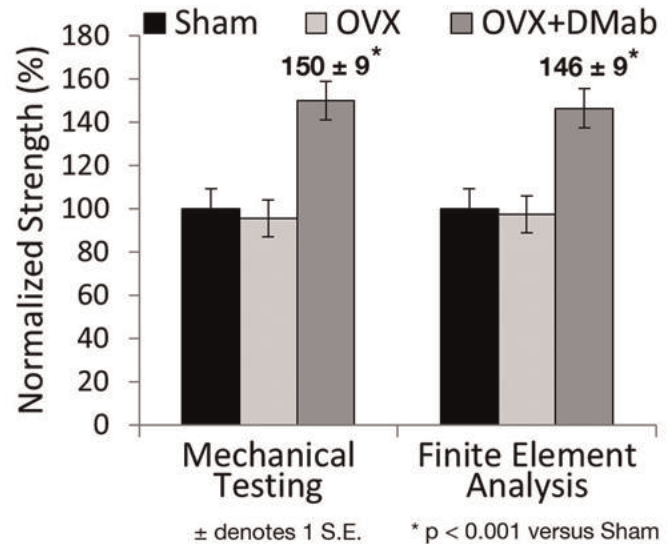
DCLee_Cyno_FEA_Fig1

SU0027

HR-pQCT based measurements of the distal tibial segment predict whole tibia stiffness. Bin Zhou*[1], Ji Wang[1], Eric Yu[1], Zhendong Zhang[2], Kyle Nishiyama[1], Elizabeth Shane[3], X Guo[1]. [1]Columbia University, USA, [2]Columbia University, USA, [3]Columbia University College of Physicians & Surgeons, USA

High-resolution peripheral quantitative computed tomography (HR-pQCT) is used to assess 3-dimensional microstructure *in vivo* of the distal tibia and radius. HR-pQCT of the distal tibia has shown thinner trabecular plates and lower cortical thickness in patients with fragility fractures and those with diseases like primary hyperparathyroidism. The standard HR-pQCT technique scans a 9.02-mm segment of the distal tibia. However, it remains to be determined whether the scanned segment is representative of bone quality of the entire tibia. In this study, we examined associations between mechanical and microstructural properties of tibia segment imaged by HR-pQCT and mechanical properties of the whole tibia.

Twenty-seven tibiae were collected from cadaver donors screened to exclude those with fracture or metabolic bone disease. The entire tibia was cleaned of soft tissue and embedded with PMMA at both ends. Non-destructive uniaxial mechanical testing with 5mm/min loading rate to 0.3% of the total length was performed after overnight curing. The standard HR-pQCT region was cut with a customized jig, immersed in saline to expel air bubbles and scanned by HR-pQCT. Volumetric BMD (vBMD), geometry and microstructure were measured by standard HR-pQCT procedures and trabecular plate/rod related microstructural parameters were evaluated by individual trabecula segmentation (ITS). Stiffness of the tibial segment was both measured by mechanical testing and predicted by finite element (FE) analysis; both correlated strongly with stiffness of whole tibia (R^2>0.9). Correlations between bone microstructure and whole tibia stiffness were also examined. The highest correlations with bone stiffness were found with total vBMD, trabecular number and cortical thickness (all R^2>0.5). Bone size, trabecular and cortical vBMD, and trabecular separation were moderately correlated with whole bone stiffness (R^2: 0.3-0.5). Several ITS measurements, including axial bone volume fraction, rod trabecular number, plate-rod, plate-plate and rod-rod junction densities, were significantly but modestly correlated with whole bone stiffness (R^2: 0.2-0.33). In summary, we detected highly significant associations between mechanical and microstructural properties of the tibial segment imaged by standard HR-pQCT scans and whole tibia bone stiffness. We conclude that the mechanical properties of the whole tibia are best approximated by estimated stiffness of the section of the tibia scanned by HR-pQCT.

Table 1. Standard HR-pQCT and ITS measurements and their correlations with the whole tibia stiffness. NS: not significant; R^2: coefficient of determination.

HR-pQCT	Mean ± SD	R^2	ITS	Mean ± SD	R^2
Total BMD (mg HA/cm³)	210.16±55.48	0.60	pBV/TV	0.08±0.04	0.15
Trabecular BMD (mg HA/cm³)	139.21±35.44	0.32	rBV/TV	0.16±0.03	0.26
Cortical BMD (mg HA/cm³)	685.59±127.49	0.49	aBV/TV	0.09±0.03	0.19
BV/TV	0.116±0.03	0.32	pTb.N (1/mm)	1.175±0.275	0.11
Tb.N (1/mm)	1.606±0.362	0.49	rTb.N (1/mm)	1.711±0.168	0.26
Tb.Th (mm)	0.074±0.019	NS	pTb.Th (mm)	0.237±0.015	NS
Tb.Sp (mm)	0.604±0.261	0.37	rTb.Th (mm)	0.224±0.012	NS
Ct.Th (mm)	0.644±0.376	0.56	pTb.S (mm²)	0.206±0.06	NS
Total Area (mm²)	747.42±164.97	0.31	rTb.t (mm)	0.76±0.15	NS
Stiffness-Experiment (N/mm)	154511±61169	0.90	R-R Junc.D (1/mm³)	2.68±0.67	0.26
Stiffness-FE (N/mm)	172520±64565	0.91	P-R Junc.D (1/mm³)	2.77±0.83	0.33
			P-P Junc.D (1/mm³)	1.45±0.48	0.29

Table 1

SU0028

Independent Measurement of Femoral Cortical Thickness and Cortical Bone Density using Clinical QCT. Graham Treece*[1], Andrew Gee[2]. [1]University of Cambridge, United Kingdom, [2]University of Cambridge, United Kingdom

Purpose: There is growing evidence that local features of cortical bone are a contributor to fracture risk. Both drug treatment and exercise regimes also result in cortical changes which are focused in particular regions rather than dispersed over the whole proximal femur. Accurate measurement of local cortical parameters is hence of importance in assessing both risk and intervention strategies. We have previously noted that both thresholding and full-width half-maximum (FWHM) techniques are incapable of measuring thickness or density for cortices less than 3 mm thick. Cortical bone mapping (CBM v1) can produce a much more accurate assessment of cortical thickness and mass (per unit cortical surface area), based on an estimate of cortical density which is presumed to be constant for each hip. However, although density varies much less than thickness, we would also like to be able to estimate the variation of density over the cortex.

Methods: A new CBM technique (v2) has been developed which makes use of the locally measured imaging blur to correct the initially global density estimate. This blur is overestimated when the initial density is too large, and underestimated when it is too small. The resulting local re-estimate of density can also be used to improve cortical thickness measurement. Performance was assessed with 70 ex vivo scans of proximal femurs (two each from 18 males and 17 females, aged from 56 to 96) from a study ethically approved by the Medical University of Vienna. True values were derived from calibrated HRpQCT data (cubic voxels of 0.082 mm) and estimates were made from QCT scans (0.33x0.33x1.0 mm) of the same femurs, each containing a BDC calibration phantom. Cortical thickness and density estimates were derived from over 700,000 matching measurements.

Results: Figure 1 shows the measurement errors for the FWHM, original CBM v1 and novel CBM v2 techniques. For thickness (in mm), range 1 to 3 mm, bias $\pm$ std was 0.48$\pm$0.37 (FWHM), -0.24$\pm$0.32 (CBM v1) and 0.12$\pm$0.39 (CBM v2), and for 0.3 to 1 mm was 1.10$\pm$0.37 (FWHM), -0.24$\pm$0.12 (CBM v1) and -0.15$\pm$0.23 (CBM v2). Density estimation (in mg/cm³) was less precise, but for range 1 to 3 mm cortex, results were -170$\pm$137 (FWHM), 195$\pm$217 (CBM v1) and -26$\pm$178 (CBM v2). Cortical density estimation for CBM v2 was relatively unbiased above 800 mg/cm³.

Conclusion: It is possible to estimate both cortical density and thickness from clinical QCT, locally over the femur, though density estimation is less precise.
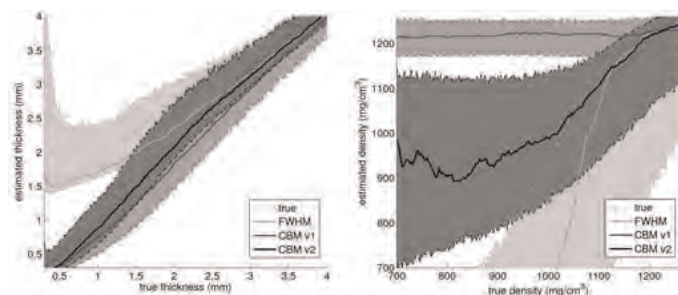

Figure 1. Estimated cortical thickness and density from QCT data compared to true values from HRpQCT data. Results are shown for FWHM, the original CBM v1 and the novel CBM v2 algorithms. The shaded regions show ± one standard deviation of many measurements from ex vivo scans of proximal femurs.

Figure 1

SU0029

Lower matrix bound water is related to compromised skeletal mechanical properties in an animal model of chronic kidney disease. Matthew Allen[1], Christopher Newman*[2], Neal Chen[1], Sharon Moe[1], Jeffry Nyman[3], Mathilde Granke[3]. [1]Indiana University School of Medicine, USA, [2]Indiana University School of Medicine, USA, [3]Vanderbilt University Medical Center, USA

Chronic kidney disease (CKD) results in an increased fracture risk, partially due to declines in bone mass and increased cortical porosity. But, bone loss alone does not fully explain the compromised mechanical properties associated with the disease. The goal of this study was to assess the impact of CKD on skeletal tissue hydration, which is known to have significant effects on bone mechanical properties. At 35 weeks of age (approximately 80% reduction in kidney function), male rats with progressive CKD and their normal littermates (NL) were examined. Key biochemical outcomes, BUN (+199%), phosphorus (+122%), PTH (+1196%), and FGF23 (+1074%) were all significantly higher in rats with CKD compared to NL. Skeletal hydration (bound and free water) of the femoral diaphysis was determined using 1H NMR spectroscopy with T2 signals normalized by bone volume as determined by Archimedes' principle. Free water was significantly higher (+58%), whereas bound water was significantly lower (-12%) in CKD compared to NL. Cortical porosity, measured by microCT, was significantly higher in CKD animals (4.16%) compared to NL (0.12%) and was significantly correlated with free water (r = 0.87). Structural mechanical properties (determined by three-point bending) were significantly reduced with CKD (ultimate strength = -31%; stiffness = -17%; energy to fracture = -26%). These properties were negatively correlated to free water (ultimate strength, r = -0.80; stiffness, r = -0.87; energy to fracture, r = -0.72), but positively related to bound water (ultimate strength, r = 0.70; stiffness, r = 0.62; energy to fracture, r = 0.70). Previous work in this same model revealed microscale and nanoscale differences in mechanical properties between CKD animals and their normal counterparts, despite similarities in composition (mineral-to-matrix ratio and mineral crystallinity) and collagen cross-linking. The results of the current work suggest that changes in tissue hydration may be driving the compromised mechanical properties associated with the disease. These data also identify bound water, which can be enhanced by agents such as raloxifene, as a new potential therapeutic target for reversing the biomechanical deficits associated with CKD.

SU0030

Multidirectional Poroelastic-Ultrasound and Structural-Anisotropy Predict Multidirectional Yield Behavior of Trabecular Bone. Paolo Palacio-mancheno*[1], Mohamad Souzanchi F[2], Sankha Ghatak S[2], Stephen Cowin C[2], Luis Cardoso[2]. [1]The City College of New York, USA, [2]The City College of New York, USA

Bone fragility increases with decreasing Bone Mineral Density (BMD) and altered bone micro architecture. While BMD is the gold standard for bone fragility assessment, it neglects the evaluation of direction-dependent mechanical behavior, which strongly contributes to bone fracture. In this study, we investigated whether multidirectional poroelastic ultrasound (PEUS) can predict direction-dependent yield properties of trabecular bone. To evaluate the direction-dependent bone fragility, bone structural-anisotropy was defined by the Fabric tensor. For this purpose, seven human calcanei were scanned by micro-CT and single volume of interests (VOIs) obtained (Fig.1a). For each VOI, structural-anisotropy magnitudes and directions were obtained from the Fabric tensor ellipsoid (Fig.1b). 31 Fabric components (Fcomp) were analyzed per VOI. New VOIs were created according to the direction of each Fcomp (Fig.1c), and then converted to numerical models. These models were uniaxially tested to yield in compression, and interrogated ultrasonically. A total of 434 simulations were completed. Quadratic fittings were evaluated against directionality (Fcomp), bulk structural mechanical properties (Young's modulus (E), yield stress (σ_y), and yield strain (ε_y)) and Ultrasonic Parameters (fast-wave speed of sound (FW-SOS), slow-wave speed of sound (SW-SOS), fast-wave velocity(FW-Vel), slow-wave velocity (SW-Vel), fast-wave attenuation (FW-BUA) and slow-wave attenuation(SW-BUA)), and correlation coefficients were quantified (Table.1). Results demonstrate that all ultrasound parameters (Fast-Wave and Slow-Wave) and Fcomp exhibited strong and statistically significant correlation with E and σ_y ($0.83 < R^2 < 0.95$), indicating that multidirectional PEUS is a good predictor of anisotropic elastic and yield mechanical properties. However, all ultrasound parameters (Fast-Wave and Slow-Wave) and Fcomp weakly predicted ε_y due to low correlation coefficients, indicating independence of yield strain to anisotropy. These results show that when bone mass structural directionality is taken into account, the anisotropic elastic and yield behavior of trabecular bone can be predicted by multidirectional ultrasound. In conclusion, multidirectional ultrasound can be used as a low cost, non-invasive, and non-radiating diagnostic tool for the assessment of direction-dependent bone fragility.

Figure 1

Table 1

SU0031

Reduced Growth-Related Trabecular Corticalization and Increased Age-Related Cortical Trabecularization: Determinants of Forearm Fragility Fractures. Yohann Bala*[1], Minh Bui[2], Sandra Iulliano[3], Tamara Rozental[4], Quinju Wang[3], Xiao-Fang Wang[5], Tara Sepehrizadeh[3], Ali Ghasem-Zadeh[6], Mary Bouxsein[7], Roger Zebaze[8], Ego Seeman[6]. [1]University of Melbourne, Dept. of Medicine, Australia, [2]Mega Center for Epidemiology, Australia, [3]Dept. Of Medicine, University of Melbourne, Australia, [4]Harvard Medical School, Beth Israel Deaconess Medical Cente, USA, [5]University of Melbourne, Austin Health, Australia, [6]Austin Health, University of Melbourne, Australia, [7]Beth Israel Deaconess Medical Center, Harvard Medical School, USA, [8]Austin Health, University of Melbourne, Australia

During growth, trabeculae emerging from the growth plate thicken. Peripherally placed trabeculae coalesce forming metaphyseal compact-appearing cortical bone (CC) while centrally placed trabeculae form cancellous bone with a transitional zone (TZ) between. Deficits in trabecular number or reduced thickening may delay corticalization leaving an enlarged and porous TZ. In adulthood, a negative bone balance and accelerated intracortical remodeling cavitates cortex. We hypothesized that these processes result in a higher porosity in women with forearm fractures across life.

We quantified microarchitecture using high resolution-peripheral quantitative computed tomography at the non-dominant or non-fractured distal forearm in cases with, and age-matched controls without, distal radius fractures with a ratio 1:2. After exclusions due to movement artefacts, we analysed: i) 110 girls (12 ± 3 yrs, range:7-18), ii) 100 pre-menopausal women (28 ± 6 yrs, range:18-44) (1) and iii) 164 post-menopausal women (65 ± 8 yrs, range:51-89). Bone compartment cross sectional areas (CSA), trabecular architecture and porosity of the, TZ and total cortex (TC) were assessed using StrAx1.0 (2) and expressed as a function of the total CSA to control for bone size.

Girls with fractures had a 3% smaller CC-CSA and a 3% reciprocally higher TZ-CSA that were 12% and 4% more porous than controls respectively (all $p \leq 0.03$). Trabecular BV/TV was 21% lower (8% fewer, 4% thicker, all $p < 0.05$). Pre-menopausal cases had normal CC- and TZ-CSA but TZ porosity was 2% higher and trabecular BV/TV was 30% lower (7% fewer, 3% thinner) (all $p < 0.05$). Post-menopausal cases had normal CC- or TZ-CSA that were respectively 25% and 5% more porous and 39% lower BV/TV (37% fewer, 10% thicker) (all $p < 0.0001$). By multivariate regression analyses, CC and TZ porosity was associated with fracture independent of trabecular vBMD in girls. In pre-menopausal women, trabecular vBMD was associated with fracture independent of porosity. In post-menopausal women CC and TZ porosity was associated with fracture independent of trabecular vBMD.

At all ages, cases had higher cortical porosity and deficits in trabecular number. Metaphyseal fragility is the result of the incomplete corticalization of fewer trabeculae emerging from the growth plate early in life leading to higher peak porosity producing more surfaces for unbalanced and rapid remodelling after menopause.

1) Rozental et al, JBJS 2013, 1) Zebaze et al, Bone 2013

SU0032

Relationship of Cortical and Endocortical-Trabecular Bone Structure to Femoral Strength in a Sideways Fall Configuration. Fjola Johannesdottir*[1], Kenneth Poole[1], Graham Treece[1], Mary Bouxsein[2]. [1]University of Cambridge, United Kingdom, [2]Beth Israel Deaconess Medical Center, Harvard Medical School, USA

The relative contribution of cortical and trabecular bone to fragility of the femur is unclear. Our goal is to determine the relationship of cortical and endocortical-trabecular bone structure to proximal femur strength during a sideways fall impact in order to improve current understanding of hip fracture etiology. We hypothesize that the relationship is stronger in areas considered 'at risk' of high load during simulation of fracture.

We obtained 70 human cadaveric proximal femurs (45 women, 25 men, range 55-98 years), scanned both using DXA and QCT, and mechanically tested the femurs to failure in a sideways fall configuration. Using a previously published method (Treece 2012), we applied a bone mapping technique (Stradwin, wxRegSurf and Surfstat) to identify regions where bone structure in the hip was significantly related to femoral strength. We spatially aligned the bone measurements onto an average femur surface and used statistical parametic mapping to analyse the results. Covariates were sex, age, height, weight and phantom type. The results are presented as percentage variation in cortical bone mass (Fig. 1A) and endocortical-trabecular density (Fig. 1B) per 1000N of failure load.

Femoral strength is predictive of both cortical bone mass and endocortical-trabecular density over large areas of the proximal femur (Fig. 1A & 1B). The increase in cortical bone mass was quite uniform (Fig. 1A), about 10-20% per 1000N of failure load. The range in increase of endocortical-trabecular density was more variable (Fig. 1B), with the strongest effect located at the femoral neck. Interestingly, both bone variables showed strong association with failure load in the regions that have been predictive of hip fractures in clinical case-control studies (marked with *). The strong relationship between endocortical-trabecular density and failure load in the femoral neck (Fig. 1B) is noteworthy because the current clinical standard for fracture prediction is femoral neck aBMD with clinical risk factors. The association between surface derived bone measurements and failure load was strongest in regions considered be 'at risk' of hip fracture.
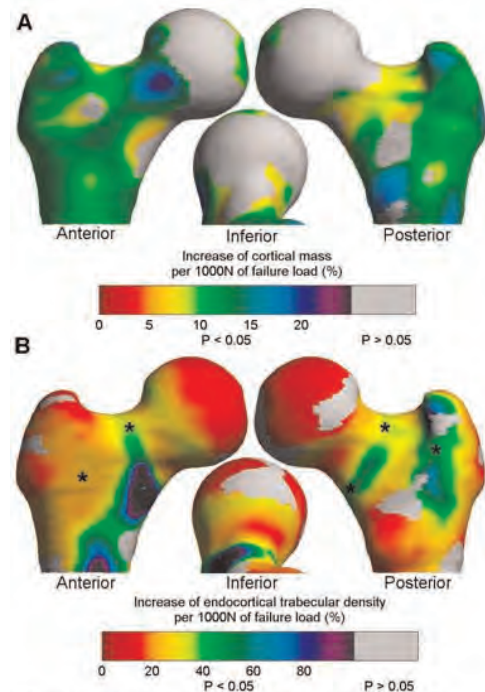
Figure 1: Relationship of cortical bone mass (A) and endocortical-trabecular density (B) to failure load. *: Locations which have been predictive of hip fractures in clinical case-control studies (Johannesdottir Bone 2011; Carballido-Gamio JBMR 2013; Poole ASBMR 2013). Only associations which were significant at p <0.05 are shown.

Figure 1

SU0033

Withdrawn

SU0034

The role of type 2 Diabetes on fracture healing in an experimental rat model. Javier La Fontaine[1], Chris Chen*[2], Lawrence Lavery[2], Ed Jude[3]. [1]UT Southwestern Medical Center, USA, [2]UT Southwestern Medical Center, USA, [3]Tameside General Hospital, United Kingdom

BACKGROUND: Persons with diabetes have a higher incidence of fractures compared to persons without diabetes. However there is very little published information concerning the deleterious effect of late stage diabetes on osseous structure and bone healing. The purpose of the study was to evaluate the role of diabetes on fracture healing in a rat femur-repair model.

Methods: 36 Lean and diabetic Zucker rats used in this study were subdivided into three groups: 1) 12 Lean rats as control (Lean), 2) 12 Diabetic rats without blood glucose control (DM), and 3) 12 Diabetic rats treated with 300mg/kg metformin to reduce blood glucose (DM+Met). The animals at the age of 14-week-old age were fractured at the right femur using a customized apparatus as previously described where the contralateral femur was sham-operated. Animal recovery, activities, and blood glucose were monitored everyday where the body weight and cytokines in serum were measured every 3-5 days. X-ray was taken every week to determine bone repair/delayed union. All the animals were sacrificed at 6-week after surgery for serum biomarkers and biomechanical properties which were evaluated using three points bending at mid-shaft diaphysis to determine Stiffness, Fracture-Load, Ultimate-Strength, and Fracture-Load/Weight.

Results: VGEF, MIP-1α and IL-2 levels were significantly elevated in all 6 weeks in the diabetic animals (DM vs. Lean). This was consistent with significant decreases of biomechanical properties in the DM. In both the sham-operated and fracture/repaired femurs, significant decreases of Fracture-load/Weight (30.3-32.3%, p=0.004, 0.02, respectively) and marginally decreases of Fracture-load (24.9-31.4%, p=0.08, 0.055, respectively) between Lean and DM groups were found. There was a delay in fracture healing found in the DM (42% vs. 83%-Lean) group at the 3 week time point. The treatment of metformin significantly reduced blood glucose and body weight after 12days post-op (DM+Met vs. DM). To our surprise, further decreases of Fracture-load (44.8%, p=0.004) and Fracture-load/Weight (21.5%, p=0.03) in the repaired femurs was also found in the DM+Met (vs. DM) group, but the factor(s) contributed to this decrease was not clear.

CONCLUSIONS: Diabetes impairs bone fracture healing. The treatment of metformin reduces blood glucose and body weight but has an adverse effect in fracture repair in diabetic rats.

Disclosures: Chris Chen, None.

SU0035

Toward non-invasive monitoring of bone infection in diabetic foot ulcers by Raman spectroscopy. Karen Esmonde-White*[1], Francis Esmonde-White[2], Michael Morris[3], Blake Roessler[4]. [1]University of Michigan, USA, [2]University of Michigan, USA, [3]University of Michigan, USA, [4]University of Michigan Medical School, USA

Introduction: Diabetics account for 8 in 10 non-traumatic amputations, and more than 80% of these amputations are preceded by foot ulcers. Diagnosis of osteomyelitis (bone infection) in diabetic foot ulcers is a challenge, especially in a point-of-care environment. Our pilot study used Raman microspectroscopy to measure composition in osteomyelitis and we discovered pathological crystals. The pathological crystals are unique to osteomyelitis and may serve as compositional markers of bone infection. We present our ongoing research in transcutaneous Raman spectroscopy (TRS) for intra-wound bone measurements. Methods: Feasibility studies were performed in human cadaveric tissue and a healthy human volunteer. Human cadaveric foot specimens were obtained from either the University of Michigan (UM) Medical School Anatomic Donations program or the UM Orthopaedic Research Laboratory. Near infrared Raman spectra were collected using our portable Raman instrument equipped with either a non-contact (~10 inch offset) or a contact (<1 cm offset) fiber optic probe. Transcutaneous measurements were collected on the plantar surface of cadaveric specimens and a healthy human volunteer. Simulated wounds were created in cadaveric specimens and examined either by the contact or non-contact probe. Results: Feasibility studies demonstrate rapid (<60s) intra-wound measurements using either a non-contact or contact probe. Probes are compatible with a single-use sterile sheath and/or hospital autoclaving protocols. No laser-induced tissue damage or localized heating was observed in the healthy human volunteer. Preclinical studies indicate that the non-contact probe is the most compatible with our clinical workflow and represents minimal risk to the patient. Conclusions: We present data from ongoing studies to translate TRS for intra-wound bone measurements, with the eventual aim of a point-of-care TRS diagnostic for osteomyelitis. Several probe designs have been evaluated in cadaveric tissue. At the time of abstract submission, we are awaiting IRB approval for a longitudinal TRS study in patients with diabetic foot ulcers. In addition to technology development, we have developed a unique clinical research workflow for the longitudinal TRS study. Co-localization of the wound clinic with clinical research facilities enables incorporation of TRS measurements into a patient's clinical visit and facilitates "bedside to bench" feedback on the TRS instrument.

Disclosures: Karen Esmonde-White, Kaiser Optical Systems, Inc., 10

SU0036

Vertebral Fracture Discrimination in Postmenopausal Women using a Subject-Specific Finite Element Model of the Disc-Vertebra-Disc Unit. Chuhee Lee*[1], Miguel Debono[2], Richard Eastell[2], Priyan Landham[3], Michael Adams[3], Patricia Dolan[3], Lang Yang[2]. [1], United Kingdom, [2]University of Sheffield, United Kingdom, [3]University of Bristol, United Kingdom

Bone Mineral Density (BMD) assessed by dual-energy X-ray absorptiometry (DXA) is low in vertebral fracture patients. In recent years, patient-specific finite element (FE) models of the vertebral body based on quantitative computed tomography (QCT) have been used to estimate vertebral strength and assess fracture risk. We developed a new patient-specific FE model of the Disc-Vertebra-Disc unit (DVD) that incorporates the vertebra and adjacent intervertebral discs. The purpose of this study was to investigate whether vertebral strength derived from the DVD FE model could discriminate between women with and without vertebral fracture.

This cross sectional case-control study included 74 postmenopausal women (age 59-82) in 3 groups: a case group (n=17) with osteopenia/osteoporosis (total hip or vertebral BMD T-score < -1) and prevalent vertebral fracture, an age- and BMD-matched control group (n=26), and an age-matched non-osteopenia/osteoporosis control group (n=31). QCT scans of L1 to L3 were used to generate DVD FE models of the L2 vertebra. Transverse-isotropic, elastic-perfectly plastic material properties were assigned to the vertebra whereas linear-elastic properties were used for the nucleus pulposus and annulus ground matrix with 4 fibre layers embedded in the annulus fibrosus. A pure compressive loading condition was simulated. Vertebral strength was defined using a 0.2% offset method in the load-displacement curve. The 2 control groups were combined to form a single control group for statistical analysis. Odds ratio (OR) for vertebral fracture for 1 SD decrease in covariates was derived from logistic regression, and area under the curve (AUC) from analysis of receiver operating characteristics.

Compared with the controls, the cases had significantly (p<0.0001) lower vertebral BMD (0.80 ± 0.02 v. 0.94 ± 0.02 g/cm^2, Z-score -0.98 ± 0.66) and FE strength (1231 ± 79 v. 1822 ± 62 N, Z-score -1.28 ± 0.69). FE strength discriminated vertebral fracture (OR 11.6, 95% CI 3.0-44.7) and after adjustment for BMD (OR 9.3, 95% CI 2.2-39.0). The AUC for FE strength (0.86, 95% CI 0.77-0.96) was higher than that for BMD (0.78, 95% CI 0.67-0.88). In a model in which we added FE strength to BMD, AUC increased to 0.88 (95% CI 0.80-0.96), significantly (p<0.05) larger than that of BMD alone.

In conclusion, vertebral strength derived from the *in vivo* DVD FE model was able to discriminate between women with and without vertebral fracture independent of BMD by DXA.

Disclosures: Chuhee LEE, None.

SU0037

What is the bilateral asymmetry of radius and tibia bone microarchitecture by HR-pQCT?. Erin Hildebrandt*, Sarah Manske, David Hanley, Steven Boyd. University of Calgary, Canada

Asymmetry is well established in human long bones on a macro scale. For example, right-side upper limbs tend to be longer and wider, regardless of hand dominance. Bone area by x-ray imaging has been shown to be significantly larger in dominant hands compared to non-dominant, presumably from an increase in mechanical loading. However, while bone microarchitecture clearly adapts to mechanical loading, scans from peripheral quantitative computed tomography (pQCT) have not found that dominance has an effect on cortical or trabecular bone mineral density (BMD) at the radius. The purpose of this study is to compare bone microarchitecture between the dominant and non-dominant radius and tibia as measured using high-resolution pQCT (HR-pQCT).

Healthy participants (average age 32.4 yrs, 43 women, 27 men) were recruited from Calgary and surrounding area and scanned at both radii and tibiae using HR-pQCT (XtremeCT, Scanco Medical). Dominance for hand and foot was determined by participant self-report. Scans were assessed using the manufacturer's standard protocol. Results were analyzed using a paired t-test and a Two-Way ANOVA of sex and limb dominance effects.

The majority of participants were right hand dominant (92.8%) and right foot dominant (94.2%). Overall, dominance was associated with an increase in cortical area (CtAr) at the radius (p=0.049) and cortical thickness (CtTh) at the tibia (p=0.04). For females, there were no microarchitectural differences at the radius, but trabecular area (TbAr) was greater at the dominant tibia (p=0.02). At the radius, males had greater CtAr (p=0.005), CtTh (p=0.001) and total BMD (TtBMD, p=0.03). Additionally, males had a greater CtAr at the dominant tibia (p=0.02). As has been previously reported, males had significantly greater TtBMD, CtAr and TbAr at the radius and tibia when compared to females (p<0.05).

This study found that dominance had an effect on structural cortical bone parameters at both the radius and tibia in a normal, healthy population. This is consistent with previous x-ray studies, but contrasts the results of pQCT studies. Our data suggest that dominance has a significant effect on cortical bone size but no significant effect on trabecular bone microarchitecture at the ultradistal radius and tibia. This work emphasizes that it is important to be consistent in the selection of either dominant or non-dominant limbs for HR-pQCT cohort studies at the ultradistal radius and tibia skeletal sites.

Disclosures: Erin Hildebrandt, None.

SU0038

Bisphosphonate Treatment During an Initial Unloading Period also Protects Against Bone Loss for a Second Unloading. Scott Lenfest*[1], Jessica Brezicha[2], Ray Boudreaux[1], Cameron Schaefer[2], Susan Bloomfield[1], Matthew Allen[3], Harry Hogan[4]. [1]Texas A&M University, USA, [2]Texas A&M University, USA, [3]Indiana University School of Medicine, USA, [4]Texas A&M University, USA

Bone response to multiple exposures of microgravity remains a concern for astronauts as more are making repeat flights, and some have taken bisphosphonates (BP) to prevent bone loss during flight. Given the long-lasting effects of these drugs it is possible that protection may persist for subsequent flights. The current study used the adult hindlimb unloaded (HU) rat model to test the hypothesis that the beneficial effects of BP treatment given during an initial HU period would also extend to a second HU. We further hypothesized that Zoledronic Acid (ZA) would be more effective than Alendronate (ALN) due to their differences in binding affinity.

Adult male rats (6 mo.) were block assigned to aging control (AC) and HU groups by body weight. HU animals were exposed to 28d of HU, followed by 56d of recovery, and then a second 28d HU exposure. Subsets of HU animals were administered ALN (HU+A), ZA (HU+Z), or no drug (HUC). ALN (2.4 µg/kg) was given 3x/week for 5 weeks, starting the week before the initial 28d of HU. ZA (60 µg/kg) was given in a single dose immediately prior to the first HU. *In vivo* pQCT scans of the proximal tibia metaphysis (PTM) were taken at baseline (BL) and every 28d. The study is ongoing, and there will ultimately be 15 animals per group. For results presented here, N varies from 3 to 15.

During the first HU, HUC showed expected losses in both total bone mineral content (BMC) and bone mineral density (vBMD) relative to BL (-10.6%, -6.7%, resp.). Total BMC and vBMD for HU+A were not different from BL or AC at day 28, indicating protection against losses. For HU+Z animals, total BMC was significantly higher than AC (+6.2%) and HU+A (+10%) at day 28, and total vBMD was significantly higher than BL (+8.5%), AC (+8.8%), and HU+A (+6.3%). This potency of ZA continued throughout the 56d recovery period, with both total BMC and vBMD significantly higher for HU+Z compared to BL, AC, and HU+A. For the second HU, total vBMD was unchanged for HU+Z and remained significantly higher than BL (+13.1%), AC (+13.8%), and HU+A (+13.2%). Total vBMD for HU+A was similar to AC at the start and end of the second HU. Total BMC was lower for HU compared to AC at the end of the second HU, but HU+Z and HU+A were not different from AC.

In summary, both ALN and ZA protected against disuse-induced losses in total BMC and vBMD for both bouts of disuse, but ZA was more potent as evidenced by enhanced mass and density above age-matched control values.

SU0039

Effects of Hind Limb Unloading and Sclerostin Antibody on Femoral Neck Strength Estimated by Finite Element Analysis. Lindsay Sullivan*[1], Eric Livingston[2], Rachel Ellman[3], Jordan Spatz[4], Louis Stodieck[5], Mary Bouxsein[6], Virginia Ferguson[5], Ted Bateman[7], Anthony Lau[1]. [1]University of North Carolina at Chapel Hill, USA, [2]University of North Carolina-Chapel Hill, USA, [3]Beth Israel Deaconess Medical Center, USA, [4]Harvard-MIT Division of Health Sciences & Technology (HST), USA, [5]University of Colorado, USA, [6]Beth Israel Deaconess Medical Center, Harvard Medical School, USA, [7]Univesity of North Carolina, USA

Skeletal unloading during spaceflight reduces bone volume and bone mineral density. Hind limb unloading is a ground based technique developed to mimic the effects of microgravity on bones. The relationship between bone loss seen in the ground based model and during spaceflight has not been extensively characterized. This study uses finite element modeling (FEM) to assess changes in femoral neck stiffness due to hind limb unloading and sclerostin antibody treatment (Scl-Ab).

Thirty mice were suspended by their hind limbs for 13-days (HLU). Half the mice were treated with placebo (n=15) and half were treated with a Scl-Ab (n=15). Corresponding control (GC) groups were similarly treated. In this study, subject specific FE models were meshed from microCT images from the same mice (down sampled from 10 to 20µm resolution) for a 3.25mm segment of the proximal femur, which was taken from the top of the femoral head. All bone elements were modeled as linear elastic (E=10GPa, *v*=0.3). A downward displacement of 50µm was applied to the entire femoral head and the femoral neck bending stiffness was calculated from the measured load at 50µm.

FEM of the proximal femur found a 12% decrease in stiffness in the HLU mice compared to the GC mice. Scl-Ab treatment resulted in an increased stiffness by 31% in the HLU and 29% in the GC. When compared to the results for mice flown on STS-135, the HLU mice exhibited a similar trend. However, the HLU mice had a larger response to the sclerostin antibody than the STS-135 mice. The increased response seen in the hind limb unloaded mice may occur due to the fact that the mice still experience some gravitational force.

Conclusion: The unloading of the mouse hind limbs caused a significant loss of femoral neck stiffness in the proximal femur. Scl-Ab prevented the loss of bone strength, and increased femoral neck stiffness in both HLU and GC mice. The results of FEM from the hind limb unloading study showed the same trend as the previous STS-135 study in the proximal femur region
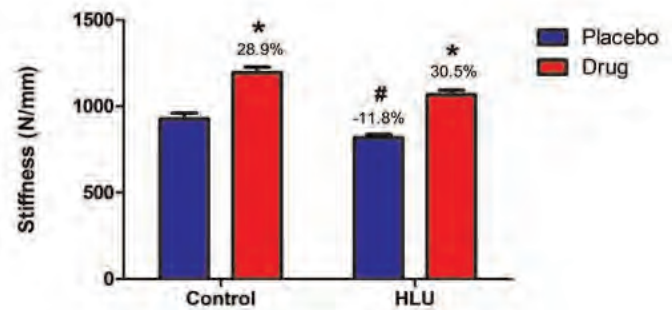
Changes in Femoral Neck stiffness caused by the sclerostin antibody(*) and HLU(#)

SU0040

Bone morphology in 46 BXD Recombinant Inbred Strains and femur-tibia correlation. Yan Jiao*[1], Yueying Zhang[2], Jinshong Huang[3], Valentin David[2], Weikuan Gu[1]. [1]University of Tennessee Health Science Center, USA, [2]UTHSC, USA, [3]UTHSC.edu, USA

Osteoporosis is recognized as the most common bone disease in the world. It is characterized with a reduction in bone mass and an alternation of bone micro-architecture, which have been approved to be the major determinants of bone strength. The inbred strains of mice have proven to be useful models for studies of genetic effects on bone structure. In current study, we evaluated the bone mass and microstructure of femurs and tibias in BXD RI mouse strains.

We examined the bone properties of BXD RI mice using High-resolution µCT by analyzing femur and tibia and compared their phenotypes of different compartments. 46 BXD RI mouse strains were analyzed including progenitor C57BL/6J (n=16) and DBA/2J (n=15), and two first filial generations (D2B6F1 and B6D2F1). Strain differences were observed in bone quality and structural properties (p<0.05) in each bone profile (whole bone, cortical bone, or trabecular bone). Additionally, strains differences were revealed in bone stiffness (p<0.0001).

It is well-known that skeletal phenotypes are largely affected by genetic determinants and genders, such as bone mineral density (BMD). While genetics and gender appear expectedly as the major determinants of bone mass and structure, significant correlations were also observed between femur and tibia. More importantly, positive and negative femur-tibia associations indicated that genetic makeup had an influence on skeletal integrity. We conclude that a) femur-tibia association in bone morphological properties significantly vary from strain to strain, which may be caused by genetic differences among strains; b) strain-wise variations were seen in bone mass, bone morphology, bone micro-architecture along with bone structural property.

Key words: Bone mineral density, Femur, Tibia, Mouse, Recombinant inbred strain

SU0041

Cx43 Scaffolding C-Terminus Intracellular Domain Is Required for Achieving Proper Bone Architecture and Strength, but It Does Not Mediate the Effect of Osteocytic Cx43 on Cortical Bone. Rafael Pacheco*[1], Iraj Hassan[2], Chad Sorenson[2], Hannah Davis[2], Max Hammond[3], Rejane Reginato[4], Eduardo Katchburian[4], Joseph Wallace[5], Teresita Bellido[6], Lilian Plotkin[6]. [1]Indiana University School of Medicine, Federal University of São Paulo, USA, [2]Indiana University School of Medicine, USA, [3]Purdue University, USA, [4]Federal University of São Paulo, Brazil, [5]Indiana University Purdue University Indianapolis (IUPUI), USA, [6]Indiana University School of Medicine, USA

Connexin (Cx) 43, a transmembrane protein abundantly expressed in bone cells, forms gap junction channels and hemichannels responsible for intercellular communication among osteocytes, osteoblasts and osteoclasts. The C-terminus intracellular domain (CT) of Cx43 acts as scaffold for structural and signaling proteins hence impacting intracellular signaling; and its phosphorylation status regulates Cx43 channel activity. Earlier *in vitro* studies demonstrated that channels formed by a mutant lacking the CT (Cx43DCT) remains open; and that Cx43 promotes osteocyte viability but Cx43DCT does not, demonstrating the requirement of the CT for survival signaling in osteocytes. Here we examined the function of this CT domain in bone *in vivo* using mice in which CT was removed, rendering a truncated Cx43DCT. First, we generated mice in which one allele of Cx43 was replaced by Cx43DCT (Cx43fl/DCT). Compared to Cx43fl/fl littermate controls, Cx43fl/DCT mice exhibit low BV/TV and

trabecular number and high trabecular spacing in the distal femur, measured by μCT. In contrast, cortical thickness in the femoral mid-diaphysis was increased, and mechanical testing by femoral 3-point bending revealed increased mechanical strength (stiffness, yield force, and ultimate force). The macro-scale toughness measured by 3-point bending was not changed; however, the micro-scale toughness index average energy dissipation was increased, measured in the tibia by reference point indentation (RPI). These findings indicate that in the presence of one allele encoding full length Cx43, the truncated $Cx43^{DCT}$ has a dominant effect, affecting cancellous and cortical bone architecture in opposite ways and increasing cortical bone strength. We next generated mice in which the truncated $Cx43^{DCT}$ was expressed in osteocytes in the absence of endogenous Cx43, by crossing mice lacking Cx43 in osteocytes ($Cx43^{fl/fl}$;DMP1-8kb-Cre) with $Cx43^{fl/DCT}$ mice. Expression of the truncated $Cx43^{DCT}$ reversed the cortical thinning measured by μCT and the defective material strength, measured at the macro- and micro-scale levels by 3-point bending and RPI, exhibited by $Cx43^{fl/fl}$;DMP1-8kb-Cre mice to levels similar to $Cx43^{fl/fl}$ littermate controls. We conclude that the Cx43CT domain is required for acquisition of normal cancellous bone volume and architecture, but negatively affects cortical bone strength. Moreover, the Cx43CT is dispensable for the maintenance of cortical bone dependent on Cx43 expression in osteocytes.

Disclosures: Rafael Pacheco, None.

SU0042

Do African-Americans and Caucasians build long bones in fundamentally different ways. Stephen Schlecht*[1], Karl Jepsen[2]. [1]University of Michigan, USA, [2]University of Michigan, USA

Ethnic differences in bone morphology and BMD are well documented and often used to identify traits contributing to fracture susceptibility. On average, African-Americans (AA) have wider, thicker cortices compared to Caucasians (CN). However, it remains unclear whether AA and CN build bones in fundamentally different ways. Cortical area (Ct.Ar) correlates positively and tissue mineral density (TMD) correlates negatively with the natural variation in robustness (total bone area/length) in both populations. We tested whether these interactions explain ethnic differences in bone structure and composition.

Cross-sectional morphology and TMD were assessed for 7 long bone mid-diaphyses of 125 CN and 115 AA adult men and women (20-40 yrs) using pQCT. AA had more robust (wider relative to length) bones compared to CN for all sites except the femora, in both sexes (p<0.05). Comparing linear regressions between Ct.Ar and robustness, AA had a slightly greater Ct.Ar for a given robustness compared to CN for all sites except the femora (Fig.1a-b) in both sexes (ANCOVA, y-int, p<0.0001). Differences in regressions were small, suggesting that the lower Ct.Ar of CN long bones was consistent with the differences in robustness. Comparing linear regressions between TMD and robustness revealed that AA bones had greater TMD for a given robustness (ANCOVA, y-int, p<0.0001) (Fig.1b-d). This was a novel finding since AA bones were expected to show reduced TMD, not increased, given that TMD correlates negatively with robustness. Finally, both ethnicities showed similar degrees of functional inequivalence, with slender bones being 1.5–2.8 times less strong compared to robust bones, independent of body size. This 50-180% natural variation in strength among individuals within each ethnicity is 5-10 times greater than the mean bone strength between ethnicities. Morphologically, CN bones are simply a more slender version of AA bones. However, AA bones have a proportionally greater TMD compared to CN, independent of robustness, which may result from reduced porosity arising from ethnic differences in intracortical bone remodeling (Cho et al., AJPA, 2006). Insignificant findings between femoral Ct.Ar and robustness among ethnicities suggest trait covariance is highly conserved within this bone. By taking the functional interactions among traits into consideration, we provide new insight into differences in bone strength that may contribute to ethnic differences in fracture incidence
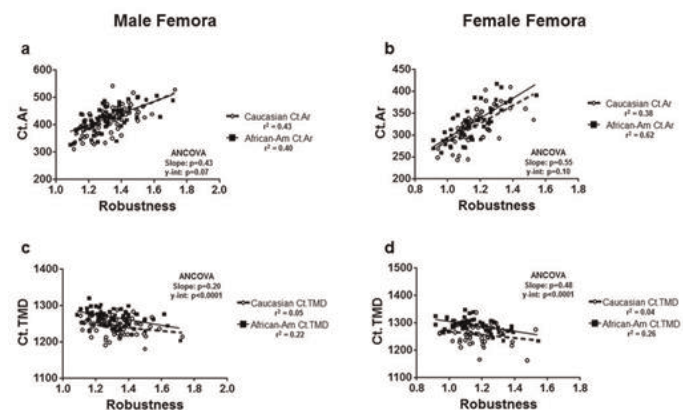

Figure 1a-d. Example of linear regressions between covarying traits for both African-American and Caucasian males and females. a) Ct.Ar versus robustness in male femora; b) Ct.Ar versus robustness in female femora; c) TMD versus robustness in male femora; d) TMD versus robustness in female femora.

Figure 1a-d

Disclosures: Stephen Schlecht, None.

SU0043

Effects of Preventive Long Term Treatment with Strontium Ranelate and Zoledronic Acid to Ovariectomized Rats on Bone Biomechanics. Marta Martín-Fernández*[1], Marina Gómez-Chinchón[1], David Guede[2], Jose Caeiro[3], Manuel Díaz-Curiel[4], Concepcion De La Piedra Gordo[5]. [1]Bioquímica Investigación, Instituto de Investigación Sanitaria Fundación Jiménez Díaz, Spain, [2]Trabeculae,Technology Based Firm, Technological Park of Galicia, Spain, [3]Orthopaedic Surgeon, Spain, [4]Medicina Interna, Instituto de Investigación Sanitaria Fundación Jiménez Díaz, Spain, [5]Instituto de Investigación Sanitaria Fundación Jiménez Díaz, Spain

Many pharmacological treatments have been developed in order to prevent or treat postmenopausal osteoporosis. There is not any study in the literature comparing long-term treatments of osteoporosis. The aim of this work was to study the effects of long-term prevention treatment with Zoledronic Acid (ZA) and Strontium Ranelate (SrR) on biomechanical parameters in ovariectomized rats.

Sixty 6-month-old female Wistar rats were used in this study and divided into four groups: SHAM (n=15), simulated intervention; OVX (n=15), ovariectomized; OVX+ZA (n=15), ovariectomized and treated with ZA (0.08mg/kg i.v. at the begining of the study); OVX+SrR (n=15) ovariectomized and treated with SrR (0.033 g/kg/day by oral gavage). Treatments started one day after ovariectomy. Eight months later all rats were sacrificed and right femora were mechanically tested to failure in three-point bending to evaluate the mechanical properties of the midshaft. All mechanical tests were performed using a 1kN load cell on a material testing machine (Microtest EM1/10/FR/m) at a constant displacement of 10mm/min until the bone fracture. Extrinsic or structural properties: ultimate load, extrinsic stiffness and work to failure; and intrinsic or material properties: ultimate stress, Young's modulus and toughness were analyzed.

Young modulus was statistically decreased in OVX and SrR groups, without significant difference between them. Levels of ZA group were similar to those of SHAM group. Extrinsic stiffness was significantly higher in ZA treated rats as compared to all other groups. No significant differences between groups were observed in the other studied parameters.

SrR long-term preventive treatment is no capable of avoid the effects of ovariectomy on bone biomechanics. Long term treatment of ovariectomized rats with ZA prevented effects of ovariectomy preserving Young's modulus.

Disclosures: Marta Martín-Fernández, None.

SU0044

New Tool for Accurate Cortical Bone Analysis in pQCT Images. Tomas Cervinka*[1], Lora Giangregorio[2], Deena Lala[3], Angela M. Cheung[4], Eva Szabo[5], Harri Sievanen[6], Jari Hyttinen[7]. [1]Tampere University of Technology, Finland, [2]University of Waterloo, Canada, [3]University of Waterloo, Canada, [4]University Health Network-University of Toronto, Canada, [5]University Health Network, Canada, [6]The UKK Institute for Health Promotion Research, Finland, [7]Department of Electronics & Communications Engineering, Tampere University of Technology, Finland

Peripheral quantitative computed tomography (pQCT) allows a reasonable option to assess the bone cross-sectional geometry and separation of the trabecular and cortical compartments. Although commonly used pQCT systems lack sufficient spatial resolution to capture specific structural traits compared with high-resolution pQCT (HR-pQCT) systems, they are cheaper and still widely used among bone researchers. However, the need for better accuracy in the detection of coarse bone structural traits in pQCT images is evident.

The aim of this study was to evaluate the agreement between pQCT and HR-pQCT measurements of cortical geometry at the distal tibia. More specifically, we addressed to what extend can our novel segmentation method, called OBS, improve the analysis of cortical CSA (CoA), thickness (CoTh) and density (CoD) from pQCT images. The OBS is a robust threshold free segmentation method developed for reliable cortical bone detection in pQCT images.

We used pQCT and HR-pQCT images of distal tibia obtained from 15 dry human tibia specimens. All scans for both modalities were taken from the same location (22.5 mm proximal to the endplate of the tibia). The pixel size of the pQCT image was 0.5x0.5 mm and the slice thickness was 2.2 mm. The HR-pQCT images were obtained with the standard acquisition approach and an isotropic voxel size of 82 μm. The performance of the OBS method, applied on pQCT data, was compared with results of standard analysis of HR-pQCT data. As descriptive statistics, the means and standard deviation (SD) of CoA, CoTh and CoD are given. In addition, we determined the mean error and its SD, and used Pearson correlations and Bland-Altman plots to describe the relationships between pQCT- and HRpQCT-derived variables.

The OBS method showed good performance for detection of CoA, CoTh and CoD in pQCT data when compared with HR-pQCT data (Table 1). The mean error and limits of agreement of these traits were $-2.8\pm16.7\%$, $4.9\pm16.2\%$ and $-0.6\pm7.9\%$, and correlation with HR-pQCT data was 0.94, 0.95 and 0.88, respectively.

In conclusions, this study showed that the OBS method offers a promising practical tool for more accurate evaluation of cortical bone geometry in pQCT images. Nevertheless, a comparison of the same volumes in pQCT and HR-pQCT data needs to be performed before the true accuracy of OBS analysis of cortical traits in pQCT images can be determined.

Table 1: Descriptive data of CoA, CoTh, and CoD (mean, SD) as obtained from analysis of pQCT and HR-pQCT images together with an agreement between obtained results:

	pQCT$_{OBS}$	HR-pQCT	Error
CoA [mm²]	139.0 (18.8)	144.8 (28.0)	-5.8 (12.1)
CoTh [mm]	1.31 (0.24)	1.26 (0.27)	0.05 (0.09)
CoD [mg/cm³]	838.1 (63.3)	844.1 (70.4)	-5.9 (34.0)

Table 1

Disclosures: Tomas Cervinka, None.

SU0045

Once Daily and Once Weekly Regimens of Teriparatide have Different Effects on Cortical Bone. <u>Roger Zebaze</u>*[1], <u>Ryoko Takao-Kawabata</u>[2], <u>Yu Peng</u>[3], <u>Ali Ghasem-Zadeh</u>[4], <u>Aya Shimomura</u>[5], <u>Hiroshi Yamane</u>[5], <u>Kyoko Hirano</u>[5], <u>Yukihiro Isogai</u>[6], <u>Toshinori Ishizuya</u>[5], <u>Ego Seeman</u>[4]. [1]Austin Health, University of Melbourne, Australia, [2]Asahi Kasei Pharma Co., Japan, [3]StraxCorp Pty Ltd, Australia, [4]Austin Health, University of Melbourne, Australia, [5]Asahi Kasei Pharma Corporation, Japan, [6]Asahi Kasei Pharma Corporation, Japan

The pharmacokinetic profile of PTH determines its relative anabolic/resorptive effects. We hypothesized that less frequent administration of teriparatide may favor a lesser effect on resorption than daily administration. As cortical bone consists of a compact cortex (CC), and a more porous outer and inner transitional zone (OTZ, ITZ) with more surface area/matrix volume formed by varying degrees of corticalization of trabeculae, we proposed that the effects of teriparatide vary according to the cortical compartment.

We studied 17 female New Zealand white rabbits, aged 6 months treated for 1 month with teriparatide [human PTH(1-34)] (Asahi Kasei Pharma; Japan) as follows. (i.) Vehicle (DV; n=4); (ii.) 20 µg/kg/day (D20; n=3); (iii.) 40 µg/kg/day (D40; n=3); (iv.) Once weekly 140 µg/kg (W140; n=3); (v.) and once weekly 280 µg/kg (W280; n=4). Proximal femurs were imaged ex vivo using micro-CT (Scanco Viva CT-40) at 15 µm voxel size. Structure was quantified in a 10mm length ROI starting at the midshaft using StrAx1.0. StrAx1.0 segments the CC, the TZ (outer & inner) and, trabecular bone.

In rabbits treated with 20 µg/kg/d, CC porosity was unchanged. OTZ and ITZ porosity increased (9.0%; p=0.02, 5.4%; p=0.07 respectively). 40 µg/kg/d increased CC and OTZ porosity respectively by 49.9 and 19.3% (p<0.05) . The increase in porosity in CC and OTZ was greater than those in D20 group (all p<0.05). Porosity in ITZ was increased but not significantly so, (5.0%; p=0.13). Bone volume fraction decreased with 40 µg/kg/d (7.9%; p=0.005). Increments in bone volume fraction with 20 µg/kg/d and weekly therapies were modest respectively 0.76, 1.4 and 2.0% (NS).

By contrast, treatment with either dose of weekly teriparatide decreased CC porosity by 6.8% and 7.3% respectively (NS). Porosity was unchanged in TZs.

Teriparatide effects on the cortex depend on the treatment regimen and on the cortical region measured. Weekly regimens did not increase porosity. Daily regimens increased porosity in TZ, and the larger dose did so both in CC and TZ. We suggest that TZ porosity may be a 'pseudo-porosity' caused by bone formation on trabeculae abutting the cortex, which have not completely fused, and therefore this may not be associated with fragility as occurs with porosity due to remodeling imbalance.

Disclosures: Roger Zebaze, StraxCorp, 4; Amgen, 3; MSD, 3; GSK, 3; Servier, 3; Asahi Kasei Pharma, 3
This study received funding from: Asahi Kasei Pharma Corporation

SU0046

Synchrotron mCT evaluation of peri-implant hard tissues -A review of the literature and preliminary results. <u>Camilla Neldam</u>*[1], <u>Else Marie Pinholt</u>[2], <u>Niklas Rye Jørgensen</u>[3]. [1]PhD student, Denmark, [2]DDS, M Sci, dr. odont, Professor & Head, Denmark, [3]MD, PhD, DMSc, Denmark

SRmCT is considered gold standard for evaluating bone microarchitecture, and it possess major advantages in comparison to laboratory-based microtomography due to its high resolution, high contrast, and excellent of high signal-to-noise-ratio. Hence, giving us the very highest spatial resolutions achieved today.

A review of the literature included 17 studies concerning animal, experimental and human studies, with SRmCT on bone substitutes and dental titanium implants. Reviewing the literature emphasizes the need, within dental practice, for more detailed evaluations in higher resolutions than previously obtained. SRmCT is required for evaluation of osseointegration of dental implants, comparison of osseointegration of different bone substitutes, and bone microarchitecture at the bone-to implant interface.

Using SRmCT at a voxel size of 5 µm in an experimental goat mandible model, bone-to-implant contact was found to around 5%, and the bone volume fraction

increased at radial distance from the implant surface up to 50% and levelled out to approximately 70% at a 300 µm radial distance.

This method has been successful in depicting the bone and cavities in three dimensions thereby enabling us to give a much more precise answer to the fraction of the bone-to-implant contact compared to previous methods.

Disclosures: Camilla Neldam, None.

SU0047

Matrix protein biglycan mediates suture expansion osteogenesis via potentiation of β-catenin. <u>Hua Wang</u>*[1], <u>Wen Sun</u>[2], <u>Lin Wang</u>[3], <u>Wei-Bing Zhang</u>[4]. [1]Institute of Stomatology, Nanjing Medical University, Peoples Republic of China, [2]Nanjing Medical UniversityThe Research Center for Bone & Stem Cells, Peoples Republic of China, [3]Institute of Stomatology, Nanjing Medical University, China, [4]School of Stomatology, Nanjing Medical University, Nanjing, China, USA

To investigate the involvement of extracellular matrix glycoprotein biglycan and β-catenin in bio-mechanical osteogenesis during suture expansion. We evaluated the changes in biglycan and β-catenin signaling over time using a mouse midpalatal suture expansion model in vivo. Furthermore, we examined the effect of tensile strain (2% magnitude, 0.5 Hz), which represents clinical expansion force on biglycan and β-catenin signaling in primary calvarial osteoblasts whose biglycan was silenced in vitro. Our data showed that expansive force significantly induced new bone formation at the edge of palatal sutures. The sutures prominently widened peaking on day 7. The immunopositive areas of biglycan peaked on day 7, showed a similar spatio-temporal pattern with ALP and Col-1. Biglycan, β-catenin, and osteogenic markers such as Runx2, ALP and Col-1 increased both at protein and mRNA levels together. Meanwhile, mechanical strain sufficiently induced up-regulation of biglycan and nuclear β-catenin in vitro. Silencing biglycan resulted in an attenuated up-regulation of nucleus β-catenin and Runx2 in response to mechanical strain; however, Wnt3a treatment was able to partly reverse this disruption. Our results demonstrated that biglycan as a component of extracellular matrix mediates suture expansion osteogenesis via potentiation of β-catenin.

Disclosures: Hua Wang, None.

SU0048

A realistic musculoskeletal model of the thoracolumbar spine and ribcage produces spinal loading patterns that may help explain the non-uniform distribution of vertebral fractures along the spine. <u>Alexander Bruno</u>*[1], <u>Dennis Anderson</u>[2], <u>Xiangjie Meng</u>[3], <u>Mary Bouxsein</u>[4]. [1]Harvard-MIT, USA, [2]Beth Israel Deaconess Medical Center, USA, [3]Tsinghua University, China, [4]Beth Israel Deaconess Medical Center, Harvard Medical School, USA

Vertebral fractures (VFx) are the most common complication of osteoporosis, and occur most frequently in the mid-thoracic and thoracolumbar regions of the spine. However, the mechanisms underlying this site-specific occurrence of VFx are not known. Our working hypothesis is that the locations of VFx may be explained by the pattern of spine loading, such that during daily activities the mid-thoracic and thoracolumbar regions see preferentially higher mechanical loading compared to other spine regions. Prior estimates of vertebral loading are limited as they have used relatively simple models that did not incorporate explicit contributions of the ribcage and thoracolumbar trunk muscles. To address these limitations and test our hypothesis we developed a realistic musculoskeletal model of the thoracolumbar spine that includes the thoracic and lumbar vertebrae, ribs, sternum, arms, and head. The model, implemented in OpenSim musculoskeletal modeling software, uses 700 Hill-Type muscle fascicles to simulate major muscle groups affecting the trunk. Intervertebral and costovertebral joints are modeled as ball and pin joints, respectively. The ribs are connected to the sternum by actuators to account for the load transfer facilitated by the costal cartilage. We also examined whether incorporation of intra-abdominal pressure (IAP) into the model affects the magnitude or pattern of spine loading. To do so, we simulated abdominal pressure (10 kPa) by exerting forces on the diaphragm, pelvis, and abdominal wall, which the major abdominal muscle groups then had to balance. We used the model to simulate a lifting activity (10 kg weights in each hand with the elbows flexed 90°) with and without IAP present, and computed the compressive force in the axial direction of each vertebral body. We found that without IAP, vertebral compressive load increased progressively from upper to lower thoracic spine, peaking at T11 (Figure 1). Inclusion of IAP reduced vertebral compressive loading, with the largest reduction occurring at T10 and T11 (~38% reduction). The highest load in the model with IAP occurred at L1, with a smaller secondary peak at T8, corresponding to the locations of peaks in VFx occurrence. In sum, our realistic thoracolumbar spine model provides evidence that variations in spine loading may partly explain observed fracture patterns, and that intra-abdominal pressure plays an important role in vertebral loading.
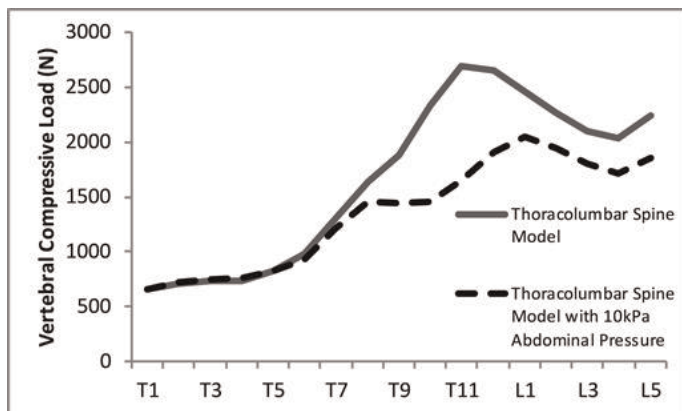
Figure 1: Vertebral compressive loading on T1 through L5 for standing with 10 kg weights

Disclosures: Alexander Bruno, None.

SU0049

Four Year Vibration Therapy Reduces Age-related Bone Loss and Improves Lower Extremity Function. <u>Belinda Beck</u>*. Griffith University, Australia

Purpose: Whole body vibration (WBV) reduces fall risk in older adults and improves bone in animal models, however, human bone responses have been inconsistent. Some have suggested the inability to detect vibration-induced skeletal adaptation is a function of inadequate trial duration and that longer term stimulus is required. The study aim then was to determine the effect of 4 years of daily WVB on risk factors of hip fracture.

Methods: Four postmenopausal women (61.8 $\pm$ 9.8 y) with low bone mass (mean femoral neck [FN] t-score: -2.9 $\pm$ 0.92) undertook daily 10-20min WBV for 4 years (VIB) (Juvent, Parsippany). Four age-, sex-, and BMI-matched controls (58.8 $\pm$ 7.4 y) continued usual activities (CON). At baseline (T0) and annually to 4 years (T4), biometrics, whole body (WB), lumbar spine (LS) and FN BMD and BMAD (DXA, XR-800, Norland), parameters of tibial geometry (pQCT, XCT3000, Stratec), and lower extremity muscle function and balance were tested. Physical activity and calcium consumption were recorded. Effects were examined by repeated-measures ANOVA controlling for calcium, and by t-test comparison of measures taken at T0 and T4.

Results: The groups were similar at baseline, except VIB had lower LS and FN t-scores (p=0.005 and p=0.03, respectively). VIB maintained all measures between T0 and T4, with the exception of chair rise time, which improved (p=0.02), and tibial trabecular content and area, which decreased (p<0.05). CON did not improve any measure and lost FN BMC, BMD, BMAD and strength as well as tibial cortical bone content (p<0.05). Controlling for calcium, significant within-subject effects (time) were detected for LS BMC, (p=0.03) and tibial endosteal circumference (p=0.0001). Despite low participant numbers, power was adequate for significant outcomes (1-ß=0.73 and1-ß=0.99, respectively). Young's modulus of the LS (p=0.06, 1-ß=0.61) and tibial cortical density (p=0.06, 1-ß=0.62) approached significance. In all cases, CON lost more than VIB.Conclusion: Long term low intensity WBV tempers age-related skeletal loss and improves lower extremity function which may reduce the risk of falling

Disclosures: Belinda Beck, None.

SU0050

Effectiveness of Community Group and Home Based Falls Prevention Exercise Programmes on Bone Health in Older People: the ProAct65+ Bone Study. <u>Rachel Duckham</u>[1], <u>Katherine Brooke-Wavell</u>*[2], <u>Tahir Masud</u>[3], <u>Rachael Taylor</u>[4], <u>Denise Kendrick</u>[5], <u>Hannah Carpenter</u>[5], <u>Dawn A Skelton</u>[6], <u>Susann Dinan</u>[7], <u>Heather Gage</u>[8], <u>Richard Morris</u>[7], <u>Steve Iliffe</u>[7]. [1]Deakin University, Aus, [2]Loughborough University, United Kingdom, [3]Nottingham University Hospitals NHS Trust, United Kingdom, [4]Nottingham University Hospitals NHS Trust, United Kingdom, [5]University of Nottingham, United Kingdom, [6]Glasgow Caledonian University, United Kingdom, [7]University College London, United Kingdom, [8]University of Surrey, United Kingdom

Exercise may reduce osteoporotic fracture risk through both increasing bone strength and reducing fall risk. Falls prevention exercise programmes can reduce fall incidence, and also include some strengthening exercises suggested to load bone but there is little information as to whether these programmes influence bone mineral density (BMD) and strength. The study compared home (Otago Exercise Programme, OEP) and group (Falls Management Exercise, FaME) falls prevention exercise programmes with usual care in older people to determine whether these interventions can improve bone strength.

Men and women aged over 65 years were recruited through primary care. They were randomised by practice to OEP, FaME or usual care. Bone mineral density (BMD) was measured by dual X-ray absorptiometry (GE-Lunar Prodigy) prior to randomisation and following the 24 week intervention. Comparisons between treatment arms were made using random effects linear regression models to allow for clustering by practice, adjusted for baseline values, gender, medication use and comorbidities.

Participants were 319 older people (193 women and 126 men), aged (mean + SD) 72 + 5 years. 92% of participants completed the trial. The OEP group completed 58 + 43 minutes/week of home exercise, whilst the FaME group completed 39 + 16 and 30 + 24 minutes/week of group and home exercise respectively. Femoral neck BMD changes did not differ between treatment arms, with mean effect sizes in OEP and FaME relative to usual care arms being -0.003 and -0.002 g/cm^2 respectively (P = 0.44 and 0.53). Effect sizes for section modulus were -8.5 and -6.9 mm^3 in OEP and FaME respectively (P=0.21 and 0.28). There were no significant changes at other skeletal sites, or in sensitivity analyses excluding those taking medication or poor compliers with exercise.

The OEP and FaME programmes did not influence bone mineral density in older people, although they have an important role in preventing fractures by preventing falls. To increase bone strength, programmes may need to incorporate exercise that exerts higher strains on bone and/or have a longer duration.

Disclosures: Katherine Brooke-Wavell, None.

SU0051

Effects of Whole-Body Vibration Therapy on Bone, Muscle and Metabolism in Obese Adolescents. <u>Rickard Zeijlon</u>*[1], <u>Bojan Tubic</u>[2], <u>Staffan Mårild</u>[3], <u>Göran Wennergren</u>[4], <u>Jovanna Dahlgren</u>[4], <u>Per Magnusson</u>[5], <u>Diana Swolin-Eide</u>[6]. [1], Sweden, [2]Department of Pediatrics, Gothenburg University, Sweden, [3]The Queen Silvia Children's Hospital, Sahlgrenska Academy at the University of Gothenburg, Sweden, [4]The Queen Silvia Children's Hospital, Sweden, [5]Linkoping University,Sweden, Sweden, [6]Queen Silvia Children's Hospital, Sweden

Purpose: Mechanical loading is osteogenic and whole-body vibration therapy (WBV) is an emerging method for muscular training. WBV results in increased muscle power and decreased blood pressure in postmenopausal women. Previous WBV studies in obese women have demonstrated increased growth hormone levels, increased oxygen uptake, lowered BMI and increased muscular strength. This prospective pilot study is the first to investigate the effects of a 3-month WBV on bone mass, muscle, anthropometry and metabolic parameters in obese adolescents.

Methods: Seven obese patients, age 11-17 years (girls=3/boys=4), mean weight 92 kg (67-119 kg) and mean BMI 32 kg/m2 (26-39 kg/m2), were included and six completed 3 months of WBV. Three sessions (10-13 min per session) per week were performed on a side-alternating Galileo® (Stratec) vibration plate, frequency 18-24 Hz and amplitude +/-3.9 mm. Measurements were made at baseline and after 3 months of heel bone mineral density (BMD) and heel bone mineral content (BMC) by DXL (Demetech), muscle strength and balance with Leonardo Mechanography® (Stratec), weight and body fat with Tanita® (Tanita Corp.). Blood pressure, anthropometrics and metabolic parameters were followed.

Results: WBV was well tolerated but compliance varied and the reasons for skipping sessions were that patients regarded the WBV training to be boring or too strenuous. We observed decreased levels of total cholesterol (-0.76 mmol/L, *p*=0.046) and triglycerides (-0.39 mmol/L, *p*=0.028). A decrease was found for serum insulin in five patients, from pathological to normal levels, with a reduction with 10% to 72%. The decreased fasting insulin levels (mean -10.8 mU/L), did, however, not reach statistical significance, *p*=0.12. There was a tendency of decreased abdominal girth (-2.4 cm, *p*=0.07) and decreased body fat (-1.6%, *p*=0.07). No change was observed for the Leonardo-measurements of muscle strength (single two leg jump, multiple one leg hopping and chair rising test). Calcaneal BMD and BMC, body weight, BMI, blood pressure and pulse did not change over the study period.

Conclusion: This prospective pilot study of whole-body vibration therapy demonstrated reduced fasting insulin levels for most patients and an improved lipid profile. There was, however, no effect on calcaneal bone mass. The number of patients was small and larger randomized studies are warranted.

Disclosures: Rickard Zeijlon, None.

SU0052

Hand grip strength, leg extensor power and cardiorespiratory fitness are associated with bone mineral density in men aged 18-60 years: the Health2008 study. <u>Peter Schwraz</u>[1], <u>Niklas Rye Joergensen</u>[2], <u>Barbara Rubek Nielsen</u>*[3], <u>Anne Sofie Dam Laursen</u>[4], <u>Allan Linneberg</u>[4], <u>Mette Aadahl</u>[4]. [1]Research Centre of Ageing & Osteoporosis, Department of Medicine, Copenhagen University Hospital, Glostrup, Denmark.Faculty of Health Sciences, University of Copenhagen, Copenhagen,Denmark, Denmark, [2]Research Centre of Ageing & Osteoporosis, Department of Medicine & Diagnostics, Copenhagen University Hospital, Glostrup, Denmark, Denmark, [3]Research Centre of Ageing & Osteoporosis, Department of Medicine, Copenhagen University Hospital, Glostrup, Denmark, Denmark, [4]Research Centre for Prevention & Health, Denmark

Background & Purpose: Osteoporotic fracture represents a growing economical burden to society, not only caused by fractures in women, but also due to an increasing number of fractures in men.

In this cross-sectional study we aimed to investigate the association of muscular and cardio-respiratory fitness with BMD at the lumbar spine and hip in men.

Material & Methods: The association between independent variables VO_{2max}, leg power and hand grip, and dependent variables BMD at the lumbar spine and total hip, was explored in a series of linear regression models successively adjusted for age, weight and height, smoking, alcohol intake and leisure time physical activity level.

Results: In the fully adjusted model we found a significant association of VO_{2max} with BMD at the lumbar spine, $p<0.0089$. Furthermore we observed significant associations of VO_{2max} ($p<0.0022$) and leg power ($p<0.011$) with BMD at total hip.

Conclusion: We found that cardiorespiratory fitness was associated with BMD. Furthermore, hand grip strength and leg power were associated with increasing BMD at the lumbar spine and total hip, respectively. These results lend support to the mechanostat hypothesis. Further prospective studies are needed to further investigate the association between physical activity and BMD.

Disclosures: Barbara Rubek Nielsen, None.

SU0053

Loading during Growth is Associated with Radius Marrow Density and Sector-specific Cortical Properties. <u>Jodi Dowthwaite</u>*[1], <u>Tomas Cervinka</u>[2], <u>Charity Ntansah</u>[3], <u>Harri Sievanen</u>[4], <u>Tamara Scerpella</u>[5]. [1]SUNY Upstate Medical University;Syracuse University, USA, [2]Tampere University of Technology, Finland, [3]Syracuse University, USA, [4]The UKK Institute for Health Promotion Research, Finland, [5]University of Wisconsin, USA

Purpose: Pediatric loading is considered osteogenic, but marrow and sector-specific cortical properties have not been evaluated. We hypothesized that extreme pediatric loading exposure and local lean mass and muscle strength would predict 33% radius marrow and cortical properties.

Methods: DXA (whole body) and non-dominant radius pQCT (33%) scans were performed, yielding data for 125 females, age 8 to 25 yrs. Cross-sectional moments of inertia (CSMImax, CSMImin), marrow density (MaD) and sector-specific cortical properties were evaluated: density (mean (CoD), medial (CoDmed)); cross-sectional area (mean (CoA), medial (CoAmed)); thickness (mean (CoTh), medial (CoThMed)). Annual mean non-aquatic physical activity and gymnastic training (h/wk) were calculated for the year prior. GYM were defined based on annual mean training ≥6 h/wk for ≥2 years (others= NON). Tanner breast stage was self-reported. Ipsilateral grip strength (GRIP) was recorded (n= 101/125). Continuous variables were log-transformed, except GRIP. Backward stepwise regressions were run, entering Tanner Breast stage, ln age (squared), ln ulna length, ln ipsilateral arm non-bone lean mass, ln ipsilateral arm fat mass, ln total body % fat, ln annual mean physical activity (lnPAL) and GYM history; separate regressions added GRIP (n=101).

Results: Subjects ranged from pre-puberty to early adulthood (mean age 15.7yrs, sd 4.3). Dependent variables increased with age ($p<0.05$), except MaD and CoAmed (positive trends); CSMI (max and min: no relationship). GYM was a negative predictor of MaD, CoD and CoDmed, but a positive predictor of CoA, CoAmed, CSMImax and CSMImin ($p<0.05$). PAL was a negative predictor of CoA, CoAmed, CoTh, CoThmed and CSMImax, whereas arm fat mass was positively related to CoA, CoAmed, CSMImax and CSMImin ($p<0.05$). Arm lean mass was positively related to all ($p<0.05$), except MaD, CoD and CoDmed. In the GRIP subsample, GRIP, GYM, lean and fat mass were positive predictors of CoA, CoAmed, CSMImax and CSMImin ($p<0.05$); in those 4 models, PAL was a negative predictor of all but CSMImin ($p<0.05$).

Conclusions: Gymnastic exposure during growth was associated with greater bone strength and geometry, except cortical thickness; GYM was negatively associated with mean and medial cortical density. As predicted, GRIP, local lean mass and GYM history were positively associated with bone area and strength indices. In contrast, marrow density was negatively associated with GYM loading history.

Disclosures: Jodi Dowthwaite, None.

SU0054

Visceral adiposity is independently and inversely associated with bone mineral density. <u>Mark Peterson</u>*, <u>Palak Choksi</u>. University of Michigan, USA

Background

Despite ample evidence to confirm that increased visceral adipose tissue (VAT) deposition occurs with higher BMIs, the interrelationships between altered fat partitioning and regional bone quality is less understood. The purposes of this study were to examine the associations between adiposity and bone mineral density (BMD) across a large, heterogeneous cohort of adults, as well as to determine the mediating influences of age, race, sex, metabolic abnormalities, and objectively measured physical activity.

Methods

A population representative sample of 5,268 individuals, aged 20-85 years, was included from the combined 2003-2006 NHANES datasets. Body mass index, percent body fat and VAT as determined by dual energy X-ray absorptiometry (DXA), accelerometry-derived objectively measured physical activity, and markers of cardiometabolic risk were examined as potential predictors of whole body and lumbar BMD, after adjusting for sociodemographic data (i.e., age, race, sex, household income, etc.). Cardiometabolic abnormalities included elevated blood pressure, levels of triglycerides, fasting plasma glucose, C-reactive protein, home-ostasis model assessment (HOMA) of insulin resistance value, hemoglobin A1c (GHB), and low HDL-cholesterol level.

Results

Females had lower whole body ($\beta=-0.10$; $p<0.001$) and lumbar ($\beta=-0.01$; $p<0.001$) BMDs. Age was a negative predictor of whole body BMD among men ($\beta=-0.001$; $p<0.001$), and of both whole body ($\beta=-0.003$; $p<0.001$) and lumbar ($\beta=-0.002$; $p<0.001$) BMD in women. BMI was independently and positively associated with BMD at the whole body ($\beta=0.01$; $p<0.001$) and lumbar ($\beta=0.007$; $p<0.001$) levels. Conversely, after adjusting for all demographic variables and BMI, VAT was negatively associated with BMD at the whole body ($\beta=-0.03$; $p<0.001$) and lumbar ($\beta=-0.02$; $p=0.002$) levels. Moderate to vigorous physical activity (i.e., per 10 minute) was positively associated with BMD at the whole body ($\beta=0.002$; $p=0.02$), but not the lumbar level ($p=0.49$). Among women, elevated fasting glucose was inversely associated with whole body BMD ($\beta=-0.02$; $p=0.04$); yet, this became non-significant after controlling for VAT.

Conclusions

Our data demonstrate a significant negative association between VAT and BMD at the whole body and lumbar levels, even after adjustment for BMI, age, sex, and other sociodemographic predictors. Moreover, moderate to vigorous physical activity was a positive predictor of whole body BMD in both men and women.v

Disclosures: Mark Peterson, None.

SU0055

The association of pediatric fractures with serum vitamin D25 [25(OH)D] levels compared to non-fracture community controls. <u>Barbara Minkowitz</u>*[1], <u>Barbara Cerame</u>[2], <u>Eileen Poletick</u>[3], <u>Tim Leier</u>[3], <u>Sherri Luxenberg</u>[3], <u>Lior Fusman</u>[3], <u>Jonathan Chevinsky</u>[3], <u>Nicole Formoso</u>[3], <u>Renee Eng</u>[3], <u>Samantha Easton</u>[3], <u>Scott Musial</u>[3], <u>Ben Lee</u>[2]. [1]Pediatric Orthopaedics, USA, [2]Goryeb Children's Hospital, USA, [3]Morristown Medical Center, USA

Background: There is growing concern over a relationship between severity of pediatric fractures and low 25(OH)D. Goals: Compare 25(OH)D levels and lifestyle of children with fractures to controls, determine if 25(OH)D is associated with fractures and determine the 25(OH)D fragility fracture threshold.

Methods: Pediatric fracture and community control patients included. Survey and medical data used. Parameters included 25(OH)D, calcium, PTH, age, gender, fracture history, severity, location, mechanism, ethnicity, skin tone, multivitamin, diet, sunscreen, outdoors time. Analyses performed, ANOVA with Tukey HSD, Chi Square test for fractures with 25(OH)D cut-off groups: 25(OH)D <12, <20, <30, and <40 ng/ml.

Results: 379 fracture patients, 754 controls ≤ 21 years. Fracture and controls mirrored comparable 25(OH)D (27.7 ±9.3 ng/mL). Lower 25(OH)D in Hispanics (23.1 ± 7.3 ng/mL), African-American (20.76 ± 7.9 ng/mL), dark skinned (22.2 ± 8.7 ng/mL). Low 25(OH)D in "poor eater" children < 5 years (23.1 ± 9.2 ng/mL, p< .01). 25(OH)D higher with multivitamins (29.0 ± 9.3 ng/mL, p< .05), and in "healthy eater" < 5 years (30.7 ± 9.3 ng/mL). Sunscreen, outdoor time not correlated. Surgical fractures with lower 25(OH)D (24.1 ± 9.6 ng/mL, p< .001) vs. nonsurgical. Past history of fracture and mechanism not correlated to 25(OH)D. Femur fractures trended to lower 25(OH)D (Mean 24.4 ng/mL, +/- 9.5). Association 25(OH)D to fracture severity (surgical fractures) is seen. OR (odds ratio) for surgical fracture within fracture groups by 25(OH)D: <12 OR 5.3 (95% confidence Cl 1.3-22.7) p < .024, <20 OR 3.8 (95% confidence Cl 2.2-6.8) p < .001, <30 OR 2.7 (95% confidence Cl 1.5-4.6) p < .001 and <40 not significant (95% confidence Cl 0.8-4.7) p < 0.1. Not pathologic with VitD >30ng/mL.

Clinical Relevance: Occurrence of surgical pediatric fractures is associated with low 25(OH)D levels, a new target serum level of 25(OH)D of at least 30ng/mL (40ng/ml being more inclusive) was noted, which is associated with reduction in surgical severity of pediatric fractures.

Disclosures: Barbara Minkowitz, None.

SU0056

Distal one-third forearm bone mineral density of healthy young children is more highly related to lumbar spine than whole body bone mineral density. <u>Catherine Vanstone</u>[1], <u>Jonathon Maguire</u>[2], <u>Hope Weiler</u>[3], <u>Paula Lavery</u>[1], <u>Neil Brett</u>*[1]. [1]McGill University, Canada, [2]University of Toronto, Canada, [3]McGill University, USA

The recommended clinical assessment of bone density in children includes dual-energy x-ray absorptiometry (DXA) scans of lumbar spine or whole body bone mineral density (BMD). However, childhood fractures in otherwise healthy children are typically in the long bones, yet data on forearm DXA scans are limited. The objective was to examine whether distal one-third forearm BMD relates to whole body and lumbar spine BMD in healthy children (2-8 y). Participants were recruited through daycares and media advertisements in Montreal, Canada. Children with mobility problems or medical conditions affecting bone health were excluded. Body mass index Z-Scores for age (BAZ) were calculated using the WHO growth standard. Lumbar spine 1-4, distal forearm (non-dominant) and whole body BMD were acquired using DXA array mode (Hologic Discovery QDR series). All measurements were taken during winter months (January and February). Relationships among BMD values were tested using Pearson correlations for normal data and Bland Altman plots of agreement. Differences among age and sexes were tested using ANOVA; data are mean $\pm$ SD. Average age was 4.6 $\pm$ 1.9 y, BAZ 0.5 $\pm$ 0.8 kg/m^2 and > 65% had at least one Caucasian parent. Distal one-third forearm BMD was more highly related (r=0.83, p<0.0001, n=68) to lumbar spine BMD than with whole body BMD (r=0.67, p<0.001, n=63). BMD at all sites varied according to age (p<0.05), but differences among one-year increments were not significant (table). From Bland-Altman plots, the bias between BMD values from whole body and distal one-third forearm was greater (0.367; 95% CI 0.212-0.521) than it was between lumbar spine and forearm (0.178; 95% CI 0.099-0.257). This study suggests that distal one-third forearm DXA scans offer an alternative assessment of BMD that is readily attainable in healthy children. Further work is needed to establish normative values.

Age (y)	Whole body BMD*	Lumbar spine BMD*	Forearm BMD*
2	0.628 ± 0.082 (10)	0.482 ± 0.073 (12)	0.298 ± 0.050 (11)
3	0.617 ± 0.082 (10)	0.501 ± 0.073 (11)	0.316 ± 0.050 (11)
4	0.714 ± 0.094 (12)	0.528 ± 0.080 (12)	0.319 ± 0.051 (12)
5	0.718 ± 0.097 (15)	0.521 ± 0.080 (12)	0.331 ± 0.052 (12)
6	0.805 ± 0.084 (4)	0.514 ± 0.072 (4)	0.324 ± 0.050 (4)
7	0.807 ± 0.097 (15)	0.557 ± 0.076 (13)	0.349 ± 0.045 (14)
8	0.872 ± 0.084 (4)	0.571 ± 0.072 (4)	0.379 ± 0.050 (4)

*mean ± SD (n)

*no significant differences between 1 year increments

Table: BMD (g/cm2) at each site for each age category

Disclosures: Neil Brett, None.

SU0057

Effect of adiposity and trabecular bone microarchitecture on vibration transmission in the lower limb of children with spastic CP. <u>Harshvardhan Singh</u>*[1], <u>Daniel Whitney</u>[2], <u>Freeman Miller</u>[3], <u>Christopher Knight</u>[2], <u>Christopher Modlesky</u>[2]. [1]University of Delaware, USA, [2]University of Delaware, USA, [3]AI duPont Hospital for Children, USA

There is evidence that a high-frequency, low-magnitude vibration (HLV) stimulus has an anabolic effect on bone in children with cerebral palsy (CP). Whether the composition of the tissue in the lower extremities affects the transmission of HLV in children with CP is unknown. Children with spastic CP (n = 11; 4 to 11 y) with a gross motor function classification (GMFC) scale of I-III and able to stand participated in the study. Triaxial accelerometers (PCB Piezotronics Inc) were secured to the skin at the lateral condyle of the distal femur and at the medial malleolus of the distal tibia in the more affected limb. A uniaxial accelerometer was secured to the center of a plate (Juvent Inc) that was programmed to emit an HLV signal (0.3 g, 30 Hz). As the children stood on the plate, accelerations were sampled (2 kHz) at the plate, distal tibia and distal femur for 30 seconds while the plate was at rest and for 30 seconds while the plate was vibrating. Markers of trabecular bone microarchitecture [apparent trabecular bone volume to total volume (appBV/TV), trabecular number (appTb.N), trabecular thickness (appTb.Th) and trabecular separation (appTbSp)] at the distal femur and distal tibia (700 x 175 x 175 μm3) were estimated in the more affected limb using magnetic resonance imaging (1.5 T, GE). The concentration of fat in the more affected leg was estimated using dual-energy X-ray absorptiometry (Hologic Inc). Compared to the acceleration measured at the plate, the accelerations were 23 $\pm$ 9 % greater at the distal tibia and 41 $\pm$ 22 % lower at the distal femur. Distal tibia appBV/TV, appTb.Th and appTbSp were significantly related to transmission of HLV to the distal tibia (r = 0.664, 0.736 and -0.736, respectively, all p < 0.05). Markers of trabecular bone microarchitecture were not significantly related to HLV transmission to the distal femur (p > 0.25). Fat concentration in the leg was not significantly related to HLV transmission to the distal femur or the distal tibia (p > 0.4). The findings suggest that the floor-based HLV plate evaluated in this study transmits higher signal to the distal tibia but only ~60 % of the signal to the distal femur in ambulatory children with spastic CP. The degree of amplification of HLV signal at the distal tibia in children with CP is less pronounced in children with less developed trabecular bone microarchitecture. Whether this amplification of HLV signal affects the adaptation of bone to HLV requires further investigation..

Disclosures: Harshvardhan Singh, None.

SU0058

Effects of exposure to oral contraceptive use on bone mineral accrual and bone density between 12 and 30 years of age: A longitudinal study. <u>Adam Baxter-Jones</u>*[1], <u>Stefan Jackowski</u>[1], <u>Ashlee McLardy</u>[2], <u>Carol Rodgers</u>[3]. [1]University of Saskatchewan, Canada, [2]College of Kinesiology, University of Saskatchewa, Canada, [3]University of Saskatchewan, Canada

Introduction: Although genetic factors are a key determinant of bone mass accrual, hormonal levels are also documented to play a major role. Hormonal based oral contraceptives (OC) are primarily designed with the intention to regulate circulating endogenous estrogen and progesterone levels to maintain endometrial stability. However, the effects of OC use on bone mass development are controversial. The purpose of this longitudinal study was to investigate the long-term effect of OC exposure on bone mass accrual from adolescence to young adulthood.

Methods: One hundred and ten female participants were drawn from the University of Saskatchewan's Pediatric Bone Mineral Accrual Study (PBMAS) (1991-2011). Height, weight, body composition, maturation (years from peak height velocity (PHV - biological age [BA]), diet, physical activity (PA) and OC use were measured annually between 12 and 30 years of age. DXA measures included total body (TB), lumbar spine (LS), femoral neck (FN) bone mineral content (BMC) and areal bone mineral density (aBMD). Site specific multilevel models were constructed for both BMC and aBMD development controlling for BA, size, body composition, PA and OC exposure.

Results: A significant negative independent OC use by biological age interaction (-4.94 $\pm$ 2.41 g, p<0.05) was found in the model of TB BMC but not TB aBMD (p>0.05). For the LS, significant BA by OC use interactions were observed for BMC (-0.29 $\pm$ 0.11 g, p<0.05) and aBMD (-3.07 $\pm$ 1.09 g/cm2, p<0.05). At the FN, no significant BA by OC use interactions were observed for either BMC or aBMD (p>0.05).

Conclusions: The effects of exposure to OC were site and age specific. When exposed to OC during the period 5 years post PHV, TB and LS BMC increased. However, from 6 years post PHV, TB and LS BMC decreased with increasing age. FN BMC showed no OC use effects. Only LS aBMD increased prior to 5 years post PHV in OC users and decreased thereafter. These results indicate that OC may be beneficial if taken within five years of obtaining PHV but thereafter may have negative effects on bone accrual and bone density.

Disclosures: Adam Baxter-Jones, None.

SU0059

Is adolescent body composition development associated with bone structural strength at the proximal femur in males at 50 years of age?. <u>Stefan Jackowski</u>*[1], <u>Donald Bailey</u>[1], <u>Joey Eisenmann</u>[2], <u>Lauren Sherar</u>[3], <u>Adam Baxter-Jones</u>[1]. [1]University of Saskatchewan, Canada, [2]Michigan State University, USA, [3]Loughborough University, United Kingdom

Purpose: Although, body composition (fat and fat-free mass) is documented to influence skeletal strength throughout life, the potential role of fat mass accrual on bone structural strength remains controversial. Additionally, there is a paucity of information regarding the associations between adolescent body composition development and mid-adulthood bone structural strength. Therefore, the purpose of this study was to investigate whether adult bone structural strength at the proximal femur at 50 years of age was associated with the development of adolescent fat and fat-free mass.

Methods: Two hundred and seven males aged 7-17 years from the Saskatchewan Growth and Development Study (SGDS) had annual skinfolds measurements from 1964-1973. The sum of 5 skinfolds were used to estimate adolescent percent body fat (%BF) and percent fat free mass (%FFM). In adulthood (52.0 $\pm$ 0.5 years) 37 male participants were reassessed and hip bone strength measures which included cross sectional area (CSA) and section modulus (Z) at the narrow neck (NN) and femoral shaft (S) were determined using hip structural analysis (HSA). Adult bone strength measures were ranked and used to categorize individuals into low and high bone strength groupings. Multilevel models were constructed to examine the independent development of %FFM and %FM between adult bone strength groups.

Results: When age and body size were controlled, males with greater SZ in adulthood had developed significantly greater %BF during adolescence (1.65 $\pm$ 0.70 %, p<0.05). No significant differences in adolescent %FFM development were observed for NNCSA, NN Z and S CSA bone strength groupings (p>0.05).Conclusions: Males with greater bending strength at the femoral shaft in adulthood had significantly higher trajectories of fat mass development relative to overall body weight during adolescence. This suggests that the development of relative fat mass in adolescence may be associated with greater bending strength at the proximal femur in mid-adulthood. Further investigations are warranted to confirm the impact of adolescent body composition on adult bone structural strength.

Disclosures: Stefan Jackowski, None.

SU0060

Risk of vitaminD insuficiency and inadequate bone mineral status in newcomer immigrant and refugee children in Canada, data from Healthy Immigrant Children study. <u>Hassanali Vatanparast</u>*[1], <u>Virginia Lane</u>[2]. [1]University of Saskatchewan, Canada, [2]University of Saskatchewan, Canada

Nutrition and physical activity are two main important factors influencing bone mineral mass accumulation during childhood and adolescence. Newcomer immigrant/refugee children are at a high risk of poor nutritional status. Vitamin D deficiency, in particular, and its related diseases is a major concern due to minimal sun exposure in countries in high latitude and limited dietary sources. Using Healthy Immigrant Children (HIC) pilot data (n=72), we previously reported vitamin D and bone mineral status of sample of newcomer children. No large scale study is available in Canada to evaluate the relationship between nutrition, physical activity and bone mineral status on newcomer immigrant and refugee children. Objective: to evaluate the association between nutrition, physical activity and bone mineral status in immigrant and refugee newcomer children to Canada. Methods: In a cross-sectional design, we recruited 299 immigrant (n=133) and refugee (n=166) children aged 3-13 years who had been living in Saskatoon and Regina, Canada for no more than five years. Measurements included serum 25OHD using LC-MS/MS method, total body bone mineral content (TBBMC) using DXA, dietary assessment using three 24-h recalls, physical activity and USDA food security questionnaires. Results: The mean age of children was 8.0 ± 2.8 y. The rate of childhood food insecurity was 18.8% and 32.3% in immigrants and refugees respectively. Most children (83.7%) were meeting the recommended level of physical activity ($\geq$60 minutes/day). Over 40% of children had the TBBMC lower than the predicted optimal values for their age, sex and ethnicity. We found 63.7% of participants had inadequate levels of serum vitamin D (<50nmol/L) for bone health. Prevalence of inadequacy in vitamin D intake was 92%. In stepwise regression analyses, after controlling for all potential covariates; height and serum vitamin D status were found to be determinants of TBBMC (R^2=0.82, p<0.001). Children who were taller and had significantly greater serum vitamin D also had greater TBBMC with β=0.93 for height and β=0.12 for serum vitamin D. In accordance with HIC pilot data, a considerably high rate of vitamin D deficiency and insufficiency in newcomer immigrant and refugee children and its association with bone mineral mass during this important stage of life requires immediate preventive interventions to minimize the risk of serious vitamin D related diseases.

Disclosures: Hassanali Vatanparast, None.

SU0061

Associations between Vitamin D Status, Undercarboxylated Osteocalcin, and Glucose Metabolism in American Children. <u>Kelly Giudici</u>*[1], <u>Berdine Martin</u>[2], <u>Emma Laing</u>[3], <u>George McCabe</u>[4], <u>Linda McCabe</u>[5], <u>Dorothy Hausman</u>[6], <u>Ligia Martini</u>[7], <u>Richard Lewis</u>[3], <u>Connie Weaver</u>[2], <u>Munro Peacock</u>[8], <u>Kathleen Hill Gallant</u>[2]. [1]Department of Nutrition, School of Public Health, University of São Paulo, Brazil, [2]Purdue University, USA, [3]The University of Georgia, USA, [4]Department of Statistics, College of Science, Purdue University, USA, [5]Department of Nutrition Science, College of Health & Human Sciences, Purdue University, USA, [6]Department of Foods & Nutrition, University of Georgia, USA, [7]University of São Paulo, Brazil, [8]Indiana University Medical Center, USA

Objective: We have previously reported a lack of relationship between total OC and insulin resistance in American children. However, there are suggestions in the literature that it may be undercarboxylated OC (ucOC) that is related to insulin resistance. The purpose of this study was to investigate the relationships among serum 25 hydroxyvitamin D [25(OH)D], ucOC, and insulin resistance in American children. Methods: This cross-sectional analysis included baseline data from 318 children who participated in a randomized controlled trial of vitamin D supplementation. Relationships among fasting serum 25(OH)D, HOMA-IR (insulin resistance), and ucOC were analyzed. Results: The prevalence of vitamin D deficiency and insufficiency was <1% and 14%, respectively, by IOM definitions, and 43.1% of participants were overweight/obese based on BMI-for-age percentiles. Serum 25(OH)D was positively associated with ucOC (r = 0.46, p < 0.0001), and this relationship persisted after adjusting for fat mass. However, a preliminary analysis of prospective data from a subset of subjects who were supplemented with 4000 IU/d vitamin D3 for 12 weeks and subjects who were given placebo for 12 weeks did not show an effect of increasing serum 25(OH)D on serum ucOC [12 week Δ25(OH)D = +132 $\pm$ 16 ng/mL with 4000 IU/d and -24 $\pm$ 8 ng/mL with placebo]. Additionally, while there was a weak negative relationship between serum 25(OH)D and HOMA-IR (r=-0.267 p<0.0001), there was no relationship between ucOC and HOMA-IR. Conclusions: This cross-sectional analysis agrees with some previous reports of associations between vitamin D status, bone, and energy metabolism. 25(OH)D was negatively associated with insulin resistance and positively associated with ucOC. However, the absence of association between ucOC and insulin resistance suggests that ucOC does not link vitamin D status, bone, and energy metabolism. Additionally, while there was a moderately strong cross-sectional association at baseline between serum 25(OH)D and ucOC, our preliminary prospective data analysis of the effect of increasing serum 25(OH)D on change in serum ucOC suggests that this is not a causal relationship.

Disclosures: Kelly Giudici, None.

SU0062

Effects of 2 years on treatment with Zoledronic acid given every 6 months on bone mineral density, bone turnover and skeletal architecture in children with secondary osteoporosis. <u>Craig Munns</u>*[1], <u>Craig Coorey</u>[2], <u>Julie Briody</u>[1], <u>Andrew Biggin</u>[2]. [1]The Children's Hospital at Westmead, Australia, [2]The Children's Hospital at Westmead, Australia

Background/Aims: Intravenous bisphosphonates are administered increasingly for treatment of childhood osteoporosis. Zoledronic acid (ZA) has potential advantages over pamidronate with a shorter infusion time and longer duration of action.

We aimed to evaluate the safety and efficacy of twenty-four months of ZA administered every six months to children with osteoporosis.

Methods: Retrospective cohort study of 28 patients (17 male, 11 female) with secondary osteoporosis treated with zoledronic acid (0.05mg/kg/dose) every six months for minimum of 24 months. Nineteen patients were immobile, 3 steroid induced osteoporosis, 3 idiopathic osteoporosis, 1 coeliac disease, 1 Girault syndrome and 1 neurofibromatosis type 1. Thirteen patients had vertebral fractures alone (vertebral wedging fractures defined as >20% reduction in anterior-posterior ratio), 9 had nonvertebral fractures alone and 6 had both vertebral and nonvertebral fractures. Mineral homeostasis, bone mineral density (BMD) via DXA and pQCT and vertebral shape were evaluated at baseline and 24 months. We compared these data to that of a similar cohort treated with zoledronic acid 0.025mg/kg every three months.

Results: Median age at start of treatment was 11.6 years (range 8.8-14.0). Following the first infusion, 2 developed asymptomatic hypocalcemia, 14 developed temperature >38℃, 13 aches/pain and 6 nausea. At 24 months, there was reduced bone turnover and improvement in BMD (DXA and pQCT) and vertebral shape. One patient fractured after starting ZA. Growth was normal. There was a significantly greater increase in lumbar spine BMD in those children who received 3 monthly zoledronic acid compared to 6 monthly zoledronic acid.

Conclusion: ZA administered six monthly was associated with acute phase reaction to the first dose and improvement in BMD, reduction in bone turnover and improved vertebral shape at 24 months. The 3 monthly zoledronic acid regimen resulted in a greater increase in BMD.

Disclosures: Craig Munns, Novartis, 7

SU0063

Osteocyte-mediated parathyroid hormone signaling restrains the long-term hematopoietic stem cell pool in the bone marrow. <u>Benjamin Frisch</u>*[1], <u>Alexandra Goodman</u>[2], <u>Olga Bromberg</u>[2], <u>Xiaolin Tu</u>[3], <u>Teresita Bellido</u>[3], <u>Laura Calvi</u>[4]. [1]University of Rochester School of Medicine & Dentistry, USA, [2]University of Rochester School of Medicine & Dentistry, USA, [3]Indiana University School of Medicine, USA, [4]University of Rochester School of Medicine, USA

The microenvironment, including osteocytes, is known to play a critical role in the regulation of hematopoiesis and hematopoietic stem cells (HSCs). Pharmacologic treatment with parathyroid hormone, PTH (1-34) increases HSCs in mice through microenvironmental signals, as HSCs do not express the PTH receptor (PTH1R). However, to date there is no evidence of a physiologic role for PTH in HSC regulation. To study the physiologic role of osteocyte-mediated PTH signaling to HSCs we utilized cre recombinase driven by the 8kb-DMP1 promoter and conditionally deleted PTH1R in osteocytes (OCy-PTH1Rko mice). There was no significant difference in PTH levels in OCy-PTH1Rko and WT mice. In 5-week-old OCy-PTH1Rko mice there was a significant decrease in long-term HSCs measured by flow cytometric analysis (.0029 $\pm$ 0..00028 vs. .0021 $\pm$ .00021 % of cells, WT vs. OCy-PTH1Rko p≤0.05 N≥19 mice/group). Confirming the phenotypic changes, OCy-PTH1Rko mice had a loss of long-term engraftment capacity, demonstrated by 12 weeks post-transplant myeloid cell engraftment was 10 fold lower than in WT littermate controls (32.68 $\pm$ 6.10 vs. 3.65 $\pm$ 1.02 % donor derived, WT vs. OCy-PTH1Rko donors p≤0.05 N≥3 mice/group). In contrast, short-term engraftment 4 weeks post-transplant was increased in OCy-PTH1Rko mice compared to WT littermate controls (10.81 $\pm$ 0.8904 vs. 25.13 $\pm$ 4.415 % donor derived, WT vs. OCy-PTH1Rko donors p≤0.01 N=9 mice/group) suggesting a shift from long to short-term HSC potential. The difference in engraftment was multilineage suggesting HSCs as the source. Five-month-old adult mice were also analyzed. At this age, OCy-PTH1Rko mice had decreased phenotypic multipotent progenitors (MPPs) compared to WT littermate controls measured by flow cytometric analysis (0.10 $\pm$ 0.01 vs. 0.07 $\pm$ 0.01 % of cells, WT vs. OCy-PTH1Rko donors p≤0.05 N≥19 mice/group). Despite this decrease, like the 5-week-old mice, at 5 months of age OCy-PTH1Rko mice showed an increase in levels of short-term engraftment 4 weeks post transplant (4.939 $\pm$ 1.367 vs. 14.34 $\pm$ 1.884 % donor derived, WT vs. OCy-PTH1Rko donors p≤0.001 N=10 mice/group). The difference in early engraftment was observed in both myeloid and lymphoid lineages, and was lost by 12 weeks post transplant. Our findings demonstrate a physiologic role of PTH signaling through osteocytes in the restraint of HSCs, indicating that osteocytes contribute to maintenance of the long-term repopulating pool.

Disclosures: Benjamin Frisch, None.

SU0064

Fibronectin from the Osteoblastic Niche Modulates Myelopoiesis and the Response to Cancer. Sabrina Kraft*[1], Carla Sens[1], Anja von Au[1], Inaam Nakchbandi[2]. [1]University of Heidelberg & Max-Planck Institute of Biochemistry, Germany, [2]Max-Planck Institute of Biochemistry & University of Heidelberg, Germany

Fibronectin (FN) is a matrix protein that stimulates osteoblast (Ob) differentiation and can bind to immune cells. The aim of this work is to characterize the role of osteoblast fibronectin in hematopoiesis.

Fibronectin was conditionally deleted in osteoblasts (cKO: colα1(I)-cre FN$^{fl/fl}$). In the bone marrow (BM) of cKO the precursors to myeloid cells (GMPs) were increased by 43% and the myeloid CD11b+ cells decreased by 53% (p<0.05). Culturing CT Ob with CT or cKO BM induced a comparable increase in the percentage of CD11b+ cells, while cKO Ob failed to induce an increase. Osteoblasts produce an isoform of fibronectin called EDA. Purified EDA, but not plasma-FN increased the percentage of CD11b+ cells *in vitro*. Thus EDA supports CD11b+ differentiation.

CD11b+ cells define a population called myeloid-derived suppressor cells (MDSCs) that inhibit the immune response to cancer. Induced subcutaneous B16 melanoma lesions were smaller in cKO (by 73%, p<0.05). Injection of MDA-MB-231B/luc+ in the tibia of T-cell deficient mice similarly resulted in hampered early tumor growth (68%, p<0.05). To establish a causal relationship between decreased CD11b+ in cKO and suppression of cancer growth we isolated CD11b+ cells from cKO and CT BM. Injection of equal numbers of these cells together with B16 cells subcutaneously in CT animals resulted in smaller lesions when CD11b+ cells from cKO animals were used. This suggests that CD11b+ cells already underwent epigenetic changes in the absence of EDA during their development. In line with this, isolated CD11b+ cells from cKO tumors showed a cytokine expression profile consistent with an immune active environment compared to cells originating from CT tumors (e.g. IFNγ increased 2x, p<0.05). Finally, in order to establish that EDA normalizes the response of CD11b+ cells, CT and cKO BM was depleted from CD11b+ cells and treated with EDA or plasma-FN for 24 hours. Developing CD11b+ cells were isolated, mixed with B16 and injected in CT mice. CD11b+ from cKO animals that were differentiated *ex vivo* in the presence of EDA normalized their response towards the tumor. Thus EDA exposure during early differentiation of myeloid cells affects their behavior.

In summary, EDA fibronectin originating from the osteoblasts controls the differentiation of myeloid cells in the bone marrow and affect their later response towards cancer. Our data also suggest the presence of myeloid cells that affect cancer growth without interacting with T-cells.

Disclosures: Sabrina Kraft, None.

SU0065

High plasma osteocalcin associates with low blood Hb and anemia in elderly men; The MrOS Sweden Study. Catharina Lewerin*[1], Helena Johansson[2], Ulf Lerner[3], Magnus Karlsson[4], Mattias Lorentzon[5], Elizabeth Barrett-Connor[6], Ulf Smith[7], Claes Ohlsson[8], Dan Mellstrom[9]. [1]Västra Götaland, Sweden, [2]Center for Bone & Arthritis Research, Sweden, [3]Sahlgrenska Univesity Hospital, Sweden, [4]Skåne University Hospital Malmö, Lund University, Sweden, [5]Geriatric Medicine, Center for Bone Research at the Sahlgrenska Academy, Sweden, [6]University of California, San Diego, USA, [7]Department of Molecular & Clinical Medicine, Sahlgrenska Academy, Sweden, [8]Center for Bone & Arthritis Research at the Sahlgrenska Academy, Sweden, [9]Sahlgrenska University Hospital, Sweden

Purpose

Osteoblasts have been suggested to be involved in the regulation and proliferation of hematopoetic stem cells. Blood hemoglobin (Hb) declines with age in healthy elderly men but the reason for this is not fully understood. Osteocalcin has previously been demonstrated to be associated with diabetes and blood glucose. The association between Hb and serum osteocalcin is unknown. Our aim was to determine whether serum osteocalcin is associated with anemia or low Hb in elderly men.

Methods

Men without diabetes participating in the Gothenburg part of the (cross-sectional), population-based MrOS (Osteoporotic Fractures in Men) Sweden cohort were included in the present study (n=821, median age 75.3 years, age range 69-81 years). Osteocalcin was evaluated in relation to Hb before and after adjustments for potential covariates (i.e. age, body mass index (BMI), erythropoietin (EPO), total estradiol, fasting insulin, adiponectin and cystatin C).

Results

Hb (r=-0.12, p<0.001), but not osteocalcin decreased with age. Hb correlated (age adjusted) negatively with osteocalcin (r=-0.18, p<0.0001). After adjusting for age, men with higher osteocalcin levels were more likely to have Hb in the lowest quartile of values (OR per SD decrease in osteocalcin = 1.35 (95% CI 1.15-1.59) and this was still significant after further adjustment for BMI, fasting insulin, EPO, and estradiol [OR per SD decrease in osteocalcin = 1.21 (95% CI 1.01-1.44)]. There was a negative linear trend (age adjusted) between quartiles of Hb and osteocalcin (p<0.001). Anemic men (age adjusted) (47/812) (Hb<130 g/L) had significantly higher mean osteocalcin than non anemic men (33.9 µg/L vs. 27.1 µg/L, p<0.001). In multiple stepwise linear regression analyses (adjusted for age, EPO, estradiol, fasting insulin,

BMI, cystatin C, and adiponectin) osteocalcin was an independent predictor of Hb (p<0.05).

Conclusion

We present novel data showing that high osteocalcin is associated with low Hb and anemia in non-diabetic subjects. This association was unaffected by adjustment for age, BMI, EPO, estradiol, fasting insulin, cystatin C, and adiponectin. However, causality between osteocalcin and Hb cannot be assumed due to the cross-sectional design of the study.

*Disclosures: Catharina Lewerin, None.*

SU0066

Simultaneous Measurement of Changes in Bone Remodeling and Microvasculature in Response to Estrogen Deficiency-Induced Bone Loss and Intermittent PTH-Induced Bone Gain. Wei-Ju Tseng*[1], Chantal De Bakker[1], Tiao Lin[1], Wei Tong[2], Haoruo Jia[3], L. Scott Levin[4], Ling Qin[1], Xiaowei Liu[1]. [1]University of Pennsylvania, USA, [2]Perelman school of medicine, USA, [3]University of Pennsylvania, USA, [4]Hospital of the University of Pennsylvania, USA

The bone remodeling process works in conjunction with the microvascular network within bone marrow to regulate calcium and phosphate homeostasis. Because of their drastic effects on bone remodeling, it is likely that both ovariectomy (OVX) and intermittent parathyroid hormone (iPTH) treatment will also affect bone vasculature. However, simultaneous visualization of the effect of bone remodeling in the trabecular and vascular microstructures remains challenging. The objective was to investigate the changes in bone remodeling and microvasculature in response to estrogen deficiency-induced bone loss and iPTH-induced bone gain in rat tibiae.

6 intact and 9 OVX female SD rats (12-wk old) were purchased. Starting at 14-wk old, 3 intact rats (PTH group) received iPTH daily for 2 weeks (60&micro;g/kg/day). At wk 15 and 16, 2 sequential scans of the proximal tibia were performed by *in vivo* µCT (Scanco, 10.5 µm) for 3 groups of rats: OVX (n=9), PTH (n=3), and control (CON, n=3). After the wk16 scan, rats were perfused with Microfil (MV122), a radiopaque contrast agent, to form a vascular cast inside bone. The tibiae were then harvested, fixed and scanned at 6-µm pre- and post- decalcification followed by a novel registration procedure to distinguish vessels from bone (Fig 1 Top). Finally, bone resorption and formation were identified and measured based on the sequential *in vivo* µCT scans (Fig 1 Bottom).

After 4-wk osteopenia development, OVX rats had 74% lower bone volume fraction (BV/TV, p<0.05), 80% lower trabecular number (Tb.N, p<0.05), 360% higher trabecular spacing (Tb.Sp, p<0.05) compared to the CON group; vessel volume fraction (Ves.V/TV) was 30% lower (p<0.05) than that of the CON group. After 2-wk iPTH treatment, Tb.Th and Ves.Th were 12% and 30% greater (p<0.05) than the CON group, respectively. µCT-based *in vivo* bone dynamic histomorphometry indicates that bone resorption rate was highly elevated after OVX (942%, p<0.05); bone formation rate increased 266% after iPTH treatment (p<0.05) compared to the CON group. The resorption and formation map with vessels (Fig 1) provides a platform for our future analysis between vessels and bone formation/resorption.

This study establishes a novel technique that simultaneously visualizes the 3D microstructures of bone and microvasculature using standard µCT. Combined with measures of bone formation and resorption, this may help improve our understanding of the effects of OVX and iPTH on the bone-blood vessel function unit.
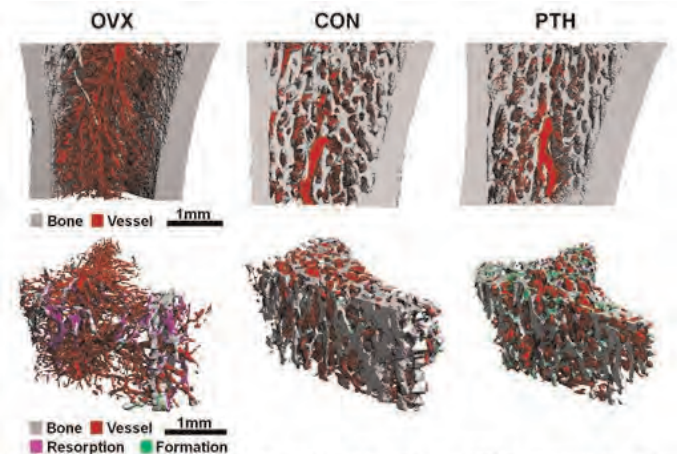
Fig 1. (Top) 3D representative bone and blood vessel images of the proximal tibia of OVX, control, and PTH groups. (Bottom) The 3D trabecular bone and blood vessel images with bone formation and resorption labeled in green and purple, respectively.

Fig 1

Disclosures: Wei-Ju Tseng, None.

SU0067

The Effect of Phosphate Deficiency on Callus Composition. Amira Hussein*[1], Kyle Lybrand[2], Anthony De Giacomo[2], Kamolnat Tabattanon[3], Brenna Hogue[2], Chantal De Bakker[4], Marie Demay[5], Elise Morgan[6], Louis Gerstenfeld[1]. [1]Boston University School of Medicine, USA, [2]Boston University School of Medicine, USA, [3]Boston University, USA, [4]Boston University, USA, [5]Massachusetts General Hospital & Harvard Medical School, USA, [6]Boston University, USA

Introduction: Fracture healing is a complex sequence that requires coordinated development of cartilage and bone, as well as tissue mineralization, to regain mechanical competence. Failure of these processes results in impaired healing. Phosphate is essential for bone growth and fracture repair; normal fracture healing is impaired in phosphate-deficient animals. This study's goal was to assess the effects of phosphate deficiency on cartilage development, cartilage resorption, and tissue mineralization.

Methods: Closed, stabilized fractures were generated in the right femora of C57BL/6J (B6) male mice. Phosphate deficiency was initiated in the diet two days prior to fracture and was maintained for 5 (5DR) or 20 (20DR) days post-fracture. Phosphate was then replenished and bone healing was allowed to continue until 14 or 21 days post-fracture. Control mice were provided with normal diet throughout the study. Cartilage volume was quantified with contrast-enhanced computed tomography using a cationic contrast agent. Cartilage volume, mineralized tissue volume, and tissue mineral density (TMD) were quantified.

Results: Phosphate deficiency impaired healing and resulted in lack of callus bridging for the longer period of diet restriction. The 20DR calluses had higher cartilage content, lower mineralized tissue volume and lower TMD than control calluses (p<0.021). The properties of the 5DR calluses were intermediate to those of the control and 20DR calluses. At 14 days post-fracture, the 5DR calluses had similar cartilage volume and TMD (p>0.693), but lower mineralized tissue volume than control calluses (p<0.001), and greater mineralized tissue volume compared to the 20DR calluses (p<0.005). At 21 days post fracture, the cartilage volume in the 5DR calluses was not different from that of the controls or 20DR (p>0.113). Further, the 5DR calluses had lower mineralized tissue volume and TMD than control calluses (p<0.001), and greater TMD than 20DR calluses (p<0.001).

Discussion: Phosphate restriction had an inhibitory effect on bone healing by impairing cartilage development and callus mineralization. More severe effects were seen with a longer duration of restriction. These results further showed that while cartilage tissues formed and resorbed, subsequent mineralization and bone replacement were progressively inhibited. The data suggest that long dietary restriction of phosphate can be used as a model of nutritionally induced delayed union.

Figure 1. For control and phosphate deficient (PI) calluses at 14 and 21 days post-fracture: (A) Representative 3-D rendering showing pre-existing bone (white) mineralized tissue (yellow), and cartilage (red); (B) Cartilage volume, mineralized tissue volume and tissue mineral density (*: p<0.05)
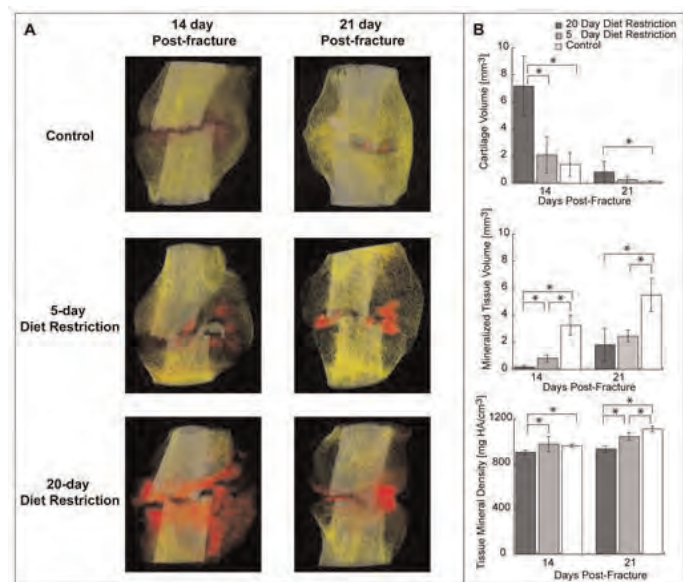

Figure 1

SU0068

Engineering an Ex Vivo Analogue of Bone Tissue for Studies of Bone Metastasis. Eliza Fong*[1], Xinqiao Jia[2], Antonios Mikos[3], Daniel Harrington[3], Mary Farach-Carson[4]. [1]BioScience Research Collaborative, USA, [2]University of Delaware, USA, [3]Rice University, USA, [4]Rice University, USA

Elucidating the survival and growth mechanisms used by metastatic tumors in the bone/bone marrow microenvironment is key to the discovery of novel therapeutics specifically targeting bone metastasis. Currently, the study of cell-cell and cell-extracellular matrix (ECM) interactions that influence cancer cell adaptation and growth in bone is hampered by a lack of physiologically relevant ex vivo preclinical models. Hyaluronan (HA) is a major component of bone marrow ECM, and hydrogels made from HA reflect the low modulus of the tissue. Having previously demonstrated the ability of HA hydrogels to support the three-dimensional growth of bone metastatic prostate cancer cells, we next sought to modify the HA matrix further via the incorporation of other ECM moieties to enable the culture of bone marrow stromal cells (BMSC) or osteoblasts (OB) – critical cell types in the bone metastatic microenvironment. Given that hyaluronan-only hydrogels lack integrin-binding ECM motifs needed for the survival of mesenchymal cells, the cell binding domain present in many adhesive proteins such as osteopontin and fibronectin, GRGDS, was selected to confer adhesive properties to the hydrogel. Additionally, the matrix metalloproteinase 2 and 9 – sensitive peptide, PQGIWGQ, was chosen so that the resulting hydrogel matrix could be remodeled by cells expressing these proteases. Using thiolated HA, we conjugated acrylated GRGDS as pendant motifs, and crosslinked the HA chains using acrylated PQGIWGQ. By modulating the concentration of GRGDS and PQGIWGQ peptides, conditions that optimized the 3-dimensional spreading and growth of human bone marrow stromal cells and murine osteoblast-like cells within the hydrogels were identified. Figure 1 shows the ability of the modified hydrogels to support extensive spreading of MC 3T3 murine osteoblast-like cells encapsulated within. Additionally, this system is suitable for 3D co-cultures of bone metastatic cancer cells with bone resident cells. This engineered 3D system provides a suitable tool to study bone metastasis in a physiologically relevant, controlled, biomimetic system, overcoming many limitations of current models.
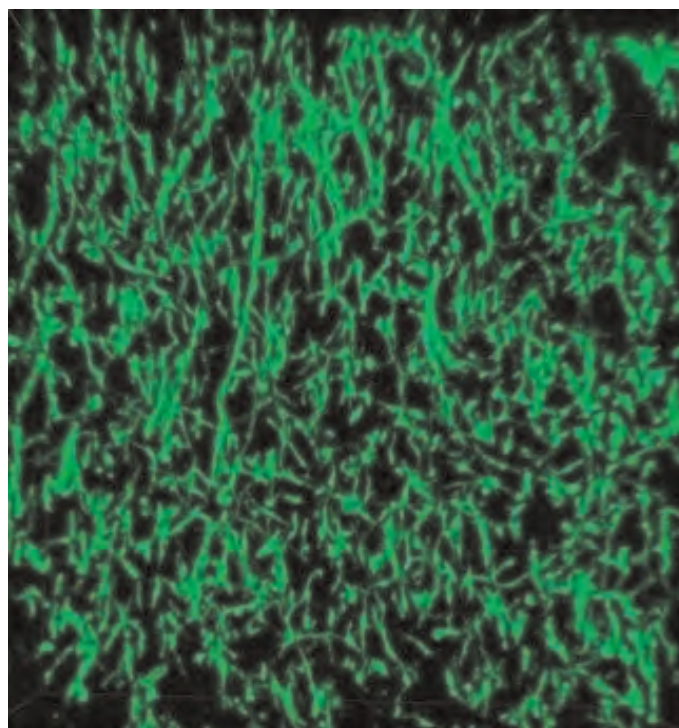

Figure 1. Volumetric rendering (~0.7 mm thickness) of hydrogel-encapsulated MC 3T3 cells

SU0069

Withdrawn

SU0070

The Bone Microenvironment Modulates ERα Positive Mammary Cancer Cells Favoring Estrogen Independent Skeletal Metastasis. Aude-Helene Capietto*[1], Szeman Ruby Chan[2], Julie Allen[2], Robert Schreiber[2], Roberta Faccio[3]. [1]Washington University School of Medicine, USA, [2]Washington University School of Medicine, USA, [3]Washington University in St Louis School of Medicine, USA

Human breast tumors expressing the estrogen receptor-α (ERα) often develop osteolytic bone metastases. Despite successful therapeutic options for ERα+ breast cancer, resistance to endocrine therapy frequently occurs and leads to tumor recurrence at skeletal locations even in patients treated with anti-resorptive therapies. To further understand how the bone microenvironment modulates ERα+ breast cancer cells towards estrogen-independency, we generated a clinically relevant mouse model of bone metastasis. ERα+ SSM2 and SSM3 cell lines are derived from spontaneous mammary tumors in STAT1-/- mice. Both cell lines developed luminal mammary tumors when injected in the mammary fat pads of WT129S6 female mice and their growth is completely prevented by estrogen deprivation. When injected intratibially (i.t.), SSM2 and SSM3 cells developed lytic bone metastases within 30 days, as visualized by X-Rays, microCT and histology. Furthermore, if inoculated in the arterial system, SSM2 tumor cells showed high bone tropism, in particular to spine (60%), and developed lytic bone lesions by 56 days. The goal of endocrine therapies, including ovariectomy (OVX), is to deprive tumor cells of estrogen thus inhibiting their growth. To determine if ERα+ SSM cells could grow in bone independent of estrogen, cells were injected i.t. in sham-operated or OVX mice. Similarly to the orthotopic location, SSM3 tumor cells are sensitive to estrogen deprivation and fail to grow in OVX mice. Surprisingly, SSM2 cells develop osteolytic bone lesions within 2 months in 6/6 OVX mice indistinguishable to sham-operated controls. Because OVX induces bone loss through osteoclast activation, we injected SSM cells into male mice. Similarly to OVX, SSM3 cells did not grow in males, while 100% of males injected with SSM2 cells displayed osteolytic lesions. To gain more insights into the ability of SSM2 cells to become estrogen resistant once they reach the bone, we compared by gene array the genetic profile of SSM2 and SSM3 cells from in vitro cultures. Surprisingly, we found no differences in expression of genes modulating bone cell activation between the two lines. In conclusion our data highlight the crucial role of the bone environment in modulating permissive tumor cell growth and acquisition of estrogen insensitivity. Future inquiries at understanding mechanisms of hormonal resistance of ERα+ SSM2 cells may help define new therapeutic targets for breast cancer patients with skeletal metastases.

Disclosures: Aude-Helene CAPIETTO, None.

SU0071

The role of Insulin-like growth factor-I and Focal adhesion kinase in angiogenesis of tumor induced bone metastasis. Naito Kurio*[1], Tsuyoshi Shimo[2], Hiromasa Kuroda[3], Kenichi Matsumoto[3], Tatsuo Okui[3], Akira Sasaki[4]. [1]Japan, Japan, [2]Okayama University Graduate School of Medicine, Dentistry & Medical Sci, Japan, [3]Okayama university, Japan, [4]Okayama University, Japan

Introduction: Insulin-like growth factors (IGFs), which are the most abundant growth factors stored in bone, have been involved in progression of many types of cancers. Recently we have reported thata novel dual inhibitor for Focal adhesion kinase (FAK) Tyr^{397} and IGF-IR, TAE226, inhibited breast cancer bone metastasis in vivo. However, the relationship between FAK Tyr^{397} and IGF-1 in angiogenesis of tumor bone microenvironment has not been revealed yet. Using both *in vivo* and *in vitro* approaches, we investigated how FAK Tyr^{397} and IGF-1 is involved in tumor progression in bone metastasis site.

Methods: A mouse model of bone metastasis was prepared by inoculating mice with tumor cell suspensions of breast cancer cell line MDA-MB-231 cells via the left cardiac ventricle. Oral administration of TAE226 was carried out at a dose of 30 mg/kg every day. A cell cycle was analyzed by flow cytometry. The expression of IGF-I and FAK related signals were confirmed by Western blot analysis. To evaluate the effects of IGF-I *in vitro*, proliferation, migration, and angiogenesis assays were performed.

Results: Oral administration of TAE226 in mice significantly decreased bone metastasis and CD31 positive endothelial cells in bone metastasis site. When the endothelial cells were exposed of 1uM of TAE226, the number of cells in sub-G_1 population increased to about 18% in flow cytometric analysis. Treatment of TAE226 increased TUNEL positive cells within 48h compared with control. IGF-I upregulated pFAK Tyr^{397} activity, and stimulated proliferation, migration and tube formation of endothelial cells *in vitro*, and these effects were inhibited in the presence of IGF-1R inhibitor.

Conclusion: IGF-I was critically involved in breast cancer progression in bone metastasis site through pFAK Tyr^{397} activation in endothelial cells.

Disclosures: Naito Kurio, None.

SU0072

Cell-to-Cell Crosstalk Between Multiple Myeloma Cells and Osteocytes Activates Notch Signaling and Triggers Osteocyte Apoptosis. Jesus Delgado-Calle*[1], Judith Anderson[2], Lilian Plotkin[1], G. David Roodman[3], Teresita Bellido[1]. [1]Indiana University School of Medicine, USA, [2]Indiana University, USA, [3]Indiana University, USA

Multiple myeloma (MM) is a malignancy characterized by accumulation of monoclonal plasma cells in the bone marrow, which grow in bone and weaken the skeleton. Hallmarks of MM bone disease are exacerbated resorption, reduced formation, and increased osteocyte apoptosis. Osteocytes regulate bone remodeling but their contribution to cancer in bone is unclear. We report that co-culture of murine osteocytic MLO-A5 cells with human JJN3 MM cells activated Notch signaling in MLO-A5 cells, with increased expression of the Notch target genes Hes/Hey1. This effect was suppressed by the Notch inhibitor GSIXX and did not occur when the MM and MLO-A5 cells were not in direct cell-to-cell contact. Similar activation of Notch signaling in osteocytic cells was induced by interaction of MLO-A5 or Y4 osteocytic cells with murine 5TGM1 MM cells or human MM.1S cells. Further, co-culture of JJN3 MM cells with MLO-A5 cells increased the percent of apoptotic MLO-A5 cells, which was inhibited by the caspase inhibitor DEVD. Importantly, human CD138+ MM cells purified from marrow aspirates from MM patients also induced MLO-A5 osteocytic cell apoptosis. MM-induced apoptosis of MLO-A5 osteocytic cells in co-culture was as early as 8h and increased for up to 48h. Interestingly, inhibition of Notch signaling with GSIXX blocked MM-induced osteocyte apoptosis at 8-24h but not at 48h. Further, culture of MLO-A5 cells on plates coated with the Notch Delta ligand 1 fused to IgG2 increased the percentage of dead cells compared to cells cultured on IgG2 control, and the effect was inhibited by GSIXX. Overexpression of the Notch intracellular domains 1 or 2 known to be sufficient to activate Notch signaling also increased MLO-A5 cell apoptosis. In contrast, MM-derived conditioned medium (MM-CM) only induced apoptosis in MLO-A5 cells at 24 and 48h but not at 8h, and GSIXX did not prevent osteocyte apoptosis induced by MM-CM. These results demonstrate that 1) cell-to-cell crosstalk between MM and osteocytes induces osteocyte apoptosis, 2) MM-induced osteocyte apoptosis is triggered by activation of Notch signaling through direct cell-cell contact and maintained by MM-derived soluble factors, and 3) Notch activation per se is sufficient to trigger osteocyte apoptosis. Together with evidence presented in a separate abstract demonstrating MM-induced changes in osteocytic gene expression, these findings suggest a critical role of osteocytes in the initiation and development of MM bone disease.

Disclosures: Jesus Delgado-Calle, None.

SU0073

Diagnostic microRNA Biomarkers Differentiate Benign Ostblastoma and Malignant Osteosarcoma. Scott Riester*[1], Amel Dudakovic[1], Eric Lewallen[2], Jorge Torres-Morra[2], Emily Camilleri[2], Peter Rose[2], Michael Yaszemski[3], Franklin Sim[2], Thomas Shives[2], Sanjeev Kakar[2], Andre Van Wijnen[1]. [1]Mayo Clinic, USA, [2]Mayo Clinic, USA, [3]Mayo Clinic College of Medicine, USA

The purpose of this investigation is to identify novel microRNA biomarkers that can reliably distinguish between osteoblastoma and osteosarcoma. Osteoblastoma is a benign primary bone tumor that is histologically very similar to malignant osteosarcoma. It is clinically difficult to distinguish between these two tumors using current techniques and misdiagnosis is common resulting in unacceptable clinical outcomes for patients.In this investigation next generation RNA sequencing was used to evaluate microRNAs expressed in fresh frozen and formalin fixed paraffin embedded (FFPE) tumor samples. RNA sequencing analysis included four fresh and four FFPE osteosarcoma samples, and two fresh frozen and five FFPE osteoblastoma specimens. A subset of microRNAs that showed differential expression in both the fresh frozen and formalin fixed paraffin embedded tumor specimens were selected for validation using TaqMan qPCR assays. In total, six microRNAs showed a statistically significant difference in expression between osteosarcoma and osteoblastoma by both RNA sequencing and qPCR. Two microRNAs showed higher expression in osteosarcoma, while four had higher expression in osteoblastoma. One of the FFPE samples examined in this study was from a case where an osteosarcoma was misdiagnosed as an osteoblastoma. These six microRNA biomarkers were able to correctly identify the FFPE tumor sample as an osteosarcoma demonstrating the potential clinical utility of these markers. MicroRNAs show differential expressed between osteoblastoma and osteosarcoma in both fresh frozen and formalin fixed paraffin embedded tumor samples by both RNA-sequencing and qPCR analysis. These differentially expressed microRNAs have the ability to clinically differentiate benign and malignant tumors which are frequently misdiagnosed in clinical practice. MicroRNA biomarkers are highly promising for the evaluation of bone tumors and have the potential to improve clinical outcomes for patients.

Disclosures: Scott Riester, None.

SU0074

NELL-1 expression in benign and malignant bone tumors and correlation with malignant potential. Jia Shen[1], Kevork Khadarian[2], Greg Asatrian[2], Xinli Zhang[1], Sarah Dry[2], Kang Ting[1], Chia Soo[2], Aaron James*[1]. [1]University of California, Los Angeles, USA, [2]UCLA, USA

NELL-1 is a secreted osteoinductive protein that binds Integrinβ1 to activate Wnt/β-catenin signaling. Recent interest has grown in using recombinant NELL-1 as both a local or systemic agent to induce bone formation. However, the expression and role of NELL-1 in benign and malignant bone tumors is entirely unknown. Our purpose was to examine the expression patterns of NELL-1 in a comprehensive analysis of bone-forming skeletal tumors, accompanied by an examination of the effects of NELL-1 in osteosarcoma (OS) cells.

First, the expression of NELL-1 was assessed across a diverse set of human bone-forming skeletal tumors by immunohistochemistry. This included benign tumors (osteoid osteoma, osteoblastoma) and malignant tumors (osteosarcoma and its variants, including osteoblastic OS, chondroblastic OS, fibroblastic OS, periosteal OS, parosteal OS, telangiectatic OS). Semi-quantitation was performed to describe the distribution and intensity of immunostaining. Next, the Saos-2 OS cell line was treated with NELL-1, and the effects on osteogenic differentiation were assessed via standard methods.

Results showed that NELL-1 was expressed to some degree in all types of bone-forming tumors (Fig. 1). Diffuse, intense staining for NELL-1 was observed in all benign bone tumors, and was localized to bone-lining osteoblasts, osteocytes and bone matrix (Table 1). A relative loss of NELL-1 expression was observed in osteosarcoma specimens, with predominant weak, patchy NELL-1 immunostaining. Among OS subtypes, fibroblastic OS demonstrated the highest NELL-1 immunostaining. *In vitro*, NELL-1 significantly induced the osteogenic differentiation of Saos-2 OS cells by all markers examined (*$p<0.01$).In summary, NELL-1 is an osteoinductive protein that is widely expressed in both benign and malignant bone-forming skeletal tumors. NELL-1 is diffusely and robustly expressed in benign tumors, and its expression is much reduced in malignant bone tumors. NELL-1 induces osteodifferentiation of OS cells, and may represent a novel approach to induce the differentiation of sarcoma stem cells in combination with traditional chemotherapeutic regimens. Future areas of investigation include the specificity of NELL-1 in bone-forming tumors, and the *in vivo* effects of NELL-1 on osteosarcoma disease progression.
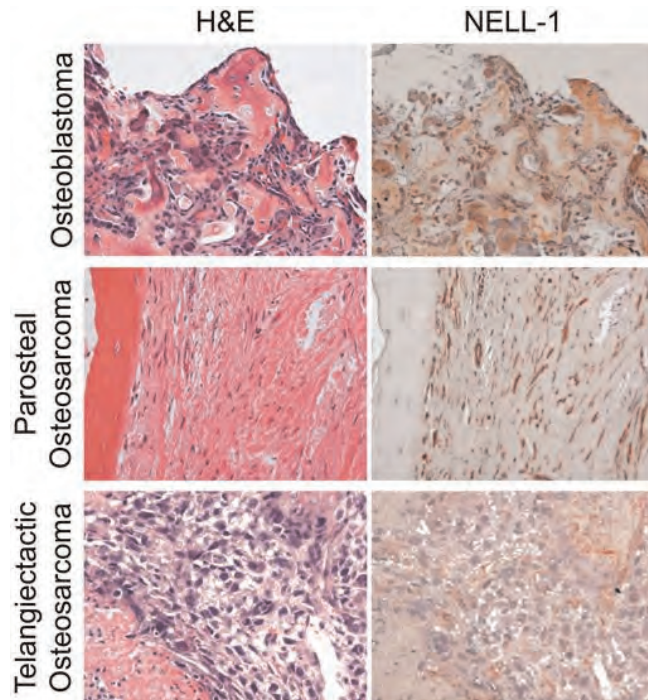

Figure 1

	Staining Intensity (fraction of cases)				Staining Distribution
	0	1+	2+	3+	% of cells stained
Osteoid Osteoma	---	---	---	5/5	76%
Osteoblastoma	---	---	2/5	3/5	71%
Fibroblastic OS	1/6	---	3/6	2/6	52%
Chrondoblastic OS	2/4	---	2/4	---	25%
Osteoblastic OS	2/4	1/4	1/4	---	18%
Parosteal OS	---	2/6	4/6	---	26%
Telangiectactic OS	---	2/3	---	1/3	18%

Table 1

Disclosures: Aaron James, None.

SU0075

Serum Dickkopf-1 is a prognostic marker in prostate cancer. Tilman Rachner*[1], Stefanie Thiele[2], Andy Göbel[2], Susanne Füssel[2], Martina Rauner[3], Lorenz Hofbauer[4]. [1]University Hospital Dresden, Germany, [2]University Hospital Dresden, Germany, [3]Medical Faculty of the TU Dresden, Germany, [4]Dresden University Medical Center, Germany

Prostate cancer is the most prevalent malignancy in men and up to 80% of affected patients develop skeletal metastases in the course of their disease. Dickkopf-1 (DKK-1) is a secreted Wnt inhibitor that has been associated with the pathogenesis of bone lesions in multiple myeloma by impairing Wnt promoted osteoblast differentiation and activity. There is emerging evidence to suggest that DKK-1 also affects the biology of prostate cancer. However, detailed knowledge regarding the contribution of DKK-1 to prostate cancer biology remains elusive.

We determined the DKK-1 tissue expression in prostate cancer using a prostate cancer tissue microarray (n=400) by IHC and DKK-1 serum levels in 80 patients with prostate cancer. DKK-1 expression in prostate cancer tissue was significantly increased (p<0.0001) compared to BPH, with no differences between different tumor stages. Increased DKK-1 expression was also observed in healthy tissue adjacent to the tumor, with no apparent difference between the mean DKK-1 expression of malignant and adjacent normal cells. There was no correlation between Gleason score, PSA values, the presence of lymph node metastases, age and DKK-1 tissue expression. Furthermore, there was no correlation between tumor DKK-1 (high vs. low) and patient overall or disease specific survival.

Detectable DKK-1 serum levels were found in 76/80 prostate cancer patients. Patients were divided into two groups according to their DKK-1 serum levels. Mean DKK-1 serum levels of all patients were 33.9 ± 10.7 pmol/l. Patients with the higher 50% of DKK-1 levels (38.4 ± 7.2 pmol/l) were found to have a significantly lower overall (p=0.015) and disease specific survival (p=0.031) than those with low DKK-1 levels (16.2 ± 7.5 pmol/l). Univariate Cox regression analyses revealed significant associations between survival and T stage, lymph node involvement, Gleason score and DKK-1. There was no association for age and PSA. An additional stepwise multivariate Cox proportional hazard analyses revealed that high DKK-1 serum levels were independently associated with a poor survival (p= 0.007; HR 3.73; 95%CI 1.44-9.66).

In summary, these observations suggest that serum DKK-1 may serve as a prognostic marker in prostate cancer.

Disclosures: Tilman Rachner, Novartis, 7

SU0076

The protein tyrosine phosphatase Rptpz suppresses osteosarcoma development in Trp53-heterozygous mice. Christina Baldauf*[1], Anke Jeschke[2], Vincent Kanbach[2], Philip Catala-Lehnen[2], Peter Nollau[3], Michael Amling[4], Sheila Harroch[5], Thorsten Schinke[6]. [1]University of Hamburg, Germany, [2]Department of Osteology & Biomechanics, University Medical Center Hamburg Eppendorf, Germany, [3]Department of Clinical Chemistry, University Medical Center Hamburg Eppendorf, Hamburg, Germany, [4]University Medical Center Hamburg-Eppendorf, Germany, [5]Department of Neuroscience, Institute Pasteur, France, [6]Department of Osteology & BiomechanicsUniversity Medical Center Hamburg Eppe, Germany

Osteosarcoma (OS), an aggressive tumor derived from osteoblasts, belongs to the most common types of cancer in growing children. Since specific molecular targets for OS treatment remain to be identified, surgical excision combined with radiation and/or chemotherapy is still the only way to help affected individuals. We have previously identified the protein tyrosine phosphatase Rptpz as a marker of terminally differentiated osteoblasts, which negatively regulates their proliferation *in vitro*. Here we have addressed the question if Rptpz can function as a tumor suppressor protein inhibiting OS development *in vivo*. We therefore analyzed the skeletal phenotype of mice lacking *Ptprz1*, the gene encoding Rptpz, on a tumor-prone genetic background, i.e. *Trp53*-deficiency or *Trp53*-heterozygosity. Since we failed to detect any type of bony tumors in 12 weeks old mice lacking both, *Ptprz1* and *Trp53*, we screened a large number of 52 weeks old *Trp53*-heterozygous mice (n ≥ 20 for each genotype) by contact radiography. In this context *Ptprz1*-deficiency significantly enhanced OS development with 25 % of the mice being affected, whereas *Trp53*-heterozygous littermates carrying two functional *Ptprz1* alleles did not display obvious skeletal abnormalities. The tumors in *Ptprz1*-deficient *Trp53*-heterozygous mice were present in various locations (spine, long bones, ribs), and their OS nature was confirmed by undecalcified histology. Likewise, cell lines derived from the tumors were able to undergo osteogenic differentiation *ex vivo*. An initial comparison between *Ptprz1*-heterozygous and *Ptprz1*-deficient cultures further revealed that the latter ones displayed increased proliferation together with a higher abundance of tyrosine-phosphorylated proteins. These findings underscore the relevance of Rptpz as an attenuator of proliferation in differentiated osteoblasts and raise the possibility that activating Rptpz-dependent signaling could specifically target osteoblastic tumor cells.

Disclosures: Christina Baldauf, None.

SU0077

Effects of PGE2 receptor EP4 antagonist on breast cancer-induced bone metastasis and bone destruction in the metastasis region. <u>Kenta Watanabe</u>[1], <u>Chiho Matsumoto</u>[2], <u>Michiko Hirata</u>[3], <u>Takayuki Maruyama</u>[4], <u>Masaki Inada</u>[2], <u>Chisato Miyaura</u>*[2]. [1]Tokyo University of Agriculture & Technology, Japan, [2]Tokyo University of Agriculture & Technology, Japan, [3]Tokyo University of Agriculture & Technology, Japan, [4]Ono Pharmaceutical Co., Ltd, Japan

Prostaglandin E2 (PGE2) is a lipid mediator, and associated with local bone destruction with inflammation. We have reported that PGE2-induced bone destruction was mediated by increased RANKL expression in osteoblasts, and that EP4 is the most effective PGE2 receptor rather than the other EP subtypes (EP1, EP2 and EP3) in bone tissues. In bone metastasis of breast cancer, however, the functional role of EP4 is still unclear. In this study, we examined the effects of EP4 antagonist in case of *in vivo* administration on the model of breast cancer bone metastasis. When the cloned breast cancer cells with luciferase expression (4T1-Luc) were inoculated into mouse tail vein, the cells metastasized to the distal femur with severe bone destruction that was detected by both imaging of bioluminescence and soft X-ray. In tibial inoculation model of 4T1-Luc cells, the oral administration of EP4 antagonist clearly protected 4T1-induced bone destruction in both cancellous and cortical bone. To examine the further mechanism of 4T1-induced bone resorption, we invented the experimental system to evaluate the effects of cell-to-cell interaction. When bone marrow cells were co-cultured with osteoblasts on the fixated cancer cell layer, we detected numerous osteoclast formation, and the treatment of EP4 antagonist completely inhibited the osteoclast formation. In calvarial organ cultures with 4T1 cells, the number of osteoclasts and following bone resorption were elevated, and the resorbing trail was clearly detected on the surface of calvaria by 3D-micro CT analysis. The 4T1-induced osteoclastic bone resorption in calvarial organ culture was attenuated by the treatment of EP4 antagonist. These results suggest that the EP4-mediated signaling induces RANKL expression in osteoblasts that leads osteoclast differentiation and following osteolysis. EP4 antagonist is a possible candidate for the therapy of breast cancer with bone metastases.

Disclosures: Chisato Miyaura, None.

SU0078

Heparanase elicits a bone resident cell-like phenotype in multiple myeloma cells and promotes myeloma bone metastasis. <u>Timothy Trotter</u>*[1], <u>Haiyan Chen</u>[1], <u>Patrick Rowan</u>[2], <u>Qianying Pan</u>[2], <u>Mei Li</u>[2], <u>Larry Suva</u>[3], <u>Amjad Javed</u>[1], <u>Yang Yang</u>[4]. [1]University of Alabama at Birmingham, USA, [2]University of Alabama at Birmingham, USA, [3]University of Arkansas for Medical Sciences, USA, [4]The University of Alabama At Birmingham, USA

Multiple myeloma (MM) is a plasma cell malignancy that thrives in the bone marrow microenvironment and frequently metastasizes between bones. Heparanase (HPSE), an endo-β-D-glucuronidase that cleaves heparan sulfate chains on proteoglycans, is upregulated in MM. Indeed, MM cells expressing high levels of HPSE exhibit a significantly higher rate of bone metastasis. We hypothesized that this enhanced MM colonization of bone is related to bone marrow specific changes in the phenotype of MM cells. To test this idea, we transfected CAG MM cells that have low endogenous levels of HPSE with empty vector (HPSE-low) or with human HPSE cDNA (HPSE-high) and evaluated the expression levels of a series of bone markers in these cells. Western blots demonstrated increased expression of both the osteoblast marker Runx2 and the osteoclast marker RANK in HPSE-high cells compared to HPSE-low cells. In addition, using ELISA we detected higher levels of bone stroma growth factors VEGF and HGF in conditioned media of HPSE-high compared to HPSE-low cells. Similarly, HPSE-high cells secreted significantly higher levels of RANKL, MMP-9, osteocalcin, and DKK-1 – all of which are associated with the character and function of bone cells. We then investigated the consequences of Runx2 upregulation in HPSE-high cells by performing ChIP assays and found Runx2 occupancy of the promoters of both MMP-9 and RANKL genes was significantly increased in HPSE-high cells compared to HPSE-low cells. This directly implicates Runx2 as a mediator of HPSE induced changes in MM cell phenotype. Finally, immunohistochemical staining of HPSE-low and HPSE-high tumors harvested from *in vivo* models of myeloma revealed significantly higher expression of RANK, RANKL, Runx2, MMP-9, Osteocalcin, VEGF, HGF and DKK-1 in the HPSE-high tumors. Interestingly, this enhanced expression by HPSE-high tumors was observed at both primary and metastatic sites. These data demonstrate that the expression of HPSE induces a bone resident cell-like phenotype in MM cells. Such a change provides MM cells with the ability to avoid immune surveillance in the bone marrow, thereby facilitating tumor survival and growth in the bone (such as seen with HPSE-high cell tumors). Importantly, our data also suggest that MM cells expressing high levels of HPSE gain the ability to directly regulate the functions of osteoblasts (DKK-1), osteoclasts (RANKL), and stromal cells (HGF, VEGF), further supporting myeloma progression.

Disclosures: Timothy Trotter, None.

SU0079

Osteocytes' Response to Mechanical Loading Supports Breast Cancer Cell Growth and Migration. <u>Yu-Heng Ma</u>*[1], <u>Lidan You</u>[2]. [1]University of Toronto, Canada, [2]Mechanical & Industrial Engineering, University of Toronto, Canada

Bone metastases are common and severe complications of cancers. It is estimated that 69% of patients died from breast cancer have developed bone metastases [1]. Cancer cells have such devastating impact on bones due to their ability to alter bone remodeling [2]. Exercise, often used as an intervention for patients suffering from breast cancer [3], regulates bone remodeling. Yet, information on the relationship between bone metastases and mechanical loadings is limited. Since osteocytes are mechanosensors of the bone that signals to reduce bone resorption in response to mechanical loading, this study focuses on the effect of this response on bone metastasis development. To achieve this, MLO-Y4 osteocyte-like cells were subjected to oscillatory fluid flow (1Pa 1Hz for 2 hours) and media from flow experiments were extracted (conditioned medium; CM). Controls were MC3T3 osteoblasts and glass slides with no cells. Migration of MDA-MB-231 breast cancer cells towards the CM was assayed with Transwell assay. Viability of MDA-MB-231 cells in the CM was measured with trypan blue, apoptosis with APOPercentage, and proliferation with CyQuant. It was observed that significantly more MDA-MB-231 cells migrated towards the CM from MLO-Y4 cells with exposure to flow in comparison to CM from MLO-Y4 cells not exposed to flow (figure 1). MDA-MB-231 cells apoptosis rate was significantly lower in CM from MLO-Y4 cells exposed to flow (figure 2). The current data (not reported) showed no difference in MDA-MB-231 cells viability and proliferation rate between any two groups. Overall, this study suggests that osteocytes subjected to mechanical loading can promote metastases. This gives insight on the potential effects of exercises on patients suffering from cancers. Further investigation on the mechanisms (figure 3) may provide potential targets for bone metastases.

[1] Coleman et al. 1987. Br. J. Cancer. 55(1): 61-66.
[2] Chen et al. 2010. Breast Cancer Res. 12(6): 215.
[3] McNeely et al. 2006. CMAJ. 175 (1): 34–41.

Figure 1. Breast cancer cell migration towards condicioned medium

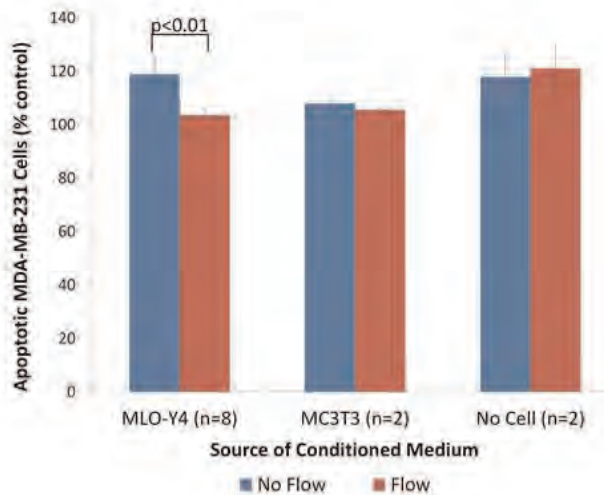## Figure 2. Breast cancer cell apoptois in conditioned medium

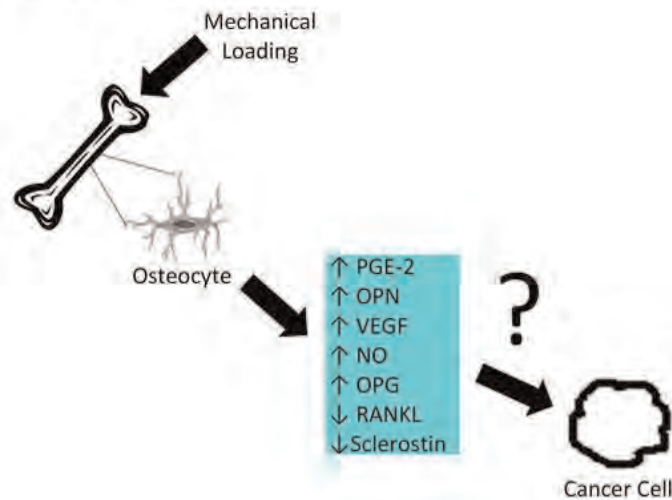Figure 2. Breast cancer cell apoptosis in conditioned medium

Figure 3. Potential mechanism

Figure 3. Potential mechanism

Disclosures: Yu-Heng Ma, None.

SU0080

Molecular Mechanisms of Bone Invasion by Oral Squamous Cell Carcinoma (OSCC). Jingjing Quan*[1], Nigel Morrison[2], Newell Johnson[3], Jin Gao[4]. [1]Guanghua Dental Hospital of Sun Yat-sen University, Peoples Republic of China, [2]Griffith University, Gold Coast Campus, Australia, [3]Griffith Univeristy, Australia, [4]James Cook University, Australia

Invasion of bone is a common complication of OSCC. This three-part study, aims to investigate signalling pathways involved in the crosstalk between OSCC cells, osteoblasts and osteoclasts. Firstly, conditioned medium (CM) was collected from OSCC cells (SCC15 and SCC25), and from osteoblasts of hFOB, then used for indirect co-culture: OSCC cells were treated with CM from osteoblasts and vice versa. Zymogenic activities of both MMP-2 and -9 were increased in OSCC cells following culture with CM from hFOB. The RANKL/OPG ratio, zymogen and protein expression of MMP-9 were increased in hFOB cultured with CM from OSCC cells. All targeted molecules were validated in clinical samples. Secondly, to determine which component of CM caused gene expression changes, OSCC cells of SCC25, HN5, and Tca8113 were artificially induced to display epithelial-mesenchymal transition (EMT) by adding 5 ng/mL of TGF-β to culture media for 1-3 days. Minimal immunochemical staining of VIM was found in SCC25 and HN5, while Tca8113 cells were strongly stained. In all cells assessed by real-time PCR, expressions of EMT markers Twist1 and N-cad were up-regulated; Snail1 and E-cad down-regulated. For osteoclast-related molecules, both MT1-MMP and RANKL were up-

regulated while OPG down-regulated. CM of OSCC cells pre-treated with TGF-β could prolong the survival of mature osteoclasts up to 4 days. Thirdly, strong staining of MCP-1 protein was observed in OSCC cells and osteoclasts from clinical samples. SCC25 cells were found to have the highest expression of MCP-1 mRNA. A plasmid with the inhibitor of MCP-1 (7ND) was transfected into SCC25 cells, and stabilized SCC25 cells with 0.6 μg of 7ND vector (SCC25-7ND) were generated. 10% CM of SCC25-7ND cells efficiently inhibited the formation of human osteoclasts, comparing with 10% CM of SCC25 cells. Additionally, OSCC cells were injected onto the surface of calvariae of nude mice to establish an animal model of bone invasion. Well-differentiated SCC was formed in both groups of SCC25 and SCC25-7ND cell injections, with tumour cells invading bone, osteoclasts locating in typical resorption lacunae. TRAP staining indicated significantly fewer osteoclasts were found in calvariae with cells of SCC25-7ND in comparison to cells of SCC25. These studies prove that crosstalk between different types of cell appears to exist in invasion of bone by OSCC. Understanding, and ultimately interfering with these pathways, may provide therapeutic approaches.

Disclosures: Jingjing Quan, None.

SU0081

PTHrP Abrogates CARP-1 Functional Mimetics (CFMs) Induced Growth Inhibition of Differentiated Osteoblasts. Sahiti Chukkapalli[1], Arun Rishi[2], Nabanita Datta*[3]. [1]Wayne State University School of Medicine, USA, [2]Wayne State University, USA, [3]Wayne State University School of Medicine, USA

The effectiveness of chemotherapeutic agents often limits their use due to negative effects on normal cells. Therefore development of new anti-cancer agents that have superior efficacy and minimal toxicity is warranted. Cell cycle and apoptosis regulatory protein (CARP)-1 (aka CCAR1) is a novel regulator of signaling by diverse agents including cell growth and differentiation factors, and chemotherapy-dependent apoptosis. CARP-1 functional mimetics (CFMs)-4 and -5 were previously shown to inhibit growth of human breast cancer (HBC) cells. In HBC, the over-production of parathyroid hormone-related peptide (PTHrP) and the bone forming osteoblasts play a critical role in facilitating colonization of metastatic cancer cells to bone. Our recent in vitro and in vivo studies revealed that CARP-1 was present in osteoblasts. PTHrP regulated CARP-1 expression in primary osteoblasts and in cultured MC3T3-E1 clone-4 (MC-4) cells. In this study we investigated the effects and mechanism of CFM-4 and -5 on growth and differentiation of MC-4 cells and the role of PTHrP in this process. Performing MTT assays our studies showed that the inhibitory effects of CFMs were dependent on the maturation stage of the MC-4 osteoblasts. While the growth of immature MC-4 cells was unaltered, CFMs suppressed growth of mature differentiated MC-4 cells. PTHrP (100 nM) abrogated MC-4 growth inhibition caused by 4 μM dose of CFM-4 and CFM-5 up to 98% and 75% respectively. Western blot analyses revealed that induction of CARP-1 protein by CFM-4 (60%) and -5 (35%) was partially attenuated by PTHrP. Importantly, while CARP-1 increase by CFM-4 or -5 correlated with activated caspase-3, PTHrP remarkably blocked caspase-3 activation (>50%). CFMs down-regulated (80-90%) cyclin D1 protein expression and was unaffected with PTHrP treatment. Together, CFM-4 and -5 induced G1-phase growth arrest as well as osteoblast apoptosis. We propose that PTHrP interferes with apoptosis signaling by CFMs in part by diminishing CARP-1 expression and caspase-3 inactivation. On the other hand PTHrP maintains G1-phase arrest of mature osteoblasts that permits continued extracellular matrix production. Thus elucidation of CARP-1 mediated osteoblast growth and differentiation mechanisms in the presence of CFMs and PTHrP will have a positive impact not only in the treatment of HBC but also in variety of other cancers which adversely affect bone.

Disclosures: Nabanita Datta, None.

SU0082

The Mevalonate Pathway Inhibitors Atorvastatin and Zoledronic Acid Exhibit Synergistic Anti-Tumor Effects in Bone-Seeking Human Tumor Cells. Andy Goebel*[1], Stefanie Thiele[2], Andrew Browne[2], Martina Rauner[3], Lorenz Hofbauer[4], Tilman Rachner[5]. [1]University Hospital Carl Gustav Carus, Germany, [2]Division of Endocrinology, Diabetes & Metabolic Bone Diseases, Germany, [3]Medical Faculty of the TU Dresden, Germany, [4]Dresden University Medical Center, Germany, [5]University Hospital Dresden, Germany

Bone metastases are a frequent complication of breast and prostate cancer as well as melanoma. Aminobisphosphonates inhibit osteoclast function and are an established therapy for skeletal metastases. Similar to statins, they block the mevalonate pathway which is important for posttranslational protein modifications. Direct anti-tumor effects of amino-bisphosphonates have been described in preclinical models of bone metastases. However, concentrations required often exceeded those achievable in the clinical setting. Here, we report on the anti-tumor potential of a combined treatment with atorvastatin (ATO) and zoledronic acid (ZOL) in human bone-seeking cancer cell lines.

We treated MDA-MB-231 (breast), MDA-435s (melanoma) and PC3 (prostate) cell lines with ATO and ZOL, respectively. The combination of 10 μM ZOL and 1 μM

ATO induced at least a two-fold increase of caspases 3 & 7 activation and a decrease of vitality by 50% after 48 h, whereas no significant effects were observed with individual treatments. The apoptotic effect was further underlined by the induction of caspase 3 and poly ADP ribose polymerase (PARP) cleavage and a significant reduction of the anti-apoptotic genes *BCL-2* and *SVV* by 50%. The observed anti-cancer effects could be reversed by geranylgeranyl-pyrophosphate, but not by farnesyl-pyrophosphate highlighting that inhibited geranylgeranylation mediates the induction of apoptosis. As small Rho GTPases (RhoA, Rac1, and CDC42) need to be geranylated for being anchored in the cell membrane to exert their function, we assumed an inactivation by the ATO and ZOL treatment. Surprisingly, a concomitant treatment with a Rho/Rac/CDC42 activator which increases the levels of GTP-bound forms of the Rho GTPases led to an even higher induction of apoptosis. In accordance with this, a pull down assay revealed an accumulation of the GTP-bound forms of the Rho GTPases RhoA, Rac1 and CDC42 upon combined treatment with ATO and ZOL. Furthermore, this effect was accompanied by an increased phosphorylation of NFκB which points to a possible mechanism of the apoptosis induction by blocking the mevalonate pathway. In line, a pre-treatment with inhibitors of Rac1, CDC42 and NFκB partially rescued the anti-cancer effects elicited by ATO and ZOL.

Our results indicate the mevalonate pathway as a potential therapeutic target for the treatment of human cancer-induced bone metastases and warrant further research by using appropriate animal models.

Disclosures: Andy Goebel, None.

SU0083

The Pain Mediator NGF is Induced by Multiple Myeloma *in vivo*, and Relieved by Therapeutic Activation of Adiponectin Signalling. <u>Sam Olechnowicz</u>*[1], <u>Megan Weivoda</u>[2], <u>Seint Lwin</u>[3], <u>James Edwards</u>[4], <u>Claire Edwards</u>[3]. [1]University of Oxford, GBR, [2]Mayo Clinic, USA, [3]University of Oxford, United Kingdom, [4]University of Oxford, United Kingdom

Multiple myeloma (MM) is a plasma cell neoplasm characterised by osteolytic bone disease. Bone pain is the most common symptom of MM at diagnosis, yet the molecular mechanisms responsible are poorly characterised. Adiponectin (Adpn) is an adipokine expressed by adipocytes and osteoblasts that is protective against MM *in vivo*. Adpn has also been shown to negatively correlate with bone pain and the major pain mediator, Nerve Growth Factor (NGF), in osteoarthritis. We sought to determine the mechanism of NGF-regulation in MM, and the potential for Adpn-targeted therapies to reduce MM bone pain *in vivo*. We combined the 5TGM1 murine model of MM with activation of the endogenous Adpn pathway by an ApoAI-mimetic peptide, L-4F. Adpn signalling in osteoblasts was disrupted by molecular inhibition of Adpn receptors 1 and/or 2. KaLwRij or *Rag2*^{-/-} mice were inoculated with 5TGM1 MM cells. In both strains, the resultant increase in tumour burden after 4 weeks was associated with a significant increase in serum NGF (KaLwRij: *p*<0.001; *Rag2*^{-/-}: *p*<0.01) as compared to baseline levels. Treatment of 5TGM1MM-bearing mice with L-4F, or existing therapeutics bortezomib or melphalan, resulted in an increase in serum Adpn in response to L-4F (*p*<0.01) and a similar reduction in tumour burden in response to all three treatments (L-4F; 36%, bortezomib; 34%, melphalan; 36%, *p*<0.01). Notably, only treatment with L-4F induced a significant 2-fold reduction in serum NGF (*p*<0.01). 5TGM1 MM cells did not express NGF mRNA, but high levels of NGF transcript were detected in osteoblasts and bone marrow stromal cells *in vitro*. Mimicking the *in vivo* findings, coculture of 2T3 osteoblasts with MM cells induced a significant 1.8-fold increase in NGF transcription from osteoblasts. Adpn inhibited an LPS-induced increase in NGF, while MM-derived cytokines such as TNFα induced a 3-fold increase in NGF expression in osteoblasts (*p*<0.05). Blockade of Adpn signalling by Adpn receptor 1 or 2 siRNA resulted in a significant 2-fold increase in NGF, which was further increased in combination with recombinant TNFα. Our results demonstrate that NGF is increased in MM *in vivo*, with osteoblastic NGF regulated by MM cells, TNFα and Adpn signalling. MM-induced NGF expression by osteoblasts is likely to be a cause of nerve dysregulation and bone pain. Adpn-based therapies may provide an improvement over traditional drugs by not only reducing tumour burden and bone disease, but also acting to reduce bone pain.

Disclosures: Sam Olechnowicz, None.

SU0084

***In Vitro* Effects of Strontium on the Proliferation Process of Human Articular Chondrocytes.** <u>Cecilia Romagnoli</u>*[1], <u>Roberto Zonefrati</u>[2], <u>Carmelo Mavilia</u>[2], <u>Anna Maria Carossino</u>[2], <u>Annalisa Tanini</u>[3], <u>Maria Luisa Brandi</u>[4]. [1]University of Florence, Italy, [2]University of Florence, Italy, [3]University of Florence, Italy, [4]DIRETTORE MALATTIE DEL METABOLISMO MINERALE E OSSEOAZIENDA OSPEDALIERA UNIVERS, Italy

Purpose: Articular cartilage defects are characterized by the lack of spontaneous resolution because of the limited regenerative capacity of adult articular chondrocytes. Based on previous studies showing that Strontium (Sr^{2+}) modulates proliferation in some cell types, it could be hypothesized that this ion is also effective on human articular chondrocytes. Therefore, aim of this study was to investigate whether different concentrations of Sr^{2+} affect the proliferation process in primary culture of human articular chondrocytes.

Methods: Slices of articular cartilage were harvested from a patient undergoing to a knee arthroplasty, after an informed consent approved by the Local Ethical Committee. Cartilage specimens were minced and digested at 37℃ in 0.3 mg/ml collagenase type I in F12 nutrient mixture, overnight. Cell aggregates were mechanically dispersed, washed, resuspended in growth medium (Ham's F12 Coon's modification medium) with 10% FBS and 1% antibiotics and cultured at 37℃ and 5% CO_2. After verification of the expression of cartilage-specific genes (COL Type II, Aggrecan, Biglycan, COL Type X) in qPCR and the collagen type II protein in immunocytochemistry, expanded monolayers of human articular chondrocytes, at passages 2 and 3, were used in the experiments. The proliferation was evaluated in presence of scalar concentrations of $SrCl_2$ from 0.1 to 5 mM in growth medium containing 1% FBS by cell counting at 24-48-72 hours. Statistical analysis was performed by linearity test and parallelism test of the linear regressions of the obtained growth curves, using Student's t-test.

Results: Characterization of human articular chondrocytes was confirmed by the presence of cartilage-specific genes and the collagen type II protein. Cells proliferation analysis has shown that Sr^{2+} significantly increases chondrocyte proliferation at concentrations 1 mM (p<0.025) and, in particular, at 3 mM (p<0.005) with respect to the control group without Sr^{2+}, while no significant results were obtained using lower (0.1-0.5 mM) or the highest (5 mM) concentrations.

Conclusion: The present results have shown that articular chondrocytes at early passages can be used as models for *in vitro* studies in the field of cell therapy. Moreover, our results suggest that Sr^{2+} has the capacity to stimulate cell growth, opening future application in cartilage repair. Studies are in progress to evaluate the effect of Sr^{2+} on COL type II gene expression and cartilage matrix formation.

Disclosures: Cecilia Romagnoli, None.
This study received funding from: I.F.B.Stroder srl

SU0085

A potential role for TGFβ-RII/MCP-5/ PTHrP axis in post-traumatic osteoarthritis. <u>Lara Longobardi</u>*[1], <u>Nunzia D'Onofrio</u>[2], <u>Tieshi Li</u>[1], <u>Joseph Temple</u>[3], <u>Huseyin Ozkan</u>[4], <u>Alessandra Esposito</u>[3], <u>Helen Willcockson</u>[5], <u>Timothy Myers</u>[5], <u>Ping Ye</u>[1], <u>Billie Moats-Staats</u>[6], <u>Lidia Tagliafierro</u>[3], <u>Marialuisa Balestrieri</u>[2], <u>Anna Spagnoli</u>[1]. [1]University of North Carolina at Chapel Hill, USA, [2]Second University of Naples, Italy, [3]UNC-Chapel Hill, USA, [4]Gulhane Military Medical Academy, Etlik, Turkey, [5]University of North Carolina, USA, [6]University of North Carolina- Chapel Hill, USA

We have previously shown that increasing expression levels of the chemokine MCP5 correlated with osteoarthritis (OA) severity in a murine model of OA (DMM). By using a Tgfbr2-β-Gal-GFP-BAC reporter mouse, we characterized the TGFβ-Receptor II (TβRII) expressing cells as joint progenitors. We previously demonstrated that early blockage of MCP-5 signaling by using either a MCP-5-receptor antagonist or by intra-articular implants of isolated TβRII+ cells into DMM knees, were able to decrease articular cartilage lesions and bone sclerosis during OA (Longobardi et al., ASBMR 2013). Several studies support the hypothesis that TGF-β and PTHrP act in a common signaling cascade to inhibit the development of a calcifying phenotype in articular chondrocytes. The aim of this study is to determine the expression pattern of TβRII and PTHrP in articular cartilage during DMM and analyze whether PTHrP could mediate MCP-5 signaling.

Methods. 1)In vivo studies. Tgfbr2-β-Gal-GFP-BAC mice were subjected to DMM and euthanized 4, 8 and 12-weeks after DMM. Knees were decalcified and paraffin embedded for histological studies and OA grading. Adjacent sections were subjected to double-immunofluorescence for GFP(TβRII)/MCP-5 or PTHrP/MCP-5 proteins and in-situ hybridization for PTHrP mRNA. 2)In-vitro studies. FACS sorted TβRII+ cells from Tgfbr2-β-Gal-GFP-BAC limb buds were micromass cultured +/- MCP-5 for 3 days, cDNA was isolated and subjected to qRT-PCR.

Results. During DMM-induced OA, TβRII expression is increased 2 weeks after DMM but is abolished by 4 weeks, when MCP-5 starts to be expressed. Consistently with TβRII pattern, we found that PTHrP protein and mRNA expression levels in the periarticular chondrocytes increase 2 weeks after surgery but such expression is disorganized and decreased at later stages after DMM. Derangement of PTHrP expression is accompanied by increase in MCP-5 expression. In-vitro, we show that MCP-5 has a direct inhibitory effect on PTHrP mRNA in TβRII+ joint progenitors.

Conclusions. Our findings show that progression of OA after trauma is associated with derangement of TβRII-progenitors and PTHrP expressing cells in the periarticular chondrocytes, accompanied by increase of MCP-5 levels. In vitro data show a direct regulation of MCP-5 on PTHrP mRNA in joint progenitors. Taken together our results suggest that during post-traumatic OA, TβRII, MCP-5 and PTHrP may act together on articular chondrocytes, regulating their commitment toward mineralization.

Disclosures: Lara Longobardi, None.

SU0086

Evaluation of cartilage based on second harmonic generation microscopy.
Hiroshi Kiyomatsu*[1], Takeshi Imamura[2], Atsuhiko Hikita[3], Tadahiro Iimura[4], Tsuyoshi Miyazaki[5], Yusuke Ohsima[6], Takashi Saitou[7], Hiromasa Miura[8]. [1]Ehime University Hospital, Japan, [2]Ehime University Graduate School of Medicine, Japan, [3]Ehime University, Japan, [4]Ehime University, Proteo-Science Center (PROS), Japan, [5]Tokyo Metropolitan Geriatric Hospital & Institute of Gerontology, Japan, [6]Translational Research Center, Ehime University Hospital, Japan, [7]Department of Molecular Medicine for Pathogenesis, Ehime University Graduate School of Medicine, Japan, [8]Department of Orthopaedic Surgery, Ehime University Graduate School of Medicine, Japan

greatly restricts daily activities of patients. For the patients at the late stage of the disease, replacements of cartilages with prostheses are performed, because there is no method to regenerate articular cartilage and to detect early stage of disease. New methods to detect the affected lesions sensitively and to evaluate them quantitatively must be established for early detection of the disease and for the development of new treatments by understanding the mechanism of the disease. Second harmonic generation (SHG) imaging is useful tool at biological fields, because non-centrosymmetric molecular assemblies such as collagen fibers can be detected without staining. The SHG signal is affected by the minute changes in localization and orientation of the type II collagen fiber which is one of the major components of cartilage matrix, and thus degeneration of cartilages can be detected sensitively. To establish a new evaluation method for degeneration of articular cartilage in experimental and clinical setting, SHG and two-photon excited fluorescence imaging were performed for articular cartilage matrix and chondrocytes of H2B-GFP mice which express green fluorescence protein (GFP) in nuclei. At first, enzyme-induced degeneration of mouse articular cartilage was observed for the same samples in the same field of view. Reduction of SHG signals by collagenase treatment was observed, suggesting that SHG signal reduction is related to the degeneration of the cartilage. Chondrocytes were found to be dislocated from some region of articular cartilage, showing the destruction of the structures of extracellular matrices (ECM). We also observed the cartilages of the femurs of aged mice by using SHG imaging. We could divide those degenerative cartilages into 2 types. One of them showed rough surfaces of articular cartilage, and the other showed very strong SHG signals. We also developed OA model of H2B-GFP mice induced by destabilization surgery to evaluate the degeneration of cartilage, which were similar to human OA. In some samples, we observed empty lacunae with no GFP signal in cartilage matrix, rough surfaces of articular cartilage, and micro-cracks in ECM. In other samples showed very strong SHG signals running fibrous, suggesting hyperplasia of hyaline cartilage. The SHG imaging of cartilage matrix is promising technique for osteoarthritis study.

Disclosures: Hiroshi Kiyomatsu, None.

SU0087

NFAT1 is an Upstream Regulator of Specific Anabolic and Catabolic Genes in Mouse Articular Cartilage.
Mingcai Zhang*[1], Qinghua Lu[2], Andrew Miller[2], Clayton Theleman[2], Jinxi Wang[3]. [1]Department of Orthopedic Surgery, University of Kansas Medical Center, USA, [2]University of Kansas Medical Center, USA, [3]University of Kansas Medical Center, USA

Purpose: Despite that osteoarthritis (OA) is the most common form of joint disease, no disease-modifying pharmacologic therapy is currently available largely because the pathogenetic mechanisms of OA remain unclear. NFAT1 is a member of the nuclear factor of activated T-cells (NFAT) family of transcription factors. Our previous studies demonstrated that mice lacking *Nfat1* exhibited normal skeletal development but began to show OA-like changes at the age of 3-4 months. This study aimed to test our hypothesis that *Nfat1* deficiency causes OA-like changes in 3 to 4-month-old mice because the NFAT1 transcription factor regulates specific anabolic and catabolic genes in articular cartilage of young adult mice.
Methods: Total RNA was isolated from femoral head articular cartilage of 3 to 4-month-old wild-type (WT) or *Nfat1*-deficient (*Nfat1*^{-/-}) mice for gene expression analysis by quantitative real-time PCR (qPCR). Chromatins were isolated from the articular cartilage of femoral and humeral heads of 3 to 4-month-old WT BALB/c mice for chromatin immunoprecipitation (ChIP) assay. Normal mouse IgG was used as negative control.
Results: The expression levels of *Acan, Col2a1, Bmp7, Tgfb1* (anabolic genes) were down-regulated but the expression levels of *Admats5, Mmp13, Il1b, and Col10a1* (catabolic genes) were up-regulated in the articular cartilage of *Nfat1*^{-/-} mice. NFAT1 ChIP assays were performed followed by qPCR analyses using specific primers encompassing the NFAT1 binding site in the promoters of selected genes (Table 1). The ChIP data demonstrated that NFAT1 directly binds to the promoter region of these candidate target genes whose expression was affected by *Nfat1* deficiency (Figure 1).
Conclusions: These results suggest that NFAT1 is an upstream factor regulating the expression of specific anabolic and catabolic molecules in articular cartilage of mice. *Nfat1* deficiency causes decreased expression of the anabolic genes and increased expression of the catabolic genes, leading to degradation of articular cartilage and OA-like changes. Thus, anti-OA agents that target NFAT1 could be more effective than drug candidates that target a single catabolic or anabolic molecule.

Key Words: NFAT1, Articular Cartilage, Gene Expression, Osteoarthritis, ChIP Assay

Table 1. Primers used for ChIP assay

Gene	Forward	Reverse	Location
Acan	AAATCACTGTATGCTGCAACTAGC	GCCTGGCCTCTACAACACTC	-1028 to -925
Adamts5	GACCGACTGGAGAGAACCAG	GCTCTGGCCTTGTAGACCTG	-536 to -440
Bmp7	CGCAGGGCCCTTGTATTG	CGAACCCTAGCTCCCTCCT	-208 to -106
Col10a1	TCATTCCATCATGAACCAACA	TTAATAGCTTCGGCTGTGCAT	-285 to -198
Col2a1	ATGGGTTAGGGAGGCTGTG	GGGGACAGTTTTCCAGACCT	-560 to -463
Il1b	TCCCCTAAGAATTCCCATCA	GCTGTGAAATTTTCCCTTGG	-144 to -55
Mmp13	CTGCTGCTTCTCCCCACTAT	GAGGGAAATGGAAAATGAAGG	-244 to -133
Tgfb1	GGACGAGCTGGTTGAGAGAAGA	CCCACGTCTCTGACTTGCAGTA	247 to 319

Table 1

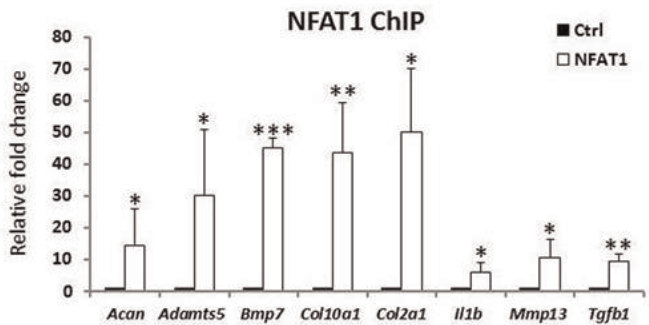Figure 1. NFAT1 binds to the gene promoter.
* p<0.05, **p<0.01, ***p<0.001

Figure 1

Disclosures: Mingcai Zhang, None.

SU0088

Role of estrogen and estrogen receptor beta signaling in mediating mandibular condylar growth in young male mice.
Sunil Wadhwa[1], Jing Chen[2], Manshan Xu*[2], Helen Lu[2], Thomas Choi[2]. [1]Columbia University, USA, [2]Columbia University, USA

Abstract- Mandibular growth abnormalities approximately afflict 20 million Americans. There is a great need in the dental research community to develop alternative economical treatments for mandibular growth abnormalities. We have previously found that estrogen receptor beta deficiency caused increased mandibular condylar cartilage growth in female mice. The goal of this study was to determine the role of estrogen and estrogen receptor beta signaling in regulating the growth of the mandibular condyle in male mice. *Materials and Methods*- 21 day old male WT and ER beta KO mice were treated with placebo or estradiol (100ng/gram body weight) for 4 weeks. Histomorphometry, micro ct analysis, proliferation, and Col2 expression of the mandibular condyle was assessed. *Results*- There was no difference in the size of the mandibular condylar cartilage and microarchitecture of the subchondral bone between 49-day-old placebo treated male WT and ER beta KO mice. Estradiol treatment caused significant increases in condylar cartilage thickness, trabecular thickness and trabecular number in male WT mice but only trabecular thickness in male ER beta KO mice compared to placebo treated male mice. There was no difference in proliferation between estradiol treated male WT and ER beta KO compared to placebo treated male mice. Estradiol also caused superior localization of Col2 in the mandibular condylar cartilage in both male WT and ER beta KO mice. *Conclusion*- Estrogen via ER beta signaling pathway promoted increased mandibular condylar cartilage thickness, while estrogen independent of ER beta increased trabecular thickness in the mandibular condylar subchondral bone in male mice.

Disclosures: Manshan Xu, None.

SU0089

Effects Of Extracellular Calcium In Human And Porcine Adipose Derived Stem Cell Differentiation For Osteochondral Tissue Engineering.
Liliana Mellor*[1], Elizabeth Loboa[2], Farshid Guilak[3], Jorge Piedrahita[2], Sehwon Koh[2], John Williams[2]. [1]North Carolina State University, USA, [2]North Carolina State University, USA, [3]Duke University, USA

Joint injury often leads to the onset of osteoarthritis (OA), a degenerative joint disease that limits mobility of the affected joint due to the degradation of articular

cartilage. The limited regenerative capacity of cartilage tissue presents significant challenges to repair or reverse the effects of damaged articular cartilage. Current methods for cartilage repair include autologous chondrocyte implantation, microfracture, and autograft and allograft osteochondral transplantation. Tissue engineering approaches using stem and/or primary cells have not been clinically proven. The majority of stem cell based approaches to cartilage or osteochondral tissue engineering, have used bone marrow derived mesenchymal stem cells (MSC) and have focused predominantly on cartilage regeneration as opposed to full osteochondral tissue regeneration.

Our goal is to use the more abundant and easily accessible adipose derived stem cell (ASC) to generate a full osteochondral construct using a gradient calcium concentration in a biodegradable poly-lactic acid (PLA) scaffold. Our laboratory has previously shown that elevated calcium concentration in human ASC induces osteogenesis and inhibits chondrogenesis. We have used this approach to seed hASC in a tricalcium phosphate (TCP) gradient scaffold, containing a 20% TCP concentration in the deep layers to induce osteogenesis, and 0%TCP in the superficial layers to induce chondrogenesis to mimic native osteochondral tissue. We are developing the same technique in a large animal model (porcine) to evaluate *in vivo* the ability to use our engineered osteochondral construct to replace damaged articular cartilage.

Our novel approach using hASC to create a full osteochondral construct would bring an alternative and less invasive treatment to patients suffering from osteochondral injuries, and would allow us to use stem cells from the patient's own fat tissue to create a full osteochondral construct designed to fit the size and shape of the injury. This technique would be less invasive as none of the healthy remaining cartilage tissue would be removed, and the use of autologous stem cells minimize tissue rejection.

Disclosures: Liliana Mellor, None.

SU0090

Epigenetic Regulatory Role of KDM4B in TGFβ-Mediated Chondrogenic Differentiation of Human MSCs. <u>Christine Hong</u>*[1], <u>HYELIM Lee</u>[2], <u>Cun-Yu Wang</u>[3]. [1]UCLA School of Dentistry, USA, [2]SEOUL NATIONAL UNIVERSITY, South Korea, [3]UCLA, USA

The biomedical burden of arthritis and cartilage defects has grown over the past decades due to the inadequate treatment options currently available. While existing efforts in tissue engineering approaches utilizing human mesenchymal stem cells (MSCs) show enormous potential, a comprehensive understanding of the intricate mechanisms that govern the fate of MSCs is required for therapeutic applications of MSCs specific for cartilage regeneration. TGFβ is a potent inducer of chondrogenesis by activating the Smad signaling pathway and inducing chondrongenic genes such as SOX9, however, the involvement of epigenetic regulation in TGFβ-mediated induction of chondrogenic gene expression is not known. Recently, the histone demethylase, KDM4B, was shown to play a key role in promoting MSC osteogenic commitment by removing repressive epigenetic marks, H3K9me3. Therefore, we examined the role of KDM4B in TGFβ-mediated chondrogenic differentiation of MSCs. TGFβ significantly induced the expression of KDM4B by 70 fold. When KDM4B was overexpressed in MSCs, chondrogenic differentiation was induced more significantly as assessed by Alcian Blue staining and mRNA expression of chondrogenic marker genes, Collagen2a1, Sox9, and Aggrecan. Conversely, KDM4B depletion using shRNA technique led to a significant reduction in chondrogenic potential. When KDM4B expression was rescued in KDM4B-knockdown MSCs, chondrogenic differentiation was restored, further confirming the facilitating role of KDM4B in chondrogenic commitment. Mechanistically, upon TGFβ stimulation, KDM4B was recruited to the SOX9 promoter region and the subsequent epigenetic modulation by removal of silencing H3K9me3 marks led to the activation of this chondrogenic master gene. In addition, the occupancy of Smad3 was also increased in the SOX9 promoter region confirming Smad signaling dependent SOX9 induction. When KDM4B was knocked down, demethylation of H3K9me3 and occupancy of Smad3 in the SOX9 promoter region were significantly diminished, suggesting that TGFβ-mediated chondrogenic differentiation is directly regulated by KDM4B's epigenetic activity on the promoter of SOX9. Taken together, our results demonstrate the critical role of a histone demethylase, KDM4B, in the epigenetic regulation of chondrogenic differentiation of MSCs. Since histone demethylases are chemically modifiable, KDM4B may present as a novel therapeutic target in cartilage regenerative therapy.

Disclosures: Christine Hong, None.

SU0091

Osteoclasts regulate chondrocyte metabolism through the inhibition of the Wnt canonical pathway. <u>Chahrazad Cherifi</u>*[1], <u>Wafa Bouaziz</u>[2], <u>Martine Cohen-solal</u>[3], Eric Hay[4]. [1]Inserm U1132, France, [2]INSERM U606, France, [3]Hôpital Lariboisière, France, [4]INSERM u1132, France

Purpose: Enhanced osteoclastogenesis is observed at early stages of osteoarthritis (OA). We have demonstrated that cartilage damage is prevented when osteoclastogenesis is inhibited in murine models. We speculate that Wnt activity, known to regulate the bone and chondrocyte cell function, might contribute to promote cartilage catabolism. Our purpose was to evaluate whether osteoclast-secreted

molecules affect the chondrocyte metabolism and to assess the contribution of Wnt pathway.

Methods: Osteoclasts were obtained from RAW cells cultures in the presence of RANKL. Primary murine chondrocyte (Ch) were cultured in the presence of osteoclast conditioned medium (Oc-CM) for 48h. The gene and protein expressions of catabolism and anabolism were analyzed by RT-qPCR and western blot. To investigate the regulation of canonical Wnt pathway, transactivation assay was performed in primary chondrocytes derived from Topgal mice and cultured with Oc-CM. Western blot and immunocytochemistry were used to confirm the activation of β-catenin canonical Wnt signaling pathway. Finally, the role of Wnt canonical signaling was investigated through the b-catenin translocation in the presence of lithium chloride (LiCl) in addition to the Oc-CM.

Results: Oc-CM induced a marked decrease in proteoglycan release by chondrocytes. Oc-CM reduced the expression of anabolic genes (collagen type II, Aggrecan and Sox-9) while increased the expression of catabolic genes (MMP-3, -13, Adamts-4,-5). We then monitored the nuclear translocation of β-catenin induced by Oc-CM. Oc-CM abolished the translocation of β-catenin and subsequently the Topgal activity in line with the reduction of Wnt target genes (Axin, Wisp1 C-Myc). Moreover, LiCl reduces the expression of catabolic genes induced by Oc-CM, indicating the contribution of the canonical pathway in the regulation of catabolic genes.

Conclusion: We have here demonstrated that osteoclasts secrete soluble factors capable to disrupt chondrocyte metabolism and the anabolic / catabolic balance via the inhibition of the Wnt canonical signaling. Therefore, our data indicate that manipulating bone may affect chondrocyte function.

Disclosures: Chahrazad Cherifi, None.

SU0092

Preferentially expressed genes in synovium derived stromal cells include atypical genes not expressed highly in mouse synovium but in embryonic cartilages. <u>Yoichi Ezura</u>*[1], <u>Tadayoshi Hayata</u>[2], <u>Takuya Notomi</u>[3], <u>Ichiro Sekiya</u>[4], <u>Masaki Noda</u>[5]. [1]Tokyo Medical & Dental University, Medical Research Insititute, Japan, [2]Organization for Educational Initiatives, University of Tsukuba, Japan, [3]Department of Pharmacology, Osaka Dental University, Japan, [4]Tokyo Medical & Dental University, Japan, [5]Tokyo Medical & Dental University, Japan

The synovium derived stromal cells (SSCs), also named as synovial mesenchymal stem cells (SMSCs) in human is a type of stromal progenitor cells resident in various adult tissues. We have reported that human SSCs are more potent for chondrogenesis in vitro than the other types of hMSCs. Gene expression profiles of the SSCs and bone marrow derived stromal cells (BMSCs) are consistently different in human and mouse, and thus a list of 113 genes significantly expressed more in SSCs than in BMSCs was made (ASBMR annual meeting 2013). To investigate if this expression profile of the signature genes in SSCs reflects the expression in adult synovial tissue, global gene expression was analyzed for adult and embryonic (E17.5) mouse synovium, menisci, epiphyseal and articular cartilage. Indeed, about 80% of these signature genes are expressed more in adult synovial tissue than in adult articular cartilage, whereas such preferential expression was not obvious when it was compared between the synovium and the meniscus. Preferential expression was also not clear between the embryonic synovial tissue and epiphyseal cartilage or the menisci. These results indicate that most synovial stromal signature genes preferentially expressed in SSCs may reflect their expressions in adult synovium, but not reflect their potential for expression in developing tissues. However, among the list of 113 genes, we could also detect several genes whose expression was paradoxically high in embryonic cartilaginous tissues i.e., epiphyseal cartilage and menisci compared to that in synovium. Those genes including *Prg4, Prelp, Comp,* and *Sfrp1* may be the candidate factors contributing to the higher potential of the SSCs for chondrogenesis than the other types of mesenchymal stromal cells.

Disclosures: Yoichi Ezura, None.

SU0093

The enzymatic activity of IRE1a modulates chondrocyte differentiation. <u>Fengjin Guo</u>*[1], <u>Zhangyuan Xiong</u>[2], <u>Peng Zhang</u>[3], <u>Xiaofeng Han</u>[3]. [1]Chongqing Medical University, Peoples Republic of China, [2]Department of Cell Biology & Genetics,Core Facility of Development Biology, Chongqing Medical University, China, [3]Department of Cell Biology & Genetics,Core Facility of Development Biology,Chongqing Medical University,Chongqing 400016,China, China

Growth and development of endochondral bones is controlled through the highly coordinated proliferation and differentiation of growth plate chondrocytes.BMP2 is known to activate UPR signaling molecules, such as BiP,ATF4 and IRE1α in chondrogenesis.IRE1a,as one of three unfolded protein sensors in UPR signaling pathways,can be activated during ER stress.GEP,also known as progranulin,is a 593–amino acid secreted glycoprotein with an apparent molecular weight of 80kDa.More evidence implicated that GEP is involved in the regulation of differentiation,development and pathological processes.We previously reported that GEP induced and promoted chondrocyte differentiation,endochondral bone formation and cartilage

repair.However,whether IRE1a influences GEP-mediated chondrogenesis remains undetermined.Specifically,the molecular mechanism by which IRE1a regulates chondrogenesis also remains unknown.Here we present evidences demonstrating that overexpression of IRE1a inhibits chondrocyte differentiation,as revealed by expression of Col?,SOX9,Col?,MMP-13,IHH,Runx2,PTHrP. Furthmore,IRE1a-mediated inhibition of chondrogenesis depends on its enzymatic activity,since its point mutant lacking enzymatic activity completely loses this activity.The RNase and Kinase domains of IRE1a C-terminal is necessary for its full enzymatic activity and inhibition of chondrocyte differentiation.Mechanism studies demonstrate that GEP induced IRE1a expression in chondrogenesis.The expression of IRE1a is depended on GEP signaling,and IRE1a expression is hardly detectable in GEP-/- embryos.IRE1a inhibits GEP-mediated chondrocyte differentiation as a negative regulator.Altered expression of IRE1a in chondrocyte hypertrophy was accompanied by altered levels of IHH and PTHrP.

Collectively,we report that IRE1α adversely mediates chondrocyte differentiation based on the following observations:(1)Overexpression expression of IRE1a dramatically inhibits the chondrocyte differentiation;(2)the enzymatic activity and the C-terminal RNase and Kinase domains of IRE1a are important for its full enzymatic activity and IRE1a-mediated inhibition of chondrogenesis;(3)IRE1α demonstrates prominent expression in proliferating and prehypertrophic chondrocytes in the wildtype embryonic growth plate,whereas its expression is hardly detectable in GEP-/- embryos;(4)IRE1a inhibits GEP-mediated chondrocyte differentiation as a negative regulator;(5)Promoting IHH/PTHrP signaling.
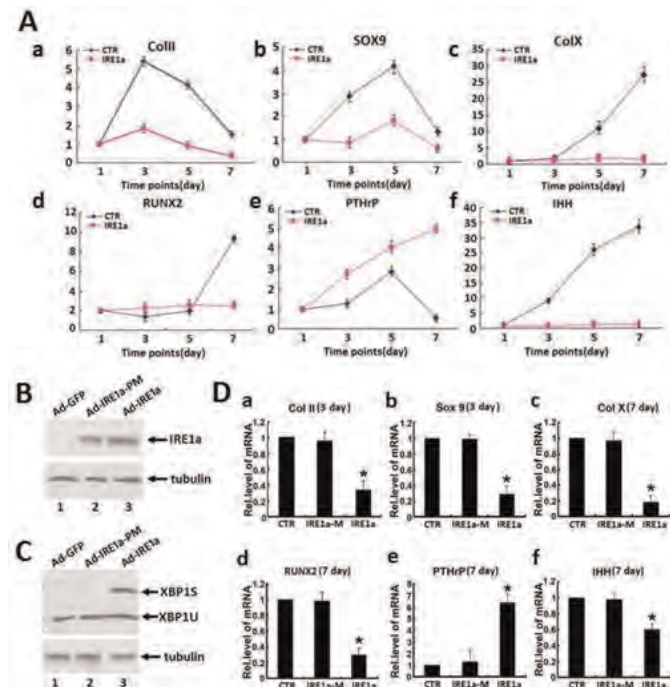
Figure 1.IRE1a inhibition of chondrogenesis is required for its enzymatic activity.
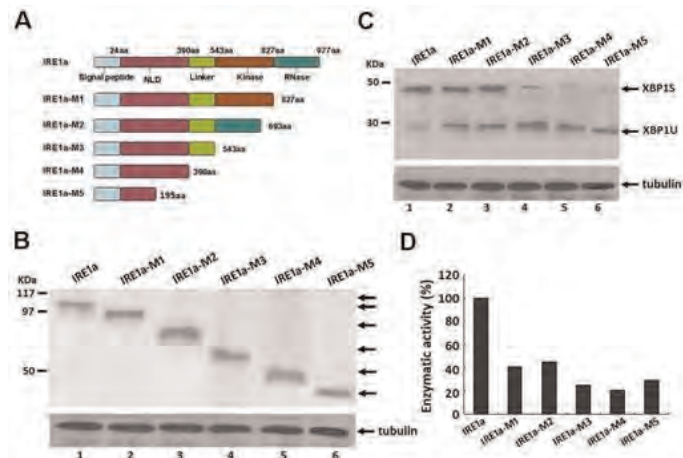
Figure 2. Effects of IRE1a functional domains and enzymatic activity.
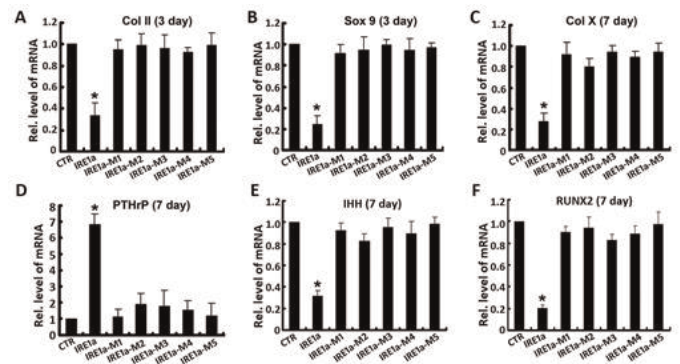
Figure 3.Kinase and Nuclease domain of IRE1a is important for its regulation of chondrogenesis.
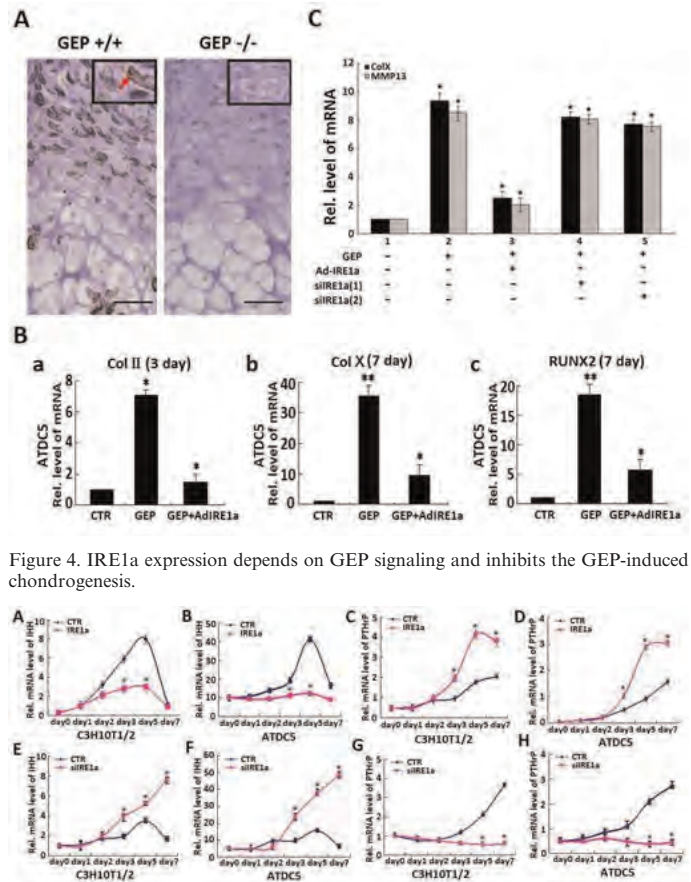
Figure 4. IRE1a expression depends on GEP signaling and inhibits the GEP-induced chondrogenesis.
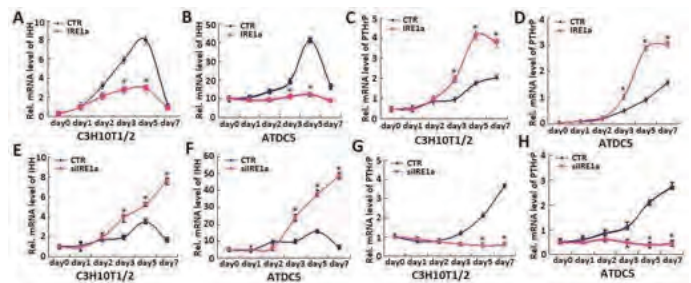
Figure 5. Altered expression of IRE1a affects the expression of IHH and PTHrP.

Disclosures: Fengjin Guo, None.

SU0094

W9 peptide repaired full-thickness articular cartilage defects in rabbits. - Mechanism of chondrogenic differentiation by W9 peptide -. Yuriko Furuya*[1], Hisashi Mera[2], Maki Itokazu[3], Hiroaki Nakamura[4], Kohji Uchida[5], Shigeyuki Wakitani[2], Hisataka Yasuda[6]. [1]Oriental Yeast Co.,Ltd, Japan, [2]Mukogawa Women's University, Japan, [3]Osaka City University Graduate School of Medicine, Japan, [4]Osaka City University Gradulate School of Medicine, Japan, [5]Oriental Yeast Co., Ltd., Japan, [6]Oriental Yeast Company, Limited, Japan

WP9QY (W9) peptide is known to accelerate osteogenesis and inhibit osteoclastogenesis in vitro and in vivo. W9 inhibits osteoclastogenesis by binding receptor activator of NF-kB ligand (RANKL) as a RANKL antagonist. Recently we reported that short hairpin RNA (sh RNA)-mediated RANKL gene knock-down using lentivirus suppressed W9-induced calcification in mouse mesenchymal stem cells (MSCs), suggesting an important role of RANKL in osteogenesis by W9. We hypothesized that reverse signaling through RANKL regulated osteogenesis. We also

reported that W9 enhanced chondrogenesis in ATDC5 cells and human MSCs in this meeting previously. We observed robust matrix accumulation in three-dimensional pellet culture by W9 using human MSCs. Moreover, we ascertained that a feature of W9 in in vitro chondrogenesis was accelerating production of cartilage matrix in chondrocytes and their culture supernatants, but not proliferation of the cells.

Here we evaluated whether W9 had a chondrocyte differentiative effect in vivo using rabbit model of full-thickness articular cartilage defects. Full-thickness defects (5 mm width and 5 mm depth) in knee joints were created by a surgical drill in male Japan White rabbits (18-20 weeks of age, n=8). Two weeks after the formation of defects, W9 or PBS (vehicle) was administrated to rabbits intraarticularly once per week for 2 weeks. After formalin fixation and decalcification of knee joints, paraffin sections were stained by hematoxylin-eosin, toluidine blue, and safranin-O, respectively. Histological analysis revealed that W9 repaired the full-thickness defects. Histological grading was performed using the modified Wakitani score. Total score of W9 was lower than that of vehicle significantly.

Moreover, to clarify the mechanism of W9, we investigated its signaling pathway in C3H10T1/2 cells and ATDC5 cells with chemical or protein inhibitors and by western-blotting using phosphorylated antibody. Phosphorylated p38 MAP kinase enhanced in C3H10T1/2 cells and ATDC5 cells treated with W9, suggesting an involvement of p38 signal in the mechanisms. W9 peptide may be useful for and applicable to the treatment of chondropathy such as osteoarthritis and cartilage injury. By analogy with the important role of RANKL in W9-induced osteoblastogenesis, we will elucidate whether W9 stimulated chondrocytes differentiation via membrane RANKL on MSCs.

Disclosures: YURIKO FURUYA, Oriental Yeast Co.,Ltd., 4

SU0095

Leptin increases VEGF expression and enhances angiogenesis in human chondrosarcoma cells. Yi-chin Fong*[1], Wei-Hung Yang[2], Jui-Chieh Chen[3], Chih-Hsin Tang[4]. [1]China Medical University Hospital, Taiwan, [2]China Medical University Hospital, Taiwan, [3]China Medical University, Taiwan, [4]China Medical University, Taiwan

Leptin, a 16 kDa product of the obese gene, is an adipocytokine that plays a critical role in the regulation of body weight. In recent years, leptin is also defined as a potent angiogenic factor, which is involved in tumorigenesis, angiogenesis, and metastasis. However, it is unknown whether leptin regulates VEGF production in human chondrosarcoma and contributing the tumor-associated angiogenesis. In the present study, we found that both leptin and VEGF are highly expressed in human chondrosarcoma tissues, which are positively correlated with histopathological grade. Thus, we examined the effects of exogenous leptin on chondrosarcoma cells. In addition, the intracellular signaling pathways were also investigated by pharmacological and genetic approaches. Our data show that leptin increases VEGF production by activating OBRl receptor and MAPKs (p38, ERK, and JNK), which in turn enhances the binding of AP-1 transcription factor to the VEGF promoter, resulting in the transactivation of VEGF expression and subsequently promoting migration and tube formation in endothelial progenitor cells (EPC). Further, we have also evaluated the effect of leptin on angiogenesis and tumor growth using the in vivo models. The results show that knockdown of leptin attenuates neovessel formation and arrests chondrosarcoma tumor growth in vivo. These findings may provide a better understanding of the pathogenesis of chondrosarcoma and can utilize this knowledge to design a new therapeutic strategy.

Disclosures: Yi-chin Fong, None.

SU0096

Influence of Beta-Aminoproprionitrile on Morphology of Type I Collagen Produced by MC3T3-E1 Osteoblasts and Measured Using Atomic Force Microscopy. Silvia Canelon*[1], Joseph Wallace[2]. [1]Purdue University, USA, [2]Indiana University Purdue University Indianapolis (IUPUI), USA

Type I collagen can be morphologically characterized through measurements of the fibril D-spacing which can be used to detect differences in collagen structure across tissue types and disease. The D-spacing describes the axially repeating bands of gap and overlap regions of collagen fibrils arranged into a quarter-staggered array. This fibrillar structure is stabilized by enzymatic cross-links initiated by the lysyl oxidase enzyme, and disrupted by the beta-aminoproprionitrile (BAPN) toxin which inhibits lysyl oxidase. Murine in vivo studies have confirmed effects of BAPN on collagen nanostructure and the objective of this study is to evaluate the mechanisms of these effects in vitro by using atomic force microscopy (AFM) to measure D-spacing.

Osteoblastic cells (MC3T3-E1) were differentiated in culture, in the presence or absence of BAPN, resulting in the synthesis of extracellular matrix. Cells were grown in complete alpha-MEM medium and then cultured for 7 days at a density of 500,000 cells/60mm plate. Differentiation was induced by supplementing the medium with 50μg/mL, and also with 25mM BAPN for the BAPN-treated group. Medium was replaced every 2 days for both control (n=3) and treated groups (n=3). At the end of the 7 days, medium was removed from the plate and cells dissociated from the matrix with an EDTA buffer. The matrix was allowed to dry in the dish and imaged in air using AFM. The matrix was imaged in tapping mode using silicon cantilevers and 5 locations were imaged in each plate. The Fourier transform of 3.5μm x 3.5μm images

was taken and D-spacing analysis was performed on 10 collagen fibrils per location for a total of 50 fibrils per plate and approximately 200 fibrils per group.

The D-spacing distribution of collagen produced in the presence of BAPN was found to be shifted toward higher D-spacing values by a statistically significant degree. These results indicate that BAPN indeed has an effect on morphology of collagen produced in vitro and support aforementioned in vivo experiments. Relevant future studies address further characterization of in vitro synthesized collagen by evaluating gene expression as well as biochemical and mechanical properties. In addition, studies are underway to analyze the effect of mechanical loading on collagen produced by osteoblasts under fluid shear stress, particularly relating to the recovery of properties altered by BAPN.

Disclosures: Silvia Canelon, None.

SU0097

Sc65 is a novel ER protein and a regulator of bone mass homeostasis. Roy Morello*[1], Roberta Besio[1], Patrizio Castagnola[2], Milena Dimori[3], Yuqing Chen[4], Dana Gaddy[1], Larry Suva[1]. [1]University of Arkansas for Medical Sciences, USA, [2]IRCCS AOU San Martino – IST, Italy, [3]University of Arkansas for Medical Sciences, USA, [4]Baylor College of Medicine, USA

Members of the Leprecan family of proteins include enzymes, prolyl 3-hydroxylase 1 (P3h1), P3h2 and P3h3, and non-enzymatic proteins, Crtap and Sc65. Mutations in *CRTAP* and *LEPRE1* (encoding P3H1) are associated with human disease such as recessive osteogenesis imperfecta. However, the function of Sc65 which is closely related and highly homologous to Crtap is unknown. Sc65 was described as a synaptonemal complex protein, a nucleolar protein, and a cytoplasmic adapter protein. In light of its similarity with Crtap, an endoplasmic reticulum (ER)-associated protein and an important mediator of collagen post-translational modifications, we hypothesized that Sc65 was also an ER-resident protein with a potential role in bone homeostasis. Here we demonstrate that Sc65 is a previously unrecognized ER protein, and that it does not localize in the nucleus of somatic cells. Sc65 is expressed during mouse skeletal development and its loss due to a gene-trap insertion results in a progressive osteopenia that affects both trabecular and cortical bone. Low bone mass is due to increased osteoclastogenesis and bone resorption. Interestingly, Sc65 is highly expressed in chondrocytes and osteoblasts but not in osteoclasts or their precursors. Osteoblast/osteoclast co-culture experiments suggest that lack of Sc65 in osteoblasts is sufficient to mediate increased osteoclastogenesis, and point to a non-cell autonomous osteoclast defect. To assess if lack of Sc65 in osteoblasts is responsible for the observed bone phenotype we generated Sc65 floxed mice and crossed them with Osterix-Cre transgenic mice. Interestingly, micro-CT analysis of distal femur and spine (males, n=10) did not reveal significant architectural differences between Osterix-Cre and Osterix-Cre;Sc65[FL/FL] mice. However, volumetric bone density was significantly reduced in Osterix-Cre;Sc65[FL/FL] femurs (850 vs 810 mg HA/ccm, p=0.001), suggesting a potential material defect. Current studies are evaluating the distribution of collagen, the diameter of individual collagen fibrils in skin and bone at the ultra-structural level as well as characterizing specific Sc65 interactors within the ER.

Disclosures: Roy Morello, None.

SU0098

Monoosteophils Accelerate Nonunion Bone Repair by Using Intracellular Apatite Formation. Zhifang Zhang*[1], Keith Le[2], Frances Chang[2], Zhuo Li[2], Ricardo Zerda[2], Marcia Miller[2], John Shively[2]. [1]City of hope, USA, [2]City of Hope, USA

BACKGROUND: Monoosteophils, derived from LL-37-treated monocytes, are a novel type of calcifying/bone forming cells. We have shown that monoosteophils have the ability to form bone-like nodules in vitro and ectopic bone in vivo and accelerate bone repair in a drilled bone repair model. Here, a critical-sized defect model was used to further investigate bone repair function of monoosteophils and mechanism of nodule formation of monoosteophils was studied.

Results: Critical-sized (5 mm) calvarial defects were created in the parietal bone of adult male NOD/SCID mice. Defects were treated with either 1 day human monocytes, 1 day human monoosteophils, or 1 day human monoosteophils with gel hydroxyapatite. Our results showed that significant healing was observed among monoosteophil engrafted calvarial defects with microCT scanning (Figure 1). In vitro study showed monoosteophils release 1-2 μm bone-like nodules on osteologic disc in low Ca2+ concentration 10% FBS RPMI1640 medium after 3 weeks by using scanning electronic microscopy. Transmission electron microscopy showed that monoosteophils, harvested from osteologic discs, express intracellular vesicles of calcium phosphate (Figure 2). When monoostophils were cultured in the 10% FBS αMEM medium with 2.5mM CaCl2 instead of osteologic disc for 3 weeks, significant intracellular calcium phosphate formations were observed by Alizarin Red S staining and elemental analysis by EDS/SEME (Figure 3). Furthermore, confocal fluorescence microscopy showed calcium phosphate vesicles of monoosteophils were positive for FAM labeled bisphosphonate or FITC labeled HABP19 staining and a small percentage of FAM-bisphophonate positive vesicles were colocalized with mitochondria, but not with Golgi, endosomes, endoplasmic reticulum, lysosomes, or autophagosomes (Figure 4), which suggest that calcium phosphate vesicles, as an unique vesicle in monoosteophil, may be associated with mitochondria.

Conclusion: Our observations highlight the bone repair function and the unique mechanism of bone formation of monoosteophils. These observations may have important implications in deciphering both how normal bone forms and in understanding pathological mineralization.
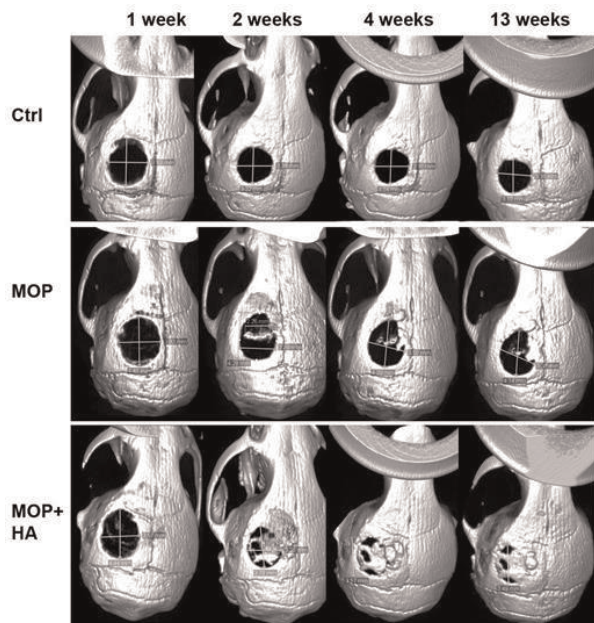
Fig 1. Monoosteophils accelerate bone repair. Critical-sized (5 mm) calvarial defects were created in the parietal bone of adult male NOD/SCID mice. Defects were treated with either 1 day monocytes (Ctrl), 1 day monoosteophils (MOP), or 1 day monoosteophils with gel hydroxyapatite.(MOP+HA) and observed using micro CT.

Fig 1
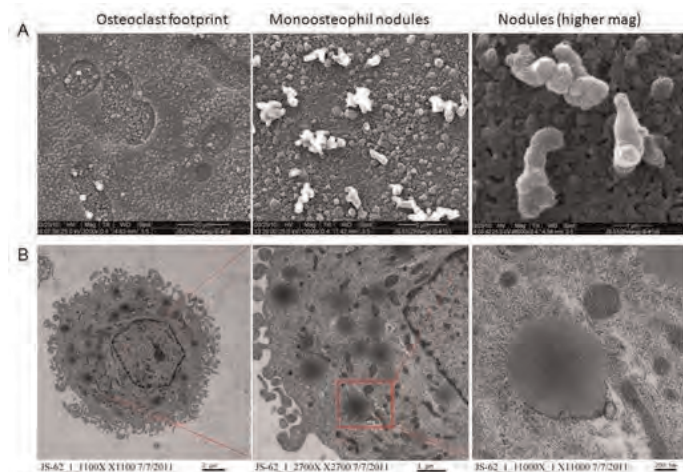
Fig 2. In vitro nodule formation of monoosteophils on BioCoat Osteologic Discs. Monocytes were incubated in the presence of M-CSF/RANKL (both at 25 ng/mL for osteoclast differentiation) or LL-37 (5µM for monoosteophil differentiation) in RPMI 1640 media on BioCoat Osteologic Discs in 5% CO2 atmosphere. After incubation for three weeks, cells were removed with bleach and observed by SEM (A) and monoosteophils were harvested and observed by TEM (B).

Fig 2
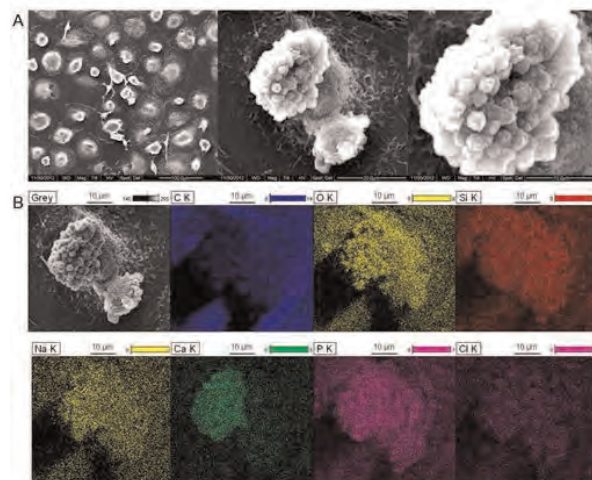
Fig 3. Intracellular nodules of monoosteophils consist of phosphorus, calcium, oxygen, and sodium. Monocytes were differentiated to monoosteophils using 5 µM LL-37 in plastic plate in αMEM with 2.5mM CaCl2 for three weeks. Elements of intracellular nodule were analyzed using SEM (A) and SEM/EDS (B).

Fig 3
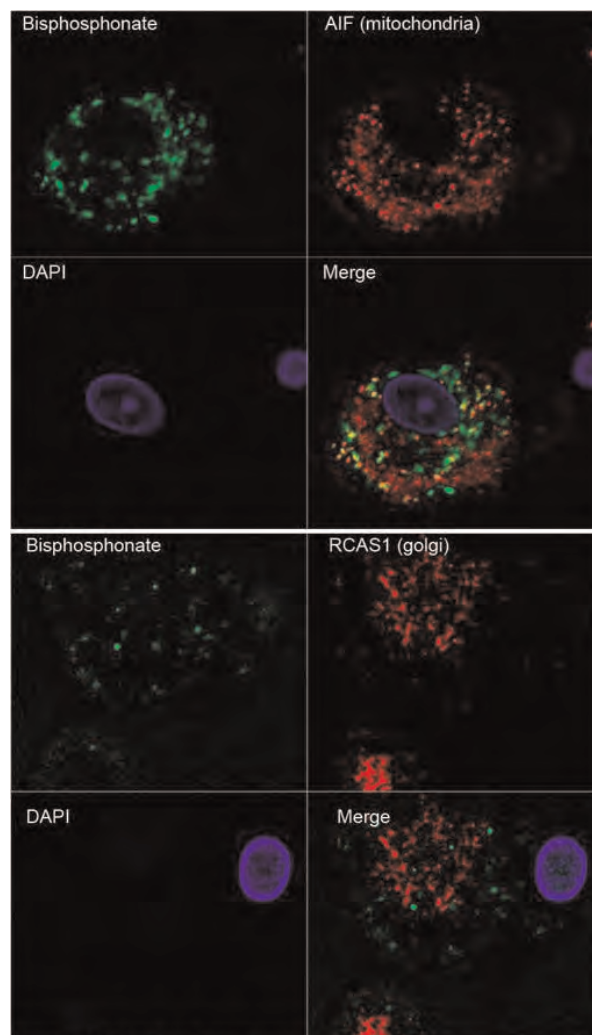
Fig 4. FAM-bisphophonate positive vesicles of monoosteophils were partly colocalized with mitochondria, but not with Golgi. Monoostophils were cultured with aMEM with 2.5 mM CaCl2 for 3 weeks and fixed/permeablized and stained shown in the fugure.

Fig 4

Disclosures: Zhifang Zhang, None.

SU0099

An insulin-sensitizing thioglitazone, which fails to activate PPARγ, does not cause bone loss. <u>Tomohiro Fukunaga</u>*[1], <u>Wei Zou</u>[2], <u>Nidhi Rohatgi</u>[3], <u>Jerry Colca</u>[4], <u>Steven Teitelbaum</u>[2]. [1]Washington University in St. Louis School of Medicine, USA, [2]Washington University in St. Louis School of Medicine, USA, [3]Washington University in St. Louis, USA, [4]Metabolic Solutions Development Company, USA

Rosiglitizone (BRL) is an insulin-sensitizing thioglitazone (TZD) drug which exerts its effect by activating the transcription factor, PPARγ. While BRL is an effective oral treatment of type II diabetes mellitus, it carries substantial complications including increased fracture risk. This predisposition to fracture is consistent with the fact that PPARγ preferentially promotes formation of adipocytes at the cost of osteoblasts. Surprisingly however, BRL-activated PPARγ also stimulates osteoclast formation. Recently, a new TZD analog with low affinity for binding and activation of PPARγ has been developed whose insulin-sensitizing properties mirror those of BRL. In this study, we investigated the effects of this new TZD analog (MSDC-0602) on osteoclast function and differentiation, in vitro and in vivo. BRL dramatically increases PPARγ activity in a PPRE reporter assay system and enhances expression of the PPARγ target gene, CD36 in osteoclast. MSDC-0602, in contrast, minimally activates PPARγ and does not alter CD36 expression. Consistent with this finding, BRL increases RANKL-induced osteoclast differentiation and number but MSDC-0602 fails to do so. To determine if this new TZD analog is bone sparing, in vivo, we fed adult male C57BL/6 mice MSDC-0602 or BRL. 6-months of a BRL diet results in a 35% decrease in bone mass whereas that of MSDC-0602 fed mice is indistinguishable from control. Thus PPARγ-sparing TZDs could reduce the skeletal side effects of TZD drugs while maintaining their insulin-sensitizing properties.

MSDC-0602 does not Induces Osteoporosis

Disclosures: Tomohiro Fukunaga, None.

SU0100

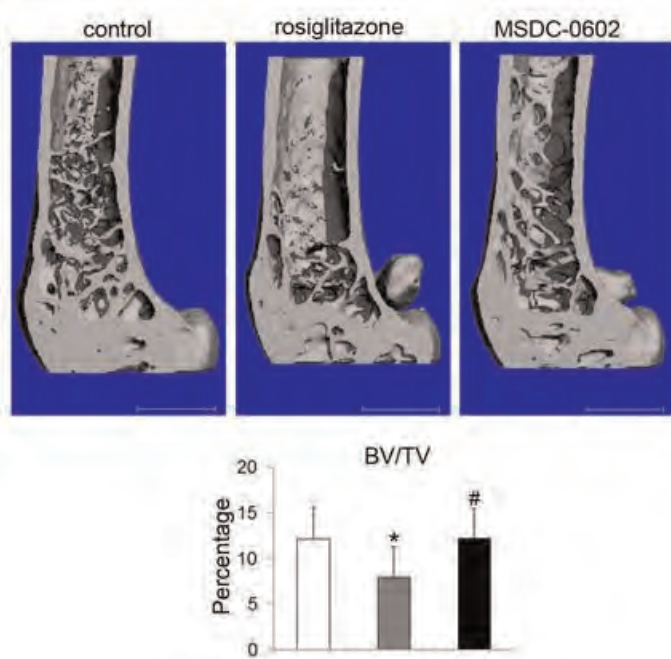**Dramatic effects of high and low glucose on osteocytes: A model for the effects of glucose on bone loss.** <u>Donna Pacicca</u>*[1], <u>Tammy Brown</u>[2], <u>Lynda Bonewald</u>[3]. [1]Children's Mercy Hospital, USA, [2]Children's Mercy Hospital, USA, [3]University of Missouri - Kansas City, USA

Fluctuations in glucose have a detrimental effect on multiple tissues in patients with diabetes mellitus. While diabetic patients are known to have an increased fracture risk, the effect of glucose variability on bone tissue has not been as well-established. We hypothesized that high and low glucose levels regulate gene expression responsible for bone loss and lack of bone gain. We tested the effects of exposure to high and low glucose on the IDG-SW3 cell line which initially express an osteoblastic phenotype before transitioning to an osteocytic phenotype in culture. The IDG-SW3 cells were cultured under low (2.5 mM), normal (10mM), and high (25mM) glucose. A mannitol control was included for high osmolarity (glucose 10mM with mannitol 15mM). Media was changed daily and cells were harvested at 3, 7, 14, 21, 28 and 35 days. Glucose and lactate levels were measured, and LDH assay was used to evaluate cell viability. After RNA extraction, qPCR was performed on samples from the six time points to evaluate expression of glucose transport proteins, insulin

receptor, E11, type 1 collagen, sclerostin, keratocan, RANKL and OPG. Glucose utilization and lactate production increased over time. PCR demonstrated expression of insulin receptor and glucose transport proteins 1 and 3 that increased under low glucose conditions and decreased with high glucose. Little or no GLUT2 and 4 was detected under any conditions (Ct values >36). Dramatic effects were observed on the osteocytic cells at days 21, 28, and 35. High glucose increased expression of sclerostin from day 21 to 35 by 3800%. RANKL was increased at days 28 and 35 in low glucose by 200%. Keratocan was increased in high glucose 350% but decreased in low glucose 65%. No significant differences were noted in E11, Col1, SOST or Kera at days 3 or 7 with either high or low glucose showing little effect on the early osteoblast cells. In summary, high glucose increased sclerostin while low glucose induced the expression of RANKL. Keratocan was increased by high glucose but decreased by low glucose suggesting effects on differentiation and dedifferentiation. These data suggest that glucose variability may affect bone health through several mechanisms, including the anti-anabolic effect of sclerostin, the osteoclastic-stimulating effect of RANKL, and an interference with normal osteoblast/osteocyte differentiation. These mechanisms could be targets for treatment of fracture due to diabetes.

Disclosures: Donna Pacicca, None.

SU0101

Glucose Intolerance Attenuates Bone Accrual in Young Growing Skeleton by Promoting the Maturation of Osteoblasts through Beclin1-Mediated Autophagy. <u>Elizabeth Rendina-Ruedy</u>*[1], <u>Jennifer Graef</u>[2], <u>Stan Lightfoot</u>[3], <u>Jerry Ritchey</u>[4], <u>Stephen Clarke</u>[2], <u>Edralin Lucas</u>[2], <u>Brenda Smith</u>[2]. [1]Vanderbilt University Medical Center, USA, [2]Oklahoma State University, USA, [3]Center for Cancer Prevention & Drug Development, University of Oklahoma Health Sciences Center, USA, [4]Department of Veterinary Pathology, Oklahoma State University, USA

Patients with type 2 diabetes mellitus (T2DM) have demonstrated a 1.5-3.5 fold increase in fracture risk, but the mechanisms responsible for these skeletal changes remain elusive. Macroautophagy, referred to hereafter as autophagy, is regulated by signaling downstream of the insulin receptor. Metabolic changes associated with the initiation and progression of glucose intolerance have been shown to alter autophagy in various tissues, but limited information is available in relation to bone cells. The aim of this study was to (1) investigate whether autophagy is altered in the bone during the initiation and progression of T2DM and (2) determine how autophagy impacts osteoblast differentiation, activity, and maturation. To accomplish this aim, 4-week old, male C57BL/6 mice were fed a control (Con) or high fat (HF) diet for 2, 8, and 16 wks. Consistent with reduced insulin sensitivity, mice on the HF diet demonstrated elevated fasting blood glucose and impaired glucose tolerance. Micro-computerized tomography (microCT) analyses revealed reduced trabecular bone at 8 and 16 wks in the femoral neck, which resulted in lower trabecular bone volume compared to Con mice. Histological evaluation of the tibia and characterization of osteoblast-related genes in the flushed femur suggested that hyperglycemia decreased bone mineralization and may promote terminal osteocyte differentiation. This shift of the osteoblasts towards a non-mineralizing, osteocyte phenotype appears to be coordinated by Beclin1 mediated autophagy during impaired glucose tolerance. However, long-term glucose intolerance resulted in an increase in apoptosis of the osteoblast based on an increase in *Casp3* mRNA. Consistent with changes occurring in the osteoblast *in vivo,* the induction of autophagy by rapamycin was able to direct MC3T3-E1 cells towards a more mature osteoblast phenotype. The current study provides evidence that glucose intolerance contributes to the skeletal dysregulation of bone metabolism by up-regulating autophagy in osteoblasts, directing this cell towards a non-mineralizing osteocyte, ultimately attenuating bone accrual. Further investigation is warranted to determine if Beclin1-mediated autophagy is essential for the terminal differentiation of the osteoblasts and whether autophagy is having a protective or deleterious effect on bone in T2DM.

Disclosures: Elizabeth Rendina-Ruedy, None.

SU0102

mTOR-dependent Reactive Oxygen Species Contribute to Diabetic Bone Pathology. <u>Nandini Ghosh-Choudhury</u>*[1], <u>Balakuntalam S Kasinath</u>[2], <u>Kavithalakshmi Sataranatarajan</u>[3], <u>Hanna E Abboud</u>[3], <u>Jameela Banu</u>[4], <u>Goutam Ghosh Choudhury</u>[3]. [1]University of Texas Health Science Center at San Antonio, USA, [2]University of Texas Health Science Center at San Antonio, USA, [3]University of Texas Health Science Center, USA, [4]University of Texas-Pan American, USA

Diabetes is reaching an epidemic stage among people aged 20 years and older in the United States. Prolonged hyperglycemia significantly augments fracture risk and increases the healing time in diabetic patients. Role of mechanistic target of rapamycin (mTOR) and oxidative stress is established in many complications of diabetes. However, their role in diabetic bone pathology is not known. We probed the role of mTOR in compromised bone quality found in db/db mouse model of type 2 diabetes and in osteoblasts exposed to high glucose conditions. High glucose induced activation of mTORC1 (mTOR complex1) in preosteoblasts as measured by increase in phosphorylation of S6 kinase and 4EBP1, two downstream effectors of mTORC1. We show that mTORC1 is activated in bones of db/db mice with type 2 diabetes.

These mice were fed a diet containing rapamycin (2.24 mg/Kg/day), a pharmacological inhibitor of mTORC1, for 4 months starting at 7 months of age. Rapamycin blocked mTOR activation and reversed overall defect in mineralized bone formation. MicroCT analysis of the distal femur from db/db mice showed reduction in trabecular thickness, trabecular number and BV/TVand increase intrabecular separation compared to the control mice. Rapamycin treatment restored these bone parameters at this late stage of diabetes in mice. To identify the downstream effector of mTOR signaling in diabetic bone we investigated the involvement of reactive oxygen species (ROS). We detected increased production of ROS, as determined by DCF fluorescence, in osteoblasts incubated with high glucose. We also show that the NADPH oxidase activity, determined by lucigenin assay, is increased by high glucose in osteoblasts. Interestingly, rapamycin inhibited both ROS production and NADPH oxidase activity induced by high glucose. These results provide the first evidence for the presence of a cross-talk between mTORC1 and ROS in diabetic bone pathology.

Disclosures: Nandini Ghosh-Choudhury, None.

SU0103

Protective effect of ion zinc on bone strength and flexibility: Bone biomechanical and molecular analyses in type 1 diabetes model. <u>Raul H Bortolin</u>*[1], <u>Marcela A G Ururahy</u>[2], <u>Flávio S Silva</u>[2], <u>Angelica A S Batista</u>[3], <u>Giselle Oliveira</u>[3], <u>Karla S C Souza</u>[2], <u>Melina B Loureiro</u>[2], <u>Valeria M G Duarte</u>[4], <u>Bento J Abreu</u>[2], <u>Maria G Almeida</u>[2], <u>Luciana A Rezende</u>[3], <u>Adriana Rezende</u>[5]. [1]Federal University of Rio Grande do Norte, USA, [2]Federal University of Rio Grande do Norte, Brazil, [3]University of Ribeirão Preto, Brazil, [4]State University of Paraiba, Brazil, [5]Federal University of Rio Grande De Norte-UFRN, Brazil

Osteopenia is one of the diabetes-induced chronic complications. Studies have showed the importance of supplementation with minerals and vitamins in preventing bone loss. Thus, the aim of this study was to evaluate the protective effect of zinc on bone in a diabetic osteopenic model. Male Wistar rats were distributed in three groups (five rats per group): Control (C), Diabetic (D; STZ-induced; 40mg/Kg i.v.) and Diabetic supplemented with 500 mg/day of zinc during 90 days (DS). Serum glucose concentration, tibia biomechanical parameters (Maximum Load, Stiffness, Ultimate Strain and Youngs modulus) and femur mRNA expression of *RANKL, OPG, OC, COL1A, MMP2, MMP9* and *TGFB* were evaluated. Animals were considered diabetic by serum glucose concentration ($\geq$ 250 mg/dL) associated with polyphagia, polydipsia and polyuria. The Maximum Load, Stiffness, Ultimate Strain and Youngs modulus parameters were found decreased in the D group (p<0.05) when compared to C group. However, for DS group, all biomechanical parameters were similar to C group, except Stiffness parameter that was reduced (p<0.05). In relation to the molecular parameters the mRNA expression of the *OPG, OC, COL1A* and *MMP9* was increased (37, 17, 17 and 344 folds, respectively) in D group when compared to C Group (p<0.05). In addition, no differences were found for *RANKL, MMP2* and *TGFB* mRNA expression between the groups. Considering DS group, we also observed results similar to C group for molecular parameters, showing an important effect of the zinc ion in preventing bone loss in diabetes condition. Our results associated important analyses, such as Maximun load and Stiffness showing a decrease in the bone strength supported by the up regulation of *OPG* and *OC* mRNA as an attempt to avoid bone loss onset. When supplemented with zinc the DS group showed similar results with C group, suggesting the maintenance of bone strength. Considering Ultimate Strain and Youngs Modulus we may suggest a reduced bone flexibility associated with the up regulation of *COL1A* and *MMP9* mRNA expression, showing a tendency to try to compensate the alteration of bone architecture associated with collagen. Similarly to bone strength, bone flexibility was maintained in zinc-supplemented group. In conclusion, our results may suggest that zinc supplementation have a protective and benefic effect on preventing bone strength and flexibility reduction over a 90 days period.

Disclosures: Raul H Bortolin, None.

SU0104

Type 2 diabetes increases infection severity, impairs humoral immunity, and alters bone remodeling following orthopaedic implant associated *S. aureus* **infection.** <u>Christopher Farnsworth</u>*[1], <u>Robert Maynard</u>[2], <u>Edward Schwarz</u>[1], <u>Michael Zuscik</u>[3], <u>Robert Mooney</u>[4]. [1]University of Rochester, USA, [2]University of Rochester, USA, [3]University of Rochester School of Medicine & Dentistry, USA, [4]University of Rochester Medical Center, USA

Purpose: Type 2 diabetes (T2D) is the greatest risk factor for infection following total joint arthroplasty. T2D is also a risk factor for osteoarthritis. With the number of type 2 diabetics expected to double by 2050, a dramatic increase in infection rates following total joint replacement is projected for the coming years. It is critical to determine the mechanism underlying increased infection rates in T2D. T2D is associated with both an impaired innate immune response and multiple bone diseases. Therefore we hypothesize that T2D increases the susceptibility of orthopedic implant recipients to infections, specifically by *Staphylococcus aureus,* by compromising immunity and altering bone remodeling.

Methods: Animals: C57BL/6J mice were fed a high fat diet (60% Kcal from fat) or lean diet (10% Kcal from fat) for 12 weeks. Osteomyelitis model: tibiae were surgically exposed and pre-drilled medially to laterally with a 27G needle. A stainless steel wire was pre-coated with bioluminescent Xen36 *S. aureus* and was placed through the defect. Bioluminescent imaging (BLI): analyses were performed up to 14 days post infection using a Xenogen IVIS camera. Total IgG and IgM titers were determined by ELISA. Antibodies to eight *S. aureus* antigens were titered by Luminex-based assays. Cortical bone was measured using uCT and confirmed with histology.

Results: Mice fed a high-fat diet developed obesity and T2D. Following implantation of a *S. aureus*-coated implant through the tibia, diabetic mice had higher bacterial loads than control mice as indicated by BLI. These results were confirmed by isolating and counting colony forming units of *S. aureus* from both bone and muscle. Furthermore, diabetic mice had an impaired antibody response to *S. aureus* infection compared to control mice as indicated by a decrease in total IgG and an increase in IgM. Antibody titers to 8 *S. aureus* antigens were also decreased in infected diabetic mice. uCT and histology revealed impaired bone remodeling and cortical thinning at the surgical site in diabetic mice.Conclusion: These data indicate that T2D causes more severe *S. aureus* infections in a mouse model of joint arthroplasty. Diabetic mice have an impaired humoral immune response and impaired bone remodeling to *S. aureus* infection. These defects may underlie the susceptibility, severity, and pathogenesis of orthopedic implant- associated infections in diabetics.

Diabetic, infected mice have worse *S. aureus* infection than lean fed, control mice. Mice were given either a control diet, or a high fat (HF) diet to induce type 2 diabetes, and were infected through the right tibia with an orthopedic implant coated with bioluminescent Xen36 *S. aureus*. BLI was measured longitudinally over a 14 day experiment. Results were confirmed by counting colony forming units from infected tibiae.

Figure 1

Diabetic, HF-fed mice have an impaired antibody response and cortical thinning. A. Antibody levels were measured to 8 *S. aureus* antigens 14 d post infection by luminex based assay. B. Cortical bone thickness was measured by microCT 14 days post implantation of either a sterile pin or a pin coated with *S. aureus*.
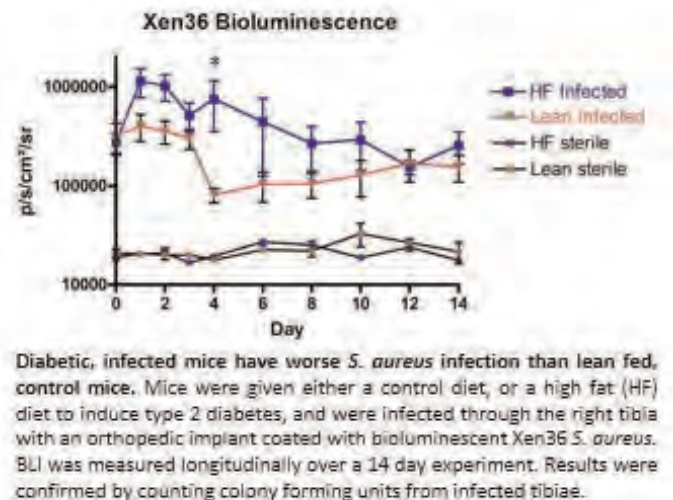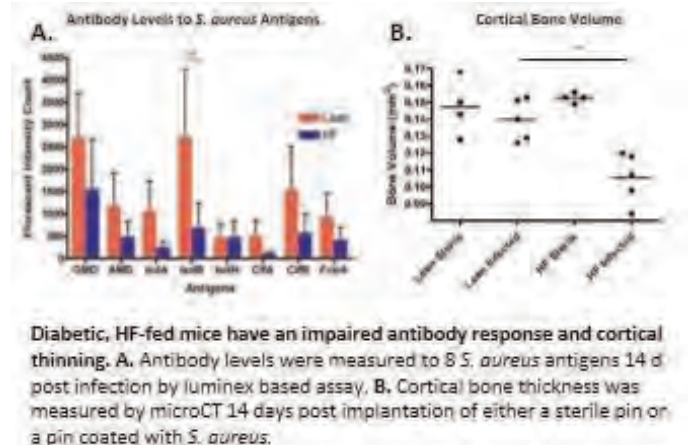
Figure 2

Disclosures: Christopher Farnsworth, None.

SU0105

Apolipoprotein E protects mice from osteoporosis by promoting osteoblasts differentiation and inhibiting osteoclasts induction. <u>Takaaki Noguchi</u>*[1], <u>Kosuke Ebina</u>[2], <u>Masafumi Kashii</u>[3], <u>Yohei Matsuo</u>[4], <u>Tsuyoshi Sugiura</u>[5], <u>Jun Hashimoto</u>[6], <u>Hideki Yoshikawa</u>[7]. [1]Osaka university, Japan, [2]Osaka University, Graduate School of Medicine, Japan, [3]Osaka University Graduate School of Medicine, Japan, [4], Japan, [5]Faculty of Medicine, Graduate School of Medicine, Osaka University, Japan, [6]National Hospital Organization, Osaka Minami Medical Center, Japan, [7]Osaka University Graduate School of Medicine, Japan

Purpose

It is well known that hyperlipidemia is frequently associated with osteoporosis, but its detailed mechanism remains unknown. Apolipoprotein E (ApoE) forms complex with lipids called lipoprotein and plays a major role in removing excess cholesterol from the blood, and its knockout mice presents severe lipidosis and arteriosclerosis. Meanwhile, effects of ApoE on bone metabolism still remains unkown.

Method

48-weeks olds ApoE knockout mice (ApoEKO) (n=8 females) and control wild type C57BL6 mice (WT) (n=8 females) which were fed with normal chaw were examined. 3D trabecular structure was measured by microCT, and the number of osteoclasts was evaluated by Tartrate-Resistant Acid Phosphatase (TRAP) staining. RNA was extracted by radius, and serum concentration of osteocalcin and CTX-1 was measured by ELISA. The effect of ApoE in osteoblasts differentiation was evaluated by using MC3T3-E1 cell, and its effect in osteoclasts differentiation was evaluated by using mice spleen cells with RANKL and M-CSF.

Results

MicroCT revealed that ApoE KO mice presents severe osteoporosis compared to wild type mice, which were evaluated by cancellous bone quantity (BV/TV) (3.3% v.s. 16.6% ; P <0.001), number of the trabecular (Tb.N) (1.2/mm v.s. 3.8/mm ; P<0.001), and cortical bone quantity (Cv/Av) (31.8% v.s. 37.9% ; P<0.01). In addition, ApoE KO mice showed larger number of osteoclasts (8.6/mm v.s. 4.5/mm ; P<0.05) and lower serum osteocalcin (52.7±13.5ng/ml v.s. 38.2±11.4ng/ml ; P=0.087) and CTX-1 (2.4±0.2ng/ml v.s. 2.0±1.5ng/ml ; P=0.58) . In vitro, human ApoE4 recombinant protein (0 v.s. 5μg/ml) inhibited osteoclasts formation(111.8±9.2 v.s. 84.8±11.3 ; P<0.05) and relative mRNA expression of c-Fos(1.1±0.07 v.s. 0.75±0.08 ; P<0.05), NFATc1(0.99±0.03 v.s. 0.92±0.07 ; P<0.05), TRAP(1.07±0.1 v.s. 0.83±0.02 ; P<0.05), and CathepsinK (0.98±0.04 v.s.0.59±0.05 ; P<0.05). In addition, human ApoE4 recombinant protein promoted ALP activity of MC3T3-E1 cell on day 7(0 v.s. 5μg/ml ; 1.0±0.03 v.s. 1.23±0.16 ; P<0.01).

Conclusions

Our findings revealed that ApoE plays a crucial role in connecting hyperlipidemia and osteoporosis by promoting osteoblasts differentiation and inhibiting osteoclasts differentiation, showing possibility as a dominant treating target of both desease.
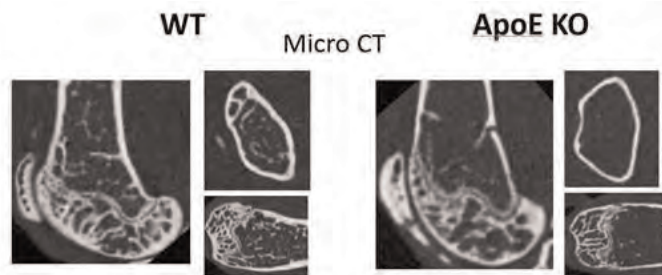
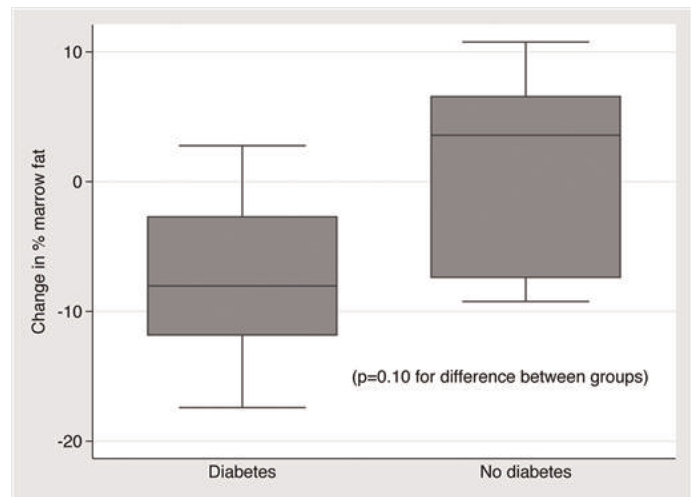ASBMR figure

Disclosures: Takaaki Noguchi, None.

SU0106

Changes in Bone Marrow Fat During Gastric Bypass Surgery-Induced Weight Loss. <u>Anne Schafer</u>*[1], <u>Ann Schwartz</u>[2], <u>Dennis Black</u>[2], <u>Amber Wheeler</u>[2], <u>Lygia Stewart</u>[3], <u>Stanley Rogers</u>[4], <u>Jonathan Carter</u>[4], <u>Andrew Posselt</u>[4], <u>Dolores Shoback</u>[5], <u>Xiaojuan Li</u>[2]. [1]University of California, San Francisco & the San Francisco VA Medical Center, USA, [2]University of California, San Francisco, USA, [3]San Francisco VA Medical Center & the University of California, San Francisco, USA, [4]University of California, San Francisco, USA, [5]VA Medical Center, USA

Osteoblasts and adipocytes share a common mesenchymal stem cell precursor within the bone marrow, and greater marrow fat is associated with lower bone mineral density (BMD). Marrow fat may serve a metabolic role distinct from other fat depots. Longitudinal effects of weight loss on marrow fat in humans have not been studied. In young mice, caloric restriction increases marrow fat. In humans, women with anorexia nervosa have higher marrow fat than controls despite having much lower visceral and subcutaneous fat. We hypothesized that marrow fat increases after Roux-en-Y gastric bypass (RYGB) surgery, even while other fat depots decrease markedly.

In a pilot study of 11 morbidly obese women (6 diabetic, 5 nondiabetic), we measured vertebral marrow fat before and 6 months after RYGB using magnetic resonance spectroscopy (MRS) at 3T. Six healthy, normal weight control women also underwent MRS at baseline and after 6 months. Marrow fat as saturated lipid content (%) was calculated as $I_{methylene}/(I_{methylene}+I_{water})$ x100, where $I_{methylene}$ and I_{water} are the signal amplitudes of the bulk methylene and water peaks, respectively. Other measures included BMD and body composition by dual-energy X-ray absorptiometry (DXA).

Surgery patients had mean pre-op body mass index 40 kg/m^2. Median pre-op marrow fat was 49% and 46% among diabetic and nondiabetic patients, respectively. Older patients had higher pre-op marrow fat (p=0.04). By DXA, fat mass declined in all patients (mean 19 kg, a 36% decrease, p<0.001). Among those with diabetes, there was a trend towards decreased marrow fat after RYGB, with a median 8% decline (p=0.07; Figure). In nondiabetic women, marrow fat did not change (median change +4%, p=0.89). There was a trend for difference in change between diabetics and nondiabetics (p=0.10). Changes in marrow fat and fat mass by DXA were inversely correlated among nondiabetic (ρ=-0.90, p=0.04) but not diabetic patients. BMD declined at the spine and hip, but changes in marrow fat and BMD were not correlated. Normal weight controls had no 6-month change in marrow fat.

In conclusion, changes in bone marrow fat are variable after RYGB, despite consistent and dramatic declines in overall fat mass. Although more investigation is necessary, our results suggest that RYGB reduces marrow fat in women with, but not without, diabetes. Marrow fat may be subject to complex regulation and may have unique metabolic behavior and kinetic properties compared with other fat depots.

Changes in bone marrow fat during gastric bypass surgery-induced weight loss

Disclosures: Anne Schafer, None.

SU0107

Differences in the Associations of Obesity with Bone Density, Microarchitecture and Strength in Younger and Older Adults. <u>Amy Evans</u>*[1], <u>Margaret Paggiosi</u>[2], <u>Richard Eastell</u>[1], <u>Jennifer Walsh</u>[3]. [1]University of Sheffield, United Kingdom, [2]University of Sheffield, United Kingdom, [3]University of Sheffield, United Kingdom

Obesity is associated with lower risk of hip and vertebral fracture, but greater risk of lower leg and proximal humerus fracture. Obese adults have greater areal BMD (aBMD) by dual energy x-ray absorptiometry (DXA). It is not known whether greater BMD in obese adults is the result of greater bone acquisition or reduced bone loss. We investigated BMD, bone structure and strength in younger and older men and women to identify age-related effects of obesity on the skeleton. We studied 100 individually matched pairs of normal weight (BMI 18.5-24.9 kg/m^2) (NW) and obese (BMI>30 kg/m^2) (OB) adults aged 25-40 (n=80) and 55-75 years (n=120). We measured whole body, hip and lumbar spine aBMD by DXA, distal radius and distal tibia volumetric BMD (vBMD) by HR-pQCT and bone strength of the radius and tibia by micro FEA from HR-pQCT. Younger OB had greater hip, lumbar spine and tibia BMD than NW, while older OB had greater BMD than NW at all sites (all p<0.001). BMD was approximately 0 to 1 SD scores greater in younger OB than NW and 1 to 2 SD scores greater in older OB than NW (Table). There was greater trabecular density at the radius (younger p<0.05, older p<0.001) and tibia (younger and older p<0.001) in OB, due to greater trabecular number (younger and older p<0.001) and lower trabecular spacing (younger and older p<0.001) in OB than NW. Cortical density was also greater in older OB than NW (p<0.001). OB had thicker cortices at the tibia (young p<0.01, older p<0.001) and radius (older p<0.001). Univariate GLM showed an interaction of age and BMI on cortical density and cortical area at both sites and on vBMD, trabecular density and cortical thickness at the radius, with a larger difference between NW and OB in older adults. Bone size did not differ between OB and NW in younger or older adults. Bone strength was greater in OB at all sites (younger p<0.05, older p<0.001). There was no interaction of age and BMI on bone strength. Obesity is associated with higher BMD, favourable microstructure and greater bone strength in younger and older adults, but there is a greater difference in

BMD and microstructure between OB and NW in older adults than in younger adults. The higher BMD in obesity is explained by both higher peak bone mass and lower rates of bone loss

	Total Hip aBMD	Lumbar Spine aBMD	Whole Body aBMD	Distal Radius vBMD	Distal Tibia vBMD
Young women (n=44)	1.33 (0.72-1.93)	0.23 (-0.38-0.84)	0.05 (-0.49-0.58)	0.33 (-0.13-0.78)	0.754 (0.01-1.50)
Young men (n=36)	1.06 (0.49-1.63)	0.56 (-0.11-1.22)	0.56 (-0.01-1.13)	0.36 (-0.37-1.09)	1.301 (0.86-1.74)
Older women (n=60)	2.83 (2.08-3.58)	2.00 (1.44-2.57)	1.27 (0.57-1.97)	1.09 (0.64-1.54)	1.597 (1.09-2.10)
Older men (n=60)	1.29 (0.78-.1.81)	1.09 (0.4701.71)	0.93 (0.29-1.56)	0.91 (0.41-1.42)	0.81 (0.19-1.44)
				Data shown as mean (95% CI) SD scores	

Table: Difference in BMD between OB and NW as SD scores of the NW, age and gender matched group

Disclosures: Amy Evans, None.

SU0108

Relationships Between Total Body and Regional Adiposity and Cortical and Trabecular Architecture in Late Adolescent Females. <u>Joseph Kindler</u>*[1], <u>Hannah Ross</u>[2], <u>Emma Laing</u>[1], <u>Christopher Modlesky</u>[3], <u>Norman Pollock</u>[4], <u>Clifton Baile</u>[5], <u>Mark Punyanitya</u>[6], <u>Richard Lewis</u>[1]. [1]The University of Georgia, USA, [2]The University of Georgia, USA, [3]University of Delaware, USA, [4]Georgia Regents University, USA, [5]University of Georgia, USA, [6]Image Reading Center, Inc., USA

Adolescents who are obese are at increased risks for skeletal fractures. However, it is unclear whether general obesity rather than site-specific adiposity is implicated in higher fracture risk. The relationships between site-specific fat deposition and bone quality have been explored in older adults, but limited data exist in adolescents. We aimed to identify relationships between total body fat mass (FM), visceral (VAT) and subcutaneous adipose tissue (SAT) and bone architecture in obese and normal weight adolescent females (18-19 years old; N=24). Magnetic resonance imaging (MRI; 3.0 Tesla magnet) was used to measure VAT and SAT, as well as trabecular and cortical bone architecture at the non-dominant tibia and radius. Total body fat-free soft tissue (FFST) and FM were determined via DXA (Hologic Discovery A). FM and SAT were transformed for normality. Unadjusted Pearson's correlations and partial correlations controlling for FFST were used to examine relationships. Significant inverse correlations were observed between FM, SAT and VAT and trabecular thickness at the proximal tibia and bone volume/total volume at the distal radius. FM and SAT were positively related to trabecular separation at the distal radius (Table 1). After adjustment for FFST, FM was additionally inversely associated with bone outcomes at the mid-tibia and mid-radius, SAT at the mid-radius and VAT at the mid-radius only. These data support a potentially negative influence of adipose tissue on trabecular bone quality regardless of fat location at habitually loaded and unloaded skeletal regions in adolescents.

Table 1. Unadjusted Pearson's correlations (r) and FFST-adjusted partial correlations between total body and regional adiposity and cortical and trabecular architecture at the non-dominant tibia and radius

	Total Body Fat Mass				SAT				VAT			
	Unadjusted		FFST-Adjusted		Unadjusted		FFST-Adjusted		Unadjusted		FFST-Adjusted	
	r	p	r	p	r	p	r	p	r	p	r	p
Proximal Tibia												
Apparent Bone Volume to Total Volume (mm³)	-0.32	0.13	-0.10	0.64	-0.22	0.30	0.05	0.81	-0.33	0.11	-0.17	0.45
Apparent Trabecular Number (mm⁻¹)	0.29	0.17	0.44	0.04	0.35	0.10	0.50	0.02	0.12	0.56	0.14	0.54
Apparent Trabecular Thickness (mm)	-0.49	0.02	-0.34	0.11	-0.40	0.05	-0.19	0.38	-0.43	0.04	-0.26	0.23
Apparent Trabecular Separation (mm)	0.07	0.75	-0.15	0.48	-0.03	0.89	-0.29	0.17	0.17	0.44	0.05	0.82
Mid-Tibia												
Cortical Volume (mm³)	-0.12	0.59	-0.45	0.03	-0.09	0.67	-0.38	0.06	-0.12	0.56	-0.33	0.13
Polar Moment of Inertia (mm⁴)	-0.05	0.83	-0.47	0.02	0.01	0.98	-0.35	0.10	-0.05	0.81	-0.32	0.13
Section Modulus (mm³)	-0.02	0.91	-0.46	0.03	0.02	0.92	-0.35	0.10	-0.04	0.86	-0.32	0.14
Cross-Sectional Moment of Inertia (mm⁴)	-0.05	0.83	-0.47	0.02	0.01	0.98	-0.35	0.10	-0.05	0.81	-0.32	0.13
Distal Radius												
Apparent Bone Volume to Total Volume (mm³)	-0.53	0.01	-0.43	0.04	-0.62	0.00	-0.58	0.00	-0.41	0.05	-0.26	0.24
Apparent Trabecular Number (mm⁻¹)	0.00	1.00	0.44	0.04	0.09	0.68	0.54	0.01	0.10	0.65	0.41	0.05
Apparent Trabecular Thickness (mm)	-0.39	0.06	-0.50	0.02	-0.50	0.01	-0.66	0.00	-0.35	0.09	-0.37	0.08
Apparent Trabecular Separation (mm)	0.42	0.04	-0.01	0.96	0.43	0.04	0.02	0.92	0.26	0.23	-0.14	0.51
Mid-Radius												
Cortical Volume (mm³)	0.01	0.98	-0.43	0.04	-0.05	0.82	-0.49	0.02	-0.28	0.19	-0.66	0.00
Polar Moment of Inertia (mm⁴)	-0.17	0.43	-0.44	0.04	-0.17	0.42	-0.41	0.05	-0.31	0.14	-0.51	0.01
Section Modulus (mm³)	-0.24	0.27	-0.46	0.03	-0.24	0.29	-0.44	0.04	-0.39	0.06	-0.55	0.01
Cross-Sectional Moment of Inertia (mm⁴)	-0.17	0.43	-0.44	0.04	-0.17	0.42	-0.41	0.05	-0.31	0.14	-0.51	0.01

FFST, fat-free soft tissue; VAT, visceral adipose tissue; SAT, subcutaneous adipose tissue

Table 1

Disclosures: Joseph Kindler, None.

SU0109

Skeletal response to caloric restriction differs in male vs. female mice. <u>Maureen Devlin</u>*[1], <u>Miranda Van Vliet</u>[2], <u>Leeann Louis</u>[3], <u>Christine Conlon</u>[3], <u>Mary Bouxsein</u>[4]. [1]University of Michigan, USA, [2]Beth Israel Deaconess Medical Center, USA, [3]Beth Israel Deaconess Medical Center, USA, [4]Beth Israel Deaconess Medical Center, Harvard Medical School, USA

Previously we showed that caloric restriction (CR) impairs bone acquisition and increases bone marrow adiposity in growing male mice, but effects of CR in female mice have not been well studied. The female skeleton may be more tolerant of CR due to females' metabolic flexibility during reproduction and/or the osteoprotective effects of estrogen. To test this hypothesis, male and female C57Bl/6J mice (N=8-13/grp) were fed normal (N) diet ad libitum or 30% calorie restricted diet from weaning (3 wks of age) to 12 or 20 wks of age. Outcomes included body mass and body length, %body fat, whole body bone mineral density (BMD), and cortical (Ct) and trabecular (Tb) bone architecture at midshaft and distal femur. Both male and female CR mice were lighter and shorter compared to N, but females were less affected than males (e.g. body mass 22-52% lower in female vs. 40-82% lower in male CR vs. N, p<0.05 for all). BMD was 10-21% lower in both male and female CR vs. N from 6-20 wks (p<0.05 for both). Body fat did not differ in CR vs. N females from 9-20 wks, but was 20-26% lower in CR males vs. N from 12-20 wks (p<0.05). In females, CR did not influence distal femur Tb.BV/TV (Figure), and led to higher Tb.N (+6-19%) and Conn.D (+32-44%) vs. N (p<0.05 for both). In contrast, male CR had markedly lower distal femur Tb.BV/TV (-75-77%, Figure), Conn.D (-24-41%), and Tb.N (-17-19%) vs. N (p<0.05 for all). Midshaft Ct.Th and polar moment of inertia did not differ in male or female CR vs. N after body mass adjustment, while mass-adjusted cortical bone area was lower in female CR vs. N (p<0.05). Thus, CR resulted in normal body fat and Tb.BV/TV and higher Tb.N and Conn.D in females, but lower body fat, Tb.BV/TV, Tb.N and Conn.D in males, suggesting that relatively higher body mass and body fat in CR females as compared to males may protect trabecular bone acquisition. These data support our hypothesis that females are more tolerant of caloric restriction than males, perhaps reflecting their higher estrogen levels or their metabolic flexibility during energetic stressors such as pregnancy and lactation.
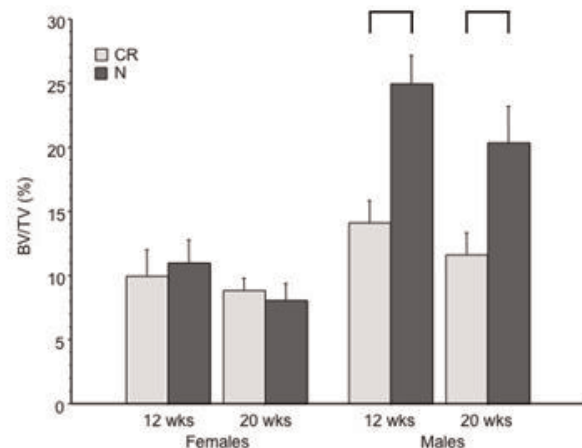
Figure

Disclosures: Maureen Devlin, None.

SU0110

Effect of dietary Fe on FGF23 level of adriamycin-treated mice. <u>Masanori Takaiwa</u>*[1], <u>Kosei Hasegawa</u>[2], <u>Kunihiko Aya</u>[3], <u>Hiroyuki Tanaka</u>[4], <u>Yoichi Kondoh</u>[5], <u>Nobuyuki Kodani</u>[5]. [1]Dept. of Pediatrics, Matsuyama Red Cross Hosp., Japan, [2]Okayama University Graduate School of Medicine, Dentistry & Pharmaceutical Sciences, Japan, [3]Kurashiki Chuou Hospital, Japan, [4]Okayama Saiseikai General Hospital, Japan, [5]Dept. of Pediatrics, Matsuyama Red Cross Hosp., Japan

Parenteral Fe therapy for CKD patients could increase FGF23 and cause hypophosphatemia. However, Fe deficiency worsens FGF23 elevation in patients with inherited hypophosphatemia. It has been documented that FGF23 is associate with poor prognosis of CKD. Since FGF23 elevates during the early CKD, we created an early CKD model by intermittent administration of adriamycin (ADR) to C57BL/6J mice (C57) and examined the effect of dietary Fe on FGF23 during the early CKD. Using 6 groups (control and 0.6%-Fe-AN groups – fed a 0.6% Fe diet; 2%-Fe and 2%-Fe-AN groups - fed a 2.0% Fe diet; 0.02%-Fe and 0.02%-Fe-AN groups - fed a 0.02% Fe diet), 10-week-old male C57 were administered serine (the control, 2%-Fe and

0.02%-Fe) or ADR weekly (0.6%-Fe-AN, 2%-Fe-AN and 0.02%-Fe-AN) for 28 days. Data were expressed as the mean $\pm$ SEM. A value of p<0.01 was considered significant (Tukey's test). After treatment, Fe for 2%-Fe and 2%-Fe-AN (275 ± 9 and $280 \pm 13 \mu g/dl$) were higher, and that of 0.02%-Fe-AN was lower ($115 \pm 10 \mu g/dl$) than the control ($161 \pm 6 \mu g/dl$). Hb of 0.02% Fe-AN (11.5 ± 0.1 g/dl) was markedly lower than the control (13.5 ± 0.1 g/dl). The kidneys of the ADR treated groups were smaller in size. Although not significant, Cr for 0.6%-Fe-AN, 2%-Fe-AN and 0.02%-Fe-AN were higher (1.8 ± 0.2, 2.3 ± 1.7 and 2.8 ± 0.3mg/dl) than the control (0.9 ± 0.1mg/dl). FGF23 tended to be higher among all ADR treated groups, only 0.02%-Fe-AN showed significant elevation (670 ± 134pg/ml) compared with the control (159 ± 10pg/ml). Ca, Pi and PTH showed no significant difference. The intermittent ADR injection caused the small kidneys associated with slight Cr increase. The ADR treatment caused mild increase in FGF23 without affecting Pi and PTH, hence serving as a reasonable early CKD model. Only the ADR treatment of the Fe depleted mice increased FGF23, hence the negative regulatory effect of Fe on FGF23 was significant during early CKD. Our results suggest that the initiation of oral Fe during early CKD suppresses FGF23 production and has a favorable effect on progression of CKD.

Disclosures: Masanori Takaiwa, None.

SU0111

Impact of Common Variants in Type 2 Diabetes Genes on Fracture Risk and Measures of Bone Quality in African American Children. Courtney Sprouse*[1], Joseph Devaney[2], Heather Gordish-Dressman[2], Leticia Ryan[3], Laura Tosi[1]. [1]Children's National Medical Center, USA, [2]Children's National Health System, USA, [3]Johns Hopkins University, USA

Purpose: Type 2 Diabetes (T2D) is a serious health problem; morever the incidence rate of type 2 diabetes is twice as high in African Americans (AA) than those of European descent. It is associated with numerous complications, including reduced bone quality and increased fractures risk in adulthood. The purpose of our study was to determine if single nucleotide polymorphisms (SNPs) previously associated with increased risk of developing T2D are also associated with measures fracture risk and bone quality in AA children.

Methods: DNA was isolated from 142 AA children, aged 5 to 9 years. Cases (n=71) had an isolated forearm fracture (radius, ulna or both) and age-matched control participants (n=71) had no prior fracture. Sixty-six SNPs previously found to be highly associated with pre-diabetic phenotypes or increased risk of developing T2D from genome wide association studies (GWAS) studies were selected for analysis. The 66 SNPs were then genotyped, using Taqman allelic discrimination assay or the Illumina Human Exome BeadChip. SNPs were analyzed for associations with Total Body minus head bone mineral density (BMD), Total Body minus head Z-score, Lumbar Spine BMD, and Lumbar Spine Z-score obtained from dual energy x-ray absorptiometry. Mean continuous phenotypes were compared among genotypes from each SNP using analysis of covariance models adjusted for gender and age. Associations between SNPs and fracture status were tested using logistic regression adjusted for gender. All regression models used a dominant genetic model.

Results: Significant associations with fracture status were found with rs17036101 located in the *SYN2* gene (OR= 3.54; 95% CI=1.21-10.34; p=0.021), rs896854 located in the *TP53INP1* gene (OR= 1.98; 95% CI=1.02-3.86; p=0.045), and rs11634397 located in the *ZFAND6* gene (OR=0.40; 95% CI=0.19-0.85; p=0.018). Furthermore, significant associations were found between rs13266634 in the *SLC30A8* gene and total body minus head BMD [CC: 0.673 ± 0.015 g/cm^3; CT/TT: 0.711 ± 0.021 g/cm^3; p=0.020] and lumbar BMD [CC: 0.549 ± 0.018 g/cm^3; CT/TT: 0.593 ± 0.025 g/cm^3; p=0.020]; and rs7542900 in the *SYN2* gene with both total BMD [CC: 0.651 ± 0.018 g/cm^3; CT/TT: 0.681 ± 0.014 g/cm^3; p=0.019] and lumbar BMD [CC: 0.549 ± 0.018 g/cm^3; CT/TT: 0.518 ± 0.022 g/cm^3; p= 0.006].

Conclusion: Our study suggests that AA children possessing alleles associated with increased risk of developing T2D in adulthood also have reduced BMD and increased risk of fracture.

Disclosures: Courtney Sprouse, None.

SU0112

A 'conditional-ON' mouse model of Fibrodysplasia Ossificans Progressiva (FOP). Sarah Hatsell*[1], Lily Huang[2], Liqin Xie[3], Trikaldarshi Persaud[2], Peter Yang[2], Lili Wang[4], Xialing Wen[2], Kalyan Nannuru[2], Vincent Idone[2], Aris Economides[5]. [1]Regeneron Pharmaceuticals, USA, [2]Regeneron Pharmaceuticals Inc, USA, [3]Regeneron Pharmaceutical company, USA, [4]Regeneron Pharmaceuticals Inc, USA, [5]Regeneron Pharmaceuticals, Inc., USA

FOP is an autosomal dominant disorder characterized by early onset, episodic and progressive ossification of skeletal muscle and associated connective tissue (Pignolo et al., 2011). FOP is driven by mutations in the intracellular domain of *ACVR1* (also known as *ALK2*), with the great majority altering Arginine 206 to Histidine (R206H). In order to enable the development of therapeutic approaches to FOP, as well as mechanistic studies of the disease process, we have engineered a Cre-regulated 'conditional-ON' allele of *ACVR1[R206H]* in the mouse – *ACVR1[R206H]COIN* – using a FlEx- (Schnutgen et al., 2003) or COIN-like design (Economides et al., 2013). (A conditional approach was necessitated because an unregulated *ACVR1[R206H]*

knock-in allele cannot be transmitted through the germline in mice (Chakkalakal et al., 2012).)

ACVR1[R206H]COIN was generated by introducing the R206H mutation in exon 5 of *mmuACVR1*, placing the mutated exon and flanking intronic sequence in the antisense strand. The corresponding region from human *ACVR1* (Chr2:158628593-158632803) was inserted into in the sense strand of *mmuACVR1* upstream of the inverted exon. To enable Cre-dependent replacement of the wild type exon 5 with its R206H version, the introduced human sequence was flanked by a 'FlEx' array of Lox2372 and LoxP sites in parallel orientation, whereas the mutant exon is followed by Lox2372-LoxP placed in antiparallel orientation with the Lox2372 and LoxP sites flanking human exon 5. This arrangement allows Cre-mediated inversion of the mutant exon into the sense strand and simultaneous deletion of the wild type human exon 5.

We show that the *ACVR1[R206H]COIN* allele is wild type prior to activation of its mutant form by Cre. Body-wide activation of the FOP allele in *Acvr1[R206H]COIN+;Gt(ROSA26)Sor[CreERt2]/+* adult mice resulted in progressive ossification resembling that of FOP, evident radiographically as early as 2 weeks after dosing with tamoxifen. MicroCT analysis at 12 weeks after tamoxifen injection revealed dense heterotopic ossification of the axial skeleton, as well as long bones and thorax, whereas untreated *ACVR1[R206H]COIN/+;Gt(ROSA26)Sor[CreERt2]/+* mice were normal in phenotype. The development of heterotopic ossification in tamoxifen-treated *ACVR1[R206H]COIN+;Gt(ROSA26)Sor[CreERt2]/+* mice was spontaneous, and did not require experimentally induced inflammation. The FOP phenotype was expressed in adult mice, uncoupling the process observed in these mice from development. Detailed studies deciphering the molecular and cellular mechanisms that underlie FOP are currently under investigation using this physiologic mouse model of FOP, along with testing of candidate therapeutic regimens.

Disclosures: SARAH HATSELL, None.

SU0113

Withdrawn

SU0114

A Transgenic Mouse Model of OI Type V Suggests the IFITM5 c.-14C>T Mutation Is Neomorphic. Ronit Marom*[1], Caressa Lietman[1], Ming Ming Jiang[2], Elda Munivez[2], Brian Dawson[2], Terry Bertin[2], Yuqin Chen[2], MaryAnn Weis[3], David Eyre[4], Brendan Lee[1]. [1]Baylor College of Medicine, USA, [2]Baylor College of Medicine, USA, [3]University of Washington, USA, [4]University of Washington Orthopaedic Research Labs, USA

Osteogenesis Imperfecta (OI) type V, characterized by increased bone fragility, long bone deformities, hyperplastic callus formation and calcification of interosseous membranes, is caused by a recurrent mutation in the 5' UTR of *IFITM5* gene (c.-14C>T). This mutation introduces a new start codon, adding 5 amino acid residues to the N-terminus of the protein. The mechanism whereby this novel IFITM5 protein causes OI type V – is yet to be defined. We present here a transgenic mouse model of OI type V that overexpresses the mutant *Ifitm5* allele.

The *IFITM5* transgenic construct, carrying either wild type (control) or mutant *Ifitm5* allele under the Col1a1 2.3kb promoter, was introduced into FVBN mice. The resultant transgenic mice carrying mutant *Ifitm5* exhibited perinatal lethality, whereas non-transgenic littermates and wild-type transgenic litters exhibited no lethality. Skeletal preparations and radiographs performed on E15.5 and E18.5 embryos revealed delayed/abnormal mineralization and skeletal defects including abnormal rib cage formation, long bone deformities and fractures. Primary osteoblast cultures, derived from mutant mice calvaria at E18.5, showed decreased mineralization by Alizarin-Red staining, as compared to non-transgenic littermates and wild-type mice calvaria cultures, consistent with the in vivo phenotype. Importantly, overexpression of wild-type *Ifitm5* did not result in significant bone phenotype, as evident by micro-CT studies of adult transgenic mice.

Collectively, our results suggest abnormal skeletal development, loss of bone mineralization and abnormal bone cell phenotype in this transgenic mouse model. Since overexpression of the mutant *Ifitm5* in bone resulted in perinatal lethality, we were unable to see the post-natal phenotype of hyper callus formation and interosseous membrane calcification. Given that neither overexpression of the wild type *Ifitm5*, as shown in our model, nor knock-out of *Ifitm5*, as previously published, were consistent with this overt bone phenotype, we suggest a neomorphic effect of *IFITM5* mutation as the cause of abnormal bone formation in OI type V.

Disclosures: Ronit Marom, None.

SU0115

Abnormal Bone Morphology in a Feline Model of Sandhoff Disease.
Margaret McNulty*[1], Patricia Beadlescomb[2], Miguel Sena-Esteves[3], Ashley Randle[4], Aime Johnson[5], D. Ray Wilhite[6], Douglas Martin[2]. [1]Louisiana State University School of Veterinary Medicine, USA, [2]Auburn University College of Veterinary Medicine, Scott-Ritchey Research Center, Dept. of Anatomy, Physiology, & Pharmacology, USA, [3]University of Massachusetts Medical School, Department of Neurology & Gene Therapy Center, USA, [4]Auburn University College of Veterinary Medicine, Scott-Ritchey Research Center, USA, [5]Auburn University College of Veterinary Medicine, Department of Clinical Sciences, Scott-Ritchey Research Center, USA, [6]Auburn University College of Veterinary Medicine, Dept. of Anatomy, Physiology, & Pharmacology, USA

Lysosomal storage disorders are characterized by abnormal accumulation of molecular waste in all cells due to defects in lysosome function, however neurons are most affected. GM2 gangliosidoses, a subgroup of the disorders, including Sandhoff disease (SD), is caused by a deficiency in the enzyme β-N-acetylhexosaminidase (Hex) and presents with severe neurological effects in humans resulting in death at an early age. With advancements in treatments to prolong lifespan, research must be conducted on the potential effects of SD on other tissues that may impact quality of life. In this study, a feline model of infantile SD was used to evaluate boney changes secondary to the disease. Affected (known deficiency in Hex) cats received an intracranial injection of adeno-associated virus vector. This treatment has been shown to significantly increase the lifespan by reducing the neurological effects of the disease. As lifespan increased, skeletal abnormalities including dysplasias & luxations were clinically identified. Long bones from 21 cats (age: 3.9-37 months), both affected (treated & untreated) and normal (not deficient in Hex) were scanned with microCT. Trabecular architecture in the distal femur & proximal humerus, and cortical geometry in the midshaft of the femur was evaluated. Affected cats (treated & untreated) displayed abnormal skeletal changes. Overall morphology indicated a significant retardation in epiphyseal development. In young (<6 months) affected cats, there was severe lack of development of the epiphyses. The physes of older (>17 months) affected cats persisted, though the epiphyses appeared to be mostly developed. The boney articular surfaces of affected cats were roughened and had subchondral bone lesions. Periarticular osteophytes were also present. Trabecular bone volume was decreased in affected (treated & untreated) cats of all ages. This difference was significant in the young cats (BV/TV femur: p=0.03; humerus: p=0.023), but not other ages due to a small sample size. Other significant differences between affected & normal cats were found in structural model index, connectivity density, and degree of anisotropy. No significant differences were identified in cortical geometry. This study shows that Hex deficiency in cats has a significant effect on bone development, particularly secondary centers of ossification and may affect bone remodeling. This has implications for studies aimed to improve the lifespan of those affected with SD.

Disclosures: Margaret McNulty, None.

SU0116

Activation of FGF/FGF Receptor Signaling in the Primary Osteocytes Isolated from Hypophosphatemic *Hyp* Mice. Kazuaki Miyagawa*[1], Miwa Yamazaki[2], Masanobu Kawai[3], Takao Koshimizu[2], Jin Nishino[4], Yasuhisa Ohata[5], Kanako Tachikawa[2], Yuko Mikuni-Takagaki[6], Mikihiko Kogo[7], Keiichi Ozono[8], Toshimi Michigami[9]. [1]Osaka University Graduate School of Dentistry, Japan, [2]Osaka Medical Center & Research Institute for Maternal & Child Health, Japan, [3]Osaka Medical Center & Research Institute for Maternal & Child Health, Japan, [4]Osaka Medical Center & Research Institute for Maternal & Child Health, Japan, [5]Osaka University Graduate School of Medicine, Japan, [6]Kanagawa Dental University Graduate School of Dentistry, Japan, [7]Osaka University Graduate School of Dentistry, Japan, [8]Osaka University Graduate School of Medicine, Japan, [9]Osaka Medical Center & Research Institute for Maternal & Child Health, Japan

Osteocytes express multiple genes involved in mineral metabolism including PHEX, FGF23, DMP1 and FAM20C. In *Hyp* mice, a murine model for X-linked *Hyp*ophosphatemia (XLH), it has been established that *Phex* deficiency results in the overproduction of FGF23 in osteocytes, which leads to *Hyp*ophosphatemia and impaired vitamin D metabolism. However, the role of osteocytes in the pathogenesis of *Hyp* mice is still not fully understood. In this study, to further clarify the abnormality in osteocytes of *Hyp* mice, we obtained detailed gene expression profiles in osteoblasts and osteocytes isolated from 20-week-old *Hyp* mice and wild-type (WT) control mice, using cells freshly isolated from the long bones based on the differentiation stage by sequential digestion with collagenase and decalcification with EGTA. The expression of *Fgf23*, *Dmp1*, and *Fam20c* was higher in osteocytic cells than in osteoblastic cells in both genotypes, and was up-regulated in *Hyp* cells. Interestingly, the up-regulation of these genes in *Hyp* bones began before birth. On the other hand, the expression of *Slc20a1* encoding the sodium/phosphate (Na$^+$/Pi) co-transporter Pit1 was increased in osteoblasts and osteocytes from adult *Hyp* mice, but

not in *Hyp* fetal bones. *Dmp1* expression in osteocytic cells was increased due to the 24-hour treatment with 10 mM Pi and was suppressed by 10^{-8} M $1,25(OH)_2D_3$ in WT. The up-regulation of *vitamin D receptor (Vdr)* by the treatment with $1,25(OH)_2D_3$ was smaller in *Hyp* cells than in WT cells, suggesting that the responsiveness to $1,25(OH)_2D_3$ might be reduced in *Hyp* cells. Previous studies suggest that induction of FGF23 in *Hyp* bone may be attributed to the activation of FGFR signaling. Therefore, we next examined the expression of the genes encoding Fgf1, Fgf2, Fgfr1–3, and a-Klotho in the osteocytic cells freshly isolated from WT and *Hyp* long bones. The expression of *Fgf1*, *Fgf2*, *Fgfr1*, and *Fgfr3* was significantly increased in *Hyp* cells, while that of a-*Klotho* was low in both genotypes. The expression of *Egr-1*, a target gene of FGF/FGFR signaling, was two-fold higher in *Hyp* osteocytic cells than in WT cells. These results provide the evidence for the activation of FGF/FGFR signaling in *Hyp* osteocytes, which might play a role in the pathogenesis of *Hyp* mice through the dysregulation of multiple genes. Since the expression of Fgf1 and Fgf2 was increased in *Hyp* osteocytic cells, these FGF ligands rather than Fgf23 might be responsible for the activation of the signaling.

Disclosures: Kazuaki Miyagawa, None.

SU0117

Development of Refined Methods to Induce Heterotopic Ossification in the Alk2^{Q207D} Mouse Model of Fibrodysplasia Ossificans Progressiva. Nicole Fleming[1], Satoru Hayano[2], Yuji Mishina[3], Charles Hong[4], Paul Yu[5], Daniel Perrien*[6]. [1]VUIIS, Vanderbilt University, USA, [2]Dept. of Biologic & Materials Sciences, University of Michigan School of Dentistry, USA, [3]Dept. of Biologic & Materials Sciences, University of Michigan School of Dentistry, USA, [4]Department of Cardiovascular Medicine, Vanderbilt University, USA, [5]Division of Cardiology, Harverd Medical School & Brigham & Women's Hospital, USA, [6]Vanderbilt University Medical Center, USA

Fibrodysplasia ossificans progressiva (FOP) is an untreatable rare congenital disorder characterized by progressive heterotopic ossification (HO) causing pain, immobility, and eventual death. FOP is caused by mutations in the *ACVR1* that produce constitutively active Alk2, a BMP Type 1 Receptor. Creating accurate and reliable animal models of FOP is a key step in developing therapies. Germline expression of activating mutations in Alk2 are embryonic lethal in mice, requiring a conditional approach. The Alk2^{Q207D}-floxed (caAlk2$^{fl/fl}$) mouse carrying a cre-inducible caAlk2 transgene was one of the first FOP models. However, it is unclear which methods and at what age HO can reliably induce HO in these mice. Hence, these studies sought to characterize multiple methods for inducing HO in caAlk2$^{fl/-}$ and caAlk2$^{fl/fl}$ mice. Local expression of caAlk2 was achieved by injection of adenovirus expressing cre recombinase (Ad-cre) into the calf muscles of mice with or without injections of cardiotoxin (CTX) at the same location to cause muscle damage. Weekly digital radiographs were acquired and the volume of HO was measured by *ex vivo* microCT. In the first study, 9-day old caAlk2 mice received i.m. injections of various titers of Ad-cre alone. HO was seen on x-ray at 2 wk only in the 10^9, $2x10^9$, and $5x10^9$ PFU groups, although the incidence of HO was lower with 10^9 PFU. The volume of HO at 3 wk was significantly greater with $5x10^9$ PFU (p<0.05). Induction of HO was significantly greater in caAlk2$^{fl/fl}$ mice vs. caAlk2$^{fl/-}$. The effect of CTX on HO in 9-11 day old caAlk2$^{fl/-}$ mice was tested using 10^9 PFU Ad-cre and injecting 0.3 µg of CTX per day for 3 days with Ad-cre on the 3rd day (3xCTX group), 1.0 µg CTX at same time of Ad-cre (1xCTX), or 1.0 µg CTX the day after Ad-cre (Delayed 1xCTX). The 3xCTX protocol significantly reduced HO vs. Ad-cre alone (p<0.05). The 1xCTX and Delayed 1xCTX protocols significantly enhanced HO, with lesions detectable within 1 wk and greater HO volume at 2-wk versus Ad-cre alone (p<0.05). Finally, 21-day old caAlk2$^{fl/-}$ mice were used to determine the reliability of HO induction in adolescent mice. Co-injection of $5x10^9$ PFU Ad-cre and 1.0 µg of CTX in the calf muscle resulted in rapid and aggressive HO detectable at 1 wk and maturing by 2 wk. These studies illustrate multiple methods for reliable induction of localized HO in the caAlk2 mouse model of FOP that should accelerate progress in research and drug development to treat this disease.

Disclosures: Daniel Perrien, None.

SU0118

Dystrophic Systemic Milieu Plays an ImportantRole in the Muscle and Bone Abnormalities in Duchenne Muscular Dystrophy. Hongshuai Li*[1], Aiping Lu[2], Ying Tang[2], Bing Wang[2], Johnny Huard[3]. [1]University of Pittsburgh, USA, [2]University of Pittsburgh, USA, [3]Orthopaedic Surgery, USA

Background: Duchenne muscular dystrophy (DMD) is a degenerative muscle disorder characterized by a lack of dystrophin expression in the sarcolemma of muscle fibers. DMD patients acquire osteopenia, fragility fractures, and scoliosis indicating a deficiency in skeletal homeostasis; however, little is known about the mechanism of the degenerative changes in the bone tissues during the process of DMD pathogenesis. We hypothesized that the DMD systemic milieu is an influencing factor that contributes to the degenerative muscle and bone pathologies observed in a severely affected model of DMD, the dystrophin/utrophin double knockout (dKO) mouse. Materials: Three animal models of DMD were utilized: mdx (dystrophin-/-), dKO-homo (dystrophin-/-, utrophin-/-), and dKO-hetero (dystrophin-/-, utrophin+/-). A

parabiotic model was used to test the influence that the systemic milieu had on the pathologic changes in the bone and skeletal muscle of dKO-hetero and -homo mice. Results: The old dKO-hetero mice (12-14 months) were surgically paired with young mdx mice (3-5 months) to examine the influence that the young DMD systemic milieu had on the pathological changes in the muscle and bone. Significant improvements in the histopathological changes were observed in the skeletal muscle and bone. Healthier vertebral structures, epiphysis of proximal tibia, and mid-shaft of the femur were observed in the old dKO-hetero mice in the old/young pairings when compared with the old dKO-hetero mice in the old/old pairings (Fig. 1 &2). The dKO-homo mice were paired with WT mice to test the influence of the systemic milieu on the development of muscle pathology and bone healing. Significant improvements in the histopathological changes in the skeletal muscle and bone volumes in the defect areas were observed in both non-critical sized tibia and cranial defects created in the dKO-homo mice in the dKO-homo/WT pairings compared to dKO-homos in the dKO homo/homo pairings (Fig.3). The dKO-hetero mice were paired with WT GFP mice to examine the engraftment of circulating progenitor cells from the WT partner. None of the regenerating myofibers in the dKO-hetero mice were GFP-positive (Fig.4). Furthermore, the quantity of hematopoietic stem cells, not bone marrow-derived mesenchymal stem cells, was significantly increased in the dKO-homo mice in the dKO homo/WT pairings when compared to the dKO homo/homo pairings (Fig.5). These data indicate that improved muscle pathology and bone healing is due to circulating factors. Conclusion: These observations demonstrated that the systemic milieu is an influential factor that contributes to the degenerative muscle and bone phenotype observed in the dKO mice. These results indicate that the defect in the somatic cells in dKO mice could be driven by the dystrophic microenvironment and might be, in part, attributable to changes in blood-borne factors.

Figure 1: Improved muscle histology in old dKO-hetero mice exposed to young mdx circulation.

Fig. 1

Figure 2: Heterochronic parabiosis reduces bone loss in old dKO-hetero mice. (A): representative 3-D reconstructions. (B) Quantitative histomophometric analysis (p<0.05, n=8).

Fig. 2

Figure 3: Pairing with WT mice improves bone healing in dKO-homo mice. (A): representative 3-D reconstructions. (B) Quantitative histomophometric analysis (p<0.01, n=6).

Fig. 3

WT-GFP/dKO-hetero   WT-GFP/dKO-hetero

Figure 4: Engraftment of circulating progenitor cells from the WT-GFP partner. None of the regenerating myofibers in the dKO-hetero mice were GFP-positive.

Fig. 4
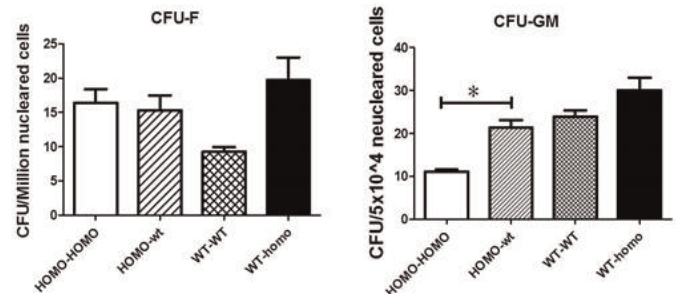
Figure 5: Quantification of bone marrow mesenchymal stem cells (CFU-F) and hematopoietic stem cells (CFU-GM) isolated from the bone marrow.
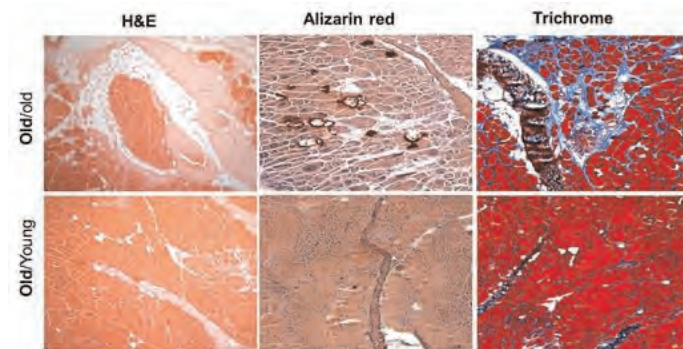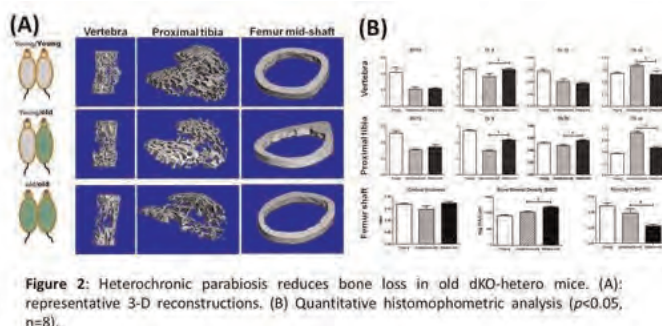
Fig. 5

SU0119

Enhanced TLR-MYD88 Signaling Stimulates Autoinflammation in SH3BP2 Cherubism Mice and Defines the Etiology of Cherubism.

Teruhito Yoshitaka[1], Tomoyuki Mukai[2], Mizuho Kittaka[3], Bjorn Olsen[4], Ernst Reichenberger[5], Yasuyoshi Ueki*[6]. [1]University Missouri-Kansas City School of Dentistry, USA, [2]University of Missouri - Kansas City, USA, [3]University of Missouri-Kansas City School of Dentistry, USA, [4]Harvard School of Dental Medicine, USA, [5]University of Connecticut Health Center, USA, [6]University of Missouri-Kansas City, School of Dentistry, USA

Cherubism (OMIM#118400) is a rare genetic disorder characterized by bilateral jawbone destruction due to proliferation of inflammatory/fibrous lesions that often regress after puberty. Heterozygous gain-of-function mutations in the adaptor protein SH3-domain binding protein 2 (SH3BP2) are responsible for the disorder. Analysis of the knock-in (KI) mouse model for cherubism revealed that, while heterozygous cherubism mice ($Sh3bp2^{KI/+}$) exhibit mild osteoporosis due to increased osteoclasto-genesis induced by RANKL, homozygous mutant mice ($Sh3bp2^{KI/KI}$) spontaneously develop macrophage-rich inflammation in face, lung, stomach, and liver as well as inflammatory bone destruction in calvariae and joints in a TNF-α-dependent manner. Since $Sh3bp2^{KI/KI}$ mice deficient in T/B cells develop the inflammation, this inflammation is regarded as autoinflammation. However, these studies failed to explain the reason why human cherubism lesions are restricted to jaws and regress with age. We discovered that the elevation of serum TNF-α levels and the systemic inflammation in $Sh3bp2^{KI/KI}$ mice are MYD88-dependent and are rescued in the absence of toll-like receptor (TLR) 2 and TLR4 ($Tlr2^{-/-}/Tlr4^{lps-del/lps-del}/Sh3bp2^{KI/KI}$). IL-1R1-deficient $Sh3bp2^{KI/KI}$ mice exhibited only a partial reduction of liver lesions. Interestingly, germ-free $Sh3bp2^{KI/KI}$ mice still developed the inflammation. *In vitro* studies showed that bone marrow-derived M-CSF-dependent macrophages (BMMs) from mutant mice are hyper-responsive to PAMPs (pathogen-associated molecular patterns) and DAMPs (damage-associated molecular patterns) that activate TLRs, resulting in TNF-α overproduction. NF-κB pathway was more activated in $Sh3bp2^{KI/KI}$ BMMs stimulated with Pam3CSK4 and LPS than in $Sh3bp2^{+/+}$ BMMs. Tyrosine 183 residue in SH3BP2 was critical for TNF-α overproduction in RAW264.7 cells. Finally, SYK depletion in macrophages ($LysM-cre/Syk^{ΔM/ΔM}/Sh3bp2^{KI/KI}$) prevented the inflammation. These data suggest that presence of a large amount of oral bacteria and increased release of DAMPs during active jawbone remodeling phase resulting from, for example, tooth eruption that activate TLRs may cause the jaw-specific development of human cherubism lesions. Reduced levels of DAMPs after stabilization of jaw remodeling and potential maturation of MYD88-independent
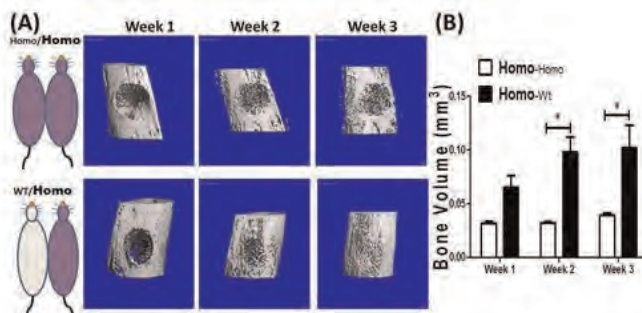
immunity with age may contribute to the age-dependent regression. Therapeutically, our data suggest that SYK inhibitors may be effective in the treatment of cherubism.

SU0120

Iroquois Homeobox Factors 3 and 5 Regulation of Skull Mineralization. Corey Cain*[1], Nathalie Gaborit[2], Wint Lwin[3], Edward Hsiao[1]. [1]University of California, San Francisco, USA, [2]Inserm 1087/CNRS UMR 6291, Institut du Thorax, France, [3]University of California, San Francisco, USA

Purpose: Osteoporosis affects over 10 million people in the United States and contributes to 1.5 million fractures each year. While osteoblast (OBC) dysfunction is thought to be one major contributor to osteoporosis, the genetic complexity of bone loss poses a major challenge to understanding how OBCs lose their ability to synthesize bone matrix. Iroquois homeobox transcription factors (IRX) are expressed early in bone tissues and facilitate patterning and mineralization of the skeleton. Recently, mutations in IRX5 have been associated with Hamamy syndrome, which presents in humans with osteoporosis, hip dysplasia, facial abnormalities, and cardiac malformations. Although $Irx3^{-/-}$ mice are asymptomatic, dual loss of both $Irx3$ and $Irx5$ in mice phenocopies the cardiac malformations found in humans with Hamamy syndrome, but causes embryonic lethality. Here, we used the $Sp7$-Cre to drive OBC-specific deletion of $Irx3$ in $Irx5^{-/-}$ mice to study the bone specific functions of the IRX genes.Methods: Newborn $Irx3^{flox/flox}$; $Irx5^{-/-}$; $Sp7$-Cre^+ mice were measured for body mass and length. 3D microCT image reconstruction was then performed on $Irx3^{flox/flox}$; $Irx5^{-/-}$; $Sp7$-Cre^+ mice to determine total body skeletal defects. $Irx3^{flox/flox}$; $Irx5^{-/-}$; $Sp7$-Cre^+ skeletons were stained with alizarin red and alcain blue to visualize bone and cartilage. We used histological analysis of sectioned skulls to determine mineralization and cartilaginous arrangement within the skull. Finally, qPCR analysis of mineralization and cartilaginous genes were performed on whole $Irx3^{flox/flox}$; $Irx5^{-/-}$; $Sp7$-Cre^+ calvaria.Results: Approximately 43% of newborn $Irx3^{flox/flox}$; $Irx5^{-/-}$; $Sp7$-Cre^+ mice die at birth. $Irx3^{flox/flox}$; $Irx5^{-/-}$; $Sp7$-Cre^+ mice had significant reductions in body mass even though body length was not significantly reduced. MicroCT, in conjunction with alizarin red and alcain blue staining, showed decreased mineralization in parietal, occipital, and mandible bones of $Irx3^{flox/flox}$; $Irx5^{-/-}$; $Sp7$-Cre^+ mice but relatively unaffected long bones. Furthermore, there were significant reductions in calvarial expression of Col1A1 and Aggrecan.Conclusion: Mineralization in the skulls of $Irx3^{flox/flox}$; $Irx5^{-/-}$; $Sp7$-Cre^+ mice was markedly reduced despite no major differences in cartilaginous formation in the skull. Our findings indicate that IRX3 and IRX5 are important for mineralization of mesenchymal-derived intramembranous bones.

SU0121

Mechanisms of Mineral Metabolism During Pregnancy in Mice with X-Linked Hypophosphatemia (XLH). Steven Tommasini*[1], Meina Wang[1], Helen King[2], Catherine Skinner[1], Carolyn Macica[3]. [1]Yale University, USA, [2]Yale University, USA, [3]Frank H. Netter School of Medicine Quinnipiac University, USA

During pregnancy, maternal adaptations to high mineral demand include more than doubling intestinal calcium absorption by increasing vitamin D production. However, in patients with XLH, vitamin D production and intestinal calcium absorption are impaired. Previously, we showed that to accommodate the increased mineral demands of lactation, Hyp mice, a murine model of XLH, increase intracortical remodeling similar to that described in post-menopausal osteoporotic bone. As vitamin D biosynthesis is impaired in Hyp mice, we hypothesized that the skeletal contribution to mineral homeostasis begins during pregnancy. Serum analysis in Hyp and C57BL/6 (B6) mice revealed that maternal 1,25(OH)$_2$D levels were lower in Hyp compared to B6 at different time points across pregnancy (p<0.05, t-test). However, consistent with human data, both groups showed an increase in 1,25(OH)$_2$D early and then a decrease at E18.5. One possibility is that increases in levels of prolactin may drive the potentiation of vitamin D. Hyp and B6 maternal PTH levels also were consistent with normal human pregnancy where PTH is suppressed during the first trimester and then increases steadily to the mid-normal range by term. However, Hyp PTH levels remained consistently 50-100% higher than B6. Despite sustained elevated levels of PTH in pregnant Hyp mice, these levels are likely to be insufficient to overcome the inhibitory effect of increased FGF23 on vitamin D production. Analysis of the femoral diaphysis by high resolution μCT (resolution=1.55μm), revealed that at the end of pregnancy, Hyp porosity (14.5±1.2%) was increased relative to virgin Hyp (8.8±0.4%) and similar to lactating Hyp (12.5±1.2%). This increase in porosity was due to an increase in large unmineralized spaces comprised of vasculature or demineralized matrix. Pregnant B6 mice had lower overall intracortical porosity (0.9±0.2%) compared to Hyp including smaller lacunae (176μm^3 vs. 234μm^3). We further characterized the matrix composition of cortical bone using FTIR and Raman spectroscopy. Compared to pregnant B6, pregnant Hyp cortical bone had similar collagen cross-linking (3.1±0.2 vs. 3.6±1.1), lower mineralization (4.1±0.4 vs. 5.3±0.3, p<0.0001), lower amounts of acid phosphate (p<0.0001), higher carbonate ion substitution (0.027±0.001 vs. 0.020±0.001, p<0.0001), and increased crystallinity (0.89±0.01 vs. 0.87±0.01, p<0.05). Taken together, these data suggest that increased intracortical remodeling

also contributes in maintaining phosphate levels during periods of high mineral demand in patients with XLH.

SU0122

Mouse Model with Mutant Type I Collagen C-propeptide Cleavage Site has Brittle Bones and Increased Osteoblast Mineralization. Aileen Barnes*[1], Joseph Perosky[2], M. Helen Rajpar[3], Kenneth Kozloff[4], Joan Marini[5]. [1]NICHD/NIH, USA, [2]University of Michigan, USA, [3]NICHD/NIH, USA, [4]University of Michigan Department of Orthopaedic Surgery, USA, [5]National Institute of Child Health & Human Development, USA

Classical dominant osteogenesis imperfecta (OI) is caused by mutations in type I collagen. Mutations in the C-propeptide cleavage site of both *COL1A1* and *COL1A2* were shown to cause high bone mass OI, characterized by bone hypermineralization and normal to increased DXA Z-scores. We generated a mouse with a heterozygous C-propeptide cleavage site defect (high bone mass, HBM) in which the Ala-Asp residues of the COL1A1 cleavage site were mutated to Thr-Asn to prevent cleavage by BMP1. We utilized this mouse to elucidate the role of type I procollagen C-propeptide processing in bone formation.

Collagen from newborn HBM calvarial osteoblasts had normal biochemistry and the collagen was incorporated normally into trimers. However, osteoblasts deposited only about 50% of WT matrix. Additionally, an *in vitro* mineralization assay showed that calvarial HBM osteoblasts had a 15% increase in mineralization (p=0.006), ± BMP2 treatment. Conditioned media from newborn HBM fibroblasts showed decreased processing of the C-propeptide. Dermal fibril diameters were smaller and more homogeneous in HBM than WT, with a loss of large fibrils.

At 2 months of age, male HBM mice are significantly smaller in weight (77%) and length (92%) and have shorter femurs (92%). Femoral areal BMD in HBM mice is decreased 25% (p<0.001), but vertebral BMD is normal. All 2 month HBM mice have pelvic deformities, and 40% have kyphosis. On μCT, HBM femora have a thinner cortex with decreased cortical area; the distal femoral metaphysis is notably thinner. Four point bending revealed an extremely brittle phenotype; post-yield displacement is only ~10% of WT (0.23 vs 0.03, p<0.001). HBM femoral stiffness, yield load, and ultimate load are also significantly decreased.

The bone phenotype of the HBM mouse is similar to that of the $Bmp1^{-/-}/Tll1^{-/-}$ mouse (Muir, et al, *Hum Mol Genet*, 2014, doi:10.1093/hmg/ddu013), in which cleavage of types I, II, III and V procollagen as well as bone-related factors such as DMP1, biglycan, lysyl oxidase, and TGFβ1 are defective. The $Bmp1^{-/-}/Tll1^{-/-}$ mouse has small size, thin cortices, reduced failure energy and maximum load and a dramatic decrease in post-yield displacement. The HBM mouse demonstrates that the essential elements of the broader enzyme deficiency can be reproduced by a substrate defect in type I C-propeptide cleavage. These data show the importance of the type I procollagen C-propeptide to both collagenous and mineral properties of bone.

SU0123

The Collaborative Cross, a Next-Generation Genetic Analysis Platform for Complex Skeletal Traits. Charles Farber[1], Larry Mesner*[2], Gina Calabrese[3], Steven Tommasini[4], Mark Horowitz[5], Clifford Rosen[6]. [1]University of Virginia, USA, [2]University of Virginia, USA, [3], USA, [4]Yale University, USA, [5]Yale University School of Medicine, USA, [6]Maine Medical Center, USA

Complex skeletal traits such as bone mineral density (BMD), trabecular microarchitecture and biomechanical strength are primarily determined by genetic factors. Genome-wide association studies (GWAS) in human cohorts have begun to identify large numbers of genetic variants associated with bone traits; however, due to the need for large cohorts (tens of thousands), GWAS is only capable of investigating the genetics of clinically accessible traits, such as areal BMD. The Collaborative Cross (CC) is a new, next-generation mouse genetic mapping population designed to facilitate gene discovery for complex phenotypes. The CC provides a platform for ultra-high resolution mapping of traits that cannot be feasibly interrogated using GWAS. The CC consists of a set of inbred strains derived from eight genetically diverse founder strains. As a result of the CC breeding design, full genome sequences on the founders and advanced analytics, the mapping resolution in the CC is sufficient to identify quantitative trait loci (QTL) containing single genes. Here, we utilized the CC to investigate the genetic basis of ~60 skeletal traits, including trabecular and cortical microarchitecture, histomorphometry, marrow adiposity and biomechanics. To date, we have phenotyped 40 CC strains (N=6, 12-week old males per strain) and across these strains high levels of variation were observed for all traits. For example, trabecular bone volume fraction (BV/TV) of the distal femur varied from 1.5% to 34.8% between the strains with the lowest and highest trait values, respectively. Heritability (H^2) estimates were significant (P<0.05) for all traits, ranging from H^2=0.20 (P=3.6 x 10^{-4}) for marrow adiposity to H^2=0.76 (P=6.8 x 10^{-42}) for BV/TV of the distal femur. QTL scans revealed a number of significant loci, many of which implicated a small number of candidate genes. Thus, the CC is a powerful new genetic mapping population in the mouse with the potential to significantly increase our understanding of the genetics of a wide-range of complex skeletal phenotypes.

SU0124

A Peptide-functionalized delivery system to target osteoclasts. <u>Ge Zhang</u>[1], <u>Lei Dang*</u>[2], <u>Baosheng Guo</u>[2], <u>Defang Li</u>[3], <u>Jin Liu</u>[2], <u>Chao Liang</u>[2], <u>Xiaojuan He</u>[4], <u>Heng Wu</u>[2], <u>Zhijun Yang</u>[2], <u>Zicai Liang</u>[3], <u>Aiping Lu</u>[2]. [1]Ge Zhang' S Lab, Hong Kong, [2]Hong Kong Baptist University, China, [3]Kunshan Industrial Technology Research Institute, China, [4]China Academy of Chinese Medical Sciences, China

Introduction: The dyregulated miRNAs in osteoclasts could contribute to osteoclastic dysfunction and even cause skeletal disorders[1]. Synthetic miRNAs antagomir could modulate the endogenous miRNAs in targeted cells. But there is lack of systems for delivering therapeutic miRNAs to osteoclasts *in vivo*[2]. Thus, it is desirable to develop a delivery system selectively targeting osteoclasts for therapeutic modulation of miRNAs.

Objective: To develop a delivery system specifically approaching bone resorption surfaces to target osteoclasts.

Methods: The D-Asp$_8$ can selectively bind to bone resorption surfaces for meeting osteoclasts nearby and miR-29a antaogmir can suppress osteoclastogenesis[3]. The D-Asp$_8$ was conjugated to the surface of liposome confirmed by HPLC. (D-Asp$_8$)-modified liposome encapsulated the miR-29a antagomir. Its hydrodynamic diameter and zeta potential were detected by the Delsa® Nano HC Particle Analyzer. Its encapsulation efficiency was measured by Quant-iT^{TM} RiboGreen® RNA assay and serum stability was determined by agarose gel electrophoresis. Its tissue-selective delivery and cell-selective delivery of miR-29a antagomir *in vivo* were analyzed by biophotonic imaging system and immunohistochemistry, respectively[4].

Results: The D-Asp$_8$ was successfully conjugated to the liposome surfaces, as confirmed by HPLC (Fig. A & B). The delivery system has a average diameter of 150 nm (Fig. C), zeta potential of -10 mV and encapsulation efficiency of 80%. The miR-29a antagomir in (D-Asp$_8$)-liposome was detectable at 24 hours after incubation in serum, while the free miR-29a antagomir was vanished at 1 hour after incubation in serum. The fluorescence signals of the labeled miR-29a antagomir were relatively stronger in bone tissues and lower in liver and kidney, but barely detected in heart, spleen and lung from the (D-Asp$_8$)-liposome group in comparison with liposome group (Fig. D). More instances of co-localization of the labeled miR-29a antagomir with OSCAR$^+$ cells were found in (D-Asp$_8$)-liposome group compared with liposome group (Fig. E).

Conclusion: The D-Asp$_8$ could facilitate miR-29a antagomir encapsulated within liposome to selectively target osteoclasts (HKBU479111 and HKBU261113).
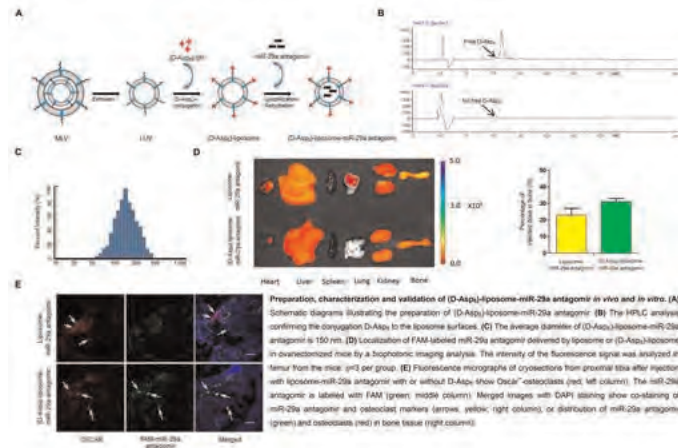
Reference:

Helfrich et al., Microsc Res Tech. 61:6, 2003.
Tautzenberger et al., Int J Nanomedicine. 7, 2012.
Franceschetti et al., J Biol Chem. 288:46, 2013.
Zhang et al., Nat Med, 18:2, 2012.

Figures-final

Disclosures: Lei Dang, None.

SU0125

Improvement of enamel and skeletal defects in murine hypophosphatasia via lentiviral gene therapy. <u>Seiko Yamamoto*</u>[1], <u>Carmen Huesa</u>[2], <u>Eri Yokoi</u>[3], <u>Chika Endo</u>[4], <u>Yumi Obi</u>[4], <u>Kei Ogawa</u>[5], <u>Takehiko Shimizu</u>[3], <u>Takashi Shimada</u>[6], <u>Jose Luis Millan</u>[7]. [1]Nihon University, Japan, [2]University of the West of Scotland, United Kingdom, [3]Nihon University School of Dentistry at Matsudo Department of Pediatric Dentistry, Japan, [4]Nihon University School of Dentistry at Mastudo Department of Pediatric Dentistry, Japan, [5]Nihon University School of Dentistry at Mastudo Department of Pediatric Dentistry, Japan, [6]Nippon Medical School, Japan, [7]Sanford-Burnham Medical Research Institute, USA

Hypophosphatasia (HPP) is an inherited skeletal disease caused by mutations of the gene (*ALPL* in humans, *Alpl* in mice) encoding tissue-nonspecific alkaline phosphatase (TNAP). Although TNAP is expressed in various tissues, the HPP symptoms appear primarily in bones and teeth. The clinical severity of HPP is varies widely; the most severe to the mildest forms are perinatal, infantile, childhood, adult, and odonto-hypophosphatasia. There is no established treatment. We reported that enzyme replacement therapy (ERT) using daily injections of bone-targeted TNAP is effective in preventing all the skeletal and dental manifestations of HPP in TNAP knockout mice (*Alpl*$^{-/-}$ mice) (Millán *et al.*, 2008; Yadav *et al.*, 2012). We also showed that a single injection of either a lentiviral vector (Yamamoto *et al.*, 2011) or an adeno-associated viral vector (Matsumoto *et al.*, 2011) harboring bone-targeted TNAP (TNAP-D$_{10}$) was equally effective in preventing all the manifestations of HPP.

Objectives: In this study we evaluated improvement of the hard tissues of *Alpl*$^{-/-}$ mice using a lentiviral vector to administer bone-targeted TNAP. We also investigated the feasibility of using mineral-targeting placental alkaline bone (PLAP-D$_{10}$), instead of TNAP-D$_{10}$.Methods : *Alpl*$^{-/-}$ mice develop skeletal disease at day 6-8 and usually die of their disease at postnatal day 20. We injected 1 day-old *Alpl*$^{-/-}$ mice with 100 ul of lentiviral vector expressing TNAP-D$_{10}$ or PLAP-D$_{10}$ (5.0 x 10^7 TU) via the jugular vein and collected and examined their tissues after 20 days of treatment and compared them to those of WT and untreated *Alpl*$^{-/-}$ mice. The tibias were used for histomorphometrical analysis. μCT imaging and analyses were used to evaluate the effect of treatment on the enamel, dentin, cementum and surrounding alveolar bone.

Results: Bone growth rates were improved compare with untreated *Alpl*$^{-/-}$ mice using TNAP-D$_{10}$. The mineral content, enamel, cementum layer and bone volume of the mandible were also improved. PLAP-D$_{10}$ was less effective than TNAP-D$_{10}$, but still provided benefit over vehicle-treatment.

Conclusion : These results indicate that targeted delivery of alkaline phosphatase(s) to dental tissues mediated via a lentiviral vector can correct the dental defects and enhance bone growth in this murine model of infantile HPP.

Disclosures: Seiko Yamamoto, None.

SU0126

Withdrawn

SU0127

Identification of a novel PCSK5 frameshift mutation in a patient with the VACTERL association. <u>Yukio Nakamura*</u>[1], <u>Shingo Kikugawa</u>[2], <u>Hidehito Inagaki</u>[3], <u>Tatsuya Kobayashi</u>[4], <u>Hiroki Kurahashi</u>[3], <u>Hiroyuki Kato</u>[5]. [1]Dept of Orthopaedic Surgery Shinshu University School of Medicine, Japan, [2]DNA Chip Research Inc., Japan, [3]Fujita Health University, Japan, [4]Massachusetts General Hospital, USA, [5]Shinshu University School of Medicine, Japan

The VACTERL association is a sporadic, non-random collection of congenital anomalies that includes vertebral defects, anal atresia, cardiac defects, tracheoesophageal fistula, renal anomalies, and limb abnormalities. Although several chromosomal aberrations and gene mutations have been reported as disease-causative, these findings have not been replicated to date. In the present study, whole exome sequencing of 2 families with the VACTERL association and 2 unrelated patients uncovered a novel frameshift mutation in the PCSK5 gene in 1 patient that was confirmed by Sanger sequencing. This mutation is suspected to disrupt PCSK5 function either by producing an abnormal protein that is missing an essential cysteine-rich motif (CRM) or by leading to nonsense-mediated mRNA decay. As several other non-synonymous variants in the CRM domain of the PCSK5 gene have been detected in patients with the VACTERL association, our finding further implicates loss-of-function mutations of PCSK5 in disease etiology.

Disclosures: Yukio Nakamura, None.

SU0128

New Lessons From An Old Disease – What Alkaptonuria Teaches Us About Cartilage and Bone Remodelling. Craig Keenan*[1], Alan Boyde[2], Lakshminarayan Ranganath[1], James Gallagher[3], Nathan Jeffery[1], Jonathan Jarvis[1], Adam Taylor[4]. [1]University of Liverpool, United Kingdom, [2]Barts & The London School of Medicine & Dentistry, Queen Mary University of London., United Kingdom, [3]University of Liverpool, United Kingdom, [4]Lancaster University, United Kingdom

Alkaptonuria (AKU) was the first human disorder recognised to conform to Mendelian inheritance by Sir Archibald Garrod in 1901. AKU is characterised by deposition of pigmented polymers in connective tissues, a process called ochronosis. Cartilage is most severely affected causing early onset arthropathy in weight bearing joints. We investigated the origin and progression of arthropathy in AKU patient tissue samples obtained at joint replacement surgery and in an AKU mouse model. Light and electron microscopy studies reveal collagen fibres are initially resistant to pigmentation but become susceptible through organisational and compositional changes, including proteoglycan loss. Onset of ochronosis appears to be associated with high mechanical loading. In joint tissues the first pigment is laid down in the pericellular matrix of hypertrophic chondrocytes in calcified articular cartilage. The hypertrophic lacunae are surrounded by previously unrecognised concentric lamellae. Ochronosis then spreads to the non-mineralised hyaline cartilage causing it to stiffen. This phase is accompanied by development of classical osteoarthritic lesions including erosions, tidemark duplication and osteophytes. The increased stiffness in cartilage also elicits a spectrum of changes in the subchondral plate and underlying bone. Some areas are subjected to aggressive local resorption possibly a mechanotransduction response to stress shielding. This can lead to complete subchondral plate resorption by osteoclastic action. In other areas there is cracking of the subchondral plate and extrusion of an unknown matrix, which becomes hypermineralised, into the hyaline cartilage. Finite element analysis predicts that this and other changes in microarchitecture in the deep cartilage have a profound effect on the strain distribution throughout the hyaline cartilage leading to the generation of potentially damaging loads. The underlying trabeculae undergo non-Frostian remodelling with areas of hypo- and hypermineralised deposition which we have named trabecular excrescences. These latter structures are templated by adipocytes. All these features, which except ochronosis per se, were first identified in the severe AKU phenotype have subsequently been observed at lower frequency in aged and osteoarthritic joints. These findings demonstrate that studying syndromes with extreme phenotypes can help elucidate the pathophysiological mechanisms in more common diseases of cartilage and bone.

Disclosures: Craig Keenan, None.

SU0129

Relationship between SQSTM1 mutations status and severity of Paget disease of Bone (PDB). Manuel Diaz Curiel*[1], m jesus moro alvarez[2], marjorie andrade[3], M Jose Trujillo[4], Ignacio Mahillo Fernandez[5], Camilo Velez[6], Nerea Carvajal[7]. [1]Jimenez Diaz Fundacion, Spain, [2]Department of Internal Medicine. Metabolic Bone Disease. Hospital Infanta Leonor., Spain, [3]Bone Diseases Service. IIFJD., Spain, [4]Genetic Department IIFJD, Spain, [5]IIFJD. Epidemiology Research, Spain, [6]Genetic Department. IIFJD, Spain, [7]Genetic Department, Spain

Paget disease of bone (PDB) is a common disorder characterized by increased bone turnover at one of more sites throughout the skeleton. Genetic factors play an important role in the pathogenesis of PDB, and the most important predisposing gene is SQSTM1.

We investigated the relationship between SQSTM1 mutation status and disease severity in 50 patients who took part in a retrospective analysis.

Mutations of SQSTM1 were detected in 5 of 50 (10 %) patients. Mutation carriers had a similar age at diagnosis (75.4 $\pm$ 11.5 versus 70.0 $\pm$ 10.1 years) and a similar rate in bone turnover with CTX 0.840 $\pm$ 0.259 versus 0.730 $\pm$ 0.429 (n.s.), alkaline phosphatase (AP) 206.80 $\pm$ 127.024 versus 168.00 $\pm$ 130.430 (n.s.), P1NP 109.75 $\pm$ 30.527 versus 140.66 $\pm$ 142.217 (n.s.).

Only one of these five patients with positive mutation of SQSTM1, presented a monostotic Pagets disease and 4 patients corresponded to poliostotic Pagets disease. In the total population 20 patients had a monostotic Pagets disease and 30 patients had a poliostotic Pagets disease. Bisphosphonate therapy was not more commonly required (86.3% versus 75.2%, p = .01) than those without mutations. Genetic testing for SQSTM1 mutations may be not of value in identifying individuals at risk of developing severe disease, therefore a program of genetic testing and early intervention in these individuals couldn ot be cost-effective.

Conclusions: We did not found a relationship between SQSTM mutation and severity of Paget disease.

Disclosures: Manuel Diaz Curiel, None.

SU0130

***Bicc1* Regulates the Expression of *Pkd2* in Osteoblasts and Genetic Variants in both are Associated with BMD.** Larry Mesner[1], Yi-Hsiang Hsu[2], Ani Manichaikul[3], Elizabeth Bryda[4], Guanqing Wu[5], Stephen Rich[3], Clifford Rosen[6], Michael Criqui[7], Matthew Allison[7], Matthew Budoff[8], Thomas Clemens[9], Charles Farber*[10]. [1]University of Virginia, USA, [2]Hebrew SeniorLife Institute for Aging Research & Harvard Medical School, USA, [3]University of Virginia, USA, [4]University of Missouri, USA, [5]Vanderbilt University, USA, [6]Maine Medical Center, USA, [7]University of California at San Diego, USA, [8]Los Angeles Biomedical Research Institute at Harbor-UCLA Medical Center, USA, [9]Johns Hopkins University, USA, [10]University of Virginia, USA

Bicaudal C homolog 1 (*Bicc1*) is an RNA-binding protein implicated in the post-transcriptional regulation of gene expression. Recently, we identified *Bicc1* as a novel genetic determinant of BMD in the mouse. Here, we sought to determine how *Bicc1* influences BMD and whether *BICC1* plays a role in the regulation of BMD in humans. To elucidate *Bicc1* function, we used a network-based approach to determine that *Bicc1* was a member of a co-expression module enriched for genes involved in osteoblast function. The network connections between *Bicc1* and genes with a known role in osteoblastogenesis were stronger than its connections with other module genes, suggesting a role for *Bicc1* in osteoblast differentiation. Consistent with this prediction, knockdown of *Bicc1* in primary calvarial osteoblasts decreased osteogenic gene expression, alkaline phosphatase activity and mineralized nodule formation. In the co-expression network, *Bicc1* was most strongly connected to the polycystic kidney disease 2 (*Pkd2*) gene. *Pkd2* encodes Polycystin-2 (PC2), a calcium channel located on the surface of primary cilium in a complex with PC1, a protein implicated in the regulation of BMD. Knockdown of *Bicc1* decreased *Pkd2* transcript levels and, similar to perturbation of *Bicc1*, *Pkd2* knockdown also decreased markers of osteoblast differentiation. Overexpression of *Pkd2* in *Bicc1* null osteoblasts rescued impaired differentiation, whereas overexpression of *Bicc1* in *Pkd2* null osteoblasts did not, suggesting that *Bicc1* acts upstream of *Pkd2*. Lastly, in two human BMD genome-wide association study (GWAS) meta-analyses, single nucleotide polymorphisms (SNPs) in *BICC1* and *PKD2* were associated with BMD. These results identify *Bicc1* as a genetic determinant of BMD and osteoblastogenesis, and suggest that it does so by regulating *Pkd2* transcript levels.

Disclosures: Charles Farber, None.

SU0131

Withdrawn

SU0132

hiPSCs from Patients with Craniometaphyseal Dysplasia are Refractory to *in vitro* Osteoclast Differentiation. I-Ping Chen*[1], Zhifang Hao[2], Ernst Reichenberger[1]. [1]University of Connecticut Health Center, USA, [2]University of Connecticut Health Center, USA

Craniometaphyseal dysplasia (CMD), characterized by progressive hyperostosis of craniofacial bones and widening metaphyses, is one of more than 500 rare genetic bone disorders (NIH Office of Rare Disease Research). Molecular mechanisms and treatment for these rare bone diseases are mostly unknown. Major obstacles for studying rare genetic bone disorders are the lack of animal models and human specimens. Our group generated a knock-in (KI) CMD mouse model carrying a Phe377del *Ank* mutation and integration-free hiPSCs from CMD patients and healthy controls. We showed that defective osteoclastogenesis is the major reason for the CMD phenotype in *Ank*[KI/KI] mice. To study the osteoclast defects in the human system, we developed protocols to differentiate hiPSCs into osteoclasts (OC).

We differentiated hiPSCs into OCs using a previously published hiPSC/OP9 coculture method or via embryoid body (EB) formation. Briefly, 3 control and 3 CMD hiPSCs were grown on matrigel-coated plates for 5 days. EBs were developed by plating 10,000 cells/well on Lipidure-coated 96 well plates for 4 days to promote primitive streak induction. EBs cultured for 1, 2, 3 and 4 days in various media under ambient or low O2 conditions were selected for expression of *hT, hSCL, hCD34, hCdx2 and hHand1*. EBs were then cultured with cytokines under various conditions to induce hematopoiesis. A CD43^{+}CD45^{+}CD14^{+} population was enriched with magnetic beads and cultured in the presence of hM-CSF, hRANKL and hTGF-β to form mature OCs, defined as TRAP^{+} multinucleated cells.

Expression of *hSCL, hCD34* and *hCdx2* genes were lower in EBs derived from CMD hiPSCs when compared to EBs from control hiPSCs suggesting reduced mesoderm induction of CMD hiPSCs. Mature OCs could be differentiated from control hiPSCs but not from CMD hiPSCs using hiPSCs/OP9 cocultures or EB methodologies. Control OCs were capable of resorbing hydroxyapatite-coated plates and showed intact actin rings. We concluded that CMD hiPSCs were refractory to *in vitro* OC differentiation. Differentiated OCs from hiPSCs will help to study bone disorders caused by defective osteoclastogenesis in a human system.

Disclosures: I-Ping Chen, None.

SU0133

Menaquinone-4 (Vitamin K$_2$) in Bone Originates from Menadione (Vitamin K$_3$) Released from Oral Phylloquinone (Vitamin K$_1$) During Intestinal Absorption. <u>Kimie Nakagawa</u>*[1], <u>Yoshihisa Hirota</u>[2], <u>Naoko Tsugawa</u>[3], <u>Yuri Uchino</u>[2], <u>Yoshitomo Suhara</u>[4], <u>Toshio Okano</u>[4]. [1]Kobe Pharmaceutical University, Japan, [2]Kobe Pharmaceutical University, Japan, [3]Kobe Pharmaceutical University, Japan, [4]Shibaura Institute of Technology, Japan

Aims: Vitamin K plays an important role in bone metabolism. Mice have the ability to convert dietary vitamin K$_1$/phylloquinone (PK) into vitamin K$_2$/menaquinone-4 (MK-4) and store the latter in many tissues. Previously, we identified a novel enzyme UbiA prenyltransferase domain containing 1 (UBIAD1) that catalyzes this conversion. Our previous study showed that UBIAD1 has a weak side chain cleavage activity for PK but a strong prenylation activity for vitamin K$_3$/menadione (MD) that has long been postulated as an intermediate or catabolic product of PK in this conversion process. Further evidence indicates that when intravenously administered in mice, PK can enter into tissues, but is not converted further to MK-4. These findings raise the question whether dietary PK is absorbed in the intestine, delivered to tissues in its original form, and converted to MK-4 or whether the phytyl side chain of PK is cleaved to release MD in the intestine, followed by delivery of MD to tissues via a mesenteric lymphatic system and subsequent conversion to MK-4. At present, the locations where release of MD from PK occurs and where MD is converted to MK-4 remain unclear. To elucidate this, it is necessary to identify PK-derived MD generated in the course of the intestinal absorption of PK and elucidate the relationship between the concentrations of MD in the mesenteric lymphatic system and blood circulation and the concentrations of MK-4 in tissues.

Methods: Cannulation experiments were conducted using stable isotope tracer technology in rats. Rats were divided into 2 groups of 4 animals and each group was used for either portal vein cannulation or thoracic lymph duct cannulation after oral administration of deuterium-labeled PK (PK-d$_7$) as a single dose of 10 µmol/kg body of weight. We measured the concentration of PK-d$_7$ and deuterium-labeled MK-4 (MK-4-d$_7$) in tissues, and conducted structural assignments and measurements of PK-derived MD using high-resolution MS (HR-MS) analysis and a bioassay using recombinant UBIAD1 protein.

Results and Discussion: We confirmed that the phytyl side chain of PK is cleaved off to release MD in the intestine, followed by delivery of MD via a mesenteric lymphatic system to tissues, where it is converted to MK-4. These results provide unequivocal evidence that MD is not only a catabolic product of PK but also a circulating precursor of tissue MK-4.

Disclosures: Kimie Nakagawa, None.

SU0134

Regulation of Osteocytic Osteolysis by the Calcitonin Receptor During Lactation in Mice. <u>Rachel Davey</u>*[1], <u>Michele Clarke</u>[2], <u>Patricia Russell</u>[2], <u>David Findlay</u>[3], <u>Jeffrey Zajac</u>[4]. [1]University of Melbourne, Australia, [2]Department of Medicine, Austin Health, University of Melbourne, Australia, [3]University of Adelaide, Australia, [4]Austin Hospital, Australia

We have shown previously, that the calcitonin receptor (CTR) plays a physiological role to protect against induced hypercalcemia in mice. In order to determine whether the CTR also protects the skeleton from excessive resorption in times of high calcium demand, we assessed the maternal skeleton of global-CTRKO and littermate control mice following pregnancy and lactation.

Viable Global CTRKO mice were generated by breeding floxed CTR mice with CMV-Cre mice, resulting in >94% but <100% global deletion of the CTR. Global-CTRKO and littermate control females were time-mated to C57BL/6 males at 8 weeks of age and their bone phenotype assessed by microCT and histomorphometric analyses at the end of pregnancy (E18) and at the end of lactation (P21). For the lactation group, following the birth of pups, litter sizes were made equal (n=4) by sacrificing the necessary number of pups in order to normalize the requirements of breast milk from each mother.

MicroCT analyses showed no effect on trabecular and cortical bone in the distal femur and L5 vertebra by global CTR deletion during pregnancy and lactation in the Global CTRKOs, compared to controls, at a resolution of 6.5µm. However, global CTRKO mice were hypercalcemic following pregnancy (Control: 2.17 ± 0.22mmol/L; Global CTRKO: 3.34 ± 0.30mmol/L; *P*<0.05), indicating a role for the CTR to regulate calcium homeostasis during pregnancy. In the absence of any changes in osteoclast number or activity, cathepsin K mRNA levels were elevated 2 fold in the bone of lactating Global-CTRKO females compared to controls (*P*<0.05). Given the recently identified function of osteocytes to resorb their surrounding bone matrix during lactation, together with their reported expression of the CTR, we assessed osteocytic osteolysis in the Global-CTRKOs and controls by determining osteocyte lacunae area in cortical bone. The top 20% of osteocyte lacunae area was increased by 10% following lactation in global-CTRKOs compared to controls (*P*<0.05). Consistent with the increased osteocytic osteolysis, serum calcium was elevated in global-CTRKOs following lactation compared to controls (Control: 2.43 ± 0.21mmol/L; Global CTRKO: 3.00 ± 0.17mmol/L; *P*=0.05). These data provide strong evidence for a significant physiological role of the CTR to protect the maternal skeleton during lactation by a direct action on osteocytes to inhibit osteolysis.

Disclosures: Rachel Davey, None.

SU0135

Fibroblast growth factor 23 impairs aortic relaxation: role of reactive oxygen species. <u>Neerupma Silswal</u>*[1], <u>Chad Touchberry</u>[1], <u>Jon Andresen</u>[1], <u>Michael Wacker</u>[2]. [1]University of Missouri-Kansas City School of Medicine, USA, [2]University of Missouri-Kansas City School of Medicine, USA

Recent clinical studies of chronic kidney disease (CKD) patients have demonstrated associations between increased plasma fibroblast growth factor 23 (FGF23) levels and impaired flow-mediated dilation of the vasculature, impaired vasoreactivity, reduced ejection fraction, and heart failure. CKD patients also have elevated levels of reactive oxygen species (ROS) which is a risk factor for the development of endothelial dysfunction by reducing nitric oxide (NO) bioavailability. However, there have been no mechanistic studies to connect these clinical observations. Recently, we have found that FGF23 directly impairs vasorelaxation of mouse aorta by inhibiting endothelial NO bioavailability. Based on the high levels of ROS found during CKD, we hypothesize that FGF23 directly increases vascular ROS which leads to impaired endothelial function. To test this hypothesis, intracellular ROS was measured by dihydroethidium-based epifluorescence microscopy of primary endothelial cells isolated from mouse aorta as well as lucigenin chemiluminiscence assay of isolated aortic rings. Pretreatment of aortic endothelial cells with FGF23 (9000 pg/ml) increased superoxide levels by an average of 78% vs vehicle (p<0.05, n=3) compared to only a 15% increase after pretreatment with the superoxide scavenger, tiron (p>0.05, n=3). Similarly, FGF23-treated aortic rings resulted in increased ROS levels that were inhibited by tiron pretreatment (p<0.05, n=3). To further define the physiological role of increased ROS in FGF23-mediated impairment of vascular function, we preincubated mouse aortic rings with tiron prior to FGF23 incubation for isometric tension myography experiments. Specifically, endothelium-dependent relaxation to acetylcholine was determined after precontraction with PGF$_{2\alpha}$ (10^{-5} M). Tiron treatment was able to rescue the impaired endothelium-dependent vasorelaxation caused by FGF23 (p<0.05, n=5). Therefore, our data suggest that FGF23-mediated increases in ROS impair NO-mediated aortic relaxation and that the antioxidant, tiron, can rescue these effects. These findings have clinical implications for therapeutic intervention to prevent cardiovascular disease in CKD patients.

Disclosures: Neerupma Silswal, None.

SU0136

MEPE-ASARM, a Substrate of Phex, Decreases Bone Volume Independently of Serum Phosphate Levels. <u>Kaoru Sakurai</u>*[1], <u>Tomoko Minamizaki</u>[2], <u>Yoko Fujino</u>[1], <u>Yuichiro Takei</u>[3], <u>Hirotaka Yoshioka</u>[4], <u>Mitsugi Okada</u>[3], <u>Katsuyuki Kozai</u>[3], <u>Yuji Yoshiko</u>[3]. [1]Hiroshima University Graduate School of Biomedical & Health Sciences, Japan, [2]Hiroshima University Institute of Biomedical & Health Sciences, Japan, [3]Hiroshima University Institute of Biomedical & Health Sciences, Japan, [4]Hiroshima University Graduate School of Biomedical Sciences, Japan

Matrix extracellular phosphoglycoprotein (MEPE), a member of the small integrin-binding ligand N-linked glycoprotein (SIBLING) family, is originally identified in tumor-induced osteomalacia and involved in bone mineralization and phosphate metabolism. This polypeptide contains the acidic serine- and aspartate-rich motif (ASARM) that exhibits high affinity to hydroxyapatite and inhibits matrix mineralization *in vitro*. Some of ASARM peptides are phosphorylated at several sites (pASARM), which appear to be relevant to its biological activities. pASARM is released in MEPE processing and presumably degraded by the phosphate regulating endopeptidase homolog, X-linked (Phex), suggesting that the accumulation of pASARM in bone may cause mineralization defects in X-linked hypophosphatemic rickets. Recently, we showed that pASARM is accumulated in bone in Klotho mutant (*kl/kl*) mice with osteopenia. pASARM had no detectable effects on rat calvaria cell proliferation and differentiation and the generation of osteoclasts from RAW 264.7 cells, which differed from results in a mouse bone marrow stroma cell model. To clarify the effects of pASARM on bone and phosphate metabolism in normal mice, C57BL/6 male mice (6-week-old) were implanted with osmotic pumps releasing pASARM for two weeks. pASARM did not impinge on body weight, serum calcium and phosphate levels, and renal *Slc34a3* and *Cyp27b1* mRNA levels; *Slc34a1* in kidney was slightly downregulated by pASARM. Neither gene expression profiling in bone nor serum markers showed significant effects of pASARM on bone formation and resorption. µCT analysis indicated that pASARM decreased tissue volume, bone volume, tissue surfaces, bone surfaces and trabecular thickness and increased trabecular bone pattern factor, with a concomitant decrease in calcein labeling of bone surfaces. Mice treated with pASARM also exhibited an increase in TRAP-positive multinucleated cells. Because non-phosphorylated ASARM has little effect on bone, the phosphorylation is necessary for ASARM to exert its actions in bone. Taken together, these results suggest that pASARM may inhibit bone mineralization independently of serum phosphate levels and increase bone resorption through an undefined mechanism.

Disclosures: Kaoru Sakurai, None.

SU0137

Role of renal phosphate excretion in the pathogenesis of renal stone disease and nephrocalcinosis: insights from the Npt2a knockout mouse model. <u>Yuwen Li</u>[1], <u>Chuanlong Zhu</u>[1], <u>Jun Guo</u>[2], <u>Marie Demay</u>[3], <u>Harald Jueppner</u>[2], <u>Clemens Bergwitz</u>*[3]. [1]Massachusetts General Hospital, USA, [2]Massachusetts General Hospital, USA, [3]Massachusetts General Hospital & Harvard Medical School, USA

Mutations in the sodium phosphate co-transporters, NPT2a and NPT2c have been reported in kindreds with renal stone disease and nephrocalcinosis. These individuals have phosphate-wasting, high circulating levels of $1,25(OH)_2D$ and hypercalciuria. Since hypophosphatemia is often observed in hypercalciuric stone formers this raises the possibility that allelic variants in NPT2a and NPT2c might contribute to the pathogenesis of calcium stone disease in the general population. Oral phosphate supplementation is thought to reduce risk for renal calcifications. As in humans, a high phosphate/normal calcium diet (HP, 0.6% calcium, 1.20% phosphate) reverses hypercalciuria in Npt2a-null mice when administered from age two to four months. However, despite this treatment, these mice develop nephrocalcinosis, albeit to a lesser degree than animals fed a high phosphate/high calcium diet (HPC, 20% lactate, 2% calcium, 1.25% phosphate). Nephrocalcinosis is not observed in wild-type animals on the HPC diet, or in Npt2a-null mice fed a normal phosphate/normal calcium diet (CO, 0.6% calcium, 0.4% phosphate). These findings suggest that oral phosphate supplementation can contribute to renal calcification despite a reduction in urine calcium at least in the setting of impaired proximal tubular function. Excessive phosphaturia even with normal or low urinary calcium can cause nephrocalcinosis in humans as is seen in XLH or after treatment with phosphate enema, and Npt2a-null mice on HP diet may serve as a model to better understand its pathophysiology. We are currently evaluating the hypothesis that phosphate supplementation causes (possibly transient) increases in PTH and FGF23. Either hormone could be targeted to reduce the phosphaturia when Npt2a is absent in mice or mutated in humans.

Table 1: All diets are egg-white based: SEM, standard error of mean; WT, wild-type; BUN, blood urea nitrogen; sCa, serum calcium; sP, serum phosphate; CEI, urine calcium excretion index; PEI, urine phosphate excretion index; calc. area, calcified area in kidney sections.

	Diet	n	weight (g) Average	SEM	calc. area (%) mean	SEM	BUN (mg/dl) Average	SEM	sCa (mg/dl) Average	SEM	sP (mg/dl) Average	SEM	CEI (1/mg) Average	SEM	PEI (1/mg) Average	SEM
Npt2a⁻/⁻	HPC	8	26.0	1.8	0.00576	0.00028	19.3	1.3	13.8	0.5	13.0	5.0	1.4	0.2	5.0	1.5
	HP	10	25.6	0.9	0.00259	0.00016	13.0	0.8	15.0	0.9	11.8	2.5	0.2	0.0	17.8	4.6
WT	CO	7	31.3	2.3	0.00115	0.00014	8.3	0.7	9.1	1.3	8.3	1.9	1.4	0.4	9.4	4.3
	HPC	7	27.8	1.8	0.00004	0.00002	9.1	0.8	8.4	0.6	8.0	1.0	1.0	0.3	0.6	0.2
p-values	HPC vs. HP		8.5E-01	ns	7.6E-07	*	1.1E-03	*	2.5E-01	ns	8.4E-01	ns	3.8E-03	*	2.3E-02	*
	HPC vs. CO		1.1E-01	ns	4.4E-08	*	1.1E-05	*	1.3E-02	*	4.0E-01	ns	7.4E-03	*	3.7E-01	ns
	HPC MT vs. WT		4.8E-01	ns	1.7E-07	*	2.1E-05	*	1.2E-04	*	3.6E-01	ns	3.5E-01	ns	2.2E-02	*
	HP vs. CO		7.2E-02	ns	5.5E-06	*	3.6E-04	*	3.6E-03	*	2.7E-01	ns	3.6E-02	*	2.1E-01	ns
	HP MT vs. WT		3.0E-01	ns	5.4E-08	*	3.4E-03	*	1.8E-05	*	1.8E-01	ns	7.8E-02	ns	4.6E-03	*
	CO MT vs. WT		2.8E-01	ns	1.6E-04	*	4.4E-01	ns	6.5E-01	ns	9.1E-01	ns	9.2E-01	ns	8.7E-02	ns

Table 1

SU0138

Chronic Inhibition of RANKL Induces an Osteoclast-Independent Mechanism of PTH-induced Calcium Mobilization. <u>Hila Bahar</u>*[1], <u>Akira Maeda</u>[2], <u>Monica Reyes</u>[3], <u>Thomas Dean</u>[3], <u>Ernestina Schipani</u>[4], <u>Paola Divieti Pajevic</u>[1], <u>Robert Neer</u>[2], <u>Paul Kostenuik</u>[5], <u>John Potts</u>[2], <u>Thomas Gardella</u>[2]. [1]Massachusetts General Hospital & Harvard Medical School, USA, [2]Massachusetts General Hospital, USA, [3]Massachusetts General Hospital, USA, [4]University of Michigan, USA, [5]Amgen Inc., USA

Acute administration of Parathyroid Hormone (PTH) into animals or humans is well known to induce rapid (within 30 minutes) and robust (>10%) increases of blood ionized calcium (Ca). The rise in blood Ca is likely due in large part to the actions of PTH on bone, as this is the largest store of Ca in the body. PTH is known to induce the release of Ca from bone via the indirect activation of bone-resorbing osteoclasts (OCs) by RANKL. Whether or not other mechanisms and cell types can also contribute to the PTH-induced release of Ca from bone is currently unclear. This question has relevance not only to basic understanding of how PTH modulates bone and Ca metabolism, but also to patients being treated with anti-resorptive drugs, such as denosumab, that target the RANKL/OC pathway, and their capacities to maintain Ca homeostasis. We reported last year that a single co-injection of the RANKL inhibitor, osteoprotegerin-Fc (OPG-Fc) in mice markedly blunted the acute (within 1-2 hours) calcemic response to co-injected PTH(1-34), suggesting that the RANKL/OC pathway of bone-resorption can be rapidly activated by PTH. Surprisingly, however, when mice were pre-treated with OPG-Fc for seven days to deplete OC populations, their acute calcemic response to PTH(1-34) was not blunted but rather was equivalent to that observed in OPG-Fc-naive mice. The results suggest that in the absence of OCs, PTH may induce Ca mobilization from bone into blood via a novel RANKL/OC-independent mechanism. Ocsteocytes (Ocys) were recently suggested to have the capacity to mediate bone resorption in response to PTH ligands under certain conditions. To assess the potential role of Ocys in this putative novel mechanism of PTH-induced Ca release, we are utilizing mice that lack the PTH receptor (PTHR1) specifically in Ocys via the DMP1(10kb promoter)-Cre/PTHR1(exonE1)-floxed alleles. The acute calcemic response to PTH(1-34) injection will be assessed in these OcyPTHR1^KO mice following seven days of OPG-Fc pre-treatment. If the above hypothesis is correct, then the calcemic response to PTH in the OPG-Fc-pre-treated OcyPTHR1^KO mice should be blunted, as compared to that in vehicle-pre-treated OcyPTHR1^KO mice. Such findings would suggest that an adaptive mechanism by which PTH mediates Ca mobilization from bone via actions on Ocys is induced under conditions of OC depletion. The results could help explain how patients treated with OC-targeted anti-resorptive drugs generally maintain normocalcemia.

SU0139

Localization of parathyroid hormone-related protein and its receptor in MIN6 cells, a mouse insulinoma cell line. <u>Syu Mi Sam</u>*[1], <u>Kristi Milley</u>[2], <u>Peter Little</u>[1], <u>Jeffrey Zajac</u>[3], <u>Mathis Grossmann</u>[4], <u>Janine Danks</u>[5]. [1]School of Medical Sciences, RMIT University, Australia, [2]RMIT University, Australia, [3]Austin Hospital, Australia, [4]The University of Melbourne, Department of Medicine, Australia, [5]School of Medical Sciences, RMIT University, Australia

Parathyroid hormone-related protein (PTHrP) is a protein first discovered in the 1980's in the search to find the cause of humoral hypercalcemia of malignancy (HHM). Since then, this molecule has been shown to be involved in many physiological roles in the body. These functional roles include calcium homeostasis, a smooth muscle relaxant and its role in cellular proliferation, survival and differentiation in tissues such as skin, mammary gland, skeleton and the islets of the pancreas. The binding of PTHrP to its receptor, the parathyroid hormone-related protein receptor 1 (PTHR1), a G-protein coupled receptor, allows PTHrP to have its many functions in the body.

The mouse insulinoma cell line MIN6 is derived from a transgenic mouse expressing the large T-antigen of SV40 in pancreatic beta cells. PTHrP has been demonstrated previously in this cell line but localization patterns have not been performed on these cells. Based on this, the aim of this project is to localize both PTHrP and PTHR1 in the MIN6 cell line and examine whether PTHR1 is functional.

The presence of PTHrP and PTHR1 protein and mRNA in MIN6 cells were localized using immunohistochemistry (IHC) and chromogenic *in situ* hybridization (CISH) on formalin-fixed agar-embedded cell blocks, respectively. IHC for glucagon and insulin were also carried to characterize the MIN6 cells. Cyclic adenosine monophosphate (cAMP) assay has been performed on cultured MIN6 cells to examine PTHR1 functionality with UMR106 cells used as an assay control.

PTHrP and PTHR1 protein have been localized in the MIN6 cells using IHC. The localization pattern of PTHrP and PTHR1 mRNA was observed using CISH. A combination of nuclear and cytoplasmic staining was observed for PTHrP and PTHR1 in both methods of detection. Preliminary cAMP data from cultured MIN6 cells indicate that PTHR1 is not functional, as there is no cAMP production after stimulation with PTH.

PTHrP and its receptor proteins and mRNA were shown to be present in the MIN6 cell line. PTHrP has been suggested to play a role in growth and differentiation of b-cells (Sawada et al Mol Cell Endocrinol 182:265, 2001) with a responsive PTHR1. So far we have demonstrated that the MIN6v cells contain both PTHrP and PTHR1 protein and mRNA but not been able to show a functional PTHR1 in these cells. PTHrP may play in glucose regulation but further characterization of this cell line is required.

SU0140

Mechanisms controlling duration of signaling at the PTH receptor 1. <u>Tomoyuki Watanabe</u>*[1], <u>Alexandre Gidon</u>[2], <u>Thomas Dean</u>[3], <u>John Potts</u>[1], <u>Jean-Pierre Vilardaga</u>[4], <u>Thomas Gardella</u>[1]. [1]Massachusetts General Hospital, USA, [2]University of Pittsburgh, School of Medicine, USA, [3]Massachusetts General Hospital, USA, [4]University of Pittsburgh, School of Medicine, USA

We have recently reported a series of PTH analogs that bind to the PTHR1 with high affinity and induce sustained cAMP signaling responses in PTHR1-expressing cells, as wells as prolonged calcemic and phosphaturic responses in animals (Maeda, A. et al., PNAS 2013). To understand better the mechanisms by which such analogs mediate prolonged signaling responses, we investigated the functional properties of one of the long-acting analogs, LA-PTH, in GP-2.3 cells, which are HEK-293-derived cells that stably express the hPTHR1 along with a Glosensor cAMP reporter. The cAMP response to LA-PTH persisted for several hours after ligand wash-out, and was thus considerably prolonged, as compared to PTH(1-34). Cell internalization patterns were assessed using confocal microscopy and fluorescently labeled FAM-LA-PTH and FAM-PTH(1-34). By 30 minutes after addition, each ligand was observed mainly in cytoplasmic vesicles. To further assess the relationship between ligand internalization and signal duration/termination, we treated cells with Bafilomycin A1 (Baf), a specific inhibitor of the vacuolar-type H^+-ATPase, which mediates vesicle acidification. Short-term (15') Baf treatment blocks endosomal acidification but not internalization, whereas long-term (24 hr) Baf treatment also blocks vesicle internalization due to inhibition of membrane lipid recycling. FAM-LA-PTH

internalized normally in cells treated with Baf for 15', whereas it remained surface-associated in cells treated for 24hr. Short-term (15') treatment with Baf prolonged cAMP signaling by PTH(1-34) but did not affect signal duration by LA-PTH. Longer-term (24hr) treatment with Baf shortened cAMP signal duration by PTH(1-34), as well as by LA-PTH, such that signaling duration was similar for the two ligands. Cell membrane-based binding assays revealed that PTH(1-34)-PTHR1 complexes were unstable at the low pH levels found in endosomes (~pH 6.0), whereas LA-PTH-PTHR1 complexes were stable. The data suggest that LA-PTH forms complexes with the PTHR1 that are more acid-resistant than those formed by PTH(1-34), and that this acid-resistance contributes to the capacity of LA-PTH to mediate more prolonged signaling responses by enabling active signaling complexes to be maintained within endosomes.

Disclosures: Tomoyuki Watanabe, None.

SU0141

Osteoblast number is dependent and bone formation independent of osteoblast-specific CaSR and calcium availability. <u>Saja Al-Dujaili</u>*[1], <u>Amy Koh</u>[2], <u>Ming Dang</u>[3], <u>Xue Mi</u>[4], <u>Wenhan Chang</u>[5], <u>Peter X. Ma</u>[3], <u>Laurie McCauley</u>[6]. [1]University of Michigan, USA, [2]University of Michigan, USA, [3]University of Michigan, USA, [4]Tianjin University, China, [5]Endocrine Unit, VA Medical Center, University of California, San Francisco, USA, [6]University of Michigan School of Dentistry, USA

While the mechanisms of PTH anabolic actions in bone are not yet entirely clear, calcium availability and the calcium sensing receptor (CaSR) are potential cofactors. *We hypothesize that bone formation depends on calcium availability, and the CaSR plays a critical role in the anabolic actions of PTH.*
Calvarial osteoblast numbers increased dose-dependently with calcium chloride administration in vitro. In vivo *bioluminescent imaging of scaffolds seeded with luciferase-tagged bone marrow stromal cells showed similar trends with a 2.5-fold increase in bone volume in scaffolds containing 0.6mg Ca vs. 0mg Ca via microCT (p<0.05) and histologic analyses.*
To determine the role of the CaSR in cell proliferation, osteoblasts were cultured from osteoblast-specific CaSR knock-out (KO) and wildtype (WT) mice. No difference in the number of WT and KO cells was observed initially. However, after confluence, WT cells increased and KO plateaued (33% increase in WT vs. KO; p<0.05). *In vitro* treatment of WT cells with calcimimetic (R-568) or calcilytic (NPS 2143) did not affect osteoblast number during early stages, but after 14 days a 32% reduction of cells was seen with calcilytic versus vehicle (p<0.05) and no difference with calcimimetic. Increased apoptosis with calcilytic treatment (1.7-fold vs. vehicle, 6-fold vs. calcimimetic; p<0.05) suggested that the CaSR is critical for protection against cell death at later stages in culture.
When vertebral bodies from CaSR KO and WT pups were implanted in athymic mice, no difference in bone volume was found via microCT or histological analyses at 4wks. Intact CaSR KO mice had 58% lower serum P1NP levels vs. WT (p<0.05). PTH treatment of young WT and KO mice increased P1NP levels in WT mice by 43% (p<0.05). In KO mice, PTH increased P1NP by 127%, normalizing the levels to WT. MicroCT and radiographic analyses were similar to P1NP trends, where basal differences between vehicle-treated CaSR KO and WT mice were rescued with PTH treatment.
In summary, osteoblast numbers *in vitro* and bone volume *in vivo* depend on calcium suggesting the CaSR is important for proliferation and protection from apoptosis in mature osteoblasts. Osseous implants from CaSR KO mice developed normally in WT hosts suggesting the CaSR is dispensable for bone formation. Intact mice with osteoblast-specific CaSR KO had a compromised bone phenotype which was rescued by PTH suggesting that the CaSR is part of a larger pathway involving PTH and endocrine feedback.

Disclosures: Saja Al-Dujaili, None.

SU0142

Reduced Differentiation of Bone Marrow Stromal Cells May Contribute to Attenuated Response to Long-term Intermittent Administration of PTH. <u>Jun Guo</u>*[1], <u>Forest Lai</u>[2], <u>Daniel Brooks</u>[3], <u>Joel Finkelstein</u>[1], <u>Mary Bouxsein</u>[4], <u>Henry Kronenberg</u>[1]. [1]Massachusetts General Hospital, USA, [2]Massachusetts General Hospital, USA, [3]Beth Israel Deaconess Medical Center, USA, [4]Beth Israel Deaconess Medical Center, Harvard Medical School, USA

Intermittent administration of teriparatide (hPTH 1-34) is currently the only approved anabolic agent for the treatment of osteoporosis. In humans, teriparatide stimulates bone formation dramatically for 6-12 months after which, for unknown reasons, bone formation declines, presumably limiting the anabolic potential of teriparatide. To investigate potential explanations for this phenomenon, we attempted to create an animal model that mimicked the decline in bone formation during long-term teriparatide administration and then assessed selected cellular and molecular mechanisms that may contribute to this pattern. 10-wk old C57BL/6J male mice (n=10/group) were treated with vehicle (VEH) or PTH (60 μg/kg/d; 5x/wk) for 16 wk, or VEH for 12 wk and then PTH for 4 wk. Long-term iPTH increased BMD progressively, though the increase was more robust in the initial 4-wk of iPTH

administration (13.5 ± 1.3%) than in the 2nd (5.0 ± 0.6%), 3rd (1.9 ± 1.9%), or 4th (2.9 ± 2.7%) 4-wk period. BMD increased 9.5 ± 1.6% in mice given iPTH only in the last 4 wk. Peak serum P1NP and CTX levels were observed at 2 or 4 wk of iPTH administration after which levels declined or remained steady. μCT analysis and histological examination revealed that long-term iPTH dramatically increased metaphyseal bone mass, associated with substantial increases in primary spongiosa and in cortical bone with increases in cortical porosity. iPTH increased the number of osteoblasts and osteoclasts per trabecular bone surface. Urine cAMP stimulation by acute PTH was not attenuated in mice with long-term iPTH, indicating no generalized desensitization or downregulation of PTH1R by long-term iPTH. iPTH administration increased levels of mRNAs encoding Runx2, osterix, Col1a1, osteocalcin, Bsp, MMP9 and TRAP in bone after16 or 4 wk, suggesting that long-term iPTH promotes osteoblast and osteoclast differentiation. After 16-wk iPTH, bone marrow cells formed fewer colonies of fibroblastic cells and, under osteogenic conditions, incorporated less calcium into osteoblastic colonies, than after VEH or 4-wk iPTH; such reduced differentiation of BMSCs may contribute to the attenuated response to long-term iPTH. Our results provide an insight into the reduced response to PTH after long-term therapy.
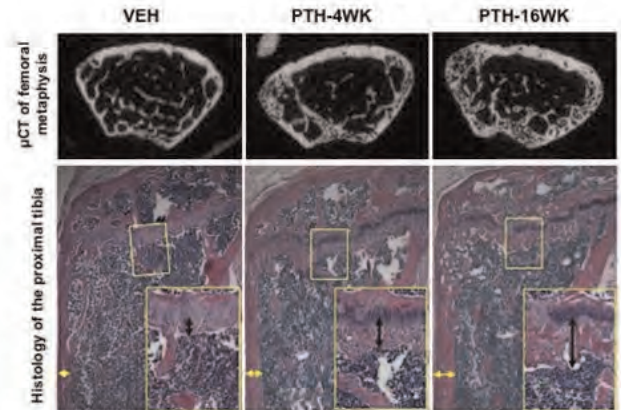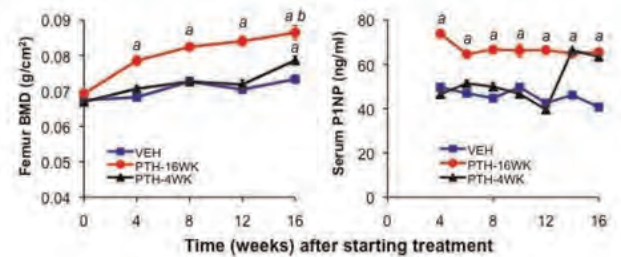
Bone Volume (% TV)	VEH	PTH-4WK	PTH-16WK
Femoral metaphysis (μCT)*	38.61 ± 0.96	45.99 ± 1.03[a]	51.01 ± 1.91[a,b]
Tibial primary spongiosa	21.22 ± 1.06	37.08 ± 1.61[a]	48.43 ± 3.42[a,b]
Cortical Thickness (mm)			
Femoral diaphysis (μCT)	0.166 ± 0.002	0.168 ± 0.002	0.176 ± 0.002[a]
Tibial metaphysis	0.116 ± 0.002	0.152 ± 0.005[a]	0.191 ± 0.01[a,b]

Data are expressed as mean ± SEM (n = 10); a: p < 0.05 vs VEH; b: p < 0.05 vs PTH-4WK
TV: total volume. * This measurement includes both trabecular and cortical bone.

Effect of long-term intermittent PTH on bone turnover

Disclosures: Jun Guo, None.

SU0143

Segment specific role of Gsα in mediating parathyroid hormone actions in the renal proximal tubule. <u>yan zhu</u>*[1], <u>Cumhur Aydin</u>[2], <u>Isabelle Rubera</u>[3], <u>Michel Tauc</u>[3], <u>Min Chen</u>[4], <u>Lee Weinstein</u>[5], <u>Vladimir Marshansky</u>[6], <u>Murat Bastepe</u>[7]. [1]Massachusetts General Hospital, Harvard Medical School, USA, [2]Endocrine Unit, Massachusetts General Hospital & Harvard Medical School, USA, [3]LP2M CNRS 7370 Université de Nice Sophia Antipolis, France, [4]National Institute of Diabetes & Digestive & Kidney Diseases, USA, [5]National Institute of Diabetes & Digestive & Kidney Diseases, USA, [6]Program in Membrane Biology, Massachusetts General Hospital & Harvard Medical School, USA, [7]Massachusetts General Hospital, Harvard Medical School, USA

The paternal promoter of the alpha-subunit of the stimulatory G protein (Gsα), is silenced in the renal proximal tubule (PT), and this silencing, together with maternal inactivating mutations in the Gsα gene, lead to Gsα deficiency and proximal tubular PTH resistance, as seen in pseudohypoparathyroidism type-I characterized by hypocalcemia, hyperphosphatemia, and elevated serum PTH. PT consists of three

functionally and anatomically distinct segments, but the spatial distribution of allelic Gsα silencing and the roles of Gsα along PT have remained unknown. We thus examined allelic Gsα expression in S1 and S3 segments in mice heterozygous for maternal (E1[m-/+]) or paternal (E1[+/p-]) *Gnas* exon 1 ablation, in which Gsα expression is exclusively paternal or maternal, respectively. We have shown that Gsα mRNA levels were $65 \pm 6\%$ of wild-type (p<0.05) in kidneys of E1[+/p-] mice when analyzing all PT segments isolated by laser cut microdissection. We now analyzed S3 segments only and showed that the levels were not significantly different from that in wild-type littermates ($83 \pm 3.5\%$; p=0.50). Moreover, immunostaining of kidney sections from E1[m-/+] mice indicated that, whereas Gsα protein levels in outer cortical PT, populated mostly by S1, were similar in E1[m-/+] and wild-type littermates, the levels in S3 were significantly lower in E1[m-/+] mice than wild-type littermates ($51.6 \pm 4.7\%$;p<0.05). These results indicate that the allelic silencing of Gsα is more prominent in S3 than the other segments. In addition, we ablated Gsα conditionally in S1 segments (S1rptE1^{-/-} mice) by using *Gnas* exon 1 floxed mice and Cre driven by the promoter of type 2 sodium glucose transporter (Sglt2-Cre). Western blot analysis of PT-enriched renal cortices, which include all PT segments and other contaminating tubules and blood vessels, showed that Gsα levels were diminished by ~50% in S1rptE1^{-/-} mice compared to controls. Offspring of Sglt2-Cre and *mTmG* reporter mice showed strong Cre activity in S1 segments. However, S1rptE1^{-/-} mice and control littermates did not appear to have significantly different ionized calcium (1.15 ± 0.02 [n=6] vs 1.18 ± 0.01 [n=13] mmol/l, respectively; p=0.12) or serum PTH (227 ± 62 [n=5] vs 165 ± 36 [n=12] pg/ml, respectively; p=0.41), suggesting that Gsα may be dispensable for PTH actions in S1. Together, our findings indicate that the allelic Gsα silencing and the role of Gsα in mediating PTH actions in PT differ in a segment-specific manner.

Disclosures: yan zhu, None.

SU0144

The Calcium-Sensing Receptor Supports the Growth of Breast Cancer Cells in High Calcium Environments By Stimulating Parathyroid Hormone-related Protein Production. Wonnam Kim*[1], Joshua VanHouten[2], Karena Swan[3], John Wysolmerski[2]. [1]Yale School of Medicine, USA, [2]Yale University School of Medicine, USA, [3]Yale School of Medicine, USA

Bone metastases from breast cancer cause pain, hypercalcemia, pathologic fractures and, ultimately, death. In order for breast cancer cells to grow in the bone microenvironment, they must adapt to high levels of extracellular calcium. Cells respond to extracellular calcium by activating the calcium-sensing receptor (CaSR), a G protein-coupled receptor that binds and signals in response to extracellular calcium. Previous reports have demonstrated that the CaSR is expressed in the lactating mammary gland and regulates parathyroid hormone-related protein (PTHrP) production and calcium transport into milk. In addition, the CaSR has been shown to be expressed in many breast cancer cell lines and its expression has been shown to be higher in bone metastases than in primary tumors in patients. Therefore, we studied the role of the CaSR in breast cancer cell behavior. First, we identified that activation of the CaSR with high extracellular calcium stimulated proliferation in human BT474 breast cancer cells. Knocking down expression of the CaSR inhibited proliferation in response to extracellular calcium. In addition, BT474 cells treated with the CaSR antagonist, NPS2143, showed decreased proliferation in a dose dependent manner. Furthermore, activation of the CaSR increased intracellular cyclic adenosine monophosphate (cAMP) levels and increased the production of PTHrP. Since PTHrP has been reported to increase proliferation in some breast cancer cell lines, we also knocked down PTHrP expression in BT474 cells, which reduced proliferation in response to increasing doses of calcium. Interestingly, BT474 cells treated with NPS2143 showed dramatic increase in apoptosis in response to increasing doses of extracellular calcium. Knocking down either the CaSR orPTHrP also dramatically increased apoptosis in response to extracellular calcium in BT474 cells. These studies suggest that the CaSR promotes the survival and proliferation of breast cancer cells under calcium-rich conditions such as those found in the bone microenvironment, and that PTHrP acts as an important mediator of these effects. Ongoing studies are examining the consequences of altering CaSR expression on the growth of breast cancer cells in bone in vivo, but our preliminary studies suggest that the CaSR-PTHrP axis may be a useful therapeutic target to treat bone metastases in breast cancer.

Disclosures: Wonnam Kim, None.

SU0145

The transcription factor, Mef2c participates in PTH stimulated MMP-13 gene expression in osteoblastic cells through the AP-1 site and c-Fos. Teruyo Nakatani*[1], Nicola Partridge[2]. [1]New York University College of Dentistry, USA, USA, [2]New York University College of Dentistry, USA

Parathyroid hormone (PTH) regulates transcription of many genes in osteoblasts. One of these is matrix metalloproteinase-13 (MMP-13), which is involved in bone remodeling and early stages of endochondral bone formation. Previously we reported that PTH induces MMP-13 transcription by causing the repressor, histone deacetylase 4 (HDAC4), to dissociate from Runx2 bound to the MMP-13 promoter. It is known that as well as Runx2, HDAC4 associates with the transcription factor, Mef2c, and represses its activity. To determine whether Mef2c is involved in the transcriptional regulation of MMP-13 by PTH, Mef2c expression was transiently knocked down in UMR cells by siRNA transfection. Knockdown of Mef2c decreased MMP-13 mRNA

expression and promoter activity with or without PTH treatment. ChIP assays showed that Mef2c associated with the MMP-13 promoter and this increased after 4 h of PTH treatment. ChIP-reChIP results indicated that endogenous Mef2c was shown to associate with HDAC4 at the promoter region and after PTH treatment this association was found to be decreased. Gel shifts showed that Mef2c associated with the AP-1 site and not the Runx2 binding site (RD) of the MMP-13 promoter. Mutation of the AP-1 site, but not the RD site, abolished the stimulatory effect of Mef2c in MMP-13 promoter-reporter assays. Immunoprecipitation demonstrated that Mef2c associated with c-Fos (but not c-Jun). In conclusion, Mef2c is necessary for PTH-induced MMP-13 gene transcription and acts by increased binding to the AP-1 site through c-Fos. This is the first description of Mef2c interaction with c-Fos and an AP-1 element.

Disclosures: Teruyo Nakatani, None.

SU0146

High Estradiol to Testosterone Ratio is Associated with Higher Baseline Bone Mineral Density but Poorer Response to Testosterone Treatment in Hypogonadal Males. Lina Aguirre*[1], Irum Jan[2], David Robbins[3], Dennis Villareal[4], Reina Armamento-Villareal[4]. [1]New Mexico VA Health Care System, USA, [2]New Mexico VA Health Care System, USA, [3]New Mexico VA Health Care System, USA, [4]University of New Mexico School of Medicine, USA

Estrogen has been recognized as the more important hormone to the male skeleton than testosterone. Despite higher levels of testosterone, deficiency in the enzyme aromatase (which is responsible for the conversion of testosterone to estradiol) is associated with low bone density which readily responds to estrogen supplementation. In this study we evaluated the role of estradiol to testosterone ratio on the response to testosterone in hypogonadal males participating in a genetic study of the enzyme aromatase. Bone mineral density (BMD) by DXA and serum total testosterone, estradiol sex hormone binding globulin and sclerostin by ELISA were measured at baseline and at six months. All participants were treated with testosterone cypionate with a starting dose of 200 mg every 2 weeks to achieve normal testosterone levels.

Results: To date, 90 patients have been enrolled in the study, with a mean age of 59.7 ± 8.6 years, and mean body mass index (BMI) of 31.4 ± 6.1 k/m^2. There were no correlations between free testosterone, free estradiol and sclerostin levels with baseline BMD at any skeletal site. However, baseline BMD of the lumbar spine increased with increasing tertiles of estradiol to testosterone ratio (1.063 ± 0.04, 1.098 ± 0.04, and 1.209 ± 0.04, for first, second and third tertiles respectively (p=0.04). In sixty patients with 6 month follow-up data to date, those in the lower tertiles for estradiol to testosterone ratio actually experienced a significant increase in the femoral neck BMD relative to the upper 2 tertiles (Fig. 1). A similar trend was observed for BMD at the trochanter and intertrochanter althought the difference did not reach statistical significance (p=>0.05). There was no correlation between changes in BMD and changes in estradiol levels or testosterone levels. Furthermore estradiol/ testosterone ratio did not correlate with sclerostin levels at baseline and at 6 months.

Conclusion: While a higher estradiol to testosterone ratio may have a positive influence on BMD in hypogonadal men at baseline, our results suggest that with testosterone treatment those in the lower tertile of estradiol/testosterone ratio actually experience greater increases in BMD relative to those in the upper tertiles. Our findings need confirmation in a larger sample size of men on testosterone treatment.

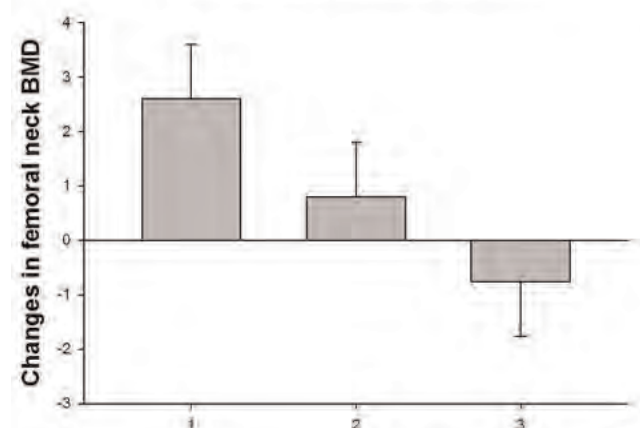Fig. 1. Changes in femoral neck BMD according to tertiles of estradiol to testosterone ratio

Figure 1

Disclosures: Lina Aguirre, None.

SU0147

A Common Polymorphism in the *CYP2R1* Gene Reduces Promoter Activity: Relevance to GWAS for 25(OH)D. <u>Jeff Roizen</u>*[1], <u>Alex Casella</u>[2], <u>Michael Levine</u>[3]. [1]The Childrens Hospital of Philadelphia, USA, [2]1Division of Endocrinology & Diabetes, The Children's Hospital of Philadelphia, Philadelphia, PA, University of Pennsylvania Perelman School of Medicine, Philadelphia, PA, United States, 19104, USA, [3]Children's Hospital of Philadelphia, USA

Optimal bone and mineral metabolism, as well as immune and cardiovascular function, depend on normal vitamin D metabolism. Ineffective sunlight exposure and inadequate dietary vitamin D intake each have well understood roles in the pathophysiology of vitamin D deficiency; however, the extent to which common variations or polymorphisms in genes encoding vitamin D metabolizing enzymes contribute to vitamin D homeostasis remains undefined. Several recent genome wide association studies (GWAS) have identified significant associations between serum [25(OH)D] and single nucleotide polymorphisms (SNPs) in or near the locus for *CYP2R1,* the gene encoding the principal vitamin D 25-hydroxylase enzyme. To examine whether common SNPs in the human *CYP2R1* gene promoter affect transcriptional activity, we generated a reporter construct in which expression of firefly luciferase was under the control of the proximal 5 kb of the *CYP2R1* promoter. The wild type *CYP2R1* promoter reporter or reporter constructs containing one of five promoter SNPs (rs2060793, rs10741657, rs1562902, rs16930609 and rs7949459) plus a Renilla luciferase reporter (to correct for transfection efficiency) were used to transfect LnCap cells, a human prostate carcinoma cell line previously shown to express CYP2R1 in a regulated fashion. The wild-type promoter showed significantly (p < 0.001 one way ANOVA) greater activity than a promoterless luciferase reporter (3.58 $\pm$ 0.51 vs 1.00 $\pm$ 0.00, mean $\pm$ SD). Four of the five polymorphic promoters (rs2060793, rs10741657, rs1562902, and rs16930609) showed luciferase activity (2.73 $\pm$ 0.35 to 3.51 $\pm$ 0.29) that was similar to the wild-type promoter. By contrast, SNP rs7949459 showed markedly reduced luciferase activity compared to the wild type promoter (0.58 $\pm$ 0.07 vs 3.58 $\pm$ 0.51, p < 0.001). *In silico* analysis of the promoter sequence using ENCODE revealed that the rs7949459 SNP is located in a DNase I hypersensitivity site, indicating that SNP rs7949459 may play a role in transcription factor binding to the *CYP2R1* promoter. Because the 1000 Genomes database indicates that this SNP occurs in more than 10% of the population, our results provide evidence that common genetic variations in *CYP2R1* may influence expression of 25-hydroxylase activity and thereby play a role in vitamin D homeostasis. Moreover, our results provide a functional context for interpreting GWAS that show relationships between circulating 25(OH)D and *CYP2R1*.

Disclosures: Jeff Roizen, None.

SU0148

Anabolic Bone Effect Of PGE₁ On The Rabbit Orthodontic Palate Disjunction. <u>Francisco Valasquez-Forero</u>*. Hospital Infantil De Mexico Federico Gomez, Mexico

Purpose: The purpose of this study was to evaluate, the PGE_1 anabolic effects on the rabbit orthodontic palate disjunction.

Methods: To evaluate the effects of the PGE_1 on the rabbit orthodontic disjunction, 30 rabbits were divided in 3 groups for study, ten control, 10 sham and ten PGE_1 subjects. Basal Rx evaluation was repeated on day 3 and 22. Using an orthodontic appliance sham and PGE_1 groups were subject to palate disjunction for five days, after wich it was filed with a steel bar. All animals received double tetracycline bone labeling. Control and sham groups were given a daily IV dose of vehicle solution, and the third group, vehicle with 50 mg of PGE_1 in vehicle and orthodontic appliance. On day 22 blood and urine samples were taken to all animals to analyze hormones, electrolytes and bone biochemical remodeling markers and the animals were sacrificed. Bone palate samples were taken and processed, undecalcified and the sutural bone modelation was histomorphometric evaluated using a digitalizing table with Osteomesure software parameters, following the recommendations of the American Society for Bone and Mineral Research. Data were statistically analyzed.

Results: Radiology verified the suture palate disjunction. In the PGE_1 group, blood exhibited significant calcitriol increments. The other calciotropic hormones and calcemia were normal (Table 1). In the urine the hypercalciuria was significantly high and the resorption bone marks (N-telopeptides) were normals (Table 1). Histomorphometric modelation on sutural bones was analyzed. It is exhibiting a significant increase percentage on structural formation parameters (SBWi: 142%, SBAr: 66%, SbTh:123%, SBV/TV;86%) when compared with control. The mineralization parameters (Omt,MLT) accelerated their function and the modelation activity (BFR/BS) is increased. Table 2. On the contrary, the resorption indexes (ES/BS and OcS/BS) showed decreased activity table 2.

Conclusions: This model suggests that PGE_1 can be an important osseous anabolic molecule. An ideal anabolic molecule is one that can optimize bone formation while producing no resorption, as we have observed in the present model. Hopefully this finding guide research to options for osteopenies treatment.

Table 1
BLOOD AND URINE BIOCHEMICAL BONE TURNOVER MARKERS

BLOOD		A (control)	B (sham)	C (with PGE₁)	p value
Ca	(mg/dL)	11.55 ± 0.72	11.55 ± 0.6	11.85 ±0.42	N.S.
Mg	(mg/dL)	2.48 ± 0.27	2.61 ±0.54	2.26 ± 0.23	N.S.
P	(mg/dL)	5.17 ± 0.65	5.03 ±0.43	5.00 ± 16.2	N.S.
Bone AkPh (%)		53.12 ±10.5	56.50 ± 9.38	50.00 ± 16.2	N.S.
PTHi (pg/mL)		28.1 ± 15.6	30.2 ± 26.0	27.4 ± 10.1	N.S.
Calcitonin (pg/mL)		32.2 ± 11.3	40.1 ± 20.5	28.4 ± 15.1	N.S.
Calcitriol (pg/mL)		50.5 ± 13.15	48.0 ±13.8	82.1 ± 13.5*	<0.01
	URINE				
Ca (mg/dL)		186 ±68.5	178 ± 53.3	376 ±102.2*	<0.01
P (mg/dL)		28 ± 15.3	29 ± 14.1	42 ±21.6	N.S.
N-telopeptides (NmBCE)		32 ± 14.1	38 ±16.5	30 ±12.0	N.S.

One way ANOVA were used to performed comparison between groups

Table 1

Table 2
STRUCTURAL BONE HISTOMORPHOMETRIC PARAMETERS

Structurals	Control	Sham	With PGE₁	p
SBWi μ	107.49 ± 26.49	201.32 ± 96.91	260.08 ± 66.85	0.001
SBAr mm²	0.06 ± 0.01	0.13 ± 0.08	0.14 ± 0.09	0.014
SBTh μ	452.47 ± 86.14	810.03 ± 373.80	1007.83 ± 246.40	0.001
SBV/TV %	26.32 ± 10.89	39.39 ± 15.78	49.07 ± 10.93	0.007
Static Bone Formation				
O.Th μ	2.90 ± 2.41	4.47 ± 1.64	4.22 ± 1.86	0.265
Ob.S/BS %	4.75 ± 2.39	7.46 ± 5.32	4.80 ± 2.26	0.251
SBOt/TAr mm²	187.83 ± 93.52	290.73 ± 125.34	383.33 ± 119.60	0.009
Dynamic Bone Formation				
MS/BS %	67.67 ± 13.56	281.85 ± 56.37	273.07 ± 54.61	0.001
MAR μ/d	2.85 ± 0.49	4.73 ± 1.13	4.81 ± 8.77	0.001
Omt d	5.11 ± 1.35	3.00 ± 0.69	1.72 ± 0.77	0.001
MLT d	23.30 ± 4.03	22.21 ± 3.18	10.38 ± 2.95	0.001
BFR/BS μ²/μ²/y	703.94 ± 140.78	4865.99 ± 973.19	4794.15 ± 958.83	0.001
SB Resorption				
ES/BS %	3.64 ± 1.44	4.04 ± 3.15	3.18 ± 0.64	0.742
OcS/BS %	1.12 ± 0.52	1.34 ± 0.98	0.87 ± 0.38	0.388

SBWi= sutural bone width; SBAr= sutural bone area; SBTh= sutural bone thickness; SBV/TV= sutural bone volume/tissue volume; O.Th= osteoide thickness; Ob.S/BS= osteoblast surface bone surface; SBOt/TAr= sutural bone osteocitos/tissue area; MS/BS= mineralizing surface/bone surface; MAR= mineral apposition rate; Omt= osteoide maduration time; MLT= mineralization lag time; BFR/BS= bone formation rate/bone surface; ES/BS=eroded surface/bone surface and OcS/BS= osteoclast surface bone surface. One way ANOVA allowed the comparison between groups by means of p values (showed in the last column).

Table 2

Disclosures: Francisco Valasquez-Forero, None.

SU0149

Effect of Dietary Calcium and Sodium on Blood Pressure and Its Related Gene Expression in *Cyp27b1* Knockout Mice. <u>Naoko Tsugawa</u>*[1], <u>Shiho Hiraiwa</u>[2], <u>Kanako Ohara</u>[2], <u>Kimie Nakagawa</u>[2], <u>Toshio Okano</u>[3]. [1]Kobe Pharmaceutical University, Japan, [2]Kobe Pharmaceutical University, Japan, [3]Kobe Pharmaceutical University, Japan

Introduction: Based upon the observation that vitamin D receptor knockout mice exhibit high blood pressure, 1,25-Dihydroxyvitamin D (1,25-D) is thought to play a role in controlling blood pressure. To clarify the role of 1,25-D in the regulation of blood pressure, we examined the effect of dietary calcium (Ca) and sodium (Na) on blood pressure and its related gene expression in *Cyp27b1* knockout mice (*Cyp27b1*-KO). Methods: [Experiment 1] Wild-type (WT) and *Cyp27b1*-KO littermates were divided into two groups. After weaning (3-week-old), they were fed a normal Ca diet (N-Ca) or a high Ca containing rescue diet (2% Ca, 1.25% phosphorus, and 20% lactose: H-Ca) for 32 weeks (age: 35-week-old). In this feeding condition, *Cyp27b1*-KO fed N-Ca and *Cyp27b1*-KO fed H-Ca showed hypocalcemia and normocalcemia, respectively. Blood pressure was measured using a noninvasive computerized tail-cuff system. [Experiment 2] Mice raised in experiment 1 were subsequently fed a high Na diet (8% NaCl: N-Ca&H-Na) or a rescue diet with 8% NaCl (H-Ca&H-Na) for further 4 weeks, respectively. Animals were sacrificed and mRNA levels of brain natriuretic peptide (BNP) in hearts and renin in kidney were measured by real-time PCR. Results: [Experiment 1] No significant difference of blood pressure was observed between *Cyp27b1*-KO and WT fed N-Ca or H-Ca for 32 weeks. [Experiment 2] Blood pressure of *Cyp27b1*-KO fed N-Ca&H-Na was significantly higher than that of WT fed the same diet. On the other hand, no significant difference of blood pressure was observed between *Cyp27b1*-KO and WT fed H-Ca&H-Na. Renal renin mRNA expression of *Cyp27b1*-KO was higher than that of WT in both feeding of N-Ca&H-Na and H-Ca&H-Na. BNP mRNA expression in the heart of *Cyp27b1*-KO fed N-Ca&H-Na was lower than that of WT fed the same diet, but no significant

difference was observed between WT and *Cyp27b1*-KO fed H-Ca&H-Na. Both WT and *Cyp27b1*-KO fed H-Ca&H-Na showed the tendency of high blood pressure and low expression of BNP. Conclusion: These results suggest that *Cyp27b1*-KO fed N-Ca&H-Na is likely susceptive to high Na containing diet. However, the susceptibility to high Na diet was not observed in *Cyp27b1*-KO fed H-Ca&H-Na, which suggests that susceptibility to high Na diet was due to hypocalcemia. Low BNP expression observed in *Cyp27b1*-KO fed N-Ca&H-Na was thought to associate partly with high susceptibility to dietary Na. However, further investigations will be needed to clarify the mechanism of these phenomenon.

SU0150

Alterations of volumertic bone density, bone microarchitecture and bone strength in patients with ankylosing spondylitis: a case-control study using high-resolution peripheral quantitative computerized tomography. Nisha Nigil Haroon*[1], Eva Szabo[2], Janet Raboud[3], Robert Josse[4], Robert. D. Inman[5], Angela M. Cheung[6]. [1]University of Toronto, Canada, [2]Osteoporosis Program, University Health Network, Canada, [3]Dept of Biostatistics, University of Toronto & Toronto General Research Institute, Canada, [4]St. Michael's Hospital, University of Toronto, Canada, [5]Department of Medicine, University of Toronto, Canada, [6]University Health Network-University of Toronto, Canada

Background: Patients with ankylosing spondylitis (AS) have high fracture risk. Bone mineral density (BMD), bone microarchitecture and bone strength determine fracture risk. However, in AS, DXA-based BMD measurements of the lumbar spine may be falsely normal due to the presence of syndesmophytes. Also, DXA cannot differentiate between trabecular and cortical bone. The effect of AS on bone microarchitecture and bone strength is unknown.

Objectives: To assess bone microarchitecture and strength in patients with AS and to compare these parameters with non-AS controls.

Methods: AS was defined by the modified New York criteria. Disease activity of AS was measured by BASDAI (clinical severity), mSASSS (radiological severity), serum ESR and CRP levels. Volumetric BMD (vBMD) and microarchitecture were measured using HRpQCT, and bone strength was estimated using finite element analysis (FEA). Multivariable linear regression was used to analyze the effect of AS on HRpQCT parameters.

Results: There were 44 cases (82% Caucasian). The mean (+SD) age and BASDAI were 44+2 and 6.3+ 1.8 respectively. Median (IQ) disease duration was 20 (7.3-27.8 years). Twenty-three subjects had mSASSS >0. Four cases (9%) reported a history of fragility fracture. Use of TNF inhibitors (none), bisphosphonates (n=2) and corticosteroids (n=2) was negligible. Mean serum ESR, CRP and SAP levels were 22.0+23.6, 12.6 +15.6 and 96.2 +43.2 IU respectively. In multivariable linear regression models adjusted for age and gender, cases (n=44) had lower vBMD (trabecular, cortical and total), cortical thickness, BV/TV, bone stiffness and stress, and higher cortical porosity and trabecular separation at the radius (Table 1) when compared to non-AS controls (n=85). Tibial vBMD, BV/TV and cortical porosity were also abnormal in cases. But trabecular architecture at tibia was not different between cases and controls.

Conclusions: This study documents abnormalities of bone structure and bone strength in patients with AS. Patients with AS had lower volumetric BMD and worse microarchitecture at the trabecular and cortical regions compared to controls. Bone stiffness and stress at the radius and tibia, as estimated by FEA, also tended to be lower in cases than controls. These abnormalities might partly explain the high fracture risk in patients with AS.

Table 1: Multivariable linear regression showing abnormal bone microarchitecture and strength in patients with AS (44 cases and 85 controls).

Outcome variables		Exposure variable Cases vs. controls		Covariate 1 Age		Covariate 2 Gender	
Site		Beta	p	Beta	p	Beta	p
Radius	Trabecular vBMD	-.232	.032	-.211	.048	.444	.000
	Cortical vBMD	-.294	.008	-.530	.000	-.143	.092
	Total vBMD	-.351	.003	-.394	.001	.128	.148
	Trabecular number	-.208	.071	-.057	.613	.328	.000
	Trabecular thickness	-.195	.068	-.310	.003	.421	.000
	Trabecular separation	.242	.035	.090	.422	-.318	.000
	BV/TV	-.231	.033	-.210	.049	.443	.000
	Cortical thickness	-.327	.003	-.604	.000	-.019	.822
	Cortical porosity	.215	.029	.661	.000	.298	.000
	Stiffness, *K* (kN/mm)	-.337	.004	-.254	.028	.136	.129
	Stress	-.337	.004	-.254	.028	.137	.129
Tibia	Trabecular vBMD	-.232	.044	-.103	.359	.328	.000
	Total vBMD	-.271	.019	-.403	.000	.136	.122
	Cortical vBMD	-.246	.019	-.636	.000	-.008	.918
	Trabecular number	-.153	.182	-.040	.722	.333	.000
	Trabecular thickness	-.122	.313	-.076	.521	.101	.276
	Trabecular separation	.213	.067	.050	.660	-.299	.001
	BV/TV	-.233	.043	-.104	.353	.329	.000
	Cortical thickness	-.176	.065	-.719	.000	-.191	.010
	Cortical porosity	.227	.025	.685	.000	.092	.233
	Stiffness, *K* (kN/mm)	-.209	.073	-.361	.002	.109	.222
	Stress	-.212	.068	-.363	.002	.108	.228

Table 1

SU0151

Circulating Osteoblast Precursors in Peripheral Blood Were Decreased after TNF-α Blocker Therapy in Patients with Ankylosing Spondylitis. Seong-Ryul Kwon*[1], Won Park[1], Min-Jung Son[2], KoWoon Joo[2], Mie-Jin Lim[2], Kyoung-Hee Jung[2]. [1]INHA University Hospital, South Korea, [2]INHA University Hospital, South Korea

Background

The relationship between inflammation and new bone formation is unsolved question in area of spondylitis. First hypothesis is that inflammation is the process that sets in motion the chain of events that leads to ankylosis; an opposite one has proposed that an unknown pathogenic trigger simultaneously induces both inflammation and activation of new bone formation.

Objective

We investigated the circulating osteoblast precursors in peripheral blood with cell culture technique before and 14 weeks after infliximab therapy in patients with ankylosing spondylitis.

Methods

Male Fifteen individuals with ankylosing spondylitis were enrolled. They met the modified New York criteria and the candidates of infliximab therapy, refractory to non-steroidal anti-inflammatory drugs or disease modifying anti-rheumatic drugs. Peripheral blood mononuclear cells were collected and cultured in osteoblast growth medium. Once cell multilayering has been observed (about 7 days later), cells were moved to osteoblast differentiation medium and cultured for 3 weeks more. Then, cells were fixed and stained with alizarin S red to detect any calcified nodules. The optic density measurement of alizarin S red was performed to quantitative analysis.

We evaluated the changes of 1) the number of circulating osteoblast precursors, 2) the optic density of alizarin S red staining of circulating osteoblast precursors, 3)the osteocalcin, c-terminal telopeptide (CTX-1), receptor activator of NFkB ligand (RANKL) with enzyme linked immunosorbent assay (ELISA) in peripheral blood before and after 14 week infliximab therapy in patients with ankylosing spondylitis.

Results

The number of osteoblast precursor cells (Figure-1) and optic density of alizarin S were decreased after infliximab therapy (p = 0.018 for optic density of alizarin S, Figure-2). The serum level of osteocalcin was increased after infliximab therapy (p = 0.01); but, that of CTX and RANKL was not changed significantly.

Conclusion

The circulating osteoblast precursors in peripheral blood were decreased significantly after 14 weeks of infliximab therapy. This result can support inflammation and activation of new bone formation occurs simultaneously in patients with ankylosing spondylitis.

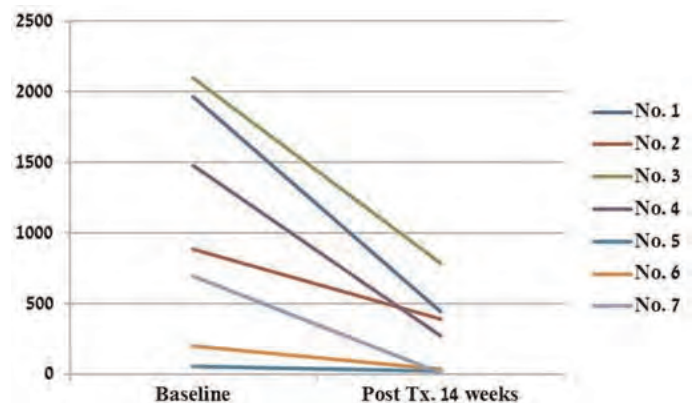Figure-1. The number of osteoblasts in peripheral blood at baseline and post infliximab therapy

Figure-2. The optic density changes of Alizarin S staining of osteoblasts

SU0152

Serum Sclerostin in Juvenile Idiopathic Arthritis. <u>Jan Stepan</u>*[1], <u>Kristyna Brabnikova Maresova</u>[2], <u>Katerina Jarosova</u>[3], <u>Karel Pavelka</u>[3]. [1]Charles University, Czech Republic, [2]Institute of Reheumatology, Czech Republic, [3]Institute of Rheumatology, Czech Republic

Background: The study was aimed to evaluate the clinical value of serum sclerostin in adult patients with active juvenile idiopathic arthritis (JIA) treated with biologicals. This group of young patients was used to avoid an overlap of changes in serum sclerostin due to disease and aging. JIA is the most common chronic rheumatic multifactorial autoimmune disorder of childhood. Sclerostin is a potent antagonist of bone morphogenetic proteins critical for osteoblastogenesis. Serum sclerostin levels are higher in males and in both sexes across the adult lifespan. Although widely thought to be an osteocyte-specific protein, the SOST mRNA is expressed by other cells including articular chondrocytes.

Methods: Adult patients (12 male and 19 female, age 25 ± 6.1 years) with active JIA (DAS 28, 6.36 ± 0.64, hsCRP, 18.36 ± 16.95 mg/l) and 84 healthy age- and gender- matched controls were enrolled into the study. Before the initiation of treatment with biologics, the patients were treated with DMARDs, and 12 patients were on glucocorticoids ($6.6 \pm$, 4.3 mg/day). After baseline evaluation, the patients were treated for 2 years with biologics (18 infliximab, 8 etanercept, 5 adalimumab). Areal bone mineral density (BMD) at the lumbar spine, proximal femur, and femoral neck was assessed using DXA, and correlated with clinical and laboratory characteristics of the disease. Sclerostin was measured using the Human SOST ELISA, Uscn Life Science Inc.

Results: At baseline, compared to healthy controls, BMD in JIA patients was lower at all measured sites (p<0.001), and serum sclerostin was increased (p<0.001). An increase in lumbar spine BMD after 2 years of therapy (Table) was predicted by decrease in DAS28 during the first year (p=0.003, after adjustment for sex, age, height, glucocorticoid therapy and disease duration). Serum sclerostin was decreased after 12 and 24 months of therapy as compared with baseline values (Table). A significant positive correlation was found between DAS28 and serum sclerostin concentrations (r=0.32, p=0.002), and between number of swollen joints and sclerostin (r=0.33, p=0.001). However, no correlation was found between sclerostin and hrCRP (r=0.01, p=0.92).

Conclusion. The association between serum sclerostin concentrations and number of swollen joints rather than CRP suggests that circulating sclerostin is a reflection of the number of sclerostin-producing cells, either subchondral bone or chondrocytes.

Table Disease activity, BMD and serum sclerostin in patients with JIA during biologics treatment and in controls. Median and 75% CI

	0 (n=31)	12 months (n=31)	24 months (n=31)	Controls (n=83)
Lumbar spine BMD (g/cm²)	1.065 ª	1.089 ᵃᵇ	1.093 ᵃᵇ	1.209
	0.972; 1.221	1.044; 1.248	1.053; 1.161	1.175; 1.279
Femur total BMD (g/cm²)	0.909 ᵇ	0.918 ᵇ	0.886 ᵇ	1.134
	0.776; 0.984	0.776; 1.015	0.790; 0.996	1.061; 1.202
Femoral neck BMD (g/cm²)	0.899 ᵇ	0.903 ᵇ	0.905 ᵇ	1.118
	0.819; 1.017	0.806; 1.033	0.821; 1.019	1.042; 1.201
Sclerostin (ng/ml)	7.42 ᵇ	2.06 ᵃ	1.22 ᵃ	1.94
	3.57; 15.49	1.00; 3.48	0.30; 3.26	0.62; 5.71
CRP (mg/l)	12.09 ᵇ	5.19 ᵇ	4.28 ᵇ	0.73
	6.28; 25.17	1.30; 12.89	0.89; 13.44	0.27; 1.78
DAS 28	6.26	2.93 ᵃ	2.51 ᵃ	
	5.87; 6.82	1.13; 3.69	1.25; 3.64	

a: probability by use of repeated measures one-way analysis of variance within JIA group, as compared with baseline, p<0.05; b: probability by use of one-way analysis of variance, as compared with control subjects, p<0.05.

Tab

*Disclosures: **Jan Stepan**, None.*

SU0153

Comparison of the effect of 18-months daily teriparatide administration on patients with rheumatoid arthritis and postmenopausal osteoporosis patients. <u>Kosuke Ebina</u>*[1], <u>Jun Hashimoto</u>[2], <u>Masafumi Kashii</u>[3], <u>Takaaki Noguchi</u>[4], <u>Yohei Matsuo</u>[5], <u>Tsuyoshi Sugiura</u>[6], <u>Hideki Yoshikawa</u>[7]. [1]Osaka University, Graduate School of Medicine, Japan, [2]National Hospital Organization, Osaka Minami Medical Center, Japan, [3]Osaka University Graduate School of Medicine, Japan, [4]Osaka Univieristy, Graduate school of medicine, Department of Orthopaedic Surgery, Japan, [5], Japan, [6]Faculty of Medicine, Graduate School of Medicine, Osaka University, Japan, [7]Osaka University Graduate School of Medicine, Japan

Purpose

The aim of this study is to clarify the effect of 18 months daily Teriparatide (TPTD; 20µg/day) administration on osteoporosis patients with rheumatoid arthritis (RA; n=70) by comparing with that of postmenopausal osteoporosis patients (Porosis; n=62).

Methods

RA group (age 68.4, prior bisphosphonate (BP) 77.1%, lumbar spine (LS) T-score -2.5, femoral neck (FN) T-score -2.7, previous vertebral fracture 72.9%, DAS28-CRP 2.8, 84.3% taking prednisolone (PSL) 4.4mg/day, 25.7% taking biologics) and Porosis group (age 71.3, prior BP 77.4%, LS T-score -3.0, FN T-score -2.5, previous vertebral fracture 71.0%) were enrolled. BMD and Bone metabolism markers including PINP,

bone ALP, TRAP-5b, uDPD, and ucOC were monitored. The relationship between baseline and changes in these markers and 18-months BMD changes in LS and FN were evaluated using Spearman correlation analysis and multivariate logistic regression analysis.

Results

Absolute increase of bone formation markers at 1-month were significantly greater in RA group compared to Porosis group, which were 101.8 v.s. 50.2 µg/L for PINP (P=0.0001), and 5.6 v.s. 2.1 U/L for bone ALP (P=0.007). Increase in FN BMD from baseline at 18 months were significantly greater in RA group compared to Porosis group, which was 4.7% v.s. 0.7% (P=0.035), while increase in LS BMD were 9.7% v.s. 7.9%, which did not reached significant difference. In RA group, increase in 18-months BMD was positively correlated with baseline ucOC (P<0.05 for LS; P<0.01 for FN) and change in PINP at 3-months (P<0.05 for LS; P<0.01 for FN) and 6-months (P<0.05 for LS ; P<0.01 for FN). The increase in FN BMD at 18-months was negatively correlated with baseline PSL dose (P<0.05), although prior use of BP, disease duration, disease activity, autoantibody titers, and combined biologics didn't show significant correlation with 18-months BMD increase. There was no significant difference between RA and Porosis group in the incidence of vertebral fractures (3.7% versus 3.9%) and nonvertebral fractures (1.9% versus 2.0%). Multivariate logistic regression analysis revealed that significant indicator of 18-months BMD change of LS and FN was baseline and 3-months change (Δ3) of ucOC in RA group, whereas Δ1 bone ALP in Porosis group.

Conclusions

Our findings indicate that RA group showed grater response to TPTD administration, especially in increase of 1-month bone formation markers, and increase of 18-months FN BMD compared to Porosis group.
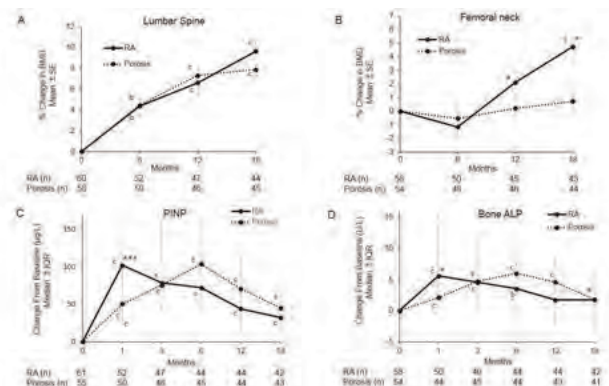
TPTD figure

*Disclosures: **Kosuke Ebina**, None.*
This study is funded by Japan Osteoporosis Foundation

SU0154

Role of the A2B Adenosine Receptor in the Degradation of Bone in Rheumatorid Arthritis. <u>Lauren Mangano</u>*[1], <u>Dana Daukss</u>[2], <u>Shannon Carroll</u>[3], <u>Katya Ravid</u>[4], <u>Louis Gerstenfeld</u>[5], <u>Elise Morgan</u>[6]. [1]Boston Univeristy, USA, [2]Boston University, USA, [3]Boston Univerisyt, USA, [4]Boston University School of Medicine, USA, [5]Boston University School of Medicine, USA, [6]Boston University, USA

Introduction: Adenosine receptors are known to mediate the activity of cytokines involved in the inflammatory processes of rheumatoid arthritis (RA) and have been connected to production of matrix metalloproteinases and differentiation of osteoblasts. The goal of this study is to determine the role of the A2B adenosine receptor (A2BAR) in degenerative changes to cartilage and bone using a mouse model of collagen antibody-induced arthritis (CAIA).

Methods: A2BAR knockout (KO) mice (n=11) were bred into a C57BL6/J background. C57BL6/J mice (n=12) were used as a wild type (WT) reference. At 16 weeks of age, female mice were injected with a collagen antibody cocktail (ArthritoMab, MD Bioproduts) and lipopolysaccharide (LPS) to induce arthritis (CAIA) or with saline (control). Ankle width, as a measure of joint swelling, was recorded on days 4, 8, and 10. Mice were sacrificed after 8 and 10 days. The forepaws and hindpaws were imaged with µCT (µCT40, Scanco Medical, Brüttisellen Switzerland) at resolution of 16 µm/voxel. The bone mineral density (BMD) and bone fraction (BV/TV) of the 2nd-4th metatarsal phalangeal (MTP) joints were measured. The distal femora and proximal tibiae were imaged with contrast-enhanced µCT (6 µm/voxel), a technique involving performing a µCT scan both before and after a 14-hourincubation in an iodinated contrast agent (CA4+) that labels cartilaginous tissues.

Results: Ankle width was higher at days 8 and 10 vs. day 4 in both WT CAIA (p<0.05), but not KO CAIA mice (p>0.05). As compared to control mice, CAIA mice—both WT and KO— showed increased porosity and roughness of the endosteal surface in the distal metatarsal metaphyses (Fig 1). Correspondingly, tissue mineral density (TMD) and bone volume fraction (BV/TV) in these regions were lower with CAIA (p<0.0001, p<0.005). TMD was also lower in the entire metatarsal-phalangeal (MTP) joints in CAIA (p<0.0001) and trended higher in KO vs. WT mice (p=0.0962).

Contrast-enhanced μCT indicated a greater loss of articular cartilage in WT vs. KO CAIA mice at day 10 (Fig 2).

Discussion: Evidence of increased bone resorption in MTP joints was seen with CAIA irrespective of genotype. Loss of articular cartilage in the knee was also seen in both genotypes with CAIA but to a lesser extent in A2BAR KO mice, suggesting a protective effect of the loss of this receptor. Pharmacological antagonism of this receptor may be a potential treatment to mitigate the destruction of bone and cartilage associated with RA.
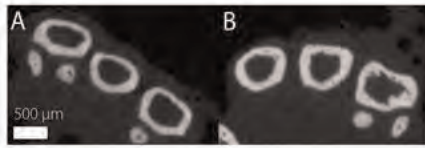
Figure 1. μCT scan of the 2nd-4th metatarsal of WT mice. A) control day 10, B) CAIA day 10.
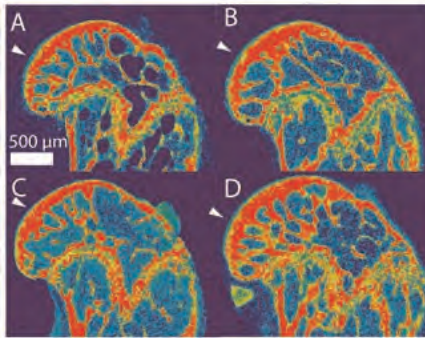
Figure 2. Contrast-enhanced μCT scan of the distal femur of CAIA mice. A) WT day 8, B) KO day 8, C) WT day 10, D) KO day10. Arrowheads indicate the articular surface.

LaurenMangano_Figure

Disclosures: Lauren Mangano, None.

SU0155

***In Vivo* Fatigue Damage in Bone Linked to Cytokine Expression.** <u>Travis McCumber</u>*[1], <u>Bryan Hackfort</u>[2], <u>Mohammed Akhter</u>[3], <u>Diane Cullen</u>[2]. [1]Creighton University, USA, [2]Creighton University, USA, [3]Creighton University Osteoporosis Research Center, USA

Long bone fractures result in cytokines that regulate the formation and/or remodeling of fracture callus; however, cytokine production is not associated with typical mechanical loading and exercise. Repetitive ulna compression that causes bone fatigue in rats induces tissue microdamage with subsequent remodeling. This project examines the cytokine response to *in vivo* fatigue loading. We have reported that IL-2 is elevated in serum and bone blood spaces after fatigue loading. IL-2 is produced by T cells and increases T cell number, suggesting that T-cells may play a role in the bone response to tissue damage and repair. We hypothesize that overloading of bone to cause fatigue damage, activates cytokines and osteoclastogenesis leading to bone resorption. In Sprague Dawley female rats (6 mo) the right ulna was fatigue loaded in compression (< 4000 με, < 20,000 cyc, 4 Hz) to 40% loss of ulna stiffness. Right and left ulnae were collected at 48 hrs post-fatigue, fixed, decalcified, and embedded in paraffin (N=8). Immunohistochemistry was used to identify Th17 cells (IL-23 receptor) and TRAP staining was used to identify osteoclasts. IL-23r was expressed strongly in *bone* blood spaces in load and nonload legs at 48 hours similar to the IL-2 pattern. TRAP stained osteoclasts were numerous in fatigue loaded bone, located in blood spaces, periosteum, and tissue in the vicinity of microcracks. Compared to loaded, the nonloaded legs had fewer osteoclasts that were randomly distributed in the tissue. The up-regulation of IL-2 and IL-23r are novel findings that implicate inflammatory signals in the bone response to fatigue damage. IL-2 is not known to be produced by osteocytes or osteoblasts. While IL-2 is a non-specific T-cell signal, it demonstrates that T-cells in the loaded limb are activated and that the response can be detected at the serum level. Th17 cells can stimulate osteoclastogenesis via IL-17. Unlike complete fracture, an inflammatory response with an influx of white blood cells typically is not associated with microdamage. These data are the first to show a rapid increase in cytokines in blood and bone tissue following ulnar fatigue damage in rats. If T cell activation and subsequent cytokines contribute to remodeling of bone tissue damage, this would provide a new paradigm for studying tissue damage and repair.

Disclosures: Travis McCumber, None.

SU0156

Continuous and intermittent hypergravity induce a bone compartment-specific anabolic response and affect differently osteocyte Sclerostin expression. <u>Vasily Gnyubkin</u>*[1], <u>Alain Guignandon</u>[2], <u>Norbert Laroche</u>[2], <u>Arnaud Vanden-Bossche</u>[2], <u>Fiona Louis</u>[2], <u>Marie-Helene Lafage-Proust</u>[3], <u>Laurence Vico</u>[4]. [1]INSERM U1059, LBTO, Faculty of Medicine, University of Lyon, France, [2]INSERM U1059, LBTO, Faculty of Medicine, University of Lyon, France, [3]INSERM Unit 1059, France, [4]University of St-Etienne, France

Bone fragility is a major obstacle to the long-term spaceflights. Adequate mechanical loading is necessary for bone status preservation. Possible countermeasure can be exposure to hypergravity (hyperG) either continuous by centrifugation or intermittent by whole body vibration (WBV). We investigated how the bones reacted to different modes of G-load and which G level was the most effective. Firstly, we studied effects of 21-d continuous hyperG at 2 and 3G on the skeleton of 7 w-old male C57/BL6 mice. We analyzed the structural parameters by μCT and cellular activities by histomorphometry in femur. At 3G, significant difference (p<0.05 vs control group) were found for femoral cortical thickness (-6%). Although trabecular bone was maintained, resorption activity (TRAcP+ Oc.S/BS,%) increased by 41% whereas bone formation activity decreased (OS/BS,%:-42%; dLS/BS,%:-20%; MAR, μm/d:-16% and BFR, μm3/μm2/day:-30%). In contrast, 2G exposure improved trabecular volume (BV/TV, %:+18%), number (Tb.N, mm-1:+15%) and connectivity density (Conn.D,1/mm3:+32%). In 2G, resorption activity decreased by 36% and osteoblast recruitment increased (OS/BS:+33%; dLS/BS:+31%). Because 3G caused negative effects and 2G was beneficial we repeated 2G experiment to investigate osteocyte Sclerostin and DMP1 levels, and bone vascularization (Roche B. et al, Bone. 2012). In femur cortex DMP1 increased by 7.2%, Sclerostin decreased by 15% (automated image analysis, 7500 osteocytes p/group, p<0.02). In distal metaphysis of femur the number and area of vessels/mm2 of bone marrow increased by 22% and 44%, respectively (p<0.02). Secondly, we studied effects of intermittent hyperG at 90Hz,15 min/d,5 d/wk, 9 wks, 3 WBV modes: 0.5G, increment from 0.5 to 2G, and 2G. Because PIXImus BMD showed 11% (p<0.02) increase in femur of 2G group only, this mode was selected for a 21-d experiment. After 21-d of WBV cortical thickness (μm) increased by 5%, area (μm2) by 6%, and porosity (%) decreased by 6% (p<0.05). Both resorption and formation activities increased (Oc.S/BS:+41%; OS/BS:+47% and BFR:+124%, p<0.02). Sclerostin and DMP1 increased by 26% and 33% respectively (p<0.001). Also, WBV led to 23% increase of vessels number (p<0.02). In summary: while continuous 2G improved trabecular, intermittent 2G improved cortical bone and both stimulated angiogenesis. Resorption activity and Sclerostin decreased after continuous 2G and increased after WBV. DMP1 increased in both cases although much more after WBV.
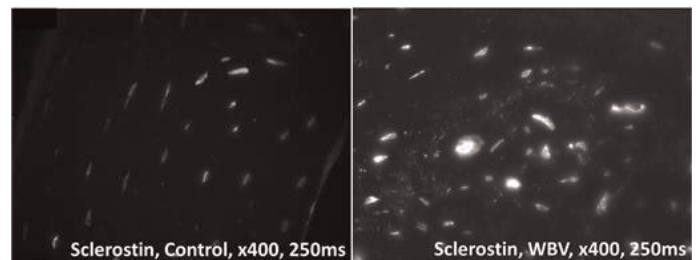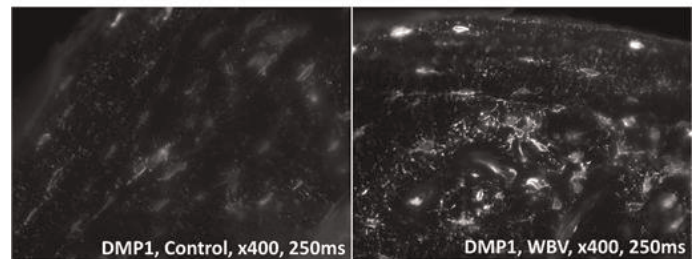
IHC of DMP1 and Sclerostin, Control vs WBV

Disclosures: Vasily Gnyubkin, None.

SU0157

Deficit in the Adaptation of Old Bone to Loading is Associated with Reduced Retention of Wnt Activity. Nilsson Holguin*[1], Michael Brodt[2], Matthew Silva[3]. [1]Washington University Department of Orthopaedic Surgery, USA, [2]Washington University in St Louis, USA, [3]Washington University in St. Louis School of Medicine, USA

Tibial compression increases bone mass in mice but aging reduces the response. Wnt signaling is a key anabolic pathway in bone, where suppression of antagonist Sost is necessary for load-induced bone formation. We hypothesized that aging diminishes the activation of Wnt signaling by mechanical loading. First, we subjected a range of adult (5-, 12- and 22-month; n=5-8/age/time) C57Bl/6 mice to 1-5 days of tibial compression (1200 cycles, peak compressive strain -2200 $\mu\varepsilon$). Multiple days of loading enhanced the gene expression of matrix production (Col1a1) (Fig. 1a), osteoblast-differentiation (Osx), late-osteoblast (Osc), and Wnt-related markers (Wnt1, Dkk1, Sost) (Fig. 1b) towards activation of the pathway. The enhanced expression of Col1a1 was age-dependent at day 5, which corroborates the age-dependent decline in mineralizing surface at day 5. Next, noting suppression of all the common bone formation markers after a single bout of loading, we determined the kinetic profile for the same above-mentioned genes. Following a single day of loading, the expression of bone formation markers and Sost (Fig. 1c) remained down-regulated for longer in young-adults than older mice (n=5-7/age/time). In order to account for control levels of Sost with aging, we ran a three-way ANOVA to demonstrate an interaction between age and loading. A post-hoc test removing time as a factor showed that aging diminished the Sost expression in control tibiae and the loading response, suggesting that heightened suppression of Sost may not be as necessary in old age (Fig. 1d). Lastly, we determined the activation of Wnt signaling in osteocytes from Wnt-reporter mice (TOPGAL, n=7-10/age/time) after 1 and 5 d of anabolic loading. We confirmed that aged TOPGAL have an age-related decline in loading-induced bone formation. Two weeks of tibial compression at -650 $\mu\varepsilon$ increased periosteal MS/BS in 5-month and 12-month mice (n=4-7/age), and the periosteal response was 5-fold greater in 5-month mice (Fig. 1e). Following tibial compression of young-adults, 1 and 5 d of loading doubled the percentage of Wnt-active cells. By contrast, 1 d of loading activated Wnt signaling in cells of 12-month mice, but 5 d of loading did not (Fig. 1f). Tibial compression at a higher strain (-2200 $\mu\varepsilon$) similarly increased activation of Wnt signaling. In conclusion, the reduced bone formation response of aged mice to tibial compression may be due to a reduced retention of Wnt activity.
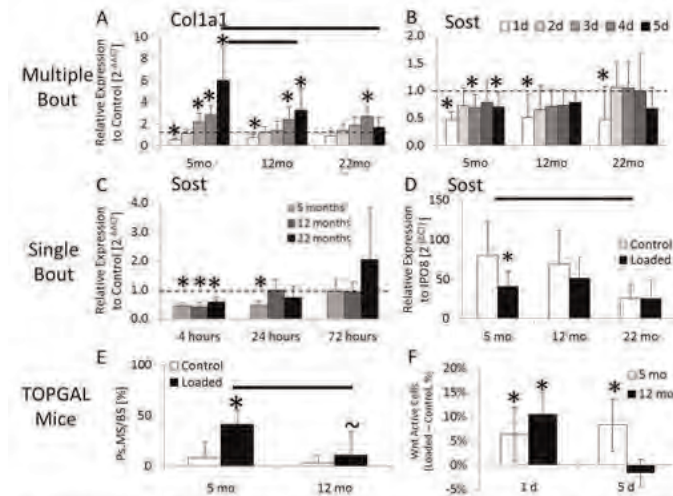

Fig. 1 Multiple bouts of loading increased (a) Col1a1 expression in a range of adult mice, with the greatest response determined in young-adult 5-month mice at day 5. (b) Similarly, Sost expression was down-regulated in 5-month mice up to the 5th day, but not reduced in older mice following multiple bouts. (c) A single session of tibial compression reduced Sost expression for longer in 5-month mice than older mice. (d) When the 4, 24 and 72 hour time points were pooled, loading did not suppress Sost expression in 22-month mice as it had in younger mice but the expression in the control tibiae of these old mice declined compared to younger mice. Tibial compression in TOPGAL mice increased (e) periosteal MS/BS more so in 5-month mice than 12-month mice. (f) Similarly, loading increased activation of Wnt in osteocytes from 5 month mice following both 1 and 5 days, whereas 12-month old mice had greater activation after 1 day but not 5 days. *: vs control, Bar: between ages, p<0.05; ~:vs control, p<0.1.

Figure 1

*Disclosures: **Nilsson Holguin**, None.*

SU0158

Differential effects of involuntary running on bone structure of high-fat diet-induced obese rats. Jay Cao*[1], Matthew Picklo[2]. [1]USDA ARS, USA, [2]Grand Forks Human Nutrition Research Center, USA

The aim of the study was to examine how exercise and exercise plus anti-oxidant supplementation with vitamin E and vitamin C alter bone structural properties at different skeletal sites and markers of bone metabolism in a high-fat diet induced obese rat model. Fourteen 5-wk old obese prone Sprague Dawley rats were fed a normal-fat diet (NF, 10% kcal as fat), and 41 rats were fed a high-fat diet (HF, 45% kcal as fat from lard) *ad libitum* for 15 wks. Then, rats on the high-fat diet were assigned randomly to three treatment groups for additional 12 wks: (1) high-fat diet (n=14); (2) high-fat diet + exercise (HF-Ex, n=14); (3) high-fat diet with vitamin E (0.4 g α-tocopherol acetate/kg diet) and vitamin C (0.5 g ascorbate/kg diet) supplementation + exercise (HF-Ex-Aox, n=13). Animals were forced to exercise by running wheel for 5 days/wk for 8 wks at a graduated rate until reaching 1.2 km/ 2 hr session and maintained at the same rate by another 4 wks. Body weight and fat (%) were similar among NF, HF-Ex, and HF-Ex-Aox whereas HF had greater body weight and fat (%) than other groups. Compared to NF, HF had elevated serum leptin, tartrate-resistant acid phosphatase (TRAP), and IGF-1, increased trabecular separation, and structural model index, decreased bone mineral density, trabecular connectivity density, and trabecular number in distal femur, while HF-Ex and HF-Ex-Aox had elevated serum TRAP, decreased bone volume/total volume and trabecular number of distal femurs. Compared to HF, HF-Ex and HF-Ex-Aox had decreased serum TRAP and osteocalcin, and improved bone structural properties of distal femur but similar bone parameters of 2nd lumbar vertebrae (L2) and cortical variables of mid-shaft femurs. HF-Ex and HF-Ex-Aox had similar bone structural properties at distal or mid-shaft femurs, or L2. These findings suggest that exercise improves but does not fully protect against negative skeletal effects of excessive adiposity induced by a high-fat diet at certain skeletal sites and that vitamin E and C supplementation has no additional benefits on bone structural properties during exercise.

*Disclosures: **Jay Cao**, None.*

SU0159

Prolonged Performance of A High Repetition High Force Task Induces Bone Degradation in Young Adult Rats. Vicky Massicotte[1], Michele Harris[2], Paul W Fisher[3], Steven Popoff[1], Mary Barbe*[1]. [1]Temple University School of Medicine, USA, [2]Temple University School of Medicine, USA, [3]Temple University, USA

Overuse injuries are the most reported types of athletic and occupational disorders. Only a few studies have examined changes occurring in upper extremity bones as a consequence of occupational tasks, although it is well known that chronic cyclical tissue over-load affects bone quality and morphometry. We have reported, using a rat model of repetitive grasping and pulling, that high repetition high force (HRHF) task for 12 weeks leads to bone loss. We have also shown that pro-inflammatory cytokines (TNF-α, IL1-β and IL-6) are increased in 6 and 12 weeks HRHF rats, but that inflammation resolves thereafter. These cytokines are known to affect osteoblasts (bone forming cells) and osteoclasts (bone resorbing cells) homeostasis. Although not yet investigated with occupational overuse injuries, RANKL is another cytokine linked to osteoclast activation during remodeling and increases in bone after osteocyte apoptosis due to microdamage. We hypothesized that performance of HRHF task for 18 weeks will induce detrimental bone remodeling, increase RANKL and osteoclast numbers. Thus, using micro-computed tomography, we investigated the impact of HRHF task performance for 18 weeks on young adult rat bones. We observed detrimental trabecular bone remodeling in the radius due to impaired bone formation and increased resorption observed as decreased bone volume, trabeculae number and thickness, increased bone surface and trabeculae separation, increased anisotropy and rod shaped trabeculae in HRHF 18W rats, compared to food restricted control rats (FRC). Osteoblast cell numbers decreased and osteoclasts increased, concomitant with an increase in empty osteocytes lacunae due to augmented apoptosis (increased TUNEL staining) in HRHF 18W, compared to FRC. Serum osteocalcin (a bone formation biomarker) was reduced (p<0.01) while CTX1 (a bone resorption biomarker) increased (p<0.01), compared to FRC. ELISA and qPCR show increases in both RANKL protein and mRNA levels. Immunohistochemistry show increased cartilaginous matrix with augmented diffused RANKL staining in HRHF 18W rat radii, while FRC rats had lower levels of RANKL that was concentrated to osteocyte's lacunae only. We can conclude that HRHF prolonged task performance leads to detrimental histomorphometric changes due to increased RANKL-mediated bone resorption.

*Disclosures: **Mary Barbe**, None.*

SU0160

Congenic Strains Confirm a Pleiotropic Bone QTL on Mouse Chromosome 4.
Jasmin Kristianto*[1], Michael Johnson[2], suzanne litscher[3], Forum Patel[3], Robert Blank[4]. [1]University of Wisconsin–Madison, USA, [2]University of Wisconsin, USA, [3]University of wisconsin Madison, USA, [4]Medical College of Wisconsin, USA

Osteoporosis is an important health problem that affects more than 75 million people worldwide. Although the etiology of osteoporosis is multifactorial, genetics contribute ~70% to its development. We and others previously identified a pleiotropic quantitative trait locus (QTL) on mouse chromosome 4 that affects bone size, shape, and strength. The QTL includes *Ece1*, the gene encoding endothelin converting enzyme 1 and in recombinant congenic HcB-8 and HcB-23 mice having widely divergent femoral biomechanical performance, *Ece1* is differentially expressed. To study the QTL in isolation from other segregating loci, we bred two congenic strains carrying overlapping segments of chromosome 4 from C57BL/10ScSnA (B10) within the locus on a C3H/DiSnA (C3H) background. The long and short congenic strains harbor a ~10 Mb and a ~1 Mb B10-derived chromosome segment, respectively. We tested femoral diaphysis biomechanical performance by quasi-static 3-point bending and measured bone geometry in (C3H x congenic) F2 mice. We analyzed the results via 2-way ANOVA, using sex and genotype as factors. In the long congenic, C3H/C3H male (M) and female (F) mice have greater shape factor (M= 1.42 $\pm$ 0.05, F= 1.38 $\pm$ 0.02) than C3H/B10 (M=1.40 $\pm$ 0.02, F=1.35 $\pm$ 0.02) and B10/B10 (M=1.40 $\pm$ 0.02, F=1.33 $\pm$ 0.02) mice, p < 0.001. Both M and F C3H/C3H mice also have greater cross-sectional area (CSA) (p= 0.022) than C3H/B10 and B10/B10 mice. C3H/C3H mice have greater total displacement relative to B10/B10 mice (p=0.023) but not C3H/B10. In the short congenic, C3H/C3H F mice (1.05 $\pm$ 0.03) and C3H/B10 F mice (1.07 $\pm$ 0.03) have greater CSA than B10/B10 F mice (0.95 $\pm$ 0.05), p=0.045. Both M and F C3H/C3H and C3H/B10 mice also have greater maximum load (p=0.015) and yield load (p=0.041) than M and F B10/B10 mice. We have also shown that autocrine endothelin signaling by osteoblasts *in vitro* and in organ culture increases IGF1 secretion, providing a mechanism that could account for the development of these phenotypes. Our findings confirm our prior intercross results and motivate further study of *Ece1*'s biological role in bone development and modeling.

Disclosures: Jasmin Kristianto, None.

SU0161

Interleukin-11 is an important factor for mechanical stress-induced osteoblast differentiation and bone formation.
Takeshi Kondo*[1], Bingzi Dong[1], Takashi Omatsu[1], Yukiyo Ohnishi[1], Itsuro Endo[2], Masahiro Abe[3], Shinichi Aizawa[4], Hiroshi Sakaue[5], Toshio Matsumoto[2]. [1]Department of Medicine & Bioregulatory Sciences, University of Tokushima Graduate School of Medical Sciences, Japan, [2]University of Tokushima Graduate School of Medical Sciences, Japan, [3]University of Tokushima, Japan, [4]not yet, Japan, [5]Department of Nutrition & Metabolism, Institute of Health Biosciences, University of Tokushima Graduate School, Japan

Background: We have previously reported that interleukin (IL)-11 expression is markedly enhanced by mechanical stress, and plays a role in mechanical stress-induced stimulation of osteoblast differentiation and bone formation. Increased IL-11 down-regulates dikkopf 1/2 (Dkk1/2) expression and stimulates canonical Wnt signaling in primary osteoblasts. The present study was undertaken to clarify the physiological role of IL-11 in osteogenesis in response to mechanical stress by creating IL-11 deficient (IL-11KO) mice.
Methods: We measured bone mineral density (BMD) and performed bone morphometric analysis of IL-11KO and WT mice. Mechanical unloading by tail suspension for 2 weeks and reloading by forced running were performed in both IL-11 KO and wild-type (WT) mice. Expression of osteoblastic and osteoclastic marker genes, and Wnt inhibitors including Dkks and sclerostin was also examined.
Results: IL-11 KO mice exhibited low BMD in weight-bearing bones such as femurs and vertebrae after weaning, which was aggravated with aging. In contrast, BMD of non-weight bearing calvarial bone was slightly increased in IL-11 KO mice. Serum osteocalcin was lower in IL-11KO than in WT mice, while serum TRAP5b was similar in both groups. Bone morphometric analysis revealed that Tb.Th, Ob.S/BS, N.Ob/BS and BMR were reduced in IL-11KO mice, but there was no significant difference in N.Oc/BS or Oc.S/BS between IL-11KO and WT mice. Expression of osteocalcin and Runx2 mRNA was reduced, while SOST and Dkk1/2 mRNA expression was elevated in bones of IL-11KO mice. Up-regulation of sclerostin expression in bones of IL-11KO mice was confirmed by immunohistochemical analysis. After unloading, BMD of weight-bearing bone and osteocalcin mRNA expression decreased in both IL-11KO and WT mice. After reloading, increase in BMD and osteocalcin mRNA was significantly lower in IL-11KO mice. SOST mRNA was higher in both unloading and reloading conditions in IL-11KO mice compared with that in WT mice. Furthermore, bone morphometric analysis revealed that bone formation parameters after reloading was significantly lower in IL-11KO mice than in WT mice.
Conclusion: IL-11 is an important factor for mechanical stress-induced osteoblast differentiation and bone formation by suppressing the expression of Wnt inhibitors in response to mechanical stress.

Disclosures: Takeshi Kondo, None.

SU0162

M1/M2-like Macrophage Polarization Contributes to Mechanical Force-induced Orthodontic Root Resorption.
Danqing He*[1], Xiaoxing Kou[2], Yanheng Zhou[3]. [1]Department of Orthodontics, Peking University School & Hospital of Stomatology, Peoples Republic of China, [2]Orthodontic Department, Peking University School of Stomatology, Beijing, China, [3]Orthodontic Department, Peking University School of Stomatology, China

Mechanical force-induced orthodontic root resorption is a major clinical challenge in orthodontic treatment, but the underling mechanism remains largely unknown. In this study we show that M1/M2-like macrophage polarization affects root resorption accompanied with orthodontic tooth movement.
Mechanical force was applied to the upper first molars of rats using NiTi springs for 14 days and then maintained for 14 days by placing resin between first and second molars. Root resorption was observed from day 3 to day 14 after force application (active resorption stage), then showed a resting stage from day 3 to day 14 of retention. Meanwhile, CD68^{+}/iNOS^{+} M1-like macrophages persistently increased in the compression side of the roots from day 3 to day 14 after force application, matching the active resorption stage, while CD68^{+}/CD163^{+} M2-like macrophages were detected upregulated in the resorption resting stage. In addition, increased expression of IFN-γ, a major M1 activator, was detected in the periodontal ligament cells (PDLCs) after force application both *in vivo* and *in vitro*, while M2 activator IL-4 was mainly observed in the resorption resting stage. Besides, M1-associated pro-inflammatory cytokine TNF-α was highly expressed during active resorption stage and persisted to the resting stage, while M2 associated anti-inflammatory cytokine IL-10 was upregulated in the resorption resting stage. Furthermore, systemic injection of TNF-α inhibitor etanercept or systemic injection of IL-4 attenuated the severity of root resorption, along with decreased numbers of iNOS^{+} M1-like macrophages and increased numbers of CD163^{+} M2-like macrophages, respectively.
These data imply that the balance between M1/M2-like macrophages may influence orthodontic root resorption, M1-like macrophages promote orthodontic root resorption in the active resorption stage and M2-like macrophages inhibit it in the resting stage.

Disclosures: Danqing He, None.

SU0163

Streptomycin inhibits effects of electrical stimulation-induced muscle force on reducing disused bone loss.
Hiroyuki Tamaki*[1], Kengo Yotani[2], Hikari Kirimoto[3], Kazuhiro Sugawara[4], Atsuhiro Tsubaki[4], Hideaki Onishi[4], Noriaki Yamamoto[5], Norikatsu Kasuga[6]. [1]Niigata University of Health & Welfare, Japan, [2]National Institute of Fitness & Sports in Kanoya, Japan, [3]Niigata University of Health & Welfare, Japan, [4]Niigata University of Health & Welfare, Japan, [5]Niigata Rehabilitation Hospital, Japan, [6]Aichi University of Education, Japan

Limb disuse due to denervation causes musculoskeletal atrophy accompanied by a large reduction in bone mass and changes in trabecular architecture. Findings from animal studies suggest that electric muscle stimulation (ES)-induced muscle force with an appropriate regimen reduces muscle deterioration caused by disuse and bone loss caused by denervation; however, whether these effects of ES are associated with mechanosensors in bone tissue or with stimulated skeletal muscle mass remains unknown. We tested the hypothesis that streptomycin, a stretch-activated channel (SAC) blocker, can essentially abolish the reduction in bone loss elicited by ES.
Direct ES with an intensity of 16 mA and a frequency of 10 Hz for 30 min/day for 6 consecutive days was applied to the tibialis anterior (TA) muscle after unilateral sciatic denervation in 7-week-old male rats as follows: control (CON); denervation (DN); DN with direct ES (DN-ES); and DN with ES treated with streptomycin (DN-ES-Str). The weight of the TA muscle and the tension force induced by ES were determined, and the metaphyseal trabecular regions of the tibiae were analyzed using micro CT and histomorphometry.
Significant losses in trabecular bone in the tibiae and TA muscle were evident in the DN rats. Trabecular bone volume fraction (BV/TV), thickness (Tb.Th), and number (Tb.N.), as well as connectivity density (Conn.D.) and osteoid thickness were increased in DN-ES compared with DN rats at 1 week after denervation. However, these parameters were lower in the DN-ES-Str than in the DN-ES group, without the differences in TA muscle weight and tension force induced by ES at 10 Hz.These findings suggest that streptomycin inhibits the ability of ES-induced muscle force to reduce the loss of disused bone. Activation of SACs might thus explain why ES-induced muscle tension applied to bone reduces bone loss in the denervated rat hindlimb.

Disclosures: Hiroyuki Tamaki, None.

SU0164

Structured Fibronectin Surfaces to Guide Migration of Mesenchymal Stem Cells. <u>Annika Kasten</u>[1], <u>Rolf Brenner</u>[2], <u>Tamara Naser</u>[2], <u>Jörg Fiedler</u>[2], <u>Petra Müller</u>[1], <u>Jürgen Groll</u>[3], Joachim Rychly*[4]. [1]Rostock University Medical Center, Germany, [2]Department of Orthopaedics, Germany, [3]Department of Functional Materials in Medicine, Germany, [4]University of Rostock, Germany

Design of chemical as well as physical modification of implant surfaces to control functions of mesenchymal stem cells (MSC) is a great challenge in regenerative medicine. Fibronectin (FN) or RGD peptides as ligands for integrins are often used to coat surfaces for controlling adhesion mediated mechanisms in cells. Beside proliferation and osteogenic differentiation, migration of MSC to a defect site is critical for regeneration of bone. We generated lines of FN with varying width and distances between them to explore migration of MSC and a number of cell parameters involved in mechanisms of cell adhesion.

The material surfaces were prepared by coating cover slips using NCO terminated six armed star shaped polymers (NCO-sP (EO-stat-PO) to prevent protein adsorption and cell adhesion. Using a microprint technique, FN was immobilized to this surface, forming lines of 10-80 μm and gaps between them of 5-20 μm. Bone marrow derived human MSC were used in the experiments. Speed and directionality of cell migration were tested and correlated with a number of cellular parameters, like morphology of cells and nuclei, cell spreading, formation of the actin cytoskeleton, as wells as size and shape of focal contacts.

With decreasing line width, cells migrated faster with a stronger directionality. On 80 μm lines, two or three cells were able to adhere in parallel and formed cell-cell contacts, which enable a collective migration. On smaller FN lines, single cells adhered in a line and at smaller gaps between the lines of 10 or 5 μm, cells were able to bridge the lines, which mimic the situation of matrix fibrils in vivo. With reducing the width of FN lines, the actin cytoskeleton formed few strongly aligned fibers. Characteristic alterations in the formation of focal adhesions were also measured in dependence on the sizes of FN lines. On lines with lower width, focal adhesions became smaller and formed a round shape.

In conclusion, using lines of FN with varying sizes and gaps between them we were able to tune speed and directionality of stem cell migration. Further, the geometry of the adhesion substrate was translated into an internal organization of significant components of cell adhesion. The generation of defined adhesive surface patterns, like lines of FN, is suitable to control the biological responses of MSC for applications in regenerative engineering.

Disclosures: Joachim Rychly, None.

SU0165

β2-adrenergic Receptor Plays an Important Role in Sympathetic Nervous System-regulated Orthodontic Tooth Movement. <u>Haifeng Cao</u>*[1], <u>Xiaoxing Kou</u>[2], <u>Yanheng Zhou</u>[3]. [1]Peking University School & Hospital of Stomatology, Peoples Republic of China, [2]Peking University School & Hospital of Stomatology, China, [3]Department of Orthodontics. Peking University School & Hospital of Stomatology, China

Sympathetic nervous system (SNS) may regulate skeletal homeostasis, but whether and how SNS contributes to the mechanical force-induced orthodontic tooth movement (OTM) remains unclear. In this study, we showed that β2-adrenergic receptor (Adrb2) mediated the enhancing capacity of SNS on OTM. We first confirmed that blocking SNS activity in jawbones by sympathectomy of superior cervical ganglion ectomy (SCGx) was capable of significantly reducing OTM. We next revealed that Adrb2-/- mice displayed significantly reduced OTM when compared to the control group. Adrb2 agonist isoproterenol (ISO) treatment accelerated OTM. Histopathological analysis showed that the number of Adrb2 positive cells increased in compressive region of periodontal ligament (PDL) after application of orthodontic force in rats. We further confirmed that the expression of Adrb2 in periodontal ligament cells (PDLCs) was upregulated by mechanical force through increase of intracellular Ca^{2+} concentration ($[Ca^{2+}]_i$). Furthermore, activation of Adrb2 in PDLCs promoted osteoclastogenesis via elevating RANKL/OPG ratio thus accelerated OTM. In summary, this study suggested that mechanical force-induced Adrb2 expression in PDLCs contributed to SNS-regulated OTM.

Disclosures: Haifeng Cao, None.

SU0166

Anti-sclerostin Antibody Treatment of Renal Osteodystrophy. <u>Sharon Moe</u>*[1], <u>Neal Chen</u>[1], <u>Christopher Newman</u>[2], <u>Jason Organ</u>[1], <u>Vincent Gattone</u>[3], <u>Michaela Kneissel</u>[4], <u>Ina Kramer</u>[4], <u>Matthew Allen</u>[1]. [1]Indiana University School of Medicine, USA, [2]Indiana University, USA, [3]Indiana University School of Medicine, USA, [4]Novartis Institutes for Biomedical Research, Switzerland

Chronic Kidney Disease (CKD) is associated with abnormalities in bone quantity and quality leading to increased fractures. Recent studies suggest abnormalities of wnt signaling in animal models of CKD and elevated sclerostin levels in patients with CKD. The goal of this study was to evaluate the effectiveness of anti-sclerostin antibody treatment in an animal model of progressive CKD with low and high parathyroid hormone (PTH) levels. Cy/+ male rats (CKD) were treated without or with calcium in the drinking water at 25 weeks of age to stratify the animals into high PTH and low PTH groups, respectively, by 30 weeks. Animals were then treated with anti-sclerostin antibody at 100 mg/kg IV weekly for 5 doses, a single 20 ug/kg subcutaneous dose of zoledronic acid, or no treatment and sacrificed at 35 weeks. As a positive control, the efficacy of anti-sclerostin antibody treatment was also evaluated in normal littermates. The results demonstrated that the CKD animals with high PTH had lower calcium, higher phosphorus, and lower FGF23 compared to the CKD animals with low PTH. Treatment with anti-sclerostin Ab had no effect on any of the biochemistries, while zoledronic acid lowered dkk-1 levels. The anti-sclerostin antibody increased trabecular BV/TV in animals with low, but not high, PTH. Neither anti-sclerostin antibody nor zoledronic acid improved biomechanical properties in the animals. Cortical porosity was severe in high PTH animals and unaffected by either treatment. In contrast, in normal animals treated with anti-sclerostin antibody, there was an improvement in bone volume and biomechanical properties.

In summary, this is the first study to test the efficacy of anti-sclerostin Ab treatment on animals with advanced CKD. We found efficacy in improving bone volume only when the PTH levels were low.

Disclosures: Sharon Moe, Novartis, 3
This study received funding from: Novartis Institutes for Biomedical Research

SU0167

Dabigatran etexilate, a new direct thrombin inhibitor, enhances bone mass, inhibits bone resorption and stimulates bone formation in mice. <u>Judy Kalinowski</u>[1], <u>Sandra Jastrzebski</u>[1], <u>Hee Yeun Won</u>[1], <u>Faryal Mirza</u>[2], <u>Sun-Kyeong Lee</u>[2], Joseph Lorenzo*[2]. [1]University of Connecticut Health Center, USA, [2]University of Connecticut Health Center, USA

Thrombin converts fibrinogen to fibrin to form a fibrin clot. The commonly used anticoagulants, heparin and warfarin, act as direct or indirect thrombin inhibitors. Heparin therapy is a well-known risk factor for osteoporosis. Warfarin's effects are variable with studies showing either no effect or an increased osteoporotic risk. Recently, a newer class of thrombin inhibitors was approved for clinical use. Dabigatran etexilate (DE) is a direct inhibitor of thrombin's catalytic activity. We investigated the effects of DE on bone mass, bone turnover and osteoclast precursor cell number in mice. Eight-week-old male C57BL/6 mice were injected intraperitoneally with DE (8.5/mg/Kg twice daily) for 6 weeks. Control mice were injected with vehicle. Bone mass in the femurs of the DE-treated mice increased by 10% (p<0.05) as measured by DXA. Using μ-CT analysis, we found that trabecular bone mass in the femurs increased by 71% (p<0.01) with no change in cortical bone mass. We also found that serum CTX was decreased by 43-53% at 3 and 6 weeks (p<0.01 for both) and serum P1NP was increased by 52% in DE-treated mice (p<0.01). In addition, we found that DE-treatment significantly decreased the number of precursors of osteoclasts in the bone marrow of the mice as measured in two assays: in vitro culture, and flow cytometry. In the in vitro culture assays bone marrow macrophage cultures were treated with M-CSF (30 ng/ml) and either 10 or 30 ng/ml of RANKL for 4 days and TRAP-stained. We found that for both RANKL concentrations, the number of osteoclasts that formed in the cultures was decreased in cultures of cells from DE-treated mice (by 42 or 35%, respectively, p<0.01 for both). The percentage of osteoclast precursor cells in bone marrow was identified by flow cytometry (CD45R-, CD3-, CD11b-/lo, CD115+) and was decreased by 36% in DE treated mice (p<0.01). We also measured the serum levels of stromal cell-derived factor 1 (SDF-1) by ELISA in the mice since this cytokine regulates osteoclast migration and resorption as well as osteoblast formation. Surprisingly, DE treatment decreased serum SDF-1 levels by 74% (p<0.01), which may be one mechanism for its effects on bone resorption and bone formation. We conclude that DE-treatment in mice markedly stimulated bone formation and inhibited bone resorption, resulting in a significant net gain in bone mass. These results imply that DE may also enhance bone mass in treated patients who are at high risk for osteoporosis.

Disclosures: Joseph Lorenzo, None.

SU0168

Dose response study of the effects of sclerostin antibody on cortical bone mass and strength in Brtl/+ mouse. <u>David Barton</u>*[1], <u>Benjamin Sinder</u>[1], <u>Yuchen Yang</u>[2], <u>Joan Marini</u>[3], <u>Michelle Caird</u>[2], <u>Kenneth Kozloff</u>[4]. [1]University of Michigan, USA, [2]University of Michigan, USA, [3]National Institute of Child Health & Human Development, USA, [4]University of Michigan Department of Orthopaedic Surgery, USA

In a number of animal studies, sclerostin antibody (Scl-Ab) has demonstrated its effectiveness for increasing bone mass and strength. Potential uses may be expanded beyond osteoporosis to other diseases including osteogenesis imperfecta (OI). We previously demonstrated a significant bone forming response of Scl-Ab in Brtl/+ mice, a model for OI, when administered for 2 weeks at 25 mg/kg, twice weekly (Sinder et al, JBMR 2013 28:73). To better understand the impact of dose on the response to Scl-Ab, a dose-response study was done to determine what dose(s) affect Brtl/+ such that

both geometric and mechanical characteristics of bone strength are sufficient to match those of untreated wild-type (Wt) mice.

In this study, 100 mice (50 WT; 50 Brtl/+) were separated into 5 dose-response cohorts and compared to a control group administered saline. Scl-Ab was administered twice per week from 3 weeks of age to 14 weeks at doses of 3, 6, 12.5, 25, and 50 mg/kg (n= 8-9 per group). Following euthanasia, femora were dissected and scanned by μCT. Mid-femoral cortical regions of interest were assessed for cross sectional geometric parameters. Femora were then tested to failure in 4-point bending, from which mechanical properties were assessed.

Brtl/+ and WT mice both showed a significant dose response in geometric measures including total area, cortical area and thickness, and bending moment of inertia (Fig 1). No significant difference in dose response between genotypes was found for these measures by linear regression models. Cortical thickness and cross-sectional area in Brtl/+ significantly exceed untreated Wt at doses of 25 and 50 mg/kg respectively. Mechanically, dose responses were found both in pre-yield measures of stiffness and yield load, and post-yield measures of ultimate load (Fig 2) and energy. Similarly, no significant dose response differences were found between genotypes by linear regression models. Brtl/+ stiffness, yield load, and ultimate load all significantly exceeded untreated Wt at 25 mg/kg.

In this study, doses less than 25 mg/kg, 2x/week for 11 weeks were sufficient to provide restoration of Brtl/+ function to untreated WT levels. These studies provide data supporting the dose response of Scl-Ab in a mouse model of OI.

Disclosures: David Barton, None.

SU0169

MVNP Expression in Osteoblast Induces IGF1 to Increase EphrinB2/EphB4 and Osteoblast Differentiation. Jumpei Teramachi[1], Yukio Kitagawa[2], Jolene Windle[3], Laetitia Michou[4], Jacques P. Brown[5], Noriyoshi Kurihara*[6], G. David Roodman[6]. [1]The University of Tokushima, Japan, [2]Indiana University, USA, [3]Virginia Commonwealth University, USA, [4]Université Laval, Canada, [5]CHU de Québec Research Centre, Canada, [6]Indiana University, USA

We reported that 70% of patients with Paget's bone disease (PD) expressed measles virus nucleocapsid protein (MVNP) in their osteoclasts (OCLs) and that MVNP is not expressed in their osteoblasts (OBs). Further, transgenic mice with targeted expression of MVNP to cells in the OCL lineage form pagetic-like bone lesions that display both increased bone resorption and rapid new bone formation. In contrast, mice with p62^{P394L} mutation (p62^{MUT}) linked to PD have increased bone resorption but do not have increased bone formation *in vivo*. EphrinB2/EphB4 were identified as key coupling factors for OCL/OB. EphrinB2 is produced by OCL and enhances OB function and bone formation through specific interactions with EphB4 on OB. We previously demonstrated by immunohistochemistry that EphrinB2 expression in OCL, and EphB4 expression in OB were dramatically increased in MVNP mice compared to WT mice. Further the gene-expression profiling studies by highly purified OCLs derived from MVNP, p62^{MUT} and WT mice revealed that IGF1 expression was significantly enhanced in MVNP expressing OCL precursors compared to the other genotypes. We hypothesized that MVNP expressing OCL play a crucial role in the promotion of bone formation in PD via IGF1 signaling and EphrinB2/EphB4 coupling. We found that MVNP expressing OCL from patients with PD and MVNP transduced human OCL highly expressed EphrinB2 and IGF1 as compared to normal or EV transduced OCLs. To examine how IGF1 signaling contributes EphrinB2 expression in MVNP expressing OCL, we treated MVNP expressing OCL with anti-IGF1 which decreased their EphrinB2 levels. The expression level of EphrinB2 in MVNP OCL was decreased by anti-IGF1 (5μM). Further the PI3K inhibitor (LY294002) (5μM) and MEK inhibitor (V112A) (10μM) completely blocked EhrinB2 expression in OCL. We tested if purified mature OCL from MVNP or WT mice stimulated mesenchymal cell migration and differentiation toward the OB lineage from MVNP or WT mice bone as measured by EphB4 and osteocalcin levels by Western blot. Co-cultures of mature OCL and mesenchymal cells from MVNP mice bone significantly increased Eph4 and osteocalcin levels compared to co-cultures of WT OCL with WT mesenchymal cells or MVNP OCL with WT mesenchymal cells. Eph4 expression in co-cultures with MVNP OCL/mesenchymal cells were blocked with anti-mouse IGF1 (5μM). These results suggest that IGF1 contributes to increased bone formation induced by MVNP by enhancing EphrinB2 expression.

Disclosures: Noriyoshi Kurihara, None.

SU0170

Bone turnover markers in a 24-month treatment study comparing efficacy of a cathepsin K inhibitor, MK-0674, to alendronate and denosumab in ovariectomized cynomolgus monkeys. Maureen Pickarski*[1], Mary Belfast[2], Brenda Pennypacker[3], Le Duong[3]. [1]Merck & Co., Inc., USA, [2]Merck & Company, USA, [3]Merck Research Laboratories, USA

Odanacatib (ODN), a selective and reversible inhibitor of cathepsin K (CatK), is currently in development for the treatment of postmenopausal osteoporosis. Here, we compared the effect of MK-0674, a highly orally bioavailable CatK inhibitor with similar potency and selectivity to ODN, to that of alendronate (ALN) and denosumab (Dmab) on bone turnover markers in ovariectomized (OVX) monkeys in treatment mode.Cynomolgus monkeys (10-27 yrs. old) were OVX-d 2 yrs prior to randomization into one of five groups (N=14-16/group): untreated control, MK-0674 at 0.6 mg/kg or 2.5 mg/kg (p.o., q.d.), ALN (30μg/kg; wkly, s.c.) or Dmab (2.5 mg/kg, wkly, s.c.) for 24 mo. A cohort of age-matched sham-operated animals was also included. Both doses of MK-0674 and ALN rapidly reduced bone resorption markers uNTX and sCTX to 70 to 90% vs. untreated control at month 5, and the reduction of these markers was maintained between 55 to 90% vs. control for the duration of the study. Dmab initially reduced uNTx and sCTx by 50-60% up to month 5; yet, these markers returned to baseline levels by study termination. Anti-Dmab antibody was confirmed to develop in 10 out of 14 monkeys treated with Dmab at month 12. As expected, ALN consistently reduced serum bone formation markers, BSAP and P1NP, by 60% and 70% relative to control, respectively. Dmab also reduced BSAP (30-50%) and P1NP (45-55%) compared to control. However, treatment with MK-0674 at both doses trended towards less reduction of BSAP and P1NP compared to ALN or Dmab. Trap-5b levels, a marker of osteoclast number, were reduced by ALN by 60% within 5 months post-dosing and levels remained suppressed for the duration of the study. In contrast, Trap-5b levels in animals treated with the low and high doses of MK-0674 continuously increased from 10-60% and 55-100% above control, respectively. Detectable Trap-5b levels in the Dmab group were consistent with the progressively reduced efficacy of this drug in monkeys. In summary, ALN reduced both bone formation and resorption markers in OVX-monkeys, while the modest effects of Dmab on bone turnover markers may be due to anti-drug antibody developed in this species. In treatment mode, MK-0674 reduced bone resorption markers similarly to ALN. Consistent with previous preclinical and clinical reports with ODN, MK-0674 showed less reduction of bone formation markers in these estrogen-deficient monkeys in treatment mode, suggesting that the bone formation sparing effects of CatK inhibitors differentiate this mechanism from those of currently available inhibitors of bone resorption.

Disclosures: Maureen Pickarski, Merck & Co., Inc, 4; Merck & Co., Inc, 8
This study received funding from: Merck & Co., Inc

SU0171

Comparison of the Efficacy of Cathepsin K inhibitor MK0674 versus Alendronate and Denosumab in Restoring Bone Mass in the Treatment of Estrogen-deficient Cynomolgus Monkeys. Brenda Pennypacker*[1], Maureen Pickarski[2], Nancy Doyle[3], Aurore Varela[4], Le Duong[1]. [1]Merck Research Laboratories, USA, [2]Merck & Co., Inc., USA, [3]Charles River Laboratories, Canada, [4]Charles River Laboratories, Canada

Selective inhibitors of cathepsin K (CatK) are currently developed for the treatment of postmenopausal osteoporosis. The aim of this study was to evaluate efficacy of MK-0674 (MK), a highly orally bioavailable CatK inhibitor with similar potency and selectivity profile to odanacatib, compared to alendronate (ALN) and denosumab (Dmab) in ovariectomized (OVX) cynomolgus monkeys in treatment mode. Adult monkeys (10-27 yrs-old) were sham- (N=12) or OVX'd for 2-years prior to randomizing the OVX animals (N=14-16/group) into 5 groups: untreated-control, treated with MK (0.6 or 2.5mg/kg, q.d., p.o.), alendronate (ALN, 30μg/kg, wkly, SC) or denosumab (Dmab, 2.5mg/kg, weekly, SC) for 24-mo. DXA scans (Hologic Discovery A) for acquiring bone mineral density (BMD) of the whole body (WB), lumbar vertebrae (LV1-4), distal radius, hip and distal femur were performed at baseline, 6, 12, 18, and 24 mo. of treatment. Cortical and cancellous BMD were also examined concurrently in the distal radius by pQCT (XCT Research SA). LVBMD loss of 13% was observed in OVX- versus Sham-animals prior to the start of treatment. MK at both doses and ALN significantly increased LVBMD by mo.-6 vs. untreated controls. By mo.-18, MK at 0.6 or 2.5 mg/kg restored BMD of all sites to the respective levels of sham animals. At mo.-24, MK at both doses and ALN significantly increased BMD (8, 11, and 5% at WB; 11, 14, and 9% at LV; and 9, 18, and 13% at total hip, respectively vs. untreated-controls). MK at both doses significantly increased BMD in femoral neck (15 and 22%), distal femur (5 and 9%), and distal radius (7 and 11%), respectively, while BMD at these sites in ALN group were not different from controls. MK 0.6 mg/kg and ALN showed equivalent efficacy at most bone sites. However, MK at 2.5 mg/kg resulted in superior BMD gains at WB (p<0.05), femoral neck (p<0.05), and distal femur (p<0.05) compared to that in ALN. Due to anti-drug antibodies developed in 10 of 14 monkeys by mo.-12, the Dmab group showed only modest increases in LVBMD by 4% (p<0.05) and total hip BMD by 6% (p<0.05) vs. controls at mo.-24. Total and cortical BMD in the distal radius was significantly increased with MK 2.5 mg/kg compared to ALN and Dmab by pQCT at mo.-24. In conclusion, treatment with this CatK inhibitor rapidly and dose-dependently restored cortical and cancellous bone mass to Sham levels. The accrued BMD gains by MK-0674 at the high dose were generally greater than that achieved by ALN or Dmab in OVX-monkeys in treatment mode.

Disclosures: Brenda Pennypacker, Merck and Co., 4

SU0172

Increased Periostin in Cortical Bone of Cathepsin K Knock-Out Mice is Responsible for Higher Cortical Bone Mass and Strength. <u>Nicolas Bonnet</u>*[1], <u>Le Duong</u>[2], <u>Serge Ferrari</u>[3]. [1]University Geneva Hospital (HUG), Switzerland, [2]Merck Research Laboratories, USA, [3]Geneva University Hospital & Faculty of Medicine, Switzerland

Cathepsin K (CatK, Ctsk) inhibition in preclinical models results not only in lower bone resorption but also in higher bone formation (BF) on both remodeling and modeling surfaces. The mechanisms for greater BF at modeling surfaces, including the periosteum, remain unexplained. Periostin (Postn) is a matricellular protein expressed in periosteum and osteocytes that mediates inhibition of sclerostin, beta-catenin signaling and skeletal response to loading. In vitro data suggest that periostin is a substrate for proteolytic degradation by CatK. We hypothesized that higher BF at modeling surfaces in Ctsk-/- mice might be related to high periostin levels in cortical bone. For this purpose, BMD, microstructure and cortical strength were evaluated in the progeny of Postn-/- x Ctsk-/- mice. Periostin protein and gene expression were analyzed by immunocytochemistry and qRT-PCR, respectively, on femur samples. Postn protein by immunostaining was more intense in Ctsk-/- osteocytes and periosteum surfaces vs WT, whereas Postn mRNA levels were similar in presence and absence of CatK. Postn-/-;Ctsk +/+ have lower femoral BMD, cortical volume (CtBV) and thickness (CtTh) whereas Postn+/+;Ctsk-/- have higher BMD, BV/TV, CtBV and CtTh compared to WT. Double heterozygous mice present similar phenotype as of Postn+/+;Ctsk+/- which tend to increase cortical and trabecular bone (NS). Removing both Postn alleles in Ctsk-/- mice, i.e. Postn-/-;Ctsk-/-, restored a WT cortical bone phenotype. Hence, the increases in ultimate force, stiffness and elastic energy in Postn+/+;Ctsk-/- (+15.9%, +19.2% and +40.5% vs WT, p<0.01) were absent in Postn-/-;Ctsk-/-. Plastic energy was significantly decreased in the double KO (-24.6% vs WT, p<0.05). In contrast, trabecular parameters at the distal femur and vertebrae were not affected by the ablation of periostin in Ctsk-/- mice. For example, at the vertebrae, Postn-/-;Ctsk-/- and Postn+/+;Ctsk-/- exhibit high BV/TV, respectively 25.1±1.1% and 27.2±2.4% vs 18.2±1.8 for WT, both p<0.001. In conclusions, Cstk-/- mice present high levels of periostin in periosteum and in osteocyte. Postn deletion abrogates the high cortical structure of Cstk-/- mice without affecting the high trabecular bone phenotype. This implies that periostin could be a novel CatK-mediated physiological substrate in the periosteum, and in the absence of this protease, high periostin levels enhance the cortical bone adaptation to loading.

SU0173

Osteoactivin/Gpnmb, A Negative Regulator of Osteoclastogenesis. <u>Hilary Stinnett</u>*[2], <u>Samir Abdelmagid</u>[1], <u>Fouad Moussa</u>[2], <u>Gregory Sondag</u>[2], <u>Matthew Matthew Khol</u>[2], <u>Kimberly Novak</u>[2], <u>Nagat Frara</u>[3], <u>Fayez Safadi</u>[1]. [1]Northeast Ohio Medical University, USA, [2]Northeast Ohio Medical University, USA, [3]Temple University, USA

Osteoactivin (OA/*Gpnmb*) was first identified by differential gene display in mutant osteopetrotic rats. The role of OA/*Gpnmb* in osteogenesis has been characterized and reported by our group. A recent study reported on OA/*Gpnmb* expression during osteoclastogenesis. To specify the critical role and mechanism of action of OA/Gpnmb in osteoclastogenesis, we characterized osteoclast phenotype of three genetically modified mouse models for OA/*Gpnmb*. These mice are: *D2J*, mutant for OA/*Gpnmb* characterized with nonsense loss-of-function mutation generating a truncated protein sequence; *D2J* wild-type (WT), *D2J/Gpnmb*+, generated by knocking in OA/*Gpnmb* alleles into *D2J* mouse; OA-null mouse (OA-KO), where OA is disrupted within the coding exons; and OA/*Gpnmb* transgenic mice (OATg), where OA/*Gpnmb* is overexpressed under the CMV-promoter. We hypothesized that OA/*Gpnmb* is a negative regulator of osteoclastogenesis. Osteoclastic phenotype examined by μ-CT analysis revealed a decrease in bone mass in the *D2J* and an increase in bone mass in OA-KO mice and OATg mice. Cortical thickness of *D2J* was significantly increased compared to *D2J/Gpnmb*+ WT mice. Cortical thickness of OATg mice was decreased, and no difference was observed between OA-KO and their wild-type littermates. Serum ELISA of CTX-1 was significantly lower in *D2J*, however, RANKL/OPG ratio were not different. In contrast, in OATg mice there was a decrease in RANKL/OPG ratio. Whereas, OA-KO mice displayed an increase in RANKL/OPG ratio. Bone marrow-derived osteoclast-progenitors (BM-OCP) isolated from mouse femurs and tibiae were differentiated into osteoclasts using RANKL and MCSF. In *ex vivo* cultures, number and surface area of TRAP-positive multinucleated osteoclasts were substantially increased in *D2J* and OA-KO compared to their WT counterparts. q-PCR analysis show increased expression of osteoclast markers in *D2J* and OA-KO compared to WT. Additionally, in *ex vivo* cultures, osteoclasts of *D2J* and OA-KO show increased ability to survive in the absence of MCSF due to delayed onset of apoptosis. RANKL signaling is enhanced in *D2J* and OA-KO osteoclasts as determined by increased phosphorylation of ERK, P38 and JNK in MAPK pathway. Most interestingly, AKT and GSK-3β phosphorylation in *D2J* and OA-KO osteoclasts were up-regulated, suggesting that mutation or lack of OA/*Gpnmb* results in increased osteoclast survival. Taken together, these data suggest that OA/*Gpnmb* works as a negative regulator of osteoclastogenesis.

SU0174

Skeletal Retention and Urinary Excretion of Nitrogen-Containing Bisphosphonates Including Fluorescently-labeled Bisphosphonates in Rats. <u>Mark Lundy</u>*[1], <u>Shuting Sun</u>[2], <u>Xuchen Duan</u>[3], <u>Charles McKenna</u>[4], <u>Gwyn Jeans</u>[5], <u>Roy Dobson</u>[5], <u>Michael Quijano</u>[5], <u>James Triffitt</u>[6], <u>R Graham Russell</u>[7], <u>Frank Ebetino</u>[8]. [1]Indiana University School of Medicine, USA, [2]BioVinc LLC, USA, [3]Department of Developmenta Biology, Harvard School of Dental Medicine, USA, [4]Department of Chemistry, University of Southern California, USA, [5]Procter & Gamble, USA, [6]University of Oxford Nuffield Orthopaedic Centre, United Kingdom, [7]University of Oxford, United Kingdom, [8]University of Rochester, USA

InThe antiresorptive mechanism of action of nitrogen-containing bisphosphonates (N-BPs) used in the treatment of osteoporosis is comprised of a combination of bone affinity characteristics, which target BPs to bone, and inhibition of farnesyl pyrophosphate synthase (FPPS) within osteoclasts and osteoclast precursor cells. Their prolonged presence in bone is related to their affinity for hydroxyapatite (HAP) (Ebetino). Differences in distribution of BPs have been demonstrated in vivo using fluorescent BPs encompassing a range of mineral affinities (Roelofs, Turek). Fluorescent-BPs provide information on localization of BPs in cortical and cancellous bone, as well as penetration at bone surfaces and within osteocyte canaliculi. We have determined the mineral affinity of both parent BPs and fluorescent-BPs by measuring their binding on HAP columns and disks. The mineral affinity was determined relative to risedronate (RIS = 1.0). Zoledronate (ZOL) had higher affinity than RIS, while minodronate (MIN) was similar. The addition of fluorescent groups to RIS can increase (rhodamine 2 (RhR) = 1.45) or decrease (alexafluor 647 (AF647) = .75) mineral affinity relative to RIS in the order: ROX-RIS > ZOL > RhR-RIS > RIS = MIN > fluorescein (FAM)-RIS = 800CW-ZOL > FAM-ZOL > AF647-RIS > deoxyRIS > NE10790, although high affinity to HAP is retained for the entire group. We further explored the impact of bone affinity in vivo on 24 hour urinary excretion after iv administration. Compounds were simultaneously injected in rats in one of the first reported head to head studies of N-BPs. This non-radioactive study was facilitated by LC-MS techniques. Approximately 90% of the amount excreted within 24 hours of both parent and fluorescent-BPs was excreted within 4 hours. The excretion within a 24 hour period relative to RIS, in order from high to low in vivo retention, was: alendronate > ZOL > RIS > etidronate > MIN > Ox-14 > neridronate > ibandronate = FAM-RIS > clodronate = AF647-RIS >> NE-10790. There was a similar but inverse relationship between urinary excretion and affinity to HAP, indicating that binding of BPs to HAP strongly influences their in vivo distribution and excretion profiles. The ability to alter bone affinity among BPs using fluorescent tags is a useful tool for exploring the localization and pharmacology of BPs.

Ebetino FH., et al (2011) Bone 49:20-33
Roelofs AJ., et al (2012) J Bone Min Res 27:835-847
Turek J., et al (2012) Calcif Tissue Int 90:202-210

SU0175

Absence of Complement Component 3 Protects Against Bone Loss in a Murine Model of Postmenopausal Osteoporosis. <u>Danielle MacKay</u>*[1], <u>Thomas Kean</u>[2], <u>Kristina Bernardi</u>[2], <u>Feng Lin</u>[3], <u>Jim Dennis</u>[4]. [1]Benaroya Research Institute, USA, [2]Benaroya Research Institute, USA, [3]Cleveland Clinic Foundation, USA, [4]Baylor College of Medicine, USA

Recent studies indicate that crosstalk between the immune system and bone extends far beyond what occurs during primary lymphopoiesis. Notably, we and others have demonstrated that differentiation of osteoblasts or osteoclasts, the two cell types maintaining bone homeostasis, is regulated by complement, an important part of the innate immune system. It is hypothesized that deficiency of complement component 3 (C3), the central part of the complement activation cascade, will reduce bone loss that results from estrogen deprivation in a model of postmenopausal osteoporosis. In addition to its contribution to our understanding of the role of complement in bone remodeling, this study points to a potential new target for osteoporosis therapy. Wild type and C3$^{-/-}$ mice on a C57BL/6 background were obtained from The Jackson Laboratory and bred and housed in accordance with the guidelines of the ACUC of Benaroya Research Institute. Only mice born on site were used in this study. At 6 weeks of age, ovariectomy or sham surgeries were performed under isoflurane anesthesia. At 12 weeks of age (6 weeks post-surgery), animals were sacrificed by CO_2 asphyxiation, and their uteri, hindlimbs, and vertebrae were harvested. Uterine mass validated successful ovariectomies. Hindlimbs and vertebrae were fixed for 72 hours in 10% formalin before being processed for micro-computed tomography or histomorphometry, respectively. The former was performed on a Scanco vivaCT 40 desktop scanner with a threshold of 300. Data are presented as a percentage and standard deviation with calculations made by dividing individual ovariectomized values by the mean sham operated value. Significance was calculated by unpaired Student's t-test. Micro-computed tomography revealed that the trabecular bone volume fraction retained in both proximal tibia metaphyses and distal femurs of ovariectomized C3$^{-/-}$ mice is significantly greater than that of their wild type counterparts (a, b). The increased trabecular number is clearly visible in 3-dimensional reconstructions from distal femur scans of ovariectomized C3$^{-/-}$ animals (c). This protection against bone deterioration is also evident in the lumbar vertebrae

of C3^{-/-} mice, as reflected by significantly greater osteoid content and mineral apposition rates (d, e). Using a murine model of postmenopausal osteoporosis, our results demonstrate that absence of C3 protects against bone loss in key anatomical locations.
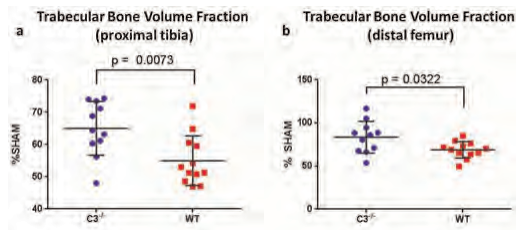
Figs a, b

Fig c

Figs d, e

For all graphs, data are presented as % sham, with each data point representing the value for each ovariectomized C3^{-/-} mouse (blue circles) and each ovariectomized wild type mouse (red squares). Horizontal lines indicate the mean ± SD. (a) μCT values for the trabecular bone volume fraction as a percentage of mean sham values in the proximal tibia (b) μCT values for the trabecular bone volume fraction as a percentage 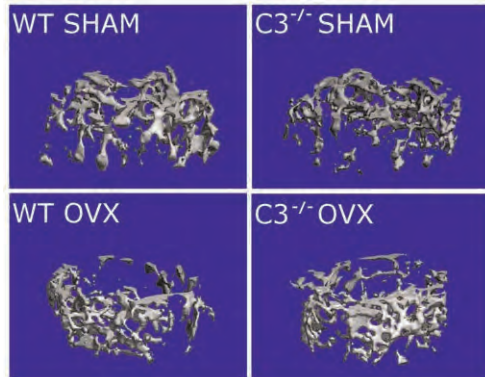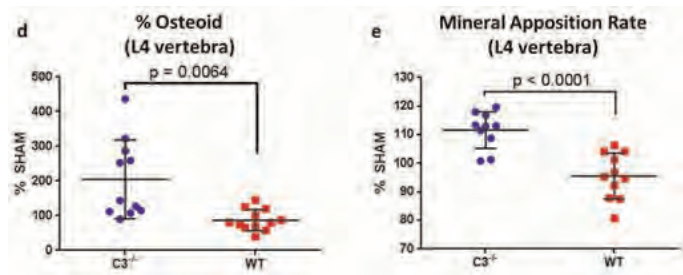of mean sham values in the distal femur (c) Images of 3D reconstructions of distal femur μCT scans (d) Histomorphometry values for the osteoid portion of the measured region of lumbar vertebra 4 as a percentage of mean sham values (e) Histomorphometry values for the mineral apposition rate in lumbar vertebra 4 as a percentage of mean sham values

legend

Disclosures: Danielle MacKay, PFE, 8

SU0176

Chronic administration of Liraglutide, a glucagon-like peptide-1 receptor agonist, improves trabecular bone mass and architecture in ovariectomised mice. Marie Pereira*[1], Jeshmi Jeyabalan[1], Mark Hopkinson[1], Mark Cleasby[1], Pascale Chavassieux[2], Jean Paul Roux[3], Chantal Chenu[4]. [1]Royal Veterinary College, United Kingdom, [2]INSERM UMR1033, Université De Lyon, France, [3]INSERM UMR1033 & Universite de Lyon, France, [4]Royal Veterinary College, United Kingdom

The increased incidence of type 2 Diabetes Mellitus among the aged is associated with an impaired skeletal structure and a higher prevalence of bone fractures. In addition, anti-diabetic therapies can also negatively affect bone mass. In this study, we tested the skeletal effects of chronic administration of two Glucagon-like peptide-1 receptor (GLP-1R) agonists and examined the expression of GLP-1R in bone tissue and cells. Twelve week-old female C57Bl/6N mice were ovariectomised (OVX) to induce bone loss. Four weeks after OVX, mice were treated with either: Liraglutide (LIR) 0.3 mg/kg/d, Exenatide (Ex-4) 10 μg/kg/d or saline for four weeks (n=10/group). Mice were injected with calcein and alizarin red at days 8 and 3 respectively, prior to euthanasia, to label bone-forming surfaces. Tibiae were harvested from these mice, bone micro-architecture determined by micro-CT and bone formation and resorption parameters measured by histomorphometric analysis. Serum was collected for evaluation of sclerostin levels, an inhibitor of bone formation. RNA was extracted from bone, bone marrow and bone cells for detection of GLP-1R using RT-PCR. GLP-1R distribution in bone was also examined using immunohistochemistry. Our results show that LIR significantly increases bone mass compared to controls, manifested by higher trabecular bone volume percent (+61%, P<0.01) and trabecular number (+46%, P<0.05). Trabecular pattern factor (-15%, P<0.05) and structure model index (SMI) (-9%, P<0.05) were significantly decreased, reflecting improvement in trabecular bone structure and connectivity, respectively. The cortical indexes were not significantly affected by LIR. Ex-4 treatment induced a similar tendency for improvement of trabecular mass and architecture, although the effects were non-significant, except for SMI (-9%, P<0.05). We found no significant effect of LIR on bone-forming and resorption surfaces, suggesting that bone turnover is not affected by LIR. We did not detect GLP-1R mRNA in bone devoid of bone marrow, osteoblasts and osteocyte cell lines, but it was expressed in bone marrow cells and mouse primary osteoclasts. The expression of GLP-1R in those cells was confirmed by immunocytochemistry. Serum sclerostin levels were significantly decreased by Ex-4 (-23%, P<0.05) but not by LIR. Our data suggest that GLP-1R agonists have beneficial effects on bone although their effects may be indirect. Further studies will determine their mechanisms of action in bone.

Disclosures: Marie Pereira, None.

SU0177

Combination Treatment of 1-34 PTH and Eldecalcitol Showed Synergistic Effect on BMD without Severe Hypercalcemia. Sadaoki Sakai*[1], Satoshi Takeda[2], Tomomaya Yamamoto[3], Tomoka Hasegawa[4], Norio Amizuka[5], Koichi Endo[6]. [1]Chugai Pharmaceutical Co., Ltd., Japan, [2]Chugai Pharmaceutical Co., Ltd., Japan, [3]Hokkaido University, Japan, [4]Hokkaido University, Japan, [5]Hokkaido University School of Dentistry, Japan, [6]Chugai Pharmaceutical Co., Ltd., Japan

Teriparatide and eldecalcitol (ELD, active vitamin D_3 derivative) have been used in osteoporosis treatment. It is suggested that teriparatide increases immature osteoblasts and ELD enhances differentiation into mature osteoblasts. On the basis of these actions of teriparatide and ELD on osteoblast differentiation, a combination treatment of teriparatide and ELD for osteoporosis may have additional effect on bone formation compared to mono-therapy of these drugs. However, combination treatment is possibly associated with a risk of hypercalcemia. In this study, we examined the effect of combination treatment of 1-34 PTH (PTH) and ELD on BMD, osteoblast number, bone histomorphometry and serum calcium concentration using a rat osteoporosis model.

Nine-week-old rats were ovariectomized (OVX) and either vehicle, PTH (10 μg/kg, s.c.), ELD (20 ng/kg, p.o.) or both were administered 5 days a week for 8 weeks from 4 weeks after surgery. Femur and serum were collected after 4 and 8 weeks treatment.

BMD of distal femur was lower than sham in vehicle treated group (vehicle) at 4 and 8 weeks. PTH, ELD and combined therapy (combination) BMD at 4 and 8 weeks and combination was higher than both PTH and ELD at 8 weeks. ES/BS was increased in vehicle and recovered in both PTH and ELD at 4 and 8 weeks, and further decreased in combination than PTH at 8 weeks. Ob.S/BS was increased in vehicle. PTH showed additional increase but ELD is lower than vehicle. Combination is comparable as vehicle. Meanwhile, MS/OS in ELD was higher than vehicle. The number of osteoblast, especially cuboidal-shaped osteoblasts, was increased in PTH. ELD decreased the total number of osteoblast but the ratio of flat-shaped osteoblasts was increased. Serum calcium was increased in ELD but there was no difference between ELD and combination.

In conclusion, combination treatment of PTH and ELD had aditive effect on BMD upregulation in OVX rats without hypercalcemia. These two drugs had different actions on regulation of osteoblast maturation. Further investigations are required but we suppose that PTH increases cuboidal-type osteoblasts and upregulates bone matrix production, whereas ELD normalizes bone remodeling cycle

and helps to mineralize the matrix through controlling the ratio of flat-shaped osteoblasts.

SU0178

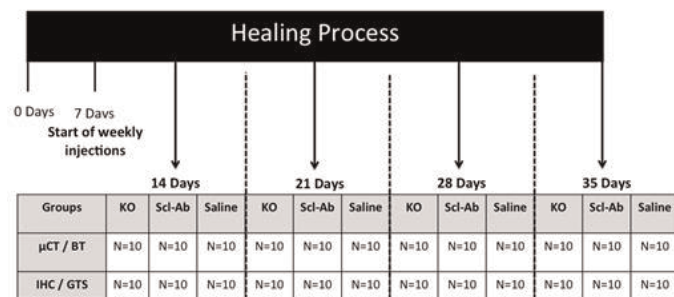**Effect of Sclerostin Depletion on Fracture Healing in the Mouse Model.** Mohammad Alzahrani*[1], Frank Rauch[2], Reggie Hamdy[3]. [1]McGill University, Canada, [2]Shriners Hospital for Children, Montreal, Canada, [3]Shriners Hospital for Children, Canada

Purpose: Sclerostin is a secreted glycoprotein that interacts with LRP5 receptor on osteoblasts and inhibits the intracellular Wnt signaling pathway, leading to decreased bone formation activity by osteoblasts. When sclerostin is inactivated bone formation is therefore stimulated. This stimulation has been proven in fracture studies showing that sclerostin deficient mice have larger and stronger calluses with accelerated fracture healing. Also sclerostin antibody (Scl-Ab) injection has been studied in its ability to promote fracture resulting in accelerated and enhanced bone volume.These observations suggest that sclerostin inhibition and depletion show improved and accelerated fracture healing, but the effect of these two mechanisms have not been compared to asses the accurate effect of Scl-Ab. Therefore we designed a study to compare the effect of sclerostin depletion (sclerostin knockout) and inhibition (Scl-Ab injection).

Methods: 10-week-old male SOST knockout (KO) (N=40) and Wild-type (WT) (N=80) mice underwent insertion of a tibial intramedullary pin after which a tibial osteotomy was performed. The mice were divided into three groups: SOST KO (N=40), WT with Scl-Ab injection (N=40) and WT with saline injection (control) (N=40). The Scl-Ab group received an intravenous dose of 100mg/kg weekly starting on day 7. Each group was managed and sacrificed according to the specified protocol (Fig.1).

Results: The Scl-Ab group showed similar callus formation and density to the sclerostin KO group, especially on microCT results. At 28 days post-fracture there was no significant difference in callus BV/TV ratio (p=0.1) between both groups. Amount of trabecular thickness between the Scl-Ab group and KO group showed no significant difference at both 28 and 35 days post-fracture (p=0.16 and p=0.92, respectively). In addition the bone surface density (BS/TV) was comparable between the two groups (Scl-Ab group mean= 15.7 and KO group mean=17.5, p=0.06) at day 28 post-fracture, a similar result was apparent also at day 35 post-fracture. Also at day 28 post-fracture Bone Mineral density difference was not significant between the two groups (p=0.32).

Conclusion: Scl-Ab injections showed promising results, which were comparable to the complete depletion of sclerostin in this model. This may be implicated in management of different types of fractures in humans and also be applied in the treatment of fracture nonunions in combination with other management options.

Groups	14 Days			21 Days			28 Days			35 Days		
	KO	Scl-Ab	Saline	KO	Scl-Ab	Saline	KO	Scl-Ab	Saline	KO	Scl-Ab	Saline
μCT / BT	N=10	N=10	N=10	N=10	N=10	N=10	N=10	N=10	N=10	N=10	N=10	N=10
IHC / GTS	N=10	N=10	N=10	N=10	N=10	N=10	N=10	N=10	N=10	N=10	N=10	N=10

Abrev:
μCT: microCT, BT: Biomechanical testing, IHC:immunohistochemistry, GTS: Goldner trichrome staining,
KO: Sclerostin Knockout Group, Scl-Ab: Sclerostin Antibody Group, C: Control Group

Fracture model protocol and study timeline.

SU0179

Estrogen replacement but not dietary antioxidants from beetroot juice preserves alveolar bone in ovariectomized rats. Bryan D. Johnston*, Amanda B. Longo, Wendy E. Ward. Centre for Bone & Muscle Health, Faculty of Applied Health Sciences, Brock University, St. Catharines, Ontario, L2S 3A1, Canada

Introduction: Tooth loss is correlated with a greater decrease in whole body and femoral neck bone mineral density (BMD) in postmenopausal women. The loss of hip and vertebral BMD are likely mirrored by the loss of tooth-supporting, alveolar bone. Individuals with fewer teeth have limited food choices, compromising nutritional status and thereby may be at higher risk of chronic disease development, such as osteoporosis. While estrogen replacement is known to attenuate deterioration of bone tissues in postmenopausal women, the response of alveolar bone has not been studied. Moreover, given concerns with estrogen replacement, dietary approaches to maintain

bone mass are of interest. Such dietary approaches could involve foods that are rich sources of antioxidants and nitrates as both are individually associated with higher BMD in postmenopausal women. Beetroot juice is an abundant source of dietary antioxidants and nitrates and thus may preserve alveolar bone. The objective of this study was to determine the potential bone sparing effect of estrogen replacement as well as a dietary strategy (beetroot juice) on alveolar bone in the well-characterized ovariectomized rat model.

Methods: Sprague Dawley rats were ovariectomized at 12 weeks and randomized to one of three groups (*n* = 14 per group): ovariectomy alone (OVX), estrogen replacement (E2) (17-β estradiol, 1.5 mg, 90-day, subcutaneous pellet from Innovative Research of America), and beetroot juice (BR) (provided as gelatinized beetroot juice containing 18.75 mg/day nitrates from James White Drinks). Rats were fed semi-purified diet (AIN93M) for 12 weeks at which time mandibles were collected. Hemimandibles were scanned at a 9μm resolution using micro-CT (Skyscan 1176). The following scanning parameters were used: 2 mm aluminum filter, 180˚ scanning rotation and 0.20˚ rotation step at 82 kV/298 μA. The region analyzed was the alveolar bone supporting the first mandibular molar.

Results: The E2 but not the BR group had a higher (p<0.001) bone volume fraction (BV/TV) than the OVX group. Trabecular separation was lower in the E2 group compared to both the OVX (p<0.05) and BR (p<0.01) groups. Trabecular thickness was higher (p<0.01) in the E2 group compared to the BR group alone. Trabecular number did not vary among groups.

Conclusion: E2 but not a beetroot intervention prevented deterioration of alveolar bone. The ability of other dietary components to preserve alveolar bone is an area of future study.

SU0180

Maintenance of Proximal Tubule Phosphate Homeostasis Requires the Transcription Factor Ebf1. Jackie Fretz*[1], Tracy Nelson[2], Yougen Xi[2], Mark Horowitz[1]. [1]Yale University School of Medicine, USA, [2]Yale School of Medicine, USA

The transcription factor Early B Cell Factor 1 (Ebf1) is not only important for maturation of B lymphocytes, but has also been revealed to be integral for maturation of several cell lineages from mesenchymal progenitors. Whole body knockout mice have many problems including low bone mineral density and are severely runted. While there is a significant *in vivo* differentiation and mineralization defect in Ebf1-deficient BM cells, recent reports using Runx2- and Osx-cre specific deletions of Ebf1 have no bone phenotype. Our investigations have revealed that Ebf1-deficient mice have deficient renal maturation and function. Urine analysis revealed that Ebf1-deficient mice waste phosphate and calcium. While the ionized serum calcium level is normal, the mice are hypophosphatemic, have reduced expression of proximal tubule phosphate transporters, and alterations in proximal tubule maturation in the peripheral cortex. Administration of a high phosphate diet (1.5%) was able to partially reverse the runting present in these animals, increase bone density and quality (as assessed by micro-CT, histomorphometry, and biomechanical testing), as well as improve survival of the KO mice. Ebf1 deficient mice are also lipodystrophic (mediated by a direct role of Ebf1 in adipocyte maturation), and a combination diet of high fat (45%) and high phosphate improved survival, bone quality, and growth better than either high phosphate or high fat diet alone. These results identify a role for Ebf1 in the complex system of renal phosphate homeostasis and provides a mechanism for Ebf1 action in kidney to explain the mineralization deficiency seen *in vivo*.

SU0181

Methylphenidate Impairs Skeletal Development In Female Rats. David Komatsu*[1], Lisa Robison[2], Melissa Vitale[2], Junho Lee[2], Michalis Michaelos[2], Jason Gandhi[3], Soyeh Paeng[2], Panayotis Thanos[2], Michael Hadjiargyrou[4]. [1]Stony Brook University, Dept. of Orthopaedics, USA, [2]Department of Psychology, Stony Brook University, USA, [3]Department of Physiology & Biophysics, Stony Brook University, USA, [4]New York Institute of Technology, USA

Methylphenidate (MP) is widely used to treat Attention Deficit Hyperactivity Disorder (ADHD), the most commonly diagnosed adolescent psychological disorder with a US incidence of ~9.5%. We previously showed MP to be detrimental to skeletal development in male rats. This study was conducted to test the hypothesis that MP adversely affects skeletal development in female rats. Four-week old female Sprague-Dawley rats were randomized to 5 groups (n=12/T$_x$): Water, Low-Dose MP (LD MP), High-Dose MP (HD MP), Water Pair-Fed to LD MP (Water LD PF), and Water Pair-Fed to HD MP (Water HD PF). Water groups received no MP. LD and HD MP received MP via their drinking water. Pair-fed groups had food restricted to their corresponding treatment groups' ad-lib consumption. After 13 weeks of treatment, HD MP rats gained less weight than Water (16%), LD MP (23%), and Water HD PF (19%) rats. Open field behavioral testing showed that HD MP rats were more active, with increases in movement time, distance, and velocity compared to Water, LD MP, and Water HD PF rats from 25 to 310%. LD MP rats were 10-52% more active than Water and Water LD PF. Length, anterior-posterior (AP) and medial-lateral (ML)

diameter were measured in tibiae, femora, and L5 vertebrae using calipers. Only tibiae showed differences with HD MP 4% shorter than LD MP and wider than Water on AP (10%) and ML (8%) axes. LD MP was 8% narrower than Water on the AP axis. Water HD PF showed ML increases of 9% and 7% compared to Water and Water LD PF, respectively. Femora were assessed by microCT at cortical (mid-diaphysis) and trabecular (distal metaphysis) regions. A 6% reduction in cortical thickness was seen for HD MP as compared to LD MP. Trabecular bone mineral density (BMD) was reduced by 2% in HD MP rats compared to both LD MP and Water. Water HD PF rats showed a similar 2% reduction in BMD compared to Water LD PF and Water. Compared to Water, trabecular volume was increased by ~12% in Water, Water HD PF, and HD PF. Three-point bending tests of femora revealed no differences. Overall, the effects of MP on skeletal development in adolescent female rats were mild. Pair-feeding removed body weight as a confounding variable at the low dose, but not at the high dose. This is likely due to the tremendous increases in activity seen in the high dose rats. This increase in activity was significantly higher than seen previously in male rats and may account for milder skeletal phenotype seen in female rats exposed to MP.

SU0182

Osteoclastogenesis–inhibiting peptide W9 delivery stimulates new bone formation in expanded mid-palatal suture. <u>Wei-Bing Zhang</u>*. School of Stomatology, Nanjing Medical University, Nanjing, China, USA

Objective – The aim of the present study was to assess the effects of the WP9QY peptide on bone formation in the expanded palatal suture model.

Materials and Methods – Expanded palates of 6-week-old male C57BL 6 mice were either unstimulated or stimulated with W9 for 7 days. Histological observations and the Raman microspectroscopy assessments of the palatal bone as well as bone mineral density measurements were performed.

Results – Raman microspectroscopy analysis demonstrated that W9 (%increase = 35.33 $\pm$ 1.82, p = 0.007) formed significantly more bone at the palatal suture compared with vehicle samples at day 7. Alkaline phosphatase activity along the bone edges was markedly greater in the W9 groups compared with that in vehicle group at day 7. The levels of Trap activity of vehicle group were higher than of W9 group.

Conclusion-These results suggest that W9 delivery stimulates new bone formation in expanded mid-palatal suture.

SU0183

PEGylation of NELL-1 Improves Pharmacokinetics and Systemic Osteogenic Therapy. <u>Yulong Zhang</u>*[1], <u>Jin Hee Kwak</u>[2], <u>Juyoung Park</u>[3], <u>Chirag Chawan</u>[3], <u>Omar Velasco</u>[4], <u>Kambiz Khalilinejad</u>[5], <u>Jia Shen</u>[1], <u>Eric Chen</u>[3], <u>Pia Bayani</u>[3], <u>Sepideh Dolatyar</u>[3], <u>Greg Asatrian</u>[3], <u>Xinli Zhang</u>[1], <u>Chia Soo</u>[6], <u>Benjamin Wu</u>[7], <u>Kang Ting</u>[1]. [1]University of California, Los Angeles, USA, [2]Department of Craniofacial Research Institute, School of Dentistry, University of California, Los Angeles, USA, [3]Department of Craniofacial Research Institute, School of Dentistry, University of California, Los Angeles, USA, [4]UCLA & Orthopaedic Hospital Department of Orthopaedic Surgery & the Orthopaedic Hospital Research Center, University of California, Los Angeles, USA, [5]Division of Associated Clinical Specialties & Section of Orthodontics, School of Dentistry, University of California, Los Angeles, USA, [6]Division of Plastic & Reconstructive Surgery, Department of Surgery, David Geffen School of Medicine, University of California, Los Angeles, USA, [7]Weintraub Center for Reconstructive Biotechnology, School of Dentistry, University of California, Los Angeles, USA

NEL-like molecule-1(NELL-1) is a pro-osteogenic secretory molecule shown to successfully prevent osteoporosis through intramedullary injection in ovariectomy-induced osteoporotic rats. However, the short half-life of native NELL-1 limits its application as a systemic therapy. Thus, the purpose of this study was to modify the structure of NELL-1 by PEGylation technology in order to improve its pharmaco-kinetics while maintaining its bioactivity and osteogenic potential *in vitro* and *in vivo*. PEGylated NELL-1 was prepared using three different types of polyethylene glycols (PEG):linear 5KDa, 20KDa, and branched 40KDa.First, when characterized by GPC and fluorometric assay, NELL-PEG-5K was found to yield the greatest amount of PEGylation (PEG degree increased from 14.2% up to 72.6%) and the most thermally stable conjugate (denature temperature increased from 49.75ºC to 63.42ºC) while maintaining a bioactivity *in vitro* comparable to that of unmodified NELL-1.Next, the pharmacokinetics and biodistribution of PEGylated NELL-1 was examined in CD-1 mice. The half-life of PEGylated NELL-1 *in vivo* was significantly improved from 5.5h to 15.5h, up to 31.3h(6-fold), while the biodistribution of NELL-PEG-5k at 48h revealed that more than 2-3 times amount of protein was distributed into bone tissue (femur, tibia, vertebrae, calvaria) compared to controls. Next, the systemic osteogenic capacity of NELL-PEG-5k was investigated by systemic administration in B6 mice(n=16, 1.25 mg/kg, q4d and q7d schedules) for 4 weeks. The femoral bone mineral density (BMD) measured by DXA showed a gradual and significant increase

(16% for q4d, 17% for q7d) in the NELL-PEG-5k group compared to the baseline. Live-microCT and F-18 microPET revealed increased BMD and bone turnover rate in the NELL-PEG-5k group. MicroCT analysis revealed significant improvements in trabecular BMD volume(BV/TV), and structural values(Tb.Th, Tb.N, Tb.Sp) compared to control. In addition, H&E staining confirmed increased bone formation and trabeculation.OCN and TRAP immunostaining demonstrated increased osteo-blastic and decreased osteoclastic activities in the NELL-PEG-5k group. These data suggest that PEGylation of NELL-1 not only improves its pharmacokinetics, but also preserves its bioactivity and systemic osteogenic effect *in vitro* and *in vivo*. The current findings hold promise for developing an effective systemic therapy of various osteodeficient disorders including osteoporosis and dysostosis syndromes.

SU0184

Sharpin-deficient *Cpdm* mice display cortical thinning due to loss of osteoblasts and osteal macrophages. <u>Anke Jeschke</u>*[1], <u>Philip Catala-Lehnen</u>[2], <u>Sabrina Sieber</u>[3], <u>Michaela Schweizer</u>[4], <u>Kristofer Wintges</u>[2], <u>Thomas Bickert</u>[2], <u>Michael Amling</u>[5], <u>Hans-Jürgen Keienkamp</u>[3], <u>Thorsten Schinke</u>[6]. [1]Department of Osteology & Biomechanics, Germany, [2]Department of Osteology & Biomechanics, University Medical Center Hamburg Eppendorf, Germany, [3]Department of Human Genetics, University Medical Center Hamburg Eppendorf, Germany, [4]Center of Molecular Neurobiology, University Medical Center Eppendorf, Germany, [5]University Medical Center Hamburg-Eppendorf, Germany, [6]Department of Osteology & BiomechanicsUniversity Medical Center Hamburg Eppe, Germany

Cpdm mice, carrying a mutation of the *Sharpin* gene, are primarily known as a model of multi-organ inflammation. A previous study additionally revealed a low bone mass phenotype, yet the underlying causes remained to be identified. Here we have applied non-decalcified histology and histomorphometry to perform a thorough skeletal phenotyping of *Cpdm* mice. We show that defects of bone formation, but not increased osteoclastogenesis, are causative for osteopenia and thinning of cortical bone in *Cpdm* mice. This phenotype is associated with a near absence of osteal macrophages, a cell type identified recently as a positive regulator of endocortical bone formation. *Ex vivo* experiments demonstrated that calvarial osteoprogenitor cells from *Cpdm* mice lack osteal macrophages and fail to differentiate into osteoblasts. Likewise, bone marrow cells from *Cpdm* mice display impaired osteogenic differentiation, also confirmed by genome-wide expression analysis. Here we additionally found that *Cpdm* bone marrow stromal cells produce higher levels of Cxcl5 and lower levels of IL1-ra, an IL1 receptor antagonist preventing chronic inflammation. Taken together, these data do not only identify Sharpin as a physiological regulator of bone formation, they also provide additional evidence for the critical role of bone and immune cell interactions in skeletal remodeling. In particular, the *Cpdm* mice represent the first model, where a spontaneous deficiency of osteal macrophages is associated with cortical thinning, thereby further underscoring the physiological relevance of this particular cell type.

SU0185

Soy Protein Isolate Inhibits High Fat Diet-Induced Senescence Pathways in Osteoblasts to Maintain Bone Acquisition in Rats. <u>Jin-Ran Chen</u>*[1], <u>Oxana P. Lazarenko</u>[2], <u>Michael L. Blackburn</u>[3], <u>Thomas M. Badger</u>[3], <u>Martin J. J. Ronis</u>[3]. [1]University of Arkansas for Medical Science, Arkansas Children's Nutrition Center, USA, [2]Arkansas Children's Nutrition Center, & The Department of Pediatrics, University of Arkansas for Medical Sciences, USA, [3]Arkansas Children's Nutrition Center, & The Department of Pediatrics, University of Arkansas for Medical Sciences, USA

Chronic consumption by experimental animals of a typical Western diet high in saturated fats and cholesterol during postnatal life has been demonstrated to impair skeletal development. However, the underlying mechanism by which high fat, energy dense diets affect bone forming cell phenotypes is poorly understood. Using peripheral quantitative computerized tomography (pQCT) analysis of the proximal tibial and vertebrae compression testing, we show that male weanling rats fed a diet containing 45% fat and 0.5% cholesterol made with casein (HF-Cas) for 6 weeks displayed lower bone mineral density and strength compared to AIN-93G-fed dietary controls. Substitution of casein with soy protein isolate (SPI) in the high fat diet (HF-SPI) prevented these effects. The bone sparing effects of SPI were associated with prevention of HF-Cas-induced osteoblast senescence pathways through suppression of p53/p21 signaling pathways. HF-Cas-fed rats had increased caveolin-1 and down-regulated Sirt1 leading to activation of PPARγ and p53/p21; whereas, rats fed HF-SPI suppressed caveolin-1and activated Sirt1 to de-acetylate PPARγ and p53 in bone. Treatment of osteoblastic cells with non-esterified free fatty acid (NEFA) (a mixture of NEFA with individual NEFA ratio and concentration similar to their appearance in HF rat serum) increased cell senescence signaling pathways. An isoflavone mixture

(at concentrations identical to that found in SPI diet rat serum) significantly blocked activation of senescence-associated β-galactosidase (SA-β-gal) and PPARγ/p53/p21 by NEFA. Over expression of PPARγ in osteoblastic cells triggered p53/SA-β-gal senescent signaling. Finally, replicative senescent osteoblastic cells and bone marrow mesenchymal ST2 cells exhibited similar behavior to cells treated with NEFA and bone cells *in vivo* in rats fed HF-Cas diet. These results suggest that: 1) high concentrations of NEFA occurring with HF intake are mediators of osteoblast cell senescence leading to impairment of bone development and acquisition; and 2) the molecular mechanisms underlying the SPI-protective effects involve isoflavone-induced inhibition of osteoblastic cell senescence to prevent HF-induced bone impairments. *Supported in part by ARS CRIS #6251-51000-005-03S (JRC).*

Disclosures: Jin-Ran Chen, None.

SU0186

Staphylococcal lipoprotein is a potent inhibitor of osteoblast differentiation. <u>Ok-Jin Park</u>*[1], <u>Jiseon Kim</u>[2], <u>Cheol-Heui Yun</u>[2], <u>Seung Hyun Han</u>[1]. [1]Seoul National University School of Dentistry, South Korea, [2]Seoul National University, South Korea

Streptococcus aureus can cause osteomyelitis and septic arthritis resulting in the bone destruction where its lipoprotein is considered as a major bone-resolving component by stimulating osteoclast formation. We previously demonstrated that synthetic diacylated lipopeptide, Pam2CSK4 mimicking Gram-positive bacterial lipoproteins, increased osteoclast differentiation through up-regulation of RNAKL and down-regulation of osteoprotegerin in osteoblasts. In order to further elucidate the action mechanism, we investigated whether the bacterial lipoprotein affects osteoblast differentiation using Pam2CSK4 together with *S. aureus* wild-type (WT) and the lipoprotein-deficient mutant (*S. aureus-Δlgt*). When mouse osteoblast cell line MC4 was treated with *S. aureus*-WT or Pam2CSK4, the osteoblast differentiation was significantly attenuated which such effect was not observed in the cells treated with *S. aureus-Δlgt* under the same condition. Furthermore, Pam2CSK4 decreased the transcriptional activity of Runx2 and β-catenin, which are important transcriptional activators for osteoblast differentiation. In addition, Pam2CSK4 attenuated the expression of osteogenic marker genes, including alkaline phosphatase and bone sialoprotein. In contrast, IL-6 negatively affecting osteoblast differentiation was increased in the cells treated with *S. aureus*-WT or Pam2CSK4, but not with *S. aureus-Δlgt*. In conclusion, these results suggest that lipoprotein is an important component of *S. aureus* for the attenuation of osteoblast differentiation through down-regulation of the Runx2 and β-catenin.

Disclosures: Ok-Jin Park, None.

SU0187

Velcade Inhibits the Ubiquitin Proteasome System in Mesenchymal Stem Cells to Enhance Fracture Repair. <u>Xing Li</u>*[1], <u>Hengwei Zhang</u>[2], <u>Hani Awad</u>[3], <u>Matthew Hilton</u>[4], <u>Zhenqiang Yao</u>[5], <u>Michael Zuscik</u>[6], <u>Brendan Boyce</u>[3], <u>Lianping Xing</u>[5]. [1]University of Rochester, USA, [2]Univeristy of Rochester, USA, [3]University of Rochester Medical Center, USA, [4]Duke University Musculoskeletal Research Center, USA, [5]University of Rochester, USA, [6]University of Rochester School of Medicine & Dentistry, USA

The Ubiquitin Proteasome System (UPS) regulates osteoblast (OB) differentiation from mesenchymal stem cells (MSCs) by promoting ubiquitination and proteasomal degradation of OB positive regulators, including Runx2, JunB and b-catenin, but it is not known if it or agents affecting its activity regulate fracture repair. To test this, we used an open tibial fracture model in C57B6 WT mice and found significantly increased expression of the ubiquitin E3 ligases, Smurf1, Itch and Wwp1 (fold increase vs day 0: 26±2, 17±3, 4±0.4, respectively) and of ubiquitinated proteins in callus tissues at day 7 post-fracture. We treated fractured mice with VELCADE (a proteasome inhibitor used to treat patients with multiple myeloma) or vehicle and found that VELCADE significantly increased callus volume (3.5±1.1 vs 1.1±0.4 mm[3] by mCT), bone area within callus (1.2±0.3 vs 0.7±0.2 mm[2] by histomorphometry), and bone strength (torsional rigidity: 1017±215 vs 688±214 N.mm/rad/mm; maximum torque: 28±4 vs 21±3 N.mm by biomechanical testing). We also fractured Nestin-GFP mice and found large numbers of Nestin^{+} cells in tissue sections of fracture calluses and a >10-fold increase in Nestin^{+} cells isolated from calluses compared to non-fractured tibial bone. FACS analysis showed that 70% of Nestin^{+} cells from calluses are CD105^{+}Sca1^{+} (surface markers of MSCs) and 80% of the CD105^{+}Sca1^{+} cells are Nestin^{+}. VELCADE increased the % of Nestin^{+} cells in fractured Nestin-GFP mouse calluses by 4-10-fold, but it had no effect on the % of CD3^{+} T cells, B220^{+} B cells or CD11b^{+} macrophage/monocytes. Finally, we treated OB/myoblast progenitor C2C12 cells with VELCADE and found that it had no effect on cell migration to a CXCL12 gradient or on apoptosis, but it significantly increased cell growth (2±0.13-fold increase vs Ctl) and % of cells in the G2 phase of cell cycle (13±2 vs 8±0.6). Cells from calluses of mice or C2C12 cells treated with VELCADE had higher levels of ubiquitinated proteins and proteins known to be degraded via the proteasome, such as Runx2, JunB, and β-catenin, consistent with proteasome inhibition. In conclusion, our findings reveal a novel role for the UPS system in fracture repair to regulate MSC proliferation and OB differentiation. Thus,

VELCADE or other UPS inhibitors may have utility as potential new therapeutic agents to enhance fracture repair in patients with impaired bone healing.

Disclosures: Xing Li, None.

SU0188

Withdrawn

SU0189

The Role of LXR in Glucocorticoid-Induced Muscle Wasting and Bone Loss. <u>Jasmine Williams-Dautovich</u>*[1], <u>Rucha Patel</u>[2], <u>Carolyn L. Cummins</u>[2]. [1]University of Toronto, Canada, [2]University of Toronto, Canada

Background: Glucocorticoids (GCs) have profound anti-inflammatory properties that are critical for the treatment of a wide range of diseases. Unfortunately, major metabolic side-effects, including osteoporosis and muscle wasting, remain a key limitation for the long-term therapeutic use of GCs. The glucocorticoid receptor (GR) and liver X receptor (LXR) are members of the nuclear receptor superfamily that regulate distinct but overlapping transcriptional programs. Our lab has found that LXRα/β-/- mice are resistant to developing hyperglycemia and hepatic steatosis, two detrimental side effects of long-term GC therapy, while retaining their therapeutic anti-inflammatory effect. The aim of this study was to determine whether LXRs are also involved in modulating GC-induced bone loss and muscle wasting.

Methods: Wildtype and LXRα/β-/- mice were given Dexamethasone (Dex, 50µg/day) in drinking water for 14 days and plasma osteocalcin and Trap-5b were measured. In vitro studies were performed with mouse myotube (C2C12), osteocyte (MLO-Y4), and osteoblast (MC3T3-E1) cell lines treated with Dex (100nM, 1µM) ± LXR antagonist (GSK2033, 100nM). Wildtype and LXR knockout mice were treated in vivo with Dex (5mg/kg), ± GSK2033 (40mg/kg) for 10 days. Gene expression was measured by QPCR for MuRF1, MAFbx and myostatin (muscle); and RANKL, OPG, osteocalcin, Col1a1 and TRAP (bone).

Results: The osteoblast marker osteocalcin was decreased with Dex treatment in both WT mice and LXRα/β-/- mice; whereas, the osteoclast marker TRAP-5b was increased only in Dex-treated WT mice. When cultured in the presence of LXR antagonist, in vitro cultured osteocytes were not protected against Dex-induced changes in osteocyte gene expression. Analysis of bone markers from Dex ± GSK2033 treated mice found no protective role for LXR antagonists on bone markers. However, it was found that the exposure of bone to the LXR antagonist was minimal, likely due to extensive hepatic metabolism of GSK2033. In vitro and in vivo studies in muscle found that the LXR antagonist treated groups were slightly protected from GC-induced muscle wasting, however, the effect did not reach statistical significance. Together, these data suggest that LXRs may play a role in modulating Dex-induced osteoclastogenesis (in vivo) but does not appear to significantly modulate GR target genes in osteocyte or muscle cell lines. Future studies are aimed at assessing the contribution of LXRs to GC-induced osteoclastogenesis.

Disclosures: Jasmine Williams-Dautovich, None.

SU0190

Wnt3a potentiates myogenesis in C2C12 myoblasts through changes of signaling pathways including Wnt and NFκB. <u>Jian Huang</u>*[1], <u>Chenglin Mo</u>[2], <u>Lynda Bonewald</u>[3], <u>Marco Brotto</u>[3]. [1]University of missouri kansas city, USA, [2]University of Missouri-Kansas City, USA, [3]University of Missouri - Kansas City, USA

As bone cells produce Wnt3a, we postulated that Wnt3a might be a candidate molecule signaling from bone cells to muscle cells. To test this hypothesis, we have conducted a series of studies with concentrations of Wnt3a ranging from 0.1 to 10ng/ml on C2C12 myogenesis. A concentration as low as 0.5ng/ml can consistently increase both the number and the size of myotubes during differentiation, a finding that was confirmed morphologically (4,299 ± 594 µm2 untreated, vs.7,957 ± 1,269 µm2 for Wnt3a treated myotubes, p < 0.001) and also with the concomitant double staining of myosin heavy chain (MHC) and nuclei. When C2C12 myoblasts were exposed to 10ng/ml Wnt3a in differentiation media, this led to a 2-fold increase in the translocation of β-catenin to the nucleus compared to control suggesting that Wnt3a might stimulate the activation of the β-catenin signaling pathway in muscle cells. Under these conditions, increased number and size of myotubes (4,319 ± 642 µm2 untreated, vs. 9,833 ± 1,013 µm2 for Wnt3a treated C2C12, p < 0.001) was also observed. Furthermore, these potent effects of Wnt3a strongly correlated with the appearance of intracellular calcium oscillations (ranging from 150-500nM free calcium) in myotubes measured with Fura-2. To study the potential molecular signaling mechanism of Wnt3a function in C2C12 myoblast differentiation, we used the Mouse Signal Transduction PathwayFinder PCR Array which monitors the activity of 10 signaling pathways to quantitate changes in gene expression between the control and the Wnt3a-treated C2C12 cells. In Wnt3a treated C2C12 cells, compared to control, the expression of Axin2, Wnt5a, Gata3 and Adm was increased by 7.05 fold, 2.53fold, 2.85fold and 2.35 fold, respectively, while the expression of Hey2, Ifng, Icam1, Tnf and Lrg1,Tnf decreased by 2.23 fold, 4.56 fold, 2.79 fold, 2.79 fold and 4.85 fold, respectively. Genes that were increased with Wnt3a were components of the Wnt signaling pathway (Axin2, Wnt5a), JAK1, 3/Stat6 signaling pathway (Gata3) and Hypoxia signaling pathway (Adm). Genes that were decreased include the Notch

signaling pathway (Hey2), NFκB signaling pathway (TnF, Ifng, Icam1), and the Stat3 signaling pathway (Lrg1). These results suggest that Wnt3a may function through these pathways to regulate C2C12 myoblast differentiation.

SU0191

Withdrawn

SU0192

Longitudinal Changes in Distal Lower-Extremity Muscle Area and Density after Chronic Spinal Cord Injury. <u>Cameron Moore</u>[1], <u>B. Catharine Craven</u>[1], <u>Lehana Thabane</u>[2], <u>Jonathan Adachi</u>[3], <u>Alexandra Papaioannou</u>[4], <u>Lindsie Blencowe</u>[5], <u>Milos Popovic</u>[6], <u>Lora Giangregorio</u>*[7]. [1]Toronto Rehabilitation Institute, Canada, [2]McMaster University, Canada, [3]St. Joseph's Hospital, Canada, [4]Hamilton Health Sciences, Canada, [5]Toronto Rehabilitation Institute, Canada, [6]University Health Network - Toronto Rehabilitation Institute, University of Toronto, Canada, [7]University of Waterloo, Canada

Background: Lower-extremity skeletal muscle atrophy and fatty-infiltration are linked to poor bone quality after spinal cord injury (SCI) and may offer potential therapeutic targets for treating osteoporosis. This study prospectively measured lower-extremity skeletal muscle cross-sectional area (CSA) and muscle density in a group of adults with chronic SCI and diverse impairment. Methods: Seventy individuals [50/20 m/f, mean ($\pm$ standard deviation) age 48.9 ± 11.5 years; duration of injury 15.5 ± 10.0 years] with chronic (>2 years post-injury) SCI (C1-T12, AIS A-D) had a pQCT scan of the 66%-site of the calf at baseline and annually for 2 years. Mixed-effects models were used to examine longitudinal changes in muscle CSA and density. Linear regression models were created to identify baseline characteristics associated with 2-year muscle CSA and density change. Possible correlates selected *a priori* included: gender, age, height, weight, waist circumference (WC), age at injury, level of injury, injury duration, leg spasm frequency and severity scale score, calf-muscle lower-extremity motor score, wheelchair use, serum vitamin D level, and physical activity level. Results: Significant reductions in muscle CSA and density were observed over a 2-year period (adjusted mean difference $\pm$ standard error: -1.8 ± 0.8 cm^2, p<0.05 and -1.2 ± 0.5 mg/cc, p<0.01, respectively). High individual variability in 2-year muscle CSA change (range: -22.6 to 8.5 cm^2) and 2-year muscle density change (range: -8.6 to 6.4 mg/cc) were observed. A greater WC at baseline was associated with a reduction in CSA (R^2 = 0.14, p<0.05), and a lower weight and WC at baseline were associated with a reduction in muscle density (R^2 = 0.26, p < 0.001 and R^2 = 0.20, p < 0.01, respectively). Conclusion: Muscle CSA and density do not reach a "steady-state" after chronic paralysis. Continued atrophy and fatty-infiltration of skeletal muscle may have adverse implications for bone quality. Rehabilitation or pharmacological interventions able to prevent progressive declines in muscle status may have therapeutic potential for augmenting bone quality. We were able to explain a small proportion of the variability in muscle change; continued investigation to determine the cellular mechanisms responsible for ongoing changes in muscle CSA and density are warranted.

SU0193

Lower Extremity Muscle Size, Density and Function Is Associated with Indices of Bone Quality in Individuals with Chronic Spinal Cord Injury. <u>Jenna Gibbs</u>*[1], <u>Catharine Craven</u>[2], <u>Cameron Moore</u>[3], <u>Lehana Thabane</u>[4], <u>Alexandra Papaioannou</u>[5], <u>Jonathan Adachi</u>[6], <u>Milos Popovic</u>[2], <u>Neil McCartney</u>[7], <u>Lora Giangregorio</u>[1]. [1]University of Waterloo, Canada, [2]University Health Network - Toronto Rehab - Lyndhurst Centre, Canada, [3]University of Waterloo, Canada, [4]McMaster University, Canada, [5]Hamilton Health Sciences, Canada, [6]St. Joseph's Hospital, Canada, [7]Brock University, Canada

Individuals with spinal cord injury (SCI) experience substantial losses in muscle cross-sectional area (CSA), density and function in the lower extremities, which may have significant implications for bone quality several years post-injury. Purpose: To examine the association between muscle CSA, density and function, and indices of bone quality among a sample of adults with chronic SCI. Methods: Baseline data from sixty-five participants (45 men and 20 women) with chronic SCI (C2-T12 ASIA Impairment Scale [AIS] A-D; $\geq$2 years post-injury) in a two-phase prospective, observational study were examined. Calf muscle CSA (adjusted for tibia length, cm^{2}m) and density (mg/cm^3), and indices of bone quality (trabecular bone mineral density (BMD) (mg/cm^3) at the distal tibia (4% tibia length) and cortical thickness (CTh) (mm), cortical CSA (mm^2), cortical BMD (mg/cm^3) and polar moment of inertia (PMI) (mm^4) at the tibial shaft (66% tibia length)) were measured using peripheral quantitative computed tomography. Plantar flexor lower extremity motor scores (pf-LEMS) were used as clinical measures of muscle function. Pearson's correlations and linear regression were performed to determine the strength of the muscle-bone relationships. Results: Participants had a mean age of 49.2 ± 11.9 years and were 15.3 ± 9.8 years post-injury (LEMS: 11.8 ± 16.1; 30.8% LEMS>20). Positive correlations were found between indices of bone quality and muscle CSA (r=0.458-

0.563, p<0.001), muscle density (r=0.245-0.473, p<0.05), and pf-LEMS (r=0.410-0.678, p<0.001). Muscle density was the only muscle variable associated with cortical BMD (r=0.383, p=0.002). When controlling for gender and duration of injury, pf-LEMS had the strongest associations with trabecular BMD (b=7.21 [5.06, 9.37], p<0.001) and CTh (b=0.08 [0.04, 0.13], p<0.001). When controlling for gender, duration of injury, and injury completeness, muscle CSA had the strongest association with PMI (b=744.7 [240.6, 1248.7], p=0.004) and cortical CSA (b=2.53 [0.43, 4.62], p=0.019); whereas, muscle density had the strongest association with cortical BMD (b=1.87 [0.70, 3.05]). Conclusion: Our findings demonstrate that lower extremity muscle CSA is more strongly associated with bone geometry and cortical CSA at the tibial shaft; whereas, muscle density and function are more strongly associated with tibial BMD and structure. Future prospective research is needed to assess the role of muscle atrophy in the manifestation of osteoporosis in SCI.

SU0194

Mechanical Stimulation Induced Musculoskeletal Adaptations Are Responses to Manner of Loading via Oscillatory Electrical Muscle Contraction and Dynamic Hydraulic Flow Stimulation. <u>Minyi Hu</u>*[1], <u>Hoyan Lam</u>[2], <u>Robbin Yeh</u>[2], <u>Morgan Teeratananon</u>[2], <u>Yi-Xian Qin</u>[3]. [1]Stony Brook University, USA, [2]Stony Brook University, USA, [3]State University of New York at Stony Brook, USA

Mechanotransductive signals through fluid flow stimulation, e.g., intramedullary pressure (ImP), have been shown effective in bone adaptation. Muscle compressions may increase vessel pressure gradient that can directly increase ImP. To elucidate the bone-muscle relationship aided by mechanical loading, the aim of this study was to evaluate the effects of oscillatory electrical muscle stimulation (MS) and dynamic hydraulic flow stimulation (DHS) on musculoskeletal adaptation in a rat functional disuse model. For MS, 6-months-old female SD retired breeder rats were divided to groups with n=8: 1) baseline, 2) age-matched, 3) hindlimb suspended (HLS), 4) HLS+1Hz, 5) HLS+20Hz, 6) HLS+50Hz, and 7) HLS+100Hz. For DHS, 5-month-old female SD virgin rats were assigned to 5 groups: 1) baseline (n=15), 2) age-matched (n=12), 3) HLS (n=10), 4) HLS+static (n=10); 5) HLS+DHS (n=14). Stimulations were given to right quadriceps (MS) and tibiae (DHS) of the experimental rats for 10min/day (MS) and 20min/day (DHS), 5 days/week for 4 weeks. Distal metaphysis of the femur (MS) and proximal metaphysis of the tibia (DHS) were scanned for trabecular bone morphology using a microCT. Right quadriceps (MS), soleus and gastrocnemius (DHS) were cross-sectioned and H&E stained. Muscle fiber areas were determined by Image J. HLS significantly reduced trabecular bone quantity and quality. MS at 20Hz and 50Hz led to increases in BV/TV by 143% (p<0.05) and 147% (p<0.01), respectively. Stimulation at 100 Hz showed an 86% increase in BV/TV. Conn.D, Tb.N and Tb.Sp were also significantly affected by MS at 20Hz, 50Hz and 100Hz (Figure 1A). Animals with DHS at 2Hz showed an increase in BV/TV by 83% (p<0.001). Conn.D, Tb.N, and Tb.Sp were also significantly affected by DHS at 2Hz (Figure 1B). HLS led to muscle atrophy and strongly reduced muscle fiber cross-sectional areas compared to age-matched control. Load-induced improvements on muscle fiber growth were observed with MS treatment at 50Hz (Figure 2B), but not with DHS (Figure 2A). DHS provides a relatively passive stimulation on muscle compared to MS, and was insufficient to reduce muscle atrophy. Moreover, as a relatively more active stimulation, MS was only effective at certain optimal loading condition. The current effective DHS loading parameters may be suitable for bone cell responses but not for muscle fiber responses. Further investigations are needed to optimize loading conditions and to determine downstream mechanisms.
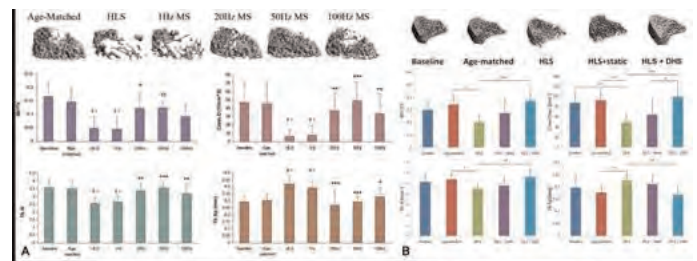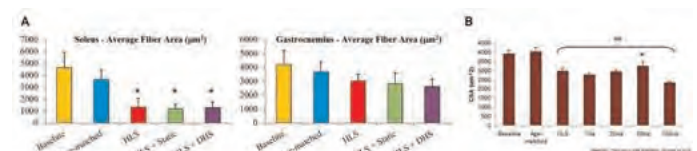

Figure 1

Figure 2

SU0195

Dkk-1 secreted by bone cells prevents mice against osteoarthritis. <u>Thomas Funck-Brentano</u>*[1], <u>Wafa Bouaziz</u>[2], <u>Caroline Marty</u>[1], <u>Valerie Geoffroy</u>[3], <u>Eric Hay</u>[4], <u>Martine Cohen-solal</u>[5]. [1]Inserm U1132, France, [2]INSERM U606, France, [3]INSERM Unit 1132, France, [4]INSERM u1132, France, [5]Hôpital Lariboisière, France

Objective: Characteristics of osteoarthritis (OA) are cartilage loss and subchondral bone changes. The regulation of Wnt pathway is crucial for bone and cartilage metabolism and homeostasis. We have previously shown that the Wnt/β-catenin pathway is activated mainly in bone structures and in articular cartilage in mice with OA. As a crosstalk takes place between bone and cartilage, we here investigated the impact of the inhibition of the Wnt pathway specifically in bone cells during the development of OA.

Methods: OA was triggered in mice by joint instability by induced partial meniscectomy (MNX). We investigated the impact of the inhibition of bone Wnt pathway in mice overexpressing Dkk1 in bone cells (2.3 Col1-Dkk1Tg) at baseline and 6 weeks after MNX. Moreover, we tested the effects of Dkk-1 in chondrocyte metabolism using the supernatant transfer assays and the expression of matrix metalloproteinases.

Results: The Wnt/β-catenin pathway was activated in both bone and cartilage, predominantly in osteocytes of subchondral bone and in osteophytes, and in articular cartilage throughout the development of OA. The number of Dkk1(+) chondrocytes was high at baseline (84.2 $\pm$ 3.1%) and decreased markedly during the course of OA from week 4 (14.4 $\pm$ 3.8%) to week 6 (5.7 $\pm$ 1.6%). At baseline, Dkk1-Tg mice had lower bone volume which was further reduced in MNX knees. Dkk1-Tg experienced a lower OA score than WT mice (5.1 $\pm$ 0.63 vs 8.4 $\pm$ 0.6, p=0.002) independently of the expression of Dkk1 in chondrocytes. This was accompanied by a reduction of the subchondral bone and osteophyte volume. However, addition of rhDkk1 or of supernatant of osteoblasts derived from Dkk-1-Tg mice in chondrocyte cultures promoted the chondrocytic expression of MMP-3, -13 and ADAMTS-4. In contrast, a decreased expression of proteases was observed in the supernatant of pre-exposed osteoblasts with Dkk1. Because Dkk1-Tg osteoblasts produced low VEGF, we tested whether VEGF could mediate the anti-catabolic effect observed in vivo. We found that blocking VEGF in the supernatant of osteoblast cultures reversed the expression of MMPs by chondrocytes.

Conclusion: We here confirm that Wnt is mainly activated in bone of OA joints. Inhibition of Wnt pathway by Dkk1 overexpression in bone decreased the severity of OA by reducing VEGF production. Our data show that targeting bone could be an efficient approach for the treatment of OA.

***Disclosures: Thomas Funck-Brentano**, None.*

SU0196

Early Diagnosis of Osteoarthritis through Detecting Articular Chondrocyte Apoptosis Using a Minimally Invasive Fluorescent Peptide Probe. <u>Xiang-Guo Che</u>*[1], <u>Lian-Hua Chi</u>[1], <u>Gyoung-Ho Cho</u>[1], <u>Na-Rae Park</u>[2], <u>Min-Su Han</u>[1], <u>Clara Park</u>[3], <u>Seung-Hee Han</u>[1], <u>Gyoung-Hwa Kim</u>[1], <u>Byung-Heon Lee</u>[1], <u>Je-Yong Choi</u>[4]. [1]Kyungpook National University, School of Medcine, South Korea, [2]Kyungpook National University School of Medcine, South Korea, [3]Kyungpook National University School of Medicine, South Korea, [4]Kyungpook National University, School of Medicine, South Korea

Early diagnosis of osteoarthritis (OA) at a reversible period of disease progression is essential to prevent further cartilage degeneration and for treatment of OA. However, current methods of OA diagnoses depend on radiography or MRI, which can only detect late-stage OA or is costly for popular use. As apoptosis of articular chondrocytes occurs during the early phase of OA, detection of early chondrocyte apoptosis may allow for the diagnosis of OA within its reversible period. ApoPep-1 is a peptide that binds to apoptotic and necrotic cells and seldom binds to live cells. The receptor for ApoPep-1 is the histone H1.2 that is exposed on the surface of apoptotic cells. Here we test the use of ApoPep-1 to serve as a specific and easily accessible diagnostic tool for early, reversible OA. *In vitro* analyses of ApopPep-1 resulted in its binding to staurosporine-induced apoptotic chondrocytes.For *in vivo* analyses, C57BL/6 mice (n=6/group) received sham or destabilization of the medial meniscus surgery. In the latter mice, OA is considered to be reversible between 1 and 4 weeks post-surgery based on the OARSI criteria. Mice were injected a Cy7.5-labeled ApoPep-1 probe or control substance intravenously at 1, 2, 4, and 8 weeks after surgery. In vivo imaging was performed at 0.5, 2, 4, 8, 12, 24 hours post injection. Higher levels of ApoPep-1 signals were detected in the knees of OA mice as early as 2 weeks post surgery and intensified with OA progression. Signals were detectable in OA mice from 30 minutes post-injection, and disappeared within 12 hours of injection. No signals in the kidney or liver were detected by 12 hours after injection, indicating the rapid removal of ApoPep-1 from the body. TUNEL and immuno-fluorescence staining at 4 weeks post-surgery revealed that ApoPep-1 signals were strongly correlated with degenerative cartilage areas and reduced type II collagen, and were co-localized with MMP13, a marker of cartilage degradation. These results suggest that the ApoPep-1 probe binds to apoptotic chondrocytes even at early stages of OA, which indicate that ApoPep-1 may be used as a novel imaging probe to detect OA at its reversible state.
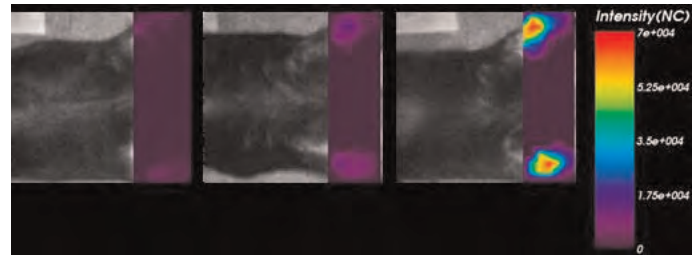

Figure. Early osteoarthritis (OA) is detected in mice 2 weeks after OA surgery by the ApoPep-1 probe

***Disclosures: Xiang-Guo Che**, None.*

SU0197

Estrogen status in experimental osteoarthritis determines extent of chondrocyte apoptosis following injury. <u>Paul Fanning</u>*[1], <u>Linda Xie</u>[2], <u>Christopher Raskett</u>[2], <u>David Ayers</u>[3]. [1]University of Massachusetts Medical School, USA, [2]UMass Medical School, USA, [3]UMass Memorial Medical Center, USA

Small animal models of osteoarthritis (OA) have shown that female mice develop less OA than males, and that ovariectomized (OVX) female mice develop worse OA than female mice with intact ovaries. One hypothesis is that estrogen (E2) may be a chondro-protective molecule. We have tested this hypothesis by surgical induction of OA in female mice and quantified articular chondrocyte apoptosis using the TUNEL methodology. The following experimental conditions were combined with surgical induction of OA (destabilization of the medial meniscus; DMM) and ovariectomy surgery (OVX) or sham-OVX and/or 17beta-estradiol 3- benzoate (E2) injections as follows: 1) OVX was performed on female mice 2 weeks prior to the DMM surgery (n=7). 2) OVX were performed on mice 2 weeks prior to DMM and treated with E2 injections (s.c.) of 1.92mg/kg every 4 days following OVX (n=7). 3) The control group consisted of sham-OVX performed 2 weeks prior to DMM (n=7). All mice were sacrificed at 4 days after DMM surgery. Results showed that female mice with intact ovaries developed significantly less apoptosis (TUNEL positive cells) than OVX-DMM females (34% reduction; p<0.01). There were significantly less total apoptotic cells in the superficial-middle zone as well as less apoptotic cells in a clearly defined lesion area within the superficial-middle zone. Additionally, mice with intact ovaries developed smaller cross sectional OA lesion areas (48% reduction; p<0.01), as well as smaller width (36% reduction; p<0.01) and height (24% reduction; p<0.01) of the lesion margins compared to OVX-DMM mice. There was significantly less apoptosis (31% reduction; p<0.01) in OVX-DMM mice with E2 injection as compared to OVX-DMM mice without E2 injection. There was no significant difference in apoptosis between the intact ovaries group and OVX-DMM + E2 treatment group. E2 treatment did have a modest but significant reduction in lesion width (9% reduction; p<0.05). These results indicate that estrogen presence results in significantly less numbers of apoptotic chondrocytes following DMM compared to OVX-DMM mice. These data suggest that estrogen may have direct anti-apoptotic effects after an induction of injury to the joint. We also propose that since early estrogen intervention in OVX-DMM mice can reduce apoptosis in OA mice, more acute anti-apoptotic based medical interventions following knee injury can be made that may alter the progression of later OA stages.

***Disclosures: Paul Fanning**, None.*

SU0198

Subchondral Bone Health is Compromised in Post-Traumatic Osteoarthritis. <u>Brett Tonkin</u>[1], <u>Natasha Jansz</u>[2], <u>Evange Romas</u>[3], <u>Natalie Sims</u>[4], <u>Nicole Walsh</u>*[5]. [1]St Vincent's Institute of Medical Research, Australia, [2]St Vincent's Institute of Medical Research, Australia, [3]St. Vincent's Hospital Melbourne, Australia, [4]St. Vincent's Institute of Medical Research, Australia, [5]St Vincent's Institute of Medical Research, Australia

Purpose: The destabilisation of the medial meniscus (DMM) mouse osteoarthritis (OA) model is a commonly used model of post-traumatic OA. We sought to determine how DMM-induced joint injury impacts tibial subchondral bone, and how this relates to onset and progression of articular cartilage damage.

Methods: 12-week old male C57BL/6 mice underwent DMM or sham surgery on the right knee; left knees served as contra-lateral controls. In vivo micro-CT was performed prior to surgery and at 4, 8, and 12 weeks post-surgery. Bone volumes were quantified using novel a method optimized to assess bone of varying mineralization states. Limbs from separate groups of mice were also collected for OARSI histologic assessment.

Results: Pre-surgery bone volume/tissue volumes (BV/TV) were similar in all limbs. Consistent with increased loading, a focal increase in medial subchondral bone BV/TV was observed in DMM-OA tibiae compared to sham from 4 weeks post-surgery. BV/TV in the lateral subchondral bone and tibial metaphyseal trabecular bone were similar in all limbs, indicating no systemic effect of DMM-OA on bone structure.

However, medial subchondral BV/TV of DMM-OA tibiae and contra-lateral tibiae were similar, suggesting an influence of altered gait on the contralateral limb. Aggrecan loss and cartilage erosion was evident in the medial compartment of DMM-OA tibiae from 4 weeks post-surgery. Interestingly, the medial subchondral bone in DMM-OA tibiae from 4 weeks post surgery was not healthy: it resembled osteonecrotic bone with many empty osteocyte lacunae present. Furthermore, the number of empty osteocyte lacunae at this site, negatively correlated with the width of overlying aggrecan-positive (healthy) cartilage suggesting a relationship between aggrecan loss and subchondral bone health in DMM-OA.

Conclusions: Focal accrual of medial subchondral bone occurs early in DMM-OA tibiae alongside cartilage damage. Similar to human OA, osteocyte cell death in subchondral bone is a feature of DMM-OA and may be in part a result of mechanical changes or biochemical signals induced by aggrecan loss in articular cartilage. This osteocyte cell death could also contribute to local changes in bone integrity, vascularization or cartilage. Finally altered bone structure in the contra-lateral tibiae of DMM-OA mice, suggests that increased subchondral bone per se does not affect overlying cartilage, and serves to highlight the need to include sham-operated mice when using this model.

Disclosures: Nicole Walsh, None.

SU0199

A High Resolution Musculoskeletal Gene Expression Atlas for Characterizing Bone and Cartilage Diseases. Eric Lewallen*[1], Scott Riester[2], Carolina Bonin[1], Amel Dudakovic[1], Emily Camilleri[2], Noelle Larson[2], Aaron Krych[2], Jay Smith[2], Sanjeev Kakar[2], Jennifer Westendorf[1], Hee-Jeong Im Sampen[3], Andre Van Wijnen[1]. [1]Mayo Clinic, USA, [2]Mayo Clinic, USA, [3]Rush University Medical Center, USA

Novel high-throughput molecular techniques have the potential to enhance our understanding of the mechanisms underlying tissue differentiation and musculoskeletal disease. The purpose of this investigation is to characterize variation within and among different types of musculoskeletal tissues, including both normal and diseased states. With this information, novel biomarkers can be identified and used directly for tissue engineering and molecular therapeutic applications. In this investigation, RNA sequencing was performed on 118 primary musculoskeletal tissues including bone, cartilage, muscle, ligament, and tendon. Multiple disease states, including but not limited to diabetes, degenerative rotator cuff, osteoporosis and osteoarthritis are represented. Molecular findings based on RNA-seq data were correlated with clinical grades of diseased osteoarthritic cartilage. Cartilage specimens were graded using a modified 5-point scale of Collins. Grade 0 tissues were considered normal non-arthritic tissues, while grades 1 through 4 reflected increasing levels of degeneration. Normal and diseased cartilage tissues were prepared using a novel zero-gravity digestion method. RNAseq profiles for each grade of osteoarthritis were subjected to a series of quality control and data filtering measures to reduce the potential impact of any sampling artifacts. Both uni- and multi-variate statistical approaches (ANOVA, Bayesian Inference, hierarchical clustering, and PCA), assisted by recent and versatile software packages (PVClust, EdgeR, DESeq, BaySeq, Bioconductor, and Partek) were used to resolve gene expression differences between grades of osteoarthritis. Our data confirms the known validity of osteoarthritic biomarkers, and identifies novel therapeutic targets for the treatment of osteoarthritis. These techniques can be applied to the identification of novel therapeutic targets for the treatment of other musculoskeletal disease states beyond osteoarthritis. High-throughput RNA-seq has important implications for the fields of tissue engineering and therapeutic drug discovery because of the ability to rapidly conduct comprehensive assessments of the molecular mechanisms that define tissue-specific phenotypes.

Disclosures: Eric Lewallen, None.

SU0200

Elevated Mean Arterial Pressure Is Associated With Higher Rate of Subchondral Bone Turnover in Patients With Knee Osteoarthritis. Yan Chen*[1], Min Guan[2], Frankie Leung[3], Xu Cao[4], Xiaohua Pan[5], William Lu[6]. [1]The University of Hong Kong, Hong Kong, [2]Center for Human Tissues & Organs Degeneration, Shenzhen Institutes of Advanced Technology, CAS, China., China, [3]Department of Orthopaedics & Traumatology, Faculty of Medicine, the University of Hong Kong, Hong Kong; China, China, [4]Johns Hopkins University, USA, [5]Department of Joint Surgery, Shenzhen People's Hospital, Jinan University Second College of Medicine, China., China, [6]The University of Hong Kong, Hong Kong

Purpose: Epidemiologic data showed that frequency of OA is much higher (40%) in hypertensive patients than in non-hypertensive individuals (25%). We previously demonstrated that hypertensive patients displayed bone loss at subchondral plate, indicated possible association between blood pressure and subchondral bone turnover. Furthermore, our animal study found that elevated level of TGF-ß1 signaling in subchondral bone induced higher rate of subchondral bone turnover and OA progression. However, the pathological relationship between hypertension and OA is still not clear. Therefore, this study investigated the association between mean arterial pressure (MAP) and subchondral bone turnover in knee OA patients.

Methods: Seventy patients undergoing total knee arthroplasty (TKA) for primary OA were recruited and divided into two groups according to their MAP: normal (n=33) and elevated (n=37). The tibial plateaus removed during TKA were collected and evaluated using micro-CT, histology and immunohistochemistry. Patients' clinical data were also collected and analyzed.

Results: No significant differences were detected in patients' age, gender, BMI, etc. between OA patients with normal or elevated MAP (table 1). Patients with elevated MAP presented lower bone volume fraction(BV/TV) and trabecular number(Tb.N) while higher structure model index(SMI) of medial subchondral bone than normal MAP group. However, the results were reverse on lateral side. (Fig.1 & table 2). Histology showed more obvious formation of new bone and osteoid islets in subchondral bone marrow in elevated MAP group(Fig.3). Compared with normal MAP group, elevated MAP group showed higher number of TRAP+ osteoclasts on the medial side. However, the numbers of TRAP+ osteoclasts showed no significant difference on lateral side between the two groups (Fig.4). Immunohistochemistry revealed that the number of pSMAD2/3+, Osterix+ and Osteocalcin+ cells were significantly lower in medial subchondral bone in elevated MAP group than normal MAP group. Nevertheless the inverse results were observed on lateral side.

Conclusions: Our data show that elevated MAP is associated with higher rate of subchondral bone turnover in patients with advanced knee OA. Moreover, uneven local distribution of osteoprogenitors in subchondral bone marrow mediated by TGF-ß1 signaling may be involved in this pathogenesis. These findings provide a possible mechanism by which hypertension may correlate with OA progression.

Table 1. Demographic, radiological and clinical data of OA patients with normal or elevated MAP

Parameters		OA patients with normal MAP (n=33)	OA patients with elevated MAP (n=37)	P
MAP (70-110 mm Hg)		101±7	119±6	0.000
Gender (Female/Male, Female %)[a]		27/6, 81.8	30/7, 81.1	0.564
Age (year)		73±8	70±9	0.291
Body Weight (kg)		63±9.4	64.9±12.5	0.516
Body Height (mm)		151.7±6.2	149.6±7	0.292
Body Mass Index (kg/m^2)		27.5±4.2	28.6±4.8	0.406
Sanding X-ray	Alignment of lower limb (degrees)	166.8±8.9	169.3±12.6	0.412
	Kellgren-Lawrence grade (grade 4/grade 3, grade 4 %)[a]	14/19, 42.4	20/17, 54.1	0.331
Knee Society Knee Score	Pain (0-50)[b]	25(22,28)	22(19,25)	0.175
	Passive range of motion (PROM) (0-25)[b]	19(18,21)	19(17,20)	0.754
	Stability (0-25)	23(21,25)	23(22,24)	0.191
	Fixed flexion contracture (FFC) (-15-0)[b]	-2(-4,-1)	-3(-5,-2)	0.45
	Extension lag (-15-0)[b]	-1(-1,0)	0(-1,0)	0.327
	Alignment (-20-0)[b]	-15(-18,-12)	-17(-20,-13)	0.453
	Sum[b]	50(43,56)	43(36,49)	0.221
Knee Society Functional Assessment	Walking (0-50)[b]	22(20,25)	21(17,24)	0.665
	Stairs (0-50)[b]	28(25,32)	22(17,27)	0.058
	Aids (-20-0)[b]	-4(-5,-3)	-7(-9,-4)	0.277
	Sum[b]	46(42,51)	36(26,45)	0.613

Table 1
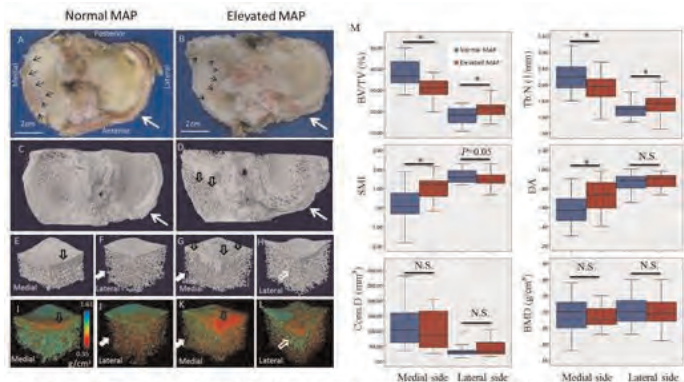
Fig. 1 Micro-CT images of tibial plateau from OA patients with normal or elevated MAP. **BV/TV**=bone volume/tissue volume; **SMI**=structure model index; **BMD**=bone mineral density; **Tb.N**=trabecular number; **Conn.D**=connectivity density; **MAP**= mean arterial blood pressure. **N.S.**= no significant difference.

Figure 1

Table 2 Linear regression analyses of the association of MAP with BV/TV, Tb.N and SMI of tibial subchondral trabecular bone from OA patients

Dependent variables	Unadjusted						Adjusted by age, gender and BMI						Adjusted by age, gender, BMI and alignment*					
	Unstandardized Coefficients	Standardized Coefficients		95% CI for B			Unstandardized Coefficients	Standardized Coefficients		95% CI for B			Unstandardized Coefficients	Standardized Coefficients		95% CI for B		
	B	Beta	P	Lower Bound	Upper Bound		B	Beta	P	Lower Bound	Upper Bound		B	Beta	P	Lower Bound	Upper Bound	
Medial BV/TV (%)	-6.261	-.453	.005	-10.488	-2.035		-6.945	-.379	.03	-13.17	-.72		-7.519	-.580	.000	-11.452	-3.586	
Lateral BV/TV (%)	3.487	.400	.004	1.194	5.780		2.701	.316	.042	0.108	5.295		2.855	.342	.023	.411	5.299	
Medial Tb.N (1/mm)	-0.369	-.389	.013	-0.655	-0.082		-.378	-.381	.026	-0.709	-.05		-0.411	-.416	.013	-.730	-.093	
Lateral Tb.N (1/mm)	0.184	.315	.020	0.030	0.338		.194	.34	.024	0.027	0.36		0.222	.383	.009	.059	.385	
Medial SMI	0.872	.488	.001	0.360	1.383		.942	.525	.003	0.338	1.546		0.989	.545	.003	.357	1.621	
Lateral SMI	-0.193	-.270	.050	-0.387	0.000		-.228	-.311	.049	-0.455	-0.001		-0.220	-.298	.071	-.460	.020	

BV/TV=bone volume/tissue volume; Tb.N=trabecular number; SMI=structure model index; MAP=mean arterial pressure. 95% CI =95% confidence interval. *Alignment= alignment angle of the lower extremity on standing X-ray

Table 2

Fig. 2 Histological images of OA patients with normal or elevated MAP.

SP= subchondral plate;
AC= articular cartilage;
⇨ =newly formed bone;
⬇ =osteoid-like tissue;
➤ =fiber tissue;
* =p<0.05

Figure 2

Fig. 3 Activities of TRAP⁺ osteoclasts in subchondral bone of OA patients with normal or elevated MAP

SB =Subchondral bone;
BM=Bone marrow;
⬅ = TRAP⁺ multiple nuclear osteoclasts;
➤ =Fracture of trabecular;
* = p<0.05
N.S.=no significant difference

Figure 3

SU0201

Individuals with Primary Osteoarthritis Have Different Musculoskeletal Phenotypes Depending on Affected Joint. Magnus Karlsson*[1], Caroline Karlsson[2], Håkan Magnusson[3], Maria Cöster[4], Jan-Åke Nilsson[3], Bjorn Rosengren[1]. [1]Skåne University Hospital Malmö, Lund University, Sweden, [2]Department of Clinical Sceinces, Lund University, SUS, Sweden, [3]Department of Orthopedics & Clinical Sciences, Lund University, SUS, Sweden, [4]Department of Orthoepdics & Clinical Sciences, Lund University, SUS, Sweden

Purpose: Primary osteoarthritis (OA) in the hip in associated with high BMD and obesity. It has then been postulated that the obesity will confer a high joint surface load and the high BMD a stiff skeleton that transfer an abnormal proportion of the mechanical load to the cartilage. If the same phenotype applies to patients with OA in all joints and if the obesity is the result of high fat or high lean mass is unclear. We therefore evaluate if primary OA, independent on affected joint, is associated with same abnormal musculoskeletal phenotype as in patients with hip OA.

Method: We included 30 women and 32 men (mean age, 66 years; range, 42–84) with primary hip OA, 38 women and 74 men (mean age 61 years; range 34–85) with primary knee OA, 42 women and 19 men (men age 64 years, range 42–87) with primary ankle or foot OA, 20 women and 19 men (mean age 66 years, range 47-88) with primary hand or finger OA and 122 women and 118 men as controls. We measured total body BMD (g/cm^2) and proportion fat and lean mass (%) with DXA and height, weight and BMI (kg/m^2) by standard equipment.

Results: Individuals with hand OA and controls had similar phenotype in respect of BMD, weight, height, BMI, fat and lean body mass. Individuals with OA in hip, knee and ankle/foot joint had all similar weight, BMI and BMD, but these values were significantly higher than in individuals with hand/finger OA and controls (all p<0.05). Individuals with OA in hip, knee and ankle/foot had also higher fat mass and lower lean mass than individuals with hand OA and controls (all p<0.001).

Conclusions: A higher BMD may lead to stiffer bone, a higher BMI to a greater joint load and a lower lean body (muscle) mass to lower joint-protective capacity, all conditions predisposing for OA in the lower extremity. There seem to be different pathophysiological pathways for primary OA in the upper and lower extremity.

SU0202

Osteoclast Regulatory Factors in Human Osteoarthritic Chondrocytes. Julie Glowacki*[1], Shuanhu Zhou[1], Thomas Thonhill[2]. [1]Brigham & Women's Hospital, USA, [2]Brigham & Women's Hospital, USA

Articular chondrocytes have capacity for anabolic and catabolic activities. Osteoarthritis (OA) is associated with increases in lytic proteinases, aggrecanases, and cytokines. We used tissue discarded during arthroplasty to partition zones of cartilage by disease severity/Grade and to identify the molecular signature of human cartilage representing OA progression.

With IRB approval, discarded tissue was obtained during knee replacement. Zones with sufficient homogeneity were ranked and partitioned according to the Outerbridge classification from Grade 0 (normal-appearing) to Grade 3 (significant fragmentation/ fissuring). Chondrocytes were isolated by sequential digestions with 0.1% hyaluronidase, 0.25% trypsin, and 0.3% collagenase. The influence of OA grade on constitutive gene expression was tested with RT-PCR and was compared with the *in vitro* effect of Interleukin (IL)-1b in normal human chondrocytes.

Clinical grade was correlated with histological score, p=0.043. Expression analysis showed expected and unexpected Grade-dependent differences. Genes encoding lytic enzymes [Adamts-5, cathepsin K (catK), and matrix metalloproteinases (MMP-8, MMP-13)] showed low/no expression in Grade 0 and upregulation in advanced Grades. There was Grade-associated upregulation of TNF-a, IL-1b, -6, and -11, and TNF receptors RI and RII. Finding CatK, a known marker of typical osteo/ chondroclasts, in OA cartilage stimulated our analysis for tartrate-resistant acid phosphatase (TRAP) and for regulators of osteoclastogenesis, including Receptor Activator of Nuclear factor-kB (RANK), Receptor Activator of Nuclear factor kB Ligand (RANKL), and osteoprotegerin (OPG). There was no or low expression of TRAP, RANK, and RANKL in Grade 0 chondrocytes, but all three were dramatically upregulated in advanced Grades. OPG was expressed similarly for all Grades. Brief treatment (24 h) of normal human chondrocytes with IL-1β upregulated RANK, RANKL, CatK and the expected lytic enzymes. These *in vitro* data support the conclusion that osteoclastogenic regulatory factors play a cell-autonomous role in cartilage pathology. In sum, these studies identified differences in constitutive gene expression in human chondrocytes based upon regional OA disease severity. Beside the expected upregulation of lytic enzymes and mediators/receptors, we found OA Grade-dependent induction of RANK, RANKL, CatK, and TRAP, proteins that are involved in typical osteoclast differentiation and function.
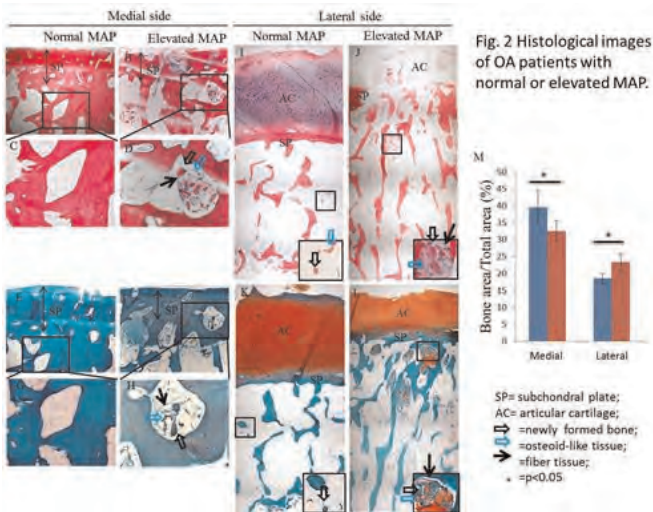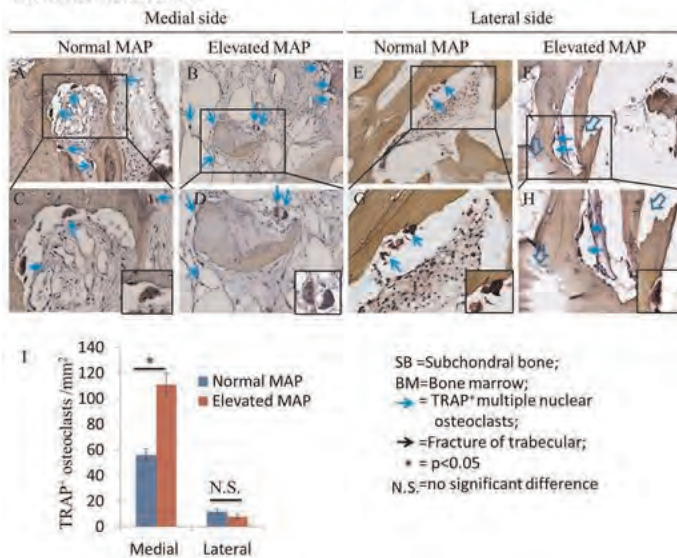
SU0203

Subchondral Bone Underlying Degenerated versus Normal Cartilage Has Greater Bone Mineral Density but No Difference in Structural Stiffness.

James Johnston*[1], Saija Kontulainen[1], Tuhina Neogi[2], Bassam Masri[3], David Wilson[3]. [1]University of Saskatchewan, Canada, [2]Boston University, USA, [3]University of British Columbia, Canada

Introduction: Thickening of subchondral bone as a part of the osteoarthritis (OA) disease process has been proposed to increase bone's overall structural stiffness, leading to higher internal cartilage stresses, and eventual cartilage breakdown. However, the proposed role of bone stiffness in OA has been primarily based upon isolated analyses of excised tissues samples (e.g., subchondral cortical or trabecular bone), typically after complete cartilage erosion. It is unclear if altered subchondral bone properties are associated with a) overlying cartilage degeneration prior to complete cartilage erosion, or b) overall structural stiffness—a measure most closely reflecting bone's response to cartilage loading. The purpose of this study was to compare regional proximal tibial bone mineral density and structural stiffness at subchondral bone sites underlying normal and degenerated cartilage. Methods: Thirteen proximal tibia compartments (4 medial, 9 lateral) from 10 male donors (age: 73+/-11 years) were scanned using Quantitative CT. Cartilage was intact with both normal (International Cartilage Repair Society (ICRS) grades 0-1) and degenerated regions (ICRS 2-3). After removing cartilage, indentation stiffness testing was performed directly at the subchondral surface (3.5mm diameter flat indentor, 3-6 sites per compartment, 51 sites in total). Each site was characterized as having minimal cartilage degeneration (ICRS 0-1, n=26) or moderate degeneration (ICRS 2-3, n=25). At each site, average subchondral bone density within a 3.5mm diameter region of interest was assessed at depths of 0-2.5, 2.5-5, and 5-10mm from the subchondral surface. Multivariate analysis of variance with Bonferroni adjustment was used to compare subchondral bone density and structural stiffness between normal and degenerated sites. Results: Density across the 0-2.5mm depth did not differ between sites (95% CI: -29 to 101 mg/cm3; p=0.27). In degenerated sites, density was 25% higher across the 2.5-5mm depth (+59 mg/cm3; 95% CI: 11-107 mg/cm3; p=0.018) and 34% higher across the 5-10mm depth (+39 mg/cm3; 95% CI: 5-72 mg/cm3; p=0.026). Structural stiffness did not differ between sites (95% CI: -132 to 1070 N/mm, p=0.12). Conclusion: Subchondral bone underlying degenerated versus normal cartilage had greater bone density at depths beyond 2.5mm from bone surface. No structural stiffness differences were observed; though, a larger sample size is likely needed to account for high mechanical testing variability.

Disclosures: James Johnston, None.

SU0204

TBRII/IL36α Axis is Involved in the Osteoarthritic Process in Mice and Humans.

Tieshi Li*[1], Joseph D. Temple[2], Lara Longobardi[1], Susan Chubinskaya[3], Helen Willcockson[4], Timothy Myers[4], Ping Ye[1], Billie Moats-Staats[5], Alessandra Esposito[6], Arnavaz A Hakimiyan[3], Daniel J. Del Gaizo[6], Christopher W. Olcott[6], Anna Spagnoli[1]. [1]University of North Carolina at Chapel Hill, USA, [2]University of North Carolina-North Carolina State University Joint Department of Biomedical Engineering, USA, [3]GME, Graduate College, Rush Medical College, USA, [4]University of North Carolina, USA, [5]University of North Carolina- Chapel Hill, USA, [6]University of North Carolina at Chapel Hill, USA

The interplay between TGF-beta type II receptor (TBRII) signaling and cytokines in osteoarthritis (OA) is complex. We have reported that the conditional inactivation of TBRII signaling in embryonic mesenchyme limb progenitors (TBRIIPrx1KO) leads to failure of joint development and its inducible postnatal inactivation (TBRII-ER-Prx1KO) to progressive OA that was associated with an increase of IL36α. To determine the interplay between TBRII and IL36α signaling in OA, we have performed intra-articular injections of IL36α or IL36Ra (receptor antagonist) in TBRII mutants and control mice starting at postnatal age 3 months (P3M). In TBRII mutants, sacrificed at P4M and P6M, injection of IL36Ra halted the loss of Safranin O staining and also the increase of Collagen10 and Mmp13 expressions. By contrast, injection of IL36α exacerbated the OA development in TBRII mutants. To determine if the TβRII/ IL36α axiswas also involved in human cartilage degeneration, histological sections of full-thickness articular cartilage from knee joints obtained from human tissue donors (Collins grade 0-1 defined as normal and grade 2-4 as asymptomatic degenerative) and from subjects with end-stage OA undergoing total joint replacement surgery were subjected to IL36α, IL36R and TBRII immunohistochemistry and Safranin O staining analyses. Our results revealed a consistent increase of IL36α expression within the degenerative lesions (from grade 0 to 3) that was associated with a parallel decrease of TBRII expression. Results were confirmed by RT-PCR analyses of isolated RNA from shaved cartilage from human tissue donors. In severely damaged articular cartilage of subjects with end-stage OA, we found high expression of IL36α in the cell clusters which is a histological hall mark of arthritic cartilage but low expression in deep-zone chondrocytes. Our studies provide a novel perspective for the prevention and treatment of cartilage degeneration by manipulating the TBRII/IL36α axis.

Disclosures: Tieshi Li, None.

SU0205

The development of articular cartilage thickness, impeded by obesity in high weight bearing regions, is protected by daily exposure to low intensity vibration.

Tee Pamon*[1], M. Ete Chan[1], Vincent Bhandal[2], Clinton Rubin[3]. [1]Stony Brook University, USA, [2]Stony Brook University, USA, [3]State University of New York at Stony Brook, USA

Obesity is a risk factor for osteoarthritis (OA), a degenerative joint disease characterized by the thinning of articular cartilage (AC), abnormal subchondral bone (SB) remodeling, joint pain, and reduced mobility. Considering that obesity has been associated with the suppression of bone formation, it is possible that cartilage formation is also impeded, contributing to relatively thin AC. Recent evidence has shown that low intensity vibration (LIV) protects mesenchymal stem cell (MSC) lineage selection towards the formation of higher order connective tissues such as bone—we sought to determine if LIV could enable the formation of AC despite the obese phenotype. C57BL/6 male, 5w mice were separated into 3 groups (n=9): Regular diet (RD), High fat diet (HF), and High fat diet + LIV (HFv). Part I of the protocol consisted of 2w of high fat diet for HF and HFv. In part II, HFv were also subject to LIV for 6w (90Hz, 0.2g, 30 m/d, 5 d/w). At end of protocol, the R tibial condyles were extracted, and the AC and SB were scanned using contrast agent enhanced μCT. The medial condyle was separated into 2 equal areas: the high-weight bearing region (HWB), adjacent to the midline of the plateau, and the lower weight bearing region (LWB), towards the joint periphery. Bone marrow from the R hindlimb was flushed and FACS used to quantify MSC number. After 8w of high fat diet, HF & HFv were 17.2% heavier than RD (p=0.006). AC thickness of the HWB of HF mice was 28.2% below RD (p=0.02). LIV had a protective effect on AC in this region, as evidenced by a 26.7% thicker AC compared to HF (p=0.13). While there was nsd between RD and HF mice in AC thickness of the LWB, LIV resulted in a 50% increase in AC thickness compared to HF (p=0.002). Despite increases in AC thickness, LIV did not compromise SB mineralization or thickness. Within the bone marrow, LIV increased MSCs by 14.2% compared to HF (p=0.16), and 17.7% compared to RD mice (p=0.03). Given that MSCs have the ability to differentiate into chondrocytes, the increase in MSCs in the HFv group could contribute increased cartilage thickness. Since the HF and HFv groups did not differ in weight, these results suggest that the OA associated with obesity may be, to an extent, the result of suppressed cartilage formation rather than excessive joint loading. The protective effect of LIV appears to be the restoration of cartilage development, due to elevated chondrocyte activity or increased MSC differentiation to chondrocytes.
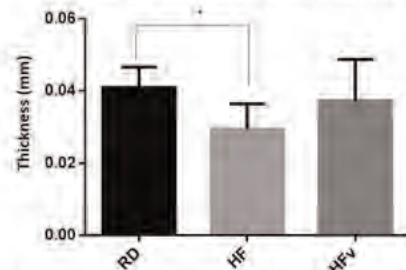

Fig 1: Articular cartilage thickness is reduced in HF with a trend towards recovery in the LIV treatment group. *p<0.05 compared to RD. Mean ± SD shown.
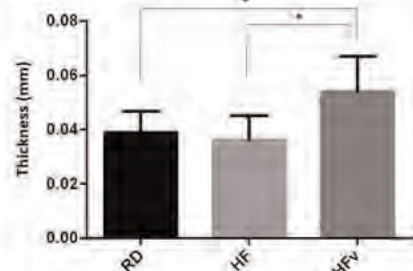
Figure 1

Fig 2: Articular cartilage thickness is increased in the LIV treatment group. *p<0.05, Mean ± SD shown.

Figure 2

Disclosures: Tee Pamon, None.

SU0206

Cortical Expansion in Connexin43 (Cx43) Deficient Bones: Potential Role of Reduced *Sost* Expression. Susan Grimston*, Marcus Watkins, Roberto Civitelli. Washington University in St. Louis School of Medicine, USA

We and others have shown decreased *Sost* expression in mice with a conditional deletion of the connexin43 (Cx43) gene (*Gja1*) specifically in osteogenic lineage cells (cKO). Similar to germline *Sost* deletion (*Sost*^{-/-}), *Gja1* cKO bones exhibit cortical expansion secondary to accentuated periosteal bone formation. Unlike *Sost*^{-/-} mice, marrow area of *Gja1* cKO is expanded rather than reduced, the consequence of increased endocortical osteoclast activity. To explore whether *Sost* down-regulation and Wnt signaling activation may in part explain periosteal expansion in *Gja1* deficient bone, we tested a genetic interaction between *Gja1* and *Sost*. We generated double *Gja1*^{+/-};*Sost*^{+/-} heterozygotes (double Hets), and compared their cortical structure and strength to *Gja1* and *Sost* heterozygous mice, which are phenotypically normal. In vivo microCT studies at 3 months demonstrated a trend towards increased Tissue Area in the double Hets, although not as evident as in the *Sost*^{-/-}. Marrow Area was similar among all groups and Cortical thickness (Ct.Th) was significantly larger in *Sost*^{-/-}. Nonetheless, Polar Moment of Inertia (pMOI) a geometric index of bone strength, in the double Hets tended to increase implying a changed cortical geometry compared with other genotypes. pMOI was significantly higher in *Sost*^{-/-}. Ultimate Force (index of bone strength) by 3-point bending was not significantly changed in the double Hets relative to single Hets, whereas it was 40% higher in *Sost*^{-/-} bones, as expected. While the modestly expanded Tt.Ar and pMOI in the double Hets would be consistent with a genetic interaction between *Gja1* and *Sost*, the contribution of decreased sclerostin in the mechanism leading to cortical expansion in *Gja1* deficient bones would be modest, based on these data.

Variable	*Gja1*^{+/-};*Sost*^{+/+}	*Gja1*^{+/+};*Sost*^{+/-}	*Gja1*^{+/-};*Sost*^{+/-}	*Gja1*^{+/-};*Sost*^{+/-}	*Sost*^{-/-}
Marrow Area (mm²)	0.68±0.06	0.71±0.07	0.69±0.08	0.72±0.05	0.69±0.06
Tissue Area (mm²)	1.45±0.05	1.46±0.01	1.42±0.01	1.54±0.14	1.64±0.13*
Ct. Th (cm)	0.15±0.01	0.15±0.01	0.14±0.02	0.16±0.02	0.21±0.02*
pMOI (mm⁴)	0.33±0.03	0.32±0.05	0.29±0.05	0.35±0.08	0.39±0.07*
Ultimate Force (N)	13.27±1.68	13.18±3.52	14.07±3.05	15.48±4.69	20.68±2.36*

p<0.05 versus all genotypes

Table

Disclosures: Susan Grimston, None.

SU0207

Sphingomyelin Synthase 2 Promotes Osteoclast Differentiation by Enhancing retinoid X receptor a Expression. Yoshihiro Yoshikawa*[1], Eisuke Domae[2], Seiji Goda[2], Isao Tamura[2], Aiko Kamada[1], Takashi Ikeo[3]. [1]Osaka Dental University, Japan, [2]Osaka Dental University, Japan, [3]Osaka Dental University, Japan

For treatment with implants, long-term survival and rapid recovery of the socket bone are necessary, and determining the mechanism of alveolar bone regeneration is important. 1,25-dihydroxyvitamin D_3 (1,25(OH)$_2$D$_3$) plays a central role in bone regeneration. A deficiency in this compound has profound negative effects on implant osseointegration and stimulates osteoclastogenesis through osteoblasts. In addition, several studies have reported that 1,25(OH)$_2$D$_3$ induces turnover of sphingomyelin, which plays vital roles in stabilizing the membrane structure and in cell-cell recognition. However, whether sphingomyelin is involved in osteoclast differentiation is unclear.

To examine the effects of sphingomyelin on osteoclast differentiation, we cocultured bone marrow cells isolated from mouse tibia and sphingomyelin synthase 2 (SMS2) siRNA-transfected primary osteoblasts (POB) isolated from calvaria of newborn mice and performed tartrate-resistant acid phosphatase (TRAP) staining. We evaluated expression of genes with real-time PCR and proteins with western blotting in the presence of 10^{-8} M 1,25(OH)$_2$D$_3$ in POB transfected with SMS2 siRNA.

Formation of TRAP-positive multinucleated osteoclasts was significantly suppressed by SMS2 siRNA. In addition, mRNA expression of the Vitamin D receptor (VDR) target gene receptor activator of nuclear factor-κB ligand (RANKL) was significantly suppressed by SMS2 siRNA in POB in the presence of 1,25(OH)$_2$D$_3$.- Next, we examined whether SMS2 affected nuclear translocation of VDR and retinoid X receptor a (RXRa), which play a profound role in VDR genomic signaling. SMS2 siRNA did not affect VDR expression but reduced RXRa expression in POB.

We suggest that SMS2 is important for osteoclast differentiation by regulating RANKL expression via RXRa.

Disclosures: Yoshihiro Yoshikawa, None.

SU0208

Biomechanical Analysis of Fibronectin Fibril Assembly Dynamics in Living Osteoblasts. Bhargav Javvaji*[1], Sarah Dallas[2], Ganesh Thiagarajan[2]. [1]University of Missouri Kansas City, USA, [2]University of Missouri - Kansas City, USA

Fibronectin (FN) is an extracellular matrix (ECM) protein expressed in bone and connective tissues. We have shown that FN regulates osteoblast differentiation and controls assembly of multiple bone ECM proteins. Therefore, understanding its mechanism of assembly is key to understanding how bone matrix is formed. To gain new insight into the kinetics of FN assembly, we have used time lapse imaging of FN assembly in living osteoblasts. This was combined with biomechanical analysis to determine the strains experienced by FN fibrils during assembly and maturation of the matrix and to quantify their motions.

FN assembly was imaged in 2T3 osteoblasts over 48hr by time lapse imaging using an alexa555 labeled FN probe, which enabled imaging from a baseline of no FN fibrils to formation of a well organized fibril network. FN assembly was highly dynamic and was associated with extensive cell motion, which subjected FN fibrils to tensile and compressive forces. 6 independent movie fields were analyzed using a previously validated cross correlation based Digital Image Correlation algorithm developed in Matlab. The 0-12h movie segment shows rapid FN deposition, generation of many new fibrils and abundant cell and fibril motion. The 12-24h segment shows some new fibrils and continued cell and fibril motion. The 24-36h and 36-48h segments show fewer new fibrils and reduced cell motion. Analysis of 20 fibrils in the 12-24h movie segment showed average strains ranging from -42,000 to 36,000 µɛ and analysis of 30 fibrils in the 24-36h segment showed average strains from -32,000 to 29,000 µɛ. Fibrils in the 36-48h segment showed average strains from -23,000 to 24,000 µɛ. Individual fibrils had unique strain profiles, driven by the underlying cell motion and experienced both tension and compression. Maximum strains were higher in shorter vs. longer fibrils and the average fibril strains decreased as a function of time, suggesting that fibril strains decrease with ECM maturation. This may be due to reduced cell motility and/or increased ECM crosslinking. Together these data show that ECM assembly is more dynamic than previously known and suggest that FN fibrils are subjected to significant strains and displacements during assembly due to cell motion. Mechanical stretching of ECM fibrils may expose binding sites for other ECM molecules, may result in shedding of ECM bound growth factors and may physically organize/reshape the ECM.

Disclosures: Bhargav Javvaji, None.

SU0209

Ciliary protein Bbs3 positively regulates the induction of ALP activity by Hedgehog signaling in MC3T3-E1. Makiri Kawasaki*[1], Tadayoshi Hayata[2], Yoichi Ezura[3], Masaki Noda[1]. [1]Tokyo Medical & Dental University, Japan, [2]Organization for Educational Initiatives, University of Tsukuba, Japan, [3]Tokyo Medical & Dental University, Medical Research Insititute, Japan

Primary cilium (PC), a hair-like organelle protruding from cell surface, is known to exist in most of the mammalian cells. The recent intensive studies revealed that this organelle plays an important role in signal transduction in osteoblasts. To date there are about 600 genes identified to be involved in the formation and function of PC. The deletion of proteins engaged to the transportation inside PC frequently causes disappearance of this structure and thus prevents us from systematic analysis. We focused on BBS3 (ADP ribosylation factor-like 6), one of the causative genes of Bardet-Biedl Syndrome, since this protein doesn't intervene in the formation of PC, while its lack disturbs the proper translocation of some GPCRs in/to PC. However, function of Bbs3 in osteoblasts is largely unknown. So, in this study we examined the effect of Bbs3 depletion in the differentiation of osteoblastic cell line MC3T3-E1.

First we examined the mRNA level of Bbs3 in skeletal tissues. Among bone tissues, Bbs3 was expressed the most highly in calvaria and less in bone marrow. We extracted bone marrow cells and cultured them in osteogenic medium for 3 weeks. The expression of Bbs3 was gradually increased along with the differentiation of bone marrow cells to osteoblasts. To know the role of Bbs3 in osteoblasts, we depleted Bbs3 in MC3T3-E1 using RNAi system (siControl/siBbs3). We performed immunocyto-chemistry and observed the PC in MC3T3-E1. We found that the knockdown of Bbs3 in MC3T3-E1 didn't affect the ratio of ciliated cells. Then we evaluated the differentiation of MC3T3-E1 on ALP activity in cells transfected with siControl or siBbs3. In the cells cultured in osteogenic medium, the induction of ALP activity was significantly suppressed in Bbs3-silenced cells, while the induction of ALP activity by BMP2 treatment wasn't suppressed in those cells, suggesting that the suppressed ALP activity was not due to the disturbed BMP2 signaling. Indeed, BRE-luc activity was comparably induced by BMP2 in Bbs3-silenced cells. PC is well known to be a signal center of Hedgehog signaling, so we cultured MC3T3-E1 in the presence of SAG, Smoothened agonist, and examined the ALP activity. In control cells, the SAG treatment up-regulated the ALP activity but this effect was diminished in the Bbs3-silenced cells.

Our data indicates that Bbs3 is positively involved in the induction of ALP activity by Hedgehog signaling during the differentiation of MC3T3-E1.

Disclosures: Makiri Kawasaki, None.

SU0210

Dock7 is a Novel Regulator of Osteoblast Differentiation and Function. Kathleen Bishop*[1], David Maridas[1], Katherine Motyl[1], Clifford Rosen[2]. [1]Maine Medical Center Research Institute, USA, [2]Maine Medical Center, USA

Dock7 is a guanine nucleotide exchange factor (GEF) involved in the activation of the small GTPases Rac1 and Cdc24. While Dock7 is best known for its role in neuronal cell function, mice lacking the Dock7 protein, the *Misty* mice, have low bone mass and accelerated age-related bone loss. Uncoupled bone remodeling was also observed, with decreased osteoblast and increased osteoclast numbers. However, it is unclear whether the *Misty* bone phenotype is a direct result of loss of Dock7 in bone remodeling cells or an indirect effect from other cell types. In order to elucidate the role of Dock7 in the osteogenic lineage and bone formation process, proliferation and differentiation markers were analyzed. Calvarial osteoblasts (COBs) displayed a decrease in the proliferation marker *Cyclin D1* and osteoblast markers *Runx2*, *Osteocalcin*, and *Alkaline Phosphatas*e when compared to wild type controls. Cell proliferation is currently being assessed by Brdu staining *in vivo*. Furthermore, COBs isolated from *Misty* mice demonstrated decreased osteogenic differentiation and mineralization as well as reduced Wnt3a-induced β-catenin nuclear localization. These data suggest that decreased osteoblast numbers observed in the *Misty* mice may be a result of decreased proliferation and impaired differentiation, potentially through modulation of Wnt signaling. Additionally, we hypothesized that if Dock7 controlled GTPase activation, GTPase-dependent processes such as cell mobility may also be affected. *Misty* bone marrow stromal cells (BMSCs) had a pronounced decrease in migration and increase in adhesion onto a collagen I matrix when compared to wild type; however, mobility in *Misty* COBs was only minimally reduced. Changes in BMSC mobility suggest an alteration in adhesion complex proteins such as integrins whose actions are dependent on the activation of small GTPases. Modulation of Rac1 and Cdc42 signaling would provide a strong rationale for the altered proliferation, differentiation, and migration observed in the osteoblast progenitors. These data indicate a direct role for Dock7 in the osteogenic lineage, specifically in the MSC to early osteoblast transition. To further determine if Dock7 deficiency in the osteogenic lineage contributes to the bone pathophysiology observed in *Misty* mice, we have generated a Dock7 conditional knockout using CRISPR, which will be used to elucidate the cell type-specific role for Dock7 modulating the bone formation and remodeling processes.

Disclosures: Kathleen Bishop, None.

SU0211

Hira, a histone chaperone, regulates bone mass. Pablo Roman-Garcia*[1], Virginia Piombo[2], Vijay Yadav[2]. [1]Systems Biology of Bone, Wellcome Trust Sanger Institute, United Kingdom, [2]Systems Biology of Bone, Wellcome Trust Sanger Institute, United Kingdom

Deletions of chromosome 22q11.2 also known as diGeorge or Velocardiofacial syndrome affect nearly one in 3000 births with an autosomal dominant inheritance. A region of at least 20 genes is lost and many clinical features, including low bone mass, are associated with this deletion. However, the genes in 22q11.2 underlying the skeletal disorders are not known.

In this study, we investigated the effect of loss of function of genes implicated in "22q11 syndromes" on osteoblast lineage and bone mass.

siRNA was used in OB6 cells to test if the silencing of genes involved in 22q11 deletion affects osteoblasts proliferation and/or differentiation. Gene expression was measured by qRT-PCR. Proliferation was measured as DNA synthesis (BrDu incorporation) and differentiation as alkaline phosphatase activity. Knockout mice generated using EUCOMM resources were used to investigate the implications of the deletion of candidate gene(s). Embryonic bone development was evaluated using whole mount skeletal preparations. Serum osteocalcin and glucose levels were measured using ELISA. Bone histology and histomorphometry was performed on undecalcified vertebral sections in adult mice using osteomeasure analysis system.

Ten genes involved in 22q11.2 deletion, with detectable levels in tibia, were silenced in OB6 osteoblastic cells. Gene expression was significantly decreased to ≥20% in all of the genes. Out of these genes only loss of function in *Hira*, which codes for a histone chaperone, was found to have a negative effect on both the proliferation (-25.5%) and differentiation (-30.2%) of osteoblasts. Generation of knock out mice for *Hira* revealed that homozygous mice were embryonically lethal, and heterozygous mice had normal skeletal mineralization during embryonic development. Analysis of 8 week-old *Hira*+/- mice showed a significant decrease in bone mass: 34% less bone volume/total volume compared to wild-type littermates. This low bone mass was caused by a severe suppression in the number and function of osteoblatsts associated with a major decrease in serum osteocalcin levels. *In vitro* osteoblast cultures showed that *Hira*+/- primary osteoblasts have impaired ability to proliferate and differentiate (-40% and -42% respectively).This study identifies a role for *Hira* in regulating osteoblast functions and bone mass, and suggests that this gene is likely involved in the low bone mass observed in diGeorge syndrome patients.

Disclosures: Pablo Roman-Garcia, None.

SU0212

Lack of Wnt16 Exerts Gender-Specific Effects on Cortical Bone Diameter in Mice. Chandrasekhar Kesavan*[1], Jon Wergedal[1], Robert Brommage[2], Subburaman Mohan[1]. [1]Jerry L. Pettis Memorial VA Medical Center, USA, [2]Lexicon Pharmaceuticals, USA

Periosteal bone formation (BF) is the primary determinant of bone diameter and canonical Wnt signaling is a major pathway regulating periosteal BF. Recent studies in our and other laboratories have shown that targeted knockout (KO) of the Wnt16 gene in mice results in reduced cortical bone thickness and strength. The C57BL6/J – 129SvEv hybrid Wnt16 KO mice examined in our laboratory have small cortical bone diameters and reduced periosteal BF. Since estrogen receptor α (ERα) can physically interact with β-catenin and genetic interactions between ERα and β-catenin signaling occur in vivo, we determined if Wnt16 exerts gender-specific effects on cortical bone size. As expected, cross-sectional area (CSA) of the tibia mid-diaphysis was significantly lower in female than male mice in both wild type (WT) and Wnt16 KO genotypes at 12 weeks of age. Compared to WT mice, lack of Wnt16 caused a greater reduction in tibia CSA in female mice (25%, P < 0.01) versus male mice (8%, P < 0.05). Similarly, cortical thickness was reduced by 10% and 20%, respectively, in male and female Wnt16 KO mice. Two-way analyses for genotype-gender interactions revealed a "p" value of 0.09 and 0.11, respectively, for CSA and cortical thickness. To examine mechanisms for the Wnt16-estrogen interaction, we evaluated the effect of estrogen on Wnt16 expression. 17β-estradiol treatment for 21 days using time release pellets (0.05 mg/21 days) implanted subcutaneously to three week-old WT ovariectomized C57BL/6J mice increased expression levels of both Wnt16 and β-catenin in the femur more than 6-fold (P < 0.01) compared to placebo treatment. Since estrogen effects on BF are mediated in part via upregulation of IGF-I signaling, we evaluated the effects of IGF-I treatment on Wnt16 expression in cultured (serum free) WT periosteal cells. IGF-I treatment at 10 ng/ml increased Wnt16 expression 10-fold but did not affect expression of Wnt4 and Wnt5a. Consistent with these in vitro data, Wnt16 mRNA level was reduced 50% (P < 0.05) in femur shafts from osteoblast-specific IGF-I conditional KO mice compared to control mice. We conclude that Wnt16 is required for the maximal effects of estrogen on cortical bone diameter and the estrogen dependence of Wnt16 expression may be mediated via IGF-I signaling.

Disclosures: Chandrasekhar Kesavan, None.

SU0213

Mechanisms for Specificity of Wnt16 Actions on the Periosteum. Jon Wergedal*[1], Chandrasekhar Kesavan[1], Karthikeyan Muthusamy[2], Robert Brommage[3], Subburaman Mohan[1]. [1]Jerry L. Pettis Memorial VA Medical Center, USA, [2]Alagappa University, India, [3]Lexicon Pharmaceuticals, USA

Human genome-wide association and mouse genetic studies revealed that Wnt16 is an important determinant of bone strength and fracture risk. Recent studies in our and other laboratories have shown that targeted knockout (KO) of the Wnt16 gene in mice results in reduced cortical bone thickness and strength. The C57BL6/J – 129SvEv hybrid Wnt16 KO mice examined in our laboratory have small cortical bone diameters and reduced periosteal bone formation. Furthermore, at the 2013 ASBMR meeting, we demonstrated that mechanical strain-induced periosteal bone formation was abrogated by a lack of Wnt16 in mice. Since numerous Wnts are expressed in bone and act via modulation of canonical β-catenin signaling, we examined the specificity of Wnt16 signaling in the periosteum. By RT-PCR, total RNA extracted from periosteal tissue of 5 week-old female wild-type (WT) mice showed several-fold higher expression of Wnt16 compared to Wnt1, Wnt2a, Wnt5a, Wnt7a, Wnt9a and Wnt10b. There were no differences in periosteal expression of Wnt1, Wnt2a, Wnt7a, Wnt9a and Wnt10b between WT and Wnt16 KO mice. Expression of Wnt5a was 30% higher (P < 0.05) in KO compared to WT mice. Wnt receptors Fzd1 and Fzd8 showed higher expression than other Frizzled receptors (Fzd3, Fzd4, Fzd5 and Fzd7), with Fzd8 expression upregulated in periosteum from Wnt16 KO mice. These findings, and structural modeling studies with two protein docking program, GRAMM-X, showing a Fzd8 binding pocket for Wnt16, suggest Fzd8 mediates Wnt16 canonical β-catenin signaling in bone. Proliferation of cultured periosteal cells obtained from Wnt16 KO mice is reduced and addition of exogenous Wnt16 but not Wnt3a rescued this defect. Supporting the importance of muscle – bone interactions, Wnt16 expression was observed to be high in muscle and elevated in both muscle (2-fold, P < 0.05) and periosteum (4-fold, P < 0.01) of mice subjected to increased mechanical strain (9N force producing 4800 µε strain was applied to the right tibia using a four-point bending loading method for 2 weeks [6 days/week] at 2 Hz frequency, for 36 cycles). Together, these studies demonstrate that the anabolic action of Wnt16 on periosteal bone formation results from high expression of Wnt16 in periosteal and surrounding muscle cells as well as high expression of the Wnt16 receptor Fzd8.

Disclosures: Jon Wergedal, None.

SU0214

Mechanisms Underlying the Effect of Melatonin, Strontium citrate, Vitamin D3 and Vitamin K2 on Bone Marrow Stem Cells and Peripheral Blood Monocytes Grown as Co-cultures. <u>Sifat Maria</u>*[1], <u>Holly Lassila</u>[2], <u>Christine O'Neil</u>[3], <u>Mark Swanson</u>[4], <u>Paula Witt-Enderby</u>[5]. [1]Duquesne University Division of Pharmaceutical Sciences, USA, [2]Duquesne University Division of Clinical, Social & Administrative Science, USA, [3]Duquesne University Division of Clinical, Social & Administrative Sciences, USA, [4]Private practice, Heart Preventics, LLC, USA, [5]Duquesne University,School of Pharmacy, USA

The bone remodeling system preserves the integrity of bone by balancing the activities of bone-forming osteoblasts and bone-resorbing osteoclasts. A shift in this equilibrium towards bone resorption could lead to bone loss. A clinical trial, the Melatonin-micronutrients Osteopenia Treatment Study (MOTS), was designed to assess the efficacy of a combination of bone tropic agents: melatonin, strontium citrate, vitamin D_3 and vitamin K_2 (MSDK) on bone health and quality of life in post-menopausal osteopenic women to address the rise in osteopenia-induced fracture. One aspect of this translational study examined the mechanisms underlying MSDK's effects on osteoblasts and osteoclasts using a co-culture system containing human bone marrow stem cells (hMSCs) and human peripheral blood monocytes (hPBMCs). Using a novel treatment paradigm that closely mimics the *in vivo* condition, hMSC/hPBMC co-cultures were exposed to vehicle or MSDK in osteogenic (OS+) or growth medium (OS-) for 21 days. These effects of MSDK on osteoblast and osteoclast differentiation were measured by alizarin red and TRAP staining, respectively. Co-cultures grown in OS+/MSDK enhanced osteoblast differentiation but inhibited osteoclast differentiation when compared to OS-/MSDK. To identify potential signaling mechanisms underlying MSDK's action, osteoprotegerin (OPG) and RANKL levels were measured in both hMSC/hPBMC co-cultures and in hMSC monocultures by ELISA and western blot analyses. In hMSC/hPBMC co-cultures exposed to OS+/vehicle or OS+/MSDK, the ratio of secreted OPG:RANKL decreased compared to cells grown in OS-/MSDK; this was due to an increase in RANKL secretion since secreted RANKL levels but not OPG levels increased when compared to OS-/MSDK. Interestingly, in hMSC monocultures, the ratio of secreted OPG:RANKL as measured by ELISA, decreased due to increases in RANKL with a concomitant decrease in OPG vs. OS-/MSDK; however, as measured by western blot, this ratio of OPG:RANKL increased in hMSC monocultures due to increases in OPG. From these data, we conclude that MSDK has dual actions on bone cells in-vitro to enhance osteoblast differentiation while inhibiting osteoclast differentiation through a modulation of OPG and RANKL expression and release from the osteoblast. These findings also suggest that the presence (co-culture) or absence (hMSC monoculture) of the osteoclast plays a significant role in MSDK-mediated expression and release of RANKL and OPG from the mature osteoblast.

Disclosures: Sifat Maria, None.
This study received funding from: Pure Encapsulations, Inc provided the study supplements and placebo

SU0215

PEPTIDE-MEDIATED α5β1 INTEGRIN ACTIVATION INTEGRATES WNT/β-CATENIN SIGNALING TO PROMOTE MESENCHYMAL CELL OSTEOGENIC DIFFERENTIATION. <u>Zuzana Saidak</u>*[1], <u>Sofia Azzi</u>[1], <u>Caroline Marty</u>[1], <u>Sophie Da Nascimento</u>[2], <u>Pascal Sonnet</u>[2], <u>Isabelle Dupin-Roger</u>[3], <u>Pierre J. Marie</u>[1]. [1]UMR-1132 Inserm, Paris, France, Université Paris Diderot, Sorbonne Paris Cité, France, [2]Equipe Théra, Laboratoire des Glucides-UMR-CNRS 6219, Université de Picardie Jules Verne, France, [3]Institut De Recherche Servier, France

Identifying mechanisms upregulating mesenchymal skeletal progenitor cell (MSC) osteogenic differentiation is an important issue for promoting bone formation during aging. We previously showed that the integrin α5β1 is essential for osteogenic differentiation in MSCs. However, the mechanisms underlying this effect are poorly understood. We thus investigated the mechanisms induced by α5β1 activation by CRRETAWAC, which interacts specifically with this integrin, and by two related peptides (GACRRTAWACGA, GACRETAWACGA) lacking the full RRET sequence that is believed to play a role similar to RGD to activate integrin signaling. These two peptides were less active than CRRETAWAC at reducing MSC attachment to fibronectin. All peptides significantly increased FAK activity (+10% in the presence of Mn2+), Runx2 transcriptional activity (+ 50-130%), osteoblast gene expression (1.2-4-fold) and in vitro matrix mineralization, showing promotion of in vitro osteogenic differentiation, irrespective of the RGD-like RRET sequence. Mechan-istically, all peptides enhanced β-catenin-dependent TCF/LEF transcriptional activity by ~50% in MSCs, an effect that was abolished by α5 integrin siRNA. Western blot analysis showed that the activation of Wnt/β-catenin signaling by the peptides was related to PI3K and GSK3 phosphorylation. To investigate the in vivo effects of the selected peptides, the purified cyclic peptides, or an inactive peptide used as negative control were coupled to (Asp-Ser-Ser)$_6$ which binds to active bone surfaces, and were administered (i.v., 100 mg/kg body weight/day, 5 days/week, 6 weeks) to 8-week old senescent osteopenic mice (SAMP6). Histological analysis showed that the peptide that was the most efficient at increasing Wnt/β-catenin signaling in vitro increased femoral bone volume (15%) and trabecular number (17%) in SAMP6 mice. This effect did not

result however from increased bone formation rate but was associated with decreased trabecular separation (17%), suggesting decreased bone resorption. Overall, the data indicate that RRET-independent activation of α5β1 integrin promotes MSC osteogenic differentiation in vitro in part by activating Wnt/β-catenin signaling, and increases bone mass in senescent osteopenic mice possibly through decreased osteoclastogenesis. This reveals a novel cross-talk between α5β1 integrin and Wnt/β-catenin signaling, which may serve as a basis for increasing bone mass in age-related bone disorders.

Disclosures: Zuzana Saidak, None.

SU0216

Pre-clinical screening of novel two-photon photopolymerized biomaterials for bone implantation. <u>Oskar Hoffmann</u>[1], <u>Tristan Fowler</u>*[2], <u>Carina Kampleitner</u>[3], <u>Leander Poocza</u>[4], <u>Andrea Markus</u>[5], <u>Christian Dullin</u>[5], <u>Gerhard Hildebrand</u>[4], <u>Frauke Alves</u>[5], <u>Klaus Liefeith</u>[4]. [1]University of Vienna, Austria, [2]Universität Wien, Aut, [3]Universität Wien, Austria, [4]Institute for Bioprocessing & Analytical Measurement Techniques (iba), Germany, [5]University Medical Center Göttingen, Germany

The development of biomaterials for bone repair is essential for non-healing large bone lesions. We sought to investigate the effects of novel scaffolds consisting of lactide (LA), caprolactone (CL), and methacrylate (MA) using 2-photon photo-polymerization (PP) on *in vitro* osteoblast (OB) function and osteoclast (OC) development and *in vivo* bone healing. We evaluated 3 formulations comprised of varying [LA : CL] ratio and different MA% as follows:
  1) LCM3 contains 8 LA : 2 CL and 85% MA
  2) LCM4 contains 9 LA : 1 CL and 90% MA
  3) LCM6 contains 9 LA : 1 CL and 40% MA
To determine the effect on OB differentiation, proliferation, and mineralization, we tested murine calvarial-derived OBs in MTT and alkaline phosphatase assays and stained them with alizarin red. We found that LCM3 and LCM4, but not LCM6, supported OB attachment, proliferation, and matrix mineralization when compared to cells plated on plastic. We then tested murine co-culture-derived OCs and human blood-derived CD14+ OC precursors and observed that mouse and human OCs attached and differentiated on LCM3 and LCM4, but not on LCM6 compared to tissue culture plastic. To evaluate *in vivo* scaffold integration, we implanted the scaffolds into 5mm calvarial defects in 3-month old BALB/c mice. We observed that all implants were well tolerated and all recipients survived without weight loss. At 12 weeks post-implantation, Quantum FX μCT and histological sections demonstrated that OVF and scaffolds enabled cellular integration and attachment. In animals re-implanted with syngeneic calvarial bone, there was a mean bone re-growth of $77.3 \pm 0.75\%$ compared with $25.7 \pm 4.29\%$ in animals without implant. Implantation of LCM3, LCM4 and LCM6 scaffolds led to a net change in mean bone re-growth of $20.1 \pm 2.76\%$, $23.7 \pm 4.17\%$, and $-7.5 \pm 1.42\%$, respectively. Thus, animals implanted with LCM3 and LCM4 scaffolds had normal bone re-growth which was identical to animals without implant, whereas LCM6 caused a significant reduction in bone formation. Using this pre-clinical screening approach, our results illustrate that LCM biomaterials with greater than 40% MA promote *in vivo* and *in vitro* OB and OC function leading to normal bone re-growth. In conclusion, these data suggest that novel 2-PP LCM biomaterials provide new opportunities for the treatment of non-healing large bone lesions.

Disclosures: Tristan Fowler, None.

SU0217

RANKL-binding peptides increased bone formation in a murine calvarial defect model. <u>Yasutaka Sugamori</u>*[1], <u>Masashi Honma</u>[2], <u>Genki Kato</u>[3], <u>Yukihiko Tamura</u>[3], <u>Yuriko Furuya</u>[4], <u>Hisataka Yasuda</u>[5], <u>Yasuhiko Tabata</u>[6], <u>Nobuyuki Udagawa</u>[7], <u>Keiichi Ohya</u>[8], <u>Hiroshi Suzuki</u>[9], <u>Kazuhiro Aoki</u>[8]. [1]Tokyo Medical & Dental University, Japan, [2]The University of Tokyo Hospital, Japan, [3]Tokyo Medical & Dental University, Japan, [4]Oriental Yeast Co.,Ltd, Japan, [5]Oriental Yeast Company, Limited, Japan, [6]Kyoto University, Japan, [7]Matsumoto Dental University, Japan, [8]Tokyo Medical & Dental University, Japan, [9]The University of Tokyo Hospital, Japan

Back ground
We have shown that the RANKL binding peptide W9 (MW: 1226.4) promotes bone formation as well as inhibiting bone resorption. We hypothesized that the increase of bone formation by the peptide is RANKL dependent since the anabolic effects of W9 on bone formation by the peptide was blunted in the RANKL deficient mice.

Purpose
In this study, we compared anabolic effects of W9 with another RANKL-binding peptide X (MW: 1448.7), which has been already known as an inhibitor of osteoclastogenesis, on local bone formation, and investigated the mechanism of the anabolic effects.
Materials and Methods
 For *in vitro* study, we used calvarial osteoblasts and ST-2 cells to compare W9 with peptide X on osteoblast differentiation. For *in vivo* study, we used murine

calvarial defect model. Gelatin hydrogel sheets were used as a carrier for these peptides. The mice were sacrificed 4 weeks after the operation, and the local bone formation was analyzed radiologically and histologically. In order to elucidate the signal transduction pathway upon the stimulation of peptide after binding to RANKL, we used ST-2 cells and investigated the phosphorylation of Akt and S6K1, which was considered as the RANKL downstream signaling molecules, by Western blotting.

Results

Peptide X could promote osteoblast differentiation more than W9 *in vitro*. Micro-CT analyses at the calvarial defects showed that peptide X (0.56 mg) could promote local bone formation to almost fully repairing extent, whereas W9 (0.56 mg) could only recover partially at the defects (See attached figure). The BMD measurement and histomorphometric analysis confirmed these Micro-CT data. Interestingly, peptide X could stimulate Akt and S6K1 phosphorylation more than W9.

Discussion

Since the phosphorylation of S6K1 is known as a signal-indicator of mTORC1 activation and mTORC1 activation is also known to lead the increase of Runx2 expression in osteoblasts, our data suggest that RANKL-binding peptides bind to the membrane-bound RANKL on the surface of osteoblasts and stimulate osteoblasts directly, promoting bone formation.

Conclusion

A RANKL-binding peptide may be a useful template to develop a therapeutic reagent for promoting local bone formation.

Anabolic effects of the RANKL-biniding peptides in the murine calvarial defects model

Disclosures: Yasutaka Sugamori, None.

SU0218

Runx2 Deficiency in Committed Osteoblasts Impairs Postnatal Skeletogenesis. Mitra Adhami*[1], Harunur Rashid[2], Haiyan Chen[3], Amjad Javed[3]. [1]UAB, USA, [2]University of Alabama Birmingham, USA, [3]University of Alabama at Birmingham, USA

Runx2 transcription factor is critical for mesenchymal cell commitment to the osteoblast lineage and skeletogenesis. Mice with global deletion of Runx2 exhibit a complete absence of osteoblasts and mineralized tissue. However, early lethality of Runx2-null mice precludes identification of cell and tissue-specific requirements of Runx2 in postnatal bone development. Moreover, it remains unclear if Runx2 is necessary after mesenchymal cell commitment to the osteoblast lineage. We specifically deleted the Runx2 gene in committed osteoblasts using 2.3kb collagen1-Cre transgenic mice. Surprisingly, homozygous mice were born alive and indistinguishable from WT littermates. Runx2 deficiency did not alter chondrocyte differentiation, cartilage growth and proliferative capacity of osteoblasts during embryonic development. However, histological analysis revealed a poorly calcified skeleton and severely disrupted cranial development in mutant mice. Runx2 mutants showed progressive retardation in postnatal growth and exhibited significantly low bone mass in cortical and trabecular bones by 1 month of age. Poor bone synthesis was associated with decreased gene expression of osteoblast markers BSP, OC and OSX and impaired collagen assembly in the extracellular matrix. In addition, 3-point bend testing revealed a 35% decrease in stiffness and 37% decrease in the ultimate force displacement of mutant femurs. Interestingly, TRAP staining showed a decrease in both osteoclast number and activity; thus, the low bone mass in mutant mice is not associated with increased bone resorption. Consistent with this observation, Runx2 mutant bones showed a decrease in RANKL, along with an increase in expression of OPG, an inhibitor of osteoclastogenesis. The altered RANKL/OPG ratio is consistent with loss of osteoclast differentiation. By 3 months of age, bone acquisition in mutant mice was roughly half of WT littermates. We also noted a 60% decrease in osteoclast number and 55% decrease in osteoclast activity. Interestingly, the number of osteoblasts was unchanged but the osteoblast surface to bone surface ratio was decreased in mutants. Our result indicate that osteoblast function, and not number, is disrupted in Runx2 mutant mice. Consistent with these findings, we observed a 50% decrease in the bone formation rate of 3-month old homozygous mice. In conclusion, Runx2 activity is critical for function after commitment to the osteoblast lineage and postnatal bone development.

Disclosures: Mitra Adhami, None.

SU0219

Static Magnetic Fields Affect Biological Behaviors of Bone Cells. Peng Shang*[1], Jian Zhang[2], Chong Ding[2], Airong Qian[3], Zhe Wang[2], Lifang Hu[2]. [1]Northwestern Polytechnical University, Peoples Republic of China, [2]Key Laboratory for Space Bioscience & Biotechnology, Institute of Special Environmental Biophysics, School of Life Sciences, Northwestern Polytechnical University, China, [3]Northwestern Polytechnical University, Peoples Republic of China

All the living beings live and evolve under geomagnetic field (25~65 µT). Besides, opportunities for human exposed to different intensities of static magnetic fields (SMF) in the workplace have increased progressively from hypo-magnetic field (HpMF, < 5 µT) environment, weak magnetic field (WMF, 5 µT~1 mT), moderate SMF (MMF, 1 mT~1 T) to high SMF (HiMF, > 1 T). Numerous studies have indicated that magnetic fields can influence our skeleton systems. However, the mechanisms of SMF environment on bone tissue are still poorly understood till now. In this study, HpMF of <500 nT, MMF of 0.2~0.4 T and HiMF of 16 T were used to investigate the effects of SMF on bone cells including osteoblasts, osteocytes and osteoclasts.

Our results showed that HiMF did not affect the morphology of osteocyte like cells of MLO-Y4, but increased cell viability. Accordingly, MLO-Y4 apoptosis decreased in MMF, but increased in the HpMF. HiMF promoted the expression of cox-2, Cx43 and some differentiation markers such as osteocalcin, sclerostin. In osteoblasts, the morphology and proliferation of osteoblastic MC3T3-E1 cells was influenced by SMF with different responses. HiMF promoted the differentiation of MC3T3-E1 cells at both early and mineralization stages. Besides, HiMF altered neither the height nor the distribution of both cytoskeleton and cytoskeleton-associated proteins. However, lots of cytoskeleton-associated genes in osteoblastic MG63 cells were sensitive to strong SMF identified by cDNA microarray. As for osteoclast, SMFs decreased the survival of preosteoclasts Raw264.7. Besides, Raw264.7 cell showed elevated osteoclastogenesis in HpMF and MMF, but reduced in HiMF.

These results suggest that exposure to the environments with magnetic intensity far away the geomagnetic field was harmful to bone metabolism such as HyMF and MMF. On the contrary, HiMF had positive effects on bone remodeling. It indicated that HiMF may be a potential physical therapy to for both maintenance and treatment of bone health. Above all, these results will improve our further understandings of the exact mechanisms of bone tissues under SMF and have potential application value in treating or preventing human bone disorders on the Earth or in outer space.

Disclosures: Peng Shang, None.

SU0220

Tension force-induced ATP promotes osteoblast differentiation-related transcription factors and osteogenesis through P2X7 receptor in osteoblasts. Natsuko Tanabe*[1], Taro Kariya[2], Chieko Shionome[2], Takayuki Kawato[2], Masao Maeno[2], Noriyoshi Shimizu[2], Naoto Suzuki[1]. [1]Nihon University School of Dentistry, Japan, [2]Nihon University School of Dentistry, Japan

Orthodontic tooth movement induced alveolar bone resorption and formation by mechanical stimuli. In particular, the force exerted on the traction side promotes bone formation. Nucleotides, such as adenosine triphosphate (ATP), are thought to be key mediators in the response of bone cells to mechanical stimuli. It has been reported that Fluid shear stress induces ATP release in the osteoblastic MC3T3-E1 cells, and also has been reported that ATP promotes bone formation through P2X7 receptor in rat calvarial cells (Panupinthu et. al., J.Cell.Biol, 181, 2008, Genetos et. al., J.Bone.-Miner.Res, 20, 2005). However, the effect of Tension force (TF) -induced ATP in osteogenesis is poorly understood. Thus, our purpose was to determine the effect of TF on ATP release, the expression of differentiation related-factors and extracellular matrix, ALPase activity and osteogenesis in osteoblasts. MC3T3-E1 cells were plated on flexible-bottom plate, incubated in the presence or absence of P2X7 antagonist A438079, then stimulate with cyclic TF (6 or 18%, that is 6 cycles/min: 5 sec strain, 5 sec relaxation) for maximum 24hs using a Flexercell Strain Unit 3000. ATP release is from the culture medium was measured by the luciferin/luciferase assay. The expression of osteogenesis-related transcription factors, P2X7, and extracellular matrix proteins was determined by real-time PCR, Western blotting or ELISA. ALPase activity was estimated by ALP staining is assessed as red stains indicating the products of enzyme activity.The calcium content in mineralized nodules was determined by using a calcium E-test kit. 6% TF induced ATP production, the gene expression of P2X7, and the expression of osteogenesis-related transcription factor and extracellular matrix protein. 6% TF also significantly increased the calcium content in mineralized nodules and ALP activity staining. Moreover, P2X7 antagonist A438079 was blocked these increases of 6% TF stimulation. These results suggest that the production of ATP which is stimulated by 6% TF promotes differentiation and osteogenesis through P2X7 in osteoblasts.

Disclosures: Natsuko Tanabe, None.

SU0221

Regulation of bone formation and mineralisation by ATP-induced ATP release from osteoblasts. <u>James Gallagher</u>*[1], <u>Jane P Dillon</u>[2], <u>Lakshminarayan R Ranganath</u>[2], <u>Peter JM Wilson</u>[2]. [1]University of Liverpool, United Kingdom, [2]University of Liverpool, United Kingdom

Extracelluar ATP appears to play a major role in the regulation of bone physiology, signalling through P2 purinergic receptors. There are almost certainly more receptor subtypes responsive to ATP expressed in bone than for any other single ligand and the receptors are expressed on osteoblasts, osteoclasts and osteocytes. Despite the dominant presence of this complex signalling system in bone, the physiological role is relatively unelucidated. Polymorphisms in several P2 receptors including P2X7 are associated with bone mass. Osteoblasts are known to release ATP both constitutively and in response to stimuli including shear stress, indicating that purinergic signalling plays a role in mechanotransduction. In this study we investigated if activation of P2 receptors influences the subsequent release of ATP from human osteoblasts in vitro. We investigated primary human osteoblasts and three osteosarcoma cell lines MG-63, TE-85 and Saos-2, which represent different stages of osteoblastic differentiation. We used the luciferin/luciferase assay to measure ATP in conditioned medium. When exogenous ATP was added to osteoblastic cells at concentrations below 10^{-5} M it was rapidly broken down with a half life of less than 1h. However when we raised the concentration of exogenous ATP above 10^{-4} M, in cultures of primary osteoblasts or MG-63 and Saos-2 cells, there was a massive release of ATP from the cells into the conditioned medium. The concentration of ATP reached millimolar level, which could only be achieved by an almost complete depletion of ATP in the cells. This release of ATP was not associated with cell death. ATP-induced ATP release was not observed in the Te-85 cells which are devoid of functional P2X7 receptors, indicating that this ionotropic, pore forming receptor might be the conduit for release of ATP. However, we could not completely replicate the effects of ATP in primary osteoblasts, or the other two osteosarcoma cell lines with BzATP, a prototypical P2X7 agonist. Taking into account the large dilution effect of tissue culture medium, the ATP released from osteoblasts could reach concentrations where it would have a significant effect on mineralisation as a source of local phosphate ions or through degradation to the mineralisation inhibitor pyrophosphate. In summary ATP-induced ATP release from osteoblasts is an unusual example of positive feedback in bone homeostasis and may play a major role in regulating formation and mineralisation of bone.

Disclosures: James Gallagher, None.

SU0222

Vitamin B$_{12}$-dependent liver taurine synthesis regulates growth and bone mass. <u>Isabel Quiros-Gonzalez</u>*[1], <u>Pablo Roman-Garcia</u>[2], <u>Liesbet Lieben</u>[3], <u>Vijay K. Yadav</u>[3]. [1]Wellcome Trust Sanger Institute, United Kingdom, [2]Systems Biology of Bone, Wellcome Trust Sanger Institute, United Kingdom, [3]Wellcome Trust Sanger Institute, United Kingdom

Purpose: Vitamin B$_{12}$ (B$_{12}$) is an essential water-soluble vitamin that regulates a multitude of cellular processes. Absortion of B$_{12}$ from the gut lumen into the blood stream requires gastric intrinsic factor (Gif), a stomach-specific protein, and following absorption B$_{12}$ is stored in the liver. A decrease in the production of functional Gif therefore causes B$_{12}$ deficiency. In humans, B$_{12}$ deficiency is associated with lower bone mineral density and increased fracture risk. In the present study we investigated the importance of B$_{12}$ in the regulation of bone mass homeostasis.Methods: A mouse genetic model of B$_{12}$ deficiency was generated by deleting *Gif* gene. Liver and bone tissues or cell lines were studied for mRNA and protein expression. Liver HepG2 cell line with alterations in B$_{12}$ levels [Transcobalamin-oleosin (TCOL) based B$_{12}$ sequestration] or in GH signaling pathway (shSTAT5) was used as an *in vitro* model to investigate effect of B$_{12}$ deprivation on in hepatocytes by metabolomic analysis. In addition, pre-osteoblast cell line MC3T3 was used to investigate the direct effect of B$_{12}$ on osteoblast proliferation and differentiation.Results: *Gif-/-* mice showed growth retardation and early onset osteoporosis during post-weaning period. Analysis of GH-Igf1 axis that regulates grwoth and bone mass revealed a major decrease in Igf1 levels and an increase in GH levels in mutant mice. These results suggested that B$_{12}$ deficiency in *Gif-/-* mice results in a block in GH signaling pathway. Consistent with this hypothesis, phosphorylation levels of STAT5 the major mediator of GH signaling showed a drastic decrease in the liver of *Gif-/-* mice. Similarly, sequestration of B$_{12}$ by TCOL transfection in HepG2 cells caused a decrease in STAT5 phosphorylation mimicking shSTAT5 transfected HepG2 cells. Both TCOL and shSTAT5 transfected cells showed disruption of Igf1 expression in response to GH. Metabolomic analysis in HepG2 cells transfected with TCOL or *Gif-/-* liver samples showed that taurine, produced mainly in the liver, is a critical metabolite affected upon B$_{12}$/GH signaling disruption. Further experiments showed that taurine increases osteoblast proliferation directly by increasing IGF1 signaling in osteoblast and when given *in vivo* can rescue growth retardation and osteoporosis observed upon B$_{12}$ deficiency.Conclusions: Together these results show that liver B$_{12}$/Taurine pathway is essential for normal functioning of GH/Igf1 axis in the regulation of growth and bone mass

Disclosures: Isabel Quiros-Gonzalez, None.

SU0223

Analysis of Runx2 and LRP5 Along the hFOB Differentiation. <u>Susana Balcells</u>*[1], <u>Behjat Gholami</u>[1], <u>Judith Garcia-Gonzalez</u>[1], <u>Roser Urreizti</u>[1], <u>Natalia Garcia-Giralt</u>[2], <u>Robert Guerri Fernandez</u>[3], <u>Leonardo Mellibovsky</u>[4], <u>Xavier Nogues</u>[5], <u>Adolfo Diez-Perez</u>[6], <u>Daniel Grinberg</u>[7]. [1]Dept. Genetics, Univ. Barcelona, CIBERER, IBUB, Spain, [2]IMIM, Spain, [3]Fundacio IMIM, Spain, [4]Institut Municipal d'Investigació Mèdica, Spain, [5]Institut Municipal D'Investigació Mèdica, Spain, [6]Autonomous University of Barcelona, Spain, [7]The University of Barcelona, Spain

Osteoblasts are bone-forming cells, derived from mesenchimal progenitors through differentiation in which Runx2 plays a crucial role. LRP5 is a Wnt coreceptor, which has been involved in determining bone mass, both in humans and in mice. Gain of function mutations in *LRP5* determine high bone mass and loss of function mutations cause osteoporosis. Five Runx2 binding sites have been described in the upstream region of *LRP5*, one of which –BS1- contains the SNP rs312009, associated with bone mineral density. The aim of this study was to characterize the expression of these genes in the human fetal osteoblast cell line hFOB, along 21 days of differentiation.hFOB cells were grown in Ham's medium with G418 and 10%FBS at 33.5℃. At 80% confluence, they were shifted to 39.5° to promote osteoblast differentiation. Viability (MTT test) and mineralization (Alizarin staining) were monitored at days 0, 3, 7, 14 and 21. Protein, RNA and fixed chromatin samples were collected at each time point. Proteins were screened by western blot and mRNAs by RT-qPCR using GAPDH as normalizer. Saos2 cells were grown in standard conditions and protein, RNA and fixed chromatin was obtained and analyzed in parallel.At day 0, hFOBs underwent rapid cell division. Upon temperature shift, cell division slowed down and at day 3 they stained positive for mineralization. Cells, initially elongated and fusiform (day 0-3), changed to a planar rectangular aspect and with pseudopodes at the borders (day 14-21). Concomitantly, viability decreased starting at day 7 and at each subsequent time point was reduced about 50%.At mRNA level, Runx2 was almost undetectable in hFOB at d.0, when compared to the very high levels present in Saos2. Along differentiation, Runx2 transcript levels raised 6.5 x at day 3 and stayed stable up to day 21. LRP5 mRNA was 3.7 x higher in hFOB d.0, when compared to Saos2, and it increased moderately along differentiation. Between d.3 and d.14, levels were 1.5 x and at d.21 they were 2 x higher than at d.0. Runx2 and LRP5 proteins were detected in hFOB at any day of differentiation. Runx2 was very abundant in Saos2, and very low, although detectable, in hFOB (any day), paralleling the mRNA profile. ChIP with anti-Runx2 in Saos2 chromatin showed occupancy of all 5 BS sites of the *LRP5* promoter.In conclusion, both Runx2 and LRP5 were detected at mRNA and protein levels along the hFOB differentiation. A ChIP assay is underway to test the occupancy of the 5 BSs in hFOB chromatin.

Disclosures: Susana Balcells, None.

SU0224

Bio-active silica nanoparticles promote osteoblast differentiation though stimulation of autophagy and direct association with LC3 and p62. <u>Shin Ha</u>[1], <u>M. Neale Weitzmann</u>[2], <u>George Beck</u>*[2]. [1]Emory University, USA, [2]Emory University School of Medicine, USA

Nanotechnology is a multidisciplinary field involving the development of engineered "devices", including particles, at the nanometer size (typically 1-200 nm). Recent advances in nanotechnology have raised exciting possibilities for use of nanoparticles as therapeutic interventions. Silica based nanoparticles have been demonstrated to alter biological processes in the nano form, dependent on size, and are generally thought to be non-toxic in vivo. Consequently, they are good candidates for use in biomedical applications. We have engineered a novel 50 nm silica-based fluorescent nanoparticle (designated herein as NP1) that potently stimulates in vitro differentiation and mineralization of osteoblasts, the cells responsible for bone formation, and increases bone mineral density in young mice in vivo. The results demonstrate that these nanoparticles have intrinsic biological activity, however the intracellular fate and a complete understanding of the mechanism(s) involved remains to be elucidated. Here we investigated the cellular mechanism(s) by which NP1 stimulates differentiation and mineralization of pre-osteoblasts. We determine that NP1 enters the cells through a caveolae mediated endocytosis followed by stimulation of the mitogen activated protein kinase ERK1/2 (p44/p42). Our findings further revealed that NP1 stimulates autophagy including the processing of LC3β-I to LC3β-II, a key protein involved in autophagosome formation, which is dependent on ERK1/2 signaling. Using a variant of NP1 with cobalt ferrite magnetic metal core (NP1-MNP) to pull down associated proteins, we demonstrate direct binding of LC3β and p62, two key proteins involved in autophagosome formation, with silica nanoparticles. Interestingly, NP1 specifically interacts with the active and autophagosome associated form of LC3β (LC3β-II). Taken together, the stimulation of autophagy and associated signaling provides a cellular mechanism for the stimulatory effects of our nanoparticles on osteoblast differentiation and mineralization.

Disclosures: George Beck, None.

SU0225

Indirubin-3'-oxime Reverses Bone Loss in Ovariectomized and Hindlimb-Unloaded Mice via Activation of the Wnt/β-Catenin Signaling. Muhammad Zahoor*[1], Pu-Hyeon Cha[2], Kang-Yell Choi[2]. , [2]Yonsei University, South Korea

Osteoporosis is a major global health issue in elderly people. Increasing evidence suggests that current anti-osteoporosis agents have adverse effects, including high risk of cancer, micro-fracture, and jaw osteonecrosis. Because Wnt/β-catenin signaling plays a key role in bone homeostasis, we screened activators of this pathway through cell-based screening, and investigated indirubin-3'-oxime (I3O), one of the positive compounds known to inhibit GSK3β, as a potential anti-osteoporotic agent. Here, we show that I3O activated Wnt/β-catenin signaling via inhibition of the interaction of GSK3β with β-catenin, and induced osteoblast differentiation *in vitro* and increased calvarial bone thickness *ex vivo*. Intraperitoneal injection of I3O increased bone mass and improved microarchitecture in normal mice and reversed bone loss in an ovariectomized mouse model of age-related osteoporosis. I3O also increased thickness and area of cortical bone, indicating improved bone strength. Enhanced bone mass and strength correlated with activated Wnt/β-catenin signaling, as shown by histological analyses of both trabecular and cortical bones. I3O also restored mass and density of bone in hindlimb-unloaded mice compared to control, suspended mice, demonstrating bone-restoration effects of I3O in non-aged–related osteoporosis as well. Overall, I3O, a pharmacologically active small molecule, could be a potential therapeutic agent for the treatment and prevention of osteoporosis.

Figure lagend:
(A): ALP staining of I3O treated murine primary osteoblasts. (B) Alizarin red stainin of I3O treated murnine primary osteoblasts. (C) I3O treated calvaria. (D). TRAP stained RANKL and I3O treated RAW264.7 cells. (E). Micro CT images of I3O treated ovarectmized mice femur. (F). Micro CT images of I3O treated hind-limb-unloaded mice femur.
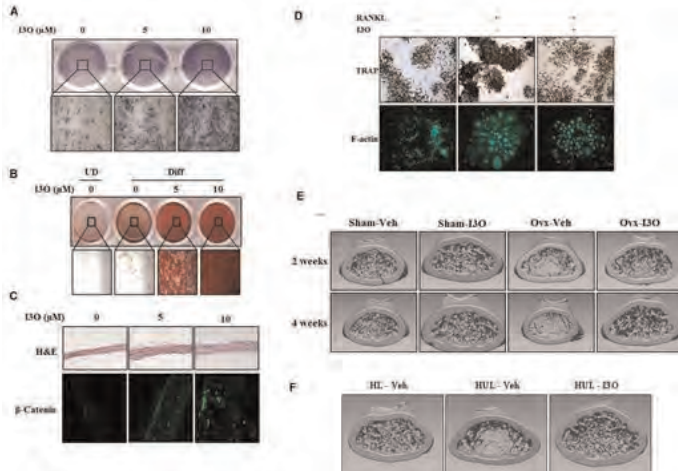
figure

Disclosures: Muhammad Zahoor, None.

SU0226

MAPK-Mediated Epigenetic Regulation of Gene Expression During Osteoblast Differentiation. Yan Li*[1], Chunxi Ge[2], Guisheng Zhao[3], Renny Franceschi[1]. [1]University of Michigan, USA, [2]Pom Univ of Michigan School of Dentistry, USA, [3]University of Michigan School of Dentistry, USA

BMPs, FGF2, mechanical loading and cell-ECM contact stimulate osteoblast differentiation in part by activating the ERK/MAP kinase pathway, which subsequently phosphorylates a number of substrates including the Runx2 transcription factor. However, the relationship between MAP kinase activation and epigenetic regulation of chromatin has not been previously examined. In this study, we used chromatin immunoprecipitation (ChIP) to examine early histone modifications during osteoblast differentiation and compared these changes with chromatin occupancy by p300 histone acetyltransferase, AOF1 histone demethylase, P-ERK and phosphorylated Runx2. Studies focused on chromatin regions containing Runx2 binding sites present in osteocalcin (Bglap2) and bone sialoprotein (Ibsp) genes. Osteoblast differentiation was induced in MC3T3-E1c4 cells using ascorbic acid (AA) and gene expression measured with quantitative RT-PCR. Initial AA-dependent induction of Bglap2 and Ibsp mRNAs was seen at 3 days and continued to increase at 6 days. Chromatin was isolated at 6 days for ChIP analysis using antibodies specific to AcH3k9, AcH4K5, H3K4dm, H3K9m, P-ERK, Runx2, P-Runx2 (S319-P), Pol II, p300 histone acetyltransferases and AOF1 histone demethylase. Osteogenic stimulation increased histone H3K9 and H4K5 acetylation near the two Runx2-binding elements of Bglap2 (OSE2a, OSE2b) and at a proximal Runx2 binding region of Ibsp. The level of H3K4 di-methylation, another gene activation-associated histone marker,

was also increased in both genes. However, the level of H3K9 mono-, di-, and tri-methylation in the same regions was reduced. Similarly, chromatin-bound P-ERK, P-Runx2, p300 and RNA polymerase II all increased. In contrast, no changes were observed in total Runx2 and AOF1. Inhibition of MAP kinase signaling blocked chromatin modifications and Bglap2 and Ibsp induction. To evaluate the role of Runx2 phosphorylation, Runx2-deficient C3H10T1/2 cells were transduced with adenovirus encoding wild type or phosphorylation-deficient Runx2 (S301A/S319A mutant). Wild type Runx2 increased H3K9 and H4K5 acetylation as well as chromatin-associated P-ERK, p300 and polymerase II. In contrast, the phosphorylation-deficient Runx2 mutant had much less activity. Taken together, this study reveals a molecular mechanism through which osteogenic genes are epigenetically controlled by a MAPK-mediated, Runx2-requiring complex associated with specific promoter regions.

Disclosures: Yan Li, None.

SU0227

Sp7 is Obligatory for Stability and Function of Runx2 Protein During Bone Formation. Harunur Rashid*[1], Haiyan Chen[2], Ching-Fang Chang[3], Krishna Sinha[4], Benoit DeCrombrugghe[4], Amjad Javed[2]. [1]University of Alabama Birmingham, USA, [2]University of Alabama at Birmingham, USA, [3]University of Alabama at Birmingham, USA, [4]UT MD Anderson Cancer Center, USA

Targeted disruption of specificity protein-7 (Sp7) and Runx2 genes results in complete failure of bone formation. Molecular reasons for surprisingly similar phenotype from two structurally unrelated proteins remain unknown. Sp7 is not expressed in Runx2-null mice reflecting a compound phenotype of both Runx2 and Sp7 loss. Sp7-null mice, however fail to form bone, despite normal levels of Runx2 mRNA in skeletal tissues. Here we identified molecular mechanisms underlying the functional incompetency of Runx2 in Sp7 null model. Human and mouse osteoblasts expressing both proteins were treated with Sp7 specific siRNA. We observed a dose dependent inhibition of Sp7 protein. To our surprise, a concomitant reduction of Runx2 protein was also noted. To assess if decrease in Runx2 protein is due to transcriptional regulation of Runx2 by Sp7, we isolated RNA. The siRNA treatment only decreased Sp7 mRNA but the levels of Runx2 mRNA remain unchanged. Thus regulation of Runx2 protein by Sp7 is post-transcriptional. We next determine if Sp7 is necessary for stability of Runx2 protein by co-transfecting cells with fixed amount of Runx2 and increasing concentration of Sp7 plasmid. We observed a dose dependent increase in Sp7 protein. Surprisingly, a progressive increase in Runx2 protein ~20 fold was also noted. Importantly, the half-life of Runx2 protein was significantly extended in the presence of Sp7. Interestingly, Co-IP studies revealed that in osteoblasts, endogenous Sp7 protein forms a molecular complex with Runx2. The physical interaction requires RHD of Runx2 and transactivation domain of Sp7 protein. Moreover, MAPK mediated phosphorylation of both Runx2 and Sp7 protein is essential for their interaction. Reciprocal interaction between Sp7 and Runx2 protein prompted us to examine how Sp7 stabilizes Runx2 protein. We found both ubiquitination and degradation of Runx2 protein by smurf1 is strongly inhibited by the presence of Sp7. Runx2-Sp7 physical interaction is an integral component of this process, as mutant Sp7 that lack Runx2 interaction domain, fail to block degradation of Runx2 protein by smurf1. Importantly, phosphorylated Runx2 and Sp7 functionally cooperate for maximal induction of osteoblast genes. Finally, we demonstrate that Runx2 protein is highly unstable and rapidly degrade in both intramembranous and endochondral bones of Sp7 null mice. In conclusion Sp7 regulate Runx2 protein stability and function through molecular interaction in bone cells.

Disclosures: Harunur Rashid, None.

SU0228

Suppression of p38alpha MAPK Signaling in Mature Osteoblasts Impairs PTH-Induced Bone Anabolism. Cyril Thouverey*[1], Joseph Caverzasio[2]. [1]University Hospital of Geneva, Switzerland, [2]Division Bone Diseases, Switzerland

Intermittent PTH administration (iPTH) increases bone mass in humans and animals. PTH exerts its effects by binding to PTH type 1 receptor (PTHR1) predominantly expressed by osteoblasts, resulting in activation of multiple downstream signaling pathways. *In vitro* investigations have suggested that p38 mitogen-activated protein kinase (MAPK) signaling is an important mediator of PTH-induced osteoblast functions. To evaluate the contribution of p38alpha MAPK signaling in iPTH-induced bone anabolism, 3-month-old male mice lacking *p38alpha* in osteoblasts (*Ocn-Cre;p38alpha[f/f]*) and their control littermates (*p38alpha[f/f]*) were treated with daily subcutaneous injections of either 40 µg/kg PTH (1-34) or its vehicle. After 4 weeks of treatment, bone phenotypes were assessed by dexa, microCT, histomorphometry and quantitative gene expression analyses (n=7 per group). Data were analyzed by two-way ANOVA and *post hoc* analyses were performed using the Holm-Sidak method. iPTH treatment increased total bone mineral density (+8.5 %, p=0.003 versus Veh), femoral cortical thickness (+10.9 %, p=0.005), femoral cancellous bone volume (+35.4 %, p=0.007) and trabecular thickness (+21.9 %, p=0.008) in control mice but did not induce significant changes of those parameters in *Ocn-Cre;p38alpha[f/f]* mice. Consistent with this, iPTH significantly stimulated mineralizing surfaces (1.5-fold), mineral apposition rate (1.9-fold) and bone formation rate (2.8-fold) in control animals, whereas it only enhanced mineralizing surfaces (1.5-

fold) in *Ocn-Cre;p38alpha^{fl/f}* mice, indicating a functional defect of *p38alpha*-deficient osteoblasts in response to iPTH. Furthermore, iPTH significantly increased osteoblast marker gene expressions (*Col1a1*, *Alp*, *BspII* and *Ocn*) in control mice but not in *Ocn-Cre;p38alpha^{fl/f}* mice. Finally, *p38alpha*-deficient osteoblasts exhibited normal *Pthr1* gene expression in comparison to control osteoblasts, but displayed reduced elevations of *Alp*, *BspII* and *Ocn* expressions and matrix mineralization in response to PTH *in vitro*. Our findings indicate that the p38alpha MAPK in osteoblasts plays an important role in PTH-induced bone anabolism in mice.

SU0229

Transcription factor SP1 regulates Frizzled 1 expression in osteoblasts. <u>Shibing Yu</u>*[1], <u>Laura Yerges-Armstrong</u>[2], <u>Yanxia Chu</u>[3], <u>Joseph Zmuda</u>[4], <u>Yingze Zhang</u>[5]. [1]University of Pittsburgh Medical Center, USA, [2]University of Maryland School of Medicine, USA, [3]University of Pittsburgh Department of Medicine, USA, [4]University of Pittsburgh Graduate School of Public Health, USA, [5]University of Pittsburgh, USA

Frizzled 1 (FZD1) is a co-receptor for Wnts and plays a role in osteoblast differentiation and mineralization. The expression of FZD1 is regulated by multiple transcription factors including Egr1 and E2F1. Promoter variants of FZD1 affect its transcriptional regulation and are associated with bone mineral density (BMD) in humans. Specificity protein 1 (Sp1) is an important transcription factor regulating gene expression in different tissues including bone. We performed in silico analysis of the promoter variant rs2232158 and identified putative differential binding of Sp1 with the G and C alleles. To assess the potential regulatory role of Sp1 in FZD1 expression in osteoblasts, we cloned the FZD1 promoter luciferase reporter plasmid containing the rs2232158 variant G or C alleles and transfected the reporter constructs into Saos2 cell lines with Sp1 or control expression plasmids. Our experiments demonstrated that Sp1 significantly increases FZD1 promoter activity, but this regulation was not affected by rs2232158 allelic variants. Overexpression of a loss-of-function Sp1 mutant plasmid did not affect the FZD1 promoter activity, indicating Sp1 specifically up-regulates FZD1 expression in Saos2 cells. Moreover, quantitative PCR and Western blot results showed that overexpression of Sp1 leads to higher FZD1 mRNA and protein expression. Further studies are needed to ascertain the specific Sp1 binding site(s) in FZD1 promoter region. Taken together, our study demonstrates that Sp1 is a transcriptional activator of FZD1 in osteoblasts.

SU0230

Transcriptional Profiling of Laser Capture Microdissected Subpopulations of the Osteoblast Lineage Provides Insight Into the Molecular Mechanism of Action of Sclerostin Antibody. <u>Paul Nioi</u>*, <u>Scott Taylor</u>, <u>Rong Hu</u>, <u>Efrain Pacheco</u>, <u>Yudong He</u>, <u>Hisham Hamadeh</u>, <u>Chris Paszty</u>, <u>Ian Pyrah</u>, <u>Mike Ominsky</u>, <u>Rogely Boyce</u>. Amgen Inc., USA

Sclerostin antibody (Scl-Ab) increases bone formation that is dependent upon activation of canonical Wnt signaling, though the specific in vivo signaling in the osteoblast lineage is largely unknown. To gain insight into the signaling pathways acutely modulated by Scl-Ab, the acute transcriptional response of subpopulations of the osteoblast lineage was assessed by microarray analysis of mRNA isolated from laser capture microdissection (LCM)-enriched samples from the vertebrae of aged ovariectomized (OVX) rats following exposure to Scl-Ab.

Six-month-old rats were OVX, and after 2 months, received a single dose of vehicle or 100 mg/kg Scl-AbVI (n=20/group). Rats were administered fluorochrome labels at 72h predose and 48h and 120h postdose to label active forming surfaces. At 6h, 24h, 72h, and 168h postdose, 5 rats/group were euthanized. Lumbar vertebrae were collected, snap-frozen, and cryosectioned undecalcified for LCM. Osteoblasts and lining cells (LC) from cancellous bone were enriched by capturing bone surfaces with and without fluorochrome label, respectively, and osteocytes were enriched by capturing bone matrix. mRNA was isolated from the LCM samples, amplified, and profiled by microarray.

Analyses revealed that Scl-Ab resulted in a strikingly similar transcriptional profile in all 3 cell types, evident as early as 6h and sustained through 168h. A limited number of Wnt target genes were found to be upregulated, with *Wisp1, Twist1, connexin 43, osteocalcin,* and *Mmp2* being the most responsive. These genes have known functions in bone including regulation of osteoblastogenesis, cell-to-cell communication, mechanotransduction, and bone matrix production and remodeling. There was coincident upregulation of numerous extracellular matrix (ECM) genes, heralding the onset of bone matrix synthesis. Several of the ECM genes have a consensus Wnt response element, suggesting these are potential canonical Wnt target genes in bone. The acute and sustained upregulation of transcripts related to bone matrix synthesis in LC supports activation of quiescent LC into matrix-producing osteoblasts consistent

with modeling-based bone formation. This same transcriptional profile in osteocytes may indicate that Scl-Ab stimulates perilacunar/pericanalicular matrix deposition.

These data demonstrate the focused nature of canonical Wnt signaling in bone in response to Scl-Ab that is acutely shared by all the mature osteoblast subpopulations.

SU0231

Hippo pathway in cranial neural crest is required for normal cranial bone and suture growth. <u>Jun Wang</u>*[1], <u>Yang Xiao</u>[2], <u>Jianning Tao</u>[3], <u>Margarita Bonilla-Claudio</u>[4], <u>Brian Dawson</u>[4], <u>Eric Olson</u>[5], <u>Brendan Lee</u>[3], <u>James Martin</u>[4]. [1], USA, [2]Baylor College of Medicine, USA, [3]Baylor College of Medicine, USA, [4]Baylor College of Medicine, USA, [5]University of Texas Southwestern Medical Center, USA

Cranial neural crest (CNC) contributes to multiple cells types including cartilage, bone, neurons, and glia. CNC defects cause different congenital defects such as craniosynostosis. The function of Hippo signaling, an ancient organ size control pathway, in CNC is poorly understood. To investigate Hippo signaling in CNC derivatives such as calvarial bones and sutures, we specifically inactivated the Hippo component *Salv*, as well as downstream Hippo pathway effectors *Yap* and *Taz* in CNC using the Wnt1 Cre driver. Our observations reveal that 1) *Wnt1^{Cre}*; *Salv^{fl/f}* mutants had dramatically enlarged calvarial bones and cranial sutures with increased calvarial bone density; 2) *Wnt1^{Cre}*; *Taz^{fl/+}*; *Yap^{fl/f}* and *Wnt1^{Cre}*; *Taz^{fl/f}*; *Yap^{fl/f}* mutants were embryonic lethal and had severe frontonasal and mandibular structural defects; 3) *Wnt1^{Cre}*; *Taz^{fl/f}*; *Yap^{fl/+}* mutants had a range of survival times from E14.5 to postnatal 8 weeks with a range of calvarial bone defects with Wormian bones and decreased calvarial bone density; 4) *Taz^{fl/f};Yap^{fl/f}* CKO mutant CNC had reduced cellular proliferation but no obvious change in apoptosis as compared to controls; 5) Yap expression level and subcellular location changed in response to matrix stiffness. Together, our findings indicated the crucially important requirement for Hippo pathway in normal cranial bone and suture growth.

SU0232

Bmp2 Gene in Stem Cell Biology of the Periodontium. <u>Stephen Harris</u>*[1], <u>Audrey Rakian</u>[2], <u>Jelica Gluhak-Heinrich</u>[1], <u>Marie Harris</u>[1], <u>Yong Cui</u>[3], <u>Ivo Kalajzic</u>[4]. [1]University of Texas Health Science Center at San Antonio, USA, [2], USA, [3]UTHSCSA, USA, [4]University of Connecticut Health Center, USA

Understanding how stem cells in the periodontium differentiate into the 3 major components of the periodontium, alveolar bone, periodontal tendon like ligament (PDL), and cementum (links PDL to teeth), will lead to new paradigms to regenerate this lost tissue in disease. Cells labeled by a-smooth muscle actin (aSMA+) in the periodontium have recently been found by lineage tracing studies to be a major class of stem cells that differentiate into these 3 major periodontium components (Roguljic et al, 2013, J. of Dental Res.). Using the conditional knock-out of the Bmp2 gene with the αSMACreERt2 model, we discovered major defects in formation of the alveolar bone, cementum, both cellular and acellular, as well as formation of periodontal ligaments or PDL in the absence of the Bmp2 gene in these stem cells. We observed decreased expression of Scleraxis, Tenomodulin, and Periostin, as well as Osterix in the Bmp2 cKO model. Utilizing Ai9 allele, (Rosa26-loxP-stop-loxP-tdTomato), we have demonstrated by lineage tracing methods, in the absence of the Bmp2 gene, that there are major defects in growth and expansion of these stem cells noted as early as 17 days after a single Tamoxifen injection (Cre activation at 6 days). By 1 month, we quantitated colocalization (Fiji/coloc2 program) of bone/cementum marker, Osterix (green FITC labeled antibody), and the td-Tomato+ (red) cells, and find a 60-70% reduction in aSMA+ cells differentiating to either alveolar osteoblasts or cellular cementoblasts. We used the Periostin antibody for periodontal ligament (PDL) cells, to also quantitate a 50% reduction in tdTomato+ stem cells capable of differentiating to mature PDL cells. Sirius red histology demonstrated that major regions of the PDL and cellular cementum are lacking or dysmorphic at 3 months of age. Purified αSMA+ periodontal stem cell differentiation, with and without the Bmp2 gene is now being used to characterize the transcriptome using RNA-seq methods. Thus, the Bmp2 gene in the periodontal stem population is required for expansion and differentiation of all three major mesodermal derived components of the period-ontium.

SU0233

Connectivity Map-Based Discovery Of Parbendazole As A Novel Osteogenic Compound. Andrea Brum*[1], Jeroen van de Peppel[2], Cindy van der Leije[2], Marco Eijken[3], Johannes Van Leeuwen[4], Bram Van Der Eerden[5]. [1]Erasmus MC, The Netherlands, [2]Erasmus MC, Netherlands, [3]Arcarios, Netherlands, [4]Erasmus University Medical Center, The Netherlands, [5]Erasmus MC, The Netherlands

Osteoporosis is a common skeletal disorder characterized by low bone mass leading to increased bone fragility and fracture susceptibility. Little is currently known about what specific factors stimulate osteoblast differentiation from human mesenchymal stem cells (hMSCs). Our aim was therefore to determine novel factors and mechanisms involved in human bone production, which can be targeted to treat osteoporosis, using gene expression profiling and bioinformatic analyses, including the Connectivity Map (CMap), as an *in silico* approach.

The gene signature of osteogenic hMSCs (top significantly regulated genes 6 hours after induction by dexamethasone as assessed by Illumina microarrays) was uploaded into CMap (www.broadinstitute.org/cmap/). Osteogenic differentiation was assessed by analyses of alkaline phosphatase (ALP) activity and mineralization by calcium assay and alizarin red staining. Gene expression was determined by qPCR and BMP activity was assessed by reporter assay. Immunofluorescent analyses were performed to examine changes in the cytoskeleton.

The CMap identified parbendazole as a compound with the most significantly correlating gene signature to osteogenic hMSCs. Parbendazole stimulated osteogenic hMSC differentiation as indicated by increased ALP activity, mineralization and upregulation of ALP, osteopontin, and bone sialoprotein II, which interestingly occurs independent of the presence of glucocorticoids (GC). Moreover, strong upregulation of GC receptor (GR) target genes by GC is absent in parbendazole-treated cells and the effect was not inhibited by GR antagonist mifepristone. Parbendazole caused profound cytosketetal changes including strong inhibition of microtubules and increased number of focal adhesions. Stabilization of microtubules by pretreatment with taxol abolished osteoblast differentiation. Additionally, BMP-2 gene expression and activity is upregulated by parbendazole. Treatment of hMSCs with the BMP antagonist DMH1 in combination with parbendazole limited mineralization.

By combining genomic and bioinformatic tools against the backdrop of highly characterized human osteogenic MSCs we have identified a novel bone anabolic candidate that induces osteoblast differentiation through a combination of cytoskeletal changes and increased BMP-2 activity, and independent of GC stimulation. In addition, the results demonstrate the significance of cytoskeletal organization in osteogenic differentiation and the power of the CMap.

Disclosures: Andrea Brum, None.

SU0234

Cross-Species Transcriptomic Analysis Reveals Conserved Osteogenic Signatures During Zebrafish and Rat Bone Regeneration. Ronald Kwon*[1], Amarjit Virdi[2], D. Rick Sumner[2]. [1]University of Washington, USA, [2]Rush University Medical Center, USA

Modern advances in large-scale biological research underscore the potential impact of novel in vivo models of bone disorders that are genetically tractable, optically transparent, and amenable to high-throughput approaches. By virtue of its capacity to recapitulate the major phases of mammalian bone formation, the regenerating zebrafish tail fin provides a compelling system for such studies. In this investigation, our goal was to utilize cross-species transcriptomic analysis to quantify the extent to which gene expression signatures underlying mammalian bone formation are conserved during zebrafish fin regeneration. We compared genome-wide gene expression during zebrafish tail fin regeneration (d1, d3, and d5; GEO accession # GSE3667) and rat marrow ablation-induced intramembranous bone formation (d0, d1, d3, d5, d7, d10, d14, d28, and d56; GSE22321) using custom meta-analysis software that mapped zebrafish and rat protein sequence homology pairings to their respective genome microarray probe sets. Analysis revealed 1778 and 14,845 significantly altered genes during zebrafish and rat bone regeneration, respectively, between which 720 were identified as orthologous gene pairs. Genome-wide correlations (Fig 1) during zebrafish and rat initial healing (r=0.31 for d1 in zebrafish & d1 in rat, p<1e-16) and early osteogenesis (r=0.33 for d5 in zebrafish & d10 in rat, p<1e-16) were highly significant, approaching the 95% confidence interval for inter-sample correlations within each species (r=0.36-0.87 in zebrafish and r=0.51-0.64 in rat). Lower correlations were observed during zebrafish blastema formation (r=-0.15 to 0.17 for d3 in zebrafish and d1-d10 in rat), suggesting zebrafish and rat bone regeneration occur through distinct transcriptomic trajectories that converge during osteogenesis. Analysis of ortholog gene pairs revealed a number of genes implicated in disorders of bone mineralization (phex, lemd3, fkbp10, crtap, mmp2, sost, col1a1, col1a2, sparc, periostin), craniofacial disorders (msx2, twist1), and skeletal dysplasias (col10a1 ,col11a1, col11a2, fgr3), suggesting the potential to map gene regulatory networks underlying these disorders through cross-species strategies. Collectively, these studies identify genome-wide correlations and conserved gene expression signatures in zebrafish and rat intramembranous bone formation, an essential step toward cross-species examinations of bone anabolic pathologies in the zebrafish and mammalian skeletons.
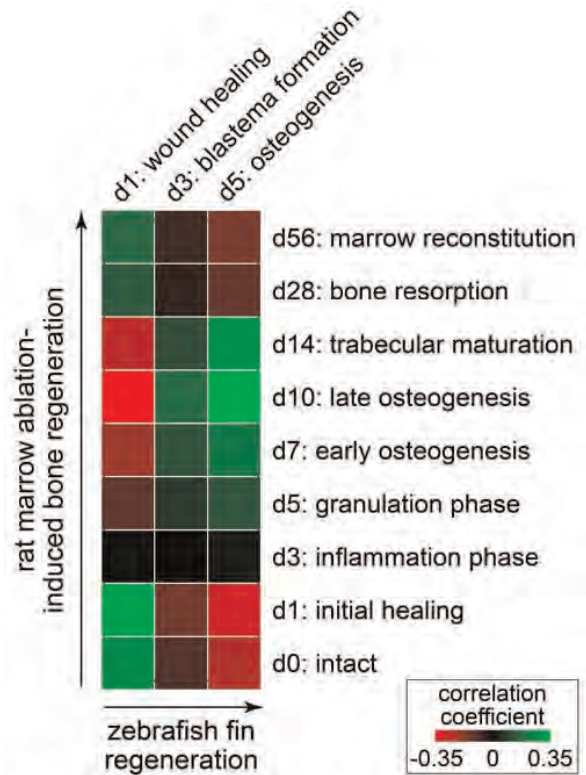
Fig 1: Correlation coefficients for genome-wide gene expression during zebrafish fin regeneration and rat marrow ablation-induced bone regeneration. Transcriptomes converge during initial healing (d1 in zebrafish and d1 in rat) and osteogenesis (d5 in zebrafish and d10 in rat).

Figure 1

Disclosures: Ronald Kwon, None.

SU0235

Evaluation of Potential Dried Plum Bioactive Components and their Effects on Osteoblast and Osteoclast Differentiation and Activity. Jennifer Graef*[1], Elizabeth Rendina-Ruedy[2], Jarrod King[3], Robert Cichewicz[4], Edralin Lucas[1], Brenda Smith[1]. [1]Oklahoma State University, USA, [2]Vanderbilt University Medical Center, USA, [3]Natural Products Discovery Group, University of Oklahoma, USA, [4]Natural Products Discovery Group, Department of Chemistry & Biochemistry, University of Oklahoma, USA

Osteoporosis treatment strategies utilizing naturally occurring phytochemicals that are abundant in certain functional foods may provide cost-effective alternatives with fewer side effects. Previously, we reported a biphasic effect of dried plum (DP) treatment *in vivo*, characterized by an initial suppression of osteoblast and osteoclast number followed by a rebound of osteoblast activity occurring later. The purpose of this study was to begin to identify the bioactive components in DP and to examine their effects on osteoblast and osteoclast differentiation and activity under normal and inflammatory conditions. A polyphenolic extract from DP was fractionated via chromatography using HP-20 resin and increasing concentrations of methanol to yield 8 fractions of interest. Toxicity was determined by evaluating the dose-escalating effects of the fractions on the viability of RAW 264.7 (monocytes/macrophages) and MC3T3-E1 (osteoblast precursor) cells using the MTT (3-[4,5-dimethylthiazol-2-yl]-2,5 diphenyl tetrazolium bromide) assay. Doses that were not detrimental to cellular growth/viability were studied. Osteoblast differentiation and activity were determined by assessing extracellular alkaline phosphatase (ALP) and quantifying ALP staining density and an Alizarin Red stain for mineralization. Osteoclast differentiation was assessed by culturing RAW 264.7 cells in the presence of receptor activator NF-kappa B ligand (RANKL) and quantifying the large, multi-nucleated TRAP-positive stained cells. Under normal conditions, there was no change in osteoblast activity at day 1 of treatment, but by day 3, suppression of extracellular ALP was occurring with most of the fractions. Osteoclastogenesis, as indicated by the number of TRAP-positive cells, was reduced. Mineralization by osteoblasts was not affected by treatments under normal conditions, but certain fractions were able to restore mineralization under inflammatory conditions to that of the control. In contrast, the fractions did not

restore the LPS-induced increase in osteoclast differentiation to that of the control. Together, these data support the notion that compounds within these fractions initially suppress bone turnover, similar to that observed in our previous *in vivo* study. Certain fractions have a more robust response in the osteoblast cell line, and these fractions will be further studied to determine how they alter osteoblast and osteoclast activity using primary cells cultures and *in vivo* models.

Disclosures: Jennifer Graef, None.

SU0236

Foxp1 Regulaes Osteogenic/Adipogenic Cell Fate Commitment in Bone Marrow Mesenchymal Stem Cell. <u>Xizhi Guo</u>[1], <u>Hanjun Li</u>*[2], <u>Sixia Huang</u>[2]. [1]Shanghai Jiao Tong University, Peoples Republic of China, [2]Bio-X Institutes, Shanghai Jiao Tong University, China

Mesenchymal stem cells (MSCs) in bone marrow are capable to differentiate into osteoblasts and adipocytes. And more, the differentiative preference of MSCs between osteoblastic and adipogenic lineages is dynamic as bone aging. However, the molecular mechanisms underlying the determination process is not fully clarified. Here we showed that the transcription factor Foxp1 plays an important role in the cell fate determination of bone marrow MSCs. Elevated fat formation and decreased bone formation bone marrow was observed in mice with MSC-targeted deletion of Foxp1. Foxp1-deficient MSCs in both Nestin-Cre; Foxp1c/c and Prx1-Cre; Foxp1c/c mice differentiated into adipocytes at expense of osteoblasts in CFU assays. Conversely, over-expression of Foxp1 in C3H/10T1/2 cells resulted in a severe blockage of adipocyte differentiation, accompanied by an increase of osteoblast differentiation. Molecularly, Foxp1 suppressed the transcactvation of Pparg (one of the master activators in adipogenesis) through interacting with and antagonizing Cebpβ/δ proteins, which are two important inducers during early adipogenic commitment. In addition, Foxp1 repressed adipogenic differentiation in its synergistical association with another adipogenic suppressor Hdac7. Taken together, Foxp1 modulates MSC differentiation as a novel switch between adipogenic and osteoblastic commitment.

Disclosures: Hanjun Li, None.

SU0237

IGBBP-2-Regulated Sequential Activation of AMP-Activated Protein Kinase is Required for Osteoblast Differentiation. <u>Gang Xi</u>*[1], <u>Christine Wai</u>[1], <u>Victoria Demambro</u>[2], <u>Clifford Rosen</u>[3], <u>David Clemmons</u>[1]. [1]Department of Medicine, University of North Carolina at Chapel Hill, USA, [2]Maine Medical Center Research Institute, USA, [3]Maine Medical Center, USA

AMP-activated protein kinase (AMPK) regulates skeletal muscle differentiation but studies analyzing its role in osteoblast differentiation have given contradictory results therefore, we determined the temporal sequence of AMPK activation during differentiation using mouse calvarial osteoblasts. The results showed that differentiation medium stimulated AMPK activation at the early stages of differentiation (e.g. days 3-9) but this change was significantly attenuated at the later stages of differentiation (e.g. days 12-21). To definitively determine the role of AMPK, we manipulated AMPK activation using chemical compounds and mutagenesis. Addition of compound C (an AMPK inhibitor) on day 0 or 3 significantly reduced differentiation but had no effect at later time points. In contrast overexpression of constitutively activated AMPK (T172D) dramatically inhibited cell differentiation (e.g., $88 \pm 10\%$ suppression compared to control cells, p<0.01) and this inhibition could be rescued by addition of compound C on days 9 or 12. In contrast stimulation of AMPK activation on days 9 and 12 with Metformin significantly inhibited differentiation. Therefore there appears to be a critical window of AMPK activation between days 3-9 that is required for differentiation.

Since our previous studies have shown that IGFBP-2 stimulates osteoblast differentiation, we determined whether IGFBP-2 regulates AMPK activation. Analysis of IGFBP-2 expression showed that it was increased on days 3-6 and declined days 9 - 12, which paralleled the decline in AMPK activation. Overexpression of IGFBP-2 enhanced AMPK activation (e.g., $35 \pm 6\%$ and $87 \pm 9\%$ increases on days 3 and 6, respectively, p<0.05). A peptide containing the heparin binding domain of IGFBP-2, a sequence that mediates the effect of IGFBP-2 on osteoblast differentiation, enhanced AMPK activation at the early stage (e.g., $76 \pm 18\%$ increase on day 6, compared to control cultures, p<0.05). The inhibitory effect of compound C added on days 0 or 3 was less effective in IGFBP-2 overexpressing cells compared to control cells. Consistently, AMPK activation was significantly impaired from days 3 to 9 in IGFBP-2 knockdown cells and in calvarial osteoblasts isolated from IGFBP-2 -/- mice. We conclude that AMPK activation followed by its down regulation after day 9 is required for osteoblast differentiation and that IGFBP-2 stimulation of AMPK activation is one of the mechanisms by which regulates osteoblast differentiation.

Disclosures: Gang Xi, None.

SU0238

Withdrawn

SU0239

Parathyroid Hormone (1-34) Increases the Numbers and Differentiation of Osteoblast Progenitor Cells *in Vivo*. <u>Deepak Balani</u>*[1], <u>Noriaki Ono</u>[2], <u>Henry Kronenberg</u>[3]. [1]Massachusetts General Hospital & Harvard Medical School, USA, [2]University of Michigan School of Dentistry, USA, [3]Massachusetts General Hospital, USA

A once daily injection of hPTH (1-34) to mice increases trabecular and cortical bone by prolonging the lifespan of osteoblasts by suppressing their apoptosis and activating quiescent lining cells. However, very little is known about the effects of PTH on progenitors of osteoblasts *in vivo*. We investigated whether once daily injections of PTH have effects on osteoblast progenitors. In col2α1-creERT mice, shortly after tamoxifen administration, Rosa26-tomato reporter expression is observed in chondrocytes, perichondrial cells and cells in primary spongiosa. After a prolonged chase, the tomato label is found in mature osteoblasts and adipocytes. We hypothesized that this system could be used to study the effects of hPTH (1-34) on early cells of the osteoblast lineage *in vivo*. 6-8 week old triple transgenic mice carrying col2α1-creERT, Rosa26-tomato reporter, and osteocalcin (Ocn)-GFP received 2 mg tamoxifen once. After 24h, once daily subcutaneous injections of 100 and 500ug/kg hPTH (1-34) or vehicle was begun. Mice were sacrificed 3, 7 and 21d after the tamoxifen injection and hind limbs were dissected. Long bones were utilized for flow cytometry or processed for histology. Flow cytometry analysis showed a dose dependent increase of tomato+ cells on day 3, 7 and 21. We chose mice treated with 500ug/kg hPTH (1-34) for all subsequent experiments. Compared to control mice PTH-treated mice showed a 6-fold increase in the number of tomato+ cells. After 3d there was no tomato/GFP+ cell, suggesting that no tomato+ cell had differentiated into Ocn-GFP+ osteoblast yet. After 7 and 21d in PTH-treated mice, tomato+ cells showed a 3- and 7-fold increase respectively over control mice. We also observed a 6-fold increase in the number of GFP/tomato+ cells after 7 and 21d. Assessment of tomato+ cells using epifluorescent/ confocal microscopy was consistent with the observations from flow cytometry. After 3w of daily PTH injections, compared to control mice, a 6-fold higher number of tomato+ cells were seen throughout the metaphyseal region extending towards the diaphysis. Counting of tomato/GFP+ cells showed a 4-fold increase in the PTH-treated mice compared to the control mice. These data suggest that the col2α1-creERT promoter is active in 6-8 week old mice in osteoblast progenitor cells. Administration of once daily injections of PTH to such mice significantly increases the number of tomato-positive cells that, over time, become Ocn-GFP expressing osteoblasts.

Disclosures: Deepak Balani, None.

SU0240

PDGF-AA promotes osteogenic differentiation and migration of mesenchymal stem cell by down-regulating PDGFRa and derepressing BMP-Smad1 signaling. <u>Qian Cong</u>*[1], <u>James Yeh</u>[2], <u>Xuechun Xia</u>[3], <u>Yuji Mishina</u>[4], <u>Aijun Hao</u>[5], <u>Baojie Li</u>[6], <u>Huijuan Liu</u>[3]. [1]Bio-X institute, Key laboratory for the Genetics of Developmental & neuropsychiatric Disorders, Ministry of Education, Shanghai Jiao Tong University, China, [2]Winthrop University Hospital, USA, [3]The Bio-X Institutes, Key Laboratory for the Genetics of Developmental & Neuropsychiatric Disorders, Ministry of Education, Shanghai Jiao Tong University, China, [4]University of Michigan School of Dentistry, USA, [5]Key Laboratory of the Ministry of Education for Experimental Teratology, Shandong University, China, [6]Shanghai Jiao Tong University, Peoples Republic of China

Platelet-derived growth factors (PDGFs) play important roles in skeletal development and bone fracture healing, yet how PDGFs execute their functions remains incompletely understood. Here we show that PDGF-AA, but not -AB or -BB, could activate the BMP-Smad1/5/8 pathway in mesenchymal stem cells (MSCs), which requires BMPRIA as well as PDGFRa. PDGF-AA promotes MSC osteogenic differentiation through the BMP-Smad1-Runx2/Osx axis and MSC migration via the BMP-Smad1-Twist1 axis. Mechanistic studies show that PDGF-AA activates BMP-Smad1 signaling by feedback down-regulating PDGFRa, which frees BMPRI and allows for BMPRI-BMPRII complex formation to activate smad1/5/8, using BMP molecules in the microenvironment. This study unravels a physical and functional interaction between PDGFRa and BMPRI, which plays an important role in MSC differentiation and migration and establishes a link between PDGF-AA and BMPs pathways, two essential regulators of embryonic development and tissue homeostasis.

Disclosures: Qian Cong, None.

SU0241

Comparative Multi-lineage Differentiation of Mandible and Femur Canine Mesenchymal Stem Cells. <u>Juan Bugueno</u>[1], <u>Weihua Li</u>[1], <u>Pinky Salat</u>[1], <u>Sunday Akintoye</u>*[2]. [1]University of Pennsylvania School of Dental Medicine, USA, [2]University of Pennsylvania School of Dental Medicine, USA

BACKGROUND: Mesenchymal stem cells (MSCs) are promising donor grafts for tissue regeneration. MSCs are phenotypically and functionally skeletal site-specific based on extensive studies using human and rodent MSCs but there is paucity of information on canine MSCs (cMSCs) and their regenerative applications in veterinary care. We hypothesized that cMSCs are functionally skeletal-site specific and that canine mandible MSCs (cmMSCs) are highly osteogenic relative to femur MSCs (cFMSCs).

Methods: Trabecular bone samples were obtained from mandible and femur of normal healthy dogs. Primary cmMSCs and cFMSCs were established in culture. Using early passage cells, colony-forming units (CFU), cell proliferation and population doubling capacity were assessed. Using established induction culture conditions, _in vitro_ osteogenesis, chondrogenesis, and adipogenesis were assessed. Western blotting and real time PCR were used to assess the following osteogenic markers: alkaline phosphatase (ALP), bone sialoprotein (BSP), osteocalcin (OCN) and osteopontin (OPN). Chondrogenesis was assessed using pellet culture method and histologic sections were stained with Alcian blue; adipogenically induced-cultures were stained with Oil Red O. Furthermore, _in vivo_ osteogenesis was assessed using the mouse model of _in vivo_ bone regeneration. Transplants were harvested at 6, 8 and 12 weeks for histological analysis.

Results: The cmMSCs demonstrated 1.5 to 2 fold increases in CFU, proliferation and population doublings relative to cFMSCs. Similar pattern was displayed by cmMSCs based on expression levels of BSP, ALP and OCN but OPN levels were not significantly different. Adipogenesis based on number of stained lipid droplets per unit area in cmMSCs were also moderately higher than cFMSCs but chondrogenic response were similar in both cell types. Evaluation of _in vivo_ bone formation by transplanted cells is still pending.

CONCLUSIONS: cmMSCs are apparently more responsive to multi-lineage differentiation relative to cFMSCs and can potentially serve as donor graft materials for oral bone regeneration.

Disclosures: Sunday Akintoye, _None._

SU0242

BMP2 induced _de novo_ bone formation utilizes different progenitors in rats versus mice and humans. <u>Corinne Sonnet</u>*[1], <u>Eleanor Davis</u>[2], <u>ZaWaunyka Lazard</u>[1], <u>Eric Beal II</u>[2], <u>Elizabeth Salisbury</u>[1], <u>Alan Davis</u>[1], <u>Elizabeth Olmsted-Davis</u>[1]. [1]Baylor College of Medicine, USA, [2]Baylor College of Medicine, USA

We developed a cell-based gene therapy approach for inducing _de novo_ bone formation at a targeted site as a means of rapidly inducing spine fusion. We tested this therapy through direct injection into the paraspinous musculature in a murine model of posterolateral spine fusion and observed stable fusion as early as 2 weeks. To further suppress any immunological response and provide the ability to re-inject the materials, we have encapsulated the cells in a PEG-DA hydrogel. Studies in which control adenovirus transduced cells were injected prior to delivery of the AdBMP2 transduced cells (therapy), demonstrated the ability of the hydrogel encapsulation to rescue the bone formation. In these studies, bone formation was similar in the primed animals with the encapsulated therapy as those without priming and no encapsulation. Surprisingly, unlike the mouse _de novo_ bone formation did not occur in rat spine, without inclusion of periosteal cells. Characterization and comparison of the bone formation in mice and rats showed that they utilize a different source of osteogenic progenitors. Further, studies which included either the mouse osteogenic cells or mesenchymal stem cells (MSCs) did not result in rescuing the bone formation although the MSCs did incorporate into bone when included in the mouse. Detailed analysis of the mechanism of the two systems reveals significant differences. Further, comparison of human osteogenic cells observed in patients with early heterotopic ossification, showed more similarities to the mouse progenitors. In conclusion, rats may not accurately reflect human physiology with respect to BMP2 induced _de novo_ bone formation. Thus significant biological consideration may be required for selecting an appropriate preclinical model for these types of therapies.

Disclosures: Corinne Sonnet, _None._

SU0243

Culture of Human BM-MSC in Physiological O2 Improves Robustness of Bone Formation in a Mouse Calvarial Defect Model. <u>Xiaonan Xin</u>*[1], <u>Xi Jiang</u>[2], <u>Liping Wang</u>[1], <u>Paiyz Mikael</u>[3], <u>Kyle Shin</u>[3], <u>Syam Nukavarapu</u>[3], <u>David Rowe</u>[1], <u>Alexander Lichtler</u>[1]. [1]University of Connecticut Health Center, USA, [2]University of Connecticut Health Center, USA, [3]University of Connecticut Health Center, USA

Human bone marrow derived mesenchymal stem (or stromal) cells (hBM-MSC) are a valuable source of cells with bone-forming potential for basic science and for therapy of human bone disease. However, their bone forming potential has often been found to be inconsistent, with dependence on passage number, age and medical condition of the bone marrow donor, and, in the case of in vivo bone formation assays, the scaffold used. It has been reported that cell culture under 5% O_2 produces a dissolved O_2 concentration that is more similar to physiological O_2, and that this decreases the production of reactive oxygen species, which decreases cell stress and genetic damage. We have compared the ability of hBM-MSC cultured under 5% O_2, to cells grown under ambient O_2 for their ability to form bone in our calvarial defect model. hBM-MSC were obtained from 20-30 year old commercial donors, or from 50 to 60 year old patients. We also tested cells that had been plated directly from whole bone marrow under standard bone marrow culture conditions, and cells that were enriched for white blood cells using the Magellan automated cell separator (Arteriocyte Medical Systems). We tested cells cultured for 1, 2 and 3 passages, and whole, uncultured bone marrow. We also tested hBM-MSCs from a commercial source that had been passaged 2-3 times before we obtained them. Cells were tested in our calvarial defect model. In some cases, cultured cells were transduced with a ubiquitin promoter driven RFPcherry expressing lentiviral vector to aid in identifying human cells. The implants were harvested after 8 weeks, and analyzed using our frozen section tape transfer method. Human bone formation was indicated by cells staining for human nuclear antigen that were alkaline phosphatase positive, associated with newly formed bone that contained human antigen positive osteocytes and stained with a human specific bone sialoprotein antibody. Our results were that uncultured bone marrow, and commercial passaged cells, never formed bone. Cultured cells from older surgical patients formed bone at passage 1 but not after 3 passages in ambient O_2, but formed bone robustly after 3 passages in 5% O_2. Cells from younger BM donors formed bone after 3 passages in both 5% and ambient O_2, although the bone formed by 5% O_2 cells had a more mature appearance. Thus low O2 culture seems to improve the robustness of in vivo bone formation.

Disclosures: Xiaonan Xin, _None._

SU0244

Early reversal cells: osteoblastic nature, catabolic function and interaction with osteoclasts. <u>Mohamed Essameldin Abdelgawad</u>[1], <u>Jean-Marie Delaisse</u>*[2], <u>Maja Hinge</u>[1], <u>Ragad Walid Hamid</u>[1], <u>Lars Rolighed</u>[3], <u>Lars H Engelholm</u>[4], <u>Niels Marcussen</u>[5], <u>Thomas Levin Andersen</u>[1]. [1]Department of Clinical Cell Biology (KCB), Vejle Hospital – Lillebaelt Hospital, IRS, University of Southern Denmark, Denmark, Denmark, [2]Vejle Hospital, IRS, University of Southern Denmark, Denmark, [3]Aarhus University Hospital, Denmark, [4]The Finsen Laboratory, Rigshodpitalet/Biotech Research & Innovation Centre (BRIC), University of Copenhagen, Denmark, [5]Department of Clinical Pathology, Odense University Hospital, Odense, Denmark, Denmark

The reversal phase is an intermediate phase in the bone remodelling process, needed to prepare the eroded surfaces vacated by the osteoclasts for bone formation. The reversal cells colonizing the vacated eroded surfaces during the reversal phase are mononuclear cells that are immunoreactive for osteoblastic markers, and whose function and interaction with the osteoclasts remains poorly investigated. Herein, we studied the reversal cells in human cancellous bone biopsies from 25 controls, confirming that reversal cells are of osteoblastic nature, even though they sometimes are immunoreactive for TRAcP, which in comparative immunostainings and in situ hybridisations was shown to be taken up from neighbouring TRAcP-expressing osteoclasts. The early osteoblastic reversal cells were also shown to have direct cell-cell contacts with the neighbouring osteoclasts, and shown to interact with the demineralised resorption debris left behind by the osteoclasts. Collectively, these data supports that early osteoblastic reversal cells interact both directly and indirectly with the neighbouring osteoclasts. The early reversal cells appear to have a catabolic/collagenolytic function, involving: extracellular collagenases of the MMP family generating defined ¾-collagen fragments, including MMP-13 (collagenase-3), and to some extent the endocytic collagen receptor uPARAP/Endo180, supporting the notion that they clean the eroded surfaces from resorption debris. Interestingly, the presence of MMP-13 in reversal cells decreased with age, indicating that the cleaning activity of reversal cells may become less efficient with age. Late reversal cells next to osteoid surfaces are functionally and phenotypically different from early reversal cells next to osteoclasts, as they show less immunoreactivity for the ¾-collagen fragment, MMP-13 and uPARAP and have a morphological resemblance to mature bone forming osteoblasts, supporting that the reversal cells gradually change during the reversal phase. Collectively, this study stresses that the early osteoblastic reversal cells as a privileged partner of the osteoclasts in the bone resorption-bone formation coupling mechanism during the bone remodelling.

Disclosures: Jean-Marie Delaisse, _None._

SU0245

Intravital Multiphoton Imaging of Skeletal Progenitor Cells in Bone Tissue-Engineered Constructs. Pieter-Jan Stiers*[1], Nick Van Gastel[1], Karen Moermans[2], Ingrid Stockmans[2], Geert Carmeliet[3]. [1]Laboratory of Clinical & Experimental Endocrinology, KU Leuven, Belgium, Belgium, [2]Laboratory of Clinical & Experimental Endocrinology, KU Leuven, Belgium, Belgium, [3]Katholieke Universiteit Leuven, Belgium

Bone tissue engineering using scaffolds, skeletal progenitor cells and osteogenic growth factors is a promising therapy for non-healing bone defects, but still largely depends on a trial and error approach. A major reason is that the in vivo behavior of the implanted cells and the response of the host tissues are still poorly understood. Insight in the early stages of the healing process are crucial because once the bone formation process is started it will largely recapitulate the bone development pathways. Analysis of these early time points using conventional techniques however does not provide dynamic information on cell behavior and on the interactions with the host tissue. To obtain insight in these processes, we developed an intravital imaging setup based on an established model for ectopic bone formation.

First, we analyzed whether the imaging windows had any influence on bone formation using microCT and histological analysis. There was only a small delay in the formation of cartilage and mineralized matrix compared to ectopically implanted scaffolds after 21 days of implantation. In addition, the inflammatory reaction at early time points was comparable between the imaging windows scaffolds and the ectopically implanted scaffolds. Next, scaffolds seeded with fluorescently labeled murine periosteum-derived cells were implanted and repeatedly imaged with a multiphoton microscope. A procedure was developed to trace the same cell population over a 2 week implantation period in relation to the collagen matrix, visualized through second harmonics generation. Seeded cells displayed diverse behavior and fate across scaffold types, which correlated to different outcomes at later time points. Changes in host blood vessels, perfused with FITC-dextrans, were observed within 6 days after implantation, but vascularization of the scaffold did not occur until day 11. Further optimization of this technique and use of reporter constructs will provide new insight into the mechanisms of bone regeneration and of therapeutic growth factors.

In conclusion, multiphoton intravital imaging is a promising technique that will allow us to study cell behavior and scaffold-host interactions non-invasively inside an implanted tissue engineered construct.

Disclosures: Pieter-Jan Stiers, None.

SU0246

LARG GEF and ARHGAP18 GAP Control Cytoskeletal Dynamics to Influence MSC Lineage Allocation. William Thompson*[1], Sherwin Yen[2], Gunes Uzer[1], Zhihui Xie[2], Buer Sen[3], Maya Styner[4], Keith Burridge[5], Janet Rubin[4]. [1]University of North Carolina, USA, [2]University of North Carolina, USA, [3]University of North Carolina At Chapel Hill, USA, [4]University of North Carolina, Chapel Hill, School of Medicine, USA, [5]University of North Carolina, USA

Bone density depends on mesenchymal stem cell (MSC) lineage allocation where adipogenic commitment depletes the pool available for osteogenesis. Cell architecture influences lineage decisions, as the cytoskeleton aligns critical elements that underwrite cellular responses to the mechanical and physical environment. Disruption of the actin cytoskeleton and RhoA activity tip MSC fate in favor of adipogenesis. We have shown that application of mechanical strain suppresses MSC adipogenesis by enhancing cytoskeletal structure through activation of RhoA via Fyn/mTORC2/AKT signaling. RhoA activity is directed by two distinct protein families, GEFs (RhoA activators) and GAPs (RhoA deactivators). In fibroblasts, ARHGAP18, a little studied GAP, suppresses RhoA leading to decreased actin stress fiber formation and motility, while the GEF LARG regulates RhoA activation in response to force. We hypothesized that ARHGAP18 and LARG determine MSC commitment by altering RhoA and cytoskeletal architecture. We observed no alteration in MSC lineage following siRNA knockdown of LARG; however, basal RhoA activity was significantly decreased and mechanical activation of RhoA was almost entirely prevented. This implicates LARG as the major GEF responding to substrate strain in MSCs. In contrast, stable shRNA knockdown of ARHGAP18 both increased basal RhoA activity and enhanced the response to mechanical strain. Additionally, actin stress fiber formation was enhanced in ARHGAP18 knockdown cells. As the actin cytoskeleton is known to modulate MSC fate, we reasoned that ARHGAP18 should affect MSC differentiation. In ARHGAP18 null MSCs adipogenesis was significantly suppressed, as assessed by Oil-Red-O staining and Western blot. Additionally, when cultured in osteogenic media, ARHGAP18 knockdown enhanced osteogenic commitment, confirmed by alkaline phosphatase staining and PCR. This suggests that ARHGAP18 is a critical tonic inhibitor of MSC cytoskeletal assembly, returning RhoA to an "off state". In contrast, LARG is recruited during active mechanical strain, and as such its absence has less effect on the resting RhoA state. In summary, control of RhoA cycling between on and off states relies on ARHGAP18 when quiescent, with LARG playing a predominant role in the active mechanical control of actin remodeling. Thus, both of these GTP exchangers converge on RhoA to regulate the MSC response to static and dynamic physical factors, influencing lineage allocation.

Disclosures: William Thompson, None.

SU0247

Temporal Nocturnin expression leads to impaired peak bone acquisition. Anyonya Guntur*[1], Phuong Le[1], Jeremy Stubblefield[2], Carla Green[2], Clifford Rosen[3]. [1]Maine medical center research institute, USA, [2]Department of Neuroscience, University of Texas Southwestern Medical Center, USA, [3]Maine Medical Center, USA

Osteoporosis is associated with an increase in marrow adiposity and reduced bone mass resulting in increased fracture risk. Allocation of bone marrow mesenchymal stromal cells towards the adipogenic lineage is one potential mechanism for age-related bone loss. Nocturnin (*Noc*), a circadian deadenylase induced by *Pparg* activation, can regulate lineage allocation. Previously, we showed that *Noc*-/- mice have higher bone mass compared to controls and are protected from Rosiglitazone induced bone loss. To test whether activation of *Noc* results in bone loss, we utilized a Doxycycline (Dox) inducible (Tet-ON) mouse model to overexpress *Noc in vivo*. In this model, the tetracycline responsive element (TRE) is fused to the *Noc* open reading frame (with a C-terminal 3x FLAG-Tag), and a Rosa promoter fused to the reverse-tetracycline trans-activator (rtTA) was used for regulating expression. Male mice were put on either 2mg/mL of Dox supplemented with 1mg/mL of saccharin (Dox+Sacch) or saccharin (Sacch) water starting at 4 weeks of age. Areal bone mineral density (aBMD) and bone mineral content (aBMC) were measured by DEXA; femur trabecular and cortical microarchitecture were measured using MicroCT. DEXA revealed that the *Noc* overexpressing mice on Dox+Sacch had a significant decrease in total aBMD and aBMC (n=6-8, p=0.001 and p=0.02 respectively) compared to Sacch mice at 12 weeks. MicroCT analysis (n=3) showed that trabecular BV/TV and trabecular thickness was significantly lower in the Dox+Sacch treated group (p=0.01 and p=.0009 respectively) although there was no difference in trabecular number or trabecular spacing. In addition, cortical thickness was significantly decreased in the Dox+Sacch treated group (p=0.0007). To determine if Dox or Sacch has an effect on the skeleton, we treated male C57BL/6J (B6) mice with Dox+Sacch and Sacch in similar manners. DEXA revealed no skeletal differences between the two groups (n=10-12). In conclusion, temporal *Noc* expression results in impaired peak bone acquisition, in part due to changes in lineage allocation.

Disclosures: Anyonya Guntur, None.

SU0248

Dibenzazepine, a gamma-secretase inhibitor, inhibits osteoclastic bone resorption by suppressing c-Src activation. Bong Jun Kim*[1], Won Jong Jin[1], Hong-Hee Kim[2], Hyunil Ha[3], Zang Hee Lee[4]. [1]Department of Cell & Developmental Biology, School of Dentistry, Seoul National University, South Korea, [2]Seoul National University, South Korea, [3]Korean Medicine-Based Herbal Drug Development Group, Korea Institute of Oriental Medicine, South Korea, [4]Seoul National University School of Dentistry, South Korea

Tyrosine kinase c-Src plays an important role in actin ring formation and bone resorption activity in osteoclast. Therefore, c-Src has been targeted for the treatment of osteolytic disorders. In the present study, we found that dibenzazepine (DBZ), one of the γ-secretase inhibitors (GSIs), has bone protective effect against osteoclast-mediated excessive bone resorption both in vitro and in vivo. Although DBZ did not affect osteoclast differentiation, DBZ significantly suppressed non-receptor tyrosine kinase c-Src phosphorylation at tyrosine 416 and proline-rich tyrosine kinase 2 (PYK2) phosphorylation at tyrosine 402. Moreover, c-Src binding ability as a adaptor protein also suppressed by DBZ treatment. Therefore, inhibitory effects of DBZ on osteoclast exhibited abnormal spreading and disturbed actin ring formation with inhibition of resorption activity. Competitively treatment of Src family activator rescued the anti-resorptive effects of DBZ, suggesting that DBZ mainly attributed to the c-Src-mediated bone resorption. Consistent with the *in vitro* results, interleukin-1 (IL-1) induced bone destruction was strongly suppressed by administration of DBZ. Collectively, we demonstrated that DBZ has inhibitory effects on bone resorptive activity by targeting disruption of c-Src activity in osteoclast and our results suggest that DBZ may serve as a useful agent for osteoclast-mediated excessive bone resorption.

Disclosures: Bong Jun Kim, None.

SU0249

Effect of IL-4 on mechanical loading-induced osteoclastogenesis and bone resorption. Hideki Kitaura*[1], Zaki Hakami[2], Keisuke Kimura[3], Masahiko Ishida[4], Jafari Saeed[2], Haruki Sugisawa[2], Teruko Takano-Yamamoto[5]. [1]Tohoku University, Japan, [2]Tohoku University, Japan, [3]Tohoku university, Japan, [4]Tohoku UniversityGraduate School of Dentistry, Japan, [5]Tohoku University, Japan

Mechanical loading exerts important effects on the skeleton by controlling bone mass and strength. Osteoclasts are required for bone resorption and remodeling. Two cytokines are required for osteoclasts formation, M-CSF and RANKL. TNF-α has also been recognized as important factor for osteoclastogenesis. It also been reported

that TNF-α plays an important role in mechanical loading-induced osteoclastogenesis and bone resorption. IL-4 is a recognized immunomodulatory cytokine that regulates bone hemostasis. However, its influence on mechanical loading-induced osteoclastogenesis and bone resorption is still unknown. Orthodontic tooth movement is a good model for exploring the mechanism underlying the mechanical loading-induced bone changes. Thus, the purpose of this study was to investigate the effect of IL-4 on orthodontic movement and associated root resorption in mice model. Mouse orthodontic tooth movement model was established, and investigate whether IL-4 inhibit osteoclastogenesis and bone resorption on mechanical loading. The maxillary first molars of male mice were subjected to mesial force by A Ni-Ti coil spring. Varying doses of IL-4 from 0 to 1.5 µ/day were injected locally adjacent to the first molar every other day. After 12 days of experimental tooth movement, the amounts of orthodontic movement and the number of tartrate-resistant acid phosphatase (TRAP)-positive cells along the loaded alveolar bone and root surface was counted as osteoclasts and odontoclasts, respectively, in histological sections. The root resorption associated orthodontic movement was also evaluated by scanning electron microscope. Orthodontic tooth movement and the number of osteoclasts were significantly decreased in IL-4 treated mice. IL-4 inhibited tooth movement in dose-dependent manner. IL-4 significantly suppressed the mechanical loading-induced odontoclasts and root resorption. These results suggest that IL-4 might be a useful adjunct to regulate the extent of orthodontic tooth movement and control root resorption.

Disclosures: Hideki Kitaura, None.

SU0250

Estrogen does not Facilitate Apoptosis, but Inhibit Bone Resorption by Regulation of V-ATPase in Avian Medullary Bone Osteoclasts. Shinji Hiyama*[1], Yumiko Kadoyama[2], Mineo Watanabe[2], Takashi Uchida[2]. [1]Hiroshima University Institute of Biomedical & Health Sciences, Japan, [2]Hiroshima University, Japan

Medullary bone (MB) of female birds acts as a calcium reservoir of egg-shell formation and is remodeled in the bone marrow cavity under the control of circulating estrogen. MB forms by a single injection of estrogen even in the male bird and is resorbed vigorously by osteoclasts with diminished circulating estrogen level. In this process, increased circulating estrogen does not facilitate apoptosis of osteoclasts, while this hormone induces mammalian osteoclasts apoptosis, which may be implicated in postmenopausal bone loss. Clarifying the role of estrogen in avian osteoclasts may be helpful to identify additional roles of estrogen in bone. We previously reported that estrogen had not effect on apoptosis of MB osteoclasts, while their activity and morphology were affected. Therefore, focusing on the effects of estrogen to bone resorption activity, we examined the expression of vacuolar H⁺-ATPase (V-ATPase) by use of the osteoclastogenesis induced by estrogen in the male avian *in vivo* and *in vitro*. Five days after first injection of estrogen (E2) into male Japanese quails, second injection of E2 was given to same quails. The femurs of these quails were analyzed histochemically. After second E2 injection, osteoclasts on the MB surface became smaller and flat-shaped and the immunoreactivity of V-ATPase was reduced in these cells progressively. Following this, after 3 days of single injection of E2, bone marrow cells were collected and cultured with or without 17β-estradiol (17β-E) in the presence of RANKL/M-CSF for a week. The expression of V-ATPase in these cells was examined by RT-PCR analysis and immunocytochemistry. The expression level of V-ATPase mRNA was decreased in the presence of 17β-E. Correspondingly, although V-ATPase immunoreactivity was also observed in these cultures, the immunereactivity was reduced in 17β-E-exposed cells. These results suggest that estrogen may inhibit bone resorption activity by the decrease of V-ATPase activity in avian osteoclasts. Further studies are needed to reveal the relationship between estrogen and the regulation of bone resorption including V-ATPase in avian osteoclasts.

Disclosures: Shinji Hiyama, None.

SU0251

Stromal cell-derived factor-1 (SDF-1) Elevations are Associated with Increased Osteoclast Formation and Bone Resorption in Transgenic or Ovariectomized mice. Philip Osdoby[1], Patricia Collin-Osdoby*[1], Linda Rothe[2], Xuefeng Yu[3]. [1]Washington University in St. Louis, USA, [2]Washington University, USA, [3]Tongji Hospital, China

SDF-1 (CXCL12), a multifunctional chemokine constitutively expressed by bone marrow stromal cells, has essential roles in lymphocyte, hematopoietic stem cell, and vascular biology through regulating cell homing, survival, mobilization, and angiogenesis. Previously, we and others have shown that SDF-1 promotes the chemotactic recruitment, fusion and development of avian, murine and human osteoclast precursors, as well as the survival of mature resorptive osteoclasts in vitro. To further examine SDF-1 roles in bone physiology or pathology in vivo, we have utilized three different model systems. First, in a chick chorioallantoic developmental model, focally administered SDF-1 dose-dependently increased avian osteoclast formation (numbers) and bone pit resorption on implanted bone chips concurrent with stimulating localized angiogenesis. Second, transgenic mice overexpressing SDF-1 (under an RSV promoter) demonstrated 2-fold more TRAP+ osteoclasts in metaphyseal regions of tibial bone sections compared to wild-type mice. Third,

microarray gene expression analyses of ovariectomized (OVX) mice, which undergo rapid bone loss following estrogen depletion, revealed increased expression of SDF-1 and its signaling receptor, CXCR4, for at least 4 months following OVX. Estrogen supplementation to prevent OVX-induced bone loss was found to also reduce OVX-stimulated SDF-1 expression. Moreover, an alternative receptor, CXCR7, that binds SDF-1 to sequester it away from CXCR4 and potentially interfere with SDF-1/CXCR4 responses, was downregulated by OVX but not if estrogen supplementation was provided. Finally, preliminary data suggest that elevated SDF-1 expression occurs in another murine bone osteolytic condition characterized by increased osteoclasts, bone resorption, and osteopenia. These and other findings lead us to conclude that elevated SDF-1 levels may be linked to pathological bone loss. If so, targeting the SDF-1/CXCR4 axis may be a novel therapeutic approach for the treatment of bone loss in osteoporosis or other osteolytic disorders.

Disclosures: Patricia Collin-Osdoby, None.

SU0252

BMP Responsive Smads Are Required for Osteoclast Differentiation. Amy Tasca*[1], Melissa Stemig[2], Aaron Broege[3], Brandon Huang[1], Eric Jensen[3], Kim Mansky[3], Raj Gopalakrishnan[3]. [1]University of Minnesota, USA, [2]University of Minnesota School of Dentistry, USA, [3]University of Minnesota, USA

Osteoclasts are regulated by numerous cytokines and growth factors including bone morphogenetic proteins (BMPs). BMPs bind to type I and type II receptors. Type I receptors then phosphorylate the receptor activated Smads (R-Smads), SMADs 1, 5 and 8 in the case of BMP signaling. The R-SMADs then bind Smad 4, a common Smad (co-Smad) and alter transcription. Our recent work indicates that osteoclasts express BMP receptors, BMP ligands, and that BMP signaling directly stimulates osteoclast formation in vitro and in vivo. Most recently we reported that loss of expression of BMP receptor type II (BMPRII) in osteoclasts results in an osteopetrotic phenotype primarily due to a change in noncanonical signaling by BMP receptors. While our BMPRII null osteoclasts confirmed the importance of BMPs in osteoclast differentiation, they did not allow us to address the importance of Smad 1, 5 and 8 expression and activation during osteoclast differentiation. In our current study intended to evaluate the role of SMADs, osteoclasts were isolated from Smad 1/5 or Smad 4 floxed mice and infected with control or CRE-expressing adenoviruses. Loss of either Smad 1/5 expression or Smad 4 expression resulted in fewer and smaller multinuclear osteoclasts compared to control infected cells. Smad 1/5 and Smad 4 null osteoclasts had less *DC-STAMP* and *cathepsin K* expression; however, *Nfatc1* expression was only changed in Smad 4 null osteoclasts and not in Smad 1/5 null cells. Lastly, we detected a significant decrease in resorption pits and area resorbed in both the Smad 1/5 and Smad 4 null osteoclasts. From this we conclude that SMAD signaling in required for osteoclast differentiation. Since osteoclast differentiation is inhibited in the Smad 1/5 and Smad 4 null osteoclasts, to better test SMADs' functional role in bone resorption, we treated fully mature wild-type osteoclasts with BMP2 with and without dorsomorphin, a chemical inhibitor that selectively blocks canonical BMP signaling. We found that BMPs stimulated resorption by mature osteoclasts whereas treatment with dorsomorphin blocked BMP's enhancement of osteoclast activity. Thus our work shows that the canonical BMP/SMAD pathway regulates both the formation and resorptive activity of osteoclasts and suggests that this pathway might be a novel target for antiresorptive therapies.

Disclosures: Amy Tasca, None.

SU0253

Ligand-mediated Notch Signaling Enhances Osteoclastogenesis and Resorption. Jason Ashley*[1], Jaimo Ahn[2], Kurt Hankenson[3]. [1]University of Pennsylvania, USA, [2]University of Pennsylvania, USA, [3]University of Pennsylvania, USA

Regulated Notch signaling is required for bone growth and healing. There are, however, conflicting reports on the role of Notch signaling in osteoclasts and their precursors. There is evidence for both stimulatory and inhibitory roles for Notch signaling in osteoclast differentiation. Based on studies by others using Notch activating antibodies, we hypothesized that Notch signaling can promote osteoclastogenesis. To address this, we investigated the effects of two Notch ligands, Jagged1 (JAG) and Delta-like1 (DLL), and two Notch inhibitors, DAPT and SAHM1, on the differentiation and function of osteoclasts.

Notch signaling was stimulated by culturing marrow-derived osteoclast precursors in tissue culture plates coated with immobilized goat anti-human Fc IgG (control), JAG-Fc, or DLL-Fc. Notch signaling was inhibited by adding DAPT or SAHM1 to the culture medium. Under M-CSF/RANKL-stimulated osteoclastogenesis, JAG, but not DLL, promoted a significant increase in osteoclast size and TRAP-stained well area compared to IgG. Conversely, both DAPT and SAHM1 significantly reduced osteoclast size and stained area compared to DMSO control. As measured by quantitative RT-PCR, JAG stimulation resulted in a significant increase in TRAP, cathepsin K, and MMP9 expression, while DAPT significantly decreased in cathepsin K expression.

To assess the function of osteoclasts under Notch stimulation and inhibition, osteoclasts were differentiated on hydroxyapatite-coated surfaces, and resorbed area was measured after 4 and 6 days. Both JAG and DLL significantly increased resorbed area compared to IgG control at day 4. At this time, DMSO control, DAPT, and SAHM1

groups were similar. At 6 days, however, IgG resorption matched JAG resorption, though DLL stimulation still showed significantly higher resorption than IgG control. DAPT and SAHM1 groups had significantly less resorption than DMSO control. In partial explanation for the enhanced osteoclast size and resorption seen in JAG and DLL stimulated osteoclasts, JAG and DLL both significantly increased expression of pro-fusion genes CD200 and DC-STAMP. DAPT significantly reduced expression of both CD200 and DC-STAMP, and SAHM1 significantly reduced expression of CD200.

These data indicate that Notch signaling is necessary for normal osteoclast differentiation and function, and Notch stimulation by JAG and DLL can increase osteoclast formation and function potentially by enhancing the fusion of osteoclast precursors.

SU0254

Bone substrate and Integrin beta 3 regulate critical pathways of cell cycle progression, proliferation and survival during terminal osteoclast differentiation. Ed Purdue*[1], Jonathan Hill[2], Steven Goldring[1], Tania Crotti[3], Gerald Nabozny[2], Kevin McHugh[4]. [1]Hospital for Special Surgery, USA, [2]Boehringer Ingelheim Pharmaceuticals, Inc., USA, [3]University of Adelaide, Australia, [4]University of Florida, USA

Background. Multiple lines of evidence have established that osteoclasts are required for physiologic bone resorption and pathological bone loss in inflammatory disorders. In vivo, analysis of osteoclasts at sites of bone resorption reveals that functionally activated osteoclasts are almost exclusively localized to the immediate bone surface, indicating that cell-substrate interactions contribute to terminal osteoclast differentiation. However, in vitro approaches to the delineation of osteoclastogenesis have almost always neglected to take into account the role of bone substrate in this process, and have been limited to the differentiation of multinucleated osteoclasts from myeloid precursor cells on tissue culture plastic substrate. In this study, we have employed a unique in vitro osteoclastogenesis system using authentic bone substrates coupled with expression profiling and pathway analysis to identify critical bone substrate-mediated pathways of osteoclast formation and activation. To further dissect the signaling pathways involved, we have also characterized the involvement of integrin beta 3 (itgb3), a critical cell surface mediator of osteoclast-bone interaction, in this process.

Methods Murine bone marrow derived macrophages from wildtype and itgb3 deficient mice were cultured in the presence or absence of RANKL on plastic, hydroxyapatite, or calvarial bone discs. RNA was isolated at different stages of osteoclast generation and subjected to microarray analysis. Pathway analysis was performed using GSEA and Ingenuity pathway analysis.

Results Of 1490 genes identified as upregulated by RANKL in differentiated osteoclasts, 5.4% were further upregulated by culture on the bone substrate; an additional 8.5% were downregulated. Pathway analysis identified that several key pathways including those regulating cellular function, death, survival, growth and proliferation, were profoundly impacted by the choice of substrate, and were further modulated by the presence or absence of itgb3 in cells growing on bone substrate.

Conclusions. Interaction of osteoclasts with the bone surface regulates multiple critical pathways of osteoclast formation and activation. Most notably, bone substrate regulates the transition from proliferation to activation during late stages of osteoclastogenesis. This suggests that developing osteoclasts can sense and respond to signals derived from bone substrate, and that these signals regulate the life cycle of the cell.

SU0255

The microRNA-26a regulates RANKL- induced osteoclast differentiation. Kabsun Kim*[1], Jung Ha Kim[2], Nacksung Kim[3]. [1]Chonnam National University Medical School, South Korea, [2], South Korea, [3]Chonnam National University Medical School, South Korea

Osteoclasts are multinucleated giant cell resulting from cell-cell fusion of monocyte/macrophage osteoclast precursor cells. Osteoclast fusion process is critical for osteoclast function. MicroRNAs (miRNAs) are small, noncoding ribonucleic acids (ncRNAs), which regulate gene expression by binding the 3'-untranslation region (3'UTR) of their target mRNAs, leading to translational repression or mRNA degradation. The role of miRNAs in osteoclastogenesis has not yet been understood. In this study, we examined the role of miRNA-26a in RANKL-induced osteoclastogenesis. The expression of miR-26a was extremely upregulated by RANKL at late stage of osteoclastogenesis. Ectopic expression of miR-26a mimic in osteoclast precursor cells suppressed osteoclast formation, actin-ring formation, and bone resorption. On the other hand, overexpression of miR-26a inhibitor slightly enhanced RANKL-induced osteoclastogenesis. Through a bioinformatics approach, we identified CCN family 2 /connective tissue growth factor (CCN2/CTGF), which can promote osteoclast differentiation via upregulation of DC-STAMP, as a candidate target gene of miR-26a. Overexpression of miR-26a mimic decreased the protein level of CTGF, whereas overexpression of miR-26a inhibitor increased the protein level of CTGF. In addition, we found putative target sites of miR-26a in the 3'-UTR of CTGF mRNA. The inhibitory effect of miR-26a on osteoclastogenesis was prevented by the treatment with recombinant CTGF. Taken together, our results suggest that

miR-26a is involved in the last stage of osteoclast formation and function through regulation of CTGF.

SU0256

Inherent Activation of Apoptosis is a Determinant of Osteoclast Lifespan. Robert Jilka*[1], Toshifumi Fujiwara[1], Kanan Vyas[2], Michela Palmieri[2], Haibo Zhao[1], Stavros Manolagas[1]. [1]Central Arkansas VA Healthcare System, Univ of Arkansas for Medical Sciences, USA, [2]Central Arkansas VA Healthcare System, Univ of Arkansas for Medical Sciences, USA

Because of their destructive potential, the lifespan of osteoclasts must be under strict control; however the mode of osteoclast death is poorly understood. We therefore investigated death pathways in cultures of murine bone marrow macrophage-derived osteoclasts. We report that the number of TRAP-positive multinucleated osteoclasts reached a maximum between 5 and 6 days of culture, and then declined to less than 25% of initial number between day 7 and 10 of culture. This occurred despite the continuous presence of RANKL and M-CSF, which activate anti-apoptotic pathways in osteoclasts. The decrease in osteoclasts coincided with a 5-10-fold increase in caspase-8 and caspase-3 activity, and a 10-fold increase in the number of ghost-like osteoclast remnants attached to the substratum. Live cell imaging of multinucleated osteoclasts by time lapse microscopy distinguished two morphologic modes of death. Some exhibited classic features of apoptosis, notably retraction of cells from the substratum, extensive blebbing of the entire plasma membrane, and phagocytosis of the small cellular remnant by macrophages. Others exhibited highly localized transient blebbing of the plasma membrane followed by rapid necrosis-like death, accounting for the formation of the osteoclast ghosts. The pan-caspase inhibitor z-VAD-fmk caused a 40% reduction in the number of osteoclast ghosts, indicating that caspases initiate this form of death, despite their necrotic appearance. Apoptosis often depends on activation of either Bak or Bax – pro-apoptotic proteins that increase mitochondrial outer membrane permeability, leading to activation of caspases. We investigated this pathway using Bak/Bax-deficient osteoclasts generated from bone marrow macrophages obtained from Bak^{-/-} mice bearing a floxed Bax gene, followed by infection with adeno-Cre. Western blotting confirmed absence of Bax in these cells. Bak/Bax-deficient osteoclasts failed to exhibit increased caspase-3 activity during prolonged culture, and the number osteoclast ghosts was reduced, compared to adeno-Cre infected Bak^{-/-} control osteoclasts. Based on these findings, we propose that the survival signaling initiated by M-CSF and RANKL during osteoclast differentiation is overwhelmed by inherent programmed death cues that ensure a limited osteoclast lifespan. Among these cues are activation of Bak and Bax leading to activation of caspases.

SU0257

A critical role of *Tet2* in osteoclastogenesis by maintaining the level of 5-hydroxymethylcytosine in the genome. Mingjiang Xu*[1], Ling Li[2], Zhigang Zhao[3], Feng-Chun Yang[4]. [1]Indiana University School of Medicine, USA, [2]Indiana University School of Medicine, USA, [3]Indiana University, USA, [4]Indiana University, USA

As an epigenetic landmark, DNA methylation plays an important role in regulating gene expression. TET protein family members enzymatically convert 5-methylcytosine into 5-hydroxymethylcytosine and play a critical role in active DNA demethylation pathway, thus, regulating gene expression. We and others have reported that deficiency of Tet2 altered myelogenesis, leading to the development of myeloid malignancies in mice. Osteoclasts, the progeny of myeloid lineage play an important role in maintaining the bone remodeling and the physiologic integrity of the skeleton. However, the role of Tet family in bone remodeling remains unknown. In this study, using both qPCR and a Tet2:GFP reporter knock-in murine model, we found that Tet2 is expressed in preosteoclasts (pre-OCLs) at high levels. Deletion of Tet2 led to dramatic reduction in the 5-hydroxymethylcytosine levels and increase in the 5-methylcytosine levels in the genomic DNA of pre-OCL. Interestingly, Tet2-/- mice are slightly smaller is size and gradually develop osteosclerosis with significantly higher BMD, increased trabecular BV/TV, conn D and direct Tb N as compared to WT littermates. Macrophages of Tet2-/- mice exhibited impaired osteoclastogenesis as shown by less osteoclast formation following tartrate-resistant acid phosphatase staining. To delineate if deletion of Tet2 alters the expression levels of critical gene that are critical for osteoclastogenesis and differentiation, RNA-Seq was performed and genomic 5-hmC profiling were surveyed in Tet2-/- pre-OCLs compared to their respective WT counterparts. Several differentially expressed genes were found in Tet2-/- pre-OCLs (Gata2, Sin3a). In addition, genome-wide 5-hmC distribution in WT and Tet2-/- pre-OCLs allowed us to correlate expression levels of selected genes with their promoter 5-hmC/5-mC status. In addition, the genomic distributions of Tet2 were mapped by Chip-Seq in pre-OCLs derived from a Tet2:Flag/V5 Tag knock-in mouse model with well-tested anti-Tag antibodies. These data indicate that deletion of Tet2 in mice leads to dysregulated hydroxylation of 5-methylcytosine and gene expression profiling in pre-OCLs, which subsequently altered cellular functions of osteoclasts, which eventually altered skeletal development. These results indicate an important role of DNA demethylation in the regulation of bone homeostasis.

SU0258

Activation of G protein-coupled receptor 84 with capric acid inhibits RANKL-induced osteoclast differentiation via the suppression of NF-κB signaling and blocks cytoskeletal organization and survival in mature osteoclasts. Hyun Ju Kim*[1], Hye-Jin Yoon[2], Shin-Yoon Kim[3], Young-Ran Yoon[2]. [1], South Korea, [2]Kyungpook National university, South Korea, [3]Kyungpook National University Hospital, South Korea

Osteoclasts are bone-resorbing cells that are generated by the differentiation of myeloid lineage progenitors. To evaluate new regulators of osteoclast development, we performed a microarray analysis, and we found that G protein-coupled receptor 84 (GPR84), a molecule known to function as a specific receptor for medium-chain fatty acids, was down-regulated by 10-fold in osteoclasts compared to their precursors. In this study, we investigated the impact of GPR84 activation on osteoclast development and addressed its possible mechanisms. Activation of GPR84 with a potent ligand, capric acid, inhibited RANKL-mediated osteoclast differentiation from bone marrow-derived macrophages. Capric acid suppressed the RANKL-induced phosphorylation of IκBα, p65 nuclear translocation, and NF-κB transcriptional activity. Capric acid further blocked the RANKL-stimulated activation of ERK without affecting JNK or p38. The induction of NFATc1 in response to RANKL was also attenuated by capric acid. In addition, GPR84 activation abrogated M-CSF and RANKL-stimulated cytoskeleton reorganization, which is crucial for efficient bone resorption of osteoclasts, and increased apoptosis in mature osteoclasts through the induction of Bim expression and the suppression of ERK activation by M-CSF. Together, our data demonstrate that GPR84 activation inhibits osteoclast differentiation and function. We therefore suggest that GPR84 may be a potential therapeutic target for the treatment of bone resorption-associated disorders.

Disclosures: Hyun Ju Kim, None.

SU0259

C-reactive protein inhibited TRAP-positive multinucleated cell formation and induced cytokine expression through TLR signaling. Ho-Yeon Chung[1], In-Jin Cho*[2], Kyung Hee Choi[2], Yoo-Chul Hwang[2], In-kyung Jeong[2], Kyu Jeung Ahn[2], Hyoung-moo Park[3]. [1]Kyung Hee University, South Korea, [2]Kyung Hee University, South Korea, [3]Chung-ang University, South Korea

Inflammatory processes play a role in osteoclastogenesis. C-reactive protein (CRP), an acute phase reactant that reflects different degree of inflammation. More recently, accumulating evidence suggest that CRP is not only an inflammatory marker but also direct cause of diseases. Therefore, we examined the direct effects of CRP on osteoclast formation using mouse bone marrow cells or RAW 264.7. CRP significantly inhibited RANKL-induced TRAP-positive multinucleated cell formation in RAW 264.7 cell cultures in a dose-dependent manner (1 ug/ml to 30 ug/ml). We observed suppression of ERK and p38 mitogen-activated protein kinases induced by RANKL in Western blotting after CRP treatment in RAW 264.7 cells. Furthermore, CRP increased TNFa and IFNb expression in RAW 264.7 cells. OxPAPC, inhibitor of toll-like receptor signaling, decreased CRP-induced TLR signaling and expression of TNFa and IFNb. Furthermore, OxPAPC reduced CRP-induced inhibition of TRAP-positive multinucleated cell formation. These data indicated that CRP may have a direct role on osteoclastogenesis via MAPK and TLR-dependent pathway.

Disclosures: In-Jin Cho, None.

SU0260

Feedback regulation of osteoclastogenesis by exosomes. Lexie Holliday*[1], Lindsay VonMoss[2], Nancy Huynh[2], Pooja Patel[2], Wellington Rody[2], Kevin McHugh[3]. [1]University of Florida College of Dentistry, USA, [2]University of Florida College of Dentistry, USA, [3]University of Florida, USA

Exosomes are 30-120 nm secreted vesicles that function in intercellular signaling. Exosomes have been shown to be involved in cell-cell communication in the immune system, nervous system and are a mechanism by which cancer cells trigger angiogenesis. The purpose of this study was to characterize changes in the composition of exosomes produced by osteoclasts as they differentiate, and to test whether exosomes regulate osteoclastogenesis by adding them to calcitriol-stimulated mouse marrow cultures.

Exosomes were isolated from CSF-1/RANKL-stimulated primary hematopoetic cell cultures or RANKL-stimulated RAW 264.7 cells either by filtration and differential centrifugation or by ExoQuick TC™ (System Biosciences). Exosomes were characterized by positive/negative contrast transmission electron microscopy and Western and Lectin blots. Various concentrations of exosomes were added to calcitriol-stimulated mouse marrow cultures on Days 1 and 4 of a 6 Day culture period. After 6 Days, cells were fixed and osteoclasts were identified as multinuclear cells expressing tartrate-resistant acid phosphatase (TRAP) activity.

Exosomes isolated from primary osteoclasts or RAW 264.7 osteoclast-like cells displayed characteristic exosome size and morphology by electron microscopy and expressed the exosome marker proteins CD63 and EPCAM. The peanut agglutinin binding proteins in exosomes changed dramatically as osteoclasts differentiated from

precursors. Only exosomes from resorbing osteoclasts contained V-ATPase subunits. When added to calcitriol-stimulated mouse marrow cultures, exosomes from osteoclast precursors increased osteoclast numbers in the mouse marrow up to 4-fold. Exosomes from mature osteoclasts decreased osteoclast numbers up to 3-fold.

Conclusions: Osteoclast precursors and osteoclasts produce exosomes that vary compositionally and functionally depending on the differentiation and activation state of the cells. Exosomes are involved in positive and negative feedback regulation of calcitriol-stimulated osteoclastogenesis in mouse marrow cultures.

Disclosures: Lexie Holliday, None.

SU0261

Identification and analysis of function of a novel splicing variant of receptor activator of NF-kB. Riko Kitazawa*[1], Ryuma Haraguchi[2], Yosuke Mizuno[3], Sohei Kitazawa[1]. [1]Ehime University, Japan, [2]Ehime University, Japan, [3]Ehime University Hospital, Japan

Receptor activator of NF-κB (RANK) is a member of the tumor necrosis factor receptor (TNFR) family expressed in osteoclast precursors, and RANK-RANK ligand (RANKL) signaling is a key system for differentiation, activation and survival of osteoclasts. We have identified a novel alternative splicing variant of mouse RANK gene (vRANK) that contains a new intervening exon between exons 1 and 2 of mouse full-length RANK (fRANK) mRNA. Since this novel exon contains the stop codon, vRANK encodes truncated 45 amino acids that have a portion of the signal peptide of fRANK and an additional 19 amino acids that show no homology to previously reported domains. By transient transfection with vRANK-GFP and -Flag expressing constructs, vRANK was found localized mostly in the cytoplasm and partly in the cell membrane, but was not secreted into the culturesupernatant. Under the stimulation of various factors, the expression of mouse vRANK mRNA was almost parallel to that of fRANK in RAW264 cells. Overexpression of vRANK in RAW cells decreased the formation of TRACP-positive multinucleated giant cells and negated the anti-apoptotic effect of sRANKL. The human RANK gene also contains an intervening exon that yields vRANK mRNA containing 38 amino acids. In the presence of Vitamin D3, PMA or TGF-b induced vRANK mRNA in HL60 cells through the ERK-dependent pathway. To examine the *in vivo* effect of mouse vRANK, we generated a systemically overexpressed CAGcre+/svRANK mouse that showed high fatality before weaning; a 13-week survivor displayed bronchopneumonia and cardiac dilatation with cardiomyopathy. Taken together, these results suggest that vRANK is a novel bioactive peptide that not only reduces the number of RANKL-induced mature osteoclasts, but also exhibits profound systemic cytopathic effects.

Disclosures: Riko Kitazawa, None.

SU0262

Iron Homeostasis is Critical for Osteoclast Differentiation. Toshifumi Fujiwara*[1], Jian Zhou[2], Shiqiao Ye[1], Stavros Manolagas[1], Haibo Zhao[1]. [1]Central Arkansas VA Healthcare System, Univ of Arkansas for Medical Sciences, USA, [2]UAMS, USA

Iron is essential for osteoclast (OC) differentiation, and iron overload in a variety of hematologic diseases is associated with excessive bone resorption. Iron uptake by OC precursors, via the transferrin (Tf) cycle, has been shown to increase mitochondrial biogenesis, reactive oxidative species (ROS) production, and activation of CREB – a critical transcription factor downstream of RANKL-induced calcium signaling. However, the molecular mechanisms regulating cellular iron metabolism in OC lineage cells remain largely unknown. Most mammalian cells acquire iron from the extracellular fluid through the Tf cycle, in which ferric iron (Fe^{3+})-loaded Tf binds to TfR on the cell surface, and the complex is then internalized via receptor-mediated endocytosis. Fe^{3+} is released from Tf due to acidic pH in endosomes. Fe^{3+} is then reduced to ferrous iron (Fe^{2+}) by the six-transmembrane epithelial antigen of prostate (Steap) family of ferrireductases. Fe^{2+} is transported across the endosomal membrane to the cytosol by divalent metal transporter 1 (DMT1). Fe^{2+} is mainly utilized by mitochondria and the rest of Fe^{2+} is pumped out of the cell by Ferroportin at the plasma membrane. Mammalian cells can also obtain iron by non-Tf-dependent mechanisms through uptake of Hemes and Ferritins which are transported by Flvcr2-Slc46a1 and Scara5-Timd2, respectively. In order to identify the molecular mechanisms of iron metabolism in OC we examined the expression of major regulators of iron homeostasis in bone marrow macrophages, pre-OCs, and mature OCs by quantitative real-time PCR. The expression of both TfR1 and TfR2 increased during OC differentiation, with TfR1 being the major isoform. Of 4 Steap family members, Steap4 was the highest expressed isoform and was increased 5-fold during OC differentiation. An increase in DMT1 expression with a simultaneous reduction of Ferroportin may be a mechanism by which OCs raise intracellular Fe^{2+}. The expression of genes involved in other iron uptake pathways such as Scara5, Timd2, Flvcr2, Slc46a1 is either undetectable or there is no significant change during OC differentiation. These results indicate that Tf-dependent iron uptake plays an essential role in iron homeostasis in OCs. Consistent with this scenario, knockdown of Steap4 and DMT1 in macrophages by lentivirus-mediated shRNAs markedly inhibits iron uptake and OC formation. Hence, iron homeostasis regulated by Steap4 and DMT1 is critical for osteoclastogenesis.

Disclosures: Toshifumi Fujiwara, None.

SU0263

Psychosine inhibits osteoclastogenesis and bone resorption via G-protein coupled receptor 65 by regulating intracellular cAMP levels in osteoclasts.

Eun-Hee Ha*[1], Seong Hee Ahn[2], Hyeonmok Kim[3], Sun-Young Lee[4], Ji-Eun Baek[4], Sook-Young Park[5], Su-Youn Lee[4], Young-Sun Lee[5], Beom-Jun Kim[6], Seung Hun Lee[2], Jung-Min Koh[6], Ghi Su Kim[2]. [1]Asan Institute for Life Sciences, South Korea, [2]Asan Medical Center, University of Ulsan College of Medicine, South Korea, [3]Division of Endocrinology & Metabolism, Asan Medical Center, University of Ulsan College of Medicine, South Korea, [4]Asan Institute for Life Science, South Korea, [5]Asan Institute for Life Sciences, South Korea, [6]Asan Medical Center, South Korea

Recently, the inhibitory effects of G-protein coupled receptor 65 (GPR65) on ovariectomy induced bone resorption have been demonstrated. Psychosine, a lysosphingolipid, has been reported to be a ligand for the GPR65. We investigated a role of psychosine on osteoclastic differentiation and bone resorption via GPR65. Osteoclasts were differentiated from mouse bone marrow macrophages. Tartrate-resistant acid phosphatase-positive multinucleated cells were considered as osteoclasts, and the resorption area was determined by incubating the cells on dentine discs. The expression levels of markers for osteoclast differentiation were assessed by qRT-PCR. GPR65 siRNA and scrambled RNA were transfected with lipofectamine reagent (Invitrogen). The intracellular cAMP levels were determined using a direct enzyme immunoassay. Psychosine inhibited both osteoclastogenesis and in vitro bone resorption, without any significant effect on the viability of preosteoclasts. Consistently, the expressions of osteoclast differentiation markers were significantly decreased by psychosine. The knockdown of GPR65 by its siRNA ameliorated the psychosine-suppressed osteoclastogenesis, and expressions of osteoclast differentiation markers. Psychosine increased the levels of intracellular cAMP, with reversal by the knockdown of GPR65. Psychosine inhibited osteoclastogenesis by increasing intracellular cAMP levels via GPR65.

Disclosures: Eun-Hee Ha, None.

SU0264

Serum calcium-decreasing factor, caldecrin, suppresses osteoclastogenesis by regulation for the RANKL-mediated Src family kinase. Akito Tomomura*[1], Mineko Tomomura[2]. [1]Meikai University, School of Dentistry, Japan, [2]Meikai University School of Dentistry, Japan

We have reported that caldecrin inhibits osteoclast differentiation by inhibition of RANKL-mediated Ca^{2+} oscillation, leading to suppression of NFATc1 activation. We have also reported that caldecrin inhibits RANKL-mediated actin ring formation and bone resorptive activity of mature osteoclasts. Caldecrin inhibits RANKL-stimulated c-Src kinase activity and c-Src-Syk association of mature osteoclasts, leading to inhibition of phosphorylation of c-Src, Syk, PLC, SLP-76, and Pyk2, and inhibition of transient receptor potential vanilloid channel 4-mediated Ca^{2+} entry. These results suggest that caldecrin inhibits RANKL-stimulated c-Src activation in mature osteoclast. C-Src is critical to the function of mature osteoclasts, but not osteoclastogenesis. Other Src family including Fyn, and Lyn are regulate osteoclast differentiation.

Here, we investigated the effects of caldecrin on the RANKL-stimulated Fyn and Lyn activation of the pre-osteoclasts. Immunoprecipitation studies indicated that caldecrin inhibited the phosphorylation of Fyn stimulated by RANKL treatment, but not those of Lyn in the pre-osteoclasts. These results suggest that caldecrin inhibits osteoclast differentiation by suppression of RANKL-stimulated Fyn phosphorylation.

Disclosures: Akito Tomomura, None.

SU0265

The Effect of Vascular Endothelial Growth Factor (VEGF) on Osteoclastogenesis in Rheumatoid Arthritis. Sang-Heon Lee*[1], Hae-Rim Kim[2], Youngil Seo[3]. [1]Konkuk University Medical Center, South Korea, [2]Konkuk University Medical Center, South Korea, [3]Hallym University Sacred Heart Hospital, South Korea

Objective. This study was aim to determine the specific role of VEGF, which is originally known to be involved in the angiogenesis, on the osteoclastogenesis in RA.

Methods. The expression of VEGF, receptor activator of nuclear factor κB ligand(RANKL) and CD55 in RA synovial tissues was analyzed using confocal microscopy. VEGF and RANKL concentrations in synovial fluid and their correlation were determined by ELISA. VEGF-induced RANKL expression was determined in RA synovial fibroblasts using RT-PCR, luciferase assay and ELISA, Peripheral blood CD14+ monocytes were cultured with VEGF, and then osteoclastogenesis was assessed by counting tartrate-resistant acid phosphatase(TRAP)-positive multinucleated cells. Osteoclastogenesis was also determined after co-culutre of monocytes with VEGF-pretreated synovial fibroblasts.

Results. We found co-expression of VEGF, RANKL and CD55 in lining and sublining areas of RA synovium. RANKL concentration correlated with VEGF concentration in synovial fluid of RA patients. VEGF stimulated the expession of RANKL mRNA and protein in RA synovial fibroblasts, and RANKL promoter activity was upregulated by VEGF in the synovial fibroblasts transfected with RANKL reporter plasmids. The VEGF-induced RANKL expression was decreased by the inhibition of Src and PKC pathways. VEGF induced osteoclast differentiation from monocytes in the absence of RANKL. When monocytes were co-cultured with VEGF-prestimulated RA synovial fibroblasts, monocytes were differentiated into osteoclasts, which was downregulated by Src and PKC inhbtion.

Conclusion. VEGF plays dual roles on osteoclastogenesis in RA: direct induction of osteoclastogenesis from the precursors and indirect stimulation of RANKL producing synovial fibroblasts, which may mediate Src and PKC pathway. The axis of VEGF and RANKL could be a potential therapeutic target to prevent bone destruction in RA.

Disclosures: Sang-Heon Lee, None.

SU0266

A bacterial artificial chromosome-based SOST-Cre transgene is active in mature osteocytes as well as an early hematopoietic progenitor. Jinhu Xiong*[1], Marilina Piemontese[2], Priscilla Baltz[3], Stavros Manolagas[1], Charles O'Brien[1]. [1]Central Arkansas VA Healthcare System, Univ of Arkansas for Medical Sciences, USA, [2]University of Arkansas for Medical Sciences, USA, [3]University of Arkansas for Medical Sciences, USA

RANKL is essential for osteoclastogenesis and RANKL expressed in Dmp1-Cre transgene-expressing cells is required for cancellous bone remodeling in adult mice. However, the Dmp1-Cre transgene used to obtain these findings is active in both osteocytes and matrix-synthesizing osteoblasts, leaving open the possibility that RANKL produced by osteocytes, osteoblasts, or bone lining cells contributes to osteoclast formation in cancellous bone. To distinguish between osteocytes, osteoblasts, and lining cells as sources of RANKL, we created transgenic mice expressing the Cre recombinase under the control of regulatory elements of the Sost gene contained in a bacterial artificial chromosome. Activity of the Sost-Cre transgene in vivo was determined by crossing Sost-Cre mice with Rosa26R reporter mice, which express LacZ only in cells expressing Cre recombinase or their progeny. X-gal staining of bones of these mice, which had also been injected with calcein to identify surfaces with active bone formation, showed that the Sost-Cre transgene is active in osteocytes but not osteoblasts. However, we also observed lacZ positive cells in the bone marrow. To determine the identity of these cells,we crossed Sost-Cre mice with another Cre reporter strain that expresses tandem dimer (td)-Red fluorescent protein upon Cre-mediated recombination and then analyzed bone marrow cells by flow cytometry. Due to the large number of lacZ positive cells in the bone marrow of Sost-Cre;R26R mice, we focused the sorting on hematopoietic cells using anti-CD3 to identify T cells, anti-CD19 to identify B cells, anti-CD11b to identify monocyte/macrophage lineage cells, and anti-TER119 to identify erythroid progenitors. Flow cytometry revealed that 27.3 percent of the cells in the bone marrow expressed the tdRed reporter gene. Among those tdRed-positive cells, 1.6 percent were T cells, 20.5 percent were B cells, 48.2 percent were monocytes, and 33.3 percent were erythroid cells. The distribution of each cell type within the tdRed-positive population is similar to that in total bone marrow population suggesting that Sost-Cre transgene activity is restricted to a subpopulation of early hematopoietic progenitors. Consistent with this, endogenous Sost mRNA was undetectable in T cells, B cells, or monocytes. Whether the activity of the transgene accurately reflects the activity of the endogenous Sost gene in hematopoietic progenitors will require further analysis.

Disclosures: Jinhu Xiong, None.

SU0267

A Novel Bone Metabolic Role for the Acute Phase Protein A-SAA/Saa3. Roman Thaler*[1], Monika Rumpler[2], Ines Sturmlechner[2], Silvia Spitzer[2], Klaus Klaushofer[3], Amel Dudakovic[4], Andre Van Wijnen[4], Franz Varga[2]. [1]Mayo Clinic, USA, [2]Ludwig Boltzmann Institute of Osteology at the Hanusch Hospital of WGKK & AUVA Trauma Centre Meidling. 1st Medical Department, Hanusch Hospital, Austria, [3]Hanusch HospitalLudwig Boftzmann Institute of Osteology, Austria, [4]Mayo Clinic, USA

Collagen triple helix disruption in osteoblasts significantly stimulates expression of the acute-phase protein Serum Amyloid A (A-SAA/Saa3), which is known to be elevated in cardiovascular diseases, rheumatoid arthritis or insulin resistance. We have previously shown that induction of SAA3 affects bone metabolism by modulating the expression of genes involved in bone matrix remodeling, inflammation and apoptosis. Here, we further investigated the regulatory role of *Saa3* during osteogenic differentiation and bone turn-over.

We observed that C3H10T1/2 mesenchymal progenitor cells do not express appreciable amounts of SAA3 protein levels. However, pre-osteoblastic MC3T3-E1 osteoblasts, late osteoblastic MLO-A5 cells and MLO-Y4 osteocytes each exhibit detectable expression of SAA3. Each of these cell types represent models for osteogenic differentiation at progressive stages of lineage-commitment. Our results

suggest that SAA3 expression positively correlates with increased cellular maturation towards the osteocyte phenotype. These findings with immortalized bone cell lines were validated with primary pre-osteoblasts, osteoblasts and early osteocytes from newborn mouse calvaria. Functionally, administration of recombinant SAA3 protein significantly reduces expression of mature osteoblast markers *Bglap2 (osteocalcin)*, *Runx2*, *Col1a1* or *Alpl* expression during osteoblasts differentiation. In contrast, SAA3 protein treatment of primary mouse macrophages/monocytes increases the number of multinuclear cells (>5 nuclei/cell), and in RAW264.7 pre-osteoclasts the number of TRAP positive cells and *Calcr* mRNA expression. Thus, SAA3 is suppressive of osteoblast differentiation and promotes osteoclast differentiation. siRNA mediated depletion of *Saa3* in MLO-Y4 osteocytes down-regulates the osteocyte biomarkers *Dmp1*, and *Mepe*. Remarkably, administration of recombinant osteocalcin, a key extracellular matrix protein produced by osteoblasts, decreases *Saa3* expression in MLO-Y4 osteocytes. These data suggests that SAA3 may function as a coupling factor between osteoblasts, osteoclasts and osteocytes to control their biological properties. We demonstrate that SAA3 produced by MLO-Y4 osteocytes is clearly deposited and integrated into the extra cellular matrix of MC3T3 osteoblasts. Importantly, mineralization is significantly decreased in newborn mouse calvaria treated for 12d with recombinant SAA3.

We propose that A-SAA/Saa3 is a novel regulator of bone metabolism and homeostasis.

Disclosures: Roman Thaler, None.

SU0268

Expression of c-fms in osteocytes is differentiation-dependent and plays an important role in regulating Tissue Mineral Density *in vivo*. Meiling Zhu[1], Joanne Walker*[2], Benhua Sun[3], Steven Tommasini[1], Christine Simpson[3], Joshua VanHouten[3], Karl Insogna[3]. [1]Yale University, USA, [2]Yale School of Medicine, USA, [3]Yale University School of Medicine, USA

Selective deletion of c-fms in osteocytes results in a marked increase in tissue mineral density (TMD) *in vivo*. TMD is an intrinsic property of bone that makes an important contribution to fracture risk. Toluidine blue staining and FTIR analyses demonstrated focal areas of hypermineralization in knock out cortical bone. This occurred despite unaltered serum levels of CTX in the knock out mice indicating that a change in the rate of skeletal remodeling was not the basis for the change in TMD. Besides altering the rate of skeletal remodeling osteocytes can influence TMD by regulating osteocyte lacunar size and the density of the perilacunar bone. Indeed, in an initial study using high-resolution microCT osteocyte lacunae size tended to be smaller. Since we have not observed expression of c-fms protein in osteoblasts we wondered if its expression in osteocytes was differentiation-dependent. When cultured in mineralizing media, primary murine osteoblasts form mineralized extracellular matrix that is reminiscent of bone and contains cells that have an osteocyte phenotype. We found that mineralizing but not non-mineralizing osteoblast cultures express c-fms protein and coincident with that mineralized cultures evidenced a marked increase in expression of DMP1 and sclerostin, two key osteocyte markers. Further, we found using the osteocyte cell line IDG-SW3, that undifferentiated IDG-SW3 cells do not express c-fms protein but when these cells were induced to differentiate to an osteocytic phenotype they also express c-fms protein. Interestingly, in both the mineralization experiments and during IDG-SW3 differentiation, the levels of c-fms transcript did not change, indicating that the expression of c-fms protein during the transition from osteoblasts to osteocytes is post-transcriptionally regulated. Phosphotyrosine western blotting of cell lysates from CSF-1-treated differentiated IDG-SW3 cells demonstrated selective phosphorylation of certain proteins indicating that c-fms was functional in these cells. Taken together with the *in vivo* data summarized above, our findings indicate that c-fms plays a direct and important role in osteocyte biology and in regulating Tissue Mineral Density.

Disclosures: Joanne Walker, None.

SU0269

Gender specific effects of β-catenin on trabecular bone with unloading. Delphine Maurel*[1], Peipei Duan[2], Ning Zhao[3], Mark Johnson[4], Lynda Bonewald[5]. [1]Department of Oral & Craniofacial Sciences, USA, [2]Oral & Craniofacial Sciences, USA, [3]univ of missouri kansas city, USA, [4]University of Missouri, Kansas City Dental School, USA, [5]University of Missouri - Kansas City, USA

Deletion of both alleles of β-catenin in bone cells results in a fragile skeleton highly susceptible to fracture. In contrast, deletion of one allele using Dmp1-Cre results in a relatively normal skeleton at 8 weeks of age with minor reductions in trabecular bone but no effect on bone density or other properties. Interestingly, anabolic response to ulnar mechanical loading was absent in Dmp1-Cre x β-catenin heterozygote (cKO) animals at 6 months of age, suggesting that β-catenin also plays a role in the response of bone to mechanical loading. In this study we asked whether β-catenin could also play a role in the response of bone to unloading.

In 18 week old female mice, tibial cortical bone volume was significantly less by a modest amount in cKO mice compared to controls (Con/cKO: Ct. BV/TV = $91.2 \pm 0.2/90.5 \pm 0.1\%$, Ct. Th. = $0.206 \pm 0.004/0.193 \pm 0.002$mm), but no differences in trabecular bone. In contrast, in 18 week old male mice, no differences were observed in cortical bone, but tibial trabecular bone volume was significantly less in cKO mice

compared to controls (Con/cKO: Tb. BV/TV = $14.4 \pm 1.2/9.1 \pm 0.5\%$, Tb. N. = $4.97 \pm 0.23/3.81 \pm 0.09$/mm, Tb. Sp. = 0.20 ± 0.01 /0.26 ± 0.01mm, a 37%, 23% and 30% change respectively), suggesting that β-catenin is essential for maintaining normal bone mass in males under normal ambulatory conditions (SPSS 21.0, independent t-test). To test the effects of unloading, mice were either suspended (SUS) or attached but not suspended (NS) using a tail ring starting at 14 weeks of age for 4 weeks. Male control mice lost significant amounts of trabecular bone with unloading (NS/SUS: BV/TV = $15.7 \pm 1.8/8.1 \pm 0.8\%$, Tb. Th. = $0.053 \pm 0.004/0.039 \pm 0.002$mm), however the cKO mice did not (One-way ANOVA with Tukey post-hoc test). The lack of bone loss in male mice may have been due to the fact that their trabecular bone mass was much less than control prior to unloading. As expected, female control mice lost significant tibial trabecular bone with unloading (NS /SUS: Tb.Th. = $0.055 \pm 0.003/ 0.048 \pm 0.002$mm), but female cKO mice had greater trabecular bone loss with unloading (Con/cKO: Tb. N. = $2.30 \pm 0.06/1.82 \pm 0.08$/mm, Tb. Sp. = 0.46 ± 0.01 / 0.57 ± 0.03 mm). These differences of a 9% decrease for controls and a 21% decrease for cKO for Tb. N. and a 12% increase for controls and a 27% increase for cKO for Tb. Sp. suggests that β-catenin is protective against the effects of unloading in females. In males, β-catenin appears necessary for normal bone mass.

Disclosures: Delphine Maurel, None.

SU0270

IGF-1 induces the differentiation of mouse and human osteoblasts in 3D culture to mature osteocytes expressing sclerostin and FGF-23. Nicole Scully*[1], Sam Evans[2], Carole Elford[2], Deborah Mason[3], Bronwen Evans[3]. [1]Cardiff University, United Kingdom, [2]Cardiff University, United Kingdom, [3]Cardiff University, United Kingdom

Osteocytes differentiate from osteoblasts, are mechano-sensitive, and are difficult to isolate with a dependence on cell lines for *in vitro* studies of osteocyte biology. Recent publications have indicated that osteoblasts maintained in *in vitro* 3D collagen gels may differentiate to osteocytes. We have developed a novel, 3D, mineralised culture system enabling the differentiation of osteoblasts to osteocytes, which can then be applied to the study of osteocyte biology and function, including responses to mechanical loading. Since IGF-1 plays a key role in bone homeostasis and regulates osteoblast differentiation from osteoprogenitor cells, we hypothesised that IGF-1 added to our 3D model in basal and/or mineralising medium regulates osteoblast differentiation and function.

We maintained osteoblasts (mouse MC-3T3; human primary hOB) in 3D type I collagen gels (48-well plates; 15 days) in basal or mineralising medium $\pm$ IGF-1 (50 ng/μl). Cell number, viability and phenotype (IHC, confocal), IL-6, VEGF and FGF-23 secretion (ELISA), and gene expression (*e.g.* sclerostin, FGF-23; qRTPCR) were measured. Results presented are combinations of at least 2 independent experiments.

Both cell types appeared more dendritic in mineralising medium compared to basal medium, and cell viability was >92% throughout. IGF-1 treatment did not affect cell number in MC-3T3s or hOBs in basal medium. MC-3T3 cells in basal medium with IGF-1 significantly increased RANKL (~43-fold; $p<0.01$) DMP-1; ($p<0.01$), Cx43 ($p<0.01$) and FGF-23 (~15-fold; $p<0.001$) expression from day 11. FGF-23 secretion was only detected with IGF-1 treatment from day 11. In mineralising medium with IGF-1 cell number increased ($p<0.05$), E11 ($p<0.05$) and MEPE ($p<0.05$) expression decreased, and VEGF secretion increased ($p<0.01$) at day 15. hOBs in basal medium with IGF-1 increased ($p<0.05$) DMP-1 and sclerostin expression from day 11, whereas VEGF, IL-6 and RANKL secretions were reduced with days in culture.

IGF-1 modulated cell differentiation and secretion, with broadly similar results obtained with both cell types tested. FGF-23 and sclerostin production, as well as the large increase in RANKL expression, in the presence of IGF-1 highlights the possible role of IGF-1 in osteocyte differentiation and function. This novel 3D *in vitro* system provides a tool to further study the role of IGF-1 in osteocyte function, especially those related to the mechano-sensing signaling pathways.

Disclosures: Nicole Scully, None.

SU0271

Multiple tissue targets revealed in a transgenic mouse model for inducible and specific osteocyte ablation. Ahmed Aljazzar*[1], Andy Pitsillides[2]. [1], United Kingdom, [2]Royal Veterinary College, United Kingdom

Many approaches highlight a potential for osteocyte-mediated control of bone remodeling. Direct in vivo support for this pivotal role stems mostly from osteocyte-selective ablation achieved following diphtheria toxin (DT) injection in mice harbouring a DMP1 promoter-regulated human diphtheria toxin receptor (hDTR) transgene. These DTR-DMP1 mice have been to support multiple osteocyte roles: in mechanical unloading responses and in regulating primary lymphoid organs, fat metabolism and hematopoietic stem cell mobilization. To explore osteocyte roles more fully we sought to confirm the selectivity of DT effects and DMP1-driven hDTR expression in bone.

Fifty-three 8-50wk-old WT and DTR-DMP1 mice were DT-injected (50ng/g), calcein double-labelled and sacrificed within 8days. hDTR, DMP1 and endogenous murine-DTR mRNA levels were assessed in multiple tissues by standard- and qRT-PCR. Tibia/femur were processed for histomorphometric analysis and samples collected for histology and assessment of EF-2 activity (DTR activation target). Health status was evaluated daily for signs of modified welfare.

hDTR (and DMP1) mRNA was detected in muscle, spleen, marrow, heart, liver, brain, lung, kidney and bone in DTR-DMP1, but not WT mice, and levels correlated with histopathology (mDTR did not). Histopathological changes included liver vacuolation, acute kidney necrosis and splenic/thymic atrophy in DTR-DMP1 only after DT-treatment within 3days. Marked DT-induced distension and congestion of bone marrow sinusoids was also evident in DTR-DMP1. Histomorphometry revealed significantly reduced bone formation rate on endosteal, not periosteal, surfaces in DTR-DMP1 mice (not WT) after DT-treatment. This was not, however, linked with expected widespread osteocyte ablation (<20% in DTR-DMP1 mice 6days after single DT (WT, <6%) and only 50% after five daily DT-doses). Whilst DT-treated WT showed little ill-health, surprisingly marked deterioration was observed (condition score, weight loss, low temperature, rough coat, staggered gait and signs of pain) in all DTR-DMP1 mice after DT-treatment.

Our data question the utility of DTR-DMP1 mouse model for inducible and specific osteocyte ablation. We find hDTR expression in multiple tissues and ill-health in response to DT treatment, suggesting that conclusions regarding osteocyte function, based solely on this model, are premature.

Disclosures: Ahmed Aljazzar, None.

SU0272

Mutual Enhancement of Differentiation of Osteoblasts and Osteocytes Occurs Through Direct Cell-cell Communication. Qian Xing[1], Koji Fujita[2], Sundeep Khosla[3], David Monroe*[4]. [1]Mayo Clinic, USA, [2]Mayo Clinic, USA, [3]Mayo Clinic College of Medicine, USA, [4]Mayo Foundation, USA

There is increasing evidence that osteocytes regulate multiple aspects of bone remodeling through communication with osteoblasts. This bi-directional communication may occur through the secretion of specific factors or through direct cell-cell contact, via osteocytic dendritic processes. We used a novel transwell model whereby calvarial osteoblasts were co-cultured (but physically separated) with IDG-SW3 osteocytes, or each cell type cultured on either side of a permeable membrane that allows direct cell-cell contact. Both conditions permit crosstalk between the osteoblastic and osteocytic cells via secreted factors, with the latter also allowing for direct cellular communication. The SW3 cells were allowed to differentiate under osteogenic conditions for 3 weeks before being placed into the transwell model with the osteoblasts, and both were allowed to continue differentiation for 1 week. At that point, the cells were separated and analyzed for specific osteoblastic and osteocytic gene expression signatures using RT-QPCR. Direct cell contact resulted in a marked upregulation of osteoblast differentiation markers, such as *Col1a1*, *Runx2*, *osterix*, *osteocalcin* (*Ocn*) and *alkaline phosphatase*, when compared to osteoblasts cultured with osteocytes without cell contact. Interestingly, the SW3 osteocytes exhibited increased osteocyte differentiation markers, such as *Phex*, *Mepe*, *Sost* and *Dmp1* expression, when in direct contact with osteoblasts. These data suggest that physical contact mutually enhances both the osteoblastic and osteocytic character of each respective cell type. We also found that *connexin 43* (*Gja1*) expression was increased in the osteoblasts only when in direct contact with the SW3 cells, suggesting that Gja1 may mediate some of the phenotypic effects of direct cell contact. To test this, we treated the direct contact system with the gap junction inhibitor 18-alpha-glycyrrhetinic acid (AGA) and found that *Ocn* expression was significantly inhibited, suggesting that osteocytes may regulate late osteoblast differentiation via Gja1. These data indicate that the pro-differentiative effects of direct osteoblast/osteocyte contact are mostly likely mediated through both gap junction signaling and presumably through cytokine secretion. Identification of the specific factors involved in the enhancement of osteoblastic/osteocytic differentiation will uncover new biology concerning how these bone cells communicate and respond to direct cell contact.

Disclosures: David Monroe, None.

SU0273

Pannexin 1 Knockout Mice Have Reduced RANKL Expression Following Focal Microinjury: Possible Mechanism Involving Pannexin 1 Channels for Osteoclast Recruitment?. Wing-Yee Cheung*[1], Eliana Scemes[2], David Spray[2], Jelena Basta-Pljakic[3], Robert Majeska[4], Mitchell Schaffler[1]. [1]City College of New York, USA, [2]Albert Einstein College of Medicine, USA, [3]City College of New York, USA, [4]City College of New York, USA

Osteocyte apoptosis is essential to recruit osteoclasts to bone microdamage sites. However apoptosis only occurs near the damage sites, while viable osteocytes surrounding the dying cells upregulate their RANKL expression to promote osteoclastogenesis. How apoptotic cells communicate with their surviving neighbors to induce pro-osteoclastogenic signal expression is unknown.

In cardic and brain ischemia, Pannexin 1 (PANX1) channels mediate the release of "find-me" signals that recruit phagocytes to clear apoptotic debris. To test whether PANX1 channels might play similar roles in recruiting osteoclasts to damaged bone, we assessed the patterns of osteocyte apoptosis and RANKL expression in mice lacking PANX1 (PANX-/-, n=4) and in C57/BL6 wild-type (WT) controls following focal microinjury in vivo.

A microindentation probe (5N, 10 cycles) was used to create a single microcrack in mouse tibiae at the indent apex. After 24 hours, bones were harvested, fixed, decalcified and analyzed by immunohistochemistry (Fig 1A). Apoptotic (cleaved caspase-3-positive) and RANKL-expressing osteocytes were counted as a function of

distance from the microcrack sites. Non-damaged regions from the same tissue sections were used to assess baseline levels of osteocyte apoptosis and RANKL expression. Differences between groups were determined by Mann-Whitney U tests ($p<0.05$).

In WT mice, focal microinjury induced osteocyte apoptosis and osteocyte RANKL expression near microdamage sites (Fig 1B; 3 to 4 fold above baseline), consistent with previous fatigue-loading studies. In PANX1 deficient mice, the numbers of apoptotic osteocytes near focal microinjury were the same as WT. However, numbers of osteocytes expressing RANKL were indistinguishable from baseline (Fig 1B, $p<0.05$). These results indicate that deficiency of PANX1 channels prevents dying osteocytes near microdamage sites from inducing their surviving neighbors to express RANKL. How PANX1 channels mediate this signaling process remains unclear, but PANX1 channels have been implicated in nucleotide release during apoptosis. Moreover, ATP has been shown to upregulate RANKL experssion in osteoclasts. Thus, PANX1 channels are likely candidates to mediate "find-me" signaling needed to activate osteoclast recruitment.
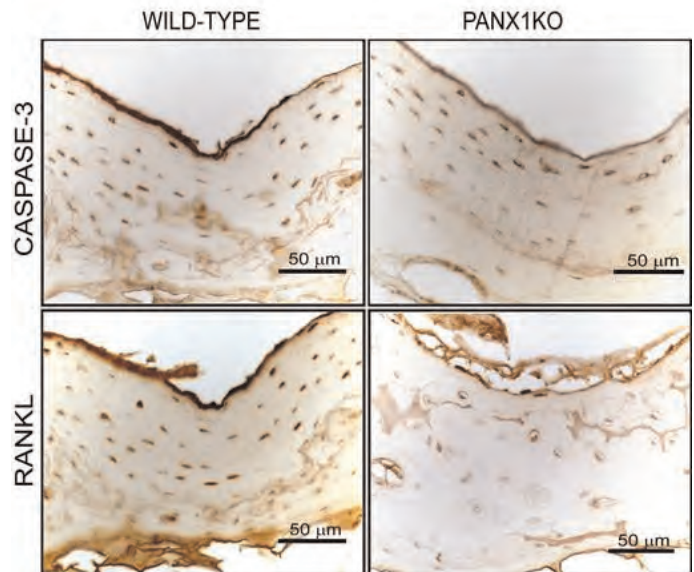
Figure 1A - IHC images of focal micro-injury sites
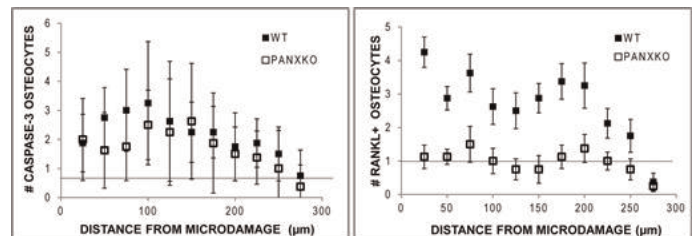
Figure 1B - Histomorphometry results for apoptotic and RANKL+ expressing osteocytes

Disclosures: Wing-Yee Cheung, None.

SU0274

Strontium Ranelate is more efficient when combined with *physical* activity. Priscilla Aveline[1], Eric Lespessailles[2], Claude Laurent Benhamou[3], Thomas M Best[4], Hechmi Toumi*[1]. [1]Univ. Orléans, I3MTO Laboratory, EA 4708, Hospital of Orleans, 1 rue Porte Madeleine, F-45032 Orléans, France, France, [2]Centre Hospitalier Regional Orleans, France, [3]CHR ORLEANS, France, [4]3-Division of Sports Medicine, Department of Family Medicine, Sports Health And, USA

Physical exercise is known to exert beneficial effects on bone status. Strontium Ranelate (SrRan) on the other hand has been shown to have anti-osteoporotic properties in both animal models and clinical trials. PURPOSE: Investigate the effects of SrRan, physical exercise (E) and a combination of SrRan and E on bone formation in sedentary and ovariectomized rats. METHODS: Ninety six female Wistar rats, aged 6 weeks, were randomly assigned to 8 groups: (1) (Sham): sedentary rats + saline, (2) (SH/ SrRan): sedentary rats + SrRan, (3) (SH/E): sedentary rats + saline + E, (4) (SH/SR/E): sedentary rats + SrRan + E, (5) (OVX): ovariectomized rats + saline, (6): (OVX/SR): ovariectomized rats + SrRan, (7) (OVX/E): ovariectomized rats + saline + E and (8) (OVX/ SrRan /E): ovariectomized rats + SrRan + E. Exercise involved 10 impacts drop landing exercises per day from 45 cm, 5 days a week over 8 weeks.

SrRan treatment consisted of 625 mg/kg of SrRan per gavage in 0.5 % carboxymethylcellulose daily. Body composition, whole bone, and left femur BMDs were analysed using µCT. Bone strength was assessed at the femur mid-shaft in 3-point bending. Osteocyte apoptosis was studied by cleaved caspase-3 immunostaining. RESULTS: Jump exercises and SrRan increased Bone/Tissue ratio in the left femur of the OVX and control groups. Similarly, a cumulative effect was observed when SrRan was combined with physical exercise. The same results were mirrored for trabeculea thickness except only the OVX rats benefited from cumulative effects when SrRan was combined with exercise. Ultimate strength increased with SrRan in the control rats, however it decreased with exercise in the OVX groups. In the OVX rats, both exercise and SrRan increased Osteocalcin expression. However, in control rats, osteocalcin increased only when SrRan was combined with exercise. Exercise and SrRan decreased amino-terminal telopeptide of type I collagen only in the OVX rats and the effect of SrRan was more prominent. Both jump exercise and SrRan decreased Osteocyte apoptosis in the OVX and control groups. SrRan decreased lipid cells in OVX rats, however in control rats, this effect was observed only when SrRan was combined with exercise. CONCLUSION: Our findings demonstrate that both jump exercise and SrRan have a positive influence on bone status, however the SrRan effects are more substantial. SrRan could have an important role in postmenopausal osteoporosis particularly when combined with jump exercise.

SU0275

Extracellular Inorganic Phosphate Functions as a Potent Inducer of the *Dmp1* Expression and Facilitates the Transition of Osteoblasts to Osteocytes.
Jin Nishino*[1], Kazuaki Miyagawa[2], Masanobu Kawai[3], Miwa Yamazaki[4], Kanako Tachikawa[4], Yuko Mikuni-Takagaki[5], Mikihiko Kogo[6], Keiichi Ozono[7], Toshimi Michigami[8]. [1]Osaka Medical Center & Research Institute for Maternal & Child Health, Japan, [2]Osaka University Graduate School of Dentistry, Japan, [3]Osaka Medical Center & Research Institute for Maternal & Child Health, Japan, [4]Osaka Medical Center & Research Institute for Maternal & Child Health, Japan, [5]Kanagawa Dental University Graduate School of Dentistry, Japan, [6]Osaka University Graduate School of Dentistry, Japan, [7]Osaka University Graduate School of Medicine, Japan, [8]Osaka Medical Center & Research Institute for Maternal & Child Health, Japan

Several molecules responsible for hypophosphatemic rickets, including FGF23, PHEX, DMP1 and FAM20C, are highly expressed in osteocytes, indicating the critical roles of osteocytes in phosphate metabolism. In the current study, to elucidate how the extracellular inorganic phosphate (Pi) modulates the osteocyte function, we first examined the direct effects of Pi on the gene expression in primary osteocytes isolated from mouse long bones. The expression of *Dmp1* was markedly increased by 24-h treatment with high (10 mM) Pi, which suggests that osteocytes are responsive to the alteration in extracellular Pi concentration. However, the expression of *Fgf23*, *Phex*, and *Fam20c* was not obviously changed by 24-h treatment with 10 mM Pi. Then, we next examined whether high extracellular Pi induced the expression of *Dmp1* in osteoblasts as well, using a murine osteoblastic cell line MC3T3-E1. We treated the cells with various concentrations (1-10 mM) of Pi for 48 h, and found that the *Dmp1* expression and phosphorylation of ERK1/2 were induced by the increased Pi in a dose-dependent manner. Interestingly, treatment with U0126, an MEK inhibitor, abolished the up-regulation of *Dmp1* by the increased Pi. Treatment with phosphonoformic acid (PFA), an inhibitor of Na^+/Pi co-transporter cancelled the increase in the *Dmp1* expression by the elevated Pi, either. These results suggest that the signaling triggered by extracellular Pi leads to an increased expression of *Dmp1* via Na^+/Pi co-transporter and MEK/ERK pathway. Since these findings indicate that Pi functions as a potent inducer of the *Dmp1* expression, we further examined the effects of longer treatment with Pi. To recapitulate the bone microenvironment, MC3T3-E1 cells were embedded in type I collagen gel and cultured in the presence of various concentration of Pi. In addition to *Dmp1*, the expression of *Fgf23*, *Fam20c*, *Hif1α*, *Connexin43*, *Fgf1*, *Fgf2*, and a Na^+/Pi co-transporter *Pit1*, was increased in the presence of 10 mM Pi compared to 1 mM Pi after 2 weeks of culture. The increase in the *Fgf23* expression was preceded by that in the *Dmp1* expression, implying that it may take long before Pi induces the expression of *Fgf23*. The expression of an osteoblastic marker *Keratocan* was decreased in the presence of 10 mM Pi. Taken together, these results indicate that Pi directly exerts its effects on osteoblast/osteocyte lineage cells to induce the expression of *Dmp1* and facilitates the differentiation of osteoblasts to osteocytes.

SU0276

Further Characterization of a Novel Cell Line Expressing a Membrane Targeted GFP in Osteocytes, Which Forms "Mini-bone"Structures in vitro.
Kun Wang*[1], Brad Chun[2], Richard Campos[3], Vladmir Dusevich[2], Sarah Dallas[1]. [1]University of Missouri - Kansas City, USA, [2]University of Missouri - Kansas City, USA, [3]University of Missouri - Kansas City, USA

With the increasing interest in osteocytes as multifunctional regulators of both osteoblast and osteoclast activity, as well as their role as endocrine cells, there is a need for new tools to study their biology and function. We have previously described the generation of a novel immortalized cell line, OmGFP66, which has the unique property of forming highly organized "mini-bone" structures in culture that closely mimic osteocytes and trabecular bone structure in normal bone tissues. Here we describe the further characterization of this novel cell line.

The OmGFP66 cell line was derived from calvarial cells isolated from transgenic mice expressing a membrane targeted GFP variant driven by the 10kb dentin matrix protein-1 promoter for selective expression in osteocytes. The cells were immortalized by stable transfection with SV40T antigen and clone OmGFP66 was found to have the unique property of forming well organized mini-bone structures in long term culture with highly dendritic GFP-positive osteocytes embedded in well defined lacunae. We have previously shown by western blotting that over a 28 day time course these cells progress from expressing early osteocyte markers E11/gp38 and dentin matrix protein-1 to expressing the late osteocyte marker, sclerostin. The cells also express alkaline phosphatase, suggesting that they represent a late osteoblast/early osteocyte cell line that can be differentiated to mature embedded osteocytes. qPCR analysis confirmed expression of these early and late osteocyte marker genes and showed that omGFP66 cells also express other osteocyte marker genes, such as FGF23, MEPE and PHEX, which increased over the 28 day time course. Expression of Cx43 was also detected as well as high expression of HIF-1α. Transmission electron microscopy revealed a highly organized mineralized matrix that appeared very similar to bone structure in vivo, with mineral deposited on collagen fibrils. Embedded cells resembling in vivo osteocytes were observed within mineralized lacunae and canaliculi containing dendrites were observed throughout the mineralized matrix. This novel cell line provides a useful tool for examining osteocyte function in vitro within a mineralized microenvironment that closely resembles the osteocyte microenvironment in vivo.

SU0277

Prevention of Osteocyte Apoptosis and the Increase in Osteocytic RANKL Are Not Sufficient to Restrain Osteoclastic Bone Resorption and Stop Bone Loss Induced by Reduced Mechanical Forces.
Lilian Plotkin*[1], Arancha Gortazar[2], Keith Condon[3], Hugo Gabilondo[3], Marta Maycas[4], Teresita Bellido[1]. [1]Indiana University School of Medicine, USA, [2]Universidad San Pablo-CEU School of Medicine Madrid Spain, Spain, [3]Indiana University School of Medicine, USA, [4]Indiana University School of Medicine, USA

Apoptosis of osteocytes precedes osteoclast-mediated resorption and bone loss induced by reduced mechanical forces, and RANKL expression is increased with unloading in mice. Because osteocytes are the major producers of RANKL, we hypothesized that apoptotic osteocytes signal to neighboring cells to increase RANKL expression, which in turn increases osteoclast formation and bone resorption. We tested herein whether inhibition of osteocyte apoptosis alters osteocytic RANKL expression and stops resorption and bone loss induced by unloading. Female 4 month old C57Bl/6 mice were tail-suspended for 28d and received daily injections of the bisphosphonates (BPs) alendronate (Aln) or IG9402 at 2.3µmol/kg/day, or placebo, starting 3d before unloading. Earlier studies showed that Aln inhibits both osteocyte apoptosis and resorption, whereas IG9402 only prevents osteocyte apoptosis. Unloading increased the prevalence of apoptotic, TUNEL+ osteocytes by 2-fold compared to ambulatory controls; and Aln and IG9402 prevented this increase. Unloading also increased the number of RANKL+ osteocytes by 2-fold, detected by immunohistochemistry with sc-7628 antibody; and both BPs equally prevented this effect. Further, unloaded mice exhibited elevated osteoclasts on cancellous vertebral bone surfaces, increased osteoclastogenesis in *ex vivo* bone marrow cultures (plus RANKL/M-CSF), and increased levels of the bone resorption marker CTX in serum. Aln prevented all these effects, whereas IG9402 was ineffective. Unloaded mice also exhibited a reduction in spinal and femoral BMD (-11%) by DXA; spinal BV/TV (-25%) and trabecular thickness (-14%) by micro-CT; and mechanical strength (-46% ultimate load, N) as well as material strength (-62% maximum stress, MPa). Aln treatment prevented the loss of both bone mass and strength. In contrast, IG9402 did not prevent the loss of bone mass, but partially prevented the loss of both mechanical and material strength (-38%) suggesting a contribution of osteocyte viability to strength independent of bone mass. These results demonstrate that inhibition of osteocyte apoptosis and prevention of the increase in osteocytic RANKL are not sufficient to restrain osteoclastic bone resorption and stop bone loss induced by unloading. We conclude that osteocyte apoptosis is not the main cause of increased resorption and that osteocytic RANKL is not the sole mediator of osteoclastogenesis and bone loss induced by lack of mechanical forces.

SU0278

Continuous PTH Administration Stimulates Osteoclasts and Leads to Increased Cortical Bone Resorption at the Endosteal Surface, Widening of the Porosities, and Osteoclasts Contact with Osteocytes. Nobuhito Nango*[1], Shogo Kubota[2], Wataru Yashiro[3], Atsushi Momose[3], Makoto Morikawa[4], Koichi Matsuo[5]. [1]Ratoc System Engineering Co., Ltd., Japan, [2]Ratoc System Engineering Co., Ltd., Japan, [3]Institute of Multidisciplinary Research for Advanced Materials, Tohoku University, Japan, [4]Laboratory of Cell & Tissue Biology, School of Medicine, Keio University, Japan, [5]School of Medicine, Keio University, Japan

With age, cortical bones tend to become more porous and thinner, which may lead to a higher risk of bone fracture. A similar phenomenon occurs by continuous PTH administration. However, the mechanism of porosity increasing in cortical bone remains unclear. We previously reported that osteocytes dissolve bone mineral through bone canaliculi, and cement lines and calcified cartilage matrices appear because of the formation of a high mineral wall (HMW) following a single administration of PTH. In this report, the effects of continuous PTH administration were evaluated to clarify the mechanism of increased porosity in cortical bone. We examined responses of microstructures and bone cells such as osteoclasts. Seven-week-old mice with implanted osmotic pumps were continuously dosed with PTH at 40 μg/kg/day for 12, 24, 48, and 144 h to maintain serum PTH levels. The tibial bones were isolated prior to and after administration. We scanned the tibial diaphysis using μCT with a voxel size of 7 μm (N = 4). Furthermore, we built a multi-scan synchrotron X-ray microscope at the SPring-8 (Hyogo, Japan) to observe the bone microstructures at 9 keV (N = 1–3). This method enables three-dimensional observation (0.2-μm voxel size) of the canaliculi and degree of bone mineralization. In the group that received continuous PTH administration for 144 h, the bone marrow volume was increased by 1.5-fold and the cortex was thinned by 28% compared with controls. Moreover, the bone canal was extended and porosity volume increased by 2.2-fold. A HMW was formed, which suggests that the osteocytes reacted to continuous PTH administration. Following continuous PTH administration, deep and wide resorption cavities were observed at the endosteum rather than the periosteum. This finding suggested that osteoclast activity was enhanced at the endosteum by continuous PTH administration. Therefore, the number of porosities on the endosteum extended the bone marrow and made cortical bone thinner. The bone canal ran through cortical bone from the endosteum (left) to the periosteum (right), and deep resorption cavities were formed on the endosteum (Fig.). Osteoclasts in the bone canal made contact with canalicular networks of osteocytes and made cell-cell contact with the osteocytes. The formation of this structure suggested that the osteoclasts may find the location of osteocytes within bone.
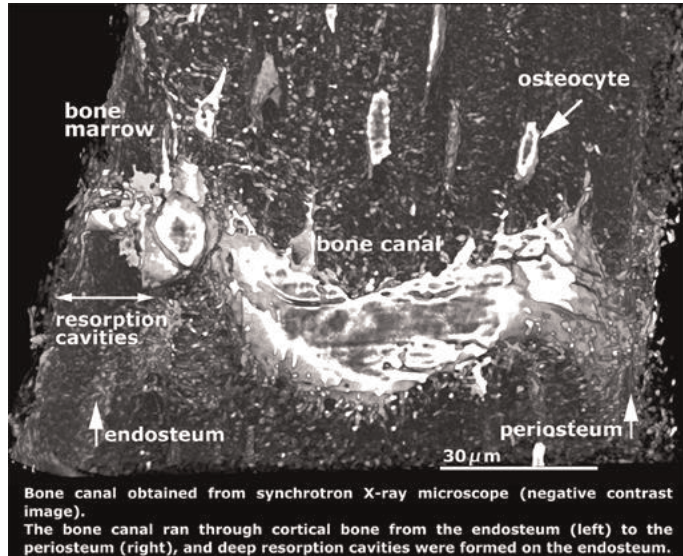

Bone canal obtained from synchrotron X-ray microscope (negative contrast image).
The bone canal ran through cortical bone from the endosteum (left) to the periosteum (right), and deep resorption cavities were formed on the endosteum.

Fig.

Disclosures: Nobuhito Nango, None.

SU0279

Circulating sclerostin as a predictor of cardiovascular events in Type 2 diabetes patients. Manuel Muñoz-Torres*[1], Cristina Novo-Rodriguez[2], Rebeca Reyes-Garcia[3], Pedro Rozas-Moreno[4], Antonia Garcia-Martin[5], Veronica Avila-Rubio[2], Sonia Morales-Santana[2], Beatriz Garcia-Fontana[2], Fernando Escobar-Jimenez[2]. [1]Bone Metabolic Unit (RETICEF), Endocrinology Division, Hospital Universitario San Cecilio, Instituto de Investigación de Granada., Spain, [2]Bone Metabolic Unit (RETICEF), Endocrinology Division, Hospital Universitario San Cecilio, Instituto de Investigación de Granada, Spain, [3]Bone Metabolic Unit (RETICEF), Endocrinology Division, Hospital Universitario San Cecilio, Instituto de Investigación de Granada. Endocrinology Unit. Hospital General Universitario Rafael Mendez, Lorca, Murcia., Spain, [4]Bone Metabolic Unit (RETICEF), Endocrinology Division, Hospital Universitario San Cecilio, Instituto de Investigación de Granada. Endocrinology. Hospital General de Ciudad Real, Spain, [5]Bone Metabolic Unit (RETICEF), Endocrinology Division, Hospital Universitario San Cecilio, Instituto de Investigación de Granada. Endocrinology. Hospital Comarcal de Moroeste, Caravaca de la Cruz, Murcia., Spain

Background: Sclerostin is an osteocyte-secreted protein, which acts as an endogenous inhibitor of Wnt/ β-catenin pathway. Recent studies have shown that type 2 diabetes patients have high sclerostin concentrations, and in type 2 diabetes sclerostin concentrations are related to prevalent atherosclerotic disease.
Aims: To evaluate the predictive ability of circulating sclerostin on the incidence of cardiovascular events in type 2 diabetes patients.
Patients and methods: We performed a prospective study with a follow-up of seven years (2007-2014). We included 133 subjects: 77 with type 2 diabetes (mean age 57 ± 6 years), and 56 subjects without diabetes (mean age 55 ± 7 years). We measured baseline sclerostin concentrations by ELISA (Biomedica), and we evaluated cardiovascular events (acute myocardial infarction, unstable angina, stroke and peripheral vascular disease) and cardiovascular event-related admissions during the follow-up.
Results: Subjects with incident cardiovascular events showed higher baseline sclerostin concentrations. Further, we found a significant difference in sclerostin concentrations (p<0.025) when we considered subjects with cardiovascular event-related admissions. The incidence of cardiovascular event-related admissions was 36.5% in the diabetic group and 14.3% for non-diabetic group. In the entire group, sclerostin concentrations above the percentile 50 ($\geq$ 43.6 pmol/L) were associated with an increase of cardiovascular events (p<0.065) and also with cardiovascular event-related admissions (p<0.001). The relative risk of suffering a cardiovascular event in patients with sclerostin concentrations above 43.6 pmol/L was 1.4 (CI 95%: 1.01-1.95). The relative risk of a cardiovascular event-related admission was 1.74 (CI 95%: 1.36-2.2).
Conclusions: Serum concentrations of sclerostin are associated with an increase of the risk of cardiovascular events in type 2 diabetes patients. According to these results, the determination of sclerostin may help in the identification of high-risk patients.

Disclosures: Manuel Muñoz-Torres, None.

SU0280

Higher serum carcinoembryonic antigen level is associated with increased development of incident fractures in Korean women: a longitudinal study using the national health insurance claim data. HyeonMok Kim*[1], Seong Hee Ahn[2], Beom-Jun Kim[3], Seung Hun Lee[2], Ghi Su Kim[2], Jung-Min Koh[3]. [1], South Korea, [2]Asan Medical Center, University of Ulsan College of Medicine, South Korea, [3]Asan Medical Center, South Korea

Pro-inflammatory cytokines play important roles in bone metabolism, and several studies revealed that carcinoembryonic antigen (CEA) has a pro-inflammatory feature. We aimed to investigate the relationships of serum CEA with osteoporosis and incident fracture risk.
We performed a small cross-sectional study in the 302 Korean women and a large, longitudinal study in the 7,192 Korean women with an average 3-years. Bone mineral density (BMD) and bone turnover markers (BTMs) were measured in the cross-sectional study. Incident fractures were identified using selected ICD-10 codes in the nationwide claims database of the Health Insurance Review and Assessment Service of Korea in the longitudinal study. In the cross-sectional study, serum CEA negatively correlated with BMD at lumbar spine (γ = -0.023, P = 0.029), and positively correlated with BTMs (γ = 0.122 to 0.138, P = 0.002 to <0.001). In the longitudinal study, 254 (3.5%) women developed incident fractures. After adjustment for potential confounders, the hazard ratio (HR) per 1 ng/mL increment of the baseline CEA level for the development of incident fracture was 1.22 [95% confidence interval (CI) = 1.05 - 1.42]. The HR was markedly higher in subjects in the highest CEA quartile category compared with those in the lowest CEA quartile category (HR = 1.54, 95% CI = 1.04 – 2.28).
These findings suggest that serum CEA may be a biomarker for the risk of incident fracture in Korean postmenopausal women.

Disclosures: HyeonMok Kim, None.

SU0281

How accurate is your sclerostin measurement? Comparison between two commercially available sclerostin ELISA kits. Isabelle Piec*[1], Emily Fisher[2], Christopher Washbourne[3], Jonathan Tang[4], William Fraser[3]. [1]BioAnalytical Facility, University of East Anglia, United Kingdom, [2]University of East Anglia, United Kingdom, [3]University of East Anglia, United Kingdom, [4]University of East Anglia, Norwich, UK, United Kingdom

Introduction: Sclerostin (SOST), osteocyte-secreted soluble antagonist of the Wnt/β-catenin signaling pathway, is a potent inhibitor of osteoblastogenesis. Circulating SOST levels have been measured in a plethora of disorders such as ankylosing spondylitis, chronic kidney disease, diabetes, fractures, hypercortisolism, multiple myeloma and spinal cord injury. SOST is a crucial regulator of the skeletal anabolic action of PTH and as so, anti-sclerostin antibodies are being investigated as potential therapeutic molecules for metabolic bone diseases. Accurate measurement of SOST is therefore of utmost importance for the diagnosis of bone disorders and therapy effectiveness. However, reports so far suggests further study is needed before SOST measurements are introduced into routine clinical practice.

Objective: To compare two commercially available assays for measurement of circulating SOST.

Method: EDTA-plasma samples from 36 anonymised healthy individuals were analyzed using ELISA kit for circulating SOST from Biomedica (Vienna, Austria) and TecoMedical (TECO, Sissach, Switzerland). Both assays are based on immuno-capture using two antibodies which have been raised against human recombinant SOST and are highly specific for this molecule.

Results: Circulating SOST levels in EDTA plasma samples were found to be significantly different between TECO and Biomedica assays (36.9 ± 2 and 21.3 ± 1 pmol/L, respectively, p<0.001) with discrepancies of up to 32pmol/L. The TECO assay demonstrated less variability between duplicates (2.6 ± 2.4 % and 7.4 ± 6.3 % respectively) and dilution study showed that the biomedical kit over-recovered diluted samples by up to 60%. When samples containing various concentrations of endogenous sclerostin were spiked with a known amount of SOST, recovery was 88.5% and 104% respectively. Conclusion: The variability in values generated from Biomedica and TECO assays has raised questions regarding the specificity of antibodies used by the two manufactures, and whether there is possible interference affecting one of the assays remains unclear. Cross-reactivity experiments are being conducted to determine the source of variation between the two kits. Until such issues are resolved, measurement of sclerostin remains invaluable for understanding the mechanism by which osteocytes regulate bone turnover but should be used in discretion and interpretation should be carried out with guided clinical evidence.

Disclosures: Isabelle Piec, None.

SU0282

LC-MS/MS Measurement of Urine Free Collagen Crosslinks Pyridinoline and Deoxypyridinoline: Urine Markers of Bone Resorption. Jonathan Tang*[1], John Dutton[2], Darrell Green[3], Isabelle Piec[4], Emily Fisher[5], Christopher Washbourne[3], William Fraser[3]. [1]University of East Anglia, Norwich, UK, United Kingdom, [2]Royal Liverpool & Broadgreen University Hospital, United Kingdom, [3]University of East Anglia, United Kingdom, [4]BioAnalytical Facility, University of East Anglia, United Kingdom, [5]University of East Anglia, United Kingdom

Background: The pyridinium cross-links Pyridinoline (PYD) and Deoxypyridinoline (DPD) are markers of bone resorption. Primarily found in bone and cartilage, PYD and DPD are the major stable cross-links only present in mature Type I collagen. Breakdown of cross-links are a result of osteoclast resorption, normally excreted in the urine, and in larger quantities when bone resorption is increased. In contrast, when bone resorption is inhibited by bisphosphonate, oestrogen or calcitonin therapy, the excretion of PYD and DPD is decreased. The main application for DPD and PYD is in assessing and monitoring response to osteoclast inhibitory treatment (mainly bisphosphonates) in osteoporosis and Paget's disease of bone. A decrease in value obtained pre-treatment is indicative of a good response in osteoporosis. Normalisation of DPD and PYD is the ultimate goal when treating Paget's disease of bone.

Objective: To develop a sample clean up protocol to extract PYD and DPD from urine and quantify by LC-MS/MS. The method was used to assay urine samples from healthy individuals and patients samples requested for bone turnover markers.

Method: PYD and DPD were measured by reversed-phase, ion-paired high performance liquid chromatography with MS/MS detection. Solid phase extraction was carried out by passing acidified urine mixed with cellulose slurry through a column containing a frit, then washed with butanol and tetrahydrofuran then followed by elution with heptafluorobutyric acid. Mass detection and quantification were performed by a triple quadrupole tandem mass spectrometer.

Results: The method was able to be fully resolved PYD and DPD. The intra assay and inter assay CVs for PYD and DPD were <10%. PYD was linear up to 2000 nmol/L, DPD up to 1000 nmol/L. Typical standard curve fit $r^2 \geqslant 0.998$. Spiked recovery was determined by adding a known quantity of PYD/DPD urine samples containing different levels of endogenous PYD/DPD, percentage recovery were ranged between 98.4-116.5%. The method was compared with two commercial immunoassays for

urine total PYD and DPD, with correlation coefficients r^2 of 0.862 and 0.832 respectively.

Conclusion: The presented LC-MS/MS method have been fully validated and showed excellent assay characteristics that is suitable for routine clinical hospital laboratory. Ratio of PYD:DPD is also a valuable diagnostic tool for Ehlers-Danlos Syndrome (EDS), where a reverse ratio is specific and diagnostic for the kyphoscoliotic type of EDS.

Disclosures: Jonathan Tang, None.

SU0283

Using Bone Turnover Markers to Predict Changes in BMD After Alendronate Therapy in Postmenopausal Women. Brian Mcnabb*[1], Eric Vittinghoff[2], Ann Schwartz[3], Douglas Bauer[3], Kristine Ensrud[4], Elizabeth Barrett-Connor[5], Richard Eastell[6], Dennis Black[3]. [1]San Francisco VA Medical Center, University of California, San Francisco, USA, [2]University of California, San Francisco, USA, [3]University of California, San Francisco, USA, [4]University of Minnesota & Minneapolis VA Health Care System, USA, [5]University of California, San Diego, USA, [6]University of Sheffield, United Kingdom

Context: Many women with osteoporosis are candidates for therapy cessation after 5 years of alendronate. Little information exists to guide monitoring women who stop alendronate with bone turnover markers (BTMs).

Objective: To determine if BTMs measured early after alendronate discontinuation can predict subsequent loss of bone mineral density (BMD).

Methods: We analyzed women who had received an average of 5.1 years of alendronate during the Fracture Intervention Trial (FIT) and were subsequently followed for 5 treatment-free years (on placebo) during the FIT Long Term Extension (FLEX) trial. Repeated measures analysis of annual BMD measurements was used to estimate 5-year changes in total hip and femoral neck BMD during the 5-year treatment-free period following alendronate use (FLEX). BMD was measured by 2D dual-energy X-Ray absorptiometry (DXA). The BTMs bone specific alkaline phosphatase (bone ALP) and N-propeptide of type-I collagen (NTX) were measured at baseline, year-1, and year-3 of FLEX. Linear regression was used to assess the associations of BTM values with 5-year changes in BMD. Models were adjusted for age, body mass index (BMI), vertebral fracture status, calcium intake, walking for exercise, smoking status, alcohol intake, general health status, and falls history.

Results: There were 392 women with analyzable BMD and BTM data. Bone ALP measured at FLEX baseline, year-1, and year-3 predicted 5-year changes in total hip BMD (Table 1), explaining 6.5% or less of the variability. Femoral neck BMD was only predicted by baseline and year-1 bone ALP measurements (data not shown), explaining 11% or less of the variability. NTX predicted total hip BMD change (Table 1), but only when measured at year-1 and year-3, and explained 6.3% or less of the variability. NTX did not predict femoral neck BMD change (data not shown). Models assessing BTMs over multiple time-points or changes in BTMs did not improve prediction over measuring at a single time-point. Measuring both BTMs improved prediction at the total hip, but not the femoral neck.

Conclusions: Bone ALP and NTX measured after alendronate discontinuation are associated with future BMD losses. However, because these BTMs only explain a small amount of the variability of BMD losses, their predictive ability is modest. Assessing changes in BTMs provides no added value over a single measurement at 1 year off therapy.

Table 1: Difference in 5-year % Change in Total HIP BMD per SD Increase in Bone ALP or NTX Measured at Different Time-points After ALN Discontinuation

BTM (SD)	Change in BMD (Percentage Points)	P	CV-R² (%)
Bone ALP, ng/mL **Years Post-ALN**			
0 (2.4)	-0.53	0.001	6.5
1 (4)	-0.43	0.002	6.1
3 (4.1)	-0.4	0.004	3.0
NTX, nmol BCE/mmol Cr **Years Post-ALN**			
0 (16.3)	-0.12	0.41	2.5
1 (12.8)	-0.51	0.001	6.3
3 (12.8)	-0.46	0.002	3.2

Abbreviations: ALN, alendronate; BMD, bone mineral density; SD, standard deviation; Bone ALP, bone specific alkaline phosphatase; NTX, N-propeptide of type 1 collagen; BTM, bone turnover marker; CV-R², 10 times cross-validated R².

Table1

Disclosures: Brian Mcnabb, DocMatter, 8

SU0284

Factors Involved in Cortical Porosity Formation in Males: Analysis of Distal Radius by HR-pQCT. Ko Chiba*[1], Andrew Burghardt[2], Narihiro Okazaki[3], Makoto Osaki[4], Sharmila Majumdar[2]. [1]Nagasaki University School of Medicine, Japan, [2]University of California, San Francisco, USA, [3]University of California, San Francisco, USA, [4]Nagasaki University, Japan

[Introduction]

Cortical porosity at the distal radius was measured using HR-pQCT in males aged between 50 to 78, and the factors involved in its formation were analyzed.

[Methods]

The subjects were 49 healthy males (60 ± 8 year-old, 50 ∼ 78 year-old).

The ultradistal radius was scanned by HR-pQCT at 82 μm in voxel size, and the volume density of cortical porosity (Ct.Po) was measured. Correlations with the following factors were analyzed: age, height, weight, body mass index, smoking/drinking habits, serum calcium, vitamin D and testosterone value, bone mineral density value of the lumbar vertebra, proximal femur, distal radius measured by dual-energy x-ray absorptiometry (DXA), and bone microstructural parameters at the ultradistal radius measured by HR-pQCT.

[Results]

The factors that significantly correlated with Ct.Po were age and height, and each of them had a weak correlation (P<0.01, R=0.39, 0.40).

[Conclusion]

The cortical porosity of the distal radius tended to be seen with aging. However, cortical porosity does not have a significant correlations to local bone loss as indicated by DXA or HR-pQCT. Rather, it can be caused by general factors.

Disclosures: Ko Chiba, None.

SU0285

Microarchitectural Deterioration of Lumbar Spine Estimated by Trabecular Bone Score (TBS) is Associated with Vertebral Fractures Independent of Bone Mineral Density in Patients with Type 2 Diabetes Mellitus. Masahiro Yamamoto*[1], Toru Yamaguchi[2], Nobuaki Kiyohara[3], Noriko Nakata[3], Toshitsugu Sugimoto[4]. [1]Shimane University Faculty of Medicine, Japan, [2]Shimane University Faculty of Medicine, Jpn, [3]Shimane University Faculty of Medicine, Japan, [4]Shimane University School of Medicine, Japan

Purpose: Patients with type 2 diabetes mellitus (T2DM) have an increased risk of vertebral fractures compared to non-T2DM controls independent of bone mineral density (BMD) (JBMR 2009), suggesting that increased bone fragility is caused by poor bone quality. Bone quality consists of bone material properties and bone structural properties. Exacerbation of bone material properties such as accumulation of advanced glycation end-products in bone tissue and aggravation of bone structural properties such as increased porosity of cortical bone are associated with bone fragility in patients with T2DM. However, impact of structure of trabecular bone on bone fragility still remains unclear in these patients. The aim of this study is to investigate whether deteriorated bone microarchitecture estimated by trabecular bone score (TBS) which is a DXA-derived index that focuses on the cancellous architecture is attributed to bone fragility in these patients.

Methods: We compared parameters of bone metabolic markers including TBS and lumbar spine BMD between Japanese T2DM patients with and without vertebral fractures [278 postmenopausal women and 334 men over 50 years old, whose creatinine levels were within normal range].

Results: There was no significant difference in TBS values between the sexes. Multiple regression analysis including independent variables of HbA1c, creatinine, BAP and duration of T2DM showed that TBS values were significantly and positively correlated with lumbar spine BMD and inversely related with age and BMI in both genders (women: r = 0.44, P < 0.04, r = -041, P < 0.01, r = -0.17, P < 0.01; men: r = 0.50, P < 0.01, r = -0.31, P < 0.01, r = -0.28, P < 0.01, respectively). Logistic regression analysis adjusted for age showed no relationship between spine BMD and the presence of vertebral fractures. In contrast, TBS values were significantly associated with vertebral fractures after adjustment for age, BMI, HbA1c, creatinine, phosphate, duration of T2DM and spine BMD [women: odds ratio (OR) 0.67 (95%CI 0.45-0.93), P =0.02; men: OR 0.70 (0.50-0.99), P = 0.04, per 0.1 increase in TBS].

Conclusion: This study demonstrated that TBS values were associated with vertebral fractures independent of BMD in both genders. This finding suggested that microarchitectural deterioration of trabecular bone may cause poor bone quality and result in elevated fracture risk in patients with T2DM.

Disclosures: Masahiro Yamamoto, None.

SU0286

Multi-Row Detector CT Imaging with Image Analysis using an Advanced Tensor Scale Algorithm Provides a Robust Assessment of Trabecular Bone Micro-Architecture for Human Studies. Punam K. Saha*[1], Yinxiao Liu[2], Chadi Calarge[1], Ryan Amelon[2], Cheng Chen[2], Elena Letuchy[2], Trudy Burns[2], James Torner[2], Steven Levy[1]. [1]University of Iowa, USA, [2]University of Iowa, USA

Recent evidence implicates serotonin in bone metabolism and selective serotonin reuptake inhibitors (SSRIs) in bone-loss and increased fracture-risk. Low bone mineral density (BMD) is the hallmark of osteoporosis, a leading cause of low-trauma fracture. However, increasing evidence suggests that the micro-architectural quality of trabecular bone (TB) is an important determinant of bone strength and fracture risk. This makes robust and sensitive measures of TB micro-architecture at *in vivo* resolution of significant interest in early detection and characterization of bone loss. Thus, a tensor scale-based *in vivo* characterization of TB micro-architecture at the distal tibia using multi-row-detector CT (MD-CT) imaging was developed.

Tensor scale provides an optimized ellipsoidal approximation of individual trabeculae, assessing their micro-architecture on the continuum between a perfect plate and a perfect rod, as well as their orientation. Repeat MD-CT scan reproducibility and the sensitivity of the method were examined by evaluating its ability to predict bone strength of cadaveric specimens. Additionally, the method was evaluated in a pilot human study involving healthy young-adult participants from the Iowa Bone Development Study (IBDS) (19 to 21 Y; 51 F, 46 M) and age-similar patients treated with SSRIs (6 F, 6 M).

Observed repeat scan intraclass correlation coefficients were greater than 95% for regional MD-CT TB measures (VOI diameter≥1.05mm). Tensor scale-based TB measures demonstrated stronger linear association with bone strength (correlation coefficient r=0.96) than did volumetric BMD (vBMD) (r=0.89). Results of the pilot human study showed that SSRI-treated participants had 8% (inner region) and 14% (peripheral region) reduced TB plate-width and also 5% (inner) and 4% (peripheral) reductions in tensor scale-measured transverse BMD as compared to healthy controls (Figure 1, Table 1). In contrast, only a 4% reduction in whole body BMD was observed in the SSRI-treated participants, suggesting that DXA is much less sensitive than TB micro-architectural measures.

In vivo MD-CT imaging, together with the advanced algorithm of tensor scale, is suitable for robust assessment of plate-rod micro-architecture and orientation of TB at a peripheral site. Long-term SSRI treatment may be associated with skeletal effects more sensitively captured by MD-CT imaging.

Color-coded illustration of trabecular bone (TB) plate/rod classification for a healthy female IBDS control (a) and a female patient on continuous treatment with a selective serotonin reuptake inhibitor (b). (c,d) A male control and a male SSRI-treated patient. Male and female IBDS participants have more TB plates (colored in green) as compared to the two patients.

Figure 1. Color-coded illustration of trabecular bone (TB) plate/rod classification.

Paired comparisons for selected trabecular bone measures (over an axial VOI covering 4-6% of tibia) computed using MD-CT imaging and tensor scale and the whole body BMD from DXA.				
	Matched (min=1, max= 4 controls /1 case)[a]			
	Paired (N=12)		t-test	Wilcoxon
Variable	Diff (μm)[b]	% Diff[b]	p-value	p-value
TB plate-width (peripheral)	-183	-13.6	0.03	0.04
TB plate-width (central)	-92	-8.1	0.15	0.20
Transverse BMD (peripheral)	-17.17	-3.9	0.20	0.15
Transverse BMD (central)	-23.00	-5.2	0.14	0.18
Whole body BMD (DXA)	-0.048	-4.0	0.07	0.08

[a] Matching algorithm with variable number of controls per case subject (1 to 4 controls) was used for optimal matching by sex, height, and weight. Paired t-test and non-parametric Wilcoxon signed ranks test were used for comparison.
[b] Mean value of differences between SSRI participants and average value for matched controls (across all pairs). Percent difference is calculated the same way relative to average value for matched controls.

Table 1. Paired comparisons for selected trabecular bone measures.

Disclosures: Punam K. Saha, None.

SU0287

Non-invasive assessment of longitudinal changes in bone microarchitecture and bone strength over eighteen months in lung transplant recipients using high-resolution peripheral quantitative computed tomography (HR-pQCT).

Daniela Kienzl[1], Lukas Fischer[1], Thomas Gross[2], Matthew DiFranco[3], Michael Weber[1], Alexander Valentinitsch[4], Peter Jaksch[1], Walter Klepetko[1], Rodrig Marculescu[5], Peter Pietschmann[6], Claudia Schueller-Weidekamm[1], Franz Kainberger[1], Georg Langs[1], Janina Patsch*[3]. [1]Medical University of Vienna, Austria, [2]Vienna University of Technology, Austria, [3]Medical University of Vienna, Austria, [4]Klinikum rechts der Isar, Technische Universität München, Germany, [5]Medical university of Vienna, Austria, [6]Department of Pathophysiology & Allergy Research, Medical University of Vienna, Austria

With additive effects of pre-existing secondary bone disease and post-transplantion bone loss, lung transplant (LuTX) recipients are highly susceptible to fragility fractures. Using HR-pQCT, we have previously reported cross-sectional data on poor cortical and trabecular microarchitecture and deficits in bone strength in LuTX recipients after surgery [1]. Bearing in mind the particularly high fracture risk in the first year after transplantation, we hypothesized to find significant longitudinal bone loss. To gain insight into structural and biomechanical changes at the ultradistal radius over time, we have thus followed up LuTX recipients (n=18) over eighteen months after surgery. We performed densitometric and morphometric standard HR-pQCT analyses for baseline and follow-up scans. We carried out extended cortical analyses including quantification of cortical porosity, 3D-texture-based clustering of trabecular bone [2] and micro-finite element analyses. Serum markers of bone turnover were analyzed along with clinical data including incident fractures and episodes of graft rejection. Paired t-tests were used to compare mean differences between baseline and follow-up. LuTX patients exhibited significant decreases in total bone mineral density (BMD; -3.1%,p=0.001), trabecular BMD (-2.9%,p=0.027) and cortical BMD (-2.1%,p=0.003). Cortical area decreased (-3.2%,p=0.015) and trabecular area increased (+0.6%,p=0.020). Changes in cortical porosity were not statistically significant (+9.4%,p=0.419). Trabecular heterogeneity (+5.6%,p=0.023) and intermediate trabecular quality cluster size (TMAC2;+7.6%,p=0.015) increased. Vice versa, the size of the trabecular high quality cluster (TMAC1) decreased by 7.1% (p<0.001). There were pronounced decreases in stiffness (-6.8%,p=0.004), failure load (-5.9%,p=0.004), and bone strength (-5.2%,p=0.001). Serum osteocalcin and P1NP increased (+254.8%,p=0.006;+123.5%,p=0.001), changes in CTX were not significant (+23.8%,p=0.348). Patients with incident fractures (17%; 3/18) had significantly greater declines in BMD than those without (p=0.034). Densitometric and microarchitectural changes did not differ between patients with (22%; 4/18) and without severe rejection episodes. Our results indicate significant bone loss, declining biomechanical properties, and increasing bone turnover in LuTX recipients in the first eighteen months after surgery.

[1] Valentinitsch A.ASBMR 2013/MO0440
[2] Valentinitsch A. Bone (2013) 54;133–140

Disclosures: Janina Patsch, None.

SU0288

Systemic and local bone loss in Psoriasis and Psoriatic Arthritis. Roland Kocijan*[1], Matthias Englbrecht[2], Arnd Kleyer[2], Judith Haschka[3], David Simon[2], Stephanie Finzel[2], Sebastian Kraus[2], Christian Muschitz[4], Heinrich Resch[5], Klaus Engelke[6], Juergen Rech[2], Georg Schett[2]. [1]St. Vincent Hospital Vienna, Austria, [2]Department of Internal Medicine 3 & Institute of Clinical Immunology, University of Erlangen-Nurnberg, Germany, [3]University Hospital Erlangen-Nuremberg, Deu, [4]St. Vincent's Hospital, Austria, [5]Medical University Vienna, Austria, [6]University of Erlangen, Germany

Purpose: Psoriatic arthritis (PsA) is a chronic inflammatory joint disorder characterized by local bone loss. However, data on systemic bone loss and bone mineral density (BMD) in PsA as well as in psoriasis are inconsistent. Moreover, data on bone quality are missing. The aim of this study was to evaluate bone microstructure and volumetric bone mineral density (vBMD) in patients with PsA and psoriasis by HR-pQCT (high resolution peripheral quantitative computed tomography).

Methods: HR-pQCT scans were performed at the periarticular and the non-periarticular radius in patients with PsA (n=50), patients with psoriasis without any signs of arthritis (n=30) and healthy, age- and sex-related controls (n=70). We assessed vBMD and parameters of microstructure including trabecular bone volume (BV/TV), trabecular number (Tb.N), inhomogeneity of the trabecular network, cortical thickness (Ct.Th) and cortical porosity (Ct.Po). Moreover, HR-pQCT scans of the metacarpophalangeal joints (MCP) were performed to detect bone erosions.

Results: At the non-periarticular radius trabecular BMD (p=0.009), cortical BMD (p=0.031), BV/TV (p=0.009) and Tb.N (p=0.0013) were significantly decreased in PsA patients compared to healthy controls. In addition, Tb.Sp (p=0.014) and inhomogeneity of the network (p=0.040) were increased in PsA. No differences were found regarding cortical thickness and cortical porosity between the three subgroups.

Similar results were found at the periarticular radius. Patients with psoriasis without arthritis had a bone phenotype comparable to healthy controls. Nonetheless, duration of skin disease was found to be associated to low BV/TV and Tb.N in patients with PsA. Bone erosions were detected in 70% of patients with PsA, 47% of patients with psoriasis and 30% of healthy controls.

Conclusion: Trabecular and cortical vBMD as well as trabecular bone microstructure are decreased in PsA. Our data suggest a skin-bone-axis linked to duration of psoriasis and a pre-PsA status in patients with psoriasis without arthritis. However, systemic bone loss seems to be triggered by additional factors linked to arthritis.

Disclosures: Roland Kocijan, None.

SU0289

Trabecular Bone Microarchitecture of lumber spine is Deteriorated in Patients with Type 2 Diabetes Mellitus. Kenichiro Matsuzaki*[1], Toshihide Kawai[2], Takeshi Miyamoto[3], Kensuke Mio[4], Hironori Kaneko[5], Keisuke Horiuchi[6], Morio Matsumoto[6], Koichi Nemoto[4]. [1]National Defense Medical College, Japan, [2]Dept. of Internal Medicine, Keio Univ., Japan, [3]Keio University School of Medicine, Japan, [4]Dept. of Orthopaedic Surgery, National Defense Medical College, Japan, [5]Keio University, Japan, [6]Dept. of Orthopaedic Surgery, Keio Univ., Japan

Introduction: Fracture risk is increased in type 2 diabetes mellitus, although areal bone mineral density is elevated. There is a possibility that some aspect of bone quality plays a role here. These include bone turnover, material property such as cross-links of collagen, cortical and trabecular microarchitecture. We investigated the trabecular microarchitecture of lumber spine of patients with type 2 diabetes mellitus (T2DM).

Methods: 33 postmenopausal women with BMD < 80%-YAM with T2DM and 33 control postmenopausal women with BMD < 80%-YAM without T2DM were evaluated in a cross-sectional study. Clinical multi-detector row CT (MDCT) was applied to capture differences in three-dimensional (3D) trabecular bone architecture and cortical or trabecular volumetric density in lumber supine. We measured/calculated 3D trabecular bone architecture parameters. Statistical significance was set at P<0.05.

Results: Trabecular and cortical vBMD significantly increased in T2DM patients. On the other hand, BV/TV was lower in T2DM patients significantly compared with control patients. V*tr, which indicates the connectivity of trabecular, was significantly decreased inT2DM compared with control. All other parameters did not reach significance but showed the tendency related to decreased bone strength in T2DM patients. These tendencies were greater at upper part of vertebra than at middle part.

Discussion: It is suggested that deterioration of trabecular bone microarchitecture may be one of the reasons why fracture risk is elevated despite high BMD in T2DM patients.

Disclosures: Kenichiro Matsuzaki, None.

SU0290

Trabecular bone score (TBS), vitamin d and biochemical measures of bone metabolism in men. Mário Rui Mascarenhas*[1], Ana Paula Barbosa[2], Didier Hans[3], Manuel Bicho[4]. [1]Lisbon's Faculty of Medicine, Santa Maria University Hospital, CHLN,EPE, Portugal, [2]Endocrinology, Santa Maria Hospital & Faculty of Medicine, Portugal, [3]Lausanne University Hospital, Switzerland, [4]Genetic Laboratory, Lisbon's Medical School, Portugal

Despite the use of DXA, biomarkers and fracture clinical risk factors, many older people are at risk for fractures, as the BMD does not provide total info on bone quality; the TBS is a diagnostic tool developed recently and at the moment is used to supplement DXA and may provide information about bone quality; together, TBS and DXA may evidence the strength of bone, which is determined by material composition and configuration. The BMD and vitamin D decline with age. Inadequate vitamin D levels may be associated to the high prevalence of osteoporosis and low vitamin D concentration may be related to an increased falls number and subsequent fragility fractures among older persons. The role of microarchitecture of bone tissue in relation to Vitamin D and PTH is relatively unkown. The TBS (trabecular bone score) may allow to estimate bone microarchitectural texture.

OBJECTIVES: To evaluate the BMD at L1-L4, the TBS at the spine and their associations with some biochemical bone and inflammatory markers and in men and post-menopausal women.

MATERIAL AND METHODS: The BMD (g/cm^2) and the BMC (g) at the L1-L4 in a group of 106 ambulatory men and post-menopausal women of were evaluated by DXA and the spine TBS was derived from each spine DXA scan.

The blood osteocalcin (ng/ml), bone alkaline phosphatase (mcg/l), 25(OH)D$_3$ (ng/ml), iPTH (pg/ml) and reactive C-protein or RCP (mg/dl) concentrations were measured.

Adequate statistical tests were used.

Results: The means($\pm$SD) obtained in men were: L$_1$-L$_4$ TBS= 1.310 ($\pm$0.1), BMC= 68.8 ($\pm$12.8) and BMD= 1.032($\pm$0.2), 25(OH)D3= 22.6($\pm$8.6), iPTH= 52.9($\pm$23.1) and RCP= 0.19 ($\pm$0.17) and the means($\pm$SD) in the post-menopausal women were: the L$_1$-L$_4$ TBS= 1.3172($\pm$0.1), L$_1$-L$_4$ BMC= 49.0 ($\pm$10.8), BMD= 0.928($\pm$0.2), 25(OH)D3= 20.3($\pm$8.8), iPTH= 57.1($\pm$34.7) and RCP= 0.34 ($\pm$0.47).

The significant correlation coefficients were detected, in men, between the spine TBS and the BMC at L$_1$-L$_4$, the osteocalcin, 25(OH) vit. D$_3$ and the PCR blood levels. In women significant correlation coefficients were observed between the spine TBS and the BMC at L$_1$-L$_4$, the 25(OH) vit. D$_3$ and the PCR blood levels.

CONCLUSIONS: The vitamin D3 may play a role on the bone quality, as normal men and post-menopausal women with low 25(OH)D$_3$ may have TBS and thus worse bone quality; it is possible that RCP may also act in the bone quality.

Further studies are needed on a larger cohort and it might be worth to investigate also patients with osteomalacia.

Disclosures: Mário Rui Mascarenhas, None.

SU0291

Comparison between normative spine TBS data for men and women: LAVOS Mexican Cohort. Patricia Clark*[1], Renaud Winzenrieth[2], Margarita Deleze[3], Fidencio Cons-Molina[4], Jorge Morales[5], Didier Hans[6], Bruno Muzzi Camargos[7]. [1]Hospital Infantil Federico Gomez-Facultad de Medicina UNAM, Mexico, [2]Med-imaps, Hôpital X. Arnozan, PTIB, Pessac, France, France, [3]Hospital Angeles Puebla, Mexico, [4]Centro de Investigacion en Artritis y Osteoporosis, Mexico, [5]Hospital Aranda de la Parra, Mexico, [6]Lausanne University Hospital, Switzerland, [7]Densimater Hospital Mater Dei, Brazil

Introduction: Analyzing the Mexican site of the LAVOS Cohort and the mexican men vertebral fracture study, we have investigated the difference between age related changes of the lumbar vertebrae micro-architecture in women and men assessed by TBS.Methods: Subjects in the study were Mexican women and men (LAVOS, Mexican centers) aged 50 and older with a BMD Z-score at spine L1-L4 within $\pm$ 2SD. Individuals were excluded if they had fractures or were on any osteoporosis treatment and/or had any illness that would be suspected to impact bone metabolism. All data have been obtained from Prodigy DXA devices (GE-Lunar, Madison, WI, USA). BMD and TBS (TBS insight v2.1, Med-Imaps, France) were evaluated at spine L1-L4.

Results: A database of 370 men and 339 women ages 50 to 90 years was created. TBS value at L1-L4 was not correlated with BMI r=0.05 and r=0.06 in women and men respectively. TBS values obtained for at lumbar spine decreased significantly with age (see figure below at L1L4) in both gender. There was a linear decline of 17% (-2.7 SD) and of 7.9% (-1SD) in the micro-architectural texture at L1-L4 between 45 and 90 years of age in women and men respectively. Similar results were obtained for other ROIs of the lumbar spine.

Conclusion: A TBS bone microarchitectural texture impairement with ageing has been observed in both women and men. As expected, TBS decrease is more marked in women than in men to reach -1.7 SD difference at 90 years old. Results in women are consistent with previously published data.
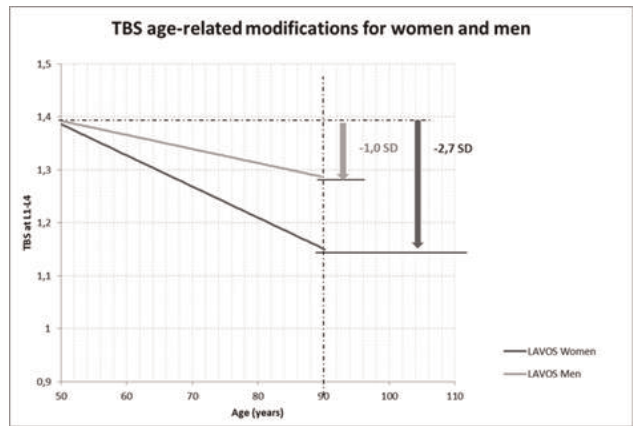

Figure 1

Disclosures: Patricia Clark, None.

SU0292

Glucocorticoid-induced osteoporosis in patients with pulmonary diseases, 4-year observation of treatment compliance. Vaclav Vyskocil*[1], Monika Honnerova[2]. [1]Center for Metabolic Bone Diseases, Czech Republic, [2]Metabolic Bone Disease Center, Czech Republic

Authors observed the group of 207 patients treated by oral corticoids indicated for pulmonary diseases within the period of last 5 years. Authors retrospectively evaluated the rate of patients where DEXA measurement was performed before corticoid therapy and who were supplemented by either calcium plus vitamin D or treated with bisphosphonates (oral as well as i.v.)

115 pateints (75 women and 40 men) out of the study group of 207 were observed further in the 5 year period. 40 patients died (24 women and 16 men) and 48 patients (28 women and 20 men) did not come back for examination after corticoid therapy cessation. This group of patients (115) who were exposed to corticoids for the whole study period was split based on corticoid equivalent > 7,5 mg Prednison and < 7,5 mg daily. BMD increased in patients with lower dose by 3,25% (female); 2,3 % (male) in spine and changed by -0,72% (female); +0,51 (male) in femur in comparison with higher dose group where change of BMD was 0,57% (female); 1,75% (male) in spine and decrease 0,38%(female); 0,62 % (male) in femur.

Authors discus the reason of low treatment compliance of pneumology patients as well.

Disclosures: Vaclav Vyskocil, None.

SU0293

Subject Position on Accuracy of Vertebral Measurement. Bo Fan*[1], Meng Lian[2], Cassidy Powers[2], Neda Sarafrazi Isfahani[3], Mita Patel[4], John Shepherd[1]. [1]University of California, San Francisco, USA, [2]University of California San Francisco, USA, [3]Nutritional Epidemiologist National Health & Nutrition Examination Survey National Center for Health Statistics Centers for Disease Control & Prevention, USA, [4]Westat, USA

Background: Advanced vertebral morphometry is an attempt to describe the projected shape of the vertebral body using many peripheral points (i.e. > 14). Vertebral shape can be assessed on lateral views of dual-energy X-ray absorptiometry (DXA) scans, either by using a rotating arm (Hologic QDR 4500 A, QDR Delphi) or by placing the patient on their side (Lunar Prodigy, Hologic Discovery W). Because all of these are fan beam systems, the inaccurate position of the subject may result in image amplification and geometric distortion.

Purpose: To investigate effect of subject's position on vertebra morphometric shape measurements.

Methods: Using the Hologic spine phantom, we tested three different positions: normal (at center of scanner table), 5 cm away from table edge of technologist (Away) and 5 cm toward the table edge of technologist (Toward). The same scanning protocol was used for the phantom scans as is used participant scans. The individual vertebra's posterior height, mid height, anterior height, superior depth and inferior depth were measured using Optasia SpinalAnalyer software. Multiple tests with bonferroni adjustments were used to test the measurement difference between three different phantom positions.

Results: Five scans in normal position and 3 scans in each of off centered position were acquired on the same DXA scanner at an NHANES examination center. The vertebra height differences between the normal and off center scans were not consistent across the individual vertebrae. Differences ranged from 0.03 (0.05%) to 1.52 (2.28%) mm (Table 1). However, the superior and inferior depth differences were consistent across individual vertebrae and between normal to off centered scans (Table 1, Figure 1, 2). The average difference was 1mm/per cm change of position from Toward to Away. The difference could be up to 8.5%.

Discussion and Conclusion: DXA equipment allows quantitative morphometric vertebral analysis with very low exposure to ionizing radiation. However, our study results show that careful positioning of the subject is a must. Otherwise, the accuracy of the measurement will be reduced.

Table 1: The absolute and percent difference between the Normal, 5cm Away and 5cm Toward.

| Position/Measures	Difference (mm) (% difference)			
	L1	L2	L3	L4
Normal to Away				
Anterior Height	0.87(1.31%)*	0.70(0.99%)*	-0.12(0.15%)	0.72(0.94%)
Posterior Height	0.87(1.28%)*	1.52(2.28%)*	0.72(1.04%)*	-0.12(0.18%)
Mid Height	0.57(0.92%)*	0.17(0.28%)	0.03(0.05%)	-0.83(1.24%)*
Superior Depth	5.02(6.19%)*	4.77(5.67%)*	6.37(7.48%)*	4.54(5.30%)*
Inferior Depth	5.46(6.66%)*	5.31(6.29%)*	6.26(7.20%)*	7.20(8.51%)*
Toward to Normal				
Anterior Height	-0.70(1.06%)	0.23(0.33%)	0.38(0.51%)	0.05(0.07%)
Posterior Height	0.33(0.49%)	-0.15(0.23%)	1.02(1.48%)*	1.02(1.54%)
Mid Height	-0.47(0.76%)	-0.30(0.50%)	0.63(0.99%)*	0.37(0.54%)
Superior Depth	6.49(8.01%)*	6.97(8.28%)*	6.87(8.06%)*	6.85(7.99%)*
Inferior Depth	6.64(8.10%)*	6.84(8.10%)*	7.29(8.37%)*	6.69(7.90%)*

*P<0.05.

Table 1
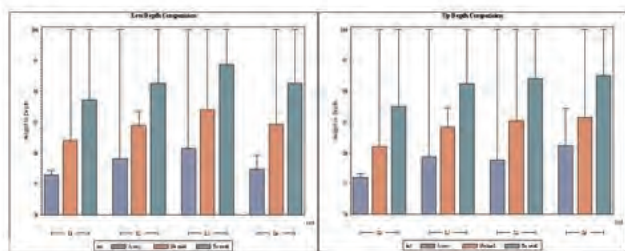
Figure 1: The superior (left) and inferior (right) depth measurement results from normal and off centered positions.

Figure 1

(A, away)   (B, Normal)   (c, Toward)
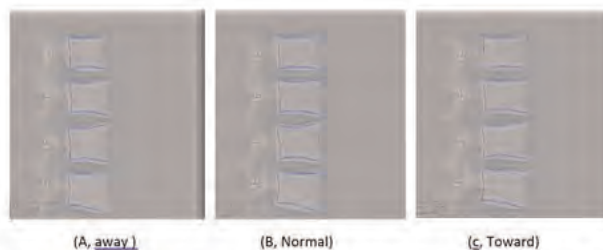
Figure 2: The outline and six points measurement of the Phantom vertebrae body. A: 5cm away from normal position to the table edge, B: Normal position, in the center of scanner, C: 5cm toward from normal position to the table edge

Figure 2

Disclosures: Bo Fan, None.

SU0294

A Comparison of Trabecular Bone Microarchitecture as Determined by Quantitative MRI in Caucasian versus Asian American Young Adults at Peak Bone Mass. Albert Shieh*[1], Jacqueline Hollada[2], Edgar Rios Piedra[2], Ameer Elbuluk[2], Alex Bui[2], John Adams[1]. [1]University of California, Los Angeles, USA, [2]University of California, Los Angeles, USA

Purpose: Trabecular microarchitecture is not well characterized in young adults at peak bone mass. The primary aim of this study was to use quantitative MRI to characterize and compare trabecular microarchitecture in Caucasian (CA) versus Asian American (AA) young adults. The secondary aim was to determine the effects of correcting vitamin D deficiency on trabecular microarchitecture.

Methods: Healthy CA and AA female and male subjects between 21 and 30 years of age were recruited. Baseline evaluation included: 1) collection of demographic and anthropomorphic data [age, gender, BMI], 2) serum biochemical evaluation [metabolic panel, 25-hydroxyvitamin D (25D), immunoactive parathyroid hormone (iPTH)], and 3) trabecular microarchitecture evaluation by calcaneal MRI [apparent bone volume/total volume (app.BV/TV), trabecular thickness (app.Tb.Th, mm) and trabecular separation (app.Tb.Sp, mm)]. Subjects with baseline 25D levels <20 ng/mL received 500,000 IU of vitamin D3 over 10 weeks, after which calcaneal MRI was repeated.

Results: Trabecular microarchitecture was not significantly different between 17 CA versus 17 AA subjects with 25D levels >20 ng/mL matched by age, gender, and BMI [structural parameter: mean (SD) (CA) vs. mean (SD) (AA), p-value; app.BV/TV: 0.479 (0.037) vs. 0.478 (0.034), p=0.534; app.Tb.Th (mm): 1.304 (0.271) vs. 1.237 (0.132), p=0.368; app.Tb.Sp (mm): 1.247 (0.267) vs. 1.189 (0.184), p=0.467]. Five AA subjects had baseline 25D levels <20 ng/mL [25D: 16.2 (2.3) ng/mL; iPTH: 39.8 (16.5) pg/ml]. 25D increased to 34.4 (3.8) ng/mL following vitamin D repletion. Trabecular microarchitecture at follow-up was not significantly different than that at baseline [structural parameter: mean (SD) (follow-up) vs. mean (SD) (baseline), p-value; app.BV/TV: 0.479 (0.047) vs. 0.468 (0.069), p=0.775; app.Tb.Th: 1.417 (0.276) vs. 1.369 (0.337) mm, p=0.812; app.Tb.Sp: 1.191 (0.236) vs. 1.237 (0.301), p=0.796]. Neither baseline 25D nor iPTH levels were significant predictors of percent change in trabecular structural parameters.

Conclusions: Trabecular microarchitecture as assessed by quantitative MRI was not significantly different between CA and AA subjects with 25D levels >20 ng/mL; this may help explain why AA women do not fracture more than CA women despite having lower areal bone mineral density. Correction of vitamin D deficiency did not elicit, in the short term, a change in trabecular microarchitecture in AA subjects with baseline 25D levels <20 ng/mL.

Disclosures: Albert Shieh, None.

SU0295

A New Method for Peripheral 3D QCT of the Distal Forearm using Clinical Whole Body CT Scanners: Preliminary Results. Bastian Gerner*[1], Dominique Töpfer[1], Oleg Museyko[1], Alexander Mühlberg[1], Wolfgang Kemmler[1], Klaus Engelke[2]. [1]University of Erlangen, Germany, [2]University of Erlangen, Germany

Introduction: For peripheral QCT typically dedicated scanners are used. However, scan times of the XtremeCT (Scanco Medical AG, Switzerland) are long and with the XCT2000 device (Stratec Medizintechnik GmbH, Germany) single slices can be acquired, only. In contrast, with clinical whole-body CT scanners, which are widely available, a scan of both distal forearms with a length of 10 to 20 cm covering the trabecular rich ultra distal region to the mid region containing pure cortical bone can be acquired in seconds. Here we developed a new 3D analysis approach based on the MIAF (Medical Image Analysis Framework, University of Erlangen) concept using 3D segmentation, anatomic coordinate systems (ACS) and an automatic placement of analysis volumes of interest (VOIs). The VOIs are adapted to the individual anatomy of the radius, for determining integral, cortical and trabecular BMD, BMC and volume as well as cortical thickness.

Material und Methods: CT datasets of both distal forearms of 16 professional male climbers (26 ± 5 years) were scanned on a SIEMENS VolumeZoom (80 kV, 122 mAs, 24 cm FOV, 15 cm scan length, 1.0 mm slice thickness, convolution kernel B60s). The Siemens Osteo Phantom was used for BMD calibration. Endosteal and periosteal surfaces of radius and ulna were segmented for both arms using a multi step local adaptive thresholding procedure. The ACS of the radius is determined as follows: (1) In each CT slice the center of mass (CM) of the radius is determined. (2) A center curve (CC) is fitted to the CMs. (3) A plane perpendicular to the CC is moved from proximal to distal direction. (4) A distinct increase in area marking the transition into the tapered part of the distal radius together with the CC is used to define the ACS origin.

Results: The figure shows periosteal and endosteal segmentation of radius and ulna along with the 4 VOIs (ultra-distal, distal, mid and proximal) defined relative to the ACS. The table shows mean BMD and BMC values for various bone compartments of the 16 subjects along with inter-operator analysis precision results (3 operators).

Discussion: A new 3D QCT analysis program for the distal forearm was developed that specifically exploits the advantages of clinical whole-body CT scanners and can be used to determine integral cortical and trabecular BMD at any position along the radius or ulna (data not shown) included in the scan. Preliminary findings show good results for inter-operator analysis precision.
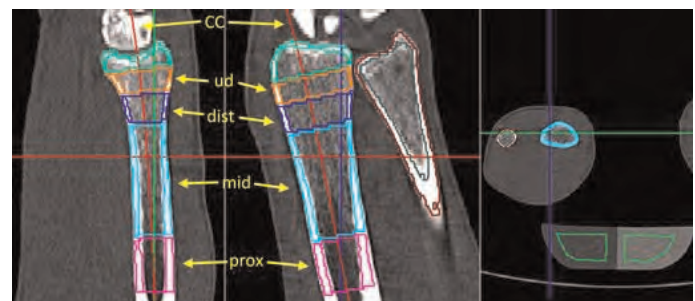
Left and center: sagittal and coronal view. Right: transversal view (both arms and calib. phantom).

VOI		Int BMD	Int BMC	Trab BMD	Trab BMC	Cort BMD	Cort BMC
ud	mean±SD	268±36	786±161	231±32	549±115	423±61	238±57
	precision	1.3±1.7	4.3±4.6	1.2±1.7	5.1±5.9	2.4±2.8	2.3±2.6
dist	mean±SD	368±42	1023±202	270±41	574±110	691±75	449±111
	precision	1.8±2.4	3.4±5.1	1.2±1.7	3.2±4.4	2.6±3.3	3.2±3.6
mid	mean±SD	612±60	3536±749			1116±53	2198±498
	precision	1.3±2.0	2.8±3.2			0.7±1.1	3.6±4.4
prox	mean±SD	801±58	1682±364			1228±34	1276±285
	precision	0.8±1.1	3.0±3.5			0.2±0.3	3.5±4.1

Mean~SD for integral, trabecular and cortical BMD [mg/cm3] and BMC [mg] with precision as rmsCV [%].

Disclosures: Bastian Gerner, None.

SU0296

Bindex® Technology for Osteoporosis Diagnostics in US Primary Care. <u>Janne Karjalainen</u>*[1], <u>Ossi Riekkinen</u>[2], <u>John Schousboe</u>[3]. [1]Bone Index Finland Ltd., Finland, [2]Bone Index Finland, Ltd., Finland, [3]Park Nicollet ClinicUniversity of Minnesota, USA

Currently, majority of the osteoporotic patients are not diagnosed (1). A new ultrasound based point of care device (Bindex®) has been recently introduced for osteoporosis (OP) screening and diagnostics at primary healthcare (2). Bindex measures cortical thickness and determines parameter called density index (DI). Thresholds for DI (90% sensitivity and specificity for OP) in OP assessment have been determined in Finnish Caucasian population (n= 448) along the International Society of Clinical Densitometry (ISCD) guidelines (3). In this study, these thresholds are tested in American-Caucasian population.

Elderly American-Caucasian females under osteoporosis suspicion were examined (n = 430, age = 67.7 $\pm$ 9.7 years). Subjects were measured with dual energy x-ray absorptiometry (DXA) to determine bone mineral density (BMD) at proximal femur. Further, the cortical thickness was measured at three locations (distal radius, distal and proximal tibia) with Bindex®. Subjects were diagnosed with OP when T-score at femoral neck or total proximal femur was below -2.5 (NHANES III reference database). Density index was calculated either by using measurement at one location (DI_1, proximal tibia) or all three locations (DI_3). By using the diagnostic thresholds, subjects were classified as healthy, osteoporotic or in need of DXA examination to verify diagnosis.

A total of 69.0% and 71.6% of the subjects could be directly diagnosed by using Bindex® measurement, with DI_1 and DI_3, respectively. Both parameters showed significant linear correlation with total proximal femur BMD (r = 0.60 - 0.65, $p <$ 0.001). Sensitivity in OP diagnostics was 81.4% and 84.3% for DI_1 and DI_3, respectively. Specificity was 86.4% and 84.0% for DI_1 and DI_3, respectively. Positive predictive values were 81.9% and 80.0% and negative predictive values were 86.1% and 88.1% for DI_1 and DI_3, respectively. OP was diagnosed in 185 subjects in total. Average reproducibility of 2.0% in DI_3 was observed with two ultrasound operators.

The correlation between BMD and DI was similar than previously observed. These results suggest that Finnish-Caucasian thresholds may be applicable for American-Caucasian population. The use of triage approach and the pocket size technology with no ionizing radiation the treatment of OP would significantly increase.

Disclosures: Janne Karjalainen, Bone Index Finland Ltd., 4
This study received funding from: Bone Index Finland Ltd.

SU0297

Can identification of vertebral fractures on lateral spine x-rays be improved by workflow software?. <u>Jeri Nieves</u>*[1], <u>Peter Steiger</u>[2], <u>Patricia Garrett</u>[3], <u>Marsha Zion</u>[3], <u>Robert Lindsay</u>[4], <u>Felicia Cosman</u>[4]. [1]Columbia University & Helen Hayes Hospital, USA, [2]Paroxel, United Kingdom, [3]Helen Hayes Hospital, USA, [4]Helen Hayes Hospital, USA

Background: Both the number and severity of vertebral fractures predict the risk of future fractures. Therefore, their identification is key to comprehensive risk assessment and development of an appropriate treatment plan. Objective: The purpose of this study was to evaluate the consistency of reporting of a dedicated vertebral fracture workflow tool that measures vertebral deformity and directs the reader to record location, type and severity of vertebral fractures (SpineAnalyzer, Optasia Medical Ltd.), compared to clinical radiology reports. Methods: 49 postmenopausal women with osteoporosis were evaluated on 2 or 3 different occasions, resulting in 123 pairs of lateral lumbar and thoracic x-rays. All x-rays were read by a physician (FC) using SpineAnalyzer and compared to the clinical radiology reports. Results: Overall, there was excellent agreement with a kappa of 0.74 in thoracic region (32 fractures by radiologist / 30 by SpineAnalyzer) and a kappa of 1.00 in the lumbar region (22/22). Severity was frequently not noted by the radiologist (31% thoracic / 8% lumbar), while where severity was noted by both approaches, SpineAnalyzer tended to grade fracture more severely (17%/33%) than vice-versa (3%/5%). Longitudinal consistency of fracture evaluation was better by SpineAnalyzer

than by radiology reading. In one case the radiologist noted several lower thoracic mild compressions of 3 adjacent vertebrae that were followed by a reading of "no compression fractures" two years later. In this patient no fractures were identified using SpineAnalyzer at either time. In another case, the radiologist noted no fracture in the first x-ray and then a fracture at T10 two years later. Again SpineAnalyzer found that neither of the x-rays had evidence of a fracture. The fractures found by SpineAnalyzer, but not by the radiologist, included a mild wedge at T7 and a mild biconcave at T10. Conclusion: We found that the workflow discipline imposed by using SpineAnalyzer and the clarity of the resulting report helps consistently quantify number and severity of vertebral fractures, thereby improving risk assessment and treatment of patients with osteoporosis.

Disclosures: Jeri Nieves, None.

SU0298

Clinical Ultrasonic Bone Assessment of the 1/3 Radius. <u>Emily Stein</u>*[1], <u>Fernando Rosete</u>[2], <u>Gangming Luo</u>[3], <u>Mariana Bucovsky</u>[2], <u>Jonathan Kaufman</u>[4], <u>Elizabeth Shane</u>[1], <u>Robert Siffert</u>[5]. [1]Columbia University College of Physicians & Surgeons, USA, [2]Columbia University College of Physicians & Surgeons, USA, [3]CyberLogic, Inc., USA, [4]CyberLogic, Inc., USA, [5]The Mount Sinai School of Medicine, USA

The objective of this study was to evaluate a new clinical ultrasound device (*UltraScan 650*, CyberLogic, Inc., NY, USA, Fig. 1) in terms of its ability to estimate BMD at the 1/3 radius (1/3R), as well as to investigate its ability to discriminate fracture and non-fracture cases. The device (Fig. 1) rests on a desktop and is portable, and permits real-time evaluation of the radial bone mineral density (BMD). The device measures in thru-transmission two (2) net time delay (NTD) parameters, NTD_{DW} and NTD_{CW}. NTD_{DW} is defined as the difference between the transit time of an ultrasound pulse through soft-tissue, cortex and medullary cavity, and the transit time through soft tissue only of equal overall distance. NTD_{CW} is defined as the difference between the transit time of an ultrasound pulse through soft-tissue and cortex only, and the transit time through soft tissue only, again of equal overall distance. The square root of the product of these two parameters is a measure of the BMD at the 1/3R as would be measured by DXA. A clinical IRB-approved study was carried out in which 77 adults (age range 21-83, 75% female) were measured at the 1/3R using ultrasound and DXA (range = 0.45-0.92 g/cm^2). An age and sex-matched subset (28 fracture cases and 16 controls) of these subjects was used to determine the capability of DXA and ultrasound to discriminate between fracture and non-fracture cases. A linear regression showed that BMD_{US}^{TM} = 0.19 * {NTD_{DW}* NTD_{CW}}$^{1/2}$ + 0.28 and that the linear correlation between BMD_{US} and BMD_{DXA} was 0.93 (P<0.001, Fig. 2). We found that forearm ultrasound measurements yield results that are very closely associated with those from DXA. These results are consistent with previous computer simulation and *in vitro* studies, in terms of the ability to estimate radial bone mass. In the case-control cross-sectional fracture study, we found a small decrease in mean BMD_{DXA} (1/3R) for the fracture cases (P=0.20) but a somewhat greater decrease in mean BMD_{US} (P=0.05). This latter result raises the possibility that BMD_{US} may contain additional information on fracture risk. In conclusion, although x-ray methods can estimate BMD, osteoporosis remains one of the world's most undiagnosed diseases. This research should enable significant expansion of the identification of bone loss as occurs in osteoporosis using an ultrasonic desktop device that can serve as a proxy for BMD_{DXA} at the 1/3R and may ultimately provide further data on fracture risk as well.

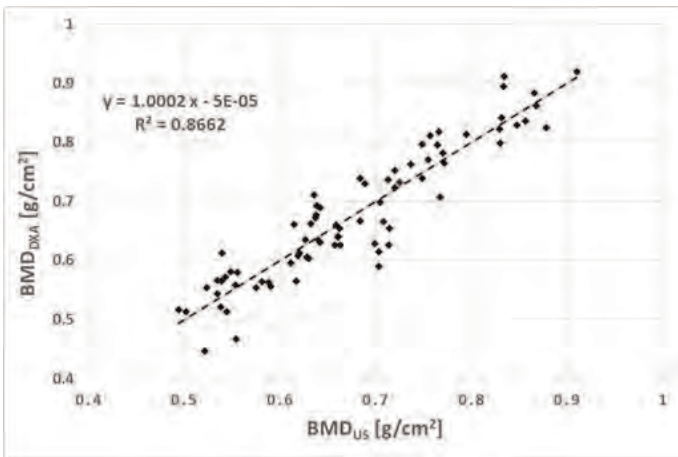Fig. 1. UltraScan 650 device for measuring radial BMD.

$y = 1.0002 x - 5E-05$
$R^2 = 0.8662$

Fig. 2. BMD-DXA vs BMD-Ultrasound

SU0299

Diagnostic performance for identifying osteoporotic postmenopausal women without prevalent fractures by dental panoramic radiographs. Akira Taguchi*[1], Noriyuki Sugino[2], Shinichiro Yamada[2], Yae Iwamoto[2], Keiichi Uchida[2], Mikio Kamimura[3]. [1]Matsumoto Dental University, Japan, [2]Matsumoto Dental University, Japan, [3]Center of Osteoporosis & Spinal Disorders, Japan

Purpose: Cortical shape and trabecular pattern of the mandible on dental panoramic radiographs (DPRs) may be useful indices for identifying asymptomatic postmenopausal women with osteoporosis. The aim of this study was to clarify the diagnostic performance in identifying postmenopausal women, who visited medical practitioners and was diagnosed as osteoporosis without prevalent fractures, by DPRs.

Methods: Of 739 women age $\geq$ 50 years who visited our hospital and underwent DPRs, 250 women participated in this study with informed consent. A structured questionnaire including a history of several diseases, lifestyle, and food consumption was mailed to all subjects. The ethics committee reviewed and approved the study protocol. Cortical shape was categorized as normal, moderately eroded, or severely eroded. The trabecular pattern was categorized as sparse, mixed, or dense. An experienced oral radiologist evaluated them. Since observer agreements for cortical shape were good in many previous studies, 3 oral radiologists assessed trabecular pattern on 30 DPRs twice with 1 week interval to calculate observer agreements by weighted Kappa. Logistic regression analysis adjusted for covariates was used to calculate the odds ratios for identifying subjects who had osteoporosis without prevalent fractures, compared to normal cortex and dense trabecular pattern. Diagnostic performances were calculated for both DPR measures when normal cortex and mixed/dense trabeculations were considered normal.

Results: Thirty-three (13.2%) had osteoporosis without prevalent fractures. Mean intra- and inter-observer agreement for trabeculation was 0.74 and 0.063, respectively. The odds ratio for identifying subjects associated with moderately and severely eroded cortices was 1.98 (95% CI, 0.59 to 6.66) and 7.85 (95% CI, 2.41 to 25.5). That for identifying subjects associated with mixed and sparse trabeculations was 1.75 (95% CI, 0.63 to 4.87) and 0.54 (95% CI, 0.19 to 1.59). Positive and negative likelihood ratios were 1.42 (95% CI, 1.15 to 1.59) and 0.32 (95% CI, 0.12 to 0.73) for cortical shape and 1.57 (95% CI, 1.01 to 2.23) and 0.75 (95% CI, 0.51 to 1.00) for trabeculation.

Conclusions: There was no significant difference in diagnostic performance between cortical shape and trabeculation. However, inter-observer agreement for trabeculation suggests that this may not be used for identifying women who will visit medical practitioners and be diagnosed as osteoporosis.

SU0300

QCT as a problem-solving diagnostic tool for individuals other than post-menopausal Caucasian females. Bruno Camargos*[1], Marlon de Faria[2], Renata Diniz[2], Alan Brett[3], Keenan Brown[4]. [1]Hospital Mater Dei, Brazil, [2]Hospital Mater Dei, Brazil, [3]Mindways Software, Inc., USA, [4]Mindways Software, USA

Introduction: Compared to DXA, QCT has a number of advantages including true volumetric measurements that have no bone size dependency, less susceptibility to degenerative spine changes and higher sensitivity to changes in bone mass. Disadvantages include the higher radiation doses and less experience with fracture prediction and therapy monitoring. QCT may be utilized in situations where the availability of DXA is restricted and it is not infrequently used as a problem solving technique for a number of clinical indications.

Methods: A male, Caucasian, 42 yo, 170cm height, 106.9kg weight, complained of back pain. No evidence of fractures on MRI, CT or plain X-Ray screening. History of high trauma fractures (car accident and sports): clavicles, left tibia, ribs, fingers. No clinical fracture risk issues other than central obesity. No surgeries. No family history of fragility fractures. Biochemical screening included liver, renal and thyroid, cortisol, testosterone, 24h urine calcium, serum minerals (Pi, Mg, Na, Ca, Cl), vitamin D > 35 ng/mL, CBC and others. All of them were normal. DXA performed on a LUNAR Prodigy Advance (GE, Madison, WI) showed L1-L4 BMD 0.904 g/cm^2 with T-score and Z-score of -2.6 (both); Femoral Neck BMD 1.075 g/cm^2 T-score = 0.0 and Z-score = -0.1; Total Femur 1.065 g/cm^2 T-score = -0.3 and Z-score = -0.5; Left forearm 33% Radius 0.791 g/cm^2 T-score = -0.2 and Z-score = -0.2. QCT at L1-L2 was then performed using QCT Pro 5.1 (Mindways, Austin, TX) according to manufacturer's instructions.

Results: QCT results showed no signal of low bone density (vBMD = 128.0 g/cm^3), despite low T and Z-scores at lumbar spine by DXA. The QCT results show better correlation to forearm and femur DXA results.

Discussion: DXA results may be influenced by excessive overlying soft tissue. This may cause high soft tissue attenuation values compromising the bone results. Male obese patients may be specifically more affected than normal weight female patients who comprised the majority part of the normal DXA reference curves available on DXA devices' software. It may act as a background "noise" and cause an abnormal low bone density reading at the involved region.Conclusion: QCT is helpful on selecting individual patients, other than female Caucasian subjects, whose lumbar DXA might be influenced by adipose and soft tissue concentration at this site. Further research is needed to determine what DXA patients should be considered for a QCT evaluation.

SU0301

Self-directed Training for Recognition of Vertebral Fractures. Sharon Chou*[1], Jessica Hwang[2], Peter Steiger[3], Tamara Vokes[1]. [1]University of Chicago, USA, [2]University of Chicago, USA, [3]PAREXEL International, USA

Although vertebral fractures (VFx) are common and associated with increased mortality and morbidity[1], only 1/3 of vertebral fractures are clinically recognized[2]. Chest x-rays are frequently performed for other indications, but as few as 18% of VFx on x-rays are mentioned in the radiology report[3,4]. Increased recognition of VFx by disciplines such as Endocrinology would improve the diagnosis and care of osteoporosis. We assessed the effect of self-directed training in VFx recognition. The training included a web-based, self-study of VFx (www.iofbonehealth.org/vertebral-fracture-teaching-program), a 60-minute lecture summarizing key points, and a demonstration of SpineAnalyzer™, a commercially available software application that generates multi-point outlines of vertebral bodies. The training did not stress the controversy of equivocal VFx (e.g. short vertebral height versus mild morphometric fracture). Two Endocrinology fellows completed the training. Fellow A is a third-year fellow familiar with VFx diagnosis. Fellow B is a second-year fellow who has not had prior training. Both fellows evaluated the same 55 images (45 chest x-rays, 10 spine x-rays) twice in random order before and after training. Among these 55 images, 26 had clear VFx, 14 had no VFx, and 15 had equivocal VFx. The first reading of each image was compared before and after training using area under the receiver operator curves. Intra- and inter-rater reliability were assessed by percent agreement and Cohen's kappa statistic. Both fellows had similar intra-rater reliability for pre-training and post-training. Training showed a trend for improvement in the recognition of clear VFx for Fellow B (p=0.13), and concordance between Fellow A and Fellow B improved from 80% (?=0.56) to 93% (?=0.83). Thus, this training program tended to improve the inexperienced fellow's ability to recognize VFx. Our findings suggest that self-directed learning tools can be used to teach VFx recognition and ultimately improve the quality of the osteoporosis care. However, additional instruction regarding the classification of equivocal VFx should be included in the training.

[1]Cummings SR,Melton LJ. 2002 Epidemiology and outcomes of osteoporotic fractures. Lancet. 359:1761-1767.
[2]Kado DM, Browner WS, Palermo L, Nevitt MC, Genant HK,Cummings SR. 1999 Vertebral fractures and mortality in older women: a prospective study. Study of Osteoporotic Fractures Research Group. Arch Intern Med. 159:1215-1220.
[3]Lansdown D, Bennet B, Thiel S, Ahmed O, Dixon L,Vokes TJ. 2010 Prevalence of vertebral fractures on chest radiographs of elderly African American and Caucasian women. Osteoporos Int. 22(8):2365-2371.
[4]Gehlbach SH, Bigelow C, Heimisdottir M, May S, Walker M, Kirkwood JR. 2000 Recognition of vertebral fracture in a clinical setting. 11(7):577-82.

Table 1

	Fellow A (first read)				Fellow B (first read)			
	All patients		Excluding equivocal cases		All patients		Excluding equivocal cases	
	Pre	Post	Pre	Post	Pre	Post	Pre	Post
Sensitivity	0.93	1.0	0.92	1.0	0.93	0.93	0.92	0.96
Specificity	0.73	0.73	0.93	0.79	0.65	0.54	0.79	0.93
PPV	0.79	0.81	0.96	0.90	0.75	0.69	0.89	0.96
NPV	0.91	1.0	0.87	1.0	0.90	0.88	0.85	0.93
AUROC	0.83	0.87	0.93	0.89	0.79	0.74	0.85	0.95
	p=0.60		p=0.67		p=0.35		p=0.13	
% agreement	81%	84%	90%	90%	82%	82%	85%	85%

Table 1

SU0302

Why we should think differently about cancer survivors'bone health - multi-modality imaging reveals gradual decreased bone mineral density but rapid and heterogeneous expansion of marrow fat from cancer therapy. Susanta Hui*[1], Luke Arentsen[2], Keenan Brown[3], patrick Bolan[2], Rahel Ghebre[2], Levi Downs[2], Ryan Shanley[2], Karen Hansen[4], Anne Minenko[2], Yutaka Takahashi[2], Masashi Yagi[2], Yan Zhang[5], Sharon Allen[1], Bruno Beomonte Zobel[6], Chap Le[2], Jerry Froelich[2], Clifford Rosen[7], Douglas Yee[8]. [1]University of Minnesota, USA, [2]University of Minnesota, USA, [3]Mindways Software, USA, [4]University of Wisconsin, USA, [5]Medtronic, USA, [6]Campus Bio-Medico University, Italy, [7]Maine Medical Center, USA, [8]University of Minnesota, USA

Cancer survivors have a high risk of fractures, but the effect of cancer treatments on marrow fat (MF) and bone mineral density (BMD) are poorly understood. The purpose is to develop multimodality imaging for quantitative monitoring of bone and marrow damage and repair over time. We used dual energy CT (DECT), water-fat MRI (WF-MRI), quantitative CT (QCT) and DXA to measure one-year changes in MF and BMD associated with three cancer treatments: oophorectomy, radiotherapy or chemotherapy. We also measured changes in circulating adiponectin levels. Twenty-nine patients with gynecologic malignancies underwent DECT and DXA at 0, 6 and 12 months after initial treatment; 15 were also imaged by WF-MRI. BMD and MF percent and distribution were quantified in lumbar vertebrae (L3, L4, and L5) and the right femoral neck (FN). We observed a high overall correlation (r = 0.77, 95% CI: 0.69, 0.83) between DECT and WF-MRI based MF quantification at L3, L4, and L5 for 15 subjects (Figure A) with r = 0.80 (95% CI: 0.65, 0.89) at baseline; r = 0.68 (95% CI: 0.47, 0.81) at 6 months; r = 0.66 (95% CI: 0.44, 0.80) at 12 months. Likewise, changes in MF from 0 to 12 months were highly correlated by both imaging methods (r = 0.91, 95% CI: 0.84, 0.95). MF increased significantly from 0 to 12 months (p<0.002 at L3, L4, L5, and FN). All three treatments increased MF (p<0.032), but chemotherapy and radiation caused greater increases than oophorectomy (Figure B &C). L4 BMD measured by DECT decreased the most after chemotherapy (p=0.01), followed by radiation (p=0.09) and oophorectomy (p=0.24). L4 BMD decreased 14% by DECT, 20% by QCT, but only by 5% by DXA (p<0.002 for all) (Figure D). At baseline, we observed a statistically significant, inverse association between MF and BMD. By contrast, at 12 months the inverse association between MF and BMD was dramatically attenuated (Figure E &F). Adiponectin increased from 0 to 12 months without changes in total body fat. Our study demonstrated rapid increases in MF following radiotherapy and chemotherapy. Additionally, DECT detected much greater changes in BMD than did conventional DXA. Our results suggest that, contrary to the general population, MF and BMD cannot be used interchangeably to monitor skeletal health following cancer therapy. Longitudinal studies in larger population are needed to determine if increases in MF and adiponectin are associated with long-term sustained bone damage and ultimate ability to predict fracture risk.
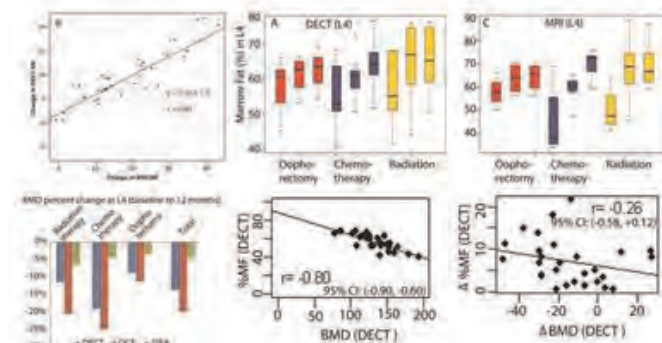
Rapid marrow and bone damage

Disclosures: Susanta Hui, None.

SU0303

Association between polymorphisms of the tissue non-specific alkaline phosphatase gene with serum alkaline phosphatase and fragility fractures in Italian population. Laura Masi*[1], Gigliola Leoncini[2], Francesco Franceschelli[3], Maria Luisa Brandi[4]. [1]University of Florence, Italy, [2]Department of Surgery & Translational Medicine, University Hospital of Florence, Italy, [3]Department of Surgery & Translational Medicine, University Hospital of Florence, Italy, [4]DIRETTORE MALATTIE DEL METABOLISMO MINERALE E OSSEOAZIENDA OSPEDALIERA UNIVERS, Italy

The process of bio mineralization that occurs in bone tissue takes place throughout an individual's life. Complex biological systems carefully orchestrating the crosstalk between skeletal tissue and modulator of mineralization. The physiological role of Alkaline Phosphatase (ALP) is not fully understood, and a useful model is provided by the rare genetic disease hypophosphatasia (HPP), an inherited disorder characterized by a defect in skeletal mineralization caused by Tissue Non Specific ALP (TNSALP) deficiency due to TNSALP gene mutations. It is highly variable in its clinical presentation and patients with the adult form present with osteomalacia, chondrocalcinosis, non-healing fractures, and premature tooth loss. Bone mineral density is often osteopenic, and the disease is misclassified as primary osteoporosis. In the present study, the clinical records of a population of 2850 patients referring to the Bone and Mineral Diseases Unit at the University of Florence Hospital is revisiting in order to mark subjects with low serum ALP before any osteoporotic treatment, with history of non-healing fractures, with metatarsal fractures, premature tooth loss, periodontal diseases Additional clinical symptoms: fatigue, chronic pain, nephrocalcinosis, hypercalciuria. As the osteoporosis patients referred to our Unit undergo blood withdrawal to be stored for genetic analysis when informed consent is obtained. TNSALP gene was evaluated. Of the populations we have so far analyzed 276 subjects with a mean age 62,3 yrs. (min 21 and max 82 yrs.). The biochemical investigations of these patients showed serum and urine calcium and phosphate in the normal range. The levels of serum vitamin D (25 OH D3) were below the optimal range (mean: 15.6 $\pm$ 6.1 ng /ml, n.v. 30-70). The mean value of Total and Bone Alkaline Phosphatase before to start any osteoporotic fracture were in the normal range (54 ± 6 IU/L n.v.: 50-126 IU/L and 12 ± 4 mcg/L n.v: 4-22.5 mcg/L). Bone resorption markers were in the normal range. BMD measured at the lumbar spine and femoral neck by DXA showed an osteopenia or osteoporosis. From the fracture's history we observed 12 women with metatarsal , 18 with wrist, 69 with spine and 5 with "other " fractures. The results of the genetic analysis showed the presence of a variant in exon 5 codon 152 (CGC > CAC , Arg > His) in heterozygosity in 16 patients , a variant of exon 9, codon 292; (CCA > GCC; Pro > Pro) in 2 patients , an intronic deletion IVS5 +14 ex 5 in 81 patients. Applying Anova analysis we found that patients with intronic deletion and exon 5 polymorphisms had a significantly lower Total and Bone Alkaline Phosphatase (45 vs. 59 IU/L and 6 vs.12 mcg/L respectively). These preliminary data, open up to the possibility that polymorphic variants of the ALP gene may be associated with a low BMD with a tendency to spontaneous fractures and insufficient response to drugs used to date in the treatment of osteoporosis.

Disclosures: Laura Masi, None.

SU0304

Association of *C6orf97* and *ESR1* region with Bone mineral density in postmenopausal Mexican women. Alma Parra-Torres[1], Humberto García-Ortiz[2], Manuel Castillejos-López[3], Rogelio Jiménez-Ortega[4], Nelly Patiño[5], Quiterio Manuel[6], Lorena Orozco[7], Jorge Salmerón[8], Rafael Velazquez-Cruz*[4]. [1]Laboratorio Genómica del Metabolismo Óseo, Instituto Nacional de Medicina Genómica, Mexico, [2]Laboratorio de Inmunogenómica y Enfermedades Metabólicas, Instituto Nacional de Medicina Genómica, Mexico, [3]Unidad de Vigilancia Epidemiológica Hospitalaria, Instituto Nacional de Enfermedades Respiratorias, Mexico, [4]Laboratorio de Genómica del Metabolismo Óseo, Instituto Nacional de Medicina Genómica, Mexico, [5]Subdirección de Desarollo de Aplicaciones Clínicas, Instituto Nacional de Medicina Genómica, Mexico, [6]Centro de Investigación en Salud Poblacional,Instituto Nacional de Salud Pública, Mexico, [7]Laboratorio de Inmunogenómica y Enfermedades Metabolicas, Instituto Nacional de Medicina Genómica, Mexico, [8]Unidad de Investigación Epidemiológica y en Servicios de Salud, Instituto Mexicano del Seguro Social, Mexico

Mexican population is admixed with a complex genetic structure including genes of Native American, European and a small percentage of African ancestries. Osteoporosis, a disease characterized by low bone mineral density (BMD), is a common health problem in Mexican population. To date, few genes affecting BMD variation in the Mexican population have been identified. The aim of this study was to investigate the possible association of single-nucleotide polymorphisms (SNPs) of *C6orf97* and *ESR1* region with BMD variation in postmenopausal Mexican-Mestizo women. Four hundred unrelated postmenopausal women were included in the study. Risk factors were recorded and BMD was measured in total hip, femoral neck and lumbar spine using dual-energy X-ray absorptiometry. Seven SNPs in *C6orf97* (rs9479055, rs7753676, rs4870044, rs712219, rs851993, rs3020331 and rs851982) and four in *ESR1* genes (rs1999805, rs2504063, rs3020404, and rs2228480) were studied. Real time PCR and TaqMan probes were used for genotyping. The pattern of association and linkage disequilibrium data in this region is very similar to previously observed in European population, suggesting four LD blocks. Each LD block was associated with total hip and/or neck femoral. Linear regression analyses adjusted by age, body mass index, blood glucose levels and ancestry showed that five SNPs were significantly associated with BMD: rs9479055, rs7753676, rs4870044, rs3020331, rs2504063 in the *C6orf97* gene (p<0.0004). In addition, rs3020331 and rs851982 SNPs of the *ESR1* gene were associated with BMD of the total hip and neck femoral under dominant and recessive models, respectively (*P*=0.006 and *P*=0.008). Our data replicate previous associations found between SNPs in the *C6orf97* and *ESR1* region and BMD and suggest that this region may contribute to variation in BMD across multiple ethnic groups.

Disclosures: Rafael Velazquez-Cruz, None.

SU0305

Association of P2Y$_2$ Receptor Single-Nucleotide Polymorphism with Bone Mineral Density in Elderly Men. Maria Ellegaard*[1], Magnus Karlsson[2], Mattias Lorentzon[3], Claes Ohlsson[4], Dan Mellstrom[5], Osten Ljunggren[6], Peter Schwarz[7], Niklas Jorgensen[1]. [1]Copenhagen University Hospital Glostrup, Denmark, [2]Skåne University Hospital Malmö, Lund University, Sweden, [3]Geriatric Medicine, Center for Bone Research at the Sahlgrenska Academy, Sweden, [4]Center for Bone & Arthritis Research at the Sahlgrenska Academy, Sweden, [5]Sahlgrenska University Hospital, Sweden, [6]Uppsala University Hospital, Sweden, [7]Glostrup Hospital, Denmark

Background and aim: The P2Y$_2$ receptor is a G-protein-coupled receptor, which is activated by adenosine 5-triphosphate and involved in signalling between bone cells. The P2Y$_2$ receptor single-nucleotide polymorphism (Leu46Pro) has been shown to be associated with high BMD in women. As gender-specific effects of P2 receptors have been suggested, the aim of this study was to investigate whether P2Y$_2$ receptor polymorphisms are associated with BMD and fracture prevalence in elderly men.

Materials and Methods: A total of 3014 men (age 69-81 years) from the MrOS Sweden study were genotyped for three P2Y$_2$ receptor polymorphisms (Leu46Pro, Ser359Pro and Arg312Ser). Genotyping was performed using Sequenom MassAR-RAY platform. BMD of lumbar spine, total hip and femoral neck was measured by DXA. Vertebral fractures were analyzed by spinal x-ray in 1428 of the participants. Furthermore, previous sustained fractures (any type) were recorded from questionnaires. Differences in BMD and fracture prevalence in wildtype allele carriers, heterozygous and homozygous variant allele carriers were assessed using analysis of covariance (covariates: BMI and age) and Chi Square test. Data are presented as mean (SD).

Results: At baseline the study population presented with an age of 75.4 (3.2) years; BMI of 26.4 (3.6) kg/m^2; spine BMD of 1142 (201) mg/cm^2; femoral neck BMD of 831 (132) mg/cm^2 and total hip BMD of 936 (144) mg/cm^2. Fifteen percent (of the 1428) had experienced one or more vertebral fractures. Age and BMI was compared within genotypes of each polymorphism and no significant differences were found between the genotypes (p>0.05). BMD of the femoral neck was significantly different between genotypes for the Leu46Pro polymorphism, with hetero- and homozygous variant allele carriers showing higher BMD compared to wildtype allele carriers (wildtype: 827 (132) mg/cm^2; heterozygous: 850 (131) mg/cm^2; homozygous: 848 (95) mg/cm^2; p=0.018). The Arg312Ser and Ser359Pro polymorphisms showed no significant difference in BMD at any site between the different genotypes (p>0.05). None of the polymorphisms were significantly associated with prevalent vertebral fractures or all reported fractures (p>0.05).

Conclusion: The Leu46Pro polymorphism of the human P2Y$_2$ receptor was in our cohort associated with BMD of the femoral neck in elderly men. Further experimental studies are required in order to establish the effect of the polymorphism on receptor and bone cell function.

Disclosures: Maria Ellegaard, None.

SU0306

Associations Between Polymorphisms in ALOX12 and ALOX15 and Bone Properties in Young and Elderly Women. Maria Herlin*[1], Fiona McGuigan[2], Holger Luthman[3], Kristina Akesson[4]. [1]University of Lund, Malmö, Skane University Hospital, Malmö, Sweden, [2]University of Lund, Malmö, Skane University Hospital, Malmö, Sweden, [3]Medical Genetics Unit, Department of Clinical Sciences, Malmö, Lund University, Sweden, [4]Skåne University Hospital, Malmö, Sweden

Purpose: The ALOX12 and ALOX15 genes encode arachidonate lipoxygenases, which produce endogenous ligands for PPARγ. Activation of the PPARγ pathway stimulates adipogenesis at the expense of osteoblastogenesis. Arachidonate lipoxygenases also produce leukotrienes with pro-inflammatory effects, and may be involved in inflammatory bone loss. In this study, genetic variation at the ALOX12 and ALOX15 loci were analyzed for associations with bone properties in two population based cohorts of Swedish women.

Methods: The PEAK-25 cohort consists of 1061 women aged 25 years, and the OPRA cohort consists of 1044 women aged 75 years and prospectively followed for 10 years. Bone mineral density (BMD) was measured with dual-energy x-ray absorptiometry (DXA) at femoral neck, lumbar spine, hip and total body. Quantitative ultrasound (QUS) measurements (SoS, BUA and stiffness) were performed on the right calcaneus. Fractures were assessed in OPRA only. Three SNPs in ALOX12 (rs1126667, rs2292350, rs312466) and five SNPs in ALOX15 (rs8074545, rs748694, rs9894225, rs2619112, rs916055) were genotyped in both cohorts. Differences between genotypes were analyzed by ANOVA and linear regression analysis, and the Chi-Square test was used to analyze genotype differences in fracture incidence.

Results: Genotype frequencies of ALOX12 and ALOX15 were similar in both cohorts. rs2292350_ALOX12 was associated with lumbar spine BMD (AA: 1.224 vs. GG: 1.240, p = 0.023) in PEAK-25, but this association did not remain significant after adjustment for weight, height and smoking. There were no associations observed for ALOX12 with BMD, QUS or fracture in OPRA. rs748694_ALOX15 was associated with QUS parameters SoS (CC: 1573.5 vs. TT: 1580.7, p = 0.024) and

stiffness (CC: 98.6 vs. TT: 102.0, p = 0.017) in PEAK-25, and remained significant after adjustment for weight, height, femoral neck BMD and smoking (p = 0.022 and p = 0.026, respectively). Further, a trend for higher total BMD with the rare allele of rs748694_ALOX15 was observed. In OPRA, rs2619112_ALOX15 was associated with incident fracture (p = 0.014), while there were no associations with BMD or ultrasound parameters.

Conclusions: A common variant in ALOX15 was associated with ultrasound parameters, indicating a role in bone microarchitecture independent of BMD, in young women. In elderly women, ALOX15 was associated with fracture independent of BMD in this cohort.

Disclosures: Maria Herlin, None.

SU0307

Common and Rare Variants in the Exons and Regulatory Regions of Osteoporosis-Related Genes Improve Osteoporotic Fracture Risk Prediction. Seung Hun Lee*[1], Moo Il Kang[2], Seong Hee Ahn[1], Kyeong-Hye Lim[3], Gun Eui Lee[4], Eun-Soon Shin[4], Jong-Eun Lee[4], Beom-Jun Kim[5], Eun-Hee Cho[6], Sang-Wook Kim[6], Tae-Ho Kim[7], Hyun-Ju Kim[8], Kun-Ho Yoon[2], Won Chul Lee[9], Ghi Su Kim[1], Jung-Min Koh[5], Shin-Yoon Kim[10]. [1]Asan Medical Center, University of Ulsan College of Medicine, South Korea, [2]Seoul St. Mary's Hospital, The Catholic University of Korea, South Korea, [3]Asan Medical Center, University of Ulsan College of Medicine, South Korea, [4]DNA Link, South Korea, [5]Asan Medical Center, South Korea, [6]Kangwon National University College of Medicine, South Korea, [7]Kyungpook National University School of Medicine, South Korea, [8]Skeletal Diseases Genome Research Center & Kyungpook National University School of Medicine, South Korea, [9]The Catholic University of Korea, South Korea, [10]Kyungpook National University Hospital, South Korea

Osteoporotic fracture risk is highly heritable, but genome-wide association studies have explained only a small proportion of the heritability to date. Genetic data may improve prediction of fracture risk in osteopenic subjects for early intervention and management. We aimed to detect common and rare variants in coding and regulatory regions related to osteoporosis-related traits, and to investigate whether genetic profiling improves the prediction of fracture risk. We performed targeted resequencing of 198 genes in 982 individuals with extreme phenotypes and then replicated sequencing of the promising variants in 3,895 participants. Genetic risk scores from common variants (GRS-C) and from common and rare variants (GRS-T) were calculated. Nineteen common variants in 17 genes (of the discovered 34 functional variants in 26 genes) and 31 rare variants in 5 genes (of the discovered 87 functional variants in 15 genes) were associated with one or more osteoporosis-related traits. Accuracy of fracture risk classification was improved in the osteopenic patients by adding GRS-C to fracture risk assessment models (6.8%, P < 0.001) and was further improved by adding GRS-T (9.6%, P < 0.001). GRS-C improved classification accuracy for vertebral and non-vertebral fractures by 7.3% (P = 0.005) and 3.0% (P = 0.091), and GRS-T further improved accuracy by 10.2% (P < 0.001) and 4.9% (P = 0.008), respectively. Our results suggest that both common and rare functional variants may contribute to osteoporotic fracture, and that adding genetic profiling data to current models could improve the prediction of fracture risk in an osteopenic individual.

Disclosures: Seung Hun Lee, None.

SU0308

BMD Genome-Wide Association Studies (GWAS) loci are enriched in tissue-specific DNase I hypersensitive sites in human muscle, skin, blood and osteoblast cells. Wen-Chi Chou*[1], Gosia Trynka[2], David Karasik[3], Douglas Kiel[1], Yi-Hsiang Hsu[4]. [1]Hebrew SeniorLife, USA, [2]Broad Institute, USA, [3]Hebrew SeniorLife; Bar Ilan University, USA, [4]Hebrew SeniorLife Institute for Aging Research & Harvard Medical School, USA

Most reported genetic loci associated with BMD are located in non-coding regions, making it difficult to interpret their functions. DNase I hypersensitive sites (DHS) have been reported to overlap with tissue-specific regulatory elements (such as enhancers and promoters) in non-coding regions, suggesting DHS is a functional-genomic marker to predict tissue-specific regulatory activities. To determine whether BMD loci are enriched in tissue-specific regulatory elements, we performed a systematic enrichment analysis of DHS data across 26 cell types (see table).

Using an algorithm developed by Trynka et al. that assesses chromatin data enrichment of cell types for a given SNP set, we tested DHS enrichment of 26 non-cancer and non-stem cell lines selected from 97 cell lines in the ENCODE project for the top 56 reported significa-nt GWAS SNPs associated with BMD. DHS signals were captured by a SNP-DHS score defined as the height of a DHS peak closest to a SNP (a GWAS SNP or a SNP in LD, $r^2 > 0.8$, of the GWAS SNP) divided by the distance of the summit of the DHS peak to the SNP. A higher DHS-SNP score has greater probability of the SNP being closer to a higher DHS peak. To test for significant cell type enrichment, summary SNP-DHS scores of BMD SNPs in each cell were compared to a null distribution of

10,000 permutations of random SNPs sets that were required to have the same number of DHS peaks in LD across all cell types as the BMD SNPs.

Across a total 7,285 DHS peaks from 26 cell types, BMD loci were observed to be significantly enriched with DHS in aortic smooth muscle ($P=1\times10^{-5}$), skin fibroblast ($P=1\times10^{-4}$), ureter cell ($P=6\times10^{-4}$), B cell ($P=0.0011$) and osteoblast ($P=0.0015$) after Bonferroni correction. Enriched BMD loci in aortic smooth muscle included *SFRP4, DNM3,* and *OPG.* Enriched BMD loci in osteoblast included *CCDC170, FAM210A,* and *MARK3.* BMD loci were found to be enriched with DHS data not only in osteoblast, but also in other cell types, suggesting genetic factors may contribute to the variation of BMD via bone cells and other tissues. In addition, 54% of 56 BMD GWAS loci were enriched in DHS in at least one enriched cell type, suggesting that the majority of non-coding GWAS loci are located in regulatory elements. This approach holds promise for characterizing the functional significance of GWAS findings located in non-coding regions.

Table: Identification of enriched cell types for BMD loci (significant P < 0.0019 = 0.05/26).

Tissue	Cell Types	Permutation p-value	Part of the most enriched GWAS Loci
Bone	Osteoblasts	0.0015	*CCDC170, FAM210A, and MARK3*
Muscle	Aortic Smooth Muscle	0.00001	*SFRP4, DNM3, and OPG*
Muscle	Myometrial Cells	0.0042	*MBL2*
Muscle	Skeletal Muscle Myotubes differentiated From HSMM	0.0909	*TNFRSF11A*
Muscle	Skeletal Muscle Myoblasts	0.2399	*LOC400950*
Muscle	Psoas Muscle tissue	0.9676	*IDUA*
Heart	Heart	0.7206	*CPN1*
Epithelium	Ureter Cell	0.0006	*DCDC5, SUPT3H, and CDKAL1*
Epithelium	Primary tracheal Epithelial Cells	0.0705	*NTAN1*
Blood	B Cells	0.0011	*SUPT3H, SP7, and SOX9*
Blood	CD77 Germinal Center B Cells	0.4122	*AKAP11*
Blood	CD14-positive Cells	0.4452	*LRP5*
Blood	CD4 Adult Th1	0.7657	*AKAP11*
Brain	Brain Frontal Cortex	0.3211	*JAG1*
Brain	Brain Cerebellum	0.3639	*SPTBN1*
Brain	Brain Cerebrum	0.6734	*C6orf97*
Breast	Mammary Epithelial Cells	0.0247	*RSPO3*
Skin	Skin Fibroblast	0.0001	*DNM3, IDUA, and RSPO3*
Skin	Epidermal Melanocytes	0.0043	*FUBP3*
Skin	Epidermal Keratinocytes	0.4982	*PTX4*
Tonsil	Naïve B Cells	0.2018	*AKAP11*
Pancreas	Pancreatic Islets	0.8624	*AXIN1*
Prostate	Prostate Epithelial	0.0295	*FLI42280*
Nasal biopsy	Olfactory Neurosphere-derived Cells	0.0587	*SMG6*
Liver	Hepatic stellate Cells	0.3737	*MEPE*
Liver	Hepatocytes	0.9693	*SALL1*

Table_Identification of enriched cell types for BMD loci

Disclosures: Wen-Chi Chou, None.

SU0309

Combined Hormonal Contraceptive Use Associated with Less Positive BMD Change in Adolescent Women in CaMOS Population-based Cohort—BMD loss significantly greater in women 20-24 using CHC at baseline. Jerilynn Prior*[1], Katharina Schlammerl[2], William Mercer[3], David Hanley[4], Jonathan Adachi[5], Christopher Kovacs[6]. [1]University of British Columbia, Canada, [2]Technical University of Munich, Germany, [3]Centre for Menstrual Cylce & Ovulation Research, Canada, [4]University of Calgary, Canada, [5]St. Joseph's Hospital, Canada, [6]Memorial University of Newfoundland, Canada

Combined hormonal contraception (CHC) is widely used by adolescent/ young women for birth control or treatment of menses related problems (PMS, heavy flow, cramps, irregular cycles or acne). Peak bone mineral density (BMD) is primarily attained by late adolescence. Baseline CaMOS BMD data in ages 25-45 found values 2.3-3.7% lower in CHC ever-users[1]. Prospective observational[2-4] and RCT data[5;6] show CHC use reduces adolescent age-appropriate BMD gain. No population-based prospective CHC BMD change data are available and no BMD change data related to contraceptive/ therapy indications for first CHC use are published. Methods—The CaMOS Youth Cohort included 527 women ages 16-24 recruited by random residential sampling in 9 Canadian centres (2004-6). Extensive interviewer-administered questionnaires and BMDs (L1-4, femoral neck, total hip [TH]) were obtained at 0 and 2-y. Results, due to sample size, are based on CHC ever/never use at baseline and y-2 and indication for first CHC use at y0. Ever CHC use was reported by 66% of

women ages 16-24 at both y0 and y2. At baseline, CHC ever vs. never users were significantly older (20 vs. 18.5 y), similar in BMI (22.6 vs 23), not different in total calcium intake and vitamin D intakes or kcal exercise/d but were more likely to smoke (P=0.000). CHC was started for contraception by only 45% of 391 ever-CHC users (55% for therapy). Two year BMD change data were available for 326. L1-4 increased as age-expected in the 57 adolescents (16-19 y) who had never used CHC; those adolescent ever-CHC users tended to gain less BMD than never-users (+.0026 vs. +.0116g/cm^2, respectively; P=.204) (Figure). Women ages 20-24 who were ever (n=127) or never (n=24) CHC users had similar L1-4 2-y changes (+.0072 vs. +.0037g/cm^2; P=.653). BMD changes were also importantly different in ages 20-24 by current vs. no CHC use at y0. Although current contraceptive CHC users ages 20-24 at baseline were younger and smoked less, CHC users showed BMD loss. L1-4 (-.007 vs. +.011, P=.028) and TH (-.009 vs. +.007, P=.005) changes were significantly different in these CHC users. In conclusion, these population-based data support previous data showing CHC decreases optimal peak BMD in those 16-19. In addition, in 20-24 y olds y0 current use of CHC was associated with significant BMD loss. References: [1]Prior *CMAJ* 2001; [2]Cromer *Fert Ster* 2008; [3]Scholes *JCEM* 2011; [4]Gai *Contraception* 2012; [5]Polatti *Contraception* 1995; [6]Cobb *Med Sci Sports Exerc* 2007.
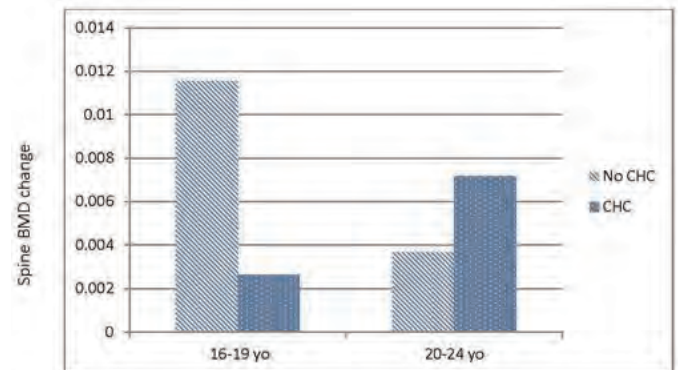
Spine BMD change

Disclosures: Jerilynn Prior, None.

SU0310

Different Relationships between Body Compositions and Bone Mineral Density According to Gender and Age in Korean Populations (KNHANES 2008–2010). Seong Hee Ahn*[1], Seung Hun Lee[1], Hyeonmok Kim[2], Beom-Jun Kim[3], Jung-Min Koh[3]. [1]Asan Medical Center, University of Ulsan College of Medicine, South Korea, [2]Asan Medical Center, University of Ulsan College of Medicine, South Korea, [3]Asan Medical Center, South Korea

Fat and muscle are linked to bone metabolism. We investigated the association of fat mass (FM) and lean mass (LM) with bone mineral density (BMD) according to gender and age. This is a population-based, cross-sectional study from Korea National Health and Nutrition Examination Surveys, including 15,036 Koreans (6,692 men and 8,344 women) aged 10–95 years. BMD and body compositions were measured using a dual-energy X-ray absorptiometry. BMD was determined at the femoral neck, total hip, and lumbar spine. Body compositions included total FM (TFM), percentage FM (PFM), truncal FM (TrFM), total LM (TLM), and appendicular skeletal muscle mass/weight (ASM/Wt). We categorized each man and woman into one of three age groups, based on changes in age-related BMD and the hormonal status. In all gender and age groups, TFM, PFM and TrFM associated inversely with BMD (*P*<0.001–0.034), while TLM and ASM/Wt associated positively (*P*<0.001–0.037) after adjusting for confounders. The negative contribution of FM (*P*=0.001–0.034), and the positive contribution of LM (*P*<0.001–0.035) on BMD were significantly stronger in men than in women. The associations were strongest in men of growing age (*P*=0.003–0.040). When we subdivided the subjects into four groups based on median values of PFM and TLM, FM had a greater effect than LM on BMD in men (*P*<0.001–0.024). These results demonstrate that the effects of FM and LM on BMD may be based on gender and age.

Disclosures: Seong Hee Ahn, None.

SU0311

Hip Structural Analysis Predicts Hip Fracture in Women Independent of BMD: A Meta-Analysis. <u>Preeti Kohli</u>*[1], <u>Chia-Ho Cheng</u>[2], <u>Marian Hannan</u>[3], <u>Yi-Hsiang Hsu</u>[4], <u>Lisa Strano-Paul</u>[5], <u>Michael Lavalley</u>[6], <u>Thomas Beck</u>[7], <u>Douglas Kiel</u>[8], <u>David Karasik</u>[9]. [1]Stony Brook University, USA, [2]Hebrew SeniorLife, USA, [3]HSL Institute for Aging Research & Harvard Medical School, USA, [4]Hebrew SeniorLife Institute for Aging Research & Harvard Medical School, USA, [5]Stony Brook University, USA, [6]Biostatistics, Boston University Sch of Public Health, USA, [7]Beck Radiological Innovations, Inc., USA, [8]Hebrew SeniorLife, USA, [9]Hebrew SeniorLife; Bar Ilan University, USA

Objective: The current gold standard to identify patients at risk for hip fracture is to use bone mineral density (BMD) measurements by Dual Energy X-Ray Absorptiometry (DXA). Though there is a strong association between BMD and hip fractures (HFx), there is also a substantial overlap in BMD between individuals with and without HFx. The reason that BMD alone does not sufficiently differentiate fracture risks may be because BMD does not account for the cross-sectional distribution of bone mass, suggesting a role for factors such as femoral geometry. Measurements of femoral geometry by Hip Structural Analysis (HSA) may improve the prediction of HFx independently of BMD. Our aim was to combine systematically assembled published data with our own data, and through meta-analysis, understand the ability of HSA to predict HFx.

Methods: PubMed, Web of Science, and Embase databases were searched in accordance with the PRISMA Statement for publications on the association of femoral geometry and HFx using a combination of key terms. Criteria for eligible studies included the measurement of HSA by DXA, odds ratios for risk of HFx at proximal femur sites, and publication after 1999 in English language journals. We extracted bibliographic information, demographics, study design, number of HFx cases and controls, exclusion criteria, method of HSA calculations, bone parameters, type of hip fracture, and average years of follow up. Similar characteristics were derived for the Framingham Cohort (unpublished). Odds Ratios (OR) and 95% CIs, unadjusted and adjusted for hip BMD, were used as input data. We performed sex-stratified meta-analyses for each bone parameter using random effects meta-analysis and evaluated heterogeneity between studies using I^2.

Results: In men, none of the HSA measures were significantly associated with HFx (not shown). In women, the following bone parameters predicted HFx risk (see Table): hip axis length (HAL), neck shaft angle (NSA), femoral neck width (FNW), and buckling ratio (BR). After adjusting for BMD, ORs for FNW and BR became non-significant, while the femoral neck cortical thickness (CT) became significant. Heterogeneity was lower in the BMD-adjusted analyses than unadjusted.

Conclusions: Although limited by substantial heterogeneity, in women, HAL, NSA, and CT showed modest strength in HFx prediction independent of BMD. Therefore, HSA indices could potentially be used in addition to BMD, to screen high-risk patients for hip fractures.

TABLE 1 Results for Women

Bone Parameter	# studies	Unadjusted for BMD (OR, 95% CI)	I^2	Adjusted for BMD (OR, 95% CI)	I^2
HAL	10	1.39 [1.09, 1.77]	70.9%	1.42 [1.19, 1.68]	63.2%
NSA	5	1.52 [1.08, 2.14]	83.2%	1.58 [1.13, 2.20]	82.3%
FNW	5	1.30 [1.08, 1.57]	54.2%	1.17 [0.97, 1.40]	33.1%
BR	3	1.76 [1.04, 2.98]	94.4%	1.12 [0.98, 1.29]	0.0%
CT	4	1.22 [0.51, 2.92]	96.4%	1.22 [1.02, 1.46]	0.0%

table1

***Disclosures: Preeti Kohli**, None.*

SU0312

Idiopathic and Secondary Osteoporosis in Premenopausal Women. <u>Alicia Bagur</u>*[1], <u>Silvina Mastaglia</u>[2], <u>Beatriz Oliveri</u>[3], <u>Diana González</u>[4], <u>Elizabeth Sarnacki</u>[5], <u>Candela Fernández</u>[5], <u>Carlos Mautalen</u>[6]. [1]Mautalen Salud e Investigacion, Argentina, [2]Laboratorio De Enfermedades Metabólicas Oseas, CONICET-UBA, Argentina, [3]Mautalen, Salud e Investigación, Argentina, [4]Mautalen Salud e Investigación, Argentina, [5]Mautalen, Salud e Investigación, Argentina, [6]Centro de Osteopatías Médicas, Argentina

Premenopausal (preMP) osteoporosis (OP) may be idiopathic or due to diseases or treatments that affect bone mineral density (BMD). Aim: To identify the clinical characteristics and the evolution of BMD over two years in women with preMP OP. We reviewed the clinical records of 95 preMP women who were referred during the last 6 years for evaluation of BMD to an Institute of Metabolic Bone Diseases. Patients were either self-referred due to concern for the disease or referred from other physician. We analyzed personal and familiar history of fractures (Fx), BMD, biochemical bone markers, diagnosis and their treatments. BMD was considered normal as a Z score above -2.0 in the lumbar spine and/or total femur. Results: 41 out 95 (43%) were in the BMD osteoporotic values. In 22 out of 41 (54%) a diagnosis of idiopathic or primary (1♂) OP was made. Nineteen patients (46%) had secondary (2♂) OP due to the following diseases: pregnancy (6), anorexia nervosa (4), celiac disease (2), hypercalciuria (1), 1♂ hyperparathyroidism (1), hypothalamic amenorrhea (1),

glucocorticoid (1), osteogenesis imperfecta (1), excess of T4 (1), and congenital adrenal hyperplasia (1). Two out 22 women (9%) with 1♂ OP had Fx (1 vertebrae and 1 wrist). Four out 19 women (21%) with 2♂ OP had Fx at the following site: wrist (1), vertebrae (2), and metatarsal (1). Eleven (50%) of the 1♂ OP women and 6 (32%) with 2♂ OP had a familiar history of Fx. Table 1 show the significant differences between 1♂ and 2♂ OP. The 1♂ OP patients received the following treatments: Calcium and vitamin D (Ca+D) (17), bisphosphonate (5). Secondary OP patients received: Ca+D and treatment according to the underlying disease.About fifty percent of preMP women with low BMD were idiopathic standing out less bone formation and vitamin D vs. 2♂ OP. In a preliminary analysis, follow up of this group showed an increase in bone mass.

Table1: Baseline Characteristic between 1°OP and 2°OP (X±SD)

	Age (years)	TF (z-score)	sCa	BAP	25OHD
NV	-	-	8.5-10.4mg%	31-95UM	>30ng/ml
1°OP	39±7	-1.8	9.2±0.4	37±13	24±11
2°OP	30±10	-2.2	9.5±0.4	67±44	37±17
p	0.006	0.04	0.04	0.009	0.03

sCa: serum calcium; BAP: bone alkaline phosphatase; 25OHD:25-hydroxivitaminD. NV: normal values

Table

***Disclosures: Alicia Bagur**, None.*

SU0313

The association of vitamin D and parathyroid hormone with bone mineral density in Korean adults. <u>Seong-Woo Choi</u>[1], <u>Sun-Seog Kweon</u>[2], <u>Jin-Su Choi</u>[2], <u>Jung-Ae Rhee</u>[2], <u>Young-Hoon Lee</u>[3], <u>Hae-Sung Nam</u>[4], <u>Hee Nam Kim</u>[5], <u>Min-Ho Shin</u>*[6]. [1]Department of Preventive Medicine, Chosun University Medical School, Gwangju, Republic of Korea, South Korea, [2]Department of Preventive Medicine, Chonnam National University Medical School, South Korea, [3]Department of Preventive Medicine & Institute of Wonkwang Medical Science, Wonkwang University College of Medicine, South Korea, [4]Department of Preventive Medicine, Chungnam National University Medical School, South Korea, [5]Center for Creative Biomedical Scientists, Chonnam National University, South Korea, [6]Chonnam National University Medical School, South Korea

The purpose of this study is to investigate the association of serum 25-hydroxyvitamin D(25(OH)D) and parathyroid hormone with bone mineral density in Korean general population. The study population consisted of 8,700 subjects (3464 men and 5236 women) aged 50 years and older who participated in the baseline survey of the Dong-gu Study conducted in Korea between 2007 and 2010. Bone mineral density (BMD) was measured by dual-energy X-ray absorptiometry at the spine and hip. Serum 25(OH)D and parathyroid hormone were measured by chemiluminescent microparticle immunoassay. Multiple linear regression analyses were used to evaluate the association of the quartiles of 25(OH)D and parathyroid hormone with BMD, after adjusting for age, height, smoking, alcohol intake, physical activity, education, medication of hypertension, and medication of diabetes. To evaluate the independent effect of parathyroid hormone and 25(OH)D levels on BMD, we further adjusted for 25(OH)D or parathyroid hormone. In multiple adjusted models, low 25(OH)D levels were associated with low BMD at both hip and spine in males and females. High parathyroid hormone levels were associated with low BMD at both spine and hip in males and females. Parathyroid hormone and 25(OH)D levels were associated with BMD independently of each other except for lumbar spine in females. In females, the association between 25(OH)D and lumbar spine BMD was attenuated and remained statistically non-significant after adjustment for covariates and parathyroid hormone. In conclusion, we found that vitamin D and parathyroid hormone were significantly associated with BMD in community-dwelling Korean adults.

Table Bone mineral density according to serum 25-hydroxyvitamin D

25 (OH)D ng/ml		Male			Female		
		Model 1	Model 2	Model 3	Model 1	Model 2	Model 3
Lumbar (L1-L4)	Q1	1.137±0.007	1.137±0.006	1.140±0.007	0.975±0.004	0.975±0.004	0.978±0.004
	Q2	1.156±0.006	1.155±0.006	1.155±0.006	0.986±0.004	0.986±0.004	0.987±0.004
	Q3	1.163±0.006	1.162±0.006	1.161±0.006	0.989±0.004	0.988±0.004	0.987±0.004
	Q4	1.184±0.006	1.186±0.006	1.184±0.006	0.991±0.004	0.991±0.004	0.988±0.004
	p for trend	<0.001	<0.001	<0.001	0.006	0.006	0.122
Femoral neck	Q1	0.864±0.004	0.865±0.004	0.867±0.004	0.778±0.003	0.779±0.003	0.782±0.003
	Q2	0.877±0.004	0.876±0.004	0.877±0.004	0.785±0.003	0.785±0.003	0.786±0.003
	Q3	0.884±0.004	0.884±0.004	0.883±0.004	0.791±0.003	0.791±0.003	0.790±0.003
	Q4	0.898±0.004	0.898±0.004	0.896±0.004	0.796±0.003	0.796±0.003	0.793±0.003
	p for trend	<0.001	<0.001	<0.001	<0.001	<0.001	0.002

All values are given as mean (standard error).
Model 1 is adjusted by age, weight and height, and month of collection.
Model 2 is adjusted by Model 1 variables plus smoking, alcohol intake, physically activity, education, medication of hypertension, medication of diabetes.
Model 3 is adjusted by Model 2 variables plus parathyroid hormone.

Table

***Disclosures: Min-Ho Shin**, None.*

SU0314

The trends in bone mineral density is reversed by body weight adjustment — a study of 12,401 Chinese women. Edith Lau*[1], Rick Chung[2], Peng Cheng Ha[3], Hai Tang[4], Dicky Lam[5]. [1]Center for Clinical & Basic Research (CCBR) (Hong Kong), Hong Kong, [2]Center for Clinical & Basic Research (CCBR) (Hong Kong), Hong Kong, [3]CCBR Beijing, China, [4]Department of Orthopedics, Friendship Hospital, Beijing, China, [5]CCBR Hong Kong, Hong Kong

Background and objective

The hip fracture incidence in Hong Kong (Southern Chinese) women is around two times that of Beijing (Northern Chinese) women. The objectives of the current study are to compare the bone mineral density (BMD) of Hong Kong Chinese and Beijing Chinese women, and to investigate how the trends were affected by adjustment for body weight. The prevalence of osteoporosis in these populations was also studied.

Subjects and materials

A total of 12,401 postmenopausal Chinese women were recruited from the community in Hong Kong and Beijing. BMD was measured by Lunar Dual X-ray Densitometry (DEXA) machines. Multiple regression was used to study the effects of adjustment for age, height and weight on the BMD comparison, and to deduce the variance in BMD accounted by the anthropomorphic factors in the two populations. The percentage prevalence of osteoporosis in the two populations was calculated using Asian normal values and the World Health Organization criteria for osteoporosis.

Results

Although the BMD of Beijing Chinese women was found to be higher than that of Hong Kong Chinese women; this trend was reversed once the body weight was adjusted for. Using the multiple analysis of ANCOVA, body weight accounted for 13.3% of the difference between lumbar spine BMD and 14.6% of the total hip BMD between Hong Kong Chinese and Beijing Chinese women respectively. The prevalence of osteoporosis at any site was extremely high: 24.9% in Hong Kong Chinese women and 20.3% in Beijing Chinese women.

Conclusion

We conclude that osteoporosis is a highly prevalent health problem in Hong Kong Chinese and Beijing Chinese women. It is extremely important to adjust for body weight when comparing BMD, even for subjects of the same ethnicity. The adjusted BMD of Hong Kong Chinese women was higher than that of Beijing Chinese women; implying that the higher hip fracture incidence in Hong Kong Chinese women could be due to factors related to bone strength and falls.

Site	Mean of BMD (g/cm²) (SD)			
	Hong Kong women (N=6099)		Beijing women (N=6302)	
	Unadjusted	Adjusted[1]	Unadjusted	Adjusted[1]
Lumbar Spine	0.956 (0.168)[2]	0.996(0.002)[3]	0.978 (0.166)	0.949(0.002)
Total hip	0.779 (0.123)[2]	0.835(0.001)[3]	0.850 (0.133)	0.813(0.001)
Femoral neck	0.732 (0.110)[2]	0.765(0.001)[3]	0.789 (0.122)	0.755(0.001)

[1] Adjusted for age, height and weight

[2] $P<0.001$ by Student's t-test in comparing the unadjusted BMD of Beijing and Hong Kong Chinese women

[3] $P < 0.001$ by ANCOVA in comparing the adjusted BMD of Beijing and Hong Kong Chinese women

Bone mineral density with and without adjustment in Beijing and Hong Kong Chinese women

Disclosures: Edith Lau, None.

SU0315

Obesity Was Not Protective Against Fractures in Post-Menopausal Women: a Cross-Sectional Study at Santa Maria, Brazil. Rafaela Copes[1], Felipe Langer[1], Karen da Costa[1], Luana Marchesan[1], Giovani Sartori[1], Aline Cocco[1], Jose de Carvalho[1], Rafael Moresco[1], Fabio Comim[1], Melissa Premaor*[2]. [1]Federal University of Santa Maria, Brazil, [2]Federal University of Santa Maria, Brazil

Recent studies have challenged the paradigm that high BMI is always protective against bone fractures. The prevalence of fractures has been reported similar between obese and non-obese people in the GLOW study[1]. Nevertheless, others did not reproduce this lack of association. In this study we aimed to evaluate the association between BMI/obesity and fractures in post-menopausal women. In order to do so, we carried out a cross-sectional study at Santa Maria (parallel 29° South), Brazil. Post-menopausal women aged 55 years or older who had at least one appointment at their GP practice in the two years prior the study were recruited from March 1st to August 31st, 2013. Women with cognitive impairment were excluded. The GLOW study questionnaire was applied with permission of The Center for Outcomes Research, University of Massachusetts of Medical School[1,2]. Height and weight were measured according the WHO protocol. Bone fractures (excluding hand, feet, and head) that occur after age 45 years were considered as the outcome. Overall, 1301 women were invited to participate of the study. In total, 1057 women completed the questionnaire; of whom, 973 had their BMI measured. The mean [mean (SD)] age and BMI were

67.2(7.6) years and 29,3(5,5) kg/m², respectively. The prevalence of fractures and obesity (BMI ≥ 30 kg/m²) were, respectively, 17% and 39.6%. The BMI was not different in women with and without fractures [29.5(5.8) kg/m² vs. 29.2(5.5) kg/m², $P=0.66$]. The power of the study for this endpoint was 99%. Of the obese women, 17.4% presented a bone fracture; it was not different from the non-obese women prevalence of fractures (16.2%, $P = 0.62$). The odds ratio of fracture in obese women was 1.09 (95% CI 0.74,1.54; $P = 0.56$). There were no association between fracture site and BMI. Moreover, age and impaired mobility were associated with fractures in obese women. Although the BMI of this population was high, the study had sufficient power to evaluate its association with fracture. In conclusion, obesity was not protective against fracture in post-menopausal women in our study. Efforts to modify the misconception that obesity is always protective against fracture are needed.

References:

COMPSTON, JE; et al. Obesity is not protective against fracture in postmenopausal women: GLOW. Am J Med (2011) 124:1043-50

HOOVEN, FH; et al. The Global Longitudinal Study of Osteoporosis in Women (GLOW): rationale and Study design, Osteoporos Int (2009) 20:1107-16

Disclosures: Melissa Premaor, None.

SU0316

Bone mineral density and association between BMI and fracture risk: a mediation study. Mei Chan*[1], Steve Frost[2], Jacqueline Center[3], John Eisman[3], Tuan Nguyen[3]. [1]Osteoporosis & Bone Biology, Australia, [2]Garvan Institute of Medical Research, Australia, [3]Garvan Institute of Medical Research, Australia

Aim The relationship between body mass index (BMI) and fracture risk is controversial. We sought to delineate the causal structure of the relationship between BMI, bone mineral density (BMD) and fracture risk by mediation analysis

Methods The study involved 2,199 women and 1,351 men aged 60 years or older. BMI was derived from baseline weight and height. Femoral neck BMD was measured by dual energy X-ray absorptiometry (GE-LUNAR, Madison, WI). The incidence of fragility fracture was ascertained by X-ray reports during 1991-2012. Mediation analysis was used to assess the direct and indirect effects of BMI, and the mediated effect of BMD, on fracture risk within the framework of the Cox's proportional hazards model.

Results Overall, 774 women (35% of total women) and 258 men (19%) had sustained a fracture. Approximately 21% of women and 20% of men were considered obese (BMI ≥ 30). In univariable analysis, greater BMI was associated with reduced fracture risk in women (HR 0.92; 95% CI, 0.85-0.99) and in men (HR 0.77; 95% CI, 0.67-0.88). After adjusting for femoral neck BMD, higher BMI was associated with greater risk of fracture in women (HR 1.21; 95% CI, 1.11-1.31) but not in men (HR 0.96; 95% CI, 0.83-1.11). However, in mediation analysis, the direct effect of BMI on fracture risk was not statistically significant, and the majority of BMI effect on fracture risk was mediated by femoral neck BMD. The overall mediated effect estimates were -0.048 (95% CI, -0.059 to -0.036; $P < 0.001$) in women and -0.030 (95% CI, -0.042 to -0.018; $P < 0.001$) in men.

Conclusion These analyses suggest that there is no significant direct effect of BMI on fracture, and that the observed association between BMI and fracture risk is mediated by femoral neck BMD in both men and women.

Disclosures: Mei Chan, None.

SU0317

Degree of Trauma Differs for Major Osteoporotic Fracture Events in Older Men vs. Older Women. Kristine Ensrud*[1], Terri Blackwell[2], Peggy Cawthon[3], Dawn Mackey[4], Douglas Bauer[5], Howard Fink[6], John Schousboe[7], Dennis Black[5], Eric Orwoll[8], Deborah Kado[9], Jane Cauley[10]. [1]University of Minnesota & Minneapolis VA Health Care System, USA, [2]California Pacific Medical Center Research Institute, USA, [3]California Pacific Medical Center Research Institute, USA, [4]Simon Fraser University, Canada, [5]University of California, San Francisco, USA, [6]GRECC, Minneapolis VA Medical Center, USA, [7]Park Nicollet ClinicUniversity of Minnesota, USA, [8]Oregon Health & Science University, USA, [9]University of California, San Diego, USA, [10]University of Pittsburgh Graduate School of Public Health, USA

Purpose: Examine the role of trauma in major "osteoporotic" fracture (MOF) events in older men vs. older women.

Methods: We used data from 15698 adults aged ≥65 years (yrs) enrolled in the prospective community-based MrOS (5994 men) and SOF (9704 women) studies. In each study, participants were contacted every 4 months to ascertain incident fractures confirmed by radiographic reports. When a fracture was reported, research staff interviewed participants about circumstances of the event and coded the fracture according to degree of trauma. Degree of trauma was classified as LOW (fall from standing height or less; fall on stairs, steps or curb; minimal trauma other than fall (coughing, turning over); MODERATE (collisions with objects during normal activity without associated fall); or HIGH (fall more than standing height; severe trauma [motor vehicle accident, assault]). Fractures missing trauma status (n=274) or

coded as pathologic (peri-prosthetic or due to malignancy, n=17) were excluded. Fracture (hip, clinical vertebral, wrist, humerus, MOF [any of the preceding 4 types]) follow-up was from baseline until 10 yrs or until time of death or termination from study (mean follow-up 9.1 yrs in SOF and 8.7 yrs in MrOS).

Results: 307 of the 465 (66.0%) MOF events in men compared with 1408 of the 1880 (74.9%) MOF events in women were due to fall from standing height or less (p<0.001). 14.6% of the MOF events in men compared with 6.3% of the MOF events in women were classified as high trauma (p<0.001) (Figure); men vs. women more often experienced both fractures due to fall more than standing height and fractures due to severe trauma. High trauma fractures were more significantly common in men vs. women at the hip (p=0.002) and wrist (p<0.001), but not at the spine or humerus. After adjustment for baseline age, race, clinical center, health status, fall history, body mass index and femoral neck bone density, the odds ratio of a high trauma fracture among men vs. women was 3.12 (95% CI 1.70-5.71) among participants with MOF, 3.34 (95% CI 1.04-10.67) among participants with hip fracture, and 5.68 (2.03-15.85) among participants with wrist fracture.

Conclusion: Among community-dwelling older adults, major osteoporotic fracture events are more likely to be related to high trauma in men as compared with women. These findings are not explained by sex differences in traditional risk factors and may reflect a greater propensity among men to engage in risky behavior.
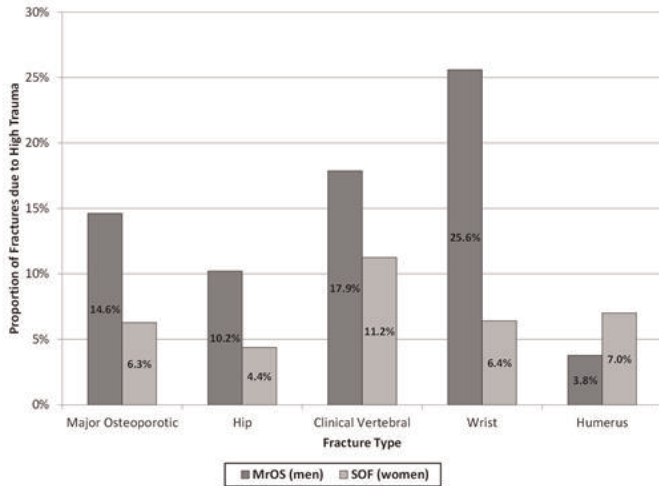

Figure. Proportion of Fracture Events Due to High Trauma According to Sex

SU0318

Withdrawn

SU0319

Identification of Osteoporosis Cases in Administrative Healthcare Databases: A Validation Study in the Province of Quebec,Canada. Sonia Jean*[1], Jacques P. Brown[2], Philippe Gamache[3], Suzanne Morin[4], Siobhan O'Donnell[5], William Leslie[6], Louis Bessette[7]. [1]Institut National De Santé Publique Du Québec, Canada, [2]CHU de Québec Research Centre, Canada, [3]INSPQ, Canada, [4]McGill University, Canada, [5]PHAC, Canada, [6]University of Manitoba, Canada, [7]CHU de Quebec Research Centre, Canada

Purpose: Administrative healthcare databases (AHDs) capture information during routine clinical care that can be used to track disease incidence, prevalence, outcomes, resources utilization and indicators of quality of care. This study assessed the validity of several case definitions to identify osteoporosis cases from AHDs, as compared with self-reported diagnosis, in a cohort of women who sustained fragility fractures as the gold standard.

Methods: Women (≥50y) without previous osteoporosis diagnosis or treatment who suffered a recent fragility fracture were recruited to the Recognizing Osteoporosis and its Consequences in Quebec (ROCQ) project. For this study, these women were used to compare several AHD case definitions for osteoporosis ascertainment. Participants were contacted at 6 and 18 months post fracture to complete questionnaires on personal and clinical characteristics related to osteoporosis (including diagnosis, treatment, co-morbidities, risk factors). BMD reports were also obtained. Each ROCQ participant's data were linked to population-based AHDs for the Province of Quebec, Canada. AHD case definitions for osteoporosis diagnosis were constructed using combinations of the number osteoporosis diagnosis codes (ICD-9 733.x and ICD-10 M80-81) from physician claims (P), hospitalizations (H), prescriptions for osteoporosis medications (Rx) and BMD tests during pre-specified time periods. The accuracy of the AHD case definitions were determined using ROCQ questionnaire data and BMD reports (gold standard). We calculated prevalence, sensitivity (Sn), specificity (Sp), positive predictive value (PPV), negative predictive

value (NPV), area under the receiver operative curve (AUC), and the ratio of number of women who test positive to the number of women who have the condition (TAP).

Results: The cohort included 557 women (mean age: 61.7 years; ≥65 years: 31.4%). During the follow-up period (mean 20.7 months), 29.1% of the women (36% of women ≥65y) self-report an osteoporosis diagnosis on the ROCQ questionnaire. The most accurate case definition to identify women with diagnosed osteoporosis from AHDs was 1H or 1P or 1RX (Sn=0.70, Sp=0.83, PPV=0.63, NPV=0.87, AUC=0.77, TAP=1.11; Table1) In women ≥65 years, the performance of this case definition was even higher (Sn=0.89, Sp=0.81, PPV=0.73, NPV=0.93, AUC=0.84, TAP=1.22; Table 2).

Conclusions: We demonstrated a higgh level of accuracy for identifying patients with diagnosed osteoporosis using AHDs.

Case Definition	Prevalence %	Sn All cases	Sp With/ Without osteopenia non-cases	PPV With/ Without osteopenia non-cases	NPV With/ Without osteopenia non-cases	AUC All cases	TAP With/ Without osteopenia non-cases
1- Rx	14.4	0.44	0.98/0.98	0.90/0.91	0.81/0.76	0.71	0.48/0.48
2- 1H or 1P	26.4	0.52	0.85/0.87	0.58/0.69	0.82/0.77	0.69	0.90/0.75
3- 1H or 2P	13.1	0.31	0.94/0.95	0.69/0.76	0.77/0.71	0.63	0.45/0.41
4- 1H or 1P or 1Rx	32.1	0.70	0.83/0.85	0.63/0.72	0.87/0.84	0.77	1.11/0.97
5- 1H or 2P or 2Rx	21.2	0.56	0.93/0.94	0.77/0.83	0.84/0.79	0.75	0.72/0.67
6- 1H or 1P or 2 BMD in 24 months	27.5	0.54	0.84/0.86	0.57/0.69	0.81/0.77	0.69	0.95/0.78
7- 1H or 1P or 2 BMD in 36 months	29.3	0.55	0.81/0.85	0.55/0.67	0.82/0.77	0.68	1.00/0.82
8- 1H or 1P or 2 BMD in 60 months	34.7	0.62	0.76/0.81	0.52/0.65	0.83/0.79	0.69	1.19/0.95
9- 1H or 2P or 2 BMD in 24 months	14.4	0.33	0.93/0.94	0.66/0.76	0.77/0.72	0.63	0.50/0.43
10- 1H or 2P or 2 BMD in 36 months	17.1	0.35	0.90/0.92	0.60/0.71	0.77/0.72	0.63	0.58/0.49
11- 1H or 2P or 2 BMD in 60 months	24.2	0.42	0.84/0.87	0.54/0.66	0.78/0.74	0.65	0.83/0.68
12- 1H or 1P or 1Rx or 2 BMD in 24 months	32.9	0.70	0.82/0.85	0.62/0.72	0.87/0.84	0.76	1.13/0.97
13- 1H or 1P or 1Rx or 2 BMD in 36 months	34.7	0.71	0.80/0.84	0.60/0.71	0.87/0.84	0.76	1.18/1.0
14- 1H or 1P or 1Rx or 2 BMD in 60 months	39.3	0.75	0.75/0.80	0.56/0.67	0.88/0.85	0.75	1.34/1.12

Table 1: Accuracy of the case definitions (All women)

Case Definition	Prevalence %	Sn All cases	Sp With/ Without osteopenia non-cases	PPV With/ Without osteopenia non-cases	NPV With/ Without osteopenia non-cases	AUC All cases	TAP With/ Without osteopenia non-cases
1- Rx	29.1	0.71	0.95/0.94	0.88/0.90	0.86/0.82	0.83	0.81/0.79
2- 1H or 1P	32.0	0.60	0.84/0.85	0.68/0.75	0.79/0.75	0.72	0.88/0.80
3- 1H or 2P	17.7	0.38	0.94/0.94	0.77/0.83	0.73/0.68	0.66	0.49/0.46
4- 1H or 1P or 1Rx	44.0	0.89	0.81/0.81	0.73/0.78	0.93/0.91	0.84	1.22/1.14
5- 1H or 2P or 2Rx	33.7	0.78	0.91/0.92	0.83/0.88	0.88/0.85	0.84	0.94/0.89
6- 1H or 1P or 2 BMD in 24 months	34.3	0.64	0.82/0.84	0.67/0.74	0.80/0.76	0.73	0.96/0.86
7- 1H or 1P or 2 BMD in 36 months	35.4	0.64	0.80/0.83	0.65/0.73	0.80/0.76	0.72	0.98/0.88
8- 1H or 1P or 2 BMD in 60 months	38.9	0.65	0.76/0.78	0.60/0.68	0.79/0.75	0.71	1.08/0.96
9- 1H or 2P or 2 BMD in 24 months	20.0	0.41	0.92/0.93	0.74/0.81	0.74/0.68	0.67	0.55/0.51
10- 1H or 2P or 2 BMD in 36 months	22.9	0.44	0.89/0.91	0.70/0.78	0.74/0.69	0.67	0.62/0.56
11- 1H or 2P or 2 BMD in 60 months	28.0	0.49	0.84/0.86	0.63/0.72	0.75/0.70	0.67	0.78/0.68
12- 1H or 1P or 1Rx or 2 BMD in 24 months	45.1	0.89	0.80/0.80	0.71/0.77	0.93/0.91	0.84	1.25/1.16
13- 1H or 1P or 1Rx or 2 BMD in 3 years	46.3	0.89	0.78/0.79	0.69/0.76	0.93/0.91	0.83	1.29/1.17
14- 1H or 1P or 1Rx or 2 BMD in 5 years	49.1	0.89	0.73/0.74	0.65/0.72	0.92/0.90	0.81	1.37/1.24

Table 2: Accuracy of the case definitions (Women 65 years and older)

SU0320

Serum 25-hydroxy vitamin D levels and fracture risk: The Dubbo Osteoporosis Epidemiology Study. Weiwen Chen*[1], Nguyen Nguyen[2], Tuan Nguyen[2], Jacqueline Center[2], John Eisman[2]. [1]St Vincent's Hospital (Sydney), Australia, [2]Garvan Institute of Medical Research, Australia

Background: Hypovitaminosis D is common in osteoporotic patients. Vitamin D deficiency leads to secondary hyperparathyroidism and possibly reduced postural stability with increased falls risk. However, the relationship between vitamin D and fracture risk is not well documented, especially in the ambulant healthy elderly population. Objectives: To examine the relationship between serum 25-hydroxyvitamin D levels and fracture risk Methods: Nested case-control study within the Dubbo Osteoporosis Epidemiology Study (DOES), a prospective cohort of men and women aged 60+ that commenced in 1989. Participants attended bi-annual follow-up. At each visit, a DXA bone density, anthropometric measures and lifestyle questionnaire, including dietary calcium intake and physical activity were completed. Participants with a minimal trauma fracture and a random sample of a non-fractured control were selected. Both groups had had serum taken and archived at -70°C. Samples from cases prior to fracture and comparable samples from controls had 25-OHD, PTH and creatinine measured. Differences in baseline measures between the fracture and non-

fracture cases were tested by paired t-test for normally distributed data and by the non-parametric Wilcoxon sign rank test for non-parametric data. Results: Fracture cases (n = 305) and non-fracture controls (n = 318) were included for analysis. The median length of follow-up was 4.52 years (IQ: 1.80 – 8.68). Of this healthy elderly cohort, < 5.3 % had 25-OH D levels of < 30 nmol/L (<12 ng/mL). 25-OH D levels were correlated with age (r=-0.16, P<0.0001), FNBMD (r=0.14, P=0.0003), serum PTH levels (r=-0.26, P=0.0001) and quadriceps strength (r=0.22, P=<0.0001). However median vitamin D levels were 67 nmol/L in both cases (IQ: 49.3-83.5) and controls (IQ: 47.1-83.1). Moreover, 25-OH D levels were not associated with increased fracture (OR: 1.00, 95 CI: 0.86-1.17, P=0.968) or falls after (OR: 1.22, 95% CI: 0.79-1.89, P=0.37) before or after adjustment for seasonal variation. Conclusion: In this sample of community dwelling elderly, serum 25-OH vitamin D levels were correlated with bone density and quadriceps strength. However, in these healthy elderly, 25-OH D levels were not associated with risk of fracture or of falls. This may be due to most participants being vitamin D sufficient.

Disclosures: Weiwen Chen, None.

SU0321

Serum Periostin Improves Fracture Prediction in Older Men: the STRAMBO Study. Pawel Szulc*[1], Olivier Borel[2], Jean Charles Rousseau[2], Roland Chapurlat[3]. [1]INSERM UMR 1033, University of Lyon, Hopital E. Herriot, Pavillon F, France, [2]INSERM UMR 1033, University of Lyon, France, [3]E. Herriot Hospital, France

Identification of older men at high risk of fracture is a public health problem. Periostin is a protein synthesized by several tissues including bone. Its serum concentration may predict fractures in postmenopausal women *(Rousseau et al. J Clin Endocrinol Metab, 2014, online)*. Therefore, our aim was to assess the predictive value of serum periostin for fracture in older men. In a cohort of 716 men aged 60 to 87 years, 80 men sustained at least one fracture (including 68 fragility fractures) during a prospective follow-up (median 6 years). Serum periostin level was measured using a sandwich ELISA assay (USCN, Wuhan, China). At baseline, serum periostin did not correlate with bone mineral density (BMD) measured by dual energy X-ray absorptiometry (HOLOGIC Discovery A) or with serum and urinary levels of biochemical bone turnover markers. After adjustment for age, weight, femoral neck BMD as well as prior falls and fractures, the risk of fragility fracture increased with decreasing periostin level (HR=1.39 per SD decrease, 95%CI: 1.06-1.82, p<0.05). The fracture risk was higher in the lowest quartile of periostin level compared with three higher quartiles combined (HR=2.08, 95%CI: 1.26-3.43, p<0.005). In men who had periostin concentration in the lowest quartile and femoral neck BMD <0.776 g/cm^2 (median), the fracture risk was higher compared with men who did not have these characteristics (HR=3.97, 95%CI: 1.92-8.23, p<0.001). The results were similar in the analyses adjusted for BMD of other skeletal sites (e.g. adjusted for mid-radius BMD: HR=1.71, 95%CI: 1.06-2.77, p<0.05 for the first quartile vs three lower quartiles of periostin level). The results were also similar when all incident fractures were included in the analysis (HR=1.57, 95%CI: 1.01-2.45, p<0.05 for the first quartile vs three lower quartiles).

In conclusion, our data show that, in older men, lower serum periostin concentrations are associated with higher risk of fracture after adjustment for age, weight, BMD, history of falls and prior fracture.

Disclosures: Pawel Szulc, None.

SU0322

Determinants of serum sclerostin in postmenopausal women. Pedro Rozas-Moreno*[1], Rebeca Reyes[2], Manuel Munoz-Torres[3], Antonia Garcia-Martin[4], Ines Luque-Fernandez[4], Verónica Avila-Rubio[4], Beatriz García-Fontana[4], Sonia Morales-Santana[4]. [1]Endocrinology Division. Hospital General de Ciudad Real. Ciudad Real, Spain., Spain, [2]Bone Metabolic Unit., Spain, [3]Hospital Universitario San Cecilio, Spain, [4]Bone Metabolic Unit, Spain

Background: Sclerostin is a 213 amino-acid glycoprotein that antagonize Wnt signaling. Some studies have demonstrated that higher concentrations of serum sclerostin are associated with increased fracture risk, particularly if coexisting with low bone mineral density. There is limited information about the determinants of sclerostin in postmenopausal women, and conflicting data have been reported.

Objectives: This study was performed to determine the predictive factors of serum sclerostin in postmenopausal women. We also analysed differences according to the presence of densitometric osteoporosis.

Patients and methods: We performed a cross-sectional study. We measured baseline serum sclerostin concentrations by ELISA (Biomedica) in 132 postmenopausal women without osteoporosis treatment. We analysed its relationship with age, weight, renal function, calciotropic hormones, bone mineral density (BMD), morphometric vertebral fractutes, prevalent fragility fracture and the presence of type 2 diabetes mellitus (T2DM).

Results: Sclerostin levels were significantly higher in T2DM patients (43.13 ± 17,08 vs 36.7 ± 14.4 pmol/L, p=0.001) and non-osteoporotic women (41,24 ± 16,2 vs 31,71 ± 10,48 pmol/L p=0.000). In the total sample, the values of serum sclerostin were positively associated with BMD at all sites analysed (r=0.316, p=0.000; r=0.426, p=0.000; r=0.429,p=0.000, lumbar spine, femoral neck and total hip respectively). We

found a negative correlation between circulating sclerostin and age (r=- 0.198, p=0.023). In stepwise multiple linear regression analysis, only the presence of densitometric osteoporosis was correlated with serum sclerostin concentrations (β=-0.374, p=0.002). There were no differences according to the presence of morphometric vertebral fractures or prevalent fragility fractures. In the subgroup of osteoporotic women, we did not find a significant relationship between serum levels of sclerostin and any of the parameters analysed.

Conclusions: In our study, the main determinant of serum sclerostin levels was the presence of densitometric osteoporosis.

Disclosures: Pedro Rozas-Moreno, None.

SU0323

Hypothyroidism, thyroxine replacement and major osteoporotic fractures – The OPENTHYRO register cohort. Bo Abrahamsen*[1], Henrik L Jørgensen[2], Anne Sofie Laulund[2], Mads Nybo[3], Douglas Bauer[4], Thomas H Brix[3], Laszlo Hegedüs[3]. [1]University of Southern Denmark, Denmark, [2]Bispebjerg Hospital, Denmark, [3]Odense University Hospital, Denmark, [4]University of California, San Francisco, USA

Introduction: The long term relationship between hypothyreosis and fracture risk is challenging to dissect due to the modifying influence of subsequent thyroxine replacement with the potential for excessive replacement doses. We studied changes in serum thyrotropin (TSH) levels over time and association with fracture risk in real world patients who presented with initially elevated TSH.

Population and methods: Register-based cohort study including all patients with a TSH measurement in the region of Funen 1996-2010. All TSH determinations were done in the same lab, which served all hospitals and GP practices in the region. The study population consisted of all adults with a first measurement of TSH > 4.0 mIU/l (N=8,414) or normal TSH (N=222138, comparator). We used a Cox PH analysis incorporating additional time dependent covariates to represent initiation of thyroxine replacement and cumulative number of periods with high vs low TSH after index date.

Results: While the risk of major osteoporotic fractures was significantly higher in patients with longer cumulative time with raised TSH (TSH> 4 mIU/l, table 1, "hypothyroid time"), cumulative time with low TSH (TSH<0.3 mIU/l, "hyperthyroid time") was a much stronger predictor of fracture risk. Hyperthyroid (OR 1.09, 95% CI 104-1.15, p=0.0012) but not hypothyroid time was significantly associated with the risk of hip fractures.

Conclusions: Among patients who present with an elevated TSH, the long term risk of hip and other osteoporotic fractures is strongly related to the cumulative duration of periods with low TSH- likely from excessive replacement- while the independent effects of elevated TSH do not appear to be clinically significant.

	Hip fracture (N$_{event}$ = 5,994)	Major osteoporotic fracture (N$_{event}$ = 15,984)
Per 6 mo of TSH > 4 mIU/l	0.99 (0.95-1.03) p=0.600	1.03 (1.01-1.06) p=0.005
Per 6 mo of TSH < 0.3 mIU/l	1.09 (1.04-1.15) p=0.0012	1.13 (1.08-1.15) p<0.0001
Thyroxine prescription	0.95 (0.77-1.17) p=0.620	0.89 (0.79-1.01) p=0.0787

Table 1. Cox analysis adjusted for age, sex, prior major osteoporotic fracture, comorbidity and use of Prednisolone or osteoporosis drugs.

Table 1

Disclosures: Bo Abrahamsen, Eli Lilly, 10; Novartis, 7; Merck, 3; Amgen, 3; UCB, 7

SU0324

Inflammatory Markers and Change in Bone Mineral Density among Older Men. Kamil Barbour*[1], Stephanie Harrison[2], Kristine Ensrud[3], Peggy Cawthon[4], Nancy Lane[5], Thuy-Tien Dam[6], Joseph Zmuda[7], Steven Cummings[2], Jane Cauley[7]. [1]CDC, USA, [2]San Francisco Coordinating Center, USA, [3]University of Minnesota & Minneapolis VA Health Care System, USA, [4]California Pacific Medical Center Research Institute, USA, [5]University of California, Davis Medical Center, USA, [6]Division of Geriatric Medicine & Aging, Columbia University, USA, [7]University of Pittsburgh Graduate School of Public Health, USA

Cytokines play a major role in bone remodeling with in vitro and rodent studies showing the involvement of inflammation in the pathogenesis of osteoporosis. Several longitudinal studies have found an association between high levels of inflammatory

makers and greater bone mineral density (BMD) loss in primarily older postmeno-pausal women. To test this hypothesis in older men, we followed 702 participants (mean age= 73.8 ± 5.9 years) from the Osteoporotic Fractures in Men Study (MrOS) for a median (range) follow-up period of 4.6 (3.7, 6.0) years. Inflammatory markers interleukin-6 (IL-6), tumor necrosis factor alpha (TNF-α), C-reactive protein (CRP) and soluble receptors (SR) for IL-6 (IL-6 SR) and TNF-α (TNF SR1 and TNF SR2) were measured at the baseline visit (2000-2002) using enzyme-linked (ELISA) with the exception of CRP which used an immunoturbidimetric assay. Total hip and femoral neck BMD were measured at baseline and visit 2 (2005-2006) using dual energy x-ray absorptiometry (DXA). Linear regression models were used to assess the association between these inflammatory markers and bone loss and included variables associated with inflammation at p<0.1. Multivariate models were adjusted for age, race, BMI, clinic site, smoking, physical activity, health status, diabetes, and congestive heart failure. The annualized rate of hip or femoral neck BMD loss did not vary by quartiles of individual inflammatory markers. In multivariable models, among men with 3-6, 2, and 0-1 inflammatory marker(s) in the highest quartile, the annualized rate of total hip BMD loss was 0.48%, 0.38%, and 0.36%, respectively, p-trend=0.16. The findings were similar for annualized rate of femoral neck BMD loss. While the average rate of bone loss appeared to higher among men with greater inflammatory marker burden, the test for trend did not reach significance. Future studies with larger sample size are needed to provide more definitive data on the association, and determine if this relationship truly varies by sex.

Table. Mean annualized rate of BMD change (95% CI) by number of inflammatory markers in the highest quartile.

	0-1	2	3-6	p-trend
Total hip BMD				
Base model[§]	-0.35 (-0.42, -0.27)	-0.39 (-0.55, -0.23)	-0.51 (-0.65, -0.37)	0.049
Multivariate model[†]	-0.36 (-0.44, -0.28)	-0.38 (-0.54, -0.23)	-0.48 (-0.62, -0.34)	0.16
Femoral neck BMD				
Base model[§]	-0.34 (-0.44, -0.24)	-0.41 (-0.61, -0.20)	-0.48 (-0.66, -0.30)	0.19
Multivariate model[†]	-0.35 (-0.45, -0.25)	-0.39 (-0.60, -0.19)	-0.46 (-0.64, -0.28)	0.30

[§]Base model controlled for age and clinic site
[†]Multivariate models controlled for age, race, BMI, clinic site, smoking, physical activity, health status, diabetes, and congestive heart failure

Inflammatory Markers and BMD Change in Older Men

Disclosures: Kamil Barbour, None.

SU0325

Is the Swedish FRAX Model Appropriate for Immigrants to Sweden?. <u>Helena Johansson</u>*[1], <u>Anders Odén</u>[2], <u>Mattias Lorentzon</u>[3], <u>Eugene McCloskey</u>[4], <u>Nicholas Harvey</u>[5], <u>John Kanis</u>[6], <u>Magnus Karlsson</u>[7], <u>Dan Mellstrom</u>[8]. [1]Centre for Metabolic Bone Diseases, University of Sheffield Medical School, Sweden, [2]Sheffield University, United Kingdom, [3]Geriatric Medicine, Center for Bone Research at the Sahlgrenska Academy, Sweden, [4]University of Sheffield, United Kingdom, [5]MRC Lifecourse Epidemiology Unit, University of Southampton, United Kingdom, [6]University of Sheffield, Belgium, [7]Skåne University Hospital Malmö, Lund University, Sweden, [8]Sahlgrenska University Hospital, Sweden

FRAX tools are country-specific since age-specific fracture and mortality rates vary between countries. This leads, in the case of immigrants, to the question of whether the model for the original or the new country is most appropriate. The aim of this study was, therefore, to compare the incidences of hip fractures in foreign-born and Swedish-born individuals living in Sweden.

We studied the incidence of hip fracture in all men and women aged 25 years or more in Sweden between 1987 and 2002. The population comprised 5 million Swedish-born and 770,000 foreign-born individuals. The effects of age, sex, and time from immigration, on hip fracture were examined by an extension of Poisson regression.

Incident hip fractures occurred in 249,850 Swedish-born and 13,612 foreign-born individuals. The hip fracture incidence rose with age for both groups and was higher for women than men (Hazard Ratio [HR] 1.6, 95% CI 1.6-1.6)) for Swedish-born and for foreign-born (HR 1.3, 95% CI 1.3-1.4). The hip fracture incidence for the Swedish-born cohort was approximately twice that of the foreign-born cohort. For example, at the age of 50 years the annual hip fracture incidence (per 100,000) was 39 (95% CI 38-39) for a Swedish-born woman and 19 (95% CI 18-21) for a foreign-born woman at 5 years after immigration. At the age of 90 years, the respective incidences were 5629 (95% CI 5523-5738) and 3611 (95% CI 3356-3886). The age-specific hip fracture incidence rose slowly with time from immigration for foreign-born men and women (0.6% per annum, 95% CI: 0.5-0.8%) but remained significantly lower than rates for Swedish-born individuals even after 40 years of residence.Our results indicate that hip fracture incidence in Sweden is substantially lower in immigrants than in the population born in Sweden. Although there is a small rise in incidence after immigration, the incidence remains markedly lower than that observed in Swedish-born individuals. Thus, the use of a FRAX model for Sweden will overestimate the risk of fracture for a foreign-born individual living in Sweden.

Disclosures: Helena Johansson, None.

SU0326

Multimorbidity in Men with and without Osteoporosis:Results from a Large US Retrospective Cohort Study. <u>Cynthia O'Malley</u>*[1], <u>Nguyet Tran</u>[1], <u>Carol Zapalowski</u>[2], <u>Nadia Daizadeh</u>[1], <u>Thomas Olenginski</u>[3], <u>Jane Cauley</u>[4]. [1]Amgen Inc., USA, [2]Amgen, USA, [3]Geisinger Health System, USA, [4]University of Pittsburgh Graduate School of Public Health, USA

Introduction: As men age, the risk of osteoporosis (OP) and other morbidities increases. Multimorbidity is recognized as a critical element in treatment and management decisions for OP. As data on multimorbidity incidence in this population are few, this study was designed to inform the interpretation of adverse events in clinical trials of OP therapies.

Methods:Using 2004-2009 electronic health records data from an integrated healthcare system, we identified men aged 55–89 with and without OP. OP was defined by OP diagnosis, physician orders for anti-osteoporosis medicine or a fragility fracture. Men with OP were matched to controls on age and length of follow-up. For each condition, incidence rates (IR) were calculated by dividing the number of men with the condition by the total follow-up person-years (P-Y) at risk. Exact Poisson 95% confidence intervals (CI) were also generated.

Results: In this predominantly white population, 3,600 men with OP and their controls were identified. In these matched groups, the mean (standard deviation, SD) age was 70.9 (9.0) years with an average follow-up time of 2.2 years. Compared to the controls, more men with OP had at least 5 comorbidities (94% of men with OP vs. 71% of controls). Hospitalizations were identified in 49% of men with OP and 29% of controls. Overall, coronary artery disease and hypertension were lower in the OP group (Table 1). Hypertension had the largest IRs difference (IR [95% CI] = 45.9 per 1,000 P-Y [40.7–51.6] in the OP group vs.118.7 [108.5–129.7] in the control group). Cerebrovascular disease was slightly lower in the OP group (29.9 [26.0-34.2] vs. 35.9 [31.6- 40.6]; transient ischemic attacks were lower (9.6 [7.5-12.0] vs. 13.1 [10.7-15.9]) but stroke incidence was slightly higher in the OP group (17.5 [14.7-20.8] vs. 15.8 [13.1-18.9]). Men with OP had a higher incidence of deep vein thrombosis/pulmonary emboli (27.8 [24.2-31.9] vs. 19.1 [16.1-22.5]). IRs for depression/anxiety and migraine/headache were higher in the OP group. Diabetes IR was lower in the OP group. In the OP group, IRs for influenza and pneumonia were twice those in the control group (Table 2). Cystitis, sepsis and pancreatitis IRs were 50% higher in the OP group. Vision and musculoskeletal diagnoses IRs were higher in the OP group than the controls.

Conclusion: Multimorbidity burden in older men with OP is considerable. Effective management of OP requires a clear understanding of the medical complexity of these men.

Table 1. Selected comorbidities in men with and without osteoporosis, U.S. 2004–2009

Disease(s)	OP Group N=3,600		Non-OP Group N=3,600	
	IR per 1,000 Person-years	95% CI	IR per 1,000 Person-years	95% CI
Osteoarthrosis/Spinal osteoarthritis	66.1	59.9, 72.9	47.9	42.6, 53.7
Osteoarthritis/Arthalgia	60.9	54.9, 67.3	45.0	39.9, 50.6
Spinal stenosis	27.8	24.1, 31.9	8.7	6.7, 11.1
Intervertebral disc disorder	32.7	28.6, 37.2	20.5	17.4, 24.1
Sciatica	14.7	12.1, 17.7	7.1	5.4, 9.3
Neuritis/radiculitis	11.1	8.9, 13.8	3.2	2.1, 4.7
Low back pain	62.3	56.2, 68.8	30.4	26.5, 34.7
Musculoskeletal pain	90.9	83.2, 99.0	53.8	48.4, 59.7
Rheumatoid arthritis	5.0	3.5, 6.9	1.3	0.6, 2.3
Psoriasis	3.3	2.2, 4.9	2.0	1.2, 3.3
Headache/Migraine	20.1	17.0, 23.5	9.1	7.1, 11.5
Dementia	12.2	9.9, 14.9	13.5	11.1, 16.4
Syncope/Dizziness/Loss of consciousness	38.2	33.8, 43.0	33.4	29.4, 37.9
Depression/Anxiety	41.7	37.0, 46.8	27.6	23.8, 31.7
Coronary Artery Disease	37.6	33.1, 42.5	49.5	44.2, 55.4
Angina	10.6	8.4, 13.1	10.6	8.5, 13.2
Acute myocardial infarction	11.0	8.8, 13.6	13.1	10.6, 15.9
Arteriosclerosis, cardiovascular disease NOS	18.4	15.5, 21.7	12.4	10.0, 15.1
Coronary atherosclerosis	33.3	29.1, 37.9	45.6	40.7, 51.4
Congestive heart failure	29.4	25.6, 33.6	32.1	28.1, 36.5
Aortic valve disorders	12.7	10.3, 15.5	11.7	9.4, 14.4
Dysrhythmias	50.3	45.1, 55.9	57.8	52.2, 63.9
Atrial fibrillation	28.6	24.9, 32.7	28.3	24.5, 32.4
Hypertension	45.9	40.7, 51.6	118.7	108.5, 129.7
Cerebrovascular disease	29.9	26.0, 34.2	35.9	31.6, 40.6
TIA	9.6	7.5, 12.0	13.1	10.7, 15.9
Stroke	17.5	14.7, 20.8	15.8	13.1, 18.9
Deep vein thrombosis/ Pulmonary embolism	27.8	24.2, 31.9	19.1	16.1, 22.5
COPD/Emphysema/Asthma	29.8	25.8, 34.1	33.3	29.1, 37.9
Diabetes mellitus (Type I or II)	17.2	14.3, 20.5	31.7	27.5, 36.4

IR = incidence rate; CI = confidence interval

Table 1. Selected comorbidities in men with and without osteoporosis, U.S. 2004-2009

Table 2. Selected comorbidities in men with and without osteoporosis, U.S. 2004–2009

Disease(s)	OP Group N=3,600		Non-OP Group N=3,600	
	IR per 1,000 Person-years	95% CI	IR per 1,000 Person-years	95% CI
Influenza	3.7	2.5, 5.3	1.9	1.1, 3.1
Pneumonia	48.6	43.6, 54.0	24.3	21.0, 28.1
Sepsis	12.9	10.5, 15.6	7.6	5.8, 9.8
Cellulitis and abscess, all sites	42.2	37.6, 47.3	22.9	19.6, 26.6
UTI/Cystitis	39.3	34.9, 44.1	24.2	20.8, 28.0
Herpes zoster	15.0	12.3, 18.0	6.3	4.6, 8.3
Pancreatitis (acute/chronic)	3.7	2.5, 5.3	2.4	1.4, 3.7
Anemia	75.5	68.9, 82.5	50.4	45.2, 56.0
GERD/gastritis	52.8	47.3, 58.7	44.5	39.6, 50.0
Urinary incontinence	13.8	11.3, 16.7	7.2	5.4, 9.4
Renal insufficiency/ Chronic kidney disease	39.7	35.2, 44.5	28.5	24.8, 32.7
Liver disease	7.4	5.6, 9.5	10.0	7.9, 12.5
Cholethiasis/Cholecytitis	9.3	7.3, 11.7	10.3	8.2, 12.8
Glaucoma	12.1	9.7, 14.8	7.3	5.5, 9.5
Cataract	43.0	38.2, 48.2	32.0	27.9, 36.5
Macular degeneration	12.5	10.1, 15.3	8.8	6.9, 11.2
Hearing loss	26.0	22.5, 30.0	21.0	17.8, 24.6
Alopecia	0.8	0.3, 1.6	0.3	0.0, 0.9
Rash	10.6	8.4, 13.2	5.2	3.8, 7.1
Eczema	55.8	50.3, 61.7	34.6	30.4, 39.2

IR = incidence rate; CI = confidence interval

Table 2. Selected comorbidities in men with and without osteoporosis, U.S. 2004-2009

SU0327

Nationwide Osteoporosis Awareness and Screening Campaigns in Taiwan. <u>Rong-Sen Yang</u>[1], <u>Ding-Cheng Chan</u>*[2]. [1]National Taiwan University Hospital, Taiwan, [2]National Taiwan University Hospital, Taiwan

Objectives: To report the preparation and implementation of large scale nationwide osteoporosis awareness and screening campaigns in Taiwan.

Material and Methods: In 2013, the Wang Jhan-Yang Public Trust Fund (WJYPTF) donated grant to the Taiwanese Osteoporosis Association (TOA) for conducting series of osteoporosis awareness and screening campaigns for the entire country. A press conference was help before inauguration of the campaign to promote public awareness and to attract potential participants. The campaign was divided into four sub-studies with common core theme on osteoporosis/fracture risk screening, fall preventions, and nutrition assessments. Osteoporosis awareness was assessed in most sub-studies. Participants were screened with varies instruments including FRAX®, One-Minute Osteoporosis Risk Test (OMORT), etc. High risk individuals (definitions varied by studies) were referred to hospitals for further assessments and managements. Four sub-studies were analyzed separately because of heterogeneity of the data and participants.

Results: Overall, 74 courses were provided and 4,808 effective questionnaires were collected. Study one found that more than 70% of participants worried about their bone health but fewer than 50% received bone mineral density (BMD) test. Study two found that roughly 60% were considered high risks from FRAX® but only 1/5 of high risk group were referred for further assessments. Supplementation rate of Vitamin D$_3$ was about 20% and calcium was 35%. Osteoporosis knowledge and awareness significantly improved. Study 3 found that 1/5 of those screened with calcareous ultrasound had low BMD value. Among those referred to hospital with low BMD from ultrasound, 84% had low BMD from DXA. It also found that kyposcoliosis in patients was associated with 3.5 times the risks of having osteoporosis among participants. Study 4 found that 35-70% of participants were screened high risks with the OMORT in Southern Taiwan. More than 40% of men had smoking or drinking history and more than 40% of women had inadequate intake of calcium/dairy products. Participant satisfactions were high across studies.

Conclusions: This nationwide osteoporosis awareness and screening campaigns were flexible to fit local needs and highly appreciated by participants. However, wide variations existed among study protocols. Efforts should be made to collect common variables for comparisons across study sites.

SU0328

Rapid resting heart rate is associated with low bone mineral density in Korean adults: the Dong-gu Study. <u>Hee Nam Kim</u>*[1], <u>Sun-Seog Kweon</u>[2], <u>Jin-Su Choi</u>[2], <u>Jung-Ae Rhee</u>[2], <u>Min-Ho Shin</u>[3]. [1]Center for Creative Biomedical Scientists, Chonnam National University, South Korea, [2]Department of Preventive Medicine, Chonnam National University Medical School, South Korea, [3]Chonnam National University Medical School, South Korea

A previous study reported that rapid resting heart rate (HR) was associated with an increased risk of osteoporotic fracture. However, there is no study on the association between HR and bone mineral density. We aimed to evaluate the association between resting HR and bone mineral density (BMD) in the general population. Our study included a total of 8835 Korean (3504 men and 5331 women) community-dwelling individuals aged 50 years and over enrolled between 2007 and 2010. Bone mineral density (BMD) was measured by dual-energy X-ray absorptiometry at lumbar spine and femoral neck skeletal sites. Resting HR was measured via a 12-lead electrocardiogram with participants in the supine position. Multiple linear regression analysis was used to evaluate the relationship between the quartiles of HR and BMD, adjusting for age, height, weight, smoking, alcohol consumption, physical activity, education, medication of hypertension, medication of diabetes, systolic blood pressure, fasting glucose, total cholesterol, parathyroid hormone, 25-hydroxyvitamin D, high-sensitivity C-reactive protein, and estimated glomerular filtration rate. In the fully adjusted model, femoral neck BMD decreased with increasing quartiles of HR (p for trend <0.001). Compared with subjects in the highest HR quartile, those in the lowest quartile had a significantly lower femoral neck BMD (0.832±0.002 vs. 0.815±0.002, p<0.001). In conclusion, we found that HR was inversely associated with femoral neck BMD but not lumbar spine BMD. Our results suggest that HR is a likely predictor of osteoporosis in middle- and old-aged Korean adults.

Table Association between resting heart rate and bone mineral density

Heart rate (/min)	Lumbar spine		Femoral neck	
	Model 1	Model 2	Model 1	Model 2
Q1 (≤57)	1.060±0.004	1.059±0.004	0.832±0.002	0.832±0.002
Q2 (58-63)	1.055±0.003	1.055±0.003	0.828±0.002	0.828±0.002
Q3 (64-69)	1.056±0.004	1.057±0.004	0.823±0.002	0.823±0.002
Q4 (≥70)	1.049±0.004	1.049±0.004	0.814±0.002	0.815±0.002
p for trend	0.050	0.062	<0.001	<0.001

All values are given as mean (standard error).
Model 1, adjusting for age, sex, weight and height
Model 2, adjusting for age, sex, weight, height, smoking, alcohol consumption, physical activity, medication of hypertension, medication of diabetes, systolic blood pressure, fasting glucose, total cholesterol, log-transformed parathyroid hormone, log-transformed 25-hydroxyvitamin D, log-transformed high-sensitivity C-reactive protein, and estimated glomerular filtration rate.

Table

SU0329

Serum 25-Hydroxivitamin D, Skin Phototype, Sun Exposure and the Metabolic Risk in a Large Sample of Subjects Living in the Tropics. <u>Francisco Bandeira</u>[1], <u>Maria Azevedo</u>[2], <u>Aline Correia</u>[3], <u>Larissa Pimentel</u>*[4], <u>Sirley Vasconcelos</u>[5]. [1]University of Pernambuco, Brazil, [2]endocrinology & diabetes, Brazil, [3]Endocrinology & diabetes unit of agamenon Magalhães Hospital, Brazil, [4], Brazil, [5]Hospital Agamenon Magalhães - Recife, Brazil

Background: Vitamin D deficiency is associated with extraskeletal disorders, including insulin resistance, metabolic syndrome, obesity and type 2 diabetes, but few studies have evaluated this association taking into account sun exposure and skin phototype.

Methods: Cross-sectional study involving 729 adults living in the tropics with the aim of evaluating serum 25OHD levels, skin phototype and the sun index and their association with the metabolic risk.

Results: Out of 729 subjects, 77.8% had hypertension and 74.5% had metabolic syndrome. Mean age: 65.13 ± 9.18 years; sun index: 5.71 ± 5.06; skin phototypes (Fitzpatrick's classification) III and IV in 60.6%, BMI: 27.60 ± 5.34; abdominal circumference: 97.29 ± 12.08cm. Mean serum 25OHD was 25.72 ± 10.91 ng/ml and the percentage of patients with 25OHD below 20ng/ml was 31.% and 25OHD below 30ng/ml was 73.1%. Although there were no significant differences between groups with vitamin D deficiency or sufficiency regarding age, BMI and waist circumference, in the group with 25OHD < 20 and sun index of 4.5 ± 4.08, higher levels of triglycerides and lower HDL-C levels were evidenced, compared to the group with 25OHD ⩾20 and sun index: 6.25 ± 5.36: triglycerides: 179.14 ± 103.53mg/dL vs 161.63 ± 90.23, p = 0.029 and HDL-C 43.48 ± 12.38mg/dL vs 45.94 ± 14.14mg/dl, p = 0.018.The group with 25OHD above P25th (18.7 ng/ml) had higher levels of triglycerides than the group with 25OHD < P75th: 176.63 ± 103.79 vs 157.47 ± 80.49,p=0.049.

Conclusion:We found a high prevalence of vitamin D deficiency, which is associated with higher levels of triglycerides and lower levels of serum HDL-C in

individuals with high rates of sun exposure, irrespective of age, BMI or waist circumference, suggesting a direct association between vitamin D deficiency and the mechanisms involved in the insulin resistance syndrome.

Disclosures: Larissa Pimentel, None.

SU0330

The 10-year probability of major osteoporotic fracture of FRAX is useful as a screening item for osteoporosis patients. A cross sectional study of Japanese women. <u>Shinya Tanaka</u>*[1], <u>Sawako Moriwaki</u>[2], <u>Kiyoshi Tanaka</u>[3], <u>Yoshitaka Ikeda</u>[4], <u>Kazuhiro Uenishi</u>[5], <u>Shunpei Niida</u>[2]. [1]Saitama Medical University, Japan, [2]Biobank, National Center for Geriatrics & Gerontology, Japan, [3]Kyoto Women's University, Japan, [4]Department of Biomolecular Sciences, Faculty of Medicine, Saga University, Japan, [5]Kagawa Nutrition University, Japan

Objective; Osteoporotic fractures give rise to deterioration of ADL and QOL. Although medication of osteoporosis is conclusively effective for preventing fracture, 70% of Japanese patients were left in no treatment. We performed cross-sectional study in aim to test the usefulness of FRAX to screen osteoporosis patients

Materials and Methods; Total 237 women, age from 43- to 75-y-o, living in a local governments in Aichi, Japan, were included in this study. They were performed anthropometry, analyzed bone mineral density from the 2nd to the 4th lumbar spine and left femoral neck, took X-ray of the thoracic and lumbar spine, and calculated the 10-year probability of fracture of FRAX. Osteoporosis was diagnosed in accordance with a 2012 revised version of primary osteoporosis of Japan. Multiple logistic regression analysis was performed using body height, body fat percentage, muscle volume, BMI and the 10-year probability of fracture as explanation factors to clarify predictive factors of osteoporosis. The ability in discriminate subjects with either osteoporosis or non-osteoporosis was made sure by making receiver operating characteristic (ROC) curve and calculation of sensitivity and specificity at adequate cutoff points.

Results: Seventy two in 237 (30.4%) women were diagnosed as osteoporosis. Only the 10-year probability of fracture was selected as predictive factor for osteoporosis (odds ratio: 1.26; 95%CI: 1.16~1.37). The AUC of ROC was 0.777. If cutoff point was set at 7%, sensitivity and specificity were 74.3% and 65.7% respectively. When women aged over 70-y-o were excluded, 62 in 210 (29.5%) women were diagnosed as osteoporosis. The 10-year probability of fracture was selected as predictive factor osteoporosis (odds ratio: 1.34; 95%CI: 1.21~1.49). The AUC of ROC was 0.797. If cutoff point was set at 7%, sensitivity and specificity were 69.4% and 72.3% respectively

Conclusion; FRAX is useful for screening osteoporosis patients in group examinations.

Disclosures: Shinya Tanaka, None.

SU0331

Trabecular Bone Score as an Indicator for Skeletal Deterioration in Diabetes. <u>Jung Hee Kim</u>*[1], <u>Hyung Jin Choi</u>[2], <u>Eu Jeong Ku</u>[3], <u>Kyoung Min Kim</u>[4], <u>Sang Wan Kim</u>[5], <u>Nam H. Cho</u>[6], <u>Chan Soo Shin</u>[1]. [1]Seoul National University College of Medicine, South Korea, [2]Chungbuk National University Hospital, South Korea, [3]Seoul National University College of Medicine, South Korea, [4]Seoul National University Bundang Hospital, South Korea, [5]Seoul National University College of Medicine, Boramae Hospital, South Korea, [6]Ajou University School of Medicine, South Korea

Type 2 diabetic patients have paradoxically high bone mineral density (BMD) but increased fracture risk. Trabecular bone score (TBS) is a novel texture index that evaluates pixel gray-level variations in lumbar spine dual energy X-ray absorptiometry (DXA) images, and is related to bone microarchitecture independent of bone mineral density (BMD). We investigated the ability of lumbar spine TBS to predict skeletal deterioration in diabetic patients including men, and elucidated the underlying mechanism in a community-based Korean cohort.

We included 1,229 men and 1,529 postmenopausal women over 50 years old in the Ansung cohort. Cross-sectional data were collected from subjects participating in an ongoing prospective community-based cohort study from 2009 to 2010. Biochemical parameters, lumbar spine TBS and BMD from DXA image were measured.

The prevalence of diabetes was 325 (26.7%) in men and 370 (24.4%) in women. Lumbar spine TBS was lower in men with diabetes than in non-diabetic men (1.287 $\pm$ 0.005 vs. 1.316 $\pm$ 0.003, p<0.001), whereas lumbar spine BMD was higher in men with diabetes (1.135 $\pm$ 0.010 vs.1.088 $\pm$ 0.006 g/cm^2). Lumbar spine TBS was lower in women with diabetes than in non-diabetic women only in an unadjusted model (1.333 $\pm$ 0.004 vs. 1.353 $\pm$ 0.003). However, women <60 years (n=507) with diabetes had lower TBS than those without diabetes even after adjusted for covariates (p=0.032). Diabetes was not associated with BMD at femur sites in both genders. TBS was negatively correlated with HbA1c, fasting plasma glucose, fasting insulin, and homeostasis model assessment -insulin resistance (HOMA-IR), but not with HOMA-β cell function in both genders. Only serum triglycerides among lipid parameters were negatively associated with TBS in both genders in unadjusted and adjusted models. TBS was also inversely related to hs-CRP, an inflammatory marker, in both genders irrespective of age and BMI

The inverse association between lumbar spine TBS and insulin resistance may make it an indicator for determining skeletal deterioration in diabetic patients who have high BMD.

Disclosures: Jung Hee Kim, None.

SU0332

Unintentional Weight Loss and Fracture: The Global Longitudinal Study of Osteoporosis in Women. <u>Juliet Compston</u>*[1], <u>Allison Wyman</u>[2], <u>Stephen Gehlbach</u>[3], <u>Nelson Watts</u>[4], <u>Ethel Siris</u>[5], <u>Coen Netelenbos</u>[6], <u>Adolfo Diez-Perez</u>[7], <u>Cyrus Cooper</u>[8], <u>Roland Chapurlat</u>[9], <u>Silvano Adami</u>[10], <u>Jonathan Adachi</u>[11], <u>Gordon FitzGerald</u>[12]. [1]University of Cambridge School of Clinical Medicine, United Kingdom, [2]UMASS Medical School, USA, [3]University of Massachusetts, USA, [4]Mercy Health Osteoporosis & Bone Health Services, USA, [5]Columbia University College of Physicians & Surgeons, USA, [6]VU Medical Center, The Netherlands, [7]Autonomous University of Barcelona, Spain, [8]University of Southampton, United Kingdom, [9]E. Herriot Hospital, France, [10]University of Verona, Italy, [11]St. Joseph's Hospital, Canada, [12]UMASS Medical School, USA

Background: The adverse effects of weight loss on bone mineral density in postmenopausal women are well documented, and increased risk of distal forearm and hip fractures has been reported in studies with average follow-up periods of around 6 years after weight loss. The aim of this study was to investigate the effects of unintentional weight loss in postmenopausal women on the incidence of clinical fractures at multiple sites in the year following weight loss.

Methods: GLOW is an observational longitudinal study of non-institutionalized women aged ≥55 years recruited from 723 primary physician practices in 10 countries. Self-administered questionnaires were mailed and data collected included demographics, medical history, fracture occurrence, medications and weight loss of 10 lb (4.5 kg) or more over the preceding year. Cox models treating weight loss as a time-varying covariate were used to predict fracture in the following survey year, adjusting for factors such as age, prior fracture, co-morbidities, and falls that we have previously shown to be associated with the specific fracture.[1]

Results: Unintentional weight loss of of ≥10 lb during the previous 12 months was reported in Year 2 by 3405 (8.0%) of 42,756 and in Year 3 by 3322 (7.7%) of 43,004 women. After adjustment for clinically relevant variables, a significantly increased risk was seen for hip (HR 1.83, 95% CI 1.25–2.69, p<0.01) and spine fracture (HR 1.46, 95% CI 1.02–2.09, p=0.04) in the year following the unintentional weight loss.

Conclusions: Unintentional weight loss in postmenopausal women is associated with increased risk of hip and spine fracture within the year following weight loss. The rapid time course of this increase in risk has not previously been reported and emphasizes the need for prompt fracture risk assessment and appropriate management in women with unintentional bone loss.

Reference

1. FitzGerald G, Boonen S, Compston JE, Pfeilschifter J, LaCroix AZ, Hosmer DW Jr, Hooven FH, Gehlbach SH; GLOW Investigators. Differing risk profiles for individual fracture sites: evidence from the Global Longitudinal Study of Osteoporosis in Women (GLOW). J Bone Miner Res. 2012 Sep;27(9):1907-15.

Disclosures: Juliet Compston, The Alliance for Better Bone Health, 3
This study received funding from: The Alliance for Better Bone Health

SU0333

Use of the Safe Functional Motion-6 test to predict incident osteoporotic fractures at any site. <u>Christopher Recknor</u>*[1], <u>Julie Recknor</u>[2], <u>Norma MacIntyre</u>[3]. [1]United Osteoporosis Center, USA, [2]United Osteoporosis Centers, USA, [3]McMaster University, Canada

Purpose: In the osteoporosis (OP) population, we have shown that physical performance of daily activities, as assessed by the Safe Functional Motion test-6 tasks (SFM-6), predict incident morphometric vertebral fractures after adjusting for known risk factors. The total SFM-6 score is calculated as a percentage of the maximum points possible such that a score of 100 reflects consistent use of 'safe' movement patterns. The current study determines if 'safe' physical functioning, as measured by the SFM-6, is necessary to consider in addition to factors known to influence the risk of any osteoporotic fracture.

Methods: A prospective review of an OP clinic database was conducted to identify men and women with an initial SFM-6, history of prevalent osteoporotic fracture at any site, history of injurious falls, femoral neck bone mineral density (fnBMD), and 1- and 3-y follow-up data (n=1490 and 884, respectively) for medication use and incident osteoporotic fracture. Multiple logistic regressions, adjusted for gender, age, prevalent fracture at any site, injurious fall(s), fnBMD at baseline, and bone sparing medication use, were used to determine whether SFM-6 score predicted incident osteoporotic fracture at follow-up visits.

Results: Table 1 summarizes the characteristics of the sample. Baseline SFM-6 score was a significant independent predictor of incident osteoporotic fracture at any site at 1-y follow-up (adjusted odds ratio (95%CI) = 0.80 (0.71-0.90) for each 10-pt increase in score; p < 0.001) and 3-y follow up (adjusted odds ratio (95%CI) = 0.77 (0.69-0.85) for each 10-pt increase in score; p < 0.0001). Baseline fnBMD and OP

medication use were also significant predictors at 1-y (p = 0.01 and p < 0.05, respectively) and 3-y (p < 0.0001 and p = 0.0001, respectively).

Conclusions: For every 10-pt increase in SFM-6 score (i.e., 'safer' movement patterns), the odds of a future osteoporotic fracture at any site decreases by 20% at 1-y and 23% at 3-y after adjusting for factors known to impact fracture risk. We conclude that, in the OP population, it is necessary to consider the quality of habitual functional movements when assessing the risk of incident fracture at any site.

	1-y Follow Up (n=1490)		3-y Follow Up (n=884)	
	Incident Fracture (n=87)	No Incident Fracture (n=1403)	Incident Fracture (n=186)	No Incident Fracture (n=698)
Female, n (%)	76 (87%)	1261 (90%)	165 (89%)	633 (91%)
Age, y*	70.4 ± 10.5	67.9 ± 10.5	71.0 ± 10.1	66.5 ± 10.0
No injurious falls, n (%)	73 (84%)	1274 (91%)	163 (88%)	644 (92%)
fnBMD, g/cm²*	0.71 ± 0.09	0.75 ± 0.12	0.71 ± 0.11	0.76 ± 0.12
On bone meds, n (%)	65 (75%)	1111 (79%)	156 (84%)	625 (90%)
SFM-6 score*	67.6 ± 21.7	77.4 ± 17.1	60.7 ± 20.7	80.0 ± 15.2

*Mean±SD

Table 1. Participant Characteristics

Disclosures: Christopher Recknor, IONmed Systems, 9

SU0334

BONE HEALTH COLLABORATIVE FRACTURE PREVENTION PLATFORM: *New tools that will enable the rapid implementation of a Fracture Liaison Service program focused on provider performance, quality improvement, care coordination and community.* <u>Debbie Zeldow</u>[1], <u>David Lee</u>*[2]. [1]National Bone Health Alliance, USA, [2]NBHA, USA

Due to the advent of healthcare reform, the healthcare system is shifting from one rooted in episodic care to one that focuses on better managing chronic disease conditions and improving the overall health status of the patient population with value and performance as the two key drivers for success.

The proven Fracture Liaison Service (FLS) model of care provides a unique opportunity to address the nearly 80% post-fracture care gap while helping providers, practices and organizations transition to the new pay-for-performance models and federal mandates that tie payment and reimbursement more closely to the health of their patients.

CECity, National Osteoporosis Foundation (NOF), and the National Bone Health Alliance (NBHA) are partnering with UPMC, MedStar Georgetown University and Creighton Alegent to launch a 15 month, Fracture Liaison Service (FLS) Demonstration Study through funding support by Merck & Co. to:

implement the proven FLS model of post-fracture care coordination in the open system

utilize CECity's cloud-based *MedConcert®* platform that will create a means for sites to automate, benchmark and improve their performance around selected osteoporosis/post-fracture quality measures and patient care

create a registry that can collect and report on each site's data

Through the MedConcert FLS platform, participating providers, practices and organizations will be able to utilize a secure social network to share best practices and connect in meaningful ways to address a variety of critical needs, including pay for performance, population health management, performance improvement, professional certification, patient experience and outcome surveys, care coordination, and much more.

The suite of MedConcert FLS platform tools built with input from the sites includes:

Patient registry

Patient task tracker

Quality measure performance dashboard (which allows for real-time tracking of performance by site or in comparison with other sites and national averages)

Quality improvement tools, resources and interventions to drive performance change

Coordination of care application that allows all members of the care team, regardless of institution, to coordinate patient care and follow-up

Disclosures: David Lee, None.
This study received funding from: Merck

SU0335

Differences in Characteristics of Osteoporosis Patients Treated by Endocrine and Non-Endocrine Specialties. <u>Leyda Callejas</u>*[1], <u>Philip Orlander</u>[2], <u>Kelly Wirfel</u>[3], <u>Nahid Rianon</u>[4]. [1]University of Texas at Health Science Center, USA, [2]Department of Endocrinology Diabetes & Metabolism, University of Texas Health Science Center, USA, [3] Department of Endocrinology Diabetes & Metabolism, University of Texas Health Science Center, USA, [4]UTHealth The University of Texas Medical School at Houston, USA

Inadequate treatment of osteoporosis remains a challenge for physicians managing patients with this chronic disease. There was an increase in number of osteoporosis related office visits by older patients in the past decade, and similar percentages of these visits were made to the primary care physicians and other specialties. Many specialties are treating osteoporosis including OB/GYN, Internal Medicine and its subspecialties, and Orthopedics. A prior study at our institution noted that majority of osteoporosis patients were seen by endocrinologists. As a follow up, we investigated differences in characteristics of osteoporosis patients treated by endocrine and non-endocrine specialties.

A cross-sectional study collected information on demographics, co-morbidities, bone mineral densities in femur neck and spine regions and duration of osteoporosis treatment for 100 men and women 50 years or older who visited UT Health outpatient clinics (Internal Medicine, Endocrinology, Rheumatology, Geriatrics and Family Medicine) for osteoporosis care between January and December of 2012. Electronic chart review identified patients with a diagnosis of osteoporosis or related fractures using ICD 9 codes. A bivariate analysis described patient characteristics by specialty (endocrine vs. non-endocrine). A multivariate regression model determined patient characteristics associated with visit made to Endocrinologist.

Mean (SD) age for all patients was 70 (11) years with majority being women (89%), Caucasians (51%) and seen by endocrinologist (59%). Mean age of patients seen by endocrine was younger than those seen by other specialty (68 vs 73 years, p <0.05). Younger age (beta coefficient, 95% confidence interval = 0.03, 0.01 to 0.05) and longer duration of osteoporosis treatment (-0.06, -0.10 to – 0.02) were significantly (p<0.05) associated with patients being seen by Endocrinologists.

Given their specific training in the field, endocrinologists may be more comfortable managing patients at risk of known side effects from long duration use of available medications for osteoporosis treatment. We also presume that a relative unfamiliarity in managing osteoporosis in younger age group by other specialties may be attributable to younger patients being seen by endocrine specialty. Our results need confirmation with a larger study. Physician characteristics from various specialties treating osteoporosis may also shed more light on our findings.

Disclosures: Leyda Callejas, None.

SU0336

Factors Associated with Non-Receipt of Osteoporosis Therapy Following an Osteoporotic Fracture. <u>Delia Scholes</u>*[1], <u>Do Peterson</u>[2], <u>Akhila Balasubramanian</u>[3], <u>Cynthia O'Malley</u>[4], <u>Jane Grafton</u>[2], <u>Jackie Saint-Johnson</u>[2], <u>Denise Boudreau</u>[2]. [1]Group Health CooperativeGroup Health Research Institute, USA, [2]Group Health Research Institute, USA, [3]Amgen Inc., USA, [4]Amgen, Inc., USA

Purpose: The two- to three-fold increased risk of future fracture after an initial osteoporotic fracture offers an important intervention opportunity. However, rates of post-fracture osteoporosis (OP) care are low. We evaluated factors associated with non-receipt of post-fracture OP pharmacotherapy in a population-based sample of female health plan enrollees.

Methods: The study population consisted of women aged >55 years who were diagnosed with an osteoporotic fracture between 2005 and 2012 and who were enrollees of Group Health Cooperative (GH), a Pacific Northwest health plan. Patient characteristics, diagnoses, medications, and healthcare utilization for the 12 months prior to the index fracture were accessed from GH administrative databases. Their associations with non-receipt of pharmacotherapy in the 6 months following the index fracture were assessed using Poisson regression to estimate age-adjusted relative risks (RR) and 95% confidence intervals (CI).

Results: Of 7,186 women diagnosed with osteoporotic fractures (mean age 79 years; 84% white), 20% received post-facture OP pharmacotherapy within 6 months. Non-receipt of pharmacotherapy increased over calendar time (RR=1.07, CI 1.04-1.10 for 2011-2012 vs 2005-2008)(Table). Women who had already received OP pharmacotherapy in the prior 12 months had significantly lower risk of non-receipt of post-fracture pharmacotherapy (RR=0.34, CI 0.32-0.38), as did those with more than one primary care visit (RR 0.93, CI 0.90-0.97 for 5-10 visits) and those with a pharmacy benefit (RR=0.92, CI 0.90-0.95) in the prior 12 months. Risks of non-receipt of pharmacotherapy also were lower with previous DXA testing, use of glucocorticoids or calcitonin, and with cancer, rheumatoid arthritis or OP diagnoses. Risks of non-receipt of care were higher for index fractures of the humerus and forearm relative to other sites, younger age, Black race, higher BMI, and prior diabetes or dementia diagnoses.

Conclusions: Women who received OP therapy or who had DXA in the 12 months prior to index fracture were far more likely to receive post-fracture therapy, as were other at-risk groups. However, the low proportion of women, overall, who received post-fracture pharmacotherapy points to further opportunities for future fracture prevention. Results also suggest that receipt of post-fracture therapy can be enhanced by continuity of primary care and by provision of a pharmacy benefit.

Characteristic in the 12 Months prior to index fracture or at fracture index date		Relative Risk[1]	95% CI
Year of Index Fracture	2005 – 2008	(referent)	
	2009 – 2010	1.07	1.04, 1.10
	2011 – 2012	1.07	1.04, 1.10
Index Fracture Site	Hip	(ref)	
	Distal Radius/Ulna	1.03	1.00, 1.07
	Spine	0.86	0.83, 0.90
	Humerus	1.09	1.05, 1.13
Age at Index Date (Years)	55 – 64	1.08	1.05, 1.12
	65 – 74	1.01	0.98, 1.04
	75 – 84	0.95	0.92, 0.98
	85+	(ref)	
Race/Ethnicity	Hispanic Ethnicity	1.04	0.97, 1.11
	Non-Hispanic White, Caucasian	(ref)	
	Asian	0.84	0.76, 0.98
	Native American	1.01	0.91, 1.13
	Black, African Am.	1.15	1.07, 1.23
	Hawaiian, Pac. Isl.	0.94	0.62, 1.40
	Unknown Race	1.04	1.01, 1.08
BMI	Underweight, <18.5	1.00	0.94, 1.07
	Normal, 18.5 - <25.0	(ref)	
	Overweight, 25 - <30	1.05	1.02, 1.09
	Obese, 30+	1.13	1.10, 1.17
	Unknown	1.09	1.06, 1.13
Prior Diagnoses	Osteoporosis	0.71	0.68, 0.73
	Diabetes	1.09	1.06, 1.12
	Dementia or AD	1.08	1.05, 1.12
	Rheumatoid Arthritis	0.98	0.97, 0.99
	Cancer, Metastases	0.93	0.88, 0.99
Prior Medications	Systemic Glucocorticoids	0.93	0.91, 0.96
	Calcitonin	0.80	0.73, 0.87
	Osteoporosis Pharmacotherapy	0.34	0.32, 0.38
Prior DXA Testing	Yes	0.78	0.74, 0.83
Prior Primary Care Visits	None	(ref)	
	1-4	0.97	0.94, 1.01
	5-10	0.93	0.90, 0.97
	11+	0.92	0.88, 0.96
Pharmacy/Co-Pay Coverage	Yes	0.92	0.90, 0.95
Treatment Setting at Fracture Index Date	Inpatient	0.95	0.93, 0.98

BMI = body mass index AD = Alzheimer's disease DXA = dual-energy x-ray absorptiometry
[1] All risk estimates, except for age, are adjusted for age.

Table: Factors Associated with Non-Receipt of Post-Fracture Osteoporosis Pharmacotherapy

SU0337

Relationship of Spine Fracture Burden to Reduced Lung Volume in Postmenopausal Women With Osteoporosis. John Krege*[1], David Kendler[2], Kelly Krohn[3], Harry Genant[4], Pierre-Yves Berclaz[5], Corina Loghin[5]. [1]Eli Lilly & Company, USA, [2]Associate Professor University of British Columbia, Canada, [3]Lilly USA, LLC, USA, [4]UCSF/Synarc, USA, [5]Eli Lilly & Company, USA

Purpose: Pulmonary function may be compromised in patients with osteoporosis due to the presence of vertebral fractures. The aim of this study was to assess the relationship between burden of vertebral fractures and pulmonary function in elderly women with osteoporosis. Methods: This was a single-visit study measuring pulmonary function via spirometry in women (70 to 91 years of age) with osteoporosis and at least 1 moderate or severe vertebral fracture. Spinal deformity index (SDI) score was calculated as the sum of the semi-quantitative (SQ) scores of T4 to L4 from lateral spine radiographs (no fracture = 0, mild = 1, moderate = 2, severe = 3). Arm span-height was assessed as a measure of height loss, and current back pain was evaluated by a 100-point visual analog scale (VAS). Results: Forty-one women were enrolled in the study. The mean age was 78 years, arm span 161 cm, height 157 cm, weight 59 kg, and SDI 7 (range 2 to 22). SDI positively correlated with arm span-height (r=0.438, P=0.004). Height decreased and arm span-height increased each by about 0.5 cm per unit increase in SDI. SDI negatively correlated with forced inspiratory vital capacity (r=-0.41, P=0.008) and inspiratory time (r=-0.407, P=0.008). Forced inspiratory vital capacity and inspiratory time decreased by 1.6% and 2.4%, respectively, for each unit increase in SDI. SDI did not significantly correlate with forced inspiratory flow at 50% of forced inspiratory volume, forced inspiratory volume in 1 second, or peak inspiratory flow rate (all P-values >0.5). SDI also was not correlated with current back pain VAS score (P=0.403). Conclusion: Increased spine fracture burden was associated with decreased inspiratory lung volume, decreased duration of inspiration, and height loss. However, increased spine fracture burden was not associated with a change in inspiratory flow. These findings are consistent with increasing spine fracture burden reducing the lung volume. This study highlights the clinical relevance of vertebral fracture burden and quantifies its impact on lung volume.

SU0338

Rural distribution and scope of a centralized, electronic consult program for patients with recent fracture. Richard Lee*[1], Megan Pearson[2], Kenneth Lyles[3], Patricia Jenkins[2], Cathleen Colon-Emeric[4]. [1]Duke University, USA, [2]Durham VAMC, USA, [3]Duke University Medical Center, USA, [4]Duke University Medical Center, USA

Background: While Fracture Liaison Services have been shown to significantly improve osteoporosis treatment, they require accurate and timely identification of recent fracture patients by the specialty team, which may be less feasible for people living in rural areas. We sought to determine whether a regional post-fracture E-consult program through a single, centralized Veterans Affairs Medical Center (VAMC) was adequately identifying rural and highly rural patients. Over 43 percent of the Veterans in this region live in rural or highly rural areas.
Objective: To evaluate the geographic distribution of the patients who received an E-consult and to assess if the E-consult program preferentially served urban patients.
Method: The E-consult program identified Veterans with potential osteoporotic fractures from inpatient and outpatient encounter data, based on ICD9 diagnosis codes (800-829) from the central data warehouse. The medical record of an eligible patient was reviewed by a bone health specialist, and an E-consult note was sent to the patient's primary care provider that specified recommendations for further management. Patients were identified as living in a rural or highly rural area if their ZIP code was not in a US Census Bureau-defined urban area, population density greater than 1000-persons per square mile.
Results: From Oct 2013 through March 2014, 176 E-consults were completed. Of those, 88 (50%) were for patients residing in a rural or highly rural area. Fifty-four (61%) of these resided outside of the central VAMC's catchment area. There was no statistical difference between the number of rural and highly rural E-consults completed and the number expected (P = 0.17).
Conclusion: A centralized, E-consult program can impartially provide specialty bone health services to patients residing in rural and highly rural areas.

SU0339

Trends in Glucocorticoid-Induced Osteoporosis Management Among Seniors in Ontario, 1996-2012. Jordan Albaum*[1], Linda Levesque[2], Andrea Gershon[3], Guoyuan Liu[2], Yan Yun Liu[1], Suzanne Cadarette[4]. [1]University of Toronto, Canada, [2]Queen's University, Canada, [3]Sunnybrook Health Sciences Centre, Canada, [4]University of Toronto, Canada

Glucocorticoid (GC) therapy is the most common cause of secondary osteoporosis. Since 1996, North American osteoporosis practice guidelines recommend that all patients starting chronic oral GC therapy receive bone mineral density (BMD) testing and/or osteoporosis treatment. We sought to examine trends in GC-induced osteoporosis management over time. We identified all community-dwelling chronic oral GC users aged 66 years or older in Ontario using healthcare utilization data from 1996 to 2012. Chronic oral GC use was defined as ≥ 2 oral GC prescriptions dispensed and ≥ 450 mg prednisone equivalent over a 6-month (180-day) period. Osteoporosis management by BMD test (sensitivity=98%, 95%CI=95.9-99.1; specificity=93%, 95%CI=89.9-95.4) and/or osteoporosis treatment within 6 months of starting chronic oral GC therapy was examined by sex and year. Results were summarized using descriptive statistics. We identified 72,099 male (mean age=74.6, SD=6.3) and 95,975 female (mean age 75.1, SD=6.6) patients on chronic oral GC therapy. Over three quarters of patients (n=131,602) received ≥ 675 mg, and two thirds (n=109,888) received ≥ 900 mg within the 6-month window. Overall, 15% (7% BMD, 12% treatment) of men and 36% (13% BMD, 30% treatment) of women on chronic GC therapy received osteoporosis management. GC-induced osteoporosis management increased steadily from 2% (men) and 10% (women) in 1996, to a high of 23% (men) and 48% (women) in 2007, with a gradual decline to 17% (men) and 38% (women) in 2012. Rates of GC-induced osteoporosis management improved significantly over time in both sexes yet remain low, particularly among men. This represents a missed opportunity for fracture prevention among patients requiring prolonged GC therapy. Targeted interventions are needed to reduce the burden of fracture-related morbidity associated with GC-induced osteoporosis.

SU0340

An Early Development Budget Impact Model for the Use of Melatonin in the Treatment and Prevention of Osteoporosis. <u>Corry Bondi</u>*[1], <u>Rahul Khairnar</u>[1], <u>Khalid Kamal</u>[1], Paula Witt-Enderby[2]. [1]Duquesne University Clinical, Social & Administrative Sciences, USA, [2]Duquesne University,School of Pharmacy, USA

The National Osteoporosis Foundation estimates approximately 9 million adults with and an additional 43 million adults at-risk for developing osteoporosis (OP). By 2030, 68 million adults (>50 years), will either have osteoporosis or be at-risk. The economic impact of OP is estimated to be $25.3 billion by 2025, which includes direct medical and non-medical expenses as well as indirect expenses like loss of work productivity. This OP burden underscores the importance of developing novel OP therapies, like melatonin, that have a high safety profile and that are well tolerated. Many studies demonstrate an association between melatonin and bone where a decline in circulating melatonin levels negatively impacts bone (e.g., shift work) while supplementation with melatonin improves bone marker turnover in perimenopausal women (Melatonin Osteoporosis Prevention Study, MOPS; NCT01152580). Given the chronic nature of osteoporosis coupled with high treatment costs, economic evaluation of melatonin over existing treatments could be very useful for those who manage and plan for health-care budgets. Budget impact models (BIM) provide necessary and sometimes unavailable evidence to understand both costs and outcomes of various treatment scenarios that may involve providing a new therapy. The goal was to determine the budgetary impact of addition of melatonin to treat and prevent OP in the US population from a payer perspective. A 1-year BIM with a hypothetical plan population of one million was utilized for the analysis for osteoporosis and osteopenia. Drug prices (WAC) for melatonin and comparators were taken from the Red Book; market share and prevalence data were taken from the literature. Univariate sensitivity analysis was integrated in the model and uncertainty in market share and drug prices was assessed. All costs were adjusted to 2013 US dollars. The model predicted 37,000 members with osteoporosis while 133,760 members with osteopenia. Market share for comparators in osteopenia were ibandronate (24.4%), alendronate (25.2%), zolendronate (16.2%), teriperatide (23.2%) and risedronate (10.96%) and for osteoporosis were ibandronate (51.3%) and teriperatide (48.7%). In osteopenia, the introduction of melatonin produced a per member per month (PMPM) change of -$2.92 suggesting major cost savings and in osteoporosis, a PMPM change of -$0.06 was estimated. As newer data on efficacy, costs and utilization on treatments gets available, the BIM can be updated to reflect the changes and estimate the economic impact of new treatments.

Disclosures: Corry Bondi, None.

SU0341

Reduction of fracture rate for treatment based on quality metrics in glucocorticoid-induced osteoporosis (GIO). <u>Robert Overman</u>*[1], <u>Bradley Layton</u>[2], <u>Joel Farley</u>[3], <u>Alan Brookhart</u>[3], Chad Deal[4], Margaret Gourlay[1]. [1]University of North Carolina, USA, [2]University of North Carolina, USA, [3]University of North Carolina, USA, [4]Cleveland Clinic Foundation, USA

Quality metrics have been proposed for glucocorticoid-induced osteoporosis (GIO) including receipt of anti-osteoporosis medications (AOM) following initiation of oral glucocorticoids (GC). However, fracture has not been a primary endpoint in any GIO trial. We created a cohort of new-users of GC based on first observable GC fill (index date) with a washout period (365 days) and having a prednisone equivalent daily dose of ≥10mg and used chronically (≥90 days). The cohort was comprised of 7,887 women from the Truven Health Analytics' MarketScan® Commercial and Medicare Supplemental databases (2000-2012) ≥50 years of age at index date. Patients were continuously enrolled in their health plan and had no fracture, GC, or AOM (bisphosphonate, denosumab, teriparatide) fills during the washout period. Continuous health plan enrollment and a GC fill for ≥90 days post-index date were also required. The quality measure (QM) period was 90 days post-index fill and receipt of QM was based on an AOM fill during this period or within 14 days before GC fill. Fractures included in the composite outcome were hip, humerus, pelvis, spine, and wrist. Covariates measured during washout: diseases and drugs associated with osteoporosis, Charlson comorbidity index, age, region, fracture, and healthcare utilization. Measured during both washout and QM period: DXA scan and diagnosis of osteoporosis. To reduce confounding, we created a propensity score of the likelihood of receipt of a QM using the measured covariates which was converted into stabilized IPTW (inverse probability of treatment weights), and the weights were applied to statistical outcome models. Cox proportional hazards models were used to estimate hazard ratios (HR) with 95% confidence intervals (95% CI) using the IPTW weights. Follow-up began at the end of the QM period (90 days post-index), and patients were followed for a maximum of 3 years until fracture, end of continuous enrollment, or AOM use after QM window. After weighting, mean age was 66.7 (95% CI 66.5, 67.0), 3.9% had osteoporosis, and 11.6% received AOM during the QM period. Mean days follow-up for QM was 639 days, and non-QM was 541 days. Fractures occurred in 3.2% of QM patients and 4.0% of non-QM patients. The weighted fracture HR was 0.67 (95% CI 0.46, 0.98). In women 50 and older, receipt of AOM within 90 days of chronic glucocorticoid initiation is associated with a 33% reduction in fracture risk by 3 years.

Table 1. Fracture Hazard Ratios (HR) for initiation of an anti-osteoporosis medication within 90 days of chronic high-dose oral glucocorticoids in women ≥50 years of age

Hazard Ratio (HR) Method	HR (95% Confidence Interval [CI])
Unadjusted	0.79 (95% CI 0.56, 1.11)
Adjusted using measured covariates	0.77 (95% CI 0.54, 1.12)
IPTW weighted	0.67 (95% CI 0.46, 0.98)

Adjusted HR and Weighted HR include diseases and drugs associated with osteoporosis, DXA scan use, Charlson comorbidity index, age, region, fracture, and healthcare utilization.

Table 1

Disclosures: Robert Overman, None.

SU0342

The Effect of Dietary Calcium versus Supplemental Calcium on Vascular and Bone Markers in Healthy Postmenopausal Women: Results of A 12-Month Pilot Clinical Trial. <u>Angel Ong</u>*[1], <u>Hope Weiler</u>[2], <u>Michelle Wall</u>[3], <u>Rouba Haddad</u>[4], <u>Emily Rose Hamilton-Leavitt</u>[4], <u>Stella Daskalopoulou</u>[5], <u>David Goltzman</u>[6], Suzanne Morin[6]. [1]McGill University Health Centre Research Institute, Canada, [2]McGill University, USA, [3]McGill University Health Centre Research Institute, Canada, [4]School of Dietetics & Human Nutrition, McGill University, Canada, [5]McGill University, Canada, [6]McGill University, Canada

Purpose: Calcium supplements are reported to be associated with increased rates of cardiovascular events. Whether dietary calcium has similar effects to calcium from supplements on vascular and bone markers is unknown. This 12-month trial was piloted to determine the feasibility of an RCT and to estimate the effect of dietary calcium versus supplemental calcium on selected vascular and bone markers in postmenopausal women.

Methods: Healthy postmenopausal women ≥ 55 years not taking calcium or vitamin D supplements were randomized to: a dietary intervention (DI) of 1200 mg calcium from food + 400 IU vitamin D supplement, or a supplemental intervention (SI) with 750 mg calcium from $CaCO_3$ supplements (and 450 mg calcium from food) + 800 IU vitamin D supplement daily. Correlations were assessed between baseline dietary intakes of calcium and vitamin D and arterial stiffness measured as carotid-femoral pulse wave velocity (cfPWV). Using repeated measures ANOVA, between-group differences in cfPWV (primary outcome), BP, anthropometric measures, vascular and bone biomarkers were examined at 0, 6, and 12 months. Dietary calcium and vitamin D intakes and compliance with supplements were determined every month.

Results: Thirteen participants were randomized (mean age 63 [SD 7] years; BMI 25 [SD 3] kg/m²; waist circumference 81 [SD 8] cm; systolic BP 111 [SD 5] mmHg; diastolic BP 71 [SD 10] mmHg). At baseline, no associations were found between calcium and vitamin D intakes and cfPWV. Four participants were lost to follow-up early in the study. Results of the remaining 9 participants are presented. There were no significant between-group differences in cfPWV, BP, anthropometric measures, vascular or bone markers at any time points (final data in Table 1). Source of calcium and vitamin D did not significantly affect cfPWV nor 25(OH) vitamin D and PTH concentrations over the study period (Figure 1). Higher dietary calcium and vitamin D intakes were observed in the DI group as compared to the SI group throughout the trial and each group met their target intake. Overall compliance with supplements was 93%.

Conclusion: Although the sample size was small, we found no differential effect of dietary calcium intake as compared to supplemental calcium intake on vascular or bone markers. Subsequent to these findings and the high level of compliance of the participants with the interventions, a randomized control trial is currently ongoing (*ClinicalTrials.gov* ID: NCT01731340).

Table 1. Anthropometric measures, vascular and bone markers measured at 12-months in each intervention group

	Dietary intervention (n=4)	Supplemental intervention (n=5)	P Value
Energy intake (kcal)	1856 (1595-2319)	1862 (1537-3082)	0.605
BMI (kg/m²)	24 (3)	26 (3)	0.357
Waist circumference (cm)	80 (9)	86 (11)	0.379
Systolic BP (mmHg)	104 (9)	125 (15)	0.054
Diastolic BP (mmHg)	70 (6)	76 (14)	0.464
cfPWV (m/s)	7.3 (1.1)	8.7 (1.8)	0.239
Cholesterol (mmol/L)	6.10 (0.84)	5.78 (0.51)	0.501
Triglycerides (mmol/L)	0.80 (0.38)	1.22 (0.87)	0.403
HDL-cholesterol (mmol/L)	1.84 (0.41)	1.98 (0.81)	0.763
LDL-cholesterol (mmol/L)	3.90 (1.04)	3.25 (0.61)	0.277
Total/HDL ratio	3.53 (1.41)	3.34 (1.27)	0.842
Apo A1 (g/L)	1.59 (0.28)	1.76 (0.33)	0.447
Apo B (g/L)	1.20 (0.32)	1.07 (0.26)	0.551
Apo B/Apo A1 ratio	0.78 (0.31)	0.62 (0.25)	0.431
hsCRP (mg/L)	0.38 (0.24)	0.76 (0.49)	0.194
Ionized calcium (mmol/L)	1.25 (0.03)	1.26 (0.03)	0.647
25(OH)D (nmol/L)	79.1 (25.4)	63.6 (13.9)	0.278
PTH (pmol/L)	2.84 (0.29)	2.89 (0.72)	0.903
Phosphate (mmol/L)	1.29 (0.17)	1.27 (0.11)	0.855
Urinary calcium (mmol/L)	1.2 (0.4)	2.9 (2.4)	0.206
Urinary calcium/creatinine ratio	0.2 (0.05)	0.2 (0.2)	0.497

Data are presented as mean (SD) or median (IQR), as indicated.

Table 1. Anthropometric measures, vascular and bone markers
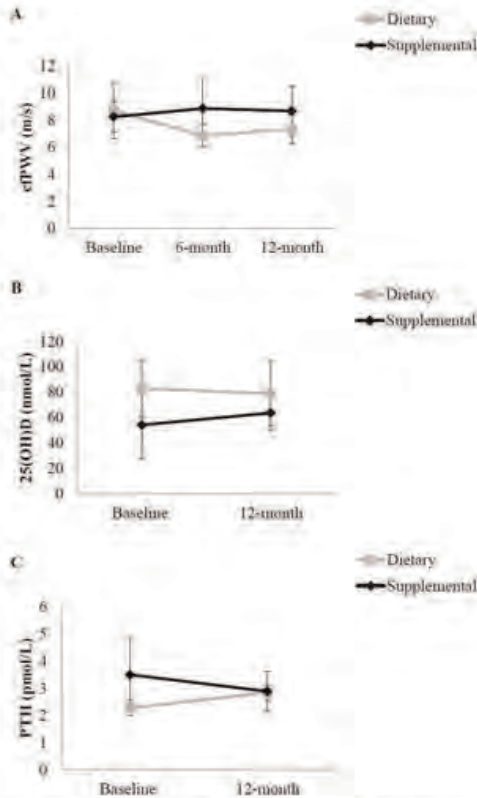

Figure 1. Change in cfPWV (A), 25(OH) vitamin D (B) and PTH (C) in supplemental and dietary intervention groups. Data are presented as mean ± SD.

Figure 1. Change in cfPWV, 25(OH) vitamin D and PTH in supplemental and dietary interventions

Disclosures: Angel Ong, None.

SU0343

Associations between serum parathyroid hormone concentrations, bone turnover markers and bone traits in Caucasian pre-menopausal females and males with fairly high dietary calcium intake. Suvi Itkonen*[1], Elisa Saarnio[2], Virpi Kemi[3], Heini Karp[3], Minna Pekkinen[4], Juha Risteli[5], Marja-Kaisa Koivula[6], Harri Sievanen[7], Christel Lamberg-Allardt[1]. [1]University of Helsinki, Finland, [2]University of Helsinki, Finland, [3]Calcium Research Unit, Department of Food & Environmental Sciences, University of Helsinki, Finland, [4]Folkhälsan Institute of Genetics, University of Helsinki, Finland, [5]University of Oulu, Finland, [6]Northern Finland Laboratory Centre Nordlab & Department of Clinical Chemistry, Institute of Diagnostics, University of Oulu, Finland, [7]The UKK Institute for Health Promotion Research, Finland

Dietary phosphorus (P) intake increases serum parathyroid hormone (S-PTH) concentrations acutely, thus, S-PTH can be considered as a surrogate marker of short-term dietary phosphorus intake. Earlier studies have shown that dietary P intake has negative effects on bone metabolism, and in some studies high P intake has also been associated with lower bone mineral density (BMD).

The aim of the study was to investigate the associations between S-PTH levels, certain bone turnover markers, and bone traits measured by peripheral quantitative tomography (pQCT) among 37-47-year old premenopausal females and males (n=550). Bone traits were measured in distal tibia and radius, as well in radial and tibial shaft. Serum PTH, intact pro-collagen type I amino-terminal propeptide (S-iPINP), and collagen type 1 cross-linked C-terminal telopeptide (S-CTX) were determined. Background and nutrient intake data were collected by a questionnaire. The data was analyzed by regression models, and the final model included S-PTH, weight, height, calcium (Ca) intake, smoking, physical activity, and serum 25-hydroxy vitamin D concentrations (among females also contraceptive use). Among females, S-PTH was negatively associated with bone mineral content and cortical bone area in distal radius (p=0.015, p=0.012) and distal tibia (p=0.010, p=0.050). In the model including height, age, and weight, S-PTH was negatively associated with total area of distal tibia (p=0.042), but the significance disappeared when other confounding factors were introduced to the model. Further, S-PTH was associated with increased S-CTX concentrations (p=0.005), indicating increased bone resorption. No results were found between S-PTH and bone formation marker S-iPINP, or S-PTH and BMD (p for all >0.05). Among males, no associations between S-PTH and bone turnover markers or pQCT bone traits were found (p for all >0.05).

Notable is that Ca intake among our study subjects was fairly high (approximately 1200 mg/d among both sexes), which may hide the negative associations between P-related S-PTH and the measured bone traits. Among other factors, in this study height and weight were the most important determinants of bone traits. To conclude, these results indicate that high Ca intake may protect bone from the detrimental effects of high P intake and accelerated bone degradation indicated by increased S-PTH concentrations, but the results may be different in a population with lower Ca intake or post-menopausal females.

Disclosures: Suvi Itkonen, None.

SU0344

GPR40 limits bone loss induced by ovariectomy upon high fat diet. Claire Philippe*. INRA, France

In the current context of longer life expectancy, the prevalence of age-related diseases such as osteoporosis is increasingly important. The cost of treatment of these diseases is a major public health problem and the implementation of strategies tailored nutritional prevention appears to be an excellent alternative to conventional treatments. However, the study of biological activities of nutrients is too marginal for some tissues and certain types of molecules; this is particularly the case of bone and lipids, especially fatty acids. They are however capable of modulating the fate of bone either indirectly or directly by systemic mechanisms at the bone cell.

Descriptions of the direct effects of fatty acids at the cellular level by activating specific receptors are becoming increasingly common in the literature. Recently, the membrane receptor GPR40 (G Protein Coupled Receptor 40) was highlighted for its interaction with the free long-chain fatty acids as well as the existence of an osteoporotic phenotype in mice invalidated for GPR40.We formerly demonstrated that GPR40 prevents from osteoporosis establishment using synthetic agonist. Here, we questioned whether stimulation of GPR40 by fatty acids, the natural ligands for GPR40, may parallel with its described beneficial effects on bone. In this study we demonstrated for the first time that GPR40 limits bone loss induced by ovariectomy upon high fat diet. Taken together, our results demonstrate that GPR40 mediates beneficial effects of high fat diets mainly by targeting the bone cell coupling and subsequent osteoclastic bone resorption.

Disclosures: Claire Philippe, None.

SU0345

A New Paradigm for Vitamin D Supplementation: Treat to Target Using a Vitamin D Panel. <u>Neil Binkley</u>*[1], <u>Ravinder Singh</u>[2], <u>Joan Lappe</u>[3], <u>Diane Krueger</u>[1], <u>Marc Drezner</u>[4], <u>Robert Blank</u>[5]. [1]University of Wisconsin, Madison, USA, [2]Mayo Clinic, USA, [3]Creighton University Osteoporosis Research Center, USA, [4]University of Wisconsin, USA, [5]Medical College of Wisconsin, USA

Variability in 25(OH)D response to vitamin D supplementation is widely recognized. It is possible that this variability reflects, in part, differences in vitamin D absorption and/or degradation. However, all expert group recommendations, and most randomized prospective studies, endorse a single fixed dose for all individuals, an approach that does not assure attainment of any pre-defined, "target" 25(OH)D level. To improve the ability to individualize vitamin D supplementation, we measured serum 25(OH)D, cholecalciferol (D_3), and 24, 25(OH)$_2$D levels in women prior to and following vitamin D administration, to determine if baseline concentrations of these compounds explain the 25(OH)D increment following supplementation. In 91 postmenopausal women who received 2300 or 2500 IU of daily D_3 supplementation for 4-6 months, a "vitamin D panel" consisting of serum D_3, 25(OH)D and 24, 25(OH)$_2$D was measured in a single analytical run at baseline and study conclusion. At study entry, subjects had a 25(OH)D level that ranged from 10-30 ng/mL. Following supplementation, 25(OH)D levels ranged from 12-62 ng/mL. From these data, we developed a multiple linear regression model for post-treatment 25(OH)D with the equation: final 25(OH)D = 8.3 + (1.05* initial 25(OH)D) – (7.7* initial 24,25(OH)$_2$D) + (0.53* final D_3) + (4.2* final 24,25(OH)$_2$D). This model has an adjusted R^2 = 0.55, thus accounting for approximately half of the observed variance in the final 25(OH)D level. Neither dose nor duration of treatment was associated with the increment in 25(OH)D. Initial serum D_3 level could not be included in this model because its distribution did not satisfy the assumptions of normality and equal variance, even after transformation. The contributions of circulating D_3 and 24,25(OH)$_2$D to the regression model can be understood heuristically as representing the contributions of intestinal absorption and clearance, respectively. Incorporation of vitamin D panel data from larger studies of supplementation into the regression model may allow the development of approaches to determine the dose of vitamin D supplement, based on initial D_3, 25(OH)D and 24, 25(OH)$_2$D levels. This approach may allow efficient "treat to 25(OH)D target" strategies for use in both clinical practice and, importantly, in prospective randomized studies. Vitamin D dosing based on these data needs to be tested prospectively.

Disclosures: Neil Binkley, None.

SU0346

Association Between Serum Levels of Vitamin D and Osteocalcin In Older Patients with Osteoporosis. <u>Matthew Hnatow</u>*[1], <u>Jonash Loh</u>[2], <u>Catherine Ambrose</u>[3], <u>Nahid Rianon</u>[4]. [1]Univeristy of Texas Health Science Center at Houston - Medical School, USA, [2]UT Medical School - Houston, USA, [3]University of Texas Health Science Center at Houston, USA, [4]UTHealth The University of Texas Medical School at Houston, USA

There is a need for better understanding of bone turnover markers (BTM) and their relationship with factors affecting bone metabolism including vitamin D. Deficiency of vitamin D, an essential nutrient for bone health, is prevalent in older patients with osteoporosis and the relationship between vitamin D and BTM, e.g., osteocalcin (OC) remains inconclusive. We investigated associations between serum levels of OC and 25-hydroxy-vitamin D (25-HD) in older ambulatory women evaluated for osteoporosis.

Chart review identified 202 women (≥50 years) evaluated between August 2010 and May 2013 (81 excluded from analysis for not having 25-HD available). Clinical parameters obtained as part of our standard osteoporosis workup included age, ethnicity, height, weight, use of calcium and vitamin D supplements and use of bone promoting medications (bonemed), serum thyroid stimulating hormone (TSH), serum creatinine, femoral neck and spine (L1-L4) bone mineral density (BMD), and OC. Bivariate analysis described patient characteristics by low 25-HD (<30 ng/mL, N = 73) or normal 25-HD (≥30 ng/mL, N=48). A regression model adjusting for all the above variables determined associations between 25-HD and OC.

The mean (SD) age of the women was 79 (9) years. There were no significant differences between the two groups in age, height, weight, co-morbidities, femoral and spinal BMD, alcohol or tobacco use and bonemed. There was a significant difference in serum OC between the groups (p=0.039) with mean (SD) of 23.64 (10.12) ng/ml for the low and 17.58 (7.98) ng/ml for the normal serum 25-HD groups. Significant differences, seen in bivariate model, in serum 25-HD (<0.05) between patients from various racial/ethnic backgrounds and between patients using or not using calcium and vitamin D supplements did not remain significant in the regression model. An inverse relationship remained significant between serum OC and serum 25-HD in the regression model after adjusting for all variables mentioned above (beta coefficient -0.36, 95% confidence interval 0.72 to -0.01).

We report associations between higher OC (indicating high bone turnover) and lower serum 25-HD in our study patients. While high bone turnover may indicate high risk of fracture in older patients, lower serum 25-HD may also indicate sub-optimal bone health maintenance contributing to their higher risk of fracture. Future studies are needed to determine if vitamin D supplementation can significantly affect OC levels.

Disclosures: Matthew Hnatow, None.

SU0347

BMD changes in accordance with serum vitamin D changes in postmenopausal Korean women. <u>Duck Joo Lee</u>[1], <u>Sanghyun Je</u>*[2], <u>Beomtek Kim</u>[2]. [1]Ajou University School of Medicine, South Korea, [2]Ajou University Hospital, South Korea

Serum vitamin D has been considered to play one of the major roles in bone health. Postmenopausal women whose initial serum vitamin D level was measured and grouped to evaluated the how one year serum vitamin D change would influence their one year bone density in various sites.

Our hypothesis include that the increase in serum vitamin D regardless of their initial vitamin D level will increase bone mineral density in various sites. This could be evaluated in more than one thousand postmenopausal women who had been enrolled in annual health check up in one of the University Hospital Health Care Center in Seoul. These women provided full health information as well as annual physical check up and health behavior.

The four initial serum vitamin D quartile; low-10ng/%, 11-20ng, 21-30ng, 30ng-higer, consisted of 25% of total number of study subjects. Each quartile were subgrouped into 1, those whose serum vitamin D was increased from the initial serum level, 2, those whose serum vitamin D level was decreased from the initial serum level.

More than one thousand postmenopausal women who had both initial serum vitamin D, bone mineral density and their annual follow up. Our hypothesis is being tested and will be presented. This data will support the effect of serum vitamin D changes on postmenopausal women bone health with various physical and behavioral conditions considered.

Disclosures: Sanghyun Je, None.

SU0348

Dairy products consumption and serum 25-hydroxyvitamin D level in Saudi children and adults. <u>Nasser Al-Daghri</u>*[1], <u>Omar Al-Attas</u>[2], <u>Soundararajan Krishnaswamy</u>[2], <u>Hanan Alfawaz</u>[2], <u>Naji Aljohani</u>[3], <u>Shaun Sabico</u>[2], <u>Majed Alokail</u>[2]. [1]King Saud University, Saudi Arabia, [2]King Saud University, Saudi Arabia, [3]King Saud University for Health Sciences, Saudi Arabia

Background
Vitamin D deficiency is common around the world and is implicated in calcium deficiency related conditions like secondary hyperparathyroidism and fracture risk and several chronic diseases, including type II diabetes, autoimmune conditions and cancer. We aimed to investigate the vitamin D status and its association with consumption frequencies of various dairy products in Saudi population.
Methods
Subjects of our study consisted of 820 children (327 boys; mean age 14.9 yrs and 493 girls; 14.8 yrs) and 565 adults (249 men, 27.9 yrs and 316 women 32.2 yrs). We estimated the consumption frequencies of various dairy food products (fresh milk, powdered milk, laban, yoghurt and cheese) using a qualitative food frequency questionnaire (FFQ) and also measured serum level of 25-hydroxyvitamin D (25(OH)D). Associations between variables of interest were assessed by Pearson correlation analysis.
Results
Approximately, 80% of the boys and 90% of the girls and 64% of men and 50% of women participants had deficient/insufficient levels of vitamin D. Modest associations were found between mean serum 25(OH)D concentration and consumption frequencies of fresh milk in children (r=0.11), more specifically in girls (r=0.12), and to the overall consumption of dairy products in women (r=0.12).
Conclusions
The results of this study indicate widespread vitamin D deficiency in children and adults of Saudi Arabia, and a lack of strong correlation between dairy product consumption frequency and serum level of vitamin D strongly implies a need for adequate fortification of milk and other dairy products with vitamin D.

Disclosures: Nasser Al-Daghri, None.

SU0349

Does Vitamin D Affect Femoral Cartilage Thickness? An Ultrasonographic Study. <u>Aysen Akinci-tan</u>*[1], <u>Serdar Güven</u>[2], <u>Fevziye Unsal malas</u>[3], <u>Murat Kara</u>[4], <u>Lale Aktekin</u>[3], <u>Murat Ersoz</u>[3], <u>Levent Ozcakar</u>[5]. [1]Hacettepe University, Turkey, [2]Hacettepe University School of Medicine, Turkey, [3]Ankara PMR Training & Research Hospital, Turkey, [4]Ankara PMR Training & Rehabilitation Center, Turkey, [5]Hacettepe University dept of PMR, Turkey

Aim: To investigate the association between vitamin D levels and distal femoral cartilage thickness in healthy subjects. Methods: Eighty patients who admitted to our outpatient clinic between May-July 2013 were classified into three subgroups according to their 25-OH vitamin D levels as <10 ng/ml, 10-20 ng/ml and ≥ 20 ng/ml. Distal femoral cartilage thickness was measured from the mid-points of right medial condyle (RMC), right lateral condyle (RLC), right intercondylar area (RIA), left medial condyle (LMC), left lateral condyle (LLC) and left intercondylar area (LIA) by using musculoskeletal ultrasonography (US). Results: The group with severe vitamin D deficiency (<10 ng/mL) had thinner femoral cartilage thickness at LMC (p=0.005).

Positive correlations were determined only between vitamin D levels and US measurements for the group with a severe vitamin D deficiency (<10 ng/mL) at RLC (r=444, p=0.020), LMC (r=357, p=0.067) and LLC (r=568, p=0.002). Conclusion: Low levels of vitamin D (<10 ng/mL) seem to affect the femoral cartilage thickness negatively. Further studies are necessary to ascertain the clinical relevance of this change in cartilage thickness and whether vitamin D supplementation can reverse the cartilage thinning process or the allied clinical symptoms in case of knee osteoarthritis.

Disclosures: Aysen AKINCI-TAN, None.

SU0350

Optimal Dose of Vitamin D Replacement in Middle Eastern and North African Population: a Systematic Review and Meta-analysis. Marlene Chakhtoura*[1], Ghada El-Hajj Fuleihan[2], Asma Arabi[3], Sara El-Ghandour[4], Elie Akl[4], Khaled Shawwa[4]. [1]American University of Beirut, Lebanon, [2]American University of Beirut-Medical Center, Lebanon, [3]Calcium Metabolism & Osteoporosis Program, American University of Beirut, Lebanon, [4]American University of Beirut, Lebanon

Background: Hypovitaminosis D, defined as <20 ng/ml, is highly prevalent worldwide more so in the Middle East and North Africa (MENA) region (1,2). Relevant risk factors in adults, and similarly to other countries, include advancing age, female gender, multiparity, clothing style, season, socio-economic status and urban living (3). The latest Institute of Medicine (IOM) recommendations for dosing vitamin D targeted populations from North America, and may not necessarily apply to the MENA region.
Objectives:
A. Determine the mean 25-hydroxyvitamin D (25(OH)D) level reached with low (≤ 800IU), moderate (800-2000 IU) or high (>2000IU) daily dose of vitamin D in subjects in MENA countries, by age and reproductive status.
B. Estimate:
1) Mean serum 25(OH)D level reached by 97.5% of individuals in above treatment groups.
2) Proportion of subjects who reach a mean 25(OH)D ≥20 ng/ml in above treatment groups.
C. Investigate the applicability of the IOM recommended daily allowance to subjects in MENA countries. Other outcomes investigated are fracture rates, mortality, hypercalcemia-hypercalciuria, bone mineral density, kidney stones and muscle strength.
Eligibility criteria: We included randomized clinical trials comparing different doses of oral vitamin D supplementation or placebo in MENA countries, of both genders and all age categories, including pregnant and lactating women.
Search method: A systematic search was conducted using Medline, PubMed, the Cochrane Library, EMBASE, Popline, Global Health Library, Index Medicus for WHO Eastern Mediterranean without any time or language restriction. Additional studies were identified on ClinicalTrial.gov and the WHO registry for clinical trials. Authors were contacted for unpublished data.
Selection and data abstraction process:References retrieved were reviewed in duplicate by 2 independent reviewers. We abstracted data, and assessed risk of bias using the Cochrane risk of bias tool in duplicate and independently. We used RevMan software for data entry and analysis.
Results:2542 articles were screened for title and abstract, 192 full texts were assessed for eligibility. We judged 20 studies as eligible: 10 in adults, 4 in children, 2 in neonates and infants, and 4 in pregnant women. The analysis is currently under progress to be completed by September 2014.
Keywords: vitamin D, Middle East and North Africa
References:
1. Hilger J, Br J Nutr. 2014
2. Arabi A, Nat Rev Endocrinol. 2010
3. Bassil D, Dermatoendocrinol. 2013

Disclosures: Marlene Chakhtoura, None.

SU0351

Quantification of total 25-hydroxyvitamin D: Acomparison between the Elecsys® Vitamin D Total assay and LC-MS/MS. Christopher Washbourne*[1], Darrell Green[1], Emily Fisher[2], Isabelle Piec[3], Jonathan Tang[4], William Fraser[1]. [1]University of East Anglia, United Kingdom, [2]University of East Anglia, United Kingdom, [3]BioAnalytical Facility, University of East Anglia, United Kingdom, [4]University of East Anglia, Norwich, UK, United Kingdom

Background: Increasing demand for vitamin D testing has led to a plethora of semi- and fully-automated methodologies for quantification of serum 25-hydroxyvitamin D (25OHD) concentrations. The ability of an assay to measure 25OHD with precision and accuracy is essential in assessing vitamin D status of an individual. Liquid chromatography-mass spectrometry (LC-MS/MS) has been identified as the gold-standard method for determination of 25OHD due to its capacity to distinguish $25OHD_3$ and D_2. Immunoassays (IM) and competitive protein binding assays (CBP) remain popular due to a user-friendly format that can be easily automated. The CBP assay from Roche Diagnostics offers total 25OHD measurement in 27 minutes with high specificity to $25OHD_3$ and D_2.

Objectives: To evaluate the Roche Diagnostics Elecsys Vitamin D total and compare the results with a fully validated, NIST-aligned (LC-MS/MS) method.
Method: 293 routine patient samples with serum 25OHD that were determined by LC-MS/MS were selected in this comparison study. Of those samples, 153 contained both $25OHD_2$ and D_3 ranging between 2.6-128.7 and 5.7-166.9 nmol/L, respectively, and 140 exhibited $25OHD_3$ ranging between 7.6-234.8 nmol/L with undetectable $25OHD_2$. The samples were analysed on a COBAS 6000 using the Elecsys method according manufacturer instructions.
Results: Intra-assay imprecision of the Elecsys method was 3.5% (53.4±1.9 nmol/L) (CV% (±S.D)) and 2.4% (89.3±2.2 nmol/L). Interassay imprecision was 7.5% (51.2±3.8 nmol/L) and 5.1% (84.1±4.3 nmol/L). Bias plots comparing the mean concentration against the percentage difference between the Elecsys and LC-MS/MS methods showed an overall negative bias of 11.6% in total 25OHD concentrations. The sample group that consisted solely of $25OHD_3$ showed a negative bias of 2.2%, whereas the sample group that contained both $25OHD_3$ and D_2 were found to have a significantly higher negative bias of 20.2%.
Conclusions: We showed the Elecsys method is precise at the concentrations of 25OHD tested. However, when compared with a fully validated LC-MS/MS method, the Elecsys method was found to underestimate total 25OHD. This is exacerbated by the presence of $25OHD_2$ in the sample, suggesting there is a lower binding affinity for $25OHD_2$ in the Elecsys method resulting in lower recovery. Our findings were in accordance with current publications on comparison studies between other commercially available IM, CBP assays and LC-MS/MS.
Sponsor: Roche Diagnostics GmbH

Disclosures: Christopher Washbourne, None.
This study received funding from: Roche Diagnostics GmbH

SU0352

Probiotic treatment prevents bone loss in type 1 diabetic mice. Laura McCabe[1], Sandi Raehtz*[2], Katherine Motyl[3], Jing Zhang[2], Robert Britton[2], Narayanan Parameswaran[2], Regina Irwin[2]. [1]Michigan State University, USA, [2]Michigan State University, USA, [3]Maine Medical Center Research Institute, USA

Type 1 diabetes (T1D) causes osteoporosis characterized by a predominant suppression of osteoblast number/activity and increased bone marrow adiposity. However, the fundamental mechansim and alternative treatments with fewer side-effects for T1D bone loss remain undetermined. Recent studies by our lab and others indicate that probiotics can be beneficial for bone. Here we demonstrate that T1D mice lose 35% femur trabecular bone volume. Surprisingly, treatment of T1D mice with L. reuteri, a probiotic with anti-inflammatory and bone health properties, completely prevented bone loss and marrow adiposity. The changes suggest a defect in Wnt10b levels which were reduced in T1D mice. This suppression was prevented with L. reuteri treatment. Taken together, probiotics may benefit T1D bone health.

Disclosures: Sandi Raehtz, None.

SU0353

Oxytocin is not a determinant of bone mineral density in men: analysis of the MINOS cohort. Veronique Breuil*[1], Eric Fontas[2], Roland Chapurlat[3], Patricia Panaia-Ferrari[2], Hedi Ben Yahia[4], Sylvie Faure[2], Yacine Allam[2], Liana Euller-Ziegler[2], Ez Zoubir Amri[4], Pawel Szulc[5]. [1]Chu De Nice, France, [2]Nice University Hospital, France, [3]E. Herriot Hospital, France, [4]CNRS, iBV UMR 7277, France, [5]INSERM UMR 1033, University of Lyon, Hopital E. Herriot, Pavillon F, France

Introduction: We previously showed that oxytocin (OT), a neurohypophysial hormone regulated by estrogen, leptin, testosterone and alcohol, is a determinant of bone mineral density (BMD) in post-menopausal women. The aim of our study was to assess the relationship between OT and bone status in men.
Subjects and methods: In 552 men aged 50 and older, included in the MINOS cohort, we measured OT serum levels (Phoenix Pharmaceuticals, Strasbourg, France) after a solid-phase extraction (Phoenix Pharmaceuticals, Strasbourg, France) and leptin (TECOmedical Group, Swizerland); estradiol and testosterone serum levels were already available. We examined the association between OT serum levels BMD (lumbar, femoral neck and hip, Hologic 1000W) and bone remodeling (PINP, BSAPand CTX).
Results: The median age of this population was 64.5 years (IQR 60 – 70); 6% were osteoporotic (OP), 49% osteopenic, 45% had normal BMD, 13% had at least 1 prevalent fragility fracture and 72% had an alcohol intake ≥3 unit/day. In univariate analysis, OT serum level was not associated with BMD at any site or with any bone turnover marker. OT serum level was significantly but weakly associated with total estradiol (r=0.087; p=0.04), bioavailable estradiol (r=0.20; p<0.0001), free testosterone (r=0.17; p<0.0001) and leptin (r=0.15; p=0.0002); but not significantly related to age, alcohol intake or total testosterone. After adjustment for age, total and bioavailable estradiol, leptin, total and free testosterone, BMI or alcohol, the association was still not significant. When examining therelationship across quartiles of estradiol, bioavailable estradiol, free testosterone or leptin, we also found no significant association.
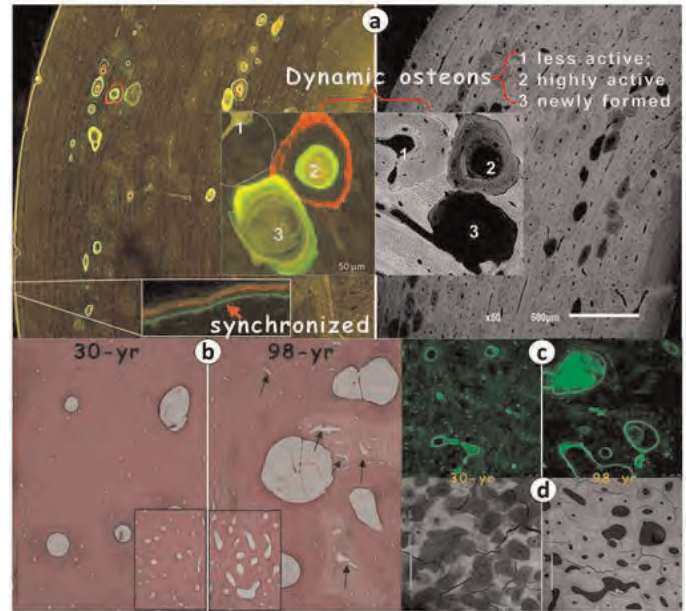Conclusion: In men, OT serum levels are not associated with BMD and bone turnover. These results point out an additionaldifference in the pathophysiology of bone loss between men and women.

Disclosures: Veronique Breuil, None.

SU0354

Pathologically Altered Osteocytes (Ocys) are Responsible for Osteoporosis.
Yinshi Ren*[1], Baozhi Yuan[2], Ying Liu[3], Marc Drezner[2], Jian Feng[3]. [1]Baylor college of dentistry,Texas A&M Health Science Center, USA, [2]University of Wisconsin, USA, [3]Baylor college of dentistry,Texas A&M Health Science Center, USA

For a long time the osteocyte (Ocy) has been considered a mechanosensor, rather than a true bone builder, despite its ideal anatomic location to regulate bone mineralization. Using acid-etched and backscattered SEM, we found a close relationship between Ocy maturation and bone mineralization. The mature Ocy volume was 50% reduced, but its surface was >50% increased, due to increased dendrites, leading to replacement of the decreased cell volume by well-defined mineral, present in individual spheres and mineral sheets. Confocal microscopy of DAPI nuclear-stained bone, labeled with calcein and alizarin red, confirmed mineral deposition in the matrix surrounding Ocys, and at the mineralization front surrounding Ocy canaliculi, in both trabecular/cortical bone from rats, mice, rabbits, and dogs. In contrast, osteoblasts (Obs) were not located in areas of active mineralization, challenging the dogma that Obs regulate mineralization. We also identified two types of mineralization processes in dog cortical bone, synchronized mineralization on the non-osteon bone surface and highly dynamic mineralization in the osteon-rich interior bone. We confirmed these observations, using confocal double-labeled images to directly assess mineral deposition from Ocys, and backscattered SEM images to define mineral resorption. We found various degrees of mineral remodeling in different osteons of the cortical bone, in contrast to the non-osteon bone surface that displayed only one mineral deposition pattern. We also identified newly formed osteons and estimated their de nova formation rate as ~9.5%. These observations define a new role for Ocys in bone remodeling and suggest a possible role for alterations of Ocy structure and function in the genesis of osteoporosis. Several lines of evidence support this concept: 1) advanced osteoporosis in compact bone is due to an increase in the Haversian canal area (>2-fold), a change that correlates with significantly reduced Ocy numbers/osteon, altered Ocy shape, from spindle to round, and a reduced number, surface area, and volume of Ocy dendrites; and 2) a lack of cortical bone remodeling and abundant microcracks in aged cortical bone, which are directly linked to defective Ocys, not to abnormally functioning Obs or osteoclasts. Collectively, these data indicate that Ocys are the cells maintaining bone mineralization and remodeling, and poorly maintained bone remodeling, due to defective Ocys, plays a key causal role in osteoporosis.

Figure 1. Bone mineralization is directly linked to osteocyte. (a). Acid-etched SEM images show mouse calvaria osteocyte maturation from newborn to 5 months of age. As it matured, the osteocyte volume was reduced by nearly 50%, but its surface area increased by >50%, due to an increased number of dendrites, which led to well-defined mineral filling the decreased cell volume. (b). Double labeling + Dapi staining revealed by confocal microscopy shows mineral deposition in the matrix surrounding the Ocys, and at the mineralization front surrounding the Ocy canaliculi.

ASBMR abstract figure 1

Figure 2. Double labeling revealed a dual mineralization pattern in osteon (dynamic, including active, inactive, and newly formed) and non-osteon area: (synchronized) within dog cortical bone (a, left); which is confirmed by the backscatter SEM imaging technique on the same bone slide (a, right); H&E stains showed increased micro-cracks in a 98-yr-old osteoporosis patient compared to a 30-yr-old male cortical bone (b); The confocal FITC stained images revealed much enlarged Haversian canals with reduced Ocy number in each osteon in 98-yr-old bone (c); and the backscatter SEM image revealed highly active remodeling in the same 30-yr-old male cortical bone, as reflected by a mixed pattern of light shade (less active) and dark (active, dominant) (d, left) in comparison with the 98-yr-old bone, in which most osteons were in light shade, indicating a lack of bone remodeling (d, right).

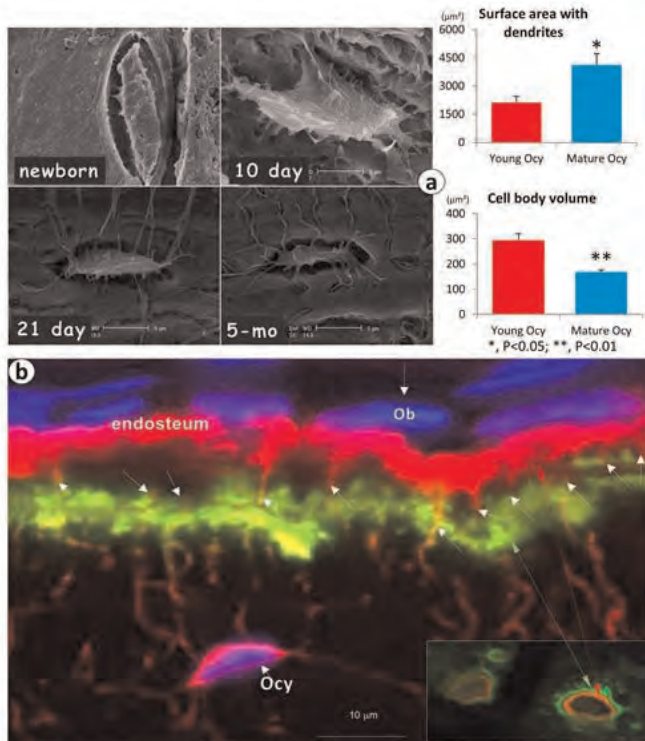ASBMR abstract figure 2

Disclosures: Yinshi Ren, None.

SU0355

Effects of the Combination of Eldecalcitol, an Analog of Active Vitamin D$_3$, and Parathyroid Hormone in Ovariectomized Rat Bones.
Tomomaya Yamamoto*[1], Tomoka Hasegawa[2], Sadaoki Sakai[3], Satoshi Takeda[4], Kimimitsu Oda[5], Minqi Li[6], Koichi Endo[7], Norio Amizuka[8]. [1]Hokkaido University, Japan, [2]Hokkaido University, Japan, [3]Chugai Pharmaceutical Co., Ltd., Japan, [4]Chugai Pharmaceutical Co., LTD, Japan, [5]Niigata University, Japan, [6]The School of Stomatology, Shandong University, Japan, [7]Chugai Pharmaceutical Co., Ltd., Japan, [8]Hokkaido University School of Dentistry, Japan

In works using rodent models, we have shown that intermittent hPTH (1-34) administration enhanced bone remodeling while promoting preosteoblastic proliferation (JBMR 2009). In addition, we have reported that eldecalcitol, an analog of active vitamin D$_3$, induced new bone formation via "minimodeling", a type of bone formation that is not coupled with osteoclastic bone resorption (Bone, 2011). Since both reagents appear to have anabolic effects in bone, we have histologically examined the biological effects of a combination of eldecalcitol and hPTH(1-34) on ovariectomized (OVX) rat bones.

Seventy-one 13-weeks old OVX Wistar rats received vehicle (OVX group), 10μg/kg of PTH (PTH group), 20 ng/kg of eldecalcitol (eldecalcitol group) or 10μg/kg of hPTH(1-34) and 20 ng/kg of eldecalcitol (combination group) for 4 or 8 weeks. Rats were then fixed with a paraformaldehyde solution, and their femora and tibiae were assessed in terms of histology, histochemical profile for alkaline phosphatase (ALP) and tartrate-resistant acid phosphatase (TRAP), and calcein labeling.

The eldecalcitol group revealed a rapid increase in metaphyseal trabecular number compared with the OVX group after 4 weeks. After 8 weeks, however, both PTH and combination groups had higher trabecular numbers than did the eldecalcitol and the OVX groups. PTH group showed a thick layer of ALP-positive preosteoblasts nearby several TRAP-reactive osteoclasts, suggesting accelerated bone remodeling. Unlike PTH, the eldecalcitol group showed increased bone volume while not developing a thick preosteoblastic layer. Eldecalcitol administration promoted a reduction in the number of TRAP-positive osteoclasts and stimulated minimodeling, defined as a focal budding of new bone deposited upon smooth arrest lines. Therefore, the mechanisms through which hPTH(1-34) and eldecalcitol promote bone anabolism seem to be different: PTH stimulates bone remodeling, while eldecalcitol both supports minimodeling and suppresses bone resorption by inhibiting osteoclast formation. The combination group displayed the highest increases in bone mass, but the osteoblast/preosteoblast numbers lied midway between those found in the PTH and in the eldecalcitol groups. Thus, it appears that the combination of hPTH(1-34) and

eldecalcitol augments the anabolic effects of both reagents on the osteoporotic rat model.

SU0356

Experimental Hepatic Osteodystrophy: The Reciprocal Influence of Glucose Metabolism and Pamidronate Treatment on Bone Microstructure and Strength. Francisco Jose De Paula*[1], Fernando Cunha[2], Leandra Ramalho[2], Ariane Ariane[2], Antonio Shimano[2], Marcello Nogueira-Barbosa[2], Ingrid Dick-de-Paula[2], Vanda Jorgetti[3], Sandra Fukada[4], Adriano Spirlandeli[2]. [1]School of Medicine of Ribeirao Preto - USP, Brazil, [2]Ribeirao Preto Medical School, USP, Brazil, [3]University of São Paulo, Brazil, [4]School of Pharmaceutical Sciences of Ribeirao Preto, USP, Brazil

Introduction: The liver has a central role on energy metabolism, is the main source of endocrine IGF-1 and participates in vitamin D metabolism. Recent studies have shown a complex interplay between bone and energy metabolism. However, the reciprocal influence of glucose metabolism and bisphosphonate therapy in hepatic osteodystrophy has scarcely been studied. Objective: To evaluate bone microstructure and strength, glucose and insulin tolerance in mice with hepatic disease induced by carbon tetrachloride (CCl4) and treated with pamidronate (P). Methods: C57BL6 mice were divided in 4 groups (n=40). Controls [treated with vehicle (V) or V and P (V+P)] and mice subjected to CCl4+V or CCl4+P treatment. The CCl4 was injected for 8 weeks; at the end of the fourth week the animals received V or P (1.25 mg/kg). Histological analysis of liver was obtained in all animals. Biomechanical test was performed on tibia and femur. Quantitative μCT was performed in femur and L5. Bone histomorphometry was performed in tibia. GTT was done with a 1g of glucose/Kg (IP) and ITT with an insulin dose of 1UI/Kg (IP). Results: Histological analysis showed that all mice subjected to CCl4 injections presented cirrhosis. The body weight was similar in all groups. While the weight of epididymal fat was lower in both groups with cirrhosis (p<0.01), the weight of brown fat and liver was lower in both control groups (p<0.01). The GTT was similar in all groups. However, the decrease in glucose levels, after insulin administration, was lower in mice with liver disease. The force at the time of fracture was higher in the two control groups (e.g., tibia: V=15.2±1.2; V+P=17.2±1.0; CCl4+V=12.3±1.5 N; CCl4+P=13.5±3.2 N, p<0.001). Data from μCT and histomorphometry showed reduced values of BV/TV and Tb.N, as well as increased values of Tb.S in CCl4+V group in comparison to control (p<0.005). However, pamidronate successfully reversed this bone profile in all bone sites (e.g., L5 (BV/TV): V= 6.17±0.64; V+P=7.96±0.56; CCl4= 5.76±0.19; CCl4+ HP= 6.99±0.80%, p<0.01), decreasing bone resorption parameters, namely Oc.S/BS and ES/BS. There was no association between energy metabolism with bone parameters.

Conclusion: Our data show that pamidronate efficiently reverses bone alterations in chronic liver disease. Cirrhosis is associated with insulin resistance, but there is no relationship between insulin resistance with bone microstructure and fragility in mice with liver disease.

SU0357

Integrative Analysis of GWASs, Human Protein Interaction and Gene Expression Identified Gene Modules Associated with BMDs. Hao He*[1], Lei Zhang[1], Jian Li[1], Yu-Ping Wang[1], Ji-Gang Zhang[1], Jie Shen[1], Yan-Fang Guo[1], Hong-Wen Deng[2]. [1]Center of Genomics & Bioinformatics, Tulane University, USA, [2]Tulane University, USA

To date, few systems genetics studies in bone field have been performed. We designed our study from a systems-level perspective by integrating GWASs, human protein-protein interaction (PPI) network and gene expression to identify gene modules contributing to osteoporosis risk. First we searched for modules significantly enriched with BMD-associated genes in human PPI network by using two large meta-analysis GWAS datasets through a dense module search algorithm. One was an imputation-based meta-analysis (referred to as Meta7), including seven individual GWAS samples. The other was the GWAS meta-analysis from Genetic Factors for Osteoporosis Consortium (GEFOS2). One was assigned as a discovery dataset and the other as an evaluation dataset, and *vice versa*. Through such a discovery-evaluation strategy, in total 42 modules and 129 modules were identified significantly in both Meta7 and GEFOS2 dataset, for femoral neck (FN) and spine (SPN) BMD respectively. 3340 modules were identified for Hip BMD only in Meta7, as Hip BMD weren't available in GEFOS2 for evaluation. Next, as candidate modules, they were assessed the biological relevance to BMD by gene set enrichment analysis (GSEA) in two independent microarray expression datasets (26 Chinese and 80 Caucasian subjects). Both expression profiles were generated from circulating monocytes isolated and purified in subjects with low versus high BMD. Interestingly, there were two final candidate modules significantly enriched in monocytes from low BMD group in both gene expression datasets (nominal *p* value < 0.05) (Table 1). Two modules had 16 nonredundant genes, including *ESR1, LRP5, TNFRSF11B, SMAD3, SFRP1, SFRP2, MDFI, LRP5, WNT1, WNT4* and *DKK1, etc*. These 16 genes were submitted for gene ontology (GO) term enrichment analysis in the WebGestalt website (http://

bioinfo.vanderbilt.edu/webgestalt/) to compute the enrichment *p* value for each GO term. It revealed that both modules were enriched for genes involved in Wnt receptor signaling and osteoblast differentiation. The present study uncovered interactions among *DKK1, LRP5* and *SFRP* in both final candidate modules. These genes and their interactions had a great impact on Wnt signaling pathway, which may result in loss of bone mass. From a system-level analysis above, we highlighted two modules as well as genes in modules playing important roles in the regulation of bone mass, providing important clues for therapeutic approaches for osteoporosis.

Table 1. GSEA results of the two final candidate modules in gene expression datasets.

Trait	Module	Genes in the module	Gene expression sample	ES[a]	NES[a]	NOM p value[a]
SPN	Module 1	SMAD3, ESR1, DKK1, FN1, SFRP2, TNFRSF11B, SMAD9, LRP5, WNT1, SE CISBP2, WNT4	Caucasian	-0.583	-1.500	0.049
			Chinese	-0.621	-1.722	0.024
Hip	Module 2	MDFI, ESR1, TAP1, DKK1, LRP5, ZNF408, SFRP1, EXOSC2, WNT1, WNT4	Caucasian	-0.685	-1.618	0.023
			Chinese	-0.657	-1.577	0.021

[a] Results in low BMD group.
Note: ES: enrichment score; NES: normalized enrichment score; NOM: nominal

Table 1

SU0358

Refining Isolation Methods of Human Osteoblastic Cells from Small Needle Bone Biopsies Without In Vitro Culture: Exclusion of Quiescent Bone Lining Cells. Joshua Farr*[1], David Monroe[2], Sundeep Khosla[3]. [1]Mayo Clinic, USA, [2]Mayo Foundation, USA, [3]Mayo Clinic College of Medicine, USA

Historically, the inability to directly study mature human osteoblasts *in vivo*, or *ex vivo* following minimal manipulation, has represented a major technical problem. Indeed, most human studies to date have either used whole bone biopsies, containing a heterogeneous cell population, or cultured bone marrow stromal cells (MSCs). While potentially useful for some purposes, bone MSCs represent early progenitor cells and it is unclear how *in vitro* culture may alter their phenotype and/or mRNA expression profile. We have circumvented this problem by developing methods to rapidly isolate (without *in vitro* culture) highly enriched osteoblastic cells from small human needle bone biopsies (Osteo Int 2014;25:887-95). These isolation techniques can then be coupled to analytic tools to study genes and pathways unique to human osteoblastic cells *in vivo*. While these techniques should provide novel insights into the pathogenesis of osteoporosis and other skeletal disorders, a potential limitation of this isolation method is that quiescent bone lining cells may still be present within our osteoblast-enriched cell population, and therefore could act as a confounder. Thus, we utilized CD54 (ICAM-1), a unique cell surface marker expressed by bone lining cells, but not osteoblasts (JBMR 2002;17:77-90), to investigate whether bone lining cells exist in our human osteoblastic cell population. A small needle bone biopsy (1-2 mm by 1 cm) was obtained from the posterior iliac crest of a healthy 63 yr old male, and was subjected to sequential collagenase digests. We previously demonstrated that the 2nd fraction contains most of the osteoblasts; thus, we used magnetic-activated cell sorting of the 2nd fraction cells to rapidly isolate the alkaline phosphatase (AP)+ cells, which are capable of *in vitro* mineralization. The next level of purification involved selection for CD45/34/31- cells, a population completely devoid of hematopoietic/endothelial markers yet highly enriched for key osteoblast markers. Finally, we stained the AP+/CD45/34/31- cells with CD54 and used flow cytometry to establish that, relative to an isotype control, 11.5% of the human AP+/CD45/34/31- cells were ICAM-1+ (Figure). In conclusion, while relatively few ICAM-1+ cells are present in the AP+/CD45/34/31- cell population, CD54 should be included as an additional marker to ensure removal of any bone lining cells. Thus, AP+/CD45/34/31/54- cells represent a further enriched human osteoblastic cell population.
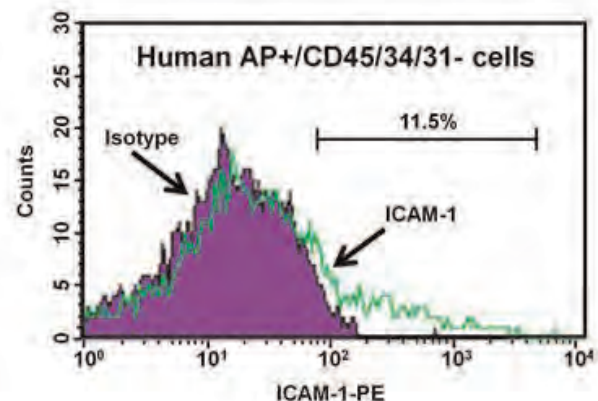
Figure

SU0359

Serum Proteomic Profiles and Incident Vertebral Fracture in Older Men: The MrOS Study. <u>Douglas Bauer</u>*[1], <u>Jian Shen</u>[2], <u>Jodi Lapidus</u>[3], <u>Peggy Cawthon</u>[4], <u>Andy Hoffman</u>[5], <u>Steven Cummings</u>[6], <u>Eric Orwoll</u>[2]. [1]University of California, San Francisco, USA, [2]Oregon Health & Science University, USA, [3]OHSU, USA, [4]California Pacific Medical Center Research Institute, USA, [5]Stanford, USA, [6]San Francisco Coordinating Center, USA

The biologic pathways that mediate vertebral fracture (VF) in men are not well defined, and no established serum biomarkers are available. We utilized a novel approach to identify serum peptides and proteins associated with incident vertebral fracture in a cohort of older men.

A1923 men ≥65 (mean age 73) were randomly selected from the Osteoporotic Fractures in Men Study (MrOS). Fasting baseline serum archived at -70C was analyzed using high throughput mass spectrometry. Incident VF (Genant grade ≥1, n=86) were detected by review of paired lateral spine radiographs from baseline and after a mean follow-up of 4.5 years. After excluding men with a history of fracture after age 50 or taking osteoporosis treatments (23 men with incident VF and 390 men without), we used ANCOVA and linear regression models adjusted for age, BMI and clinical center to compare peptide abundance between men with and without new VF. We adjusted for multiple comparisons using the false discovery rate (FDR) calculated via the Storey method (q-value). Peptide abundance was considered significantly different when FDR≤0.1 and fold differential ≥10%. A meta-analytic approach that combines p-values from peptides within the same protein was applied to generate an overall significance level and fold change for specific proteins. The abundance of selected peptides and risk of incident VF were further analyzed using adjusted logistic regression models.

Serum proteomic analysis identified 3099 unique peptides that mapped to 458 known proteins. None of the identified peptides or proteins met our predefined threshold for differential abundance but one peptide related to plasminogen, a coagulation protein that modulates expression of OPG in rodents, was less abundant among men with incident VF (p=$4.7*10^{-5}$, FDR q-value=0.13, fold differential= 1.29). Each SD decrease in the adjusted abundance of this peptide was associated with a 47% higher risk of new VF (OR=1.47, 95% CI: 1.20, 1.78). Two other peptides related to serum plasminogen were also less abundant among men with VF (p<0.004, FDR q-value=0.99, fold differential>1.15 for both), but meta-analysis of plasminogen peptide abundance did not differ among men with and without VF (p=0.04, FDR q-value=0.99, fold differential= 1.08).

Using novel, in depth proteomic methods in older men, we did not identify peptides or proteins significantly associated with incident vertebral fracture, but several peptides related to plasminogen appear promising and should be evaluated in larger studies.

Disclosures: Douglas Bauer, None.

SU0360

Simvastatin action on bone repair after fracture in experimental surgical protocol. <u>João Paulo Mardegan Issa</u>*[1], <u>Conrado Ingraci de Lucia</u>[2], <u>Fellipe Augusto Tocchini de Figueiredo</u>[3], <u>Junia Ramos</u>[4], <u>Daniela Mizusaki Iyomasa</u>[3], <u>Mamie Mizusaki Iyomasa</u>[5], <u>Ana Paula Macedo</u>[4], <u>Roberta Carminati Shimano</u>[3]. [1]USP- University of São Paulo, Brazil, [2]Professor, Brazil, [3]University of São Paulo, Brazil, [4]Technician of University of São Paulo, Brazil, [5]Professor of University of São Paulo, Brazil

Statins are able to inhibit the osteoblast apoptosis, osteoclasts activities and this process might be good for osteoporotic bone tissue. The number of experimental studies which investigate the hypothesis that osteoporosis can difficult fractures repair are considerable. Ovariectomized animals models are the most commonly model used for bone metabolism evaluation in osteoporosis. This study evaluated the interaction between simvastatin and a metabolic disorder represented by ovariectomization on biochemical, immunohistochemical (BSP, OCN, VEGF, MMP-2 and MMP-9) and histological parameters for bone remodeling in female Wistar rats submitted to fracture on femur. Ninety female animals were divided into six experimental groups (n=15). SH, SH5mg, SH20mg, OVX, OVX5mg and OVX20mg, which SH means, sham operated simulating ovariectomy, and OVX was the ovariectomized rats, the 5mg/kg and 20mg/kg means the concentration of simvastatin. The drug was administrated on drinking water for 7, 14 and 21 days post-fracture, and both femurs were used for analyses. According to the histological data, statistical significance was found for time x medication (P = 0.002), surgery x medication (P < 0.000), and time x surgery x medication (P = 0.001). According to MMP-2 expression, experimental time was significant (P<0.000), but the surgery (P = 0.427) and medication (P = 0.420) were not significant. For MMP-9, experimental time (P < 0.000) and medication (P = 0.042) were significant, but not the surgery (P = 0.662). Immunostaining showed positive reaction as brownish color predominantly on the cytoplasm of some cells and extracellular matrix. In conclusion, the simvastatin executes a positive action for bone repair, especially on groups affected by osteometabolic disorder and those with 20 mg of this drug, and the process was strongly expressed on 14th day and after this period the bone maturation occurred, as evidenced by analyses on 28th day.

Disclosures: João Paulo Mardegan Issa, None.
This study received funding from: FAPESP and CAPES

SU0361

Effects of intermittent administration of teriparatide on bone mineral density and bone strength in autochthonous transgenic mice for diabetes mellitus (Akita mice). <u>Kentaro Ohuchi</u>*[1], <u>Naohisa Miyakoshi</u>[1], <u>Yuji Kasukawa</u>[1], <u>Hayato Kinoshita</u>[2], <u>Yoichi Shimada</u>[3]. [1]Akita University Graduate School of Medicine, Japan, [2]Akita University, Japan, [3]Akita University Graduate School of Medicine, Japan

Introduction: Diabetes mellitus (DM) causes secondary osteoporosis, which reduces bone mineral density (BMD) or bone strength, and increases the risk of fracture. Akita mice (AM) are a model of autochthonous transgenic mouse for DM, and are used to evaluate sugar metabolism. However, the variation of BMD and bone strength in AM remains unclear. The objectives of this study were to measure BMD and bone strength in AM and to evaluate the effects of intermittent administration of PTH on BMD and bone strength in AM.

Materials and Methods: Female AM and control mice (C57/BL/6NCrSlc: CM) at 14 weeks old were divided into four groups: 1) AM+PTH (n=8), AM treated with PTH; 2) AM+vehicle (n=8), AM treated with vehicle; 3) CM+PTH (n=8), CM treated with PTH; and 4) CM+vehicle (n=8), CM treated with vehicle. PTH (80 μg/kg) or vehicle alone (0.1% mouse albumin) was administered subcutaneously 3 times/week for 4 or 8 weeks. Blood sugar (BS) and BMD of the tibia were measured after 4 or 8 weeks treatment. Bone strength of the femoral shaft was evaluated using a 3-point bending test at 4 or 8 weeks.

Results: BS was significantly higher in the AM-group than in the CM-group with both PTH (4 weeks, p=0.001; 8 weeks, p=0.001) and vehicle (4 weeks, p=0.001; 8 weeks, p=0.001). BMD was significantly lower for AM+vehicle than for CM+vehicle at 8 weeks (p=0.003). Intermittent administration of PTH significantly increased BMD in both AM-groups (4 weeks, p=0.001; 8 weeks, p=0.001) and CM-groups (4 weeks, p=0.01; 8 weeks, p=0.005) compared with vehicle-treated groups. Bone strength tended to be lower for AM+vehicle than for CM+vehicle, but the difference was not significant. Maximum load (p=0.01), breaking power (p=0.01) and stiffness (p=0.04) were significantly higher in AM+PTH than in AM+vehicle at 8 weeks.

Conclusion: BMD was lower in the AM-group than in the CM-group. Intermittent administration of PTH also significantly increased BMD and bone strength in AM.

Disclosures: Kentaro Ohuchi, None.

SU0362

Osthole inhibits osteoclast formation and exerts an osteoprotective effect in mice model of 5/6 nephrectomy. <u>Bing Shu</u>*[1], <u>Xiaofeng Li</u>[2], <u>Chunchun Xue</u>[2], <u>Yongjian Zhao</u>[2], <u>Weiwei Da</u>[2], <u>Sheng Lu</u>[2], <u>Dezhi Tang</u>[3], <u>Qi Shi</u>[2], <u>Yongjun Wang</u>[4]. [1]Longhua Hospital, Peoples Republic of China, [2]Longhua Hospital, Spine Research Institute, Shanghai University of TCM, China, [3]Shanghai University of Traditional Chinese Medicine, Peoples Republic of China, [4]Othopedic Surgery, Peoples Republic of China

The objective of this study is to observe the function of osthole on osteoclast formation, and bone loss in mice model of 5/6 nephrectomy. 3-month old C57BL/6 were randomly divided into model group and osthole group, and were treat with placebo or osthole one week after 5/6 nephrectomy. Sham-operated group were set as control. Two month after treatment, L4 vertebre were harvested. BMD of cortical bone and cancellous bone were detected with micro-CT. Bone histomorphology was revealed by HE staining. Osteoclasts were shown with TRAP staining and quantified. c-fos, NFATc1, MMP9 and Cathepsin K expressions were detected with IHC staining. The L4 vertebre BMD of mice was significantly reduced after 5/6 nephrectomy(p<O.O5)with reduced number and thickness of trabecula. Osteoclast number was significantly increased(p<O.O5). c-fos, NFATc1, MMP9 and Cathepsin K expressions were increased.Compared with model group, mice in osthole group showed increased BMD of L4 vertebre(p<O.O5), reduced osteoclast number(p<O.O5)and c-fos, NFATc1, MMP9 and Cathepsin K expressions. The histomorphology of L4 vertebre was also improved. Osthole can inhibit osteoclast formation and partially reverse bone loss induced by 5/6 nephrectomy in mice.

Disclosures: Bing Shu, None.

SU0363

An herbal formula prevents postmenopausal osteoporosis via DHEA suppressing osteoclastogenesis. <u>Ling Wang</u>*[1], <u>Xuemin Qiu</u>[2], <u>Hans-Jürgen Gober</u>[3], <u>Dajin Li</u>[2]. [1]Fudan University, Institute of Obstetrics & Gynecology, Obstetrics & Gynecology, Peoples Republic of China, [2]Laboratory for Reproductive Immunology, Hospital & Institute of Obstetrics & Gynecology, China, [3]Department of Cell Signaling, Graduate School of Medical & Dental Sciences, Tokyo Medical & Dental University, Japan

Bu-Shen-Ning-Xin Decoction (BSNXD), a traditional Chinese medicinal composition, has been used as a remedy for postmenopausal osteoporosis, but the efficient mechanisms on bone metabolism remain not fully understood. We sought to identify

whether BSNXD could regulate osteoclast differentiation. BSNXD administration ameliorated the osteoporotic phenotype of ovariectomized (OVX) mice, evidenced by an increase in bone mineral density (BMD), bone volume, and a decrease in osteoclast bone resorption; these effects could not be abolished by aromatase inhibitor letrozole. BSNXD-derived serum suppressed RANKL-activated osteoclastogenesis in a dose-dependent manner, and this suppressive effect could be reversed by estrogen receptor (ER)a antagonist Methyl-piperidino-pyrazole (MPP). The serum suppressed RANKL-induced NF-kappa B transcription, and inhibited accumulation of the nuclear factor of activated T-cells, cytoplasmic 1 (NFATc1) in osteoclast precursor cells; the inhibitory effect was abolished by MPP. Administration of BSNXD increased serum DHEA but not E2 concentration. DHEA treatment inhibited RANKL-induced osteoclastogenesis in BMMs via ERa-dependent pathway and ameliorated the bone phenotype of OVX mice. These results collectively suggest that administration with BSNXD increases serum DHEA that presents inhibitory effects on osteoclast differentiation by abrogation of RANKL-induced NFATc1 and NF-kappa B signaling pathway as downstream of ERa, which contributes to the inhibitory role in bone resorption.

Disclosures: Ling Wang, None.

SU0364

Changes in Cortical and Trabecular vBMD After 5 Months of Ovarian Hormone Suppression in Premenopausal Women. <u>Vanessa Sherk</u>*[1], <u>Karen Shea</u>[2], <u>Pamela Wolfe</u>[2], <u>Robert Schwartz</u>[2], <u>Wendy Kohrt</u>[3]. [1]University of Colorado - Denver, USA, [2]University of Colorado Anschutz Medical Center, USA, [3]University of Colorado Denver, USA

Cortical and trabecular bone loss accelerates during menopause and with aging. Menopause is a process with large variability in its rate of progression and the effects of aging may confound the effects of the loss of ovarian function on BMD. GnRH agonist (GnRH$_{AG}$) therapy can be used as a model of menopause to isolate effects of ovarian function. The purpose of this pilot study was to determine the magnitude of the loss in volumetric BMD (vBMD) in response to the suppression of ovarian function and whether the loss is mitigated by exercise. Healthy premenopausal (20-40 y) women (n=27) with normal menstrual function started GnRH$_{AG}$ (leuprolide acetate 3.75 mg) therapy as monthly injections and were randomized to receive transdermal placebo GnRH$_{AG}$+PL or GnRH$_{AG}$+E$_2$ (0.075 mg/d) therapy for 5 months. Women in each treatment arm were also randomized to an exercise (EX) program or non-exercise control (CON). The exercise intervention was 4 days/week of progressive high-intensity resistance training with days split between upper and lower body exercises. Total (ToD), trabecular (TrD), and cortical (CoD) vBMD was measured at 4, 33, and 66% of the length of the tibia with pQCT. Differences in change from baseline to 5 months between groups were tested using an ANCOVA model conditioned on baseline. Planned contrasts were: GnRH$_{AG}$+PL vs. GnRH$_{AG}$+E$_2$, GnRH$_{AG}$+PL+CON vs. GnRH$_{AG}$+PL+EX, and GnRH$_{AG}$+PL+EX vs. GnRH$_{AG}$+E$_2$+CON. Decreases in vBMD in response to GnRH$_{AG}$ treatment were largest in trabecular regions (Table 1) and EX appeared to have a small benefit (TrD: GnRH$_{AG}$+E$_2$+CON vs. GnRH$_{AG}$+PL+EX, p=0.02; GnRH$_{AG}$+PL+EX vs. GnRH$_{AG}$+E$_2$+CON, p=0.09). The benefit of EX was not detected in cortical regions (33% CoD: GnRH$_{AG}$+PL+EX vs. GnRH$_{AG}$+E$_2$+CON, p=0.06). Given the small sample sizes, results must be interpreted cautiously.

Table 1. Relative (%) changes in vBMD. Mean±SD

	GnRH$_{AG}$+PL+CON (n=7)	GnRH$_{AG}$+PL+EX (n=6)	GnRH$_{AG}$+E$_2$+CON (n=7)	GnRH$_{AG}$+E$_2$+EX (n=7)
4% ToD	-2.0±2.9	-0.2±1.9	-1.7±2.1	0.3±1.1
4% TrD	**-1.1±2.5**	**1.2±1.3**	-0.3±0.7	0.7±0.4
33% ToD	-0.2±0.9	**-0.8±1.1**	**0.2±0.9**	0.2±0.8
33% CoD	-0.3±1.2	-0.9±1.3	0.2±0.6	-0.1±1.1
66% ToD	-0.8±1.6	-1.1±1.6	-0.7±2.3	0.5±1.5
66% CoD	-0.3±0.6	-0.9±1.6	-0.8±2.3	0.5±1.6

Means in bold are significantly different from each other within site, p=0.02.

Sherk Changes in vBMD After GnRH Agonist Table 1

Disclosures: Vanessa Sherk, None.

SU0365

Adefovir-induced nephrotoxicity with osteomalacia - cases series. <u>Su Jin Lee</u>*[1], <u>Kwang Joon Kim</u>[2], <u>JO EUN Kim</u>[3], <u>Yumie Rhee</u>[4], <u>Sung-Kil Lim</u>[3]. [1]Yonsei University Health System, South Korea, [2]Severance Hospital, South Korea, [3]Yonsei University College of Medicine, South Korea, [4]Department of Internal Medicine, College of Medicine, Yonsei University, South Korea

Background: Adefovir dipivoxyl (ADF) has been prescribed for patients with chronic hepatitis B (CHB) and increasingly used due to high prevalence of lamivudine resistance. Although adefovir-induced nephrotoxicity (AIN) has been reported in CHB, it is still uncertain the progress or prognosis of AIN. Hence, we report 4 cases of AIN and summarize the progress of AIN.

Method: Retrospective chart review was performed. The patients with abnormal liver function or have history of chronic kidney disease, cancer were excluded. From 2010 to 2013, four patients were diagnosed as AIN. Laboratory parameters including bone turnover markers, whole body bone scan (WBBS), bone mineral density (BMD) were measured at the time of diagnosis.

Result: Chief complaint of four patients was bone pain after taking ADF. All of the patients have taken lamivudine more than 3 years and after that taken ADF for more than 2 years. Laboratory parameters showed hypophosphatemia, hyperphosphateuria, decreased GFR and increased bone turn over markers. Two patients were osteoporotic and another two patients were diagnosed as osteopenia. Two patients had fractures. WBBS showed increased uptake at multiple sites. After diagnosed as AIN, all patients stopped taking ADF and entecavir (ECV) was prescribed. Phosphate supplement was recommended until serum phosphate level would be normalized (K-Phos® neutral 4g daily). After two months, the symptoms of all patients were subsided by changing medication and phosphate replacement.

Conclusion: Based on the results, risk factors for the development of AIN are previous lamivudine use, usage of adefovir more than 2 years. Changing ADF into ECV is effective to prevent progression of renal dysfunction. Phosphate replacement could be effective to control hypophosphatemia and bone pain. Patients undergoing long-term treatment with ADF should be monitored in order to detect renal dysfunction.

Disclosures: Su Jin Lee, None.

SU0366

High circulating sclerostin levels and low bone formation in primary biliary cirrhosis. <u>Ana Monegal</u>[1], <u>Silvia Ruiz-Gaspà</u>[2], <u>Laia Gifre</u>[3], <u>Albert Pares</u>[4], <u>Rosa Miquel</u>[5], <u>Pilar Peris</u>[6], <u>Marta Dubreuil</u>[7], <u>Ana Arias</u>[8], <u>Nuria Guanabens</u>*[9]. [1]Hospital Clinic Barcelona, Spain, [2]Centro de Investigación Biomédica en Red de Enfermedades Hepáticas y Digestivas (CIBERehd). Hospital Clínic Barcelona., Spain, [3]Hospital Clinic Barcelona, Spain, [4]Centro de Investigación Biomédica en Red de Enfermedades Hepáticas y Digestivas (CIBERehd). Hospital Clínic Barcelona. 3Liver Unit. Hospital Clínic of Barcelona.University of Barcelona., Spain, [5]4Department of Pathology, Hospital Clínic of Barcelona, Spain, [6]Hospital Clínic of Barcelona, Spain, [7]Centro de Investigación Biomédica en Red de Enfermedades Hepáticas y Digestivas (CIBERehd). Hospital Clínic Barcelona, Spain, [8]Department of Rheumatology. Metabolic Bone Diseases Unit. Hospital Clínic of Barcelona, Spain, [9]Universitat De Barcelona, Spain

Background and aims: Low bone formation is the main pathogenic mechanism of osteoporosis in primary biliary cirrhosis (PBC). Sclerostin, an inhibitor of the Wnt pathway, is involved in the regulation of osteoblastogenesis and little is known about its role in the development of bone disease in PBC. Thus, we evaluated the circulating levels of sclerostin and its relationship to bone mass, the parameters of mineral metabolism and liver disease severity. Methods: Serum sclerostin levels were measured in 83 women with PBC (mean age: 60 ± 12 years) treated with ursodeoxycolic acid and 101 control women of the same age. In patients with PBC, we assessed the degree of cholestasis, lumbar and femoral BMD (DXA), as well as parameters of mineral metabolism (Ca/P, PTH, 25OHD, PINP, bone ALP, sCTX, NTX and osteocalcin). In 20 PBC patients sclerostin levels were measured again after 5 years. Results: 77% of patients had low BMD (22% osteoporosis and 55% osteopenia). PBC patients showed higher sclerostin levels than controls (76.7 ± 38.6 vs. 32.5 ± 14.7 pmol/L, p<0.001). Sclerostin levels were higher in patients with less severe cholestasis. A direct correlation between sclerostin and lumbar (r=0.354, p=0.002) and femoral BMD (r=0.336, p=0.003), and age (r=0.256, p=0.002) was observed. In the 65 patients not receiving bisphosphonates at the time of the evaluation, there was an inverse correlation of sclerostin with bone formation markers, PINP (p=0.05) and osteocalcin (p=0.037) and bone resorption, NTX (p=0.01) and sCTX (p=0.03). Sclerostin significantly decreased in patients who were evaluated 5 years later (99.5 ± 35.9 vs. 60.1 ± 30.9 pmol/L, p=0.001). Conclusion: In primary biliary cirrhosis there is an increase in sclerostin, related to bone mass and liver disease severity. The inverse association with bone formation markers may indicate that sclerostin plays a role in the decreased bone formation in this liver disease.

Disclosures: Nuria Guanabens, None.

SU0367

Analysis of age among clinical risk factors in patients with glucocorticoid-induced osteoporosis (GIO). Ikuko Tanaka*[1], Mari Ushikubo[2], Harumi Kuda[3], Yuki Takane[3], Kumiko Akiya[3], Shigenori Tamaki[4], Hisaji Oshima[5]. [1]NAGOYA Rheumatology Clinic, Japan, [2]National Tokyo Medical Center, Japan, [3]National Tokyo Medical Center, Japan, [4]National Tokyo Medical Center, Japan, [5]Tokyo Medical Center, Japan

Background) Although management against GIO has been progressed, little data were available for younger patients with GIO.

Purpose) To clarify clinical relevant factors for management in younger patients with GIO.

Patients and Methods) Patients (n=137) with connective tissue diseases other than rheumatoid arthritis were recruited and observed for 2 years. The means of age, disease duration, total prednisolone (PSL) dosage, and daily PSL dosage during the study period were 61+/-15 (SD), 12+/-11 years, 34+/-34g, and 8+/-6mg/day, respectively. Prevalent vertebral fractures were seen in 44% of the patients. Agents used for prevention and treatment of GIO were Bis (54%), active vitamin D3 (7%), vitamin K2 (6%). Bone mineral densities (BMD) were measured with DXA.

Results) 1) The incident vertebral fracture determined with deteriorating grades by the SQ method was seen in 64 patients (47%). 2) In all subjects, logistic regression analysis showed the age (1.4(OR)/5yo), total PSL dosage (1.1/5g), daily PSL dosage (2.4/5mg), and BMD (1.3/5% decrease) as independent risk factors for the incident fracture, and treatments with Bis (0.02) and vitamin K2 (0.06) as preventing factors (P<0.05). 3) The older patients (age; ≥65) and the middle age patients (age; >40, <65) showed high incident fractures in 2 years (60% and 51%, respectively). Same risk factors for the incident fracture were found in these groups. 4) In younger patients (premenopausal women or age <50 for men), the incident fracture was observed in 17% of the patients, and was not found in patients treated with Bis. The dose of PSL was found a possible risk factor in this group.Conclusions) Because clinical importance of known risk factors in GIO might not be similar in younger patients as compared from those of older patients, careful individual management in younger patients should be considered

Disclosures: Ikuko Tanaka, None.

SU0368

Effects of teriparatide (TPT) on bone mineral density and vertebral fractures in patients with severe glucocorticoid-induced osteoporosis (GIO) pretreated with bisphosphonates (BP). Mari Ushikubo*[1], Harumi Kuda[2], Yuki Takane[2], Kumiko Akiya[2], Shigenori Tamaki[3], Ikuko Tanaka[4], Hisaji Oshima[5]. [1]National Tokyo Medical Center, Japan, [2]National Tokyo Medical Center, Japan, [3]Nagoya Rheumatology Clinic, Japan, [4]NAGOYA Rheumatology Clinic, Japan, [5]Tokyo Medical Center, Japan

Background) Although BP and TPT are both recommended for prevention and treatment of GIO, it was not clear whether immediate switch from BP to TPT is effective or not.

Purpose) To clarify effects of immediate switch from BP to TPT on BMD and vertebral fractures in patients with severe GIO.

Patients and Methods) Patients (n=28, 89% women) with connective tissue diseases and severe GIO (low BMD or fragile fractures), who had been treated with alendronate or risedronate and switched to TPT, were recruited and observed for 2 years. The means of age, daily prednisolone (PSL) dosage during the study period were 71+/-11 (SD), 8.0+/-4.9 mg/day, respectively. Prevalent vertebral fractures were seen in 44% of the patients. Bone mineral densities (BMD) of the lumbar spine were measured with DXA. Prevalent vertebral fractures were found in 26 (93%) patients.

Results) 1) The BMD was increased from 77.9+/-11.3 (%YAM) to 80.7+/-11.5 and 79.7+/-11.4 after 1 and 2 years, respectively (p<0.02). 2) The levels of serum Ca and IP were not changed significantly. Serum NTX, TRACP-5b, PINP, BAP, ucOC were increased to 152 to 373% after 6 months to 1 year but tended to decrease in the 2nd year. 3) Incident vertebral fractures determined with deteriorating grades by the SQ method were seen in 29% of patients at the 1st year and 22% in the 2nd year (44% in 2 years).

Conclusions) PTP was effective to increase the lumbar spine BMD and to prevent vertebral fractures in severe GIO. Because significant percentages of ineffective cases were seen, a novel treatment strategy for a long time should be developed in GIO.

Disclosures: Mari Ushikubo, None.

SU0369

Rapid changes in bone metabolism and clinical benefits of alendronate in patients with systemic rheumatic diseases treated with high dose glucocorticoid: Early DIagnosis and Treatment of OsteopoRosis in Japan (EDITOR-J) Study. Yoshiya Tanaka*[1], Hiroko Mori[2], Takatoshi Aoki[3], Tatsuya Atsumi[4], Yutaka Kawahito[5], Hisanori Nakayama[6], Shigeto Tohma[7], Hitoshi Hasegawa[8], Kazuhide Tanimura[9], Nobuo Negoro[10], Yuji Yamanishi[11], Yukitaka Ueki[12], Atsushi Kawakami[13], Katsumi Eguchi[14], Kazuyoshi Saito[15], Yosuke Okada[16]. [1]University of Occupational & Environmental Health, Japan, Japan, [2]University of Occupational & Environmental Health, Japan, Japan, [3]Department of Radiology, University of Occupational & Environmental Health, Japan, Japan, [4]Hokkaido University School of Medicine, Japan, [5]Kyoto Prefectural University of Medicine, Department of Inflammation & Immunology, Japan, [6]Samihara National Hospital, Department of Rheumatology, Japan, [7]Sagamihara National Hospital, National Hospital Organization, Department of Rheumatology, Clinical Research Center for Allergy & Rheumatology, Japan, [8]Ehime University Graduate School of Medicine, Department of Rheumatology, Japan, [9]Hokkaido Medical Center for Rheumatic Diseases, Japan, [10]Clinical Immunology & Rheumatology, Osaka City University, Japan, [11]Department of Rheumatology, Hiroshima Rheumatology Clinic, Japan, [12]Sasebo Chuo Hospital, Rheumatic & Collagen Disease Center, Japan, [13]Nagasaki University Graduate School of Biomedical Sciences, Department of Immunology & Rheumatology, Japan, [14]Sasebo Municipal Hospital, Department of Internal Medicine, Japan, [15]The First Department of Internal medicine, University of Occupational & Environmental Health, Japan, Japan, [16]University of Occupational & Environmental Health, Japan

Although glucocorticoids are widely used for the treatment of rheumatic diseases, osteoporosis is the most common and serious side effect in glucocorticoid therapy and bone fracture occurs in 30% to 50% of patients on long-term glucocorticoid therapy. However, there is not enough evidence for the prevention of osteoporosis induced by high-dose glucocorticoid therapy. We conducted a prospective multicenter study to assess early changes in the dynamics of bone metabolism in patients with systemic connective tissue diseases following commencement of high-dose glucocorticoid and the benefits of early treatment with bisphosphonate and a vitamin D analog. The subjects of this randomized controlled trial were 106 female, including 37 SLE, 42 vasculitis syndrome and 27 DM/PM, treated for the first time with PSL ?20 mg/day. One week after initiation of glucocorticoid therapy, patients were randomly assigned to treatment with alfacalcidol, a vitamin D analog, at 1 μg/day, alendronate, a bisphosphonate, 35 mg/week, and alfacalcidol plus alendronate. The primary endpoints were changes in lumbar spine bone density at 6 months of treatment and the frequency of bone fracture at 12 months. The study included 58 premenopausal and 48 postmenopausal women, with a mean age of 47.8 years; the initial dose of PSL was 45.5 mg/day, bone mineral density (BMD) for L2-4 was 0.976 g/cm^2, BMD for femoral neck 0.737 kg/m^2. Significant and rapid increases in bone resorption markers (serum CTx, serum NTx and urinary NTx) were observed after 1 week of glucocorticoid therapy. There were no significant differences in baseline characteristics among the treatment groups. After the intervention, bone resorption makers were significantly lower at 24 weeks in the alendronate group and the combination group, compared to the alfacalcidol group. Although the BMD for lumbar spine and femoral neck was markedly lower at 24 weeks after the treatment of alfacalcidol, alendronate and the combination significantly prevented the decrease in BMD. At 12 months after the glucocorticoid therapy, vertebral and non-vertebral bone fractures were observed in 6 (21.4%) patients of the alfacalcidol group, in 2 (6%) of the alendronate group, and in none (0%) of the combination group. Among the various factors at baseline, multivariate analysis identified treatment type as the single significant determinant of the rate of change in lumbar BMD as well as bone fractures. Taken together, we first observed that rapid and marked enhancement of bone resorption was induced within 1 week of the start of glucocorticoid therapy in patients with systemic connective tissue diseases. The combination of alfacalcidol and alendronate administered after the first week of glucocorticoid therapy increased bone density and reduced the incidence of bone fracture for 12 months.

Disclosures: Yoshiya Tanaka, Mitsubishi-Tanabe, Chugai, MSD, Astellas, Novartis, 7; Abbvie, Chugai, Astellas, Takeda, Santen, Mitsubishi-Tanabe, Pfizer, Janssen, Eisai, Daiichi-Sankyo, UCB, GlaxoSmithKline, Bristol-Myers ,

SU0370

Abaloparatide (BA058), a Human PTHrP Analog: Correlation of In vivo Bone Mass Gains and Improved Bone Strength in an Osteopenic Rat Model. <u>Aurore Varela</u>*[1], <u>Elisabeth Lesage</u>[2], <u>Susan Y. Smith</u>[1], <u>Gary Hattersley</u>[3]. [1]Charles River Laboratories, Canada, [2]Charles River, Canada, [3]Radius, USA

Abaloparatide (ABL) is a PTHrP(1-34) analog being developed for the treatment of osteoporosis. Long-term effects of ABL on bone mass and bone strength were studied in ovariectomized (OVX) skeletally mature rats. Four groups were OVX and one group underwent Sham surgery. After a 3-month bone depletion period, animals received daily subcutaneous injections of either vehicle (Sham and OVX controls) or ABL at 1, 5 or 25 µg/kg for 12 months. DXA and pQCT were performed at the end of the bone depletion period (EBD) and after 12 months of treatment. Lumbar vertebrae and femurs were retained for biomechanical tests. In order to assess the relationship between bone mass change with bone strength, correlation analyses within all OVX groups were performed between % change from the EBD and strength data (L1-L4 DXA vs. L4-L5 compression, proximal femur DXA vs. femoral neck shear, mid-femur DXA vs. femur 3-pt bending and tibia diaphysis cortical pQCT data vs. femur 3-pt bending). Marked gains in bone mass after 12 months of ABL treatment resulted in positive effects on bone strength at all sites. At the lumbar spine, these changes in strength parameters correlated strongly with in vivo gains in BMC/BMD (yield load vs. DXA BMC, r=0.89, yield stress vs. DXA BMD, r=0.90). At the femur diaphysis, strength parameters correlated strongly with in vivo gains in BMC/BMD (peak load vs. DXA BMC, r=0.78, ultimate stress vs. DXA BMD, r=0.76). A positive association was also obtained at another cortical site: the tibia pQCT diaphysis vs. femur diaphysis 3-point bending (peak load vs. pQCT cortical BMC, r=0.84, ultimate stress vs. pQCT cortical BMD, r=0.59). At the femoral neck, gains in bone strength were slightly less marked vs. the in vivo gains in bone mass, resulting in positive but more modest correlations (peak load vs. DXA BMC, r=0.45, ultimate stress vs. pQCT cortical BMD, r=0.54). Individual correlation plots showed a clear dose-response with increased values in both densitometry and strength data as dose increased. Correlations were positive for both primary strength parameters (influenced by geometry) and also for material bone properties, showing positive effects of ABL not only on bone mass but also on bone quality. In summary, ABL resulted in dose-related in vivo bone mass gains and improved bone strength, with strong positive correlations at clinically relevant sites, illustrating the potential clinical impact to mitigate fracture risk.

SU0371

Abaloparatide (BA058), a Human PTHrP Analog: Correlation of In Vivo Bone Mass Gains and Improved Bone Strength in the Osteopenic Cynomolgus Monkey. <u>Nancy Doyle</u>*[1], <u>Aurore Varela</u>[1], <u>Susan Y. Smith</u>[1], <u>Gary Hattersley</u>[2]. [1]Charles River Laboratories, Canada, [2]Radius, USA

Abaloparatide (ABL) is an analog of hPTHrP (1-34) undergoing clinical development for the treatment of osteoporosis. Long-term effects of ABL on bone mass and bone strength were evaluated in aged osteopenic, ovariectomized (OVX) monkeys. Four groups were ovariectomized (OVX) and one group underwent Sham surgery. Treatment commenced after a 9-month bone depletion period. Animals received daily subcutaneous injection of either vehicle (Sham and OVX controls), or ABL at 0.2, 1 or 5 µg/kg for 16 months. DXA and pQCT scanning were performed at the end of the bone depletion period (EBD) and after 16 months of treatment. Lumbar vertebrae and femurs were retained for biomechanical testing (compression and femoral neck shear). In order to assess the impact of bone mass gains on bone strength, correlation analyses were performed between % change in bone mass from the EBD and strength data for all OVX animals for L1-L4 DXA vs. L5+L6 vertebral core compression, L1-L4 DXA vs. L3+L4 vertebral body compression, and for all OVX groups for proximal femur DXA vs. femoral neck shear. Marked gains in bone mass after 16 months of ABL treatment at the lumbar spine and femoral neck resulted in positive effects on bone strength at these sites. At the femoral neck, these changes in strength parameters correlated strongly with gains in BMC (peak load vs. femoral neck DXA BMC, r=0.89, stiffness vs. femoral neck DXA BMC, r=0.71). For the vertebral cores, strength parameters correlated positively with gains in BMC/BMD (yield load vs. DXA BMC, r=0.50, apparent strength vs. DXA BMD, r=0.53). For the vertebral bodies, gains in bone strength were slightly less marked vs. the gains in bone mass, resulting in positive but more modest correlations (yield load vs. DXA BMC, r=0.38, apparent strength vs. DXA BMD, r=0.50). Correlation analyses generally showed increased values in both densitometry and strength data as dose increased, with strength values at ≥1 µg/kg being generally comparable to sham controls. Correlations at the spine were greater for strength parameters adjusted for bone geometry. The overall correlation analysis not only showed positive effects of ABL on bone mass but also on bone quality. In summary, ABL resulted in dose-related bone mass gains and improved bone strength, with positive correlations at the spine and femoral neck, two clinically relevant sites, illustrating the potential clinical impact to mitigate fracture risk.

SU0372

Activation of the cAMP/PKA Pathway is Dominant During Vasodilation of the Femoral Principal Nutrient Artery to PTH 1-84 and PTHrP, While Activation of PKC and cAMP/PKA are Equally Important for Vasodilation to PTH 1-34. <u>Jahyun Kim</u>*[1], <u>Brianna Hood</u>[2], <u>Ashley Bice</u>[3], <u>Rhonda Prisby</u>[1]. [1]University of Delaware, USA, [2]University of Delaware, USA, [3]University of Delaware, USA

BACKGROUND: Nitric oxide (NO) blockade with the endothelial nitric oxide synthase (eNOS) inhibitor L-NAME reduced vasodilation of the femoral principal nutrient artery (PNA) by 81%, 92% and 54% in response to PTH 1-84, PTH 1-34 and PTHrP, respectively (Benson et al., 2012). Further, endothelial cell removal eliminated vasodilation to PTHrP (Prisby & Bice, 2013) and PTH 1-84 (Benson & Prisby, 2013) and dramatically impaired vasodilation to PTH 1-34 (Prisby & Bice, 2013). In human umbilical vein endothelial cells, PTH 1-34 stimulated eNOS via the protein kinase C (PKC) and A (PKA) pathways (Rashid et al., 2007). Thus, we sought to determine the pathways of eNOS activation in response to PTH 1-84, PTH 1-34 and PTHrP in intact bone blood vessels. *METHODS:* Right femoral PNAs were dissected from male Wistar rats (4-6 mon) and cannulated to assess vasodilation to PTH 1-84 ($10^{-13} – 10^{-8}$ M; n=9), PTH 1-34 ($10^{-13} – 10^{-8}$ M; n=9) and PTHrP ($10^{-13} – 10^{-8}$ M; n=8) in the presence of 1) PSS buffer, 2) PSS buffer with the PKC inhibitor, Calphostin, 3) PSS buffer with the cAMP antagonist, Rp-cAMP and 4) PSS buffer with the PTH1 receptor blocker, [Nle ^{8,18}, Tyr^{34}]-PTH(7-34) amide. *RESULTS:* Blockade of PKC, cAMP/PKA and PTHR1 reduced (*p*<0.05) vasodilation by 65%, 86% and 104%, respectively, to PTH 1-84. PTH1 receptor and cAMP/PKA blockade reduced (*p*<0.05) vasodilation to PTHrP by 88% and 80%, respectively, and tended (p=0.08) to reduce vasodilation to PTH 1-34 by 42% and 67%, respectively. *CONCLUSION:* The PKC and PKA pathways are equally important for vasodilation to PTH 1-34. Activation of cAMP/PKA is the dominant vasodilator pathway in response to PTH 1-84 and PTHrP. Finally, vasodilation of the femoral PNA to PTH 1-84, PTH 1-34 and PTHrP occurs via the PTH1 receptor.

SU0373

Characteristics of premenopausal women with idiopathic osteoporosis who experience significant bone loss after teriparatide cessation. <u>Adi Cohen</u>*[1], <u>Mafo Kamanda-Kosseh</u>[2], <u>Robert Recker</u>[3], <u>Joan Lappe</u>[4], <u>David Dempster</u>[5], <u>Hua Zhou</u>[6], <u>Serge Cremers</u>[2], <u>Mariana Bucovsky</u>[2], <u>Julie Stubby</u>[7], <u>Elizabeth Shane</u>[8]. [1]Columbia University Medical Center, USA, [2]Columbia University, USA, [3]Creighton University, USA, [4]Creighton University Osteoporosis Research Center, USA, [5]Columbia University, USA, [6]Helen Hayes Hospital, USA, [7]Creighton University, USA, [8]Columbia University College of Physicians & Surgeons, USA

We conducted an open-label pilot study of teriparatide (TPTD; 20 mcg daily for 2 years) in 21 premenopausal women with idiopathic osteoporosis (IOP), and reported substantial BMD increases at the lumbar spine (LS; mean$\pm$SD: 10.8$\pm$8.3%), total hip (TH; 6.2$\pm$5.6%) and femoral neck (FN; 7.6$\pm$3.4%). Although postmenopausal women treated with TPTD lose bone mass after therapy is stopped, BMD remains stable after TPTD cessation in postmenopausal women taking estrogen. We hypothesized that our subjects, who by definition had sufficient endogenous estrogen production to menstruate regularly, would maintain the BMD gains associated with TPTD therapy. Of 21 women who completed the pilot study, 4 declined further participation and 2 were perimenopausal and began antiresorptive therapy. BMD was remeasured 2.0$\pm$0.6 years after TPTD cessation in the remaining 15 women. LS BMD declined by 4.8 $\pm$ 4.3% (p=0.0007) overall and by 3.9 $\pm$ 3.9% (p=0.004) after excluding 2 women who became menopausal during follow-up. On average, BMD was stable at the FN (-1.5 $\pm$ 4.2), total hip (-1.1 $\pm$ 3.7%) and 1/3 radius (+0.2 $\pm$ 2.5%). Those who sustained significant LS bone loss, defined as >3% (-7.3 $\pm$ 2.9%; n=10), did not differ from those with stable LS BMD (0.1 $\pm$ 1.1%; n=5) with regard to baseline BMI, BMD at any site or duration of follow-up (2.1 $\pm$ 0.5 vs 1.7 $\pm$ 0.8 yrs; p=0.2). Those with LS bone loss tended to be older at baseline (41 $\pm$ 3 vs 34 $\pm$ 7; p=0.1) and TPTD completion (44 $\pm$ 3 vs 36 $\pm$ 7; p=0.07), and were significantly older at re-evaluation (46 $\pm$ 3 vs 38 $\pm$ 7; p=0.046). Those who lost bone mass had larger increases in LS BMD during TPTD treatment (12.7 $\pm$ 6.4% vs 5.8 $\pm$ 4.2%; p=0.047) and had higher cancellous bone remodeling (mineralized perimeter) on transiliac biopsy at baseline (4.4 $\pm$ 2.9 vs 1.7 $\pm$ 1.3%; p=0.07) and completion of TPTD treatment (3.4 $\pm$ 2.2 vs 0.9 $\pm$ 0.8%; p=0.049). However, serum bone turnover markers (BTMs) did not differ at baseline, TPTD completion or follow-up. In summary, 2 years after completing a course of TPTD, the majority of premenopausal women with IOP sustain partial loss of lumbar spine BMD, while gains at the hip are maintained. Those with significant bone loss were usually older, had a more robust response to TPTD and had higher bone turnover on transiliac biopsy, though not by serum BTMs. These findings lead us to conclude that premenopausal women with IOP, particularly those over 40 may require antiresorptive treatment to prevent bone loss after TPTD.

	>3% LS BMD loss N=10	< 3% LS BMD loss N=5	p
Before TPTD treatment			
Age at baseline	40.8 ± 2.8	33.8 ± 7.4	0.1
BMI	22.6 ± 3.9	20.3 ± 3.9	0.3
BMD Z Score Lumbar spine	-1.9 ± 0.8	-1.8 ± 1.0	0.7
Total hip	-1.9 ± 0.4	-1.5 ± 0.5	0.1
Femoral neck	-2.0 ± 0.7	-1.6 ± 0.6	0.3
Cancellous bone remodeling:			
Bone formation rate (mm²/mm/yr)	0.010 ± 0.007	0.005 ± 0.004	0.1
Mineral apposition rate (μm/d)	0.63 ± 0.08	0.65 ± 0.20	0.8
Mineralized perimeter (%)	4.4 ± 2.9	1.7 ± 1.3	0.07
Serum bone turnover markers:			
CTX (ng/mL)	0.320 ± 0.121	0.317 ± 0.178	0.9
PINP (mcg/L)	51.6 ± 16.0	41.8 ± 19.3	0.3
At TPTD Treatment Completion			
Age	43.9 ± 2.8	36.0 ± 7.2	0.07
BMD % change from baseline:			
Lumbar Spine	12.7 ± 6.4	5.8 ± 4.2	0.047
Total Hip	6.4 ± 7.2	3.7 ± 3.7	0.4
Femoral Neck	5.7 ± 4.7	7.1 ± 6.0	0.6
Cancellous bone remodeling:			
Bone formation rate (mm²/mm/yr)	0.008 ± 0.006	0.002 ± 0.002	0.08
Mineral apposition rate (μm/d)	0.61 ± 0.13	0.54 ± 0.04	0.4
Mineralized perimeter (%)	3.39 ± 2.16	0.90 ± 0.80	0.049
Serum bone turnover markers:			
CTX (ng/mL)	0.363 ± 0.226	0.308 ± 0.204	0.7
PINP (mcg/L)	44.5 ± 20.7	37.8 ± 10.0	0.5
At Re-evaluation			
Age	45.9 ± 3.1	37.6 ± 6.7	0.046
BMD % change from TPTD completion:			
Lumbar Spine (*variable used for group determination)	-7.3 ± 2.9	0.06 ± 1.1	0.0001
Total Hip	-1.2 ± 4.2	-0.7 ± 1.4	0.8
Femoral Neck	-2.0 ± 4.5	0.3 ± 2.9	0.4

TableBMDfollowup

SU0374

Effect of Teriparatide on Trabecular Bone Microarchitecture Assessed by the Trabecular Bone Score (TBS) in Patients with Osteoporosis. Oksana Davydov*[1], Didier Hans[2], Richard Bockman[3]. [1]New York Presbyterian Hospital/ Weill-Cornell Medical Center, USA, [2]Lausanne University Hospital, Switzerland, [3]Hospital for Special Surgery, Weill Cornell Medical College, USA

Bone mineral density (BMD) is the main measure of bone strength that is used clinically to diagnose osteoporosis. However, it does not always accurately predict fracture risk. Evaluating the trabecular bone microarchitecture increases the accuracy and sensitivity of bone quality examinations. TBS, a texture measurement of 2D projections of existing lumbar spine dual-energy X-ray absorptiometry (DXA) images, is a surrogate measure of trabecular microarchitecture. It has been shown to predict fracture risk independent of BMD. The goal of this study was to analyze the effects of teriparatide (TPTD) treatment on BMD and TBS in a population of patients with osteoporosis.

Bone densities were collected retrospectively for 30 patients treated for osteoporosis with TPTD at the Hospital for Special Surgery. Patients were treated for an average of 24 months. All participants were given calcium and vitamin D supplementation to meet their daily calcium requirements and to maintain 25-hydroxy-vitamin D (25-OH Vit D) levels within normal range. Each patient underwent a baseline and a follow up DXA at the end of the treatment period. BMD at the lumbar spine was assessed by DXA using GE-Lunar Prodigy in 11 participants and Hologic Discovery in 19 patients. The standardized BMD (sBMD) for lumbar spine was calculated using the formula proposed by Hui, et. al. in JBMR (1997) to cross-calibrate the BMD for differences in DXA machines. Twenty-five participants had BMD measured by DXA in the femoral neck (17 Hologic and 8 GE-Lunar). The femoral neck BMD was standardized using the formula in Fan, et. al. in Osteoporosis Int (2010). TBS was determined by TBS INsight software version 2.1.

Twenty-six out of 30 participants were women (Results, Table 1). Percent change in TBS and sBMD did not significantly change if men were excluded from the analysis. The changes in TBS and sBMD did not correlate. Nineteen out of the 30 patients were previously treated with bisphosphonates for an average of 6 years. Baseline and post-TPTD TBS and sBMD values were not affected by prior bisphosphonate (Bisph) exposure, Table 2.

In conclusion: Teriparatide treatment resulted in independent increases in lumbar spine sBMD and TBS, with a greater effect seen on the lumbar spine bone mineral density. Prior exposure to bisphosphonates did not affect the improvement in trabecular bone microarchitecture as measured by the TBS.

	Baseline (mean ± SD)	Post TPTD (mean ± SD)	p-value	Percent Change from Baseline (%)
Age (years)	65 ±10.35			
BMI (kg/m2)	22.6 ±3.6			
25-OH Vit D (ng/mL)	39 ±13	42 ±11	NS	
LS sBMD	0.835 ±0.15	0.887 ±0.15	<0.001	6.72
FN sBMD (n= 25)	0.660 ±0.08	0.674 ±0.10	NS	2.01
TBS	1.286 ±0.11	1.321 ±0.11	0.013	2.92

Table 1.

	Bisph n=19 (mean)	no Bisph n=11 (mean)	p-value
TBS Baseline	1.274	1.307	NS
TBS Post TPTD	1.309	1.343	NS
% chg TBS	2.91[a]	2.93[a]	NS
LS sBMD Baseline	0.806	0.883	NS
LS sBMD Post TPTD	0.855	0.942	NS
% chg LS sBMD	6.44[b]	7.21[b]	NS

[a] The change in TBS from baseline is not significant, p= 0.08.

[b] The change in BMD is significant.

Table 2.

SU0375

Effects of Sclerostin antibody on osteoblast and osteocyte viability/autophagy in mouse model of glucocorticoid-induced bone loss. Weiwei Dai[1], Yu-An Lay[2], Li Jiang[3], Xiaodong Li[4], Hua Zhu (David) Ke[5], Nancy Lane[6], Wei Yao*[6]. [1]Longhua Hospital Shanghai University of Traditional Chinese Medicine, USA, [2]UC Davis Medical center, USA, [3]UC Davis Medical Center, USA, [4]Amgen, Inc., USA, [5]Amgen Inc., USA, [6]University of California, Davis Medical Center, USA

Objective. Sclerostin is a negative regulator of bone formation. A monoclonal antibody to sclerostin (Scl-Ab) is a new anabolic agent that builds bone by stimulating bone formation and decreasing bone resorption. We have previously demonstrated that glucocorticoids (GCs) over -stimulate sclerostin expression in bone and, accordingly, inhibits bone formation. Furthermore, high dose or prolong GC treatments inhibit osteoblast and osteocyte cell viabilities through autophagy, an intracellular degradative mechanism that removes dysfunctional organelles and/or oxidized proteins to maintain cell viability. To understand the effects of Scl-Ab on autophagy in response to GC excess *in vivo*, we have generated transgenic mice systemically expressing dsRed fused to LC3, a protein marker for autophagosomes. We then studied the effects of GCs and Scl-Ab on autophagic osteoblasts and osteocytes, bone structure, and strength in these mice.

Methods. Two-month-old male dsRed-LC3 reporter mice received placebo (PL) or prednisolone (2.8mg/kg/d) implantation and then were treated immediately with Scl-Ab (25mg/kg, 2x/wk) for three weeks. Bone volume (BV/TV) and bone formation were measured at the distal femur (DF), lumbar vertebral body (LVB), and mid-femoral shaft (FS) by μCT and bone histomorphometry (n=8-10/group). LC3+ osteoblast surface/bone surface (Ob.S/BS) was determined at LVB and LC3+ osteocyte density was determined at the femoral shaft (FS) in all the study animals. Autophagic RNA and protein levels were determined by RT-PCR and western blotting (WB) on the FS (n=3).

Results. - GC significantly lowered osteoblast surface and inhibited bone formation at both LVB and FS as compared to PL. These changes were associated with reduced bone volume and strength. Scl-Ab completely prevented the decrease in bone formation and the vertebral and femoral strength due to GC excess. GC excess reduced the gene expression in the autophagy pathway by 3-5-fold at the FS and Scl-Ab maintained autophagic gene expression at the PL level. Autophagy of the osteoblast surface (Auto.Ob) was observed at bone surface and frequently co-localized with double-labeled surface. The Auto.Ob was reduced at the trabecular bone surface by nearly 70% in GC group as compared the PL group and was not significantly affected in Scl-Ab group. The autophagic osteocyte density was 39% lower in GC group than in the PL group, whereas it was not significantly affected in Scl-Ab group. Western blot analyses performed at the FS demonstrated that GC reduced the expression of ATG-7, ATG-16L and LC3-II, by more than 50%, indicating reduced formation of autophagosome. Scl-Ab preserved expressions of ATG- 7 and ATG -16L and LC3-II at the PL levels.

Conclusion. GC reduced bone formation, bone mass and osteoblast and osteocyte autophagy. Scl-Ab prevented the detrimental effects of GC on bone formation, bone mass and osteoblast and osteocyte autophagy.

SU0376

Factors related to the response rate of bone mineral density (BMD) to osteoanabolic therapy (teriparatide/PTH) in patients with severe osteoporosis.

Laia Gifre*[1], Ana Monegal[2], Xavier Filella[3], Africa Muxi[4], Nuria Guanabens[5], Pilar Peris[6]. [1]Hospital Clinic Barcelona, Spain, [2]Hospital Clinic Barcelona, Spain, [3]Department of Biochemistry & Molecular Genetics, Hospital Clinic., Spain, [4]Nuclear Medicine Department. Hospital Clinic, Spain, [5]Universitat De Barcelona, Spain, [6]Hospital Clínic of Barcelona, Spain

Background: Factors related to the magnitude of BMD response to osteoanabolic treatment (teriparatide/PTH) remain unclear.

Aim: To evaluate the long-term BMD response rate to osteoanabolic treatment in patients with severe osteoporosis and the factors related to "inadequate" response (IR) to therapy.

Methods: 49 patients (46F:3M) with a mean age of 69.5 ± 11.1 years treated with teriparatide (41) or PTH1-84 (8) during 18 or 24months were included (84% had vertebral fractures [mean 5 ± 4], 71% non-vertebral fractures, 86% had been previously treated with bisphosphonates [mean duration 5.7 ± 4.5 years, time range of discontinuation 0-29 months] and 22% were receiving glucocorticoid treatment). Bone turnover markers (BTM)(formation: P1NP, bone ALP; resorption: sCTx, NTx) and 25OH vitamin D (25OHD) levels were assessed before and at 3, 6, 12 and 18/24 months of treatment. Lumbar and femoral BMD and spinal X-ray were assessed at baseline, and at 12 and 18/24 months. Previous and incidental fractures, previous antiosteoporotic treatment, risk factors and cause of osteoporosis were recorded in all patients. IR was defined by a lumbar BMD increase <3% at 18/24 months. BTM were also evaluated in fold-number over/under normal values and as a normalized bone formation/resorption index.

Results: 29% of patients showed IR to therapy. No significant differences were observed in age, length of previous bisphosphonate use or discontinuation, baseline BMD and BTM or bone formation/resorption index, and 25OHD levels between patients with or without IR. As expected, IR patients presented worse BMD evolution in lumbar spine and femur at 18/24 months (Lumbar BMD: -3.4% vs. 12.8%, p <0.001; femur total -0.6% vs. 4.5%, p=0.012). Nevertheless, no significant differences were observed in the magnitude of changes in BTM (formation and resorption markers) throughout the study or in the evolution of their corrected values (by normal range) or the normalized bone formation/resorption index. 25OHD serum levels were similar in both groups of patients throughout the study as was the incidence of new fractures.

Conclusions: In patients with severe osteoporosis previously treated with other antiosteoporotic therapies no factors to predict the efficacy of osteoanabolic agents were identified.

Disclosures: Laia Gifre, None.

SU0377

FRAX and the effect of teriparatide on vertebral and non-vertebral fracture.

John Kanis[1], Anders Oden[2], Helena Johansson[3], Russel Burge[4], Bruce Mitlak[4], Eugene McCloskey*[5]. [1]University of Sheffield, Belgium, [2]University of Sheffield, United Kingdom, [3]Centre for Metabolic Bone Diseases, University of Sheffield Medical School, Sweden, [4]Eli Lilly & Company, USA, [5]University of Sheffield, United Kingdom

Daily administration of 20 µg or 40 µg teriparatide has been shown to significantly decrease the risk of vertebral and non-vertebral fracture compared with placebo. The aim of the present study was to evaluate fracture risk assessed at baseline using the FRAX® tool and to determine the efficacy of teriparatide as a function of baseline fracture risk. Because there was no difference in fracture efficacy of 20 and 40 µg teriparatide daily, the two active groups were merged. Baseline clinical risk factors (age, BMI, prior fracture, glucocorticoid use, rheumatoid arthritis, smoking and maternal history of hip fracture) were entered into country-specific FRAX models to compute the 10-year probability of major osteoporotic fractures with or without input of femoral neck BMD. The interaction between probability of a major fracture and treatment efficacy was examined by Poisson regression.The 10-year probability of major osteoporotic fractures (with BMD) ranged from 2.2-67.2%. Treatment with teriparatide was associated with a 37% decrease in all non-vertebral fractures compared to placebo treatment (95% CI = 10-56 %). In patients in whom fractures were characterised as low energy, the decrease in fracture risk was more marked (RRR=56%; 95% CI = 24-75 %). The risk of vertebral fractures decreased significantly by 66% (50-77 %). There was no significant effect on hip fracture. Hazard ratios for the effect of teriparatide on the fracture outcome did not change significantly with increasing fracture probability (p>0.30). Similar findings were noted for the interaction when BMD was excluded from the FRAX model. Comparable findings were also noted for the interaction between probability of a hip fracture and treatment efficacy. We conclude that teriparatide significantly decreases the risk of non-vertebral and morphometric fractures in women by a similar extent, irrespective of baseline fracture probability.

Disclosures: Eugene McCloskey, Eli Lilly and Company, 3
This study received funding from: Eli Lilly and Company

SU0378

Indirubin-3′-oxime, an activator of Wnt/β-catenin pathway, induces osteogenic lineage commitment of ST2 cells and reverses bone loss in high-fat diet-induced obese mice.

Jeong-Ha Hwang*[1], Zahoor Muhammad[2], Kang-Yell Choi[2], Pu-Hyeon Cha[2]. [1]Translational Research Center for Protein Function Control, Yonsei University, South Korea, [2]Translational Research Center for Protein Function Control, Yonsei University, South Korea

Obesity is a global issue of the modern world, and its negative impact on bones in obese male patients has been recently reported. The Wnt/β-catenin pathway has an established role in the regulation of body fat content and bone density. We investigated the effects of indirubin-3′-oxime (I3O), the GSK3β inhibitor that activates Wnt/β-catenin signaling, on trabecular bone in high-fat diet (HFD)-induced obese male mice. I3O reverses the downregulating effect of fatty acid (FA) on Wnt/β-catenin signaling and enhances the osteogenic commitment of the bone marrow-derived stromal cell line ST2. FA induces the adipogenic differentiation of bone marrow stromal cells in vitro. In a male mouse model of HFD-induced obesity, trabecular bone loss was observed in the femora, with a gross increase in abdominal fat; however, the HFD effects were rescued with the activation of Wnt/β-catenin signaling by I3O treatment. I3O administration also reversed the increase in the number of HFD-induced adipocytes in the femur bone marrow in trabecular bone. Taken together, our results indicate that I3O could be a potential therapeutic agent for obese male patients through downregulation of abdominal fat and net increment in trabecular bone density.

Indirubin-3′-oxime, an activator of Wnt/β-catenin pathway, induces osteogenic lineage commitment of ST2 cells and reverses bone loss in high-fat diet-induced obese mice

Muhammad Zahoor,[1,2] Jeong-Ha Hwang, [1,2] Pu-Hyeon Cha,[1,2] Kang-Yell Choi[1,2]

[1]Translational Research Center for Protein Function Control, College of Life Science and Biotechnology, Yonsei University, Seoul, South Korea
[2]Department of Biotechnology, College of Life Science and Biotechnology, Yonsei University, Seoul, South Korea

Abstract
Obesity is a global issue of the modern world, and its negative impact on bones in obese male patients has been recently reported. The Wnt/β-catenin pathway has an established role in the regulation of body fat content and bone density. We investigated the effects of indirubin-3′-oxime (I3O), the GSK3β inhibitor that activates Wnt/β-catenin signaling, on trabecular bone in high-fat diet (HFD)-induced obese male mice. I3O reverses the downregulating effect of fatty acid (FA) on Wnt/β-catenin signaling and enhances the osteogenic commitment of the bone marrow-derived stromal cell line ST2. FA induces the adipogenic differentiation of bone marrow stromal cells in vitro. In a male mouse model of HFD-induced obesity, trabecular bone loss was observed in the femora, with a gross increase in abdominal fat; however, the HFD effects were rescued with the activation of Wnt/β-catenin signaling by I3O treatment. I3O administration also reversed the increase in the number of HFD-induced adipocytes in the femur bone marrow in trabecular bone. Taken together, our results indicate that I3O could be a potential therapeutic agent for obese male patients through downregulation of abdominal fat and net increment in trabecular bone density.

Abstract

Disclosures: Jeong-Ha Hwang, None.

SU0379

Noninvasive Quantification of Focal Osteogenesis Induced by Mechanical Loading.

Brandon Ausk*[1], Philippe Huber[2], Ted Gross[1], Sundar Srinivasan[1]. [1]University of Washington, USA, [2]University of Washington, USA

Exercise holds potential to focally enhance bone mass at skeletal sites most at risk for fracture. However, current imaging techniques do not permit the noninvasive assessment of exercise induced focal alterations in bone mass. We have previously developed an image registration technique capable of quantifying focal resorption in a model of profound osteoclastogenesis. Here, we sought to extend this technique to noninvasively quantify focal alterations in osteoblast activity induced by mechanical loading of bone. Five female C57 mice (22 mo) underwent cyclic cantilever bending of the right tibia (50 cycles, 1700 µε) on M, W, F for 9 wks. A primary µCT scan of the right tibia midshaft (4.45 mm starting 1.78 mm distal to tib-fib junction) was obtained on d 0, with secondary scans obtain on d 21, d 42 and post-sacrifice (d 63). To enable histomorphometric validation of the image registration technique, all mice received calcein (day 10 and 19) and alizarin (day 52 and 61) injections. Based upon previous data, the distal 2.0 mm of the scanned tibia that displays minimal periosteal adaptation was defined as the invariant registration volume (IRV) critical for registration of scans obtained over time. We assessed bone adaptation throughout the scan volume by registering the primary and secondary scans of the tibia segments. As an initial proof of concept, µCT based focal bone alterations were then compared at 3 wks to dynamic histomorphometry parameters at the mid-shaft cross-section (2.0 mm proximal to tib-fib) around 16 circumferential sectors. In this time period, the registration accuracy of the primary and secondary IRVs was consistent with our previous data (1.9 ± 0.3% misalignment). Focal periosteal bone formation rates, as quantified by µCT, was highly correlated with that determined via dynamic histomorphometry (r=0.76, p<0.001; Fig 1). In addition to quantifying osteoblast activity, the image registration technique enabled the tracking of focal osteoclastic bone resorption as well (Fig 1). These results demonstrate that when temporally invariant bone volumes can be identified, image registration enables the accurate quantification of focal bone alterations arising over time from the accumulated activity of bone cells. As this goal can be achieved regardless of whether the intervention is anabolic or catabolic, these data underscore its potential use in clinical trials where it is not possible to quantify bone cell responses via histomorphometry.

Fig 1: Within the first three weeks, focal periosteal bone formation quantified through µCT image registration (A) was highly correlated to that determined through traditional dynamic histomorphometry (mean ± s.e., B) and allowed for temporal quantification of bone formation (orange, C) and bone resorption (red, C) on all bone surface throughout the 9 wk study.

Figure 1

Disclosures: Brandon Ausk, None.

SU0380

PTH-CBD, a Long-Acting Parathyroid Hormone Analog, restores normal bone formation after cyclophosphamide therapy in mice. <u>Ranjitha Katikaneni</u>[1], <u>Robyn Goforth</u>[2], <u>Andrew Seymour</u>[3], <u>Robert Gensure</u>[4], <u>Tulasi Ponnapakkam</u>*[5]. [1]Childrens Hospital at Montefiore/Albert Einstein College of Medicine, USA, [2]BiologicsMD, Inc, USA, [3]Department of Pathology, Montefiore Medical Center, USA, [4]Children's Hospital at Montefiore, Albert Einstein College of Medicine, USA, [5]Childrens Hospital at Montefiore, New York/Albert Einstein College of Medicine, USA

PTH-CBD is a hybrid protein of PTH(1-33) and a bacterial collagen binding domain designed to accumulate in collagen rich areas such as bone. We have previously shown that PTH-CBD can improve bone mineral density (BMD) in chemotherapy osteoporosis. We now investigate the time course of this response, examining effects on bone formation and bone removal evident in serology and histological analysis, paired with measurements of BMD, in a mouse model with chemotherapy-induced impairments in bone formation. 8 week old C57BL/6 mice were treated with cyclophosphamide (50 mg/kg/wk IP x 3 weeks), cyclophosphamide plus PTH-CBD (320 mcg/kg SQ x1), or vehicle alone. BMD was measured every 2 weeks. Animals were sacrificed at baseline, 1 month, 2 months, or 3 months to provide blood and tissue samples throughout the expected time of the treatment response. BMD measurements confirm that cyclophosphamide treatment prevented the normal increases in BMD expected in young mice (BMD at 6 weeks: 68.2+/-1.2 chemo vs. 74.4+/-1.1 mg/cm2 no chemo, p<0.05), presumably because of impairments in bone formation. PTH-CBD therapy restored the normal pattern of increases in BMD in cyclophosphamide-treated mice (BMD at 6 weeks: 72.9+/-1.2 PTH-CBD + Chemo vs. 68.2+/-1.2 mg/cm2 chemo, p<0.05), such that there was no difference between animals which did not receive chemotherapy. Serum samples will be processed for alkaline phosphatase, osteoproteregin, TRAP to assess effects of cyclophosphamide and PTH-CBD on bone turnover. Calcium will also be measured to assess for potential side effects. Histological samples will be processed for histomorphometry and TRAP staining. Together, these data will provide confirmation of the effects of cyclophosphamide on bone formation and bone removal, and will define which of these processes is most important in mediating the restoration of normal BMD seen with PTH-CBD treatment.

Disclosures: Tulasi Ponnapakkam, None.

SU0381

Safety of daily subcutaneous administration of teriparatide with regard to calcium metabolism in patients with serum procollagen type 1 N-terminal propeptide elevation above the upper limit of normal range. <u>Takanori Yamamoto</u>*[1], <u>Mika Tsujimoto</u>[2], <u>Hideaki Sowa</u>[3]. [1]Eli Lilly, Japan, [2]Asia Pacific Statistical Science, Eli Lilly Japan K.K., Japan, [3]Lilly Research Laboratories Japan, Eli Lilly Japan K.K., Japan

Purpose: Daily administration of teriparatide enhances bone formation-precedent and -dominant bone metabolism. Procollagen type 1 N-terminal propeptide (P1NP), which is produced in the course of bone metabolism, is a useful marker of therapeutic efficacy. On the other hand, elevation of P1NP over the upper limit of normal range may indicate adverse effects such as calcium metabolism disorders. Thus, we evaluated the relationship between serum P1NP elevation and patient safety using data from a phase 3 study in Japanese patients with osteoporosis. Methods: A randomized clinical trial of teriparatide 20 µg/day was previously conducted in Japanese patients with osteoporosis at high risk of fracture (Full Analysis Set, n = 203; ClinicalTrials.gov identifier: NCT00433160). This study consisted of a 12-month placebo-controlled double-blinded period and a 12-month treatment period in which all patients received open-label teriparatide. Vitamin D and calcium were also administered throughout the study period. Serum P1NP and serum calcium levels were measured at baseline, and 1, 3, 6, 12 and 24 months after starting treatment (24 hours after dosing). Adverse events related to calcium metabolism disorders, metastatic bone neoplasms, and other metabolic bone disorders were analyzed using MedDRA ver.12.0. Results: Median value of serum P1NP increased in the teriparatide group from 52.5 µg/L at baseline to 95.5 µg/L at 1 month after starting treatment and remained high until 24 months. In either treatment group, there was no significant difference in albumin-corrected serum calcium between patients who had a P1NP level >200 µg/L at least once during the study period or those who had P1NP levels ≤200 µg/L over the entire study period. One patient in teriparatide group and 1 patient in placebo-teriparatide group had hypercalcemia during the teriparatide treatment period, but recovered without changing teriparatide dosage or requiring additional medication. Other adverse events possibly related to calcium metabolism disorders included periarthritis calcarea (1 patient in teriparatide group) and chondrocalcinosis pyrophosphate (2 patients in teriparatide group), but none of these were accompanied by significant increases in serum P1NP or serum calcium. Conclusion: Serum P1NP elevation after daily subcutaneous teriparatide treatment indicates efficacy for osteoporosis, however, its relationship with safety concerns related to bone metabolism disorders was not determined.
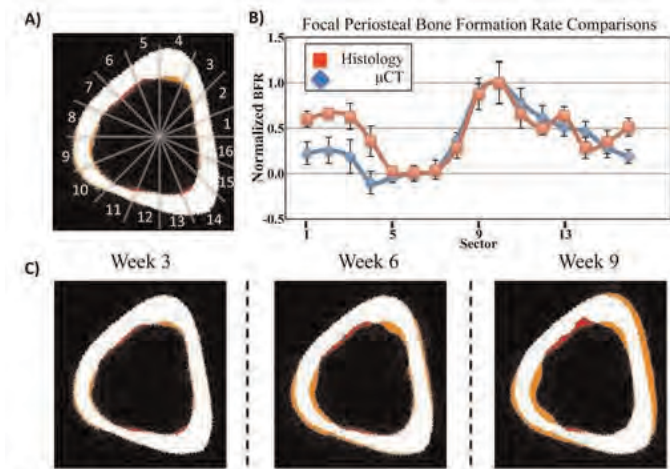
Disclosures: Takanori Yamamoto, Eli Lilly Japan K.K., 4
This study received funding from: Eli Lilly Japan K.K.

SU0382

Thapsigargin increases bone volume in mice in vivo by inhibiting Notch signaling in mesenchymal progenitors and promoting osteoblast differentiation. <u>Hengwei Zhang</u>*[1], <u>Xing Li</u>[2], <u>Brendan Boyce</u>[3], <u>Lianping Xing</u>[4]. [1]Univeristy of Rochester, USA, [2]University of Rochester, USA, [3]University of Rochester Medical Center, USA, [4]University of Rochester, USA

Notch plays critical roles in osteoblasts (OBs) and osteoclasts (OCs) to maintain bone homeostasis under physiological conditions. TNF transgenic (TNF-Tg) mice (a model of rheumatoid arthritis and inflammatory osteoporosis) have sustained Notch activation in their mesenchymal stem cells (MSCs) associated with decreased bone formation. Treatment of these mice with DAPT, a Notch inhibitor, resulted in increased OB differentiation and bone volume, indicating a beneficial effect of Notch inhibition on inflammation-associated bone loss. Thapsigargin (THAP), a long-known regulator of OB and OC function in vitro via effects on intracellular Ca^{++} and ER stress and which is in phase I clinical trials for treatment of solid cancers, was shown recently through complementary genomic screening to also be a Notch inhibitor (Cancer Cell, 2013), but no studies to date have examined its effects on bone volume in vivo. We treated TNF-Tg mice and WT littermates long-term with THAP (0.4mg/kg/injection ip/day for 2 months) and found using in vivo microCT that it slightly increased BV/TV in lumbar vertebrae at 1 month and this increase was significant at 2 months in both TNF-Tg and WT mice: 32 ± 6 vs $27 \pm 5\%$ in WT; 24 ± 3 vs $18 \pm 2\%$ in TNF-Tg (p<0.05 vs. vehicle-treated mice). Histomorphometric analyses showed increased BV/TV (15 ± 4 vs $9 \pm 2\%$ in WT; 13 ± 3 vs $5 \pm 2\%$ in TNF-Tg, p<0.05) and OB numbers (50 ± 9 vs 41 ± 7/mm bone surface in WT; 38 ± 5 vs 22 ± 3/mm in TNF-Tg, p<0.05) in tibial sections from THAP-treated mice. Unlike DAPT, which increases OC numbers, THAP significantly decreased OC numbers (1 ± 0.8 vs 2.8 ± 0.7/mm in WT; 1.4 ± 0.7 vs 5.7 ± 1.2/mm in TNF-Tg, p<0.05). THAP decreased mRNA levels of the Notch target gene, Hes1, in CD45-MSC-enriched cells from THAP-treated WT (by $90 \pm 5\%$) and TNF-Tg (by $95 \pm 8\%$) mice and increased the formation of CFU-ALP+ colonies (57 ± 5 vs 24 ± 4/dish in PBS-treated WT; 22 ± 2 vs 11 ± 3 in PBS-treated TNF-Tg mice) and nodule formation (68 ± 4 vs 47 ± 6/well in PBS-treated WT; 41 ± 4 vs 8 ± 2 in PBS-treated TNF-Tg) from bone marrow stromal cells from the mice. Long-term Thapsigargin treatment did not affect body weight or survival. Thus, THAP increases bone volume and inhibits Notch signaling in both TNF-Tg and WT mice. THAP has several advantages over DAPT: it more efficiently suppresses Notch signaling, increases bone volume in both TNF-Tg and WT mice, and decreases OC formation. Thus, THAP is a potential new anabolic agent to increase bone mass by inhibiting Notch signaling.

Disclosures: Hengwei Zhang, None.

SU0383

The LRP5 Variants rs312024 and rs312009 are not Associated with Teriparatide Efficacy in the Treatment of Osteoporosis. <u>Hou-Feng Zheng</u>*[1], <u>Lauren Morkry</u>[2], <u>Lee O'Brien</u>[3], <u>Bente Langdahl</u>[4], <u>Brent Richards</u>[1]. [1]McGill University, Canada, [2]McGill University, Canada, [3]Eli Lilly & Company, USA, [4]Aarhus University Hospital, Dnk

Results from a teriparatide pharmacogenetics study [ASBMR Abstract, Presentation Number 1172, 2012], indicated that genetic variants in LRP5 may be associated with a change in femoral neck (FN) bone mineral density (BMD) following 12 months of teriparatide treatment. The rationale for this study was to replicate these results in a second cohort of teriparatide treated patients. DNA samples from two well-characterized cohorts of osteoporosis patients receiving teriparatide for at least 6 months (Canadian cohort, n = 44 and Danish cohort, n= 121), were genotyped by Taqman for 2 SNPs in LRP5 (rs312009 and rs312024). Changes in BMD from baseline to the BMD measurement collected closest to 12 months was assessed using linear regression where the model included covariate adjustments for baseline BMD, BMI, age, gender and years since menopause. Each SNP was tested under a dominant mode of inheritance in the combined Canadian/Danish cohorts (since the primary analysis was for the combined analysis population) and in each individual cohort. The baseline demographics between the Canadian and Danish cohorts were similar; however, an increase in FN BMD was only observed in the Canadian cohort (P = 0.59 vs <0.0001 for Danish and Canadian cohorts, respectively). The rs312009 variant was not associated with changes in FN BMD in the overall analysis population or the individual cohorts. The rs312024 variant was not associated with changes in FN BMD in the overall analysis population or the Danish cohort; however an associated with teriparatide induced changes in BMD was observed in the Canadian cohort (p = 0.02). However, the effect in the Canadian cohort was in the opposite direction than the discovery cohort, where the GG genotype group had a larger BMD increase in the discovery cohort, and the AA/AG genotype group had a larger BMD increase in the Canadian cohort. The conflicting results may be due to limited power in the current study as the Canadian cohort analysis only included 28 subjects with genotype and relevant clinical information. Analyses in larger cohorts will be necessary to discern the conflicting results. In the current study, we find no evidence that the LRP5 variants rs312009 and rs312024 are associated with teriparatide treatment in the overall analysis population.

Disclosures: Hou-Feng Zheng, None.

SU0384

Treatment of Severe Osteoporosis in Youngs with Teriparatide And Denosumab. <u>Jose Manuel Quesada Gomez</u>*[1], <u>Concepción Muñoz</u>[2], <u>Maria Angeles Galvez</u>[2], <u>Adolfo Diez-Perez</u>[3]. [1]Quesper R&D, Spain, [2]SAS, Spain, [3]Autonomous University of Barcelona, Spain

Osteoporosis treatment with bone-active drugs is a challenge in young and premenopausal patients with severe osteoporosis. The conventional therapeutic strategy is to stimulate bone formation (anabolic treatment) or inhibit bone turnover (anti-catabolic treatment). The combined treatment of the monoclonal anti RANKL denosumab (Dab) every six months with teriparatide (TPT) every day would maintain the anabolic effects of TPT, inhibiting its catabolic activity.

We have carried out a proof-of-concept study in young patients with severe osteoporosis treated with TPT and Dab to assess bone mineral density (BMD) and bone turnover markers (BTM).

We studied twelve patients (38 $\pm$ 15 yr.) with low BMD (lumbar spine (LS) of 0.77 $\pm$ 0.1 g/cm^2; total femur (TF) 0.77 $\pm$ 0.12 g/cm^2 and increased bone turnover markers and/or spine fracture at baseline. Treated for one to two years with TDP (s.c.) 20 mg/day and denosumab (s.c.) 60 mg/six months. BMD significantly increased at 12 months compared with baseline: CL (0.87 $\pm$ 0.9 cm^2, P <0.0001) and TF (0.8 $\pm$ 0.13 g/cm^2, P <0.0001) with a gain of 16% after the first year, even reaching a normalized BMD in patients after two years. This treatment was associated with suppression of BTM.

Thus,the combined treatment of teriparatide and denosumab provides a significant and fast gain in BMD. This combinationconstitutes an interesting therapeutical approach for young patients with osteoporosis (low BMD) or high risk of osteoporotic fracture.Acknowledgements: Grant of Intensification of Research in Andalusia and Institute of Health Carlos III (Ministry of Science and Innovation) PI08/1692 project. Thematic Network of Cooperative Research on Aging and Fragility (RETICEF).

Disclosures: Jose Manuel Quesada Gomez, None.

SU0385

Bisphosphonate drug holiday: results from the ESTRATOS survey. <u>Enrique Casado</u>*[1], <u>Jorge Malouf</u>[2], <u>Esteban Salas</u>[3], <u>Manuel Caamaño</u>[4], <u>Santos Castañeda</u>[5], <u>Juan Sánchez-Bursón</u>[6], <u>Gabriel Herrero-Beaumont</u>[7]. [1]University Hospital Parc Taulí, Spain, [2]Hospital de la Santa Creu i Sant Pau, Spain, [3]Hospital Universitario de San Juan de Alicante, Spain, [4]Hospital Clínico Universitario Santiago de Compostela, Spain, [5]Hospital Universitario de la Princesa, Spain, [6]Hospital Universitario Nuestra Señora de Valme, Spain, [7]Fundación Jiménez Díaz, Spain

Introduction: Long-term treatment with bisphosphonates (BP) has been associated with some complications. Therefore, although scientific evidence is scarce, some experts recommend a temporary discontinuation of these drugs in patients with osteoporosis who are receiving them for several years.

Purpose : To evaluate the opinion of bone specialists regarding the concept "BP drug holiday" and to ascertain their routine clinical practice.

Methods: The ESTRATOS (from Spanish: Treatment Strategy in Osteoporosis) is a 19-item survey regarding the concept "BP drug holiday" and decision-making criteria in clinical practice, addressing members of the Spanish Bone Mineral Metabolism and

Research Society (SEIOMM). SPSS v.13.00 software (Chicago, IL) was used for data analysis. Categorical variables were expressed as absolute and relative frequencies; and continuous variables as mean and standard deviation or, as median and range.

Results: We collected 146 completed surveys from bone specialists (62% Rheumatologists, and the remaining 58% from Internal Medicine, General Practitioners, Orthopaedic Surgeons and others). About 88% of the participants had good knowledge of the concept "BP drug holiday", and only 3% stated this should never or exceptionally be considered. More than half (57%) of the participants usually take a time off BP after several years of treatment because of the sustained efficacy of BP after withdrawal, while 40% of them due to the risk of long-term complications, especially atypical femoral fractures. DXA and spine X-ray are the most used tools to make a decision of BP discontinuation, and 1 out of 3 participants believe both are necessary. According to 55% of the participants, BP drug holiday should be considered after 5 to 10 years of treatment, although 35% thought it should be considered after 3-5 years. 99% of the participants have already recommended drug holiday to some of their patients, and 90% consider that it should last 2 or more years, regardless of the type of BP. The main indicators for reintroducing treatment are the occurrence of a new fragility fracture or a significant decrease in BMD.

Conclusions: According to our survey bone specialists withdraw temporarily the treatment with BP (drug holiday) in their osteoporotic patients after 3 to 10 years of treatment. Nevertheless, for them it is important to monitor BMD and the incidence of new fragility fractures during the untreated period.

Disclosures: Enrique Casado, None.
This study received funding from: Lilly

SU0386

Bisphosphonate ISS Flight Experiment. <u>Adrian LeBlanc</u>*[1], <u>Toshio Matsumoto</u>[2], <u>Jeffrey Jones</u>[3], <u>Jay Shapiro</u>[4], <u>Thomas Lang</u>[5], <u>Linda Shackelford</u>[6], <u>Scott Smith</u>[7], <u>Harlan Evans</u>[8], <u>Elisabeth Spector</u>[8], <u>Robert Ploutz-Snyder</u>[9], <u>Jean Sibonga</u>[7], <u>Joyce Keyak</u>[10], <u>Toshitaka Nakamura</u>[11], <u>Kenjiro Kohri</u>[12], <u>Hiroshi Ohshima</u>[13], <u>Gilbert Moralez</u>[14]. [1]Baylor College of Medicine, USA, [2]University of Tokushima Graduate School of Medical Sciences, Japan, [3]Baylor College of Medicine, USA, [4]Kennedy Krieger Institute, Johns Hopkins, USA, [5]University of California, San Francisco, USA, [6]NASA JSC, USA, [7]NASA, USA, [8]Wyle, USA, [9]USRA, USA, [10]Department of Radiological Sciences, University of California, Irvine, USA, [11]National Center for Global Health & Medicine, Japan, [12]Nagoya City University, Japan, [13]JAXASpace Biomedical Research Office, Japan, [14]UNTHSC, USA

Elevated bone resorption is a hallmark of human spaceflight and bed rest (common zero G analog). In a collaborative effort between the NASA and JAXA space agencies, we tested whether an antiresorptive drug in combination with in-flight exercise would ameliorate bone loss and hypercalciuria during long-duration spaceflight. Measurements of bone loss included DXA, QCT, pQCT, urine and blood biomarkers. We have completed analysis of R+1year data from 7 crewmembers treated with alendronate during flight, as well as immediate post flight (R+<2wks) data from 5 of 10 controls without treatment. Both the treated and current control group used the Advanced Resistive Exercise Device (ARED) during their missions.

We previously reported the pre/post flight results of crew taking alendronate during flight (Osteoporosis Int. 24:2105–2114, 2013). The purpose of this report is to present the 12-month follow-up data in the treated astronauts and to compare these results with preliminary data from untreated crewmembers exercising with ARED (ARED control) or without ARED (Pre-ARED control, previously published). Results: the table presents DXA and QCT BMD expressed as % change from preflight in the control astronauts (18 Pre-ARED and the current 5 ARED-one year data not yet available) and the 7 treated subjects. As shown previously the combination of exercise plus antiresorptive is effective in preventing bone loss during flight. Bone

measures for treated subjects, 1 year after return from space remain at or near baseline values. Except for one region, the treated group maintained or gained bone one year after flight. Biomarker data are not currently available for either control group and therefore not presented. However data from other studies with or without ARED show elevated bone resorption and urinary Ca excretion while bisphosphonate treated subjects show decreases during flight. Comparing the two control groups suggests significant but incomplete improvement in maintaining BMD using the newer exercise protocols compared to earlier resistive exercise protocols. Quantitative characterization of this improvement requires additional measurements in the ARED control group which we are currently collecting. In conclusion, these results indicate that an antiresorptive may be an effective adjunct to exercise during long-duration spaceflight.

%Change from Pre-Flight (Mean ± SD)

	Pre-ARED Control (n=18)	ARED Control (n=5)	Alendronate Treated (n=7)	
	R+<2 week	R+<2 week	R+<2week	R+1 year
DXA BMD				
Total Hip	-6.2 ± 2.8*	-2.7 ± 3.2	-0.2 ± 1.5	0.8 ± 1.4
Trochanter	-6.8 ± 4.8*	-3.8 ± 2.9*	0.02 ± 2.3	2.1 ± 1.2*
Femur Neck	-6.6 ± 3.0*	0.8 ± 4.6	-0.7 ± 1.2	1.5 ± 1.7*
Lumbar Spine	-3.9 ± 3.2*	-3.7 ± 2.3*	2.8 ± 4.0	3.9 ± 3.8*
QCT BMD				
Trabecular Total Hip	−13.6 ± 6.4*	-6.9 ± 8.0	-1.1 ± 9.8	-1.1 ± 12.1
Cortical Total Hip	−3.2 ± 3.5*	-3.6 ± 0.4*	-0.6 ± 4.7	-2.9 ± 3.7
Trabecular Trochanter	−13.5 ± 6.5*	-5.6 ± 7.8	-1.9 ± 9.9	-1.2 ± 12.4
Cortical Trochanter	−3.2 ± 3.3*	-4.6 ± 1.4*	-0.5 ± 5.0	-3.2 ± 4.3
Trabecular Femur Neck	−15.0 ± 9.8*	-15.8 ± 15.8*	6.5 ± 14.8	2.8 ± 7.2
Cortical Femur Neck	−4.0 ± 5.5*	-3.2 ± 2.6	-1.0 ± 4.8	-3.9 ± 3.1*

*P < 0.05, uncorrected for multiple comparisons

ASBMR abstract table

Disclosures: Adrian LeBlanc, None.

SU0387

Bone Benefit of Fish Oil Supplementation Depends on Its EPA and DHA Content. <u>Md Rahman</u>*[1], <u>Xiao Yang</u>[2], <u>Mohiuddin Rasel</u>[3]. [1]University of Texas Health Science Center, USA, [2]University of Texas at San Antonio, USA, [3]UT Health Science Center at San Antonio, USA

The goal of this study is to determine the effective minimal dose of eicosapenaenoic acid (EPA) and docosahexaenoic acid (DHA) in fish oil (FO) supplementation to maintain better bone health during aging. FO is one of the most popular dietary supplements used by American people for various health benefits. We earlier showed that 9% regular fish oil (RFO) with low content of EPA and DHA could maintain better bone mineral density (BMD) during aging. However, this amount of FO is not feasible for human consumption. To determine if low dose RFO can maintain the bone health during aging, 6 month old C57BL/6 female mice were fed either with 4% RFO or 4% corn oil (representative of American diets which have high content of linoleic acids) fed for 6 months and 14 months. All mice were DXA scanned at 6 month of age as a baseline value. Mice were again DXA scanned after 6 and 14 months of feeding. BMD was analyzed using PIXIMUS software. We did not see any significant improvement of BMD in different bone regions of 4% RFO fed mice as compared to CO fed mice in both age groups. Mice were sacrificed at 12 and 20 month of age and performed the digital x-ray of bones for histomorphometric analysis. No significant difference was found between the groups. We hypothesized that low content of EPA and DHA in 4% RFO may not be sufficient to maintain bone mineral density during aging. Recently, concentrated FO (CFO) with high content of EPA and DHA are available. We further examined if 4% CFO can maintain BMD during aging. Twelve month old female C57BL/6 mice were divided into 4 groups and supplemented for 12 months with 1) 4% CO, (2) 4% RFO, (3) 4% CFO and (4) 1% CFO. Mice were DXA scanned once at 12 month and again at 24 month of age. Interestingly, 4% CFO could maintain higher BMD in lumber, proximal tibial metaphysis, tibial diaphysis, distal femoral metaphysis and femoral diaphysis regions as compared to 4% CO and 4% RFO. This bone beneficial effect of 4% CFO was even more effective than seen in our earlier 9% RFO fed aging mice. Better BMD in 4% CFO was also correlated with reduced pro-inflammatory and enhanced anti-inflammatory cytokine levels in bone marrow cells treated with LPS. Bone marrow cells from 4% CFO mice also exhibited lower levels of NF-κB and MAPK signaling activation. 4% CFO, in fact supplies more amount of EPA and DHA than 9% RFO. These data indicate that bone benefit of FO may depend on how much EPA and DHA consumed through the supplementation.

Disclosures: Md Rahman, None.

SU0388

Comparative Characteristics of Subtrochanteric Fracture cases fulfilling and not fulfilling the ASBMR Task Force Criteria. <u>Angela Juby</u>*[1], <u>Sean Crowther</u>[2], <u>Marilyn Cree</u>[2]. [1]University of Alberta, Canada, [2]University of Alberta, Canada

Purpose

Atypical femoral fractures (AFF) are rare, but still have significant impact on quality of life. Association with antiresorptive therapy and duration of treatment is not absolute. Identification of potential subjects at increased risk for these fractures is important. Recent publications suggests that AFF subjects are younger, more likely to be Asian, have fewer co-morbidities, have a diagnosis of osteoporosis, have exposure to bisphosphonates (BP) for >6 years, and are less likely to be men. This study was done to see if the suggested risk criteria from other studies and population groups, are similar in a Canadian population of AFF patients.

Methods

An eleven year review of data from two referral hospitals in Alberta, Canada for subtrochanteric fracture, identified 79 cases. 70 cases were available for radiographic review for assessment of the 2013 ASBMR Task force criteria. The Charlson/Deyo comorbidity index was calculated from the chart review, all cases over 18 years were included (men and women).

Results

There were 41 cases fulfilling the ASBMR criteria, including one male. They were significantly younger (69.9 vs 80.9 years) than the 29 non criteria fracture patients. Also, 27% had prodromal pain compared to 0% in the non ASBMR criteria fracture group. The percentage of Asian patients was low (5%) and not different between the groups. There were similar rates of osteoporosis diagnosis and Charlson co-morbididty, but there were significantly more cases of COPD in the non criteria group (12 vs 4). There were no differences in documented numbers exposed to corticosteroids, or BP, although the AFF group had significantly more cases with BP exposure >10 years, but not with exposure > 6 years. Significance was calculated at 0.05 level.

Conclusion

Our study corroborates some of the data in the literature about potential risk factors for AFF. However, it does not suggest Asian ethnicity, or BP exposure <10 years to be risk factors, but the numbers of non Caucasians was very low in both groups. COPD was suggested as a risk factor for the non AFF group, although there was no clear link with oral glucocorticoid use. Research in this area needs to continue to identify those at risk of AFF with antiresorptive therapy.

Disclosures: Angela Juby, None.

SU0389

Comparative Effects of Raloxifene and Bisphosphonate on Bone Marrow Density and Osteoporotic Fracture Outcomes in Rheumatoid Arthritis Patients. <u>Kowoon Joo</u>*[1], <u>Won Park</u>[1], <u>Seong-Ryul Kwon</u>[2], <u>Mie-Jin Lim</u>[2], <u>Kyong-Hee Jung</u>[2]. [1]Inha University Hospital, South Korea, [2]Inha University Hospital, South Korea

Purpose: Rheumatoid arthritis (RA) accelerates bone loss, increasing the risk of osteoporosis and osteoporotic fractures. We evaluated the effect of raloxifene and bisphosphonate on bone marrow density (BMD) and osteoporotic fractures in RA patients.

Method: We retrospectively examined data of 112 seropositive RA patients who were diagnosed with osteoporosis and started on either raloxifene or bisphosphonate from January 2006 to December 2010 with no prior history of either medication. Patients with baseline BMD and at least one follow up BMD were included. The patients were examined for maximum of 3 years. Bisphosphonates consisted of risendronate, alendronate or oral ibandronate. Vertebral fractures were defined using Genant's semiquantitative classification.

Results: Forty-four patients were in the raloxifene group and 68 patients were in the bisphosphonate group. The patients in the raloxifene group were older and lighter in weight compared to the bisphosphonate group (Table 1). The patients in the bisphosphonate group consumed higher doses of calcium and vitamin D through medication compared to the raloxifene group. There was no significant difference in duration of RA, the daily dosage of prednisolone and medication possession ratio between the 2 groups. Thirty-six patients in the raloxifene group and 67 patients in the bisphosphonate group had follow up BMD at 1 year of treatment. Nineteen patients in the raloxifene group and 40 patients in the bisphosphonate group had follow up BMD at 2 years of treatment. There was no significant difference in the mean change of lumbar, total hip and femoral neck BMD from baseline and the number of vertebral fractures between the 2 groups at 1 year and at 2 years of treatment. Eighteen patients in the raloxifene group and 29 patients in the bisphosphonate group had follow up BMD at 3 years of treatment. There was no significant difference in the mean change of lumbar and femoral neck BMD from baseline and the number of vertebral and non-vertebral fractures between the 2 groups at 3 years of treatment. However the mean change of total hip BMD was higher in the bisphosphonate group compared to the raloxifene group (Table 2).

Conclusion: There was no significant difference in BMD changes and osteoporotic fractures in RA patients treated with raloxifene and bisphosphonate.

	Raloxifene (n = 44)	Bisphosphonate (n = 68)	P value
Female (%)	45 (100)	46 (68)	< 0.001
Age (yr)	62 ± 9	58 ± 9	0.023
Weight (kg)	52.3 ± 10.3	55.8 ± 9.0	0.04
Height (cm)	152.5 ± 6.2	157.9 ± 7.6	< 0.001
Alcohol	0	0	
Smoking (%)	1 (2)	11 (16)	0.026
Diabetes mellitus (%)	1 (2)	7 (10)	0.107
Menopause (%)	43 (98)	38 (56)	<0.001
Rheumatoid arthritis duration (mo)	70 ± 80	66 ± 67	0.666
Follow up duration (yr)	2 ± 1	2 ± 1	0.629
Methotrexate (%)	17 (39)	34 (50)	0.238
Cyclosporine (%)	1 (2)	5 (7)	0.244
Selective serotonin reuptake inhibitors	0	0	
Proton pump inhibitors	2 (4)	3 (4)	0.973
Calcium (mg/day)	253.2 ± 120.8	284.2 ± 89.2	0.012
Vitamin D (IU/day)	341 ± 310	535 ± 348	0.003
Prednisolone (mg/day) None	12 (27)	13 (19)	
<2.5	3 (7)	5 (7)	
2.5 ≤ P<7.5	27 (59)	38 (57)	0.454
≥7.5	3 (7)	11 (16)	
ESR	36 ± 29	36 ± 28	0.945
CRP	1.49 ± 2.42	1.98 ± 3.18	0.714
Medication possession 1 year	90 ± 12	87 ± 21	0.865
ratio (%) 2 year	92 ±9	89 ± 18	0.576
3 year	89 ± 15	92 ± 12	0.331

Table 1. Baseline characteristics

		Raloxifene (n = 44)	Bisphosphonate (n = 68)	P value
No. of BMD 1yr (%)		n = 36 (82)	n = 67 (99)	P value
Mean change from baseline	Lumbar spine	5.5 ± 12.6	7.1 ± 11.1	0.203
	Total Hip	5.6 ± 8.1	3.7 ± 8.7	0.198
	Femoral Neck	6.0 ± 15.0	5.8 ± 14.4	0.836
Fracture (%)	Vertebral	3 (8)	3 (4)	0.419
	Nonvertebral	0	0	
No. of BMD 2yr (%)		n = 19 (43)	n = 40 (59)	P value
Mean change from baseline	Lumbar spine	7.8 ± 12.7	13.6 ± 14.1	0.253
	Total Hip	7.4 ± 12.2	8.29 ± 9.35	0.604
	Femoral Neck	14.4 ± 20.8	13.3 ± 17.7	0.922
Fracture (%)	Vertebral	2 (11)	0	0.1
	Nonvertebral	0	0	
No. of BMD 3yr		18 (41)	29 (43)	P value
Mean change from baseline	Lumbar spine	10.6 ± 16.2	19.5 ± 14.9	0.078
	Total Hip	5.5 ± 10.3	12.5 ± 10.7	0.038
	Femoral Neck	13.1 ± 19.6	21.1 ± 15.2	0.12
Fracture (%)	Vertebral	3 (17)	3 (10)	0.662
	Nonvertebral	2 (11)	1 (3)	0.549

Table 2. Mean change of bone marrow density from baseline and fracture outcomes.

Disclosures: Kowoon Joo, None.

SU0390

Comparison of Bone Turnover in Patients with Prodromal Bone Deterioration (Pbd) and Atypical Femoral Fracture (AFF). Shijing Qiu*[1], George Divine[2], Mahalakshmi Honasoge[1], Saroj Palnitkar[2], Sudhaker Rao[1]. [1]Henry Ford Hospital, USA, [2]Henry Ford Hospital, USA

Background: It is now well established that AFF is one of the most serious complications after long-term bisphosphonate (BP) treatment, which may be linked to severely suppressed bone turnover (SSBT). A lateral femoral cortical crack, which we refer to as PBD, usually precedes AFF. PBD is characterized by a focal bump on the lateral cortex of the femur in which a horizontal fracture line is often present. However, it is unclear if there are differences in bone turnover between patients with PBD and AFF.

Methods and Results: We examined trans-iliac bone biopsies obtained from 12 white women with long-term (>5 years) BP treatment with either PBD (n = 6) or AFF (n = 6). In order to better define the change in bone turnover in PBD and AFF patients, iliac bone biopsies from 48 age-matched healthy white women were used as controls. Histomorphometric measurements were conducted on cancellous bone. AFF patients were significantly younger than PBD patients (57.8 ± 11.2 vs 71.5 ± 6.0 years; p<0.05). There were no significant differences in the variables examined between PBD and AFF patients, although the bone turnover values in AFF patients were lower than in PBD patients (Table 1). More importantly, compared to the healthy women, the bone turnover-related variables were all significantly decreased in both PBD and AFF patients (p< 0.05-0.001; see-Table 1).Conclusions: Both PBD and AFF are associated with SSBT without a significant difference in bone turnover between them. This implies that SSBT appears much earlier than the occurrence of PBD, which in turn precedes AFF. The occurrence of AFF in younger women is likely to be due to the greater amount of physical activity and exercise that would accelerate the damage of bone, resulting in PBD and thus predisposing to AFF. To the best of our knowledge this is the first report on comparative bone turnover status in PBD and AFF. We propose the following sequence for the pathogenesis of AFF: SSBT-PBD-AFF.

Table 1. Comparison of histomorphometric values for iliac cancellous bone between patients with PBD and AFF as well as between PBD/AFF patients and normal postmenopausal women

	PBD n = 6	AFF n = 6	p	PBD/AFF n = 12	Normal n = 48	p
BV/TV	13.9 (4.26)	16.7 (7.51)	0.436	15.3 (6.01)	20.2 (6.06)	0.015
Tb.Th	113 (14.9)	122 (35.0)	0.591	118 (26.0)	134 (32.3)	0.099
Tb.N	1.22 (0.277)	1.33 (0.256)	0.486	1.27 (0.261)	1.50 (0.303)	0.019
ES/BS	4.94 (3.88)	3.34 (3.85)	0.491	4.14 (3.78)	7.30 (2.93)	0.003
OS/BS	1.39 (1.14)	2.28 (3.39)	0.558	1.84 (2.46)	20.0 (11.0)	<0.001
O.Th	3.84 (2.15)	5.01 (3.45)	0.497	4.42 (2.81)	8.21 (2.17)	<0.001
Ob.S/BS	0.283 (0.390)	0.208 (0.325)	0.589	0.246 (0.345)	6.01 (3.98)	<0.001
MS/BS	1.54 (1.91)	0.430 (0.800)	0.132	0.984 (1.51)	7.39 (5.18)	<0.001
Oc.S/BS	0.794 (0.765)	0.341 (0.272)	0.394	0.567 (0.596)	0.968 (0.777)	0.051
MAR	0.190 (0.115)	0.074 (0.118)	0.116	0.132 (0.127)	0.520 (0.122)	<0.001
BFRs	1.16 (1.31)	0.367 (0.776)	0.132	0.763 (1.11)	14.7 (10.6)	<0.001
Ac.f	0.024 (0.019)	0.002 (0.005)	0.056	0.013 (0.017)	0.426 (0.286)	<0.001

Table 1

Disclosures: Shijing Qiu, None.

SU0391

Effect of Denosumab Three Years Therapy in Women with Osteoporosis and Contraindications to Oral Bisphosphonates on Bone Mineral Density. Andrzej Sawicki*[1], Radoslaw Janiak[2], Ireneusz Nawrot[3], Piotr Sawicki[4]. [1]Synexus Poland, Poland, [2]Medical Centre Synexus, Poland, [3]Medical University of Warsaw, Poland, [4]Medical Centre Synexus, Poland

Objectives: Denosumab is a fully human monoclonal antibody that inhibits bone resorption by neutralizing RANKL, a key mediator of osteoclast formation, function, and survival. In clinical trials denosumab treatment was well-tolerated and increased BMD. The aim was to evaluate whether osteoporotic women with contraindication to oral bisphosphonates treatment (e.g. GERD) or intolerance or resistance, have similar positive effect on bone mass after denosumab have positive effect on bone mass after denosumab as in FREEDOM study patients , in open study in out-patients clinic. We report observational BMD results from the 3 years of treatment. Materials/Method: The study was performed in 138 women with osteoporosis aged 29 to 93 with contraindication to oral bisphosphonates treatment or intolerance or resistance. Bone Mineral Densitometry (BMD) was assessed in AP Spine, Femur Neck and Femur Total regions by Hologic 4500 W before and after 6, 12, 18, 24 and 36 months denosumab treatment and calcium 400-800 mg and vitamin D 800- 1000 i.u. daily. Results: Table 1. Percentage change in BMD from baseline and after 6, 12, 18 , 24. 36 months of denosumab treatment in 138 women with osteoporosis and contraindications to oral bisphosphonates. Note: number of patients in 6, 12, 18, 24, 36 months groups is not the same. Conclusions: These data demonstrated that denosumab treatment for up to 3 years in patients with contraindication to oral bisphosphonates treatment or intolerance or resistance was associated with continued gains in Spine BMD in patients and have good effect in beginning of treatment at 6 months. Denosumab treatment has positive effect on femur BMD up to 3 years of treatment. Denosumab have similar positive effect on bone mass as in FREEDOM study patients.

Months Region	0 m	6 m	12m	18 m	24 m	36 m
L1-L 4 % (n=106)		+ 3,8 (71)	+ 5,5 (76)	+ 7,4 (44)	+ 12,9 (26)	+ 10,6 (19)
F Neck % (n=101)		+ 3,4 (66)	+ 2,8 (71)	+ 5,5 (44)	+ 2,4 (23)	+ 2,2 (10)
Total Hip % (n=101)		+ 4,1 (65)	+ 2,1 (70)	+ 3,5 (46)	+2,4 (23)	+ 4,1 (13)

Table

Disclosures: Andrzej Sawicki, None.

SU0392

Effects of denosumab on microarchitecture and bone mineral density in a Swiss outpatient women population. Berengere Aubry-rozier*[1], Delphine Stoll[2], Olivier Lamy[3], Didier Hans[1]. [1]Lausanne University Hospital, Switzerland, [2]Centre a bone diseases, Che, [3]University Hospital, Switzerland

Introduction

Bone mineral density (BMD) is a standard for osteoporosis diagnosis and fracture risk prediction. The trabecular bone score (TBS) is a new parameter obtained after a

re-analysis of a DXA exam. TBS is a texture measurement that correlates with parameters of bone microarchitecture. Spine TBS and BMD predict osteoporotic fracture independently and their combination is superior to either measurement alone. TBS and BMD seem to react differently to different treatments for osteoporosis. The subcutaneous administration of denosumab reduces bone turnover and increases bone mineral density and is associated with a reduction of vertebral, nonvertebral and hip fracture. The aim of our study was to evaluate the effect of two years treatment of six-monthly subcutaneous denosumab on TBS and BMD parameters in our post-menopausal women outpatient population.

Method

We selected all consecutive women treated for 2 years with denosumab (60 mg subcutaneously every 6 months) for osteoporosis between October 2010 and December 2013. Patients who had not at least one DXA scan before and one after 2 years of treatment were excluded.

Results

Thirty eight women were included. Mean age was 65 yo (57-80) before treatment with denosumab. Mean body mass index was 24.7 kg/m2 (17.9-36.2) before treatment. It did not significantly change after 2 years. 70% had a prevalent major osteoporotic fracture and 35% already received a previous specific treatment against osteoporosis. After 2 years, TBS increased significantly from 1.283 to 1.307 (+1.8%; p<0.05). Spine BMD increased significantly from 0.799 to 0.861 g/cm2 (+7.7%; p<0.05) and neck BMD from 0.609 to 0.631 g/cm2 (+3.6%,p<0.05).

Conclusion

In our clinical routine population, we found that two years of six-monthly injections of denosumab increased significantly spine BMD, neck BMD and spine TBS.

Disclosures: Berengere Aubry-rozier, None.

SU0393

Effects of local administration of zoledronate for the local osteoporotic lesion of ovariectomized rats. Yohei Matsuo*[1], Masafumi Kashii[2], Tsuyoshi Sugiura[3], Masayuki Furuya[4], Tokimitsu Morimoto[5], Takahiro Makino[4], Takaaki Noguchi[4], Kosuke Ebina[6], Takashi Kaito[4], Motoki Iwasaki[4], Hideki Yoshikawa[7]. [1], Japan, [2]Osaka University Graduate School of Medicine, Japan, [3]Faculty of Medicine, Graduate School of Medicine, Osaka University, Japan, [4]Department of Orthopaedic Surgery, Osaka University Graduate School of Medicine, Japan, [5]Department of Orthopaedic Surgery, Osaka University Graduate School of Medicine, Japan, [6]Osaka University, Graduate School of Medicine, Japan, [7]Osaka University Graduate School of Medicine, Japan

Management of local osteoporotic or osteolytic lesions is a clinical challenging problem, and intravenous administration of bisphosphonates has a limited effect for local pathological lesions. We hypothesized that local administration of high-dose zoledronate (ZOL) for local osteoporotic or osteolytic lesions enables to improve local bone structure with little systemic adverse effects. To examine the efficacy and safety of local administration of ZOL on local osteoporotic lesion of ovariectomized rats.6 weeks later after ovariectomy, 30 six-months-old female SD rats were divided into the 3 groups (group L, S, and C). In the group L, 50μl ZOL at a dose of 67μg/kg were locally injected into the bone marrow between the 2 drilled holes and 50μl saline was systemically administrated by subcutaneous injection. In the group S, 50μl saline was locally injected, and 50μl ZOL at a dose of 67μg/kg was systemically administrated. In the group C, 50μl saline was locally and systemically administrated, respectively. 2 local osteoporotic lesions (Area 1: cancellous bone area of right proximal tibia between the two holes where ZOL or saline were injected, Area 2: left side mirror area) were analysed using in vivo micro-CT at 2, 4, 6, and 8 weeks after administration. Histological evaluations of proximal tibiae (Area 1 & 2) were evaluated using HE and TRAP staining. In the group C, vBMD of the Area1 and 2 continuously decreased until week 8 (Area 1: -9%, Area 2: -10%) and local osteoporotic lesion developed. In the group L, vBMD of Area 1 where ZOL was locally administrated increased continuously until week 8 (+40%), but vBMD increased and stayed constant in the group S (+16%). In the group L, vBMD of the Area 2 continuously decreased until week 8 (-9%), but vBMD maintained at the pre-treated level in the group S. TRAP positive osteoclast surface at Area 1 was significantly reduced in the group L compared with the other 2 groups. However, serum TRACP-5b level continuously decreased in the group L, and there were no significant differences in serum TRACP5b level between the group L and S. ZOL is the most potent bisphosphonate that strongly inhibits osteoclast function with high binding affinities for bone. Taking advantage of these characteristics, we showed that local administration of high-dose ZOL for local osteoporotic lesion have more beneficial effects on local bone structure than the systemic administration, and have a little influence on other bone tissue.

Disclosures: Yohei Matsuo, None.

SU0394

Long-term Oral Bisphosphonate Use for Osteoporosis Among Older Women – US and Canadian Perspective. Nicole Wright*[1], Suzanne Cadarette[2], Wilson Smith[3], Andrea Burden[2], Amy Warriner[1], P. Jeffrey Foster[3], Huifeng Yun[1], Mary Melton[3], Jeffrey Curtis[1], Kenneth Saag[1]. [1]University of Alabama at Birmingham, USA, [2]University of Toronto, Canada, [3]University of Alabama at Birmingham, USA

Purpose: Bisphosphonates (BPs) have been widely used for the treatment and prevention of osteoporosis for two decades. Although new parenteral preparations have been introduced, oral BPs still represent the vast majority of osteoporosis treatments. Little is known about the characteristics of or regional differences in long-term oral BP users.

Methods: We evaluated the long-term use of oral BPs in the national US Medicare and Ontario (ON) Canada data systems. The US Medicare cohort consisted of women aged ≥65 years with an osteoporosis or fracture diagnosis code, or BP prescription fill. The ON data consisted of women aged ≥66 years who were new users of oral BPs. We identified women with three years of continuous medical and pharmacy coverage. Long-term BP users were those with exposure to an oral BP (alendronate, risedronate, ibandronate, and etidronate) in each of the three most recent years of available data (2009-2011). We evaluated demographic and BP utilization data including, BP exclusivity (no exposure to another BP agent in three year period) and compliance to therapy using proportion of days covered (PDC) (days of drug supplied in 3 years/ 3*365.25) . Users with a PDC of ≥70% were considered compliant.

Results: We identified 888,704 US and 99,530 ON women meeting the inclusion criteria with at least one oral BP prescription in the most recent data. We then identified 698,012 US and 54,656 ON long-term oral BPs users (Table). Alendronate was primarily used by Medicare patients (78.0%), whereas risedronate was the primary oral BP in ON (56%). Based on the available data, the mean duration of us among the long-term BP users was five years in both US (SD: 1.1) and ON (SD: 2.2). In the US, risedronate users were more likely to be exclusive users (83%) compared to alendronate users; whereas in ON, a higher proportion of alendronate users were considered exclusive users than risedronate users. All ibandronate users were exclusive users in US data. Compliance was higher in ON (80% alendronate, 78% risedronate) than in US (63% alendronate, 63% risedronate).

Conclusion: Although alternative preparations of BPs and new non-BP drugs have emerged in the market, the prevalence of oral BP use is high. In the data evaluated, the prevalence of long-term use (≥3years), was also high in both countries. However, compliance differed by country. Evaluations in more recent data would determine if and how drug holidays have altered these characteristics.

Table. Characteristics of Long-term Oral Bisphosphonate Users

	US, 2009-2011 (n=698,012)	ON, 2009-2011 (n=54,656)
Age, mean (SD)	79.3 (7.4)	74.0 (6.4)
Mean BP duration[a], yrs (SD)	5.0 (1.1)	4.9 (2.2)
Most recent BP, (n,%)		
Alendronate	544,656 (78.0)	24,056 (44.0)
Risedronate	96,795 (13.9)	30,600 (56.0)
Ibandronate	56,561 (8.1)	-
Exclusive BP users[b], (n,%)		
Alendronate	419,496 (77.2)	22,596 (93.9)
Risedronate	80,314 (83.0)	26,981 (88.2)
Ibandronate	56,561 (100.0)	-
Compliant BP users[c], (n,%)		
Alendronate	262,125 (62.5)	18,173 (80.4)
Risedronate	50,880 (63.4)	20,981 (77.8)
Ibandronate	33,981 (60.1)	-

[a]Mean duration based on first BP dispensed in each data system. US = 2006-2011; ON: 2002-2011
[b]Exclusive users are those who only filled a prescription for each oral BP among most recent BP users
[c]Compliance estimated at proportion of days covered (PDC) of ≥70% among exclusive BP users

Table

Disclosures: Nicole Wright, None.

SU0395

The Positive Effects of Bisphosphonate on the Biomechanics of Human Bone Are Not Seen with Long-Term Treatment. Jonathan Ward[1], Constance Wood[2], Keith Rouch[3], David Pienkowski[4], Hartmut Malluche*[5]. [1]University of Kentucky, Department of Biomedical Engineering, USA, [2]University of Kentucky, Department of Statistics, USA, [3]University of Kentucky, Department of Mechanical Engineering, USA, [4]University of Kentucky, USA, [5]University of Kentucky Medical Center, USA

Oral bisphosphonates (BPs) are an established treatment modality for osteoporosis. Although the short-term beneficial effects of BPs on bone mass are known, concerns exist that long-term BP use may predispose to atypical fractures. To address this concern, this study quantified the load-bearing competence of human bone versus the duration of BP treatment.

Fifty-three anterior iliac crest bone biopsies from Caucasian women with osteoporosis (diagnosed by DXA t-scores) were obtained from the Kentucky Bone Registry; 45 from women treated with oral BPs for 1 to 16 years and 8 from women before the start of treatment. Bone samples were scanned using micro-computed

tomography (Scanco µCT 40). A 3D image of trabecular bone from each sample was derived from this micro-CT and subjected to uniaxial compression simulation using finite element analysis (ANSYS 14.0). The apparent elastic modulus (Eapp, reflective of sample rigidity) and failure stress (Pfail, reflective of fracture propensity) of each sample were calculated. A general linear model was then used to fit response curves relating the square root transformed biomechanical response variables to patient characteristics and BP treatment duration at time of biopsy.

The fitted models showed that patient age, BP treatment duration, and BP treatment duration-squared adequately described and were significant predictors of the response variables Eapp and Pfail. Specifically, the prediction equation for the square root of Pfail was: $0.265 - 0.032$ age $+ 0.239$ duration $- 0.017$ duration^2. All p-values for these coefficients were <0.0047. This response curve increased, reached a maximum at 7.06 ± 0.65 years of BP treatment, and then declined. The prediction equation for Eapp also initially increased with BP treatment duration, reached a maximum at 7.16 ± 0.67 years, and then declined.

This study provides relevant and much needed information on the relationship between human bone mechanics and BP treatment duration spanning the period of 1 to 16 years. Based on these fitted models showing the relationship between BP treatment duration and bone biomechanics, an initial increase is observed followed by a decline after an estimated 7 years (95% C.I. 5.76 – 8.35 years) of treatment. Mechanistic insights regarding these long-term BP treatment-related changes await prospective studies and complementary evaluation of bone material properties.

SU0396

Treatment of Nonunion of Long Bones in Bisphosphonate users vs Non Bisphosphonate users with Concentrated Autogenous Iliac Crest Bone Marrow Aspirate (BMAC) and Demineralized bone matrix(DBM) and/or Bone Morphogenic Protein. Pingal Desai*[1], Lester Zambrana[2], Saad Hasan[2], Joseph Nguyen[3], Libi Galmer[3], Joseph Lane[1]. [1]Hospital for special surgery, USA, [2]Weil Corneil medical college, USA, [3]Hospital for special surgery, USA

Bisphosphonates are the antiresorptive drugs used to treat osteporosis and various metabolic bone conditions. They reduce bone resportion and so are useful in the treatment of osteoporosis. A long term use of the drug causes alterations to normal pattern of collagen cross-linking in bone, increased mineralization, reduced heterogeneity of mineralization, reduced vascularity and eventually reduced bone turnover. A reduction in bone turnover causes ineffective curing of cracks in the bone. This results in delayed fracture healing in patients with bisphosphonate use.

While the current gold standard of treatment of nonunion is open autologous bone grafting, studies have shown that concentrated percutaneous autologous bone marrow grafting (BMAC) with osteoinductors is an effective treatment for nonunions.

Methods
We hypothesized that BMAC with osteoinductors would be equally effective in treatment of nonunions in patients with bisphosphonate users as compared to nonusers.

We used BMAC with demineralized bone matrix (DBM) and/or recombinant human bone morphogenic protein-2 (BMP) in 82 consecutive patients for delayed union or nonunion fractures between 2006 and 2012 by one surgeon at two institutions. Patients were at least on bisphosphonate therapy for a year prior to the fracture to qualify to be in bisphosphonate user group. Patients were age and sex matched between two groups and followed until radiographic union was achieved, nonunion or another procedure was performed. Differences in clinical characteristics and healing of nonunion between bisphosphonate users and nonusers were evaluated using independent sample t-tests and chi-square tests.

Results
Forty nine patients met the inclusion criteria.There was no significant difference in clinical characteristics between bisphosphonate users and nonusers (p> 0.05). The rate of healing bisphosphonate users was 75% and nonusers was 82.7% (p =0.5). The time to union in bisphosphonate user was 6.1 months and in nonuser was 4.0 months (p=0.03).

Conclusion
This study shows that use of BMAC with osteoinductors is minimally invasive, cost-effective and useful in healing of nonunion in both bisphosphonate users and nonusers. However, time to union of long bone in bisphosphonate user is long as compared to nonusers.

Level of Evidence: Level II, prospective comparative study

Bibliography
1. Black DM el al
2. Rschger P et al
3. Van der Meulen MC et al
4. Desai PA et al

Characteristics of Bisphosphonate users vs nonusers

Characteristics between Bisphosphonate users and nonusers

	Bisphosphonate user	Bisphosphonate nonuser
Age in years	67.7	44.9
Time to intervention after original procedure		
Within 6 months	12/20 (60%)	18/29 (62%)
After 6 moths	8/20 (40%)	11/29 (38%)
Fracture gap		
≤ 5 mm	14/20 (70%)	12/29 (41.3%)
> 5 mm	6/20 (30%)	17/29 (59.7%)
P > 0.05		

Results

Results

	Bisphosphonate user	Bisphosphonate nonuser	P value
Healing	15/20 (75%)	24/29 (82.7%)	0.5
Non Healing	5/15 (25%)	5/29 (17.3%)	
Time to healing (in months)	6.1	4.0	0.03

Preoperative imaging of nonunion

Post procedure imaging

SU0397

Why don't we treat her right? Documentation from physicians when not prescribing medications for women with osteopenia, osteoporosis, or osteoporosis-suspicious fractures. Meg Durbin*[1], Miriam Rotman[2], Bradley Stolshek[3], Harold Luft[4]. [1]Palo Alto Medical FoundationSutter Health, USA, [2]Palo Alto Medical Foundation, USA, [3]Amgen, USA, [4]Palo Alto Medical Foundation Research Institute, USA

Background: National Osteoporosis Foundation (NOF) guidelines recommend screening and treating women for low bone mineral density and high fracture (fx) risk to prevent such fx. Despite proven efficacy, prescription medications (Rx) are inconsistently prescribed. Few studies explore why physicians do not prescribe guideline-consistent treatment (tx).

Objective: To describe physicians' documented reasons for tx not consistent with NOF guidelines for women age ≥ 50 years with osteopenia, osteoporosis, or osteoporosis-suspicious fx.

Methods: Data were obtained from 2009-10 electronic health records (EHR) in a large multispecialty practice. We identified 9047 patients (pts) with osteopenia, 3112 with osteoporosis, and 2748 with fx. "Rx" included prescriptions from the EHR medication list. "No Rx" reflects no Rx or Rx stopped between 2 mo before and 1 mo after DXA or fx. Pts without Rx included 61% of the 4718 pts with osteopenia and high or no FRAX (2878), 29% of pts with osteoporosis (891), and 59% of pts with fx (1635). We randomly selected and reviewed charts and categorized reasons discernible for tx not consistent with NOF guidelines among 412 pts: 47 pts with severe osteopenia (-2.5 <T score <-2.0) + high FRAX, 218 with osteoporosis; and 147 with fx.

Results: In pts with severe osteopenia + high FRAX (Fig. 1), reasons documented included: prior bisphosphonates > 5 yrs, 14%, pt declined Rx, 9%, MDs noted risk but did not prescribe Rx, 23%; and MD did not document risk or follow up, 53%. In pts with osteoporosis (Fig. 2), pt declined Rx, 15%; prior bisphosphonates > 5 yrs, 17%; MDs noted risk but did not prescribe Rx, 45%; and MDs did not document risk or follow up, 18%. In all 218 pts reviewed with fx (Fig. 3), reasons included: pt frailty, 14% (26% in hip fx); pt declined Rx 5% (10% in upper extremity fx), prior bisphosphonates > 5 yrs, 4% (10% in rib fx); MD noted risk but did not Rx, 49% (60% in rib fx), and MD did not document risk or follow up, 27% (35% in spine fx).

Conclusion: The proportion of different reasons documented for tx that is not guideline-consistent differed across groups. In pts with osteopenia or osteoporosis without fx, MDs most commonly did not document risk or follow up. In pts with fx, MDs most commonly noted risk but did not prescribe Rx. Frailty was more often noted as a reason for no Rx in pts with fx vs. those without fx. Opportunity exists to improve how MDs identify, document and treat patients at high risk for fx.
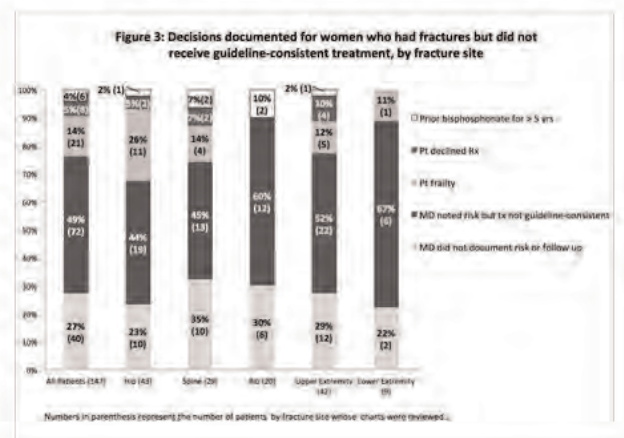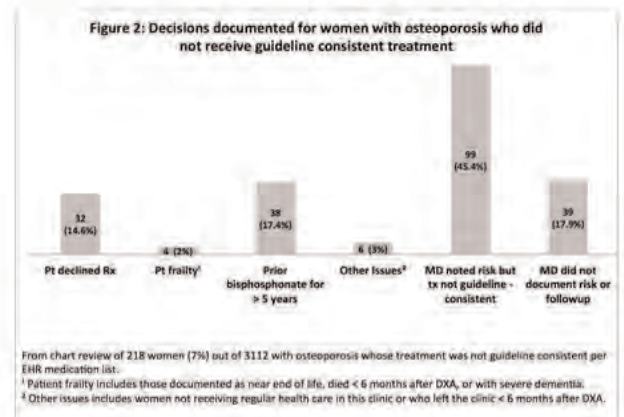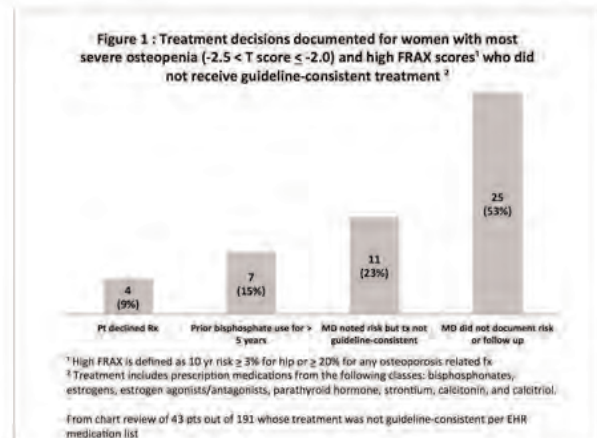
Figures for Abstract "Why don't we treat her right?"

SU0398

Factors associated with Hardware Failure, Non-union and other Complications of Atypical Femoral Fractures. R Bleakney*[1], Linda Probyn[2], Leon Lenchik[3], Jonathan Adachi[4], Aliya Khan[5], Earl Bogoch[6], Catherine Lang[7], Robert Josse[8], Angela M. Cheung[9]. [1]Mount Sinai Hospital, Canada, [2]University of Toronto, Sunnybrook Health Sciences Centre, Dept Medical Imaging, Canada, [3]Wake Forest University, USA, [4]St. Joseph's Hospital, Canada, [5]McMaster University, Canada, [6]St. Michael's Hospital, Canada, [7]University of Toronto, Canada, [8]St. Michael's Hospital, University of Toronto, Canada, [9]University Health Network-University of Toronto, Canada

Purpose: Long-term bisphosphonate use has been associated with Atypical Femoral Fractures (AFFs). The purpose of this study is to evaluate the association of fracture morphology and hardware type with hardware failure in patients with AFFs.

Materials and Methods: Imaging studies of 100 patients from the Ontario AFF cohort with 131 AFFs (4 men, 96 women, mean age 68.1 years) with hardware instrumentation from July 2004 to February 2014 were reviewed. Type of instrumentation, fracture morphology (overall fracture morphology (OFM), lateral cortical fracture angle (LCFA), lateral cortical thickness, femoral angle), and fracture location were compared in the hardware complication group and control group using the Wilcoxon rank sum test or Fisher's exact test.

Results: 131 AFFs had instrumentation (98 for complete and 33 for incomplete fractures). Instrumentation included intramedullary (IM) nailing (117), dynamic hip screw (7), lateral plate (2), short gamma nail (3), total hip arthroplasty (1), compression plate (1). Hardware complications occurred in 15.3% (21/131) and were more common in complete (18/21) than incomplete (3/21) fractures. Complications included screw fractures in 19%(4/21), plate fractures in 14.3%(3/21), loosening of hardware in 28.6%(6/21), nonunion in 9.5%(2/21), and combination of complications in 28.6%(6/21). Hardware failure was significantly less common after IM nailing (12.8%) compared to other hardware (35.7%) (p=0.04). Comparing failure to non-failure group, the mean OFM 31.9 degrees (vs 36.3), LCFA 7.0 degrees (vs 11.3), lateral cortical thickness 12.1 mm (vs 12.1), medial cortical thickness 8.9 mm (vs 7.8), femoral angle 133 degrees (vs 133). Comparing failure to the non-failure group, the location of fracture was 14.9 cm (vs 16.8) from the greater trochanter. Of all measured parameters, only LCFA was significantly associated with hardware failure (p= 0.03).

Conclusion: In patients with AFFs, hardware complications are not uncommon. Hardware failure is more common in AFFs with smaller LCFA and when fixation other than IM nailing is used.

Disclosures: R Bleakney, None.

SU0399

Withdrawn

SU0400

Withdrawn

SU0401

Concentration of Urinary C-terminal Telopeptide of Type I Collagen Predicts Bone Mineral Density in Modeling and Simulation Analysis: MOVER Study with Monthly Intravenous Administration of Ibandronate. Kiyohiko Nakai*[1], Satofumi Iida[2], Masato Tobinai[2], Junko Hashimoto[3], Takehiko Kawanishi[2], Yoshiaki Matsumoto[4]. [1], Japan, [2]Chugai Pharmaceutical CO., LTD., Japan, [3]Chugai Pharmaceutical Corporation Limited, Japan, [4]Nihon University, Japan

Purpose: Modeling & simulation (M&S) based on population pharmacokinetics/pharmacodynamics contributes to the efficient development of new drugs; by predicting efficacy, it allows the optimization of clinical trial design, including dose/dosage, observation period, and patient population. Previously conducted M&S has shown links between ibandronate (IBN) dosage, urinary C-terminal telopeptide of type I collagen (uCTx), and lumbar bone mineral density (BMD). In this study, the potential of uCTx as an early response marker was explored by using M&S based on data from the MOVER study.

Methods: Modeling was performed based on the uCTx and BMD values obtained in the MOVER study, where IBN (0.5?or 1 mg) was intravenously administered monthly for 3 years to 758 Japanese osteoporosis patients. The model used nonlinear mixed effects modeling software (NONMEM version 7.2) with a first-order conditional estimation method to link the dosage of IBN, uCTx, and BMD. In addition to modeling using the full data set, modeling was also performed using subsets of the uCTx data up to 3, 6, 12, or 24 months after the first administration of IBN. The BMD values for 3 years were simulated based on the model parameters estimated from each cut-off set of data. These simulated BMD values were compared with the observed ones.

Results: Goodness-of-fit and visual predictive check plots showed that the predictions were in good agreement with the observations. When the absolute BMD values for 3 years simulated from uCTx data until 3, 6, 12, or 24?months were compared with corresponding observed values, median absolute simulation error (representing precision of simulation) was approximately 3% and median simulation error (representing bias of simulation) was approximately 1%. On the other hand, with respect to change in BMD from baseline, the simulated and observed values were not as comparable due to high variability.

Conclusions: This model was successfully applied to the results of the MOVER study. Moreover, the absolute BMD values for 3 years simulated by the model based on uCTx levels until 3 months well reflected the observed results. This suggests that uCTx would be useful as a quantitative early response marker with which to predict the efficacy of long-term IBN treatment. An ultimate objective of osteoporosis treatment is to reduce the risk of fractures. We are currently working on expanding the model to incorporate fracture risk by a time-to-event model.

Disclosures: Kiyohiko Nakai, None.

SU0402

The Effect of Food on Odanacatib Pharmacokinetics. Stefan Zajic*[1], Aubrey Stoch[2], David Hreniuk[3], Filipos Kesisoglou[4], Fang Liu[5], Deborah Panebianco[5], Stefaan Rossenu[6], Julie Stone[5], Rose Witter[5], Sachiko Yama[7], Randall Stoltz[8]. [1]Merck Research Laboratories, USA, [2]Merck & Co., Inc., USA, [3]Akros Pharma, USA, [4]Merck Research Labs, USA, [5]Merck Research Labs, USA, [6]Merck Research Labs, Netherlands, [7]Merck Research Labs, Japan, [8]Covance, Inc., USA

Odanacatib (ODN) is a selective inhibitor of human cathepsin K being developed for the treatment of osteoporosis in men and women. ODN is an oral, once-weekly drug being studied at the anticipated marketed dose of 50 mg in pivotal trials. The effect of dosing with food on ODN pharmacokinetics (PK) was evaluated in four Phase (Ph) I studies. In addition to study-specific PK analyses, food effect was assessed via absorption modeling based on data from an absolute bioavailability study and via pooled population PK (pop-PK) analysis of data from Ph I, II and III studies. Dosing in Ph II and III clinical trials was done without respect to food.

ODN exposure was increased when dosed with food compared to fasted, with increasing meal fat content corresponding to greater increases in exposure. The effect of food on AUC0-∞ was generally less than that on Cmax. When administered with a high-fat meal, ODN AUC0-∞ was increased by 63% at 50 mg and Cmax by 76 to 136% at 25 to 200 mg compared to fasted. Administration of 25 mg with a Japanese meal of moderate fat content resulted in an increase in AUC0-∞ of 34% and in Cmax of 70% compared to fasted. For doses of 50 to 100 mg with a low-fat meal, AUC0-∞ was increased by 15 to 39% and Cmax by 16 to 20% compared to fasted.

The bioavailability of 50 mg ODN was 30% in the fasted state, and was increased to 36% and 49% when dosed with low-fat and high-fat meals, respectively. An absorption modeling analysis showed that dosing ODN with food appeared to affect primarily the extent of bioavailability, with minor effects on the rate of absorption (ka). These findings are consistent with the hypothesis that ODN absorption, and thus bioavailability, is limited by solubility, and that administration with meals containing dietary lipids increases the solubility of ODN, due to its lipophilicity (logP 3.12). In addition, a pop-PK analysis based on data from Ph I, II, and III studies indicated that meal state was not a meaningful covariate for ODN exposure, suggesting that in patients, dosing ODN with or without food would not be an effective way to control food-related variability in exposure.

Taken together, Ph I, II, and III data support that meal state is not a meaningful determinant of ODN exposure. In light of the available safety and BMD efficacy data obtained in Phase II and III studies in which odanacatib was dosed without respect to food, it is appropriate to recommend that odanacatib may be dosed with or without a meal.

Disclosures: Stefan Zajic, Merck & Co., Inc., 4; Merck & Co., Inc., 8
This study received funding from: Merck & Co., Inc.

SU0403

The Effect of Raloxifene on Sclerostin, Bone Turnover and Bone Balance in Postmenopausal Women with Osteopenia. Fatma Gossiel*[1], Kim Naylor[1], Richard Jacques[2], Nicola Peel[3], Richard Eastell[4]. [1]The University of Sheffield, United Kingdom, [2]University of Sheffield, United Kingdom, [3]Sheffield Teaching Hospitals, United Kingdom, [4]University of Sheffield, United Kingdom

Sclerostin is a regulator of bone formation produced by the osteocytes. In postmenopausal women estrogen therapy reduces sclerostin production. Raloxifene is a selective estrogen receptor modulator (SERM) which acts as an agonist on bone, reduces bone turnover and may restore the imbalance between resorption and formation in postmenopausal women with osteopenia. These effects may be mediated by levels of circulating sclerostin. The aims were to investigate the effects of raloxifene on i) sclerostin in postmenopausal women with osteopenia and ii) bone turnover and bone balance compared to healthy premenopausal women.We studied postmenopausal women with osteopenia (mean age 62 years) from a parallel open trial, n=21 receiving 60mg/day of raloxifene (Evista Eli Lilly & Co) and n=23 untreated. Lumbar spine BMD T-score was between -1 and -2.5. Fasting serum was collected at baseline

and up to 48 weeks. Sclerostin was measured by ELISA (TECO Medical Group). The data were $\log_{10}$ transformed and the change from baseline was back transformed and expressed as a percentage change. Fasting serum was also collected from healthy premenopausal women (n=205) (mean age 38 years). We measured PINP and CTX by automated assay (iSYS IDS) and calculated the multiple of the median (MoM) for bone formation (PINP) and bone resorption (CTX) at baseline. The rate of bone turnover was calculated as the square root of the sums of the squared MoMs. Bone balance was calculated from the ratio of the formation MoMs to the resorption MoM. The data were log transformed. After 2 weeks of treatment the mean levels of sclerostin were different between the treated and non-treated groups (p<0.001). Sclerostin continued to decrease significantly by 10 to 15% throughout the treatment period, (p<0.001), figure. Osteopenic women had higher rates of bone turnover and a more negative balance than premenopausal women (Mahalanobis distance 1.29, p<0.001). After 48 weeks of treatment there was no difference in balance and turnover as compared to premenopausal women (Mahalanobis distance 0.15, p=0.802). Raloxifene decreases bone turnover and restores bone balance to levels shown by healthy premenopausal women. These effects may be mediated by sclerostin.
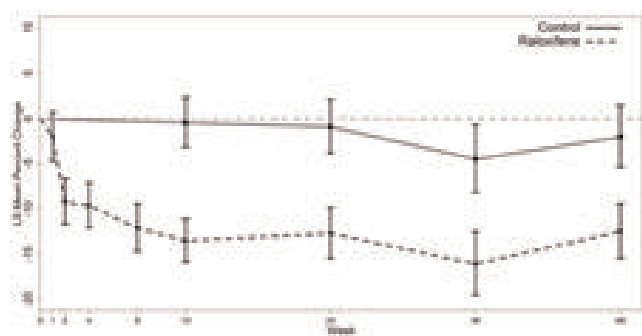
Figure: The effect of raloxifine treatment on sclerostin

Disclosures: Fatma Gossiel, None.

SU0404

The effects of combination therapy of Raloxifene with Eldecalcitol in postmenopausal osteoporosisswitch from Alfacalcidol to Eldecalcitol.

Kozaburo Inoue*[1], Shoichi Ichimura[2], Masaichi Hasegawa[1], Tomoo Inoue[3]. [1]Kyorin Univercity school of Medicine Department of Orthopedic Surgery, Japan, [2]Kyorin University School of MedicineDepartment of Orthopedic Surgery, Japan, [3]Yamanasi Hospital Orpthopedic Surgery, Japan

Objective : The aim of this study was to compare bone mineral density(BMD) and biochemical markers of bone turnover in patients receiving lomg-term raloxifene(RLX) therapy with alfacalcidol(ALF) who continued with ALF or were switched to combination therapy with eldecalcitol(ELD).

Patients and study design : We conducted a randomized, open-labeled, multicenter study with 132 postmenopausal osteoporosis women. A total of 119 women who were diagnosed with postmenopausal osteoporosis and treated with RLX(60mg/d) and ALF(0.5-1?/d) for a mean period of months were randomized into the two groups, continuation of RLX with ALF (n=58, Group RA) or switching combination therapy with RLX and ELD (0.75?/d; n=61, Group RE). Patients continued their assigned treatment in a 12-months study phase.

Outcome measures : BMD (lumbar spine and total hip) was measured at baseline and after the 6 and 12 months. Biochemical parameters (serum Tartrate Resistant Acid Phosphatase-5b; TRACP-5b, Bone specific Alkaline Phosphatase; BAP, calcium; Ca, and urinary Ca excretion) were assessed at baseline and after the 3, 6 and 12 months.

Results : The switching to RLX with ELD therapy, compared with continuation of RLX with ALF, prevented lumbar spine BMD loss (percent cange from baseline at 12 months: +2.16% vs -0.61% ; p<0.001). Continuation of combination therapy with RLX and ALF resulted in a decrease in lumbar spine BMD at 12 months, but increased total hip BMD. The percent changes of total hip BMD at 12 months in the both group caused a similar increase (+1.26% and +1.00%; not significant). At 3 months after switching, the percent changes of TRACP-5b and BAP from baseline in the RE group was significantly lower than the RA group (TRACP-5b: -20.2% vs +3.4% ; p<0.001). The significant differences of these bone markers among the two groups were also observed at 6 and 12 months. Throughout the sturdy period, in the RA group, the mean value of change in TRACP-5b and BAP remained unchanged. Bone turnover markers in all patients of the both group were not less than the normal premenopausal reference values. The values of the corrected serum Ca and urinary Ca excretion in all patients remained unchanged during the sturdy period, and no significant change was observed among the two groups.

Conclusions: Combination therapy with RLX and ELD switched from RLX and ALF demonstrated beneficial effects on BMD and bone turnover after long-term RLX therapy with ALF.

Disclosures: Kozaburo Inoue, None.

SU0405

Age and gender differences in the treatment of different osteoporotic fractures.

Hans-Christof Schober*[1], Reimer Andresen[2], Kathrin Baessgen[3], Thomas Mittlmeier[4]. [1]Klinikum Südstadt RostockKlinik Für Innere Medizin I, Germany, [2]Westküstenklinikum, Germany, [3]Klinikum Suedstadt Rostock, Germany, [4]University of Rostock, Dept Traumatology, Germany

Introduction: Osteoporotic fractures represent a major health problem. Treatment of femur-,humerus-,distal radius and vertebral fractures comprises a large economic burden. In order to prevent complications immediate and appropriate treatment is necessary. The aim of the study presented was to identify medical and surgical treatment procedures concerning the above mentioned 4 fracture types in women and men in different age groups.

Methods: Between October 2008 and October 2009 we prospectively collected all patients sutaining a fracture of the proximal femur, the proximal humerus, the distal radius and clinically vertebral fractures presenting to all health care institutions in the city of Rostock (200 413 inhabitants, located at the baltic sea). For every patient the type of fracture was ensured by X-Ray. All of the health care reports were reviewed. The different treatment methods were determined.

Results: We detected 242 fractures of the proximal femur (f.162, m.80), 190 of the proximal humerus (f.127, m.63), 395 of the distal radius (f.293,m.102) and 152 clinically vertebral fractures (f.109, m.43).

Treatment options were conservative or surgical procedures. The following options were used:

proximal femur fractures: surgery: female 97 %, male: 100 %
proximal humerus fractures: surgery: female 57%, male 52%
distal radius fractures: surgery: female 24%, male 31 %
vertebral fractures: kyphoplasty: female 33%, male 23 %.

Differences in the duration of hospitalization concerning age groups and gender were observed:

Distal radius fractures: age 75 -89 y. female $7,8 \pm 1,7$ days, male $12,2 \pm 3,2$ days (p< 0,05).

Vertebral fractures: age 70 -74 y: $4,2 \pm 0,7$ days vs 85-89y:$9,4 \pm 2,3$ days (p<0,05)

Kyphoplasty: $5,9 \pm 0,6$ days vs conservative: $7,2 \pm 0,9$ days (ns)

Conclusion:Despite the different behaviour of women and men especially in different age groups no real differences concerning the treatment aspects could be observed. The longer duration of hospitalization in older age groups should lead to methods with the potential of a faster recovery.

Disclosures: Hans-Christof Schober, None.

SU0406

Bone Mineral Density and Vitamin D Status in Antiretroviral-naïve HIV-infected Thais: A Preliminary Result from a Five-Year Prospective Cohort Study.

Lalita Wattanachanya*[1], Jureeporn Jantrapakde[2], Anchalee Avihingsanon[3], Reshmie Ramautarsing[3], Nipat Teeratakulpisarn[2], Tanate Jadwattanakul[4], Nittaya Phanuphak[2], Praphan Phanuphak[3]. [1]Kingchulalongkorn memorial hospital, Thailand, [2]Thai Red Cross AIDS Research Centre, Thailand, [3]The HIV Netherlands Australia Thailand Research Collaboration (HIV-NAT), Thai Red Cross AIDS Research Centre, Thailand, [4]Queen Savang Vadhana Memorial Hospital, Thailand

Background: Low bone mineral density (BMD) has been commonly documented in HIV-infected patients from many Western countries, however, there are scant published studies regarding bone mass in Asian populations, especially in females.

Methods: We have conducted a five-year prospective cohort study to determine the prevalence of low BMD, rates of BMD decline and possible risk factors for bone loss in HIV-infected Thais of both sexes. Here, we report cross-sectional analyses of the baseline visit of the study. BMD was performed by dual-energy x-ray absorptiometry scan (Hologic®). CD4+ T-cell count, blood HIV RNA, bone turnover markers, serum 25OHD, parathyroid hormone, calcium, phosphate and sex hormones were measured.

Results: A total of 453 Thai participants were recruited from HIV-NAT and the Thai Red Cross Anonymous Clinic in Bangkok and the Queen Savang Vadhana Memorial Hospital in Chonburi: 117 HIV-infected men, 111 HIV-uninfected men, 103 HIV-infected women and 122 HIV-uninfected women. All HIV-infected individuals were antiretroviral therapy (ART) naïve. Mean age was comparable for all groups (39 ± 6 vs.40 ± 6 years in HIV-infected and uninfected men and 39 ± 4 vs. 41 ± 5 years in HIV-infected and uninfected women). For HIV-infected men, average duration since HIV diagnosis was 2.57 ± 1.3 years, mean CD4+ T-cell count was 339 ± 203 cells/mm^3 and mean HIV RNA was 4.49 ± 0.9 copies/ml. HIV-infected men have lower body mass index (BMI; 22 ± 3 vs.24 ± 3 kg/m^2) but similar lumbar spine Z score [median (IQR) -0.1 (-0.7, 0.5) vs. -0.2 (-0.7, 0.3)] and total hip Z score [0.1 (-0.7, 0.8) vs. 0 (-0.5, 0.5)], compared to controls. Serum 25OHD among men was not significantly different (32.6 ± 13 vs.27.7 ± 11 ng/ml). For HIV-infected women, average duration since HIV diagnosis was 2.58 ± 1.1 years, mean CD4+ T-cell count was 357 ± 188 cells/mm^3 and mean HIV RNA was 4.32 ± 0.9 copies/ml. There was no significant difference in BMD between HIV-infected women and controls with Z score (median, IQR) of -0.1(-0.7, 0.6) vs. 0.1 (-0.6, 0.7) at lumbar spine and 0.4(-0.4, 1.2) vs. 0.6 (0, 1.1) at total hip. No significant difference was observed in 25OHD level

between HIV-infected women and controls (22.7±7 vs.26.4±9 ng/ml). There was no history of previous fracture in any participants.

Conclusion: Low BMD is not detected in middle-aged, ART naïve HIV-infected Thais of both sexes. Vitamin D deficiency was not more prevalent in these patients.

Key words: Bone mineral density, Vitamin D, HIV, Asia

SU0407

Adequate Glucose Control Attenuates the Effects of Longstanding Type 2 Diabetes on Bone. <u>Tomaz Kocjan</u>*[1], <u>Ana Tomc</u>[2], <u>Jan Zmuc</u>[2], <u>Mojca Jensterle</u>[2], <u>Andrej Janez</u>[2], <u>Ajda Bicek</u>[2], <u>Janez Prezelj</u>[3]. [1]University Medical Centre Ljubljana, Slovenia, [2]University Medical Centre Ljubljana, Slovenia, [3]University Medical Centre Ljubljana, Slovenia

Objective: Longer disease duration and poor glycemic control are among main determinants of the increased fracture risk in patients with type 2 diabetes (T2D). Our aim was to examine the impact of adequately controlled longstanding T2D on established and potential new surrogate predictors of fracture risk.

Methods: This was a cross-sectional study. We compared 25 postmenopausal women with longstanding T2D (average time since diagnosis 10.14 years) on oral antihyperglycemic agents without microvascular complications (mean ± SD, aged 63.4 ± 5.4 years, with BMI 28.6 ± 2.8 kg/m²) and 25 controls with normal glucose homeostasis matched for age, time since menopause and BMI. Their fasting venous blood samples were taken for the determination of HbA1c, procollagen type 1 N-terminal propeptide (P1NP), C-terminal cross-linked telopeptide of type-I collagen (CTX), osteocalcin, undercarboxylated osteocalcin and osteopontin. Bone mineral density (BMD) at lumbar spine, total hip, femoral neck and distal radius was measured by DXA and trabecular bone microarchitecture was assessed by trabecular bone score (TBS) in both groups.

Results: Glycemia was well controlled in 48.3% of T2D patients (HbA1c ≤ 7.0%) and the average serum HbA1c value of the group was still acceptable at 7.42%. TBS was lower in the T2D patients, however the difference reached only borderline statistical significance (mean ± SD; 1.264 ± 0.107 vs. 1.318 ± 0.104; p=0.074). There were no statistically significant differences in BMD values at all sites between the two groups. The same was true for all measured bone markers with the probable exception of CTX and P1NP where a tendency for lower values in T2D patients was indicated (mean ± SD; 3,707 ± 1,800 pmol/L vs. 4,500 ± 1,599 pmol/L; p=0.072 and 43.9 ± 20.4 μg/L vs. 46.5 ± 13.8 μg/L; p=0.079, respectively).

Conclusions: Our results suggest that adequate glucose control indicated by absence of microvascular complications and satisfactory HbA1c values attenuates the effects of longstanding T2D on bone. However, some negative consequences of the disease reflected in lower TBS and lower bone formation seem imminent.

SU0408

Defects in cortical microarchitecture among postmenopausal African-American women with DM2. <u>Elaine Yu</u>*[1], <u>Melissa Putman</u>[2], <u>Nicolas Derrico</u>[3], <u>Gabriela Abrishamanian-Garcia</u>[3], <u>Joel Finkelstein</u>[1], <u>Mary Bouxsein</u>[4]. [1]Massachusetts General Hospital, USA, [2]Massachusetts General HospitalChildren's Hospital Boston, USA, [3]MGH, USA, [4]Beth Israel Deaconess Medical Center, Harvard Medical School, USA

PURPOSE: Fracture risk is increased in patients with type 2 diabetes mellitus (DM2) despite normal bone mineral density (BMD). In populations comprised predominantly of Caucasians, cortical porosity is higher in diabetics than in non-diabetics. DM2 is more common in African-Americans than in Caucasians. We tested whether postmenopausal African-American women with DM2 have cortical bone deficits as compared to non-diabetic African-American women.

Methods: We measured BMD at the spine, hip, and total body by DXA, and volumetric bone density and microarchitecture at the distal radius and tibia by HR-pQCT in 22 type 2 diabetic and 78 non-diabetic postmenopausal African-American women participating in the Study of Women Across the Nation (SWAN). Microfinite element analysis was performed to estimate bone strength. We measured fasting glucose and insulin and calculated HOMA-IR.

Results: There were no significant differences in age (60 ± 3 yr vs. 59 ± 3 yr, p=NS) or weight (87 ± 20 kg vs. 84 ± 19 kg, p=NS) between the diabetic and non-diabetic groups. DXA BMD was similar in the diabetics and non-diabetics at all bone sites. At the radius, cortical porosity and cortical pore volume were greater (P<0.04 for both) and cortical BMD and tissue mineral density were lower (p<0.05 for both) in diabetics than in non-diabetics (Table). There were no differences in radius total BMD or trabecular BMD between groups. Measures of cortical bone strength were significantly lower in the diabetic women though overall failure load was similar (Table). There were no significant associations between cortical parameters and either the duration of DM2 or with HOMA-IR. In the full cohort, fasting glucose levels were associated with worse cortical porosity (r=0.25, p=0.02) and lower cortical BMD (r=-0.35, p<0.01). In particular, cortical porosity and cortical pore volume were higher among those who had fasting glucose >100 mg/dL (p<0.05 for both). There were no differences in tibial bone density or microarchitecture between diabetic and non-diabetic women. These findings remained similar after adjustment for use of diabetes or osteoporosis medications.

CONCLUSIONS: DM2 and higher fasting glucose are associated with unfavorable changes in cortical bone at the non-weight-bearing radius in postmenopausal African-American women. These structural deficits may contribute to the increased fracture risk among women with DM2. Further our results suggest that hyperglycemia may be involved in mechanisms of skeletal fragility associated with DM2.

Table. Radius HR-pQCT in postmenopausal African-American women with and without DM2

	DM2 n=22	Non-DM2 n=78	t-test p-value	Correlation with fasting glucose
Cortical Porosity, %	2.9 ± 1.5	2.3 ± 1.1	0.03	R = 0.25 p = 0.02
Cortical Pore Volume, mm³	14.8 ± 7.5	11.5 ± 6.2	0.04	R = 0.21 p = 0.04
Cortical Tissue Mineral Density, mgHA/cm³	976 ± 40	994 ± 35	0.05	R = -0.34 p < 0.01
Cortical Bone Mineral Density, mgHA/cm³	933 ± 53	958 ± 47	0.04	R = -0.35 p < 0.01
Cortical Von Mises Stress, N/mm²	80.6 ± 3.6	82.3 ± 3.3	0.04	R = -0.26 p-value = 0.01
Failure Load, N	3191 ± 765	3268 ± 719	NS	NS

Table

SU0409

Sex-specific differences in the relationship between glycemic status and hip geometry: The Baltimore Longitudinal Study of Aging. <u>Kendall Moseley</u>*[1], <u>Chee Chia</u>[2], <u>Eleanor Simonsick</u>[2], <u>Josephine Egan</u>[2], <u>Deborah Sellmeyer</u>[3]. [1]Division of Endocrinology, Johns Hopkins Bayview Medical Center, USA, [2]NIA, USA, [3]The Johns Hopkins Bayview Medical Center, USA

Despite normal to high bone mineral density (BMD) compared to age and weight-matched controls, older men and women with type 2 diabetes mellitus (T2DM) are at increased risk for fracture. The discordance between bone quantity and skeletal fragility has prompted investigation into measures of bone quality in T2DM. The aim of this study was to determine differences in bone quantity, as measured by dual energy X-ray absorptiometry (DXA) and parameters of bone quality, as measured by Hip Structure Analysis (HSA), among older men and women with normal glucose tolerance (NGT), impaired glucose tolerance (IGT) and T2DM. The HSA method utilizes data derived from DXA scans to estimate hip geometry and strength parameters. Older (age > 55 years) men (n=472) and women (n=473) participating in the Baltimore Longitudinal Study of Aging (BLSA) were classified as NGT, IGT or T2DM based on 2-hour oral glucose tolerance testing. Individuals on diabetes medications were categorized as having T2DM and did not undergo oral glucose tolerance testing. Bone quantity was measured using BMD of the spine and hip. Bone quality was measured using DXA and standardized HSA equations. Specifically, bone quality parameters of hip geometry and strength included section modulus (Z), cross sectional area (CSA), and buckling ratio (BR). Men had higher bone quantity (BMD) and quality (hip geometry) than women on all measures. Men and women with T2DM (n=128) had higher BMD of the spine and total hip than those with NGT (n=512, p=0.01). In multivariate models controlling for demographic, anthropometric, biochemical and medication variables, T2DM remained positively associated with BMD of the total hip (R² = 0.012; p=0.01). In analyses stratified by sex, both IGT and T2DM were negatively associated with CSA (both p <0.01), Z (both p<0.01) and hip BR (both p<0.05) in women only. There was no observed association between glycemic status and hip geometry parameters in men. In summary, among women over age 55 years, T2DM was positively associated with BMD; however, both IGT and T2DM were inversely associated with the hip geometry and strength parameters CSA and Z although also associated with lower BR. These results indicate a sex-specific association between impairment in hip geometry and the evolution of T2DM. Additionally, the findings in women with IGT suggest that impairments in bone quality may begin early in the development of glycemic derangement.

SU0410

Musculoskeletal Effects of Two Functional Electrical Stimulation Cycling Paradigms for People with Spinal Cord Injury. <u>Therese Johnston</u>*[1], <u>Mary Schmidt-Read</u>[2], <u>Ralph Marino</u>[3], <u>Christina Oleson</u>[4], <u>Benjamin Leiby</u>[3], <u>Christopher Modlesky</u>[5]. [1]Thomas Jefferson University, USA, [2]Magee Rehabilitation Hospital, USA, [3]Thomas Jefferson University, USA, [4]Thomas Jefferson University, USA, [5]University of Delaware, USA

Purpose: People with spinal cord injury (SCI) rapidly lose bone mass following injury. Rate of loss slows within 2 years but bone loss continues, increasing fracture risk especially in the distal femur and proximal tibia. To attempt to increase load on the lower extremities, the objective of this study was to compare the musculoskeletal effects of a novel low cadence cycling paradigm (LOW-CAD) with functional electrical stimulation (FES) to a high cadence paradigm (HIGH-CAD) for people

SCI. It was hypothesized that LOW-CAD would show greater changes in bone and muscle as greater resistance and thus greater loading could be obtained. Methods: Fourteen men and 3 women ages 22-67 years with C4-T6 motor complete chronic SCI participated. Nine subjects were randomized to LOW-CAD and eight to HIGH-CAD. Subjects cycled with FES 1 hour, 3 times/week for 6 months. LOW-CAD cycled at 20 rpm and HIGH-CAD at 50 rpm. Resistance increased automatically if cadence was maintained. Pre and post training, bone changes were measured via dual-energy x-ray absorptiometry to assess areal bone mineral density (distal femur/proximal tibia), magnetic resonance imaging (MRI) to assess microarchitecture (mid/distal femur), and biochemical bone markers to assess bone formation and resorption. Thigh muscle volume was measured via MRI. Results: LOW-CAD obtained maximal resistance of 2.9 $\pm$ 2.8 Nm and HIGH-CAD of 0.8 $\pm$ 0.2 Nm. Over time, LOW-CAD showed greater decreases (p<0.05) in bone-specific-alkaline-phosphatase (BALP) compared to HIGH-CAD (LOW-CAD: 12.9 $\pm$ 3.6 to 10.6 $\pm$ 3.4 µg/L; HIGH-CAD: 13.4 $\pm$ 4.9 to 14.7 $\pm$ 6.1 µg/L) indicating less bone formation. However, N-telopeptide decreased within LOW-CAD (p<0.05, 53.4 $\pm$ 25.3 to 34.1 $\pm$ 15.5 mg/dL), suggesting less bone turnover. BALP to N-telopeptide ratio (formation/resorption) increased non-significantly from 0.29 $\pm$ 0.14 to 0.36 $\pm$ 0.16 for LOW-CAD and 0.35 $\pm$ 0.21 to 0.39 $\pm$ 0.21 for HIGH-CAD, indicating less bone turnover for LOW-CAD. Both groups increased muscle volume (LOW-CAD: 1193 $\pm$ 603.7 to1361.1 $\pm$ 546.4 cm3; HIGH-CAD: 1215.6 $\pm$ 331.8 to 1335.1 $\pm$ 342.6 cm3). LOW-CAD showed a non-significant increase (1.08 $\pm$ 0.23 to 1.13 $\pm$ 0.22) in trabecular bone number (measured at 12 images proximal to condyles) while HIGH-CAD showed a non-significant decrease (1.17 $\pm$ 0.33 to 1.14 $\pm$ 0.27). Conclusion: This preliminary study suggests that LOW-CAD may stimulate greater musculoskeletal changes. Research is needed with a larger sample size.

Disclosures: Therese Johnston, None.

SU0411

Combined Effects of Spaceflight and Age in Astronauts as Assessed by Areal Bone Mineral Density [BMD] and Trabecular Bone Score [TBS]. Jean Sibonga*[1], Elisabeth Spector[2], Robert Ploutz-Snyder[3], Harlan Evans[2], Lisa King[2], Nelson Watts[4], Didier Hans[5], Scott Smith[2]. [1]NASA Johnson Space Center, USA, [2]Wyle, USA, [3]USRA, USA, [4]Mercy Health Osteoporosis & Bone Health Services, USA, [5]Lausanne University Hospital, Switzerland

Spaceflight is a potential risk factor for secondary osteoporosis in astronauts. Although lumbar spine (LS) BMD declines rapidly, more than expected for age, there have been no fragility fractures in astronauts that can clearly be attributed to spaceflight. Recently, astronauts have been returning from 6-month spaceflights with absolute BMD still above young adult mean BMD. In spite of these BMD measurements, we project that the rapid loss in bone mass over long-duration spaceflight affects the bone microarchitecture of the LS which might predispose astronauts to premature vertebral fractures. Thus, we evaluated TBS, a novel texture index correlated with vertebral bone microarchitecture, as a means of monitoring changes to bone microarchitecture in astronauts as they age. We previously reported that TBS detects an effect of spaceflight (~6-month duration), independent of BMD, in 51 astronauts (47+/-4 y) (Smith et al, J Clin Densitometry 2014). Hence, TBS was evaluated in serial DXA scans (Hologic Discovery W) conducted triennially in all active and retired astronauts and more frequently (before spaceflight, after spaceflight and until recovery) in the subset of astronauts flying 4-6-month missions. We used non-linear models to describe trends in observations (BMD or TBS) plotted as a function of astronaut age. We fitted 1175 observations of 311 astronauts, pre-flight and then post-flight starting 3 years after landing or after astronaut's BMD for LS was restored to within 2% of preflight BMD. Observations were then grouped and defined as follows: 1) LD: after exposure to at least one long-duration spaceflight > 100 days and 2) SD: before LD and after exposure to at least one short-duration spaceflight < 30 days. Data from males and females were analyzed separately. Models of SD observations revealed that TBS and BMD had similar curvilinear declines with age for both male and female astronauts. However, models of LD observations showed TBS declining with age while BMD appeared stable or trending upward. For females (n=8) LD observations were too few to discern a trend. Notably, models describing trends in TBS appeared to be more sensitive to the effects of age than the models for BMD. We conclude that TBS may provide an additional index for the lumbar spine to monitor the combined changes due to spaceflight and due to aging. This increased knowledge may enhance the ability to identify an intervention trigger for premature vertebral fractures in astronauts.

Disclosures: Jean Sibonga, None.

SU0412

Cortical and trabecular bone microarchitecture after severe burn injury. Christian Muschitz*[1], Gabriela Katharina Muschitz[2], Roland Kocijan[3], Gerald Ihra[4], Heinrich Resch[5], Lukas A. Fischer[6], Thomas Rath[2]. [1]St. Vincent's Hospital, Austria, [2]Division of Plastic & Reconstructive Surgery Department of Surgery, Medical University Vienna, Austria, [3]St. Vincent Hospital Vienna, Austria, [4]Department of Anesthesia & Intensive Care, Medical University Vienna, Austria, [5]Medical University Vienna, Austria, [6]CIR Lab, Department of Radiology, Medical University of Vienna, Austria

Purpose:
Extensive thermal injury causes immediate and severe katabolic metabolism, increased inflammatory cytokines and glucocorticoids, alterations in calcium levels as well as an early detoriation of bone matrix. The objective of this study was to evaluate prolonged alterations in bone microarchitecture and bone metabolism.
Methods:
Male Caucasian patients, who had sustained at least a burn injury stage IIb – III°, were included in this single center case-control study. The minimum timeframe from trauma to evaluation was 24 months. Exclusion criteria were a high-voltage injury, any prior or ongoing antiresorptive or anabolic therapy, any calcium and vitamin D supplementation, any endocrine disease affecting bone metabolism or permanent immobilization. All patients had a HR-pQCT examination of the radius and tibia and an evaluation of fasting serum markers of bone formation (P1NP) and resorption (CTX) as well as 25-OH vitamin D and iPTH levels.
Results:
20 male patients (mean age: 38.0 $\pm$ 10.6 years, mean burn total body surface area: 43.9 $\pm$ 12.3 %) were and compared to 30 age-matched healthy male controls (HC). The mean time after trauma was 27.5 $\pm$ 2.9 months, the mean time of immobilization directly after trauma was 35.9 $\pm$ 11.6 days. At both, the radius and the tibia, CtBMD (p<0.05) and CtTMD (p<0.005) was significantly lower, CtPo was significantly higher (p<0.001) when compared to HC. No differences were observed in CtTh at the radius, but CtTh was decreased by trend at the tibia (p=0.078). At the radius and tibia EndoCtPm (p<0.05) and TbAr (p<0.01) were increased. Serum markers were comparable, but vitamin D was decreased (19.3 $\pm$ 6.4 vs 34.5 $\pm$8.4 ng/ml, p<0.001). Five patients had fragility fractures after trauma (radius: 2, humerus: 2, rib 1).
Conclusions:
In this study young male patients who had sustained a severe trauma more than two years prior to all examinations show altered cortical and trabecular bone microstructure. These differences are likely due to the impaired and highly increased bone metabolism in the early stage after trauma. Bone turnover markers do not reflect these alterations and are of less validity. Decreased cortical structures, increased cortical porosity, trabecular area and endocortical perimeter enhance the vulnerability of these patients for fragility fractures.

Disclosures: Christian Muschitz, None.

SU0413

Hepatitis C Infection is Associated with Lower Bone Mineral Density. Naim Maalouf*[1], Xilong Li[2], Beverley Huet[2], James Cutrell[3], Roger Bedimo[3]. [1]University of Texas Southwestern Medical Center, Dallas, USA, [2]University of Texas Southwestern Medical Center, USA, [3]VA North Texas Health Care System, USA

Background: Hepatitis C virus (HCV) infection, either as mono-infection or as co-infection in HIV-positive individuals, has been associated with an increased risk of fracture in several studies. However, the mechanisms underlying the skeletal effects of HCV are not clearly understood, and the impact of HCV infection on bone mineral density (BMD) has not been well-studied.
Objectives: To compare BMD in HCV-infected (HCV+) vs. non-infected (HCV-) controls, and evaluate the impact of liver disease activity and systemic inflammation on BMD among HCV+.
Methods: Using the National Health and Nutrition Examination Survey (NHANES) 2007-2010 surveys, we identified 205 HCV+ individuals (defined by presence of HCV antibody and confirmed by detectable HCV RNA viral load in blood) who had BMD measurement. For each HCV+ participant, two control (HCV-) subjects matched for gender, race, age ($\pm$5 years) and body mass index (BMI, $\pm$5 Kg/m^2) and available BMD measurement were randomly selected. Liver disease activity was assessed by serum alanine aminotransferase (ALT). Systemic inflammation was assessed by serum C-reactive protein (CRP).

Results: By design, HCV+ and HCV- participants were well-matched with respect to gender, race, age, and BMI (Table). Prevalence of family history of osteoporosis was 7% in both groups. HCV+ were significantly more likely to be current smokers, to consume ⩾ 3 alcoholic drinks daily, to be past drug users, and to have higher serum ALT (61 ± 42 vs. 26 ± 24 IU/L, p<0.001). After adjusting for age, gender, race and BMI, HCV+ had significantly lower BMD at the lumbar spine, femoral neck and total hip (p<0.05, Table). A significant gender x HCV status interaction was detected for BMD. In subgroup analysis, HCV+ men and postmenopausal women had significantly lower BMD at all sites after adjusting for age, race, BMI, tobacco and alcohol use (p<0.05), whereas BMD was similar in HCV+ and HCV- premenopausal women. Among HCV+, there was no significant correlation between BMD and serum ALT or serum CRP.

Conclusions: HCV infection is associated with low BMD independent of age, race, BMI, tobacco and alcohol use in men and postmenopausal women. Severity of systemic inflammation and of liver disease activity (as assessed by serum CRP and ALT respectively) do not explain BMD lowering in HCV+. Additional mechanisms by which HCV impacts bone health and the role of HCV therapy on BMD and fracture risk remain to be determined.

	HCV+ (N=205)	HCV- (N=410)
Age, years	50.4 ± 10.4	50.3 ± 11.4
Gender, % Female/Male	36 / 64	36 / 64
Race, % AA/Cauc/Hisp/Other	39/41/17/3	39/41/17/3
BMI, Kg/m^2	28.0 ± 6.1	27.9 ± 5.8
Family History of Osteoporosis,%	7	7
Smoking, %Current/Former/Never	59/26/15 *	26/24/50
Alcohol, %Heavy/Moderate/Non	21/60/19 *	4/73/23
Drug Use, % Ever	45*	1
Serum ALT (IU/L)	61 ± 42 *	26 ± 24
Lumbar spine BMD (g/cm^2)	1.04 ± 0.14 *	1.06 ± 0.15
Femoral Neck BMD (g/cm^2)	0.84 ± 0.13 *	0.86 ± 0.14
Total Hip BMD (g/cm^2)	0.97 ± 0.14 *	1.01 ± 0.15

* p<0.05 for HCV+ vs HCV-

Table: Comparison of HCV+ vs. HCV-

Disclosures: Naim Maalouf, None.

SU0414

Risk Factors for Fractures in Women with Breast Cancer, the WHI Bone Density Study. <u>Beatrice Edwards</u>*[1], <u>Zhao Chen</u>[2], <u>Wenjun Li</u>[3], <u>Carolyn Crandall</u>[4], <u>Marilyn Kwan</u>[5], <u>Meryl Leboff</u>[6], <u>Jane Cauley</u>[7]. [1]MD Anderson Cancer Center, USA, [2]University of Arizona College of Public Health, USA, [3]University of California, San Francisco, USA, [4]University of California, Los Angeles, USA, [5]Kaiser Permanente, USA, [6]Brigham & Women's HospitalProfessor of Medicine, Harvard Medical School, USA, [7]University of Pittsburgh Graduate School of Public Health, USA

Background: Fractures are common in women with breast cancer (BC)
Objective: To assess risk factors for fractures in women with prevalent BC
Methods: prospectve cohort study, WHI Bone Density Study
Results: Within the 11,006 participants, 211 women with prevalent BC were identified at enrollment. During follow up, women with BC sustained 33 fractures (16%). Fractures sites included wrist (11/33), other sites (11/33), hip fractures (6/33) and clinical vertebral fractures (5/33). Women with BC who fractureed were older ($67 \pm$ 6 yr. v. $64 \pm$ 7 yr., p=0.03), had lower BMI ($26 \pm$ 4 v. $28 \pm$ 7, p=0.03), were white (90% v. 63%, p=0.003), and had a history of prior fracture (33% v. 8 %, p=0.001). Few participants were receiving gonadotropin releasing hormones agonists or aromatse inhibitors. Fractures were observed approximatley 4 years after study enrollment (1 - 5 yr). In multivariate logistic regression, being white (O.R.= 5.15, 95% C.I. 1.45, 18.25, p=0.01), and having a prior fracture (O.R. = 3.8, 95% C.I. 1.46, 9.83, p= 0.006) were significant risk factors for fracture, while there was a trend for a higher bMD (O.R. 0.669, 95% C.I. 0.43, 1.04, p=0.07) to be protective in women with BC. Bone density was lower in women with fractures (hip T-score -1.61 $\pm$ 0.9 v. -1.03 $\pm$ 1.1, p=0.004) than in women with BC without fractures.

Conclusion: Fractures are common in women with BC who have low bone mass. Traditional risk factors such s white ethnicity and a prior fracture are present in women with BC. HIgher BMD was protective in women with BC.

Disclosures: Beatrice Edwards, None.

SU0415

serum sclerostin change after exercise in breast cancer patients. <u>Seong-Bin Hong</u>*[1], <u>Soo Hyun Kim</u>[2], <u>Joo Young Han</u>[3], <u>So Hun Kim</u>[4], <u>Moonsuk Nam</u>[4], <u>Yong Seong Kim</u>[4]. [1]INHA University, South Korea, [2]Department of Nursing, Inha University, South Korea, [3]Inha University hospital, South Korea, [4]Inha University School of Medicine, South Korea

Sclerostin, an endogenous regulator of the Wnt pathway and bone formation has been investigate the role in cancer induced bone loss. Its levels increase with age and regulated by PTH. However, there are no data regarding the relationship between sclerostin and bone mineral density in the breast cancer and effect of exercise on the sclerostin level.

Objective: To assess relationships between serum sclerostin level and BMD, and serum sclerostin change after 6 month exercise program in breast cancer patients.

Methods: Serum sclerostin, Ntx and 25(OH) vitamin D were measured in breast cancer patients who hadn't done active exercise. Subjects were divided into exercise and normal activity group. Vitamin D 800 IU and calcium 1000 mg were supplied in both groups. BMD was measured by DXA at baseline and 6 month. Serum sclerostin and bone turnover marker repeated at 6 month.

Results: 46 patients were enrolled. Mean age was 55 7 $\pm$ 7 years, Serum sclerostin was measured twice in 24 patients. Serum sclerostin 17.22 $\pm$ 9.81 pg/mL, Circulating sclerostin was positively associated with bone mineral density in the spine (r=0.286, P<0.05). However its change was not different in two groups. Sclerostin and 25(OH)D3 level increased in both groups (p<0.05).

Conclusions: In this cross-sectional study, circulating sclerostin was positively associated with BMD in the spine. Although exercise did not effect change of sclerostin, sclerostin may play a role in skeletal mineral metabolism in breast cancer patient.

Disclosures: Seong-Bin Hong, None.

SU0416

The Effect of Kidney Function on the Performance of FRAX: A Population-based report from CaMos. <u>Kyla Naylor</u>*[1], <u>William Leslie</u>[2], <u>Amit Garg</u>[3], <u>Guangyong Zou</u>[3], <u>Lisa-Ann Fraser</u>[1], <u>Suzanne Morin</u>[4], <u>Jonathan Adachi</u>[5], <u>Brian Lentle</u>[6], <u>David Goltzman</u>[4], <u>Stuart Jackson</u>[7], <u>Sophie Jamal</u>[8]. [1]Western University, Canada, [2]University of Manitoba, Canada, [3]Western University, Canada, [4]McGill University, Canada, [5]St. Joseph's Hospital, Canada, [6]University of British Columbia, Canada, [7]University of Alberta, Canada, [8]The University of Toronto, Canada

Background: Individuals with chronic kidney disease (CKD) are at an increased risk for fracture. The World Health Organization's Fracture Risk Assessment Tool (FRAX) is widely used in clinical practice to predict the 10-year probability of fracture in the general population. It is not known if FRAX accurately predicts fracture in CKD.

Methods: We examined the discrimination and calibration of FRAX (Canadian tool) using data from the Canadian Multicentre Osteoporosis Study. We included men and women 40 years of age or older who had an estimated glomerular filtration rate (eGFR) value at baseline (eGFR <60 mL/min/1.73 m^2 *vs.* ⩾60 mL/min/1.73 m^2) and followed subjects for a mean of 4.7 years for an incident major osteoporotic fracture (clinical spine, hip, forearm/wrist, or humerus).

Results: Our analyses included 320 individuals with an eGFR <60 mL/min/1.73 m^2 and 1787 individuals with an eGFR ⩾60 mL/min/1.73 m^2; mean age was 67 ± 10 years and 70.5% were women. There were 20 (6.6%, 95% confidence interval [CI], 4.3 to 10.1%) major osteoporotic fractures over 4.7 years of follow-up in individuals with an eGFR <60 mL/min/1.73 m^2 which was similar to the FRAX predicted fracture risk (5.8% with bone mineral density [BMD]; 7.4% without BMD). FRAX major osteoporotic fracture prediction was slightly lower in individuals with an eGFR <60 mL/min/1.73 m^2 compared to individuals with an eGFR ⩾60 mL/min/1.73 m^2. For example, in individuals with an eGFR <60 mL/min/1.73 m^2 the area under the curve (AUC) value for FRAX with BMD was 0.67 (95% CI, 0.54 to 0.80) compared to those with an eGFR ⩾60 mL/min/1.73 m^2 (AUC: 0.75, 95% CI, 0.69 to 0.81); however, this did not reach statistical significance (p-value=0.257). In individuals with an eGFR <60 mL/min/1.73 m^2 the AUC value for FRAX without BMD was 0.65 (95% CI, 0.51 to 0.78) and in individuals with an eGFR ⩾60 mL/min/1.73 m^2 the AUC was 0.73 (95% CI, 0.67 to 0.80).

Conclusions: In individuals with an eGFR <60 mL/min/1.73 m^2 FRAX demonstrated major osteoporotic fracture predictive discrimination which was slightly lower than individuals with an eGFR ⩾60 mL/min/1.73 m^2. Observed and FRAX predicted fracture rates were similar in individuals with an eGFR <60 mL/min/1.73 m^2. If confirmed by larger studies, FRAX may become a helpful tool for clinicians to use to assess fracture risk in individuals with reduced kidney function.

Disclosures: Kyla Naylor, None.

SU0417

Assessment of mineral bone diseases in adult post-pancreas transplantation recipients in Japan. Megumi Shibata*[1], Atsushi Suzuki[2], Izumi Hiratsuka[3], Mizuho Kondo-Ando[3], Hiroyuki Hirai[4], Sahoko Sekiguchi-Ueda[2], Takeshi Takayanagi[5], Masaki Makino[6], Hitomi Sasaki[7], Mamoru Kusaka[7], Taihei Itoh[8], Takashi Kenmochi[8], Kiyotaka Hoshinaga[7], Mitsuyasu Itoh[9]. [1]Fujita Health University Division of Endocrinology, Japan, [2]Fujita Health University, Division of Endocrinology, Japan, [3]Division of Endcrinology & Metabolism,Department of Internal Medicine, Fujita Health University School of Medicine,Toyoake, Japan, [4]Fujita Health University Division of Endocrinology, Japan, Japan, [5]Division of Endocrinology & Metabolism, Department of Internal Medicine, Fujita Health University School of Medicine, Toyoake, Japan, [6]Division of Endcrinology & Metabolism, Department of Internal Medicine, Fujita Health University School of Medicine, Toyoake, Japan, [7]Department of Urology, Fujita Health University School of Medicine, Toyoake, Japan, [8]Department of Organ Transplant Surgery, Fujita Health University School of Medicine, Toyoake, Japan, [9]Division of Endocrinology & Metabolism, Department of Internal Medicine, Fujita Health University School of Medicine, Toyoake, Japan

Background: Type 1 diabetes (T1DM) is known to be a risk factor for osteoporotic fracture. Pancreas transplantation is nowadays one of good therapeutic option for unstable T1DM patients, especially when they have end-stage renal diseases (ESRD). Recovery of insulin secretion from transplanted pancreas must give beneficial effect on bone metabolism, but pre-existing chronic kidney disease-mineral and bone disease (CKD-MBD) and other clinical risk factors such as hyperparathyroidism and glucocorticoid therapy would make osteoporosis as a serious problem in post-transplant patients. The aim of this study is to estimate the MBD in post-pancreas transplant recipients. Subjects and Methods: Post-pancreas transplant recipients of Fujita Health University Hospital were recruited (n=14, M/F=4/10, age, 45.9 ± 7.2 years old, 10 SPK and 2 PTA). Mean age of onset of T1DM was 13.2 ± 6.5 years old. Simultaneous pancreas-kidney transplantation (SPK) was performed in 11 cases, pancreas-after-kidney transplant (*PAK*) was in 2 cases, and 1 other case had pancreas transplant alone (PTA). Measurement of bone mineral density at lumbar spine and hip were performed during their stay in the hospital for the transplantation. When we examined bone turn over markers, all the patients took continuous glucocoritioid therapy. The data were shown as median with interquartile range. Results: Pre-existing vertebral fracture on x-ray was found in 3 cases. Median hip BMD was 0.59 [0.52 - 0.68] g/cm^2 (Z-score:-1.40[-1.80 - -0.60]), while median lumbar BMD was 0.92 [0.76 -0.99] g/cm^2 (Z-score: -0.50[-1.48 – 0.23]). Serum intact PTH level and TRACP-5b were high (intact PTH, 103.7 [63.6-191.9] pg/mL; TRACP-5b, 508 [343-640] mU/dL). On the other hand, serum osteocalcin level was low (6.1 [3.1-8.0] ng/mL). Serum BAP was 14.0 [9.0-26.2] mg/L. Serum iPTH level was negatively correlated with hip BMD but was not associated with lumbar BMD. These results suggest that post-pancreas transplantation recipients seem to have relatively high risk of osteoporosis, especially when they have secondary hyperparathyroidism after transplantation.

***Disclosures: Megumi Shibata**, None.*

SU0418

Utility of trabecular bone score in kidney transplantation recipients. Sahoko Sekiguchi-Ueda*[1], Atsushi Suzuki[1], Hitomi Sasaki[2], Midori Hasegawa[3], Hiroyuki Hirai[4], Megumi Shibata[5], Tamotsu Sugita[6], Masashi Sugimoto[7], Yutaka Kinomura[7], Hiroshi Toyama[7], Yukio Yuzawa[8], Kiyotaka Hoshinaga[2], Mitsuyasu Itoh[9]. [1]Fujita Health University, Division of Endocrinology, Japan, [2]Department of Urology Fujita Health University, Japan, [3]Devision of Nephrology, Department of Internal Medicine Fujita Health University, Japan, [4]Fujita Health University Division of Endocrinology, Japan, Japan, [5]Fujita Health University Division of Endocrinology, Japan, [6]Department Radiology Fujita Health University, Japan, [7]Department of Radiology Fujita Health University, Japan, [8]Department of Nephrology Fujita Health University, Japan, [9]Division of Endocrinology & Metabolism, Japan

Background: Despite Kidney transplantation (KTx) could restore many disorders in end-stage renal diseases (ESRD) patients, pre-existing chronic kidney disease-mineral and bone disease (CKD-MBD) and other clinical risk factors such as hyperparathyroidism and glucocorticoid therapy would make osteoporosis as a serious problem in post-KTx patients. The bone density (BMD) measurement by DXA is a "golden standard" technique of bone quantity evaluation, but it's not useful for evaluating about bone microstructure and bone quality. Trabecular bone score (TBS) is new type of analysis to evaluate bone microstructure by using lumbar spine front view taken by DXA. The aim of this study is to explore the utility of TBS in post-KTx patients.

Subjects and Methods: Post-KTx recipients in outpatient clinic of Fujita Health University Hospital were recruited (n=32, M/F=20/12, age 51 ± 1.8 years old, mean duration from KTx, 136 ± 16 months). Prednisolone or methylprednisolone were prescribed to all patients, and 20 patients (20/32) took oral bisphosphonate.

Result : Mean BMD of lumber spine evaluated by DXA was 0.84±0.03 g/cm^2, Mean TBS score was 1.29 ± 0.01. Seven patients were categorized in the range of osteoporosis by lumbar BMD, while 3 patients were by TBS. Only one patient was diagnosed as osteoporosis by both methods. There was significant association between lumbar BMD and TBS in female post-KTx patients (p<0.01), but not in male population. Femoral neck BMD was also measured in 25 cases (mean TBS was 1.29 ± 0.07). Mean femoral neck BMD evaluated by DXA was 0.65±0.02 g/cm^2 (mean T-score was -1.55±0.2 SD, and mean Z-score was -0.88 ± 0.2 SD). TBS was not correlated with hip BMD, its T-score or Z-score regardless of gender. Discussion: TBS is considered to assess bone microstructure independently from BMD. The present study showed that lumbar BMD was correlated with TBS in only female population of post-KTx patients. As MBD in post-KTx patients was modulated by CKD-MBD, medication and treatment for co-existing diseases, more precise assessment of bone and further prospective study should be needed for the prevention of osteoporotic fracture. In post-KTx patients.

***Disclosures: Sahoko Sekiguchi-Ueda**, None.*

SU0419

SDF-1β / BMP-2 Co-Therapy Augments BMSC-Mediated Healing of Critical-Size Mouse Calvarial Defects. Samuel Herberg*[1], Alexandra Aguilar[2], Sudharsan Periyasamy-Thandavan[3], R. Nicole Howie[4], Mohammed Elsalanty[5], Xing-Ming Shi[5], Mark Hamrick[6], Carlos Isales[5], William Hill[7], James Cray[8]. [1]Case Western Reserve University, USA, [2]UCC School of MedicineGeorgia Regents University, USA, [3]Georgia Regents University & Charlie Norwood VAMC, USA, [4]Georgia Regents University, USA, [5]Georgia Regents University, USA, [6]Georgia Health Sciences University, USA, [7]Georgia Regents University & Charlie Norwood VAMC, USA, [8]Medical University of South Carolina, USA

Purpose: Bone has the potential for spontaneous healing. However, this regenerative process often fails in patients with underlying impairments requiring clinical intervention. Numerous experimental and clinical studies have revealed that bone marrow-derived mesenchymal stem/stromal cells (BMSCs) hold great potential for regenerative therapies. Increasing evidence suggests that stromal cell-derived factor-1 (SDF-1) is involved in bone formation. We have shown that SDF-1β, the second most abundant splice variant, enhances osteogenesis by regulating bone morphogenetic protein-2 (BMP-2) signaling *in vitro* and *in vivo*. Here we investigated healing of critical-size mouse calvarial defects following transplantation of GFP-positive Tet-Off BMSCs that overexpress SDF-1β, either alone or co-delivered with BMP-2, on acellular DermaMatrix (ADM). We tested the hypothesis that SDF-1β/BMP-2 co-therapy augments BMSC-mediated bone formation.

Materials: Critical-size (5-mm) calvarial defects were created in 2-month-old male C57BL/6J mice. 70 animals randomized in 7 groups (n=10) received Tet-Off-EV (empty vector) or Tet-Off-SDF-1β BMSCs alone or co-delivered with 542.5 ng BMP-2 soak-loaded onto ADM. Controls included sham, vehicle, and BMP-2. Animals were euthanized 4-weeks post-surgery. Surgical sites were explanted and subjected to radiographic, μCT, and histomorphometric analyses.

Results: Radiographic and μCT analyses (e.g. BV/TV) revealed significant BMP-2-induced bone formation relative to vehicle controls (p<0.01) and BMSCs (p<0.05). Both Tet-Off-EV and Tet-Off-SDF-1β BMSCs showed limited healing, comparable to vehicle controls. Co-delivery of BMP-2 promoted the BMSC-mediated regenerative effects, which were significantly enhanced with SDF-1β overexpression (p<0.05). However, BMSCs+BMP-2 produced less bone than BMP-2 alone. Quantitative histomorphometry (e.g. B.Ar/T.Ar) confirmed the microstructural bone evaluation. Immunohistochemistry for GFP showed significantly greater signal intensity in ADM soak-loaded with BMSCs+BMP-2 compared to BMSCs alone. *In vitro* cell culture studies suggested that the decrease in BMP-2 osteoinduction with co-delivery of BMSCs is due to both cell adsorption and uptake, reducing the bioavailable BMP-2 dose on the ADM carrier.

Conclusion: Our data suggest that SDF-1β/BMP-2 co-delivery provides significant synergistic effects supporting BMSC-mediated bone healing and appears a suitable strategy for optimization of clinical bone augmentation.

Figure 1. Representative 3-D reconstructions of çCT images 4-weeks post-transplantation

**p<0.01
***p<0.0001 vs. Control
bp<0.01
cp<0.0001 vs. Tet-Off-EV or Tet-Off-SDF-1β
$p<0.05
%p<0.01 vs. Tet-Off-SDF-1β

Figure 2. 3-D bone morphometry within the craniotomy defects 4-weeks post-transplantation

Disclosures: Samuel Herberg, None.

SU0420

Acute inflammatory response in macrophages induced by titanium particles released from ultrasonic scaling of surface-treated dental implants. Michal Eger*[1], Nir Sterer[2], Tamar Liron[1], David Kohavi[2], Yankel Gabet[3]. [1]Department of Anatomy & Anthropology, Sackler Faculty of Medicine, Tel Aviv University, Israel, [2]Department of Prosthodontics, Goldschleger School of Dental Medicine, Sackler Faculty of Medicine, Tel Aviv University, Israel, [3]Department of Anatomy & AnthropologySackler Faculty of Medicine, Israel

Titanium and its alloys are widely used as dental implants due to their biocompatibility, mechanical strength, high corrosion resistance and above all osseointegration (direct bone-titanium bonding). To date, virtually all available implants undergo surface roughening in order to accelerate osseointegration and shorten healing time before loading. Peri-implantitis is a major clinical concern and main cause of long term implant failure. Triggered by specific oral bacteria, it consists of an inflammatory process that leads to bone resorption around dental implants. Once the process starts it can hardly be controlled and often results in implant loss. Treatment includes mechanical cleaning of the surrounding oral flora by ultrasonic scaling. We hypothesize that the scaling process releases titanium particles into the implant micro environment and that these particles aggravate or even trigger the inflammatory response. To test this hypothesis, we performed ultrasonic scaling (NanoSight®) of titanium discs that had a sand-blasted/acid etched (SLA) surface. The released particles were then added to bone marrow-derived mouse macrophages (BMDM) cultures. Bacterial lipopolysaccharides (LPS) were added to parallel cultures as positive control and in addition to titanium particles to assess additive/synergistic effects. RT-qPCR indicated that titanium particles stimulated gene expression of pro-inflammatory cytokines (TNFα, IL1β, IL6) to a greater extent than LPS. We then compared the profile and quantity of titanium particles obtained from 3 different surface types, namely machined, SLA and sand-blasted (SB). Using SEM, we found implant surfaces differed in the micro-roughness and quantity of titanium particles released during scaling but not their average size. BMDM were then cultured with the particles released from each surface type. Particles originating from SB implants yielded the most severe inflammatory response, while particles from machined implants induced the mildest inflammasome. This was mainly due to differences in the number of released particles. These data suggest that scaling of titanium implants, intended at preventing peri-implantitis, may actually aggravate the catabolic inflammatory response by causing an accumulation of titanium particles in the peri-implant environment. This adverse reaction is likely to be even more severe around roughened titanium implants.
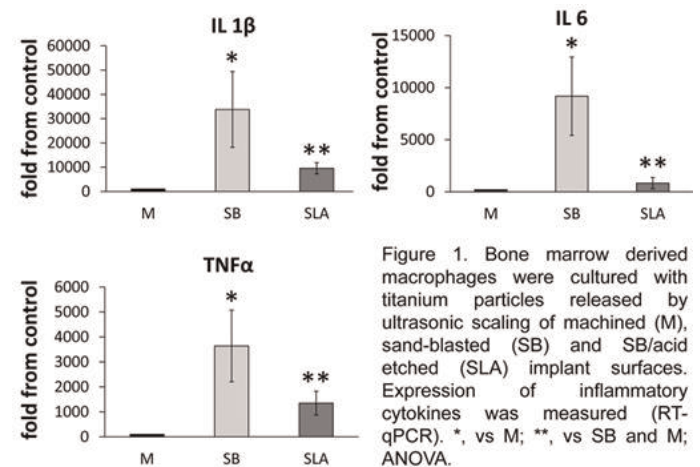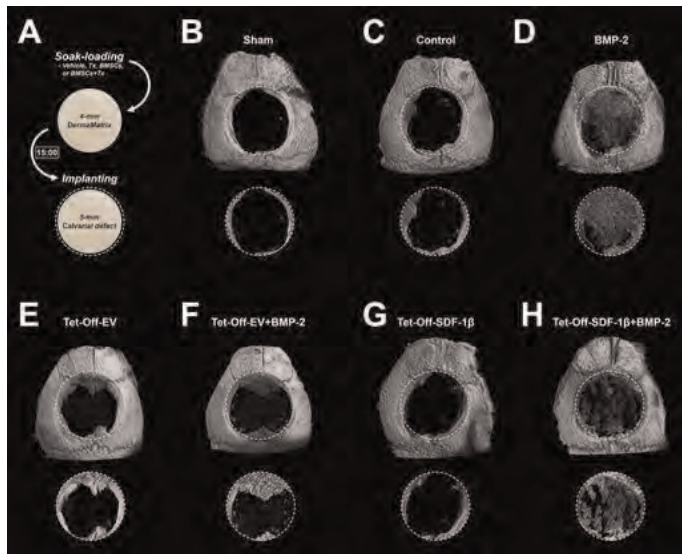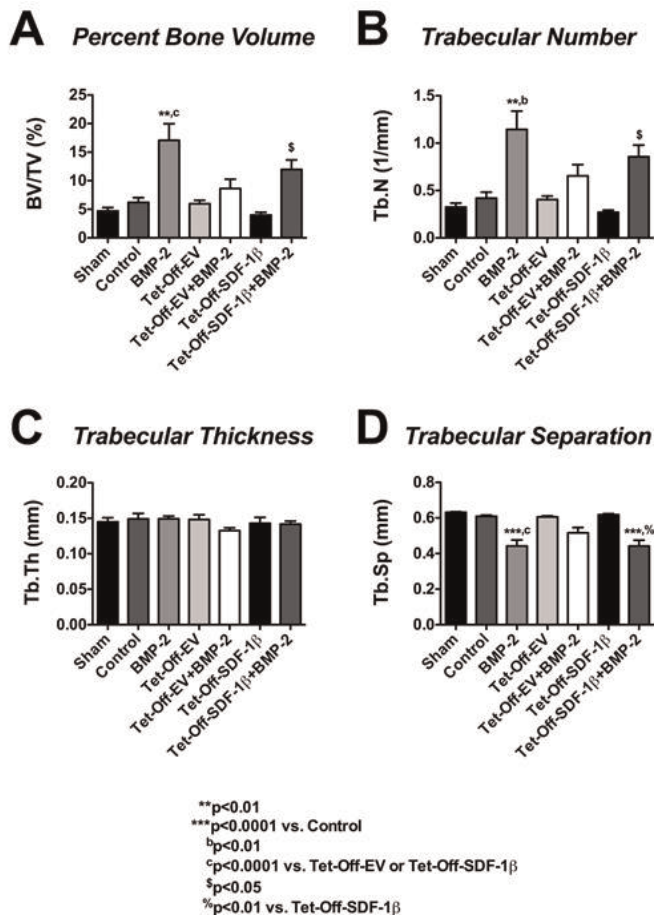

Figure 1. Bone marrow derived macrophages were cultured with titanium particles released by ultrasonic scaling of machined (M), sand-blasted (SB) and SB/acid etched (SLA) implant surfaces. Expression of inflammatory cytokines was measured (RT-qPCR). *, vs M; **, vs SB and M; ANOVA.

Figure 1

Disclosures: Michal Eger, None.

SU0421

Inflammatory Factors in the Circulation of Patients with Active Rheumatoid Arthritis Stimulate Osteoclastogenesis via Endogenous Cytokine Production by Osteoblasts.

Janak L Pathak[1], Nathalie Bravenboer[2], Patrick Verschueren[3], Willem F Lems[4], Frank P Luyten[5], Jenneke Klein-Nulend*[6], Astrid D Bakker[7]. [1]ACTA-University of Amsterdam & VU University Amsterdam, Dept Oral Cell Biology, MOVE Research Institute Amsterdam, Netherlands, [2]VU University Medical Center, The Netherlands, [3]Skeletal Biology & Engineering Research Center, KU Leuven, Belgium, [4]Department of Rheumatology, VU University Medical Center, MOVE Research Institute Amsterdam, Netherlands, [5]Skeletal Biology & Engineering Research Center, KU Leuven, Belgium, [6]ACTA-VU University AmsterdamDept Oral Cell Biology (Rm # 11N-63), The Netherlands, [7]Department of Oral Cell Biology, Academic Centre for Dentistry Amsterdam (ACTA), University of Amsterdam & VU University Amsterdam, MOVE Research Institute Amsterdam, Netherlands

Introduction: Generalized bone loss, as occurs in patients with rheumatoid arthritis (RA), is related to elevated levels of circulating cytokines. Individual cytokines have deleterious effects on proliferation and differentiation of osteoblast cell lines, but little is known about the effect of the interaction between inflammatory factors in the circulation of patients with active RA on human osteoblast function, including their communication towards other bone cells. The purpose of this study was to investigate whether serum from patients with active RA enhances cytokine production by osteoblasts, thereby effectively altering osteoblast-stimulated osteoclastogenesis.

Methods: Serum was obtained from 20 patients with active RA (active RA-sera) and from the same patients in clinical remission (remission RA-sera). Primary human osteoblasts (OB) were cultured with 10% active or remission RA-sera. Osteoblast proliferation, differentiation as well as cytokine gene expression was analyzed. To determine osteoclastogenesis, RA-sera-pretreated primary human osteoblast cultures were established in direct contact with human peripheral blood mononuclear cells (PBMCs) in the presence or absence of osteoprotegerin or IL-6 inhibitor.

Results: Compared to remission RA-sera, active RA-sera inhibited osteoblast proliferation and differentiation *in vitro* as demonstrated by a reduced DNA content and decreased gene expression of KI-67, collagen type 1, osteopontin, and osteocalcin. Active RA-sera inhibited osteoprotegerin expression and enhanced RANKL and IL-6 expression (Fig. 1), but did not alter IL-8 expression in osteoblasts. IL-1β, IL-17 and TNF-α expression were undetectable. In co-culture, active RA-sera treatment of osteoblasts stimulated (Fig. 2), while addition of osteoprotegerin or IL-6 inhibitory antibodies significantly reduced the number of osteoclasts (Fig. 3).

Conclusion: Active RA-sera contain circulating factors, likely cytokines and chemokines that might contribute to bone loss by directly inhibiting osteoblast proliferation and differentiation. Especially these factors modulate endogenous cytokine (i.e. RANKL and IL-6) production by osteoblasts, thereby affecting osteoclastogenesis.
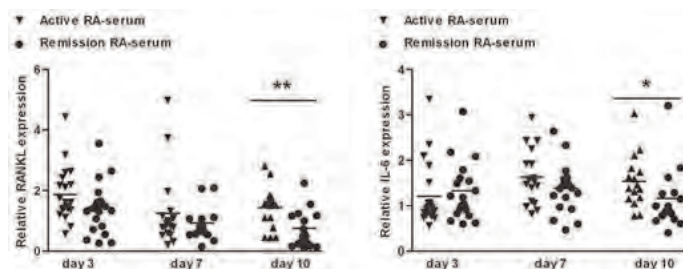
Active RA-sera enhanced RANKL and IL-6 gene expression in osteoblasts
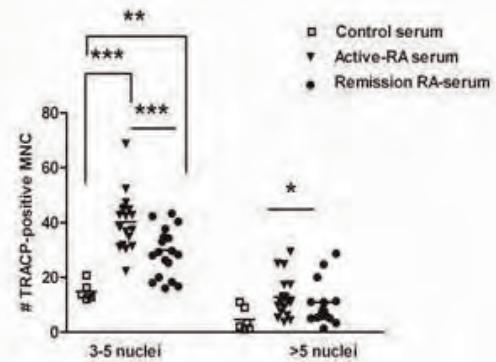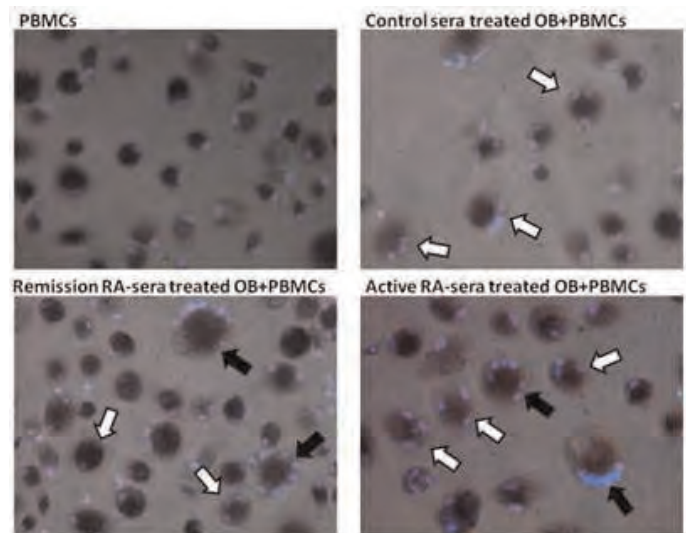
Active RA-sera-pretreated osteoblasts enhanced osteoclastogenesis
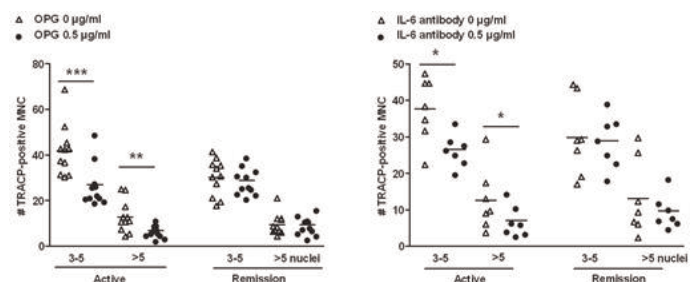
OPG and IL-6 antibody reduced osteoclastogenesis enhanced by active RA-sera-pretreated osteoblasts

Disclosures: Jenneke Klein-Nulend, *None.*

SU0422

Prevention of hyper-active PTH signaling and function by VPS35.

Lei Xiong[1], Wen-Fang Xia[2], Fu-Lei Tang[1], Shan Xiong[1], Wen-Cheng Xiong*[3]. [1]Georgia Health Sciences University, Charlie Norwood VA Medical Center, USA, [2]Georgia Health Sciences University, Charlie Norwood VA Medical Center, Union Hospital, Tongji Medical College, Huazhong University of Science & Technology, USA, [3]Georgia Regents University, USA

PTH plays a critical role in bone remodeling. Although the signaling and function of PTH have been investigated extensively, much less is known about negative regulatory mechanisms of its signaling. We demonstrate here that PTH1R trafficking, signaling, and function are negatively regulated by VPS35, a major component of retromer essential for selective endosome-to-Golgi retrieval of membrane proteins. VPS35 loss-of-function altered PTH-induced PTH1R distribution, enhanced PTH signaling, and suppressed it's catabolic response. Although hemizygous deletion of Vps35 gene in mouse at young adult age decreased bone formation, such an osteoporotic deficit was ameliorated by intermittent injections of PTH. These results

indicate that VPS35 critically deregulates PTH1R signaling, thus restraining increased anabolic response and promoting adequate bone remodeling.

Disclosures: Wen-Cheng Xiong, None.

SU0423

PTHrP Induces Lactation in the Absence of Pregnancy and Affects Breast Cancer Initiation and Progression Differentially in Two Murine Models. <u>Farzin Takyar</u>*[1], <u>Kata Boras-Granic</u>[2], <u>Pamela Dann</u>[3], <u>Christina Marmol</u>[3], <u>Alexzandrea Buscarello</u>[3], <u>John Wysolmerski</u>[4]. [1]Yale University, School of Medicine, USA, [2]Yale School of Medicine, USA, [3]Yale University, School of Medicine, USA, [4]Yale University School of Medicine, USA

PTHrP affects mammary development and breast cancer. PTHrP is expressed in basal myoepithelial cells until late pregnancy,when it also becomes expressed in alveolar epithelial cells.During lactation, PTHrP is secreted into milk and into the circulation, where it regulates systemic calcium and bone metabolism. When PTHrP is secreted by breast cancers, it stimulates bone resorption, promoting the growth of skeletal metastases and/or the development of hypercalcemia. Less is known about the contribution of PTHrP to the development and/or progression of primary breast cancers. However, recent GWAS reports have identified the PTHrP gene as a breast cancer susceptibility locus. In order to test the effects of PTHrP overexpression on the development of mammary tumors in mice, we developed a tetracyline-regulated, MMTV-*driven transgenic model of PTHrP overexpression targeted to mammary epithelial cells (*MMTV-rtTA;tetO-hPTHrP*). Surprisingly, we found that PTHrP overexpression in luminal epithelial cells causes alveolar hyperplasia, secretory differentiation and milk production in virgin mice. This phenotype was associated with an increase in the number of both luminal progenitor cells and basal stem cells upon FACS analysis of mammary stem/progenitor cell populations. Overexpression of PTHrP for 7 days in virgin mice was associated with activation of Stat5, but not Jak2 in mammary epithelial cells. Initial studies demonstrate activation of Focal Adhesion Kinase (FAK), but not integrin-linked kinase (ILK).Mammary secretory differentiation requires cooperation between prolactin and integrin signaling and these data suggest that PTHrP may act to enhance matrix-related signaling in these cells.Overexpression of PTHrP in* MMTV-PyMT *mice, a transgenic model of breast cancer,dramatically accelerated the formation of mammary tumors reducing the latency of tumor formation and survival of the mice dramatically. All* MMTV-rtTA;tetO-hPTHrP;MMTV-PyMT *mice developed palpable tumors in all mammary glands within 3 weeks of age, became hypercalcemic and died before 4.5 weeks of age. However, PTHrP overexpression in* MMTV-Neu *mice, another model of breast cancer, had no effect on tumor latency or survival, suggesting that PTHrP influences only certain pathways of transformation. Ongoing profiling of gene expression in these two tumor models will hopefully define the molecular pathways through which PTHrP acts to accelerate breast cancer formation.*

*FT and KBG contributed equally

Disclosures: Farzin Takyar, None.

SU0424

PTHrP-Induced BMP Signaling Contributes to Specification of The Mammary Mesenchyme. <u>Minoti Hiremath</u>[1], <u>Pamela Dann</u>[2], <u>Wei Shi</u>[3], <u>John Wysolmerski</u>*[4]. [1]Boise State University, USA, [2]Yale University, USA, [3]Children's Hospital Los Angeles, USA, [4]Yale University School of Medicine, USA

PTHrP regulates mammary cell fate by specifying the mammary mesenchyme during embryonic mammary development. Loss of PTHrP (PTHrP^{-/-}) or its receptor (PTH1R^{-/-}) causes epithelial cells within the mammary bud to revert to an epidermal fate and disrupts mammary bud outgrowth. In contrast, overexpression of PTHrP in the epidermis (K14-PTHrP) induces inappropriate differentiation of the ventral epidermis into nipple-like skin. In previous studies, PTHrP-mediated upregulation of BMPR1a was implicated in mammary bud outgrowth. Therefore, we hypothesized that PTHrP might regulate levels of BMP signaling in the mammary mesenchyme. We first examined BMP-signaling in the embryonic mammary mesenchyme expression using a transgenic Bre-*lacZ* reporter mouse. X-gal staining of whole embryos detected Bre-*lacZ* expression in the mammary mesenchyme as early as day 12 and up to day 18 of embryogenesis. To determine whether PTHrP regulates BMP signaling, we examined expression of the BMP reporter in PTHrP^{-/-} mice. Our studies show that loss of PTHrP abolishes reporter expression of BRE-*lacZ* in mammary mesenchyme, demonstrating that PTHrP regulates BMP signaling. To determine the contribution of BMP signaling in mammary mesenchyme specification, we conditionally deleted BMPR1a using the Dermo1 promoter to drive Cre recombinase expression in the mammary mesenchyme of BMPR1a[lox/lox] mice. We confirmed that BMPR1a deletion almost completely abolishes Bre-*LacZ* expression in the mammary mesenchyme of the second and third pairs of mammary buds. Furthermore, deletion of BMPR1a in the mammary mesenchyme caused a delay in bud outgrowth and reduced mesenchymal proliferation, resulting in fewer layers of cells in the condensed mammary mesenchyme. Deletion of BMPR1a in the mesenchyme reduces the expression of mammary mesenchyme markers such as Lef1, estrogen receptor, b-catenin and androgen receptor but not to the same degree as does loss of PTHrP. Despite this, the androgen-mediated apoptosis of the male

mammary buds is severely retarded, demonstrating loss of mammary mesenchyme function. Taken together, our studies suggest that BMP signaling via BMPR1a is required for functional differentiation of the mammary mesenchyme and for mammary bud outgrowth. Our studies suggest that BMP signaling acts downstream of PTHrP to specify the mammary mesenchyme.

Disclosures: John Wysolmerski, None.

SU0425

Regulation of bone metabolism by Semaphorin 3A derived from osteoblast lineage cells. <u>Mikihito Hayashi</u>*[1], <u>Tomoki Nakashima</u>[2], <u>Hiroshi Takayanagi</u>[3]. [1]Tokyo Medical & Dental University, Japan, [2]Tokyo Medical & Dental University, Japan, [3]The University of Tokyo, Japan

Cells in bone, including osteoblasts, osteoclasts and osteocytes, mutually influence each other to achieve bone homeostasis. We previously demonstrated that Sema3A plays an important role in the regulation of bone homeostasis (Hayashi *et al.*, Nature, 2012). However, a recent publication showed that osteoblast–specific Sema3A–deficient mice had normal bone mass, even though the expression of Sema3A in bone was substantially decreased (Fukuda *et al.*, Nature, 2013). They concluded that neuron–derived Sema3A regulates bone remodeling indirectly through the modulation of sensory nerve development, but not directly through the action on osteoblasts. However, they could not explain why does osteoblast lineage cell--derived Sema3A have no effect on bone homeostasis and innervation into bone although *Sema3a* is highly expressed in osteoblast lineage cells.

To examine the role of osteoblast lineage cell–derived Sema3A, we crossed *Sema3a* floxed mice with *Osx–Cre*[+] and *Dmp1–Cre*[+] mice. In contrast to the results obtained by Fukuda *et al.*, the deletion of *Sema3a* in *Osx*–expressing cells recapitulates the low bone mass phenotype of long bone as observed in *Sema3a*^{-/-} mice, due to an increase in bone resorption accompanied by decreased bone formation. Interestingly, these mice have normal bone phenotype in vertebrae. In addition, *Sema3a* deletion in osteoblasts from newborn or adult mice, by means of *Osx-Cre*-tTA, led to low bone mass phenotype, indicating that Sema3A expression in osteoblasts is important for the regulation of bone homeostasis.

In contrast, *Dmp1–Cre*[+] *Sema3a*[flox/Δ] mice had normal bone mass at 10 weeks of age. However, the bone volume of these mice decreased with age and aged *Dmp1–Cre*[+] *Sema3a*[flox/Δ] mice developed an extremely low bone mass phenotype. These observations suggest that Sema3A expression in osteoblast lineage cells (especially osteocytes) is essential for the maintenance of bone homeostasis.

Disclosures: Mikihito Hayashi, None.

SU0426

Quality of life assessment of adults patients with X-Linked Hypophosphoremia. <u>Hélène Che</u>[1], <u>Adrien Etcheto</u>[2], <u>Anya Rothenbuhler</u>[3], <u>Peter Kamenicky</u>[3], <u>Agnès Linglart</u>[3], <u>Christian Roux</u>[4], <u>Karine Briot</u>*[5]. [1]Paris Descartes University, Cochin Hospital, France, [2]Paris Descartes Uniiversity, Cochin Hospital, France, [3]Hôpital Bicêtre, France, [4]Hospital Cochin, France, [5]Paris Descartes University, Cochin hospital, Rheumatology Hospital, France

X-Linked Hypophosphatemia (XLH) is the most common form of heritable rickets. Although disease severity is variable, adults with XLH may suffer from skeletal symptoms leading to function disability. There are no data on the consequences of these symptoms on quality of life (QoL) of adults with XLH. The objective was to evaluate the QoL and the variables associated with low QoL in adult patients with XLH

We conducted a cross sectional study in adult patients with XLH, who consulted in rheumatology, for skeletal symptoms, between 2013 and 2014. We assessed the intensity of pain (VAS Visual Analogic Scale) and QoL using 3 Patient Reported Outcomes: HAQ (Health Assessment Questionnaire, high if >0.5), RAPID3 (Routine Assessment of Patient Index Data 3, high if >6) and 36-item short-form health (SF36) survey. We also collected demographic and disease characteristics, radiographic features and data on treatments of XLH. We described the QoL of XLH patients and analysed the variables associated with low QoL.

Thirty two patients with XLH (27 women; mean age of 42.8 yrs) with PHEX mutations were included. 15 (48.4%), 16 (51.6%), 12 (40%) received respectively phosphate supplements, vitamin D analogues, and 25 OH-vitamin D supplements, at the time of assessment. X-rays showed osteoarthritis (knee, hip or spine) (n=27, 90%), enthesopathies (n=19, 61.3%) and sequelae of insufficiency fractures (n=4, 14.8%). Skeletal pain was reported by 64.3% of patients with a mean VAS of 4.6 (+/-2.6). Age is significantly associated with low QoL ($p \leq 0.05$), indicated by high scores of HAQ (mean value 0.71 ± 0.6, HAQ>0.5 in n=19), RAPID3 (mean value 11.32 ± 6.4, RAPID3>6 in n=23), and physical domains of SF36 (physical functioning (mean value 58.4 ± 23.6) and physical role (mean value 37.5 ± 39.1)). Osteoarthritis was associated with low QoL indicated by high HAQ ($p \leq 0.05$). Radiographic enthesopathies were significantly higher in patients with high RAPID3 and low bodily pain scale of SF36 (mean value 55 ± 24) ($p \leq 0.05$). Phosphate supplements, vitamin D analogues and physiotherapy treatments were associated with high general health (mean value 40.23 ± 17.1) and social functioning (mean value 70.31 ± 21.7) scales of SF36 ($p \leq 0.05$).

This study showed that QoL of adults with XLH is altered; age and radiographical involvement (osteoarthritis and enthesopathies) are significantly associated with low QoL; adults treated for XLH reported better general health and social functioning scores.

Disclosures: Karine Briot, None.

SU0427

Bone Material Properties in Osteogenesis Imperfecta: a Matter of Quantity Over Quality. Carolyne Albert*[1], John Jameson[2], Peter Smith[3], Gerald Harris[4]. [1]Marquette University, USA, [2]Lawrence Berkeley National Lab, USA, [3]Shriners Hospitals for Children, USA, [4]Marquette University, USA

Osteogenesis Imperfecta (OI) is a collagen-related genetic disorder resulting in a high susceptibility to bone fracture. The mechanisms behind bone fragility in OI are not yet well understood. In addition to a characteristic low bone mass, i.e., structural deficiency, studies in mice suggest that the material properties of bone tissue may also be compromised in OI [1, 2]. However, little is known about bone material properties in humans with this disorder. The objectives of this study were investigate relationships between bone material properties, bone volume fraction, volumetric tissue mineral density (vTMD), and donor age in children with OI.

Ten small diaphyseal specimens from long bones of eight children with mild to severe OI (ages 3-16) were obtained during routine osteotomy procedures. Longitudinal beams were machined from these specimens, and elastic modulus and yield strength were measured in bending. Bone volume fraction (1 – intracortical vascular porosity), representing the quantity of bone material per unit volume, and vTMD, representing the density of the bone material, were determined by synchrotron microcomputed tomography.

Average elastic modulus and flexural strength were 4.8 GPa (SD 2.0 GPa) and 91 (39 MPa), respectively. Bone volume fraction was 0.80 (0.12), and vTMD 1.58 g/cm^3 (0.12 g/cm^3). Each property was associated significantly with volume fraction, but not with vTMD or donor age (Table 1, Figure 1).

Reduced modulus and flexural strength were observed compared to typical values for children and adolescents [3]. Volume fraction and vTMD were also lower than in normal pediatric bone [4]. Unlike in normal bone tissue [3], bone properties in children and adolescents with OI did not appear related to age. Results of this preliminary study indicate that bone material properties at the mesoscale in OI may be associated more with bone quantity (volume fraction) than with the quality (density) of the bone material itself. These results offer valuable insight toward a better understanding of bone fragility in OI.

References:

1. Misof et al. 2005, Bone 36:150-8.
2. Jepsen et al. 1997, J Biomech 30:1141-7.
3. Currey and Butler 1975, JBJS Am 57:810-4.
4. Jameson et al. 2013, Proc SPIE Vol. 8672.

Table 1. Pearson's correlation coefficients between bone material properties, bone volume fraction (V$_f$), volumetric tissue mineral density (vTMD), and donor age in children and adolescents with OI. (*P<0.05)

Material property	Factor	Slope	P value	R
Elastic modulus (GPa)	V$_f$ (-)	15.1	0.002*	0.86
	vTMD (g/cm3)	7.41	0.186	0.46
	Age (years)	-0.113	0.503	-0.24
Flexural strength (MPa)	V$_f$ (-)	260	0.010*	0.76
	vTMD (g/cm3)	27.8	0.809	0.09
	Age (years)	-0.971	0.771	-0.11

Table
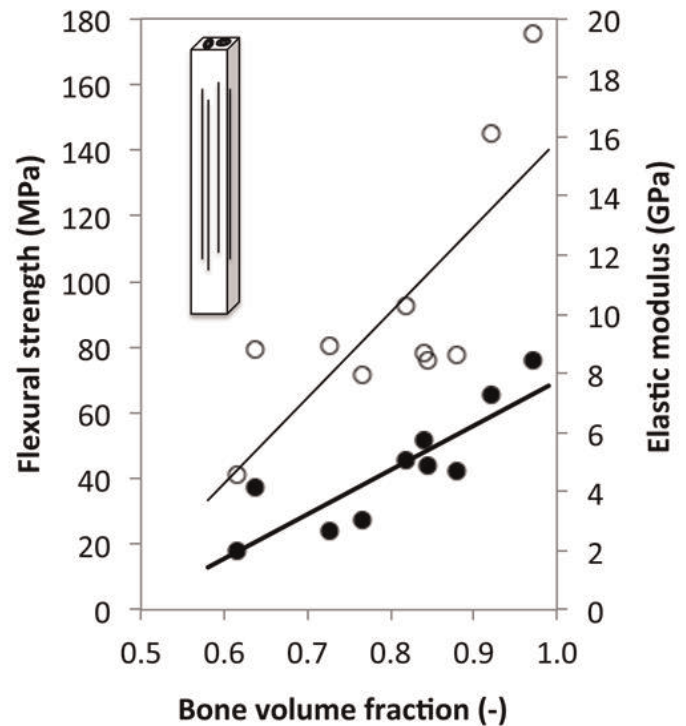
Figure 1. Relationships between diaphyseal bone material properties and volume fraction in pediatric OI bone: elastic modulus (black circles), strength (white circles).

Figure

Disclosures: Carolyne Albert, None.

SU0428

Demographics, bone mass density, lifetime fractures and bisphosphonate use in an adult Osteogenesis Imperfecta cohort: a cross-sectional explorative study. Anton Franken*[1], Luuk Scheres[2], Guus Janus[3], Fleur van Dijk[4]. [1]Isala clinics, The Netherlands, [2]Isala clinics, Netherlands, [3]Isala, Netherlands, [4]VU medical center, Netherlands

We present data from one of the largest adult Osteogenesis Imperfecta (OI) patient cohorts ever reported. A database was created which stores data on all adult OI patients which have visited our expert center for OI adult patients. Over 200 adult patients have visited our outpatient-clinic already. This is the first report on data retrieved from this database. We present extensive demographical features of this cohort and results on bone mass density (BMD) measured at different sites of the body. We collected data from 149 (106 type I, 20 type III and 23 type IV) adult OI patients.

There was a discrepancy between BMD measured at lumbar spine and hip region by means of dual-energy X-ray absorptiometry (DXA). In all three types the lumbar spine measurement yielded lower BMD levels than the measurement of the hip region

For type I and IV patients the total amount of fractures did not seem to increase in adulthood. In type III the total mean fractures almost double from early adulthood to the age of 65. For type I patients there was no difference in fracture total per decade of life, independently of bisphosphonates (BP) use. Half of all type I and IV patients had never used BP's in their lifeThese findings suggest that the effectiveness of BP's solely in terms of fracture reduction in type I adult patients is questionable. OI in adults is not just a form of osteoporosis where loss of bone mass and structure predominate. OI is characterized by increased bone fragility due to defective matrix quality caused by defective collagen

Disclosures: Anton Franken, None.

SU0429

HSP47 and FKBP65 cooperate in the synthesis of type I procollagen. Ivan Duran*[1], Lisette Nevarez[2], Anna Sarukhanov[3], Sulin Wu[3], Katrina Lee[4], Maryann Weis[5], David Eyre[5], Deborah Krakow[6], Daniel H. Cohn[2]. [1]University of California Los Angeles, USA, [2]Department of Molecular, Cell, & Developmental Biology. UCLA, USA, [3]Orthopaedic Surgery, USA, [4]Department of Molecular, Cell, & Developmental Biology, USA, [5]Department of Orthopaedics & Sports Medicine, University of Washington, USA, [6]Orthopaedic Surgery, UCLA, USA

Osteogenesis Imperfecta (OI) is a genetic disorder that results in low bone mineral density and brittle bones. Most cases result from dominant mutations in the type I procollagen genes, but about 10% of cases result from primarily recessively inherited mutations. The latter cases include mutations in the genes *SERPINH1* and *FKBP10* which encode the type I procollagen chaperones HSP47 and FKBP65, respectively, and which produce a mild to moderately severe form of OI, similar to OI type IV. Little is known about the biochemical consequences of the mutations and how they produce OI. We identify a new OI mutation in *SERPINH1* that results in destabilization and mislocalization of HSP47, and that secondarily has similar effects on FKBP65. We found evidence that HSP47 and FKBP65 act cooperatively during posttranslational maturation of type I procollagen. Furthermore, mutations in either *SERPINH1* or *FKBP10* alter type I procollagen trafficking through the ER and Golgi, triggering an Unfolded Protein Response and ER-associated degradation of mislocalized molecules. These findings suggest that a chaperone complex including HSP47 and FKBP65 act downstream from the CRTAP complex during the maturation of fibrillar collagens.

***Disclosures: Ivan Duran**, None.*

SU0430

Improved Bone Density in a patient with Osteogenesis Imperfecta using Denosumab. Jessica Abramowitz*[1], Stuart Weinerman[2]. [1]Hofstra North Shore LIJ, USA, [2]Division of Endocrinology, USA

Introduction: Osteogenesis imperfecta is a rare inherited disease caused by a defect in collagen formation. Bone histology reveals increased bone remodeling in types I, III and IV. The syndrome is characterized clinically by low bone density and fractures. Treatment goals are to: reduce fracture rates, skeletal deformities and maximize mobility while reducing pain. The mainstay of treatment has been bisphosphonates. Denosumab binds RANKL and inhibits osteoclast formation and thereby decreases bone resorption, increases bone density and thus reduces fractures. It is known to be effective in the treatment of postmenopausal osteoporosis and bone metastases of cancer but its use in treatment of adults with osteogenesis imperfect has not been reported.

Case presentation: A 38 yo male with type IV osteogenesis imperfecta presented for evaluation in our department for management of osteoporsis. He had been diagnosed with osteoprosis 3 years prior and had been on Alendronate since the time of diagnosis. He had a history of multiple fractures which subsided after starting bisphosphonate treatment. After 10 years of treatment with Alendronate treatment was held for 1 year. Bone density prior to drug holiday showed a T score of -3.5 in the lumbar spine, -2.7 in the femoral neck, -1.8 in the total hip and 1.2 in the radius. Following 1 year off treatment for osteoporosis the patient was started on Denosumab 60mg every 6 months. After 3 doses bone density was stable or improved, with a T score of -3.2 (+4.8%) in the lumbar spine, -2.6 (+2.3%) in the femoral neck, -1.9 (-1.7%) in the total hip and 2.4 in the radius. Bone specific alkaline phsophatase was 10 mcg/L and calcium 9.8 mg/dL. After 6 doses of Denosumab lumbar spine bone density T score was -2.8 (+5.2%), femoral neck was -2.5 (+1.5%), and -1.9 (-0.5%) in the total hip, and 2.9 (+2.7%) in the radius. In addition to improvement in bone density the patient reported decreased bone pain during treatment with Denosumab.

Conclusions: Denosumab is a potential agent for use in osteogenesis imperfecta. We report a case of decrease in fractures and increase in bone density in a patient with type IV osteogenesis imperfecta.

***Disclosures: Jessica Abramowitz**, None.*

SU0431

Intravenous bisphosphonate therapy prevent the development and progression of spinal deformity associated with osteogenesis imperfecta. Masafumi Kashii*[1], Sadaaki Kanayama[2], Taichi Kitaoka[3], Takahiro Makino[4], Takashi Kaito[2], Kosuke Ebina[5], Tsuneo Shigi[6], Takuo Kubota[7], Noriyuki Namba[3], Motoki Iwasaki[4], Takehisa Yamamoto[8], Keiichi Ozono[9], Hideki Yoshikawa[10]. [1]Osaka University Graduate School of Medicine, Japan, [2]Osaka University, Graduate School od Medicine, Japan, [3]Osaka University Graduate School of Medicine, Japan, [4]Osaka University Graduate School of Medicine, Japan, [5]Osaka University, Graduate School of Medicine, Japan, [6]Minoh City Hospital, Japan, [7]Osaka University Graduate School of Medicine & Dentistry, Japan, [8]Minoh City Hospital, Japan, [9]Osaka University Graduate School of Medicine, Japan, [10]Osaka University Graduate School of Medicine, Japan

Osteogenesis imperfecta (OI) is characterized by fragile bone and hypermobility of the spinal ligaments, and is often associated with spinal deformities. Bisphosphonate (BP) is used to prevent fragility fractures and subsequent bony deformities of the limbs, but there are no studies to examine the effect of BP on spinal deformities associated with OI. The purpose of this study is to analyze the development and progression of spinal deformities in OI patients treated by intravenous BP therapy.

Ninety-one OI patients were enrolled in this study and 40 patients who were treated by intravenous pamidronate alone (mean age: 9.8 years, range 2-20) were studied to clarify the prevalence of scoliotic deformities and to determine risk factors for scoliotic deformities. Scoliotic angle (L1-4 Cobb angle) was measured using the DXA scout view, and scoliotic deformities were defined by the presence of a curvature 10 or larger. We examined the relationship between scoliotic deformities and age, BMI, OI type, physical activities and lumber L2-4 BMD (Z-score).

Cyclic intravenous pamidronate was administrated for an average of 3.8 years. The mean lumber Z-score was -2.4 (-7.7 to 2.2). The prevalence of scoliotic deformities was 23%, and vertebral deformities were found only in 5 patients (5 vertebras). OI patients with scoliotic deformities had a higher BMI (p<0.01) and a higher proportion of OI type3 by Sillence classification (p=0.01). Lower lumber Z-score tended to be related to a larger scoliotic curve, but there were no statistical significances in OI patients with scoliotic deformities. In 16 OI type3 patients without scoliotic deformities, time of initiation of BP therapy is significantly younger (average age 2 years). The retrospective longitudinal study of 6 OI patients with scoliotic deformities revealed that coronal vertebral deformity caused by fragile vertebral fracture lead to the development and progression of scoliotic deformities.

The prevalence of scoliotic deformity and coronal vertebral deformity were extremely lower compared with previous reports (50-100%). This study firstly shows that BP administration effectively prevents coronal vertebral deformity due to bone fragility and subsequently decreases the development and progression of scoliosis in OI patients. BP administration from early childhood prevents the development and progression of scoliosis in OI type3.

***Disclosures: Masafumi Kashii**, None.*

SU0432

Physical Activity and Muscle Function in Children with Osteogenesis Imperfecta Type I. Louis-Nicolas Veilleux*[1], Annie Pouliot-Laforte[2], Martin Lemay[2], Frank Rauch[3]. [1]McGill University/Shriners Hospital for Children, Canada, [2]Université du Québec à Montréal; Marie Enfant Rehabilitation Center, Canada, [3]Shriners Hospital for Children, Montreal, Canada

Context: Osteogenesis imperfecta (OI) type I is a heritable bone fragility disorder that is caused by mutations affecting collagen type I. In addition to bone fragility, recent evidences showed that patients with OI type I frequently have muscle weakness. The cause of this weakness remains unclear at present. One hypothesis is that patients with OI type I are hypoactive due to fractures or fear of fracture. Objective: To evaluate the relationship between physical activity and muscle function in patients with OI type I and in healthy age and gender-matched controls. Patients and other participants: Fourteen children with OI type I (mean age [SD]: 12.72 [4.57] years, 9 females) and 14 age- and gender-matched controls (mean age [SD]: 12.75 [4.62] years) took part in this study. All participants were between 6 and 21 years of age. Main Outcome Measures Muscle force and muscle power were determined through mechanography. Physical activity (sedentary, light and moderate to vigorous) was measured with an accelerometer whereas energy expenditure was estimated with the 'Bouchard' questionnaire on physical activity. Results: Compared to age- and gender-matched controls, patients with OI type I had lower muscle force (p<0.001) and power (p<0.04) than controls. However, in contrast with our expectations OI type I patients were as active as their age- and gender-matched controls with a daily average of 36 minutes and 39 minutes of moderate to vigorous physical activity for the OI group and the control group respectively (p>0.31). Regression analysis showed that within all three type of physical activity only the time spend in the light physical activity was found to be negative predictor of the power tests but not of the force tests. Conclusion: This is the first study evaluating physical activity in children and adolescent with OI type I. The difference in muscle function and the similarities in the volume of physical activity between the two groups suggest that hypoactive lifestyle is not the primary cause of muscle weakness in the study participants.

***Disclosures: Louis-Nicolas Veilleux**, None.*

SU0433

A Case of Tumor-Induced Osteomalacia and Hyperparathyroidism: Primary vs.Tertiary?. Racha Dermesropian*, Pamela Taxel. university of connecticut health center, USA

We present a 10-year postoperative follow up of a patient with oncogenic osteomalacia.

The patient is a 60-year-old male who initially presented at age 47 years with a 6 months history of severe joint pain and a new onset gait instability resulting in recurrent falls.

He was found to have multiple bilateral fractures of his ribs, heels, and metatarsals as well as a right femoral neck fracture. Biochemical testing showed low levels of serum phosphate, increased serum alkaline phosphatase, reduced renal tubular reabsorption of phosphorus and inappropriately normal levels of 1,25-dihydroxyvitamin D. Octreotide scan showed increased uptake in the right shoulder. An MRI showed a 1.8 cm suspicious lesion in the greater tuberosity of the right humerus . Over the next 2-3 years, the patient underwent surgical resection x two with incomplete excision, as well as radiation therapy and eventual complete right shoulder replacement. Medical therapy during that time included oral phosphorous and calcitriol. Ultimately, normalization of serum phosphate and resolution of symptoms occurred.

The patient was lost to follow-up for 7 years until he presented recently with recurrent generalized body aches. His biochemical profile showed elevated FGF23 with normal serum phosphorus, elevated serum calcium and PTH levels. His differential diagnosis included primary vs. tertiary hyperparathyroidism due to long-term therapy with phosphorus and vitamin D. Investigation of his hyperparathyroidism is ongoing.

Tumor induced osteomalacia is a rare paraneoplastic syndrome caused by unregulated secretion of FGF23. It can be associated with tertiary hyperparathyroidism due to prolonged treatment with phosphorous that is unopposed by calcitriol. This outcome was not anticipated in this patient who had appropriate medical therapy for 2-3 years. Thus we suspect that his hyperparathyroidism is likely a primary event.

Disclosures: Racha Dermesropian, None.

SU0434

Assessment of Adverse Effects Associated with Zoledronic Acid Use in Children and Young Adults with Metabolic and Genetic Bone Disease. Sobenna George*[1], David Weber[2], Heather Bodenstab[3], Kelly Hummel[3], Paige Kaplan[3], Jaya Ganesh[3], Michael Levine[1]. [1]Children's Hospital of Philadelphia, USA, [2]Golisano Chilldren's HospitalThe University of Rochester, USA, [3]The Children's Hospital of Philadelphia, USA

PURPOSE: The intravenous bisphosphonate zoledronic acid (ZA) is increasingly used to treat children with a variety of bone disorders due to its greater potency, shorter infusion time, and longer dosing interval than pamidronate. However, data related to the safety and efficacy of ZA in this population are limited. The goal of this study was to describe the prevalence of adverse events (AE) and identify risk factors for AEs in children treated with ZA at The Children's Hospital of Philadelphia.

METHODS: We systematically evaluated medical charts of all children treated with ZA for bone disorders between July 2010 and January 2014. Charts were reviewed for diagnoses, dose of ZA and adjunct medication, type of AEs, and potential risk factors for AEs. Chi-square tests and multivariate regression were used to analyze data.

RESULTS: We examined charts for 83 children (55% male; mean age 11.6 ± 5.6 yrs) who had a total of 210 ZA infusions. 27% had osteogenesis imperfecta (OI), accounting for 42% of the infusions. Remaining patients had osteoporosis (34%), chronic recurrent multifocal osteomyelitis (16%), avascular necrosis (7%) and other genetic or metabolic bone diseases (16%). Median ZA dose was 0.025 mg/kg (IQR:0.025-0.075). AEs occurred after 29% of all infusions and were more common after a first than a subsequent infusion (50% vs 17%; p<0.0001). In previously bisphosphonate naive patients, the most common AEs after the first ZA infusion were acute phase reaction (43%),hypophosphatemia (41%), and hypocalcemia (32%). Risk of AEs with initial infusion was similar between patients with and without OI (58% vs 62%, p=0.8). However, the risk of AEs with subsequent infusions was less in patients with OI than non-OI (7% vs 25%, p = 0.002). AEs were not associated with ZA dose, baseline blood chemistries (including serum 25(OH)D and calcium), parathyroid hormone or calcium/vitamin D supplementation

CONCLUSIONS: Our study found that children with OI and non-OI have similar risks of AEs after the initial infusion, but non-OI have significantly greater risk of experiencing AEs after subsequent infusions, for reasons that are not obvious. Prospective longer term studies to evaluate the underlying risk factors that are associated with AEs in youths receiving ZA are necessary.

Disclosures: Sobenna George, None.

SU0435

Paternal Uniparental Isodisomy Involving Chromosome 20q (patUPD20q) as a Cause of Japanese Patients Affected by Sporadic Pseudohypoparathyroidism Type Ib. Rieko Takatani*[1], Masanori Minagawa[2], Kaori Kinoshita[3], Tomozumi Takatani[3], Angelo Molinaro[4], Harald Jueppner[5]. [1]Massachusetts General Hospital & Harvard Medical School, USA, [2]Chiba Children's Hospital, Japan, [3]Chiba University, Japan, [4]Massachusetts General Hospital & Harvard Medical School, USA, [5]Massachusetts General Hospital, USA

Context: Pseudohypoparathyroidism type Ib (PHP-Ib) is caused by proximal tubular resistance to parathyroid hormone that occurs in most cases in the absence of Albright's Hereditary Osteodystrophy (AHO). Patients affected by PHP-Ib have epigenetic changes that involve one or multiple differentially methylated regions (DMRs) in *GNAS*, the gene encoding Gsα and several splice variants thereof. Maternally inherited microdeletions within *STX16*, the gene encoding syntaxin 16, or within *GNAS* cause familial forms of PHP-Ib. Most sporadic cases of PHP-Ib show broad *GNAS* methylation abnormalities, but the underlying molecular mechanism remains unknown. Paternal uniparental isodisomy involving chromosome 20q (patUPD20q), which includes the *GNAS* locus, can be a rare cause of sporadic PHP-Ib.

Objective: To determine whether patUPD20q can be a cause of Japanese patients affected by sporadic PHP-Ib.

Methods: We investigated 23 Japanese sporadic PHP-Ib cases, who had presented with PTH-resistant hypocalcemia and hyperphosphatemia, some of whom had mild AHO. The *GNAS* methylation status was evaluated by Southern blot analysis after digestion of DNA with methylation-sensitive endonucleases, Methylation-Specific PCR (MS-PCR), and Methylation-Specific Multiplex Ligation-dependent Probe Amplification (MS-MLPA) followed by analysis of single nucleotide polymorphism and microsatellite markers across the entire chromosome 20.

Result: All investigated sporadic PHP-Ib patients showed broad *GNAS* methylation changes. Several patients were homozygous for SNPs within the NESP55 region and a pentanucleotide repeat in exon A/B, and two of these individuals revealed homozygosity for numerous microsatellite markers on chromosome 20q raising the possibility of patUPD20q; this was confirmed for one PHP-Ib patient through the analysis of parental DNA.

Conclusion: Our findings suggest that patUPD20q may be a more frequent cause of sporadic PHP-Ib than initially thought.

Disclosures: Rieko Takatani, None.

SU0436

The Type 2 Diabetes associated rs7903146 T allele within *TCF7L2* is significantly under-represented in Hereditary Multiple Exostoses: insights into pathogenesis. Federica Sgariglia*[1], Elena Pedrini[2], Jonathan Bradfield[3], Tricia Bhatti[3], Pio D'Adamo[4], John Dormans[3], Aruni Gunawardena[3], Hakon Hakonarson[3], Jacqueline Hecht[5], Luca Sangiorgi[2], Maurizio Pacifici[6], Motomi Enomoto-Iwamoto[6], Struan Grant[7]. [1]Children's Hospital of Philadelphia, USA, [2]Rizzoli Orthopaedic Institute, Italy, [3]Children's Hospital of Philadelphia, USA, [4]Institute for Maternal & Child Health, IRCCS "Burlo Garofolo", Italy, [5]UTHealth School of Dentistry, USA, [6]Children's Hospital of Philadelphia, USA, [7]Children's Hospital of Philadelphia / University of Pennsylvania, USA

TCF7L2 and *EXT2* are among the earliest associated loci reported in genome wide appraisals of type 2 diabetes (T2D). Intriguingly, *EXT2* is one of two genes, the other being *EXT1*, to carry heterozygous loss-of-function mutations that account for the vast majority (~80-90%) of the primary genetic component of Hereditary Multiple Exostoses (HME), an autosomal-dominant disorder characterized by benign cartilage tumors (exostoses), causing skeletal deformations, growth retardation and chronic pain. Despite the wide clinical heterogeneity presented by patients, no clear genotype-phenotype correlation has been described so far suggesting that modifier genes contributing to severity still need to be found. Our previous work has implicated Wnt signaling in HME etiology, pointing to an imbalance of b-catenin signaling being involved in the pathogenesis of osteochondroma formation. Activation of Wnt signaling results in b-catenin nuclear translocation, where it forms a transcriptional complex with members of TCF family, including TCF7L2; indeed TCF7L2 is highly expressed in both human and mouse cartilage. Thus, we investigated if the key T allele of SNP rs7903146 within *TCF7L2*, strongly over-represented among T2D cases, was also associated with HME. We leveraged genotype data available from ongoing GWAS efforts from orthopaedic centers in the US, Canada and Italy. Collectively 213 cases and 1,890 controls were analyzed and, surprisingly, the T allele was significantly under-represented in the HME patient group [*P*=0.009; OR=0.737 (95% C.I. 0.587 - 0.926)] and the direction of effect was consistent within each individual cohort. Immunohistochemical analyses revealed that TCF7L2 is differentially expressed and distributed in the human growth plate and is exclusively observed in resting and hypertrophic chondrocyte zones. Furthermore, TCF7L2 expression exhibited substantial variability in human exostosis surgical specimens in terms of staining intensity and distribution. These observations resonate with our previous reports that b-catenin levels are lower in human exostoses specimens and that deficiency in murine cartilage leads to formation of osteochondroma-like masses, supporting the notion of

a role of the Wnt/b-catenin pathway in HME pathogenesis. In summary, the data in this study indicate that there is a putative genetic connection between *TCF7L2* and *EXT* in the context of HME, as well as T2D, orchestrated by the modulation of shared pathways, in particular with respect to b-catenin.

Disclosures: Federica Sgariglia, None.

SU0437

To determine the prevalence of osteonecrosis of the jaw in patients who take bisphosphonate for osteoporosis treatment. Tak Kee Dicky Choy*. The Chinese University of Hong Kong, Hong Kong

Dicky Choy[1], Timothy Kwok[1], Jason Leung[1], Anthony Kwok[2], [1]Jockey Club Centre for Osteoporosis Care and Control, School of Public Health, Chinese University of Hong Kong, Hong Kong; [2]Department of Orthopaedics and Traumatology, Chinese University of Hong Kong, Hong Kong

Osteonecrosis of the Jaw (ONJ) is a serious condition which is difficult to treat. Bisphosphonate-Related Osteonecrosis of the Jaw (BRONJ) is a well known complication in patients receiving high dose intravenous bisphosphonate for the treatment of metastatic bone disease. In recent years, there have been reported cases of BRONJ in post-menopausal women receiving oral bisphosphonate for the treatment of osteoporosis as well.

Determine the prevalence of osteonecrosis of the jaw in patients on chronic bisphosphonate for osteoporosis treatment.

Patients with history of 3 years or more of oral bisphosphonate treatment for osteoporosis will be invited to the telephone interview using a dental screening questionnaire. The questionnaire was designed by a dental surgeon experienced in managing BRONJ. For those who report any suspicious symptoms of BRONJ, we tried to find out the dental records for BRONJ confirmation. If those records were not available or the records did not contain clear information about the diagnosis, the subjects were invited to have a dental examination for the confirmation of ONJ.

One thousand two hundred and eighty four eligible subjects completed the screening questionnaire by telephone, the response rate being 62.8%. There were four clinically confirmed cases of BRONJ. The prevalence of BRONJ in our study was 0.3% with a frequency of 73.53 per 100,000 person-years of oral bisphosphonate treatment. Three of the patients had tooth extraction and none of them had regular dental visits.

In conclusion, the prevalence of BRONJ in our study was relatively high. Most of them were related to tooth extraction.

Table 1. Baseline clinical characteristics of the study respondent (n=1,284)

Table 2. Characteristics of the 4 cases of BRONJ

Characteristic	Respondents
Mean age ± SD (yr)	74.6 ± 7.9
Women	1224 (95%)
Mean BP duration ± SD (yr)	4.2 ± 1.2
BP type	
Alendronate	758
Risedronate	566
Ibandronate (oral)	57
Regular dental check	295 (23%)

Abbreviation: BP, bisphosphonate

table1

No.	Sex	Age (yr)	Dental extraction	DM	Regular dental visit	Duration of BP (yr)
1	F	69	Yes	No	No	5
2	F	74	Yes	No	No	6
3	F	78	Yes	Yes	No	5
4	F	84	No	No	No	5

Abbreviation: BP, bisphosphonate

table2

Disclosures: Tak Kee Dicky Choy, None.

SU0438

Body Composition Analysis in Brazilian Men: Normative Data. Marcela Ushida[1], Vera Szejnfeld*[2], Marcelo Pinheiro[3]. [1]Universidade Federal de São Paulo, Brazil, [2]UNIFESF/EPM, Brazil, [3]Sao Paulo Federal University/ Unifesp/ Escola Paulista De Medicina, Brazil

Background: Dual-energy x-ray absorptiometry (DXA) is the gold-standard method to evaluate bone mineral density (BMD) and to estimate risk of osteoporotic fracture. Recently, it has also used to measure body composition (BC), including fat and lean mass. Considering ethnic and anthropometric differences among populations, it is interesting to have specific normative data for each population.

Objective: To assess BC's normative data in Brazilian healthy men.

Patients and Methods: A total of 284 Brazilian healthy men aged 20 years or over were enrolled in this study. Details about concomitant diseases, alcohol intake, smoking and physical activity were evaluated in all subjects. Black and Asian individuals were excluded as well as those with any condition that could interfere on bone, fat or lean mass, including drugs. All of them performed BC measurements by DXA (DPX MD+, version 8.5; GE-Lunar). $P<0.005$ was considered as significant.

Results: Mean age, BMI, weight and height were 40.0 ± 15.1 years, 26.1 ± 3.4 kg/ m^2, 77.6 ± 11.2 kg, 172 ± 7cm, respectively. Almost 80% was White and almost 50% was considered as physically active and only 10% was current smokers. Mean appendicular lean mass (ALM) was 8.48 ± 0.87 kg/ m^2. Regarding fat mass, more than 60% was overweight by BMI. Total body fat and fat mass index (FMI) were 27% and 6.93 ± 2.82kg/ m^2, respectively. There was negative and significant association between ALM (p=0.005) and FMI (p=0.004) with age. Besides, there was positive association among ALM, FMI and BF with physical activity evaluated by Baecke's Sport Index (p<0.005).

Conclusion: This is the first study to determine the BC's normative data in Brazilian healthy male. Reduction of ALM and higher fat mass were associated with increasing age.

Disclosures: Vera Szejnfeld, None.

SU0439

Bone, muscle, fat triad in women: Determining the threshold at which body fat becomes harmful for bone. Pei-Yang Liu[1], Jasminka Z. Ilich*[2]. [1]University of Akron, USA, [2]Florida State University, USA

Objective: To investigate the relationships among lean mass (LM), fat mass (FM), and bone mineral density (BMD) in women stratified by body mass index (BMI – normal-weight, overweight, obese) and to determine threshold at which body fat becomes harmful for bone. Methods: BMD, LM, and FM were measured by iDXA. ANOVA with Bonferroni corrections was used to test BMI group differences. Regression models were used to examine independent contributions of LM and FM on BMD of various skeletal sites (controlling for age and height). In overweight/obese women PROC LOESS plots (adjusted for age) were used to determine the inflection points at which either LM or FM relationship with BMD changes direction. Results: Spine and femoral neck BMD were not different among three BMI groups while total body, femur and radius BMD were statistically different (the highest in the obese group). Linear regression revealed that LM had significant positive association with BMD of various skeletal sites in all groups. FM showed a negative association with BMD of femoral neck and femur in normal-weight and overwight women and spine in overweight women but a positive association with radius in obese women. Inflection points showed that body fat between 33-38% assumed negative relationship with BMD for most skeletal sites. Conclusions: While LM has strong positive relationship with BMD, FM above 33% in overweight/obese women is negatively related to BMD of most skeletal sites. Therefore, overweight/obesity after certin amount of FM, may not be a protective factor against osteoporosis in females. For clinical practice, it is important to maintain LM and keep FM accrual below ~30% body fat to maintain good skeletal health in women.

Disclosures: Jasminka Z. Ilich, None.

SU0440

Development of a QCT- and MRI-compatible Muscle Phantom. Andy Kin On Wong*[1], Zamir Merali[2], Jonathan Adachi[3]. [1]McMaster UniversityUniversity Health Network, Canada, [2]University of Toronto, Canada, [3]St. Joseph's Hospital, Canada

Objectives: To determine the optimal concentrations of CuCl$_2$, EDTA and agar to yield physiologically similar values to muscle density on peripheral quantitative computed tomography (pQCT) and muscle T2 relaxation time on 1.0T peripheral magnetic resonance imaging.

Methods: Evaporated milk (50 mL) was heated to 50°C. Agar was dissolved in 0.08% v/v 50 mL ethanol heated to 90°C and pH adjusted to 9.0. This solution was cooled to 50°C, mixed with the evaporated milk and reheated to 80°C before rapidly dissolving EDTA, CuCl$_2$ (Table I) and 80 μL of ProClin 150 with continued mixing. The completed solution was cooled to room temperature until hardened. Phantoms were prepared with varying concentrations of EDTA and CuCl$_2$, sequentially altered to achieve different T2 relaxation times and linear attenuation values.

T2 relaxation times were quantified using a 4 mm single-slice fast spin echo sequence repeated for 6 serial echo times at 937 μm resolution. MRMap software compiled T2 relaxation maps using the Levenberg-Marquardt equation. A pQCT scanner measured density of phantoms. Five 2.3 ± 0.5 mm thick slices were acquired at 15 mm/s scan speed and 500 μm resolution. A linear regression model was fitted to data for QCT-density regressed on $[CuCl_2]$. Logarithmic functions were fitted to T2 relaxation time regressed on each of $[CuCl_2]$ and $[EDTA]$.

Results: Density (D) was linearly dependent on $[CuCl_2]$ ($D = 0.27[CuCl_2] + 63.92$, $R^2 = 0.84$, $p = 0.01$) and invariant to $[EDTA]$. T2 relaxation time was related negatively to $[CuCl_2]$ ($T2 = -10.13\ln[CuCl_2] + 66.70$, $R^2 = 0.91$, $p<0.01$) and positively to $[EDTA]$ ($T2 = 5.72 \ln[EDTA] + 54.47$, $R^2 = 0.86$, $p<0.01$). For an average muscle T2 relaxation time of 45 ms as determined from in vivo fast spin echo scanning of the calf muscles, an $[EDTA]$ of 0.79 mM was required if $[CuCl_2]$ was fixed at 22.52 mM, yielding a mean density of 70 mg/cm^3. Two other scenarios are illustrated in Table I.Conclusions: This phantom optimization protocol provides a means for altering a soft-tissue mimic phantom to be suited for calibrating MRI and QCT signals within the range of a muscle. The proposed composition adjustment equations (Figure 1) apply only for density values as low as 64 mg/cm^3 as this lower limit results when $[CuCl_2]$ approaches 0.00 mM and T2 relaxation time approaches the upper limit of muscle values (79.9 ms in the gluteus maximus). Any lower density must be calibrated by altering the agar composition, thus affecting gelatination power.

Table I. Example of muscle phantom values representing different muscle quality

Phantom Properties	Fatty Muscle	Average Muscle	Lean Muscle
$[CuCl_2]$	4.00 mM	22.52 mM	41.04 mM
$[EDTA]$	0.73 mM	0.03 mM	0.01 mM
T2 relaxation time	52.65 ms	35.15 ms	29.07 ms
Density	65 mg/cm^3	70.00 mg/cm^3	75.00 mg/cm^3

Phantom Calibration

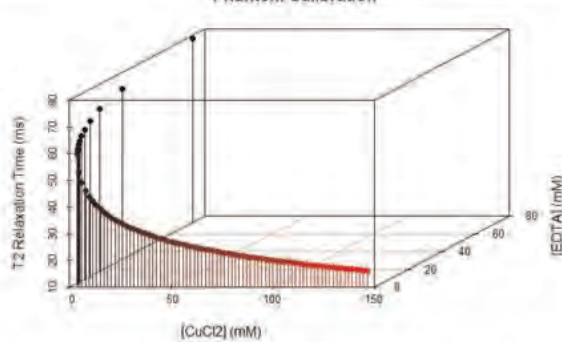**Figure 1. Combined logarithmic relation among [EDTA], [CuCl$_2$] concentrations and T2 relaxation time.** Density was not included in this three-dimensional plot since it depends mostly on [CuCl$_2$] only.

Table I. Figure 1.

Disclosures: Andy Kin On Wong, None.

SU0441

Dietary protein patterns are not associated with lean mass or strength among adults from the Framingham 3rd Generation Study. Kelsey Mangano*[1], Shivani Sahni[2], Robert McLean[3], Alyssa Dufour[4], Douglas Kiel[4], Katherine Tucker[5], Marian Hannan[6]. [1]Institute for Aging ResearchHebrew SeniorLifeHarvard Medical School, USA, [2]Hebrew SeniorLife, Institute for Aging Research & Harvard Medical School, USA, [3]Hebrew SeniorLife Institute for Aging Research & Harvard Medical School, USA, [4]Hebrew SeniorLife, USA, [5]University of Massachusetts Lowell, USA, [6]HSL Institute for Aging Research & Harvard Medical School, USA

Background: Total protein intake has been shown to benefit lean mass and muscle strength among adults, yet little is known about the influence of protein food source on muscle. It is essential to examine food sources of protein due to their different nutritional profiles and synergy with other nutrients consumed in the diet, which may affect muscle health differentially. Purpose: To examine the cross-sectional association of dietary protein patterns with quadriceps strength and appendicular lean mass (aLM) among adults. Methods: Quadriceps strength (n=2,846) and aLM (n=2,926) were measured in Framingham 3rd Generation Study participants (2008-2011). Isometric quadriceps strength (kg) of the right leg was measured using the Lafayette Manual Muscle Test System. aLM was calculated as the sum of leg and arm lean mass (kg) from whole body dual energy x-ray absorptiometry scans, and normalized for body size by dividing height (m^2). Dietary intakes were estimated using the Willett food frequency questionnaire (2002-2005). Cluster analysis (fastclus procedure, k-means method) classified participants into clusters, determined by major source of dietary protein. Linear regression was used to compare crude and multivariable-adjusted least-squares mean aLM and quadriceps strength across dietary protein

clusters. Results: Average age was $41 \pm 9y$ (range: 19-72y); 46% were men; mean total protein intake was 93 ± 32g/d; mean aLM, 22 ± 6kg and mean quadriceps strength, 28 ± 9kg. Five dietary protein clusters were identified (Table). Crude models showed significantly greater aLM in the red/processed meat cluster compared to the fish/plant/whole grains and low-fat milk clusters. The fish/plant/whole grains cluster had the lowest aLM. Similar results were observed with aLM/m^2. However, following multivariable adjustment, no significant differences were observed. No statistically significant differences in mean quadriceps strength were observed in crude or adjusted models. Results were similar when men and women were analyzed separately. Conclusions: In this cohort of men and women across a wide age range, dietary protein patterns were not associated with measures of lean mass or strength following adjustment for other factors associated with muscle health. These results suggest the benefit of dietary protein to muscle health occurs apart from protein food source in the context of the whole diet.

Least squares means ± SD^1 for appendicular lean mass (aLM) and quadriceps strength by dietary protein pattern

Variable	n	Cluster 1 Fish, plant & whole grains	Cluster 2 Processed foods	Cluster 3 Low fat milk	Cluster 4 Red meat & processed meat	Cluster 5 Chicken
Total protein (g/d)	2934	86 ± 32	92 ± 30	98 ± 30	95 ± 29	95 ± 36
Muscle Measures						
aLM (kg)	2926					
Unadjusted		21.2 ± 0.29^a	22.6 ± 0.19^{b,c}	21.8 ± 0.29^{a,c}	23.1 ± 0.27^b	22.4 ± 0.24^{b,c}
Adjusted^2		21.6 ± 0.13	21.6 ± 0.09	21.5 ± 0.13	21.4 ± 0.13	21.6 ± 0.11
aLM/height (kg/m^2)	2926					
Unadjusted		7.2 ± 0.07^a	7.6 ± 0.05^b	7.4 ± 0.07^{a,c}	7.8 ± 0.07^b	7.6 ± 0.06^{b,c}
Adjusted^3		7.3 ± 0.04	7.3 ± 0.03	7.3 ± 0.04	7.2 ± 0.04	7.3 ± 0.04
Quadriceps strength (kg)	2846					
Unadjusted		27.6 ± 0.45	27.8 ± 0.29	27.5 ± 0.46	27.6 ± 0.43	27.3 ± 0.37
Adjusted^3		27.4 ± 0.49	27.1 ± 0.36	27.1 ± 0.49	26.5 ± 0.48	26.7 ± 0.42

^{1} The analyses were adjusted for multiple comparisons using Tukey's test (different superscripts denote means that are significantly different. P<0.05)

^{2} Adjusted for: age, sex, estrogen status, total energy, physical activity, body mass index, height

^{3} Adjusted for: age, sex, estrogen status, total energy, physical activity, body mass index

Table

Disclosures: Kelsey Mangano, None.

SU0442

Do Strong Women Have Strong Bones?. Julie Pasco*[1], Sharon Brennan[1], Kara Holloway[2], David Moloney[2], Mark Kotowicz[3]. [1]Deakin University, Australia, [2]Deakin University, Australia, [3]Deakin University School of Medicine, Australia

Purpose: Resistance training and high impact exercises are promoted for building and maintaining a healthy skeleton. However, the linkages between muscle and bone are not yet fully understood. We aimed to investigate the relationship between hip flexor strength and areal bone mineral density (BMD) in women.

Methods: This cross-sectional study utilises data from 865 women (age 26-97 years) assessed for the 6-year follow-up phase of the Geelong Osteoporosis Study. Isometric hip flexor strength was measured three times on each leg, using a hand-held dynamometer (Nicholas Manual Muscle Tester). The maximal measure was used for analyses. BMD was measured at multiple skeletal sites using dual energy x-ray absorptiometry (DXA; Lunar DPX-L). Appendicular lean mass and body fat mass were determined from whole body DXA scans. Height and weight were measured. Relationships were analysed using linear regression techniques, with muscle strength as the independent variable and BMD as the dependent variable of interest.

Results: Muscle strength was negatively correlated with age and positively with appendicular lean mass (r=-0.49 and r=0.40; both p<0.001). Age-adjusted hip flexor strength was positively associated with BMD at all sites; for each standard deviation (SD) increase in muscle strength, the increase in BMD (SD) was 12.3% at the PA-spine (p=0.013), 10.4% at the total hip (p=0.009), 16.2% for the whole body (p<0.001), 14.3% at the ultra-distal forearm (p=0.003) and 21.5% at the mid forearm (p<0.001). The associations were independent of height and remained significant after adjustment for appendicular lean mass and body fat mass only at the mid-forearm.

Conclusion: The positive association between muscle strength and BMD was explained by differences in body composition at all sites except the mid-forearm. The findings suggest that the muscle-bone interaction might reflect muscle quantity rather than muscle strength.

Disclosures: Julie Pasco, None.

SU0443

How Does the Frailty Status of a Population-based Cohort Change? Results from the Longitudinal Canadian Multicentre Osteoporosis Study (CaMos).
Courtney Kennedy*[1], George Ioannidis[2], Jonathan Adachi[3], Lehana Thabane[4], Kenneth Rockwood[5], Susan Kirkland[5], Andy Kin On Wong[6], Laura Pickard[1], Alexandra Papaioannou[7]. [1]McMaster University, Canada, [2]McMaster University, Canada, [3]St. Joseph's Hospital, Canada, [4]McMaster University, Canada, [5]Dalhousie University, Canada, [6]McMaster UniversityUniversity Health Network, Canada, [7]Hamilton Health Sciences, Canada

Purpose: A Frailty Index is a continuous measure which considers the degree of frailty as proportional to the number of accumulated "health deficits" (symptoms, signs, diseases, and disabilities). The CaMos Frailty Index (CFI) was developed using a cumulative deficits framework and consisted of 30 items including co-morbidities, cognition, energy, functional and mobility measures. We examined frailty status of all CaMos participants at baseline and after 10-years of follow-up. Methods: CaMos began in 1995 and is a prospective cohort study of randomly selected Canadian men and women aged 25 years and older. Total CFI scores were derived by summing the deficit score on individual variables (0=absent, 1=maximal expression of deficit) and dividing by the total number of variables (n=30), yielding a continuous score between 0 (least frail) and 1 (most frail). We examined the prevalence of frailty among those in the cohort at baseline and at 10-years, with a CFI score $\geqslant 0.25$ considered as frail. We also examined the change in frailty scores over ten years for individuals who completed the 10-year follow-up; a change of 0.03 in CFI was considered clinically significant. Results: The CaMos baseline cohort was 9423 non-institutionalized individuals aged 25 years and older, including 6539 women (70.7%). The mean baseline CFI was 0.13 [standard deviation (SD)=0.11] in the entire cohort and 0.11 (SD=0.09) in participants completing the 10-year follow-up (n=5566). Of 1386 individuals (mean age=71.2 years, SD=11.2) classified as frail at baseline, 66.7% died/dropped out, 14.7% were also frail at year 10, and 18.6% were non-frail by year 10. Of 8037 individuals (mean age=61.1 years, SD=13.2) not frail at baseline, 36.5% died/dropped out, 4.5% were frail at year 10, and 59% were also non-frail at year 10. In the cohort reaching 10-years (n=5566), the mean change in frailty scores ranged from -0.37 to +0.46 (mean =0.004, SD=0.08). Overall, 32% increased their frailty status (i.e., >0.03 CFI increase), 30% decreased frailty status (i.e., >0.03 CFI decrease) and 38% did not change. Conclusion: As we would expect, the frailest participants died/dropped-out during the study period. The dynamic nature of frailty is indicated, with similar proportions of individuals who increased and decreased their frailty status over 10-years.

Disclosures: Courtney Kennedy, None.

SU0444

Identification of a Particular Clinical, Functional and Biochemical Profile in Sarco-Osteoporotic Older Persons.
Ruth Huo*[1], Pushpa Suriyaarachchi[2], Piumali Gunawardene[2], Oddom Demontiero[3], Gustavo Duque[4]. [1]University of New South Wales, Australia, [2]Ageing Bone Research Program, The University of Sydney, Australia, [3]The University of Sydney Nepean Clinical School, Australia, [4]Ageing Bone Research Program, University of Sydney, Australia

In older persons, the combination of sarcopenia and osteopenia/osteoporosis has been proposed as a subset of frailer individuals at higher risk of falls and fractures. However, the particular clinical, functional and biochemical characteristics of the sarco-osteoporotic patients remain unknown. In this study, we aimed to identify a standard definition of sarco-osteoporosis (SOP) and to determine the clinical, functional and biochemical features that are unique to SOP within a population of older persons. 680 subjects (mean age=79, 65% female) were assessed between 2009-2012 at the Falls & Fractures Clinic, Nepean Hospital (Penrith, Australia). Assessment included physical examination, bone densitometry and body composition by DXA, posturography, grip strength, gait assessment (GaitRITE), and blood tests for nutrition and secondary causes of SOP. Patients were divided in 4 groups: 1) osteopenia/osteoporosis (BMD<-1.0 SD); 2) sarcopenia (following the European Consensus criteria); 3) SOP and; 4) normal. Difference between groups was assessed with one-way ANOVA and chi square analysis. Multivariable linear regression evaluated the association between the groups and measures of physical function. Multivariable logistic regression evaluated risk factors for being in the SOP group. Sarcopenia was present in 47.4% of those with osteopenia (167/352) and 62.7% in those with osteoporosis (91/145). Mean age of the SOP was 80.4 ± 7 years. Univariate analyses showed that SOP are older, mostly female (OR 6.0, CI95% 3.67 – 9.87, p<0.001), at high risk for depression and malnutrition, BMI <25, and showed higher prevalence of peptic disease, inflammatory arthritis, history of maternal hip fracture, previous atraumatic fracture, and impaired mobility. Levels of parathyroid hormone were higher in SOP subjects (p<0.01). In summary, we have identified a set of clinical, functional and biochemical characteristics that are highly prevalent in SOP. This study could be used to inform the design future trials and to develop interventions for this particular syndrome.

Disclosures: Ruth Huo, None.

SU0445

Longitudinal Decline of Quality of Life is Determined by Loss of Muscle Mass and Reduced Physical Functioning in Older Adults.
Andrea Trombetti*[1], Kieran Reid[2], Mélany Hars[1], François Herrmann[1], Roger Fielding[3]. [1]Division of Bone Diseases, Geneva University Hospitals & Faculty of Medicine, Switzerland, [2]Jean Mayer USDA HNRCA At Tufts University, USA, [3]Jean Mayer USDA HNRCA At Tufts University, USA

Purpose: The age-related loss of skeletal muscle mass and function are critical determinants of independent physical functioning in later life. Longitudinal studies examining how decrements in these parameters impact quality of life in older adults are lacking.

Methods: Twenty-six healthy older subjects (age (mean $\pm$ SD), 74.1 $\pm$ 3.7; Short Physical Performance Battery (SPPB) score, 11.0 $\pm$ 0.9) and twenty-two older mobility-limited subjects (age, 77.2 $\pm$ 4.4; SPPB score, 7.9 $\pm$ 1.3) underwent evaluations of mid-thigh by computed tomography to estimate total muscle cross-sectional area (CSA), leg extensor muscle power, and 400m walk performance at baseline and after 3 years of follow-up. Quality of life was assessed at both timepoints using the Physical Component Score (PCS) of the Short-Form 36 questionnaire.

Results: At 3-year follow-up, muscle CSA decreased by 3% (p < 0.01), muscle power decreased by 9.4% (p < 0.001), while time to complete 400m increased by 22 $\pm$ 46 seconds (p < 0.001). Using linear mixed-effects regression models to adjust for study group (healthy/mobility-limited), gender, duration of follow-up and depressive symptoms, the decline of muscle mass (β = 0.10; p < 0.05) and decreased 400m walk time (β = -0.04; p < 0.003) were independent determinants of PCS at follow-up.

Conclusions: In older adults with and without mobility-limitations, declining muscle mass and physical function are independent factors that compromise quality of life over a 3 year follow-up period. Future studies should evaluate how intervention strategies designed to maintain muscle mass or restore physical functioning impact quality of life in older adults.

Disclosures: Andrea Trombetti, None.

SU0446

MMP-2 Mediated Degradation of Titin in Muscle Atrophy Study.
Shu Sun*[1], Anders Nedergaard[2], Morten Karsdal[1], Kim Henriksen[1], Gabriele Armbrecht[3], Daniel L. Belavý[4], Dieter Felsenberg[5]. [1]Nordic Bioscience A/S, Denmark, [2]Nordic Bioscience Biomarkers & Research, Denmark, [3]Centre of Muscle & Bone Research, Charite-CBF, Germany, [4]Center for Muscle & Bone Research, Charite Campus Benjamin Franklin, Free University & Humboldt-University Berlin, Germany, [5]Charité - Campus Benjamin Franklin, Germany

Background: Muscle loss is a problem which is getting increased clinical awareness, as loss of muscle mass and function are important predictors of mortality, morbidity and quality of life. In muscle loss syndromes, there is a pronounced lack of biochemical biomarkers that can predict or monitor pathological progress. In order to identify novel biomarkers of muscle loss, we set out to test if a cleavage fragment of the muscle protein titin identified in urine could be used as such a marker and we raised an antibody and constructed an ELISA assay for serum detection of said fragment.

Methods: A competitive ELISA assay measuring the titin fragment was developed. For biological validation of the assay, it was measured in rat tissue extractions and in vitro rat muscle enzymatic cleavage model, in order to characterize how the fragment is produced in vivo. Then the titin degradation marker was validated in a human 56-day bed rest study.

Results: The ELISA measuring titin fragment was technically robust and the fragment was shown to be produced by MMP-2 cleavage. This titin-MMP2 degradation fragment had higher expression in rat EDL muscle extraction compared to extractions from soleus and cardiac muscle. In a human bed rest study, the titin-MMP2 fragment was initially decreased about 10% after 1 day of bed rest, and then gradually increased until day 47, up to an average of 17% increase. On the last day of bed rest, the concentration did not significant differ to day 47.

Conclusions: We developed an ELISA measuring titin-MMP2 degradation fragment in human serum. We proposed that the titin-MMP2 marker during bed rest process may potentially reflect compensatory mechanisms to the catabolic immobilization stimulus. The gradually increased titin-MMP2 may reflect aspects of the catabolic processes in human long-term bed rest-induced muscle loss.

Disclosures: Shu Sun, Nordic Bioscience, 4
This study received funding from: salary from Nordic Bioscience

SU0447

Nutritional and Laboratory Associations with Skeletal Muscle Mass in Postmenopausal Women. Karen Hansen*[1], Sheeva Marvdashti[2], Christina Lemon[2], Kaitlin Chambers[2], R. Erin Johnson[2], Bjoern Buehring[3]. [1]University of Wisconsin, USA, [2]University of Wisconsin School of Medicine & Public Health, USA, [3]University of Wisconsin, Madison, USA

Sarcopenia, an age-associated decline in skeletal muscle mass and function, associates with falls, fractures, hospitalization and death. We evaluated relationships between height-corrected appendicular lean mass (ALM/Ht^2), physical function, nutritional habits and laboratory studies in ambulatory postmenopausal women.

Subjects were 231 postmenopausal women age 61 ± 6 years old randomized into a double-blind, placebo-controlled trial evaluating changes in calcium absorption, bone mineral density and physical function with treatment of vitamin D insufficiency. Subjects' baseline data were analyzed. ALM/Ht^2 was determined by whole body DXA (GE Lunar), using appendicular lean mass and height measured without shoes using a wall-mounted stadiometer. Nutritional habits were determined by 4–day diet diaries, and physical function was assessed by Timed Up and Go (TUG) and 5 Sit to Stand (STS) tests. Subjects completed questionnaires (Physical Activity Scale for the Elderly, PASE and Health Assessment Questionnaire, HAQ) assessing daily activities. Spearman correlation coefficients and linear models were used to evaluate associations between ALM/Ht^2 and subject characteristics.

Subjects' mean $\pm$ SD ALM/Ht^2 was 7.29 ± 1.15 kg/m^2; 55% had sarcopenia (ALM/Ht$^2 \leq 7.23$ kg/m^2). Body weight was strongly associated with ALM/Ht^2 ($\rho=0.821$, p<0.001) and accounted for 73% of its variance (R^2). Additionally, ALM/Ht^2 was associated with the TUG, STS and Health Assessment Questionnaire scores, consumption of alcohol and sodium, use of supplemental calcium, iron and potassium, and serum parathyroid hormone and estradiol levels (Table). In linear models controlling for weight and age, ALM/Ht2 was positively associated with the TUG and PASE scores, dietary magnesium and use of magnesium and potassium supplements. Addition of the STS test, serum calcium and albumin improved the model and together, these 10 variables explained 79% of the variance in ALM/Ht^2.

Body weight is the largest factor associated with ALM/Ht^2. Like other researchers, we found that alcohol, parathyroid hormone levels and estradiol were associated with muscle mass in univariate analyses. Both univariate and multivariate analyses identified potassium and magnesium intake as statistically significant. Future studies are needed to clarify the role of magnesium and potassium intake in skeletal muscle mass.

Table: Correlation between Muscle Mass (ALM/Ht2) and Subject Characteristics		
	Spearman	p-value
Physical Attributes		
Age, years	-0.083	0.206
Weight, kg	0.852	<0.001
Height, cm	-0.022	0.747
Timed Up and Go, seconds	0.270	<0.001
5 Sit to Stand Test, seconds	0.236	<0.001
Physical Activity Score	0.006	0.933
Health Assessment Questionnaire Sco	0.191	0.004
Pain in past week (0-10 VAS)	0.088	0.186
Dietary Habits (units/day)		
Kilocalories	0.069	0.294
Protein, g	0.102	0.122
Fat, g	0.088	0.180
Carbohydrates, g	0.032	0.620
Fiber, g	-0.001	0.999
Calcium, mg	0.041	0.529
Vitamin D, IU	-0.098	0.139
Magnesium, mg	-0.027	0.703
Iron, mg	0.037	0.569
Sodium, mg	0.216	<0.001
Phosphorus, mg	0.046	0.480
Potassium, mg	-0.071	0.294
Oxalate, servings	0.067	0.307
Caffeine, mg	0.015	0.828
Alcohol, g	-0.215	0.001
Supplemental Intake (mg/day)		
Calcium	-0.142	0.031
Magnesium	0.106	0.111
Iron supplement	0.131	0.049
Potassium	0.177	0.007
Laboratory Data		
Serum Calcium, mg/dL	-0.021	0.755
Parathyroid Hormone, pg/mL	0.265	<0.001
25(OH)D, ng/mL	-0.134	0.054
Serum Creatinine, mg/dL	0.169	0.010
Estradiol, pg/mL	0.225	0.002

Table

SU0448

Prevalence of 'Dysmobility Syndrome' in Community Dwelling Older Adults: Findings from the UK and US. Bjoern Buehring*[1], Mark Edwards[2], Rebecca Moon[3], MA Clynes[4], Celia Gregson[5], Ellen Fidler[6], Nicholas Harvey[7], Elaine Dennison[8], Neil Binkley[1], Cyrus Cooper[9]. [1]University of Wisconsin, Madison, USA, [2]MRC Lifecourse Epidemiology Unit, University of Southampton, United Kingdom, [3]MRC Lifecourse Epidemiology Unit, University of Southampton, United Kingdom, [4]MRC Lifecourse Epidemiology Unit, University of Southampton, UK, United Kingdom, [5]University of Bristol, United Kingdom, [6]University of Wisconsin, USA, [7]MRC Lifecourse Epidemiology Unit, University of Southampton, United Kingdom, [8]MRC Lifecourse Epidemiology Unit, United Kingdom, [9]University of Southampton, United Kingdom

Sarcopenia and osteoporosis become common with advancing age, often coexist, and increase risk for adverse outcomes such as falls and fracture. We recently proposed a score-based system to diagnose "dysmobility syndrome" in an attempt to combine adverse musculoskeletal phenotypes to identify older individuals at risk for falls and fractures. This report compares the prevalence of dysmobility, and sarcopenia using conventional definitions, in two cohorts of community dwelling older adults; a group from the Hertfordshire Cohort Study in the UK and a convenience sample from the US.

In both cohorts, body composition was measured by DXA, gait speed and grip strength were assessed in routine manner. Participants completed a questionnaire detailing self-reported falls and fracture history. Dysmobility syndrome was arbitrarily defined as 3 or more of low appendicular lean mass/height ratio, low grip strength, low gait speed, low leg lean/fat mass ratio, osteoporosis, and fall in the last year. Sarcopenia prevalence was determined using the European Working Group on Sarcopenia in Older People (EWG) and International Working Group on Sarcopenia (IWG) definitions. The UK cohort included 156 men and 142 women of mean (SD) age 76.1 (2.6) years and BMI of 27.4 (4.1) kg/m^2; the US cohort included 48 men and 49 women with mean (SD) age 80.7 (5.9) and BMI 25.6 (4.1). Sarcopenia prevalence (EWG/IWG) was 7%/8% in the UK and 20%/10% in the US group. Dysmobility prevalence was 25% in the UK and 41% in the US cohort. Dysmobility syndrome was more common (p<0.05) in women than men in both cohorts (33.1% vs. 17.3% in the UK and 59.2% vs. 22.9% in the US). The higher dysmobility syndrome prevalence in women was associated with a higher frequency of abnormal parameters in several of the chosen factors. In the UK cohort, those with dysmobility reported a higher number (p <0.01) of falls than counterparts without dysmobility, but no increased fracture rate was observed in the dysmobility group (p=0.96). No significant differences in falls and fracture prevalence were found in the US cohort (all p>0.1).

In conclusion, dysmobility syndrome is common among older community dwelling adults in the UK and US, with higher rates observed in the US cohort. Prevalence was higher in women than men. Further work is needed to optimally define how muscle mass/function, in combination with body composition assessment, can be used to identify older adults at risk for falls and fractures.

SU0449

Use of the Safe Functional Motion-6 test to classify individuals at risk for functional decline following a distal radius fracture. Norma MacIntyre*[1], Joy MacDermid[2], Julie Richardson[2], Ruby Grewal[3], Christopher Recknor[4]. [1]McMaster University, Canada, [2]McMaster University, Canada, [3]St Joseph's Health Care, Canada, [4]United Osteoporosis Center, USA

Purpose: A distal radius fracture (DRF) may mark the onset of osteoporosis (OP) and/or functional decline. This study determines the effects of age and physical functioning on functional recovery in individuals followed for 1 year after DRF.

Methods: Adults with recent DRF completed the 6-task Safe Functional Motion test (SFM-6) at follow-up clinic visits. The SFM-6 quantifies observed physical performance during activities typical of daily living with a score calculated as a percentage of the maximum points possible where higher scores reflect better movement patterns. Prevalence of OP at the time of the DRF was defined as DXA-based total hip t-score <-2.5, where available, and use of bone sparing medications. Since assessments were done at varying time intervals, hierarchical linear modeling was used to determine if the pattern of functional recovery, as measured by the SFM-6, was predicted by age (<60 vs ≥60yr) and initial SFM-6 score (≥80 vs <80 points).

Results: Seventy-nine DRF patients (mean(SD) age=61.3(6.8)yr; 8 men), completed the SFM-6 on at least 2 occasions. Musculoskeletal conditions were the most prevalent comorbidities (osteoarthritis: n=32 and back pain: n=20). Few had prevalent OP (t-score < -2.5: n=3; on bone sparing medications: n= 8). Figure 1 illustrates individual SFM-6 scores over 1 year for the cohort according to age and physical functioning at baseline. Age and baseline SFM-6 score were significant predictors of functional recovery (^{2}=41.74, p<0.001). The ≥ 60yr group scored 3 points lower than the <60yr group at baseline (p = 0.038); age was not a significant predictor of the linear or nonlinear slopes modelling functional recovery. Those with SFM-6 scores <80 points at baseline had a steeper linear slope than those with scores ≥80 points at baseline (β coefficient=11.3, p<0.001). The rate of change in SFM-6 scores was attenuated in those ≥60yr with low physical functioning at baseline but this difference was not statistically significant.Conclusions: Whereas age was a

predictor of physical functioning, only baseline physical functioning predicted patterns of functional recovery in our sample. The SFM-6 may be useful for classifying those at risk for functional decline following DRF. Few participants had an elevated risk for OP fracture and long-term follow-up is required to determine if SFM-6 scores predict future fracture in the DRF population.
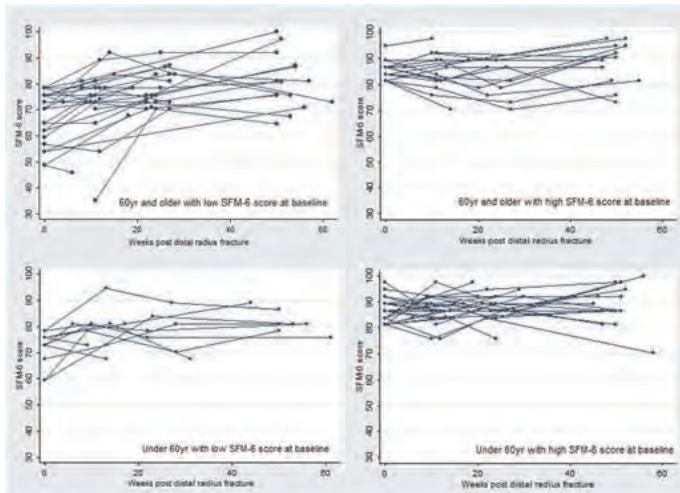

Figure 1. SFM-6 scores for participants followed over 1 year post distal radius fracture.

Disclosures: Norma MacIntyre, None.

SU0450

Compartment Specific Changes in Bone Mass with Advanced Age in a Mouse Model with Enhanced Sympathetic Tone and Impaired Brown Adipose Tissue Function. Phuong Le*[1], Katherine Motyl[1], Kathleen Bishop[1], David Maridas[1], Daniel Brooks[2], Mary Bouxsein[3], Clifford Rosen[4]. [1]Maine Medical Center Research Institute, USA, [2]Beth Israel Deaconess Medical Center, USA, [3]Beth Israel Deaconess Medical Center, Harvard Medical School, USA, [4]Maine Medical Center, USA

'Browning' of white adipose tissue (WAT) is a critical goal for novel weight loss drugs; however, these agents may have deleterious effects on the skeleton. The *Misty* mice (*m/m*) have a spontaneous mutation leading to a loss of function in the *Dock7* gene which acts downstream of the EGFR to activate Rac1 and Cdc42. *Misty* at 16wk have low trabecular bone mass, loss of brown adipose tissue (BAT) function, increased sympathetic tone (SNS), and marked browning of WAT depots. As predicted, *m/m* are resistant to high fat diet-induced obesity. In this study, we hypothesized *m/m* would have accelerated age-related bone loss in conjunction with progressive browning of peripheral WAT depots. Female *m/m* and their littermate controls (WT) were aged to 78wk on a regular chow. Body composition and areal bone mineral density (aBMD) were measured by DXA; femur trabecular and cortical microarchitecture were measured by μCT. Total aBMD and trabecular BV/TV were significantly reduced in *m/m* and remained at low levels beyond 1 year (p<0.001, age x genotype interaction). With regard to cortical bone, *m/m* have greater total area (TtAr) younger ages, but smaller TtAr at 78 wk, suggesting impaired age-related periosteal apposition. Cortical thickness and cortical bone area fraction (CtAr/TtAr) are consistently lower in *m/m* than WT, though with increasing age, WT CtAr/TtAr declines at a faster rate. This suggests *m/m* are less susceptible to age-related endosteal resorption, which could explain in part, their lower rate of periosteal expansion. Body weight increased with age in both strains, but *m/m* were slightly thinner than WT. From 52 to 78wk, *m/m* did not increase body weight but the WT did. Inguinal fat depots in *m/m* had smaller adipocytes and more UCP-1 staining at 52 and 78wk *vs.* WT mice. In both genotypes, BAT weight increased with age. *Misty* BAT had larger lipid droplets than WT, with less UCP-1 staining at 78wk. Thus, progressive browning of WAT continues unabated in *m/m*. Age-related changes in trabecular bone are likely related to the high SNS drive from impaired BAT function, while cortical bone loss may be associated with the absence of weight gain in the older *m/m* mice. The absence of periosteal compensation with age in *m/m* may also be due to a cell autonomous effect of the *Dock7* mutation. In conclusion, although SNS activation may protect against diet-induced obesity, the long term effects on body composition and bone mass are profound.
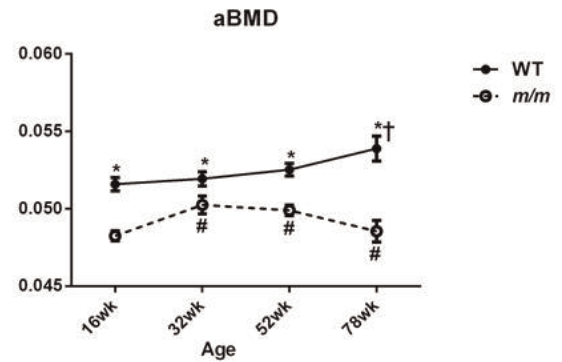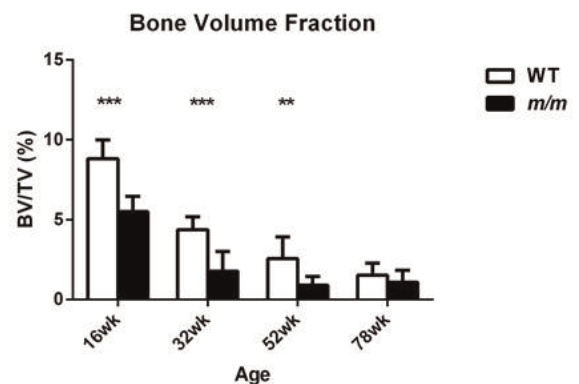

* *vs. m/m*; † *vs.* 16wk WT; # *vs.* 16wk *m/m*

Misty aBMD
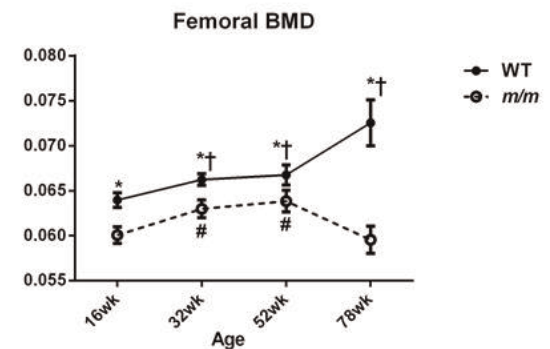
* *vs. m/m*; † *vs.* 16wk WT; # *vs.* 16wk *m/m*

Misty fBMD

*p = 0.01-0.05, **p = 0.001-.01, ***p <.001 vs. WT

Misty BV/TV

Disclosures: Phuong Le, None.

SU0451

Cortical porosity increases with age in murine long bones and is associated with elevated RANKL and reduced OPG expression in osteocytes. Charles O'Brien*[1], Jinhu Xiong[1], Marilina Piemontese[2], Stuart Berryhill[3], Priscilla Baltz[3], Robert Weinstein[1], Maria Jose Almeida[1], Stavros Manolagas[1], Robert Jilka[1]. [1]Central Arkansas VA Healthcare System, Univ of Arkansas for Medical Sciences, USA, [2]University of Arkansas for Medical Sciences, USA, [3]Central Arkansas VA Healthcare System, Univ of Arkansas for Medical Sciences, USA

Increased cortical porosity is now recognized as an important contributor to skeletal fragility in elderly humans. However, the cellular and molecular mechanisms responsible for the increase in cortical porosity associated with advanced age are

unclear. Here we have investigated changes in structure and gene expression in cortical bone of aged mice. Cortical bone architecture was investigated in the femur, tibia, and humerus of C57BL/6 female mice at 6, 18, and 24 months of age using micro-CT. Cortical thickness of the femur was reduced at the two older ages compared with 6-month-old mice and this was associated with increases in both the inner and outer diameters of the cortical bone. Porosity, as observed in full-length scans of the femoral cortical bone, also increased with age and was especially prominent at both the distal and proximal metaphyses. Moreover, porosity in the region of the third trochanter increased. In the tibia, porosity increased throughout the proximal region. The humerus of aged mice exhibited the same pattern of porosity, along with a striking increase in the porosity of the deltoid tuberosity. These changes in bone structure were associated with increased levels of the osteoclast-specific mRNAs cathepsin K, calcitonin receptor, and TRAPase in cortical bone, consistent with increased remodeling. Notably, RANKL mRNA was increased and OPG mRNA was decreased in osteocyte-enriched cortical bone of aged mice compared with 6-month-old mice. Soluble RANKL protein was also elevated in bone marrow supernatants of aged mice as measured by both ELISA and Luminex bead assays. The highly localized porosity that develops in the murine appendicular skeleton with advancing age appears to occur at sites of high bone strain, i.e. the metaphyses and trochanteric sites of muscle attachment. In view of the evidence that osteocytes are an important source of RANKL, these results suggest that altered osteocyte function or viability with age leads to changes in the RANKL/OPG axis that promote intra-cortical bone resorption, predominantly at sites of higher loading. Moreover, since bone remodeling is reduced in the cancellous bone of aged mice, these findings suggest there are important mechanistic differences underlying the age-associated changes in bone remodeling in cortical versus cancellous bone.

Disclosures: Charles O'Brien, None.

SU0452

Galectin-3: A novel regulator of bone mass. Kevin Maupin*[1], John Wang[2], Bart Williams[3]. [1]Van Andel Institute Graduate School, USA, [2]Michigan State University, USA, [3]Van Andel Research Institute, USA

The decline of hormone production during aging leads to a gradual loss of bone mass. Over time, these bones can become porous and brittle, leading to osteoporosis. Half of all women over the age of 60 will suffer an osteoporotic fracture and of those women who fracture, nearly 40% will die within 5-years due to complications. While hormone replacement therapy is effective at reducing bone loss and preventing fractures, it also carries the risk of breast cancer, endometrial hyperplasia, and liver disease. The identification of novel non-hormonal regulators of bone mass will lead to improved treatment strategies to prevent/reverse osteoporosis. We have identified one potential target: Galectin-3 (Gal3).

Gal3 is a beta-galactoside binding protein expressed by all bone lineage cells and has been implicated as a negative regulator of both osteoblast and osteoclast differentiation. In order to understand the role of Gal3 in bone during aging, we analyzed femurs and L3 vertebrae from mice carrying a null mutation of the Gal3 gene (*Lgals3*) on a C57BL/6 background and their wildtype littermates at pre-skeletal maturity (12 wks), post-skeletal maturity (24 wks), and advanced age (36 wks). Using micro computed tomography (µCT) we found that the vertebra of female *Lgals3*-null mice have 10% higher trabecular bone mineral density (tBMD) and a 35% greater bone volume fraction (BV/TV) at both the 24- and 36-wk time points. The femurs of *Lgals3*-null females showed no difference until 36 wks when their femurs failed to show the normal age-related loss of trabecular bone. This preservation of bone resulted in 45% higher tBMD and 239% greater BV/TV compared to *Lgals3*-wildtype females. Interestingly there was no significant difference in trabecular bone parameters at any measured time point when *Lgals3* was deleted in males. Our findings indicate that Gal3 is a negative regulator of trabecular bone formation and/or a positive regulator of trabecular bone resorption in females. Additionally, genetic loss of *Lgals3* was well tolerated in mice, and therefore, pharmacological targeting of Gal3 may be an efficacious option for treating/preventing osteoporosis.

Disclosures: Kevin Maupin, None.

SU0453

Mitochondria-targeted expression of catalase does not prevent the low bone mass caused by suppression of autophagy in osteoblasts and osteocytes. Marilina Piemontese*[1], Jinhu Xiong[2], Priscilla Baltz[3], Rajamani Selvam[3], Li Han[2], Stuart Berryhill[3], Stavros Manolagas[2], Charles O'Brien[2]. [1]University of Arkansas for Medical Sciences, USA, [2]Central Arkansas VA Healthcare System, Univ of Arkansas for Medical Sciences, USA, [3]University of Arkansas for Medical Sciences, USA

Autophagy maintains cell function and homeostasis by recycling damaged intracellular components. Previous studies have shown that deletion of Atg7, a gene required for the formation of autophagosomes, with an osteoblast-specific Cre recombinase (Osx1-Cre) causes low bone mass and spontaneous fractures. Suppression of autophagy in other cells types often results in reduced recycling of mitochondria leading to accumulation of damaged mitochondria and oxidative stress. Consistent with this, we observed elevated levels of reactive oxygen species (ROS) in the bone marrow of Osx1-Cre;Atg7f/f (Atg7ΔOb) mice. To determine whether the increase in oxidative stress contributes to the low bone mass caused by

Atg7 deletion, Atg7ΔOb mice were crossed with mice harboring a conditionally-activated transgene expressing mitochondria-targeted catalase (mCAT), an antioxidant enzyme. Thus, in the offspring of this cross the Osx1-Cre transgene simultaneously deletes Atg7 and activates the catalase transgene in the same cell populations (osteoblasts and osteocytes). Serial BMD analysis up to 24 weeks of age confirmed low bone mass in the femur and spine of Atg7ΔOb mice compared to both Atg7f/f and Osx1-Cre control littermates. Expression of mCAT in Atg7ΔOb mice did not alter the low bone mass caused by suppression of autophagy. Catalase activity, measured in stromal cells cultured in osteogenic medium, was greatly elevated in mCAT;Atg7ΔOb mice compared to control littermates, confirming activation of the transgene. ROS levels measured in the bone marrow and phosphorylation of p66shc protein, an oxidative stress mediator, were increased in Atg7ΔOb mice and did not change with expression of catalase. Thus, mitochondrial expression of catalase in osteoblasts and osteocytes did not prevent the increase in oxidative stress in the bone marrow caused by suppression of autophagy. Analysis of femoral and vertebral architecture confirmed the low trabecular bone volume in Atg7ΔOb mice as well as the reduction in strength, and expression of mCAT did not prevent any of these changes. Consistent with this, the rate of spontaneous fractures occurring in tibias of conditional knockout mice was similar in conditional knockout mice expressing catalase. Together these results suggest that autophagy exerts its positive effects on the skeleton by mechanisms other than suppression of H202 levels in the mitochondria of osteoblasts and osteocytes

Disclosures: Marilina Piemontese, None.

SU0454

Osteoblast depletion increases osteoblast activity and reduces bone toughness in mice. Adeline Ng*[1], Gurpreet Baht[2], Marc Grynpas[3], Benjamin Alman[2]. [1]University of Toronto Samuel Lunenfeld Research Institute, Canada, [2]Program in Developmental & Stem Cell Biology, Hospital for Sick Children, Canada, [3]Lunenfeld-Tanenbaum Research Institute of Mount Sinai Hospital, Canada

Background: Literature has suggested factors that sustain stem cell levels in the bone marrow decline with age and this deficit may be related to age-associated bone loss. Using the Col2.3Δtk (DTK) transgenic mouse, we investigated the consequences of repeated ablation of differentiated osteoblasts on osteogenic progenitor cells in the bone marrow. The DTK transgenic mouse takes advantage of the HSV-tk (herpes simplex virus thymidine kinase)/GCV (ganciclovir) system to conditionally ablate differentiated osteoblasts.

Methods: In an osteoblast-depletion experiment, 4-month old DTK mice were repeatedly treated with ganciclovir (GCV) to conditionally ablate differentiated osteoblasts, while controls were treated with saline. All animals were sacrificed at 8 months; bone marrow stromal cells (BMSCs) were harvested for cell culture and whole bones were excised for bone quality assessment. Colony forming unit (CFU) assays were conducted to investigate BMSC osteogenic potential. RNA was extracted from cell culture and whole bones (tibias) to assess the expression of genes defining BMSC lineage. *Ex vivo* bone quality assessments included bone histomorphometry, TRAP-staining, microcomputed tomography, and biomechanical testing.

Results: Osteoblast depletion using GCV decreased CFU-F (fibroblast), CFU-ALP (alkaline phosphatase) and CFU-VK (von Kossa) counts in cell culture. *Ex vivo*, there was no difference in bone mineral density (vertebrae and femurs) between treatment groups despite differences in BMSC osteogenic capacity *in vitro*. Histology showed a decrease in bone volume and bone connectivity with repeated osteoblast depletion; this was accompanied by an increase in osteoid volume and surface, mineralizing surface, and bone formation rate. Although osteoblast depletion did not decrease the number of active osteoblasts between treatment groups, it decreased the number of TRAP-positive osteolcasts. Repeated osteoblast depletion decreased the energy to failure in vertebral compression and 3-point bending tests.

Discussion: This study aims to connect *in vitro* cell culture data with *in vivo* skeletal phenotypes. Results suggest that the number of healthy bone marrow stromal cells (BMSCs) and the osteogenic potential of those healthy BMSCs decline with repeated osteoblast ablation. Activity of the remaining osteoblasts increases to compensate for this loss in osteogenic potential, but mechanical properties remain compromised with repeated osteoblast ablation.

Disclosures: Adeline Ng, None.

SU0455

PTH/PTHrP Receptor (PPR) Signaling in Osteocytes Delays Osteocyte Senescence and Protects from Age-related Osteopenia. Vaibhav Saini*[1], Keertik Fulzele[2], Xiaolong Liu[3], Christopher G Dedic[3], Vladimir Zoubine[3], Jordan Spatz[4], Hiroaki Saito[5], Katharina Jahn[5], Saman F Khaled[3], Kathryn D Held[3], Eric Hesse[6], Paola Divieti Pajevic[7]. [1]MGH, Harvard Medical School, USA, [2]Massachusetts General Hospital; Harvard Medical School, USA, [3]MGH, USA, [4]Harvard-MIT Division of Health Sciences & Technology (HST), USA, [5]University Medical Center Hamburg-Eppendorf, Germany, [6]University Medical Center Hamburg-Eppendorf, Deu, [7]Massachusetts General Hospital & Harvard Medical School, USA

We have previously shown that PPR signaling in osteocytes is essential for bone remodeling and generating anabolic and catabolic skeletal responses to parathyroid hormone (PTH) administration. Herein, to understand age-induced osteoporosis, we investigated the effect of ablated PPR signaling in osteocytes on aged skeleton. Towards our goal, we used mice lacking PPR in osteocytes (OcyPPRKO), generated, as in the previous study, by mating 10kb-DMP1-Cre mice with PPR floxed mice. Littermates lacking Cre-expression were used as control. To investigate the role of PPR signaling in aging, we analyzed adult (4 months (mo)) and aged (12mo) OcyPPRKO. Histological analysis of long bones showed increased trabecular bone at 4mo which was dramatically decreased by 12mo in OcyPPRKO. High resolution μCT of L5 vertebrae and distal femurs showed increased trabecular bone at 4mo ($p<0.05$, N=6-12) which was decreased by 12mo ($p<0.05$, N=7-12) in OcyPPRKO than control. Histomorphometric analysis showed reduced osteoclast number and bone resorption in OcyPPRKO at 4mo ($p<0.05$, N=6-10) which were increased by 12mo ($p<0.05$, N=8-10). Osteoblasts and bone formation, on the other hand, were unchanged, as was SOST mRNA level in osteocyte-enriched calvariae from OcyPPRKO and control. Immunohistochemistry on tibiae showed reduced RANKL expression in osteocytes at 4mo ($p<0.05$) in OcyPPRKO, possibly accounting for decreased osteoclasts at 4mo; however RANKL expression was unchanged at 12mo between OcyPPRKO and control. TNFα mRNA level in osteocyte-enriched calvariae was similar between OcyPPRKO and control at 4mo; however it was increased by 62% ($p<0.05$) at 12mo in OcyPPRKO, possibly accounting for increased osteoclasts at 12mo. To investigate PPR signaling in osteocytes, we knocked-down PPR expression by lentiviral-delivered shRNA in Ocy454, a murine osteocyte cell line established in our laboratory. As compared with Ocy454-shGFP (control), Ocy454-shPPR cells showed reduced proliferation by time-lapse microscopy upon sequential passaging, intense senescence-associated ß-galactosidase staining at 11 and 21 days, and increased p53 mRNA level (270%, $p<0.05$) at 11 days *in vitro*. Furthermore, there was a 650% increase ($p<0.05$) in TNFα mRNA level in Ocy454-shPPR at 11 days. Our results demonstrate that PPR signaling in osteocytes delays senescence by decreasing p53 expression and protects from age-related osteopenia by decreasing TNFα expression and preventing osteoclast activation.

Disclosures: Vaibhav Saini, None.

SU0456

TNFα modulates cholesterol transport protein synthesis and efflux in osteocytes. Kent Wehmeier*[1], Salma Makhoul-Ahwach[2], Melanie Thomas[3], William Kurban[3], Harshit Shah[3], Aiham Chamseddin[4], Michael Haas[5], Arshag Mooradian[6], Luisa M. Onstead-Haas[6]. [1]University of Florida, College of Medicine, Jacksonville, USA, [2]Division of Endocrinology, Diabetes & Metabolism. University of Florida, College of Medicine Jacksonville, USA, [3]Division of Endocrinology, Diabetes & Metabolism, University of Florida, College of Medicine Jacksonville, USA, [4]Division of Endocrinology, Diabetes & MetabolismUniversity of Florida, College of Medicine Jacksonville, USA, [5]Division of Endocrinology, Department of Medicine, University of Florida, College of Medicine Jacksonville, USA, [6]Department of Medicine, University of Florida, College of Medicine Jacksonville, USA

Hip fracture and myocardial infarction cause significant morbidity and mortality. In vivo studies raising serum cholesterol levels as well as pro-inflammatory cytokines such as TNFα manifest bone loss and atherosclerotic vascular disease, suggesting that abnormalities of cholesterol transport may contribute to osteoporosis. We used the mouse osteocyte cell line (MLO-Y4) to investigate the effects of TNFα on the expression of cholesterol acceptor proteins such as apolipoprotein A-I and apolipoprotein E, as well as on ATP-binding cassette-1 (ABCA1) and scavenger receptor class B type 1 (SRB1). MLO-Y4 cells do not express apolipoprotein A-I or apolipoprotein E; however they do express the cholesterol transporters ABCA1 and SRB1. Treatment of MLO-Y4 cells with TNFα had no effect on osteocalcin levels; however TNFα reduced ABCA1 protein levels and cholesterol efflux to apolipoprotein A-I. Interestingly, TNFα treatment increased ABCA1 mRNA levels 1.8-fold and increased liver-x-receptor-alpha (LXRα) protein expression but had no effect on retinoid-x-receptor-alpha (RXRα) and retinoic acid receptor alpha (RARα) protein levels. TNFα treatment suppressed SRB1 mRNA levels (18%) but there was no

change in SRB1 protein expression. TNFα induced p38 mitogen-activated protein (MAP) kinase activity, but had little effect on c-jun N-terminal kinase 1 and extracellular regulated kinase 1/2. Pharmacological inhibition of p38 MAP kinase restored ABCA1 protein levels. These results demonstrate that pro-inflammatory cytokines regulate cholesterol transport in osteocytes. Understanding cholesterol movement within bone cells may suggest novel therapeutic approaches to osteoporosis.

Disclosures: Kent Wehmeier, None.

SU0457

Factors Associated with Kyphosis and Kyphosis Progression in Older Men: the MrOS Study. Deborah Kado*[1], Mei-Hua Huang[2], Peggy Cawthon[3], Howard Fink[4], John Schousboe[5], Elizabeth Barrett-Connor[1]. [1]University of California, San Diego, USA, [2]UCLA, USA, [3]California Pacific Medical Center Research Institute, USA, [4]GRECC, Minneapolis VA Medical Center, USA, [5]Park Nicollet ClinicUniversity of Minnesota, USA

Hyperkyphosis, or increased thoracic curvature, is common in older men and women. While it is thought that vertebral fractures are the major cause of increased kyphosis, only about a third of those with the worst degrees of kyphosis have underlying vertebral fractures. In older men, hyperkyphosis is associated with increased risk of worse physical function, injurious falls, and earlier mortality. Thus, it would be useful to better understand the determinants of kyphosis progression in older men. Therefore, we studied 1051 men from the MrOS Study aged 64 – 92 (mean age 72.7) who had repeated standardized measures of Cobb angle kyphosis calculated from lateral spine x-rays taken at baseline and an average of 4.6 years later (SD = 0.4). Using multivariable linear regression, we analyzed the association between known and hypothesized risk factors of kyphosis and kyphosis progression. Specifically, we examined the association of age, family history of stooped posture, prevalent radiographic thoracic and lumbar vertebral fractures (RVF), incident RVF (longitudinal analyses only), degenerative disc disease (DDD), hip bone mineral density (BMD), bone density loss, BMI, weight, weight loss, co-morbidities such as diabetes, and health behaviors. Men had an average baseline kyphosis of 38.8° (SD = 11.2); over 4.6 years, they progressed an average of 1.4° (SD = 4.6). In cross-sectional analyses, older age (p = 0.002), DDD (p = <0.0001), lower hip BMD (p = 0.007) and lower body weight (p = 0.015) were associated with increased kyphosis, but prevalent vertebral fracture was not. In multivariable longitudinal analyses, incident vertebral fracture, lower hip BMD and DDD were the factors that significantly associated with increasing kyphosis (Table).

Other factors not included in the Table such as diabetes, smoking, alcohol use, and self-reported physical activity did not affect kyphosis progression. In contrast to the associations in older women, prevalent vertebral fracture was not associated with kyphosis while DDD was a significant predictor of both baseline kyphosis and kyphosis progression, possibly reflecting sex differences in the causes of worsening age-related posture. Common to both sexes, however, was the importance of BMD and incident vertebral fractures, suggesting that identifying and treating osteoporosis in both older men and women may help prevent or delay age-related kyphosis progression.

Variable	Parameter Estimate	95% CI	P-value
Baseline kyphosis (per degree)	-0.046	(-0.07, -0.02)	0.0003
Prevalent RVF	0.69	(-0.71, 2.09)	0.33
Incident RVF	1.60	(0.0003, 3.16)	0.05
Hip BMD (per SD)	-0.55	(-0.82, -0.27)	0.0001
Degenerative Disc Disease (DDD)	0.60	(0.031, 1.17)	0.04

Table. Multivariable-Adjusted Beta Coefficients for Association Between Selected Characteristics and Kyphosis Progression over 4.6 years

Above model also adjusted for age, clinic, weight change, and family history of stooped posture.

Table

Disclosures: Deborah Kado, None.

SU0458

Self-reported Estrogen Use, Kyphosis and Kyphosis Progression in Older Women: the Study of Osteoporotic Fractures. Deborah Kado[1], Gina Woods*[2], Mei-Hua Huang[3], Corinne McDaniels-Davidson[4], Peggy Cawthon[5], Howard Fink[6]. [1]University of California, San Diego, USA, [2]UCSD, USA, [3]UCLA, USA, [4]SDSU/UCSD Joint Doctoral Program in Public Health (Epidemiology), USA, [5]California Pacific Medical Center Research Institute, USA, [6]GRECC, Minneapolis VA Medical Center, USA

Hyperkyphosis (HK), or increased thoracic spine curvature, tends to progress with age and is associated with poor physical and pulmonary function and earlier mortality. Although closely associated with osteoporosis, only 1/3 of older persons with the worst degrees of kyphosis have underlying vertebral fractures (VF) and the underlying biological correlates of kyphosis progression are not known. Rodent

models of kyphosis suggest that there is a link between sex steroid hormones and HK and we have recently reported that older men with lower serum estradiol have worse kyphosis. Therefore, to test the hypothesis that estrogen may play a role in kyphosis and kyphosis progression in older women, we studied 983 women from the Study of Osteoporotic Fractures aged >65 (mean age 69.4, SD = 4.0) who provided detailed information on estrogen use and who had their Cobb angle of kyphosis measured from baseline and follow-up lateral spine x-rays done an average of 3.7 and 15 years later. Using linear mixed effects regression, we examined the correlation between self-reported estrogen use (categorized as current, past or never), adjusting for factors thought to influence kyphosis alone or both estrogen use and kyphosis. Women had an average kyphosis of 44.9° (SD = 11.8) that progressed an average of 7° over 15 years. At baseline, 154 (16%) women reported current, 324 (33%) reported past, and 505 (51%) women reported never use of estrogen replacement. While we found no cross-sectional association between self-reported estrogen use and HK, there was a strong association between baseline reported estrogen use and kyphosis progression over the next 15 years. In age and clinic adjusted models, baseline reported current estrogen use was associated with 2.5° less (p = 0.0007) and past use with 1.6° less kyphosis progression (p = 0.005) than those who reported never using estrogen. In fully adjusted multivariable models that included BMD, degenerative disc disease, prevalent & incident VF's, weight, weight change, smoking, alcohol and self-reported physical activity, women who reported current or past estrogen use at baseline experienced 1.8°(95% CI: 0.47, 3.2, p = 0.0081) or 1.3° (95% CI: 0.28, 2.35, p = 0.014) less kyphosis progression, respectively, compared with those who reported never using estrogen. Confirming results from the animal literature and recent findings in older men, we conclude that estrogen may play an important role in the development of age-related HK.

Disclosures: Gina Woods, None.

SU0459

Statement of Changes in Muscle Mass during Life by DXA. <u>Silvana Di Gregorio</u>[1], <u>Jorge Malouf</u>[2], <u>Luis Del Rio</u>*[3], <u>Beatriz Oliveri</u>[4]. [1]Ph, Spain, [2]Hospital de la Santa Creu i Sant Pau, Spain, [3]Cetir Centre Medical, Spain, [4]Mautalen, Salud e Investigación, Argentina

Aging is a physiological process that involves a progressive, generalized impairment of the functions of various systems. Muscle mass decreases especially in the lower extremities, leading to impairment in gait speed, stability and an increased fall risk. Thus, the clinical relevance of sarcopenia is widely recognized, but currently there is no universally accepted definition of this disorder. Muscle mass assessment, as the main item of the diagnostic definition of sarcopenia, needs to be feasible for both research and clinical practice, and accurate in older people. The study of Whole body composition by DXA allows the quantification of lean mass and the calculation of the appendicular fat-free mass of the upper and lower limbs. These measures divided by square body height gives us the patient's muscle mass index. Sarcopenia is diagnosed if it is >2 standard deviations (SD) below the sex-specific average in healthy young adults. There is a demographic in body composition variation due to physical and diet habits.

Objective: To evaluate the lean mass by DXA in healthy young adults, to obtain the normal values in our population, and ??to estimate the degree of lean mass lost in the elderly population to be able to identify those at risk.

Population and Methods: This is a retrospective cross sectional study. Subjects of both sexes stratified by decades of age were scanned with Hologic (965 subjects); iDXA (930subjects) and Prodigy (1110) scanners. The population was stratified by sex and decade of age , 20th-40th were used as reference category . Total Lean Mass (TLM); Legs Lean Mass (LLM); Appendicular Lean Skeletal Mass and its respective index related to (height –m-)2 , Appendicular Lean Skeletal Mass Index (ALSMI)and Lean mass index- LMI were calculated. T test was applied to establish statistical significance of media differences between the results obtained and those of the reference decade, p<0.00 was assumed as statistically significant.

Results : An increment of BMI in both genders was seen. A significant decrease in Lean mass absolute values (total, legs and extremities) along life was observed. Moreover, indices had a varied behavior (only men 80 and older had both indices lower than young men (p<0.000) regardless of the scanner used. This finding could be explained by the 10 cm height increase in Spanish population in the last century. Consequently the older subjects are compared to normal subjects, which are 10 cm higher that they were at similar age. This could explain that absolute values discriminate better the aging change.
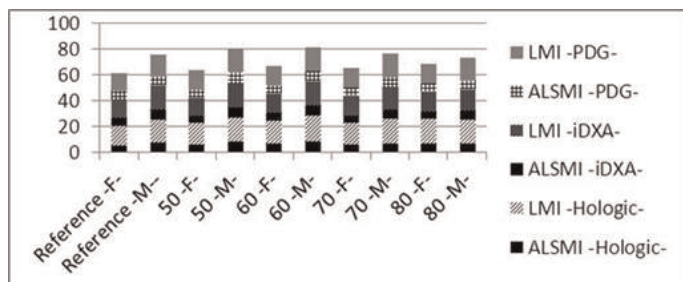
Evolution Changes

Disclosures: Luis Del Rio, None.

SU0460

How Muscle Force Shapes a Growing Mandible. <u>Donna Jones</u>*. Cincinnati Children's Hospital, USA

Alteration in muscle force brought about by a change in food texture produces shape differences in the mandible. The biochemical and cellular mechanisms by which this occurs, however, is not well understood. This research aims to empirically determine the specific anatomic locations affected by differential muscle milieus through three dimensional multivariate shape analyses to elucidate which cell populations are responsible for producing altered shape (pre-osteoblasts, osteoblasts, and/or osteocytes).

Prx1-CreER-GFP mice were grown with two different diet consistencies. Animals were weaned at 3 weeks of age to a hard (standard chow) or soft (DietGel7A) diet. Four males from each diet were sampled weekly from 4 to 12 weeks of age. After sacrifice, µCT scans and 3D reconstructions were produced and 12 landmarks were localized to capture mandibular shape differences among the two treatments. A generalized Procrustes superimposition was performed, and the full set of residuals that were regressed on age, within treatment groups. Principal components analysis was used to visualize the major dimensions of variation. Growth trajectories (i.e., the direction through shape space with age) for each treatment were calculated. To determine whether the trajectories between the treatments altered direction by more than expected by chance, the angle between them was calculated. By resampling and recalculating trajectories, 95% confidence intervals of variance in the data were established, indicating a statistically significant difference among treatments. Thin plate spline analyses were then employed to elucidate the anatomical pattern of shape change correlated with increasing age.

The diets produced differently shaped mandibles, with shape differences localized in the angle, position of the condyle, and length of the diastema. The three dimensional analyses also captured shape differences in the breadth of the mandible and integration with the skull base, missed in previous analyses. The shape trajectories differed significantly, with the greatest disparity generated before 6 weeks of age.

Histological analyses of the identified areas were used to identify differences in osteoblastogenesis (Prx1 expression), osteogenesis (increased mineralization; Von Kossa), and/or osteoclastic activity (TRAP). These results provide data essential to discovering the etiology of a variety of orofacial myofunctional disorders, including idiosyncratic mandibular hypoplasia.

Disclosures: Donna Jones, None.

SU0461

Intermittent Parathyroid Hormone Treatment Enhances Both Trabecular and Cortical Bone Modeling in Growing Rats. <u>Allison Altman</u>*[1], <u>Wei-Ju Tseng</u>[2], <u>Abhishek Chandra</u>[1], <u>Ling Qin</u>[1], <u>Xiaowei Liu</u>[1]. [1]University of Pennsylvania, USA, [2]University of Pennsylvania, USA

Intermittent parathyroid hormone (PTH), a potent bone anabolic agent, is a treatment candidate for stunted skeletal growth and adolescent idiopathic osteoporosis. However, the mechanism of PTH's anabolic effect on the growing skeleton is unclear. The objective of this study was to delineate the effect of PTH on bone modeling in young rats. We hypothesized that PTH would enhance bone modeling in the growing skeleton in both the trabecular (Tb) and cortical (Ct) compartments.

14 1-month-old rats were treated with either saline (Veh, n=6) or PTH (n=8, 80 µg/kg) daily for 12 days. A 3 mm region of the proximal tibia, distal to growth, plate was scanned by *in vivo* µCT (Scanco, 10.5 µm) every 4 days. By overlaying 2 sequential scans based on their unaltered Tb pattern (Fig 1), we visualized periosteal bone resorption and endosteal bone accrual due to rapid bone modeling. Linear growth rate was measured to be 0.25 mm/day. Therefore, the region imaged at day 12 represented newly generated bone tissue from the growth plate that did not exist on day 0.

Compared to day 0, PTH-treated primary spongiosa had 2.1, 1.1, and 1.4-fold increase in bone volume fraction (BV/TV), Tb number (Tb.N), and Tb thickness (Tb.Th), respectively, after 12 days. Similar increases were also found in the secondary spongiosa. In contrast, no change was found in the Veh-treated group after 12 days . Histology revealed a 22% wider growth plate height in the PTH group compared to Veh due to a 30% thicker hypertrophic zone. While the number of chondrocyte columns and bone spicules was similar between groups, bone spicules had greater mineral deposition in the PTH group, resulting in 44% thicker Tb.Th and 114% higher BV/TV in the primary spongiosa than the Veh group.

The Ct bone at the proximal tibia also thickened more in the PTH group (23%) than the Veh group (14%). This was primarily driven by endosteal bone formation and coalescence of trabecular bone into the cortex (Fig 1C). As a result, the cortex after PTH treatment was 31% less porous, and had a 22% greater polar moment of inertia compared to the Veh group.

These data demonstrate that, in addition to its well defined effect on bone remodeling, PTH also enhanced bone modeling on the growing skeleton. The modeling effect is apparent by the enhanced endochondral ossification, resulting in improved Tb quality in the primary spongiosa, and more effective Tb coalescence at the endosteal surface, resulting in improved Ct bone structure.
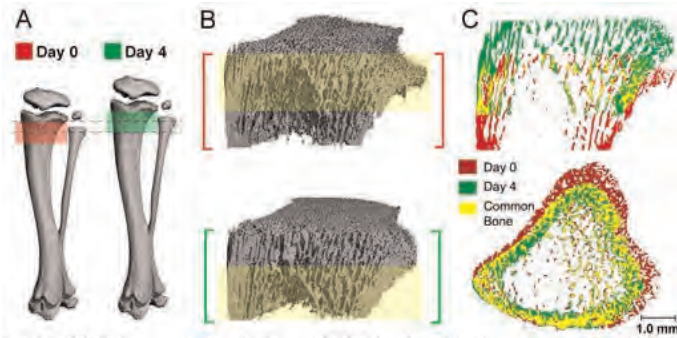
Fig. 1. (A&B) The same trabecular bone (highlighted in yellow) moves away from the growth plate due to longitudinal growth from day 0 (red) to 4 (green). (C) Overlaid 2D view of registered bone structure at days 0 (red) and 4 (green), where bone present in both images is shown in yellow (common bone), top-sagittal, bottom-coronal.

Fig 1

Disclosures: Allison Altman, None.

SU0462

C57Bl/6J mice have a lower bone mass than C3H/HeJ mice but are less sensitive to the skeletal effect of intrauterine stress by teratogens. Maria Raygorodskaya*[1], Arkady Torchinsky[2], Yankel Gabet[3], Eugene Kobyliansky[2], David Karasik[4]. [1]Faculty of Medicine, Bar Ilan University, Israel, [2]Department of Anatomy & AnthropologySackler Faculty of Medicine, Israel, [3]Department of Anatomy & AnthropologySackler Faculty of Medicine, Israel, [4]Hebrew SeniorLife; Bar Ilan University, USA

Establishment of normal structure and functioning of bones begins early in life. Several studies demonstrated that exposure of mouse embryo to different environmental factors, including teratogens at a sub-threshold dose, can detrimentally affect bone microarchitecture later in life. The purpose of our study was to investigate to what extent the genetic differences between mouse strains determine the skeletal sensitivity to 5-deoxy-2'-cidtine (5-AZA). 5-AZA is a teratogen capable of inducing phocomelia (absence of long bones of limbs).

We used mice of 2 inbred strains, C3H/HeJ (C3H, high bone mass) and C57Bl/6J (C57, low bone mass), males and females. Animals from these 4 groups (strain/sex) were 6-month old offspring of mice injected with 5-AZA at a sub-threshold dose (or saline for untreated controls) on day 10 of pregnancy. Sample size was 5 for each condition, except for treated C3H females group (n=4) totaling 39 mice. We collected the left femur from each mouse and compared treated and untreated mice within each of the strain/sex groups using micro-CT (Scanco Medical).

Analysis of bone mineral density within both strains did not reveal significant difference between treated and untreated mice, although vBMD was slightly lower in treated C3H (both males and females) compared to their respective controls. Treated C3H males demonstrated reduced cortical thickness (p<0.01), reduced trabecular number and increased trabecular spacing (p<0.05). On the other hand, treated C57 mice, both males and females, demonstrated no difference in trabecular number and spacing and a significant increase of trabecular thickness compared to the untreated groups (p<0.05).

Ultimately, this study demonstrates for the first time that the exposure to a sub-threshold teratogenic dose of 5-AZA during embryonic life causes femoral bone loss in the offspring of a mouse strain with high bone mass (C3H), but not in a low bone mass strain (C57). Furthermore, in mice with inherently weaker bones such an exposure seems to trigger some compensatory mechanisms, that is reflected in thickening of bone trabeculae.

Disclosures: Maria Raygorodskaya, None.

SU0463

Ephrin Reverse Signaling Mediates Palatal Fusion and Epithelial-to-Mesenchymal Transition Independently of Tgfß3. Maria Serrano*[1], Jingpeng Liu[2], Kathy Svoboda[1], Ali Nawshad[2], M. Douglas Benson[3]. [1]Baylor College of Dentistry, USA, [2]University of Nebraska Medical Center College of Dentistry, USA, [3]TA&M HSC Baylor College of Dentistry, USA

The mammalian secondary palate forms from shelves of epithelia-covered mesenchyme that meet at midline and fuse. Failure of the midline epithelial seam (MES) to degrade blocks fusion and causes cleft palate. It was previously thought that transforming growth factor ß3 (Tgfß3) is required to initiate fusion. Members of the Eph tyrosine kinase receptor family and their membrane-bound ligands, the ephrins, are expressed on the MES. The purpose of this study was to discover if Eph/ephrin signaling is required for mammalian palatal fusion. We discovered that activation of ephrin reverse signaling (where the ephrin acts as a receptor and transduces signals

from its cytodomain) was sufficient to cause fusion in cultured mouse palates and epithelial-to-mesenchymal transition (EMT) in palatal epithelial cells, even in the absence of Tgfß3 signaling. We cultured mouse palates in the presence of either a blocking antibody against Tgfß3 or an inhibitor of the TgfßrI serine/threonine receptor kinase. Fusion was abolished by both treatments, but was significantly rescued by the addition of EphB2/Fc recombinant protein to activate ephrin reverse signaling. Treatment with Tgfß3, however, was not able to rescue fusion when ephrin signaling was blocked. Cultured palate epithelial cells traded their expression of epithelial cell markers for that of mesenchymal cells after treatment with EphB2/Fc and became motile. They concurrently increased their expression of the EMT-associated transcription factors Snail, Sip1, and Twist1. These data confirm that ephrins direct palatal fusion in mammals and activate a gene expression program not previously associated with reverse signaling.

Disclosures: Maria Serrano, None.

SU0464

HDAC inhibitor MS-275 could attenuate phenotypes of cleidocranial dysplasia syndrome in Runx2^{+/-} mice through the activation of Runx2 activity. Han-sol Bae*[1], Won-Joon Yoon[2], Young-Dan Cho[3], Rabia Islam[4], Hea-rim Shin[1], Bong-Soo Kim[2], Kyung-Mi Woo[2], Jeong-Hwa Baek[5], Hyun-Mo Ryoo[6]. [1]Seoul National University, South Korea, [2]Seoul National University School of Dentistry, South Korea, [3]Seoul National University, South Korea, [4]School of Dentistry, Seoul National University, South Korea, [5]Seoul National University, School of Dentistry, South Korea, [6]Seoul National University School of Dentistry, South Korea

Runx2 is essential for osteogenesis and bone growth. Cleidocranial dysplasia (CCD) is an autosomal-dominant skeletal disorder caused by haploinsufficiency of Runx2. Aplastic or hypoplastic clavicles and delayed suture closure are major symptoms of CCD. Previous reports indicated that CCD phenotypes developed when Runx2 mRNA level is less than 70% that of WT littermates. We previously identified that HDAC inhibitors (HDACi) stimulated RUNX2 protein stability and its transcriptional activity. Specific aim of this study was to examine whether genetic Runx2 haploinsufficiency could be overcome by an HDACi. Runx2^{+/+} and Runx2^{+/-} mice were mated and pregnant mice were injected once with MS-275 or vehicle at 14.5 d.p.c. The MS-275 neither caused pregnant mice to die or show toxic behaviors nor did it affect littermate numbers. MS-275 remarkably improved most of the skeletal deformities associated with Runx2^{+/-}; cranial bone development and clavicle maturation, spinal bone maturations, mandible growth and ribcage development. The recovered CCD phenotypes were maintained at postnatal stage. In the in vitro study, MS-275 has positive effects on osteoblasts differentiation. MS-275 stimulated bone marker gene expression in primary calvaria cell culture. Primary calvarial osteoblast from Runx2^{+/-} mice showed a significantly lower Runx2 protein level than that from WT mice. Treatment of MS-275 increased Runx2 protein level in both genotype cells. In addition, Runx2 protein level of MS-275-treated Runx2^{+/-} mice was increased quite significantly compared to that of untreated WT mice. Lastly, Runx2 transacting activity was also increased by the MS-275 treatment both in Runx2^{+/+} and Runx2^{+/-} calvarial osteoblasts. Taken together, these results indicated that MS-275 could be applied for the intervention of CCD phenotype development. Moreover, the mechanism of action we identified in this study strongly suggests that HDACi could also be applied for bone regeneration.

Disclosures: Han-sol Bae, None.

SU0465

Involvement of PiT-1 (Slc20a1) function during endochondral ossification. Manisha Yadav*[1], Pia Kuss[2], Campbell Sheen[2], Laurent Beck[3], Colin Farquharson[4], Jose Luis Millan[1]. [1]Sanford-Burnham Medical Research Institute, USA, [2]Sanford Burnham Medical Research Institute, USA, [3]Inserm U791, France, [4]Roslin Institute, University of Edinburgh, United Kingdom

Mineralization of cartilage and bone occurs by a series of physicochemical and biochemical processes that together facilitate the deposition of hydroxyapatite in specific areas of the extracellular matrix (ECM). We have shown that tissue-nonspecific alkaline phosphatase (TNAP) plays a crucial role in restricting the concentration of extracellular inorganic pyrophosphate (PPi), a mineralization inhibitor, to maintain a Pi/PPi ratio permissive for normal bone mineralization. We have also shown that together with TNAP, PHOSPHO1 is required for proper bone mineralization. Using genetically modified mice we have found that 1) the lack of TNAP (Alpl-/- mice) leads to reduced MV calcification but mice are born with a normally mineralized skeleton and only develop hypophosphatasia at postnatal day 6. 2) The lack of PHOSPHO1 (Phospho1-/- mice) also leads to reduced MV calcification and hyperosteoidosis and the born pups show fractures in their curved long bones and in the rib cage as early as post-natal day 1. Scoliosis is a prominent feature from postnatal day 10 onwards. 3) The [Alpl-/-; Phospho1-/-] double knockout mice are embryonic lethal and the E16.5 embryos, show complete absence of skeletal mineralization and MVs devoid of mineral.

We hypothesized that HA crystals appear inside the MVs favored by Pi accumulation resulting from a dual mechanism, i.e. PHOSPHO1-mediated intra-

vesicular production and transporter-mediated influx of Pi produced extra-vesicularly primarily by TNAP's ATPase activity. To test this hypothesis, we generated mice with a conditional ablation of PiT-1, the major Pi-transporter in chondrocytes, in the Phospho1-/- background, [Phospho1-/-; PiT-1flox/flox; Col2a1-Cre]. While mice with a conditional deletion of PiT-1 in chondrocytes, [PiT-1flox/flox; Col2a1-Cre], did not show any phenotypic abnormalities at 1 month of age, severe skeletal deformities were observed in the [Phospho1-/-; PiT-1flox/flox; Col2a1-Cre] double knockout mice, which were more pronounced than those in the Phospho1-/- mice. Histological analysis showed growth plate abnormalities with a shorter hypertrophic chondrocyte zone in the double knockout samples and extensive unmineralized osteoid was observed both in the vertebrae, tibial and femoral sections. These data support the involvement of PiT-1 in the initiation of endochondral ossification.

Supported by grant AR053102 from the National Institutes of Health, USA.

Disclosures: Manisha Yadav, None.

SU0466

Mechanism of Longitudinal Overgrowth of Femur of Developing Rat Following Circumferential Periosteal Division. Shinjiro Takata*. Tokushima National Hospital,National Hospital Organization, Japan

We showed the mechanisms of longitudinal overgrowth of femur of developing rat aged 8 weeks following circumferential periosteal division (CPD). The previous study have shown that CPD of rat tibia produces an increase in its growth rate and in the activity of both the proliferative and hypertrophic zones (Taylor FJ et al. J Anat 151:221-231,1987).

Eigthteen male Wistar rats aged 8 weeks were used for this study. Periosteum of diaphysis of the right femur was divided circumferentially (CPD group), and the left femur was control (Control group). Rats were sacrificed 4 weeks after CPD. The longitudinal length of femur (n=6) and rate of longitudinal growth and bone turnover by bone histomorphometry were compared between CPD group and Control group 4 weeks after CPD (n=6). Histological and immunohistological analyses in distal growth plate of femur were performed with hematoxylin and eosin (HE), alcian blue (AB), tartrate-resistant acid phosphatase (TRAP), collagen X, indian hedgehog (IHH), parathyroid hormone-related protein (PTH-rP), runt-related transcription factor 2 (Runx2) staining.

Longitudinal length of rat femur of CPD group and Control group were 39.4 ± 1.2 mm and 38.5 ± 0.8mm, respectively (p=0.0086), showing that CPD for 4 weeks produced an approximately 2.5% increase of rat femur compared with Control group.

Bone histomorphometry shows that the rate of longitudinal growth of femur of CPD group and Control group 4 weeks after CPD was 92.3 ± 5.3 and 54.4 ± 4.6 μm/day, respectively (p<0.0001). Mineral apposition rate of femora of CPD group and Control group 4 weeks after CPD was 3.90 ± 0.38 and 3.07 ± 0.25 μm/day, respectively (p=0.0004). Osteoclast surface/bone surface of CPD group and Control group 4 weeks after CPD was 13.1 ± 1.0 and $9.1 \pm 1.8\%$, respectively (p<0.0001).

HE and AB staining analysis in distal growth plate of rat femur showed an increased number of hypertrophic chondrocytes and width of hypertrophic zone of the distal growth plate of rat femur of CPD group compared with Control group. Immunohistogical expression of Runx2 and IHH of CPD group in the growth plate was higher than that of Control group.

The major finding of this study was that CPD of diaphysis of rat femur stimulates endochondral ossification to produce longitudinal overgrowth. The results suggest that periosteum of tubular bone plays an critical role in endochondral ossification of growth plate.

Disclosures: Shinjiro Takata, None.

SU0467

Osterix-Cre Transgene Causes Craniofacial Bone Development Defect. Li Wang*[1], Fei Liu[2]. [1]School of dentistry, University of Michigan, USA, [2]University of Michigan School of Dentistry, USA

The Cre/loxP system has been widely used to generate bone-targeted gene knockout mice. One of the most widely used Cre mouse lines that targets osteoblasts is Osx-GFP::Cre (Osx-Cre) mouse line, which contains a tTA and a tetracycline responsive element-controlled GFP/Cre fusion protein under the control of osterix (Sp7) promoter. Recently, defective intramembranous bone development phenotype was reported in several conditional knockout mouse models with Osx-Cre. However, it is unknown to what extent that Osx-Cre transgene itself may contribute to these defects. In this study, we investigated the effect of Osx-Cre on early postnatal bone development (from birth to day 21). Osx-Cre mice exhibited reduced body weight at all time-points except at birth. Osx-Cre mice and control mice at different ages (at birth, p7, p14 and p21) were analyzed by whole skeletal staining. Despite normal development pattern in the axial and appendicular bones, Osx-Cre mice showed severe hypomineralization in parietal, frontal, and nasal bones and the integrity of cranial sutures were also compromised compared to control mice at birth. Among the craniofacial bones, the nasal bone had the severest defect shown by 30.5% (N=10, SD=6.21%) decrease of the mineralized area at birth. The defects became less severe when mice grew older. At postnatal day 21, the major defects disappeared while sporadic hypomineralization spots were still present. Interestingly, Doxycycline treatment could completely eliminate the craniofacial defects at birth, indicating that the Cre expression may be responsible for the phenotype. To determine the potential effect of Osx-Cre transgene on osteoblast differentiation, we isolated primary calvaria

osteoblasts from Osx-Cre and control neonatal mice and found that Osx-Cre transgene did not affect osteoblast differentiation and mineralization *in vitro* (by Day 7 ALP staining and Day 21 AR staining). In conclusion, Osx-Cre transgene can cause craniofacial bone defect at early development stages and this defect is gradually resolved at later stages. In addition, Osx-Cre does not affect in vitro osteoblast differentiation. This study reinforces the necessity of including Cre transgenic littermate controls for in vivo phenotyping and validates the use of primary calvarial osteoblasts isolated from CKO mice with Osx-Cre for in vitro differentiation study.

Disclosures: Li Wang, None.

SU0468

Quantitative Micro-CT Analysis of Bone in Zebrafish: Accessing an Untapped Resource. Julia Charles*[1], Katrin Henke[2], Kelly Tsang[3], Ruby Russell[4], Matthew P. Harris[2], Jeffrey Duryea[5], Antonios Aliprantis[6]. [1]Brigham & Women's Hospital & Harvard School of Medicine, USA, [2]Department of Genetics Harvard Medical School, Department of Orthopedics, Boston Children's Hospital, USA, [3]Department of Medicine, Brigham & Women's Hospital & Harvard Medical School, USA, [4]. Department of Radiology, Brigham & Women's Hospital, USA, [5]Department of Radiology, Brigham & Women's Hospital, USA, [6]Brigham & Women's Hospital, USA

Zebrafish are a commonly used research model to investigate the genetic and developmental causes of disease. Similar to higher vertebrates, bone formation and remodeling in zebrafish rely on the coordinated activity of osteoclasts, osteoblasts and osteocytes. Given this, many of the key genes regulating bone differentiation are likely conserved. Several zebrafish mutants correlating to human bone disorders (e.g. osteogenesis imperfect, Raine syndrome) recently identified in forward genetic screens supports this concept. However, the use of zebrafish (and other small laboratory fish models) to investigate skeletogenesis and skeletal dysplasias has been limited by the lack of systematic analytical techniques to assess bone quality and shape. We performed mutagenesis screens in the zebrafish and have identified a large number of mutants having specific defects in skeletal differentiation and patterning. In order to characterize these mutants, we set out to develop a standardized micro-computed tomography (μCT) analysis method to quantify bone parameters at two anatomic sites: the parasphenoid bone of the skull base and the last precaudal and first 2 caudal vertebral bodies. Ontological series of male and female siblings at 3, 5 and 10 months of age (n=5) were imaged by μCT at 6 micron resolution (Scanco μCT35). Scanco software was utilized to measure parasphenoid length, volume, and mg HA/mm^3. Vertebrae were analyzed using custom software to determine length, bone volume, and radius of vertebral opening. No sex difference was apparent, thus males and females were combined for analysis. We show that these measures are robust, as within group variance is low and show consistent isometry during development allowing for within and between strain comparisons (Fig.1). As a proof of the utility of this application, analysis of the hypermineralization mutant *Khronos* identified significant differences in bone density and size, demonstrating the utility of our standardized analysis methods for quantification of skeletal phenotypes in zebrafish. These techniques can be expanded to include quantitative analysis of vertebral morphology and regional variation in mineralization, as well as to characterize more subtle skeletal phenotypes that qualitative assessment by Alizarin red staining cannot provide. These analyses lay the foundation to tap into the power of zebrafish to better understand the genetic and cellular mechanisms regulating skeletal biology in vertebrates.
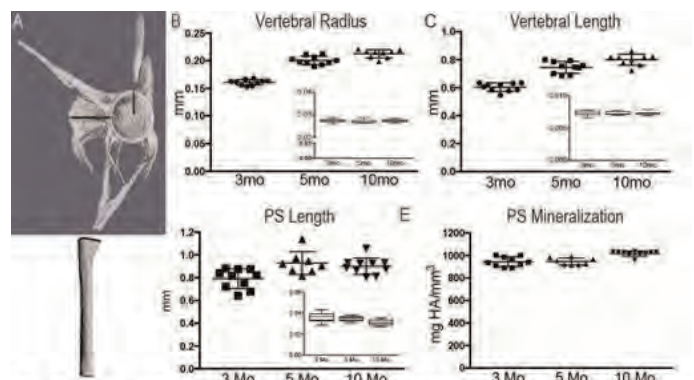
Fig. Standardized Quantitation Method for Zebrafish Bone. A. Representative images of vertebrae (top) and parasphenoid (PS) showing measurement parameters (black lines). **B-C.** Quantitative analysis of first caudal vertebrae demonstrates age related increase in (B) radius and (C) length but stable ratio of radius/length:standard length (insets) consistent with isotropic growth; 1 way ANOVA p<0.0001 for radius and length. **D-E.** Analysis of parasphenoid similarly demonstrates age dependent increases in (D) length and (E) mineralization as determined by mg HA/mm^3 of bone volume; 1 way ANOVA p<0.005 for each.

Fig. Micro-CT Analysis of Zebrafish Bone

Disclosures: Julia Charles, None.

SU0469

Stat3 signaling modulates the osteochondro transcription factor Sox9 in vivo to influence endochondral ossification and is important in the pathology of campomelic dysplasia. Michael Hall*[1], Alan Perantoni[2]. [1]National Cancer Institute, USA, [2]National Cancer Institute, USA

Campomelic dysplasia (CD) is an often-fatal human congenital abnormality characterized by a hallmark bowing of the long bones and features such as short stature, cleft palate, and laryngotracheomalacia. The pathology of CD is frequently underpinned by mutations in and around the coding region of the Sry-box gene Sox9, a master regulator of multipotent osteochondro progenitor cells. Beyond this, little is known about the normal regulation of Sox9 or, in cases where Sox9 mutations have not been detected, if CD is also caused by alterations in the control of Sox9 expression. To elucidate novel regulators of Sox9, we analyzed its proximal promoter region and discovered several potential Stat DNA response elements (DRE). Stat3 has been implicated in stem cell maintenance, and disruption of Stat3 signaling through deletion of leukemia inhibitory factor (LIF) receptor causes a defect in bone mineralization, suggesting the possible involvement of Sox9. Indeed, we found that a Sox9 promoter-driven reporter is activated in cells by oncostatin M in a Stat3-dependent fashion. Further, reporter activation is mediated by the Stat DREs, and Stat3 physically binds the promoter of Sox9. In the developing mouse, Stat3 is expressed in somites and early limb buds, mesodermal compartments where Sox9 mediates endochondral ossification of vertebrae and limbs, respectively. We engineered mesodermal Stat3 loss of function mutant mice, which, as neonates, yielded a phenotype consistent with CD, i.e., limb bowing, labored breathing, and mortality. The histology of Stat3 mutants was also consistent with Sox9 heterozygous mutants, including shortening of the long bones, and expansion of the hypertrophic chondrocyte zone, suggesting modulation of Sox9 function. Furthermore, Sox9 levels were decreased in Stat3 mutant mice, as was the direct target Col2a1, a marker for a functional decrease in Sox9 in vivo. Other skeletal features such as reduced trabecular mineralization, regional restriction and death of osteoblasts, and elevated osteoclast activity were also observed, indicating a critical role for Stat3 in skeletogenesis. We posit that Stat3 instructs bone development by fine-tuning Sox9 expression in mesenchymal stem cells to drive the differentiation of osteochondro progenitors. These findings demonstrate for the first time a role for Stat signaling in regulating SRY-box factors in vivo and provide a potential alternative mechanism for CD where Sox9 mutations are not detected.

Disclosures: Michael Hall, None.

SU0470

Targeted Deletion of Atg5 or Atg7 in Chondrocytes Impairs Cell Viability and Bone Growth. Karuna Vuppalapati*[1], Thibault Bouderlique[2], Vitaliy Kaminskyy[3], Phillip Newton[2], Lars Sävendahl[4], Boris Zhivotovsky[3], Andrei Chagin[5]. [1]Department of Physiology & Pharmacology, Karolinksa Institutet, Sweden, [2]Department of Physiology & Pharmacology, Karolinska Institutet, Sweden, [3]Institute of Environmental Medicine, Karolinska Institutet, Sweden, [4]Department of Women's & Children's Health, Karolinska Institutet, Sweden, [5]Karolinska Institutet, Swe
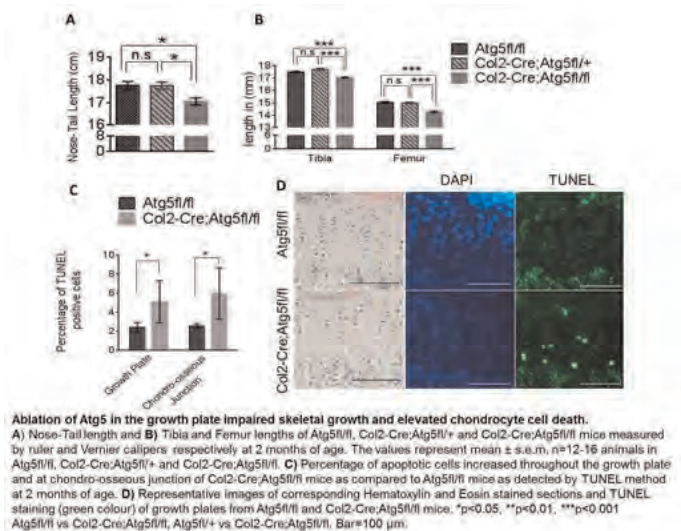
Background: Longitudinal bone growth takes place in the epiphyseal growth plate, a cartilage structure located in the ends of long bones. The growth plate consists of chondrocytes traversing from undifferentiated (resting zone) to terminally differentiated (hypertrophic zone) stage. Chondrocytes in the middle of the growth plate are hypoxic and nutritionally depleted due to the avascular nature of the growth plate. Autophagy is activated during nutritionally depleted or hypoxic conditions in order to facilitate cell survival Autophagy is an intracellular catabolic process of lysosome dependent recycling of protein complexes and intracellular organelles.

Objective and hypotheses: We hypothesized that chondrocytes may utilize autophagy for their survival.

Methods: To explore the role of autophagy in chondrocyte survival and longitudinal bone growth we generated mice with cartilage-specific ablation of either Atg5 (Atg5 cKO) or Atg7 (Atg7 cKO) by crossing Atg5 or Atg7 floxed mice with cartilage-specific collagen type 2 promoter driven Cre. To delineate the underlying mechanisms we employed *ex vivo* cultures of human growth plate tissue, mouse metatarsal bones and the RCJ3.IC5.18 rat chondrogenic cell line and exposed them to autophagy inhibitors Bafilomycin-A1 (Baf) or 3-Methyladenine (3MA).

Results: Both Atg5 cKO and Atg7 cKO mice showed growth retardation associated with enhanced chondrocyte cell death and decreased cell proliferation. Furthermore, pharmacological inhibition of autophagy by Baf or 3MA promoted cell death in cultured slices of human growth plate tissue. Baf or 3MA impaired metatarsal bone growth associated with activation of caspase-3 and caspase-9 as well as massive cell death. Similarly, treatment of RCJ3.IC5.18 chondrogenic cells with Baf also showed massive cell death as well as caspase-3 and caspase-9 processing. This effect was associated with cytochrome C release.

Conclusion: Altogether our data suggest that autophagy is important for chondrocyte survival and inhibition of this process leads to stunted growth and caspase dependent death of chondrocytes.

Ablation of Atg5 in the growth plate impaired skeletal growth and elevated chondrocyte cell death.
A) Nose-Tail length and B) Tibia and Femur lengths of Atg5fl/fl, Col2-Cre;Atg5fl/+ and Col2-Cre;Atg5fl/fl mice measured by ruler and Vernier calipers respectively at 2 months of age. The values represent mean ± s.e.m. n=12-16 animals in Atg5fl/fl, Col2-Cre;Atg5fl/+ and Col2-Cre;Atg5fl/fl. C) Percentage of apoptotic cells increased throughout the growth plate and at chondro-osseous junction of Col2-Cre;Atg5fl/fl mice as compared to Atg5fl/fl mice as detected by TUNEL method at 2 months of age. D) Representative images of corresponding Hematoxylin and Eosin stained sections and TUNEL staining (green colour) of growth plates from Atg5fl/fl and Col2-Cre;Atg5fl/fl mice. *p<0.05, **p<0.01, ***p<0.001 Atg5fl/fl vs Col2-Cre;Atg5fl/fl, Atg5fl/+ vs Col2-Cre;Atg5fl/fl. Bar=100 µm.

Ablation of Atg5 in the growth plate impaired skeletal growth and elevated chondrocyte cell death

Disclosures: Karuna Vuppalapati, None.

SU0471

The Transcriptional Regulator Jab1 Is Essential for Osteoblast Differentiation *In Vivo*. Lindsay Bashur[1], Zhijun Chen[2], Shunichi Murakami[1], Guang Zhou*[1]. [1]Case Western Reserve University, USA, [2]Case Western Reserve University, USA

The transcriptional regulator Jab1 controls cell proliferation, apoptosis, and differentiation in diverse developmental processes. Still very limited, however, is our understanding of Jab1's physiological role in skeletal development. Osteoblast differentiation is a finely-tuned process governed by a spatiotemporal-specific transcriptional circuit. Interestingly, *Jab1* knock-down in primary osteoblasts resulted in impaired osteoblast differentiation. To elucidate Jab1's function at successive steps of osteogenesis *in vivo*, we mated *Jab1floxlflox* mice with various *Cre* drivers to ablate *Jab1* expression at different stages of osteoblast differentiation. To determine the role of Jab1 during early limb development, we generated *Jab1floxlflox*; *Prx1-Cre* conditional knockout (*Prx1-Cre/cKO*) mutant mice in which *Jab1* was deleted in the osteochondral progenitor cells of the limb buds. At E18.5, *Prx1-Cre/ cKO* mutants exhibited significantly shorter limbs with: very few hypertrophic chondrocytes, much smaller primary ossification centers with reduced von Kossa staining, and significantly decreased expression of *Runx2* and *Col1a1*. Thus, Jab1 is required for early differentiation of osteochondral progenitor cells. To determine a more specific role of Jab1 in osteoblasts, we generated *Jab1floxlflox*; *Osx-Cre* conditional knockout (*Osx-Cre/cKO*) mutant mice in which *Jab1* was deleted in the osteoblast precursor cells. *Osx-Cre/cKO* mutants appeared grossly normal in size at birth. However, histological study revealed greatly reduced trabecular thickness and fewer trabecular areas in newborn *Osx-Cre/cKO* mutant long bones. Furthermore, *Osx-Cre/cKO* mutant long bones grew less after birth and all the mutants died before weaning age. Thus, Jab1 is likely to be required for the proliferation and function of osteoblast precursor cells. Finally, to specifically target differentiating osteoblasts, we generated *Jab1floxlflox*; *Col1a1-Cre* conditional knockout (*Col1a1-Cre/ cKO*) mutant mice, using a *2.3 Col1a1-Cre* driver. *Col1a1-Cre/cKO* mice were viable, fertile, and showed no gross phenotype until 12-month age, indicating that Jab1 plays a less prominent role at later stage of osteoblast differentiation. In summary, our study revealed the crucial and stage-specific role of Jab1 in osteoblast differentiation. We are further characterizing these novel *Jab1* mutant models to elucidate the underlying mechanism of Jab1's function during osteogenesis.

Disclosures: Guang Zhou, None.

MO0001

Biological and clinical benefits of a systematic protocol of bone evaluation and treatment in kidney transplantation. Rose-Marie Javier*[1], Clotilde Kiener[2], Peggy Perrin[2], Sophie Caillard[2], Bruno Moulin[2]. [1]Department of Rheumatology, University Hospital, France, [2]Nephrology-Transplantation Department , University Hospital Strasbourg, France

Introduction: Over the last years, clinical practice for Chronic Kidney Disease-Mineral and Bone Disorders has changed. The impact of a systematic bone evaluation before transplantation and 25OHD normalization, cinacalcet if needed and prophylactic bisphosphonates treatment in renal transplant recipients with T-score lower –2.5 has not been evaluated yet, in particular on the incidence of fractures.

PATIENTS AND METHODS: We have analyzed the mineral and bone disorders during the first posttransplant year in 141 patients who underwent kidney transplantation between 2009 and 2011 in our center compared to 152 other patients transplanted five years earlier (2004-2006). Biochemical parameters were prospectively determined before transplant, at M3 and M12 and in our routine pretransplant evaluation, bone mineral density was systematically measured (Hologic Delphi densitometer) at lumbar spine and hip. Since February 2006, a systematic scheme of 25OHD normalization is applied. In the presence of a T-score<–2.5 and/or osteoporotic fractures before transplant, our local practices recommended a preventive treatment with pamidronate (two 30 mg intravenous infusions 15 and 45 days after transplantation) in the absence of adynamic bone and severe kidney dysfunction. All the collected clinical fractures are documented after a clinical rheumatologic assessment (RMJ).

Results: At time of transplantation, hyperparathyroidism rate and vitamin D insufficiency have decreased in the more recent cohort (PTH>585ng/L in 13.2% versus 28%; p=0.002 and 25OHD 28.1 versus 14.3 ng/mL; p<0.001). In the first posttransplant year, 25OHD is twice higher and near to 30 μg/L with a better control of HPT at M3 and M12. At one year, the incidence of fractures is three-fold lower (3.1% versus 9.1%, p=0.0036) and patients with pretransplant OP were more treated by BP. Nevertheless, fracture risk seems to be higher in subjects with pretransplant osteopenia in the recent cohort.

Conclusion: The evolution of our clinical practice have led to reduction in fracture risk, persistent hyperparathyroidism and vitamin D insufficiency in the first posttransplant year. However, we have to reconsider the management of renal transplant recipients with osteopenia.

Disclosures: Rose-Marie Javier, None.

MO0002

Bone Adiposity and Magnetic Resonance Spectroscopy in Kidney Disease. Ranjani Moorthi*[1], Chen Lin[2], Kristen Ponsler-Sipes[2], Sharon Moe[1]. [1]Indiana University School of Medicine, USA, [2]Indiana University School of Medicine, USA

Chronic Kidney Disease (CKD) is an important public health problem affecting more than 26 million Americans. Fractures are 2-4.4 times more prevalent in CKD compared to the general population. Histologically, bone remodeling is abnormal in CKD with extremes such as adynamic bone disease and osteitis fibrosa cystica. However, changes within the bone marrow are not well characterized in CKD. We propose that there is excessive fat deposition in the marrow of patients with CKD and that this can be demonstrated by magnetic resonance spectroscopy (MRS). Our project aims were to 1) determine reproducibility of bone marrow fat assessment in CKD patients by MRS 2) determine differences in bone marrow fat% at various skeletal sites in CKD and 3) in a pilot study, compare marrow fat% in CKD patients compared to matched controls with normal kidney function.

Methods: This is a case-control study of 5 subjects with CKD and 5 age, sex and race matched controls. MRS of the iliac crest, the tibia and L2-4 vertebrae were performed. Each subject underwent 2 scans per site with repositioning between measurements. The coefficient of repeatability for marrow fat% at each site was calculated. Graphs were plotted to compare fat content at different skeletal sites. T-tests were used to compare marrow fat% between CKD subjects and controls at each location.

Results: The mean age of CKD subjects in the study was 64.3+6.3 years and mean eGFR was 25.6+7.8 ml/min. In CKD subjects, 58% of marrow was composed of fat in the L2-3 area, as compared to most of the tibia(86%). The coefficient of repeatability was low at all sites in CKD, ranging from 2.4-13% (see Table). There was no significant difference between CKD subjects and controls in bone marrow fat% at any of the sites studied.

Conclusion: Bone marrow fat assessment can be performed at the iliac crest (the site of traditional histomorphometry) in patients with CKD by MRS and it is highly reproducible at all skeletal sites. In CKD, patterns of marrow fat deposition are different at the tibia, vertebrae and iliac crest. MRS is suitable to study changes in marrow fat over time at various skeletal sites in CKD patients. Preferential differentiation of adipocytes in bone marrow from mesenchymal stems cells may lead to alterations in bone remodeling in patients with CKD as well as in normal aging. This needs to be explored in future studies that relate bone quality and marrow fat assessment in CKD compared to healthy controls..

Skeletal Site	CKD		Controls	
	Mean+SD (%)[¶]	COR (%)*	Mean+SD (%)[¶]	COR (%)*
L2	58.1+11.2	13.0	47.5+9.9	4.9
L3	58.6+10.7	6.1	51.4+8.9	6.6
L4	60.9+11.4	3.5	51.8+9.9	6.6
Iliac crest	59.4+15.5	5.5	52.4+8.8	7.1
Tibia	86.4+1.35	2.4	84.8+2.6	3.9

*Coefficient of Repeatability (COR) is the value under which the difference between any two repeat measurements on the same patient acquired under identical conditions should fall with 95% probability
[¶]Paired t-test for marrow fat% between CKD and controls at all sites were not significant at a level of 0.05

Marrow fat% at Different Sites in CKD and Controls by MRS and Coefficients of Repeatability

Disclosures: Ranjani Moorthi, None.

MO0003

Determination of FGF23/FGFR3 Interfacing Domains; Insights into Developing Novel Therapeutics. Abdulhafez Selim*[1], Mohamed Hafez[2], Mourad Ali[3], Osama Yasin[3], Tarek El-Ghandour[3]. [1]Center for Chronic Disorders of Aging, PCOM, USA, [2]Inspire, Egypt, [3]Ain Shams University, Egypt

Fibroblast growth factor 23 (FGF23) is a phosphaturic factor that suppresses both sodium-dependent phosphate transport and production of 1,25-dihydroxyvitamin D [1,25(OH)$_2$D] in the proximal tubule. *In vitro studies indicated that FGF23 can activate FGFR1, 3, and 4. Liu et al demonstrated that neither* FGFR3 nor FGFR4 is the principal mediator of FGF23 effects in the proximal tubule, and co-localization of FGFR1 and Klotho suggests that the distal tubule may be an effector site of FGF23 through the FGFR1.

Gutierrez et al, demonstrated that in chronic kidney disease (CKD), circulating FGF-23 levels gradually increase with declining renal function such that by the time patients reach end-stage renal disease, FGF23 levels can be up to 1000-fold above the normal range. Wahl et al demonstrated that it is also possible that markedly increased FGF23 levels in CKD could contribute directly to tissue injury in the heart and vessels. Moreover, it has been hypothesized by Razzaque et al, that FGF-23 at very high serum concentrations (as observed in CKD patients) may exert certain nonspecific and presumably adverse effects through low-affinity, Klotho-independent binding to FGF-R, for example, on endothelial cells. Therefore, it is of great importance to characterize FGF23 interactions with other receptors including FGFR3 and FGFR4.

Since no previous studies characterized the FGF23/FGFR3 or FGF23/FGFR1 complexes, we decided to address this task. Three dimensional models for the complexes were constructed and validated. This was followed by protein-protein interface analytical studies. The FGF23/FGFR3 complex interface data showed that four regions of FGF23 (A, B, C and D) were involved in the interface. In contrast to that, the FGF23/FGFR1 interface data revealed that three regions only (A, B and C) were involved in the interaction. Data suggested that region D and its complementary sequences are attractive candidates for drug development.These findings could pave the way for designing novel specific inhibitors including peptides, mono-clonal antibodies, or small molecules. Those inhibitors could be used to prevent and/or reduce FGF23-related complications in CKD patients.
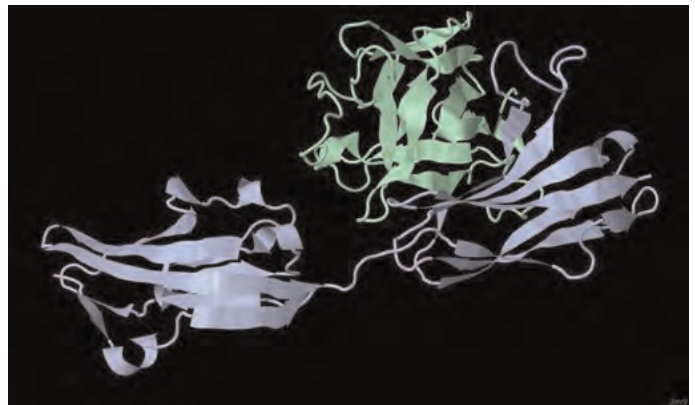
FGF23-R3 Complex: Ligand is green and Receptor is blue

Disclosures: Abdulhafez Selim, None.

MO0004

Low Bone Mineral Density and Fractures in Stages 3-5 CKD: An Updated Systematic Review and Meta-Analysis. Roxana Bucur*[1], Dilshaan Panjwani[2], Lucy Turner[3], Tamara Rader[4], Sarah West[5], Sophie Jamal[6]. [1], Canada, [2]Women's College Research Institute, Women's College Hospital, The University of Toronto, Canada, [3]Ottawa Hospital Research Institute, Canada, [4]Cochrane Musculoskeletal Group, Centre for Global Health, University of Ottawa, Canada, [5]University of Toronto, Canada, [6]The University of Toronto, Canada

Chronic kidney disease (CKD) is associated with an increased risk of fracture. The utility of dual energy x-ray absorptiometry (DXA) to assess fracture risk in CKD is unknown.

We performed an updated meta-analysis and systematic review of published studies (from 1946 to April 12, 2013) that reported on the association between DXA and fracture (morphometric spine or clinical non-spine) in predialysis and dialysis CKD. We identified 2894 potential publications, retrieved 292 for detailed review and included 13 in our analysis. There were a total of 1785 subjects; 989 men. All but one study was cross-sectional and 3 reported on the ability of DXA to discriminate fracture status in predialysis CKD. Results were pooled using a random effects model and statistical heterogeneity was assessed using the I2 statistic.

BMD was statistically significantly lower at the femoral neck, lumbar spine, the 1/3 and ultradistal radius in subjects with fractures compared to those without, regardless of dialysis status. For example, compared to those without fractures, femoral neck BMD was 0.06 g/cm2 lower in dialysis subjects with fractures and 0.102 g/cm2 lower in predialysis subjects with fractures. Lumbar spine BMD was 0.05 g/cm2 lower in dialysis subjects and 0.108 g/cm2 lower in predialysis subjects with fractures compared to those without. In predialysis subjects, BMD at the total hip was lower in those with fractures but there was no difference in BMD at the total hip by fracture status in those on dialysis. BMD at the mid radius was lower in dialysis subjects with fractures compared to those without fractures and was not reported in predialysis subjects. We performed further subgroup analyses comparing pooled effects across studies that adjusted for age and weight. Data allowed for BMD at the femoral neck, total hip and lumbar spine to be compared. We found no difference in the overall effect for any these sites, regardless of dialysis status. Our meta-analysis was limited to studies with small numbers of subjects and even smaller numbers of fractures. All of the studies were observational and only one was prospective. There was statistical heterogeneity at the lumbar spine, 1/3 and ultradistal radius.

Our findings suggest that BMD can discriminate fracture status in predialysis and dialysis CKD. Larger, prospective studies are needed.

Disclosures: Roxana Bucur, None.

MO0005

Vitamin D2 vs. Vitamin D3 in Stage 5 Chronic Kidney Disease Patients on Dialysis. Valentina D. Tarasova*[1], Laura Armas[2], Robert Dunlay[3]. [1]Creighton University, USA, [2]Creighton University, USA, [3]Creighton University, USA

Background: Studies in healthy people have shown differences in 25(OH)D response to large doses of ergocalciferol (D2) or cholecalciferol (D3), but there were no studies estimating such response in patients with Stage 5 CKD on hemodialysis.

Methods: This was a randomized, single blind, placebo controlled study of a single oral dose of 47,095 IU D2 or 43,730 IU D3. 26 subjects (17 males, 9 females), with average age 53 years, from two hemodialysis centers in Omaha, Nebraska completed the study. 25(OH)D levels were measured at days 0, 2, 4, 7, 14, 21, 28, 42, 56, 70, 84, 96 and 112, prior to a hemodialysis session. 25(OH)D was measured by the DiaSorin Liaison method (DiaSorin, Inc., Stillwater, MN). The 25(OH)D levels were adjusted for the difference between doses in the 2 intervention groups and for seasonal change seen in the placebo group. Area under the serum curves (AUC) of 25(OH)D increments at 56, 84 and 112 days were calculated by the trapezoidal method individually for each subject. The study was approved by the IRB at Creighton University and registered on clinicaltrials.gov in August 2012 (NCT01675557).

Results: The median (IQR) for all participants baseline 25(OH)D level was 18.1 (13.6-29.4) ng/ml. The placebo group's 25(OH)D level decreased 3.4 (6.0-0.7) ng/ml over the course of the study. The median (IQR) maximum 25(OH)D AUC was 919 (676-1204) ng·day/ml in the D3 group at day 112 and 621(332-797) ng·day/ml in the D2 group. There was wide interindividual variation and because of the small sample size, AUC_{56}, AUC_{84} and AUC_{112} between the 2 types of vitamin D did not reach statistical significance (P=0.07, 0.07 and 0.08, respectively (Mann Whitney U).

Conclusion: Ergocalciferol (D2) and cholecalciferol (D3) likely produce different 25(OH)D pharmacokinetic profiles, but a larger sample size is needed to show an effect.

Disclosures: Valentina D. Tarasova, None.

MO0006

Low Circulating 25 Hydroxyvitamin D in Obesity is not Associated with Lower 24-hour Urine Calcium, Higher Bone Turnover or Lower Bone Mineral Density. Jennifer Walsh*[1], Amy Evans[2], Kim Naylor[3], Fatma Gossiel[4], Simon Bowles[4], Richard Jacques[4], Richard Eastell[2]. [1]University of Sheffield, United Kingdom, [2]University of Sheffield, United Kingdom, [3]The University of Sheffield, United Kingdom, [4]University of Sheffield, United Kingdom

The aims of this study were to determine if lower 25OHD in obesity is associated with higher PTH, lower calcium absorption (assessed by 24-hour urine calcium), higher bone turnover or lower bone density.

We conducted a cross-sectional study of 216 healthy Caucasian adults (ages 25 to 40 and 55 to 75) from Sheffield and South Yorkshire, UK. Participants were recruited in three body weight categories: normal weight (BMI 18.5 to 24.9 kg/m²), overweight (BMI 25 to 29.9 kg/m²), or obese (BMI >30 kg/m²). Vitamin D measurements were made in autumn or spring by immunoassay and results were adjusted for date of sample collection, age group and gender.

25OHD was lower in overweight and obese people. PTH and 24 hour urine calcium:creatinine did not differ by BMI group. CTX and osteocalcin were lower in obese people, but PINP and bone ALP did not differ by BMI group.

BMD by DXA at the whole body, lumbar spine and hip were higher in obese people (all ANCOVA p<0.001). In regression models of DXA BMD, including age, gender and BMI, 25OHD was not a significant predictor of BMD. Total, cortical and trabecular BMD by HR-pQCT at the distal radius and tibia and were higher in obese people (all ANCOVA p<0.001).

We conclude that the lower circulating 25OHD in obesity is not associated with higher PTH, lower intestinal calcium absorption, higher bone turnover or lower BMD. Therefore, it is not clear whether there would be skeletal benefits from treating obese people to the same serum vitamin D targets as normal weight people.

Table

Disclosures: Jennifer Walsh, None.

MO0007

Conditional ablation of *Alpl* in osteoblasts and mesenchymal cells leads to murine models of adult hypophosphatasia. Pia Kuss*[1], Manisha C. Yadav[2], Sonoko Narisawa[1], Jose Luis Millan[3]. [1]Sanford Burnham Medical Research Institute, USA, [2]Sanford Burnham Medical Research Institute, USA, [3]Sanford-Burnham Medical Research Institute, USA

Hypophosphatasia (HPP) is a rare inherited disease that features rickets or osteomalacia due to loss-of-function mutation in the gene for tissue-nonspecific alkaline phosphatase (TNAP). The clinical severity in HPP patients varies widely, from severe life-threatening perinatal and infantile forms to the milder childhood, adult and odonto-HPP. The phenotypes range from complete absence of bone mineralization and stillbirth to spontaneous fractures and loss of teeth in adult life. Adult HPP usually manifests during middle age, with a history of rickets and/or early loss of teeth. Recurrent metatarsal stress fractures and arthritis are common. TNAP knockout mice (*Alpl^{-/-}*) phenocopy infantile HPP, and their rickets/osteomalacia is caused by extracellular accumulation of PP_i, a substrate of TNAP and a potent calcification inhibitor. Epileptic seizures, caused by pyridoxal deficiency, lead to early lethality in that model. To phenocopy the milder forms of HPP, we analyzed mice with tissue-specific ablation of TNAP function in both chondrocytes and osteoblasts in the appendicular skeleton (*Alpl[floxlflox]; Prx1-Cre*), and in osteoblasts only (*Alpl[floxl flox]; Col1a1-Cre*). Both mouse strains are viable, fertile and display normal growth curves, while displaying drastically reduced levels of plasma alkaline phosphatase activity, without manifesting seizures. Histomorphometry revealed the presence of osteomalacia in both conditional knockout strains. These new mouse models will enable us to investigate aspects of HPP pathophysiology not manifested by the *Alpl^{-/-}* model due to their short life span, such as chondrocalcinosis, and to evaluate the potential use of enzyme replacement with mineral-targeting TNAP for the improvement of adult HPP disease.

Disclosures: Pia Kuss, None.

MO0008

Direct and indirect effect of cytokines on osteoclast differentiation. Enver Aydilek[1], Martina Blaschke[1], Regine Koepp[1], Ute Hempel[2], Sabine Blaschke[3], Heide Siggelkow*[4]. [1]Clinic of Gastroenterology, Germany, [2]Institute of Physiological Chemistry, Greenland, [3]Clinic for Nephrology & Rheumatology, Germany, [4]University Medicine of Goettingen, Dep. of Gastroenterology & Endocrinology, Germany

The pathogenesis of osteoporosis in Crohn's disease is still controversial, yet disease activity is thought to be one of the main contributing factors, especially the cytokines interleukin-6 (IL-6), interleukin-1 (IL-1) and tumor necrosis factor alpha

(TNF-α) seemed to be involved. We now investigated the effect of a cytokine combination in a concentration as measured in patients with active CD on osteoclasts. In parallel, conditioned medium from identically incubated SCP-1 cells were applied.

Immortalized osteoblastic cells (SCP-1 cells) were incubated with a cytokine combination for 48 hours at day 14 of culture at 7 days after confluence. The concentration of cytokines was 0.01 ng/ml IL-6, 0.001 ng/ml IL-1 beta and 0.005 ng/ml TNF-α in 0.1% bovine serum albumin (BSA). After 48 hours medium was collected for osteoclast experiments and cells were prepared for mRNA analysis. For osteoclast culture monocytes obtained from healthy individuals were isolated by MACS cell separation method (CD14) and differentiation to mature osteoclasts was achieved by the addition of RANKL (100 ng/ml) and M-CSF (25 ng/ml) in 6 well plates for 14-17 days. Osteoclasts expressed the characteristic protein profile and resorbed osteoblast-derived matrix in a bone resorption assay. On day 6, 9 and 13 cells were treated with either (a) control medium, (b) the cytokine combination (IL-1, IL-6, TNF-α) or (c) with the supernatants obtained from SCP-1 cells. After 17 days mRNA from osteoclasts was isolated. In three independent experiments marker expression was determined by real-time PCR and beta-actin was used as housekeeping gene.

The cytokine combination decreased cathepsin K significantly by about 25%. No significant effect on osteoclast activity as measured by vitronectin, RANK or TRAP mRNA expression was shown. In contrast, the supernatant of SCP-1 decreased cathepsin K significantly and also affected TRAP. In SCP-1 cells RANKL/OPG was increased to 1.57 fold by the combination of cytokines.

We can show a direct effect of the cytokine combination on mRNA expression of cathepsin K as osteoclast specific marker. The conditioned medium revealed additional effects on osteoclast differentiation possibly by an increased RANKL/OPG ratio as shown by mRNA levels in SCP-1 cells. These results suggest, that bone resorption in CD is mediated by a direct effect of the involved cytokines on the osteoclast but primarily by osteoblast-osteoclast interaction.

Disclosures: Heide Siggelkow, None.

MO0009

SQSTM1 Mutations Lead to Enhanced Immunoglobulin Production in Paget's Disease of Bone. <u>Daniela Merlotti</u>*[1], <u>Luigi Gennari</u>[1], <u>Fernando Gianfrancesco</u>[2], <u>Niccolò Pengo</u>[3], <u>Domenico Rendina</u>[4], <u>Riccardo Muscariello</u>[4], <u>Laura Oliva</u>[5], <u>Teresa Esposito</u>[6], <u>Stefano Rotatori</u>[7], <u>Maria Beatrice Franci</u>[7], <u>Barbara Lucani</u>[7], <u>Maria Stella Campagna</u>[7], <u>Ranuccio Nuti</u>[1], <u>Simone Cenci</u>[8]. [1]University of Siena, Italy, [2]National Research Council of Italy, Italy, [3]MRC LMCB; University College London, United Kingdom, [4]Department of Clinical & Experimental Medicine, Federico II University, Italy, [5]Division of Genetics & Cell Biology; San Raffaele Scientific Institute & University Vita-Salute San Raffaele, Italy, [6]Institute of Genetics & Biophysics, National Research Council of Italy, Italy, [7]Department of Medicine, Surgery & Neurosciences, University of Siena, Italy, [8]Fondazione Centro San Raffaele, Italy

Mutations in *SQSTM1* gene encoding p62 have been associated with Paget's disease of bone (PDB) in up to 50% and 15% of familial and sporadic cases, respectively. Among other functions, p62 is the prototypical cargo receptor for autophagy, a lysosomal recycling process recently implicated in plasma cell ontogenesis and immunoglobulin (Ig) production. Apart from one report of elevated Ig levels in a subset of PDB patients, whether antibody immunity is altered in PDB has not been explored. To address this issue, we assessed serum Ig levels in a cohort of 154 patients with active PDB in relation to *SQSTM1* mutation status. Compared with age-matched controls (n=60), PDB cases showed higher IgG (p<0.05) and gamma globulin levels by protein electrophoresis (p<0.05). This effect was mainly driven by patients with *SQSTM1* mutations (n=27) and became non-significant when patients without *SQSTM1* mutation were considered. A similar but not significant trend was observed in IgM levels in *SQSTM1* mutated patients versus controls (p=0.09). Moreover, among *SQSTM1* mutation carriers, patients with truncating mutations (Y383X and E396X) were associated with the highest serum IgG levels. Since treatment with nitrogen containing bisphosphonates may exert adjuvant, immune-modulating effects, Ig levels were monitored in 10 and 15 patients with and without *SQSTM1* mutations, respectively, before and after 1, 3, 6, and 12 months from intravenous treatment with zoledronic acid. In both treatment groups, IgG and IgM levels increased between 1 and 3 months from treatment and then decreased towards pretreatment levels. At each time-point, IgG levels were higher in *SQSTM1* mutation carriers than in patients without mutation. To conclusively assess whether *SQSTM1* mutations affect plasma cell activity in a cell-autonomous fashion, we lentivirally engineered the IgM-producing B18 plasmocytoma and the IgG-producing OKT3 hybridoma cell lines to stably express wild type and mutant (E396X) p62. Standard 4 hr Ig secretion assays demonstrated increased rates of Ig secretion in cell lines expressing mutant p62, as compared to controls engineered to express wild type p62. In conclusion, our clinical and experimental data indicate that PDB-associated *SQSTM1* mutations affect plasma cell activity and humoral immunity. The possible implications of these findings in the pathogenesis of the disorder and the occurrence of comorbidities in mutated PDB patients warrant further investigation.

Disclosures: Daniela Merlotti, None.

MO0010

Functional study of *OPTN* variants associated with Paget's disease of bone. <u>Iris A. L. Silva</u>*[1], <u>Natércia Conceição</u>[2], <u>Laetitia Michou</u>[3], <u>M. Leonor Cancela</u>[4]. [1]University of Algarve - PhD program in Biomedical Sciences; Dept of Biomedical Sciences & Medicine, Portugal, [2]University of Algarve - Centre of Marine Sciences (CCMAR), Portugal, [3]Université Laval, Canada, [4]University Algarve - CCMAR, Portugal

Paget's disease of bone (PDB) is the second most frequent metabolic bone disease after osteoporosis. Genetic factors play an important role in PDB, but to date the only PDB causal gene identified was the Sequestosome 1 gene. A significant association was identified between PDB and Optineurin (OPTN) gene in 10p13 (PDB6 locus). Several groups replicated the strong association of rs1561570 with PDB, but no functional studies on OPTN and PDB were reported to date. We proposed here to assess the functional contribution of rs1561570, as well as other variants to PDB pathogenesis. First, we screened OPTN gene to search for additional relevant variants associated with PDB. We found that rs2234968, a SNP in an OPTN coding exon, was associated with PDB but functional data did not reveal any functional effect. Using a combination of in silico and expression analysis, we concluded that there were two SNPs in linkage disequilibrium with rs2234968 - rs10906303 and rs79529484 - that changed the OPTN splicing pattern, altering the reading frame and creating a premature STOP codon. In addition, we predicted that rs1561570 C allele - the most frequent in controls - was methylated. Using bisulfite sequencing and qPCR techniques, we showed that the C allele was indeed methylated in all samples and it was also responsible for lower levels of OPTN transcription when compared to the T allele. Since methylation is known to be related to transcription inhibition, the methylated rs1561570 C allele in healthy controls was probably inhibiting OPTN expression, which was confirmed by our qPCR results. Since OPTN has a NEMO functional domain and NEMO proteins are responsible for the degradation of NFKB inhibitor along with IKK, controls will have an increase in the levels of the inhibitor and thus a decrease in NFKB. In contrast in patients where the T allele is no longer methylated, this would lead to higher levels of OPTN expression, higher levels of NFKB inhibitor degradation and also higher levels of NFKB translocation to the nucleus, which will increase the expression of genes related to osteoclastogenesis and thus may contribute to the PDB phenotype. In conclusion, our work clarifies the effect of rs1561570 in PDB and also describes other functional SNPs in OPTN gene potentially important for PDB pathophysiology.

Disclosures: Iris A. L. Silva, None.

MO0011

Withdrawn

MO0012

Changes in Trabecular Bone Score up to Two Years After Parathyroidectomy in Primary Hyperparathyroidism. <u>Alice Abraham</u>*[1], <u>Chiyuan Zhang</u>[2], <u>Barbara Silva</u>[3], <u>Fan Wen-Wei</u>[4], <u>Didier Hans</u>[5], <u>Natalie Cusano</u>[6], <u>John Bilezikian</u>[7]. [1]Endocrinology fellow, USA, [2]Columbia University, USA, [3]Federal University of Minas Gerais, Brazil, Brazil, [4]Columbia University College of Physicians & Surgeons, USA, [5]Lausanne University Hospital, Switzerland, [6]Columbia University College of Physicians & Surgeons, USA, [7]Columbia University College of Physicians & Surgeons, USA

Following parathyroidectomy (PTX), BMD improves in patients with primary hyperparathyroidism (PHPT), but little is known about changes in microarchitectural texture by trabecular bone score (TBS). We have recently shown that TBS is associated with HRpQCT measures of bone microstructure in PHPT. Moreover, TBS predicts fracture risk, independent of BMD.

In this study, we investigated site, time and sex-specific changes in BMD and TBS up to 24 months after PTX. We studied 31 subjects with PHPT after PTX, of whom 21 were followed for 6 months, 16 were followed for 12 months, 14 were followed for 18 months and 9 were followed for 24 months after surgery. Site-matched spine TBS was extracted from the DXA image (Hologic) using TBS iNsight software. Linear mixed model was performed to assess the % change in BMD and TBS relative to the baseline over 24 months.

The mean age was 61 ± 13 yrs. Our cohort included 20 women and 11 men. At baseline, the mean TBS was low at 1.309 ± 0.129 (normal ≥ 1.35). TBS was lower in men than in women (1.242 ± 0.144 vs 1.346 ± 0.106; p<0.001). Overall, there was an increase in BMD at the lumbar spine at 6 months ($+2.1 \pm 5.1\%$, p=0.001), which was sustained at 12 months ($+4.3 \pm 7.5\%$; p=0.000), 18 months ($+4.5 \pm 8.8\%$; p=0.000) and 24 months ($3.0 \pm 10.3\%$; p=0.009). There were similar significant increases at 6, 12, 18 and 24 months at the femoral neck and total hip. We found sex-specific changes at the lumbar spine and total hip. In men, there were significant increases in BMD at all time points at the lumbar spine and hip. In contrast, women had a significant increase in BMD at the lumbar spine alone at 12 months. At the hip, women significantly gained BMD at 6 and 12 months. Overall, there were no significant changes in BMD at the radius and 33% radius. Among all subjects, there was a trend toward significant increase in TBS at 12 months ($+2.2 \pm 11.9\%$; p=0.088).

While TBS markedly improved at 6 ($+6.1 \pm 8.0\%$; p=0.003) and 12 ($+6.0 \pm 11.7\%$; p=0.013) months post PTX in men, it did not change in women ($-1.2 \pm 7.6\%$; p=0.323

at 6 months; $-0.4 \pm 8.1\%$; p=0.750 at 12 months). There were no significant changes in TBS at 18 or 24 months.

TBS increases after PTX in men up to 12 months, while it does not change in women. The results confirm the previous findings by HRpQCT of similar or better trabecular microstructure after PTX, and also reveal differences between men and women. We demonstrate that TBS has potential clinical utility in evaluation of patients following PTX.

Disclosures: Alice Abraham, None.

MO0013

No Seasonal Variation in 25-Hydroxyvitamin D in Mild Primary Hyperparathyroidism. <u>Elaine Cong</u>*[1], <u>Marcella Walker</u>[2], <u>Anna Kepley</u>[2], <u>Chiyuan Zhang</u>[2], <u>Donald McMahon</u>[3], <u>Shonni Silverberg</u>[2]. [1]Columbia Presbyterian Medical Center, USA, [2]Columbia University, USA, [3]Columbia University College of Physicians & Surgeons, USA

Population-based studies have demonstrated seasonal variability in 25-hydroxyvitamin D (25OHD) levels with a nadir in the winter and a peak in the summer which inversely correlate with serum parathyroid hormone (PTH), markers of bone turnover and areal bone mineral density (aBMD). In 1999, we reported similar seasonal variability in 25OHD and PTH levels in mild primary hyperparathyroidism (PHPT) at our latitude (New York City: 40.67°N, 73.9°W). Given the increased awareness of vitamin D deficiency and widespread use of supplements, we sought to determine if seasonal variability in 25OHD is still present in PHPT patients.

In a cross-sectional study of 100 PHPT patients (79% female, 87% white, 84% non-Hispanic, 1 black, age [mean $\pm$ SD] 62 ± 12 years, calcium 10.7 ± 0.6 mg/dl, PTH 83 ± 41 pg/ml), mean 25OHD was 29 ± 10 ng/ml, and vitamin D insufficiency and deficiency were common (54%<30 ng/ml; 20%≤20 ng/ml). No differences in the levels of 25OHD, PTH or 1,25(OH)2D, or in the prevalence of vitamin D deficiency or insufficiency were seen by season of enrollment as defined by the almanac (see Table). To compare 25OHD in winter vs summer seasons, we combined winter/spring vs summer/fall to reflect the time-lag of 25OHD production in response to sunlight exposure and found no differences. Patients enrolled in different seasons did not differ in age, gender, race, ethnicity or BMI. In addition, no seasonal differences were observed in serum calcium, CTX, aBMD (spine, hip, radius) or cortical and trabecular indices by high resolution peripheral QCT (radius, tibia). No seasonal variations were observed in any parameter when subgroups were analyzed by gender or race. Omitting the single African-American participant did not affect the results.

Vitamin D intake was high. Supplementation was common (64%; mean 1414 ± 1489 IU/d [range:71-7143 IU]). The average combined dietary and supplemental intake was 2045 ± 1680 IU daily (range:181-8000 IU). Patients not on supplements had an average dietary vitamin D intake of 401 ± 42 IU daily (range:1-2000 IU). No difference was seen in the use or quantity of vitamin D supplementation, dietary intake or both by season.

In conclusion, in a cohort with mild PHPT, we no longer see evidence for seasonal variability in 25OHD levels or markers of PHPT disease activity. This change is likely due to high vitamin D supplement intake, which can mask the effect of season on serum 25OHD levels.

Measurement (mean±SD)	Spring (N=26)	Summer (N=20)	Fall (N=24)	Winter (N=32)	P-value
25OHD≤20 (N,%)	4 (15%)	4 (20%)	3 (13%)	9 (28%)	0.40
25OHD>30 (N,%)	12 (46%)	9 (45%)	13 (54%)	20 (63%)	0.49
25OHD ng/ml	31±11	31±12	29±6	26±11	0.20
PTH pg/ml	88±48	65±30	89±42	84±38	0.27
1,25(OH)2D pg/ml	70±24	60±27	83±36	62±23	0.21
Calcium mg/dl	10.6±0.6	10.7±0.5	10.6±0.5	10.8±0.7	0.74

Prevalence of Vitamin D Deficiency and Insufficiency in Two PHPT Cohorts

Disclosures: Elaine Cong, None.

MO0014

Plasma PTH levels measured with the 3rd generation 1-84 PTH assay in patients with different stages of chronic kidney disease. <u>Giuseppe Viccica</u>[1], <u>Simona Borsari</u>[1], <u>Elena Pardi</u>[1], <u>Filomena Cetani</u>[2], <u>Roberta Centoni</u>[3], <u>Sonia Albertini</u>[3], <u>Silvia Chiavistelli</u>[4], <u>Giordano Fumagalli</u>[1], <u>Adamasco Cupisti</u>[1], <u>Claudio Marcocci</u>*[5]. [1]Department of Clinical & Experimental Medicine, University of Pisa, Italy, [2]University Hospital of Pisa, Italy, [3]University Hospital of Pisa, Italy, [4]Azienda Ospedaliera Pisana, Italy, [5]University of Pisa, Italy

Patients with chronic kidney disease (CKD) have decreased renal function and increased plasma PTH levels. Previous guidelines based on the Allegro intact PTH assay recommended that patients with different disease stages should be managed in order to maintain plasma PTH within a given range, which was fixed between 150 and 300 pg/ml in CKD stage 5. Several methods of intact PTH assay are available and a wide inter-method variability in the PTH results has been shown and opposite therapeutic attitudes may be reached in a single patient depending on the PTH assay used. A new 3rd generation PTH assay, which measures only the full length molecule,

is currently available. Aim of the present study was to define PTH ranges using this assay in patients with different stages of CKD.

A series of 141 patients (65 females and 76 males, age 21-89 yr) with CKD stage 3-5 followed in a tertiary care center were enrolled in the study. Patients were classified according to the estimated GFR (eGFR, stage 3: n=46; stage 4: n= 42; stage 5: n=53). Plasma PTH was measured using the 3rd generation LIAISON® 1-84 PTH assay (Diasorin; normal range 5-40 pg/ml). Serum bone specific alkaline phosphatase (BASP, LIAISON®BAP OSTASE®, normal range 16-26 ng/ml), serum C-terminal telopeptide (S-CTx; Serum CrossLaps® ELISA, Nordic Bioscience Diagnostics A/S; normal range 0.07-1.43 ng/ml) and 25OH vitamin D (25OHD; LIAISON®25 OH Vitamin D TOTAL Assay, Diasorin, normal range 4-64 ng/ml) were also measured. Finally, in a subgroup of patients (n=80) plasma intact PTH was measured using the 2nd generation LIAISON® N-tact™PTH (Diasorin, normal range 15-75 pg/ml).

Plasma 1-84 PTH was increased in the majority (72%) of our patients and there was a significant negative correlation with the eGFR (r=-0.46, P<0.001). Conversely, a significantly positive correlation was found between plasma 1-84 PTH and BSAP (r= 0.23, P=0.008) and S-CTx (r=0.31, P=0.001), and a no correlation with serum 25OHD and age.

A significantly high positive correlation was found between plasma 3nd generation 1-84 PTH and intact 2nd generation PTH concentrations (r=0.94, P<0.0001).

The table summarizes our data in whole group of patients grouped according to the different CKD classes. Results are expressed as mean $\pm$ SD. [table1] The 1-84 PTH assay values nicely segregate patients with different stages of CKD and could provide a reference point for managements of CKD patients across the various stages of CKD.

CKD class	Age (yr)	eGFR (ml/min/1.73 m²)	1-84 PTH (pg/ml)	BSAP (ng/ml)	S-CTx (ng/ml)	25OHD (ng/ml)
3 (n=46)	61±14	42±9 a,b	46±26 a,b	17±9 b	0.76±0.50 a,b	17±9
4 (n=52)	66±13	21±4 a,c	89±58 a,c	20±12	2.00±1.93 a	16±7
5 (n=43)	64±14	8±3 b,c	134±103 b,c	23±10 b	2.56±2.18 b	15±10

P<0.05: a CKD class 3 vs 4; b CKD class 3 vs 5; c CKD class 4 vs 5

Tab.1

Table 1

Disclosures: Claudio Marcocci, None.

MO0015

Predictors of Depression Response in Primary Hyperparathyroidism. <u>Ann Kearns</u>*[1], <u>Rachel Espiritu</u>[2], <u>Kristin Vickers Douglas</u>[3], <u>Clive Grant</u>[3], <u>Euijung Ryu</u>[3], <u>Robert Wermers</u>[1]. [1]Mayo Clinic, USA, [2]Summa Physicians, Inc., USA, [3]Mayo Clinic, USA

Neuropsychiatric symptoms including depression are common in patients with primary hyperparathyroidism (PHPT). However, the clinical characteristics that predict improvement are not defined by existing studies.

To understand the improvement in depression symptoms, we examined the relationship between clinical and biochemical parameters and the depression response.

We previously conducted a prospective case-control study of PHPT patients with parathyroidectomy (n=88) and observation (n=81). Depression scores were assessed using a validated depression questionnaire (PHQ-9) longitudinally for 12 months. Patients were classified as depression response if their PHQ-9 scores at 12 months were less than 10. Biochemical parameters (PTH, calcium, and vitamin D) and clinical characteristics (age, sex, depression history and baseline PHQ-9 and its symptom category) were considered as potential factors associated with the depression response. Logistic regression models were used and odds ratios (ORs) and their 95% confidence intervals (CIs) were presented.

Overall, 88% of PHPT patients had PHQ-9 scores less than 10 at 12 months (i.e., depression response). These patients were slightly younger (median age 65.9 vs 68.4 yrs) and more males (18% vs 17%) compared to the patients with depression non-response. Adjusting for age and sex, parathyroidectomy was positively associated with the depression response (OR 2.52, 95% CI 0.92 – 7.61). Biochemical parameters at baseline were not associated with depression response, except for marginal impact of vitamin D values (OR 1.96, 95% CI 0.91 – 1.00). Baseline depression severity was strongly associated with the risk of depression non-response (OR 14.3, 95% CI 4.0 – 50.0). Two baseline symptom categories (cognitive or somatic) showed comparable association with the risk of depression non-response (OR 1.52, 95% CI 1.27 – 1.85).

These results show that baseline PHQ-9 scores strongly predict improvement in depression scores whereas baseline biochemical parameters do not. Our results may not be applicable to severe primary hyperparathyroidism or normocalcemic hyperparathyroidism, which are not represented in this group. This information may be useful to clinicians who are counseling patients with primary hyperparathyroidism about the benefits of parathyroidectomy.

Disclosures: Ann Kearns, None.

MO0016

Primary Hyperparathyroidism Not Confounded by Coexisting Vitamin D Deficiency. <u>Anna Kepley</u>*[1], <u>Marcella Walker</u>[1], <u>Elaine Cong</u>[2], <u>Chiyuan Zhang</u>[1], <u>James Lee</u>[3], <u>Shonni Silverberg</u>[1]. [1]Columbia University, USA, [2]Columbia Presbyterian Medical Center, USA, [3]Columbia University, USA

Vitamin D (D) deficiency and insufficiency are common in PHPT and thought to be associated with more severe disease. Because these two common conditions often coexist, our understanding of PHPT is confounded by the effect of D-deficiency. We describe the clinical, biochemical and skeletal phenotype of a PHPT cohort not confounded by D status (25OHD≥30ng/ml; mean 38 ± 6 [range: 30-54 ng/ml]). Notably, 80% were on D supplements (dose: 2043 ± 1741 IU/d). Patients (n=46; age $\pm$ SD 67 ± 9 yrs) were mostly female (87%), white (92%), and non-Hispanic (82%). Most were asymptomatic, but 15% had a history of nephrolithiasis. None had *osteitis fibrosa cystica*, but 20% had a history of fragility fracture at the spine (n=4), ankle (n=2), forearm (n=2) and metatarsal (n=1).

PHPT was biochemically mild: PTH 73 ± 38 pg/ml, serum calcium 10.7 ± 0.6 mg/dl, phosphate 3.2 ± 0.4 mg/dl, urinary calcium 219 ± 133 mg/d and $1,25(OH)_2D$ 63 ± 19 pg/ml. Markers of bone formation and resorption were normal (BSAP 37.4 ± 15 [nl: 14.2-42.7 U/L]; CTX 0.604 ± 0.374 [nl: 0.142-1.351 ng/ml]). Mean DXA T-scores were in the osteopenic range, but osteoporosis was common (n=19; 41%). T-Scores at the 1/3 radius (RAD:-1.4±1.7) were not lower than those at the lumbar spine (LS:-1.1±1.6), femoral neck (FN:-1.6±1.0) or total hip (TH:-1.3±0.9). High resolution peripheral QCT T-scores were in the osteopenic range at the radius: cortical density (Dcort) -2.2±2.3, cortical thickness (Ct.Th) -1.1±1.4, trabecular density (Dtrab) -1.2±1.2, trabecular thickness (Tb.Th) -1.9±0.8; while tibial cortical density was severely affected: Dcort T-score -4.6±2.7, Ct.Th -1.9±1.2, Dtrab -0.7±1.0, and Tb.Th –1.4±0.8.

Most (76%; n=35) met 3rd International Workshop on Asymptomatic PHPT surgical criteria: 10 (22%) had serum calcium >1.0 mg/dl above normal; 7 (15%) had stones; 10 (22%) had an estimated glomerular filtration rate <60 ml/min; 9 (20%) had fragility fractures; 19 (41%) had osteoporosis by T-score (LS n=11, 24%; TH n=4; 9%; FN n=7,15%; RAD n=9, 20%); and 1 (2%) was <50 yrs.

In summary, this D-replete PHPT cohort was nearly all Caucasian, female and taking high doses of vitamin D. Although their PHPT was biochemically mild, they had a typical prevalence of kidney stones, a high prevalence of fragility fractures and osteoporosis by DXA, and most met surgical criteria. Their fracture history and BMD do not suggest a disorder affecting only cortical bone. We find no evidence that D-replete PHPT patients have unusually mild disease.

Disclosures: Anna Kepley, None.

MO0017

PTH(1-84) Is Associated with Improved Quality of Life in Hypoparathyroidism Through 5 Years of Therapy. <u>Natalie Cusano</u>*[1], <u>Mishaela Rubin</u>[2], <u>Donald McMahon</u>[1], <u>Dinaz Irani</u>[3], <u>Laura Beth Anderson</u>[2], <u>Elizabeth Levy</u>[4], <u>John Bilezikian</u>[1]. [1]Columbia University College of Physicians & Surgeons, USA, [2]Columbia University, USA, [3]Columbia University Medical Center, USA, [4]Columbia University College of Physicians & Surgeons, USA

Hypoparathyroidism is a rare disease characterized by low serum calcium and PTH concentrations. Our group and others have shown that hypoparathyroid patients have compromised quality of life (QOL) compared to normal subjects. We have shown that QOL improves after 1 year of PTH(1-84) treatment in hypoparathyroidism. We now report our data through 5 years of therapy.

Sixty-nine hypoparathyroid subjects [age 46 ± 13 years (X $\pm$ SD); 55 women; etiology: 42 surgical, 26 idiopathic, 1 DiGeorge; duration 12 ± 11 years; serum calcium 8.7 ± 0.9 mg/dL; PTH 2.4 ± 5 pg/mL] were treated with PTH(1-84) for up to 5 years. Subjects completed the RAND SF-36 survey, a validated measure of health-related QOL covering 8 domains of physical and mental health. We analyzed data from baseline and months 2, 6, 12 (n=58), 18, 24 (n=42), 30, 36 (n=33), 42, 48 (n=26), 54 and 60 (n=25) of treatment. Some subjects dropped out before reaching the 5-year mark (n=27), while others have not yet reached 5 years of therapy (n=17). At baseline, hypoparathyroid subjects were below the normative reference range in all domains (p<0.001). With PTH therapy, intention-to-treat analysis showed significant improvement in the overall score at 2 months (386 $\pm$ 206 to 468 $\pm$ 245; p<0.0001) that persisted through 5 years (482 $\pm$ 391; p<0.0001). The mental component summary (MCS) score improved significantly at 2 months and remained significantly improved through 5 years (199 $\pm$ 121 to 246 $\pm$ 245; p=0.001), as did each of the 4 mental health domains [vitality (VT), social functioning (SF), role emotional (RE), mental health (MH)]. The physical component summary score improved significantly at 2 months and remained significantly improved through 5 years (187 $\pm$ 110 to 237 $\pm$ 210; p<0.0001), as did 3 of the physical health domains [physical functioning (PF), role physical (RF), general health (GH)]. Using T-scores, 7 of 8 domains improved early with sustained effects through 5 years: VT, -1.4 to -0.9 (p=0.001); SF, -1.1 to -0.7 (p=0.003); RE, -0.9 to -0.4 (p=0.011); MH, -0.9 to -0.4 (p=0.001); PF, -0.9 to -0.3 (p<0.0001); RF, -1.2 to -0.5 (p=0.002); GH, -1.3 to -0.9 (p=0.001).

These results document that PTH(1-84) therapy is not only associated with improvement in biochemical and skeletal indices (previously well-documented), but also in mental and physical health, among the major complaints of subjects with hypoparathyroidism.

Disclosures: Natalie Cusano, None.
This study received funding from: NPS Pharmaceuticals

MO0018

Vitamin D Status in Hyperthyroidism. <u>Ana Paula Barbosa</u>*[1], <u>Mário Rui Mascarenhas</u>[2], <u>Manuel Bicho</u>[3]. [1]Endocrinology, Santa Maria Hospital & Faculty of Medicine, Portugal, [2]Lisbon's Faculty of Medicine, Santa Maria University Hospital, CHLN,EPE, Portugal, [3]Environmental Health Institute of Lisbons Faculty of Medicine, Portugal

Hyperthyroidism is a known risk factor for reduced bone mineral density (BMD), osteoporosis and fragility fractures because of the increased bone resorption induced by the thyroid hormones. Also, the coexistence of nutrient malabsorption and urinary calcium loss can contribute to vitamin D abnormalities and consequently to BMD changes and influences in the risk of falls.

PURPOSE
To evaluate the relationships between the vitamin D status and BMD, in patients with hyperthyroidism.

MATERIAL AND METHODS
A group of 44 patients with hyperthyroidism (21 men and 23 premenopausal women) were evaluated. Fasting venous sampling was done to measure the free thyroid hormones, TSH, iPTH, calcium, phosphorus, pituitary hormones and 25(OH)vitamin D.

The BMD (g/cm^2) at the lumbar spine (L$_1$-L$_4$), at the proximal femur, at the distal radius and at the whole body and the total body soft tissues composition (lean and fat masses, Kg) were evaluated by dual X-ray absorciometry (Hologic QDR Discovery W densitometer).

No patient was previously treated for hyperthyroidism and/or osteoporosis.

According to the endocrine society and IOM criteria, the vitamin D levels (ng/mL), were divided in deficient (<20), insufficient (21-29) and normal (>30).

Descriptive and regression tests were used and statistical significance was considered for P <0.05.

RESULTS
In the men group the vitamin D deficiency was detected in 42.8%, insufficiency in 33.4% and normal in 23.8%, but in the women group the deficiency was 34.8%, the insufficiency was 39.1% and normal levels in 26.1%.

CONCLUSIONS
The results of this study suggest the presence of inadequate levels of vitamin D in almost 75% of the patients with hyperthyroidism, which, associated to an increased bone turnover, can contribute to bone mass loss and the possible increase of osteoporotic fractures risk.

Disclosures: Ana Paula Barbosa, None.

MO0019

Are left and right the same? Contralateral microstructural differences between HR-pQCT images at the radius and tibia. <u>Bin Zhou</u>*[1], <u>Eric Yu</u>[1], <u>Ji Wang</u>[1], <u>Zhengdong Zhang</u>[2], <u>Fernando Rosete</u>[3], <u>Kyle Nishiyama</u>[1], <u>Elizabeth Shane</u>[4], <u>X Guo</u>[1]. [1]Columbia University, USA, [2]Columbia university, USA, [3]Columbia University Medical Center, USA, [4]Columbia University College of Physicians & Surgeons, USA

HR-pQCT has become a popular clinical research tool to distinguish fragility fractures and assess efficacy of pharmacological interventions for osteoporosis. In general, the non-dominant radius (usually the left) along with the ipsilateral tibia is chosen for imaging. Under certain circumstances, such as prior fracture, the contralateral limbs are scanned instead. However, the variance in microstructural and mechanical properties between contralateral limbs is unknown. In this study, we investigated differences in these properties between left and right radii and tibiae.

Twenty-seven sets of paired cadaveric human left and right distal radii and tibiae were scanned by HR-pQCT and μCT. Regions corresponding to the standard HR-pQCT scan were identified in μCT images using 3D image registration. Volumetric bone mineral densities and trabecular microstructure were examined, and the trabecular compartments were subjected to individual trabecula segmentation (ITS) analysis to evaluate plate- and rod-related microstructural parameters. Whole bone stiffness was determined by image μFE analysis.

By gold standard μCT, right radius had higher BV/TV and stiffness. However, at the tibia, both parameters were similar (Table 1). By ITS-based microstructural analysis, the right radius had higher plate and rod BV/TV, while plate BV/TV was similar between left and right tibiae. By HR-pQCT, the right radius had higher total area and lower average BMD. At the tibia, only average BMD was modestly but significant different between sides (Table 2). The majority of microstructural parameters from standard and ITS analysis were significantly different at both sites. Strong correlations between microstructural parameters and stiffness were found between sides; however, the correlations were relatively lower in the radius compared to the tibia.

These data suggest the selection of the contralateral radius can introduce significant variance to *in vivo* HR-pQCT analysis. For tibia, though some microstructural parameters differed, important indicators like μCT-based BV/TV and stiffness are similar. Compared with radius, the higher correlation in tibia likely originates from routine loads that are evenly distributed on the lower limbs but may be more asymmetric in the upper limbs. In conclusion, careful consideration of the selection of the dominant or non-dominant limb for scanning is important for HR-pQCT studies. The consistency between HR-pQCT and μCT needs to be further examined.

Table 1. µCT (37µm)-based morphological, ITS analysis, µFE and the correlations between left and right radius and tibia. Bold indicates left is significantly different from right (paired-t test, p<0.05). % difference is with respect to the left limb. (Tb: trabecular; N: number; Th: thickness; BV/TV: Bone volume fraction; DA: Degree of anisotropy; p: Plate; r: Rod)

	Radius				Tibia			
	Left	Right	% difference	Correlation coefficient	Left	Right	% difference	Correlation coefficient
Standard µCT								
BV/TV	0.132±0.024	0.145±0.033	8.97	0.81	0.135±0.033	0.14±0.034	3.70	0.94
Conn.D	3.497±0.756	3.706±0.868	5.64	0.78	3.532±1.029	3.236±1.023	-8.38	0.93
SMI	1.682±0.353	1.624±0.338	-3.57	0.83	1.549±0.386	1.333±0.382	-13.94	0.92
Tb.N	1.239±0.139	1.249±0.151	0.80	0.92	1.091±0.188	1.104±0.206	1.19	0.91
Tb.Th	0.16±0.01	0.163±0.012	1.84	0.49	0.172±0.017	0.169±0.016	-1.74	0.93
Tb.Sp	0.798±0.104	0.784±0.114	-1.79	0.91	0.944±0.259	0.936±0.321	-0.85	0.91
BS/BV	17.246±1.385	16.36±1.587	-5.42	0.67	16.027±1.917	16.001±1.979	-0.16	0.87
DA	2.091±0.171	2.031±0.168	-2.95	0.78	2.143±0.141	2.209±0.342	3.08	0.62
ITS								
pBV/TV	0.098±0.025	0.107±0.031	8.41	0.84	0.106±0.03	0.112±0.031	5.66	0.95
rBV/TV	0.033±0.007	0.038±0.009	13.16	0.88	0.032±0.011	0.026±0.008	-18.75	0.70
aBV/TV	0.096±0.022	0.104±0.029	7.69	0.87	0.099±0.026	0.105±0.028	6.06	0.93
pBV/BV	0.74±0.073	0.729±0.073	-1.51	0.88	0.763±0.077	0.806±0.068	5.64	0.80
rBV/BV	0.26±0.073	0.271±0.073	4.06	0.88	0.237±0.077	0.194±0.068	-18.14	0.80
pTb.N	1.798±0.136	1.8±0.137	0.11	0.85	1.739±0.118	1.764±0.121	1.44	0.91
rTb.N	1.561±0.107	1.558±0.11	-0.19	0.90	1.462±0.128	1.383±0.143	-5.40	0.90
pTb.Th	0.131±0.008	0.138±0.01	5.07	0.69	0.143±0.011	0.136±0.012	-4.90	0.92
rTb.Th	0.128±0.01	0.138±0.011	7.25	0.89	0.13±0.015	0.132±0.014	-0.75	0.84
pTb.S	0.127±0.012	0.129±0.012	1.35	0.78	0.137±0.016	0.147±0.021	7.30	0.86
rTb.I	0.603±0.017	0.602±0.019	-0.17	0.86	0.615±0.029	0.614±0.029	-0.16	0.85
RR func.D	1.351±0.408	1.39±0.446	2.81	0.90	1.321±0.547	0.942±0.452	-28.69	0.87
PR func.D	6.005±1.079	6.103±1.19	1.61	0.83	5.59±1.435	4.914±1.464	-12.09	0.85
PP func.D	5.446±1.126	5.502±1.202	0.67	0.81	5.347±1.28	5.159±1.328	-3.52	0.87
Stiffness	61528±26158	70416±29932	12.62	0.87	151387±57357	150741±59243	-0.43	0.94

Table 1

Table 2. HR-pQCT (82µm)-based morphological, ITS analysis, µFE and the correlations between left and right radius and tibia. Bold indicates left is significantly different from right (paired-t test, p<0.05). % difference is with respect to the left limb. (Tb: trabecular; N: number; Th: thickness; BV/TV: Bone volume fraction; DA: Degree of anisotropy; p: Plate; r: Rod)

	Radius				Tibia			
	Left	Right	% difference	Correlation coefficient	Left	Right	% difference	Correlation coefficient
Standard HR-pQCT								
Average BMD	248.9±49.7	226.7±58.6	-8.92	0.85	210.7±54.5	213.7±62.3	1.40	0.96
Trabecular BMD	145.2±27.2	130.7±38.765	-9.96	0.82	139.3±34.8	140.4±37.4	0.75	0.94
Cortical BMD	711.0±98.4	702.3±111.8	-1.23	0.88	687.5±125.5	678.2±147.5	-1.36	0.96
Tb.N	1.409±0.725	1.338±0.725	-5.04	0.87	1.61±0.356	1.279±0.342	-20.56	0.92
Tb.Th	0.086±0.01	0.08±0.014	-6.98	0.32	0.074±0.019	0.09±0.015	21.62	0.90
Tb.Sp	0.643±0.127	0.686±0.136	6.69	0.87	0.6±0.26	0.829±0.6	38.17	0.91
Ct.Th	0.527±0.225	0.476±0.221	-9.68	0.88	0.647±0.369	0.68±0.403	5.10	0.97
Total Area	299.5±87.1	338.1±91.3	12.89	0.95	744.8±162.5	734.2±171.8	-1.42	0.98
ITS								
pBV/TV	0.072±0.029	0.081±0.041	12.50	0.85	0.081±0.035	0.101±0.041	24.69	0.94
rBV/TV	0.134±0.021	0.123±0.02	-8.21	0.86	0.15±0.028	0.117±0.025	-22.00	0.89
aBV/TV	0.084±0.024	0.087±0.034	8.75	0.87	0.085±0.025	0.301±0.082	18.82	0.94
pBV/BV	0.339±0.08	0.378±0.104	11.50	0.81	0.342±0.098	0.451±0.116	31.87	0.93
rBV/BV	0.661±0.08	0.622±0.104	-5.90	0.81	0.658±0.098	0.549±0.116	-16.57	0.93
pTb.N	1.214±0.156	1.254±0.183	3.29	0.88	1.267±0.161	1.362±0.158	7.50	0.94
rTb.N	1.643±0.103	1.583±0.102	-3.65	0.84	1.769±0.165	1.572±0.141	-11.14	0.90
pTb.Th	0.223±0.007	0.219±0.008	-1.79	0.47	0.227±0.009	0.224±0.01	-1.32	0.82
rTb.Th	0.225±0.007	0.227±0.008	0.89	0.91	0.218±0.006	0.226±0.008	3.67	0.90
pTb.S	0.171±0.01	0.173±0.011	1.17	0.61	0.165±0.011	0.168±0.017	1.82	0.85
rTb.I	0.701±0.033	0.707±0.038	0.86	0.83	0.666±0.029	0.692±0.034	3.90	0.94
RR func.D	2.067±0.414	1.791±0.377	-13.26	0.76	2.603±0.678	1.738±0.548	-33.23	0.89
PR func.D	2.349±0.733	2.393±0.768	1.87	0.90	2.781±0.776	2.556±0.663	-8.09	0.90
PP func.D	1.192±0.441	1.285±0.543	7.80	0.88	1.39±0.648	1.465±0.456	5.40	0.93
Stiffness	72848±28153	80501±34896	10.51	0.90	172064±63404	192101±69824	11.65	0.96

Table 2

Disclosures: Bin Zhou, None.

MO0020

Bone Density, Geometry, and Strength Changes after Lower Limb Amputation. Debra Bemben*[1], Vanessa Sherk[2], Michael Bemben[1], William Ertl[3]. [1]University of Oklahoma, USA, [2]University of Colorado - Denver, USA, [3]University of Oklahoma Health Sciences Center, USA

We have previously documented in cross-sectional and longitudinal studies that there are large losses in areal BMD (aBMD) for the hip sites after lower limb amputation. There is a lack of information about the changes that occur to bone quantity and quality at the end of the amputated bone, which is important for prosthesis fit and long term ambulation. The purpose of this study was to assess changes in at the end of the amputated bone using pQCT that occur in the early stages post-amputation of a lower limb. Nine participants (1 premenopausal female, 8 males), ages 23 to 53 years were enrolled immediately prior to their amputation surgery. They all were traumatic unilateral amputees (1 above-knee, 7 below-knee) who had undergone the Ertl procedure. pQCT was used to assess volumetric BMD (vBMD), bone content (BMC), bone area, bone strength (SSI, Imax, Imin), and muscle cross-sectional area (MCSA) at 5% of the residual limb length proximal to the top of the bone-bridge and at the same distance on the contralateral limb. Changes in cortical bone porosity were estimated by determining the proportion of the bone area that was contained within different vBMD cutoffs (>650, >480 mg/cm^{3}). Bone measurements were obtained at 3 time points: after amputation prior to prosthesis fitting (pre-ambulatory baseline); at 6 months walking with prosthesis; and at 12 months walking with prosthesis. There were no significant changes for bone or muscle variables in the intact bone. The amputated bone had significant decreases (p<0.01) in BMC (-28%) and vBMD (-24%) from pre-ambulatory to 6 and 12 month time points, but there were no differences between the 6 and 12 month time points (Table 1). SSI, Imin and MCSA showed the same pattern of results, but Imax decreased only at the 6 month time point. On the amputated bone, there was a decrease (p<0.05) in the proportion of bone area that was > 650 mg/cm^{3} (56.2% to

41.5% of total area) or > 480 mg/cm^{3} (63.4% to 51.3%), suggesting that the cortical bone became more porous after amputation. In conclusion, rapid and substantial losses in bone content and bone strength occur early after amputation and are not regained by 12 months of becoming ambulatory. It is unclear whether bone loss from amputation can be recovered; early post-amputation appears to be the most critical window for potential efforts to prevent bone loss.

Table 1. Changes (Mean ± SE) in the Amputated Bone (n=9)

Variable	Pre-Ambulatory	6 Months with Prosthesis	12 months with Prosthesis
BMC (mg/mm)	430.63 ± 19.66	329.37 ± 24.49**	310.45 ± 27.44**
vBMD (mg/mm^{3})	683.63 ± 37.03	550.96 ± 49.01**	530.50 ± 55.80**
SSI (mm[3])	2521.30 ± 148.08	1871.42 ± 209.66*	1793.53 ± 224.37*
Imax (mm[4])	28433.24 ± 3021.45	19193.67 ± 2283.35*	19813.31 ± 3008.43
Imin (mm[4])	21756.06 ± 2121.51	15718.71 ± 2240.35*	13754.19 ± 2458.04*

* p<0.05; ** p<0.01 vs. Pre-Ambulatory

Table 1

Disclosures: Debra Bemben, None.

MO0021

Comparison of short term *in vivo* precision of cortical bone micro-architecture between two HR-pQCT assessment methods at the distal radius and tibia in postmenopausal women and young adults. Chantal Kawalilak*[1], James Johnston[1], David Cooper[1], W.P. Olszynski[2], Saija Kontulainen[1]. [1]University of Saskatchewan, Canada, [2]Midtown Professional Center (#103), Canada

Introduction. Precise measurement of cortical bone micro-architecture is fundamental when monitoring cortical bone changes and treatment effects. At present, it is unknown how endocortical boundary contour definition influences precision of cortical bone micro-architecture using HR-pQCT. Our purpose was to assess whether HR-pQCT precision of cortical bone micro-architecture in postmenopausal women and young adults differed when using the automatic and modified endocortical contouring methods.

Methods. We scanned the distal radius and tibia at two time points in 30 young adults (mean age 27, SD ± 9 years) and 34 postmenopausal women (74 ± 7 years) using HR-pQCT (XtremeCT). Standard protocols were used to define the periosteal surface. Dual-threshold technique was used to define endocortical surface. Cortical bone outcomes of repeated scans were determined using a) automatically generated contour line, and b) manual correction of the endocortical contour line. Precision error (CV%$_{RMS}$), Least Significant Change, and 95% Limits of Agreement were calculated for the following cortical bone outcomes: perimeter, endocortical perimeter, porosity, porosity volume, pore diameter, pore diameter distribution, total volume, bone volume, density, and thickness. We used Wilcoxon sign rank tests to compare precision error between the two contour protocols for non-parametric variables. Paired samples *t*-tests were used to compare parametric variables. Bonferroni adjustments for multiple comparisons were used for all analyses. Significance was accepted at $P<0.005$.

Results. No significant differences were found between the two methods apart from the endocortical perimeter measure in the distal tibia of postmenopausal women (Automatic CV%$_{RMS}$: 0.6, Modified CV%$_{RMS}$: 3.2; $P<0.0001$).

Discussion. The automatic endocortical contouring method appeared to provide as precise cortical bone outcomes as manually modified endocortical contours in both postmenopausal women and young adults. Based on these results, automatic contouring of the endocortical surface can be recommended to save time and costs in cortical bone image analysis from HR-pQCT scans.

Disclosures: Chantal Kawalilak, None.

MO0022

Composite but Not Individual Tissue-Level Bone Traits Differ Significantly Between Femurs that are Stronger vs. Weaker for Body Size. Daniel Nicolella*[1], Arthur Nicholls[2], Don Moravits[2], Jennifer Harris[3], Shayna Levine[3], Travis Eliason[2], Jeffry Nyman[4], Todd Bredbenner[1], Lorena Havill[5]. [1]Southwest Research Institute, USA, [2]Southwest Research Institute, USA, [3]Texas Biomedical Research Institute, USA, [4]Vanderbilt University Medical Center, USA, [5]Texas Biomedical Research Institute, USA

The structural integrity of bone is an integrative function of a multitude of complex and interrelated traits of the bone matrix, microstructure, macroscopic bone morphology, and bone density. Co-adaptation of these traits provides for redundant combinations of traits through which the skeleton is able to provide nominally equivalent functionality under "normal" loading conditions; however, particular

combinations of traits sufficient for everyday loading could be suboptimal when subjected to atypical, traumatic loads such as those encountered in a fall. We measured the following compositional and biomechanical traits in cortical bone from 45 pedigreed baboons: porosity, apparent density, ash and water content, collagen crosslinks (pyridinoline, deoxypyridinoline, pentosine, and total collagen content), elastic modulus, yield and peak strain, yield and ultimate stress, toughness, and post yield toughness. We also measured robustness, polar moment of inertia, anterior-posterior (AP) and medial-lateral (ML) section modulus, and AP and ML slenderness ratios. We used principal components analysis to identify independent composite traits (combinations of the compositional, biomechanical, and morphological traits) that describe variability within the group. The strength of the proximal femur was measured in 3-point bending in a loading direction orthogonal to the predominant daily functional load direction then normalized by body mass. Femurs were ranked from high to low based on strength/mass ratio. The highest ranking half and the lowest ranking half were compared as the "stronger" vs. the "weaker" group and tested for significant differences in individual and PCA-derived composite traits. None of the individual tissue-level traits differed significantly between groups (p>0.05) while all morphology traits did differ significantly (p=0.002-0.016). However, the composite traits of bone tissue-level properties (porosity, ash and water content, collagen crosslinks, modulus, tissue yield properties) together with morphology differed significantly between groups (p=0.001-0.023). Our results support that bone traits co-adapt to functional loading in a complex multivariate manner at multiple hierarchical length scales, and indicate that multivariate discriminators (composite traits) that encompass variation at all of these levels are most appropriate for rapidly advancing our understanding of bone fragility and identifying novel targets for therapeutic intervention.

MO0023

Effects of strontium ranelate on the intrinsic quality of human bone tissue.
Sebastien Rizzo*[1], Delphine Farlay[2], Audrey Doublier[1], Georges Boivin[3]. [1]INSERM, UMR 1033, Université de Lyon, France, [2]INSERM, UMR1033; Université De Lyon, France, [3]INSERM, UMR1033 ; Universite De Lyon, France

To assess precisely the effects of strontium ranelate (SrRan) on bone tissue, intrinsic quality (mineralization, microhardness, mineral and organic characteristics) was analyzed in women with postmenopausal osteoporosis before and after prolonged treatment with SrRan. This treatment reduces the risk of fracture (1,2) via a mechanism of action partially elucidated. Thirty eight iliac bone biopsies were taken from women with postmenopausal osteoporosis before (N=10) or after 3-8 yrs of SrRan (N=28), then were embedded in methyl methacrylate (3). Degree of bone mineralization, heterogeneity index of mineralization and microhardness were measured by quantitative microradiography and microhardness (4). Mineral and organic characteristics were assessed by Fourier transform infrared microspectroscopy (5,6). Degree of mineralization was not significantly modified by SrRan [before, cortical bone (cort): 1.05 ± 0.07 g/cm^3, cancellous bone (canc): 1.09 ± 0.09 g/cm^3; after 3 yrs, cort: 1.16 ± 0.09 g/cm^3, canc: 1.18 ± 0.08 g/cm^3; after 8 yrs, cort: 1.21 ± 0.07 g/cm^3, canc: 1.22 ± 0.03 g/cm^3]. Bone microhardness was also unchanged after SrRan (before, cort: 52.05 ± 2.73 kg/mm^2, canc: 52.93 ± 2.01 kg/mm^2; after 3 yrs, cort: 50.81 ± 3.50 kg/mm^2, canc: 52.96 ± 3.23 kg/mm^2; after 8 yrs, cort: 58.15 ± 1.80 kg/mm^2, canc: 56.76 ± 2.76 kg/mm^2). Mineral and organic characteristics of newly formed bone (mineralization index, mineral maturity, crystallinity index, carbonation and collagen maturity) were not significantly modified whatever duration of SrRan. Thus, in cortical and cancellous bone, intrinsic quality was not modified by a treatment, even prolonged, with SrRan. Present data are in agreement with those related on apatite crystals [crystallinity (size and/or perfection), lattice parameters (a) and (c), inter-reticular distances 002 (d$_{002}$) and 310 (d$_{310}$)] showing that these variables were not modified either by duration (3 yrs vs before) or type (SrRan vs placebo) of treatment (7). In conclusion, intrinsic quality of bone tissue was maintained at a physiologically normal level after different durations of treatment with SrRan at therapeutic dose.

1. Meunier et al. 2004, N Engl J Med 350:459-68 ; 2. Reginster et al. 2005, J Clin Endocrinol Metab 90:2816-22 ; 3. Doublier et al. 2011, Eur J Endocrinol 165:469-76 ; 4. Boivin et al. 2008, Bone 43:532-8 ; 5. Farlay et al. 2010, J Bone Miner Metab 28:433-45 ; 6. Farlay et al 2011. PLoS One 6:e28736 ; 7. Doublier et al. 2013, Osteoporos Int 24:1079-87

MO0024

High Resolution 3D-Printing of Trabecular Bone based on microCT data.
Volker Kuhn*[1], Nikola Ivanovic[2], Wolfgang Recheis[3]. [1]Medical University Innsbruck, Austria, [2]Medical University Innsbruck, Austria, [3]Medical University Innsbruck, Austria

Introduction:
Modern high-end 3D-printers enable resolutions up to 16µm. Purpose of the presented study was firstly, to investigate the quality and difference of microCT-based 3D-printed trabecular bone structures, and secondly, the biomechanical properties of such 3D-printed trabecular bone samples.
Material and Methods:
MicroCT scans of human trabecular samples with different bone quality were performed with a vivaCT40 (Scanco/CH) and analyzed according the standard settings. Based on these data typical STL-files were created for 3D-printing purpose for the use with a high-end 3D-printer. The washing-out procedure of the necessary supporting material was optimized with appropriate chemical solutions. In the next step original bone structures were compared with the 3D-printed copies from microCT based data by image registration.
Results:
The selected procedure enables high conformity between original and high resolution 3D-printed trabecular bone structures. The conformity is affected by image and printing resolution, thresholding and filtering parameters.
Conclusion:
After further optimization of the selected 3D-printing materials it is possible to achive appropriate E-modulus values of different trabecular bone qualities. Such artificial created bone samples may be helpful for future standardized biomechanical testing of newly developed osteosynthesis screws and implants for osteoporotic fractures.

MO0025

Menopause is Not Followed by Increased Mineral Loss but Increase in Bone Size. Magnus Karlsson*[1], Henrik Ahlborg[2], Ola Svejme[3], Jan-Åke Nilsson[4], Bjorn Rosengren[1]. [1]Skåne University Hospital Malmö, Lund University, Sweden, [2]Malmo University Hospital, Sweden, [3]Lunds Universitet, Sweden, [4]Department of Orthopedics & Clinical Sciences, Lund University, SUS, Sweden

Purpose: Bone mineral density (BMD) is the clinical used estimate of bone mass, incorporated in the World Health Organization definition of osteoporosis. However, BMD (sometimes called areal BMD) depends not only on the amount of mineral but also bone size. The increased postmenopausal decline in BMD could thus hypothetically be the result of increased bone mineral loss, increased bone size, or both, to our knowledge never being evaluated.
Methods: We measured the amount of bone mineral, bone mineral content (BMC; mg), BMD (mg/cm^2) and bone width (mm) by single-photon absorptiometry at the cortical site of the forearm in a prospective observational study that included a population-based sample of 105 Caucasian women without medication or disease interfering with bone metabolism. We conducted 12 measurements during a 28-year period from mean 5 years (range 2 to 9) before to mean 24 years (range 18–28) after menopause. Menopause was defined according to World Health Organization criteria, i.e. permanent cessation of menstruation due to the loss of ovarian follicular activity. The onset of menopause was therefore determined retrospectively when 12 months of spontaneous amenorrhea was reported in conjunction with elevated serum levels of follicle-stimulating hormone.We calculated individual slopes for changes in the periods before, 0 to <8, 8 to <16 and 16 to 28 years after menopause. Data are presented as means with 95% confidence intervals.
Results: The were in all four periods a significant annual BMC loss of respectively 1.4% (–0.1, –2.6), –1.1% (–0.9, –1.4), –1.2% (–0.9, –1.6) and –1.1% (–0.8, –1.4). That is, that were no different loss in BMC in the four periods. In contrast, the was an annual increase in bone width only in the immediate postmenopausal period; the increase in bone width was in the four periods 0.4% (–1.2, 1.9), 0.7% (0.5, 0.9), 0.1% (–0.2, 0.4) and 0.1% (–0.2, 0.4), respectively. The increase in bone width was also significantly higher in the first than in the second (p=0.003) and the third (p=0.01) postmenopausal period.
Conclusion: Menopause is followed by an increase in bone with but no increased mineral loss.

MO0026

Micro-Architectural Parameters other than BV/TV and Fabric Bring No Further Contribution to Stiffness of Human Trabecular bone. Sarah Khadri[1], Ghislain Maquer[1], Jasmin Wandel[2], Philippe Zysset*[3]. [1]University of Bern, Switzerland, [2]Bern University of Applied Sciences, Switzerland, [3]University of Bern, Switzerland

Degradation of trabecular bone architecture belongs to most definitions of osteoporosis, but its actual contribution to bone fragility remains unclear. Although several studies reported statistically significant effects for the influence of morpho-logical parameters on trabecular bone stiffness and/or strength, no systematic analysis was performed to compare the relative importance of these parameters on multi-axial stiffness at relevant fracture sites.
Seven hundred and one trabecular bone cubes of 5.3 mm edge length from 44-82 years old male and female proximal femora, vertebral bodies and distal radii were scanned with 18 microns resolution. Classical morphometric indices such as bone volume fraction (BV/TV), mean intercept length based fabric tensor, degree of anisotropy (DA), bone surface (BS), connectivity density (Conn.D), structure model index (SMI), trabecular number (Tb.N), thickness (Tb.Th), spacing (Tb.Sp) and their

standard deviations (Tb.Th.SD, Tb.Sp.SD) were calculated. The homogenized stiffness tensors of all cubes were computed by linear micro finite element analysis using kinematic uniform boundary conditions. Relationships of the morphological parameters with the orthotropic elastic constants were investigated by linear models after log transform. Their relative contribution to the orthotropic model was established via ANOVA.

For the pooled data, all morphological parameters exhibit significant and sometimes high correlation with BV/TV, except DA derived from the fabric tensor (r=0.032 p>0.05). In single regressions, BV/TV achieves higher coefficients of determination with the elastic constants than any other parameter. In multiple regressions, parameters other than BV/TV and fabric are often significant, but contribute less to the total sum of squares of the bone elastic properties than the residuals (Table 1).Thirty years after introduction of bone histomorphometry, these results from a large sample database suggest that architectural parameters other than BV/TV and fabric do not further contribute to the prediction of trabecular stiffness at 3 major fracture sites. This implies that in terms of stiffness, there is no identifiable degradation in architectural quality beyond bone loss. In other words, trabecular bone remodelling maintains an optimally stiff structure for a given bone mass. Further studies are needed to test if this finding holds for yield strength and for bone altered by specific metabolic diseases.

	Femur	Radius	Vertebra	All
n	264	81	356	701
BV/TV	91.4	73.1	86.7	88.7
Fabric	6.9	23.4	8.9	8.1
Other parameters	1.3	1.3	1.2	0.8
Residuals	1.4	2.2	3.2	2.4
TOTAL	100.0	100.0	100.0	100.0

Table 1. Percentage of total variation of the elastic constants explained by architecture.

Disclosures: Philippe Zysset, None.

MO0027

Modulation of material property and composition parameters that contribute to impaired bone quality in Osteogenesis Imperfecta by anti-TGFβ treatment.
Xiaohong Bi*[1], Hao Ding[2], Ingo Grafe[3], Stefanie Alexander[4], Elda Munivez[4], Ming-Ming Jiang[4], Brian Dawson[4], Annie Abraham[5], Brendan Lee[6], Catherine Ambrose[7]. [1]University of Texas Health Science Center at Houst, USA, [2]Department of Nanomedicine & Biomedical Engineering, University of Texas Health Science Center, USA, [3]Department of Molecular & Human Genetics, Baylor College of Medicine, USA, [4]Department of Molecular & Human Genetics, Baylor College of Medicine, USA, [5]Department of Orthopaedic Surgery, University of Texas Health Science Center, USA, [6]Baylor College of Medicine, USA, [7]University of Texas Health Science Center at Houston, USA

Osteogenesis Imperfecta (OI) is characterized by low bone mass, deformities and fractures. In mouse models of OI some studies have demonstrated significant changes in bone mechanical properties and molecular composition compared with wildtype (WT) controls. Anti-TGFβ treatment using the neutralizing antibody 1D11 (Genzyme) improved the bone phenotype in OI mice with improved mechanical properties in a previous report. This study seeks to identify the material factors substantially contributing to the impaired bone quality in OI, and to characterize the response of such factors to anti-TGFβ treatment. For this, we utilized mice harboring a G610C mutation in the *Col1a2* gene that model a dominantly inherited form of OI. Femurs from 16 week old female mice (8 week old mice treated for 8 weeks: control WT, control OI and 1D11 treated OI) were analyzed with biomechanical testing and Raman spectroscopy.

When compared to WT, the control OI bones were significantly less stiff, withstood less energy and underwent less displacement after yield before failure. The parameters associated with bone plasticity (post-yield (PY) energy, displacement, toughness and strain) were also significantly reduced, consistent with increased brittleness. Collagen mineralization was significantly increased in OI bones and demonstrated a positive correlation with ultimate strength and elastic modulus and a negative correlation with PY energy and toughness. Decreased collagen density, carbonation, and mineral crystallinity were observed in OI compared to WT femurs. Collagen density was significantly correlated with bone plasticity. Carbonation and mineral crystallinity also correlated positively with PY energy and toughness.

With 1D11 treatment, the OI bones demonstrated a slightly higher ultimate strength and an increased elastic modulus, as well as a more normal carbonation, collagen density and mineral crystallinity. In the OI control and treated animals, enhanced mineral crystallinity and carbonation significantly correlated with bone plasticity, indicating an inverse relationship with brittleness. Increased collagen mineralization correlated to bone stiffness and the improved elastic modulus.

In summary, we find that collagen density, carbonate substitution and mineral crystallinity likely play critical roles in the inferior bone quality in OI. Anti-TGFβ treatment improved those parameters and could potentially be useful for reducing the fracture risk in OI patients.

Disclosures: Xiaohong Bi, None.

MO0028

Patients with stress fractures exhibit impaired bone material properties by microindentation. Daysi Duarte Sosa*[1], Erik Fink Eriksen[2]. [1]Ph.D., Norway, [2]Oslo University Hospital, Norway

Bone material properties are one of the key determinants of bone quality. Stress fractures are considered to result from microdamage accumulation secondary to repetitive strains exerting negative effects on bone material properties. We therefore wanted to test, whether subjects with stress fractures show impaired bone material properties. Bone material properties were assessed by microindentation, which measures the indentation distance increase (IDI) into the thick cortex of the tibia. We used a new instrument (Osteoprobe®, Active Life Scientific, Santa Barbara, CA) to measure IDI in 16 subjects with stress fractures (age range, 18-74 yrs, males 3, females 13) and 41controls (age range 23-76 yrs, males 3, females 38). The IDI measured was standardized against a calibration phantom of methyl methacrylate, and results expressed in BMS (Bone Material Strength) units as percentage of this reference value.

Average BMS values were lower in stress fracture patients than controls (68.9 $\pm$ 9.9 % vs 76.7 $\pm$ 7.3% p= 0.01)(Figure). Total hip BMD was increased in controls 1.206 $\pm$ 0.160g/cm2 vs subjects with stress fracture 1.042 $\pm$ 0,166g/cm2 p= 0,005). Patients with stress fracture exhibited increased serum PINP (61$\pm$(30)) vs. controls, (43$\pm$(17); p=0,04), but revealed similar vitamin D levels (61$\pm$19 vs 64$\pm$31; p=0,72). No correlations between BMS and BMD at the hip, bone turnover, S-calcium and vitamin D were demonstrable.

Subjects with stress fracture show impaired bone material properties and reduced Bone Mineral Density. This combination may contribute to the increased fracture propensity in these patients.
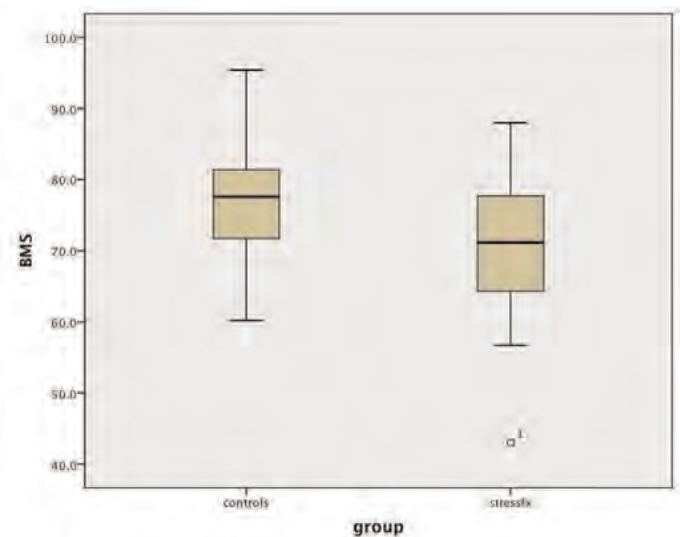

Figure BMS: Stress fx vs controls

Disclosures: Daysi Duarte Sosa, None.

MO0029

Proximal Femoral Strengths in Men and Women Age 27 to 90+: A Subject-Specific Finite Element Modeling Study. Joyce Keyak*[1], Tadashi Kaneko[2], Sundeep Khosla[3], Shreyasee Amin[4]. [1]Department of Radiological Sciences, University of California, Irvine, USA, [2]University of California, USA, [3]Mayo Clinic College of Medicine, USA, [4]Mayo Clinic, USA

Subject-specific finite element (FE) modeling is a robust tool for evaluating proximal femoral strength and hip fracture risk. However, interpreting FE strength values can be difficult, requiring a reference database containing FE-computed strengths for subjects with and without hip fractures. Unfortunately, most FE studies have focused on older subjects, making FE assessment of fracture risk in younger subjects, e.g. astronauts, problematic. Thus, the purpose of this study was to create a reference database containing FE-computed proximal femoral strengths of adult men and women of all ages.

QCT scans of the hips of 216 women and 181 men [mean age (range): 61 (27 to over 90) years, and 60 (28 to over 90) years, respectively] were obtained, with no exclusions, from a previous study of an age-stratified, random sample of Rochester, MN residents, the majority of whom were white (≥96%). The QCT scans (Light Speed QX-I; GE Medical Systems, Wakesha, WI, USA; 120kVp; 80mA; 3-mm-thick slices) were obtained using a K_2HPO_4 calibration phantom (Model 3, Mindways Software, Inc., San Francisco, CA, USA).

For each subject, FE models of the left proximal femur were generated using heterogeneous nonlinear material properties computed from QCT density (Keyak, Bone, 2013). Displacement was applied incrementally to the femoral head, and proximal femoral strength (the maximum femoral head reaction force) was computed for single-limb stance loading and for a posterolateral fall onto the greater trochanter.

Multiple linear regression was performed to relate strength in each loading condition to age (years) and sex (women=0, men=1).

Proximal femoral strengths (N) were associated with age (p<0.001) and sex (p<0.001) [Stance=19,973−137.5(Age)+3278(Sex), R^2=0.39; Fall=4763−18.2(Age)+685(Sex), R^2=0.37], indicating that, on average, stance and fall strengths, respectively, are 3278N and 685N greater in men than in women and demonstrate age-related decreases of 138N/year and 18N/year, with no age-sex interaction (p>0.4). From these rates, reductions in stance and fall strengths associated with fracture (Keyak, Bone, 2013) are respectively equivalent to 17 and 27 years of aging in men, and 7 and 11 years of aging in women. For comparison, mean reductions in stance (1648N) and fall (459N) strengths from long-duration spaceflight astronauts (age 40 to 55) (LeBlanc, Osteoporos Int, 2013) are equivalent to strength reductions normally associated with 12 and 25 years of aging, respectively.
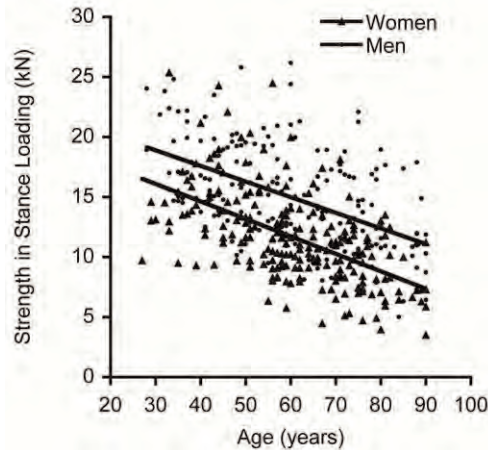
Proximal femoral strength in single-limb stance loading
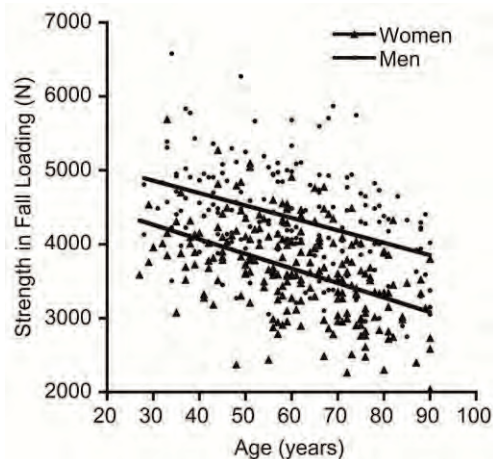
Proximal femoral strength in fall loading

Disclosures: Joyce Keyak, Finite element modeling method for fall loading is patent pending, 10

MO0030

Structural and Mechanical Properties of Trabecular Bone in the Distal Extremities Studied by Micro-MRI in Postmenopausal Women. Mahdieh Bashoor-Zadeh*[1], Mona Al Mukaddam[2], Wenli Sun[2], Eual Phillips[2], Chamith Rajapakse[3], Felix Werner Wehrli[4]. [1]University of Pennsylvania, USA, [2]University of Pennsylvania, USA, [3]University of Pennsylvania School of Medicine, USA, [4]University of Pennsylvania Medical Center, USA

Trabecular bone integrity is known to decline rapidly following menopause, resulting in compromised mechanical competence. There is evidence these effects are systemic but less is known whether bone loaded during daily living (tibia) is affected differently than unloaded bone (radius). This cross-sectional study examined µMR-derived trabecular structural parameters in the tibia and radius and determined the ability of these parameters to predict axial stiffness (AS). In addition, associations were examined between µMR-derived parameters at the two peripheral sites and DXA BMD in the central skeleton.

75 postmenopausal women, ages 55-78 years, were evaluated by µMRI of the left distal tibia and radius and DXA BMD at the spine and hip. High-resolution µMR images (137x137x410 μm^3 voxel size, 32 slices) were acquired at 3T field strength using

a 3D spin-echo sequence with a 4-element receive coil (tibia) and elliptical birdcage transmit-receive coil (wrist) at the distal metaphysis. Structural parameters (bone volume fraction (BV/TV), surface-to-curve ratio (S/C), trabecular thickness (Tb.Th) and number (Tb. N)) were measured. Finite-element analysis (FEA) was performed to compute trabecular AS by converting each voxel into hexahedral finite elements. AS was computed as the ratio of the stress on the proximal face to the applied axial strain.

MicroMR-derived structural parameters correlated with AS; the strongest explanatory variable was BV/TV at both distal sites (tibia R^2=0.89; radius R^2=0.55, p<0.0005); the association was stronger at the load-bearing site (tibia) than radius (Table1). Mean AS ($\pm$SD) of the tibia (917 $\pm$ 99 MPa) was much greater than that of the radius (358 $\pm$ 95 MPa, p<0.0005). AS of the tibia weakly correlated with DXA BMD at spine and hip (R^2=0.07 and 0.09, respectively, p<0.05), however those involving the radius did not.

BV/TV map of trabecular region of the tibia and radius, from two subjects (A, 59-YO, B,79-YO) highlight the loss of trabecular connectivity with age (Fig.1). The degree of structural integrity is reflected by the structural and mechanical parameters that are higher in subject A. In contrast, DXA BMD at the lumbar spine was greater in subject B (Table2), likely the result of aortic calcification or osteophytes.

In conclusion, µMRI-derived BV/TV is a strong predictor of mechanical competence (AS) of trabecular bone. Inclusion of other structural parameters into the model did not significantly improve that association.

Table1 Correlation (R^2, n=75) between µMR-derived structural parameters and AS at tibia and radius (* indicates p<0.0005).

Structural Parameters	Axial Stiffness	
	Tibia	Radius
BV/TV	0.89*	0.55*
S/C	0.66*	0.16*
Tb. Th.	0.47*	—
Tb. N	0.86*	0.65*
BV/TV & S/C	0.89*	0.58*
BV/TV & Tb.Th	0.91*	0.67*
BV/TV & Tb.N	0.91*	0.66*

Table2. µMR-derived structural and mechanical parameters at distal tibia and radius of subject A (59-YO) and subject B (79-YO)

Parameters	Subject A		Subject B	
	Tibia	Radius	Tibia	Radius
BV/TV(%)	9.85	8.41	8.88	6.90
S/C	6.67	5.70	5.25	3.97
Tb. Th (µm)	104	105	103	100
Tb. N (mm⁻¹)	0.95	0.80	0.86	0.69
Axial Stiffness (MPa)	912	472	854	413
DXA-BMD Spine (g/cm²)	0.792		0.915	
DXA Spine T-Score	-2.3		-1.9	

Figure 1. Computed grayscale maps of BV/TV map images of trabecular region of distal tibia and radius from subject A (59-YO) and subject B (79-YO), highlighting the loss of trabecular connectivity in subject B.

Table1_Table2_Figure1

Disclosures: Mahdieh Bashoor-Zadeh, None.

MO0031

The Effect of Diabetes on Bone Strength and Collagen Cross-linking. Stephen Warner*[1], Heather Hunt[2], Jonathan Jo[3], Kate Meyers[3], Edward DiCarlo[3], Joseph Lane[1], Eve Donnelly[4]. [1]Hospital for Special Surgery, USA, [2]Cornell University, USA, [3]Hospital for Special Surgery, USA, [4]Cornell University, USA

Patients with diabetes have an increased fracture risk compared to non-diabetics even after accounting for changes in bone mineral density (BMD), suggesting that diabetes affects not only the quantity of bone but also the quality. Studies using diabetic animal models demonstrate that diabetic animal bone is weaker than non-diabetic bone, and this may correlate with changes in collagen advanced glycation end products (AGEs). However, an extension into humans is lacking. Because of the high and increasing prevalence of diabetes, in addition to the morbidity that results from fractures, insight into how diabetes affects bone quality in humans has significant clinical implications. Our objective was to examine whether diabetes is associated with changes in bone mechanical properties and collagen AGEs.

Cancellous bone cores were removed from femoral neck specimens of patients undergoing total hip arthroplasties for osteoarthritis. All patients included in the study had a glycated hemoglobin (HbA1c) measurement within one month of surgery. Specimens were allocated to the control group (HbA1c < 6.0) or the pre-diabetic and diabetic group (HbA1c > 6.0). Each core was imaged using micro-computed tomography to assess bone microarchitecture and density. Unconfined compression testing was performed to obtain load-displacement data. Subsequently, specimens were assayed for AGEs and total collagen content.

Based on power analyses from animal studies, a total of 18 specimens underwent complete testing, including 9 control and 9 pre-diabetic and diabetic age- and gender-matched specimens. The average HbA1c was 5.52 in the control patients and 6.86 in the pre-diabetic and diabetic group (p < 0.001). Average elastic modulus was decreased by 20% in the diabetic patients compared to controls (214.6 MPa versus 267.3 MPa) and average AGE content was 23% increased in the diabetic samples compared to controls (1193 versus 972). However, these differences were not statistically significant. Bivariate regression analyses did not demonstrate a significant association between HbA1c and core mechanical properties.

In our cohort of patients, HbA1c did not significantly correlate with changes in bone mechanical properties or with local AGE content in the femoral neck. Additional studies will be useful to determine if differences exist with a larger subset of patients or in different anatomic areas. Alternatively, other clinical measures of diabetes other than HbA1c may be more representative of altered bone metabolism.

Disclosures: Stephen Warner, None.

MO0032

The Femoral Neck Strength of Post-menopausal Women is Predicted by Factors at Multiple Length Scales. Adam Abraham*[1], Simon Tang[2], Avinesh Agarwalla[3]. [1]Washington University at St.Louis, USA, [2]Washington University in St Louis, USA, [3]Washington University in St.Louis, USA

As a hierarchical structure, bones' overall ability to resist fracture is determined by factors at multiple length scales. Although bone mineral density is routinely used to assess fracture risk, recent clinical evidence show that patients with altered bone material properties and structure, such as those with diabetes mellitus, have an elevated risk of fracture independently of BMD. It is thus critical to assess fracture risk at multiple scales. We sought to understand the relative contributions of material level properties (reference point micro-indentation, RPI), tissue structure (cortical porosity), and bone mass (DeXA T-score) on the femoral neck strength of postmenopausal women. Using these relationships we aim to improve to predictive fidelity of femoral neck strength by incorporating these clinically measurable factors at multiple scales. 48 whole lower limbs from fresh postmenopausal female cadavers (57-97y) were used for this study. T-score was acquired using a clinical DeXA system (Hologic). RPI (BioDent Hfc) was performed *in situ* at the tibia mid-diaphysis for each leg through the skin (15 sites/limb), and the parameter indentation distance increase (IDI) was averaged for each leg. Micro-CT (Scanco Medical Ag, 30μm^3 voxel size) was used to determine the cortical porosity at the anterior tibial mid-diaphysis. Femoral neck strength was assessed by compressively loading at the femoral head to failure at adduction 12° using a material test stand (Instron). Linear correlations were examined between the predictors T-score, cortical porosity, and IDI and response variables ultimate strength and work-to-failure. T-score ranged from -4.6 to +0.5. T-score, cortical porosity, and IDI were significantly linearly correlated with ultimate strength (r=0.74; r=-0.51; r=-0.46, respectively) and work-to-fracture (r=0.51; r=-0.45; r=-0.44, respectively). Multivariate regression analysis incorporating each permutation for predictors of strength improved the correlation (IDI+Porosity, r=0.63; IDI+T-score, r=0.80; IDI+Porosity, r=0.83; IDI+Porosity+T-score, r=0.88). Although the T-score is the strongest single predictor of strength, our findings reveal that factors at other scales are also significant predictors. Moreover, the prediction of an individual's bone strength is improved by incorporating multiple personalized quantitative factors, demonstrating the diagnostic potential of such a multi-scale approach.
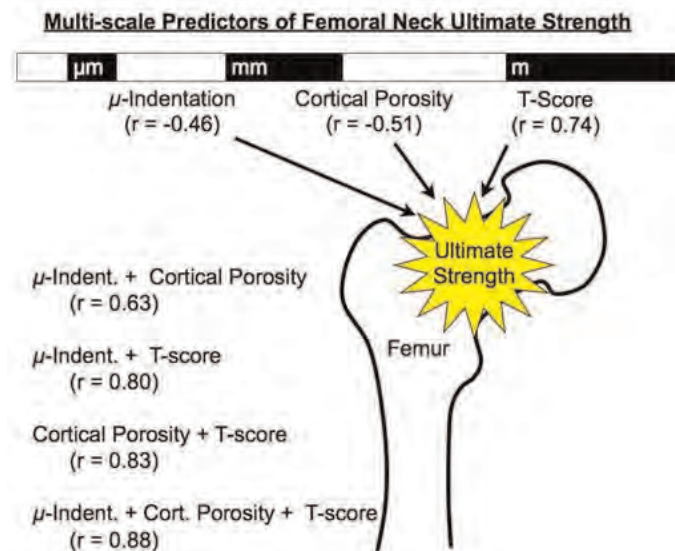
Multi-scale predictors of femoral neck ultimate strength

*Disclosures: **Adam Abraham**, None.*

MO0033

Validation of a digitized device of microradiography for the characterization of bone mineralization. Florian Montagner*[1], Valérie Kaftandjian[2], Delphine Farlay[3], Daniel Brau[4], Georges Boivin[5], Helene Follet[5]. [1]INSERM UMR 1033, Université de Lyon, France, [2]Laboratoire Vibrations Acoustique, INSA de Lyon, France, [3]INSERM, UMR1033; Université De Lyon, France, [4]Photonic Science, France, [5]INSERM, UMR1033 ; Universite De Lyon, France

The quantitative microradiography is an imaging technique for the study of variables characterizing the quality of bone mineralization. Until now, photographic films were used for their high power of resolution. New digital detectors, now allow to obtain an image quality close to that of films. Our aim is to validate the replacement of films by a digital detector for bone mineralization analysis. A prototype has been developed in collaboration with Photonic Science. The X-ray source is a copper anode associated with a nickel filter (similar to the photographic system). The parameters chosen to evaluate the quality of the image are: the contrast-to-noise ratio (CNR) and spatial resolution. CNR evaluates the quality of the information provided by the gray levels contained in the image. CNR was calculated between two aluminum steps whose attenuations are close to those obtained with a 100 μm-thick section of bone. With a power of 2 W, the best CNR (i.e., 6) was obtained at 50 kV, 40 μA and with an averaging of 6 images. The spatial resolution concerns the ability to separate details in an image. It is generally measured by curves representing the contrast obtained for a periodic object whose spatial frequency is expressed in pair of lines per millimeter (lp/mm). The modulation transfer function (MTF) when the profile of the object is sinusoidal and the contrast transfer function (CTF) when the profile is rectangular, were used. The MTF is defined by the modulus of the Fourier transform of the impulse response of the system and obtained by deriving a straight edge profile. MTF and CTF have been obtained by imaging respectively a straight object and a calibration pattern engraved lp/mm. Both curves showed that with the digital system, a magnification factor of 4 is necessary to have an equivalent resolution of the photographic system. It represents a resolution of 100 lp/mm. Photographic and digital systems had a similar image quality. The digital system has advantages: easy to use and absence of supplies, reduced acquisition time and digital data storage. The reproducibility was also improved by removing the photographic processing. Digitized microradiography has been validated to measure the different variables characterizing bone mineralization. These variables are validated by comparing the measurements with both systems for the same group of samples and calculating the level of uncertainty associated with the measurements.

*Disclosures: **Florian Montagner**, None.*

MO0034

Vertebral Fracture Load Predicted with Finite Element Model from Bi-planar X-rays Absorptiometry for Osteoporosis Assessment. Julie Choisne*[1], Christophe Travert[1], Jean-Marc Valiadis[2], Anabela Darbon[3], Philippe Rouch[2], Wafa Skalli[1]. [1]Arts et Metiers ParisTech, France, [2]Arts et Metiers ParisTech, LBM, France, [3]EOS imaging, France

Finite element models (FEM) derived from QCT-scans were developed to evaluate vertebral strength, and fracture load. However, the high dose, time and cost of CT-scanner are limitations for routine osteoporotic diagnosis. A new approach considers using bi-planar dual energy (BP2E) X-rays absorptiometry to build vertebral FEM using synchronized lateral and frontal radiographs. A previous pilot study showed the feasibility of estimation of the 3D bone mineral density (BMD) distribution within vertebrae using a BP2E model from EOS radiographs. The purpose of this study was to confirm the predictability of the vertebral fracture load calculated from a BP2E-based FEM compared to a QCT-scan based FEM which is considered as a gold standard.

Eighteen vertebrae were used for the pilot study and were QCT scanned with a mindway calibration phantom. In addition, 28 vertebrae were scanned with the European Spine Phantom (ESP). All the forty six lumbar vertebrae (8 women and 5 men, donor age 83 ±9 years) were imaged in BP2E using the EOS imaging dual energy prototype device along with the ESP phantom for bone mineral density calibration. In the QCT-based FEM, the geometry was obtained by segmentation of the QCT-scan slices, and material properties were assigned to each element of the mesh according to the BMD value measured in the corresponding voxels of the calibrated QCT-scans. In the BP2E based FEM, the geometry was reconstructed in 3D using bi-planar EOS images acquired simultaneously in the frontal and sagittal planes. First a generic BMD distribution is applied to this geometry from an independent vertebral model database, and then each element's BMD values are adjusted to fit the BMD value measured in the lateral dual energy image. Vertebral fracture load prediction from the BP2E based FEM and the CT scan based FEM were compared.

The average vertebral fracture load was 3321N ±1657 and 4030N ±1728 for the QCT scan based FEM and BP2E based FEM respectively with a root mean square error of 641N. The coefficient of determination was 0.92 with a standard error of the estimate of 461N in fracture load prediction from the BP2E model.With a Pearson's correlation of 0.96, the bi-planar dual energy X-rays absorptiometry model appears to be a good alternative to QCT FEM. With its fast acquisition and analysis time, this low-dose technique could be used in routine clinic for osteoporotic fracture risk assessment after *in vitro* and *in vivo* validation.
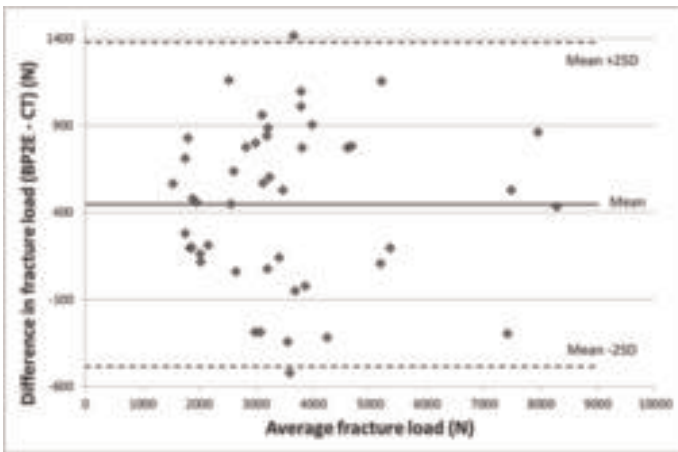
Bland Altman plot of the differences in vertebral fracture load prediction between the 2 models

Disclosures: Julie Choisne, None.

MO0035

Differences in Bone Microarchitecture and the Degree of Bone Loss during Hindlimb Unloading between C57BL/6J and C57BL/6N Mice. Jeyantt Srinivas Sankaran*[1], Alyssa Tuthill[2], Leah Rae Donahue[3], Stefan Judex[1]. [1]Stony Brook University, USA, [2]Stony Brook University, USA, [3]Jackson Laboratory, USA

Differences in the amount of bone loss induced by unloading can be large between inbred strains of mice. While environmental factors may account for some differences, genetic variability is a principal determinant of bone's sensitivity to unloading. C57BL/6 knockout (KO) mice are often used to investigate gene-effects on the musculoskeletal response to hindlimb unloading (HLU). C57BL/6J (B6J) and C57BL/6N (B6N) are the two main sub-strains used to generate genetic KO. These sub-strains exhibit slight variations in their genome including 34 single nucleotide polymorphisms (SNP) and 2 insertion-deletion (INDELS) in coding regions and 15 gene linked chromosomal structural variations (SV). We recently identified one SNP and one SV as potential modulators of bone's sensitivity to unloading in a genetic linkage study. We therefore hypothesized that B6J and B6N will respond differently to HLU. 9wk old female B6J and B6N mice (n=34) were assigned to baseline control, age matched control and hindlimb unloaded (HLU) groups. Mice were HLU for 2wk and variables indicative of bone quantity and architecture were analyzed by μCT in the distal metaphysis and midshaft of the femur. In the metaphysis, at baseline, B6N mice had 21% lower bone volume (BV), bone volume fraction and 6% lower trabecular number and thickness when compared to B6J mice (all P<0.05) while total volume (TV) and connectivity density were similar between strains. The cortical compartment of the metaphysis was similar between the two strains at baseline. In the midshaft, however, cortical bone morphology was different in B6N including a 9%, 10% and 14%, lower cortical thickness, cortical area, and porosity when compared to B6J (all P<0.01) while marrow area and the total area remained similar. Upon HLU, tissue losses were similar between B6J and B6N in the trabecular metaphysis and cortical bone in the midshaft. However, cortical bone in the metaphysis of HLU B6N was more susceptible with 18%, 9% and 3% lower BV, TV and marrow volume when compared to its respective controls. In contrast, B6J mice displayed only 15%, 6.5% and 1% reductions in these indices (Gene*HLU, all P<0.05). These data show complex differences in trabecular architecture and its response to unloading between B6N and B6J mice. Together, they highlight the importance of even very subtle genomic differences between inbred sub-strains and emphasize that the genetic background of C57BL/6 knockout mice needs to be selected carefully.

Disclosures: Jeyantt Srinivas Sankaran, None.

MO0036

Zolendronic Acid Administered Before Disuse Conserves Cancellous Bone Microarchitecture by Suppressing Turnover. Corinne Metzger*[1], Michael Junior[1], Ramon Boudreaux[1], Jacqueline Perticone[1], Harry Hogan[2], Susan Bloomfield[3]. [1]Texas A&M University, USA, [2]Texas A&M University, USA, [3]Texas A&M University, USA

Periods of disuse such as bed-rest, injury, or long-duration spaceflight induce rapid bone loss, especially in cancellous compartments. Through independent mechanisms, bisphosphonates and exercise can mitigate bone loss due to disuse. However, our group's previous data demonstrated that a bisphosphonate blunted the anabolic effect of exercise on bone during rodent hindlimb unloading (HU). The goal of this study was to quantify the effects of simulated exercise [impact loading (IL)] and a single administration of Zoledronic acid (ZA) immediately prior to a period of disuse. We

hypothesized this novel sequential pre-treatment would better protect against disuse-induced cancellous bone loss than either treatment alone. Male Sprague Dawley rats (6 mo.) were block assigned by weight to cage control (CC), hindlimb unloading without any pre-treatment (HU), 5 weeks of IL prior to HU (IL+HU), ZA administration prior to HU (ZA+HU), and IL plus ZA prior to HU (IL+ZA+HU). IL consisted of 25 high-impact, free fall drops from 60 cm per session 3x/week. A single dose of ZA (60 μg/kg) was given immediately following IL and just prior to 28 days of HU. Standard histomorphometry at the proximal tibia metaphysis revealed that ZA treated HU groups had greater cancellous bone mass (BV/TV %), higher trabecular number, and lower trabecular separation than both non-ZA treated HU groups (p<0.05). Osteoclast surface increased 2-fold in HU compared to CC, but was 4-fold lower with ZA treated groups vs. HU (p<0.001); IL alone mildly reduced osteoclast surface compared to HU (47% lower, p<0.05). IL mitigated the HU-induced increase in serum TRAcP 5b, but ZA treatment exhibited the lowest TRAcP 5b values of all groups – 5-fold lower than HU alone (p<0.05). Serum TRAcP 5b and osteoclast surface were positively correlated (R^2 = 0.58). Bone formation rate was 2-fold lower in HU vs. CC and ZA treated groups were significantly lower compared to HU and IL+HU. In conclusion, we found pre-treatment with IL improved measures of osteoclast activity compared to HU, but did not maintain optimal microarchitecture. ZA prior to a period of disuse successfully preserved cancellous microarchitecture while suppressing overall bone turnover. There was no synergistic effect of IL and ZA pre-treatments. ZA appears to be a potent inhibitor of disuse-induced bone loss and may be a valuable pre-treatment in clinical populations to mitigate the detrimental impact of prolonged periods of bed rest.

Disclosures: Corinne Metzger, None.

MO0037

A comprehensive study of long-term skeletal changes after spinal cord injury in adult rats. Tiao Lin*[1], Wei Tong[2], Abhishek Chandra[1], Shao-Yun Hsu[3], Haoruo Jia[4], Wei-Ju Tseng[1], Ji Zhu[5], Xiaowei Liu[1], Dongming Sun[3], Wise Young[3], Ling Qin[1]. [1]University of Pennsylvania, USA, [2]Perelman school of medicine, USA, [3]Rutgers, The State University of New Jersey, USA, [4]University of Pennsylvania, USA, [5]University of Pennsylvania, School of Medicine, USA

Rapid bone loss in low extremities after spinal cord injury (SCI) represents one of the most severe forms of osteoporosis. Almost all previous rodent studies have examined bone damage at the acute SCI stage in adolescent rodents. To mimic the clinical scenario that SCI patients are normally adults and to search for possible remedy, we performed a comprehensive analysis of long-term structural and mechanical changes in axial and appendicular bones in skeletally mature rats with or without olfactory ensheathing glia (OEG) transplantation, a treatment accelerating axonal regeneration in the central nerve system. Four-month old Fischer 344 male rats received a spinal cord contusion injury at T13 were divided into two groups (n=5/group) injected with either vehicle or OEG cells (400,000/rat). Four months later, femurs, tibiae, humeri, L4 and T8 vertebrae, were collected from these SCI rats and age-matched uninjured controls (n=6) for microCT, micro-finite element, and histomorphology analyses. We found extreme losses of bone mass (65%) and mechanical competence (90%), accompanied by reductions in trabecular number (36%) and thickness (26%) and an increase in structure model index (SMI, 3.9-fold), in the metaphysis of sublesional bones, particularly distal femur and proximal tibia, in SCI rats compared to controls. Interestingly, the subchondral trabecular bone had a much milder bone loss (20%) and structural deterioration, implying that the mechanism for SCI-induced trabecular bone loss is site-specific even within the same bone. In contrast, SCI mildly affected supralesional humeri with only a trend of trabecular bone loss. In regards to axial bones, significant decreases in bone mass and strength were observed in both superlesional T8 and sublesional L4 vertebrates with more severer bone damage in L4. Histomorphometry revealed that SCI resulted in a 71% decrease in osteoblast number and a 3.7-fold increase in osteoclast number, which were consistent with changes in serum bone markers. OEG treatment did not significantly improve bone structure and mechanical property after SCI. In conclusion, our data revealed site-specific effects of SCI on bone and demonstrated sustained inhibition of bone formation and elevation of bone resorption at the chronic stage of SCI. Hence, bone anabolic agents that greatly stimulate new bone formation should be suitable treatments for long-term SCI-induced osteoporosis.

Disclosures: Tiao Lin, None.

MO0038

Age-related calcification may increase the stiffness of costal cartilage. Dennis Anderson*[1], Daniel Brooks[2], Alexander Bruno[3], Mary Bouxsein[4]. [1]Beth Israel Deaconess Medical Center, USA, [2]Beth Israel Deaconess Medical Center, USA, [3]Harvard-MIT, USA, [4]Beth Israel Deaconess Medical Center, Harvard Medical School, USA

The mechanical properties of costal cartilage, which connects the bony ribs to the sternum, have not been well studied. Age-related changes may alter mechanical properties. In particular, calcification within the cartilage is known to increase with age. We hypothesized that larger amounts of calcification would increase the measured bending modulus of costal cartilage. We tested 12 fresh frozen human cadaveric costal cartilage from 5 donors (2 men, 3 women, age range 47 – 93 years).

Cartilages were from left ribs 3 – 6, and were potted at each end in polymethylmethacrylate cement, and mechanically tested in a four-point bending configuration with the posterior side up. Images were taken during testing and analyzed to determine the curvature of the specimen. Specimens also underwent pQCT scans to determine cross-sectional geometry and quantify the amount of calcification in each specimen. Bending modulus for each specimen was calculated, and correlated with amount of calcification. Mean bending modulus was 121 ± 111 MPa, and mean amount of calcification was $15.0 \pm 13.9\%$. Modulus was positively correlated with amount of calcification ($r = 0.61$, $p = 0.035$). This indicates that cartilage stiffness is affected by calcification in the cartilage, a known age-related change, which may result in altered thoracic biomechanics.

Disclosures: Dennis Anderson, None.

MO0039

Alterations in vertebral endplate microarchitecture and adjacent disc health in the UCD-T2DM rat model of type 2 diabetes. Aaron Fields*[1], Britta Berg-Johansen[2], Lionel Metz[2], James Graham[3], Kimber Stanhope[3], Peter Havel[3], Jeffrey Lotz[2]. [1]University of California, San Francisco, USA, [2]University of California, San Francisco, USA, [3]University of California, Davis, USA

Type 2 diabetes adversely affects many tissues, and the greater incidence of intervertebral disc pathologies among diabetics suggests that the disc is affected too. Although diabetes-related complications in the disc may relate to the increased accumulation of advanced glycation end products (AGEs) with hyperglycemia, hyperinsulinemia could also be important. For example, increased insulin levels during the pre-diabetic state can have an anabolic effect on bone metabolism. Any increases in bone formation in the vertebral endplate, i.e. sclerosis, could negatively impact disc health since the disc is avascular and thus, sclerosis could hinder nutrient transport to the disc. The purpose of this study was to test the hypothesis that T2DM compromises disc health, and that these changes associate with diminished endplate microarchitecture and with increased AGE accumulation. Caudal motion segments were harvested from 6-month-old lean Sprague Dawley rats, non-diabetic obese Sprague Dawley rats, and diabetic obese UCD-T2DM rats (diabetic for 69 ± 7 days; $n = 6$ rats/group). At sacrifice, the obese diabetic and non-diabetic rats had significantly higher insulin levels than age-matched controls (Table). Diabetic rats also had substantially higher glucose and HbA1c concentrations. Diabetes but not obesity caused dramatic changes in disc composition that were consistent with the early stages of degeneration. Diabetes reduced disc nucleus glycosaminoglycan (GAG) content by 51% ($p < 0.005$) and water content by 12% ($p < 0.005$); these degenerative changes correlated with a 21% increase in endplate thickness and 41% decrease in endplate porosity (Figure 1). GAG content decreased with increasing endplate thickness ($r = -0.56$, $p = 0.02$) and with decreasing endplate porosity ($r = 0.47$, $p = 0.05$). Also, diabetes but not obesity significantly increased AGE concentrations in the disc. In the annulus, AGE concentration was elevated by 50% ($p < 0.001$); in the nucleus, by 140% ($p < 0.0001$). As expected, increased AGE concentrations were independently correlated with lower GAG contents ($r = -0.72$, $p = 0.002$). These findings indicate that in addition to increased AGE levels in the disc, adjacent endplate sclerosis could also be an important factor for explaining the higher incidence of disc pathology in type 2 diabetes.

Table 1: Body weight, glucose, insulin, and HbA1c data (mean ± SEM) for 6-month-old lean Sprague Dawley (SD), obese SD, and UCD-T2DM rats.

	Lean SD (n = 5 rats)	Obese SD (n = 6 rats)	UCD-T2DM (n = 6 rats)
Diabetes duration (days)	NA	NA	69 ± 7
Body weight (g)	426.0 ± 12.1	693.7 ± 29.0[a]	563.5 ± 18.9[c,d]
Non-fasting glucose (mg/dl)	112.2 ± 3.4	112.2 ± 4.7	546.2 ± 18.5[a,b]
Fasting glucose (mg/dl)	91.8 ± 3.2	98.7 ± 2.8	246.4 ± 52.6[c,d]
Fasting insulin (ng/ml)	0.6 ± 0.07	1.4 ± 0.2[c]	1.4 ± 0.3[c]
HbA1c (%)	4.5 ± 0.09	4.3 ± 0.06	11.8 ± 1.28[a,b]

ANOVA w/ Tukey-Kramer test; [a] $p < 0.0001$ vs. lean SD; [b] $p < 0.0001$ vs. obese SD; [c] $p < 0.05$ vs. lean SD; [d] $p < 0.05$ vs. obese SD

Table 1
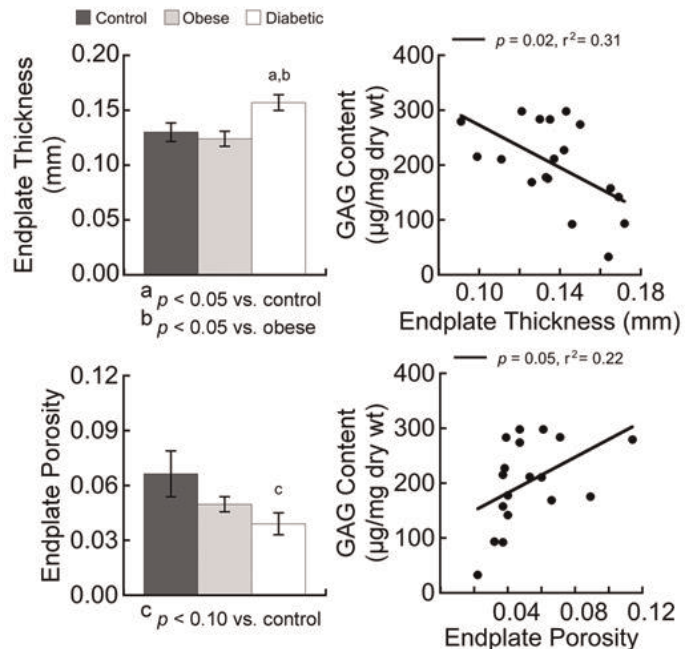
Figure: Diabetes-related changes in endplate thickness and porosity correlated with reduced disc GAG content.

Figure 1

Disclosures: Aaron Fields, None.

MO0040

Differential effects of strontium ranelate on bone microarchitecture in vivo and osteogenic differentiation in vitro - role of vitamin D. Claudia Sedlinsky*[1], Juan Manuel Fernandez[2], María Silvina Molinuevo[2], León Schurman[2], Ana María Cortizo[2], Anthony Desmond McCarthy[2]. [1]Universidad Nacional de La Plata, La PlataHospital Cesar Milstein, Buenos Aires, Argentina, [2]LIOMM, Universidad Nacional de La Plata, Argentina

Advanced glycation end products (AGEs) are increased in diabetes, and this has been associated with bone fragility and vascular calcifications. Strontium ranelate (SrRan) has been approved in several countries as a therapeutical option for osteoporosis treatment. We evaluated the effects of SrRan on bone microarchitecture in diabetic rats, and of SrRan and/or 25-OH-vitamin D (VD) on the osteogenic potential of vascular smooth muscle cells (VSMC). Diabetic Sprague Dawley rats were either untreated (D) or treated with 625 mg/kg/day SrRan (DR). Untreated non-diabetic rats (C) were also evaluated. Femora were dissected for histologic examination. VSMC were isolated from the aorta of C rats, and incubated with 100 µg/ml of either bovine serum albumin (BSA) or AGEs-BSA, in the presence or absence of 100 µM SrRan and/or 70 ng/ml VD. Cell proliferation (MTT bioassay) and cell migration (wound assay) were assessed. VSMC were also cultured in an osteogenic medium, after which collagen production, mineral nodules, Runx-2 and alpha-actin were determined. Results: bone histology was altered in D group (trabecular area: 71% vs. C, p<0.01; osteocytes: 69% vs. C, p<0.01; marrow adiposity: 1339% vs. C, p<0.001); SrRan significantly prevented Diabetes-induced trabecular area loss (p<0.01) and bone marrow adiposity (p<0.05). SrRan increased VSMC proliferation and migration (125% and 150% vs. BSA respectively, p<0.01), as did incubation with AGEs (130% and 150% vs. BSA respectively, p<0.01). Co-incubation with SrRan and AGEs showed an additive effect on proliferation: 160% vs. BSA and migration: 200% vs. BSA, p<0.01). After osteogenic induction of VSMC, the presence of SrRan and/or AGEs increased collagen and mineral vs. BSA in an additive manner (p<0.01). SrRan and AGEs also increased the Runx2/alpha-actin ratio (180% and 250% vs. BSA, respectively, p<0.01). Co-incubation with physiological levels of VD abolished all the effects of SrRan and/or AGEs on VSMC *in vitro*. In conclusion, our *in vivo* results show that SrRan treatment may prevent diabetic bone disease by improving trabecular microarchitecture and decreasing bone marrow adiposity. Our *in vitro* results show that SrRan may promote VSMC proliferation, migration and osteoblastic trans-differentiation, particularly in the context of diabetic AGEs accumulation. Nevertheless, these effects can be prevented by physiological levels of VD. Our *in vitro* results remain to be confirmed in a diabetic animal model.

Disclosures: Claudia Sedlinsky, None.

MO0041

Effects of Single vs. Hypofractionated Focused Radiation Therapy on Vertebral Structure and Biomechanical Integrity. Christina Holmes*[1], Ioan Lina[2], Jason A Liauw[2], Sheng-fu Larry Lo[2], Annie Mao[2], Matthew Naumann[2], Debebe Theodros[2], Varun Puvanesarajah[2], Benjamin Elder[2], Timothy F Witham[2]. [1]Johns Hopkins School of Medicine, USA, [2]Johns Hopkins School of Medicine, USA

Stereotactic radiosurgery has shown great promise in the treatment of metastatic lesions within the spine. However, recent clinical studies have indicated that the procedure may increase the risk of developing vertebral compression fractions, particularly in osteoporotic patients [1, 2]. There is thus a critical need for research examining the effects of focused radiation on bone quality and mechanical properties. We have developed a rabbit model which enables the analysis of the effects of focused radiation on vertebral osteonecrosis, structure and biomechanical integrity. Using this model we are testing the hypothesis that fractionation of radiation dosing can reduce radiation osteonecrosis and preserve structural and biomechanical integrity of the spine.

The L5 vertebral body of New Zealand White (NZW) rabbits was treated, under computerized tomography (CT) guidance, with either a single 24 Gy dose of radiation or three fractionated doses over three days of 8 Gy radiation via the small animal radiation research platform (SARRP) [3]. Effects of radiation treatment on L2, L4, L5 and L6 vertebral osteonecrosis, structure and biomechanical integrity were evaluated 6 months post-irradiation via high-resolution CT-imaging, histology, and non-destructive biomechanical compression testing and compared to non-irradiated controls. Vertebral bone volume over total volume (BV/TV), trabecular thickness (Tb.Th.) and trabecular spacing (TB.Sp) were evaluated from CT images via the BoneJ plugin (4) of ImageJ software (NIH, Bethesda, MD).

Preliminary data suggests that the L5 vertebra from rabbits that underwent single-dose irradiation exhibits osteopenia, as indicated by decreased BV/TV and Tb.Th and increased Tb.Sp, compared to both non-irradiated controls and rabbits who received hypofractionated radiation. Whether these changes in bone morphology translate into reduced mechanical integrity is currently under analysis. Future work will utilize this rabbit focused irradiation model to evaluate the efficacy of various therapies, such as teriparatide (PTH (1-34)), in the prevention of radiation induced osteonecrosis.

References: (1) Rose PS, et al., 2009. J Clinical Onc. 27(29):5075-79; (2) Boehling NS, et al., 2012. J Neurosurg Spine. 16:379-386; (3) Wong J, et al, 2008. Int J Radiat Oncol Biol Phys. 71(5): 1591–1599; (4) Doube M, et al, 2010. Bone. 47:1076-9
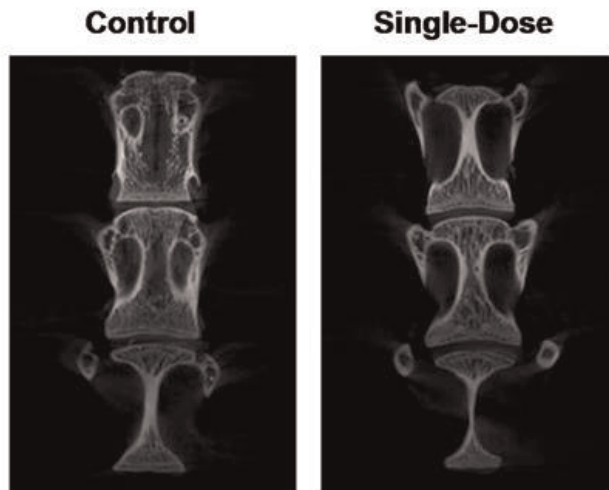
CT images of L4-L6 vertebrae 6 months post-irradiation. Controls=non-irradiated, Single-dose=24 Gy

Disclosures: *Christina Holmes, None.*

MO0042

New Approach to Analysis of Bone Loss Patterns in Longitudinal Studies. Tomas Cervinka*[1], Harri Sievanen[2], Jörn Rittweger[3], Jari Hyttinen[4]. [1]Tampere University of Technology, Finland, [2]The UKK Institute for Health Promotion Research, Finland, [3]Institute of Aerospace Medicine, German Aerospace Center, Germany, [4]Department of Electronics & Communications Engineering, Tampere University of Technology, Finland

The aim of this study was to perform a robust and threshold-free analysis of pQCT-measured traits in the same bone cross-sectional areas. The analysis employed recently developed segmentation algorithm, called OBS, and a fast rigid image registration on longitudinal pQCT data. More specifically, we addressed whether our analysis approach would reveal changes that remained masked in conventional analysis.

In this study, we reanalysed pQCT image data from control group of the 56-day 1st Berlin Bed Rest study (N = 10) that was carried out in Berlin/Germany in 2003 and 2004. The analysed images were obtained from the left leg at the 4% distal site of the tibia. The pixel size of the pQCT images was 0.5 x 0.5 mm and the slice thickness was 2.5 mm. For each participant, the raw data from the first baseline pQCT image was used for the determination of an individual reference template for the cortical cross-sectional area (CoA). The reference template was made with use of OBS method that accurately detected CoA and an additional enlargement of detected CoA to compensate possible small alignment differences between the baseline and follow-up images. In order to determine changes in cortical and trabecular bone mass within the same cross-sectional area through the study, the reference template was applied to all follow-up images of the given participant. As descriptive statistics, the means and standard error of the mean (SEM) of relative changes of bone mineral content (BMC) in the cortical and trabecular area are given.

The novel analysis approach revealed that cortical and trabecular bone loss might have different time responses to the immobilization (Figure 1). While bone loss in the trabecular compartment linearly increases, the cortical loss seems to be more sudden. In addition, in contrast with previously published results, this approach suggests that magnitude of bone loss in both cortical and trabecular compartments is similar at the end of immobilization. However, at the onset of a recovery period, the cortical loss continues with the same rate and exceeds the trabecular loss by ~2%.In conclusion, in this study we demonstrated that OBS method in conjunction with image registration procedure is a promising approach for analysis of longitudinal bone studies and newly opened question whether bone loss induced by immobilization is more pronounced in the cortical or trabecular compartment.
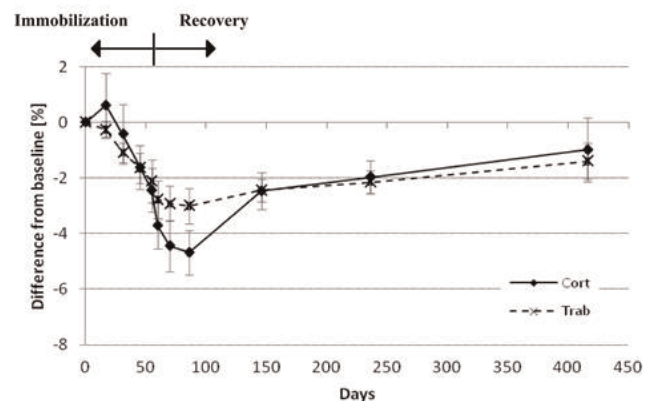
Figure 1: Assessment of the distribution of relative bone losses in the cortical and trabecular compartments of distal tibia. Values are given as the differences from baseline and SEM

Figure 1

Disclosures: *Tomas Cervinka, None.*

MO0043

The Effect of a High Resolution Flat Panel Detector on a Single X-Ray Absorptiometry (SEXA) system versus the Lower Resolution Detector on a Dual X-ray Absorptiometry (DEXA) system in-vitro in the Calculation of Mouse Bone Mineral Density (BMD). Chester Lowe*[1], Li Sun[2], Jianhua Li[3]. [1]KUB Technologies, Inc, USA, [2]Mount Sinai School of Medicine, USA, [3]Tount Sinai School of Medicine, USA

OBJECTIVE: To evaluate the effect of a high resolution detector on the efficacy and accuracy of mouse bone mineral density (BMD) measurements utilizing a single-energy absorptiometry (SEXA) system versus a lower resolution detector Dual X-ray Absorptiometry (DEXA) system in vivo.

Methods: (1) The coefficients of variation (CV) for BMD measurements at various skeletal regions were repeatedly determined by DEXA and SEXA in a preliminary study of mice and were analyzed on both a DEXA machine and a SEXA machine equipped with high resolution flat panel detector. (2) Identical Regions of Interest, Lumbar Region L3-L5, Lumbar Region >L6, both sides of femurs and tibias, were visualized and the BMD calculated on both the SEXA and DEXA machines. And (3) resultant calculations were compared.

Results: (1) The CVs of the preliminary BMD measurements in different regions of mice weighing between 17.4 grams to 38.5 grams by SEXA calculations versus the DEXA calculations were as follows, 99.88% for lumbar vertebra (L3-L5), 100.13% for lumbar vertebra >L6, 99.91% for left femur, 99.08% for right femur, 99.40% for left tibia, and 99.42% right tibia, respectively. (2) The mean BMD values of the 25 mice were (51.1 +/- 8.2 SEXA; 50.7 +/- 7.0 DEXA) mg/cm2 in lumbar vertebra L3-L5, (51.0 +/- 13 SEXA; 50.2 +/- 11.2 DEXA) mg/cm2 in lumbar vertebra >L6 , (66.8 +/- 12.5 SEXA; 63.5 +/- 16.9 DEXA) mg/cm2 in left femur and (57.3 +/- 14.8 SEXA; 57.1+/- 14.5 DEXA;) mg/cm2 in right femur, (41.9 +/- 8.4 SEXA; 42.7 +/- 10.4 DEXA) mg/cm2 in left tibia and (37.2+/- 8.5 SEXA; 39.8+/- 8.2 DEXA;) mg/cm2 in right tibia, respectively., (3) The BMD values calculated and recorded were consistent

between the SEXA and DEXA unit on the ROIs selected with variations between the 2 techniques being accounted for by the higher resolution and the 16-bit output of the SEXA detector versus the lower resolution and 8-bit output of the DEXA unit.

DISCUSSION: Measurement of MOUSE BMD in vitro by a system utilizing a higher resolution detector and SEXA is a useful method, it can produce repeatable results, and it can reflect the changes in mouse bone masses with good precision and as accurately as can the tried and true low resolution detector system utilizing DEXA.

SIGNIFICANCE: The Kubtec DIGICOM BMD calculates BMD utilizing a high resolution flat panel detector and Single X-ray Absorptiometry (SEXA), where only a short single exposure of the subject, thereby reducing radiation exposure, and from the resultant image the X-ray absorption in the bone is used for determining the BMD of the bone.

ACKNOWLEDGEMENTS: I would like to acknowledge the help of Li Sun, M.D. Ph.D. and Jianhua Li – Mt Sinai Medical Center Division of Endocrinology, Diabetes & Bone Disease Department of Medicine with the collection of my data.

Disclosures: Chester Lowe, KUB Technologies, Inc., 3

MO0044

The Role of Osteocalcin Carboxylation on Bone Fragility. <u>Timothy Cleland</u>*[1], <u>Caren Gundberg</u>[2], <u>Deepak Vashishth</u>[1]. [1]Rensselaer Polytechnic Institute, USA, [2]Yale University School of Medicine, USA

Recently, osteocalcin (OC) has been shown to play an integral role in the mechanical properties of bone based on differences in toughness between wild type and osteocalcin knockout mice models. However, the full knockout of this protein does not provide evidence for the effect of OC carboxylation level on bone mechanical properties. This may be especially important in humans where the levels of carboxylation in bone have been shown to be variable likely due to long-term variations in vitamin K nutrition (Cairnes and Price, 1994 JBMR). The variation in carboxylation may provide lesser affinity of OC for the mineral and thereby lead to a change in the organic-inorganic interface and the resulting mechanical properties of bone.

Tibiae from six donors (48M, 68M, 82M, 44F, 62F, 81F) were used to extract bone osteocalcin and measure bone toughness. Extracted osteocalcin was further digested using trypsin to analyze the variation in carboxylation by mass spectrometry. Carboxylation shows a +44 Da mass shift between the undercarboxylated and carboxylated peptides, allowing for direct quantification of carboxylation level (Fig. 1).

Using newly developed sample preparation and mass spectrometry methodology, we have evaluated the levels of OC carboxylation from donor bone of varying age and sex. Through this study, we found that bone fragility increases (toughness values decrease from 0.6 to 0.1) with age and this fragility increase is accompanied by variation in carboxylation level. For example, we found that the first carboxyglutamic acid (Gla) residue is only 23% carboxylated in the 48M (Fig. 1).
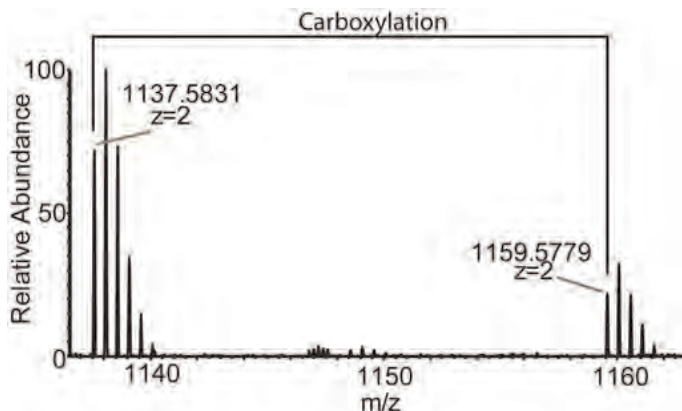

Figure 1

Disclosures: Timothy Cleland, None.

MO0045

Biomechanical Analyses of Bone Tissue Damage from Fatigue Loading *In Vivo*. <u>Mohammed Akhter</u>*[1], <u>Diane Cullen</u>[2], <u>John Danforth</u>[3], <u>Gwendolin Alvarez</u>[2], <u>Bryan Hackfort</u>[2], <u>Robert Recker</u>[2]. [1]Creighton University Osteoporosis Research Center, USA, [2]Creighton University, USA, [3]Creighton University, USA

It is hypothesized that fatigue loading-related micro damage is responsible for bone tissue inflammation response and subsequent targeted remodeling. Rat ulna model was used to induce micro damage using a fatigue loading technique in vivo. We present biomechanical analyses of fatigue loading to reduce ulnar strength/stiffness by 40%. Six-month-old, retired breeder (Sprague Dawley, n=12) female rats were used. Right ulna of each rat was fatigue loaded in vivo in compression at 4 Hz until the ulnar stiffness declined by 40%, which is an indication of structural damage. During

this in vivo loading the lateral ulnar surface was in tension, the medial surface in compression. After the completion of fatigue loading, rats were euthanized. Both left (contra lateral control) and right (loaded) mid-shaft ulnae were scanned at 6 micron resolution using microCT (Scanco) to investigate presence of damage in the loaded ulnae. This is an ongoing work and will be pursued at even submicron level with the new MicroXCT-200. The data suggest that at 15N and 20N compression loads, the induced average surface strain in the mid-shaft (medial side) region was 3000 and 4000 microstrain (um) respectively. Most of the ulnae reached 40% stiffness decline by an average of 20,000 fatigue cycles. Initial ulnar stiffness (@1000 cycles) at the start of the actual fatigue loading and final stiffness (@ 22,600 cycles) for one rat is shown in Figure 1. Mid-shaft ulna (right loaded) shows an ~18 micron deep microcrack along the lateral region of the cross section (Figure 2). These biomechanical data are important to understand the bone response with respect to signaling molecules in blood and bone tissue resulting from fatigue damage in vivo. These data will be helpful in understanding the mechanism of fatigue-related damage that results in significant strength/stiffness decline. This work will help characterize the relationship between the magnitude of microdamage and stiffness decline in bone tissue. The current work in this animal model is highly applicable to humans in understanding targeted bone remodeling resulting from excessive skeletal loading/exercise.
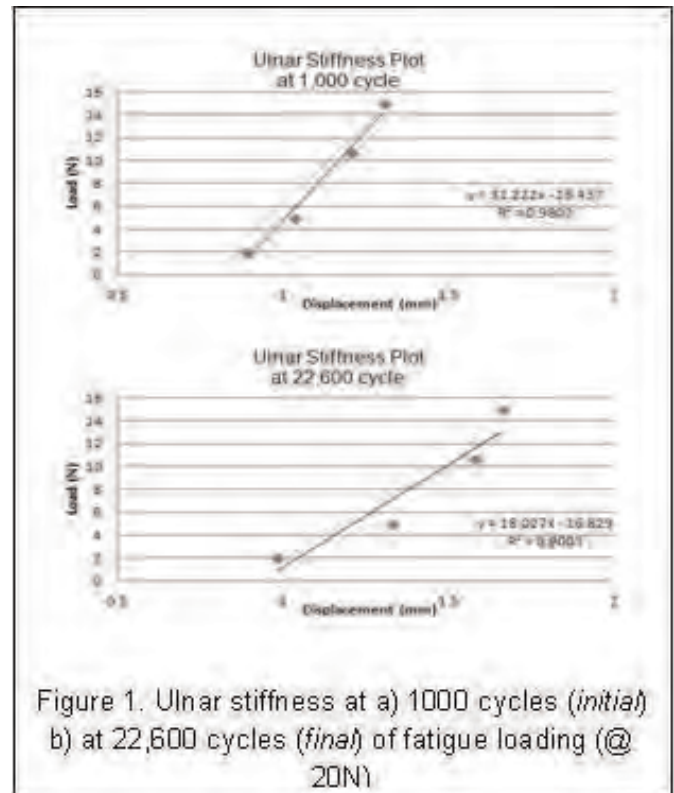

Figure 1. Ulnar stiffness at a) 1000 cycles (*initial*) b) at 22,600 cycles (*final*) of fatigue loading (@ 20N)

Figure-1

Figure-2. Mid-shaft ulnae (Left-contra lateral control and Right-fatigue loaded *in vivo*). Mid-shaft section in the loaded ulna shows an 18micron deep micro-crack (at the lateral surface) that contributes to the stiffness decline during *in vivo* fatigue loading. These ulnae were scanned at 6um resolution using MicroCT40 (Scanco).

Figure-2

Disclosures: Mohammed Akhter, None.

MO0046

Cyclooxygenase Response to Multiple Mechanical Loads. <u>Bryan Hackfort</u>*[1], <u>Mohammed Akhter</u>[2], <u>Diane Cullen</u>[1]. [1]Creighton University, USA, [2]Creighton University Osteoporosis Research Center, USA

Cox-2 inhibitors are used for daily treatment of arthritis and chronic pain. Cox-2 inhibition blocks the bone formation response to a single mechanical load, but not to multiple loads. We hypothesized that Cox-1 is up-regulated in response to mechanical loading under chronic Cox-2 inhibition. Immunohistochemistry (IHC) was used to visualize Cox expression after loading. The right tibia of C57Bl6 mice (N = 7/grp) were loaded in compression (360 cycles, 2 Hz, 1450 ??) either 1 time and collected 1, 6, or 12 hrs post loading or loaded 1, 2, or 3 times and collected 24 hours post load. Bones were fixed in 4% paraformaldehyde, decalcified, and paraffin embedded. Sections were cut 3 mm proximal to the tibia-fibula junction and stained for Cox-1 or Cox-2. Sections were quantified for percent positive periosteal and endocortical perimeter and positive osteocyte density. We used qPCR to investigate the PTGS (Cox) gene response to load with vehicle and Cox-2 inhibition over time. Tibias were loaded in compression (100 cycles, 2 Hz, 1450 ??) 3 d/wk and groups (N = 10) were collected after 1, 5, and 10 loads. Cox-2 inhibitor (NS-398) or control (DMSO) was given daily (3 hrs prior to load). Tibias from two mice were pooled, dissected of all soft tissue, RNA was extracted and cDNA was obtained for qPCR of PTGS1 (Cox-1), PTGS2 (Cox-2) and GAPDH (control). Loading did not increase Cox-1 or Cox-2 positive osteocytes. Cox-1 and Cox-2 periosteal expression were similar (2%) but Cox-2 endocortical expression was two-fold greater than Cox-1 (8.8 vs 4.1%). Cox-1 positive periosteal and endocortical surface increased with time and load, the greatest expression occurred after day 3 (P < 0.05). Cox-2 positive periosteal label was increased at 12 and 48 hours (P < 0.03) after the first load. Neither PTGS1 nor PTGS2 mRNA differed with number of days loaded. PTGS1 increased 1.5 fold in vehicle versus no increase with NS398. PTGS2 increased 2.0 fold (P < 0.03) after loading in NS398 and DMSO groups. In conclusion, periosteal cells increased Cox-1 expression after 3 loads while endocortical cells increased both Cox-1 and Cox-2. Loading did not increase Cox-1 or Cox-2 osteocyte staining with up to 3 days of loading. PTGS1 mRNA was up-regulated after loading in cortical bone of only the vehicle group. PTGS2 increased similarly in both groups in response to loading. Given these results, we reject our hypothesis since Cox 1 did not increase with Cox-2 inhibition.

Disclosures: Bryan Hackfort, None.

MO0047

Mechanical Loading as an Anabolic Stimulus After Exposure to Ionizing Radiation. <u>Yasaman Shirazi-Fard</u>*[1], <u>Joshua Alwood</u>[1], <u>Alesha Castillo</u>[2], <u>Ruth Globus</u>[1]. [1]NASA Ames Research Center, USA, [2]VA Palo Alto Health Care System, USA

Long-term spaceflight leads to extensive changes in the musculoskeletal system attributable, in large part, to unloading during microgravity exposure. Additionally, irradiation at doses similar to those of solar particle events or a round-trip sojourn to Mars (1-2 Gy) may cause significant depletion of stem/progenitor cell pools throughout the body as well as skeletal tissue degradation. Previously, we demonstrated that irradiation leads to rapid bone loss as a function of cumulative dose. Exposure to 50 or 200 cGy of high Z, high energy (LET) 56Fe (600-100MeV, 50-100cGy/min) can cause significant bone loss 30 days after irradiation and progressive bone loss continues even after 180 days. Ex vivo culture to assess growth and terminal differentiation of osteoblast lineage cells shows that 56Fe exposure impairs osteoblastogenesis and causes persistent defects in progenitor and stem cells. We hypothesized that heavy ion radiation damages skeletal tissue despite a prolonged recovery period and depletes the ability of osteoblasts to respond to anabolic stimuli. Male, 16-week old, C57BL6/J mice were exposed to 0 (sham) or 200 cGy 56Fe total body irradiation at NASA Space Radiation Laboratory/Brookhaven National Lab. We used the axial loading model for anabolic stimulation of the tibia 5 months post-irradiation, where %Bone Volume (BV/TV) was 20% lower in irradiated compared to sham animals. A rest-inserted (10s) prescription was used to load the right tibia (9N in compression, 60cycles/day, 3days/wk, for 4 wks). The left tibia was used as the contralateral control. At the end of the loading period, the cancellous bone microarchitecture was quantified and a 2-factor ANOVA was performed. The data show a main effect of mechanical loading for BV/TV, Trabecular Thickness (Tb.Th), and Trabecular Number (Tb.N.). Microarchitectural parameters for the loaded tibia were normalized to the contralateral control tibia for each animal. The axial loading paradigm increased BV/TV by 41% and 25%, Tb.Th by 17% and 23%, and Tb.N. by 20% and 2% in sham and irradiation groups, respectively. More detailed histomorphometric analyses are in progress to yield further insight. Based on these preliminary results, high LET radiation did not impair ability of the bone to respond to a mechanical anabolic stimulus. Anabolic mechanical stimulation of the skeleton has the potential to mitigate persistent, adverse effects of radiation and improve bone microarchitecture.

Disclosures: Yasaman Shirazi-Fard, None.

MO0048

Tamoxifen does not affect the anabolic response to tibial compression in male mice 3 weeks after initial injection. <u>Heather Zannit</u>*[1], <u>Michael Brodt</u>[2], <u>Matthew Silva</u>[3]. [1]Washington University St. Louis, USA, [2]Washington University in St Louis, USA, [3]Washington University in St. Louis School of Medicine, USA

As the use of reporter mice driven by tamoxifen (TMX) inducible Cre-mediated recombination increases, it is important to evaluate the effects of TMX on the murine skeleton. Our goals were to (1) evaluate how tamoxifen affects bone formation in Osx-Cre-ERT2;mTmG mice, (2) determine if there is a sex-dependent effect, (3) evaluate the effect of recovery time, and (4) determine if TMX persists in the bone.

In each experiment, TMX or vehicle was administered i.p. for 5 consecutive days (3mg/40g BW/day), a protocol shown to turn reporter. In an initial study, the right tibia of 5 month old male and female mice were scanned by in vivo micro-computed tomography (μCT), administered TMX or vehicle, and 26 days later re-scanned and euthanized. We found no interaction of TMX on temporal changes in cortical and trabecular bone morphology (BV, TV, BV/TV, and BMD). In addition, dynamic histomorphometry at the mid-diaphysis revealed no significant effect of TMX on Ps.MS/BS, Ps.MAR, Ps.BFR, Ec.MAR, and Ec.BFR.

Next, to determine if TMX affects loading-induced bone formation, 5 month old male and female mice were administered TMX or vehicle, allowed a 1 or 3 week recovery, and then the right tibia was subjected to axial tibial compression for 1 week (1200 cycles/day; -2200 με peak strain). After a 1 week recovery, both male and female relative Ec.MS/BS were less in the TMX treated group than the in the vehicle treated group (Fig. 1). However, in males after a 3 week recovery period, there was no TMX effect on cortical bone formation indices. In both male TMX and vehicle treated groups with a 3 week recovery, tibial loading increased Ps.MS/BS, Ps.MAR, Ps.BFR, Ec.BFR (p<0.05), Ec.MAR, and Ec.MS/BS (p<0.08) in the right tibias compared to contralateral controls (Fig. 2).

Finally, to determine the persistence of TMX in the bone, a set of mice were administered TMX, euthanized corresponding to the start of tibial loading, and tibias prepared for mass spectrometry. After a 1 week recovery, the presence of TMX was found in all bones (n=4 of 4), but after 3 weeks, half of the bones had none (n=2 of 4) and half had only trace amounts of TMX (n=2 of 4).

In conclusion, TMX administered in a manner sufficient to turn on reporter expression, did not affect bone structure. Nor did it affect loading induced bone formation of males after a 3 week recovery. This corresponds with a decrease in the presence of TMX in bones after a 3 week recovery as assessed by mass spectrometry.
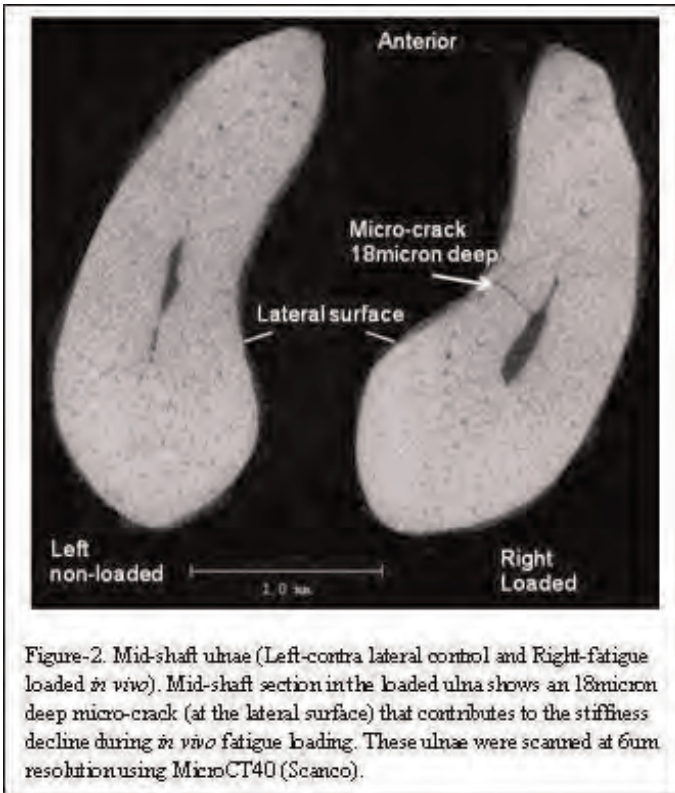
Figure 2

Figure 1

Disclosures: Heather Zannit, None.

MO0049

Withdrawn

MO0050

Human Tibia Bone Strength is Unaffected Following Long-Term Spinal Cord Injury or Bed Rest. <u>Alex Ireland</u>[1], <u>Ricardo Capozza</u>[2], <u>Gustavo Cointry</u>[3], <u>Jose Ferretti</u>*[4], <u>Jorn Rittweger</u>[5]. [1]Manchester Metropolitan University, United Kingdom, [2]Center of P-Ca Metabolism Studies (CEMFoC); National University of Rosario, Argentina, [3]Center of P-Ca Metabolism Studies (CEMFoC); National University of Rosario, Argentina, [4]National University of Rosario, Argentina, [5]Division of Space Physiology, Institute of Aerospace Medicine, German Aerospace Center, Germany

The tibia bears over 80% of compressive loading in the shank in humans (Wang et al, Clin Orthop Rel Res, 1996). Given this high level of habitual loading, it is unsurprisingly highly responsive to disuse. Long-term spinal cord injury is associated with a 60% reduction in tibial bone mass (Eser et al, Bone, 2004), and 90 days' bed rest results in up to 4.4% loss of bone mass dependent on site (Rittweger et al, Bone, 2005). Conversely the fibula contributes to only -6 to +19% of shank compressive force transmission, with greater contributions observed during pronounced foot eversion and plantar flexion (Goh et al, Clin Orthop Rel Res, 1992) and as absolute load increases. However, the influence of disuse on the human fibula has not previously been explored. To investigate fibular response to disuse, re-analysis of two previous pQCT datasets were completed. First, serial scans at 5% increments from 5% to 95% distal-proximal tibia length in 9 long-term spinal cord injury (SCI) patients aged 39.2 ± 6.2y taken 9-32 years post-injury, and in 9 age, height and mass-matched controls were compared. Also, scans taken in 25 young male volunteers aged 33.7 ± 3.7y prior to and 14 days after 90 days of 6° head-down tilt bed rest were examined. No significant differences or group-site interactions in total & cortical BMC, and bone area, cortical vBMD, periosteal and endocortical circumferences and cortical thickness of the fibula were found between SCI patients and controls (P > 0.16 for all parameters). In contrast, tibial BMC was 22-51% lower in SCI patients with group-site interactions revealing more pronounced differences in distal and proximal sites as opposed to shaft measures (both P < 0.001). There was no effect of bed rest on tibial bone mass, with only fibular trabecular BMD differing significantly (-1.4%, P = 0.04) from baseline measures. Tibial analysis revealed significant 0.9%-4.4% lower tibia bone mass following bed rest (all P < 0.01). Results suggest that the fibula is affected little by disuse, with diaphyseal sites in particular displaying no effects of reduced physical activity in either SCI or bed rest data. This may be a result

of the fibula's comparatively small contribution to load-bearing in the shank. Exercise models involving high compressive shank loads and pronounced eversion and /or plantarflexion may be effective in elucidating substantial exercise response in the fibula.

Disclosures: Jose Ferretti, None.

MO0051

Evaluation of Bone Density and Muscle Function in Mitochondrial Respiratory Chain Disorders. <u>Anna Middleton</u>*[1], <u>Craig Munns</u>[1], <u>John Christodoulou</u>[2], <u>Hiran Selvadurai</u>[2]. [1]The Children's Hospital at Westmead, Australia, [2]The Children's Hospital at Westmead, Australia

Purpose: Mitochondrial respiratory chain disorders (MRCD) are common inborn errors of metabolism where mitochondria exhibit impaired ability to generate energy. Reduced mobility and physical activity cause a decline in muscle mass and strength over time with resultant disuse osteoporosis. Alterations in bone, biomechanics and physical activity have not been investigated in this population.

Methods: Participants (n=19, 5-65 years) were recruited from one adult and one paediatric tertiary referral hospital. Participants performed a 6 minute walk test (6MWT) and parameters of muscle function (power, force and coordination) using the single two leg jump (S2LJ), multiple one leg jump (M1LJ) and chair rise test (CRT) on the Leonardo Jumping Platform. Bone mineral density (BMD) and bone mineral content (BMC) were assessed using duel energy x-ray absorptiometry (DEXA) of the total body and lumbar spine and peripheral quantitative computed tomography (pQCT) of the tibia at 4% and 66% of the tibial length. One-sample t-tests were used to explore difference from zero in parameters of bone density, biomechanics and physical activity in the MRCD population. Correlations between these parameters were assessed using Pearson Correlations (significance p<0.05).

Results: Parameters of muscle mass and function and bone mass and density are significantly altered in MRCD (Table 1). Performance in the S2LJ correlated strongly with BMD measured by DEXA (r=0.8, p<0.00), BMC (r=0.7, p<0.00) and muscle CSA (r=0.5, p<0.04) at the 66% pQCT site and vBMD (r=0.6, p<0.02) at the 4% site. Cortical vBMD at the 66% site correlated most strongly with M1LJ force (r=0.7, p<0.01). Distance achieved during the 6MWT showed moderate to strong correlations with parameters of muscle function, especially the time taken to complete the CRT (r=-0.8, p<0.00).

Conclusions: Muscle and bone parameters are altered in children and adults with MRCD. There is an obvious correlation between physical activity, biomechanics and bone despite the underlying impairments in muscle function. Therapies supporting normal skeletal loading and physical activity may be beneficial in this population.

One-Sample t-test	Mean Diff	95% CI	p Value
Muscle Function Parameters			
S2LJ Esslinger Fitness Index Z-score	-3.6	-4.5 – -2.7	0.00
S2LJ Force Efficiency Z-score	-3.9	-4.9 – -2.9	0.00
M1LJ Maximum Force Z-score	-4.7	-6.0 – -3.4	0.00
DEXA Parameters			
Total BMD Z-score	-0.8	-1.5 – -0.1	0.02
Lumbar spine BMD Z-score	-1.0	-1.7 – -0.3	0.01
pQCT Parameters			
4% Trabecular vBMD Z-score	-1.2	-1.7 – -0.7	0.00
66% Cortical vBMD Z-score	1.9	1.1 – 2.8	0.00
66% Cortical BMC Z-score	-2.8	--4.1 – -1.4	0.00
66% Muscle CSA Z-score	-1.8	-2.7 – -0.9	0.00

Table 1: One Sample t-tests

Table 1: One Sample t-tests

Disclosures: Anna Middleton, None.

MO0052

Increasing Bone and Reducing Fat with Modified Capoeira in the Primary School Setting: The CAPO Kids Trial. <u>Rossana Nogueira</u>*[1], <u>Benjamin Weeks</u>[2], <u>Belinda Beck</u>[3]. [1]Griffith University - Gold Coast CampusSchool of Allied Health Sciences, Australia, [2]Griffith University, Australia, [3]Griffith University, Australia

Introduction: The increasing incidence of both chronic bone and obesity-related disease places a heavy burden on health economies. Both conditions may arise in childhood. While exercise in youth is beneficial for both bone and metabolism, the nature of exercise recommendations for each traditionally differs.

Aim: Our goal was to determine the effect of a brief, novel, enjoyable, school-based exercise regimen targeting both bone and fat in primary school children.

Methods: A controlled exercise intervention trial was conducted over a full school year (9 months). The intervention comprised 10 minutes of thrice-weekly capoeira and jumping activities. Anthropometrics, waist circumference (WC), calcaneal broadband ultrasound attenuation (BUA) and stiffness index (SI) (Lunar Achilles, GE), maximum vertical jump (VJ), cardiovascular endurance (predicted VO2 max), resting heart rate (HR), blood pressure (BP) and maturity (YAPHV) were recorded at baseline and 9 months. A subset of whole body (WB), lumbar spine (LS) and femoral neck (FN) BMD, lean and fat mass (DXA, XR800, Norland), and indices of tibial and radial morphology and density (pQCT, XT3000, Stratec) was also collected. Changes in outcome variables were compared between groups using two-way ANOVA,
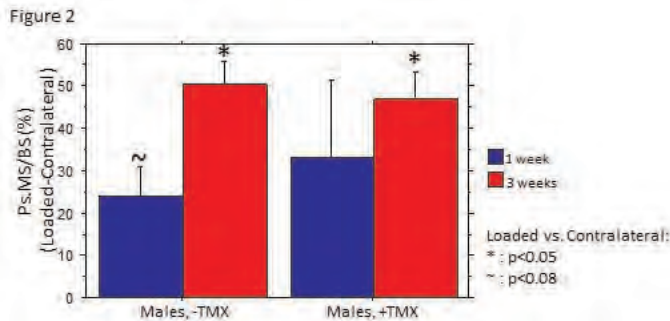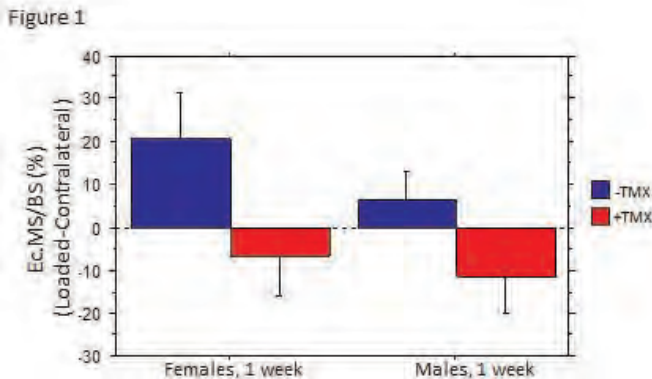
controlling for YAPHV and initial values. Stepwise linear regression were performed to determine the relationships between bone parameters.

Results: 296 children, including 130 control (CON) (10.7 ± 0.6yo; YAPHV -1.9 ± 0.9y) and 166 treatment (EX) (10.5 ± 0.5yo, YAPHV -2.1 ± 0.9y) participated. EX improved WC (EX: 1.95 ± 2.82 cm; CON: 4.09 ± 4.05 cm; p = 0.001), HR (EX: -4.11 ± 3.35 BPM; CON: 0.22 ± 3.8 BPM; p = 0.001), VJ (EX: 3.47 ± 4.01; CON: -0.59 ± 5.16; p = 0.001), predicted VO2 max (EX: 2.68 ± 3.96; CON: -0.20 ± 3.38 ml/kg/min; p = 0.001), SI (EX: 6.25 ± 10.04%; CON: 4.09 ± 6.99%; p = 0.05) and BUA (EX: 3.99 ± 9.06 dB/MHz; CON: 1.33 ± 8.3 dB/MHz; p = 0.01) compared to control. Sex-specific effects largely mirrored those findings. Baseline BUA and maturity predicted 32.2% of the variance in BUA change (p = 0.001) for boys; while BMI and baseline BUA accounted for 16.4% of the variance in BUA change (p = 0.006) for girls.

Conclusion: School-based capoeira with jumping improved markers of metabolic and musculoskeletal health in primary school children. The exercise program was safe, enjoyable and easily incorporated into the school schedule.

Disclosures: Rossana Nogueira, None.

MO0053

Individually Tailored Rehabilitation Regimen Did Not Prevent Tibial Bone Weakening Following Hip Fracture in Elderly Patients. Leg Bone Structural Analysis of a 12-Month Randomized Controlled Intervention. Ari Heinonen*[1], Tuuli Suominen[2], Tapio Senne[3], Johanna Edgren[3], Anu Salpakoski[3], Maija Pesola[4], Maria Arkela[5], Markku Kauppinen[3], Mauri Kallinen[6], Sarianna Sipilä[3]. [1]Department of Health Sciences, University of Jyväskylä, Finland, [2]Gerontology Research Center, Department of Health Sciences, University of Jyväskylä, Finland, [3]Gerontology Research Center Department of Health Sciences, University of Jyväskylä, Finland, [4]Department of Ortopedic, Central Finland Central Hospital, Finland, [5]Department of Physical & Rehabilitation Medicine, Central Finland Central Hospital, Finland, [6]Department of Medical Rehabilitation, Oulu University Hospital, Finland

The purpose of this study was to examine the effects of a home-based rehabilitation program on leg bone traits in elderly hip fracture patients. Population-based clinical sample of men and women operated for hip fracture (n=81, mean age 80 years, 78% women) were randomly assigned into a control (Standard Care, n=41) and an intervention (n=40) groups on average 70 (SD 28) days after discharged to home. The year-long intervention included an evaluation and modification of environmental hazards, guidance for safe walking, non-pharmacological pain management, progressive home exercise program, physical activity counseling and Standard Care. Distal tibia compressive strength (BSId, mm[3]), total density (ToD, mg/cm^{3}) and total area (ToA, mm[2]), as well as tibial mid-shaft bending strength (SSI, g[2]/dm[4]), CoA (mm[2]) and total density (ToD, mg/cm^{3}) were measured from fractured and non-fractured side with pQCT. Assessments were performed at baseline and in 3, 6 and 12 months. Effect of the intervention was analyzed by GEE and longitudinal repeated measures mixture path model.

Intervention had no effect (group x time) on tibial mid-shaft and distal tibia bone traits, neither in the fractured leg nor in the non-fractured leg.

Fractured side tibial mid-shaft SSI (time effect, p=0.001) ToD (p<0.020) and CoA (p=0.035) decreased significantly in both group from -1.2% to -1.9% in the intervention group and from -0.4% to -0.9% in the control group. Fractured side distal tibia ToD (time effect, p=0.004) decreased significantly in both group, -1.7% in the intervention group and -0.7% in the control group. In the non-fractured tibial mid shaft, ToD (time effect, p=0.004) and SSI (p=0.001) decreased significantly in both group, from -0.5% to –1.0% in the intervention and from -1.0% to -1.1% in the control group.

At baseline there were no side-to-side differences in tibial mid-shaft bone traits in the whole group. However, at baseline in distal tibia, there were significant side-to-side difference in BSId (p=0.005) and in ToA (p=0.006). In mid tibia, significant side-to-side difference developed in CoA, SSI and ToD. In distal tibia, the significant side-to-side difference continued in BSId and developed in ToD.

Leg bone traits weakened after hip fracture in both fractured and non-fractured side in trabecular and cortical bone. The year-long progressive and individually tailored rehabilitation program or standard care was not able to prevent leg bone weakening after hip fracture.

Disclosures: Ari Heinonen, None.

MO0054

Overhand Throwing Athletes as a Model for Exploring the Skeletal Benefits of Exercise during Growth. Alyssa Weatherholt*[1], Robyn Fuchs[1], Stuart Warden[2]. [1]Indiana University, USA, [2]Indiana University School of Health & Rehabilitation Sciences, USA

Exercise influences bone properties in pre-pubertal children, but few studies demonstrate the rate of response. Most longitudinal studies either follow subjects for 12 months or require participants to perform some form of forced exercise (i.e. jumping exercises) to show an exercise effect. This longitudinal pilot study investigated the skeletal influence of voluntary exercise in the form of overhand

throwing in male pre-pubertal baseball players (n=13; age=10.4 ± 0.7 yrs, Tanner stage= 1.6 ± 0.5) followed over one competitive season (6 months). Throwing athletes are a useful model as they unilaterally expose their throwing arm to elevated loads enabling the contralateral, nonthrowing arm to serve as an internal control site for growth. pQCT of the distal humerus diaphysis (75% of humerus length) was performed to assess: cortical volumetric bone mineral density (Ct.vBMD), cortical bone mineral content (Ct.BMC), total area (Tt.Ar), cortical area (Ct.Ar), medullary area (Me.Ar) and polar moment of inertia (IP). One sample t-tests were used to assess baseline percent differences between the throwing and nonthrowing arms, whereas paired t-tests were used to compare throwing-to-nonthrowing arm percent differences over time (baseline vs. 6 months). At baseline, the throwing arm had 20.2% (95%CI, 13.7 to 26.7%) greater Ct.BMC (p<0.001) than the nonthrowing arm. The extra mass was distributed on the periosteal and endosteal surfaces, as indicated by 7.2% (95%CI, 4.5 to 9.9%; p<0.001) greater Tt.Ar and 14.5% (95%CI, 7.3 to 21.7%; p=0.001) smaller Me.Ar within the throwing arm. There was no throwing-to-nonthrowing arm difference in Ct.vBMD (-0.6%; 95%CI, -1.3 to 0.2%; p=0.13). The mass and structural changes resulted in the throwing arm having 18.2% (95%CI, 11.9 to 24.5%; p<0.001) greater IP than the nonthrowing arm. Over the course of 6 months, the throwing arm gained 4.2% (95%CI, 0.1 to 8.5%) and 5.2% (95%CI, 0.2 to 10.3%) more Ct.BMC and Ct.Ar than the nonthrowing arm, respectively (all p<0.05). Gains in Tt.Ar (3.8%; 95%CI, -1.0 to 8.6%) and IP (10.0%; 95%CI, -2.5 to 22.5%) were not significant (all p=0.11). These data indicate that pre-pubertal throwing athletes have side-to-side differences in humeral cortical bone properties, with throwing-related changes in some bone properties being detectable with as little as 6 months follow-up. This suggests throwing athletes may be a useful within-subject controlled model for exploring the skeletal effects of exercise during growth.

Disclosures: Alyssa Weatherholt, None.

MO0055

Physical performance, handgrip strength, functional limitations and 10-year mortality in a representative sample of the elderly Dutch population, a LASA-study. Joseph Biedermann[1], Natasja Van Schoor[2], Mirjam Oosterwerff[1], Nathalie Bravenboer[3], Mireille Van Poppel[2], Dorly Deeg[2], Elisabeth Eekhoff*[4]. [1]Department of Internal Medicine, Section Endocrinology, VU University Medical Center, Netherlands, [2]EMGO Institute for Health & Care Research, VU University Medical Center, Netherlands, [3]VU University Medical Center, The Netherlands, [4]VU University Medical Center, Amsterdam, The Netherlands, The Netherlands

Background: Prior studies have shown a relationship between decreased physical functioning and various negative health outcomes in the elderly, including all-cause mortality.

The comparative predictive ability of often used measurements of physical functioning, including physical performance (tests), grip strength and functional limitations, for all-cause and cause-specific, cardiovascular related disease (CVD) and non-CVD related, mortality in older men and women is unknown.

Objective: To assess the predictive values of both objective (physical performance, handgrip strength) and self-reported (functional limitations) measures of physical functioning on 10-year mortality risk (all-cause, CVD and non-CVD) in a representative sample of older persons.

Design: Data from the second cycle of the Longitudinal Aging Study Amsterdam, an ongoing cohort study in a population based sample of the elderly Dutch population were used. A total of 1,242 subjects between the age of 65 and 88 years were included in this study.

Methods and measurements: Physical performance was defined as the sum of the scores on chair stand, tandem stand and walk tests. Handgrip strength was measured using a size-adjusted hand-held dynamometer (HHD). Functional limitations were assessed by asking about difficulty doing six activities.

Cox regression analysis and Cox proportional hazard models were used to determine the predictive value of the three measures of physical functioning on (cause-specific) mortality risk during 10 years follow-up.

Results: 585 deadly events, of which 203 CVD related and 382 non-CVD related, occurred over an average of 8.4 (SD ± 3.3) years of follow-up. In men, after adjustments for confounders, all measurements (HR 1.35-1.56 P<0.005) were predictors but only of all-cause mortality. In women, only physical performance (HR 2.25 P=0.001) and handgrip strength (HR 1.75 P=0.007) predicted all-cause mortality, while for CVD-related mortality physical performance (HR 2.72 P=0.012) and functional limitations (HR 2.40 P=0.012) were the significant predictors.

Conclusion: In men, all measurements of physical functioning predict only all-cause mortality. In contrast, in older women physical performance are proved the best predictor of all-cause mortality and the only measure related to all and CVD-related causes of mortality.

Disclosures: Elisabeth Eekhoff, None.

MO0056

Bone remodeling compartment canopies in pediatric renal osteodystrophy.
Renata Pereira*[1], Thomas Andersen[2], Peter Friedman[3], Isidro Salusky[4], Katherine Wesseling-Perry[5]. [1]UCLA, USA, [2]Vejle Hospital - Lillebaelt Hospital, IRS, University of Southern Denmark, Denmark, [3]University of Pittsburgh School of Medicine, USA, [4]University of California, Los Angeles School of Medicine, USA, [5]UCLA Medical Center, USA

Absence of BRC canopies—a layer of flat cells which are lifted from the bone surface to form an enclosed compartment over the remodeling surface, separating osteoclasts and osteoblasts from the bone marrow—is associated with impairments in bone formation despite increased bone resorption (i.e. osteolysis) in patients with normal kidney function. Their role in bone remodeling in chronic kidney disease (CKD) remains undefined. To characterize the role of these structures in ROD, BRC canopies were assessed in 106 bone biopsies of pediatric patients with CKD stages 2-5. BRC canopy histology was quantified by a trained observer (RCP) on a subjective scale of 0 to 4 (0: no surfaces with canopy lift; 0.5: 1-2 surfaces; 1: 3-4 surfaces; 2: 5-6 surfaces; 3: 7-9 surfaces; 4: > 10 surfaces). The presence of PTHR1 immunoreactivity in undecalcified bone was assessed simultaneously by immunohistochemistry using polyclonal rabbit anti-human PTHR1 and quantified on the same subjective scale. Biochemical values were obtained at bone biopsy (Table 1). PTHR1 immunoreactivity was observed in canopies as well as in bone lining cells, but not in osteoblasts, osteoclasts, or osteocytes. Circulating PTH values were lower and fewer canopies were seen in pre-dialysis CKD than in dialysis patients. Circulating PTH levels correlated with canopies (r=0.54, p<0.01). The osteoid surface to eroded surface (OS/ES) ratio was higher in patients with BRC canopies than in those without, suggesting a role for BRC canopies in coupling of bone formation and resorption. In summary, disruption of BRC canopies appears to coincide with disrupted coordination of bone formation and resorption in CKD. BRC canopies, may play a role in PTH mediated bone formation and resorption in CKD. The role of BRC canopies in the pathogenesis of ROD, including in the development of skeletal PTH resistance, warrants further investigation.

Parameter	CKD stages 2-4 (n=18)	Dialysis (n=88)
Biochemicals		
Calcium (mg/dL)	9.2 + 0.2	9.0 + 0.1
Phosphorus (mg/dL)	4.8 + 0.3	6.5 + 0.2 *
Alkaline phosphatase (IU/L)	212 + 38	246 + 25
1st PTH (pg/mL)	68 (48, 137)	508 (310, 930) *
2nd C-terminal FGF23 (RU/ml)	228 (101, 462)	1989 (617, 7345) *
Histomorphometry		
Bone Volume (BV/TV) (%)	29.8 + 2.1	33.3 + 1.0
Osteoid Volume (OV/BV) (%)	5.1 + 2.5	5.1 + 0.5
Osteoid Surface (OS/BS) (%)	19.4 + 3.8	31.4 + 1.7 *
Osteoid Thickness (O.Th) (um)	10.1 + 1.8	11.1 + 1.1
Osteoid Maturation Time (OMT) (d)	14.5 (8.4, 19.5)	12.5 (9.6, 16.0)
Mineralization Lag Time (MLT) (d)	24.6 (11.9, 45.2)	35.1 (21.1, 88.7)
Bone Formation Rate (BFR/BS) (um³/ um²/yr)	14.0 (5.4, 17.8)	25.6 (7.8, 63.2)
Eroded Surface (ES/BS) (%)	4.8 + 0.8	9.6 + 0.6 *
Osteoclast surface (Oc.s/BS) (%)	0.4 + 0.1	2.2 + 0.3 *
BRC Canopy and PTHR1		
PTHR1 (subjective scale: 0-4)	1.0 (0.5, 2.0)	1.0 (0.5, 2.0)
BRC Canopy (subjective scale: 0-4)	0 (0, 0.5)	0.75 (0.5, 2.0) *

Table 1

MO0057

Adult Bone Density Loci and Sex Specific Bone Mass in Childhood.
Jonathan Mitchell*[1], Alessandra Chesi[2], Okan Elci[2], Shana McCormack[2], Heidi Kalkwarf[3], Joan Lappe[4], Vicente Gilsanz[5], Sharon Oberfield[6], John Shepherd[7], Andrea Kelly[8], Babette Zemel[9], Struan Grant[10]. [1]University of Pennsylvania, USA, [2]Children's Hospital of Philadelphia, USA, [3]Cincinnati Children's Hospital Medical Center, USA, [4]Creighton University Osteoporosis Research Center, USA, [5]Children's Hospital Los Angeles, USA, [6]Columbia University Medical Center, USA, [7]University of California, San Francisco, USA, [8]Children's Hospital of Philadelphia / University of Pennsylvania, USA, [9]Children's Hospital of Philadelphia, USA, [10]Children's Hospital of Philadelphia / University of Pennsylvania, USA

Osteoporosis is a heritable condition that is particularly prevalent among postmenopausal women. Adult bone mineral density (BMD) and osteoporotic susceptibility loci have been identified; however, it is not known if these loci affect bone mass in childhood or if they affect bone mass equally in boys and girls. We therefore tested if adult BMD susceptibility loci played a role in the pediatric setting and if they interacted with sex.

Our sample comprised of 694 subjects (331 boys and 363 girls) of European ancestry, aged 5-20y at baseline who enrolled in the Bone Mineral Density in Childhood Study. Participants completed annual dual energy X-ray absorptiometry scans (up to 7y) and we calculated BMD or bone mineral content (BMC) z-scores (adjusted for age, sex and height) for the total hip (hip-BMD), femoral neck (FN-BMD), distal $1/3$ radius (radius-BMD), spine (spine-BMD), and whole body less head (WB-BMC). We used mixed-effects linear regression models accounting for correlations arising from the repeated measures and siblings and tested for sex interactions with each of the 77 single nucleotide polymorphisms (SNPs) after adjusting for age, Tanner stage, BMI, dietary calcium and self-reported physical activity.

Nineteen sex-SNP interactions were observed at one or more skeletal sites, with P-values $<1.3x10^{-4}$. SNPs in/near *MBL2* (radius-BMD, $P=6.46x10^{-11}$ and spine-BMD, $P=1.03x10^{-4}$), *CPED1* (radius-BMD, $P=1.76x10^{-8}$), *C12orf53* (spine-BMD, $P=5.46x10^{-7}$ and FN-BMD, $P=3.61x10^{-6}$), *AXIN1* (spine-BMD, $P=7.31x10^{-7}$) and *LEKR1* (WB-BMC, $P=6.46x10^{-6}$ and spine-BMD, $P=6.56x10^{-5}$) were more strongly associated with bone mass in girls. SNPs in/near *WNT16* (radius-BMD, $P=1.22x10^{-6}$ and WB-BMC, $P=3.12x10^{-6}$), *SOX9* (WB-BMC, $P=5.16x10^{-5}$) and *XKR9* (radius-BMD, $P=6.29x10^{-5}$) were more strongly associated with bone mass in boys. For example, per rs13245690 risk allele (*CPED1*) mean radius-BMD z-score was lower in girls by 0.38 (girls: b=-0.38, $P=7.04x10^{-10}$; boys: b=-0.05, $P=0.51$). Whereas, per rs3779381 risk allele (*WNT16*) mean radius-BMD z-score was higher in boys by 0.30 (girls: b=0.03, $P=0.12$, boys: b=0.30, $P=4.55x10^{-13}$).

This is the first study to show that specific adult BMD susceptibility loci associate with pediatric bone mass in a sex specific manner, suggesting that different biological pathways contribute to bone mass in boys and girls. The reason for the dichotomous findings will need further investigation.

MO0058

Withdrawn

MO0059

Effect of Dietary Calcium on Phosphorus Balance and Net Absorption in Healthy Adolescent Girls.
Colby Vorland*[1], Berdine Martin[2], Connie Weaver[2], Munro Peacock[3], Kathleen Hill Gallant[2]. [1], USA, [2]Purdue University, USA, [3]Indiana University Medical Center, USA

Phosphorus is an essential nutrient which plays a critical role in energy metabolism as ATP and as a major structural component of bone. Phosphorus deficiencies are extremely rare as it is widespread in the food supply. Conversely, there is increasing concern over potential harms of dietary phosphorus excess. Inorganic forms of phosphorus are commonly used as food additives, which contributes to an increased intake in the U.S. Emerging evidence shows that elevated serum phosphorus and high dietary phosphorus intake may increase the risk of cardiovascular disease and mortality in patients with chronic kidney disease as well as the general population. However, few phosphorus balance studies have been conducted, and are needed to examine factors that influence whole body phosphorus metabolism.

The purpose of this study was to determine the effect of dietary calcium on phosphorus balance and net phosphorus absorption in healthy adolescent girls, utilizing a unique resource of banked urine, fecal, and diet samples from a controlled calcium balance study previously conducted at Purdue University. Eleven healthy girls ages 11-14y participated in a randomized crossover study conducted in 2007 which consisted of two 3-week periods of a controlled diet with low (817 ± 62 mg/d) or high (1418 ± 35 mg/d) calcium, separated by a 1-week washout period. Phosphorus intake was the same on the low and high calcium diets (1531 ± 29 and 1534 ± 30 mg/d, respectively, p = 0.83). Results show urinary phosphorus excretion was lower on the high calcium diet (649 ± 41 vs 535 ± 42 mg/d, p = 0.01). However, fecal phosphorus (553 ± 60 vs 678 ± 63 vs mg/d, p = 0.14), net phosphorus absorption (980 ± 56 vs 859 ± 58 mg/d, p = 0.14), and overall phosphorus balance (339 ± 72 vs 329 ± 74 mg/d, p = 0.90) were not significantly different between low and high calcium intake. This agrees with our previously published study of phosphorus balance in adult moderate-stage chronic kidney disease patients, where increased calcium intake modestly reduced urinary phosphorus, but did not affect overall phosphorus balance or absorption. Combined, these balance studies suggest that increasing dietary calcium is not an effective strategy for reducing phosphorus absorption or retention.

MO0060

Preeclampsia and gestational hypertension are associated with adolescent offspring bone mineral density in a UK population based cohort.
Kim Hannam*[1], Jon Tobias[2], Debbie Lawlor[2]. [1]University of Bristol, United Kingdom, [2]University of Bristol, United Kingdom

Introduction: Intra uterine insufficiency has been postulated to have long term effects on health, including risk of osteoporosis, via fetal programming. Since preeclampsia (PE) and to a lesser extent gestational hypertension (GH) are associated with impaired placental dysfunction we postulated that these represent hitherto unrecognised risk factors for reduced bone mineral density (BMD) of the off spring. *Objective:* To investigate if exposure to PE or GH in utero influences BMD of

the offspring as measured in late adolescence. *Methods:* Mother-offspring pairs from the UK population based cohort study ALSPAC were investigated (N=3224 with relevant data). PE and GH were determined by abstracting every antenatal blood pressure (BP) and proteinuria record and applying the International association of hypertension in pregnancy guidelines to the measurements; PE was defined as systolic BP >139mmHg or diastolic BP >89mmHg on at least two occasions after 20wks gestation with proteinuria and GH as the same elevated BP without proteinuria. Multivariable linear regression was used to examine associations between PE/GH and BMD as measured by whole body and hip DXA at age 17. Fully adjusted analyses included gender, age at scan, maternal age, parity, maternal smoking (self-reported in 3rd trimester), maternal socioeconomic status (based on highest parental occupation) and maternal pre-pregnancy body mass index. *Results:* Of the 3224 mother-offspring pairs 2% (n=64) of the mothers fulfilled criteria for PE and 14% (n=433) for GH. In unadjusted analyses, GH was positively associated with BMD of the total hip, spine sub-region and total body; these associations remained after adjustment at the spine (mean SD difference= 0.12, 95% CI= 0.02-0.22 p=0.02) and total hip (mean SD difference= 0.10, 95% CI= 0.01-0.20 p=0.04). In contrast, in unadjusted analyses, there was evidence of a negative association between PE and total hip BMD (mean SD difference= -0.23, 95% CI= -0.48-0.02 p=0.07), which was strengthened after confounder adjustment (mean SD difference= -0.35, 95%CI=-0.58 - -0.11 p=0.003). There was no evidence of association between PE and BMD at other sites. *Conclusion:* Whereas PE appears to represent a risk factor for low BMD of the off-spring, if anything GH may be protective, possibly reflecting distinct effects of these two hypertensive disorders of pregnancy on placental function and/or intra uterine insufficiency.

Disclosures: Kim Hannam, None.

MO0061

Osteocyte Dysfunction After Burns: Possible Role of Bisphosphonates. Gordon Klein*[1], David Herndon[2], Phuong Le[3], Debra Benjamin[2], Clark Andersen[2], Clifford Rosen[4]. [1]University of Texas Medical Branch, USA, [2]University of Texas Medical Branch & Shriners Burns Hospital, USA, [3]Maine Medical Center Research Institute, USA, [4]Maine Medical Center, USA

We previously reported that burned children receiving pamidronate in a randomized controlled trial (RCT) had sparing of both resorptive bone loss (Bone 2007; 41: 297) and muscle protein breakdown (J Bone Miner Res pub online 18 Dec 2013). Based on the hypothesis that bisphosphonates prevent osteocyte apoptosis, possibly permitting release of paracrine factors that prevent muscle catabolism, we measured serum concentrations of sclerostin (SOST) and fibroblast growth factor (FGF)23 in 18 children originally enrolled in the RCT using blood obtained 6-60d post-burn. FGF23, which can cause left ventricular hypertrophy, was undetectable in both groups starting at day 6 post-burn. SOST concentrations in serum were normal in both groups. However, SOST vs time post-burn was significantly different between controls (n=9) and the pamidronate group (n=9), p=0.016 by ANCOVA. The control group had a slope of -2.5 while the pamidronate group had a slope of +3.5. Normal range of the assay is 67-300 pg/ml. The explanation for the undetectable levels of FGF23 is uncertain but would appear to precede osteoblast apoptosis, which occurs at approximately 14d post-burn (Osteoporos Int 2004; 15: 468). All subjects were hypoparathyroid, not improved with bisphosphonates (Osteoporos Int 2005; 16: 631). Since serum SOST varies inversely with serum PTH concentrations, the low PTH could be driving the normal levels of SOST. The negative slope of the SOST concentrations in the controls and the positive slope of SOST concentrations in the pamidronate group are consistent with the hypothesis that pamidronate preserves osteocytes following burn injury. However, FGF23 is not the osteocytic paracrine factor that preserves muscle protein from breakdown post-burn.

Disclosures: Gordon Klein, None.

MO0062

Bisphosphonate Treatment and Dental Development in Children with Osteogenesis Imperfecta. Ilkka Vuorimies*[1], Heidi Arponen[2], Helena Valta[1], Outi Tiesalo[2], Marja Ekholm[2], Outi Makitie[3], Janna Waltimo-Sirén[1]. [1]Hospital for Children & Adolescents, University of Helsinki, Helsinki Finland, Finland, [2]Institute of Dentistry, University of Helsinki, Helsinki, FINLAND, Finland, [3]Children's Hospital, Helsinki University Central Hospital, Finland

Osteogenesis imperfecta (OI) is an inherited disorder characterized by bone fragility. Bisphosphonates (BPs) have become an established therapy for paediatric OI patients. As tooth eruption requires resorption of alveolar bone and roots of the deciduous teeth, it has been hypothesized that antiresorptive BPs might delay tooth eruption. This phenomenon has been established in rats, but in OI patients evidence for such an effect is lacking. The purpose of the present study was to assess whether BP treatment affects eruption of permanent teeth in children with OI.

We analyzed dental panoramic tomograms for 22 OI patients (age 3-16 yrs, mean 10.4 yrs) treated with BPs (pamidronate, zoledronic acid or risedronate) for a minimum period of a year. We performed dental age assessment using the method introduced by Demirjian et al., evaluated the number of erupted left mandibular permanent teeth and assessed the resorption rate of the persistent deciduous teeth using a method described by Haavikko with some modification. Radiographs of 50 age-matched OI patients naïve to BPs were used as controls. In addition, we used published and own normative data for healthy Finnish children.

In OI patients without BPs the dental age and the number of left mandibular permanent teeth were significantly advanced (mean difference 0.55 years, P<0.001 and 0.29 teeth, P=0.048, respectively) but were similar to healthy children in the BP-treated group. No statistically significant difference was found between the OI groups. Furthermore, no difference was found between the OI groups in resorption rate.

In conclusion, OI children treated with BPs were similar to healthy control children in terms of rate of dental development. OI patients who have not received BPs have somewhat advanced dental development, and BPs seem to slow it down to a rate comparable to normal.

Disclosures: Ilkka Vuorimies, None.

MO0063

Vibration Induced Cytoskeletal F-Actin Alignment and Molecular Gene Expression Patterns of Human Bone Marrow Mesenchymal Stem Cells are Influenced by Vibration Direction. Suphannee Pongkitwitoon*[1], Gunes Uzer[2], Janet Rubin[3], Stefan Judex[4]. [1]Stony Brook University, USA, [2]University of North Carolina, USA, [3]University of North Carolina, Chapel Hill, School of Medicine, USA, [4]Stony Brook University, USA

Human bone marrow derived mesenchymal stem cells (hBMSCs) are sensitive to mechanical stimulation in vitro and in vivo but the transduction pathway by which hBMSCs can respond to vibrations at very low intensities is unclear. We recently showed in vitro that vibration enhanced hBMSC proliferation, and osteogenic differentiation is similar between vibrations applied in the horizontal and vertical direction. Here, we investigated the molecular and cytoskeletal response between the two directions. hBMSCs were subjected to two bouts of vibrations in horizontal or vertical direction using vibration frequency/acceleration combinations of 100Hz-0.15g and 30Hz-1g and compared to non-vibrated controls. Gene expression analysis was performed with 96-gene PCR arrays while two-photon laser confocal microscopy visualized cytoskeletal elements. Gene expression of many skeletal transcription factors, growth factors and matrix molecules was up-regulated in vibration groups compared to non-vibrated controls. Adiponectin and PPARg were down regulated in most vibration groups compared to non-vibration. Osteoblast markers (e.g. ALP, BMP2, COL1 and RUNX2) were up-regulated up to 6-fold with vibrations. Genes for cytoskeletal fibers (e.g. talin, tubulin up-regulated 2-4 fold) and nuclear fibers (e.g., NESPRIN-1,2 and SUN1,2 up-regulated 2-4 fold) were also up-regulated. Cluster analysis grouping up- or down-regulated gene transcripts showed that horizontal vibrations tended to up-regulate osteoblast differentiation markers more effectively than vertical vibrations. For instance, up-regulation of alkaline phosphate, collagen-I, RUNX2 was up to 2x greater in horizontally vibrated (100Hz-0.15g) than in vertically vibrated (100Hz-0.15g) hBMSCs. Further, two-photon microscopy revealed that cytoskeletal F-actin became more aligned in one direction with horizontal vibrations (100Hz-0.15g) than with vertical vibrations (100Hz-0.15g) or in non-vibrated control hBMSCs. Reflecting this cytoskeletal reorientation, lamins, nesprins and sun proteins were up-regulated primarily with horizontal vibrations. β-catenin and wnts were up-regulated with both horizontal and vertical vibrations. Across the two loading directions, the 100Hz-0.15g vibration signal generally elicited a greater molecular response than the 30Hz-1g signal. The data show the rapid molecular response of hBMSC to vibrations and suggest that the direction in which the vibration is applied may play a role in 2D culture.

Disclosures: Suphannee Pongkitwitoon, None.

MO0064

Increased type II diabetes indices and compromised bone marrow niche caused by obesity is salvaged by inclusion of refractory periods in low intensity mechanical vibrations in adult C57BL/6 mice. Vihitaben Patel*[1], Meilin Chan[2], Clinton Rubin[3]. [1]Stony Brook University, USA, [2]Stony Brook University, USA, [3]State University of New York at Stony Brook, USA

Obesity-induced type II diabetes (T2D) has been shown to degrade bone health. In addition, current drug treatments for T2D may also inadvertently deteriorate bone quality. This study aims to investigate whether various loading regimes for mechanical stimulation, as an element of exercise, can serve as a non-pharmacologic treatment to cure T2D and improve bone health simultaneously. Thirty-four, 17 weeks old, male C57BL/6 mice were separated in four groups, regular diet (RD, n=8), high fat diet (HF, n=8), high fat diet with 30 minutes of mechanical stimulation (HFv, n=8), high fat diet with two 15 minute bouts of mechanical stimulation with 5 hour refractory period (RHFv, n=9). The mechanical stimulation was delivered via low intensity vibration (LIV) protocol (90Hz frequency and 0.2g peak acceleration) for 5 days/week. While the RD mice were fed regular diet (10kcal% fat), the HF, HFv and RHFv mice were fed high fat diet (45kcal% fat) for 2 weeks to induce obese phenotype. Continuing on the same diets, the HFv and RHFv mice were subjected to their respective LIV treatment, whereas RD and HF mice were sham handled for 6 weeks. At the end of the experiment, HF had increased glucose intolerance (+15%, p=0.005), a typical characteristic of T2D, paralleled with crippled bone marrow mesenchymal stem cell (MSC, Sca1+ CD90.2+ Ckit+ CD44+ CD105+) population (-56%, p=0.002), B cell (B220+) population (-50%, p=0.0001) and T cell (CD4+) population (-52%, p<0.0001) suggesting compromised bone marrow niche. While 30 minutes of mechanical stimulation without a refractory period was capable of only salvaging B cell population (+56%, p=0.037), inclusion of 5-hour refractory period between two bouts of 15 minutes mechanical stimulation resulted in parallel normalization of both T2D and bone marrow niche. Compared to HF, RHFv

resulted in decreased glucose intolerance (-7.8%, p=0.055) and increased bone marrow MSC population (+90%, p=0.046), B cell population (+59%, p=0.026) and T cell population (+43%, p=0.05). In summary, this study suggests the potential benefit of refractory period incorporation in the mechanical stimulation loading regime to simultaneously improve T2D and bone marrow niche by affecting bone marrow MSC, B cell and T cell population in adult mice.

Disclosures: Vihitaben Patel, None.

MO0065

Regional Variability in Radius Marrow Density- A pQCT Study in Females Aged 8 to 58. Jodi Dowthwaite*[1], Tomas Cervinka[2], Charity Ntansah[3], Paula F. Rosenbaum[4], Harri Sievanen[5], Tamara Scerpella[6]. [1]SUNY Upstate Medical University;Syracuse University, USA, [2]Tampere Institute of Technology, Finland, [3]Syracuse University, USA, [4]SUNY Upstate Medical University, USA, [5]The UKK Institute for Health Promotion Research, Finland, [6]University of Wisconsin, USA

Purpose : Bone marrow density may indicate the proportion of osteogenic versus adipogenic progenitor cells, with higher marrow density indicating greater osteogenic propensity. However, the homogeneity of marrow density assessments within a single bone is unknown. The current analysis examined relationships between 33% and 65% radius marrow and cortical properties across a broad subject age and maturity range (pre-puberty through post-menopause).

Methods: We evaluated pQCT scan results for 33% and 65% radius sites from 160 females. Marrow and cortical properties were evaluated using threshold definitions of 550 mg/cm^3 for bone and 80 mg/cm^3 for marrow. Coefficients of variation were calculated from duplicate, repositioned pQCT scan results for 31 adult women. Kolmogorov-Smirnov tests indicated non-normal data distributions. Spearman correlations quantified associations among variables. Wilcoxon signed-rank tests assessed site-to-site differences for marrow (M) and cortical (C) tissue densities (vBMD). Bland-Altman plots evaluated agreement between 33% and 65% marrow vBMD, labeling data points by subject age group (8-13yrs, 13.1-18yrs, 18.1-30yrs, 30yrs+).

Results: Subject ages ranged from 8.1 to 57.8yrs (mean 22.3, sd 13.2). No relationship was detected between sites for marrow density (rho= 0.00, p=0.99; Figure 1; 33% site MvBMD greater, Wilcoxon p<0.001). In contrast, site-to-site correlations for cortical density (CvBMD), thickness (CTh) and cross-sectional area (CCSA) were strong (rho: CvBMD= +0.85, CTh= +0.75, CCSA= +0.90; p<0.001), despite inequality (33% greater, Wilcoxon p<0.001). Coefficients of variation for pQCT outcomes were <2% for all but MvBMD (33%= 2.5%, 65%= 5.6%).

Conclusions: No associations were detected between marrow densities at 33% and 65% radius sites, whereas site-to-site cortical properties were strongly positively correlated. Thus, marrow density results are not interchangeable. As 65% medullary cavity area is larger than 33% medullary area, the 65% site may be preferable for marrow density assessment in small subjects. However, cortical thickness is lower at 65% than 33% radius, making 33% radius preferable for cortical density assessment in small subjects. To maximize data quality for assessment of radius marrow and cortical properties, scans should be performed at both sites (33% cortex, 65% marrow). The significance of site-to-site marrow density variation within bone has yet to be determined.
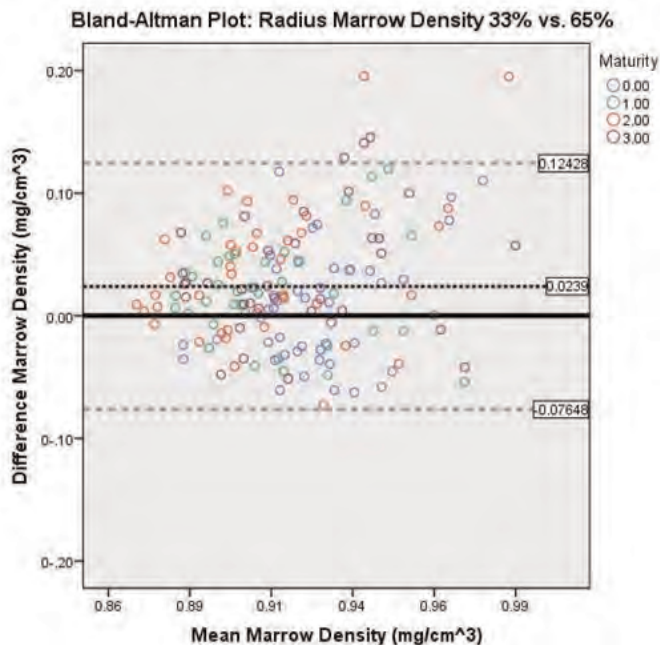
Bland-Altman Plot: 33% vs 65% Radius Marrow Density

Disclosures: Jodi Dowthwaite, None.

MO0066

Macrophagic cells are abundant along the bone marrow envelope in human and mice cancellous bone. Thomas Andersen*[1], Maja Hinge[2], Jean-Marie Delaisse[3]. [1]Vejle Hospital - Lillebaelt Hospital, IRS, University of Southern Denmark, Denmark, [2]Department of Clinical Cell Biology (KCB), Vejle Hospital – Lillebaelt Hospital, IRS, University of Southern Denmark, Denmark, [3]Vejle Hospital, IRS, University of Southern Denmark, Denmark

Recent studies identified several bone physiology-relevant features at the marrow-bone interface. (i) Very thin elongated mesenchymal cells surround the bone marrow, forming a bone marrow envelope (BME), which get the appearance of a canopy above the remodeling sites. (ii) Marrow cell activities in an area within 50 μm of the BME/canopy correlate with bone surface events. Recently, the canopies were proposed to consist of a mixture of osteoblastic and macrophagic cells, and the latter were also ascribed a role in bone formation.

Here we clarified the position of the macrophagic cells both in relation with the canopy/BME and bone surface events. Immunolocalizations were performed in cancellous iliac crest biopsies of 9 human controls and in vertebrae, tibiae and femur of 4 aged mice. Macrophagic and osteoblastic markers were respectively, CD68/CD163 and CD56/Runx2 for the humans, and F4/80 and CD56/β-catenin for the mice.

In humans, we consistently observed that none of the BME/canopy cells were immunoreactive for the macrophagic markers (<1%), while basically all the BME/canopy cells were immunoreactive for the osteoblastic markers (>98%). This confirms that the BME contains only osteoblastic cells and no macrophagic cells. The same conclusion was drawn for the cells on the bone surface, except for the osteoclasts, which were positive for CD68. Interestingly however, 57% of the BME/canopy was found in contact with CD68$^+$ cells at its marrow side, but only 5% of it was found in contact with CD163$^+$ cells. This suggests that CD68$^+$CD163$^-$ macrophagic cells are abundant in the bone marrow right next to the BME/canopy. Furthermore, 37% of the bone marrow cells within 50 μm of the BME/canopy were immunoreactive for CD68 and/or CD163. Of note, the CD68 $^+$ macrophagic cells in the bone marrow appeared most abundant above osteoid surfaces, less abundant above eroded surfaces, and least abundant above quiescent surfaces.

In mice, the BME/canopy is more difficult to detect. When detectable, the BME/canopy cells were only immunoreactivity for the osteoblastic markers CD56 and β-catenin, and not stained with the macrophagic marker F4/80. As in humans F4/80$^+$ macrophagic cells were found lining the marrow side of the BME/canopy and were abundant in neighboring bone marrow.

In conclusion, macrophagic cells are abundant right next to the osteoblastic BME/canopy both in human and mouse cancellous bone - a position compatible with a role at the marrow-bone interface.

Disclosures: Thomas Andersen, None.

MO0067

The Other Side of Osteoimmunology: Osteoclasts as Myeloid Derived Immune Regulator. Ichiro Nishimura*[1], Keiichi Kanayama[2], Han-Ching Tseng[2], Shuting Sun[3], Charles McKenna[3], Sil Park[4], Anahid Jewett[2]. [1]University of California, Los Angeles, USA, [2]UCLA School of Dentistry, USA, [3]USC Department of Chemistry, USA, [4]UCLA, School of Dentistry, USA

The interaction between immune cells and bone has suggested important regulatory processes for physiological bone remodeling and pathological bone diseases. Osteoimmunology has identified the role of immune cells for osteoclast development. Osteoclasts are originated from myeloid-derived immune cells that regulate lymphocytic inflammatory activities. In this study, we have tested the hypothesis that fully differentiated osteoclasts may still retain the myeloid immune cell characteristics. Human peripheral blood mononuclear cells from volunteer subjects were used to purify CD14+ monocytes. Monocytes were then differentiated to different lineages by medium containing M-CSF/RANKL (osteoclasts), GM-CSF/IL-4 (dendritic cells), LPS/IFN-gamma (M1 macrophages) or M-CSF (M2 macrophages). The condition medium of each group was subjected to multiplex cytokine profiling. Osteoclasts were found to secrete cytokines and chemokines that showed a similar profile as that of monocytes and M2 macrophages but not of dendritic cells and M1 macrophages. By determining cell surface markers using FACS analysis, osteoclasts were found to express CD14^{dim}CD11b+. The cytokine profile and cell surface markers indicated that osteoclasts resembled the characteristics of myeloid-derived suppressor cells (MDSC). Thus, osteoclasts' conditional medium was further subjected to ELISA, which revealed the secretion of anti-inflammatory IL-10. After the exposure to Zoledronate or Alendronate, the secretion of IL-10 was significantly decreased. By contrast, these nitrogen-containing bisphosphonates dose dependently increased the osteoclastic secretion of pro-inflammatory cytokines, IL-6 and TNFa. The cytokine modulations were not induced by Etidronate. In a mouse model for osteonecrosis of the jaw (ONJ) using Zoledronate, some oral osteoclasts were detached from the jawbone and positively stained by anti-IL-6 antibody. The detached osteoclasts were shown to contain fluorescent-labeled Zoledronate and surrounded by inflammatory infiltrates in the oral mucosa. This study demonstrated that osteoclasts retained an MDSC-like characteristic with a potential to mediate immune suppressive effect, but nitrogen-containing bisphosphonates changed it to

pro-inflammatory characteristics. These findings suggest a potential role of osteoclasts in supporting bone marrow tumors by MDSC-like mechanism and also a role as pro-inflammatory regulator in bisphosphonate-related ONJ.

Disclosures: Ichiro Nishimura, None.

MO0068

Diet-induced obesity promotes a myeloma-like disorder *in vivo*. Seint Lwin*[1], Sam Olechnowicz[2], Jessica Fowler[3], Claire Edwards[1]. [1]University of Oxford, United Kingdom, [2]University of Oxford, GBR, [3]University of California, Los Angeles, USA

The relationship between obesity and bone biology is complex, with evidence to support an association between obesity and risk of multiple myeloma (MM). The mechanisms that mediate this association remain unknown. In the present study, we have combined the well-characterized 5TGM1 murine model of MM with diet-induced obesity (DIO) and a genetic model of obesity to determine the effect of increased adiposity on MM development *in vivo*. In the 5TGM1 MM model, MM only develops if 5TGM1MM cells are inoculated into C57Bl/KaLwRij (KaLwRij) mice and not in closely related C57Bl6 mice. Non-permissive C57Bl6 or permissive KaLwRij mice were fed a high fat diet (42% kcal from fat) or control diet (10% kcal from fat) for 5 weeks, when a significant increase in body fat was detected. Mice were then inoculated with 5TGM1MM cells. C57Bl6 mice on a high-fat diet developed features of MM, including a 3.7-fold increase in serum paraprotein (p<0.001), GFP-positive cells in bone marrow (5.75%, p<0.001) and a 10% decrease in trabecular bone volume. Removal of the high fat diet upon detection of MM reduced tumour burden (p<0.05). Inoculation of MM-permissive KaLwRij mice resulted in MM, but no significant difference in serum paraprotein, tumour burden within bone marrow or trabecular bone volume was detected in mice on a high fat diet as compared to control, despite a significant increase in body fat at time of tumour inoculation. This suggests that the obese host microenvironment created by DIO is not directly promoting tumour growth or survival, but may instead be creating and maintaining a permissive environment. In support of this, analysis of MM-permissive KaLwRij mice revealed a 29% increase in body weight (p<0.05), an 82% increase in body fat (p<0.05), and a 58% decrease in trabecular bone volume (p<0.01) as compared to age-and sex-matched C57Bl6 mice. To investigate whether general adiposity in the absence of a high-fat diet would provide a supportive niche, mice deficient in leptin (ob/ob) were inoculated with 5TGM1MM cells. Surprisingly, no evidence of tumour burden or bone loss was detected, suggesting that distinct differences in the obese microenvironments created by DIO and leptin deficiency. Our studies demonstrate that DIO creates a permissive environment for the development of a MM-like disorder. Furthermore, the reduction in tumour burden following removal of the high fat diet suggests the potential for dietary intervention strategies.

Disclosures: Seint Lwin, None.

MO0069

Expression and role of sonic hedgehog in oral squamous cell carcinoma induced jaw bone destruction. Tsuyoshi Shimo*[1], Naito Kurio[2], Masahiro Iwamoto[3], Tatsuo Okui[4], Hiromasa Kuroda[5], Kenichi Matsumoto[5], Soichiro Ibaragi[5], Norie Yoshioka[5], Yuichirou Takebe[5], Hitoshi Nagatsuka[5], Akira Sasaki[6]. [1]Okayama University Graduate School of Medicine, Dentistry & Pharmaceutical Sci, Japan, [2]Japan, Japan, [3]Children's Hospital of Philadelphia, USA, [4]Okayama University, Japan, [5]Okayama University Graduate School of Medicine, Dentistry & Pharmaceutical Sciences, Japan, [6]Okayama University, Japan

Introduction: Sonic hedgehog (Shh) and its signaling have been identified in several human cancers, and increased levels of its expression appear to correlate with disease progression and metastasis. However, the role of Shh in bone destruction associated with oral squamous cell carcinomas is still unclear. In this study we have analyzed the expression and how hedgehog signaling is involved in the gingival carcinoma induced jaw bone destruction.
Methods: From surgically resected lower gingival squamous cell carcinoma mandible samples, decalcified, immunohistochemical staining was performed. To evaluate the effects of SHH on osteoclastogenesis and activity in vitro, osteoclast formation assay and pit formation assays were performed by using RAW264.7 cells and CD11b+ cells from mouse bone marrow cells. The expression of SHH related signals were confirmed by Western blot analysis.
Results: We found that SHH was highly expressed in stromal cells and osteoblsts near the tumor cell that had invaded bone matrix. On the other hand, hedgehog signal Gli-2 was highly expressed in the preosteoclasts and mature osteoclasts. SHH stimulated osteoclast formation and pit formation in the presence of receptor activator for nuclear factor-κB ligand (RANKL). SHH upregulated phosphorylation of ERK1/2 and p38 MAPK, NFATc1, tartrate-resistant acid phosphatase (TRAP), and cathepsin K expression in RAW264.7 cells.
DISCUSSION: Our results suggest that tumor derived growth factors stimulated the SHH in the stromal cells and osteoblasts near the bone invaded tumor cells, and regulated osteoclast formation and bone resorption in the tumor bone microenvironment.

Disclosures: Tsuyoshi Shimo, None.

MO0070

Increased Expression of TAF12 in the Bone Microenvironment in Multiple Myeloma Enhances Tumor Cell Growth and Osteoclast Formation. Yukiko Kitagawa[1], Jumpei Teramachi[2], Jolene Windle[3], John Chirgwin[1], G. David Roodman[1], Noriyoshi Kurihara*[1]. [1]Indiana University, USA, [2]The University of Tokushima, Japan, [3]Virginia Commonwealth University, USA

Vitamin D has been implicated in the progression of many cancers; however, its role in multiple myeloma (MM) is unclear. Vitamin D insufficiency or deficiency has been reported in the majority of MM patients, but it is unknown how Vitamin D levels affect disease activity. We reported that TAF12 expression, a VDR coactivator, was induced in bone marrow stromal cells (BMSC) by pagetic osteoclasts (OCL) that have increased NFκB signaling. Further, the increased TAF12 expression in BMSC enhanced their production of RANKL in response to low concentrations of 1,25-D_3 (10^{-10}M). MM cells also have increased NFκB signaling analogous to pagetic OCL. Therefore, we determined if TAF12 was also increased in BMSC of MM patients (MM-BMSC) and enhanced RANKL production or VCAM1 expression in BMSC treated with 1,25-D_3. We found that MM-BMSC expressed increased TAF12 levels compared to normal BMSC. TAF12 expression in MM-BMSC was increased by TNFα and IL-6, and TAF12 enhanced RANKL and VCAM1 expression by MM-BMSC in response to 10^{-10}M 1,25-D_3. Further, 1,25-D_3 enhanced adhesive interactions between MM cells and BMSC to increase the growth of human myeloma cells. To confirm that TAF12 increased MM cell growth by BMSC in response to 1,25-D_3, we generated TAF12 heterozygous knock-out (TAF12$^{+/-}$) mice, because TAF12$^{-/-}$ mice die during gestation. BMSC from TAF12$^{+/-}$ mice expressed 50% lower TAF12 levels compared to WT, and had decreased RANKL and VCAM1 production, and CYP24A1 accumulation in response to 1,25-D_3. VDR content in BMSC from TAF12$^{+/-}$ mice treated with 1,25-D_3 (10^{-10} to 10^{-8}M) was also decreased compared to WT cells. Co-culture of JJN3 human MM cells with TAF12$^{+/-}$ BMSC treated with 1,25-D_3 resulted in decreased MM cell growth as compared to co-cultures with WT BMSC. WT mouse OCL precursors co-cultured with TAF12$^{+/-}$ BMSC formed fewer OCL with 1,25-D_3 treatment compared to normal BMSC and the increased OCL formation was blocked by OPG. These results show that increased expression of TAF12 in the MM microenvironment upregulates VDR transcription in response to low levels of 1,25-D_3 to enhance MM cell growth and osteoclast formation. Since we have shown that primary myeloma cells from patients also express increased TAF12 levels, these results suggest that TAF12 may be a novel target for treating MM bone disease.

Disclosures: Noriyoshi Kurihara, None.

MO0071

Acid sensing and survival signaling in myeloma cells in acidic bone lesions: formation of acid-induced vicious cycle. Ryota Amachi*[1], Masahiro Hiasa[2], Jumpei Teramachi[3], Keiichiro Watanabe[4], Takeshi Harada[5], Shiro Fujii[5], Shingen Nakamura[5], Hirokazu Miki[5], Asuka Oda[5], Eiji Tanaka[6], Itsuro Endo[7], Toshio Matsumoto[7], Masahiro Abe[1]. [1]University of Tokushima, Japan, [2]Indiana University School of Medicine, USA, [3]The University of Tokushima, Japan, [4]Tokushima University Hospital, Japan, [5]Dept. of Medicine & Bioregulatory Sciences, Tokushima Univ., Japan, [6]Dept. of Orthodontics & Dentofacial Orthopedics, Tokushima Univ., Japan, [7]University of Tokushima Graduate School of Medical Sciences, Japan

In osteolytic lesions in myeloma (MM), MM cells and osteoclasts (OCs) interact with each other to enhance their growth and activity. The interaction creates an acidic milieu by protons produced by OCs and lactate by MM cells, which further confers drug resistance in MM cells. We found that such mutual interaction enhanced the expression of Pim-2 in MM cells as a prosurvival mediator. However, precise mechanisms of acid sensing in MM cells and its role in tumor survival are largely unknown. In the present study, we therefore explored the relationship between acid sensing and survival signaling in MM cells in acidic conditions. MM cell lines as well as primary MM cells variably expressed extracelluar pH sensors, TDAG8, OGR1, and TRPV1, at pH7.4; the expression of these pH sensors was up-regulated at mRNA levels in MM cells cultured at pH6.8 or cocultured with acid-producing OCs. The pH sensor levels were further up-regulated in the MM cells cocultured with OCs in acidic conditions. The acidic conditions also induced Pim-2 expression and phosphorylated Akt in MM cells. The addition of the PI3K inhibitor LY294002 abolished the up-regulation of these pH sensors along with the suppression of Akt phosphorylation at pH6.8. The Pim inhibitor SMI16a also reduced the expression of these pH sensors in MM cells at pH6.8. Acid-induced activation of the PI3K-Akt pathway enhanced the nuclear localization of the transcription factor Sp1 in MM cells. Among the pH sensors up-regulated in MM cells in acidic conditions, treatment with terameprocol, a competitive inhibitor of Sp1 binding, selectively abolished the expression of TRPV1, a sensor for lower ranges of pH to sense pH as low as pH4.0. LY294002 and SMI16a in combination cooperatively induced MM cell death more markedly in acidic conditions than at pH7.4. These results suggest that MM cells respond to acid and activate the PI3K-Akt and Pim-2-mediated survival pathways, which in turn up-regulates their expression of pH sensors, thereby forming a positive feedback loop between the edition of pH sensors and activation of the survival pathways in MM cells under acidic conditions. Besides skewed cellular microenvironment surrounding MM

..

cells, protons and/or lactate may act as niche factors for MM cells to elicit their drug resistance while adapting to acidic environment. Combinatory treatment with PI3K and Pim inhibitors may be a good therapeutic option against MM cells in acidic bone lesions in MM.

Disclosures: Ryota Amachi, None.

MO0072

C-11-Acetate Metabolic PET Imaging uncovers a Role for Acetate Metabolism in Multiple Myeloma. Francesca Fontana*[1], Michelle Hurchla[2], Kooresh Shoghi[3], Walter Akers[3], Simone Cenci[4], Michael Tomasson[5], Andre D'Avignon[6], Monica Shokeen[7], Roberto Civitelli[8], Katherine Weilbaecher[8]. [1]Bone & Mineral Diseases, USA, [2]Washington University in St. Louis, USA, [3]Washington University School of Medicine Department of Radiology, USA, [4]Fondazione Centro San Raffaele, Italy, [5]Division of Oncology - Washington University School of Medicine, USA, [6]Department of Chemistry - Washington University in St Louis, USA, [7]Washington University School of Medicine - Department of Radiology, USA, [8]Washington University in St. Louis School of Medicine, USA

Multiple Myeloma (MM), a bone marrow (BM) plasma cell malignancy, is characterized by high levels of monoclonal immunoglobulins (Ig), bone osteolytic lesions and systemic symptoms. 18FDG-Positron Emission Tomography (PET) is the current gold standard for metabolic imaging of MM, yet it can fail to detect nearly 40% of lesions, particularly in intramedullary disease. We hypothesized that membrane biosynthesis and lipid metabolism may represent novel targets for developing better diagnostic tools and new therapeutic modalities, as these are key biologic processes for MM cells, which produce large amounts of Ig and undergo fast cell replication. We applied dynamic PET imaging using 11C-acetate to preclinical models of MM. 18F-Sodium fluoride scans were performed for co-registration with the skeleton. High 11C-acetate uptake was demonstrable in subcutaneous grafts of 5TGM1-GFP tumor cells in immunodeficient mice, and areas of uptake matched the optical imaging signal for the same tumors. Upon intravenous injection, 5TGM1 cells engraft to the bones of syngeneic KaLwRij mice; in this orthotopic model we found a significant increase of 11-C-acetate SUV (standardized uptake value) in tumor-bearing vs. control bones (p<0.05). The presence of tumor cells at sites of increased 11C-acetate uptake was then demonstrated by in vivo and ex-vivo optical imaging, flow cytometry, histology, and immunohistochemistry for IgG. To directly address acetate utilization by tumor cells, we analyzed by 1H/13C-NMR in the supernatant of MM cells incubated with13C-acetate, and found a consistent uptake depending on incubation time and cell density. As Fatty Acid Synthase (FASN) is a key enzyme in acetate metabolism, we further hypothesized that targeting FASN may result in anti-myeloma effects, and potentiate the effects of proteasome inhibitors. Indeed, the FASN-inhibitor orlistat was toxic for a panel of myeloma cell lines (p<0.01). Importantly, at comparable doses, bone marrow mesenchymal stem cells were affected by orlistat with respect to adipogenic differentiation, but did not undergo apoptosis. Additionally, FASN synergized in MM cells with proteasome inhibitors and with tunicamycin, an endoplasmic reticulum stressor. Thus, we identified acetate metabolism as crucial to MM biology. This holds potential for a new, clinically robust diagnostic tool for tumor identification by PET imaging, and represents a promising new therapeutic target for this bone invading tumor.

Disclosures: Francesca Fontana, None.

MO0073

Comparing the Incidence of Bone Tumors in Rats Chronically Exposed to Abaloparatide (BA058) or PTH(1-34). Jacquelin Jolette*[1], Aurore Varela[2], Bassem Attalla[3], Susan Y. Smith[2], Gary Hattersley[4]. [1]Charles River Laboratories, Preclinical Services Montreal, Canada, [2]Charles River Laboratories, Canada, [3]Charles River, Canada, [4]Radius, USA

Prolonged treatment with rhPTH(1-34) or rhPTH(1-84) in rats results in development of bone tumors. However to date, this rodent response has not translated into evidence of an increased osteosarcoma risk in patients treated with these drugs or in diseases associated with chronic PTH elevation. This study was conducted to evaluate the potential for abaloparatide (ABL) to induce bone tumors in rats exposed for up to 2 years. Six-week old F344 rats (60/sex/dose) were subcutaneously injected with 0, 10, 25, or 50μg/kg ABL or 30μg/kg PTH(1-34) daily. PTH(1-34) served as positive control. Whole body radiographs were taken from all rats to facilitate tumor detection at necropsy. Systemic hyperostosis, increased bone radiopacity and BMD (Table) were observed in rats treated with ABL at ≥10μg/kg or PTH(1-34), consistent with expected pharmacodynamics. A comparable continuum of proliferative changes in bones, mostly osteosarcoma, were observed in both ABL and PTH(1-34) treated rats. Comparison of these findings for ABL and PTH(1-34), at similar exposure multiples to the human therapeutic dose (25μg/kg ABL and 30μg/kg PTH), showed marked similarities in osteosarcoma-associated mortality, tumor incidence (Table), age at first occurrence and metastatic potential. Females were less sensitive than males to bone tumor development with both compounds. In conclusion, close to whole life treatment with ABL in rats resulted in the dose and time dependent formation of osteosarcomas, with a comparable response to PTH(1-34) at similar exposure. These results suggest no increased risk of bone tumors would be expected in patients treated with ABL compared to PTH(1-34).

Treatment	Veh	Male BA058			PTH	Veh	Female BA058			PTH
Dose (μg/kg/day)	0	10	25	50	30	0	10	25	50	30
DXA–Mean BMD (g/cm²)										
Femur : global	0.258	0.417	0.464	0.508	0.493	0.245	0.368	0.417	0.429	0.417
Lumbar spine : L1-L4	0.285	0.408	0.426	0.449	0.467	0.255	0.364	0.418	0.413	0.421
No. of rats examined	60	60	59	60	60	60	60	61	60	60
No. of rats affected										
Osteoblastoma	0	1	15c	20c	10c	0	8c	7b	9b	4
Osteosarcoma										
primary	1	31c	46c	52c	39c	1	11b	22c	37c	24b
metastasis	1	14	17	35	21	0	2	3	16	9

Pairwise comparison p-values to Vehicle controls (Veh) shown in bold for DXA data: p < 0.001
Pairwise comparison p-values to Veh using one-sided Peto's test: b < 0.01, c < 0.001

Table

Disclosures: Jacquelin Jolette, Charles River, 8; Charles River, 4
This study received funding from: Radius Health Inc.

MO0074

Histomorphometric Assessment of Breast Cancer Bone Metastases with the 2mm Jamshidi Trephine Reveals Intense Woven Bone Formation and Resistance to Bisphosphonates. Richard Kremer*[1], Iryna Kuchuk[2], Monzur Murshed[3], Nathaniel Bouganim[2], Natasha Kekre[2], Susan Robertson[2], Lisa Vandermeer[2], Jin Li[4], Christina Addison[2], Roanna Segal[2], Mark Clemons[2]. [1]McGill University, Royal Victoria Hospital, Canada, [2]Ottawa Hospital Research Institute, Canada, [3]McGill University, Canada, [4]McGill University, Canada

Despite widespread use of bisphosphonates in breast cancer patients with metastatic spread to the skeleton, relatively little is known about their effects on tumor growth within bone and on the surrounding bone microarchitecture. A major limitation to better understand these histomorphometric changes is the invasiveness of the traditional 7mm trephine to obtain routine transiliac bone biopsies. In this study we examined these histomorphometric changes using a 2 mm "Jamshidi" bone biopsy trephine in a series of breast cancer patients with and without metastatic spread to the skeleton. Patients were divided into 4 groups based on histological evidence of tumor invasion in the skeleton and on IV administration of pamidronate(PM): group 1(n=1) no evidence of bone invasion and no treatment with PM, group 2(n=1) evidence of bone invasion and not treatment with PM, group 3(n=3) no evidence of bone invasion and treatment with PM, group 4(n=6) evidence of bone invasion and treatment with PM. Three dimensional micro-computed tomography revealed significant architectural disruption in bone samples with evidence of tumor invasion with variable indices of bone volume(BV/TV) ranging from low to high. Biopsies were embedded in methylmethacrylate and sections were stained with haematoxylin and eosin, Von Kossa, tartrate-resistant acid phosphatase (TRAP) for osteoclasts and toluidine blue or alkaline phosphatase for osteoblasts. Histomorphometric analysis of group 1 showed number of osteoclasts (Oc) and osteoblasts (Ob) consistent with postmenopausal bone turnover (mean NOc/T.Ar=2.2, mean NOb/T.Ar=138). Group 2 was characterized with very high Oc number (mean NOc/T.Ar=30) and normal Ob number (mean NOb/T.Ar=111). Group 3 was characterized by an almost absence of Oc (mean NOc/T.Ar=0) with apparently normal Ob number (mean NOb/T.Ar=101). Group 4 had very high Oc number (mean NOc/T.Ar =14) with normal Ob number (NOb/T.Ar=102). Furthermore, in group 4 tumor invasion was accompanied by disruption of the trabecular bone structure immediately juxtaposed to tumor cells as well as large areas of unmineralized woven bone characteristic of osteoblastic bone metastases. In conclusion our data support the mixed osteolytic/osteoblastic nature of metastatic skeletal lesions in breast cancer and their apparent resistance to bisphosphonate therapy. Our minimally invasive approach should prove useful in monitoring the efficacy of bone targeting agents in patients with skeletal metastases.

Disclosures: Richard Kremer, None.

MO0075

Human CD138+ myeloma cells suppress osteoblastogenesis when co-cultured with human mesenchymal stem cells. Wei Zhang[1], Moustapha Kassem[2], Matthew Drake*[3]. [1]Mayo Clinic, USA, [2]Odense University Hospital, Denmark, [3]College of Medicine, Mayo Clinic, USA

Multiple myeloma (MM) is a malignancy of terminally differentiated plasma cells. MM cells undergo clonal expansion in the bone marrow cavity in close proximity to mesenchymal stem cells (MSCs), a dynamic population of self-renewing multi-potent progenitor cells capable of differentiation along the osteoblast (OB) lineage. Osteolytic lesions affect nearly all patients with MM, and result from localized bone resorption unmatched by bone formation. As such, MM cell suppression of MSC to OB differentiation is critical for the development of MM bone disease.

We developed an *in vitro* system in which the immortalized human MSC line hMSC-TERT was cultured in a transwell system with human MM cells. hMSC-TERT cells co-cultured with hMSC-TERT cells served as a negative control. We employed whole transcriptome sequencing (RNA-seq) to identify differentially expressed genes (defined as p < 0.05 and a false discovery rate < 0.10) between hMSCs co-cultured with or without human MM cells.

Co-culture significantly reduced hMSC matrix mineralization and the expression of known OB differentiation marker genes including alkaline phosphatase, col1α1, osteoprotegerin, and osteonectin. RNA-seq identified 97 specific pathways uniquely regulated in the MSCs during MM cell co-culture, including signaling pathways involving interleukin (IL)-1, IL-6, tumor necrosis factor-alpha, NFκB, ephrin B, BMP, RANK, and apoptosis. Further cluster analyses of pre-specified gene sets identified statistically significant suppression of pathways involved in OB differentiation, Wnt/Wnt-related signaling, and proliferation, with up-regulation of pathways involving NFκB and inflammation. Collectively, these data demonstrate the validity of this model for assessing the effects of monoclonal plasma cell-secreted factors on hMSC function. In summary, MM cells significantly inhibited the OB lineage differentiation of hMSCs via regulation of both known and novel pathways in a co-culture model used to simulate human MM cell/hMSC interactions. These results are consistent with the OB suppression that occurs *in vivo* in humans with osteolytic myeloma. Whether similar gene expression changes also occur when hMSCs are co-cultured with CD138+ monoclonal plasma cells from patients with the myeloma precursor condition monoclonal gammopathy of undetermined significance (MGUS) are unknown, but if found may provide insight into the bone loss and increased fractures known to occur in this common condition.

Disclosures: Matthew Drake, None.

MO0076

Interactions Between Multiple Myeloma Cells and Osteocytes Alter Osteocytic Gene Expression: Evidence for Osteocyte-Driven Dysregulation of Bone Remodeling in Multiple Myeloma. <u>Jesus Delgado-Calle</u>*[1], <u>Lilian Plotkin</u>[1], <u>Teresita Bellido</u>[1], <u>G. David Roodman</u>[2]. [1]Indiana University School of Medicine, USA, [2]Indiana University, USA

Multiple myeloma (MM)-induced bone disease is characterized by exacerbated bone resorption with osteolytic lesions that do not heal due to a concomitant reduction in bone formation. Osteocytes are major producers of the pro- and anti-osteoclastogenic cytokines RANKL and OPG and also secrete sclerostin, a potent inhibitor of bone formation. In MM, monoclonal plasma cells grow into bone allowing the exchange of soluble factors as well as direct cell-to-cell contact between MM cells and osteocytes. We investigated whether direct contact or soluble factors produced by MM cells alter osteocytic gene expression. Human JJN3 MM cells were cultured in direct cell-to-cell contact with murine osteocytic MLO-A5 cells, or cells were cultured separated by a membrane that only allows the passage of soluble factors. Direct cell-to-cell contact with JJN3 MM cells up-regulated Sost mRNA expression in MLO-A5 osteocytic cells by 3-fold as early as 4h and remained elevated up to 24h. Simultaneous with Sost upregulation, OPG mRNA was decreased by 30-50%. The expression of other Wnt target genes including Axin2 and Smad6 was also decreased. In contrast, Sost/Wnt target gene expression was not altered when MM and MLO-A5 cells were not in direct cell-to-cell contact; however, RANKL gene expression was upregulated suggesting that molecules secreted by MM cells stimulate RANKL. Treatment with TNFα, known to be secreted by MM cells, increased RANKL expression in osteocytic cells after 4 and 24h. However, addition of TGFβ or IL-6, other potential RANKL regulators secreted by MM cells, did not affect RANKL mRNA expression. Further, OPG protein was reduced by 25 and 50% at 4 and 24h respectively, and soluble RANKL was increased by 3-fold at 24h compared to media of MLO-A5 cells cultured alone. These findings demonstrate that direct interactions between osteocytes and MM cells, upregulate the expression of the bone formation inhibitor Sost in osteocytes, which in turn decreases Wnt signaling and reduces osteocytic OPG expression. In addition, soluble factors secreted by MM cells increase osteocytic RANKL expression. Our results suggest that direct contact with MM cells or MM-derived soluble factors alter osteocytic gene expression, which drives the dysregulated bone remodeling in MM.

Disclosures: Jesus Delgado-Calle, None.

MO0077

Cross-talk between Runx2 regulatory network and IGF-1R pathway: A novel regulatory mechanism of bone metastasis. <u>Jitesh Pratap</u>[1], <u>Manish Tandon</u>*[2], <u>Zujian Chen</u>[2], <u>Amarjit Virdi</u>[1]. [1]Rush University Medical Center, USA, [2]Rush University Medical Center, USA

Bone is one of the most common target sites of distant metastasis of epithelial cancers, resulting in cancer-related deaths and skeletal complications. The paracrine signaling between tumor cells and the bone microenvironment leads to a selective growth advantage for the cancer cells. The bone-derived insulin-like growth factor-1 (IGF-1) binds to insulin-like growth factor receptor (IGF-1R) to initiate intracellular signaling. The downstream signaling events in response to IGF-1 stimulation include activation of phosphatidyl inositol 3' kinase and mitogen activated protein kinases that regulate survival and proliferation of cancer cells. However, the inhibition of these signaling pathways has shown modest benefit in recent clinical trials
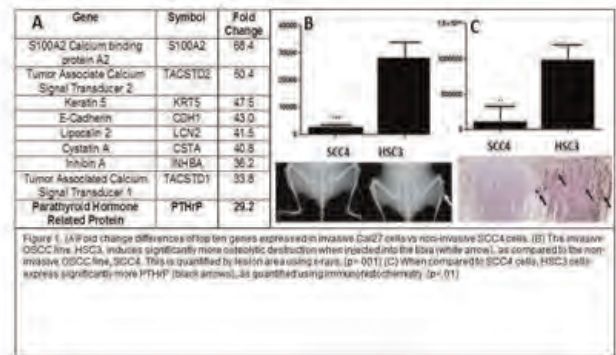
necessitating the need to understand the regulatory mechanisms of the IGF-1R pathway and to block bone metastasis. The Runt-related transcription factor, Runx2, is required for bone development but is also aberrantly expressed at higher levels in invasive mammary epithelial cells and promotes invasive properties. Recently, we have shown that Runx2 promotes survival of invasive breast cancer cells by increasing phosphorylation of serine/threonine kinase Akt (pAkt-Serine 473) via mammalian target of rapamycin complex-2. To determine the implications of Runx2-mediated pAkt regulation in bone metastasis of breast cancers, we isolated Runx2 knockdown or control MDA-MB-231 cells from bones 7-8 weeks post intracardiac injections in SCID mice. The expression profiling of IGF-1R/Akt signaling pathway showed increased IGF-1Rβ, pIGF1R-β and pAkt levels in bone-seeking Runx2 knockdown cells compared to controls and that could be inhibited with IGF-1Rβ inhibitor OSI-906 (Linsitinib). However, despite inhibition of IGF-1R and Akt activity with OSI-906, no apparent phenotypic alterations were observed. Interestingly, in contrast to IGF-1Rβ and pAkt, the Erk 1/2 levels were reduced in bone-seeking Runx2 knockdown cells compared to parental MDA-MB-231 cells. The treatment with Erk 1/2 inhibitor reduced clonogenic potential of these cells. Taken together, our studies indicate a temporal requirement of Runx2-mediated regulation of IGF-1R/Akt/Erk signaling during bone metastasis of breast cancer and suggest that the inhibition of Runx2 could enhance sensitivity of cancer cells towards Erk inhibitors targeting bone metastasis with high IGF-1R.

Disclosures: Manish Tandon, None.

MO0078

Hedgehog and mechanical signaling regulate PTHrP expression and bony invasion of oral squamous cell carcinomas. <u>Shellese Cannonier</u>*[1], <u>Cara Gonzales</u>[2], <u>Jonathan Page</u>[3], <u>Scott Guelcher</u>[4], <u>Julie Sterling</u>[5]. [1], USA, [2]UT Health Science Center, USA, [3]Department of Cehmical & Biomolecular Engineering, Vanderbilt University, USA, [4]Vanderbilt University, USA, [5]Department of Veterans Affairs (TVHS)/Vanderbilt University Medical Center, USA

Oral Squamous Cell Carcinoma (OSCC) frequently invades the mandible, which dramatically reduces survival rates while increasing associated morbidity. Despite decades of research, the molecular mechanisms of OSCC mandibular invasion are not well understood. PTHrP is expressed in OSCC biopsies with mandibular invasion and PTHrP knock-down in a murine OSCC line prevented invasion. Clinical data shows that the Hedgehog (Hh) signaling pathway regulator, Gli2, correlates with invasion and poor overall survival, and we have shown that in tumors that metastasize to bone, Gli2 activates PTHrP expression. Based on this data and our preliminary microarray data showing that PTHrP is over-expressed 29-fold by invasive OSCC cells (Fig 1), we hypothesized that Gli2 controls PTHrP expression in bony invasive OSCC. Therefore, we examined a panel of 10 OSCC cell lines, and found that 8 lines expressed both Gli2 and PTHrP. To determine if this increased expression correlated with bony invasion, we injected SCC4 cells, a non-invasive OSCC line with low PTHrP expression, or HSC3 cells, an invasive OSCC line with high PTHrP expression similar to that of Cal27, into the tibia of mice. HSC3 cells induced a 12-fold increase in osteolytic lesion area by X-ray and 8-fold more PTHrP by IHC than SCC4 cells (Fig 1). To explore the regulation of Gli2 and PTHrP expression, we examined pathways known to regulate both in other tumors, including rigidity, TGF-β, Hh, and Wnt signaling. Firstly, using 2D polyurethane films of varying rigidities, we found that PTHrP expression was increased 13-fold in cells grown on films approximating the rigidity of the mandible compared to soft tissue rigidities (Fig 2). To determine the upstream modulators of Gli2 and PTHrP, we used agonists and antagonists against known regulators of Gli2. Using promoter assays and qPCR, we found that while the activation of Hh, Wnt, and TGFβ signaling pathways all modulate PTHrP expression, only Hh signaling is required, as cyclopamine treatment (Hh inhibitor) completely blocked PTHrP stimulation by other pathways. To determine if this effect was specific to Gli2, we examined the efficacy of Gli inhibitors, Gant58 and HPI-1, both of which reduced PTHrP expression by 5 to 6 fold. Together, our data demonstrate that PTHrP expression in bony-invasive OSCC is regulated by Gli2, and Hh inhibition reduces PTHrP expression, suggesting Gli2 as a potential therapeutic target for inhibiting bony invasion of OSCC.

Figure 1. (A)Fold change differences of top ten genes expressed in invasive Cal27 cells vs non-invasive SCC4 cells. (B) The invasive OSCC line, HSC3, induces significantly more osteolytic destruction when injected into the tibia (white arrow), as compared to the non-invasive OSCC line, SCC4. This is quantified by lesion area using x-rays. (p= 001) (C) When compared to SCC4 cells, HSC3 cells express significantly more PTHrP (black arrows), as quantified using immunohistochemistry. (p<.01)

1

Figure 2. SCC4 cells grown on 2D films with a rigidity similar to that of the mandible show increased basal expression of PTHrP as compared to cells grown on compliant films with a rigidity similar to that of soft tissue. SCC4 cells stimulated with TGF-β show significantly more PTHrP expression when seeded on rigid films as compared to compliant films. This appears to be synergistic, as cells stimulated on rigid scaffolds show more PTHrP expression than the combined levels of PTHrP when cells are either grown on rigid scaffolds or stimulated with TGFβ.

2

Disclosures: Shellese Cannonier, None.

MO0079

Withdrawn

MO0080

Inhibition of Autophagy Increases Cytotoxic Effects in Chondrosarcoma Cells. Stephan Reumann[1], Kristen Shogren[1], Michael Yaszemski[2], Avudaiappan Maran*[2]. [1]Mayo Clinic College of Medicine, USA, [2]Mayo Clinic College of Medicine, USA

Chondrosarcoma is a cancer of cartilage cells and is the second most common type of bone tumor in the United States. Unlike other musculoskeletal tumors, chondrosarcomas are resistant to conventional chemotherapy and radiotherapy. Autophagy is a homeostatic mechanism through which cellular proteins and organelles are subjected to lysosomal degradation and recycling and could play a dual role in cancer by facilitating either cell death or cell survival. Although autophagy has been shown to contribute to chemoresistance in several cancers, its involvement in chondrosarcoma has not yet been investigated. To determine whether autophagy plays a role in chondrosarcoma, we have studied the individual effects of 2-methoxyestradiol (2-ME) and cis-platin, two compounds that have been shown to induce cell death. Transmission electron microscopy imaging indicates that 2-ME treatment resulted in the accumulation of autophagosomes in human chondrosarcoma cells. Both 2-ME and cis-platin induced the conversion of microtubule-associated protein LC3-I to LC3-II, a protein marker that is correlated with the formation of autophagosomes. In addition, our results show that treatment with Bafilomycin and 3-methyl adenine, the inhibitors of autophagy, further increased the cell death in 2-ME and cis-platin-treated chondrosarcoma cells. Together, this study demonstrates that 2-ME and cis-platin induce autophagy in chondrosarcoma cells which might contribute to the chemoresistance. Thus, our studies show that the targeted treatment and the efficacy of chemotherapeutic drugs in chondrosarcoma could be further improved by modulating autophagy.

Disclosures: Avudaiappan Maran, None.

MO0081

Withdrawn

MO0082

Interleukin-6 receptor inhibitor suppresses bone metastases in a breast cancer cell line. Hiroki Wakabayashi*[1], Takahiko Hamaguchi[2], Takahiro Iino[2], Akihiko Matsumine[2], Akihiro Sudo[2]. [1]Mie University Graduate School of Medicine, Japan, [2]Mie University, Japan

Background. Interleukin-6 (IL-6) is a multipoietic cytokine produced by many cell types. IL-6 acts on a wide range of tissues and cell lines and induces cell growth and differentiation, production and expression of other cytokines, and acute phase protein synthesis. IL-6 is a potent inflammatory cytokine that appears to play a key role in cancer growth and metastasis. In the present study, the effects of IL-6 receptor (IL-6R) inhibitor on breast cancer aggressiveness and bone metastases were investigated.

Methods. MDA-MB-231 (MDA-231) cells were injected into the left heart ventricle of mice, and then anti-human IL-6R monoclonal antibody or saline was administered intraperitoneally for 28 days. After 28 days, incidence of bone metastases was evaluated in the hindlimbs by radiography and histology. MDA-231 cells were treated in presence or absence of IL-6R inhibitor and were examined with respect to cell survival. The appearance of signal transducer and activator of transcription 3 (Stat3) and vascular endothelial growth factor (VEGF) was analyzed by SDS-PAGE and immunoblotting.

Results. In X-ray, osteolytic bone metastases appeared around the knee joints in the mice without tocilizumab treatment. 93.8% (15/16) of untreated mice developed metastases per mouse. In contrast, 60% (9/15) of treated mice developed metastases per mouse. In histomorphometric analysis, the area of metastases per hind limb bone was 22.7% ± 6.1% and 8.3% ± 4.5% in untreated and treated mice, respectively. Radiological and histomorphometric analysis showed that the area of metastatic bone tumor was decreased significantly in treated mice. The mechanism of bone metastasis inhibition involved inhibited cell proliferation and decreased expressions of phospho-Stat3 and VEGF in MDA-231 cells.
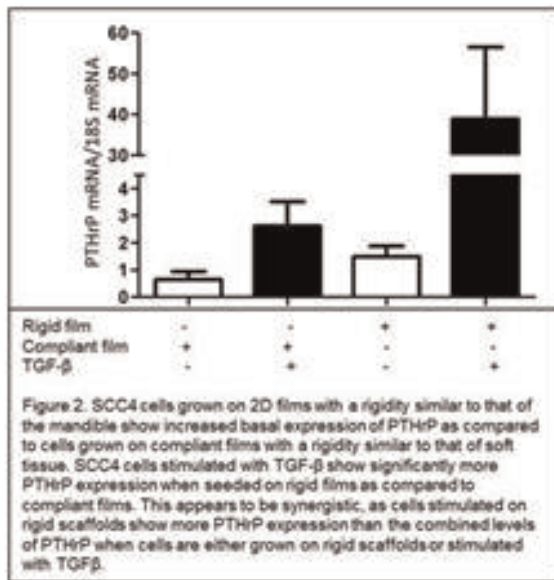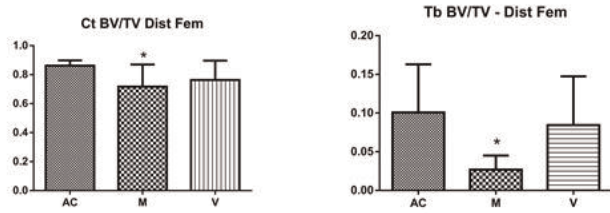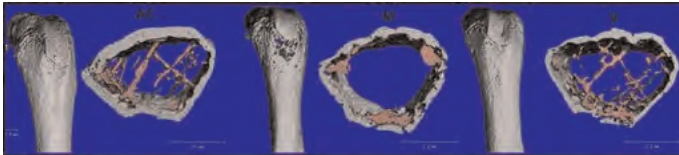
Conclusions. IL-6R inhibitor reduced bone metastases in an animal model injected with MDA-231 cells. These results suggest a novel role for IL-6 signal inhibition in the reduction bone metastases in this breast cancer model. The results of the present study suggest that inhibition of IL-6 signal may become a preventive therapeutic option for breast cancer.

Disclosures: HIROKI WAKABAYASHI, None.

MO0083

Osteopenia and Osteolysis Resulting from Multiple Myeloma Partially Suppressed through Low Intensity Mechanical Signals. Gabriel Pagnotti*[1], Benjamin Adler[1], M. Ete Chan[1], Mallory Korman[2], Kenneth R Shroyer[2], Clinton Rubin[3]. [1]Stony Brook University, USA, [2]Stony Brook Medicine Department of Pathology, USA, [3]State University of New York at Stony Brook, USA

Multiple myeloma promotes osteopenia and osteolysis while causing marked destruction of healthy marrow, elevating fracture risk while simultaneously compromising the capacity for bone repair. In this study, we evaluated the capacity of low intensity vibration (LIV) as a means to harness bone's sensitivity to mechanical signals and protect skeletal quantity and quality put at risk as a consequence of multiple myeloma. Twenty-five 7w old immunocompromised mice (*NSG*, The Jackson Laboratory) were tail-injected with 2 x 10^6 U266β1 (ATCC) human myeloma cells, while 8 controls (AC) were saline-injected. Of the 25 myeloma injected animals, 13 were subject to 15 minutes per day of low intensity vibration (V; 0.3g @ 90Hz), while 12 received sham handling (M). At 9w post-injection, histological assessment of the femoral and tibial bone marrow revealed extensive plasma cell infiltration throughout the medullary cavity in both M and V as compared to AC, resulting in displacement of healthy marrow constituents, phenotypically consistent with gross anemia and leukopenia. As reviewed by a pathologist, evaluation of the marrow space estimates a 75% infiltration of the disease in M, with a 61% invasion in V. FACS analysis of marrow isolated from the femur showed a +180% (p<0.002) greater number of early-stage hematopoietic stem cells (KLS) in M versus AC, while a -6% decrease was observed in V as compared to M. Micro-CT of the distal femora demonstrated a -73% (p<0.04) lower trabecular bone volume fraction (BV/TV) in M as compared to AC. In contrast, the mechanically stimulated V group had a +36% greater BV/TV (p<0.05) as compared to M. Cortical BV/TV of the femoral diaphysis was -16% (p<0.03) lower in M as compared to AC, while V was +6% greater than M (nsd). Cross-cortical perforation of the metaphysis observed in many M mice was not evident in V or AC. This murine model of multiple myeloma demonstrates the rapid invasion of the tumor through the marrow, and the resulting erosion of both bone quality and quantity. These preliminary experiments suggest that the introduction of mechanical signals – perhaps as a surrogate to exercise – helps slow the progress of the disease by potentially protecting the bone marrow microenvironment.

Micro-CT Analyses of Femoral Diaphysis

Micro-CT Reconstructions of the Distal Femur

Disclosures: Gabriel Pagnotti, *None.*
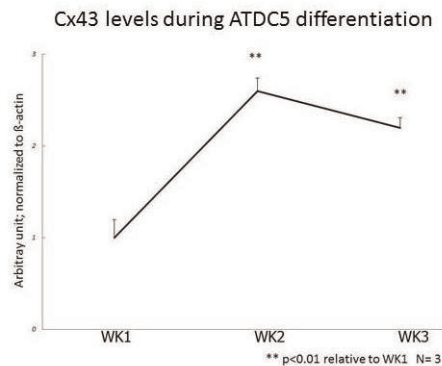
MO0084

Connexin 43 Regulates Chondrocyte Differentiation. <u>Yue Zhang</u>[1], <u>Alayna Loiselle</u>[2], <u>Yanghue Xing</u>[3], <u>Jun You</u>[4], <u>Henry Donahue</u>*[4]. [1]Pennsylvania State University College of Medicine, USA, [2]University of Rochester, USA, [3]Pennsylvania State University College of Medicine, USA, [4]The Pennsylvania State University College of Medicine, USA

Osteoarthritis (OA) is the most common joint disorder. Recent studies suggest connexin 43 (Cx43) and gap junctions (GJs) are increased in human OA cells. GJs are membrane-spanning channels which facilitate intercellular communication. It has been reported that Cx43 and GJ regulate differentiation of musculoskeletal cells including osteocytes, osteoblasts and osteoclasts, however, it is unknown whether Cx43 regulates chondrocyte differentiation, a key step in initiating OA. In this study, we used mouse primary chondrocytes and a chondrocytic cell line, ATDC5, as models to study the function of Cx43 during chondrocyte differentiation. We examined the hypothesis that Cx43 regulates chondrocyte differentiation.

Our qPCR data showed that Cx43 mRNA levels in ATDC5 cells significantly increased during 3 weeks culture in differentiation media. Interestingly, over expression of Cx43 in ATDC5 cells prevented chondrocyte differentiation, as demonstrated by inhibition of Alcian blue staining and prevention of increases in Col2, Aggrecan, and Sox9 mRNA levels. Col10 mRNA levels also did not increase, suggesting inhibition of chondrocyte hypertrophy. To verify these results, we transiently ablated Cx43 from mouse primary chondrocytes (Cx43-) using a Cre-loxp system. Despite low primary cell transient transfection efficiency, our data showed that Cre transfection inhibited Cx43 mRNA levels about 44%. After culturing in differentiation media, Cx43- cells showed moderate non-significant increases in Col10, Col2, AGN and Sox9 mRNA levels relative to control cells, suggesting an increase in chondrocyte differentiation and hypetrophy.

By using gain and loss of function approaches, we examined the function of Cx43 during chondrocyte differentiation. Our results clearly demonstrated that Cx43 is closely related to chondrocyte differentiation, a step initiating OA. We showed that Cx43 mRNA levels increased during chondrocyte differentiation and overexpression of Cx43 prevents chondrocyte differentiation and hypertrophy. These results suggest that normal (non OA) chondrocyte Cx43 levels increase as the cells differentiate and eventually this moderates, in a negative feedback manner, chondrocyte differentiation and development of hypertrophic chondrocytes. The increased levels of Cx43 in OA chondrocytes previously reported suggest that OA chondrocytes are resistant to the moderating effect of Cx43 and Cx43 levels increase further to overcome this resistance.

Cx43 expression during ATDC5 cell differentiation
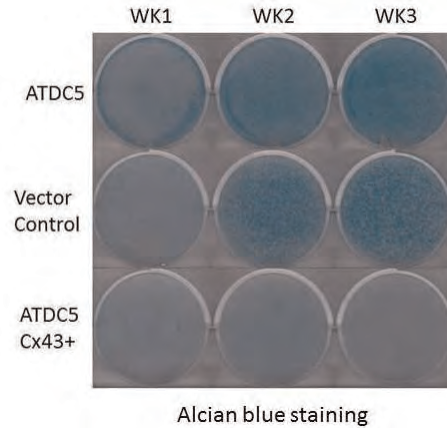
Alcian blue staining

Disclosures: Henry Donahue, *None.*

MO0085

Pulsed Electromagnetic Field (PEMF) Treatment Reduces Expression of Genes Associated with Disc Degeneration in Human Intervertebral Disc Cells. <u>Stephanie Miller</u>*[1], <u>Rachel Bradshaw</u>[2], <u>Dezba Couglin</u>[3], <u>Jeffrey Lotz</u>[2]. [1]University of California, San Francisco, USA, [2]UCSF, USA, [3]UCSF, USA

Imbalances in inflammation, innervation, and extracellular matrix maintenance are potential unifying clinical features of intervertebral disc (IVD) degeneration and low back pain (LBP). Pulsed electromagnetic field (PEMF) therapies have been applied to stimulate bone health and healing as well as to reduce the symptoms of arthritis, but the effects of PEMF on IVD biology is unknown.

Human IVD tissues were collected from patients being surgically treated for discogenic pain or spinal instability. The IVD tissues of annulus fibrosus (AF) and nucleus pulposus (NP) were separated by blunt dissection, incubated, and cultured separately until use at passage 4. Each cell type was separately encapsulated in 1.2% alginate beads, and the cells were acclimated for 24 hours before treatment. Cells were treated with IL-1α (10 ng/mL) to stimulate an inflammatory environment associated with chronic LBP. Cells were also exposed to an FDA-approved PEMF waveform (Orthofix, Inc., Lewisville, TX) for four hours daily. At each terminal incubation point (1, 4, 7 days), RNA was isolated from cells from each treatment group to assess IL-1α- and PEMF-induced changes in gene expression. NuGEN Pico V2 was used for amplification, fragmentation and biotin-labeling of cDNA, and the labeled cDNA was hybridized to Human GeneChip Gene 2.0 ST microarrays. Linear models were fitted for each gene using the Bioconductor Limma package in R, and moderated t-statistics, fold-change and the associated p-values were calculated for each gene.

PEMF treatment lessened the IL-1-induced upregulation of particular genes known to play a role in IVD degeneration and LBP. Consistent with our previous results, PEMF tended to reduce IL-1α-associated expression of IL-6 (25%, p=0.069) in NP cells and MMP13 (26%, p=0.10) in AF cells. Additionally, PEMF treatment significantly diminished IL-1α-induced expression of IL-17A (33%, p=0.011) and MMP2 (24%, p=0.0059) in NP cells. In AF cells, PEMF treatment significantly decreased IL-1α-linked NFκB (11%, p=0.042) expression. These results demonstrate that disc cells are responsive to PEMF, and motivate future studies to determine whether PEMF may be helpful for patients with IVD degeneration and LBP.

Disclosures: Stephanie Miller, *None.*
This study received funding from: Orthofix Inc.

MO0086

The dynamics of mineralized cartilage formation. <u>David Rowe</u>[1], <u>Nathaniel Dyment</u>*[2], <u>Yusuke Hagiwara</u>[1], <u>Andrew Breidenbach</u>[3], <u>David Butler</u>[3], <u>Thomas Thomopoulos</u>[4], <u>Andrea Schwartz</u>[4], <u>Lindsey Aschbacher-Smith</u>[5], <u>Han Liu</u>[5], <u>Rulang Jiang</u>[5]. [1]University of Connecticut Health Center, USA, [2]University of Connecticut Health Center, USA, [3]University of Cincinnati School of Engineering, USA, [4]Washington University, Department of Orthopedics, USA, [5]Cincinnati Children's Hospital Research Foundation, USA

The boundary that separates subchondral bone from the mineralized portion of articular cartilage (AC) and the fibrocartilage (FC) that attaches tendon/ligaments to bone (enthesis) juxtaposes two tissues with distinctly different cell environments and mechanical functions. Both undergo a mineralization process that is driven by different cells and molecular processes. Using non-decalcified cryohistology, appositional mineral deposition is found in rapidly growing mice in both types of mineralizing cartilage (MC). The mineralization lines of bone and MC are formed in opposite directions indicating that a mineralized interface is being created. Collagen fibers run vertically through the MC where they juxtapose with horizontally oriented

subchondral bone. Bone formation is characterized by Col3.6GFP+ osteoblasts overlying a mineralization label in close association with TRAP+ osteoclastic activity. In contrast, ColX-RFPchry+, alkaline phosphatase (AP+), and occasionally TRAP+ chondrocytes are located at the tidemark and extend into the MC zone. Using a Gli1-CreERT2/Ai14 lineage tracing strategy, cells in the unmineralized zone can be chased into the mineralized zone indicating that the mineralization front extends into the tendon/ligament/cartilage as cell differentiation progresses away from the MC (fig 1). This concept is strengthened by the observation that Scx-Cre:Smof/- mice have severely underdeveloped entheses, suggesting that hedgehog signaling is crucial for MC formation (fig 2). After skeletal maturity, minimal mineralization activity is observed, but in the case of the enthesis (not AC), it can reactivate when abrupt mechanical forces are experienced. Using an ACL transection model, the enthesis initiates appositional mineral growth with the ColX-RFP/AP+ cells extending ahead of the tidemark. Chondrocytes in the unmineralized cartilage just above the tidemark become TRAP+ showing a punctate morphology that is distinctly different from osteoclasts (fig 3). These changes are prominent in the uninjured MCL and can be observed within two weeks after surgical intervention. Osteophytes subsequently develop reflecting the loss in the barrier between the two tissues. Understanding the molecular and cellular environment of the FC that produces the barrier and the limitations it has in maintaining this boundary when a new mechanical load is experienced may be an avenue of research for understanding the pathogenesis of degenerative arthritis.
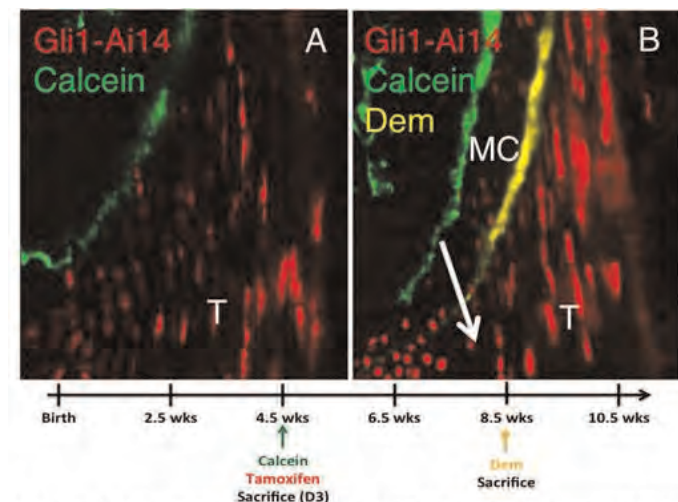

Figure 1. Lineage trace of Gli1-Ai14+ cells from unmineralized fibrocartilage (A) in the patellar tendon enthesis to mineralized fibrocartilage (B). Tamoxifen and calcein were delivered at 4 weeks of age followed by demeclocycline (Dem) at 8 weeks of age. Mice were analyzed at 3 days (A) and 28 days (B) following tamoxifen injection. Tendon (T), Mineralized Fibrocartilage (MC).

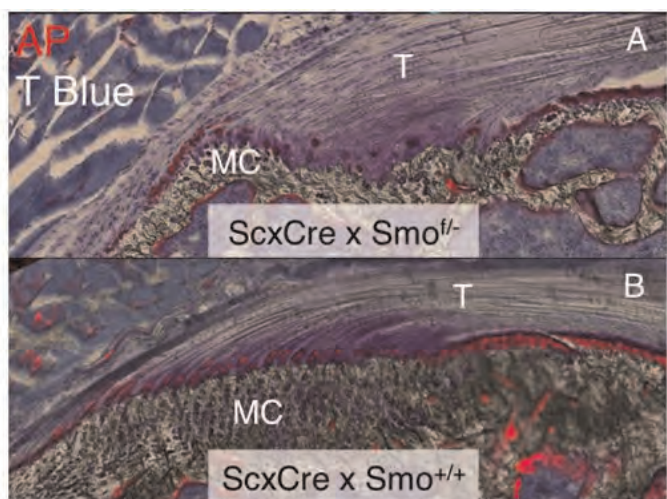Figure 1. Lineage trace of Gli1-Ai14+ cells from unmineralized fibrocartilage

Figure 2. Targeted knockdown of hedgehog signaling (A) in the enthesis through deletion of smoothened gene (Smo) by scleraxis (Scx) Cre driver yields severely impaired mineralized fibrocartilage (MC) formation with reductions of alkaline phosphatase (AP, red) activity near the tidemark of the supraspinatus tendon (T).

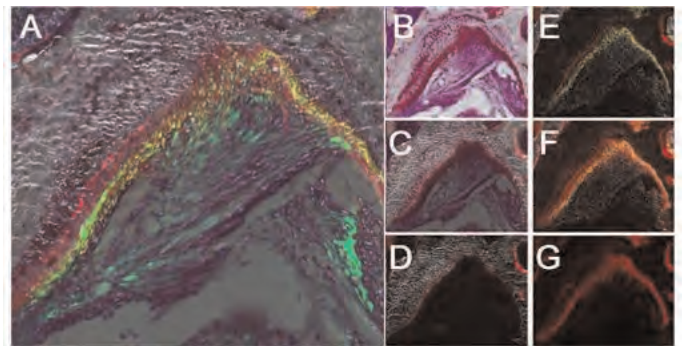Figure 2. Targeted knockdown of hedgehog signaling

Figure 3: Femoral insertion of the PCL 1 month after ACL transection. A. Overlay of the individual images shown in B-G. B. Toluidine blue and alkaline phosphatase (AP, red); C. Accumulated mineral (gray), alizarin complexone (AC) mineralization line of the tidemark (red) and toluidine blue/AP; D. Mineral (gray and AC mineralization line; E. AC mineralization line (red) and TRAP stain (yellow). Enlarge panel A to appreciate the morphology of the TRAP stain within the chondrocytic cells. F and G show the addition of alkaline phosphatase activity (red) that is in the same area as the TRAP positive cells.

Figure 3: Femoral insertion of the PCL 1 month after ACL transection

Disclosures: Nathaniel Dyment, None.

MO0087

The Effects of Reduced Gravity On Subchondral Bone And Articular Cartilage: Are They Good Neighbors?. <u>Liliana Mellor</u>*[1], <u>Elizabeth Loboa</u>[2], <u>Julia Oxford</u>[3], <u>Travis Baker</u>[4], <u>Minoti Hiremath</u>[5]. [1]North Carolina State University, USA, [2]North Carolina State University, USA, [3]Boise State University, USA, [4]Boise State University, USA, [5]Boise State University, USA

Astronauts are exposed to prolonged periods of microgravity during spaceflight. Lack of gravity is known to negatively affect the musculoskeletal system, mainly bone and skeletal muscle, which are constantly exposed to mechanical loading on Earth. However, another important component of the musculoskeletal system, the synovial joint, has not been fully investigated in space-like conditions. Unlike bone and muscle, the articular cartilage of the synovial joint has limited regenerative capacity. Cartilage degradation leads to a severe disease known as osteoarthritis (OA). OA is the leading cause of disability in the US, and one of the few chronic diseases of aging without a cure. Little is known about the effects of microgravity on the synovial joint and changes in cartilage homeostasis. The goal of this project is to elucidate the molecular changes triggered by microgravity that cause degradation of articular cartilage and subchondral bone, and to investigate the interactions between these adjacent tissues. Changes in subchondral bone density are commonly associated with the onset of cartilage degradation in OA. Aberrant cross-talk between signaling pathways in the two tissues may precipitate pathological conditions. This is the first study to address interactions between these two tissues in reduced gravity conditions.

The Wnt pathway plays a crucial role in bone and cartilage mechanotransduction. It has been shown that inhibitors of the Wnt pathway are up-regulated in bone during unloading conditions, contributing to a decrease in bone formation that leads to bone density loss. We used primary chondrocytes and Rat Chondrosarcoma cells (RCS) cultured under reduced gravity conditions using a Rotating Wall Vessel bioreactor to determine changes in chondrocyte gene expression and Wnt signaling in response to simulated microgravity. Our data shows that similar to bone, Wnt inhibitors are also up-regulated in chondrocytes in response to reduced gravity; however, this may be a chondro-protective mechanism to prevent further cartilage degradation. We have found that Wnt activation and inhibition appear to have opposite effects on adjacent subchondral bone and articular cartilage; therapeutic targeting against Wnt inhibitors to prevent bone loss needs to be further investigated.

Disclosures: Liliana Mellor, None.

MO0088

An *in Vitro* Chondrogenic Differentiation Model Using KS483 Mouse Mesenchymal Progenitor Cell Line. <u>Katja Fagerlund</u>*[1], <u>Natalia Habilainen-Kirillov</u>[2], <u>Clemens Lowik</u>[3], <u>Alan Chan</u>[4], <u>Jussi Halleen</u>[5]. [1]Pharmatest Services Ltd, Finland, [2]Pharmatest Services Ltd, Finland, [3]Department of Radiology, Leiden University Medical Center, Netherlands, [4]Percuros BV, Netherlands, [5]Pharmatest Services Ltd, Fin

KS483 cells are multipotent mouse mesenchymal progenitor cells that are able to differentiate into chondrocytes, adipocytes and osteoblasts and are a well-characterized model for the study of osteoblast differentiation and bone formation. We have studied the use of KS483 cell line in an *in vitro* model of chondrogenic differentiation. The cells were cultured in three-dimensional (3D) pellet culture system in serum-free differentiation medium in the presence and absence of BMP-6 for 17-28 days. The pellets were cultured in 96-well plates and the medium was changed in 2-3 day intervals. The pellets were embedded in paraffin, sectioned and stained for

Safranin O and Alcain blue for assessment of sulfated glycosaminoglycan (sGAG) content, and processed for immunohistochemistry to visualize type II collagen. For biochemical analysis, the pellets were digested with proteinase K and assayed for sGAG at days 17, 24 and 28. Type II collagen carboxyterminal propeptide (CP-II) was determined in the culture medium collected at day 17. Based on histological analysis, BMP-6 showed concentration-dependent stimulatory effects on chondrogenic differentiation, increased sGAG content of the pellets, and increased CP-II released into the culture medium. These results suggest that the KS483 cell line can be used for setting up an *in vitro* model for studying chondrogenic differentiation and for identifying novel compounds with anabolic effects on chondrogenesis. As these cells can rapidly proliferate, they provide an unlimited source of easily expanded progenitor cells for conducting large number of replicates and studies.

Disclosures: Katja Fagerlund, Pharmatest Services Ltd, 9; Pharmatest Services Ltd, 4

MO0089

Antiangiogenic Drug, TNP-470, Inhibited Early Chondrocyte Condensation During Ectopic Bone Formation. Beth Bragdon*[1], Stephanie Lam[2], Sherif Aly[3], Elise Morgan[4], Louis Gerstenfeld[5]. [1]Boston University School of Medicine Department of Orthopaedics, USA, [2]Department of Orthopaedic Surgery, Boston University School of Medicine, USA, [3]Department of Orthopaedic Surgery, Boston University School of Medicine, USA, [4]Boston University, USA, [5]Boston University School of Medicine, USA

Introduction: Angiogenesis is required for endochondral ossification where vessels invade hypertrophic cartilage and facilitates the replacement of cartilage with mineralized bone tissue during embryological skeletal development. Blocking angiogenesis impedes fracture repair and BMP2-induced ectopic bone formation. Although angiogenesis and bone formation is a coupled process, little is known about the angiogenic role during endochondral ossification in ectopic bone formation.

Methods: Human Demineralized Bone Matrix(DBM) was obtained with an MTA from Medtronics Inc. Fifty milligrams were implanted at the periosteum of the femur of male B6,129S7-Rag1[tm1/MOM]/J. Antiangiogenic drug, TNP-470 (EMD Millipore), was subcutaneously injected (25mg/kg) daily starting the day of surgery. Ectopic bone formation was followed for 16 days. Micro-CT quantified new bone. RNA was isolated from the implant at post-operative day 2, 8 and 16. RT-qPCR was used to quantify mRNA expression for stem cell recruitment (*Sox2*, *Nanog*), chondrocyte commitment and condensation (*Sox9*, *Sox5*, and *NCam1*), chondrocyte (*Aggrecan* and *Collagen10a*), osteoblast (*Osterix* and *Osteocalcin*), and vascular (*VEGFA*, and *Pecam1*) development.

Results: Ectopic bone was induced by the DBM implant by days 8 and 16. TNP-470 significantly decreased bone volume at both time points (Fig1A). Molecular assessment showed stem cell marker expression was present at day 2 for control and TNP-470. This was followed by peak expression of chondrocyte differentiation at day 8 and osteoblasts at day 16 for control implants. While TNP-470 treated implants showed expression for chondrocyte commitment marker, *Sox9*, there was a significant decrease in gene expression for early chondrocyte condensation, *N-Cam1*, and progression of chondrocyte differentiation (Fig1B). Endothelial maker, *Pecam1*, was significantly decreased whereas *VEGFA* expression was increased at day 2 and 4 with TNP-470.

Discussion: Consistent with prior findings inhibition of angiogenesis with TNP-470 decreased ectopic bone. While inhibition of angiogenesis had no effect on stem cell recruitment to the implant site and commitment to the chondrogenic lineage, subsequent chondrogenesis failed to progress. Most striking, however, is that chondrogenic progression was halted prior to chondrocyte condensation, noticeably earlier than the expected hypertrophic chondrocytes. These results suggest an earlier role for angiogenesis for postnatal endochondral ossification.
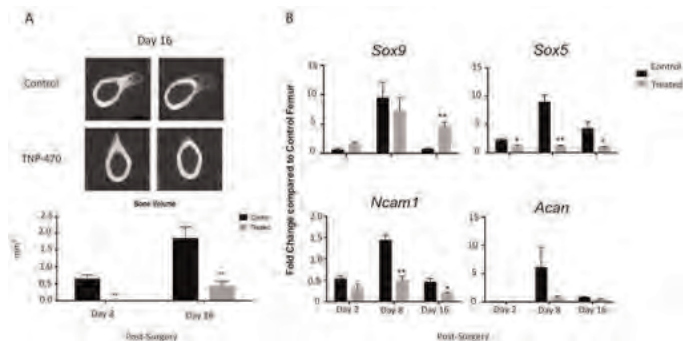
FigureI A. Micro-CT individual bone slices show cross-sectional view of bone in white and surrounding implant in textured grey. Bone volume at day 8 and 16 for control and TNP-470-treated samples. * = p<0.05, ** = p<0.005. **B.** qRT-PCR analysis of cartilage genes. n= 3-7.

Fig1_TNP

Disclosures: Beth Bragdon, None.

MO0090

Environmental Stress Promotes Chondrogenic Commitment of Skeletal Progenitor Cells by Activating Autophagy. Nick Van Gastel*[1], Sophie Torrekens[2], Patrizia Agostinis[3], Geert Carmeliet[4]. [1]Laboratory of Clinical & Experimental Endocrinology, KU Leuven, Belgium, Belgium, [2]Laboratory of Clinical & Experimental Endocrinology, KU Leuven, Belgium, Belgium, [3]Laboratory of Cell Death Research & Therapy, KU Leuven, Belgium, Belgium, [4]Katholieke Universiteit Leuven, Belgium

Skeletal progenitor cells present in the periosteum are crucial for successful bone fracture healing, making them an attractive cell source for bone regeneration strategies. Insight in the signaling pathways regulating the activation and differentiation of these cells remains however limited. In the current study, we determined how environmental stress controls the fate of periosteal progenitor cells.

Periosteal progenitor cells were isolated from adult mice and exposed to low nutrient availability (reduced serum, glucose, glutamine and oxygen or low serum alone), which induced activation of autophagy, as determined by measuring LC3 conversion and degradation and p62 protein levels. No changes in AMPK signaling were noted, indicating that the cells were able to maintain their energy balance. Inhibition of autophagy by chloroquine showed that the increased autophagic flux allowed periosteal cells to survive the stressful conditions. Surprisingly, we found that nutrient reduction also alters the fate of periosteal cells and upregulates chondrogenic markers, an effect that was blocked by pharmacological inhibition of autophagy. We observed a similar chondrogenic switch *in vivo* using a new mouse model for compromised bone healing, in which we physically prevented early blood vessel ingrowth from the muscle to the expanding periosteal region, confirming that nutrient availability controls the fate of periosteal cells. Further dissection of the autophagic process using a range of pharmacological compounds indicated that not macro-autophagy but rather chaperone-mediated autophagy, a highly selective form of autophagy, is responsible for the chondrogenic switch of periosteal cells upon nutrient deprivation.

Taken together, our data show that the change in the autophagic flux induced by environmental stress not only acts as a survival mechanism, but is also actively involved in determining the fate of periosteal cells, an exciting finding with important implications for skeletal biology and regenerative medicine.

Disclosures: Nick Van Gastel, None.

MO0091

Enhanced ST2 Expression in Late Stages of Chondrocyte Differentiation in Growth Plate is Regulated by Transcriptional Activity of Runx2. Ehsan Bonyadi Rad*[1], Karin Pichler[2], Giuseppe Musumeci[3], Egon Marth[4], Annelie Weinberg[2]. [1]Medical University Graz, Austria, [2]Medical University Graz, Austria, [3]University of Catania, Italy, [4]Medical University of Graz, Austria

The primary response gene ST2 which is also known as IL1RL1 or T1 is expressed in various cell types including preosteoblasts. It is suggested that ST2 plays a role in early differentiation stages in osteogenic cells and ST2 receptor regulates osteogenic potential in mouse osteosarcoma cells. Evidently, there are no studies about importance of ST2 in cartilaginous tissue therefore we aimed to investigate expression, regulation and possible biological role of this gene, in murine growth plate chondrocytes. Reverse transcription PCR (RT-PCR) confirmed mRNA expression of ST2 receptor (ST2L) and secreted ST2 (sST2) in murine chondrogenic cell line ATDC5. Immunohistochemistry (IHC) of murine tibiae of euthanized three week old mice showed increased ST2 expression at pre-hypertrophic to strong persistent expression at hypertrophic chondrocyte in the growth plate. Interestingly, consistent with significant ST2 upregulation at pre- and hypertrophic growth plate chondrocyte, mRNA expression of ST2L and sST2 were increased to several folds in ATDC5 cells after differentiation. In these cells, markers of chondrocyte hypertrophy, e.g. ColX and MMP-13 were also significantly increased. Previous studies reported that Runx2 a master transcription factor for osteoblast differentiation controls hypertrophic chondrocyte differentiation. Moreover, Runx2 upregulation in differentiated ATDC5 cells were documented before. In an evaluation for possible effect of Runx2 on ST2 expression, quantitative RT-PCR of ATDC5 cells stably transfected with Runx2 cDNA showed significant upregulation of both ST2L and sST2 mRNA expressions. Accordingly, selective knockdown of Runx2 by siRNA led to substantial down-regulation of both variants in ATDC5 cells. Expression of ST2 splice variants are regulated by alternative promoters (distal and proximal) which is cell dependent. Whereas our results demonstrated that both ST2L and sST2 are transcribed from proximal promoter, low mRNA expressions produced from distal promoter were observed in Runx2 overexpressing cells. Using genomic analysis we identified putative Runx2 binding sites on both distal and proximal promoters and electrophoretic mobility shift assay demonstrated binding of Runx2 to both promoters. Overall, our data so far suggest that Runx2 is involved in transcriptional activation of ST2 in pre- and hypertrophic chondrocytes and further investigations might lead to better understanding of ST2 function in the growth plate.

Disclosures: Ehsan Bonyadi Rad, None.

MO0092

Expression and function of CCAAT/enhancer-binding protein family in chondrocytes. <u>Tomotake Okuma</u>*[1], <u>Makoto Hirata</u>[2], <u>Sakae Tanaka</u>[3], <u>Hiroshi Kawaguchi</u>[4], <u>Taku Saito</u>[5]. [1]University of Tokyo, Japan, [2]University of Tokyo, Japan, [3]The University of Tokyo, Japan, [4]JCHO Tokyo Shinjuku Medical Center, Japan, [5]University of Tokyo, Graduate School of Medicine, Japan

CCAAT/enhancer-binding protein (C/EBP) is a member of the leucine zipper family of transcription factors. Among six isoforms of C/EBP family members, C/EBPα, C/EBPβ, C/EBPδ and C/EBPε have a transactivation domain (TAD) and exert redundant functions in many physiological processes such as cell differentiation, cell proliferation, cell cycle regulation, inflammation and immunity. We previously reported that C/EBPβ is abundantly expressed in chondrocytes and regulates skeletal growth and osteoarthritis through the induction of cell cycle-related genes and metalloproteinases. Since the roles of C/EBPα, C/EBPδ and C/EBPε remain unclear, we examined expressions and functions of these C/EBPs in chondrocytes. Among the four C/EBPs with TAD, expression of C/EBPβ and C/EBPδ in mouse primary costal chondrocytes was abundant compared to C/EBPα, while C/EBPε was hardly expressed at the mRNA level. Immunofluorescence showed that C/EBPβ and C/EBPδ proteins were predominantly localized in the prehypertrophic and hypertrophic zones of mouse embryonic limb cartilage, while C/EBPα protein was localized in the proliferative zone. Retroviral overexpression of each of the three C/EBPs in ATDC5 cells suppressed expressions of early differentiation markers including *Col2a1* and *Sox9*, enhanced those of late differentiation markers including *Mmp13* and *Vegfa*, and decelerated cell proliferation, indicating their redundant functions in chondrocytes. To investigate loss-of-function of the three C/EBPs, we used A-C/EBP which exerts a dominant-negative effect against all C/EBPs. Lentiviral overexpression of A-C/EBP into ATDC5 cells increased expressions of *Col2a1* and *Sox9*, decreased those of *Mmp13* and *Vegfa*, and accelerated cell proliferation, confirming that these three C/EBPs suppress the early stage of chondrocyte differentiation and proliferation while enhancing the late stage. Finally, microarray and gene ontology analyses identified many genes regulated by the A-C/EBP overexpression: 19, 17, 35 and 13 genes were upregulated while 26, 41, 97 and 62 genes were downregulated in the skeletal development-related, cell cycle-related, apoptosis-related, and inflammation-related gene groups, respectively. In conclusion, C/EBPβ, C/EBPδ and C/EBPα regulate proliferation and differentiation of chondrocytes and may possibly be involved with apoptosis and inflammation. C/EBPs may play a variety of roles in the homeostasis of joint cartilage under physiological and pathological conditions.

Disclosures: Tomotake Okuma, None.

MO0093

LSD1-Mediated Demethylation of Histone H3 Lysine 9 Contributes to Interleukin 1-Induced Microsomal Prostaglandin E Synthase-1 Expression. <u>Fatima Ezzahra El Mansouri</u>*[1], <u>Sarah Nebbaki</u>[1], <u>Hassan Afif</u>[2], <u>Johanne Martel-Pelletier</u>[2], <u>Jean-Pierre Pelletier</u>[2], <u>Mohamed Benderdour</u>[3], <u>Hassan Fahmi</u>[2]. [1]Research Center-CHUM, Canada, [2]Osteoarthritis Research Unit, CR-CHUM, Canada, [3]Hopital Sacre-Coeur, Canada

Objective: Microsomal prostaglandin E synthase-1 (mPGES-1) catalyzes the terminal step in the biosynthesis of PGE$_2$, a critical mediator in the pathophysiology of osteoarthritis (OA). Histone methylation plays an important role in epigenetic gene regulation. In this study, we investigated the roles of histone H3 (H3K9) methylation in interleukin-1β (IL-1)-induced mPGES-1 expression in human chondrocytes.

Methods: Chondrocytes were stimulated with IL-1 and the expression of mPGES-1 mRNA was evaluated using real-time reverse transcriptase-polymerase chain reaction (RT-PCR). H3K9 methylation and the recruitment of the histone demethylase LSD1 to the mPGES-1 promoter were evaluated using chromatin immunoprecipitation (ChIP) assays. The role of LSD1 was further evaluated using the pharmacological inhibitors, tranylcypromine and pargyline, and siRNA-mediated gene silencing. The LSD1 level in cartilage was determined using RT-PCR and immunohistochemistry.

Results: The induction of mPGES-1 expression by IL-1 correlated with decreased levels of mono- and dimethylated H3K9 at the mPGES-1 promoter. These changes were concomitant with the recruitment of the histone demethylase LSD1. Treatment with tranylcypromine and pargyline, potent inhibitors of LSD1, prevented IL-1-induced H3K9 demethylation at the mPGES-1 promoter and mPGES-1 expression. Consistently, LSD1 gene silencing with siRNA prevented IL-1-induced H3K9 demethylation and mPGES-1 expression, suggesting that LSD1 mediates IL-1-induced mPGES-1 expression via H3K9 demethylation. Finally, we showed that the level of LSD1 was elevated in OA compared to normal cartilage.

Conclusion: These results indicate that H3K9 demethylation by LSD1 contributes to IL-1-induced mPGES-1 expression and suggest that this pathway could be a potential target for pharmacological intervention in the treatment of OA and possibly other arthritic conditions.

Disclosures: Fatima Ezzahra El Mansouri, None.

MO0094

PTHrP Uses HDAC4 and 5 to Suppress Mef2 Action and Inhibit Chondrocyte Hypertrophy. <u>Shigeki Nishimori</u>*[1], <u>Forest Lai</u>[2], <u>Marc Wein</u>[1], <u>Elena Kozhemyakina</u>[3], <u>Andrew Lassar</u>[3], <u>Eric Olson</u>[4], <u>Henry Kronenberg</u>[1]. [1]Massachusetts General Hospital, USA, [2]Massachusetts General Hospital, USA, [3]Harvard Medical School, USA, [4]UT Southwestern Medical Center at Dallas, USA

PTHrP (Parathyroid Hormone-related Peptide) is a powerful inhibitor of chondrocyte hypertrophy. In the chondrocyte-specific PTHrP transgenic mouse (Weir, PNAS 1996), the long bones are composed of only round proliferating chondrocytes without hypertrophic chondrocytes until 7 days after birth. In contrast, the PTHrP KO mouse (Karaplis, Genes Dev 1994) dies just after birth due to respiratory failure caused by abnormal chondrocyte hypertrophy and ossification in the rib cartilage.

Olson's group reported that the transcription factor, Mef2c, drives the hypertrophic program and that Histone Deacetylase 4 (HDAC4), a class IIa HDAC, suppresses this activity (Vega, Cell 2004, Arnold, Dev Cell 2007). Using cultured cells, Lassar's group proposed that PTHrP suppresses hypertrophy by increasing HDAC4 suppression of Mef2c action through a kinase/phosphatase cascade (Kozhemyakina, MCB 2009). Here, we test the validity of these hypotheses *in vivo*.

The HDAC4 KO mouse shows a lethal chondrocyte phenotype similar to that of the PTHrP KO mouse. However, to explain the longer life span (around 10 days) and the delayed onset of the phenotype in the HDAC4 KO mouse, we found that another Class II HDAC member, HDAC5 also mediates the action of PTHrP. The double HDAC4, 5 KO mouse dies at birth with the same phenotype as the PTHrP KO mouse. Even though the HDAC5 KO mouse has normal chondrocyte differentiation, removal of only one allele of the HDAC5 gene in the context of the HDAC4 KO mouse dramatically changes Collagen II and Collagen X mRNA expression in the rib cartilage (Figure).

To exclude the possibility of systemic effects by HDAC4 expressed in other tissues, we compared the phenotypes of the universal HDAC4 KO and the chondrocyte-specific (Collagen II-Cre) conditional HDAC4 KO mouse. We confirmed similar phenotypes in the tibial growth plates, suggesting that the growth plate phenotype in the universal KO mouse is a consequence of deletion of HDAC4 in chondrocytes.

Rib chondrocytes never normally differentiate into hypertrophic chondrocytes, but these chondrocytes have a potential to become hypertrophic chondrocytes, as we can see in Figure. Thus, chondrocyte differentiation is regulated by the balance between the activator (Mef2) and the suppressors (PTHrP/HDAC4/HDAC5) in each cartilage.

in situ hybridization (Rib, P0)
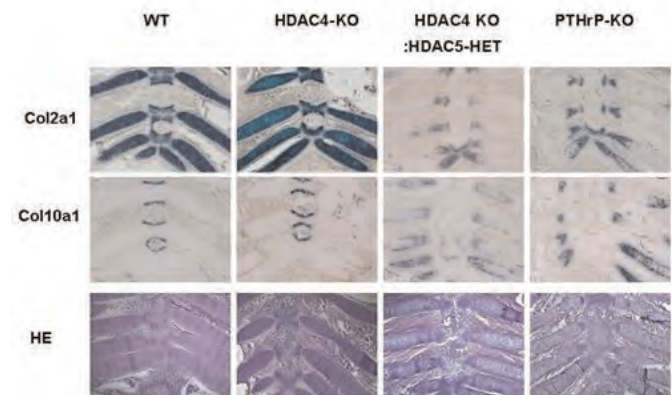
Shigeki Nishimori-ASBMR2014

Disclosures: Shigeki Nishimori, None.

MO0095

Deletion of Connexin 43 in osteocytes blunts the response to intermittent PTH administration in the bone matrix. <u>Rafael Pacheco Da Costa</u>[1], <u>Iraj Hassan</u>[2], <u>Eduardo Katchburian</u>[3], <u>Hannah Davis</u>[4], <u>Lilian Plotkin</u>[5], <u>Rejane Reginato</u>*[6]. [1]Indiana University/Universidade Federal de Sao Paulo - Brazil, Brazil, [2]Indiana University School of Medicine, USA, [3]Federal University of São Paulo, Brazil, [4]Indiana University School of Medicine, USA, [5]Indiana University School of Medicine, USA, [6]UNIFESP - Federal University of São Paulo, Brazil

Connexin (Cx) 43 form gap junction channels and hemichannels, which mediate intercellular communication in osteoblasts, osteocytes and osteoclasts. Earlier studies showed that mice lacking Cx43 have impaired bone mineralization and a defective anabolic response to intermittent PTH administration (iPTH). However, the role of osteocytes on the response of Cx43 deficient mice to iPTH is unknown. To address

this question, we generated mice lacking Cx43 in osteocytes (Cx43^{fl/fl};DMP1-8kb-Cre). Longitudinal DXA analysis in males from 1 to 4 months of age (N=6-11) did not show differences in BMD between Cx43^{fl/fl};DMP1-8kb-Cre and Cx43^{fl/fl} littermate controls expressing Cx43 in osteocytes. Similarly, the expression of genes associated with bone matrix glycosaminoglycans (has1-3, chsy1, chpf and chsy3), proteoglycans (luminican, decorin and biglycan), collagens (col1a1, col3a1, lox and loxl1-loxl4) and mineralization (osteocalcin, alp and runx2) was not changed by deleting Cx43 from osteocytes in vertebral bone (L6), measured by qPCR. Daily iPTH injections (100ng/g for 14d) increased vertebral, femoral and total BMD by DXA and BV/TV in the lumbar vertebra (L4) by μCT in mice from either genotype in a similar fashion, indicating that Cx43 in osteocytes is not required for increased bone mass induced by iPTH. We next examined the expression of matrix-associated proteins by qPCR and we found that, whereas iPTH induced an increase in the expression of bone sialoprotein in vertebral bones obtained from mice of either genotype; Runx2 and osteocalcin were only increased in Cx43^{fl/fl} mice. Collagen analysis in bone sections stained by picrosirius red under polarized light microscopy did not show changes in the pattern of birefringence in femoral bone sections from vehicle-treated Cx43^{fl/fl};DMP1-8kb-Cre compared to Cx43^{fl/fl} mice. On the other hand, iPTH administration increased the predominance of greenish birefringence, suggesting an intense collagen remodeling in Cx43^{fl/fl}, but not in Cx43^{fl/fl};DMP1-8kb-Cre mice. In summary, deletion of Cx43 from osteocytes renders the bone less susceptible to the effects of iPTH administration on the bone matrix. These findings suggest that the inability of PTH to modify the bone matrix in the absence of osteocytic Cx43 expression might contributes to the defective anabolic response to the hormone in mice lacking Cx43.

Disclosures: Rejane Reginato, None.

MO0096

Healing of the bone and tendon interface: an in vivo study using a lactoferrin seeded biomaterial scaffold. David Musson*[1], Matthew Street[2], Michael Dray[3], Ashvin Thambayah[2], Karen Callon[2], Donna Tuari[2], Brendan Coleman[4], Jillian Cornish[5]. [1]University of Auckland, New Zealand, New Zealand, [2]University of Auckland, New Zealand, [3]Waikato District Health Board, New Zealand, [4]Counties Manukau District Health Board, New Zealand, [5]University of Auckland, New Zealand

Healing of hard-soft tissue interfaces are a significant clinical problem. Up to 40% of people over 60yrs of age experience rotator cuff tears, which predominantly occur at the bone-tendon interface. Due to the complex nature of the osteotendinous junction surgical repair is challenging and re-tear rates are about 70%. A potential approach for the improvement of surgical outcomes is the insertion of scaffold materials and growth factors that accelerate the healing. Decellularized extracellular matrix (ECM) scaffolds are known to improve soft tissue regeneration and our preliminary studies demonstrated that a novel ovine forestomach ECM scaffold is cytocompatible and has low immunogenicity. In addition, our group established that lactoferrin (LF) is a potent bone anabolic factor. The aim of this study was to assess the potential use of the decellularized forestomach ECM scaffold, in combination with LF, for augmenting bone and tendon repair.

Complete unilateral supraspinatus tears were surgically created in 46 Sprague-Dawley rats. The tendons were surgically repaired via a single row technique and the rats were randomised into 3 groups. Group 1 (control), received surgical repair only; group 2 received an augmented repair using the ECM scaffold; and group 3 received the ECM scaffold with LF. The repairs were assessed 6 and 12 weeks postoperatively. Primary endpoints were biomechanical testing and blinded histological scoring of bone-tendon interdigitation, collagen fibre density and alignment, inflammatory response and vascularity of the tendon.

At 6 weeks the ECM scaffolds had completely degraded in all animals. Group 3 scored highest in the overall histological evaluation of healing. Both groups 2 and 3 scored significantly higher than group 1, with improved collagen fibre orientation and bone and tendon interdigitation at 6 and 12 weeks. Both stiffness and modulus were increased in group 2, compared to groups 1 and 3 at both time points, although this did not reach significance (11.8N/mm stiffness in group 2 vs. 9.1N/mm in and 9.5N/mm in groups 1 and 3, respectively, at 12 weeks).

This study demonstrated that combining the positive effects of LF and a decllularized ovine forestomach ECM scaffold augments rotator cuff tendon repair in a rat model, and thus has the potential to improve clinical outcomes. Therefore further continuing research is required to identify the ideal augment for delivering LF and improving bone and tendon healing.

Disclosures: David Musson, None.

MO0097

The Leader Tripeptide of Mature DMP1 Guides the Transportation of Secretory DMP1 from Endoplasmic Reticulum to Golgi Apparatus. Suzhen Wang[1], Tian Meng[1], Chunlin Qin[2], Yongbo Lu*[3]. [1]Texas A&M University Baylor College of Dentistry, USA, [2]Texas A & M University Baylor College of Dentistry, USA, [3]Texas A&M University Baylor College of Dentistry, USA

Dentin matrix protein 1 (DMP1) is highly expressed in tooth and bone. The secretory DMP1 is processed into a 37 kDa amino-terminal fragment and a 57 kDa carboxyl-terminal fragment. Previous in vivo studies have demonstrated that the 57 kDa fragment is the biological functional form of DMP1 that rescues the Dmp1-null mouse skeletal and serum biochemical abnormalities, but the function of the 37 kDa fragment remains unknown. The purpose of this study was to examine the function of the 37 kDa amino-terminal region in the secretion of DMP1. Polymerase chain reaction (PCR) and site-directed mutagenesis were employed to generate various DMP1-expressing constructs. These DNA constructs were then transfected into a preosteoblast cell line, MC3T3-E1 cells, and immunofluorescent staining was performed to determine the expression and subcellular localization of various DMP1 proteins. Immunofluorescent staining showed that the full-length DMP1 proteins and 37 kDa amino-terminal fragments were predominantly localized in the Golgi apparatus, whereas the 57 kDa carboxyl-terminal fragments were largely accumulated in the endoplasmic reticulum (ER). However, when the leader tripeptide, leucine-proline-aspartic acid (LPD), of the mature DMP1 was fused to the 57 kDa carboxyl-terminal fragment, the resulting fusion proteins were mainly located in the Golgi apparatus, suggesting that the leader tripeptide was sufficient to guide the transportation of the 57 kDa carboxyl-terminal fragment from the ER to the Golgi apparatus. Furthermore, when the proline (P) residue in the leader tripeptide was substituted with a leucine (L) residue, the mutated full-length DMP1 proteins were primarily found in the ER. These data indicate that the 37 kDa amino-terminal region, particularly the leader tripeptide LPD, plays an essential role in directing the transportation of the secretory DMP1 from the ER to the Golgi apparatus.

Disclosures: Yongbo Lu, None.

MO0098

Tartrate-Resistant Acid Phosphatase – a Potential Regulator of Bone Mineralization Controlled by Osteopontin. Cecilia Halling Linder*[1], Michael Krumpel[2], Barbro Ek-Rylander[2], Göran Andersson[2], Per Magnusson[1]. [1]Department of Clinical Chemistry, Linköping University, Sweden, [2]Division of Pathology, Department of Laboratory Medicine, Karolinska Institute, Sweden

Osteopontin (OPN) is a phosphoprotein secreted by osteoblasts and osteocytes that can act as an inhibitor of hydroxyapatite (HA) crystal formation and growth when extensively phosphorylated. Consequently, dephosphorylation of OPN is an important trigger of mineralization. Bone alkaline phosphatase (ALP) is an important promoter of mineralization by degradation of the mineralization inhibitor inorganic pyrophosphate (PPi) and by acting as an OPN phosphatase. Tartrate-resistant acid phosphatase (TRAP), secreted from osteoclasts and osteoblasts, has also been shown to exert phosphatase activity towards OPN; however, its potential capacity as a regulator of mineralization has not been addressed. Moreover, a model to explain the differential roles of the two phosphatases, their possible functional interplay or how they might substitute for each other as regulators of mineralization is missing. Our aim was to investigate ALP and TRAP regarding their substrate specificity and their impact on mineralization in vitro by dephosphorylation of OPN.

Phosphatase activity for bone ALP extracted from human SaOS-2 osteosarcoma cells and TRAP extracted from rat bone was assessed by the Malachite green-based phosphate assay. Kinetic properties were evaluated using the physiological substrates for ALP, PPi and pyridoxal 5'-phosphate (PLP), as well as fully phosphorylated OPN purified from bovine milk. SaOS-2 cells were cultured for 10 days in the presence of β-glycerophosphate to initiate mineralization. After treating the cells with fully phosphorylated OPN and OPN dephosphorylated by ALP or TRAP, the degree of mineralization was quantified using the OsteoImage fluorescent dye, which specifically binds to HA nodules.

TRAP showed higher phosphatase activity towards phosphorylated OPN and PPi than ALP, whereas the activity for TRAP towards PLP was significantly lower in comparison with ALP. Phosphorylated OPN was able to inhibit mineralization in cell culture, whereas OPN dephosphorylated by either ALP or TRAP showed a decreased inhibitory capacity on the formation of mineralized HA nodules.

In conclusion, TRAP has similar, if not superior kinetic properties towards OPN and PPi compared with ALP, but PLP seems to be a better substrate for ALP compared with TRAP. Similarly to ALP, TRAP can modify the mineralization inhibitory property of OPN in an in vitro system. Further studies are warranted to explore the possible physiological relevance of TRAP in bone mineralization.

Disclosures: Cecilia Halling Linder, None.

MO0099

Age-Related Soft Tissue Body Composition Changes in CD-1 Mice. Nancy Doyle*[1], Luc Chouinard[2], Ousmane-Noel Diallo[3], Angela Keightley[3], Lewis Gruber[4], Susan Y. Smith[1]. [1]Charles River Laboratories, Canada, [2]Charles River Laboratories, PCS Montreal, Canada, [3]Charles River Laboratories, Canada, [4]SIWA Regenerative Medicine Corporation, USA

Aging is a complex process associated with metabolic changes that ultimately contribute to terminal metabolic dysfunction and or disease. Some studies have characterized the clinical and metabolic aspects of aging in animal models. Understanding the age-related soft tissue composition in a rodent model is valuable to characterize the senescence process and evaluate novel therapeutic intervention. The objectives of this study were to compare soft tissue body composition and evaluate expression of p16Ink4a mRNA, a marker of senescence, in adipose tissue in

young and old CD-1 Mice. Old mice were approximately 92 weeks (~21 months) old while young mice were 10 weeks old at the initiation of the study. Young mice were observed for 3 weeks and old mice were observed for 3 months and euthanized at the end of the observation period. Body composition (lean/fat mass) was measured at baseline, Week 3 and 12 by dual energy X-ray absorptiometry (DXA), and body weights were evaluated weekly during the in life phase. Gastrocnemius muscle weights were recorded at necropsy, adipocyte and muscle fiber size were measured with histomorphometry, and quantitative determination of p16Ink4a mRNA was performed in inguinal adipose tissue using real-time reverse transcription quantitative PCR (RT-QPCR). Compared to young mice, old mice showed statistically significant age-related effects, higher body weights (45g vs 30g at Week 3), lower whole body lean mass (relative to body weight) (55 vs 73% at Week 3) corroborating the lower gastrocnemius muscle weights (relative to body weight) (0.77 vs 1.1%), smaller muscle fiber size (Fiber area – 1139 vs 1317 μm^2), higher fat mass (relative to body weight) (32 vs 16 % at Week 3) and larger adipocyte size (Cytoplasm Area – 1952 vs 828 μm^2). p16Ink4a mRNA expression was significantly increased in inguinal adipose tissue of old mice (approximately 2.6-fold) compared to young mice. Based on these results, the old CD-1 mice can be considered a good model for the evaluation of new therapeutics targeting age-related muscle or fat metabolic changes.

Disclosures: Nancy Doyle, Charles River Laboratories, 4

MO0100

Enhanced Mitochondrial Oxygen Consumption by Noncanonical Wnt5a is Reversed in Aortic Myofibroblasts From LRP6-Null Mice. John Stabley*[1], Abraham Berhmann[2], Karen Krchma[2], Su-Li Cheng[2], Bindu Ramachandran[2], Megan Mead[2], Bart Williams[3], Dwight Towler[1]. [1]Sanford-Burnham Medical Research Institute, USA, [2]Sanford-Burnham Medical Research Institute at Lake Nona, USA, [3]Van Andel Research Institute, USA

Msx-Wnt signaling regulates osteogenic differentiation during bone formation and the pathological mineralization of arterial calcification. Multiple Wnt ligands are upregulated in the aorta of mice lacking the LDL receptor (LDLR) when fed an arteriosclerotic high fat diet, entrained to TNF. The complex I inhibitor rotenone reduces TNF-dependent induction of mitochondrial reactive oxygen species and downstream osteogenic Msx2-Wnt programs in aortic myofibroblasts. To investigate the effects of canonical and noncanonical Wnt signaling on mitochondrial function in aortic myofibroblasts, the present study measured oxygen consumption rate (OCR) in myofibroblasts isolated from LRP6(fl/fl);LDLR$^{-/-}$ mice with (LRP6-CKO) and without (CON) an active Cre recombinase directed by the SM22 promoter. Primary myofibroblasts from 6-8 wk old mice with and without LRP6 were treated for 6 hr with Wnt3a (15 ng/mL), Wnt5a (15 ng/mL), or vehicle (Veh) prior to measurement of OCR (XF96, Seahorse Bioscience). The canonical ligand Wnt3a had no effect on basal OCR in CON (Veh: 86±3, Wnt3a: 79±3 pmol/min) or LRP6-CKO (Veh: 69±2, Wnt3a: 78±4 pmol/min) cells. However, while the noncanonical ligand Wnt5a produced an increase in basal OCR of CON cells (Veh: 86±3, Wnt5a: 126±6 pmol/min; p<0.0001), it reduced basal OCR in LRP6-CKO cells (Veh: 69±2, Wnt5a: 43±2 pmol/min; p<0.0001). When ATP synthase was arrested by acute treatment with oligomycin (1 µM), OCR remained unchanged in myofibroblasts treated with Wnt3a from CON (Veh: 47±3, Wnt3a: 43±3 pmol/min) and from LRP6-CKO (Veh: 37±2, Wnt3a: 38±2 pmol/min) cells. However, similar to the basal condition, Wnt5a increased OCR in CON cells (Veh: 47±3, Wnt5a: 62±6 pmol/min; p<0.001) and decreased OCR in LRP6-CKO cells (Veh: 37±2, Wnt5a: 24±2 pmol/min; p<0.01). Disruption of the proton motive force with carbonyl cyanide-p-trifluoromethoxyphenylhydrazone (FCCP, 1 µM) did not alter OCR in response to Wnt3a in CON (Veh: 347±39, Wnt3a: 300±29 pmol/min) or LRP6-CKO (Veh: 253±4, Wnt3a: 274±2 pmol/min) cells. Similar again to the basal condition, Wnt5a increased OCR in CON cells (Veh: 347±39, Wnt5a: 475±57 pmol/min; p<0.001) and decreased OCR in LRP6-CKO cells (Veh: 253±4, Wnt5a: 119±6 pmol/min; p<0.001) following acute FCCP treatment. Thus, noncanonical Wnt signaling activates mitochondrial respiration in vascular myofibroblasts, modulated by LRP6 expression.

Disclosures: John Stabley, None.

MO0101

The Effect of PTH Treatment on Bone Tissue Mechanics, Mineral Density and Non-enzymatic Glycation in Rats with Type 2 Diabetes Mellitus. Graeme Campbell*[1], Christine Hamann[2], Ann-Kirstin Picke[2], Martina Rauner[3], Sanjay Tiwari[4], Gerd Huber[5], Jaime Peña[6], Timo Damm[6], Reinhard Barkmann[7], Michael Morlock[5], Lorenz Hofbauer[8], Claus-C Glueer[9]. [1]University Hospital Schleswig-Holstein, Kiel Campus, Germany, [2]Dresden Technical University Medical Center, Germany, [3]Medical Faculty of the TU Dresden, Germany, [4]University Hospital Schleswig-Holstein, Campus Kiel, Germany, [5]Technical University of Hamburg, Germany, [6]University Hospital Schleswig-Holstein, Kiel Campus, Germany, [7]Universitaetskinikum Kiel, Germany, [8]Dresden University Medical Center, Germany, [9]Christian Albrechts Universitaet zu Kiel, Germany

Diabetes mellitus results in increased skeletal fragility through reduced bone mineral density and altered collagen structure. How these changes affect bone mechanics at the tissue level remains largely unclear. Anti-osteoporosis medications improve bone mass, but it is not known whether these treatments can fully restore tissue strength in diabetic bone. The objective of this study was to determine the effect of type 2 diabetes mellitus and bone-anabolic treatment on bone mechanics, tissue mineral density (TMD) and non-enzymatic glycation (NEG) in Zucker Diabetic Fatty (ZDF) rats. We hypothesized that diabetic rats have inferior tissue mechanics, which cannot be fully restored with anabolic treatment due to diabetes-induced changes in the organic phase of the bone.

Eleven-week old ZDF diabetic and non-diabetic rats were given 75 µg/kg PTH(1-84) or vehicle five days per week for 12 weeks (4 groups, N=7 per group). L4 vertebrae were excised, micro-CT scanned, and tested to failure in compression. The TMD was calculated as the mineral content within the bone tissue volume in the micro-CT scans. From the mechanical tests, stress-strain curves were produced, and tissue mechanical properties including elastic modulus (intrinsic stiffness), yield and failure strain, and toughness were determined. To determine NEG content, the samples were demineralized, papain-digested and analysed for fluorescence at 370nm excitation and 440nm emission wavelength standardized against a quinine sulphate solution. The NEG content was normalized to the amount of collagen determined from hydroxyproline content after hydrolysis.

Diabetic rats showed significantly reduced failure strain (–22%) and toughness (–42%), but not yield strain, elastic modulus or NEG compared to controls. In the healthy animals, PTH treatment increased the failure strain, (+24%) and reduced NEG content (-81%) compared to the untreated controls. In the PTH-treated diabetic animals, no significant changes in mechanical or NEG properties compared to untreated diabetic animals were observed. TMD was reduced with PTH treatment in both healthy (-7%) and diabetic (-6%) animals. This study shows that diabetes weakens the post-yield biomechanics of ZDF rat bone, and that there is a differential effect of PTH treatment on healthy and diabetic animals. The lack of improved mechanics after PTH treatment in diabetic animals may be due to an inability to reduce non-enzymatic glycation, as was observed in healthy bone.

Disclosures: Graeme Campbell, None.

MO0102

Induction of Heterotopic Ossification is Severely Curtailed in Mice lacking Apolipoprotein E. Eric Beal*[1], Elizabeth Salisbury[1], Zbigniew Gugala[2], Elizabeth Olmsted-Davis[1], Alan Davis[1]. [1]Baylor College of Medicine, USA, [2]University of Texas Medical Branch, USA

Evaluation by plain X-ray or microCT shows that heterotopic ossification is severely curtailed in mice lacking apolipoprotein E. Additionally, we find that injection of BMP2-producing cells into the quadriceps of wild type C57BL/6 mice induces the appearance of a "new" population of CD31-containing endothelial cells, separable from the CD31-positive cells present in untreated wild type mice by fluorescent-activated cell sorting. This population increases 6-fold 2 days after BMP2 induction and 8-fold 4 days after BMP2 induction in wild type mice. In the ApoE (-/-) mouse this population increases similarly at two and four days after BMP2 induction. However, unlike the wild type mouse, this population of CD31-positive cells (e.g. analogous to those present in untreated wild type controls) decreases 2 to 3-fold 4 days after BMP2 induction of ApoE (-/-) mice. We interpret this to mean that the ApoE (-/-) mouse is perhaps incapable of supplying the new vasculature necessary to transport these cells to areas where new cartilage and bone would form.

Both wild type and ApoE (-/-) mice were also evaluated for hypoxic regions in tissue around the site of injection of BMP2-producing cells using Hypoxyprobe®. At both 2 and 4 days after BMP2 induction areas of hypoxia were both more extensive and more intense in the ApoE (-/-) mice. Surprisingly, vessels were also found that were profoundly hypoxia in the ApoE (-/-) mice, but not in their wild type counterparts. This result also points to dysfunctional endothelial cells in the ApoE (-/-) mice in that these endothelial cells seem unable to maintain a normoxic environment in the vessel. Whether this deficiency is due to the endothelial cells themselves or to deficiencies in other cells interacting with the endothelial cells, such as astrocyte-like cells produced after BMP2 induction, is currently unknown.

Disclosures: Eric Beal, None.

MO0103

Influence of obesity on the prevalence of osteoporosis and low-impact fractures in Brazilian women. Marcelo Pinheiro[1], Bruna Castro*[2], Edgard Reis Neto[2], Jacob Szejnfeld[2], Vera Szejnfeld[3]. [1]Sao Paulo Federal University/ Unifesp/ Escola Paulista De Medicina, Brazil, [2]Federal University of Sao Paulo (Unifesp/ EPM), Brazil, [3]UNIFESF/EPM, Brazil

Background: Several studies have emphasized the protective role of body weight on the risk of osteoporosis (OP) and low-impact fractures (Fx). However, more recently, higher rate of fragility fractures has been shown in overweight and obese individuals, especially of the lower limbs.Aim: To determine the prevalence of Fx and OP in women, according to the stratification by body mass index (BMI). Furthermore, we investigated the relationship between obesity, OP and Fx, as well as the performance of the SAPORI (Sao Paulo Osteoporosis Risk Index) tool in each BMI category, according to the World Health Organization (WHO) classification. Patients and Methods: A total of 6.182 women over 40 years old, regardless menopausal status, from Brazilian primary care centers were enrolled in this research. All of them answered detailed questionnaires about clinical risk factors for OP and Fx, as well as they underwent spine and femur bone mass measurements by DXA (DPX NT, GE-Lunar).

Results: The prevalence of osteoporosis in overweight and obese women was 33.6% and 20.8%, respectively. The increase of BMI played a protective role for osteoporosis (OR=0.88, 95%CI 0.87-0.89, p<0.001), according DXA. On the other hand, the prevalence of low-impact Fx was quite similar among the categories of BMI (13.7% for underweight, 12.3% for healthy weight, 11.8% for overweight and 12.7% for obese women; p=0.81). Wrist fractures were the most prevalent (24.9%), followed by metatarsal (24.5%), humerus (11%) and ankle (11.1%). After excluding women with low weight, it was observed the obese women had lower risk of hip fracture than non-obese women (OR=0.44, 95%CI 0.2-0.97, p=0.03). Regarding SAPORI tool's performance, there was impairment of sensitivity to identify women with low bone mineral density (BMD), according to increase of BMI (from 67% to 41% for femur and from 93.8% to 51.7% for spine BMD; p<0.001). Conclusion: Our data showed that anthropometric measures had a significant impact on BMD measurements in women, but not on the prevalence of low-impact fractures. These findings suggest that other factors, regardless BMD, may be involved with higher risk of fractures in overweight and obese individuals. Moreover, our results point out the need of identifying new cut points to improve the clinical performance of SAPORI tool.

Disclosures: Bruna Castro, None.

MO0104

Mechanisms of reduced bone mineral density are diet- and strain-dependent. Casey Doucette*[1], Clifford Rosen[2]. [1]Maine Medical Center Research Institute, USA, [2]Maine Medical Center, USA

The relationship between energy status and bone mineral density (BMD) is well-studied, but not well understood. Mechanical loading during obesity is thought to have a positive effect on bone density, but the effects of endocrine factors released by adipocytes are unclear. On the other hand, anorexia nervosa causes a dramatic reduction in BMD and visceral adipose tissue with a paradoxical increase in marrow adipose tissue (MAT) volume. Here, we have tested the effects of calorie insufficiency and calorie excess to compare their profiles in two strains of mice, C57BL/6J (B6) and C3H/HeJ (C3H), which are innately different in their bone properties; C3H mice have significantly higher BMD and MAT volume. Male mice from both strains were given a 30% calorie restricted diet (30%CR), 60% high fat diet (HFD), or control diet from 3-15 weeks of age. Calorie-restricted mice from both strains had significant loss of femoral trabecular and cortical bone as compared to control (n=10, p<0.01). Interestingly, we also found compartment-specific loss of BMD in HFD-fed mice, with C3H mice displaying a loss of BMD in the cortical region of the femur (n=10, p<0.04), while B6 mice on a HFD had a reduction in trabecular parameters as compared to control (n=10, p<0.03). Serum analysis showed increased insulin levels and a decrease in osteoprotegerin (OPG) in HFD-fed B6 mice (p<0.03), supporting a mechanism for decreased cancellous bone mass through insulin-mediated inhibition of OPG expression and subsequent increase in RANKL-mediated bone resorption. We also noted an increase in serum levels of osteocalcin (OC) and insulin in B6 mice on a 30%CR diet as compared to controls (p<0.01), which may be indicative of OC release from the bone matrix during resorption and subsequent stimulation of insulin secretion by β-cells. Changes in OC serum levels were not seen in C3H mice on a 30%CR diet and may indicate that, during adolescence in this strain, 30%CR may result in a lowered rate of bone formation rather than increased resorption as compared to controls, resulting in lower bone mass. Our results demonstrate that HFD has strain-dependent and compartment-specific effects on BMD, which may be mediated by insulin-dependent inhibition of OPG expression. We also conclude that differential mechanisms of reduced BMD in response to 30%CR between the two strains are likely due to underlying genetic differences and may have implications for a genetically heterogeneous human population.

Disclosures: Casey Doucette, None.

MO0105

Nerve Growth Factor and Brain-derived Neurotrophic Factor are differently expressed in energy stores, bone and reproductive organs. Claudia Camerino*[1], Maria Cannone[2], Elena Conte[2], Domenico Tricarico[2]. [1]School of Medicine, University of Bari, Italy & University of Cincinnati, USA, [2]Dept. of Pharmacy-Drug Sciences, University of Bari, Italy

That gonadal failure favors the appearance of osteoporosis while obesity seems to protect from osteoporosis shows that bone mass, energy metabolism, and reproduction are linked. On this regard, recent data indicate that the bone derived hormone Osteocalcin favors insulin sensitivity and male fertility by promoting testosterone production in Leydig cells. It has also been reported that the neurotrophin Nerve Growth Factor (NGF) is the ovulation inducing factor in the seminal plasma that following an endocrine route, crosses the Blood Brain Barrier of the female and elicit the surge of LH. This sparked our interest since NGF is also involved in energy regulation, upregulating the adipocyte-derived hormone leptin and increases bone turnover. To further investigate the role of NGF in these tissues we analyzed by RT-PCR the mRNA levels of NGF and its receptor p75NTR and NTRK1 in white and brown fat, bone and reproductive organs of 3 months old mice of both genders with brain as positive control. We compared these data with the expression of the Brain-derived Neurotrophic Factor (BDNF) and its receptor TRKb. Interestingly our preliminary data show that NGF as well as p75NTR mRNA is expressed in brown fat at levels greater than the positive control. NGF is expressed also in white fat and bone at levels comparable in both genders. BDNF and TRKB expression in bone is higher than in the brain, but lower in white and brown fat, conversely TRKB is down-regulated in bone and up-regulated in adipose tissue. Furthermore, NGF as well as p75NTR is highly expressed in ovaries and uterus. Differently NGF is down-regulated in testes while p75NTR is expressed at levels higher than the brain. NTRK1 is down-regulated in all tissues. Neither BDNF or TRKB are expressed in the ovaries, uterus or testis excluding a main role in this organ. In sum, our work shows that NGF is expressed in brown fat, white fat and bone and with an opposite trend comparing to BDNF. NGF is also expressed in reproductive organs in a gender specific fashion. The pattern of expression of NGF and receptors in the fat stores is consistent with our hypothesis, of NGF as a regulator of energy metabolism, and the inverse correlation of NGF and BDNF in these tissues, confirms a previous study that shows NGF and BDNF exerting opposite effect on leptin with BDNF playing a relevant role in bone. Further studies will clarify the role of NGF in energy and bone metabolism and its correlation with the reproductive function.

Disclosures: Claudia Camerino, None.

MO0106

Oleic acid protects hMSC from healthy donors and osteonecrotic patients against lipotoxicity by inducing intracellular lipid droplet formation and preventing ERK activation. Céline Gillet*[1], Delphine Spruyt[1], Jessica Berlier[2], Sabrina Rigutto[1], Antoine Dalla Valle[1], Caroline Louis[3], Cathy Debier[3], Nathalie Gaspard[1], Willy J Malaisse[1], Valerie Gangji[4], Joanne Rasschaert[5]. [1]Université libre de Bruxelles, Belgium, [2]Université Libre de Bruxelles, Belgium, [3]Université catholique de Louvain, Belgium, [4]Hôpital Erasme, Université Libre de Bruxelles, Belgium, [5]Laboratory of Bone & Metabolic Biochemistry, Belgium

Osteoporosis and osteonecrosis are characterized by adipocyte accumulation in bone marrow. Adipocytes are not inert cells; they release cytokines, adipokines and free fatty acids (FFAs) that modify the bone marrow niche and may alter the biology of adjacent cells. Although it is known that FFAs affect the viability and function of various cell types, only a few studies examined their effect on human mesenchymal stem cells (hMSC) and osteoblasts (Ob). In a previous work, we showed that palmitic acid (PAL), a saturated FFA, exerted a cytotoxic action on hMSC and Ob via activation of NF-κB and initiation of endoplasmic reticulum stress. We demonstrated that oleic acid (OL), a monounsaturated FFA, fully neutralized lipotoxicity in both cell types.

In the present study,hMSC were obtained from bone marrow of healthy donors or patients with non-traumatic osteonecrosis of the femoral head (ON-MSC). Cells were cultured in standard medium or in osteogenic conditions. Viability was evaluated by nuclear staining and detection of caspases 3/7 activation. ERK phosphorylation was quantified by Western blot. Triglyceride (TG) content was measured by gaz chromatography and cellular neutral lipids were stained by Oil Red. Gene expression was analyzed by qPCR. IL-6 secretion was quantified by ELISA.

We showed that OL rescued hMSC and Ob from PAL-induced toxicity by inducing a preferential channeling of PAL into the TG cellular pool via restoration of DGAT-2 (diacyl-glycerol acyl-transferase) expression which controls the last step of TG synthesis. OL thus promoted the formation of lipid droplets (LD) which are now considered as highly dynamic organelles. In parallel, we observed that PAL decreased Runx2 expression, a key osteogenic factor, whilst it upregulated PPARγ, a regulator of adipogenesis. OL abolished PAL-induced gene modifications. PAL also stimulated ERK and secretion of IL-6, a cytokine favoring osteoclast activity. The presence of OL restored ERK activity and IL-6 level to basal values. Lastly, we demonstrated that ON-MSC displayed a higher sensitivity to lipotoxicity than healthy hMSC. This was correlated to a 2-fold higher basal phosphorylation level of ERK in ON-MSC.

In conclusion, we demonstrated that in hMSC and Ob OL prevents lipotoxicity via increasing LD formation and blocking ERK-activation. OL also abolished

PAL-induced cytokine expression and adipogenesis. Of interest, the susceptibility to lipotoxicity is enhanced in hMSC of osteonecrotic patients.

Disclosures: Céline Gillet, None.

MO0107

Stem Cell Transplantation in Type 1 Diabetes Mellitus: Influence on Bone Marrow Fat (BMF) and Bone Mineral Density (BMD). Adriana Carvalho*[1], Bianca Massaro[2], Marcello Nogueira-Barbosa[2], Carlos Salmon[2], Belinda Simões[2], Maria Carolina Rodrigues[2], Clifford Rosen[3], Francisco Jose De Paula[4]. [1], Brazil, [2]University of São Paulo, Brazil, [3]Maine Medical Center, USA, [4]School of Medicine of Ribeirao Preto - USP, Brazil

Introduction: Type 1 diabetes mellitus (T1D) is classically one of the secondary causes of osteoporosis. Enhanced osteoclastogenesis from myeloid progenitors cells and suppressed bone formation contribute to low bone mass. Recently, hematopoietic stem cell transplantation (HSCT) was reported as an alternative treatment for T1D. However, there is no study regarding the impact of this treatment on bone mass or turnover. Our aim was to investigate BMD and bone marrow fat (BMF) in conventionally treated T1D as well as in patients subjected to HSCT. Material and Methods: The study comprised three groups: T1D (10M/6F; 31 ± 12 years; 73 ± 11 Kg; 1.71 ± 0.08m, 24.9 ± 3.5 Kg/m^2, 16 ± 11 years of diagnosis), T1HSCT (7M/5F; 26 ± 6 years; 64 ± 10 Kg; 1.69 ± 0.09m, 22.3 ± 2.1 Kg/m^2, 4.4 ± 3.4 years of diagnosis) and Control group (11M/10F, 29 ± 6 years; 67 ± 15Kg; 1.70 ± 0.07m, 23.0 ± 3.8 Kg/m^2). Blood samples were collected for measurement of glucose, HbA$_1$C, IGF-1. BMD was assessed in the lumbar spine, proximal femur and total body by DXA. ^{1}H magnetic resonance spectroscopy (1,5T) was used to evaluate BMF in the lumbar spine (L3). Results: T1D and T1HSCT showed higher HbA$_1$C and serum levels of glucose than C group. T1HSCT group had better glycemic control than T1D group (T1=8.9 ± 1.4 vs T1HSCT=6.7 ± 0.8 vs C=5.2 ± 0.3 %; p<0.0001). BMD was similar in all sites for the three groups (e.g., L1-L4: T1=0.982 ± 0.124 vs T1HSCT=0.986 ± 0.117 vs C=0.999 ± 0.137 g/cm^2). There was no difference in total body fat (T1=20 ± 7 vs T1HSCT=17 ± 6 vs C=19 ± 6 Kg) and android fat mass (T1=1.5 ± 0.8 Kg vs T1HSCT=1.2 ± 0.4 Kg vs C= 1.4 ± 0.6 Kg) between groups. T1HSCT exhibited a trend to have higher BMF than the other groups (T1=23 ± 7 vs T1HSCT=30 ± 7 vs C=23 ± 9 %; p=0.07). Also, there was no association between lumbar BMD with android fat and HbA$_1$C, neither in T1D nor in the T1HSCT group. Lumbar BMD correlated negatively with total fat in T1D (r= -0.52; p=0.04). Additionally, BMF had no relationship with lumbar BMD, android and total body fat in both diabetic groups. Conclusion: The present results suggest that well controlled T1D have normal BMD, independent of metabolic control and previous HSCT. There was no relationship of body composition and glycemic control to BMF. Despite the lower dose of insulin therapy, T1HSCT group has better metabolic control than T1. T1HSCT had slightly higher BMF but lower body fat. Our results support the need for further studies to uncover the mechanism for the relationship between T1D and osteoporosis.

Disclosures: Adriana Carvalho, None.

MO0108

A General Theory of Metabolism Demonstrating an Organizing Principle for Calciotropic Signals. Robert Fredericks*. Endocrine Associates, USA

Metabolism modeled as heterostatic organization of heat provides insight for the role of calciotropic signals in the maintenance of health. Hierarchical structure increases complexity, but conserves the heterostatic principle where positive feed forward and negative feedback create multiple basins of attraction functioning as authorities governing system behavior, contrasting with the single authority of homeostasis. Validation rests on coherently organizing available data and demonstrating utility in finding solutions for problems. Application of genome wide sequencing (GWS) to healthcare personalization is facilitated with metabolic modeling at the case level.

Utilizing a field study directed toward clarification of metabolism as influenced by calciotropic signals, GWS has been engaged to explore causality of phenotypes and discover appropriate utilization of interventions, including repurposing of existing modalities. Outcomes are assessed at the case level in accordance with the dictates of the Helsinki Accords.

A case of normocortisolemic Cushing's syndrome demonstrated mutations in creb binding protein and its closely related signal EP300. An additional mutation in ISX that modifies vitamin A signaling appears to have rescued the patient from the expected myodystrophic phenotype. Initial interventions unmasked a predisposition to febrile seizures associated with mutations causal of Dravet's syndrome also present in the patient. These interactions can be explained in the context of the metabolic models engaging the heterostatic organization of heat as an organizing principle.

It is proposed that hydroxylations of vitamin D evolutionarily originated from non-enzymatic interactions with metabolism. Interactions of the metabolites with receptors for vitamin D create a complex sensing device for the interface between physiology and metabolism that accounts for the findings in this and many other informative cases.

Investigating informative cases with GWS and a metabolic evaluation in the context of structural equation models clarifies the clinically expressed variance in phenotypes and demonstrates the effectiveness of this strategy for the understanding of functionalities of calciotropic hormones in the organization of heat. Appropriate personalization of healthcare delivery based on available technology becomes apparent when findings in osteo-immunology and osteo-endocrinology are incorporated into the models.

Disclosures: Robert Fredericks, None.

MO0109

Insulin Resistance and Bone Strength in Children. Joseph Kindler*[1], Norman Pollock[2], Emma Laing[1], Kathleen Hill Gallant[3], Stuart Warden[4], Berdine Martin[3], Connie Weaver[3], Munro Peacock[5], Richard Lewis[1]. [1]The University of Georgia, USA, [2]Georgia Regents University, USA, [3]Purdue University, USA, [4]Indiana University School of Health & Rehabilitation Sciences, USA, [5]Indiana University Medical Center, USA

Given that type 2-diabetes (T2D) is a potential risk factor for fracture, combined with recent evidence indicating that 1 in 4 adolescents will most likely develop impaired glucose tolerance, it is important to understand the effects of insulin resistance (a key pathology in T2D) on bone strength in children during the early stages of puberty. This ancillary study investigated the relationships between insulin resistance and cortical bone strength at the radius and tibia in 314 early pubertal children aged 9 to 13 years (50% male, 49% black) participating in a multi-site clinical trial. Serum glucose and insulin were measured and used to calculate homeostasis model assessment of insulin resistance (HOMA-IR). Peripheral QCT (Stratec XCT-2000) scans of the radius and tibia were obtained at the 66% site from the distal metaphyses. Bone strength was estimated by calculating the polar strength-strain index (SSIp) from volumetric BMD and bone geometry. Comparability of bone data at different study sites was accomplished using a cortical bone phantom. Total body fat mass (FM) and fat-free soft tissue (FFST) mass were measured by DXA and data from different study sites were cross-calibrated for the specific DXA instrument used. Multiple linear regression analyses, adjusting for race, sex, pubertal maturation stage, FM, and FFST, revealed that HOMA-IR was negatively correlated with SSIp at the radius (β = -0.12) and tibia (β = -0.10) (both P < 0.01). These findings in children suggest a negative influence of insulin resistance on bone strength in the growing skeleton. Future studies should examine the influence of chronic insulin resistance on cortical and trabecular bone development.

Disclosures: Joseph Kindler, None.

MO0110

Protection from Fracture Risk in Long Term Type 1 Diabetes: 50- Year Medalist Study. Hillary Keenan*[1], Stephanie Hastings[2], George King[3]. [1]Joslin Diabetes CenterHarvard Medical School, USA, [2]Joslin Diabetes Center, USA, [3]Joslin Diabetes Center, USA

Studies of individuals with type 1 diabetes (T1D) have demonstrated a 12-fold increased risk of fragility fractures over their age-matched peers. As hospitalization for fracture is highly associated with decreased quality of life, morbidity and mortality, this is an important, yet little studied diabetic complication particularly amongst those with extreme duration T1D. The 50-Year Medalist Study has extensively characterized over 800 individuals with a mean age of 69 years and duration of 55 years of T1D. The purpose of the Medalist Study is to determine how individuals with long term T1D have resisted complications. Early examination of self-reported rates of hip, vertebral, and wrist fractures show extraordinarily low rates (0.33%, 0%, and 1.7%, respectively) in stark contrast to the expected 12-fold increased prevalence compared to non-diabetic individuals. To further examine these findings, 63 participants received DXA scans, 32 females, 31 males with a mean $\pm$SD HbA1c of 7.2 ± 0.8% and 7.1 ± 1.3%, age 62.7 ± 7.3 years and 66.1 ± 7.2 years, and duration of 52.7 ± 2.9 years and 55.1 ± 4.8 years, respectively. BMI for this age group was low with 25.6 ± 5.2 kg/m^2 for females and 26.2 ± 7.5 kg/m^2 for males. T-scores, indicative of risk for fracture, for females at the hip was -0.63 ± 0.82 and lumbar spine (LS) 0.1 ± 1.2. For males the hip T-score was -0.56 ± 0.88 and at the LS was -0.1 ± 1.8. Total vitamin D, D2, D3 and calcium did not correlate with T scores among females or males, except for D3 among male and the LS T-score (R=0.5, p=0.03). There was no association of T scores with HbA1c, BMI, age or duration in either gender, p>0.05. As BMIs were low in males and females, the lower than expected risk T scores are likely not due to increased weight bearing as seen in T2D patients. These pilot data suggest protection from fracture, and low risk in this group with long term T1DM suggestive of a protective factor preventing bone health deterioration.

Disclosures: Hillary Keenan, None.

MO0111

Reduced Biomechanical Loading may Contribute to the Bone Phenotype of FGF21 Overexpressing Mice. <u>Yanfei Ma</u>*[1], <u>Armando R. Irizarry</u>[2], <u>Tamer Coskun</u>[2], <u>Qianqiang Zeng</u>[2], <u>Mattew Hamang</u>[2], <u>Venkatesh Krishnan</u>[1], <u>Henry Bryant</u>[1], <u>Vincent L Reynolds</u>[2], <u>Malgorzata Gonciarz</u>[2], <u>Libbey O'Farrell</u>[2], <u>Alexei Kharitonenkov</u>[2], <u>Ruth E Gimeno</u>[2], <u>Andrew Charles Adams</u>[2]. [1]Eli Lilly & Company, USA, [2]Eli Lilly & Company, USA

FGF21 is known for its beneficial effects on glucose and lipid metabolism. However, a recent report showed that FGF21 transgenic (Tg) mice have lower bone mass compared to wild-type mice (WT). The goal of our studies was to characterize the bone phenotype of our independently generated FGF21Tg mice. Tg mice had substantially lower body weight compared to WT (-32% at 3 month and -43% at 6 month age), primarily due to reduced fat mass. In vivo μCT scanning of Tg mice at 3 and 6 months of age revealed significantly lower bone mineral content (BMC) in lumbar vertebrae (LV, -26%, -17%), proximal tibial metaphysis (PTM, -30%, -20%), tibial shaft (TX, -20%, -23%), and bone mineral density (BMD) in LV (-9, -5%). Because bone growth readily adapts to mechanical loading, we normalized bone values to body weight. When data were normalized, Tg mice at 3 and 6-months of age had significantly higher LV-BMC (16% to 45%), PTM-BMC (37% to 41%) and TX-BMC (19% to 34%) than WT. The bone formation biomarkers PINP (26%, 48%) and intact OCN (106%, 176%), were higher in Tg mice at 3 and 4 month age, and no different from WT at 6 months of age. The bone resorption biomarker CTX-1 was -13% lower in Tg mice at 3 months of age and no different at 4-6 months age. Ex vivo studies at 6-months of age showed a similar pattern of bone changes as observed in vivo, where absolute values of BMC and bone strength were lower but body weight normalized values were higher in Tg mice. Bone histomorphometry showed that mineralizing surface, osteoblast surface and bone formation rate (BFR/BS) were higher in LV of Tg mice. While endocortical mineral appositional rate was -30% lower in Tg mice, no other differences were observed in bone formation indices of cortical bone. In a separate study, hFGF21 infusion for 14 days resulted in body weight loss in both 8 month old diet induced obese (DIO, -23%) and chow fed control (-21%) mice. A significant reduction -10% in BMD was seen in the distal femur of hFGF21 treated chow fed mice but not in DIO mice. Bone histomorphometric analyses revealed the only significant change was a reduced periosteal BFR/BS in both cohorts of hFGF21 treated mice. Finally, in a separate mouse food restriction study aimed to address directly the role of reduced body weight on bone, bone mass declined in parallel with reduced body weight. Our data suggest that lower mechanical loading plays a contributory role in the bone phenotype of FGF21 overexpressing mice.
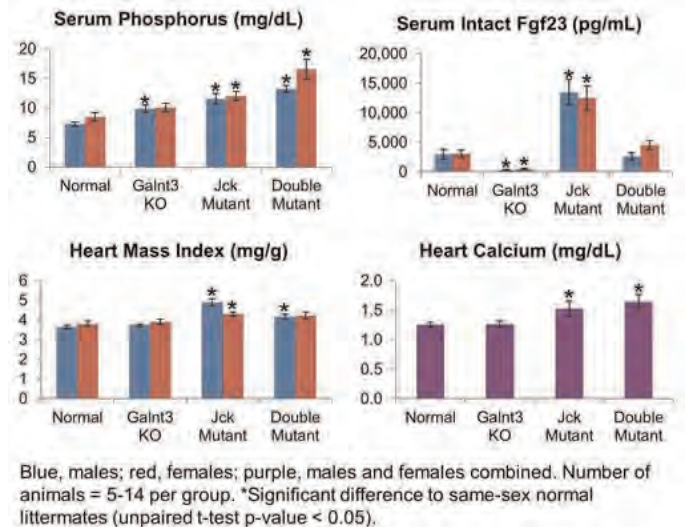
Disclosures: Yanfei Ma, Eli Lilly and Co., 4

MO0112

A Murine Model of CKD Has Increased Heart Mass, Even in the Absence of Elevated Fgf23. <u>Shoji Ichikawa</u>*[1], <u>Tyler Unsicker</u>[2], <u>Amie Gray</u>[2], <u>Sharon Moe</u>[1]. [1]Indiana University School of Medicine, USA, [2]Indiana University School of Medicine, USA

Background: In early stages of chronic kidney disease (CKD), a phosphaturic hormone, fibroblast growth factor 23 (FGF23), begins to rise in order to maximize renal phosphorus excretion. As the kidney function declines, phosphorus excretion becomes insufficient despite continuously increasing FGF23, and hyperphosphatemia ensues. Due to the concomitant rise in both Fgf23 and phosphorus, it is difficult to distinguish relative contributions between elevated FGF23 and hyperphosphatemia to cardiovascular and skeletal abnormalities associated with CKD.

Materials and Methods: To determine independent effects of phosphorus and Fgf23, we created high and low Fgf23 states in the *jck* mutant mouse, a naturally progressive CKD model. By crossing *jck* mice with *Galnt3* knockout mice, we could induce low Fgf23 levels despite CKD and hyperphosphatemia. We then compared serum biochemistries, heart mass index, heart calcium and phosphorus, and bone volume and mineralization.

Results: Compared to normal mice, serum phosphorus was higher in all three mutant mice. As expected with CKD, the *jck* mice had a 4 fold increase in Fgf23 levels. *Galnt3* knockout mice had 87% reduction in intact Fgf23, whereas the *jck/Galnt3* double mutants had normal Fgf23 levels. *Jck* mutant mice had cardiac hypertrophy with significantly higher heart mass index (25% increment compared to normal animals). Double mutant mice also had on average 13% higher heart mass than the *jck* mice despite normal Fgf23. In addition, both CKD mice – *jck* and double mutant mice – had 21 and 31% increases in heart calcium, respectively, suggesting the presence of cardiovascular calcification. Micro CT analysis of the femurs showed that trabecular thickness was also significantly lower in female double mutant mice. Compared to *jck* mutant mice, double mutants had decreased bone volume and trabecular thickness.

Conclusion: The *jck* mice with CKD had increased heart mass index and elevated Fgf23. The double mutants also had increased heart mass despite normal Fgf23 levels. Thus, even in setting of normal Fgf23, the CKD mice have increased heart mass, perhaps due to elevated phosphorus, deposition of calcium or other kidney disease-related factors. The severe bone defects in the double mutants also suggest that non-Fgf23 factors in the setting of CKD may have an adverse effect on bone.

Blue, males; red, females; purple, males and females combined. Number of animals = 5-14 per group. *Significant difference to same-sex normal littermates (unpaired t-test p-value < 0.05).

Biochemical and cardiovascular measures of jck/Galnt3 double mutants and littermate controls

Disclosures: Shoji Ichikawa, None.

MO0113

A Quantitative Trait Loci Analysis for BMD using the Diversity Outbred Mouse Population. <u>Hayley Britz</u>*[1], <u>Denise Liberton</u>[2], <u>Fernando de Villena</u>[3], <u>Benedikt Hallgrimsson</u>[1]. [1]University of Calgary, Canada, [2]University of Calgary, Canada, [3]University of North Carolina, USA

Osteoporosis is a heritable bone disease characterized by a decreased bone mineral density (BMD) and a deterioration in bone microarchitecture. The genetic determinants of osteoporosis remain largely unknown and without these we cannot begin to develop more effective treatments or a cure for this disease. Multiple studies using quantitative trait loci (QTL) analysis to map the chromosomal location of genes affecting BMD have been conducted; however, the mouse crosses utilized often result in large haplotype blocks, meaning that many of the biologically significant QTLs for BMD have occurred within large regions and thus may not have been fully described.

To partially overcome this limitation, I will be using 500 mice from the Diversity Outbred (DO) mouse population for the QTL analysis. The DO mice are derived from the eight founder strains of the Collaborative Cross (CC) instead of two strains like the recombinant inbred mice most commonly used for this type of analysis. The breeding scheme employed for developing the DO leads to increased recombination, resulting in a level of genetic diversity that better mirrors what is seen in human populations and leads to a higher, sub-Mb mapping resolution for detecting QTL. The aim of this study was to investigate whether the increased variation in the DO mice will allow for the detection of new QTLs in narrower intervals and better localize the regions of QTLs that have been previously observed.

In the DO mice, we found a broad range of BMD values, with a 95% confidence interval of 653 +/- 10.3 mg HA/cm^3, which is larger compared to what was seen in the CC parental mice (520 +/- 12.3 mg HA/cm^3). Using SNPs from the MegaMUGA genotyping array (~75K SNPs), we performed a QTL analysis for BMD using the DOQTL package in R. First, a Hidden Markov Model was used to reconstruct haplotype blocks from the eight founder populations. BMD measures were then regressed on the allelic dosage for each of the founder alleles. Additionally, given the complex pedigree of the DO mice, we accounted for the effects of relatedness via a kinship matrix calculated directly from the genotypes to better improve mapping power. Our results indicate several regions of interest associated with BMD after controlling for the effects of multiple testing. This suggests that the DO continues to be a useful resource for mapping the genetics of complex traits, including those related to bone diseases such as osteoporosis.

Disclosures: Hayley Britz, None.

MO0114

Altered osteoclast homeostasis responsible for bone changes in progressive myoclonus epilepsy EPM1. <u>Otto Manninen</u>*[1], <u>Elina Harittu</u>[2], <u>Tiina Laitala</u>[2], <u>Riku Kiviranta</u>[3], <u>Anna-Elina Lehesjoki</u>[4], <u>Outi Kopra</u>[4]. [1]Folkhalsan Institute of Genetics, Finland, [2]University of Turku, Finland, [3]Medical Biochemistry & Genetics & Turku PET Centre, University of Turku, Finland, [4]Folkhalsan Research Center, Finland

Unverricht-Lundborg type progressive myoclonus epilepsy (EPM1, OMIM 254800) is an autosomal recessive disorder, characterized by myoclonus and epileptic seizures. EPM1 is caused by mutations in the gene encoding cystatin B (CSTB).

Cystatin B is an inhibitor of one of the key enzymes in bone resorbtion, cathepsin K, and has been shown to modulate bone resorbtion *in vitro*. In line with these findings patients with EPM1 exhibit various skeletal abnormalities including changes in skull bones and appendicular skeleton. The purpose of this study was to elucidate the molecular mechanismsby which lack of cystatin B alter bone metabolism.

In the study, we utilized male cystatin B deficient (*Cstb*^{-/-}) mice (129-[*Cstbtm1Rm/J*]; stock 003486; Jackson Laboratories) between 1 of 6 months of age and wild-type animals of the same background served as controls. Microtomography of perfusion fixed hindlegs revealed thicker trabeculae in *Cstb*^{-/-} mice when compared to controls, indicating that the bone changes in EPM1 patients do not result of anti-epileptic drugs, as suggested previously, but in fact are connected to the lack of cystatin B. Subsequently, histology from hindlegs and calvarie was performed, revealing changes in trabecular bone morphology, thinner growthplates and lower osteoclast number in *Cstb*^{-/-} animals. Furthermore, immunohistochemistry showed more TRACP 5b and Cathepsin K staining in osteoclasts of *Cstb*^{-/-}bone, indicating higher resorbtion activity by *Cstb*^{-/-} osteoclasts. As expected, culturing bonemarrow derived osteoclasts did not reveal cross changes in *Cstb*^{-/-} osteoclast morphology, when compared to controls. We did, however, detect elevated Cathepsin K expression in *Cstb*^{-/-} cells, and counting of osteoclasts showed significantly reduced number of mature *Cstb*^{-/-} osteoclasts. These findings indicate that lack of cystatin B affects the bone morphology through changes in osteoclast homeostasis and resorbtion activity, and the results warrant further studies on the role of cystatin B in bone and osteoclasts.

Disclosures: Otto Manninen, None.

MO0115

An *Fkbp10* mouse model recapitulates joint contractures found in Bruck syndrome. Caressa Lietman*[1], Keren Machol[2], Elda Munivez[2], Brian Dawson[2], Terry Bertin[2], Yuqing Chen[2], Deborah Krakow[3], Brendan Lee[1]. [1]Baylor College of Medicine, USA, [2]Baylor College of Medicine, USA, [3]UCLA, USA

Osteogenesis Imperfecta (OI) is the most commonly inherited form of brittle bone disease and displays a spectrum of severity from mild phenotypes to severe early lethality. Mutations in FK506 Binding Protein 10 (*FKBP10*) that encode the FKBP65 protein result in recessive OI as well as Bruck Syndrome, characterized with congenital joint contractures in addition to the low bone mass phenotype. FKBP65 is thought to act as a collagen chaperone and possesses PPIase activity for proper trimer formation. Currently, we do not understand the consequences of *FKBP10* loss and its role in collagen and ECM formation. Therefore our goal is to elucidate the role of *FKBP10* in the skeleton and how null mutations lead to progressively deforming OI and Bruck syndrome. We generated a mouse model using the EUCOMM allele to further elucidate the function of *Fkbp10* in connective tissues. We have utilized the LacZ knockin allele to assess expression during development as well as the knockout allele to discern the phenotypic outcomes of FKBP65 loss in the mouse. Furthermore, mouse embryonic fibroblasts (MEFs) have been used for comparison to human cells and for collagen studies and analysis. We found that *Fkbp10* is expressed at low levels at E13.5 particularly in skeletal tissues and increasing through E17.5 with expression in not only skeletal tissues, but also other mesothelial lined tissues, and vessels. Postnatally, expression is limited to developing bone, tendons and ligaments, suggesting a more restricted role at this timepoint. Null mice display neonatal lethality with viable embryos isolated up to E18.5 but not after birth, growth delay and generalized tissue fragility. *Fkbp10*^{-/-} mouse embryonic fibroblasts show retention of procollagen in the cell layer, similar to what is seen in patient fibroblasts. These data suggest a requirement for *Fkbp10* function during embryonic connective tissue development in mice but restricted expression postnatally in bone, ligaments, and tendons correlating with the bone fragility and contracture phenotype in humans. Furthermore, we generated conditional knockout mice with scleraxis Cre in order to further investigate the tendon/ligament requirement for *Fkbp10*. We show that these mice recapitulate human features of Bruck syndrome and characterize this phenotype. Together, we suggest that this is a model mimicking joint contractures in humans due to alterations in tendons and ligaments.

Disclosures: Caressa Lietman, None.

MO0116

Calcium Absorption Efficiency Protects Bone from Dietary Ca Restriction During Growth: Evidence for Common Genetic Control. Perla Reyes*, Rebecca Replogle, James Fleet. Purdue University, USA

Habitual low dietary Ca intake during growth limits peak bone mass but physiological adaptation can limit the adverse effects of dietary Ca restriction on bone. We previously reported that bone parameters and their adaptation to dietary Ca restriction are significantly variable across a genetically diverse panel of 11 inbred mouse lines. We conducted a forward genetic study in 51 BXD recombinant inbred mouse lines fed with either 0.5% (normal) or 0.25% (low) Ca diets from 4-12 wks of age (n=8/line/diet) to identify the genetic loci controlling bone/mineral metabolism and their response to low Ca intake. Ca absorption (CaAbs) was measured by an oral gavage test ([45]Ca, 0.1 mM/L Ca, 10 min absorption) while femur BMD and BMC were measured by DEXA. After correcting phenotypes for confounding effects of body size, Analysis of Variance was used to detect significant line/diet main effects, line-by-diet interactions, and to provide heritability estimates. Genetic mapping was conducted for each corrected phenotype using composite interval mapping (CIM) for

each diet and for an additional parameter reflecting adaptation to Ca restriction. Phenotypes on the 0.5% Ca diet (basal), on the 0.25% Ca diet, and after adaptation to low Ca had moderate heritability estimates (h^2) of 32%-51%. Interestingly, the adaptive responses of BMD or BMC to Ca restriction were significantly correlated to CaAbs on low (r=0.52 and r=0.33 respectively) and normal Ca diets (r=0.36 and r=0.33 respectively). This indicates that in a genetically diverse population, the ability to protect bone under dietary Ca stress depends on high CaAbs efficiency. Genetic mapping identified multiple significant quantitative trait loci (QTL) for each diet and adaptation phenotype. Several QTL were linked to both bone and CaAbs phenotypes. For example, significant peaks affecting basal BMC (39 cM, 45.8 cM) and BMC adaptation (49.2 cM) on chromosome (Chr) 4 overlap with a significant QTL for basal CaAbs (49.4 cM). This suggests a cluster of genes may exist on Chr 4 to regulate multiple interdependent bone metabolism-related phenotypes. Similarly, a significant peak for basal BMC on Chr 1 (88.3 cM) and a putative peak for basal BMC on Chr 10 (66 cM) were also close to loci controlling basal CaAbs (Chr 1, 90.6 cM; Chr 10, 64.6 cM), suggesting novel relationships between bone and Ca metabolism during growth. Our data reveal novel gene-by-diet interactions that may ultimately have relevance to human bone health.

Disclosures: Perla Reyes, None.

MO0117

Dysregulated TGF-β signaling alters bone microarchitecture in a mouse model of Loeys-Dietz Syndrome. Ashvin Dewan*[1], Ryan Tomlinson[2], Brian Goh[3], Stuart Mitchell[1], Rachel Yung[1], Sarvesh Kumar[4], Eric Tan[1], Harry Dietz[1], Thomas Clemens[2], Paul Sponseller[1]. [1]Johns Hopkins University, USA, [2]Johns Hopkins University, USA, [3]Johns Hopkins University School of Medicine, USA, [4]Johns Hopkins University, Baltimore MD, USA

Loeys-Dietz Syndrome (LDS) is a complex connective tissue disorder characterized by vascular, craniofacial, and musculoskeletal abnormalities that is most commonly caused by heterozygous mutations in the genes encoding the transforming growth factor β (TGF-β) receptor type I or II subunits (TGFBR1 or TGFBR2, respectively). Patients with LDS commonly show osteoporosis with a predisposition for pathologic fracture. In this study, we characterized the skeletal phenotype of mice harboring a very severe LDS mutation, Tgfbr2[G357W/+]. Morphometric analysis by micro-computed tomography (CT) revealed reduced tissue area, bone area, and cortical thickness along with increased eccentricity in the cortical bone of LDS mice, but no detectable alterations in the trabecular compartment. Mechanical testing using three point bending showed that LDS femora had reduced strength and fracture resistance, a common characteristic of bone in patients with LDS. Histomorphometric analysis showed that LDS mice had a decreased mineral apposition rate but normal numbers of osteoblasts and osteoclasts. Primary osteoblasts cultured from LDS mice had impaired TGFβ1 induced Smad2 phosphorylation, an effector of signal transduction, compared to controls, confirming that G357W is a loss-of-function mutation in osteoblasts. Surprisingly, however, LDS osteoblasts demonstrated more mineralization and had increased expression of osteoblast differentiation markers compared to controls. These changes were associated with increased expression of TGFβ1 ligand. Finally, immunohistochemistry revealed increased pSmad2 in cortical osteocytes from LDS mice. Our findings in this mouse model mimic the principal structural features of bone observed in humans with LDS and consequently provide a useful model with which to further investigate the role of dysregulated TGF-β signaling in this bone disorder.

Disclosures: Ashvin Dewan, None.

MO0118

Mice with Sclerostin Gene Deficiency are Resistant to Bone Loss after Acute Spinal Cord Injury. Weiping Qin*[1], Xiaodong Li[2], Jay Cao[3], Lauren Collier[4], Yuanzhen Peng[5], Jerry Feng[6], Jiliang Li[7], Yiwen Qin[4], Tom Brown[8], Hua Zhu (David) Ke[9], William A. Bauman[4], Christopher Cardozo[1]. [1]James J. Peters Va Medical Center, USA, [2]Amgen, Inc., USA, [3]USDA ARS, USA, [4]James J. Peters VA Medical Center, USA, [5]The Mount Sinai School of Medicine, USA, [6]Baylor College of Dentistry, TX A&M, USA, [7]Indiana University Purdue University Indianapolis, USA, [8]Amgen Inc., USA, [9]Amgen Inc., USA

The bone loss secondary to spinal cord injury (SCI) has several unique pathological features that are different from other forms of osteoporosis. These features include the permanent immobilization, neurological dysfunction, systemic hormonal alternations and associated metabolic disorders. It remains unclear how these complex pathophysiological changes are linked to molecular alterations that influence bone formation and bone resorption. Sclerostin is considered as a key negative regulator of bone formation and bone mass. Thus, we hypothesized that sclerostin could function as a major mediator of bone loss following acute SCI. To test this hypothesis, 10 week-old sclerostin knockout (SOST ko) and wild type (WT) mice underwent complete spinal cord transection at T10 or sham operation and were followed for 8 weeks. As expected, significant loss of bone mineral density was observed at the distal femur and proximal tibia in WT-SCI mice. However, no such loss was observed in SOST ko-SCI mice compared with the SOST ko-sham animals. Trabecular bone volume of the distal femur by μCT was markedly decreased by 40%

in WT-SCI mice compared with WT-sham mice. In striking contrast, there was no significant reduction of bone volume in SOST ko-SCI mice compared with SOST ko-sham mice, whose trabecular bone volume was 4-fold higher than that in WT-sham mice. The trabecular bone thickness, number and connectivity density were not significantly altered in SOST ko-SCI animals, relative to the SOST ko-sham animals. Histomorphometry of trabecular bone in SOST ko-sham mice revealed a significant increase in bone formation rate (BFR) and significant decrease in osteoclast surface. Notably there was no reduction of BFR in SOST ko-SCI mice when compared to SOST ko-sham mice. Finally, the differentiation potential of bone marrow stem cells was studied and revealed no difference in the number of TRAP+ multinucleated cells or osteoblast number between SOST ko animals with or without SCI. In summary, our findings demonstrated that SOST ko mice were protected from the dramatic bone loss associated with SCI. The evidence indicates that sclerostin is an important mediator of the marked sublesional bone loss after acute SCI, and that pharmacological inhibition of sclerostin may represent a promising novel approach to this challenging problem.

MO0119

Oxidative DNA damage as the cause for osteoporosis in gerodermia osteodysplastica, a premature aging disorder. Hardy WL Chan*[1], Magdalena Steiner[2], Uwe Kornak[1], Michael Amling[3], Stefan Mundlos[2], Björn Busse[4], Jan Pestka[5], Thorsten Schinke[6], Till Köhne[4], Danny Chan[7]. [1]Charité-Universitaetsmedizin Berlin, Germany, [2]Institut für Medizinische Genetik und Humangenetik, Germany, [3]University Medical Center Hamburg-Eppendorf, Germany, [4]University Medical Center Hamburg-Eppendorf, Germany, [5]Department f.Orthopädie u.Traumatologie, Universitätsklinikum Freiburg, Germany, [6]Department of Osteology & BiomechanicsUniversity Medical Center Hamburg Eppe, Germany, [7]Department of Biochemistry, The University of Hong Kong, Hong Kong

Gerodermia Osteodysplastica (GO) is a premature ageing disorder characterized by wrinkled, lax skin and osteoporosis. It is caused by loss of function mutations in *GORAB*, encoding a golgin with poorly understood function. In order to understand the pathomechanism, a conditional Gorab mouse model was created and crossed with Prx1cre to inactivate Gorab starting from limb bud development. The *Gorab*[Prx1cre] mutants showed mild growth retardation, a reduction of trabecular and cortical bone volume, mineralization defects, and spontaneous fractures. Histomorphometric analysis revealed a significant increase in osteoblast and osteocyte numbers, but expression analysis showed a block in terminal osteoblast differentiation. This was also mirrored by strongly abnormal osteocyte morphology. There were no significant changes in osteoclast number, suggesting low turnover osteoporosis. *In vitro*, GORAB-deficient fibroblasts exhibited an accumulation of DNA damage and cellular senescence, which was also identified in *Gorab*[Prx1cre] mutant bone cells. Adding N-acetyl cysteine (NAC) to the culture medium rescued the accumulation of DNA damage after loss of GORAB, suggesting oxidative stress as the cause of DNA damage. Furthermore, NAC treatment also increased the trabecular bone volume and improved the organization of collagen fibers in the cortical bone of *Gorab*[Prx1cre] mice. Taken together, our results demonstrate that oxidative DNA damage and cellular senescence plays a pivotal role for the pathomechanism of GO and that antioxidants might be a treatment option.

MO0120

Pathologically increased osteoclastogenesis in a mouse model of MPS-I following bone marrow transplantation. Sonja Kuehn*[1], Thorsten Schinke[2], Michael Amling[3], Till Koehne[3], Thomas Braulke[4], Kerstin Cornils[5], Boris Fehse[5], Sandra Breyer[6], Ralf Stuecker[6], Nicole Muschol[4]. [1]University of Hamburg, Germany, [2]Department of Osteology & BiomechanicsUniversity Medical Center Hamburg Eppe, Germany, [3]University Medical Center Hamburg-Eppendorf, Germany, [4]Department of Biochemistry, Childrens Hospital, University Medical Center Hamburg Eppendorf, Germany, [5]Department of Stem Cell Transplantation, University Medical Center Hamburg Eppendorf, Germany, [6]Childrens Hospital Hamburg-Altona, Germany

Mucopolysaccharidosis-I (MPS-I) is a lysosomal storage disorder associated with various skeletal defects. The disease is caused by inactivating mutations of the *IDUA* gene, encoding the lysosomal enzyme a-L-Iduronidase, which is involved in glycosaminoglycan degradation. Most affected individuals are currently treated by bone marrow transplantation (BMT) in early childhood, and in some cases this is followed by enzyme replacement therapy (ERT). To study bone remodeling in MPS-I we analyzed *Idua*-deficient mice by non-decalcified histology and histomorphometry. We found that bone remodeling was unaffected in 6 weeks old *Idua*-deficient mice, yet at 24 and 52 weeks of age these mice displayed a high bone mass phenotype. Although bone formation was not significantly reduced in 24 weeks old *Idua*-deficient mice,

there was a shift in the distribution of osteoblasts at the bone surface, as their average number within the bone-forming units was significantly decreased. Most importantly however, osteoclastogenesis and bone resorption were significantly reduced in 24 weeks old *Idua*-deficient mice, indicative of an osteopetrotic phenotype. In sharp contrast to these findings, a histomorphometric analysis of an iliac crest biopsy from an 8 years old individual with MPS-I revealed low bone mass with pathologically increased eroded bone surfaces. Since this patient underwent BMT at 1 year of age and received ERT for the last three years prior to biopsy, we addressed the question, how these two types of treatment affect bone remodeling in *Idua*-deficient mice. We found that ERT (weekly IDUA injection from 12 to 24 weeks of age) did not significantly influence the bone remodeling phenotype of *Idua*-deficient mice. In contrast, the high bone mass of 24 weeks old *Idua*-deficient mice did not develop after BMT (performed at 8 weeks of age), thereby confirming that it is primarily explained by an osteoclast defect. Most importantly however, the reduced osteoclastogenesis in *Idua*-deficient mice was not only corrected by BMT, but instead, osteoclast number in transplanted mice was more than 4-fold higher compared to non-transplanted or transplanted wildtype mice. Collectively, these findings do not only demonstrate that Idua-deficiency causes an osteopetrotic phenotype, they also show that BMT negatively affects skeletal integrity in MPS-I. It is therefore important to study if a combination of BMT with ERT is the preferable treatment for the affected individuals.

MO0121

Previously unsuspected defects in the cranial base of a mouse model of Hereditary Multiple Exostoses. Federica Sgariglia*[1], Paul Billings[2], Hyo-bin Um[2], Kevin Jones[3], Eiki Koyama[4], Maurizio Pacifici[4]. [1]Children's Hospital of Philadelphia, USA, [2]Children's Hospital of Philadelphia, USA, [3]University of Utah, USA, [4]Children's Hospital of Philadelphia, USA

Hereditary Multiple Exosostes (HME) is an autosomal-dominant pediatric disorder caused by mutations in *EXT1* or *EXT2* that synthesize heparan sulfate (HS). The patients are HS-deficient and display benign cartilaginous tumors – exostoses- next to, but never within, the growth plates. Exostoses are observed in long bones, ribs and vertebral body and arches, but have never been described in the skull that contains several endochondral structures. Thus, we re-examined the skulls of conditional *Ext1*-deficient mice (*Ext1fl/fl;Col2CreER)* that were tamoxifen-injected at P10, focusing on cranial base synchondroses. These are dual mirror-image growth plates that share a resting chondrocyte zone and sustain cranial base elongation by a combination of chondrocyte proliferation and hypertrophy. Growth in cranial base thickness occurs by chondrocyte apposition from flanking perichondrium. We found that multiple exostoses were present intra-cranially and/or extra-cranially along mutant synchondrosis growth plates at sphenoidal and occipital locations. The initial phase of exostosis formation was often associated with displacement of peripheral prehypertrophic and/or hypertrophic chondrocytes from growth plate into perichondrium, followed by the apparent apposition of immature chondrocytes from the flank. We found also that mutant cranial bases were shorter and thinner than controls, and their growth plates exhibited fewer resting and proliferative chondrocytes, irregular column formation at the periphery, suboptimal subchondral and perichondral bone and fewer osteoblasts. These events were accompanied by decreased expression of genes encoding HS proteoglycan core proteins such as *Perlecan* and *Syndecan 3* particularly in growth plate proliferating zone. To uncover mechanisms, we examined hedgehog signaling, using *Ext1*-deficient mice in a *Gli1LacZ* background. LacZ activity was much stronger and widespread along mutant synchondrosis perichondrium at early stages, thus closely connected to -and possibly triggering- exostosis formation at later time points. In sum, our data reveal that the skull is also affected by the loss of Ext1, displaying large exostoses and other defects, at least in mouse. It will be interesting to re-examine radiographic skull scans and data from HME patients to determine whether exostoses or other skeletal changes are present. If so, the data could lead to new clinical practice principles in the diagnosis, care and prognosis of HME patients.

MO0122

SDF-1/CXCR4 Axis in Endothelial Progenitor Cells Regulates Both Vasculogenesis and Osteogenesis for Bone Fracture Healing. Yohei Kawakami*[1], Msaaki Ii[2], Tomoyuki Matsumoto[3], Atsuhiko Kawamoto[4], Yutaka Mifune[5], Ryosuke Kuroda[6], Takayuki Asahara[4], Masahiro Kurosaka[6]. [1]Kobe University Graduate School of Medicine, Japan, [2]Department of Pharmacology, Faculty of Medicine, Osaka Medical College, Japan, [3]University of Pittsburgh, USA, [4]Group of Vascular Regeneration, Institute of Biomedical Research & Innovation, Japan, [5]Kobe university, Japan, [6]Department of Orthopaedic Surgery, Kobe University Graduate School of Medicine, Japan

Introduction: CXC chemokine receptor 4 (CXCR4) is a specific receptor for stromal-derived-factor 1 (SDF-1). SDF-1/CXCR-4 interaction is reported to play an important role in vascular development. On the other hand, the therapeutic potential of endothelial progenitor cells (EPCs) for fracture healing has been demonstrated with

mechanistic insight of vasculogenesis and osteogenesis enhancement at sites of fracture. The purpose of this study is to investigate the influence of the SDF-1/CXCR4 pathway in EPCs in bone formation.

Methods: We created CXCR4 gene conditional knockout mice using the Cre/loxP system and set two groups of mice: Tie2-Cre[ER] CXCR4 knockout mice (CXCR4-/-) and wild type mice (WT).

Results: We report here, in vitro, EPCs derived from CXCR4-/- mouse bone marrow demonstrated severe reduction of migration activity and EPC colony forming activity when compared with those derived from WT mouse. In vivo, radiological and morphological examinations showed fracture healing was delayed in the CXCR4-/- group and the relative callus area at weeks 2 and 3 was significantly smaller in CXCR4-/- group mice. (Fig.1) Quantitative analysis of capillary density at peri-fracture sites also showed a significant decrease in CXCR4-/- group. Especially, CXCR4-/- group mice demonstrated significant reduction of blood flow recovery at fracture sites compared with the WT group in Laser Doppler Perfusion Imaging analysis.(Fig.2) Real time RT-PCR analysis showed that the gene expressions of angiogenic markers (CD31, VE-cadherin, VEGF) and osteogenic markers (osteocalcin, collagen1A1, BMP2) were lower in the CXCR4-/- group. In the EPC incorporation assay, double immunofluorescent staining for isolectin B4 and DiI demonstrated that double stained cells were found in the mice injected EPCs from wild type mice, but not in the mice injected EPCs from CXCR4 KO mice. In the gain-of-function study, the fracture in the SDF-1 intraperitoneally injected WT group healed significantly faster from fracture with enough callus formation comparing them with SDF-1 injected CXCR4-/- group.

Discussion: We demonstrated that an EPC SDF-1/CXCR4 axis plays an important role in bone fracture healing using Tie2-Cre[ER] CXCR4 conditional knockout mice. This study also suggested that he promotion of EPC CXCR4/SDF-1 axis leads to the acceleration of bone fracture healing for a novel therapeutic application for genetic bone diseases and fracture repair.
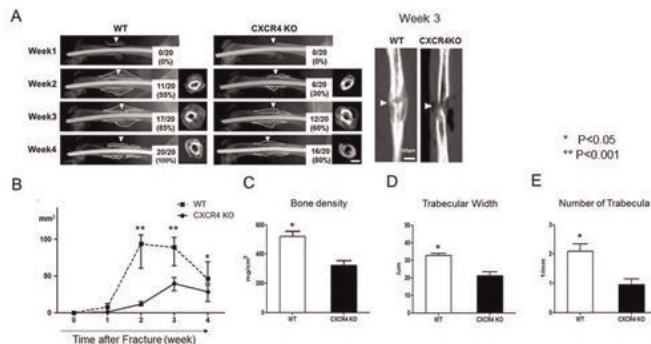

Figure 1

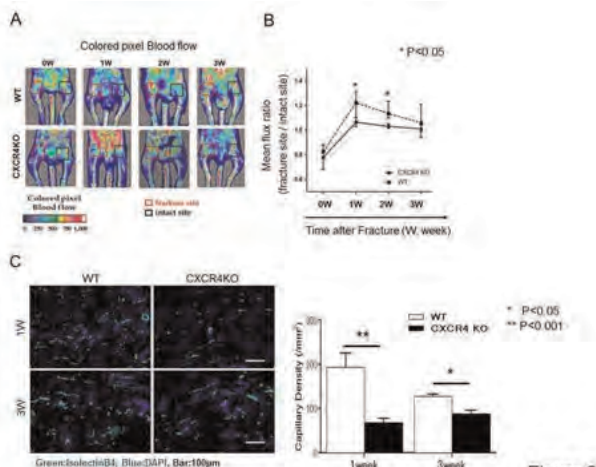Figure 2

Disclosures: *Yohei Kawakami*, None.

MO0123

The FOP R206H ACVR1 mutation is sufficient to cause heterotopic ossification in mouse limbs and is inhibited by a selective RARγ agonist treatment. Salin Chakkalakal*[1], Kenta Uchibe[2], Deyu Zhang[3], Andria Culbert[1], Michael Convente[4], Frederick Kaplan[1], Maurizio Pacifici[5], Masahiro Iwamoto[5], Eileen Shore[1]. [1]University of Pennsylvania, USA, [2]Division of Orthopaedic Surgery, Children's Hospital of Philadelphia, USA, [3]University of Pennsylvania, USA, [4]University of Pennsylvania School of Medicine, USA, [5]Children's Hospital of Philadelphia, USA

Fibrodysplasia ossificans progressive (FOP) is a rare autosomal dominant genetic disorder characterized by extensive heterotopic ossification (HO). Most cases of FOP are caused by the same gain-of-function mutation of the ACVR1/ALK2 type I BMP receptor (R206H). In the present study, we conditionally-activated the ACVR1 R206H mutation in skeletal mesenchymal progenitor (Prrx1^{+}) cells in mice to examine the effects of this cell population on HO and skeletal development. We also tested palovarotene, a phase II selective RARγ agonist, as an inhibitor of ACVR1 R206H-induced heterotopic ossification. Heterozygous Prrx1-Cre;ACVR1 R206H (Prrx1;R206H) mice are viable, but show reduced body length at birth. Histology revealed shorter growth plates with increased proliferative cells and a decreased hypertrophic chondrocyte zone. Consistent with FOP patients, Prrx1;R206H mice at P0 had hind-limb specific great toe malformations and no HO. Soft x-ray and microCT analyses showed that all Prrx1;R206H mice spontaneously developed HO within 2 weeks, with most occurring in the hind limbs. By 4 weeks, HO formation occurs in both hind limbs and fore limbs where Prrx1 is most highly expressed, then progressed to severely impair movement over time. Histological examination confirmed that the HO occurs through endochondral ossification, as in FOP patients. Of note, when the ACVR1 R206H mutation was globally expressed post-natally by a doxycycline-inducible system beginning at P5, all mice developed HO, however the onset and progression were substantially delayed compared to mice with embryonic expression of ACVR1 R206H in Prrx1^{+} cells. Palovarotene, a RARγ agonist that inhibits chondrogenesis, was administered to Prrx1;R206H mice from P3-P14 and significantly reduced spontaneous HO in a dose dependent manner, rescued longitudinal bone growth, and improved limb movement.Our data demonstrate that ACVR1 R206H expression in skeletal progenitor cells supports the induction and progression of heterotopic endochondral ossification as well as being sufficient to induce the characteristic great toe malformations that are characteristic of FOP. While Prrx1^{+} cells appear to be major contributors to HO formation, given the localized expression of Prrx1, additional cell populations likely also contribute to HO in patients. Palovarotene was able to inhibit both the skeletal and HO effects of ACVR1 R206H, providing strong preclinical data for RARγ agonists in clinical trials for FOP.

Disclosures: *Salin Chakkalakal*, None.

MO0124

1,25 dihydroxyvitamin D treatment improves bone microarchitecture in Hyp mice. Eva Liu*[1], Adalbert Raimann[2], Daniel Brooks[3], Mary Bouxsein[3], Marie Demay[4]. [1]Brigham & Women's Hospital & Massachusetts General Hospital, USA, [2]Medical University Vienna, Austria, [3]Beth Israel Deaconess Medical Center, USA, [4]Massachusetts General Hospital & Harvard Medical School, USA

X-linked hypophosphatemia (XLH) is characterized by elevated serum FGF-23, which inhibits the 25-hydroxyvitamin D 1-alpha-hydroxylase, resulting in inappropriately low 1,25 dihydroxyvitamin D (1,25(OH)$_2$D) levels. In both mice and humans, this disorder is accompanied by rickets and osteomalacia. Treatment of affected children with 1,25(OH)$_2$D has been reported to increase trabecular, but not cortical, bone density in the radius as assessed by pQCT. 1,25(OH)$_2$D treatment of Hyp mice, the murine homolog of XLH, has been shown to normalize bone ash weight, a surrogate for bone mineral content.

Investigations were undertaken to examine the effect of 1,25(OH)$_2$D therapy on bone microarchitecture in Hyp mice. 1,25(OH)$_2$D (175 pg/g/day) was administered daily to Hyp mice from post-natal day 2 to day 75. Hyp and wild type mouse controls were injected daily with vehicle. 1,25(OH)$_2$D treatment led to a significant increase in serum phosphate relative to Hyp controls (6.3 ± 0.5 mg/dL vs 4.9 ± 0.4 mg/dL, $p < 0.05$). Compared to wild type mice, control Hyp mice had shorter femurs, reduced bone cross-sectional size, cortical thickness, and trabecular (Tb) bone volume, as well as increased cortical porosity (Table 1). 1,25(OH)$_2$D treatment of Hyp mice normalized their diaphyseal bone shape, such that femoral midshaft moments of inertia were similar to those of wild type controls. Treatment partially rescued several other parameters including femoral length, cortical thickness, cortical area, and metaphyseal combined cortical and trabecular bone volume (adjacent to the growth plate) ($p < 0.05$ vs Hyp controls for all). However, these parameters remained significantly different from those of wild type controls. Neither cortical porosity nor trabecular bone volume in the secondary spongiosa was altered by 1,25(OH)$_2$D treatment of Hyp mice.

These studies demonstrate that 1,25(OH)$_2$D improves femoral diaphyseal shape and cortical microarchitecture in Hyp mice without leading to hypercalcemia or nephrocalcinosis. They also reveal a unique region of increased mineralization adjacent to the growth plate.

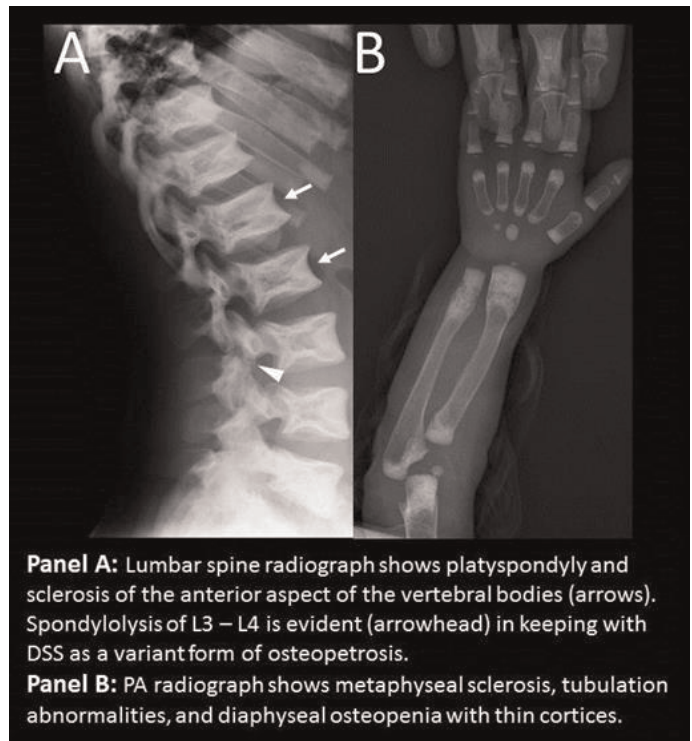Table 1: Bone microarchitecture of Hyp mice treated with daily 1,25 dihydroxyvitamin D

microCT Parameter	Wild Type (vehicle, n=8)	Hyp Control (vehicle, n=5)	Hyp Treated (1,25(OH)$_2$D, n=5)
Femur Length (mm)	14.81±0.31	10.91±0.49[b]	12.64±0.43[*, a]
Midshaft Cortical			
Ct.Th (mm)	0.145±0.008	0.055±0.01[b]	0.074±0.01[*, a]
Ct.TMD (mgHA/ccm)	1122.46±8.17	993.12±9.70[b]	983.48±18.36[a]
Ct.Ar (mm^2)	0.75±0.07	0.39±0.07[b]	0.63±0.13[*, a]
Ma.Ar(mm^2)	1.44±0.11	1.82±0.15[b]	1.96±0.17[a]
Tt.Ar(mm^2)	2.19±0.16	2.21±0.17	2.58±0.21[*, a]
Ct.Ar/Tt.Ar (%)	34.12±1.74	17.39±2.80[b]	24.17±3.95[*, a]
Cortical Porosity (%)	5.83±0.42	31.80±5.11[b]	26.72±5.40[a]
pMOI (mm^4)	0.45±0.07	0.25±0.05[b]	0.46±0.11[*]
I$_{max}$ (mm^4)	0.30±0.05	0.16±0.03[b]	0.30±0.08[*]
I$_{min}$ (mm^4)	0.15±0.02	0.09±0.02[b]	0.15±0.04[*]
Distal Femur Trabecular			
BV/TV (%)	16.83±5.01	10.20±1.85[b]	10.09±3.37[a]
Distal Femur (Ct + Trab)			
BV/TV (%)	48.99±4.65	18.49±2.47[b]	40.29±2.86[*, a]
BMD (mgHA/ccm)	436.42±41.77	166.43±19.19[b]	320.52±22.69[*, a]

Values are represented as average±SD
* p value < 0.05 for Hyp Treated vs Hyp Control
a p value < 0.05 for Hyp Treated vs Wild Type
b p value < 0.05 for Hyp Control vs Wild Type

Liu et al. Table 1

Disclosures: Eva Liu, None.

MO0125

Dysosteosclerosis: Evidence for Genetic Heterogeneity. Gary Gottesman*[1], Steven Mumm[2], William McAlister[3], Serap Turan[4], Katherine Madson[1], Angela Nenninger[5], Murat Bastepe[6], Harald Jueppner[7], Michael Whyte[1]. [1]Shriners Hospital for Children-Saint Louis, USA, [2]Washington University School of Medicine, USA, [3]Washington University School of Medicine, USA, [4]Marmara University Istanbul-Turkey, Turkey, [5]Shriners Hospital for Children-Saint Louis, USA, [6]Massachusetts General Hospital, Harvard Medical School, USA, [7]Massachusetts General Hospital, USA

Dysosteosclerosis (DSS) (OMIM #224300) is the extremely rare (< 25 reports) autosomal recessive disorder characterized during childhood by platyspondyly with diffuse osteosclerosis especially evident in the expanded metaphyses of tubular bones. In 2010, we reported (JBMR 25:2527) that DSS is an "osteoclast-poor" form of osteopetrosis. In 2012, we discovered mutations in the nucleoside transporter gene, *SLC29A3*, in two unrelated DSS patients (Hum Mol Genet: 21:4904). In 2013, genetic heterogeneity for DSS was suggested by absence of a mutation in *SLC29A3* in a single subject with DSS (Osteoporos Int 24: 2253). Molecular studies of the two patients described below provide evidence for genetic heterogeneity of DSS. Our most recent patient, of Amish descent, showed characteristics of DSS when diagnosed at 15 years of age: short stature, fractures, visual loss, cranial nerve palsies, and oligodontia, but no developmental delay or bone pain. Radiographs revealed a generalized skeletal disorder featuring a sclerotic skull base, broad ribs with sclerotic ends, platyspondyly (Figure-Panel A), long bones with horizontal bands of sclerosis (especially in the metaphyseal regions) bordering hypodensity, failure of modeling at the ends of the long bones, synostosis of the left coronal suture, and absent sinuses. Our second patient, a Turkish child, had the clinical and radiographic phenotype of DSS including: a generalized skeletal disorder with platyspondyly, tubulation failure, sclerosis of regions of endochondral growth with dense metaphyses bordering relatively transparent diaphyses, and thin diaphyseal cortices (Figure-Panel B). Bone biopsies were not performed on either patient. Mutation analysis of coding sequence and exon-intron splice sites did not reveal mutations in *SLC29A3*. In particular, the Turkish patient did not show the mutations found in our previously reported DSS patient of Turkish heritage. Our findings suggest that alterations may lie elsewhere in the *SLC29A3* gene (untranslated regions) or that there is locus heterogeneity involving another gene causing DSS.

*Dr. Gottesman and Dr. Mumm contributed equally to this work.

Panel A: Lumbar spine radiograph shows platyspondyly and sclerosis of the anterior aspect of the vertebral bodies (arrows). Spondylolysis of L3 – L4 is evident (arrowhead) in keeping with DSS as a variant form of osteopetrosis.
Panel B: PA radiograph shows metaphyseal sclerosis, tubulation abnormalities, and diaphyseal osteopenia with thin cortices.

DSS Figure

Disclosures: Gary Gottesman, None.

MO0126

R990G mutation of CASR gene in the autosomal dominant hypocalcemia. JO EUN Kim*[1], Hanseok Choi[2], Sihoon Lee[3], Yumie Rhee[4], Sung-Kil Lim[1]. [1]Yonsei University College of Medicine, South Korea, [2]Dongguk University Ilsan Hospital, South Korea, [3]Gachon University School of Medicine, Rok, [4]Department of Internal Medicine, College of Medicine, Yonsei University, South Korea

Autosomal dominant hypocalcemia (ADH) is a congenital isolated hypoparathyroidism caused by activating mutations in the calcium-sensing receptor (CASR) gene. ADH is characterized by mild-to-moderate hypocalcemia, a tendency towards hyperphosphatemia, low-to-normal serum PTH levels and hypercalciuria. A 35-year-old female patient who diagnosed with hypocalcemia 15 years ago was referred to us for further evaluation. At the time of diagnosis, her serum calcium was 7.6 mg/dL (reference value 8.0-10.5), phosphate was 5.1 mg/dL (2.5-4.5), magnesium was 1.5 mEq/L (1.5-2.4), iPTH was 8.01 pg/mL (10-65), and 24 hour urine calcium was 174.9 mg (70-180). In family history, her farther and her younger brother were also diagnosed with hypocalcemia and hypoparathyroidism, and recently, her new-born baby was suffered from tetany due to hypocalcemia (Baseline of biochemical results for family members are shown in Table 1). She was suspected ADH, thus we sequenced all coding exons and intron-exon junctions of CASR, GNA11 and PTH gene. Direct sequencing of genomic DNA revealed only two nucleotide alterations in the CASR gene, C-to-G transition at nucleotide position 47 and G to A transition at nucleotide position 2968. The 2968G>A transition produces an amino acid change from Arg to Gly at codon 990 (R990G) on exon 7. No mutation was found in GNA11 and PTH gene. R990G was reported as benign polymorphism at first in 1996, but thereafter the evidence of R990G was associated with hypercalciuria, lower levels of serum PTH and ionized calcium have been reported. Moreover, Vezzoli et al. demonstrated that transfection of the 990G variant in HEK-293 cells induced a gain-of-function of the receptor. We are about to study CASR gene analysis in rest of the family members. Our result suggests that the potential role of R990G mutation of CASR gene in autosomal dominant hypocalcemia.

Table1. Baseline of biochemical results for family members at the time of diagnosis

Family (sex/age)	Ca (8.5-10.5 mg/dL)	P (2.5-4.5 mg/dL)	Mg (1.5-2.4 mEq/L)	iPTH (10-63 pg/mL)	24hr Urine Ca (70-180 mg)
Index patient (F/20)	7.6	5.1	1.5	8.01	174.9
Father (M/41)	7.5	4.5	1.6	5.63	158.7
Brother (M/18)	7.6	5.2	1.6	5.88	123.8
Son (M/1month)	8.0	7.1	NA	9.17	NA

Table 1

Disclosures: JO EUN KIM, None.

MO0127

An Alignment of ChIP-seq-Defined MEF2C Binding Sites and Genome Wide Polymorphisms Reveals a Risk Genotype Associated with Low Bone Mineral Density (BMD). David Karasik*[1], Jaeyoon Chung[2], Yi-Hsiang Hsu[3], L. Adrienne Cupples[4], Izhak Haviv[5], Douglas Kiel[6], Ching-Ti Liu[4]. [1]Hebrew SeniorLife; Bar Ilan University, USA, [2]Bioinformatics Program, Boston U, USA, [3]Hebrew SeniorLife Institute for Aging Research & Harvard Medical School, USA, [4]Biostatistics, Boston U Sch Public Health, USA, [5]Faculty of Medicine, Bar-Ilan University, Israel, [6]Hebrew SeniorLife, USA

MEF2C encodes a Myocyte Enhancer Factor 2C, a transcription factor which fulfills a critical role in the differentiation of vascular smooth muscle cells and is essential for the transcriptional activation of the bone formation inhibitor, SOST. We hypothesized that variation in *MEF2C* regulates binding throughout the genome and this affects skeletal function. Thus we investigated potential epistatic association between genetic variation of *MEF2C* with its binding sites and BMD traits, including femoral neck (FN) and lumbar spine (LS).

We first extracted Chromatin ImmunoPrecipitation Sequencing (ChIP-Seq) data from the ENCODE consortium for MEF2C to characterize its global genomic binding pattern in GM12878 B lymphocytes and K562 CML cell lines. The aligned read density of the sequencing across the reference human genome and peak finder algorithm, produced a total of 6775 MEF2C-binding sites. We analyzed data from 6,624 Framingham Osteoporosis Study participants with Affymetrix 550K array genotype data using regression analysis to model the association between BMD and interactions between 28 tagging SNPs in the *MEF2C* gene and 358 SNPs in MEF2C-binding sites defined in ENCODE (2kb upstream and downstream of the binding site). We implemented linear mixed effects model to account for sample relatedness and adjusted for covariates, including age^2, weight and sex. In addition, we included principal components as covariates to account for population stratification.

There were 10,024 pairwise interactions between the SNPs in the *MEF2C* and MEF2C-binding sites. Interaction between rs13188739 (G/C) and rs7161172 (G/A) was found to be strongly associated with FN-BMD (p=9.96*10^{-5}). Both SNPs were common (minor allele frequency 26.7% and 49%, respectively). Participants with the CC/GG genotype (n=109) were similar to the rest of the sample in age, sex, total body lean mass, and BMI, while their BMD was significantly lower for both FN and LS. SNP rs13188739 is located in the intron of *MEF2C*. rs7161172 is 18,620 bps from 5' of *RNASE10* (involved in ribonuclease activity and nucleic acid binding) and 13,844 bps from 3' of *PNP* (purine nucleoside phosphorylase, active in Purine metabolism). Comparing the MEF2C elements that exhibit epistasis with the *MEF2C* gene, over all MEF2C binding elements in the genome, identified an enrichment of the NFkB elements, confirming a role for inflammatory processes in the BMD phenotype.

In conclusion, using ChIP-seq data, we found a suggestion of interaction between the variants in the *MEF2C* and its binding sites. The risk interactive genotype, which corresponds to a significantly lower BMD, needs to be replicated in other cohorts.

Disclosures: David Karasik, None.

MO0128

Characterization of small molecule activators and inhibitors of the mutated G$_s$α responsible for Fibrous Dysplasia of Bone. Nisan Bhattacharyya*[1], Marek Kucka[2], Catherine Z. Chen[3], Xin Hu[3], Noel T. Southall[3], Andrea Estrada[4], Michael T. Collins[5]. [1]NIDCR, NIH, USA, [2]NICHD, NIH, USA, [3]NCATS, NIH, USA, [4]National Institutes Of Health, USA, [5]NIDCR, NIH, USA

Mutations in *GNAS* (R201C/R201H), the gene encoding for the small G-protein, G$_s$α, (*gsp* oncogene), result in constitutively active G$_s$α, and increased cAMP levels. These mutations cause fibrous dysplasia of bone/McCune-Albright syndrome (FD/MAS). Patients with FD/MAS exhibit ligand-independent over-secretion of growth hormone, prolactin, thyroid hormone, and/or sex steroids and a skeletal dysplasia characterized by fibro-osseous tissue. Identification of small molecule modulators of G$_s$α may lead to the development of treatments for FD/MAS. To isolate small molecule activators and inhibitors of *gsp*, high-throughput screening (HTS) was performed by measuring cAMP levels in Chinese hamster ovary (CHO) cells stably expressing the wild-type (WT) or mutant G$_s$α proteins. Chemical libraries comprised of more than 3x10^5 compounds were screened in CHO and then in patient-derived bone marrow stromal cells. A total of 114 inhibitory and 132 stimulatory compounds were identified. The aim of this study was to develop a hormone-based rat pituitary cell culture model (GH3 cells) for secondary screening of the small molecule modulators identified in the HTS.

GH3 cell lines stably overexpressing either the WT or mutant G$_s$α, were selected based on equivalent G$_s$α protein expression but low or high cAMP levels, respectively. Cells were treated with varying concentrations of agonists and antagonists using known adenylyl cyclase activators and inhibitors as controls and optimized for prolactin or growth hormone (GH) secretion. 36% of the selected inhibitors could inhibit prolactin secretion; including 7 that reduced prolactin levels by ≥ 50% at 10 µM concentrations. Three of these compounds were confirmed to also inhibit growth hormone (GH) secretion. Decreases in prolactin and GH secretion correlated with decreased cAMP levels. Cytotoxicity assays confirmed test compounds had no effect on cell viability. Results from activator studies indicated that 8 compounds increased prolactin levels in both wild-type and mutant protein-expressing cells. *In silico*

analyses of activators/inhibitors suggest some compounds may compete for the GTP/GDP binding pocket of G$_s$α. In conclusion, this secondary, orthogonal screening system confirmed that a significant number of the molecules previously identified in HTS have inhibitory activity and that 3 compounds have selective activity on mutant G$_s$α. Further testing is necessary to determine which molecules may have potential for drug development.

Disclosures: Nisan Bhattacharyya, None.

MO0129

Somatic Neurofibromin Deficiency and Transcriptional Dysregulation in Tibial Pseudoarthrosis with Neurofibromatosis Type 1. Nandina Paria[1], Tae-Joon Cho[2], In Ho Choi[3], Nobuhiro Kamiya[4], Kay Kayembe[5], Rong Mao[6], Rebecca Margraf[6], Gerlinde Obermosser[7], Ila Oxendine[1], David Sant[6], Mi Hyun Song[8], David Stevenson[9], David Viskochil[9], Carol Wise[1], Harry Kim[10], Jonathan Rios*[4]. [1]Texas Scottish Rite Hospital for Children, USA, [2]Seoul National University Hospital, South Korea, [3]Seoul National University Children's Hospital, South Korea, [4]Texas Scottish Rite Hospital for Children, USA, [5]Baylor Institute for Immunology Research, USA, [6]ARUP Institute for Clinical & Experimental Pathology, USA, [7]Baylor Institute for Immunology Research, USA, [8]Jeju National University Hospital, South Korea, [9]University of Utah, USA, [10]Scottish Rite Hospital for Children, USA

Neurofibromatosis type 1 (NF1) is an autosomal dominant syndrome caused by mutations in *NF1*. Among the earliest manifestations in individuals with NF1 is tibial pseudoarthrosis and persistent nonunion after fracture. The pathogenesis of pseudoarthrosis was proposed to result from tissue-specific (somatic) loss-of-heterozygosity (LOH) resulting in bi-allelic inactivation of *NF1*, though subsequent studies were inconclusive. We sought to determine the extent of somatic mutation in pseudoarthrosis and to characterize the transcriptional dysregulation potentially underlying the persistent bone remodeling defect in individuals with NF1.

To identify somatic mutations, we performed whole-exome sequencing and genomewide microarray analysis of blood and pseudoarthrosis samples from 16 individuals. Only five (31%) samples had somatic LOH, which encompassed the entire q-arm of chromosome 17 and included the *NF1* gene. Somatic mutations were not identified in four samples. The remaining seven (44%) samples had somatic sequence mutations in *NF1*. In several samples, further genetic analysis confirmed the somatic mutations resulted in bi-allelic *NF1* inactivation and predicted pseudoarthrosis-associated neurofibromin deficiency.

Genomewide transcription was assessed using whole-transcriptome sequencing, and results from pseudoarthrosis- and iliac crest-derived cultured cells from individuals with NF1 as well as control bone samples from individuals without NF1 were compared. Transcriptome analysis identified upregulation of multiple pathways associated with neurofibromin deficiency: phosphoinosital-3-kinase (PI3K) and mitogen-activated protein kinase (MAPK) signaling pathways. Specific upregulation of *EGFR* (2.5-fold, p=4.8e-4), *KITLG* (3.4-fold, p=1.9e-4) and *EREG* (55.7-fold, p=2.49e-11) in pseudoarthrosis cells suggest a tumor promoting, though not tumorigenic, transcriptional profile, and this upregulation was associated with neurofibromin deficiency rather than quantitative differences in ERK activation compared to *NF1*-haploinsufficient iliac crest cells.

The transcriptional profile described in pseudoarthrosis-derived cells and the lack of extensive somatic mutation, other than in the *NF1* gene, suggest a potential for FDA-approved receptor tyrosine kinase (RTK)-inhibitors, which may specifically target neurofibromin-deficient pseudoarthrosis cells, to promote proper bone remodeling and bone union after fracture in individuals with NF1.

Disclosures: Jonathan Rios, None.

MO0130

Targeted sequencing of the Paget's disease associated 14q32 locus identifies several missense coding variants in *RIN3* that predispose to Paget's disease of bone. Maheva Valett[1], Dinesh Soares[1], Sachin Wani[1], Jon Warner[2], Stuart Ralston[3], Omar Albagha*[3]. [1]University of Edinburgh, United Kingdom, [2]south east Scotland Clinical Genetics Service, Western General Hospital, United Kingdom, [3]University of Edinburgh, United Kingdom

Paget's disease of bone (PDB) is a common disorder with a strong genetic component characterised by increased but disorganised bone remodelling. Previous genome-wide association studies identified a locus on chromosome 14q32 tagged by rs10498635 which was significantly associated with susceptibility to PDB in several European populations. Here we conducted fine-mapping and targeted sequencing of the candidate locus to identify possible functional variants. Imputation using 1000 genomes data as reference in 741 PDB patients and 2,699 controls confirmed that the association was confined to a 60 kb region in the RIN3 gene and conditional analysis adjusting for rs10498635 identified no new independent signals. Sequencing of the *RIN3* gene identified a common missense variant (p.R279C) that was strongly associated with the disease (OR=0.64; P=1.4 x 10^{-9}), and was in strong linkage disequilibrium with rs10498635. A further 13 rare missense variants were identified, seven of which were novel and detected only in PDB cases. When combined, these rare

variants were over-represented in cases compared to controls (OR=3.72; P=8.9 x 10^{-10}). Most rare variants were located close to p.R279C in exon 6 in a region that encodes a proline-rich, intrinsically disordered domain of the protein. The common p.R279C variant and many of the rare variants were predicted to have deleterious effects on the protein structure. We conclude that susceptibility to PDB at the 14q32 locus is mediated by a combination of common and rare coding variants in RIN3 and indicate that RIN3 may have a previously unsuspected role in the regulation of bone metabolism.

Disclosures: Omar Albagha, None.

MO0131

Unraveling the Skeletal Pathophysiology in Gaucher Disease and Gba2 as a Therapeutic Target. <u>Mone Zaidi</u>*[1], <u>Li Sun</u>[2], <u>Tony Yuen</u>[2], <u>Ping Lu</u>[3], <u>Se-Min Kim</u>[4], <u>Peng Liu</u>[5], <u>Kate Zhang</u>[6], <u>Ruhua Yang</u>[7], <u>Jianhua Li</u>[8], <u>Yiaoting Ji</u>[4], <u>Wei-Lien Chuang</u>[9], <u>Joan Keutzer</u>[6], <u>Agens Stachnik</u>[7], <u>Albert Mennone</u>[6], <u>James Boyer</u>[7], <u>Dhanpat jain</u>[7], <u>Roscoe Btady</u>[10], <u>Maria New</u>[11], <u>Jun Liu</u>[7], <u>Pramod Mistry</u>[7]. [1]Mount Sinai Medical Center, USA, [2]Mount Sinai School of Medicine, USA, [3]Bone Program, USA, [4]Mount Sinai School of Medicine, USA, [5], USA, [6]Genzyme, USA, [7]Yale University School of Medicine, USA, [8]Tount Sinai School of Medicine, USA, [9]Genzyme Corporation, a Sanofi Company, USA, [10]4National Institute of Neurological Disorders & Stroke, National Institutes of Health, USA, [11]Mount Sinai School of Medicine,Departments of Pediatrics, USA

In non-neuronopathic type 1 Gaucher disease (GD1), mutations in the *GBA1* gene result in glucocerebrosidase deficiency leading to a complex phenotype involving the viscera, bone marrow and skeleton. The prevailing macrophage-centric view, however, does not explain emerging aspects of the disease, including malignancy, autoimmune disease and osteoporosis. To understand the pathophysiology of the multi-system involvement in GD1, we conditionally deleted the *Gba1* gene in hematopoetic and mesenchymal cell lineages using an *Mx1* promoter. The Gba1 mouse fully recapitulated human GD1. Cytokine measurements, microarray analysis, and cellular immunophenotyping revealed widespread dysfunction not only in macrophages, but also in other cell types, notably T- and B-cells, NK cells, and dendritic cells, among others. Moreover, we found that the severe osteoporosis in these mice arose not from osteoclastic defects, but rather from defects in osteoblastic bone formation. Mechanistically, GBA1 deficiency causes the accumulation of two key sphingolipids, glucosylceramide (GL-1) and glucosylsphingosine (LysoGL-1). However, it is not known whether downstream metabolites of GL-1 or LysoGL-1 produced by extralysosomal glucocerebrosidase Gba2 contribute to GD1 pathophysiology. We show that the deletion of *Gba2* significantly rescues the GD1 phenotype, including the reduced bone volume, suggesting that metabolism of GL-1 or LysoGL-1 are major contributors to the bone formation defect. Direct testing revealed a strong inhibition of osteoblast viability by nanomolar concentrations of sphingosine, but not ceramide. These findings are consistent with toxicity of high circulating sphingosine levels in GD1 patients, which we show decline upon enzyme replacement therapy; serum ceramide levels remain unchanged. This study provides direct evidence for the involvement in GD1 of cell lineages other than mononuclear phagocytes and defines sphingosine as an osteoblast toxin, setting forth Gba2 as a viable therapeutic target for inhibitors to ameliorate certain disabling consequences of GD1.

Disclosures: Mone Zaidi, Genzyme, 3

MO0132

Insulin-like Growth Factor Binding Protein 4 in the Development and Metabolism of Bone and Fat Tissues. <u>David Maridas</u>*[1], <u>Victoria Demambro</u>[1], <u>Phuong Le</u>[1], <u>Casey Doucette</u>[1], <u>Clifford Rosen</u>[2]. [1]Maine Medical Center Research Institute, USA, [2]Maine Medical Center, USA

Insulin-like Growth Factor Binding Protein 4 (BP4) is the most abundant BP produced by osteoblasts. While BP4 inhibits IGF actions on pre-osteoblasts *in vitro*, it is unclear whether BP4 enhances or inhibits IGF-I activity *in vivo*. Previous reports showed that locally injected BP4 diminishes IGF-I effects on bone while systemic injection induces bone formation. The purpose of this study was to determine how BP4 mediates adipose differentiation and if this impacts skeletal acquisition. Thus, we investigated the skeletal and adipose phenotypes of BP4 null (BP4^{-/-}) mice at 8 and 16 wks of age using DXA, MicroCT, gene expression and protein analysis. At 8 wks, BP4^{-/-} males and females had significant growth retardation (p<0.05) compared to BP4^{+/+} littermates. At 16 wks, BP4^{-/-} mice of both genders displayed reductions in femur length, inguinal (iWAT) and gonadal white adipose depots. Interscapular brown fat depots did not differ. Whole body DXA confirmed a marked decrease in fat and lean masses in 8 and 16 wk-old mice of both genders (p<0.05). Additionally, areal and femoral BMD and BMC were reduced in females (p<0.05) but surprisingly not in males at 16 wks of age. MicroCT revealed decreased BV/TV (p=0.06) and trabecular thickness (p=0.046) in the femurs of BP4^{-/-} females. However, the males had increases in connectivity density (p=0.02) and trabecular number (p=0.005) with decreased trabecular spacing (p=0.02). Serum IGF-I and BP6 were both increased in BP4^{-/-} females (p=0.03). However, in males, serum IGF-I was decreased (p=0.02) and BP6 was unchanged. Femoral expression of *SOST* was decreased in BP4^{-/-} males but not in females. *CyclinD1*, *CDKN1a* and *CDKN1b* mRNA were downregulated in iWAT and

whole bone of BP4^{-/-} males but only in iWAT for females. *PPARγ* expression was reduced in iWAT of both genders. In sum, our data suggests that BP4 is an important modulator of bone and fat development, but there is clear gender and tissue specificity. Gene expression analysis indicates that the reduction of *SOST* expression may contribute to the preservation of bone in males but not in females. Alterations of serum IGF-I suggest that the skeletal phenotype might be IGF-I independent. Also, impaired adipocyte proliferation and function may partially explain the generalized reduction of WAT. Taken together, our results support the hypothesis that BP4 likely mediates mesenchymal cell progress through several mechanisms, which may be linked to IGF-I and tissue specificity.

Disclosures: David Maridas, None.

MO0133

Association with Fetuin-A and Ectopic Calcification in Alpha-klotho Mutant Mice. <u>Hironori Yamamoto</u>*[1], <u>Nozomi Yokoyama</u>[2], <u>Rina Onishi</u>[2], <u>Shiori Fukuda</u>[2], <u>Otoki Nakahashi</u>[2], <u>Yuichiro Takei</u>[3], <u>Yutaka Taketani</u>[2], <u>Eiji Takeda</u>[2]. [1]University of Jin-ai, Japan, [2]University of Tokushima School of Medicine, Japan, [3]Hiroshima University, Japan

Background: α-klotho mutant (kl/kl) mice exhibit hyperphosphatemia, hypercalcemia and hypervitaminosis D. These abnormalities are associated with growth retardation and ectopic calcification. Fetuin-A is a hepatic secretory protein acting as a systemic calcification inhibitor. However, it is still unknown about the role of fetuin-A in kl/kl mice. In this study, we examined the expression of fetuin-A in kl/kl mice. Methods: Wild-type (WT) mice and kl/kl mice at 3- or 6-wk-old were used and given free access to regular chow and water. For histology using paraffin sections of kidney, aorta and heart tissues, calcification sites and fetuin-A expression were detected by von Kossa staining and immunohistochemistry (IHC), respectively. Gene expression analysis were performed using western blots (WB) and Real-time RT-PCR methods. Results: Analysis of serial kidney, aorta and heart sections by IHC and von Kossa staining showed a high regional expression of fetuin-A protein in 6-wk-old kl/kl mice and its localization merged with calcifying sites. We also confirmed its co-localization with the calcified lesions in aorta and heart of chronic kidney disease (CKD) rats. Interestingly, the high regional expression of fetuin-A in kidney was also observed at 3-wk-old kl/kl mice without ectopic calcification. Although WB analysis observed markedly high expression of fetuin-A in kidney of kl/kl mice, its renal mRNA levels were no significant differences between WT and kl/kl mice. In contrast, fetuin-A mRNA levels in liver of kl/kl mice were significantly increased than WT mice from 3-wk-old. Moreover, we found that plasma fetuin-A levels in kl/kl mice were significantly higher than WT mice. Conclusions: These results suggest that the up-regulation of hepatic fetuin-A mRNA expression in kl/kl mice contributes to increase plasma fetuin-A levels and co-localize with calcified lesions as an inhibitor of hyperphosphatemia-induced ectopic calcification.

Disclosures: Hironori Yamamoto, None.

MO0134

FGF23 deficiency ameliorates progression of chronic kidney disease in mice. <u>Olena Andrukhova</u>*[1], <u>Svetlana Slavic</u>[2], <u>Sathish Kumar Murali</u>[2], <u>Reinhold Erben</u>[3]. [1]INST. OF PHYSIOLOGY, PATHOPHYSIOLOGY & BIOPHYSICS, Austria, [2]1Dept. of Biomedical Sciences, University of Veterinary Medicine, Austria, [3]University of Veterinary Medicine, Austria

Clinical studies have shown that circulating fibroblast growth factor 23 (FGF23) is associated with disease progression, cardiovascular risk, and mortality in patients with chronic kidney disease (CKD). Here, we sought to elucidate further the vitamin D independent role of FGF23 in the pathogenesis of CKD in a mouse model. CKD was induced by 5/6 nephrectomy in 3-month-old wild-type (WT) mice, vitamin D receptor (VDR) mutant mice, and Fgf23/VDR compound mutant mice. Sham-operated (SHAM) WT, VDR, and Fgf23/VDR mice served as controls. Both WT and VDR mutant mice developed progressive CKD by 8 weeks after 5/6 nephrectomy as evidenced by reduced glomerular filtration rate (GFR), increased serum creatinine, increased albuminuria, hypertension, increased serum FGF23 and serum parathyroid hormone (PTH) levels, as well as reduced body weight and increased mortality, relative to SHAM controls. Lack of Fgf23 in Fgf23/VDR mice showed higher GFR and lower urinary albumin but unchanged serum PTH levels as compared to WT and VDR CKD mice. Furthermore, Fgf23/VDR compound mutant CKD mice were partially protected against the CKD-induced weight loss and increase in mortality. In addition, the CKD-induced volume expansion, hypernatremia, hypercalcemia, hyperphosphatemia, hypertension, left ventricular functional impairment, and increase in heart-to-body weight ratio observed in WT mice were ameliorated in Fgf23/VDR compound mutants. Consistent with the recently described function of Fgf23 as a sodium- and calcium-conserving hormone, urinary excretion of sodium and calcium was higher in Fgf23/VDR compound mutant CKD mice as compared to WT and VDR mutant CKD mice. Collectively, our data suggest that elevated FGF23 contributes to the pathogenesis of CKD in VDR-ablated mice, and may provide a mechanistic explanation for the association between circulating FGF23 and disease progression in CKD patients.

Disclosures: OLENA ANDRUKHOVA, None.

MO0135

HMW FGF2 isoforms mediate renal phosphate wasting by modulating FGF23/FGFR/MAPKinase signaling in kidney. <u>Erxia Du</u>*[1], <u>Liping Xiao</u>[2], <u>Marja Marie Hurley</u>[3]. [1], USA, [2]University of Connecticut Health Center, USA, [3]University of Connecticut Health Center School of Medicine, USA

We previously reported that transgenic mice overexpressing nuclear high molecular weight isoforms of Fibroblast growth factor 2 (HMWFGF2) in osteoblastic lineage cells had phenotypic changes including dwarfism, hypophosphatemia, osteomalacia and increased FGF23 that plays an important role both in bone mineralization and renal phosphate homeostasis. The purpose of the current study was to examine the effect of short-term blocking of FGF23 using FGF23 neutralizing antibody on phosphate homeostasis in kidney of HMWTg mice. One-month-old male HMWTg mice were injected with FGF23 neutralizing antibody (10mg/kg body weight) or Isotype IgG. One-month-old male VectorTg mice were treated with IgG only as control. After 24 hours, mice were sacrificed. DEXA analysis, serum biochemistry, and harvesting of kidneys for mRNA and protein analysis of the genes of interest were performed. Consistent with our previous reports, at baseline, there were significant reductions in bone mineral density and bone mineral content in HMWTg compared with VectorTg mice. In addition, compared with VectorTg, serum phosphate (Pi) was significantly reduced (P<0.05) in HMW Tg mice. In HMWTg mice treated with IgG there was no increase in serum Pi. In contrast FGF23 neutralizing antibody significantly increased serum Pi in HMWTg mice (Fig A). There was no statistical difference observed in serum calcium between VectorTg and HMWTg mice. We also examined the effect of FGF23 signaling in kidney of HMWTg mice. We observed that excess FGF23 in HMWTg mice increased protein expression of FGF Receptors (FGFR1&FGFR3), klotho, phospho-Erk (pERK1/2), c-fos and decreased the sodium phosphate transporter (Npt2a) in kidneys to cause Pi wasting. By blocking FGF23 function in kidneys of HMWTg, we observed significantly decreased FGFR1(Fig B), FGFR3, and P-ErK based on immunoflurencent staining. Furthermore Western blot revealed that p-Erk was dramatically reduced and the ratio with total Erk changed from 4.3 to 1.9 (Fig C). There was also a significant reduction in c-Fos mRNA (P<0.05), as well as significantly increased Npt2a mRNA (P<0.05) (Fig D). Taken together, these data suggests that HMWFGF2 acts on the kidney via FGF23/FGFR/Klotho/MAPK/c-Fos and Npt2a to regulate Pi homeostasis.

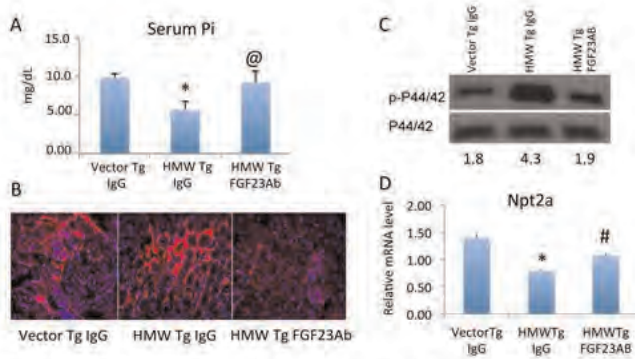Keywords: HMWFGF2, Pi wasting, FGF23, FGF23 neutralizing antibody, MAPKinase signaling.

Figure. Effect of FGF23 neutralizing antibody on serum phosphate (Pi) and kidneys from one-month-old male Vector Tg and HMW Tg mice. (A) Serum Pi, (B) FGFR1 protein expression by immunofluorescent staining,(C) P-ErK protein by Western blotting, and (D) Npt2a mRNA by qPCR.
n=3-8 per group. Values are mean + SE. *: Vector Tg IgG vs. HMW Tg IgG p<0.05; #: Vector Tg IgG vs. HMW Tg FGF23AB p<0.05; @: HMW Tg IgG vs. HMW Tg FGF23AB p<0.05.

Figure. Effect of FGF23 neutralizing antibody on serum phosphate (Pi) and kidneys.

Disclosures: Erxia Du, None.

MO0136

Calcemic actions of a long-acting PTH analog in PTH knockout mice. <u>Tomoyuki Watanabe</u>*[1], <u>Monica Reyes</u>[2], <u>David Goltzman</u>[3], <u>John Potts</u>[1], <u>Thomas Gardella</u>[1]. [1]Massachusetts General Hospital, USA, [2]Massachusetts General Hospital, USA, [3]McGill University, Canada

Parathyroid hormone (PTH) plays a critical role in regulating blood concentrations of ionized Ca via activation of the PTH receptor 1 (PTHR1). We recently have reported on a series of PTH analogs that bind to the PTHR1 with high affinity, induce sustained cAMP signaling responses in PTHR1-expressing cells, and mediate prolonged calcemic and phosphaturic responses when injected into animals (Maeda et al., PNAS 2013). Given their prolonged duration of action in vivo, such PTH analogs could potentially be used as treatments for hypoparathyroidism. We assessed this possibility for one such long-acting PTH analog, called LA-PTH, in an animal model of hypoparathyroidism. We thus tested the capacity of the analog to modulate blood calcium concentrations in PTH-deficient knock out mice (PTH-KO) mice. The base-line levels of blood ionized Ca in these KO mice are about 10% lower than those

in normal mice, consistent with hypoparathyroidism. The mice were injected subcutaneously with either vehicle, LA-PTH (10 nmol/kg) or PTH(1-34) (50 nmol/kg), and blood ionized calcium concentrations were measured at times thereafter. Both LA-PTH and PTH(1-34) injections caused blood Ca++ levels to increase to similar levels (~10% above the levels in vehicle-injected mice), but the duration of the response induced by LA-PTH was significantly greater than that induced by PTH(1-34), despite the five-fold lower dose of LA-PTH. These data support the view that modified PTH analogs can indeed be developed to have prolonged actions on PTHR1 target cells in vivo and to be thus potentially useful as agents for treating hypoparathyroidism.

Disclosures: Tomoyuki Watanabe, None.

MO0137

Evolution of a Long-Acting Parathyroid Hormone Analog for the Treatment of Hypoparathyroidism. <u>Henry Bryant</u>*[1], <u>Charles Benson</u>[2], <u>Venkatesh Krishnan</u>[1], <u>Masahiko Sato</u>[3], <u>Ricky Cain</u>[2], <u>Qianqiang Zeng</u>[2], <u>Deborah Robins</u>[2], <u>Nora Yang</u>[4], <u>Yanfei Ma</u>[1]. [1]Eli Lilly & Company, USA, [2]Eli Lilly & Company, USA, [3]Indiana University School of Medicine, USA, [4]NIH, Therapeutics for Rare & Neglected Diseases, National Center for Advancing Translational Sciences, USA

LSN2561553 is a long-acting PEGylated analog of human parathyroid hormone 1-34 (PTH) that was originally developed as a potential once per week bone anabolic therapy for osteoporosis. The peptide binds with high affinity to the PTH1 receptor and activates cAMP signaling in a manner comparable to PTH, although with some in vitro effects distinct from PTH (e.g. PTH1 receptor internalization/recycling dynamics). In 7-month old rats that were osteopenic (4-week post-ovariectomy), once every 6 day dosing of LSN2561553 for 8 weeks produced dose-related bone anabolic effects as demonstrated by increased serum P1NP levels, bone mineral density, bone biomechanics, and a dynamic histomorphometry profile consistent with bone anabolism. These effects on bone were comparable to the bone effects observed with PTH given as once daily injections, but were accompanied by transient hypercalcemia. LSN2561553, subcutaneously administered to postmenopausal osteopenic women at a dose range of 10 – 100 mcg/w over a 4-week period, increased serum P1NP and osteocalcin at the 100 mcg/kg dose. Doses greater than 65 mcg were accompanied by hypercalcemia and its associated clinical symptoms, including nausea, vomiting, headaches and fatigue. These adverse effects were observed after the first and each subsequent weekly dose of LSN2561553 over the 4-week study and led to termination of further development of the molecule for osteoporosis. Follow-up work in parathyroidectomized (PTX) rats suggested potential efficacy of LSN2561553 as replacement therapy. PTX rats confirmed to have low circulating PTH(1-84) and low serum calcium levels were treated with either daily vehicle or various doses of LSN2561553. Subcutaneous LSN2561553 at 10 mcg/kg and higher, elevated serum calcium within 24 hours. Subsequent daily doses of LSN2561553 normalized serum calcium in PTX rats between 36 and 48 hours, which were sustained over a 5 day period. These studies suggested that while LSN2561553 had little value as a bone anabolic therapy for osteoporotic patients with normal PTH status, therapeutic potential was possible for patients deficient in PTH (1-84). This therapeutic potential as a treatment for hypoparathyroidism is being investigated as part of the NIH Therapeutics for Rare and Neglected Diseases program at the National Center for Translational Sciences.

Disclosures: Henry Bryant, Eli Lilly Company, 4

MO0138

Serum Amyloid A3 Secreted by Osteoclasts Inhibits PTH-Stimulated cAMP Production and Osteoblast Differentiation *In Vitro*. <u>Shilpa Choudhary</u>*[1], <u>Thomas Estus</u>[2], <u>Joseph Lorenzo</u>[1], <u>Hector Aguila</u>[1], <u>Carol Pilbeam</u>[1]. [1]University of Connecticut Health Center, USA, [2]University of Connecticut Health Center, USA

Cyclooxygenase-2 (Cox-2) is the major enzyme responsible for prostaglandin (PG) E_2 production in bone. In contrast to wild type (WT) mice, *Cox-2* knockout (KO) mice increase their trabecular bone mass with continuous PTH infusion. *In vitro*, Cox-2 produced PGE$_2$ inhibits PTH-stimulated osteoblast (OB) differentiation. This inhibition is mediated by a factor secreted from RANKL-stimulated bone marrow macrophages (BMMs). Conditioned medium (CM) from these BMMs inhibits PTH-stimulated cAMP production, cAMP-mediated early gene expression and OB differentiation. The goal of this study was to identify the inhibitory factor in the CM. Microarray analysis of gene expression in RANKL-stimulated BMMs showed that the gene for Serum amyloid a3 (*Saa3*) was the most highly differentially expressed gene in WT BMMs compared to *Cox-2* KO BMMs. In the presence of M-CSF alone, *Saa3* was barely detectable by real time PCR in WT BMMs but was markedly increased by RANKL. Similar results were seen in an osteoclast (OC) progenitor population (B220⁻ CD3⁻ CD11b⁻/low CD115⁺) isolated by flow sorting. Saa3 protein, measured by ELISA in CM, was detectable only in RANKL-stimulated WT BMMs and OC progenitor cells. Saa3 belongs to the family of four secreted, acute phase apolipoproteins. None of the other *Saa* genes were detectable or induced by RANKL. Addition of recombinant human homolog of Saa3 to primary osteoblasts (POBs) inhibited PTH-stimulated cAMP-mediated early gene expression and OB differentiation. A 99% knockdown of *Saa3* gene and protein expression was achieved in WT

BMMs by lentiviral transduction of shRNA constructs. CM from RANKL-stimulated BMMs with Saa3 knockdown did not inhibit PTH-stimulated cAMP production, cAMP-mediated early gene expression or OB differentiation in POBs. Saa3 has been shown to act via the FPRL-1 receptor, which activates the GPCR/Gαi/o signaling pathway that can be blocked by pertussis toxin (PTX). Addition of PTX to POBs prevented the inhibitory effect of recombinant SAA on PTH-stimulated OB differentiation. We conclude that Saa3 is likely to be the OC-secreted factor that acts on OBs to inhibit PTH-stimulated cAMP signaling and OB differentiation and may act via GPCR/Gαi/o signaling. We speculate that Saa3 may also suppress the bone formation response to PTH when PTH is given continuously *in vivo*.

Disclosures: Shilpa Choudhary, None.

MO0139

Activity and Gene Expression of Steroid Sulfatase During Differentiation of the Human MG-63 Preosteoblastic Cell Line. <u>Kyle Selcer</u>[1], <u>Natasha Dias</u>*[2]. [1]Duquesne University, USA, [2]Duquesne University, USA

Estrogen plays an important role in regulation of bone turnover by inhibiting osteoclastic bone resorption. Postmenopausal women have low estrogen production, but inactive sulfated steroids, particularly estrone sulfate (E1S) and dehydroepiandrosterone sulfate (DHEAS), are present in considerable levels in postmenopausal circulation. Conversion of these precursors to active estrogens may help maintain bone density in postmenopausal women. The enzyme steroid sulfatase converts sulfated steroids into their active form in peripheral tissues. Steroid sulfatase is known to occur in bone, but little is known about the regulation of this enzyme. In this study, we investigated the activity and expression of steroid sulfatase in a human preosteoblastic cell line (MG-63). MG-63 cells progress through the various stages of bone cell differentiation under the influence of estrogen and osteogenic supplement, passing through a well-defined sequence of proliferation, matrix maturation, and extracellular mineralization. Cells were grown for 21 days in whole medium alone (OS-) or whole medium containing an osteogenic supplement (OS+) known to enhance differentiation. Growth of cells in OS- medium was nearly exponential, whereas that of cells treated with OS+ was considerably slower. Steroid sulfatase activity, as determined by a whole-cell 3H-E1S conversion assay, increased substantially over time in OS- cells, but increased little in OS+ cells. Steroid sulfatase gene expression, as measured by real-time quantitative rtPCR, revealed a 75% increase in steroid sulfatase mRNA expression in the OS- cells over the OS+ cells, across all time points. Alkaline phosphatase activity increased in the OS+ cells over time, but did not increase in the OS- cells. Osteocalcin gene expression was increased in OS-cells on days 5-21, but was increased in OS+ cells on days 2-8. Our data reveals that activity and expression of steroid sulfatase varies during bone cell differentiation, being higher in the early stages. These results suggest that steroid sulfatase is regulated during bone differentiation and may play a role in bone development.

Disclosures: Natasha Dias, None.

MO0140

Compartmental, temporal and functional interaction of the *cis*-acting heterogeneous nuclear ribonucleoprotein D₀ (AUF1) and estrogen receptor-α in osteoblasts. <u>Alejandro Garcia</u>*[1], <u>John Adams</u>[2], <u>Martin Hewison</u>[2], <u>Rui Zhou</u>[3]. [1]Univ. of California, Los Angeles, USA, [2]University of California, Los Angeles, USA, [3]University of California, Los Angeles, USA

We analyzed the coupled intermolecular, locational, and functional association among the ERE-interacting heterogeneous nuclear ribonucleoprotein D₀ (hnRNP D₀, AUF1), the estrogen receptor alpha (ERα) and estradiol (E2) in the osteoblastic cell line MC3T3-E1. AUF1, also known as the estrogen response element binding protein (ERE-BP), exerts a dominant–negative effect on ERα–E2-directed transcription and E2 resistance *in vivo*. Co-immunoprecipitation and chromatin immunoprecipitation (ChIP) experiments with AUF-1 and ERα were preformed in the presence or absence of E2 to ascertain association between these two proteins in the cytoplasmic and nuclear compartments of the cell in context with their potential to regulate bone-activating genes *in trans*. Immunoprecipitation of AUF1 from MC3T3-E1 cells treated with 10nM E2 for 5, 15, 30, or 180 min and probing for ERα demonstrated AUF1–ERα association exclusively in the nuclear fraction of the cell before and after E2 stimulation. Maximal nuclear AUF1–ERα association was observed 15 min post introduction of E2, suggesting that nuclear association of AUF1-ERα was due to translocation of E2-ERα complex from the cytoplasm. In synchronized cells prolonged exposure to E2 at 30 min led to a 22% decrease in the association between AUF1 and ERα; this is reminiscent of the liganded ERα's cyclical interaction with regulatory *cis* elements. Suprisingly, immunoprecipitation of AUF1 from the cytoplasmic fraction failed to pull down ERα in the presence or absence of E2. ERα is known to interact with the intracellular estradiol-binding protein (IEBP; hsc70) in the cytoplasm, an event that could obscure the anti-AUF1 binding epitope. ChIP of the ERα or AUF1 followed by quantitative PCR (qPCR) of an enhancer element upstream of the Fas ligand gene (FasL; E2-ERα-induced *FasL* expression in osteoblasts is a direct mediator of osteoclast apoptosis) demonstrated 3.4 fold enrichment of ERα 45 minutes after E2 stimulation and ~300% increase in E2-driven *FasL* mRNA expression after 24 hours of E2 stimulation. This event was reciprocally associated with AUF1 occupancy at the same cis element. These data are the first to show a direct association between AUF1 and the ERα in its E2-activated state in the nucleus and suggest that AUF1 can function as a transacting mediator of bone remodeling in a native *Auf1* expression state.

Disclosures: Alejandro Garcia, None.

MO0141

Prednisolone Treatment Reduces the Osteogenic Effects of Loading in Female Mice. <u>Ingrid Bergstrom</u>*[1], <u>Hanna Isaksson</u>[2], <u>Riccardo Chiusaroli</u>[3], <u>Christina Perdikouri</u>[2], <u>Neashan Mathavan</u>[2], <u>Maria Norgård</u>[4], <u>Antti Koskela</u>[5], <u>Juha Tuukkanen</u>[6], <u>Claes Ohlsson</u>[7], <u>Goran Andersson</u>[8], <u>Sara Windahl</u>[9]. [1]Karolinska Institutet, Sweden, [2]Department of Solid Mechanics & Orthopedics, Lund University, Sweden, [3]Rottapharm Biotech, Italy, [4]Department of Laboratory Medicine, Karolinska Institutet, Sweden, [5]Department of Anatomy & Cell Biology, Institute of Biomedicine, University of Oulu, Finland, [6]University of Oulu, Finland, [7]Center for Bone & Arthritis Research at the Sahlgrenska Academy, Sweden, [8]Karolinska Institute, Sweden, [9]Center for Bone & Arthritis Research, Sahlgrenska Academy, Sweden

Glucocorticoids have deleterious effects on the skeleton leading to osteoporosis and an increased fracture risk while mechanical loading increases bone mass. The aim of the present study was to investigate whether high-dose Prednisolone treatment reduces the beneficial effect of loading on cortical bone mass.

Three-month-old female C57BL/6 mice (n=8-9 in each experimental group) were treated with high-dose Prednisolone (15mg/60d.pellets/mouse) or vehicle. The right tibiae were subjected to short periods of cyclic compressive loading three times a week for two weeks (40 cycles, peak strain 3,000με). Micro-computed tomography was used to assess the osteogenic response in the cortex of the loaded (right) versus the non-loaded (left) tibia. Three-point bending was used to assess the bone strength. Alterations in gene expression were investigated by real-time PCR.

As expected, loading increased the cortical bone area in vehicle treated mice (11.8 ± 1.8% vs non-loaded, p<0.01%). Importantly, Prednisolone-treatment substantially reduced the loading response on cortical bone area (-81.7 ± 8.0%, p<0.01%) compared to vehicle-treated mice. Bone-strength measured by 3-point bending was significantly increased by loading in vehicle-treated mice (force at yield point +37%, p<0.05), while no significant effect of loading was observed in Prednisolone-treated mice. The expression of osteoblast-associated genes was significantly reduced by prednisolone-treatment in non-loaded tibia. Several osteoblast and early osteocyte associated genes were induced by loading in vehicle-treated but not in prednisolone-treated mice (Figure 1).

These findings demonstrate that the stimulatory effect of loading on cortical bone mass is reduced by high-dose Prednisolone-treatment. These data suggest that loading may not be beneficial for the skeleton in patients on high dose glucocorticoid treatment.
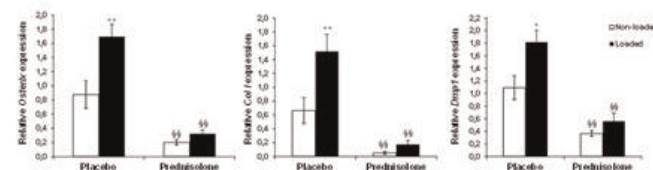
Figure 1. The load-related increase in osteoblast and early osteocyte genes, is blunted in Prednisolone-treated female mice. N=8-9. *p<0.05 and **p<0.01 vs non-loaded tibiae. §§p<0.01 vs placebo control of the same loading regime.

Figure 1

Disclosures: Ingrid Bergstrom, None.

MO0142

A Reverse J-shaped Association Between Serum 25-hydroxyvitamin D and Cardiovascular Disease Mortality – the CopD Study. <u>Darshana Durup</u>*[1], <u>Henrik L. Jørgensen</u>[2], <u>Jane Christensen</u>[3], <u>Anne Tjønneland</u>[3], <u>Anja Olsen</u>[3], <u>Jytte Halkjær</u>[3], <u>Bent Lind</u>[4], <u>Anne-Marie Heegaard</u>[5], <u>Peter Schwarz</u>[6]. [1]Faculty of Pharmaceutical Sciences, University of Copenhagen, Denmark, [2]Department of Clinical Biochemistry, Copenhagen University Hospital Bispebjerg, Denmark, [3]Danish Cancer Society Research Center, Denmark, [4]The Elective Laboratory of the Capital Region, Denmark, [5]Faculty of Health & Medical Sciences, University of Copenhagen, Denmark, [6]Glostrup Hospital, Denmark

PURPOSE

Cardiovascular disease is the major cause of death in the Western World, but the association between 25-hydroxyvitamin D levels and the risk of cardiovascular disease mortality remains unclear

METHODS

We examined the association 25-hydroxyvitamin D levels and mortality from cardiovascular disease, stroke and acute myocardial infarct among 161,428 women

and 86,146 men in the Copenhagen vitamin D study (CopD study) in age, time of blood sample and gender-adjusted Cox regression models.

RESULTS

During follow-up between 2004 and 2011 a total of 16.645 subjects died. 5,454 died from cardiovascular disease including 1,574 from stroke and 702 acute myocardial infarct. 25-hydroxyvitamin D level of 70 nmol/L was associated with the lowest cardiovascular disease mortality risk. Compared to that level the hazard ratio for cardiovascular disease mortality was 2.0(95% CI 1.8-2.1) at the lower extreme (~12.5 nmol/L) with higher risk for men 2.5(95% CI 2.2-2.9), than for women 1.7(95% CI 1.5-1.9). At the higher extreme (~125 nmol/L), the hazard ratio of cardiovascular disease mortality was 1.3(95% CI 1.2-1.4), with similar risk among men and women. Results were similar for stroke and acute myocardial subgroups.

CONCLUSIONS

In this large prospective study low and high levels of 25-hydroxyvitamin D were associated with cardiovascular disease, stroke and acute myocardial mortality in a non-linear, reverse J-shaped manner, with highest risk at lower levels. Whether this was a causal or associational finding cannot be determined from our data. There is a need for randomized clinical trials which include information on the effects of 25-hydroxyvitamin D levels above 100 nmol/L

Disclosures: Darshana Durup, None.

MO0143

Adipose Derived Stem Cells Combined With Beta-Tricalcium Phosphate Is a Potential Therapeutic Approach for Bone Defects Under Systemic Administration of 1,25(OH)$_2$D$_3$. Shengyu Lv*[1], Jian Cui[1], Hongrui Liu[1], Wei Feng[1], Juan Li[1], Bao Sun[1], Kefeng Wang[2], Xiong Lu[3], Minqi Li[4]. [1]Shandong University, China, [2]Sichuan University, China, [3]Southwest Jiaotong University, China, [4]The School of Stomatology, Shandong University, Japan

We have examined a new therapeutic approach for the restoration of bone defects. Adipose derived stem cells (ADSC) isolated from adipose tissue of 8-week-old Vista rats were cultured in the osteogenic induction medium. After osteoblastic properties were verified, ADSC were loaded onto beta-tricalcium phosphate (β-TCP) and co-cultured for another 3 days. The ADSC-β-TCP complexes were then implanted into $5 \times 3 \times 5$mm femoral defects of the same ADSC donate rats. Meanwhile, 1,25(OH)$_2$D$_3$ (120ng/kg body weight) was administrated intraperitoneally once every other day. Animals were divided in 4 groups in this study: i. Bone defects restored with β-TCP and treated with normal saline (NS); ii. Bone defects restored with ADSC-β-TCP complex and treated with NS; iii. Bone defects restored with β-TCP and treated with 1,25(OH)$_2$D$_3$; iv. Bone defects restored with ADSC-β-TCP complex and treated with 1,25(OH)$_2$D$_3$. At day 7, 14 and 28 after operation, rats were perfused with 4% paraformaldehyde in 0.1M phosphate buffer (pH 7.4), and their femurs were harvested for histochemical analysis (n=6). The histochemisty of alkaline phosphatase (ALP), Runx2, cathepsin K and tartrate resistant acid phosphates (TRAP) were performed in this study. Groups treated with 1,25(OH)$_2$D$_3$ showed more newly formed bone than the other corresponding two groups treated with NS. The largest volume of new bone was observed in group iv at day 28 (BV/TV: $34.3 \pm 1.3\%$, $49.2 \pm 3.5\%$, $56.1 \pm 2.3\%$ and $65.0 \pm 5.2\%$ for group i, ii, iii and iv respectively). In a respect of osteogenic activity, immunolocalization of ALP and Runx2 were more seen in the bone defects restored with ADSC-β-TCP, especially at the time point of day 7. However, groups treated with 1,25(OH)$_2$D$_3$ showed no obvious effect on the expression of these proteins according to our data. On the other hand, TRAP-positive osteoclasts number showed significant difference at day 7 and day 14 between groups treated with 1,25(OH)$_2$D$_3$ or NS (day 7: 81.80 ± 6.40, 67.70 ± 7.60, 12.10 ± 1.97 and 8.90 ± 1.79; day 14: 88.90 ± 6.98, 105.30 ± 8.34, 31.50 ± 2.59 and 28.40 ± 2.50 in group i, ii, iii and iv respectively, cells/mm2). Importantly, immunolocalization of cathepsin K also revealed obvious decline in the groups treated with 1,25(OH)$_2$D$_3$ at day 7 and day 14 when compared with the corresponding groups treated with NS. Thus, osteogenic-activity-possessing ADSC loaded β-TCP is a potential therapeutic approach for bone defects under systematic administration of 1,25(OH)$_2$D$_3$.

Disclosures: Shengyu Lv, None.

MO0144

Evidence that C/EBP alpha, PU.1 and the SWI/SNF complex are key mediators of 1,25-dihydroxyvitamin D$_3$ regulation of innate immune responses in lung epithelial cells. Puneet Dhawan*[1], Ran Wei[2], Cheng Sun[2], Adrian F. Gombart[3], H. Phillip Koeffler[4], Gill Diamond[5], Sylvia Christakos[2]. [1]Rutgers - New Jersey Medical School, USA, [2]Rutgers - New Jersey Medical School, USA, [3]Oregon State University, USA, [4]Cedars Sinai Medical Center, USA, [5]University of Florids, USA

Although vitamin D has been reported to have an important role in the regulation of innate immunity, little is known regarding the role of vitamin D in host defense in the airway. We earlier reported that the cathelicidin antimicrobial peptide is induced by 1,25(OH)$_2$D$_3$ in human bronchial epithelial cells with a resultant increase in antimicrobial activity against airway pathogens. In this study we identify key factors that cooperate with the vitamin D receptor (VDR) in the regulation of the human cathelicidin antimicrobial peptide (CAMP) gene. We found that C/EBPα is induced by

1,25(OH)$_2$D$_3$ in human lung epithelial cells and is a potent enhancer of 1,25(OH)$_2$D$_3$ induced CAMP transcription and mRNA and peptide expression. A C/EBP activation domain was identified at -628/-620 within the hCAMP promoter, adjacent to the vitamin D response element (VDRE; -616/-601). Mutation of the C/EBP site markedly attenuated the transcriptional response to C/EBPα as well as to 1,25(OH)$_2$D$_3$, further indicating cooperation between these two factors in the regulation of CAMP expression. C/EBPα has been shown to cooperate with Brm (a component of the SWI/SNF chromatin remodeling complex). Brm dominant negative inhibited the stimulatory effect of C/EBPα and the induction by 1,25(OH)$_2$D$_3$ of CAMP transcription. ChIP/re-ChIP assays showed that Brm functionally cooperates with C/EBPα by direct protein-protein interaction at the C/EBP site in the CAMP promoter. We found that the PU.1 myeloid cell transcription factor is present in lung epithelial cells and cooperates with VDR and C/EBPα to enhance CAMP transcription and mRNA expression. Results of PCR arrays indicate that the two genes most induced by 1,25(OH)$_2$D$_3$ in human bronchial epithelial cells are cathelicidin (38 fold induction) and the TLR4 coreceptor CD14 (46 fold). We found similar cooperative effects between VDR, C/EBPα, PU.1 and the SWI/SNF complex in the regulation of CD14 transcription. These findings indicate that C/EBPα, PU.1 and the SWI/SNF complex are key mediators involved in the regulation by 1,25(OH)$_2$D$_3$ of innate immune responses in lung epithelial cells. The mechanisms involved in the enhanced activation of the CAMP gene suggest potential candidates, including vitamin D, for the development of innate immune responses to augment current therapies to treat or prevent bacterial airway infections.

Disclosures: Puneet Dhawan, None.

MO0145

Gene expression profiles identify selective transcriptome responses of the duodenum and distal intestine to modulation by calcium or vitamin D. Vaishali Veldurthy*[1], Puneet Dhawan[2], Tanya Seth[1], Kiin Kim[1], Angela Porta[3], Patricia Soteropoulos[1], Saleena Ghanny[1], Sylvia Christakos[2]. [1]Rutgers - New Jersey Medical School, USA, [2]Rutgers - New Jersey Medical School, USA, [3]Kean University, USA

Intestinal calcium absorption is important for maintaining calcium homeostasis. However, as indicated in knock out mice studies, an understanding of the mechanisms responsible for intestinal calcium absorption remains incomplete. To identify key genes involved in the intestinal calcium absorptive process RNA was isolated from the duodenum as well as from distal intestinal segments and studied by Affymetrix microarray. In studies using vitamin D deficient (-D) mice and –D mice injected with 1,25(OH)$_2$D$_3$ (+D) [(1ng/g bw) 3 times over 48h] the genes most strongly affected by 1,25(OH)$_2$D$_3$ in the intestine were CYP24A1, TRPV6 and calbindin-D$_{9k}$. There was a 5 – 10 fold greater induction of TRPV6 and calbindin-D$_{9k}$ by 1,25(OH)$_2$D$_3$ in the distal intestine compared to the duodenum. Similar findings were observed using RT-PCR and Western blot analysis. Transcript levels for S100A8 and S100A9 antibacterial proteins were induced 3 – 6 fold (2 fold greater induction in the distal intestine). A significant 1.4 fold decrease in gene expression of cadherin-17 (important for cell to cell contact) by 1,25(OH)$_2$D$_3$ was also observed using –D and +D WT mice as well as –D and +D mice null for both calbindin-D$_{9k}$ and TRPV6 (DKO mice). Using WT or DKO mice the transcript levels for claudin-2, claudin-12 and Cav1.3 voltage gated Ca^{++} channel (previously suggested to be involved in vitamin D regulated calcium transport) were unaffected by 1,25(OH)$_2$D$_3$. In previous studies we showed that transgenic expression of VDR restricted to the distal ileum, cecum and colon of VDR KO mice rescues rickets. Microarray analysis indicated that the genes most strongly affected by VDR expression in the distal intestine are TRPV6 (100 -115 fold induction) and calbindin-D$_{9k}$ (10 – 71 fold induction). Transcript levels for claudin-2, 12, and Cav1.3 were similar in VDR KO and transgenic mice. In VDR KO mice that were fed a rescue diet (high in Ca, P and 20% lactose), which normalizes mineral homeostasis, TRPV6 and calbindin-D$_{9k}$ genes were down-regulated in the duodenum. Most notable was the suppression of genes for intra and intercellular matrix proteins including aquaporin 8 and claudin 8 in the ileum under rescue diet conditions. In summary, our findings provide new insight into genes regulated by 1,25(OH)$_2$D$_3$ and high calcium/ lactose in intestine and further emphasize the importance of the distal as well as the proximal intestinal segments in order to understand intestinal effects of calcium and vitamin D.

Disclosures: Vaishali Veldurthy, None.

MO0146

Hypercalcemia and Nephrocalcinosis in Two Infants with Glucose Galactose Malabsorption: The Role of 1,25 Vitamin D. Melissa Fiscaletti*[1], Marie-Jeanne Lebel[2], Nathalie Alos[3], Prevost Jantchou[4], Geneviève Benoit[5]. [1]University of Montreal, Canada, [2]University of Montreal, Canada, [3]CHU Sainte Justine, Canada, [4]Unviersity of Montreal, Canada, [5]Univerity of Montreal, Canada

Hypercalcemia and nephrocalcinosis have been reported in infants with congenital carbohydrate malabsorption - disorders that are potentially fatal if not promptly diagnosed. Yet the mechanisms that produce calcium imbalance in glucose galactose malabsorption (GGM) are incompletely understood.We report two cases of non-related caucasian infants with GGM who both presented with hypercalcemia and nephrocalcinosis. One patient consulted for failure to thrive while the other was first

seen for macroscopic hematuria. In both cases, the osmotic diarrhea was misidentified as polyuria which delayed the diagnosis of malabsorption. The investigations showed hypercalcemia and bilateral nephrocalcinosis in both patients with high levels of 1,25 OH vitamin D despite suppressed PTH and normal 25 OH vitamin D levels. Hypercalciuria was present in one case. After a one-year follow-up, nephrocalcinosis remained stable and hypercalcemia normalized with the introduction of an appropriate diet.

These two cases demonstrate that when hypercalcemia and nephrocalcinosis are detected, the clinician must rule out a malabsorption disorder. Hypercalcemia and nephrocalcinosis in GGM have classically been attributed to dehydration, metabolic acidosis and increase calcium absorption from vitamin D independent pathways. Our cases highlight the possible implication of 1,25 OH vitamine D in this process possibly through the activation of the TRPV6 transcellular pathway. Genotype-phenotype studies are necessary to better understand the variable clinical presentation of GGM.

Disclosures: Melissa Fiscaletti, None.

MO0147

Obese premenopausal women have lower serum total, free and bioavailable 25(OH)D status and higher vitamin D binding protein (DBP) and parathyroid hormone (PTH) concentrations compared to normal weight premenopausal women. Elisa Saarnio*[1], Minna Pekkinen[2], Suvi Itkonen[3], Virpi Kemi[4], Heini Karp[5], Christel Lamberg-Allardt[3]. [1]University of Helsinki, Finland, [2]Folkhälsan Institute of Genetics, University of Helsinki, Finland, [3]University of Helsinki, Finland, [4]Calcium Research Unit, Finland, [5]Calcium Research Unit, Finland

Recent studies have reported lower S25(OH)D mean concentrations in obese subjects than normal weight individuals. However, differences in vitamin D binding protein (DBP) or in free and bioavailable S25(OH)D concentrations between obese and normal-weight persons are not so well studied. We compared 43 obese (BMI >30) and 144 normal-weight (BMI 20-25) women aged 37-47 with mean BMI of 35.7 ± 4.3 kg/m2 (mean +SD) and 22.5 ± 1.6 kg/m2, respectively. Blood samples and data on total vitamin D and calcium intake (from food and supplements) were collected as well as life style habits including sunny holidays. Comparisons between the normal-weight and obese subjects were made with ANCOVA. Logarithmic transformation was applied to non-Gaussian variables and outliers were removed. DBP concentrations were significantly higher in obese compared to normal-weight subjects (388 ± 89 mg/L and 358 ± 88 mg/L, respectively; p= 0.033). Total S-25(OH)D concentrations were 56.7 ± 18.2 nmol/L in normal-weight subjects and 50.4 ± 17.9 nmol/L in obese subjects; p=0.004.The concentration of calculated free 25OHD was lower in obese woman compared to normal-weight women (10.7 ± 4.1 nmol/L and 12.6 ± 4.3 nmol/L, respectively; p=0.002). Also the calculated bioavailable 25(OH)D (free+albumin bound) was lower in obese persons (p<0.001). Total vitamin D intake, serum parathyroid hormone (SPTH) concentration and sunny holidays were used as covariates. SPTH was higher in obese compared to normal weight subjects (65.1 ± 29.9 and 54.0 ± 23.5 ng/L, respectively; p=0.017).Total vitamin D intake was higher in normal-weight than in obese subjects (15 µg/day and 11µg/day, respectively; p=0.012, which in both groups met the vitamin D recommendation in the Nordic European countries (10 µg/day). In conclusion, obese women had higher DBP concentrations than normal-weight subjects. The concentrations of total, free and bioavailable 25(OH)D were lower than in normal weight women, also after adjustment for total vitamin D intake. Additionally, SPTH concentration was higher in obese women. The observed associations between BMI and total- free-, bioavailable 25(OH)D, DBP and PTH suggests that obesity may modify vitamin D metabolism.

Disclosures: Elisa Saarnio, None.

MO0148

Withdrawn

MO0149

Vitamin D Deficiency and Cardiometabolic |Risks in Arab Adolescents: the "Veiled" Female Advantage. Nasser Al-Daghri*[1], Yousef Al-Saleh[2], Abdulaziz Al-Othman[3], Majed Alokail[3], Omar Al-Attas[3], Abdullah Alnaami[3], Shaun Sabico[3], George Chrousos[4]. [1]King Saud University, Saudi Arabia, [2]King Saud University for Health Sciences, Saudi Arabia, [3]King Saud University, Saudi Arabia, [4]Athens University, Greece

Objective
The recent exponential surge in vitamin D research reflects the global epidemic of vitamin D deficiency and its potential impact on several chronic diseases in both children and adults. Several subpopulations, including Arab adolescent boys and girls, remain understudied. This study aims to fill this gap.

Study Design
A total of 848 apparently healthy adolescent Saudis (334 boys and 514 girls, aged 13-17 years old) were recruited from different public schools within Riyadh, Saudi Arabia. Anthropometrics were taken and fasting blood samples withdrawn to examine serum glucose and lipid profile by routine analysis and 25-hydroxyvitamin D by ELISA.
Results: Almost half of the girls (256/514 or 49.7%) had vitamin D deficiency as compared to only 22.2% (74/334) of the boys (p<0.001). In contrast, there was a significantly higher prevalence of prediabetes in boys than girls (20.8% versus 14.6%;p<0.001). Skin color (R=-0.12;p< 0.001) was strongly inversely associated with vitamin D status in girls, but not in boys. In boys but not in girls, vitamin D status was strongly and inversely associated with BMI (R=-0.17;p<0.001), arm circumference (R=-0.14;p<0.001), systolic blood pressure (R=-0.19;p< 0.001) and triglycerides (R=-0.14;p<0.001). In neither group was fasting blood sugar associated with vitamin D status.
Conclusion: Vitamin D deficiency is more common in Arab adolescent girls than boys. However, vitamin D deficiency is mostly associated with cardiometabolic risk factors in boys, suggesting gender-specific differences that need to be taken into account as to who might benefit the most from vitamin D correction in the adolescent population.

Disclosures: Nasser Al-Daghri, None.

MO0150

An open label study of Zoledronic Acid (*Reclast/Aclasta* 5mg iv) in the treatment of Ankylosing Spondylitis. Gavin Clunie*[1], Amel Ginawi[2], Philip O'Connor[3], Philip Bearcroft[4], Steven Garber[5], Shweta Bhagat[6], Andrew Grainger[3], Hill Gaston[7]. [1]Addenbrooke's Hospital, United Kingdom, [2]Basildon University Hospital, United Kingdom, [3]NIHR Biomedical Research Unit, United Kingdom, [4]Cambridge University Hospitals NHS Foundation Trust, United Kingdom, [5]The Ipswich Hospital NHS Foundation Trust, United Kingdom, [6]West Suffolk NHS Foundation Trust, United Kingdom, [7]University of Cambridge Medical School, United Kingdom

Spinal lesions in Ankylosing Spondylitis (AS) include enthesitis, osteitis, and spondylodiscitis. Osteitis occurs frequently and is characterised by high signal on T2w fat-suppressed or STIR Magnetic Resonance (MR). Pamidronate improves spinal symptoms in NSAID-refractory AS but treatment gains are modest. Zoledronic Acid (*Aclasta/Reclast; ZA*) is more 'potent' than pamidronate but its unknown whether ZA improves osteitis in AS. The purpose of the study was to establish whether ZA reduces osteitis in AS as defined by MR.

Patients with AS (NY criteria) were recruited from two Rheumatology Units (exclusions: poor dentition, planned dental work, GFR<35ml/min). Written informed consent was obtained. Patients' progression in the protocol required osteitis in ≥2 discovertebral units (DVUs) Spondylarthropathy Research Consortium of Canada (SPARCC) definition. Eligible patients received ZA. Ethical approval was obtained and protocol authorized (MHRA; 2007-000087-25). Eligible patients had MR scan pre-treatment then 3 and 6 months after ZA. Sagittal plane spine STIR and T1w sequences were obtained. Images were anonymised and coded and scored by 2 radiologists experienced in SPARCC scoring, blinded acquisition of scans and each others' scoring. An average of the scores for each study was taken. Clinical data obtained at baseline and follow-up: Spinal pain visual analogue score (VAS), Composite Clinical Index (BASDAI), MASES enthesitis index (EI).

Of 11 patients recruited, 7 (6m/1f; age 35-54y) qualified for ZA, with the other 4 patients failing to exhibit ≥2 scorable DVUs on initial MR. Baseline SPARCC scores were between 16-67 (/108). Scores improved in 4/7 patients by 3 months remaining better than baseline at 6 months. Overall 6/7 patients had improved SPARCC scores vs baseline (19-76%) at 6 months. Inter-rater reliability scores were identical for 79% DVUs differing on 21% by maximum of 1 only. Median pain VAS improved 55% (28-63%) at 3 months, sustained in 4/7 patients through 6 months. BASDAI improved 6.3-5.3 by 3 months and to 5.1 by 6 months after ZA. Mean EI improved from 5.1-3.3 at 3 months and to 3.9 at 6 months.

This is the first study in AS to report MR change in osteitis with ZA. Although a small study, the results suggest ZA reduces osteitis in AS. The reduction in SPARCC scores at 6-months mirrors overall clinical improvement over a meaningful period of therapeutic response. ZA treatment was tolerated well and there were no adverse events.

Disclosures: Gavin Clunie, None.

MO0151

Differential expression of inflammation- and regeneration-associated markers of macrophage-polarization (M1 vs. M2) in Bisphosphonate Related Osteonecrosis of the Jaw (BRONJ) and Osteoradionecrosis (ORN). Falk Wehrhan*[1], Manuel Weber[2], Patrick Moebius[2], Raimund Preidl[2], Phillip Stockmann[2], Friedrich W. Neukam[2], Kerstin Amann[3]. [1]University of Erlangen-Nuremberg, Germany, [2]Dept. of Oral & Maxillofacial Surgery, University hospital of Erlangen-Nuernberg, Germany, [3]Institute of Pathology, University hospital of Erlangen-Nuernberg, Germany

Background and Objectives:
Suppression of the local osseous remodeling followed by local inflammation of jaw bone and soft tissue are thought to be involved in the pathogenesis of BRONJ. ORN has been described to be related to chronic inflammation, fibrotic bone remodeling and -destruction. Inflammative processes are mediated by M1-polarized macrophages (CD68-, iNOS-expression), whereas M2 macrophages (CD163-expression) are critical for tissue regeneration. Aminobisphosphonates have been shown to shift macrophage polarization towards the M1-type. Yet it is unknown, if BRONJ and ORN differ regarding the polarization of involved osteoclasts and macrophages.

The aim of this study was to compare the M1- and M2-polarization of osteoclasts and macrophages in BRONJ and ORN by immunohistochemistry analysis compared to healthy jaw bone (NB).

Material and Methods:
15 specimens of BRONJ-associated bone, 15 of ORN-bone and 15 of healty jaw bone were processed for immunohistochemmistry (Peroxidase / DAB+, DAKO Autostainer). A staining of macrophage- and osteoclast-polarization markers (M1: CD 68; iNOS; M2: CD163) was performed. The specimens were completely digitalized in 400x magnification using "Whole-Slide-Imaging" and in each case the three fields of view with the highest expression level within the bone tissue were selected for cell counting (cells/mm^2, ANOVA-Test).

Results:
A significantly ($p<0,05$) increased CD68-expression was seen in ORN compared to BRONJ and NB. Additionally a significantly ($p<0,05$) increased expression of CD163-positive cells was seen in in ORN compared to BRONJ.

The iNOS-expression in BRONJ-specimens was significantly ($p<0,05$) higher than in ORN-samples.

Conclusion:
The results indicate a differential polarization of osteoclasts and macrophages in BRONJ- and ORN-affected bone. Compared to ORN, BRONJ-samples show an increased M1- and a reduced M2-polarization.

These findings are a possible explanation for the clinically and histopathologically observed fibrotic tissue-remodelling processes in ORN compared to the dramatically impaired tissue proliferation and regeneration in BRONJ-affected bone.

Disclosures: Falk Wehrhan, None.

MO0152

Regulatory T cells-mediated arrest of inflammatory bone loss involves the chemoattraction of MSCs and the improvement of its pro-reparative and -immunosuppressive phenotype. Gustavo Garlet*[1], Ana Claudia Araujo-Pires[2], Claudia Biguetti[2], Ana Paula Trombone[3], Andrew Glowacki[4], Sayuri Yoshizawa[4], Steven Little[5], Charles Sfeir[6]. [1]School of Dentistry of Bauru, São Paulo University -FOB/USP, Brazil, [2]FOB/USP, Brazil, [3]USC, Brazil, [4]University of Pittsburgh, USA, [5]University of, USA, [6]University of Pittsburgh, USA

Previous studies demonstrate that regulatory T cells (Tregs) chemoattraction arrest experimental periodontitis (ePD), attenuating the inflammatory bone loss that characterize such condition, and promoting the healing (at least partially) of periodontal tissues. Since mesenchymal stem cells (MSCs) are supposed to interact with Tregs towards the generation of a immunoregulatory and regenerative milieu g, in this present study we investigated the potential modulation of MSCs fate and function by Tregs in ePD model in C57Bl/6 mice.

In the absence of functional Tregs (anti-GITR treatment), the levels of MSCs (CD29, CD44, CD73, CD90, CD105, CD106, CD166, NANOG, Stro-1 and CXCR4) and wound healing (SERPINE1, TIMP1, COL1A1, TGFB1, and ITGA4) markers mRNA (qPCR) were significantly reduced, being associated with increased ePD severity (i.e. increased inflammation and bone loss) and increased levels of osteoclasts markers (RANK, RANKL, catepsin K) expression.Conversely, Tregs chemoattraction by a CCL22-releasing formulation, increases the levels of MSCs and wound healing markers expression along the decrease of bone resorption and osteoclast markers expression. Interestingly, the CCL22/Tregs protective effect is significantly diminished by blocking MSCs mobilization with a CXCR4 inhibitor (AMD3100), indicating an active role for MSCs in ePD arrest. MSCs extracted from periodontal tissues (sorted by magnetic beads) in the presence of active Tregs present higher MFI levels of MSCs and healing markers expression (when analyzed by FACS/qPCR), as well increased immunosuppressive properties in vitro, when compared to MSCs from tissues without Tregs. This results were confirmed using a reverse strategy, when MSCs were attracted to periodontal tissues by CXCL12 in the presence or absence of functional Tregs (Tregs disable by anti-GITR treatment or in CCR4KO mice strain), the absence of Tregs resulted in decreased migration of MSCs, as well in decreased

levels of healing markers expression (when analyzed by FACS/qPCR) and reduced immunosuppressive properties in vitro.

The results demonstrated that Tregs and MSCs cooperates to suppress inflammatory bone loss in vivo; where the presence of Tregs boosts the chemoattraction of MSCs, as well improves of its pro-reparative and pro- immunosuppressive phenotype, which actively contributes to the attenuation inflammatory bone loss along experimental periodontitis.

Disclosures: Gustavo Garlet, None.

MO0153

Bone Geometry and Volumetric Density of Femoral Shaft in postmenopausal Patients with Rheumatoid Arthritis and Bisphosphonate Therapy. Rahel Meinen*[1], Inna Galli-Lysak[1], Daniel Aeberli[2]. [1]Dept. of Rheumatology & Clinical Immunology/Allergology University Hospital, Switzerland, [2]Dept. of Rheumatology & Clinical Immunology/Allergology University Hospital, Switzerland

Background: Rheumatoid Arthritis (RA) leads to synovial hyperplasia, bone erosions, periarticular bone loss, and systemic osteoporosis. Approximately 25% of patients with early RA show osteopenic BMD, and 10% are osteoporotic. There is evidence that postmenopausal women with RA receiving glucocorticoid and bisphosphonate (BP) therapy are at increased risk for atypical subtrochanteric and diaphyseal femoral fracture. To date, the underlying mechanism has not been elucidated. The present study compared femoral shaft bone geometry and volumetric density in postmenopausal RA patients with and without BP therapy using peripheral quantitative computed tomography (pQCT).

Methods: Consecutive postmenopausal RA patients were recruited at the Department of Rheumatology of the Inselspital Bern. PQCT measurements were performed according to a standard protocol at 33% of the femoral bone, and total bone cross-sectional areas (CSA), cortical CSA, and cortical BMD were determined. Primary outcome was cortical thickness, calculated on the basis of a cylindrical model using total CSA and total bone marrow area. Secondary outcomes were cortical BMD and CSA of total bone, cortex, and bone marrow. Mann-Whitney tests were used for group comparisons.

Results: 91 postmenopausal women were recruited for pQCT measurement. Thirty-one patients were excluded due to comorbidities or medications. Of the remaining 60 patients, 20 were on BP and 40 were BP-naïve. Mean disease duration was 14.2 years (range 0–46). Height and weight were comparable between the two groups. Mean age was 62.5 years (range 48–84). On average, women in the BP group were 8.5 years older (p=0.02). Mean cortical thickness was 10.8% lower in the BP group (BP: mean 3.89 mm, 95%CI 2.65–5.12 mm; BP-naïve: mean 4.36 mm, 95%CI 2.90–5.82 mm; p=0.03). Mean cortical CSA was 9.1% lower in the BP group (BP: mean 296.83 mm2, 95%CI 246.37–347.29 mm2; BP-naïve: mean 326.72 mm2, 95%CI: 283.99–414.0 mm2; p=0.01). Differences remained significant when corrected for age. The BP group showed a trend for increased marrow and total femoral shaft CSA (+18% and +2%, respectively), and for lower cortical BMD (-3%).

Conclusion: This cross-sectional pQCT study comparing postmenopausal RA patients with and without BPs supports the hypothesis that BP therapy affects femoral bone shaft geometry and may lead to a lower cortical thickness and area. Further longitudinal prospective pQCT studies are needed.

Disclosures: Rahel Meinen, None.

MO0154

***In Situ* Osteocyte Modulation of β_3 Integrin in Response to Hindlimb Unloading.** Pamela Zuckerman*[1], Damien Laudier[2], Robert Majeska[3], Stefan Judex[4], Mitchell Schaffler[1]. [1]City College of New York, USA, [2]City College of New York, USA, [3]City College of New York, USA, [4]Stony Brook University, USA

β_3 integrin (β_3) adhesions linking osteocyte (OCY) processes to canalicular walls appear to be critical sites of mechanotransduction. However, the structure and behavior of these complexes *in situ* are incompletely understood. We used Structured Illumination Microscopy (SIM), providing 100nm fluorescence resolution, to i) characterize the number and distribution of β_3 foci along OCY processes *in situ*, ii) test whether the foci contained vinculin (Vin), as a marker for the cytoskeletal linking proteins found in typical focal adhesions, and iii) determine whether the foci are altered due to changes in mechanical loading. Bones of C57Bl/6 mice (4 m.o. male, N=6/grp) subjected to hindlimb unloading (HLU) for 5 or 14 days or left as cage controls were studied. Fixed and demineralized femoral mid-diaphyseal cross sections (5μm) were double stained for β_3 and Vin, and images acquired via SIM. 10 OCYs/animal were analyzed with ImageJ for β_3 cluster number & size in 3 concentric areas (L1-L3) extending 0.5, 2.5 and 3.5mm from the OCY lacunar margins. ANOVA & post hoc Mann-Whitney U-test were used to compare data by distance from cell bodies and by unloading group. In control animals, β_3 staining was punctate and localized in cell processes as previously observed (Fig 1). Focal number and size were highest in L1, closest to the OCY bodies, and 70% and 50%, respectively, in L3 (Fig 2). Vin staining was also punctate, but located exclusively in OCY cell bodies, consistent with earlier findings for paxillin (Fig 1). HLU reduced the number of β_3 foci after 5 and 14 days (by over 50% in L2, $p<0.05$), but did not alter their size. In contrast, the area stained by Vin was unchanged with HLU, though Vin focal size was

reduced at 14 days (Fig3). These results show that β_3 adhesion foci in OCY processes are not typical focal adhesions, and suggest that β_3 mechanotransduction in these sites must be mediated by non-cytoskeletal pathways like ion channels. In addition, β_3 foci *in situ* are dynamic, changing markedly in response to mechanical unloading while Vin foci in the cell body do not. Whether these changes are reversible with remobilization remain to be determined.
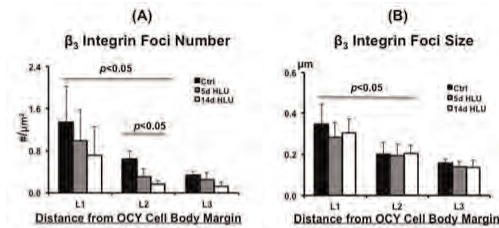

Figure 1

SIM Image of Cortical Bone Osteocytes Stained for β_3 Integrin & Vinculin

β_3-integrin (Red) was observed along osteocyte processes throughout the bone matrix (arrows), seen as discrete punctate staining.

Vinculin (Green) staining was present only in osteocyte cell bodies, and not in cell processes.

Figure 1

Figure 2

β_3 Integrin in Cortical Bone Tissue Osteocytes of Unloaded Mice

(A) The number of β_3 integrin foci decreased with distance from the lacuna margin and with days of HLU.

(B) Integrin foci size remained unchanged with HLU, plotted as a function of distance from the OCY cell body: L1=0-0.5 µm, L2=0.5-2.5µm & L3=2.5-3.5µm.
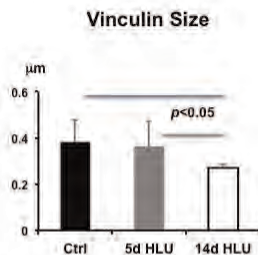
Figure 2

Figure 3

Vinculin in Cortical Bone Tissue Osteocytes of Unloaded Mice

Vinculin was found exclusively within osteocyte cell bodies. Vinculin cluster size was not changed with unloading until after 14 days of HLU, when it was reduced by a third.

Figure 3

Disclosures: Pamela Zuckerman, *None.*

MO0155

Withdrawn

MO0156

Effects of Early Axial Compressive Loading on Cortical Bone Defect Healing in Mice. Robert Carrera*[1], David Wagner[2], Benson George[3], Philipp Leucht[4], Daniel Hunter[3], Gary Beaupre[5], Jill Helms[3], Alesha Castillo[5]. [1]Department of Bioengineering, Stanford University, USA, [2]VA Palo Alto Health Care System, USA, [3]Department of Surgery, Stanford University School of Medicine, USA, [4]Department of Orthopaedic Surgery, Stanford University School of Medicine, USA, [5]VA Palo Alto Health Care System, USA

Introduction: The purpose of this study was to determine the effects of early loading on bone healing. Mechanical stimulation is a known regulator of fracture repair and early weight-bearing is an important aspect of post-surgical care, though very little is known about its effects on the underlying mechanisms of healing. Our hypothesis is that early loading regulates proliferation and differentiation during bone repair. Methods: All procedures were approved by the VAPAHCS IACUC. Under isoflurane anesthesia, bilateral 1-mm monocortical defects were created in ante-romedial tibiae in 16 wk-old B6 mice (n=10). The right tibia was subjected to four consecutive days of *in vivo* axial compressive loading (4 N, 2 Hz, 60 cycles) (Fig. 1A) beginning at post-surgery day (psd) 2. Left tibiae served as nonloaded controls. *In vivo* transverse µCT images of bilateral defects were acquired (55 kVp, 300 ms int time, 10.5 µm isotropic voxel) on days 2, 5, 8, 10, and 14. The region of interest included the regenerate and surrounding cortices, and extended up to 50 slices (0.525 mm) on either side of the defect. Percent change in bone volume (BV) at each time point, relative to psd 2, was calculated for each tibia. Groups of animals were euthanized on days 5, 10, and 14. Four-micron longitudinal sections at mid-defect were assessed for histological appearance and proliferation (PCNA, Invitrogen). A linear elastic finite element model of the defect at psd 2 was created (Scanco FE Software), and strains in the longitudinal direction were computed for an applied 4 N point load (Fig 1B). Results: Estimated cortical strains at the edge of the defect reached 800 µɛ in tension (Fig 1B). Percent change in BV was significantly lower in loaded versus control tibias at psd 8 and psd 10 relative the first day of loading (psd 2) (Fig 2) by a Student's t-test. Loaded defects displayed increased proliferation (Fig 3) and greater amounts of cartilage and fibrocartilage (Fig 4) at the periosteum and within the regenerate at psd 10 and 14. Conclusion: Defect-adjacent periosteum and the early regenerate respond to modest levels of cortical bone strain. Loading in the inflammatory and early soft callus phase delays mineralization and remodeling possibly by initiating a robust cartilaginous response and prolonging the proliferative phase. Load-induced increases in callus size may mechanically stabilize the regenerate, which would have implications in clinical rehabilitation protocols.
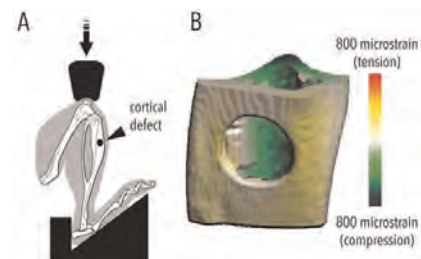

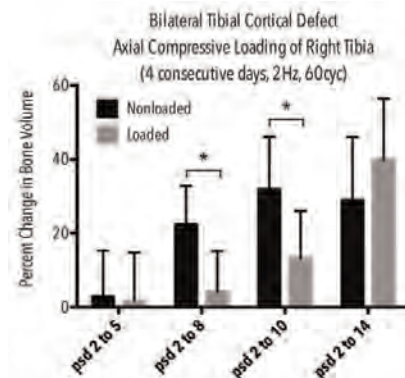Figure 1. (A) Tibial cortical defect subjected to axial loading. (B) Estimated longitudinal strain.

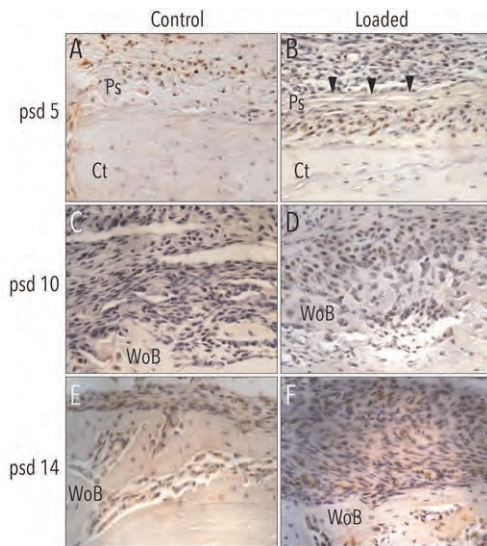Figure 2. Percent change in bone volume in loaded and control defects.

Figure 3. Proliferating cells observed at the periosteal surface and adjacent to the defect.
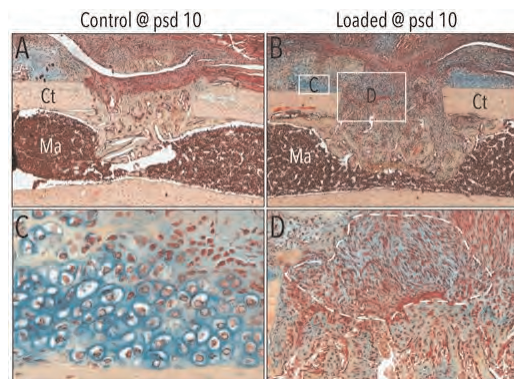

Figure 4. Histological appearance of the defect in loaded and control tibiae at psd 10.

Disclosures: Robert Carrera, None.

MO0157

Effects of Mechanical Stimulation on Differentiation of Human Adipose-Derived Stem Cells. Kai Megerle*[1], Whitney Cole[2], Ian Mahaffey[2], Philipp Leucht[3], James Chang[4], Alesha Castillo[5]. [1]Technische Universität München, Germany, [2]VA Palo Alto Health Care System, USA, [3], USA, [4]Department of Surgery, Stanford University School of Medicine, USA, [5]VA Palo Alto Health Care System, USA

Introduction: The goal of this project was to determine the effects of oscillatory fluid flow (OFF) and orbital shaking (OS) on lineage commitment of adipose-derived stem cells (ASCs). Traditional treatment strategies for delayed- and non-union include internal fixation and autologous bone graft, but challenges with donor site morbidity and limited tissue harvest highlight the need for unique sources of osteogenic precursors for orthopaedic applications. We hypothesized that short- and long-term mechanical stimulation enhanced ASC osteogenic differentiation, alkaline phosphatase (ALP) activity, and mineralization. Methods: Human adipose-derived stem cells were obtained from a commercial source and expanded in proliferation media (PM). Passages 1-5 were used for all experiments. At 80% confluence, cells were cultured in either PM or osteogenic media (PM+100nM dexa+10mM b-glycerolphosphate+0.05mM ascorbic acid), and subjected to static conditions or mechanical stimulation (MS). MS consisted of orbital shaking (OS) in a 6-well plate at 200 rpm, 10 dyne/cm^2 or oscillatory fluid flow (OFF), 1 Hz, 20 dynes/cm^2 for given periods. Gene expression, ALP activity, and mineralization were assessed. Data were analyzed by a one-way ANOVA with a Tukey's post-hoc analysis.Results: OFF (3hr, 2Hz) resulted in an increase in Osx and OPN expression and a decrease in PPARγ and Sox9 expression. OS (3hr, 200 rpm) resulted in an increase in Osx, OPN, PPARγ and Sox9 (Fig 1). Runx2 expression did not change in response to OFF or OS. ALP activity of the PM+OS group was not significantly different from the PM group (Fig 2). The OM group exhibited a significant increase in ALP activity compared to PM and PM+OS groups, and the OM+OS group exhibited a significantly lower ALP activity compared to OM alone. Mineralization (RFU 492/520, arbitrary units) was significantly enhanced by OM (140.9 ± 14.1) compared to PM (2.8 ± 0.2). Orbital shaking did not affect mineralization of ASCs grown in PM (3.19 ± 0.4) or OM (131.5 ± 28.8). Conclusion: OFF is capable of inducing osteogenic differentiation of

ASCs. The increase in both osteogenic and adipogenic genes in response to OS suggests that OS may regulate transcription factors involved in unique lineage pathways. Long-term OS either attenuated or had no effect on osteogenic activity suggesting that OS at tested protocols does not represent an effective method for inducing long-term osteogenic lineage commitment of human ASCs.
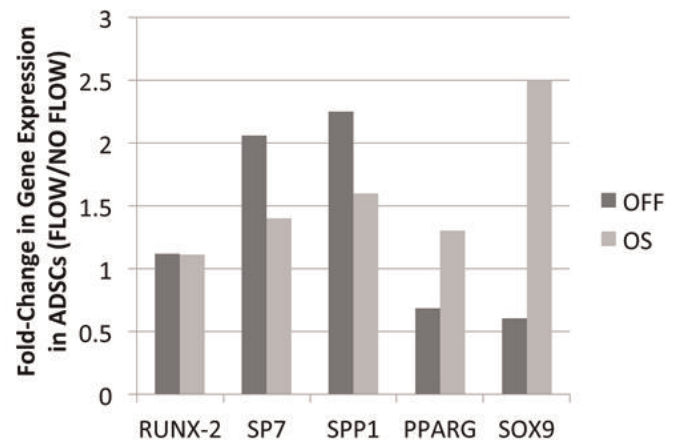

Figure 1. Gene expression in ASCs following 3hr of mechanical stimulation
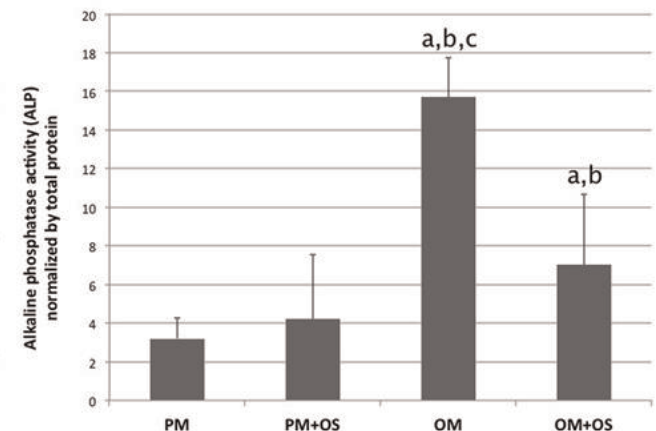

Figure 2. ALP activity in ASCs in response to orbital shaking (OS) in PM or OM

Disclosures: Kai Megerle, None.

MO0158

Load-Induced Changes in Corticocancellous Gene Expression, Bone Formation, and Resorption Are Regulated by an Applied Load Threshold and Mechanical Unloading. Haisheng Yang*[1], Whitney A Bullock[2], Alexandra Myhal[2], Daniel Duffy[2], Philip DeShield[2], Maxime Gallant[1], Russell Main[1]. [1]Purdue University, USA, [2]Purdue University, USA

The anabolic cortical tissue response to mechanical stimuli is regulated by a load threshold. To establish the time-dependent cellular basis for the threshold-regulated response in cortical bone and to determine whether corticocancellous tissues respond similarly, successively greater dynamic compressive loads (-3.5N, -5.2N, -7.0N) were unilaterally applied to the tibiae of three groups of 16wk old female C57Bl/6 mice. MicroCT-based finite element analyses were performed to determine the tissue-level strain environments in the diaphyseal cortical and proximal metaphyseal cortico-cancellous bone at these load levels. Peak principal compressive strains of -1470, -2180, -2940µε were found at the tibial mid-diaphysis and -1320, -1960, -2640µε in the proximal cancellous tissues. Load-related changes in gene expression regulating osteoblast and osteoclast function were examined at 3hr and 24hr following a single loading session, following 3 daily loading sessions (3d), and after 2wks of daily loading (5d/wk). The timecourse for the effects of mechanical disuse (unloading) on skeletal gene expression were examined through hindlimb suspension of 16wk old female C57Bl/6 mice for 3hr, 24hr, and 3wks. Dynamic histomorphometry and microCT were used to quantify the mechanobiological response at the cellular and tissue levels, respectively, following 2wks of loading and 3wks of unloading. Short-term downregulation of *Sost* (3hr) and upregulation of *Col1a1* (24hr, 3d, 2wks) at the High Load are consistent with increased mineral apposition rates, bone formation rates, cancellous bone mass, and cortical geometry in the High Load group. The ratio of *Rankl/Opg* expression was reduced in corticocancellous tissues 3hr following High Load and increased at all timepoints in the Unload group. Consistent with increased mid-diaphyseal cortical geometry and endocortical bone formation following loading,

diaphyseal *Sost* expression in the Medium Load group decreased following 3d of loading and *Col1a1* expression increased following load (24hr, 2wks), though less than in the High Load group at 2wks. There were no cancellous cellular or tissue level responses observed in the Medium Load group. Taken together, these results suggest that changes in gene expression associated with load-induced bone formation and resorption in cortical and corticocancellous bone are regulated by a load or strain threshold that may differ in magnitude between cortical and cancellous tissues.

Disclosures: Haisheng Yang, None.

MO0159

Rearing Medaka Fish in International Space Station (ISS) for Bone Metabolism Study. Masahiro Chatani*[1], Akiko Mantoku[2], Kazuhiro Takeyama[2], Kazuhiro Aoki[3], Yasutaka Sugamori[4], Keiichi Ohya[3], Satoko Uchida[5], Hiromi Suzuki[5], Toru Sakimura[5], Yasushi Kono[6], Fumiaki Tanigaki[7], Masaki Shirakawa[7], Keiji Inohaya[8], Dawud Abduweri[4], Yoshiro Takano[4], Akira Kudo[1]. [1]Tokyo Institute of Technology, Japan, [2]Tokyo Institute of Technology, Japan, [3]Tokyo Medical & Dental University, Japan, [4]Tokyo Medical & Dental University, Japan, [5]Japan Space Forum, Japan, [6]Mitsubishi Heavy Industries, Japan, [7]Japan Aerospace Exploration Agency (JAXA), Japan, [8]Tokyo Institute of Technology, Japan

Introduction: Astronaut bone density decreases partially during space flight because of an imbalance between the activities of osteoclasts and osteoblasts. However, the molecular mechanism how these activities change in long-term space flight remains unclear. Medaka fish serve as a model for research of microgravity environment on osteoclasts and osteoblasts. In particular, we have focused on the pharyngeal bone, which is the active bone remodeling tissue.

Aim: To examine the cellular activities related to bone formation and resorption and elucidate the mechanism of decreased mineralization under microgravity.

Method: Medaka fish were rearing in the aquatic habitat for 2 months at "Kibo", Japanese experimental module in the ISS. To investigate the bone formation and resorption, we established the TRAP promoter-GFP/Osterix promoter-DsRed double transgenic medaka. Fish were either fixed with 4 % paraformaldehyde at day 16 and day 58, or preserved in RNAlater at day 2 and day 62. Bone mineral density (BMD) was measured by Soft X-ray and μCT. The activity of osteoclasts and osteoblasts was examined by confocal microscopy and histological analysis. The gene expression level was examined by the whole transcriptome analysis using HiSeq.

Results: Medaka fish were sometimes swimming vertically and upside down, indicating unique regulation in swimming position under microgravity. In 58 days-rearing medaka, BMD of the pharyngeal bone region was decreased, compared to 1G control (-30%; 1G control: 213.833 $\pm$ 10.095 mg/cm3 n=6, flight: 149.2 $\pm$ 18.094 mg/cm3 n=5, p<0.0001). In 16 days-rearing medaka, the volumes of both GFP and DsRed fluorescence area were decreased (GFP; -49%, DsRed; -68%, p<0.05) and the volume of osteoclasts per that of osteoblasts was elevated 1.45 folds, compared to 1G control (p<0.05).

Conclusion: These results show that, while osteoclasts and osteoblasts were inactive in 16 days, the ratio of osteoclasts per osteoblasts was increased, compared to 1g control, which is accompanied with the decreased BMD in 58 days. Taken together, the increased bone resorption under microgravity is similar to the low bone-metabolic rotation osteoporosis.

Disclosures: Masahiro Chatani, None.

MO0160

Elevation of Glucose to Levels Associated with Type 1 Diabetes Profoundly Diminished Bone Cell Mechanosignaling. Zeynep Seref-Ferlengez*[1], Stephanie Maung[2], Xiaonan Wang[2], Jelena Basta-Pljakic[3], Mitchell Schaffler[4], David C. Spray[2], Sylvia O. Suadicani[2], Mia M. Thi[1]. [1]Albert Einstein College of Medicine, USA, [2]Albert Einstein College of Medicine, USA, [3]City College of New York, USA, [4]City College of New York, USA

Patients with insulin dependent diabetes mellitus (IDDM; Type 1 diabetes) manifest a range of bone problems, including increased risk for bone fractures and defective bone healing. However, the underlying mechanisms are still not well understood. Given that the maintenance of skeletal integrity in response to daily physical activity relies on the regulation of the bone forming cells, osteoblasts, and the primary load sensing cells, osteocytes, we hypothesized that bone loss in Type 1 diabetes is primarily triggered by exposure to high glucose levels which in turn compromises ability of bone cells to perceive and respond to mechanical loading as a result of altered expression of mechanosignaling mediators: specific purinergic receptor (P2Rs) and pannexin 1 (Panx1) channels. To simulate the extracellular glucose levels to which bone cells are exposed in healthy vs. diabetic bones *in vitro*, we cultured MOB-C osteoblasts and MLO-Y4 osteocytes for 10 days in medium (α-MEM) containing 1 or 4.5 g/L glucose. Changes in the expression of P2Rs and Panx1 were determined using Western Blot analysis. Cells were subjected to oscillatory fluid shear stress (OFSS; $? = \pm$ 10 dyne/cm^2) at 1 Hz in μ-Slide VI$^{0.4}$ chambers (ibidi). We used the ratiometric Ca^{2+} indicator (Fura-2 AM) to image OFSS-induced changes in intracellular Ca^{2+} levels. ATP concentration in each flow sample was measured using

the Luciferin-luciferase bioluminescence assay. Cells were also exposed to selective agonists (BzATP, UTP) to evaluate the effects of high glucose (HG) on function of each P2R subtype. The Akita mouse model of Type 1 diabetes (C57BL/6J-Ins2^{Akita}) was used in parallel to evaluate the effects of HG on bone integrity and mechanosignaling system *in situ*. Micro-CT analysis from male Akita (16-week old) and age- and sex-matched wildtype (WT) femurs revealed reduced diaphyseal cross sectional size in Akita compared to WT mice (Fig. 1A). Immunoblots of protein harvested from long bones of Akita (8-week old) and age-matched WT mice (Fig. 1B) and *in vitro* cultures indicated altered expression of P2R (specifically P2Y$_2$R, P2Y$_4$R and P2X$_7$R) and Panx1 expression in diabetic compared to controls. Moreover, HG exposure blunted normal OFSS-induced Ca^{2+} and ATP signaling. Our findings indicate that Type 1 diabetes impairs the proper response of bone cells to mechanical loads, which is required to maintain bone health.
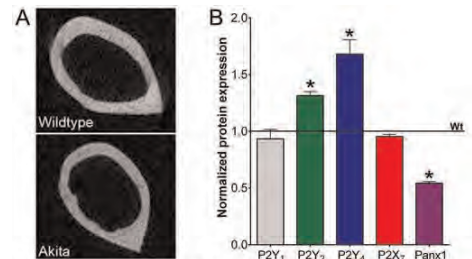

Figure 1. (A) Micro-CT cross-section images of femoral mid-diaphyseal from 16-week old Akita and age-matched wildtype control mice showing reduced diaphyseal cross sectional size in Akita mice. (B) Expression of P2Y$_1$R, P2Y$_2$R, P2Y$_4$R, P2X$_7$R and Panx1 in long bones of Akita and age-matched wildtype mice. All data are presented as $\pm$ SEM. *P < 0.05.

Figure 1

Disclosures: Zeynep Seref-Ferlengez, None.

MO0161

A Novel In Vivo Loading Model to Study Microdamage in Subchondral Bone Following Acute Knee Injury. Oran Kennedy*[1], Bryan Beutal[2], Matin Lendhey[2]. [1]New York University School of Medicine, USA, [2]Department of Orthopaedic Surgery, New York University School of Medicine, Hospital for Joint Diseases, NY, NY 10003, USA

Introduction:Acute knee injury, such as Anterior Cruciate Ligament (ACL) rupture, may result in microscopic damage in subchondral bone. ACL rupture increases the risk of post-traumatic osteoarthritis (PTOA) within 5-10 years. Whether microdamage plays a specific role in this process is unknown. The presence of microdamage is important since recent data showed that, in cortical bone, it can induce production of pro-resorptive factors in osteocytes following fatigue loading. Also, the unique microarchitecture of the subchondral region, means the spatial distribution of microdamage among Calcified Cartilage (CC), Cortical Plate (CP) and Trabecular Bone (TB) will likely be a crucial factor. If microdamage in this system stimulates an osteoclastogenic response as it does in the fatigue system, this represents a novel paradigm for subchondral bone involvement in PTOA. Here we characterize an in vivo model for ACL rupture, and quantify resultant subchondral microdamage.

Methods: We modified the standard in vivo tibial axial loading configuration to include rotational and valgus components (Fig 1A), which contribute to ACL rupture in humans. Under anesthesia, the knees of female Sprague Dawley rats (n=8, IACUC approved) were fixed at 80-85˚ flexion and subjected to a loading ramp (rate 0.1 mm/s) until ACL rupture. Animals were sacrificed and knee joints were harvested, with contralateral limbs as controls. Samples were imaged by MRI to confirm rupture, then fuchsin stained for histology.

Results and Discussion: Animal weight was 278.94 $\pm$ 18.4[g] and ACL failure load was 65.8 $\pm$ 11.4 [N] (Fig 1D) with coefficients of variation at 6.6 and 17.3[%]. MRI confirmed rupture of ACL in all tested joints, with no evidence in controls (Fig1 B,E). Microdamage was found in all subchondral compartments (Fig1 C,F) of tested joints and crack density was 6.69 $\pm$ 3.64, 2.65 $\pm$ 0.65 and 2.84 $\pm$ 0.80 [#/mm^2], in CC, CP and TB, regions respectively. This suggests that microdamage in CC, which has not been well described previously, may be a significant consideration in knee injury – and in particular the biological consequences, such as PTOA.

Conclusion: We report a novel animal model for ACL rupture and subchondral bone microdamage. Damage was differentially distributed among the subchondral mineralized tissue zones. This represents a powerful new approach for examining the role of subchondral bone in PTOA following knee injury.
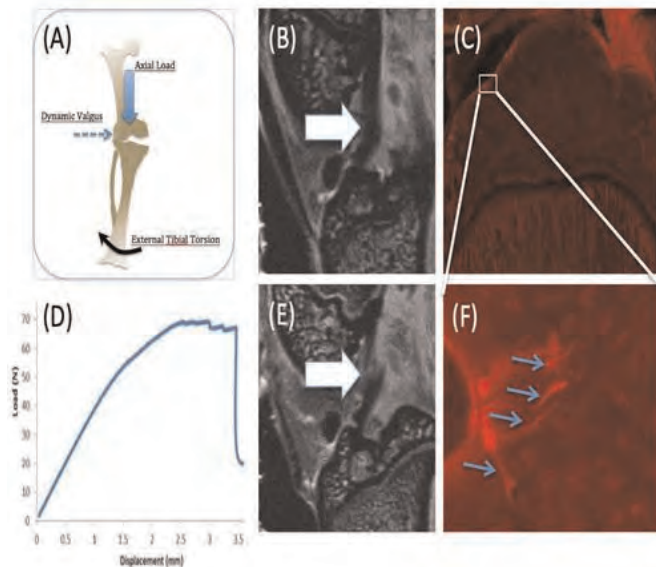
Figure 1

*Disclosures: **Oran Kennedy**, None.*

MO0162

Interrelation between External Oscillatory Muscle Coupling Amplitude and In Vivo Intramedullary Pressure Related Bone Adaptation. Minyi Hu*[1], Jiqi Cheng[2], Neville Bethel[2], Frederick Serra-Hsu[3], Suzanne Ferreri[2], Liangjun Lin[3], Yi-Xian Qin[3]. [1]Stony Brook University, USA, [2]Stony Brook University, USA, [3]State University of New York At Stony Brook, USA

Bone interstitial fluid flow (BIFF) is suggested as a communication media that bridges external physical signals and internal cellular activities within the bone, which thus regulates bone remodeling. Intramedullary pressure (ImP) is one main regulatory factor of BIFF and bone adaptation related mechanotransduction. Our group has recently observed that dynamic hydraulic stimulation (DHS), as an external oscillatory muscle coupling, was able to induce local ImP with minimal bone strain as well as to mitigate disuse bone loss. The current study aimed to further evaluate the interrelationship between DHS's amplitude and *in vivo* ImP induction, as well as this correlation on bone's phenotypic change in conjunction with functional disuse. Simultaneous measurements of ImP and DHS cuff pressures were obtained from the experimental rats under DHS that was driven by loading voltages of 0V ~ 2.4V with a constant frequency of 2Hz. The observed responding trend of the ImP values against DHS cuff pressure amplitudes showed a linear fashion during DHS loading. The ImP reached the peak at 2.4V that was equivalent to 33.75mmHg cuff pressure (Figure 1). The interrelationship between ImP and DHS cuff pressure was evaluated and shown to be proportional, in which ImP was raised with increases of DHS cuff pressure amplitudes. In addition, 4-week *in vivo* experiment using a rat hindlimb suspension model demonstrated that the mitigation effect of DHS on disuse trabecular bone was highly related to DHS's amplitude, where a higher loading dose (30mmHg) led to a more pronounced effect than the lower loading lose (15mmHg). Animals with 15mmHg DHS showed an increase in BV/TV by 80.20% ($p<0.05$) while 30mmHg DHS showed an increase in BV/TV by 100.30% ($p<0.01$). Measures of Conn.D, Tb.N, and Tb.Sp were also significantly affected by DHS treatments with amplitude dependency. There were up to 59.41% ($p<0.05$) and 132.99% ($p<0.05$) increases for Conn.D respected to 15mmHg and 30mmHg of DHS; up to 16.61% ($p>0.05$) and 32.33% ($p<0.001$) increases for Tb.N respected to 15mmHg and 30mmHg of DHS; and up to 21% ($p<0.05$) and 30.99% ($p<0.001$) decreases for Tb.Sp respected to 15mmHg and 30mmHg of DHS (Figure 2). This study provides valuable information for DHS loading optimization, and confirms the regulatory effect of oscillatory DHS on local fluid dynamics.
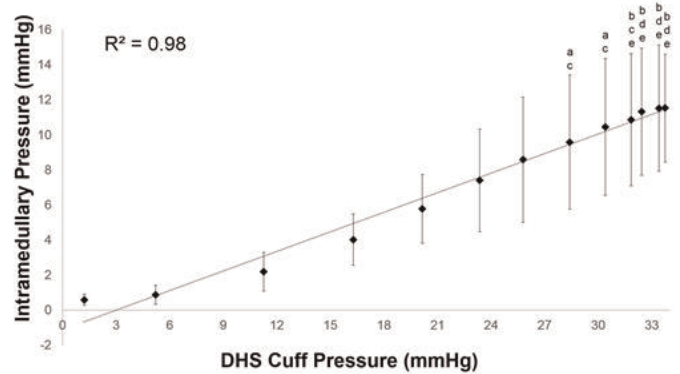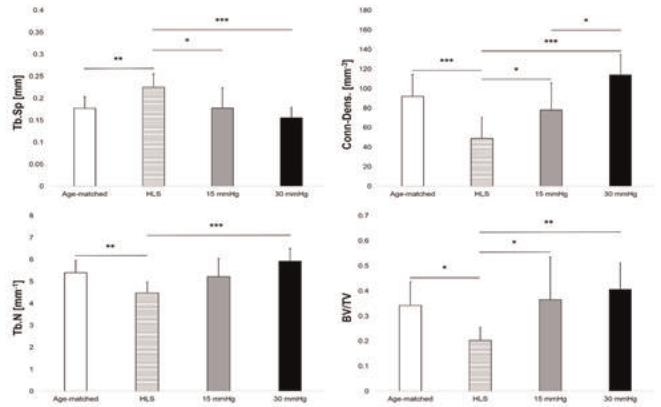

Figure 1

Figure 2

*Disclosures: **Minyi Hu**, None.*

MO0163

Load Represses TGFβ Signaling in Bone through a CYLD and PGE2-dependent Mechanism. Jacqueline Nguyen*, Tamara Alliston. University of California, San Francisco, USA

Mechanical load induces an anabolic response in bone through a sequence of steps consisting of mechanical strain detection, signal transduction, regulation of effector cells, and finally bone formation (Duncan R.L. and Turner C.H., 1995). We demonstrated that load-induced bone formation requires intact TGFβ signaling in bone (Nguyen J. et al., 2013). DNTβRII mice, which express a dominant negative TGFβ receptor type II under the control of the osteocalcin promoter, failed to induce maximal bone formation in a hindlimb-loading model. Furthermore, we found that load represses TGFβ signaling through Smad3 in osteocytes within 5 hours after load. Although this rapid mechanosensitive repression of TGFβ signaling is essential for new bone formation, the responsible mechanisms remain elusive. To identify the most proximal steps in mechanoregulation of TGFβ signaling, we examined TGFβ ligand, receptor, and effector mRNA and protein expression in bone at 1, 3, and 5 hours after *in vivo* loading. Load inhibits TGFβ1 and TGFβ2 mRNA expression by 24% and 54% respectively at 1 hour after load (p<0.05; t-test). The level and phosphorylation of Smad2 and Smad3 proteins were also reduced (n=4) within 1 hour after *in vivo* loading. Likewise in MLO-Y4 cells, fluid flow shear stress rapidly represses Smad3 stability and phosphorylation. The rapid change in Smad2/3 stability led to the hypothesis that mechanosensitive regulation of TGFβ signaling requires load-dependent regulation of ubiquitin ligases that target Smads for proteosomal degradation. In the lung, the deubiquitinase CYLD induces Smad3 degradation through AKT and GSK3β (Lim JH et al., 2012). We find that CYLD protein expression is induced (2.5 fold; n=3) in cortical bone within 1h of hindlimb loading. Furthermore, CYLD siRNA stabilizes Smad3 protein in MLO-Y4 osteocytes. Using chemical inhibitors of other pathways known to respond rapidly to load, we found that load-induced prostaglandin signaling regulates Smad2 phosphorylation, possibly through a CYLD-dependent mechanism. These studies identify CYLD as a novel mechanosensitive protein and, in particular, a novel pathway in load-mediated regulation of TGFβ and Smad3 signaling in bone. Since CYLD regulates molecular pathways involved in load-induced bone formation, understanding the role of CYLD in bone could yield novel drug targets for low bone mass diseases.

*Disclosures: **Jacqueline Nguyen**, None.*

MO0164

Numerical Characteristics of Overloaded Vertebra L[1]. <u>Oleg Ardatov</u>[1], <u>Vidmantas Alekna</u>*[2], <u>Algirdas Maknickas</u>[3], <u>Marija Tamulaitiene</u>[2], <u>Rimantas Kacianauskas</u>[3]. [1]Department of Biomechanics, Vilnius Gediminas Technical University, Lithuania, [2]Faculty of Medicine, Vilnius University, Lithuania, [3]Institute of Mechanics, Vilnius Gediminas Technical University, Lithuania

Aim: Osteoporosis impacts the micro-architectural structure of bone tissue and increases fracture risk. Although osteoporosis affects the entire skeleton, many fragility fractures occur in the lumbar spine. Vertebral fractures in particular result in a high mortality rate. The present study is aimed to investigate the influence of osteoporosis on the mechanical behavior of the vertebra L[1].

Methods: The three-dimensional continuum boundary value problem was formulated and a finite element model (FEM) of L[1] lumbar vertebra was applied. Model was meshed with volume finite elements. The inhomogeneous model consists of two basic parts – cancellous bone and outer cortical shell with anatomical geometry. Impact of osteoporosis on cortical and cancellous bone was modeled by varying transversal elasticity modulus. Cancellous bone and cortical shell are modelled transversally isotropic. Also, two isotropic inter-vertebral disks were modeled on purpose to simulate distributed external load on the boundaries. The value of bending moment was in the range from 3 to 15 Nm. This model was validated according to experimental results of research of healthy lumbar vertebrae.

Results: Model was tested under bending load on both frontal and sagittal planes. A yield stress criterion is chosen to predict the risk of failure of the model. The risk of failure is evaluated according to von Mises stress. It was found, that the critical load for normal bone is 25% higher than for the high degree of osteoporosis (HDO) model and 13% higher for average degree of osteoporosis (ADO) model during forward bending. The highest values of von Mises stress occurred during lateral bending. The critical load for healthy bone is 26% higher than for the ADO model and approximately 60% higher than for HDO model.

Conclusions: Obtained numerical results show large dependence between stress and state of physical properties of cancellous bone. Numerical comparison of frontal and lateral bending showed that during lateral bending stress values in osteoporotic cortical shell are twice greater than in normal cortical shell.

Disclosures: Vidmantas Alekna, None.

MO0165

Spontaneous Activity from Access to Running Wheels Stimulates Bone Gain at Multiple Sites in Mice. <u>Robert Brommage</u>*[1], <u>Sabrina Jeter-Jones</u>[2], <u>Andrea Thompson</u>[3], <u>Jeff Liu</u>[3]. [1]Lexicon Pharmaceuticals, USA, [2]Lexicon Pharmaceuticals, USA, [3]Lexicon Pharmaceuticals, USA

Resetting the bone mechanostat in rodents by increasing mechanical forces typically involves forced treadmill exercise or defined cycles of limb compression. Although these procedures are highly successful, they do not perfectly mimic forces acting on bone during normal activity and are usually employed during the daily sleep phase. Rodents voluntarily run several km each day when given access to running wheels and this physiological exercise regimen stimulates bone formation.

Male C57BL/6J-129SvEv hybrid mice were singly housed with (N = 10) or without (N = 8) running wheels (23 cm diameter, MiniMitter system) from 4 through 18 weeks of age. For 5 of 10 running mice, wheel weight was increased by 26% (with a greater increment in moment of inertia) to increase the work required per revolution. Running wheel revolutions were recorded each minute and summed in two hour increments throughout the study. Bone architecture was determined by standard microCT techniques using a Scanco μCT40. Statistical significance was defined as P < 0.01.

Mice ran an average of 4.0 (SD = 1.3) km daily with most running occurring nocturnally. There was no effect of running wheel weight on bone parameters and data for these two groups were combined. Femoral length was identical in running and non-running mice.

Running produced a cancellous bone anabolic response in both spine LV5 and distal femur metaphysis, with increases in trabecular bone BV/TV (24% spine, 21% femur) and thickness, but not trabecular number.

The femur responded to running with elevated bone areas in the femoral neck (17%), proximal shaft at the third trochanter (9%) and midshaft (20%). Total areas (diameter) were higher at both femoral shaft sites (10%, 16%) with an elevated cortical thickness (7%) at the midshaft. The tibia midshaft, tibia-fibula junction and distal shaft responded to running with elevated total (19%, 17%, 11%) and bone (20%, 17%, 10%) areas and greater cortical thickness (10%, 7%, 4%). There was no evidence of endocortical bone formation, as marrow cavity areas were consistently elevated and statistical significance achieved for midshaft femur (15%), midshaft tibia (18%) and the tibia-fibula junction (19%).

These results show a consistent beneficial effect of physiological running exercise on bone mass at every site examined, including both cancellous and cortical bone. The cortcal bone respose primarily involved periosteal formation. There was no major effect of running wheel weight.

*Disclosures: **Robert Brommage**, Lexicon Pharmaceuticals, 10*
This study received funding from: Lexicon Pharmaceuticals

MO0166

Using Novel 3D Bone Mimicking Scaffolds to Investigate Tumor-Induced Bone Disease. <u>Ushashi Dadwal</u>*[1], <u>Jonathan Page</u>[2], <u>Alyssa Merkel</u>[3], <u>Michael Kessler</u>[4], <u>Julie Sterling</u>[5], <u>Scott Guelcher</u>[6]. [1]Vanderbilt Center for Bone Biology, Vanderbilt University Medical Center, USA, [2]Department of Chemical & Biomolecular Engineering, Vanderbilt University, USA, [3]Department of Veterans Affairs (TVHS), USA, [4]School for Math & Science, Vanderbilt University, USA, [5]Department of Veterans Affairs (TVHS)/Vanderbilt University Medical Center, USA, [6]Vanderbilt University, USA

Tumor Induced Bone Disease (TIBD) is common in patients with advanced metastatic disease originating from primary breast, prostrate and lung cancer. While many studies have elucidated multiple mechanisms that influence TIBD, most have focused on the interactions between the tumor cells and bone cells (osteoclasts and osteoblasts). Recent studies from our group and others have begun to investigate other facets of the bone microenvironment and demonstrate that both the bone marrow cells and the physical rigidity of bone can influence tumor cell behavior, gene expression, and bone destruction. The majority of these studies have relied on 2D culture, which while valuable, limits our ability to recapitulate complex interactions between multiple cells and physical properties of the bone microenvironment. Therefore we have developed a novel 3D bone mimicking model using polyurethane scaffolds (PURS).

Since our previous 2D data demonstrated that matrix rigidity regulated the expression of genes important in TIBD (TGF-βRII, PTHrP, Integrin β3 and Gli2) in the bone metastatic breast (MDA-MB-231) and lung (RWGT2) cells, we first examined the effect of rigidity in 3D on gene expression. 3D scaffolds were made by printing an inverse mold using a 3D printer (MakerBot). Liquid PUR was then cast into the mold and compressed. The resulting 3D PUR scaffolds have a defined interconnected architecture (Fig. 1a&b) with rigidity ranging from Rigid (2600 MPa: trabecular bone) to Complaint (10 MPa: basement membrane) as determine by nanoindentation (Agilent, g200 nanoindentor).

3D scaffolds were seeded with tumor cells both in vitro (Fig.1c&d) and in vivo. A live cell imaging system was used to track migration of individual cells on rigid and compliant scaffolds to demonstrate tumor cells migrate faster on rigid scaffolds as compared to compliant scaffolds (Fig1e). In vitro data from a bioreactor (3D Biotek) which mimics dynamic cellular environment using physiologically relevant flow rate (2.1 rpm) shows increased expression of PTHrP in rigid vs. compliant scaffolds (Fig.1f) Additionally, In vivo studies were conducted with tumor cells seeded scaffolds implanted into the mammary fat pads of athymic mice. Scaffolds were explanted after 21 days and analyzed for PTHrP expression using RT PCR and histomorphometry (Fig.1h) Thus, we successfully demonstrate 3D PUR scaffolds can be used to analyze the osteolytic potential of tumor cells during TIBD.
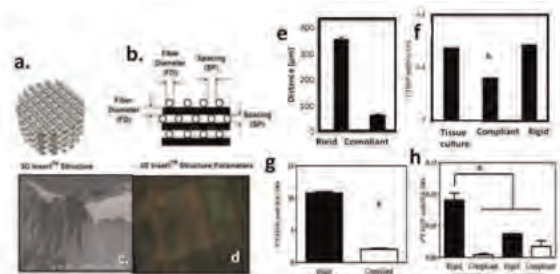
Fig. 1 3D PUR scaffolds have a defined architecture **a.** with interconnected pores and **b.** modifiable Fiber Diameter and Spacing. MDA MB 231 GFP tumor cells were seeded in 3D PUR scaffolds as seen by **c.** SEM imaging that shows cells adhere to the scaffolds and **d.** in vitro using fluorescence imaging seeded inside the scaffolds. **e.** MDA 231 MB cells seeded on rigid scaffolds migrated significantly faster than tumor cells on the compliant scaffolds as determined by live cell imaging. Osteolytic gene expression (PTHrP) measured by RT PCR demonstrates tumor cells have increased expression of PTHrP on rigid scaffolds vs. compliant scaffolds in **f.** static culture as well as **g.** dynamic culture using a perfusion based bioreactor with 2.1 rpm. **h.** in vivo, 10⁶ tumor cells were seeded into the scaffolds that were transplanted into mammary fat pads of athymic mice. PTHrP expression is increased on rigid scaffolds.

abstract figure

Disclosures: Ushashi Dadwal, None.

MO0167

Bone Regeneration in a Rat Model of Type 2 Diabetes and Aging is Improved by PTHrP Loaded in a Biopolymer-coated Hydroxyapatite. Juan Antonio Ardura*[1], Sergio Portal-Nuñez[1], Irene Gutierrez-Rojas[1], Daniel Lozano[2], Ana Lopez-Herradon[1], Francisca Mulero[3], Maria Vallet-Regi[4], Pedro Esbrit[5]. [1]Instituto de Investigación Sanitaria-Fundación Jiménez Díaz, Spain, [2]Instituto de Investigación Sanitaria-Fundación Jiménez Díaz, Spain, [3]Centro Nacional de Investigaciones Oncológicas (CNIO), Spain, [4]Universidad Complutense de Madrid, Spain, [5]IIS-Fundación Jiménez Díaz, Spain

Type 2 diabetes, which predominates in older individuals, is associated to an increase in fracture risk. The N-(1-37) and C-terminal (107-111) epitopes of parathyroid hormone-related protein (PTHrP) exhibit osteogenic properties. Biopolymer-coated nanocrystalline hydroxyapatite (HA) made as macroporous foams are promising candidates as scaffolds for bone tissue engineering applications. The main aim of this study was to evaluate whether PTHrP (1-37) or (107-111) loading into gelatin-glutaraldehyde biopolymer-coated HA (HAGlu) scaffolds improve bone regeneration in a model of aging and type 2 diabetes.

Type 2 diabetes was induced in male rats by a single dose of streptozotocin intraperitoneally administered on the day of birth. At the age of 18-20 months, those rats showing a glucose disappearance constant below 2.5×10^{-2}/minute during a glucose tolerance test were selected. A cavitary defect was performed in both distal tibial metaphysis of diabetic or control aged rats and HAGlu scaffolds with and without PTHrP (1-37) or (107-111) were implanted into the cavitary defects. Animals were sacrificed after 4 weeks and femurs and tibiae were extracted for μ-computerized tomography and histomorphometry analysis.

Femurs from diabetic aged rats showed decreased bone volume/tissue volume (BV/TV) and trabecular thickness and increased trabecular separation compared to control aged rats. No differences in trabecular number and body weight were observed between groups. Four weeks after performing the surgery, the cavitary defect in tibiae of diabetic aged rats presented decreased bone regeneration compared to control aged rats as shown by decreased BV/TV and increased trabecular separation and bone surface/bone volume (BS/BV).In contrast, the bone defect was healed in the presence of PTHrP (1-37) and PTHrP (107-111)-containing HAGlu implant in both diabetic and control rats aged, related to an increase of cortical and trabecular BV/TV, bone thickness and decreased trabecular separation and BS/BV compared to unloaded HAGlu implants.

Our findings suggest the suitability of PTHrP (1-37) and (107-111) loaded into HAGlu scaffolds to produce promising biomaterials as implants in fractures in older adults with type 2 diabetes.

Disclosures: Juan Antonio Ardura, None.

MO0168

Improving Parathyroid Hormone (PTH) Therapy In An Osteoporotic Mouse Model. Joseph Bidwell[1], Paul Childress*[2], Yu Shao[3], Selene Hernandez-Buquer[2], Yongzheng He[2], Daniel Horan[2], Alexander Robling[4], Stuart Warden[5], Feng-Chun Yang[4], Matthew Allen[1]. [1]Indiana University School of Medicine, USA, [2]Indiana University School of Medicine, USA, [3]Indiana University School of Medicine, USA, [4]Indiana University, USA, [5]Indiana University School of Health & Rehabilitation Sciences, USA

Nmp4/CIZ (Nmp4)-knockout (KO) mice have a normal skeletal phenotype but show an exaggerated response to anabolic parathyroid hormone (PTH). Despite unremarkable bone marrow (BM) and peripheral blood (PB) profiles, KO mice have elevated numbers of BM osteoprogenitors (CFU-F[Alk Phos+] and CD45-/CD105+/CD146+/nestin+ cells), BM CD8+ T cells, and a modest increase in CFU-GM cells, all of which drive PTH-induced bone anabolism. We asked whether the cellular profile and PTH-responsiveness persisted in an osteoporosis model. Wild type (WT) and KO mice were ovariectomized (ovx) at 12wks of age 4wks before therapy initiation (16wks-old, hPTH[1-34] 1μg/kg/day or vehicle). Endpoint parameters were obtained after 4wks (20wks-old) and/or 8wks (24wks-old) of treatment. MicroCT profiles included femoral bone volume/total volume (BV/TV) and connectivity density (Conn D). FACs was employed to obtain BM and/or PB profiles of osteoprogenitors, CD8+ and CD4+ T cells. Histomorphometry for mineralization apposition rate (MAR), mineralizing surface (MS/BS), and bone formation rate (BFR) were evaluated after 4wks of therapy. We employed a two-factor ANOVA for analyses using genotype and treatment as independent variables followed by a Tukey HSD post hoc test. The ovx WT and KO mice showed equivalent bone loss 4wks post-op as we previously reported. The KO mice exhibited a significantly enhanced PTH-induced gain in BV/TV and Conn D at the end of 4wks and 8wks therapies. There was no difference in these parameters between the vehicle-treated genotypes. PTH equally increased WT and KO MAR and BFR after 4wks therapy. The ovx KO mice had an elevated number of BM osteoprogenitors at the end of 4wks therapy but not at 8wks. The ovx null mice had augmented numbers of BM and PB CD8+ T cells compared to WT mice throughout treatment. The CD4+ T cells profiles were similar in both genotypes. PTH had no influence on the T cells with the exception of equally decreasing the number of WT and KO BM CD8+ T cells at 8wks. We conclude that the enhanced PTH response in *Nmp4*-KO mice persists with ovx perhaps sustained by the elevated numbers of osteoprogenitors and CD8+ T cells. This confirms that Nmp4 provides a novel therapeutic target for osteoporosis.

Disclosures: Paul Childress, None.

MO0169

Inactivation of Tgfbr2 in osteoclasts causes osteopenia due to impaired coupling of bone formation to bone-resorption. Megan Weivoda*[1], Ming Ruan[2], Christine Hachfeld[2], Larry Pederson[2], Rachel Davey[3], Jeffrey Zajac[4], Jennifer Westendorf[1], Sundeep Khosla[5], Merry Jo Oursler[1]. [1]Mayo Clinic, USA, [2]Mayo Clinic, USA, [3]University of Melbourne, Australia, [4]Austin Hospital, Australia, [5]Mayo Clinic College of Medicine, USA

In the adult skeleton, osteoclast-mediated bone resorption is coupled to osteoblast-mediated bone formation to maintain skeletal mass. While the pathways by which osteoblasts regulate osteoclast differentiation and activity are well established, the mechanisms by which osteoclasts recruit osteoblasts to sites of bone resorption remain unresolved. TGF-ß1 is enriched in the bone microenvironment and is released from the bone matrix during bone resorption. We recently reported that osteoclasts treated with TGF-β1 secrete factors that promote osteoblast migration and mineralization. Using a genetic mouse model, we tested the hypothesis that disrupting TGF-β receptor (Tgfbr) signaling in mature osteoclasts would impair the coupling of bone formation to bone resorption. Transgenic Ctsk promoter Cre mice were utilized to generate animals expressing dominant negative Tgfbr2 specifically in osteoclasts (Tgfbr2[OclKO]). Inactivation of Tgfbr signaling in osteoclasts led to significant reductions in bone mineral density in the spine and femur at 20 weeks of age. Mice were sacrificed at 22 weeks; *ex vivo* microCT analysis showed a significant decrease in bone volume per total volume and trabecular number, with an increase in trabecular spacing in Tgfbr2[OclKO] femurs. Histomorphometric analysis revealed no change in osteoclast number with inactivation of osteoclast Tgfbr signaling, and serum TRAP levels were unaltered. Of interest, osteoblast numbers were significantly reduced in Tgfbr2[OclKO] mice. Tgfbr2[OclKO] mice exhibited significantly decreased bone formation rate (BFR), and a significant decrease in serum P1NP. Mineral apposition rate was unchanged, indicating that the reduced BFR in Tgfbr2[OclKO] mice is due to reduced osteoblast number, rather than altered osteoblast function. Wnt1 is crucial to normal skeletal development. TGF-β1 caused a 100-fold increase in osteoclast Wnt1 expression *in vitro*. Immunohistochemistry for Wnt1 showed a significant reduction in osteoclast membrane Wnt1 in Tgfbr2[OclKO] femurs. These data show that impaired Tgfbr signaling in osteoclasts causes osteopenia by reducing osteoblast numbers and establish a novel paradigm in which TGF-ß stimulated osteoclasts are a key source of factors, such as Wnt1, that promote osteoblastic bone formation at sites of bone resorption.

Disclosures: Megan Weivoda, None.

MO0170

Intermittent PTH after Prolonged Bisphosphonate Treatment Improves Trabecular Bone Microarchitecture and Alleviates Bone Tissue Hypermineralization by Inducing Substantial New Bone Formation. Allison Altman*[1], Carina Lott[2], Wei-Ju Tseng[2], Chantal De Bakker[1], Sy-Dar Liou[2], Tiao Lin[1], Ling Qin[1], Xiaowei Liu[1]. [1]University of Pennsylvania, USA, [2]University of Pennsylvania, USA

Postmenopausal osteoporosis is often treated with bisphosphonates (BP), such as alendronate (ALN). However, long-term BP therapy may lead to hypermineralized bone tissue and atypical femoral fractures. Intermittent parathyroid hormone (PTH) therapy promotes bone formation and reduces tissue mineral density (TMD). We hypothesized that switching from ALN to PTH would improve trabecular bone microstructure and alleviate high TMD.

18 6-mo-old ovariectomized (OVX) rats (OVX at 4 mo-old) were assigned to 3 groups (n=6/group). The Veh+PTH group was treated with saline from wk 0 to 12 and then switched to PTH (40 μg/kg 5x/wk) from wk 12 to 16. The ALN group was treated with ALN (28 μg/kg 2x/wk) throughout wk 0 to 16. The ALN+PTH group received ALN for 12 wks followed by PTH for 4 wks. The right proximal tibia of each rat was scanned by *in vivo* μCT (VivaCT40, 10.5μm) to track changes in trabecular bone over time (Fig 1).

Bone volume fraction (BV/TV) was 0.13 ± 0.03 at wk 0 across all groups. From wk 0 to wk 12, the BV/TV decreased by 57% ($p < 0.001$) in Veh-treated rats. No bone was lost in ALN-treated rats. From wk 12 to 16, BV/TV increased 40% in the Veh+PTH group, 42% in the ALN+PTH group, and did not change in the ALN group ($p < 0.001$). The increase in BV/TV was accompanied by an increase in trabecular thickness (Tb.Th, 33% Veh+PTH and 25% ALN+PTH, $p < 0.001$). Structure model index (SMI) decreased by 10% and trabecular number (Tb.N) increased by 5% in the ALN+PTH group, indicating more plate-like trabeculae. In contrast, Veh+PTH had no change in SMI or Tb.N from wk 12 to 16. μCT-based *in vivo* dynamic histomorphometry showed a 4-fold increase in bone formation rate in the Veh+PTH group and 3-fold in the ALN+PTH group after 2 wks of PTH treatment. Serum osteocalcin in the Veh+PTH and ALN+PTH groups were 155% and 132% greater than the ALN group.

Left tibia (Tib) and lumbar vertebra L2 were scanned by ex vivo μCT (Tib-6μm, L2-3.5μm). TMD at the trabecular surface was lower in the ALN+PTH group than in the ALN group at both sites (4% p = 0.07, and 3% p < 0.001).

Our results suggest that intermittent PTH substantially stimulates new bone formation regardless of inhibited osteoclast resorption activities by prior treatment with BP. Pre-treatment with ALN may improve the skeletal response to PTH by promoting plate-like trabeculae. Moreover, switching to PTH after prolonged ALN treatment helped to alleviate hypermineralization of trabecular bone tissue.

Fig 1. Left: Registered comparison of tibia bone segments at each timepoint with treatment indicated by the arrows between time-points. Right: μCT-based *in vivo* bone dynamic histomorphometry, green indicates areas of new bone (formation), and red indicates lost bone (resorption).

Fig 1

Disclosures: Allison Altman, None.

MO0171

Osteolineage Jagged1 maintains bone homeostasis by regulating osteoblast and osteoclast. <u>Rialnat Lawal</u>*[1], <u>Mary Georger</u>[2], <u>Alexandra Goodman</u>[2], <u>Laura Calvi</u>[3]. [1]University of Rochester Medical Center, USA, [2]University of Rochester, USA, [3]University of Rochester School of Medicine, USA

Notch signaling maintains the progenitor compartment of both osteoblasts and osteoclasts, however a critical Notch ligand in osteoblastic cells is unknown.The Notch ligand Jag 1 is present in osteoblastic cells, where its expression peaks coincidentally with osteocalcin.To determine if osteolineage Jag1 is the critical ligand maintaining the balance of osteoprogenitors and mature bone cells, we examined mice with osteolineage Jag1 deletion (Prx1-cre;Jag1fl/fl: PJ1ko mice). In 2 week old PJ1ko and wildtype (wt) mice there were no skeletal differences by μCT, indicating that osteolineage Jag1 is not required for bone modeling.We next examined 2 month old mice, where lack of osteolineage Jag 1 increased trabecular bone, trabecular number and trabecular thickness by μCT (BV/TV:0.3633 $\pm$ 0.03165 N=5 vs. 0.4996 $\pm$ 0.04582 N=5 Wt.vs.KO p=0.0400). Quantification of osteoprogenitors by colony forming unit osteoblast (CFU-OB) assay in limiting dilution demonstrated a significant decrease in CFU-OB in PJ1ko mice compared to wt. Conversely, the mature osteoblast pool was increased, as shown by increased osteocalcin+ cells by IHC and increased osteocalcin expression by qRT-PCR in osteoblastic cells (1.011 $\pm$ 0.1904 N=9 vs. 1.786 $\pm$ 0.2314 N=7 Wt.vs.KO p=0.0206). Since an increase in BV/TV could also be due to decreased osteoclastic cell numbers and/or function, we examined bone resorption and found that marrow CTX was increased significantly in PJ1ko compared to wt (0.7168 $\pm$ 0.1034 N=6 vs. 1.514 $\pm$ 0.1851 N=5 Wt. vs. KO p=0.0034), while TRAP+ staining multinucleated cells in the metaphyseal region were not increased, suggesting that Jag1 regulates osteoclast function. These data indicate that during peak bone formation Jag1 is a critical Notch ligand, which maintains trabecular bone volume by restricting osteoblastic differentiation, preserving progenitor pools and limiting excess osteoclast function. Since in mice lacking osteolineage Notch signaling the initial bone was succeeded by significant bone loss at 6 mons, we examined PJ1ko and wt at 6-8 mons and found no significant changes in trabecular bone mass. Therefore, loss of Jag1 increases trabecular bone during active skeletal remodeling by enhancing the differentiation of osteoblasts in spite of increased osteoclastic function without age-dependent bone loss by 6-8 mons. These observations may provide a Notch ligand-specific therapeutic strategy for achieving increased bone mass without adverse bone loss.

Disclosures: Rialnat Lawal, None.

MO0172

Sost Antibody Treatment Improves Fracture Healing in Type 1 Diabetes. <u>Cristal Yee</u>*[1], <u>Liqin Xie</u>[2], <u>Deepa Murugesh</u>[3], <u>Sarah Hatsell</u>[4], <u>Aris Economides</u>[5], <u>Gabriela Loots</u>[6], <u>Nicole Collette</u>[7]. [1]University of California, Merced, USA, [2]Regeneron Pharmaceutical company, USA, [3]Lawrence Livermore National Laboratory, USA, [4]Regeneron Pharmaceuticals, USA, [5]Regeneron Pharmaceuticals, Inc., USA, [6]Lawrence Livermore National Laboratory, UC Merced, USA, [7]Lawrence Livermore National Laboratory, USA

Type 1 diabetes mellitus (T1DM) patients suffer from low bone mass, increased fracture risk, and impaired fracture healing due to reduced osteoblast activity. Available treatments can improve bone mineral density (BMD) in T1DM, however, no treatment can adequately restore the fracture healing phenotype. Since over 8% of the US population suffers from T1DM, a great need exists to explore new opportunities to treat orthopedic complications. Sclerostin (*Sost*), a Wnt antagonist, is secreted by osteocytes and inhibits bone formation. *Sost* knockout mice (*Sost KO*) have 3X higher BMD than normal and enhanced fracture healing due to increased Wnt signaling. Hematoxylin and Eosin (H&E) stained paraffin sections of STZ treated *Sost KO* calluses at 21 days post fracture showed enhanced bony bridging compared to *WT* (C57Bl6/J) and *STZ* calluses, confirming the likely positive effects of SostAb treatment in T1DM fracture healing. We hypothesized that elevated Wnt signaling imparted *via* pharmacologic inhibition of Sost with a blocking anti-Sost antibody (SostAb) can improve repair of difficult fractures in Streptozotocin (STZ)-induced T1DM mice. Mid-femoral fractures were generated in a closed Einhorn model and SostAb (25 mg/kg) was administered twice weekly up to 21 days post-fracture (*sham control, STZ, sham+SostAb,* and *STZ+SostAb* groups). MicroCT analysis at 21 days post fracture showed *STZ* calluses had a significant ~50% decrease in total volume (*p*-value 0.0155) in comparison to *sham control,* consistent with delayed healing. Histologically, there was less bridging and woven bone in *STZ* compared to *sham control* calluses, suggesting that *STZ* calluses are smaller with less mineralized bone, similar to published reports of poor osteogenesis. Bone volume/total volume ratios at 21 days post fracture showed that *STZ+SostAb* calluses had significantly increased mineralized bone relative to both *sham control* and *STZ* groups (*p*-value < 0.0008), suggesting that SostAb treatment is able to rescue the reduced osteogenesis caused by T1DM through a mechanism different from glucose regulation. Further analysis at 42 days post-fracture will determine the long term effects of SostAb on diabetic fractures. Our results suggest that SostAb may potentially help heal problematic fractures associated with T1DM.
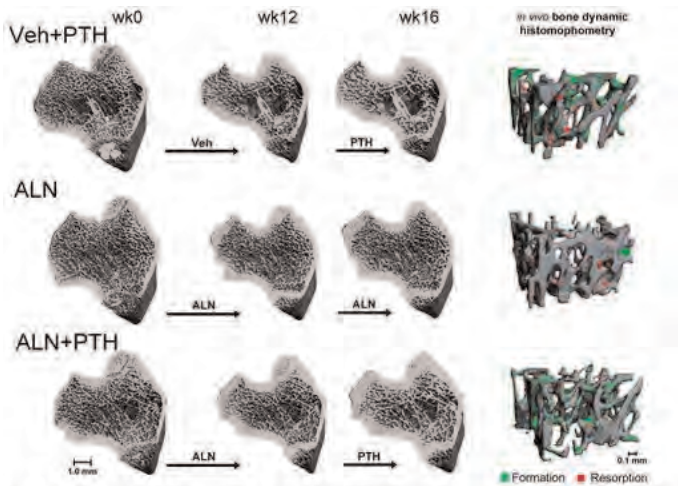
Disclosures: Cristal Yee, None.
This study received funding from: LDRD 11-ERD-060

MO0173

The P2X7 Antagonist AFC-5261 rescues Ovariectomy-induced Bone Loss in Mice. <u>Susanne Syberg</u>*[1], <u>Ankita Agrawal</u>[2], <u>Solveig Petersen</u>[3], <u>Jens-Erik Beck Jensen</u>[4], <u>Peter Schwarz</u>[5], <u>Alison Gartland</u>[6], <u>Michael Bös</u>[7], <u>Niklas Jorgensen</u>[8]. [1]Research Centre for Ageing & Osteoporosis, Denmark, [2]The Mellanby Centre for Bone Research, The University of Sheffield, United Kingdom, [3]Research Centre for Ageing & Osteoporosis, Departments of Diagnostics & Medicine, Copenhagen University Hospital Glostrup, Denmark, [4]Department of Endocrinology, Copenhagen University Hospital Hvidovre, Denmark, [5]Glostrup Hospital, Denmark, [6]The Mellanby Centre for Bone Research, The University of Sheffield, United Kingdom, [7]Affectis Pharmaceuticals AG, Fraunhoferstrasse 13, Germany, [8]Copenhagen University Hospital Glostrup, Denmark

The regulatory role of the purinergic receptor P2X7 in bone metabolism is well known, but the effects in bone of pharmacologic modification of P2X7 receptor function in animal models has not yet been reported. Aim: To investigate the influence of a P2X7 receptor antagonist, AFC-5261 (N-[4-Chloro-1-(2-hydroxyethyl)-1H-indol-3-yl]-2-cyclohexylacetamide) on bone cell function and its therapeutic potential in a murine model for osteoporosis (ovariectomy (OVX)-induced bone loss). Method: Primary osteoblasts and osteoclasts were isolated from mice, rat and humans and cultured with AFC-5261 for determination of gene expression of osteoblast markers, ability to produce mineralized bone matrix (AR-S) or perform resorption pits on dentine discs. To evaluate the effect of AFC-5261 in the murine OVX model we measured bone strength, analyzed serum bone markers and performed DXA on female BALB/cJ mice either OVXed or sham-operated. The OVXed animals were treated twice daily with vehicle (PEG) or AFC-5261 (400 mg/kg/day) for four weeks.

Results: *In vitro*, the bone formative activity of the individual osteoblast was stimulated by AFC-5261 in all three species. murine osteoblasts deposited mineralized matrix corresponding to 477.8 nmol Ca^{2+}/well when treated with AFC-5261 (125 nM) compared to 272.1 nmol Ca^{2+}/well in control cultures (p=0.002). AFC-5261 (500 nM) increased gene expression of Runx2 (2.7 fold, p<0.001), ALP (1.7 fold, p=0.004), collagen (2.2 fold, p=0.005) and OPG up to 4.0 fold (p<0.001) in trabecular derived human osteoblastic cells. In opposite, RANKL expression was decreased to a third of the level in control cultures (p=0.022). In murine osteoclast cultures AFC-5261 (400 nM) reduced the area resorbed with 58.5 % (p<0.001), without affecting the number of osteoclasts. *In vivo* BMD increased in the group treated with AFC-5261 to 0.0513 from 0.0488 g/cm² (p=0.016) and bone strength was increased at femoral neck from 12.6 to 19.4 N (p<0.001), but not at femoral midshaft (from 22.3 to 22.2 N, p=0.359). AFC-5261 induced bone formation as an increase was seen in both ALP (from 77.7 to 110.0 nmol/ml, p<0.001) and P1NP (from 1.18 to 2.32 ng/ml, p<0.001), while bone resorption (CTX-I) was reduced (from 21.9 to 14.9 ng/ml, p<0.001). Conclusion: AFC-5261 was shown anabolic and anti-resorptive both *in vitro* and *in vivo*. Further studies are necessary in order to determine the potential effects of AFC-5261 on the regulation of human bone metabolism.

Disclosures: Susanne Syberg, None.

MO0174

The Sirtuin1 Activator SRT3025 Down-regulates Sclerostin in Vivo and in Vitro and rescues OVX-induced bone loss and biomechanical deterioration in mice. <u>Hanna Artsi</u>[1], <u>Einav Cohen-Kfir</u>[2], <u>Irina Gurt</u>[1], <u>Yankel Gabet</u>[3], <u>Ron Shahar</u>[4], <u>Teresita Bellido</u>[5], <u>Rivka Dresner-Pollak</u>*[6]. [1]Hadassah-Hebrew University Medical Center, Israel, [2]HEBREW UNIVERSITY Medicine Faculty, Israel, [3]Department of Anatomy & AnthropologySackler Faculty of Medicine, Israel, [4]The Hebrew University, Israel, [5]Indiana University School of Medicine, USA, [6]Hadassah-Hebrew University Medical Center, Israel

Estrogen deficiency leads to rapid bone loss and skeletal fragility. Sclerostin, encoded by the *sost* gene, is a negative regulator of bone formation, and blocking its action increases bone mass and strength in animals and humans. Sirtuin1 (Sirt1), a major player in aging and metabolism, regulates bone mass and was shown by us to inhibit *sost* gene expression by deacetylating histone 3 at its promoter (*Endocrinology; 152:4514-4524, 2011*). These findings prompted us to ask if activation of Sirt1 by a synthetic Sirt1-activating compounds (STAC), previously shown to be allosteric activator of Sirt1, can down-regulate sclerostin and reverse ovariectomy (OVX)-induced bone loss and biomechanical deterioration.

Nine-week-old C57BL/6 female mice underwent OVX or SHAM operation and were left untreated for 6 weeks to allow bone loss. SRT3025 at 50,100 mg/kg/day or a vehicle was administered daily by gavage to OVX mice for 6 weeks. Upon sacrifice L4 and one femur were analyzed by microCT, and the 3 point bending test was conducted in the other femur. Trabecular and cortical bone histomorphometry analyses were conducted. Bone markers were determined in serum 1, 6, 9 weeks post OVX. Protein was isolated from whole tibiae extracts. Serum drug levels and uterine weight were determined.

Ovariectomy induced a a rapid bone loss accompanied by a substantial decrease in tibial Sirt1 protein level accompanied by increased sclerostin. SRT3025 administration fully reversed the deleterious effects of ovariectomy on vertebral bone mass, micro-architecture and femoral biomechanical properties-stiffness and the material's Young's modulus of elasticity. Treatment with SRT3025 decreased tibial sclerostin expression and increased femoral cortical periosteal mineralizing surfaces as well as serum P1NP but not CTX, allowing for an anabolic window. In MLO-Y4 osteocyte-like cells SRT3025 down-regulated sclerostin and inactive beta-catenin while a reciprocal effect was observed with EX-527, a Sirt1 inhibitor.

Sirt1 activation by a sirtuin1 activating compound is a potential novel pathway to down-regulate sclerostin and design anabolic therapies for osteoporosis concurrently ameliorating other metabolic and age-associated conditions.

Disclosures: Rivka Dresner-Pollak, None.

MO0175

Effect of Green Tea on Socket Repair of Rats Treated with Bisphosphonates. <u>Mariza Matsumoto</u>*[1], <u>Alana Santos</u>[2], <u>Angelica Fonseca</u>[2], <u>Roberto Kawakami</u>[2], <u>Edson Mada</u>[2], <u>Fernando Neves</u>[2], <u>Patrícia Saraiva</u>[2]. [1]Sagrado Coração University, Brazil, [2]Sagrado Coração University, Brazil

A number of systemic disturbances can lead to bone remodeling imbalance demanding treatment with drugs such as bisphosphonates (BP). Due to the popularity of green tea because of its anti-oxidant activity and also on bone tissue, the aim of this study was to evaluate its effects in association with a nitrogenate BP on socket healing repair. Sixty male albinus Wistar rats were divided in 3 groups, according to the treatment: Group C – Control, animals treated with endovenous (EV) 0.9% saline solution, Group GT – treated with 1% green tea in drinking water, Group BP – treated with EV zoledronic acid, and Group BP + GT – treated with EV zoledronic acid and 1% green tea. It was administered 0.035mg/Kg of the drug, every two weeks.

After six weeks of the beginning of the BP administration, right upper molars were extracted, and the green tea started to be offered for Groups GT and BP+GT. After 7, 14, and 28 days the animals were euthanized and the maxillas removed for histological analysis. No significant differences were observed among the groups at day 7 when the extraction site was still exposed, with any mucosal coverage. At day 14, while Group C presented granulation tissue inside the sockets, the other groups presented non-viable bone tissue still exposed, covered by a thick layer of bacterial biofilm. At day 28, Group C the extraction site was predominantly covered by the mucosa and primary bone could be seen inside the sockets around a focus of granulation tissue. Specimens from Group GT still presented exposed sockets, covered by biofilm; however, osteoblastic activity resulting in primary bone formation could be seen in the third apical of the socket and granulation tissue in the middle third. Groups BP and BP + GT were very similar, showing thick biofilm covering and invading non viable bone tissue, which was still exposed, associated with neutrophilic infiltrate. An epithelial bridge could be seen under the infected bone fragment coming from the adjacent mucosa. The newly formed bone in deep regions was marked by strong basophilic reversal lines, and evident osteocytes lacunae. Eventual osteoclastic activity was observed when using the BP. From the microscopic morphological results, the association of the green tea had no beneficial effects on socket healing in rats under BP administration.

Disclosures: Mariza Matsumoto, None.

MO0176

Effects of Risedronate, Alendronate and Minodronate in Combination with Eldecalcitol in Ovariectomized rats. <u>Hirotaka Wagatsuma</u>*[1], <u>Tetsuo Yano</u>[2], <u>Mei Yamada</u>[2], <u>Daisuke Inoue</u>[3]. [1]Ajinomoto Pharmaceuticals Co., Ltd., Japan, [2]Ajinomoto Pharmaceuticals Co., LTD, Japan, [3]Teikyo University Chiba Medical Center, Japan

Background/Aim: Eldecalcitol (ELD) is a derivative of calcitriol with antiresorptive activity. Although evidence suggests that combined treatment with active vitamin D3 and some bisphosphonates (BPs) is clinically beneficial, combination therapy with ELD and BP has not been validated in the clinical setting. Preclinical studies have shown that simultaneous treatment with ELD and BP is more effective in increasing bone mineral density (BMD) and bone strength than monotherapy. However, relative potency of various BPs, when used in combination with ELD, remains unknown. In this study, we examined effects of treatment with risedronate (RIS), alendronate (ALN) and minodronate (MIN) in combination with ELD on bone mass, microarchitecture and strength in ovariectomized (OVX) rats.

Methods: Female Sprague Dawley rats at 13 weeks old were divided into one sham-operated and eight OVX groups (1: vehicle, 2: RIS, 3: ALN, 4: MIN, 5: ELD, 6: RIS+ELD, 7: ALN+ELD, 8: MIN+ELD). RIS (0.07 µg/kg s.c.), ALN (0.14 µg/kg s.c.), MIN (0.014 µg/kg s.c.) and ELD (0.004 µg/kg p.o.) were given 5 times per week for 16 weeks. Then BMD and bone architecture of the 4th lumbar vertebrae (L4) and the femur were measured by micro-CT, and bone mechanical strength was evaluated by three-point bending of the femur and axial compression of the L4.

Results: Trabecular BMD in the L4 was significantly increased in RIS+ELD, ALN+ELD and MIN+ELD by 56%, 60% and 62%, respectively, compared with the vehicle group. Cortical BMD and connectivity density in the L4 of all BP+ELD combination groups were also significantly increased compared with the vehicle group. On mechanical testing of the L4, the maximum load was significantly decreased in the vehicle group compared with the sham group, and significantly increased in RIS+ELD and ALN+ELD by 59% and 55%, respectively, compared with the vehicle group. MIN+ELD showed a 44% increase without statistical significance. In the femur, every combination therapy significantly improved trabecular BMD and architecture compared with the vehicle group, but no significant inter-group differences were observed in cortical bone mass, architecture and bone strength.

Conclusions: Treatment of RIS, ALN and MIN in combination with ELD improved BMD and bone structural properties to approximately the same extent. And at least RIS and ALN improved bone strength as well. These results suggest that combination therapy of BP and ELD is valid, and further warrant clinical trials.

Disclosures: Hirotaka Wagatsuma, None.

MO0177

Intermittent interleukin-10 administration prevents early radiation- and combined trauma-induced bone loss by altering RANKL/OPG and Sclerostin. <u>Joshua Swift</u>*[1], <u>Aminul Islam</u>[2], <u>William Danchanko</u>[3], <u>Min Zhai</u>[2], <u>Joan Smith</u>[2], <u>Rossitsa Owens</u>[2], <u>Juliann Kiang</u>[2], <u>Sibyl Swift</u>[1], <u>Matthew Allen</u>[4]. [1]Armed Forces Radiobiology Research Institute, USA, [2]Armed Forces Radiobiology Research Institute, USA, [3]Uniformed Services University of the Health Sciences, USA, [4]Indiana University School of Medicine, USA

Ionizing radiation, when combined with another trauma (i.e. skin wounding), accelerates and prolongs radiation-induced bone loss for at least 120 days post-exposure. These effects arise from early and sustained increases in bone resorption and prolonged suppression of osteoblast activity. The purpose of this study was to determine the efficacy of interleukin-10 (IL-10), an anti-inflammatory cytokine and

potent inhibitor of osteoclastogenesis, to mitigate or prevent negative alterations in bone due to radiation and/or radiation combined with skin wounding (combined injury; CI). Female B6D2F1/J mice (16-wk-old) were exposed to a either a sub-lethal dose of 8 Gy γ radiation (RI) or 0 Gy (SHAM) followed by skin wound (W and CI only), and administered either IL-10 (15 ng/d, s.c.) or an equal volume of sterile saline (VEH; 0.2 mL) 3x/wk for 7 or 30 days. RI significantly lowered distal femur cancellous bone volume fraction (BV/TV; -35% vs. SHAM), trabecular thickness (Tb.Th; -8%), and trabecular number (Tb.N; -29%) by Day 7, which continued to decline through Day 30. CI resulted in similar alterations in bone microarchitecture as RI on Day 7, however these changes were exacerbated by Day 30 (BV/TV: -54% vs. SHAM; Tb.N: -40%). IL-10 treatment after RI and CI resulted in greater BV/TV (+15-16%), Tb.Th (+5%), and Tb.N (+10%) vs. VEH treated mice on Day 7; CI+IL-10 mitigated reductions in BV/TV (+15% vs. VEH) on Day 30. RI and CI significantly reduced mid-diaphysis femur ultimate force (-8% and -19% vs. SHAM, respectively) on Day 7, which was restored by IL-10 administration (+12% and +19% vs. VEH). CI resulted in greater bone tissue concentration (measured by ELISA) of RANKL (+67%), sclerostin (+181%) and RANKL/OPG ratio on Day 7 vs. SHAM. IL-10 treatment after CI reduced RANKL (-68% vs. VEH) and sclerostin (-47%), increased OPG (+52%), and lowered RANKL/OPG on Day 7. On Day 30, increased bone concentrations of RANKL and sclerostin, and reductions in OPG persisted after CI and RI, which were not affected by IL-10 treatment. IL-10 treatment attenuated reductions in cancellous BFR (-40% vs. SHAM) after RI and CI by Day 7 but not Day 30. These data demonstrate the potential involvement of RANKL-OPG signaling in bone loss after irradiation and combined trauma. Furthermore, although IL-10 effectively inhibits early negative effects on bone after these traumas, there does not appear to be a long-term beneficial effect of IL-10 treatment for bone health.

Disclosures: Joshua Swift, None.

MO0178

Orally Administered Bisphosphonates Alleviate Colonic Inflammation and Bone Loss in a Mouse Model of Acute Colitis. Maria K. Tsoumpra*[1], Hans-Anton Lehr[2], F. Hal Ebetino[3], Jeffrey D. Neighbors[4], R Graham Russell[5], Sylvie Ferrari-Lacraz[6], Serge Ferrari[7]. [1], Switzerland, [2]Institute of Pathology, Medicine Campus Bodensee, Germany, [3]Structural Genomics Consortium, Oxford University, United Kingdom, [4]Terpenoid Therapeutics Inc., USA, [5]University of Oxford, United Kingdom, [6]Departments of Paediatrics & Internal Medicine & the Transplantation Immunology Unit, Geneva University Hospital, Switzerland, [7]Geneva University Hospital & Faculty of Medicine, Switzerland

Inflammatory bowel diseases arise by altered immune responses to enteric antigens and are characterized by progressive extra-intestinal manifestations that may compromise the quality of life of patients. Bisphosphonates (BPs) may hinder the activation of pro-inflammatory signaling pathways and have been shown to improve bone mineral density (BMD) in colitis animal models. To examine this further, we have evaluated the effects of two novel lower bone affinity BPs, OX14 and digeranyl bisphosphonate (DGBP), on colonic inflammation and bone loss in a mouse colitis model induced by dextran sulfate sodium (DSS) using risedronate (RIS) as a comparator. OX14 has similar anti-resorptive potency to RIS and strongly inhibits farnesyl diphosphate synthase, whereas DGBP selectively inhibits geranylgeranyla-tion. Mice (n=6/group) received RIS or DGBP (25 mg/kg/day) or OX14 (12.5 mg/kg/day) or PBS (control) via oral administration for 10 days, as well as 2% DSS in their drinking water from day 3 onwards. Bone turnover, architecture and mass were evaluated by serum CTX quantification, micro-computed tomography and DXA respectively. The severity of colitis was assessed by blood in stool, body weight and colon length and histology at sacrifice. The anti-inflammatory response was assessed by qPCR on colonic RNA and FACS analysis of bone marrow cells. RIS and OX14 lowered the CTX levels (8.12 ng/ml in RIS, 9.91 ng/ml in OX14 vs 20.38 ng/ml in DGBP, 24.42 ng/ml in control, p<0.001) and increased the bone volume fraction at the distal femur metaphysis (9.92% in RIS, 9.65% in OX14 vs 6.62% in control, p<0.01). All BPs tested attenuated bone loss in the spine but RIS also increased the femur and body BMD. At sacrifice, colon length was non-significantly greater in OX14 and DGBP treated mice (75 mm in OX14, 72 mm in DGBP vs 68.2 mm in RIS, 65.8 mm in control, ns), in agreement with the histological scoring of decreased inflammation (0 in OX14, 2.5 in DGBP vs 3.3 in RIS, 5 in control, ns). RIS enhanced the expression of the anti-inflammatory cytokine IL10 and decreased the percentage of monocytic and osteoclast progenitors, while OX14 decreased the TNF and IFNγ levels. Collectively, the data indicate that the novel BPs were more potent modulators of local colonic inflammation while RIS better preserved BMD, consistent with its higher affinity for bone. Interestingly, the ability of DGBP to attenuate colonic inflammation was independent of its modest anti-resorptive potency.

Disclosures: Maria K. Tsoumpra, None.
This study received funding from: Warner Chilcott Pharmaceuticals, Dundalk, Ireland

MO0179

Targeting osteoclast sealing zone to prevent bone degradation while maintaining bone formation: *in vivo* proof of concept with a small chemical compound. Anne Blangy*[1], Virginie Vives[2], Gaelle Cres[2], Christian Richard[2]. [1]CNRS CRBM Montpellier University, France, [2]CNRS CRBM Montpellier University, France

Current anti-osteolytic medical treatments target osteoclast survival and differ-entiation. But molecules secreted by the osteoclast or clastokynes are essential to stimulate bone formation by osteoblasts. Suppression of osteoclasts blunts bone turnover, which is suspected to increase the risk of atypical fractures in the long term. A solution to overcome this would be to develop novel therapeutic strategies that target selectively the bone-resorbing activity of osteoclasts without affecting their survival or differentiation.

To reach this goal, we propose here to specifically target the organization of podosomes in osteoclasts. Preventing sealing zone formation by affecting podosome patterning impairs the acidification of the extracellular medium by osteoclasts and renders bone resorption ineffective. We report here the *in vivo* proof of concept that this approach allows to protect against bone resorption while preserving bone formation.

As a model we used C21, a small chemical compound inhibitor of Rac activation by Dock5, which is essential for sealing zone formation. We show here in cultured osteoclasts that C21 destabilizes podosomes organization rapidly and reversibly. We further used C21 in three established mouse models of pathological bone loss: post menopause osteoporosis, rheumatoid arthritis and bone metastases. We demonstrate that administration of C21 efficiently protected mice against bone loss in those three models and that this had no noticeable adverse effect in the mouse. Most interestingly, bone formation parameters (MS/BS, MAR and BFR/BS) were not affected by C21, while they were severely diminished in mice treated with Alendronate.

Our results provide the proof of concept that a chemical compound that destabilizes podosome organization in osteoclasts efficiently protects against pathological bone loss without affecting bone formation. Our findings open new avenues to develop innovative strategies for the treatment of osteolytic bone diseases.

Disclosures: Anne Blangy, None.

MO0180

Ablation of Tak1 in monocyte leads to defects in skeletal growth and bone remodeling in mice. Huihuan Liu*[1], Bing Qi[2], Qian Cong[1], Ping Li[1], Micheal Schneider[3], Baojie Li[4]. [1]The Bio-X Institutes, Key Laboratory for the Genetics of Developmental & Neuropsychiatric Disorders, Ministry of Education, Shanghai Jiao Tong University, China, [2]School of Biological Science, Taishan Medical University, China, [3]Cardiovascular Science National Heart & Lung Institute, United Kingdom, [4]Shanghai Jiao Tong University, Peoples Republic of China

Tak1 is a MAPKKK that can be activated by TNFa, RANKL, TGFb, and BMPs. It forms a complex with Tab2 and Tab3 and activates the downstream NF-kB and JNK/p38 MAPK pathways. Tak1 is essential for mouse embryonic development and plays critical roles in homeostasis of tissue such as liver, cartilage, and the immune system. Previous studies have implicated Tak1 as a positive regulator of osteoclastogenesis, yet there lacks a mouse model to study the function of Tak1 in bone remodeling, as mature osteoclast-specific Tak1 deletion resulted in runtedness, postnatal lethality, and severe osteopetrosis, phenotypes that were not even observed in RANK or RANKL deficient mice. Here we generated monocyte-specific Tak1 knockout mice and found that these mice show normal body weight, limb size, and fertility, and osteopetrosis with severity level close to that of RANK or RANKL deficient mice. Mechanistically, Tak1 deficiency altered the signaling of NF-kB, p38MAPK, and Smad1/5/8 and the expression of transcriptional factors required for osteoclastogenesis including PU.1, MITF, c-Fos, and NFATc1, suggesting that Tak1 regulates osteoclast differentiation at multiple stages via multiple signaling pathways. Moreover, the Tak1 mutant mice also showed skull overgrowth, an increase in articulate cartilage thickness, and an increase in the number of mesenchymal stromal/stem cells in vivo. Ex vivo Tak1-/- monocytes also showed enhanced ability in promoting osteogenic differentiation of mesenchymal stromal cells. These findings indicate that Tak1 functions in osteoclastogenesis in cell-autonomous manner and in osteoblastogenesis and chondrogenesis in non-cell-autonomous manners.

Disclosures: Huihuan Liu, None.

MO0181

Biglycan and fibromodulin deficiency leads to increased bone remodeling that can be rescued by exogenous osteoprotegerin. <u>Vardit Kram</u>*[1], <u>Tina Kilts</u>[2], <u>Kenn Holmbeck</u>[2], <u>Marian Young</u>[1]. [1]National Institutes of Health, USA, [2]NIH/NIDCR, USA

Biglycan (bgn), a class I SLRP, is highly expressed in bone and cartilage and has been shown to play an important role in the proliferation, survival and differentiation of osteoblasts, acting as a positive regulator of bone formation and bone mass. Fibromodulin (fmod), a class II SLRP is also highly expressed in the skeleton, but its function in bone is unclear. In order to examine the combined roles of bgn and fmod in mineralized tissue, double-deficient mice, lacking both *bgn* and *fmod* (*bgn-/0; fmod-/-* DKO) were generated. These mice are smaller in size compared to WT, and have reduced bone mass, detectable as early as 3 weeks of age, which becomes more pronounced with age. Morphological differences in femoral bone of DKO mice were observed, which may be the result of abnormal shear forces due to weak tendons and mis-articulation of joints, leading to impaired gait. These mice also develop early onset osteoarthritis as well as ectopic bone formation and tendon ossification. Dynamic histomorphometry showed that the low bone mass phenotype was not the result of decreased bone formation, as the bone formation rate (BFR) of DKO mice was not significantly different from that of WT littermates, implying that the low bone mass was not due to defective osteoblast proliferation or action. Both *in vivo* and *in vitro*, TRAP staining indicated that the DKO mice had increased osteoclast number and activity. Since neither bgn nor fmod is made by osteoclasts, and because decreased levels of the RANKL decoy receptor, osteoprotegerin (opg), which is made by BMSCs and decreased in the serum of the DKO mice, we concentrated on opg as a potential mediator of the increased osteoclast number seen in the DKO mice. Long-term (6 weeks) injections of both WT and DKO mice with rat opg-Fc, a truncated form of opg consisting of the RANKL binding site of opg fused to the Fc domain of IgG, showed it was able to cure the age-related bone loss in the DKO mice, bringing the bone mineral density (BMD) and bone mineral content (BMC) of the DKO mice to comparable levels of the WTs. Thus, while the DKO produce and accumulate less opg, they are able to respond to it when added exogenously. Considering that SLRPs have previously been shown to have roles in binding and regulating extracellular components in bone, we speculate that bgn and fmod may control osteoclast differentiation by potentially mediating the stability and storage of opg in the ECM compartment of mineralized tissue.

Disclosures: Vardit Kram, None.

MO0182

Bone Quality Changes in The Streptozocin-induced Diabetes Rat and The Effect of Zoledronic Acid Through Up-regulating The Expression of The Osteogenic Genes. <u>Lingzhi Yu</u>*[1], <u>Min Cui</u>[2], <u>Jing Sun</u>[3]. [1]"shandong University ,jinan Central Hospital", , [2]Shandong University,Jinan Central Hospital, China, [3]Binzhou Medical college,affiliated Hospital, China

Aims:To evaluate the bone quality and the osteogenes changes and the short term effect of zoledronic acid (ZOL) on bone remodeling in the streptozotocin (STZ) induced diabetes rats.Methods:One hundred and twenty female Wistar rats aged 8-10 weeks were randomly divided into four groups: C, D, Z-I and Z-II. C was the control group. Rats in group D were suffered streptozotocin-induced diabetes. Those in group Z-I and Z-II received a bolus injection of zoledronic acid (0.1mg/kg) at the onset of diabetes and 2 weeks later, respectively. Rats were sacrificed at 1, 2, 3, 4 and 5 weeks after diabetes onset. The serum osteocalcin (OC), bone alkaline phosphatase (BALP) and tartarate-resistant acid phosphatase (TRAP) were measured. Real–time PCR and western blot were performed to detect the expression of the mRNAs and their proteins of bone morphogenetic proteins 2 (BMP-2), Runx-2, Osterix and Noggin on the right femur metaphysis. The left femurs were used to measure the bone mineral density (BMD) and the mechanical resistance test. The bone histomorphology of left tibiae were observed.Results: Rats in group D displayed significantly lower serum BALP and OC, higher serum TRAP levels. ZOL administration showed restorative effect on BALP and OC. The expression of Runx-2 and Osterix mRNA in group D had regulated down since the 1st week and BMP-2 mRNA since the 2nd week. Z-I treatment could completely reverse the result. However group Z-II showed only a transient reversing effect on the 4th week and could not be sustainable. The expression of Noggin mRNA regulated up continuously in group D. But the reducing influences began to show until the 4th week both in group Z-I and Z-II. The protein expressions of BMP-2, Runx2 and Osterix in group D lowered at the 5th week to about 64%, 71% and 57% respectively of the control level, while those in group Z-I were obviously

higher than all the other groups include Z-II, which was also higher than those of group D. Contrary, Noggin protein expression regulated up markedly than the control level and only Z-I treatment showed a slightly decrease. On the 5th week in group D, the BMD decreased. Z-I treatment restored the alterations. The same trend was observed in Z-II group. Conclusions:Zoledronic acid could prevent the osteopenia. The underlying mechanisms might be associated with its effects of increasing the expression of BMP-2, Runx-2 and Osterix, inhibition of the expression of Noggin.Keywords: Bisphosphonates, diabetic osteoporosis
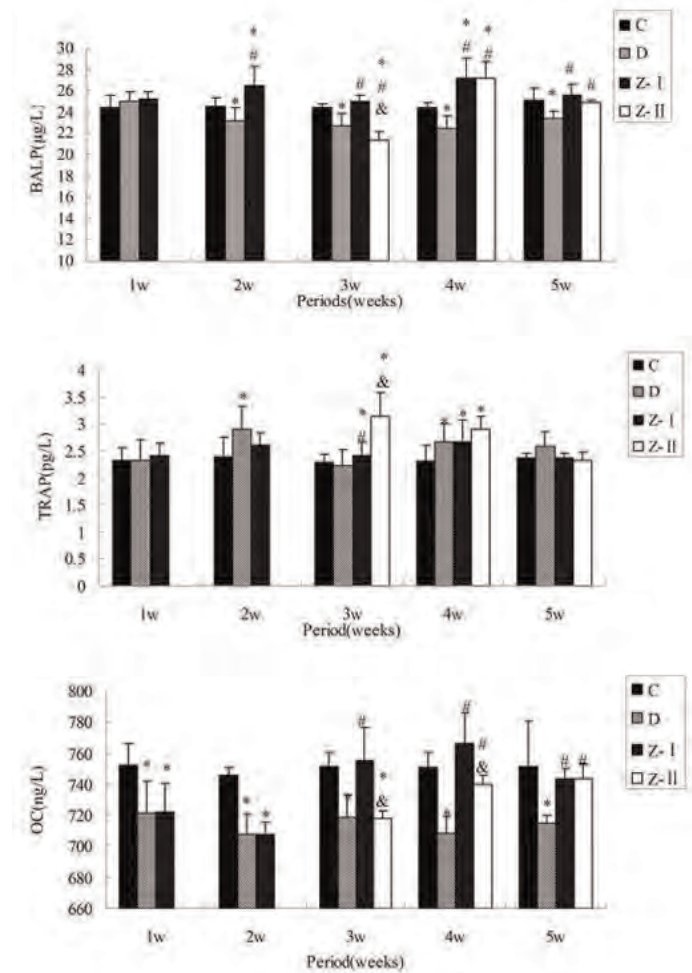

Fig 1 At 1,2,3,4 and 5 weeks after the onset of diabetes, serum OC, BALP and TRAP were determiner as described in Material and methods. Values are the mean±SD .*Significantly different from the control value (P<0.05). # Significantly different from the diabetes (P<0.05). & Significantly different from the Z-I group (P<0.05).
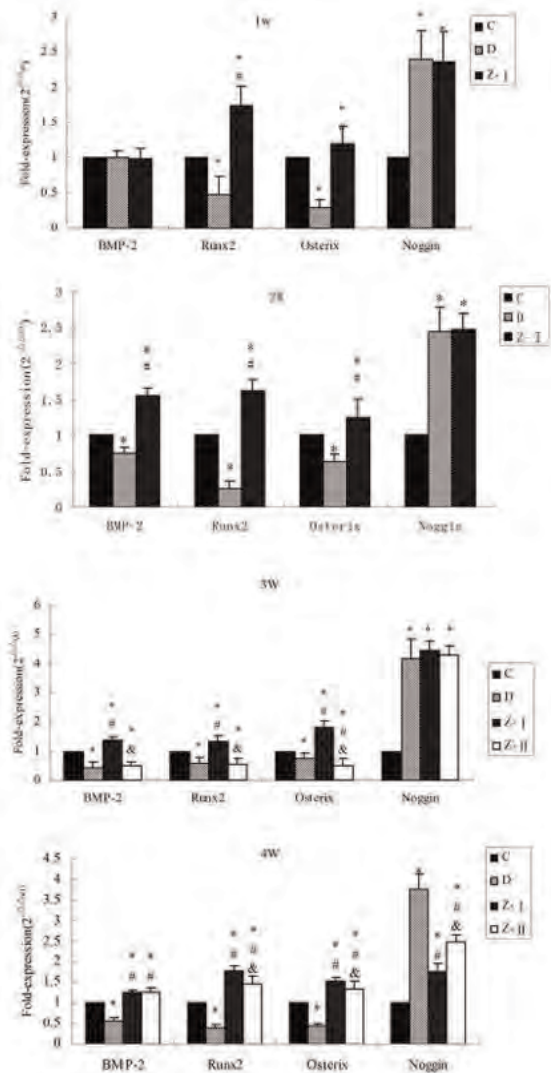
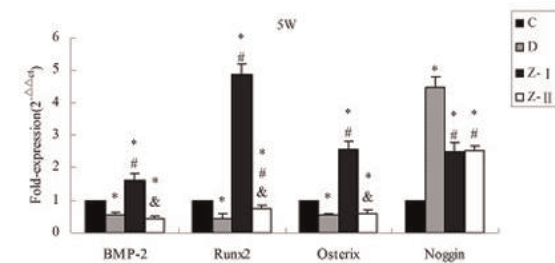figure 1

figure 2

figure 2

Fig 2 Effects of the ZOL treatment on the mRNA levels of BMP-2, Runx2, Osterix and Noggin in the distal femurs. Total RNA was extracted from distal femurs of rats at 1, 2, 3, 4 and 5 weeks after the onset of diabetes. The mRNA levels of BMP-2, Runx2, Osterix and Noggin were determined by real-time RT-PCR and were expressed relative to an internal standard, actin. Values represent the means±SD for 4 independent experiments. *Significantly different from the control value (P<0.05). # Significantly different from the diabetes (P<0.05). & Significantly different from the ZOL-I group (P<0.05).
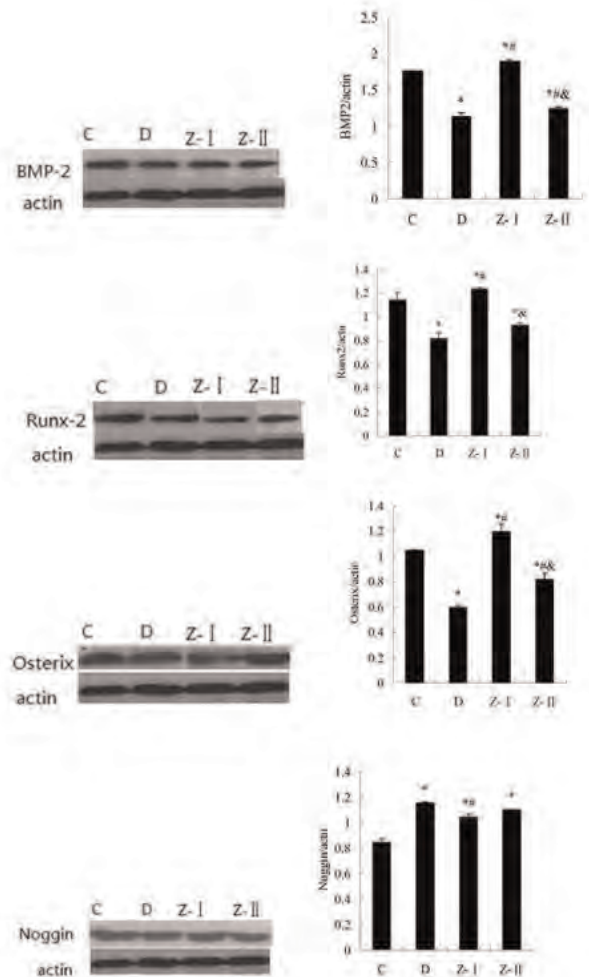

Fig 3 Effects of the ZOL treatment on the protein levels of BMP-2, Runx2, Osterix and Noggin in the distal femurs. Total protein was extracted from distal femurs of rats at 5 week after the onset of diabetes. The protein levels of BMP-2, Runx2, Osterix and Noggin were determined by Western Blot and were expressed relative to an internal standard, actin. Values represent the means±SD for 4 independent experiments. *Significantly different from the control value (P<0.05). # Significantly different from the diabetes (P<0.05). & Significantly different from the ZOL-I group (P<0.05).

figure 3
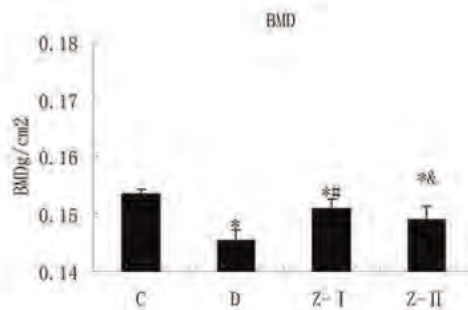

Fig 5 Bone mineral density measurements of the whole femur (g/cm²). The C group had the highest BMD value among all the groups. The BMD value of Z-I group was significantly higher from the D and Z-II group. *significantly different from the control value (P<0.05). #Significantly different from the diabetes (P<0.05). & significantly different from the Z-I (P<0.05).

figure 4

MO0183

Combined Treatment with Ascorbic Acid and Thyroid Hormone Promotes Healing of a Non-union Tail Vertebra Defect in Mice. Kevin DeLeon*[1], Hongrun Yu[2], Heather Watt[1], Catrina Alarcon[1], Subburaman Mohan[2]. [1]VALLHCS, USA, [2]Jerry L. Pettis Memorial VA Medical Center, USA

Bone injuries are a serious health problem. Healing is impaired in 10-20% of fractures with seriously delayed union or non-union, causing morbidity for patients and enormous healthcare costs. Thus, there is a compelling need to find novel effective therapies to promote fracture healing. Based on the findings that ascorbic acid (AA) deficiency in mice resulted in spontaneous fractures (Sfx) and that thyroid hormone (TH) deficiency caused impaired skeletal growth both acting via regulating osterix (Osx) expression, we proposed the hypothesis that a combination of AA and TH will produce a synergistic effect on skeletal healing in mice. Treatment of MC3T3-E1 cells with 10 ng/ml of triiodothyronine (T3) or 50 ug/ml AA increased ALP activity less than 3-fold compared to vehicle while combined treatment with both T3 and AA increased ALP activity by 20-fold. Similarly, combined treatment increased Osx expression 20-fold, which was significantly greater than the additive effect of individual treatments. To test if TH and AA play an important role in skeletal healing, we generated gulonolactone oxidase gene disrupted Sfx mutant mice and subjected them to transient AA deficiency (by removing AA from drinking water) and TH deficiency (via methimazole treatment) at 4 wks of age. At 6 wks of age, AA/TH-deficient mice and control wild type (WT) mice were subjected to a 0.8 mm diameter drill hole in the mid-diaphysis of the third tail vertebra. Mice were treated with vehicle, AA (330 μg/ml in drinking water), T3 (1 μg)/T4 (10 μg) via I.P. injection or a combination of AA and T3/T4 for 30 days after the drill hole procedure. At day 1 and 30 after defect, in vivo μ-CT scans of anesthetized mice were performed at 10.5 micron resolution and changes in bone volume (BV) to tissue volume (TV) at the defect site were determined. Bone regeneration was reduced dramatically (56%, P<0.01) in vehicle treated Sfx mice with transient AA/TH deficiency compared to WT mice. In WT mice, only the combination of AA/TH produced a significant increase (28%, P=0.02) in BV/TV compared to vehicle. In deficient mice, AA, TH and the combination caused a 70%, 106% and 163% increase (all P<0.01 vs vehicle; P<0.05 in AA/TH vs AA or TH) in BV/TV during the 30 day treatment. Based on these data, we conclude that a combination of AA/TH caused a greater increase in osteoblast differentiation and Osx expression in vitro and bone regeneration ability in vivo compared to individual treatments.

Disclosures: Kevin DeLeon, None.

MO0184

Delay in Fracture Healing by Phosphate Restriction Displays Uniform Recovery in AJ and C57B6 Strains Independent of Genetic Variability. Kyle Lybrand*[1], Brenna Hogue[2], Heather Matheny[2], Amira Hussein[3], Anthony De Giacomo[1], Elise Morgan[4], Thomas Einhorn[5], Louis Gerstenfeld[3]. [1]Boston University Dept of Orthopaedic Surgery, USA, [2]Boston University School of Medicine, USA, [3]Boston University School of Medicine, USA, [4]Boston University, USA, [5]Boston Medical Center, USA

Introduction: Phosphate is essential for bone growth and fracture repair. Although phosphate deficiency has been shown to impair fracture repair, it is unknown how genetic factors interact with this deficiency to affect healing. It is also unknown if healing will be re-initiated once phosphate is replenished, or if initial phosphate deficiency will irreversibly affect healing even after phosphate has been restored. The aims of this project addressed these two questions.

Methods: Closed stabilized fractures were generated in the femora of 3 strains of male mice, A/J (AJ), C57BL/6J (B6), and C3H/HeJ (C3). Phosphate deficiency was initiated 2 days prior to fracture and was maintained for 15 days. Phosphate was then replenished and bone healing was allowed to continue until 35 days. RNA expression for marker genes of chondrogenesis and osteogenesis was assessed by qRT-PCR analysis over this time course. Callus microstructural properties, cartilage content and torsional strength were measured by micro-computed tomography (CT), contrast-enhanced CT and mechanical testing at 21 days post-fracture.

Results: All three strains had impaired expression of cartilage and bone associated genes during the period of phosphate deficiency. Once phosphate was replenished, osteogenic genes showed a burst of late expression in all three strains. Compared to control calluses phosphate deficient calluses were stronger for AJ and B6 strains (p<0.003). Even though tissue mineral density (TMD) was lower in these calluses (p <0.03), the standard deviation in TMD was lower (p<0.001) and for AJ calluses the tissue was located closer to the bone axis (p=0.03) indicating a more even distribution of mineralized tissue compared to controls. Further, the phosphate deficient AJ calluses were more brittle than controls (p<0.02). No differences in mineralization and mechanical strength were found for C3 calluses (p>0.30) suggesting that healing does not recover upon phosphate repletion.

Conclusions: The phosphate restriction in the C3 strain delayed the regain of mechanical strength relative to AJ and B6 strains suggesting that C3 mice respond differently to a rachitic state. These results suggest strain dependent bone repair that is more osteogenic in the C3 strain, which is more effected by phosphate deficiency, while the more chondrogenic strains (AJ and B6) are more responsive to return to the normal metabolic state independent of genetic variability.
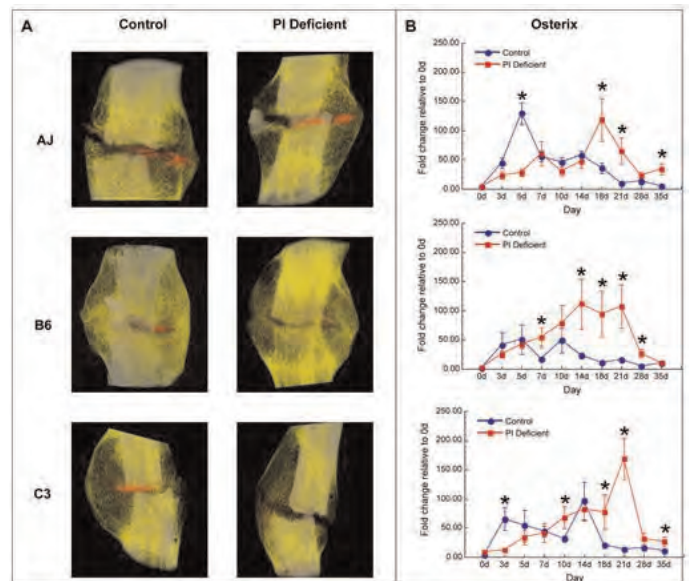

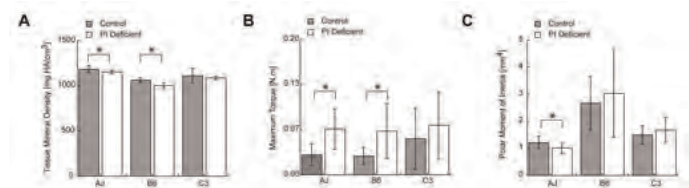Figure 1. For each strain: (A) 3-D rendering of callus; (B) Osterix mRNA expression (*p<0.05)

Figure 2. Callus mechanical properties: (A) TMD; (B) Max Torque; (C) Moment of Inertia (*p<0.05)

Disclosures: Kyle Lybrand, None.

MO0185

Differing effects are exerted by the Vitamin E isomers gamma-tocotrienol (GT3) and delta-tocotrienol (DT3) on indices of bone remodeling in mice following exposure to non-lethal ionizing radiation. Sibyl Swift*[1], Joshua Swift[1], Shukla Biswas[2], Merriline Satyamitra[2], Venkataraman Srinivasan[2], Sanchita Ghosh[2]. [1]Armed Forces Radiobiology Research Institute, USA, [2]AFRRI, USA

Exposure of normal skeletal tissue to ionizing radiation, at even low doses similar to those administered for cancer treatment, results in significant bone loss and increased risk of fracture at weight bearing skeletal sites in short periods of time. Vitamin E isomers, such as gamma-tocotrienol (GT3) and delta-tocotrienol (DT3), stimulate osteoblastogenesis and inhibit osteoclast formation and activity. We sought to determine whether the administration of DT3 or GT3 prior to radiation exposure would attenuate radiation-induced bone loss. Male CD2F1 mice (8-10 wk old) were exposed to either a single dose of 7 Gy ionizing radiation (Co[60], γ-rays; 0.6 Gy/min) or SHAM (0 Gy). Mice from each group were treated (s.c.) with either VEH (5% Tween-80), DT3 (300 mg/kg), or GT3 (100 mg/kg) 24 hrs prior to radiation exposure or SHAM. Serum biomarkers were assessed 1, 3, 7, 10, 14, and 30 days post-irradiation and compared to sham controls. Radiation injury (RI) resulted in early increases in serum TRACP 5b by Day 7 (+114% vs. VEH), which remained elevated on Days 14 (+121%) and 30 (+69%). This response was diminished with the administration of GT3 at Day 10 (-25%), but did not restore TRACP 5b levels to those of VEH. DT3 had no detectable effect on TRACP 5b levels. DT3 down-regulated serum osteocalcin levels from Day 7 (-44%) through Day 14 (-56%). DT3 treatment restored osteocalcin levels to those of the VEH group; GT3 treatment had not detectable effect on osteocalcin levels. These data suggest that bone remodeling is initially up-regulated following exposure to non-lethal γ-radiation (7 Gy). These data indicate opposing effects of DT3 and GT3 on bone, when given prior to radiation exposure. The administration of DT3 before RI appears to stimulate overall bone metabolism by increasing TRACP 5b and osteocalcin. However, GT3 treatment in combination with RI, down-regulates RI-induced increases TRACP 5b. Further research into the precise mechanisms by which GT3 and DT3 affect bone after ionizing radiation exposure is necessary to characterize the efficacy of these agents as countermeasures to RI-induced osteoporosis.

This work was supported by AFRRI Grant RAB2GP to SPG and RAB2GY to VS.

MO0186

Mushroom polysaccharides improve bone microarchitecture and strength in diabetic rats. Chung-Hwan Chen*[1], Hui-Chen Lo[2], Yi-Shan Lin[3], Zai-Jie Wang[3], Lin Kang[4], Chwan-Li Shen[5]. [1]Kaohsiung Medical University Hospital & Kaohsiung Medical University, Taiwan, [2]Fu Jen Catholic University, Taiwan, [3]Kaohsiung Medical University, Taiwan, [4]National Cheng Kung University, Taiwan, [5]Texas Tech University Health Sciences Center, USA

Patients with DM exhibit osteopenia and osteoporosis. Trametes versicolor (L.:Fr.) Pilát (TV), a medicinal mushroom with a wide range of applications, formerly known as Coriolus versicolor, and named Yunzhi in China, has been successfully grown in submerged fermentation as mycelial biomass. Recently, a novel TV strain LH-1, originally collected in Taiwan, has been successfully cultured. Up to now, no study has ever been conducted to show the effects of mushroom polysaccharides on bone health, especially in DM. Therefore, the present study was designed to investigate the potential benefit of TV LH-1 on bone health, in terms of bone microstructure and bone turnover biomarkers, in diabetic rats with impaired glucose tolerance. Male Wistar rats weighing approximately 280 g were used in this study. 27 rats were fed with high fat chow dietand the rest rats (n=10) were fed with normal chow diet during the experimental period served as control (CON) group. The diabetic animals were then divided into 2 groups and intragastrically administered with 0.5 ml of distilled water (the IGT group) (n=12) or TV LH-1 (0.1g/kg of body weight, the TV group) (n=15) daily for 28 days. The rats were sacrificed after treatment. All proximal tibiae were assessed by μ-CT and bending test at the end of study. Bone volume and trabecular number decreased and trabecular separation increased in the IGT group compared with the CON group while TV increased bone volume and trabecular number and decreased trabecular separation compared with the IGT group. The maximal load, stiffness and Young's modulus decreased in IGT group compared with the CON group while TV increased maximal load, stiffness and Young's modulus compared with the IGT group. The anti-hyperglycemic activity of TV LH-1 has also been demonstrated in diabetic rats previously. In this study, bone microarchitecture and bone markers deteriorated after DM induction while TV rescue the deleterious effects of DM on bone microarchitecture and bone marker. This is the first report that TV can improve bone microarchitecture and maximal load, stiffness and Young's modulus of bone in rats with DM. Though DM is a risk factor in osteoporosis, well-control of DM is not exactly known to rescue osteoporosis. The protective effect of TV on bone microarchitecture and bone strength was through the improvement of DM or/and directly on the bone was not elucidated. The protective mechanism of TV in rat with DM on bone required further studies.

MO0187

Role of CCR2+ Cells in the Alveolar Bone Repair Process in Mice. Claudia Biguetti*[1], Andreia Vieira[2], Priscila Maria Colavite[3], Carlos Eduardo Repeke[3], Franco Cavalla[3], Ana Paula Trombone[4], Gustavo Garlet[5]. [1]Universidade de São Paulo, Brazil, [2]Bauru School of Dentistry - University of Sao Paulo (FOB - USP), Brazil, [3]Universidade de São Paulo, Brazil, [4]Universidade do Sagrado Coração, Brazil, [5]School of Dentistry of Bauru, São Paulo University -FOB/USP, Brazil

The bone repair process depends of an initial and transitory inflammatory response, which involves the participation of various leukocytes subsets, as the monocyte/macrophage lineage. The CCR2 receptor is important to macrophage recruitment during inflammatory and immune responses, and play an active role in the regulation of osteoclastogenesis. However, its role in bone repair process remains unknown. Thereby, the purpose of this study was to investigate the role of CCR2+ cells in the alveolar bone repair process in mice, by means of microscopic - histomorphometry, birefringence analysis and immunohistochemistry), tomographic (MicroCT) - and molecular (PCRArray) comparative analysis between C57BL / 6 (WT) and CCR2KO mice during periods of 0 hour, 7, 14 and 21 days post-extraction of the right upper incisor. Our results demonstrated that CCR2 is in fact associated with monocyte/macrophage influx to bone repair site, since the CCR2+ cells are present in the inflammatory infiltrate developed along the alveolar bone repair in WT mice, with a kinetics similar to F4/80+ and CCR5+ cells. Furthermore, F4/80+ and CCR5+ cell number was significantly reduced in CCR2KO mice, suggesting that F4/80+ cells are double positive for CCR2 and CCR5. While CCR5 receptor may account for the remaining (but reduced) migration of the F4/80 + cells in CCR2KO mice, the reduced F4/80+ cells number suggests that CCR2 may be the primary receptor required for its migration. Also, the microscopic analysis demonstrated that CCR2 absence resulted in an increase of inflammatory infiltrate, collagen fibers, osteoblasts and osteoclasts counts and decrease of blood vessels in CCR2KO mice compared to WT mice. Birefringence analysis did not demonstrate major changes in extracellular matrix maturation dynamics in WT vs CCR2KO mice comparison. The

molecular analysis demonstrated that CCR2 absence resulted in an altered expression of different markers in CCR2KO mice. While growth factor TGFβ1, bone markers RUNX2 and CTSK, immunological markers TNFα, CCR1 and CCR5, and several MSCs markers (CD106, OCT4, NANOG, CD146, CXCL12 and CD105) were decreased in CCR2KO mice, RANK, RANKL, DMP1, IL6 and CXCR1 mRNA levels were increased. In conclusion, these results indicate that CCR2+ cells play an active role in alveolar bone repair in mice controlling F4/80+ cells migration, which in turn consequently influences inflammatory and healing response events throughout the repair process.

MO0188

Sheep Model Reflecting Glucocorticoid-induced Osteoporosis in Postmenopausal Women. Christina Andreasen*[1], Søren Overgaard[2], Ming Ding[3], Peter Bollen[4], Thomas Levin Andersen[5]. [1]Odense University Hospital, Institute of Clinical Research, Denmark, [2]Department of Orthopedics & Traumatology, Institute of Clinical Research, University of Southern Denmark, Denmark, [3]Department of Orthopedics & Traumatology, Institute of Clinical Health, University of Southern Denmark, Denmark, [4]Biomedicine Laboratory, University of Southern Denmark, Denmark, [5]Department of Clinical Cell Biology, Institute of Regional Health Services Research, University of Southern Denmark, Denmark

Large animal models are often used for studying orthopedic implants and biomaterial research. In the present study, we investigate whether the bone loss in glucocorticoid treated ovariectomised sheep results from a similar bone remodeling defect as in osteoporotic postmenopausal women treated with glucocorticoids. Ten female sheep were ovariectomised and treated with prednisolone (0.6 mg/kg/day, 5 times weekly) for 7 months. Ten untreated sheep served as control. The bone structure and selected histomorphometric parameters were evaluated in iliac crest biopsies, whereas blood samples were used to evaluate serum levels of bone biomarkers. Ovariectomy and glucocorticoid-treatment induced a significant loss of cancellous bone (19.7 %) after 7 months. During these 7 months the extent of bone surfaces colonized by osteoclasts was unchanged, while the resorption marker carboxy-terminal collagen crosslinks (CTX) on the other hand had a significant periodically elevation that peaked after one month. This suggests that the presence of osteoclasts was unchanged, but that their resorption activities were temporary enhanced or changes. In contrast, the bone formation marker osteocalcin was consistently reduced after one week, and the extent of formative osteoid surfaces was significant reduced after 1 month and almost undetectable after 7 months. The extent of reversal surfaces that reflects the reversal phase coupling bone formation and resorption were significant increased after 1 month, and covered as much as 50% of the bone surfaces after 7 months. Most of these accumulated surfaces were arrested reversal surfaces without any neighboring osteoclasts or osteoid surfaces, supporting that the bone formation and resorption were uncoupled during the reversal phase. As recently described in osteoporotic patients the arrested reversal surfaces had a significantly decreased cell density and reduced immunoreactivity for the osteoblastic markers runx2, osterix, and smooth muscle actin (SMA) when compared to the active reversal surfaces with neighboring osteoclasts and osteoid surfaces. In conclusion, the bone loss in glucocorticoid-treated ovariectomised sheep results from an uncoupling of the bone formation and resorption during the reversal phase, as recently described in osteoporotic postmenopausal women treated with glucocorticoids. This makes it a relevant preclinical model for studying orthopedic implant and biomaterial research under osteoporotic conditions.

MO0189

WISP1/CCN4 controls bone mass by uncoupling osteoblast and osteoclast function potentially by regulation of Wnt signaling. Azusa Maeda*[1], Mitsuaki Ono[2], Tina Kilts[2], Li Li[2], Kenn Holmbeck[2], Pamela Robey[3], Marian Young[1]. [1]National Institutes of Health, USA, [2]National Institutes of Health, USA, [3]National Institute of Dental & Craniofacial Research, USA

WISP1/CCN4 (WISP1) is highly expressed during bone development however, its function in bone is not clear. To study this, we created *Wisp1* knockout (*Wisp1*-KO) mice and results from micro-CT indicated that the bone mass of the *Wisp1*-KO mice was lower and the cortex was thinner compared to wild type (WT) mice. We also previously showed that the osteogenic differentiation of bone marrow stromal cells (BMSCs) was diminished in *Wisp1*-KO-BMSCs.

To learn more about the cellular basis for the phenotypes that we uncovered in the *Wisp1*-KO mice, we next examined the effect of *Wisp1*-deficiency on osteoclastgenesis. When osteoclast progenitors were isolated from bone marrow and cultured with RANKL and M-CSF, more TRAP positive cells were observed in *Wisp1*-KO bone marrow compared to WT. Next, BMSCs were transplanted under the skin of immunocompromised mice in a gelatin vehicle and harvested after 6 weeks. TRAP staining of the transplants showed more osteoclasts in the transplant

containing *Wisp1*-KO-BMSCs. Finally, using 6-month-old ovariectomized mice, we found whole-body bone mineral density was significantly lower in *Wisp1*-KO mice compared to WT, indicating that promotion of osteoclast activity caused by a loss of estrogen is accelerated by *Wisp1*-deficiency. These results suggest that lower bone mass in *Wisp1*-KO mouse is caused by over active osteoclast function.

To further decipher the molecular mechanisms causing lower osteogenesis and higher osteoclastgenesis in the *Wisp1*-KO mouse, we focused on the Wnt pathway since *Wisp1* is a downstream target of this pathway. We measured the differences in expression of genes specifically related to the canonical Wnt pathway and osteogenic differentiation. Our experiment showed the level of mRNAs encoding *β-catenin* (*β-cat*), *Axin2*, *Matrix metalloproteinase 14* (*Mmp14*) and *Cyclin D1* (*Ccnd1*) was significantly lower in *Wisp1*-KO-BMSCs, suggesting that *Wisp1* is not only a target but also an effector of the Wnt pathway. To determine where *Wisp1* functions in the pathway, BMSCs were cultured with osteogenic differentiation media and treated with LiCl which activates the Wnt pathway by inhibiting Gsk3-β. LiCl treatment increased the expression level of *Axin2* mRNA in *Wisp1*-KO-BMSCs but to a lower extent than that found in WT-BMSCs. These results suggest that *Wisp1* could function both up- and downstream of Gsk3-β in the Wnt pathway to regulate bone mass.

Disclosures: Azusa Maeda, None.

MO0190

COX-1,2 and EP1,2 expression in chronic spinal cord injured patients and healthy controls skeletal muscle tissue. Marco Invernizzi*[1], Manuela Rizzi[2], Claudio Molinari[3], Carlo Cisari[4], Stefano Carda[5], Filippo Renò[2]. [1]University of Eastern Piedmont, Novara, Italy, [2]Innovative Reasearch Laboratory for Wound Healing, Department of Health Sciences, University of Eastern Piedmont "A.Avogadro", Novara, Italy, [3]Human Physiology, Department of Translational Medicine, University of Eastern Piedmont "A.Avogadro", Novara, Italy, [4]Physical & Rehabilitation Medicine, Department of Health Sciences, University of Eastern Piedmont ''A.Avogadro'', Novara, Italy, [5]Department of Neurorehabilitation & Neuropsychology, Centre Hospitalier Universitaire Vaudois (CHUV), Lausanne, Switzerland

INTRODUCTION: Muscle tissue biology is regulated by a wide array of bioactive compounds among which Prostaglandins (PG), and in particular prostaglandin E_2 (PGE$_2$) play a pivotal role. PG are a family of active compounds produced by the ubiquitous cyclooxygenase (COX) enzymes (COX 1 and 2) and in skeletal muscle they regulate protein synthesis/degradation, tissue injury recovery and bone-muscle crosstalk. EP1-4 are G protein coupled PGE$_2$ receptors, and EP1 and 2 represent the most ubiquitous ones. The aim of this study was to evaluate, for the first time, the different expression of COX1,2 and EP1,2 in athrophic skeletal muscle obtained by a new mini-invasive muscle tissue biopsy technique in chronic spinal cord injured (SCI) patients and healthy controls.

MATERIALS AND METHODS: Skeletal muscle biopsies were collected from 6 chronic complete SCI patients and 3 healthy controls vastus lateralis muscle with a tri-axial end cut needle (Biopince© - Angiotech). Correct needle positioning in the target muscle was confirmed by ultrasound guide. All biopsies were performed under local anesthesia. Muscle samples were stained for ATPase to determine fibers composition, while COX1,2 and EP1,2 expression were evaluated by immunofluorescence.

RESULTS: All the bioptic procedures were perfomed easily without failures. Control muscle tissue was macroscopically thicker than SCI one. Moreover SCI sample microscopically displayed some structural degradation (vacuolization). Control specimen displayed an equal distribution of type I and type II fibers, while SCI sample displayed a high prevalence of type II fibers. COX1,2 and EP1 expression in muscle tissue did not display any significant difference between SCI patients and healthy controls. EP2, indeed, was significantly less expressed in SCI patients.

CONCLUSION: The observed shift from type I to type II fibers in SCI specimen was consistent with the results previously described in literature. Moreover in this work, for the first time, attention was focused on PGE$_2$ synthesis and signalling pathway in human skeletal muscle showing a significant difference in EP2 expression in SCI muscle compared to healthy controls.

Disclosures: Marco Invernizzi, None.

MO0191

GPR55 Regulates Peak Bone Mass and Steroid Hormone Levels in Male Mice. Lauren Whyte*[1], Aysha Khalid[2], Graeme Finnie[2], Selina Chiu[2], David Baker[3], Richard Aspden[4], Ruth Ross[1]. [1]University of Toronto, Canada, [2]University of Aberdeen, United Kingdom, [3]Blizard Institute, Barts & The London School of Medicine & Dentistry, United Kingdom, [4]University of Aberdeen, United Kingdom

Peak bone mass is generally associated with bone mineral density in older age, therefore accrual of bone mass during childhood and adolescence is an important determinant of osteoporosis risk later in life. Previously we characterised an osteopetrotic phenotype in 3 month old male GPR55$^{-/-}$ mice due to a decrease in osteoclast function (Whyte *et al*, 2009). It is not known whether this high bone mass phenotype is maintained with age and equates to increased bone strength. This study investigated the structural and mechanical bone properties of GPR55$^{-/-}$ mice at 3, 5 and 12 months.

µCT analysis of the proximal tibia and distal femur demonstrated a significant increase in trabecular bone volume in male GPR55$^{-/-}$ mice compared to wildtype mice at 3 months (P<0.05 tibia, P<0.01 femur), 5 months (P<0.01 tibia, P<0.01 femur) and 12 months (P<0.0001 tibia, P<0.0001 femur). The increased trabecular volume was associated with significantly increased trabecular number, decreased trabecular separation and increased trabecular connectivity at all ages. Additionally, a significant decrease in structural model index, indicative of a more plate like trabecular structure, was noted at 3 and 12 months. Together these parameters infer increases in bone strength and this was confirmed by mechanical testing of cortical bone. Three point bending demonstrated significantly increased stiffness and increased failure load in 3 and 12 month old GPR55$^{-/-}$ mice.

Although GPR55$^{-/-}$ mice have increased bone mass and strength at 12 months relative to wildtype mice, loss of bone mass still occurs with age. No differences in osteoclast activity were observed between wildtype and GPR55$^{-/-}$ mice at 12 months as determined by measurement of plasma CTx. This likely indicates that the high bone mass phenotype is a result of increased peak bone mass attained in early months, offering protection against the effects of bone loss with age. Interestingly, plasma testosterone levels were significantly increased in GPR55$^{-/-}$ mice at 12 months (wildtype = 26 nmol/L and GPR55$^{-/-}$ = 53 nmol/L (P<0.01)). In line with this, epididymal sperm counts revealed a 2.2 fold increase in GPR55$^{-/-}$ mice (P<0.05). No changes in estradiol levels were observed. These results suggest that GPR55 may negatively regulate testosterone levels in mice and further extends the therapeutic potential of GPR55 antagonists. Together these data may have implications for understanding the value of GPR55 antagonists to preserve bone loss.

Disclosures: Lauren Whyte, None.

MO0192

Maternal Myostatin Deficiency Improves Bone Quality of Wildtype Murine Offspring. Arin Oestreich*[1], Marcus McCray[1], William Kamp[1], Laura Schulz[1], Charlotte Phillips[2]. [1]University of Missouri, USA, [2]University of Missouri-Columbia, USA

During fetal development, changes in the uterine environment can have effects on offspring bone quality that persist throughout life; however the biochemical and molecular mechanisms involved remain unknown. Myostatin, a TGF-β family member, is a transcription factor that circulates in the serum and is well known as a negative regulator of muscle mass. Myostatin alters placental glucose transfer and is dysregulated in a model of developmental programming. Additionally, maternal myostatin deficiency increases muscle mass in offspring, but paternal myostatin deficiency does not, suggesting an intrauterine effect of myostatin. The goal of this study was to investigate whether decreased maternal myostatin levels in mice impact adult offspring bone quality. Femora of 4 month old wildtype male offspring from myostatin deficient dams were evaluated by µCT and torsional loading to failure and found to have an 18% increase in torsional ultimate strength compared to genetically identical, age-matched offspring from wildtype dams. Tensile strength, a measure of the bone material strength, was also increased by 20%, suggesting the increased whole bone strength may be due to changes in the bone material. Collagen, the main structural protein in bone, was also increased 8.95% in the offspring from myostatin deficient dams compared to those from wildtype dams, as measured by hydroxypro-line content. Taken together, our results suggest that the decrease of myostatin in the maternal environment impacts the developmental programming of bone to increase bone strength and material properties of wildtype mice at 4 months of age.

Disclosures: Arin Oestreich, None.

MO0193

Musculoskeletal effects of a 246-km ultramarathon race. Peter Pietschmann*[1], Elisabeth Weiss[2], Ursula Föger-Samwald[2], Markus Thalmann[3], Maria Tsironi[4], Katerina Skenderi[5], Katharina Kerschan-Schindl[6]. [1]Department of Pathophysiology & Allergy Research, Medical University of Vienna, Austria, [2]Department of Pathophysiology & Allergy Research, Center for Pathophysiology, Infectiology & Immunology, Medical University of Vienna, Austria, [3]Department of Cardiovascular Surgery, Hospital-Hietzing, Austria, [4]School of Nursing, University of Peloponnese, Greece, [5]Department of Nutrition & Dietetics, Harokopio University, Greece, [6]Department of Physical Medicine & Rehabilitation, Medical University of Vienna, Austria

Background: Although it is commonly accepted that regular physical exercise is beneficial for the skeleton, relatively little is known about musculoskeletal effects of extreme forms of exercise. In previous work [Bone 45 (2009) 1079-1083] we had demonstrated that a 246-km ultra-distance race ("Spartathlon") transiently suppressed bone formation and increased bone resorption. The aim of this study was to analyze effects of the Spartathlon race on novel musculoskeletal markers.

Methods: In 19 participants of the Spartathlon venous blood samples were obtained before and after the race; serum levels of myostatin (an inhibitor of myogenic differentiation), follistatin (an antagonist of myostatin) and markers/

regulators of bone (including the wnt signaling inhibitors sclerostin and dickkopf-1) were determined by ELISA.

Results: After the race a significant four-fold increase of serum follistatin levels was observed; myostatin increased by 12%. Whereas sclerostin levels were not significantly different before and after the race, dickkopf-1 levels had significantly decreased by 15%. In 9 participants also serum samples taken on the day after the race were available; interestingly, at this time point a decrement of sclerostin and dickkopf-1 levels was seen. Serum cathepsin K levels did not differ before and after the ultramarathon.

Conclusion: We speculate that the marked increase of follistatin and the decline of dickkopf-1 after a 246-km ultramarathon race reflect important anabolic signals for muscle and bone.

Disclosures: Peter Pietschmann, None.

MO0194

The amino acid tryptophan increases skeletal muscle IGF-1 and follistatin in mice, and induces the expression of exercise-related factors. Mona El Refaey[1], Colleen Davis*[1], Phonepasong Arounleut[2], Sunil Upadhyay[1], Amy Dukes[3], Maribeth Johnson[3], William Hill[4], Carlos Isales[1], Mark Hamrick[5]. [1]Georgia Regents University, USA, [2]Georgia Regents University (formally Georgia Health Sciences University), USA, [3]Georgia Regents University, USA, [4]Georgia Regents University & Charlie Norwood VAMC, USA, [5]Georgia Health Sciences University, USA

Nutrition plays a key role in the maintenance of muscle and bone mass, and dietary protein deficiency has in particular been associated with catabolism of both muscle and bone tissue. One mechanism thought to link protein deficiency with loss of muscle mass is deficiency in specific amino acids that play a role in muscle metabolism. We tested the hypothesis that the essential amino acid tryptophan, and its metabolite kynurenine, might impact muscle metabolism in the setting of protein deficiency. Adult mice (12 mo) were fed a normal diet (18% protein), as well as diets with low protein (8%) supplemented with increasing concentrations (50, 100, and 200 uM) of kynurenine or with tryptophan (1.5 mM). Results indicate that all mice on the low protein diets weighed less than the group fed normal protein (18%) but that the tibialis anterior muscle, relative to body weight, was larger in those mice on the high kynurenine diets. ELISA assays showed significant increases in skeletal muscle IGF-1, leptin, and the myostatin antagonist follistatin with tryptophan supplementation, and the low dose of kynurenine also increased muscle-derived IGF-1. Reverse-phase protein analysis revealed that tryptophan increased activation of several factors known to be induced with exercise in skeletal muscle, including p21 which promotes myocyte terminal differentiation and stat5a, which is involved in IGF-1 and androgen signaling in skeletal muscle. Together, these findings suggest that dietary amino acids can directly impact molecular signaling in skeletal muscle, further indicating that dietary manipulation with specific amino acids could potentially attenuate muscle loss with aging or dietary protein deficiency.

Disclosures: Colleen Davis, None.

MO0195

The osteogenic effects of swimming, jumping and vibration on the protection of bone quality from disuse bone loss. Mauricio Falcai[1], Ariane Zamarioli*[2], Francisco Jose de Paula[1], Graziela Leoni[3], Manoel Sousa Neto[3], Jose Batista Volpon[1]. [1]School of Medicine of Ribeirao Preto, University of Sao Paulo, Brazil, [2]University of Sao Paulo, Brazil, [3]Dental School of Ribeirao Preto, University of Sao Paulo, Brazil

Purpose: We investigated whether swimming activity associated with a three-week period of unloading could prevent the deleterious effects of disuse on the tibias of hindlimb-suspended rats. Methods: Forty-five Wistar rats were randomly divided into 5 groups: (HS) permanently hindlimb suspended rats; (HS+Swim) rats submitted to unloading interrupted by swimming exercise; (HS+WB) suspended rats with interruption for regular weight bearing for the same length of time as the HS+Swim rats; (Con) control rats; and (Con+Swim): control rats that underwent swimming exercise. Results: The HS rats exhibited a substantial loss of bone quality and uncoupled bone turnover, whence resorption was up-regulated and formation was down-regulated (HS vs Con). In tibias, we observed a significant decrease in BMD (-15%), in bone strength (-28%) and a marked deterioration in the trabecular architecture (-67% in BV/TV, -52% in TbN, -19% in TbTh and -72% in ConnD, p<0.01). In femurs, we found a significant reduction of -47% in the number of osteoblasts and a significant increase in bone resorption (i.e. osteoclasts number and eroded surface). We also found a significant decrease in the osteocalcin level (-17%) in the HS rats. Conversely, swimming mitigated bone quality loss induced by hypogravity in the suspended rats submitted to swimming exercise (vs HS). In tibias, swimming significantly increased in +11% the bone mass, in +23% the bone strength, in +32% trabecular thickness, in +50% bone volume and in +89% trabeculae number. In femurs, swimming caused a significant increase of +9.5% in the bone mass, +27% in the bone strength, +12% in the trabecular thickness, +16% in the trabecular volume and a significant reduction in the bone resorption. We found a significant increase of +30% in the osteocalcin serum level and +28% in the IGF-I level. The rats submitted to the suspension interrupted by periods of regular weight-bearing (HS+WB) also showed a slight improvement in bone quality when compared to the permanently suspended rats, but to a lesser degree than those submitted to periods of swimming exercise. Curiously, swimming did not increase bone health in non-osteopenic rats when compared to the control rats, leading to the hypothesis that swimming plays an important role with an osteogenic action in bones ongoing loss. Conclusions: We concluded that swimming activity was shown to be effective at preventing and even reverting the deleterious effects of unloading on the bone quality of osteopenic rats.
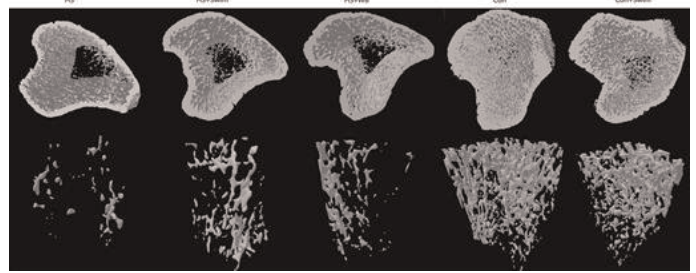
Micro-CT images

Disclosures: Ariane Zamarioli, None.

MO0196

A Novel mimetic peptide CK2.1 that induces chondrogenesis and cartilage repair *in vivo*. Hemanth Akkiraju*[1], Jeremy Bonor[2], Padma Srinivasan[2], Catherine Kirn-Safran[1], Randall Duncan[1], Anja Nohe[1]. [1]University of Delaware, USA, [2]University of Delaware, USA

Here we demonstrated the effect of a novel mimetic peptide of Bone Morphogenetic Protein Receptor type Ia (BMPRIa) on cartilage formation and repair. Bone Morphogenetic Proteins (BMPs) are crucial for the formation of articular cartilage and are known to differentiate mesenchymal stem cells to chondrocytes that secrete its extracellular matrix (ECM). The ECM consists of proteoglycans and collagen, including collagen II, IX and XI, and form the functional framework of the articular cartilage. However, a drawback for BMP use as therapeutics is that they also initiate the differentiation of chondrocyte hypertrophy and cartilage degradation. This is evidenced by the up-regulation of collagen X and MMP-13. Recently we identified a new BMPRIa receptor interacting protein, Casein Kinase 2 (CK2). We designed blocking peptides CK2.1, CK2.2, CK2.3 that release CK2 from the BMP receptor type Ia (BMPRIa) isoform activating the downstream BMP signaling pathways in the absence of BMP2. Here we show that CK2.1 alone but not CK2.2 and CK2.3 induced chondrogenesis and the expression of collagens II and IX but not collagen X in adult bovine chondrocytes. This effect was in contrast to BMP2 stimulation which induced collagen X synthesis. Systemic injections of CK2.1 *in vivo* via the tail vein in 8 week old mice resulted in cartilage growth in comparison to controls. Furthermore, Immuno-staining of processed cartilage sections with collagen IX, X and MMP-13 revealed increased collagen IX expression among CK2.1 injected mice, while collagen X and MMP-13 expression was only increased in BMP2 injected mice. We further destabilized the medial meniscus in mice and determined the effect of peptide CK2.1 to repair the damaged cartilage. Intra-articular injections of CK2.1 conjugated to a slow release system resulted in complete regeneration of the damaged tissue. Moreover, immuno-staining of processed samples with collagen IX, X and MMP-13 resulted in the up-regulation of collagen IX synthesis in CK2.1 injected but not in the control. However, more research is required to identify the specific mechanism of CK2.1 in cartilage repair. These data suggests that CK2.1 a novel mimetic peptide could be a possible future therapeutic for cartilage growth and repair.

Disclosures: Hemanth Akkiraju, None.

MO0197

An Rescue Effect of Altering Subchondral Bone Architecture on the Temporomandibular Joint Cartilage Degradation Induced by an Aberrant Dental Occlusion. Yundong Liu[1], Lifan Liao[1], Kai Jiao[1], Hongyun Zhang[1], Lei Lu[1], Mian Zhang[1], Jing Zhang[1], Jianjun He[1], Yaoping Wu[2], Meiqing Wang*[1]. [1]College of Stomatology, Fourth Military Medical University, China, [2]Xijing Hospital, Fourth Military Medical University, China

Aberrant biomechanical stimulation from abnormal dental occlusion plays an important role in temporomandibular joint (TMJ) OA development. Recently, we developed a unilateral anterior crossbite (UAC) prosthesis in rats and mice and found a significant degenerative change in the TMJ cartilage and subchondral bone loss (1). Subchondral bone remodeling played an important role in the onset and development of osteoarthritis. Therefore it is conceivable to test whether UAC induced TMJ cartilage degradation could be attenuated by administration of a specific classic NF-κB pathway inhibitor and/or strontium via targeting abnormal TMJ subchondral bone resorption.Methods: 6-week-old female C57BL/6J mice were randomly divided into blank control group (withou UAC, without any injection/gavage), and five

experimental (EXP) groups which were treated with UAC and additionally: (1) Saline Group: daily gavage of 0.9% saline; (2) Control Peptide Group: intra-peritoneal injection of control peptide 5 mg/Kg, 1 time/2d; (3) $SrCl_2$ Group: daily gavage of $SrCl_2$, 4 mmol/Kg; (4) NBD Peptide Group: intra-peritoneal injection of NBD peptide, 5 mg/Kg, 1 time/2d; (5) $SrCl_2$ + NBD Peptide Group: combination of daily gavage of $SrCl_2$, 4 mmol/Kg and intra-peritoneal injection of NBD peptide, 5 mg/Kg, 1 time/2d. All UAC additional treatment were appied from day 7 to day 21. The TMJs were sampled and analized 3 weeks after installing of UAC by histomophormetry, histochemistry, real-time PCR, and immunohistochemistry assays.

Results: Thinner and degraded cartilage, reduced cartilage cellular density, decreased expression levels of Collagen II and Aggrecan and increased ADAMTS-5, TNF-α/IL1-β/NFIKBA and NF-κB p-p65, loss of subchondral bone and enhanced osteoclast activity with decreases in OPG/RANKL ratio both in condylar cartilage and subchondral bone were observed in mouse TMJs of Saline Group, Control Peptide Group. However, a mild change were found in mouse TMJs of $SrCl_2$ Group, NBD Peptide Group and $SrCl_2$ + NBD Peptide Group.

Conclusions: The present UAC induced TMJ cartilage degradation could be attenuated via administration of a specific classic NF-κB pathway inhibitor and/or strontium targeting abnormal TMJ subchondral bone resorption, suggesting that inhibiting pathological subchondral bone resorption would be theraputically significant for occlusal original TMJ OA.

References

1. Liu YD, et al. Osteoarthritis Cartilage 2014; 22: 302-312.

Disclosures: Meiqing Wang, None.

MO0198

Characterization of Monosodium Iodoacetate Induced Osteoarthritis in Rat Knee, Including Tibiofemoral and Patellofemoral Joints. <u>Zhiqi Peng</u>*[1], <u>Jukka Vääräniemi</u>[2], <u>Katja Fagerlund</u>[1], <u>Jukka Rissanen</u>[1], <u>Jenni Bernoulli</u>[2], <u>Jussi Halleen</u>[3], <u>Jukka Morko</u>[1]. [1]Pharmatest Services Ltd, Finland, [2]Pharmatest Services Ltd, Finland, [3]Pharmatest Services Ltd, Fin

Monosodium iodoacetate (MIA) injection in rat knee induces osteoarthritis (OA) symptoms and is used as a preclinical model of OA. Most data of MIA-induced damage in rat knee has been obtained from tibiofemoral joint and not much information is available from patellofemoral junction. In this study, we characterized the effects of intra-articular MIA on entire rat knee, including both tibiofemoral and patellofemoral joints. One mg of MIA was injected into the knee of male Lewis rats in 50 µl of saline. Static mechanical allodynia was used for determining OA-related pain and measured as paw withdrawal threshold. The pain was detected in MIA-injected hind limbs after the injection and continued for 4 weeks until the end of the experiment. X-ray analysis indicated that bone mineral density was decreased in the metaphysis of distal femur and proximal tibia in MIA-injected hind limbs when compared with healthy control limbs. The density of subchondral bone was also decreased in the patella and femoral condyle of MIA-injected knees, whereas their patellofemoral joint space exhibited higher intensity than was observed in the x-rays of control limbs. Histology revealed that eroded or degraded cartilage fragments were distributed in the patellofemoral joint space of MIA-injected knees and that articular cartilage was completely lost at some sites of their patella and femoral condyle. Histological changes were less severe in the tibiofemoral joint, including mainly the loss of proteoglycans in entire articular cartilage and destroyed chondrocytes and collagen matrix in the superficial layer of articular cartilage in the tibial plateau of MIA-injected knees. Double fluorescence labeling demonstrated an endochondral ossification under articular cartilage both in the tibiofemoral and patellofemoral joints of control knees. The endochondral ossification was impaired in the tibiofemoral joint and totally ceased in the patellofemoral joint of MIA-injected knees. When comparing the effects of the same acidic state of the environment on both joints of the knee, the patellofemoral joint exhibited much stronger damage than the tibiofemoral joint. Probably, also the patellofemoral joint plays a substantial role in inducing symptomatic OA pain. This study suggests that the patellofemoral joint should not be ignored when studying the preclinical efficacy of disease modifying OA drugs in the rat MIA model.

Disclosures: Zhiqi Peng, Pharmatest Services Ltd, 4

MO0199

Chondroprotective Effects of Salubrinal in a Mouse Model of Osteoarthritis. <u>Kazunori Hamamura</u>*[1], <u>Akinobu Nishimura</u>[1], <u>Akihiro Sudo</u>[2], <u>Hiroki Yokota</u>[3]. [1]Indiana University Purdue University Indianapolis, USA, [2]Mie University Graduate School of Medicine, Japan, [3]Indiana University Purdue University Indianapolis, USA

Salubrinal is a synthetic chemical agent that elevates phosphorylation of eukaryotic translation initiation factor 2 alpha (eIF2α) and alleviates stress on the endoplasmic reticulum. Previously, we reported that in chondrocytes salubrinal attenuates expression and activity of matrix metalloproteinase 13 (MMP13) through downregulation of p38 MAPK and NFkB signaling. In this study, we determined whether administration of salubrinal prevents degradation of articular cartilage in a mouse model of osteoarthritis (OA). We hypothesized that progression of OA is reduced by salubrinal through downregulation of inflammatory responses and activities of proteolytic enzymes including MMP13. In order to test this hypothesis,

OA was surgically induced in the left knee of C57/BL6 female mice (approximately nine weeks old) by transecting the medial collateral ligament and removing the medial meniscus. Three animal groups were age-match control, OA placebo, and OA treated with salubrinal. Three days after the induction of OA, administration of salubrinal (1.5 mg/kg) was conducted daily into an intra-articular space of the left knee of the OA salubrinal group, while a solvent for salubrinal (49.5% PEG 400 and 0.5% Tween 80 in PBS) was injected to the OA placebo group. In 3 weeks (N = 6) and 6 weeks (N = 5-8) after the induction of OA, femora and tibiae were isolated and stained with Safranin O. OA progression was quantitatively evaluated based on the scoring system previously reported by Glasson et al. (Grade 0, 0.5, 1, 2, 3, 4, 5, or 6), and data were expressed as mean ± SD. For comparisons among multiple samples, ANOVA followed by post hoc tests was conducted. The results revealed that injection of salubrinal decreased the progression of OA for samples harvested both in 3 and 6 weeks. In particular, compared to the OA placebo group the statistically significant attenuation of OA progression was observed in the 3-week femur samples (3.8 ± 1.2 for placebo and 2.5 ± 0.5 for salubrinal; $p = 0.016$) and 6-week tibia samples (5.3 ± 0.7 for placebo and 3.7 ± 1.8 for salubrinal; $p = 0.041$). The results demonstrate that administration of salubrinal has chondroprotective effects in arthritic joints, and that salubrinal can be considered as a potential agent for alleviating OA symptoms.

Disclosures: Kazunori Hamamura, None.

MO0200

Osteoarthritis in Mice Overexpressing High Molecular Isoforms of FGF2. <u>Patience Meo Burt</u>*[1], <u>Liping Xiao</u>[1], <u>Caroline Dealy</u>[2], <u>Marja Marie Hurley</u>[3]. [1]University of Connecticut Health Center, USA, [2]University of Connecticut Health Center, USA, [3]University of Connecticut Health Center School of Medicine, USA

Osteoarthritis (OA) is a debilitating joint disease that affects over 27 million adults in the U.S., characterized by the loss of articular cartilage and changes in underlying bone. Currently, there is no permanent treatment for OA and a better understanding of the molecular mechanisms that lead to cartilage degradation will be useful in identifying therapeutic targets to help treat the disease. Patients with X-linked hypophosphatemic rickets (XLH) have increased fibroblast growth factor 23 (FGF23) in bone which results in hypophosphatemia, osteomalacia and osteoarthropathy, leading to problems associated with degenerative joint disease. Thus, FGF23 may play a role in OA development. We have developed novel transgenic mice overexpressing nuclear high molecular weight (HMW) isoforms of fibroblast growth factor 2 (HMWTg) in pre-osteoblasts. These mice phenocopy XLH since they have rickets/osteomalacia, hypophosphatemia, and increased FGF23 in serum and bone. We therefore hypothesized that mice overexpressing FGF2 HMW isoforms, in which FGF23 is increased, will develop more severe OA signs than Vector control mice at 18 months of age. To asses for signs of OA, the knee joints from 18 month old HMWTg and Vector male mice were collected. Digital x-ray imaging and microCT analysis were performed to visualize changes in bone. To determine articular cartilage integrity, histological analysis of proteoglycan expression by Safranin-O staining was performed. Immunohistochemistry was used to establish the expression of OA markers, such as metalloproteinases MMP-13 and ADAMTS-5, which are typically increased during joint degeneration. Examination of the knees revealed that HMWTg mice had increased osteophyte formation and subchondral thickening, compared to Vector mice, as indicated by x-ray images. MicroCT analysis of HMWTg revealed that trabecular number in the tibia and femur was decreased, whereas, trabecular thickness and separation were increased while subchondral sclerotic bone was observed. By immunohistochemistry, Safranin-O staining was decreased and metalloproteinase labeling was increased in the knee joint cartilage of HMWTg mice compared to the Vector. These changes imply that the osteoarthritic phenotype is more severe in HMWTg mice. Overall, these results suggest that overexpression of HMWFGF2 leads to signs of severe OA and offers insight into a molecular mechanism that causes the disease, while being a potential therapeutic target to treat it.
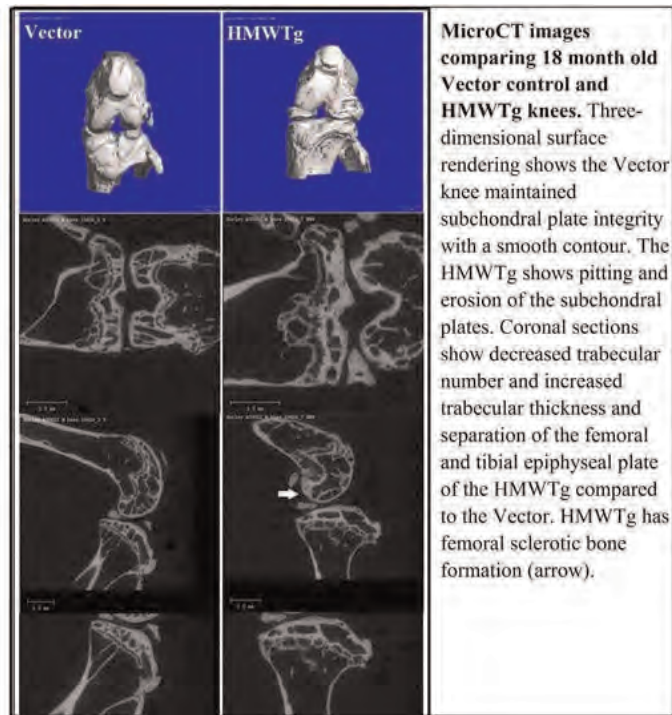
MicroCT images comparing 18 month old Vector control and HMWTg knees. Three-dimensional surface rendering shows the Vector knee maintained subchondral plate integrity with a smooth contour. The HMWTg shows pitting and erosion of the subchondral plates. Coronal sections show decreased trabecular number and increased trabecular thickness and separation of the femoral and tibial epiphyseal plate of the HMWTg compared to the Vector. HMWTg has femoral sclerotic bone formation (arrow).

Figure 1

Disclosures: Patience Meo Burt, None.

MO0201

Withdrawn

MO0202

Bone Marrow Lesions Are Characterized by Increased Bone Turnover and Increased Vascularity. Maziar Shabestari*[1], Erik Fink Eriksen[2], Janne Reseland[1], Jarle Vik[3]. [1]University of Oslo, Norway, [2]Oslo University Hospital, Norway, [3]Martina Hansens Hospital, Norway

Bone Marrow Lesions (BMLs), previously denoted Bone Marrow Edema, are detected as water signals on MR scans (low intensity on T1 weighted images and high intensity on T2 weighted scans). Previous histologic studies were unable to demonstrate any edematous changes at the tissue level, which led us to hypothesize that the water signal stems from increased vascularization accompanying a high turnover state in bone. To test this hypothesis we performed tetracycline labeling in addition to T1-weighted and STIR MR scans of 28 patients planned for total hip replacement surgery. Among 14 femoral heads studied so far, 8 revealed BMLs on MR, while 6 were negative. The latter acted as controls in the analysis. On the femoral heads we took out cylindrical biopsies guided by the MR images taken in two perpendicular planes. These biopsies were stored in 70% alcohol prior embedding in methyl methacrylate. Subsequently 7 um sections were prepared and subjected to histomorphometric analysis of the cancellous bone envelope using commercially-available software (BioQuant Osteo). We chose to focus on mineralizing surface (MS/BS) and vascular area (sinusoids + blood vessels), but also evaluated mineral apposition rate (MAR), bone formation rate (BFR/BS), bone volume (BV/TV) and trabecular thickness (Tb.Th).

The analysis revealed that compared to controls bone tissue from patients with BMLs exhibited increased bone turnover: MS/BS (median (95% Confidence interval)) 8.1% (3.41 – 33.29) vs 0.3% (0.06 – 1.64) ($p < 0.0007$) and increased vascular area 0.29 mm2 (0.17 – 1.14) vs 0.03 mm2 (0.004 – 0.16) ($p < 0.03$). None of the other variables of interest were different between the two groups.

In conclusion, this study confirms that Bone Marrow Lesions are characterized by increased bone turnover and increased vascularity in keeping with it being a reparatory process. Thus, the water signal, which is the hallmark of BMLs on MR, is most probably reflecting increased tissue vascularity accompanying increased remodeling activity.

Disclosures: Maziar Shabestari, None.

MO0203

Correlates of Knee Bone Marrow Lesions in Younger Adults. Benny Samuel Eathakkattu Antony*[1], Graeme Jones[2], Alison Venn[3], Lyn March[4], Leigh Blizzard[3], Andrew Halliday[5], Terence Dwyer[6], Flavia Cicuttini[7], Changhai Ding[3]. [1]Menzies Research Institute Tasmania, University of Tasmania, Australia, [2]Menzies Research Institute, Australia, [3]Menzies Research Institute Tasmania, University of Tasmania, Australia, [4]Institute of Bone & Joint Research, University of Sydney, Australia, [5]Department of Radiology, Royal Hobart Hospital, Australia, [6]Murdoch Childrens Research Institute, Australia, [7]Department of Epidemiology & Preventive Medicine, Monash University, Australia

Purpose: Bone marrow lesions (BMLs) of the knee joint are a key player in osteoarthritis of the knee. However, little is known of their determinants, especially in young adults . The aim of this study was to examine the structural and functional correlates of BMLs in younger adults including physical activity and to determine whether bone mass, cholesterol and hormones measured 5 years prior are associated with current BMLs.

Methods: Subjects broadly representative of the Australian population (n=330, aged 31-41 years, female 48.7%) were selected from the Childhood Determinants of Adult Health study. They underwent T1 and T2-weighted fat- supressed magnetic resonance imaging in their knee. BMLs, cartilage defects, meniscal tears and cartilage volume were measured. Knee pain was assessed by self-administered Western Ontario and McMasters osteoarthritis index (WOMAC) questionnaire. Physical activity was measured by IPAQ questionnaires at the time of MRI. Heel bone mass, lipids and hormone levels (in females) were assessed 5 years prior.

Results: The prevalence of any BMLs in the knee joint was 17%. Cross-sectionally, any BML in the knee was associated with age (PR: 1.09, 95% CI: 1.00, 1.19), previous knee injury (medial tibiofemoral BMLs PR: 2.20, 95% CI: 1.03, 4.71) and total WOMAC knee pain (PR: 1.05, 95% CI: 1.02, 1.09). BMLs were associated with other structural abnormalities such as total knee cartilage defects (PR: 2.65, 95% CI: 1.47, 4.80) and total meniscal tears (PR: 1.70, 95% CI: 0.99, 2.94).

High Density Lipoprotein (HDL) cholesterol measured 5 years prior was negatively associated with any BML (PR: 0.36, 95% CI: 0.15, 0.87). Testosterone measured 5 years prior in females (PR: 0.99, 95% CI: 0.99, 1.00) and speed of sound (bone mass) (PR: 0.98, 95% CI: 0.97, 0.99) were negatively associated with femoral BMLs. Moderate physical activity was protective (PR: 0.93, 95% CI: 0.87, 0.99) while vigorous activity showed a deleterious trend (PR: 1.01, 95% CI: 1.00, 1.02) with BMLs as we reported in older and middle aged adults. All these models were adjusted for age, gender, BMI, duration of follow-up and injury.

Conclusions: BMLs in young adults are associated with increased knee symptoms, a history of injury and other knee structural lesions. Moderate physical activity (not vigorous) may be protective with BML. A higher bone mass and HDL cholesterol in both sexes and testosterone in women may be protective with the devolpment of BMLs in young adults.

Disclosures: Benny Samuel Eathakkattu Antony, None.

MO0204

Knee osteoarthritis patients with severe pain while lying down have higher local subchondral tibial bone mineral density. Wadena Burnett*[1], Saija Kontulainen[1], Christine McLennan[2], Diane Hazel[3], Carl Talmo[3], David Hunter[4], David Wilson[5], James Johnston[1]. [1]University of Saskatchewan, Canada, [2]Hebrew SeniorLife, USA, [3]New England Baptist Hospital, USA, [4]University of Sydney, Australia, [5]University of British Columbia, Canada

Introduction: Knee osteoarthritis (OA) is a painful and debilitating joint disease. Knee pain while lying down is of particular concern to patients as it disturbs sleep and quality of life. The subchondral bone is innervated and could be of particular importance in OA-related pain. The objective of this study was to investigate associations between proximal tibial subchondral bone mineral density (BMD mg/cm^3) and pain while lying down in patients with OA.

Methods: The preoperative knee of 42 knee arthroplasty patients was scanned using quantitative computed tomography (QCT). Pain was measured using the Western Ontario and McMaster Universities Arthritis Index (WOMAC) and participants were categorized into three groups: 'no pain', 'moderate pain', and 'severe pain' while lying down. We assessed tibial subchondral BMD at normalized depths of 0-2.5mm, 2.5–5mm and 5-10mm relative to the subchondral surface. Regional analyses of each medial and lateral plateau included total BMD and maximum BMD within a 10mm diameter 'focal' region of interest. The association between WOMAC pain scores and BMD measurements was assessed using Spearman's rank correlation. Regional BMD was compared pairwise between pain and no pain groups using multivariate analysis of covariance with age, sex, and BMI as covariates and Bonferoni adjustment for multiple comparisons.

Results: Lateral focal BMD at the 2.5-5mm depth was related to pain while lying down ($\rho=0.388$, $p=0.011$). Lateral focal BMD was 33% higher in participants with 'severe pain' than participants with 'no pain' at the 2.5-5mm depth (adjusted mean difference: 114mg/cm^3; 95%CI: 9.6 to 218mg/cm^3; $p=0.028$) and 32% higher at the 5-10mm depth (adjusted mean difference: 60mg/cm^3; 95% CI: 0.3 to 120mg/cm^3; $p=0.049$) (Figure 1). There were no lateral BMD differences at 0-2.5mm from the subchondral surface and no medial BMD differences across all depths.

Conclusion: Higher lateral focal BMD was found in patients with 'severe pain' while lying down compared to patients with 'no pain' at depths of 2.5-5mm and 5-10mm from the tibial subchondral surface. This alteration in lateral plateau BMD may be due to patient self-adjustment in gait or alignment, where actively shifting loading from medial to lateral tibial plateau may help alleviate pain, but may result in higher local lateral BMD at deeper regions from the subchondral surface. This study suggests that local subchondral bone density may have a role in OA-related pain pathogenesis.
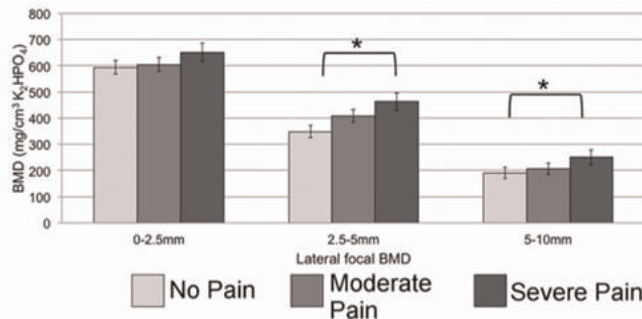
Adjusted mean lateral focal BMD of each pain group at three depths from subchondral surface.

Disclosures: Wadena Burnett, None.

MO0205

Structure of Femoral Neck in Hip Osteoarthritis: Texture Analysis Improvement in Cortical Evaluation. <u>Gustavo Davi Rabelo</u>[1], <u>Jean-Paul Roux</u>*[2], <u>Nathalie Portero-Muzy</u>[1], <u>Stephanie Boutroy</u>[3], <u>Roland Chapurlat</u>[4], <u>Pascale Chavassieux</u>[5]. [1]INSERM UMR1033, Université de Lyon, France, [2]INSERM, UMR 1033, Université de Lyon, France, [3]INSERM U1033 & Université de Lyon, France, [4]E. Herriot Hospital, France, [5]INSERM UMR1033, Université De Lyon, France

Cortical porosity (Ct.Po) and cortical thickness (Ct.Th) contribute to the cortical bone strength. When compared to osteoporosis, femoral neck (FN) in hip osteoarthritis (OA) is characterized by thicker cortices, that may contribute to the reduced fracture risk (Blain et al, 2008), with the highest Ct.Th and the lowest Ct.Po in the inferior part, when compared with upperquadrants (Boutroy et al, 2011). However, the isotropic pixel size being 82 µm in the computed tomography images, the smallest cortical bone channels could not been taken into account. The aim of this study was to analyze additional 3D characteristics of the cortices in FN in hip OA and evaluate topological distribution of bone elements in each quadrant.

FN samples were obtained during arthroplasty for hip OA in 18 postmenopausal women (mean age 66 ± 8 yrs). 3D measurements of the bone cortices were assessed from HR-pQCT (Xtreme CT, Scanco Medical) and analyzed by computational routines using Ctan software (Skyscan, Belgium) and Fraclac running in ImageJ (NIH, USA) in the four FN quadrants (Inferior, Superior, Anterior and Posterior). Classical analyses were performed with thresholded methods from binary images to obtain Ct.Th and its heterogeneity (Ct.ThSD), Ct.Po and Fractal Dimension (Ct.FDbin). In addition, texture analysis using unthresholded methods was applied to measure Fractal Dimension (Ct.FDgray) and Lacunarity (Ct.Lac) from gray-scale images.

When compared to the upperquadrants, the inferior quadrants was characterized by a higher and more heterogeneous Ct.Th (Ct.Th p<0.0001, Ct.ThSD p<0.0001), with a lower Ct.Po (p<0.0001). These data were confirmed by higher Ct.FDbin (p<0.0001) and Ct.FDgray (p<0.0001) and a lower Ct.Lac (p<0.0009). There was a significant correlation between Ct.FDbin and Ct.Th (p<0.001, r=0.73) and Ct.Po (p<0.009, r=-0.60).

In conclusion, in hip OA, besides a greater thickness and lower porosity, the cortex of the inferior quadrants presents with higher complexity of structure as shown by the Fractal dimension, with more topological homogeneity as shown by the lacunarity in relation to the distribution of bone channels.

Disclosures: Jean-Paul Roux, None.

MO0206

The comparison study of quality of sleep(QOS) in rheumatoid arthritis and osteoarthritis. <u>Sang-Hyon Kim</u>*[1], <u>Sang-Il Lee</u>[2]. [1]Chief of Rheumatology, South Korea, [2]M.D., South Korea

Introduction: Patients with musculoskeletal disorders such as rheumatoid arthritis (RA) and Osteoarthritis (OA) suffer from insomnia and other sleep disturbance. However, in the previous study, there was lesser data about comparison of quality of sleep (QOS) in RA and OA. In this study, we aimed to assess (1) the impact of RA on QOS comparing with that of OA patients and control subjects and (2) the impact of these two musculoskeletal disorders on various components of QOS using PSQI (Pittsburgh sleep quality index) Survey. Methods: Ninety three patients with RA, 38

patients with OA, and 126 voluntary control subjects were included in the study. The groups were comparable in terms of demographic characteristics. QOS was evaluated by using PSQI Health survey in all study participants. ESR (Erythrocyte Sedimentation Rate) and CRP (C-Reactive Protein), which is a specific inflammatory marker for RA, was used in RA patients, and McGill Pain Questionnaire be used to evaluate experiencing significant pain in RA and OA. Results: Sleep disturbance, use of sleeping medication, daytime dysfunction score were higher in OA than RA patients and control subjects (p<0.05). The between-groups comparisons revealed that RA patients had significantly higher sleep duration scores than OA patients (0.95 ± 1.06 vs 0.61 ± 1.05, respectively), (p<0.05). The CRP level correlated with PSQI score (p<0.05). The parameters of McGill Pain score, sensory pain, affective pain, and VAS score had significantly higher in OA than RA patients (p<0.05). Especially, all parameter of McGill Pain score correlated significantly with PSQI score in RA (p<0.01), and only sensory pain related to PSQI score in OA (p<0.05). Conclusion: Taken together, we need a slightly different approach on evaluating the patients with arthritis suffer from sleep disturbance, either RA or OA. And the CRP level associated with QOS in RA patients.

Disclosures: Sang-Hyon Kim, None.

MO0207

Connexin45 is Involved in Cancellous but not Cortical Bone Homeostasis. <u>Marcus Watkins</u>*[1], <u>Susan Grimston</u>[1], <u>Bing Wang</u>[2], <u>Xiaowen Zhang</u>[2], <u>Roberto Civitelli</u>[1]. [1]Washington University in St. Louis School of Medicine, USA, [2]Washington University in St. Louis School of Medicine, USA

Intercellular communication via gap junctions is an important method of coordinating cellular processes. Gap junctions are composed of connexin hexamers that allow passage of small molecules between cells. The biophysical properties of these transcellular channels are dictated by the connexin that forms the gap junction. We and others have previously shown that genetic ablation of connexin43 (Cx43) – the most abundant gap junction protein present in bone – specifically in osteoblasts alters cortical modeling via modulation of both osteoblast and osteoclast activity. Connexin45 (Cx45) is less abundantly expressed in bone cells; and unlike Cx43, whose abundance increases during osteoblast differentiation; Cx45 expression remains relatively stable as osteoblasts differentiate. To examine the role of Cx45 in bone we have induced a conditional deletion of its gene (*Gjc1*) in osteo-chondroprogenitor, using Cre recombinase driven by the *Twist2* (*Tw2*) promoter. *Gjc1*^{fl/fl}::*Tw2-Cre* (cKO) mice were recovered at the expected Mendelian frequency and showed no overt phenotype. Examination of femurs from 2-month-old cKO and control (*Gjc1*^{fl/fl}) mice by µCT revealed an unexpected $60 \pm 12\%$ (p<0.05) increase in trabecular bone volume/tissue volume. This was associated with $20 \pm 6\%$(p<0.05) increase in trabecular number and $15 \pm 7\%$ (p=0.06) decrease in trabecular spacing. Cancellous bone mineral density was also increased in cKO mice ($24 \pm 10\%$) compared to control littermates. By contrast, no significant changes were observed in cortical parameters. Results were consistent among genders. *In vitro* analysis of bone marrow stromal cells (BMSC) using colony forming unit (CFU) assays revealed no change in CFU-fibroblast, CFU-osteoblast nor CFU-adipocyte; thus excluding an abnormality at earlier steps of the osteogenic differentiation program. Thus, Cx45 is involved in cancellous bone homeostasis, whereas Cx43 primarily controls cortical bone modeling. Surprisingly, the function of Cx45 appears to be opposite to Cx43 in modulating skeletal homeostasis.

Disclosures: Marcus Watkins, None.

MO0208

Osterix Has a Critical Role in BMP2-induced Cx43 Promoter Activity in vitro. <u>Dong Jin Chung</u>*[1], <u>Dong Hyeok Cho</u>[2], <u>Jin Ook Chung</u>[2], <u>Min Young Chung</u>[2], <u>Kwang Youl Lee</u>[3]. [1]Chonnam National University Medical School, South Korea, [2]Chonnam National University Medical School, South Korea, [3]College of Pharmacy, Chonnam National University, South Korea

Osterix is a transcription factor specifically expressed by osteoblasts and is important for osteoblast differentiation. Although Osterix has been shown to be induced by BMP2, the molecular basis of the regulation, expression and function during osteoblast differentiation are not fully understood. Connexin43 (Cx43) is a major gap junction (GJ) protein in bone and plays a critical role in osteoblast differentiation. Recessive or dominant disruption of connexin43 function results in osteoblast dysfunction and abnormal expression of osteoblast genes. However, little is known about the functional interactions between Osterix and the Cx43 promoter. Previously, we showed that aminobisphosphonates as well as the pro-osteogenic transcription factors, Runx2, Osterix or Dlx5, increased transcriptional activity of the Cx43 promoter. In this study, we investigated further the relationship between Osterix and Cx43 using the cell lines HEK 293 and C2C12. Osterix increased transcriptional activity of the Cx43 promoter in a dose-dependent manner with peak of 4 and 5 folds in HEK 293 and C2C12 cell lines, respectively. Western blot analysis confirmed that Osterix increased protein expression of Cx43 in a similar pattern. Mutagenesis and chromatin immunoprecipitation assay also showed similar results. These results suggest that Osterix has a critical role in increase in BMP2-induced Cx43 promoter activity.

Disclosures: Dong Jin Chung, None.

MO0209

Pyk2 Isoforms in Osteoblasts: Mechanism of Regulation by Phosphorylation, Translocation, and Pin1 Activity. Pierre Eleniste*, Angela Bruzzaniti. Indiana University School of Dentistry, USA

Deletion of the protein tyrosine kinase Pyk2 in mice results in high bone mass. We previously demonstrated that Pyk2 and the shorter Pyk2-S isoform are highly expressed in osteoblasts (OBs), with Pyk2 mRNA expression declining during OB differentiation, while Pyk2-S mRNA levels increase with time. In addition, deletion of both Pyk2 isoforms promotes OB bone formation. Tyrosine Y402 phosphorylation is important for Pyk2 kinase activity, whereas serine phosphorylation may control subcellular localization. In the current study, we examined the mechanism action of Pyk2 and Pyk2-S by examining tyrosine (pTyr) and serine phosphorylation (pSer), subcellular localization and the activation of OB signaling pathways. Pyk2 and Pyk2-S were transiently expressed in MC3T3-E1 cells, which lack endogenous Pyk2. The pY402 and pSer levels of Pyk2-S were significantly higher than Pyk2 under basal conditions. We also found that the prolyl isomerase Pin1 formed a protein complex with Pyk2 and PyK2-S. Juglone, a Pin1 inhibitor, increased pY402 levels in Pyk2 to a greater extent than Pyk2-S. In contrast, juglone increased the pSer level of Pyk2-S to a much greater extent than Pyk2. Subcellular protein fractionation revealed that Pyk2 is most abundant in the cytoskeleton fraction, followed by the nucleus, membrane and cytosol. Although Pyk2-S was localized mostly in the cytosol under basal conditions, juglone led to the translocation of Pyk2-S to the cytoskeleton. We also examined the effect of Pyk2 and Pyk2-S expression on OB signaling. Western blotting revealed that Pyk2 activated the Notch1 signaling pathway, leading to increased levels of cleaved Notch1. In contrast, Pyk2-S led to the activation of ERK and b-catenin pathways in OBs. Collectively, our studies reveal isoform-specific differences in Pyk2/Pyk2-S phosphorylation, localization and signaling in OBs. Further, Pin1 plays an important role in regulating both the serine phosphorylation and intracellular translocation of Pyk2-S. Serine or tyrosine phosphorylation of the Pyk2 isoforms may also contribute to the activation of specific OB signaling pathways.

Disclosures: Pierre Eleniste, None.

MO0210

Adiponectin Enhances Fracture Repair. Liping Wang*[1], Theresa M. Roth[2], Robert Nissenson[3]. [1]VA Medical Center, San Francisco, USA, [2]Endocrine Unit, VA Medical Center, USA, [3]VA Medical Center & University of California, San Francisco, USA

Adiponectin (APN) is the most abundant adipokine secreted from adipose tissue. Clinical studies have shown an inverse relationship between circulating APN levels and total body bone mineral density in humans. Circulating APN is also positively associated with fracture (FX) risk, suggesting a role for APN as a negative regulator of bone mass and strength. However, the influence of APN on FX healing is not known. To investigate this, fracture studies were carried out on male mice with adipocyte-specific overexpression of APN (AdTg) compared with wild type male littermate controls (WT). Four month old mice were subjected to FX at the mid-shaft of the right tibia by three point bending. The analysis of the healing process was carried out using μCT 28 days post FX. AdTg displayed a 59% increase in callus bone fractional volume (BV/TV) (WT vs. AdTg: 28.62 ± 1.45 vs. $45.50 \pm 2.82\%$, p<0.01), a 31.9% increase in trabecular thickness (Tb.Th) (WT vs. AdTg: 67.17 ± 2.09 vs. $88.63 \pm 3.99 \mu m$, p<0.01), and a 31.6% decrease in total callus volume (TV) (WT vs. AdTg: 3.68 ± 0.34 vs. $2.52 \pm 0.40 mm^3$, p<0.05). To determine the effects of APN on bone structure and bone formation within the callus, we performed histomorphometry and found that APN over-expression resulted in significantly increased callus BV/TV by 73.8% (WT vs. AdTg: 20.99 ± 3.10 vs. $36.49 \pm 2.14\%$, p<0.01), Tb.Th by 49.3% (WT vs. AdTg: 13.15 ± 0.41 vs. 19.63 ± 3.54 μm, p<0.05), mineral appositional rate by 43.1% (WT vs. AdTg: 1.19 ± 0.16 vs. 1.71 ± 0.13 μm/d, p<0.05), and bone formation rate by 153.7% (WT vs. AdTg: 0.07 ± 0.01 vs. 0.19 ± 0.05 μm^3/μm^2/day, p<0.05). Finally, we assessed markers of the osteogenic process by quantitative real time PCR of callus RNA samples at 10 and 28 days after FX. AdTg mice displayed increased expression of the endothelial markers, Tie2 (1.98-fold) and VEGFD (3.0-fold) at 10 days after FX and, at day 28 post FX, increased expression of osterix (1.86-fold) and osteocalcin (2.13-fold), and decreased expression of PPARγ (0.8-fold). Taken together, our results demonstrate that over-expressed endogenous APN produces a positive effect on FX healing by stimulating the function of osteoblasts and callus remodeling. These results raise the possibility that APN or small molecule APN mimetics currently in development for treatment of type 2 diabetes might be effective in promoting FX repair.

Disclosures: Liping Wang, None.

MO0211

Autophagy in Osteoblasts is involved in Mineralization and Bone Homeostasis. Valérie Pierrefite-Carle[1], Marie Nollet[1], Sabine Santucci-Darmanin[1], Véronique Breuil[2], Rasha Al-Sahlanee[1], Michel Samson[1], Sophie Pagnotta[3], Séverine Battaglia[4], Delphine Farlay[5], Romain Dacquin[6], Pierre Jurdic[7], Georges Boivin[8], Dominique Heymann[9], Shi Shou Lu[10], David Dempster[11], Georges Carle*[12]. [1]Université Nice-Sophia Antipolis, CEA, UMR E4320 MATOs, France, [2]CHU Nice, Université Nice-Sophia Antipolis, CEA, UMR E4320 MATOs, France, [3]Université Nice Sophia-Antipolis, CCMA, France, [4]INSERM UMR 957, Université de Nantes, France, [5]INSERM, UMR1033; Université De Lyon, France, [6]IGFL, Université de Lyon, CNRS, Ecole Normale Supérieure de Lyon, France, [7]Ecole Normale Superieure de Lyon, France, [8]INSERM, UMR1033 ; Universite De Lyon, France, [9]INSERM U957, University of Nantes, France, [10]Regional Bone Center, Helen Hayes Hospital, USA, [11]Columbia University, USA, [12]Université Nice-Sophia Antipolis, CEA, France

Autophagy is the major catabolic process of eukaryotic cells that degrades and recycles damaged macromolecules and organelles. During this process, the cytoplasmic material targeted to degradation is delivered to lysosomes upon sequestration within double-membraned vesicles called autophagosomes. Autophagosomes and their contents are cleared upon fusing with late endosomes or lysosomes, and products of these catabolic reactions can then re-enter anabolic and/or bioenergetic metabolisms. Autophagy occurs at low level in all cells to ensure the homeostatic turnover of long-lived proteins and organelles and is upregulated under stressfull conditions.

In the present work, we analyzed the role of autophagy in osteoblasts (OB). We first show that the autophagic process is induced in OB during mineralization. Then, using knockdown of autophagy-essential genes and OB-specific autophagy-deficient mice, we demonstrate that autophagy deficiency reduces mineralization capacity. Moreover, our data suggest that autophagic vacuoles are used as vehicles in OB to secrete hydroxyapatite crystals. In addition, autophagy-deficient OB exhibit increased oxidative stress and receptor activator of NF-kB (RANKL) secretion, favoring generation of osteoclasts (OC), the cells specialized in bone resorption. In vivo, we observed a 50% reduction in trabecular bone mass in OB-specific autophagy-deficient mice.

Taken together, our results show for the first time that autophagy in OB is involved both in the mineralization process and in bone homeostasis. These findings are of importance for mineralized tissues which extends from corals to vertebrates and uncovers new therapeutics targets for calcified tissue related metabolic pathologies such as osteoporosis.

Disclosures: Georges Carle, None.

MO0212

Withdrawn

MO0213

ECE1 Dependent Endothelin Signaling Regulates the Production of IGF-1, the WNT Signaling Inhibitors Sclerostin and DKK1, and is Critical for Osteogenesis. Michael Johnson*[1], Jasmin Kristianto[2], Baozhi Yuan[1], Everett Smith[1], Luisa Meyer[3], Caitlin Collins[4], Heidi Ploeg[4], Robert Blank[5]. [1]University of Wisconsin, USA, [2]University of Wisconsin–Madison, USA, [3]University of Wisconsin - Madison, USA, [4]University of Wisconsin, USA, [5]Medical College of Wisconsin, USA

Osteoblasts produce, process, and respond to endothelin 1 (ET1), expressing all the proteins required for autocrine ET1 signaling to occur. Previously we demonstrated that exogenous big endothelin (big ET1), increases mineralization by TMOb osteoblasts and acts through increasing production of IGF-1 and decreasing the production of the WNT signaling inhibitors DKK-1 and sclerostin (SOST). Furthermore, the effects of big ET1 supplementation could be blocked by inhibiting endothelin converting enzyme 1 (ECE1) or the ET A type receptor (EDNRA). Earlier studies on the effect of ET1 on bone were done in the context excess ET1 and pathology. It remains unknown whether deficits in ET1 signaling have an impact on bone. To determine the role of ET1 signaling in normal bone physiology we blocked ENDRA and ECE1 using BQ-123 and phosphoramidon, respectively. In both cases, we saw decreased mineralization (p<0.05). Concordantly, these treatments also decreased production of IGF-1 (p<0.001). While inhibition of EDNRA produced the expected increases of DKK1 and SOST, inhibition of ECE1 either pharmacologically or by transfection with ECE1 specific siRNA led to decreases of both DKK-1 and SOST. In human bone cores exposed to exogenous big ET1, we saw a similar molecular footprint with increased IGF-1 (p<0.001), decreased SOST (p<0.008) and a trend decreased DKK1. These data indicate that ET1 signaling contributes to osteoblasts' developmental program. In addition, they suggest that ECE1 may have additional substrates whose actions are mediated by non-ET1 signaling pathways. Identifying these pathways will require further investigation.

Disclosures: Michael Johnson, None.

MO0214

Evidence that adiponectin negatively regulates skeletal homeostasis by direct panacrine effects on osteoblasts. <u>Linh Ho</u>*[1], <u>Marcia J Abbott</u>[2], <u>Dylan O'Carroll</u>[3], <u>Liping Wang</u>[3], <u>Theresa Roth</u>[4], <u>Robert Nissenson</u>[5]. [1]UCSF, USA, [2]SFSU, USA, [3]SF VAMC, USA, [4]SF VAMC, USA, [5]VA Medical Center & University of California, San Francisco, USA

Adiponectin is a regulator of skeletal homeostasis with an inverse correlation between circulating adiponectin levels and BMD. Whether adiponectin systemically regulates bone formation and skeletal homeostasis or these skeletal effects are direct on osteoblasts and site-specific due to local production of the adipokine by marrow adipocytes have yet to be fully understood. To address these issues, we use FVB/N adiponectin transgenic mouse model in which secretion of endogenous adiponectin is increased by adipocytes (AdTg), kindly provided by Philipp Scherer, U. Texas Southwestern Medical School. We found that adiponectin exerts its negative effects on skeletal homeostasis by local regulation and this effect may involve the Beta catenin/PPARγ signaling axis. Tissue volume (TV) and bone volume (BV) by uCT were significantly lower in female distal femurs in AdTg mice (P<0.05). The cancellous TV, BV, and BV/TV at the proximal tibia was significantly lower in AdTg females (P<0.05). Proximal tibia in female AdTg mice by dynamic histomorphometry displayed a decrease in mineral apposition rate and bone formation rates at the proximal tibia (P<0.05). Cortical thickness was significantly smaller at both the mid shaft of the femur and tibia in female AdTg mice compared to WT (P<0.05). In female AdTg mice cortical thickness at the TFJ was significantly smaller than in WT (P<0.05). Static histomorphometry analysis revealed a decrease in osteoclast surface in the proximal tibia of female AdTg mice (P<0.05). AdTg female mice exhibited increased number of adipocytes in the proximal tibia compared to WT. Treatment with adiponectin on differentiating osteoblastic cells, day 14-28, impaired their ability to fully differentiate (P<0.05), reached maximal levels at 2.5 ug/ml. Osterix, runx2, alkaline phosphatase, osteocalcin, and collagen type I were significantly lower in adiponectin treated osteoblastic cells compared to control cells (P<0.05). Additionally, the RANKL:OPG ratio was significantly lower in the cells treated with adiponectin compared to the vehicle control cells (P<0.05). Adiponectin treatment on mature differentiating osteoblastic cells resulted in increasing in oil red O and Nile red staining (P<0.05) and in mRNA levels of PPARγ and C/EBPa (P<0.05). Adiponectin treatment on differentiating osteoblastic cells resulted in a decrease in Beta Catenin and cyclin D1 (P<0.05). In conclusion, adiponectin has negative effects on bone formation in vivo and in vitro. The in vivo effects are likely to involve direct paracrine actions of adiponectin to suppress osteoblastogenesis and promote adipogenesis.

Disclosures: Linh Ho, None.

MO0215

miR-665 Regulates Dentinogenesis by miRNA and Epigenetic Mechanism. <u>Mohammad Hassan</u>*[1], <u>Austin Kemper</u>[2], <u>Harunur Rashid</u>[3], <u>Amjad Javed</u>[2], <u>Austin Kemper</u>[2], <u>Christopher Clarke</u>[4]. [1]University of Alabama, USA, [2]University of Alabama at Birmingham, USA, [3]University of Alabama Birmingham, USA, [4]UNIVERSITY OF ALABAMA, SCHOOL OF DENTISTRY, USA

MicroRNAs (miRNAs or miRs) are evolutionarily conserved, non-coding RNA which regulate gene expression by translational repression or mRNA degradation. Studies have proven the pivotal role miRNA plays in biological processes including tooth development. In our current study, we discovered microRNA-665 (miR-665) to be a potential repressor of odontoblast maturation. Stable overexpression of miR-665 in odontoblast cells inhibits, while knock-down promotes, matrix maturation marker (Col1A1) and mineralization markers Dspp, Dmp1 and osteocalcin. Similar inhibition was observed for the expression of enamelysin (MMP-20) and kallikrein 4 (KLK4), the early and late proteases for dentin and enamel maturation. Consistent with this finding, miR-665 suppressed, whereas anti-miR increased, Runx2 and osterix two essential tooth specific transcription factors. Hence, we determined that miR-665 inhibition of odontoblast maturation could lead to innovative mechanisms that would further our understanding of odontoblast gene function by miR 665. To understand the mechanism by which this miR-665 inhibits odontoblast differentiation, we sought to determine the following mechanisms for miR-665 relevant to dentinogenesis. MiRNA mechanism: Homeodomain gene Dlx3 is highly critical for tooth development. No study of miR regulation of Dlx3 expression during dentinogenesis has been reported to date. We found that miR-665 directly binds to the 3'UTR of Dlx3 mRNA and robustly decreases Dlx3 mRNA and protein in primary and culture odontoblasts cells. Epigenetic mechanism: Analysis of miR-665 guided silencing complex revealed that Kat6A, a MYST family of histone acetyltransferase is endogenously associated with miR-665. Stable expression of miR-665 in odontoblast cells significantly inhibits Kat6A expression (mRNA and protein) and acetylated H3K9 protein level. Kat6A physically interacts with Runx2 and activates tooth specific DSPP promoter activity synergistically. MiR-665 noticeably reduces the recruitment of Kat6A, Runx2, Ing4, osterix and acetylated H3K9 and, induces the recruitment of methylated H3K9 at DSPP promoter close to transcriptional start site (TSS). Regulation of this chromatin remodeling switch (H3K9Ac to H3K9me) by miR-665 clearly demonstrates a repressive state of DSPP gene transcription. When taken together, our results for the first time provide molecular evidence for miR-665 regulation in a miRNA-epigenetic regulatory network to control odontoblast differentiation.

Disclosures: Mohammad Hassan, None.

MO0216

Naringenin stimulates mineral formation by human osteoblast-like cells at levels attainable by consuming fruits and vegetables. <u>Bryan D. Johnston</u>*, <u>Dylan W. Johnston</u>, <u>Wendy E. Ward</u>. Centre for Bone & Muscle Health, Faculty of Applied Health Sciences, Brock University, St. Catharines, Ontario, L2S 3A1, Canada

Introduction: A diet high in flavanones, or citrus flavonoids, has been correlated with higher hip and vertebral BMD, and lower bone resorption in perimenopausal women. Naringenin is one of the citrus flavonoids, and by consuming between 2-3 servings of grapefruit juice it is possible to achieve plasma levels of naringenin in the μM range. The stability of naringenin in plasma makes it a good candidate to potentially modulate human osteoblast function. In the present study, naringenin was screened in the long-term culture of human osteoblast-like cells (SaOS-2) for positive effects on the formation of mineral.

Materials/Methods: SaOS-2 cells were seeded at 1.0×10^4 cells per well in 12 well plates with phenol red free DMEM/F-12 media (10% fetal bovine serum, 1% antibiotics, 10nM dexamethasone (DEX)). The cells were differentiated for 7 days in media supplemented with both 10nM DEX and 50mg/ml ascorbic acid. Naringenin treatment (1, 5, 10, 25, 50, and 75μM) was started after differentiation and the media was supplemented with 10μM β-glycerophosphate to encourage matrix mineralization for 14 days. Media was changed every 2-3 days. To measure mineral formation, cells were fixed in 4% paraformaldehyde (pH 7.4), incubated with Alizarin Red Stain (ARS) (40mM, pH 4.2) and incubated with 10% cetylpyridinium chloride (pH 7.0) to extract the ARS. Since ARS binds to calcium at a molar ratio of 1:2, the amount of calcium per well was determined. The same fixed cell layers were also treated with von Kossa (VK) staining and images of the wells were used to quantify the area of mineral per well. Based on previous research, epigallocatechin-3-gallate (EGCG) treatment at 5μM was used as a positive control.

Results: Naringenin treatment at 1, 5, 10, and 25μM resulted in 12.4%, 25.4%, 25.6%, and 20.5% higher mineral formation compared to control, respectively. These higher levels of mineral formation were similar to the 26.3% higher mineral formation with the positive control, EGCG. The 50μM naringenin treatment resulted in no difference in mineral formation while the 75μM treatment reduced mineral formation. Naringenin treatment at 5 and 10μM and the EGCG control all resulted in higher mineral formation as assessed by VK staining.

Conclusions: At concentrations attainable through diet alone (1-10μM), naringenin stimulated mineral formation by human osteoblast-like cells. Future studies aim to examine the mechanism underlying the observed increase in mineral formation.

Disclosures: Bryan D. Johnston, None.

MO0217

N-linked Glycosylation: a Critical Mechanism of PTH-Resistance in Osteoblasts under High Glucose Conditions. <u>Ann-Kristin Picke</u>*[1], <u>Christine Hofbauer</u>[2], <u>Martina Rauner</u>[3], <u>Lorenz Hofbauer</u>[4]. [1]Dresden University Medical Center, Germany, [2]Dresden Technical University Medical Center, Germany, [3]Medical Faculty of the TU Dresden, Germany, [4]Dresden University Medical Center, Germany

Type 2 diabetes mellitus impairs bone quality and increases fracture risk. We showed that diabetic ZDF rats have low bone mass due to impaired osteoblastogenesis, which can be partially reversed with an intermittent parathyroid hormone 1-84 (PTH) therapy. It remains unclear, why PTH treatment does not fully restore osteoblast (OB) function in diabetic conditions. Here, we tested if high glucose (HG) conditions lead to a partial PTH resistance in osteoblasts *in vitro*.

Pre-osteoblastic MC3T3-E1 cells were cultured in osteogenic medium in HG concentrations (100 mM) for 21d. Intermittent PTH treatment was performed by treating the cells with 50 ng/ml PTH for 8h every other day.

HG decreased the production of mineralized matrix by -69% as compared to control cells. Intermittent PTH treatment reversed this effect (+115%), but did not reach the level of control cells. The Ca/P-ratio (quality) of the mineralized matrix was decreased in HG (-83%) compared to control, and PTH treatment increased the Ca/P-ratio by 30% under HG conditions. PTH dose dependently increased cAMP levels up to 2.5-fold, whereas in HG conditions cAMP levels were even decreased after PTH stimulation (4-fold). Similarly, PTH-induced activation of protein kinase A and cAMP response element-binding protein (CREB), the downstream targets of cAMP, were blunted in HG conditions. Gene expression of insulin-like growth factor-1, alkaline phosphatase, osteopontin, connexin43 and RANKL significantly increased after intermittent treatment of PTH in control and HG conditions. To determine whether the blunted cAMP activation was due to a decreased expression of the PTH receptor 1 (PTHR1), we determined protein levels of PTHR1 using Western blot. However, PTHR1 expression was not affected by HG or PTH. Instead N-linked glycosylation was increased in HG. Combined treatment of HG and PTH with tunicamycin to block N-linked glycoprotein synthesis elevated the amount of mineralization in HG-treated cells similarly to PTH treatment alone (4-fold). Interestingly, tunicamycin alone was able to reverse the inhibition of mineralization of HG-treated OB. Tunicamycin treatment also significantly increased gene expression of OB markers.

These results suggest that increased N-linked glycosylation is a critical mechanism of OB function in HG conditions in MC3T3-E1 cells. Thus, preventing these posttranslational modifications may improve OB function and augment the response to PTH treatment in type 2 diabetes mellitus.

Disclosures: Ann-Kristin Picke, None.

MO0218

Parathyroid Hormone Regulates Osteoblast Bioenergetics Through its Actions on Glycolysis. Anyonya Guntur*[1], Phuong Le[1], Clifford Rosen[2]. [1]Maine medical center research institute, USA, [2]Maine Medical Center, USA

We recently measured the bioenergetic pathways utilized by C57BL/6J neonatal calvarial osteoblasts (COBs) at various stages of differentiation. We reported that differentiating COBs use both Oxidative phosphorylation (OxsPhos, measured via Oxygen Consumption Rates) and Glycolysis (Glyc, measured via Extra Cellular Acidification Rates) for optimal differentiation. Intermittent Parathyroid hormone (PTH) is anabolic to bone through enhancement of osteoblast (OB) differentiation *in vivo*, although *in vitro* chronic exposure may impair differentiation. We hypothesized that PTH would regulate COB bioenergetic pathways. To test this hypothesis, we treated C57BL/6J COBs with Vehicle (VEH) or 20nM PTH for 21 days in the presence of OB differentiation media. In the presence of PTH both OCR and ECAR were inhibited as was nodule formation during in vitro osteoblast differentiation. Furthermore, we performed *in vitro* calvarial organ culture from 4 days old C57BL/6J pups in the absence (VEH) or presence (100nM) of PTH added one day after plating the calvariae. Three days after PTH treatment, calvariae were assayed using the Seahorse XF24. PTH treatment led to a significant increase in ECAR levels compared to VEH treated samples. To test whether Glyc plays a key role in regulating osteoblast differentiation, we utilized 2-DeoxyGlucose a specific inhibitor of Glyc at 0.1mM concentration in the presence of OB differentiation media. In the presence of the Glyc inhibitor we observed a dramatic decrease in ECAR and OB nodule formation compared to cells in differentiation media. In sum these data suggest that glycolysis is a critical component in OB differentiation and that chronic PTH treatment can suppress OCR and ECAR in vitro but induce ECAR in whole calvaria.

Disclosures: Anyonya Guntur, None.

MO0219

Role for Chloride and Potassium Channels Supporting Na/H Exchange in Bone Formation. Harry Blair[1], Li Liu*[1], Deborah Nelson[2], Peter Friedman[3], Paul Schlesinger[4]. [1]University of Pittsburgh, USA, [2]University of Chicago, USA, [3]University of Pittsburgh School of Medicine, USA, [4]Washington University, USA

We are investigating u*ncharacterized steps of bone mineral synthesis.* Mineral deposition is not fully defined; many cases of osteopenia or osteoporosis have no known cause. Disordered bone formation also contribute to slowly-developing skeletal defects such as kyphoscoliosis. *Bone mineral is precipitated from phosphate and calcium in an isolated extracellular compartment*: the surface layer of osteoblasts is linked by tight junctions. Phosphate and Ca^{2+} cannot move by diffusion because of the tight junctions. Thus, ion transport is obligatory. The bone forming unit, surface cells and osteocytes, is also unified by gap junctions, allowing coordinated bone synthesis. Calcium is transported across osteoblasts by facilitated transport; phosphate is actively produced from ATP and PPi, with high concentrations of free phosphate liberated by phosphatases at the secretory osteoblast surface by alkaline phosphatase and ENPPs. These create a large phosphate gradient. *Formation of mineral from this calcium and phosphate requires H^+ counter-transport*, as seen in the equation of state:

$$6\ HPO_4^{2-} + 2\ H_2O + 10\ Ca^{2+} ?\ Ca_{10}(PO_4)_6(OH)_2 + 8\ H^+$$
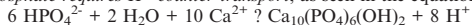
Since bone mineral forms in a closed space, as Ca^{2+} precipitates acid accumulates, lowering the pH. This would stop precipitation if H^+ is not removed. This stoichiometry was recognized with experimental evidence of an alkaline bone compartment long ago. But how H^+ transits the osteoblast tight epithelium is uncharacterized. Osteoblasts do have massive basolateral Na^+/H^+ exchange capacity. We recently showed that this is mediated by Na^+/H^+ exchangers (NHEs) 1 and 6. But how H^+ enters the barrier layer of osteoblasts is unknown. We used direct osteoblast membrane transport study to characterize key acid transport mechanisms. This used membrane fragments from mineralizing osteoblasts made by nitrogen cavitation. We show that *osteoblast membranes have massive CLC-type Cl^-/H^+ exchange*, which depends on K^+; thus Cl/H exchange very likely is driven by a membrane voltage from K^+ channels. Studies of mRNA and antibody labeling show massive expression of *both* CLC3 and CLC5 at the secretory membranes of osteoblasts. This expression carries through the entire haversian system. We hypothesize that this allows maintenance of the osteon's mineral by maintaining a slight alkaline gradient during the life of the bone unit. Sudies of CLC3 KO mice show a mild mineralization delay; we hypothesize that CLC3/5 double KO mice will show a severe phenotype.

Disclosures: Li Liu, None.

MO0220

The Function of MicroRNA miR-23a Cluster in Osteogenesis. Huan-Chang Zeng*[1], Yangjin Bae[1], Jordan Kho[1], Yuqing Chen[2], Terry Bertin[2], Elda Munivez[2], Brendan Lee[1]. [1]Baylor College of medicine, USA, [2]Baylor College of Medicine, USA

MicroRNAs are negative regulators of target genes and are involved in various biological processes. The miR-23a cluster is a group of microRNA which is highly enriched in bone tissues but the function of this cluster during osteogenesis is not yet clear. To study the function of miR-23a cluster in bone development *in vivo*, we generated a transgenic mouse model overexpressing miR-23a cluster using the osteoblast (Ob)-specific Col1a1-2.3kb promoter. Micro-computed tomography (uCT) and histomorphometric analysis showed that transgenic mice exhibited low bone mass with decreased Ob number and decreased mineral apposition rate. Interestingly, we also found that osteocytes were significantly increased in transgenic mice supporting dysregulation of both early Ob fate commitment and late Ob terminal differentiation into osteocytes. To study the loss of function of miR-23a cluster *in vivo*, we also generated transgenic mice expressing decoys for miR-23a, miR-27a or miR-24-2 individually driven by the Col1a1-2.3kb promoter. Mice with the miR-23a decoy and miR-27a decoy showed dental fractures and low bone mass by μCT while miR-24 decoy lines had no apparent abnormalities. RNASeq analysis of mouse models showed that TGF-β signaling pathway may be directly regulated by the miR-23a cluster.

Disclosures: Huan-Chang Zeng, None.

MO0221

Transgenic Over-expression of Vitamin D Receptor in Mature Osteoblasts Enhances Anabolic and Catabolic Activities Depending on Dietary Calcium and Phosphate Levels. Rahma Triliana*[1], Howard Morris[2], Paul Anderson[3]. [1]SA Pathology/IMVSthe University of Adelaide., Australia, [2]SA Pathology, Australia, [3]Musculoskeletal Biology Research, University of South Australia, Australia

1,25-dihydroxyvitamin D (1,25D) action in osteocytes has been reported to actively inhibit mineralisation in mice in addition to its actions to enhance RANKL-mediated bone resorption. However, osteocalcin-promoter driven over-expression of vitamin D receptor (VDR) in mature osteoblasts and osteocytes (OSVDR mice) has also been demonstrated to enhance bone formation as well as reduce bone resorption. While these complex observations are not easily reconciled, the physiological conditions which determine the nature of vitamin D activity is likely to be an important factor. To address this, 3-week-old female OSVDR and WT mice were fed standard semi-synthetic diet containing either 1% calcium and 0.625% Phosphorus (NCaP) or 0.03% calcium and 0.08% phosphorus (LCaP) until 20 weeks of age, at which time they were killed for subsequent analyses. When compared to NCaP fed WT mice, LCaP fed WT mice exhibited marked reduction in femoral cortical bone volume (24%, P<0.001) due to increased endosteal circumference and reduced metaphyseal trabecular bone volume (70%, P<0.001) due to reduced trabecular number, which is consistent with osteopenia due to enhanced bone resorption. Consistent with previous findings, OSVDR mice fed NCaP diet demonstrated increased cortical (8%, P= 0.056) and trabecular (64% P=0.003) bone volumes when compared to WT fed NCaP diet. However, OSVDR mice fed LCaP diet demonstrated markedly reduced femur length, reduced trabecular bone volume and cortical thinning which was splayed towards the metaphyseal region. In addition, these mice frequently demonstrated disturbed growth plate structure, marked intra-cortical porosity which was associated with pronounced osteoclastic activity. The pronounced catabolism of bone in OSVDR mice fed LCaP occurred despite normocalcemia and normophosphatemia. However, serum FGF23 levels were 2-fold lower and serum 1,25D levels were 2-fold higher in OSVDR mice when compared with WT mice fed LCaP suggesting that the enhanced catabolism mediated by 1,25D activity may be due, at least in part to altered feed-back on renal 1,25D synthesis. These findings support the notion that 1,25D activity in osteoblasts/osteocytes mediates anabolic and catabolic activities depending on the physiological challenge of calcium and phosphate demand.

Disclosures: Rahma Triliana, None.

MO0222

Membrane-bound prostaglandin E synthase (mPGES)-1-mediated prostaglandin E_2 (PGE_2) production plays a critical role in the ligand for toll-like receptor 2 heterodimer (TLR1/2, TLR 2/6) induced bone resorption. Chiho Matsumoto[1], Tsukasa Tominari[2], Michiko Hirata[3], Chisato Miyaura[1], Masaki Inada*[1]. [1]Tokyo University of Agriculture & Technology, Japan, [2]Tokyo University of Agriculture & Technology, Japan, [3]Tokyo University of Agriculture & Technology, Japan

Toll-like receptors (TLRs) play critical roles in innate immunity, and various ligands for TLRs are thought to regulate the host defense mechanisms against pathogens. TLR2 generally forms heterodimers with TLR1 or TLR6. TLR2 heterodimers have different biological response, the TLR2-TLR1 heterodimer recognizes triacylated lipopeptides from gram-negative bacteria, whereas the TLR2-TLR6 heterodimer recognizes diacylated lipopeptides from gram-positive bacteria. We have reported that bone resorption associated with inflammation such as bacterial infection of periodontitis was attenuated in prostagrandin E2 synthethase deficient mice (*mPges*1-/-) due to the lack of PGE_2 production by osteoblasts. In this study, we examined the roles of PGE_2 in various TLR2 ligands induced bone resorption using the models of *mPges*1-/-. TLR1/2 and TLR 2/6 synthetic ligands markedly increased bone resorbing activity in wild-type derived calvarial organ cultures, and that the activity was attenuated in the cultures derived from *mPges*1-/-. In the cultures of *mPges*1-/- osteoblasts, both PGE_2 production and the following RANKL expression were attenuated. The activation of NFkB in osteoblast is critical for the induction of various inflammation related genes, such as COX-2 and mPGES-1. In luciferase assay, TLR1/2 and TLR2/6 ligands induced NFkB activation in wild type derived osteoblasts.

To examine the direct effects of TLR1/2, 2/6 ligands on the survival in mature osteoclasts, we used the models of RANKL induced osteoclasts derived from bone marrow macrophage. Mature osteoclasts expressed RANK, cathepsin K, NFATc1, and the treatment of TLR 2/6 ligand enhanced NFATc1 expression and osteoclast life span. Finally we investigated the possible roles of a gram positive bacteria derived native TLR2 ligand in bone resorption. Lipoteichoic acid from gram positive bacteria stimulated bone resorption in the calvarial cultures with increased production of PGE2. These results suggest that synthetic and native ligands for TLR2 heterodimer promotes RANKL expression via mPGES-1-mediated PGE_2 synthesis, leading to bone resorption. mPGES-1 may play a key role in the inflammatory bone destruction via TLR2 heterodimer signaling pathway.

Disclosures: Masaki Inada, None.

MO0223

Osteoblast-Speci R≥c IGF-1 signaling deficiency causes delayed endochondral bone formation during fracture healing. Tao Wang*[1], Yongmei Wang[2], Candice GT Tahimic[3], Chak Fong[4], ALICIA MENENDEZ[4], Daniel Bikle[3]. [1]University of California, San Francisco, SAN FRANCISCO, CA, USA, [2]Endocrine Unit, University of California, San Francisco/VA Medical Center, San Francisco, CA, USA, [3]Endocrine Research Unit, Division of Endocrinology UCSF & VAMC, San Francisco, CA, USA, [4]University of California, San Francisco, San Francisco, California, USA

Insulin-like Growth Factors (IGFs) are important local regulators during fracture healing. Although IGF signaling deficiency is known to increase the risk of delayed union or non-union fractures in the elderly population, the mechanism has received little attention. We hypothesize that the loss of the IGF-1 receptor (IGF-1R) results in decreased bone formation and impaired healing following fracture. To test this hypothesis, we mated conditional knockout (CKO) mice harboring a tamoxifen-inducible Cre under the control of the osteoblast-specific promoter, 2.3-kb fragment of α1(I) collagen, with floxed IGF-IR mice. Using the inducible Cre-LoxP system, disruption of the IGF-1R gene in osteoblasts at the time of fracture impaired both autocrine/paracrine and endocrine IGF-1 effects on osteoblasts only during fracture healing. Gene disruption was induced by 5 i.p. injections of tamoxifen in oil (2mg per mouse), and fracture was performed after the second tamoxifen injection. A unilateral closed tibial fracture was made in CKO mice and IGF-IR $^{flox/flox}$ (CON) mice aged 12 weeks. Non fractured tibial diaphysis (basal line control) and fracture callus samples were collected and analyzed by micro-CT, histomorphometry and gene expression. The results demonstrated that non fractured tibia in CKO mice were not significantly different from CON mice,but smaller callus size, decreased bone formation and a higher percentage of cartilage were found in the callus of CKO mice at day 10 post-fracture (p<0.05). Gene expression analysis showed that levels of osteoblast differentiation markers (OCN, Col1α1) were significantly reduced in the CKO callus compared to CON at day 10, 15, 21 post-fracture (p<0.05). Relative gene expression of Col2a1 and Col10a1, early and late markers of chondrocyte differentiation, showed that Col2a1 was significantly upregulated at day 10, 15, 21 and 28, and Col10a1 was significantly increased in the CKO callus at day 15 and 21 post-fracture. Two key osteoblast transcription factors, Runx2 and Osterix, acting sequentially to initiate osteoblast differentiation and highly expressed in the preosteoblast and immature osteoblast population, were significantly increased in the CKO callus at day 15 and 21 post-fracture (p<0.05). Our data indicate that IGF-1 signaling deficiency in this transgenic mouse model hindered osteoblast formation and maturation, and delayed endochondral ossification at the early stages of fracture healing. Enhancing IGF-I signaling may provide a means to enhance endochondral bone formation resulting in improved fracture healing.

Disclosures: Tao Wang, None.
This study received funding from: VA Program Project Award

MO0224

Use Of MC3T3 Cells For Native High-Level Production Of Carboxylated Mouse Osteocalcin. Patricia Buckendahl*[1], Daniel Benjamin[2]. [1]Rutgers University, USA, [2]Cenoxys Corporation, USA

Studies of *in vitro* and *in vivo* function of fully carboxylated native osteocalcin (OC) in the mouse require greater quantities of pure protein than are available commercially. Purification of native OC from mouse bone can be complicated by extensive glycation of the protein, as indicated by MALDI-TOF analysis, particularly from bone of older mice. To avoid this problem we cultured MC3T3-E1 cells and harvested the media. MC3T3-E1 cells were obtained from ATCC, plated in proliferation conditions in αMEM, 10% FBS, without ascorbic acid in 75 cm^2 culture flasks. When cells were confluent, flasks were changed to serum free advanced MEM containing ascorbic acid, 10 mM β-glycerophosphate, and 10 µM vitamin K1 to promote differentiation. To stimulate a further increase of OC production, we exposed some cultures to bioactive glass conditioned medium (GCM). Serum free medium was exposed to 45s5 Bioactive glass (MO-SCI Healthcare, Rolla MO), 100 mg/50 ml, for at least 3 days, to leach Si^{4+} and Ca^{2+} into the medium. Plain or GMC media were harvested every 3 to 7 days, frozen and lyophilized prior to purification. Under these conditions, cells continued to secrete OC for more than 5 months. Separation of OC from the media initially followed Sephadex G25 gel filtration and ion-exchange protocols. However, this was hampered because several

red to yellow colored components, including phenol red, vitamin B12 and riboflavin co-eluted with the OC. These bound irreversibly to the ion-exchange resin (Biorad Macro-Prep High Q Anion Exchange), rendering separation unreliable. A preliminary step of separation of reconstituted media on a bulk C18 reverse phase column was added. Elution with 30% methanol eliminated most of the phenol red and vitamins as well as some unwanted proteins. Additional protein, including OC, was then eluted with 80% methanol. After evaporation of the methanol and lyophilization, the protein was dissolved and assayed for OC content by RIA. At this stage, media from cells cultured without GCM yielded about 3 ng OC/ml of culture media. Cultures with GCM yielded a 10 to 20-fold increase in OC secretion into the media, up to 60 ng OC/ml of media after 7 days. Presence of GLA in chromatographic fractions was confirmed qualitatively by reaction with diazobenzene sulfonic acid. Culture of MC3T3 cells with GCM can be easily scaled up to yield large quantities of native mouse OC and purified by standard chromatographic methods.

Disclosures: Patricia Buckendahl, None.

MO0225

Cation activation of G-class signalling in human osteoblasts. Mark Rybchyn[1], Wendy Green[1], Arthur Conigrave[2], Rebecca Mason[3], Tara Brennan-Speranza*[4]. [1]Bosch Institute, Physiology & School of Medical Sciences, University of Sydney, Australia, [2]University of Sydney, Australia, [3]University of Sydney, Australia, [4]University of Sydney, Australia

We have previously shown that treatment of primary human osteoblasts (HOBs) with pharmacologically relevant concentrations of divalent cations including Ca^{2+} and Sr^{2+} resulted in an increase in osteoprotegerin (OPG) release, whilst decreasing the expression of membrane-associated receptor activator of NFκB Ligand (RANKL) (1,2). The present study investigated whether the calcium-sensing receptor (CaSR) and/or a related class C GPCR, GPRC6A, mediate these responses.

HOBs were transfected with siRNA directed at the CaSR (HOB/CaSR^{kd}) or GPRC6A (HOB/GPR^{kd}) or with a scrambled sequence (HOB/SCR) for 24h. Transfected cells were then exposed to zero or 1 mM strontium in the presence of 1 mM calcium for 24h. OPG and RANKL mRNA were measured by qRT-PCR. Strontium induced ~2-fold increase in OPG expression and ~2.5-fold decrease in RANKL expression in HOB/SCR cells (p<0.05; p< 0.01) but had little effect in HOB/CaSR^{kd} cells. There was no significant difference in the strontium-induced increase in OPG mRNA expression between HOB/SCR and HOB/GPR^{kd} cells. However, the strontium-induced reduction in RANKL mRNA expression was not observed in HOB/GPR^{kd} cells and, instead, a paradoxical increase in RANKL expression was observed when compared to HOB/SCR cells (p<0.001). PI-3-kinase inhibitor wortmannin inhibited strontium-induced changes in both OPG and RANKL, but only changes in RANKL were inhibited by ERK-inhibitor peptide. Furthermore, Co-IP investigations show that treatment of HOBs with Ca^{2+}, the natural ligand for CaSR, results in dimerization of the CaSR with GPRC6A. GPRC6A also appears to support *osteocalcin*-sensing in at least some tissues. However, recent results in Chinese Hamster Ovary (CHO) cells that stably express GPRC6A, have raised doubts regarding its role in osteocalcin sensing while confirming the role of GPRC6A in sensing basic amino acids and divalent cations. Our studies show that it might be necessary for the GPRC6A to dimerize with the CaSR or another receptor in order for it to signal to downstream pathways.

Refs:
1. Brennan TC, Rybchyn MS, Green W, Atwa S, Conigrave AD, Mason RS. *Osteoblasts play key roles in the mechanisms of action of strontium ranelate.* Br J Pharmacol. 2009 Aug;157(7):1291-300
2. Rybchyn MS, Slater M, Conigrave AD, Mason RS.*An Akt-dependent increase in canonical Wnt signaling and a decrease in sclerostin protein levels are involved in strontium ranelate-induced osteogenic effects in human osteoblasts.* J Biol Chem. 2011 Jul 8;286(27):23771-9.

Disclosures: Tara Brennan-Speranza, None.

MO0226

HIF-1α Dependent Metabolic Reprogramming of Periosteal Cells Improves Bone Repair. Steve Stegen*[1], Nick Van Gastel[2], Guy Eelen[3], Annelies Quaegebeur[4], Riet Van Looveren[5], Peter Carmeliet[4], Geert Carmeliet[3]. [1]Laboratory of Clinical & Experimental Endocrinology, KU Leuven, Belgium, [2]Laboratory of Clinical & Experimental Endocrinology, KU Leuven, Belgium, Belgium, [3]Katholieke Universiteit Leuven, Belgium, [4]Angiogenesis & Neurovascular Link, Vesalius Research Center, KU Leuven, Belgium, [5]KU Leuven, Belgium

Cell-based bone tissue engineering represents a promising strategy for the treatment of large bone defects. However, the low survival rate of the osteogenic cells implanted in an environment deprived of oxygen and nutrients remains a therapeutic challenge. We hypothesized that metabolic preconditioning by activation of the hypoxia signaling (HIF) pathway may protect these cells from cell death and hereby improves bone repair.

To stimulate the HIF-pathway, the PHD2 oxygen sensor was genetically inhibited in murine periosteum derived cells (*Phd2*^{low} mPDC). The bone formation (ectopic model) and bone repair capacity (large bone defect model) was assessed by implanting mPDC-seeded calcium phosphate-collagen scaffolds in nude mice. Histomorphometric and microCT analysis revealed enhanced bone formation, especially within the

scaffold center, in the *Phd2*^{low} mPDC-seeded scaffolds 8 weeks after implantation compared to control. In addition, we observed an increase in the number and size of blood vessels closely associated with the sites of bone formation.

In contrast to the later time points, blood vessels were absent in both control and *Phd2*^{low} mPDC-seeded scaffolds 3 days after implantation. However, *Phd2*^{low} mPDC survived better in the hypoxic center of the scaffold and showed reduced oxidative stress, suggesting the involvement of metabolic reprogramming. Indeed, several metabolic adaptations contributed to this prosurvival effect *in vivo*. We observed a redistribution of metabolic intermediates necessary for supplying energy and regulating redox homeostasis during cell stress. Furthermore, inhibition of enzymes responsible for maintaining these processes significantly reduced the prosurvival capacity of *Phd2*^{low} mPDC *in vitro* and *in vivo*.

Lastly, the effects of *Phd2* inactivation were HIF-1α dependent, as inhibition of *Hif-1α* transcription using a shRNA approach completely abrogated the prosurvival and bone forming properties of *Phd2*^{low} mPDC.

In conclusion, activation of the HIF-pathway in periosteal cells by genetic inactivation of *Phd2* preserves cellular bioenergetics and redox homeostasis during stress and hereby improves cell survival and ultimately bone formation in a tissue-engineered construct.

Disclosures: Steve Stegen, None.

MO0227

Induction of single nucleotide polymorphisms in the purinergic P2X7 receptor and subsequent investigation of changes in function and gene expression of specific bone markers. <u>Barakat Ali Nasir Ali</u>[1], <u>Jan Rune Larsen</u>*[2], <u>Solveig Petersen</u>[2], <u>Niklas Jorgensen</u>[3], <u>Ole Vang</u>[4], <u>Susanne Syberg</u>[5]. [1], Denmark, [2]Research Center for Ageing & Osteoporosis, Diagnostic Department, Glostrup Hospital, Denmark, [3]Copenhagen University Hospital Glostrup, Denmark, [4]Department of Science, Systems & Models, 18.1 Roskilde University, Denmark, [5]Research Centre for Ageing & Osteoporosis, Denmark

The investigation of bone is an interesting field in research involving crosstalk between several cells of different origins including several pathways of which many are still to be discovered and characterised. Through this system, a constant remodelling of the skeleton throughout the lifespan of a human is administered. If this system is no longer in homeostasis, it can lead to osteoporosis – a very invasive disease of which many elderly people suffers, in particular post-menopausal women. Involvement of the purinergic P2X7 receptor in regulation of bone formation has been reported. In addition, a subsequent identification of several single nucleotide polymorphisms (SNPs) within its gene has also been documented. This project has its basis in indicative findings of the negative and positive effect from SNPs in the P2X7 receptor gene and the subsequent risk of developing osteoporosis.

As a result, it is the aim of this report to investigate the cellular effect of three selected SNPs transfected into an osteoblastic cell line in order to determine functional changes in the receptor followed by an analysis of the pattern of expression in selected bone markers. This was approached by inducing a single point mutation using site directed mutagenesis in the P2X7 receptor gene whilst it sits in a plasmid. This is followed by transfection of the plasmid into ROS 17/2.8 cells using Lipofectamine 2000 and a subsequent examination of change in receptor function by looking at changes in intracellular calcium concentration using calcium assay. In addition, seven bone markers are tested for change in gene expression by RT-qPCR.

A functional change of the P2X7 receptor observed by a change in intracellular calcium concentration was found for two SNPs according to their gain- or loss-of-function character when compared to WT. In contrast, the third SNP induced no significant change in function of the P2X7 receptor when compared to WT.

For the seven bone markers, although significant differences between SNPs and WT was observed, no tangible patterns of increase or decrease in boneformation seen as a result of change in bone markers was observed.

Disclosures: Jan Rune Larsen, None.

MO0228

Mice Deficient in Osteoblast Smad4 Exhibit Impaired Collagen Fibrillogenesis. <u>Cynthia Brecks</u>*[1], <u>Gabriel Mbalaviele</u>[2], <u>Roberto Civitelli</u>[2]. [1]Washington University In St Louis, USA, [2]Washington University in St. Louis School of Medicine, USA

Previous work from our lab demonstrates that Smad4, a key component of the TGF-β and BMP pathways, regulates skeletal development. Indeed, osterix (OSX)-Cre-driven osteoblast-specific ablation of *Smad4* (cKO) causes stunted growth, spontaneous fractures and a combination of features seen in osteogenesis imperfecta and cleidocranial dysplasia. Here, we further explored the nature of the collagen matrix abnormalities caused by osteoblast *Smad4* deficiency. All markers of osteoblast differentiation downstream of Osx, measured by qPCR in calvaria cells, were significantly decreased in bone extracts from cKO mice relative to wild type (WT) littermates, including type I collagen. We have also shown that fibrillar collagen organization is abnormal in cKO bones by picrosirius red staining. This was corroborated by transmission electron microscopy, showing significantly larger cross-sectional diameter of collagen fibers in cKO relative to WT mice, suggestive of aberrant collagen fiber assembly and processing. This is consistent with our previous observation of reduced *Lox* expression by *Smad4* deficient cells. Indeed, we observed

reduced deposition of collagen into the extracellular matrix in cKO mice relative to WT mice. However, collagen processing enzymes were not altered in cKO mice. However, collagen fiber assembly is also regulated by small leucine-rich proteoglycans (SLRPs) such as biglycan, as they are associated with collagen fibrils and contribute to their assembly. Indeed, biglycan protein expression was significantly down-regulated in the calvaria of cKO compared to WT mice, consistent with published data showing that biglycan expression is Smad4-dependent. Thus, Smad4 is a key regulator of organic bone matrix, by modulating collagen synthesis, post-translational modification and assembly in a proper fibrillar structure; its absence recapitulates matrix abnormalities found in some forms of osteogenesis imperfecta.

Disclosures: Cynthia Brecks, None.

MO0229

Odd-skipped related 1 transcription factor modulates skull closure and cranial bone formation. <u>Shinji Kawai</u>*[1], <u>Masashi Yamauchi</u>[1], <u>Ikumi Michikami</u>[2]. [1]Osaka University Graduate School of Dentistry, Japan, [2]Osaka University Graduate School of Dentistry, Japan

The odd-skipped gene is initially identified as a Drosophila segmentation gene, and contains three DNA-binding C2H2-type zinc fingers in the C-terminal half of the molecule as a pair-rule transcription factor. Mammalian homologues, Odd-skipped related 1 (Osr1) and Osr2, are cloned from both mice and humans. Human OSR1 is detected in fetal lungs, adult colon, small intestine, prostate, and testis. Osr1 is known to play important roles in embryonic, heart, and urogenital development. To elucidate the in vivo function of Osr1 in bone formation, we generated transgenic mice overexpressing full-length Osr1 under control of 2.8kb Osr1 promoter. Osr1 transgenic mice were smaller than wild-type littermates. Especially, abnormality was found in skull of Osr1 transgenic mice by soft X-ray analysis, skeletal preparation, and morphological analysis. Round skull and cranial dysraphism were observed in transgenic mice. Further, primary calvarial cells obtained from Osr1 transgenic mice showed increased proliferation and increased expression of chondrocyte markers, but decreased expression of osteoblast markers. BMP2 reduced Osr1expression and Osr1 knockdown by siRNA induced ALP and osteocalcin expressions in mesenchymal and osteoblastic cells. Thus, Osr1 negatively functioned in bone formation. Our genetic observations show that the Osr1 gene plays a role in appropriate skull closure and cranial bone formation.

Disclosures: Shinji Kawai, None.

MO0230

Osteoblast differentiation causes a switch in the primary mechanism that regulates activity of the cAMP/PKA signaling pathway. <u>Bryan Hausman</u>*[1], <u>Xin Chen</u>[1], <u>Guang Zhou</u>[1], <u>Guangbin Luo</u>[2], <u>Shunichi Murakami</u>[1], <u>Edward Greenfield</u>[1]. [1]Case Western Reserve University, USA, [2]Case Western Reserve University, USA

The cAMP/Protein Kinase A (PKA) pathway is essential for regulation of many genes and cellular processes and is therefore tightly controlled by multiple mechanisms including secretion/degradation of the initiating hormones, activity of their cognate receptors, cAMP production/degradation, levels of the PKA regulatory subunits and their binding to A-kinase anchoring proteins, nuclear import/export of the PKA catalytic subunit, transcription factor phosphorylation/dephosphorylation, production of inhibitory transcription factors, and histone acetylation/deacetylation. However, we previously showed that inhibition of nuclear PKA activity by Protein Kinase Inhibitorγ (PKIγ) is the primary mechanism that regulates activity of the cAMP/PKA pathway in mesenchymal precursor cells and in osteoblast-like ROS17/ 2.8 cells. Thus, PKIγ terminates PKA activity and expression of primary response genes (*c-fos*, *LIF*, and *IL6*) induced by parathyroid hormone (PTH) or isoproterenol. As a result, PKIγ reduces production of LIF protein and thereby restrains osteogenesis and enhances adipogenesis by mesenchymal precursor cells. In our current studies, we investigated the effects of PKIγ in mature osteoblasts *in vitro* and *in vivo*. Before and after differentiation into osteoblast-like cells (7 days with ascorbic acid and β-glycerol phosphate), wild-type murine embryonic fibroblasts (MEFs) exhibit equivalent forskolin (Fsk)-induced increases in nuclear PKA activity and expression of *c-fos*, *LIF*, and *IL6* mRNAs. In contrast, undifferentiated PKIγ^{-/-} MEFs exhibit greater Fsk-induced increases in nuclear PKA activity (3-fold, p<0.001) and expression of the mRNAs (2- to 10-fold, p<0.05). However, upon differentiation into osteoblast-like cells, the effects of PKIγ deficiency are compensated as wild-type and PKIγ^{-/-} MEFs are indistinguishable. This compensation occurs in the absence of major up-regulation of PKIα or PKIβ mRNAs. Similar to MEFs after differentiation into osteoblast-like cells, no differences are detected between wild-type and PKIγ^{-/-} calvarial osteoblasts in PTH- or Fsk-stimulated gene expression. Similarly *in vivo*, PTH-induced gene expression in femoral osteoblasts is not different between PKIγ^{-/-} and wild-type littermates; and no major skeletal phenotype is detected in adult or embryonic PKIγ^{-/-} mice. These data suggest that PKIγ is most important early in the osteoblastic lineage and that other mechanisms to regulate cAMP/PKA signaling predominate in mature osteoblasts.

Disclosures: Bryan Hausman, None.

MO0231

Osteoclast-derived coupling factor Cthrc1 stimulates osteoblast differentiation through Rac1/PKCδ/ERK. <u>Kazuhiko Matsuoka</u>[1], <u>Kyoji Ikeda</u>[2], <u>Sunao Takeshita</u>*[2]. [1]National Center for Geriatrics & Gerontology, Japan, [2]National Center for Geriatrics & Gerontology, Japan

Various regulatory molecules relaying between bone resorption and formation have been reported, including matrix-derived growth factors, secreted and membrane factors derived from osteoclasts themselves. We have recently reported that Cthrc1 secreted from active bone-resorbing osteoclasts stimulates bone formation and acts as a coupling factor in vivo. In this study, we examined signal transduction pathways of Cthrc1 to clarify the mechanism how it transmits anabolic signals to osteoblasts using ST2 cells that are induced into osteoblastic differentiation by recombinant Cthrc1.

We found that recombinant Cthrc1 phosphorylates PKCδ, ERK and JNK, and activates Rac1 on ST2 cells. Cthrc1 induces alkaline phosphatase (ALP) activity in ST2 cells, which is dose-dependently reduced by the addition of pharmacological inhibitors of PKCδ, ERK and Rac1, i.e. Rottlerin, U0126 and EHop-016, respectively. PLC and JNK inhibitors, U73122 and SP600125, however, did not affect ALP activity by Cthrc1 stimulation. Knockdown of PKCδ by siRNA abrogated the stimulation of ALP activity induced by Cthrc1. Cthrc1 dose-dependently inhibited β-catenin dependent signals assessed with a TOP Flash system. These data suggest that Cthrc1 may cross-talk with not only Wnt/PCP pathway, but also canonical Wnt/β-catenin pathway. In order to search for a Cthrc1 receptor, ST2 cell lysates were applied to an affinity column of recombinant Cthrc1 protein, and a membrane protein was identified by mass spectrometry.

Taken together, these results suggest that Cthrc1 stimulates osteoblast differentiation through Rac1/PKCδ/ERK pathways.

Disclosures: Sunao Takeshita, None.

MO0232

RUNX2 O-GlcNAcylation Links Osteogenesis and Nutrient Metabolism in Mesenchymal Stem Cells. <u>Alexis Nagel</u>*[1], <u>Lauren Ball</u>[2]. [1]Medical University of South Carolina, USA, [2]The Medical University of South Carolina, USA

The *runt*-related transcription factor 2 (RUNX2) is the master switch controlling osteoblast differentiation and formation of the mineralized skeleton. The post-translational modification (PTM) of RUNX2 by phosphorylation, ubiquitinylation, and acetylation modulates its activity, stability, and interactions with transcriptional co-regulators and chromatin remodeling proteins downstream of osteogenic signals. We report for the first time novel sites of O-linked N-acetylglucosamine (O-GlcNAc) modification on human type II RUNX2 identified by tandem mass spectrometry, as well as interaction of RUNX2 with the nutrient responsive enzyme O-GlcNAc transferase (OGT) which modulates the action of numerous transcriptional effectors. Mass spectrometric characterization also revealed novel sites of arginine methylation, as well as sites of lysine acetylation. A chemoenzymatic labeling approach demonstrated that ~40% of RUNX2 isolated from nuclei of osteogenic bone marrow derived mesenchymal stem cells (BMMSCs) treated with the pharmacological OGA inhibitor, Thiamet G, was O-GlcNAc modified. Levels of O-GlcNAcylated RUNX2 were increased in BMMSCs after 1 and 2 days of rhBMP2/7-treatment (50 ng/mL), and the presence of rhBMP2/7 significantly decreased activity of the O-GlcNAcase (OGA) cycling enzyme by 39.0% after 8 days. Differentiation of BMMSCs in the presence of Thiamet G enhanced expression (24.3%) and activity (65.8%) of alkaline phosphatase (ALP) after 6 days, and rhBMP2/7-induced effects on ALP activity were enhanced by 35.6% in the presence of Thiamet G. These data suggest that decreased OGA activity is associated with increased activity of the early osteogenic marker ALP and that the effects of BMP2/7 are mediated in part by modulation of protein O-GlcNAc modification. These findings support a role for the nutrient responsive O-GlcNAc PTM in the regulation of osteoblast function, and have implications for pathological bone loss observed under conditions of altered nutrient metabolism such as type I and type II diabetes.

Disclosures: Alexis Nagel, None.

MO0233

Sr stimulating effect on mineralization is modified by calcimimetic R568 in UMR 106.1 osteoblast like cells. <u>Nicole Nijs-De Wolf</u>*[1], <u>Rafik Karmali</u>[2], <u>Pierre Bergmann</u>[3]. [1]Université Libre de Bruxelles, Belgium, [2]CHU Brugmann, Université Libre de Bruxelles, Belgium, [3]Centre Hospitalier Universitaire Brugmann, Belgium

Introduction: Strontium ranelate is used to treat osteoporosis and acts on bone resorption, which is inhibited, while it stimulates bone formation. Sr^{++} increases the mineralization of UMR106.1 OB like cells cultivated in mineralizing conditions. Osteoblasts express PTHrP, a bone anabolic agent, and the expression of PTHrP in osteoblasts is stimulated by divalent cations. We have shown previously that Sr^{++} increased the relative abundance of the mRNA of PTHrP in UMR 106.1 osteoblast like cells and that PTH 7-34, an inhibitor of PTH action on the parathyroid hormone receptor 1 (PTHR1) decreased the stimulating effect of Sr^{++} on OB-like cells mineralization. To get more insight into the mechanism of action of Sr^{++}, we investigated in this work if its effect on UMR106.1 mineralization was modified by agents which modulate the sensitivity of the calcium sensing receptor (CaSR) to divalent cations.

Methods: UMR-106.1 were cultivated in MEM containing 10 % FCS. At confluence, the cells were trypsinized, plated at 10^5 cells/cm^2 density and cultivated in

mineralizing conditions for 6 days without SrCl$_2$ or with SrCl$_2$ 0.25, 0.5, 1.0, 1.5 or 2 mmol/L. The calcimimetic R568 (generous gift of Amgen) was added from the beginning at a concentration 0, 100, 300 and 1000 nmol/l. Control experiments were performed with the enantiomer S568. In some experiments, the calcilytic NPS 2143 (purchased from Sigma) was added at the concentrations 100 and 1000 nmol/L. At the end of the culture, alizarin 2% was added for 15 min; the plates were washed and the color dissolved in cetyl pyrimidin-HCl 10%. The optical density of the supernatant was measured at 562 nm.

Results: Sr^{++} increased significantly mineralization for concentrations $\geq$ 0.5 mmol/L. The calcimimetic R568 had no effect per se on mineralization except at the highest concentration, for which mineralization was maximally stimulated. The effect of Sr^{++} on mineralization was sensitized, with a significant increase for a concentration of 0.25 mmol/L of Sr at a R568 concentration of 100 nmol/L, and a maximal effect of this low Sr concentration when the calcimimetic was added at a concentration of 300 nmol/L. With the enantiomer or the calcilytic NPS 2143, we observed a moderate increase of mineralization in the absence of Sr, but the stimulatory effect of Sr was abolished.

Conclusion: Our data show that the stimulating effect of Sr^{++} on UMR 106.1 mineralization is at least in part transduced through the CaSR.

Disclosures: Nicole Nijs-De Wolf, None.

MO0234

Alternative Splice Variants Of The Osteogenic Cytokine SDF-1 Differentially Mediate CXCR4 and CXCR7 Expression in Bone Marrow MSCs. <u>Alexandra Aguilar</u>*[1], <u>Samuel Herberg</u>[2], <u>Sudharsan Periyasamy-Thandavan</u>[3], <u>Brian Volkman</u>[4], <u>Galina Kondrikova</u>[5], <u>Xing-Ming Shi</u>[6], <u>Mark Hamrick</u>[7], <u>Carlos Isales</u>[6], <u>William Hill</u>[8]. [1]UCC School of MedicineGeorgia Regents University, USA, [2]Case Western Reserve University, USA, [3]Georgia Regents University & Charlie Norwood VAMC, USA, [4]Medical College of Wisconsin, USA, [5]Georgia Regents University, USA, [6]Georgia Regents University, USA, [7]Georgia Health Sciences University, USA, [8]Georgia Regents University & Charlie Norwood VAMC, USA

Purpose: Stromal cell-derived factor-1 (SDF-1/CXCL12) has six known alternative mRNA splice variants. SDF-1α and SDF-1β are the main isoforms. SDF-1a has been implicated in bone marrow-derived stem/stromal cell (BMSC) mobilization and osteogenic differentiation. We have previously shown that SDF-1b, the second most abundant splice variant, is also important for regulating osteogenesis. It is unclear whether there is a difference in the activation of gene expression and signaling pathways between these two constitutively expressed isoforms in BMSCs. We assessed the effects of SDF-1α & β on the expression of SDF-1 ligands and receptors using a dose range know to differentially affect CXCR4 signaling by SDF-1α due to ligand biased GPCR activation. Hypothesis: SDF-1 splice variants have different affects on BMSC SDF-1 ligand & receptor expression. Materials: BMSCs were derived from 18-month-old male C57BL/6J mice. Cells were treated for 24 and 48 h with increasing doses (50, 100, 200, 400 and 800ng/mL) of rhSDF-1a or SDF-1b. mRNA expression of SDF-1a, SDF-1b, CXCR4 and CXCR7 were analyzed by qRT-PCR. SDF-1a protein levels in cell lysates and supernatants were assessed by ELISA. Results: mRNA levels of SDF-1a and SDF-1b at 24 and 48 h were comparable, independent of the exogenous stimulus. SDF-1a treatment induced expression of CXCR4 at 24 h in a dose-dependent manner. In contrast, BMSCs responded to SDF-1b treatment only at a higher dose (400ng/mL) to increase CXCR4 levels. At 48 h, SDF-1b still did not increase CXCR4 expression below 200ng/ml. Both isoforms induced the expression of CXCR7 in a similar fashion at both time points; however, SDF-1b significantly increased the overall mRNA level at 48 h. SDF-1a protein levels in cell lysates significantly increased (p<0.01) with SDF-1b treatment at 24 h relative to controls and decreased with both isoforms at 48 h. SDF-1a levels in the supernatant increased significantly (p<0.0001) with SDF-1a treatment at both time points. SDF-1b treatment also increased the expression of SDF-1a at 24 h (p<0.05) and 48 h, however, to a lesser extent compared to SDF-1a treatment. Conclusions: Our data suggest that there is a distinct difference in the mechanisms by which the expression of CXCR4 and CXCR7 is induced in BMSCs depending on the SDF-1 splice variant, and dose, cells are exposed to. This suggests potentially a difference in GCPR ligand biased signaling between SDF-1 isoforms that may alter BMSC osteogenesis.

Disclosures: Alexandra Aguilar, None.

MO0235

IRE1a,forming a control loop with BMP2 and GEP,regulates osteoblastogenesis. <u>Fengjin Guo</u>*[1], <u>Zhangyuan Xiong</u>[2], <u>Peng Zhang</u>[3], <u>Xiaofeng Han</u>[4], <u>Meiling Li</u>[4], <u>Fei Xia</u>[4]. [1]Chongqing Medical University, Peoples Republic of China, [2]Department of Cell Biology & Genetics,Core Facility of Development Biology, Chongqing Medical University, China, [3]Department of Cell Biology & Genetics,Core Facility of Development Biology, Chongqing Medical University, Chongqing 400016,China, China, [4]Department of Cell Biology & Genetics,Core Facility of Development Biology, Chongqing Medical University, Chongqing 400016,China, China

Osteoblast differentiation is a multi-step process where mesenchymal cells differentiate into osteoblast lineage cells including osteocytes.All is known that the differentiation of uncommitted mesenchymal cells to osteoblasts is a fundamental process in embryonic development and the repair of bone defect.The BMPs are

important regulators of this process and play a key role in the BMP-induced osteogenic differentiation and bone formation.Recently,BMP2 is known to activate unfolded protein response(UPR) signaling molecules,such as BiP,PERK,IRE1α.IR-E1a,as one of three unfolded protein sensors in UPR signaling pathways,can be activated during ER stress.

GEP is an autocrine growth factor that has been implicated in embryonic development,tissue repair,tumorigenesis,and inflammation.We previously reported that GEP induced chondrocyte differentiation,endochondral bone formation and cartilage repair.GEP was reported to promote bone regeneration and bone formation.However,little is known about the modulation and physiological significance of IRE1a in osteoblast differentiation.Specifically,whether IRE1a influences GEP mediated osteoblastogenesis have not been delineated,the molecular mechanism on how to regulate GEP-mediated osteoblastogenesis by IRE1a is also remains unknown.Herein,we demonstrate that overexpression of IRE1a inhibits osteoblast differentiation,as revealed by reduced activity of ALP and OCL.Mechanistic studies revealed that the expression of IRE1a during osteoblast was a consequence of JunB transcription factor binding to several AP1 sequence(TGAG/CTCA) in the 5'-flanking regulatory region of the IRE1a gene,followed by transcription.In addition,GEP induces IRE1a expressions and this induction of IRE1a by GEP depends on JunB;Furthermore,IRE1a inhibition GEP-induced osteoblastogenesis relies on JunB;Besides,GEP is required for IRE1a inhibition of BMP2-induced bone formation.Collectively,these findings demonstrate that (1)IRE1a Inhibits the BMP2-mediated Osteogenic Differentiation;(2)JunB upregulates endogenous IRE1a expression and enhanced this inhibition;(3)GEP induces IRE1a expressions and this induction depends on JunB; (4)GEP is required for IRE1a inhibition of BMP2-induced bone formation;(5)IRE1a inhibition of GEP induced osteoblastogenesis is,at least partially,mediated by the transcription factor JunB.Thus,IRE1a,BMP2,GEP,and JunB constitute a regulatory feedback loop and act in concert during osteoblast differentiation and bone formation.

Figure 1. IRE1a inhibits the BMP2-induced osteogenesis assayed by ALP and OCL.

Figure 2. JunB binds to the AP1 of the IRE1a promoter and upregulation of IRE1a reporter constructs.

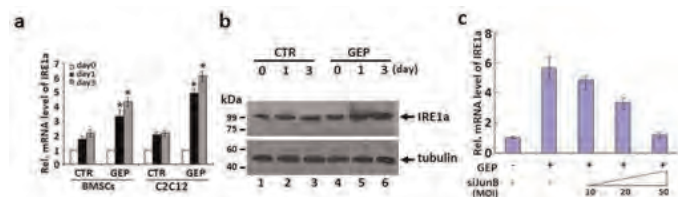

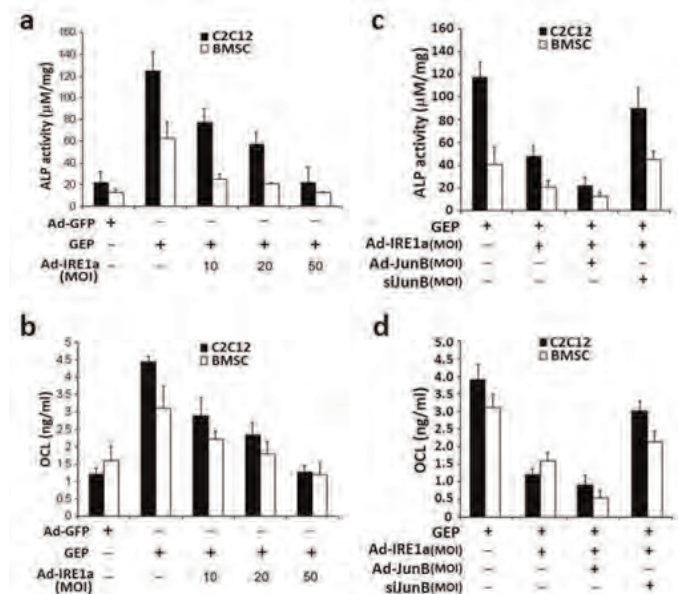Figure 3. IRE1a expression induced by GEP is depended on JunB.

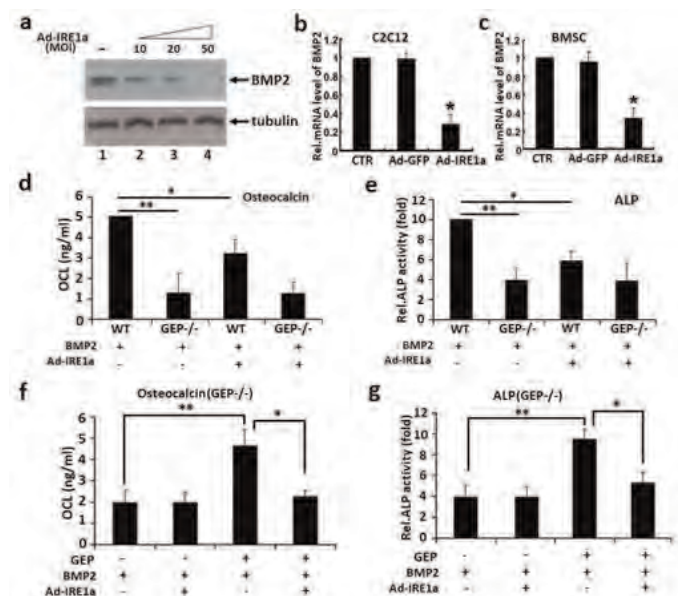Figure 4. IRE1a inhibits GEP-mediated osteogenesis assayed by ALP and OCL.

Figure 5. GEP is required for BMP2-induced osteoblastogenesis and IRE1a inhibition in vitro.

Disclosures: Fengjin Guo, None.

MO0236

The canonical Wnt/β-catenin signaling improves osteoblast and osteocyte survival by enhancing DNA repair. Abhishek Chandra*[1], Tiao Lin[1], Ji Zhu[2], Wei Tong[3], Xiaowei Liu[1], Keith Cengel[4], Bing Xia[5], Ling Qin[1]. [1]University of Pennsylvania, USA, [2]University of Pennsylvania, School of Medicine, USA, [3]Perelman school of medicine, USA, [4]University of Pennsylvania, USA, [5]Rutgers Cancer Institute of New Jersey & Robert Wood Johnson Medical School, USA

Focal radiotherapy for cancer patients has detrimental effects on tumor adjacent bones and currently there is no curative treatment available. We previously reported that focal radiation causes massive cell death in osteoblasts and a modest reduction of osteocyte number in rat bone, and that daily injection of parathyroid hormone (PTH, 1-34) alleviates radiation-induced bone loss by promoting the survival of osteoblasts and osteocytes. Osteoblastic cell culture and calvarial organ culture experiments demonstrated that the anti-apoptotic effect of PTH on osteoblast lineage cells after radiation is mainly mediated through the β-catenin pathway. Consistently, we found that Wnt3a, a canonical Wnt ligand, almost completely mitigated the 10-fold increase in radiation-induced apoptosis in osteoblasts and osteocytes by activating β-catenin. Radiation exposure rapidly generates DNA lesions, among which DNA double strand break (DSB) is the most deleterious form that causes cell death. Using immuno-fluorescence staining of γ-H2AX and the comet assay, we found that Wnt3a greatly reduced the number of nuclear γ-H2AX foci (a DSB marker) and the percentage of comet tail (corresponding to damaged DNA) in irradiated osteoblasts and osteocytes and that Dkk1 abolished both effects of Wnt3a, suggesting that canonical Wnt pathway promotes the DSB repair. Most radiation-induced DSBs are repaired through non-homologous end-joining (NHEJ), which requires the binding of Ku70/80 heterodimer to DSB ends. Interestingly, we found that Wnt3a modestly elevated Ku70 amount and remarkably stimulated nuclear heterodimer formation of Ku70/80 by activating the b-catenin pathway. In addition, Wnt3a suppressed the activation and nuclear localization of cleaved caspase-3, a main effector caspase responsible for cell death. Osteoblast and osteocyte apoptosis is also the major cause for glucocorticoid-induced osteoporosis. We found that dexamethasone greatly stimulated ostebolast apoptosis accompanied by a strong increase in γ-H2AX foci number and that addition of Wnt3a completely reversed such DNA damage and cell death. In conclusion, we have demonstrated a strong anti-apoptotic effect of canonical Wnt/β-catenin on osteoblasts and osteocytes and a novel role of this pathway in regulating DSB repair machinery. Our data also suggest that Wnt agonist, such as Sclerostin neutralizing antibody, could be a potential therapeutic treatment for radiation- and steroid-induced osteoporosis.

Disclosures: Abhishek Chandra, None.

MO0237

A Glimpse into MicroRNA 23a~27a~24-2 Regulation of Bone Development. Austin Kemper*[1], Mohammad Hassan[2]. [1]University of Alabama at Birmingham, USA, [2]University of Alabama, USA

Previously we have shown that miR 23a~27a~24-2 (miR-cluster) is involved in a regulatory network with Runx2 and Satb2, two key transcription factor for osteoblast differentiation. During differentiation of osteoblasts we have observed reciprocal expression levels of miR-cluster and Hoxa5, Hoxa10, and Hoxa11; spatially and temporally regulated transcription factors. Further investigations have uncovered regulation of these Hox factors by miR-cluster. Reporter and ChIP assays revealed binding of these factors to the promotors of Runx2 and Osteocalcin to promote osteogenesis. These experiments have indicated a regulatory role for miR-cluster in skeletal and craniofacial development. Recently we have developed two mouse lines for studying this cluster. The first is a global knockout mouse for the cluster and the second is a drug inducible anti-miR-cluster (miR-ZIP) transgenic knockdown mouse to investigate how loss of the miR-cluster impacts embryonic and postnatal development. We found that heterozygous knockout mice have higher bone mineralization, narrower cranial sutures, and extended zygomatic arches in alcian blue and alizarin red stained skeletal preparations at birth. MicroCT has revealed higher cortical bone volume, bone mineral density and cortical thickness in these mice. RNA sequencing in MC3T3 mouse preosteoblast cells overexpressing miR-cluster has revealed many potential targets of the cluster including many chromatin binding transcription factors such as Phf10 and Lin9. Validation of Phf10 in miR-cluster overexpression cells revealed significantly increased expression. Overexpression of Phf10 was found to increase expression of p21, an important regulator of cell cycle progression and an inhibitor of cellular proliferation. Further characterization and identification of the molecular mechanisms involving miR 23a~27a~24-2 contributing to regulation of bone and craniofacial development could have a strong impact on research into osteoporosis and other human diseases.

Disclosures: Austin Kemper, None.

MO0238

Bisphosphonate Suppress Mesenchymal Cells Proliferation and Differentiation into Osteoblast via Attenuation of Wnt Signaling. Seungwoo Han[1], Hye-Ri Park*[2], Min-Su Han[2], Youn-Kwan Jung[2], Eun-Ju Lee[2], Ji-Ae Jang[2], Gun-Woo Kim[2]. [1]Daegu Fatima Hospital, South Korea, [2]Laboratory for arthritis & bone biology, Fatima research institute, South Korea

Bisphosphonates (BPs) are widely used for osteoporosis, but its long term use can cause a femoral insufficiency fracture which is mainly responsible for decreased bone turnover by BP-mediated suppression of osteoclast. As a farnesyl pyrophosphate synthase inhibitor, BP can attenuate various farnesylated and geranylgeranylated GTPase proteins, such as Rab, Rac, Rap, Ras and Rho. Among them, especially Rho GTPase signaling is critical in mesenchymal cell commitment into osteoblast by RUNX2 induction, but the role of BP in osteoblast differentiation is still controversial. We investigated the effect of BP on osteoblast and bone marrow stromal cells in vivo and underlying mechanisms. Mice with zolendronate (ZA) administration (0.1 mg/kg intraperitoneal weekly) showed higher bone mass and decreased osteoclast number per bone surface. Further, ZA-administrated mice revealed an attenuated mineral deposition rates and decreased expression of osteogenic marker such as Runx2, osterix, and osteocalcin in RNA and protein level. ZA significantly decreased the number of fibroblast colony-forming units (CFU-F) from bone marrow stromal cells (BMSCs), suggesting the decreased proliferation of BMSCs by ZA. That was repeated in vitro BrdU incorporation assay using mouse mesenchymal cell line, C3H10T1/2 cells and BMSCs. In addition, ZA diminished the osteoblast differentiation in both C3H10T1/2 cells and BMSCs. ZA significantly decreased the expression of canonical Wnt target protein, Lef1, and increased Dkk2 expression. Furthermore, the nuclear translocation of β-catenin was markedly decreased by ZA, suggesting that the inhibition of canonical Wnt signaling is associated with reduced mesenchymal commitment to the osteoblast lineage by BPs. Together, these results provide the evidence of BPs-induced impairment of mesenchymal cell proliferation and osteoblast differentiation, and a mechanistic insight into how BPs lead to the impaired bone quality causing insufficiency fracture.

Disclosures: Hye-Ri Park, None.

MO0239

Bobby Sox homology regulates osteogenic/odontogenic differentiation of human dental pulp stem cells. Eui Kyun Park[1], Young-Ae Choi*[2], Hye Jung Ihn[3], Jiwon Lim[2], Ju Ang Kim[2]. [1]Kyungpook National University, South Korea, [2]Department of Oral Pathology & Regenerative Medicine, School of Dentistry, Kyungpook National University, South Korea, [3]Department of pharmacology, School of medicine, Kyungpook National University, South Korea

Transcription factors have been implicated in regulating the differentiation of odontoblasts from dental pulp stem cells (DPSCs) but their regulatory network is not completely understood. In this study, new transcription factors that control the odontoblast differentiation of human DPSCs were identified using a microarray. The results revealed bobby sox homolog (BBX) was expressed most strongly during odontoblast differentiation. Validation using RT-PCR revealed the strong expression of BBX during the odontoblast differentiation of DPSCs. BBX expression was also detected in adult molar odontoblasts and other tissues, including the heart, kidney, testis and bone marrow. To understand the role of BBX in odontoblast differentiation, BBX variant 1 and 2 cDNAs were cloned and overexpressed in DPSCs. The overexpression of BBX cDNA in DPSCs induced substantial mineralization and expression of the odontoblast marker genes, such as alkaline phosphatase (ALP), osteopontin (OPN), bone sialoprotein (BSP), dentin matrix acidic protein 1 (DMP1), and Dentin sialophosphoprotein (DSPP). Moreover, the knock-down of BBX using shRNA substantially decreased the expression of ALP and DSPP. Overall, these results suggest that BBX plays an important role during the odontoblast differentiation of human DPSCs.

Disclosures: Young-Ae Choi, None.

MO0240

Comprehensive profiling of gene expression temporal dynamics during osteoblastogenesis in the context of differing genetic backgrounds. Kwangbom Choi[1], Dana Godfrey[1], Matthew Hibbs[2], Cheryl Ackert-Bicknell*[3]. [1]The Jackson Laboraotry, USA, [2]The Jackson Laboratory, USA, [3]University of Rochester, USA

The proper maturation and function of osteoblasts is critical for maintaining bone mass. However, the differentiation of osteoblasts is inadequately characterized at a molecular level and the impact of genetic background on this process is largely unknown. To address this, we measured whole genome transcriptional dynamics using RNA-seq throughout differentiation from the pre-osteoblast stage to mature osteoblasts. Specifically, neonatal mice were generated by breeding male C57BL/6J (B6) mice expressing cyan florescent protein (CFP) under the control of the Col3.6 promoter to female mice of each of four inbred strains: B6 itself, 129S1/SvImJ, C3H/

HeJ and CAST/EiJ. Calvarial cells were obtained via standard protocols, cells cultured for 4 days, and the FACS sorted to enrich for pre-osteoblasts based on the presence of CFP. CFP+ cells were returned to culture, differentiated into osteoblast by culturing in the presence of 50 mg/ml ascorbic acid, 4 mM beta-glycerol phosphate and RNA was collected at 2, 4, 6, 8, 10, 12, 14, 16 and 18 days post differentiation. mRNA profiles for each time point for each of the four strains were generated by Next-Gen RNA sequencing, using an Illumina HiSeq 2000. The alignments for abundance estimation of transcripts was conducted using Bowtie (0.12.9) and expression level per gene was calculated using RSEM (1.2.0). In order to identify co-expressing genes based on temporal expression pattern, we utilized Weighted Gene Co-expression Network Analysis and hierarchical clustering. We were able to find only two groups (or modules) of genes, whose expression levels monotonically increase or decrease within the measured time frame. A logistic growth model was fit to each gene in these two modules and the time of maximal increase or decrease was estimated. This allowed us to order genes relative to one another across osteoblastogenesis with regards to when expression increased or decreased and this temporal ordering was compared between strains. We observed that the major impact of genetic background was on the pace of differentiation, and that the ordering of genes was only minimally influenced by strain with some notable exceptions. These outliers in gene expression timing may be potential drug targets and should be further evaluated. From this data we can, in detail, define the gene expression steps associated with the maturation of pre-osteoblasts to mature mineralizing osteoblasts thus increasing our understanding of the process.

Disclosures: Cheryl Ackert-Bicknell, None.

MO0241

COUP-TFII suppression by miR-194 determinates fate of mesenchymal stromal cells. <u>Jeong-Tae Koh</u>*[1], <u>Byung-Chul Jeong</u>[2], <u>In-Hong Kang</u>[3], <u>Hyuck Choi</u>[4], <u>Sin-Hye Oh</u>[5], <u>Yu-Ri Kim</u>[3]. [1]Chonnam National University, South Korea, [2]Chonnam National University School of Dentistry, South Korea, [3]Department of Pharmacology & Dental Therapeutics, School of Dentistry, Chonnam National University, South Korea, [4]Research Center for Biomineralization Disorders & Dental Science Research Institute, School of Dentistry, Chonnam National University, South Korea, [5], South Korea

Mesenchymal stromal cells (MSCs) have the capacity to differentiate into adipocytes and osteoblasts. Differentiation of MSCs is tightly controlled by various growth factors, transcriptional factors, and other intracellular molecules. The chicken ovalbumin upstream promoter-transcription factor II (COUP-TFII) has been introduced to be a regulator of MSC fate. In this study, we aimed to investigate if microRNAs targeting COUP-TFII can determinate the fate of MSCs. In the present study, we observed that miR-194 was involved in the reciprocal regulation of osteoblast and adipocyte differentiation from MSC lineage cells. In the cultures of mesenchymal lineage C3H10T1/2 and bone marrow stromal cells, osteogenic stimuli increased miR-194 expression with the decreases in COUP-TFII expression, whereas adipogenic stimuli reduced miR-194 expression with the increases in COUP-TFII expression. A luciferase assay with COUP-TFII 3′-UTR reporter plasmid, including miR-194 binding sequences, showed that miR-194 reduced the luciferase activity. However, miR-194 did not affect the activity of mutated COUP-TFII 3′-UTR reporter. Enforced expression of miR-194 significantly enhanced osteoblast differentiation, but inhibited adipocyte differentiation with decreasing COUP-TFII mRNA and protein level. In contrast, inhibition of the endogenous miR-194 reduced matrix mineralization in the MSC cultures, and promoted the formation of lipid droplets by rescuing COUP-TFII expression. Furthermore, overexpression of COUP-TFII reversed the effect of miR-194 on the cell fates. Taken together, our data demonstrated that miR-194 acts as a critical regulator of COUP-TFII and can determinate the fate of MSCs into osteoblasts.

Disclosures: Jeong-Tae Koh, None.

MO0242

Genome-wide DNase hypersensitivity analysis reveals novel transcriptionally active regions during osteoblastogenesis. <u>Phillip Tai</u>*[1], <u>Hai Wu</u>[2], <u>Jonathan Gordon</u>[2], <u>Troy Whitfield</u>[3], <u>Andre Van Wijnen</u>[4], <u>Jane Lian</u>[5], <u>Gary Stein</u>[6], <u>Janet Stein</u>[7]. [1]University of VermontCollege of MedicineDepartment of Biochemistry, USA, [2]University of Vermont, USA, [3]University of Massachusetts Medical School, USA, [4]Mayo Clinic, USA, [5]University of Vermont College of Medicine, USA, [6]University of VermontCollege of Medicine, USA, [7]University of Vermont, USA

The discovery and characterization of regulatory sequences that control bone-related genes during development have been limited by the classical approaches for identifying *cis*-regulatory modules. These approaches relied primarily on sequence conservation in promoters and the identification of disease-causing, non-coding mutations near critical genes. New technologies have revealed the extent to which regulatory sites can reside far beyond promoter regions. To identify novel and dynamic *cis*-regulatory modules, we probed the presence of open chromatin using DNase hypersensitivity analysis on a genome-wide scale during MC3T3 osteoblast

differentiation using high-throughput sequencing. We demonstrate that DNase hypersensitivity profiling can accurately define the boundaries of active regulatory sequences across the genome. More than 220,000 unique DNase hypersensitive sites (DHSs) were identified, with a majority being highly dynamic throughout differentiation. DHSs that overlap promoters are generally constitutive throughout differentiation, while dynamic DHSs are found predominantly in intronic and intergenic regions. This observation coincides with the regulatory nature of intronic and intergenic enhancer regions.

To understand the function of dynamic DHSs, we examined the representation of osteogenic regulatory motifs within these regions, revealing specific motif rules for osteoblast-related transcription factors. One striking finding is that at peak levels of *Runx2* expression in committed osteoblasts (d9), RUNX2 binds distinct motifs according to preference rules defined by genomic position. Intronic sequences enriched for RUNX2 are overrepresented by both TGTGGT and TGCGGT motifs at equal ratios, while in intergenic sequences, only the TGTGGT motif is over-represented, suggesting a functional distinction between intronic and intergenic recruitment of RUNX2. Some of these RUNX2 enriched regions appear to precede DHS regions that emerge later during differentiation. The importance of position-dependent motif preferences is under investigation. In summary, DHS profiling of the osteoblast genome has identified highly dynamic regulatory modules at non-promoter regions. Additionally, the discovery of distinct binding patterns of bone-essential transcription factors in intronic versus intergenic sequences further enriches our understanding of the concerted regulatory network that drives bone differentiation.

Disclosures: Phillip Tai, None.

MO0243

High Osteogenic Potential of fibroblast from FOP Patients. <u>Nathalie Bravenboer</u>*[1], <u>Dimitra Micha</u>[2], <u>Huib van Essen</u>[3], <u>Coen Netelenbos</u>[4], <u>Gerard Pals</u>[2], <u>Marelise Eekhoff</u>[5]. [1]VU University Medical Center, The Netherlands, [2]Department Clinical Genetics, VU University Medical Center, Netherlands, [3]Department Clinical Chemistry, VU University Medical Center, Netherlands, [4]VU Medical Center, The Netherlands, [5]Deparment Internal Medicine, VU University Medical Center, Netherlands

Fibrodysplasia ossificans progressiva (FOP) is a rare, extremely disabling genetic disorder characterized by progressive heterotopic ossification preceded by episodic inflammatory soft tissue swellings, leading to early death. There is no effective treatment. We have developed an in vitro system to investigate trans-differentiation towards the osteogenic cell lineage using platelet lysate (PL). PL contains many growth factors and cytokines important for cell growth and differentiation. Since osteogenic potential is high in FOP, we hypothesize that lower concentrations of PL are necessary for osteogenic differentiation of cells from FOP patients compared to control cell lines.

Skin biopsies were obtained from four patients with FOP. Sub-dermal fibroblasts were cultured in Ham F10 media. Fibroblast cell lines from 4 age- and sex-matched healthy individuals were used as controls. Osteogenic trans- differentiation was induced by culturing in osteogenic medium containing beta glycerol phosphate, ascorbic acid and different concentrations of PL (2%, 1%, 0.5%) or FCS (10%). Osteogenic differentiation was determined by mRNA expression of runx2, alkaline phosphatase and osteocalcin at day 0,3, 7, 14 and 21. Mineralization capacity was detected at day 21 by alizarin red staining.

In all four cell lines the classical mutation in the activin receptor-like kinase2 (Alk2) receptor was confirmed. Runx2 and alkaline phosphatase mRNA expression started to increase 3 days after addition of osteogenic medium with a maximum increase at day 7, both in control and FOP cell lines with all PL concentrations. Runx2 was significantly higher in FOP cell lines compared to controls at t=7 for 2% PL, at T=14 for all PL concentrations and at t=21 for 1% PL. Alkaline phosphatase was not different in FOP cell lines compared to controls. Osteocalcin mRNA expression was not increased osteogenic medium, but the mRNA expression was higher in FOP cell lines compared to controls at t=0 for 2%PL. After 21 days of culture calcium deposits were detected with alizarin red staining in FOP cell lines, similarly to the control cell lines.

We demonstrated osteogenic differentiation both in fibroblasts from FOP patients and controls. The concentration of platelet lysate required to trigger the cells into the osteocytic lineage is not relevant. FOP cell lines express higher amounts of runx2 during the trans-differentiation process which suggests a higher osteogenic potential.

Disclosures: Nathalie Bravenboer, None.

MO0244

IL-17 inhibits osteoblast differentiation and bone regeneration in rat. <u>Youngkyun Lee</u>*[1], <u>Yong-Gun Kim</u>[2], <u>Jae-Young Kim</u>[3]. [1]Kyungpook National University School of Dentistry, South Korea, [2]School of Dentistry, Kyungpook National University, South Korea, [3]Kyungpook National University, South Korea

Objective: The interleukin-17 (IL-17) family is a group of pro-inflammatory cytokines that are produced by a subset of helper T cells. IL-17 family members are not only involved in the immune response of tissues but also play a role in bone

metabolism. Although the role of IL-17 in osteoclast-mediated bone resorption has been extensively studied, its role during osteoblast-mediated bone formation has rarely been investigated. In this study, we examined the effect of IL-17 on osteogenesis in rats both *in vitro* and *in vivo*.

Design: To evaluate osteogenesis *in vitro*, rat calvarial osteoblast precursor cells were cultured for 14 days in osteogenic medium with or without 50 ng/mL IL-17. Osteogenic activity was evaluated by alkaline phosphatase and alizarin red staining. The mRNA expression of alkaline phosphatase, osteocalcin, and osterix was also measured by using real-time PCR. To test whether IL-17 affects bone formation *in vivo*, bone filling was examined by micro-computed tomography and histological observations at 8 weeks after critical-sized defects were made in rat calvaria.

Results: Rat calvarial cells expressed distinct IL-17R isoforms compared with human mesenchymal stem cells and mouse calvarial cells. The presence of IL-17 significantly reduced alkaline phosphatase and alizarin red staining and the expression of alkaline phosphatase, osteocalcin, and osterix *in vitro*. IL-17 also significantly inhibited the filling of calvarial defects *in vivo*.

Conclusion: IL-17 exerted a negative effect on osteogenesis in a rat model. In contrast to the previously reported beneficial effect on osteogenic differentiation of human mesenchymal stem cells, our results suggest a species or cell type-specific role for IL-17 in bone formation.

Disclosures: Youngkyun Lee, None.

MO0245

Inhibition of Adipogenic and Osteogenic Differentiation of hBM-MSCs by FGF1 and FGF2 in 3D Collagen Gels. Solange Le Blanc*[1], Meike Simann[2], Franz Jakob[3], Norbert Schuetze[4], Tatjana Schilling[5]. [1]University of Wuerzburg, Orthopedic Center for Musculoskeletal Research, Germany, [2]University of Wuerzburg, Orthopedic Center for Musculoskeletal Research, Germany, Germany, [3]University of Wuerzburg, Orthopedic Center for Musculoskeletal Research, Germany, [4]University of Wuerzburg, Orthopedic Center for Musculoskeletal Research, Germany, [5]University of Wuerzburg, Germany

Existing evidence suggests that there is an inverse relationship between osteogenesis and adipogenesis in the bone marrow; enhanced differentiation in one pathway results in a diminished differentiation in the other. This is particularly relevant in the pathogenesis of osteoporosis, the most prevalent disorder of bone remodeling, in which the loss of bone is accompanied by a parallel increase of adipose tissue in the bone marrow.

Previous results of our group suggested that fibroblast growth factor 1 (FGF1) signaling might act as a molecular check point and switch of differentiation. Based on this, the main objective of this work was to study the effect of FGF signaling on adipogenic and osteogenic differentiation of primary human bone marrow mesenchymal stem cells (hBM-MSCs) in 3D type I collagen gels, in order to better mimic the environment of native bone marrow.

hBM-MSCs embedded in 3D collagen gels were chemically induced to differentiate into adipocytes or osteoblasts in the absence and presence of recombinant FGF1 or FGF2. Differentiation was evaluated by histochemical staining of cryosections for lipid vesicles, alkaline phosphatase activity, and matrix mineralization and by measuring the expression levels of differentiation markers by quantitative PCR.

Both, FGF1 and FGF2 exerted a dose-dependent negative effect on adipogenic differentiation. A reduction in lipid droplet formation and in the gene expression of adipogenic markers was observed for FGF-treated samples. Similarly, FGF1 and FGF2 had got a dose-dependent negative effect on osteogenic differentiation in 3D. Alkaline phosphatase activity and matrix mineralization were inhibited by high concentrations of FGFs, as was the gene expression of osteogenic markers.

Taken together, these results indicate that the continuous stimulation with FGFs during the differentiation induction of hBM-MSCs in 3D collagen gels results in the inhibition of both, adipogenesis and osteogenesis.

Disclosures: Solange Le Blanc, None.

MO0246

Microarray Analysis of Pulsed Electromagnetic Field (PEMF) Stimulatory Effects on Human Bone Marrow Stromal Cells. Nicola Partridge[1], Zhiming He*[2], Nagarajan Selvamurugan[3]. [1]New York University College of Dentistry, USA, [2]New York University, USA, [3]University of Medicine & Dentistry of New Jersey, USA

The fundamental mechanism of the osteogenic effect of pulsed electromagnetic field (PEMF) is currently not fully understood. We proposed that it is caused by the regulation of gene expression by an extracellular signal. Thus, in this study we performed Affymetrix microarray and RT-PCR analyses to systematically investigate the patterns of gene expression with PEMF using human bone marrow stromal cells (hBMSCs). Fresh bone marrow from a 27 year old healthy female donor was purchased (Lonza) to obtain hBMSCs. PEMF (Cervical-Stim by Orthofix, Inc.) treatment was initiated 24 h after BMSCs were seeded, with 4 h daily exposure every day throughout the experimental period. Cell samples from both PEMF and sham (control) groups were collected simultaneously at different time points corresponding to pre-osteoblast proliferation, differentiation and mineralization phases. Total RNAs

were analyzed using Affymetrix Human U133 plus 2.0 Gene Chips and qRT-PCR. ERK/MAPK activation was observed after 30-60 min of PEMF exposure on day 5 of culture and paralleled by stimulation of cyclin D1 at 2h which was chosen for the subsequent microarray analysis. After fully evaluating PEMF-regulated gene expression and intense gene ontology analysis, our results indicate that PEMF stimulation of hBMSCs' proliferation mainly affect genes of cell cycle regulation, structure and some growth receptors or kinase pathways. There were a total of 114 known genes up regulated and 17 known genes down regulated at this time point. During the differentiation (day 23) and mineralization (day 33) stages, a total of 37 and 173 known genes, respectively, were identified as significantly regulated. In these two stages, PEMF-regulated osteoblast gene expression mainly involved down regulation of transcriptional regulators, metabolism, proteases and regulators, and also cell adhesion and binding proteins, cytoskeletal and structural proteins. Notably, the transforming growth factor beta (TGF-β) signaling pathway seems to be most highly regulated by PEMF. TGFB2 gene expression was up regulated at both stages, while TGF-β regulator-1(TBRG1) was increased at 23 days. PEMF also affected Fibrillin-2 (FBN2) expression which regulates osteoblast maturation through binding to TGF-β and controlling its bioavailability. Taken together, our results provide insights into PEMF-regulated gene expression of the entire human genome, which provides the fundamentals to reveal the mechanism of action of PEMF therapy.

MO0247

Connective Tissue Growth Factor Reporter Mice Label a Subpopulation of Mesenchymal Progenitor Cells that Reside Around Trabecular Bone. Peter Maye*[1], Wen Wang[2], Sara Strecker[3], Yaling Liu[3], Mark Kronenberg[1], Spenser Smith[1], Liping Wang[1], Fayekah Assanah[3]. [1]University of Connecticut Health Center, USA, [2]University of Connecticut, USA, [3]University of Connecticut Health Center, USA

Few gene markers selectively identify skeletal progenitor cells inside the bone marrow. We have investigated a cell population located in the mouse bone marrow labeled by *Connective Tissue Growth Factor* reporter expression (CTGF-EGFP). Bone marrow flushed from CTGF reporter mice yielded an EGFP+ stromal cell population. Interestingly, the percentage of stromal cells retaining CTGF reporter expression decreased with age and was half the frequency in females compared to males. Relative to past fate mapping strategies to mark bone marrow skeletal progenitors *in vitro*, including Twist2-Cre and Osterix-Cre approaches, CTGF reporter expression and endogenous CTGF expression marked largely overlapping cell populations in culture. Consistent with this past work, sorted EGFP+ cells displayed multipotent skeletal potential being able to differentiate into osteoblasts, chondrocytes, and adipocytes *in vitro* and osteoblasts, adipocytes, and stromal cell lineages after transplantation into a calvaria defect. Examination of CTGF reporter expression in bone tissue sections showed that EGFP+ cells were highly localized to regions around trabecular bone and were rarely detected in the periosteum, endocortical surfaces, or the central marrow space. Comparison of CTGF and Osterix reporter expression in bone tissue sections indicated an inverse correlation between strength of CTGF expression and osteoblast maturation. Down regulation of CTGF reporter expression also occurred during in vitro osteogenic differentiation. Collectively, our studies indicate that CTGF reporter mice selectively identify a subpopulation of bone marrow skeletal progenitor cells that reside around trabecular bone.

Disclosures: Peter Maye, None.

MO0248

3D Scaffolding with Adipose Derived Mesenchymal Stem Cells – Their Osteogenicity and Osteoblast Mineralization. Morten Dahl*[1], Susanne Syberg[2], Niklas Jorgensen[3], Else Marie Pinholt[4]. [1], Denmark, [2]Research Centre for Ageing & Osteoporosis, Denmark, [3]Copenhagen University Hospital Glostrup, Denmark, [4]Department of Maxillofacial Surgery, Denmark

Purpose: Adipose derived mesenchymal stem cells (ADMSCs) can differentiate into mineralizing osteoblasts and may generate neoangiogenesis. Three-dimensional (3D) scaffolds like titanium granules and dense collagen matrix may be suitable carriers for these cells. The aim of the current in vitro experiment was to demonstrate the osteogenic potential of ADMSCs seeded on 3D titanium granules and 3D dense collagen matrix.

Materials and methods: ADMSCs were isolated, cultured in osteoblast-differentiating medium and evaluated with alkaline phosphatase (ALP) assay, osteogenic gene expression, and ALP staining. ADMSC-derived osteoblasts were seeded on oxidized and non-oxidized titanium granules (TiO_2 and Ti granules) and dense collagen matrixes and the cultures were evaluated for in vitro mineralized matrix formation (Alizarin Red assay) and gene expression of osteoblast-related genes. Results are presented as mean $\pm$ SEM.

Results: ADMSCs expressed osteoblastic lineage genes, CBFA-1 and stained strongly for ALP. Mineralization measured as absorbance was significantly higher for cells seeded on TiO_2 granules on day 10 (0.1883 ± 0.0342), 14 (0.2738 ± 0.0854) and 17 (0.3152 ± 0.1077) than on cells seeded on Ti granules (0.0421 ± 0.0213, 0.473 ± 0.0143

and 0.478 ± 0.0102, respectively) or cells alone (0.0129 ± 0.0046, 0.0275 ± 0.0189 and 0.0230 ± 0.0057, respectively) after correcting for controls (empty wells, TiO_2 and Ti granules without cells). Relative ALPL expression was significantly higher for cells seeded on TiO_2 granules on day 1 (1.90 ± 0.18) compared to cells alone (1.04 ± 0.07). On day 4 relative ALPL expression was significantly higher for cells seeded on Ti granules (1.20 ± 0.10) compared to cells alone (0.88 ± 0.05). Relative RUNX2 expression was significantly higher for cells seeded on TiO_2 granules on day 1 (2.48 ± 0.27) compared to cells seeded on Ti granules (1.35 ± 0.23) and cells alone (1.41 ± 0.13). Relative COL1α1 expression was significantly higher for cells alone on day 1, (5.60 ± 0.78), 4 (2.12 ± 0.42) and 8 (1.69 ± 0.43) than for cells seeded on TiO_2 granules (1.35 ± 0.36, 0.17 ± 0.02 and 0.14 ± 0.01, respectively) and Ti granules (1.02 ± 0.31, 0.45 ± 0.07 and 0.56 ± 0.07, respectively).

Conclusion: ADMSCs have osteogenic potential especially when seeded on TiO_2 granules evidenced by increased mineralization. TiO_2 granules may be used as carrier for ADMSCs from laboratory bench to the patient within bone defects in maxillofacial surgery.

Disclosures: Morten Dahl, None.

MO0249

Loss of Notch Signaling in Skeletogenic Mesenchymal Stem Cells Results in Fracture Nonunion. Cuicui Wang*[1], Jason Inzana[2], Michael Zuscik[3], Regis O'Keefe[4], Hani Awad[1], Matthew Hilton[5]. [1]University of Rochester Medical Center, USA, [2], USA, [3]University of Rochester School of Medicine & Dentistry, USA, [4]University of Rochester, USA, [5]Duke University Musculoskeletal Research Center, USA

Although the vast majority of the fractures progress to union, fracture non-union develops in 10-20% of all patients. It is believed that fracture non-union or inappropriate fracture repair is due to the inadequate regenerative potential of the tissue on the cellular level. This regenerative potential is largely dictated by stem cell populations that reside in the bone marrow and periosteal tissue surrounding the bone. Recently, our laboratory identified the Notch signaling pathway as a critical maintenance factor for bone marrow derived mesenchymal stem cells (BMSCs) during development. To determine whether Notch signaling in MSCs or more mature osteoblasts is required during the process of bone fracture repair, we preformed open, non-stabilized tibial fractures on *Prx1Cre;RBPjk^f/f*, *Col1Cre(2.3Kb);RBPjk^f/f*, and control mice. Following injury, bone fractures were analyzed via radiographs, biomechanical torsion testing, histology, immunohistochemistry, TRAP staining, and real-time qPCR at multiple time-points post fracture. We also assessed the number of BMSCs present in mutant and control mice. Our data demonstrate that *Prx1Cre;RBPjk^f/f* mutant mice display characteristics most commonly observed in human hypertrophic non-unions, while *Col1Cre(2.3Kb);RBPjk^f/f* and control fractures heal normally. Although the *Prx1Cre;RBPjk^f/f* mutants did form a substantial external callus involving periosteal stem cells, they did not develop an appropriate internal callus which ultimately resulted in fracture non-union. Furthermore, *Prx1Cre;RBPjk^f/f* mutants exhibited a dramatic reduction in the pool of BMSCs. We also performed stabilized or rigidly fixed femur fractures on *Prx1Cre;RBPjk^f/f* mutants to determine whether fracture instability was required for fracture non-union. Stabilized femur fractures of *Prx1Cre;RBPjk^f/f* mutants also resulted in fracture non-union, suggesting that insufficient fracture stabilization is not absolutely required for fracture non-union in these mutant mice. Therefore, all fracture non-unions observed in *Prx1Cre;RBPjk^f/f* mutants likely resulted from BMSC pool depletion or loss of Notch signals within BMSCs. Collectively, our data reveal that BMSCs are a vital component of fracture repair and act to form the internal callus providing stability to the fracture and promoting healing, and that loss of Notch signaling in MSCs and depletion of BMSCs results in bone fracture non-unions.

Disclosures: Cuicui Wang, None.

MO0250

Aging Effects of Advanced Glycation End Products on Osteoclast Resorption on Human Bone. Xiao Yang*[1], Chintan Gandhi[2], Rahman Md mizanur[3], Mark R. Appleford[4], Lian-Wen Sun[5], Xiaodu Wang[6]. [1]University of Texas at San Antonio & Beihang University, USA, [2]Department of Mechanical Engineering, University of Texas at San Antonio, USA, [3]Department of Medicine - Clinical Immunology & Rheumatology, University of Texas Health Science Center at San Antonio, USA, [4]Department of Biomedical Engineering, University of Texas at San Antonio, USA, [5]School of Biological Science & Medical Engineering, Beihang University, China, [6]UTSA, USA

Advanced glycation end-products (AGEs) are products of non-enzymatic glycation and oxidation of long-lived proteins (e.g. collagen) and lipids [1]. AGEs are reported to accumulate in extracellular matrix as seen in bone tissues of elderly people and affect bone resorption/formation during remodeling process, thus leading to skeletal fragility [2]. However, it has been controversial in the previous studies regarding the age-related influences of matrix AGEs on osteoclastic resorption activities in bone.

In this study, we collected bone slices from mid-diaphysis of human cadaveric femurs of three age groups: young, middle-aged and elderly group, respectively. The bone slices were polished and sterilized, and then human osteoclast precursor cells (Lonza Walkersville Inc., MD) were seeded onto the bone slices. The precursor cells were activated with medium supplemented with M-CSF and RANKL and differentiated into osteoclasts. After terminating the cell culture in 14 days, osteoclastic resorption pits on the bone slices were stained and imaged. Next, the bone slices were demineralized to determine the areal AGEs distribution based on its autofluorescence intensity. The local resorption pit number and area were measured in regions with different AGEs concentrations. Moreover, the matrix AGEs distribution (autofluorescence intensity) in interstitial and osteonal regions was also measured for the three age groups.

The results showed that 1) AGEs concentration in both osteonal and interstitial bone regions was significantly less in young bone than in middle-aged and elderly bones, suggesting that matrix AGEs accumulation is related to donor age; 2) the total resorption pits number/area were similar for all bone slices irrespective of age-related differences in local AGEs concentrations, suggesting that the average osteoclastic resorption activities are not dependent on matrix AGEs concentrations; 3) the resorption pit number/area in the interstitial bone regions were significantly less in young group than in elderly group, while such differences were not observed in the osteonal regions, thus suggesting that age-related changes in osteoclastic resorption activities were manifested only in biologically older bone tissues (interstitial bone). In summary, donor age induced changes in osteoclast resorption activities occur only in biologically older bone tissues.

Disclosures: Xiao Yang, None.

MO0251

Effect of Zoledronate on Particle-Induced Osteolysis In Vitro and In Vivo. Yue Ding*[1], Maolin Zhang[2], Huiyong Shen[2], Changchuan Li[2], Chi Zhang[2]. [1]Sun Yat-sen Memorial Hospital, , [2]Sun Yat-sen Memorial Hospital, China

Aseptic loosening is a key factor that causes implant failure of joint replacement. This study was aimed to investigate the effect of zoledronate on particle-induced osteolysis in vitro and in vivo. First, osteoclast precursors were isolated from the long bones of six-week-old C57BL/6J mice and assigned into 6 groups with different component: in Group A, the culture solution was added; in Group B, the macrophage colony stimulating factor(M-CSF), the receptor activator of nuclear factor kappa ligand(RANKL) and culture solution was added; in Group C, the titanium particles and culture solution was added; in Group D, the solution(the supernatant of cultured mouse macrophages induced by titanium particles after 24h) and culture solution was added; in Group E, the M-CSF, RANKL, ZOL and culture solution was added; in Group F, the solution, ZOL and culture solution was added. After 10 days coverslips were stained by the tartrate-resistant cultured acid phosphatase (TRAP). And the activity of the osteoclast cells was detected with the area of osteo-assay surface resorption. The TRAP positive multinucleated cells and the resorpion lacunae were observed in group B, group D, group E and group F. In group F($5.54\% \pm 1.25\%$), the area of resorption lacunae was smaller than that in group D($10.34\% \pm 1.69\%$, $P<0.01$,$t=5.61$).It suggested that the zoledronate could inhibit the activation of osteoclasts induced by the titanium particles in vitro. On the other hand, the model of particle-induced osteolysis in mice skull was established, and then a single dose of zoledronate was locally administered to investigate its effect on particle-induced osteolysis. Ninety-six 12-week-old C57BL/6J mice were equally allocated into eight groups, and different dosages of zoledronate were added. Fourteen days after operation, the animals were sacrificed in CO_2. According to the CT scan and Micro-computed Tomography, it showed an inverse correlation between dosage of zoledronate and the extent of bone resorption. According to these results, zoledronate may have the potential to be a therapeutic target for particle-induced osteolysis.

Disclosures: Yue Ding, None.

MO0252

Glucocorticoids Enhance Mature Osteoclast Activity Without Affecting RANKL Induced Osteoclast Formation. Ulf Lerner[1], Petra Henning*[2], Jan Tuckermann[3], Howard Conaway[4]. [1]Sahlgrenska Univesity Hospital, Sweden, [2]Centre for Bone & Arthritis Research, Sahlgrenska Academy, University of Gothenburg, Sweden, [3]University of Ulm, Germany, [4]University of Arkansas for Medical Sciences, USA

Glucocorticoid (GC) therapy is the greatest risk factor for secondary osteoporosis. Pathogenetic mechanisms involve an initial increase in bone resorption followed by decreased bone formation. In an effort to gain a better understanding of the resorptive activity of GC, we have used mouse bone marrow macrophages (BMM) to determine if GCs can directly modulate RANKL stimulated osteoclast formation and/or activity. Experiments performed in plastic wells showed that GCs (dexamethasone, hydrocortisone, and prednisolone) inhibited osteoclast number and size during the initial phases of RANKL stimulated osteoclastogenesis. In more prolonged cultures, escape from GC induced inhibition occurred and an enhanced number of osteoclasts was formed, many with an increased area. These changes were not associated with any effect by dexamethasone on RANKL stimulated mRNA expression of several osteoclastic genes. When BMM cells were seeded on bone slices, no inhibition or

stimulation by GCs of RANKL induced osteoclast formation was observed, nor was the release of Trap5b affected. However, GCs (dexamethasone, hydrocortisone, and prednisolone) robustly enhanced RANKL stimulated formation of resorption pits and release of CTX. Release of CTX was concentration dependent, occurring at and above 1 nM of dexamethasone. The stimulation of pit formation was not associated with an effect on the mRNA expression of several osteoclastic genes (Acp5, Ctsk, Oscar) or osteoclastogenic transcription factors (c-fos, Nfatc1). The potentiation of RANKL induced CTX release by dexamethasone was significantly less in BMM cells from mice with conditional knockout of the glucocorticoid receptor (GRLysMCre). No effect by dexamethasone on CTX release was observed in RANKL stimulated BMM from GRdim mice, which are unable to dimerize the GC receptor. These data suggest that: 1. GCs do not have a direct effect on RANKL stimulated osteoclast formation, and 2. a direct enhancement of RANKL mediated resorption is stimulated by the dimeric GC receptor.

Disclosures: Petra Henning, None.

MO0253

Kinase Activity of Leucine Rich Repeat Kinase 1 (LRRK1) Is Essential for Osteoclast Resorptive Activity. Weirong Xing*[1], Bo Liu[2], Shaohong Cheng[3], Robert Brommage[4], Subburaman Mohan[5]. [1]Musculoskeletal Disease Center, Jerry L. Pettis Memorial Veteran's Admin., USA, [2]VALLHCS, USA, [3]VA Loma Linda Health Care Systems, USA, [4]Lexicon Pharmaceuticals, USA, [5]Jerry L. Pettis Memorial VA Medical Center, USA

LRRK1 belongs to the ROCO protein family, and contains ankyrin repeats and leucine-rich repeats, a GTPase-like domain of Roc, a COR domain, and a serine/threonine kinase domain. We have shown that knockout (KO) of Lrrk1 in mice causes severe osteopetrosis. Precursors derived from Lrrk1 KO mice differentiate normally into multinucleated osteoclasts (OCs) in response to M-CSF/RANKL treatment, but these OCs fail to resorb bone due to defects in cytoskeletal rearrangement, peripheral sealing zones and ruffled borders. While bone resorption in KO mice is reduced dramatically, bone formation is not significantly affected. Lrrk1 KO mice have normal teeth, are healthy through one year of age and respond to anabolic PTH treatment, but are resistant to ovariectomy-induced bone loss. We characterized calvarial and mandibular bones of 6-wk old male Lrrk1 KO mice and control WT littermates (N = 4 pairs) by μCT analyses. In contrast to dramatically elevated trabecular BV/TV in long bones and vertebra (2- to 5-fold), deficiency of Lrrk1 had only a mild effect on the skull. Calvaria from Lrrk1 KO mice had normal TV, 20% higher BV and 17% higher BV/TV than control mice (all P < 0.05). For the mandible, TV, BV and BV/TV in Lrrk1 KO mice were increased 25%, 34% and 7%, respectively (all P < 0.01). To determine if LRRK1 regulation of OC function depends on kinase enzymatic activity, OC precursors derived from Lrrk1 KO mice were transduced with lentivirus containing 3xFlag/hLRRK1, 3xFlag/K650A hLRRK1 that abolishes GTP/GDP binding and kinase activity or GFP control. Transduced cells were differentiated to OCs on bone slices in the presence of M-CSF/RANKL before determining resorptive activity by pit formation. Comparable expression of WT hLRRK1 and K650A mutant hLRRK1 proteins in transduced OCs was confirmed by Western blot analyses with a Flag tag antibody. Ectopic expression of full length WT hLRRK1/Flag fusion protein in Lrrk1 null OCs completely rescued resorptive activity. In contrast, OCs with the kinase dead K560A hLRRK1/Flag mutant protein had no enhanced resorptive activity as compared to GFP expressing cells. Conclusions: 1) The modest skull and mandible phenotypes of Lrrk1 KO mice compared to long bones and vertebra are consistent with evidence that regulation of OC function is different in membranous and endochondral bone. 2) The requirement for LRRK1 in functional OCs depends upon its enzymatic kinase activity in addition to presumed scaffolding functions.

Disclosures: Weirong Xing, None.

MO0254

WASH complex subunit FAM21 is required for efficient osteoclast formation. Jian Zuo[1], Edgardo Toro[2], John Neubert[1], Kevin McHugh[2], Lexie Holliday*[3]. [1]University of Florida College of Dentistry, USA, [2]University of Florida, USA, [3]University of Florida College of Dentistry, USA

Our previous studies have suggested that binding between the vacuolar H$^+$-ATPase (V-ATPase) and microfilaments is vital for osteoclast function. Recent work in *Dictyostelium discoideum* showed that the Wiscott Aldrich and Scar Homolog (WASH) complex is involved in a process that sorts V-ATPases between membrane compartments which involves V-ATPase binding to microfilaments. In mammalian cells the WASH complex is known to function by regulating actin polymerization and is linked to vesicle sorting by the retromer complex. The purpose of this study was to test the hypothesis that the WASH complex plays a role in osteoclast function which may be tied to specialized sorting of V-ATPases.

We found by quantitative real time PCR and Western blotting that multiple subunits of the WASH complex were upregulated up to 3-fold during osteoclastogenesis. FAM21, a subunit of the WASH complex, was localized to a tubulovesicular network and, surprisingly, to the plasma membrane-associated actin rings of resorbing osteoclasts. This is the first description of FAM21 (or any subunit of the

WASH complex) being localized to a plasma membrane domain. FAM21 co-localized with V-ATPase after treatment of resorbing osteoclasts with wortmannin, which stimulates internalization of V-ATPases from the ruffled plasma membrane into cytosolic vesicles. Immunoaffinity purification using an anti-V-ATPase antibody pulled down FAM21 only after treatment of osteoclasts with wortmannin. This association remained even when actin filaments were depolymerized with latrunculin A, a result consistent with a direct interaction between the WASH complex and V-ATPase as was reported in *Dictyostelium*. Knockdown of FAM21 by RNA interference in RAW 264.7 cells resulted in reduction of osteoclast formation by 85% even though it had no effect on the viability of the cells.

These data support the hypothesis that the WASH complex has a role that is vital for osteoclast formation, and may be crucial for specialized membrane trafficking required for bone resorption. As in *Dictyostelium,* the WASH complex may be involved in sorting V-ATPases between membrane compartments. This idea is supported by co-precipitation of FAM21 with V-ATPase during the retrieval of V-ATPases from the ruffled plasma membrane, but further studies are required to test this concept. These studies are the first to identify FAM21 and the WASH complex as important components of the bone resorptive machinery of osteoclasts.

Disclosures: Lexie Holliday, None.

MO0255

Exosome-encapsulated miR-214 secreted from osteoclast to inhibit osteoblastic activity. Defang Li*[1], Chao Liang[2], Baosheng Guo[2], Jin Liu[2], Lei Dang[1], Liang Xu[3], Xiaojuan He[4], Zicai Liang[5], Aiping Lu[1], Ge Zhang[1]. [1]Institute for Advancing Translational Medicine in Bone & Joint Diseases, School of Chinese Medicine, Hong Kong Baptist University, Hong Kong SAR, China, [2]Institute for Advancing Translational Medicine in Bone & Joint Diseases, School of Chinese Medicine, Hong Kong Baptist University, Hong Kong SAR, China, [3]nstitute for Advancing Translational Medicine in Bone & Joint Diseases, School of Chinese Medicine, Hong Kong Baptist University, Hong Kong SAR, China, [4]Institute of Basic Research in Clinical Medicine, China Academy of Chinese Medical Sciences, Beijing, China, [5]Academician Chen Xinzi Workroom for Advancing Translational Medicine in Bone & Joint Diseases, Kunshan RNAi Institute, Kunshan Industrial Technology Research Institute, Kunshan, Jiangsu, China

Introduction

A number of miRNAs have been found to be present in body fluids of humans (mice) and mediate intercellular communication, suggesting that the potential role of miRNAs in mediating intercellular communication from osteoclasts to osteoblasts deserves intense investigation. Exosomes (50-100 nm) can function as efficient vectors to protect miRNAs from RNase-induced degradation to mediate intercellular communication. However, the functional role of exosomes in miRNAs transfer between osteoclasts and osteoblasts is unknown. Recently, our study implied that the increased miR-214 could regulate osteoblastic activity (Wang XG, et al., Nat Med, 2013), and miR-214 was abundant in primary osteoclasts other than primary osteoblasts. Therefore, it is highly desirable to study the role of exosomes in miR-214 transfer from osteoclast to osteoblast.

Methods

Experimental Design: (1) Study 1: The influence of miR-214 within osteoclasts in regulating the osteoblastic activity was investigated *in vitro*. (2) Study 2: The transferred miR-214 from osteoclasts to osteoblasts encapsulated in exosomes was confirmed *in vitro*. (3) Study 3: The role of DNM3, which was implicated in pinch off of exosomes and co-expressed with miR-214, in exosome-mediated miR-214 transfer from differentiating osteoclasts was investigated *in vitro*. Refer to http://sdrv.ms/1ay09xO for experimental protocols online.

Results

In study 1, the mRNA expression levels of osteoblast marker genes (*Bglap*, *Alp*, *Collagen-I*, *Opn*, *Runx2*, *Osx* and *Atf4*) in osteoblasts were down-regulated by increased miR-214 with osteoclasts. In study 2, the miR-214 levels in exosomes were increased after increasing the miR-214 level in differentiating osteoclasts by transfer of miR-214-expressing lentiviral vector (LV-miR-214), which could be inhibited by an exosome inhibitor GW4869. Further, flow cytometry data and confocal microscope analysis demonstrated that the exosomes from osteoclasts could be internalized into osteoblasts. In study 3, *DNM3* silencing by transfection of LV-DNM3 siRNA attenuated extracellular transfer of miR-214 in osteoclasts and promoted the expression of bone formation marker genes (*Bglap* and *Osx*) in osteoblasts *in vitro*.

Conclusions

The *in vitro* experiments demonstrated that miR-214 was transferred from osteoclast to osteoblast in exosome-encapsulated form, and DNM3 participated in the intercellular transfer of exosome-encapsulated miR-214.

References

Wang XG, et al. *Nat Med* 2013;19:93-100.

Figure 1 Role of miR-214 within osteoclasts in regulating osteoblastic activity (a) The schematic of the co-culture system for the interaction between osteoblasts and differentiating osteoclasts. (b) The miR-214 level within differentiating osteoclasts after the transfection of LV-miR-214 and LV-miR-NC, respectively. (c) Time course change of miR-214 level in the supernatant after co-culture of osteoclasts-transfected with LV-miR-214 and osteoblasts. (d) Time course change of miR-214 level in the osteoblasts after co-culture with LV-miR-214-transfected osteoclasts. (e) The mRNA expression levels of marker genes (Bglap, Alp, Collagen-I, Opn, Runx2, Osx and Atf4) in osteoblasts after the co-culture with the LV-miR-214- and LV-miR-NC-transfected osteoclasts, respectively. The data was presented as the mean ± standard deviation. *P <0.05 for comparison with LV-miR-NC.

Figure 2 miR-214 from osteoclasts in vesicles encapsulation (a) The two-dimension morphology of the vesicles imaged by cryo-electron microscopy. (b) The three-dimension morphology of the vesicles imaged by cryo-electron microscopy. (c) Quantitative analysis of the electron micrographs showing the diameter of the vesicles. (d) The miR-214 levels in differentiating osteoclasts transfected with LV-miR-214 and LV-miR-NC, respectively. (e) The miR-214 levels in supernatant exosomes from osteoclasts transfected with LV-miR-214 and LV-miR-NC, respectively. The data was presented as the mean ± standard deviation. *P < 0.05 or **P < 0.01 for comparison with the corresponding LV-miR-NC control.

Figure 3 Osteoclasts-derived exosomes internalized by osteoblasts. (a) The miR-214 levels in osteoclast lysates or exosomes after 24 hours treatment with exosome inhibitor (GW4869) at different concentration levels. (b) The mRNA expression levels of marker genes (Alp, Collagen-I, Opn, BSP and Bglap) in osteoblasts after the co-culture with the exosomes from LV-miR-214- or LV-miR-NC-transfected osteoclasts or pretreatment with exosome inhibitor (GW4869), respectively. (c) Capture of osteoclasts-derived exosomes labeled with PKH26 by osteoblasts. Numbers indicate percentage of cells. (d) PKH26-labeled exosomes (green) rapidly internalized into early endosomes labeled with Texas red-transferrin (yellow indicates colocalization of green and red). (e) Later, PKH26-labeled exosomes (green) trafficked to late endodome/lysosomes labeled by DiI-LDL (red). Data are representative of 3 independent experiments. Data are representative of 3 independent experiments. The data was presented as the mean ± standard deviation. *P<0.05 or **P<0.01 for comparison with the corresponding LV-miR-NC control.

Figure 4 Participation of DNM3 in exosome required for extracellular transfer of miR-214 from osteoclasts in vitro. (a) The DNM3 mRNA expression in osteoclasts transfected with LV-DNM3 siRNA and LV-siRNA NC, respectively. (b) The miR-214 level in supernatant exosomes from osteoclasts transfected with LV-DNM3 siRNA and LV-siRNA NC, respectively. (c) The miR-214 level in supernatant exosomes from osteoclasts transfected with LV-miR-NC, LV-miR-214, LV-DNM3 siRNA and LV-miR-214 plus DNM3 siRNA, respectively. (d) The mRNA levels of marker genes (Bglap and Osx) in osteoblasts after the co-culture with osteoclasts transfected with LV-miR-NC, LV-miR-214, LV-siRNA NC, LV-DNM3 siRNA and LV-miR-214 plus DNM3 siRNA, respectively. The data was presented as the mean ± standard deviation. *P <0.05 or **P < 0.01 for comparison with LV-siRNA-NC.

Results-Figure

Disclosures: Defang Li, None.

MO0256

Interleukin-1 receptor-associated kinase-4 (IRAK4) promotes inflammatory osteolysis by activating osteoclasts and inhibiting formation of foreign body giant cells. <u>Eri Katsuyama</u>*[1], <u>Takeshi Miyamoto</u>[2], <u>Yoshiaki Toyama</u>[3]. [1]Keio University, Japan, [2]Keio University School of Medicine, Japan, [3]Keio uni., Japan

[objective and methods]

Foreign body giant cells (FBGCs) and osteoclasts, both of which are derived from bone marrow macrophages (BMMs), have been implicated in osteolysis and implant failure associated with inflammation or microbial infection. FBGCs are induced following implantation of biomaterials, however, we have little understanding about the regulation of FBGC differentiation. In this study, we focused on interleukin-1 receptor-associated kinase-4 (IRAK4), which plays a role in IL-1R/TLR signaling, and examined the differentiation of FBGCs and osteoclasts in IRAK4-deficient mice under an inflammatory condition.

[results and discussion]

FBGCs from wild-type (WT) BMM did not have bone resorbing activity but rather expressed *yellow mottled (YM)* and *arachidonate 15-lipoxygenase (Alox15)*, M2 macrophage-like wound-healing and inflammation-terminating molecules. By adding IL-1β, FBGC and osteoclast formation were significantly inhibited and promoted, respectively; however, such effects were cancelled when FBGCs and osteoclasts were generated from IRAK4-deficient BMMs. Furthermore, calvarial bone resorption promoted by LPS, an infection mimetic of a gram-negative bacteria, was abrogated in IRAK4-deficient mice *in vivo*. IRAK4-deficiency did not alter physiological osteoclast formation *in vitro* and bone mineral density *in vivo*. In contrast, IRAK4-deficiency restored FBGC formation and M2 macrophage like molecule expression in condition with LPS *in vivo*.

[conclusion]

Our results identify IRAK4 as a therapeutic target to inhibit the stimulated osteoclastogenesis and to rescue the inhibited FBGC formation under an inflammatory and an infectious condition without affecting physiological bone resorption.

Disclosures: ERI KATSUYAMA, None.

MO0257

Lhx2 regulates bone remodeling in mice by modulating RANKL signaling in osteoclasts. <u>Jung Ha Kim</u>*[1], <u>Bang Ung Youn</u>[2], <u>Kabsun Kim</u>[3], <u>Nacksung Kim</u>[4]. [1], South Korea, [2]Chonnam National University, South Korea, [3]Chonnam national university, South Korea, [4]Chonnam National University Medical School, South Korea

The LIM homeobox 2 transcription factor Lhx2 has a variety of functions, including neural induction, morphogenesis, and hematopoiesis. Here we show the involvement of Lhx2 in osteoclast differentiation. Lhx2 was strongly expressed in osteoclast precursor cells but its expression was significantly reduced during receptor activator of nuclear factor-kB ligand (RANKL)-mediated osteoclastogenesis. Over-expression of Lhx2 in bone marrow-derived monocyte/macrophage lineage cells (BMMs), which are osteoclast precursor cells, attenuated RANKL-induced osteoclast differentiation by inhibiting the induction of nuclear factor of activated T cells c1 (NFATc1). Interestingly, interaction of Lhx2 proteins with c-Fos attenuated the DNA binding ability of c-Fos and thereby inhibited the transactivation of NFATc1. Furthermore, Lhx2 conditional knockout mice exhibited an osteoporotic bone phenotype, which was related with increased osteoclast formation *in vivo*. Taken together, our results suggest that Lhx2 acts as a negative regulator of osteoclast formation *in vitro* and *in vivo*. The anti-osteoclastogenic effect of Lhx2 may be useful for developing a therapeutic strategy for bone disease.

Disclosures: Jung Ha Kim, None.

MO0258

The elementary fusion modalities of osteoclasts. <u>Kent Soe</u>*[1], <u>Anne-Sofie Hobolt-Pedersen</u>[2], <u>Jean-Marie Delaisse</u>[3]. [1]Vejle Hospital, University of Southern Denmark, Denmark, [2]Vejle Hospital, University of Southern Denmark, Denmark, [3]Vejle Hospital, IRS, University of Southern Denmark, Denmark

The last step of the osteoclast (OC) differentiation process is cell fusion. Most efforts to understand the fusion mechanism have focused on the identification of molecules involved in cell fusion. Surprisingly, the basic fusion modalities, which are well known for fusion of other cell types, are not known for the OC. Here we characterize the partners involved in a fusion event with respect to their mobility, number of nuclei, and differentiation level.

OCs were generated from buffy coat monocytes exposed to RANKL. Time-lapse videos were recorded on OC preparations of three donors. A total of 174 videos, representing 3,468h, 656 fusion events, and 100 mm2 were analyzed by two observers. Fusion partners were categorized according to number of nuclei and mobility. Furthermore, nucleus tracing tests were performed by co-culturing cells from male and female donors, at early or late differentiation stages.

Fusions between a mobile and immobile partner were most frequent. They represented 62% of the fusion events, while fusion between two mobile or two immobile partners represented only 26% (p<0.001) and 12% (p<0.001), respectively. The immobile fusion partner contained on average significantly more nuclei than the mobile one (p<0.01). Enrichment in nuclei of an OC with three or more nuclei resulted from fusion with a mononucleated cell in 67% of the cases (p<0.001), while mononucleated cells fused with a multinucleated cell in 61% of the cases (p<0.05). This observation suggests that fusion is more likely to occur between a more mature (multinucleated) fusion partner and a less mature (mononucleated) partner. This hypothesis was supported by an independent approach based on nucleus tracing. These experiments showed that more differentiated cells have a higher propensity to fuse with less differentiated cells mixed at a 1:1 ratio (p=0.002), when compared to conditions where cells of male and female donors had been exposed to RANKL for the same amount of time.
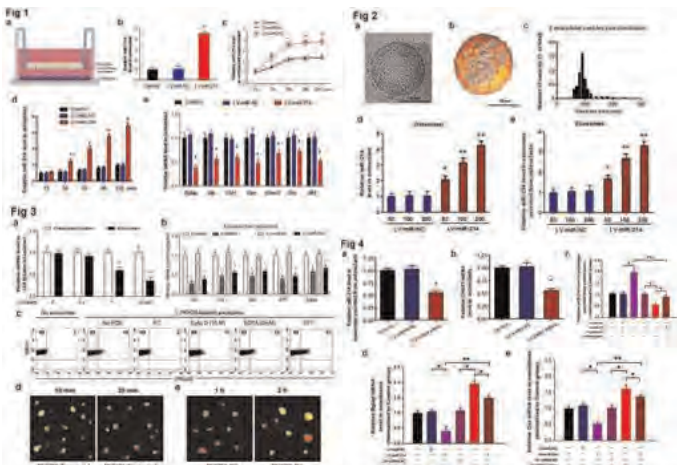
We conclude that OCs most often gain nuclei by addition of one nucleus at a time, and that this nucleus is most often delivered by a moving cell to an immobile cell. This conclusion appears relevant to the in vivo situation where mononucleated cells migrating from the bone marrow fuse with more mature OCs on the bone surface. These results also fit the fusion modalities reported for other cell types and may in addition help to elucidate how hyper-nucleated OCs are generated in some clinical situations.

Disclosures: Kent Soe, None.

MO0259

Connexin 43 Hemichannels are Important Regulators of Osteoclast Differentiation. <u>Danielle Callaway</u>*[1], <u>Manuel Riquelme</u>[2], <u>Jean Jiang</u>[1]. [1]University of Texas Health Science Center at San Antonio, USA, [2]University of Texas Science Center, San Antonio, USA

Connexin 43 (Cx43) is a membrane protein that forms gap junctions and hemichannels for communication between the cell and adjacent cells or the extracellular environment, respectively. Although the function of Cx43 in osteocytes and osteoblasts has been extensively investigated, its role in the osteoclast remains largely unknown. In this study, we found that Cx43 is expressed in the osteoclast and macrophage precursors, localized on the cell surface in mononuclear cells during

osteoclastogenesis. Conversely, in the osteoclast, Cx43 was found in the cytoplasm. In order to evaluate the function of Cx43 during the differentiation process, gap junction and hemichannel activity were assessed. Gap junction activity was analyzed with the dye coupling assay where we failed to detect dye transfer between cells during differentiation. However, both osteoclasts and precursors possessed functional hemichannels that could be blocked by the Cx43(E2) antibody developed by our laboratory that is specific for Cx43 hemichannels. Dye uptake analysis measuring hemichannel activity revealed that upon RANKL addition, Cx43 hemichannels were opened suggesting that hemichannels could serve as regulators during the osteoclast differentiation process. In agreement with the previous results showing a lack of Cx43 at the cell surface, dye uptake in the osteoclast was significantly attenuated compared to mononuclear precursors. Next, we assessed whether Cx43 plays a role in osteoclast differentiation with models of reduced Cx43 including RAW264.7 cells with Cx43 knockdown by siRNA and the heterozygous ($Cx43^{+/-}$) mouse model. In both models, there was a significant decrease in total numbers of osteoclasts formed compared to controls. In order to determine whether hemichannels were important in osteoclast differentiation, we applied Cx43(E2) antibody during differentiation, which led to a reduction in total osteoclast numbers and TRAP activity. Levels of nuclear factor of activated T-cells, cytoplasmic 1 (NFATc1), which activates mature osteoclast and pro-fusion genes, were then evaluated to assess if it could be regulated by hemichannels. However, because there was no evident reduction in NFATc1, the mechanisms mediating Cx43 hemichannel activity and its impact on osteoclastogenesis could be downstream of NFATc1 or part of a separate pathway. In total, this data indicates that Cx43 hemichannels have important contributions as regulators of osteoclast differentiation.

Disclosures: Danielle Callaway, None.

MO0260

Duffy Antigen Receptor for Chemokines (DARC) Modulates Inflammation-induced Recruitment of Osteoclast Precursors. <u>Mohamed Elgendy</u>[1], <u>Yan Hu</u>[1], <u>Subburaman Mohan</u>[2], <u>Bouchra Edderkaoui</u>*[2]. [1]Jerry L Pettis Memorial Veterans Administration Medical Center, USA, [2]Jerry L. Pettis Memorial VA Medical Center, USA

Inflammatory reactions observed after many, if not all, bacterial infections have been shown to be powerful activators of monocytes and macrophages and potent inducers of pro-inflammatory cytokines and chemokines. Because Duffy antigen receptor for chemokines (Darc) is known to bind to a number of the pro-inflammatory chemokines of the CC and CXC families and because chemokines are known to regulate osteoclast (OC) trafficking, we have predicted that Darc regulates OC recruitment to the sites of inflammation by modulating chemokine actions. We have used mice that lack Darc expression (Darc-KO) and wild type (WT) mice to assess the role of Darc in the response to bacterial Lipopolysaccharide (LPS) infections. Animals were administered with subcutaneous LPS injections on mouse calvaria bone. Five hours post-LPS injection, the expression of CD14 which is a marker of inflammatory monocytes, was found to be increased significantly in response to LPS injection. Histological sections were prepared at the injection sites, and the sections were stained for tartrate-resistant acid phosphatase (TRAP), 3 days post-LPS injection. The percentage of bone surface covered by OCs (Trap stained surface) was measured. As expected, LPS injection caused a significant increase in the percentage of bone surface covered by OCs in both lines of mice compared to the saline injected animals at three days post-LPS injection. While, the % TRAP labeled OC surface was significantly reduced in KO mice compared to WT mice in saline injected animals, the magnitude of increase in OC surface in response to LPS was greater in Darc-KO mice compared to WT mice. Based on these data and the previous data that showed Darc mediates trancytosis of chemokines to vascular lumen promoting chemokine-mediated leukocyte transmigration, we predicted that blocking Darc function enhances the response of OC precursors to bacterial infections. To test this hypothesis, we evaluated the expression levels of CD11b, an established marker of OC precursors, around the injection site for the two lines of mice and found greater increase in the expression of CD11b in response to LPS injection in KO mice compared to WT mice. Based on these findings, we conclude that Darc regulates recruitment of OC precursors at the inflammation site, probably through regulation of chemokines transcytosis that consequently regulate leukocytes migration.

Disclosures: Bouchra Edderkaoui, None.

MO0261

Withdrawn

MO0262

Loss of HDAC7 in Osteoclasts Increases Bone Mass Through Interactions with MITF and PU.1. <u>Melissa Stemig</u>[1], <u>Kristina Astleford</u>[2], <u>Ann Emery</u>[2], <u>Tsang-hai Huang</u>[3], <u>Janice Cho</u>[2], <u>Raj Gopalakrishnan</u>[4], <u>Kim Mansky</u>*[4], <u>Eric Jensen</u>[4]. [1]University of Minnesota School of Dentistry, USA, [2]University of Minnesota, USA, [3]National Cheng-Kung University, Taiwan, [4]University of Minnesota, USA

We recently identified histone deacetylase 7 (HDAC7) as a novel regulator of osteoclast formation. Our in vitro data indicated that suppression of HDAC7 enhanced differentiation of osteoclasts from bone marrow macrophage cultures, while overexpression of HDAC7 inhibited osteoclast formation. In reporter assays, HDAC7 repressed the activity of the microphthalmia-associated transcription factor, MITF. Physical interaction between MITF and HDAC7 was attenuated by stimulation with RANK Ligand (RANKL), a factor that enhances MITF activity.

To further characterize the role of HDAC7 in osteoclast differentiation in vivo, we created mice null for HDAC7 expression in osteoclasts using LysM-CRE. Micro-CT at 1, 3 and 6 months indicates that mice null for HDAC7 expression are osteopenic at 3 and 6 months compared to their wild type littermates, with increased osteoclast activity as measured by CTX ELISA but with no significant change in the rate of bone formation. When osteoclasts from the HDAC7 null mice are cultured in vitro, they are larger in size and display increased resorption activity. They also exhibit increased expression of MITF/PU.1 target genes including *DC-STAMP*, *OSCAR*, *cathepsin K* and *v-ATPase V_0 subunit d2*. New biochemical studies show that HDAC7 interacts with both MITF and PU.1 transcription factors. Deletion analysis identifies a specific region in the HDAC7 amino-terminal domain that mediates MITF and PU.1 binding. Further, we found by ChIP analysis that HDAC7 is located at MITF-responsive promoter elements. These data suggest a model in which HDAC7 regulates bone resorption and the onset of osteoclast differentiation by repressing the activities of MITF and PU.1 at target gene promoters. Unexpectedly, targeted mutations in HDAC7 reveal that constitutively nuclear, constitutively cytoplasmic, as well as deacetylase inactive forms of HDAC7 all can inhibit osteoclast differentiation. Thus, the mechanism(s) used by HDAC7 to regulate osteoclast formation represent an active area for ongoing investigations.

Disclosures: Kim Mansky, None.

MO0263

RANK cytoplasmic IVVY535-538 motif activates C/EBPα which plays a crucial role in osteoclast lineage commitment. <u>Joel Jules</u>*, <u>Wei Chen</u>, <u>Xu Feng</u>, <u>Yi-Ping Li</u>. University of Alabama at Birmingham, USA

The receptor activator of NF-κB (RANK) ligand (RANKL) plays an essential role in osteoclast (OC) formation by stimulating its receptor, RANK, leading to the activation of many critical OC transcription factors (TFs), such as FBJ osteosarcoma oncogene (c-fos), SFFV proviral integration 1 (PU.1), Runt-related transcription factor 1 (Runx1), and CCAAT/enhancer binding protein α (C/EBPα). However, it is not fully known whether all of these factors are essential for OC lineage commitment. In this study, we first confirmed that the expression of C/EBPα, Runx1, cFos or PU.1 was significantly up-regulated by transient stimulation of bone marrow macrophages (BMMs) with RANKL and macrophage-colony stimulating factor (M-CSF) to induce osteoclastogenesis, suggesting the potential involvement of these factors in OC lineage priming. In addressing this issue, we found that whereas overexpression of all four TFs in BMMs could stimulate the expression of many OC marker genes in the absence of RANKL, C/EBPα played a more striking role in mediating OC formation when attended by permissive levels of RANKL. This finding indicates that C/EBPα may play a stronger role than the other 3 in OC lineage commitment. RANK contains an IVVY (535-538) motif which plays a critical role in OC formation by committing BMMs into OC lineage. Hence, we investigated the role of the IVVY motif in the activation of these four TFs during OC lineage commitment via a mutational strategy. We utilized a chimeric receptor system containing the human Fas external domain linked to transmembrane and cytoplasmic domain of normal mouse RANK (ChA) or mouse RANK bearing an inactivating mutation in the IVVY motif (ChB), which were activated by a specific human-Fas activating antibody. We showed that the IVVY motif plays a dispensable role in the activation of PU.1, cFos, and Runx1, but it is critical for C/EBPα activation during OC lineage priming. Consistently, the ChA, but not the ChB, expressers could mediate osteoclastogenesis. Finally, despite its critical role in OC lineage commitment, we found, unexpectedly, that overexpression of C/EBPα in the ChB expressers failed to rescue osteoclastogenesis, indicating that C/EBPα may not be the sole factor responsible for OC lineage commitment. Collectively, these findings reveal C/EBPα is the most critical of the known OC TFs for OC lineage commitment. Significantly, C/EBPα has the potential to serve as a therapeutic target for bone loss from excessive OC formation.

Disclosures: Joel Jules, None.

MO0264

RANKL Enhances TNF Induced Osteoclast Differentiation by Degrading TRAF3 in the Absence of TRAF6. <u>Zhenqiang Yao</u>*[1], <u>Yanyun Li</u>[2], <u>Bryant Darnay</u>[3], <u>Lianping Xing</u>[1], <u>Brendan Boyce</u>[4]. [1]University of Rochester, USA, [2]University of Rochester Medical Center, USA, [3]University of Texas M.D. Anderson Cancer Center, USA, [4]University of Rochester Medical Center, USA

TNF receptor associated factors (TRAFs) regulate osteoclastogenesis. For example, TRAF6 is essential for RANKL-induced osteoclast (OC) formation, while TRAF3 limits both RANKL- and TNF-induced OC formation by promoting proteasomal degradation of NF-κB-inducing kinase thereby negatively regulating NF-κB signaling. We have used TRAF6-/- and generated TRAF3-Cathepsin K conditional KO (cKO) mice to further investigate the roles of TRAF6 and TRAF3 in RANKL- and TNF-induced osteoclastogenesis. We confirmed that RANKL does not induce OC formation from TRAF6-/- OC precursors (OCPs), but surprisingly it significantly increased OC formation induced by TNF alone from these cells (135+/-14 vs. 51+/-6/well). Also surprisingly, RANKL induced OC formation (152+/-21/slice) and bone resorption when TRAF6-/- OCPs were cultured on bone slices (resorption pit 0.07+/-0.02 mm2/slice). This effect was blocked by a TNF inhibitor, but not by a TGFbeta1 neutralizing antibody or an IL-1 receptor antagonist. WT and TRAF6-/- spleen cells cultured on bone slices with OC-inducing medium produced equal amounts of TNF (169+/-43 vs. 151+/-17 pg/ml) and these were significantly higher than those from cells cultured on plastic (26+/-4 vs 19+/-2 pg/ml). TRAF3 protein levels increased in TRAF6-/- OCPs in response to TNF, similar to WT cells, and these levels were significantly reduced by concomitant RANKL treatment. OC formation induced by RANKL+TNF from TRAF6-/- OCPs (65+/-7/well) was blocked by TRAF3 over-expression (3+/-1/well) and dose-dependently by an antagonist of cellular inhibitor of apoptosis proteins (cIAPs), which function along with TRAF2 to degrade TRAF3 in B cell. Consistent with this, the cIAP antagonist inhibited RANKL-induced TRAF3 degradation in TRAF6-/- OCPs. Finally, TNF induced significantly more OCs from TRAF3-CatK cKO OCPs (157+/-9/well) than from WT cells (43+/-5/well), and TRAF6 levels were low in cKO OCPs and, unlike in WT cells, they did not increase in response to RANKL or TNF. We conclude that OCP interaction with bone matrix increases their expression of TNF to stimulate OC formation and that RANKL enhances TNF-induced osteoclastogenesis by promoting degradation of TRAF3, both through a TRAF6-independent mechanism, while TRAF3 appears to be required for induction of TRAF6 by these cytokines. Thus, strategies to increase TRAF3 levels in OCPs should inhibit RANKL- and TNF-induced osteoclastogenesis.

Disclosures: Zhenqiang Yao, None.

MO0265

Regulation of Osteoclastogenesis by Integrated Signals from Toll-Like Receptors. <u>Tamar Krisher</u>*[1], <u>Zvi Bar-Shavit</u>[2]. [1]Hebrew University of Jerusalem, Israel, [2]Hebrew University of Jerusalem Faculty of Medicine, Israel

Toll-like-receptors (TLRs) in immune cells sense and are activated by pathogen-derived molecules to initiate the innate immune response. TLRs are also expressed by osteoclasts (OCs) and modulate their differentiation in a dual manner: stimulation of committed precursors which is the mechanism by which pathogen-induced bone loss occurs and inhibition of early precursors that could serve as a mechanism for down-regulating excessive resorption, and as a switch for promoting the differentiation of common precursor cells into inflammatory cells. TLRs 3, 4 and 9 are activated by viral double stranded RNA, LPS and bacterial DNA, respectively. Since infections may contain more than one pathogen we studied the simultaneous stimulation of different TLRs on OC differentiation. The TLR ligands used were Poly-IC (P), LPS (L) and CpG-ODN (C) activating TLRs 3, 4 and 9, respectively. To examine a synergy among the TLR ligands we used suboptimal doses of the ligands. Combinations of L+C and L+P, but not of C+P resulted in a synergistic effect on the inhibition of osteoclastogenesis (reduction of RANKL-induced TRAP + multinucleated cells). The role of induction of cFos in RANKL-induced OC differentiation is well documented, and consistent with the differentiation data, the combinations of L+C and L+P, but not of C+P resulted in a synergistic effect on inhibition of RANKL-induced cFos expression. Similar conclusions were obtained when the induction of the expression of the osteoclastogenesis inhibitory cytokine, IL-12 was examined. In contrast, all 3 combinations exhibited synergistic effects on inhibition of MCSF-receptor expression. We then examined the stimulatory effect. Combinations of L+C and C+P, but not of L+P exhibited synergy in stimulation of osteoclastogenesis, in increase of cFos expression, its downstream target NFATc and in the expression of the osteoclastic genes, MMP9 and cathepsin K. MCSF receptor expression was not altered significantly in stimulation protocols. Finally, the effects of each ligand on the 3 TLRs were examined. The 3 ligands increased the expression of TLR3 and TLR9, while no significant effects were observed on the expression of TLR4. In summary, cFos plays a role in the two effects while MCSF receptor plays a role only in the inhibitory effect. Increasing TLRs expression by other TLR ligands may cause part of the synergy. The synergism between TLR ligands enables the individual to initiate response at a lower level of pathogen.

Disclosures: Tamar Krisher, None.

MO0266

SUMOylation of NEMO Differentially Regulates Osteoclastogenesis and Bone Loss. <u>Yousef Abu-Amer</u>[1], <u>Kyuhwan Shim</u>*[2], <u>Kuljeet Seehra</u>[3], <u>Yi-Ping Li</u>[4]. [1]Washington University in St. Louis School of Medicine, USA, [2]Washington University school of medicine, USA, [3]Washington University School of Medicine, USA, [4]University of Alabama at Birmingham, USA

The role of NF-κB in osteoclastogenesis (OCG) has been established. However, the role of IKKγ/NEMO; the NF-κB essential modulator, in this process and in bone development has not been studied. Based on clinical case reports, wherein various mutations in *nemo* gene elicit Incontinentia Pigmenti and skeletal defects in humans, we surmised that this gene may regulate skeletal development. Indeed, conditional deletion of *nemo* from the myeloid compartment caused osteopetrosis owing to defective OCG. To unveil the molecular mechanism underlying this phenotype, we performed domain structure-functional analysis of NEMO. The function of NEMO is governed by oligomerization which is regulated by Ubiquitination (UB) and SUMOylation events at multiple lysine residues occurring in cell and signal specific manners. To this end, we identified lysine (K)-270 and K302, known as SUMOylation sites, as critical differential regulators of NEMO function during OCG. Specifically, expression of K270A-NEMO (K270 SUMOylation-deficient) elicited higher OCG in NEMO-null compared to wild type NEMO expressing cells. In contrast, expression of the mutant K302A-NEMO in NEMO-null cells failed to restore OCG, indicating that K302-modification is essential for NEMO stability and function. More prominently, introduction of K302A mutation in concert with K270A abrogated the robust OCG observed by the latter form. Consistently, localization of WT and mutant NEMOs in HEK cells shows that K270A-NEMO forms condensed multimer in perinuclear compartments whereas K302A-NEMO was diffusely distributed throughout the cytoplasm. Importantly, introduction of K302A mutation in concert with K270A significantly disrupted the multimeric appearance of NEMO. These findings suggest that K270A increases oligomerization and OCG, a gain of function, and K302A impairs oligomer formation and impedes OCG, a loss of function mutation. Because K270 and K302 are SUMOylation sites for SUMO2/3 and SUMO1, respectively, we examined their effect directly by co-expression with the various forms of NEMO WT and mutants. Our findings indicate that SUMO1 coexpression enhances NEMO function and OCG whereas SUMO2 acted as a negative regulator. Additional experiments show that SUMO2 acts in a K270 site-specific manner whereas SUMO1 has no site preference and can still function when c-terminally fused with NEMO. Thus, we provide evidence that SUMO1 and SUMO2/3 differentially regulate OCG and maybe viable to regulate bone resorption.

Disclosures: Kyuhwan Shim, None.

MO0267

The Notch modulators Lnx2, Tspan5/10, and Msi2 play a critical role in osteoclast differentiation. <u>Toshifumi Fujiwara</u>*[1], <u>Jian Zhou</u>[2], <u>Shiqiao Ye</u>[1], <u>Haibo Zhao</u>[1]. [1]Central Arkansas VA Healthcare System, Univ of Arkansas for Medical Sciences, USA, [2]UAMS, USA

Genetic studies in human and mice have pinpointed an essential role of Notch signaling in osteoblast and osteoclast proliferation and differentiation during skeletal development and remodeling. However, the factors and pathways regulating Notch activation in bone cells remain largely unknown. Each Notch receptor is present at the cell surface as a heterodimer. When the cognitive ligand binds to the extracellular domain of Notch, a disintegrin and metalloprotease (ADAM), such as ADAM10, cleaves the juxtamembrane S2 proteolysis site of the Notch receptor. The γ-secretase subsequently cleaves the S3 site within the transmembrane domain and releases the Notch intracellular domain (NICD). NICD then translocates to the nucleus, where it functions as a transcriptional co-activator of Notch target genes, including Hes and Hey. Numb, a membrane-associated adaptor protein critical for cell-fate determination, inhibits Notch signaling through the regulation of Notch endocytosis/recycling and the ubiquitin/proteasome degradation of NICD. In this study, we demonstrate that the expression of Notch activators, Lnx2 (Ligand of Numb protein X2), Tspan 5, Tspan 10 (Tetraspanin 5 and 10), and Msi2 (Musashi 2), are up-regulated during osteoclast differentiation as measured by quantitative real-time PCR. Lnx2, an E3 ubiquitin ligase, promotes Notch signaling by lowering the level of Numb. Tspan5 and 10, two of the TspanC8 subfamily members of tetraspanins, regulate ADAM10 maturation and cell surface expression. Msi2 is a mRNA binding protein and may inhibit Numb gene translation. Knocking down the expression of these four genes in bone marrow macrophages by lentivirus-mediated shRNAs markedly inhibits osteoclast formation, as exhibited by decreased TRAP+ multinucleated osteoclasts and declined mRNA and protein expression of osteoclast markers, TRAP, Cathepsin K, and NFATc1. Mechanistically, loss of these Notch activators in osteoclast precursors diminishes intracellular level of NICD, especially NICD2, and attenuates the expression of Notch targeting gene Hes1 and Hey1. Thus, Lnx2, Tspan 5, Tspan 10, and Msi2 are previously unidentified Notch modulators in osteoclast lineage cells that play a critical role in osteoclast differentiation.

Disclosures: Toshifumi Fujiwara, None.

MO0268

The stimulation-dependent internalization of RANK is crucial for osteoclast differentiation. Yuu Taguchi*[1], Jun-ichiro Inoue[2]. [1]The Inst. of Med. Sci., Univ. of Tokyo, Japan, [2]The Inst. of Med. Sci., Univ. of Tokyo, Japan

Bone remodeling involves bone formation by osteoblasts and bone resorption by osteoclasts. Excess formation of osteoclasts leads to pathological bone resorption observed in osteoporosis and rheumatoid arthritis. Therefore, elucidating the molecular mechanisms of osteoclastogenesis is crucial for developing drugs and therapeutic strategies to treat such diseases. Osteoclast differentiation requires activation of the signal transduction emanated from RANK expressed on cell surface of osteoclast-precursor cells, whish are differentiated from hematopoietic stem cells upon M-CSF stimulation. We have previously demonstrated that RANK has the unique domain, HCR, essential for osteoclastogenesis. The HCR domain works as a platform for forming the long-termed signal complex that links to the PLCγ2-Ca^{2+} pathway, which together with the RANK signal to activate NFATc1, a master transcriptional factor for osteoclastogenesis. Here we report a novel mechanism for the HCR-mediated activation of the osteoclastogenic signal. Our immunofluorescence analysis revealed that RANK was located only on cell surface before RANKL-stimulation, but that subpopulation of RANK subsequently became internalized and localized to peri-nuclear region at 48 hours after stimulation. However, RANK mutant lacking the HCR-region remains on cell surface even at 48 hours after stimulation, indicating that HCR mediates the RANK internalization. More importantly, inhibition of RANK-internalization by treating with Dynasore, an inhibitor of the dynamin-dependent receptor internalization, blocked osteoclast differentiation. Similarly, treatment with Methyl-β-cyclodextrin, a selective inhibitor of lipid-raft formation, and that with Pitstop2, a specific inhibitor of clathrin, inhibited the RANK-internalization, and resulted in failure of osteoclastogenesis. These results suggest that RANK-internalization is crucial for osteoclastogenesis. Interestingly, the inhibition of RANK-internalization by treatment with such drugs had no effect on the RANK-mediated activation of NF-κB and MAPKs and the induction of NFATc1 expression. Taken together, these results strongly suggest the HCR-mediated novel signal pathway that is coupled with the RANK internalization and involved in the osteoclastogenic signal.

Disclosures: Yuu Taguchi, None.

MO0269

A Microfluidic System to Study the Effects of Mechanically Loaded Osteocytes on Osteoclast recruitment and formation. Kevin Middleton*[1], Lidan You[2]. [1]University of Toronto, Canada, [2]Mechanical & Industrial Engineering, University of Toronto, Canada

Introduction

It has been well established that bone remodels to accommodate the mechanical loads under which it is placed [1]. This remodeling process occurs through the action of a basic multicellular unit (BMU) that consists of a head of bone resorbing osteoclasts, a tail of bone matrix secreting osteoblasts, and an axially aligned blood vessel supplying precursor cells, signals, and nutrients [2]. However, the mechanisms that link macro-scale mechanical loading to the activation and development of this BMU have yet to be fully elucidated. One cell of particular interest is the osteocyte, which is a mechanosensing cell that is well distributed throughout the bone matrix [3]. In this work we have developed a microfluidic system to overcome the limitations of current in vitro studies [4] and test the hypothesis that unloaded osteocytes promote osteoclast precursor migration and osteoclastogenesis in a physiologically relevant environment.

Methods

MLO-Y4 and RAW264.7 cells were seeded in a microfluidic device consisting of three cell seeding channels (16mm long x 1mm wide x 60μm high), separated by side channels (200μm long x 50μm wide x 60μm high). One channel of MLO-Y4 cells is exposed to a stimulatory fluid shear stress for 1 hour every day, while the other channels are exposed only to a perfusion flow to replace waste media. Every day cells are imaged to determine any net change in the location of cell populations. At the end of 7 days, RAW cells are TRAP stained to quantify the degree of osteoclastogenesis across the width of the central channel.

Results

Using a computational model of our device, we show that our system can produce a stimulatory flow to one channel while keeping the other channels in static conditions. Additionally, we demonstrated that signals produced in one channel are able to diffuse to a neighbouring channel, generating a concentration gradient across that channel. Furthermore, preliminary data shows that RAW cells preferentially migrate towards a RANKL source as compared to a control. Additionally, increased osteoclastogenesis was found closer to the RANKL supplying channel, validating the existence of a chemical gradient across the channel width.

Reference

1 van Oers, R., et al., Bone 48 1210-1215 (2011).
2 Kular, J., et al., Clin. Biochem. 45 863-873 (2012).
3 Bonewald, L., J. Bone Miner. Res. 26 (2) 229-238 (2011).
4 Heino, T., et al., Exp. Cell Research 294 458-468 (2004).
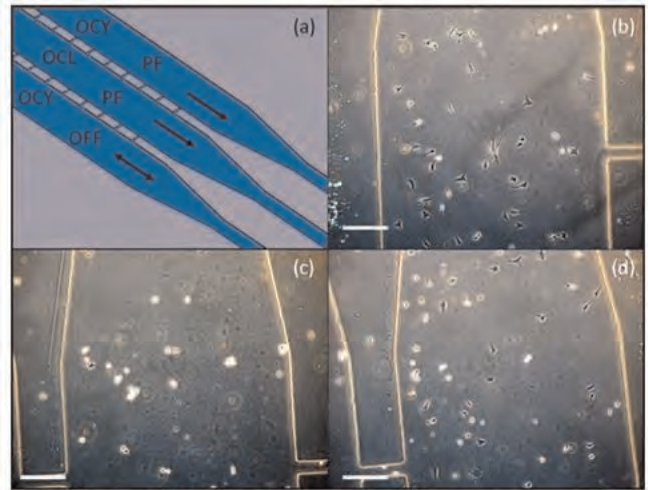
Figure 1 – (a) 3D SolidWorks model of 3-channel microfluidic device cell culture region. Channels are separated by 200μm wide side channels to prevent convective fluid flow while allowing diffusive fluid flow. Presents experimental set-up of osteocytes (OCY) seeded in the two outer channels, and osteoclast precursors (OCL) seeded in the central channel. One channel of osteocytes undergoes mechanically stimulatory oscillatory fluid flow (2Pa, 1Hz). Not to scale. Microfluidic channels seeded with osteocytes (b,d) and osteoclast precursor cells (c). Scale bar represents 200μm.

Device Design and Cell Loading
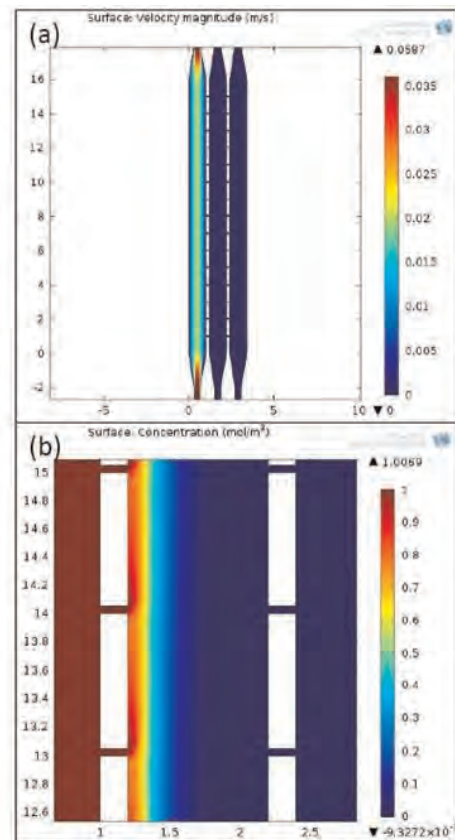
Figure 2 - Comsol multiphysics model results of device. (a) Applying a stimulatory fluid flow (1Pa) through one channel while the other channels simultaneously undergo no significant flow. (b) Generation of a chemical gradient within the central channel coming from signal (60kDa) generated in left-hand channel.

Model Results

Figure 3 – (a,b) RAW cells exposed to no RANKL from parallel channel at 5 days and 7 days respectively. As expected, no sign of osteoclastogenesis. (c,d) RAW cells exposed to a RANKL gradient produced from a side channel at 5 and 7 days respectively. At 7 days see strong evidence of osteoclastogenesis. All scale bars represent 200μm. (e) Plot showing relative cell densities along the width of the cell channel after 5 days compared to the original density. Observable trend that a RANKL gradient drives increased cell densities towards it. (f) Normalized osteoclast count across the width of a channel exposed to a RANKL gradient. Statistically significant (p<0.05) groups designated by a different letter. N = 2.

Study Results

Disclosures: Kevin Middleton, None.

MO0270

Connexin 43 Hemichannels are Important in Maintaining Normal Bone Structure and Osteocyte Viability. Huiyun Xu[1], Sumin Gu[2], Manuel Riquelme[3], Sirisha Burra[4], Danielle Callaway[5], Hongyun Cheng[2], Teja Guda[6], James Schmitz[4], Roberto Fajardo[7], Sherry Abboud Werner[5], Hong Zhao[8], Peng Shang[9], Mark Johnson[10], Lynda Bonewald[11], Jean Jiang*[5]. [1], Peoples Republic of China, [2]University of Texas Health Science Center at San Antonio, USA, [3]University of Texas Science Center, San Antonio, USA, [4]University of Texas Health Science Center, USA, [5]University of Texas Health Science Center at San Antonio, USA, [6]University of Texas at San Antonio, USA, [7]UT Health Science Center, San Antonio, USA, [8]University of Missouri, USA, [9]Northwestern Polytechnical University, Peoples Republic of China, [10]University of Missouri, Kansas City Dental School, USA, [11]University of Missouri - Kansas City, USA

Connexin (Cx) 43 plays important roles in bone function and development. Targeted deletion of Cx43 in osteoblasts or osteocytes leads to increased osteocyte apoptosis, osteoclast recruitment, and reduced biomechanical properties. Cx43 forms both gap junctions and hemichannels, which mediate the communication between adjacent cells or between cytoplasm and extracellular environments, respectively. Two transgenic mouse models driven by a 10 kb-DMP1 promoter with the overexpression of dominant negative Cx43 mutants were generated to dissect the functional contribution of Cx43 gap junctions as compared to hemichannels in osteocytes. The R76W mutant blocks gap junction, but not hemichannel function, and the ?130-136 mutant inhibits activity of both types of channels. ?130-136 mice showed a significant increase in bone mineral density compared to WT and R76W mice. MicroCT analyses revealed a significant increase in tissue and bone area in midshaft cortical bone of ?130-136 mice. The bone marrow cavity was expanded, whereas the cortical thickness was increased and associated with increased bone formation along the pericortical area. Histologic sections of the midshaft showed increased numbers of empty osteocyte lacunae and apoptotic osteocytes in ?130-136, but not in WT and R76W, mice which correlated with altered biomechanical and estimated bone material properties. There was a trend for reduced osteoblasts along the endosteal surface in ?130-136 mice. Osteoclasts were increased along the endosteal surface in both transgenic mice with a greater effect in ?130-136 mice which likely

contributed to the increased marrow cavity. These findings suggest that osteocytic hemichannels play a dominant role in regulating osteocyte survival and balance between endocortical bone resorption and periosteal apposition that is crucial for maintaining bone mass and strength.
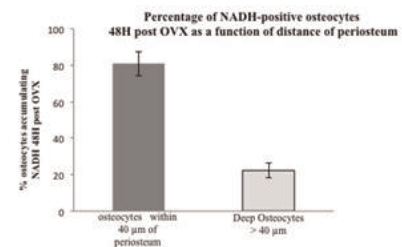
Disclosures: Jean Jiang, None.

MO0271

Estrogen loss causes mitochondrial stress in Osteocytes in vivo. Dorra Frikha-Benayed*[1], Jelena Basta-Plajkic[2], Robert J Majeska[3], Mitchell Schaffler[4]. [1]The City University of New York, USA, [2]City Collage New York, USA, [3]City Collage New York, USA, [4]City College of New York, USA

Estrogen loss was shown to cause osteocyte (OCY) apoptosis that triggers bone resorption. The mechanism by which estrogen loss leads to osteocyte death is not clear. However, studies from our laboratory and others suggest that increased oxidative damage could play a role, since estrogen was reported to exhibit anti-oxidant effects that can attenuate harmful effects of reactive oxygen species (ROS). Mitochondrial (Mt) oxidative metabolism is a major source of ROS, and we previously showed that hypoxia-induced oxidative stress in OCY leads to impaired Mt function and NADH accumulation that could be monitored in situ by multiphoton microscopy (MPM). In this study, we tested the hypothesis that estrogen loss results in a similar stress response in OCY in vivo. We adapted our previous approach to assess OCY NADH levels in situ after estrogen withdrawal. OVX or Sham surgery was performed on C57BL/6J mice (17 wk old, n=6, IACUC approved). OCY NADH levels were investigated at 2 days post-OVX from metatarsal diaphyses of anesthetized mice using in vivo MPM (40X Objective; Excitation: 833 nm; Emission: 460 nm). In separate studies, OCY mitochondrial content was also assessed by IHC in metatarsals mid-diaphyses of control mice by staining with antibody to mitochondrial ATPase V. Results: NADH fluorescence was absent from OCY in Sham animals, consistent with our previous findings for OCY at baseline conditions in vivo. In contrast, OCY in OVX bones showed high levels of NADH fluorescence (Fig 1). NADH accumulation was greatest in OCY located with approximately 40 μm of the periosteal surface (Fig 2). IHC studies revealed that the more NADH responsive cells closest to the periosteal surface also expressed high levels of ATPase V, indicating greater Mt content. This study shows that estrogen loss causes dramatic and region-specific NADH accumulation in OCY in vivo. The increase in NADH is consistent with impaired mitochondrial electron transport, such that NADH produced by cellular catabolic pathways cannot be re-oxidized to NAD+. How estrogen regulates mitochondrial is not yet clear; however, OCY express estrogen receptors and estrogen has been shown to act directly on mitochondrial DNA (in nonskeletal systems), so multiple mechanisms are possible.
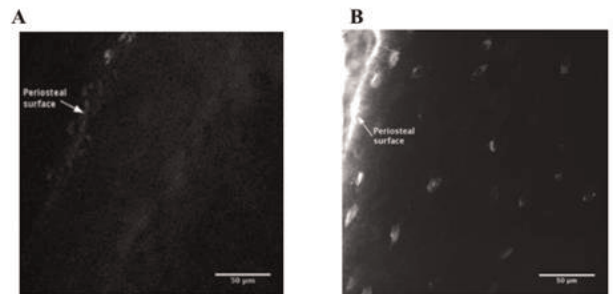
Figure1: (A) In vivo imaging of metatarsal cortex of Sham operated animal shows no NADH fluorescence in osteocytes. **(B)** Strong NADH fluorescence seem in osteocytes near periosteum at 48 hours post OVX.
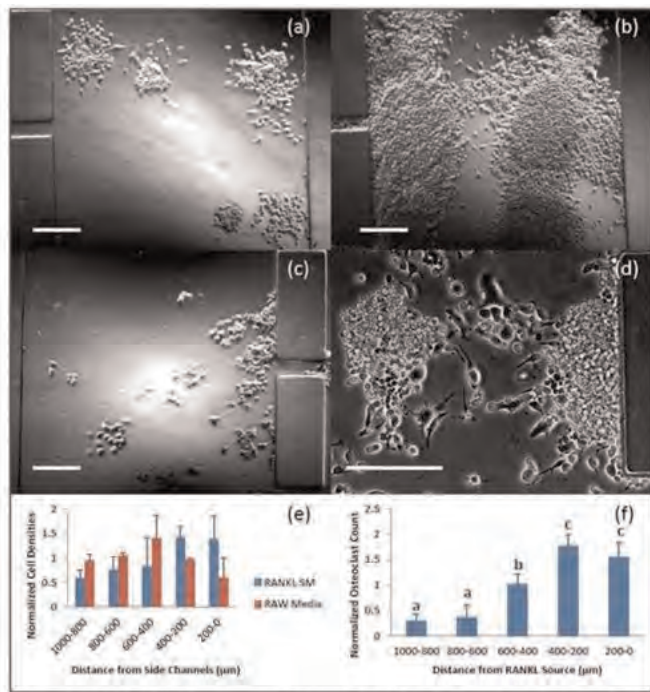
Figure1

Figure2: Percentage of osteocytes accumulating NADH 48H post OVX function of their location: within 40 μm from periosteum or deeper region in the cortex.

Figure2

Disclosures: Dorra Frikha-Benayed, None.

MO0272

IDG-SW3 early osteoblasts in mineralising 3D collagen gels differentiate to osteocytes that respond to mechanical loading. <u>Nicole Scully</u>*[1], <u>Lynda Bonewald</u>[2], <u>Sam Evans</u>[3], <u>Deborah Mason</u>[4], <u>Bronwen Evans</u>[4]. [1]Cardiff University, United Kingdom, [2]University of Missouri - Kansas City, USA, [3]cardiff university, United Kingdom, [4]Cardiff University, United Kingdom

Osteocytes *in vivo* are derived from osteoblasts, embedded in mineralised matrix and mechano-sensitive. They are difficult to isolate and models for *in vitro* osteocyte studies are limited. IDG-SW3 mouse early osteoblasts differentiate (35 days) in monolayer to mature osteocytes expressing sclerostin and FGF-23.[1] These are DMP1-GFP[(-)] under immortalizing conditions but DMP1-GFP[(+)] under osteogenic conditions. We investigated osteocytic differentiation of IDG-SW3 in mineralising 3D gels, thus mimicking osteocytes *in vivo*, and assessed their responses to mechanical loading.

Cells were set up in 3D type I collagen gels (48-well plates), incubated at 33°C (4 days), then placed in osteogenic medium at 37°C (22 days). Cell number/viability and phenotype (trypan blue, qRTPCR, confocal), and VEGF and IL-6 protein secretion (ELISA) were quantified over time. Following mechanical loading (10 Hz, 5 mins, 2.5 N, day 10), putative mechano-sensitive factors (DMP1, VEGF, IL-6, RANKL, LRP-5) were measured at 0.5–48 hrs (qRTPCR, ELISA). All results presented are combinations from3 independent experiments.

Cells were viable (>90%) but did not proliferate in osteogenic medium. They were DMP1 GFP[(+)] from day 2 (confocal microscopy), and DMP1 mRNA steadily increased, peaking at day 21 ($p<0.05$). Phalloidin labelling confirmed actin organisation and osteocytic processes (day 21). E11 and PHEX mRNA both peaked at day 14 ($p<0.01$, $p<0.001$ respectively) before decreasing, whilst MEPE expression was the same throughout. Sclerostin expression peaked at day 7 with little expression at other timepoints. VEGF and IL-6 protein increased during differentiation (IL-6, day 21, $p<0.001$). Following mechanical loading, DMP1 (48 hrs, $p<0.05$), VEGF (30 mins, $p<0.05$), IL-6 (24 hrs $p<0.01$), LRP-5 (48 hrs, $p<0.05$) and RANKL (24 hrs, $p<0.01$) mRNA, as well as VEGF and IL-6 protein secretion increased (IL-6, 24 hrs $p<0.01$) compared to unloaded controls.

This mineralising 3D collagen gel model enables differentiation of osteoblasts to osteocytes in an environment akin to osteocytes *in vivo*. Differentiation is accelerated in 3D compared to monolayer, with sclerostin detected after 7 days. The 3D model enables mechanical loading of osteocytes, as demonstrated by up-regulation of putative mechano-sensitive factors. This model will further our understanding of mechano-sensitive pathways in osteocytes and could also be applied to human primary osteoblasts.

[1]Woo SM *et al.,* J Bone Miner Res. 26:2634–46, 2011

Disclosures: Nicole Scully, None.

MO0273

Local Bone Tissue Mechanical Properties Change Without Remodeling: A Study Of Lactating Mice. <u>Serra Kaya</u>*[1], <u>Jelena Basta-Pljakic</u>[2], <u>Zeynep Seref-Ferlengez</u>[2], <u>Wing-Yee Cheung</u>[1], <u>Robert Majeska</u>[3], <u>Susannah Fritton</u>[4], <u>Shoshana Yakar</u>[5], <u>Mitchell Schaffler</u>[1]. [1]City College of New York, USA, [2]City College of New York, USA, [3]City College of New York, USA, [4], USA, [5]New York University COLLEGE OF DENTISTRYDavid B. Kriser Dental Center, USA

Introduction: Osteocytes can dynamically remodel their pericellular bone matrix through osteocytic osteolysis, leading to increases in lacunar and canalicular size. Furthermore, these increases are reversible. It is well established that cortical bone modulus depends strongly on its vascular porosity, but whether the resulting changes in osteocyte pericellular void space can also alter local material properties of bone is unknown. In the current study, we tested whether bone elastic modulus and lacunar-canalicular space (LCS) change at the microscopic level in response to lactation and post-lactation recovery.

Methods: C57/B6 mice (n=15, 3 m.o.) were mated and allowed to nurse their pups. After 2 wks of lactation (Lac), mice were divided into three groups. *Group 1* was sacrificed after 2 wks Lac; *Groups 2* and *3* were allowed to recover for 1 wk and 4 wks post-Lac (after forced-weaning), respectively. Age-matched controls (n=5/group) were also examined. Femurs were stored at -20°C until testing. Tissue level elastic modulus (Ei) was measured using microindentation on femoral mid-diaphyseal cross-sections. For osteocyte LCS studies, femoral cross-sections were imaged using super resolution microscopy (100 nm resolution fluorescence imaging) and lacunar and canalicular areas measured.

Results: Two weeks of Lac caused marked reductions in bone Ei (10% and 15% at Posterior and Anterior regions, respectively) compared to controls. After 1 wk post-Lac, Ei returned to pre-Lac levels and did not increase further at 4 wks post-Lac (Fig 1). Lac did not cause intracortical resorption or increases in vascular spaces. Lacunar and canalicular areas increased by 2 wks Lac (19% and 15%, respectively) and retuned to baseline levels after 1 wk post-Lac (Fig 2).

Conclusion: These results reveal that tissue-level cortical bone material properties are reversibly modulated in response to physiological challenge without bone remodeling. Small changes in LCS appear sufficient to alter local material. In addition, these studies demonstrate that Lac-induced reductions in Ei and increased in LCS void space reverse quickly once Lac stops. The precise mechanisms underlying osteocytic osteolysis and lacunar/canalicular are as yet unknown. Nevertheless, our studies reveal that bone possesses an intrinsic ability for rapid and dynamic regulation of its material properties, accomplished by the action of osteocytes.
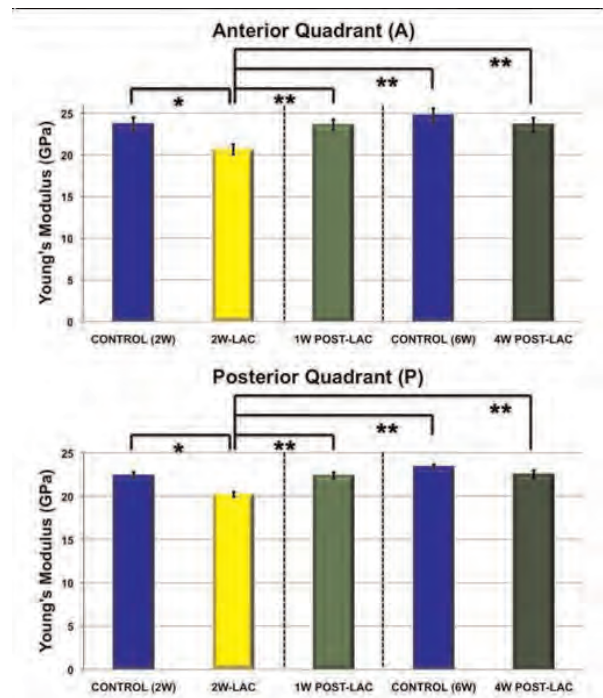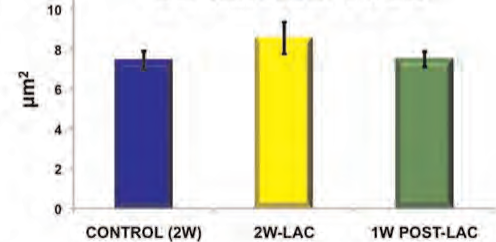

Fig.1. Microindentation Ei values (GPa) of (A) and (P) quadrants of mice femur. Statistical Analysis: ANOVA, Mann-Whitney post-hoc
*: $p<0.005$ vs Control (2W),   **: $p<0.005$ vs 2W-LAC

Elastic Modulus
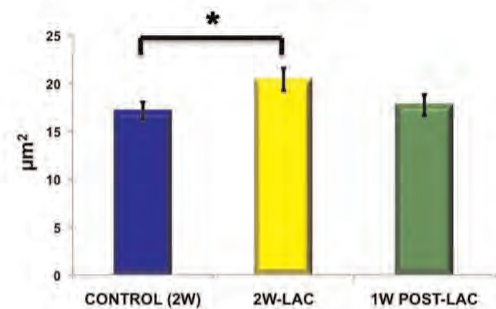
Fig.2. LCS Super resolution microscopy results. Lacunar and Canalicular Area (μm^2).
*: $p<0.05$ vs Control (2W)

Lacunar-Canalicular Area

Disclosures: Serra Kaya, None.

MO0274

Osteocyte Signaling and Perilacunar Remodeling during Exercise. Joseph Gardinier*[1], Alexander Khmaladze[2], Michael Morris[1], David Kohn[1]. [1]University of Michigan, USA, [2]University of Michigan, USA

The ability to improve the quality of bone, as defined by its mechanical properties, reduces the risk of fracture and development of musculoskeletal diseases later in life. The mechanical properties of cortical bone gained during exercise despite no significant changes in bone geometry are often attributed to local adaptation of existing tissue. Given that osteocytes are ideally located to modify the intrinsic properties of bone during exercise, the purpose of this study was to determine if exercise increases osteocyte remodeling of the perilacunar matrix and identify changes in their gene expression. Under the University Committee on Use and Care of Animals approval, 16 week old male mice were weight-matched and assigned to sedentary or exercise groups. Exercise involved 30 minutes of treadmill running at 12 m/min on a 5° incline. After 6 consecutive days of exercise, mice were sacrificed and the tibia extracted, cleaned, and flushed of excess tissue to reduce the presence of non-osteocyte cells for qRT-PCR. Additional mice were subjected to 21 days of exercise and then sacrificed to extract tibia samples for mechanical testing and Raman spectroscopy, which consisted of a locally constructed microprobe with a line focused laser beam. After 6 days of exercise, tartrate-resistant acid phosphatase (TRAP), matrix metalloproteinases (MMP), and SOST expression were significantly reduced, while FGF-23 significantly increased by 3.5 fold. Raman spectroscopy revealed a higher mineral-to-matrix ratio after 21 days of exercise (15.8 ± 0.8 vs. 14.1 ± 0.6) that was predominately located within the perilacunar matrix (tissue within 5μm of the lacunae wall) compared to non-perilacunar matrix (tissue 15μm away from any lacunae wall). In sedentary controls, the carbonate-to-phosphate ratio of the perilacunar tissue was larger compared to non-perilacunar (0.156 ± 0.002 vs. 0.150 ± 0.003), while exercise demonstrated an opposite trend (0.160 ± 0.001 vs. 0.165 ± 0.003). The changes in composition coincided with an increase in stiffness (95 ± 4.7 N/m vs. 83 ± 4.6 N/m) and ultimate strength (206 ± 6 MPa vs. 180 ± 6 MPa) compared to sedentary controls. Overall, these data demonstrate that exercise suppresses TRAP and MMP expression, which osteocytes can utilize to alter the perilacunar tissue composition. As a result, the perilacunar remodeling observed during exercise is considered a key determinate of the mechanical properties gained without changes in tissue geometry.

Disclosures: Joseph Gardinier, None.

MO0275

**Pigment epithelium derived factor reduces sclerostin expression by osteocytes.** Feng Li*[1], Na Song[2], Joyce Tombran-Tink[2], Christopher Niyibizi[3]. [1]Penn State College of Medicine, USA, [2]Penn State College of Medicine, USA, [3]The Pennsylvania State University College of Medicine, USA

Pigment epithelium-derived factor (PEDF) encoded by serpinf1 is a strong antiangiogenic factor found in a variety of fetal and adult tissues. Lack of PEDF expression has been reported to be the cause of a recessive form of osteogenesis imperfecta type VI whose hallmark is a defect in mineralization (1, 2). The mechanisms by which PEDF leads to defective mineralization are not known. We and others reported that PEDF enhances mesenchymal stem cell (MSCs) differentiation and osteoblastic mineralization in osteogenic cultures(3, 4). Reduction or absence of PEDF expression by MSCs resulted in the inability of the cells to efficiently mineralize bone matrix upon differentiation. The mechanisms by which PEDF regulates matrix mineralization however, remain unclear; in present study, weexamined expression of factors that play a role in matrix mineralization in osteoblastic osteogenic cultures. Osteoblasts harvested from human bone and maintained in osteogenic medium to day 14 expressed PHEX, MEPE and Sost/sclerostin suggesting that the cells differentiated into osteocytes at this time point (Fig 1). Supplementation of the cultures with PEDF reduced expression Sost and MEPE while promoting expression of Collagen I indicating that PEDF regulates factors that play a role in matrix mineralization. We then focused on sclerostin expression and its suppression by PEDF. Osteoblasts incubated in osteogenic medium to day 7 did not show any sost expression, however by day 14, sost/sclerostin expression was observed confirming the data that at this time point osteoblasts giverise to osteocytes in osteogenic cultures (Fig. 2). Presence of PEDF in osteogenic cultures reduced production of sclerostin by osteocytes in culture to 50% in comparison to the protein produced by osteocytes in osteoblastic cultures incubated in absence of PEDF (Fig. 2). To confirm that PEDF reduced expression of sost/sclerostin by osteocytes, primary osteocytes were isolated from human bone. Isolated cells expressed DMP-1 and sclerostin; incubation of the cells with PEDF for 48, reduced expression of sost/sclerostin confirming the data that PEDF suppresses expression of sost by osteocytes. Sclerostin is a known potent inhibitor of bone formation through its inhibition of Wnt signaling. Taken together, these data suggest that reduction in Sost expression by osteocytes as a result of exposure to PEDF may be one of the mechanisms by which PEDF increases mineralization of bone matrix. The mechanisms by which PEDF regulates sclerostin expression by osteocytes are currently under investigation.
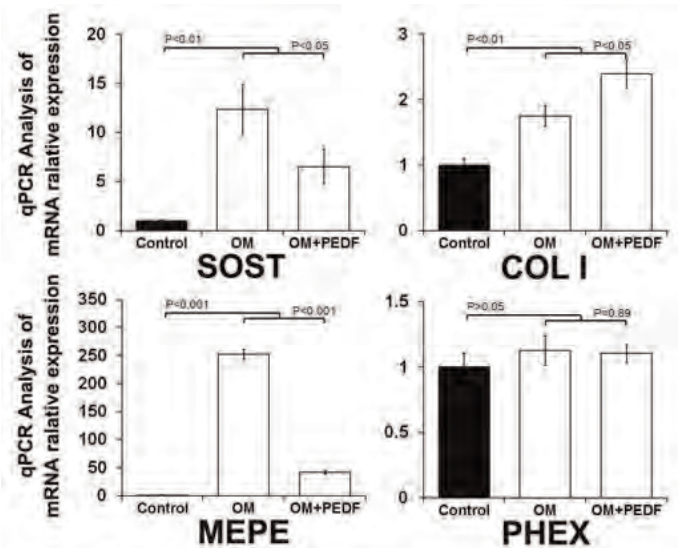
Figure 1. Supplementation of osteoblastic culture with PEDF regulated mRNA expression of osteoblasts and osteocytes related genes at 2 weeks.

Figure 1. Supplementation of osteoblastic culture with PEDF regulated mRNA expression
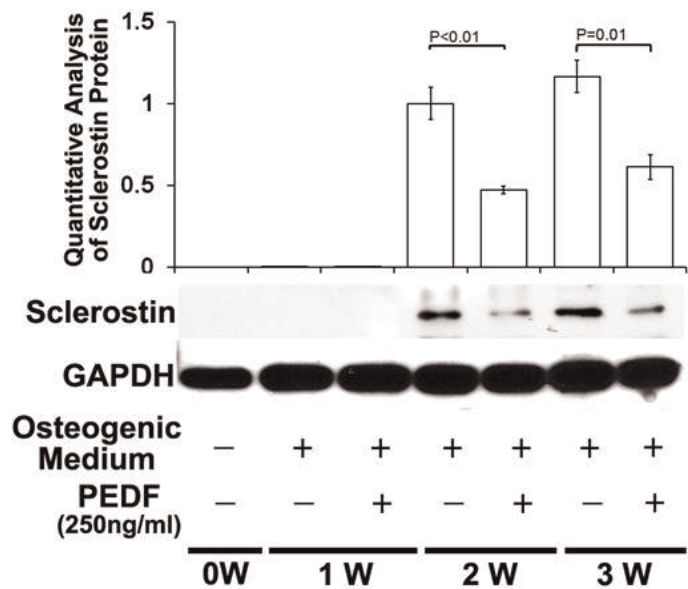
Figure 2. Presence of PEDF in osteogenic cultures reduced production of sclerostin by osteocytes in culture to 50% in comparison to the protein produced by osteocytes in osteoblastic cultures incubated in absence of PEDF.

Figure 2. Presence of PEDF in osteogenic cultures reduced production of sclerostin by osteocytes

Disclosures: Feng Li, None.

MO0276

E11 protein stabilisation promotes osteocyte differentiation and protects against osteoarthritis pathology. <u>Katherine Staines</u>*[1], <u>Matt Prideaux</u>[2], <u>Nigel Loveridge</u>[3], <u>David Buttle</u>[4], <u>Andrew Pitsillides</u>[5], <u>Colin Farquharson</u>[6]. [1]The Roslin Institute & R(D)SVS, The University of Edinburgh, United Kingdom, [2]University of Adelaide, Australia, [3]University of Cambridge, United Kingdom, [4]University of Sheffield, United Kingdom, [5]Royal Veterinary College, United Kingdom, [6]Roslin Institute, University of Edinburgh, United Kingdom

The mechanisms which govern osteoblast-to-osteocyte transitions are yet to be elucidated, however their dysregulation are likely to contribute to osteoarthritic (OA) subchondral bone (SCB) sclerosis. The transmembrane glycoprotein E11 is critical in early osteocytogenesis, however its function and regulatory mechanisms are still unknown. Here we established the regulation of E11 expression during osteocytogenesis and examined whether this expression is compromised in OA. Using the late osteoblast MLO-A5 cell line we reveal increased expression of E11 protein/mRNA (P<0.001) concomitant with extensive osteocyte dendrite formation and matrix mineralisation (P<0.001). Whilst overexpression of E11 significantly increased mRNA expression (P<0.001), western-blotting failed to detect any correlative increases in protein expression, suggestive of post-translational regulation. We therefore treated E11-overexpressing cells with calpeptin and ALLN, inhibitors of calpains (cysteine proteases) and found that both promoted E11 protein expression, with ALLN having the greatest effect. However, whilst exogenous treatment of MLO-A5 cells and osteocytic IDG-SW3 cells with 10μM ALLN induced a profound increase in stellate cell morphology (50%, P<0.001) and increased E11 protein expression (69%), treatment with calpeptin failed to promote similar osteocytogenesis; the calpain inhibitors E64d/Z-FA-FMK also failed to modify MLO-A5 cell morphology or gene/protein expression. Similarly, the protein expression of calpain 1 and 2 remained unchanged over a 15-day MLO-A5 time course. Due to the dual roles for ALLN in calpain and proteasome inhibition, this characterised proteasomal degradation as the key pathway in E11 post-translational targeting and degradation. This was supported by studies using proteasomal-selective inhibitors (MG132/lactacystin) which produced similar dose-dependent increases in E11 expression in MLO-A5 cells. These data implicate proteasome degradation in controlling E11 stability which will be confirmed using the therapeutic proteasome inhibitor Bortizomib in MLO-A5, and human osteoblast cultures. In a natural model of OA (STR/Ort mouse) we revealed decreased E11 protein expression in the SCB osteocytes in regions of the joint where OA pathology is observed. Together these data suggest that proteasome-mediated E11 protein degradation limits acquisition of the osteocyte phenotype and this contributes to the SCB sclerosis observed in OA.

Disclosures: Katherine Staines, None.

MO0277

Deletion of ephrinB2 in osteocytes leads to increased trabecular bone mass, but reduced bone strength. <u>Christina Vrahnas</u>[1], <u>Stephen Tonna</u>[2], <u>Huynh Nguyen</u>[3], <u>Mark Forwood</u>[4], <u>T John Martin</u>[5], <u>Natalie Sims</u>*[6]. [1], Australia, [2]St Vincent's Institute, Australia, [3]Griffith University, Australia, [4]Griffith University, Australia, [5]St. Vincent's Institute of Medical Research, Australia, [6]St. Vincent's Institute of Medical Research, Australia

EphrinB2 is a receptor tyrosine kinase expressed by osteoblasts and osteocytes; in these cells its production is stimulated by parathyroid hormone (PTH) and IGF-1. Osteoblastic ephrinB2 signalling has been reported to prevent osteoblast apoptosis, and is required for osteoblast maturation and their support of osteoclast formation. Furthermore, we have reported that the bones of mice lacking ephrinB2 throughout the osteoblast lineage (Osx1Cre.efnB2$^{f/f}$) displayed greater compliance in 3 point bending tests compared to controls, indicating that osteoblastic ephrinB2 maintains cortical modelling during growth. The present study examined the effect of targeted deletion of ephrinB2 in osteocytes on bone mass and strength.

Bones were collected from 12-week-old female mice with ephrinB2 deleted in osteocytes (Dmp1Cre.efnB2$^{f/f}$) and littermate controls (Dmp1Cre.efnB2$^{w/w}$);n=7-12/group. Tibiae were analysed by histomorphometry and femora by both microCT and 3-point bending tests. Dmp1Cre.efnB2f/f mice showed significantly greater tibial trabecular bone volume (BV/TV by 40%, p<0.01), trabecular thickness (by 10%, p<0.05) and trabecular number (by 20%, p<0.01). Both femoral and tibial trabecular separation were significantly lower by 12% and 23% respectively, p<0.01, p<0.05). While neither osteoblast number nor bone formation rate were significantly altered, osteoclast surface/bone surface (OcS/BS) and osteoclast size were both ~12% greater in Dmp1Cre.efnB2$^{f/f}$ mice compared to control (p<0.01), without any significant change in RANKL or OPG mRNA levels. The combination of a high OcS/BS with normal bone formation rate and increased BV/TV suggests impaired bone matrix destruction in mice lacking osteocytic ephrinB2.

Dmp1Cre.efnB2$^{f/f}$ femora also had significantly thinner cortices (p<0.01) and were more brittle than controls when assessed by 3 point bending tests. They showed a significant reduction in post-yield deformation (by 24%, p<0.01), toughness (33%, p<0.001), yield stress (10%, p<0.05), ultimate deformation (20%, p<0.001) and energy absorbed to failure (35% less, p<0.001) compared to controls. This indicates increased brittleness of the bone matrix.

These data indicate that although ephrinB2 in osteoblasts is required for their ongoing differentiation, osteocytic ephrinB2 does not mediate this effect. Rather, osteocytic ephrinB2 provides signals that limit osteoclastogenesis, stimulate osteoclast function, and maintain compliance of the bone matrix.

Disclosures: Natalie Sims, None.

MO0278

Osteocyte differentiation is delayed by low dose TNF. <u>Mark Nanes</u>*[1], <u>Linda Gilbert</u>[2]. [1]VA Medical Center & Emory University, USA, [2]Atlanta VA Medical Center, USA

Inflammation causes bone loss in arthritis, menopause, and aging. TNF contributes to systemic bone loss by suppressing osteoblast (Ob) differentiation. We reported that low levels of TNF in TgTNF mice (2-5 pg/ml) suppress osteoblast numbers and diminish bone accrual at 4 weeks of age without affecting osteoclasts or bone resorption. By 12 weeks of age TgTNF and WT mice had the same number of Ob [Gilbert *et al.* Bone 56(1):174-183 2013]. Despite the similarity of Ob number between TgTNF and WT mice at at12 weeks of age, TgTNF show persistently less bone by micro computed tomography.

Since it is known that osteocytes (Ot) play a key role in regulating bone formation and resorption, we examined the effect of TNF on the appearance of Ot in young TgTNF mice. At 4 weeks of age TgTNF mice had 40% fewer Ot vs. WT by histomorphometry. By 6 weeks of age Ot number was not different between groups and by 12 weeks TgTNF had a trend for more Ot than WT mice. Thus, delayed appearance of Ob was followed by delayed appearance in Ot that later catch up to that observed in Wt.

To determine the effect of TNF on expression of Ot phenotypic markers, IDG-SW3 osteocyte-like cells (gift from Dr. Lynda Bonewald) were treated with TNF either beforeor after their consecutive differentiation to the Ob and Ot phenotype. Real time RT-PCR of cultured IDG-SW3 cells showed early expression of the Ob markers alkaline phosphatase (AP), osteocalcin (OC), and bone sialoprotein (BSP) followed by the Ot markers dentin matrix acidic phosphoprotein 1 (DMP1), phosphate regulating endopeptidase homolog, X-linked (Phex), and sclerostin (SOST). TNF dose-dependently inhibited expression of the Ot markers even after cells had achieved expression of the Ob phenotype (days 9-12). IC$_{50}$ for the Ot markers (DMP1, Phex, SOST) was 2.3 ng/ml and IC$_{50}$ was 1 ng/ml for the Ob markers (AP, OC, BSP). Interestingly, IDG-SW3 cells did not respond to TNF with increased expression of SOST as reported in other cells lines and in TgTNF mice. TNF inhibited expression of Dickkopf-related protein 1. Cell viability throughout the 12 day culture period was demonstrated by TNF stimulation of RANKL and Alamar Blue assay. These results suggest that Ot are extremely sensitive to TNF. Ot may mediate chronic inhibitory effects of TNF on bone formation.

Disclosures: Mark Nanes, None.

MO0279

Sclerostin Expression can be Induced by Enforced Expression of Defined Transcription Factors in Human Fibroblasts. <u>Makoto Fujiwara</u>*[1], <u>Wei Wang</u>[2], <u>Yasuhisa Ohata</u>[2], <u>Kouji Miura</u>[2], <u>Taichi Kitaoka</u>[3], <u>Takuo Kubota</u>[4], <u>Yasuji Kitabatake</u>[2], <u>Noriyuki Namba</u>[3], <u>Toshimi Michigami</u>[5], <u>Keiichi Ozono</u>[6]. [1]Osaka University graduate school of medicine, Japan, [2]Osaka University Graduate School of Medicine, Japan, [3]Osaka University Graduate School of Medicine, Japan, [4]Osaka University Graduate School of Medicine & Dentistry, Japan, [5]Osaka Medical Center & Research Institute for Maternal & Child Health, Japan, [6]Osaka University Graduate School of Medicine, Japan

Background: Sclerostin, coded by *SOST*, is a secretory protein expressed specifically in osteocytes and suppresses osteogenesis by inhibiting the Wnt signaling. Regulatory mechanism of *SOST* expression remains unclear mainly due to difficulty in using osteocytes in vitro.

Purpose: We aim to induce sclerostin expression in human fibroblasts, which are easily available, by retroviral gene transduction.

Methods: Human sarcoma cell line SaOS-2, which expresses *SOST* during long-term differentiation culture, was cultured in differentiation medium or maintenance medium. We compared and analyzed RNA expression pattern in each medium by RNA microarray and searched for candidate transcription factor (TF) genes which increased more than two-fold higher in differentiation medium than maintenance medium. Furthermore, we narrowed down the TFs by (1) IPA upstream regulator analysis which expects effective causal TFs on the microarray data in reference to empirical gene expression data, (2) prediction of binding ability to *SOST* promoter and enhancer with TRANSFAC database, and (3) previous reports that showed some association between the TF and osteogenesis. After determining the candidate TFs, we cloned these genes into retrovirus pMXs vector, induced them into human fibroblasts, and analyzed *SOST* expression by real time PCR on day 7. Finally, we measured screlostin concentration in conditioned medium by ELISA.

Results: Twenty TFs were selected from 70 candidates. Among them, enforced expression of the seven TFs, ATF3, DLX3, IRF7, MXI1, KLF4, PAX4 and SP7, induced *SOST* expression in fibroblasts. Gradual reduction of the number of TFs

demonstrated significantly high *SOST* expression, approximately 200 folds than control at four TFs. Sclerostin secretion was also confirmed in conditioned medium by ELISA.

Conclusion: We have established the method to induce sclerostin expression in human fibroblasts by inducing defined TFs. The method is applicable to analyze the pathological role of sclerostin in bone metabolic disorders such as various kinds of hereditary rickets.

Disclosures: Makoto Fujiwara, None.

MO0280

Sclerostin is Mechanically and Hormonally Regulated in a Novel *in vitro* Osteocyte Model. William Thompson*[1], Gunes Uzer[1], Sherwin Yen[2], Buer Sen[3], Zhihui Xie[4], Kaitlyn Brobst[2], Maya Styner[5], Janet Rubin[5]. [1]University of North Carolina, USA, [2]University of North Carolina, USA, [3]University of North Carolina At Chapel Hill, USA, [4]University of North Carolina, USA, [5]University of North Carolina, Chapel Hill, School of Medicine, USA

Osteocytes modulate bone density through both osteoblast and osteoclast effectors, and "reach out" to interact with cells in the marrow compartment. The stellate morphology and spatial organization of osteocytes are optimal for sensing force and transmitting biochemical signals through their interconnected lacuno-canalicular system. In addition to the paracrine effects of sclerostin and RANKL on bone effector cells, osteocytes secrete endocrine signals including DMP1 and FGF23, which alter matrix mineralization and renal phosphate homeostasis. To understand how osteocytes respond to hormonal and physical signals there is a need for cell models that faithfully replicate the *in vivo* osteocyte phenotype. Current osteocyte cell lines present limitations that inaccurately represent *in vivo* conditions. We have developed a novel osteocyte model expressing the defining markers of these cells while displaying a stellate morphology within a mineralized matrix. Primary polyclonal murine marrow-derived mesenchymal stem cells were grown in osteogenic medium. Within 15 days, expression of early osteocyte markers E11, DMP1, and Phex were significantly increased compared to culture day 10. Genes found later in osteocyte differentiation, including Dmp1 and Fgf23, were also measurable at 15 days. Importantly, Sost rose approximately 100 fold, plateauing at d15. At this time, electron microscopy revealed osteocyte-like cells encased in matrix with a defined pericellular space and dendritic extensions. Staining for actin or with an anti-E11 antibody revealed numerous cellular projections connecting adjacent cells. Mimicking *in vivo* osteocyte secretory responses, our cell model responded to PTH and $1,25(OH)_2D_3$. PTH treatment significantly repressed Sost, Dmp1, and Opg mRNA expression, and reductions in sclerostin protein were also observed. Exposure to $1,25(OH)_2D_3$ increased expression of Fgf23, Dmp1, and Rankl, and decreased that of Opg. As it is known that mechanical loading suppresses osteocyte Sost *in vivo*, we tested whether twice daily low intensity vibration treatment reduced Sost production *in vitro*. After two days of LIV, Sost mRNA expression was decreased by $23 \pm 8\%$, while Dmp1, E11 and Phex were unaffected. In summary, we have developed a novel osteocyte model that faithfully replicates the morphology, gene expression profile, and hormonal and mechanical responses of osteocytes observed *in vivo* that will enable molecular and biochemical studies of sclerostin regulation.

Disclosures: William Thompson, None.

MO0281

Withdrawn

MO0282

FREE CIRCULATING miRNAS AND BONE TISSUE miRNAs ARE NOVAL BIOMARKERS FOR OSTEOPOROSIS. Mohammed-Salleh Ardawi*[1], Mohammed Qari[2], Talal Bahksh[3], Abdulrahman Sibiani[4], Ali Ahmad[5], Mohammad Noaman[5], Abdulrahim Rouzi[6]. [1]Center of Excellence for Osteoporosis Research & Department of Clinical Biochemistry & KAU Hospital, Faculty of Medicine, King Abdulaziz University, Saudi Arabia, [2]Center of Excellence for Osteoporosis Research & Department of Haematology & KAU Hospital, Faculty of Medicine, King Abdulaziz University, Saudi Arabia, [3]Center of Excellence for Osteoporosis Research & Department of General Surgery, Faculty of Medicine & KAU Hospital, King Abdulaziz University, Saudi Arabia, [4]Center of Excellence for Osteoporosis Research & Department of General Surgeryand KAU Hospital, Faculty of Medicine, King Abdulaziz University, Saudi Arabia, [5]Center of Excellence for Osteoporosis Research, King Abdulaziz University, Saudi Arabia, [6]Center of Excellence for Osteoporosis Research & Faculty of Medicine, Saudi Arabia

Background: Many patients at risk of osteoporosis or osteoporotic fracture will be missed based on bone mineral density (BMD) assessment alone. Accordingly, there is a need to identify new biomarker(s) independent of BMD to improve fracture prediction. The identification of specific micro-RNA (miRNA) signatures is

considered as possible new diagnostic and therapeutic targets. Several free circulating extracellular miRNAs identified as biomarkers that were associated with various types of cancer. The objective of the present study is to identify specific miRNAs in patients with osteoporotic fractures compared with non-osteoporotic fractures.

Methods: Isolated miRNAs were examined from the serum of 26 patients with hip fractures that were transcribed and the samples were studied among 15 osteoporotic and 15 non-osteoporotic samples. With each pool of samples, human serum and plasma miRNA PCR Arrays were performed. A total of 90 different miRNAs were identified. miRNA samples were isolated from the serum and bone tissues of 45 osteoporotic and 45 non-osteoporotic patients and studied. Two-tailed Mann-Whitney test was used to compare between the groups. ROC-curve analysis was used to determine diagnostic miRNAs appility.

Results: A total of 13 miRNAs that were regulated were identified following the validation analysis including: miR-19b, miR-21, miR-221, miR-23a, miR-24, miR-93, miR-100, miR-122a, miR- 124a, miR-125b and miR-148a. These were significantly up-regulated in the serum of osteoporotic patients. In the bone tissue of osteoporotic patients, the following were identified: miR-21, miR-23a, miR-24, miR-25, miR-27a, miR-93, miR-100 and miR-125b that were significantly highly expressed. A total of 7 miRNAs displayed an up-regulation both in serum and bone tissue.

Conclusions: The present study demonstrates a significant role for several miRNAs in patients with osteoporosis and suggests that they may be useful biomarkers for diagnostic purposes and possible target(s) for treating bone loss and optimizing fracture healing among osteoporotic patients.

Disclosures: Mohammed-Salleh Ardawi, None.

MO0283

Very Early Responses of Biochemical Markers of Bone Turnover to Teriparatide. Deborah Robins[1], Benjamin Leder*[2], Kelly Krohn[3], Jahangir Alam[4], Heather Murphy[5], Alan Chiang[6], John Krege[6]. [1]Eli Lilly & Company, USA, [2]Massachusetts General Hospital Harvard Medical School, USA, [3]Lilly USA, LLC, USA, [4]Lilly USA, LLC, USA, [5]inVentiv Health Clinical, LLC, USA, [6]Eli Lilly & Company, USA

Purpose: Few data are available on the early response of biochemical bone turnover markers (BTMs) to teriparatide. This open-label, single-site study in healthy postmenopausal women measured immediate and short-term effects of single and multiple doses of teriparatide on serum PINP, osteocalcin (OC), CTX, and NTX. Methods: 18 women enrolled and completed the study. Mean age was 57 yrs (range 47-77 yrs); 2 were of African descent and 16 were Caucasian. In Period 1, subjects received a single subcutaneous (SQ) dose of 40 mcg teriparatide. In Period 2 (after a 3-4 week washout), subjects received daily 20 mcg teriparatide SQ injections for 28 days. In both periods, serum for BTM evaluations was collected at 4 timepoints throughout the day prior to dosing. In Period 1, BTMs were measured postdose at 0, 2, 6, 10, and 24 hrs, and at 3 and 7 days. In Period 2, BTMs were measured at 0, 2, 6, 10, and 24 hrs following the first dose, and then every week pre-dose for the remaining 28-day dosing period. Comparisons used paired t-test. Results: Prior to teriparatide treatment, PINP and OC showed little change in diurnal variation or food effect when compared with baseline, whereas significant decreases were noted in CTX and NTX (p<0.001, compared with baseline). In Period 1, two significant increases in bone formation markers were noted: PINP increased from 53 ± 18 (mean $\pm$ SD) at baseline to 56 ± 19 mcg/L at 24 hrs postdose (p=.002); OC increased from 23 ± 11 at baseline to 26 ± 13 ng/ml at 3 days postdose (p=.017). In Period 2, PINP increased steadily, reaching 102 ± 34 mcg/L at 28 days (p<0.001), and OC levels increased to 40 ± 20 ng/ml (p<0.001). Both 40 and 20 mcg of teriparatide partially blocked the decrease in NTX and CTX otherwise observed with food and diurnal variation in the absence of treatment. Serial fasting concentrations of BTMs showed progressive increases in bone formation markers (PINP and OC) but not bone resorption markers (CTX and NTX) through 28-day dosing. No new or serious adverse events were reported during this study. Conclusions: Teriparatide increased PINP and OC, while preventing decline of CTX and NTX normally observed with food and diurnal variation. These findings suggest early anabolic effects of teriparatide may involve progressive stimulation of bone formation and an acute, but not progressive, stimulation of bone resorption. This study also supports PINP as a useful early formation marker to assess the bone anabolic effect of teriparatide.

Disclosures: Benjamin Leder, Eli Lilly and Company, 4; Eli Lilly and Company, 8 This study received funding from: Eli Lilly and Company

MO0284

We Are Not On The Same Page: Variation of PTH and Vitamin D Binding Protein Measurement in 2014. Neil Binkley*[1], Gretta Borchardt[2], Diane Krueger[1], Ravinder Singh[3], Donald Wiebe[4]. [1]University of Wisconsin, Madison, USA, [2]University of Wisconsin, USA, [3]Mayo Clinic, USA, [4]University of Wisconsin, USA

Standardization of 25(OH)D measurement is recognized as necessary to define vitamin D (D) status. However, other related analytes, e.g., PTH and vitamin D binding protein (DBP), may also require standardization. PTH measurement is often used to determine D adequacy and recent work suggests that bioavailable 25(OH)D (Bio-25D) measurement may be needed to define D status. Methodologic differences exist for both PTH and DBP. We hypothesized that standardization of PTH and DBP

is currently inadequate and thus compared current PTH and DBP measurements. Common PTH methods were compared with a nominal gold standard, liquid chromatography tandem mass spectroscopy (LC-MS/MS). DBP results from 3 commercially available kits were compared.

PTH comparability was assessed in a QA study of 14 plasma pools derived from clinical lab residual specimens selected to span from low to high PTH values. Seven clinical labs measured PTH in routine manner (6 by automated immune-based methods, 1 by LC-MS/MS). DBP was measured in 30 serum specimens (10 in duplicate) with 3 commercial kits. Results were compared using linear regression and Bland-Altman analyses.

Immunoassay based PTH results were consistently higher than a LC-MS/MS method (mean bias of +18-28 pg/mL). Good correlation was observed between LC-MS/MS and the other labs ($R^2 = 0.90$ to 0.94) and between the immune based assays (R^2 from 0.99 to 1.00) with mean bias of -2 to +12 pg/mL. However, the normal range for the laboratories differed; the reported upper limit of normal ranged from 53.5 to 90 pg/mL. As a result, a variable number (from 5 to 10) of these 14 specimens were classified as "high" by the various labs. The 3 DBP assays were quite reproducible (%CV from 4 to 7%). However, there was no significant correlation between results from the 3 DBP kits ($R^2 = 0.003$ to 0.022).

In conclusion, there is good between-lab correlation of PTH results, suggesting that harmonization of these assays is possible. However, if the LC-MS/MS values are correct, all clinical labs tested here report PTH results that are variably "too high." As PTH measurement will likely continue to assist in defining D sufficiency, development of a reference measurement procedure and subsequent standardization (along the lines currently being undertaken for 25(OH)D by the Vitamin D Standardization Program) is necessary. Similarly, standardization of DBP and Bio-25D measurement will be needed if this analyte is validated to have clinical utility.

Disclosures: Neil Binkley, None.

MO0285

Abnormal Trabecular Plates and Cortical Thinning at the Distal Radius and Tibia in Postmenopausal Women with Vertebral Fractures.

Ji Wang*[1], Emily Stein[2], Bin Zhou[1], Kyle Nishiyama[1], Elizabeth Shane[2], X Guo[1]. [1]Columbia University, USA, [2]Columbia University College of Physicians & Surgeons, USA

Postmenopausal women with fragility fractures have deterioration of trabecular microstructure and cortical thinning, independent of areal BMD by DXA. In postmenopausal women with vertebral fractures, lower volumetric BMD, fewer and more widely separated trabeculae, thinner cortex and reduced stiffness have been observed at the distal radius and distal tibia by HR-pQCT. While previous studies have demonstrated the importance of trabecular plates in mechanical integrity of trabecular bone, whether vertebral fracture is associated with deficiencies in trabecular plate microstructure is unknown. Postmenopausal women with vertebral fractures (n=40) and non-fracture controls (n=40) were scanned by HR-pQCT. Trabecular and cortical compartments were separated by an automatic segmentation algorithm. Trabecular type, orientation and connectivity were measured by individual trabecula segmentation (ITS) analysis. Cortical thickness, porosity and area were measured by a customized cortical evaluation script (Nishiyama et al. 2013). Whole bone and trabecular bone stiffness were estimated by finite element analysis. The fracture and control groups were similar in age (69 ± 8 and 69 ± 7 yrs), race (82.5% and 92.5% Caucasian, respectively), and body mass index (27 ± 6 and 26 ± 5). Group differences in microstructure and stiffness are shown in Figure 1. Compared to controls, women with vertebral fractures had lower cortical thickness, smaller cortical area, and larger trabecular area. Cortical porosity and pore size did not differ. By ITS, fracture subjects had lower plate bone volume, fewer trabecular plates, less axially aligned trabeculae and less trabecular connectivity. Group differences in trabecular microstructure were greater at the radius than at the tibia, while cortical differences were more pronounced at the tibia. Whole bone stiffness and trabecular bone stiffness were lower in women with vertebral fractures by 17% and 25%, respectively at the radius, and by 18% and 19% at the tibia. In summary, postmenopausal women with vertebral fractures had both trabecular and cortical microstructural deterioration at the peripheral skeleton, with preferential loss of trabecular plates and cortical thinning. These microstructural deficits translated into lower whole bone and trabecular bone stiffness at the radius and tibia. Our results suggest that abnormalities in trabecular plate and rod microstructure may be important mechanisms of vertebral fracture in postmenopausal women.
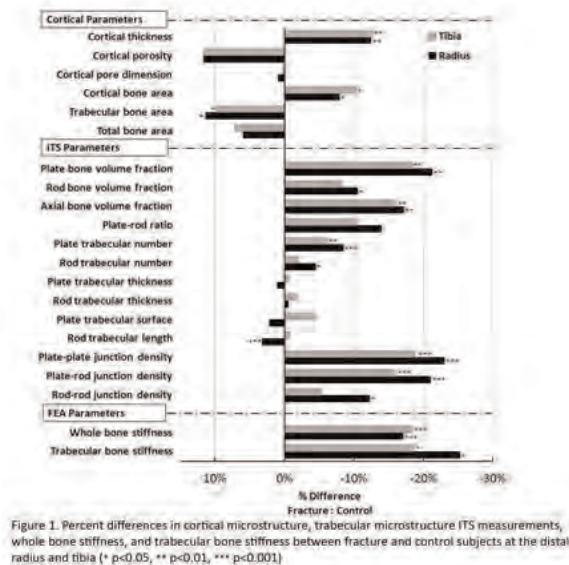

Figure 1. Percent differences in cortical microstructure, trabecular microstructure ITS measurements, whole bone stiffness, and trabecular bone stiffness between fracture and control subjects at the distal radius and tibia (* p<0.05, ** p<0.01, *** p<0.001)

Figure 1

Disclosures: Ji Wang, None.

MO0286

Advanced *In Vivo* Bone Quality Assessment Using the Next Generation of HR-pQCT.

Sarah Manske*[1], Ying Zhu[2], Clara Sandino[3], Steven Boyd[1]. [1]University of Calgary, Canada, [2]University of Calgary, Canada, [3]Faculty of KinesiologyBone Imaging LabUniversity of Calgary, Canada

While HR-pQCT scanners have been readily adopted for 3D bone quality assessment, the spatial resolution (82 μm) was insufficient for direct morphological assessment of trabecular thickness (Tb.Th) and separation (Tb.Sp). The second generation scanner (HR-pQCT2, XtremeCTII, Scanco Medical) can perform *in vivo* scans at 61 μm nominal isotropic resolution using a shorter acquisition time and similar radiation dose as the previous generation. We assessed whether the HR-pQCT2 can provide results similar to the original HR-pQCT (XtremeCT) in order to support ongoing longitudinal studies, and whether the accuracy of HR-pQCT2 is sufficient to perform a direct assessment of trabecular bone microarchitecture.

We evaluated 20 human cadaveric radii (mean age 70 yrs, 9 male). We compared a standard patient evaluation performed on the HR-pQCT system (X1, 82 μm) and a mimicked HR-pQCT evaluation performed on the HR-pQCT2 system (X1M, 82 μm). We also compared an HR-pQCT2 patient evaluation (X2, 61 μm), and a gold standard, high resolution *ex vivo* protocol on HR-pQCT2 (HR, 30 μm). Additionally, we scanned a microCT spatial resolution phantom (mCTP610, Shelley Automation). All scans were 3D registered to ensure a common region of analysis. For X1 and X1M we applied the manufacturer's standard patient evaluation to assess total BMD (Tt.BMD), trabecular BMD (Tb.BMD), trabecular number (Tb.N), and derived Tb.Th[d] and Tb.Sp[d]. For X2 and HR we applied a direct morphological assessment of Tb.N, Tb.Th, and Tb.Sp.

X2 could resolve the coil spaced at 100 μm (Figure 1A) better than X1 (Figure 1B), with a 30% improvement in spatial resolution. All outcomes of X1 agreed well with X1M scans ($R^2 = 0.93$ to 0.99). In our setup, Tt.BMD and Tb.BMD were significantly higher in X1M than X1, which resulted in significantly higher Tb.Th[d] in X1M than X1. In contrast, Tb.N and Tb.Sp[d] did not differ between X1 and X1M. Directly assessed Tb.N and Tb.Sp were highly correlated ($R^2 = 0.93$ to 0.98) and did not differ between HR and X2. However, despite an excellent association for Tb.Th ($R^2 = 0.97$), differences in spatial resolution caused systematic overestimation by X2.

Our results suggest that compatibility between X1 and X1M scans will require accurate density calibration. Importantly, spatial resolution of HR-pQCT2 is sufficiently accurate to assess trabecular microarchitecture directly, which opens new possibilities for understanding of bone microarchitectural changes with aging and treatment.
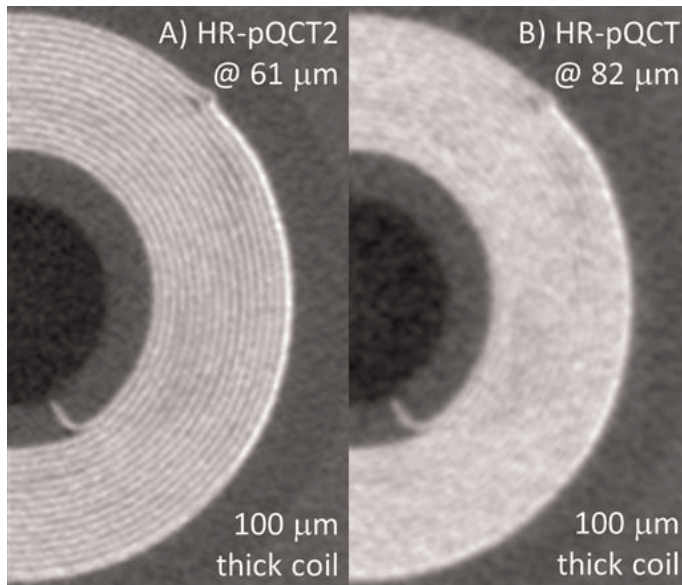
Figure 1 - 100 um coil in HR-pQCT2 and HR-pQCT

Disclosures: Sarah Manske, None.

MO0287

Comparability of HR-pQCT Bone Quality Measures Improved by Scanning Anatomically Standardized Regions. Serena Bonaretti[1], Margaret Holets[2], Isra Saeed[3], Louise McCready[2], Thomas Lang[1], Sundeep Khosla[4], Andrew Burghardt*[1]. [1]University of California, San Francisco, USA, [2]Mayo Clinic College of Medicine, USA, [3]University of California, San Francisco, USA, [4]Mayo Clinic College of Medicine, USA

Current HR-pQCT protocols do not account for limb length despite tremendous variation in bone density and geometry along the radius and tibia. Consequently, limb length adds considerable variability that confounds the interpretation of biological effects and increases scatter in cross-sectional and normative data. We measured the variability in bone quality parameters due to limb length and propose a protocol for scanning anatomically-standard regions based on measured limb-length. HR-pQCT scans covering twice the typical length of the distal radius and tibia were acquired in adult men (n=17) and women (n=13). Percutanous limb length was measured using standard anthropometric protocols. Bone parameters were calculated for three subvolumes equivalent to the normal scan length (110 slices) based on the following positioning scenarios: (1) the standard fixed distance from the jointline; (2) the average % location of the standard position based on measured limb-length; (3) the average % location of the standard position estimated from height data of previous HR-pQCT population studies in the literature. The standard deviation of differences between fixed and anatomic positions, and percent difference for representative bone parameters (BMD, Tb.BMD, Ct.Th, Tb.N) measured in subvolumes based on the default and either anatomic scan position, were calculated. The average anatomic position in the study population was $4.0\pm0.5\%$ in the radius and $7.2\pm0.6\%$ at the tibia, corresponding to a variance of ±1.1 and ±2.2 mm in the scan position, respectively. The height-estimated anatomic position for optimal comparability to previous HR-pQCT population data was 4.1% and 7.4%. Average differences in bone measurements between fixed and anatomic scan regions were minimal by design; however individual differences exhibited substantial variability (Table 1). The large distribution of differences between bone parameters measured at a fixed distance from the joint and an anatomically relative distance indicates limb length contributes significant variance to bone quality measurements. This strongly recommends the use of scan protocol that is adjusted for measured limb length, particularly for cross-sectional studies and normative database generation. The minimal average differences between fixed distance scanning and the literature-derived relative distance suggest that anatomically-standardized scan positioning can maintain a high degree of comparability to legacy population data.

Table 1: Summary of variability in HR-pQCT measures associated with limb length

| | Relative position based on limb length measured in current study participants [Radius: 4.0% \| Tibia: 7.2%] | | Relative position estimated from height of existing HR-pQCT population data in the literature [Radius: 4.1% \| Tibia: 7.4%] | |
	Difference vs. Fixed: Population Averages	Variance and Range of Differences	Difference vs. Fixed: Population Averages	Variance and Range of % Differences
Radius				
BMD	-0.6%	6.7% [-9.8, +20.8]	1.2%	6.6% [-10.2, +19.5]
Ct.BMD	0.4%	5.6% [-5.7, +20.2]	0.0%	5.4% [-6.2, +19.1]
Ct.Th	-0.9%	18.8% [-18.6, +66.7]	2.1%	18.6% [-19.8, +66.7]
Tb.BMD	0.5%	2.4% [-5.3, +5.1]	-0.5%	2.5% [-5.2, +5.6]
Tb.N	-0.6%	5.2% [-15.0, +3.4]	0.4%	5.2% [-14.6, +3.5]
Tibia				
BMD	-0.1%	3.1% [-6.0, +6.6]	-1.2%	3.2% [-7.4, +5.4]
Ct.BMD	0.1%	2.3% [-3.9, +5.4]	-0.7%	2.3% [-5.1, +5.0]
Ct.Th	-0.3%	11.8% [-24.1, +27.5]	-3.4%	11.5% [-28.6, +22.2]
Tb.BMD	0.2%	4.0% [-11.6, +7.4]	1.3%	4.3% [-10.9, +9.8]
Tb.N	-0.4%	5.0% [-20.4, +8.3]	0.6%	4.6% [-16.1, +10.4]

Table 1

Disclosures: Andrew Burghardt, None.

MO0288

Focal Osteoporosis in the Trabeculae of the Femoral Head in Hip Fracture. Linda Skingle[1], Fjola Johannesdottir[2], Paul Mayhew[2], Karen Blesic[1], Kenneth Poole*[2]. [1]Cambridge University Hospitals NHS Foundation Trust, United Kingdom, [2]University of Cambridge, United Kingdom

Objective: In cases of femoral neck fracture there is thinning of the femoral cortex in a focal patch near the anterolateral head-neck junction compared with the rest of the femoral head (Poole et al. PLoS One 2012). We took femoral heads at operation from this hip fracture population and tested whether the volume of trabecular bone beneath the thinned cortex was also osteoporotic by histomorphometric criteria. We used microCT to calculate bone volume/tissue volume (BV/TV) and compared it with another subcortical site within the same femoral head.

Method: Sixteen femoral heads were obtained at hip replacement (with appropriate ethics approval) following femoral neck fracture. The heads were halved and a core was taken from each half: one through the focally thin patch of the head and the other from the opposite, subfoveal, part of the head. These two cores were microCT scanned (XTEK HMX CT 300 - 23μm/pixel). Measurements of BV/TV were made using Image J/Bone J (Doube et al. Bone 2010) along the length of the core starting at the endocortical trabeculae and progressing through in 100x23μm slice segments through the core. Paired t tests were performed to compare the BV/TV in 100 slice segments for the subfoveal and focally thin areas (Fig.1).

Results:The results show a significant difference between the first hundred slices of each pair of cores, after this point in the core no significant difference was found between the two sites (Fig.1).Conclusion: We conclude that there is focal osteoporosis (by histomorphometric criteria) in the trabecular bone immediately beneath the focally thin areas of cortex (identified previously using in vivo CT imaging (Poole et al. PLoS One 2012)). In cases of femoral neck fracture this may be a factor in fracture initiation and propagation. We plan to elucidate the mechanism (be it disuse or fatigue) for this focal osteoporosis with further histological studies on these same core biopsies.
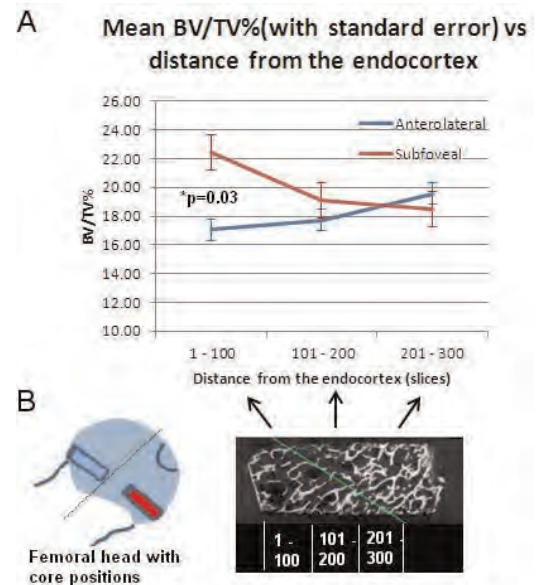

Fig. 1: A) Comparison of BV/TV from 2 sites within the femoral head. B) Core positions.

Disclosures: Kenneth Poole, None.

MO0289

Intra- and Inter-Operator Variability in HR-pQCT Scan Positioning. <u>Serena Bonaretti</u>*[1], <u>Margaret Holets</u>[2], <u>Nicholas P. Derrico</u>[3], <u>Kyle Nishiyama</u>[4], <u>Danmei Liu</u>[5], <u>Stephanie Boutroy</u>[6], <u>Roland Chapurlat</u>[7], <u>Heather McKay</u>[5], <u>Elizabeth Shane</u>[8], <u>Mary Bouxsein</u>[9], <u>Thomas Lang</u>[1], <u>Sundeep Khosla</u>[10], <u>Andrew Burghardt</u>[1]. [1]University of California, San Francisco, USA, [2]Mayo Clinic College of Medicine, USA, [3]Beth Israel Deaconess Medical Center, USA, [4]Columbia University, USA, [5]University of British Columbia, Canada, [6]INSERM U1033 & Université de Lyon, France, [7]E. Herriot Hospital, France, [8]Columbia University College of Physicians & Surgeons, USA, [9]Beth Israel Deaconess Medical Center, Harvard Medical School, USA, [10]Mayo Clinic College of Medicine, USA

The role of the operator in HR-pQCT precision has not been evaluated and may be critical for multicenter cross-sectional studies. At scan time, the operator acquires a 2D projection of the limb (scout image) and manually identifies an anatomic landmark, which determines the scan region. Variability in landmark identification impacts bone measurements, especially in the radius where morphological variations are greater. In this study, our goal was to quantify long-term and short-term intra-operator precision of landmark placement, variability among operators at multiple imaging centers, and the corresponding effect on bone measurements.

We reproduced the acquisition interface of the HR-pQCT system (XtremeCT, Scanco Medical AG) to simulate the process of identifying anatomic landmarks in the scout image. To evaluate intra-and inter-operator precision, 56 double stack scans (220 slices, centered on the standard scan region) and corresponding scout images were acquired at two imaging centers. We were thus able to virtually localize standard 110-slice sub-volumes for analysis, based on landmark positions retrospectively identified in the simulation environment. For both radius and tibia, we evaluated (1) long-term intra-operator variability for 2 operators (over 6-24 months); (2) short-term intra-operator precision for 7 operators in a subset of 15 images, positioned three times in a random order; (3) inter-operator precision for 5 operators. For each experiment, we calculated standard deviation of the landmark position (SDRMS) and coefficient of variation (CVRMS) of primary bone densitometric and structure parameters.

Precision results are in Table 1. Positioning for the tibia was highly reproducible, even across multiple operators (CVRMS<1.8%). In contrast, errors for the radius were significantly greater (p<0.05), and particularly high across multiple operators (SDRMS=0.56mm, CVRMS=6.6% for Ct.Th). At both sites, Ct.Th was considerably more sensitive to position variability than density and structure measures.

In conclusion, we found that HR-pQCT scan positioning for the tibia is highly reproducible over time and across operators. Greater positioning variability is observed for the radius, leading to relatively high precision errors. Efforts to define more reproducible landmarks, establish more rigorous operator training procedures, and develop automated scan positioning methods should be pursued to minimize the effects of operator variability in the radius.

Table 1

Disclosures: Serena Bonaretti, None.

MO0290

Is TBS different in healthy European Caucasian men and women ?: Creation of normative spine TBS data for men. <u>Vladyslav Povoroznyuk</u>*[1], <u>L. Del Rio</u>[2], <u>S. Di Gregorio</u>[2], <u>F. Michelet</u>[3], <u>N. Dzerovych</u>[4], <u>A. Musiienko</u>[4], <u>R. Winzenrieth</u>[5]. [1]Institute of Gerontology AMS Ukraine, Ukraine, [2]Cetir Group Mèdic, Spain, [3]R&D department, Med-Imaps, France, [4]Institute of Gerontology NAMS, Ukraine, [5]R&D department, Med-Imaps, Ukraine

Introduction: Trabecular Bone Score (TBS, Med-Imaps, France) is an index of bone microarchitectural texture extracted from antero-posterior spine DXA. In this cross-sectional analysis from two facilities in Ukraine and Spain, we have investigated the age-related changes of the lumbar vertebrae microarchitecture assessed by TBS in a cohort of Caucasian men and compare the results to TBS reference data for Caucasian women.

Methods: Subjects in the study were Ukrainian and Spanish men aged 40 and older with a BMD Z-score at spine L1-L4 within ± 2SD. Individuals were excluded if they had fractures, were on any osteoporosis treatment and/or had any illness that would be expected to impact bone metabolism. All data have been obtained from GE-Lunar DXA devices (Prodigy and iDxa, Madison, WI, USA). Cross-calibration between the two centers was performed for TBS. TBS was evaluated at spine L1-L4 but also for all possible vertebrae combinations.

Results: A database of 368 men aged 40 to 90 years was created. TBS and BMD values at L1-L4 were poorly correlated with BMI (r=0.16 and 0.22). TBS was poorly correlated with weight (r=-0.1) and height (0.03) whereas higher correlations were obtained for BMD (r=0.3 and 0.2). TBS values obtained for all lumbar vertebral combinations decreased significantly with age (see figure below, at L1-L4 for men and women). There was a linear decline of 13.5% (~-1.75 T-score) in TBS at L1-L4 between 40 and 90 years of age in men whereas a decline of 16.7% (~-2.58 T-score) was observed in women *(Dufour et al., OI 2012)*. Conversely to women, there is no modification of TBS decline rate after 65 years in men.

Conclusion: This study established for the first time TBS age related curve in European men at lumbar spine. The decrease seen in lumbar TBS reflects age-related micro-architecture texture changes at spine. Within 40-65 age range, similar TBS decline was observed in both European Caucasian men and women (p=0.8). After 65, TBS decline rate is significantly higher for women than for men (p<0.01). This study confirms the need for using gender dedicated reference data.
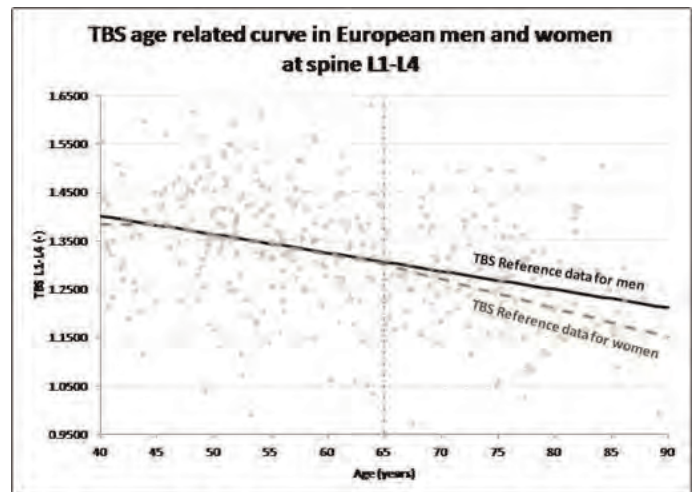
grafik

Disclosures: Vladyslav Povoroznyuk, None.
This study received funding from: Renaud Winzenrieth and F. Michelet have disclosures: Med-Imaps employees

MO0291

Static postural stability and hip fracture in elderly individuals. <u>Hua Lin</u>*[1], <u>Changchang Liu</u>[2], <u>Brian Lin</u>[3], <u>Xiufen Zhu</u>[2]. , [2]Center of Bone Metabolic DiseasesAffiliated Drum Tower Hospital of Nanjing University Medical School, China, [3]Johns Hopkins University, USA

Objective: To study the effect of static postural stability and its correlation with hip fracture in elderly individuals.

Methods: We carried out a retrospective study comprising 141 elderly individuals aged more than 60 years old. Static postural stability was assessed in participants with or without prior history of hip fracture.

Results: The mean age of participants was 71.12 ± 7.08. There were 65 participants (46.10%) with history of hip fracture. The logistic regression analysis showed significantly positive correlation between NO-WDI (OR=8.458,P=0.004) or HF-F4 (OR=6.883,P=0.009) and history of hip fracture incidence.

Conclusion: In elderly individuals with history of hip fracture, the ability to remodel the body's center of gravity and the ability of lower-extremities to maintain balance were both decreased. The data suggest NO-WDI and/or HF-F4 may be effective parameters in early prediction and rehabilitation for hip fracture in elderly individuals.

Disclosures: HUA LIN, None.

MO0292

Acromegaly induces bone microarchitectural alteration as assessed by TBS (Trabecular Bone Score) at lumbar spine without impacting bone mineral density (BMD). <u>Giuseppe Guglielmi</u>[1], <u>Claudia Battista</u>[2], <u>Francesca di Chio</u>[1], <u>Antonio Salcuni</u>[2], <u>Michelangelo Nasuto</u>[1], <u>Renaud Winzenrieth</u>[3], <u>Alfredo Scillitani</u>*[4]. [1]Department of Radiology, University of Foggia, Italy, [2]Department of Endocrinology, Scientific Institute Hospital "Casa Sollievo della Sofferenza", Italy, [3]Department of Clinical Research, Medimaps Group, Switzerland, [4]Casa Sollievo Della Sofferenza Scientific Institute, Italy

Subjects with acromegaly (AG) were more susceptible to sustained fractures. It has been reported in the literature that subjects suffering from AG have a high prevalence of vertebral fractures even for subjects with normal BMD. Sparse information exists on the effect of AG on bone microarchitecture and no at axial sites. The aim of our study was to examine bone quality and quantity assessed by TBS (Trabecular Bone Score) and BMD in subject with AG at lumbar spine.

We present a cross-sectional study on 46 subjects with AG (26 women and 20 men) with mean age and BMI of 54.9 ± 11.5 years and 29.3 ± 4.2 Kg/m^2 respectively. Among them, 41% were in active phase of the disease, 74% suffered from hypogonadism (Hy) and 22% sustained at least a fracture (Fx). BMD and TBS were evaluated at PA Spine (L1-L4) using an iDxa DXA device (GE-Lunar) and TBS iNsight® (v2.1, Med-Imaps, France).

BMD and TBS were correlated together (p<0.0001), with 49% of TBS explained by spine BMD. Subjects with Hy have a significant lower BMD and TBS (p<0,002). Those with fracture have a lower TBS (p=0.02) whereas no difference has been observed on spine BMD (p>0.5). TBS was associated with the presence of the fracture with an odd-ratio per one SD decrease of 2.64 [1.1-6.3] and an area under the ROC curve of 0,71 [0.56-0,84]. BMD, Age, presence of Hy, or duration of Hy were not associated with the presence of fractures. Compared to normative TBS values, AG subjects have a significant TBS impairment (-6%, p<0,001). Those with Hy or the presence of the fractures have a lower TBS values when compared to normative values: -8% (p<0,001) and -13% (p<0,02) respectively.

The present study is the first to report data on changes in spine BMD and TBS at lumbar spine in Subject with acromegaly. AG induces bone microarchitectural texture impairment at lumbar spine. Presence of hypogonadism or fractures worsens such ann impairment. As previously obtained, TBS seems to be more sensitive to bone modification than BMD.

Disclosures: Alfredo Scillitani, None.

MO0293

Association Between the Risk of Distal Ulnar Fracture Complicated with Low-Energy Distal Radial Fracture among Postmenopausal Women and Bone Mineral Density of the Forearm Shaft. <u>Kayoko Furukawa</u>*[1], <u>Akinori Sakai</u>[2]. [1], Japan, [2]University of Occupational & Environmental Health, Japan

Background: The presence or absence of distal ulnar fracture as a complication with distal radial fracture greatly influences the surgical procedure employed and the patient's postoperative course. In the present study, we aimed to compare the bone mineral density (BMD) following low-energy distal radial fracture among Japanese postmenopausal women aged >65 years who also had distal ulnar fracture with those women who did not.

Method: In total, 78 postmenopausal women aged >65 years who experienced distal radial fractures after a fall were enrolled in this study. Of these patients, 10 had distal ulnar fractures as a complication with distal radial fractures (ulnar fracture group), whereas the remaining did not (non-ulnar fracture group). Along with the patient characteristics, we compared the BMD at 6 sites—lumbar, proximal hip, entire forearm, ultra distal forearm, mid distal forearm, and forearm shaft—between the groups. No significant differences in age, body height, and weight were noted between the 2 groups. The ulnar fracture group had a significantly greater body mass index than the non-ulnar fracture group.

Result: The BMDs of the proximal hip and the entire forearm were significantly lower in the ulnar fracture group than in the non-ulnar group. Stepwise regression analysis indicated that the BMD of the forearm shaft was the most significant factor associated with ulnar distal fracture; moreover, MID, UD, entire forearm BMD, and lumbar BMD were significantly associated with ulnar distal fracture complicated with distal radial fracture, in decreasing order.

Disclosures: Kayoko Furukawa, None.

MO0294

Normative Spine TBS Data For Latin American Women. <u>Bruno Camargos</u>*[1], <u>Luis Jaime Elizondo-Alanís</u>[2], <u>Ben-Hur Albergaria</u>[3], <u>Patricia Clark</u>[4], <u>Carlos Eduardo Magro</u>[5], <u>Fidencio Cons-Molina</u>[6], <u>Jorge Morales-Torres</u>[7], <u>Renaud Winzenrieth</u>[8]. [1]Hospital Mater Dei, Brazil, [2]Centro de Investigación Clínica, Mexico, [3]CEDOES, Brazil, [4]Laboratorios Clinicos De Puebla, Mexico, [5]Clinica Densito, Brazil, [6]Centro de Investigacion en Artritis y Osteoporosis, Mexico, [7]Hospital Aranda de la Parra, Mexico, [8]Med-imaps, Hôpital X. Arnozan, PTIB, Pessac, France, France

Introduction: Trabecular Bone Score (TBS, Med-Imaps, France) is an index of bone microarchitecture texture extracted from postero-anterior spine DXA. In this cross-sectional analysis from six facilities in Mexico and Brazil, we have investigated the age related changes of the lumbar vertebrae micro-architecture assessed by TBS in a cohort of Latin American women. METHODS: Subjects in the study were Mexican and Brazilian women (LAVOS cohort, Mexican and Brazilian centers) aged 30 and older with a BMD Z-score at spine L1-L4 within $\pm$ 2SD. LAVOS MEXICO included patients from Puebla Mexico and the data source for this TBS values were from Mexicali Baja California, Ciudad Obregon Sonora and Leon, Guanajuato. LAVOS BRAZIL included patients from Vitoria. Individuals were excluded if they had fractures or were on any osteoporosis treatment and/or had any illness that would be expected to impact bone metabolism. All data have been obtained from Prodigy DXA devices (GE-Lunar, Madison, WI, USA). Cross-calibrations between the six centers were performed for TBS and BMD. BMD and TBS (TBS insight v2.1) were evaluated at spine L1-L4 but also for all possible vertebrae combinations.RESULTS: A database of 941 women ages 30 to 90 years was created. TBS and BMD values at L1-L4 were not correlated with BMI r=0.02 and r=0.1 respectively, both non significant. TBS and BMD values obtained for all lumbar vertebral combinations decreased significantly with age (see figure below). There was a linear decline of 20% (-3.2 SD) in the micro-architectural texture at L1-L4 between 45 and 90 years of age whereas a decline of 27% (-3.3 SD) was observed in BMD. Before 45 years old, TBS is slightly increasing (+0.95% between 30 and 45 years). Similar results were obtained for other ROIs of the lumbar spine.CONCLUSION: The decrease seen in lumbar TBS reflects age-related micro-architectural texture changes at spine. These findings suggest that TBS normative data can be used in clinical practice to assess bone micro-architectural texture deterioration over time and improve patient management.
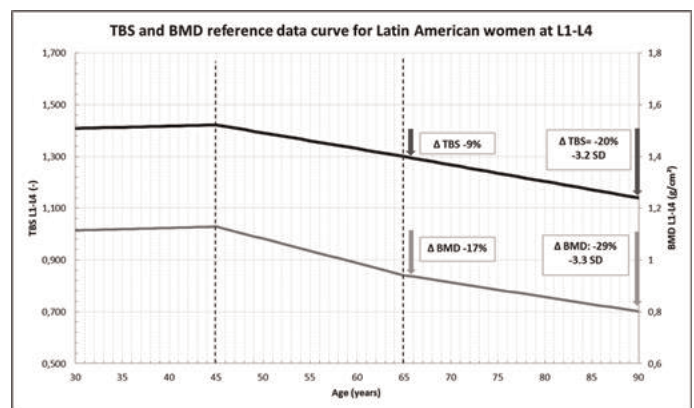
TBS LATAM CURVE ASBMR 2014

Disclosures: Bruno Camargos, None.

MO0295

Bone structure assessed by TBS reflects trabecular microarchitecture of transiliac bone biopsies in idiopathic osteoporotic females with fragility fractures. <u>Christian Muschitz</u>*[1], <u>Heinrich Resch</u>[2], <u>Roland Kocijan</u>[3], <u>Olivier Lamy</u>[4], <u>Angela Trubrich</u>[5], <u>Dieter Pahr</u>[6], <u>Wolfgang Schima</u>[7], <u>Fritz Lomoschitz</u>[7], <u>Stylianos Kapiotis</u>[8], <u>Didier Hans</u>[9]. [1]St. Vincent's Hospital, Austria, [2]Medical University Vienna, Austria, [3]St. Vincent Hospital Vienna, Austria, [4]University Hospital, Switzerland, [5]BHS, Austria, [6]Institute of Lightweight Design & Structural Biomechanics, Vienna University of Technology, Austria, [7]Department of Diagnostic & Interventional Radiology, St. Vincent Hospital Vienna, Austria, [8]Labcon – Medical Laboratories Ltd., St. Vincent Group, Austria, [9]Lausanne University Hospital, Switzerland

Purpose:Trabecular Bone Score (TBS) is a novel grey-scale textural analysis used in estimating trabecular structure from the lumbar spine DXA. It has been shown that TBS correlates well with direct measures of bone microarchitecture independent of BMD in human cadaver vertebrae.

Methods:The aim of this cross-sectional study was to evaluate correlations between TBS of the spine and microarchitectural parameters of transiliac bone biopsies in females with idiopathic osteoporosis and fragility fractures. As a result, the

clinical impact and precision of TBS in bone quality assessment was evaluated. The following structural parameters of transiliac bone biopsies from 12 consecutive treatment-naïve and otherwise healthy females (mean 47; range 34 to 69.5 years) with recent fragility fractures were analyzed by a microtomographic imaging system: Bone volume/total volume (BV/TV), trabecular thickness (TbTh), trabecular separation (TbSp), number of trabeculi (TbN), connectivity density (ConnD) and structure model index (SMI). Spine BMD was assessed by DXA and site-matched spine TBS parameters were extracted from the DXA image using the TBS iNsight calculator.

Results:Laboratory tests did not reveal any evidence of metabolic disorder in any of our subjects. There was a correlation between TBS and the following 3D parameters: TBS and BV/TV: r=0.70 (p<0.01), TBS and TbSp: r=-0.70 (p<0.01), TBS and TbN: r=0.58 (p<0.05), and TBS and SMI: r=-0.75 (p<0.01). Even after adjustment for spine BMD, the correlation between TBS and BV/TV, TbN, TbSp and SMI remained significant. Using the stepwise regression approach the best models combining density and microarchitecture predicted 97% of the TBS parameters.

Conclusion:The association between TBS and microarchitectural parameters indicated that low TBS showed a marked deteriorated microarchitecture related to low TbN, high TbSp, altered SMI as well as low BV/TV. Hence, TBS is a feasible non-invasive surrogate technique for the assessment of bone mircorarchitecture texture from DXA scans in clinical routine that would not satisfy the definition of osteoporosis when solely based on T-scores or BMD values.

Disclosures: Christian Muschitz, None.

MO0296

Characterization of the osteocyte lacuno-canalicular network using ptychographic X-ray nanotomography. Cameron Kewish[1], Antonia Ciani*[1], Manuel Guizar-Sicairos[2], Ana Diaz[2], Mirko Holler[2], Stephane Pallu[3], Zahra Achiou[4], Rachid Jennane[5], Hechmi Toumi[5], Eric Lespessailles[6], Claude Laurent Benhamou[7], Jean-Pierre Samama[1]. [1]Synchrotron Soleil, France, [2]Paul Scherrer Institut, Switzerland, [3]EA 4708 - I3MTO Orléans, France, [4]Univ Orléans, I3MTO, Ea 4708, France, [5]Univ Orléans, I3MTO, Ea 4708, France, [6]Centre Hospitalier Regional Orleans, France, [7]CHR ORLEANS, France

Osteocytes are the last differentiated state of the osteoblast lineage, the longest living cells in the skeleton, and they play various functions including a crucial role in the mechanotransduction pathway. The osteocyte network, a system of extra cellular spaces, including lacunae and lacuno-canalicular network (LCN) is implicated in perilacunar mineralization and localized changes in bone strength. Thus, the geometrical three-dimensional (3D) characterization of this network might be of crucial importance in understanding bone pathologies. [1]

The recent development of ptychographic X-ray nanotomography exploits the penetrating power of hard X-rays and the high resolution of coherent lensless imaging to produce quantitative 3D images of the electron density within objects. [2] This has provided biomedical science with a new tool for characterization of the LCN with a resolution of tens of nanometers, for bone specimens currently up to 100 micrometers in diameter. We present here the application of ptychographic nanotomography for the morphometric characterization of the LCN, and nano-densitometry within the vicinity of the osteocyte lacunae. Tibial diaphysis cortical bone samples were taken from glucocorticoid-induced osteopenic, and control rats.

Results from this study can offer critical information on how osteoporosis and current drug treatments alter a measure of matrix quality and, ultimately, may provide insight into why drug treatments have shown variable clinical effectiveness across different studies. The shape of the lacunae and morphological parameters of the LCN have been extracted from 3D images using a newly developed data processing method. Network changes are discussed in connection with the biological impact.

Disclosures: Antonia Ciani, None.

MO0297

Cushing Disease: Gain in Bone Mineral Density and also Bone texture assessed by Trabecular Bone Score after cure of Cushing Disease. Eugenie Koumakis*[1], Renaud Winzenrieth[2], Laurence Guignat[3], Catherine Cormier[4]. [1]Hôpital Cochin, France, [2]Med-imaps, Hôpital X. Arnozan, PTIB, Pessac, France, France, [3]Service d'Endocrinologie, Hôpital Cochin, France, [4]AP-HP Groupe Hospitalier Cochin, France

Cushing disease (CD) is considered as a true model of a glucocorticoïds (GCs) effects on bone metabolism because of the minimization of confounding factors. Hypercortisolism frequently induces bone loss which is more pronounced at the lumbar spine than at the femoral neck due to a higher content in trabecular bone. This bone loss results in osteoporosis and leads to an increase in fracture risk. Several studies have shown bone mass restoration in patients with CD after treatment. The aim of our study was to examine treatment effects on bone mineral density (BMD) and on bone texture assessed by TBS in subjects with CD.

Patients and methods. We present a longitudinal study on 31 subjects (20 women and 11 men) with CD with mean age and BMI of 36.8 ± 12.4 years and 27.8 ± 4.0 Kg/m², respectively. Mean 24h urinary cortisol before treatment was $589 \pm 1301 \mu g/24h$. All subjects were completely cured, i.e. 24h urinary cortisol normalization after treatment. Cure of CD was obtained following transsphenoidal surgery (TSS) only

(n=17), TSS in combination with medical treatment (n=3), TSS and bilateral surrenalectomy (n=8), bilateral surrenalectomy (n=1), medical treatment only (n=1). BMD and TBS were evaluated at AP Spine (L1-L4) with DXA prodigy (GE-Lunar), QDR 4500 (Hologic), and TBS iNsight® (Med-Imaps) before and after treatment. Both DXA were cross-calibrated using a custom-made phantom. Linear regression was used to evaluate TBS and BMD modifications over time. Results were normalized at 1 and 2 years after treatment. BMD and TBS gains were expressed in % in comparison to baseline.

Results. Absolute TBS and BMD gains were significant (p<0.0001, and p<0.01, respectively). Normalized gains of TBS and BMD in % are presented figure 1 (mean + SEM). After treatment, BMD and TBS increased by 3.1 and 6.9% respectively after 1 year, and by 6.2 and 13.8% after 2 years. Before treatment, BMD and TBS were not correlated (p=0.43). After treatment, this correlation remained non significant (p=0.53). TBS gain was correlated with BMI and weight before treatment: r=0.46 (p=0.009) and r=0.44 (p=0.01).

Conclusion. The absence of correlation between TBS and BMD and the more significant improvement of microarchitecture assessed by TBS than BMD suggest qualitative rather than quantitative bone alterations in hypercorticism-induced osteoporosis. Bone microarchitecture assessment could therefore be a useful and supplementary tool for fracture risk evaluation in GC induced bone loss.
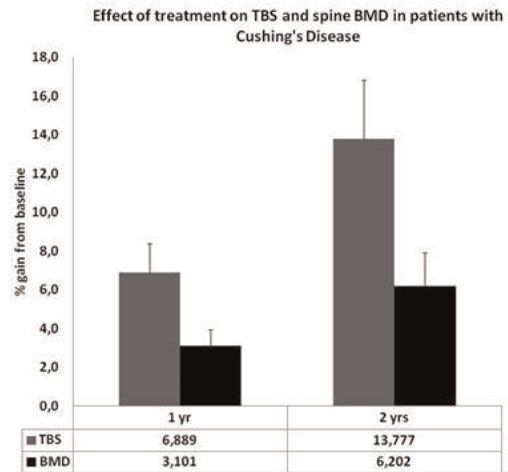

Figure 1

Disclosures: Eugenie Koumakis, None.

MO0298

Diagnosis of vertebral fractures by the EOS X-ray imaging system. Karine Briot*[1], Jacques Fechtenbaum[2], Adrien Etcheto[3], Sami Kolta[2], Antoine Feydy[3], Christian Roux[4]. [1]Paris Descartes University, Cochin hospital, Rheumatology Hospital, France, [2]Centre D'Evaluation, Des Maladies Osseuses, France, [3]Paris Descartes University, Cochin Hospital, France, [4]Hospital Cochin, France

Vertebral fractures (VF) are independent risk factors for both vertebral and peripheral fractures. However, for both cost and radiation concern, spine radiographs cannot be done neither as a screening method for at risk patients, nor as a follow-up tool. Vertebral fracture assessment (VFA) is a reliable technique with low radiation (3 µSv) to assess vertebral deformities but with a poor visualization of the upper thoracic spine. EOS® X-ray imaging system allows the acquisition of biplane images while the patient is in an upright weight-bearing position with a low radiation dose (80µSv).The objective of the study was to evaluate the sensitivity and specificity of EOS radiographs compared to VFA for the diagnosis of VF.

We conducted a cross sectional study in subjects aged above 50 years with indication for spine radiograph (risk factors for postmenopausal osteoporosis, height loss,..). EOS radiographs and VFA of the spine from T4 to L4 using DXA were performed the same day. EOS images were independently compared with VFA scans by two rheumatologists, for the diagnosis of VF. We assessed the sensitivity, specificity, predictive values and the interobserver precision of EOS compared to VFA images.Two hundred patients (mean age of 66.2 years were included; 62.5% were osteoporotic (T≤-2.5 at at least one site) and 38% has scoliosis with a mean BMI of 23.7 (3.8) kg/m² . At the vertebral level (n=5200), the percentage of unreadable vertebrae was 2.4% and 3.6% using EOS radiographs and VFA, respectively (p=0.0007). Unreadable vertebrae were located at T4, T5, T6. The legibility of spine was significantly affected by scoliosis (OR=2.845, p<0.0001,for EOS radiographs and OR= 1.85, p= 0.0041, for VFA). Using VFA, 66 patients (33.0%) had at least one VF whereas 69 patients (34.5%) had at least one VF using EOS radiographs. At the patient level, sensitivity, specificity and VPN for the diagnosis of VF of EOS radiographs were 0.797, 0.916 and 0.895, respectively. At the vertebral level, sensitivity, specificity and VPN were 0.657, 0.994 and 0.895, respectively. Concordance between both observers was very good for EOS radiographs (kappa-score=0.89), higher than for VFA (κ= 0.67).

This study shows that EOS X-rays have a good diagnostic value for the diagnosis of VF with a better legibility of upper thoracic spine and a higher concordance between readers compared to VFA, suggesting that this method could improve screening and follow-up of patients.

Disclosures: Karine Briot, None.

MO0299

Effects of Glucocorticoid Treatment on Bone BMD and TBS in Men. <u>Edward Leib</u>*[1], <u>Renaud Winzenrieth</u>[2]. [1]University of Vermont, USA, [2]Center of Bone diseases, Lausanne University Hospital, Lausanne, Switzerland, France

Aim: The aim of the study is to evaluate whether microarchitectural texture changes as measured by Trabecular Bone Score (TBS) can identify those male patients exposed to glucocorticoid (GC) therapy who are more likely to fracture.

Material and Methods: This mono-centric study involves US white men aged 45 and older who at the time of bone density testing gave a history of present or past use of GC. They were compared to a group of control subjects. Control subject exclusions included one or more historical fractures, or a past or present treatment or illness influencing bone metabolism. Subjects included in the GC treated group received prednisone $\geq$ 5mg/day for $\geq$3months or equivalent treatment. BMD was assessed at the lumbar spine (L1-L4) using a Prodigy device (GE-Lunar, Madison, USA). TBS was calculated at L1-L4 using the TBS iNsight® (Medimaps, France). Clinical data, presence of osteoporotic fracture (OPF), GC treatment and common clinical risk factors (CRFs) were documented.

Results: From the database, 73 men treated with GC and 90 control men were matched for age and BMI (p>0.4). Characteristics of the patients are shown in table. No correlation was observed when comparing spine TBS, spine BMD and BMI in either treated or cont. groups (-0.16 $\leq$ r $\leq$ 0.23). When compared to normal values, no TBS difference was observed in the control group whereas the GC group had a significantly lower TBS value (see table). GC subjects had a lower TBS compared to healthy subjects (ΔTBS =-4.1%, p<0.02) whereas no significant difference was observed for BMD (p>0.07). The negative effects of GCs was even more marked when fracture status was taken into account. We observed a TBS decrease of 9.3% in GC-patients with fracture (p<0.01) compared to control group whereas no differences was observed for BMD (p>0.5).

Conclusion: GC induces a microstructural texture impairment whereas no effect was observed on BMD. This result is consistent with previous TBS studies on GC treatment in women. Presence of an osteoporotic fracture worsens the GC effects on microarchitectural texture. TBS outperformed BMD in its ability to identify a population at risk for fracture and therefore should be a reliable tool for management of glucocorticoid-treated men.

Table: Characteristics of patients and controls

	GC-treated group	Control group
No. Of subjects	73	90
No. Of subjects with OP fracture	10 (13.7%)	0%
Age (years)	62.6±10.7	63.4±9.9
Height (cm)	173.6±6.1	174.8±6.5
Weight (kg)	80.1±12.7	81.7±12.0
BMI (kg/m²)	26.5±3.6	26.8±4.1
L1L4 BMD (g/cm²)	1.134±0.183	1.181±0.125
L1L4 TBS	1.244±0.146	1.298±0.124
L1L4 TBS reference value	1.316±0.108	1.313±0.108
L1L4 TBS comparison with reference values	*p<0.001*	*p=0.3*
Past use of GC	19%	0%
Renal disease	18%	0%
Rheum. Arthritis	20%	0%
Previous Fracture	14%	0%

Leib_TBS_Steroid_Table

Disclosures: Edward Leib, None.

MO0300

Evaluation of Patients' Intervention Following Osteoporosis Screenings at Health Fairs. <u>Frances Tepolt</u>*[1], <u>Susan Hassenbein</u>[2], <u>Edward Fox</u>[3]. [1]Penn State Hershey Bone & Joint Institute, USA, [2]Penn State Bone & Joint Institute, USA, [3]Pennsylvania State Hershey Medical Center, USA

Introduction: Osteoporosis, a systemic skeletal disease resulting in the deterioration of the micro architecture of bone tissue, affects 15-20 million people in the U.S. Screening methods, although improving, remain inadequate, leaving the disease underdiagnosed and undertreated. The purpose of this study is to determine the effectiveness of calcaneal quantitative ultrasound (US) scanning in prompting osteoporosis evaluation with a health care provider. Similar studies investigating the utility of heel US in the community setting to promote bone health are lacking in currently published research.

Materials and Methods: Male and female subjects 18 years of age or older presenting at health fairs/ community events May 2012 - October 2013 were asked to participate in the study, providing consent for US scanning of the calcaneus and future telephone contact. Interested subjects with abnormal scan results (T-score less than or equal to -1) were contacted via telephone at least three months post-screening and asked a series of questions regarding their health and follow-up with a care provider.

Results: 67 subjects provided consent for participation and qualified for the study (T-score by heel US less than or equal to -1). 48/67 (71.6%) had phone screenings completed, and, of those, 42/48 (87.5%) were female and 6/48 (12.5%) male, mean age 53.9 years (range 29-84 years). 23/48 (47.9%) had follow-up with a health care professional. The average T-score of those with follow-up (-1.7 +/- 0.4) was significantly lower (p=0.03) compared to those without follow-up (-1.4 +/- 0.3). There was no significant difference in age. Of those who sought follow-up, 21/23 (91.3%) did so with a primary care physician, and 19/23 (82.6%) received recommendation for further evaluation/treatment. Recommendations included calcium/Vit D supplementation (12/19, 63.2%), DEXA scan (12/19, 63.2%), laboratory testing (2/19, 10.5%), or pharmacotherapy (2/19, 10.5%). None of the patients contacted for follow-up (0/48) suffered a fracture between time of heel US and phone screening.

Conclusions: Osteoporosis screening with heel US effectively prompts patients at high risk for osteoporosis to seek further osteoporosis workup from a health care professional in near half (47.9%) of cases and, of those, further evaluation/treatment in the vast majority (82.6%). Heel US screenings are therefore highly effective in improving the diagnosis and treatment of osteoporosis in the community.

Disclosures: Frances Tepolt, None.

MO0301

HR-pQCT, Finite Element Analysis, and Machine Learning with Support Vector Machines Improved Classification of Postmenopausal Women with Fragility Fractures. <u>Kyle Nishiyama</u>*[1], <u>Emily Stein</u>[2], <u>Stephanie Sutter</u>[3], <u>Donald McMahon</u>[2], <u>Edward Guo</u>[4], <u>Elizabeth Shane</u>[2]. [1]Columbia University, USA, [2]Columbia University College of Physicians & Surgeons, USA, [3]Columbia University Medical Center, USA, [4]Columbia University, USA

Measurement of areal bone mineral density (aBMD) by dual-energy x-ray absorptiometry (DXA) is the current standard for diagnosis of postmenopausal osteoporosis. However, the majority of fractures occur in women who do not have osteoporosis by DXA criteria. Fracture is a complex, multifactorial event affected by many factors not measured by DXA, such as age, race, height, weight, falls, as well as bone structure and strength. The interaction among these factors is not well understood. We hypothesized that high-resolution peripheral quantitative computed tomography (HR-pQCT) combined with DXA and demographic data would improve classification of women with and without prior fragility fracture. To account for the complex interactions among measurements, we used support vector machines (SVM), in which models are trained on a subset of data and tested on the remaining data. We studied 101 women with previous low-trauma fracture (age 68 $\pm$ 8) and 101 fracture-free controls (age 68 $\pm$ 7). Demographic data and historical information were obtained by questionnaire. We measured aBMD by DXA at the spine, total hip, femoral neck, 1/3 and ultradistal radius. We also measured bone microarchitecture and volumetric BMD by HR-pQCT and estimated bone strength by finite element (FE) analysis at the radius and tibia. We compared a logistic regression model based on DXA parameters with five different models using SVM's and 10-fold cross validation. These included: 1) demographic data only, 2) DXA only, 3) HR-pQCT and FE only, 4) demographic and DXA data, and 5) all parameters. We also classified participants with wrist fractures only (N=40) and spine fractures only (N=35) compared to controls using all parameters. Sensitivity, specificity, accuracy, kappa, and area under the ROC curve (AUC) are presented (Table). The highest performance was achieved using all parameters and SVM models (AUC=0.71). The lowest was achieved with DXA only and logistic regression (AUC=0.56). DXA only slightly outperformed the model based on demographics alone. HR-pQCT alone outperformed both of these models. Performance was high for forearm fractures only, using all parameters (AUC=0.76). We conclude that SVM models that integrate information from DXA, demographics, HR-pQCT and FE perform better at discriminating fracture. Such models may be used as a basis to identify critical parameters for assessing fracture risk and to predict individuals at increased risk of fracture in future prospective studies.

Model	AUC	Accuracy (%)	Sensitivity (%)	Specificity (%)	PPV (%)	NPV (%)	Kappa
Logistic: DXA only	0.560	55.4	55.6	55.3	54.5	56.4	0.11
SVM: Demographics	0.579	57.9	58.2	57.7	56.4	59.4	0.16
SVM: DXA	0.609	60.9	59.2	63.4	70.3	51.5	0.22
SVM: demographics and DXA	0.649	64.9	63.2	67.0	71.3	58.4	0.29
SVM: HR-pQCT	0.658	65.8	64.5	67.4	70.3	61.4	0.32
SVM: all parameters	0.708	70.8	69.1	72.8	75.2	66.3	0.42
SVM: forearm fx only	0.757	77.1	64.1	84.8	71.4	80.0	0.5
SVM: spine fx only	0.647	71.3	59.1	75.4	44.8	84.5	0.31

Results classifying women with and without fractures using machine learning.

Disclosures: Kyle Nishiyama, None.

MO0302

Multimodality Radiographic Characteristics and Complications of Atypical Femoral Fractures: the Ontario AFF Cohort. R Bleakney*[1], Linda Probyn[2], Jonathan Adachi[3], Leon Lenchik[4], Aliya Khan[5], Earl Bogoch[6], Robert Josse[7], Catherine Lang[8], Angela M. Cheung[9]. [1]Mount Sinai Hospital, Canada, [2]University of Toronto, Sunnybrook HSC, Dept. of Medical Imaging, Canada, [3]St. Joseph's Hospital, Canada, [4]Wake Forest University, USA, [5]McMaster University, Canada, [6]St. Michael's Hospital, Canada, [7]St. Michael's Hospital, University of Toronto, Canada, [8]University of Toronto, Canada, [9]University Health Network-University of Toronto, Canada

Background: Atypical femoral fractures (AFFs) are increasingly recognized in patients on long term bisphosphonate therapy. There are many complications of AFFs including delayed healing, progression from incomplete to complete fractures, and fracture of the contralateral femur. Hardware fixation may be performed prophylactically or for management of complete AFFs and hardware complications are important to recognize.

Objective: To demonstrate characteristic radiographic findings using multimodality imaging (SE-femur, conventional radiographs, CT femur, MRI and bone scintigraphy scans) so as to aid clinicians with the diagnosis of AFFs and their complications.

Results: Included are images showing delayed healing, progression of incomplete to complete fractures, bilateral fractures, surgical management with complication and other cases. (See figure)Conclusion: AFFs and their complications have characteristic radiographic findings. Radiologists and clinicians should familiarize themselves with these findings so as to better diagnose AFFs and their complications.
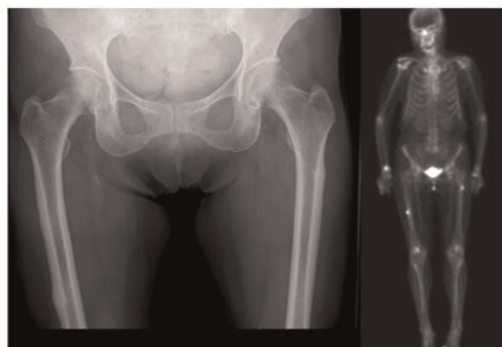
Bilateral incomplete AFFs on plain film and bone scan.
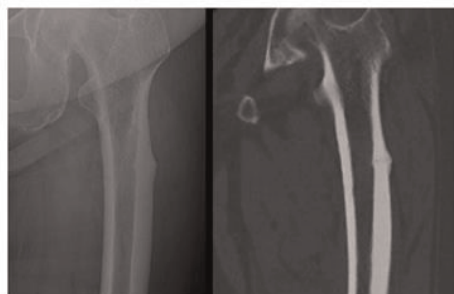
Incomplete AFF with focal lateral cortical thickening on plain film. CT demonstrates a focal lucent cleft / fracture line

page 1 image

Complete AFF treated with lateral compression plate, with subsequently failure and ultimately treated with a Gamma nail.
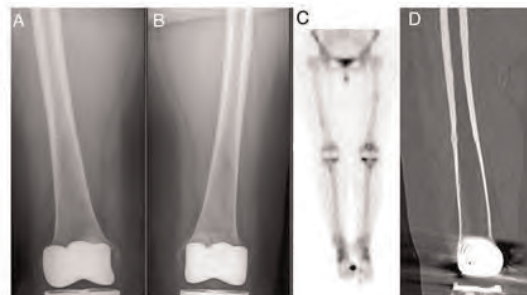
Subtle incomplete AFFs on plain film (A and B), areas of increased uptake on bone scan (C) and focal lucent cleft identified with CT (D)

page 2 image
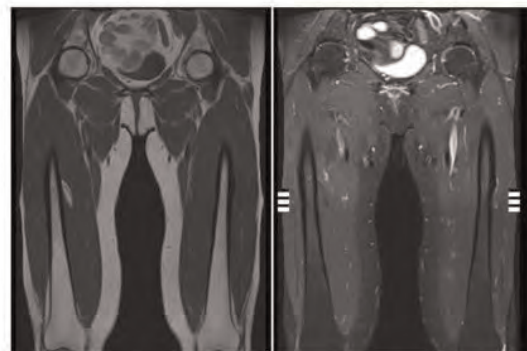
Bilateral incomplete AFFs on MRI showing focal cortical thickening and periosteal / surface oedema.

page 3 image

Disclosures: R Bleakney, None.

MO0303

Normative Data of TBS for Healthy Postmenopausal African American Women. John Aloia[1], Mageda Mikhail[2], Gianina Usera*[1], Ruban Dhaliwal[3], Shah Islam[4]. [1]Winthrop University Hospital, USA, [2]Winthrop University Hospital, USA, [3]SUNY Upstate Medical University, USA, [4]Winthrop University Hospital, USA

Purpose: African American women have fewer incidences of fractures than do their Caucasian counterparts, for any given bone density. Studies conducted on TBS have used data from Caucasian women. The purpose of this study is to provide a reference range for postmenopausal African American women.

Methods: Baseline data of 418 healthy postmenopausal African American women was obtained from two clinical trials, one previously conducted and one ongoing, conducted at the Bone Mineral Research Center at Winthrop University Hospital. Exclusion criteria included bone disease or any co-morbidity that impacts bone metabolism. Health status was determined through medical history, physical exam, and screening laboratory tests. Spine BMD was obtained with DXA Hologic (model Discovery A) scans. TBS was calculated for L1-L4 as those used for BMD using TBS iNsight software by Med-Imaps (Version 2.0). All calculations were performed using SAS 9.3. Results were considered significant if $p < 0.05$.

Results: The correlation coefficient was 0.40 for the relationship between spine BMD and TBS (L1-L4) (p-value<0.0001). Mean(SD) age of the subjects was 66(7) years. Mean(SD) TBS was 1.304(0.101), and mean(SD) spine BMD was 1.009(0.159). Significant correlations were found between TBS and age (p-value<0.003), as well as BMI (p-value<0.0001). There were no significant correlations found between TBS

and bone-specific alkaline phosphatase, parathyroid hormone, C-terminal telopeptide, 24-hr urine calcium, and serum 25(OH) D.

Conclusion: TBS, which is a measure of the micro architecture of bone, may indicate structural differences not apparent from BMD. Here we provide a reference range of TBS for healthy postmenopausal African American women.

Selected model R-Square: 0.34

Variable	Model Estimate(SE)	95%CI of estimates	p-value
Intercept	1.323(0.049)	1.227, 1.419	<.0001
Age	-0.002(0.001)	-0.003, -0.001	0.002
BMI	-0.008(0.001)	-0.009, -0.006	<.0001
BMD (Spine)	0.334(0.027)	0.281, 0.387	<.0001

Table 1

Fig1. Relationship between Age and Spine Trabecular Bone Score (TBS)

Spearman rho= -0.14, p-value=0.003

Regression Equation
Spine TBS=1.4359629179 + -0.002011442*AGE

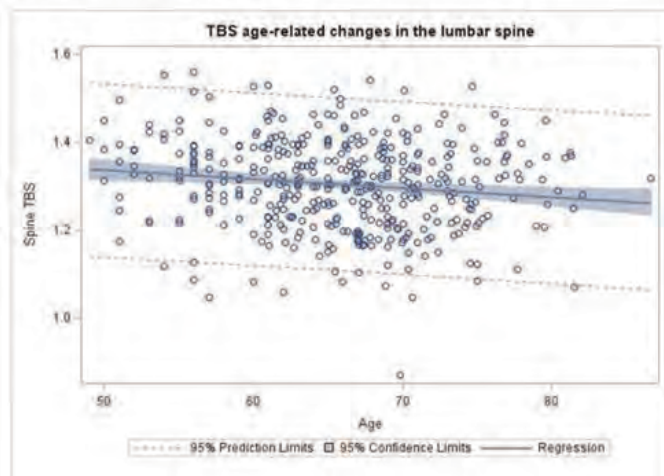Figure 1

Fig3. Relationship between Spine BMD L1L4 and Spine Trabecular Bone Score (TBS)
Spearman rho= 0.40, p-value=<.0001

Regression Equation
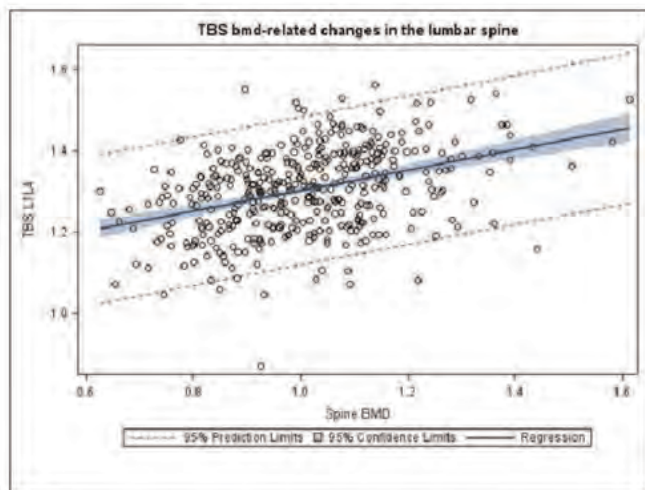Spine TBS=1.0501437838 + 0.2511936066*SpineBMD

Figure 3

Disclosures: Gianina Usera, None.

MO0304

Osteoporosis assessment at hip with Bindex®. Janne Karjalainen*[1], Ossi Riekkinen[2], Heikki Kroger[3]. [1]Bone Index Finland Ltd., Finland, [2]Bone Index Finland, Ltd., Finland, [3]Kuopio University Hospital, Finland

Currently, majority of the osteoporotic patients are not diagnosed (1). Efficient osteoporosis diagnostics would require novel approaches at primary healthcare. An ultrasound based device (Bindex®) has been recently introduced for osteoporosis screening and diagnostics. Bindex measures cortical thickness and determines parameter called density index (DI). Thresholds for DI in osteoporosis assessment have been determined in Finnish Caucasian population ($n= 448$) along the International Society of Clinical Densitometry (ISCD) guidelines (2,3). In this study, these thresholds are tested in Finnish caucasian female population.

A total of 100 females were recruited from private primary healthcare centers (Suomen Terveystalo Ltd., Finland) to the study (age 61.5 ± 8.1 years). Subjects were measured with dual energy x-ray absorptiometry (DXA) to determine bone mineral density (BMD) at proximal femur . Further, the cortical thickness was measured at three locations (distal radius, distal and proximal tibia) with Bindex. Subjects were diagnosed with osteoporosis when T-score at femoral neck or total proximal femur was below -2.5. Density index was calculated either by using measurement at one location (DI_1, proximal tibia) or all three locations (DI_3). By using the diagnostic thresholds, subjects were classified as healthy, osteoporotic or in need of DXA examination to verify diagnosis.

An average of 27% of the patients would require additional axial DXA examination when using thresholds and triage approach with DI_1 and DI_3. Sensitivity in osteoporosis diagnostics was 71.4% and 85.7% for DI_1 and DI_3, respectively. Specificity was 90.3% and 89.1% for DI_1 and DI_3, respectively. Osteoporosis at the hip was diagnosed in 7 and osteopenia in 40 subjects by DXA.

In this study, preliminary findings suggest good performance of previously determined thresholds in the current population. More data is needed to verify findings, especially more osteoporotic patients need to be included in the study.

[1] Nguyen, Med J Aust., 2004
[2] Karjalainen JP, ASBMR, Baltimore, 2013
[3] Hans, J Clin Densitom., 2008

MO0305

The better prediction of vertebral fractures using Trabecular Bone Score and FRAX than Bone Mineral Density in postmenopausal diabetic women. Yoon-Sok Chung*[1], So Young Ock[2], Yong Jun Choi[2]. [1]Ajou University School of Medicine, South Korea, [2]Ajou University School of Medicine, South Korea

Background: Increased fracture risk in diabetes is related to bone quality rather than bone mineral density (BMD). The trabecular bone score (TBS) derived from the dual x-ray absorptiometry (DXA) image is proposed as an index of bone microarchitecture that associated with bone quality. The aim of this study is to investigate whether TBS improves the prediction of radiographic vertebral fractures compared to BMD or FRAX alone.

Methods: Total 118 Korean postmenopausal diabetic women were enrolled. Lateral plain radiographs of the thoracolumbar spine, and lumbar vertebral BMD (GE Lunar) were obtained. The FRAX® probability was computed using the algorithm available online at http://www.shef.ac.uk/FRAX (South Korea version). We classified the subjects with and without radiographic vertebral fracture. TBS was obtained by TBS iNsight Software program with BMD DXA images (GE Lunar). We compared the performance of TBS, BMD, FRAX and the combination with TBS and FRAX, by using receiver operator characteristics (ROC) analysis with area under the curves (AUCs).

Results: Among the subjects, 55 women (46.6%) had vertebral fractures and 63 women (52.5%) not. The TBS was lower in subjects with VFs (1.28 ± 0.11) than without VF (1.33 ± 0.10), (p=0.10). However, there was no difference in BMD between the subjects with VFs (1.00 ± 0.18) and without VFs (1.03 ± 0.14), (p=0.241). For radiographic vertebral fractures, TBS and lumbar spine (LS) BMD had similar predictive power (AUC: 0.381 versus 0.407) but the combination of TBS and lumbar spine BMD increased the performance over LS BMD alone (AUC: 0.619). FRAX score for major osteoporotic fracture showed good predictive power (AUC: 0.642). Furthermore, the prediction improved with the combination of TBS and FRAX score (AUC: 0.667).

Conclusion: These results suggest that combination of TBS with FRAX or BMD improves the performance of LS BMD or FRAX alone for the prediction of radiographic vertebral fractures in postmenopausal diabetic women.

MO0306

A Trans-ethnic Genome-wide Association Study Identifies Gender Specific Loci Influencing Pediatric BMD and BMC at the Distal Radius. Alessandra Chesi*[1], Jonathan Mitchell[2], Heidi Kalkwarf[3], Jonathan Bradfield[4], Joan Lappe[5], Shana McCormack[4], Vicente Gilsanz[6], Sharon Oberfield[7], Hakon Hakonarson[5], John Shepherd[8], Andrea Kelly[4], Babette Zemel[1], Struan Grant[9]. [1]Children's Hospital of Philadelphia, USA, [2]University of Pennsylvania, USA, [3]Cincinnati Children's Hospital Medical Center, USA, [4]Children's Hospital of Philadelphia, USA, [5]Creighton University Osteoporosis Research Center, USA, [6]Children's Hospital Los Angeles, USA, [7]Columbia University Medical Center, USA, [8]University of California, San Francisco, USA, [9]Children's Hospital of Philadelphia / University of Pennsylvania, USA

Osteoporosis, a condition with a strong heritable component, likely has origins in childhood when bone accrual is rapid. Childhood fractures are common, with the forearm being the most common site. Genome-wide association studies (GWAS) have identified >70 loci associated with BMD in adults but less is known about genetic influences specific to bone in childhood. To identify novel genetic factors that influence pediatric bone strength at the one-third distal radius, we performed a GWAS of BMC and BMD expressed as sex-, age-, population ancestry (black vs. non-black) specific Z-scores, adjusted or unadjusted for height Z-score, in a multicenter, multi-ethnic cohort of 1,399 healthy children (720 girls and 679 boys; 53% Caucasian, 22% African American, 14% Hispanic) aged 5-20y from the Bone Mineral Density in Childhood Study. BMC/BMD was measured using Hologic bone densitometers, with scans analyzed centrally. Biospecimens were genotyped using the Illumina OmniExpress BeadChip. We performed a sex-stratified analysis on ~16.43 million SNPs (directly genotyped or imputed) using a univariate linear mixed model as implemented in the software GEMMA to account for population stratification. Among females, variation at one locus (*CPED1*, also known as *C7orf58*) yielded association at the level of genome wide significance (rs7797976, $P=1.2 \times 10^{-10}$, β=0.34; BMD-Z height-adjusted). In males, one locus on 9p21.3 yielded suggestive association (rs7035284, $P=2.8 \times 10^{-7}$, β=-0.28; BMC-Z height-adjusted). Results were tested for replication in an independent, same-age cohort of 486 Caucasian children (245 girls and 241 boys). Both loci achieved at least nominal significance in this cohort within the relevant gender (rs7797976; $P=0.047$; rs7035284; $P=0.015$), and reached genome-wide significance when combining the cohorts (rs7797976; combined $P=2.4 \times 10^{-11}$; rs7035284; combined $P=1.2 \times 10^{-8}$).

Signals in the *CPED1* region were previously associated with BMD at other skeletal sites in adults and children. Our result at the distal radius underscores the importance of this locus at multiple skeletal sites. The 9p21.3 is within a gene desert, with the nearest gene flanking each side being *MIR31HG* and *MTAP*, neither of which has been implicated in BMD or BMC previously.

In summary, we report a novel locus for pediatric BMC at the distal radius in males, and implicate the *CPED1* locus in pediatric radius BMD in females. The difference in genetics between genders warrants further investigation.

Disclosures: Alessandra Chesi, None.

MO0307

Association between osteoporosis susceptibility genes and bone mineral density in Vietnamese population. Lan T Ho-Pham*[1], Bich Tran[2], Sing Nguyen[3], Tuan Nguyen[2]. [1]Pham Ngoc Thach University of Medicine, Vietnam, [2]Garvan Institute of Medical Research, Australia, [3]Garvan Institute of Medical Research, Australia

Background and Aim: Bone mineral density (BMD) is under strong genetic control. However, it is not clear which specific genes are involved in the genetic regulation. Moreover, data on the genetics of osteoporosis in Asian population are very limited. This study sought to determine the contribution of osteoporosis genes discovered by genome-wide association studies in Caucasian populations to the variation in BMD in the Vietnamese population.

Methods: The study involved 564 Vietnamese men and women aged 18 years and over (average age: 47 years) who were randomly recruited from the Ho Chi Minh City (formerly Saigon). Demograpic data and clinical history were obtained by a structured questionnaire. BMD at the femoral neck, lumbar spine, total hip and whole body were measured by DXA (Hologic QDR4500, Bedford, MA, USA). Thirty-two single nucleotide polymorphisms (SNPs) in 29 genes were genotyped using Sequenom MassArray technology. We used the Bayesian Model Average (BMA) method to identify a set of SNPs that are independently associated with BMD.

Results: The distribution of genotypes of all SNPs included in this analysis was consistent with the Hardy-Weinberg's equilibirum law. After adjusting for age, gender and weight, 3 SNPs were associated with BMD: rs2016266 (SP7 gene), rs7543680 (ZBTB40 gene), and rs1373004 (MBL2/DKK1 gene). Among the three genetic variants, the SNP rs2016266 had the strongest association, with each minor allele being associated with ~0.02 g/cm2 increase in BMD at the femoral neck and whole body. Each of these genetic variant explained about 0.2 to 1.8% variance of BMD. All other SNPs were not significantly associated with BMD.

Conclusion: These results suggest that genetic variants in the SP7, ZBTB40 and MBL2/DKK1 genes are associated with BMD in the Vietnamese population, and that the effect of these genes on BMD is likely to be modest.

Disclosures: Lan T Ho-Pham, None.

MO0308

Association between polymorphisms in Glucose-dependent insulinotropic poly-peptide (GIP) and GIP receptor (GIPR) genes and bone quality in young and elderly Swedish women. Gaurav Garg*[1], Jitender Kumar[2], Fiona McGuigan[3], Mattias Callréus[4], Maria F. Gomez[5], Paul Gerdhem[6], Holger Luthman[7], Valeriya Lyssenko[8], Leif Groop[9], Kristina Akesson[10]. [1]Clinical Research Center, Lund University, Sweden, [2]Dept of Medical Sciences, Molecular Epidemiology & Science for Life Laboratory, Uppsala University, Sweden, Sweden, [3]University of Lund, Malmö, Skane University Hospital, Malmö, Sweden, [4]Skåne University Hospital, Sweden, [5]Department of Clinical Sciences, University Hospital Malmö, Lund University, Sweden, [6]Dept of Clinical Science, Intervention & Technology, Karolinska Institutet, Sweden, [7]Medical Genetics Unit, Dept. of Clinical Sciences Malmö, Lund University, Sweden, [8]Department of Clinical Sciences, Diabetes & Endocrinology, University Hospital Malmö, Lund University, Sweden, [9]Department of Clinical Sciences, Diabetes, & Endocrinology, University Hospital Malmö, Lund University, Sweden, [10]Skåne University Hospital, Malmö, Sweden

Introduction: Glucose-dependent insulinotropic polypeptide (GIP) is an anabolic gastro-intestinal hormone that potentiates glucose-induced insulin secretion thereby stimulating bone formation and mineralization. Hormone activity is induced via GIP binding to the GIP receptor (GIPR). GIPR gene is widely expressed including on osteoblasts. Mice studies have shown that deficiency in GIP or GIPR leads to low bone mass and bone strength. To date, only one genetic association study for GIPR gene with bone phenotype in human has been published.

The aim of this study was to determine the age-related association between genetic variation in the GIP and GIPR genes and bone strength and bone mineral density (BMD) in young and elderly women and investigate relationship between serum GIP and bone.

Methodology: Two SNPs rs229172_GIP and rs10423928_GIPR were studied in two cohorts of Swedish women: PEAK-25 (all 25 yrs, n=1061) and OPRA (all 75 yrs, n=1044) and analyzed for their association with BMD, bone mineral content (BMC), ultrasound measures, trabecular bone score (TBS), body composition parameters and serum GIP levels. We also analyzed the association between serum GIP and bone related phenotypes.

Results: Women with the minor 'A' allele of rs10423928_GIPR had significantly lower ultrasound values (BUA: TT: 117.1 vs. AA: 115.4, p=0.011; SI: TT: 97.8 vs. AA: 94.5, p=0.03) after adjustment (p=0.004; 0.014) in PEAK-25 only. No association was observed with BMD and BMC in either cohort. rs10423928_GIPR was associated with lower serum GIP levels (β value = -6.93) (unadj. p=0.019; adj p=0.03).

In the OPRA cohort, women with minor 'A' of rs2291725_GIP had lower ultrasound values (SoS: TT: 1525.3 vs AA: 1516.2, p = 0.03; SI: TT: 71.2 vs. AA: 69.0, p = 0.04) at baseline as well as at 10 years follow-up (SoS: GG: 1516.9 vs. AA: 1507.7, p = 0.02; SI: GG: 64.9 vs. AA: 57.0, p = 0.018). rs2291725_GIP was associated with FN BMD, TB BMC and FN BMC after adjusting for fat mass (p=0.016; 0.02; 0.03) in the OPRA cohort only. No association was found between SNPs in either genes with TBS in PEAK-25 and fracture incidence in the OPRA women. No relation was found between serum GIP and bone phenotypes.Conclusion: This is a first genetic study where we have identified the genetic association between rs2291725_GIP and rs10423928_GIPR with lower bone strength. However, the association appears to be age-dependent, suggesting the involvement of yet unknown gene-environment interaction

Disclosures: Gaurav Garg, None.

MO0309

Association of VDR, COL1A1 and LCT gene polymorphisms with bone mineral density in Lithuanian women with postmenopausal osteoporosis. Pavel Marozik[1], Marija Tamulaitiene*[2], Irma Mosse[1], Vaidile Strazdiene[3], Vidmantas Alekna[2]. [1]Institute of Genetics & Cytology NAS Belarus, Belarus, [2]Faculty of Medicine, Vilnius University, Lithuania, [3]National Osteoporosis Center, Lithuania

The purpose of this study was to investigate the frequency of genes predisposing to osteoporosis (OP) in postmenopausal Lithuanian women.

Methods. This case-control study included 73 women from National Osteoporosis Center, Lithuania. Dual-energy X-ray absorptiometry (iDXA, GE Lunar) was used to measure bone mineral density (BMD). DNA was extracted from bloodspots dried on special NucleoSafe cards (Macherey-Nagel, Germany). OP predisposition gene polymorphisms (VDR *ApaI, BsmI, TaqI* and *Cdx2*, COL1A1 *G2046T* and LCT *T-13910C*) were determined using PCR analysis.

Results. Case group included 28 postmenopausal women with severe OP (age 74.1 ± 1.2 years in average), the control group included 45 women (average age 72.9 ± 0.9 years, p>0.05). Genotyping results showed that the total frequency of unfavorable risk alleles (predisposing to OP) in case group (52.1%) was higher comparing to controls (48.6%). The analysis of *Cdx2* polymorphism of VDR gene did not reveal any statistically significant difference between groups analysed, although the frequency of protective A allele in control group was 1.6 times higher compared to patients with OP. The frequency of risk allele *B* (42.9%, 1.6 times) and *BB* homozygotes (17.9%, 1.4 times) of VDR *BsmI* gene polymorphism was higher in

patients with OP compared to controls (p>0.05). The same was found for COL1A1 *G2046T* and LCT *T-13910C* polymorphisms.

In further analysis, control Lithuanian population was compared with control Belarusian population. No statistically significant difference was shown between them, and both were in correspondence with the one expected from the Hardy-Weinberg equilibrium. This allows us to compare Lithuanian patients with Belarusian control population. Statistically significantly higher risk allele *C* (OR=2.38, 95% CI, 1.39–4.07) and homozygotes *CC* (OR=3.32, 95% CI, 1.53–7.22) of LCT *T-13910C* gene polymorphism were found in patients compared to control group.

The analysis of the relationship between gene polymorphisms and BMD in Lithuanian population revealed a statistically significantly higher BMD at lumbar spine in *CT* heterozygotes of LCT *T-13910C* gene polymorphism compared to unfavorable *CC* homozygotes (1.06 ± 0.03 and 0.98 ± 0.02, correspondingly, p=0.05).

Conclusion. The findings of this study suggest that analysed gene polymorphisms are associated with postmenopausal OP in Lithuanian women, and insufficient statistical power may be due to small number of investigated subjects.

Disclosures: Marija Tamulaitiene, None.

MO0310

Genome-wide Association Study of Trabecular Bone Score Reveals Several Candidate Loci for Bone Quality. Hyung Jin Choi*[1], Jung Hee Kim[2], Nam H Cho[3], Chan Soo Shin[2]. [1]Chungbuk National University Hospital, South Korea, [2]Seoul National University College of Medicine, South Korea, [3]Preventive Medicine, Ajou University School of Medicine, South Korea

Several large-scale genome-wide association studies of bone mineral density have been performed. However, genetic factors influencing bone quality has not been investigated. To identify genetic factors for bone quality, we conducted a genome-wide association study in 2,987 samples from a community-based cohort. After sample quality control, 2,587 samples were analyzed. The discovery analysis revealed several candidate loci for trabecular bone score ($P<1\times10^{-5}$). One locus in chromosome 13 near SERP2 showed highest statistical significance ($P=1.0\times10^{-6}$) in combined analysis. Another loci in chromosome 1 near SLC4A1 and chromosome 9 near KLF4 were associated with trabecular bone score in combined analysis ($P=1.8\times10^{-6}$ and $P=3.7\times10^{-6}$). One locus in chromosome 9 near DBC1 showed highest statistical significance ($P=6.0\times10^{-7}$) in female specific analysis. Our result reveals several candidate loci for bone quality.

Disclosures: Hyung Jin Choi, None.

MO0311

Polymorphisms in Cannabinoid Receptors Genes and Bone Mineral Density in Postmenopausal Korean Women. Jung-Gu Kim*[1], Jae Hee Woo[2], Hoon Kim[3], Jong Hak Kim[2]. [1]Seoul National University Hospital, South Korea, [2]Department of Anesthesiology & Pain Medicine, School of Medicine, Ewha Womans University, South Korea, [3]Department of Obstetrics & Gynecology, Seoul National University College of Medicine, South Korea

Purpose: The purpose of this study was to investigate the association between single nucleotide polymorphisms (SNPs) in cannabinoid receptor genes and bone mineral density (BMD) in postmenopausal Korean women.

Methods: The seven polymorphisms (CNR1c.*2394A>G, c.*3475A>G, c.1359C>A, rs2023239 C>T, rs2180619A>G, rs7766029C>T, rs806379A>T) in CNR 1 gene and sixteen polymorphisms (CNR2 c.188A>G, c.189A>G, c.465C>T, c.660G>A, c.751T>C, c.846T>C, c.946C>T, c.999G>A, c.1014C>G, rs2229583, rs2229584, rs229585, and rs229586, CNR2 rs4237, rs7530595, and rs16828926) in CNR2 gene were analyzed in 405 postmenopausal Korean women. Serum levels of osteoprotegerin (OPG), soluble receptor activator of the nuclear factor-κB ligand (sRANKL) and bone turnover markers were measured and BMDs at the lumbar spine and femoral neck were also examined.

Results: The CNR2 c.465C>T, c.660G>A, c.946C>T, and c.*263G>A polymorphisms among polymorphisms measured in CNR genes, were associated with BMD of lumbar spine. The AA genotype of thec.660G>A, and c.*263G>A polymorphism in the CNR2 gene was found to have significantly lower BMD of the lumbar spine compared to non AA genotype. BMD of lumbar spine in the TT genotype of CNR2 c.465 C>T, and c.946C>T polymorphism was lower, compared to non TT genotype. The TT genotype of the CNR2 c.946C>T polymorphism (OR, 3.43; 95% CI, 1.28-9.19) and the AA genotype of and CNR2 c.*263G>A polymorphisms (OR, 1.74; 95% CI, 1.03-2.95) had an increased risk of osteoporosis of the lumbar spine and/or femoral neck compared with other genotype respectively. The adjusted serum levels of bone turnover markers, OPG, sRANKL, or sRANKL $\times$ 1,000/OPG ratios were not associated with the CNR polymorphisms.

Conclusion: Our results suggest that the CNR2 c.465C>T, c.660G>A, c.946C>T, and c.*263G>A polymorphisms may be genetic factors affecting BMD in postmenopausal Korean women.

Funding Support: This research was supported by Basic Science Research Program through the National Research Foundation of Korea (NRF) funded by the Ministry of Education, Science and Technology (2013052650), and by grant funded by the Seoul National University Hospital Research fund (04-2013-0320).

Disclosures: Jung-Gu Kim, None.

MO0312

Bone Mineral Density Changes Among Women Initiating ACE Inhibitors , Beta Blockers, and Thiazide Diuretics: Results from the SWAN Bone Study. Daniel Solomon*[1], Kristine Ruppert[2], Zhenping Zhao[2], YinJuan Lian[2], Gail Greendale[3], Joel Finkelstein[4]. [1]Harvard Medical School, USA, [2]University of Pittsburgh, USA, [3]University of California, Los Angeles, USA, [4]Massachusetts General Hospital, USA

Introduction: There has been substantial controversy over the potential role of several medications used to lower blood pressure and their potential effect on bone mineral density (BMD). Thiazide diuretics have been found to improve BMD in several small randomized controlled trials. As well, observational studies suggest improvement in BMD in some but not all beta-blocker analyses. The purpose of these analyses was to examine the effect of different antihypertensive agents on BMD using rigorous pharmacoepidemiologic methods.

Methods: we examined data from the Study of Women's Health Across the Nation (SWAN). 2365 women were followed for a median of 7.1 years at five SWAN sites with annual BMD assessments performed. In addition, medication use and other potential confounders – body mass index, diabetes, menopausal status, and comorbidities – were assessed annually. We performed a matched propensity score analysis examining annual rates of BMD change, comparing new users of thiazide diuretics, beta blockers, and ACE inhibitors with nonusers of any anti-hypertensive.

Results: Among the 2365 eligible women we found 1305 new users of any of the anti-hypertensive agents of interest. Propensity scores were calculated between each of the anti-hypertensive categories and non-users and then matched sets were created. 76 users of thiazide diuretics were matched with an equal number of nonusers, 69 ACE inhibitor users were matched with a similar number of nonusers, and 88 beta blocker users were matched with a similar number of nonusers. Baseline characteristics were very similar across users and nonusers for all three sets of matched cohorts. As expected, thiazide diuretic users gained bone mineral density or had a slower rate of decline compared to nonusers (Table 1). In contrast, rates of BMD loss in beta blocker(Table1) and ACE inhibitor users were similar to rates in non-users (data not shown).

Conclusions: Matched propensity score analysis of new users of thiazide diuretics produced the expected increase in BMD. The loss in BMD observed among new users of beta blockers and ACE inhibitors suggests that prior observational studies may be confounded. These methods may be helpful for estimating the effects of medications on BMD in observational cohorts.

Table 1. Annual within group change in BMD for SWAN participants starting thiazide diuretics or beta blockers.

	Annual BMD Change (95% Confidence Interval)		
	Spine	Femoral Neck	Total Hip
Base Model[a]			
Thiazide user	**+0.43% (-0.10, 1.0)**	**-0.28% (-.80, .30)**	+0.22% (-.20, 0.70)
Non-user	+0.09% (-0.5, 0.7)	-0.59% (-1.2, -0.03)	+0.22% (-0.30, 0.60)
Full Model[b]			
Thiazide user	**+0.42% (-0.16, 0.99)**	**-0.30% (-0.87, 0.27)**	+0.34% (-0.10, 0.78)
Non-user	+0.08% (-0.49, 0.65)	-0.64% (-1.20, -0.07)	0.18% (-0.26, 0.62)
Base Model[a]			
Beta blocker user	-0.66% (-1.10, -0.20)	-0.42% (-0.78, -0.05)	-0.49% (-0.80, -0.18)
Non-user	-0.69% (-1.1, -0.20)	-0.63% (-1.0, -0.26)	-0.49% (-0.80, -0.18)
Full Model[b]			
Beta blocker	-0.60% (-1.1, -0.14)	-0.42% (-0.79, -0.06)	-0.51% (-0.81, -0.20)
Non-user	-0.65% (-1.1, -0.20)]	+0.63% (-1.0, -0.27)	-0.50% (-0.80, 0.19)

[a] Base Model is adjusted for age, race, site, BMI and menstrual status. [b] Full model is Base Model + physical activity, # comorbid conditions, and propensity score. Bold italics indicate that the annualized rate of loss of BMD in the medication-using group is statistically significantly different from that of the matched, non-using comparison group; p-values range between p= 0.01 to p=0.04.

Table 1

Disclosures: Daniel Solomon, None.

MO0313

Explaining gender difference in fracture risk: the role of volumetric bone mineral density. Hanh Pham*[1], Nguyen Nguyen[2], Mei Chan[3], Jacqueline Center[2], John Eisman[2], Tuan Nguyen[2]. [1]Garvan Institute of Medical Research, Australia, [2]Garvan Institute of Medical Research, Australia, [3]Osteoporosis & Bone Biology, Australia

It has been suggested that men and women with the same age and areal bone mineral density (aBMD) have the same risk of a fragility fracture. However, such a relationship is not always true for all types of fractures. The present study aimed to determine the gender difference in fracture risk using volumetric and areal bone mineral density.

The study was designed as a population-based prospective investigation that involved 2279 women and 1379 men aged 57+ years (median: 68) who had been followed for a median of 9 years (range 1 – 25 years). Femoral neck aBMD, expressed as g/cm2, was measured by dual energy X-ray absorptiometry (GE-Lunar) at baseline. Femoral neck volumetric bone mineral density (vBMD), expressed as g/cm3, was estimated from aBMD and bone mineral content using a published algorithm. Low-trauma fracture was ascertained from X-ray reports. Hazard ratio (HR) of fracture

was estimated from the Cox's proportional hazards model to compare fracture risk between groups by BMD, age and gender.

Baseline vBMD in men is 0.31 ± 0.06 g/cm3, which was not significantly different from women (0.32 ± 0.07 g/cm3). However, baseline aBMD in men (0.93 ± 0.15 g/cm2) was significantly higher than women (0.81 ± 0.14 g/cm2). During the follow-up period, a significantly higher proportion of women (31.9%; n = 728) sustained fragility fractures compared to men (16.5%; n = 227). For a given aBMD and age, women had a higher risk of any fracture compared to men (HR: 1.4; 95%CI: 1.18 to 1.62), but not for hip or vertebral fracture. However, for a given vBMD and age, the risk of fracture was consistently greater in women than men for any fracture (HR 2.04; 95%CI: 1.76-2.36), for hip fracture (HR: 2.02; 95%CI: 1.37-2.96), and for vertebral fracture (HR: 1.93; 95%CI: 1.51-2.45).

These results indicate that women have higher risk of fracture than men for a given age and vBMD. The data also suggest that vBMD migh be a better predictor of fracture risk than aBMD, and that the diagnosis of osteoporosis should be based on vBMD rather than aBMD.

Disclosures: Hanh Pham, None.

MO0314

Influence of degenerative disorders on the lumbar spine BMD and TBS with age: the Cohort OsteoLaus. <u>Olivier Lamy</u>*[1], <u>Ivan Padlina</u>[2], <u>Berengère Aubry-rozier</u>[2], <u>Delphine Stoll</u>[3], <u>Marie Metzger</u>[2], <u>Didier Hans</u>[4]. [1]Chief of the Bone Unit, Switzerland, [2]Bone Unit, Switzerland, [3]Centre a bone diseases, Che, [4]Lausanne University Hospital, Switzerland

Introduction: After menopause, lumbar spine (LS) BMD and TBS decrease with age. In practice, we are often faced with values of LS BMD "relatively" high for the age, which can lead to erroneous interpretations. Preliminary studies have shown that osteoarthritis (oa) does not influence TBS. The aim of this study was to measure changes in LS BMD and TBS values in women 50 to 80 years, taking into account the impact of fractured vertebrae (VFx) and oa (Voa).

Material and Methods: The 1'500 women 50 to 80 years old included in the cohort OsteoLaus (Lausanne, Switzerland) have had LS BMD and TBS, and VFA. All exams were analyzed independently by two experts following the ISCD guidelines, excluding VFx and vertebra with > 1 SD difference with the vertebra immediately adjacent.

Results: We included 1'443 women: age 66.7 ± 11.7 y, BMI 25.7 ± 4.4. Participants were divided into six age groups: 50-55, 55-60, 60-65, 65 -70, 70-75 and 75-80 years. BMD was increased from 1.2 to 3.2 % before excluding VFx and Voa (p < 0.001). TBS didn't change after excluding VFx and Voa (0.0% to 0.8%, ns). BMD (Vfx and Voa excluded) was for the six age groups: 0.953 ± 0.141 g/cm2, 0.916 ± 0.155, 0.909 ± 0.158, 0.917 ± 0.167, 0.918 ± 0.168 and 0.933 ± 0.188, respectively. Loss between 52.5 and 77.5 y. was 2.10 %, or 0.09 %/y with a loss of 0.46%/y from 52.5 to 62.5 y, followed by a gain of 0.18 %/y between 62.5 and 77.5 y. The change in BMD between two consecutive age gr was significant only between gr1 and gr2 (p < 0.02). TBS (Vfx and Voa excluded) was for the six age groups: 1.357 ± 0.093, 1.317 ± 0.099, 1.289 ± 0.092, 1.269 ± 0.099, 1.253 ± 0.101 and 1.235 ± 0.105, respectively. Loss between 52.5 and 77.5 y. was 8.99 %, or 0.36 %/y with a loss of 0.50 %/y between 52.5 and 62.5 y, and 0.26%/y between 62.5 and 77.5 y. Changes in TBS between 2 consecutive age groups was highly significant (p <0.02 - p <0.0001). These results are more pronounced in a sub-analysis including only women with Voa (with and without exclusion of Voa).

Conclusion: This study shows a double interest in TBS, particularly in the older population: 1) on average, TBS is not affected by fractures or oa disorders, 2) while BMD increases after 65 years (moderate degenerative disorders cannot be excluded from the analysis), TBS continues to decline. For the LS evaluation, TBS should play a leading role not only for diagnosis but also for treatment monitoring in view of its independence to oa.

Disclosures: Olivier Lamy, None.

MO0315

Age-Related Loss of Cortical Bone in Males: Trends from the 3rd century AD to the Present Day in North-West Europe, a Study Using Archaeological Skeletons. <u>Simon Mays</u>*. English Heritage, United Kingdom

Background: Osteoporosis has been increasingly recognised as a health threat in the ageing male. Studies of osteoporosis in archaeological skeletons are useful to our understanding of the disease, particularly the impact of enviromental risk factors, because they allow comparisons to be made with populations of similar genetic make-up to the present day but with very different livestyles. To date, most studies of osteoporosis in ancient skeletons have focused on the disease in females. The aim of this study is to investigate age-related loss of cortical bone in male skeletons. British archaeological populations from three different time periods, ranging from the 3rd century to the 19th century AD, are investigated, and comparisons drawn with modern data. Over this 1600 year period there was an increase in exposure to risk factors such as cigarette smoking, sedentary lifestyle and vitamin D deficiency, which are commonly held to exacerbate osteoporotic loss of bone mass. It was thus hypothesised that there should be an increase in the severity of age-related loss of cortical bone in later compared with earlier populations.

Methods: Bone status was evaluated using measurement of cortical thickness at the midshaft of the the second metacarpal from radiographs (N=215 male skeletons). The

cortical thickness was expressed as the cortical index (100 x combined cortical thickness / bone width).

Results: peak cortical index in young male adults was less in the archaeological populations than today (p<0.001). Two-factor analysis of variance indicated no difference in age-patterning in cortical index between the three archaeological populations (F=0.54, p=0.71), and in each case the pattern of age-related loss of cortical bone in resembled that in a large modern reference group (Fig. 1). No fragility fractures were found in the archaeological populations.

Discussion and conclusions: The lesser peak cortical bone in ancient populations may reflect the poorer nutrition characteristic of earlier populations, although other unidentified factors may also be involved. There was no difference in age-related patterns of cortical bone loss between the different time periods, despite the time-progressive increase in exposure to risk factors commonly held to exacerbate loss of bone mass. The current results suggest that such factors may not exert very great effects on age-related cortical bone loss in males.
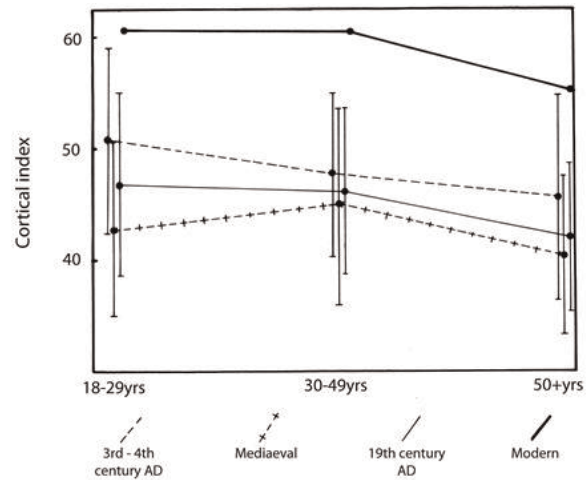
Metacarpal cortical index versus age in males from different time periods

Disclosures: Simon Mays, None.

MO0316

Osteopenia and Osteoporosis in Adult Females with Type 1 Diabetes: Results from the T1D Exchange Registry. <u>Ruban Dhaliwal</u>*[1], <u>Nicole Foster</u>[2], <u>Linda Dimeglio</u>[3], <u>Katherine Manseau</u>[4], <u>Viral Shah</u>[4], <u>Julie Kittelsrud</u>[5], <u>Jill Simmons</u>[6], <u>Lucy Mastrandrea</u>[7], <u>Maya Styner</u>[8], <u>Roy Beck</u>[9], <u>Ruth Weinstock</u>[10]. [1]SUNY Upstate Medical University, USA, [2]Jaeb Center for Health Research, USA, [3]Indiana University School of Medicine, USA, [4]Barbara Davis Center for Childhood Diabetes, USA, [5]Avera McKennan Hospital & University Health Center, USA, [6]Vanderbilt University Medical Center, USA, [7]SUNY at Buffalo, School of Medicine, USA, [8]University of North Carolina, Chapel Hill, School of Medicine, USA, [9]Jaeb Center for Health Research, USA, [10]State University of New York Health Science Center, USA

To obtain a better understanding of the relationshp between type 1 diabetes (T1D) and osteopenia/osteoporosis (OP), factors associated with bone health were examined in adult females aged 26-92 years from 38 centers in the T1D Exchange clinic registry (median age 45 years, median duration of diabetes 23 years, 91% non-Hispanic white).

Diagnoses were obtained from medical record review. Since the diagnosis of osteoporosis could not be distinguished in the registry from the diagnosis of osteopenia, the conditions were grouped for analyses into one entity (OP). Individuals with end stage renal disease or history of transplantation were excluded. Multi-variable logistic regression models evaluated associations of demographic and clinical factors with OP.

Of 2582 adult females, 295 (11%) overall; 38% ≥65 years) had an OP diagnosis. Those with OP were more likely to be older (mean 62 vs 45 years, p<0.001) and have lower BMI (mean 27 vs 34 kg/m^2, p=0.05) compared with participants without OP. Among 76 participants with a history of celiac disease (CD), 17% had OP compared with 11% of those without CD (unadjusted p=0.12). Only 27 of the 295 with OP were <50 years old. OP status was not associated with recent HbA1c (p=0.42), diabetes duration (p=0.90), youth vs later (> 18 years of age) onset T1D (p=0.62), and presence of CD (p=0.09), thyroid disease (p=0.77), and known microvascular complications of T1D (p=0.22). Use of supplements was more common in those diagnosed with OP: 86% vs 52% took vitamin D; 76% vs 32% took calcium. Limitations of these data include lack of systematic screening for OP, of bone mineral density data, and of fracture data. In conclusion, in the T1D Exchange, OP is common, particularly in older women. Further studies are needed to better understand contributing factors, impact of OP on fracture risk, and optimal approaches for prevention.

Disclosures: Ruban Dhaliwal, None.

MO0317

A small population-wide increase in BMD is associated with substantial reduction in fracture incidence. <u>Mei Chan</u>*[1], <u>Dana Bliuc</u>[2], <u>Jacqueline Center</u>[2], <u>John Eisman</u>[2], <u>Tuan Nguyen</u>[2]. [1]Osteoporosis & Bone Biology, Australia, [2]Garvan Institute of Medical Research, Australia

It is not clear whether a shift in the population distribution of bone mineral density (BMD) could have an impact on the fracture incidence in the general population. The present study sought to determine the effect of change in population-based BMD on fracture incidence in the elderly population.

The study involved two cohorts recruited from the City of Dubbo (Australia). The first cohort, DOES1, included 2204 participants who were recruited from 1990. The second cohort, DOES2, included 1516 participants who were recruited from 2000. All participants were aged 60 years and above at the time of study entry. Baseline anthropometric and demographic characteristics were ascertained at baseline by a structured questionnaire. BMI was calculated from measured height and weight. BMD at the femoral neck and lumbar spine was measured by DXA (GE-LUNAR Corp, Madison, WI). Osteoporosis was defined as femoral neck BMD T-score ≤ -2.5. Low trauma and non-pathological fractures were ascertained from X-ray reports during the follow-up (from study entry till 31/12/2013).

The prevalence of obesity (BMI≥30) increased during the follow-up period: in women, from 18% in DOES1 to 30% in DOES2. In men, the corresponding prevalence increased from 7% and 33%. During the same period, for a given age and BMI, women in DOES2 had a greater BMD (~6%) than their counterparts in DOES1. Femoral neck BMD changes were also observed in men but with a smaller magnitude (3%). In the DOES2 cohort, the prevalence of osteoporosis by BMD was 9%, a reduction of ~20% compared with the DOES1 cohort. In women, the age-standardised annual fracture incidence decreased from 3.2% in DOES1 to 2.5% in DOES2, a relative decline of 28% (P < 0.001). In men, there was a similar decline of fracture incidence: from 1.7% to 1.3% per year, a reduction of 24% (P = 0.006). Most of this reduction was in non-vertebral fractures. There was no change in the uptake of anti-osteoporosis treatment during the follow-up period. These data suggest that a modest population-wide secular increase in BMD was associated with a substantial reduction in fracture risk in the general population.

These results support the concept that a population-based approach to improve BMD distribution could be as or more effective than focusing on those at high-risk, e.g. post fracture) in reducing the community burden of fracture incidence. One aspect of these findings suggests how a modest increase in BMD induced by anti-resorptive therapy could bring larger-than-expected reduction in fracture risk reduction. An important but conflicting aspect to these findings is that an intervention that could bring substantial benefit to the population may not necessarily bring benefit to an individual.

Disclosures: Mei Chan, None.

MO0318

Correlation of Other Fracture Types with Hip Fracture: Toward a Rational Combined Hip Fracture Endpoint. <u>Cathleen Colon-Emeric</u>*[1], <u>Carl Pieper</u>[2], <u>Janet Grubber</u>[3], <u>Courtney VanHoutven</u>[3], <u>Joanne LaFleur</u>[4], <u>Kenneth Lyles</u>[5], <u>Robert Adler</u>[6]. [1]Duke University Medical Center, USA, [2]Duke University, USA, [3]Durham VA Medical Center, USA, [4]University of Utah, USA, [5]Duke University Medical Center, USA, [6]McGuire VA Medical Center, USA

Background: With ethical requirements to enroll lower risk subjects, recent osteoporosis trials are underpowered for change in hip fractures. Different anatomical sites have varying properties which confer different levels of fracture risk and response to treatment.

Objective: To identify anatomical sites which cluster with hip fracture at higher than expected frequency. If treatment is associated with similar risk reductions within the cluster, subsequent trials can use a combined endpoint to increase power.

Design: Cohort study using administrative data from Veterans Affairs and Centers for Medicare and Medicaid Services.

Population: U.S. Male Veterans (n=5,036,536) aged 50 years and over receiving primary care in the VA system between 1999-2009.

Methods: Fractures were ascertained using ICD9 and CPT codes and classified by fracture type; hip, forearm, spine, shoulder, pelvic, rib/clavicle, distal femoral, tibial/fibular, and other. To avoid double counting due to repeated coding of the same event over time, each individual was counted only once for each fracture type, and femur fracture codes must have occurred at least 6 months away from hip fracture codes. Pearson correlation coefficients for each pair of fracture types were calculated, and logistic regression was used to calculate the odds ratios and kappa statistic for each fracture type with hip fracture. Latent class analysis was used to identify clusters of highly correlated fractures.

Results: Over the study period 595,579 (11.8%) men suffered 1 or more fractures and 140,905 (2.8%) suffered 2 or more fractures. Hip fracture was the most common specific fracture type (49% of individuals with fracture), followed by spine (31%), femur (26%) and shoulder (21%). The fracture types most highly correlated with hip fracture were pelvic/acetabular (Pearson coefficient 0.25, p<0.0001), femur (0.16, p<0.0001), and shoulder (0.11, p<0.0001). Odds ratios and kappa statistics (reflecting the proportion of potential agreement above chance) for each fracture type with hip fracture are reported below. Latent class analysis revealed good loading onto a single factor (rho estimates <0.10 or >0.90).

Conclusions: Pelvic, acetabular, femur, and shoulder fractures cluster with hip fractures within individuals at greater than expected frequency. If subsequent analyses confirm similar treatment risk reductions within that cluster, then a combined endpoint could be used in subsequent trials to better estimate the effect of new therapies on hip fracture risk.

Fracture Types	Odds Ratio (95% CI)	Kappa
hip * femur	10.1 (46.5, 48.6)	0.16
hip * forearm	5.1 (5.0, 5.2)	0.06
hip * pelvic/acetabular	47.6 (46.5, 48.6)	0.20
hip * rib	4.5 (4.4, 4.6)	0.08
hip * shoulder	9.1 (8.9, 9.3)	0.10
hip * spine	5.4 (5.3, 5.5)	0.09
hip * tibia	4.7 (4.5, 4.8)	0.05

Abstract table

Disclosures: Cathleen Colon-Emeric, None.

MO0319

Fall in Elderly Cared by Undegraduate Medical Students Belonging to The Internal Medicine Academic League. <u>Fabiana Fonseca</u>[1], <u>Layla Bonfim Faleiros</u>*[2], <u>Renan Rodrigues Neves Ribeiro do Nascimento</u>[2], <u>Stéfano Franco Minohara Minohara</u>[2], <u>Estela Mion Petrillo Mion Petrillo</u>[2], <u>Tiago Marques Agostinho Marques Agostinho</u>[2], <u>Egidio Lima Dórea Lima Dórea</u>[2]. [1]PUC - SPUNICID, Brazil, [2]UNICID, Brazil

INTRODUCTION

Fall in elderly represents a serious problem in public health. Its impact has not been properly discussed in academic circles. Furthermore, many professionals believe that fall is inevitable with aging. Approximately 30% of the older populatiom fall, that figure rises to 50% above 80 years of age. This makes falling a representatuve fraction of morbidity rates and causes of death. Therefore, it raises the attetion the lack of studies about fall in elderly cared by medicine students.

OBJETIVE

To assess the number of patients cared by undergraduate medicine students belonging to an Internal Medicine Academic League that have suffered a fall, comparing to literature data and characterize the methods of fall porevention in the studied population.

MATERIALS AND METHODS

Retrospective study, encompassing 106 medical records of patients cared in LACM between 2007 and 2013. Information was retrived about the presence of falls in the last year of visits of all patients. The results were compiled in an Excel spreadsheet and analyzed as data tables.

RESULTS

Approximately 22,45% of patients cared by LACM have suffered falls, with a slight bias to the male population (54,1%). The average age was 70 yeaes of age. The patients reporting falls used in average 5 different medicines. 20,8% of the patients reporting falls did not present concurrent comorbidity, while 3 (12,5%) had two and 16 (66,7%) three or more.

CONCLUSION

The study enabled us to identify that the data of patients cared by LACM are in agreement with the literature. The use of multiple medicines was an important factor in patients that suffered falls, as well as the presence of comorbidity. Therefore, the assessment of medication and proposal for education in fallprevetion is important to reduce the incidence of falls. Furthemore, the training in fall prevention for professionals involved in elderly care can reduce fall rates and promote quality of life.

Disclosures: Layla Bonfim Faleiros, None.

MO0320

High Body Mass Index Is a Risk Factor for Low Trauma Fractures in Women Who Have Sustained an Upper Arm or Lower Leg Fracture. <u>Claudia Beaudoin</u>*[1], <u>Sonia Jean</u>[2], <u>Louis Bessette</u>[1], <u>Louis-Georges Ste-Marie</u>[3], <u>Jacques P. Brown</u>[4]. [1]CHU de Quebec Research Centre, Canada, [2]Institut National De Santé Publique Du Québec, Canada, [3]CHUM, University of Montreal, Canada, [4]CHU de Québec Research Centre, Canada

Purpose: To investigate the relationship between body mass index (BMI) and the level of trauma in a cohort of fractured women aged 50 and older. Methods: In the Recognizing Osteoporosis and its Consequences in Quebec programme, a cohort of recently-fractured women was recruited. Information on circumstances of fracture and skeletal sites were collected at baseline, and fractures were classified as low or high-energy trauma fractures. A low-energy trauma fracture was defined as occurring spontaneously, from a fall from standing height, sitting, lying (<1m high), missing three or fewer steps, coughing or sneezing or from a movement outside of the normal

range of motion. All other fractures were classified as high-energy trauma fractures. Six to eight months following fracture, women were contacted to complete a follow-up questionnaire detailing personal and clinical characteristics related to osteoporosis. Femoral neck bone mineral density (FN-BMD) of participants who reported having had a BMD measurement within 2 years of the fracture event were obtained from patients' clinics. BMD data was imputed for women who did not have a FN-BMD result available (1250/2633). To evaluate the association between BMI and the level of trauma, a multivariate logistic regression model including adjustment variables and an interaction between BMI and fracture site was constructed. Results are presented by fracture site category. Results: The analysis included 2633 women who suffered a fracture. The number of women who suffered a low and high trauma fracture is presented in Table 1 according to fracture site and BMI. Women who suffered a foot, ankle, tibia or fibula fracture were more likely to have experienced a low-energy trauma fracture if they were overweight (O.R. [95% C.I.] = 1.80 [1.20; 2.70]) or obese (O.R. [95% C.I.] = 2.91 [1.85; 4.58]) than if they had a normal BMI (Table 2). In women who suffered an upper arm fracture, those with an obese BMI tend more to have experienced a fracture following a low- than a high-energy trauma (O.R. [95% C.I.] = 2.08 [1.22; 3.55]). No significant association was detected between BMI and the level of trauma in women who suffered a hip/pelvis/femur or wrist/forearm fracture. Conclusions: This study suggests that the association between BMI and level of trauma differs depending on the fracture site. In women who have suffered an upper arm or lower leg fracture, high BMI is a risk factor for low trauma fractures.

Fracture site n₁/n₂	Body mass index (m/kg²)			
	Underweight (<18.5)	Normal (18.5-24.9)	Overweight (25-29.9)	Obese (≥30)
Foot, ankle, tibia/fibula	6/2	164/77	240/70	223/44
Hip, pelvis, Femur	18/2	121/24	71/16	34/8
Upper arm	3/3	120/57	118/44	119/33
Wrist, Forearm	13/3	351/87	277/79	159/47

Table 1: Number of women who suffered a low- (n1) and high- (n2) energy trauma fracture

Fracture site O.R. [95% C.I.]	Body mass index (m/kg²)			
	Underweight (<18.5)	Normal (18.5-24.9)	Overweight (25-29.9)	Obese (≥30)
Foot, ankle, tibia/fibula	0.95 [0.17; 5.27]	1.00 (Ref)	**1.80** [1.20; 2.70]	**2.91** [1.85; 4.58]
Hip, pelvis, femur	1.67 [0.34; 8.29]	1.00 (Ref)	1.02 [0.49; 2.13]	1.28 [0.49; 3.34]
Upper arm	0.46 [0.08; 2.59]	1.00 (Ref)	1.27 [0.77; 2.08]	**2.08** [1.22; 3.55]
Wrist, forearm	0.79 [0.20; 3.07]	1.00 (Ref)	0.94 [0.65; 1.35]	1.01 [0.66; 1.56]

*Odds ratio adjusted for the age, FN-BMD, level of physical activity and level of schooling

Table 2: Adjusted* odds ratio estimates according to BMI and by fracture site

MO0321

Is Fall Risk Indirectly Captured by FRAX?. Shreyasee Amin*[1], Kenton Kaufman[2], Jeremy Crenshaw[2], Sara Achenbach[2], Elizabeth Atkinson[2], Sundeep Khosla[3], L. Joseph Melton[1]. [1]Mayo Clinic, USA, [2]Mayo Clinic, USA, [3]Mayo Clinic College of Medicine, USA

Falls precipitate most fragility fractures, which increase with advancing age and tend to be more common in women. Many risk factors incorporated into the fracture risk assessment score, FRAX, are also associated with falls. Thus, it may be that fall risk is indirectly captured through FRAX. If not, fall risk would be important to assess separately when determining individual fracture risk.

We studied an age-stratified cohort of 125 ambulatory, community-dwelling women age ≥ 65 yrs (body mass index [±SD], 27.3 ± 5.0 kg/m²). All except one woman had femoral neck bone mineral density (FN BMD, g/cm²) measured and FRAX scores (% 10-year risk), for both major osteoporotic (OP) fractures and hip fractures, determined. Self-reported history of falls within the last year was recorded. Subjects completed various assessments for fall risk, unless prior injury or surgery precluded safe participation, including the Activities-specific Balance Confidence (ABC) Scale (0-100%) [N=125], Functional Reach Test (FRT, cm) [N=124], and maximum unipedal stance (1-Leg Stance) (0-30 s) [N=121], where higher scores are

associated with lower fall risk. In a motion analysis laboratory, we also assessed the dynamic stability margin (DSM, m) [N=119], a measure of gait stability captured while subjects performed unobstructed level walking. Negative DSM values quantify the dynamic instability that an individual allows during undisturbed gait. Using Spearman's correlation, we examined the relation between each fall risk tool with age, FN BMD and FRAX and then assessed the association between each fall risk tool with FN BMD and FRAX, adjusted for age.

The median (range) for age, FN BMD and the two FRAX scores of these women was 77 (65-92 yrs), 0.81 (0.54-1.20 g/cm²), 14.2 (3.3-56.9%, major OP fracture risk) and 3.5 (0.1-45.8%, hip fracture risk), respectively. There were 47 women who reported at least 1 fall within the prior year. The median (range) for ABC, FRT, 1-Leg Stance and DSM was 92 (43-100%), 26 (5-38 cm), 11 (1-30 s) and -0.41 (-0.65 to -0.18 m), respectively. Most assessments of fall risk were associated with age. After adjusting for age, none of the fall risk tools was associated with FN BMD or either of the two FRAX scores (Table).

In the assessment of individual fracture risk, our results suggest that fall risk would need to be considered separately from either FN BMD or FRAX score.

Fall Risk Tool	Spearman Correlation Coefficient (Unadjusted/Age-adjusted)			
	Age	FN BMD	FRAX Major OP Fractures	FRAX Hip Fractures
ABC Scale	-0.44*/--	0.18*/0.07	-0.34*/-016	-0.38*/-0.15
FRT	-0.19*/--	0.03/-0.02	-0.19*/-0.11	-0.16/-0.06
1-Leg Stance	-0.57*/--	0.13/-0.03	-0.31*/-0.05	-0.37*/-0.02
DSM	0.22*/--	0.10/0.16	0.14/0.04	0.07/-0.09
Fall History	0.03/--	-0.04/-0.03	0.08/0.07	0.08/0.08
*p-value <0.05				

Table

MO0322

Low Rate of Osteoporosis Treatment in Nursing Home Men at High-risk for Fractures. Alexandra Papaioannou*[1], Carly Skidmore[2], George Ioannidis[3], Courtney Kennedy[4], Denis O'Donnell[5], Hrishikesh Navare[5], Lora Giangregorio[6], Sharon Marr[4], Sid Feldman[7], Angela M. Cheung[8], Richard Crilly[9], Sophie Jamal[10], Robert Josse[11], Sadhana Prasad[3], Anne Braun[2], Ravi Jain[12], Lehana Thabane[2], Jonathan Adachi[13]. [1]Hamilton Health Sciences, Canada, [2]McMaster University, Canada, [3]McMaster University, Canada, [4]McMaster University, Canada, [5]Medical Pharmacies Group Limited, Canada, [6]University of Waterloo, Canada, [7]Baycrest, Canada, [8]University Health Network-University of Toronto, Canada, [9]University of Western Ontario, Canada, [10]The University of Toronto, Canada, [11]St. Michael's Hospital, University of Toronto, Canada, [12]Osteoporosis Canada, Canada, [13]St. Joseph's Hospital, Canada

Introduction: Our previous work in LTC has shown that awareness and use of clinical practice guidelines in Long-Term Care (LTC) are low. Clinicians practicing in LTC face unique challenges caring for elderly individuals including co-morbidities and prescribing contraindications. To address these challenges, the Gaining Optimal Osteoporosis Assessments in Long-Term Care (GOAL) knowledge translation initiative was implemented to improve identification and treatment. In this analysis, we examined baseline prescribing rates in residents identified as high-risk. Methods: GOAL is a stepped wedge cluster randomized controlled trial currently underway in 50 LTC homes in Ontario, Canada. De-identified clinical/prescribing data were downloaded from the database of a large pharmacy provider that services all study homes. Chart audits were performed to determine residents at high risk of fractures. Based on Osteoporosis Canada clinical practice guidelines, high-risk was defined as individuals who had at least one spine/hip fracture, 2 or more other fractures, or taking corticosteroids (>7.5 mg/d Prednisone equivalent). We calculated the proportion of high-risk residents who were receiving osteoporosis medications (including alendronate, risedronate, zoledronic acid, denosumab or parathyroid hormone), and average total daily vitamin D and calcium supplementation. Results: In 1740 residents from 13 LTC homes [mean age = 83 (standard deviation (10), 70% (1130/1607) women] randomized to the first wave, 12.2% (58/477) of men and 17.8% (201/1130) of women were identified as high-risk. Overall, 17.2% (10/58) of high-risk men and 42.3 % (85/201) of high risk women were taking an osteoporosis medication. Average total daily vitamin D and calcium supplementation in high-risk residents was 1189 IU/day (SD 857) and 306 mg/day (SD 432) respectively. Conclusion: Our results demonstrate that men, in particular, may be a group not being considered for fracture prevention. In the high-risk cohort, greater than 80% of men and 50% of women were not prescribed osteoporosis medication. Several factors contribute to low rates of treatment in nursing home elderly and the GOAL initiative aims to reduce this care gap.

MO0323

Real-World Evidence on Fragility Fractures and Treatment in Canadian Osteoporotic Patients. <u>Marie-Claude Meilleur</u>*[1], <u>Martin Cloutier</u>[2], <u>Jimmy Royer</u>[2], <u>Arun Krishna</u>[3]. [1]Merck Canada Inc, Canada, [2]The Analysis Group, Canada, [3]Merck, USA

OBJECTIVES: Patients with osteoporosis (OP) are at high risk of fragility fractures, although some treatments may help reduce that risk. This study aims to assess the prevalence of fractures in patients with OP in Quebec (Canada) and describe the use of antiresorptive agents (AAs) among patients who had a fragility fracture.

Methods: Patients ≥50 years of age with an OP-related event, defined as either a diagnosis for OP, a fragility fracture, or a prescription fill for an AA were identified in Quebec's healthcare database, *Régie de l'assurance maladie du Québec (RAMQ)* between 06/2005 and 06/2013. Patients with a diagnosis for Paget's disease or a neoplasm were excluded. The date of a patient's first OP-related event was defined as the index date. Patients were required to be continuously enrolled in the RAMQ healthcare plan for ≥36 months following the index date. Patients were observed from the index date until the end of their continuous RAMQ healthcare plan enrollment or end of data availability (observation period). Incident fractures were defined as either a newly diagnosed fragility fracture or a subsequent diagnosis of a fragility fracture occurring ≥6 months after a previous diagnosis for the same type of fracture.

Results: A total of 63,784 patients met the selection criteria. Most patients were female (82.6%) and ≥65 years old (64.3%). At the index date, 54.8% of the patients had a diagnosis for OP, 24.2% had a fragility fracture, and 21.0% had a prescription fill for an AA as their first OP-related event. The median follow-up time after index date was 5 years. Over the observation period, 19,498 (30.6%) patients experienced ≥1 fragility fracture. Among these patients, 13,064 (67.0%) did not use any AA over the entire observation period. Among the 13,064 patients with a fragility fracture and no use of AA, 37.9% had ≥2 fragility fractures, 14.3% had ≥3 fragility fractures, and 5.7% had ≥4 fragility fractures. Among patients previously treated with an AA or diagnosed for OP, 9.7% of them experienced ≥1 fragility fracture.

CONCLUSIONS: Despite available treatment options, a large proportion of OP patients experienced fragility fractures and a majority of these patients were untreated prior to their first fragility fracture and remained untreated. Further studies are warranted to better understand the rationales for not prescribing/using AAs.

MO0324

The Epidemiology of Distal Forearm Fractures in Austria Between 1989 and 2010. <u>Hans P. Dimai</u>*[1], <u>Axel Svedbom</u>[2], <u>Astrid Fahrleitner-Pammer</u>[3], <u>Thomas Pieber</u>[4], <u>Heinrich Resch</u>[5], <u>Christian Muschitz</u>[6], <u>Heinrich Thaler</u>[7], <u>Michael Szivak</u>[8], <u>Karin Amrein</u>[1], <u>Fredrik Borgström</u>[9]. [1]Medical University of Graz, Department of Internal Medicine, Division of Endocrinology & Metabolism, Austria, [2]OptumInsight, Sweden, [3]Medical University Graz, Austria, [4]Medical University of Graz, Department of Internal Medicine, Division of Endocrinology & Metabolism, Austria, [5]Medical University Vienna, Austria, [6]St. Vincent's Hospital, Austria, [7]Trauma Center Meidling, Austria, [8]Austrian Worker's Compensation Board (AUVA), Austria, [9]Quantify Research, Sweden

Purpose
To estimate the incidence of distal forearm fractures and assess trends in the entire Austrian population aged ≥50 years, from 1989-2010 for inpatient fractures, and from 1999 to 2010 for all fractures (outpatient and inpatient).

Methods
The number of inpatient forearm fractures was obtained from the Austrian Hospital Discharge Register (AHDR) for the entire population ≥ 50 years from 1989 to 2010. The total number of forearm fractures (i.e. including outpatient fractures) was modeled using patient level data on 36,327 patients with forearm fractures. The model estimated the proportions of patients treated in outpatient care based on sex, age and calendar year. The adjusted proportions were applied to the AHDR data to estimate the total number of forearm fractures in Austria. Age-standardized incidence rates (cases per 100,000) were estimated in 5-year age intervals. To analyze the change in incidence of forearm fractures over time, average annual changes expressed as incidence rate ratios (IRR) were calculated.

Results (Figure 1)
Age-standardized incidence
The age-standardized incidence rate per 100,000 person years of inpatient forearm fractures in women in 1989, 1999, and 2010 were estimated at 84, 155, and 192. The age standardized incidence of inpatient forearm fractures in men the same years were estimated at 24, 41, and 37. Overall, approximately 27% of all fractures were treated in an inpatient setting.

For all distal forearm fractures, the age standardized incidence in women in 1999 and 2009 were estimated at 709 (95% CI: 675-743), and 607 (578-637) respectively. The age standardized incidences in men the same years were estimated at 171 (156-185), and 162 (151-174) respectively.

Trend analyses
For inpatient fractures, the IRR analysis showed statistically significant increases in the incidence of inpatient fractures per year for both men (2.0% per year, p<0.01) and women (2.9%, p<0.01) over the entire time period (1989-2010) and the first ten

years (1989-1998) (7.6%, p<0.01 in men; and 8.1%, p<0.01 in women). However, for the last twelve years (1999-2010) the increase was only significant for women (2.2%, p<0.01).

For all distal forearm fractures, the IRR analyses showed a significant decrease in women (-1.1%, p<0.01) but not in men (-0.8%, p>0.05) over the last twelve years (1999-2010).

Conclusion
The incidence of distal forearm fractures in the entire Austrian population is comparable to hip fracture incidence which is known to be among the highest worldwide. However, trend analyses reveal a significant decrease for all distal forearm fractures in women, but not in men, over the last 12 years. It is noteworthy that similar trends have been observed for hip fracture incidence in several countries of the so-called Western World (including Austria) in the past few years.

Age-standardized incidence rates of distal forearm fracture
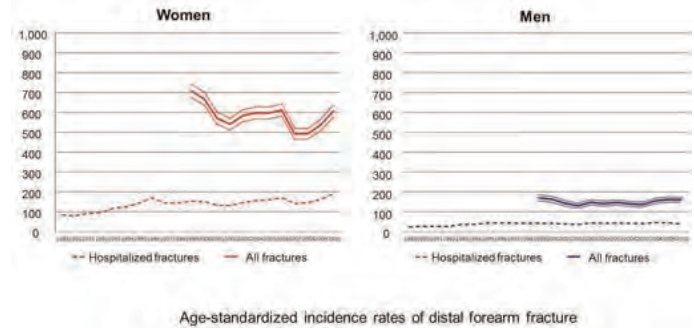
Figure

MO0325

What is the Bone Metabolic State of Patients With High Energy Trauma Fractures. <u>Debra Sietsema</u>*[1], <u>Michael Koets</u>[2], <u>Clifford Jones</u>[1]. [1]Orthopaedic Associates of Michigan; Michigan State University, USA, [2]Wayne State University School of Medicine, USA

Purpose: Osteoporosis is a metabolic bone disorder affecting 9 million adults in the United States, resulting in nearly 2 million fractures annually from low energy falls. This disease causes low skeletal mass and a decrease in bone remodeling leading to fragility and fracture. The cause of this decline in bone strength is a physiological imbalance of metabolites, most importantly calcium and Vitamin D. Yet, little is known regarding bone health of those experiencing high-energy fractures. The purpose of this study was to determine the bone metabolic health of patients with a high-energy trauma fractures.

Methods: From 2011 through 2012, 522 consecutive adults with high-energy trauma fractures were initially treated at a Level I Trauma Center, were seen in an outpatient clinic for bone health, and retrospectively evaluated. 96 patients were excluded due to insufficient chart data, resulting in 426 patients in the study. Patients had a full work up consisting of mechanism of traumatic fracture(s), health and medication history, physical exam, bone health laboratory values, and DXA.

Results: There were 231 (54%) males and 195 (46%) females with a mean age of 54 (18-90) and BMI of 27.7 (15.3-70.6) and predominance of Caucasians (405, 95%). Mechanism of injury was MVA (149, 35%), fall from height (106, 25%), MCA (53, 12%), and other (118, 28%). 19/426 (5%) had previous fracture(s) after age 50. Comorbidities included: diabetes (45, 11%), hypothyroidism (45, 11%), COPD (23, 5%), and RA (17, 4%). 92/426 (22%) were smokers and 67 (16%) were past smokers. Medication history included: bisphosphonate (10, 2%), PPI (64, 15%), Estrogen (52, 12%), Glucocorticoids (7, 2%). Lab values included: Calcium 8.9 (6.5-11.1), Vitamin D 25 (OH) 27.5 (3-65) with 262 (62%) less than 30 ng/ml. Bone turnover markers were: P1NP 52 (1-231) and CTX 0.5 (0.09-1.77). DXA T-score was -1.7 (0.4 to -4.8). Decreased T score was related to increased age (r=-0.318, p<0.001).

Conclusions: Despite having a high-energy mechanism, patients presenting with fractures at a Level 1 Trauma Center were found to have risk factors for poor bone health similar to patients presenting with low energy fractures. Vitamin D insufficiency occurred in a majority and bone turnover markers demonstrated poor bone remodeling. Previously undiagnosed osteoporosis was noted, especially with increased age. Consistent screening criteria should be implemented for all patients presenting with fractures to improve the bone-healing environment.

MO0326

Assessment of the Fracture Risk by Age Distribution in Korean Using FRAX with and without BMD. <u>JI WAN Kim</u>*[1], <u>Young-Jee Jeon</u>[2], <u>Jae Suk Chang</u>[3]. [1]Haeundae Paik Hospital, Inje University, South Korea, [2]Department of Family Medicine, Haeundae Paik Hospital, Inje University, South Korea, [3]Department of Orthopedic Surgery, University of Ulsan, College of Medicine, Asan Medical Center, South Korea

Introduction This study estimated the fracture risk according to age distribution in Korean by FRAX model and the correlation was assessed between the fracture risk with and without bone mineral density (BMD).

Methods Data collected from the 2010 Fifth Korean National Health and Nutrition Examination Survey, a cross-sectional survey of the general South Korean general population, were analyzed. The 10-year fracture risk was calculated in Korean aged 50 years or older using FRAX model with and without BMD. The correlation in relation with BMD was analyzed by evaluating the Pearson correlation.

Results The average 10-year risk was $3.9 \pm 2.4\%$ for osteoporotic fracture and $1.3 \pm 1.4\%$ for hip fracture in men over 50 years of age, while it was $8.1 \pm 4.9\%$ and $2.9 \pm 3.2\%$ respectively in women over 50 years of age. The 10-year fracture risk calculated without BMD was $4.3 \pm 14.2\%$ for osteoporotic fracture and $1.3 \pm 1.2\%$ for hip fractures in men, and those was not statistically different from the result with BMD (p=0.385, 0.591). There was a linear correlation between the risk of hip fracture with and without BMD (p<0.001), but the risk of osteoporotic fracture wasn't correlated (p=0.126). In women, the 10-year fracture risk calculated without BMD was $7.6 \pm 4.3\%$ for osteoporotic fracture and $2.6 \pm 3.1\%$ for hip fractures. The results were lower than that with BMD (p<0.001, p=0.001), and there were strong positive correlation between the risk of osteoporotic and hip fracture with and without BMD (p<0.001).

Conclusion The fracture risk was increased with age, but the increase was converted in age over than 80 years old in Korean population. The fracture risk using FRAX model with BMD was highly correlated with that with BMD, and it had a tendency to underestimate the 10-year fracture probability in women. However the FRAX risk calculator without BMD was well calibrated to hip fracture but not to major osteoporotic fracture in men.

Disclosures: JI WAN Kim, None.

MO0327

Association of serum uric acid concentration with bone: Roles of age and vitamin C intake. <u>Shivani Sahni</u>*[1], <u>Katherine Tucker</u>[2], <u>Caroline Fox</u>[3], <u>Douglas Kiel</u>[4], <u>Marian Hannan</u>[5]. [1]Hebrew SeniorLife, Institute for Aging Research & Harvard Medical School, USA, [2]University of Massachusetts Lowell, USA, [3]Framingham Heart Study, National Heart, Lung, & Blood Institute, Harvard Medical School, USA, [4]Hebrew SeniorLife, USA, [5]HSL Institute for Aging Research & Harvard Medical School, USA

Rationale: Serum uric acid (UA) has been linked with higher areal bone mineral density (BMD) but at elevated concentrations UA can act as a pro-oxidant, thus contributing to inflammation. The trabecular bone compartment may be a more sensitive indicator of changes due to inflammation-mediated osteopenia; hence, examination of associations between UA and Quantitative Computed Tomography (QCT) bone measures may provide insights into UA's metabolic effects. Further, UA increases with advancing age and vitamin C intake increases UA excretion. Yet, little is known about the role of UA on bone, accounting for these factors.

Objective: To examine the cross-sectional association of UA with QCT volumetric measures of bone [vBMD(g/cm^3), integral and trabecular vBMD] and cross-sectional area (CSA, cm^2) at the L3 level of the spine in men and women from the Framingham 3rd Generation Cohort. We further examined if these associations were modified by age and vitamin C intake.

Methods: 966 men and 800 women [mean age: 45 (31-72y) had UA (mg/dl) and QCT measures in 2002-2005. Sex-specific multivariable linear regression was used to calculate the association of UA with each of the QCT measures, adjusting for age, BMI, smoking, calcium intake, alcohol intake, physical activity, serum creatinine, vitamin C intake, and post-menopausal status (in women). Interactions with age and vitamin C intake were tested. If significant (P<0.10), then sub-groups of age (<50y; 50+y) and vitamin C intake (at median) were examined.

Results: The mean ages were 44($\pm$6) y in men and 46($\pm$6) y in women. Mean UA concentrations were 6.30 ($\pm$1.24) mg/dl in men and 4.47($\pm$1.10) mg/dl in women. UA was not significantly associated with bone measures (Table, P range: 0.07-0.98).

Significant interactions by age (men, P=0.06) and vitamin C intake (women, P=0.08) were observed for CSA. Higher UA was associated with lower CSA (P=0.02) in men ≥50 y of age, but not in men <50, Higher UA tended to be associated with lower CSA (P=0.1) in women with low vitamin C intake, but not in those with high vitamin C intake.

Conclusions: While UA was not associated with bone overall, it appeared to be important for bone in sub-sets of age in men and vitamin C intake in women. In women, vitamin C intake may modify the effect of UA on CSA, suggesting that vitamin C may protect against negative effects of elevated UA under some conditions.

Table. Association of serum uric acid with QCT measures of bone in men and women and stratified by age groups and vitamin C intake levels.

Models	QCT bone measures	Men (n=966)		Women (n=800)	
		β±SE	P value	β±SE	P value
Crude	Integral vBMD (g/cm³)	0.0015±0.001	0.08*	0.0003±0.001	0.80
	Trabecular vBMD (g/cm³)	0.0016±0.001	0.07*	0.00003±0.001	0.98
	CSA (cm²)	0.0484±0.030	0.11	0.0362±0.042	0.39
		Men (n=942)		Women (n=796)	
		β±SE	P value	β±SE	P value
Adjusted¹	Integral vBMD (g/cm³)	-0.0002±0.001	0.85	-0.0001±0.001	0.95
	Trabecular vBMD (g/cm³)	0.0001±0.001	0.97	-0.0007±0.001	0.58
	CSA (cm²)	-0.0289±0.034	0.39	-0.0828±0.051	0.10*
Age stratified		Age <50y (n=739)		Age ≥50y (n=203)		Age <50y (n=586)		Age ≥50y (n=210)	
		β±SE	P value	β±SE	P value	β±SE	P value	β±SE	P value
	Integral vBMD (g/cm³)	0.0006±0.001	0.43	-0.0027±0.002	0.17	-0.0011±0.001	0.42	0.0014±0.002	0.54
	Trabecular vBMD (g/cm³)	0.0005±0.001	0.67	-0.0020±0.002	0.27	0.0021±0.002	0.18	0.0016±0.002	0.49
	CSA (cm²)	-0.0078±0.039	0.84	-0.1604±0.060	0.02*	-0.0662±0.060	0.27	-0.1383±0.098	0.16
Vitamin C stratified		Vit C≤ median intake (n=418)		Vit C> median intake (n=544)		Vit C≤ median intake (n=399)		Vit C> median intake (n=397)	
	Integral vBMD (g/cm³)	-0.0006±0.001	0.67	-0.0001±0.001	0.92	-0.0008±0.002	0.66	0.0003±0.001	0.80
	Trabecular vBMD (g/cm³)	-0.0006±0.002	0.58	0.0002±0.001	0.88	-0.0008±0.002	0.76	-0.0011±0.002	0.48
	CSA (cm²)	-0.0338±0.052	0.52	-0.0298±0.043	0.52	-0.1278±0.077	0.10	-0.0337±0.067	0.61

¹ adjusted for age, BMI, smoking, total calcium intake, alcohol intake, PAI, creatinine and post-menopausal status (in women) and vitamin C intake.
* P≤0.05
† P>0.05

Table

Disclosures: Shivani Sahni, Unrestricted research grants from General Mills Bell Institute of Health and Nutrition , 7

MO0328

Associations between Serum Vitamin K1 and Risk of Hip Fractures in Elderly Norwegian Men and Women. A NOREPOS Study. <u>Trine Elisabeth Finnes</u>*[1], <u>Cathrine M Lofthus</u>[2], <u>Haakon E. Meyer</u>[3], <u>Anne Johanne Søgaard</u>[4], <u>Grethe Tell</u>[5], <u>Ellen M Apalset</u>[6], <u>Clara Gjesdal</u>[7], <u>Guri Grimnes</u>[8], <u>Berit Schei</u>[9], <u>Rune Blomhoff</u>[10], <u>Sven Ove Samuelsen</u>[11], <u>Kristin Holvik</u>[12]. [1]Sykehuset Innlandet Thrust, Norway, [2]Department of Endocrinology, Oslo University Hospital, Norway, [3]Norwegian Institute of Public Health/University of Oslo, Norway, [4]Department of Chronic Diseases, Division of Epidemiology, Norwegian Institute of Public Health, Norway, [5]Department of Global Public Health & Primary Care, University of Bergen, Norway, [6]Department of Global Public Health & Primary Care, University of Bergen & Department of Rheumatology, Haukeland University Hospital., Norway, [7]Haukeland University Hospital, Norway, [8]University Hospital of Northern Norway, Norway, [9]Department of Public Health & General Practice Norwegian University of Science & Technology, Norway, [10]Department of Nutrition, Faculty of Medicine, University of Oslo, Norway, [11]Department of Mathematics, University of Oslo, Norway, [12]Norwegian Institute of Public Health, Norway

BACKGROUND: Low vitamin K concentrations are associated with a higher proportion of under-carboxylated osteocalcin, and are suggested a risk factor for osteoporotic fractures. The relationship between circulating vitamin K1 and the risk of fractures is not established, and few larger studies have included both men and women.

AIM: To investigate the association between the levels of serum vitamin K1 (phylloquinone) and the risk of subsequent hip fractures in elderly men and women.

MATERIALS AND METHODS: In this case cohort study 21,774 men and women aged 65 to 79 years who attended four community based health studies during 1994-2001 were followed with regard to hip fractures for a median follow up time of 8.2 years. Hip fractures were identified through electronic discharge registers. Vitamin K1 was determined in frozen serum samples obtained at baseline in all hip fracture cases (n=1090) and in a randomly selected subcohort (n=1241). The relation between quartiles of vitamin K1 and risk of hip fracture was investigated in a Cox proportional hazards regression adapted for the case-cohort design.

RESULTS: Serum vitamin K1 levels ranged from 0 to 11.7 ng/mL (median 0.72 ng/mL). In a model adjusted for age, sex, and study centre, HR for hip fracture in the 1st (lowest) quartile of vitamin K1 compared to the 4th (highest) quartile was: 1.47 (95% CI: 1.15 – 1.87). The corresponding figures for the 2nd and the 3rd quartiles were 1.29 (95% CI: 1.01 – 1.64) and 1.09 (95% CI: 0.85 – 1.40), respectively. P for trend across quartiles was <0.001. The same pattern was seen in sex stratified analyses, and no interaction between sex and vitamin K was found. In a model also adjusting for body mass index and serum concentrations of 25OH-vitamin D, α-tocopherol and retinol, HR for hip fracture in the 1st compared to the 4th quartile was 1.30 (95% CI: 1.01 – 1.67).

CONCLUSION: Low serum concentrations of vitamin K were associated with a higher risk of hip fractures. Intake of vitamin K1 may be a surrogate marker of a healthy life style. However, the higher risk for hip fracture was still evident after adjusting for common confounders, and other fat soluble vitamins. The possible protective effect of vitamin K1 provides a preventive opportunity, which should be investigated in well-designed randomized controlled trials.

Disclosures: Trine Elisabeth Finnes, None.

MO0329

Brown adipose tissue (BAT) activity is inversely associated with bone mineral density (BMD) in healthy young adults. Robert McLean*[1], Lauren Weiner[2], Aaron Cypess[2], Douglas Kiel[3]. [1]Hebrew SeniorLife Institute for Aging Research & Harvard Medical School, USA, [2]Joslin Diabetes Center & Harvard Medical School, USA, [3]Hebrew SeniorLife Institute for Aging Research & Harvard Medical School, USA

While white adipose tissue stores energy, BAT generates energy through calorie consumption (thermogenesis), which can be activated in response to cold exposure. BAT depots have recently been identified in adults. It has been hypothesized that BAT in the bone marrow may regulate osteogenesis, or that reduced BAT activity may indirectly contribute to bone loss through increased sympathetic activity. In humans, BAT volume was positively correlated with BMD in women with anorexia, and in women, but not men, in a study of healthy adults. Identification of BAT activity as a mechanism for bone loss would suggest that activation BAT may be a potential intervention for maintaining bone. The objective of this study was to determine the association between BAT activity and BMD in healthy adults. Nine (4 men, 5 women) young (mean age 25 years, range 20-31), healthy volunteers were recruited from the community. Height and weight were measured and body mass index (BMI, kg/m^2) was calculated. Total body BMD, fat-free mass and fat mass were measured by DXA (Discovery A, Hologic). BAT activity (BAT volume [mL] x mean standard uptake value [g/mL]) was determined by ^{18}F-fluorodeoxyglucose (FDG) PET-CT (Discovery LS, GE Medical Systems) after 2 hours of cold exposure (14℃) using a cooling vest. Unadjusted correlations (r) among study variables were calculated, and linear regression was used to calculate the age- and multivariable-adjusted association between BAT activity and BMD. Mean BMI was 23 kg/m^2 (range 19-29) and mean BMD was 1.188 g/cm^2 (SD 0.122). Unexpectedly, BAT activity was negatively correlated with BMD (r=-0.72, P=0.03; Figure). BAT was also negatively correlated with age (-0.58, P=0.09), but was not correlated with BMI, fat-free mass or fat mass. BMD was positively correlated with age (r=0.74, P=0.02). After age adjustment, there was no statistically-significant association between BAT activity and BMD (β=-0.0009, P=0.18), and results were similar after adjustment for BMI, fat mass and fat free mass. These results suggest that increased BAT activity may be associated with lower BMD in young, healthy adults. Larger studies of longitudinal changes in BMD that include adults across a wider age range are needed to determine whether BAT may have a mechanistic role in bone loss.

Figure. Association of brown adipose tissue (BAT) activity after cold exposure with total body BMD among healthy volunteers (4 men, 5 women) aged 20 to 31 years.
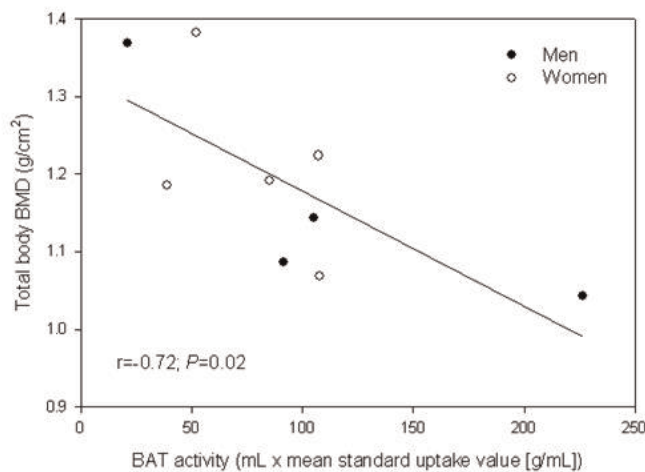
Figure

MO0330

Cancer Rates in Men With and Without Osteoporosis in a US Healthcare System. Cynthia O'Malley*[1], Nguyet Tran[2], Carol Zapalowski[3], Nadia Daizadeh[4], Thomas Olenginski[5], Jane Cauley[6]. [1]Amgen Inc., USA, [2]Amgen Inc., USA, [3]Amgen, USA, [4]Amgen Inc, USA, [5]Geisinger Medical Center, USA, [6]University of Pittsburgh Graduate School of Public Health, USA

Introduction: Osteoporosis (OP) and cancer are common age-related diseases which share some similar risk factors such as smoking and alcohol use. Moreover, bone-sparing therapies are approved to counter the bone loss associated with a number of cancer treatments. Given the co-occurrence of these common conditions, we describe the incidence of cancers in men by OP status.

Methods: We identified 3,600 men with OP (evidence of OP diagnosis, fragility fracture or OP medication order) and 3,600 age-matched controls with no evidence of OP in the electronic health records from an integrated healthcare system (2004-2009). Men were also matched by length of follow-up to allow equal opportunity to develop an incident cancer. For each cancer type, exposure time began at index until the first of the following events: a diagnosis of that cancer, death, disenrollment, end of study. For each cancer type, incidence rates (IR) were calculated by dividing the number of men with the cancer by the total follow-up person-years (P-Y) at risk for that cancer. Exact Poisson 95% confidence intervals (CI) were also generated. For comparison, we present SEER age-adjusted rates for white men age ≥65.

Results: The matched groups had a mean age of 70.9 years (standard deviation [SD], 9.0) with an average follow-up time of 2.2 years; 98% were white. The mean (SD) body mass index (BMI) was 28.1 (5.4) in the 91.4% of the OP subjects with known BMI. In the control group, the mean (SD) BMI was 29.1 (5.5); BMI was known for 67.7% of these subjects. BMI could not be calculated in men with missing height. For all malignancies combined, the IRs were similar between the OP subjects and controls, at 29.3 per 1,000 P-Y and 30.4 per 1,000 P-Y, respectively. IRs by OP status were similar for the most common cancers including prostate, lung, colorectal and bladder cancers (see table). Carcinoma in situ of skin was common in both the OP and control groups (7.1 and 6.2 per 1,000 P-Y, respectively). SEER IRs were similar to those reported here, falling within the observed CIs. The exceptions were lung/bronchus and brain tumors which were higher in our study, regardless of OP status.

Conclusion: This assessment describes the cancer burden in older men by OP status. While there were slight variations in IRs by OP status, the rates were similar overall in this study population and comparable to those reported for older men in the SEER registry.

Table. Cancer rates in men by osteoporosis status, 2004–2009

	Men with osteoporosis (N = 3,600)		Men without osteoporosis (N = 3,600)		Age- adjusted SEER[1] White Males Age ≥ 65
	IR[2] per 1,000 Person-years	95% CI[3]	IR[2] per 1,000 Person-years	95% CI[3]	IR[2] per 1,000 Person-years
All malignant neoplasms	29.3	25.6, 33.5	30.4	26.5, 34.7	27.4
Prostate	9.8	7.7, 12.3	9.1	7.0, 11.5	7.6
Lung, bronchus	6.5	4.8, 8.5	7.5	5.7, 9.7	4.5
Colorectal	3.3	2.2, 4.9	4.2	2.9, 5.9	2.7
Bladder	2.5	1.5, 3.9	2.5	1.6, 3.9	2.5
Melanoma	2.0	1.2, 3.3	2.9	1.9, 4.4	1.4
Kidney/Renal	1.8	1.0, 3.0	1.4	0.7, 2.5	0.9
Multiple myeloma	1.6	0.9, 2.8	0.6	0.2, 1.5	0.4
Lymphoma	1.5	0.8, 2.7	1.8	1.0, 3.0	1.2
Leukemia	1.4	0.7, 2.5	0.9	0.4, 1.8	0.8
Oral	1.3	0.6, 2.3	1.0	0.4, 2.0	0.6
Brain/Nervous system	1.1	0.5, 2.2	1.0	0.4, 2.0	0.3
Pancreas	1.0	0.4, 2.0	2.1	1.2, 3.4	0.8
Stomach	0.9	0.4, 1.8	0.6	0.2, 1.5	0.5
Liver	0.8	0.3, 1.6	1.0	0.4, 2.0	0.4
Larynx	0.8	0.3, 1.6	0.8	0.3, 1.7	0.3
Carcinoma in situ of skin	7.1	5.4, 9.3	6.2	4.6, 8.2	Not available

[1]Howlader et al. SEER Cancer Statistics Review, 1975-2010, National Cancer Institute. Bethesda, MD, http://seer.cancer.gov/csr/1975_2010/, based on November 2012 SEER data submission, posted to the SEER web site, April 2013
[2]IR = incidence rate; [3]CI = confidence interval
IRs are not shown for cancers with < 5 new diagnoses (Hodgkin's, gall bladder, penile, testicular, breast, endocrine, and bone).

Table. Cancer rates in men by osteoporosis status. 2004-2009

MO0331

Co-morbidities in patients with a recent fracture at the Fracture Liaison Service. Lisanne Vranken*[1], Caroline Wyers[2], Robert Van Der Velde[3], Heinrich Janzing[4], Wim Morrenhof[5], Marcel Janssen[6], Piet Geusens[7], Joop Van Den Bergh[8]. [1]VieCuri Medical Centre, The Netherlands, [2]Maastricht University, The Netherlands, [3]VieCuri Medical Center Venlo, the Netherlands, The Netherlands, [4]VieCuri Medical Centre, Department of Surgery, Netherlands, [5]VieCuri Medical Centre, Department of Orthopedic Surgery, Netherlands, [6]VieCuri Medical Centre, Laboratory of Clinical Chemistry & Haematology, Netherlands, [7]University Hasselt, Belgium, [8]VieCuri MC Noord-Limburg & Maastricht UMC, The Netherlands

Purpose
To evaluate co-morbidities and medication use in patients with a recent fracture (fx) at the Fracture Liaison Service (FLS).
Methods
Retrospective chart review of all consecutive patients with a recent fx visiting the FLS for fracture risk evaluation. Data were analysed using Chi-square tests, Fisher's Exact Test and logistic regression analysis adjusting for age, sex, BMD (normal vs. osteopenia vs. osteoporosis) and fx classification (finger & toe vs. minor vs. major vs. hip).
Results
1359 consecutive patients (≥50 yrs) were evaluated at the FLS (72% women; mean age 65 years), 57% with a minor, 29% major, 8% hip and 6% finger or toe fx. Osteoporosis was diagnosed in 30%, osteopenia in 47% and a normal BMD in 23%. In 83% one or more co-morbidities were reported in medical history; cardiovascular disease (CVD) in 27%, COPD in 7%, diabetes mellitus type 2 (DM2) in 7%, rheumatic disease in 4% and psychiatric disorders in 4%. CVD was significantly more present in men (p=0.001) at higher age (p=.000), COPD with lower BMD (p=.002), DM2 with

higher age (p=0001) and psychiatric disorders with lower BMD (p=.035) and severe fx (p=.008). In addition, in 28% of patients we detected ≥ 1 contributors to secondary osteoporosis with laboratory testing (men: 22%, women 30%); monoclonal proteinemia in 0.5%, renal insufficiency grade ≥ 3 in 11.2%, primary hyperparathyroidism in 3.0%, secondary hyperparathyroidism in 15.7%, hyperthyroidism in 5.1% of patients and hypogonadism in 1.6% of men. The presence of these contributors was significantly higher in women (p=.002) at higher age (p=.000). Medication was used by 74% of patients; 54% used 1-4 drugs and 20% used ≥ 5 drugs (polypharmacy); cardiovascular medication was used by 45%, antidepressant by 8%, benzodiazepine by 7%, proton-pump inhibitor by 17% and antiepileptic by 4%. Polypharmacy was reported more frequently in patients with higher age (p=0.000), lower BMD (p=.015) and severe fx (p=.001). After adjustments, only age was significantly related with polypharmacy.

Conclusion

One or more co-morbidities were present in 83% of patient with a recent fracture after age 50 and 74% use one or more drugs, 20% with polypharmacy. Furthermore, in 28% new contributors to secondary osteoporosis were diagnosed. Therefore careful evaluation of medical history, medication use and laboratory testing should be performed for optimal management of bone and fall related co-morbidities and risk factors.

Disclosures: Lisanne Vranken, None.

MO0332

High Prevalence of Vitamin D Insufficiency and Deficiency among Postmenopausal Women in China: Preliminary Results of a Chinese Multicenter Study. <u>Zhongjian Xie</u>[1], <u>Zhenlin Zhang</u>[2], <u>Eryuan Liao</u>[1], <u>Wen Wu</u>[3], <u>Chunyan Lu</u>[4], <u>Shuqing Tao</u>[5], <u>Lijun Wu</u>[6], <u>Julie Chandler</u>[7], <u>Senaka Peter</u>[8], <u>Ting Wu</u>[9], <u>Weibo Xia</u>*[10]. [1]Institute of Endocrinology & Metabolism, the second Xiangya Hospital of Central South University, China, [2]Department of Osteoporosis & Bone Diseases, Shanghai Jiao Tong University, Affiliated Sixth People's Hospital, China, [3]Department of Endocrinology, Guangdong General Hospital, China, [4]Department of Endocrinology, West China Hospital, Sichuan University, China, [5]Department of Orthopedics, the Second Affiliated Hospital of Garbin Medical University, China, [6]Department of Rheumatism & Immunology, People's Hospital of Xinjiang Uygur Autonomous Region, China, [7]Merck Research Laboratories, USA, [8]Department of Epidemiology, Merck Research Laboratories, USA, [9]Department of Epidemiology, Merck Research Laboratories, China, [10]Department of Endocrinology, Key Laboratory of Endocrinology, Peking Union Medical College Hospital, Chinese Academy of Medical Sciences, China

Purpose: Previous small studies exploring the prevalence of low serum Vitamin D [25(OH)D] levels among postmenopausal women in China reported inconsistent findings. The aim of this study was to determine the prevalence of low 25(OH)D levels in a large cohort of post-menopausal women in China.

Methods: This cross-sectional study recruited 960 women with a mean age of 65.8 years (55-93) from urban (N=481) and rural (N=479) areas of 7 geographically distinct regions during the summer in China. Each woman was evaluated for total serum 25(OH)D using liquid chromatography-tandem mass spectrophotometry, fracture risk using Osteoporosis Self-Assessment Tool for Asians (OSTA), and bone mineral density (BMD) using Dual energy X-ray absorptiometry. Demographic and clinical data were obtained and a questionnaire assessing general health, lifestyle habits and sun exposure was completed. Published definitions of vitamin D deficiency range from 25(OH)D < 10ng/ml to < 20ng/ml, and insufficiency from < 20ng/ml to <30ng/ml. For the present study, prevalence is reported using 25(OH)D cut-off points of < 15 ng/ml, < 20ng/ml and < 30ng/ml.

Results: Overall, 43.8 % of women had a serum 25(OH)D < 20 ng/ml, with a higher prevalence (48.1%) in women over 75 years and a lower prevalence (38.5%) in women 55-59 years.. The overall prevalence was 86.5% for 25(OH)D < 30 ng/ml and 17% for 25(OH)D < 15 ng/ml. Using a cut-off point of 25(OH)D <20 ng/ml, the prevalence was significantly higher among urban than rural dwellers (51.1% vs. 36.3%. respectively). Prevalence of low vitamin D levels increased with decreasing BMD. The prevalence of low vitamin D varied by region, but not necessarily latitude, with lower prevalence (19.2-25%) found in the Middle and Northeast regions, and higher prevalence (46.7-56.7%) found in Northwest, North, East, Southwest and South regions. There was no correlation between the prevalence of low vitamin D and fracture risk score determined by OSTA.

Conclusions: Our results show that the prevalence of Vitamin D deficiency and insufficiency, by any definition, is common among postmenopausal women in China, even during the summer, and especially among those living in urban areas. Higher prevalence of low Vitamin D is associated with lower BMD. Increased awareness of Vitamin D deficiency and insufficiency among post-menopausal women in China is necessary, and dietary and other intervention strategies should be undertaken to correct this problem.

Disclosures: Weibo Xia, None.
This study received funding from: Merck and Co, Inc was the funder and has a financial interest in Osteoporosis

MO0333

Hip Fracture Vital Signs: Simple Observations at a Medical Visit Estimate Hip Fracture Risk in Women and Men. <u>Steven Cummings</u>*[1], <u>Lily Lui</u>[2], <u>Peggy Cawthon</u>[3], <u>Jane Cauley</u>[4], <u>Susan Diem</u>[5], <u>Teresa Hillier</u>[6], <u>Kristine Ensrud</u>[7]. [1]San Francisco Coordinating Center, USA, [2]UCSF, USA, [3]California Pacific Medical Center Research Institute, USA, [4]University of Pittsburgh Graduate School of Public Health, USA, [5]University of Minnesota, USA, [6]Kaiser Center for Health Research, USA, [7]University of Minnesota & Minneapolis VA Health Care System, USA

We developed a simple assessment of a patient's risk of hip fracture that can be counted while taking vital signs and walking the patient to the exam room. Hip fracture risk would be available when the physician begins to talk with the patient.

We included 9495 women enrolled in the prospective community-based Study of Osteoporotic Fractures (SOF) and 5921 men enrolled in the companion MrOS. The two studies made similar measurements of weight and height (BMI), pulse rate, walking speed over 6 meters, and ability to rise from a chair without needing one's arms. Incident hip fractures were validated by radiographs over 12 years of 98 and >99% complete follow-up. We generated separate multivariable proportional hazards models for women and men but the associations were very similar so we pooled the data into one multivariable model. Points were based on the coefficients for each term in the multivariable model (multiplying by 2 and rounded to the nearest digit) to create a simple additive score. We then calculated the relative hazards and absolute risks of hip fracture for categories of total scores. The scores and rates warrant validation and calibration in other cohorts.

Every factor was significantly and independently associated with risk of hip fracture (Table 1). Each added point strongly increased a patient's risk of hip fracture (Table 2). 23.0% of women and 5.5% of men had a score ≥ 5 points indicating at least an 18.6% 10-year risk of hip fracture. We conclude that a patient's risk of hip fracture can be easily estimated at the beginning of any medical visit. Start with points for gender and age. From vital signs, add points for BMI and pulse rate. Then add points as the patient walks a timed distance on the way to the exam room and then sits then rises from the chair. This quickly generates a risk of hip fracture that physician sees along with other vital signs to stimulate discussion about how to reduce that risk.

Table 1. Association of individual vital signs with relative risk of hip fracture and points

Sign	Points	HR (95% CI)
Female	1	1.8 (1.5, 2.1)
Age ≥ 75	2	2.9 (2.5, 3.3)
BMI <25	1	1.6 (1.4, 1.8)
Pulse ≥80	1	1.3 (1.1, 1.5)
Gait ≤1.0 m/s	2	2.4 (1.9, 2.9)
or >1.0-1.2 m/s	1	1.5 (1.3, 1.9)
Unable to rise	1	2.1 (1.6, 2.6)

Table 2. Total points and hip fracture risk

Total	10-yr risk %	HR (95% CI)	Prevalence (%)
0	1.1	1	9.4
1	2.3	2.0 (1.2, 3.5)	12.6
2	3.8	3.4 (2.1, 5.4)	20.9
3	5.0	4.4 (2.8, 7.1)	25.4
4	9.7	8.9 (5.5, 14)	15.5
≥5	18.6	18 (11, 28)	16.3

Tables of vital signs and risk of hip fracture

Disclosures: Steven Cummings, None.

MO0334

Lack of concordance among vitamin D binding protein assays and effect on bioavailable 25OHD estimates. Carrie Nielson*[1], Priya Srikanth[2], Ying Wang[1], Christine Swanson[2], Christine Lee[1], Rene Chun[3], Martin Hewison[4], John Adams[4], Dirk Vanderschueren[5], Roger Bouillon[5], Jodi Lapidus[2], Jane Cauley[6], Eric Orwoll[1]. [1]Oregon Health & Science University, USA, [2]Oregon Health & Science University, USA, [3]UCLA/ Orthopedic Hospital Research Center, USA, [4]University of California, Los Angeles, USA, [5]Katholieke Universiteit Leuven, Belgium, [6]University of Pittsburgh Graduate School of Public Health, USA

Vitamin D binding protein (DBP) is an important determinate of vitamin D activity. Bioavailable 25OHD (bioD) varies by circulating DBP level, and DBP haplotype affects binding affinity for 25OHD. Multiple DBP assays are available, but their concordance has not been determined. We compared results of three DBP assays and evaluated their effect on resulting bioD estimates.

In a random sample of 610 men in the Osteoporotic Fractures in Men (MrOS) cohort (age $\geq$65), we measured DBP by 3 assays (R&D Systems, Genway, and Leuven). 25OHD was measured by GCMS. DBP genotyping was done for two nonsynonymous SNPs, rs4588 (Thr436Lys) and rs7041 (Asp432Glu), and these were combined into six previously characterized haplotypes, corresponding to those with the highest (1F1F) to lowest affinity (22) for 25OHD. From these, bioD was estimated using previously validated equations. Correlations and plots were used to assess concordance across the range of DBP and bioD. Differences in mean DBP and bioD by DBP haplotype were tested by ANOVA.

Mean DBP levels were similar across all three assays (4.8-5.1 µM), and SD were similar for Genway and Leuven assays (0.8 and 0.7, respectively); the R&D assay had a much broader distribution (SD=1.7). All had low CVs (2-4%). Correlations among DBP assays were generally poor: they were highest between Genway and Leuven (r=0.60) and weak for R&D and Genway (r=0.29) and R&D and Leuven (r=0.39, all p<0.0001). Correlations among calculated bioD estimates were high for those incorporating DBP from Genway and Leuven (r=0.95), but were lower for those incorporating R&D (with Genway, r=0.65; with Leuven, r=0.66; all p<0.001). All DBP assay results differed by DBP haplotype (Figure, p<0.001); for Genway and Leuven assays, DBP was lower among higher affinity haplotypes, and for the R&D assay, DBP was lowest in the highest affinity (1F1F) haplotype. Assay differences were most pronounced in the 1F1F and 1F2 haplotypes, those common in persons of African descent. These differences resulted in higher mean bioD for 1F1F and 1F2 haplotypes when R&D was used than when Genway or Leuven were used.

These results have important implications for assessing biological effects of DBP and bioD, and for understanding racial differences in vitamin D physiology. Understanding the reasons for assay discordance will be necessary before conclusions can be drawn regarding DBP and calculated bioD associations with skeletal and other outcomes.

Figure. DBP distributions differ by DBP by haplotype. Left side is Genway, and distributions are similar for Leuven (not shown); right side is R&D. All p for ANOVA < 0.001.
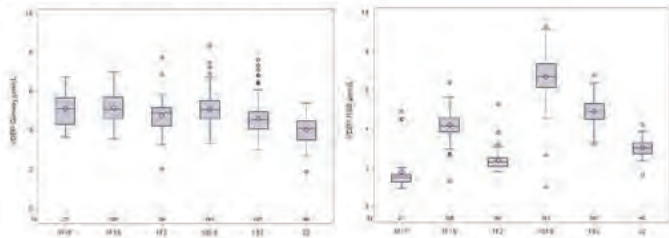
Figure. DBP distributions differ by DBP by haplotype.

Disclosures: Carrie Nielson, None.

MO0335

Risk factors for hip fracture in older men: The Osteoporotic Fractures in Men Study (MrOS). Jane Cauley*[1], Peggy Cawthon[2], Kathy Peters[3], Steven Cummings[4], Kristine Ensrud[5], Douglas Bauer[6], Brent Taylor[7], James M. Shikany[8], Andrew Hoffman[9], Nancy Lane[10], Deborah Kado[11], Eric Orwoll[12]. [1]University of Pittsburgh Graduate School of Public Health, USA, [2]California Pacific Medical Center Research Institute, USA, [3]California Pacific Medical Center Research Institute, USA, [4]San Francisco Coordinating Center, USA, [5]University of Minnesota & Minneapolis VA Health Care System, USA, [6]University of California, San Francisco, USA, [7]University of Minnesota, USA, [8]University of Alabama, Birmingham, USA, [9]Stanford University, USA, [10]University of California, Davis Medical Center, USA, [11]University of California, San Diego, USA, [12]Oregon Health & Science University, USA

Risk factors for hip fracture have been extensively studied in women have but less is known about risk factors for hip fracture in men. We performed a comprehensive overview of risk factors for hip fracture and tested whether these risk factors are independent of femoral neck bone mineral density (FN BMD).

MrOS is a prospective study of 5,994 men, age 65+. Among 5,876 men not reporting osteoporosis treatment at baseline, 178 men suffered an incident hip fracture confirmed by radiographic report during a mean of 8.64 ± 2.5 years of 99% complete follow-up. Follow-up time was truncated to 10 years. All risk factors and measurements were assessed at the baseline exam. Cox Proportional Hazards models were used to calculate the hazard ratio (HR) and 95% confidence intervals (CI).

Older age ($\geq$ 75 years), poor chair stand performance, comorbidity, current smoking, positive fracture history since age 50 , greater height and lower mental health scores were all associated with an increased risk of hip fracture, Table. Body mass index was not associated with an increased risk of hip fracture after adjustment for FN BMD. One standard deviation decrease in FN BMD was associated with 3-fold increased risk of hip fracture after adjusting for BMD most associations remained statistically significant although the magnitudes of the HRs were attenuated. Two or more major comorbidities were associated with > 2-fold risk of hip fracture. Specific comorbidities associated with an increased risk of hip fracture in a secondary multivariate + BMD model were history of myocardial infarction, HR=1.57 (1.03, 2.39), hyperthyroidism, HR=2.57 (1.18, 5.61), stroke, 1.99 (1.25, 3.16) and Parkinson's disease, HR=4.12 (1.64, 10.36). Tricyclic antidepressant use was also associated with an increased risk of hip fracture, HR=2.73 (1.26, 5.91). Education, health status, weight change, family history of fracture, diabetes, RA or OA, physical activity, alcohol, cognitive function and visual impairments were unrelated to hip fracture. Several variables unrelated to hip fracture e.g., rheumatoid arthritis and corticosteroids likely reflected low power.

Older men who smoke and have multiple comorbidities, low BMD, greater height, a positive fracture history and have poor chair stand test performance have an increased risk of hip fracture. Targeting these high risk men for intervention could prevent hip fractures.

Table: Multivariate Models of Risk Factors for Hip Fracture with and without adjusting for FNBMD

	Referent/ Unit for HR	Multivariate Model HR(95% CI)	Multivariate Model + BMD HR(95% CI)
Age(y)	65-69		
70-74		1.51 (0.84, 2.71)	1.43 (0.79, 2.57)
75-79		3.63 (2.13, 6.20)	2.76 (1.62, 4.73)
80-84		6.37 (3.65, 11.13)	4.80 (2.74, 8.39)
85+		7.98 (4.01, 15.88)	5.39 (2.70, 10.79)
FN BMD g/cm²	0.13 g/cm²*	——	3.21 (2.61, 3.95)
BMI(kg/m²)	$\geq$ 30		
25- < 30		1.20 (0.76, 1.87)	0.80 (0.51, 1.25)
< 25		1.85 (1.15, 2.98)	0.78 (0.48, 1.28)
Chair Stand	Quartile 1		
Quartile 2		1.78 (1.02, 3.11)	1.55 (0.89, 2.71)
Quartile 3		1.91 (1.10, 3.32)	1.71 (0.98, 2.98)
Quartile 4		2.48 (1.44, 4.25)	1.97 (1.15, 3.38)
Unable		4.35 (1.87, 10.12)	3.71 (1.60, 8.58)
Major Comorbidity**	None		
1		1.67 (1.20, 2.32)	1.87 (1.34, 2.61)
$\geq$ 2		1.94 (1.20, 3.12)	2.33 (1.44, 3.77)
Current Smoker	Past or Never	2.55 (1.32, 4.93)	2.08 (1.06, 4.07)
Fracture History after age 50	No	1.87 (1.38, 2.54)	1.44 (1.06, 1.97)
Fall past 12 months	No	1.12 (0.80, 1.57)	1.26 (0.90, 1.77)
Height at age 25(cm)	6.87 cm*	1.10 (0.94, 1.29)	1.24 (1.06, 1.45)
SF-12 Mental Score	6.96*	0.87 (0.76, 0.99)	0.90 (0.79, 1.02)
SF-12 Physical Score	10.20*	0.99 (0.85, 1.16)	1.05 (0.90, 1.23)

*per one standard deviation
**Major comorbidity = myocardial infarction (MI), stroke, congestive heart failure, chronic obstructive pulmonary disease, diabetes and Parkinson's disease.
All models also adjusted for race and clinic.

Table

Disclosures: Jane Cauley, None.

MO0336

Systematic evaluation of loss of renal function over 10 years in elderly Swedish women. Linnea Malmgren*[1], Fiona McGuigan[2], Sofia Berglundh[1], Kerstin Westman[1], Anders Christensson[1], Kristina Akesson[3]. [1]Skane University Hospital, Sweden, [2]University of Lund, Malmö, Skane University Hospital, Malmö, Sweden, [3]Skåne University Hospital, Malmö, Sweden

Introduction: Chronic kidney disease (CKD) has been shown to be associated with bone mineral density (BMD), bone loss and fracture, therefore identifying women at risk of CKD is an important element in fracture prevention. There is a natural decline in renal function with age, but longitudinal studies investigating the pattern of decline in elderly women are scarce. We estimated renal function using the most commonly used creatinine based algorithms in 1011 women from the population based OPRA cohort consisting of 75-year-old Swedish women, at baseline, 3-, 5- and 10 years and investigated the association with mortality and comorbidities.

Materials and methods: Serum creatinine was measured at age 75 (N=1011), age 78 (N=849) age 80 (N=679) and age 85 (N=362). Estimated glomerular filtration rate (eGFR) was calculated using each of the equations; Chronic Kidney Disease Epidemiology Collaboration (CKD-EPI), the revised Lund-Malmö (LM-rev), the Modification of Diet in Renal Disease (MDRD), the Berlin Initiative Study (BIS-1) and the Cockcroft-Gault (CG) study equations. CKD was staged as 1-5 and mortality and comorbidity compared between women with CKD stage 3 or worse and all others using Cox proportional hazard and regression.

Results: Approximately 95% of women aged 75-85 years had an eGFR equivalent to CKD stage 2-3 from CKD-EPI, with a continuous progression towards stage 3 during the follow-up. During the 10y follow-up, an overall loss of 22% of eGFR was observed, with an accelerated loss between ages 80-85y. Mean loss per decade was 16.5 mL/min (SD 12.2). Women with advanced CKD (stage 3-5) had an almost doubled risk of dying (adjusted hazard ratio 1.9 (95%CI 1.3-2.8) during the follow-up and an increased risk of comorbidities.

Conclusion: In 75-85 year old women the majority has reached CKD stage 2-3 and that it is essential to use a formula appropriate for age. Loss of renal function is not uniform over time and is related to eGFR level at baseline. The twenty percent reduction in renal function over 10 years is considerably higher than previously estimated. These studies indicate reduced kidney function is associated with impaired health and mortality, whereas the implications for bone loss and fracture will be further evaluated.

Disclosures: Linnea Malmgren, None.

MO0337

A Fracture Liaison Service specifically designed to address local government concerns can be effective. <u>Diane Theriault</u>*[1], <u>Carla Purcell</u>[2]. [1]Dartmouth General Hospital, Canada, [2]Dartmouth General Hospital, Canada

There is no Fracture Liaison Service (FLS) in Nova Scotia, Canada. The Dartmouth General Hospital (DGH) Fracture Navigator Program (FNP) was designed as a prototype that might be endorsed by government for on-going funding. Accordingly, the prototype is aligned with the 2010 Osteoporosis Canada (OC) Guidelines, uses a nurse working through protocols with minimal on-going input from physicians, lessens duplication of services and recommends limited referrals to osteoporosis specialists (only as per the indications listed in the 2010 OC Guidelines). The FNP focuses on high risk patients and ensuring that they receive effective osteoporosis medication to reduce their risk of repeat fracture.

The FNP sees fragility fractures of hip, spine, wrist, shoulder and pelvis at DGH. Initially, the patient's fracture risk is determined as per 2010 OC Guidelines: BMD and spine X-rays performed and CAROC tool used. A letter is sent to the family physicians of high risk patients recommending osteoporosis treatment. To see if effective medication has been started, these patients are contacted by phone 3 months later.

We show results for the non-spine fractures only. Fracture risk assessment is described for patients who had initial fractures from Feb 19, 2013 to Jan 13, 2014; treatment rates are described for patients who had initial fracture from Feb 19 to Dec 31, 2013. A total of 204 non-spine fractures were seen up to Jan 13, 2014. Exclusions include under the care of an osteoporosis specialist (5), bilateral total hip replacement (1), subtrochanteric femoral fracture (2), palliative care (2). 19 patients declined enrollment and 3 have yet to undergo the prescribed investigations. Of the 173 non-spine fracture patients who completed the fracture risk assessment, 123 (71.1%) were deemed at high risk and 50 (28.9%) were deemed at moderate risk as per CAROC. For the period of Feb 19 to Dec 31, 2013, there were 101 patients who were at high risk ready for phone follow-up, of which 34 could not be reached by phone by Apr 7, 2014, 1 was deceased, 1 declined further assessment and 2 were discharged as per protocol (having been referred to an osteoporosis specialist). Of the 63 remaining high risk patients, 53 (84.1%) had been initiated on treatment, 9 (14.3%) were not initiated on treatment and 1 was unsure.

Conclusion: An FLS can be designed to respond to local government concerns and still be effective at closing the post-fracture osteoporosis care gap.

Disclosures: Diane Theriault, None.

MO0338

Clinical evaluation of the appropriateness of referrals for dual energy X-ray absroptiometry: differences by physician specialty. <u>Alp Cetin</u>*. Proffessor, Turkey

OBJECTIVES

It is well established that who should be tested for dual energy X-ray absorptiometry (DXA) scan and for this purpose International Society for Clinical Densitometry (ISCD) recommendations for DXA referrals are most widely accepted guidelines. However, appropriateness of referrals for DXA has not been extensively studied so far. This study was conducted to investigate the ordering practices of physicians and appropriateness of DXA referrals in Hacetepe University Hospitals.

MATERIALS AND METHODS

The indications for DXA testing were prospectively recorded in 200 consecutive patients (174 females, 26 males) who referred for DXA scan. Indications were categorized as appropriate or inappropriate according to the ISCD recommendations; the specialty of the ordering physician was also noted.

RESULTS

DXA indications were found appropriate in 108 patients (54%) and inappropriate in 92 patients (46%). As expected most appropriate DXA scans (100%) were observed in patients referred from the department of geriatrics. This was followed by the department of physical medicine and rehabilitation (77%), rheumatology (66%), endocrinology (43%), internal medicine (42%), and obstetrics and gynecology (23%).

CONCLUSION

In this preliminary evaluation of the appropriateness of DXA testing, a considerable number of studies was classified as inappropriate. There was a great variation among different specialities who deals with osteoporosis. Educational programs should be implemented to reduce the rate of less appropriate examinations.

Disclosures: Alp Cetin, None.

MO0339

Effectiveness and feasibility of an iPad based Patient administered informed consent (IC) vs. Paper Consent for Osteoporosis Pragmatic Clinical Trials (PCT). <u>Amy Warriner</u>*[1], <u>P. Jeffrey Foster</u>[2], <u>Nicole Wright</u>[1], <u>Amy Mudano</u>[1], <u>Cora Lewis</u>[1], <u>Sebastian Sattui</u>[2], <u>Mary E. Melton</u>[2], <u>Wilson Pace</u>[3], <u>Walter Calmbach</u>[4], <u>Laura Nichols</u>[3], <u>Susan Booth</u>[5], <u>T. Michael Harrington</u>[2], <u>Jeffrey Curtis</u>[1], <u>Kenneth Saag</u>[1]. [1]University of Alabama At Birmingham, USA, [2]University of Alabama at Birmingham, USA, [3]University of Colorado Denver, USA, [4]University of Texas San Antonio, USA, [5]Mytrus, Inc., USA

Purpose: Pragmatic clinical trials (PCTs) comparing osteoporosis therapeutic options require large numbers of investigative sites for sufficient sample size and generalizability. Conducting Informed Consent (IC) constitutes a major barrier to performing PCTs in practice settings due to time and resource limitations. There is a need to improve efficiency and effectiveness of IC. To address this, we compared a patient-administered iPad IC tool to traditional paper IC in community practices and evaluated their feasibility for a mock future osteoporosis PCT of bisphosphonate discontinuation vs. continuation.

Methods: In collaboration with a software vendor experienced in direct-to-patient studies (Mytrus, Inc.), we developed an interactive iPad IC tool that included an animated video summarizing the PCT, the complete IC, and a quiz to assess and reinforce comprehension. We recruited community-based practices (n=9) from the Alabama Practice Based Research Network and the American Academy of Family Physicians National Research Network. Practices aimed to recruit 3 participants for each IC approach. Practices were randomized to start with the iPad IC, or with the paper IC. After completing 3 patient enrollments, practices were switched to the other IC process. Patient inclusion criteria included ≥ 1 year alendronate use and willingness to use an iPad for IC. Patients' comprehension and satisfaction were collected on surveys (7-point Likert scale) following the IC process. We surveyed practice staff to assess satisfaction and perceived time demands following each phase and at the end of study. Patient and provider satisfaction and patient comprehension for the 2 IC processes were compared using non-parametric methods.

Results: To date, 8 clinics have enrolled 31 women (n= 14 iPad, mean age 69.9 ± 6.5years, and n= 17 paper, mean age 72.3 ± 8.3years). Overall satisfaction and comprehension with both consent methods was high, with the iPad participants trending towards greater satisfaction and understanding of key concepts but not reaching significance (Table). Among providers, we saw similar trends in satisfaction despite a slightly longer perceived time to complete (Table). When comparing the iPad with Paper IC, providers consistently favored the iPad (Figure).

Conclusion: Patients and providers appeared more satisfied with the iPad delivered IC than traditional paper IC. Use of patient administered iPAD has potential to improve IC effectiveness in PCTs.
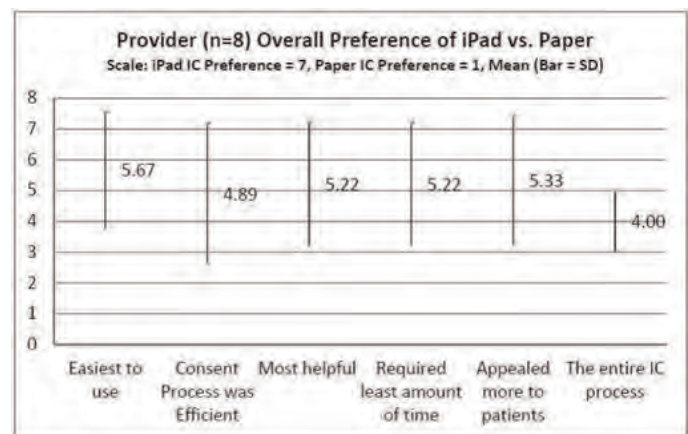
Figure

SURVEY RESPONSES (1-7, 7=EXTREMELY SATISFIED), mean (SD)	iPad	Paper
Patient Comprehension, mean (SD)	(n = 14)	(n = 17)
Study purpose	6.79 (0.6)	6.24 (1.1)
Use of PHI	6.36 (1.3)	6.24 (1.1)
Medication changes	6.64 (0.7)	6.35 (1.1)
Risks/Benefits	6.86 (0.4)	6.13 (1.5)
Randomization	6.21 (1.3)	5.76 (1.6)
Data access	6.43 (1.1)	6.06 (1.3)
Other treatment	6.79 (0.6)	6.24 (1.5)
Patient Satisfaction	(n = 14)	(n = 17)
Amount of assistance required	6.57 (0.8)	6.41 (1.1)
Overall satisfaction	6.62 (0.8)	5.82 (1.7)
Time required for completion	6.15 (1.5)	6.18 (1.4)
Perceived time to complete	22.5 (7.5)	22.9 (14.2)
Provider Satisfaction	(n = 8)	(n = 8)
Process of identifying the patients	6.56 (0.5)	6.11 (0.6)
Integration of process into workflow	6.50 (0.5)	6.25 (0.5)
Patients ability to complete w/o assistance	6.25 (0.7)	6.25 (1.0)
Patient level of understanding	6.25 (0.5)	6.13 (0.4)
Time required for patients to complete	6.31 (0.8)	6.31 (0.8)
The overall IC process	6.56 (0.5)	6.19 (0.7)
Perceived time to complete	33.1 (17.5)	19.06 (8.0)

Table

Disclosures: Amy Warriner, None.

MO0340

Secondary prevention of osteoporotic fractures: evaluation of the Amiens University Hospital's fracture liaison service between January 2010 and December 2011. Nassima Dehamchia-Rehailia[1], Daciana Ursu[1], Isabelle Henry-Desailly[1], Patrice Fardellone*[2], Julien Paccou[3]. [1]Department of Rheumatology, Amiens University Hospital, France, [2]Service de rhumatologie, CHU Hôpital Nord, France, [3]University of Picardie Jules Verne, Amiens, France

Purpose: The main goal of the present study was to assess the performance and results of the Fracture Liaison Service (FLS) at Amiens University Hospital, France.

Methods: This was an observational, single-center, ambispective study. All patients admitted to Amiens University Hospital between January 2010 and December 2011 for a low-trauma fracture (vertebral and non-vertebral fractures) were identified by a FLS nurse. Patients willing to enter the study were assessed for their osteoporosis risk factors, daily calcium intake, bone mineral density (BMD) by DXA, and clinical chemistry parameters. When necessary, the patients received a prescription for osteoporosis medication. The participation rate, osteoporosis medications, initiation rate and osteoporosis treatment persistence were assessed 12 and 18 months later.

Results: Of the 1,439 patients contacted, 872 were eligible for inclusion. A total of 335 patients (participation rate: 38.4%) were included in the study (mean age: 63.3 years; 71.9% female). All patients underwent BMD measurement and more than 90% of them were assessed for osteoporosis risk factors and daily calcium intake. Osteoporosis medication was prescribed in 182 patients (75.5% of the patients in whom it was indicated [n=241]). Bisphosphonates were the mainly prescribed osteoporosis medications (83.5%). 74.1% and 67.4% of patients were still under treatment at 12 and 18 months respectively. The main cause of treatment discontinuation was non-renewal of the prescription by the patient's general practitioner.

Conclusion: Secondary prevention of osteoporosis in Amiens University Hospital has improved since the creation of the FLS, with encouragingly high treatment initiation and persistence rates.

Disclosures: Patrice Fardellone, None.

MO0341

What Percentage of Patients in UK Nursing Homes are Suitable for and Require IV Zoledronate? Results of a Structured Nursing Home Review Programme. Eamonn Brankin*[1], Wendy Feeney[2], Robin Munro[3]. [1]NHS Lanarkshire / University of Glasgow, United Kingdom, [2]NHS Lanarkshire, United Kingdom, [3]NHS Lanarkshire / University of Glasgow, United Kingdom

Over a 2 year period all nursing homes in NHS Lanarkshire were visited by an osteoporosis specialist nurse with a view to assessing patients' fracture risk, medication compliance and suitability for IV zoledronate if appropriate. A paucity of information remains about who might be suitable for and require IV bisphosphonate therapy in this high risk population and who in particular, if

intolerant of oral therapy or contraindicated, might be precluded from receiving IV therapy due to impaired renal function. Over the 2 year period 64 nursing homes were visited and all residents assessed for the above parameters. A total of 1555 patients were assessed, of whom 268 had already had a hip fracture.477 were on calcium & vitamin D, 31% of the relevant patient population.177 were found to be already on oral alendronate.

Compliance overall with oral bisphosphonate therapy was 100% (ie those documented to be on the drug were actually taking it) although further assessment identified that there was great variation in knowledge among nursing home staff re the importance of adhering to the specific drug regime of oral bisphosphonate medication and as a result this medication was not given correctly.

Through a programme of patient and staff education a significant number of patients were actually subsequently able to take oral bisphosphonates. 52 educational sessions have been undertaken to date. After completing the programme we initiated a process of evaluation to assess the effectiveness of these sessions.

Very surprisingly only 2 of those who had been tried on oral bisphohsponate therapy were truly intolerant of this and therefore could be considered for IV therapy and / or denosumab

No patients have so far been commenced on denosumab.Two patients have been successfully treated with IV bisphosphonate therapy, with zero requiring denosumab.

Conclusions: By instituting a structured nursing home review programme, we successfully managed to review a large percentage of patients in nursing homes within the county for fracture risk, compliance and suitability for alternative therapies for those unsuitable for oral bisphosphonate therapy. Of those assessed for '2nd line' therapy, only 2 were found to be suitable for and subsequently treated with IV zoledronate and none required densoumab. Through structured staff education far more patients were found to be able to take oral alendronate than had been previously thought.

Disclosures: Eamonn Brankin, None.

MO0342

Zoledronic Acid and Denosumab Use in Ontario, Canada. Andrea Burden*[1], Mina Tadrous[2], Andrew Calzavara[3], Suzanne Cadarette[1]. [1]University of Toronto, Canada, [2]University of Toronto, Canada, [3]Institute for Clinical Evaluative Sciences, Canada

Residents aged 65 or more years in Ontario Canada receive full coverage for medications listed on the public drug formulary. Two novel extended dosing osteoporosis medications were added to the public drug formulary for the treatment of osteoporosis in the last decade: annual zoledronic acid in 2006 (access changed in 2012), and semi-annual denosumab in 2012. The objectives of our study were to: 1) describe the use of zoledronic acid and denosumab by physicians and patients over time, and 2) examine the impact of the 2012 formulary change that opened access (less restricted) to zoledronic acid. We identified new users of zoledronic acid and denosumab from 2006 to 2013 using Ontario pharmacy claims data. The number of new patients and physicians were plotted by month and examined over time. Descriptive characteristics of patients and prescribers were summarized pre- and post-formulary change for zoledronic acid; and overall for denosumab. We identified 1,508 zoledronic acid users 2006/09-2013/03 (896 pre-formulary change: 81% female, 41% prior osteoporosis treatment, mean age=76 [SD=7.0]; and 612 post-formulary change: 91% female, 26% prior osteoporosis treatment, mean age=77 [SD=6.9]) treated by 630 physicians (420 pre-formulary change), and 16,736 denosumab users 2012/02-2013/03 (79% female, 55% prior osteoporosis treatment, mean age=79 [SD=7.5]) treated by 2,904 physicians. We identified a rapid uptake of denosumab (>450 new physicians and >1,200 new patients) in contrast to zoledronic acid (<6 new physicians and <6 new patients) in the first two months on the drug formulary. Zoledronic acid use increased significantly post-formulary change with >80 new physicians and >200 new patients within 2 months of the formulary change. We document a slow increase in use of zoledronic acid over 7 years of observation, and a rapid increase in the use of denosumab in just over 1 year of observation. Drug formulary listing status and restrictions impact drug prescribing and patient characteristics. The impact of formulary restrictions on drug utilization and the study of drug effects (safety and effectiveness) deserves close attention. We anticipate that use of denosumab and zoledronic acid will continue to increase, yet the ability to compare the effects of these agents will require novel study designs given the inherent time trends and drug policy-induced selection bias.

Disclosures: Andrea Burden, None.

MO0343

Comparisons of Osteoporotic Fracture Incidence and Anti-osteoporotic Medication Expenditures after Changes of Reimbursement Policy. Rong-Sen Yang[1], Li-Wei Hung*[2]. [1]National Taiwan University Hospital, Taiwan, [2]National Taiwan University Hospital, Taiwan

Objective

Osteoporosis is a public health burden for aging society. Prevalence of osteoporosis-related fracture in Taiwan is the highest over Asia. With increasing use of anti-osteoporotic medications, our previous analysis showed concomitant decline in hip fracture prevalence with dramatic increase in anti-osteoporotic medications from 1999 to 2010 in Taiwan. However, National Health Insurance (NHI) launched a policy to restrict osteoporosis medication use since 2011. This study

aimed to analyze the prevalence of osteoporosis and its related fracture for calculate the expenditure on anti-osteoporotic medication between 2009 and 2011.

Materials and Methods

We used 2009-2011 National Health Insurance Research Database (NHIRD) to evaluate the prevalence of osteoporosis and its related fracture. Patients with a diagnosis of osteoporosis (ICD-9-CM code: 733.XX) and osteoporotic related fractures (ICD-9-CM code: hip fracture: 820.XX; vertebral fracture: 805.2, 805.4, 805.8, 806.2, 806.4; proximal humerus fracture: 812.0, 812.1, 812.2; forearm fracture: 813.4, 813.5) were identified. Using the pharmaceutical audit from IMS health, Taiwan, the expenditure of anti-osteoporotic drugs, including calcitonin, alendronate, raloxifene, teriparatide, ibandronate, zoledronic acid, strontium ranelate and denosumab, were analyzed.

Results

During the study period, prevalence of osteoporosis was slightly decreased from 3,823 to 3,509 per 100,000 people. However, the prevalence of osteoporosis-related fracture was increased from 2,258 to 2,315 per 100,000 people. The prevalence of fracture at spine and hip elevated (1,115 to 1,186 per 100,000 and 537 to 558 per 100,000 respectively) whereas the prevalence of fracture at shoulder or forearm reduced (267 to 253 per 100,000 and 475 to 459 per 100,000 respectively). Compared to the expenditure of anti-osteoporotic medication in 2009, an 11.6% decrease was found in 2011. All medication expenditure has been declined except zoledronic acid. Among them, teriparatide declined to 80% of its expenditure in 2010.

Conclusions

Between 2009 and 2011, the prevalence of osteoporosis slightly decreased. However, its related fracture increased as well as the prevalence of spin and hip. The anti-osteoporotic medication expenditures declined sharply. Further study on the prevalence of osteoporosis and its related fracture and its related expenditures is needed to evaluate the impact of the policy which restricted anti-osteoporotic medication use.

Disclosures: Li-Wei Hung, None.

MO0344

Calcium alleviation of oxidative stress. Active Absorptive Algal Calcium decreases total peroxides in blood. <u>Takuo Fujita</u>*[1], <u>Mutsumi Ohue</u>[2], <u>Ryuji Aoyama</u>[2], <u>Tomohiro Tanaka</u>[2], <u>Yoshio Fujii</u>[3], <u>Tsuyoshi Jotoku</u>[4], <u>Akimitsu Miyauchi</u>[5], <u>Yasuyuki Takagi</u>[6]. [1]Katsuragi Hospital, Japan, [2]Katsuragi Hospital, Japan, [3]Calcium Research Institute Kobe Branch, Japan, [4]Dept of Orthopedic Surgery, Osaka Medical College, Japan, [5]Miyauchi Medical Center, Japan, [6]National Hyogo Chuo Hospital, Japan

Background Severe cell injury occurs in response to oxidative stress on reperfusion as in calcium deficiency, PTH hypersecretion, Ca release from bone and osteoporosis leading to universal rise of cytosolic Ca and cell death. In an attempt to find a link between these two common phenomena, effect of Ca supplementation to overcome calcium paradox on oxidative stress was tested.

Methods Twenty postmenopausal women consulting Osteoporosis and Osteoarthritis Clinic of Katsuragi Hospital volunteering to participate the study were randomly divided into 2 equal groups : A (mean age 67 ± 9) and B (mean age 72 ± 4) without significant difference in age (p=0.2055). A but not B was supplemented with 900mg / day Active Absorptive Algal Calcium (AAACa) with a high intestinal absorbability (Nutrients 2010). To estimate the total oxidizing activity (dROMs), 20µl diethyl p-phenylendiamine and 2 ml acetate buffer at pH4.8 was added to 20µl serum and incubated for 5 min at 37C. Biological Antioxidant Potential (BAP) was measured as the total reducing activity. BAP / dROMs was calculated to evaluate antioxidant activity against the given oxidizing activity. This study was approved by the IRB of Katsuragi Hospital.

Results In contrast to a rise of dROMs by 6.2 ± 13.9 % (Mean $\pm$ SD) per month in B, it fell distinctly by -15.5 ± 13.0 % characterizing A, indicating a marked alleviation of oxidative stress in response to AAACa (p=0.0020). BAP/dROMs significantly increased in A by 27.4 ± 26.8, over B by 1.8 ± 2.4 (p=0.0335), suggesting a significant antioxidant activity of calcium. BAP failed to change significantly.

Discussion Rise of intracellular free calcium, an inevitable consequence of calcium paradox, initiates oxidative stress with increase of reactive free radical formation possibly through mitochondrial Ca accumulation. Oxygen free radicals, on the other hand, aggravate cell Ca overload through promotion of Ca entry by changing membrane phospholipid composition (Zhou et al 2009). Oxygen paradox and calcium paradox thus appears to promote each other causing a negative spiral in cell destruction, unless prevented by an effective Ca supplementation.

Conclusion Distinct alleviation of oxidative stress demonstrated in response to Ca supplementation with AAACa appears to support an important role of calcium to counteract the harmful effect of oxidative stress.

Disclosures: Takuo Fujita, None.

MO0345

The effect of calcium and vitamin D supplementation on bone mineral density in healthy males: A meta-analysis. <u>David Greene</u>*[1], <u>Leslie Silk</u>[2], <u>Michael Baker</u>[2]. [1]Australian Catholic University, Australia, [2]Australian Catholic University, Australia

Musculoskeletal diseases is an Australian national health priority however, osteoporosis remains an under-diagnosed and under-treated disorder, particularly in men. Despite the known benefits of vitamin D and dietary calcium on bone density, it is estimated that 31% of Australian adults are vitamin D deficient (<50 nmol/L) and a similar proportion of adults have inadequate dietary calcium intake [(1,2)]. Calcium and vitamin D supplementation has previously shown a small, but positive effect on bone strength and a reduction in fracture risk. However, research has focused on children and females with the preventative effects of vitamin D and/or calcium supplementation on male bone remaining largely unexplored. The aim of this meta-analysis is to examine the efficacy of calcium and vitamin D supplementation on improving bone mineral density in healthy males. Medline, EMBASE, SPORTDiscus, Academic Search Complete, CINHAHL Plus and PubMed databases were searched for all studies including healthy males which provided participants with vitamin D and/or calcium supplementation and used changes to bone mineral density (BMD) as the primary outcome measure. From 3,930 possible references, a meta-analysis was performed using 8 references. Results demonstrated significant pooled effects size (ES) for comparison between supplementation and placebo/control groups at all sites included in the meta-analysis. The largest effect was found in total body (ES=0.644; 95% CI=0.406 to 0.883; p=0.001), followed by total hip (ES=0.483, 95% CI= 0.255 to 0.711, p=0.001) and femoral neck (ES=0.402, 95% CI=0.233 to 0.570, p=0.001). The smallest impact was observed on the lumbar spine (ES=0.290, 95% CI=0.164 to 0.415, p=0.001). Evidence appears to support the use of calcium and vitamin D supplementation for improving BMD in older males however, there is a need for high quality randomised controlled trials in younger age cohorts.

1. Daly RM, Gagnon C, Lu ZX, Magliano DJ, Dunstan DW, Sikaris KA, et al. Prevalence of vitamin D deficiency and its determinants in Australian adults aged 25 years and older: a national, population-based study. Clin Endocrinol (Oxf). 2012;77(1):26-35.
2. Nowson CA, McGrath JJ, Ebeling PR, Haikerwal A, Daly RM, Sanders KM, et al. Vitamin D and health in adults in Australia and New Zealand: a position statement. Med J Australia. 2012;196(11):686-7.

Disclosures: David Greene, None.

MO0346

Supplementation with Beetroot Juice Does Not Affect Bone Microarchitecture of the Femur or Lumbar Vertebrae of OVX Rats. <u>Amanda Longo</u>*[1], <u>Bryan Johnston</u>[1], <u>Paul LeBlanc</u>[1], <u>Sandra Peters</u>[1], <u>Gregory Wohl</u>[2], <u>Wendy Ward</u>[3]. [1]Brock University, Canada, [2]McMaster University, Canada, [3]Brock University, Canada

Postmenopausal osteoporosis is characterized by a decline in the production of endogenous estrogen resulting in a decrease in skeletal mass and changes to bone microarchitecture. Hormone replacement therapy protects bone microstructure in postmenopausal women and estrogen-deplete rodent models through estrogen receptor modulated signaling. The beneficial effects of estrogen can also be mediated, in part, through the nitric oxide pathway. Moderate levels of nitric oxide result in a net positive bone balance. Flux through this pathway has been show to decrease in response to estrogen withdrawal. With digestion, dietary nitrates are converted to the bioactive ion nitric oxide, a known regulator of local osteoblast and osteoclast activity. Thus, dietary nitrates, a component found in high concentrations in beetroot, may provide an alternative therapy for the maintenance of bone microarchitecture in response to estrogen withdrawal. Three-month, ovariectomized (OVX) Sprague-Dawley rats (n=14/group) were randomized to control (no treatment), 17β-estradiol replacement (1.5mg 90-day release subcutaneous pellet from Innovative Research of America, positive control), or beetroot juice (once daily, 18.75mg nitrates, James White Drinks) for 12 weeks. Femur and lumbar vertebrae were excised and imaged using high-resolution micro-computed tomography (SkyScan 1176). Images of the femur mid-shaft, femoral neck, and third lumbar vertebrae (L3) body were acquired at a voxel size of 9µm and bone morphometry was analyzed using SkyScan CT-Analyser, v.1.13. As expected, estrogen-replacement provided significant (p<0.05) benefits to trabecular bone structure outcomes (femoral neck, L3) including BMD, percent bone volume, trabecular number, and separation compared to OVX control. For all trabecular bone outcomes at the femoral neck and L3, the beetroot group was similar to control. Beetroot intervention resulted in a lower (p<0.05) cortical area fraction of the femur mid-shaft compared to other groups. Cross-sectional thickness, bone area, tissue area, and BMD of the femur mid-shaft or L3 body were similar among all groups suggesting no change in surrogates of cortical bone structure. In summary, 12-week intervention with nitrate-concentrated beetroot juice did not preserve bone microarchitecture in the femur mid-shaft, femoral neck, or L3 body.

Disclosures: Amanda Longo, None.

MO0347

Development and validation of a food frequency questionnaire for assessment of vitamin D and calcium intake in Finnish adults. <u>Suvi Itkonen</u>*[1], <u>Maijaliisa Erkkola</u>[2], <u>Essi Skaffari</u>[3], <u>Pilvi Saaristo</u>[3], <u>Elisa Saarnio</u>[4], <u>Christel Lamberg-Allardt</u>[1]. [1]University of Helsinki, Finland, [2]Division of Nutrition, Department of Food & Environmental Sciences, University of Helsinki, Finland, [3]Calcium Research Unit, Department of Food & Environmental Sciences, University of Helsinki, Finland, [4]University of Helsinki, Finland

Adequate vitamin D (vitD) intake is important for bone health, and a low vitD status may increase the risk of many common chronic diseases. The aim of this study was to update and develop a food frequency questionnaire (FFQ) to assess dietary and supplemental vitD and calcium (Ca) intake in a Finnish population. VitD-enrichment of almost all fluid dairy products has increased vitD intake during recent years. These are now the main vitD sources, other important sources are fish products and vitD-enriched margarines. For the development of the FFQ, data on the use and supply of vitD-enriched products in the markets was examined. An interviewer-driven 98-item FFQ, including also Ca sources, was developed. The foods were divided in 8 categories, including detailed questions on the use of supplements. In addition, short questions on possible sunlight exposure were included. Trained interviewers collected information of vitD intake of 69 healthy Caucasian adults aged 20-37-years by the FFQ. Serum 25-hydroxy-vitamin D (S-25OHD) concentration, the major biomarker of vitD status, concentrations was assessed by EIA (IDS). Validity was assessed using Spearman correlation coefficients and cross-classification into quartiles of vitD intake and S-25OHD. The mean (SD) intakes of vitD were 9.8 µg/d (5.0 µg/d) from food, 9.4 µg/d (15.0 µg/d) from supplements, 19.1 µg/d (15.7 µg/d) in total, respectively. The mean concentration of S-25OHD was 68.9 nmol/L (23.9 nmol/L). A strong correlation between total vitD intake (from FFQ and supplements) and S-25OHD was observed (r=0.560, p<0.001), which did not improve when adjusted for sunny holidays (r=0.544, p<0.001). Cross-classification analyses demonstrated no major misclassification of participants into intake quartile; 83% percent of subjects were classified into the same or adjacent quartile, and 1% into the opposite quartile. In those not using vitD supplements (n=32), the correlation between the two methods was good (r=0.351, p=0.049), and 84% of subjects were classified into the same or adjacent quartile, and 9% into the opposite quartile. This FFQ provides promising validation evidence and a reasonable estimation of vitamin D intake in healthy young Caucasian adults during winter season. The validity and reproducibility of the FFQ will further be assessed with repeated measurements and with comparison to food records by triad method, and also Ca intake assessment by these two methods will be compared.

Disclosures: Suvi Itkonen, None.

MO0348

Evaluating Effects of Supplemental Vitamin D on Incident Fracture Risk in the VITamin D and OmegA-3 TriaL (VITAL). <u>Amy Yue</u>[1], <u>JoAnn Manson</u>[2], <u>Julie Buring</u>[2], <u>Nancy Cook</u>[2], <u>Douglas Bauer</u>[3], <u>Peggy Cawthon</u>[4], <u>Dennis Black</u>[3], <u>Meryl Leboff</u>*[5]. [1]Brigham & Women's Hospital, USA, [2]Brigham & Women's Hospital Professor of Medicine, Harvard Medical School, USA, [3]University of California, San Francisco, USA, [4]California Pacific Medical Center Research Institute, USA, [5]Brigham & Women's HospitalProfessor of Medicine, Harvard Medical School, USA

Although there is widespread use of supplemental vitamin D to promote bone health, data from large, randomized, placebo-controlled trials of the effects of supplemental vitamin D *alone* on fracture outcomes are sparse and inconsistent; these trials show benefit, no effect, or increased risk of supplemental vitamin D on fracture outcomes. We are conducting an ancillary bone study to the large *VIT*amin D and Omeg*A*-3 Tria*L* (VITAL) to test the safety and efficacy of high-dose supplemental vitamin D in the primary prevention of incident fractures (all, non-vertebral, and hip).

The parent VITAL is a 2x2 factorial, double-blind, placebo-controlled trial testing the effects of daily, high-dose supplemental vitamin D3 (cholecalciferol, 2000 IU/d) and/or omega-3 fatty acids (EPA+DHA; 1 g/d) in the primary prevention of cancer and cardiovascular disease (CVD). After completing a 3-month placebo run-in, men aged ≥50 and women aged ≥55 were randomized to receive either high-dose, supplemental vitamin D or placebo, permitting up to 800 IU/d of supplemental vitamin D and an intake of 1200 mg/d of elemental calcium. Randomization closed March 24, 2014. VITAL includes approximately 26,000 participants (exceeding the target of 20,000), with an oversampling of blacks (n>5,100) and high minority representation (~26% non-white).

Among VITAL participants enrolled in the parent trial, 580 reported at least one fracture event in year 1 post-randomization. Fractures reports were examined separately and according to annual questionnaires, medical record review, and fracture adjudication including review of radiological images of hip and femur fractures. Participants who fractured were older and more likely to be women than men. The cohort has broad U.S. geographic diversity. Questionnaires at run-in and baseline assessed demographic, lifestyle, physical activity, nutritional and clinical risk factors related to osteoporosis, CVD, cancer, and other health outcomes. Assessments will be repeated on an annual basis. Baseline levels of serum 25-hydroxyvitamin D, PTH, and calcium will also be measured using blood samples collected from a subset of >16,000 participants. Determination of treatment effects will be based on intent-to-treat and other analyses. Results from this large study will inform clinical and public health recommendations and clarify the role of high-dose, daily supplemental vitamin D in the primary prevention of fractures in the U.S.

Disclosures: Meryl Leboff, None.

MO0349

High prevalence of vitamin D deficiency in patients with xeroderma pigmetosum (XP)- A under strict sun-protection. <u>Akiko Kuwabara</u>*[1], <u>Naoko Tsugawa</u>[2], <u>Kiyoshi Tanaka</u>[3], <u>Yasuyo Uejima</u>[1], <u>Junko Ogawa</u>[1], <u>Natsumi Otao</u>[1], <u>Nanae Yamada</u>[1], <u>Taro Masaki</u>[4], <u>Chikako Nishigori</u>[5], <u>Shinichi Moriwaki</u>[6], <u>Toshio Okano</u>[7]. [1]Department of Health & Nutrition, Osaka Shoin Women's University, Japan, [2]Kobe Pharmaceutical University, Japan, [3]Kyoto Women's University, Japan, [4]Division of Dermatology, Clinical Molecular Medicine, Graduate School of Medicine, Kobe University, Japan, [5]Division of Dermatology, Clinical Molecular Medicine, Graduate School of Medicine, Kobe University, Japan, [6]Department of Dermatology, Osaka Medical College, Japan, [7]Kobe Pharmaceutical University, Japan

Purpose: Xeroderma pigmentosum (XP) is a rare autosomal recessive disease characterized by defective repair of ultraviolet (UV) irradiation-induced DNA damage and resultant high risk of skin cancer. Thus, these patients need photoprotection through minimization of daytime outdoor activity and constant sunscreen use. Since DNA repair is most severely impaired in XP group A (XP-A), such restrictions are most strictly applied to XP-A patients. Considering the UV-mediated cutaneous vitamin D production, rigorous photoprotection would be associated with vitamin D deficiency. Reports have been scarce, however, on the vitamin D status of patients with XP. Then, we have studied the vitamin D status in XP-A patients under most strict photoprotection.

Methods: Twenty-two XP-A patients (male;12, female;10, aged 6 to 44) were evaluated for their vitamin D intake, serum levels of 25-hydroxy-vitamin D (25OHD) and parathyroid hormone (PTH). Vitamin D intake was assessed by 2-day food weighing method.

Results: Median dietary vitamin D intake was 4.7µg/day. In 40% of the subjects, vitamin D intake was below the adequate intake (AI) of Dietary Reference Intakes (DRIs) in Japan. The median concentrations of serum 25OHD and PTH were 8.0ng/mL and 46.5pg/mL, respectively. In 73% of patients, serum 25OHD level was lower than 10ng/mL, strongly indicating vitamin D deficiency. Vitamin D intake was not significantly correlated with serum 25OHD concentration. Vitamin D intake and serum 25OHD level were significantly lower in patients under enteral nutrition (EN) than those with oral intake (OI). Multivariate analyses revealed that EN was a significant predictor of decreased serum 25OHD level.Conclusions: We have found that vitamin D deficiency is highly prevalent in XP-A patients under strict photoprotection. The implication of our finding would be two-fold. First, supplementation should be considered to avoid unfavorable skeletal consequences in these patients. Second one is related to the DRIs. Determination of dietary vitamin D requirement has been an annoying issue in the decision of DRIs because of its cutaneous production. Recently published DRIs for calcium and vitamin D 2011 from Institute of Medicine adopted the comparison of serum 25OHD level and dietary vitamin D intake in subjects from arctic region. Data from XP patients would shed light on the dietary vitamin D requirement and yield useful information on the DRIs determination.

Disclosures: Akiko Kuwabara, None.

MO0350

Measurement of Serum 1,25-dihydroxyvitamin D Levels: An Excercise in Utility or Futility?. <u>Tarlisha Holsey</u>*[1], <u>Sudhaker Rao</u>[2], <u>Arti Bhan</u>[1]. [1]Henry Ford Hospital, USA, [2]Henry Ford Hospital, USA

Background: With growing interest in vitamin D nutrition (VDN), it has become common practice to assess VDN status with measurement of vitamin D metabolites. Although the best available index of VDN is serum 25-hydroxyvitamin D (25-OHD) level, the difference between 25-OHD and 1,25-dihydroxyvitamin D (1,25-DHD) measurements, and the clinical indication and relevance of each measurement is not well appreciated in clinical practice.

Methods: As part of continuous quality improvement process in the Bone and Mineral Research Laboratory (BMRL), we conducted an audit of the number of serum 1,25-DHD measurement requests in a 3-month period (01/01/2014 to 03/31/2014). For each serum 1,25-DHD measurement, a review of the patients' records and/or personal phone contact with the ordering provider was conducted by the BMRL director (DSR) to clarify which vitamin D metabolite the provider intended to measure, and to educate the provider about the appropriate metabolite to assess VDN. In almost all instances, the intention of the providers was to measure serum 25-OHD, and not 1, 25-DHD.

Results: During the 3-month audit period, 449 serum 1,25-DHD measurements were requested: 55 came from 2 community based hospitals owned by the Henry Ford Health System (HFHS), 64 from community providers that use BMRL as reference laboratory, 246 from providers within the HFHS, and 84 from the Henry Ford Hospital inpatient setting (reasons for the latter source were not readily apparent).

The mean serum 1, 25-DHD level for the entire cohort was 61.7 ± 26.9 (range: 6-141 pg/ml). Only 71 of the 441 (or 16%) requests included simultaneous serum 25-OHD requests. Unfortunately, no provider simultaneously assessed renal function or measured serum calcium.

Conclusions: Isolated measurement of serum 1,25-DHD to assess VDN, as with 25-OHD (ASBMR Annual Meetings 2010 and 2012) appears quite pervasive, despite the well-established and publicized guidelines to measure 25-OHD to assess VDN. Many providers are ordering serum 1, 25-DHD to assess VDN when in fact they intended to measure serum 25-OHD, the best available index of VDN. Increased education and computerized "stop-gaps" is urgently needed to avoid unnecessary (and perhaps irrelevant) testing of serum 1, 25-DHD level, which is needed only in rare circumstances, and to avoid considerable health care costs, as implied in the "Choose Wisely" campaign!

Disclosures: Tarlisha Holsey, None.

MO0351

Rational Assessment of Vitamin D. Arthur Chausmer*. C/A Informatics, LLC, USA

There is some controversy regarding the use of 25 hydroxycalciferol as an assessment of vitamin D status. The aim of this presentation is to provide literature evidence based suggesting this is only a marginally viable surrogate and that it is vastly overused to justify unnecessary treatment with pharmacologic doses of vitamin D The physiology of calcium and vitamin D are reviewed and discussed in the light of decision making regarding the need and advisability of therapeutic intervention and concurrent risk of potentially life threatening hypervitaminosis D.

There is no data in any animal model regarding the measurement of the total body burden of vitamin D as calciferol, 25 OHD or 1,25 OH2D, consequently there is no test which has been demonstrated to reflect the total body stores of any element of the metabolic pathways. The measurement of an inactive metabolite, 25 OHD, although commonly used for the diagnosis of D deficiency, has some weak statistical relationship with the active metabolite, but no causal relationship with any aspect of calcium homeostasis. Multiple confounding factors are presented which make this a poor choice for determination of clinical vitamin D sufficiency.

While it is more costly than simple measurement of 25 OHD, it is concluded that the actual evaluation of vitamin D status requires different testing. This includes elements of it's interaction with calcium metabolism as a whole, which cannot be assessed by the simplistic approach of a single 25 OHD value. Rather a true assessment of vitamin D status includes measurement of 1,25 dihydroxycalciferol in concert with PTH, calcium, phosphorus and renal function testing. Simply measuring 25 OHD should not be the basis for treatment with potentially toxic doses of vitamin D.

Disclosures: Arthur Chausmer, None.

MO0352

The Effect of High-Dose Vitamin D Supplementation on Bone Mineral Density and Bone Turnover Markers in Subjects with Type 2 Diabetes and Hypovitaminosis D – a Randomized Controlled Trial. Hanne Gulseth*[1], Cecilie Wium[2], Erik Fink Eriksen[3], Kåre I. Birkeland[4]. [1]Norwegian Institute of Public Health/ Oslo University Hospital, Norway, [2]Department of Endocrinology, Morbid Obesity & Preventive Medicine, Oslo University Hospital /University of Oslo, Norway, [3]Oslo University Hospital, Norway, [4]Department of Endocrinology, Morbid Obesity & Preventive Medicine, Oslo University Hospital/ University of Oslo, Norway

Low levels of 25 hydroxy-vitamin D (25OHD) are common, and associated with increased bone turnover, risk of fractures and possibly adverse glucose metabolism. We tested whether vitamin D supplementation could improve bone mineral density (BMD) and bone turnover markers in subjects with type 2 diabetes, and if the effects of vitamin D supplementation depended on ethnicity.

In a 6-month, parallel group, placebo-controlled, double-blind randomized trial, patients of South-Asian and Nordic ethnicity, with type 2 diabetes and hypovitaminosis D (25OHD < 50 nmol/L) received oral vitamin D_3 or placebo. A dose of 400,000 IU vitamin D_3 was given at baseline, followed by 200,000 IU after 5 weeks if 25OHD <100 nmol/L. We measured 25OHD, PTH, CTX1, P1NP and osteocalcin as well as BMD of the hip and spine. Data are mean (SD).

Subjects (n=62, 48% females) of Nordic (n=43) and South Asian (n=19) ethnicity with age 57.7 (9.6) years, BMI 31.9 (5.2) kg/m2, HbA1c 7.8 (1.4)%, diabetes duration 10.3 (6.2) years and 25OHD 37.4 (12.1) nmol/L participated in the trial. After 3 and 6 months 25OHD increased significantly in the D_3 group, by 35.5 (19.4) and 14.9 (12.2) nmol/L respectively, compared to the placebo group: 6.1 (15.7) and 1.5 (15.3) nmol/L, p<0.001 and p=0.001 . The changes in bone turnover markers and BMD did not differ significantly between groups (table 1). However, in subjects of South Asian ethnicity PTH decreased (-2.0 (0.8) pmol/L, p=0.036) and spine BMD increased (0.034 (0.013) g/cm2, p=0.032) significantly in the D_3 group compared to placebo. There were no significant changes in the Nordic group.

In conclusion, in a 6-month, placebo-controlled, double-blind, randomized trial of oral vitamin D_3 versus placebo, subjects with type 2 diabetes and hypovitaminosis D did not change bone turnover markers or BMD. In subjects of South Asian ethnicity PTH concentrations fell and spine BMD improved after vitamin D supplementation.

	Vitamin D_3		Placebo		
	Baseline	Change	Baseline	Change	p-value
BMD spine (g/cm²)	1.26 (0.17)	0.014 (0.04)	1.20 (0.20)	0.001 (0.04)	0.086
BMD hip (g/cm²)	1.16 (0.13)	-0.003 (0.02)	1.09 (0.16)	0.02 (0.10)	0.18
PTH (pmol/L)	4.3 (1.9)	-0.5 (2.1)	3.7 (2.1)	0.6 (2.3)	0.13
Osteocalcin (nmol/L)	0.50 (0.38)	-0.04 (0.3)	0.53 (0.31)	0.06 (0.6)	0.62
CTX1 (µg/L)	0.26 (0.14)	-0.01 (0.11)	0.26 (0.14)	0.01 (0.10)	0.20
P1NP (µg/L)	32.0 (13.5)	-1.10 (13.4)	32.4 (15.1)	-1.67 (11.6)	0.82

Table_1

Disclosures: Hanne Gulseth, None.

MO0353

Three doses of vitamin D on bone mineral density and structural analysis in postmenopausal women: a double-blind randomized controlled pilot study. L. Claudia Pop*[1], Deeptha Sukumar[2], Christopher Gordon[3], Stephen Schneider[4], Yvette Schlussel[1], Theodore Stahl[4], Sue Shapses[5]. [1]Rutgers University, USA, [2]Drexel University, USA, [3]McMaster University, Canada, [4]Rutgers-Robert Wood Johnson Medical School, USA, [5]Rutgers University, USA

Background: Studies examining bone due to vitamin D supplementation, in a dose-dependent manner, are currently lacking. Postmenopausal women undergoing weight control to improve health outcomes, are particularly at risk for bone loss, and might benefit from additional vitamin D intake.

Objective: This one year-long study addressed whether vitamin D supplementation, in healthy overweight/obese older women, attenuates bone structural parameters with modest weight loss.

Design: Fifty-nine women (age, 58 ± 6 years; body mass index, 30.2 ± 3.8 kg/m², serum 25-hydroxyvitamin D (25OHD), 27.3 ± 4.4 ng/ml), were randomly assigned to one of 3 daily doses of vitamin D_3 (A, 600 IU; B, 2000 IU; C, 4000 IU) with total calcium intake (diet and supplement) of 1.2 g/d while counseled for weight control. Serum was analyzed for 25OHD, parathyroid hormone and bone turnover markers. Areal bone mineral density was measured by dual energy x-ray absorptiometry. Geometry, strength, and trabecular and cortical BMD and microarchitecture by high resolution three dimensional peripheral quantitative computed tomography.

Results: After one year, serum 25OHD levels increased to 26.5 ± 4.4, 35.9 ± 4.5 and 41.5 ± 6.9 ng/ml, in groups A, B and C, respectively, and the groups were different (p<0.01). Weight change was similar between groups ($-3.0 \pm 4.1\%$). Trochanter aBMD decreased more in group A ($-1.5 \pm 3.9\%$) than group B ($+0.9 \pm 2.8\%$) (p<0.05) and did not differ from C. No other BMD parameters differed between treatments. However, femoral neck aBMD decreased in the A group ($-1.0 \pm 2.8\%$) compared to baseline (p<0.05). Cortical thickness changed differently between groups, by: $-1.5 \pm 5.2\%$, $+0.6 \pm 3.2\%$ and $+2.0 \pm 4.8\%$ in groups A, B and C, respectively (p < 0.05). Also, compared to baseline, trabecular separation increased ($+2.6 \pm 5.2\%$) and trabecular number decreased (-1.6 ± 3.0) in group A (p < 0.05), but there was no change in thickness or bone volume/tissue volume.

Conclusion: There is no effect of vitamin D_3 supplementation at any dose on BMD in older women over 1 year, but a decrease in cortical geometry and the age-related changes in trabecular microstructure are attenuated with higher vitamin D supplementation.

Disclosures: L. Claudia Pop, None.

MO0354

Vitamin D replacement in patients undergoing bariatric surgery: a systematic review and meta-analysis. Marlene Chakhtoura*[1], Ghada El-Hajj Fuleihan[2], Elie Akl[3], Nancy Nakhoul[3], Bassem Safadi[3]. [1]American University of Beirut, Lebanon, [2]American University of Beirut-Medical Center, Lebanon, [3]American University of Beirut, Lebanon

Background:
Bariatric surgery is the most effective measure for weight loss. Vitamin D deficiency is common in patients undergoing bariatric surgery (1). Specific risk factors related to obesity include sedentary lifestyle and vitamin D sequestration in adipose tissue. In addition, limited intake of dairy products due to dietary intolerance and bypass of the primary absorption sites of vitamin D at the jejunum and ileum concur to result in hypovitaminosis D. This would contribute to bone loss following bariatric surgery (2). Major clinical practice guidelines on vitamin D supplementation in patients undergoing bariatric surgery are mostly based on expert opinion (3-5).

Aim:

Assess the benefits and harms of different doses of vitamin D replacement therapy in patients undergoing bariatric surgery.

Outcomes measures:

The main outcome of this study is the mean difference in serum 25-hydroxyvitamin D level reached between three vitamin D dose categories: low ($\leq$ 800IU), moderate (800-3500 IU) or high (>3500IU) daily dose of vitamin D, or placebo/no vitamin D supplementation.

Other outcomes include mortality, change in bone mineral density and muscle strength, diabetes, hypertension and dyslipidemia resolution, incidence of fracture, hypercalcemia - hypercalciuria and kidney stones, in addition to quality of life and cost economics.

Eligibility criteria:

We included randomized controlled trials (RCTs) and controlled clinical trials (CCTs) administering different oral doses of vitamin D or placebo in bariatric surgery patients.

Search methods:

We searched Medline, PubMed, Embase and the Cochrane Library for eligible trials. No time or language limitations were applied. We searched clinicaltrial.gov, ICTRP and ICRCTN for registered trials. References retrieved were reviewed in duplicate by 2 independent reviewers. Authors were contacted for unpublished data. The protocol will be submitted to the Cochrane Collaboration Group.

Results:

The search yielded 1339 articles. After duplicate removal, we screened 996 articles by title and abstract, and retained a total of 86 articles for full text screening. We also identified 8 ongoing clinical trials. The data abstraction and analysis are currently under progress, to be completed by September 2014.

Keywords: vitamin D, bariatric surgery

References:

1. Shankar P, Nutrition. 2010
2. Hage M, OI 2014
3. Heber D, JCEM 2010
4. Mechanick JI, Endocrine Practice. 2013
5. Fried M. Obesity Facts. 2013

Disclosures: Marlene Chakhtoura, None.

MO0355

Higher bone resorption across the menopause may impair trabecular micro-architecture – the prospective OFELY study. Elisabeth Sornay-Rendu*[1], Pawel Szulc[2], Stephanie Boutroy[3], Olivier Borel[4], Roland Chapurlat[5]. [1]INSERM UMR1033, Université de Lyon, France, [2]INSERM UMR 1033, University of Lyon, Hopital E. Herriot, Pavillon F, France, [3]INSERM U1033 & Université de Lyon, France, [4]INSERM UMR 1033, France, [5]E. Herriot Hospital, France

Median values of bone turnover markers (BTM) are higher in post- than in premenopausal women. As many skeletal traits track - follow in a trajectory established early in life through young adulthood to advanced age, we hypothesized that BTM levels will also track in their percentile location established before menopause into the postmenopausal years.

Seventy women aged 38 ± 4 yr had blood collected 13 ± 4 yr before the menopause and then, 6 ± 4 yr after the menopause, when they were 57 ± 4 yr. At the end of the follow-up, bone microarchitecture was assessed at the distal radius and tibia by high resolution peripheral quantitative computed tomography (XtremeCT SCANCO, Scanco AG, Brüttisellin, Switzerland).

Of women who were in the highest tertile of serum CTX-I levels before the menopause, 58% remained in the highest tertile after the menopause. Of women who were in the lowest premenopausal tertile, 63% remained in the lowest tertile after the menopause. Overall, 51% of women remained in the same tertile across menopause (weighted k= 0.40, 95% confidence interval: 0.23-0.56, p<0.001). Premenopausal CTX-I levels explained 24% of variability of CTX-I levels after menopause (p<0.001). Women from the highest premenopausal tertile had higher average CTX-I level and variance after the menopause compared with women from the lowest premenopausal tertile (0.62 ± 0.20 vs 0.39 ± 0.11 ng/mL, p<0.001).

Women who were in the highest CTX-I tertile before and after the menopause had 20% fewer trabeculae (Tb.N) at the distal tibia (1.5SD, p<0.001) than women who were in the lowest CTX-I tertile before and after the menopause (p for trend <0.001). Similar results were found for Tb.N at the distal radius (14%, 0.9SD, p<0.05, p for trend <0.05). Furthermore, trabecular distribution (Tb.Sp.SD) at the distal tibia was more heterogeneous in women in the highest CTX-I tertile before and after the menopause compared with women in the lowest CTX-I tertile before and after the menopause (42%, 2.1SD, p<0.01, p for trend <0.01). No difference were detected for cortical parameters or volumetric bone mineral density.Remodeling marker CTX does not consistently track, but tracking in the higher CTX-I levels across the menopause is associated with poorer trabecular microarchitecture, a feature that can assist in rational targeting of therapy.

Disclosures: Elisabeth Sornay-Rendu, None.

MO0356

Model Development in Ovariectomized Rabbits to Translate the Increased Bone Remodeling Associated with the 3-mg Dose of the Odanacatib Phase II Study. Tara Cusick*[1], Le Duong[2]. [1]Merck & Co., Inc., USA, [2]Merck Research Laboratories, USA

Odanacatib (ODN) is a selective and reversible CatK inhibitor currently developed for osteoporosis treatment. Results from the dose-ranging ODN phase II study revealed modest bone loss in spine and hip from patients treated with the lowest dose of ODN 3-mg once-weekly (OW) for 2-yrs. Both biochemical formation and resorption markers were elevated in these patients above baseline. The goal of this study is to develop a preclinical model to further our understanding of the mechanism of bone loss associated with this 3-mg dose. Based on pharmacokinetic (PK) profiles, we modeled the 3-mg (Cmax=64nM, Cmin=15nM) and fully efficacious 50-mg OW (Cmax=337nM, Cmin=47nM) clinical doses in ovariectomized (OVX) rabbits using food formulations. Adult rabbits received sham- (N=18) or OVX (N=47) surgery 9-mo. prior to dosing. OVX-rabbits were randomized into 4 groups (N=11-12) and fed food containing: vehicle (Veh), high dose ODN (1.5mg/kg) once-daily (OD-H) or once-wkly (OW-H) and low dose ODN (0.45mg/kg) once-wkly (OW-L). Note, ODN-food was fed only the first day of the week in the OW regimens. Study endpoints included PK, bone resorption (uHP) and formation (BSAP) biomarkers and longitudinal BMD scans at 0, 3, 6, 9 and 12 mo. Rabbits fed 1.5 or 0.45mg/kg ODN daily achieved plasma exposures of ~263 and 66nM, respectively. Hence, OD-H maintained ODN mean exposure above the IC90 at all times. To mimic the 3-mg clinical dose, OW-H achieved Cmax=83nM and Cmin=7nM and OW-L had Cmax=22nM and Cmin=2nM in rabbits over the week. Comparing Veh, OD-H showed sustained reduction of uHP 65-78% (p<0.001) at all-time points and increased BSAP up to 24.2% (p<0.05) by 9 mo. However, OW-H and OW-L regimens significantly reduced uHP up to 80% (p<0.05) early in the week and rebounded to Veh levels toward weeks end. The OW groups maintained BSAP at Veh levels at all-time points. Versus baseline, OD-H increased LV5-6 aBMD up to 12.1% (p<0.05) after 12 mo. In contrast, LV5-6 aBMD of OW-H and OW-L were unchanged or tended to decrease compared to Veh. Thus, by mimicking the PK of the 3-mg human dose, we demonstrated that cyclic intermittent dosing of ODN at sub-/clinical exposures accelerated bone remodeling rate that tended to favor modest net bone loss in OVX-rabbits. The results from this preclinical model supports the clinical finding that maintaining optimal inhibition of CatK is necessary to achieve full benefit of ODN for the treatment of osteoporosis.

Disclosures: Tara Cusick, Merck & Co., 8; Merck & Co., 4
This study received funding from: Merck & Co.

MO0357

Regulating osteogenesis via Bcl6. Takeshi Miyamoto[1], Yoshiaki Toyama[2], Atsuhiro Fujie*[3]. [1]Keio University School of Medicine, Japan, [2]Department of Orthopaedics Surgery, School of Medicine, Keio University, Japan, [3]Department of Orthopaedic Surgery, School of Medicine,Keio University, Japan

The aim of the present study is to explore a single molecule, which simultaneously regulates both osteoclasts and osteoblasts. The pathophysiology of osteoporosis is based on the imbalance between bone resorption and bone formation, which two arms are regulated by the activities of osteoclasts and osteoblasts, respectively. Because these two arms are linked each other through coupling factors, treatment with anti-resorptive agents promotes simultaneous suppression of bone formation, which frequently results in limited increment of bone volume. Myriad of therapeutic agents for osteoporosis had been developed for decades, yet no agent which can regulate both bone resorption and bone formation, had been developed. In this study, we show that B cell lymphoma6 (Bcl6) KO mice exhibited significantly reduced bone mass due to accelerated osteoclastogenesis and altered osteoblastogenesis.

Bcl6 KO mice and control littermates were necropsied at 6 weeks of age. Removed hindlimbs were fixed with 70% ethanol, and were subjected to dual-energy X-ray absorptiometry analysis to measure bone mineral density and for bone-histomorphometric analysis. Primary osteoblasts isolated from the calvarial bones of the newborn (1-3d) mice were cultured, and mRNA was extracted to perform RT-PCR, to analyze expression of osteoblast-specific genes. Expression of osteoblast-specific genes in Bcl6 over-expressed MC3T3E1 cells was also analyzed.

Bcl6 KO mice exhibited severe osteoporosis compared with WT littermates. Enhanced osteoclast development while altered bone formation by osteoblasts was simultaneously seen in Bcl6KO mice, and Bcl6 KO mice showed decreased BV/TV(%), Ob.S/BS(%),Tb/N(/mm) compared with WT littermates. Primary osteoblasts derived from Bcl6 KO mice showed inhibited expression of osteoblast-specific genes after BMP2 stimulation. On the contrary, primary osteoblasts from Bcl6 over-expressed MC3T3E1cells showed accelerated expression of osteoblast-specific genes after BMP2 stimulation. Bcl6 inhibits osteoclast differentiation, while promotes osteo-blastic bone formation.Bcl6 can be a potent therapeutic target, which simultaneously regulates both osteoclasts and osteoblasts.

Disclosures: Atsuhiro Fujie, None.

MO0358

RNA Seq-based Gene Expression in Mouse Cortical and Cancellous Bone.
Natalie Kelly*[1], John Schimenti[2], F Patrick Ross[3], Marjolein Van Der Meulen[1]. [1]Cornell University, USA, [2]Cornell University, USA, [3]Hospital for Special Surgery, USA

Osteoporotic fractures occur predominantly at corticocancellous sites [1]. Mechanical loading is a promising approach for recovery of bone mass. Cortical (Ct) and cancellous (Cn) bone respond differently to mechanical loading, dependent on waveform [2]. The ability to quantitate differential changes in gene expression separately in Ct and Cn bone, in the absence of contaminating marrow cells, would be an important advance. We aimed to isolate high quality RNA from Ct and Cn bone in the absence of marrow cells and to examine differential gene expression between these tissues with RNA-seq.

Tibiae from 11-wk-old female C57Bl/6 mice were used for histology (left leg, H&E) or RNA isolation (right leg). Tibial bone marrow was not removed, flushed with PBS, or centrifuged (n=10/group). A Cn core was removed from the Ct shell of the metaphysis and RNA was isolated from these samples and from bone marrow (n= 3). Bone- (Col1a1, Bglap) and marrow-associated genes (Icam4) were assayed by qPCR and normalized to Gapdh. mRNA from cortical and cancellous bone of 4 10-wk old female mice mouse was processed for RNA-seq (100bp, single-end). Sequences were aligned with TopHat, and differential expression (>2-fold) was determined with Cuffdiff [3].

Marrow was visible in H&E stained intact Ct and Cn bone, removed incompletely by flushing, and barely detectable in centrifuged samples. Centrifuged Ct bone had 11- and 12-fold higher expression of Col1a1 and Bglap than bone with marrow, while centrifuged Cn bone values were 26- and 29-fold higher. The expression of Col1a1 and Bglap was significantly lower in Cn than Ct bone. Marrow had very low expression of bone-related genes compared to intact bone (80- to 990-fold less). Centrifugation, but not flushing, decreased the expression of Icam4. Marrow and intact Ct and Cn bone had similar expression of Icam4 (Figure 1). On average 76% of the 18 million reads per library were mapped to the mouse genome, 95% uniquely. After removal of 11 contaminating muscle genes [4], 136 genes were over 2-fold increased (81) or decreased (55) in Cn versus Ct bone. These included osteocrin (–26-fold), Wnt16 (–10-fold), Sost (–3-fold), and Wnt10b (–2-fold).

The ability to examine gene expression by RNA-seq in marrow-free mouse Ct and Cn bone separately has the potential to impact osteoporosis and mechanotransduction research.

References:[1] Report of the Surgeon General, 2004 [2] Holguin et al. 2013 [3] Trapnell et al. 2012 [4] Ayturk et al. 2013
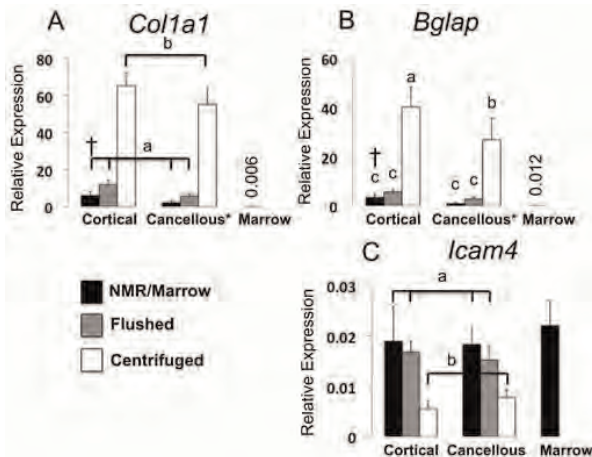

Figure 1

Disclosures: Natalie Kelly, None.

MO0359

Tissue Heterogeneity Determined by FTIR Imaging Decreases with Increasing Fracture Count.
Adele Boskey*[1], Lyudmila Spevak[2], Patrice Watson[3], Susan Bare[3], Robert Recker[4]. [1]Hospital for Special Surgery, USA, [2]Hospital for Special Surgery, USA, [3]Creighton University, USA, [4]Creighton University, USA

Fourier transform infrared imaging (FTIRI) can provide a "chemical photograph" of bone composition. We previously used FTIRI to define compositional parameters that vary with fracture risk [JBMR 29:24,1565]. We also showed that the full-width at half maximum of the pixel distribution (heterogeneity) of FTIRI parameters decreased if patients were treated with bisphosphonates [JBMR 2013;28;150; JBMR 2012; 27:172]. Increased heterogeneity is believed to retard crack propagation suggesting that a more homogeneous bone would have an increased risk of fracture. In the present study we examined FTIRI means and heterogeneities from 80 iliac crest biopsies from patients with and without prior self-reported fractures. The study objective was to test the hyothesis that tissue heterogeneity decreased with increased number of fractures. FTIRI spectra were collected from 3 sections of each biopsy with cortical and cancellous bone examined separately. Mean and standard deviation for 5 FTIRI parameters (mineral/matrix; CO_3/PO_4, crystallinity, acid phosphte content, and collagen maturity) and their respective mean heterogeneities were compared by linear regression analysis. Fracture data was initially segregated by number with 0 (n=33), 1 (n=11), 2 (n=17), 3 (n=13), and 4-7 (n=6) fractures and later, 3 groups of ~ equal size were studied. Mean age and BMD were not significantly different in these groups. FTIRI analysis showed no significant difference in any of the mean cortical or cancellous parameters with fracture number, although there was a significant linear decrease in coritcal CO_3/PO_4 ratio and a significant linear increase in collagen maturity with number of fractures for both cortical and cancellous bone. To facilitate comparion of heterogeneities, we normalized each heterogeneity values, dividing each by its parameter mean, combined cortical (co) and cancellous (ca) bonesand compared groups with 0, 1&2, and 3-7 fractures. This gave several trends but only CO_3/PO_4heterogeneity decreased with fracture number. Regression analysis of fracture number vs. heterogeneity (Fig 1) showed small but significant negative slopes for most parameters. These data, while limited due to the reliance on patient reported fracture incidence, support our hypothesis that heterogeneity decreases with increasing number of fractures. Decreased heterogeneity is associated with weaker materials, decreased energy dissipation and ability to retard microcracks, contributing to fracture risk.
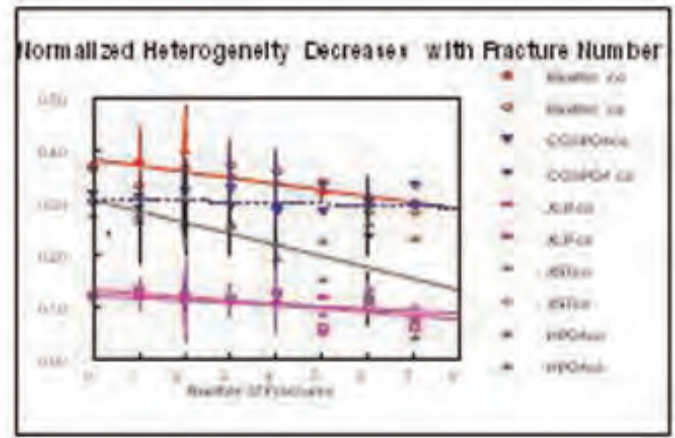

Figure 1

Disclosures: Adele Boskey, None.

MO0360

Improving bone metabolism by pomegranate seed oil in bone cells culture and in a preclinical mice model of postmenopausal osteoporosis.
Mélanie Spilmont*[1], Yohann Wittrant[2], Veronique Coxam[3], Laurent Rios[4]. [1]Equipe Alimentation, Squelette et Métabolisme, France, [2]Equipe Alimentation, Squelette et Métabolismes, INRA, UMR 1019, UNH, CRNH Auvergne, France, [3]INRA Theix, France, [4]GREENTECH SA Biopôle Clermont-Limagne, France

In the current context of longer life expectancy, the prevalence of osteoporosis is increasingly important. This is why development of new strategies of prevention is highly suitable. Some dietary fats and particularly conjugated linoleic acid have a positive impact on bone formation leading to improved bone mineral density (BMD). Pomegranate seed oil (PSO) and its major component: punicic acid, a conjugated linolenic acid specific to this fruit, have potent anti-inflammatory and anti-oxidative properties both in-vitro and in-vivo, two process strongly involved in osteoporosis establishment. In this study, we demonstrated that PSO consumption (5% of the diet) improved significantly bone BMD and prevented trabecular microarchitecture impairment in ovariectomized (OVX) mice C57bl6j, compared to OVX controls animals. Those findings are associated with transcriptional changes in bone tissue, suggesting involvement of both osteoclastogenesis inhibition and osteoblastogenesis improvement. In addition, thanks to an ex-vivo experiment, we provided evidence that serum from mice fed pomegranate seed oil (5% by gavage) had the ability to significantly down-regulate the expression of specific osteoclast differentiation markers and RANK-RANKL downstream signaling targets in osteoclast like cells (Raw264.7). Moreover, in osteoblast like cells (MC3T3-E1) it elicited significant increase in ALP activity, matrix mineralization and transcriptional levels of major osteoblast lineage markers involving the Wnt/β-catenin signaling pathways may. Our data also reveal that PSO inhibited pro-inflammatory factors expression, while stimulating anti-inflammatory ones. These results demonstrate that PSO is highly relevant regarding osteoporosis. Indeed, it offers promising alternatives in the design of new strategies in nutritional management of age-related bone complications.

Disclosures: Mélanie Spilmont, None.

MO0361

Bone Loss in a New Rodent Model Combining Spinal Cord Injury and Cast Immobilization.

Joshua Yarrow*[1], Fan Ye[2], Alexander Balaez[3], Jillian Mantione[3], Dana Otzel[3], Cong Chen[4], Luke Beggs[2], Celine Baligand[4], Jonathan Keener[3], Wootaek Lim[4], Ravneet Vohra[4], Abhinandan Batra[4], Stephen Borst[2], Prodip Bose[2], Krista Vandenborne[4]. [1]VA Medical Center, University of Florida, USA, [2]VA Medical Center, University of Florida, USA, [3]VA Medical Center, USA, [4]University of Florida, USA

Rodent contusion spinal cord injury (SCI) models are commonly used to assess preclinical interventions designed to restore musculoskeletal integrity. However, unlike humans, rodents exhibit spontaneous recovery of hindlimb function after contusion SCI, which complicates the interpretation of musculoskeletal outcomes. We have previously reported that hindlimb immobilization (IMM) subsequent to SCI exacerbates muscle atrophy in rodents due to the complete inhibition of hindlimb loading. Herein, we characterize bone loss in our newly developed SCI+IMM model and determine the influence of muscle contractility on skeletal integrity after SCI. Female Sprague-Dawley rats aged 16 weeks were randomized into the following groups: (a) Controls, (b) severe contusion SCI sacrificed at 7 days (SCI-7), (c) SCI sacrificed at 21 days (SCI-21), (d) 2 weeks IMM-alone, (e) SCI+IMM, or (f) SCI+IMM plus 2 weeks quadrupedal treadmill training (SCI+IMM+TM). SCI-7 and SCI-21 exhibited a >20% reduction in distal femoral and proximal tibial cancellous bone mineral density (vBMD) measured via μCT (p $\leq$ 0.01), characterized by reductions in cancellous bone volume (cBV/TV%), trabecular number, and trabecular thickness. IMM-alone induced no observable bone loss. However, SCI+IMM exacerbated cancellous vBMD deficits with values being 25-45% below Controls (p $\leq$ 0.01) and SCI-21 (p $\leq$ 0.05) resulting from reduced cBV/TV% and reduced trabecular number. Similarly, SCI+IMM produced the greatest cortical bone loss within the distal femoral cortical region with cortical area and cortical thickness being 14-28% below Control (p $\leq$ 0.01). SCI+IMM+TM partially alleviated cancellous vBMD deficits with values being 21% above SCI+IMM (p $\leq$ 0.01), resulting from higher cBV/TV% and increased trabecular number, and also ameliorated cortical bone deficits at the distal femur; although, SCI+IMM+TM did not restore cancellous or cortical bone to Control or SCI-21 levels. Our findings indicate that residual and/or facilitated muscle contractility ameliorate bone decrements after SCI and suggest that our novel SCI+IMM model represents a clinically-relevant means of assessing strategies to prevent SCI-induced musculoskeletal deficits.

Disclosures: Joshua Yarrow, None.

MO0362

Effects of alendronate for bone loss and pain-related behavior in the hindlimb-unloaded mouse model of osteoporosis.

Taro Nakagawa*[1], Hiroki Wakabayashi[2], Yohei Naito[2], Takahiro Iino[2], Sho Kato[2], Akihiro Sudo[2]. [1]Mie University Gaduate School of Medicine, Japan, [2]Department of Orthopaedic Surgery, Mie University Graduate School of Medicine, Japan

Background/Purpose: Factors of chronic pain due to hemiplegia or prolonged immobility are varied, there is osteoporosis (a rarefaction due to bone atrophy) as the cause. However, there have been few reports regarding the correlation between osteoporosis and pain-related behavior. We investigated the effects on bone mass and pain-related behaviors in osteoporosis model mice with hindlimb unloading, and investigated the effect of alendronate (ALN) on pain-related behaviors.

Methods: Male ddY mice (8 weeks old) were tail-suspended for 2 week and assigned to 3 groups; hindlimb-loaded mice treated with vehicle (control), hindlimb-unloaded mice treated with vehicle (HU), hindlimb-unloaded mice treated with ALN (HUA)(n=8/group). Starting immediately after tail-suspension, vehicle or 40μg/kg ALN was injected subcutaneously twice a week for 2 weeks. The bilateral femoral distal metaphyses and proximal tibial metaphyses were analyzed three-dimensionally by micro-computed tomography (μCT) 2 weeks after tail-suspension. The frequency of the withdrawal response and the withdrawal threshold to the application of von Frey filaments to the planter surface of the hindpaws was examined as mechanical hyperalgesia 2 weeks after tail-suspension.

Results: μCT analysis of the femoral distal metaphysis (Fig. 1) and the proximal tibial metaphysis showed that bone volume/tissue volume (BV/TV) and trabecular number (Tb.N) were significantly less in the HU group than in the control group, whereas trabecular separation (Tb.Sp) was significantly greater in the HU group than in the control group. In the HUA group, BV/TV and Tb.N were significantly greater than in the HU group, whereas Tb.Sp was significantly less than in the HU group. The paw-withdrawal-frequency stimulated by von Frey filaments with strength of 0.4~2.0 gwas significantly higher in the HU group than in the control group. Whereas it was significantly lower in the HUA group than in the HU group (Fig. 2). The withdrawal threshold was significantly lower in the HU group than in the control group, whereas it was significantly higher in the HUA group than in the HU group. There was no significant difference between the HUA group and the control group in μCT analysis and hyperalgesia of hindlimbs.

Conclusion: In this study, ALN prevented bone loss and mechanical hyperalgesia in hindlimbs induced by unloading. The results suggest that bone resorption is one of the causes of osteoporotic pain.
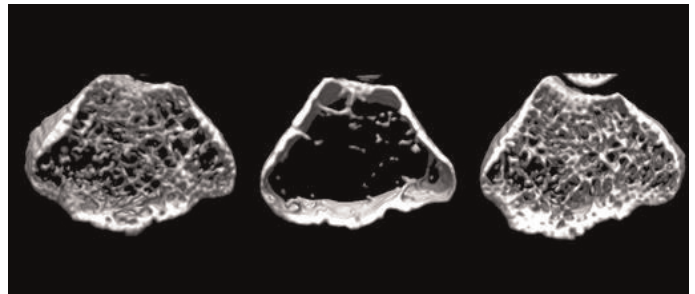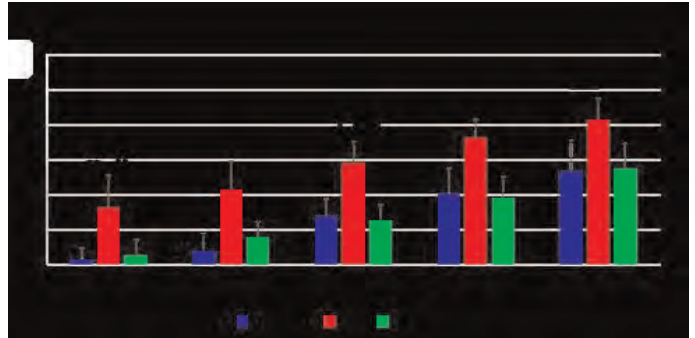

Fig.1

Fig.2

Disclosures: Taro Nakagawa, None.

MO0363

MiRNAs Involved in the Osteoblastic Function are Altered in Human Osteoporotic Bone.

Natalia Garcia-Giralt*[1], Laura De-Ugarte[2], Susana Balcells[3], Sergi Ariño-Ballester[4], Guy Yoskovitz[5], Santos Martinez-Diaz[6], Robert Guerri Fernandez[7], Leonardo Mellibovsky[8], Roser Urreizti[3], Xavier Nogues[9], Daniel Grinberg[10], Adolfo Diez-Perez[11]. [1]IMIM, Spain, [2]MSRU,IMIM (Institut Hospital del Mar d'Investigacions Mèdiques), Spain, [3]Departament de Genètica, Universitat de Barcelona, IBUB, Centro de Investigación Biomédica en Red de Enfermedades Raras (CIBERER), ISCIII, Spain, [4]MSRU,IMIM (Institut Hospital del Mar d'Investigacions Mèdiques), Spain, [5]IMIM, Parc de salut Mar, RETICEF, Spain, [6]Department Orthopaedic Surgery & Traumatology, Hospital del Mar, Spain, [7]Fundacio IMIM, Spain, [8]Servei de Medicina Interna, Hospital del Mar, Universitat Autònoma de Barcelona, Spain, [9]Institut Municipal D'Investigació Mèdica, Spain, [10]The University of Barcelona, Spain, [11]Servei de Medicina Interna, Hospital del Mar, Universitat Autònoma de Barcelona,IMIM (Institut Hospital del Mar d'Investigacions Mèdiques), Red Temática de Investigación Cooperativa en Envejecimiento y Fragilidad (RETICEF), Spain

It is well known that osteoblastic function is abnormal in osteoporotic bone. Moreover, we have observed by Real-time PCR that fresh human bone from fractured hips expresses low levels of osteoblastic markers (Alkaline phophatase, BMP2, osteocalcin and COL1A1). Our aim was to identify miRNAs differentially expressed in bone samples of fractured compared to healthy individuals. Additionally, we performed a miRNA profiling of primary osteoblasts (hOB) to assess the origin of the differentially expressed miRNAs. Total RNA was extracted from fresh femoral neck trabecular bone from women undergoing hip replacement due to either osteoporotic fracture (n=6) or osteoarthritis in the absence of osteoporosis, according to BMD measurements (n=6), age and BMI-matched, and from hOBs at passage 0, obtained from knee replacement due to osteoarthritis (n=4). Samples were hybridized to the miRCURY LNA^{TM} microRNA Array 7th (Exiqon, Denmark), in the manufacturers' facilities. For comparison of expression levels, the threshold was set at log fold change > 1.5 and a p-value < 0.05 (Benjamini and Hochberg corrected).

Overall, 790 miRNAs were detected in fresh bone samples, from which 292 (35.89%) were also detected in hOBs. A subset of 82 microRNAs was found to be significantly differentially expressed between osteoporotic and control samples. Upon validation of 8 miRNAs with the lowest p-values, and for which a validated assay was available (miRCURY LNATM Universal RT microRNA qPCR assay), two of them were confirmed: miR-320a and miR-483-5p. They were both found over-expressed in the osteoporotic samples (and expressed in hOBs). The intersection pathways involving genes targeted by miR-320a and miR-483-5p are mainly prostate cancer (4.496403e-14), PI3K-Akt signalling (5.614388e-08) and focal adhesion (6.000918e-07). It is noteworthy that these three pathways share many genes, such as: SOS2, IGF1R, PDK1, PDGFD, PIK3CA, AKT3, PTEN and MAPK1. Most of these genes are involved in cell proliferation and survival signalling, suggesting that a dysfunction in the osteoblastic cell renewal is occurring in the osteoporotic bone.

In conclusion, osteoporotic bone has an altered widespreadly osteoblast function at both key osteoblast gene expression as well as miRNAs expression levels.

Disclosures: Natalia Garcia-Giralt, None.

MO0364

Understanding Low Bone Mass In Down Syndrome Patients. <u>Archana Kamalakar</u>*[1], <u>Diarra Williams</u>[2], <u>Nisreen Akel</u>[1], <u>Tristan Fowler</u>[3], <u>Frances Swain</u>[4], <u>Kent McKelvey</u>[4], <u>Dana Gaddy</u>[1], <u>Larry Suva</u>[1]. [1]University of Arkansas for Medical Sciences, USA, [2]University of Arkansas for Medical Sciences, USA, [3]Universität Wien, Aut, [4]Department of Orthopaedic Surgery, University of Arkansas for Medical Sciences, USA

Down Syndrome (DS), trisomy of human chromosome 21, is the most common chromosomal abnormality that affects live infants, with a prevalence of around 1:700 in the US. There are currently approximately 5.6 million people with DS world-wide. DS females have ovaries containing reduced numbers of small follicles with greatly increased rates of atresia, whereas DS males are often well-masculinized, but infertile. We and others have reported an increased prevalence of low bone mass in men and women with DS. However, we have shown (in both DS mice (Ts65Dn) and humans) that the mechanism of low bone mass in DS involved low bone turnover, in the face of overt hypogonadism. In an effort to resolve this conundrum in a series of 18 euthyroid, and vitamin D and calcium replete men with DS (mean age 29 ± 7 years), we measured BMD as well as serum bone turnover markers (NTx, P1NP) and a marker of bone formation, sclerostin. NTx and P1NP were significantly decreased compared with age-matched normals, yet serum sclerostin levels were not different between DS and normals. To determine the potential influence of reproductive hormones in the Hypothalamic-Pituitary-Gonadal-Skeletal axis on low BMD, we also measured serum levels of the gonadotropins (LH, FSH) and testosterone (T). Interestingly, LH and FSH levels were both significantly elevated compared with the normal reference ranges. In all patients, BMD Z-score was less than -2.0, confirming the expected low BMD. All 18 males with DS had serum T levels within the low normal reference range. We next examined the expression of sclerostin and RANKL in the long bones of DS mice (Ts65Dn and TC1) by immunohistochemistry. RANKL staining was difficult to detect but unchanged compared with littermate controls. In addition, although more robust, sclerostin immunostaining was not different between WT and DS. In culture, the low bone turnover was replicated with decreased numbers of TRAP+ multinucleated cells as well as osteoblasts in whole bone marrow cultures. In osteoclast motility assays, a significant increase was observed in precursor motility of bone marrow macrophages from Ts65Dn mice compared to WT type mice. These data suggest that the decreased bone turnover in the face of hypogonadism in these DS patients maybe accompanied by a compensatory increase in the motility of TRAP+ osteoclast precursors. In sum, the low bone mass in these patients remains unexplained by decreased sex steroids or elevated LH and FSH levels.

Disclosures: Archana Kamalakar, None.

MO0365

The effects of androgens on cortical bone mass do not result from direct actions on osteoblasts or osteoclasts. <u>Semahat Serra Ucer</u>*[1], <u>Shoshana Bartell</u>[2], <u>Ha-Neui Kim</u>[3], <u>Srividhya Iyer</u>[2], <u>Li Han</u>[2], <u>Aaron Warren</u>[4], <u>Julie Crawford</u>[4], <u>Maria Jose Almeida</u>[2], <u>Stavros Manolagas</u>[2]. [1]University of Arkansas for Medical Sciences, USA, [2]Central Arkansas VA Healthcare System, Univ of Arkansas for Medical Sciences, USA, [3]Univ. Arkansas for Medical Sciences, Central Arkansas VA Healthcare System, USA, [4]Center for Osteoporosis & Metabolic Bone Diseases, Central Arkansas Veterans Healthcare System, University of Arkansas for Medical Sciences, USA, USA

Global deletion of the androgen receptor (AR) in male mice causes high bone turnover, increased resorption, and decreased cortical and trabecular bone mass. Targeted AR deletion in the entire osteoblast lineage, on the other hand, decreases trabecular, but not cortical, bone mass. It remains possible, therefore, that direct actions of androgens on cells of the osteoclast lineage mediate their protective effects on the cortical compartment and/or contribute to their effects on cancellous bone in males. To explore this possibility, we have generated mice with selective deletion of AR in cells of the monocyte/macrophage lineage by crossing mice harboring a floxed AR allele (exon 2) with mice expressing the Cre recombinase under the control of regulatory elements of the LysM gene (AR flox;LysM-Cre mice). Analysis of genomic DNA extracted from cultured bone marrow-derived macrophages and osteoclasts revealed >90% reduction of the AR conditional allele. The number of myeloid cells (CD11b+) were similar between AR flox;LysM-Cre and LysM-Cre littermate control mice, as determined by flow cytometry. At 12 and 26 weeks of age femoral and spinal DEXA BMD, trabecular bone volume in the distal femur and L5 vertebra, and cortical thickness in femoral mid-shaft, by μCT were also indistinguishable between the AR flox;LysM-Cre mice and their littermate wild-type controls. We next orchidectomized (ORX) AR flox;LysM-Cre and LysM-Cre controls at 20 weeks of age and examined their skeletons 6 weeks later. ORX decreased cortical thickness, trabecular bone volume and trabecular number to the same extent in both genotypes, compared to their respective sham-operated littermates. These findings indicate that the osteoclast AR plays no role in the protective effects of androgens on cancellous or cortical bone. Taken together with the evidence that the osteoblast AR affects only

cancellous bone, our results also indicate that neither the osteoblast nor the osteoclast AR are involved in the protective effects of androgens on cortical bone mass. Hence, the effect of androgens on cortical bone mass must be exerted indirectly, perhaps via effects on muscles and mechanical strains and/or changes in growth factor production.

Disclosures: Semahat Serra Ucer, None.

MO0366

Transmenopausal changes in cortical bone quality. <u>Sonja Gamsjaeger</u>*[1], <u>Wolfgang Brozek</u>[1], <u>Robert Recker</u>[2], <u>Klaus Klaushofer</u>[3], <u>Eleftherios Paschalis</u>[4]. [1]Ludwig Boltzmann Institute of Osteology at the Hanusch Hospital of WGKK & AUVA Trauma Centre Meidling, 1st Medical Department, Hanusch Hospital, Austria, [2]Creighton University, USA, [3]Hanusch HospitalLudwig Boftzmann Institute of Osteology, Austria, [4]Ludwig Boltzmann Institute for Osteology, Austria

Hormonal changes due to menopause are considered to be among the culprits of postmenopausal osteoporosis. These changes are believed to result in bone tissue loss and decrease in bone mineral density (BMD), mainly through alterations in bone remodeling rates. Specifically, bone remodeling rates (based on activation frequency of new remodeling sites) in women 1 year after cessation of menses are roughly twice those of healthy premenopausal women.

Bone strength depends on its amount and quality. Bone quality includes its structural and material properties. Bone material properties are dependent on bone turnover rates. Remodeling rates are significantly increased immediately following menopause.

We have previously reported that menopause results in changes in bone quality of human iliac crest trabecular bone. In the present study we used Raman microspectroscopic analysis of double iliac crest biopsies with a spatial resolution of 1 μm obtained before and immediately after menopause (1 year after cessation of menses) in healthy females, to investigate changes in material properties due to menopause in cortical bone. In particular, the mineral / matrix ratio, the relative proteoglycan and lipid content, the mineral maturity / crystallinity, and the relative pyridinoline collagen cross-link content were determined in cortical bone as a function of tissue age (freshly deposited bone in osteons and at endosteal surfaces based on the presence of fluorescent double labels, and older cortical interstitial bone). 2-way ANOVA statistical analysis indicated that although all monitored bone quality parameters were significantly dependent on tissue age, no significant differences due to menopause were evident at any of the cortical microanatomical locations examined, unlike what we have previously described in trabecular bone.

The results of the present study suggest that menopause does not affect the bone quality of cortical bone. Moreover, they emphasize the need to consider cortical separately from the trabecular compartment (most likely due to different turnover rates and specific surface area). Finally, these results help in understanding changes due to aging hallmarks such as menopause, which in turn facilitates the discrimination from changes due to diseases such as osteoporosis.

Disclosures: Sonja Gamsjaeger, None.

MO0367

Long-term low-molecular-weight heparin and bone health in non-pregnant patients: A systematic review. <u>Olga Gajic-Veljanoski</u>*[1], <u>Chai W. Phua</u>[2], <u>Prakesh S. Shah</u>[3], <u>Angela M. Cheung</u>[4]. [1]University Health Network, Canada, [2]Division of Hematology, Dept of Medicine, University of Toronto, Canada, [3]Departments of Paediatrics & IHPME, University of Toronto, Canada, [4]University Health Network-University of Toronto, Canada

Introduction: Patients who require long-term anticoagulation with low-molecular-weight heparin (LMWH) such as cancer patients or the elderly may be at increased risk of fractures. However, it is unclear whether long-term use of LMWH has any deleterious effect on bone health.

Objective: To determine if LMWH therapy of at least 3 months' duration adversely affects bone outcomes in non-pregnant adult populations.

Methods: We systematically searched Medline, EMBASE, the Cochrane Library, conference proceedings and bibliographies until February 2014. We included comparative studies, published in English, conducted in non-pregnant adult populations, reporting the long-term effect of LMWH (>= 3 months) on fractures or bone mineral density (BMD). Two reviewers independently extracted the data and assessed methodological quality of the included studies. We used a tool developed by the Cochrane Collaboration Back Review Group to evaluate the method quality of clinical trials and the Newcastle Ottawa Scale to evaluate the quality of observational studies. We qualitatively synthesized evidence from all studies and used random-effects meta-analysis to quantify the effect of LMWH on fractures.

Results: Of 2726 identified records, we excluded 2603 citations based on the title and abstract screening and examined 123 citations in full. Sixteen articles reporting 14 studies were included: 10 clinical trials (4865 patients) and four observational cohort studies (251 patients). Majority of studies had high risk of bias. In most studies, BMD and fractures were assessed as secondary outcomes. In a random-effects meta-analysis of the five trials (2280 patients), LMWH for 3-6 months did not significantly increase the relative or absolute risk of all fractures (pooled risk ratio=0.58, 95%CI: 0.23 to 1.43, I2=12.5%; risk difference=0.00, 95%CI: -0.02 to 0.02), when compared to unfractionated heparin, vitamin K antagonists or placebo. Qualitative synthesis of the

prospective cohort studies (166 patients) suggested that LMWH for 3-24 months decreased the mean BMD by 2.8-4.8% (depending on the BMD site) compared to vitamin K antagonists that decreased the mean BMD by 1.2-2.5%.

Conclusions: The long-term use of LMWH may not increase the risk of fractures, but may adversely affect BMD. The strength of evidence is weak and further well-designed studies are warranted.

MO0368

The Association Between Use of Antidepressants and Bone Quality Using Quantitative Ultrasound. Päivi Rauma*[1], Julie Pasco[2], Michael Berk[3], Amanda Stuart[4], Risto Honkanen[1], Heli Koivumaa-Honkanen[5], Jason Hodge[6], Lana Williams[7]. [1]University of Eastern Finland, Finland, [2]Deakin University, Australia, [3]Deakin University; The University of Melbourne, Australia, [4]Deakin University, Australia, [5]University of Eastern Finland; Kuopio University Hospital; University of Oulu, Finland, [6]Deakin University; The Geelong Hospital, Australia, [7]The University of Melbourne, Australia

Osteoporosis and depression are major public health problems worldwide. Studies have reported an association between antidepressant use, mainly selective serotonin reuptake inhibitors (SSRIs) and bone density, but the issue remains unclear.

Altogether 849 Australian men (aged 24-98 years) from the Geelong Osteoporosis Study (GOS) completed a comprehensive questionnaire in 2006-2011 and had quantitative ultrasound (QUS) heel measurements. Bone quality was indexed by Broadband Ultrasound Attenuation (BUA), Speed of Sound (SOS) and Stiffness Index (SI). The cross-sectional associations between these parameters and use of antidepressants were studied using multivariate linear regression adjusted for anthropometric, medication and lifestyle factors. The study was approved by the Human Research Ethics Committee at Barwon Health and all participants provided written, informed consent.

At the time of assessment, 61 (7.2%) men were using antidepressants, of which 44 (72.1%) used SSRIs. Mean SI values were 95.4% and 100.2% (p=0.076), BUA 115.7 dB/Mhz and 120.8 dB/MHz (p=0.020) and SOS 1566.9 m/sec and 1572.5 m/sec (p=0.32) for antidepressant users and non-users, respectively. After adjustments antidepressant use was associated with lower SI (p=0.002), SOS (p=0.010) and BUA (p=0.053). However, body weight was identified as an effect modifier; QUS values were lower for antidepressant users with low weight (<90kg) only.

In conclusion, use of antidepressants was associated with lower bone quality measures of QUS for men with low body weight. Thus, osteoporosis should be considered among men with light body weight when antidepressants are prescribed.

MO0369

Bone Marrow Fat (BMT), Energy Metabolism and Bone Mineral Density (BMD) in Young Women with Cushing Disease (CD). Sergio Luchini Batista*[1], Marcello Henrique Nogueira-Barbosa[2], Iana Mizumukai de Araújo[2], Adriana Lélis Carvalho[2], Carlos Ernesto Garrido Salmon[3], Ayrton Custódio Moreira[2], Margaret de Castro[2], Francisco José Albuquerque de Paula[2]. [1]School of Medicine of Ribeirao Preto, University of Sao Paulo, Brazil, [2]School of Medicine of Ribeirão Preto, University of São Paulo, Brazil, [3]Faculty of Science & Letters, University of São Paulo, Brazil

Introduction: Glucocorticoid-induced osteoporosis (GIO) is a multifactorial disorder involving systemic (hypogonadism, impaired GH/IGF-I and PTH secretion and decreased vitamin D action) as well as tecidual alteration in bone cells crosstalk (i.e., increased RANKL, decreased osteoprotegerin). Osteocyte and osteoblast apoptosis has also been considered an important mechanism for bone loss in this condition. Although rare, Cushing Disease is the most important cause of endogenous hypercortisolism. It typically differs from GIO due to the maintenance of adrenal androgen secretion (e.g., S-DHEA, DHEA and androstenedione). Our aim was to measure Bone Marrow Fat (BMF), Bone Mineral Density (BMD) and some energy metabolism parameters in young women with CD. Material and Methods: The study comprised 28 young women, 14 with CD and 14 controls (C), matched by age (C=35.4 ± 10.3 vs CD= 34.5 ± 9.2years) and height (C=1.65 ± 0.08 vs CD=1.62 ± 0.05m). Blood sample was collected after overnight fast for measurement of glucose, insulin, IGF-I, osteocalcin and CTX. BMD was evaluated in L1-L4, femoral neck, total hip. ^{1}H magnetic resonance spectroscopy (1.5T) in lumbar spine (L3) was used to evaluate BMF. Results: Body weight (C=60.3 ± 8.8 vs CD=89.2 ± 17.3Kg), waist circumference (C=79.5 ± 10.0 vs CD=111.8 ± 11.6cm) and BMI (C=22.4 ± 2.9 vs CD=33.9 ± 5.9Kg/m^2) were higher in CD (p<0.05). CD patients showed alteration in the circadian rhythm of salivary cortisol (9am=2510 ± 1182ng/dl, 23h=1784 ± 989ng/dl) and in response to 1mg-dexamethasone suppression test (1786 ± 1861ng/dl). CD group exhibited greater serum levels of alkaline phosphatase (C=150 ± 30 vs CD=190 ± 40U/L), glucose (C= 86 ± 7 vs CD=136 ± 59mg/dl), insulin (C=7.9 ± 3.7 vs CD=$29.7 \pm 25.2\mu$IU/ml) and HOMA-IR (C=1.68 ± 0.84 vs CD=10.31 ± 9.22). The serum levels of creatinine, calcium, phosphorus, albumin, PTH and 25-OHD (C=22.8 ± 9.6 vs CD=17.3 ± 8.4ng/mL) were similar in both groups. Despite higher BMI, BMD in L3 was slightly lower in CD group (C=1.000 ± 0.101 vs

CD=0.945 ± 0.086g/cm^2), but 57% of CD patients showed Z-score lower than -1.0, whereas this figure was 21% in C. Bone marrow fat was significantly higher in CD than in C (37.1 ± 8.7 vs 20.8 ± 8.2%; p<0.05). Conclusion: Endogenous hypercortisolism due to CD impacts trabecular bone even in young women. While trabecular bone is negatively affected, bone marrow fat is significantly enhanced in these patients. Our results encourage further studies to unveil the role of insulin resistance and BMF into bone deterioration in CD.
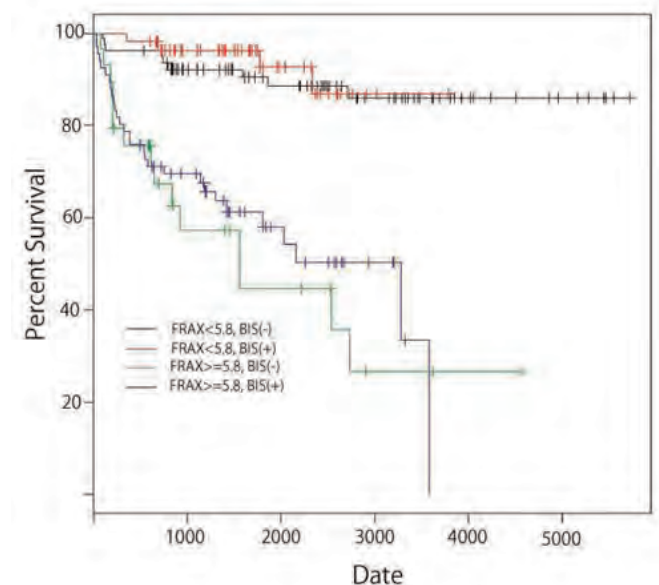
MO0370

Ineffective fracture prevention by bisphosphonate in patients undergoing high dose glucocorticoid therapy with a FRAX ten year probability greater than 5.8%. Goichi Kageyama*[1], Takaichi Okano[2], Kousaku Tsuda[2], Yuzuru Yamamto[3], Daisuke Sugiyama[4], Goh Tsuji[5], Shunichi Kumagai[5], Akio Morinobu[6]. [1]Kobe University Hospital, Japan, [2]Kobe University Hospital, Japan, [3]Kobe University Hospital, Japan, [4]Keio University, Japan, [5]Shinko Hospital, Japan, [6]Kobe University Hospotal, Japan

(Background) High dose glucocorticoid (GC) therapy (PSL>0.8mg/kg/day) is often provided to patients with systemic rheumatic disease. GC induced osteoporosis (GIO) is a common complication of high dose GC therapy and bisphosphonate(BP) is frequently used as a first-line prevention of GIO and fragile fractures. However, some patients are still at high risk of bone fractures despite bisphosphonate administration. The World Health Organization fracture risk assessment tool (FRAX) is used to calculate the 10-year probability of major (hip, clinical spine, humerus or wrist fracture) fractures and has been recently adopted to the treatment guidelines for GIO and for assessment of fracture risk. Drugs more effective than BP have recently become available, but it is unclear which patients with high dose GC therapy should be given the newer drugs for GIO prevention.

(Aim) To identify patients with high dose GC therapy at a high risk of developing fragility fracture despite bisphosphonate treatment.

(Method) We conducted a retrospective study on systemic rheumatic disease patients who were treated with PSL>0.8mg/kg/day at Kobe University Hospital from April 1988 to March 2012. The fracture risk at the start of high dose GC therapy was assessed by FRAX. Comparison between patients who remained fracture-free for over 5 years and those who suffered fractures within 5 years despite taking bisphosphonate were focused in particular.(Results) 229 (SLE 76, Vasculitis syndrome 58, PM/DM 51, AOSD 12, MCTD 7, others 25) patients were included and the mean observational period was 1819 days (95% CI 1653-1989). 57 patients (52 clinical spinal, 3 hip, 1 humerus, 1 wrist) suffered from fracture. 28 patients suffered from fracture within 5 years despite taking BP. 94 patients were fracture-free for over 5 years with or without BP. Receiver operating characteristic (ROC) analysis revealed that the optimal cut-off of FRAX ten year probability failing to prevent fracture over 5 years despite bisphosphonate treatment was 5.8% (Sensitivity 89.3%, Specificity 74.5%, Area under the curve 0.885). Kaplan-Meier analysis also revealed that bisphosphonate had no effect in reducing fractures in patients with FRAX?5.8%.

(Conclusion) BP is ineffective for preventing fractures in high-risk patients (FRAX>=5.8%) undergoing high dose GC therapy. Thus, these patients require alternative prophylactic measures for fragility fractures.

Survival.png

MO0371

Serum Levels of Growth Differentiation Factor (GDF)-15 Are Elevated, And Decreased After Introduction of Oxygen Therapy in Japanese Male Subjects with COPD-Associated Osteoporosis. Reiko Watanabe*[1], Takeshi Tanaka[2], Keisuke Aita[2], Masaaki Hagiya[2], Nobuyuki Tai[2], Junko Hirano[2], Kyoko Yokosuka[3], Hisami Yamakawa[4], Tsutomu Yarita[2], Toshiaki Homma[2], Ryo Okazaki[1]. [1]Teikyo University Chiba Medical Center, Japan, [2]Teikyo University Chiba Medical Center, Japan, [3]Yarita Hospital, Japan, [4]Yaria Hospital, Japan

Background&Aim: We have reported a high prevalence of vertebral fractures in male COPD patients in Japan. The mechanism of COPD-associated osteoporosis, however, still remains unclear. The aim of the present study is to investigate bone metabolism in COPD and its change after introduction of oxygen therapy. We also examined a role for GDF-15, a marker of congestive heart failure that has recently been shown to be induced by hypoxia in osteocytes through HIF-1α.

Subjects&Methods: In this cross-sectional study, 52 Japanese male COPD subjects (mean age 70.0 ± 8.3, BMI 21.3 ± 3.9 kg/m^2) were enrolled. The number and severity of existing vertebral fractures was assessed by lateral spine x-rays, and bone mineral density was measured by DXA. Bone metabolic markers and parameters of calcium metabolism were measured by standard assays. Serum levels of GDF-15 was measured by ELISA.

Results: We found prevalent vertebral fractures in 38 (73.1%), multiple fractures in 25 (48.1%), and SQ Grade 2 or 3 fractures in 11 (21.2%). Lumber spine and femoral neck BMD T scores were -1.13 ± 1.49 and -1.83 ± 1.26, respectively. Mean 25(OH)D levels were 23.7 ± 11.0 ng/ml, which showed no correlation with PTH levels. Mean GDF-15 levels were 1747 pg/mL (healthy male mean: 1020 pg/mL (59 years)) and correlated positively with age, creatinine, interleukin-6, pyridinoline 1CTP, and negatively with albumin, hemoglobin(Hb) and LDL-cholesterol. In multivariate linear regression analysis, Hb was the only independent determinant of GDF-15 (R^2=0.250,β=-0.459, p=0.007). When the subjects were divided into four groups according to the PTH and 25(OH)D levels, GDF-15 was significantly elevated (2714 pg/mL, p=0.024) and Hb was decreased (12.1 g/dl, p=0.00001) in subjects with PTH <42 pg/mL and 25(OH)D <20 ng/ml. Interestingly, in 4 patients who were introduced to the oxygen therapy, GDF-15 dramatically decreased (mean 6047→1779 pg/mL) within one month, while PTH tended to increase (39.5→48.5 pg/mL) and Tracp-5b significantly increased (131→379 mU/dL, p=0.030) without any appreciable changes in Hb.

Conclusions: GDF-15 was shown, for the first time, to be elevated and immediately decreased after oxygen therapy in COPD subjects. The results further suggest that systemic hypoxia affects bone metabolism at least in part indirectly through suppression of PTH secretion. Further examination is needed to elucidate pathophysiological roles of GDF-15 and PTH in COPD-associated osteoporosis.

Disclosures: Reiko Watanabe, None.

MO0372

Differential effects of teriparatide (TPTD) and zoledronic acid (ZOL) on bone mineralization density distribution (BMDD) at 6 and 24 months in the SHOTZ study. David Dempster*[1], Paul Roschger[2], Barbara M. Misof[3], Hua Zhou[4], Eleftherios Paschalis[5], Fangqiu Zhang[6], Jahangir Alam[7], Valerie A. Ruff[8], Klaus Klaushofer[9], Kathleen Taylor[10], For the SHOTZ Investigators [11]. [1]Columbia University, USA, [2]L. Boltzmann Institute of Osteology, Austria, [3]Ludwig Boltzmann Institute of Osteology, Austria, [4]Helen Hayes Hospital, USA, [5]Ludwig Boltzmann Institute for Osteology, Austria, [6]inVentiv Health Clinical, Canada, [7]Lilly USA, USA, [8]Eli Lilly & Company, USA, [9]Hanusch HospitalLudwig Boftzmann Institute of Osteology, Austria, [10]Eli Lilly & Company, USA, [11], USA

Purpose: SHOTZ assessed the progressive effects of TPTD and ZOL on bone remodeling and material properties in postmenopausal women with osteoporosis. Previously, we reported that bone formation indices were significantly higher in patients receiving TPTD versus ZOL. In this analysis, we report BMDD results − a measure that reflects bone matrix mineralization. This is the first head-to-head study to compare the effects of an anabolic versus an antiresorptive agent on BMDD over time.

Methods: Subjects from the 12-month randomized study were eligible to enroll in a 12-month extension and assigned open label to their original treatment regimen: TPTD 20 µg/d (sc injection) or ZOL 5 mg/y (IV infusion). Biopsies were obtained at month 6 (TPTD, n=28 and ZOL, n=31) and month 24 (TPTD, n=10 and ZOL, n=10). Quantitative backscattered electron imaging was used to obtain BMDD measurements from the same bone samples used for histomorphometric analyses.

Results: In cancellous bone, CaMean (mean calcium concentration), CaWidth (width of the distribution peak), and CaLow (percentage of low mineralized bone) provided the clearest distinction between TPTD and ZOL at months 6 and 24 (Table). CaMean was significantly higher while CaLow and CaWidth were significantly lower in the ZOL group at both time points, indicating higher mineralization density and more homogeneous mineral content with ZOL. Compared to TPTD, mean BMDD curves (Figure) show that bone matrix mineralization in the ZOL group increases (peak shift to the right) and becomes more homogeneous (narrower peak width) over time. Within the ZOL group, significant changes were seen in all parameters from

month 6 to 24, indicating a progressive increase in mineralization density. In sharp contrast, mineralization density did not increase over time in the TPTD group, reflecting ongoing deposition of new bone. Similar within- and between-group differences were observed in cortical bone.

Conclusions: In this study, TPTD stimulated new bone formation, producing a bone mineral matrix that remained relatively heterogeneous with a stable mean mineral content. ZOL slowed bone turnover rate and prolonged secondary mineralization, producing a more homogeneous and, over time, a more highly mineralized bone matrix. While both TPTD and ZOL increase clinical measures of bone mineral density (BMD), this study shows that the underlying mechanism for the BMD increase with each drug is fundamentally different.

Table. BMDD Findings in Subjects from the SHOTZ Trial

Parameter	Month 6 TPTD (n=28)	Month 6 ZOL (n=31)	P Values TPTD vs ZOL at Month 6	Month 24 TPTD (n=10)	Month 24 ZOL (n=10)	P Values TPTD vs ZOL at Month 24	Within Group P Values (Mo 24 vs Mo 6) TPTD	Within Group P Values (Mo 24 vs Mo 6) ZOL
Cancellous Bone								
CaMean[a] (wt% Ca)	21.66 (0.88)	22.14 (0.62)	0.018	22.04 (0.82)	22.90* (0.42)	0.009	0.240	<0.001
CaPeak[b] (wt% Ca)	22.57 (0.88)	22.84 (0.58)	0.176	22.75 (0.71)	23.34* (0.41)	0.036	0.549	0.014
CaWidth[c] (Δwt% Ca)	4.30 (0.81)	3.77 (0.39)	0.003	3.73* (0.36)	3.36* (0.15)	0.012	0.005	<0.001
CaLow[d] (% bone area)	7.48 (5.84)	4.89 (1.32)	0.029	5.43 (2.16)	3.60* (0.32)	0.025	0.123	<0.001
CaHigh[e] (% bone area)	6.06 (4.12)	7.12 (4.90)	0.374	7.07 (5.84)	12.04* (5.91)	0.075	0.556	0.012
Cortical Bone								
CaMean[a] (wt% Ca)	21.51 (0.72)	22.06 (0.57)	0.002	21.92 (0.67)	22.66* (0.34)	0.006	0.127	0.003
CaPeak[b] (wt% Ca)	22.56 (0.63)	22.82 (0.55)	0.096	22.58 (0.70)	23.20* (0.35)	0.021	0.931	0.043
CaWidth[c] (Δwt% Ca)	4.72 (1.04)	4.21 (0.46)	0.021	4.21 (0.50)	3.83* (0.24)	0.050	0.052	0.002
CaLow[d] (% bone area)	8.83 (4.68)	5.44 (1.84)	0.001	5.21 (1.36)	3.46* (0.57)	0.003	<0.001	<0.001
CaHigh[e] (% bone area)	5.96 (3.60)	7.32 (4.59)	0.213	6.72 (5.86)	9.95 (4.62)	0.188	0.705	0.125

[a]CaMean = Mean calcium concentration in the area of bone measured.
[b]CaPeak = The most frequent calcium concentration occurring in the area of bone measured.
[c]CaWidth is a measure of the variability of mineralization density (heterogeneity).
[d]CaLow is a measure of the area of bone with the least amount of calcium.
[e]CaHigh is a measure of the area of bone with the most amount of calcium.
Values are shown as mean (SD). P values are for 2-sample t-test. *P<0.05 Month 24 vs Month 6.
BMDD=bone mineralization density distribution; TPTD=teriparatide; ZOL=zoledronic acid.

Table
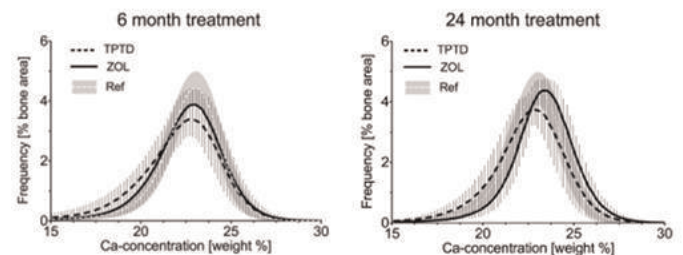
Figure. Changes in cancellous BMDD with type and duration of treatment.
The mean BMDD curves (±1SD) of treatment groups (TPTD and ZOL) show a progressively increasing difference with treatment duration. Compared to TPTD, the bone matrix mineralization becomes more homogeneous (narrower peak width) and higher (peak shift to the right) for ZOL treatment. Reference data (historical) were obtained from 52 healthy adults (Roschger et al. Bone 2003;32:316-23).

Figure

Disclosures: David Dempster, Eli Lilly, Amgen, Merck, 3; Eli Lilly, 7; Amgen, Eli Lilly, This study received funding from: Lilly USA, LLC

MO0373

Early increases in IGF-1 receptor density on circulating osteogenic progenitor cells predict responsiveness to teriparatide. Adi Cohen*[1], J. Sanil Manavalan[2], Stavroula Kousteni[1], Robert Recker[3], Joan Lappe[4], David Dempster[5], Donald McMahon[6], Mariana Bucovsky[7], Mafo Kamanda-Kosseh[7], Julie Stubby[8], Elizabeth Shane[6]. [1]Columbia University Medical Center, USA, [2]Columbia University, USA, [3]Creighton University, USA, [4]Creighton University Osteoporosis Research Center, USA, [5]Columbia University, USA, [6]Columbia University College of Physicians & Surgeons, USA, [7]Columbia University, USA, [8]Creighton University, USA

In an open-label pilot study of teriparatide (TPTD; 20 mcg daily for 2 yrs) in 21 premenopausal women with idiopathic osteoporosis (IOP), we found substantial

increases in lumbar spine (LS; mean $\pm$ SD: $10.8 \pm 8.3\%$), total hip (TH; $6.2 \pm 5.6\%$) and femoral neck (FN; $7.6 \pm 3.4\%$) BMD. However, LS BMD response to TPTD varied from -1% to +20%. Lower pre-TPTD bone turnover by serum bone turnover markers (BTM) and bone biopsy, smaller 1M increases in BTM, and higher BMI and body fat predicted lower responsiveness to TPTD. Since IGF-1 is low in obesity and is also critical for TPTD action on osteoblasts, we investigated whether differential TPTD responsiveness was mediated by IGF-1 related mechanisms. Serum IGF-1 and IGFBP3 did not change in response to TPTD. However, baseline serum IGF-1 was inversely associated with TPTD response. Prompted by these findings, we measured IGF-1 receptor (IGF-1R) density on circulating osteogenic progenitor (COP) cells. We obtained peripheral blood mononuclear cells (PBMCs) at baseline and 1, 3 and 18M of TPTD in 11 women who participated in the pilot study (38 ± 7 yrs, BMI 20.9 ± 3.0 kg/m^2). Following exclusion of hematopoietic lineage cells, COPs were identified by flow cytometry with antibodies against osteocalcin and Runx2 and designated as %COP, meaning % of PBMCs expressing these markers. IGF-1R density on COPs was measured by mean channel fluorescence (MCF) of antibodies to IGF-1R. At baseline, %COP correlated directly with cancellous wall width (r;p: 0.85;0.0008) and mineral apposition rate (0.76; 0.006) on transiliac biopsies. %COP increased with TPTD, peaking at 3M by 221% (p=0.02). IGF-1R MCF increased by 128% (p=0.009) at 3M (Figure). Baseline %COP and the increase in COP at 3M did not predict BMD response to TPTD (Table). In contrast, the increase in IGF-R MCF in COPs (3M %change) correlated directly with early BMD response to TPTD. Although baseline IGF-1R MCF did not correlate with BMI and body fat, IGF-1R increase (3M %change) correlated strongly and inversely with BMI and body fat by DXA. We conclude that both %COP and IGF-1R density on COPs rise markedly in IOP women in response to TPTD. The increase in IGF-1R density on COPs correlates inversely with body fat and directly with early BMD response. These results suggest that body fat may be inversely associated with responsiveness to TPTD mediated via the IGF-1 axis. An early increase in IGF-1R density on COPs may play an important role in the osteoanabolic response to TPTD.
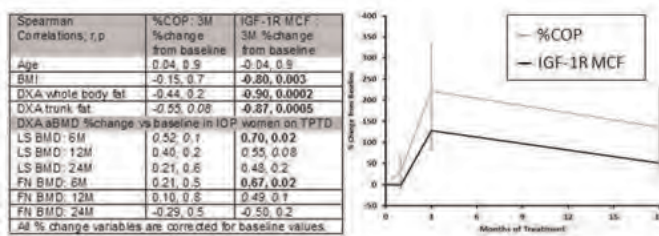
COPAbstractTableFigure

Disclosures: Adi Cohen, None.
This study received funding from: Eli Lilly & Company provided funding for the original pilot study

MO0374

Effectiveness of Teriparatide in the Treatment of Osteoporosis, Data from Real-World Clinical Practice George O. Tsoukas1, Alaa Dekis2, Philip H. Tsoukas3, Louise Ullyatt1, Fiona Vickers, George M. Tsoukas1 1 Division of Endocrinology, 2 Division of Rheumatology, McGill University Health Center; 3 Department of Medicine, University College Dublin. Georges Tsoukas*. McGill University, Canada

Although the efficacy of teriparatide in bone metabolism has been demonstrated in multiple controlled clinical trials, data from longitudinal observational studies are limited. Such studies are essential in understanding real-world effectiveness of therapeutic interventions. In this study, we aim to demonstrate true population-based benefits of teriparatide in a clinical practice setting.

We conducted a retrospective chart review on a total of 286 patients seen at 4 different osteoporosis clinics in Montreal, Canada. All patients were treated according to Canadian Osteoprosis Guidelines. Fracture data were available on 240 of these patients. All fractures were clinical and reported according to Canadian guidelines.

51% of the patients received teriparatide for 18 months, 38% for 24 months and 11% for other duration of treatment.The mean follow up after cessation of teriparatide was 36 months ranging from 5 to 106 months. All patients after teriparatide therapy received an antiresorptive.

During teriparatide treatment, new fractures occured in 9 patients, all fractures were non-hip and non-vertebral. After cessation of teriparatide, new fractures occured in 17 patients, 3 patients had 2 fractures each, with a total of 20 fractures. Of these, 15 were non-vertebral fractures, 3 vertebral and 2 hip. After 24 months, teriparatide increased the bone mineral density by 9% in the lumbar spine and 5% in the hip. the alkaline phosphatase, osteocalcin and c-terminal telopeptide increased by 26, 111 and 107% respectively at 18 months. Compliance to therapy was reported to be 85% at 18 months.

Our results suggest that treatment of osteoporosis with teriparatide significantly increased spinal bone mineral density. The fracture outcome evaluation in this retrospective review of the clinical practice data indicated that the occurence of fracture incidence during teriparatide therapy was low (3.7%) with no new vertebral fractures. In the post teriparatide therapy follow up period, an increase in the incidence of fractures was observed with most (85%) being non-vertebral.

Disclosures: Georges Tsoukas, None.

MO0375

Effects of Recombinant Human Parathyroid Hormone on Bone Structure in Premenopausal Women with Lower Extremity Stress Fractures: A Pilot Study. Ellen Almirol*[1], Lisa Gao[2], Shelley Hurwitz[3], Meryl Leboff[4]. [1]Brigham & Women's Hospital, USA, [2]Case Western Reserve University School of Medicine, USA, [3]Brigham & Women's Hospital, USA, [4]Brigham & Women's HospitalProfessor of Medicine, Harvard Medical School, USA

Stress fractures are repetitive motion injuries of the lower extremities, which are more common in women than men. Although Teriparatide (TPD) has advanced osteoporosis care, there are no randomized, placebo (PBO)-controlled trials on effects of TPD on bone structure in adults with stress fractures. In this pilot study, we evaluated the effects of TPD vs PBO on structural changes according to peripheral quantitative computed tomography (pQCT) in women with lower extremity stress fractures. We recently found early and robust rises in bone formation markers and a larger anabolic window in women treated with TPD vs PBO (ASBMR 2013). Premenopausal women (aged 21-45) with lower extremity stress fractures were randomized to daily TPD (20µg s.c.) or placebo injections for 8 weeks; women received calcium and vitamin D to achieve daily intakes of 1000 mg of calcium and 400 IU vitamin D3. To assess changes in bone structure, pQCT (XCT 3000 Stratec Germany) at the distal radius (4, 33%) and unaffected tibia (4, 38, 66%) were measured at 0, 8 and 12 weeks. Serum biomarkers of bone formation [amino terminal propeptide of type 1 collagen (P1NP) and osteocalcin (OC)] and resorption (C-telopeptide) were measured at 0, 4 and 8 weeks. Groups were compared using the Wilcoxon Rank-Sum Test or Chi Square test, as appropriate. Of 101 women screened, 13 were randomized to TPD (n=6) or PBO (n=7). Compared with PBO, the TPD-group at the 38% tibial site showed an increase in cortical thickness (TCT) and cortical area (TCA) at 8 weeks (p≤0.01). In the PBO-treated group, there was an increase at the tibial 38% cortical density (TCD) site at 8 weeks (p=0.01), with no change in the TPD-treated group, possibly related to the increase in TCA. No significant differences were observed between groups at the distal radius over the study period. Changes in P1NP and OC with TPD were positively correlated with changes at the 38% tibial TCA (p=0.03 and 0.01) and TCT (p=0.01 and 0.02) site at 8 weeks. This short-term study in women with stress fractures treated with TPD or PBO showed increases in TCA and TCT at the 38% tibial site, with an unexpected rise in the TCD in the PBO group; changes in bone formation biomarkers were positively correlated with changes in TCA and TCT, but not TCD. This 8-week pilot study showed some potential benefit of TPD on bone structure, although larger PBO-controlled studies are needed to assess the systemic effects of TPD on bone in adults with stress fractures.

Disclosures: Ellen Almirol, None.

MO0376

Er-Xian Decoction stimulates osteoblastic differentiation of bMSCs in OVX mice and its gene profile analysis. Qin Bian*[1], Yongjun Wang[2]. [1], USA, [2]Othopedic Surgery, Peoples Republic of China

Er-Xian Decoction (EXD), a traditional Chinese herbal formula, has been widely used for the treatment of postmenopausal osteoporosis. To evaluate osteogenetic effect of EXD on bMSCs in OVX mice and to search for its genes and pathways targets. Six-month-old ICR mice that underwent OVX were treated with EXD. After 3 months, bone mass was evaluated by microcomputed tomography, histological and immunohistochemical detection. The bone mesenchymal stem cells (bMSCs) from femurs and tibiaes were harvested to observe the self-renewal and differentiation capacity by Colony. forming unifibroblastic (CFU-F), Colony. forming adipocyte (CFU-Adipo) and alkaline phosphatase (ALP) staining. In addition, the expression of 26991 genes of bMSCs ex vivo at 2 weeks after EXD-treatment or of bMSCs in vitro after exposure to conditioned serum from EXD-treated rats was measured and analyzed using NimbleGen Gene Expression Profiling, Cluster and pathway analysis. Micro-CT displayed a decrease in bone mass at 3 month after OVX. EXD treatment increased bone mass, elevating osteocalcin (OC) protein levels in vivo and facilitating the self-renewal and osteoblastic differentiation of bMSCs ex vivo. Gene expression profile analysis revealed that EXD rescued several gene expressions that were dyregulated by OVX. These genes overlapped and concentrated upon ten pathways between ex vivo and in vitro experiments. EXD exerts an osteogenetic effect on bMSCs in OVX induced osteoporotic mice. Our results contribute to further study of its molecular mechanism and traditional use in the treatment of postmenopausal osteoporosis.
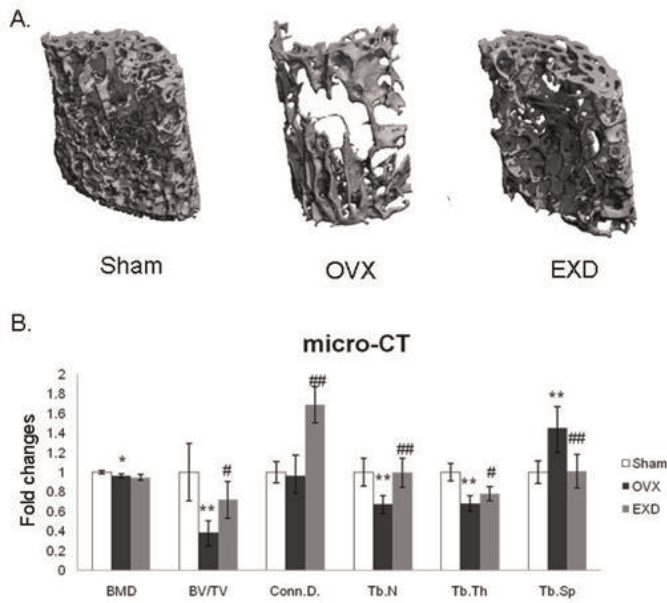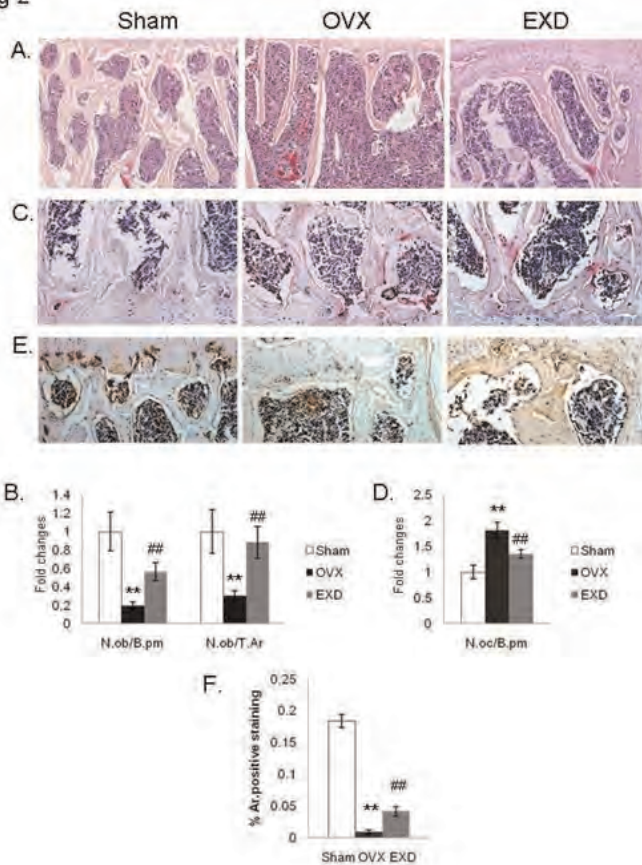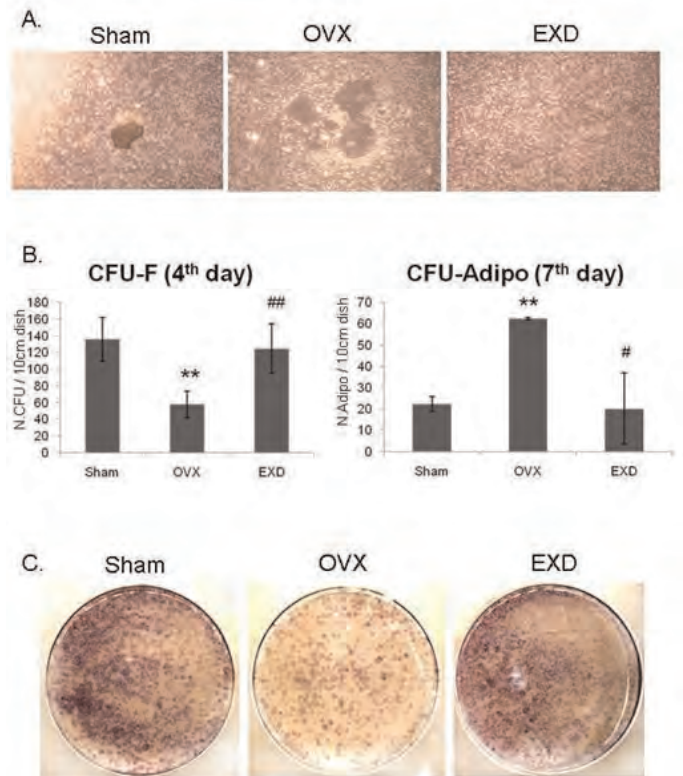
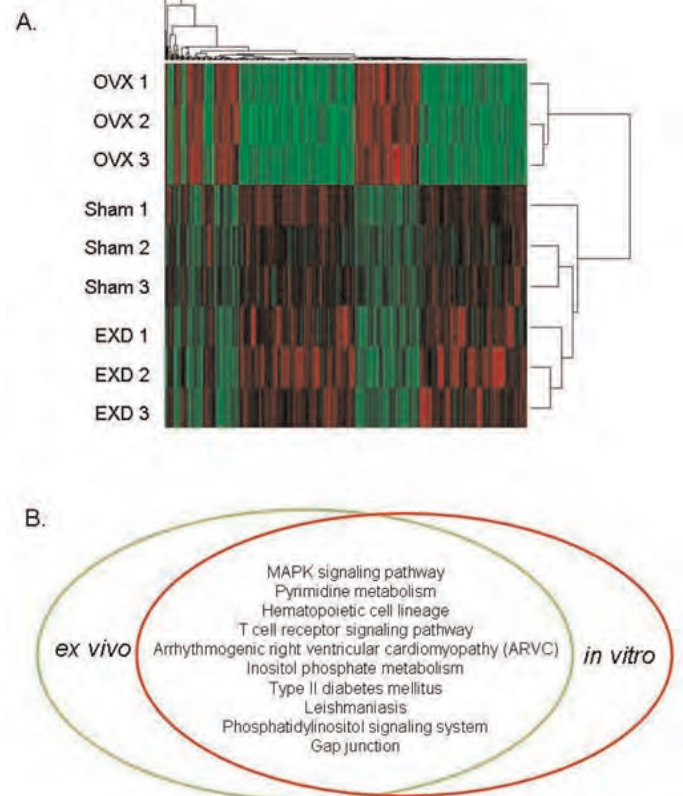Fig 1

igure 1

Fig 2

figure 2

Fig 3

figure 3

Fig 4

figure 4

*Disclosures: **Qin Bian**, None.*

MO0377

First in Man Studies of Pharmacokinetic Profiles of a Novel Oral PTH(1-34). Jonathan Tang*[1], Hillel Galitzer[2], Christopher Washbourne[3], Isabelle Piec[4], Naifang Wang[5], Gregory Burshtein[6], Phillip Schwartz[7], Yoseph Caraco[8], Ehud Arbit[6], William Fraser[3]. [1]University of East Anglia, Norwich, UK, United Kingdom, [2]Entera Bio, Israel, [3]University of East Anglia, United Kingdom, [4]BioAnalytical Facility, University of East Anglia, United Kingdom, [5]Enter Bio, Israel, [6]Entera Bio, Israel, [7]Entera Bio, Israel, [8]Hadassah Hospital, Israel

Background: PTH(1-34) (Teriparatide) is an anabolic agent used in treatment of osteoporosis. It promotes bone formation and reduces the risk of vertebral and some non-vertebral fractures. The route of administration by daily subcutaneous (sc) injection can cause problems in certain patients. A new oral delivery system for human PTH(1-34) has been developed as a possible treatment option. Galitzer *et al.* presented pre-clinical data (ASBMR 2012, MO0402) and first-in-human results (ASBMR 2013, FR0378) on safety, tolerability and absorption dynamics of oral PTH(1-34) in various dosages. We now describe the pharmacokinetics (PK) of oral PTH(1-34) compared to sc and placebo in healthy subjects.

Objective: A single-center, double blinded, triple crossover study was designed to compare the 1.8 mg optimal dose of oral PTH(1-34) against standard dosage of teriparatide injection and oral placebo.

Method: The study was conducted following and in accordance with the Hadassah Medical Center ethical approval committee.12 healthy volunteers (6m/6f), 18-50y, received three treatments: single sc injection of 20µg FORTEO®, 1.8 mg oral PTH(1-34), or placebo. Blood samples were collected at time 0, 10, 15, 20, 30, 45, 60, 75, 90, 120, 180, 240, 300 minute post dose. Plasma concentration of PTH(1-34) (IDS, Tyne and Wear, UK) and cyclic adenosine 3',5'monophosphate (cAMP) were measured on all samples.

Results: All 12 subjects on oral PTH(1-34) showed rapid, post dose increase then decrease of PTH(1-34), from baseline mean ($\pm$SD) of 5.9 (1.8) pg/mL to peak mean of 185.3 ($\pm$128.8) pg/mL. Pharmacokinetic profiles of oral PTH(1-34) showed Cmax (pg/mL), Tmax (mins), AUC_{0-last} of 238.3 (110.8), 17.5 (5.4) and 6161.7 (2726.7), respectively; whereas sc showed mean Cmax (pg/mL), Tmax (mins), AUC_{0-last} of 172.3 (55.7), 20.8 (8.7) and 13965.9 (2984.8), respectively. Plasma cAMP increased in all subjects in response to oral PTH(1-34) and sc treatment. Serum adjusted calcium in all subjects remained within normal limits throughout the studies.

Conclusion: Pharmocokinetic profiles showed a single oral dose of 1.8 mg PTH(1-34) is rapidly absorbed, and no significant difference in Cmax and Tmax when compared with 20µg of sc teriparatide. A significant difference in the rate of plasma clearance and AUC_{0-last} value was observed (fig.1). These differing profiles and modality of administration of PTH(1-34) could offer unique advantages in the treatment of calcium and metabolic bone disorders.
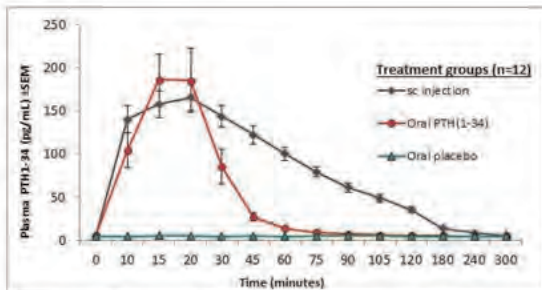
Figure 1: Pharmacokinetic profile showing changes in plasma PTH(1-34) levels in response to treatments.
One-way ANOVA analysis showed no significant difference in Cmax value achieved between oral PTH(1-34) and sc treatment. Plasma PTH (1-34) concentration declined more rapidly after oral treatment. Significant difference (p<0.05) in plasma PTH(1-34) was observed 20 minutes post treatment.

Figure1: Pharmacokinetic profile showing changes in plasma PTH(1-34) levels in response to treatment

Disclosures: Jonathan Tang, None.

MO0378

Flavonoid class compounds abrogating sclerostin induced inhibition of Wnt/beta catenin signaling. Sung-Kil Lim[1], Eun Jin Kim*[2], Bo Mi Park[2], Dongdong Zhang[2], Nam Hee Kim[2], Joohyun Bae[2]. [1]Yonsei University College of Medicine, South Korea, [2]Yonsei University, South Korea

Sclerostin, the key negative regulator of Wnt signaling in bone, has been spotlighted as a potential target for osteoporosis because of its specific expression in osteocytes. Recent studies on anti-Sclerostin antibody treatment in mouse and phase II clinical trials revealed dual effects on bone; enhancement of bone formation and inhibition of bone resorption. Our group and others identified that loop2 region is the functional domain of Sclerostin for the interaction with Lrp5/6, and the NXI motif,

and its neighboring residues play an important role for the inhibition of Sclerostin on canonical Wnt/beta catenin signaling. If NXI motif of sclerostin is a part of active binding site to LRP5/6, NXI motif mimic chemicals would abrogate sclerostin inhibition for the Wnt/beta-catenin signaling. Recently we found two flavonoid compounds abrogated sclerostin induced inhibition of Wnt/beta catenin signaling pathway. The compounds bound to E1 domain of LRP5 (IC50:39 uM). They stimulated ALP expression in ST2 stromal cells and also enhanced BMP2 induced ALP expression in C2C12 cells. In ex vivo analysis, they enhanced calvaria bone formation dose dependently. We are planning to perform in vivo bone formation analysis in OVX mouse model.

Disclosures: Eun Jin Kim, None.

MO0379

Inceased Serum Undercarboxylated Osteocalcin in use of Teriparatides could be reduced with concurrent use of vitaminK. Yoichi Kishikawa*[1], Taro Mawatari[2]. [1]Kishikawa Orthopedics, Japan, [2]Hamanomachi Hospital, Japan

BackgroundPreviously we reported changes in serum bone metabolism markers after 4 months of daily teriparatide (Forteo20µ/day) and weekly teriparatide (Teribone56.5µ/week) in treatment of vertebral fracture.

Concerning as the bone formed when teriparatide was used in the treatment of vertebral fracture, it is possible that bone with relatively increased ucOC was formed. It is expected that bone of better quality could be formed using vitaminK as an attended medicine.

A weekly chemically synthesized teriparatide (Teribone) has become available only in Japan.

Methods

162 patients with vertebral fracture were treated conservatively using soft Corset with administration of two types of Teriparatides.

Changes in serum TRACP 5b, ucOC, OC and ucOC/OC at 0, 4 and 8 months were analyzed. Intially vitamin D (alphacalcidole 0.25µ) was used for all the patients as a concurrent medicine besides Teriparatide. If ucOC increased too much in comparison to OC at 4months, switched from vitamin D to vitaminK (menateterenone45mg).

Results

Four subgroups devided by two factors are compaired statisitically, daily or weekly Teriparatide, alphacalcidole or menateterenone as a concurrent medicine. Daily with vitaminK 42 or vitaminD 50 cases, Weekly with vitaminK 21 or vitaminD 49 cases.

ucOC increased at 4months and clearly decreased at 8 months by switching from vitaminD to vitaminK. That tendency was obvious in daily Teriparatide than weekly one.

On the other hand OC was not affected by that switching.

Discussion

The meanig of ucOC icreasing after Teriparatide is not well known, but is suspected representing not only activating Osteoblasts but also lack of vitaminK when it makes a lot of new bone.

Concurrent use of vitamin K would be neccecery and could make good quallity bone when Teriparatide is used. An Animal study is expected rveal the effect of vitaminK attended.

Disclosures: Yoichi Kishikawa, None.

MO0380

Increased Endocortical Formation and Periosteal Resorption at the Distal Tibia in Premenopausal Women with Idiopathic Osteoporosis Treated with 18 Months of Teriparatide. Mary Beth Tribble*[1], Adi Cohen[2], Chantal De Bakker[3], Joan Lappe[4], Robert Recker[5], Kyle Nishiyama[6], Mishaela Rubin[6], John Bilezikian[7], Elizabeth Shane[7], Xiaowei Liu[3]. [1]University of Pennsylvania, USA, [2]Columbia University Medical Center, USA, [3]University of Pennsylvania, USA, [4]Creighton University Osteoporosis Research Center, USA, [5]Creighton University, USA, [6]Columbia University, USA, [7]Columbia University College of Physicians & Surgeons, USA

Idiopathic osteoporosis (IOP) in premenopausal (PreM) women is characterized by abnormal bone microarchitecture and reduced bone stiffness. We've reported that teriparatide (TPTD) treatment improves trabecular bone quality at the distal radius and tibia, but little is known about TPTD's effect on cortical bone. We hypothesized that significant bone remodeling occurs at both the periosteal (PS) and endosteal (ES) surfaces in IOP patients treated with TPTD.

PreM women (n=18; 41$\pm$6 years) with a history of fragility fractures and/or low BMD received 20 µg of TPTD daily for 18 months. The distal tibia was scanned using high-resolution peripheral QCT (HRpQCT, Scanco) at 0, 6, and 18 months. A novel image registration technique was applied to precisely align the baseline and follow-up scans. PS, ES, and intracortical area (IC) envelopes were isolated (Fig 1A), and the follow-up scans were subtracted from the baseline to generate a BMD differential map (ΔBMD, Fig 1B). Regional ΔBMD, bone mineral content (BMC), and cortical structure were quantified. Reproducibility of all parameters was determined in a separate group of subjects (n=15) who were scanned twice in one week.

Over 18 months, compared to ΔBMD of the IC (-2 mg HA/cm^3), ΔBMD at the PS (-57 mg HA/cm^3) indicates significant mineral loss (p<.001), and ΔBMD at the ES (48 mg HA/cm^3) indicates significant mineral gain (p<.001, Fig. 1B). BMC decreased 14% (p<.001) at the PS and increased 7% (p<.001) at the ES, with no change in the IC (Fig

1C). There were 0.2% (p<.01) and 0.4% (p<.05) decreases in PS and ES perimeters, respectively, leading to a 1% increase in Ct.Area (p<.01) and a 0.9% increase in cortical thickness (Ct.Th, p<.05). No change in polar moment of inertia (pMOI) was observed over time (Fig 1D). Reproducibility was 1-5% for BMC and 0.1-0.5% for structural measures. Our results indicate that TPTD preferentially improves new bone accrual at the ES and accelerates bone resorption at the PS of the distal tibia in PreM women with IOP. In contrast, an earlier study showed that TPTD stimulates bone accrual at both the ES and PS of the iliac crest in postmenopausal women, suggesting TPTD's effect on cortical bone is site-specific. Although both ES and PS perimeters decrease at the tibia, Ct.Th and Ct.Area significantly increase, and the cortex's mechanical function is maintained. The preferential mineral deposition at the ES may help to improve bone's resistance to endocortical trabeculation.
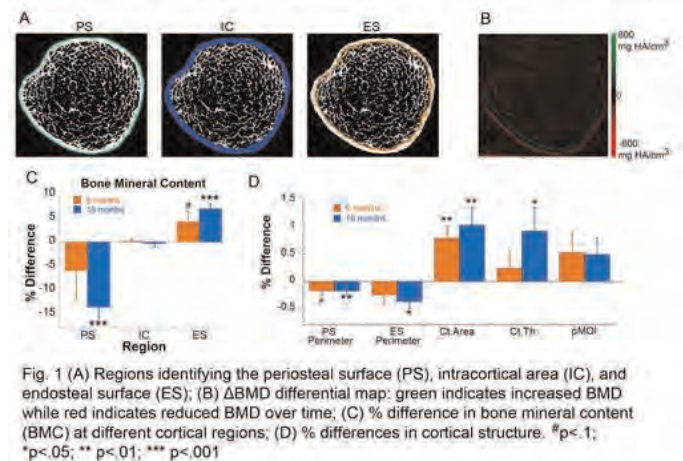

Fig. 1 (A) Regions identifying the periosteal surface (PS), intracortical area (IC), and endosteal surface (ES); (B) ΔBMD differential map: green indicates increased BMD while red indicates reduced BMD over time; (C) % difference in bone mineral content (BMC) at different cortical regions; (D) % differences in cortical structure. #p<.1; *p<.05; ** p<.01; *** p<.001

Fig 1

MO0381

Withdrawn

MO0382

Once-weekly Teriparatide Increases Bone Mineral Density in the Distal Radius using The Correction Method of Dual-energy X-ray Absorptiometry Images.

Yukihiro Isogai[1], Nobuo Urushibara[2], Harumi Nakayama[3], Ryutaro Adachi[4], Shigeru Kitagawa[4], Naoto Kato*[5], Tatsuhiko Kuroda[5]. [1], Japan, [2]Nukada Memorial Hospital, Japan, [3]Harumi clinic, Japan, [4]Hitachi Aloka Medical, Ltd, Japan, [5]Asahi Kasei Pharma Corporation, Japan

Purpose

Teriparatide increases bone mineral density (BMD) in lumbar vertebrae and femur. In radius, few study have investigated the effect of daily teriparatide on the changes of BMD, however, there are no reports of once-weekly teriparatide. In this study, the effect of once-weekly teriparatide in increasing BMD was examined in the distal 1/10 of the radius and the distal 1/3 of the radius using the correction method to avoid rotation and inclination of hands in dual-energy X-ray absorptiometry (DXA) images.

Methods:

This study is retrospective study at 2 medical sites which included the data of postmenopausal women who had a vertebral fracture and were diagnosed with primary osteoporosis with BMD of ≤70% of the young adult mean in the healthy Japanese population. The DXA scan images of the radius were taken at the start of once-weekly 56.5 μg teriparatide administration and after administration for 6, 12, and 18 months. Percentage changes of BMD from baseline in the radius (distal 1/10 and 1/3 radius) with correction method were evaluated.

Results

(Medical site 1)

9 subjects (mean age: 80.4 years) who had been not used bisphosphonates or had taken washout times if patients were used bisphosphonates were treated by once-weekly teriparatide administration for 6 months. When the corrections were made, significant increase of BMD at 6 months was found in the distal 1/10 radius (1.98 %, p = 0.001), but not in the distal 1/3 radius (0.98%, p = 0.272).

(Medical site2)

17 subjects (mean age: 77.7 years), who had been used bisphosphonates were subsequently treated by once-weekly teriparatide for 18 months. When the corrections were made, significant increase of BMD at 12 months was found in the distal 1/10 radius (2.05%, p = 0.045) and the efficacy was lasting until 18 months (2.18%). No significant increase in BMD was observed in the distal 1/3 radius, but BMD were maintained during teriparatide treatment (1.32% (6 months), 1.17% (12 months), 0.99% (18 months)).

Conclusion

Once-weekly teriparatide significantly increased BMD in the distal 1/10 radius and maintained BMD in the distal 1/3 radius. A correction method to avoid irrelevant

measurement of BMD produced by in adequate arm positioning was also useful tool to detect the efficacy of teriparatide. However, further studies are needed to provide clear evidence of the pharmaceutical efficacy of once-weekly teriparatide due to small number of patients.

MO0383

Sclerostin Antibody Administration Activated Bone Formation in Ovariectomized Rats with Concurrent Mechanical Unloading.

Dongye Zhang*[1], Minyi Hu[1], Timothy Chu[2], Liangjun Lin[3], Xiaodong Li[4], Hua Zhu (David) Ke[5], Yi-Xian Qin[3]. [1]Stony Brook University, USA, [2]Stony Brook University, USA, [3]State University of New York at Stony Brook, USA, [4]Amgen, Inc., USA, [5]Amgen Inc., USA

Severe bone loss occurs when postmenopausal osteoporosis patients had concurrent immobilization and it is challenging condition to manage. Sclerostin antibody (Scl-Ab) increased bone formation and bone mass, and decreased bone resorption in postmenopausal osteoporosis. The current study was to examine the effect of Scl-Ab in mitigating the conditions in ovariectomized (OVX) rats with concurrent hindlimb suspension (HLS). Four-month-old female Sprague Dawley rats were divided into 7 groups (n=11 per group) as shown in Figure 1, HLS was introduced 2 weeks after sham and OVX. Scl-Ab (25 mg/kg) or vehicle was injected sc twice weekly for 5 weeks starting at the time of HLS. Histomorphometry analyses were performed at metaphyseal trabecular bone of the distal femurs. OVX alone, but not HLS resulted in significant decrease in BV/TV (-36%) in comparison to sham control. HLS plus OVX showed more bone loss than OVX alone. Scl-Ab significantly increased bone mass in all three conditions (HLS, OVX alone and OVX with concurrent HLS) with relative BV/TV increase of 37%, 87% and 87% compared with respective controls (Fig. 1 & 2a). Similar trend was observed in Tb.Th (Fig. 1 & 2b). Trabecular mineralizing surface/bone surface (MS/BS), mineral apposition rate (MAR) and bone formation rate (BFR/BS) were significantly increased in Scl-Ab treated rats (HLS alone, OVX alone and HLS+OVX) compared with respective controls. In summary, Scl-Ab prevented trabecular bone loss in OVX rats with concurrent HLS. Histomorphometric analyses reveal that Scl-Ab promoted bone formation in OVX rat model with concurrent HLS. The data suggest that sclerostin antibody represents a promising therapeutic approach for osteoporosis induced by estrogen deficiency with concurrent mechanical unloading.
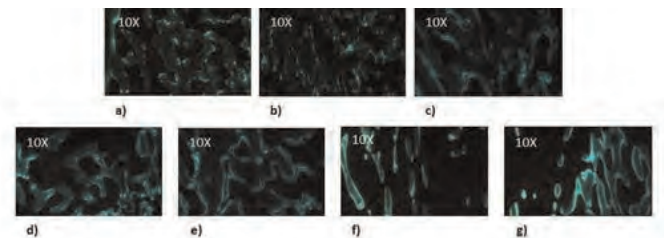
Fig. 1. Representative images of calcein labeled trabecular bone histomorphometry in distal region of femur. a) sham control. b) Sham+HLS+Veh, c) Sham+HLS+Scl-Ab, d) OVX+Veh, e) OVX+Scl-Ab, f) OVX+HLS+Veh and g) OVX+HLS+Scl-Ab.

Fig.1.
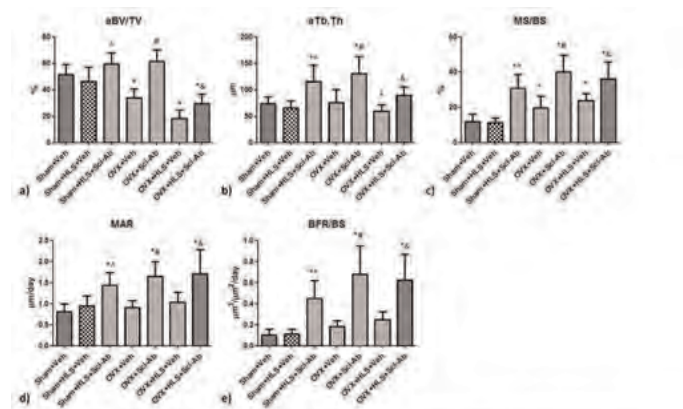
Fig. 2. a) Graphs show mean+SD values for histomorphometric bone volume fraction (aBV/TV). OVX, and HLS plus OVX showed significant decrease of aBV/TV in comparison to sham control. Scl-Ab significantly increased bone mass vs. the respective controls, i.e., vs. HLS alone(*), OVX alone(#), and HLS+OVX(&). b) Similar trend in (a) was found in the mean+SD values for trabecular thickness (aTb.Th). c), d), e) mean+SD values for Histomorphometric MS/BS, MAR, BFR/BS respectively, Scl-Ab increased bone formation rate against respective controls, i.e., vs. HLS alone(*), OVX alone(#), and HLS+OVX(&). (Overall, *p<0.05 vs. Sham+Veh; "p<0.05 vs. Sham+HLS+Veh; #p<0.05 vs. OVX+Veh; &p<0.05 vs. OVX+HLS+Veh)

Fig.2.

MO0384

Sequential anti-osteoporotic therapy against recurrence of fragility fractures: the positive clinical effects of an osteo-anabolic first choice. Costantino Corradini*[1], Francesca Boisio[2], Vittorio Macchi[2], Francesca Ingegnoli[2]. [1]State University of Milan Department of Human Science, Italy, [2]State University of Milan, Italy

Introduction - Fragility fractures daily treated in orthopaedy of general hospitals or specialized institutes represent a common problem of healing and prevention of recurrence. In particular in osteoporotic women femoral, vertebral, humeral and wrist fractures continue to be the controversy over the type of treatment and their duration, especially given the possible adverse effects of long-term use. Furthermore, pharmaceutical spending review has conditioned the treatment and social choices. In this scenario the combined or sequential use of anti-osteoporotic drugs is actually debated. Objective - To evaluate the clinical outcome of femoral and vertebral fragility fractures after sequential treatment using teriparatide (TPTD) and risedronate (RIS) or denosumab (DMAB) following the guidelines of Italian Drug Agency (AIFA). Materials and methods - 124 postmenopausal women with femoral and/or vertebral fragility fractures received teriparatide (20-µg daily) for 24 months and then risedronate (35mg weekly) or denosumab (60-mg every 6-months), for other 24 months. They were undergone at the beginning, 3rd month and variably every six months to lumbar and femoral BMD and X-ray, serum markers of bone turnover, functional ability, SF-36, EQ-5. Results: Osteocalcin increased significantly at 3rd month maintaining high levels till to 24th month in TPTD group; while it declined more in the RIS group than the DMAB group. CTX I were equally suppressed in both groups. The X-ray between 3rd and 6th evidenced fracture healing in all cases. During TPTD assumption all patients detect positive effects on quality of life; whereas in the first six month of antiresoptive agents they reduced. At 24th month in all groups any recurrence of fragility fractures was detected. At 2nd year lumbar spine BMD increased in the TPTD (8.7 ± 4.8%), DMAB (7.3 ± 2.8%,) and RIS (5.6 ± 3.4%) groups; femoral neck BMD also increased the TPTD (3.6 ± 2.9%), DMAB (4.1 ± 3.8%) and RIS (2.6 ± 1.9%) groups. Conclusions- The initiation of anti-osteoporotic treatment with anabolic agent in the fragility fractures permits to enhance fracture healing and to restore BMD with reduced functional disability and better quality of life.The treatment with an osteo-anabolic agent needs to be followed by anti-resorptive treatment in order to maintain the bone restored. The different clinical outcomes revealed in two periods of treatment suggest the need by fractured patients to have further anabolic windows.

MO0385

The Long Term Effects Of Abaloparatide (BA058) On Bone Histomorphometry in Osteopenic Rats. Luc Chouinard*[1], Elisabeth Lesage[2], Susan Y. Smith[3], Gary Hattersley[4]. [1]Charles River Laboratories, PCS Montreal, Canada, [2]Charles River, Canada, [3]Charles River Laboratories, Canada, [4]Radius, USA

Abaloparatide (ABL) is a novel analog of PTHrP(1-34) currently being developed for the treatment of osteoporosis. This study was conducted to evaluate the effects of daily subcutaneous injection of ABL for 12 months on bone historrmorphometry in ovariectomized (OVX) female Sprague-Dawley (SD) rats. Six-month old SD rats (10/sex/dose) underwent OVX or Sham surgery. Following a 3-month bone depletion period, daily subcutaneous injection of vehicle (Sham and OVX controls) or ABL at 1, 5 or 25 µg/kg, was given for 52 weeks. Rats were injected subcutaneously with fluorochrome labels 10 and 3 days prior to euthanasia. Histomorphometry of the cancellous bone was performed on the proximal tibia and lumbar vertebrae while the cortical bone histomorphometry was conducted on the tibia at mid-diaphysis. OVX induced high bone turnover by the end of the bone depletion period, that progressed to osteopenia at the cortical and both cancellous bone sites after 12 months. In cortical bone, ABL treatment resulted in a dose-related increase of periosteal formation rate and endosteal mineralizing surfaces. At the endosteal level, the effects of ABL were limited to increases in the endocortical labeled surfaces at 25 µg/kg. The increases in periosteal and endosteal formation indices, combined with the absence of effect on endosteal resorption, resulted in a reduction of the medullary area and endocortical perimeter that lead to cortical thickening despite the minimal periosteal perimeter expansion at all dosed groups, compared to OVX and Sham controls. In cancellous bone, treatment of OVX rats with ABL at $\geq$ 1µg/kg resulted in increases of all bone formation parameters. These effects, combined with the lack of effect on the osteoclast surface, resulted in dose-related increases in trabecular number and thickness that resulted in increased bone volume, decreased trabecular separation and complete reversal of the OVX-induced osteopenia in the tibia and L3. Additionally there was no abnormal cell proliferation, marrow fibrosis, osteoid accumulation and/or mineralization defect observed in the examined bone sections. Thus, the administration of abaloparatide to OVX female rats at $\geq$ 1µg/kg/day completely reversed the OVX-induced cancellous and cortical bone changes.

MO0386

A RCT Study to Compare the Short-term Biochemical Bone Metabolism Outcome of Weekly Alendronate Treatment in Osteopenic Women with or without Vibro-Therapy Intervention. Emilio Roldan*[1], Ricardo Capiglioni[2], Victor Montangero[2], Alicia Marino[2], Claudia Gomez Acotto[2]. [1]Gador S.A., Argentina, [2]Maimonides Univ, Argentina

Gómez Acotto C, Capiglioni R, Marino A, Montangero V, Roldán EJA.gomezacotto.claudia@maimonides.edu
Phospho-Calcium Unit, Maimonides University, Buenos Aires, Argentina
The outcome of alendronate treatment of osteoporosis in practice is variable depending on many factors, as therapy compliance and persistence, among the main ones. The addition of a comfortable and periodical physical program may help in many ways. In addition, the subsequent skeletal impact may favor the enlargement of the bone active surface, which in turn is the alendronate arrival area to the bone; and given the exercises in adequate "doses" it may improve the muscle driven skeletal properties, even in aged people (Bone mechanostat theory). To test the above a group of 53 postmenopausal women having little physical activities, which give consent to be randomized and receive or not 3 weekly, 15 minutes sessions of passive interventions with a vibrio-therapy (VT) equipment (Galileo(R), a footplate developing a frequency range up to 30 Hertz), during 12 months. Osteoporosis was diagnosed by standard DEXA methods, and pQCT assessments quantified muscle/bone variables. As alendronate absorption is a further bias variable we treat all the patients with a drinkable formulation of 70mg weekly alendronate, from commercial resources, as the administration of soluble alendronate reduces variations in digestive transit and absorption, and may avoid serious GI unwanted effects. Blood D-pyridinoline was used as bone resorption marker, it was reduced in both groups but was found significantly more depressed among the VT users after 6 and 12 months (from average [range] 0.905 [1.215-0.780] to 0.640 [0.860-0.500] and 0.610 [0.810-0.490] in non-VT users vs. 0.908 [1.205-0.637] to 0.510 [0.660-0.370] and 0.510 [0.660-0.365] in VT users; p<0.05). Other variables as Ca/creatinine, AlkPh, and glycaemia did not evolve differently between groups. We conclude that a VT intervention increases the benefit of alendronate therapy in postmenopausal women with customary low level of activity by achieving a more effective suppression of bone metabolism after 6 months, and further maintaining the difference steady during the year of this observation. In some other studies the value of this therapeutic approach has not been clearly distinguished, but with close monitoring of patient adherence and the administration of soluble alendronate may remark the above described benefit. We continue working in this program to assess changes in bone density and structure.

MO0387

A Study of Women with Osteoporosis who are at High Risk for Fracture despite Benefits of Oral BisphosphonateTreatment. Arun Krishna[1], Debra Eisenberg[2], Tao Gu[2], Hillary Placzek[2], Ankita Modi*[3]. [1]Merck, USA, [2]Healthcore, USA, [3]Merck & Co., Inc., USA

Background: Bisphosphonates (BIS) have been shown to significantly reduce the risk of osteoporotic fracture in women with post-menopausal osteoporosis (OP). However, there are a substantial proportion of women who remain at high risk despite being compliant to BIS therapy.

Objective: To estimate the proportion of osteoporosis patients who remain at high risk for fracture despite being compliant to BIS treatment and to estimate their disease burden in terms of healthcare resource use and costs.

Methods: This was a retrospective claims and medical chart study, focusing on women ≥55 years of age with OP and ≥2 years of oral BIS treatment identified from the HealthCore Integrated Research Environment (HIRE) between 01/01/2007-06/30/2009. Initiation date of BIS was set as the index date. The pre-index period was 6 months prior to index date and the post index period was 25-36 months after index date. Patients were designated as high risk if they were compliant (defined as Medication Possession Ratio (MPR = days supply/365 days) ≥ 70%) to BIS treatment for ≥ 24 months, had a pre-index fracture or BMD test, and were considered as high risk of fracture if they met ≥ 1 of the following criteria: a) patients experiencing a fracture or b) have a subsequent BMD score of t<-2.5 during post-index period.

Results: The total study sample was n=4,021. Of these, a total of 4.6% (n=185) experienced a fracture between index date and 36 months post-index. And a total of 1.5% (n=58) experienced a fracture during 25-36 month post index period. Also, of those with pre-index fracture (5.5%, n=220), 30% (n=66) experienced a subsequent post-index fracture despite compliance to BIS treatment. Of the total 330 charts reviewed to validate BMD test results, 124 (38%) were identified as high risk through the chart review (BMD of t<-2.5) in the post-index 25-36 months period. Within the high risk claims cohort, 38% (n=71) had an OP-related office visit during the 25-36 month post-index time period with a mean cost of $135. Among the high risk chart cohort, 69% (n=86) had an OP-related office visit during the 25-36 month post-index time period with a mean cost of $218.

Conclusions: In this study, a large proportion of women adherent to bisphosphonates for 2 years remain at high fracture risk. Although these women may have benefited from their therapy and have a lower fracture risk than if they had remained untreated, alternative treatments for osteoporosis could be considered for such patients

MO0388

Alendronate Improves Bone Material Level Properties in Paired Human Transiliac Bone Biopsy Specimens. <u>Patrick Ammann</u>*[1], <u>Rene Rizzoli</u>[2]. [1]Division of Bone Diseases, Switzerland, [2]Geneva University Hospitals & Faculty of Medicine, Switzerland

Bone strength, hence fracture risk, is dependent on bone geometry, microstructure and bone material level properties. Alendronate treatment maintains bone mass, prevents further microarchitecture deterioration and increases the mean degree of mineralization. This latter effect could potentially modify bone material level properties. We investigated the effects of Alendronate treatment on bone material level properties and bone microarchitecture of transiliac bone biopsy from postmenopausal osteoporotic patients. In a longitudinal study, 38 paired biopsies were obtained at baseline and after 6 or 12 months of treatment with Alendronate 70 mg once weekly. Elastic Modulus, Hardness and Working Energy were blindly analyzed by nanoindentation at the level of the interstitial and haversian bone of the cortex and of trabecular nodes and remodeling units under humid conditions. Parameters of microarchitecture were evaluated by microCT (Scanco Medical). Bone microarchitecture and bone mass were not influenced by Alendronate treatment. Changes in bone material level properties were observed at the level of the interstitial cortical bone at the two time points and only by 12 months in haversian bone, but not at the level of the trabecular bone. In another group of the same study, patients were treated with Strontium Ranelate which changed bone material level properties after 6 and/or 12 months at the level of the trabecular bone and cortical bone. The significant changes were of similar magnitude for both treatments. The positive effect on bone material level properties of Alendronate could be partially explained by the known increase of mean degree of mineralization and could contribute to the known improvement of bone strength since no modification of bone mass was observed. Interestingly this study indicates that bone material level properties could be selectively improved by two anti-osteoporotic treatments like Alendronate and Strontium Ranelate.

	M0 (n=19)	M6 (n=19)	M0 (n=19)	M12 (n=19)
Cort Modulus (gPa)	13.31±0.18	14.46±0.20***	13.10±0.24	13.84±0.27*
Cort hardness (mPa)	398.23±4.94	450.58±6.64***	395.49±7.57	433.20±10.47**
Cort Working Energy (pJ)	3189±37	3372±43**	3164±50	3295±57
BV/TV(1)	0.188±0.018	0.161±0.016	0.180±0.015	0.174±0.016
Cort thickness (mm)	0.555±0.041	0.572±0.029	0.513±0.028	0.547±0.042

Significance of differences are evaluated by Student's unpaired t-test.* p<0.05, **p<0.01, ***p<0.001.

table

Disclosures: Patrick Ammann, Servier, 3
This study received funding from: Servier Lab

MO0389

Differentiating effects of treatments on TBS. <u>Renaud Winzenrieth</u>*[1], <u>Luis Del Rio</u>[2], <u>Silvana Di Gregorio</u>[3], <u>E Bonel</u>[3], <u>M Garcia</u>[3]. [1]Med-imaps, Hôpital X. Arnozan, PTIB, Pessac, France, France, [2]Cetir Centre Medical, Spain, [3]Cetir Grup Medic, Spain

Purpose:. The objective of the study is to assess longitudinal effects of different osteoporosis treatments on TBS and BMD at lumbar spine.
Method: We analyzed 337 patients (men: 61; women: 276; Age range: 29 to 89 years; Follow-up: 23.5 ±13.9 months, BMI<29 kg/m^{2}). We stratified the cohort by treatments: No treatment (NT,n=82), Vitamin D+Calcium (VC, n=75), Testosterone (T,n=24), Biphosphonate (B,n=104), Denosumab (D,n=30), PTH (n=11), Raloxifene (R,n=11). The follow-up changes were analyzed by T-Test. Variation in % from baseline were assessed and normalized at 24 months. (Statistical significance was set at p< 0.05).
Results (See table): After 24 month, TBS NT group decreased by 2.4% (p<0.01) whereas a non significant decrease was observed for spine BMD (Δ=-0.3%). Compared to NT group, significant improvement (p<0.05) have been observed in both ΔTBS and ΔBMD for T, B, D, PTH groups. Significant variations have been observed in the V and R group for TBS whereas no significant variations were observed for BMD when compared to T group. At the end of the follow-up, significant improvement have been observed for BMD in T(+4.0%), B(+2.3%), D(+7.3%) and PTH(+8.5%) groups. Significant improvement was only observed in the D group (+2.1%) for TBS whereas a improvement tendency was observed in the

PTH group (+1.9%).Conclusion: Non correlated effects have been observed on BMD and TBS irrespectively to the treatment. As expected from the literature, TBS of NT subjects decreased with age. When compare to NT subjects, significant differences have been observed for TBS in all treatment groups whereas BMD underdiagnoses the follow-up changes in V and R group. As expected TBS remained stable under Biphosphonate. Significant TBS increasing was observed under Denosumab whereas a positive tendency has been observed under PTH. TBS could be a useful tool to monitor treatment effects.

	TBS Basal vs. Follow-up	p vs.No treatment	BMD Basal vs.Follow-up (g/cm2)	p vs.No treatment
Non Treatment (82) Age: 37,9-83,6. Follow-up (months): 23.4	1,301 vs. 1,270 Δ%_24months=-2.4%*		1,042 vs. 1,039 Δ%_24months=-0.3%	
Vit.D +Calcium (75) Age: 34,3-86,9 Follow-up (months): 21,5	1,238 vs. 1,243 Δ%_24months=0.5%	<0,01	0,962 vs. 0,964 Δ%_24months=0.2%	NS
Testoterone (24) Age: 47,9-67,9 Follow-up (months): 23,5	1,194 vs. 1,198 Δ%_24months=0.3%	<0,05	1,107 vs. 1,112 Δ%_24months=+4.0%*	<0,001
Biphosphonate (104) Age: 29,7-88,4 Follow-up (months): 26,5	1,223 vs. 1,224 Δ%_24months=0.1%	<0,001	0,891 vs. 0,913 Δ%_24months=2.3%*	<0,001
Denosumab (30) Age: 52,4-82,9 Follow-up (months): 19,7	1,233 vs 1,254 Δ%_24months=+2.1%*	<0,01	0,821 vs. 0,870 Δ%_24months=7.3%*	<0,001
PTH(11) Age: 52,4-82,86 Follow-up (months): 25,0	1,149 vs 1,172 Δ%_24months=+1.9%	<0,001	0,868 vs. 0,945 Δ%_24months=8.5%*	<0,001
Raloxifene (11) Age: 52,4-82,86 Follow-up (months): 18,7	1,304 vs 1,299 Δ%_24months=-0.5%	0,05	0,851 vs. 0,842 Δ%_24months=-1.4%	NS

* significant difference between baseline and follow-up

Table

Disclosures: Renaud Winzenrieth, Med-Imaps, 4

MO0390

Efficacy and Safety of Bazedoxifene in Postmenopausal Latino Women with Osteoporosis. <u>Jose A. Hernández Bueno</u>[1], <u>Lizbeth Arias</u>[2], <u>Ching-Ray Yu</u>[3], <u>Robert Williams</u>[4], <u>Barry S. Komm</u>*[4]. [1]Unknown, Mexico, [2]Pfizer Inc, Mexico, [3]Pfizer Inc, USA, [4]Pfizer Inc, USA

Introduction: After menopause, declining estrogen levels contribute to accelerated bone loss, increasing risk of osteoporosis and fracture. Bazedoxifene (BZA), a selective estrogen receptor modulator, reduces fractures and bone turnover rate in postmenopausal women with osteoporosis.Purpose: Evaluate safety/efficacy of BZA on vertebral fractures, bone mineral density (BMD), and bone turnover markers (osteocalcin, C-telopeptide [cTX]) in women from Latin American (LA) sites in the global pivotal trial.Methods: In the 3-year, phase 3, randomized, double-blind trial, healthy postmenopausal women with osteoporosis (N=7492) received BZA 20 mg/d (BZA20) or 40 mg/d (BZA40), raloxifene 60 mg/d (RLX), or placebo (PBO). This post hoc analysis included participants (n=3036) from Argentina, Chile, Brazil, and Mexico.Results: In the ITT population, incidence of new vertebral fractures at month 36 with BZA20 (1.87%) and BZA40 (1.9%) was comparable to RLX (1.43%;) and lower than PBO (2.83%); differences were not statistically significant. BZA20 and BZA40 reduced new vertebral fractures by 39% (HR, 0.61; 95% CI, 0.30-1.26) and 32% (HR, 0.68; 95% CI, 0.34-1.36) respectively vs PBO. Compared with PBO, BZA20 and BZA40 were associated with greater (*P*<0.001) adjusted mean % increases from baseline to month 36 in BMD (lumbar spine: 1.26%, 2.49%, 2.79%; total hip: -0.41%, 0.40%, 0.95%; femoral neck: -0.59%, 0.88%, 1.78%; trochanter: -0.25%, 0.90%, 1.26%). Adjusted mean % BMD changes with BZA40 were comparable to RLX (lumbar spine, 3.18%; total hip, 1.11%; femoral neck, 1.68%; trochanter, 1.43%). Except for the trochanter, BMD changes were greater (*P*<0.05) with RLX vs BZA20. Compared with PBO, BZA20 and BZA40 produced greater (*P*<0.001) adjusted median % reductions in osteocalcin (-27.0%, -43.0%, -44.1%) and cTX (-32.1%, -50.7%, -53.4%) by month 12. Except for osteocalcin in the BZA40 group, the reductions were statistically significantly smaller for BZA vs RLX (osteocalcin, -46.9%; cTX, -57.6%). There were no significant differences between groups in overall incidence of TEAEs, serious AEs, or AEs leading to study withdrawal. There were significantly higher rates of somnolence, rhinitis, vaginitis, elevated alkaline phosphatase, and hypercholesterolemia with BZA20 and vascular disorders, depression, accidental injury, hypercholesterolemia, elevated liver enzymes, and vaginitis with BZA40 vs PBO.Conclusion: BZA is effective and safe in postmenopausal LA women with osteoporosis.

Table. Efficacy of BZA in Postmenopausal Latin American Women with Osteoporosis (ITT Population)

	BZA20 (n=760)	BZA40 (n=754)	RLX (n=756)	PBO (n=760)
Incidence of vertebral fracture at month 36, n/N (%)[a]	13/695 (1.87)	13/684 (1.90)	10/699 (1.43)	20/706 (2.83)
BMD, adjusted mean % change from baseline to month 36				
Lumbar spine	2.49[b,e]	2.79[b]	3.18[b]	1.26
Total hip	0.40[b,d]	0.95[b]	1.11[b]	-0.41
Femoral neck	0.88[c,d]	1.78[b]	1.68[b]	-0.59
Trochanter	0.90[c]	1.26[b]	1.43[b]	-0.25
Bone turnover markers, adjusted median % change from baseline to month 12				
Osteocalcin	-43.0[b,e]	-44.1[b]	-46.9[b]	-27.0
cTX	-50.7[b,c]	-53.4[b,d]	-57.6[b]	-32.1

[a]n/N=number of patients with vertebral fracture/number of patients evaluable at month 36. [b]P<0.001 vs PBO.
[c]P<0.001 vs RLX. [d]P<0.01 vs RLX. [e]P<0.05 vs RLX.
BMD, bone mineral density; BZA, bazedoxifene; cTX, C-telopeptide; PBO, placebo; RLX, raloxifene.

Table. Efficacy of BZA in Postmenopausal Latin American Women with Osteoporosis (ITT Population)

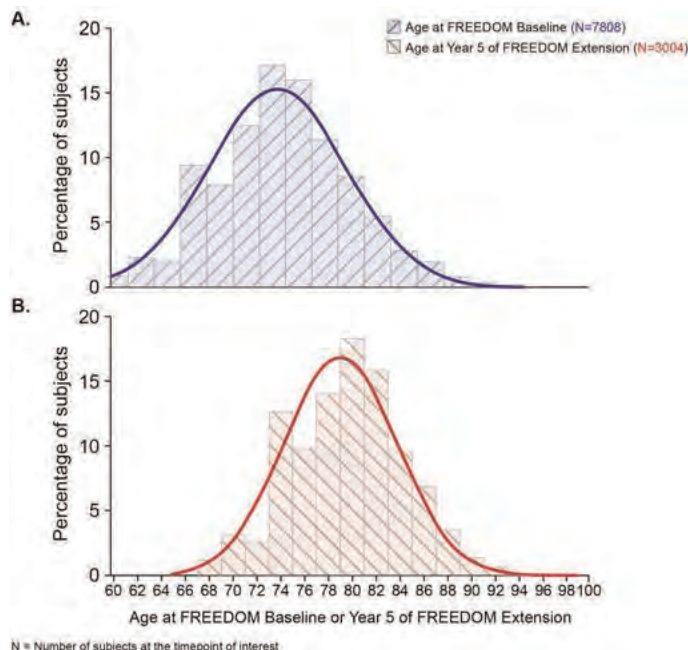## MO0391

Evolution of Subject Characteristics in FREEDOM and its Extension for Up to 8 Years. <u>JD Adachi</u>*[1], <u>PR Ho</u>[2], <u>CJF Lin</u>[2], <u>MA Bolognese</u>[3], <u>HG Bone</u>[4], <u>P Hadji</u>[5], <u>S Papapoulos</u>[6], <u>C Recknor</u>[7], <u>NS Daizadeh</u>[2], <u>P Dakin</u>[2], <u>RB Wagman</u>[2], <u>S Ferrari</u>[8]. [1]McMaster University, Canada, [2]Amgen Inc., USA, [3]Bethesda Health Research Center, USA, [4]Michigan Bone & Mineral Clinic, USA, [5]Philipps-University of Marburg, Germany, [6]Leiden University Medical Center, Netherlands, [7]United Osteoporosis Centers, USA, [8]Geneva University Hospital, Switzerland

Purpose: Changes in study population demographics enrolled in long-term osteoporosis clinical trials may affect interpretation of efficacy/safety outcomes. Denosumab (DMAb) is being evaluated for up to 10 years in the 3-year FREEDOM trial and 7-year Extension (EXT). DMAb for up to 8 years is associated with low fracture incidence, continued BMD increases, and adverse event profile similar to what has previously been reported (Papapoulos et al., *JBMR.* 2013;28:S1). We compare the FREEDOM and EXT populations at baseline and in the EXT to assess potential selection bias that might influence long-term treatment outcomes.

Methods: In FREEDOM, women were randomized to placebo (PBO) or DMAb 60 mg Q6M. All FREEDOM subjects who had not missed >1 dose of investigational product, completed the 3-year visit, and consented to enroll were eligible to receive open-label DMAb in the EXT. We assessed whether older age and incident fractures contributed to attrition at Year 5 of the EXT, representing 8 years of follow-up.

Results: In FREEDOM, 6478/7808 (83%) subjects completed the trial. Of 5928 subjects eligible for the EXT, 4550 (77%) enrolled. Through Year 5 of the EXT, 3004 (66%) remained on study. While baseline characteristics were similar in FREEDOM and EXT, all subjects were 3 years older at EXT baseline, prevalent vertebral fracture rate in PBO-treated subjects was higher at EXT baseline compared with FREEDOM baseline (25% vs 22%), and DMAb-treated subjects had higher mean BMD at EXT baseline. Age distribution after 5 years of EXT remained consistent with the antecedent 3 years in FREEDOM, with no preponderance of younger subjects (Figure). As expected, older subjects were more likely to discontinue, however, 62% of subjects who were ≥75 years at EXT baseline remained on study through Year 5. While subjects who fractured were more likely to discontinue in FREEDOM and in the EXT, 88% and 83% of PBO and DMAb fractured subjects, respectively, completed the 3-year FREEDOM trial, and 72% of fractured subjects in the EXT remained enrolled through Year 5.

Conclusion: In this large-scale, long-term study of DMAb, EXT population maintained similar characteristics to the original FREEDOM cohort. During EXT, a high percentage of subjects at increased risk for fractures due to older age and incident fracture remain on study. This suggests that the low fracture incidence and consistent safety profile reflect the long-term DMAb treatment effect.

Figure. Age Distribution at FREEDOM Baseline (A) and Year 5 of FREEDOM Extension (B)

MO0392

NSAID Efficacy in Acute-Phase Reaction Management in Chinese Postmenopausal Osteoporosis Patients after Zoledronic Acid Infusion: A Subgroup Analysis. <u>Fuxing Pei</u>*[1], <u>Xun Liu</u>[2], <u>Yingxu Gao</u>[2]. [1]West China Hospital, Sichuan University, Peoples Republic of China, [2]Novartis Pharmaceuticals (China), China

Objective: To evaluate short-term safety and access the acute phase response (APR) (fever and body pain) in an observational setting during first 4 weeks post zoledronic acid (ZOL) 5 mg single infusion in postmenopausal osteoporosis (PMO) patients of mainland China.

Methods: This was a 4-week, prospective, multicenter, open-label, non-interventional study in 2601 PMO patients. The primary outcome was the rate and severity of fever (temperature increases 1 ? compared with baseline) and body pain. The secondary outcome was efficacy of antipyretic-analgesic and anti-inflammatory drugs (NSAIDs) for treatment with APR. Patients with an APR were separated into 3 groups: prevention group (patients using NSAIDs to prevent APR on infusion day irrespective of APR); control group (patients using NSAIDs for symptom control when fever or pain severity aggravated); no therapy group (no NSAIDs usage).

Results: Data from 2583 patients with complete body temperature records and 2601 patients with pain severity data were analyzed, with an average age of 68.14 ± 9.89 years old and baseline body temperature of 36.51 ± 0.31?. There were 740 (28.65%) patients experienced fever within 1st week and 456 (17.53%) patients pain severity aggravated within 2 weeks post ZOL infusion. Within 2 weeks of infusion, 1187 patients used NSAIDs, 50.72% (602) of them used NSAIDs to prevent APR, the other 49.28% (585) patients used NSAIDs for symptom control.

Subgroup analysis showed the fever rate in patients with preventive NSAIDs usage was 8.71% less than that of patients without preventive NSAIDs (21.76% vs 30.47%) within 1st week post ZOL infusion. The percentage of patients with pain severity aggravated with preventive NSAIDs usage was 12.00% less than that in group without preventive NSAIDs usage (8.31% vs 20.31%) within 2 weeks after ZOL infusion. The detail changes of body temperatures and fever recovery time was showed in the table. There was no statistically significant result on the efficacy of NSAIDs for pain relief in patients with the severity aggravation.Conclusion: Comparing symptom control post ZOL infusion, preventive NSAID treatment could effectively reduce the rate of patients experiencing fever or body pain aggravation. Patients with preventive NSAID treatment experienced mild symptom with a shorter period. Our results could provide guidance for APR management in clinical practice.

Items		Prevention group (n=131)	Control group (n=487)	P value
Patients with elevated body temperature	1°C-≤2°C	104(79.39%)	359(73.72%)	<0.0001
	>2°C	27(20.61%)	128(26.28%)	<0.0001
Average elevated body temperature (LSMean) (°C)		1.73	1.82	<0.0001
Average fever recovery time (LSMean) (Day)		1.51	1.83	<0.0001

Table. Efficacy of NSAIDs treatment in fever patients

Disclosures: Fuxing Pei, *None.*

MO0393

Oral alendronate is associated with gastro-intestinal reflux disease and voice alterations irrespective of the presence of esophagitis. Sirley Vasconcelos*[1], Francisco Bandeira[2], Alyne Loureiro[3], Ana Catarina Araújo[3], Severino dos Santos[4], Larissa Pimentel[5]. [1]Hospital Agamenon Magalhães - Recife, Brazil, [2]University of Pernambuco, Brazil, [3]Agamenon Magalhães Hospital, Brazil, [4]Osvaldo Cruz Hospital, Brazil, [5], Brazil

Bisphosphonates (BPS) are considered first-choice drugs for the treatment of osteoporosis, and due to its low cost, alendronate is the most widely used. Esophagitis is one of the main side effects of this drug and little is known about gastroesophageal reflux disease (GERD) with its atypical features such as voice problems, as a consequence of oral BPS. The aim of this study was to identify GERD and vocal changes in postmenopausal women with osteoporosis taking alendronate, compared to a control group. One hundred eighteen postmenopausal women were studied, of whom 59 were on alendronate and 59 were not using it. The diagnosis of GERD was made by the presence of dyspeptic symptoms and signs of esophagitis on endoscopy. The presence of voice disturbances was evaluated by the Perceptual Assessment of Voice and Acoustic Evaluation of Voice. The mean age was 66.87 ± 7.78 years (range 52 – 85), mean BMI= 27.38 ± 4.63 and age of menopause was 45.35 ± 7.04 years. Regurgitation and pyrosis were more frequent in the treatment group (88.14 %) than in the control group (77.97 %), with OR = 2.09 (95% CI 0.77 to 5.71), although these differences were not statistically significant . There were significant differences for the following atypical manifestations in the cases x controls: globus pharyngeal (55.93 % vs. 33.90%, p=0.010), dysphagia (35.59 % vs. 18.64%, p=0.041), discomfort in the upper airways (23.73 % x 8.47 %, p=0.030) and odynophagia (22.03 % vs. 6.78 %, p=0.025). Voice changes were also noted more frequently in treatment group than in the control group (89.83% x 72.88 %), adjusted OR 4.4 (95% CI 1.48-13.1, p = 0.022). The most prevalent changes were vocal hoarseness (72.03 %, p = 0.154), vocal fatigue (44.07 % vs. 27.12%, p = 0.056), and difficulty in speaking (30.51 % vs. 15.25% p=0.052). Esophagitis was more prevalent in the control group (15.25 % vs. 3.39 %, p = 0.042), suggesting an independent effect of BPS on atipical GERD symptoms. Our data suggested that alendronate may be implicated in generation of laryngeal GERD symptoms.

Disclosures: Sirley Vasconcelos, *None.*

MO0394

Osteoporosis Treatment with Denosumab: Our Experience in the Real Clinical Practice. Diana González*[1], Beatriz Oliveri[2], Alicia Bagur[3], Carlos Mautalen[4]. [1]Mautalen Salud e Investigación, Argentina, [2]Mautalen, Salud e Investigación, Argentina, [3]Mautalen Salud e Investigacion, Argentina, [4]Centro de Osteopatías Médicas, Argentina

Randomized controlled trials have demonstrated that subcutaneous denosumab (DNB), a fully human monoclonal antibody against the receptor activador of nuclear factor $_k$B ligand (RANKL), ensures an effective anti-osteoporotic treatment. In the pivotal trials previous use of IV bisphosphonate was an exclusion criterion while previous oral bisphosphonates were allowed after a long wash out period. Other trials showed DNB effectiveness in patients previously treated with bisphosphonates without wash out period. The aim of this study was to report our experience with DNB in the real clinical practice in patients with osteoporosis. Subjects and Methods: osteoporotic women who received one or two doses of DNB during the period from 2011 to 2013 were included. The following issues were analyzed: a) Biochemical markers of bone turnover: serum Crosslaps (sCTX), Bone Gla Protein (BGP) and Bone Remodeling Index (BRI) at baseline, 6 (range: 5-7) months after the first dose of DNB, and at one year of treatment (six months after the second dose of DNB). b) Bone mineral density (BMD) of the lumbar spine (LS), femoral neck (FN) and total femur (TF) at baseline and one year of treatment. Results: Seventy-five postmenopausal women with mean $(X \pm SD)$ 67.0+9 years-old were included. Seven out of 75 women were naive of bisphosphonate treatment. Sixty-eight patients had been treated with bisphosphonates during 5.8 ± 4 years. The 41.3% of the patients had history of fragility fractures. Biochemical determination and BMD values at baseline, 6 months and 12 months of treatment with DNB are shown in the table. The percent change from baseline in BMD was +6.5% (p<0.0001), +8.0% (p<0.0001) and +5.6%

(p<0.0001) in LS, FN and TF respectively. S-CTX and BRI showed a very significant decrease at 6 months: sCTX -77.3% (p<0.0001), and BRI -57.3% (p<0.0001) and at 12 months: sCTX -65.9% (p<0.0001), and BRI -34.25% (p<0.05). Although mean values of BGP were in the lower normal range at baseline and during treatment, they decreased 17 % at the 6th month after DNB (p<0.01) . The change of BGP at 12 months was not significant. A negative correlation between the percent changes BMD of TF and sCTX corresponding to 6 months (r=-0.36; p<0.01) was observed. No patients suffered new fractures during the study period. DNB was well tolerated and no adverse events were recorded. Conclusion: DNB has been an effective and safety anti-osteoporotic treatment even in those patients previously treated with other antiosteolytic treatments.

Table: Biochemical markers of bone turnover values at baseline, after first and second doses of DNB. BMD values at baseline and after second doses of DNB.

	Biochemical markers of bone turnover			Bone Mineral Density		
	sCTX (80-590ng/ml)	BGP (15-45ng/ml)	BRI (100-300)	LS L2-L4 (g/cm²)	FN (g/cm²)	TF (g/cm²)
Baseline	292.54±185	13.6±10.7	110.54±105	0.880±0.15	0.656±0.19	0.708±0.13
After 1st doses DNB	66.57±53*	11.3±16.7*	46.50±38*	-	-	-
After 2nd doses DNB	99.59±82*#	16.4±21.4	72.67±28#	0.938±0.11*	0.713±0.15*	0.748±0.14*

*p<0.000 vs. baseline; #p< 0.01 vs. 6 months; #p<0.01 vs. baseline; £p<0.05 vs. baseline

Table

Disclosures: Diana González, *None.*

MO0395

Relationship between Response to Treatment with Risedronate and Baseline Characteristics Including Age, BMD, and Serum 25(OH)D Level - Subanalyses of Japanese Risedronate Phase III Trials-. Taro Mawatari*[1], Ryoichi Muraoka[2], Yukihide Iwamoto[3]. [1]Hamanomachi Hospital, Japan, [2]Ajinomoto Phamaceuticals Co, Ltd., Japan, [3]Dept. of Orthopaedic Surgery, Kyushu University, Japan

Purpose: Risedronate (RIS) increases bone mineral density (BMD) and reduces fracture risk. However, the response to the treatment may depend on the subjects' characteristics, such as baseline BMD, age, and Serum 25(OH)D Level. In this study, Japanese Phase III trials of RIS were subanalyzed to consider these issues.
Subjects and Methods: A total of 1447 subjects whose baseline BMD, serum 25(OH)D level were measured prior to RIS treatment were included in this study. RIS was administered for 12 months without vitamin D supplementation in those trials. Relationship between baseline characteristics (BMD, serum 25(OH)D level, and age) and response to RIS treatment (BMD change and new fracture) were evaluated.
Results: Subjects with a baseline 25(OH)D levels below 20ng/mL were 44.7%, and only 10.8% were above 30ng/mL. Student's t-test showed that the percent change in BMD was significantly higher when initial BMD (T-score) was < -2.5 than when it was ≥ -2.5 (mean ± SE was 5.80 ± 0.13% and 4.59 ± 0.28%, respectively; P=0.0003), and lower when baseline 25(OH)D level was < 21 ng/mL than when it was ≥ 21 ng/mL (mean ± SE was 5.39 ± 0.18% and 5.99 ± 0.17%, respectively; P=0.0138). (Figure) When subjects were divided into tertiles of age at start of RIS treatment, the percent change in BMD showed no significant difference among groups. Irrespective of baseline BMD, fracture rate was 1.5% in the population with a endpoint T-score < -2.5 and 0.8% in the population with a endpoint T-score ≥ -2.5.
Conclusions: These results suggest that bone density increases in response to RIS treatment even when the initial BMD is low, but early initiation of treatment would be more effective from the standpoint of preventing fracture. BMD response to RIS was smaller when 25(OH)D was less than 21 ng/mL than when it was not less than 21 ng/mL, suggesting the importance of vitamin D supplementation.
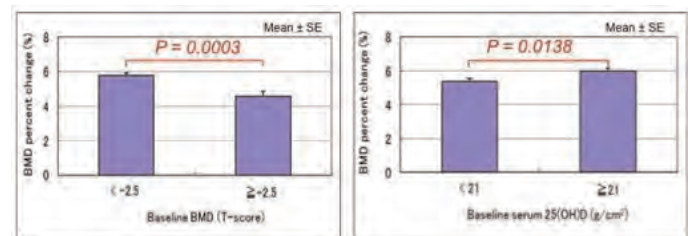
Figure

Disclosures: Taro Mawatari, *None.*

MO0396

Closing the Gap in Osteoporosis Management: Implementation and Outcome Analysis of Secondary Fracture Prevention Programs. <u>Kirtan Ganda</u>*[1], <u>Markus Seibel</u>[2]. [1]Concord Hospital, Australia, [2]Bone Research Program, ANZAC Research Institute, University of Sydney, Australia

In the majority of patients with fragility fractures, the underlying osteoporotic bone disease remains undiagnosed and untreated. We present three analyses (1) establishing the characteristics of effective Secondary Fracture Prevention programs (SFPP), (2) optimising follow-up after treatment initiation, and (3) determining factors associated with increased risk of re-fracture in patients managed within a SFPP.

(1) Systematic review and meta-analysis of 42 reports on SFPPs published between 1996-2011: Outcome measures extracted included bone mineral density (BMD) testing and osteoporosis treatment initiation rates. Studies were grouped into 4 models of care, from most intensive (Type A = assessment & treatment) through to type D (patient education only). Meta-analyses demonstrated increased BMD testing (p=0.06) and treatment initiation rates (p=0.03) with increasing intensity of intervention. Thus, fully coordinated, intensive SFPPs were more effective in improving patient outcomes than approaches involving patient education only.

(2) A 2-year RCT of 102 patients initiated on oral bisphosphonate therapy at the Concord SFPP, randomised to 6-monthly follow-up with the SFPP (group A) or primary care physician follow-up (group B). Compliance & persistence were measured using claims data and their predictors analysed. At 24-months, medication possession ratio (MPR) and persistence were high and similar in both groups. In the adjusted analysis, patients in group A were not more likely to be compliant or persistent than those in group B, indicating that initiation of therapy within an SFPP is associated with high long-term therapeutic adherence.

(3) In a 7-year prospective study, we determined the predictors of re-fracture amongst 234 subjects managed by the Concord SFPP. In multivariate analysis, co-morbidity (HR 2.04 if >3, 95%CI 1.10-3.79), corticosteroid use (HR 1.75, 95%CI 1.12-2.73), total hip BMD (HR 1.36 per $0.1g/cm^2$ decrease, 95%CI 1.08-1.70) and a MPR of less than 50% (HR 3.36, 95%CI 1.32-8.53) were significantly associated with re-fracture, indicating patients who fulfil these criteria are at very high risk of refracture, requiring intensive management.

These results demonstrate that intensive SFPPs (i.e.Type A) are effective in raising treatment rates, and that following treatment initiation by the program, patients are likely to adhere to therapy outside the SFPP. However, therapeutic compliance remains the major determinant of re-fracture risk.

Disclosures: Kirtan Ganda, None.

MO0397

DEVIDE-Study: DEnosumab Versus Intravenous IbanDronatE – a 24 months retrospective head to head real life study – Baseline Data. <u>Astrid Fahrleitner-Pammer</u>*[1], <u>Christian Muschitz</u>[2], <u>Doris Wagner</u>[3], <u>Karin Amrein</u>[3], <u>Thomas Pieber</u>[3], <u>Heinrich Resch</u>[4], <u>Hans Dimai</u>[5]. [1]Medical University Graz, Austria, [2]St. Vincent's Hospital, Austria, [3]Medical University, Austria, [4]Medical University Vienna, Austria, [5]Medical University of Graz, Austria

Purpose: Effective treatment of postmenopausal osteoporosis (PMO) is frequently dominated by poor persistence and adherence to short-term medications. Aim of this study which has been performed in a real-life setting, is to investigate the effect of parenteral ibandronate (IBN) compared to denosumab treatment in a cohort of IBN pretreated patients.

Methods: Retrospectively 808 patients with PMO who did not tolerate oral BP therapy were analyzed. All were treated with quaterly IBN injections for 27+3mos and were regularly monitored at a osteoporosis outpatients clinic. After Denosumab was launched 366 women were switched to receive this therapy whereas the remaining 422 preferred to stay on IBN. Effectiveness in terms of fracture incidence, BMD, BTM as well as adherence and safety of the two treatments will be analyzed.

Results: The baseline characteristics are given in table 1. There were no differences in any of the parameters investigated including renal and liver function, vitamin D, PTH and bone turnover markers. Laboratory testing , recording of adverse events was done every 6 months, BMD readings, soinal X-ray and fracture assessment were performed at baseline and after 12 and 24 months of ongoing IBN or Denosumab therapy.

Conclusion: The results of this study not only will provide clincans with insights into persistence with denosumab in comparison to quarterly IBN therapy, bit will also compare the effect of denosumab for the first time with a parenteral administered bisphosphonate in respect to safety, changes in BMD as well as fracture incidence and changes in spine deformity index over a time period of 2 years.

tab1:

Characteristics	Denosumab (n=366)	Ibandronate (n=442)
Age (years)	67.2 + 7	67.5 + 6
Years since menopause	22 + 3	21 + 4
Weeks on ALN	5 + 2	5 + 2
Total Hip BMD T-Score	-1.8 + 0.7	-1.7 + 0.8
Femoral neck BMD T-score	-2.1 + 0.9	-2.0 + 1
Lumbar spine BMD T-score	-2.8 + 1.2	-2.7 + 1.4
Non vertebral fracture, n (%)	26 (7.1%)	34 (7.7%)
Vertebral fracture, n (%)	69 (18.9%)	84 (19%)

Disclosures: Astrid Fahrleitner-Pammer, None.

MO0398

Persistence With Prolia® (Denosumab) for 1 Year in Relation to Patient-reported Data: Interim Results From a Prospective Observational Study of Postmenopausal Women With Osteoporosis. <u>SL Silverman</u>*[1], <u>E Siris</u>[2], <u>DL Kendler</u>[3], <u>D Belazi</u>[4], <u>JP Brown</u>[5], <u>DT Gold</u>[6], <u>EM Lewiecki</u>[7], <u>A Papaioannou</u>[8], <u>C Simonelli</u>[9], <u>G Quinn</u>[10], <u>A Balasubramanian</u>[11], <u>FM Mirza</u>[11], <u>P Ho</u>[11], <u>S Siddhanti</u>[12], <u>B Stolshek</u>[12], <u>C Recknor</u>[13]. [1]Cedars-Sinai Bone Center for Excellence, UCLA School of Medicine, & OMC Clinical Research Center, USA, [2]Columbia University Medical Center, USA, [3]University of British Columbia, Canada, [4]AlchemiPharma LLC, USA, [5]Laval University & CHU de Québec Research Centre, Canada, [6]Duke University Medical Center, USA, [7]New Mexico Clinical Research & Osteoporosis Center & University of New Mexico School of Medicine, USA, [8]McMaster University, Canada, [9]Health East Osteoporosis Care, USA, [10]Sarnia Statistics LTD, United Kingdom, [11]Amgen Inc., USA, [12]Amgen Inc., USA, [13]United Osteoporosis Centers, USA

Purpose: Persistence with osteoporosis therapy is important for optimal reduction of fracture risk. In a randomized clinical trial in women with low BMD, persistence with denosumab (DMAb) was >90% (Freemantle *Osteoporos Int* 2012). Patients who had greater perceived necessity for an osteoporosis drug had lower odds of nonadherence (Kendler *Menopause* 2013). We are conducting a prospective observational study to evaluate persistence with DMAb in routine clinical practice in Canada (CAN) and the United States (US).

Methods: In this ongoing, multicenter, observational, 2-year study, women were enrolled within 4 wk after the 1st injection of DMAb, recommended for administration every 6 mo for the treatment of osteoporosis per the local product label. Clinical sites include primary care and specialty practices. No clinical procedures, assessments, or changes to routine management of patients were required. Persistence with DMAb for 12 mo was defined as receipt of the 2nd injection no more than 6 mo+8 wk from the baseline injection. Patients completed questionnaires at baseline that included Beliefs About Osteoporosis Medicines (BMQ 11; necessity and concern), the Patient Satisfaction Questionnaire, and other questions about accessing the provider and treatment. We report interim results of 1-year persistence with DMAb in relation to these patient-reported data.

Results: Of the 935 women enrolled (CAN 303, US 632), 82% were persistent with DMAb for 1 year (CAN 88%; US 79%). Median scores (on a scale of 0.00 to 5.00) for the BMQ 11 were 3.00 for necessity of the medication and 2.33 for concern about the medication. Patients were very or quite satisfied with the frequency (87%), mode (85%), and convenience (87%) of DMAb administration. Persistence for 1 year was slightly higher in patients who perceived a higher necessity, had lower concern, or had a higher necessity-concern ratio (Table 1). There was a suggestion of increased persistence among patients who were satisfied with DMAb (Table 2). Other patient-reported data suggest that copayment >$100 (US) and payment by patient (CAN) but not household income, educational level, distance travelled, or patient-support programs might have a relationship with persistence.

Conclusion: In this study of routine clinical practice, 82% of patients persisted on therapy for 1 year. Patients' perceived need for the drug and satisfaction with the drug may lead to better overall persistence.

Table 1. Persistence With Denosumab for 1 Year by Beliefs About Osteoporosis Medication

	Canada (N=303)		US (N=632)		Overall (N=935)	
	n/N1	% (95% CI)	n/N1	% (95% CI)	n/N1	% (95% CI)
Adjusted necessity score (Canada median = 3.20, US median = 3.00, Overall median = 3.00)						
≤ Median	142/164	86.6 (80.4, 91.4)	265/340	77.9 (73.2, 82.2)	382/479	79.7 (75.9, 83.3)
> Median	117/132	88.6 (82.0, 93.5)	213/257	82.9 (77.7, 87.3)	355/414	85.7 (82.0, 89.0)
Adjusted concern score (Canada median = 2.33, US median = 2.33, Overall median = 2.33)						
≤ Median	133/150	88.7 (82.5, 93.3)	269/326	82.5 (77.9, 86.5)	402/476	84.5 (80.9, 87.6)
> Median	127/147	86.4 (79.8, 91.5)	211/273	77.3 (71.9, 82.1)	338/420	80.5 (76.4, 84.2)
Necessity-concerns differential (Canada median = 0.53, US median = 0.57, Overall median = 0.53)						
≤ Median	124/148	83.8 (76.8, 89.3)	228/298	76.5 (71.3, 81.2)	358/450	79.6 (75.5, 83.2)
> Median	135/148	91.2 (85.4, 95.2)	250/298	83.9 (79.2, 87.9)	379/442	85.7 (82.1, 68.9)

N=number of patients enrolled. n=number of persistent patients within the covariate group. N1=number of patients in the full analysis set within the covariate group. Percentages are based on N1. CI=confidence interval based on exact method.

Table 1

Table 2. Persistence With Denosumab for 1 Year by Patient Satisfaction

	Canada (N=303)		US (N=632)		Overall (N=935)	
	n/N1	% (95% CI)	n/N1	% (95% CI)	n/N1	% (95% CI)
Satisfaction with frequency of administration						
Not at all satisfied	1/2	50.0 (1.3, 98.7)	0/2	0 (0, 0)	1/4	25.0 (0.6, 80.6)
A little satisfied	2/2	100.0 (15.8, 100.0)	6/9	66.7 (29.9, 92.5)	8/11	72.7 (39.0, 94.0)
Moderately satisfied	8/9	88.9 (51.8, 99.7)	36/48	75.0 (60.4, 86.4)	44/57	77.2 (64.2, 87.3)
Quite satisfied	82/95	86.3 (77.7, 92.5)	159/198	80.3 (74.1, 85.6)	241/293	82.3 (77.4, 86.5)
Very satisfied	162/181	89.5 (84.1, 93.6)	272/342	79.5 (74.9, 83.7)	434/523	83.0 (79.5, 86.1)
Satisfaction with mode of administration						
Not at all satisfied	2/3	66.7 (9.4, 99.2)	5/7	71.4 (29.0, 96.3)	7/10	70.0 (34.8, 93.3)
A little satisfied	3/4	75.0 (19.4, 99.4)	5/8	62.5 (24.5, 91.5)	8/12	66.7 (34.9, 90.1)
Moderately satisfied	11/13	84.6 (54.6, 98.1)	48/60	80.0 (67.7, 89.2)	59/73	80.8 (69.9, 89.1)
Quite satisfied	74/86	86.0 (76.9, 92.6)	148/191	77.5 (70.9, 83.2)	222/277	80.1 (75.0, 84.7)
Very satisfied	162/181	89.5 (84.1, 93.6)	267/333	80.2 (75.5, 84.3)	429/514	83.5 (80.0, 86.6)
Satisfaction with convenience						
Not at all satisfied	0/1	0 (0, 0)	4/6	66.7 (22.3, 95.7)	4/7	57.1 (18.4, 90.1)
A little satisfied	6/6	100.0 (54.1, 100.0)	8/11	72.7 (39.0, 94.0)	14/17	82.4 (56.6, 96.2)
Moderately satisfied	11/12	91.7 (61.5, 99.8)	37/44	84.1 (69.9, 93.4)	48/56	85.7 (73.8, 93.6)
Quite satisfied	69/83	83.1 (73.3, 90.5)	147/190	77.4 (70.8, 83.1)	216/273	79.1 (73.8, 83.8)
Very satisfied	168/187	89.8 (84.6, 93.8)	279/351	79.5 (74.9, 83.6)	447/538	83.1 (79.6, 86.2)

N=number of patients enrolled. n=number of persistent patients within the covariate group. N1=number of patients in the full analysis set within the covariate group. Percentages are based on N1. CI=confidence interval based on exact method.

Table 2

MO0399

Preferences for Osteoporosis Treatment in Japan. Ikuko Tanaka*[1], Marco DiBonaventura[2]. [1]NAGOYA Rheumatology Clinic, Japan, [2]Kantar Health, USA

Introduction: Nearly 15 million people experience osteoporosis in Japan and, although there are a number of treatment options available, they all vary on a range of different attributes. Understanding patient preferences in each country is important because these can differ based on societal and cultural backgrounds as well as medical and insurance systems. The aim of this study was to investigate patient preferences for osteoporosis treatment in Japan and how these preferences might vary based on prior treatment experience. METHODS: The current study included data from an online survey that was administered to respondents of the Japan National Health and Wellness Survey, an annual general health survey of the adult Japanese population. Only those diagnosed with osteoporosis and who had osteoporosis treatment experience were included in the analyses (N=655). Patients were categorized into one of four groups based on two dimensions (bisphosphonate experience or not; currently on treatment or not). Respondents evaluated medication attributes and reported their level of agreement with various statements for a hypothetical treatment which had varied dosing frequencies of daily, weekly, or monthly. RESULTS: All attributes were considered important in absolute terms. Efficacy was rated as the most important followed by side effects, the administration process (e.g., food and posture restrictions), and dosing frequency. Cost was not considered an important attribute. In forced choice rankings, efficacy, safety, and dosing frequency were the most highly ranked attributes. Both current and former bisphosphonate users had a significant preference for weekly dosing over daily dosing. All patient groups perceived daily dosing as the most burdensome and monthly dosing to be most highly associated with missed doses. DISCUSSION: Patients place particular value on efficacy and side effects, though dosing frequency is considered the next most important attribute. There was a preference for weekly dosing over daily dosing among those with bisphosphonate experience, primarily because of the perceived burden of daily dosing as well as a greater perceived likelihood of missing doses for monthly dosing. Overall, weekly dosing was evaluated as the best balance between frequency and ease of remembering to take the medication. Physicians should be aware of patient preferences as aligning medications with preferences may be associated with better health outcomes.

MO0400

Preventing breaking bad: The impact of DXA and FRAX results on physicians' treatment decisions in a large multispecialty group practice. Meg Durbin*[1], Miriam Rotman[2], Bradley Stolshek[3], Harold Luft[2]. [1]Palo Alto Medical FoundationSutter Health, USA, [2]Palo Alto Medical Foundation Research Institute, USA, [3]Amgen, USA

Background: Osteoporosis and related fractures cause significant morbidity, mortality, and expense, but medications recommended by groups such as the National Osteoporosis Foundation (NOF) to prevent fracture (fx) are inconsistently prescribed. FRAX calculations added to dual energy x-ray absorptiometry (DXA) reports estimate fx risk, but few studies assess the impact of such reports on physician prescribing patterns.

Objective: To describe prescribing patterns for women age ≥ 50 years after 1) DXA showing low BMD (T score < -1.0) with or without FRAX (15362)- 1^0 prevention or 2) fx suspicious for osteoporosis (2748) -2^0 prevention.

Methods: All data were obtained from electronic health records (EHR) in a large multispecialty group. In the 1^0 prevention group, DXA and FRAX reports from 2009-10 were reviewed. High FRAX score is defined as 10 yr risk > 3% for hip or > 20% for any osteoporosis related fx. In the 2^0 prevention group, fxs were identified from 2009-10, with any DXAs done between 2 y before through 6 mo after fx. Prescription medication to treat low BMD ("Rx") was identified in medication lists from 6 mo before through 6 mo after DXA date (1^0 prevention) or fx (2^0 prevention).

Results: Most women with osteoporosis had Rx (71%), but Rx rates differed by FRAX score - 73% with high or no FRAX vs. 61% with low FRAX, p <0.01 (Fig. 1). Only 34% of all women with osteopenia had Rx, but greater Rx was strongly related to high FRAX and lower T scores: 46% with osteopenia and high FRAX had Rx vs. 28% with low FRAX (p <0.01), and Rx rates rose as T scores fell from the highest to lowest subgroups: 23% vs. 32% vs. 44% (Fig. 2) (test for trend, p <0.01). In women with suspicious fx, 42% overall had Rx, but Rx rates were higher in the subset with DXA: 79% with T score < -2.5 vs. 42% with higher T score vs. 37% without DXA (p <0.01) (Fig. 3).

Conclusion: Most women with osteoporosis had NOF guideline-consistent treatment. Treatment rates in osteopenia were low overall but rose with higher FRAX scores and lower BMD. Most women with osteoporosis-suspicious fractures were not prescribed Rx. However, in the subset with fracture and DXA-confirmed osteoporosis, most were prescribed Rx, even though DXA to confirm low BMD is not required before starting Rx after osteoporosis- suspicious fx. Opportunities exist to increase both physicians' recognition of fracture risk stemming from low BMD and to raise their rates of prescribing medication to prevent such fractures.

Figure 1: Primary Prevention Cohort - Treatment[1] Pattern by DXA and FRAX[2]

[1]Treatment includes prescription medications documented in the EHR medication list with start and end dates from the following classes: bisphosphonates, estrogens, estrogenagonist/antagonists (tamoxifen and raloxifene), calcitonin, parathyroid hormone, strontium, denosumab, and calcitriol.
[2]FRAX: Low = 10 year risk < 3% for hip and < 20% for any osteoporosis related fracture; high = 10 year risk ≥ 3% for hip or ≥ 20% for any osteoporosis related fracture.
[3]Rx includes continuing medications begun ≥ 2 months before DXA and continued for 6 months after DXA, and medications started ≤ 6 months after DXA. No Rx includes no medications started ≤ 6 months after DXA, and medications stopped between 2 months before through 6 months after DXA.

Figure 2: Treatment Pattern among Women with Osteopenia, by T group subscore

Numbers in bars represent number of cases

Figure 3: Treatment Patterns for Women with Suspicious Fracture, by DXA

Numbers in bars represent number of cases
DXAs were completed between 2 years before fracture through 6 months after fracture.

Figure

MO0401

Understanding Physicians Perceptions of Patients Barriers to Osteoporosis Medication Intitiation. Stuart Silverman*[1], Haiyan Qu[2], Jeffrey Curtis[3], Susan Greenspan[4], Sarah Morgan[3], Jeri Nieves[5], Ryan Outman[3], Richard Shewchuk[2], Ethel Siris[6], Amy Warriner[3], Nelson Watts[7], Kenneth Saag[3]. [1]Cedars-Sinai/UCLA, USA, [2]University of Alabama at Birmingham, USA, [3]University of Alabama at Birmingham, USA, [4]University of Pittsburgh, USA, [5]Columbia University & Helen Hayes Hospital, USA, [6]Columbia University College of Physicians & Surgeons, USA, [7]Mercy Health Osteoporosis & Bone Health Services, USA

Purpose: Despite international guidelines, osteoporosis treatment rates remain low. A better understanding is needed on how to organize and address barriers to medication initiation. We derived a cognitive map of how physicians perceive patient-identified barriers for the purpose of developing minimally invasive interventions aimed at increasing treatment initiation.

Methods: To elicit barriers to initiating osteoporosis medication, we conducted 4 nominal groups with 18 postmenopausal women with a history of fracture who were not currently receiving osteoporosis treatment. Each woman then independently ranked her 3 most important barriers creating a final list of 25 barriers. Next, physician osteoporosis experts (n=26) independently grouped these barriers into clusters of at least 2 barriers each. The data were analyzed using multidimensional scaling and hierarchical cluster analysis. The physicians also used a 5-point Likert scale to indicate their level of agreement or disagreement of the ability of each barrier to be addressed by an intervention.

Results: The physicians included 11 rheumatologists, 9 endocrinologists, 3 general internists and 3 others with significant osteoporosis management experience. A sorting exercise identified 5 distinct clusters (Figure): 1) concerns about side effects, 2) experience of side effects, 3) lifestyle changes, 4) medication access and complexity, and 5) patient uncertainty about treatment and trust in provider. Barriers were mapped along 2 dimensions: the x-axis represented patient uncertainty about osteoporosis treatment with medication side effect concerns on the left and uncertainty in trust of care providers on the right. The y-axis represented patient belief and expectations about osteoporosis treatment with lifestyle change at the top, and access and complexity of medications at the bottom. The project team named the clusters and axes based on common features. Based on the average mean ratings within clusters, physicians agreed that the concerns about side effects cluster could be addressed as elements of an intervention (M+SD, 3.9+0.9) while the uncertainty of medication and providers cluster could not be addressed easily (M+SD, 2.7+1.1).

Conclusion: The identified clusters generated by physician agreement using cognitive mapping provide a basis for a theoretical framework from which to develop future tailored interventions to address the barriers to initiating osteoporosis treatment.
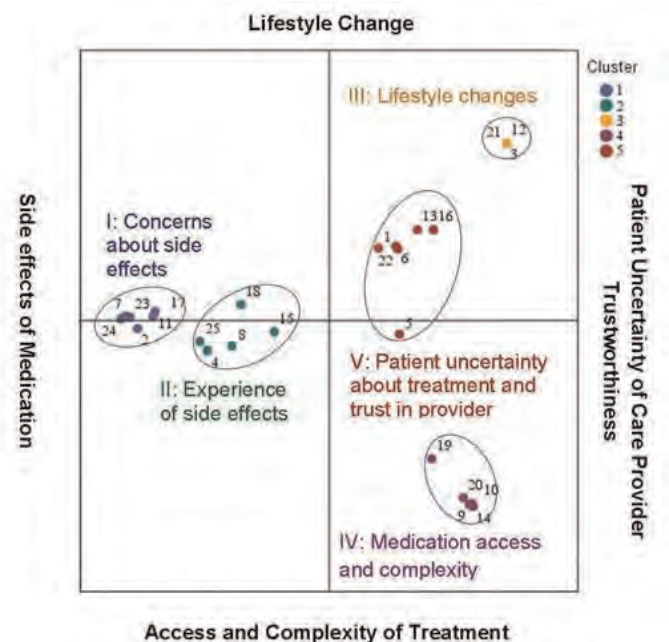

Figure. Dimensional Arrangement of Osteoporosis Treatment Barrier Clusters

MO0402

Two Years of Osteoanabolic Treatment to Heal a Non-union Fracture in a Patient with Multiple Co-Morbidities. <u>Elliott Schwartz</u>*[1], <u>Patricia Schwartz</u>[2], <u>George Tischenko</u>[3]. [1]Northern California Institute for Bone Health, Inc., USA, [2]Northern California Institute for Bone Health, Inc., USA, [3]Muir Orthopaedic Specialists, USA

Non-union of a fracture is defined as permanent failure of healing following a fracture, usually, by 6 months. The FDA defines non-union for investigative purposes as a fracture 9 months old that has shown no signs of healing for 3 months. Non-unions occur in 10-20% of the 6,000,000 annual fractures in the United States. The morbidity of non-unions is extensive and expensive. The treatment of non-unions is, usually, surgical. However, the development of osteoanabolic agents suggests there may be another approach. However, the duration of time of treatment to "heal" a non-union is unknown. Numerous individuals suggest that this treatment may take weeks to a few months.

We evaluated a 66 year old morbidly obese white male who fractured his right medial malleolus after weeks in an exercise class without obvious trauma. A CT scan of the ankle 5 months later showed a non-union. Because of morbid obesity and chronic obstructive pulmonary disease, surgical repair was deemed inadvisable. A "secondary" osteoporosis laboratory work-up showed pre-diabetes and hypogonadism. A DXA showed normal bone density. He was started on low dose pulsed ultrasound. A month later, he was started on teriparatide 20mcg subcutaneously daily. A month later, he was started on a Heart Healthy Diet and testosterone gel. He was followed with appropriate laboratory monitoring and serial CT scans at appropriate intervals. The CT scan performed at one year showed an incompletely healed medial malleolar fracture. A CT scan of the ankle performed 23 months after initiation of osteoanabolic treatment showed complete healing of the medial malleolar fracture.

Conclusion: Current osteoanabolic therapy can heal fracture non-unions but the length of time to do so may be prolonged.

Disclosures: Elliott Schwartz, Lilly, 3

MO0403

Combination therapy Denosumab and Alfacalcidol in Postmenopausal Osteoporosis - tree years experience. <u>Corina Galesanu</u>*[1], <u>Andra Iulia Loghin</u>[2]. [1]University of Medicine & Pharmacy, Romania, [2]University of Medicine & Pharmacy, Romania

Background: Analysis of data from the FREEDOM trial confirmed that Denosumab significantly improved bone mineral density, mass and strength besides significantly reducing the risk for fractures. Denosumab is a full human monoclonal antibody targeting the RANK Ligant, an essential regulator of osteoclast formation, function and survival.

Objectives: The purpose of this study was to investigate the effect of the Denosumab on change Bone Mineral Density (BMD) in postmenopausal osteoporotic women.

Methods: Twenty seven postmenopausal women with BMD T-score at lumbar spine (LS), total hip(TH) or femoral neck (FN) less than -2.5 received Denosumab 60 mg subcutaneous injection at every 6 months , plus 1000 mg calcium and alfacalcidol 1 µg/d. Mean age of our patients was 63 years old and mean age of menopause was 49.5 years old. BMD was measured by Dual-energy X- ray Absorptiometry (DXA) at baseline and 1, 2, 3 years. Adverse events were monitored.

Results: At baseline mean BMD at LS was 0.727 g/cm2 and increased to 0.781 g/cm2 (+7.8%), 0.825 g/cm^2 (+5.6%), 0.852g/cm^2 (+3.2%) after 1,2,3 years. For FN mean BMD at baseline was 0.556 g/cm2 and increased to 0.572 g/cm2 (+2.8%), 0.607g/cm^2 (+6.1%), 0.632g/cm^2 (+2.4%) after 1,2,3 years. BMD at TH increased from 0.725 g/cm2 to 0.754 g/cm2 (+4.0%), 0.792g/cm^2 (+5.0%), 0.806g/cm^2 (+1.7%) after 1,2,3 years. No adverse events or fractures under the therapy.

Discussions: Regarding combination therapy there are no studies showing that combination treatment with 2 or more osteoporosis drugs has a greater effect on fracture reduction than treatment with a single agent. Additive effects on BMD and bone turnover have been observed with combinations of 2 antiresorptive agents. We consider that the combination between Denosumab and Alfacalcidol explaned the increase of BMD more than in monotherapy.

Conclusion: Denosumab and Alfacalcidol treatment significantly increased BMD at the LS, FN and TH in our patients with postmenopausal osteoporosis. It was well tolerated by the women.

Disclosures: Corina Galesanu, None.

MO0404

Effect of Eldecalcitol on Bone Metabolism Following Alendronate Treatment in Ovariectomized Rats. <u>Satoshi Takeda</u>*[1], <u>Sadaoki Sakai</u>[2], <u>Yoshihito Tashiro</u>[3], <u>Michinori Hirata</u>[4], <u>Ken-ichi Serizawa</u>[4], <u>Kenji Yogo</u>[4], <u>Koichi Endo</u>[5]. [1]"chugai Pharmaceutical Co., Ltd.", Japan, [2]Chugai Pharmaceutical Co., Ltd., Japan, [3]Chugai Pharmaceutical Co.,Ltd, Japan, [4]Chugai Pharmaceutical Co.,Ltd., Japan, [5]Chugai Pharmaceutical Co., Ltd., Japan

Although treatment with bisphosphonate (BP) reduces the risk of osteoporotic fractures, concerns have recently emerged that long-term BP therapy is associated with an increased risk of atypical femoral fractures and osteonecrosis of the jaw. These concerns highlight the need for a drug holiday or switching to other drugs after long-term BP therapy. Eldecalcitol (ELD), an active vitamin D_3 derivative, is used to treat osteoporosis in Japan. ELD has been shown to inhibit osteoclastic bone resorption more potently than alfacalcidol, a prodrug of the active vitamin D_3, and stimulate bone minimodeling, a type of focal bone formation without prior bone resorption, in ovariectomized (OVX) rats. In this study, we examined the effects of ELD on bone mineral density (BMD), bone biomechanical strength, and bone turnover following alendronate (ALN) treatment in OVX rats.

Wistar-Imamichi rats (6-month old) were ovariectomized and treated with ALN (1µg/kg, s.c., 5 times/week) for 12 weeks. Thereafter, rats were treated with ALN (A→A group), ELD (20 ng/kg, p.o., 5 times/week; A→E group) or vehicle (A→V group) for another 12 weeks. Lumbar BMD was measured by DXA, and the biomechanical strength of the L5 vertebra was tested by the compression test. Bone histomorphometry was performed using the L3 vertebra.

The OVX-induced reduction of lumbar BMD was inhibited in the A→A, A→E, and A→V groups. BMD of the A→E group was higher than that of either the A→A or A→V group. The maximum load of L5 in the A→E group was higher than in the disease control (DC), A→A, and A→V groups. N.Oc/BS, ES/BS, N.Ob/BS, OS/BS, BFR/BS, and Ac.f were elevated by OVX and were suppressed in the A→A, A→E, and A→V groups. N.Oc/BS and ES/BS in the A→E group were lower than in either the A→A or A→V group. N.Ob/BS and OS/BS in the A→E group were higher than in the A→A group. Bone minimodeling in the A→E group was higher than in the DC group.We demonstrated that switching to ELD following 12-week treatment with ALN was more beneficial than continuing or discontinuing ALN in terms of increasing BMD and bone biomechanical strength in OVX rats. Because ALN is known to remain in bone even after treatment has been terminated, the effects of ELD following ALN treatment observed in this study may be caused by a combination effect of ELD and ALN. Bone minimodeling action of ELD may contribute to increasing BMD and bone biomechanical strength after ALN treatment.

Disclosures: Satoshi Takeda, Chugai Pharmaceutical Co.,Ltd, 4
This study received funding from: Chugai Pharmaceutical Co.,Ltd

MO0405

Intrinsic bone mineral quality in postmenopausal osteoporotic women treated for 12 months with strontium ranelate or alendronate. <u>Camille Ponçon</u>*[1], <u>Delphine Farlay</u>[2], <u>Georges Boivin</u>[3]. [1]INSERM U1033 Université de Lyon, France, [2]INSERM, UMR1033; Université De Lyon, France, [3]INSERM, UMR1033 ; Universite De Lyon, France

Strontium ranelate (SrRan) and alendronate (ALN) are anti-osteoporotic treatments reducing fracture risk. However, the mechanism of action of SrRan on bone remains partially elucidated. Its active agent, strontium ion (Sr), is exclusively fixed in bone mineral formed during treatment (1). In order to better understand its mechanism of action, early effects of SrRan were compared to those of ALN. Our goal was to analyze the intrinsic properties of bone mineral in the newly deposited tissue. One hundred twenty iliac bone biopsies were performed in postmenopausal osteoporotic women, before (M0) and after a 12 months (M12) treatment (SrRan or ALN), i.e., 30 pairs of biopsies for each treatment. After methylmethacrylate embedding, 2 µm-thick sections were analyzed by Fourier transform infrared microspectroscopy (FTIRM). The intrinsic mineral bone quality was assessed by 4 variables: mineralization index, mineral maturity, crystallinity index and carbonation. FTIRM was performed on the newest bone tissue, at M0 and M12, on the surface of trabeculae or on endocortical layer or in cortical osteons with wide Haversian canals. In SrRan group M12, Sr was localized by X-ray microanalysis to identify the recent bone formed during treatment. After SrRan (M12 vs M0), mineralization index, mineral maturity and crystallinity index were not significantly changed. Only mineral carbonation decreased significantly in cortical and trabecular sites. After ALN, only mineralization index and carbonation increased significantly in the two sites. These effects were coherent with the inhibitory action of ALN on bone remodeling, and indicated that mineral crystals were more numerous after ALN. However the mineral maturity remained unchanged at M12, suggesting the precipitation of new crystals instead of growth of the old ones. The decreased carbonation observed after SrRan, could be due to the Sr ion steric hindrance altering the incorporation of carbonates into crystals. This effect is independent of an action on bone remodeling. Our study underlined that SrRan and ALN have distinct modes of action on bone tissue. A decrease of bone mineral carbonation may be a variable contributing to the decrease of fracture risk.

Disclosures: Camille Ponçon, None.
This study received funding from: Servier

MO0406

The Effects of Pulsed Electromagnetic Field (PEMF) and/or Bisphosphonate Treatments on Vertebral Bone Mass in a Long-Term Osteoporosis Model. <u>Caroline Androjna</u>*[1], <u>Erik Waldorff</u>[2], <u>James Ryaby</u>[3], <u>Maciej Zborowski</u>[4], <u>Ronald Midura</u>[5]. [1]Lerner Research InstituteCleveland Clinic, USA, [2]Orthofix, USA, [3]Orthofix Inc, USA, [4]Cleveland Clinic, USA, [5]Lerner Research Institute of Cleveland Clinic, USA

Cervical-Stim® (Orthofix, Lewsville, TX) PEMF treatment has been shown to provide clinical benefits as an adjunct to spinal fusion in patients with risk factors for failed fusion. However, the effect on osteoporotic patients currently undergoing bisphosphonate treatments has not been established. The objectives of this study was to determine if the commercial Cervical-Stim PEMF waveform and a combinatorial treatment approach with a bisphosphonate could mitigate osteoporosis bone loss in the lumbar spine to reduce vertebral compression fracture risk in at risk patients. 120 skeletally mature (6-7 month old) ovariectomized (OVX) female Sprague-Dawley rats were equally divided into 6 cohorts being treated with a combination of alendronate (ALN, 3 s.c. injections/week at 10μg/kg BW) and/or PEMF (Cervical-Stim, 3 hrs/day, 7 days/week): age-matched normal rats (Sham OVX), Sham OVX+PEMF, OVX, OVX+ALN, OVX+PEMF, and OVX+PEMF+ALN. In-vivo microCT imaging (20 μm resolution), of the L4 vertebrae, was performed at baseline (5-7 days post OVX), 6, 12, 18 and 24 weeks post initiation of PEMF/ALN treatment. Outcome measures included bone volume fraction (BV/TV), bone mineral content (BMC), and bone mineral density (BMD). Injections of Alizarin Red and Calcein injections were done at 22 and 24 weeks, respectively, for end-point histomorphometry assessment of trabecular bone remodeling rates. Preliminary BV/TV, BMD and BMC results from the first 60 animals (10 rats/cohort) indicate that bone losses in the spine were minimal for the Sham OVX group while the OVX group experienced continual bone loss over the 24 weeks. ALN slows down bone loss as expected, but cannot prevent it. Intermediate results indicate that PEMF appears to partially mitigate OVX bone losses: analyses shows a trend of 23% and 18% mitigation at 18 and 24 weeks, respectively as compared to no treatment. While PEMF was shown to not be as effective as ALN treatment, co-treatment of OVX rats with PEMF and ALN did not demonstrate interference with ALN's effectiveness. Histomorphometric data are currently being completed. In conclusion, intermediate results suggest that daily PEMF treatment partially mitigates cancellous bone loss in the spine of long-term osteoporotic rats but not as effectively as ALN treatment. In addition, PEMF does not alter the effectiveness of ALN, and could therefore potentially be used as an adjunct treatment for osteoporotic patients currently undergoing bisphosphonate treatments.

Disclosures: Caroline Androjna, Orthofix Inc, 7
This study received funding from: OrthoFix Inc

MO0407

The role of the renin–angiotensin system in the bone metabolic response to mental stress. <u>Norman Pollock</u>*[1], <u>Laura Carbone</u>[1], <u>Monique Bethel</u>[2], <u>Yanbin Dong</u>[3], <u>Luiz Ortiz</u>[3], <u>Obioma Nwobi</u>[3], <u>Coral Hanevold</u>[4], <u>Deborah Stewart</u>[3], <u>Gregory Harshfield</u>[3]. [1]Georgia Regents University, USA, [2]Indiana University School of Medicine, USA, [3]Georgia Regents University, USA, [4]Seattle Children's Hospital, USA

Although increasing evidence suggests that mental stress may contribute to osteoporosis, it is unclear how the two comorbidities are linked. Because animal and co-culture models indicate that activation of renin-angiotensin system (RAS) causes abnormal bone metabolism, we postulate that the stress-related hormone angiotensin II (Ang II) may be a contributing factor linking mental stress to poor bone health. We tested this hypothesis in a randomized, double-blind, placebo-controlled crossover study, which examined the effect of an Ang II receptor blocker (Irbesartan, Avapro®) on the bone turnover and pressure natriuresis response to one hour of mental stress in sodium retainers and excreters. Fifteen healthy normotensive adults (7 men and 8 women; mean age, 25 y; range, 18-46 y) were randomized to either a 4-day standardized sodium diet and Irbesartan tablets (50 mg daily for 7 days) or the same diet and identical placebo tablets, each for 1 week, after a washout period of 1 week. On day 5 of each testing week, a 3-hour mental stress protocol was administered, which included 1-hour of rest, 1-hour of mental stress (competitive video game), and another 1-hour of rest. Blood pressure was collected at 15-minute intervals during the 3-hour protocol. Blood was collected hourly for assessment of procollagen type 1 amino propeptide (P1NP; bone formation marker) and C-terminal telopeptide α-1 chain of type 1 collagen (CTX; bone resorption marker). Hourly urine specimens were collected to determine urinary sodium excretion. An individual was designated as a sodium retainer if urinary sodium excretion decreased during the stress protocol in the placebo condition. In the sodium retainers, Irbesartan increased urinary sodium excretion during stress and had a beneficial effect on blood pressure levels throughout the protocol (all p< 0.05). During stress, Irbesartan also had a beneficial effect on P1NP, CTX, and the P1NP/CTX ratio in the sodium retainers (all p<0.05). In the sodium excreters, there was no effect of Irbesartan on change in urinary sodium excretion during stress or changes in blood pressure or bone turnover markers during the 3-hour protocol (all p>0.05). Our data suggest that in individuals who retain sodium under stress, suppression of Ang II inhibits sodium retention and improves bone metabolism, providing evidence of RAS in the bone metabolic response to mental stress.

Disclosures: Norman Pollock, None.

MO0408

Long-term Improvements in Bone Mineral Density and Health Related Quality of Life in Osteoporosis Patients Treated with Teriparatide. <u>Herman Bami</u>*[1], <u>Adrian Budhram</u>[2], <u>Raymond Chu</u>[3], <u>George Ioannidis</u>[4], <u>Alexandra Papaioannou</u>[5], <u>Arthur Lau</u>[1], <u>Jonathan Adachi</u>[6]. [1]McMaster University, Canada, [2]Michael G. DeGroote School of Medicine, McMaster University, Canada, [3]Faculty of Medicine, University of Toronto, Canada, [4]McMaster University, Canada, [5]Hamilton Health Sciences, Canada, [6]St. Joseph's Hospital, Canada

Purpose: To investigate the effect of Forteo ® (teriparatide) therapy on bone mineral density (BMD) and health-related quality of life (HRQL) during and up to 2 years after completion of teriparatide therapy.

Methods: We retrospectively reviewed consecutive osteoporosis patients treated with teriparatide in a Canadian rheumatology outpatient practice. We included patients that received teriparatide therapy with baseline and follow-up BMD results up to two years after completion of 18 or 24-month treatment. Patient information was reviewed via electronic medical system records (EMR). If EMR data was unavailable, paper copies of patient files were reviewed. Baseline information collected included age, gender, height and weight as well as BMD and Mini-Osteoporosis Quality of Life Questionnaire (OQLQ) data. Medications taken prior, during, and post-teriparatide therapy were also recorded. Repeated measures mixed-model analyses were used to compare baseline and follow-up measurements for BMD at the femoral neck, lumbar spine and total hip as well as each of the ten questions of the OQLQ questionnaire (five domains). The analyses were adjusted for sex and baseline age, height and weight.

Results: 167 patients were included in this study including 143 women. The baseline characteristics were: mean (standard deviation) age 65.1 (11.4) years, height 159.8 (9.1) centimeters and weight 63.0 (13.1) kilograms. Statistically significant improvement in BMD at the femoral neck, lumbar spine and total hip were demonstrated up to 2 years after teriparatide treatment (see table 1). Significant improvements were also observed at the second follow-up post-teriparatide treatment in the OQLQ domains of pain symptoms, emotional functioning and physical functioning (p < 0.05 for the first 6 questions) as well as a trend towards significance in the domains of activities of daily living and leisure.

Conclusion: This study demonstrates the efficacy of teriparatide treatment in osteoporosis patients to improve both BMD, particularly in the lumbar spine, and HRQL. Furthermore, these findings are suggestive of maintained improvement in BMD up to 2 years after completion of teriparatide therapy.

	Baseline (T-score)	1st follow-up Change in T-score From baseline	P-value*	3rd follow-up Change in T-score From baseline	P-value**
LS BMD	-2.79	0.75	<0.001	0.83	<0.001
FN BMD	-2.27	0.22	<0.001	0.22	0.029
Total hip BMD	-1.93	0.18	<0.001	0.25	0.002

*Between baseline and 1st follow-up ** Between baseline and 3rd follow-up

Table 1: BMD Comparisons to Baseline

Disclosures: Herman Bami, None.

MO0409

Differences in bone status between type 1 and type 2 diabetes mellitus patients. <u>Jakob Linde</u>*[1], <u>Søren Gregersen</u>[2], <u>Ellen Hauge</u>[1], <u>Bente Langdahl</u>[3], <u>Peter Vestergaard</u>[4]. [1]Aarhus University Hospital, Denmark, [2]Aarhus University Hospital, Denmark, [3]Aarhus University Hospital, Dnk, [4]Aalborg University Hospital, Denmark

Background: Diabetes Mellitus are associated with an increased fracture risk and underestimation of fracture risk by common predictors.

Aim: To investigate whether bone status differs between type 1 diabetes mellitus (T1D) and type 2 diabetes mellitus patients (T2D).

Methods: Ongoing cross-sectional study. Diabetes patients were consecutively recruited from diabetes outpatient clinics at Aarhus University Hospital and Aalborg University Hospital. Diabetes was diagnosed according to international guidelines. Only patients aged 50 years or more, with a recent eGFR ⩾50 mL/min, and HbA1c ⩾ 49 mmol/mol during the last six months were included. Unpaired t-test and multiple linear regression were used. Included patients were evaluated using hip, spine and forearm DXA (Hologic™ (n=112) and Lunar™ (n=14)), and a subset evaluated at forearm and ankle by HRpQCT (Scanco™) (n=112). Patients suffering from conditions and/or using medications affecting bone metabolism were excluded.

Results: 126 diabetes patients (60 T1D, 66 T2D) were included. T2D were older (mean difference: 4.54 years, P<0.01) and had a larger body mass index (BMI) (mean difference: 5.04 kg/m^2, P<0.01) than T1D. No gender differences were apparent (P=0.78). Hip T-score was -0.45 (p=0.03) lower among T1D. Spine and radius T-score did not differ between T1D and T2D (p=0.10 and 0.39, respectively).

Neither cortical nor trabecular parameters evaluated by HRpQCT differed between T1D and T2D, although the tibial cortical area tended to be lower among T1D (P=0.07).

Multiple linear regression revealed that diabetes type did not influence hip (P=0.21), spine (P=0.54), and radius (P=0.33) T-score or tibial cortical area (P=0.01) significantly after adjustment for BMI, age and gender.

Conclusion: Bone structure did not differ between T1D and T2D when evaluated by DXA and HRpQCT scans. Although T1D and T2D differ in etiology, treatment and other characteristics, these findings support that T1D and T2D share the same structural characteristics in regard of bone status and possible bone fragility.

Disclosures: Jakob Linde, None.

MO0410

FRAX Underestimates Fracture Risk in Patients with Type 1 Diabetes Mellitus. <u>Tayyab Khan</u>*[1], <u>Tamara Spaic</u>[2], <u>Lisa-Ann Fraser</u>[3]. [1]Department of Medicine, Western University, Canada, [2]Western University, Canada, [3]Western University, Canada

Individuals with type 1 diabetes (DM1) have over a 6-fold increased risk of sustaining a hip fracture compared to the general population. The WHO Fracture Risk Assessment Tool (FRAX) incorporates DM1 into its fracture risk assessment by including it as a cause of "secondary osteoporosis". We aimed to assess how well FRAX identifies fracture risk in a real-world population of patients with DM1.

We studied bone health in a sequential population of patients with known DM1 being followed by Endocrinologists at an academic centre. Patients filled out a bone health questionnaire which was used to up-date their electronic medical record (EMR). De-identified data was extracted from the EMR for all patients with DM1 over age 40. Fracture risk scores were calculated using FRAX (without BMD).The study was approved by the local Research Ethics Board.

There were 201 individuals with DM1 identified, with mean age of 53.9 years (40-82). Prior fracture was reported by 29.9% of patients, and 19.9% of these were confirmed fragility fractures (defined as a fall from standing height or less). Despite this, only 25 patients (12.4%) were identified as "high risk" for future fracture by their calculated FRAX score (>20% risk of major osteoporotic fracture or >3% risk of hip fracture over the next 10 years), and 19 (9.5%) were in the "moderate risk" category (10-20% risk). Out of the 40 patients who had sustained at least one fragility fracture, 15 (37.5%) were at "high risk" and 10 (25%) were at "moderate risk" of fracture according to their FRAX score.

We found that FRAX systematically underestimated fracture risk in a population of patients with DM1. The pathogenesis of the increased bone fragility caused by DM1 is thought to be multifactorial and complex. Our results suggest that this risk is not adequately accounted for by the FRAX tool, and highlights the limitations of using conventional fracture assessment tools in the diabetic population.

Disclosures: Tayyab Khan, None.

MO0411

Young and middle aged male with type 1 diabetes have lower vBMD and strength in femoral bone and have aging structure of the femoral neck assessed by Quantitative CT. <u>Koji Ishikawa</u>*[1], <u>Takashi Nagai</u>[2], <u>Tomoyasu Fukui</u>[3], <u>Takuma Kuroda</u>[4], <u>Katsunori Inagaki</u>[4]. [1]Department of Orthopeadic Surgery, Showa University School of Medicine, Japan, [2]Department of Orthopeadic Surgery, Showa University School of Medicine, Japan, [3]Department of Internal Medicine, Division of Diabetes & Endocrinology, Showa University School of Medicine, Japan, [4]Department of Orthopeadic Surgery, Showa University School of Medicine, Japan

Several previous studies have reported osteoporosis measured by dual-energy X-ray absorptiometry (DXA) in younger patients with type 1 diabetes (T1D). DXA, however, is unsuitable for precise measurements of bone mineral density and strength because of the limitations of two-dimensional (2D) imaging. Our group used 3D quantitative computed tomography (QCT) to obtain more precise information about bone fragility in T1D. Seventeen male T1D patients aged from 19 to 48 years, and eighteen age-matched control males (C) were studied. Patients with diabetic nephropathy (proteinuria and eGFR<60) were excluded. In QCT measurements,

T1D patients had a significantly lower cortical volumetric bone mineral density (vBMD) in the femoral neck, significantly lower total vBMD and cortical cross-sectional area (CSA, an estimator of compression strength) in the inter-trochanter. Bone strength estimated by the bucking ratio (an index of cortical instability) of the inter-trochanter was significantly higher in T1D. We also measured QCT parameters (cortical thickness, cortical vBMD, trabecular vBMD, integral vBMD) in anatomic quadrants [supero-anterior (SA), infero-anterior (IA), infero-posterior (IP), supero-posterior (SP)] of the femoral neck to reveal the structure more precisely. In IA and IP area, there were not significant difference between T1D and controls. But T1D patients had significant lower cortical thickness in SP, and cortical BMD in SA. This quadrant data suggest that structure of the femoral neck in T1D was aging bone. Bone metabolic markers were also comparable between T1D and C. There were not significant difference between T1D and C. Biochemical measurements including IGF-1 were collected too. The IGF-1 values were significantly lower in T1D than in C (130 ± 35 vs 158 ± 34 mg/dl). Furthermore, IGF-1 values were positively correlated with the total vBMD of the neck and the serum bone formation markers (r=0.49~0.71, respectively) in T1D. Indeed, in quadrant, IGF-1 values were positively correlated with cortical thickness in SA, trabecular vBMD in SP, respectively.In conclusion, young and middle-aged T1D patients had cortical weakness of the femoral inter-trochanter lesions with lower vBMD. Moreover, there already exist more aging structures at the femoral neck in T1D. Perhaps more importantly, low IGF-1 might be a causative factor for skeletal abnormality in T1D.

Disclosures: Koji Ishikawa, None.

MO0412

Prospective study of bone loss after spinal cord injury (SCI). Role of osteocyte markers. <u>Laia Gifre</u>*[1], <u>Joan Vidal</u>[2], <u>Josep Lluís Carrasco</u>[3], <u>Xavier Filella</u>[4], <u>Silvia Ruiz-Gaspà</u>[5], <u>Enric Portell</u>[2], <u>Ana Monegal</u>[6], <u>Africa Muxi</u>[7], <u>Nuria Guanabens</u>[8], <u>Pilar Peris</u>[9]. [1]Hospital Clinic Barcelona, Spain, [2]Guttmann Neurorehabilitation Institute, Spain, [3]Public Health Department. University of Barcelona, Spain, [4]Department of Biochemistry & Molecular Genetics. Hospital Clinic, Spain, [5]CIBERehd. Hospital Clínic, Spain, [6]Hospital Clinic Barcelona, Spain, [7]Nuclear Medicine Department. Hospital Clínic, Spain, [8]Universitat De Barcelona, Spain, [9]Hospital Clínic of Barcelona, Spain

Background: SCI has been associated with a marked increase in bone loss and bone remodeling. The absence of mechanical load, probably mediated by osteocyte mechanosensory function, seems to be a determinant factor related to bone loss in this condition. However, the pathogenesis and clinical management of this process remains unclear.

Aim: To analyze the effect of recent SCI on osteocyte function and its relationship with bone turnover and bone mineral density (BMD) evolution.

Methods: We prospectively included 42 patients (40M:2F, aged 35 ± 14yrs) with a recent (<6months) complete SCI (ASIA A 39:B 3). Osteocyte markers (serum sclerostin, Dkk-1 and FGF23), bone turnover markers (bone formation: P1NP, bone ALP; resorption: sCTx) and BMD (lumbar spine, proximal femur, total body and lower extremities [DXA]) were assessed in all patients at baseline, and at 6 and 12 months. The results were compared with a healthy control group of similar age and sex.

Results: 22/42 patients completed the 12-month follow-up period. At baseline SCI patients showed a marked increase in bone markers (PINP and CTx) which remained significantly increased at up to 6 months of follow-up (Table). In addition, they presented significantly increased Dkk-1 values throughout the study (Table). Sclerostin or FGF23 values did not significantly change. BMD markedly decreased at the proximal femur (-13 ± 5% at 6 months, p<0.01; -20 ± 5% at 12 months, p<0.01), total body (p<0.01 at 6 months, p<0.01 at 12 months) and lower extremities (p<0.01 at 6 months, p<0.01 at 12 months), with no significant changes at the lumbar spine. As a result, 59% of patients developed densitometric osteoporosis at 12 months. Bone markers were negatively correlated with proximal femur BMD (bone ALP: r=-0.33, p<0.01; P1NP: r=-0.26, p<0.01, adjusted for age and BMI) with a decreasing negative association throughout the study period.

Conclusions: Marked bone loss associated with increased bone turnover and increased Dkk-1 serum levels is observed shortly after complete SCI. Maintenance of increased Dkk-1 levels throughout the study coinciding with continuous BMD loss further suggest a regulatory role of this osteocyte mediator in this process.

Parameters	Healthy controls	SCI at baseline	SCI at 6 months	SCI at 12 months
	Mean (CI, 95%)	Mean (CI, 95%)	Mean (CI, 95%)	Mean (CI, 95%)
Dkk-1 (pmol/l)	39.7 (35.2 – 44.7)	59.0 * (53.1 – 65.6)	58.9 * (51.9 – 66.9)	56.7 * (48.9 – 65.7)
SOST (pmol/l)	35.1 (31.6 – 38.8)	39.7 (36.3 – 43.5)	39.2 (35.2 – 43.7)	36.23 (31.9 – 41.1)
FGF23 (RU/ml)	69.6 (56.9 – 85.1)	75.5 (62.3 – 91.4)	64.5 (52.3 – 79.6)	74.2 (58.1 – 94.8)
P1NP (ng/ml)	46.2 (37.3 – 57.3)	161.3 * (136.2 – 190.9)	98.3 *† (78.9 – 122.5)	69.2 † (53.4 – 89.6)
Bone ALP (ng/ml)	11.6 (10.0 – 13.4)	13.8 (12.3 – 15.5)	14.8 (12.9 – 16.9)	15.5 (13.3 – 18.2)
sCTx (ng/ml)	0.52 (0.35 – 0.68)	1.48 * (1.36 – 1.61)	0.85 *† (0.68 – 1.02)	0.70 † (0.5 – 0.89)

*p<0.05 compared to healthy controls
†p<0.05 compared to SCI at baseline

Bone turnover and osteocyte markers in control group and SCI patients throughout the study.

MO0413

Bone Turnover Markers and Different Dialysis Procedures.

Vladimir Palicka*[1], Sylvie Dusilova Sulkova[2], Magdalena Holeckova[2], Roman Safranek[2], Ladislava Pavlikova[2]. [1]Fakultni Nemocnice, Czech Republic, [2]Charles University, University Hospital, Czech Republic

Introduction: The role of P1NP and CTx in patients with ESRD and dialysis is not well established. Data comparing hemodialysis (HD) with on-line hemodiafiltration (HDF) are lacking. We aimed (1) to assess the relation between bone turnover markers and traditional markers of CKD-MBD in dialysis patients and (2) to compare effect of HD and HDF on serum concentrations of P1NP and CTx.

Methods: 96 clinically stable dialysis patients were studied. Regime has been stable for at least three previous months, using dialysate calcium 6 mg/dL. 54 patients were on high-volume on-line HDF; 42 patients were treated by conventional HD. Serum Ca, P, B-ALP, 25-hydroxyvitamin D, 1-84 PTH, CTx and P1NP were measured before and after single HD or HDF procedure. Results are expressed as median (interquartile range); p value < 0.05 was considered statistically significant.

Results: Only twelve patients had pre-dialysis B-ALP above the reference range for given age and sex, while P1NP was elevated in 92 patients and CTx in 94 patients, indicating a possibility of retention of P1NP and CTx in serum due to kidney failure. However, significant correlation between serum B-ALP (15.6; 10.9-23.1) and P1NP (323; 189-441) was found (r = 0.492; p<0.001). Similarly, CTx (2.05; 1.6-2.47) significantly correlated with B-ALP (r = 0.470; p<0.001) and 1-84PTH (18; 11.2-26.7) correlated with P1NP (r = 0.415, p<0.001) as well as with CTx (r = 0.420; p<0.001). All these correlations indicate that P1NP and CTx reflect bone turnover in dialysis patients.

Both dialysis procedures influenced P1NP and CTx differently. Conventional HD did not change either P1NP or CTx. HDF, on the contrary, decreased CTx by 80% (from 2.26; 1.99-2.85 to 0.53; 0.33-0.70), p<0.001 and P1NP by 32% (from 395; 255-509 to 288; 168-396), p<0.001. Serum Ca and P levels did not differ between HD and HDF procedures. Serum 25-D did not correlate with any of the bone turnover markers.

Conclusion: Serum CTx and P1NP are markedly elevated in dialysis patients, which may reflect not only the missing renal elimination, but also their high bone turnover. Different elimination strategies may be associated with procedure-dependent acute changes in bone turnover indicators. As there was no pre-dialysis difference in P1NP and CTx between HD and HDF patients, the effect of HDF is probably only temporary. However, the long-term consequences of these findings deserve further studies.

MO0414

Increased marrow adipose tissue following Spinal Cord Injury.

Tiffiny Butler*[1], Thomas Schnitzer[2], William Edwards[3], Karen Troy[1]. [1]Worcester Polytechnic Institute, USA, [2]Northwestern University, USA, [3]University of Calgary, Canada

Spinal cord injury (SCI) all but eliminates loading from the paralyzed regions, resulting in rapid loss of both bone and muscle mass. Suboptimal loading from decreased muscle mass may alter the muscle-bone crosstalk resulting in increased medullary adiposity and decreased bone mass. Marrow adipose tissue (MAT) negatively regulates bone formation and may play a synergistic endocrine related role in the loss of bone following SCI. However, the exact function of MAT and its effect on other diseases is not well understood.

Our purpose was to determine factors related to tibial MAT accumulation following spinal cord injury in acute and chronic SCI subjects. We previously exploited clinical CT data to quantify visceral and intermuscular adipose tissue in the torso. Here, we established a similar technique to quantify MAT using quantitative CT. Computed tomography (CT) data of the proximal 15 mm of the non-dominant tibia were acquired on 49 subjects with acute (13 subjects) and chronic (36 subjects) SCI (41 male), age 22-65 years, duration of injury of 0–42.5 years. A calibration phantom with known hydroxyapetite concentrations was included in each scan and was used to establish a linear relationship between Hounsfield units (Hu) and tissue mineral density. Quantitative image analysis was performed to determine integral BMD (g/cm3) and MAT volume, defined as voxels within the periosteal envelope having Hu [-205 to -50]. Pearson's correlations were used to determine relationships between MAT volume (cm^3) and: BMD, duration of injury (years), age (years) and body mass (kg).

MAT volume was 31.1 ± 23.9 cm3 for all subjects combined, 8.7 ± 6.9 cm3 for acute subjects and 38.3 ± 22.9 cm3 for chronic subjects. MAT showed an inverse relationship with BMD (r=-0.734, p<0.001) and increased with duration of SCI (r =0.51, p<0.001; Figure 1) but not with age (r=0.13, p=0.42) or body mass (r= -0.02, p=0.89).

Although few studies have investigated changes in long bone MAT in individuals with SCI, others have linked increased marrow adiposity with decreased bone mineral density and cortical bone area. MAT and osteoblasts share common precursors, and low magnitude mechanical vibration has been shown to inhibit adipogenesis in mice. Similarly, resistance exercises and whole body vibration have been shown to prevent increases in vertebral marrow fat during prolonged bed rest. Further study of MAT in SCI patients may lead to improved understanding of the role MAT plays in bone health.
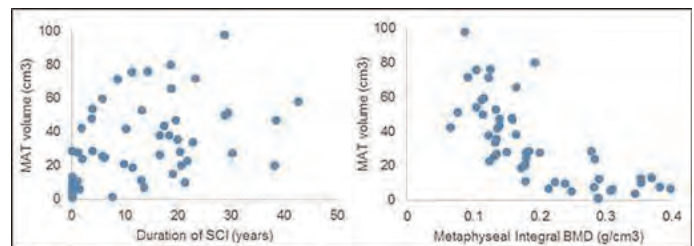

Figure 1: (a) MAT volume versus duration of spinal cord injury. (b) MAT volume versus integral BMD

MO0415

Proximal Femur Strength and Cortical Thickness Estimates in Klinefelter Syndrome and Post-Menopausal Women.

Enrico Schileo*[1], Ilaria Palmadori[2], Fulvia Taddei[3], Alessandro Coran[4], Sigurur Sigursson[5], Vilmundur Gudnason[6], Tamara Harris[7], Carlo Foresta[4]. [1]Istituto Ortopedico Rizzoli, Bologna, Italy, Italy, [2]Istituto Ortopedico Rizzoli, Italy, [3]Istituto Ortopedico Rizzoli, Italy, [4]Università di Padova, Italy, [5]Icelandic Heart Association, Iceland, [6]Icelandic Heart Association Research Institute, Iceland, [7]Intramural Research Program, National Institute on Aging, USA

The structural basis of the reported low bone mass in Klinefelter Syndrome patients (KS), and its consequences on bone strength are poorly understood.

In a very recent HRpQCT study KS exhibited, at the distal tibia (load-bearing bone), compromised bone microstructure and strength, suggesting an analogy with aging women [1].

The aim of the present QCT study was to test if proximal femur strength and bone structure of KS patients and post-menopausal women are actually similar.

Methods

QCT-based Finite Element estimates of proximal femur strength (FE-strength) were obtained for: KS patients (n= 18, aged 44 ± 8), post-menopausal women (n=83, aged 76 ± 6, composed of VPHOP (n=12) and Ages (n=71) cohorts), and aging men (Ages, n=39, aged 79 ± 5).

FE-strength was calculated with a validated procedure [2], retaining the minimum strength among a range of plausible fall directions.

In KS and VPHOP women cohort, cortical density (Ct.D) and cortical thickness (Ct.Th.) were estimated [3]. In the superior aspect of the femoral neck (i.e. the most critical as from FE results) Ct.Th. was further mapped to nine regions (cross-combinations of head-neck junction, mid-neck, trochanteric fossa levels in anterior, central, and posterior sectors).

Results

The FE-strength of KS and women was similar (KS: 2981 ± 514 N; Women: 2822 ± 627 N, % diff. < 3%, not significant, Mann-Whitney p = 0.29).

Conversely, the FE-strength of older men (4176 ± 985 N) was significantly higher compared to KS (p < 0.001), and, as expected, to similarly aged women (p < 0.001).

The women for whom CT.D and Ct.Th. were analyzed did not differ in FE-strength (2710 ± 386 N, p=0.11) from KS.

Cortical density was equivalent (p=0.38) in KS (1.128 ± 0.055 g/cm^3) and women (1.146 ± 0.054 g/cm^3).

Bone cortex was instead significantly thinner in KS [Figure], reaching a three-fold thinning in the posterior and central sectors of the head-neck junction, a site of fracture-related cortical thinning traits [4].
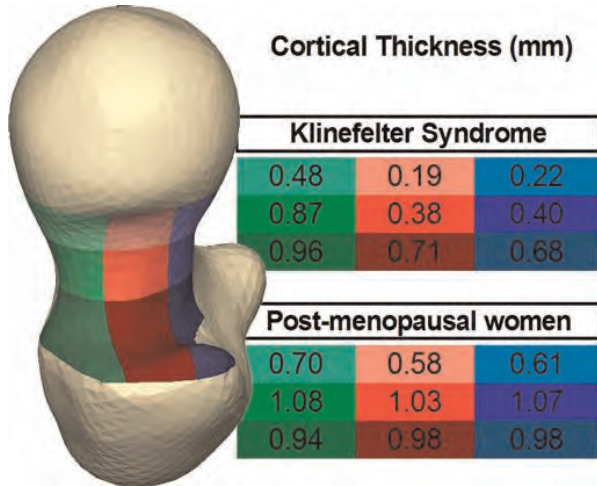
Discussion

We confirmed, for proximal femur strength, the analogy between KS and post-menopausal women. This analogy was not reflected in bone structure, being Ct.Th. much thinner in KS. This low Ct.Th. could be a starting point to explain compromised bone strength, in future studies on larger cohorts, including trabecular and metabolic parameters.

Shanbhogue et al., JBMR doi:10.1002/jbmr.2272
Schileo et al, J Biomech 2008:356-67
Treece et al., Med Image Anal. 2012;16:952-65
Poole et al., PLoS One. 2012;7(6):e38466

Bone cortex in the superior aspect of the femoral neck is thinner in KS patients compared to women

Disclosures: Enrico Schileo, None.

MO0416

The relationship between sclerostin, bone mineral density and vascular calcification in rheumatoid arthritis. <u>Julien Paccou</u>*[1], <u>Cedric Renard</u>[2], <u>Sophie Liabeuf</u>[2], <u>Said Kamel</u>[2], <u>Patrice Fardellone</u>[3], <u>Ziad Massy</u>[2], <u>Michel Brazier</u>[4], <u>Romuald Mentaverri</u>[5]. [1]University of Picardie Jules Verne, Amiens, France, [2]Amiens University Hospital, France, [3]Service de rhumatologie, CHU Hôpital Nord, France, [4]University of Picardie, France, [5]INSERM U1088, France

Introduction

Recent data indicate that serum sclerostin could be involved in vascular calcification (VC). The present study tested the hypothesis that serum sclerostin levels are associated with VC in patients with rheumatoid arthritis (RA) and control subjects matched for age and gender.

Methods

In this cross-sectional study, 75 RA patients were compared to 75 control subjects matched for age and gender. Demographic and clinical characteristics, bone mineral density (BMD) measured by DXA, cardiovascular risk factors and serum sclerostin (ELISA) were assessed. Coronary artery calcium (CAC) and abdominal aortic calcification (AAC) scores were evaluated by computed tomography in patients free of clinical evidence of coronary artery disease. Analyses were performed to identify determinants of serum sclerostin and VC.

Results

Coronary artery calcification was more prevalent in patients with RA (65.3%) than in controls (49.3%) (p=.04). The mean CAC score was 197 ± 470 in patients with RA and 109 ± 297 in controls (p=.07). However, AAC was also more prevalent in patients with RA (71.2%) than in controls (54.7%) (p=.04). The mean AAC score was 1.0 ± 1.3 in patients with RA and 0.7 ± 1.4 in controls (p=.02). Higher AAC scores (P=.02) and higher lumbar BMD (P=.03) were identified as independent determinants of higher serum sclerostin levels in RA patients, whereas male gender (P=.03), higher lumbar BMD (P<.0001) and low estimated glomerular rate (eGFR) (P<.001) were identified in controls. In RA patients, multivariate logistic regression analysis identified older age (OR per year of 1.10 [1.03-1.18]; P<.01) and male gender (OR=6.79 [1.33-34.62]; P=.02) as independent determinants of CAC, and older age (OR=1.16 [1.07-1.27]; P<.001) as an independent determinant of AAC. For controls, independent determinants were older age (OR=1.19 [1.06-1.35]; P<.01), hypertension (OR=7.31 [1.98-26.96]; P<.01) and lumbar BMD (OR per 30 mg/cm2 of 1.14 [1.01-1.29]; P=.03) for CAC and older age (OR=1.11 [1.02-1.20]; P=.01) for AAC.

Conclusion

Circulating sclerostin was significantly and independently associated with AAC in RA patients.

Disclosures: Julien Paccou, None.

MO0417

Adverse Changes in Bone Mineral Density and FRAX Score 100 Days Post Allogeneic Bone Marrow Transplant. <u>Monika Pawlowska</u>*[1], <u>Basia Pajerski</u>[2], <u>Qun Yang</u>[3], <u>Indy Sekhon</u>[2], <u>David Kendler</u>[4], <u>Raewyn Broady</u>[5]. [1], Canada, [2]University of British Columbia, Canada, [3]Prohealth Clinic Research, Canada, [4]Associate Professor University of British Columbia, Canada, [5]Clinical Associate Professor University of British Columbia, Canada

Purpose: Bone loss following allogeneic bone marrow transplant (allo-BMT) is a common complication and is multifactorial. Previous studies have demonstrated bone loss occuring 6 months after allo-BMT but few studies address earlier changes in bone mineral density (BMD). Furthermore, there are no data quantifying the impact of changes in BMD on fracture risk as calculated by FRAX. Determining BMD and performing a fracture risk assessment at baseline and 100 days after allo- BMT could identify patients with rapid bone loss and allow for early therapeutic intervention.

Methods: Patients who underwent allo-BMT (2011-2013) and had BMD testing before and 100 days post BMT were analyzed. FRAX risk factors were prospectively determined and a FRAX score was calculated at baseline and day 100.

Results: 98 patients (59 males, 39 females), mean age 49, were included. A BMD decline of 3% or more, the least significant change on many DXA instruments, was seen in 46 patients at the lumbar spine, 56 at total hip, and 55 at femoral neck at 100 days post transplant. The mean decline in lumbar spine, total hip, and femoral neck BMD was 3.27%, 4.43%, and 4.53%, respectively (P < 0.001 for all). Following transplant, 47 patients had long-term, high dose glucocorticoid exposure. The mean FRAX 10 year risk of major osteoporotic fracture was 4.2% at baseline, and 5.7 % at 100 days (p < 0.001). This represents a 1.5% increase in 10 year fracture risk over 100 days. The mean 10 year risk of hip fracture was 0.5% at baseline, and 0.8% at 100 days (p< 0.001), for a 0.3% increase in risk. Prior to BMT, 4 patients met the North American menopause society criteria for osteoporosis pharmacotherapy and at 100days, 9 patients met this threshold; 2 of whom sustained vertebral fractures during this time.

Discussion: Allo-BMT recipients have a rapid, and statistically significant, decline in hip and spine BMD, even in the first 100 days post transplant. These changes in BMD, and frequent high dose glucocorticoid use post transplant, confer a significant rise in fracture risk. Although FRAX has not been validated previously in the post transplant population, femoral neck BMD and steroid exposure are important components of risk assessment using this tool, and in this cohort, the main contributors to the significant increase in 10 year fracture risk. This new information strengthens the argument for preventive strategies to reduce bone loss subsequent to BMT.

Disclosures: Monika Pawlowska, None.

MO0418

BMD Changes after Kidney Transplantation. <u>Nicolas Segaud</u>[1], <u>Isabelle Legroux</u>[2], <u>Marc Hazzan</u>[3], <u>Christian Noel</u>[3], <u>Bernard Cortet</u>*[4]. [1]Service de Rhumatologie, France, [2]Service de Rhumatologie, France, [3]Service de Néphrologie, France, [4]Service de Rhumatologie, France

Introduction: Renal transplant patients may have bone loss related to the drugs taken but also to their past history of chronic kidney disease. The objective of the present work was to study changes in BMD 2 years after the first assessment.

Methods: This longitudinal study included patients who underwent renal transplantation realized between 2005 and 2011 and followed at the University-Hospital of Lille. Patients were included if they had a first bone evaluation (including bone densitometry, spine X-rays and biological assessment) and at least another BMD assessment. The first assessment was done on average 9 months after transplantation and 2 years later.

Results: 259 patients satisfied to the inclusion criteria, (96 women) with a mean age of 49.7 ± 12.1 years at transplantation. The mean duration of dialysis was 3.2 ± 3.3 years. 75 patients (29.0%) withdrew corticosteroid 7 days after transplantation without new introduction during follow-up. Vertebral fractures were found in 28 patients (10.8%). According to the WHO classification, 101 patients had osteoporosis and 125 had osteopenia at the first evaluation (at least at one site). Osteoporosis treatment with bisphosphonates (alendronate or risedronate) was initiated for 95 patients. In all patients, BMD gains compared with baseline were significant : $3.9 \pm 6.6\%$, 2.6 ± 7.6, $3.0 \pm 7.2\%$ at the lumbar spine, femoral neck and the total hip respectively (p <0.0001). The gains were significant for patients treated with bisphosphonates compared with baseline: 5.0% respectively (p <0.0001), 2.5% (p = 0.012) and 2.7% (p = 0.004) at the lumbar spine, femoral neck and total hip respectively. BMD gains were higher for patients treated by bisphosphonates for all the sites (p<0.015) than for patients without bisphosphonates. There was no difference in terms of BMD gains between alendronate and risedronate (p = 0.457). The patients who withdrew corticosteroids early had higher gains in BMD than patients with more prolonged corticosteroid therapy: difference between groups for the overall population = 2.1% for the lumbar spine (p = 0.019) and 2.0% for the total hip (p = 0.044). The stepwise regression analysis (patients without bisphosphonates) showed associations between BMD changes (femoral neck) and the duration of corticosteroid therapy, the level of bone alkaline phosphatase at baseline, the lack of vertebral fracture. No correlation was found between the change in BMD and the duration of dialysis or renal function.

Conclusion: Kidney transplant recipients have a pre-existing increased bone fragility. Bisphosphonates and early corticosteroid withdrawal can improve BMD.

Disclosures: Bernard Cortet, None.

MO0419

Bone Quality at the Time of Lung Transplant in Cystic Fibrosis. <u>Louis-Georges Ste-Marie</u>*[1], <u>Natalie Dion</u>[1], <u>Pasquale Ferraro</u>[2], <u>Caroline Albert</u>[3], <u>Nathalie Bureau</u>[2], <u>Audray Fortin</u>[2], <u>Valérie Jomphe</u>[2], <u>Larry Lands</u>[4], <u>Genevieve Mailhot</u>[5]. [1]CHUM, University of Montreal, Canada, [2]CHUM, University of Montreal, Canada, [3]CHUM, Canada, [4]MUCH, McGill University, Canada, [5]Research Center CHU Sainte-JustineUniversity of Montreal, Canada

In the past 20 years, cystic fibrosis patients (CF) have dramatically extended their survival due to advances in care. As CF get older, age-related complications such as fragility fractures, known to seriously undermine their quality of life, have emerged. Despite its high prevalence, pathogenesis of CF-related bone disease remains poorly understood and predicting individuals at increased risk of fracture is still difficult. Bone strength is determined by bone quantity and quality. Knowing that bone mineral density (BMD) is a poor predictor of fractures in CF, it is reasonable to postulate that alterations in bone quality will likely contribute to their propensity to fracture. In order to assess bone quality in CF, a 2 cm segment of rib was recovered during lung transplantation. For the control group, a rib sample has been taken from simlarly aged lung donors without chronic diseases (D). To date, 25 specimens were collected [12 CF: 28 $\pm$8yo and 13 D: 34 $\pm$11yo; p=0.14] which exclude CF under bisphosphonate treatment. These specimens were analysed with various techniques to evaluate: BMD by DXA, microstructure by micro-CT, bone remodelling by histomorphometry and quality of bone strength by calcein staining of microcracks. *Ex vivo* rib BMD tended to be lowered in CF compared to D (CF: 0.16 $\pm$0.05 vs D: 0.19 $\pm$0.03g/cm^2; p=0.08) as well as cortical tissue mineral density measured by micro-CT (CF: 0.84 $\pm$0.09 vs D: 0.93$\pm$0.16g HA/cm^3; p=0.12). Interestingly, trabecular BMD determined by micro-CT was significantly lower in CF than in D (CF: 0.06 $\pm$0.5 vs D: 0.11 $\pm$0.06g HA/cm^3; p=0.03). As shown in Table I, no major differences in microstructural indices (by micro-CT and by histomorphometry) were found between CF and D. Compared to D, osteoid parameters, OV/BV and OS/BS, tended to be lowered in CF whereas mean osteoid thickness was significantly reduced. Eroded surfaces were significantly decreased in CF than in D. Presence of microcraks in trabecular bone (Cr.D) was four times higher in CF than in D (p=0.009). These preliminary results suggest a possible decrease in bone remodeling in CF (both formation and resorption),which could contribute to the accumulation of micro-damage leading to the weakening of bone strength. This exploratory study confirmed the use of rib specimens as a precious tool to assess bone quality and ultimately, to better understand fracture risk in end-stage CF patients.

Table I	CF	D	
Micro-CT	(n=12)	(n=13)	*p* Value (t-test)
BV/TV (%)	9.9 ±3.2	11.6 ±4.1	0.28
Tb.Th (µm)	144 ±19	147 ±18.1	0.77*
Tb.N (per mm)	0.70 ±0.21	0.78 ±0.24	0.37
Tb.Sp (µm)	871 ±210	817 ±200	0.52
SMI	1.5 ±0.5	1.3 ±0.4	0.52
Conn.D (per mm^3)	5.5 ±4.2	6.8 ±5.4	0.38*
Ct.Th (µm)	408 ±143	398 ±98	0.84
Histomorphometry	(n=9)	(n=6)	*p* Value (t-test)
BV/TV (%)	8.0 ±3.2	11.3 ±4.2	0.11
Tb.Th (µm)	69.1 ±9.6	84.8 ±10.7	0.01
Tb.N (per mm)	1.1 ±0.3	1.4 ±0.5	0.19
Tb.Sp (µm)	891 ±352	702 ±307	0.31
OV/BV	1.1 ±0.81	2.6 ±2.6	0.12
OS/BS	5.1 ±3.4	12.1 ±11.2	0.09
O.Th	6.1 ±0.9	7.7 ±1.5	0.03
ES/BS	4.5 ±1.9	8.1 ±3.5	0.03
Cr.D (#/mm^2)	0.52 ±0.26	0.13 ±0.21	0.009
Values are expressed as mean ±SD. * non-parametric Mann-Withney test			

Table I

Disclosures: Louis-Georges Ste-Marie, Novartis, 10; Eli Lilly, 3; Merck, 10; Eli Lilly, 10; Novartis, 7; Alliance for better bone health, 10; Amgen, 7; Eli Lilly, 7; Alliance for better bone health (Warner Chilcott and Sanofi Aventis Canada inc), 3; Novartis, 3; Merck, 3; Alliance for better bone health, 7; Amgen, 10; Amgen, 3; Sanofi, 3

MO0420

Effect of Risedronate on Bone Mineral Density and Trabecular Bone Score in Liver Postransplantation patients after one year of follow-up. <u>Gonzalo Allo Miguel</u>[1], <u>María Soledad Librizzi</u>[2], <u>Sonsoles Guadalix Iglesias</u>[1], <u>David Lora</u>[3], <u>Guillermo Martinez Diaz-Guerra</u>[4], <u>Federico Hawkins</u>*[5]. [1]12 de Octubre, University Hospital., Spain, [2]12 de Octubre, University Hospital, Spain, [3]Clinical Epidemiology Unit, 12 de Octubre University Hospital., Spain, [4]University Hospital 12 Octubre, Esp, [5]Hospital Universitario, Spain

Introduction: Patients with organ transplantion have higher risk of osteoporosis and related fractures. Aminobisphosphonates are the mainstay of anti-resorptive treatment for them.Risedronate (RIS) seems to have an early and positive effect, reducing these complications. In addition to bone loss, bone quality alterations are involved in bone strength and could be assessed by the trabecular bone score (TBS).
Aim: Evaluate the effect of RIS (35 mg/weekly) on TBS and BMD in patients with liver transplantation, during one year follow-up.
Material and methods: 81 patients with liver transplantation and low BMD at baseline were randomized to RIS plus calcium and vitamin D (RIS group) vs. calcium and vitamin D (control group, CON) and followed over 1 year. LS and FN DXA (Hologic Discovery W) was perfomed at baseline, 6 and 12 months. Site matched LS TBS data was obtained using TBS iNsight 2.0 software (Medimaps, Swiss). Serum PTHi, 25(OH)D, β-CTX and P1NP were determined at baseline, 6 and 12 months. Bivariate comparisons were performed using Student's *t* test and Pearson's X^2 analysis for continuous variables.
Results: 62/19 (male/female) patients were randomized in two groups (RIS and CON). Baseline characteristics (mean$\pm$SD) were similar between groups in age (56.04$\pm$8.41), IMC (24.96$\pm$4.41), TBS (1.29$\pm$0.12), except in LS T-score (RIS -2.57$\pm$0.87; CON -2.13 $\pm$0.73, p=0.016). TBS was low in both groups at baseline (RIS 1.29$\pm$0.12; CON 1.30$\pm$0.12, p=0.84), 6 months (RIS 1.27$\pm$0.13; CON 1.30$\pm$0.10, p=0.75) and 12 months (RIS 1.27$\pm$0.11; CON 1.29$\pm$0,12, p=0.98). LS BMD increased in both groups at 12 months vs. baseline; RIS: +4.81$\pm$8,81%; CON +3,35$\pm$5,76% (p=0.385).There were no significant differences between groups in BMD at any site at 6 or 12 months. No correlations were found between BMD and TBS values, at any follow-up time point. No significant differences were found between patients with (n=6) or without vertebral fractures in their TBS values. A positive correlation (r=0.34; p=0.009) was found between β-CTX and TBS at 6 months. No correlations were found between TBS and age, sex, PTHi, 25 (OH)D and P1NP.
Conclusions: After 12 months of treatment, BMD improved at LS in both groups. We found persistently low TBS values during the follow-up, in both groups, without significant changes after RIS treatment. Our results point towards 1 year of immunosuppressive therapy does not induce bone microarchitecture degradation in liver transplant patients.

Disclosures: Federico Hawkins, None.

MO0421

Inkjet-based biopatterning of SDF-1β augments BMP-2-induced repair of critical size mouse calvarial defects. <u>James Cray</u>*[1], <u>Samuel Herberg</u>[2], <u>Galina Kondrikova</u>[3], <u>Sudharsan Periyasamy-Thandavan</u>[4], <u>R. Nicole Howie</u>[3], <u>Mohammed Elsalanty</u>[5], <u>Lee Weiss</u>[6], <u>Phil Campbell</u>[7], <u>William Hill</u>[8]. [1]Medical University of South Carolina, USA, [2]Case Western Reserve University, USA, [3]Georgia Regents University, USA, [4]Georgia Regents University & Charlie Norwood VAMC, USA, [5]Georgia Regents University, USA, [6]Carnegie Mellon University, USA, [7]Carnegie Mellon University, USA, [8]Georgia Regents University & Charlie Norwood VAMC, USA

Purpose: A major problem in craniofacial surgery is non-healing bone defects. Autologous reconstruction remains the standard of care in the treatment of these cases, however bone morphogenetic protein-2 (BMP-2) therapy has proven its clinical utility, although non-targeted adverse events occur due to the high milligram-level BMP-2 doses used. Ongoing efforts explore the use of different growth factors, cytokines, or chemokines as well as co-therapy strategies to augment healing.
Methods: Here we utilize inkjet-based biopatterning technology to controllably load acellular DermaMatrix delivery matrices with nanogram-level doses of BMP-2, stromal cell-derived factor-1β (SDF-1β), transforming growth factor-β1 (TGF-β1), or co-therapies thereof. We tested the hypothesis that bioprinted SDF-1β co-delivery enhances BMP-2- and TGF-β1-driven osteogenesis both *in vitro* and *in vivo* using a mouse calvarial critical size defect (CSD) model.
Results: Our data showed that BMP-2 bioprinted in low-doses induced significant new bone formation by four weeks post-operation. TGF-β1 was less effective compared to BMP-2, and SDF-1β therapy did not enhance osteogenesis above vehicle control levels. Co-delivery of BMP-2 + SDF-1β was shown to augment BMP-2-induced bone formation compared to BMP-2 alone. In contrast, co-delivery of TGF-β1 + SDF-1β decreased bone healing compared to TGF-β1 alone. This was further confirmed *in vitro* by osteogenic differentiation studies using MC3T3-E1 pre-osteoblasts.
Conclusions: Our data indicates that delivery of a low-dose growth factor therapy based on biopatterning technology can aid in healing CSD injuries. SDF-1β augments

the ability for BMP-2 to drive healing, a result confirmed *in vivo* and *in vitro*; however, because SDF-1β is detrimental to TGF-β1-driven osteogenesis, its' effect on osteogenesis is not universal. We are continuing work specifically investigating dose and delivery technologies within this paradigm.

Disclosures: James Cray*, None.*

MO0422

CXCL8 and CCL20 Enhance Osteoblast-Mediated Osteoclastogenesis.

Janak L Pathak[1], Astrid D Bakker[2], Patrick Verschueren[3], Willem F Lems[4], Frank P Luyten[3], Jenneke Klein-Nulend*[5], Nathalie Bravenboer[6]. [1]Department of Oral Cell Biology, Academic Centre for Dentistry Amsterdam (ACTA), University of Amsterdam & VU University Amsterdam, MOVE Research Institute Amsterdam, Netherlands, [2]Department of Oral Cell Biology, Academic Centre for Dentistry Amsterdam (ACTA), University of Amsterdam & VU University Amsterdam, Netherlands, [3]Skeletal Biology & Engineering Research Center, KU Leuven, Belgium, [4]Department of Rheumatology, VU University Medical Center, MOVE Research Institute Amsterdam, Netherlands, [5]ACTA-VU University AmsterdamDept Oral Cell Biology (Rm # 11N-63), The Netherlands, [6]VU University Medical Center, The Netherlands

Introduction: Osteoporosis is common in rheumatoid arthritis. CXCL8 and CCL20 are chemokines, which are produced by inflammatory cells around the inflamed joints in rheumatoid arthritis, and which are found at elevated levels in synovial fluid and serum. Since osteoblasts express receptors for CXCL8 and CCL20 we hypothesized that CXCL8 and CCL20 contribute to osteoporosis in rheumatoid arthritis by affecting osteoblast proliferation, differentiation, and osteoblast-osteoclast communication. The purpose of this study was to indicate a role for the chemokines CXCL8 and CCL20 in osteoclastogenesis through their effect on osteoblasts.

Methods: Primary human osteoblasts were cultured in the presence or absence of CXCL8 (2-200 pg/ml) or CCL20 (5-500 pg/ml) for 14 days. Osteoblast proliferation and differentiation were analyzed, as well as cytokine gene expression. IL-6 protein production was quantified by ELISA. Human peripheral blood mononuclear cells were cultured with conditioned medium (CM) from CXCL8 and CCL20-treated osteoblasts in the presence or absence of IL-6 inhibitor for 21 days. The number of tartrate-resistant acid phosphatase-positive osteoclasts was counted, and osteoclast activity was determined by the resorption pit assay.

Results: CXCL8 (200 pg/ml) enhanced mRNA expression of Ki-67 up to 2.7-fold, alkaline phosphatase by 1.7-fold, and IL-6 protein production by 1.2-fold in osteoblasts. CXCL8-CM enhanced the number of osteoclasts by 1.7-fold (3-5 nuclei), and 3.0-fold (>5 nuclei) (Fig. 1A). IL-6 inhibition reduced these osteoclast numbers by ~40% (Fig. 1A). CCL20 (500 pg/ml) enhanced mRNA expression of Ki-67 up to 2.5-fold, alkaline phosphatase by 1.6-fold, and IL-6 protein production by 1.3-fold in osteoblasts. CCL20-CM enhanced the number of osteoclasts by 1.3-fold (3-5 nuclei), and 2.8-fold (>5 nuclei), while IL-6 inhibition reduced these osteoclast numbers by ~30% (Fig. 1B). CCL20-CM increased osteoclast activity by 2.2-fold (Fig. 2). Neither CXCL8 nor CCL20 directly affected osteoclastogenesis.

Conclusion: CXCL8 and CCL20 did not negatively affect osteoblast proliferation or differentiation. However, both CXCL8 and CLC20 enhanced osteoblast-mediated osteoclastogenesis, partly via stimulation of IL-6 production, suggesting that CXCL8 and CCL20 contribute to localized and generalized osteoporosis in rheumatoid arthritis.
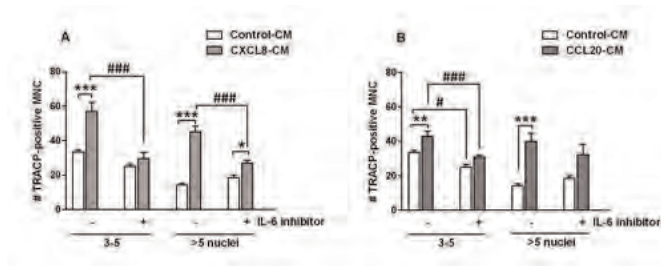
CXCL8-CM and CCL20-CM enhanced osteoclastogenesis, and inhibition of IL-6 reduced this effect
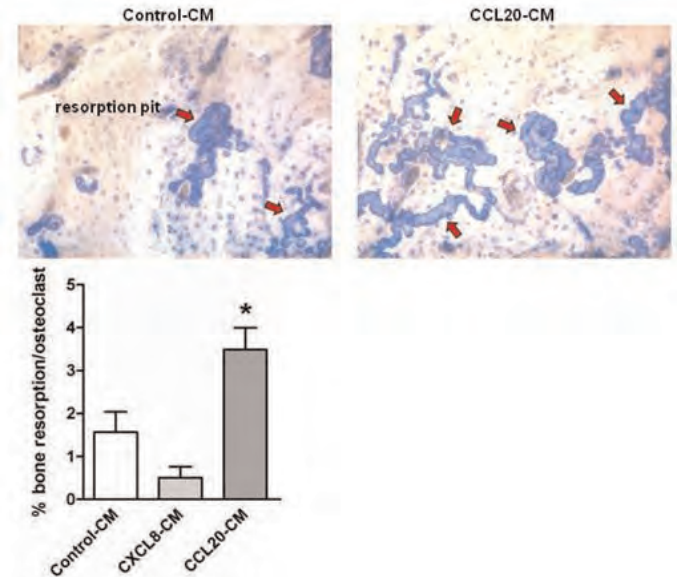
CCL20-CM, but not CXCL8-CM, enhanced osteoclastic bone resorption

Disclosures: Jenneke Klein-Nulend*, None.*

MO0423

Withdrawn

MO0424

Targeted inhibition of the Parathyroid Hormone related Protein (PTHrP) 1-173 isoform in human triple negative breast cancer (TNBC) reproduces all the effects of simultaneous inhibition of all three PTHrP isoforms on tumor growth *in vitro* and *in vivo* . Aimee-Lee Luco*[1], Dao Chao Huang[2], Ibtihal Fadhil[3], Benoit Ochietti[3], Xian Fang Huang[3], Anne Camirand[3], Richard Kremer[2]. [1]McGill University, Canada, [2]McGill University, Royal Victoria Hospital, Canada, [3]McGill University Health Center, Canada

In humans PTHrP exists in three isoforms including PTHrP 1-139, 1-41 and 1-173.PTHrP 1-173 is uniquely expressed in human tissues but its biological role remains elusive. Most human cancer tissues express the three isoforms but their specific role in breast cancer progression has not been examined. In this study we raised specific monoclonal antibodies against PTHrP 1-173 and compared their effects to monoclonal antibodies directed at all three isoforms in human triple negative breast cancer (TNBC) models. *In vitro* we examined the following PTHrP producing TNBC cell lines: MDAMB231, BT549 and MDAMB435.We also used the PTHrP negative TNBC cell line MDAMB468 as a negative control. Monoclonal antibodies were raised against PTHrP1-33(P158 and M45), PTHrP140-173(P108) and PTHrP 150-169(P6 and M18).Expression of PTHrP isoforms was examined with real time PCR and Western Blots. Cells were grown in DMEM 10% FBS and cell growth over time determined using the alamar assay. A dose dependent growth inhibition with the monoclonal antibodies was observed in PTHrP positive TNBC but not in the PTHrP negative TNBC or in PTHrP positive TNBC treated with IgG/IgM controls. A maximal growth inhibition of ≥80% was achieved with all monoclonal antibodies tested in PTHrP positive cells with no significant difference was observed between cells treated with monoclonal antibodies directed against PTHrP 1-173 (P108, P6 and M18) compared to cells treated with monoclonal antibodies raised against all three isoforms (P158 and M45) .In contrast treatment with Tamoxifen or Herceptin had no effect on TNBC growth. We next examined *in vivo* the efficacy of two monoclonal antibodies directed either at the three isoforms (M45)or specifically directed at the PTHrP1-173 isoform (M18) in female nude mice transplanted with MDAMB435 cells in the mammary fat pad. Animals received intra-peritoneal injections of 200 micrograms of antibodies three times a week for 6 weeks and tumor growth examined overtime. A significant inhibition of tumor growth (~60%, p≤0.01) was observed but was not significantly different between animals treated with M45 or M18 monoclonal antibodies. Tumor examination at sacrifice revealed significant inhibition of cell cycle and mitogenic markers (cyclinD1 and Ki67) and of the chemokine receptor CXCR4.

Disclosures: Aimee-Lee Luco*, None.*

MO0425

Detection of sonic hedgehog in a patient with orthognathic surgery. Tsuyoshi Shimo[1], Yuki Kunisada*[2], Naito Kurio[3], Masanori Masui[2], Norie Yoshioka[2], Soichiro Ibaragi[2], Tatsuo Okui[2], Akiyoshi Nishiyama[2], Akira Sasaki[4]. [1]Okayama University Graduate School of Medicine, Dentistry & Pharmaceutical Sci, Japan, [2]Okayama University Graduate School of Medicine, Dentistry & Pharmaceutical Sciences, Japan, [3]Japan, Japan, [4]Okayama University, Japan

Introduction: Previously, we have reported that sonic hedgehog (SHH) is expressed at the site of a bone fracture spatiotemporally, and activate bone remodeling. In this study, we investigated the involvement of SHH in the fractured healing processes during the perioperative period for orthognathic surgery.

Methods: Between 2012 and 2013, 34 patients (24 female and 10 male, mean age was 23.4 (16-42) years) were admitted to our institution for the orthognathic surgery (22 maxillary and mandibular, 12 mandibular). Human serum from peripheral venous and local drainage was isolated from patient at the different time points during the perioperative period. The levels of SHH, soluble receptor activator of nuclear factor-κB ligand (sRANKL) and osteoprotegerin (OPG) were assayed by ELISA and the relationship between them was analyzed. Approval for this study was obtained from the human ethics committee of Okayama University.

Results: Local serum SHH, sRANKL and OPG levels at 1 day after surgery was increased more than those of peripheral serum. The ratio of SHH/OPG in peripheral serum were decreased after 1 days of surgery, and increased on day 3 and 7. Similarly the ratio of sRANKL/OPG in peripheral serum were decreased after 1 and 3 days of surgery, and increased on day 7. SHH/OPG ratio in local serum was unchanged at 0, 1, and 2 days after surgery. On the other hand, the sRANKL/OPG ratio in local serum was decreased 2 days after surgery.

Conclusion: The level of SHH in the local serum was increased after the osteotomy. There should be further evaluation of use of SHH as a biomarker of fracture healing.

Disclosures: Yuki Kunisada, None.

MO0426

Novel ELISA for the Quantitative Measurement of Free, Bioactive, Soluble RANKL - A New Highly Sensitive Tool for Bone Research. Andreea Suciu[1], Andreas Breitwieser*[2]. [1], Austria, [2]Biomarker Design Forschungs GmbH, Austria

RANKL, the receptor activator of nuclear factor kappa B ligand is a key regulator in bone metabolism (1) and acts through binding to the transmembrane receptor RANK. RANKL is a membrane-bound protein that can be segregated to a soluble, bioactive (2) form (sRANKL). Through competitive binding to the naturally occurring decoy receptor Osteoprotegerin (OPG), the RANKL/RANK interaction can be blocked at the ligand/receptor level.

One of the biggest challenges in measuring free soluble RANKL are its low circulating levels and its nature to bind to OPG, making it difficult to measure: the accuracy of sRANKL measurement is compromised by the very low or undetectable levels, as observed in some patient cohorts (3).

Our goal was to develop a highly sensitive and specific assay that enables the direct measurement of free, bioactive, soluble RANKL in serum and plasma samples by taking advantage of the high affinity and specificity protein-protein interaction between sRANKL and OPG. Immobilized, recombinant OPG was used to capture free sRANKL, which subsequently is detected with a biotin labeled anti-sRANKL antibody.

We could show that nearly all samples (98%) from an unselected healthy population (n=210) had detectable free sRANKL values within the calibration range of the assay (0 - 2 pmol/l). The median of serum samples (prepared immediately after blood collection and stored at -25℃) was 0.14 pmol/l, with a lower limit of quantification (LLOQ) of 0.01 pmol/l. Assay characteristics, such as intra/inter-assay precision, dilution linearity and spike/recovery as well as sample stability have been analyzed and will be presented.

Our novel ELISA provides a reliable and accurate tool for the quantitative determination of free, soluble, bioactive RANKL in human samples and could help to understand the underlying regulatory mechanisms of various diseases such as rheumatoid arthritis, inflammatory bowel disease, multiple myeloma, and cardiovascular disease. Future analyses of free soluble RANKL with this highly sensitive assay could also range from drug efficacy studies to screening for the early detection of diseases.

Literature:

(1) Walsh M.C. and Choi Y. Cytokine growth factor Rec. 14(3-4):251-63, 2003.
(2) Proell V. et al., Bone 45(4):677-81, 2009.
(3) Anastasilakis A. et al., J. Clin. Endocrinol. Metab. 98(8):3206-12, 2013.
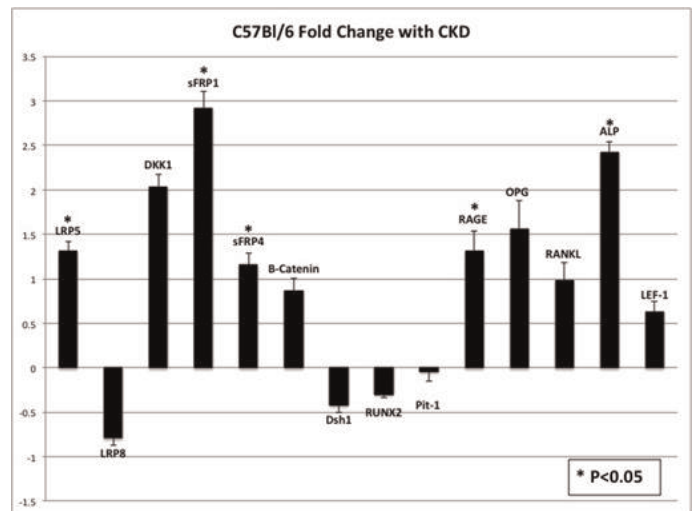
Disclosures: Andreas Breitwieser, None.

MO0427

Baseline Bone Density Modulates the Wnt Signaling Pathway in a Murine Kidney Disease Model. Ryan Clark*[1], Laura Shum[1], Xiaoxin Wang[1], Moshe Levi[2], Karen King[3]. [1]University of Colorado, USA, [2]University of Colorado Denver, USA, [3]University of Colorado School of Medicine, USA

Purpose: Chronic kidney disease (CKD) often leads to decreased bone quality. However, the mechanisms involved are not clear. One potential mechanism linking CKD to bone metabolism is the Wnt signaling pathway. We measured Wnt pathway gene expression changes due to CKD in two strains of mice: C57Bl/6, a *low* bone density strain, and FVB, a *high* bone density strain. The purpose was to answer the following: 1) Does CKD affect Wnt signaling in bone?, and 2) Does baseline bone density modulate the effect of CKD on Wnt signaling?

Methods: This study was IACUC approved. In a two-stage surgery on 10 wk. old mice, one kidney and the cortical portion of the second were removed ("5/6 Nx" N = 12 mice/strain). Control surgeries were also two-stage on 10 wk. old mice, but no renal tissue removed ("Sham" N = 12 mice/strain). Mice were euthanized at 10 wks. post-surgery. Femoral bone was cleaned, snap-frozen and analyzed by SYBR green real time RT-PCR. Data were analyzed by Mann-Whitney rank sum test; α = 0.05. The expression of [A] extracellular signaling genes, LRP5, LRP8, DKK1, sFRP1, and sFRP4; [B] intracellular signaling genes, β-catenin and disheveled-1; and [C] downstream regulation of bone turnover, RUNX2, PIT-1, RAGE, OPG, RANKL, ALP, and LEF1 were measured.

Results: [A] LRP5, sFRP1, sFRP4, and DKK1 increased in the 5/6 Nx C57Bl/6 group (P=0.03, 0.001, 0.05 and 0.07, respectively compared to Sham C57Bl/6). Expression of these genes appeared lower in the 5/6 Nx FVB group compared to Sham FVB but data were not significant. [B] Intracellular signaling genes were not significantly changed with 5/6 Nx in either strain (P>0.05); however, they all appeared to increase in the 5/6 Nx C57Bl/6 but decrease in the 5/6 Nx FVB group. [C] RAGE and ALP increased in the 5/6 Nx C57Bl/6 group (P=0.03 and 0.03 respectively). However, Pit-1 and Lef1 decreased significantly in the 5/6 Nx FVB group (P=0.03 and 0.02 respectively). Conclusion: This study demonstrates that in mice 1) CKD alteration of bone metabolism involves the Wnt signaling pathway. This study further demonstrates that in mice 2) baseline bone density likely modulates this Wnt signaling. The *low density* bone of the C57Bl/6 is resistant to changes in CKD while the *high density* bone of the FVB is more susceptible. To our knowledge, this is the first study connecting Wnt signaling with baseline bone density. This new information is important to the development of bone therapies for patients with kidney disease.

C57Bl/6 with CKD

FVB with CKD

MO0428

Induction of CXC Chemokines in Human Mesenchymal Stem Cells (hMSCs) by Stimulation with Secreted Frizzled-Related Proteins (sFRPs) through Non-Canonical Wnt Signaling. David Bischoff*[1], Jian-hua Zhu[2], Nalini Makhijani[1], Dean Yamaguchi[3]. [1]VA Greater Los Angeles Healthcare System, USA, [2]VA Greater Los Angeles Healthcare System, USA, [3]VA Greater Los Angeles Healthcare System, USA

CXC chemokines, CXCL5 and CXCL8, are elaborated from hMSCs during differentiation with osteogenic differentiation medium (OGM) and dexamethasone (DEX), and may be involved in angiogenic stimulation during bone repair. We showed that components of both canonical and non-canonical Wnt signaling are involved in the stimulation of CXCL5 in OGM. Conditioned medium (CM) from L-cells expressing Wnt5a, a non-canonical Wnt, stimulated an increase in CXCL5 mRNA expression and protein secretion in comparison to control L-cell CM. Dkk-1, an inhibitor of canonical Wnt signaling inhibited basal levels of CXCL5 expression at 7 days but not at 10 days. RoR2, a co-receptor for non-canonical Wnt signaling was also significantly up-regulated by OGM and DEX approximately 12-fold. sFRP1, which should inhibit both canonical and non-canonical Wnt signaling, surprisingly enhanced the expression of CXCL8 and to a lesser degree CXCL5 at 7 and 10 days. In addition, all four sFRPs induced CXCL8 expression in a dose- and time-dependent manner with maximum expression at ~150 nM at 7 days although the largest increases in CXCL8 and CXCL5 expression were seen with sFRP1 or sFRP2. Activation of MAPK signaling can enhance CXC ligand expression. Analysis of MAPK signaling showed sFRP1-induced phosphorylation of ERK in hMSCs maximally at 5 minutes. We used siRNA technology to decrease expression levels of several Frizzled receptors (Fzds) in an attempt to identify those receptors that could potentially be involved in sFRP stimulation of CXCL5 and CXCL8. Fzd2, 4, 5, and 7 were chosen since they are known to bind Wnt5a protein, and Fzd6 since it has been shown to bind sFRPs. hMSCs were transfected with siRNA for the Fzds and then treated with sFRPs. Screening experiments indicated that Fzd2, 4, 5 and 6 but not Fzd7 may be involved in the sFRP stimulation of CXCL5 and CXCL8. Subsequent experiments using siRNA directed against Fzd2 verified that Fzd2 is strongly involved in sFRP stimulation of both CXCL5 and CXCL8 with the effect on CXCL8 being greater than that on CXCL5. Conclusions: 1) the expression of the CXC chemokines, CXCL5 and CXCL8, was enhanced in hMSCs undergoing osteoblastogenesis; 2) the non-canonical Wnt pathway appears to be involved in CXC chemokine expression during osteogenic differentiation; 3) sFRPs which stimulated CXCL5 and CXCL8 mRNA expression may do so through the Fzd2 receptor and possibly other non-canonical Fzd receptors and perhaps through ERK signaling.

MO0429

Pharmacokinetics (PK) and Pharmacodynamics (PD) of a Human Mono-clonal Anti-FGF23 Antibody (KRN23) in a Long-Term Extension Study of Adults with X-linked Hypophosphatemia (XLH). Xiaoping Zhang*[1], Erik Imel[2], Mary Ruppe[3], Thomas Weber[4], Mark A. Klausner[5], Kavita Gumbhir-Shah[5], Takahiro Ito[5], Maria Vergeire[6], Jeffrey S. Humphrey[5], Francis Glorieux[7], Anthony Portale[8], Karl Insogna[9], Munro Peacock[10], Thomas Carpenter[9]. [1]Kyowa Hakko Kirin Pharma Inc, USA, [2]Indiana University School of Medicine, USA, [3]The Methodist Hospital, USA, [4]Duke University Medical Center, USA, [5]Kyowa Hakko Kirin Pharma Inc., USA, [6]Kyowa Hakko Kirin Pharma Inc., USA, [7]Shriners Hospital for Children & McGill University, Canada, [8]University of California San Francisco, USA, [9]Yale University School of Medicine, USA, [10]Indiana University Medical Center, USA

Objectives: In XLH, abnormally elevated serum FGF23 results in low renal maximum threshold for phosphate reabsorption (TmP/GFR), low serum phosphorus (inorganic Pi), and inappropriately normal 1,25 dihydroxyvitamin D [1,25(OH)$_2$D] with subsequent development of rachitic deformities. Single intravenous and subcutaneous (SC) and 4 monthly SC doses of KRN23 increased TmP/GFR, serum Pi, and 1,25(OH)$_2$D in adults with XLH. We previously reported PK and PK-PD relationships in the 4-month SC study. We report the PK and PK-PD relationships of KRN23 following up to 12 additional monthly SC administrations in an extension study of the initial 4-month protocol.

Methods: Up to 12 SC doses of KRN23 were given every 28 days to 22 adults with XLH who had completed the initial 4-dose study. KRN23 doses (0.05, 0.1, 0.3, 0.6 and 1 mg/kg) were based on a dosing algorithm. Blood and urine samples for assessing PK and PD variables were collected pre-dose and periodically after each dose. Serum samples for KRN23 were analyzed using a validated assay and PD parameters using commercial methods.

Results: The starting KRN23 dose was 0.3 to 1.0 mg/kg. Doses were generally increased for Doses 2 and 3. Doses within individual subjects were stable from Doses 4 to 12 and $\geqslant$ 85% received 0.6 or 1.0 mg/kg doses. Serum KRN23 levels peaked 7 days after each dose. The correlation between area under the PD effect curve (AUEC) using change from baseline, and serum KRN23 area under the curve (AUC) was better described by an E$_{max}$ model for serum Pi (E$_{max}$ = 329 mg × day/dL, EC$_{50}$=10809 µg × hr/mL), TmP/GFR (E$_{max}$ 409 mg × day/dL, EC$_{50}$ 16015 µg × hr/mL) and 1,25(OH)$_2$D (E$_{max}$ 6395 pg × day/dL, EC$_{50}$ 9146 µg × hr/mL) compared with a linear model. The AUEC for the change from baseline increased linearly with KRN23 PK exposure (AUC) for several bone biomarkers: serum bone alkaline phosphatase, osteocalcin, P1NP and CTx. There were no meaningful PK-PD relationships for a variety of additional PD and safety parameters (serum calcium, calcitonin, intact PTH, creatinine, 25-hydroxy vitamin D; and 24-hour urine calcium, calcium/creatinine ratio, phosphate and creatinine)
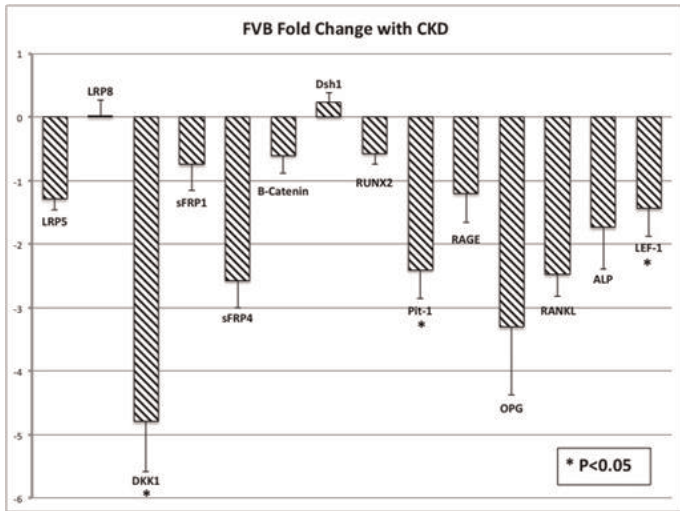
Conclusion: Stability of KRN23 doses and serum levels was achieved after approximately 3 doses of extended monthly KRN23 SC administration. An E$_{max}$ model described the relationship between KRN23 PK exposure and the key PD parameters of serum phosphorus, TmP/GFR and serum 1,25(OH)$_2$D after long-term monthly administration of KRN23 in adults with XLH.

MO0430

Osteoblast malfunction in the G610C model of osteogensis imperfecta. Lynn Mirigian[1], Elena Makareeva[1], Edward Mertz[1], Joseph Perosky[2], Kenneth Kozloff[3], Sergey Leikin*[4]. [1]National Institutes of Health, USA, [2]University of Michigan, USA, [3]University of Michigan Department of Orthopaedic Surgery, USA, [4]National Institutes of Health, USA

In this study, we investigated osteoblast dysregulation caused by misfolding of type I procollagen with a Cys substitution for Gly610 (from the N-terminal end of the triple helix) in the α2(I) chain. Mice with G610C substitution in one Col1a2 allele exhibit low bone density, hypermineralization of bone matrix, and reduced bone strength. They represent a model for moderately severe osteogenesis imperfecta (OI) caused by Gly substitutions. Calvarial osteoblasts isolated from newborn G610C mice secreted less procollagen yet had more procollagen inside the cell compared to wild type osteoblasts. Pulse-chase labeling of the cultured cells revealed a delay in folding of molecules with the G610C chain. Lower than expected fraction of these molecules in secreted procollagen suggested that they were selectively retained by the cell. The resulting procollagen accumulation is likely responsible for abnormal osteoblast differentiation and function. In bone marrow stromal cell culture, we observed abnormal activation of NFkB signaling and reduced osteoblast colony formation. In calvarial osteoblast culture, we also observed attenuated Smad2 phosphorylation and insufficient stimulation of collagen production in response to TGFb. In vivo, we observed severe osteoblast ER cisternae dilation, abnormal bone deposition (rate, location, and composition), and abnormal relative quantities of Runx2, Sp7, Bglap, and Ibsp transcripts. Osteoblasts appeared to degrade misfolded G610C molecules in lysosomes via autophagy; we found significant additional accumulation of procollagen upon treatment of cultured G610C cells with inhibitors of this pathway (chloroquine and bafilomycin) but not with inhibitors of ER associated degradation

in proteasomes (bortemozib and eeyarestatin). An important role of autophagy was further supported by improvements in bone material properties and differentiation of cultured osteoblasts from G610C mice placed on a low protein diet (8% vs. 18%), although the diet inhibited bone and overall animal growth. We propose that osteoblast adaptation to accumulation of misfolded mutant procollagen alters crucial cell signaling and functions. Better understanding of pathways involved in this cell response may lead to novel therapeutic treatments for OI and other disorders involving procollagen misfolding.

Disclosures: Sergey Leikin, None.

MO0431

Two Distinct Mutations in *IFITM5* Causing Different Forms of Osteogenesis Imperfecta Using Reciprocal Mechanisms. ADI Reich*[1], Charles Farber[2], Aileen Barnes[3], Patricia Becerra[4], Frank Rauch[5], Wayne A. Cabral[3], Alison Bae[3], Francis Glorieux[6], Thomas Clemens[7], Joan Marini[8]. [1]NIH, USA, [2]University of Virginia, USA, [3]NIH/NICHD/BEMB, USA, [4]NIH/NEI/Protein Structure & Function Section, USA, [5]Shriners Hospital for Children, Montreal, Canada, [6]Shriners Hospital for Children & McGill University, Canada, [7]Johns Hopkins University, USA, [8]National Institute of Child Health & Human Development, USA

Osteogenesis imperfecta (OI) type V is caused by a recurrent dominant mutation (c.-14C>T) in *IFITM5*, which encodes BRIL, a transmembrane ifitm-like protein most strongly expressed in osteoblasts, whose expression coordinates with mineralization. Patients with type V OI have distinctive clinical manifestations with overactive bone mineralization and include mesh-like lamellation on bone histology. Recessive null mutations in *SERPINF1* cause OI type VI, which impairs mineralization. Type VI OI patients have absence of serum PEDF, elevated alkaline phosphatase (ALPL) as children, and bone histology with broad unmineralized osteoid and fish-scale pattern.

We identified a 25-year-old woman with severe OI, who had no characteristics of OI type V. Her dermal fibroblasts (FB) and cultured osteoblasts (OB) displayed minimal secretion of PEDF, but her serum PEDF was normal. *SERPINF1* sequences were normal despite bone histomorphometry typical of type VI OI, and elevated childhood serum ALPL. Exome sequencing on the proband, parents and an unaffected sibling yielded a *de novo* mutation in *IFITM5* in one allele of the proband, causing a p.S40L substitution in the BRIL intracellular domain.

In OB with the *IFITM5* p.S40L mutation, *IFITM5* expression was normal, as was BRIL protein level on western blot and in permeabilized OB by microscopy. Notably, *SERPINF1* expression was decreased in p.S40L OB, and PEDF was barely detectable in conditioned media of S40L cells. OB with the S40L mutation also had decreased expression of *ALPL* and osteocalcin (*OCN*), as seen in primary PEDF defects. In contrast, OB from type V OI, with 5 residues added to the N-terminus of BRIL, have increased *SERPINF1* expression and PEDF secretion during differentiation, and increased *ALPL* and *OCN* expression. The *IFITM5* mutations also have opposite effects on OB mineralization in culture – OB with the 5'-terminal mutation have increased mineralization during differentiation, while mineralization was decreased in S40L OB. OB from both mutations had a collagen related defect, with decreased expression and secretion of COL1A1. Together, these data show that 2 distinct mutations in *IFITM5* generated different forms of OI with distinctive phenotypes using reciprocal mechanisms; the type V OI and p.S40L BRIL are gain- and loss-of-function mutations, respectively. Furthermore, BRIL and PEDF have a relationship that connects the genes for types V and VI OI and their roles in bone mineralization.

Disclosures: ADI REICH, None.

MO0432

Whole exome sequencing is efficient for detecting mutations in patients with osteogenesis imperfecta and children with bone fragility. Ikuma Fujiwara*. Tohoku University School of Medicine, Japan

Purpose: Most of the patients with osteogenesis imperfecta (OI) are caused by mutations in either two of the genes for type 1 collagen, *COL1A1* or *COL1A2*. Genetic analysis is useful to predict the clinical course of patients because genotype usually correlates phenotype of the disease. Since the sizes of both *COL1A1* and *COL1A2* are large, time and effort are required for analyzing the genes. In recent years, more than a dozen of genes have been revealed to cause OI, and it is difficult to tell which gene is related only by clinical manifestation except a couple of genes.

Methods: We have performed whole exome sequencing (WES) in three patients clinically diagnosed as OI and a child with bone fragility and low bone mineral density, in whom mutations in *COL1A1/COL1A2* were not detected by Sanger sequence. This study was approved by IRB of the institute, and informed consent was obtained from at least one of the parents of each patient. For WES, targeted enrichment was performed using the SureSelect Human All Exon 50Mb kit for twelve individuals. Exon-enriched DNA libraries were sequenced on the Illumina Hiseq 2000 for 101bp. BWA was used to align the sequence reads to the human genome (hg19); all parameters of BWA were kept at the default settings. Following removal of duplicates from the alignments, realignment around known indels, recalibration and SNP/indel calling were performed with Genome Analysis Toolkit (GATK) (1.5). ANNOVAR was used for the annotation against the RefSeq database and dbSNP. We searched for variants in OI causing genes (*IFITM5*, *SERPINF1*, *CRTAP*, *LEPRE1*, *PPIB*,

SERPINH1, *FKBP10*, *SP7*, *BMP1*, *WNT1*, *TMEM38B*, *CREB3L1*) in addition to *COL1A1* and *COL1A2*.

Results: A missense mutation (p.G326R) in *COL1A1* was found in an OI patient. Two rare variations in *CREB3L1* (p.G92S, p.A411T) were found in another girl with bone fragility. We have not found specific variants in OI causing genes in other patients.

Conclusion: WES is an efficient method to detect variants for OI, but more strategic and deliberate approach is necessary to find new causative genes.

Disclosures: Ikuma Fujiwara, None.

MO0433

Activities of Dysregulated ALK2 Receptor Kinases Provide Insight Into the Protein Structural-Functional Basis of Fibrodysplasia Ossificans Progressiva. Jay Groppe*[1], Mary Rose Tandang-Silvas[2], Anupama Pathi[2], Jingfeng Wu[2], Viet Le[3], Andria Culbert[4], Kristi Wharton[3], Frederick Kaplan[4], Eileen Shore[4]. [1]Texas A&M University Baylor College of Dentistry, USA, [2]TAMU Baylor College of Dentistry, USA, [3]Brown University, USA, [4]University of Pennsylvania, USA

Although structurally similar to the constitutively active type II counterparts, type I or Activin-like receptor kinases (ALKs) are set apart by the helix-loop-helix (HLH) element preceding the conserved Ser/Thr kinase domain that serves a passive role as an inhibitor-to-substrate binding switch according to the longstanding paradigm. Interestingly, signaling can be robustly activated without ligand-mediated assembly of a hetero-tetrameric complex by a single substitution with aspartate at the terminal residue of the regulatory subdomain. A single recurrent mutation in the codon of the penultimate residue, directly adjacent the position of the constitutively activating substitution, causes milder ligand-independent activation of ALK2 that leads to heterotopic bone deposition and secondary skeleton formation in patients presenting with FOP. Structure-based homology modeling showed that the recurrent mutation of classical FOP (R206H) disrupts a conserved ion pair juxtaposed between the FKBP12 inhibitory protein binding site and a loop (L45; β4>β5) conferring substrate protein specificity for the downstream effectors (R-Smads 1/5/8).

To determine the structural and functional basis of the activating effects of the recurrent FOP mutation, ALK2 receptor kinase forms have been produced at milligram scale by means of a baculovirus-insect cell expression system and purified to near homogeneity. Wildtype, R206H mutant, Q207D (aspartate-substituted) and HLH subdomain-truncated (208ntrunc) forms were compared through an array of *in vitro* kinase activity assays and diverse protein-protein interaction analyses that were complemented by comparison of signaling read-out (p-Smad) in primary mouse embryonic fibroblasts and cultured *Drosophila* S2 cells. We observed that FKBP12 buffered but did not strictly inhibit kinase activities *in vitro* and had no detectable effect on basal signaling in wildtype fibroblasts. On the other hand, the HLH subdomain alone diminished the activity of the wildtype kinase as shown by comparison with mutant and variant forms. In addition, an absolute requirement for the HLH subdomain was observed for Smad phosphorylation despite significantly elevated kinase activity upon truncation. Hence rather than passively serving as obligate sites of binding and phosphorylation, the juxtamembrane regulatory element plays active and direct roles in autoinhibition of the kinase and recruitment of substrate, safeguarding through coupling the processes.

Disclosures: Jay Groppe, None.

MO0434

Association between Nance-Horan Syndrome and Fragility fractures in a young man. Are Connexins the Connection?. Manju Chandran*[1], Bart Clarke[2], Robert D Tiegs[2], Matthew Tan[1], Peter Byers[3], Ching Lin Ho[4]. [1]Osteoporosis & Bone Metabolism Unit, Singapore General Hospital, Singapore, [2]Division of Endocrinology, Diabetes, Metabolism & Nutrition, Mayo Clinic, USA, [3]Collagen Diagnostic Laboratory, Department of Pathology & Medicine (Medical Genetics), University of Washington, USA, [4]Glaucoma Service, Singapore National Eye Centre, Singapore

Introduction: A pathogenic variant in the single copy of the *NHS* gene causes Nance-Horan (Congenital Cataract-Dental) syndrome, an X-linked disorder with ocular, dental and auricular manifestations [1]. Bone loss and osteoporosis have not been described in association with NHS before. We present the case of a young man with low bone density and multiple low trauma compression fractures of the spine that were likely associated with his cataract–dental syndrome.

Case: A clinical diagnosis of Nance Horan Syndrome was made in a 24 year old Chinese male with congenital cataracts when he presented with the characteristic phenotype of micropthalmos, sclerocornea and peg shaped teeth. His mother also was noted to have some ocular features of the disease. 3 years later, he presented with a history of falling from standing height. X-Rays of his spine revealed compression fractures of T12, L1 and L3 vertebrae and a superior end plate fracture of L2. He recalled a history of a similar fall several years ago in his teens, however he had not had X-rays done then. He was 181 cm tall and weighed 73.6 kg. He had well developed secondary sexual characteristics and there were no other obvious physical deformities or stigmata such as blue sclerae. Plasma testosterone, FSH, LH, intact PTH, calcium, phosphorus, liver function tests, alkaline phosphatase, renal function, thyroid

function, cortisol level, and blood count were normal as were the serum and urine protein electrophoresis. There was no hypercalciuria. 25-OHD level was 26.4 ng/ml. DXA scan showed a femoral neck BMD of 0.631 gm/cm2 (Z-score: -2.2). Bone Scan showed only vertebral fractures. Sequencing of COL1A1 and COL1A2 genes did not show any coding sequence mutations or mutations in the nearby splice site domains. PCR based genotyping performed on blood of the patient and his mother showed a previously unreported pathogenic variant (c.565+1G>T) in the NHS gene in both individuals.

Discussion: The genes implicated in congenital cataract syndromes include members of the connexin family of gap junction proteins [2]. Connexins 43 and 45 have been found to be associated, specifically, with osteogenesis[3]. The intriguing possibility exists that mutations in the NHS gene could be responsible for the very unusual bone fragility in this young man with no other identifiable cause. It raises very interesting questions on the hitherto unexplored connection between connexins, bone development and fragility in humans.

References:

1. Horan MB, Billson FA. X-linked cataract and Hutchinson teeth. Aust Paediatr J 1974; 10:98-102.

2. Ionides A, Francis P, Berry V et al. Clinical and genetic heterogeneity in autosomal dominant congenital cataract. Br J Opthalmol. 1999; 83;802-808.

3. Civitelli R, Beyer EC, Warlow PM et al. Connexin43 mediates direct intercellular communication in human osteoblastic cell networks. J Clin Invest 1993. 91:1888-1896.

Disclosures: Manju Chandran, None.

MO0435

Controlled local delivery of Trametinib combined to rBMP2 promotes osteoblast differentiation and bone healing in $Nf1_{Osx}^{-/-}$ mice. <u>Jean De La Croix Ndong</u>*[1], <u>David Stevens</u>[2], <u>Guillaume Vignaux</u>[2], <u>Sasidhar Uppuganti</u>[2], <u>Daniel Perrien</u>[3], <u>Xiangli Yang</u>[1], <u>Jeffry Nyman</u>[3], <u>Eva Harth</u>[2], <u>Florent Elefteriou</u>[1]. [1]Vanderbilt University, USA, [2]Vanderbilt university, USA, [3]Vanderbilt University Medical Center, USA

Neurofibromatosis type I (NF1) is an autosomal dominant disease with an incidence of 1/3000, caused by mutations in the *NF1* gene, which encodes the RAS/GTPase-activating protein neurofibromin. Non-bone union following fracture (pseudarthrosis) in children with NF1 remains a challenging orthopedic condition to treat. Recent progress in understanding the biology of neurofibromin suggested that NF1 pseudarthrosis stems primarily from defects in the bone mesenchymal lineage and hypersensitivity of hematopoietic cells to TGFb. However, clinically relevant pharmacological approaches to augment bone union in these patients remain limited. In this study, we report the generation of a novel conditional mutant mouse line used to model NF1 pseudarthrosis, in which *Nf1* can be ablated in an inducible fashion in osteoprogenitors of post-natal mice, thus circumventing the dwarfism associated with previous mouse models where *Nf1* is ablated in embryonic mesenchymal cell lineages. An *ex vivo*-based cell culture approach based on the use of *Nf1*flox/flox bone marrow stromal cells showed that loss of *Nf1* impairs osteoprogenitor cell differentiation in a cell-autonomous manner, independent of developmental growth plate-derived or paracrine/hormonal influences. In addition, *in vitro* gene expression and differentiation assays indicated that chronic ERK activation in *Nf1*-deficient osteoprogenitors blunts the pro-osteogenic property of BMP2, based on the observation that only combination treatment with BMP2 and the MEK inhibitor Trematinib promoted the differentiation of *Nf1*-deficient osteoprogenitors. The *in vivo* preclinical relevance of these findings was confirmed by the improved bone healing and callus strength observed in $Nf1_{osx}^{-/-}$ mice receiving Trematinib and BMP2 released locally at the fracture site via a novel nanoparticle and polyglycidol (PEG)-based delivery method. Collectively, these results provide novel evidence for a cell-autonomous role of neurofibromin in osteoprogenitor cells and insights about a novel targeted approach for the treatment of NF1 pseudarthrosis.

Funding Sources:

Young Investigator Award (2012-01-028) from the Children's Tumor Foundation (JN);

The National Institute of Arthritis and Musculoskeletal and Skin Diseases, part of the National Institutes of Health, under Award Number 5R01 AR055966 (FE) ;

The National Institutes of Health, Award Number S10 RR027631 (DSP)

Disclosures: Jean De La Croix Ndong, None.
This study received funding from: The Children's Tumor Foundation (CTF)

MO0436

Familial hypocalciuric hypercalcemia associated with a novel homozygous loss-of-function mutation, E671D, of the calcium-sensing receptor gene. <u>Filomena Cetani</u>[1], <u>Simona Borsari</u>[2], <u>Elena Pardi</u>[2], <u>Brunella Bagattini</u>[2], <u>Federica Saponaro</u>*[2], <u>Claudio Marcocci</u>[3]. [1]University Hospital of Pisa, Italy, [2]Department of Clinical & Experimental Medicine, University of Pisa, Italy, [3]University of Pisa, Italy

Familial Hypocalciuric Hypercalcemia (FHH) is an autosomal inherited dominant disease characterized by mild to moderate asymptomatic hypercalcemia, relative hypocalciuria, and inappropriately normal PTH levels. Fractional urinary excretion of calcium is important to distinguish patients with FHH from others forms of

primary hyperparathyroidism (PHPT). The calcium/creatinine clearance ratio is <0.01 in FHH and higher in PHPT. Heterozygous and homozygous/compound heterozygous mutations of calcium sensing receptor gene (CASR), a G-protein-coupled receptor, are responsible for FHH type 1 and neonatal severe hyperparathyroidism (NSHPT), respectively. NSHPT is a much more serious disorder characterized by marked calcemia, hypotonia, skeletal demineralization, and can occur in the offspring of patients with FHH. In this study we report the case of 61-years-old woman referred to our Department for suspected PHPT. Biochemical analysis revealed high serum calcium (13 mg/dl) and ionized calcium (1,9 mmol/l) levels, PTH moderately elevated (78 pg/ml) and calcium/creatinine clearance ratio <0.01, suggestive of FHH. Serum calcium screening of her relatives showed normal values in the mother, brother and sons, while the father and the half-sister had mild hypercalcemia (10,3 and 10,9 mg/dl, respectively). Of note, her parents were consanguineous. Germline proband and parents' DNA was extracted from peripheral blood cells and the entire coding region and splice junctions of the CASR gene were directly sequenced. The proband was homozygous for the change c.2013G>C, that resulted in a novel missense mutation, E671D. The same mutation, in a heterozygous state, was present in the her parents and absent in 100 chromosomes of healthy control subjects. In conclusion, we identified a novel homozygous mutation, located in the first extracellular loop of CASR, in an adult woman with hypercalcaemia and hypocalciuria. The proband was born in good health and has had a normal neurological growth, so we can assume that the mutation E671D could have a mild effect. So far, at least three similar cases with homozygous presentation and a FHH phenotype have been described in the literature and functional studies of the mutations showed a mild functional inactivation in-vitro, demonstrating that not all CASR mutations found in a homozygous state necessarily cause neurodevelopmental defects due to an elevated hypercalcemia in infancy and childhood, but can resemble a classical FHH phenotype.

Disclosures: Federica Saponaro, None.

MO0437

Lysinuric Protein Intolerance Presenting with Multiple Fractures. <u>Lindsay Burrage</u>*[1], <u>Jennifer Posey</u>[2], <u>Marcus Miller</u>[2], <u>Pengfei Liu</u>[2], <u>Matthew Hardison</u>[2], <u>Sarah Elsea</u>[2], <u>Qin Sun</u>[2], <u>Yaping Yang</u>[2], <u>Alecia Willis</u>[2], <u>Alan Schlesinger</u>[2], <u>Carlos Bacino</u>[2], <u>Brendan Lee</u>[1]. [1]Baylor College of Medicine, USA, [2]Baylor College of Medicine, USA

Lysinuric Protein Intolerance (LPI), an autosomal recessive disorder, is caused by mutations in *SLC7A7*, which encodes a subunit of the dibasic amino acid transporter. LPI is characterized by urinary losses of lysine, ornithine, and arginine that result in a secondary ureagenesis defect, and thus, the typical presenting features include vomiting, irritability, and symptomatic hyperammonemia after consumption of protein-rich meals. Pulmonary alveolar proteinosis, renal dysfunction, macrophage activation syndrome, and osteoporosis are other possible long-term complications of this disorder. Here, we describe a 6-year-old male with history of short stature, speech delay and fragility fractures who has been treated with bisphosphonates. Evaluation for heritable forms of brittle bone diseases including sequencing of *COL1A1/COL1A2* was normal. Whole exome sequencing identified a nonsense mutation in one allele of *SLC7A7* and array comparative genomic hybridization detected a deletion involving the second allele. Biochemical testing was consistent with the diagnosis of LPI. Our patient's atypical presentation highlights the importance of including LPI in the differential diagnosis of idiopathic osteoporosis in the pediatric population even in the absence of other typical presenting features of this disorder.

Disclosures: Lindsay Burrage, None.

MO0438

Phosphate Metabolism in Craniometaphyseal Dysplasia (CMD): Dietary Phosphate Restriction Reduces Increased Bone Mass in a CMD Mouse Model. <u>Yaling Liu</u>[1], <u>Eliane Dutra</u>[2], <u>Zhifang Hao</u>[1], <u>Ernst Reichenberger</u>[2], <u>I-Ping Chen</u>*[2]. [1]University of Connecticut Health Center, USA, [2]University of Connecticut Health Center, USA

Mutations in the pyrophosphate (PPi) transporter ANKH are responsible for craniometaphyseal dysplasia (CMD), which is characterized by progressive thickening of craniofacial bones and flared metaphyses of long bones. Mutant ANK fails to adequately transport PPi into the extracellular matrix. PPi inhibits and phosphate (Pi) promotes mineralization. Here, we examine whether an imbalance of the Pi/PPi ratio leads to an abnormal skeleton in a CMD knock-in mouse model ($Ank^{KI/KI}$) and in CMD patients.

Homozygous $Ank^{KI/KI}$ mice have lower serum Pi levels, increased *Fgf23* mRNA and hypomineralized bone. FGF23 is secreted by bone to increase Pi wasting and to decrease 1,25-(OH)$_2$D$_3$ by reducing *1-α hydroxylase*, *Npt2a* and by increasing *Cyp24a1* upon binding to *Fgfr1* and *Klotho* in kidney. Unexpectedly, the FGF23 protein level in $Ank^{KI/KI}$ femurs was immunohistochemically normal. Serum of $Ank^{KI/KI}$ mice had an increased trend of intact FGF23 and significantly higher levels of the C-terminal FGF23 fragment suggesting enhanced proteolytic processing of FGF23. Renal expression of *1-α hydroxylase*, *Npt2a*, *Npt2c*, *Cyp24a1*, *Fgfr1*, *Klotho* were not significantly different but serum levels of 25-hydroxyvitamin D were significantly lower in $Ank^{KI/KI}$ mice.

To examine the effects of dietary Pi on the skeletal phenotype, $Ank^{+/+}$ and $Ank^{KI/KI}$ mice were exposed to high Pi (1.5%) or low Pi (0.3%) diet from birth for 13 weeks. Dietary Pi restriction reduced hyperostotic mandibles and extensive diaphyseal trabeculation in femurs whereas high Pi diet aggravated massive jawbone development and decreased the endosteal and periosteal perimeters of femurs of $Ank^{KI/KI}$ mice. We suggest that dietary phosphate restriction protects against effects of an increased Pi/PPi ratio caused by impaired PPi transport activity of mutant ANK. Interestingly, osteopontin (OPN), an inhibitor of mineralization, was significantly increased in $Ank^{KI/KI}$ mice and in CMD patients suggesting that it may act as a compensatory mechanism for decreased extracellular PPi. Plasma analysis showed that 3 out of 7 CMD patients had vitamin D deficiency or insufficiency while PTH and FGF23 were normal.

In summary, changes of *Fgf23*, Pi and OPN levels are likely compensatory mechanisms rather than etiologic factors for CMD. Therefore, low Pi diet or the use of Pi binders may benefit CMD patients.

Disclosures: I-Ping Chen, None.

MO0439

Phosphaturic Mesenchymal Tumour (PMT) of the Ethmoid Sinus, Confirmed with Chromogenic In-Situ Hybridization for *FGF23*. Aliya Khan*[1], Iman M'Hiri[2], Andrew L. Folpe[3], Waleed Khan[2], Christopher Marriott[4], Chaudhry Aslam[2], Gavino Perez[5], Sebastien Hotte[6], Lach Boleslaw[7]. [1]McMaster University, Canada, [2]Oakville Bone Centre, Canada, [3]Mayo Clinic, Department of Laboratory Medicine & Pathology, USA, [4]McMaster University , Department of Nuclear Medicine, Canada, [5]McMaster University , Department of Internal Medicine, Canada, [6]McMaster University,Division of Oncology, Department of Medicine, Canada, [7]McMaster University, Division of Pathology, Department of Medicine, Canada

Oncogenic Hypophosphatemic Osteomalacia (OHO) is a rare metabolic bone condition caused in almost all instances by a fibroblast growth factor -23 (FGF-23) secreting phosphaturic mesenchymal tumour (PMT).PMTs occur in bone and in soft tissue and are usually benign with very rare malignant examples. PMTs express FGF-23 at the mRNA and protein level. Following excision of the tumour, phosphate homeostasis normalizes. An accurate diagnosis and confirmation of the presence of a PMT is clinically invaluable.

A 58-year-old man with multiple lytic lesions in the pelvis, ribs, and acetabulum was referred for assessment following exclusion of malignancy. Serum phosphate and1,25dihydroxyvitaminD (1,25D) levels were low at 0.54 mmol/L,and 26 pmol/L respectively. Hyperphosphaturia was present(Table 1).Tetracycline double labelled bone biopsy revealed osteomalacia. Bone scan showed intense sacroiliac activity with a healing insufficiency fracture of the sacrum.(fig 1) BMD was relatively well maintained.

FGF-23 assays are currently not available in Canada. CT scans of the head, chest, abdomen and pelvis were reported as normal. A whole body MRI was declined by the patient. Treatment with calcitriol and phosphate resulted in improvements in serum phosphate however urinary phosphate also increased. His bone pain, myalgias and muscle weakness progressed. An octreotide scan with tomographic CT coregistration of the head, neck, and abdomen was performed. A 1 cm lesion was identified in the left ethmoid sinus with excessive uptake of octreotide .Figure 2. In retrospect this lesion was also present on the head CT obtained in 2005 but not reported.

Following surgical resection of the ethmoid sinus tumour serum phosphate, 1,25D and alkaline phosphatase normalized.The symptoms of myalgias, arthralgias and muscle weakness resolved.BMD improved The biopsy specimen was further evaluated at the Mayo Clinic, where the diagnosis of a morphologically benign PMT was confirmed, and the tumour shown to express *FGF-23* mRNA by chromogenic in situ hybridization (CISH) on formalin-fixed, paraffin-embedded tissue sections (RNA-Scope, Advanced Cell Diagnostics, Hayward, CA, USA).

Figure 3 shows the morphological features of the tumour (A) and Figure 4 shows the *FGF23* CISH (B).

Conclusion:

Oncogenic hypophosphatemic osteomalacia is caused by PMTs. CISH for FGF-23 is a valuable diagnostic tool capable of confirming the presence of a PMT in resected tissue.

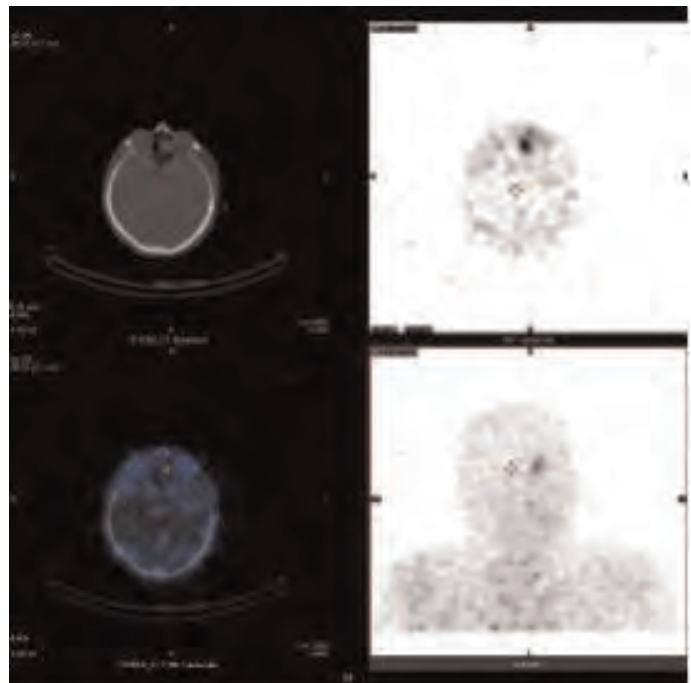Figure 1: Whole Body Bone Scan 2009 baseline and 2011 followup

Figure 2: Excess uptake of Octreotide in the left region of ethmoid sinuses
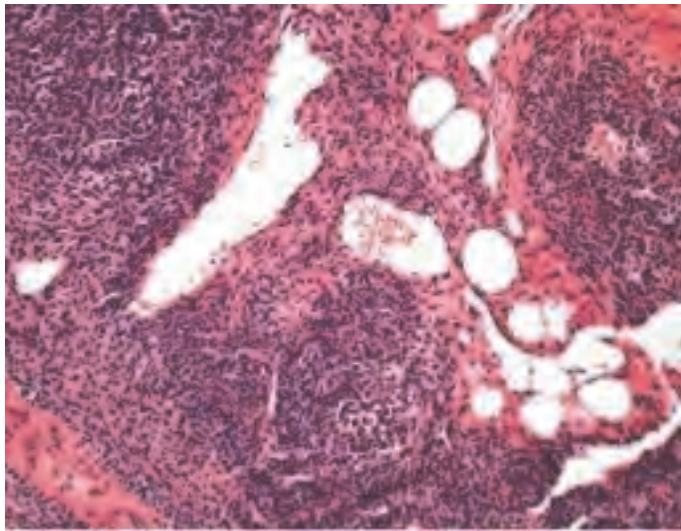
Figure 3: Phosphaturic mesenchymal tumor, consisting of bland spindled cells, blood vessels and fat
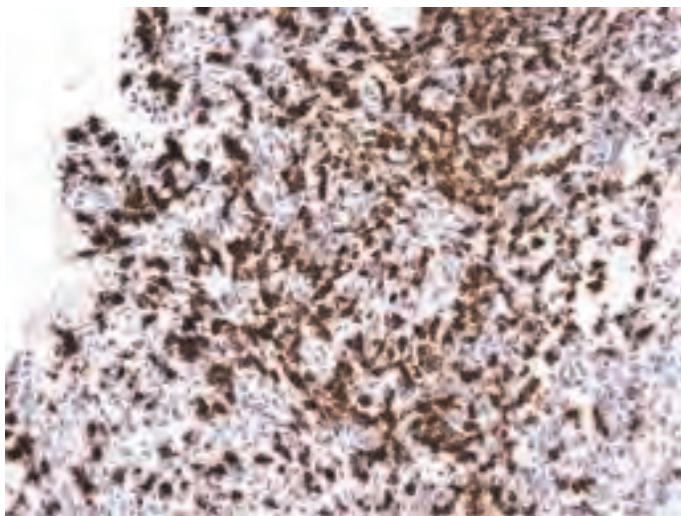

Figure 4: Chromogenic in situ hybridization for FGF23 mRNA, strongly positive in the neoplastic cells

Lab results	Normal reference	August 2009 Values	January 2014 Values
25 Hydroxy-Vitamin D	75-250nmol/l	66	103
1-25 dihydroxy vitamin D	39-193 pmol/L	26	42
Serum Phosphate	0.79-1.59 mmol/L	0.54	1.08
Alkaline Phosphatase	44-147 IU/L	229	116
Ionized Calcium (pH 7.4)	1.15-1.30 mmol/L	1.7	1.27
PTH	1.0-6.5 pmol/L	2.3	3.0
24 hour Urinary Phosphate	14-32 mmol/day	40	19

Table 1: Lab Results Baseline and Post-Resection

Disclosures: Aliya Khan, None.

MO0440

Volumetric characteristics of cortical and trabecular bone in patients with acromegaly meassured by pQCT. Jorge Malouf*[1], Elena Valassi[2], Iris Crespo[2], Jaume Llauger[3], Ana Marin[4], Susan Webb[2]. [1]Hospital de la Santa Creu i Sant Pau, Spain, [2]Endocrinology department, Hospital Sant Pau, Centro de Investigación Biomédica en Red de Enfermedades Raras, Spain, [3]Radiology department. Hospital de la Santa Creu i Sant Pau., Spain, [4]Internal Medicine Department. Hospital de la Santa Creu i Sant Pau, Spain

Growth hormone (GH) excess in acromegaly is deleterious for bone. DXA is not the optimal technique for the evaluation of bone in patients with acromegaly, since it is influenced by bone size and it does not differentiate between trabecular and cortical compartments.

The aim of this cross-sectional study was to evaluate the volumetric bone parameters in patients with acromegaly (AP) and compare them with healthy controls (HC).

Thirty-six patients were included (19 men and 17 women). Mean age was 47 ± 8 years. Sixteen patients had active acromegaly , 20 had controlled acromegaly and 21 subjects were healthy controls paired by sex, age and BMI. A volumetric quantitative CT (vQCT) was performed to each subject according to the Mindways® scan acquisition instructions. The analysis of the volumetric parameters was performed using the BIT (bone investigational tool) from Mindways.

Volumetric bone mineral density (vBMD) of L2-L4 was inferior in AP than in HC (111 ± 39 vs.132 ± 30 mg/cm3 and 105 ± 39 vs. 127 ± 32; p<0.05). When isolating trabecular bone from the total hip (THTvBMD), femoral neck (FNFTvBMD) and trochanteric region (TRTvBMD), the volumetric BMD of AP was lower than in HC (122 ± 20 mg/cm3 vs. 140 ± 20; 143 ± 21 vs. 124 ± 27 and 123 ± 18 vs. 138 ± 19; p<0.01). Regarding the cortical component, mass and volume were higher in AP than in HC (4 ± 2 vs. 3 ± 1 mg y 6 ± 4 cm3; p<0.01). None of the structural parameters of the femoral neck (cross sectional área [CSA], cross sectional moment of inertia [CSMI], average cortical thickness [ACT], section modulus [z] and buckling ratio [BR] showed statistically significant differences between AP and HC.

This study shows significant differences between cortical and trabecular compartments in AP versus HC. Even if the observed increase in the cortical mass and volume would suggest significant structural changes in AP , the geometric parameters in the femoral neck were not different as compared with HC. Further analysis is in progress to explain where the differences in both the trabecular and cortical compartments are most critical in AP.

Disclosures: Jorge Malouf, None.

MO0441

A 4-year retrospective longitudinal study: muscle mass and bone loss. Sun Mi Park*[1], Yong-Ki Min[2]. [1]Samsung Medical Center, Sungkyunkwan University School of Medicine, South Korea, [2]Samsung Medical Center, South Korea

Objective

Many studies have focused on the relationship between muscle mass and bone mass in that sarcopenia associated with low bone mass. Muscle mass could be an indicator of bone mineral density (BMD). There is no longitudinal data examined the rate of muscle declining and bone loss rate. To determine whether age-related muscle mass declining could be a predictor of the bone loss, we investigated the relationship of muscle mass and bone mass changes during a 4-year period.

Methods

We reviewed medical records of 1,053 postmenopausal women retrospectively who had undergone periodic (baseline, 1-year, 2-year, 4-year) comprehensive health examinations at the health promotion center of Samsung Medical Center from 2007 to 2012 and 497 subjects (45-81 years) were finally eligible. Lean mass and fat mass were measured with InBody 720 analyzer and BMD on lumbar spine and femur were evaluated using dual-energy X-ray densitometry. Appendicular lean mass (ALM)/height^2, lean mass percentage and ALM percentage were calculated as proposed in previous studies.

Results

Lean mass, ALM/height^2, lean mass percentage and ALM percentage were significantly positively associated with BMD (lean mass, ALM/height^2 in lumbar spine (LS), femoral neck (FN) and total hip (TH), lean mass percentage in LS and FN; $P < 0.001$, lean mass percentage in TH, ALM percentage in LS and FN; $P < 0.05$). By the fourth year of follow up period, ALM/height^2 changes significantly positively associated with BMD changes on LS, FN and TH (ΔLS; $P = 0.007$, ΔFN; $P = 0.003$, ΔTH; $P < 0.001$) after adjustment for age, smoking, exercising status and fat mass.

Conclusion

Body composition, especially lean mass and ALM/height^2, contribute to current BMD in postmenopausal women. In postmenopausal women, ALM/height^2 changes with aging were most strongly associated with bone mass loss.

Disclosures: Sun Mi Park, None.

MO0442

A Novel 3D QCT Technique to Quantify the Muscle-Lipid-Composition in the Thigh and its Association with Fracture of the Proximal Femur. <u>Alexander Muehlberg</u>*[1], <u>Oleg Museyko</u>[2], <u>Bastian Gerner</u>[2], <u>Dominique Töpfer</u>[2], <u>Valérie Danielle Bousson</u>[3], <u>Jean-Denis Laredo</u>[4], <u>Klaus Engelke</u>[1]. [1]University of Erlangen, Germany, [2]University of Erlangen, Germany, [3]Service de Radiologie OsteoArticulaire, France, [4]Service de Radiologie OstéoArticulaire, France

Introduction: The characterization of muscle morphology and function is important in sarcopenia and other muscle diseases. CT imaging has been used to quantify muscle volume and density. Here we developed a new analysis technique to also quantify the spatial muscle-lipid distribution. CT is widely available, relatively cheap, quick and in the apendicular skeleton radiation exposure is low. It was the specific aim of this study to apply this new technique to discriminate patients with acute femur fractures from unfractured controls.

Material und Methods: The 3D QCT analysis consists of a semiautomatic segmentation of the skin and of the *fascia lata* (FL), which separates subcutaneous adipose tissue (SAT) and intermuscular adipose tissue (IMAT). Inside the FL in each voxel muscle and lipid concentrations were determined based on the CT value relative to that of SAT. In addition to standard parameters (adipose tissue and muscle volume and density), the muscle-lipid-distribution was analyzed using structural descriptors such as texture, topology, or roughness. The new method was applied in QCT-Datasets (120kV, 170mAs, slice thickness 1 or 1.25mm, pitch 1) of 89 patients of the EFFECT-Study (36 patients with fresh proximal femur fractures, age 73.2 ± 9.4y and 53 controls, age 80.5 ± 11.1y) [1]. In the fractured subjects the contralateral leg and in the controls the left leg was analyzed. For fracture discrimination a best subset analysis was performed to construct multivariate models consisting of soft tissue or BMD descriptors that were selected by a univariate analysis adjusted for age and BMI.

Results: The figure shows the muscle-lipid segmentation results. The table shows Area-Under-Curve (AUC) of a BMD model (parameters: troch trab BMD & neck cort thick) and a soft tissue model (parameters: local inhomogeneity of muscle & local anisotropy (directedness) of adipocytes within the muscle). In the EFFECT cohort the soft tissue model was superior to the BMD model; the combination of the soft tissue and bone model achieved the best discrimination. A model of standard parameters like muscle density and volume added only little discriminative power compared to the bone model alone.

Conclusion: The analysis of the structural muscle-lipid distribution using a novel 3D QCT analysis technique may contribute to the understanding of hip fracture etiology. In contrast simple measurements of lean and fat volume did not give comparable results.

1. Bousson, JBMR, 2011. 26: 881-893
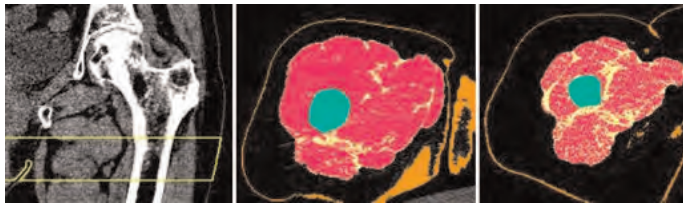
Left: VOI used for muscle analysis; Center: non-fractured subject: Right: fractured subject.

Models	AUC [CI]
Bone Mineral Model	0.81 [0.72; 0.90]
Soft Tissue Model	0.88 [0.80; 0.96]
Combined Model	0.93 [0.88; 0.99]

ROC-AUC of bone mineral model, soft tissue model and a combined model of both.

Disclosures: Alexander Muehlberg, None.

MO0443

Bioelectrical Impedance Spectroscopy: A Reproducible Method of Muscle Mass Assessment. <u>Yosuke Yamada</u>*[1], <u>Bjoern Buehring</u>[2], <u>Diane Krueger</u>[2], <u>Neil Binkley</u>[2], <u>Dale Schoeller</u>[1]. [1]University of Wisconsin, Madison, USA, [2]University of Wisconsin, Madison, USA

Loss of leg muscle mass and function with aging increases falls and fracture risk. Widely accessible methods to detect muscle loss are confounded by the presence of multiple tissues, e.g., bone, fat, skin, etc. DXA is often used to evaluate lean mass but does not directly measure muscle. In fact, DXA essentially measures water and cannot distinguish intracellular (ICW) from extracellular (ECW) water. As Bioelectrical Impedence Spectroscopy (BIS) measures ICW, it may be a more specific marker of muscle mass. We hypothesized that BIS measurements would better correlate with muscle function than DXA lean mass. The aims of this study were to assess: 1) BIS reproducibility and 2) Correlate muscle function with BIS measured ICW and DXA lean mass in adults.

BIS was measured in 15 adults mean age 40.5 ± 16.1 (range 20-72) years by 3 technologists 3 times on the same day. Additionally, in 57 healthy adults (44W/13M age 26-76 years), total body DXA was performed. Resistance of ICW (RICW) and ECW (RECW) was measured by segmental BIS to estimate leg total water (TW), ICW and ECW. Leg muscle power was measured by jumping mechanography and grip strength by dynamometer. Correlation coefficients were statistically compared using Meng's statistical method.

The %CV for duplicate BIS ICW measures taken without repositioning was negligible (0.5%). When the same technician repositioned leg electrodes, the BIS CV was 2.2% and between technician CV was 2.6%. Thus, the total CV would be 3.5%, corresponding to 1.8% of the between subject ICW range in the reproducibility cohort. DXA leg lean mass (LLM) was only weakly correlated with age (r=-0.35) while BIS leg ICW displayed a significantly stronger correlation (r=−0.51, p=0.01). Moreover, BIS indicated a greater decrease with age than DXA (12.8% vs 6.7% per decade). The ratio of BIS ECW to ICW increased with age (r=0.72, p<0.001) indicating a relative ECW expansion with age that may blunt the ability of DXA to detect muscle loss. BIS ICW correlated better (p=0.007) with muscle power than DXA LLM (r =0.88 vs r=0.79).

In conclusion, BIS very reproducibly measures ICW. In a cross-sectional study, BIS ICW was more highly correlated with age and muscle power than DXA lean mass. Thus DXA measured LLM underestimates age effects on skeletal muscle mass and function due to ECW masking a lower amount of leg muscle mass. Further research is needed to determine if/how a combination of BIS and DXA may optimize fracture risk assessment.

Disclosures: Yosuke Yamada, None.

MO0444

Fibromodulin reprogrammed progenitor cell-based therapy for skeletal muscle generation. <u>Zhong Zheng</u>*[1], <u>Pu Yang</u>[2], <u>Omar Velasco</u>[3], <u>Elisabeth Lord</u>[3], <u>Kambiz Khalilinejad</u>[3], <u>Olivia Yue</u>[3], <u>Maxwell Murphy</u>[3], <u>Soyon Kim</u>[3], <u>Min Lee</u>[3], <u>Xinli Zhang</u>[4], <u>Kang Ting</u>[4], <u>Chia Soo</u>[3]. [1]UCLA, USA, [2]Sichuan University, China, [3]UCLA, USA, [4]University of California, Los Angeles, USA

Background: Millions of people suffer from deficient muscle mass caused by congenital musculoskeletal deformities, severe trauma or salvage surgeries. Unfortunately, *de novo* formation of skeletal muscle is unsatisfactory in these scenarios due to the lack of enough endogenous myogenic progenitor cells, while current cell-based restorative strategies for skeletal muscle generation are hindered by numerous obstacles, such as inadequate cell availability, limited cell spreading, poor survival ability, and tumorigenesis. Recently, our research group reported a simple method to reprogram somatic cells, such as dermal fibroblasts, to a multipotent state using a single extracellular molecule, fibromodulin (FMOD), instead of using oncogenes or an integrative genomics approach. The FMOD reprogrammed progenitor (FReP) cells do not exhibit tumorigenicity but demonstrate exceeding potential to generate skeletal muscle both *in vitro* and *in vivo*, making them a safer candidate for *in situ* skeletal muscle generation.

Methods: To generate large volume muscle tissues *in vivo*, it is important to maintain an appropriate cellular localization and retention to preserve cell-to-cell interaction. In this study, an injectable, photopolymerizable hydrogel composed of methacrylate glycol chitosan and type I collagen (MeGC/CI) was used to encapsulate $5x10^5$ FReP cells for transplantation in tibialis anterior (TA) muscle pouch SCID mouse model to develop a simple process for *in situ* skeletal muscle generation.

Results: Immunostaining showed more than 90% of MeGC/CI gel-encapsulated FReP cells with intense myogenic signals after a 3-week *in vitro* myogenic differentiation. qRT-PCR revealed marked increased expression of muscle-specific transcription factors and reduced expression of essential pluripotent regulators in FReP cells during the *in vitro* myogenic differentiation. Furthermore, with or without *in vitro* pre-myogenic differentiation, MeGC/CI gel-encapsulated FReP cells not only survived and differentiated into skeletal muscle tissue *in vivo*, but also significantly increased (~25%) the skeletal muscle mass of SCID mouse TA muscle at 1-month post-implantation.

Conclusion: In this study, we demonstrate the feasibility and ease of using MeGC/CI gel-encapsulated FReP cells for *in situ* skeletal muscle generation without tumorigenic risk. The FMOD reprogramming technology has promising future applications in reconstructive surgery that requires muscle augmentation and regeneration.

Disclosures: Zhong Zheng, Scarless Laboratories, 10

MO0445

Macro- and Microstructural Outcomes of Leg Muscle and Bone are Similar in Postmenopausal Women With and Without Osteoporosis. <u>Amanda Lorbergs</u>*[1], <u>Michael Noseworthy</u>[2], <u>Norma MacIntyre</u>[1]. [1]McMaster University, Canada, [2]McMaster University, Canada

Bone fragility is predicted by small muscle size in combination with greater fat infiltration. It is unknown if magnetic resonance imaging (MRI)-based outcomes of muscle composition differ in women with osteoporosis. Thus, we aimed to: 1)

compare MRI-based muscle and fat outcomes in healthy postmenopausal women with and without osteoporosis, and 2) determine the associations between muscle, fat and bone outcomes.

The sample (n=35, mean(SD)age=70(4)y) included 18 postmenopausal women with osteoporosis matched for age and physical activity with 17 postmenopausal women without osteoporosis. All women with osteoporosis were taking bone sparing medications. MRI (3T GE DiscoveryMR750) was used to evaluate muscle outcomes in the tibialis anterior (TA), tibialis posterior, soleus (SOL) and gastrocnemius (GC). TA, SOL and GC muscle and intramuscular fat volumes (cm^3) and total intermuscular fat volume (cm^3) were quantified from segmented proton density weighted images. Muscle microstructure was evaluated with diffusion tensor (DT)-MRI, which assesses mean water diffusivity (MD,mm^2/s) and fractional anisotropy (FA), a structural index of diffusivity. Muscle density (MuD,mg/cm^3), volumetric bone density and geometry (polar stress strain index, SSIp) were determined at the 66% tibia site using peripheral quantitative computed tomography (pQCT, Stratec XCT2000). One-way ANOVAs were performed to compare group means for each muscle, fat and bone outcome. Between-tissue associations were assessed using Pearson correlation coefficients.

Women with and without osteoporosis were similar in height (p=0.7) and weight (p=0.9). No group differences were observed in MD or FA for any leg muscle (all p>0.1). Similarly, muscle, intramuscular fat and intermuscular fat volumes and MuD did not differ (all p>0.3). Both groups had comparable values for tibia bone density and geometry. SSIp was positively correlated with MD in the SOL (r=0.55) and GC (r=0.49), FA in the SOL (r=0.37) and muscle volume in the TA (r=0.38) and GC (r=0.38). Our cross-sectional findings suggest that muscle, fat and bone outcomes are similar our sample of postmenopausal women with and without osteoporosis. Medication use may explain the group similarities, but longitudinal evaluation is warranted to determine if these outcomes change with treatment. Between-tissue correlations indicate that bone geometry is moderately related to site-specific muscle outcomes, but not fat macro- and microstructure in the leg.

Disclosures: Amanda Lorbergs, None.

MO0446

Muscle mass and adiposity, muscle strength, and physical performance vary by gender as risk factors for hip fracture: the Age Gene/Environment Susceptibility Study-Reykjavik. <u>Thomas Lang</u>*[1], <u>Sigurdur Sigurdsson</u>[2], <u>Gunnar Sigurdsson</u>[3], <u>Kristin Siggeirsdottir</u>[2], <u>Vilmundur Gudnason</u>[4], <u>Tamara Harris</u>[5]. [1]University of California, San Francisco, USA, [2]Icelandic Heart Association, Iceland, [3]Landspitali, Iceland, [4]Icelandic Heart Association Research Institute, Iceland, [5]Intramural Research Program, National Institute on Aging, USA

Muscle loss and increased muscle adiposity are linked to poorer physical function and increased hip fracture risk in the elderly. However, little is known about how gender influences muscle mass and muscle adiposity and function as these predict risk. .

We acquired hip CT scans in 4724 subjects (57% female) aged 66-90 years in Age, Gene/Environment Susceptibility Study (AGES-REYJAVIK), a study of community-dwelling men and women in Reykjavik, Iceland. CT analyses provided lean cross-sectional area (CSA, a muscle mass measure) and attenuation (HU, a measure of fatty infiltration and muscle quality) of the hip extensor muscles. We also measured timed up and go (TUGO) and knee extensor strength. As co-variates affecting physical performance and body composition, we included age, BMI, height, self-reported health status, and self-reported physical activity. Within gender, we defined three logistic regression models. First, we computed age-adjusted odds ratios (OR/SD) individually for all of the variables listed above. Second (Model A), we computed OR/SD for CSA, HU, TUGO and strength individually after adjustment for co-variates. A third model (Model B) examined predictor values simultaneously.

Over 7.7 years of follow-up, 68 men and 134 women had hip fractures (See Table). In age-adjusted logistic regressions, lower CSA, strength, and physical activity were significant risk factors for hip fracture in both men and women, but lower HU (poorer muscle quality) and higher TUGO time were significant only in men. Poorer health, and lower BMI were significantly associated with incident hip fracture only in women. In Model A, reduced hip CSA was individually associated with incident hip fracture in both men and women, but lower HU and strength and higher TUGO time continued to be significant in men but not women. When CSA, HU, strength and TUGO were combined in Model B, higher TUGO time and lower extensor HU were independent risk factors in men. In women, no independent risk factors remained. Although men and women shared some muscle and function-related risk factors for hip fracture, several risk factors were significant in only one gender. In women, but not in men, the relationship of muscle size and strength to hip fracture appeared to be explained by a combination of poorer health, lower BMI and lower physical activity. These results support the importance of gender for the design of preventive strategies related to function and body composition.

Table		
Age-adjusted logistic regression (OR/SD)		
	Men	Women
Leg Strength	1.37 [1.11, 1.70]	1.46 [1.17, 1.82]
TUGO	0.67 [0.55, 0.84]	0.91 [0.79, 1.07]
Extensor CSA	1.40 [1.10, 1.78]	1.60 [1.29, 2.00]
Extensor HU	1.55 [1.21, 1.97]	1.06 [0.54, 3.38]
BMI	1.31 [0.94, 1.84]	1.51 [1.24, 1.86]
Less Physical Activity	1.23 [1.03, 1.50]	1.29 [1.11,1.51]
Poorer Self-Reported Health	1.19 [0.97, 1.47]	1.34 [1.15, 1.59]

	Men		**Women**	
Logistic regression adjusted by age, height, BMI ,physical activity and health (OR/SD)				
	Model A	Model B	Model A	Model B
Leg Strength	1.34 [1.06,1.68]	1.16 [0.89,1.50]	1.25 [0.98, 1.60]	1.25 [0.97, 1.63]
TUGO	0.66 [0.54, 0.84]	0.74 [0.58, 0.97]	0.96 [0.82, 1.15]	1.10 [0.89,1.38]
Extensor CSA	1.36 [1.02,1.83]	1.00 [0.71,1.42]	1.30 [1.01,1.69]	1.22 [0.91, 1.65]
Extensor HU	1.73 [1.29, 2.31]	1.74 [1.23, 2.45]	1.17 [0.96,1.43]	1.07 [0.85,1.35]

Table

Disclosures: Thomas Lang, None.

MO0447

Muscular mass (MM) diferentiates women with low bone mass (BM) and osteoporotic fractures from those with low BM and no fractures. <u>Silvina Mastaglia</u>[1], <u>Alicia Bagur</u>[2], <u>Beatriz Oliveri</u>[3], <u>Carlos Mautalen</u>*[4]. [1]Laboratorio De Enfermedades Metabólicas Oseas, CONICET-UBA, Argentina, [2]Mautalen Salud e Investigacion, Argentina, [3]Mautalen, Salud e Investigación, Argentina, [4]Centro de Osteopatías Médicas, Argentina

In a retrospectic study of 41 women over 60 years of age, 38 of them had a BMD below - 1 SD of the total skeleton. Body composition obtained by DXA was reanalyzed. Eleven of these patients had suffered an osteoporotic fracture (6 vertebral, 4 non vertebral and 1 both). Muscular strenght or performances were not assessed.

The results of the whole group were: Age 75 $\pm$ 8 y.o., body mass index (BMI) 25.4 $\pm$ 4.0 kg/m^2, fat mass (kg) 24.1 $\pm$ 6.9, lean mass (kg) 34.1 $\pm$ 3.4 and total skeleton T-score -2.03 $\pm$ 0.82. Apendicular (aMM) (kg/m^2) 5.99 $\pm$ 0.72. Arms MM (arMM) (kg/m^2) 1.44 $\pm$ 0.21 and legs MM (lMM) (kg/m^2) 4.55 $\pm$ 0.6. The T-score of the aMM was -1.16 $\pm$ 1.03.

aMM had a significant correlation with lean mass (r= 0.63; p< 0.001) but a weak correlation with fat mass (r= 0 .42;p<0.01). arMM and lMM had the same correlation with lean mass (r= 0.63; p<0.001) and somewhat reduced correlation among them (r= 0.57; p<0.001)

Nine patients (25%) had an aMM below 2 SD of young reference woman (Presarcopenia) and 12 (31%) patients had a T- score between -1 and -2 SD (low aMM)

The group of patients with osteoporotic fractures (Fx) (n=11) was compared with the group without fractures (NoFx)(n=27) Although the former had greater age, lower BMI, lower fat mass, and lower BMD T-score the differences on this items were not significant. In contrast, statistically significant differences were observed on aMM (5.49 $\pm$ 0.57 vs. 6.16 $\pm$ 0.68 < p 0.005) aMM T-score (0.86 $\pm$ 0.96 vs. 1.87 $\pm$ 0.81 p < 0.005), arms MM (1.24 $\pm$ 0.18 vs. 1.51 $\pm$ 0.15; p< 0.001), legs MM (4.7 $\pm$ 0.6 vs. 4.25 $\pm$ 0.4; p < 0.03) and total lean mass (32.3 $\pm$ 25 vs. 35.2 $\pm$ 37.0; p < 0.02)

Five out of 11 of Fx patients had Presarcopenia and 5/11 had low aMM. One obese patient of this group had a normal aMM. In contrast only 15% of NoFx patients had Presarcopenia, and 27% low aMM.

These results emphasize the need to assess MM on patients with osteopenia with or without osteoporotic fractures to detect a risk factor for bone and general health. The study should also include evaluation of muscular strength and performance.

Disclosures: Carlos Mautalen, None.

MO0448

Nutrition and Physical Activity Determinants of Muscle Adiposity and Bone Density Measured by MRI and pQCT. <u>Andy Kin On Wong</u>*[1], <u>Karen Beattie</u>[2], <u>Hardik Valand</u>[3], <u>Laura Pickard</u>[2], <u>Alexandra Papaioannou</u>[4], <u>Jonathan Adachi</u>[5]. [1]McMaster UniversityUniversity Health Network, Canada, [2]McMaster University, Canada, [3]McMaster University, Canada, [4]Hamilton Health Sciences, Canada, [5]St. Joseph's Hospital, Canada

Objectives: 1) To assess how physical activity relates to lower limb bone and muscle properties; and 2) to evaluate the relationship between the same muscle and bone outcomes and each of dietary protein and creatine intake.

Methods: Women $\geqslant$ 50 years old from the CaMOS Hamilton site completed a 1.0 tesla (T) peripheral (p) MRI (fast-spin echo) and pQCT (20 mm/s, 38 kVp) scan at 66% of the tibial length. Inter+intramuscular fat (IMF) was segmented from muscle on MR images (5x2.0 mm thick, 195 µm resolution) using a region-growing algorithm. Total IMF area (A) and volumes (Vol), as well as total muscle proton density (PD) were determined. Muscles on pQCT images (2.3 $\pm$ 0.5mm thick, 500 µm resolution) were manually segmented from subcutaneous fat and bone using a watershed algorithm to compute muscle and cortical bone areas (MCSA, Ct.A) and density (MD, Ct.vBMD). All participants completed a Food Frequency Questionnaire

(FFQ), a Paffenbarger Physical Activity Questionnaire (PPAQ) and the Physical Activity Scale for the Elderly (PASE) with reference to activities within the last 7 days. Local grocery stores were surveyed to obtain meat wet weight and protein content standardized to serving size for all meat formats. Creatine was estimated based on concentrations published previously. A linear regression analysis quantified the relationship between muscle or bone outcomes and each of PPAQ, PASE, total protein, total creatine, and meat-specific protein and creatine contents, all adjusted for age and body mass index (BMI).

Results: Among 38 women (mean age: 75.3 $\pm$ 7.9 years; BMI: 27.03 $\pm$ 4.34 kg/m^2), muscle adiposity measures were most variable. None of the women were vegetarian. Women expended a mean 2387 $\pm$ 2648 kcal within a week but this did not relate to any muscle or bone outcome. Higher PASE score related to lower IMF.Vol and higher MD (Table I). Larger amounts of fish protein and creatine related to larger muscles and lower overall muscle adiposity while total protein and creatine, or that from other individual sources did not show any relation to muscle properties. Only higher total creatine consumption related to larger Ct.A and Ct.vBMD. These relations remained robust after adjusting for age and BMI.Conclusions: Women who exercise and eat more fish demonstrate larger and leaner muscles. The source of meat for creatine may be important for maintaining muscle quantities. Bone was more influenced by total creatine consumption than overall protein intake.

Table I. Relationship between muscle/bone outcomes and each of physical activity and dietary intake.
Linear regression analyses were performed with each of physical activity scale for the elderly (PASE), fish-derived protein, fish-derived creatine, and total creatine from all food sources as exogenous variables. Muscle (inter+intramuscular fat (IMF) volume, muscle area, proton density and muscle density) and bone (cortical (Ct.) cross-sectional area and volumetric bone density (vBMD)).

PASE (per +10 unit)	Unadjusted regression coefficients					Age & BMI-Adjusted	
	B	SE	Beta	R2	P	Beta	Model R2
MRI IMF Volume (mm³)	-116	53	-0.355	0.126	**0.036**	-0.127	0.517
MRI Muscle Area (mm²)	-149	462	-0.056	0.003	0.748		
MRI proton density (U/cm³)	-0.50	0.19	-0.418	0.175	**0.012***	-0.457	0.24
pQCT muscle density (mg/cm³)	0.20	0.10	0.49	0.24	**0.004***	0.402	0.435
Creatine Fish (per +1g)							
MRI IMF Volume (mm³)	-215.697	137.763	-0.263	0.069	0.127	-0.176	0.533
MRI Muscle Area (mm²)	2231	1095	0.334	0.112	**0.05***	0.303	0.321
MRI proton density (U/cm³)	-0.96	0.5	-0.32	0.103	0.061*	-0.345	0.169
pQCT muscle density (mg/cm³)	0.18	0.23	0.144	0.021	0.425	0.146	0.312
Creatine Total (per +1g)							
Cortical area	6.27	2.12	0.317	0.214	**0.006**	0.371	0.423
Cortical vBMD	5.49	1.91	0.288	0.206	**0.007**	0.288	0.285

* = significant at 95% confidence level after adjusting for BMI and age

Table I

Disclosures: Andy Kin On Wong, None.

MO0449

Nutritional Satus in Sarco-Osteoporotic Older Persons. <u>Ruth Huo</u>*[1], <u>Sandra Bermeo</u>[2], <u>Pushpa Suriyaarachchi</u>[3], <u>Piumali Gunawardene</u>[3], <u>Oddom Demontiero</u>[4], <u>Gustavo Duque</u>[5]. [1]University of New South Wales, Australia, [2]University of Sydney, Australia, [3]Ageing Bone Research Program, The University of Sydney, Australia, [4]The University of Sydney Nepean Clinical School, Australia, [5]Ageing Bone Research Program, University of Sydney, Australia

In older persons, the combination of sarcopenia and osteopenia/osteoporosis has been proposed as a subset of frailer individuals at higher risk of falls and fractures. Nutrition could be a determinant risk factor in the pathogenesis of sarco-osteoporosis (SOP) in older persons. In this study, we aimed to identify the nutritional status that is particular of SOP older persons. 680 subjects (mean age=79, 65% female) were assessed between 2009-2012 at the Falls & Fractures Clinic, Nepean Hospital (Penrith, Australia). Assessment included physical examination, bone densitometry and body composition by DXA, posturography, grip strength, mini-nutritional assessment (MNA), gait assessment (GaitRITE), and blood tests for nutritional status. Patients were divided in 4 groups: 1) osteopenia/osteoporosis (BMD<-1.0 SD); 2) sarcopenia (following the European Consensus criteria); 3) SOP and; 4) normal. Difference between groups was assessed with one-way ANOVA and chi square analysis. Multivariable logistic regression evaluated risk factors for being in the SOP group.

There were 258 SOP (37%), 241 with osteopenia/osteoporosis (35%), 87 just sarcopenic (12%) and 94 normal (15%) individuals. Mean age of SOP individuals was 80.40 years ($\pm$7.1 SD). Univariate analyses showed that SOP were more likely than normal to have a BMI lower than 25 (OR 2.42 95%CI 1.45-4.041, p<0.001), a MNA score less than 12 (OR 2.013, 95%CI 1.158-3.497, p<0.05), serum folate less than 20 (OR 4.011 95%CI 1.355-11.876, p<0.01) and hemoglobin less than 130g/L (OR 2.056 95%CI 1.278-3.309, p<0.01). Multivariate analysis showed that a MNA score less than 12 was independently associated with SOP compared to normal when adjusted for age and gender. Hypoalbuminaemia was associated with just osteoporosis (OR: 2.034, 95%CI 1.083-3.819, p<0.01) and just sarcopenia (OR: 1.771, 95%CI 1.025 – 3.062, p<0.01) compared to normal. No differences in vitamin D, eGFR, albumin, corrected calcium, phosphate, or vitamin B12 levels were found between the subgroups.

In summary, we have fully characterized the nutritional status of SOP patients. Our results indicate that close monitoring for low hemoglobin, low serum folate, and low BMI in SOP patients should be combined with appropriate nutritional

supplementation as essential components of the clinical and therapeutic approach to SOP older persons.

Disclosures: Ruth Huo, None.

MO0450

Osteosarcopenic Obesity Is Associated with Functional Disabilities in Obese Postmenopausal Women. <u>Julia E. Inglis</u>[1], <u>Owen J. Kelly</u>[2], <u>Jasminka Z. Ilich</u>*[1]. [1]Florida State University, USA, [2]Abbott Nutrition, USA

Introduction: Recently, we defined a new condition that encompasses osteopenia/osteoporosis (loss of bone) and sarcopenia (loss of muscle mass and strength) in the presence of obesity and named it osteosarcopenic obesity. This combined condition may be associated with greater functional disabilities and increased risk for falls and fractures than each individual condition alone. The purpose of this study was to identify women with osteosarcopenic obesity, assess some of their functional performance measures and compare them with those in obese-only women.

Methods: The study included 225 obese (%body fat>30) postmenopausal women, age and BMI 61.8$\pm$8.5y and 28.9$\pm$5.0kg/m2 (mean$\pm$SD), respectively. Bone, muscle and fat mass was measured by iDXA (GE Healthcare). Sarcopenia was identified from linear regression residuals utilizing appendicular muscle mass/height2 and osteopenic/osteoporotic status from T-scores of L1-L4 vertebrae and/or femoral neck, resulting in n=37 women with osteosarcopenic obesity who were compared with n=53 obese women (without sarcopenia or osteopenia). Handgrip strength (both arms combined) and 8-meter brisk and normal walking speed/number of steps were assessed.

Results: Results showed significantly lower values for handgrip strength (44.6kg vs. 53.5kg) and slower brisk walking speed (4.4 sec vs. 3.8 sec) in osteosarcopenic obese women compared to obese-only women, p=0.0017 and p=0.0003, respectively by ANOVA adjusted for age and BMI with Scheffe's post hoc tests.

Conclusion: These results indicate a greater decline in function in the obese women diagnosed as osteosarcopenic obese, suggesting a greater need for medical recognition of the fat-bone-muscle triad and specific therapy of this combined condition.

Disclosures: Jasminka Z. Ilich, None.

MO0451

The relationship between bone and muscle and its affecting factors. <u>Sangmo Hong</u>*[1], <u>Woong Hwan Choi</u>[2]. [1]Hanyang University, South Korea, [2]Division of Endocrinology, Department of Internal Medicine, College of Medicine, South Korea

Background: Muscle mass was known to related with bone mineral density. However there were few data for affecting factor to this relationship. In this study, we investigated the affecting factor to the relationship between bone and muscle.

Subjects and Methods: The data from a population-based survey, namely, The Korea National Health and Nutrition Examination Survey (KNHANES) IV (08-09) & V(10) (18,007 subjects), were analyzed. We studied the relating factor (anthropometric data and insulin resistance) to bone mineral density(BMD)/[appendicular lean mass(ALM)/(height)^2].

Result: With increasing age, BMD/ALM(ht)^2 was increasing in men (B=0.126, p<0.001) but decreasing in women (B= - 0.408, p<0.001). After adjusting age, fat mass (men: B=-0.186, p<0.001, women: B=-0.162, p<0.001) and waist circumference (men: B=-0.186 , p<0.001, women: B=-0.162, p<0.001), fasting insulin level (men: B=-0.108, p=0.002, women: B=-0.088, p=0.016) was negatively related with BMD/ALM(ht)^2. And insulin resistance (HOMA-IR) was also negatively related with BMD/ALM(ht)^2 (men: B=-0.115 , p<0.001, women: B=-0.121, p<0.001). HDL cholesterol level had positive relation with BMD/ALM(ht)^2 (men: B=0.081, p<0.001, women: B=0.115, p<0.001).

Conclusion: In this study, bone and muscle relation was differing between men and women. And obesity and insulin resistance may be weakening the relationship between bone and muscle.

Disclosures: Sangmo Hong, None.

MO0452

Age-Related Changes in Osteocyte Connectivity and Bone Structure in a Murine Model of Aging. <u>LeAnn Tiede-Lewis</u>*[1], <u>Yixia Xie</u>[2], <u>Vladimir Dusevich</u>[2], <u>Molly Hulbert</u>[2], <u>Mark Dallas</u>[2], <u>Lynda Bonewald</u>[1], <u>Sarah Dallas</u>[1]. [1]University of Missouri - Kansas City, USA, [2]University of Missouri - Kansas City, USA

Age-related bone loss and associated increased fracture risk are major clinical problems. Although previously viewed as quiescent, osteocytes are now known to be important regulators of osteoblast and osteoclast function and play key roles in regulation of bone mass in response to hormonal signals, mechanical loading and aging. Osteocytes are interconnected, not only with each other but also with cells on the bone surface, however it is not clear if this connectivity is maintained with aging. Here we have used multiplexed 3D confocal imaging to compare osteocytes in

young adult (5Mo) and aged (22Mo) C57BL/6 mice and combined this with microCT, histological and electron microscopical analysis.

3D confocal imaging of osteocytes using phalloidin and DAPI staining showed dramatic differences in osteocyte morphology and connectivity with aging in the midshaft of the femur which were more prominent in the distal femur. Aging resulted in a 25% reduction in dendrite number per osteocyte (p<0.05) and a 17% reduction in osteocyte number/mm^3 bone (p<0.05). Extensive cortical remodeling was seen, resulting in reversal lines that appeared as discontinuities, especially in endocortical regions. Osteocyte dendrites did not connect across these discontinuities, resulting in isolated "islands" of osteocytes. Occasionally dendrites were observed without a cell body, suggesting that dying osteocytes may leave dendrite remnants behind. Confocal imaging with the membrane dye DiI confirmed reduced osteocyte dendrite number and connectivity in aged mice. We have previously shown in young mice that osteocytes deposit microvesicles into bone matrix and also found abundant vesicle-like material in bone in aged mice. MicroCT analysis showed decreased trabecular bone volume, expansion of the cortical diameter, irregular cortical thickness and intracortical remodeling in aged mice, with abundant cortical porosities that were more pronounced in females than males. Histological analysis showed that the cortical porosities contained marrow. In aged male mice the growth plate was reduced or absent. Together these data show dramatic differences in osteocyte connectivity and bone geometry and structure with aging. Discontinuities in bone may not only compromise the mechanical properties of the bone but may also impair mechan-oresponsiveness of osteocytes by decreasing their connectivity. This may partially explain the age-related reduction in skeletal responsiveness to mechanical loading.

Disclosures: LeAnn Tiede-Lewis, None.

MO0453

Autophagy is Activated in Bone and Joint Cells During Lineage Commitment and is Regulated *In Vivo* by Diet and Ageing via SirT1. Emma Morris*[1], Pradeep Sacitharan[1], Victoria Treasure[1], Tonia Vincent[1], James Edwards[2]. [1]University of Oxford, United Kingdom, [2]University of Oxford, United Kingdom

Autophagy is a process of 'good housekeeping'. Cellular debris is degraded and recycled back to preserve energy homeostasis and optimal cell function. Defective autophagy is linked to ageing where impaired clearance reduces cellular activity - a common feature in ageing tissues and age-related disorders including osteoarthritis and osteoporosis. This study uses diet modification and genetically modified mice in combination with molecular and pharmacological approaches to explore the hypothesis that impaired autophagy underlies bone and joint disorders, and may be regulated by known ageing- and energy-related factors, such as the epigenetic modifier SirT1.

Autophagy is activated by nutrient starvation. Serum starvation of chondrocyte (HTB-94) or osteoblast (2T3) cell lines increased SirT1 protein and expression of the essential autophagy-related factor LC3 (western blot and IF staining). In vivo, SirT1 expression is elevated 10-fold in bone and joint tissue of mice on a calorie restricted (CR) diet compared to ad libitum (AL)-fed controls (p<0.001). Importantly, CR-fed mice had higher BMD (mgHA/ccm) at 185.7±11.5 Vs 140.3±6.0 in AL-fed controls (p<0.01), following long bone μCT analysis. This corresponded with significantly higher trabecular BV/TV in CR-fed mice (10.8% ±0.4% Vs 6.7% ± 0.5%, p<0.0001), opposite to that observed in SirT1-deficient and ageing mice, suggesting that SirT1 regulation via nutrient sensing pathways may improve autophagy and skeletal integrity. In support of this, LC3 protein expression is decreased in osteoblasts in SirT1-deficient and ageing (24mth) mice compared to WT or young (1mth) respectively, whilst a CR diet significantly elevates LC3 expression (Vs AL).

Pharmacological inhibition of SirT1 (Ex-527; 0.2-10uM) decreased differentiation and functional activity in both cell types, evidenced by reduced gene expression (COL2A1, Aggrecan, p<0.01) and mineralisation respectively. Similarly, SirT1 siRNA significantly inhibited growth and activity, whilst pharmacological activation of SirT1 (SRT1720; 0.5-5uM) stimulated the expression of pro-differentiation markers (p<0.01). Importantly, pharmacological and molecular regulation of SirT1 con-comitantly altered the gene expression of key autophagy markers (Beclin-1, ULK-1, LC3, p<0.01) and LC3 conversion.This data suggests that the ageing-related molecule SirT1 may mediate dietary effects, such as following CR, in the bone and joint by controlling autophagy in these cells.

Disclosures: Emma Morris, None.

MO0454

Do Senescent Cells Accumulate in the Bone Microenvironment with Aging?. Joshua Farr*[1], Daniel Fraser[2], David Monroe[3], Sundeep Khosla[4]. [1]Mayo Clinic, USA, [2]Mayo Clinic, USA, [3]Mayo Foundation, USA, [4]Mayo Clinic College of Medicine, USA

With aging, there is now overwhelming evidence that cells can undergo cellular senescence, which results in the permanent arrest of proliferation. Moreover, because with advancing age senescent cells accumulate in tissues and secrete factors that cause inflammation, these "bad" cells and their senescence-associated secretory phenotype (SASP) have been hypothesized to disrupt tissue morphology and function and to promote degenerative pathologies. To date, however, age-related cellular senescence effects in bone have received insufficient attention.

To assess whether senescent cells accumulate in the bone microenvironment of aged mice *in vivo*, we measured senescence-associated β-galactosidase (SA-β-Gal) abundance – an established biomarker of cellular senescence. As evident in Figure, both the bone cortex (Panel A) and bone marrow (Panel B) of old (24 month) wild-type (WT) C57BL/6 female mice stained strongly for SA-β-Gal. By contrast, SA-β-Gal abundance was nearly undetectable in matched young (6 month) WT female mice (Figure C and D). Next, we harvested bones from young (6 month) and old (24 month) WT C57BL/6 female mice (n = 6 per group) and obtained RNA from bone marrow derived hematopoietic lineage negative (lin-) cells, which represent a highly enriched osteoprogenitor cell fraction, and from cortical bone that had been flushed to remove marrow cells. Quantitative reverse transcription-polymerase chain reaction analysis revealed that transcript levels of p16^{Ink4a}, a principle mediator of senescence, were significantly elevated in both the bone cortex (by 2.7 fold; P < 0.001) and bone marrow (by 4.1 fold; P < 0.05) of old relative to young mice. In addition, p19 and p53 expression levels were also higher in the bone marrow of aged mice. Because the SASP has not been previously characterized in bone, we also examined a panel of genes associated with SASP acquisition in various soft tissues. Interestingly, expression levels of Ccl2, Icam1, Mmp12, and Sfrp1 were significantly (all P < 0.05) higher in cortical bone cells of old versus young mice.

These findings thus indicate that senescent cells accumulate in the bone microenvironment and acquire multiple SASP components with aging. Therefore, senescent cells are present at the expected time and site of osteoporosis. Our findings point to the need to establish if and how senescent cells are causally implicated in mediating age-related bone loss and whether their removal can delay or prevent this loss.
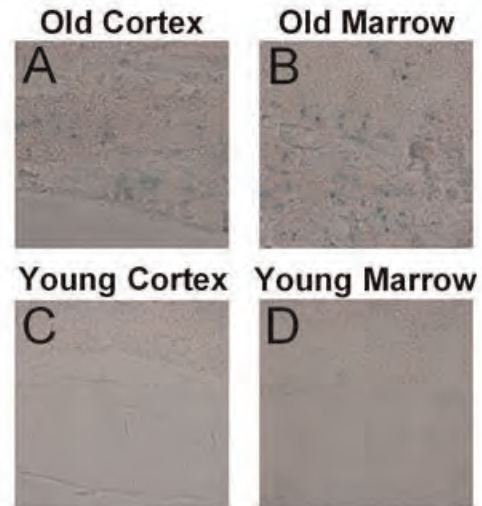
Figure

Disclosures: Joshua Farr, None.

MO0455

Withdrawn

MO0456

Role of sonic hedgehog in the process of fracture healing with aging. Tsuyoshi Shimo[1], Kenichi Matsumoto*[2], Naito Kurio[3], Tatsuo Okui[2], Yuu Horikiri[2], Akira Sasaki[4]. [1]Okayama University Graduate School of Medicine, Dentistry & Pharmaceutical Sci, Japan, [2]Okayama University Graduate School of Medicine, Dentistry & Pharmaceutical Sciences, Japan, [3]Japan, Japan, [4]Okayama University, Japan

Introduction: Previously, we have reported that sonic hedgehog (SHH) signaling was activated in osteoblasts at the dynamic remodeling site of a bone fracture. In this study, we compared and examined the distribution patterns of SHH and functional effect of SHH signaling on the osteoclastogenesis between young-aged and elderly mice during fracture healing.

Methods: The right eighth ribs of male ICR mice (8-week-old and 60-week-old) were fractured, resected, decalcified, and immunohistochemical staining and RT-PCR analysis were performed. To evaluate the effects of Hedgehog signaling on osteoclastogenesis associated with aging in vitro, osteoclast formation assay and pit formation assays were performed by using mouse bone marrow cells.

Results: SHH was expressed in bone marrow cells in the young-aged rib of mice fractured site on day 3. However, SHH protein and mRNA was barely detectable in the fractured site in the elderly rib of mice. Tartrate-resistant acid phosphatase (TRAP) positive cell number at the margin of the cortical bone were significantly greater in young-aged mice than elderly mice. On the other hand, osteoclast precursor

cells derived from bone marrow cells were cultured with receptor activator for nuclear factor-κB ligand (RANKL), TRAP positive cells were significantly greater in elderly mice than young-aged mice. Cyclopamine, anatagonist of smoothened, suppressed the RANKL upregulated osteoclast formation and resorption greater in elderly mice than young-aged mice, and SAG, agonist of smoothened, rescued the inhibition.

Conclusion: SHH signaling was suppressed in bone marrow cells and down-regulated osteoclast formation and resorption at the dynamic remodeling site of an elderly bone fracture.

Disclosures: Kenichi Matsumoto, None.

MO0457

Role of the Oxidized Tryptophan Metabolite L-Kynurenine in Age Induced Bone Loss. <u>Mona El Refaey</u>*[1], <u>Eileen Kennedy</u>[2], <u>Qing Zhong</u>[1], <u>Kehong Ding</u>[1], <u>William Hill</u>[3], <u>Xing-Ming Shi</u>[1], <u>Jianrui Xu</u>[4], <u>Wendy Bollag</u>[4], <u>Monte Hunter</u>[4], <u>Mark Hamrick</u>[5], <u>Carlos Isales</u>[1]. [1]Georgia Regents University, USA, [2]Univesity of Georgia, USA, [3]Georgia Regents University & Charlie Norwood VAMC, USA, [4]Georgia Regents University, USA, [5]Georgia Health Sciences University, USA

Age-dependent bone loss has been well documented in both human and animal models. Although the underlying causal mechanisms are not known changes in hormonal status or circulating levels of inflammatory cytokines have been implicated. We previously reported that aromatic amino acids activated signaling pathways in osteoprogenitor cells involved in protein synthesis in vitro and that in contrast the oxidized metabolites of these aromatic amino acids blocked the activation of these anabolic pathways and activated catabolic pathways instead. Our group had also previously shown that C57BL/6 mice have a characteristic pattern of bone gain with a peak around 12 months, followed by a subsequent marked decline in bone mass by 24 months of age. Since it has been proposed that aging is associated with an increase in the generation of damaging reactive oxygen species, our hypothesis was that the oxidized products of dietary aromatic amino acids could play a role in aged induced bone loss by altering osteoprogenitor cell differentiation or activating osteoclastic activity. In this study, we first examined the bone marrow concentration of the oxidized aromatic amino acids in mature (12 month) vs aged (24 months) C57Bl6 mice and found that kynurenine, the oxidized product of the aromatic amino acid tryptophan, was found in the highest concentration. Thus, we tested the effects of kynurenine, fed as a dietary supplement, on the bone mass of twelve-month-old C57BL/6 mice compared to a normal protein diet to see if it would induce a pattern consistent with age related bone loss. Twelve-month-old, male C57BL/6 mice were fed one of four diets; 18% protein diet (normal protein diet); 8% protein diet + tryptophan; 8% protein diet + kynurenine (50 μM) and 8% protein diet + kynurenine (100 μM) for 8 wks. Bone densitometry and micro-CT analyses demonstrated significant bone loss with the kynurenine diet. Histological and histomorphometric studies showed a decrease bone formation and an increase in osteoclastic activity in the kynurenine groups, these animals also had increased serum pyridinoline, a marker of bone breakdown. Thus, these data demonstrate that feeding an oxidized product of an essential amino acid induces bone loss in a pattern consistent with accelerated aging and we propose that one of the mechanisms involved in age induced bone loss may be from alterations of dietary nutrients by the increased generation of reactive oxygen species associated with aging.

Disclosures: Mona El Refaey, None.

MO0458

Effects of Aging on Bone and Muscle in Male and Female Mice Lacking a Single Allele of β–catenin in Osteocytes. <u>Nuria Lara</u>*[1], <u>Julian Vallejo</u>[2], <u>Mark Begonia</u>[3], <u>Mark Dallas</u>[3], <u>Madoka Spence</u>[3], <u>Leticia Brotto</u>[3], <u>Marco Brotto</u>[1], <u>Mark Johnson</u>[4]. [1]University of Missouri - Kansas City, USA, [2]UMKC, USA, [3]University of Missouri-Kansas City, USA, [4]University of Missouri, Kansas City Dental School, USA

We have shown previously that 6 month old mice lacking one allele of β–catenin in osteocytes (HET cKO) (β–catenin fl/+ X Dmp1-Cre mice) do not respond to anabolic loading. We also observed a greater loss of trabecular bone in females versus males. In this current study we sought to determine the effect of aging on bone loss and muscle function in these mouse models.

Analysis of femurs from 18 month old controls and HET cKO mice using microCT showed differences in the cortical compartment in male controls (n=3) versus male HET cKO (n=6) in BV/TV (%) 91.1 $\pm$ 0.78 vs 88.8% $\pm$ 1.01, cortical thickness (mm) 0.19 $\pm$ 0.01 vs 0.15 $\pm$ 0.02 and bone area (mm^2) 0.99 $\pm$ 0.08 vs 0.82 $\pm$ 0.06 respectively (p<0.05). Females showed no changes in cortical bone. Controls and HET cKO of both genders had significantly decreased trabecular bone compared to 6 month old animals. Using reference point indentation (RPI) we observed that the indentation distance increase was greater in male HET cKO mice compared to other groups. Muscle function in these mice was assessed in the Extensor Digitorum Longus (EDL) and Soleus muscles using a well-established ex-vivo contractility assay. In the female EDL specific force (N/cm^2) at submaximal frequency of stimulation (20 Hz) was greatly reduced in the HET cKO (9.7 $\pm$ 2.0) vs controls (17.5 $\pm$ 12.5) (n=12, p<.05), however, in Soleus there was no difference. In female EDL and Soleus the % of maximal tetanic force was significantly higher in HET cKO vs control at both high

(120 Hz) and low (20 Hz) levels of stimulation. In female Soleus the % force remaining at submaximal frequency of stimulation was significantly higher in controls vs HET cKO after zero Calcium or after 5 min of fatigue stimulation, while the EDL showed no differences in these functional endpoints.

These studies demonstrate that aging results in loss of trabecular bone in both genders. Deletion of a single allele of β-catenin in osteocytes in male mice also results in changes in their cortical compartment not observed in females with aging. The observed changes in muscle function with aging resulting from the loss of a single allele of β-catenin in osteocytes could reflect decreased loading of bone and/or might reflect the loss of an unknown bone-to-muscle secreted factor important for muscle function. These data support a central role of β-catenin in osteocytes in the maintenance of bone and muscle across aging and/or crosstalk between these two tissues.

Disclosures: Nuria Lara, None.

MO0459

Skeletal muscle index using height overestimate muscle mass in the elderly women: Japanese Population-based Osteoporosis (JPOS) cohort study. <u>Takahiro Tachiki</u>*[1], <u>Masayuki Iki</u>[1], <u>Jun Kitagawa</u>[2], <u>Naonobu Takahira</u>[3], <u>Junko Tamaki</u>[4], <u>Yuho Sato</u>[5], <u>Etsuko Kajita</u>[6], <u>Sadanobu Kagamimori</u>[7], <u>Yoshiko Kagawa</u>[8], <u>Hideo Yoneshima</u>[9]. [1]Kinki University Faculty of Medicine, Japan, [2]Kitasato University, Japan, [3]Kitasato University, Japan, [4]Osaka Medical College, Japan, [5]Jin-ai University, Japan, [6]Nagoya University, Japan, [7]University of Toyama, Japan, [8]Kagawa Nutrition University, Japan, [9]Shuwa General Hospital, Japan

Aim: Sarcopenia is a syndrome characterized by progressive and generalized loss of skeletal muscle mass and strength leading to an increased risk of adverse outcomes such as physical disability, poor quality of life and mortality. Skeletal muscle index (SMI: appendicular muscle mass (AMM) /height^2) is used to assess muscle mass and is included in a diagnostic criterion of sarcopenia. Muscle mass decreases with aging. In the elderly, however, SMI may not decrease with advancing in age due to age-related height reduction. Arm span is closely related to height in young adults and does not decrease in the elderly as much extent as seen in height. Therefore, use of arm span instead of height in calculation of SMI may improve accuracy of SMI in the elderly. This study aimed to evaluate the accuracy of SMI using height and arm span by comparing their relationship with aging.

Methods: The subjects were 450 women aged 50 to 91 years at baseline (mean age, 70.2 $\pm$ 7.9 years) who participated the baseline and 15- or 16-year follow-up surveys in the Japanese Population-based Osteoporosis (JPOS) cohort study. All subjects had undergone natural menopause more than 10 years before follow-up, and did not have abnormalities in bone metabolism. Subject's height was measured at baseline and at followed-up, and arm span was determined at baseline. AMM was measured by using dual-energy X-ray absorptiometry (QDR4500A, Hologic, USA) at followed-up. Height-SMI was calculated from AMM divided by height squared at followed-up. Arm span-SMI was calculated with arm span the instead of height. The Pearson correlation coefficient was used to determine the correlations of age with SMI and arm span-SMI. Statistical significance was defined a priori as p<0.05.

Results: Height of subjects was 152.7 $\pm$ 5.4 cm at baseline, and decreased to 150.6 $\pm$ 6.0 cm at follow-up. Mean SMI using baseline height was 6.66 $\pm$ 0.66, which increased to 6.85 $\pm$ 0.70 when using height at follow-up. Arm span-SMI was 6.77 $\pm$ 0.71 kg/m^2. There was no significant correlation between height-SMI at follow-up and age whereas arm span-SMI was significantly negatively correlated with age (r = –0.23, p < 0.01).Conclusions: The lack of age-related changes in height-SMI was considered to be a consequence of a reduction in height in elderly women. We conclude that height-SMI overestimates muscle mass in older people and recommend the use of arm-span SMI for them.

Disclosures: Takahiro Tachiki, None.

MO0460

Reducing Fall and Unsteadiness of Gait through Mechanical Loading of Vertebral Facet Joints. <u>Mehrsheed Sinaki</u>*. Mayo Clinic, USA

Objective: This study was conducted to determine the outcome of dynamic counterstrain and reorientation of specific vertebral facet joints to achieve reduction in risk of falls by reducing gait unsteadiness.

Subjects and Methods: Two groups of subjects were identified in our outpatient clinic. Group A consisted of 36 patients who had gait disorder and propensity to falls, referred to our outpatient clinic for fall prevention. To meet the inclusion criteria all had to have comprehensive musculoskeletal and neurological evaluations. Subjects in this group were not able to return for follow up due to the distance from our institution. They all signed the consent form and were videotaped for gait analysis.

Group B consisted of fourteen subjects who were able to return for follow up and all underwent two supervised training sessions in our outpatient clinic. They had formal laboratory gait analysis and computerized dynamic posturography at baseline and follow up. They were instructed for a 4-week spinal proprioceptive extension exercise dynamic (SPEED) program to be performed at home with use of a weighted kypho- orthosis (WKO). The WKO when applied properly accentuates a patient's perception of spinal joint position.

Intervention: All subjects had the trial of spinal proprioceptive extension exercise dynamic (SPEED) program.

Outcome: Subjects had either laboratory gait analysis, computerized dynamic posturography and strength evaluation or were videotaped.

Results: All subjects in group A were videotaped before and after WKO trial and displayed noticeable improvement often to their surprise. They decided to implement the program at home. Subjects in group B returned after a 4-week implementation of prescribed treatment and, showed a significant change in balance (P=.003) and several gait parameters (P<.05). Mean back extensor strength improved significantly from baseline (144.0±46.5 N) to follow-up (198.6±55.2 N; P<.OOl).

Conclusion: Balance, gait, and risk of falls improved significantly through mechanical stimulation of the vertebral facet joints and application of counterstrain to specific areas of spine. This method of intervention might potentially lead to novel investigations for managing patients with unsteadiness of gait and propensity to falls.

Disclosures: Mehrsheed Sinaki, None.

MO0461

Differential Bone Regeneration Starts as early as Seven Days after Marrow Ablation in Two Mouse Strains. Meghan Moran*[1], Amarjit Virdi[2], D. Rick Sumner[2]. [1]Rush Medical College, USA, [2]Rush University Medical Center, USA

It is well-established that mouse strains exhibit varied intact bone phenotypes, including bone mass, bone mineral density and mechanical properties. Various mouse strains and genetic models also exhibit differential responses to injury challenges such as ear punches, articular cartilage notches and fracture healing. However, there is limited data on intramembranous bone regeneration after an injury challenge in different mouse strains. We previously established that bone regeneration varies among different inbred wild type mouse strains using a mechanical marrow ablation model. From that study, we identified good (FVB/N) and poor (Balb/c) bone regeneration strains. There are time-dependent phases involving inflammation, repair and remodeling.

In this study, we aimed to identify during which phase the previously identified differential bony response occurred. To do this, we focused on the good (FVB/N) and the poor (Balb/c) bone regeneration strains. We performed mechanical marrow ablation of the medullary canal in 11 week old FVB/N and Balb/c virgin female mice. Animals were euthanized 7 days and 21 days post-ablation. All bone within the medullary canal in the region between 30% and 60% of the total femur length was measured by microCT (6 µm voxels). This region is normally lacking bone in intact animals. The sample size was 6 animals per strain.

We found that BV/TV differences were present by 7 days and were still present at 21 days (Table 1, ANOVA strain effect p = 0.031, time effect p = 0.005, strain X time p = 0.258). Mean BV/TV varied between 3.48% at 7 days and 9.43% at 21 days post-ablation in FVB/N mice. This is approximately a 3-fold increase in BV/TV during 21 days. Mean BV/TV values were less but also varied from 1.89% at 7 days to 4.62% at 21 days in Balb/c mice. The differences in BV/TV over time and between strains were due mainly to differences in trabecular thickness.

The findings of the present study suggest that differential bone regeneration occurs during the repair phase and persists through the remodeling phase.

Time	Strain	Mean (%)	SD (%)
7 days	FVB/N	3.48	1.27
	Balb/c	1.89	1.17
21 days	FVB/N	9.43	5.78
	Balb/c	4.62	3.05

Table 1. Mean BV/TV Values for FVB/N and Balb/c at 7 and 21 days post-ablation

Disclosures: Meghan Moran, None.

MO0462

Osteogenic Capillaries Spatially Orient Pericapillary Osteoblasts to Direct Endochondral Ossification of the Malleus. Ichiro Takada[1], Kouji Shimoda[1], Yoshiaki Kubota[1], Masatsugu Ema[2], Yoshihiro Takeda[3], Nobuhito Nango[4], Wataru Yashiro[5], Atsushi Momose[5], Latifa Bakiri[6], Erwin Wagner[6], Koichi Matsuo*[7]. [1]School of Medicine, Keio University, Japan, [2]Shiga University of Medical Science, Japan, [3]Rigaku Corporation, Japan, [4]Ratoc System Engineering Co., Ltd., Japan, [5]Tohoku University, Japan, [6]Spanish National Cancer Research Centre (CNIO), Spain, [7]School of Medicine, Keio University, Japan

Endochondral ossification is a developmental process by which cartilaginous anlagen are replaced by bone. Once cartilage is vascularized and removed, bone matrix is laid down by osteoblasts. However, the spatio-temporal relationship between capillary endothelial cells and bone-forming osteoblasts remains elusive. Here we report that clusters of osteoblasts surrounding the capillary loop in the murine

malleus produce bone matrix such that the diameter of the capillary lumen rapidly decreases over two weeks after weaning. Synchrotron X-ray tomographic microscopy demonstrated a roughly concentric, cylindrical arrangement of osteocyte lacunae along capillaries, indicative of pericapillary bone formation. Remarkably, the reduction in capillary volume was significantly inhibited by both constitutive and inducible overexpression of the transcription factor Fra-1 (*Fosl1*) in transgenic animals. Finally, a concentric relationship between osteoblasts and endothelial cells was also observed at the growth plate and fracture healing sites of long bones in Fra-1 transgenic and wild-type mice. These data support the concept that, during endochondral ossification, osteogenic capillaries accompanied by pericapillary osteoblasts establish the orientation of microscopic bone formation to fill spaces within the original cartilage.

Disclosures: Koichi Matsuo, None.

MO0463

***Fgfr*1 and *Fgfr*2 signaling in the osteoprogenitor lineage is essential for skeletal growth and development.** Kannan Karuppaiah*[1], Kai Yu[2], Craig Smith[3], David Ornitz[4]. [1]Washington University School of Medicine in St. Louis, USA, [2]Seattle Children's hospital, USA, [3]Washington University St. Louis, USA, [4]Washington University School of Medicine, USA

Cell-specific roles for Fibroblast Growth Factor (FGF) signaling in skeletal development and the requirement for FGF-signaling for skeletal homeostasis and response to injury are not well understood. To explore the functions of FGF receptors 1 and 2 (FGFR1 and FGFR2) in the osteoprogenitor-lineage, we have conditionally inactivated *Fgfr1* and *Fgfr*2 using the *Osterix-Cre* deleter allele and floxed alleles of *Fgfr1* and *Fgfr*2 (DFF) to generate double conditional knockout (DCKO) mice. Lineage-specific expression of *Osx-Cre* was examined using the *ROSA26 mT/mG* and *ROSA26R-lacZ* reporter alleles. This lineage analysis revealed expression in most of the cells lining trabecular and cortical bone, approximately 20% of cells clonally distributed in the proliferating and hypertrophic chondrocyte regions of the growth plate, and in some cells within the bone marrow stroma. At birth, DCKO mice appeared phenotypically normal, however, showed an ~50% reduction in postnatal growth (total body weight) compared to control (DFF or *Osx-Cre*) mice. DEXA analysis revealed that the DCKO mice had a normal body fat content but significantly reduced bone mineral content. X-ray analysis showed reduced bone density and a proportionally smaller skeleton. Micro-CT analysis of long bones revealed a reduced trabecular BV/TV, bone mineral density (BMD), trabecular number, trabecular thickness, an increased trabecular separation, and a reduced cortical BV/TV in DCKO compared to control mice. Histological analysis of the long bones of P21 DCKO mice confirmed the reduced cortical thickness and showed decreased mineralized bone and reduced unmineralized bone matrix (osteoid) but normal osteoclast number. To explore the mechanisms accounting for decreased longitudinal bone growth we examined growth plate histology and cell proliferation in 3-week-old (P21) DCKO mice. Interestingly, DCKO mice showed a significantly reduced proliferating zone length and an 80% reduction in growth plate chondrocyte proliferation but a normal appearing hypertrophic chondrocyte zone. Molecular analysis revealed reduced expression of Type I Collagen and *Mmp13* and increased expression of *Fgfr3*. These observations suggest a mechanism in which FGFR signaling in osteoprogenitor cells, mature osteoblasts, or bone marrow stroma indirectly regulates chondrocyte proliferation, resulting in reduced longitudinal bone growth, and in which FGFR signaling in osteoblasts impairs osteoblast maturation and anabolic activity.

Disclosures: Kannan Karuppaiah, None.

MO0464

Bivariate genetic association analysis of pediatric total-body DXA parameters identifies two novel genetic variants that jointly influence bone mineral content and bone area. John P. Kemp*[1], Carolina Medina-Gomez[2], Nicole M. Warrington[1], Denise H.M. Heppe[2], Nicholas J. Timpson[3], Ling Oei[2], Beate St Pourcain[3], Claudia J. Kruithof[2], M. Carola Zillikens[2], Albert Hofman[2], André G. Uitterlinden[2], George Davey Smith[3], Vincent WV. Jaddoe[2], Jonathan H. Tobias[4], Fernando Rivadeneira[5], David M. Evans[3]. [1]University of Queensland Diamantina Institute, Translational Research Institute, Australia, [2]Erasmus University Medical Center, Netherlands, [3]MRC Integrative Epidemiology Unit, University of Bristol, United Kingdom, [4]School of Clinical Sciences, University of Bristol, United Kingdom, [5]Erasmus University Medical Center, The Netherlands

Aim: Genome-wide association (GWA) studies of osteoporosis traditionally involve univariate genetic association analysis of bone mineral density (BMD). As BMD is influenced by changes in bone mineral content (BMC) and bone area (BA), examining BMD alone may not detect genetic variants that have similar effects on BMC and BA. Moreover, simulation studies and statistical theory suggest that bivariate association analysis can be more powerful than genetic association analysis of univariate measures. Hence, we investigated whether bivariate genetic association analysis of BMC and BA could identify novel loci.

Methods: GWA meta-analysis was performed on 9393 subjects from the Avon Longitudinal Study of Parents and Children and the Generation R Study, using

HapMap2 imputed genotype data and DXA measures of BMC and BA [measured at the upper limbs (UL), lower limbs (LL), and total-body less head (TB)]. For each cohort, canonical correlation analysis was performed using best guess genotypes, adjusting for sex, age, weight, height and ancestry informative principal components. Meta-analysis using Fisher's product of P-values was conducted for ~2.3 million autosomal SNPs and compared to univariate GWA association meta-analyses of BMD, BMC and BA.

Results: Seven known BMD-associated loci reached genome-wide significance (GWS) at one or more skeletal sites: WNT4, GALNT3, CENPW, WNT16, CPED1, PTHLH and RIN3. Two novel loci [20p11.22 (GDF5: $P_{UL}=4 \times 10^{-9}$) and 17q24.3 (KCNJ2: $P_{TB}=4 \times 10^{-8}$)] achieved GWS and an additional four loci displayed strong association in the bivariate analyses: 13q33.2 (DAOA: $P_{TB}=7\times10^{-8}$), 5q35.1 (SH3PXD2B: $P_{LL}=8 \times 10^{-8}$), 10q22.1 (ADAMTS14: $P_{LL}=5 \times 10^{-7}$) and 3q26.1 (MIR-720, $P_{UL}=3 \times 10^{-7}$). No relationship was detected between the GDF5 locus and BMD ($P \geqslant 0.3$), despite varying degrees of association being observed for BMC and BA at the UL ($P_{BMC}=2 \times 10^{-5}$, $P_{BA}=2 \times 10^{-8}$), LL ($P_{BMC}=3 \times 10^{-2}$, $P_{BA}=1 \times 10^{-7}$) and TB ($P_{BMC}=2 \times 10^{-2}$, $P_{BA}=2 \times 10^{-4}$). Nominal associations ($P \leq 5 \times 10^{-2}$) between the KCNJ2 locus and BMD were observed at the UL and TB, but not the LL ($P=0.9$), while varying magnitudes of association with BMC and BA were detected at the UL ($P_{BMC}=4 \times 10^{-8}$, $P_{BA}=4 \times 10^{-8}$), LL($P_{BMC}=2 \times 10^{-4}$, $P_{BA}=2 \times 10^{-6}$) and TB ($P_{BMC}=3 \times 10^{-8}$, $P_{BA}=1 \times 10^{-9}$).

Conclusion: Bivariate genetic association analysis appears to be a powerful method for identifying novel genetic variants (missed by univariate analyses of BMD), that may influence bone growth and development via changes in bone mineralization and bone size.

Disclosures: John P. Kemp, None.

MO0465

Functional Roles of IGF-II on Cartilage during Postnatal Bone Growth under the Normal and Inflammatory Condition. <u>Tomoya Uchimura</u>*, <u>Li Zeng</u>. Tufts University, USA

Postnatal cartilage development is an important aspect of bone development. Despite its importance, precise mechanisms that govern early postnatal growth, which is growth hormone-independent, remain largely elusive. In addition, postnatal bone growth is subject to factors that are absent in utero. Here, we show that IGF-II has a previously unidentified role in postnatal bone growth. Our data indicate that IGF-II is essential for early postnatal cartilage development in terms of growth in length and girth. In addition, IGF-II plays an important role in resisting inflammation-induced abnormal development of growth plate.

Our IHC analysis showed that IGF-II is strongly expressed in articular cartilage and proliferating chondrocytes, but weakly in hypertrophic chondrocytes in the mouse metatarsal bone. Igf-II mutant bones are shorter and thinner, particularly between P0 and P10. Mutant bones showed increased hypertrophic differentiation (Col X), but similar proliferation rates (Ki67) in the growth plate compared to wild type. In contrast, mutant bones showed delayed hypertrophic differentiation in the secondary ossification center with higher levels of Ki67 staining. The perichondrium of Igf-II mutant bones was 1-2 cell layers thinner with reduced Sox9 and Ki67 staining. These data suggest a role of IGF-II in chondrocyte maturation as well as the maintenance and chondrogenic potential of the perichondrium in postnatal bone growth.

Under inflammatory stimulation of IL-1ß in ex vivo cultures, wild type metatarsal bones had severe longitudinal growth defects, reduced Col II and increased Col I, MMP13 and NF-κB/p65 expression in the growth plate and peri-articular surface. Igf-II mutant bones showed further IL-1ß-induced growth defects and cartilage matrix destruction, and exogenous IGF-II inhibited IL-1ß activity in wild type and partially did so in the Igf-II mutant. However, exogenous IGF-I only rescued the defects in the wild type, but not Igf-II mutant. These data suggest an essential role of IGF-II in preventing inflammatory stimuli-induced growth defects and cartilage destruction and indicate a functional difference between IGF-I and IGF-II.

This work has implications in understanding growth hormone-independent bone growth in early stages of postnatal development as well as bone growth arrest in children with chronic inflammation.

Disclosures: Tomoya Uchimura, None.

MO0466

Nell-1 is a Functional Mediator of Runx2 in Regulating Chondrogenic Differentiation. <u>Chenshuang Li</u>*[1], <u>Jie Jiang</u>[1], <u>Kang Ting</u>[1], <u>Xuepeng Chen</u>[2], <u>Yanheng Zhou</u>[3], <u>Chia Soo</u>[4], <u>Xinli Zhang</u>[1]. [1]University of California, Los Angeles, USA, [2]University of California, Los Angeles, USA, [3]and Hospital of Stomatology, Peking University, China, [4]University of Carlifornia, Los Angeles, USA

Objectives: The lack of Runx2 results in delayed chondrogenesis. Nell-1 functions downstream of Runx2 in osteogenesis, which partially rescues bone defects in Runx2^{+/-} mice. This study aims to examine the functional interaction of Nell-1-Runx2 during chondrogenesis at in vitro, ex vivo and in vivo levels. Methods: Nell-1 overexpression transgenic(CMV-Nell-1) mice were crossmated with Runx2^{+/-} mice to get Runx2^{-/-}/CMV-Nell-1 and Runx2^{-/-} newborns for gross and histological comparasion. The limb explants from E14.5 Runx2^{-/-} were cultured with/without rhNELL-1 for histological and immunohistochemical evaluation. At cellular and

molecular levels, primary embryonic mesenchymal progenitor cells from limb bud of E11.5 wild-type(WT) or Runx2^{-/-} underwent chondrogenesis in pellet culture with/ without rhNELL-1. The correlation of chondrogenic markers expression and morphological evolution was assessed by qPCR, histological and immunohistochemical staining. The activation of Ihh signaling and possible involvement of Runx3 in Nell-1 induced-chondrogenesis in absence of Runx2 were also analyzed from gene and protein levels. Results: Phenotypically, Nell-1 rescues Runx2^{-/-} chondrocyte maturation partially in neonatal femurs revealed by skeletal staining, histology and Collagen X expression. This rescuing effect was recapitulated in Runx2^{-/-} limb ex vivo model with exogenous rhNELL-1 treatment. Notably, the endogenous level of Nell-1 in Runx2^{-/-} primary chondrocytes was only a fraction of that in WT cells, and the upregulation of Nell-1 was achieved in chodnrocytes by AdRunx2 transduction. The delayed chondrogenic differentiation in Runx2^{-/-} pellets at both early and late stages was partially rescued with rhNELL-1 stimulation, which were evidenced by chodrogenic markers expression and morphological changes. Interestingly, rhNELL-1 increased gene expression of Ihh, Patched and Gli in Runx2^{-/-} chondrocytes dose-dependently. The expression pattern of Ihh signaling molecules in Runx2^{-/-}/CMV-Nell-1 femur was partially restored. Furthermore, the upregulation of Runx3 and Aggrecan and downregulation of Pthrp and Pthr1 with rhNELL-1 in Runx2^{-/-} cells were also observed. Conclusion: Our data clearly demonstrate that Nell-1 functions as a key functional mediator of Runx2 in chondrogenesis in addition to osteogenesis. The activation of Ihh signaling pathway is likely an underlying mechanism Nell-1 takes among the complex signaling networks of Runx2 in regulating chondrogenesis.

Disclosures: Chenshuang Li, None.

MO0467

Parathyroid hormone receptor signaling in dental mesenchymal progenitors is essential for tooth root formation. <u>Wanida Ono</u>*[1], <u>Noriaki Ono</u>[2], <u>Henry Kronenberg</u>[1]. [1]Massachusetts General Hospital, USA, [2]University of Michigan School of Dentistry, USA

Dental root formation is a dynamic process involving a series of epithelial-mesenchymal interactions, in which neural crest-derived dental mesenchymal cells are recruited and participate in biomineralization of dentin and cementum. Parathyroid hormone-related protein (PTHrP) and its PTH/PTHrP receptor (PPR) play crucial roles in organogenesis. PPR haploinsufficiency is associated with non-syndromic primary failure of tooth eruption in humans. However, how the PTHrP-PPR system regulates dental root morphogenesis is unknown. Here we show that PPR signaling in dental mesenchymal progenitors is essential for tooth root formation. Lineage-tracing experiments using tamoxifen-inducible creER recombinases with a Rosa26-tomato reporter revealed that cells expressing osterix (Osx), but not type I collagen (Col1), were root-forming mesenchymal progenitors contributing to all relevant cell types during molar root morphogenesis. Analysis of a LacZ knock-in allele showed that cells in the dental follicle and on the root surface predominantly expressed PTHrP. Deletion of the PPR in root-forming progenitors using Osx-cre, but not in mature mineralizing cells using osteocalcin (Oc)-cre or dentin matrix protein 1 (Dmp1)-cre, led to failure of eruption and significantly truncated roots lacking the periodontal ligament that resulted in ankylosis to the alveolar bone. Overexpression of a constitutively active PPR in Col1-expressing cells (Col1-caPPR) was insufficient to rescue these phenotypes. To further understand mechanisms regarding how PPR-deficient cells contribute to root formation, we conducted lineage-tracing experiments using the Osx-creER, Rosa26-tomato reporter and PPR-floxed alleles. Deletion of the PPR in Osx[+] progenitors at postnatal day 3 led to accelerated cementoblast differentiation that formed thick cellular cementum. qPCR analysis of FACS-sorted PPR-deficient Tomato^{+} cells showed a upregulation of nuclear factor I/C (Nfic), the putative transcription factor critical to root formation, and genes associated with mineralization including Bsp, Opn and Dmp1. Histone deacetylase-4 (HDAC4) appeared to be a candidate downstream mediator of PPR signaling, as its deletion using Osx-cre partially recapitulated the PPR root phenotype. These findings indicate that PPR signaling in dental mesenchymal progenitors is essential for orchestrated differentiation of cementoblasts, underscoring the importance of the PTHrP-PPR system in dental root formation and tooth eruption.

Disclosures: Wanida Ono, None.

MO0468

Withdrawn

MO0469

The *Hox* program in adult tissues: Continuing roles for embryonic patterning genes during skeletal regeneration. Danielle Rux*[1], Ilea Swinehart[2], Daniel Lucas-Alcaraz[2], Aleesa Schlientz[2], Steven Goldstein[3], Kenneth Kozloff[4], Deneen Wellik[5]. [1]University of Michigan, USA, [2]University of Michigan, USA, [3]University of Michigan Orthopaedic Research Lab, USA, [4]University of Michigan Department of Orthopaedic Surgery, USA, [5]University of Michigan Medical Center, USA

Hox genes are a unique and highly conserved set of transcription factors whose most prominent role is to pattern the limb and body axis. The four chromosomal clusters of mammalian *Hox* genes (A, B, C, and D) are subdivided into 13 paralogous groups based on sequence similarity and cluster position. Specifically, the *Hox11* paralogous group (*Hoxa11*, *Hoxc11*, and *Hoxd11*) patterns the axial sacral region and the limb zeugopod region (radius/ulna and tibia/fibula). Complete loss of *Hox11* function results in severe patterning defects of these elements during development. Using our *Hoxa11eGFP* knock-in allele, we have shown that *Hox11* is expressed broadly in early limb bud mesenchyme and is then quickly restricted to the zeugopod. It is excluded from the condensing chondrocytes that will become the skeletal elements, but is highly expressed in the perichondrium through newborn stages. Recently, we found that *Hox11* expression is retained in periosteum in adult animals, and also becomes predominant in the endosteum and the bone marrow stroma of the zeugopod. Importantly, GFP-positive cells are absent from other regions of the limb demonstrating that the regional-restriction of *Hox* is retained through adulthood. To examine the potential roles for *Hox* genes in adult tissue, we have performed regional fracture injuries in our mutants. First, we show that *Hox11* expression is expanded at the site of fracture injuries performed in zeugopod regions, specifically. Notably, it is strongly expressed in the periosteal-derived stromal layer of cells surrounding the callus. Second, we show that loss of *Hox11* function results in aberrant callus formation and delayed bridging of the fracture site compared to controls. Cartilage deposition is significantly reduced in *Hox11* mutants at all stages of repair, while new bone formation farthest from the fracture site appears unaltered. Our results are consistent with defects in endochondral ossification while intramembranous ossification appears unaffected. Additionally, remodeling of the bony callus is severely perturbed. Of note, loss of *Hox11* function does not affect repair in other regions of the limb. Continued work is focused on identifying cell type(s) in which *Hox11* is expressed to shed light on its function during bone regeneration. Overall, data presented, demonstrate a continued role for *Hox11* in adult bone tissue and, more broadly, suggests that the regionally-restricted *Hox* program is retained from embryonic development.

Disclosures: Danielle Rux, None.

MO0470

Withdrawn

MO0471

Vitamin D dose-response in young children 2 to 8 y of age: a 12 wk randomized clinical trial to establish requirements in the absence of ultra-violet beta solar radiation. Neil Brett*[1], Paula Lavery[2], Sherry Agellon[2], Catherine Vanstone[2], Jonathon Maguire[3], Frank Rauch[4], Hope Weiler[5]. [1]McGill University, Canada, [2]McGill University, Canada, [3]University of Toronto, Canada, [4]Shriners Hospital for Children, Montreal, Canada, [5]McGill University, USA

Canadian children do not meet the recommended dietary intake for vitamin D (VTD). Both VTD and calcium are well established as fundamental nutrients for calcium homeostasis and bone health. Yogurt and cheeses have only 15-30% of the VTD that fluid milk contains. No Canadian studies have investigated longitudinally, the amounts of dietary VTD needed to support current targets of VTD status. The objective was to determine whether a dose-response will be observed in response to a regular diet, one that meets the EAR and one that meets the RDA for vitamin D intakes. Healthy children 2 to 8 y (n=77) from Greater Montreal, randomized into age strata, consumed 1 of 3 dietary VTD targets (200, 400 or 600 IU/ day) for 12 wk starting in the winter. Fasting blood was sampled at baseline and 12 weeks for measurement of total serum 25(OH)D (Liaison, Diasorin) as well as ionized calcium (ABL80 Flex, Radiometer) followed by standardized anthropometry, demographics plus activity and dietary questionnaires. Data analysis used a mixed model ANOVA accounting for fixed effects (sex, age strata, dietary group, time) and random effects (e.g. baseline 25(OH)D and demographics) with *post-hoc* Bonferroni adjustment. Data are mean $\pm$ SD unless otherwise indicated. The participants were 54.5 % male (42/77) were 72.7 % (56/77) white and had healthy mean BMI z-scores of 0.50 (+ 0.85). Seventy five (97.4%) children (5.1 $\pm$ 1.9 y) completed the study with compliance of 86% for yogurt and 84% for cheese with no difference among dietary groups or age categories. Baseline VTD intakes were not different whereas intakes significantly differed at 12 wk (Table 1). No differences were observed in baseline 25(OH)D, while at 12 wk both the EAR and RDA groups had significantly higher VTD status compared to control (Figure 1A) and had a positive change in VTD status from baseline (Figure 1B). Average ionized calcium was within normal limits (1.15-1.38 mmol/L) in all groups. However, a group by time interaction (P=0.027) suggested ionized calcium values declined in the control group by 12 wk, but did not reach

statistical significance (P=0.0585) with no differences in the EAR or RDA groups. This data in healthy young children suggests that increasing dietary VTD intakes ameliorates the negative effects of the non-VTD synthesizing winter months on VTD status.

Table 1. Vitamin D intake (IU/d) in young children.

Assessment	Control group	EAR target group	RDA target group
FFQ baseline	269 $\pm$ 136[a] (n=24)	237 $\pm$ 103[a] (n=26)	225 $\pm$ 129[a] (n=25)
FFQ follow up	239 $\pm$ 77[a] (n=24)	424 $\pm$ 141[b] (n=25)	559 $\pm$ 175[c] (n=25)
24 h follow up	247 $\pm$ 135[a] (n=24)	379 $\pm$ 152[b] (n=23)	514 $\pm$ 324[c] (n=25)

* Boxes with different superscripts are significantly different. data are unadjusted mean±SD

vitamin D intake

Figure 1. Serum 25(OH)D concentrations at baseline and 12 wk (panel A); and change in 25(OH)D concentrations over time (panel B). Bars with different superscripts are significantly different, mixed model ANOVA adjusted for age, sex, ethnicity, baseline 25(OH)D, number of days between baseline and follow up with Bonferroni post hoc testing. Data was log transformed before analysis and are unadjusted mean±SD.
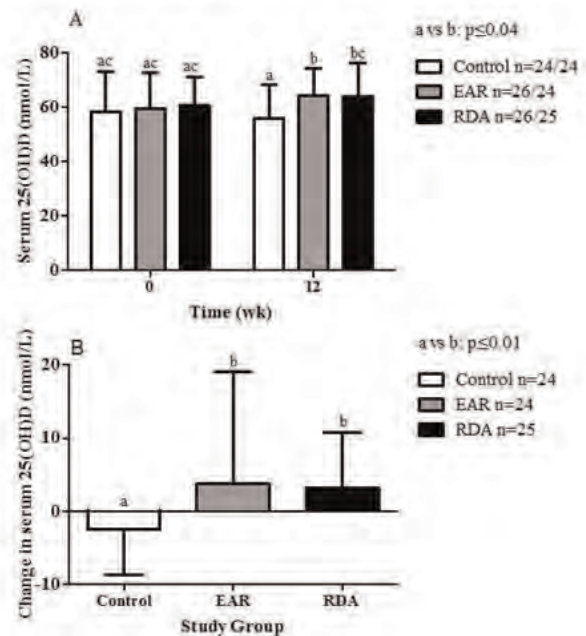
serum 25(OH)D concentrations

Disclosures: Neil Brett, None.

ADULT BONE AND MINERAL WORKING GROUP

WG1

A Case of a Family with Subclinical Hypoparathyroidism. Cory Wilczynski, MD[1]; Pauline Camacho, MD, FACE[1]. [1]Department of Endocrinology & Metabolism, Loyola University Medical Center, Maywood, Il 60157.

Introduction: Subclinical hypoparathyroidism is rare and even more if not caused surgically. The causes for hypoparathyroidism are similar to other endocrine disorder surgical, autoimmune, genetic and infiltrative. Familial hypoparathyroidism can be seen in cases of polygandular autoimmune syndrome type 1 which consists of hypoparathyroidism, chronic mucocutaneous candidiasis and adrenal insufficiency. In subclinical cases where patients have normal calcium but PTH is decreased there is thought to be increased risk of hypocalcemia after bisphosphonate therapy but not much is known about the disease genetics. Here we present three cases of subclinical hypoparathyroidism that occurred in a mother, daughter, and son. Their history, presentation, and laboratory evaluation that eventually led to their diagnosis will be discussed.

Case Description: Case 1 is a 51 year-old female was initially evaluated in endocrine clinic for history of multiple metatarsal fractures, manubrium fracture, and hypercalcuria. Dual-energy x-ray absorptiometry (DXA) one year prior was had T scores of −1.7 at the lumbar spine, 0.4 at the femoral neck, and −1.4 at the hip. Her past medical history included hypothyroidism and polycystic ovarian syndrome. Family history was significant for a mother with osteoporosis and daughter with

history of multiple fractures (case 2). Laboratory values on initial evaluation showed elevated urinary calcium of 366 mg/24 hr, serum calcium of 9.6 mg/dL, serum phosphorus of 3.8 mg/dL vitamin D 25-OH total of 72 and intact parathyroid hormone (PTH) of 3 pg/mL. After three months of treatment with hydrochlorothiazide, 24 hr urinary calcium was reduced to 275 mg/24 hr and her PTH normalized to 13 pg/ml.

Case 2 involves the 22 year old daughter of the subject in case1. Her history included numerous fractures starting two years prior to presentation. She fractured her wrist falling off a bike, 4 metacarpals after catching a football, and a metatarsal fracture. All fractures were low-trauma. During her work up, patient sustained another fracture to her left foot after a fall. She was started on teriparatide for one month but stopped because did not like injections. Laboratory evaluation revealed a normal urinary calcium of 117 mg/24 hr, serum calcium 9.4 mg/dL, vitamin D 25-OH of 23, serum phosphorus 3.8 mg/dL and intact PTH that was initially normal at 13 pg/mL but had decreased when rechecked 10 months later to 9 pg/mL. Z scores on her DXA were −1.7 at the lumbar spine, and −0.7 at the femoral neck.

Case 3 is a 22 year old male who is the son of the subject in case 1 and fraternal twin of subject in case 2. He did not present with any fracture history but rather was seen for right foot pain. His laboratory values included a serum calcium of 9.6 mg/dL, phosphorus of 3.2 mg/dL, vitamin D 25OH of 42, bone specific alkaline phosphatase of 14.8 ug/L and intact PTH of 9 pg/ml. DXA showed a normal bone mineral density with Z score of 0.5 in lumbar spine and 0.4 at the femoral neck. .

Discussion: This is a case of three family members with hypoparathyroidism. Two of the three subjects had suffered fractures. The treatment for overt hypoparathyroidism with the deficient hormone is still not approved. Treatment is symptomatic control with calcium and calcitriol. Even less is known about the usefulness for treatment of subclinical hypoparathyroidism. In this article, we discussed three family members with evidence of hypoparathyroidism and two with potentially symptomatic side effects of their disease which included fractures. The genetics and heritability of hypoparathyroidism outside of an autoimmune polyglandular syndrome needs to further investigation. Further research into the potential benefits and risks of treatment with hormone replacement is also required as that has potential to reduce hypercalcuria that was seen in case 1.

WG2

Familial Intermittent Hypercalcemia, Hypercalcuria with elevated Calcitriol, low PTH, Chronic Nephrolithiasis and Osteopenia. Derek T O'Keeffe MD PhD[1,2], Peter J Tebben MD[1,2], Rajiv Kumar MD.,[1,3] Ravinder J Singh PhD[4], Robert A. Wermers, M.D.[1,2]. [1]Department of Internal Medicine, [2]Division of Endocrinology, Diabetes, Nutrition, and Metabolism, [3]Division of Nephrology and Hypertension and [4]Department of Laboratory Medicine and Pathology, Mayo College of Medicine, Mayo Clinic, Rochester, Minnesota, USA.

Introduction:

Familial syndromes of non-PTH mediated intermittent hypercalcemia associated with hypercalcuria and elevated 1,25-dihydroxyvitamin D are rarely encountered and likely, the underlying cause often is unrecognized.

Case:

A 60 year old man presented with a history of intermittent hypercalcemia, low PTH, hypercalciuria, elevated 1,25-dihyroxyvitamin D and normal 25-hydroxyvitamin D. He also has had nephrolithiasis (>40yrs) requiring several urological interventions and ultimately causing urethral strictures. He reported two previous fractures: right clavicle, age four, after falling out of a tree and left wrist, age 14, after pole vaulting. A bone mineral density showed osteopenia with a femoral neck T-score = −1.6. His physical exam was unremarkable with a height of 178.8 cm, weight of 87.8 kg, BMI of 27.49 and blood pressure of 90/55 mmHg.

He had a significant family history (six siblings) with the same clinical picture (chronic urinary calculi, hypercalcemia, hypercalciuria, and low PTH). He denied any use of medications associated with hypercalcemia. He denied calcium or Vitamin D supplements. A chest radiograph showed a calcified aorta, but no evidence of any granulomatous disease or tumour burden.

His laboratory evaluation revealed a serum calcium = 10.6 (8.9–10.1 mg/dl), PTH = 14 (15–65 pg/ml), serum phosphorous = 3.5 (2.5–4.5 mg/dl), serum albumin = 4.3 (3.5–5 g/dl), 25-hydroxyvitamin D = 69 (20–80 ng/mL). 1,25-dihydroxyvitamin D = 70 (18–64 pg/mL), serum creatinine = 1.5 (0.8–1.3 mg/dl), eGFR 48 (>60 ml/min/BSA), serum magnesium = 1.9 (1.7–2.3 mg/dl). His CBC, electrolytes, ACE, TSH, UA and SPEP were all normal. A 24 h urine calcium was 207 (25–300 mg/spec) in the context of a diet restricted in dietary calcium intake. A urinary calculi analysis was 50% calcium phosphate (apatite), 30% calcium oxalate monohydrate, 20% calcium oxalate dihydrate.

Given his family history, a 24,25-dihydroxyvitamin D level was performed by the Mayo Medical Laboratory and was 0.15 ng/mL (based the 25-hydroxyvitamin D, expected value 4–10 ng/ml). Repeat testing confirmed this result, consistent with the inability to convert 25-dihydroxyvitamin D to 24,25-dihydroxyvitamin D due to a CYP24A1 mutation.

Conclusion:

Familial P450 (24-hydroxylase) enzyme abnormality (CYP24A1 mutation) is a rare cause of familial 1,25-dihydroxyvitamin D mediated hypercalcemia due to the reduced ability to convert 1,25 dihydroxyvitamin D to 1,24,25-trihydroxyvitamin D. It is important to recognize this entity through the measurement of 24,25-dihyroxyvitamin D, and initiate appropriate treatment measures including dietary calcium and oxalate restriction, high fluid intake, and possibly use of medications such as ketoconazole.

WG3

The Primacy of Parathyroid Hormone over Fibroblast Growth Factor 23 in Renal Phosphorus Handling. MJ McKenna[1,2], M Morrin[1], M Sloman[3], K Guegan[3], M O'Keane[1], M Kilbane[1]. [1]Metabolism Laboratory, and [2]Department of Endocrinology, St. Vincent's University Hospital, Dublin, Ireland; and [3]Molecular Genetics Laboratory, Royal Devon & Exeter NHS Foundation Trust, Exeter, UK.

Context The principal determinant of serum phosphorus is the tubular maximum reabsorption of phosphorus (TmP/GFR). This is mainly regulated by parathyroid hormone (PTH), ionized calcium, renal function, and fibroblast growth factor 23 (FGF23); all four factors are associated with lowering the (TmP/GFR). Animal studies suggest a dominant effect of PTH compared to FGF23 on renal phosphorus handling. Renal phosphorus wasting due to excessive FGF23 is seen in rare conditions such as X-linked hypophosphatemia (XLH) and tumour-induced osteomalacia (TIO). We have recently reported that total parathyroidectomy in a case of XLH ameliorated renal phosphorus wasting despite a very high FGF23 level. There are two reports of similar findings in two adults with TIO. We sought to explore the relative roles of PTH and FGF23 on renal handling of phosphorus in clinical cases.

Participants Three groups attending an endocrine bone clinic were studied: group 1, patients with FGF23-mediated hypophosphatemia (n=16); group 2, patients with bone and mineral disorders (n=37); group 3, patients with XLH and hypoparathyroidism post total parathyroidectomy (n=2) and a patient with hypophosphatemic bone disease due to congenital renal tubular acidosis.

Outcomes We measured FGF23, PTH, renal phosphate threshold (TmP/GFR), ionised calcium, 25-hydroxyvitamin D (25OHD) and a panel of bone turnover markers in all patients, as well as genetic mutation analysis in patients with congenital hypophosphatemia.

Results In group 1, *PHEX* sequencing diagnosed XLH in 12 patients, 1 patient had autosomal dominant hypophosphatemic rickets (ADHR) secondary to a mutation in *FGF23*, 1 patient had no mutation currently known to cause congenital hypophosphatemia, and 2 patients had TIO. In the combined groups 1 and 2, following partial correlation analysis, there was a significant association between TmP/GFR and PTH (r=−0.369, p=0.008) and with FGF23 (r=−0.463, p=0.001). After adjusting for disease category, there was a significant correlation between TmP/GFR and PTH (r=−0.357, p=0.001). In the patients with congenital hypophosphatemia, FGF23 levels were within the reference range (<100 RU/ml) in 5 of 14 patients. In those with elevated levels, they ranged from 115 RU/mL to 525 RU/mL, with the highest result in a 62 year old man who had a mildly elevated creatinine at 108 μmol/ml with an estimated glomerular filtration rate (eGFR) of 63 ml/min. The two cases of TIO had persistently elevated FGF23 levels but were different in terms of severity. The more severe case with persistent Looser zones had a TmP/GFR of 0.27 mmol/L and an FGF23 of 934 RU/mL; the other case had a TmP/GFR of 0.54 mmol/L and an FGF23 of 134 RU/mL. The two patients with XLH, who were rendered hypoparathyroid after surgery, had undetectable PTH levels; TmP/GFR were within the normal reference range at 0.88 mmol/L and at 0.92 mmol/L despite extremely high FGF23 levels at 13,030 RU/mL and 4,310 RU/mL, respectively. Serum creatinine levels were elevated at 157 μmol/L and 191 μmol/L giving eGFR of 37 ml/min and 29 ml/min, respectively. The third member of group 3, who had renal tubular acidosis and nephrocalcinosis, presented with waddling gait and bilateral femur shaft looser zones. His TmP/GFR was low at 0.66 mmol/L, and FGF23 was the lowest recorded at 27 RU/mL.

Conclusions While FGF23 is a determinant of TmP/GFR in congenital and acquired disorders of dysregulated FGF23 production, it would appear that the dominant regulator of renal phosphorus handling is PTH and that the FGF23 effect on TmP/GFR is dependent on PTH secretion. We conclude that the primacy of PTH over FGF23 in renal phosphorus handling is evident in both clinical cases and animal studies.

WG4

Drug Induced Fanconi's syndrome and Metabolic Bone Disease (Hypophosphatemic Osteomalacia) due to nucleotide reverse transcriptase inhibitors: Need for increased physician awareness, prospective surveillance and prompt therapy. M Honasoge, L Reddy, T Kamala, SS Srikanta. (Henry Ford Hospital Detroit, USA, and Jnana Sanjeevini Medical Centre and Diabetes Hospital, Bangalore, India).

Introduction: Hepatitis B viral infection has been successfully treated and long term viral remissions achieved over the past decade with the use of nucleotide reverse transcriptase inhibitors. Hypophosphatemic osteomalacia and Fanconi's syndrome due to renal tubular damage have been reported with the long term use of these drugs to maintain viral remission. Despite the Black Box warning, there appears to be a lack of awareness and surveillance and thus a delay in diagnosis.

Case Report: A 78 year old Asian male was evaluated in the endocrine clinic for progressive right hip pain, weakness, poor balance and weight loss over 8 months. X-ray and CT scan of pelvis were normal. MRI of the pelvis showed an undisplaced [spontaneous] subcapital fracture of the right femur. Past medical history included: ulcerative colitis (quiescent on mesacol), and hepatitis B on long term antiviral therapy with Adefovir (2005 - current), previous attempt to stop Adefovir was associated with viral relapse. Metabolic investigations: Hypophosphatemia [2.2 mg/dl (2.5–4.8)], hypouricemia [1.4 mg/dl (3.5–7.2)], normokalemia [4.1 meq/l (3.5–5.5)], elevated alkaline phosphatase [191 u/l(53–128)], normocalcemia [9.34 mg/dl (8.8–

10.6)], normal iPTH [22 pg/ml(15–68)], Serum 25(OH) vitamin D [28 ng/ml(30–199)], proteinuria [1.4 G/24 h] with aminoaciduria; HCO3 21.4 mmol/L, S creatinine 1.44 mg/dl (0.6–1.1), eGFR 49 ml/min. Bone markers: C.Telopetide [814 pg/ml(<854)], P1NP [147 ng/ml (14–86)], bone alkaline phosphatase [33 ug/L(6–30)], osteocalcin [3.1 ng/ml (upto 30)] and urine DPD/creatinine ratio [6.28 nmol DPD/nmolCr (2.3–5.4)]. BMD (T-score): Osteopenia left femoral neck (−2.3), left total hip (−1.6) and severe osteoporosis right femoral neck (− 4.1); and right total hip (−3.4), normal lumbar spine (L1 – L4: −0.6) and forearm (Ultra distal: −0.8). Dotonac PET CT (for oncogenous osteomalacia): normal; Isotope bone scan: Increased technetium uptake in right femoral neck, bilateral femoral heads, sacroiliac joints, scapulae and ribs. Management: Adefovir has been withdrawn (HBV DNA undetectable; LFT normal), and oral phosphate, 1-25(OH) vitamin D and calcium supplementation started.

Conclusion: Increased physician awareness, prospective surveillance for renal tubular dysfunction and prompt therapy for drug induced proximal renal tubulopathy and resultant metabolic bone disease are crucial in patients on long term therapy with nucleotide reverse transcriptase inhibitors group of drugs [Reported prevalence of hypophosphatemia and osteomalacia being about 35% and 12%, respectively – Adefovir], with ethnic [Asians] predisposition. Annualized prevalence of renal tubular dysfuction was 15% in a US population over 9 years with age as the main predisposing factor. The reports that newer agents such as entecavir are less prone to cause mitochondrial toxicity including renal tubular dysfucntion needs to be confirmed.

WG5

Restoration of Bone Remodeling with Teriparatide in a Patient with Severely Suppressed Bone Turnover. R. Mills[1], J.E. Brunner[2], S. Qiu[1], S. Palnikar[1], S.D. Rao[1]. [1]Division of Endocrinology, Diabetes, Bone & Mineral Disorders; Henry Ford Health System Detroit, MI. [2]Endocrinology and Diabetes Care Center; Toledo, Ohio.

Background: Severely suppressed bone turnover (SSBT) is a state in which bone mechanical property/mineral density relationships are compromised resulting in unusual fractures. Although SSBT was originally described in bisphosphonate treated patients, it shares many features of adynamic bone disease in dialysis patients and age related low-turnover osteoporosis; differing only in the degree of suppression. Bone biopsy is essential to establish SSBT. To our knowledge there are no reports describing restoration of normal bone turnover after teriparatide therapy in patients with SSBT.

Case report: A 60 year old white woman with osteoporosis and multifactorial SSBT developed multiple fractures (bi-malleolar, distal femur, intertrochanteric) over one year. Serum PTH (22 pg/mL; normal 10–75) and 25-hydroxyvitamin D levels (80 ng/mL; normal >20) were normal with mild hypercalcemia (1.37 mmol/L; normal 1–1.35). In vivo double tetracycline labeled bone biopsy established the diagnosis of SSBT. Patient was treated with teriparatide for 2 years and a repeat bone biopsy showed complete resolution of SSBT with restoration of normal bone remodeling. Relevant bone histomorphometric data are in the Table.

Measurement	Pre-Rx	Post-Rx	Ref. Mean
Cortical Bone Volume (% TV)	86.90	92.70	93.80
Cortical Thickness (mm)	0.84	0.45	1.22
Trabecular Bone Volume (% TV)	8.90	12.20	20.40
Trabecular Thickness (μm)	61.70	114.00	135.00
Osteoid Surface (% BS)	0.00	6.35	20.60
Osteoid Width (μm)	0.00	10.89	8.48
Osteoid Volume (% BV)	0.00	0.96	5.95
Osteoblast Surface (% OS)	0.00	10.67	2.63
Eroded Surface (% BS)	0.16	0.41	7.65
Osteoclast Surface (% NOS)	0.00	0.06	1.27
Mineralizing Surface (%BS)	0.00	0.60	7.66
Mineral Appositional Rate (MAR) (μm/day)	0.00	0.34	0.53
Bone Formation Rate (Surface) (μ3/μ2/year)	0.00	0.59	15.30

Conclusion: The results of the bone biopsy demonstrate the benefit of teriparatide for SSBT. To the best of our knowledge this is the first case describing reversal of SSBT confirmed by bone biopsy. We extrapolate that the use of teriparatide would be of benefit in SSBT stemming from anti-resorptive medication use.

WG6

Arterial Dissection and Associated COL1A1 Sequence Variants in Adult Osteogenesis Imperfecta. Jay Shapiro, Kennedy Krieger Institute.

Osteogenesis Imperfecta (OI) is a systemic disorder in which mutations involving type I collagen occur in 90 % of individuals. Abnormalities of the mitral or aortic valves and aortic dilatation occur in adult OI. However, Involvement of central or peripheral vessels is not appreciated. **Purpose**: This report describes: a) internal carotid, vertebrobasilar, iliac and femoral circumflex artery dissections in five adults with OI types I and IV and, b) COL1A1 and COL1A2 sequence variants. **Results**:

Case 1: A 37 year old male type I OI experienced spontaneous dissection of the distal right common iliac artery extending into the right external iliac artery with focal dissection of the left common iliac artery. Case 2: A 35 year old male, type I OI, acutely developed facial tingling. CT angiogram revealed a spontaneous right carotid artery dissection and previous bilateral focal dissections within the origins of the common iliac arteries Case 3: A 54 year-old woman, type IV OI, developed numbness of her left arm and two days later, awoke with a sharp frontal/occipital headache. CT angiogram of the head and neck demonstrated dissection of the right internal carotid artery starting at the C-1 level with mural thrombus and significant stenosis of the true lumen. Case 4: A 30 year-old woman, type I OI presented with 4 weeks of sub-acute left-sided headache, left arm weakness, dysphagia, and voice change. MRI showed marked attenuation of the internal carotid artery with bulbus ectatic dilatation distal to the left carotid artery bifurcation. There was long segment dissection involving the left vertebral artery extending from the proximal V-1 segment to V-3 junction. Case 5: A 58 year old female with type IV OI hospitalized and heparinized for DVT, experienced spontaneous dissection of the left medial femoral circumflex artery and a decrease in hemoglobin to 2.8 mg. In these patients different COL1 sequence variants were found. Case # 1: c.544-1G>T: #2: c.1405C>T, p. (Arg469*);#3: c.3505G>A, p.(Gly1169Ser): #4: c.4327_4333delinsCTGGA p.(Ala1443Leufs*107). In 3 previously reported cases of arterial dissection the following COL1 mutations occurred: Mayer, 1996; c.572G>C, p.Gly191Ala: Matouk, 2011c.3532G>A: and Kaliaperumal, 2011; *c. 3532-2A>G*. **Conclusions:** Adult OI may be associated with spontaneous vascular dissection. Arterial dissection may involve both type I collagen and other matrix proteins as yet undefined, 2) Life threatening arterial dissection in adult OI is underreported.

WG7

A Case Report: A Patient With Extensive Osseous Sarcoidosis ("Holes in Her Bones"). E Cong and SJ Silverberg. Division of Endocrinology, Columbia University Medical Center, New York, NY.

Sarcoidosis, a multi-system inflammatory disorder, affects the bones in about 3-13% of patients. Osseous sarcoidosis is usually localized to the hands and feet with preservation of the cortical borders of the bone. While generally asymptomatic and not progressive, rarely osseous sarcoid lesions may be found in other locations including the vertebra and may be progressively destructive, thereby causing fractures. There are currently no evidence based guidelines with regards to treatment for osseous sarcoidosis, and case reports illustrate that it responds poorly to corticosteroids as well as to other drugs used in treating the illness. We report a case of a patient with extensive osseous sarcoidosis.

A 49 year old premenopausal Hispanic female with no past medical history presented to Columbia University Medical Center with dyspnea on exertion, dry cough, progressive dysphagia and bone pain. On CT scan, she was found to have numerous lesions involving the lungs, liver, lymph nodes and bones. An extensive workup was negative for infectious and malignant etiologies. Biopsy of a mediastinal lymph node and left iliac crest lesion revealed non-caseating granulomas consistent with sarcoid. ACE level was 14 U/L [9–67]. Prednisone was begun at 50 mg/day with a prolonged taper, along with calcium and vitamin D supplementation. All symptoms resolved including her bony pain. Imaging at three months showed improvement in the pulmonary nodules, but skeletal lesions were unchanged.

She was referred to the endocrinology clinic for management of her bone disease, which involved the left occiput, right humeral head, left scapula, bilateral clavicles, multiple ribs, spine at L5, T4, T10, T12, right sacral hila, and bilateral ileum, acetabulum and proximal femur. Hand X-rays were negative for lytic lesions. No fractures were seen. Laboratory evaluation included: calcium 8.8 mg/dl [8.7–10.2], ionized calcium 1.23 mmol/L [1.12–1.32], phosphorous 3.6 mg/dl [2.5–4.3], parathyroid hormone 42 pg/ml [8–51], 25-hydroxyvitamin D <13 ng/ml [30–80], 1,25-dihydroxyvitamin D 29 pg/ml [15–75], alkaline phosphatase 30 U/L [33–96], GFR >60 mL/min/1.73 m², 24 hour urine calcium 37 mg/24 hrs [150–300]. Bone turnover markers included a serum c-telopeptide level of 345 pg/ml [premenopausal range: 40–465], osteocalcin 19 ng/ml [11–50], procollagen type-I peptipde 35 ug/L [20–200], bone-specific alkaline phosphatase 4.6 ug/L [4.5–16.9]. BMD by DXA at the lumbar spine, femoral neck, total hip, and 1/3 left forearm was normal [T-score: LS 0.9, FN 0.2, TH 0.5, RAD 1.4]. VFA did not show vertebral compression. HRpQCT of the left distal tibia and radius showed very low cortical density at the distal tibia (T-Score -3.7). Total density was preserved due to high trabecular density. Cortical porosity measurement is pending. Skeletal survey confirmed the lesions seen on CT without fracture. Bone scan showed multiple radiotracer avid lesions including those corresponding to her left femur lesions.

In summary, this patient with extensive osseous sarcoidosis had normal DXA BMD but markedly low cortical BMD at a weight bearing site. Steroid treatment did not improve her bony lesions, although it improved her pain. Bone turnover activity was not very elevated despite widespread high avidity lesions on bone scan, including several at sites at high risk for fracture. Previous reports suggest that patients with osseous sarcoidosis have high fracture risk even in the setting of normal BMD. She is also at risk for progressive bone loss due to incipient menopause and ongoing steroid therapy. Once she is vitamin-D replete we will consider osteoporosis therapy, and monitor for any changes in her osseous lesions.

WG8

Osteosarcoma in a patient with pseudohypoparathyroidism type 1b due to paternal uniparental disomy of chromosome 20q. Yumie Rhee*, MD, PhD, Chang Gon Kim, MD, Su Jin Lee, MD, Jo Eun Kim, MD. Department of Internal Medicine, Yonsei University College of Medicine, Seoul, Korea.

Pseudohypoparathyroidism type 1b (PHP1b) is the result of end-organ resistance to parathyroid hormone (PTH) in the absence of any features of Albright' osteodystrophy. The function of the Gs protein is solely controlled by maternally originated Gs specifically in the renal proximal tubules, thus its loss or imprinting error in the maternal GNAS give rise to impaired PTH action, resulting in reduced 1,25-OH vitamin D synthesis, increased phosphate excretion, and hypocalcemia. As PTH responsiveness is intact in the bone and parathyroid glands, theoretically it can lead to overt hyperparathyroid bone disease due to chronically elevated PTH levels, which may be exacerbated by low 1,25-OH vitamin D levels.

A 21-year-old Korean male, presenting with gum swelling at the right mandible, was referred to the Department of Oncology with the impression of sarcoma-like lesion by the tissue biopsy. Curative surgical resection by segmental mandibulectomy was performed followed by reconstruction with fibular flap of left leg. A 2.5X5.0X3.0 cm white infiltrating mass showed anaplastic and pleomorphic spindle-cells with myxoid stroma and osteoid formation fulfilling the histological criteria of conventional osteoblastic osteosarcoma.

To further investigate the reason for the low calcium level (6.1 mg/dL; normal 8.5~10.5 mg/dL) and high phosphorus level (6.3 mg/dL; normal 2.5~4.2 mg/dL), consultation to us was done. Elevated intact PTH level (250 pg/mL; normal, 15~65 pg/mL) with low 1,25-OH vitamin D level (9.7 pg/mL; normal 19.6~54.3 pg/mL) reflected the failure of target tissues to respond appropriately to the biological actions of PTH on the proximal renal tubule. Bone mineral density showed osteopenia at the lumbar spine. Additionally, thyroid function test revealed TSH resistance (Free T4 level 1.24 ng/dL; normal 0.70~1.48 ng/dL, TSH 9.61 μIU/mL; normal 0.35~4.94 μIU/mL). He revealed no specific past history except somewhat short stature (165 cm, 2.0 SD below the mean for age) with normal mentation and without any shortening of fingers. With the impression of PHP1b, conventional sequencing for GNAS was performed but with no genetic mutation identified within exon 1–13 and exon-intron boundaries. Therefore, multiplex ligation-dependent probe amplification (MLPA) for analysis was pursued revealing hypermethylation at NESP 55 and hypomethylation at GNAS A/B and XL suggesting loss of maternal methylation pattern. In a uniparental disomy (UPD) analysis using microsatellite markers on chromosome 20 (D20S117, D20S889, D20S115, D20S112, D20S107, D20S178, D20S196, D20S100, D20S496, D20S459, D20S173), there was no maternal alleles inherited at markers (D20S196 and D20S100 which represent 20q13.13 and 20q13.2) flanking the GNAS locus. Generally, most patients with sporadic PHP-1b are known to have deletions in the multiple differentially methylated regions (DMRs) of the GNAS. Rarely, paternal UPD of chromosome 20 (patUPD 20) causing PHP 1b had been reported in 8 patients up to now including this case.

In this condition, as the skeletal PTH responsiveness is untouched or even elevated, persistent stimulation of PTH on osteoblasts results in elevated bone remodeling. In preclinical rat model treated with high dose of recombinant PTH (1–34) for nearly entire life span, osteosarcoma had occurred. There were three patients having previous hyperparathyroidism out of 1234 patients with osteosarcoma investigated in the M.D. Anderson Cancer Center. Here we report an adolescence patient with osteoblastic osteosarcoma and PHP1b where the PTH resistance on renal proximal tubule with over-responsive PTH to skeleton might have incurred a bone tumor.

WG9

Transient Osteoporosis of the Hip Associated with Alcohol Consumption. K. Asadipooya, L Graves. University of Kansas Medical Center, Kansas City KS.

Background: Transient Osteoporosis of the Hip (TOH) is a condition of acute bone marrow edema of the hip without obvious cause. It is a transient clinical condition of unknown etiology and mechanism that typically affects women, especially in the last trimester of pregnancy, as well as middle-aged men. It has been represented in the literature as Bone Marrow Edema syndrome (BMES), Regional Migratory Osteoporosis (ROM) and Reflex Sympathetic Dystrophy (RSD). We present a case in which the onset and recurrence of symptoms appeared related to increased alcohol consumption.

Case Report: A 59-year-old male presented with acute right hip discomfort and limping. There was no precedent trauma and no history of underlying arthritic condition. The pain was aggravated by standing and walking and relieved by supine position with hip flexion. On physical examination he had mild limitation of motion of the right hip but no tenderness in Log Roll, FABER and FADIR test. His typical alcohol consumption was 6 units per week. Four weeks prior to the onset of pain he had increased this to 24 units per week. Following the onset of pain he reduced his alcohol consumption. Pain subsequently improved but then returned again following 1–2 days of increased alcohol. This pattern repeated itself again 1–2 weeks later. Evaluation revealed a normal general chemistry panel, complete blood count, TSH, and 25-OH vitamin D. MRI revealed extensive bone marrow edema in the right femoral head and neck, with the diagnosis being transient bone marrow edema or early avascular necrosis of the right hip. DXA of the spine and hip were normal. In consultation with his orthopedic surgeon, protected weight bearing activity using crutches for walking was recommended. Following 8 weeks of reduced weight bearing, and reduce alcohol intake, the pain resolved and with no further limp. A repeat MRI revealed no femoral head collapse, persistent but improved edema with no fracture lines present, most consistent with TOH.

Discussion: Patients with TOH or bone marrow edema syndrome involving other sites may present with a wide range of clinical and radiological manifestations, and some likely never seek medical assistance. *Lakhanpal* et al. reported 56 patients (33 men and 23 women) with transient regional osteoporosis who presented with monoarticular or oligoarticular joint pain aggravated by weight bearing. Eighteen (32%) of the patients had pain at rest and six (10%) had nocturnal pain. The joints of lower extremities were more commonly involved and hip was the most commonly affected joint. Smoking appeared to be a potential risk factor. Biopsy of the affected area has revealed edema and reactive bone formation in the marrow, high bone turnover and absence of fat necrosis, suggesting vasomotor response as opposed to osteonecrosis. The prognosis of BMES is usually good and it has a benign and self-limiting course.. The relationship to alcohol suggested by this presentation was similarly suggested in 2 of 22 patients with BMES reported by *Karantanas et al*, 2008. Though alcohol has multiple potential effects on bone formation and resorption a clear mechanism to BMES is unclear.

Conclusion: TOH or other BMES should be considered in the diagnosis of acute bone pain with findings of edema by MRI. The differential diagnosis should include ischemic injury (avascular necrosis of femoral head), infection (septic arthritis and osteomyelitis), neoplastic diseases, trauma (stress fracture), inflammatory diseases, degenerative process, metabolic diseases and neurological disorders.